FIFTH EDITION

Jatin Shah's

HEAD AND NECK SURGERY AND ONCOLOGY

JATIN SHAH | SNEHAL PATEL | BHUVANESH SINGH | RICHARD WONG

ELSEVIER

JATIN SHAH'S

HEAD AND NECK

SURGERY AND ONCOLOGY

FIFTH EDITION

Jatin Shah's HEAD AND NECK SURGERY AND ONCOLOGY

Jatin P. Shah, MD, PhD (Hon), DSc (Hon), FACS, FRCS (Hon), FDSRCS (Hon), FRCSDS (Hon), FRCSI (Hon), FRACS (Hon)
E.W. Strong Chair in Head and Neck Oncology
Memorial Sloan Kettering Cancer Center
Professor of Surgery
Weill Cornell College of Medicine
New York, NY
USA

Snehal G. Patel, MD, MS (Surg), FRCS (Glasg)
Attending Surgeon, Head and Neck Service
Memorial Sloan Kettering Cancer Center
Professor of Otolaryngology
Weill Cornell College of Medicine
New York, NY
USA

Bhuvanesh Singh, MD, PhD, FACS
Attending Surgeon, Head and Neck Service
Director, Laboratory of Epithelial Cancer Biology
Memorial Sloan Kettering Cancer Center
Professor of Otolaryngology
Weill Cornell College of Medicine
New York, NY
USA

Richard J. Wong, MD, FACS
Chief, Head and Neck Service
Memorial Sloan Kettering Cancer Center
Professor of Otolaryngology
Weill Cornell College of Medicine
New York, NY
USA

For additional online content visit ExpertConsult.com
ELSEVIER
Edinburgh London New York Oxford Philadelphia St Louis Sydney 2020

JATIN SHAH'S HEAD AND NECK SURGERY AND ONCOLOGY, FIFTH EDITION

First Edition 1990
Second Edition 1996
Third Edition 2003
Fourth Edition 2012
Fifth Edition 2020

Library of Congress Control Number: 2019934874

ISBN: 978-0-323-41518-7

eBook ISBN: 978-0-323-41789-1
Inkling ISBN: 978-0-323-41790-7

Content Strategist: Belinda Kuhn
Content Development Specialist: Nani Clansey
Project Manager: Louisa Talbott
Design: Patrick C. Ferguson
Illustration Manager: Teresa McBryan
Illustrator (Front Cover): Christine Amstrong
Marketing Manager: Claire McKenzie

Printed in China

Last digit is the print number: 9 8 7 6 5 4 3 2 1

ELSEVIER

Contents

Preface

The stimulus for the senior author to write a book on head and neck surgery came from Prof. Arnold Maran, of Scotland, at an advanced course in head and neck surgery in Singapore in 1982. This led to the publication of the first edition of the book on operative surgery in two volumes in 1987 and 1990. The surgical techniques described in the first edition were the culmination of the influence of my surgical mentors in general surgery, Drs. Manubhai Patel and A.B. Kothari from Baroda, India, and in head and neck surgery, Drs. H. Randall Tollefsen, Hollon Farr, and Elliott Strong, from Memorial Hospital in New York. Subsequent editions of the book included diagnostic workup, perioperative care, radiology, pathology, adjuvant therapies such as radiation and chemotherapy, systemic therapy algorithms on selection of therapy, and finally outcomes of treatment. The book had a global influence in head and neck surgery as exemplified by its demand for multiple language translations. Over the years, the book has been translated and published in Portuguese, Spanish, Chinese, Greek, Russian, and Polish. We anticipate that this edition will also be available for translation into other languages. From a single author book for the first two editions, the book has been enriched with the addition of Drs. Snehal Patel, Bhuvanesh Singh, and Richard Wong as authors and editors in subsequent editions. The book has maintained its leadership position in the head and neck literature for over 30 years with three major book awards.

The fifth edition of this book continues to build its strength on the previous four editions and reflects the shifting paradigms in the understanding of the etiology and biological behavior of head and neck cancers and its contemporary management. Advancing knowledge as a result of new discoveries in basic sciences and advances in technology has led to better understanding of the natural history of these tumors. Thus a new edition becomes necessary to incorporate new information and changes to the practice patterns of the past. This edition has numerous new illustrations, data, therapeutic algorithms, and shifting paradigms in the management of several tumors. As with the previous editions, the mainstay of the book is based on description of diagnostic approaches, therapeutic decisions, surgical techniques, and results of treatment. However, there is a significant expansion on the discussion of selection of therapy and the rationale behind that. In addition, principles of radiation oncology, systemic therapy, maxillofacial prosthodontics, and dental oncology have been included. New to this edition are dedicated sections on nuances in pathology and diagnostic radiology, including three-dimensional imaging and computer-aided design/computer-aided manufacturing (CAD-CAM) technology in reconstruction. This edition also includes the newly published eighth edition of the staging system for head and neck cancer of the American Joint Committee on Cancer and the International Union Against Cancer. The diagnostic approaches, therapeutic decisions, and algorithmic thought process for selection of therapy presented in this edition are a culmination of the experience of a multidisciplinary Disease Management Team (DMT), working together for over 20 years, at Memorial Sloan Kettering Cancer Center in New York. These philosophies and management strategies currently practiced by our faculty have evolved as a consensus of the multidisciplinary group of specialists working together as members of a cohesive team. Most of the outcomes presented in this book are generated from databases of patients treated by the members of the Head and Neck Disease Management Team at Memorial Sloan Kettering Cancer Center, but the treatment paradigms and information presented are relevant worldwide. Where appropriate we have added outcomes data from other global sources with stronger datasets.

Management of tumors of the head and neck has evolved into an increasingly complex specialty, demanding expertise and exposure not only in various surgical disciplines, but also in allied specialties such as radiation oncology, medical oncology, immunology, endocrinology, nuclear medicine, diagnostic radiology, pathology, and maxillofacial prosthodontics. The primary goal of contemporary management of neoplasms of the head and neck has historically been in achieving an improvement in survival. In addition, however, increasing emphasis is being placed on optimizing quality of life and limiting the sequela of treatment in the selection of treatment approaches.

The past two decades have seen major paradigm shifts in the management of tumors of the oropharynx and thyroid, as well as larynx and pharynx. The role of HPV in the genesis and management of oropharynx cancers has led to the development of new treatment strategies to minimize sequelae of treatment. Increasingly conservative approaches are applied to thyroid cancer with risk group stratification and less radical surgery and restricted use of radioactive iodine. Increasing use of minimally invasive and endoscopic laser resections has replaced open surgical procedures for conservation of voice. Failures of nonsurgical larynx preservation approaches have opened up new challenges for the surgeon in salvage surgery, with the goal of minimizing complications and improving survival. The chapter on systemic therapy includes the pharmacology of currently used drugs and evidence-based treatment recommendations from randomized clinical trials of chemotherapy, chemoradiotherapy, targeted therapy, and immunotherapy. Availability of intensity-modulated radiation therapy (IMRT) and proton beam radiation has completely changed the spectrum of radiotherapy techniques and the short- and long-term sequelae of external radiation therapy. The increasing use of IMRT and proton beam therapy is emphasized, and fundamental principles of radiation oncology essential for the surgeon are enumerated in the chapter on radiation therapy.

Surgery for neoplasms at the cranial base has reached a state of maturity, and long-term outcomes of open craniofacial surgery

have remained stable over the past three decades. In the past two decades, however, there has been increasing use of endonasal endoscopic surgery for anterior skull base lesions. These techniques are included in the current edition, and its applications and limitations are defined. Widespread application of microvascular free tissue transfer, routinely practiced for over 25 years, has matured to the state of finesse where functional restoration and aesthetic considerations are now prioritized in reconstructive techniques. These are amply demonstrated with the utility of local, regional, and free flaps. Introduction of CAD-CAM technology to facilitate accurate bone reconstruction is included with examples of mandible and maxillary reconstruction. The aesthetic impact of ablative surgical procedures has been a matter of concern for a long time. Refinements in surgical techniques have minimized the aesthetic sequelae of ablative surgery, as demonstrated in several operative procedures.

Surgical techniques demonstrated here with sequential operative photographs of actual operations performed by our faculty have evolved over the years and are continuously refined. The operative photographs taken by the authors maintain the "surgeon's view" of the operative field. Where necessary, the operative photographs are supplemented with color artwork to demonstrate the anatomic relationships and enhance the technical details of a complex surgical field. The addition of Diagnostic Radiology and Pathology to each chapter complements the comprehensive coverage of each topic by presenting the selection of a particular imaging study and the salient histologic features of tumors.

It is impossible for a surgical book of this nature to remain "up to date" for a prolonged period. Undoubtedly, improved understanding of the molecular mechanisms of oncogenesis; introduction of new technology in the operating room; newer modalities of imaging; newer techniques of delivering ionizing radiation; and the introduction of new drugs for chemotherapy, targeted therapy, and immunotherapy will change management strategies in the future. New surgical procedures, developed as a result of new technology, will be introduced to challenge old and established operations. The focus will be to minimize surgical trauma, preserve form and function, and leave minimal impact from surgical intervention. Similarly, complex multidisciplinary nonsurgical treatment programs will be aimed at reduction of morbidity, acute toxicity, and long-term sequelae of therapy in the future. The contents of this edition, though, reflect the state of the art in head and neck oncology and the craft of head and neck surgery as practiced today. The book is primarily aimed at the young head and neck surgeon who has completed basic surgical training in otolaryngology, general surgery, plastic surgery, or maxillofacial surgery. This book may also be of use to practicing surgeons in the specialty of head and neck surgery and oncology to become familiar with the current philosophies in the surgical management of tumors of the head and neck and the role of multidisciplinary approaches to certain tumors with an emphasis on optimizing oncologic and functional outcomes.

Jatin P. Shah
Snehal G. Patel
Bhuvanesh Singh
Richard J. Wong

List of Contributors

Jay Boyle, MD, FACS
Attending Surgeon,
Head and Neck Service,
Memorial Sloan Kettering Cancer Center;
Professor of Surgery,
Weill Cornell College of Medicine,
New York, NY, USA

Klaus Busam, MD, PhD
Attending Pathologist,
Director of Dermatopathology,
Memorial Sloan Kettering Cancer Center;
Professor of Pathology and Laboratory Medicine,
Weill Cornell College of Medicine,
New York, NY, USA

Diane Carlson, MD
Director, Breast and Head & Neck Pathology,
Cleveland Clinic Florida,
Weston, FL, USA;
Affiliate Associate Professor,
Charles E. Schmidt College of Medicine,
Florida Atlantic University,
Boca Raton, FL, USA

Marc Cohen, MD, MPH
Associate Attending Surgeon,
Head and Neck Service,
Memorial Sloan Kettering Cancer Center;
Associate Professor,
Weill Cornell College of Medicine,
New York, NY, USA

Peter Cordeiro, MD, FACS
Attending Surgeon,
Plastic and Reconstructive Surgery Service,
Memorial Sloan Kettering Cancer Center;
Professor of Surgery,
Weill Cornell College of Medicine,
New York, NY, USA

Jennifer Cracchiolo, MD
Assistant Attending Surgeon,
Head and Neck Service,
Memorial Sloan Kettering Cancer Center;
Assistant Professor,
Weill Cornell College of Medicine,
New York, NY, USA

Joseph Dayan, MD
Assistant Attending Surgeon,
Plastic and Reconstructive Surgery Service,
Memorial Sloan Kettering Cancer Center;
Assistant Professor,
Weill Cornell College of Medicine,
New York, NY, USA

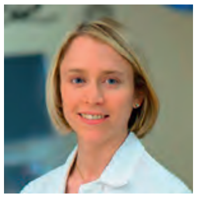

Jasmine Francis, MD, FACS
Assistant Attending Surgeon,
Ophthalmic Oncology Service,
Memorial Sloan Kettering Cancer Center;
Assistant Professor,
Weill Cornell College of Medicine,
New York, NY, USA

Ian Ganly, MD, PhD, MS, FRCS, FRCS-ORL
Associate Attending Surgeon,
Memorial Sloan Kettering Cancer Center;
Associate Professor of Otolaryngology,
Weill Cornell College of Medicine,
New York, NY, USA

Ronald Ghossein, MD
Attending Pathologist,
Director of Head and Neck Pathology,
Memorial Sloan Kettering Cancer Center;
New York, NY, USA

Alan Ho, MD, PhD
Assistant Attending Physician,
Head and Neck Oncology Service,
Memorial Sloan Kettering Cancer Center;
Instructor,
Weill Cornell College of Medicine,
New York, NY, USA

Joseph Huryn, D.D.S.
Chief, Dental Service,
Memorial Sloan Kettering Cancer Center;
Professor of Clinical Surgery (Oral and
Maxillofacial Surgery),
Weill Cornell College of Medicine,
New York, NY, USA

Nora Katabi, MD
Associate Attending Pathologist,
Memorial Sloan Kettering Cancer Center,
New York, NY, USA

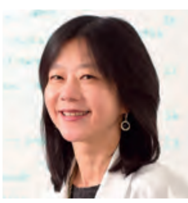

Nancy Lee, MD, FASTRO
Vice Chairman and Chief of Head and
Neck Radiation Oncology,
Director of Proton Therapy,
Memorial Sloan Kettering Cancer Center,
New York, NY, USA

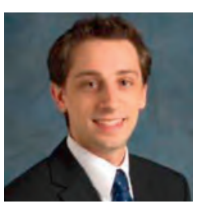

Jonathan Leeman MD
Instructor, Department of Radiation
Oncology,
Brigham and Women's Hospital;
Instructor, Department of Radiation
Oncology,
Dana Farber Cancer Institute,
Boston, MA, USA

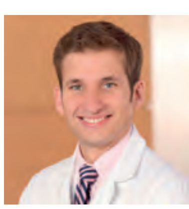

Sean McBride, MD, MPH
Assistant Attending Physician,
Department of Radiation Oncology,
Memorial Sloan Kettering Cancer Center,
New York, NY, USA

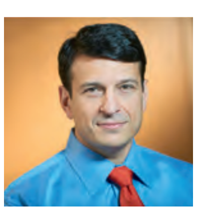

Babak Mehrara, MD
Chief,
Plastic and Reconstructive Surgery Service;
William G. Cahan Chair in Surgery,
Memorial Sloan Kettering Cancer Center;
Professor of Surgery,
Weill Cornell College of Medicine,
New York, NY, USA

Luc Morris, MD, MSc, FACS
Associate Attending Surgeon,
Head and Neck Service,
Catherine and Frederick Adler Chair for
Junior Faculty,
Memorial Sloan Kettering Cancer Center;
Associate Professor of Otolaryngology,
Weill Cornell College of Medicine,
New York, NY, USA

Kishwer Nehal, MD
Attending Physician,
Dermatology Service,
Memorial Sloan Kettering Cancer Center;
Professor of Dermatology,
Weill Cornell College of Medicine,
New York, NY, USA

Snehal G. Patel, MD, MS,
FRCS (Glasg)
Attending Surgeon,
Head and Neck Service,
Memorial Sloan Kettering Cancer Center;
Professor of Surgery,
Weill Cornell College of Medicine,
New York, NY, USA

David Pfister, MD, FACP, FASCO
Chief, Head and Neck Oncology, Solid
Tumor Service,
Deputy Physician in Chief/Partnerships,
Memorial Sloan Kettering Cancer Center;
Professor of Medicine,
Weill Cornell College of Medicine,
New York, NY, USA

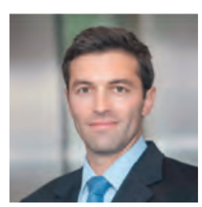

Benjamin Roman, MD, MSHP
Assistant Attending Surgeon,
Head and Neck Service,
Memorial Sloan Kettering Cancer Center;
Assistant Professor of Otolaryngology,
Weill Cornell College of Medicine,
New York, NY, USA

Evan Rosen, DMD, MPH
Assistant Attending Surgeon,
Dental Service,
Memorial Sloan Kettering Cancer Center;
Assistant Professor of Clinical Surgery
(Dentisty, Oral and Maxillofacial Surgery),
Weill Cornell College of Medicine,
New York, NY, USA

Jatin P. Shah, MD, PhD, FACS
E.W. Strong Chair in Head and Neck Surgery and Oncology,
Memorial Sloan Kettering Cancer Center;
Professor of Surgery,
Weill Cornell College of Medicine,
New York, NY, USA

Ashok Shaha, MD, FACS
Attending Surgeon,
Head and Neck Service,
Memorial Sloan Kettering Cancer Center;
Professor of Surgery,
Weill Cornell College of Medicine,
New York, NY, USA

Bhuvanesh Singh, MD, PhD, FACS
Attending Surgeon,
Head and Neck Service,
Director,
Laboratory of Epithelial Cancer Biology,
Memorial Sloan Kettering Cancer Center;
Professor of Otolaryngology,
Weill Cornell College of Medicine,
New York, NY, USA

Hilda E. Stambuk, MD
Attending Radiologist,
Clinical Head and Neck Imaging,
Memorial Sloan Kettering Cancer Center;
Professor of Radiology,
Weill Cornell College of Medicine,
New York, NY, USA

R. Michael Tuttle, MD
Clinical Director, Endocrinology Service,
Memorial Sloan Kettering Cancer Center;
Professor of Medicine,
Weill Cornell College of Medicine,
New York, NY, USA

Brian Untch, MD
Assistant Attending Surgeon,
Head and Neck and Gastric and Mixed Tumor Service,
Memorial Sloan Kettering Cancer Center,
New York, NY, USA

Richard J. Wong, MD
Chief, Head and Neck Service,
Memorial Sloan Kettering Cancer Center;
Professor of Otolaryngology,
Weill Cornell College of Medicine,
New York, NY, USA

Vivian Yin, MD, MPH
Assistant Attending Surgeon,
Ophthalmic Oncology Service,
Memorial Sloan Kettering Cancer Center;
Assistant Professor of Ophthalmology,
Weill Cornell College of Medicine,
New York, NY, USA

Acknowledgments

We are eternally grateful to our patients and their loved ones, who have suffered from and lived through the calamity of head and neck cancer and who have demonstrated exemplary courage and tenacity in the struggle to prolong life and preserve quality of life. These special human beings who joined hands with us in the dogged pursuit for a cure of their cancer and a better quality of life have a special place in our hearts and our lives. We salute them for their extraordinary courage, understanding, perseverance, and eternal hope for the conquest of cancer. We are also thankful to them for putting their lives in our hands, for giving us the opportunity to learn the natural history of this disease, and for inspiring us to strive for better methods of cancer control and quality of life, and reflect our views in writing this book.

We would like to express our sincere appreciation to our teachers, peers, and colleagues from whom we have learned and continue to learn. Every one of these individuals has contributed to our knowledge, understanding, and experience in head and neck surgery and oncology.

We would also like to acknowledge the work and support of all the contributors to various chapters in this book. Nearly all of them are members of the Head and Neck Disease Management Team at Memorial Sloan Kettering Cancer Center. Their valuable contributions form the core of this book.

Our sincere thanks to the trainees of the Head and Neck fellowship program, surgical oncology fellows, and residents in the Department of Surgery at Memorial Sloan Kettering Cancer Center who have contributed significantly to our experience and wisdom. Their thirst for knowledge of head and neck oncology and their desire to learn the craft of surgery are constant sources of inspiration.

We would like to express our appreciation to our editors on the Head and Neck Service, Jessica Massler and Raia Mohamed, and our data manager, Jocelyn Migliacci, for their invaluable assistance over the past few years; Christine Armstrong, who has consistently provided superb cover art for the current and previous editions of this book; and the Medical Graphics Department at Memorial Sloan Kettering Cancer Center for their timely help with artwork and photography.

Jatin P. Shah
Snehal G. Patel
Bhuvanesh Singh
Richard J. Wong

Dedicated to

Our Patients*, who have endured the suffering from cancer. These extraordinary individuals put their lives in our hands, in the quest for a life worth living. Their exemplary courage and resilience have taught us the meaning of perseverance and hope. They have a special place in our hearts.*

Our Trainees*, whose thirst for knowledge has been a constant source of inspiration and encouragement for us to remain at the forefront of our specialty.*

and

Our Families*, for their patience, understanding, and support, without which this work would not have been possible.*

CHAPTER 1

Introduction

Anatomically and histologically, the head and neck region is one of the most diverse and complex parts of the human body. This diversity gives rise to a myriad of neoplastic processes with diverse behaviors and outcomes. The combination of anatomic and functional intricacies combined with the neoplastic spectrum necessitates a basic understanding of cancer biology, in addition to a working knowledge of all therapeutic options for delivering optimal care to patients with head and neck neoplasms. Moreover, the head and neck surgeon must appreciate and optimize the anatomic (esthetic) and physiologic (functional) impact of treatment. The vast majority of head and neck neoplasms arise from the mucosa of the upper aerodigestive tract, including the oral cavity, pharynx, larynx, nasal cavity, and sinuses, but neoplasms also can originate from the salivary glands, thyroid and parathyroid glands, soft tissue, bone, and skin. The most common malignant neoplasms of the head and neck are squamous cell carcinoma and papillary thyroid carcinoma. Salivary gland cancers and sarcomas of the soft tissue and bone are relatively infrequent.

Surgery has been the mainstay of therapy for tumors in the head and neck for more than a century. With the introduction of ionizing radiation in the latter half of the 20th century, radiotherapy became an important modality used either independently or in combination with chemotherapy as primary treatment or as an adjuvant to surgery. Although initially chemotherapy was used primarily as palliative treatment, it is now used as a component of curative treatment approaches when combined with radiation, producing significant improvements in outcomes in patients with squamous cell carcinomas of the head and neck at certain sites. Similarly, biological or targeted agents also are evolving to become part of standard therapy. Immunotherapy also has a role in the treatment of head and neck cancers and is expected to play an increasing role in the future. Accordingly, understanding and implementing multidisciplinary management strategies are cornerstones for achieving optimal therapeutic outcomes.

ETIOLOGY

Most cancers result from a complex interplay between host and environmental factors. Environmental carcinogenic signals that promote the development of most human cancers remain ill-defined. In contrast, correlative studies have shown that alcohol and tobacco exposure are key causative factors for carcinomas of the mucosa of the upper aerodigestive tract. Head and neck cancers are typically tobacco-related cancers, with initial risk for the development of cancer and subsequent risk for additional primary cancers directly attributable to the duration and intensity of tobacco use. Similarly, the chronic consumption of alcohol is estimated to increase the risk for upper aerodigestive tract cancers by two-fold to three-fold in a dose-dependent manner. Moreover, persons who both smoke and consume alcohol regularly have a multiplicative increase in risk that is up to 10 to 20 times higher than that of nonsmokers/nondrinkers, as reflected by a geometric rise in the incidence with increasing use of tobacco and increasing consumption of alcohol (Fig. 1.1). It is now well established that human papilloma virus (HPV) is associated with the development of oropharyngeal carcinomas. Genetic predisposition to the development of head and neck cancers in patients with Fanconi anemia is thought to be related to HPV infection. Similarly, immune-compromised patients with human immunodeficiency virus infection and patients undergoing chronic immunosuppressive treatment after organ transplantation have an increased risk for the development of head and neck cancers. Several other factors also are known to play a role in the pathogenesis of tumors in the head and neck region. For example, exposure to ionizing radiation increases the risk for the development of primary malignant tumors of the thyroid gland and salivary glands as well as for cancers of the skin, soft tissues, and bone. Similarly, Epstein-Barr virus infection is thought to promote the development of nasopharyngeal cancer.

GLOBAL EPIDEMIOLOGY

Head and neck cancers form the sixth most common cancer type and cause for cancer-related deaths worldwide. Significant

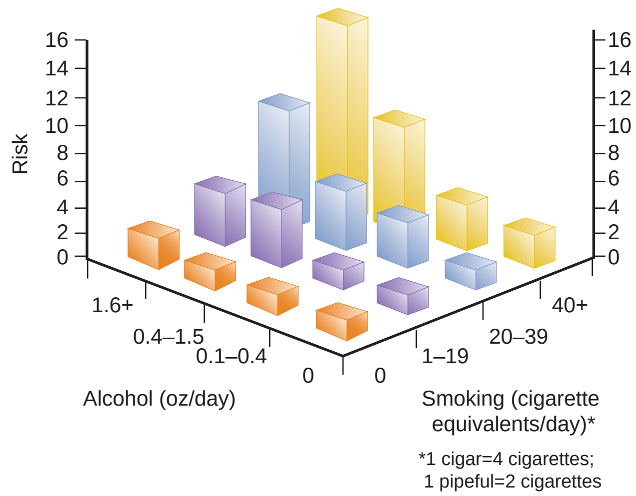

Figure 1.1 Risk of development of squamous cell carcinoma of the head and neck with alcohol and tobacco consumption.

geographic variation exists in the incidence of squamous cell carcinomas of the head and neck. The highest incidence of carcinomas of the oral cavity and hypopharynx are reported in Southeast Asia, and particularly in India, where chewing tobacco with betel quid ("paan") is a common practice. High rates of oral cancer are also reported in Brazil. The global incidence of squamous carcinomas of the oral cavity is shown in Figs. 1.2 and 1.3. Lip cancer had the highest incidence in Australia and central and eastern Europe, and rising incidence of oropharyngeal cancers in North America and Europe, especially in Hungary, Slovakia, Germany, and France, is associated with alcohol use, tobacco smoking, and HPV infection. Nasopharyngeal cancers are most commonly reported from Northern Africa and Eastern and Southeast Asia, suggestive of genetic susceptibility combined with Epstein-Barr virus (EBV) infection. On the other hand, significantly higher rates of laryngeal and hypopharyngeal carcinomas are reported in Italy, France, and Spain as a consequence of higher rates of alcohol consumption and smoking. In the past two decades a rising incidence of head and neck cancer has been reported in Eastern European countries, particularly in Hungary; the exact reasons for this phenomenon remain unclear. The global incidence of lip, oral

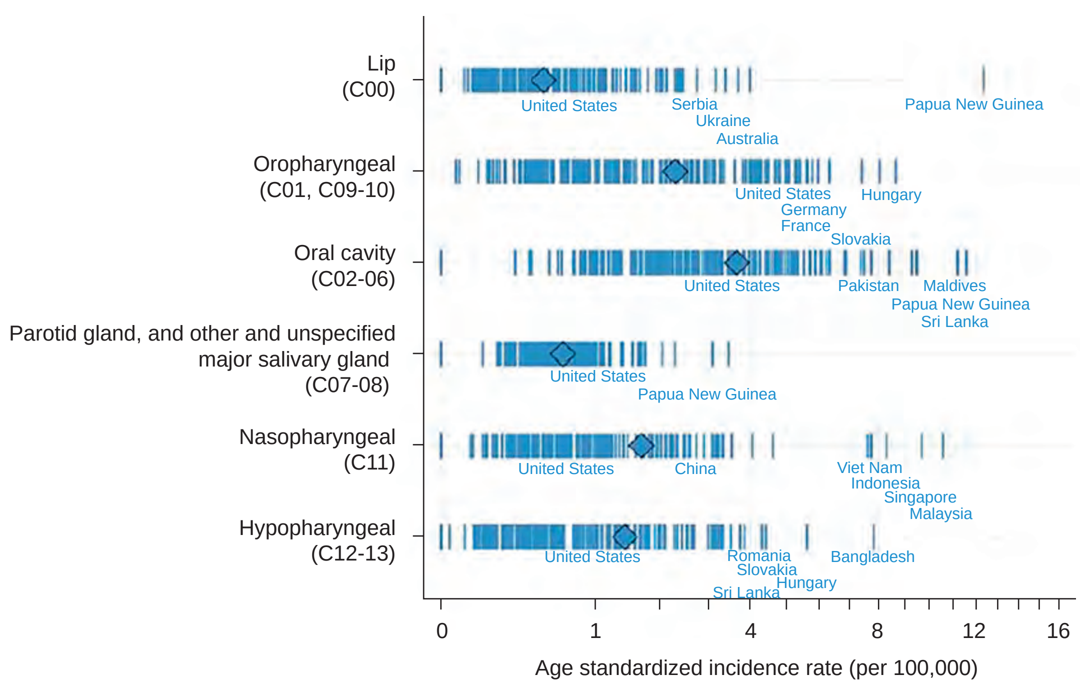

Figure 1.2 Age Standardized Incidence Rates (per 100,000) of Lip, Oral Cavity, and Pharyngeal Cancers by Subsite in 2012 Among Men. International Classification of Diseases 10th Revision codes are indicated for each subsite. *(With permission from Shield KD, Ferlay J, Jemal A et al. The global incidence of lip, oral cavity, and pharyngeal cancers by subsite in 2012. CA Cancer J Clin 2017;67(1):51–64.)*

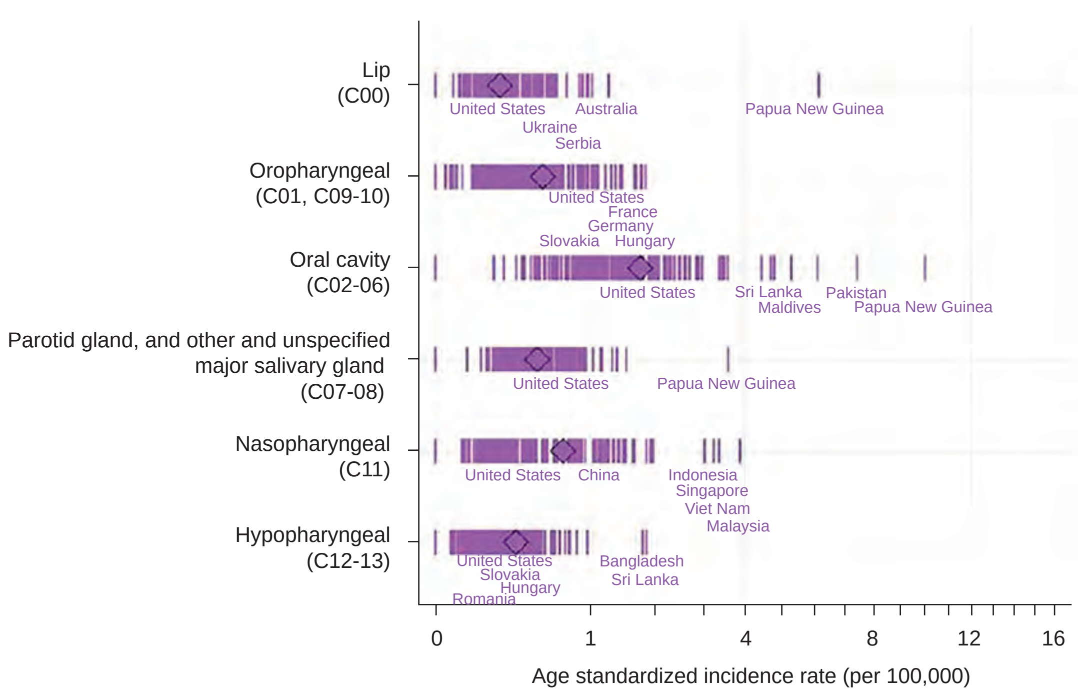

Figure 1.3 Age Standardized Incidence Rates (per 100,000) of Lip, Oral Cavity, and Pharyngeal Cancers by Subsite in 2012 Among Women. International Classification of Diseases 10th Revision codes are indicated for each subsite. *(With permission from Shield KD, Ferlay J, Jemal A et al. The global incidence of lip, oral cavity, and pharyngeal cancers by subsite in 2012. CA Cancer J Clin 2017;67(1):51–64.)*

cavity, and pharyngeal cancers of approximately 530,000 corresponds to 3.8% of all cancers. However, it is predicted to rise by 62% to 856,000 cases by 2035.

An increased incidence of differentiated carcinoma of the thyroid gland in children has been reported in Belarus and the Ukraine following the Chernobyl accident in 1986. Although initially the adult population in these areas did not show an increase in thyroid cancer, the adult population exposed to the Chernobyl accident is now manifesting an increase in thyroid cancer. It is anticipated that a similar rise in thyroid cancers may occur following the Fukushima nuclear accident in Japan. In addition, during the course of the past two decades, a rising incidence of differentiated carcinoma of the thyroid gland has been reported worldwide, likely due to the early increased diagnosis of clinically occult tumors resulting from increasing awareness and frequent utilization of routine sonography of the neck and other imaging studies.

HEAD AND NECK SQUAMOUS CELL CANCER BIOLOGY: OVERVIEW

Despite its anatomic and histologic diversity, head and neck squamous cell carcinoma (HNSCC), like all human cancers, is a genetic malady in which genetic aberrations accumulate in cells consequent to an imbalance between mutagenic signals and inherent protective mechanisms. In some cases, the development of head and neck cancer may be subject to inherited predispositions, with the strongest association observed for patients with Fanconi anemia, a disease that results from mutations in a group of genes that mediate DNA damage repair. In some patients, head and neck cancers of mucosal origin are associated with exposure to mutagens, chief among which is tobacco. Tobacco use is a strong risk factor for the development of head and neck squamous cell cancer, with alcohol use representing a comparatively smaller level of risk, but the two agents appear to work synergistically and are likely responsible for up to 75% of cases. In parts of Asia, betel quid chewing also plays a significant role in the development of squamous cancer.

More recently, in the United States and developed world, oncogenic strains of the HPV (mainly HPV-16) have been linked with the development of squamous cell cancer arising in the oropharynx; specifically, the lymphoid-rich regions of the tonsil and base of tongue. Most HPV-positive cancers occur in nonsmokers and nondrinkers and are instead associated with sexual behavior as a means of transmitting the virus. In the developed world, the incidence of HPV-associated head and neck cancer is rising, while the incidence of tobacco-associated HPV-negative cancer is declining. HPV-associated cancers differ significantly from HPV-negative cancers in their genetic complexity and content, natural history, response to treatment, and outcomes. Due to these substantial differences, HPV-positive and HPV-negative cancers are best thought of as biologically distinct entities. The differences in the behavior of these two entities has led to the development of a different and separate staging system for HPV-positive oropharynx cancers.

Finally, many patients have no history of either an inherited cancer syndrome or exposure to tobacco or alcohol. The exact cause for the development of head and neck cancer in these patients remains to be defined. Although genetic aberrations appear to develop randomly, those directly contributing to carcinogenesis are selected for in a darwinian manner through the process of clonal selection. As such, cancers are a model for cellular evolution in that they constantly adapt to environmental stimuli through alterations in their genetic complement. As genetic events accumulate, these malignancies progress through several stages, ultimately resulting in invasive cancer. Head and neck cancers, especially head and neck squamous cell carcinomas and thyroid carcinomas, represent a prototypic model for cancer progression (Fig. 1.4). Moreover, with diffuse exposure to tobacco carcinogens, it is not uncommon to see multiple lesions at varying stages of progression within the upper aerodigestive tract, representing a process of field cancerization. Preclinical changes in the cellular structure of the exposed mucosa occur several years before the manifestation of clinical features suspicious for carcinoma, making field cancerization much more common than is appreciated clinically.

Given that the behavior of a cancer is directly attributable to its genetic content, the study of cancer genetics offers an opportunity to predict cancer behavior and direct targeted therapy. The study of cancer genetics has been bolstered in

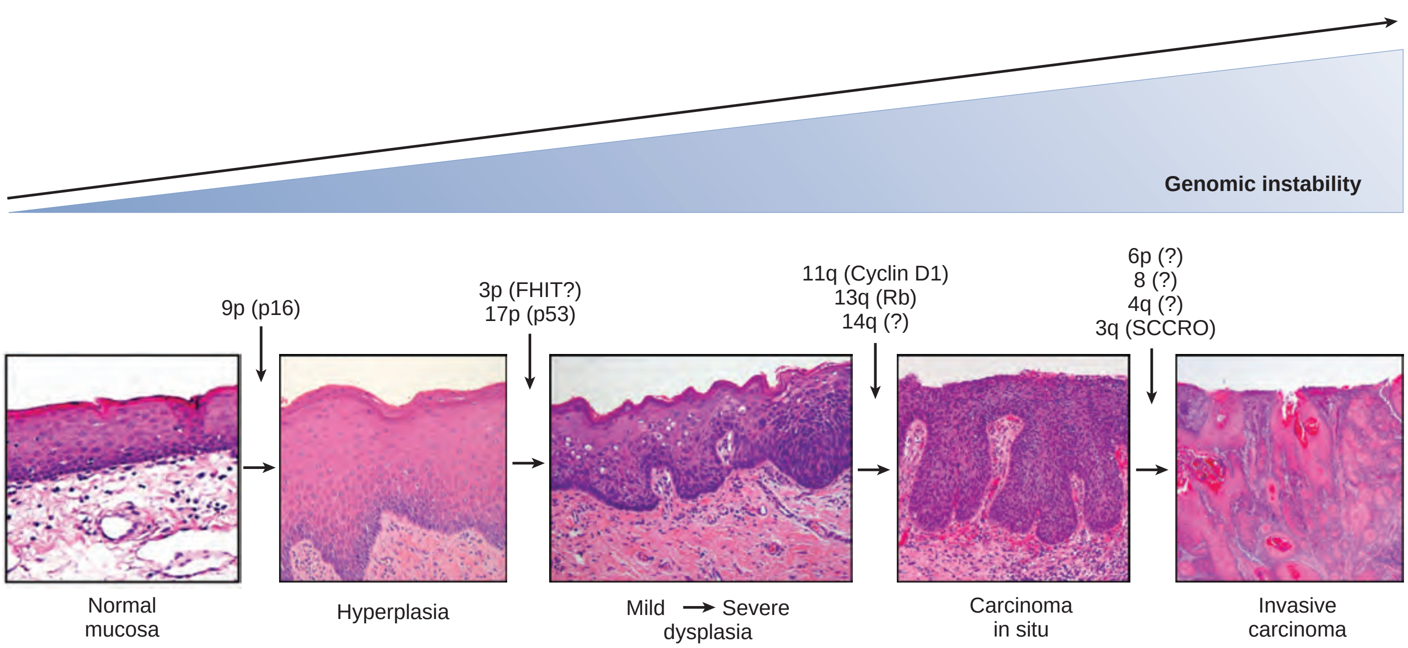

Figure 1.4 Progression model for squamous cell carcinoma of the head and neck showing increasing genomic instability from histologically normal mucosa to invasive carcinoma.

recent years by the completion of, first, the Human Genome Project and, subsequently, the large-scale tumor-sequencing studies of the Cancer Genome Atlas project. Despite these advances, the direct application of genetic information to head and neck cancer prognostication and treatment remains limited. Buoyed by successes such as anti–epidermal growth factor receptor targeting and, more recently, immunotherapy in head and neck squamous cell carcinomas and the promise of more significant contributions, the field of head and neck cancer genetics continues to advance and likely will influence cancer treatment in the years to come.

GENETIC PREDISPOSITION TO HEAD AND NECK SQUAMOUS CELL CANCER

Only a small fraction of cases are familial in nature. The clearest link is observed in patients with Fanconi anemia, an autosomal recessive genomic-instability syndrome associated with bone marrow failure, leukemia, congenital defects, and sensitivity to cross-linking chemotherapy agents. The risk of developing head and neck cancer is elevated several hundred-fold, and most patients develop a solid tumor by age 45 years. Treatment of these patients is clinically challenging, because these patients have significant hypersensitivity to chemotherapy and radiation therapy.

It is not clear whether there is any clear genetic predisposition for head and neck cancer, apart from syndromic families. While initial studies seemed to show a genetic predisposition was common in first-degree relatives, more recent analyses now demonstrate that the association is mild. It is quite possible that inherited differences in relevant cellular pathways such as DNA repair, carcinogen metabolism, and cell cycle control may modulate the risk of cell sensitivity to carcinogen exposure.

MOLECULAR SUBTYPES OF HEAD AND NECK SQUAMOUS CELL CANCER

The first analyses performing a broad molecular characterization of head and neck cancer utilized high throughput gene expression arrays. These first identified four distinct subgroups of HNSCC, which have been termed basal, atypical, mesenchymal, and classical. The "atypical" tumors are mostly HPV-associated, but the other subtypes do not have any clear association with patient factors such as age or smoking history. Of interest, however, is that these subtypes resemble similar subtypes in lung cancer, suggesting that there may be shared biology that is relevant for future research into factors that are prognostic or predict response to certain treatments.

GENETIC ALTERATIONS IN HEAD AND NECK SQUAMOUS CELL CANCER

More recently, several large-scale projects have performed DNA sequencing of the exomes (the parts of the genome that are transcribed into RNA), in order to identify genes that are mutated in HNSCC. These studies have included large studies drawing tumors from multiple international centers, carried out by the Cancer Genome Atlas and the International Cancer Genome Consortium. Overall, HNSCC has the ninth highest mutational load of the 30 tumor types studied, with an average of 5 (range of 1–100) mutations per megabase. HPV-positive tumors tend to have lower mutation rates, and smoking-related tumors tend to have higher mutation rates.

HPV-negative tumors are predominantly characterized by multiple mutations in tumor suppressor genes (genes that normally function to protect cells from developing cancer), rather than oncogenes (genes that have the potential to cause cancer if altered). It has long been recognized that the most commonly altered gene in HNSCC is *TP53,* the gene that encodes the p53 protein, a protein that normally triggers cell cycle arrest in response to DNA damage or oncogenic stress. Mutations in *TP53* can be observed early in the formation of HNSCC, for example in premalignant lesions, or in histologically normal-appearing mucosa on the margin of a tumor resection. *TP53* mutations are present in 70% to 80% of HNSCC and are associated with poorer prognosis. Other commonly altered tumor suppressor genes in HNSCC include the cell cycle gene *CDKN2A* and genes involved in the differentiation and development of squamous cells, such as *NOTCH1, TP63,* and *FAT1.* The chief oncogenes that are altered in HNSCC include *EGFR,* which encodes the epidermal growth factor, driving downstream signaling that promotes cellular growth, invasion, and metastasis and is the target of *EGFR*-inhibiting therapeutic drugs such as cetuximab. Unlike in lung cancer, *EGFR* is rarely mutated in HNSCC but is often amplified, leading to overexpression. *PIK3CA,* a kinase gene that is the second-most commonly mutated gene in human cancer, is also mutated in up to 30% of HNSCC and plays an important role in promoting cellular growth and metabolism.

BIOLOGY OF HUMAN PAPILLOMA VIRUS–ASSOCIATED HEAD AND NECK CANCERS

HPV-positive HNSCCs have a completely distinct molecular profile from HPV-negative HNSCC. The HPV family of genes include both low-risk and high-risk strains, based on the ability of a strain to lead to malignant progression of an infected cell. HPV has long been known to induce malignancies such as cervical, anal, and vulvar cancers. Definitive evidence linking HPV as a causative agent in oropharyngeal cancer only began to emerge in the early 2000s. It is now clear that HPV-related oropharyngeal cancers are a distinct entity that have a better prognosis than traditional smoking- and alcohol-related HNSCC. In the United States and the developed world, where smoking rates have declined, HPV is now the cause of up to 80% of oropharyngeal cancers. HPV16 is the main subtype associated with HNSCC.

HPV chiefly causes HNSCC through its two viral oncogenes, E6 and E7, that inactivate tumor suppressor genes in the host cell. E6 inactivates p53 (described previously), and E7 inactivates Rb (the retinoblastoma tumor suppressor gene). As a result of these driving events, HNSCCs caused by HPV tend to require far fewer other mutations to develop into cancer.

PRECISION MEDICINE AND IMMUNOTHERAPY

The only molecularly targeted therapy currently used in HNSCC targets *EGFR*. Cetuximab, one of these drugs, is approved by the Food and Drug Administration (FDA) in the United States and has a 10% to 15% response rate as a single agent in advanced HNSCC. There is significant interest in exploring other targeted therapies, but our molecular understanding of HNSCC reveals that these approaches are most likely to be effective when matched to cancers with a corresponding alteration.

In recent years, a "precision" or "personalized" molecular oncology approach to advanced cancer has begun to be practiced

in several large cancer centers. The premise of such an approach is that clinicians could use molecular or genetic approaches to comprehensively profile a patient's tumor and identify targets of vulnerabilities that could be matched with a specific therapy. These approaches are currently the subject of intense investigation to determine whether in-depth molecular profiling of advanced cancer can lead to successful matching of tumors to new therapies and improved patient outcomes.

The most recent FDA-approved drugs for HNSCC are immunotherapies, specifically drugs that target checkpoints on T cells. In HNSCC, these drugs target the PD-1 (programmed cell death-1) protein, which is a receptor expressed on T cells that suppresses T cell activity. PD-1 binds to PD-L1, a protein that can be expressed (and upregulated) by cancer cells as a means of allowing tumors to evade the immune system. By inhibiting PD-1, these drugs are able to release the brakes on the immune system and unleash adaptive immunity targeting cancer cells. Current research seeks to improve the response rates of these immune checkpoint therapies against HNSCC and understand why some tumors respond and some are resistant to these treatments.

EVALUATION

A detailed history and physical examination form the basis for initial diagnosis. In addition to tumor parameters, a complete history should include evaluation of factors that may influence the management of the primary neoplasm, including a detailed family history, lifestyle habits (including smoking and alcohol consumption), sexual behavior, and occupational exposures. The patient's comorbid conditions, such as nutritional status, chronic obstructive pulmonary disease, liver functions, and general medical condition, should be assessed carefully.

Clinical examination should be performed with the patient sitting upright. A headlight and simple instruments such as a tongue depressor should be used to facilitate examination of the oral cavity, along with a flexible fiberoptic laryngoscope to allow adequate assessment of the nasal cavity, nasopharynx, oropharynx, hypopharynx, and larynx. The examination begins with evaluation of the skin of the scalp, face, and neck, followed by palpation of the neck for masses, especially in the cervical nodal basins, and palpation of the thyroid and parotid glands. Evaluation of the external auditory canals and eardrum and anterior rhinoscopy also should be routine. Assessment of cranial nerve functions is integral and should be performed systematically. Examination of the oral cavity and oropharynx should include not only visual inspection but also palpation of the mucosa and underlying soft tissues of the tongue, floor of mouth, buccal mucosa, palate, tonsil, and base of the tongue. Flexible fiberoptic endoscopic examination should include visualization of the nasal cavity, nasopharynx, oropharynx, hypopharynx, and larynx, not only to look for mucosal and submucosal lesions but also to assess the soft palate and vocal cord function.

If a primary tumor is identified, its site of origin, visual characteristics, palpatory findings, and physical signs of local extension and invasion of adjacent structures should be meticulously assessed and documented to allow for staging and treatment planning. Adequate palpation, preferably bimanual palpation of the lesion when feasible, is necessary to assess the depth of invasion (DOI), since that is required to assign appropriate T staging of oral cancer. All malignant tumors of the head and neck region must be staged according to the staging system developed by the American Joint Committee on Cancer (AJCC) and the International Union Against Cancer (UICC), published in the eighth edition of the *AJCC Cancer Staging Manual*.

STAGING OF HEAD AND NECK CANCER

Cancers of the head and neck are staged according to their site of origin. Seven major sites are described in the AJCC/UICC (International Union Against Cancer) staging system. The seven major sites are (1) oral cavity; (2) pharynx; (3) larynx; (4) nasal cavity and paranasal sinuses; (5) thyroid gland; (6) salivary glands; and (7) skin cancers, including melanoma. The most recent revisions in the staging criteria for common tumors and the regional lymph nodes were published in the eighth edition of the AJCC staging manual and are shown in Tables 1.1 to 1.9. Because of a different biological behavior, p16+ (HPV-positive) oropharyngeal carcinomas have a separate nodal staging system (see Chapter 11).

RADIOGRAPHIC IMAGING

Imaging plays an integral role in the evaluation of head and neck tumors. Imaging can help define the extent of the primary tumor as well as the presence, volume, and location of regional and distant metastases. In addition, imaging is helpful in detecting synchronous or metachronous primary tumors that may not be evident clinically and for assessing treatment response, performing posttreatment surveillance, and obtaining tissue diagnosis by image-guided biopsy. In certain specific situations, such as paragangliomas or neurogenic tumors, a reliable diagnosis can be made on the basis of imaging alone without the need for tissue diagnosis. Imaging is able to define several salient features of the tumor that can have important implications in treatment selection, the extent of surgery, and planning of

Table 1.1 Staging for Carcinoma of the Lip and Oral Cavity

Definitions of AJCC TNM

Definition of Primary Tumor

T CATEGORY	T CRITERIA
TX	Primary tumor cannot be assessed
Tis	Carcinoma in situ
T1	Tumor ≤2 cm, ≤5 mm depth of invasion (DOI) DOI is depth of invasion and not tumor thickness
T2	Tumor ≤2 cm, DOI >5 mm and ≤10 mm *or* tumor >2 cm but ≤4 cm, and ≤10 mm DOI
T3	Tumor >4 cm *or* any tumor >10 mm DOI
T4	Moderately advanced or very advanced local disease
T4a	Moderately advanced local disease Tumor invades adjacent structures only (e.g., through cortical bone of the mandible or maxilla, or involves the maxillary sinus or skin of the face) Note: Superficial erosion of bone/tooth socket (alone) by a gingival primary is not sufficient to classify a tumor as T4
T4b	Very advanced local disease Tumor invades masticator space, pterygoid plates, or skull base and/or encases the internal carotid artery

(Used with the permission of the American Joint Committee on Cancer [AJCC], Chicago, Illinois. The original source for this material is the AJCC Cancer Staging Manual, 8th ed. Springer Science and Business Media LLC, 2016, www.springer.com.)

Table 1.2 Staging for Carcinoma of the Major Salivary Glands

Definitions of AJCC TNM

Definition of Primary Tumor (T)

TX	T CRITERIA
T0	Primary tumor cannot be assessed
Tis	No evidence of primary tumor
T1	Carcinoma in situ
T2	Tumor 2 cm or smaller in greatest dimension without extraparenchymal extension*
T3	Tumor larger than 4 cm and/or tumor having extraparenchymal extension
T4	Moderately advanced or very advanced disease
T4a	Moderately advanced disease Tumor invades skin, mandible, ear canal, and/or facial nerve
T4b	Very advanced disease Tumor invades skull base and/or pterygoid plates and/or encases carotid artery

*Extraparenchymal extension is clinical or macroscopic evidence of invasion of soft tissues. Microscopic evidence alone does not constitute extraparenchymal extension for classification purposes.

(Used with the permission of the American Joint Committee on Cancer [AJCC], Chicago, Illinois. The original source for this material is the AJCC Cancer Staging Manual, 8th ed. Springer Science and Business Media LLC, 2016, www.springer.com.)

Table 1.3 Staging for Carcinoma of the Larynx

Definitions of AJCC TNM

Definition of Primary Tumor (T)

T CATEGORY	T CRITERIA
TX	Primary tumor cannot be assessed
Tis	Carcinoma in situ
T1	Tumor limited to one subsite of supraglottis with normal vocal cord mobility
T2	Tumor invades mucosa of more than one adjacent subsite of supraglottis or glottis or region outside the supraglottis (e.g., mucosa of base of tongue, vallecula, medial wall of pyriform sinus) without fixation of the larynx
T3	Tumor limited to larynx with vocal cord fixation and/or invades any of the following: postcricoid area, preepiglottic space, paraglottic space, and/or inner cortex of thyroid cartilage
T4	Moderately advanced or very advanced
T4a	Moderately advanced local disease Tumor invades through the outer cortex of the thyroid cartilage and/or invades tissues beyond the larynx (e.g., trachea, soft tissues of neck including deep extrinsic muscle of the tongue, strap muscles, thyroid, or esophagus)
T4b	Very advanced local disease Tumor invades prevertebral space, encases carotid artery, or invades mediastinal structures

(Used with the permission of the American Joint Committee on Cancer [AJCC], Chicago, Illinois. The original source for this material is the AJCC Cancer Staging Manual, 8th ed. Springer Science and Business Media LLC, 2016, www.springer.com.)

Table 1.4 Staging for Carcinoma of the Nasal Cavity and Paranasal Sinuses

Definitions of AJCC TNM

Maxillary Sinus

T CATEGORY	T CRITERIA
TX	Primary tumor cannot be assessed
Tis	Carcinoma in situ
T1	Tumor limited to maxillary sinus mucosa with no erosion or destruction of bone
T2	Tumor causing bone erosion or destruction including extension into the hard palate and/or middle nasal meatus, except extension to posterior wall of maxillary sinus and pterygoid plates
T3	Tumor invades any of the following: bone of the posterior wall of maxillary sinus, subcutaneous tissues, floor of medial wall of orbit, pterygoid fossa, ethmoid sinuses
T4	Moderately advanced or very advanced local disease
T4a	Moderately advanced local disease Tumor invades anterior orbital contents, skin of cheek, pterygoid plates, infratemporal fossa, cribriform plate, sphenoid or frontal sinuses
T4b	Very advanced local disease Tumor invades any of the following: orbital apex, dura, brain, middle cranial fossa, cranial nerves other than maxillary division of trigeminal nerve (V2), nasopharynx, or clivus

(Used with the permission of the American Joint Committee on Cancer [AJCC], Chicago, Illinois. The original source for this material is the AJCC Cancer Staging Manual, 8th ed. Springer Science and Business Media LLC, 2016, www.springer.com.)

Box 1.1 Critical Radiologic Features of the Tumor That Can Affect Selection of Treatment

1. Submucosal/deep extension of tumor
2. Involvement or encasement of major vessels
3. Bone invasion
4. Perineural spread of disease
5. Detection of subclinical neck nodal disease
6. Lateral retropharyngeal lymphadenopathy and mediastinal lymphadenopathy

radiation therapy (Box 1.1). Selection of the appropriate imaging modality is critical for complete assessment in individual cases. Therefore the head and neck surgeon should be familiar with the strengths and weakness of each imaging modality. In addition, it is important to discuss the clinical problem with the radiologist so the investigation can be tailored to provide the desired information.

Computed tomography (CT) and magnetic resonance imaging (MRI) are the mainstay of imaging assessment of most head and neck tumors. Given their unique strengths and weaknesses, CT and MRI can complement each other to enhance the anatomic definition of selected tumors. Contrast-enhanced CT is widely used because it is readily available, less expensive than MRI, and can be performed rapidly, especially with multidetector scanners that can complete actual imaging in less than a minute. In addition, thin-section images obtained with modern scanners

Table 1.5 Staging for Carcinoma of the Pharynx

Definitions of AJCC TNM

Definition of Primary Tumor (T)

Oropharynx (p16-)

T CATEGORY	T CRITERIA
TX	Primary tumor cannot be assessed
Tis	Carcinoma in situ
T1	Tumor 2 cm or smaller in greatest dimension
T2	Tumor larger than 2 cm but not larger than 4 cm in greatest dimension
T3	Tumor larger than 4 cm in greatest dimension or extension to lingual surface of epiglottis
T4	Moderately advanced or very advanced local disease
T4a	Moderately advanced local disease Tumor invades the larynx, extrinsic muscle of tongue, medial pterygoid, hard palate, or mandible*
T4b	Very advanced local disease Tumor invades lateral pterygoid muscle, pterygoid plates, lateral nasopharynx, or skull base or encases carotid artery

*Note: Mucosal extension to lingual surface of epiglottis from primary tumors of the base of the tongue and vallecula does not constitute invasion of the larynx.

Hypopharynx

T CATEGORY	T CRITERIA
TX	Primary tumor cannot be assessed
Tis	Carcinoma in situ
T1	Tumor limited to one subsite of hypopharynx and/or 2 cm or smaller in greatest dimension
T2	Tumor invades more than one subsite of hypopharynx or an adjacent site, or measures larger than 2 cm but not larger than 4 cm in greatest dimension without fixation of hemilarynx
T3	Tumor larger than 4 cm in greatest dimension or with fixation of hemilarynx or extension to esophagus mucosa
T4	Moderately advanced and very advanced local disease
T4a	Moderately advanced local disease Tumor invades thyroid/cricoid cartilage, hyoid bone, thyroid gland, central compartment soft tissue, or infiltration muscle of esophagus*
T4b	Very advanced local disease Tumor invades prevertebral fascia, encases carotid artery, or involves mediastinal structures

*Note: Central compartment soft tissue includes prelaryngeal strap muscles and subcutaneous fat.

(Used with the permission of the American Joint Committee on Cancer [AJCC], Chicago, Illinois. The original source for this material is the AJCC Cancer Staging Manual, 8th ed. Springer Science and Business Media LLC, 2016, www.springer.com.)

Table 1.6 Staging for Metastatic Carcinoma of the Cervical Lymph Nodes

Definition of Regional Lymph Node

Clinical N (cN)

N CATEGORY	N CRITERIA
NX	Regional lymph nodes cannot be assessed
N0	No regional lymph node metastasis
N1	Metastasis in a single ipsilateral lymph node, 3 cm or smaller in greatest dimension and ENE(–)
N2	Metastasis in a single ipsilateral lymph node larger than 3 cm but not larger than 6 cm in greatest dimension and ENE(–); *or* metastases in multiple ipsilateral lymph nodes, none larger than 6 cm in greatest dimension, ENE(–); *or* in bilateral or contralateral lymph nodes, none larger than 6 cm in greatest dimension, ENE(–)
N2a	Metastasis in single ipsilateral or contralateral node larger than 3 cm but not larger than 6 cm in greatest dimension and ENE(–)
N2b	Metastasis in multiple ipsilateral nodes, none larger than 6 cm in greatest dimension and ENE(–)
N2c	Metastasis in bilateral or contralateral lymph nodes, none larger than 6 cm in greatest dimension and ENE(–)
N3	Metastasis in a lymph node larger than 6 cm in greatest dimension and ENE(–); *or* metastasis in a single ipsilateral node ENE(+) *or* multiple ipsilateral, contralateral, or bilateral nodes, any with ENE(+)
N3a	Metastasis in a lymph node larger than 6 cm in greatest dimension and ENE(–)
N3b	Metastasis in a single ipsilateral node ENE(+) *or* multiple ipsilateral, contralateral, or bilateral nodes, any with ENE(+)

Note: A designation of "U" or "L" may be used for any N category to indicate metastasis above the lower border of the cricoid (U) or below the lower border of the cricoid (L). Similarly, clinical and pathologic ENE should be recorded as ENE(–) or ENE(+).
ECS, extracapsular spread; *Eg*, gross; *Em*, microscopic; *En*, not present; *E*–, absent; *E*+, present.

(Used with the permission of the American Joint Committee on Cancer [AJCC], Chicago, Illinois. The original source for this material is the AJCC Cancer Staging Manual, 8th ed. Springer Science and Business Media LLC, 2016, www.springer.com.)

can be reconstructed in sagittal and coronal planes to allow multiplanar viewing for comprehensive definition of the extent of the primary lesion and regional metastasis. Bone and soft tissue algorithms (windows) are used to provide specific details. CT is superior to MRI in evaluating cortical bone involvement, demonstrating calcification in tumors, and detecting clinically occult nodal metastasis and early extracapsular spread. However, beam hardening artifact from dental work can limit evaluation of certain portions of the oral cavity, although modern multi-detector scanners generally can overcome this limitation. The anatomic resolution of CT is limited if the patient cannot receive iodinated intravenous contrast dye for medical reasons (e.g., renal disease or severe contrast allergy) or therapeutic reasons (e.g., planned use of radioactive iodine for thyroid cancer).

MRI is based on energy emittance from nuclei placed in a strong magnetic field. The computer-based detection and spatial localization of the released energy allows generation of an image, which is dependent on multiple factors, including the proton concentration, proton flow in vessels, and time required for stimulated nuclei to return to the basal state. The images generated by MRI are T1-weighted (based on the physical state of the material or proton density) or T2-weighted (based on loss of coherent resonance of protons). Fluid (e.g., cerebrospinal fluid and the vitreous in the eye) is bright and fat is dark on T2 images, whereas fat is bright on T1 images. Because of differences in tissue characteristics on T1 and T2 images, MRI is

Table 1.7 Staging for Carcinoma of the Thyroid Gland

Papillary, Follicular, Poorly Differentiated, Hurthle Cell, and Anaplastic Thyroid Carcinoma

T CATEGORY	T CRITERIA
TX	Primary tumor cannot be assessed
T0	No evidence of primary tumor
T1	Tumor <2 cm in greatest dimension limited to the thyroid
T1a	Tumor <1 cm in greatest dimension limited to the thyroid
T1b	Tumor >1 cm but <2 cm in greatest dimension limited to the thyroid
T2	Tumor >2 cm but <4 cm in greatest dimension limited to the thyroid
T3	Tumor >4 cm limited to the thyroid, or gross extrathyroidal extension invading only strap muscles
T3a	Tumor >4 cm limited to the thyroid
T3b	Gross extrathyroidal extension invading only strap muscles (sternohyoid, sternothyroid, thyrohyoid, or omohyoid muscles) from a tumor of any size
T4	Includes gross extrathyroidal extension
T4a	Gross extrathyroidal extension invading subcutaneous soft tissues, larynx, trachea, esophagus, or recurrent laryngeal nerve from a tumor of any size
T4b	Gross extrathyroidal extension invading prevertebral fascia or encasing the carotid artery or mediastinal vessels from a tumor of any size

**Note:* All categories may be subdivided: (s) solitary tumor and (m) multifocal tumor (the largest tumor determines the classification).

Definition of Regional Lymph Node (N)

N CATEGORY	N CRITERIA
NX	Regional lymph nodes cannot be assessed
N0	No evidence of locoregional lymph node metastasis
N0a	One or more cytologically or histologically confirmed benign lymph nodes
N0b	No radiologic or clinical evidence of locoregional lymph node metastasis
N1	Metastasis to regional nodes
N1a	Metastasis to level VI or VII (pretracheal, paratracheal, or prelaryngeal/Delphian, or upper mediastinal) lymph nodes. This can be unilateral or bilateral disease.
N1b	Metastasis to unilateral, bilateral, or contralateral lateral neck lymph nodes (levels I, II, III, IV, or V) or retropharyngeal lymph nodes

Definition of Distant Metastasis (M)

M CATEGORY	M CRITERIA
M0	No distant metastasis
M1	Distant metastasis

Differentiated

WHEN AGE AT DIAGNOSIS IS...	AND T IS...	AND N IS...	AND M IS...	THEN THE STAGE GROUP IS...
<55 years	Any T	Any N	M0	I
<55 years	Any T	Any N	M1	II
>55 years	T1	N0/NX	M0	I
>55 years	T1	N1	M0	II
>55 years	T2	N0/NX	M0	I
>55 years	T2	N1	M0	II
>55 years	T3a/T3b	Any N	M0	II
>55 years	T4a	Any N	M0	III
>55 years	T4b	Any N	M0	IVA
>55 years	Any T	Any N	M1	IVB

Table 1.7 Staging for Carcinoma of the Thyroid Gland—cont'd

Anaplastic

WHEN T IS...	AND N IS...	AND M IS...	THEN THE STAGE GROUP IS...
T1-T3a	NO/NX	M0	IVA
T1-T3a	N1	M0	IVB
T3b	Any N	M0	IVB
T4	Any N	M0	IVB
Any T	Any N	M1	IVC

Used with the permission of the American Joint Committee on Cancer (AJCC), Chicago, Illinois. The original source for this material is the AJCC Cancer Staging Manual, 8th ed. Springer Science and Business Media LLC, 2016, www.springer.com.

Table 1.8 Staging for Nonmelanoma Skin Cancer

Definitions of AJCC TNM

Definition of Primary Tumor (T)

T CATEGORY	T CRITERIA
TX	Primary tumor cannot be identified
Tis	Carcinoma in situ
T1	Tumor smaller than 2 cm in greatest dimension
T2	Tumor 2 cm or larger, but smaller than 4 cm in greatest dimension
T3	Tumor 4 cm or larger in maximum dimension or minor bone erosion or perineural invasion or deep invasion*
T4	Tumor with gross cortical bone/marrow, skull base invasion and/or skull base foramen invasion
T4a	Tumor with gross cortical bone/marrow invasion
T4b	Tumor with skull base invasion and/or skull base foramen involvement

*Deep invasion is identified as invasion beyond the subcutaneous fat or >6 mm (as measured from the granular layer of adjacent normal epidermis to the base of the tumor); perineural invasion for T3 classification is defined as tumor cells within the nerve sheath of a nerve lying deeper than the dermis or measuring 0.1 mm or larger in caliber, or presenting with clinical or radiographic involvement of named nerves without skull base invasion or transgression.

SCC, squamous cell carcinoma.

Used with the permission of the American Joint Committee on Cancer (AJCC), Chicago, Illinois. The original source for this material is the AJCC Cancer Staging Manual, 8th ed. Springer Science and Business Media LLC, 2016, www.springer.com.

Table 1.9 Staging for Melanoma of the Skin

T CATEGORY	THICKNESS	ULCERATION STATUS
TX: Primary tumor thickness cannot be assessed (e.g., diagnosis by curettage)	Not applicable	Not applicable
T0: No evidence of primary tumor (e.g., unknown primary or completely regressed melanoma)	Not applicable	Not applicable
Tis (melanoma in situ)	Not applicable	Not applicable
T1	≤1.0 mm	Unknown or unspecified
T1a	<0.8 mm	Without ulceration
T1b	<0.8 mm 0.8-1.0 mm	With ulceration With or without ulceration
T2	>1.0-2.0 mm	Unknown or unspecified
T2a	>1.0-2.0 mm	Without ulceration
T2b	>1.0-2.0 mm	With ulceration
T3	>2.0-4.0 mm	Unknown or unspecified
T3a	>2.0-4.0 mm	Without ulceration
T3b	>2.0-4.0 mm	With ulceration
T4	>4.0 mm	Unknown or unspecified
T4a	>4.0 mm	Without ulceration
T4b	>4.0 mm	With ulceration

Used with the permission of the American Joint Committee on Cancer (AJCC), Chicago, Illinois. The original source for this material is the AJCC Cancer Staging Manual, 8th ed. Springer Science and Business Media LLC, 2016, www.springer.com.

excellent at delineating the interface between normal soft tissue and a tumor. Paramagnetic substances, such as gadolinium, can alter the MRI signal and are used as a contrast agent to enhance the definition of soft tissues.

Direct multiplanar imaging can be performed on an MRI scanner without the need for computer reformatting, which allows better anatomic definition and spatial resolution. In general, MRI is also superior to CT in identifying perineural spread of disease, differentiating tumor from postobstructive mucosal disease in the paranasal sinuses, and detecting the presence of intracranial extension by tumor. MRI is therefore ideal for the evaluation of tumors of the nasopharynx, skull base, parapharyngeal space, and soft and hard palate. However, MRI is inferior to CT in delineating bony detail, and it also can give a false-positive impression of bone invasion, particularly in the maxilla and mandible in patients with underlying odontogenic disease. On the other hand, MRI is superior in showing early invasion of marrow space of the mandible, without cortical destruction. Because of the high fat content of the marrow, the medullary space is bright white on T1 sequence. When involved by tumor, the fat signal is lost, and the marrow space appears grey, indicating tumor infiltration. MRI cannot be used in patients with ferromagnetic objects embedded in the body, which precludes safe scanning. In addition, because of the limited confines of the bore of the magnet, MRI may not be suitable for patients with

claustrophobia or those with a large body habitus. "Open" MRI can overcome this limitation, but the image quality is inferior in the currently available equipment. MRI requires 30 to 45 minutes for image acquisition and therefore is susceptible to degradation of image quality from any movement by the patient during the study, including swallowing.

Ultrasound is particularly useful in the head and neck for evaluation of superficial soft tissue lesions in sites such as the parotid and thyroid gland. Ultrasound allows imaging in real time and assessment of vascularity and punctate calcification, which is especially useful in characterizing thyroid disease. Although ultrasound is the modality of choice for evaluating most thyroid lesions, it cannot detect tumor extension into bone or the airway, because ultrasound waves cannot penetrate these two media. Therefore CT or MRI is useful in evaluating more advanced disease of the thyroid gland when local invasion into the central compartment viscera or the spine is a cause for concern. Ultrasound is also sensitive in detecting nodal metastases in small lymph nodes in patients with thyroid cancer. At many institutions, ultrasound is routinely used for evaluation of cervical lymph nodes for metastatic disease and has become the standard of care for posttreatment surveillance of the neck.

Functional imaging with use of 18F-fluorodeoxyglucose positron emission tomography (PET) and particularly PET/CT adds yet another dimension that enhances and complements the anatomic information gained from CT or MRI. PET imaging is particularly helpful in evaluating patients with advanced head and neck cancers for distant metastases and posttherapy recurrence. The 18F-fluorodeoxyglucose avidity reflects metabolic activity in the lesion but is unable to differentiate between inflammation, infection, or tumor as the cause of increased metabolic activity. Whereas some nuclear medicine studies such as bone scans, gallium scans, and octreotide scans have limited use in head and neck imaging, other studies that use radioisotopes such as radioactive iodine, sestamibi, and metaiodobenzylguanidine (MIBG) have specific applications in thyroid and parathyroid disease.

Interventional applications of radiology of the head and neck include angiography and image-guided biopsy. Conventional diagnostic angiography has been essentially replaced by CT and MR angiography, and diagnosis of vascular tumors can be reliably achieved without invasive angiography. Invasive angiography is now primarily reserved for specific situations such as evaluation of the adequacy of cerebral perfusion when carotid sacrifice is a possibility, balloon occlusion testing (BOT), preoperative embolization of vascular tumors such as juvenile nasopharyngeal angiofibroma, control of hemorrhage, or delivery of intraarterial chemotherapy.

Image-guided biopsy of head and neck tumors greatly aids diagnosis and subsequent treatment in the appropriate clinical setting. Image-guided biopsy can be the least invasive approach to diagnosis, and in experienced hands it is a low-risk procedure that often obviates the need for general anesthesia and a more complicated open surgical procedure for tissue diagnosis. Obviously, the clinician or cytopathologist can obtain samples of palpable lesions easily by fine-needle aspiration (FNA). Superficial lesions such as thyroid nodules, superficial parotid gland lesions, and small lateral cervical lymph nodes are readily accessible with use of real-time ultrasound guidance, and thus accurate and expeditious FNA of suspicious lesions as small as 4 to 5 mm is feasible. Lesions that are located more deeply within the head and neck require CT or MR guidance to negotiate bone and the air-tissue interface. MR is used infrequently because it requires special nonferromagnetic MR-compatible equipment, apart from its other disadvantages compared with CT, as previously described.

Our ability to specifically image cancer cells in relation to normal tissue or posttherapy effects in tissue can be expected to improve with enhanced understanding of the biological and molecular mechanisms of cancer. In addition, the role of imaging in the management of head and neck cancer will continue to evolve with new technologic developments, newer contrast agents, and three-dimensional real-time imaging as well as in vivo confocal microscopy.

BIOPSY AND TISSUE DIAGNOSIS

Tissue diagnosis is mandatory before treatment for any malignant tumor. Diagnosis can be achieved by performing a biopsy or a fine needle aspiration cytology (FNAC) of superficial tumors or by performing a core needle or open biopsy of deeper tumors. A sufficient quantity of representative viable tissue from the tumor should be obtained to enable the pathologist to render an accurate tissue diagnosis. Obtaining a superficial biopsy specimen from an exophytic tumor, a biopsy specimen of necrotic tissue from an extensive tumor, or a biopsy specimen from tissue adjacent to the tumor that is not representative of the true nature of the lesion will result in inaccurate tissue diagnosis. If the index of suspicion for malignancy of a tumor is high and the initial biopsy is not confirmatory, then a repeat biopsy is warranted.

Deeper tumors that are not accessible for surface biopsy, such as submucosal tumors, soft tissue tumors, or tumors of the thyroid and salivary glands, as well as enlarged cervical lymph nodes, are best assessed by an FNA biopsy for cytologic diagnosis. FNA can be performed directly with palpation or under the guidance of imaging (i.e., ultrasound or CT). Whereas histopathologic diagnosis is based on tissue architecture (i.e., the relationship of cells to one another and the context in which they coexist), cytologic diagnosis is based on evaluation of characteristics of individual cells in suspension, including nuclear features. The tissue that has been aspirated is smeared onto several slides and stained, and some material may be centrifuged, fixed in formalin, and processed into a paraffin block. This "cell block" allows for hematoxylin and eosin staining and additional studies, such as immunohistochemistry or flow cytometry. FNA is highly accurate for diagnosis of most head and neck cancers, but it is important to understand that a negative cytologic diagnosis does not rule out the presence of a malignant tumor. If FNA is not conclusive, either a core or an open biopsy should be performed. A core biopsy usually provides sufficient tissue for histopathologic analysis. An open biopsy is indicated if a core biopsy is unsafe or nondiagnostic.

FROZEN-SECTION ANALYSIS

The indications for frozen-section analysis include confirmation of tissue diagnosis (e.g., parathyroid), diagnosis of malignancy, determination of the type of malignancy, evaluation of the margins, and adequacy of the tissue for further studies. Accuracy of the margins is dependent on the surgeon's judgment in sampling and the quality of the tissue submitted. Margins of surgical resection may be obtained from the specimen or from the surgical defect.

The accuracy of a frozen section is dependent on the context in which it is used. Limitations include assessment of bone, assessment of irradiated tissue (e.g., radiation-induced metaplasia

versus carcinoma), diagnosis of thyroid adenoma versus carcinoma (follicular and Hürthle cell neoplasms), differentiation of salivary tumors, and differentiation of necrotizing sialometaplasia and pseudoepitheliomatous hyperplasia from carcinoma. Lymphovascular invasion also cannot be assessed adequately with a frozen section. Other limitations include sampling error and electrocautery artifact.

TISSUE PROCESSING AND PATHOLOGY

Tissue can be submitted to the pathologist unprocessed or fixed in formalin. Most tissues can be fixed in 10% neutral-buffered formalin for routine processing. Fresh tissue is required for cytogenetic or diagnostic molecular tests. The specimen should be kept sterile for cultures for cytogenetics or for microorganisms. Banking of fresh, frozen tissue is desirable to facilitate study of tumor biology.

The patient's pertinent clinical details should be provided to the pathologist for accurate tissue processing and diagnosis. Orientation and gross description of the specimen requires communication between the surgeon and the pathologist. The gross description of the tumor is an essential component of the pathology report. Assessment of the margins of surgical resection is aided by the use of colored inks on the specimen. Decalcification is required for specimens that contain bone to allow processing. The prosector must determine the location and number of sections depending on the type of tumor for accurate histopathologic analysis.

The capsule (pseudocapsule, formed by compression of contiguous tissue) of tumors of the thyroid, salivary glands, and soft tissues should be assessed completely. Neck dissection specimens should be specifically studied, with a description of the location (levels) and number of lymph nodes. This description should be performed by the surgeon in the operating room by either pinning the specimen on a foam board with a diagram or prosecting the specimen according to designated levels. The number of lymph nodes in the neck dissection specimen depends on several factors, including the completeness of the neck dissection by the surgeon, previous radiation therapy to the neck, and the diligence of the prosector. Accurate reporting of the extent of nodal metastases requires reporting of extranodal extension (ENE), which is essential for N staging of tumors. The pathology report must also indicate whether the ENE is macroscopic (ma) or microscopic (mi).

After formalin fixation, paraffin blocks are prepared and sections that are at a thickness of 4 to 5 microns are fixed to glass slides. Hematoxylin and eosin is the gold standard for tissue diagnosis, and it is supplemented with immunohistochemistry and molecular techniques such as in situ hybridization under select circumstances (Table 1.10).

Table 1.10 Immunohistochemistry and Molecular Techniques Can Supplement Hematoxylin and Eosin Diagnosis in Certain Tumors.

ANTIBODY		SCC	PAPILLARY THYROID CARCINOMA	MEDULIARY THYROID CARCINOMA	MALIGNANT MELANOMA	ONB	CARCINOID	LYMPHOMA
34BE12	High-molecular-weight cytokeratin	++	–	–	–	–	–/–	–
Cam 5.2		+	+	+	–	–	–	–
AE1:AE3		+	+	+	–	–	–	–
4a4/p63	Basal cell or myoepithelial cell marker	++	–	–	–	+/–		–
CK7		–	+	+	–	–	–/–	–
CK20		–	–	–	–	–	–/–	–
LCA (CD45)	Leukocyte common antigen	–	–	–	–	–	–	+
CD20	B cells	–	+	–	–	–	–	+
CD5	T cells	–	–	–	–	–	–	–
HMB45		–	–	–	+/–	–	–	–
A103			–	–	+/–	–	–	–
MART-1 (MELAN A)		–	–	–	+/–	–		–
s-100		+/–	–	–	+/–	+		–
Thyroglobulin		–	+	–	–	–		–
TTF-1	Thyroid transcription	–	+	+	–	–	+/–	–
PAX B		–	+	+/–	–	–	–	–
HMBE		–	+	–	–	–	–	–
Calcitonin		–	–	+	–	–		–
Chromogranin		–	–	+	–	+/–	+	–
Synaptophysin		–	–	+/–	–	+	+	–
CEA		+/–	–	+/–	–	–	+/–	–
Mib-1 (Ki 67)	Proliferation marker	**	**	**	**	**	**	**

*Variable

Epithelial markers Lymphoid markers Melanoma markers Thyroid markers

ONB, Olfactory neuroblastoma; *SCC,* squamous cell carcinoma.

A wide variety of chromosome analysis techniques are available, ranging from basic G-banded karyotyping to 24-color spectral karyotyping as well as fluorescence in situ hybridization mapping of cloned deoxyribonucleic acids. Chromosomal translocation analysis by fluorescence in situ hybridization has become the mainstay in diagnosis of Ewing's sarcoma and rhabdomyosarcoma.

SELECTION OF THERAPY

Treatment of head and neck cancers can be divided into two broad categories: curative and palliative. With progression of the disease, curative treatment becomes less effective and integration of palliative therapy becomes increasingly important. Conventionally palliative treatment has only been used in patients with advanced tumors toward the end of their lives. On the other hand, it is preferable to integrate symptomatic palliation and pain relief early in the course of curative treatment (Fig. 1.5).

The selection of initial definitive treatment is dependent on the histologic diagnosis and the site and stage of the primary tumor as well as on its biological behavior and expected response to therapy. In general, early-stage tumors (i.e., stages I and II) are managed by a single-modality treatment such as surgery or radiotherapy. Selection of either surgery or radiotherapy depends on the site, size, and stage of the primary tumor as well as its proximity to bone and its depth of infiltration into the underlying soft tissues. In addition, the histologic features of the primary tumor and the history of any previous treatment also will affect the selection of therapy. Additional factors influencing the choice of initial treatment are complications and sequelae of treatment, the patient's compliance with treatment, convenience of the recommended therapy for the patient, the cost of treatment, and the competency of the treatment delivery team in executing the recommended therapy. In general, outcomes of therapy for early-stage tumors using single-modality treatment are comparable for either surgery or radiotherapy. On the other hand, advanced-stage tumors (i.e., stages III and IV) require multidisciplinary treatment with a combination of surgery and adjuvant radiotherapy or chemoradiotherapy. Thus in advanced-stage tumors, multidisciplinary input from all disciplines is necessary to develop an optimal therapeutic program. When a cure is not likely, attention turns to palliative treatment to control or prevent symptoms or to slow down progression of the disease. Surgery may be employed for palliation in select circumstances, including resection of fungating or bleeding tumors or resection of central compartment tumors to prevent airway compromise. Similarly, radiation can be used for palliative benefit, for example, to control effects of spinal cord compression from vertebral metastasis. Chemotherapy has an important role as a "radiation booster" when employed concurrently, or as an in vivo drug sensitivity test when employed in a neoadjuvant fashion. It also has an essential role in palliative treatment, with agents selected on the basis of risk/benefit profiles and response.

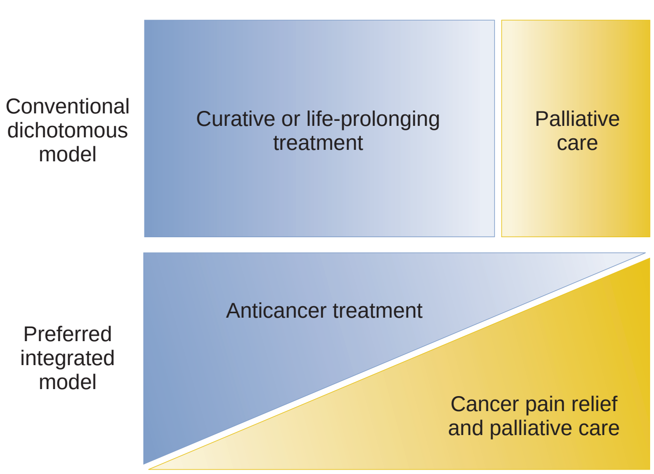

Figure 1.5 Integrating life-prolonging and palliative treatment in patients with head and neck cancer.

SURGERY

The surgeon plays a pivotal role in the management of patients with head and neck tumors. Involvement of the surgeon begins with the initial diagnosis, assessment of the extent of disease, selection of optimal treatment, and during delivery of definitive treatment and continues with rehabilitation, follow-up care, surveillance, and diagnosis and management of recurrent and new primary tumors as well as palliative and terminal care (Fig. 1.6). Surgery remains the most effective curative treatment for most head and neck neoplasms. In tumors of the salivary glands, thyroid, nasal cavity and paranasal sinuses, oral cavity, soft tissues, bone, and skin, it is the treatment of choice. In select patients with squamous cell carcinoma of the oropharynx and larynx, primary surgical resection is preferred. Surgery also becomes necessary for salvage of persistent or recurrent tumors after radiotherapy or chemoradiotherapy.

RADIATION THERAPY

Radiation therapy results in deoxyribonucleic acid (DNA) damage, leading to death during subsequent cell division. The benefits of radiotherapy include coverage of a wider area

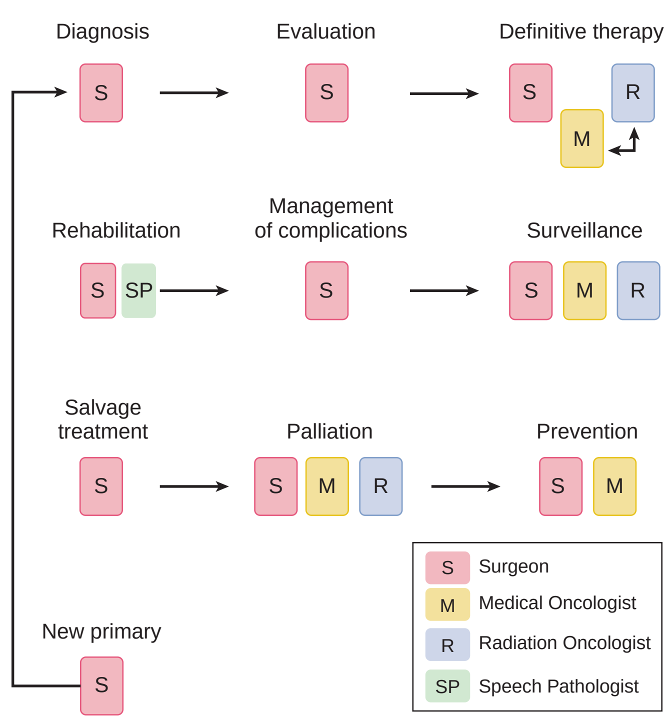

Figure 1.6 Role of the various specialists in the multidisciplinary management of patients with head and neck cancer. *M,* medical oncologist; *R,* radiation oncologist; *S,* surgical oncologist; *SP,* speech pathologist.

around the primary tumor compared with surgery, applicability to surgically inaccessible or incurable tumors or to patients who, for medical reasons, cannot undergo an operation, and the potential for anatomic organ preservation. Although radiation therapy is highly effective in the treatment of tumors such as those of Waldeyer's ring and early larynx cancer, application of radiation therapy often is limited by the sensitivity of adjacent normal tissues. Several factors need to be considered when choosing radiation as part of the treatment program. First, radiation damage to normal tissues within the field is permanent. As such, long-term sequelae are quite common. Tissues with the lowest radiation tolerance, such as the salivary glands and neural tissues, show the most profound and lasting changes, resulting in xerostomia, changes in taste and dentition, and related sequelae. Moreover, reirradiation in previously treated areas may overwhelm normal tissue tolerance, limiting use of radiation for subsequent treatment. This consideration is significant given that the overall lifetime risk for additional primary tumors approaches 30% in patients cured of the index primary head and neck cancer and who continue the life style or habits of tobacco and alcohol consumption. In addition, radiation can have mutagenic effects on normal structures, leading to the development of radiation-induced malignancies. Finally, radiation may make surgical salvage more complicated, often leading to more extensive procedures. Advances in technology such as intensity-modulated radiation therapy and the availability of proton therapy are allowing improved targeting of the primary tumor volume while limiting exposure of surrounding tissues to the damaging effects. The combination of chemotherapy with radiation has improved the therapeutic outcomes in several primary sites in the head and neck.

CHEMOTHERAPY

In the past, the role of chemotherapy in the management of head and neck cancers was primarily for palliation. With improved understanding of the impact of multimodality treatment, chemotherapy is now used as part of both definitive and adjuvant treatment regimens in conjunction with radiation therapy. For head and neck squamous cell carcinomas, platinum-based compounds are the most commonly used agents because they have shown the best responses either alone or in combination with other drugs. Platinum compounds, including cisplatin and carboplatin, traditionally have been used in combination with antimetabolites such as 5-fluorouracil and taxanes such as paclitaxel. Chemotherapy may be combined with radiation in one of several sequences, including neoadjuvant, concurrent, or induction, followed by concurrent chemoradiation therapy. Chemotherapy also is used as concurrent treatment with postoperative radiation therapy in high-risk patients.

Initially, chemotherapy was given before radiation, on the basis of the results of the Veteran's Administration larynx preservation trial. Since then, several prospective trials and metaanalyses have shown advantages of concomitant chemoradiation over sequential treatment. However, the benefits from concomitant chemoradiotherapy are tempered by higher rates of acute and long-term treatment-related sequelae. This issue is of particular concern for patients who fail to respond and who must unnecessarily endure the adverse effects of treatment and require salvage surgery. On the basis of observations that response to chemotherapy predicts radiation response, there is now renewed interest in the use of induction chemotherapy to select patients for subsequent concomitant chemoradiotherapy. The role of biological agents is evolving. Biological agents that target epidermal growth factor receptors have shown promise in combination with radiation therapy, because this approach enhances treatment response without increasing severe adverse effects.

Introduction of immunotherapeutic agents has opened a new vista in systemic therapy of many cancers. In the head and neck cancers, immune checkpoint inhibitors, including PD 1, PDL 1, and MAP kinase inhibitors are currently being tested in clinical trials.

POSTTREATMENT MANAGEMENT

Rehabilitation and Lifestyle Modification

Rehabilitation of the patient after initial definitive treatment is focused on functional, psychological, and vocational restoration. Postsurgical sequelae require intervention by physical and rehabilitation specialists (e.g., neck and shoulder exercises and speech and swallowing therapy). In addition, rehabilitation of a paralyzed face or vocal cord, stricture of the pharynx, and obstruction of the nasolacrimal duct require specific interventions. Esthetic restoration of the face is crucial to psychological rehabilitation. Postradiation sequelae require management of xerostomia, dental care, and prevention of fibrosis-related complications such as trismus and frozen shoulder. Postchemotherapy sequelae require management of renal function, hearing, and peripheral neuropathy. Support services and counseling are important for vocational rehabilitation.

Modification of lifestyle to reduce the risk of recurrence and to prevent development of new primary tumors is an integral component of posttreatment management. Involvement of psychosocial specialists for cessation of smoking and alcohol use is of great benefit. Appropriate pharmacologic and behavioral interventions are necessary to achieve this goal. Genetic counseling and screening of family members should be provided in the event of certain diseases such as medullary carcinoma of the thyroid and paragangliomas.

Posttreatment Surveillance

The patterns of tumor recurrence and risk of subsequent new primary tumors influence the frequency and intensity of surveillance. For tobacco-related cancers (such as squamous cell carcinoma of the upper aerodigestive tract), the highest risk for local/regional recurrence is within the first 2 years. Therefore regular head and neck examination at 2- to 3-month intervals is recommended for the first 2 years. Thereafter this risk diminishes gradually, but the risk of developing a new primary cancer increases at a rate of about 2% per year, reaching a lifetime cumulative risk of 35%. Long-term follow-up is therefore recommended semiannually for the first 5 years and annually thereafter. More stringent surveillance should be performed in high-risk patients such as those with field cancerization or those who continue to smoke and/or drink alcohol.

Increasing use of radiation and chemotherapy in patients with advanced-stage disease has influenced the patterns of failure with improved local/regional control but higher risk for distant metastasis. Surveillance for detection of distant metastases and new primary tumors at other locations should include annual chest imaging and/or a PET scan. Ultrasonography and biochemical surveillance (with thyroglobulin and calcitonin) is applicable in patients with thyroid cancer.

OUTCOMES

The only available registry-based data on outcomes of therapy for head and neck cancer in the United States come from the National Cancer Database of the American College of Surgeons. The AJCC has regularly published outcomes data from the National Cancer Database in each successive edition of its cancer staging manual. Therefore the outcomes data presented in each chapter are from the eighth edition of the *AJCC Cancer Staging Manual*. Single-institution data from Memorial Sloan-Kettering Cancer Center are also presented where appropriate, to highlight the differences in outcomes from a tertiary care cancer center.

CHAPTER 2

Basic Principles of Head and Neck Surgery

Because most patients with tumors of the head and neck initially present to the surgeon, it is the surgeon's responsibility to do a comprehensive examination of the head and neck area, accurately assess the tumor and assign the stage of the disease, discuss treatment options, obtain appropriate multidisciplinary input, and initiate treatment planning. Accordingly, the head and neck surgeon must have a basic understanding of the biology of the disease and the factors involved in cancer management, including tumor and host factors as well as the principles and effectiveness of available treatment modalities. If surgery is selected as the initial definitive treatment, the surgeon should focus on thorough preparation of the patient for surgery. This process includes patient education, a preoperative medical evaluation as well as a dental evaluation if required, speech and swallowing assessment, and psychological consultation as required. This is essential to obtain an informed consent from the patient.

PREOPERATIVE EVALUATION AND PREPARATION

Patient Education and Informed Consent

Before proceeding with surgery, it is essential to have a detailed discussion with the patient and provide counseling regarding the nature and severity of the disease, its impact on the selection of therapy, the treatment options available, the pros and cons of each approach, and the details of the operative procedure if surgery is recommended as the preferred choice of treatment. The sequelae and morbidity of surgery and possible complications should be discussed with the patient and appropriately documented as part of the informed consent process. Central to this discussion is the understanding and realistic expectations by the patient and family members. In addition, the patient should be informed about what to anticipate in the postoperative period. This discussion should stress the need for breathing exercises and early ambulation to prevent complications. Patients undergoing laryngectomy require specific preoperative counseling, including consultation with a speech pathologist, review of voice rehabilitation, and video education regarding expected sequelae. Similarly, patients who are expected to have significant functional or aesthetic sequelae after surgery also require specific counseling and access to support services.

Initiation of Preventive Measures

A key factor contributing to perioperative morbidity is current tobacco use. Smoking causes changes in cardiopulmonary function that can have unfavorable implications for patients undergoing prolonged anesthesia. Smokers are at an increased risk for postoperative pulmonary complications as well as free flap failure. Smoking-induced changes in cardiopulmonary function can be minimized by preoperative abstinence from smoking. Accordingly, appropriate counseling for cessation and support services are an essential part of preoperative preparation. The period before surgery is also an excellent time to initiate efforts at permanent smoking cessation. Similarly, perioperative β-blockade has been shown to reduce the incidence of myocardial ischemia, myocardial infarction, and long-term overall mortality related to cardiac events after surgery in patients at high cardiac risk. It is believed that the beneficial effects of β-blockers result from a positive balance of myocardial oxygen supply and demand. The current recommendations for perioperative β-blockade for patients at high risk for a perioperative cardiac event are to begin use of a β-blocker several weeks before a planned operation, titrate the dose to achieve a heart rate of 60 to 70 beats per minute, and taper the dose in the postoperative period.

Medical Optimization

The basic preoperative assessment includes a detailed history and physical examination, a complete blood cell count, routine biochemistry tests, urinalysis, an electrocardiogram, and a chest radiograph. In addition, overall poor general medical status and the presence of comorbid conditions warrant the need for a preoperative medical or cardiology consultation. Although advanced age by itself is not a contraindication for surgery, comorbidities that are more common in older patients may require specific preoperative evaluation and optimization. In advanced tertiary care centers, special Geriatric Services are available. If such resource is available, then a preoperative geriatrics consultation should be obtained. In general, most medications can be continued until the day of surgery with the exception of anticoagulants, such as aspirin, warfarin (Coumadin), and any other antiplatelet agents, which should be stopped 5 days before surgery if medically acceptable. For patients in whom anticoagulants cannot be stopped, warfarin should be switched to short-acting anticoagulants that can be withheld on the day of surgery. Because antihypertensive agents that target angiotensin-converting enzyme can cause severe hypotension during anesthesia, they also should be discontinued before surgery.

Preoperative Considerations for Postoperative Management

In addition to medical optimization, postoperative management issues also should be addressed before surgery. If significant or prolonged pain is expected, a pain management specialist should be consulted preoperatively. Psychological consultation and

counseling also may be considered preoperatively if a patient (or family member) is having significant problems with stress or coping. In addition, a history of heavy alcohol use warrants prophylaxis for delirium tremens, which should be instituted in collaboration with a psychiatrist. Effective treatment of delirium tremens relies on early identification of patients at risk before symptoms develop, use of benzodiazepines (e.g., lorazepam) for withdrawal prophylaxis, and then gradual tapering for detoxification.

INTRAOPERATIVE MANAGEMENT

Hair Removal

Traditionally, the preparation of patients for surgery has included shaving of hair from the intended surgical site the night before the operation. It is now recognized that shaving in advance of surgery can lead to hair follicle irritation and infection, and accordingly it is no longer recommended. When necessary, hair removal should be performed in the operating room with use of electric clippers. The use of sharp razors (even safety razors) is discouraged.

Operating Room Setup

The design of the operating room should accommodate all the required equipment and yet provide easy access to the patient. To facilitate the free flow of personnel and equipment, a minimum of 800 square feet of floor space is desirable. The operating room setup for head and neck surgery requires at least two overhead operating lights and an operating table with the flexibility to position the patient as required. Procedures that require two surgical teams working simultaneously are ideally performed in an operating room with two sets of overhead operating room lights. In contemporary operating rooms, digital imaging, operative endoscopy and microscopy, electrocautery, various energy devices for coagulation, and other basic surgical instruments should be available. A typical setup of a contemporary head and neck operating room is shown in Fig. 2.1.

Standardized operating room setup allows operations to be conducted smoothly. Most head and neck surgical procedures can be performed with a single surgical team consisting of the operating surgeon, the first and second assistant surgeons, and a scrub nurse. Complex operations of the skull base, mediastinum, or thorax and free flap procedures require more than one surgical team. Some select situations require two teams to work simultaneously. When multiple surgical teams are involved, the surgical plan and sequence should be discussed with the entire team, which includes the anesthesiologist and operating room personnel. Similarly, for robotic surgery, the setup requires specific positioning of the patient, the operating table, and the robotic console.

Setup for General Open Head and Neck Operations

As a general rule the operating surgeon stands on the side of the operative field, with the first assistant at the head end of the table and the second assistant directly across on the opposite side of the surgeon. The endotracheal tube and the anesthesia circuit are directed diagonally away from the operative field at the head end, to be connected to the anesthesia machine. In general, the scrub nurse should stand on the same side as the surgeon, with the Gerhardt instrument table brought over the operating table and up to the level of the umbilicus of the patient (Fig. 2.2). The electrocautery cords and suction tubing are directed into the operative field between the scrub nurse and the surgeon and are secured to the drapes. Wastebaskets are positioned for easy access by the surgeon and in sight of the scrub nurse so that the contents are readily visible.

Setup for Endoscopic Surgery

A sterile field generally is not required for endoscopic surgical procedures. The procedure is performed with the use of either endoscopes or an operating microscope. If a carbon dioxide laser is used, the appropriate laser precautions should be in place. Transnasal and transoral endoscopic surgery requires a full complement of endoscopes as well as specialized insulated instruments and suction coagulators. The setup and positioning of the operative equipment and personnel are shown in Fig. 2.3.

Setup for Robotic Surgery

Setup for robotic surgery requires generally a larger operating room to accommodate the robotic console and the robot itself (Fig. 2.4). The robotic console may be located in a convenient location in the room away from the operating table and anesthesia equipment. In addition, to position the robot for transoral surgery, adequate space is necessary at the head end of the table, with space for the assistant to sit and work in the oral cavity to assist the surgeon operating the robotic arms. The

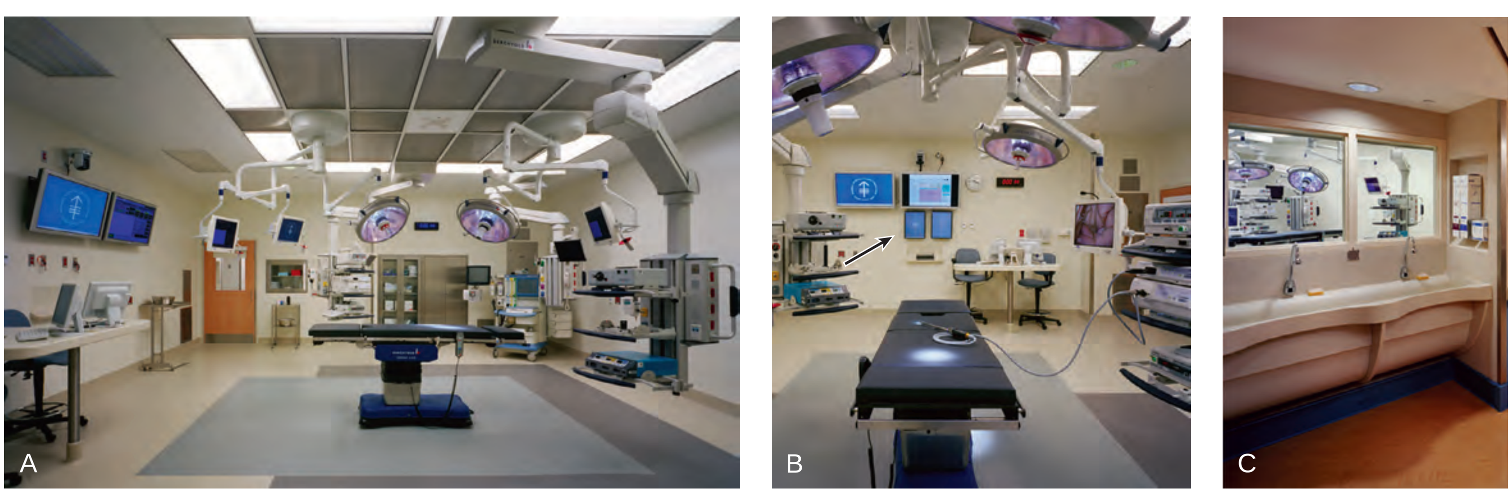

Figure 2.1 A modern operating room showing (**A**) an overview; (**B**) a "wall of knowledge" that displays surgical video images, continuous vital signs, and imaging studies (*arrow*); and (**C**) the surgical scrub area with visual access to the operating room. *(Images of MS Surgery Suite from Chuck Choi, Brooklyn, NY.)*

assistant may need to use the suction machine or may be required to provide additional retraction or to apply vascular clips for hemostasis. Thus, by necessity, the anesthesia tubing and circuit are extended to have the anesthetic equipment at a distance from the endotracheal tube.

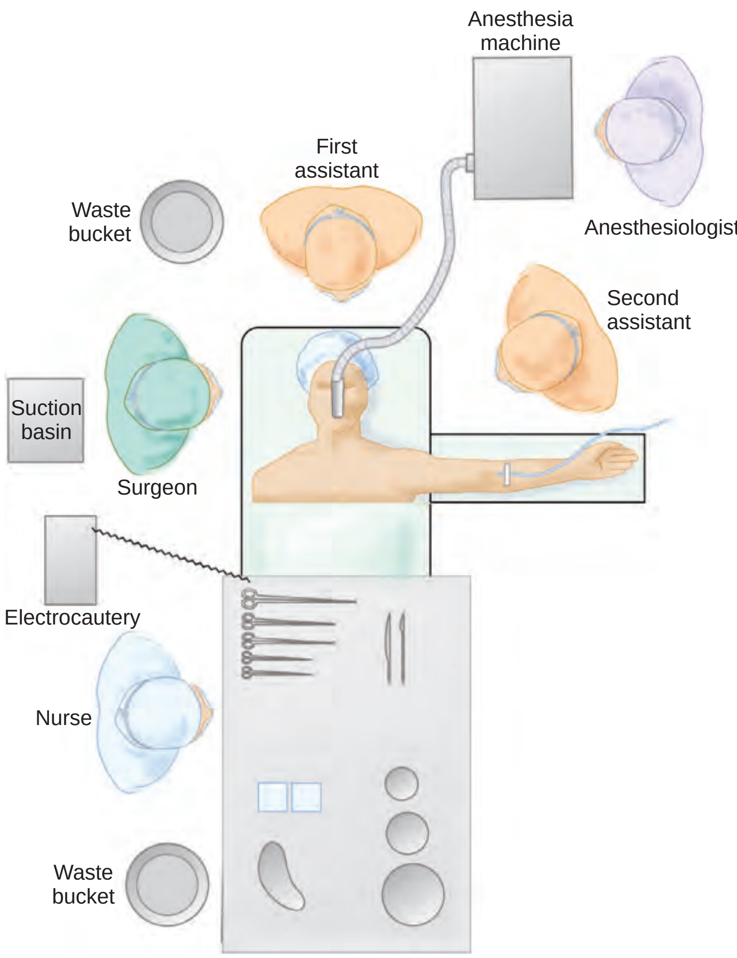

Figure 2.2 Positioning of personnel and equipment for most open head and neck procedures.

Setup for Two-Team Craniofacial Surgical Procedures

Craniofacial surgery for tumors involving the skull base requires planning of the operating sequence to prevent confusion and crowding at the operating table. The patient is prepared and draped for simultaneous access by both the neurosurgical

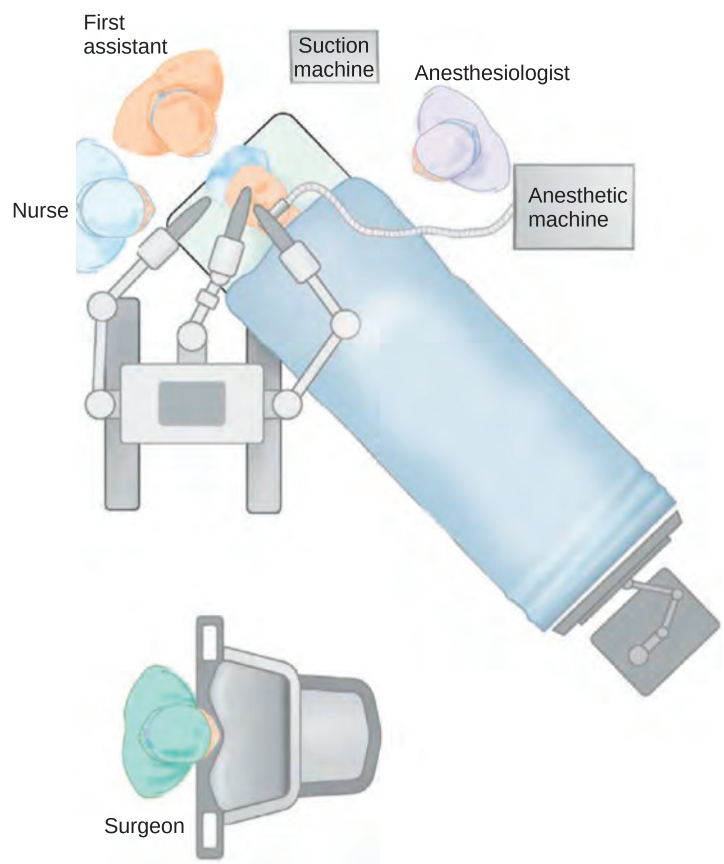

Figure 2.4 Positioning of personnel and equipment for transoral robotic surgery.

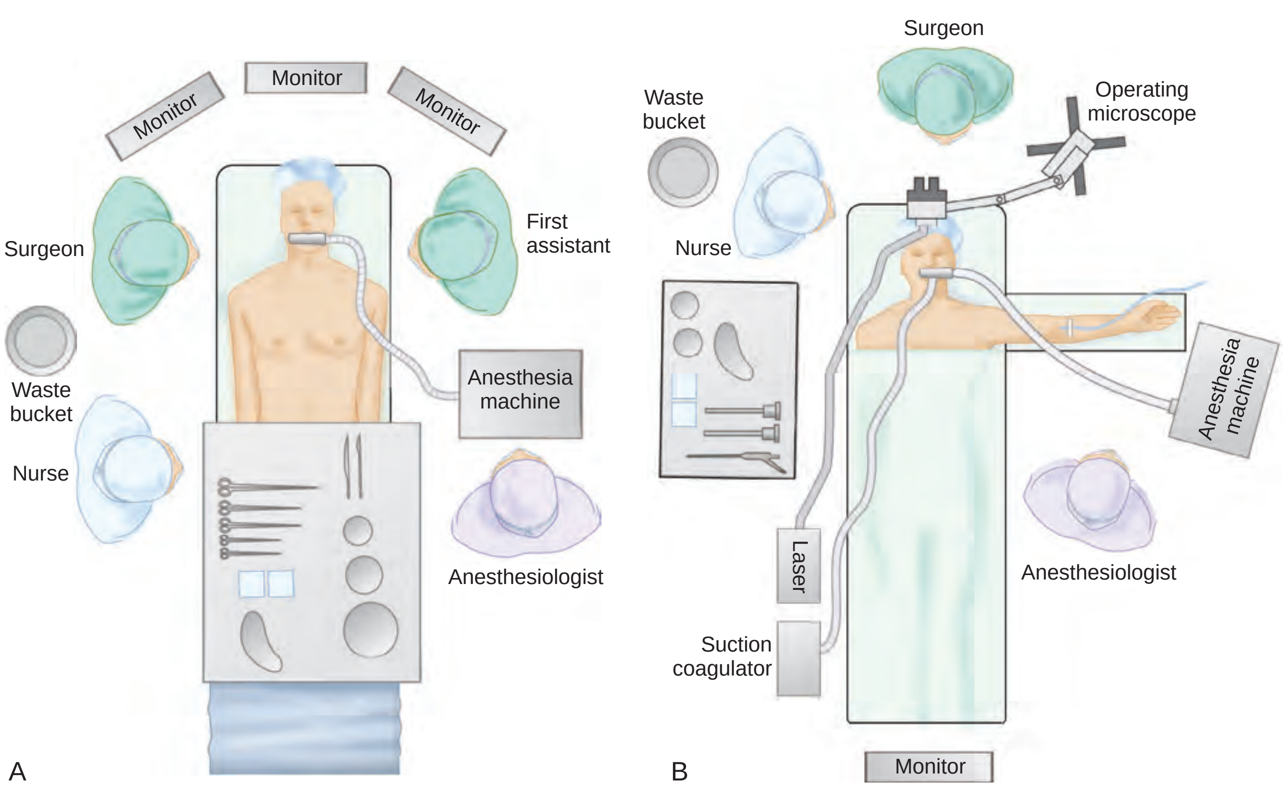

Figure 2.3 Positioning of personnel and equipment for (**A**) transnasal and (**B**) transoral endoscopic procedures.

and the head and neck teams, even though many stages of the operation are performed sequentially by one team at a time. When both teams are working simultaneously, the head and neck surgeon works from the same side as the lesion, with the first assistant between the head and neck surgeon and the neurosurgeon, who works from the head end of the table. The operative setup is depicted in Fig. 2.5. Two sets of powered instrumentation including the appropriate drills, saws, and electrocautery and suction equipment are necessary for this complex operative procedure.

Setup for Simultaneous Operations for Resection and Reconstruction With Two or More Surgical Teams

When a head and neck tumor resection is planned simultaneously with harvest of a microvascular free flap, two surgical teams need to work independently and often simultaneously, to save time, with their own separate scrub nurse. While the head and neck team is resecting the tumor, the reconstructive team can harvest the free flap in selected situations. Similarly, harvest of the jejunal graft or mobilization of the stomach for gastric transposition for reconstruction of a pharyngolaryngoesophagectomy defect may be possible simultaneously. Proper positioning of operating room personnel and equipment is especially important in these situations (Fig. 2.6).

Intravenous Access

A large-bore peripheral venous catheter should be in place for most head and neck surgical operations. As a general rule, the intravenous line should be placed in the arm opposite the side of the tumor resection so the anesthesiologist can have unimpeded access to it. However, if microvascular free tissue transfer is planned, the arm used for the intravenous line should be selected in consultation with the reconstructive surgeon so that harvest of a radial forearm flap, if such is planned, is not compromised.

Intraoperative Monitoring

Peripheral monitoring equipment, including the blood pressure cuff and pulse oximeter, generally should be placed on the arm on the side opposite the operative field. For more complex and prolonged operations, an arterial line is desirable to monitor the hemodynamic status of the patient. As with intravenous access, the arterial line should also be planned in consultation with the reconstructive surgeon. The use of an esophageal temperature probe does not interfere with the surgical field for most operations on the neck, but a rectal probe should be inserted if the operation involves the upper aerodigestive tract. A Foley catheter helps monitor urine output during prolonged operations. Proper monitoring is crucial during the operation to avoid overloading the patient's cardiovascular system with intravenous fluids, especially if there is significant blood loss that needs to be replaced with blood or blood products. Fluid balance is particularly important in older and physiologically compromised patients undergoing prolonged operations, because fluid overload can result in significant postoperative cardiopulmonary complications.

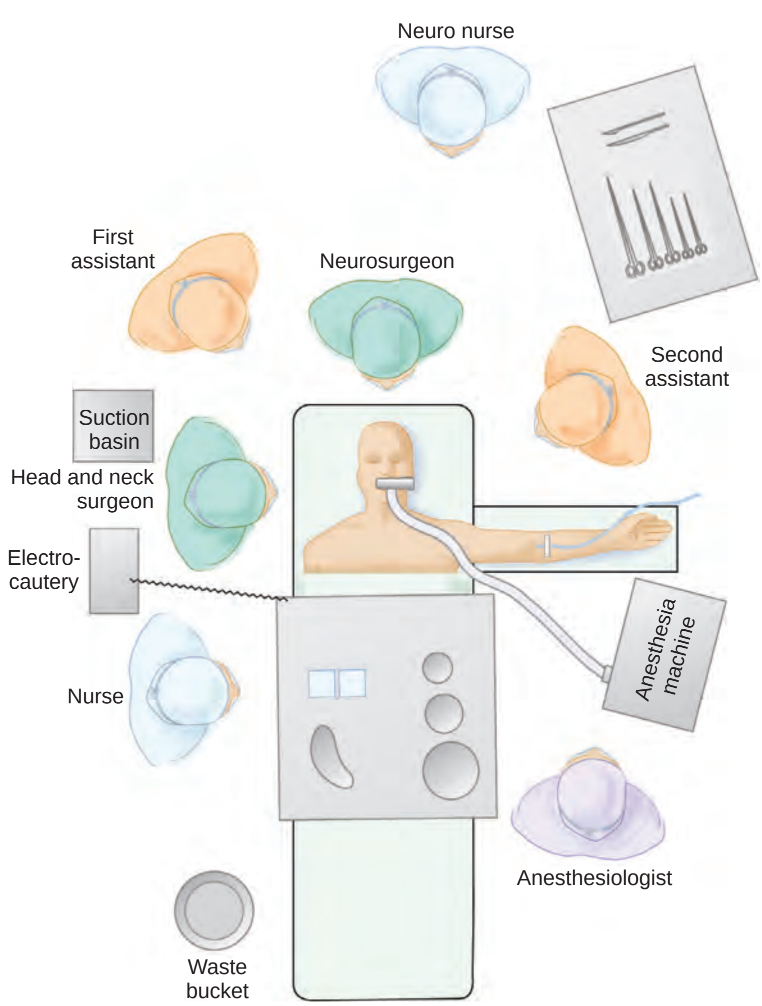

Figure 2.5 Positioning of personnel and equipment for craniofacial surgery requiring two teams.

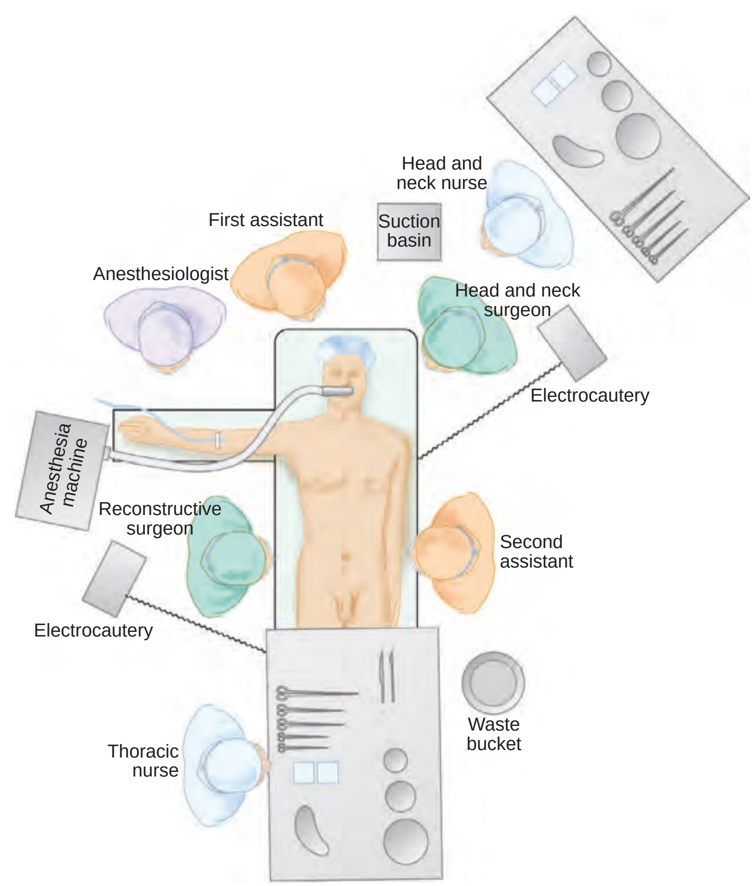

Figure 2.6 Positioning of personnel and equipment for resection and reconstructive surgery requiring two teams.

Antibiotics

Prophylactic perioperative antibiotics are administered for specific indications. In clean cases, such as thyroidectomy, parotidectomy, or neck dissection without simultaneous resection of a mucosal primary tumor, antibiotic coverage is not required. Because most operations on the upper aerodigestive tract and paranasal sinuses are considered *clean-contaminated,* appropriate antibiotic coverage should be provided before skin incision. The choice of antibiotic regimen is dictated by the type of the operation being performed. As a general rule, prophylactic use of a cephalosporin with metronidazole is preferred for most operations on the upper aerodigestive tract. Clindamycin may be used for patients who are allergic to penicillin. A combination regimen of ceftazidime, metronidazole, and vancomycin is recommended for patients undergoing craniofacial surgery. The first intravenous dose of antibiotics is given before the induction of anesthesia, and the dose should be repeated at appropriate intervals for prolonged procedures.

Anesthesia

An anesthesiologist familiar with head and neck surgery is preferred as a member of the operating team, because his or her role is critical for the smooth conduct of head and neck operations. Discussion of the operative procedure between the operating surgeon and the anesthesiologist is essential to allow for safe and expeditious surgery. The mode of anesthesia induction, type and route of intubation, need for muscle relaxation, maintenance of a desired level of blood pressure, anticipated blood loss, and the need for blood transfusion and the rate of fluid administration should be discussed before surgery.

The key anesthesia issue in head and neck surgery involves airway management. Unlike surgical operations at other sites in the body, management of the airway must be a collaborative effort between the anesthesiologist and the head and neck surgeon. Preoperative identification of a potentially difficult airway is the responsibility of the head and neck surgeon. The anesthesiologist should be alerted so that the induction of anesthesia and endotracheal intubation is accomplished safely. Moreover, it is also incumbent upon the surgeon to be proficient in endotracheal intubation techniques, because in select circumstances the head and neck surgeon should take charge and intubate the patient in collaboration with the anesthesiologist.

The surgeon should be familiar with various endotracheal tubes that are available and their applicability to the planned head and neck surgical procedures. As a general rule, the smallest size endotracheal tube that permits satisfactory ventilation should be used, especially for endoscopic surgery for laryngopharyngeal tumors. A wire-reinforced flexible endotracheal tube rather than a simple flexible plastic tube is preferred so that kinking is prevented.

Endotracheal Intubation

The mode of intubation should be planned in advance. Although transoral intubation is appropriate for most head and neck procedures, operations in the oral cavity and oropharynx are best performed with nasotracheal intubation. Similarly, nasotracheal intubation is also helpful in allowing complete excursion of the mandible during operations on the deep lobe of the parotid gland and other tumors in the parapharyngeal space. For nasotracheal anesthesia, special tubes that conform to the curve of the nasal air passage into the larynx are available. Nasotracheal tubes require flexible connections to prevent kinking between the tip of the nose and the anesthesia circuit. Moreover, transoral endoscopic procedures using the CO_2 laser require the use of a “laser safe” endotracheal tube and isolation of the endotracheal tube away from the operative field with moist patties to prevent injury to the tube or cuff and laser-induced fire. High-frequency jet ventilation via a catheter is useful in select circumstances for transoral procedures. Finally, if neuromonitoring of the recurrent laryngeal or vagus nerves is planned during thyroid surgery, an electrode-embedded endotracheal tube is required.

An airway that is difficult to manage should be approached cooperatively. Endotracheal intubation may be difficult in patients with trismus; bulky tumors that preclude a clear view of the laryngeal introitus; or a fibrotic, contracted neck resulting from chemoradiation. In these situations, flexible fiberoptic endoscope-guided nasal intubation should be considered. An elective tracheotomy performed with the patient under local infiltration anesthesia to secure the airway preoperatively may be necessary in select circumstances, such as when a bulky and friable tumor obstructs the laryngeal introitus. If the tracheotomy site is within the sterile operative field, a wire-reinforced endotracheal tube is used intraoperatively, because it is flexible enough to conform to the contour of the patient’s chest during surgery. If the tracheotomy site is not within the operative field, a regular cuffed Silastic tracheotomy tube is used and secured with silk sutures. A flexible “accordion” type plastic or metallic connector is used to connect the tracheotomy tube to the anesthesia circuit.

Nerve Monitoring

Recurrent laryngeal nerve monitoring has become an important tool in modern-day surgery on the thyroid gland. Specialized electrode-impregnated endotracheal tubes are available for this purpose. It is important for the anesthesiologist and the surgeon to ensure that the endotracheal tube is accurately positioned to have proper contact of the electrodes with the vocal cords. Inadequate placement of the tube (electrodes distal to vocal cords or above the vocal cords) will give false signals and inaccurate response to stimulation of the recurrent laryngeal nerves.

Blood Pressure Maintenance

Most head and neck surgical procedures are best conducted with a systolic pressure of approximately 90 mm of mercury. Hypertensive episodes during surgery cause unnecessary blood loss and impede smooth conduct of a safe surgical procedure. A thorough understanding between the surgeon and the anesthesiologist is crucial for maintaining systolic pressure at this level throughout the surgical procedure. Hypotensive anesthesia is particularly indicated in patients requiring craniotomy and major skull base resection. Appropriate use of hypotensive agents should be discussed with the anesthesiologist before starting the surgical procedure.

Muscle Relaxation

Most surgical procedures in the head and neck are best conducted with the patient fully relaxed and paralyzed with appropriate use of short-acting or long-acting muscle relaxants. Thus patients requiring prolonged endoscopic surgical procedures, such as endoscopic laser resections of laryngopharyngeal tumors, require complete

paralysis to achieve optimal positioning of instrumentation for ease of the operative procedure. On the other hand, muscle relaxants should be avoided during surgical procedures in which neuromonitoring is used, such as surgery of the facial nerve, and for monitoring recurrent laryngeal nerves during thyroid surgery.

Position and Draping

For head and neck surgical procedures, the patient is placed on the operating table so that extension of the neck in a partially propped-up position is possible. Preferably the operating table should be electrically controlled, and it should be able to hinge in two sections. The standard position recommended for most head and neck surgical procedures requires the table to hinge at approximately 30 degrees at the patient's waist, with the headboard dropped at least 35 degrees to provide extension of the neck (Fig. 2.7). The patient is essentially in a semisitting position, and elevation of the head serves the purpose of reducing bleeding from minor blood vessels. If possible the patient should be supported with a footboard, and all pressure points, including the heels and elbows, should be padded and protected. The arm on the side of the lesion is tucked by the patient's side so that the shoulder is drawn down, exposing the neck. A surgical hat covers the patient's hair, and a paper tape is used to secure the hat to the patient's skin along the hairline. The pinna on the surgical side is exposed, whereas the contralateral pinna is covered by the hat. The patient's head is supported by a donut cushion to prevent it from rolling from side to side during the operation.

Eye Care

Protection of the cornea during surgery is important for obvious reasons. The patient's eyes are generally not included in the operative field for most head and neck operations. In such instances, the eyes are protected with instillation of an ophthalmic methylcellulose lubricant and are taped shut with the use of a transparent plastic adhesive sheet such as Tegaderm (Figs. 2.8 and 2.9). For surgical procedures on the face that include the eye in the operative field, a 60 nylon suture through the skin of the upper and lower eyelids is recommended to keep the eyelids closed to protect the cornea. Alternatively, a ceramic corneal shield is inserted in the conjunctival sac to protect the cornea. The corneal shield rests on the sclera, and thus protects the cornea, but allows access to the eyelids and conjunctival sac. This is particularly necessary for surgery on facial skin or eyelids.

The skin at the surgical site is prepared with a bacteriostatic solution such as Betadine or chlorhexidine. In patients who are allergic to iodine, alcohol may be used for skin preparation. In general, the area prepared should include not only the immediate field of surgical intervention but also any possible extensions of the procedure. For example, the skin from the hairline of the forehead (including the skin in front of and behind the pinna) and the ipsilateral side of the face, and the neck up to the clavicles, should be prepared for a parotidectomy. In addition, the entire neck and upper chest on the surgical side should also be prepared in the event that the surgical procedure needs to be extended for a neck dissection. For surgery of facial lesions and surgery on the paranasal sinuses, the entire face on both sides is prepared from the hairline down to the clavicle. The skin of the face and neck from a line joining the tragus to the ala of the nose at the upper end and down to the nipples at the lower end should be prepared for operations on the oral cavity, pharynx, and neck. If a pectoralis major myocutaneous flap is anticipated, the skin preparation should extend down to the umbilicus. Other donor sites for harvest of skin grafts or free flaps, such as the arm, abdomen, thigh, or leg, should be prepared as necessary depending on the reconstructive plan.

Figure 2.7 Position of the table for most open head and neck procedures.

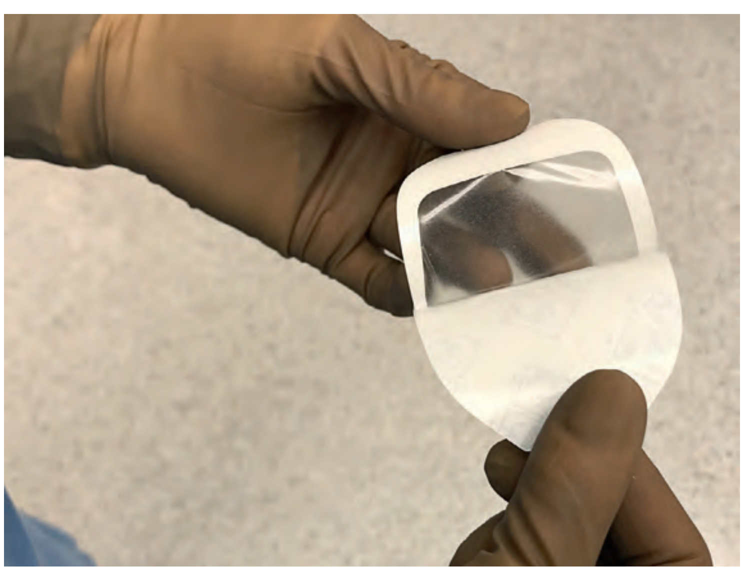

Figure 2.8 Adhesive plastic protective eye covering.

Figure 2.9 The eyes are taped shut after instillation of Lacri-Lube ointment.

Once the skin is prepared, draping of the surgical field begins. Isolation of the head with a head drape requires the use of two folded sheets, placed one over the other with a margin of approximately 10 cm between the folded edges of the two drapes. This method allows the lower drape to rest on the table while the upper drape is wrapped around the patient's head alongside the paper tape that holds the surgical hat in place (Fig. 2.10). The patient's head is lifted and the two sterile drapes are tucked under the head and down to and under the shoulders (Fig. 2.11). The anesthetic tubing must be held up in the air while this draping is taking place. The patient's head is then placed back on the drapes, and the upper drape is wrapped around the patient's head. A towel clip is applied to hold the folded drape in position over the patient's forehead (Fig. 2.12). The anesthesiologist now places the anesthetic tubing over the folded head drape and secures it in place without kinking by folding over the ends of the head drape and securing them with another towel clip (Fig. 2.13). With the head draping completed, a split sheet is placed over the anterior surface of the patient's body and is secured in place. The exposed anesthetic tubing and the upper part of the head are now isolated with a sterile transparent plastic drape, which provides easy view of the endotracheal tube and anesthesia circuit and the eyes during the operation (Fig. 2.14).

Figure 2.12 The top sheet is used to fold over the head while the bottom sheet rests on the operating table under the head.

Figure 2.10 Two flat sheets are held together for draping of the head.

Figure 2.13 The anesthesia tubing is held in the head drape with a towel clip.

Figure 2.11 Both flat sheets are placed under the head.

Figure 2.14 A sterile, transparent plastic drape is used to isolate the upper part of the head and anesthesia tubing out of the sterile field.

BASIC SURGICAL TECHNIQUE

Surgical Incision

The surgical incision for any procedure in the head and neck is planned to provide maximum exposure while allowing for the best aesthetic and functional outcome. Most incisions for head and neck surgery should be planned to respect natural skin creases (Langer's lines) to minimize unpleasant scarring. When the initial surgical incision is planned, the possible need to extend the surgical procedure intraoperatively should be considered, and any future surgical procedures that may be required should be thought of. An ill-placed incision can significantly compromise a subsequent surgical procedure (Fig. 2.15). Issues related to the planning of surgical access and incisions are addressed in detail where applicable for each operation in its respective chapter.

Surgical Procedure

The initial skin incision is made thru the epidermis into the dermis with a scalpel. The remainder of the operative procedure is performed with electrocautery, which allows safe and controlled surgical dissection with minimal blood loss. Because each electrocautery unit is unique, an appropriate wattage setting should be selected and standardized by the operating surgeon for each unit based on his or her level of comfort. Electrocautery does not work well in loose and lax tissue or in a surgical field flooded by blood or fluids. Therefore the surgical field should be dry and tense under traction or retraction for the effective use of electrocautery.

Cutting current is used to divide the dermis up to the subcutaneous tissue to prevent charring of the skin edges, after which coagulating current or a blend of cutting and coagulating current can be used for dissection. Electrocautery should be used to facilitate surgery that allows dissection in tissue planes exposed by properly applied traction and countertraction. Only the tip of the instrument should be used at an angle of 15 to 30 degrees to the tissue rather than at right angles. When used correctly, tissues undergoing electrocautery dissection should show clean, healthy cut edges without any "black" charred tissue. With appropriate use of electrocautery, nearly all surgical procedures in the head and neck can be conducted safely with minimal blood loss. Although monopolar cautery can be used near neurovascular structures, bipolar cautery is preferred to avoid the risk of thermal or conduction injury. In addition, harmonic devices are available to seal and divide blood vessels and tissues. These devices are products of new technology that function at lower temperatures than electrocautery and use ultrasonic waves rather than an electrical current, thus lowering the risk for thermal or conduction injuries.

Energy Devices

Use of energy devices for control of bleeding has entered the arena of head and neck surgery. Commercial devices include the Harmonic scalpel, Ligasure, etc. These instruments are effective in control of bleeding and securing hemostasis and do save some time during surgery. However, the tips of these devices are quite blunt and do not permit meticulous delicate dissection of tissues. In addition the "jaws" of these instruments generate heat and pose a risk of thermal injury to delicate neurovascular structures. Thus caution should be exercised when using energy devices near important nerves.

Wound Closure

Mucosal wounds are closed with interrupted sutures using chromic catgut or synthetic absorbable sutures such as Vicryl. Wound closure should not be under tension, and the sutures should be placed only a few millimeters apart to avoid large gaps in the suture line to prevent fistula formation. The skin wound is closed in layers, using absorbable material for the platysma and subcutaneous tissue and fine nylon for subcuticular tissue or sutures through the skin.

Salvage Surgery

With increasing use of chemoradiotherapy treatment protocols, employed for tumors of the larynx and pharynx, a new treatment paradigm has been established for these tumor sites. However, approximately 20% to 60% of patients being treated with chemoradiotherapy fail to respond and require salvage surgery. Embarking upon surgery in a previously treated field with chemoradiotherapy poses a significant risk of failure to heal, leading to major wound complications. Therefore special preoperative and intraoperative treatment planning is required to avoid and prevent such disastrous complications. Patients must be nutritionally adequate to undergo surgery, and are thus brought into positive nitrogen balance with preoperative nutritional supplements. Their hematocrit is optimized. Nonradiated well-vascularized regional or distant free flaps are generously employed on mucosal suture lines as a buttress to bring in new blood supply to promote healing. In spite of such measures, wound complications occur due to skin necrosis. In a situation where there is significant radiation damage to the skin, manifested by thinning of skin with lack of elastic tissue, and dermal telangiectasia, consideration should be given to excising such compromised skin and replacing it with a local, regional, or distant free flap.

Surgical Drains

The decision to place a drain and the type of drain to be used in a wound depends on the operation performed and the status of the surgical bed at the time of closure. Most procedures with dry fields, absence of large dead spaces, and no anticipated lymphatic fluid accumulation, such as thyroidectomy, do not require drain placement. A Penrose drain is used for small, superficial wounds where only a minimal amount of serosanguineous drainage is anticipated; it also is preferred for drainage after parotid surgery, because suction drain has the potential to injure the underlying facial nerve. The drainage from a Penrose drain is collected in sterile gauze dressing held in place with a stockinette. The gauze should be changed as often as required to prevent maceration of the skin.

Suction drains should always be used for patients who have had operations such as neck dissection, where draining of a larger volume of serum or serosanguinous fluid is anticipated. The perforated inner ends of the suction tubes are carefully positioned in the wound away from nerves and major vessels. A loose loop of chromic catgut suture can be used to hold the distal end of the drain in position. The drains are brought out through separate incisions in the skin of the neck and sutured in place with silk sutures. The patency of the suction drains should be checked carefully during the final stages of wound closure, and clots in the drainage tubes should be cleared. The wound should be irrigated with saline solution to verify that

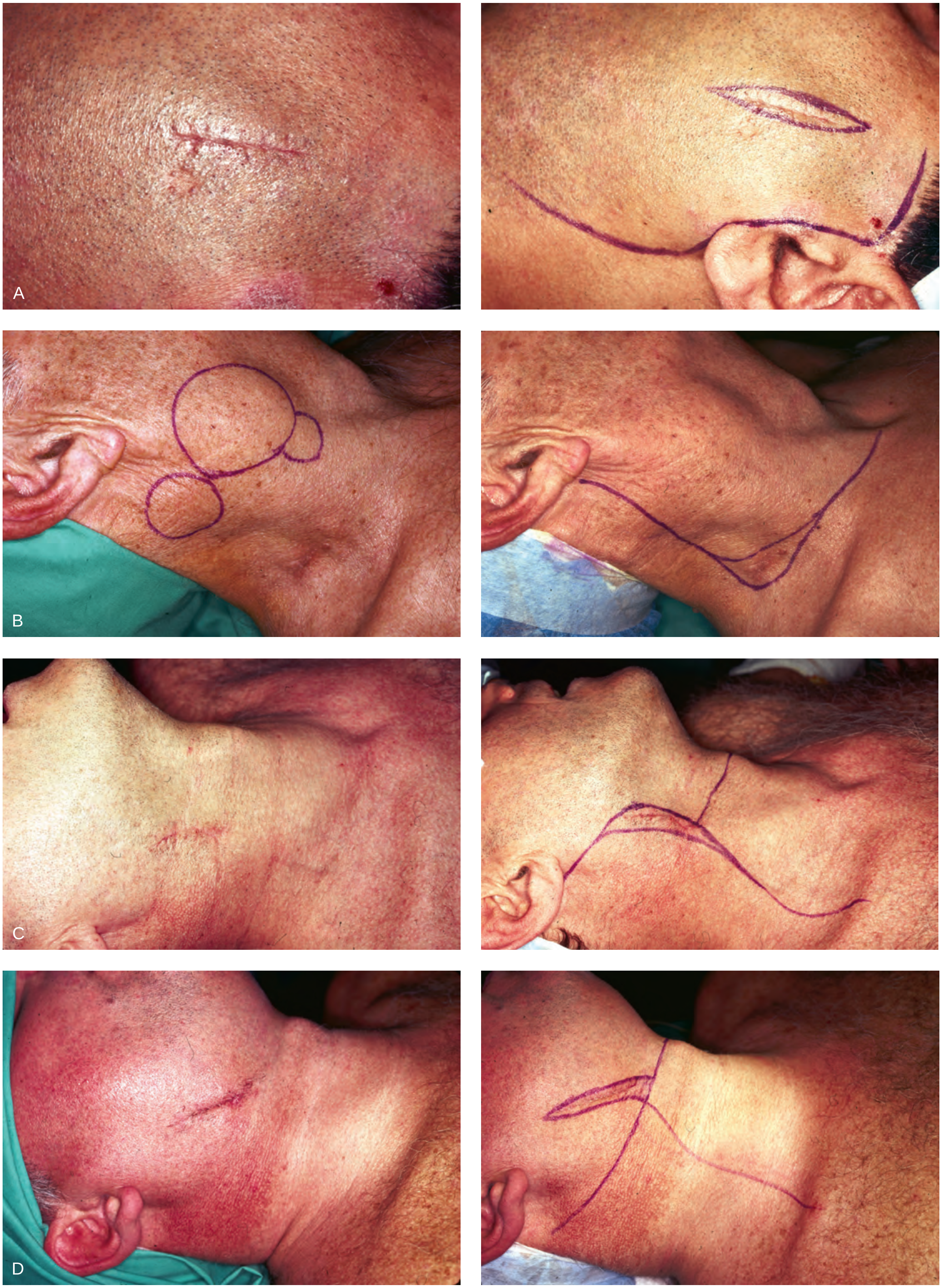

Figure 2.15 Examples of ill-placed incisions for biopsy. This requires modifications of standard incisions for subsequent definitive surgery. **A**, Parotidectomy. **B**, **C**, and **D**, Neck dissections.

the suction drains work. At the end of the operation, the skin flaps should be completely flat and the drains should be able to maintain negative pressure with suction. Any air leaks leading to loss of suction should be rectified before reversal of anesthesia. Prevention of clogging of the suction drains is crucial, because close apposition of the undersurface of the skin flaps to the raw area in the neck plays an important role in minimizing oozing. Loss of suction allows the skin flaps to lift off the surgical bed, leading to oozing and ultimately hematoma formation. Therefore the suction drains should be connected to a "high negative pressure" suction source for at least 24 to 48 hours, at which point they may be transferred to the self-suctioning canister.

POSTOPERATIVE MANAGEMENT

To minimize complication rates and recovery time, postoperative care for patients undergoing major head and neck surgery should proceed in an organized manner with established protocols. Key issues include infection control, management of the surgical site and drains, free flap monitoring, pain control, airway management, and nutrition.

Infection Control

Infection is a major risk for patients in the postoperative period. Several measures should be instituted to minimize infection risks. Early ambulation and respiratory therapy with an incentive spirometer are crucial to prevent atelectasis, pneumonia, and thromboembolic phenomena. If a Foley urinary catheter was placed, it should be removed as soon as the patient is ambulatory. Intravenous lines and narcotic analgesic drugs also should be discontinued as early as possible in the postoperative period. Perioperative antibiotics are usually discontinued within 24 to 48 hours. Longer use of prophylactic antibiotics is indicated in select circumstances such as craniofacial surgery and surgical procedures where "packing" is used, creating a contaminated "closed space," for example, for a defect after a maxillectomy.

Management of the Surgical Site and Drains

Most surgical wounds in the head and neck region do not require a dressing and can be kept open to the air. These surgical sites must be kept meticulously clean to prevent infection. Blood clots and crusting around the suture line are cleaned daily, and Bacitracin ointment is applied to keep the wound free from superficial infection. Intraoral suture lines should be cleaned beginning 2 to 3 days after surgery with hydrostatic power sprays of saline solution, with or without hydrogen peroxide. A dilute solution of hydrogen peroxide and saline is sprayed using powered equipment at least twice daily in the oral cavity to keep the area mechanically clean. In addition, the patient is taught self-care using frequent gravity-controlled oral irrigations. The surgical drain site should be kept clean, with frequent sterile dressing changes if a Penrose drain is used. Output from surgical drains should be monitored and the drain removed when output is less than 25 mL in 24 hours for closed suction drains and when output is minimal for Penrose drains.

Pain Control

Intravenous analgesic drugs are administered for pain control in the first 24 hours following surgery. For most head and neck procedures, the use of intravenous analgesic agents should be terminated as soon as the patient is able to take oral analgesic medications. In selected cases, patient-controlled analgesia (PCA) may be initiated if intense pain is anticipated or in situations in which a patient is not able to communicate analgesic needs. This system allows the patient to self-administer intravenous analgesics as required on demand and can be adjusted until pain is properly controlled. Management of prolonged pain following surgery requires consultation with a pain specialist.

Airway Management

Humidification of the airway is essential for smooth recovery from anesthesia in the immediate postoperative period. If the patient is breathing through his or her mouth or nose, humidity is delivered with the use of a face tent. The use of nasal catheters to deliver oxygen should be discouraged, because they are prone to cause drying of the nasal cavity, increasing the risk for epistaxis. If a tracheotomy is performed, humidity is delivered via a tracheotomy collar to maintain moisture in the air delivered to the lungs. The nursing staff should be familiar with the care of the tracheotomy site and the tube. The cuff of the tracheotomy tube should remain deflated if the patient is breathing spontaneously. Regular gentle suctioning of the airway is generally required for the first few days, and the patient should be encouraged to cough out secretions. The cuffed tracheotomy tube generally should be exchanged for a cuffless tube when mechanical ventilatory support is no longer required. Ties around the neck to secure the tracheostomy tube should be avoided in patients who have undergone reconstruction with a pedicled or free flap to prevent pressure on the vascular pedicle of the flap. In such instances the tracheostomy tube is secured with sutures to the skin of the neck. When the patient is able to tolerate plugging of the tracheotomy tube for 24 to 48 hours, it may be removed safely. Downsizing of the tracheotomy tube in anticipation of decannulation is not necessary. The sequence of decannulation of the tracheotomy tube in relation to the nasogastric tube depends on several factors; this issue will be addressed with each surgical procedure as applicable. Following decannulation, an occlusive dressing is applied to the tracheotomy site. The patient is instructed to apply digital pressure on the dressing when he or she coughs and phonates for the first few days. Most temporary tracheotomy wounds heal within a few days, and no special wound care is required. If a long-term tracheotomy is anticipated, the patient and the family should be educated and instructed about tracheostomy care as soon as the patient is stable.

Nutrition

Maintenance of adequate nutrition is necessary for satisfactory wound healing. An average daily intake of 2000 calories is satisfactory for most patients. Intravenous alimentation is seldom required, because the alimentary tract is physiologically intact in nearly all patients undergoing head and neck surgery. For most uncomplicated procedures in the oral cavity, oral intake can begin on the first postoperative day, starting with liquids and advancing to a full diet as tolerated. In cases in which a short restriction in oral diet is anticipated, a nasogastric feeding tube should be placed at the time of the operation. The tube should be sutured in place to the ala of the nose to minimize

risk for accidental removal. The position of the tube should be confirmed radiographically with a chest x-ray, before starting tube feedings. If prolonged use of nasogastric feeding is anticipated, placement of a percutaneous endoscopic gastrostomy (PEG) tube should be considered. Oral intake can start 7 to 10 days after most uncomplicated laryngopharyngeal surgical procedures, even when free tissue transfer is used for reconstruction. The timing of oral intake may be delayed in patients who have previously received radiation or when fistula formation is a concern. Consultation with a speech and swallowing pathologist should be considered in cases in which dysphagia or aspiration is a concern before starting an oral diet.

Rehabilitation

Successful outcome after head and neck surgery depends on multidisciplinary involvement in preoperative assessment and thorough preparation of the patient, intraoperative management, and postoperative care. Participation by the patient in understanding the disease, its natural history, and self-care after recovery from surgery are also crucial to a successful outcome. As the patient recovers from the operation, the emphasis of care should transition to education of the patient and his or her family regarding self-care and early rehabilitation. Rehabilitative measures, including speech and swallowing and physical and occupational therapy, should be initiated in the hospital and continued until satisfactory goals are achieved. Psychosocial issues often surface after treatment and should be anticipated, identified, and addressed as required. Long-term preventative measures also should be instituted in the perioperative period, including smoking and alcohol cessation with involvement of dedicated personnel if possible. Finally, lifelong follow-up is necessary for patients undergoing head and neck surgery for cancer so that they can be monitored for recurrence and new primary cancers and their psychosocial needs can be addressed.

CHAPTER 3

Scalp and Skin

The skin, by surface area, is the largest organ in the human body. In its role as a barrier to the outside environment, the skin is continuously exposed to putative carcinogens; thus it is not surprising that skin cancer represents the single most common human malignancy. The diversity of embryologic origins of the skin and its adnexal structures leads to a wide range of malignancies. Although their true incidence is difficult to determine, it is well established that basal and squamous cell carcinomas represent the most common human malignancies, accounting for more than 3 million new cases annually in the United States (Table 3.1). Melanomas are the third most common cutaneous malignancy, with approximately 73,000 new cases annually. Nonepithelial skin cancers such as adnexal carcinomas account for an additional 5000 cases. Moreover, the rates of both melanoma and nonmelanoma skin cancers are rising in the United States. The increase is most pronounced for melanoma. The precise cause for this increase is unknown, but it may be related to increased sun exposure and an increased rate of detection. In spite of the rising rates of skin cancers, mortality rates have remained relatively stable. Overall, the clinical behavior of these tumors ranges from low-risk basal cell carcinoma to the more aggressive melanoma and adnexal tumors, with squamous cell carcinoma holding an intermediate position.

Excessive and/or cumulative sunlight exposure occurring at a younger age in fair-skinned persons contributes to skin cancer pathogenesis. Ultraviolet (UV) radiation, specifically UV-B radiation in sunlight, promotes oncogenesis through deoxyribonucleic acid (DNA) damage. Innate defense mechanisms against UV-B–induced oncogenesis include melanin synthesis and active DNA repair mechanisms. Therefore fair-skinned persons with low levels of melanin or those with compromised DNA repair are at highest risk for development of skin cancers. Patients with an immune dysfunction such as acquired immunodeficiency syndrome or medical immunosuppression related to transplantation or lymphoma also have a significantly higher risk of cutaneous squamous cell carcinomas, Merkel cell carcinoma, and possibly melanomas. Moreover, heritable factors are known to play a role in skin cancer pathogenesis. For example, a family history of melanoma is associated with a twofold to eightfold increased risk for developing melanoma. In addition, several genetic syndromes predispose some persons to skin cancer, including xeroderma pigmentosum (*XPC* mutation; basal cell carcinoma and melanoma), nevoid basal cell carcinoma syndrome (*PTCH1* mutation; basal cell carcinoma), Bazex syndrome (basal cell carcinoma), and basal cell nevus syndrome (melanoma).

A wide range of genetic changes occur in human skin cancers. Mutations in specific pathways known to contribute to skin carcinogenesis include hedgehog signaling and the mitogen-activated protein kinase pathway. Mutations in the patched gene *(PTCH1),* which is the receptor for the sonic hedgehog *(SHH)* gene, have been identified both in patients with sporadic basal cell carcinomas and in patients with nevoid basal cell carcinoma syndrome. Germline mutations in cell cycle regulatory genes (*CDKN2A,* cyclin-dependent kinase 4, and the melanocortin 1 receptor gene) have been associated with melanoma development. Inactivation of *CDKN2A* by methylation and of cyclin-dependent kinase 4 by amplification is common in sporadic cases. The identification of activating somatic mutations in the *BRAF* gene in patients with melanoma has had a significant impact on our understanding of this disease and on development of novel treatment approaches. Although activation of *BRAF* mutations is common in melanomas (>50%), it also is found in high frequency in patients with benign nevi, suggesting it may be an early event in carcinogenesis. No pathognomonic or highly characterized abnormalities have been identified in other cutaneous malignancies.

Table 3.1 Annual Incidence and Mortality From Cutaneous Malignant Tumors in the United States

HISTOLOGY	ANNUAL INCIDENCE (US)	ANNUAL MORTALITY (US)
Basal cell and squamous cell carcinoma	>3 million	<5000 (<0.1%)
Melanoma (all) Invasive (2015 American Cancer Society estimates)	135,000 73,870	 9490 (12.8%)

EVALUATION

Most cutaneous malignancies present as surface lesions (Fig. 3.1). In contrast, adnexal tumors typically present as subepithelial lesions (Fig. 3.2). In most cases, a thorough clinical examination including palpation of the lesion and surrounding tissue and draining the lymph node basin is sufficient to define the extent of the tumor. Optical aids such as dermoscopy (epiluminescence microscopy) and Wood light may be used to enhance clinical evaluation. Technologic advancements, such as confocal microscopy and computer-assisted image analysis, likely will provide clinicians with additional diagnostic tools in the future. Although selected indeterminate lesions can be followed clinically and/or with photodocumentation, biopsy is the cornerstone of diagnosis of skin malignancy.

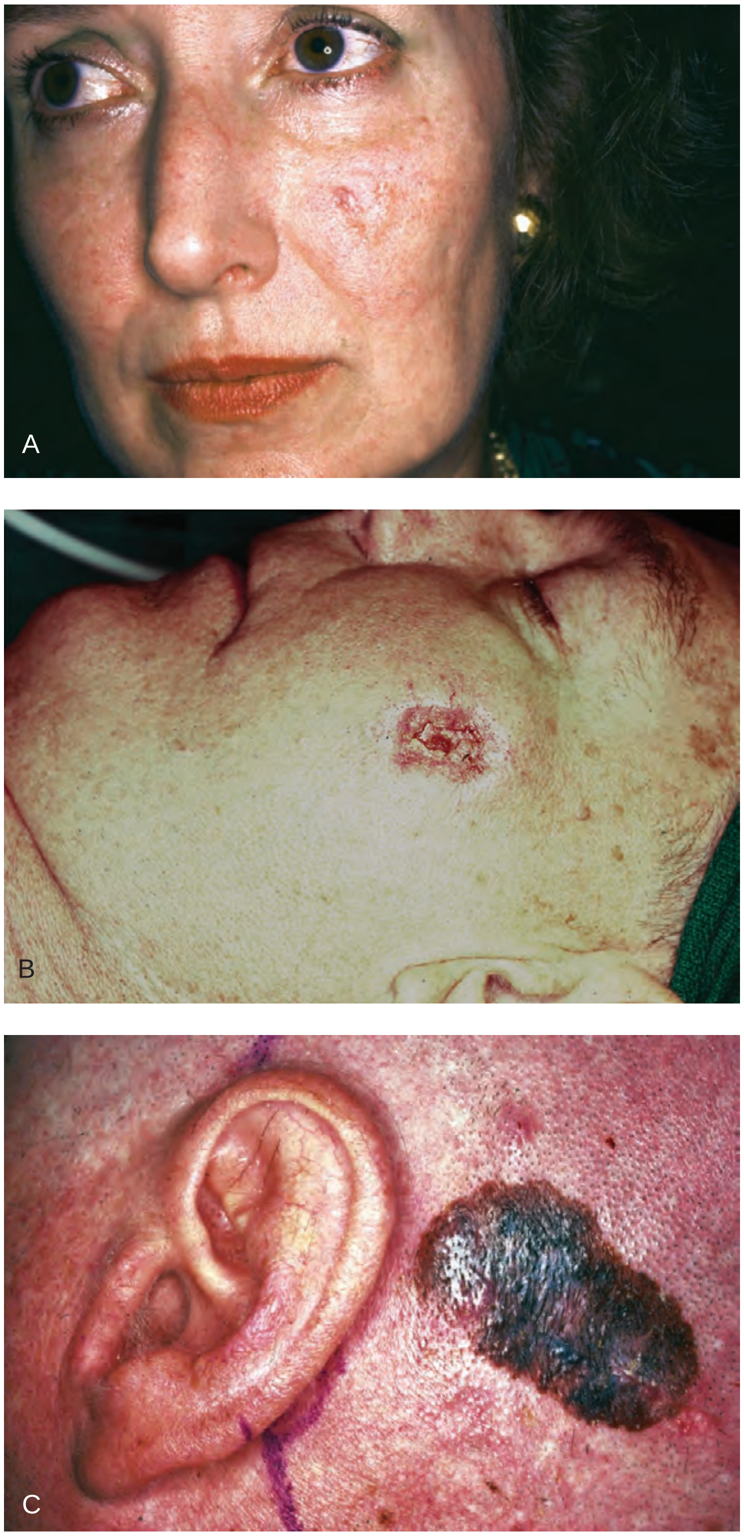

Figure 3.1 Clinical appearance of (**A**) basal cell carcinoma, (**B**) squamous cell carcinoma, and (**C**) malignant melanoma.

Radiologic evaluation is helpful in selected cases. Local extension of disease in the dermis, subcutaneous plane, and satellite nodules, along with bone erosion, can be defined by computed tomography (CT) (Fig. 3.3) or magnetic resonance imaging (MRI). Several skin malignancies can be neurotropic and manifest perineural extension. The cranial nerve most commonly at risk is the trigeminal nerve, which provides the sensory supply to the majority of the face (Fig. 3.4). MRI is useful in demonstrating the presence and extent of perineural spread of disease (Fig. 3.5). The role of positron emission

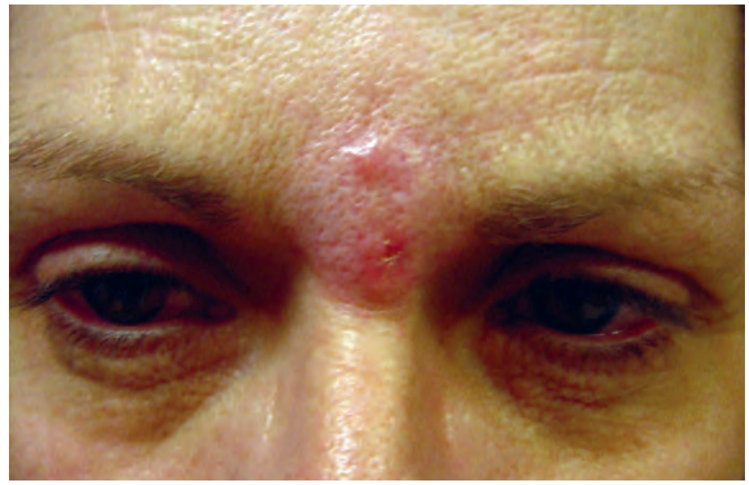

Figure 3.2 Typical appearance of an adnexal tumor.

tomography scanning is evolving, but this type of scan appears to be a valuable adjunct for assessing the extent of disease.

Basal Cell Carcinomas

Approximately 80% of basal cell carcinomas occur in the head and neck region. These tumors classically present as pearly papular lesions that can ulcerate and invade local tissues, earning them the nickname of "rodent ulcer." Because basal cell carcinomas also can be pigmented, malignant melanoma may be a consideration in the differential diagnosis. Morpheaform basal cell carcinoma can present as a flat atrophic lesion with poorly defined borders similar to a scar appearance, making clinical diagnosis challenging (Fig. 3.6). After diagnosis of a basal cell carcinoma, there is substantial risk of developing a subsequent basal cell carcinoma within a few years. These tumors rarely metastasize (only in 0.01% of cases) but can cause significant tissue destruction and disfigurement if not diagnosed and treated appropriately. Metastasis is associated with a poor clinical outcome with an expected survival of <10% at 5 years. Recent advances in hedgehog pathway inhibitor drugs offer patients with locally advanced or metastatic basal cell carcinoma another treatment option when further surgery or radiation is no longer possible. Basal cell carcinomas are derived from basal progenitor cells of the epidermis. Histologically these tumors are composed of dark, elongated cells aligned side by side with peripheral palisading and retraction from the adjacent stroma, producing a cleftlike space. This space may contain prominent stromal mucin (hyaluronic acid). The histologic growth patterns include superficial, nodular, infiltrative, morpheaform, and metatypical (Fig. 3.7), and frequently more than one pattern is present in a tumor. Infiltrative, morpheaform, and metatypical (or basosquamous) types are considered more aggressive with greater invasion and increased risk for recurrence. While immunohistochemical studies are not typically required in diagnosis, these tumors are known to be immunoreactive for Ber-EP4 and pankeratin and may even show carcinoembryonic antigen (CEA) positivity.

Although there is no formal staging system for basal cell carcinoma, the National Comprehensive Cancer Network has developed guidelines for treatment based on evidence and consensus expert opinion. The guidelines divide basal cell carcinoma into low and high risk for local recurrence based on clinical and histologic tumor features. The "mask-area" of the face (around eyes, nose, lips, ears, temple, mandible) represents

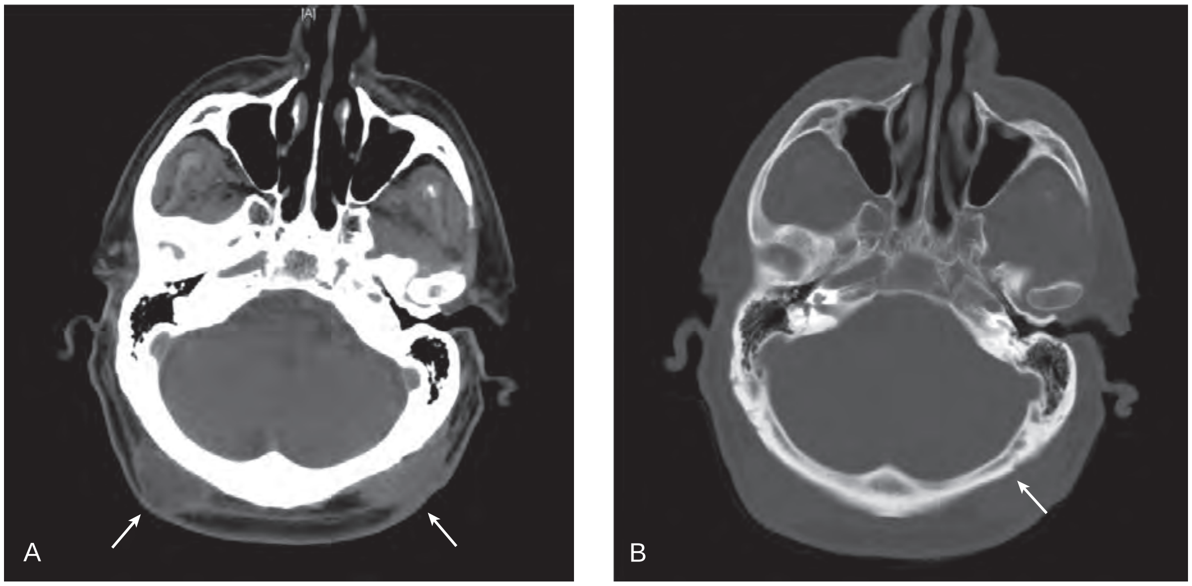

Figure 3.3 Computed tomography scan of a patient with squamous cell carcinoma of the scalp show (**A**) satellite nodules on soft tissue window (*arrows*) and (**B**) erosion of the calvarium on the bone window (*arrow*).

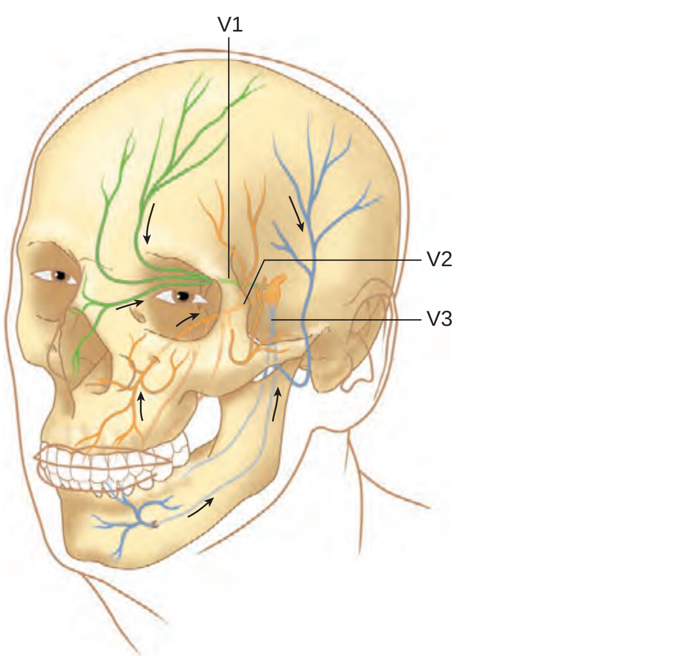

Figure 3.4 Pathways of perineural spread of cutaneous malignancies along the trigeminal nerve.

a higher risk location for skin cancer extension and recurrence. High-risk features include large size, location in "mask area," poorly defined clinical borders, recurrence, site of prior radiation, aggressive histologic subtype, and immunosuppression.

Squamous Cell Carcinomas

Squamous cell carcinomas can be variable in their presentation, ranging from erythematous scaly lesions to highly infiltrative aggressive tumors. Dermal lymphatic permeation presents as distinct intradermal nodules and have an aggressive behavior (Fig. 3.8). More than 70% of all cutaneous squamous cell carcinomas arise in the head and neck region in sun-exposed areas primarily on the ear and upper face. A small proportion of these tumors arise from preexisting actinic keratoses. Although progression has been reported to occur in as many as 25% of untreated cases, the true progression rate for actinic keratoses to squamous cell carcinoma is closer to 0.01% to 0.2% per lesion per year. When actinic damage develops on the lower lips, the term *actinic cheilitis* is used. Other causes of squamous cell carcinoma include ionizing radiation exposure, chronic nonhealing wounds, and human papilloma virus.

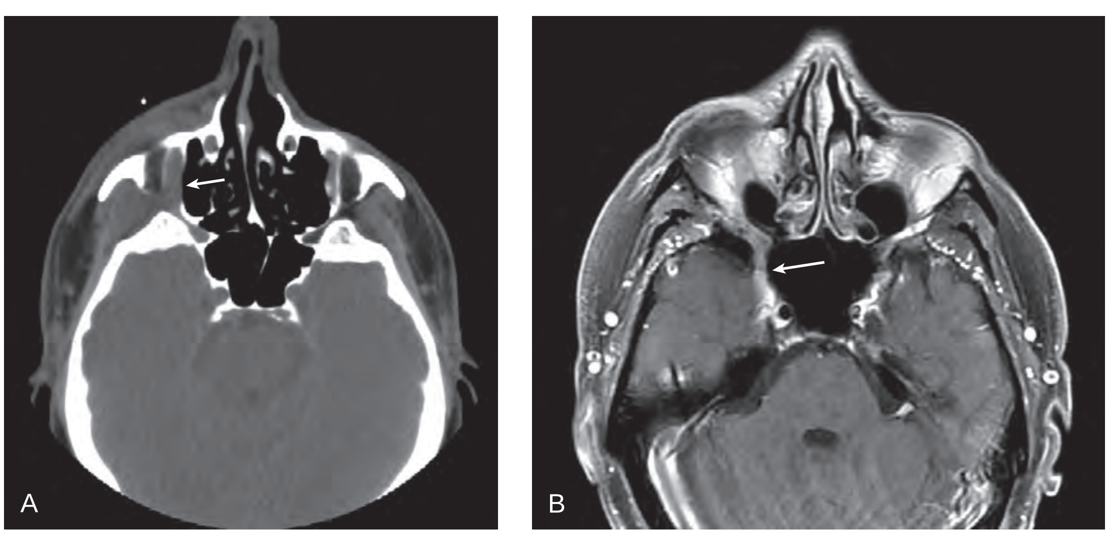

Figure 3.5 Perineural extension of a skin cancer along the second division of the trigeminal nerve. **A**, Computed tomography scan showing involvement of the infraorbital nerve (*arrow*). **B**, Magnetic resonance imaging scan showing extension into Meckel's cave (*arrow*).

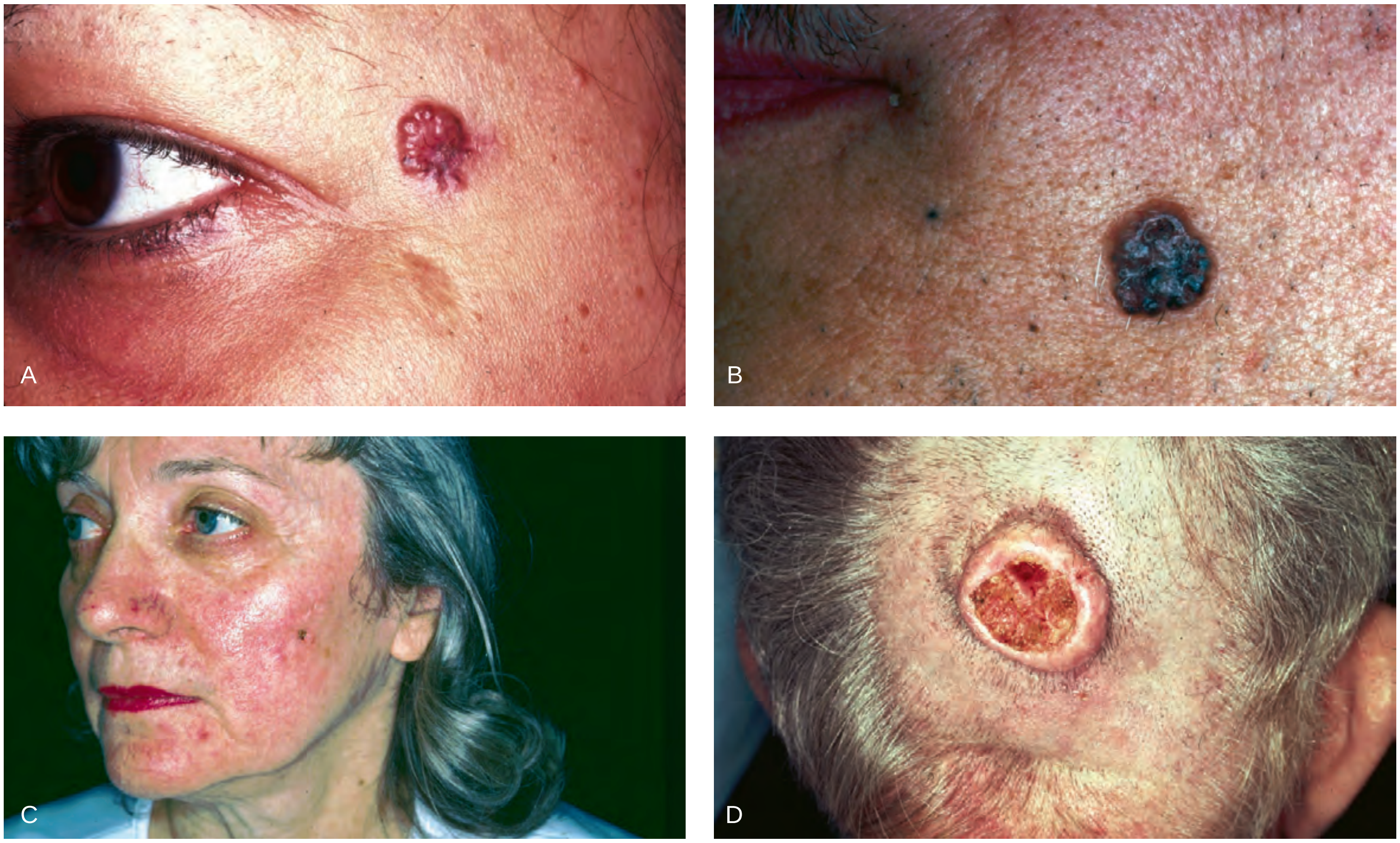

Figure 3.6 Clinical variants of basal cell carcinoma. **A**, Classic. **B**, Pigmented. **C**, Morpheaform.

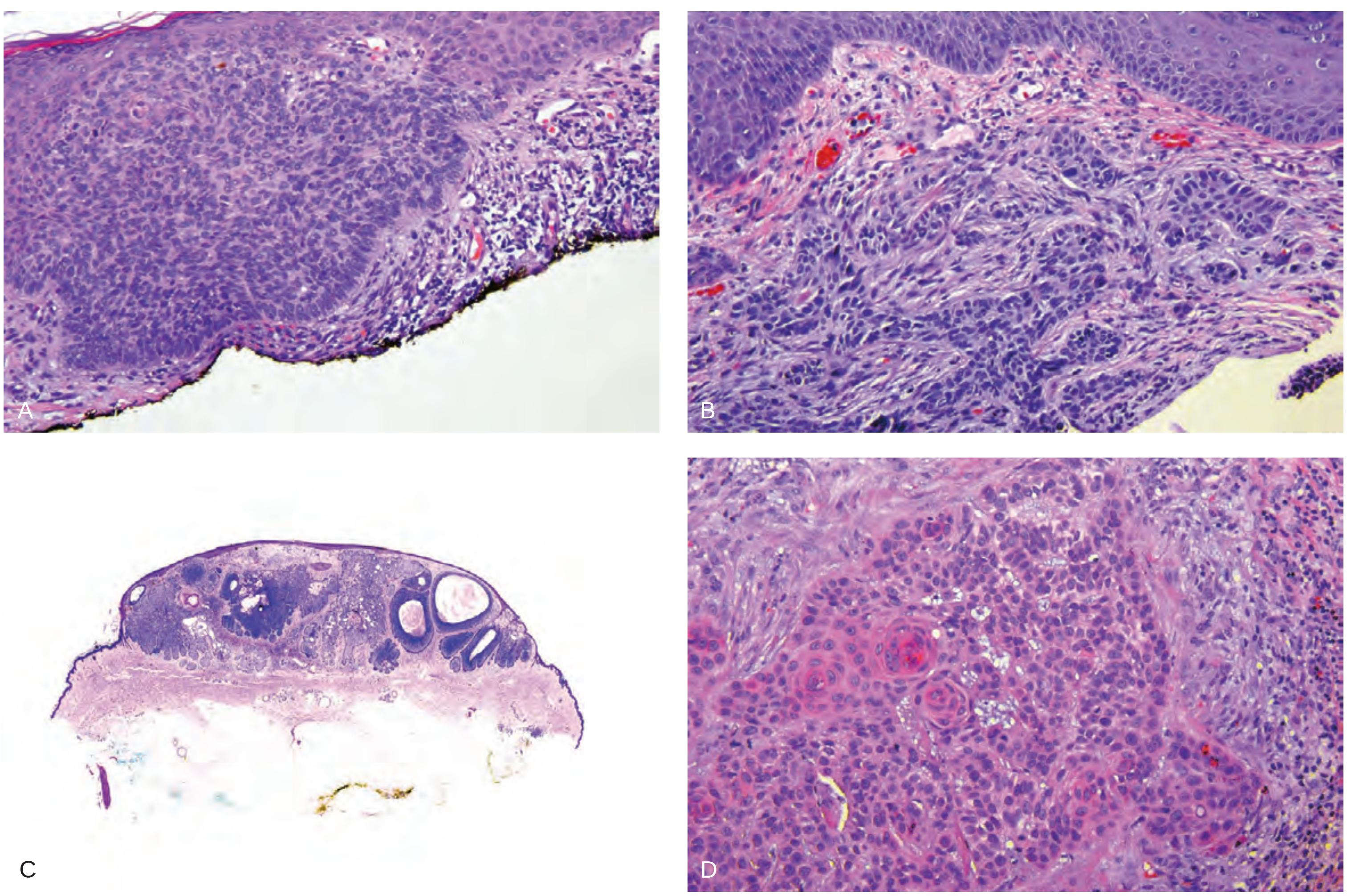

Figure 3.7 Histologic subtypes of basal cell carcinoma showing low to high risk types. **A**, Superficial. **B**, Nodular. **C**, Infiltrative. **D**, Metatypical.

Figure 3.8 Clinical appearance of squamous cell carcinoma. **A**, Multiple superficial lesions. **B**, Infiltrative. **C**, Extensive squamous cell carcinoma of the scalp with dermal nodules.

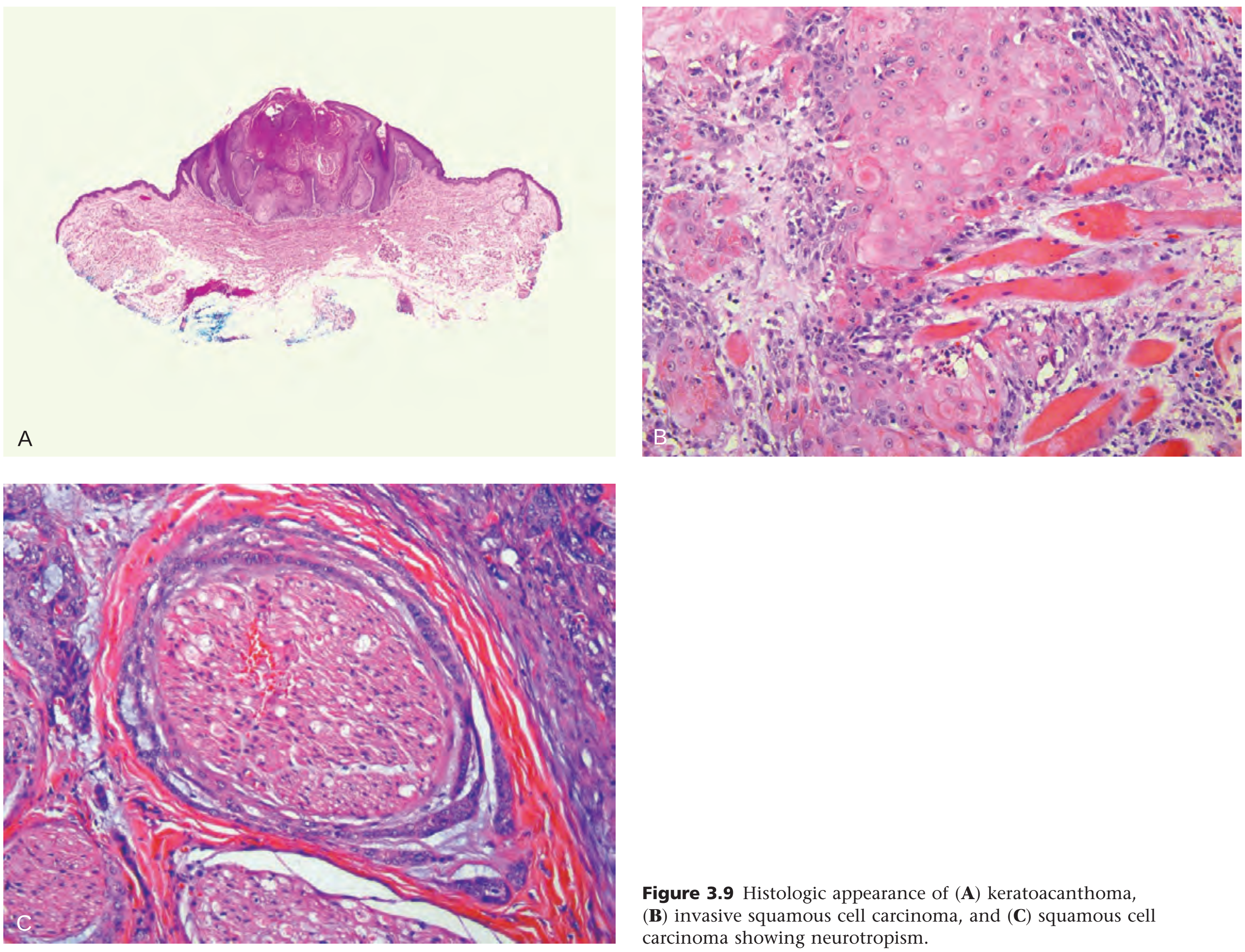

Figure 3.9 Histologic appearance of (**A**) keratoacanthoma, (**B**) invasive squamous cell carcinoma, and (**C**) squamous cell carcinoma showing neurotropism.

Bowen disease (also known as *intraepithelial squamous cell carcinoma*) and keratoacanthoma are unique variants of squamous cell carcinoma. Bowen disease is essentially an in situ squamous cell carcinoma that can progress to invasive cancer if left untreated. Keratoacanthomas are unusual neoplasms that often display rapid growth over a 2- to 4-week period, followed by involution. The precise classification of keratoacanthomas as a variant of squamous cell carcinoma or as a unique entity remains a topic of debate. Histologically, squamous cell carcinomas show a "mosaic" or tile-like pattern of cells with anastomosing intracellular bridges, or desmosomes. Tumors may grow in nests, islands, or single cells and can show variable degrees of intracytoplasmic keratinization, with keratin pearl formation in well-differentiated carcinomas (Fig. 3.9).

Overall, small squamous cell carcinomas (<2 cm) rarely metastasize (metastasis occurs in <5% of cases), but when metastasis does occur, it portends a dismal outcome. Other negative prognostic features include a size larger than 2 cm, prior

treatment, immunosuppression, tumor invasion into subcutis or greater (>6 mm), poor differentiation, and neurotropism (perineural invasion). Microscopic perineural invasion does not portend the same poor prognosis as invasion of named nerves such as the trigeminal and facial nerves. Peripheral nerve involvement is indicated by pain, paresthesia, and numbness along sensory nerves and by fasciculation or weakness of muscles of expression, denoting involvement of the facial nerve. Several staging systems have been proposed for squamous cell carcinoma using high-risk features for local recurrence and metastasis, including American Joint Committee on Cancer (AJCC) and the International Union Against Cancer (UICC; eighth edition). The most recent staging criteria include histologic criteria such as depth of invasion (DOI; >6 mm) and perineural invasion.

Melanoma

Melanomas originate from junctional or dermal melanocytes that frequently involve the skin of the head and neck. In addition to skin type and a history of sun exposure, the presence of dysplastic nevi, family history, and immune dysfunction raise the risk for melanoma. Nearly half of all melanomas occur de novo in normal skin, and the remaining ones arise from preexisting nevi. A change in the size or appearance of a preexisting nevus with itching, variegated appearance, ulceration, and bleeding should prompt examination of a biopsy specimen.

Melanomas typically present as an irregularly pigmented lesion with a macular or papular appearance. They can be amelanotic or scarlike (i.e., desmoplastic melanomas), but this presentation is rare. These nonpigmented lesions can be mistaken for the more common basal or squamous cell carcinomas. The four main subtypes of melanoma are (1) superficial spreading melanoma (70% of cases) and has a characteristic horizontal growth pattern; (2) lentigo maligna, which occurs in heavily sun-exposed regions with potential for unpredictable subclinical horizontal extension; (3) acral lentiginous melanoma, which typically occurs in the nail beds, palms, and soles of the feet and is more common in African Americans and Asians; and (4) nodular melanoma, which usually is invasive at presentation and has a predilection for the extremities and trunk, with the scalp being the most common site in the head and neck (Fig. 3.10).

The clinical behavior of melanoma typically is defined by its depth of infiltration, which is assessed microscopically by direct measurement (Breslow's thickness) and is used to define the T stage (except for T1 tumors) by the AJCC. In the past, Clark's Level of Depth of Invasion was used for staging of cutaneous melanoma. However, Breslow thickness is more accurate in prediction of prognosis for melanoma and is currently used in staging. Comparative depth of invasion between Clark's Levels and Breslow thickness are shown in Fig. 3.11. Other factors included in the staging system are ulceration, mitotic rate, nodal metastasis (i.e., number and size), and distant metastasis (i.e., location and the serum lactate dehydrogenase level). Whereas thin melanomas rarely metastasize, intermediate-thickness melanomas show a high propensity for regional nodal metastasis, and thick melanomas have equal predilection to metastasize to both regional and distant sites. Moreover, melanomas also can produce "in transit" or "satellite" metastases.

Histologically, melanomas may or may not be pigmented and are composed of round to oval or fusiform tumor cells with nuclear pleomorphism and large, cherry-red, prominent nucleoli. These cells generally are located in rounded nests or as solitary units at the dermal-epidermal junction. Within the epidermis, tumor cells may migrate upward to the surface of the epidermis (pagetoid spread). Invasive melanoma may infiltrate the dermis as single cell units or in groups of cells. In some instances the malignant cells may appear epithelioid, whereas in other instances they may appear to be elongated and spindled (fusiform). Hence numerous histologic phenotypes of melanoma exist (e.g., conventional epithelioid, spindle cell, signet ring cell, or balloon cell). Immunohistochemical staining for S-100 protein, Sox 10, Melan-A (MART-1; A103), HMB-45, tyrosinase, and microphthalmia transcription factor can help differentiate melanomas from other nonmelanotic malignant tumors. S-100 protein and Sox 10 also stain myoepithelial and dendritic cells and are found in nevi but are valuable markers for the diagnosis of desmoplastic melanomas. Melanomas are usually negative for epithelial markers. HMB-45 and Melan-A are highly specific for melanocytes, although Melan-A also can label adrenocortical carcinoma and sex cord stromal tumors of the ovary. Molecular diagnosis also may play a role in assessment of melanocytic tumors and help with treatment selection by identifying the presence or absence of a targetable mutation such as *BRAF* V600E.

Adnexal Tumors

Adnexal tumors in the head and neck region present as intradermal or subcutaneous nodules and represent a wide range of neoplasms that vary in behavior and malignant potential. Nevus sebaceous is a congenital hamartoma that probably arises from basal cells and has a small propensity for transformation to basal cell carcinoma. Cylindromas (turban tumors) can be of either apocrine or eccrine origin and typically arise in the scalp or facial region of young adults. These lesions can occur de novo or may be inherited in an autosomal-dominant pattern. The *CYLD*1 tumor suppressor gene is inactivated in both sporadic and familial forms. These tumors have a small propensity for malignant transformation to sweat gland carcinomas. Head and neck syringomas are tumors of eccrine origin that typically arise from the facial skin and eyelids. These lesions are usually multiple, yellowish in color, and have a fleshy covering. Eccrine spiradenomas usually are seen in younger patients and have a small propensity for malignant degeneration. These lesions present as expanding solitary nodules that are painful. Other benign tumors originating in adnexal structures include trichoepitheliomas and pilomatrixomas, but they are relatively rare.

Sweat gland carcinomas are skin appendage tumors derived from eccrine or apocrine glands. Unlike other skin cancers, these tumors do not have a racial predilection. These tumors typically present as 1- to 2-cm, firm, fixed, intradermal, or subcutaneous nodules that may ulcerate and become necrotic (Fig. 3.12). As they grow, they may coalesce and form larger subcutaneous lesions. Apocrine gland carcinomas are less common and occur most often in the axilla of elderly persons. In the head and neck, apocrine gland carcinomas can arise from various sites, including in the eyelid from Moll's gland, a modified apocrine gland. Apocrine gland carcinomas are highly aggressive neoplasms with a mortality rate over 50%. Metastases occur most frequently in regional lymph nodes, and local recurrence after resection is common. Eccrine gland carcinomas arise either de novo or from preexisting benign lesions. Histologic variants of sweat gland carcinomas include primary cutaneous, mucinous carcinoma, eccrine duct carcinoma, porocarcinoma, microcystic adnexal/sclerosing sweat duct carcinoma, endocrine

Figure 3.10 Clinical variants of cutaneous melanoma. **A**, In-situ. **B**, Superficial spreading. **C**, Lentigo maligna melanoma. **D**, Acral lentiginous melanoma. **E**, Nodular melanoma with satellitosis.

mucin-producing sweat gland carcinoma, cribriform adenocarcinoma, and adenocarcinomas arising in association with a cylindroma or spiradenoma. Eccrine gland carcinomas typically arise from the ocular adnexa, including the meibomian glands, Zeis' glands, or pilosebaceous glands in older women. Salivary gland–type adenocarcinoma, or a metastasis of breast, pulmonary, or even prostate origin, may come into consideration in the differential diagnosis of eccrine carcinoma such as adenoid cystic carcinoma.

Merkel Cell Carcinoma

Merkel cell carcinoma is a neuroendocrine neoplasm of the skin. The majority of these tumors in North America (80%) are caused by infections with Merkel cell polyomavirus (MCV), a double-stranded DNA virus. Nearly half of all Merkel cell carcinoma lesions occur in the head and neck region. The cheek is the most common site, followed by the upper neck and nose. These lesions typically occur in elderly white persons and appear as a red to violaceous, smooth, dome-shaped lesion with telangiectasias (Fig. 3.13). These tumors have a high propensity for metastatic spread to regional lymph nodes as well as distant sites. Histologically they are composed of basophilic cells with scant cytoplasm and dark powdery chromatin, and they may be morphologically similar to other neuroendocrine carcinomas. Hence metastatic small cell carcinoma, malignant melanoma, or primary neuroendocrine (or "small cell") carcinoma of the parotid gland may be considerations in the differential diagnosis.

Immunohistochemical stains for synaptophysin, chromogranin, and cytokeratin 20 (CK20) (demonstrating a characteristic "dotlike" pattern) or the Merkel cell polyoma virus large T antigen (recognized by the antibody CM2B4) are positive, whereas thyroid transcription factor-1 (TTF-1) is negative.

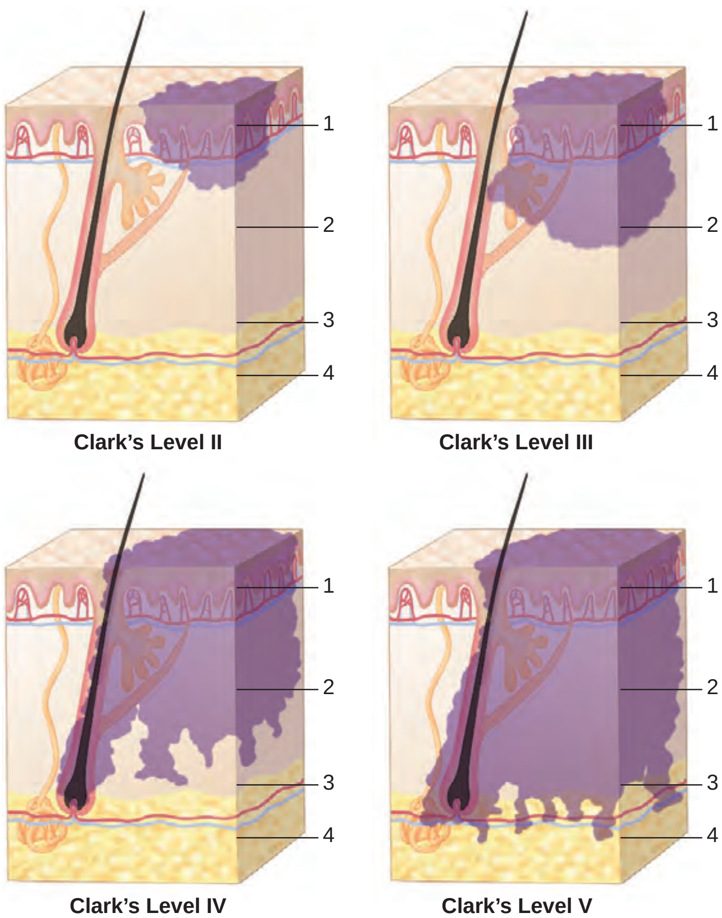

Figure 3.11 Clark's levels and Breslow thickness for histologic staging of cutaneous melanoma.

Dermatofibrosarcoma Protuberans

Dermatofibrosarcoma protuberans is an intermediate-grade sarcoma that presents as a unifocal or multifocal nodular lesion. Dermatofibrosarcoma protuberans involves the head and neck region in 10% to 20% of cases, with the scalp and supraclavicular fossae the most common sites for involvement (Fig. 3.14). These slow-growing, locally aggressive tumors have tentacle-like extensions well beyond the visible lesion, and thus the true extent of the disease is often underestimated, leading to local recurrence in more than 50% of patients. Histologically a storiform or fascicular proliferation of spindle cells extends from the dermis into the subcutis, with immunohistochemistry showing CD34 positive staining in most cases. Presence of fibrosarcomatous changes and high mitotic rate may portend a more aggressive course. This tumor frequently has a translocation of a fusion protein involving COL1A1 and PDGFB that functions like PDGFB. Wide excision with margins of ≥2 cm is generally advocated, with adjuvant radiation reserved for larger or recurrent tumors when resection is not feasible.

Figure 3.13 Clinical appearance of Merkel cell carcinoma.

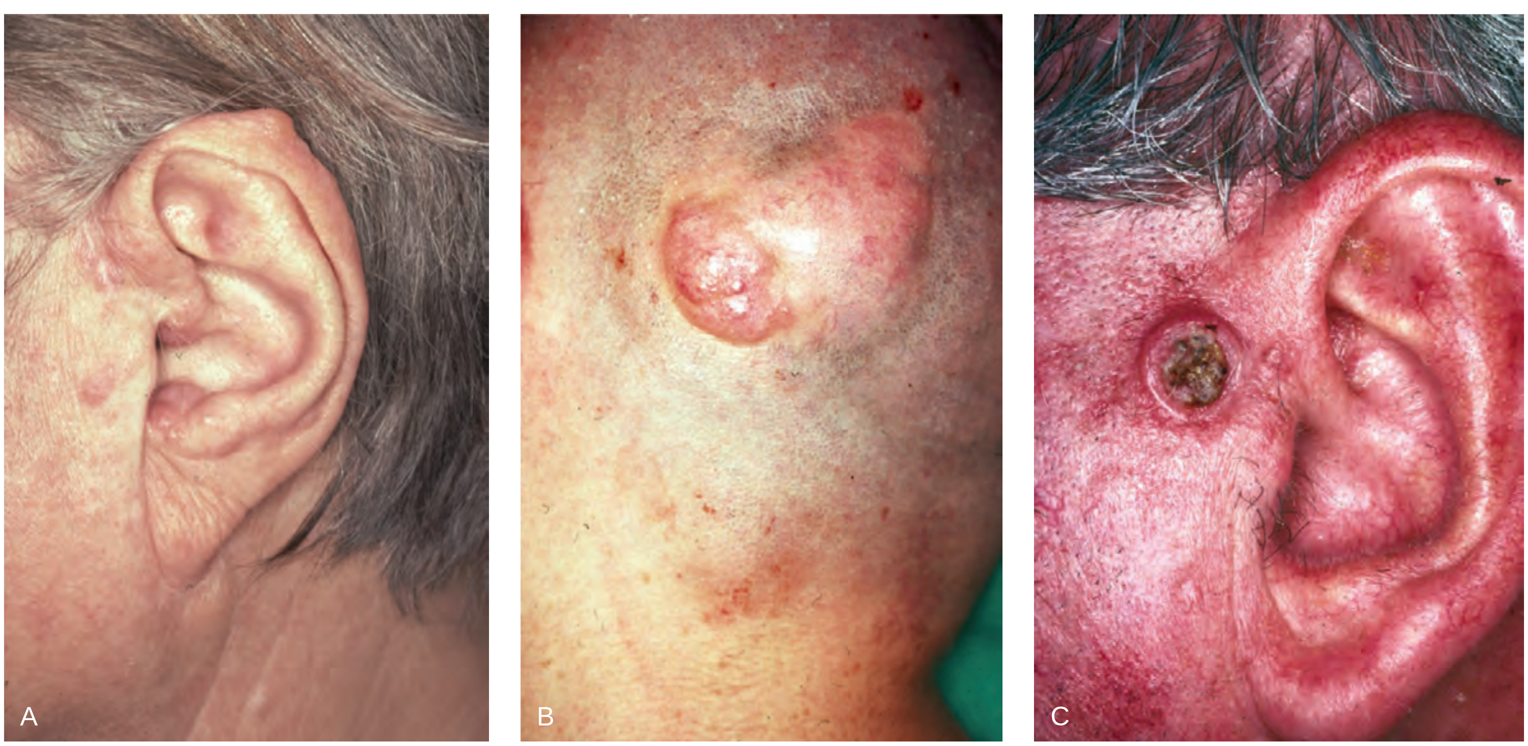

Figure 3.12 Clinical appearance of adnexal tumors. **A**, Benign cylindroma. **B**, Sweat gland carcinoma on the occipital scalp. **C**, Ulcerated adenocarcinoma.

Figure 3.14 Dermatofibrosarcoma protuberans. **A**, Unifocal. **B**, Presenting with multiple nodules on the forehead.

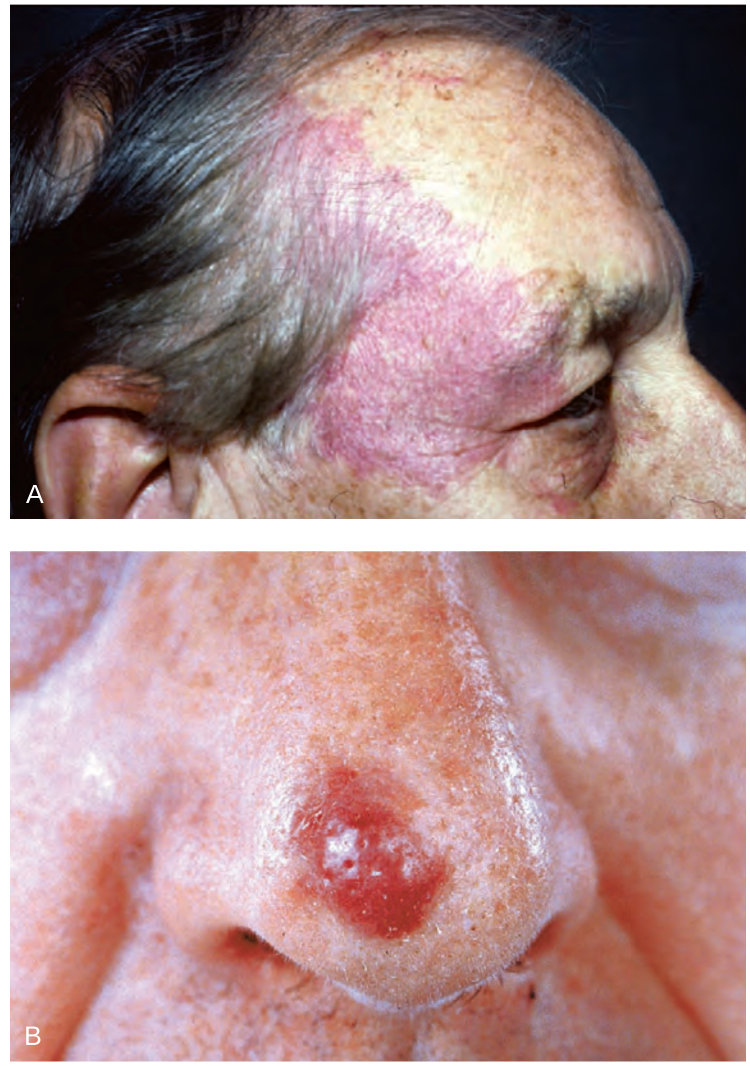

Figure 3.15 Cutaneous angiosarcoma. **A**, Macular. **B**, Nodular variant.

Angiosarcoma

Angiosarcomas typically have an innocuous presentation, appearing as a purplish bruise, whereas the actual tumor can extend well beyond the visible edge of the lesion (Fig. 3.15). These tumors are thought to arise from vascular endothelial cells and can have a heterogeneous presentation ranging from macular to papular morphology. Angiosarcomas involve the skin in about half of the cases, with 50% arising in the head and neck region. A high degree of clinical suspicion is required, and a biopsy is required to establish tissue diagnosis. These tumors have a high propensity for local recurrence and distant metastasis. Pulmonary metastases can appear as bullous lesions on chest imaging. Surgical resection is feasible only in well-demarcated, nodular lesions. The vast majority of ecchymotic macular lesions are treated with a combination of radiation and chemotherapy. Long-term prognosis is poor despite aggressive treatment.

SELECTION OF TREATMENT

Curative approaches to cutaneous malignancies include topical chemotherapy, surgery, or radiotherapy. Factors affecting choice of treatment are related to the tumor characteristics (e.g., type, location, size, and extent), the patient, and therapy-related issues. Surgery is effective and typically sufficient as a single-modality treatment for most skin cancers, and accordingly it is the mainstay of treatment. For large, recurrent, unusual, or complex skin cancers where standard treatment approaches are not feasible, a multidisciplinary evaluation and treatment plan is recommended.

NONSURGICAL MANAGEMENT

Topical Therapy

Several topical agents have been used in the management of selected premalignant and superficial skin cancers. In general, this treatment approach is used in patients with multiple lesions or lesions involving large areas of the scalp and facial skin. However, topical agents should not be used for more invasive lesions. Topical chemotherapy with 5-fluorouracil and topical immunotherapy with imiquimod have been effective for actinic keratoses, superficial basal cell carcinoma, and in situ squamous cell carcinoma. Photodynamic therapy also has been used for such lesions with high initial response rates, but the long-term control rates are lower.

Radiation Therapy

Cutaneous malignancies of the scalp and the facial skin, particularly superficial squamous cell carcinoma and basal cell carcinoma, can be treated effectively with radiotherapy. Because skin cancers are superficial in their location with respect to the

remainder of the deeper tissues in the body, these tumors preferably are treated with electron beam, superficial, or orthovoltage x-rays. With use of these modalities, an effective dose of radiation can be delivered to the tumor target without delivering excessive radiation to the deeper tissues.

Radiotherapy is an option in patients who present with lesions that require extensive surgery that would affect function and cosmesis, such as compromised oral competence with lesions located near the oral commissure and epiphora with lid retraction for lesions of the eyelid. External radiation is quite effective in basal cell carcinoma of the eyelids, particularly adjacent to the medial canthus (Fig. 3.16). The immediate results of radiotherapy are excellent, with essentially no cosmetic or functional impact on the patient (Fig. 3.17). Atrophy of the underlying cartilage can occur and may result in an unattractive scar over time. Therefore definitive radiotherapy is generally used for elderly patients, for whom cosmesis is not of great concern. Elderly and medically unfit patients with massive skin cancer requiring surgical resection are also considered for treatment with radiation. Radiotherapy can offer excellent palliation and sometimes can be curative. The patient shown in Fig. 3.18 has an extensive basal cell carcinoma of the nose that would have required nasal amputation if treated surgically. Six months after radiation therapy, complete resolution of the tumor was achieved with an excellent cosmetic result (Fig. 3.19). Radiotherapy is also used postoperatively for adverse histopathologic features of the primary tumor (e.g., inadequate surgical margins, extensive perineural invasion, or deep soft tissue infiltration) or in patients with regional lymph node metastasis.

In general, radiotherapy is not recommended in younger patients, because the long-term sequelae of treatment are progressive and can affect cosmesis as the patient gets older. These late effects include telangiectasias, atrophy, and pallor of the skin. In addition, a small risk exists for development of a radiation-induced second cancer in the irradiated field. Although radiotherapy can be curative, a prolonged treatment course, typically over 4 to 5 weeks or 5500 cGy at 250 cGy per day, may limit its applicability in some patients.

The role of radiation therapy in the treatment of head and neck cutaneous melanoma is typically only in the adjuvant setting after surgical resection. Results from in vitro experiments assessing radiation response in several human melanoma cell lines support the use of hypofractionated radiation therapy in the treatment of melanoma. Several nonrandomized studies show that doses of ≥4 Gy per fraction produce higher complete response rates. In particular, 8 Gy fractions given on days 0, 7, and 21 or 6 Gy given in five fractions over 2.5 weeks produce excellent response rates. However, the Radiation Therapy Oncology Group (RTOG) prospective randomized trial, in which measurable melanomas were treated either with 8 Gy per fraction given once every week over 4 weeks or conventional fractionation of 2.5 Gy per fraction given daily over 20 days, showed no

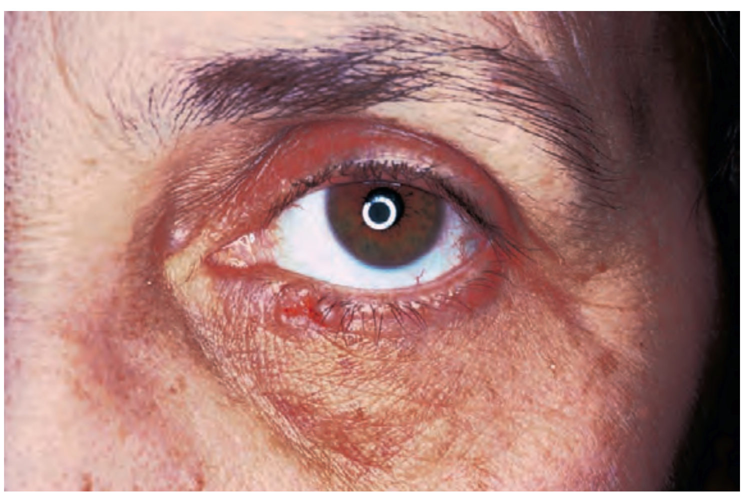

Figure 3.16 Basal cell carcinoma of the lower eyelid near the medial canthus.

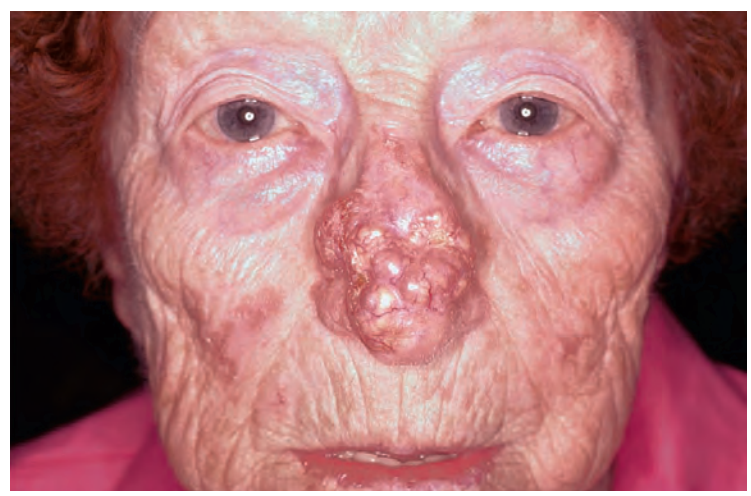

Figure 3.18 Extensive basal cell carcinoma of the dorsum of the nose.

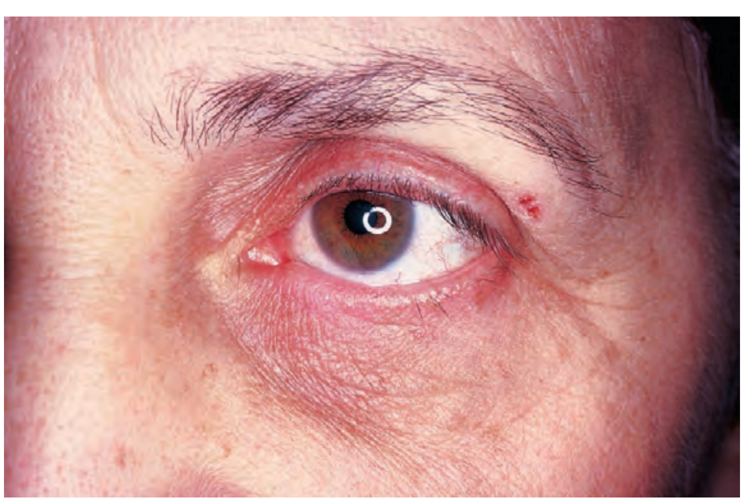

Figure 3.17 Clinical appearance 6 months after radiotherapy.

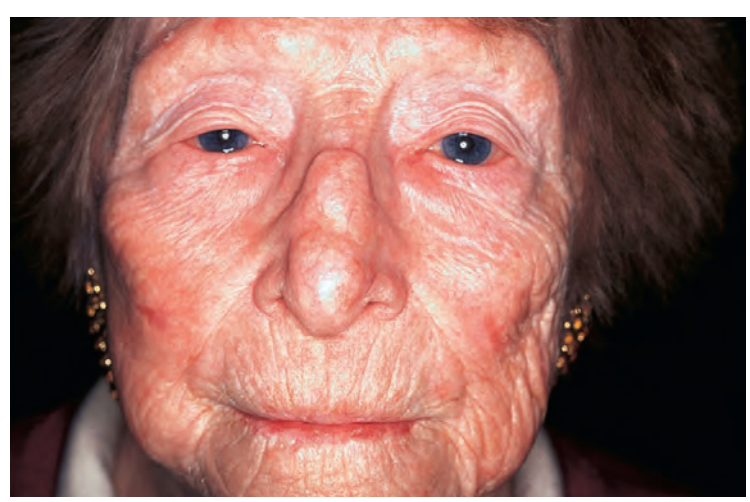

Figure 3.19 Clinical appearance 6 months after radiation therapy.

differences in outcome. Nonetheless, the shortened treatment time resulting from a hypofractionated course of radiation therapy is preferred, because it allows early initiation of systemic therapy if warranted. Radiation fields should encompass the postoperative bed at the primary site and regional nodes at risk for involvement in the N0 neck or after therapeutic neck dissection for multiple positive lymph nodes, extranodal extension, or recurrent neck disease.

The role of radiation therapy for the treatment of adnexal tumors remains to be defined. The best data are available for Merkel cell carcinoma, for which adjuvant radiotherapy has been shown to be important, especially for larger tumors that are associated with regional metastasis. More recently, reports suggest increased effectiveness with the use of concurrent chemotherapy as well as adjuvant chemotherapy, but the precise role for both these approaches remains to be defined.

SURGICAL MANAGEMENT

When performing surgery in the head and neck region for resection of skin cancers, the goal is cure of the tumor with clear surgical margins while maximally preserving function and cosmesis before definitive reconstruction. Surgical techniques include excision and examination of surgical margins with frozen sections or subsequent paraffin-embedded sections or Mohs micrographic surgery with immediate complete frozen section margin control. Small low-risk skin cancers can be removed with standard excision in the office setting if a primary linear repair of the defect is feasible. Irrespective of excision technique, it is advisable to delay complex reconstruction of surgical defects until clear surgical margins are obtained in the head and neck region.

Mohs micrographic surgery is a well-established dermatologic surgery technique to secure histologic clearance of all epidermal, intradermal, and subdermal extensions of cutaneous cancers. It is indicated for skin cancers with unpredictable subclinical extension at high risk for local recurrence. Mohs surgery is particularly advantageous for basal cell carcinomas located in the mask area of the face adjacent to vital structures or with morpheaform histology where tumor invasion is more likely but maximal tissue conservation where possible is desirable. Other indications include basal cell carcinomas that are extensive, recurrent, or in previously irradiated fields where the clinical assessment of the extent of disease is suboptimal.

The technique of Mohs surgery requires (1) initial excision of the tumor under local anesthesia in the office setting; (2) immediate grossing, inking, and mapping of excised tissue to preserve surgical margin orientation in an onsite Mohs frozen section laboratory; (3) processing of the entire circumferential surgical margin (peripheral and deep margin) with frozen sections; (4) pathologic examination of the surgical margins by the Mohs surgeon and mapping residual tumor (Fig. 3.20); and (5) reexcision of involved surgical margins and processing of tissue according to Mohs technique until tumor-free margins are achieved (Fig. 3.21). In the United States, Mohs micrographic surgery is generally practiced by dermatologic surgeons (i.e., dermatologists with special training in Mohs micrographic surgery). Because this procedure is labor and time intensive, it is best utilized for skin cancers that are at high risk for local recurrence. From a cost perspective, standard excision in the office and subsequent pathology is least expensive, with Mohs surgery incurring an intermediate cost (cost of excision and pathology is bundled) and excision in the OR setting with frozen sections, which is most expensive. Because Mohs surgery is used for high-risk skin cancers often with extensive involvement, large surgical defects can result, requiring complex reconstruction and coordination with multidisciplinary experts.

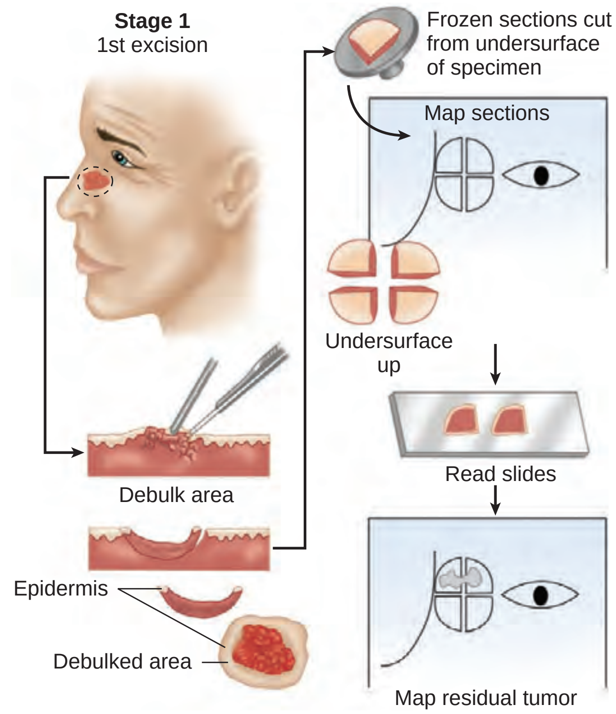

Figure 3.20 Schematic representation of the Mohs surgery technique.

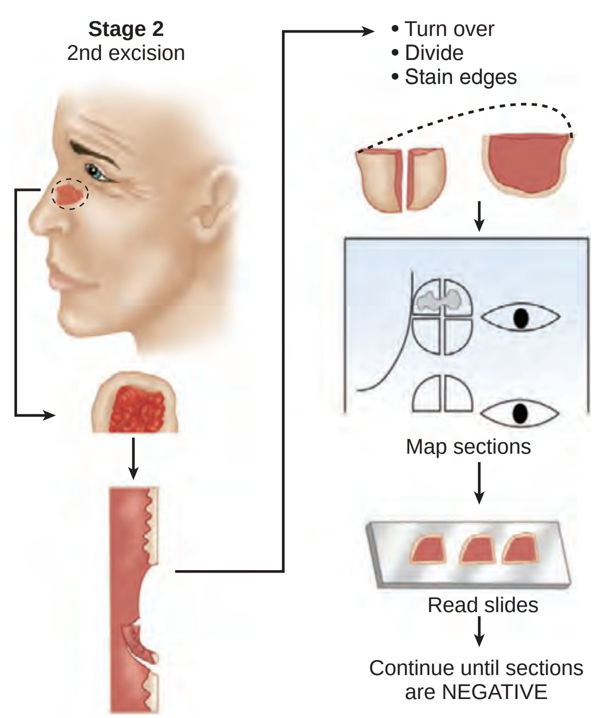

Figure 3.21 Stepwise excision with immediate histologic analysis is continued until all margins of excision are negative.

Surgical Anatomy

The scalp is a unique adaptation of the epithelial covering of the body. Anatomic variations present in the scalp modify both tumor behavior and the treatment of tumors in this

area. The hair-bearing area of the scalp consists of a thick padding of hair follicles, sweat glands, fat, fibrous tissue, and lymphatics that are interspersed with numerous arteries and veins (Fig. 3.22). This thick padding is supported by the galea, a tough aponeurotic layer that is fused in the anterior region with the frontalis muscle and in the posterior region with the occipital muscle. This inelastic layer rests loosely on the periosteum of the skull, creating a potential subaponeurotic space. Laterally, the temporalis muscle provides an additional barrier between the galea and the periosteum.

Three principal arteries provide a rich blood supply to each side of the scalp. The superficial temporal and occipital arteries are branches of the external carotid artery, whereas the supraorbital artery is a branch of the internal carotid artery (Fig. 3.23). The scalp has a rich subdermal and subcutaneous lymphatic network. The general pattern of lymphatic drainage is divided by a coronal plane at the level of the tragus. Malignant tumors located anterior to this plane drain to preauricular, parotid, and anterior triangle lymph nodes in the neck. On the other hand, lesions located posterior to this plane drain to postauricular, suboccipital, and posterior triangle lymph nodes.

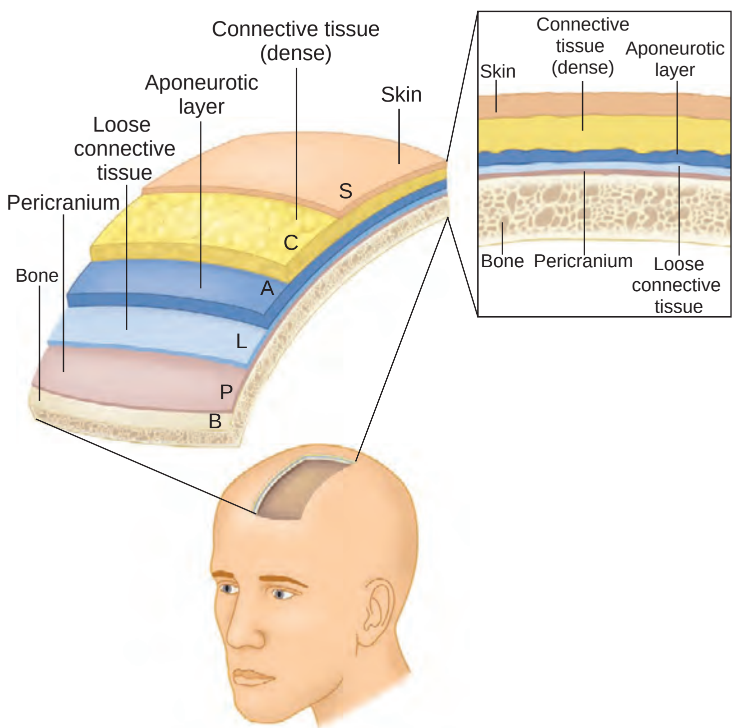

Figure 3.22 Anatomy of the scalp.

Facial skin is also unique in that it has several distinguishing characteristics on various parts of the face, with unique anatomic features providing different functions. For example, the skin around the eyelids is extremely thin, with almost no subcutaneous fat. In contrast, the skin around the central part of the face adjacent to the nose and lips is intimately attached to the underlying facial muscles and offers facial expression. Thus the skin of the central part of the face is mobile, whereas areas of facial skin along the lateral aspect of the nose, the bridge of the nose, and along the preauricular region and temple are relatively immobile. These unique characteristics of the facial skin have significant surgical implications. Similar to the scalp, the facial skin has a rich blood supply through the facial and superficial temporal arteries, and it has predictable patterns of lymphatic drainage to preauricular and periparotid lymph nodes and perivascular facial lymph nodes adjacent to the body of the mandible at level I, eventually draining into the deep jugular chain of lymph nodes.

Principles of Surgical Treatment

Surgical management of skin malignancies is dictated by the location and extent of the tumor. For lesions in the scalp, the extent of surgical resection depends on the surface dimensions of the tumor and the depth of invasion by the tumor. Excision is through partial thickness for superficial tumors or through entire thickness, including the periosteum, for deeply infiltrating tumors. Scalp tumors that are adherent to or involve the underlying cranium require removal of at least the outer table of skull or a through-and-through resection up to and including the dura (Fig. 3.24).

Small lesions of the face and neck can be excised elliptically in the plane of skin tension with excellent aesthetic results.

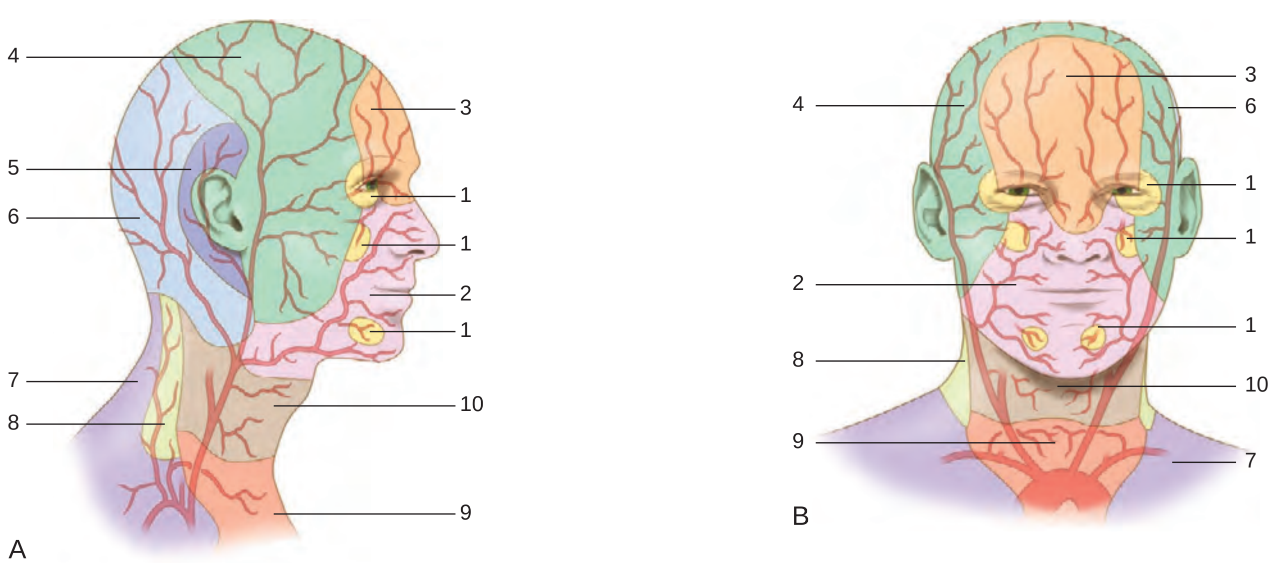

Figure 3.23 Vascular territories (angiosomes) of the scalp, face, and neck showing arterial blood supply, lateral view (**A**) and frontal view (**B**). The blood supply to various zones is from *1,* internal maxillary, *2,* facial, *3,* ophthalmic branch of internal carotid, *4,* superficial temporal, *5,* posterior auricular, *6,* occipital, *7,* transverse cervical, *8,* deep cervical branch of thyrocervical trunk, *9,* inferior thyroid, and *10,* superior thyroid.

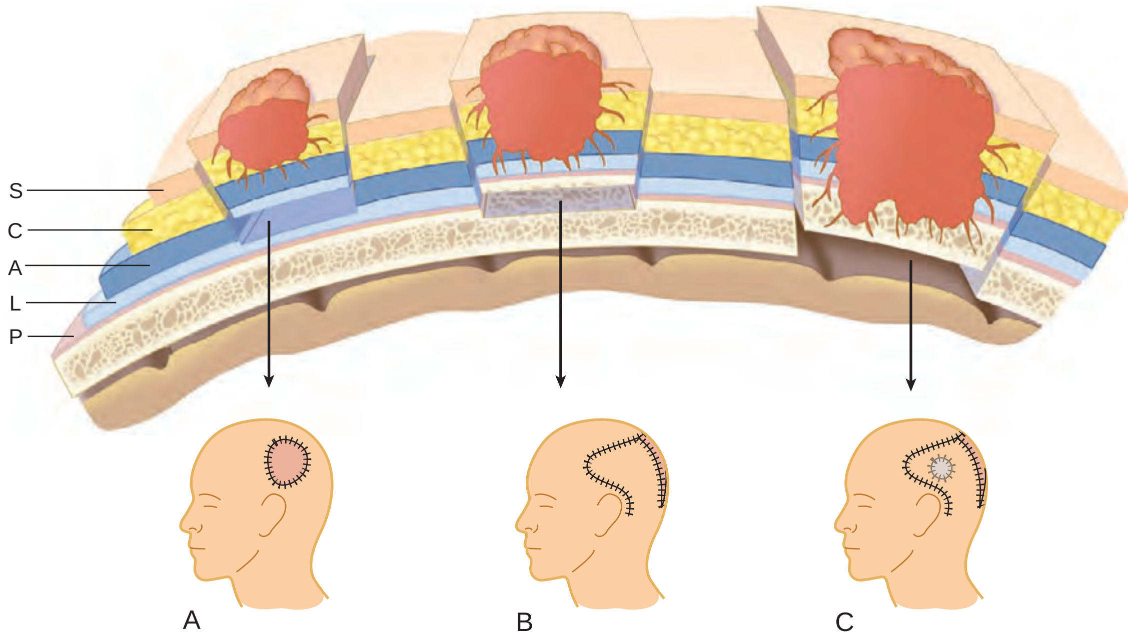

Figure 3.24 Extent of resection and reconstruction of tumors of the scalp. **A**, Tumor depth to the galea: Excision up to the pericranium and repair with a split-thickness skin graft. **B**, Tumor depth to the periosteum: Excision through the outer table and repair with a rotation scalp flap or free flap. **C**, Tumor invading the calvarium: Excision with a craniectomy with or without dural excision and repair with cranioplasty and a rotation flap or free flap, along with a dural graft if the dura is resected.

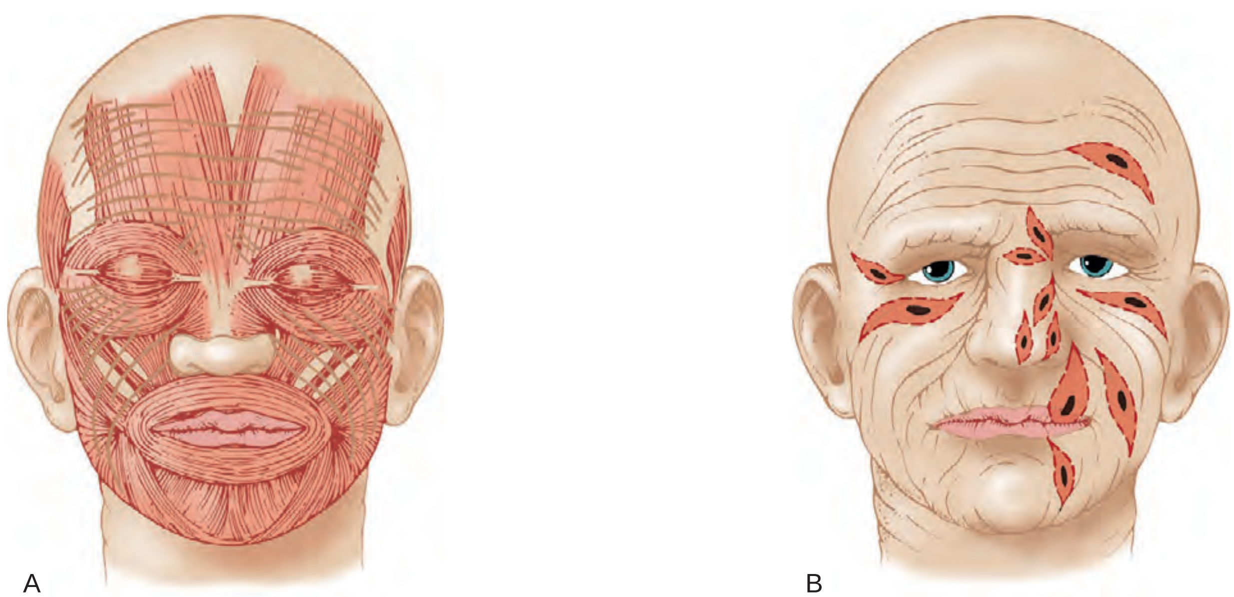

Figure 3.25 Design of facial skin incisions. **A**, The facial skin lines are at right angles to the underlying muscles of facial expression. **B**, Elliptical incisions along the facial skin lines produce optimal cosmetic results.

The facial skin lines are at right angles to underlying fibers of the muscles of facial expression. Orientation of facial skin lines and potential directions for elliptical incisions are shown in Fig. 3.25. Identification and orientation of the long axis for elliptical incision is facilitated by asking the patient to grimace. These lines are horizontal on the forehead and around the bridge of the nose and the outer canthus of the eye. Near the cheek the tension lines run obliquely or perpendicularly, near the lips they run radially from the mouth opening, and on the chin they run horizontally on the midline and obliquely perpendicular at the sides. On the sides of the neck, the wrinkles and tension lines run obliquely downward and forward (Fig. 3.26).

Elliptical excision of a small tumor of the skin of the face along the facial skin lines can be easily closed primarily, with excellent cosmetic outcomes. Meticulous attention should be paid to accurate approximation of the skin with fine sutures, which can be removed as early as 4 days postoperatively. Alternatively, one may elect to use a subcuticular suture, particularly in the area of the eyelids where the skin is very thin.

Most surgical defects resulting from resection of skin neoplasms can be closed primarily after wide undermining. Application of split-thickness or full-thickness skin grafts is best suited to the part of the face with minimal facial motion, such as the tip or lateral aspect of the bridge of the nose or the temple. Similarly, a skin graft can be used in the parotid region where facial movement is minimal with excellent cosmetic results. The most suitable donor sites for obtaining full-thickness skin grafts are from the retroauricular or supraclavicular regions. Local flaps are preferred to repair larger surgical defects or those

Figure 3.26 Skin lines of the face and neck.

Figure 3.27 In situ malignant melanoma of the skin of right cheek.

Figure 3.28 Planned surgical excision along facial skin lines.

requiring full-thickness reconstruction, because they provide the best functional and aesthetic outcome. Primary closure of the donor site defect usually can be accomplished with ease with proper planning of local skin flaps. The blood supply of facial skin and soft tissues is extremely rich, because the terminal branches of the external carotid artery provide a major source of blood to the facial skin, which allows use of axial flaps. In addition, an extensive subdermal anastomotic network facilitates the use of random flaps with relative ease. Examples of axial skin flaps are nasolabial, glabellar, Mustardé cheek, and temporal forehead. Examples of random flaps are cervical, rhomboid, and bilobed. If local flaps are not suitable, consideration should be given to regional or free flaps for appropriate repair of large surgical defects.

Metastatic dissemination to regional lymph nodes from primary squamous cell carcinomas of the scalp and face is infrequent. In general, squamous carcinomas <2 cm in diameter have an exceedingly low risk of metastasis, and therefore elective treatment of regional lymph nodes is not recommended because it does not offer significant therapeutic advantage. Lesions >2 cm have a proportionately higher risk of regional lymphatic dissemination, and elective neck dissection should be used selectively. Other more aggressive cutaneous malignancies, such as Merkel cell carcinoma and melanoma, have a higher risk of lymphatic dissemination. Currently, sentinel node biopsy is used to identify occult nodal metastasis.

PROCEDURES

Excision and Primary Closure Along Facial Skin Lines

Excellent cosmetic results are obtained for even larger skin defects repaired by primary closure, if the excision is planned along natural skin creases, and if there is sufficient laxity of facial skin to obtain a tension-free closure. The patient shown in Fig. 3.27 has a melanoma in situ of the skin of the face adjacent to the oral commissure. The surgical excision requires full-thickness resection of the skin and underlying subcutaneous soft tissue, remaining superficial to the facial muscles. The plan of excision is marked out along the facial skin lines of the nasolabial fold and the perioral and chin area (Fig. 3.28). The closure of the surgical defect is done in two layers, without any tension (Fig. 3.29). Postoperative appearance of the patient approximately 18 months following surgery shows an excellent aesthetic result (Fig. 3.30).

Even deeper excisions including some facial muscles offer an excellent aesthetic outcome, if excision is planned along skin lines. The patient shown in Fig. 3.31 has an adnexal tumor involving the skin of the face. The extent of the tumor and the planned excision along the nasolabial skin crease will permit three-dimensional excision and primary closure. The surgical defect after excision required undermining and mobilization

Figure 3.29 Primary surgical closure in two layers.

Figure 3.30 Postoperative appearance 18 months following surgery.

Figure 3.31 Adnexal carcinoma of the skin of the cheek. Extent of the lesion and planned surgical excision along facial skin lines.

Figure 3.32 Three dimensional surgical defect preserving the buccal branches of the facial nerve.

Figure 3.33 Primary closure in multiple layers.

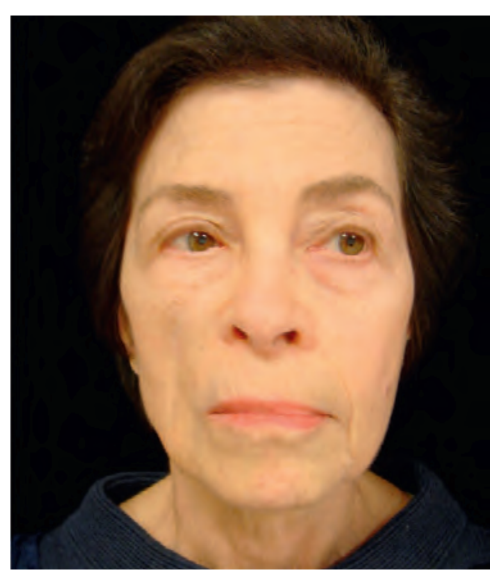

Figure 3.34 Postoperative appearance 3 years following surgery.

of both medial and lateral skin edges for a tension-free closure (Fig. 3.32). The closed incision lies along the nasolabial fold (Fig. 3.33). The patient's postoperative appearance 3 years following surgery shows excellent aesthetic outcome (Fig. 3.34).

Excision Tumor of the Scalp and Reconstruction With Split-Thickness Skin Graft

The patient shown in Fig. 3.35 has a nodular pigmented basal cell carcinoma of the scalp measuring approximately 2.5 × 4.5 cm. Because this skin tumor is freely mobile over the underlying periosteum, the galea aponeurotica will form the deep margin of the surgical specimen for this tumor.

Although most of the lesion is nodular and protuberant in nature, an additional intracutaneous component could be seen only after the scalp was shaved. The surgical procedure is performed under general endotracheal anesthesia. The scalp is shaved to expose the area of intended surgical excision (Fig. 3.36). The planned area of surgical excision is outlined with a generous margin of normal skin around the visible tumor. Generally, a margin of at least 1 cm on each side of the lesion is desirable. The incision on the scalp is made with a number 15 scalpel and is made obliquely so that the cut edge of the scalp is beveled, with the bevel sloping toward the center of the surgical defect (Fig. 3.37). This maneuver is undertaken to facilitate subsequent healing of the skin graft and to avoid an indentation between the skin graft and the scalp. The incision in the scalp is made circumferentially with a scalpel, and elevation of the specimen and dissection are performed with the use of electrocautery (Fig. 3.38).

Brisk hemorrhage as a result of the rich blood supply of the scalp is to be anticipated from the cut edges. However, the use of suction with a Frazier suction tip and prompt use of several hemostats will minimize blood loss. Major bleeding vessels will require a suture ligature, whereas fine bleeding points can be electrocoagulated safely. Once the proper plane between the galea aponeurotica and the periosteum of the skull is reached, elevation of the surgical specimen becomes very simple, because the plane consists of loose areolar tissue (Fig. 3.39). This mobilization is best accomplished digitally. Once the undersurface of the surgical specimen is completely mobilized (Fig. 3.40), the remaining circumferential incision is completed through its full thickness and the surgical specimen is removed. Complete hemostasis is secured by ligating, suture ligating, or electrocoagulating the bleeding points from the cut edges of the scalp. The surgical defect is shown in Fig. 3.41. The depth of the surgical defect shows the periosteum of the scalp, which will be the bed to receive a split-thickness skin graft. The

Figure 3.36 An area of the scalp large enough to expose the area of intended surgical excision is shaved.

Figure 3.35 Nodular pigmented basal cell carcinoma of the scalp.

Figure 3.37 The incision is made obliquely so that the cut edge of the scalp is beveled, with the bevel sloping toward the center of the surgical defect.

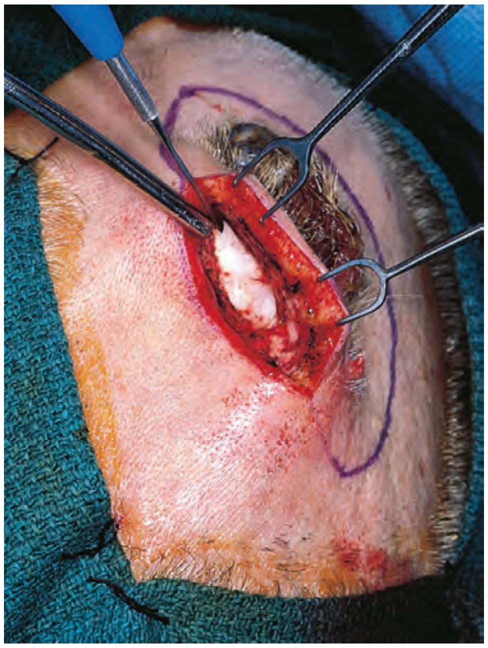

Figure 3.38 The remainder of the elevation of the specimen and dissection is performed with use of electrocautery.

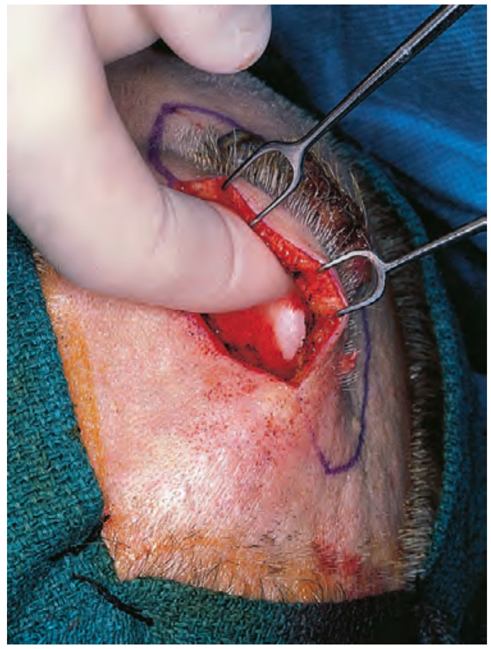

Figure 3.39 The plane consists of loose areolar tissue, which facilitates digital dissection.

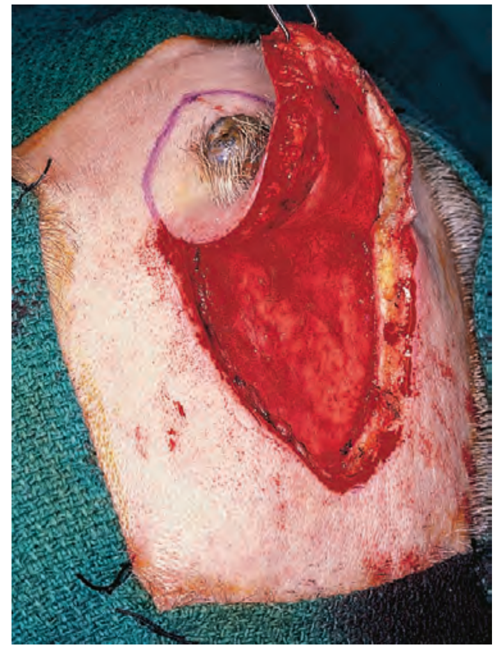

Figure 3.40 Mobilization of the undersurface of the specimen.

Figure 3.41 The surgical defect.

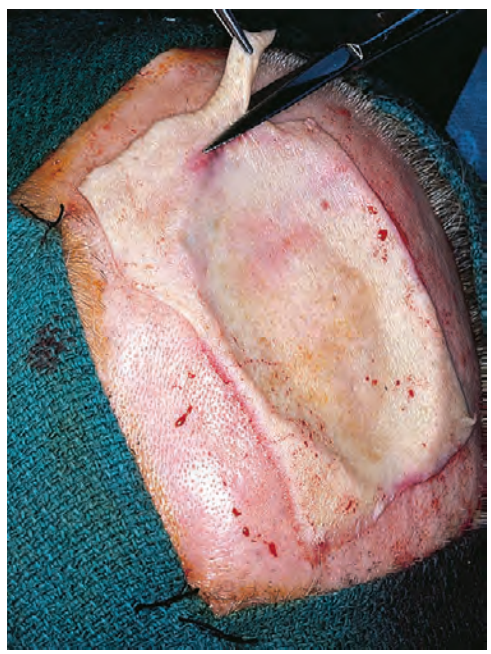

Figure 3.42 The skin graft is appropriately positioned and excess is trimmed off.

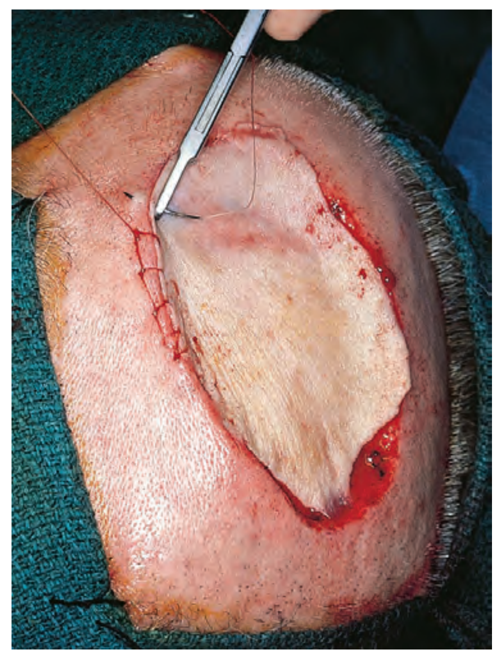

Figure 3.43 The skin graft is sutured to the edges of the surgical defect with use of continuous interlocking absorbable sutures.

previously harvested split-thickness skin graft is now brought into the field and laid over the surgical defect. A fairly thick split-thickness skin graft is desirable to avoid ulceration from trauma on the scalp. Thin split-thickness skin grafts give a very tight and shiny appearance and are prone to ulceration even with trivial trauma. The skin graft is appropriately positioned, and excess is trimmed off (Fig. 3.42). The skin graft is sutured to the edges of the surgical defect using continuous interlocking absorbable suture material (Fig. 3.43). Continuous interlocking sutures provide hemostasis and secure the graft in the proper position. Several buttonholes are made with a number 15 scalpel in the center of the graft to provide for drainage of serous material from beneath the graft. This maneuver is often called "pie crusting" (Fig. 3.44). The skin graft is further secured tightly and apposed against the periosteum with use of Xeroform gauze and a pressure dressing, with a sea sponge bolster secured with silk sutures taken on the scalp at the periphery of the surgical defect (Fig. 3.45). A layer of Xeroform gauze is applied to the skin graft (Fig. 3.46). A sea sponge is now trimmed to the required size and is wrapped in a gauze piece (Fig. 3.47). The assembly of sea sponge wrapped in gauze is now placed over the Xeroform gauze dressing and is properly positioned to exert even pressure to all areas of the skin graft (Fig. 3.48). The silk sutures taken at the periphery of the surgical defect are now

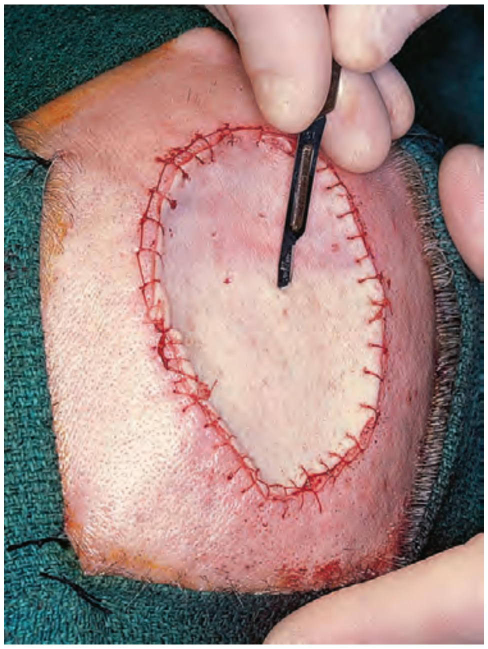

Figure 3.44 The "pie crusting" technique.

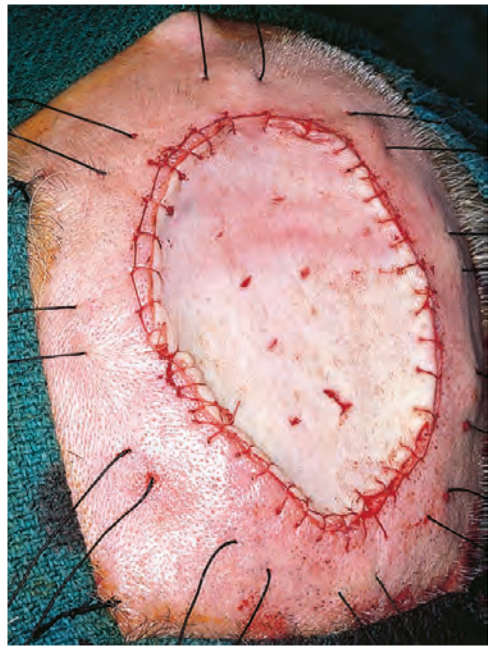

Figure 3.45 Silk sutures are applied to secure a bolster over the graft.

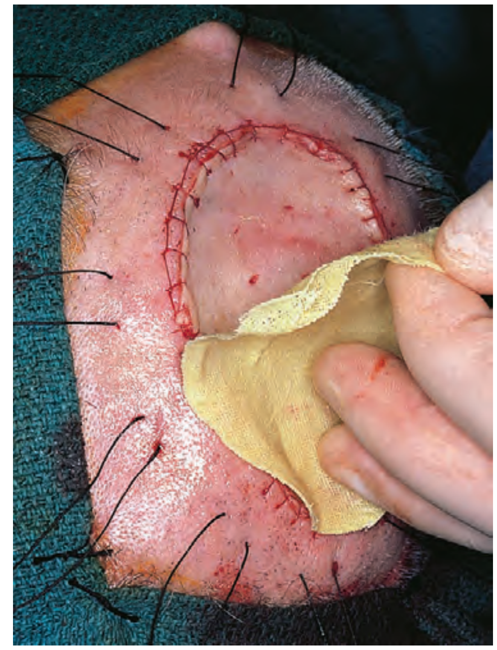

Figure 3.46 A layer of Xeroform gauze is applied to the skin graft.

Figure 3.47 A sea sponge is trimmed to the required size and wrapped in a piece of gauze.

Figure 3.48 The sea sponge wrapped in gauze is placed over the Xeroform gauze dressing.

Figure 3.49 The silk sutures taken at the periphery of the surgical defect are tied over the bolster of sea sponge.

tied over the bolster of sea sponge (Fig. 3.49). The dressing is now completely secured in position, providing adequate and even pressure over the skin graft, which remains apposed to the periosteum of the skull (Fig. 3.50). This dressing is left in position for 1 week, at which point the pressure dressing is removed.

The surgical specimen of the excised tumor shows a generous portion of normal skin around the tumor (Fig. 3.51). The deep surface of the specimen shows the galea aponeurotica, which is grossly uninvolved by tumor (Fig. 3.52). When the bolster dressing is removed, debridement of crust and clots at the edges of the surgical defect is necessary to keep it clean until full maturation of the grafted area takes place. The patient should be instructed to avoid direct trauma or injury to this area.

The postoperative appearance of the patient approximately 3 months after surgery shows 100% take of the skin graft (Fig. 3.53). A split-thickness skin graft on the scalp is a very satisfactory procedure for coverage of a surgical defect resulting from excision of a tumor when the periosteum can be preserved. If periosteum is not preserved, then split-thickness skin graft cannot be used because it will not survive over intact cortical bone. In select situations, drill holes can be made through the outer cortex of the bone to expose the diploic vessels, which can support a split skin graft; otherwise, a rotation flap or free flap is the only choice to cover a large defect.

Figure 3.50 The dressing is secured in position.

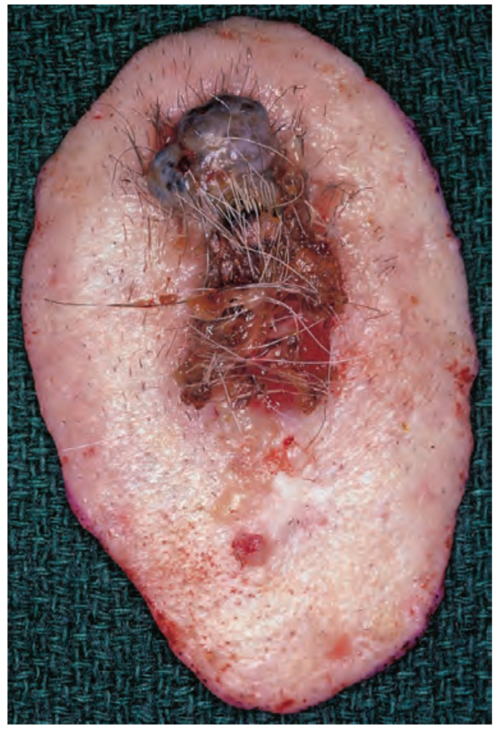

Figure 3.51 The surgical specimen shows a generous portion of normal skin around the tumor.

Figure 3.52 The deep surface of the specimen shows the galea aponeurotica, which is grossly uninvolved by tumor.

Figure 3.53 The postoperative appearance of the patient approximately 3 months after surgery.

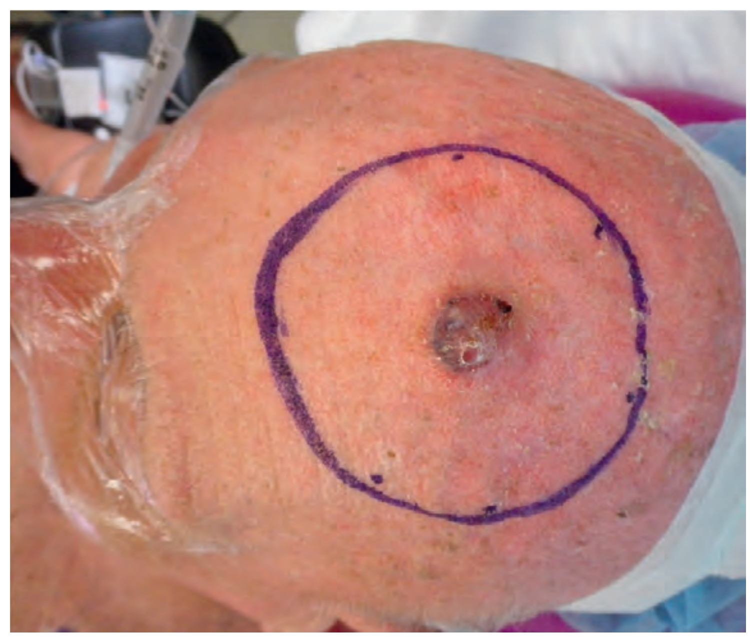

Figure 3.54 Merkel cell carcinoma of the frontal parietal scalp with planned excision marked out.

An alternative method of fixing the bolus dressing over the skin graft is to use a skin stapler to hold the bolus "tie down" sutures. This method minimizes trauma to the skin surrounding the defect and does not compromise the blood supply to the edges of the skin defect. The patient shown in Fig. 3.54 has a Merkel cell carcinoma of the frontoparietal scalp. A wide excision of the lesion is planned down to the pericranium. A split-thickness skin graft is sutured in position (Fig. 3.55). A skin stapler is used to put staples all around the periphery of the grafted area (Fig. 3.56). Silk strands are passed through each of the staples (Fig. 3.57) and are then tied over a bolus dressing (Fig. 3.58). At the time of removal of the bolus, a simple staple remover is used to release the ties. This is a painless process. Use of staples is an expeditious step during surgery and cuts down the operating time and allows quick removal of the bolus in a pain-free manner.

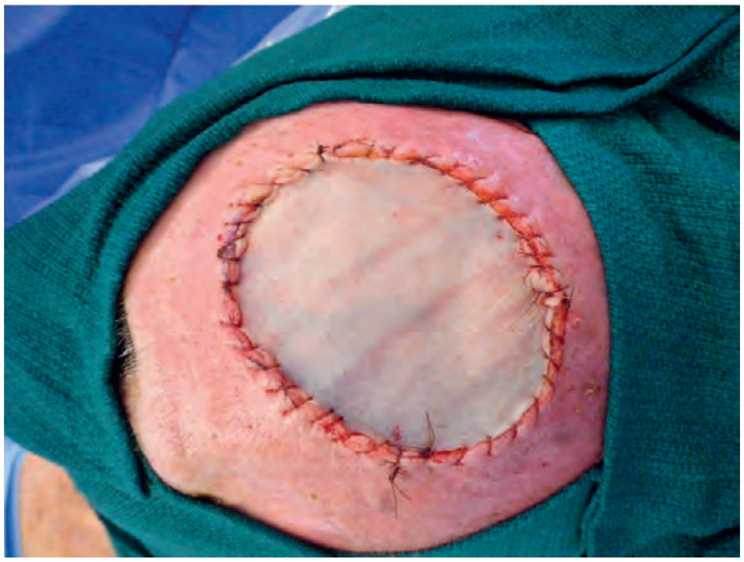

Figure 3.55 Split thickness skin graft sutured to the skin edges.

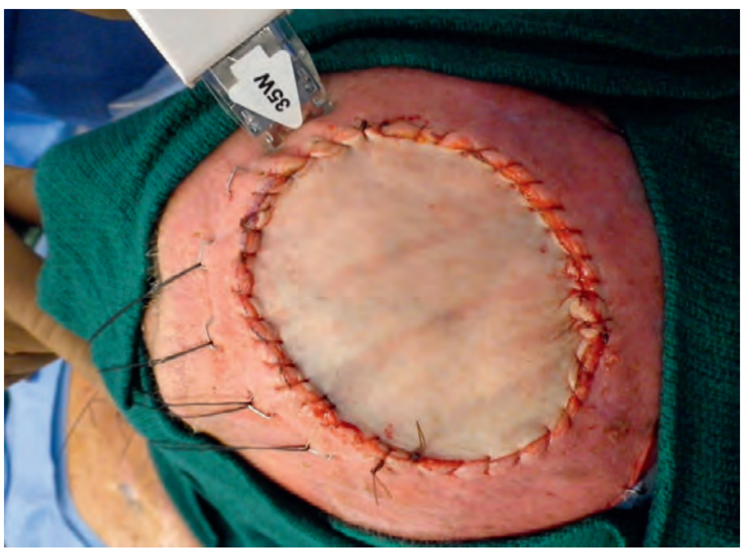

Figure 3.56 Skin stapler is used to place staples surrounding the periphery of the defect.

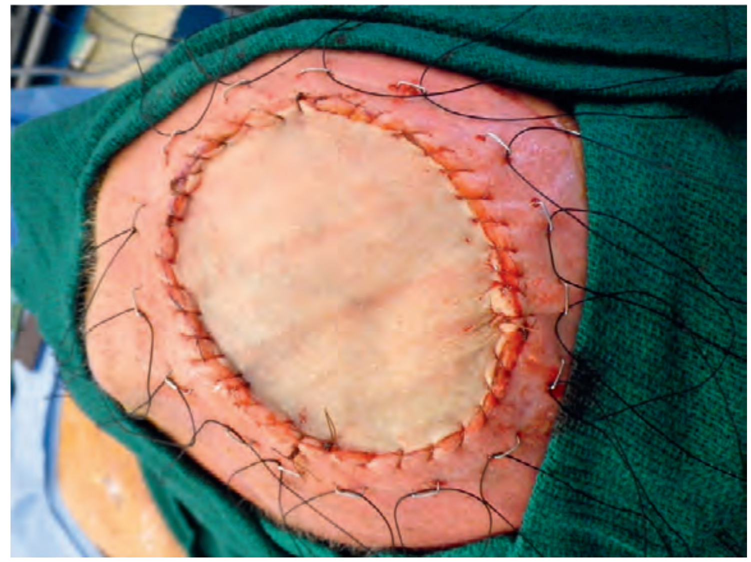

Figure 3.57 Silk strands are threaded through the staples.

Figure 3.58 The bolus is tied over with the silk strands.

Advancement Rotation Flap

Surgical excision of tumors in the non–hair-bearing areas of the scalp requires coverage of the surgical defect with tissues that resemble the normal tissues in the area for a satisfactory aesthetic appearance. Although a split-thickness skin graft can be used to cover such surgical defects, its aesthetic appearance is unacceptable. Advancement rotation scalp flaps provide a very satisfactory method of closing such surgical defects. The defect is covered with the adjacent scalp while the donor site deformity is transferred posteriorly in the hair-bearing area of the scalp, which may be closed either primarily or, on occasion, covered with a split-thickness skin graft. Alternatively, large defects of the non–hair-bearing area of the scalp or forehead can be repaired with a microvascular free flap.

When surgical excision of a scalp tumor requires excision of the underlying periosteum, bones of the calvarium are exposed. Scalp flaps or microvascular free flaps are the ideal method for covering such surgical defects.

The patient shown in Fig. 3.59 had a dermatofibrosarcoma protuberans involving the forehead at the hairline area of the scalp. A local excision was performed for biopsy purposes elsewhere before presentation. The intended extent of surgical excision and the outline of the rotation advancement flap are shown in Fig. 3.60. Even though the anticipated surgical defect is relatively small because of its inelasticity, a large area of the scalp must be elevated to provide sufficient mobilization and coverage. The blood supply of this scalp flap is through both the superficial temporal and occipital arteries. The flap is advanced anteriorly and rotated inferiorly to cover the surgical defect. Meticulous attention should be paid to the outline of the flap by appropriate measuring of the surgical defect and the rotated scalp flap, keeping the pivot point in mind. Ideally, a 4 × 8 cm gauze piece is taken, with one end being held at the pivot near the external ear and the other brought up to the apex of the surgical defect inferomedially.

Using that length as a radius, the scalp flap is outlined all the way up to the parietooccipital region. Thus if proper measurements are taken, the flap will satisfactorily rotate and cover the surgical defect. The tumor is excised in the usual fashion through the full thickness of the scalp, including the underlying periosteum (Fig. 3.61). The scalp flap is elevated through

Figure 3.59 A patient with a dermatofibrosarcoma protuberans involving the forehead at the hairline area of the scalp.

Figure 3.61 The tumor is excised in the usual fashion.

Figure 3.60 The intended extent of surgical excision and the outline of the rotation advancement flap.

Figure 3.62 The flap is reflected laterally.

the subgaleal plane, remaining superficial to the periosteum. Brisk hemorrhaging will occur from the cut edges of the scalp and should be promptly controlled. Achieving elevation of the flap through the subgaleal plane, remaining superficial to the periosteum, is very easy. Hemostasis is secured by suture ligating or electrocoagulating the bleeding from the cut edges on both sides.

The flap is reflected laterally, showing its proximal mobilization up to the vascular pedicle near the pinna (Fig. 3.62). Meticulous attention should be given to preserving the feeding vessels, which in this case are the superficial temporal artery, the posterior auricular artery, and a branch of the occipital artery. The periosteum of the entire scalp is kept intact. The flap is now rotated both anteriorly and inferiorly to cover the surgical defect (Fig. 3.63). The anterior end of the scalp flap should be adequate to match the lower border of the surgical defect. Closure is performed first with 3-0 chromic catgut interrupted subcutaneous sutures. Once the lower border of the surgical defect is completely closed, the remainder of the scalp on the left-hand side is mobilized, and appropriate spacing sutures are placed to match the convex medial edge of the scalp flap to the concave edge of the remaining scalp. These sutures are under some tension, but the scalp is vascular enough to handle this tension with no difficulty. Even spacing of sutures distributes the tension throughout the incision, which is closed primarily (Fig. 3.64). A Penrose or a suction drain is inserted. Pressure dressings are applied over the entire head. Minimal

Figure 3.63 The flap is rotated both anteriorly and inferiorly to cover the surgical defect.

Figure 3.64 Even spacing of sutures distributes the tension throughout the incision, which is closed primarily.

Figure 3.65 The postoperative appearance of the patient approximately 6 months after surgery.

Figure 3.66 Locally advanced squamous cell carcinoma of the scalp.

Figure 3.67 Extensive basal cell carcinoma of the scalp invading the orbit.

drainage is to be anticipated, and the drainage tube can be removed in approximately 48 to 72 hours. Sutures from the scalp are left for approximately 10 days and then removed in several stages to avoid disruption of the wound, which may have been closed under tension.

The postoperative appearance of the patient approximately 6 months after surgery is shown in Fig. 3.65. Excellent coverage of the surgical defect has been achieved near the hairline without any significant functional or aesthetic deformity.

Advancement rotation scalp flaps are very satisfactory for most defects of the anterior scalp. However, if these defects are of significant size, then primary closure of the donor site is not possible, and a split-thickness skin graft is necessary in the occipital region.

Extensive cutaneous malignancies of the scalp, particularly those that are either adherent to the calvarium or invade the calvarium, require major composite resections, including craniectomy and even excision of the dura to accomplish a satisfactory resection (Fig. 3.66). Such resections often are undertaken with multidisciplinary surgical teams, including head and neck surgeons, neurosurgeons, and microvascular/plastic surgeons. Surgical defects in patients such as the ones described in this section will require repair of the dura, calvarium, and a composite microvascular free flap such as the rectus abdominis or the latissimus dorsi flap to reconstruct the defect. Details of such procedures are described in Chapters 6 (Skull Base) and 17 (Reconstructive Surgery). Another patient with an extensive basal cell carcinoma of the scalp invading the forehead and orbit is shown in Fig. 3.67. This patient required a cranioorbital resection with reconstruction using a rectus abdominis free flap. The details of her operative procedure are discussed in Chapter 6.

Figure 3.68 Dermatofibrosarcoma protuberans of the scalp.

Figure 3.69 Attempted excision and a skin graft for the patient in Fig. 3.55 were unsatisfactory because of positive peripheral and deep margins.

Figure 3.70 The final postoperative result at 1 year for the patient in Fig. 3.55 after complete resection and reconstruction with a latissimus dorsi free flap and a split-thickness skin graft.

Free Flap Reconstruction of the Scalp Defect

Tumors of the scalp that either involve the periosteum or show erosion of the outer cortex of the calvarium require three-dimensional resection with underlying bone. Resection of the outer table is indicated if no gross invasion of the bone has occurred. Defects following resection of the outer table of the calvarium can be reconstructed either with a rotation flap of the scalp and a skin graft at the donor site of the rotated scalp flap or with a free flap. A full-thickness craniectomy is required if bone invasion has occurred. Cranioplasty and a free flap are necessary for reconstruction of such defects that exceed 3 to 4 cm in diameter.

The patient shown in Fig. 3.68 had a slowly enlarging tumor of 6 years' duration on the forehead at the level of the hairline. The tumor had been slowly enlarging, and a biopsy confirmed that it was a dermatofibrosarcoma protuberans. The patient had undergone an attempted excision of this tumor and skin graft repair elsewhere. However, all the margins of resection, both peripheral as well as deep, were positive for tumor. At that point, the patient was referred for definitive resection and reconstruction (Fig. 3.69). The plan of surgery at this juncture was to achieve a three-dimensional resection with generous peripheral and deep margins, which required resection of the pericranium and outer table of the calvarium.

The surgical defect in this patient was repaired with use of a latissimus dorsi muscle free flap with microvascular anastomosis of its vascular pedicle to the superficial temporal artery and its accompanying vein. The transposed free muscle flap was covered with a split-thickness skin graft. The technique of muscle transfer with a split-thickness skin graft avoids the excessive bulk of soft tissue (subcutaneous fat) that is associated with a myocutaneous flap. The postoperative appearance of the patient 6 months after surgery shows excellent healing of the surgical site with very little if any aesthetic deformity (Fig. 3.70).

Postoperative follow-up of this patient requires careful surveillance of the surgical site, because local recurrence is a feature of dermatofibrosarcoma protuberans in spite of wide resection.

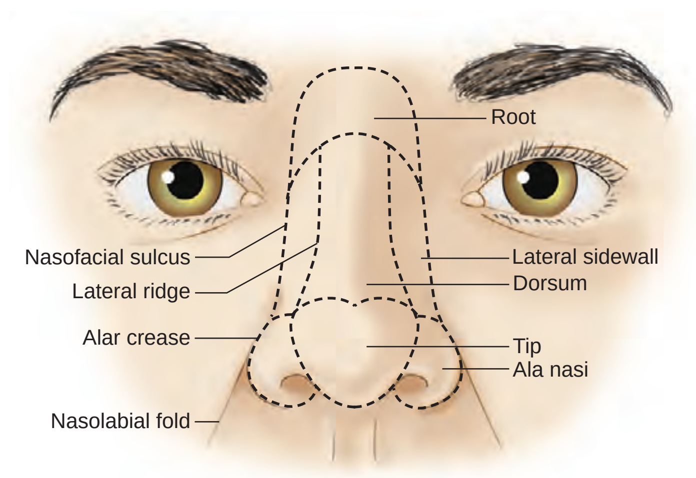

Figure 3.71 Aesthetic subunits of the nose.

Excision Lesions on the Nose and Reconstruction of Surgical Defects

Full-Thickness Skin Graft

The basic principles of reconstruction of cutaneous defects on the nose require a thorough understanding of the anatomy of the nasal aesthetic subunits to facilitate appropriate excision and reconstruction. The cutaneous surface of the nose is divided into several aesthetic subunits, shown in Fig. 3.71. The most cephalad part of the nose, also called the root of the nose, encompasses a subunit extending from the medial aspect of the eyebrow from one side to the other. The middle third of the nose is divided into the dorsum and lateral walls, and the lower third of the nose is divided into the tip of the nose, the alar subunit, and the columella. Excision of any lesion involving any part of the cutaneous surface of the nose therefore should include consideration of these subunits in planning not only the excision but also repair or reconstruction. If the nasal aesthetic subunits are not considered in treatment planning, the aesthetic result is not optimal.

Lateral Aspect of the Nose

The operative technique described in this section is for a patient who presented with Hutchinson's melanotic freckle on the left side of the nose (Fig. 3.72). The procedure is performed with the patient under general anesthesia. It is vital to estimate carefully the size of the surgical excision before embarking on the operative procedure. Good lighting and occasional optical magnification are necessary when examining subtle skin lesions such as this one to accurately assess the extent of the tumor and the desired excision. Difficulties in estimating the extent of the excision often are encountered in patients who present with lentigo maligna or morpheaform basal cell carcinomas. The desired extent of the excision is marked out with a skin-marking pen, and its dimensions are measured (Fig. 3.73). If possible, a paper template of the anticipated surgical defect should be obtained to outline the size of skin graft required. The surgical defect should not be considered final, however, until after frozen sections have been obtained from the margins of the surgical excision to ensure the adequacy of the resection.

The ideal donor site is the skin of the supraclavicular region for a defect of this size. A transverse elliptical incision is made of the desired dimensions (larger than the anticipated defect) in the loose skin in the supraclavicular fossa posterior to the sternomastoid muscle (Fig. 3.74). The skin is incised with a scalpel through its full thickness but not through the subcutaneous fat or platysma. A scalpel and fine skin hooks are used to harvest the full-thickness skin graft, remaining just deep to the dermis (the so-called "white layer" of the skin). No fat should be retained on the skin graft, and attention should be paid to remain in the same plane of subdermal dissection so the thickness of the graft is uniform. If any fat deposits are harvested inadvertently on the skin graft, they should be excised. The skin graft is preserved in a wet sponge soaked with saline solution. The resulting defect at the donor site is closed primarily in two layers after adequate hemostasis is obtained. If the skin graft is larger than 3 cm at its widest point, some tension will be present on the suture line, and it may be necessary to undermine the skin edges to facilitate closure. However, this part of the skin of the neck will heal adequately in spite of some tension on the suture line. When such tension is present, the sutures on the skin should be left in place for approximately 2 weeks.

Attention is now focused on the site of tumor excision. A skin incision is made with use of a number 15 scalpel through the previously marked outline, circumferentially through the full thickness of the skin, but remaining superficial to the nasal cartilage. Brisk bleeding from the skin incision is to be anticipated because of the rich blood supply of nasal skin. Fine, sharp hooks and suction with a Frazier suction tip are used to keep the area of advancing surgical excision dry. Once an edge of the skin is elevated, the remainder of the dissection proceeds, using needle-tip electrocautery to give a precise plane of excision without causing excessive charring or burning of tissues (Fig. 3.75). Application of adequate traction on the surgical specimen with the skin hook is important, because it will provide a uniform plane of excision remaining deep to the dermis and the soft tissues but over the cartilage. Bleeding is to be anticipated from branches of the nasolabial artery and the subdermal plexus of vessels. In general the hemorrhage can be controlled with electrocautery, but ligation of the branches of the nasolabial artery occasionally may be necessary.

After the surgical specimen is excised and complete hemostasis is achieved, several frozen sections are obtained from the margins

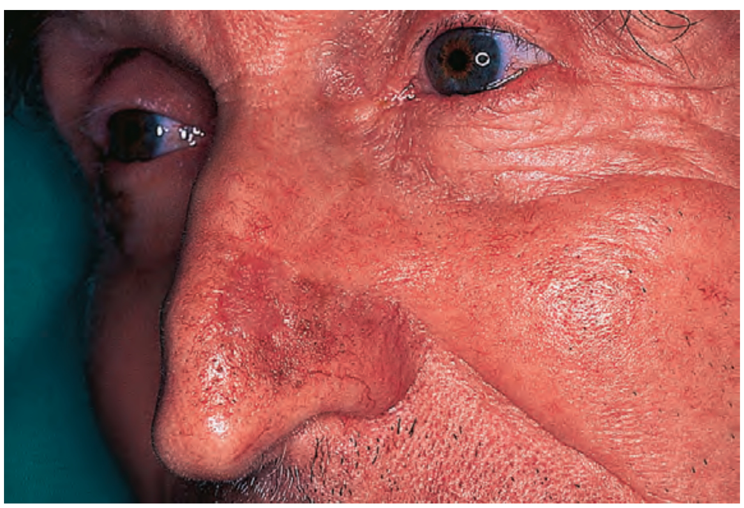

Figure 3.72 A patient with Hutchinson's melanotic freckle on the left side of the nose.

Figure 3.73 The desired extent of the excision is marked with a skin marking pen.

Figure 3.74 A transverse elliptical incision is made in the loose skin in the supraclavicular fossa to harvest a full-thickness skin graft.

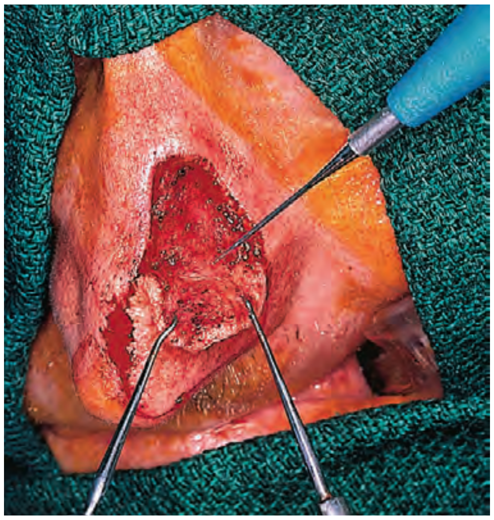

Figure 3.75 The skin lesion is excised with electrocautery, remaining superficial to the nasal cartilages.

Figure 3.76 Several frozen sections are obtained from the margins of the surgical defect to ensure the adequacy of the excision.

Figure 3.77 The skin graft is sutured with interrupted nonabsorbable sutures.

of the surgical defect to ensure the adequacy of the excision (Fig. 3.76). A frozen section also is obtained from the depth of the surgical field as its deep margin. Once the adequacy of the surgical excision is confirmed by the pathologist, the previously harvested full-thickness skin graft is brought to the surgical field and appropriately tailored to fit the surgical defect. A single-layered closure using nonabsorbable suture material is performed, paying meticulous attention to accurate approximation of the skin edge to the full-thickness skin graft (Fig. 3.77). Accurate approximation of epidermis to epidermis is of utmost importance for a desirable aesthetic result. Several interrupted skin sutures are applied, and every third suture is left with a long end that will be used to tie a bolster dressing.

After the entire skin graft is sutured in place, several stab incisions are made in the center of the graft to drain any serosanguineous material that may accumulate beneath the graft. A bolster dressing is then applied, using Xeroform gauze wrapped over plain gauze. The long ends left on select sutures are now tied over the bolster to keep it taut over the skin graft. The sutures should not be tied too tightly; otherwise, the edges of the skin on the surgical defect will "tent" and cause necrosis or disruption of sutures. Antibiotic ointment is applied at the edges of the suture line.

Postoperatively, some crusting and minor clots are to be anticipated along the suture line, and the area must be cleaned daily to prevent sepsis. Formation of a massive hematoma under the skin graft is unlikely because of the bolster dressing, but occasionally small amounts of a blood clot can accumulate under the skin graft. The bolster dressing should be inspected daily and the suture line should be kept clean with hydrogen peroxide to clear crusts and clots. The bolster dressing is removed on the seventh postoperative day, and the skin graft is left open. Over the next 2 to 3 days, the remaining skin sutures can be removed.

Initially the skin graft may look purplish-blue because of small amounts of underlying hematoma, but as it heals its color will change. Initially the skin graft is quite pale compared with the pinkish skin of the nose because of its minimal capillary vascularity. However, as neovascularization continues to develop, the skin graft takes on an essentially normal color, similar to that of the nasal skin. The postoperative appearance of the skin graft in this patient at 6 months is shown in Fig. 3.78. Because sensations are absent on this skin, the patient must avoid trauma to prevent ulceration and infection. The aesthetic result with a full-thickness skin graft is excellent on the lateral aspect of the nose with no specific donor site deformity.

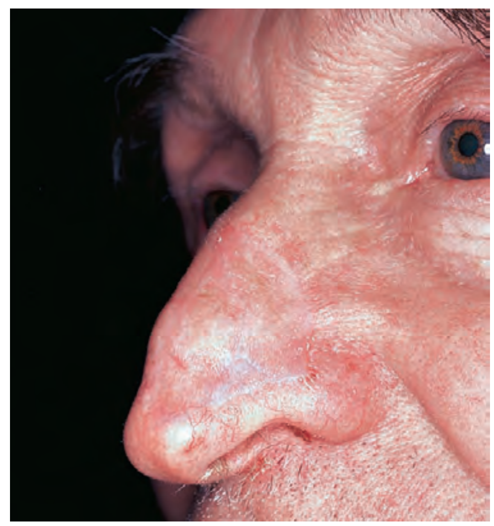

Figure 3.78 The postoperative appearance of the skin graft at 6 months.

Tip of the Nose

The patient shown in Fig. 3.79 has in situ melanoma on the skin of the nose. Accurate assessment of the extent of the lesion often requires optical magnification with a hand lens. The visible boundary of the lesion is shown in Fig. 3.80. Planning and excision around the boundaries of the lesion will give a suboptimal aesthetic result. Therefore the extent of the excision should conform to the nasal subunits laterally as well as in a cephalocaudad direction, even if it requires sacrifice of additional normal skin (Figs. 3.81 and 3.82). Surgical excision requires meticulous dissection in a plane between the undersurface of the skin and the nasal cartilages, which is accomplished with a fine-tip electrocautery. The surgical defect shows exposed nasal cartilages (Fig. 3.83). A full-thickness skin graft harvested from

Figure 3.79 In situ melanoma of the tip of the nose.

Figure 3.80 The visible boundary of the lesion is outlined with a skin marking pen.

Figure 3.81 The extent of the excision laterally to encompass the entire nasal tip up to the alar groove.

Figure 3.82 The inferior extent of the excision along the margin of the alar subunit.

Figure 3.83 Surgical defect showing the exposed nasal cartilages.

Figure 3.84 A full-thickness skin graft is sutured to the edges of the surgical defect.

the supraclavicular region is applied to the surgical defect (Fig. 3.84). The full-thickness skin graft should include the "white" dermal layer but does not include any subcutaneous fat. A Xeroform gauze bolster is applied over the skin graft and held in place with tie-over sutures for 1 week. The postoperative appearance of the patient 3 months after surgery shows a well-healed skin graft with restored nasal subunits (Fig. 3.85). Further aesthetic improvement is expected with the passage of time. With passage of time, the skin graft assumes normal color of the adjacent skin and gives an excellent esthetic outcome.

The patient shown in Fig. 3.86 had a full-thickness repair of a similar skin defect of the tip of the nose for a basal cell carcinoma. Three years following surgery, she has an excellent aesthetic outcome, with a good color match, as well as restoration of the contour of the nose in anterior as well as right and left lateral profiles (Fig. 3.87 and Fig. 3.88).

Figure 3.85 The early postoperative appearance of the nose.

Figure 3.86 Anterior view of the tip of the nose 3 years following full-thickness skin graft repair.

Excision of Lesions and Reconstruction of Defects on the Nose With Local Flaps

Glabellar "Z" Plasty

A skin lesion located in the center of the forehead is best suited for elliptical excision with primary closure, giving a midline vertical scar. However, when the lesion is off the midline and when an elliptical excision leaves a surgical defect likely to produce forehead asymmetry by primary closure, then a "Z" plasty may be considered. The lesion shown in Fig. 3.89 measures 2 × 1.5 cm and is a recurrent basal cell carcinoma. Surgical excision of this lesion is performed in the usual way, going through full thickness of the skin of the forehead but remaining superficial to the underlying frontalis muscle. Adequacy of the surgical resection is confirmed by frozen section of margins. A "Z" plasty is outlined so that the surgical defect will distribute tension on both sides of the midline equally, leaving a symmetric forehead with well-balanced eyebrows (Fig. 3.90). The skin incision is made through the outlined area, and the triangular flaps of skin that are developed at the upper and the lower part of the mobilized area are transposed so that the upper triangle is shifted to the right-hand side and the lower triangle is shifted to the left-hand side to fill the surgical defect. Tension on the suture line of the surgical defect is now distributed in such a

Figure 3.87 Right lateral view.

Figure 3.88 Left lateral view.

Figure 3.89 A recurrent basal cell carcinoma.

Figure 3.90 A "Z" plasty is outlined so that the surgical defect will distribute tension on both sides of the midline equally, leaving a symmetric forehead with well-balanced eyebrows.

Figure 3.91 Tension on the suture line of the surgical defect is distributed in such a way as to balance the forces of traction on both sides of the midline.

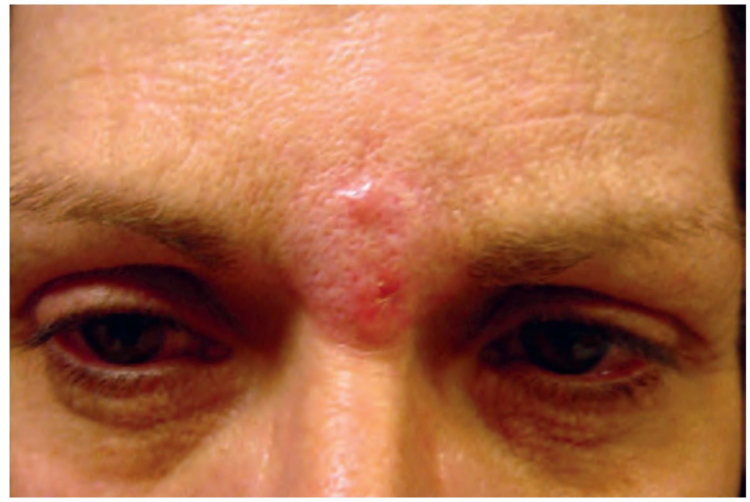

Figure 3.93 Clinical appearance of an adnexal carcinoma in the glabellar region.

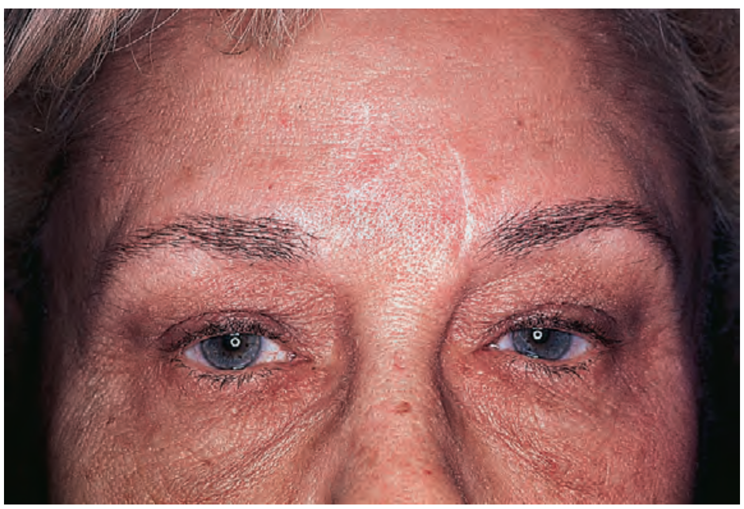

Figure 3.92 The patient's postoperative appearance 1 year later.

way as to balance the forces of traction on both sides of the midline (Fig. 3.91).

Meticulous attention to detail is necessary in closure of the subcutaneous tissues. Fine chromic catgut sutures are taken through the subcutaneous tissue, and the knots are buried. Subcutaneous sutures should be placed so they enter the undersurface of dermis on both sides at the same level to facilitate approximation of the skin edges with fine nylon sutures without tension. No dressings are necessary. Bacitracin ointment is applied to the suture line.

The same patient's postoperative appearance is shown approximately 1 year later in Fig. 3.92. Although the scar is visible, the eyebrows are well balanced and the midline of the forehead is not distorted.

Glabellar Flap

The glabellar flap is best suited for reconstruction of surgical defects at either the bridge or the upper half of the nose. It is an axial flap that derives its blood supply mainly from the supratrochlear artery but also from the dorsal nasal branches. The flap also can be used for through-and-through defects of the nasal dorsum with a split skin graft on its undersurface. Extreme care must be taken with incisions for this flap. The upper portion of the incision is carried down to the periosteum, proximal mobilization near the pedicle of the flap at the nasofrontal angle is only through the skin, and the deeper dissection on the undersurface of the flap is done bluntly to avoid injury to the supratrochlear vessels. The flap must be outlined longer than is actually necessary. Because the flap is to be turned 180 degrees, some length is lost in rotation, but in spite of this loss of length, it must be rotated without any tension to prevent compromise of its blood supply.

The patient shown in Fig. 3.93 had adnexal carcinoma of the skin of the glabellar region, for which she had undergone an open biopsy and attempted excision before presentation. Physical examination showed that the lesion was largely intradermal and subdermal in nature, with ill-defined margins and involvement of the skin extending from the medial aspect of the eyebrow on one side to that of the other. The overall dimension of the lesion was approximately 3 × 3.5 cm. Surgical repair of the defect in this location is best accomplished by an inferiorly based glabellar flap that derives its blood supply from the supratrochlear vessels. The outline of the extent of the excision and the planned flap is shown in Fig. 3.94. A grossly adequate margin of normal skin at the periphery of the lesion by inspection and palpation is performed. Frozen sections should be obtained from several margins of the periphery of the surgical defect (Fig. 3.95). Once the peripheral margins and the deep margin of the surgical defect are confirmed to be clear by frozen section, the glabellar flap is elevated. The flap is elevated in a full-thickness manner, thus preserving the underlying periosteum and the frontalis muscle fibers. The flap elevation begins at the distal tip of the flap first, with an incision on the left-hand side (the side opposite to the pedicle) first. The incision is deepened through the full thickness of the skin. Blunt dissection is then undertaken to elevate the remainder of the flap well to the right-hand side of the forehead. Blood vessels going to the flap from the left-sided supratrochlear vessels must be divided and carefully ligated. Incision of the right lateral margin of the flap then begins, starting at the tip of the flap and working caudad toward the pedicle based on the left-right supratrochlear vessels. Careful palpation of the pedicle of the flap during mobilization or, better yet, utilization of a Doppler scanner is recommended

Figure 3.94 Outline of the planned excision and glabellar flap.

Figure 3.95 Surgical defect after excision of the tumor.

Figure 3.96 Glabellar flap elevated with blood supply from the right supratrochlear vessels.

Figure 3.97 The flap is rotated 180 degrees.

Figure 3.98 The flap is trimmed to conform to the surgical defect.

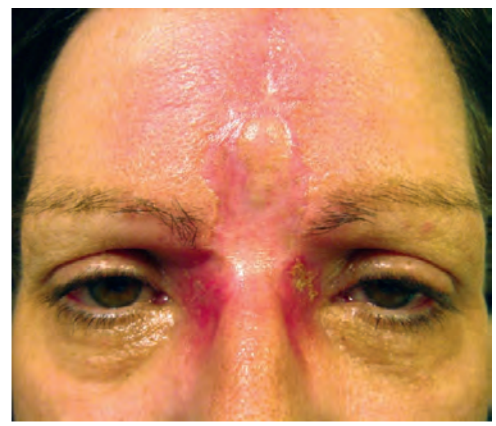

Figure 3.99 The appearance of the patient immediately after radiation therapy.

to ensure the integrity of the vascular pedicle in the narrow bridge of skin overlying the supratrochlear vessels (Fig. 3.96).

Once the flap is elevated, it is rotated caudad to see whether it would fit into the surgical defect without any tension. If excessive tension on the pedicle is noted, then further mobilization of the flap on the right-hand side is undertaken to avoid excessive tension on the pedicle (Fig. 3.97). The flap is now appropriately trimmed and sutured to the surgical defect in two layers (Fig. 3.98). The defect at the donor site of the flap is closed in two layers. Mobilization of the forehead on both sides is required to achieve midline vertical closure without any tension.

The postoperative appearance of the patient immediately after completion of adjuvant radiation therapy is shown in Fig. 3.99, and three months later in Fig. 3.100.

Figure 3.100 The appearance of the patient 3 months after completion of radiation therapy.

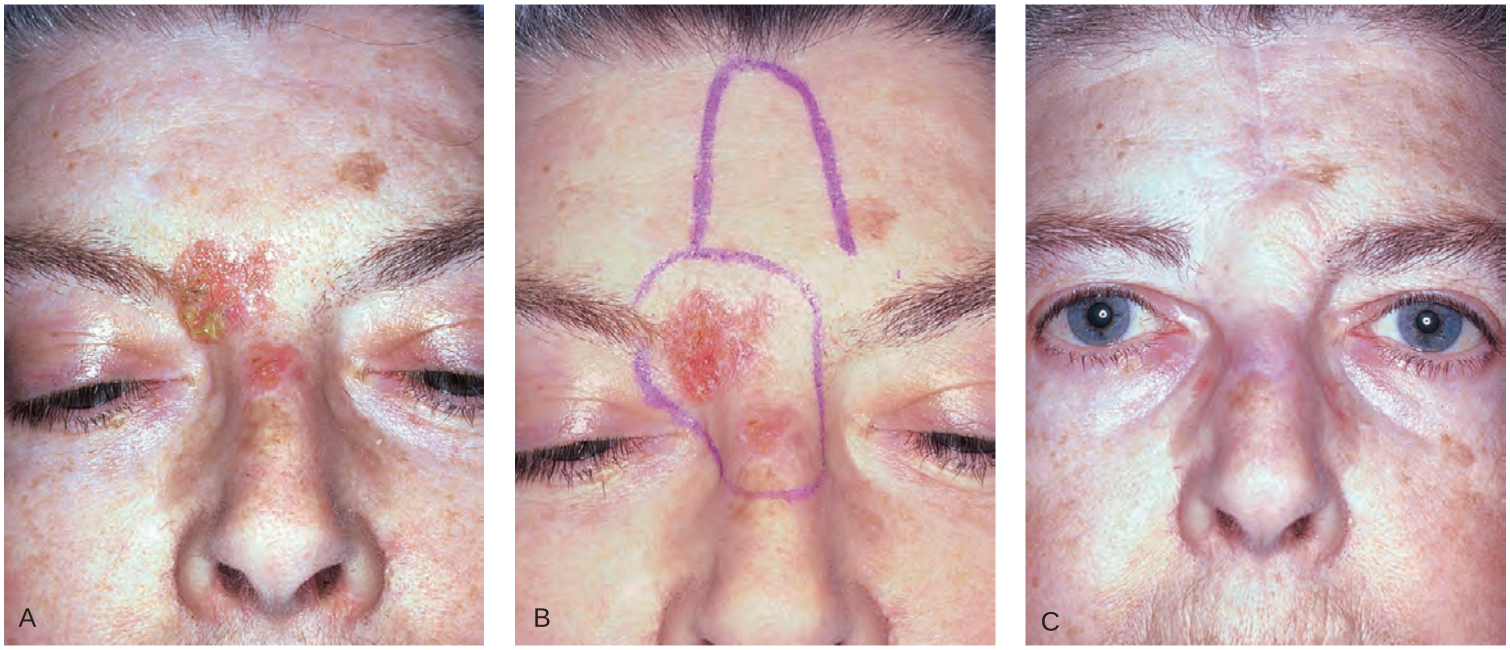

Figure 3.101 **A**, Squamous carcinoma of the glabellar region. **B**, Plan of excision and reconstruction. **C**, Postoperative appearance 1 year after surgery.

The skin flap has set well in place with well-balanced eyebrows on both sides and satisfactory coverage of the skin and soft tissue defect at the bridge of the nose. Closure of the donor site leaves an aesthetically acceptable midline vertical scar.

Another patient with multifocal squamous cell carcinoma in the glabellar region who underwent excision and reconstruction with a glabellar flap is shown in Fig. 3.101, with an excellent aesthetic result 1 year after surgery.

Sliding Rotation Degloving Nasal Flap

Full-thickness surgical defects of the skin on the front of the lower half of the nose present considerable problems for aesthetic repair. The ideal substitute for the excised skin in this area is the nasal skin itself. The patient shown here has two separate basal cell carcinomas on the skin of her face (Fig. 3.102). The basal cell carcinoma on the skin of the upper lip was excised and repaired primarily with an elliptical excision. The lesion on the nose is a deeply infiltrating lesion measuring 2.5 × 2 cm. Although the underlying cartilages are not involved, the lesion has infiltrated through the skin and the underlying soft tissues.

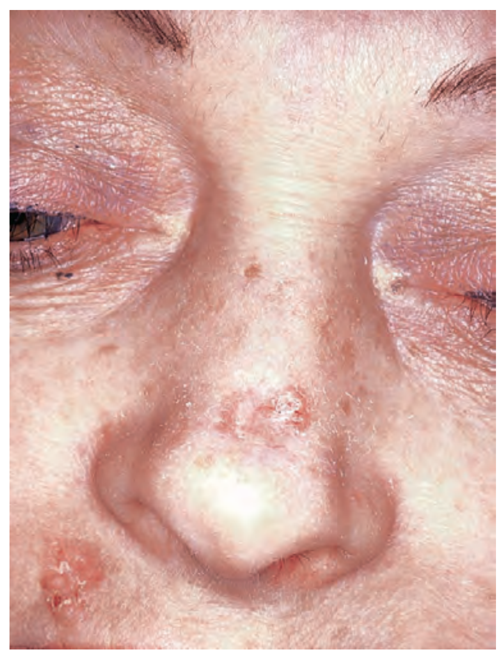

Figure 3.102 This patient has two separate basal cell carcinomas on the skin of her face.

The plan for surgical excision and reconstruction is outlined in Fig. 3.103. The degloving flap is outlined in such a fashion that the incision to mobilize the flap is on the right-hand side along the nasolabial fold going up to the glabellar region. The apex of the flap is in the midline, with its left limb remaining symmetric to the right limb. The blood supply to this flap is from the left nasolabial artery.

Excision of the lesion is performed in the usual way. In this particular patient, a generous amount of underlying soft tissue is excised down to the cartilage and nasal bone (Fig. 3.104). An adequate surgical excision is confirmed by frozen section control of margins. The degloving flap is mobilized by extending the incision on the right-hand side along the nasolabial fold up to the apex of the outlined mark. The left limb of the flap is also elevated by an incision beginning at the apex and stopping at the medial margin of the left eyebrow. The flap is elevated to lift it off the nose and nasal bones entirely, and it is mobilized well to the left side of the nose, carefully preserving the left nasolabial artery.

The flap is now ready for rotation and advancement caudad to fill the surgical defect. The lower corners of the flap at both sides, as previously outlined in the skin markings, are sacrificed and closure of the flap to the surgical defect at the tip of the nose is performed, using interrupted 3-0 chromic catgut subcutaneous buried sutures. The remaining closure of the incision is performed in the usual way so that the defect at the superior end of the flap in the center of the forehead is closed like a "V"–"Y" plasty (Fig. 3.105). Closure of the defect at the tip of the nose in the midline is difficult, because it

Figure 3.103 The plan of surgical excision and reconstruction.

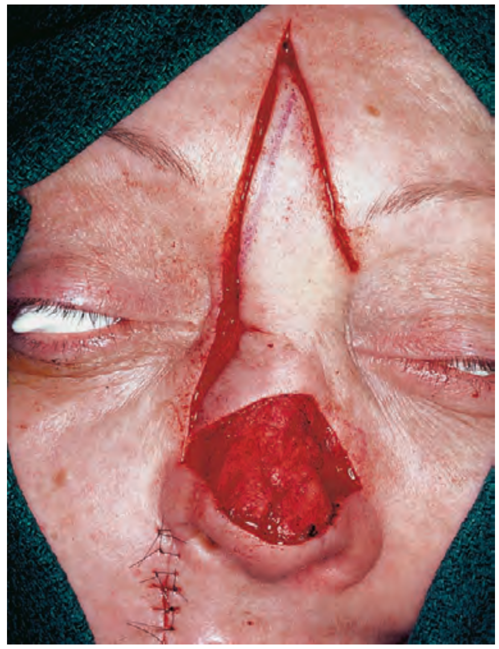

Figure 3.104 The excision is completed and the flap is elevated.

Figure 3.105 The closure of the defect is completed with advancement of the flap.

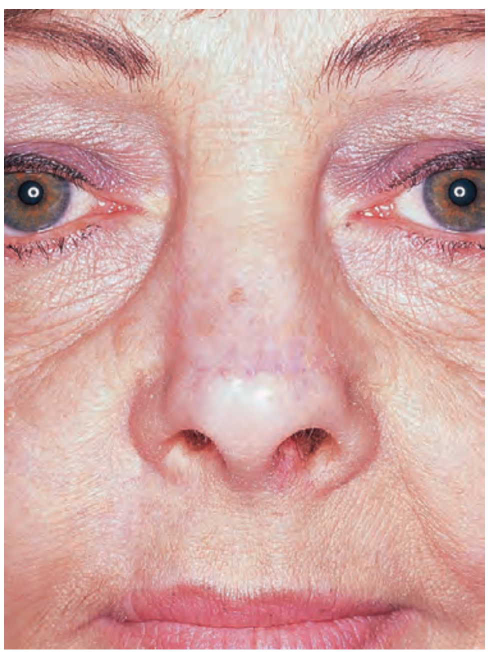

Figure 3.106 The appearance of the patient 18 months later.

significantly lifts the tip of the nose cephalad, and elevation of the tip of the nose in this way gives a "piggy" nose deformity. However, with passage of time the tip of the nose drops to its normal configuration, and the eventual aesthetic result is very acceptable.

The postoperative appearance of the patient approximately 18 months later is shown in Fig. 3.106. Note that the surgical incision is barely visible, the tip of the nose has dropped down and symmetry of the nares on both sides is restored, and the reconstructed nose has regained its essentially normal configuration. The degloving flap is of limited application for very large defects at the tip of the nose because its arc of rotation is limited. Although the blood supply to the flap is generous, its flexibility to fill the surgical defect is not very good, and therefore extreme caution should be exercised in deciding to use this flap for repair of nasal skin defects. Configuration of the nose in itself is also an important consideration for the application of this flap. For example, a patient with a nose pointing downward with a large hump would not be a suitable candidate.

Nasolabial Flap

The nasolabial flap is an axial flap that derives its blood supply from the nasolabial artery, one of the terminal branches of the facial artery. The width-to-length ratio can be as much as 1:5 in select circumstances. The nasolabial flap is a highly reliable and very versatile flap. It is generally used in reconstruction of surgical defects resulting from excision of skin cancers on the side or the ala of the nose as well as for full-thickness reconstruction of excised nasal ala, philtrum, and columella.

Inferiorly Based Nasolabial Flap. Because the vascular supply of the nasolabial flap is through the nasolabial artery, it would appear logical to have the flap based inferiorly. This flap is ideally suited for small defects of the lateral aspect of the nose in its lower half. The elevated distal part of the flap is rotated downward and anteriorly to fill the surgical defect. However, the length of the flap used in this way is limited because the skin at the root of the nose near the medial canthus is rather tight, and little flexibility is available for closure of the donor site defect.

The site of the surgical excision and the outline of the proposed nasolabial flap are marked in the patient with a basal cell carcinoma on the ala of the nose (Fig. 3.107). Appropriate measurements should be taken with a gauge to see that the flap is of adequate length and will rotate without any kink. Even though the flap is required to fill a circular defect, its apex is made triangular to allow primary closure of the donor site defect. Surgical excision of the lesion is performed using electrocautery, and care is taken to save the underlying cartilage.

If a through-and-through excision is necessary, elevation of the nasolabial flap in this way is not satisfactory. Once the adequacy of surgical excision is confirmed by histologic evaluation of the margins of the surgical defect, then the nasolabial flap is elevated. An incision is made along the previously marked outline of the proposed nasolabial flap. It is important to note

Figure 3.107 The site of surgical excision and the outline of the proposed nasolabial flap are marked.

Figure 3.108 Skin closure of the surgical defect with rotation of the flap is performed.

Figure 3.109 The postoperative appearance of the patient several months later.

that the lateral aspect of the surgical defect becomes the medial edge of the proposed skin flap.

Elevation of the flap is begun superiorly near the apex of the triangular tip. Increasing thickness of the flap is retained as dissection proceeds proximally, so that adequate soft tissue coverage will be available to repair the surgical defect satisfactorily. During this maneuver, however, it is important to note that the flap should remain superficial to the underlying facial musculature. Brisk bleeding from branches of the nasolabial artery is usually encountered, and these vessels require clamping and ligation. Delicate handling of the flap is essential during elevation so that injury to the nasolabial artery is prevented, although sharp dissection is recommended. A sufficient length of the flap should be elevated to avoid any kinking or tension on the suture line.

After elevation of the flap, and securing hemostasis, the flap is rotated anteroinferiorly to fill the surgical defect on the nose. Several interrupted inverting 4-0 chromic catgut sutures are used to secure the flap to the surgical defect. The flap is trimmed appropriately to give it a shape to fit the surgical defect. Before skin closure, the donor site defect is closed by mobilization of the skin of both the cheek and nose, which is approximated with subcutaneous chromic catgut sutures and 5-0 nylon sutures for skin. Skin closure between the skin flap and the nose is performed with use of either 5-0 or 6-0 interrupted nylon sutures (Fig. 3.108). If the flap is small, horizontal mattress sutures on both sides are not advisable because they may compromise the axial blood supply of the flap, causing necrosis of the tip. Therefore half-buried sutures, as described by Gillies, are recommended. These sutures begin on the skin of the nose, come through the dermis at the surgical defect, run horizontally through the dermis of the skin flap, and then are brought back out from the dermis and skin of the nose. Thus the knot is on the nose side and the intradermal suture in the skin flap remains parallel to the axial blood supply of the flap. This excellent suture technique is ideal for small flaps with an axial blood supply, such as this patient's.

Edema of the flap and slight duskiness are not unusual on the first postoperative day. Although the flap may look dusky or bluish, its vascularity is preserved; the discoloration is generally due to venous congestion, but the arterial blood supply of the flap is usually intact. Satisfactory healing of the skin is achieved in approximately 5 to 7 days, when the skin sutures can be removed. Excessive fat retained on the flap will result in a "fat flap" that may require defattening under local anesthesia but is not recommended for at least 6 months to 1 year. If sufficient care is taken to match the thickness of the flap to the thickness of the surgical defect with appropriate excision of excess fat from the flap at the time of the closure, a "fat flap" complication can be avoided. The postoperative appearance of the patient several months later shows an excellent cosmetic result with very little facial deformity at either the donor site or along the nasolabial skin crease (Fig. 3.109).

Superiorly Based Nasolabial Flap. Although the axial blood supply of the nasolabial flap is derived from the nasolabial artery, anastomotic communications between the angular branch of the anterior facial artery and vessels coming from the infraorbital foramen provide adequate blood supply to a superiorly based nasolabial flap.

A patient with recurrent basal cell carcinoma involving the lateral aspect of the ala and the nasolabial skin fold is shown preoperatively in Fig. 3.110. This lesion was treated previously by electrodesiccation and curettage.

The plan for surgical excision and repair using a superiorly based nasolabial flap is shown in Fig. 3.111. An adequate circumferential excision is carried out in the usual way with control of margins by frozen-section studies.

The nasolabial flap is elevated, keeping the medial incision along the nasolabial skin crease (Fig. 3.112). The generous amount of fat in the subcutaneous tissue is kept attached to the nasolabial flap for appropriate trimming before closure of the surgical defect.

The flap is elevated up to its base and is rotated anteromedially to fill the surgical defect. The flap is appropriately trimmed and sutured in two layers with 4-0 chromic catgut interrupted subcutaneous sutures and 6-0 nylon half-buried skin sutures (Fig. 3.113). The donor site is closed primarily with advancement of the skin edges.

A photograph of the patient taken 1 year later shows an excellent aesthetic result achieved by the superiorly based

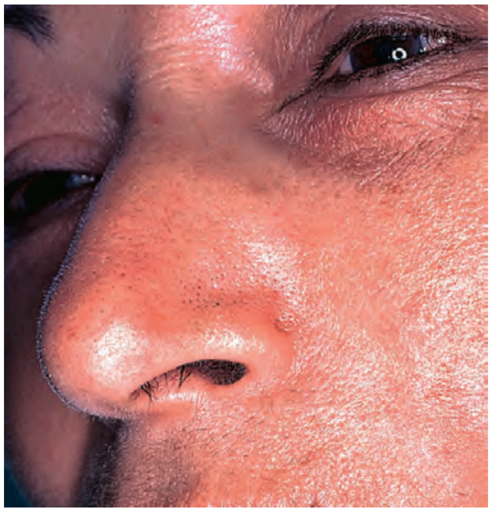

Figure 3.110 The preoperative appearance of recurrent basal cell carcinoma involving the lateral aspect of the ala and the nasolabial skin fold.

Figure 3.111 The plan of surgical excision and repair using a superiorly based nasolabial flap.

Figure 3.112 The nasolabial flap is elevated, keeping the medial incision along the nasolabial skin crease.

Figure 3.113 The flap is appropriately trimmed and closed in two layers.

Figure 3.114 The appearance of the patient 1 year later.

nasolabial flap for repair of a lateral alar defect (Fig. 3.114). The nasolabial fold skin crease is maintained in its normal position without any aesthetic deformity at the donor site.

Superiorly Based Nasolabial Flap for Reconstruction of the Ala. Skin carcinomas of the ala that involve the alar cartilage but not the underlying mucosa can be excised with the cartilage, carefully preserving the underlying mucosa. In such situations the nasolabial flap provides an excellent choice for repair of the alar defect.

A patient with basal cell carcinoma of the skin of the ala that is adherent to the alar cartilage is shown in Fig. 3.115. The underlying mucosa is intact. Surgical treatment required a circumferential excision, including the free edge of the ala at the mucocutaneous junction and the alar cartilage, preserving the underlying mucosa. The nasolabial skin flap is outlined along the nasolabial skin crease with its pedicle based superiorly.

The surgical defect is shown in Fig. 3.116. The mucocutaneous junction forms the lower margin of the surgical specimen. After ensuring adequacy of the excision by frozen section study of margins of the surgical defect, the nasolabial flap is elevated and rotated anteriorly and medially to fill the surgical defect. The flap is trimmed as necessary to obtain a satisfactory contour. A suture line between the lateral edge of the skin flap and the

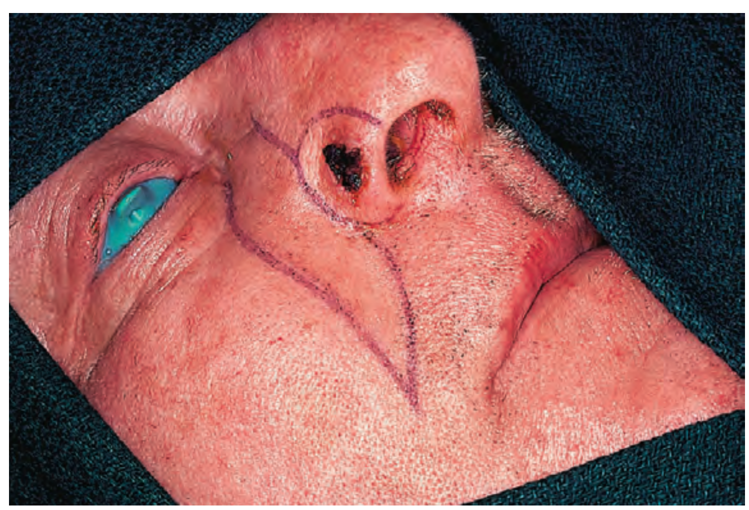

Figure 3.115 Basal cell carcinoma of the skin of the ala adherent to the alar cartilage.

mucosa reconstituted the free alar margin in this patient (Fig. 3.117). The skin flap had to be rotated anteriorly, and an angulation in its long axis required an excision of a small wedge in its middle third. The donor site defect is closed primarily by appropriate mobilization.

Figure 3.116 The surgical defect with excision of the ala to the alar groove, including the alar cartilage but sparing the mucosa of the nasal vestibule.

The postoperative appearance of the patient approximately 6 months later shows very satisfactory reconstruction of the alar defect (Fig. 3.118).

Nasolabial Flap Reconstruction for Through-and-Through Defect of the Alar Region. A patient with a recurrent basal cell carcinoma involving the skin of the ala and through the alar cartilage and nasal mucosa into the nasal vestibule is shown in Fig. 3.119. The lesion previously had been treated by electrodesiccation and curettage on two occasions.

A plan of surgical excision requiring a through-and-through resection of the ala of the nose, including the underlying mucosa, and a proposed nasolabial flap for reconstruction of the surgical defect that would provide external and inner lining is shown in Fig. 3.120.

The excision is completed, showing a through-and-through defect. The superiorly based nasolabial flap is elevated (Fig. 3.121). The flap is elevated lateral to the nasolabial crease, with a generous amount of fat on the undersurface.

The distal quarter of the flap is completely defatted, leaving only the skin and dermis behind. The tip of the flap is now

Figure 3.117 A suture line between the lateral edge of the skin flap and the mucosa reconstituted the free alar margin.

Figure 3.119 Recurrent basal cell carcinoma involving the skin of the ala, the alar cartilage, and the nasal mucosa.

Figure 3.118 The postoperative appearance of the patient 6 months later.

Figure 3.120 Outline of the extent of surgical resection and the nasolabial flap for reconstruction of the surgical defect, which will provide external and inner lining.

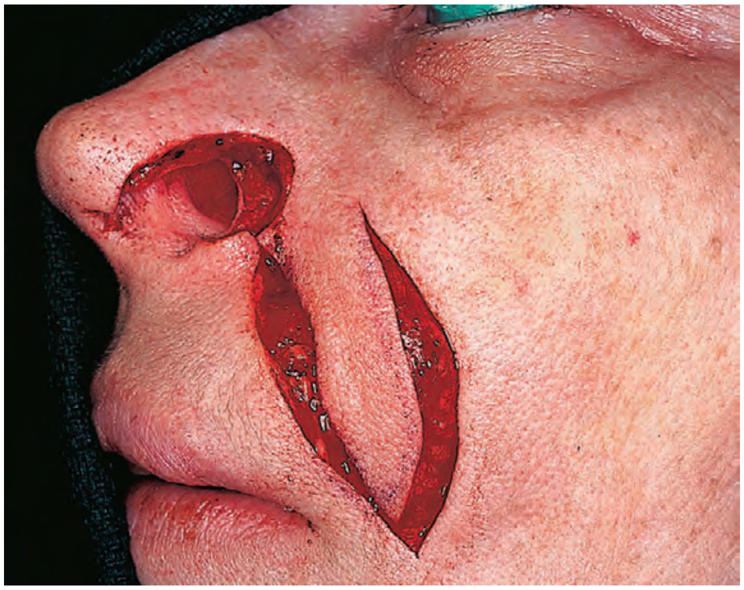

Figure 3.121 The superiorly based nasolabial flap is elevated.

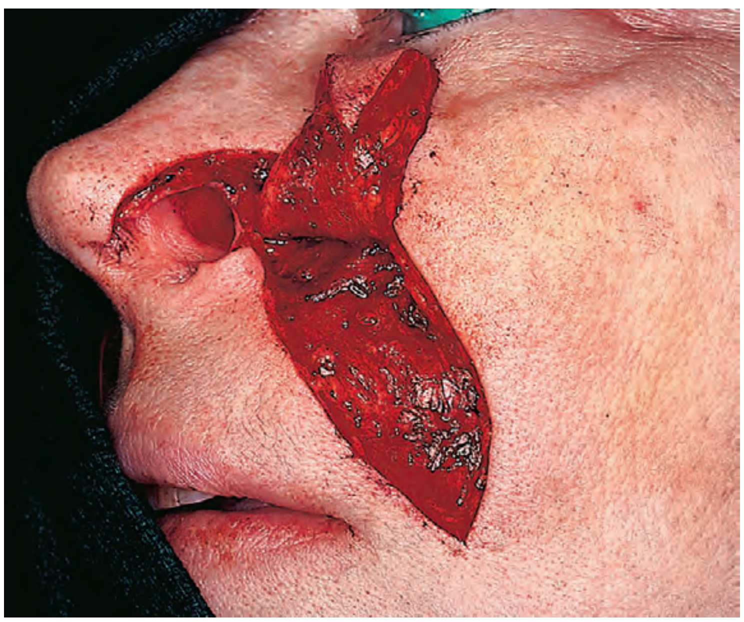

Figure 3.122 The tip of the flap is turned over itself to provide the inner lining and free edge of the ala. It is maintained in this inverted fashion with use of interrupted chromic catgut sutures.

turned over itself to provide for inner lining and the free edge of the ala, and it is maintained in this inverted fashion with use of interrupted chromic catgut sutures (Fig. 3.122). The entire distal part of the flap is now brought into the surgical defect and sutured in three layers. The skin of the tip replacing the mucosa is sutured to the mucosa of the nasal vestibule with interrupted chromic catgut sutures, and subcutaneous sutures set the flap in the surgical defect. The skin closure is performed with interrupted fine nylon sutures (Fig. 3.123).

The postoperative appearance of the patient 18 months after surgery following minor revision for defattening of the flap is shown in Fig. 3.124. The nasolabial flap used in this way is ideal for repair of a through-and-through defect of the alar region of the nose. The flap is folded over itself to replace the free edge of the ala, and aesthetically it is quite acceptable (Fig. 3.125). Cartilage support is usually not necessary unless the alar defect extends from the tip of the nose to the region of the nasolabial crease.

Figure 3.123 The skin closure is performed with interrupted fine nylon sutures.

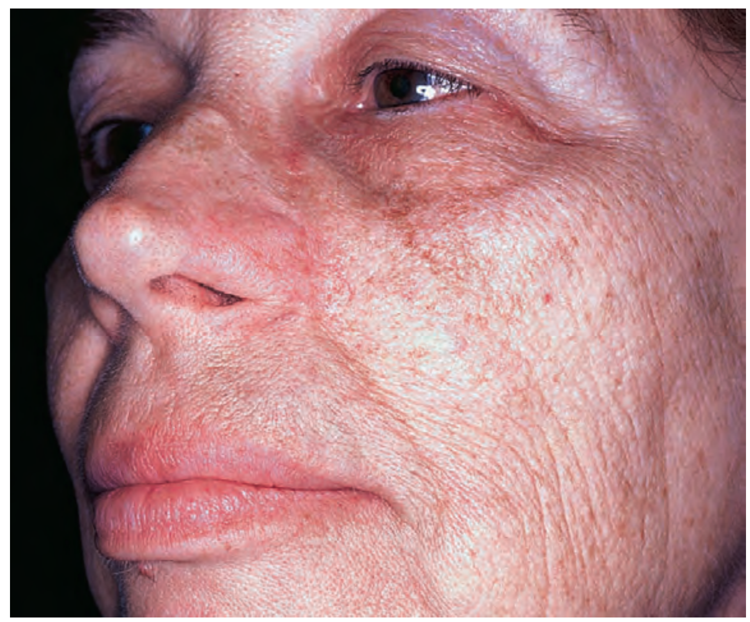

Figure 3.124 The postoperative appearance of the patient 18 months after surgery following minor revision for defattening of the flap.

Figure 3.125 The flap is folded over itself to reconstruct the free edge of the ala. Aesthetically, it is quite acceptable.

Rhinectomy and Reconstruction

Extensive cutaneous tumors of the lower third of the nose with invasion of the nasal cartilages and/or the nasal septum, floor of the nasal cavity, or the premaxilla require extensive operations, including a partial or complete amputation of the nose (rhinectomy) and rehabilitation. Surgical rehabilitation in this setting is one of the most complex operative undertakings, requiring multiple surgical procedures and multistaged refinements to achieve a satisfactory outcome.

The patient shown in Fig. 3.126 had locally extensive and invasive squamous cell carcinoma of the columella of the nose with invasion of the tip of the nose and ala of the nose on both sides, requiring amputation of the distal third of the nose in a monobloc fashion. The surgical defect on the operating table shows resection of the tip and ala of the nose as well as of the distal septum and columella (Fig. 3.127). One year after surgery and postoperative radiation therapy, the rhinectomy defect shows significant aesthetic deformity (Fig. 3.128). Reconstruction of the distal third of the nose in this patient required 11 surgical procedures of varying degrees of magnitude, including initial free tissue transfer and multistaged reconstructive efforts to achieve the optimal aesthetic outcome (Fig. 3.129). Surgical finesse of this nature is achieved only in the hands of expert reconstructive surgeons specializing in functional and aesthetic nasal reconstructive surgery.

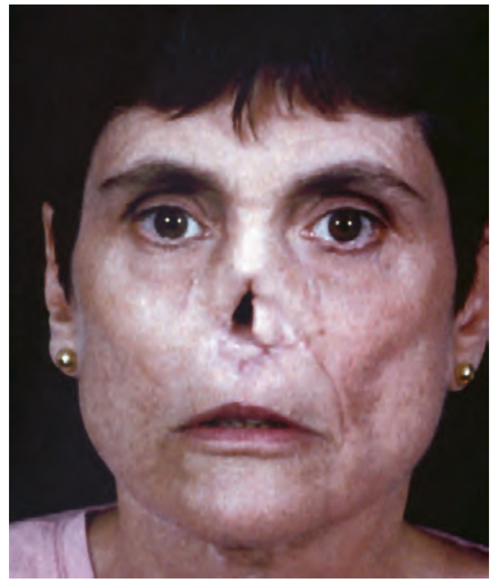

Figure 3.128 The postoperative appearance of the patient 1 year after surgery and radiation therapy indicates extensive cosmetic deformity.

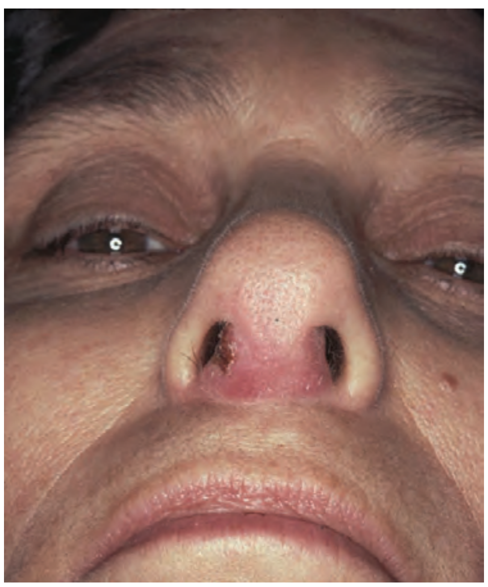

Figure 3.126 Locally extensive carcinoma of the columella of the nose.

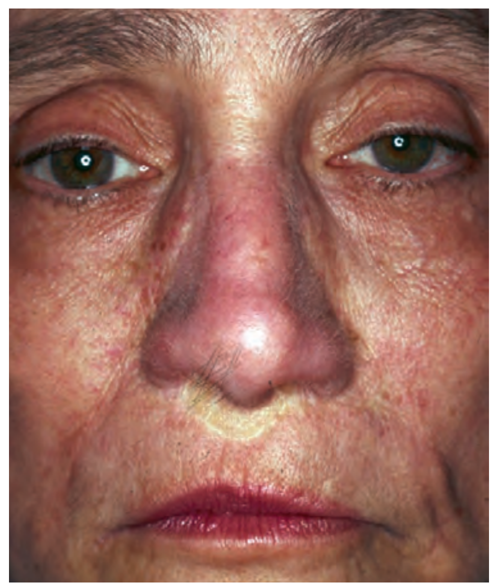

Figure 3.129 The patient's postoperative appearance after multiple reconstructive procedures 3 years after the rhinectomy.

Figure 3.127 The surgical defect on the operating table. A split-thickness skin graft is used for temporary coverage of the defect.

Rhinectomy and Nasal Prosthesis

Most patients requiring rhinectomy, however, undergo immediate and acceptable rehabilitation with the use of a nasal prosthesis. The patient shown in Fig. 3.130 had a massive adnexal carcinoma arising from the distal third of the nose with invasion of the dorsum, septum, and columella of the nose as well as the premaxilla and upper lip. A total rhinectomy and premaxillectomy were necessary to encompass resection of the entire tumor. This patient required postoperative radiation therapy

Figure 3.130 Extensive recurrent squamous cell carcinoma of the skin of the nose with invasion of the ala, septum, and nasal bones.

Figure 3.131 The patient's postoperative appearance after total rhinectomy and postoperative radiation therapy.

Figure 3.132 A nasal prosthesis offers excellent cosmetic rehabilitation.

to enhance local control. The appearance of the surgical defect approximately 6 months after surgery and the completion of radiation therapy shows a significant aesthetic deformity (Fig. 3.131). A nasal prosthesis was fabricated to accomplish aesthetic rehabilitation of this massive defect. The prosthesis is made of soft Silastic material, and appropriate coloring is performed to achieve an acceptable color match with facial skin (Fig. 3.132). Rehabilitation of rhinectomy defects with a prosthesis is the most expeditious way of achieving aesthetic rehabilitation of such massive defects. The prosthesis is retained in position either with glue applied to the skin at the periphery of the defect or by placement of osseointegrated implants into the nasal process of the maxilla, the nasal bones, or the hard palate and use of magnets in the prosthesis.

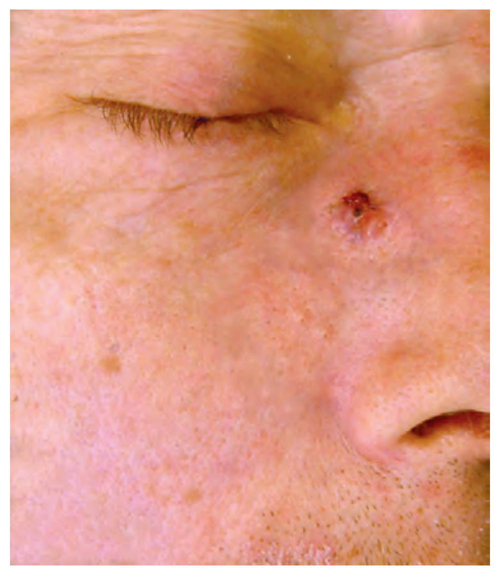

Figure 3.133 Squamous cell carcinoma of the lateral aspect of the nose.

Rhomboid Flap

The versatile, geometric rhomboid flap was described by Limberg, a mathematician. It can be used in many areas of the body and provides satisfactory closure of surgical defects, particularly in patients with lax skin. The rhomboid flap is an excellent random flap with a high degree of reliability in spite of the dependence of the blood supply to the flap from a random subdermal vascular network. Because no identifiable vessels are included in the pedicle of the flap, the length-to-width ratio of the flap should not exceed 2:1.

Rhomboid Flap Reconstruction of a Lateral Nasal Defect

The patient shown in Fig. 3.133 had a squamous cell carcinoma of the skin of the face at the junction of the lateral nasal wall and the infraorbital region of the skin of the cheek. The lesion measured approximately 1.2 cm in diameter. The planned extent of excision and the outline of the rhomboid flap are shown in Fig. 3.134. Full-thickness resection of the tumor in all three dimensions is undertaken. Frozen sections are obtained from the peripheral as well as deep margins of the surgical defect. After ensuring the adequacy of the resection, the rhomboid flap is elevated and rotated in the surgical defect to achieve coverage of the defect and primary closure of the donor site.

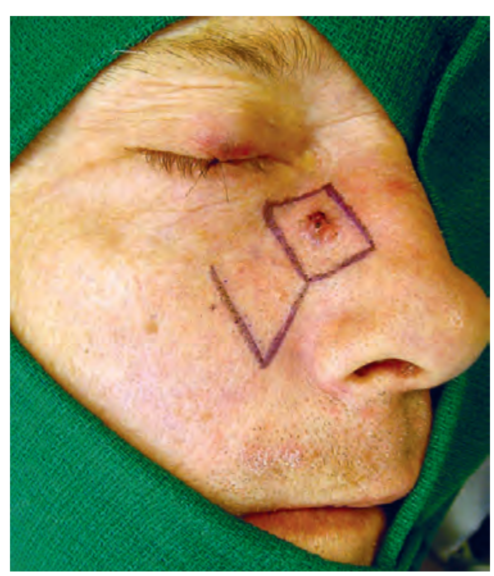

Figure 3.134 Outline of the excision and the rhomboid flap.

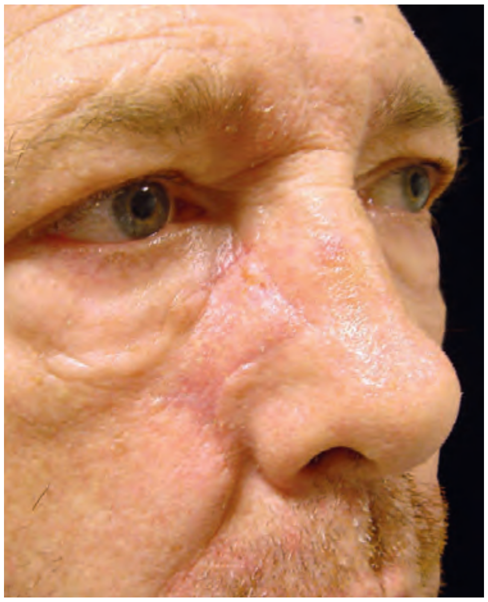

Figure 3.135 The postoperative appearance of the patient approximately 6 months after surgery.

Figure 3.136 Frontal view showing restoration of facial symmetry.

The postoperative appearance of the patient approximately 6 months after surgery shows excellent primary healing of the flap in the surgical defect with minimal aesthetic deformity (Fig. 3.135). A frontal view of the patient's face shows excellent aesthetic results with maintenance of bilateral facial symmetry, as shown in Fig. 3.136.

Rhomboid Flap Repair for a Defect of the Cheek

A patient with morpheaform basal cell carcinoma of the skin of the left cheek is shown in Fig. 3.137. A biopsy of this tumor had been performed for confirmation of tissue diagnosis. Note the hypopigmentation and very ill-defined margins of the morpheaform basal cell carcinoma outlined by a red pencil mark to show the clinically appreciable extent of the disease. Although one can consider Mohs micrographic surgery in a situation such as this, adequate surgical resection with frozen-section control of the margins and immediate reconstruction can be undertaken safely as a single-stage operative procedure. The extent of the surgical resection required for this lesion is outlined, along with a posteriorly based rhomboid flap (Fig. 3.138). Surgical excision of this lesion required wide excision around the visible and palpable margins of the tumor and was controlled by frozen section of all the margins of the surgical specimen. The flap is elevated only after negative margins are secured by frozen-section control (Fig. 3.139). The flap is elevated enough to permit its easy rotation to fill the surgical defect. A two-layered closure is performed to avoid tension on the suture

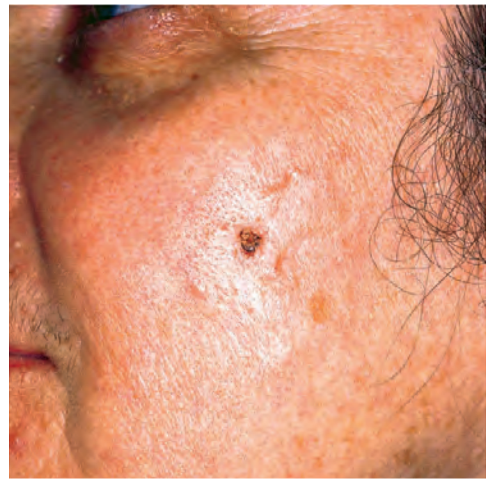

Figure 3.137 A morpheaform basal cell carcinoma of the cheek.

Figure 3.138 The outline of the surgical excision is marked with a posteriorly based rhomboid flap.

Figure 3.139 The surgical defect.

line (Fig. 3.140). The postoperative result several months after surgery shows an excellent cosmetic result with minimal deformity at the donor site. The surgical scars merge with the facial skin lines and provide an excellent aesthetic result (Fig. 3.141). Long-term follow up of the same patient 28 years later still shows an excellent aesthetic outcome (Fig. 3.142).

Figure 3.140 Rhomboid flap closure.

Mustardé Advancement Rotation Cheek Flap

Surgical defects in the infraorbital region and medial part of the cheek are best suited for repair with use of a Mustardé flap. The major blood supply of this skin flap is from the terminal branches of the facial artery.

A patient with a Hutchinson's melanotic freckle and in situ melanoma presenting on the skin of the cheek in the infraorbital region is shown in Fig. 3.143. The outline of the anticipated surgical defect and the Mustardé flap is shown in Fig. 3.144. The superior margin of the surgical defect and the Mustardé flap are kept as close to the tarsal margin as possible. Excision of the tumor is completed, preserving the orbicularis oculi and its nerve supply (Fig. 3.145). The skin incision is completed for elevation of the Mustardé flap. The superior aspect of the incision is carried cephalad toward the temple so that the tension along the suture line draws the lower lid cephalad. This procedure prevents drooping of the lateral canthus of the eye. The incision is then carried into the

Figure 3.141 The postoperative appearance of the patient 1 year after surgery.

Figure 3.143 Hutchinson's melanotic freckle and in situ melanoma presenting on the skin of the cheek in the infraorbital region.

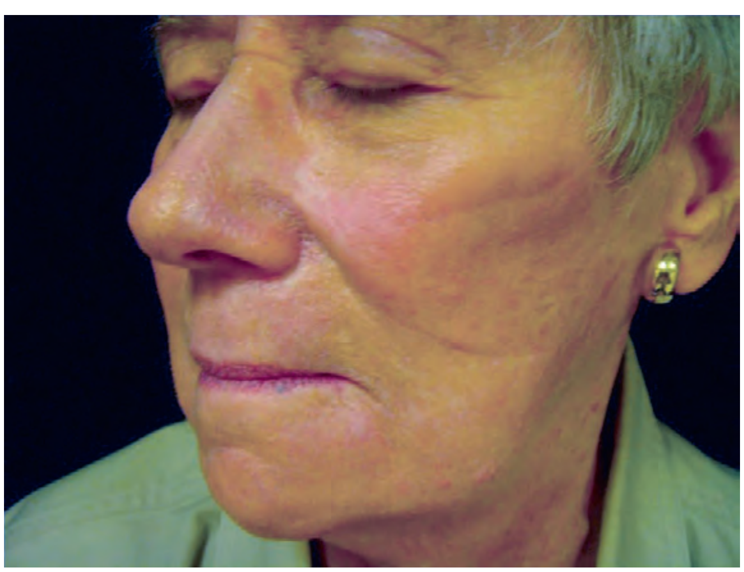

Figure 3.142 Long-term follow-up at 28 years still shows excellent cosmesis.

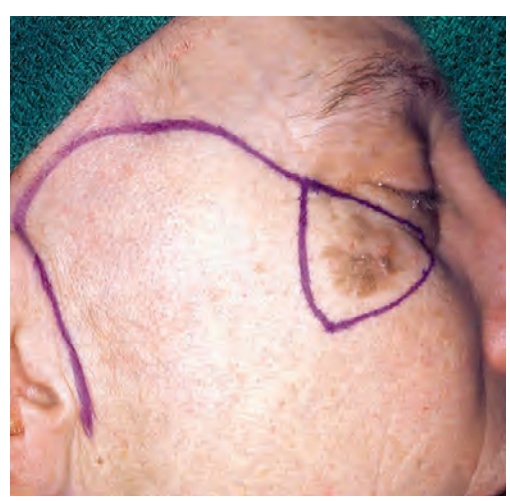

Figure 3.144 The plan for surgical excision and outline of the Mustardé flap.

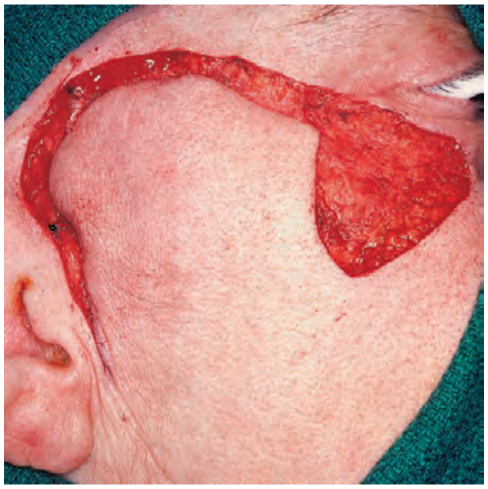

Figure 3.145 Excision of the tumor is completed, preserving the orbicularis oculi and its nerve supply.

Figure 3.146 Sutures must be appropriately spaced to provide even closure.

Figure 3.147 The postoperative appearance of the patient 9 months later.

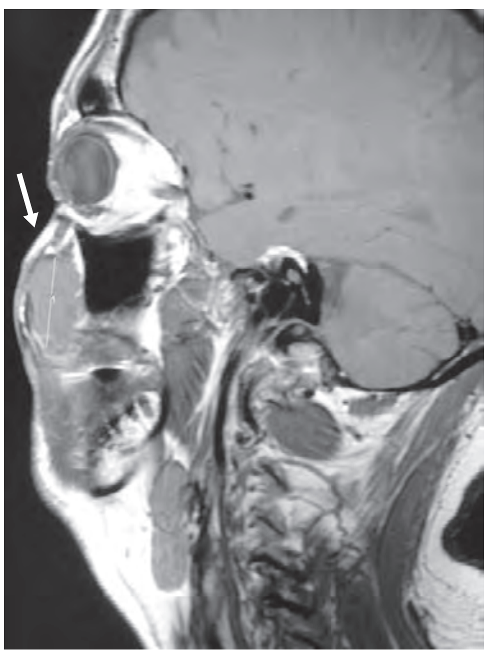

Figure 3.148 Sagittal view of MRI showing recurrent tumor occupying full thickness of the soft tissues of the cheek (*arrow*).

Figure 3.149 Wide three dimensional resection and reconstruction with a Mustardè flap is planned.

preauricular skin crease, and if additional mobilization is necessary, it can be extended into the retroauricular region like a bilobed flap. The skin flap is elevated superficial to the parotid gland, carefully preserving the blood supply in the subcutaneous tissues. Sufficient mobilization of the flap up to the angle of the mandible is often necessary to avoid tension on the suture line. Mobilization of the skin of the forehead and temporal region also may be needed to facilitate closure. The flap is now rotated anteromedially to cover the surgical defect. Absorbable inverting interrupted subcutaneous sutures are placed to minimize tension on the skin closure. Because a discrepancy usually exists between the length of the elevated flap and the surgical defect, skin sutures must be appropriately spaced to achieve even closure (Fig. 3.146). The postoperative appearance of the patient approximately 9 months later shows an excellent aesthetic result (Fig. 3.147).

Another patient with multiple recurrences of basal cell carcinoma in the nasolabial region presented with deep soft tissue multinodular recurrence involving a large area of skin of the nasolabial region and soft tissue disease up to the mucosa of the upper gingivobuccal region. A sagittal view of the MRI shows tumor occupying the entire thickness of the cheek up to the anterior wall of the maxilla and upper gum (arrow in Fig. 3.148). The extent of skin excision and Mustardè flap is marked out (Fig. 3.149). A wide three-dimensional resection required a through-and-through resection of the cheek (Fig. 3.150). The mucosal defect was repaired by primary closure (Fig. 3.151). The defect in the skin of the cheek and soft tissues was reconstructed with a Mustarde flap (Fig. 3.152). The postoperative appearance of the patient 3 years after surgery shows an excellent aesthetic outcome (Fig. 3.153).

Figure 3.150 A three-dimensional through-and-through surgical defect.

Figure 3.152 Tension free closure accomplished with the Mustardè flap.

Figure 3.151 Primary closure of the mucosal defect and Mustardè flap elevated to repair the skin and soft tissue defect.

Figure 3.153 Postoperative appearance 3 years following surgery.

Bilobed Flap

The bilobed flap is a random flap that is an excellent choice for coverage of various surgical defects throughout the body. The flap can be used very effectively on skin defects of the face and the neck, especially those overlying the zygoma and the buccinator muscles. This flap works best in patients who have lax skin, providing easy rotation of the flap and minimal donor site deformity.

The patient shown in Fig. 3.154 has a recurrent basal cell carcinoma involving the skin and subcutaneous tissues but not the underlying buccinator muscle. The area of skin at risk around the tumor measures approximately 5 cm in diameter. The plan of surgical excision and reconstruction using a bilobed flap is outlined in Fig. 3.155. A circular disk of skin measuring 5.5 cm is outlined around the ulcerated lesion for surgical excision. The bilobed flap is also outlined, using skin of the lower part of the cheek and the upper part of the neck for rotation cephalad to cover the surgical defect, with closure of the donor site along the upper skin crease in the neck.

The surgical excision is completed, with the defect exposing the zygoma in the upper part of the surgical field and the buccinator muscle, as well as other facial muscles in the lower part of the defect (Fig. 3.156). Adequacy of the surgical resection is confirmed by frozen section of margins from both the periphery and depth of the surgical defect. The buccal branch of the facial nerve had to be sacrificed because of its proximity to the undersurface of the tumor.

The bilobed flap is elevated superficial to the facial musculature, but all the subcutaneous fat is kept on the flap (Fig. 3.157). The second lobe of the flap has a triangular apex to facilitate closure of the donor site. This portion will be excised when the flap is rotated. The flap is elevated posteriorly far enough to allow rotation without tension.

Figure 3.154 Recurrent basal cell carcinoma involving the skin and subcutaneous tissues of the cheek.

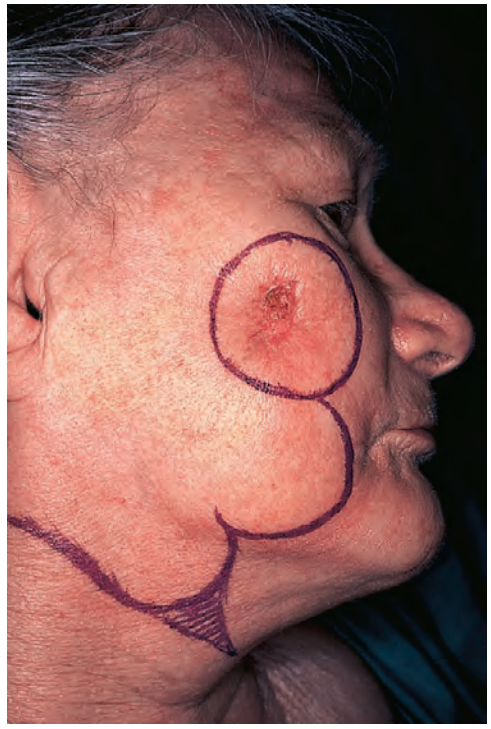

Figure 3.155 The plan of surgical excision and reconstruction with use of a bilobed flap.

Figure 3.156 The surgical excision is completed; the defect exposes the zygoma in the upper part of the surgical field and the buccinator muscle as well as other facial muscles in the lower part of the defect.

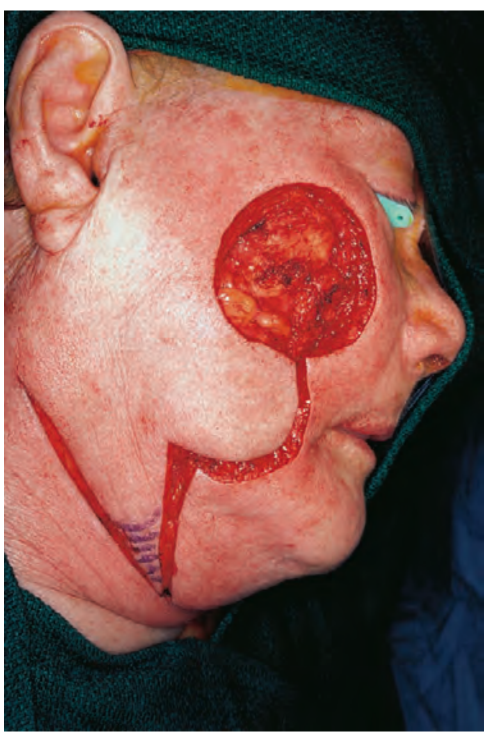

Figure 3.157 The bilobed flap is elevated superficial to the facial musculature, but all the subcutaneous fat is kept on the flap.

Figure 3.158 The flap is rotated cephalad so the first lobe of the bilobed flap fills the surgical defect at the site of excision, while the second lobe fills the defect created by the first lobe.

Figure 3.159 Interrupted chromic catgut sutures are used for subcutaneous tissue to distribute tension appropriately and set the flap in the surgical defect accurately.

The flap is now rotated cephalad so that the first lobe of the bilobed flap fills the surgical defect at the site of excision while the second lobe fills the defect created by the first lobe (Fig. 3.158). The surgical defect in the upper part of the neck created by the second lobe is closed primarily by mobilization of the skin of the neck. Interrupted absorbable sutures are used for subcutaneous closure to distribute tension and accurately set the flap in the surgical defect (Fig. 3.159). The triangular apex of the second lobe is excised, and subcutaneous sutures are placed at this point. Mobilization of the neck skin in the lower part allows closure of the donor site defect in the upper part of the neck. A small Penrose drain is inserted and brought

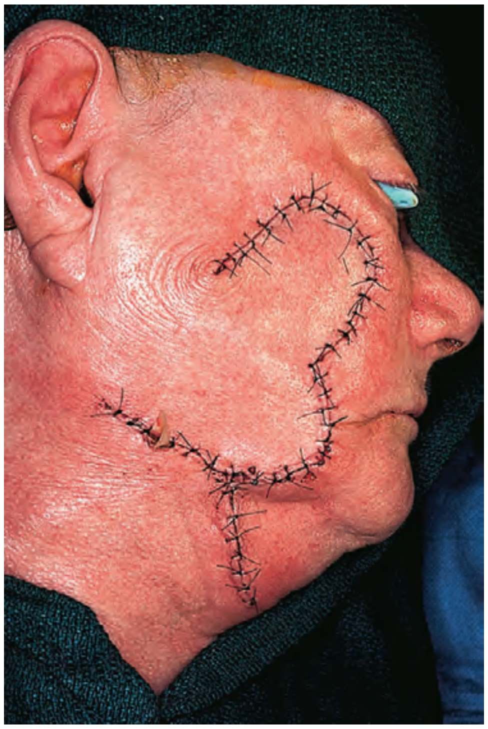

Figure 3.160 Final skin closure is performed with interrupted nylon sutures.

Figure 3.161 The postoperative appearance of the patient 1 month after surgery.

Figure 3.162 Recurrent basal cell carcinoma of the skin of the lower lip.

Figure 3.163 The surgical defect and the outline of the cervical flap.

Figure 3.164 Closure of the surgical defect is performed in two layers.

Figure 3.165 The postoperative appearance of the patient at 6 months.

out through the posterior aspect of the incision in the neck. Final skin closure using interrupted nylon sutures is shown in Fig. 3.160.

The postoperative appearance of the patient approximately 1 month after surgery shows satisfactory closure of the surgical defect with minimal donor site deformity (Fig. 3.161).

Cervical Flap

The cervical flap is a regional cutaneous flap that offers excellent skin color matching for reconstruction of surgical defects in the lower half of the face and the upper part of the neck. The flap is based on the subdermal arterial network of the skin. Therefore the length-to-width ratio of the flap generally should not exceed 3:1. The flap can be based laterally or medially, oriented in a transverse or oblique fashion, and rotated up to 180 degrees. A major advantage of the cervical flap is that its incisions allow exposure for neck dissection if required.

The patient shown in Fig. 3.162 has a recurrent basal cell carcinoma of the skin of the lower lip adjacent to the commissure of the mouth on the right-hand side. Resection of this tumor required excision of the skin and underlying soft tissues up to the orbicularis oris muscle. An outline of the advancement cervical flap is shown in Fig. 3.163. A wedge of the skin of the cheek on the lateral aspect of the surgical defect is excised to permit a satisfactory closure. The cervical flap is elevated superficial to the platysma muscle. Adequate elevation of the flap should be performed to allow satisfactory advancement and closure without tension on the suture line to avoid pulling of the lower lip or the oral commissure. A two-layered closure is performed (Fig. 3.164). The postoperative appearance of the

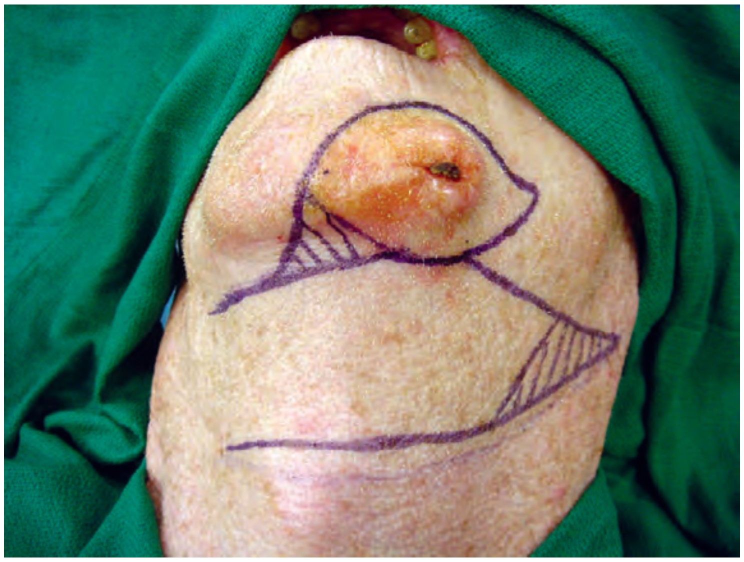

Figure 3.166 Desmoplastic melanoma involving the skin and soft tissues of the chin. The plan of surgical excision and reconstruction is outlined.

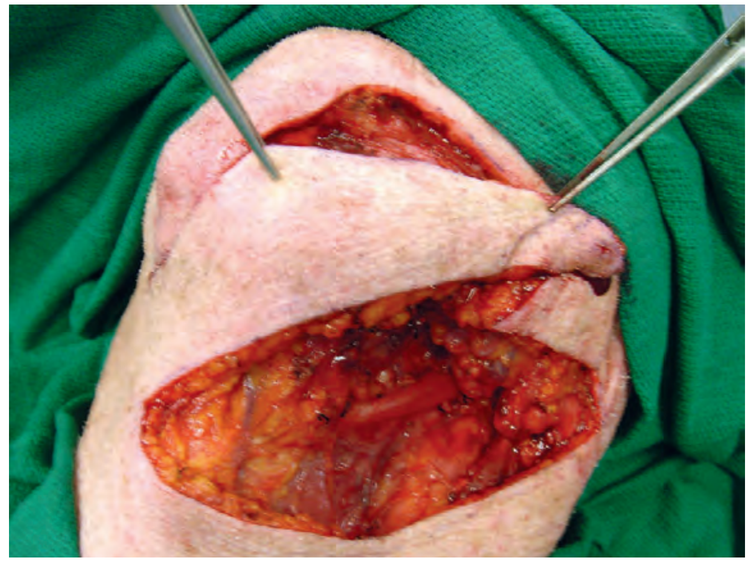

Figure 3.168 The flap is rotated cephalad and trimmed to fit the surgical defect.

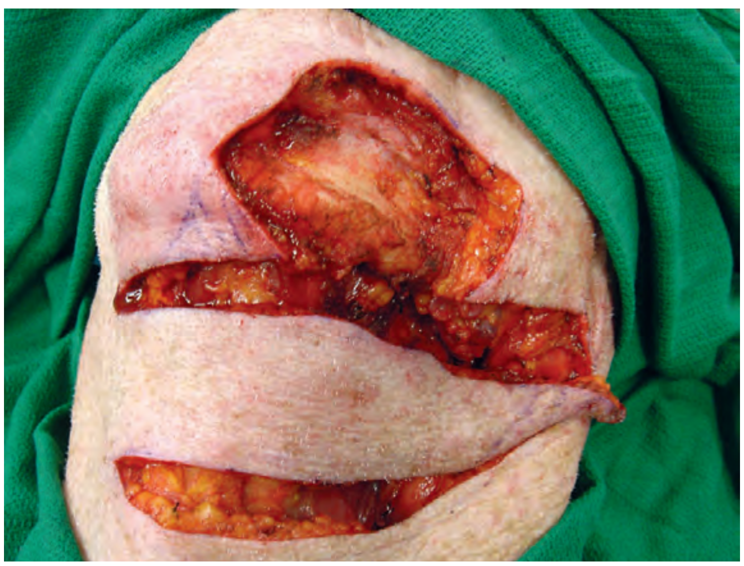

Figure 3.167 The surgical defect with the cervical flap elevated.

Figure 3.169 The donor site defect is closed in layers.

patient approximately 4 months after surgery shows satisfactory closure of the surgical defect with minimal aesthetic deformity at the donor site (Fig. 3.165).

Another patient with a desmoplastic melanoma involving the skin, soft tissues, and underlying musculature of the chin is shown in Fig. 3.166. Outline of the surgical excision and a transversely oriented cervical flap permits elective neck dissection. Two triangular wedges of skin must be excised to fill the surgical defect and provide satisfactory closure at the donor site.

Surgical excision in this patient is carried down to the underlying mandible because of the depth of tumor infiltration. The platysma is included in the flap to provide additional soft tissue. Meticulous attention should be paid to the dissection, identification, and preservation of the mandibular branch of the facial nerve during elevation of the proximal part of the cervical flap (Fig. 3.167). The flap is rotated cephalad and trimmed to fit the surgical defect (Fig. 3.168). Closure of the surgical defect is performed in two layers with use of absorbable interrupted inverting sutures for the subcutaneous layer. The donor site defect is closed similarly by mobilization of the skin of the lower part of the neck (Fig. 3.169).

Figure 3.170 The postoperative appearance of the patient at 10 months.

The postoperative appearance of the patient approximately 10 months after surgery is shown in Fig. 3.170. A satisfactory aesthetic result is accomplished in a single-stage procedure for a sizable defect of the skin of the chin. Minor revision and defattening of the flap may be undertaken later to enhance the aesthetic appearance of the patient.

Cervical Flap Reconstruction of Preauricular Skin and a Soft Tissue Defect

Surgical defects of the skin of the preauricular region as well as composite defects of the skin and underlying parotid gland can be adequately repaired with a posteriorly based cervical flap. The patient shown in Fig. 3.171 had a deeply infiltrating squamous cell carcinoma of the skin of the preauricular region with invasion of the underlying soft tissues and the superficial lobe of the parotid gland. The overall area of invasion of the skin and the soft tissues measured approximately 3 × 4.5 cm. Clinically there was no evidence of regional lymph node metastasis; however, with the extent of the primary tumor, the risk of micrometastasis to regional lymph nodes is considerably high. The plan for surgical resection is shown in Fig. 3.172. Wide excision of the skin of the preauricular area with a generous margin of skin surrounding the visible and palpable extent of the tumor was planned, in conjunction with superficial parotidectomy and modified neck dissection to include cervical lymph nodes at levels I, II, III, and IV and the apex of the posterior triangle of the neck. A posteriorly based cervical flap was planned along the skin crease of the upper part of the neck. These cervical incisions would permit completion of a modified neck dissection and superficial parotidectomy and thus removal of the primary tumor and regional lymph nodes in a monobloc fashion. The surgical defect following three-dimensional resection of the primary tumor in conjunction with the tragus of the ear and the anterior portion of the cartilaginous auditory canal, as well as superficial parotidectomy and a modified neck dissection, is shown in Fig. 3.173. The cervical flap is elevated, and its blood supply is dependent on branches of the postauricular and occipital arteries. It is then reflected laterally, preserving its soft tissue attachment to the underlying sternocleidomastoid muscle, the mastoid process, and the upper end of the trapezius muscle. The flap retains excellent circulation throughout its length, as

Figure 3.171 Advanced squamous cell carcinoma of the preauricular skin with invasion of the parotid gland.

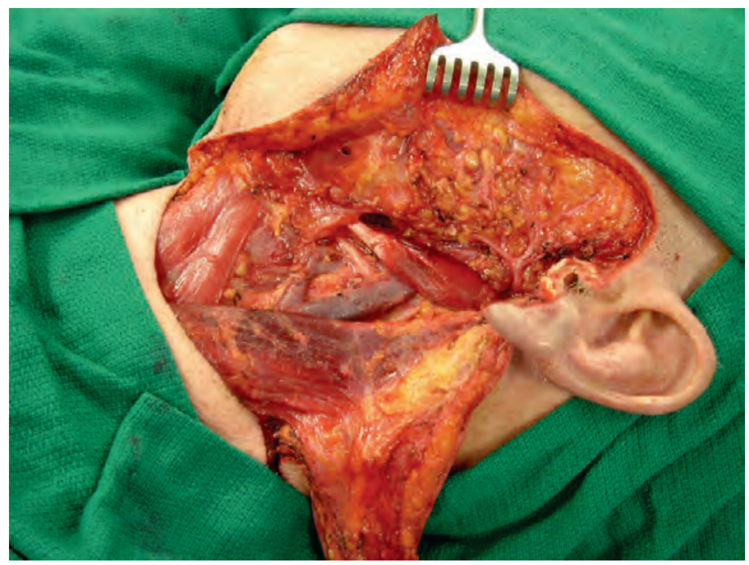

Figure 3.173 The surgical field after resection of the primary tumor with superficial parotidectomy and modified neck dissection.

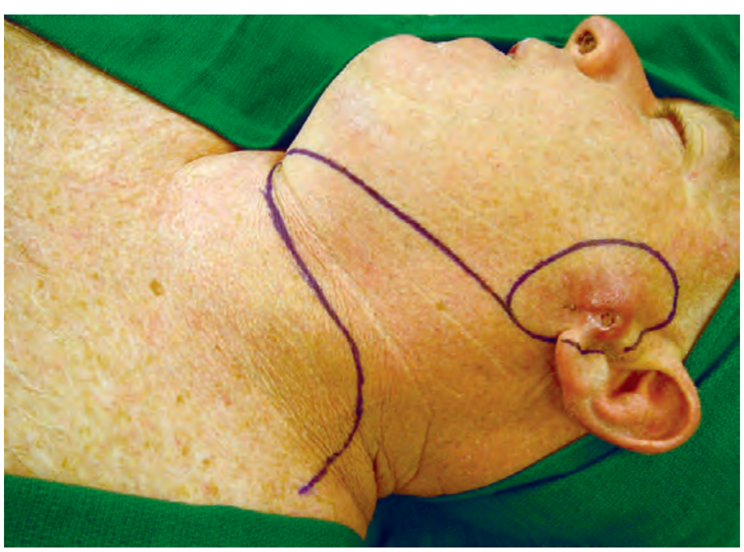

Figure 3.172 The plan of surgical excision and cervical flap reconstruction.

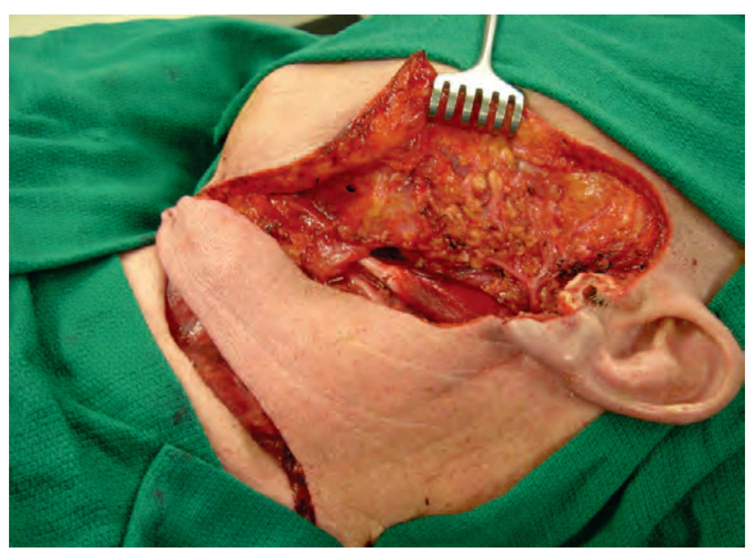

Figure 3.174 The cervical flap showing excellent perfusion throughout its length.

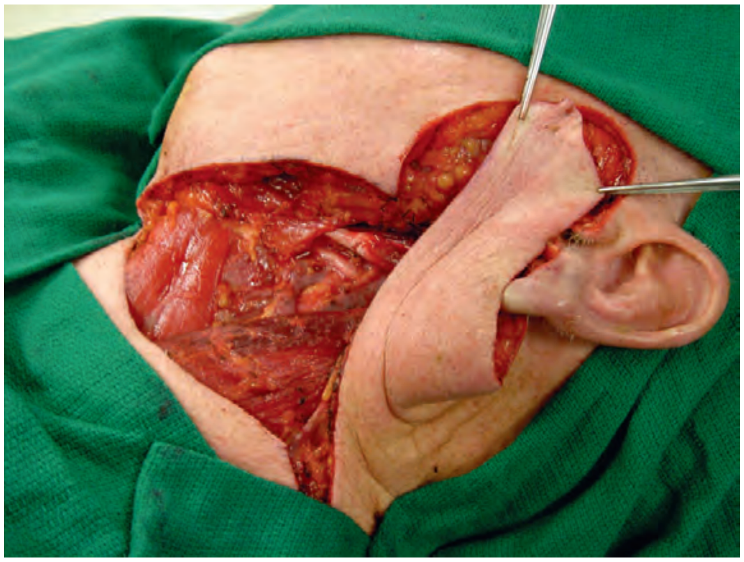

Figure 3.175 The flap is rotated cephalad to cover the surgical defect.

Figure 3.176 The postoperative appearance of the patient after minor revision of the flap.

shown in Fig. 3.174. The flap is rotated cephalad to cover the surgical defect. Note that the flap is rotated nearly 160 degrees, leaving an excess fold of skin adjacent to the lobule of the ear (Fig. 3.175). Mobilization of the upper and lower skin flaps in the neck permits primary closure of the neck incision. Appropriate trimming of the flap permits satisfactory single-stage closure of the surgical defect. The postoperative appearance of the patient approximately 1 year after surgery shows an acceptable cosmetic result (Fig. 3.176). Excess skin (sometimes referred to as a "dog ear") adjacent to the lobule of the ear can be trimmed later to optimize the aesthetic result.

Free Flaps in Facial Reconstruction

Excision and Repair of a Large Defect of Facial Skin With a Radial Forearm Free Flap

Large defects of the facial skin are best repaired with use of a microvascular free tissue transfer. The disadvantages of free tissue transfer are that the color match often is not satisfactory and occasionally the tissue may be too bulky.

Figure 3.177 This patient has recurrent dermatofibrosarcoma protuberans of the preauricular region requiring excision and a superficial parotidectomy.

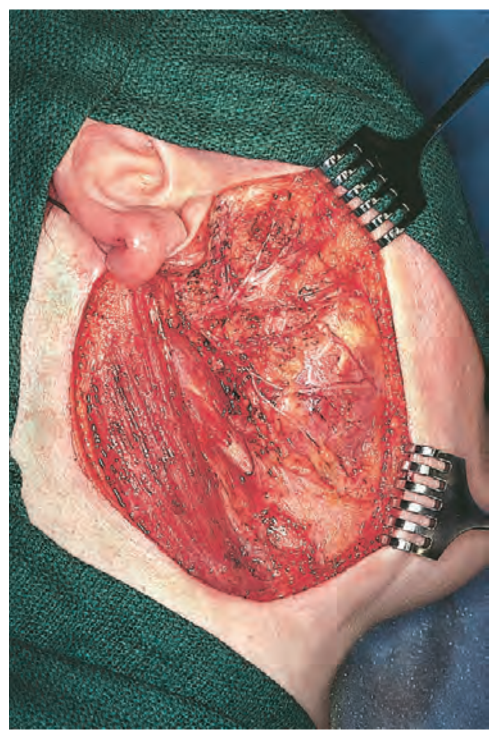

Figure 3.178 The surgical defect after excision of skin of the preauricular region and the parotid gland to encompass a three-dimensional resection.

The patient shown in Fig. 3.177 has recurrent dermatofibrosarcoma protuberans of the preauricular region that requires wide excision of the skin and a superficial parotidectomy. A generous portion of the skin in the preauricular region is excised to accomplish a three-dimensional resection (Fig. 3.178). The surgical defect thus created is repaired with a microvascular fasciocutaneous radial forearm free flap. The postoperative

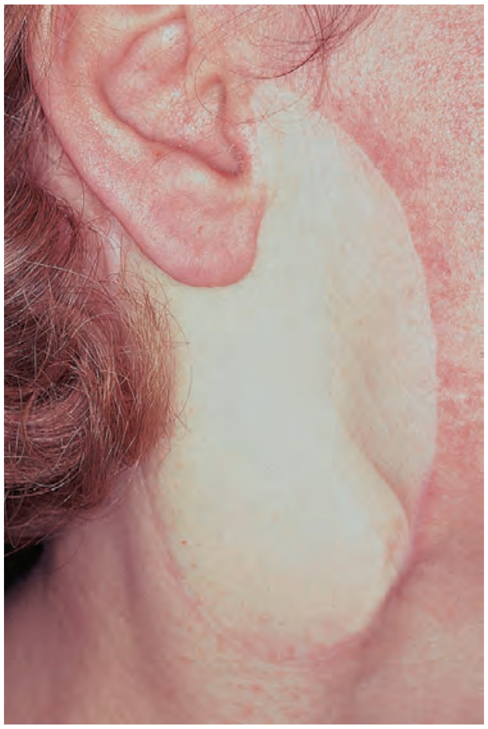

Figure 3.179 The postoperative appearance of the patient. Note the discrepancy in color between the free flap and the face.

appearance of the patient shows a satisfactory reconstruction of this large surgical defect, although the color match is not ideal (Fig. 3.179). Dermatologic tattooing can be performed to optimize the aesthetic outcome.

Repair of a Through-and-Through Defect of the Nose With an Osteocutaneous Radial Forearm Free Flap

Composite defects of the skin of the nose, its supporting framework, and the underlying mucosa require complex reconstruction. Often repair of such surgical defects using local flaps will entail multiple procedures. Single-stage reconstruction using a composite free flap is desirable to avoid delay in initiating adjuvant treatment.

The patient shown in Fig. 3.180 had an extensive squamous cell carcinoma that began on the septum of the nose and invaded

Figure 3.180 Widening of the bridge of the nose in a patient with squamous cell carcinoma of the nasal septum.

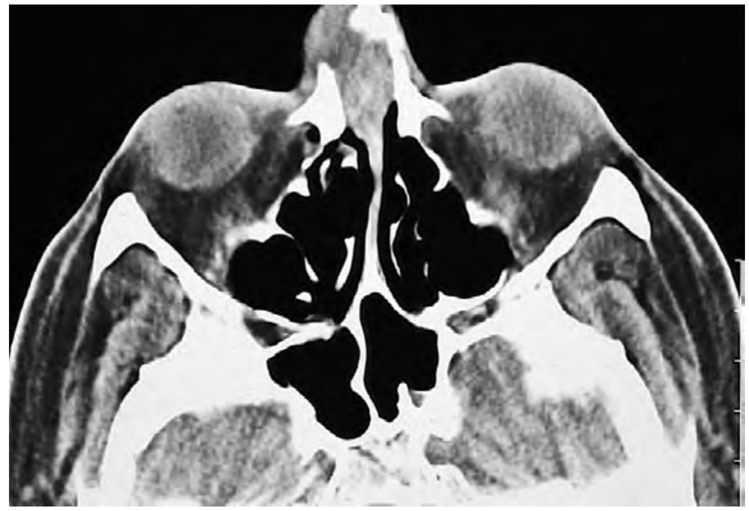

Figure 3.181 A computed tomography scan shows destruction of the nasal bone and extension into the overlying soft tissue.

Figure 3.182 Surgical defect.

the subcutaneous soft tissues and the overlying skin. This patient had not received any previous treatment but had a biopsy performed endoscopically from the nasal septum that confirmed the diagnosis of squamous cell carcinoma. A CT scan shown in Fig. 3.181 demonstrates a soft tissue mass arising from the anterior aspect of the septum of the nose with extension to the subcutaneous soft tissues and destruction of the nasal bone on the right-hand side. A through-and-through resection of the upper two thirds of the nose, including the nasal septum and the lateral wall of the nasal cavity on the right-hand side, was performed. Frozen-section analysis of the margins confirmed satisfactory resection of the tumor. The surgical defect shown in Fig. 3.182 demonstrates the need to reconstruct multiple structures to achieve a satisfactory result. A composite osteocutaneous radial forearm free flap was harvested with a split radius to provide bony support to the nose, and two islands of the skin flap were created to provide an inner lining and outer coverage. The immediate postoperative appearance of the patient approximately 8 weeks after surgery demonstrates satisfactory reconstruction of the composite nasal defect (Fig. 3.183). This patient received postoperative radiation therapy as adjunctive treatment and will require minor revisions to achieve an improved aesthetic appearance.

Figure 3.183 The patient approximately 8 weeks after surgery.

Extensive Resections for Advanced Skin Cancers of the Face

Advanced neglected or extensive recurrent skin cancers of the facial area often require three-dimensional composite resections including orbital exenteration, amputation of the nose, maxillectomy, mandibulectomy, and craniofacial or cranioorbital resection, depending on the location and extent of the tumor. Reconstruction of such massive surgical defects usually requires a composite free flap to provide bulk and surface lining. The patient shown in Fig. 3.184 has an extensive squamous cell carcinoma of the skin of the right cheek invading the underlying soft tissues, the anterior wall of the maxilla, and the orbit. A CT scan of the patient demonstrates destruction of the zygoma with infiltration of the periorbital soft tissues (Fig. 3.185). Composite resection of the tumor in this patient entailed wide excision of the skin and soft tissues of the right side of the face in conjunction with partial maxillectomy and orbital exenteration. In addition, resection of the zygoma, superficial parotidectomy, and a modified neck dissection were performed. The surgical specimen is shown in Fig. 3.186. The surgical defect was repaired with use of a rectus abdominis free flap. The postoperative appearance of the patient approximately 3 months after surgery is shown in Fig. 3.187. This patient will require an external prosthesis for the right eye to restore his aesthetic appearance.

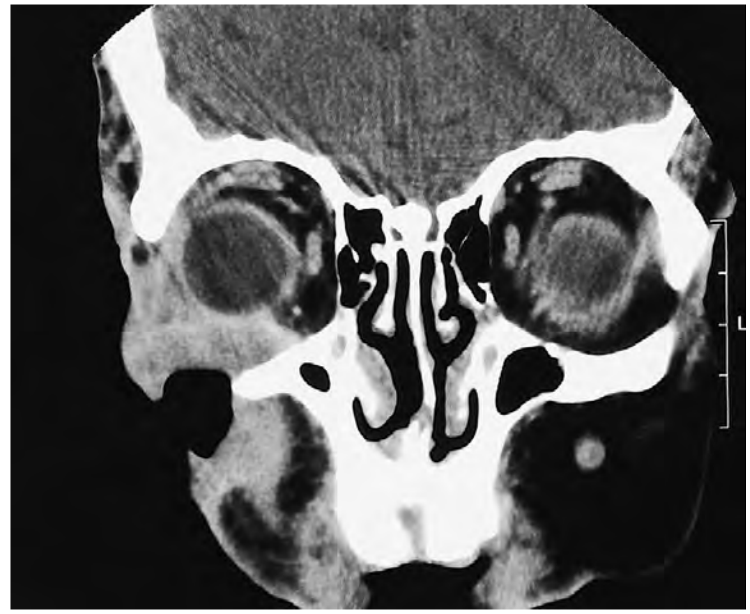

Figure 3.185 A computed tomography scan demonstrates invasion of the orbit.

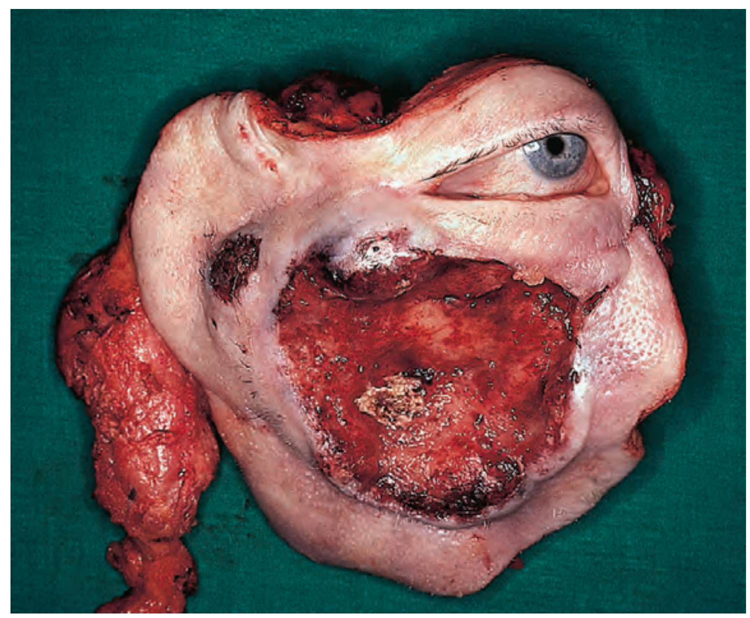

Figure 3.186 Surgical specimen.

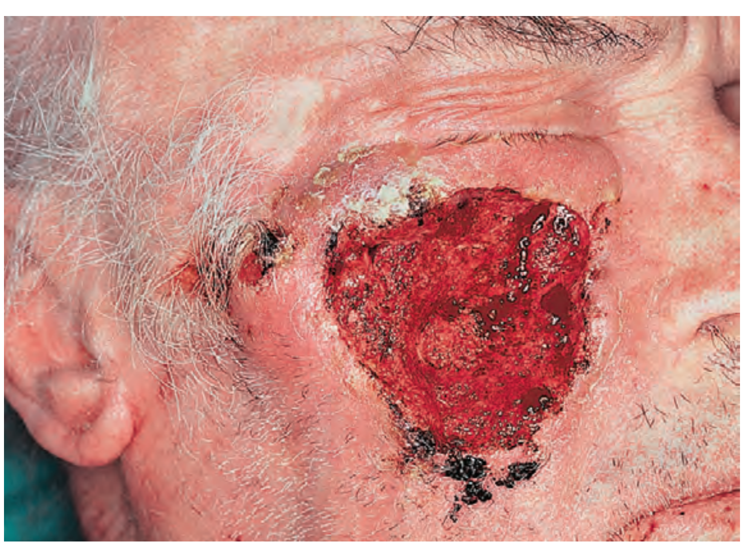

Figure 3.184 Locally advanced squamous cell carcinoma of the right cheek.

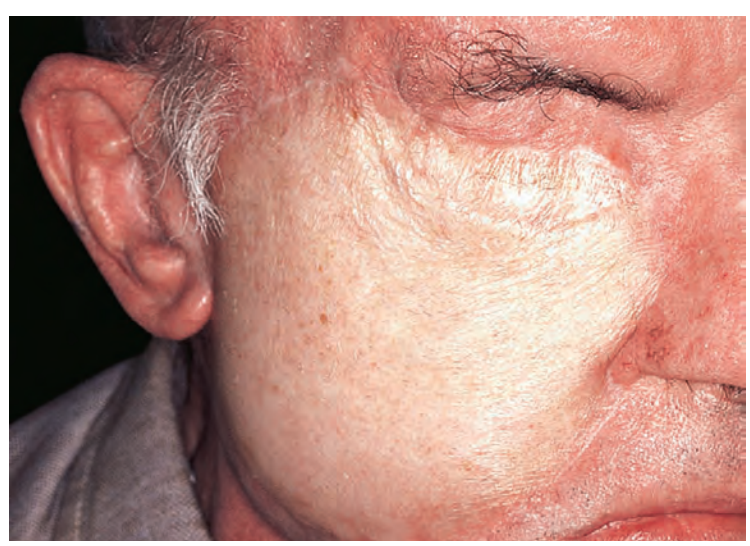

Figure 3.187 The patient approximately 3 months after surgery.

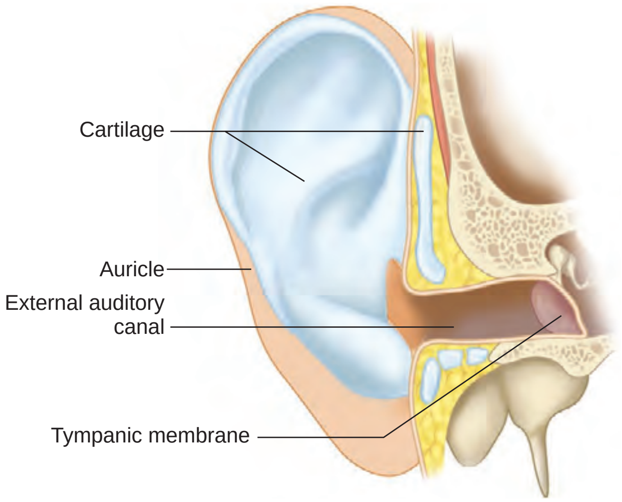

Figure 3.188 Surface and cross-sectional anatomy of the pinna and external auditory canal.

Figure 3.189 Squamous cell carcinoma of the external ear.

Excision of Tumors of the Ear

Surgical Anatomy. The unique anatomy of the external ear (auricle or pinna) requires special consideration when planning resection and reconstruction. The cartilage of the external ear is covered by the overlying skin without any subcutaneous soft tissue or fat. The tightly bound skin of the external ear retracts over the cartilage after resection of any part of the auricle. Skin cancers of the anterior or posterior surface of the external ear infrequently invade the cartilage, and therefore full-thickness resection is rarely required. Reconstruction of a composite surgical defect of skin and underlying cartilage can be accomplished with a full-thickness skin graft supported by underlying skin on the other side of the cartilage. Blood supply to the external ear is from the preauricular and postauricular branches of the external carotid artery. The surface and cross-sectional anatomy of the pinna and external auditory canal is shown in Fig. 3.188. Deeply infiltrating tumors with invasion of the underlying bone will require temporal bone resection.

Excision and Full-Thickness Skin Graft for Cutaneous Malignancies of the Skin of the External Ear

Cutaneous malignancies of the skin of the external ear that do not involve the underlying cartilage can be easily resected in a three-dimensional fashion with the cartilage of the external ear as its deep margin. Reconstruction of the defect with a full-thickness skin graft allows preservation of the shape and contour of the external ear.

The patient shown in Fig. 3.189 has a keratinizing squamous cell carcinoma of the external ear, extending up to the lateral aspect of the cartilaginous ear canal. The area of involvement is approximately 2.5 × 3 cm on the anterior surface of the skin of the external ear.

A full-thickness skin graft of appropriate dimensions is harvested from the skin of the supraclavicular region to fit the anticipated surgical defect. The required amount of skin is isolated in an elliptical fashion to match with a skin crease in the lower part of the neck (Fig. 3.190). Harvest of the full-thickness skin graft is done meticulously in the subdermal plane, remaining superficial to the subcutaneous fat. This procedure is best accomplished by applying tension to the skin of the graft over the index finger of the operating surgeon and using a sharp scalpel in an oblique fashion, remaining directly in contact with the undersurface of the dermis (Fig. 3.191). After harvest of the skin graft, adequate hemostasis is secured by electrocoagulation of fine bleeding points. The skin defect at the donor site is closed in two layers.

Figure 3.190 Outline of a full-thickness skin graft.

Excision of the tumor with the underlying cartilage, while preserving the skin of the posterior surface of the external ear, requires dissection in a plane between the cartilage and the skin of the posterior surface of the ear. A number 25 needle is used to infiltrate this plane with saline solution and epinephrine (Fig. 3.192). "Hydrodissection" of the tissue plane between the skin and the cartilage elevates the posterior skin over the cartilage and prevents perforation of the posterior skin. This skin will be the surgical "bed" that supplies blood to the full-thickness skin graft.

Excision of the primary tumor now begins with a circumferential incision around the visible and palpable extent of the lesion, with a sufficient margin of normal skin in all directions. Minor but brisk bleeding is encountered from cutaneous blood vessels immediately superficial to the cartilage. This bleeding

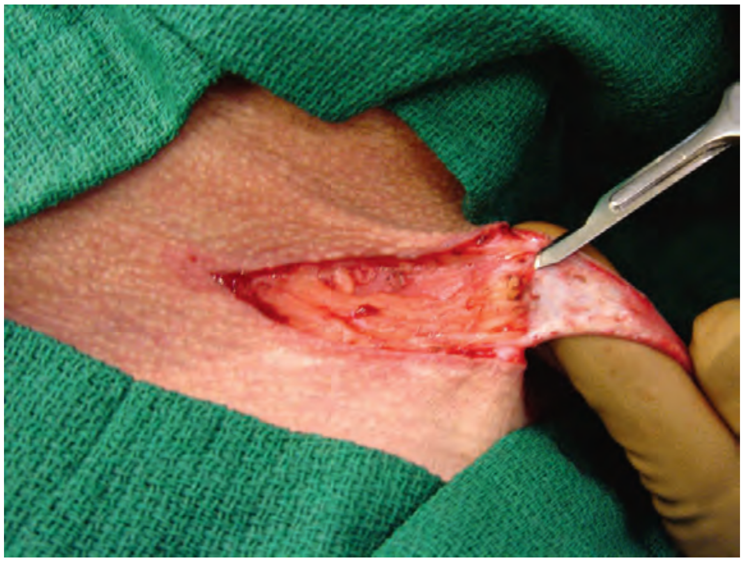

Figure 3.191 The graft is harvested in the subdermal plane.

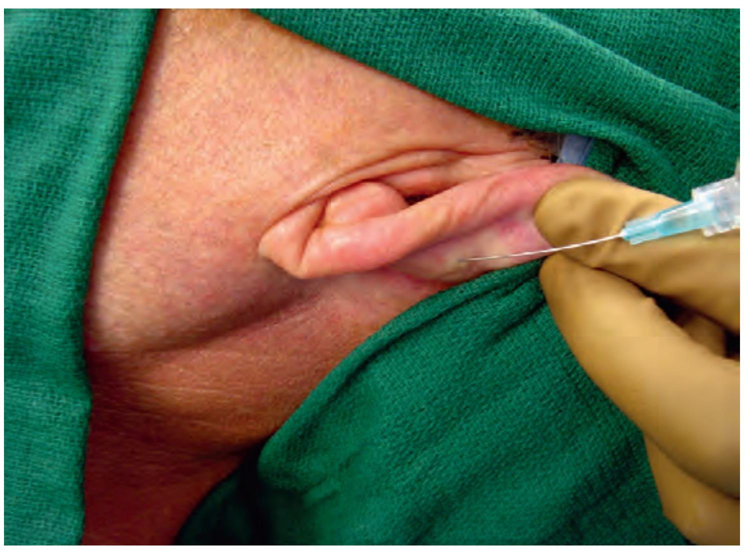

Figure 3.192 "Hydrodissection" to elevate the posterior skin off the underlying cartilage.

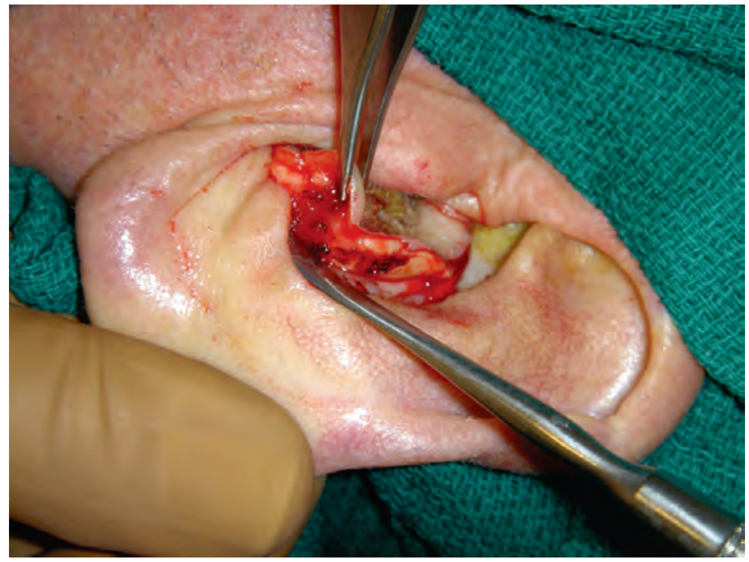

Figure 3.193 A Freer periosteal elevator is used to dissect in the plane between the cartilage and posterior skin.

Figure 3.194 The surgical defect.

is easily controlled with electrodessication. The cartilage is incised circumferentially along the skin incision, carefully remaining in the tissue plane between the posterior surface of the cartilage and the skin of the posterior part of the external ear. This dissection is facilitated by the previously created tissue plane achieved by hydrodissection as a result of the injection of saline solution in that tissue plane. Once circumferential incision of the skin and cartilage is completed, elevation of the surgical specimen between the posterior surface of the cartilage and the skin of the posterior surface of the external ear is accomplished with use of a Freer periosteal elevator (Fig. 3.193). Removal of the surgical specimen is thus accomplished in a monobloc fashion with satisfactory peripheral margins and the underlying cartilage as the deep margin. The surgical defect shows the undersurface of the posterior skin, which is the bed for receiving the full-thickness skin graft (Fig. 3.194).

The previously harvested full-thickness skin graft is now appropriately trimmed and secured in position with several interrupted 3-0 silk sutures. These sutures are left with long ends to use as tie-over sutures on the bolster to hold the skin graft in position (Fig. 3.195). Additional absorbable sutures are applied between the retaining silk sutures to achieve accurate alignment of the edges of the skin graft to the edge of the skin defect. Three to four small incisions are placed through the full-thickness skin graft to "pie crust" the graft and thus provide drainage of serosanguineous collection from below the skin graft. After completing the peripheral sutures of the skin graft, a Xeroform "bolster" dressing is applied over the skin graft and retained in position with the long ends of the silk sutures. This bolster holds the skin graft in place, allowing it to heal (Fig. 3.196). The bolster dressing is retained for 7 to 8 days. The silk sutures are removed, and the patient is instructed regarding care of the grafted area. The postoperative appearance of the surgical site 1 year following surgery. To prevent stenosis of the ear canal, a silastic tubular prosthesis may be fabricated for use in the immediate postoperative period (Fig. 3.197).

Wedge Excision of the External Ear

Malignant tumors of the skin of the external ear occasionally invade the underlying cartilage or may even perforate through to present on both sides of the external ear. These lesions require a through-and-through excision of a portion of the pinna to remove the tumor satisfactorily. Surgical defects resulting from

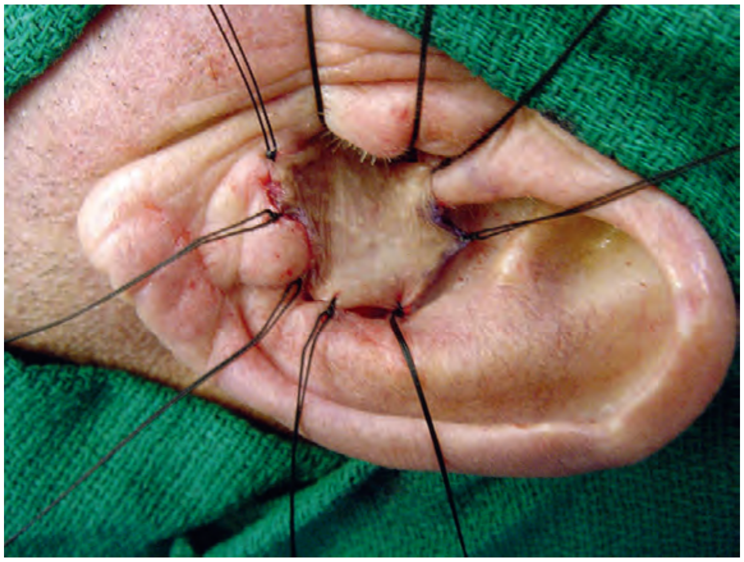

Figure 3.195 The skin graft is anchored with long silk sutures.

Figure 3.196 The bolster is secured with silk sutures.

Figure 3.197 Postoperative appearance of the external auditory canal 1 year following surgery showing excellent healing of the skin graft and normal circumference of the ear canal.

excision of up to one third of the vertical height of the pinna are suitable for primary closure by approximating the edges of the surgical defect. The height of the pinna is reduced, but the aesthetic result is acceptable.

The preoperative appearance of the anterior surface of the pinna of a patient with a recurrent basal cell carcinoma that involves the underlying cartilage and mainly presents on the posterior aspect is shown in Fig. 3.198. The lesion involves the helix and the underlying cartilage (Fig. 3.199).

The incision for wedge resection is outlined, with the apex of the wedge in the retroauricular skin crease (Fig. 3.200). A similar incision is marked out on the anterior aspect of the pinna so that the apex of the surgical defect meets at approximately the same point both anteriorly and posteriorly. Excision is made with a scalpel in a through-and-through fashion (Fig. 3.201). A wedge of the pinna is excised, including the skin of the anterior aspect, the cartilage beneath, and the skin of the posterior aspect until both skin incisions meet at the apex of the wedge. After removal of the surgical specimen, brisk hemorrhage is encountered from the dermal vessels, but it is easily controlled by electrocoagulation (Fig. 3.202). Once hemostasis

Figure 3.198 The preoperative appearance of the anterior surface of the pinna of a patient with a recurrent basal cell carcinoma involving the underlying cartilage, mainly presenting on the posterior aspect.

Figure 3.199 The lesion involves the helix and underlying cartilage.

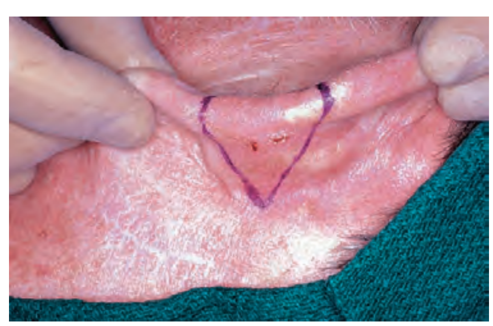

Figure 3.200 A plan for surgical excision is outlined by an incision drawn to resect a wedge of the ear, with the apex of the wedge in the retroauricular skin crease.

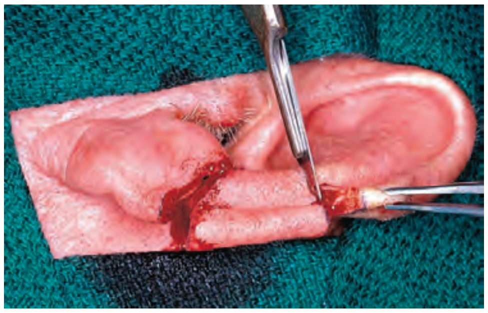

Figure 3.201 Excision is made with a scalpel in a through-and-through fashion along the predrawn skin incision.

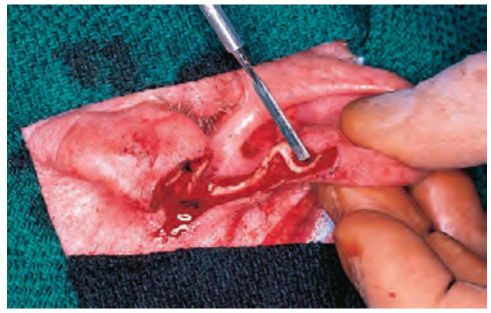

Figure 3.202 Brisk hemorrhage from the dermal vessels is easily controlled by electrocoagulation of the bleeding points from the cut edges of the pinna.

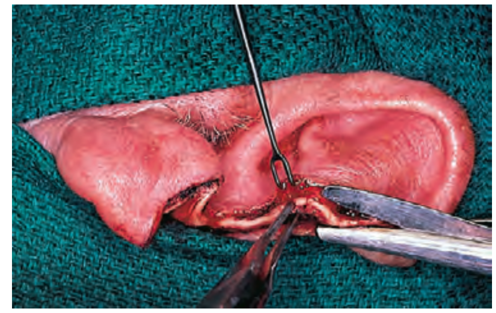

Figure 3.203 The skin edges usually retract over the cartilage immediately after excision of the tumor.

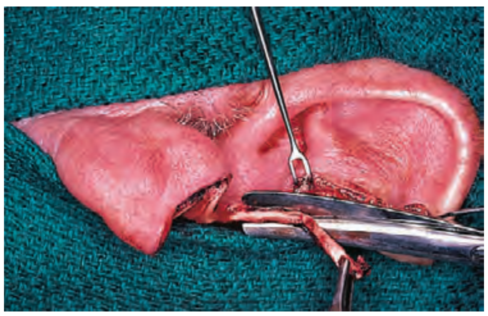

Figure 3.204 The extruded portion of the cartilage is excised using serrated scissors.

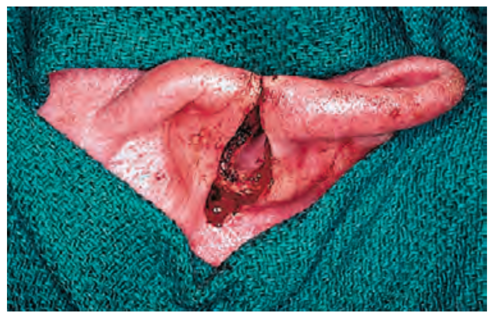

Figure 3.205 Closure of the surgical defect is begun by taking one nylon skin suture at the margin of the helix from the upper part to the lower part of the surgical defect to provide accurate approximation of the edges of the helix of the pinna.

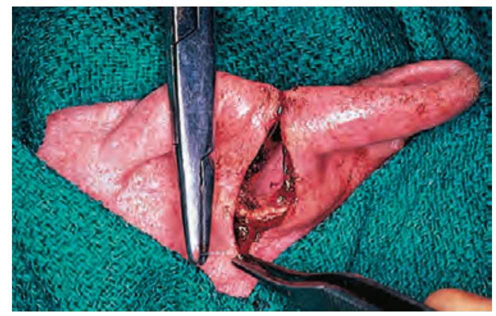

Figure 3.206 No attempt is made to suture the cartilage ends, so the closure consists exclusively of skin sutures anteriorly and posteriorly.

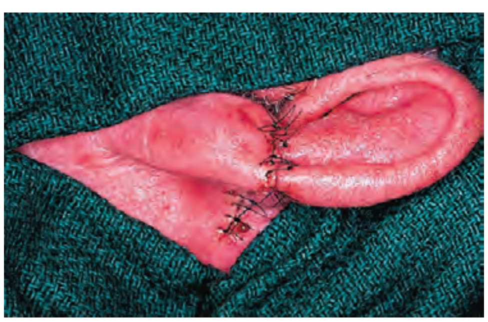

Figure 3.207 Completed skin closure.

Figure 3.208 The surgical specimen shows a through-and-through wedge of the pinna with the skin of its anterior aspect, the underlying cartilage, and the skin of the posterior aspect encompassing the entire tumor.

is obtained, an extra margin of the cartilage is removed to facilitate skin closure.

The skin edges usually retract over the cartilage immediately after excision of the tumor (Fig. 3.203). The extruded portion of the cartilage is excised with use of serrated sharp scissors so that during closure the cartilage ends do not push against each other, causing excessive tension on the suture line (Fig. 3.204).

Closure of the surgical defect is begun by first taking one nylon suture at the margin of the helix from the upper part to the lower part of the surgical defect to provide accurate alignment of the edges of the helix of the pinna (Fig. 3.205). This suture is not tied but is held in position and retracted laterally to facilitate skin closure. Both posterior and anterior skin is closed separately. No attempt is made to suture the cartilage ends (Fig. 3.206).

Bacitracin ointment is applied to the skin edges on the suture line (Fig. 3.207). The skin sutures are left in place for approximately 2 weeks to avoid wound dehiscence.

The surgical specimen shows a through-and-through wedge of the pinna encompassing the entire tumor (Fig. 3.208).

Larger defects of the external ear after partial or total amputation for more extensive tumors are difficult to reconstruct, and the cosmetic result is seldom satisfactory. Such defects therefore are best restored with use of a prosthesis.

CHAPTER 4

Eyelids and Orbit

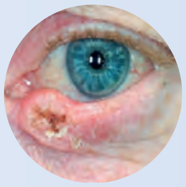

Although they are relatively rare, tumors that involve the eyelids and orbit are a therapeutic challenge because of the complex anatomy and diversity of pathologic processes that occur in this region. A systematic approach to evaluation and management and a thorough understanding of the pathologic processes of these tumors are required to optimize outcome. Within the eyelid, benign lesions include cutaneous keratosis and papillomas, inclusion and dermoid cysts, and cysts arising from the obstruction of sebaceous and sweat glands. In addition to these lesions, benign sweat gland tumors such as syringomas, myoepitheliomas, and sebaceous adenomas can also occur in the eyelids. The most frequently seen malignant lesions of the eyelids is basal cell carcinoma, accounting for over 90% of all eyelid malignancies, followed by squamous cell carcinomas, sebaceous cell carcinoma, melanomas, Merkel cell carcinomas, and sweat gland carcinomas.

Benign processes represent the most common orbital lesions. An orbital pseudotumor typically presents with eyelid edema, conjunctival chemosis, pain, and rarely visual loss. It sometimes can be misdiagnosed as a neoplasm on the basis of both clinical examination and imaging studies (Figs. 4.1 and 4.2). The most common malignant tumors involving the orbit are extensions of primary tumors from adjacent structures, including the skin, paranasal sinuses, intracranial tumors, and metastasis. Primary malignant orbital tumors represent a small proportion of cases. Despite their rarity, they comprise a wide spectrum of diseases arising from the nerves and nerve sheaths, extraocular muscles, lacrimal gland and lacrimal drainage system, orbital bones, and soft tissues, including lipomas, fibromas, hemangiomas, and their malignant counterparts. The most common primary malignant intraocular tumor is uveal melanoma in adults and retinoblastoma in children, and these can extend into the orbit. Lymphoma and metastatic tumors also can occur in the orbit and need to be included in the differential diagnosis. Clinical examples of some malignant tumors of the eyelid (Figs. 4.3 through 4.10), conjunctiva (Fig. 4.11), and orbit (Figs. 4.12 through 4.14) are shown here.

EVALUATION

Evaluation of eyelid and orbital tumors centers on an adequate history and physical examination. Orbital neoplasms may cause changes in appearance (such as lid retraction, entropion, ectropion, ptosis, proptosis, or a change in the position of the globe) or function (e.g., diplopia, blurry vision, or epiphora). Examination should focus on assessment of the position of the lid and globe, as well as their function. Functional examinations should include assessment of the opening and closing of the lid, extraocular movement, globe position, pupillary function,

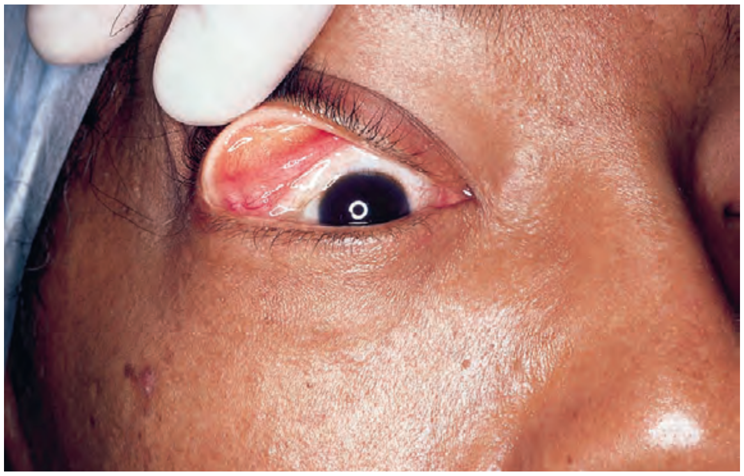

Figure 4.1 Orbital pseudotumor. (Idiopathic orbital inflammation).

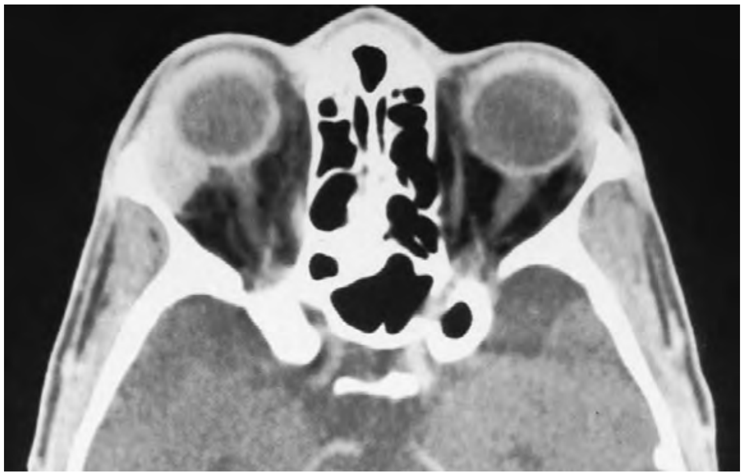

Figure 4.2 Axial computed tomography scan of the patient in Fig. 4.1.

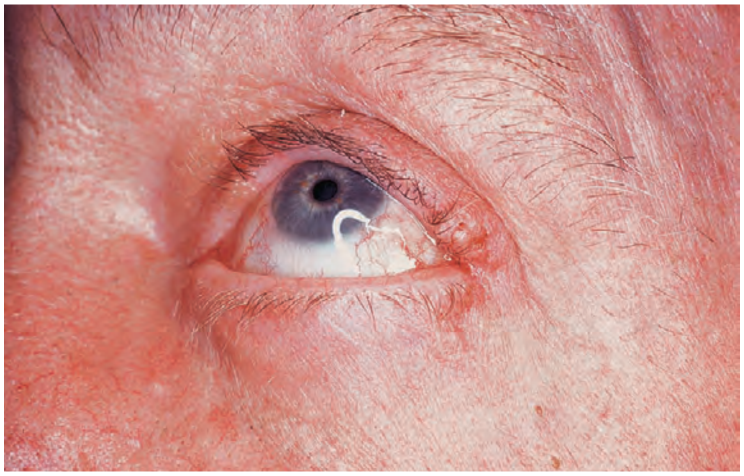

Figure 4.3 Basal cell carcinoma of the lateral canthus.

Figure 4.4 Locally advanced squamous carcinoma of the lower eyelid.

Figure 4.5 Advanced squamous cell carcinoma of the lower eyelid with metastasis to the cervical lymph nodes.

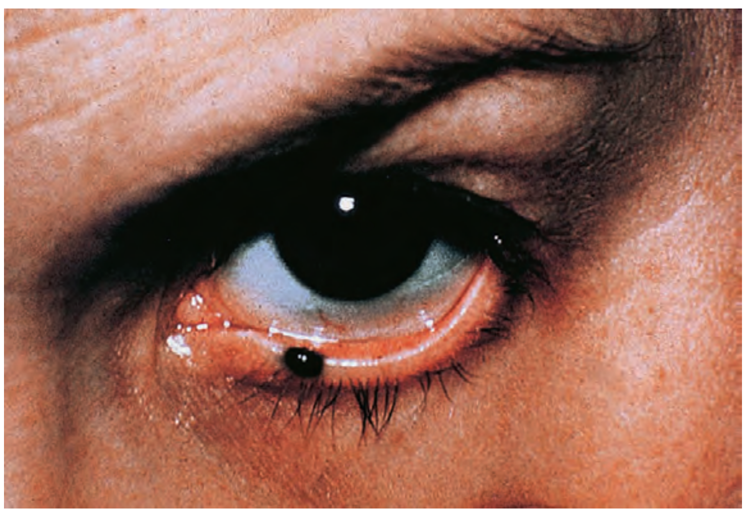

Figure 4.6 Melanoma of the lower eyelid.

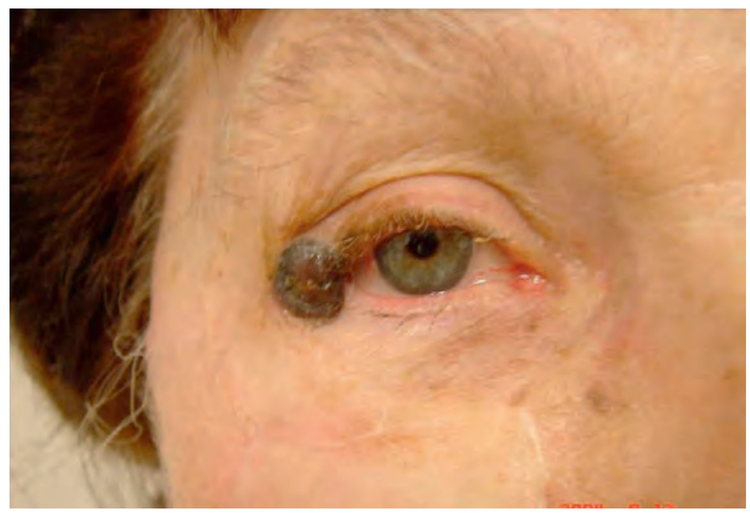

Figure 4.7 Malignant melanoma of lateral canthus.

Figure 4.8 Hemangioma of the upper eyelid.

Figure 4.9 **A**, Plexiform neurofibromatosis involving the upper eyelid and forehead. **B**, Coronal computed tomography scan demonstrating intraorbital extension of the tumor.

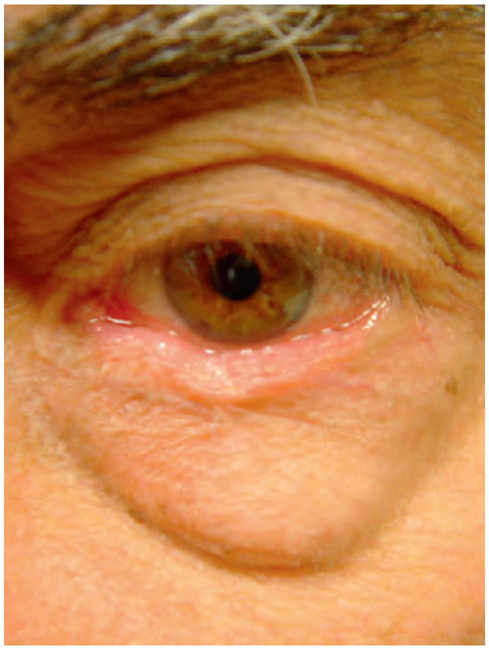

Figure 4.10 In situ squamous cell carcinoma in Bowen's disease of the lower eyelid.

Figure 4.14 Chondrosarcoma of the orbit.

Figure 4.11 Squamous cell carcinoma of the conjunctiva.

Figure 4.12 Neuroblastoma of the orbit.

Figure 4.13 Malignant fibrous histiocytoma of the orbit.

vision, and visual fields. Additional specialized ophthalmic examination may be used to look for change in intraocular pressure (tonometry); the anterior chamber or iris (slit lamp examinations); and the vitreous, retina, or optic disc (funduscopic examinations). The lacrimal system also may be examined to assess for obstruction or involvement of the nasolacrimal duct. In addition, assessment of ocular tumors should include a thorough evaluation of the sinonasal cavity, given the predilection of these tumors for orbital extension.

Radiographic imaging is essential to assess the extent of the tumor within the orbit and extension into the paranasal sinuses, cranial cavity, and infratemporal fossa. A computed tomography (CT) scan is preferred for assessment of bone involvement, whereas magnetic resonance imaging (MRI) is more accurate for defining soft tissue disease and perineural extension. Accurate assessment of invasion of the extraocular muscles, lacrimal gland, or lacrimal drainage system is crucial for surgical treatment planning. The orbital periosteum is a strong barrier to tumor infiltration, and its involvement as demonstrated by imaging studies is an important factor in planning reconstructive surgery to support the globe (Figs. 4.15 through 4.19). A positron emission tomography scan often can demonstrate a clinically occult metastatic tumor in the orbit.

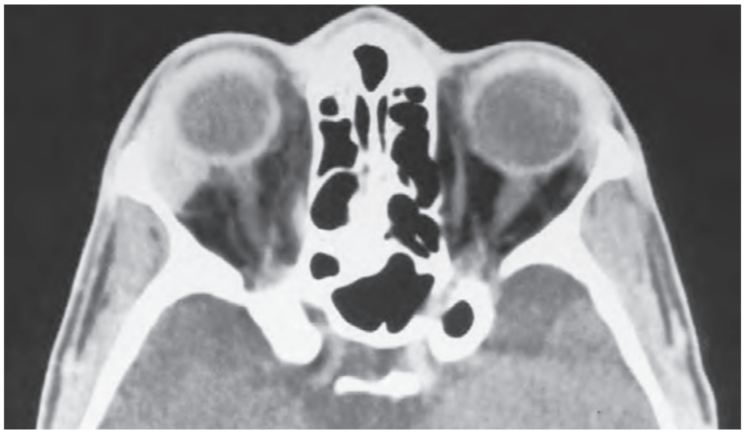

Figure 4.15 Contrast-enhanced computed tomography scan of a patient with a right-sided orbital pseudotumor.

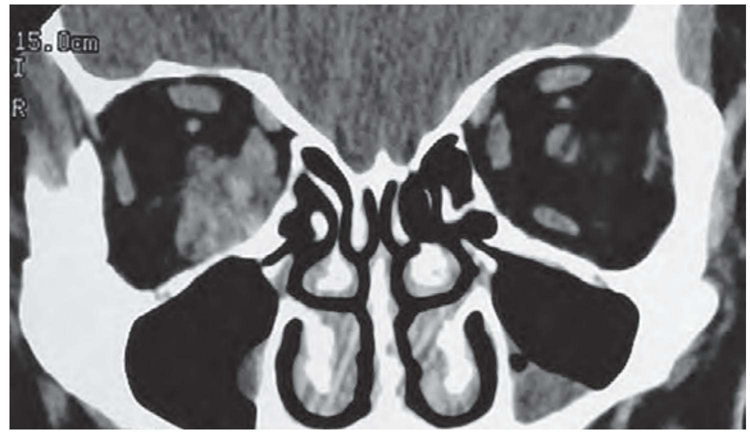

Figure 4.16 Contrast-enhanced computed tomography scan of a patient with a liposarcoma of the right orbit.

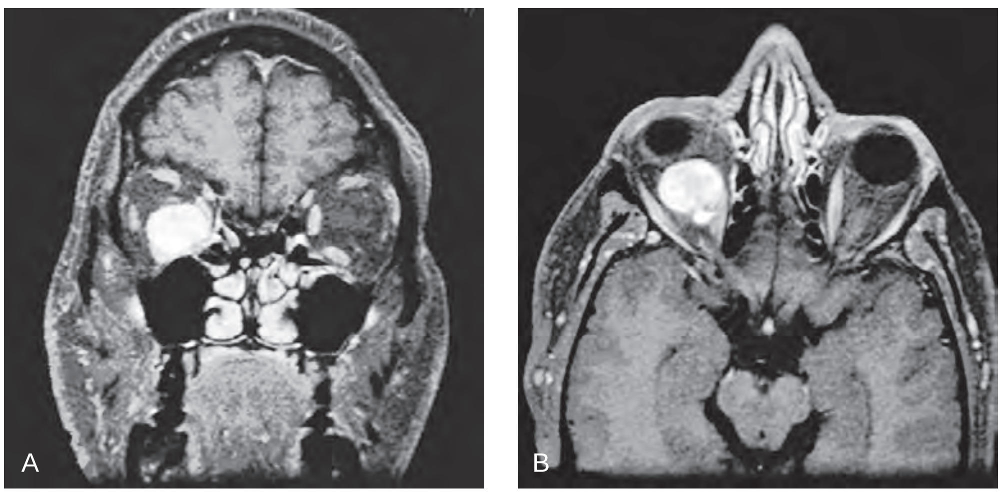

Figure 4.17 Magnetic resonance imaging scan of a patient with a liposarcoma of the right orbit. **A**, Coronal view. **B**, Axial view.

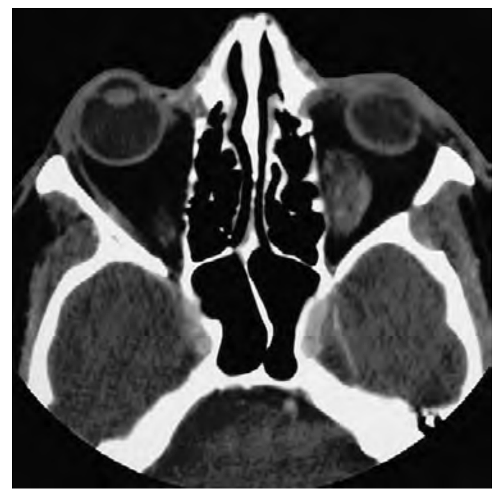

Figure 4.18 Computed tomography scan of a patient with a leiomyosarcoma of the left orbit.

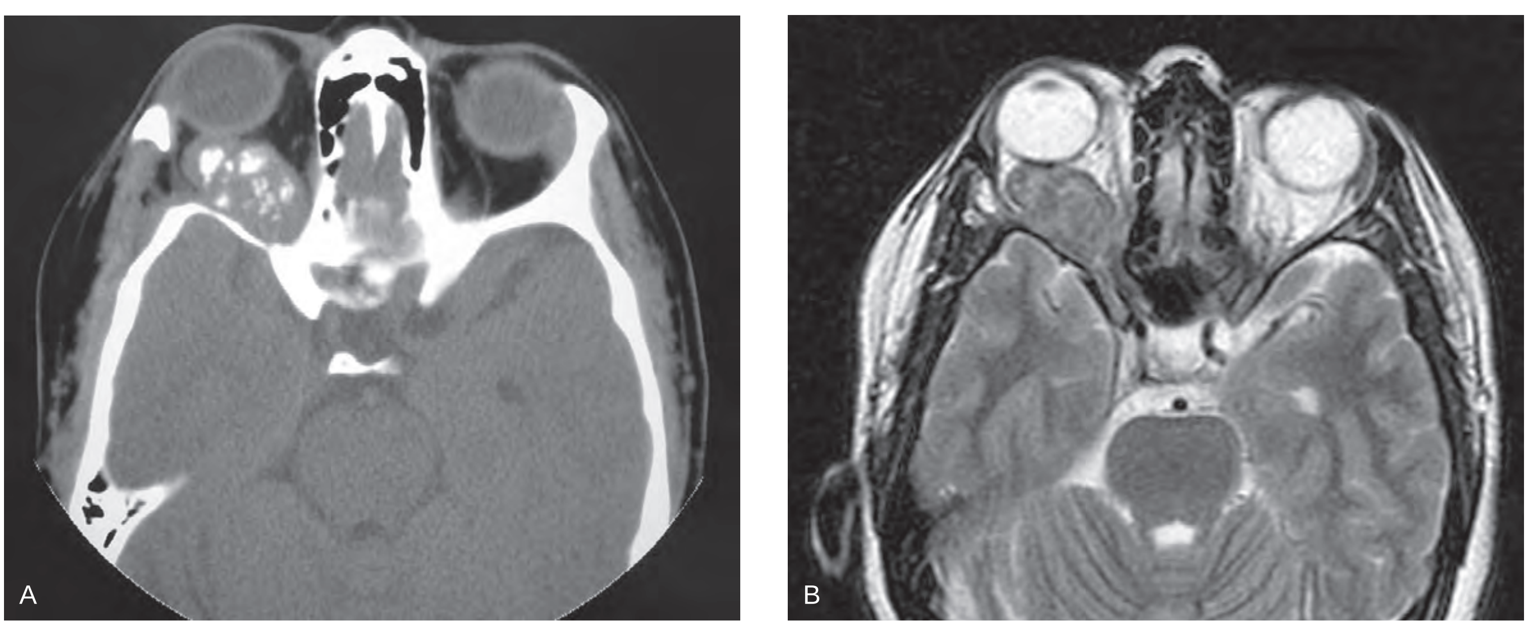

Figure 4.19 **A**, Computed tomography scan of a patient with a chondrosarcoma of the right orbit. **B**, Magnetic resonance imaging scan of the same patient showing tumor in orbit.

BENIGN NEOPLASMS

The vast majority of eyelid and orbital lesions (>80%) are inflammatory or benign neoplasms, and identifying the ones that might be malignant often poses a challenge for head and neck surgeons. Familiarity with common benign conditions that can mimic malignancies facilitates identification of malignant processes. In the eyelids, benign conditions such as inflammatory lesions (chalazia), seborrheic keratosis, pilomatrixoma, papillomas, and epidermoid inclusion cysts usually can be differentiated from malignancies by their clinical presentation. Many of these conditions require conservative surgical excision, which can be performed transcutaneously or transconjunctivally, depending on the location of the lesion.

Orbital lesions present a more complex diagnostic conundrum. Because the orbit is a confined space, different lesions in the orbit have similar presentations, including proptosis, chemosis, diplopia, and blurry vision. Imaging sometimes helps differentiate benign from malignant conditions. Idiopathic orbital inflammation, also known as *orbital pseudotumors,* include a broad category of nonspecific idiopathic inflammatory lesions in the orbit. These tumors can have a diverse clinical presentation, and their diagnosis is based on a combination of clinical, radiologic, and histopathologic findings after careful exclusion of specific systemic and local diseases. True benign neoplasms, including neurogenic tumors and hemangiomas, commonly arise from the lacrimal glands, adnexal structures, and soft tissues of the orbit. The management of these lesions is dictated by size, location, and symptoms.

MALIGNANT NEOPLASMS

Cutaneous Malignancies

Basal cell carcinomas (BCC) represent the most common eyelid malignancy, accounting for 90% to 95% of all cases, followed by squamous cell carcinomas (5%–10%) and other malignancies (e.g., sebaceous cell carcinoma, Merkel cell carcinoma, and melanomas). Local progression of these cancers may extend to involve the orbit or globe by direct extension or perineural invasion. Squamous cell carcinomas have a higher risk of orbital invasion compared with BCC. Mohs micrographic surgery is effective in controlling small basal cell carcinoma and superficial squamous cell carcinoma of the eyelids, with local control rates above 95%. Lesions at the medial canthus are often excised incompletely, leading to a high risk for local recurrence. Local recurrence is also more common in squamous cell carcinoma than in basal cell carcinoma, and it occurs in up to a third of patients. Metastasis to the regional lymph nodes from basal cell carcinoma occurs very rarely unless the tumor is large or has recurred multiple times. Squamous cell carcinomas, deeply invasive tumors, and those with perineural invasion also have a higher propensity of spread to the regional lymph nodes. Local recurrence is as high as 30% in sebaceous gland carcinoma of the eyelids due to late diagnosis and skip lesions. As with squamous cell carcinoma, these tumors need assessment of regional lymph nodes and consideration for sentinel lymph node biopsy.

Melanoma of the eyelids is relatively rare compared with basal cell and squamous cell carcinoma. The pathogenesis of cutaneous malignant melanoma of the eyelids involve melanocytes in blue-eyed, fair-skinned persons with a history of sun exposure. Surgical management of melanoma requires wide margin of excision and paraffin confirmation of margins, as frozen section is inaccurate in up to 30% of cases. Outcomes depend on histologic features of Breslow thickness, ulceration, mitotic figures, and perineural or lymphovascular invasion. Lesions that are determined to be a Clark's level IV or greater, Breslow thickness 1.5 mm or more, or greater than AJCC stage T2b are associated with a worse prognosis.

Glandular Malignancies

Given the relative abundance of sebaceous glands, it is not surprising that the eyelid is a common site for the development of sebaceous gland carcinomas. These tumors arise from meibomian glands in the tarsus, glands of Zeis in the eyelids, and secretory glands in the caruncle. They can have a varied presentation and often are misdiagnosed, most commonly as a chalazion. Sebaceous gland carcinomas are aggressive neoplasms with a high propensity for pagetoid spread and multifocal involvement with skip areas, making their management quite difficult. Conjunctival involvement is common (in up to 80% of cases) and can be associated with unilateral blepharoconjunctivitis. Lymphatic spread can occur in up to 30% of advanced cases. Local progression can extend onto the bulbar conjunctiva, requiring exenteration of the globe.

Lacrimal gland neoplasms account for 2% to 5% of all orbital tumors. These tumors are equally divided between benign and malignant neoplasms and epithelial and lymphoproliferative lesions. These neoplasms usually present with fullness of the lateral upper eyelid and proptosis and often are palpable. Typically, these symptoms have a limited effect on extraocular movement until the lesion becomes advanced. The most common benign epithelial neoplasms of the lacrimal gland are pleomorphic adenomas. They are similar to salivary tumors in that they can have a heterogeneous radiographic appearance, including the presence of cystic spaces. Adenoid cystic carcinoma is the most common epithelial lacrimal gland cancer, accounting for 30% to 40% of cases, followed by carcinoma ex-pleomorphic adenoma, adenocarcinoma, and mucoepidermoid carcinoma. In general, the behavior of these tumors mimics that seen for corresponding salivary gland cancers. For example, adenoid cystic carcinomas have a high propensity for perineural invasion and metastasis.

Intraocular Tumors

The most common primary malignant intraocular neoplasm in adults is uveal melanoma. The highest concentration of melanocytes is in the uveal tract (i.e., the iris, ciliary body, and choroid), which is by far the most common site of origin for primary ocular melanomas. Uveal melanomas may originate from preexisting pigmented lesions, including choroidal nevi and melanosis oculi (nevus of Ota). It has been predicted that 3% of uveal melanoma patients have germline mutations in *BRCA*-associated protein-1 (BAP1), which comprise a cancer hereditary syndrome that includes mesothelioma, renal cell cancer, and gastric cancer, among others. The choroid is the site of origin for approximately 80% of all uveal tract melanomas, with females typically diagnosed on routine examination and a diagnosis in males being prompted by visual symptoms. These tumors are pigmented, extend into the vitreous cavity, and may show a propensity for growth along nerves, although it can also extend into the sclera and potentially into the orbit. The diagnosis can be made by ophthalmoscopy, and the extent of the tumor can be defined by imaging studies (i.e., ultrasound, CT, and MRI).

Primary intraocular uveal melanomas have a divergent clinical course compared with cutaneous melanomas. These tumors typically spread hematogenously, primarily to the liver. Management of these tumors has been a subject of considerable debate. Two large-scale prospective randomized trials (the Collaborative Ocular Melanoma Study) have compared treatment options for small, medium, and large melanomas. The trial including large choroidal melanomas showed that the addition of preoperative radiation therapy did not improve patient outcome. For medium-sized choroidal melanomas, it was demonstrated that metastatic rates were comparable for I^{125} brachytherapy and enucleation, thereby offering an eye-preserving alternative in management. In general, smaller choroidal melanomas are typically observed and treated with plaque brachytherapy if there are signs of growth. Only 2.1% to 2.4% of uveal melanoma patients have radiographic or clinical evidence of distant disease at the time of treatment; however, they carry a significant lifetime risk of systemic disease recurrence. Overall survival ranges from more than 85% for smaller tumors to 70% to 85% for medium-sized tumors and less than 50% for larger tumors, even with aggressive treatment.

Retinoblastoma is the most common primary intraocular malignancy in children, with approximately 5000 cases occurring annually worldwide. Up to 80% of cases of retinoblastoma are diagnosed before the age of 3 years, with 20% to 30% being bilateral. Cone photoreceptors in the retina are thought to be the origin of retinoblastomas. Retinoblastomas typically involve the retina and vitreous, leading to the common presentation of white pupil (leukocoria or loss of red reflex) and strabismus (due to the loss of central vision). Funduscopically, these tumors appear as white to tan lesions and may detach the retina and can be associated with dislodged tumor into the subretinal space or vitreous ("seeds").

The study of familial retinoblastoma has provided valuable insight into cancer pathogenesis. The landmark "two-hit" model proposed by Knudsen suggests that two genetic events are required for the development of retinoblastoma. In the inherited form of the disease one hit (mutation in the *RB1* gene) is present in all cells (germline), and a mutation in the second copy of the *RB1* gene is acquired in retinal cells (somatic), leading to their malignant transformation. In contrast, in cases of sporadic retinoblastoma, both hits must occur in a single cell for retinoblastoma to develop. It is for this reason that retinoblastoma develops at a younger age in patients with the inherited form of the disease, with a higher frequency of multifocal and bilateral retinal involvement. The *RB1* gene was cloned from children with familial retinoblastoma carrying a deletion at 13q14.2. The Children's Oncology Group version of the International Classification of Retinoblastoma groups eyes into the following categories: A (<3 mm); B (>3 mm or macular or juxtapapillary location or subretinal fluid); C (presence of localized subretinal and/or vitreous seeds less than 6 mm from the tumor); D (presence of diffuse subretinal and/or vitreous seeds greater than 6 mm from the tumor); or E (no visual potential of the globe or the presence of any of the following: tumor in the anterior segment, tumor in or on the ciliary body, neovascular glaucoma, vitreous hemorrhage obscuring the tumor or significant hyphema, phthisical or prephthisical eye, orbital cellulitis-like presentation). The use of systemic chemotherapy has largely been replaced by ophthalmic artery chemosurgery (intraophthalmic arterial chemotherapy), which has the benefit of delivering a high, localized dose to the eye while reducing the complications associated with systemic exposure. Focal treatment including laser and cryotherapy can be used as primary or adjunctive treatments. Familial retinoblastomas often are discovered early. In contrast, most sporadic retinoblastomas (>75%) appear with advanced disease (group E) and often require extensive local treatment or enucleation. In some parts of the world, particularly Asia and Africa, retinoblastoma presents late with extraocular disease extending into the orbit, posing a particular treatment challenge.

Orbital Tumors

Rhabdomyosarcomas are the second most common primary intraorbital tumors in children, typically presenting before the age of 15 years. More than 95% of orbital rhabdomyosarcomas are of the embryonal type (especially the botryoid variant). These tumors manifest as rapidly growing retrobulbar masses that can cause effects on the ocular appearance and function by pressure or direct invasion. The presence of two pathognomonic translocations (t(2;13)(q35;q14) or t(1;13)(p36;q14)), resulting in the formation of oncogenic fusion proteins PAX3-FOXO1 (FKHR) and PAX7-FOXO1 (FKHR), respectively, are present in 80% to 85% of cases of embryonal rhabdomyosarcomas and can be identified by molecular-cytologic analyses. In the past, the outcome of patients with rhabdomyosarcoma was quite poor despite aggressive treatment. The findings from four consecutive Intergroup Rhabdomyosarcoma Study Group (IRSG) cooperative trials have significantly enhanced outcome, especially for patients with locoregionally advanced disease. These trials have helped define a risk-adapted treatment strategy based on the histologic subtype, primary site, extent of disease (International Society of Pediatric Oncology [SIOP] stage, International Union Against Cancer [UICC] stage, or IRSG stage), and extent of resection. All patients with rhabdomyosarcoma require chemotherapy, and surgical excision of the primary tumor is recommended whenever possible if it does not cause major functional or cosmetic deficits. When complete excision of the tumor is not possible, adjuvant radiotherapy is recommended, with the dose modified on the basis of chemotherapeutic treatment response. A 5-year survival rate of more than 70% has been achieved in recent trials for patients with localized rhabdomyosarcoma. However, the outcome for patients with metastatic disease remains poor.

Other tumors of the orbit include those arising from soft tissues and bone such as liposarcomas, malignant schwannomas, hemangiopericytomas, chondrosarcomas, and osteosarcomas. However, these tumors are rare, and the general principles of management are the same as those for such tumors that appear elsewhere in the body.

Other Tumors Invading the Orbit

Invasion of the orbit by local extension from malignancies of the paranasal sinuses, skin, and nasopharynx form the most common malignancies invading the orbit. These tumors include diverse histopathologic entities such as squamous cell carcinomas, minor salivary gland carcinomas, sinonasal undifferentiated tumors, esthesioneuroblastomas, sarcomas, and lymphomas. Management of the orbit in these cases depends on the overall stage of the tumor, the extent of orbital invasion, and available treatment alternatives.

TREATMENT

Radiation Therapy

As with other anatomic sites, the treatment of eyelid and orbital neoplasms is dictated by tumor type, location, extent, and

patient factors. Although surgery is the mainstay for most primary eyelid malignancies, radiation may be used in select cases. Because radiation in this area can incur a small risk of ocular surface disturbance and potentially corneal ulceration, excision is preferred for amenable tumors. To minimize injury to the cornea, lens, and lacrimal gland, a gold-plated lead eye shield generally is used. However, tungsten eye shields provide better protection from electrons than do lead shields and are preferred. Radiation with a treatment dose of 60 Gy offers excellent local control in more than 90% of patients with cutaneous malignancies of the eyelids. As the size of the lesion increases, the anticipated disfigurement of surgery versus a lower local control rate by radiation should be weighed when deciding on a treatment modality. Larger lesions (>4 cm) are best treated with surgery, sometimes followed by postoperative radiation.

The use of radiation in the periorbital and orbital regions requires special considerations because of the high radiosensitivity of structures in the anterior and posterior chambers of the globe. Radiation planning for orbital tumors always should attempt to exclude the cornea, lens, retina, and pituitary gland. Intensity-modulated radiation therapy or a proton beam plan can help exclude extraorbital normal structures while maintaining therapeutic efficacy.

Both brachytherapy and charged-particle radiation with helium ions or protons have been used effectively to treat uveal melanomas. Brachytherapy delivers a tumoricidal dose of 70 to 100 Gy to the tumor apex. A margin to include the thickness of the sclera (~1 mm) along with an additional 1 mm of tumor thickness is planned. A 2-mm margin surrounding the perimeter of the tumor also is included in the treatment field. The optimal dose rate has not been clearly defined; most treatment is delivered during a period of between 4 and 7 days. More recent experience suggests that the optimal minimal tumor dose rate is likely between 0.7 and 1 Gy per hour using episcleral plaques. The 5- and 10-year local recurrence rates are 11.5% and 15.8%. The efficacy of plaque brachytherapy versus proton beam has not been directly compared, but they are believed to be relatively equal in their efficacy. However, proton beam is superior at controlling peripapillary lesions, although it may result in higher anterior segment toxicity, which is particularly pertinent to ciliary body and anteriorly located tumors.

Surgical Treatment

Surgical treatment planning for excision of malignant lesions of the eyelids must include an appropriate plan for reconstruction of the surgical defect. Most lesions of the upper or lower eyelid can be repaired with use of local tissues. However, more advanced lesions require complex reconstructive procedures. The important issues in reconstructive surgery of the eyelids include prevention of exposure keratopathy resulting from the inability to close the eyelids (lagophthalmos); inadequate drainage of the lacrimal secretions, leading to epiphora; eversion or exposure of the conjunctiva; and impairment of peripheral visual fields because of excessive closure of the palpebral fissure. For more complex reconstructions, the reader is advised to consult more detailed textbooks of oculoplastic surgery. Complex reconstructive procedures are best handled by adequately trained and experienced oculoplastic surgeons.

Surgical Anatomy

The eyelids are a complex set of paired anatomic structures that protect the eye and facilitate continuous distribution of the tear film over the cornea. Because the skin of the eyelid is extremely thin and devoid of subcutaneous fat, surgical dissection between the skin and the orbicularis oculi muscle should be performed very carefully. The inner surface of the eyelid is covered by conjunctiva that is thin, transparent, nonkeratinized stratified epithelium. In between the tarsal plate and the orbicularis oculi muscle are the hair follicles of the eyelashes. The meibomian glands are located within the tarsal plate. The superior and inferior tarsal plates are crescent-shaped condensation of fibrous tissue that provides structural integrity to the eyelids. The tarsal plates also are attached to the medial and lateral canthal ligaments, which allow the eyelids to follow the curvature of the globe. The deepest fibers of the levator aponeurosis insert into the anterior surface of the tarsal plate and the smoother muscle of the Mueller's muscle attach to the superior edge of the tarsus. The levator muscle elevates the eyelid under voluntary control from the superior branch of cranial nerve III while Mueller's muscle is under sympathetic control. Most of the movement during closure of the eyelids, from contraction of the orbicularis muscle, is performed by the upper eyelid, with the lower eyelid being relatively less mobile. The posterior surface of the tarsal plates is tightly lined by conjunctiva that is continuous with the eyelid margin at the mucocutaneous junction and the fornix onto the anterior surface of the globe. The ducts of the modified sebaceous glands (meibomian glands) open on the posterior lid margin between the mucocutaneous junction and the gray line.

The rich vascular network of the eyelids arises from both the external carotid arteries (facial, superficial temporal, and infraorbital branches) and internal carotid arteries (ophthalmic artery). These arteries anastomose to form the medial and lateral palpebral arteries, which in turn form the marginal and peripheral arcades that supply the pretarsal eyelids. The small veins of the eyelids drain superficially to the facial venous system or deeply into the ophthalmic veins in the orbit. The superior and inferior ophthalmic veins of the orbit pass through the superior and inferior orbital fissures, respectively, to drain into the cavernous sinus. The lymphatics of the eyelids drain either to the preauricular nodes or the intraparotid lymph nodes and can be highly variable between individuals. The orbicularis oculi muscle is innervated by the facial nerve, its upper eyelid component is innervated by the frontal branch of the temporal division, and the lower eyelid component is innervated by the zygomatic branch.

The lacrimal drainage system consists of the upper and lower lacrimal puncta that open into the canaliculi, leading to the lacrimal sac, which continues in the lacrimal fossa as the nasolacrimal duct and eventually opens into the inferior meatus of the lateral wall of the nasal cavity. The lacrimal gland consists of two lobes: an orbital lobe and a palpebral lobe. The orbital lobe is located in the superolateral orbit in the lacrimal fossa within the zygomatic process of the frontal bone. The grayish color and firm consistency of the orbital lobe allow it to be distinguished from the orbital fat pad. The orbital and palpebral lobes of the lacrimal gland are contiguous posterolaterally but are separated anteriorly by the lateral horn of the levator aponeurosis. Because the secretory ducts of the orbital lobe traverse the smaller palpebral lobe before draining into the upper conjunctival fornix, the function of the orbital lobe can be affected by excision of the palpebral lobe. The lacrimal puncta are located within the medial canthus, the superior punctum more medially than the inferior punctum. The superior and inferior canaliculi form a common channel

that drains into the nasolacrimal sac in 90% of patients. In the remaining 10%, the two canaliculi enter the nasolacrimal sac separately. The nasolacrimal sac is located in a bony fossa on the medial wall of the orbit and is approximately 10 to 12 mm in length. The sac continues into the nasolacrimal duct, which is approximately 12 to 18 mm in length in a posterior medial direction. The lining of the outflow system transitions from the stratified squamous epithelium of the canaliculi to the columnar epithelium of the sac and the duct. The nasolacrimal duct opens at the inferior meatus under the inferior turbinate in the nasal cavity. Its opening is covered by a mucosal flap (Hasner's valve).

The bony orbital cavities contain the globes, lacrimal gland and sac, extraocular muscles, fat, blood vessels, and nerves. Seven cranial bones form the four bony walls of the pyramid-shaped orbit. The floor of the orbit forms the roof of the maxillary sinus and ends 1 cm anterior to the optic canal. Posteriorly, the floor is separated from the greater wing of the sphenoid by the inferior orbital fissure that connects the orbit to the pterygopalatine fossa (which contains the pterygopalatine ganglion and the internal maxillary artery) and to the infratemporal fossa anteriorly. The infraorbital nerve runs in a lateral to medial direction in the floor of the orbit; it is contained within a bony groove posteriorly and then a bony canal more anteriorly before it exits at the infraorbital foramen on the anterior surface of the maxilla. The rectangular medial orbital wall is composed from anterior to posterior by the maxilla, lacrimal, ethmoid, and sphenoid bones. The lacrimal fossa is formed by the maxillary and lacrimal bones. Most of the medial wall is thin ethmoid bone (lamina papyracea) that separates the orbit from the ethmoid sinuses, and thus this part of the orbit is vulnerable to infections and invasion by tumors that arise in the ethmoid sinuses. More posteriorly, the medial wall is formed by thicker sphenoid bone, and this sphenoethmoid junction is a useful landmark for the optic canal ring located about 3 to 4 mm posterior to it. The medial wall ends superiorly at the frontoethmoid suture, which indicates the position of the fovea ethmoidalis (roof of the ethmoid sinus) and the cribriform plate. The anterior and posterior ethmoidal foramina are located along the suture line approximately 24 mm and 36 mm from the anterior orbital rim.

The apex of the orbit transmits the optic nerve and other neurovascular structures from the cranial cavity. The optic canal is located medial to the superior orbital fissure and transmits the optic nerve, ophthalmic artery, and sympathetic fibers. The superior orbital fissure transmits the third and sixth cranial nerves, nasociliary nerve, ciliary ganglion (a condensation of nerves from nasociliary, sympathetic, and parasympathetic fibers from the inferior division of CN III) with postganglionic parasympathetic branches, middle meningeal artery, lacrimal nerve, superior ophthalmic vein, trochlear nerve, and frontal nerve.

The ophthalmic artery and its branches are the major arterial supply to the orbit. It passes through the optic canal and exits the muscle cone at the level of the posterior aspect of the globe. The posterior ethmoidal artery branch of the ophthalmic artery enters the posterior ethmoidal foramen approximately 6 mm anterior to the optic canal. The anterior ethmoidal artery enters its foramen approximately 12 mm anterior to the posterior ethmoidal foramen. The ophthalmic artery also supplies branches to the extraocular muscles and lacrimal gland. Its distal-most branches are the supraorbital artery that exits through the supraorbital foramen, the supratrochlear artery, and the dorsal nasal artery. The superior and inferior ophthalmic veins both drain into the cavernous sinus. Salient features of the anatomic structures in the orbit and the cross-sectional anatomy of the eyelids are depicted in Fig. 4.20.

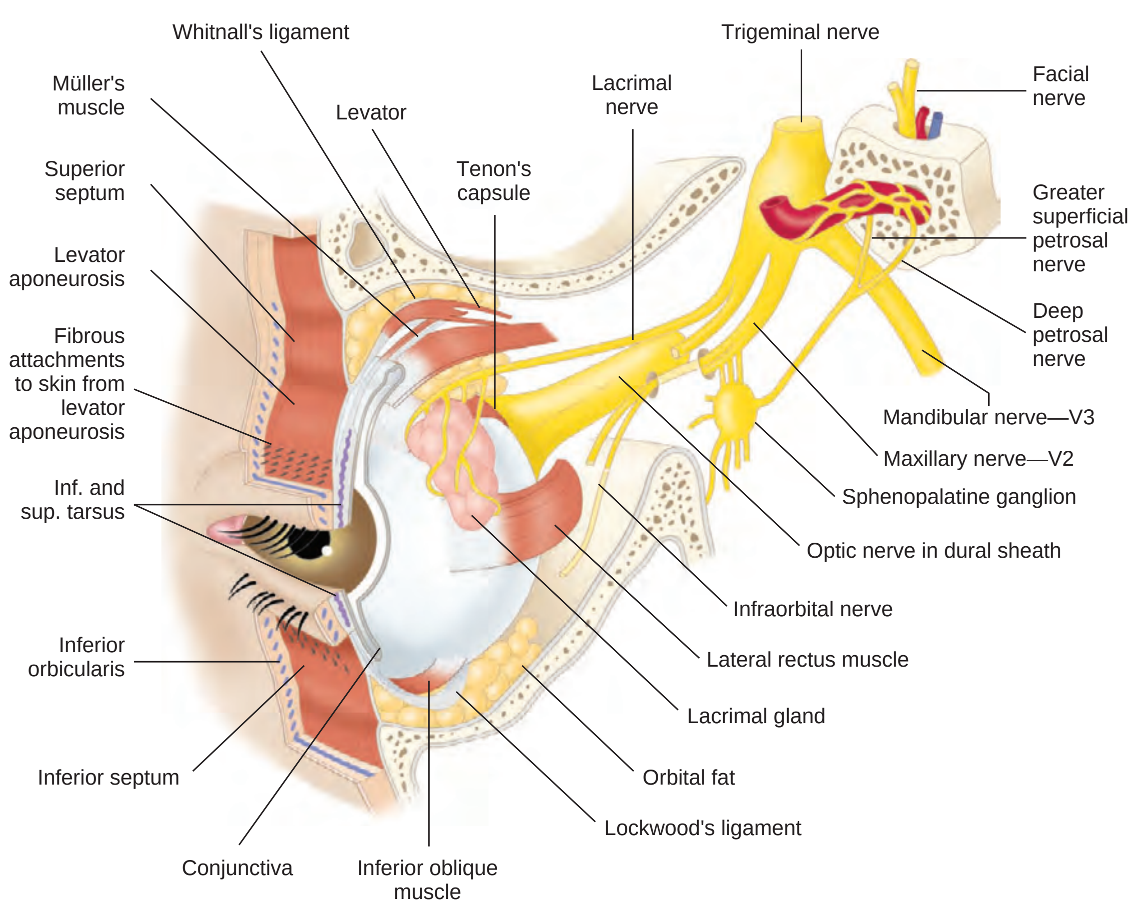

Figure 4.20 Anatomy of the orbit and eyelids.

Surgery for Eyelid Tumors

Excision of a Carcinoma of the Skin of the Upper Eyelid. Unlike the lower eyelid, the upper eyelid has a generous amount of lax skin available, making primary closure of the surgical defect possible following excision of even a large skin cancer. However, there can be loss of symmetric lid crease with this. The patient shown in Fig. 4.21 has a superficial infiltrating squamous cell carcinoma involving the skin of the upper eyelid that extends into the eyebrow. Palpation reveals that the lesion is confined to the skin and does not infiltrate into either the underlying musculature or the tarsal plate.

Upon closure of the eyelid, the true extent of the lesion becomes evident. A significant portion of the skin of the upper eyelid is involved, with extension into the eyebrows (Fig. 4.22).

Surgical excision of this lesion will require sacrifice of a large portion of the skin of the upper eyelid, including some of the eyebrow. When planning surgical excision and repair, it is important to remember that the shape of the eyebrow must be retained or restored. To maintain the shape of the eyebrow, surgical excision at that site is oriented vertically, whereas excision of the skin of the upper eyelid is oriented transversely, like an inverted letter "T."

The surgical defect following excision of the lesion is shown in Fig. 4.23. Frozen sections must be obtained from the margins of the surgical defect to ensure adequacy of excision, and care should be taken to avoid sacrifice of undue amounts of underlying musculature. After achieving satisfactory hemostasis, the skin edges are undermined on the lateral aspects of the upper portion of the surgical defect. Closure of the upper part of the surgical defect is accomplished vertically with use of interrupted 3-0 chromic catgut sutures to restore the continuity of the eyebrow between its medial and lateral parts. The remainder of the surgical defect in the skin of the upper eyelid is closed transversely in two layers, with the completely closed wound resembling an inverted letter "T." The postoperative appearance of the patient approximately 8 weeks after surgery is shown in Fig. 4.24. Note that the eyebrow has been reconstructed to its normal shape and that the upper eyelid essentially has no disfigurement because closure of the skin defect is transverse. The aesthetic result of this repair is quite satisfactory.

Full-Thickness Resection and Reconstruction of the Upper Eyelid. Full-thickness resection of any portion of the eyelid poses a significant reconstructive problem. Because the upper eyelid provides most of the lubricating function and protection to the cornea and globe, accurate reconstruction is extremely important to prevent any subsequent injury to the cornea. The patient presented in Fig. 4.25 has a pigmented basal cell carcinoma involving two-thirds of the width of the upper eyelid, the tarsal margin, and the adjacent conjunctiva. Surgical excision of the lesion will require a full-thickness through-and-through resection of that part of the upper eyelid with immediate reconstruction.

The plan of surgical excision is outlined in Fig. 4.26. A rectangular portion of the full thickness of the upper eyelid is resected. The shaded triangular areas at the two upper corners of the rectangular excision are wedges of skin that will be excised to permit advancement of the skin of the upper eyelid for reconstruction (Fig. 4.27). A corneal shield is inserted to protect the cornea. Two heavy silk sutures are taken through the full thickness of

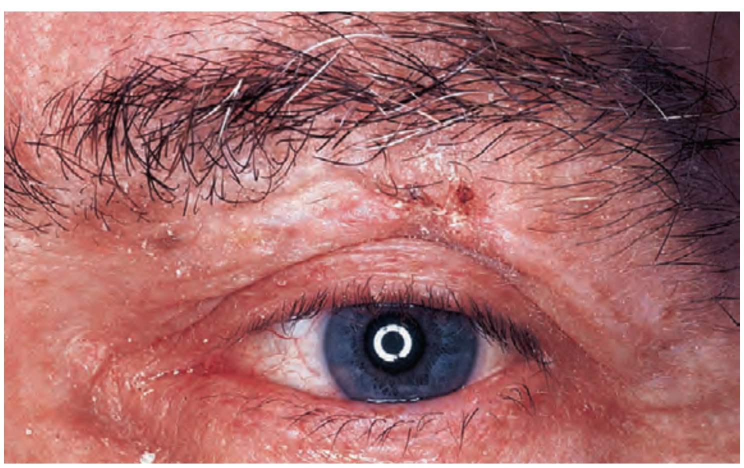

Figure 4.21 A superficially infiltrating squamous cell carcinoma involving the skin of the upper eyelid and extending into the eyebrow.

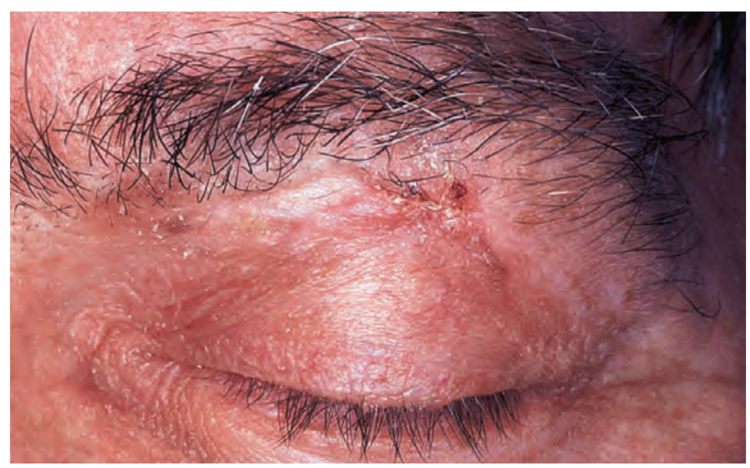

Figure 4.22 This lesion involves a significant portion of the skin of the upper eyelid with extension into the eyebrow.

Figure 4.23 The surgical defect following excision of the lesion.

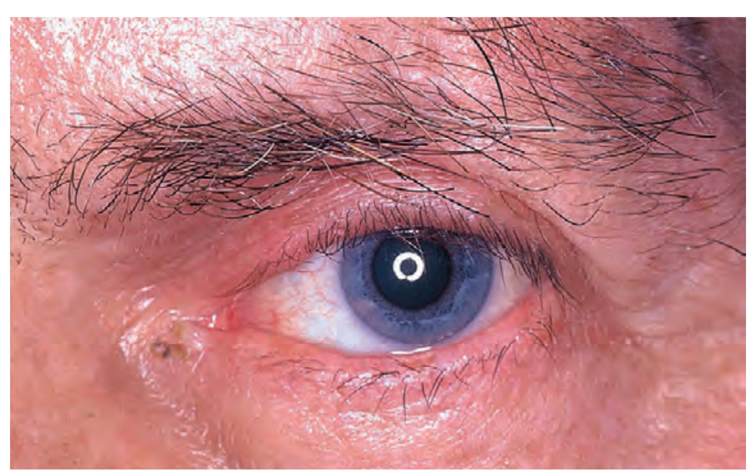

Figure 4.24 The postoperative appearance of the patient 8 weeks after surgery.

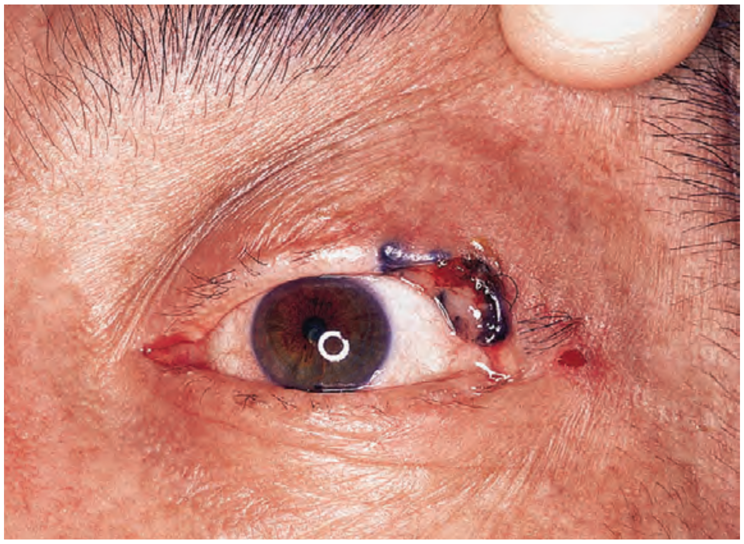

Figure 4.25 A pigmented basal cell carcinoma involving two-thirds of the width of the upper eyelid, the tarsal margin, and the adjacent conjunctiva.

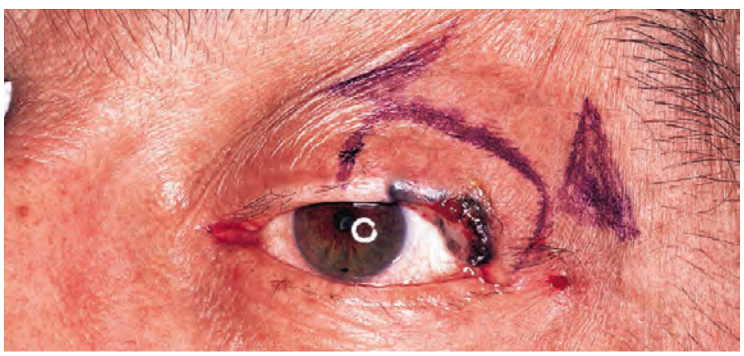

Figure 4.26 The outline of surgical excision and skin advancement on the upper eyelid.

the tarsal margin of the upper eyelid on the periphery of the intended site of excision; these stay sutures are held with hemostats to stabilize the eyelid during excision.

One approach is shown here. Through-and-through resection of the upper eyelid along the previously outlined area of rectangular excision is completed (Fig. 4.28). Note that the surgical excision is just medial to the stay sutures, which help stabilize the cut edges of the surgical defect. Complete hemostasis is obtained by ligating and/or coagulating the bleeding points during the excision. Similar silk stay sutures are applied to the tarsal margin of the lower eyelid and an incision is made through the gray line of the tarsal margin of the lower eyelid between the two stay sutures. The skin is retracted inferiorly to expose the tarsal plate (Fig. 4.29). A sharp, fine knife is used to divide the tarsal plate in a coronal plane through its thickness to retain the inner aspect of the tarsal plate attached to the palpebral conjunctiva, while its outer aspect remains continuous with the remainder of the tarsal plate.

Using sharp scissors, two incisions are made in the palpebral conjunctiva with the attached split tarsal plate to match the surgical defect of the upper eyelid, and the incision is taken down to its reflection over the globe. This procedure will provide a composite conjunctival flap that contains a portion of the split tarsal plate from the lower eyelid, which is then advanced cephalad and sutured to the horizontal cut edge of the conjunctiva of the upper eyelid in the rectangular surgical defect (Fig. 4.30). The conjunctival sutures are taken with 6-0 plain catgut sutures. Several interrupted sutures are applied, and the knots are kept on the undersurface of the conjunctiva and buried in the soft tissues.

Once this bridged conjunctival repair is completed, skin incisions are made in the upper eyelid farther cephalad from

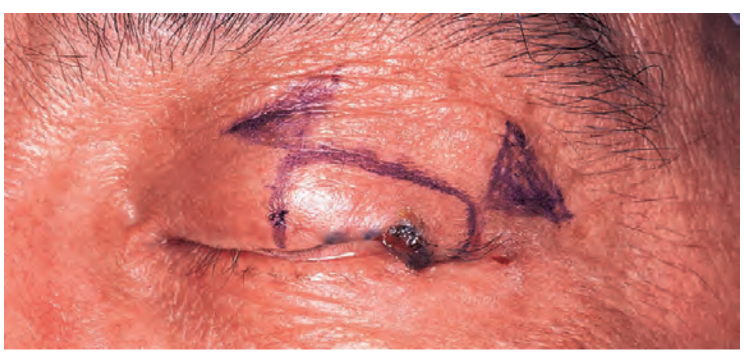

Figure 4.27 The shaded triangular areas at the two upper corners of the rectangular excision are wedges of skin that will be excised to permit advancement of the skin of the upper eyelid for reconstruction.

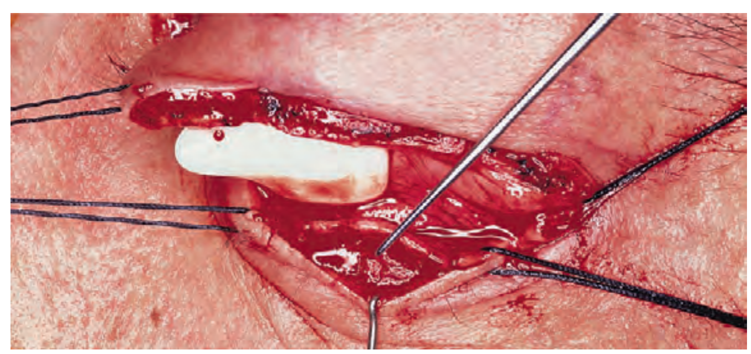

Figure 4.29 The tarsal plate of the lower eyelid is exposed through a skin incision at the gray line.

Figure 4.28 Through-and-through resection of the upper eyelid along the previously outlined area of rectangular excision is completed.

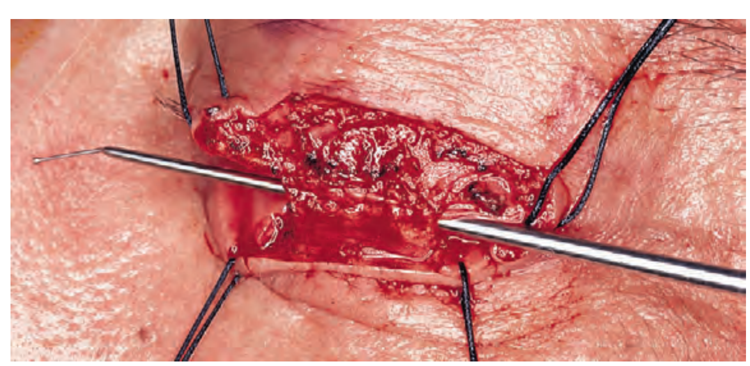

Figure 4.30 The composite conjunctival flap containing a portion of the split tarsal plate from the lower eyelid is advanced cephalad and sutured to the horizontal cut edge of the conjunctiva of the upper eyelid in the rectangular surgical defect.

the rectangular defect to match the previously outlined triangular areas of skin to be sacrificed, and these areas are excised (Fig. 4.31). This procedure allows downward advancement of the skin flap from the upper eyelid, which is sutured to the cut edge on the skin side of the tarsal margin of the lower eyelid with use of 6-0 nylon sutures. Thus approximation of the lower edge of the upper eyelid skin flap and the skin margin of the lower eyelid is completed (Fig. 4.32). The remaining skin closure is completed along the lateral aspect of the skin flap and then transversely through the region of the excised wedges of the skin. This process is the first stage of reconstruction of the upper eyelid (Fig. 4.33). At the conclusion of the operation, the upper and lower eyelids are fused and remain so for 8 weeks. Skin sutures are removed in approximately 1 week. During fusion of the upper and lower eyelids, the patient is instructed to irrigate the eye and keep the area as clean as possible.

Six to eight weeks after the first stage of the operation, the patient is returned to the operating room, where the fused eyelids are divided under topical and local anesthesia (Fig. 4.34). Two drops of a topical anesthetic are introduced into the conjunctival sac, and a local anesthetic is infiltrated along the palpebral fissure through the fused eyelids. A fine lacrimal probe is introduced from the palpebral fissure medial to the bridge of skin and is brought out through the fissure lateral to the bridge to protect the cornea during division of the fused eyelids. Sharp, curved scissors are used to divide the bridge of the fused eyelids along the line of the palpebral fissure, and full-thickness through-and-through division of the bridged reconstruction is performed to separate the reconstructed upper eyelid from the lower eyelid. Some minimal bleeding is to be expected from the cut edges of the reconstructed area but will stop with application of slight pressure.

The postoperative appearance of the patient 1 week after division of the bridged lower eyelid flap to reconstruct the upper eyelid is shown in Fig. 4.35. The functional and aesthetic restoration is complete, and the final postoperative result is very gratifying (Figs. 4.36 and 4.37). Bridged repair of upper eyelid defects with use of a split tarsal plate and a conjunctival composite flap is a very satisfactory means of performing immediate reconstruction of sizable defects of the upper eyelid.

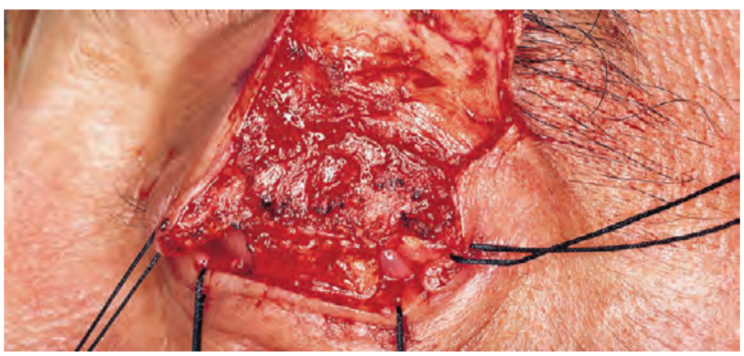

Figure 4.31 The previously marked triangular wedges of skin are excised.

Figure 4.33 The remaining skin closure is completed along the lateral aspect of the skin flap and then transversely through the region of the excised wedges of the skin.

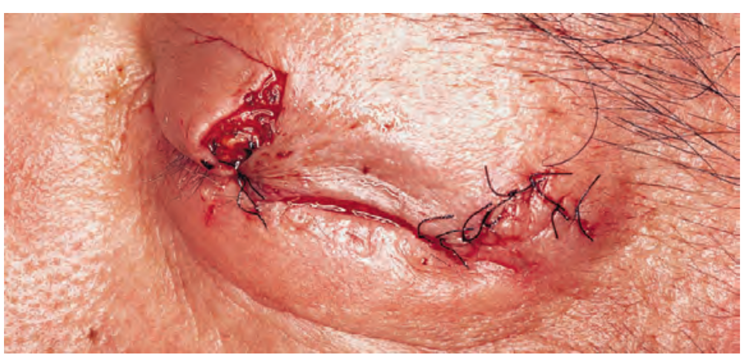

Figure 4.32 Approximation of the lower edge of the upper eyelid skin flap and the skin margin of the lower eyelid is completed.

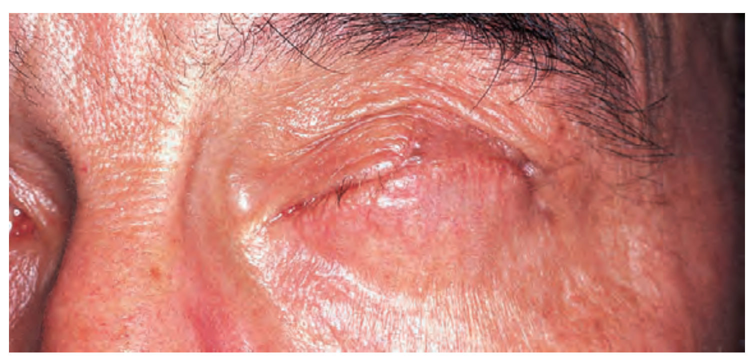

Figure 4.34 Eight weeks after the first stage of the operation, topical and local anesthetic is administered and the patient's fused eyelids are divided.

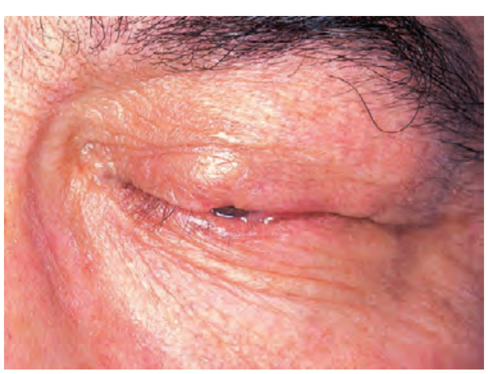

Figure 4.35 The postoperative appearance of the patient 1 week after division of the bridged lower eyelid flap.

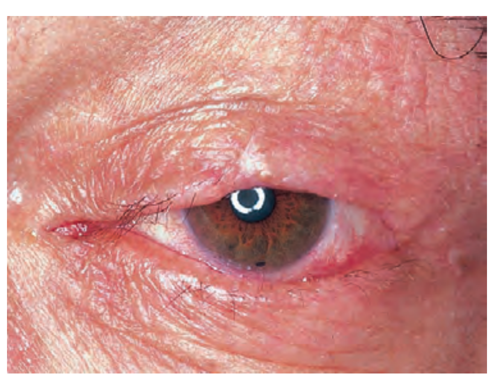

Figure 4.36 Postoperative appearance of the patient 6 months after surgery.

Figure 4.37 Symmetry of both upper eyelids is restored.

This approach of transferring the lower lid tarsus to the upper lid sometimes renders the lower lid unstable. Other approaches for upper lid reconstruction include the Cutler-Beard with a free tarsal, scleral, or AlloDerm graft and Hughes flaps, which are also useful as lid sharing procedures.

Excision of a Carcinoma of the Skin of the Lower Eyelid. Skin carcinomas involving less than two-thirds of the lower eyelid are easily managed by wide excision and closure by mobilizing skin from the lateral aspect of the cheek and the temporal region. When excision of a skin lesion of the lower eyelid is performed in a transverse axis with primary closure of the defect, ectropion often will result. Thus whenever feasible, the surgical excision should be planned in such a manner that an advancement flap from the lateral aspect can be brought in to close the surgical defect, thereby avoiding ectropion. The patient shown in Fig. 4.38 has a basal cell carcinoma involving the skin of the lower eyelid. The lesion does not reach the tarsal margin and is not infiltrating the underlying musculature or cartilage.

The plan of surgical excision is outlined in Fig. 4.39. The surgical defect resulting from this excision has a triangular shape. The upper transverse skin incision is extended along the lateral canthus into the temporal region, and the skin flap is elevated. The skin from the temporal region is thus advanced into the surgical defect. The apex of the flap slides into the surgical defect, permitting its closure. Adequate mobilization of the lateral skin is necessary to avoid tension on the suture line and secondary pull on the lower eyelid. This is also called a *Tenzel flap*.

The completed closure shows skin sutures with 6-0 nylon in place (Fig. 4.40). Note that the skin sutures beneath the lower eyelid are left long and their ends are taped or sutured to the skin of the cheek to avoid trauma to the cornea from the stumps of the sutures. No dressings are necessary, but bacitracin ophthalmic ointment is applied to the suture line.

The postoperative appearance of the patient approximately 8 weeks after surgery is shown in Fig. 4.41. Note that the scar of the surgical excision is almost imperceptible and the position of the lower eyelid remains within normal limits without any ectropion. Surgical excision of skin lesions of the lower eyelid is best managed by repair of the surgical defect with advancement of skin from the lateral aspect of the cheek.

Excision of Skin Cancer at the Medial Aspect of the Lower Eyelid. Skin lesions of the medial half of the lower eyelid that involve the tarsal margin, or are in close proximity to it, present a significant problem for the reconstructive surgeon. Advancing skin from the lateral aspect of the cheek in this setting is not satisfactory for repair, because the line of tension will draw the medial canthus downward and laterally, causing ectropion and epiphora. Therefore skin lesions requiring a limited extent of resection in this region are best repaired with use of a medially based skin flap from the upper eyelid. The patient shown in Fig. 4.42 has a pigmented basal cell carcinoma involving the skin of the lower eyelid, with involvement of the tarsal margin near the medial canthus.

The plan of surgical excision is outlined, as shown in Fig. 4.43. A corneal shield is used to protect the cornea. The tarsal plate is included in the surgical specimen near the medial third of the tarsal margin. The surgical defect is shown in Fig. 4.44. Frozen sections are obtained from the margins of the conjunctiva as well as the skin of the cheek. The medially based random skin flap from the upper eyelid, as outlined, is then elevated.

The medially based skin flap from the upper eyelid is transferred to fill the surgical defect. The donor site defect is closed primarily (Fig. 4.45). Meticulous attention must be given to the delicate handling of this skin flap, because the skin in this area is very thin and tears easily with rough handling. The skin closure is performed with 6-0 nylon sutures. The ends of the sutures are left long and taped or sutured to the skin of the cheek to avoid trauma to the cornea from the sutures. No dressings are necessary, but ophthalmic antibiotic ointment is applied to the sutures.

Figure 4.38 Basal cell carcinoma involving the skin of the lower eyelid.

Figure 4.40 The completed closure.

Figure 4.39 The plan of surgical excision.

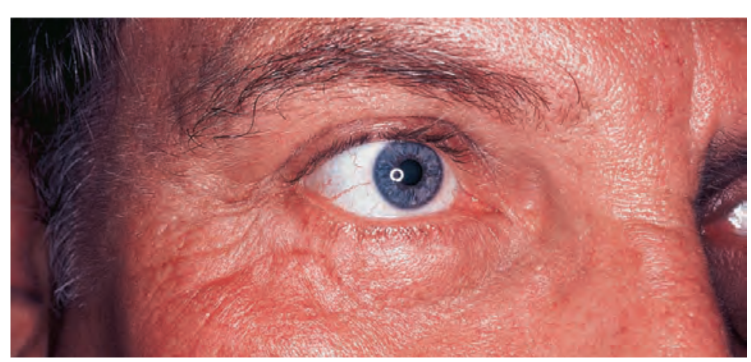

Figure 4.41 The postoperative appearance of the patient approximately 8 weeks after surgery.

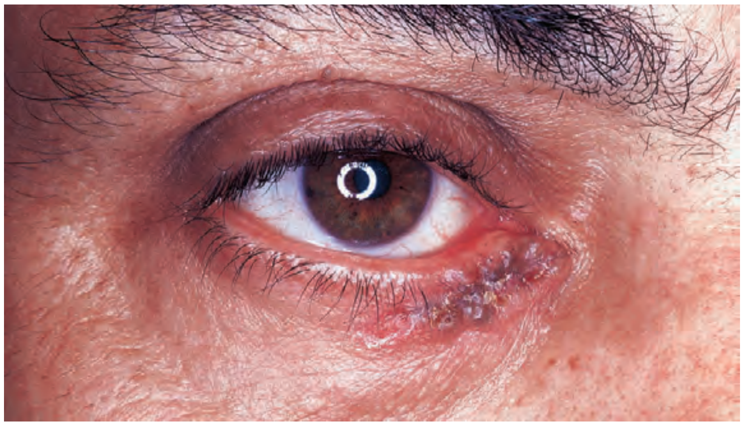

Figure 4.42 A pigmented basal cell carcinoma involving the skin of the lower eyelid, with involvement of the tarsal margin near the medial canthus.

Figure 4.43 The plan of surgical excision and repair of the surgical defect.

Figure 4.44 The surgical defect and outline of the flap.

Figure 4.45 The surgical defect is repaired with the flap, and the donor site defect is closed primarily.

Figure 4.46 The postoperative appearance of the patient 8 weeks after surgery.

The postoperative appearance of the patient 8 weeks after surgery shows satisfactory repair of the surgical defect (Fig. 4.46). The patient has no functional disability, and the aesthetic result is quite pleasing.

Excision of Skin Cancer Involving the Medial Canthus. Skin lesions involving the medial canthus of the lower eyelid can be excised and repaired with a medially based skin flap from the upper eyelid, as described in the previous operative procedure. However, if the extent of the surgical excision reaches the base of the medially based upper eyelid skin flap, then that particular method of reconstruction is not applicable. The patient shown in Fig. 4.47 has a pigmented basal cell carcinoma involving the skin of the lower eyelid and the medial canthus. Because of the extent of the surgical excision that would be necessary in this patient, a medially based upper eyelid skin flap cannot be used here. Thus the plan of surgical excision and reconstruction would include a laterally based upper eyelid skin flap that would be rotated inferiorly and medially to reach the region of the medial canthus. Medial advancement of the skin of the cheek from the lateral aspect allows repair of the resultant surgical defect in the skin of the lower eyelid. Other approaches to repairing medial canthus defects include nasal-based rotational flaps (glabella or rhomboid are examples).

Skin incisions are marked for the planned surgical excision and the anticipated skin flaps to be elevated following excision (Fig. 4.48). The surgical defect shows adequate excision of the skin cancer with resection of the medial canthus and a generous portion of skin around the primary lesion (Fig. 4.49). Frozen sections must be obtained from several margins of the surgical defect to ensure adequacy of the excision. Laterally based skin flaps are elevated as previously outlined. A flap from the upper eyelid is rotated inferiorly and medially, and the cheek flap is advanced medially to accomplish closure of the surgical defect.

The postoperative appearance of the patient approximately 3 months after surgery is shown in Fig. 4.50. Note that the patient does not have ectropion. Because eyelashes in the medial part of the reconstructed lower eyelid are missing, some aesthetic deformity is present, but functionally the patient has no other

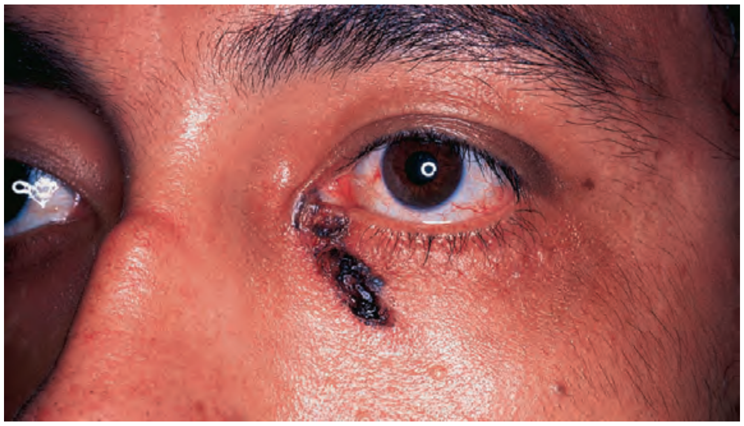

Figure 4.47 A pigmented basal cell carcinoma involving the skin of the lower eyelid and the medial canthus.

Figure 4.49 The surgical defect shows adequate excision of the skin cancer with resection of the medial canthus and a generous portion of skin around the primary lesion.

Figure 4.48 Skin incisions are marked for the planned surgical excision and the skin flaps to be elevated for reconstruction.

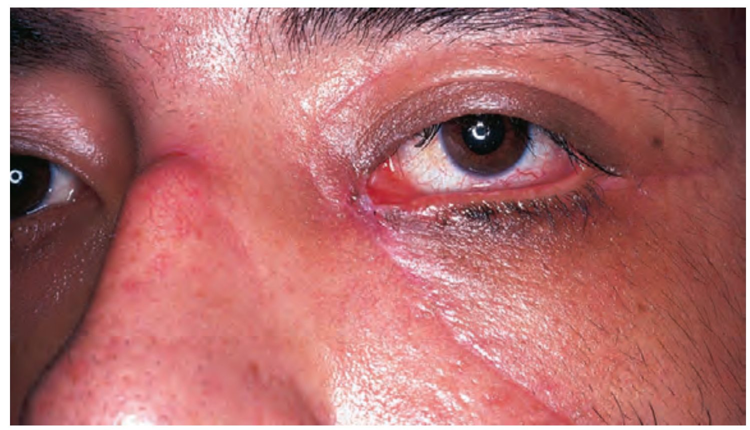

Figure 4.50 The postoperative appearance of the patient 3 months after surgery.

problems. Thus the combination of medial advancement of skin of the lateral aspect of the cheek and advancement of a rotation flap from the skin of the upper eyelid proves to be a satisfactory combination for reconstruction of surgical defects in the region of the medial canthus.

"V" Excision of the Lower Eyelid. When skin lesions involving the lower eyelid in the region of the tarsal margin demand full-thickness resection, a "V" excision is most satisfactory as long as the extent of surgical resection is limited. Up to one-third of the lower eyelid can be resected in a wedge excision with primary repair.

The patient shown in Fig. 4.51 has a nodular basal cell carcinoma involving the tarsal margin of the lower eyelid. A through-and-through wedge excision of the lower eyelid is performed, including the skin, the tarsal plate, and the conjunctiva. Frozen sections are obtained from the margins of the surgical defect, with full-thickness 1-mm section of the eyelid, to ensure the adequacy of the resection. Reconstruction of the surgical defect requires reapproximation of the tarsal plate, which is accomplished with use of a 6-0 Vicryl suture (Fig. 4.52). The suture begins at the gray line of the tarsal edge, entering through the tarsal margin and the underlying tarsal plate; it then exits through the transected edge of the tarsal plate on one side, reenters the transected edge of the tarsal plate on the opposite side, and exits from the tarsal margin at the opposite end of the surgical defect. This suture is snugly tied to reapproximate the tarsal plate, and the remaining surgical defect is closed in two layers with 6-0 nylon sutures for the skin of the lower eyelid. Meticulous attention should be given to accurate reapproximation of the tarsus and lid margin; otherwise indentation (notching) will develop at the site of the surgical closure, leading to an unpleasant appearance.

The postoperative appearance of the patient 3 months after surgery is shown in Fig. 4.53. Note that the tarsal margin is accurately reapproximated without any indentation, leaving no functional or aesthetic deformity at the site of the surgical excision. Wedge resection of the lower eyelid is best suited for lesions that need through-and-through resection of limited portions of the lower eyelid.

Full-Thickness Resection and Reconstruction of the Lateral Canthus and the Lower Eyelid. Lesions involving the tarsal margin at the lateral third of the lower eyelid require a through-and-through resection of the lower eyelid that reaches the lateral canthus. Repair of the surgical defect under these circumstances requires a structural support to restore the defect in the tarsal plate and an advancement flap of skin from the lateral aspect of the cheek to provide skin coverage. The patient shown in Fig. 4.54 has an adenocarcinoma of adnexal origin involving the lower eyelid. The lesion involves at least the lateral third of the lower eyelid, and therefore the surgical excision will entail resection of the lateral half of the lower eyelid. The planned incision for resection of the tumor and advancement of the lateral cheek flap is outlined in Fig. 4.55. A through-and-through resection of the lower eyelid, including the skin and underlying tarsal plate, is completed with preservation of the palpebral conjunctiva inferior to the tarsus of the lower eyelid because this is a skin lesion (Fig. 4.56). Frozen sections are obtained from the margins of the skin to ensure the adequacy of the surgical resection.

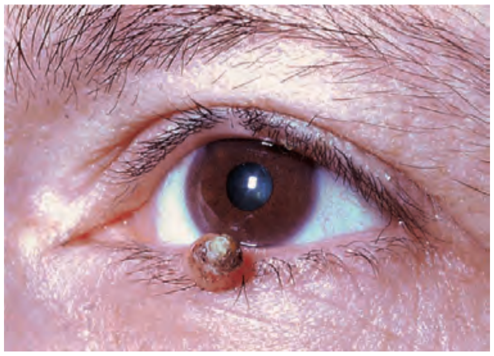

Figure 4.51 A nodular basal cell carcinoma involving the tarsal margin of the lower eyelid.

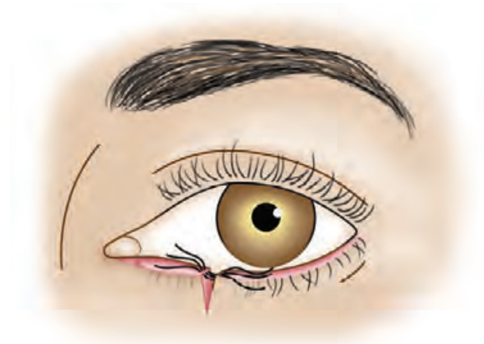

Figure 4.52 Accurate alignment of the tarsal plate with a Vicryl suture is crucial.

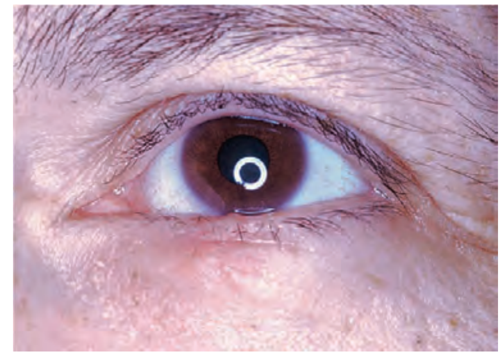

Figure 4.53 The postoperative appearance of the patient 3 months after surgery.

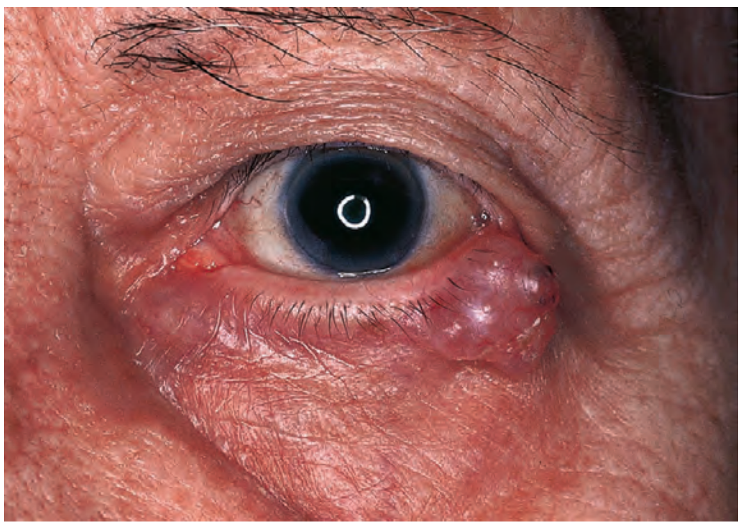

Figure 4.54 An adenocarcinoma of adnexal origin involving the lower eyelid.

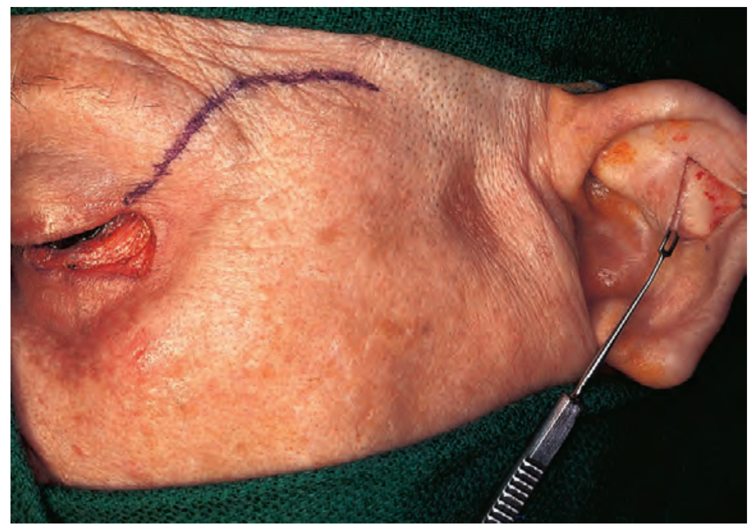

Figure 4.56 A through-and-through resection of the lower eyelid is completed. A cartilage graft is harvested from the external ear.

Figure 4.55 The outline for resection of the tumor and advancement of the lateral cheek flap.

Figure 4.57 The donor site on the ear is closed with skin sutures. The lateral cheek flap is elevated superficial to the orbicularis oculi muscle.

A cartilage graft is now harvested from the external ear on the same side. A skin incision is placed on the anterior aspect of the pinna, and the cartilage is exposed. By alternate blunt and sharp dissection, an appropriate piece of cartilage is harvested to replace the resected portion of the tarsal margin. The skin at the donor site is closed with interrupted sutures after the cartilage is harvested (Fig. 4.57).

The lateral cheek flap is now elevated, remaining superficial to the orbicularis oculi muscle along the previously drawn line of incision. The orbicularis oculi muscle is elevated from the underlying septum to create a pocket for insertion of the cartilage graft (Fig. 4.58). This dissection should be performed delicately and extremely carefully to avoid tearing of the muscle fibers or production of unnecessary hematoma. The previously harvested cartilage graft is appropriately trimmed and placed into the submuscular pocket created by elevation of the orbicularis oculi muscle (Fig. 4.59). The orbicularis oculi muscle is now returned to its previous position, and its divided fibers are reapproximated with 4-0 chromic catgut interrupted sutures to bury the cartilage completely (Fig. 4.60). The skin flap that had

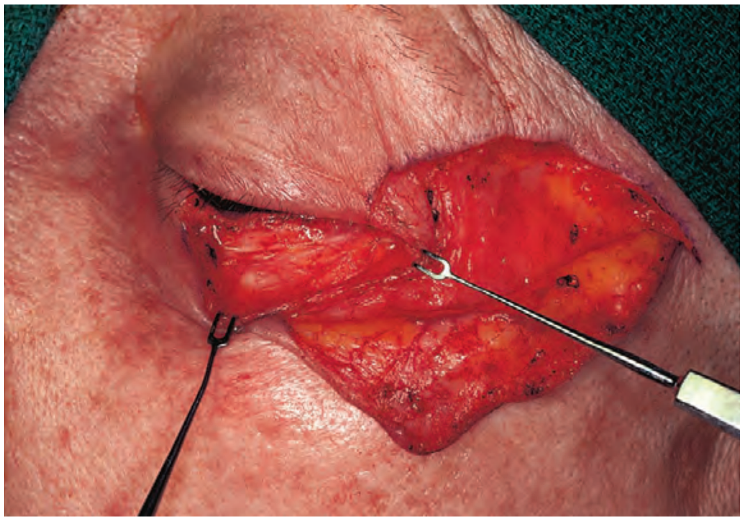

Figure 4.58 The orbicularis oculi muscle is elevated from the underlying conjunctiva to create a pocket for insertion of the cartilage graft.

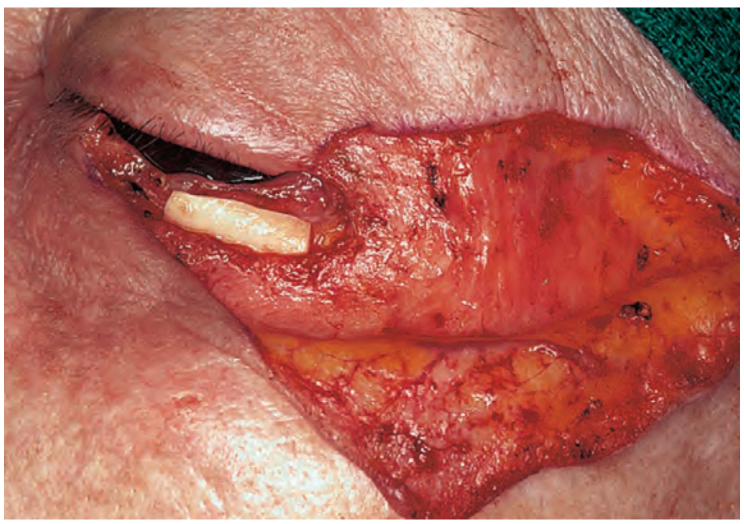

Figure 4.59 The previously harvested cartilage graft is appropriately trimmed and placed into the submuscular pocket created by elevation of the orbicularis oculi muscle.

Figure 4.60 The orbicularis oculi muscle is reapproximated to bury the cartilage graft.

Figure 4.61 The flap is appropriately trimmed and the skin incision is closed with interrupted sutures.

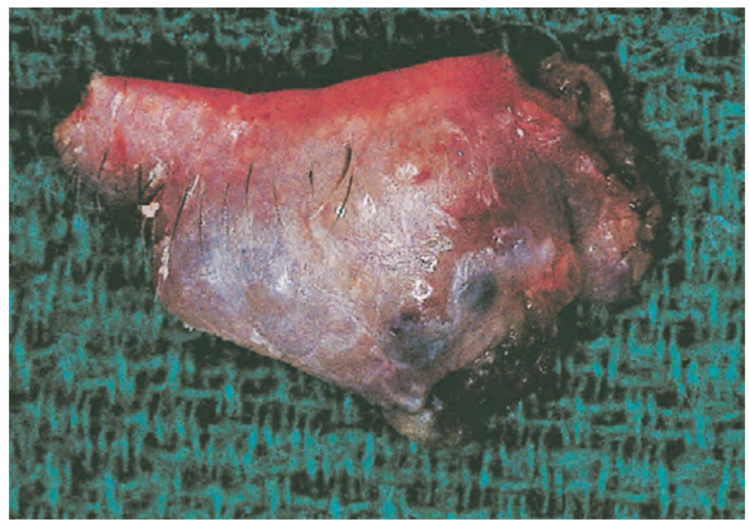

Figure 4.62 The surgical specimen demonstrates adequate excision of the cutaneous adenocarcinoma of adnexal origin.

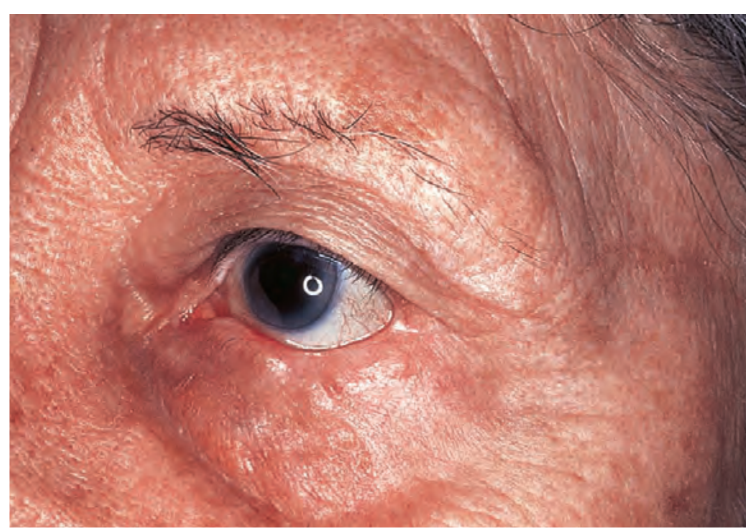

Figure 4.63 The postoperative appearance of the patient approximately 2 months after surgery.

been elevated previously is now advanced medially and inferiorly to provide skin coverage of the surgical defect. The flap is appropriately trimmed and the skin incisions are closed with interrupted sutures (Fig. 4.61). The surgical specimen shown in Fig. 4.62 demonstrates adequate excision of the cutaneous adenocarcinoma of adnexal origin. The postoperative appearance of the patient approximately 2 months after surgery shows satisfactory reconstruction of the surgical defect following through-and-through resection of the lateral half of the lower eyelid (Fig. 4.63).

Radical Resection of the Lower Eyelid and Reconstruction With a Mustardé Flap. When the entire lower eyelid must be resected to remove a malignant lesion, reconstruction becomes a significant problem. The patient shown in Fig. 4.64 has a nodular melanoma involving the skin and the tarsal margin of the lower eyelid. The extent of surgical resection for the primary tumor is outlined (Fig. 4.65). The entire lower eyelid is resected along with a generous portion of the skin of the cheek. A portion of the palpebral conjunctiva is excised, but the bulbar conjunctiva remains intact. The skin incision necessary for elevation and advancement rotation of the Mustardé flap is shown in Fig. 4.66. Note that the skin incision for the Mustardé flap must be taken higher than the lateral canthus in the temporal region to prevent downward retraction. The skin incision in the temporal region is taken high and then turned inferiorly toward the preauricular skin crease, continuing on to the upper part of the neck, where it curves anteriorly to permit satisfactory elevation and rotation of the skin flap. The skin flap is elevated superficial to the terminal branches of the facial nerve to prevent them from being injured.

The surgical defect following superficial parotidectomy and upper neck dissection with elevation of the Mustardé flap is shown in Fig. 4.67. Note that the entire lower eyelid is resected to encompass the primary tumor.

The surgical specimen following full-thickness resection of the lower eyelid with the underlying soft tissues is shown in Fig. 4.68. The appearance of the patient on the operating table following complete closure of the surgical defect with the Mustardé flap is shown in Fig. 4.69. The flap is advanced medially and rotated inferiorly to fill the surgical defect. A temporary tarsorrhaphy is performed.

The postoperative appearance of the patient 2 months after surgery is shown in Fig. 4.70. Note that because of the lack of the tarsal plate and the support necessary for the lower eyelid, some degree of lid margin ectropion is present, and eversion of the conjunctival mucosa is present. The absence of eyelashes also impairs the aesthetic restoration of the lower eyelid, but functionally the patient has no trouble with the eye. He has minimal epiphora as a result of eversion of the palpebral conjunctiva, but the cornea is fully protected. The Mustardé advancement rotation flap provides an excellent choice for reconstruction of a full-thickness defect following resection of the entire lower eyelid.

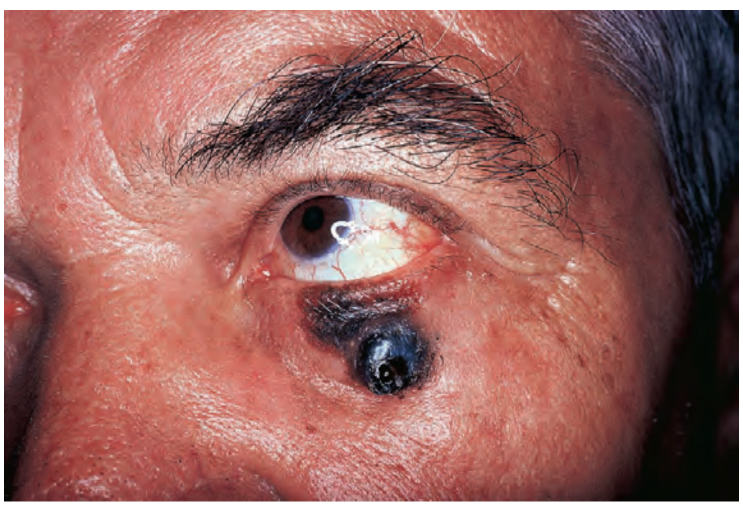

Figure 4.64 A nodular melanoma involving the skin and the tarsal margin of the lower eyelid. *(Courtesy Ronald Spiro, MD.)*

Figure 4.65 The extent of surgical resection for the primary tumor is outlined. *(Courtesy Ronald Spiro, MD.)*

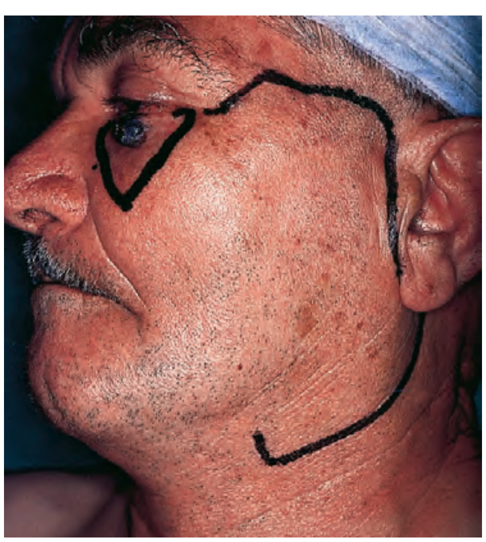

Figure 4.66 The skin incision necessary for elevation and advancement rotation of the Mustardé flap is outlined. *(Courtesy Ronald Spiro, MD.)*

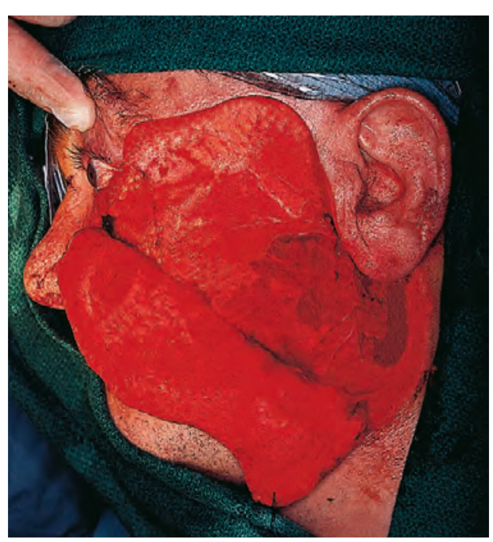

Figure 4.67 The surgical defect following resection of the tumor, superficial parotidectomy, and upper neck dissection with elevation of the Mustardé flap. *(Courtesy Ronald Spiro, MD.)*

Figure 4.68 The surgical specimen following full-thickness resection of the lower eyelid with the underlying soft tissues. *(Courtesy Ronald Spiro, MD.)*

Figure 4.69 Completed closure of the surgical defect with the Mustardé flap. A temporary tarsorrhaphy is performed. *(Courtesy Ronald Spiro, MD.)*

Figure 4.70 The postoperative appearance of the patient 2 months after surgery. *(Courtesy Ronald Spiro, MD.)*

Surgery for Orbital Tumors

Surgical approaches for tumors of the orbit vary, depending on the location and size of the tumor, as well as its tissue of origin and the proximity of other vital neurovascular structures and the globe. A presentation of the full spectrum of surgical procedures for neoplasms in the orbit is beyond the scope of this book. However, to highlight the concepts of surgical resection for orbital neoplasms, several examples of excision of benign and malignant tumors are shown here.

Surgical Approaches. The surgical approach for a tumor in the orbit depends on the location and size of the tumor, as well as the need for adequate exposure via a bony orbitotomy. A simple soft-tissue orbitotomy can be performed by making a variety of incisions along the circumference of the orbit, depending on the location of the tumor. Thus an orbitotomy may be performed along the orbital rim in the medial, lateral, superior, or inferior quadrant of the orbit. One can take advantage of the lid crease superiorly, transcaruncle or retrocaruncle incision medially, and transconjunctival incision inferiorly to achieve an aesthetically pleasant approach to the superior, medial, and inferior orbit, respectively. A wide exposure in the superior orbit can be obtained with an incision along the inferior border of the eyebrow, which can be extended laterally to add exposure to the lateral orbit. These soft-tissue orbitotomies are useful for benign lesions of the orbit or the lacrimal gland. Tumors located in the intraconal region of the orbit or that are large are best approached via a lateral orbitotomy with excision of the orbital processes of the zygomatic and frontal bones. For further exposure toward the optic cone, portions of the zygomatic arch and the greater wing of the sphenoid bone also may need to be removed. After the tumor is excised, the removed portions of the bony framework of the orbit are replaced to reconstruct the orbit. Orbital exenteration requires a circumferential incision along the orbital rim if the eyelids are to be resected en bloc with the contents of the orbit. On the other hand, if the skin of the eyelids can be preserved, an incision is made supraciliary on the upper and subciliary on the lower eyelid and is extended at the medial and lateral canthus up to the orbital rim. This incision will provide adequate access for exenteration of the orbit and allow the skin of the eyelids to be used for coverage of the bony socket. Finally, enucleation of the globe can be performed through a transconjunctival removal of the globe with preservation of the bulbar conjunctiva, orbital soft tissue, and eyelids. A 360-degree circumferential incision is made on the bulbar conjunctiva at the corneal limbus, and the extraocular muscles can be hooked, sutured, and resected to facilitate access to the optic nerve, which is transected behind the globe, allowing enucleation. An orbital implant of varying materials (silicone, Medpore, hydroxyapatite, glass, dermis-fat graft, etc.) fills the void left by the enucleated globe. The previously released extraocular muscles can be sutured to the orbital implant or implemented into the closure of Tenon's capsule, which is closed over the orbital implant followed by approximation of the conjunctival edge in a horizontal fashion with interrupted or continuous absorbable sutures. The conformer is placed in the socket to prevent contracture of the fornices.

Excision of a Hemangioma of the Orbit. The patient shown in Fig. 4.71 presented with proptosis of her left eye of several years' duration with discomfort and diplopia on right lateral gaze. The vision in her left eye was normal, although significant proptosis was evident on clinical examination. Radiographic studies of this patient entailed a CT scan with contrast in the axial and coronal planes (Figs. 4.72 and 4.73). In the axial plane, a well-demarcated contrast-enhancing mass is seen in the left orbit posterior to the globe and inferior to the optic nerve. The mass was contained within the bony orbital socket and did not infiltrate into the periorbita or the adjacent bone. On the coronal CT scan, the mass again is vividly demonstrated in the left orbit lying inferomedial to the optic nerve and between the medial and inferior recti muscles. Contrast enhancement of the lesion allowed the radiographic diagnosis of a hemangioma to be rendered.

Surgical excision of this lesion required an orbitotomy performed through the upper part of a lateral rhinotomy incision along the nasolabial skin crease extending up to the medial edge of the left eyebrow, under general endotracheal anesthetic (Fig. 4.74). The skin incision is deepened through the underlying soft tissues to expose the rim of the orbit in its inferior medial compartment. The medial canthal tendon is identified and is detached from the medial orbital tubercle and retracted with a 4-0 Nurolon suture. The nasolacrimal duct demonstrated in Fig. 4.75 is divided flush with the orbital wall at the lacrimal fossa. A periosteal elevator is now used to carefully and very slowly elevate the orbital periosteum without inadvertently entering the orbital fat or the tumor. Meticulous and diligent elevation

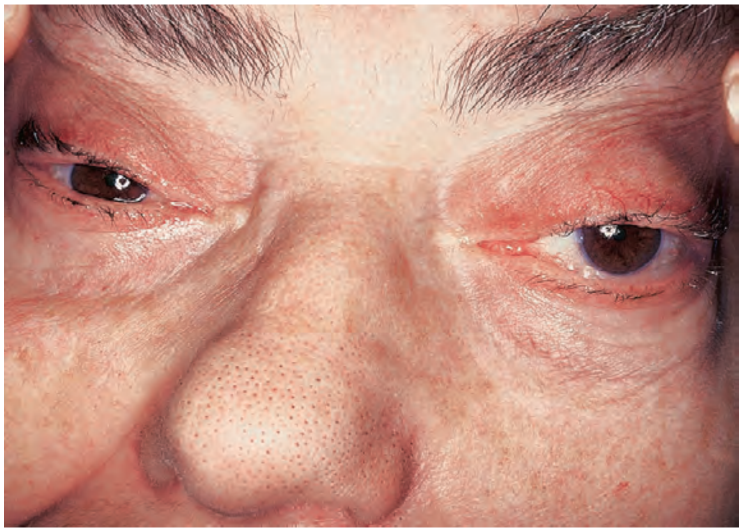

Figure 4.71 This patient presented with proptosis of her left eye of several years' duration with discomfort and diplopia on right lateral gaze.

of the orbital periosteum permits it to be retracted laterally with a malleable retractor, bringing the underlying purplish-red vascular lesion into view (Fig. 4.76). A close-up view of the surgical field clearly demonstrates a purplish, spongy lesion occupying the inferomedial quadrant of the orbit in the extraperiosteal plane (Fig. 4.77). A fine-tip electrocautery is used to perform a meticulous, slow dissection of the tumor, carefully separating it from the underlying periorbita and the bony orbital socket without inadvertent injury to the contents of the orbit or the globe. Careful mobilization and meticulous dissection permit delivery of the lesion in an en bloc fashion. The surgical field following excision of the tumor shows the empty space created by removal of the lesion in the inferomedial quadrant of the left orbit, permitting the globe to be returned to its normal position (Fig. 4.78). The medial canthal ligament is reapproximated to the bony medial wall of the orbit. No attempt is made to resuture the transected nasolacrimal duct, which rests in the lacrimal fossa and will spontaneously epithelialize along its natural course. Alternatively, a transcaruncle or retrocaruncle incision would eliminate the need to transect the nasolacrimal duct. A small Penrose drain is inserted in the inferior portion of the medial aspect of the orbit, and the skin incision is closed in two layers.

Figure 4.72 Axial view of the computed tomography scan with contrast showing a retrobulbar tumor in the left orbit.

Figure 4.73 Coronal view of the computed tomography scan shows the tumor in the left orbit in its inferomedial quadrant.

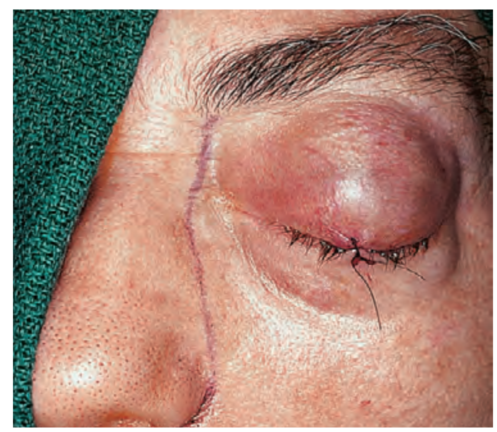

Figure 4.74 The rim of the orbit in its inferomedial compartment is exposed through a lateral rhinotomy incision.

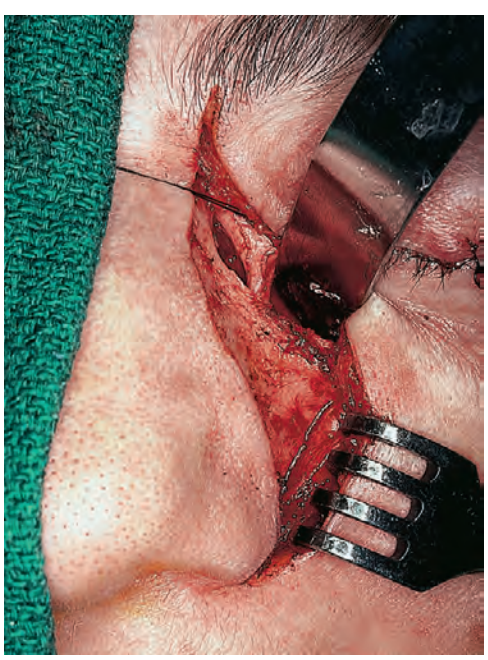

Figure 4.75 The nasolacrimal duct is divided flush with the orbital wall at the lacrimal fossa.

Figure 4.76 The purplish-red vascular lesion is brought into view.

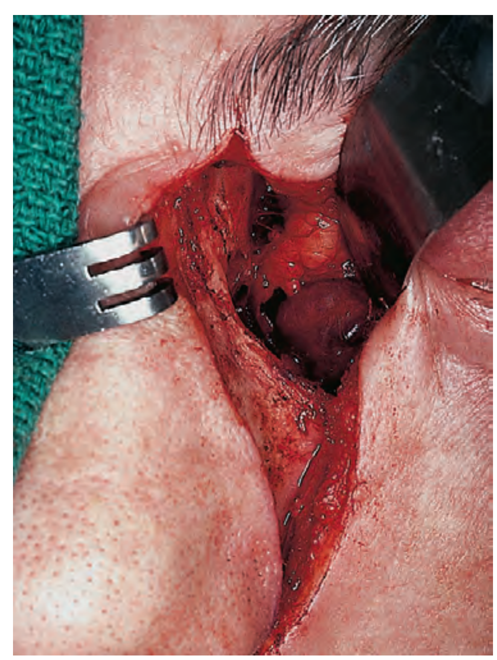

Figure 4.77 Close-up view of the surgical field showing the purplish, spongy lesion.

Figure 4.78 The surgical field following excision of the tumor.

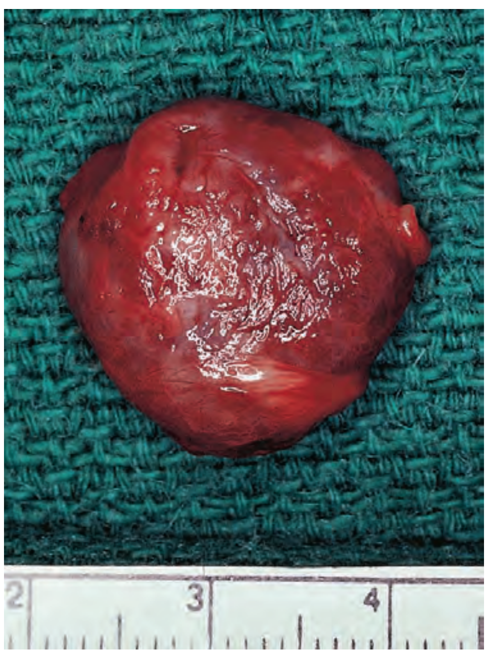

Figure 4.79 The surgical specimen.

Figure 4.80 The cut surface of the specimen.

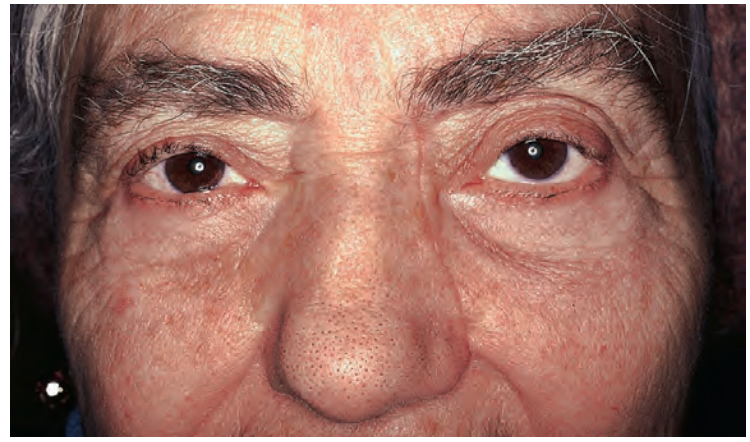

Figure 4.81 The appearance of the patient 3 months after surgery.

The surgical specimen, which measures approximately 2.5 cm, shows the entire lesion excised in an en bloc fashion in toto (Fig. 4.79). The cut surface of the specimen shows a fairly thick-walled but spongy lesion, which, upon histologic analysis, proved to be a cavernous hemangioma (Fig. 4.80). The postoperative appearance of the patient approximately 3 months after surgery shows that the globe has returned to its normal position and the patient no longer has proptosis; in addition, her discomfort has been relieved, and the diplopia has disappeared (Fig. 4.81).

Resection of a Carcinoma of the Lacrimal Sac and Reconstruction With a Glabellar Flap. Epithelial carcinomas arising from the lacrimal sac and the lining of the lacrimal drainage system (canaliculus and nasolacrimal duct) often present with obstruction of the collecting system and epiphora. Larger lesions may cause displacement of the globe laterally and cephalad, which can cause diplopia. Tissue diagnosis is easy if the tumor fungates through the skin. If the skin is intact, a fine-needle aspiration biopsy is recommended or an incisional biopsy can be performed, in a such a manner that the incision can be included in the definitive excision specimen.

The patient shown in Fig. 4.82 had a history of epiphora and a subcutaneous nodule in the region of the medial canthus of the left eye for 6 months. An incisional biopsy of the nodule was performed by the patient's local ophthalmologist. Although this biopsy established the diagnosis of mucoepidermoid carcinoma, it compromised the overlying skin, and as a result it had to be sacrificed. An MRI scan in the axial plane shows a circumferential tumor surrounding the nasolacrimal duct in the nasolacrimal canal medial to the anterior segment of the left orbit. A coronal view of the orbit at the same level shows an extensive tumor involving the lacrimal sac and the lacrimal collecting system, with extension of the tumor into the nasolacrimal duct (Figs. 4.83 and 4.84).

The plan of surgical resection and reconstruction involved a wide three-dimensional resection, including the overlying skin and the upper and lower puncta of the medial canthus of the left eye through a lateral rhinotomy incision. Immediate reconstruction of the defect was planned with use of an inferiorly based glabellar flap (Fig. 4.85). The surgical excision proceeds with through-and-through resection of the medial ends of the upper and lower eyelids, including the puncta and the skin overlying the tumor, encompassing the previous biopsy site. The surgical dissection proceeds in the orbit with excision of the orbital periosteum in its inferior medial quadrant, extending posteriorly midway through the lamina papyracea. An ethmoidectomy is performed with the primary tumor, including a portion of the nasal bone and the nasal process of the maxilla.

Figure 4.82 A patient with a mucoepidermoid carcinoma of the lacrimal apparatus showing skin invasion by the tumor.

The lacrimal fossa is resected en bloc with the entire nasolacrimal duct up to its opening in the lateral wall of the nasal cavity. The surgical specimen is removed in an en bloc fashion.

The surgical defect following removal of the specimen shows herniation of the orbital fat into the surgical defect (Fig. 4.86). Repair of the surgical defect begins with restoration of the orbital periosteum to prevent enophthalmos resulting from herniation of the globe into the nasal cavity. A dermis graft harvested from the lower extremity is used to repair the defect in the orbital periosteum with interrupted absorbable sutures (Fig. 4.87). The inferiorly based glabellar flap is elevated, preserving its blood supply through the supratrochlear vessels of the opposite side. Excellent vascularity of this flap is retained through the pedicle of the supratrochlear vessels. Nasal packing is introduced to support the repair of the orbital periosteum, and the lateral rhinotomy is closed (Fig. 4.88). The flap is rotated inferiorly and is appropriately trimmed to fit the skin defect at the site of the surgical resection. Excessive trimming of the flap should be avoided, even if a "dog ear" is left at its pedicle (Fig. 4.89). The surgical defect is repaired in two layers (Fig. 4.90).

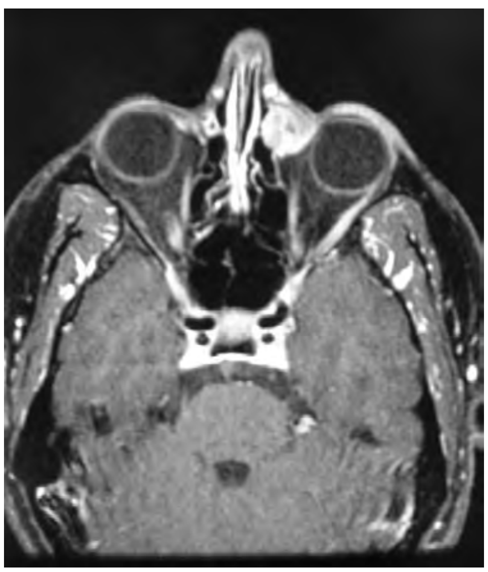

Figure 4.83 The axial view of a magnetic resonance imaging scan shows the tumor in the anteromedial compartment of the left orbit.

Figure 4.84 The coronal view of the magnetic resonance imaging scan shows the tumor involving the inferomedial quadrant of the left orbit.

Figure 4.85 The plan of exposure for surgical resection through a lateral rhinotomy and reconstruction with a glabellar flap.

Figure 4.86 The surgical defect following excision of the tumor shows herniation of periorbital fat.

Figure 4.87 The orbital periosteum reconstructed with a dermis graft.

Figure 4.88 The glabellar flap is elevated based on the supratrochlear vessels.

Figure 4.89 The flap is rotated inferiorly and trimmed to fit the surgical defect.

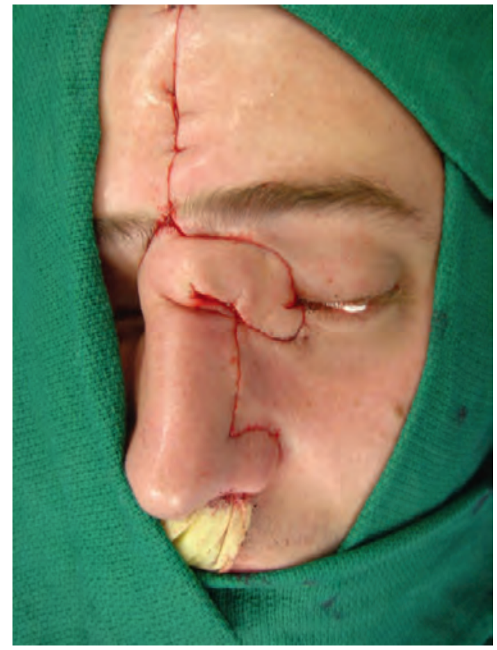

Figure 4.90 The donor site defect is closed primarily and the surgical defect of the skin is reconstructed with the flap.

Figure 4.91 The postoperative appearance of the patient 6 months after surgery.

Figure 4.92 Postoperative appearance of the patient with reading glasses on.

The postoperative appearance of the patient approximately 6 months after surgery and postoperative radiation therapy shows adequate healing of the surgical defect with restoration of the medial canthus (Fig. 4.91). The patient wears reading glasses, and with them on, the surgical scars are not readily apparent (Fig. 4.92). At this juncture, the patient may benefit from further aesthetic improvement with appropriate trimming of excess skin and soft tissue. Adjuvant radiation with or without concurrent chemotherapy should be considered 6-weeks postoperatively based on histopathologic high-risk features such as perineural invasion. In addition, the patient should be considered for reconstruction of the lacrimal drainage system through the creation of a new nasolacrimal duct and placement of a Jones tube if no adjuvant treatment is warranted at this point.

Radical Resection for a Locally Advanced Carcinoma of the Lacrimal System and Reconstruction With a Free Flap. The patient shown in Fig. 4.93 had a rapidly progressing lesion at the medial canthus of the left eye. A biopsy confirmed the diagnosis of a high-grade mucoepidermoid carcinoma. Imaging studies showed that the tumor was displacing the globe with invasion of the lacrimal fossa, lacrimal drainage system, and the adjacent ethmoid air cells without extension into the orbital soft tissue. The plan of surgical excision required wide resection of the lower eyelid along with the adjacent skin in the nasolabial region with a through-and-through resection of the medial wall of the orbit, an ethmoidectomy, a medial maxillectomy, and resection of the orbital periosteum (Fig. 4.94).

The surgical resection required excision of the bony orbit in its lower medial quadrant along with the upper punctum and medial one-fourth of the upper eyelid, the lower punctum and medial half of the lower eyelid, and the medial wall of the maxilla, along with an ethmoidectomy. The surgical defect shows the remnant lateral half of the lower eyelid, herniated fat of the orbit, and the remaining palpebral conjunctiva of the lower eyelid (Fig. 4.95). The first step in repair of this surgical defect is restoration of the orbital contents to prevent herniation of the globe into the nasal cavity and ptosis of the globe. Repair of the orbital periosteum is achieved with a dermis graft to prevent herniation of orbital fat into the maxilla and nasal cavity (Fig. 4.96). The remaining surgical defect of the ethmoidectomy and medial maxillectomy does not require any reconstructive effort, but the large through-and-through skin defect

Figure 4.93 Advanced carcinoma of the lacrimal apparatus fungating through the skin.

will require skin coverage externally and coverage of the inner lining of the nasal cavity. A radial forearm flap provides excellent coverage of the surgical defect of the skin and soft tissues externally. The undersurface of the radial forearm flap was lined with a split-thickness skin graft to provide coverage for mucosa in the nasal cavity. The postoperative appearance of the patient 1 month following surgery shows satisfactory healing of the skin defect with significant distortion of the upper and lower eyelids and lacrimal drainage system, which will require secondary revision (Fig. 4.97). This patient underwent postoperative radiation therapy, and 3 months later, secondary revisional surgery was performed to restore the medial canthus, the lower eyelid, and the lacrimal drainage system (Fig. 4.98). Complex reconstruction of such massive surgical defects restores the patient's aesthetic appearance and the function of the eye and avoids unnecessary orbital exenteration.

Figure 4.94 The plan of surgical resection includes wide resection of the cheek and medial maxillectomy through a lateral rhinotomy.

Figure 4.95 The surgical defect.

Figure 4.96 Repair of the orbital periosteum with a dermis graft.

Figure 4.97 The postoperative appearance of the patient 1 month after surgery.

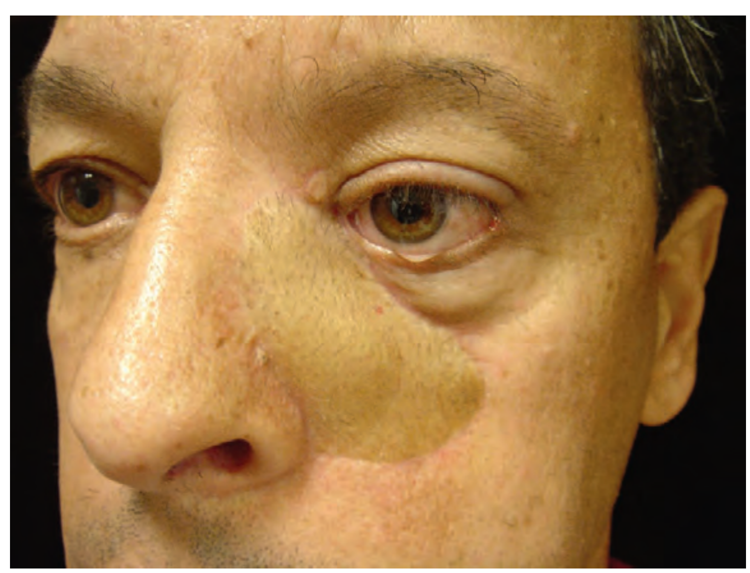

Figure 4.98 The appearance of the patient following revisional surgery for correction of the lower eyelid and reconstruction of the lacrimal drainage system.

Orbital Exenteration. Exenteration of the contents of the orbit is indicated for malignant tumors arising from the globe with significant or ill-defined invasion of the orbital soft tissue or for malignant lesions arising from the adnexal structures involving more than half of the bulbar and palpebral conjunctiva or having extensive infiltration of orbital soft tissue. The patient shown in Fig. 4.99 has a high-grade adenocarcinoma of the lacrimal sac located in the medial aspect of the left orbit with displacement of the globe laterally. The tumor has involved the extraocular muscles, causing ophthalmoplegia, and it has caused complete obstruction of the nasolacrimal drainage system, causing continuous epiphora. The tumor involves the skin overlying the medial aspect of the lower eyelid. A preoperative contrast-enhanced, axial-view of the CT scan demonstrates that the tumor involves the medial compartment of the left orbit with invasion of the subcutaneous soft tissues overlying the nasal bone and extends up to the lamina papyracea of the left orbit (Fig. 4.100).

The operative procedure is performed under general endotracheal anesthesia. The operative field is isolated with sterile drapes, and the skin incision is marked (Fig. 4.101). The skin incision extends from the lateral canthus along the tarsal margin of the upper eyelid up to the medial canthus. A similar incision is placed on the lower eyelid extending from the lateral canthus toward the medial canthus, but both the upper and the lower eyelid incisions are extended along the nasolabial fold to encompass the involved portion of the skin overlying the lacrimal fossa and nasolacrimal duct. The skin incision is deepened through the subcutaneous tissue but remains superficial to the orbicularis oculi muscle (Fig. 4.102). A generous portion of soft tissue is sacrificed under the medial aspect of the incision where the skin is involved. Here the skin incision is deepened straight down to the nasal bone medially and the anterior wall of the maxilla laterally. Elevation of the upper and lower skin flaps continues with the use of electrocautery up to the orbital rim in a circumferential fashion. In the inferomedial quadrant of the orbit, however, the soft tissues along the nasolabial fold are retained on the specimen.

Figure 4.99 This patient has an adenocarcinoma of the left lacrimal sac.

Figure 4.100 A contrast-enhanced computed tomography scan shows the tumor involving the orbit with displacement of the globe.

Using the electrocautery, a circumferential incision is made in the periosteum of the orbit at the orbital rim, extending from the supraorbital foramen superiorly up to the infraorbital foramen inferiorly, thus encompassing the lateral half of the circumference of the orbit. A Freer periosteal elevator is used to elevate the periosteum of the orbit in its outer half, as shown in Fig. 4.103. Brisk hemorrhage from small bleeding points between the bony orbit and the periosteum is to be expected and is promptly controlled with electrocautery. Mobilization of the entire orbit is carried on posteriorly as far as possible up to the apex of the orbit. Care should be exercised to avoid perforating the periosteum; otherwise, herniation of the periorbital fat will occur, compromising the exposure and adequacy of the operation. No attempt is made to mobilize the periosteum in the lower medial quadrant of the orbit, where the lacrimal apparatus and the lacrimal fossa will be resected en bloc with the orbital contents. Using a power saw, the orbital rim in its lower medial quadrant is divided, remaining lateral to the lacrimal fossa and medial to the infraorbital canal. Similarly, the medial aspect of the bony orbital rim is also divided with a power saw. Finally, the lateral aspect of the left nasal bone is divided with a power saw to completely mobilize the bony lacrimal fossa in continuity with the orbital contents. At this juncture, the apex of the orbit is nearly completely mobilized posteriorly. The attachment of the extraocular muscles and the optic nerve now needs to be divided. With use of curved orbital retractors, the apex of the orbit is exposed to permit angled scissors to divide the origin of the extraocular muscles and the optic nerve as shown in Fig. 4.104. Brisk hemorrhage is to be expected from the central retinal artery, the ophthalmic artery, and the cut ends of the extraocular muscles. This bleeding is promptly controlled with bipolar cautery for the central retinal and ophthalmic arteries, although it can also be controlled with digital pressure and occasionally the use of thrombin. Finally, the surgical specimen is removed by dividing the soft tissue attachments with heavy Mayo scissors in an en bloc fashion, encompassing the contents of the orbit and the tumor of the lacrimal apparatus in continuity with the full length of the nasolacrimal duct up to the lateral wall of the nasal cavity. The surgical defect thus shows the exenterated left orbit with resection of the lacrimal fossa (Fig. 4.105). The stump of the optic nerve and the stumps of the divided extraocular muscles can be seen at the apex of the orbit. Absolute hemostasis from the structures at the apex of the orbit can be secured with use of a chromic catgut suture ligature on a small curved needle or bipolar cautery.

A previously harvested split-thickness skin graft is now used to provide lining for the raw surfaces of the exenterated orbit. The skin graft is sutured to the edges of the skin of the upper and lower eyelids (Fig. 4.106). Xeroform gauze packing is used to snugly apply the skin graft over the bony orbital walls, permitting secure contact. The orbital socket is completely packed with Xeroform gauze, which holds the skin graft in position

Figure 4.101 The plan of surgical excision.

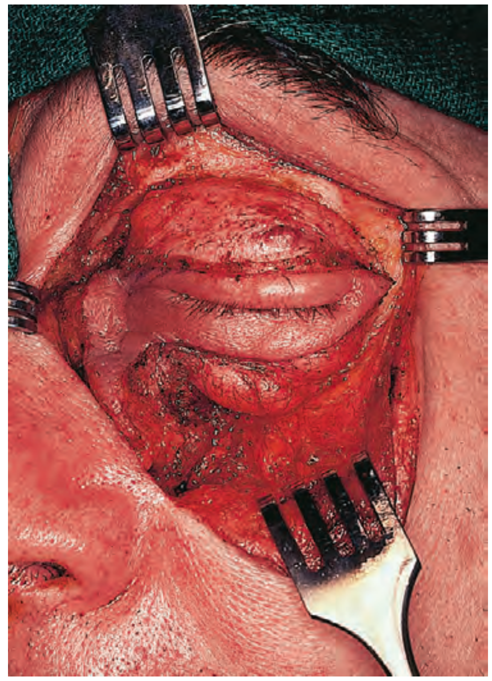

Figure 4.102 The skin incision is deepened in a plane superficial to the orbicularis oculi muscle.

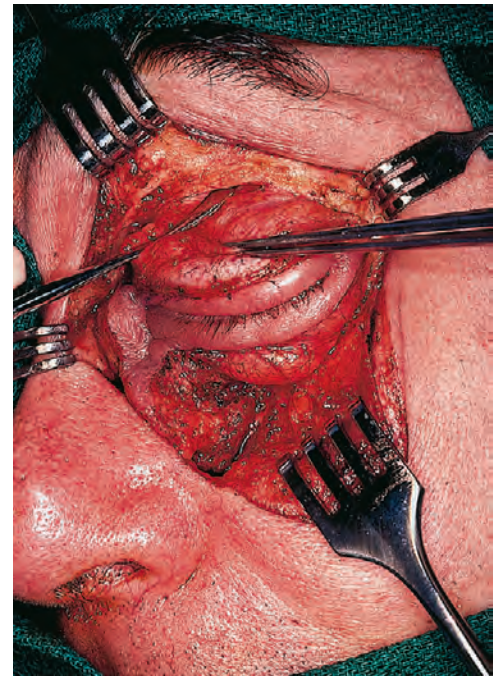

Figure 4.103 A Freer periosteal elevator is used to elevate the periosteum of the orbit.

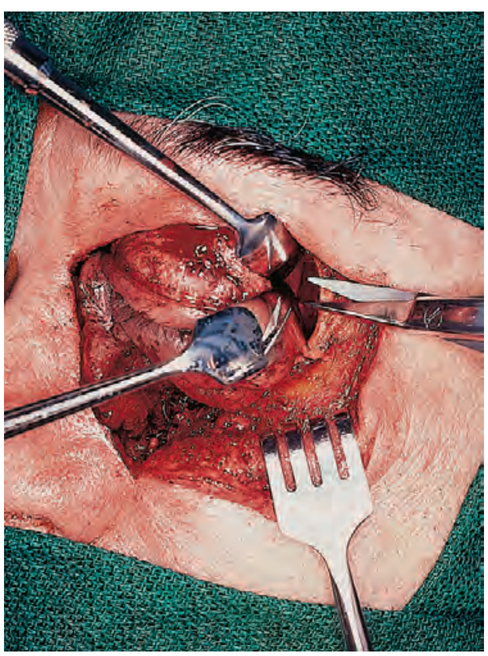

Figure 4.104 The extraocular muscles and the optic nerve are divided at the orbital apex with angled scissors.

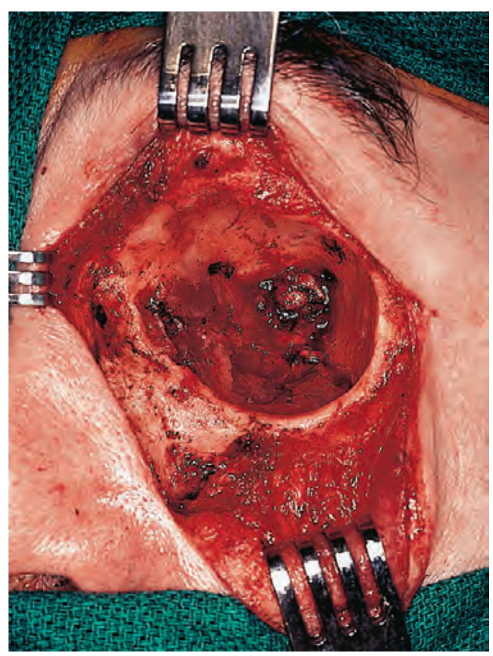

Figure 4.105 The surgical defect.

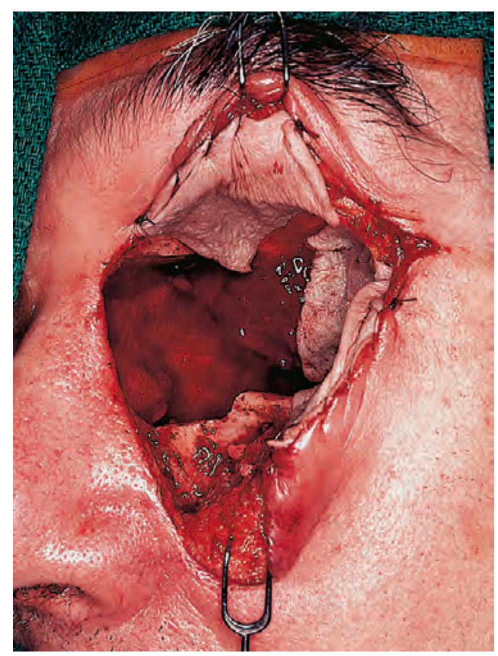

Figure 4.106 The skin graft is sutured to the edges of the skin of the upper and lower eyelids.

(Fig. 4.107). The skin incision is closed in two layers. The postoperative appearance of the patient approximately 1 month after surgery shows excellent healing of the skin graft within the orbital socket (Fig. 4.108). Minor debridement of the orbital defect is necessary until absolute healing of the skin graft is achieved. The patient is instructed regarding irrigation of the orbital defect and use of a 4×4 gauze soaked with mineral oil to maintain moisture in the orbital cavity to avoid crusting. Approximately 3 months after surgery, an orbital prosthesis is fabricated, which provides aesthetic rehabilitation of the exenterated defect (Fig. 4.109).

Figure 4.107 Xeroform gauze packing is used to support the skin graft in position.

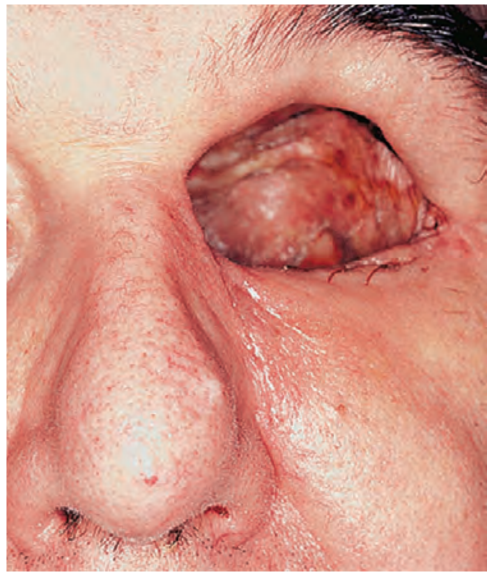

Figure 4.108 The postoperative appearance of the patient approximately 1 month after surgery shows excellent healing of the skin graft within the orbital socket.

Figure 4.109 The patient's postoperative appearance at 6 months shows excellent aesthetic rehabilitation with an orbital prosthesis.

Orbital Exenteration With Medial Maxillectomy. Orbital exenteration with extension of the operative procedure to include any part of the maxilla is indicated for tumors of the orbit that extend to adjacent paranasal sinuses or along the lacrimal collection system. Such extended procedures may require orbital exenteration with maxillectomy, ethmoidectomy, or radical maxillectomy and exenteration of the nasal cavity. When tumors of the lacrimal collecting system extend along the nasolacrimal duct into the lateral wall of the nasal cavity, orbital exenteration with a medial maxillectomy is indicated.

The patient shown in Fig. 4.110 has a poorly differentiated carcinoma of the lacrimal sac. Her presenting symptom was epiphora and nasal congestion. A contrast-enhanced MRI scan in the coronal view clearly shows the tumor in the medial lower quadrant of the right orbit with extension along the floor of the orbit inferiorly and along the nasolacrimal duct on the lateral wall of the right nasal cavity (Fig. 4.111). The axial view of the MRI shows that the tumor is confined to the medial quadrant of the orbit but abuts the globe and involves the orbital soft tissue (Fig. 4.112). The operative procedure therefore will entail an orbital exenteration with a medial maxillectomy.

The plan of surgical resection includes access through a lateral rhinotomy incision that respects the nasal subunits and extends from the floor of the nasal cavity along the alar groove and the lateral aspect of the nose up to the medial canthus. The incision is then extended along the subciliary line on the upper and lower eyelids up to the lateral canthus (Fig. 4.113). The skin incision is deepened, leaving a generous amount of soft tissue on the medial aspect of the orbit and the lateral wall of the nasal cavity to secure adequate margins around the tumor (Fig. 4.114). The skin flap is elevated laterally, directly over the zygoma and the anterior bony wall of the maxilla. Electrocautery is used to make an incision on the soft tissues at the orbital rim along the lateral half of the orbit (Fig. 4.115). A Freer elevator is used to elevate the orbital periosteum in its lateral half all the way up to the cone of the orbit. Extreme caution must be exercised in elevating the periosteum from the orbital bone to avoid perforating the periosteum and causing herniation of the orbital fat (Fig. 4.116). Complete mobilization of the orbital contents from the bone is achieved by meticulous slow dissection in the subperiosteal plane (Fig. 4.117), which allows removal of the tumor in an en bloc fashion.

The bone cuts to encompass the tumor are depicted on a skull (Fig. 4.118). A power saw is used to make bone cuts for the proposed medial maxillectomy in conjunction with orbital exenteration (Fig. 4.119). The inferior rim of the orbit is divided lateral to the infraorbital foramen to keep the lower medial quadrant in the specimen with adequate bone margins. This bone cut extends through the floor of the orbit up to the optic foramen posteriorly. The anterior wall of the maxilla is divided in the same plane up to the vestibule of the nasal cavity. Another bone cut is made on the medial wall of the orbit, above the meridian of the orbit, to keep the entire lacrimal fossa in the specimen remaining well above it to secure a satisfactory medial margin. This bone cut is extended through the lamina papyracea posteriorly up to the posterior ethmoid air cells. The next bone cut is made on the lateral aspect of the right nasal bone from the orbit up to the nasal vestibule (Fig. 4.120). Small osteotomes are used to complete the bone cuts to mobilize the bony attachments of the surgical specimen. The final bone cut at the lower margin of the lateral wall of the nasal cavity is made with an osteotome, beginning at the nasal vestibule and extending up to the posterior wall of the maxilla. This bone cut is made inferior to the inferior turbinate to excise the entire lateral wall of the nasal cavity in the surgical specimen in an en bloc fashion. Once all bone cuts are completed, the surgical specimen remains attached only at the cone of the orbit posteriorly through the attachments of the extraocular muscles and the optic nerve.

At this juncture, the orbital contents are retracted medially and the posterior attachments of the extraocular muscles and the optic nerve are transected with serrated angled scissors (Fig.

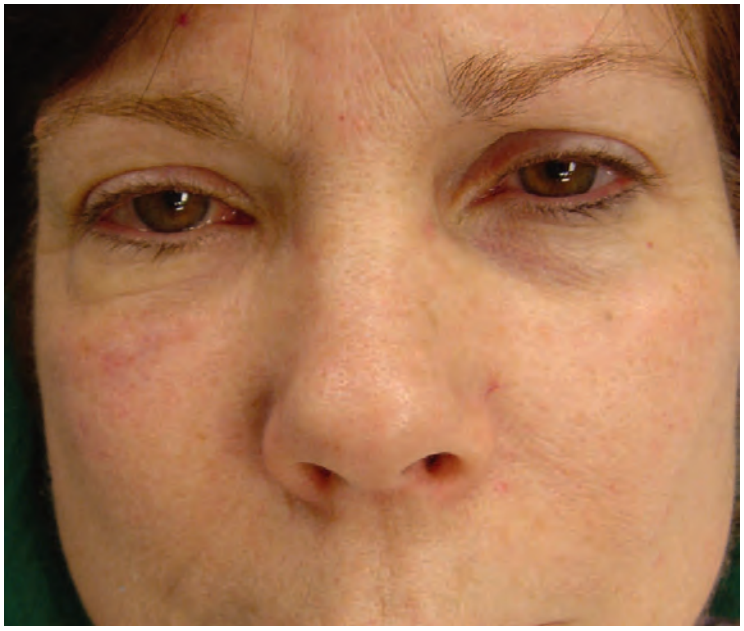

Figure 4.110 A patient with a carcinoma of the right lacrimal apparatus shows chemosis and subtle fullness of the infraorbital region.

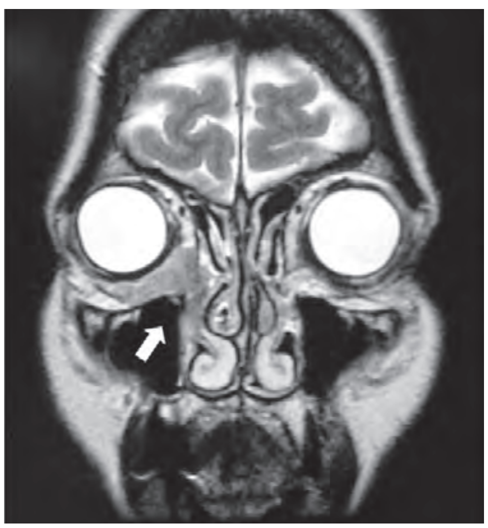

Figure 4.111 The coronal view of a magnetic resonance imaging scan shows a tumor involving the inferomedial quadrant of the right orbit and the right lateral nasal wall (*arrow*).

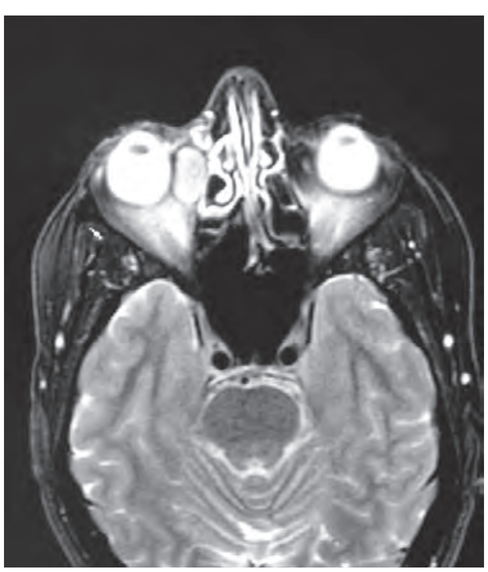

Figure 4.112 The axial view of a magnetic resonance imaging scan shows tumor invasion into the periorbital fat.

Figure 4.113 The plan of surgical resection through a lateral rhinotomy with orbital exenteration.

Figure 4.114 A surgical incision is deepened through subcutaneous soft tissues.

4.121). The anesthesiologist should be alerted before transection of the optic nerve, as traction on the optic nerve can cause significant bradycardia or even asystole. Brisk hemorrhage from the central retinal artery and the ophthalmic artery is to be expected and is controlled once the surgical specimen is removed. Attempting to clamp these vessels without removal of the surgical specimen is futile because adequate exposure is not available, and thus expediency is essential during this part of the operation. Once the soft-tissue attachments at the apex of the orbit are divided, Mayo scissors are used to incise the mucosa of the lateral wall of the nasal cavity and ethmoid air cells to deliver the specimen. At this point, the bleeding from the central retinal artery and ophthalmic artery is clamped and ligated with sutures or cauterized with bipolar cautery. All bony sharp margins are smoothed out with a burr, and hemostasis is secured by electrocoagulation or ligation of the bleeding vessels. Brisk hemorrhage from the sphenopalatine artery is to be expected at the posteromedial aspect of the defect and is controlled with electrocoagulation. The surgical defect is irrigated with warm

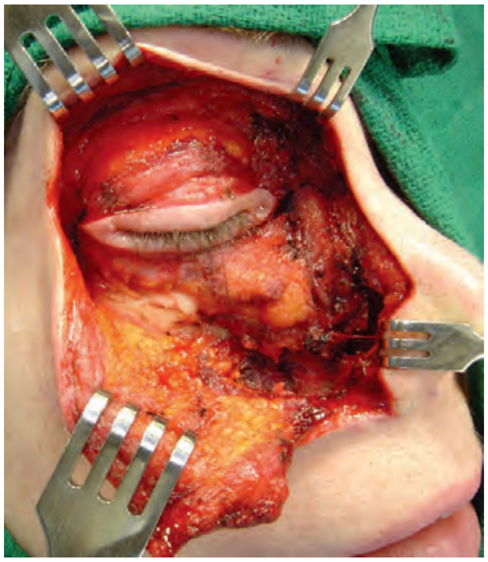

Figure 4.115 The cheek flap is elevated to expose the zygoma and anterior wall of the maxilla.

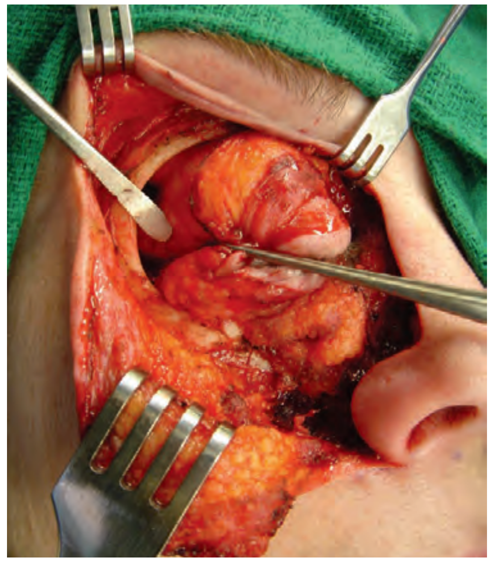

Figure 4.116 The periosteum of the lateral half of the orbit is elevated from the bone with a Freer elevator.

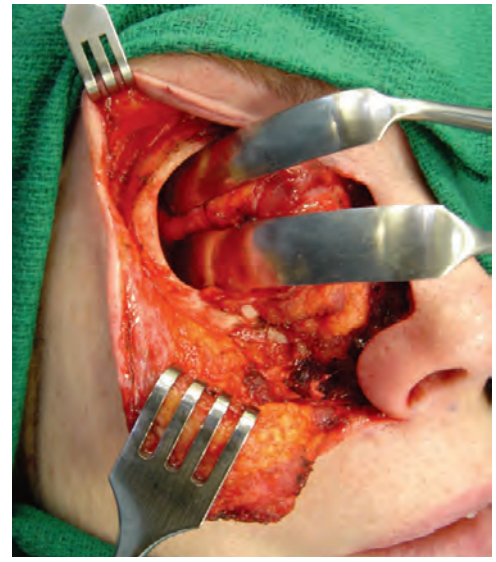

Figure 4.117 The lateral half of the orbital contents are mobilized up to the apex.

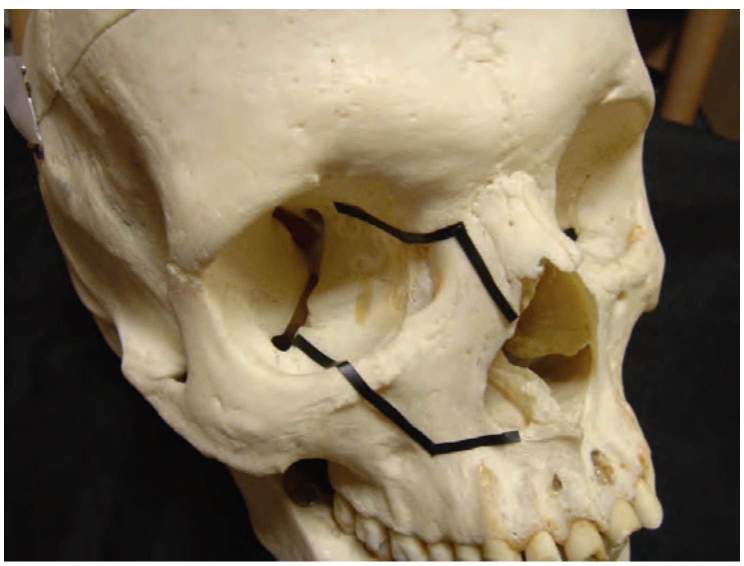

Figure 4.118 The planned bone cuts are outlined on a skull.

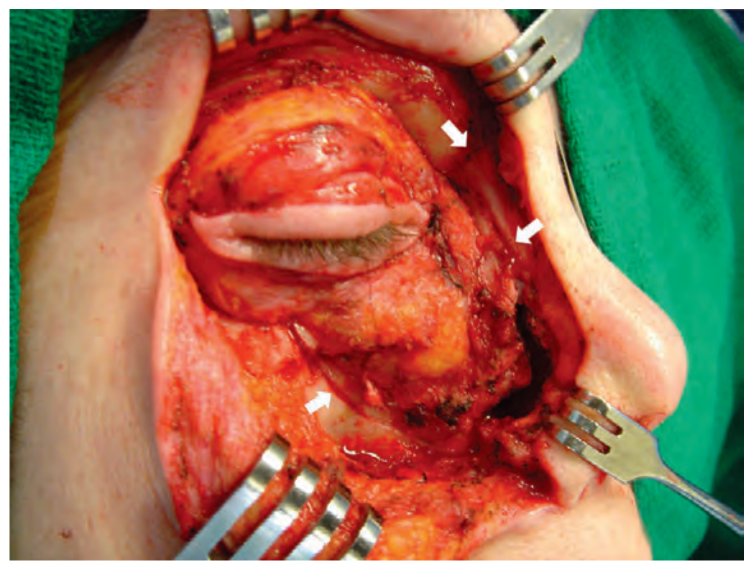

Figure 4.120 All bone cuts are completed (*arrows*).

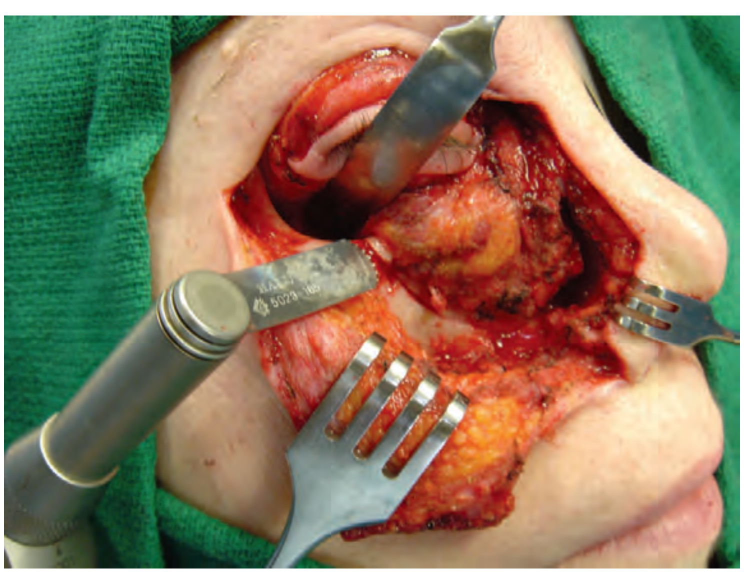

Figure 4.119 Bone cuts are made with a sagittal saw.

saline solution, and all clots are removed. The surgical defect following removal of the specimen is shown in Fig. 4.122. Note that the medial one-third of the orbital rim has been resected to encompass the tumor of the lacrimal apparatus, which is removed in an en bloc fashion with the contents of the orbit and lateral wall of the nasal cavity. At the apex of the orbit, the stump of the optic nerve and the extraocular muscles are readily visible.

A previously harvested split-thickness skin graft is now applied to the bony surface of the remnant orbital wall and the cone of the orbit to achieve primary healing. The skin graft covers all the exposed raw bone and the stump of the soft tissues at the apex of the orbit (Fig. 4.123). The skin graft is held in position with Xeroform gauze packing. The packing is applied snugly to keep the skin graft in contact with the bone to promote primary healing (Fig. 4.124). The remainder of the packing is used to fill the maxillary antrum, the orbit, and the nasal cavity. The skin incision is closed in layers, and an eye patch is applied over the packing as a dressing (Fig. 4.125).

Figure 4.121 Posterior attachments of the extraocular muscles and the optic nerve are divided with angled scissors.

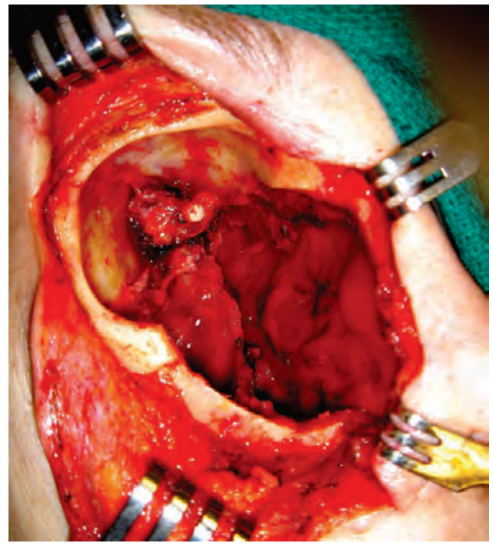

Figure 4.122 The surgical defect shows the apex of the orbit and nasal contents after resection.

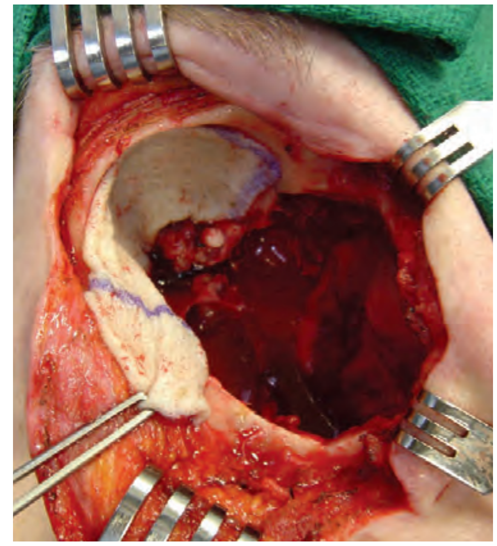

Figure 4.123 A split-thickness skin graft is applied against the bone and soft tissue of the orbital defect.

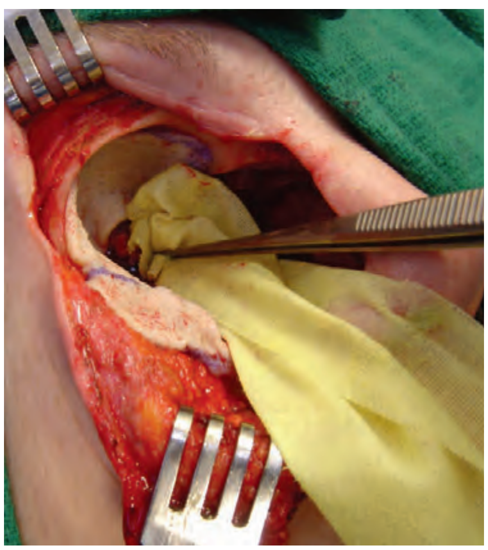

Figure 4.124 The position of the skin graft is maintained with Xeroform packing.

Figure 4.125 The skin incision is closed in layers.

Figure 4.126 The surgical specimen shows monobloc resection of the tumor with the contents of the orbit and the lateral wall of the nasal cavity.

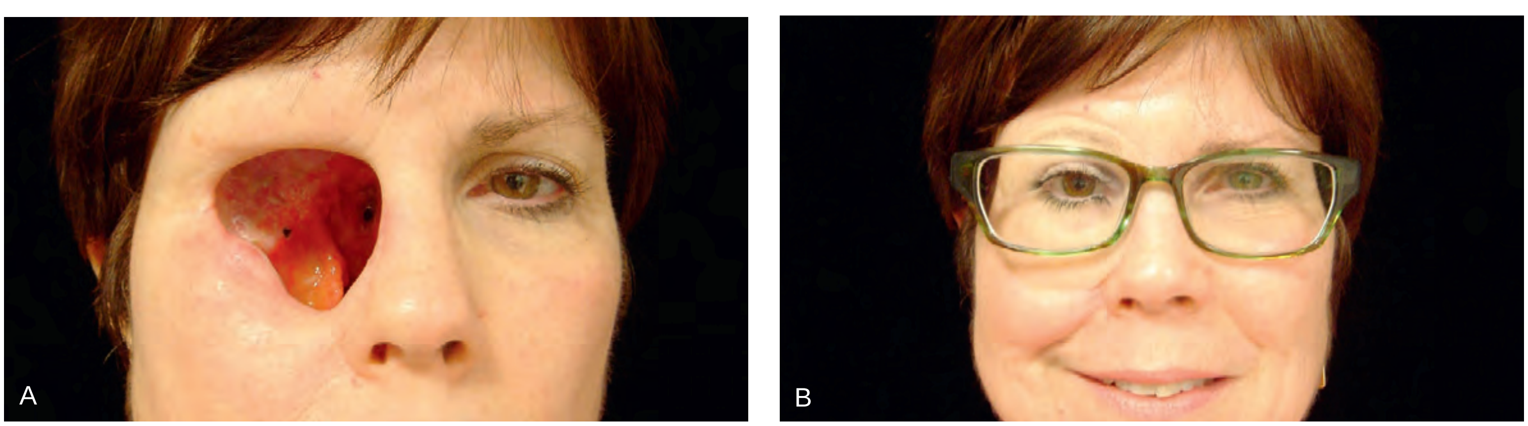

Figure 4.127 **A**, Postoperative appearance of the patient showing the healed surgical defect. **B**, The postoperative appearance of the patient with orbital prosthesis and glasses.

The surgical specimen shown in Fig. 4.126 demonstrates en bloc resection of the tumor of the lacrimal apparatus, located on the medial half of the lower quadrant of the orbit and the medial half of the floor of the orbit with extension along the nasolacrimal duct.

This patient required postoperative radiation therapy, and the surgical defect was rehabilitated with an orbital prosthesis that was fabricated approximately 3 months after completion of postoperative radiation therapy (Fig. 4.127A and B).

Cranioorbital-Zygomatic Resection With Exenteration. High-grade malignant neoplasms of the orbit often require orbital exenteration to achieve a satisfactory three-dimensional tumor resection. The extent of surgery, whether orbital exenteration or exenteration of the orbital contents with an orbitectomy (i.e., resection of a part of the bony wall of the orbit), depends on the histology of the primary tumor, its local extent, and the presence or absence of bone invasion. The CT scan of a patient with an adenoid cystic carcinoma arising in the lacrimal gland shows a large soft-tissue tumor situated posterolateral to the globe in the orbit and adjacent to and involving the lateral wall of the orbit (Fig. 4.128). The tumor extends posteriorly to involve the extraocular muscles and extends through the superior orbital fissure to the anterior aspect of the floor of the middle cranial fossa (Fig. 4.129).

The surgical procedure required a cranioorbital-zygomatic exposure (Fig. 4.130) through a coronal scalp incision to gain access to the intracranial component of the tumor. (The details of craniofacial resection are presented in Chapter 6.) After removal of the tumor, the surgical field shows the dural defect, which exposes the brain at the floor of the middle cranial fossa (Fig. 4.131). A superior and lateral orbitectomy has been performed to achieve en bloc resection of the tumor along with the contents of the orbit. The dural defect was repaired with a free graft of pericranium. The surgical defect seen from the anterior aspect shows loss of the superior orbital rim as well as the lateral wall of the orbit up to the middle cranial fossa. The floor and medial wall of the orbit are preserved (Fig. 4.132). The surgical specimen shows an en bloc resection of the tumor encompassed by orbital contents and the bony superior and lateral orbital walls (Figs. 4.133 and 4.134). The surgical defect in this patient was repaired with a rectus abdominis myocutaneous free flap with microvascular anastomosis to the superficial temporal artery and vein. Major orbitectomy, particularly when the roof of the orbit has been resected, warrants the need for free tissue transfer to avoid brain herniation. A composite free flap provides satisfactory support to the brain, obliterates the orbital defect, and provides reconstruction of the skin defect. The postoperative appearance of the patient 3 months after surgery shows satisfactory soft tissue and skin reconstruction after orbitectomy (Fig. 4.135). Free tissue transfer in this setting obviates the need for cleaning and maintenance of the orbital defect. Aesthetic rehabilitation of the reconstructed area can be optimized with a facial prosthesis.

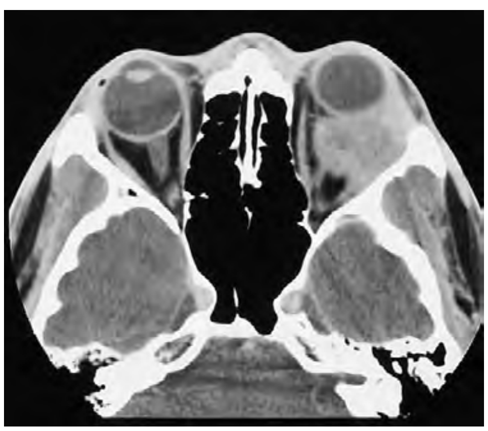

Figure 4.128 A computed tomography scan of a patient with an adenoid cystic carcinoma of the lacrimal gland.

Figure 4.129 A computed tomography scan shows involvement of the lateral orbital wall and middle cranial fossa.

Figure 4.130 Surgical incisions outlined for a cranioorbital-zygomatic resection.

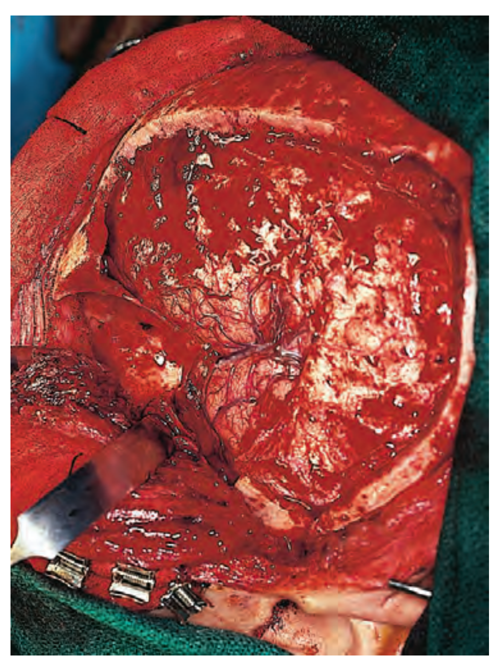

Figure 4.131 The surgical defect showing exposed brain after dural resection.

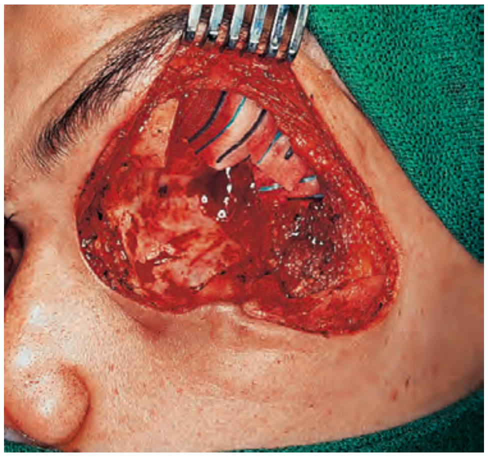

Figure 4.132 The surgical defect showing preservation of the medial wall and floor of the orbit.

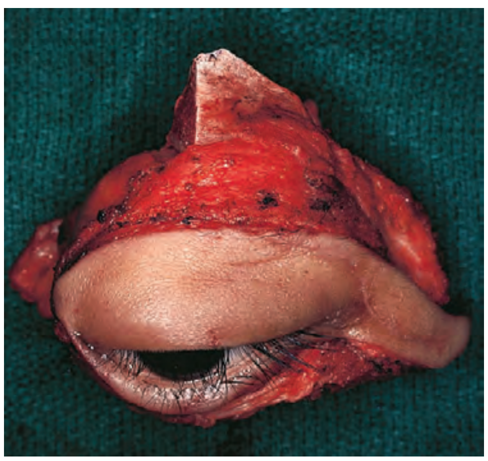

Figure 4.133 The anterior view of the surgical specimen showing orbital contents and the resected portion of the bony orbit.

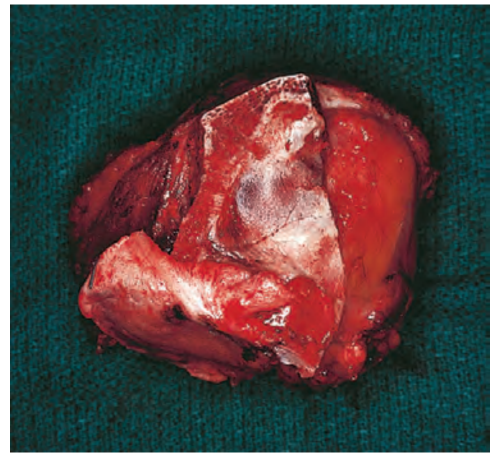

Figure 4.134 The superior view of the specimen showing the dura of the floor of the middle cranial fossa.

Figure 4.135 The postoperative appearance of the patient 3 months after reconstruction with a free flap.

Rehabilitation of Paralyzed Eyelids

Surgical sacrifice or destruction of the facial nerve as a result of tumor invasion leads to paralysis of facial muscles on the ipsilateral side. On the other hand, isolated dysfunction of a branch of the facial nerve leads to paralysis of its corresponding muscles. Thus loss of function of the frontal branch leads to paralysis of the frontalis muscle, resulting in the inability to raise the forehead and drooping of the eyebrow and reverse ptosis of the upper lid. Dysfunction of the zygomatic branch of the facial nerve causes paralysis of the orbicularis oculi muscle, which results in the inability to close the palpebral fissure and lower lid retraction or paralytic ectropion. Exposure keratopathy is a significant complication that can be prevented with appropriate management. Dysfunction of the buccal, marginal mandibular, and cervical branches of the facial nerve causes paralysis of the muscles of the lower half of the face, including the buccinator, orbicularis oris, and platysma, as well as the elevators and depressors of the commissure of the mouth.

Rehabilitation of a paralyzed eyelid is crucial to alleviate the symptom of epiphora, ocular surface irritation leading to blurring of vision and risk of corneal breakdown resulting from exposure keratopathy. Three procedures aid in restoring a paralyzed eyelid: (1) gold weight implant; (2) lateral tarsorrhaphy; and (3) lateral canthoplasty.

Gold Weight Implant. Insertion of a gold weight in the upper eyelid provides closure of the eyelid by gravity, which occurs in harmony with the opposite eye. Restoration of upper lid function in this manner works extremely well in patients while awake or upright. In older patients, additional procedures may be necessary to repair ectropion of the lower eyelid in addition to placement of the gold weight in the upper eyelid. Placement of a gold weight should be delayed for at least 3 to 4 weeks after resection of the facial nerve. In addition, placement of the gold weight also should be delayed in patients who are to undergo postoperative radiation therapy in the vicinity of the eye for at least 6 months to a year.

The postoperative appearance of a patient who required a radical total parotidectomy with sacrifice of the facial nerve shows paralysis of the upper eyelid during closure of the eye (Fig. 4.136). The procedure to place a gold weight in the eyelid generally is done under local anesthesia. Before the operative procedure is performed, however, the weight of the gold pellet insert that is required to counteract the levator palpebrae superioris muscle must be determined. A series of dummy weights are available to choose from. The correct weight for this patient is shown in Fig. 4.137. The patient should be sitting up while the assessment is being done. The weight is temporarily applied over the skin of the upper eyelid with adhesive tape, and the patient

is asked to close his or her eyes. If satisfactory closure is achieved, then that is the correct weight to be used. The weight also should be tested with the eyelids open to ensure that excessive weight does not cause drooping of the eyelid (blepharoptosis). The actual gold weight is a curved pellet with three holes in it that are used to suture the weight to hold it in place (Fig. 4.138).

An incision is marked in the natural lid crease over the upper eyelid, usually between 8 mm to 10 mm in Caucasian population but may be lower in Asian patients (Fig. 4.139). Local anesthetic is infiltrated, and the skin incision is made to expose the orbicularis oculi muscle (Fig. 4.140). The muscle fibers are spread apart with a hemostat to create a pocket between the muscular layer and the underlying tarsal plate. Careful dissection should be done following the horizontal and slightly curved fibers of the orbicularis and avoiding damage to the levator muscle underneath. The pocket created should be large enough to permit easy insertion of the weight, which should be placed in the pocket without any tension and centered on the pupillary axis, which is slightly medial from the midpoint of the lid (Fig. 4.141). The weight is anchored to the undersurface of the orbicularis oculi muscle or in partial-thickness sutures to the tarsal plate. The muscular layer is closed with interrupted 5-0 chromic catgut sutures to avoid exposure (Fig. 4.142). After complete closure of the muscular layer, the skin is approximated with 6-0 nylon interrupted sutures. Immediately after surgery, the patient is able to close the eye in harmony with the opposite eye, achieving complete closure of the palpebral fissure (Fig. 4.143). Almost all patients experience immediate relief of epiphora and irritation of the exposed cornea following the insertion of a gold weight implant. Alternative implant materials include lower-profile titanium chain.

Figure 4.136 Paralysis of the left eyelids following a radical total parotidectomy with sacrifice of the facial nerve.

Figure 4.137 A dummy of the correct weight applied to the skin of the upper eyelid is used to determine the weight of the gold pellet insert required to achieve adequate palpebral closure.

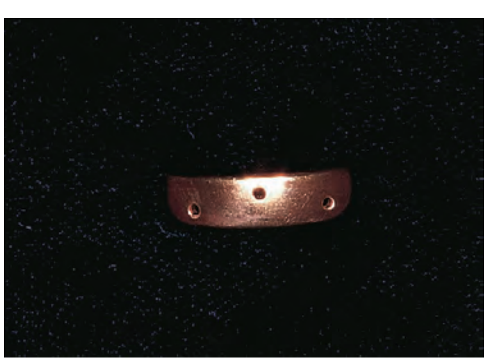

Figure 4.138 The actual gold weight is a curved pellet with three holes in it that are used to suture the weight securely in place.

Figure 4.139 A transverse incision is marked in a skin crease on the upper eyelid approximately 6 mm above the tarsal margin.

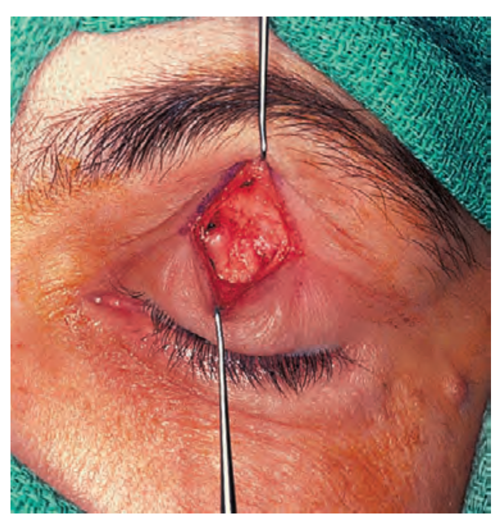

Figure 4.140 The orbicularis oculi muscle is exposed.

Figure 4.141 The gold weight is inserted in a pocket created between the orbicularis oculi muscle and the tarsal plate.

Figure 4.142 The muscle is reapproximated over the gold weight to prevent its exposure.

Figure 4.143 The patient is able to achieve complete palpebral closure in harmony with the opposite eye immediately after the procedure.

Lateral Tarsorrhaphy. The excellent results with gold weight implants seen in young patients or milder cases generally do not apply to elderly patients and those who have had long-standing facial paralysis. In addition, ectropion of the lower eyelid develops relatively soon in elderly patients after the onset of facial paralysis. Although insertion of a gold weight facilitates the ability to close the upper eyelid, complete closure of the palpebral fissure is not achieved because of ectropion. Thus in these patients a lateral tarsorrhaphy can be used in conjunction with gold weight implant.

A temporary lateral tarsorrhaphy also is recommended in patients who are candidates for a gold weight implant in the upper eyelid but are to receive postoperative radiation therapy. Placement of the gold weight should be delayed until the completion of radiotherapy.

The procedure is done under local anesthesia, with topical anesthesia of the conjunctiva and the cornea achieved by instillation of topical anesthetic eye drops in the conjunctival sac before the surgery. Anesthesia of the eyelids is achieved with injection of a local anesthetic. The opposing tarsal margins of the upper and lower eyelids are denuded in an area approximately 5 to 6 mm in length with use of a scalpel (Fig. 4.144). Only the mucocutaneous junction on the tarsal margin is denuded, without taking any part of the underlying tarsal plate. These incisions should be placed in such a manner that the limbus of the cornea is not compromised upon closure.

Two rubber booties (i.e., short segments of a No. 6 red rubber catheter) are used to achieve flat approximation of the raw areas of the upper and lower eyelids without any space in between. A 3-0 silk suture is applied as shown in Fig. 4.145. Complete hemostasis is secured. The suture is then tightened as shown in Fig. 4.146. The approximation of the upper and lower eyelid is thus achieved by completely apposing the raw areas without any space in between. The suture is then pulled snug and tied over the lower booty. The suture is left in position for approximately 3 weeks, at which time it is removed. The postoperative appearance of a patient with a lateral tarsorrhaphy is shown in Fig. 4.147. A lateral tarsorrhaphy adequately protects the cornea from exposure keratopathy and directs drainage of the tears medially to the lacrimal collecting system.

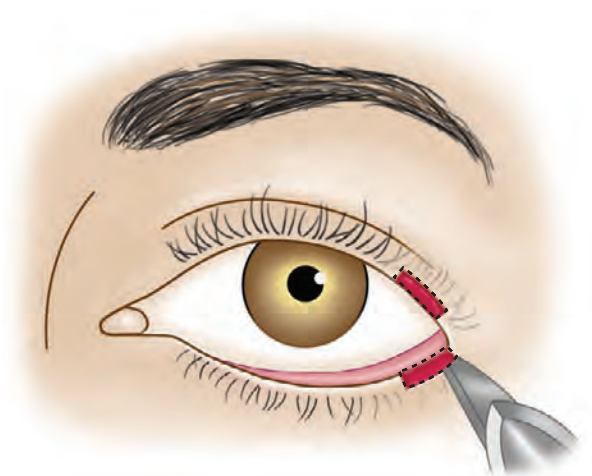

Figure 4.144 An area approximately 5 to 6 mm in length along the tarsal margins of both eyelids is denuded with a sharp scalpel without taking any of the underlying tarsal cartilage.

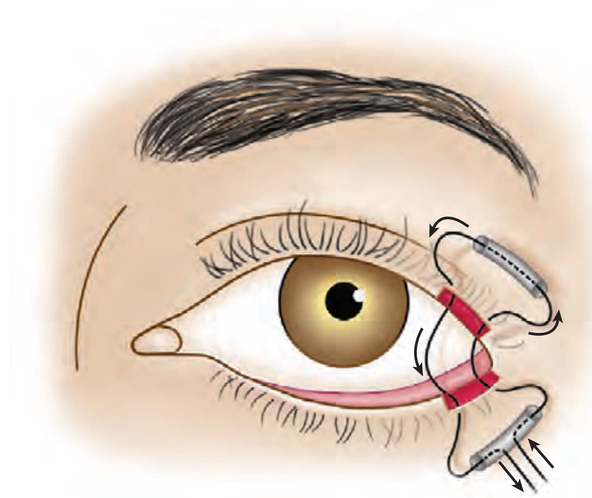

Figure 4.145 A 3-0 silk suture is used to approximate the raw areas and is passed through rubber booties to prevent it from cutting through.

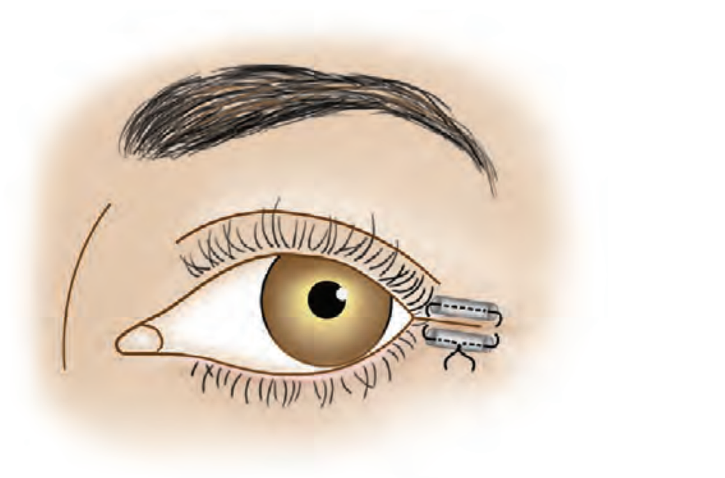

Figure 4.146 The suture is pulled snugly and tied over the lower booty.

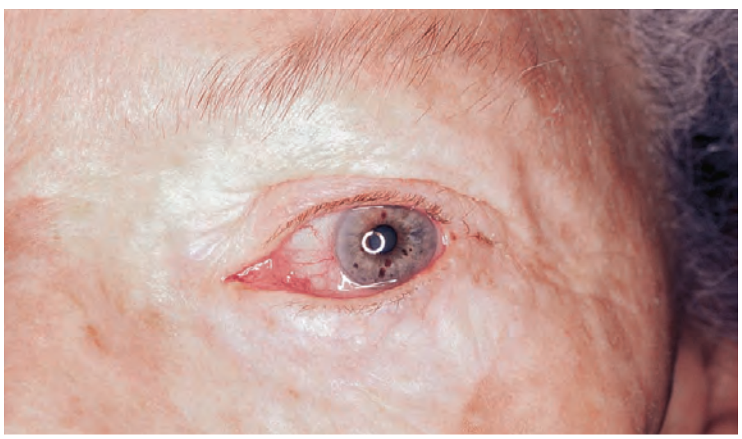

Figure 4.147 The postoperative appearance of a patient with a lateral tarsorrhaphy.

Lateral Canthoplasty. In elderly patients with significant ectropion leading to eversion of the lower eyelid, excess laxity, and epiphora, significant conjunctivitis often develops as a result of irritation of the everted lower eyelid. A lateral canthoplasty provides adequate tightening of the lower eyelid and inversion of the everted eyelid and restores satisfactory drainage of the tears into the lacrimal collecting system from the lower fornix. The operative procedure is done under local anesthesia. A common way to correct this problem is with a lateral tarsal strip. An alternative method is as follows: a wedge of the full thickness of the lower eyelid is resected at its lateral end (Fig. 4.148). The appropriate length of the lower eyelid margin to be resected should be checked to achieve satisfactory inversion and closure of the palpebral fissure upon repair. Following full-thickness wedge resection, complete hemostasis is secured. A 4-0 Vicryl suture is used to approximate the cut edge of the transected tarsal plate to the lateral canthal ligament and through the periosteum of the lateral margin of the orbit to achieve suspension and restoration of the lateral canthus (Fig. 4.149). Once this suture is applied, the remaining wound is closed in two layers using 6-0 plain catgut sutures for the conjunctiva and 6-0 nylon for the skin.

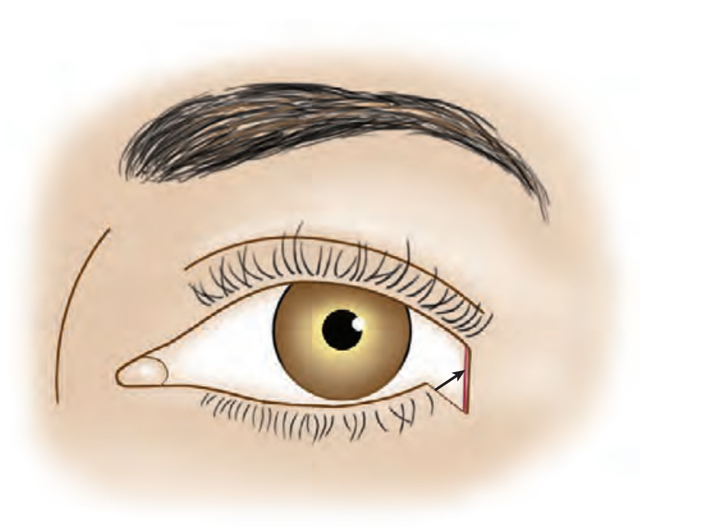

Figure 4.148 A full-thickness wedge of the lower eyelid is resected with its lateral end at the lateral canthus.

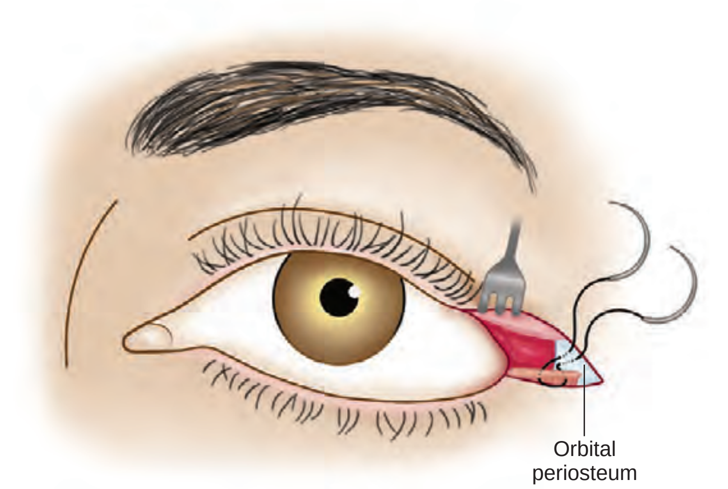

Figure 4.149 The cut edge of the tarsal plate is sutured to the lateral canthus and the periosteum of the orbit.

Nasolacrimal Duct Stent for Obstruction

Stenosis of the nasolacrimal duct often is encountered after surgical resection of malignant tumors of the maxillary antrum, the lateral wall of the nasal cavity, and the ethmoid complex. Patients who experience stenosis of the nasolacrimal duct as a result of fibrosis in the nasal cavity experience epiphora, and dacryocystitis also may develop as a result of obstruction and infection in the lacrimal sac. Repair of the stenosed duct may require cannulation, dilation, and placement of a stent. Stent placement may be performed at the time of surgery to maintain patency of the nasolacrimal drainage system. Some patients are asymptomatic despite a stenosed system, and these patients can be observed.

Cannulation of the nasolacrimal duct and placement of the stent are performed under general anesthesia. The anatomy of the nasolacrimal duct system is shown in Fig. 4.150. The stent is a fine, soft nylon tube with wirelike probes at each end of the stent to facilitate cannulation of the collecting duct system through the upper and lower punctum. The stent should be inserted in a gentle and meticulous fashion, because excessive force or rough manipulation may result in a false passage. The probes are inserted along the expected direction of the upper and lower lacrimal ducts into the lacrimal sac and then into the nasal cavity through the stump of the nasolacrimal duct in the nasolacrimal fossa at the inferior medial quadrant of the orbit. The probe is observed coming out of the stump of

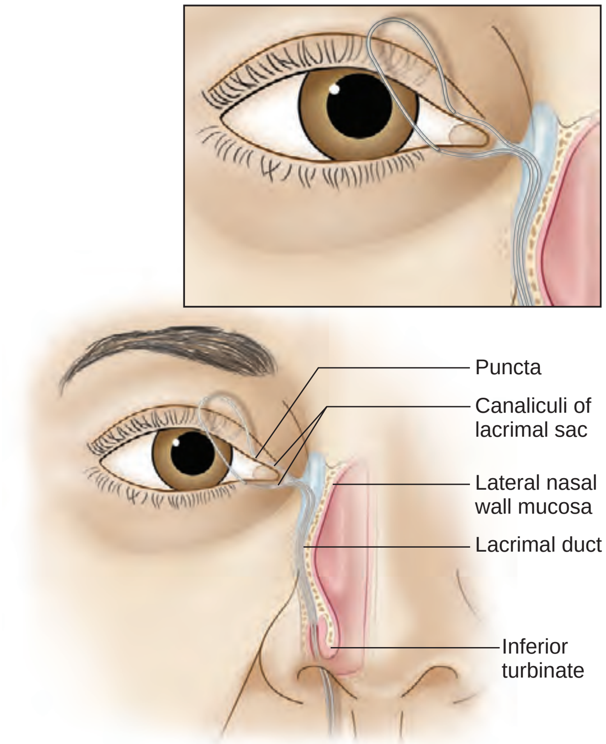

Figure 4.150 The anatomy of the nasolacrimal duct system and a schematic representation showing insertion of a stent.

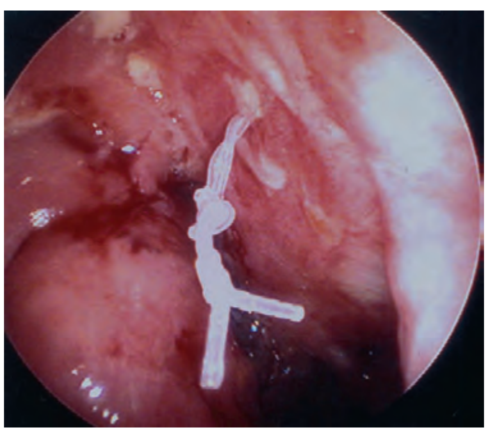

Figure 4.151 An endoscopic view of the nasal cavity showing the ends of the stent tied together.

the nasolacrimal duct in the nasal cavity. Both the upper and lower probes are retrieved in the nasal cavity, and the stent is pulled snug without excessive pressure on the punctum. If the procedure is done secondarily for stenosis, then a nasal endoscope would be required to retrieve the lower ends of the stent in the nasal cavity. The probes are detached and the two ends of the stent are tied to each other with multiple knots to prevent extrusion. The ends are cut short so the knotted ends of the stent remain high in the nasal cavity. An endoscopic view

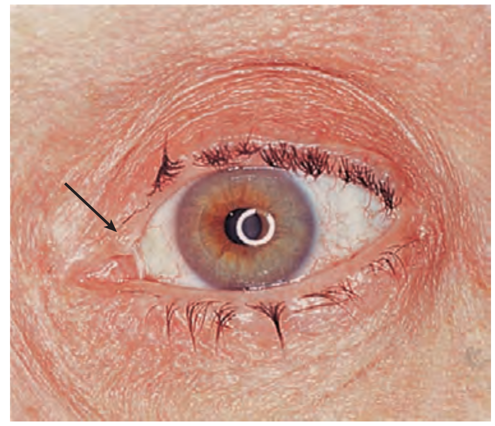

Figure 4.152 The postoperative appearance of the patient showing the stent looping across the upper and lower puncta at the medial canthus (*arrow*).

of the ends of the nasolacrimal stent tied together is shown in Fig. 4.151. The postoperative appearance of the patient shows the presence of the stent at the medial canthus in the upper and lower puncta of the left eye (Fig. 4.152). The stent provides satisfactory drainage of tears through the nasolacrimal collecting system and prevents recurrent stenosis of the nasolacrimal duct.

POSTOPERATIVE CARE AND COMPLICATIONS

Postoperative care for patients undergoing surgery for lesions of the eyelid and orbit is relatively simple. Local wound care demands most of the attention, with prevention of crusting of dried blood and serum over the suture line. Meticulous cleaning of the suture line and application of ophthalmic antibiotic ointment are generally satisfactory for wound care. Patients who have had a skin graft applied in the orbit after orbital exenteration need to take systemic antibiotics until the packing is removed. Patients who have undergone an orbitotomy for excision of orbital tumors need to be carefully observed for risk of orbital hemorrhage. Generally, these patients are given steroids to reduce orbital edema, proptosis, and compromise of vision. Any progressive swelling and proptosis should be promptly investigated with imaging studies and treated with prompt orbital decompression if warranted. Similarly, orbital cellulitis resulting from sepsis after an orbitotomy is rare but may require urgent intervention with intravenous antibiotics and orbital decompression if progressive intraorbital tension and proptosis are noted. Orbital abscess resulting from orbital cellulitis is a surgical emergency, because visual loss can occur rapidly. Finally, patients who have undergone an orbitectomy with exposure of the dura at the base of the skull are at risk of cerebrospinal fluid (CSF) leakage, which requires appropriate attention. If CSF leakage is noted, then appropriate immediate intervention is necessary for repair of the CSF leak, either by exploration of the orbit or by a craniotomy.

CHAPTER 5

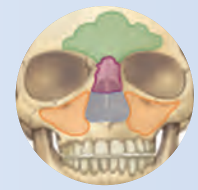

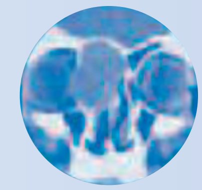

Nasal Cavity and Paranasal Sinuses

Malignancies of the sinonasal tract are rare. They account for less than 10% of head and neck cancers, with an annual incidence of 0.5 to 1.0 per 100,000 people in the United States. The nasal cavity is by far the most common site for neoplasia of epithelial origin arising in this region, followed by the maxillary antrum and ethmoid air cells. Tumors of the frontal and sphenoid sinuses are exceedingly rare. However, the exact site of origin of many advanced tumors often is difficult to ascertain because of the anatomic contiguity of the paranasal sinuses and because a significant number of tumors may involve more than one site at the time of initial diagnosis. The distribution of primary tumors of the nasal cavity and paranasal sinuses is shown in Fig. 5.1.

More than 80% of neoplasms arising in this region are of epithelial origin, and the remainder arise from the bone cartilage and soft tissues. Approximately 25% of all sinonasal tumors are benign. Benign epithelial neoplasms include squamous papillomas, inverted papillomas, adenomas, and other rare lesions. Squamous cell carcinoma is the most common malignant tumor, followed by carcinomas of minor salivary gland origin (adenocarcinoma, adenoid cystic carcinoma, and mucoepidermoid carcinoma), melanoma, and esthesioneuroblastomas. Although they are rare, a wide variety of mesenchymal tumors can arise in the sinonasal cavity, including benign lesions such as osteoma, ossifying fibroma, fibromyxoma, and angiofibroma; malignant lesions such as chondrosarcoma and osteogenic sarcoma; and, less commonly, soft-tissue sarcomas. The histologic distribution of malignant epithelial tumors of the nasal cavity and paranasal sinuses is shown in Fig. 5.2.

As with the remainder of the upper aerodigestive tract, smoking is a predisposing factor for the development of sinonasal squamous cell carcinomas. Moreover, squamous cell carcinomas may also develop from preexisting inverting papillomas in up to 10% of cases. Other etiologic factors for sinonasal malignant tumors include exposure to wood dust, nickel, and possibly chemicals used in leather processing, although the precise carcinogens have not yet been identified. Transcriptionally active high-risk human papillomavirus (HPV) has more recently been detected in a significant proportion (25%) of patients with sinonasal squamous cell carcinoma, more commonly in nonkeratinizing carcinomas. Similar to other sites, HPV-associated cancers have a favorable prognosis.

EVALUATION

Because the paranasal sinuses are air-filled structures with significant potential space, sinonasal neoplasms rarely produce symptoms at an early stage. Sinonasal tumors may be discovered incidentally on radiographic imaging performed for other reasons, or during surgery for presumptive inflammatory sinus disease. Symptoms usually develop as a result of obstruction of the involved sinus or nasal cavity or when the tumor breaks through the walls of the involved sinus and produces symptoms relating to the local invasion of adjacent tissues or bleeding (epistaxis). Thus the majority of patients present with advanced stage tumors (Fig. 5.3). Even when symptoms from sinonasal tumors are present, they may be interpreted as innocuous, such as nasal obstruction, epistaxis, or symptoms of obstructive sinusitis, including facial pain and congestion. Accordingly, a high index of suspicion should be maintained, especially in older patients with unilateral symptoms. As tumors extend beyond the bony confines of the sinonasal tract, they can affect other structures and cause swelling or a mass in the hard palate, upper gum, gingivobuccal sulcus, or soft tissues of the cheek. Loose teeth, anesthesia of the skin of the cheek and upper lip, diplopia, and proptosis are signs of local extension of disease beyond the maxillary sinus. More advanced tumors may present with trismus consequent to extension into the masticator space with infiltration of the pterygoid muscles. Posteriorly based sinonasal tumors, especially those in the sphenoid sinus, may present with anesthesia in the distribution of the fifth cranial nerve or paralysis of the third, fourth, or sixth cranial nerves with associated eye symptoms or ophthalmoplegia. Anosmia is a common symptom in patients with esthesioneuroblastoma, but it can occur with any advanced tumor of the nasoethmoid complex.

Intranasal lesions, especially those in the inferior aspect of the nasal cavity, can be assessed in the office by anterior rhinoscopy or nasal endoscopy (Fig. 5.4). Nasal endoscopy may be performed with rigid 0-degree and 30-degree endoscopes or a flexible fiberoptic endoscope. Examples of endoscopic views of sinonasal lesions are shown in Figs. 5.5 through 5.10. A topical spray of 0.5% phenylephrine and 4% lidocaine generally provides good decongestion and topical anesthesia to allow adequate examination of the nasal cavity. Care must be exercised to avoid trauma and manipulation of the tumor to prevent bleeding. It is important to keep in mind that tumors causing sinonasal obstruction can induce inflammatory, polyp-like changes in the mucosa of the nasal cavity. Consequently, endoscopic evaluation alone is not sufficient to define the nature and extent of a sinonasal tumor. Radiographic imaging is essential for all patients suspected of having a neoplasm of the nasal cavity or paranasal sinuses.

Radiographic Evaluation

A noncontrast sinus computed tomography (CT) scan is usually the initial examination obtained, because most patients present

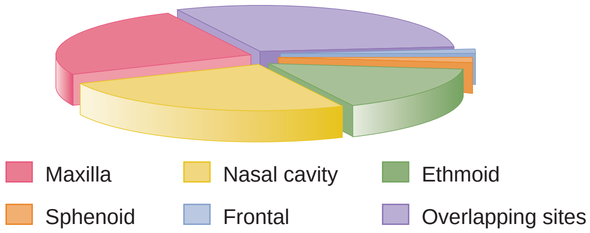

Figure 5.1 The distribution of various sites for primary tumors of the nasal cavity and paranasal sinuses.

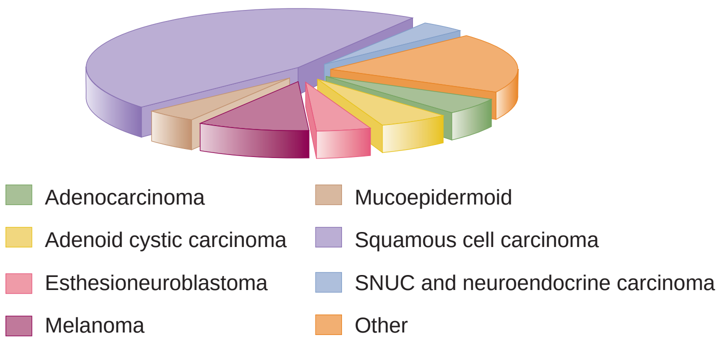

Figure 5.2 The distribution of malignant epithelial tumors of the nasal cavity and paranasal sinuses. *SNUC,* Sinonasal undifferentiated carcinoma.

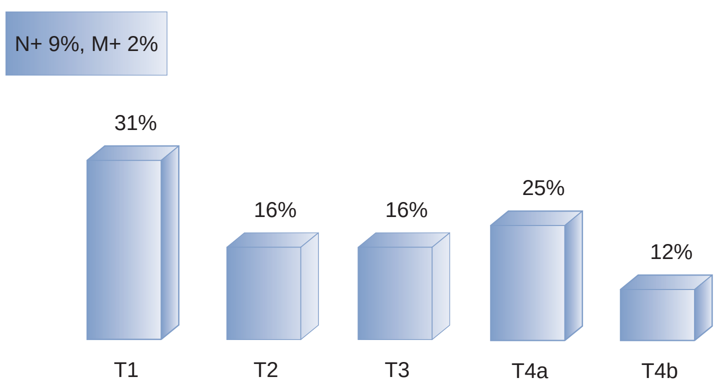

Figure 5.3 Distribution of the stages of squamous cell carcinoma of the maxilla at the time of diagnosis in the United States (National Cancer Database, USA, 2003–2012).

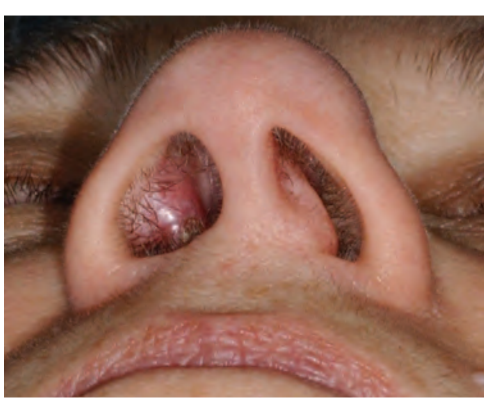

Figure 5.4 Squamous cell carcinoma of the nasal vestibule.

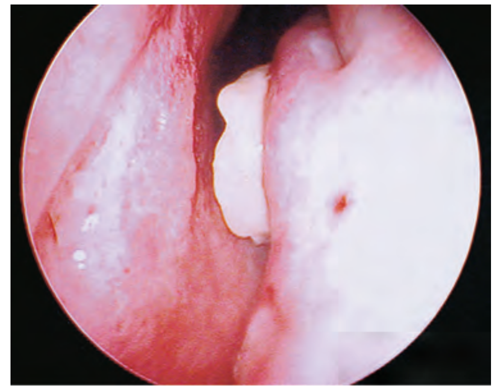

Figure 5.5 Sinonasal benign polyp at the middle meatus.

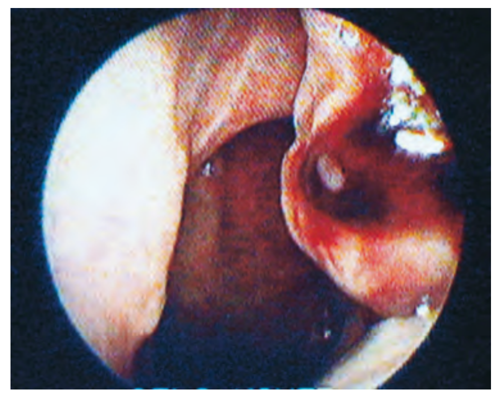

Figure 5.6 Adenocarcinoma of the lateral wall of the nasal cavity.

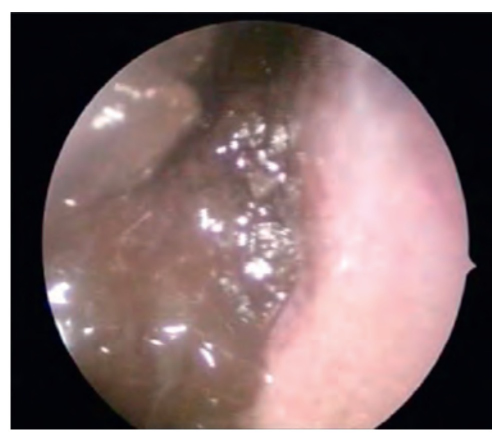

Figure 5.7 Mucosal melanoma of the ethmoid.

with nonspecific sinonasal symptoms. Although this study may raise suspicion for a tumor, it is not optimal for accurate assessment of the anatomic extent of the tumor. Further options for radiographic workup include contrast-enhanced CT and magnetic resonance imaging (MRI) of the sinuses. The important features in the assessment of sinonasal tumors are the extent of soft tissue and bone invasion, orbital and intracranial extension, and perineural invasion. CT and MRI have strengths and weaknesses that complement each other in defining the precise extent of the tumor (Box 5.1).

Modern multidetector CT scanners allow fast acquisition of data that can then be reconstructed in axial, coronal, or sagittal planes. CT is better for evaluating bone changes, including expansion, remodeling, and erosion or destruction. Bone destruction is more commonly associated with aggressive malignant tumors (Fig. 5.11). In general, tumors that cause poorly defined, destructive changes are squamous cell carcinoma, esthesioneuroblastoma, sinonasal undifferentiated carcinoma, adenocarcinoma, lymphoma, and metastatic lesions. On the other hand, regressive remodeling of adjacent bone suggests the diagnosis of benign tumors such as inverted papilloma, schwannoma, pleomorphic adenoma, and juvenile nasopharyngeal angiofibroma but can also include low-grade minor salivary gland

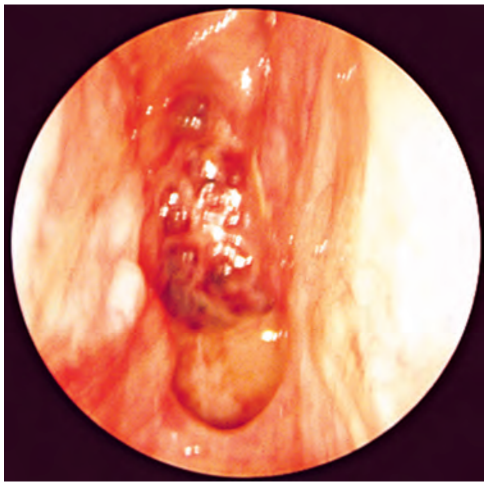

Figure 5.8 Adenoid cystic carcinoma of the ethmoid.

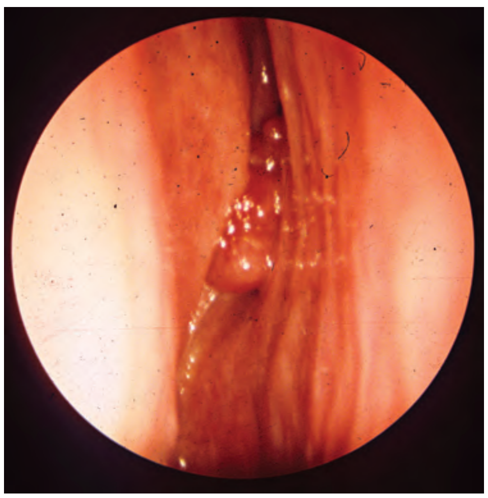

Figure 5.9 An esthesioneuroblastoma.

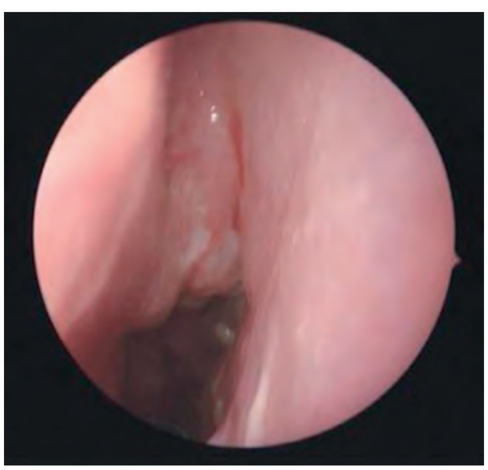

Figure 5.10 Endoscopic view of hemangiopericytoma of the ethmoid.

carcinomas, melanoma, and lymphoma (Fig. 5.12). The presence of calcification is a feature often associated with esthesioneuroblastomas (Fig. 5.13). Tumors of cartilage and bone origin exhibit cartilaginous or bony matrix (Fig. 5.14). These radiographic features can help in narrowing the differential diagnosis of a tumor. In addition, three-dimensional reconstructions of CT scans can assist in surgical treatment planning for complex lesions that involve the skull base and for planning of reconstructive surgery or a maxillofacial prosthesis (Fig. 5.15).

Box 5.1 Advantages of Evaluation of Sinonasal Neoplasms With Computed Tomography and Magnetic Resonance Imaging

- Advantages of computed tomography
  - Better delineation of bony changes: expansion, remodeling, erosion
  - Bony or cartilaginous matrix
  - Calcifications
- Advantages of magnetic resonance imaging
  - Better tumor delineation relative to adjacent tissue
  - Tumor versus inflammatory change
  - Orbital and/or intracranial extension
  - Perineural spread

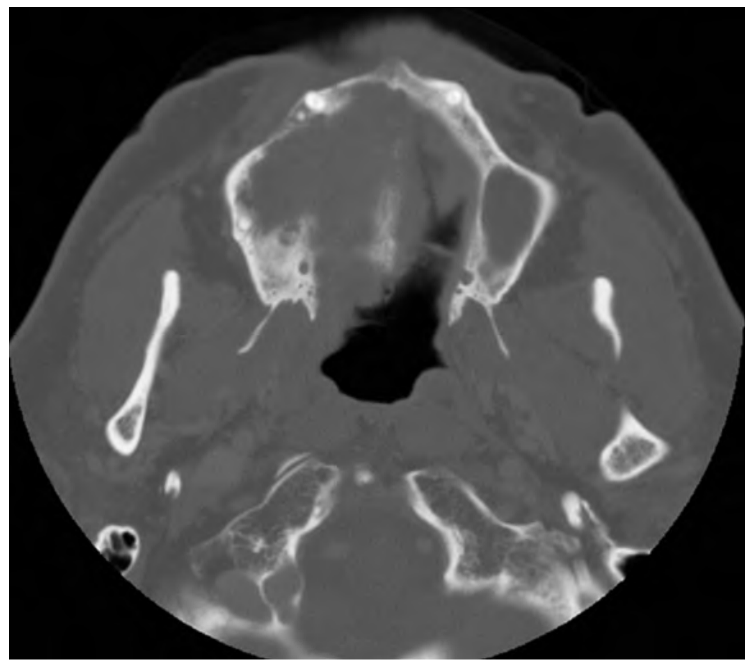

Figure 5.11 Computed tomography showing erosion of the right maxillary sinus and upper alveolus as a result of squamous cell carcinoma.

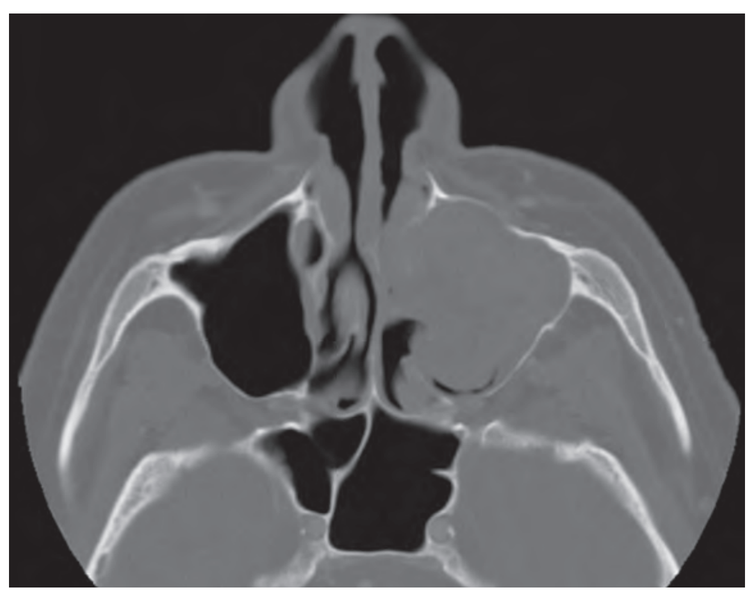

Figure 5.12 Computed tomography showing expansion and remodeling of bone around a left maxillary sinus tumor.

Figure 5.13 Intratumoral calcification in a right nasal cavity tumor, which is characteristic of an esthesioneuroblastoma.

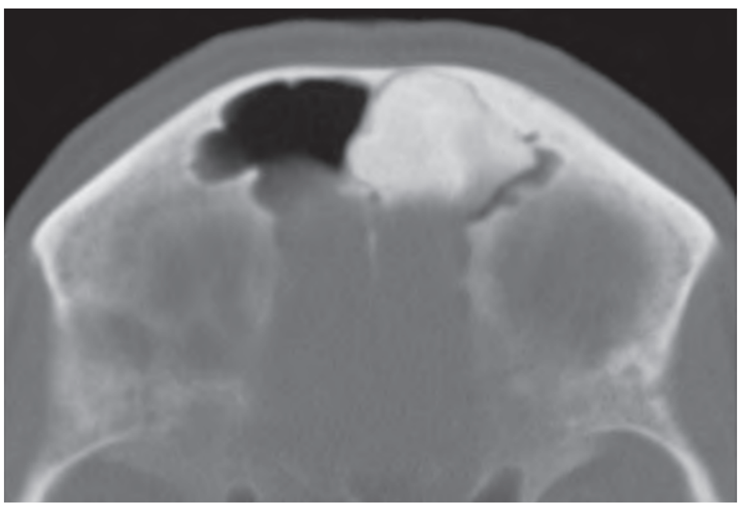

Figure 5.14 Computed tomography showing the classic appearance of an osteoma in the left frontal sinus with bony matrix.

Figure 5.15 Three-dimensional reconstruction of a computed tomography scan showing the extent of bone destruction on the anterior wall of the maxilla on the right-hand side.

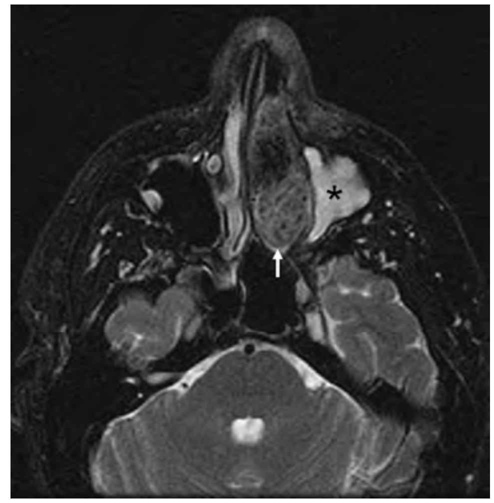

Figure 5.16 An axial T2-weighted magnetic resonance imaging of a left nasal cavity esthesioneuroblastoma (*arrow*) demonstrating high-signal postobstructive change in the left maxillary sinus (*).

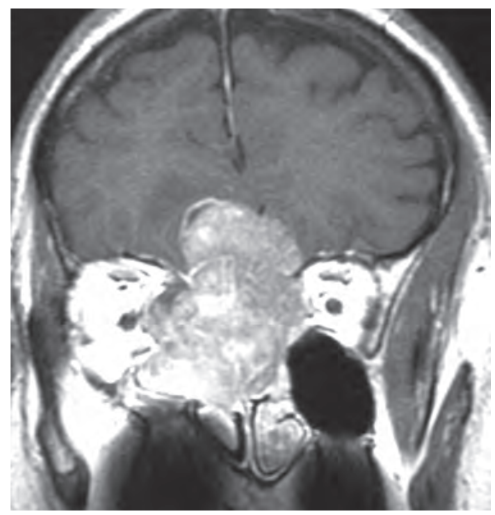

Figure 5.17 A large sinonasal tumor with extension into the anterior cranial fossa and bilateral orbits as seen on postcontrast coronal T1-weighted magnetic resonance imaging.

MRI is most advantageous in delineating a tumor relative to adjacent normal soft tissue. Most tumors are low to intermediate signal on T1-weighted MRI and intermediate on T2-weighted MRI; they enhance only moderately because they are highly cellular with little water content. On the other hand, some minor salivary gland tumors, schwannomas, and inverted papillomas have a higher water content and a characteristic bright T2-weighted signal. Most bones around the sinuses, with the exception of the hard palate, do not contain enough marrow for MRI to resolve tumor involvement. A CT scan easily demonstrates bone erosion or destruction. Obstruction of a sinus cavity by a tumor and the extent of postobstructive mucosal changes can be difficult to delineate accurately on noncontrast CT. Contrast-enhanced CT generally can differentiate a tumor from postobstructive inflammatory change. However, MRI clearly delineates a tumor from inflammatory change because of obvious differences in signal intensity between these two entities on all sequences. In particular, postobstructive change is typically very bright on T2-weighted MRI (Fig. 5.16). MRI is superior to CT in demonstrating orbital and intracranial extension (Fig. 5.17). Perineural spread of disease is better defined on MRI (Fig. 5.18). Encroachment or invasion of normal fat in locations such as the orbit, pterygopalatine fossa, pterygomaxillary fissure,

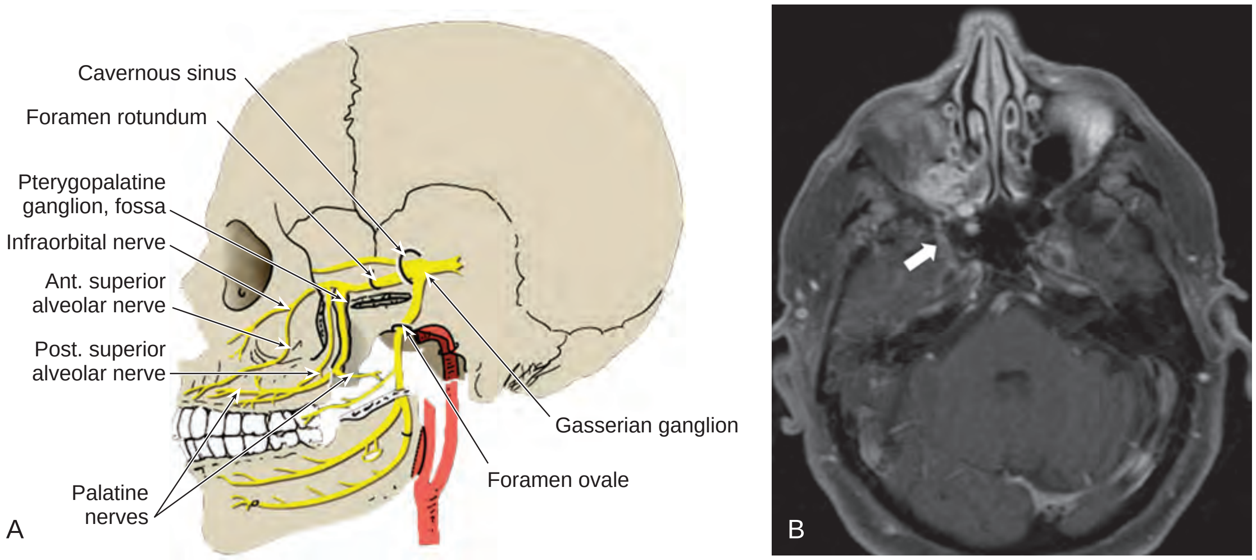

Figure 5.18 Perineural spread. **A**, Schematic representation of the anatomic course of the branches of the trigeminal nerve. **B**, Perineural spread of an adenoid cystic carcinoma of the right maxillary sinus along right V2 is seen as an abnormally enhancing and thickened nerve (*arrow*) on postcontrast fat-saturated axial T1 magnetic resonance imaging.

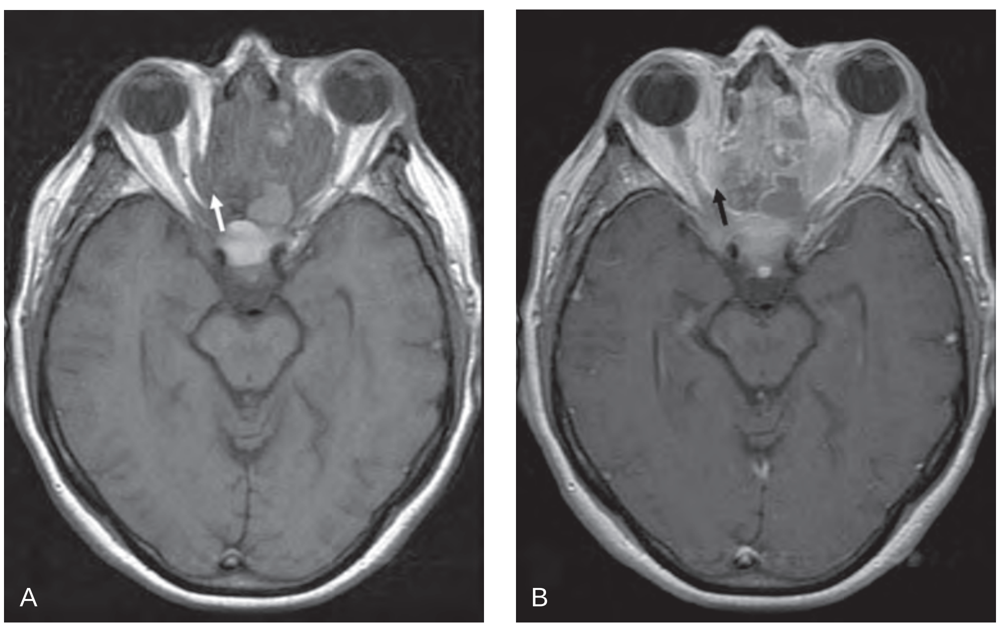

Figure 5.19 A large sinonasal tumor with bilateral intraorbital extension, on the left more than the right. Precontrast T1-weighted magnetic resonance imaging (MRI) shows obliteration of the fat plane (*white arrow*) between the medial rectus muscle and the tumor, indicating early intraorbital extension (**A**). This finding could be easily overlooked on the postcontrast T1-weighted MRI sequence without fat suppression (**B**) (*black arrow*).

or premaxillary region is easily detected on precontrast T1-weighted MRI because fat is bright while most tumors are darker. After the contrast is administered, fat tends to blend with adjacent enhancing tumor, and therefore fat suppression techniques must be used in postcontrast MRI (Fig. 5.19). The different information gained from CT and MRI is exemplified in a patient with a 10-year history of a slowly enlarging low-grade mucoepidermoid carcinoma of minor salivary origin in the hard palate. Axial, coronal, and sagittal views of the noncontrast CT scan shows a bone-destructive lesion of the hard palate and upper alveolus extending into the maxillary sinus with expansion of the maxillary antrum (Fig. 5.20A through C). Axial and coronal views of the T2-weighted images show that the content of the maxillary sinus is bright, indicating that it is fluid, secondary to an obstructive inflammatory process (Fig. 5.20D and E). A postcontrast T1-weighted image in the coronal plane shows that the lesion is confined to the hard palate and upper alveolus with clear demarcation of tissue planes from the maxillary antrum (Fig. 5.20F). The expanded maxillary sinus is filled with soft tissue and shows no contrast enhancement. On the axial and sagittal views, some air is seen in the anterior aspect of the antrum. Thus both CT and MRI in this case helped in arriving at an accurate diagnosis and facilitated treatment planning.

In contrast to CT and MRI, 18F-fluorodeoxyglucose–positron emission tomography (FDG-PET) scan generally does not play an important role in the initial local assessment of sinonasal tumors. However, PET/CT is useful for assessment of regional and distant disease (Fig. 5.21). In addition, it is particularly useful in posttreatment surveillance to diagnose viable tumors, as shown in Fig. 5.22. Further, PET scan can also draw attention to FDG-avid lesions, which when confirmed by contrast-enhanced CT scans would be considered for biopsy. The patient whose posttreatment surveillance PET scan is shown here had

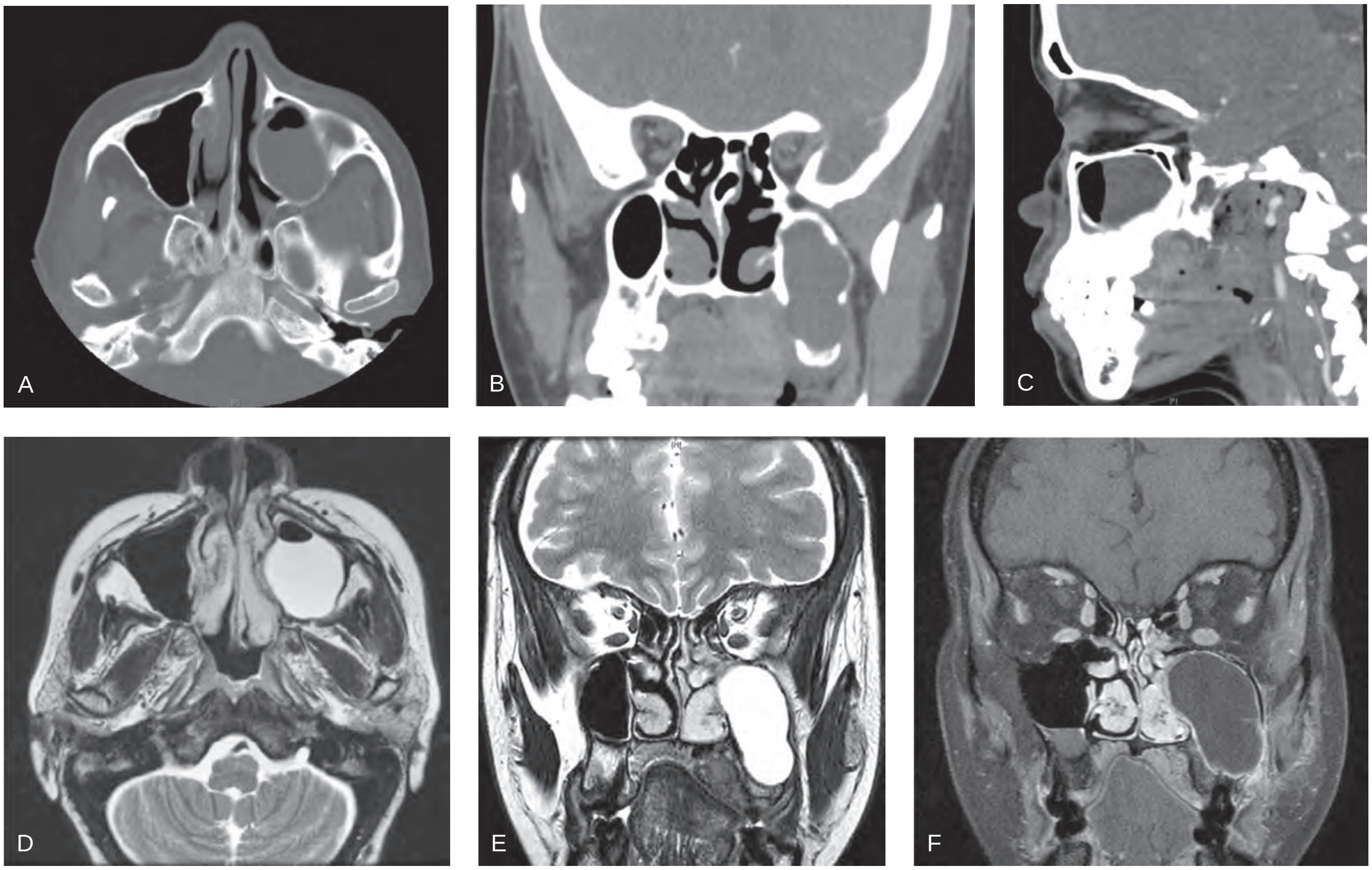

Figure 5.20 Noncontrast computed tomography (CT) and magnetic resonance imaging (MRI) of a patient with minor salivary gland carcinoma of the hard palate. Axial (**A**), coronal (**B**), and sagittal (**C**) views of the CT scan show a bone-destructive lesion of the hard palate and upper alveolus, contiguous with a mass expanding the maxillary sinus. T2-weighted MRI images in axial (**D**) and coronal (**E**) views show a bright white mass in the maxillary sinus indicating fluid without any signal characteristics of the palatal tumor. Postcontrast T1-weighted coronal view (**F**) of the MRI shows enhancement in the tumor of the palate with no contrast enhancement in the maxillary sinus.

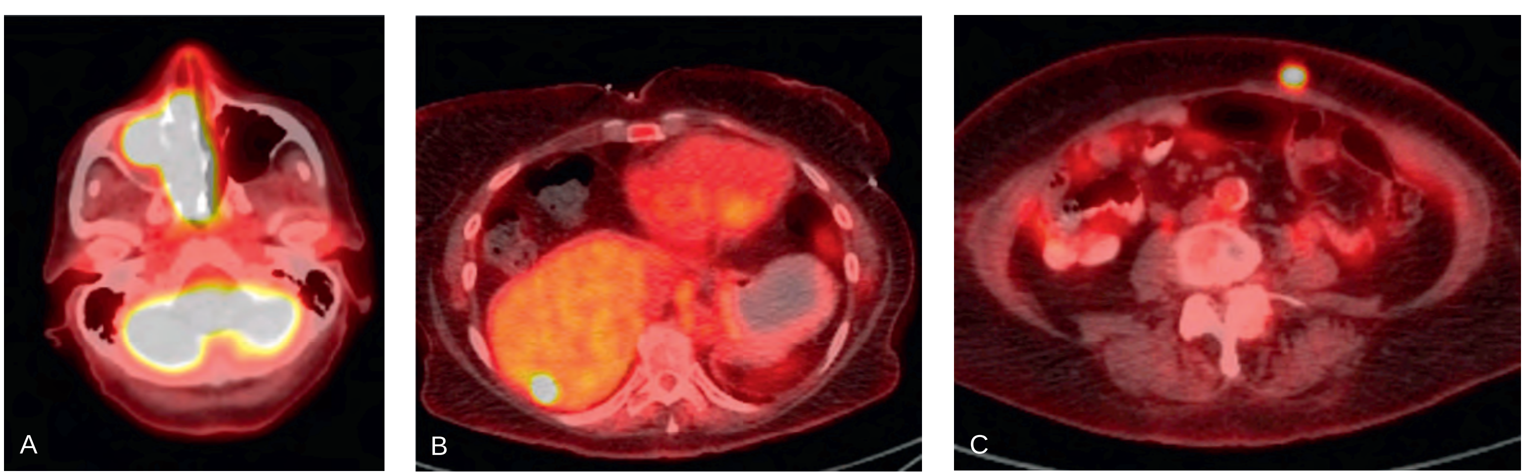

Figure 5.21 An FDG whole-body positron emission tomography (PET) scan of a patient with carcinoma of the nasopharynx showing intense FDG activity at the primary site (**A**) and distant metastases in the liver (**B**), and soft tissue of the anterior abdominal wall (**C**).

previously undergone treatment of nasopharyngeal carcinoma. The PET scan showed an FDG-avid hotspot on the left lateral wall of the nasopharynx (Fig. 5.23A). Contrast-enhanced CT scan in axial and coronal views showed a rim-enhancing lesion (Fig. 5.23B and C). These findings facilitated a precise biopsy of the lesion under CT-guided navigation (Fig. 5.23D). The biopsy in this patient showed an abscess from radiation necrosis.

Biopsy

Tissue diagnosis of a lesion of the nasal cavity or paranasal sinuses is required before undertaking definitive treatment, except in selected circumstances in which radiologic characteristics may be sufficient to establish the diagnosis (e.g., angiofibroma). The approach to the biopsy of a sinonasal tumor is dictated by the anatomic location and radiologic characteristics. For lesions that are visible through the nasal cavity or oral cavity, a simple punch

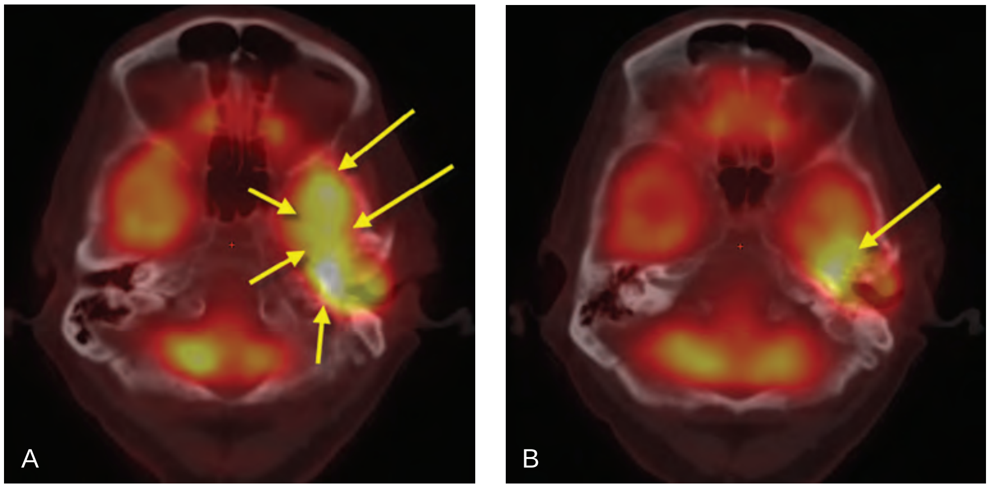

Figure 5.22 A positron emission tomography (PET) scan showing a FDG-avid left-sided lesion before chemoradiation treatment (**A**), and decreased FDG activity 8 weeks after completion of treatment (**B**).

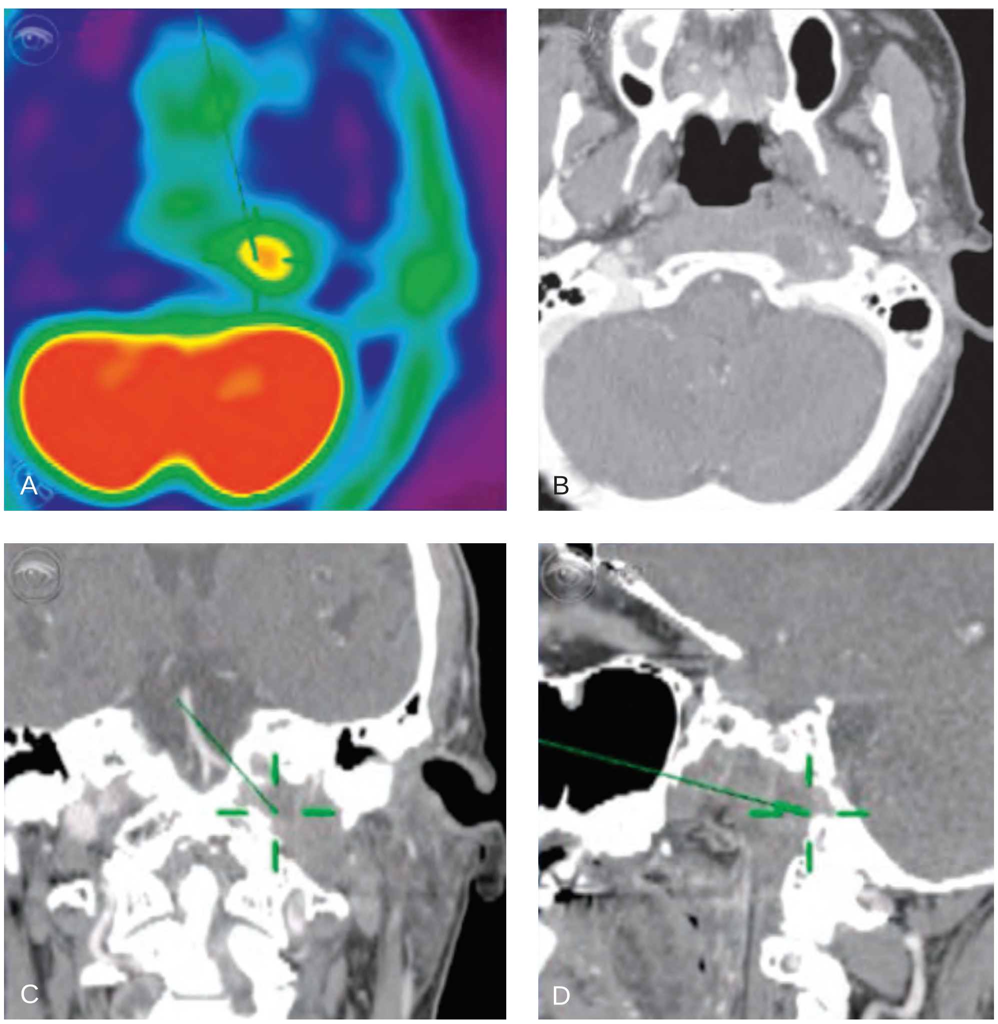

Figure 5.23 A posttreatment surveillance positron emission tomography (PET) scan in a patient with a history of nasopharyngeal carcinoma showed an FDG-avid lesion in the left lateral nasopharynx (**A**). Contrast-enhanced computed tomography (CT) showed a rim-enhancing lesion at that site (**B** and **C**). CT-guided navigation allowed an accurate biopsy at that site (**D**).

biopsy may be sufficient to establish tissue diagnosis. Transnasal biopsies should be performed in an environment with appropriate instrumentation and support, in case of unexpected bleeding. The approach to the biopsy of tumors that are not readily accessible for transnasal or transoral biopsy, such as those in the maxillary antrum, the posterior and/or superior aspect of the nasal cavity, the frontal sinus, or the infratemporal fossa, should not entail approaches that violate subsequent surgical planes. For example, a Caldwell-Luc antrotomy should be avoided, because it would contaminate the soft tissues of the cheek if it was used to obtain a biopsy specimen of a malignant tumor of the maxillary antrum, making a curative resection more complicated. In experienced hands, most nasal cavity lesions can be biopsied in the office with a straight or angled endoscope and Blakesley forceps after topical anesthesia is applied. Hemostasis is attained through direct pressure and vasoconstrictor sprays. In cases in which the

patient is unable to tolerate this biopsy under local anesthesia, the clinic has inadequate equipment, or there are concerns about a fragile tumor, transnasal endoscopy with biopsy under sedation or general anesthesia should be considered. Before embarking on in-office biopsy, it is critical to ensure that the sinonasal lesion is not an encephalocele or a primary vascular tumor. In addition, surgical biopsy under general anesthesia has the benefit of the ability to use navigation systems that provide image guidance with CT, MRI, or PET-fused images, in order to allow precise localization of tumors that are in close proximity to vital structures (see Fig. 5.23). This renders biopsy safe and accurate. This would not be possible without help from intraoperative navigation. Finally, for tissue diagnosis for otherwise inaccessible sinonasal tumors or tumors of the infratemporal fossa, a CT-guided needle biopsy should be considered.

BENIGN NEOPLASMS

A wide variety of benign neoplasms arise in the sinonasal tract. The most common benign neoplasm, the sinonasal papilloma, originates from well-differentiated ciliated columnar or respiratory epithelium with varying degrees of squamous differentiation. Papillomas can be categorized into three broad categories—exophytic, oncocytic, and inverted—or they can be categorized collectively as Schneiderian papillomas. Exophytic papillomas predominantly arise from the nasal septum (Fig. 5.24). On the other hand, columnar cell and inverted papillomas most commonly arise from the lateral nasal wall of the nasal cavity or in the maxillary sinus (Fig. 5.25). Exophytic and oncocytic papillomas are easily treated with conservative, endoscopic surgical excision. Conversely, inverted papillomas have an endophytic, infiltrative growth pattern that can cause destruction of adjacent tissue and may not be suitable for endoscopic excision, because they have a high tendency for recurrence after conservative surgical excision. Moreover, about 10% of inverted papillomas undergo malignant transformation into squamous cell carcinoma. Malignant degeneration is usually detected at the time of initial presentation, but it can also occur metachronously in up to one-third of cases.

The relationship between inverted papillomas and HPV is controversial, with studies showing variable expression of HPV in these tumors. Recent studies suggest a higher prevalence of HPV in inverted papillomas but with low transcriptional activity. Most inverted papillomas lack nuclear features associated with viral integration, namely, nuclear inclusions. Histologically they are composed of hyperplastic epithelium, both the ciliated respiratory type and squamous. Up to 20% of inverted papillomas may show surface keratinization, and anywhere from 5% to 10% may show varying degrees of dysplasia. These two latter features, although not necessarily indicative of malignancy, should reinforce the need for thorough histologic evaluation of the lesion (Fig. 5.26). Recurrence does not correlate with the subsequent development of malignancy. When malignancy does occur, it most frequently manifests in the form of squamous cell carcinoma; however, verrucous carcinoma, mucoepidermoid carcinoma, spindle cell carcinoma, and clear cell carcinoma also may be seen. Wide surgical resection is the mainstay of treatment for inverted papillomas and can be performed endoscopically or by an open approach based on the extent and

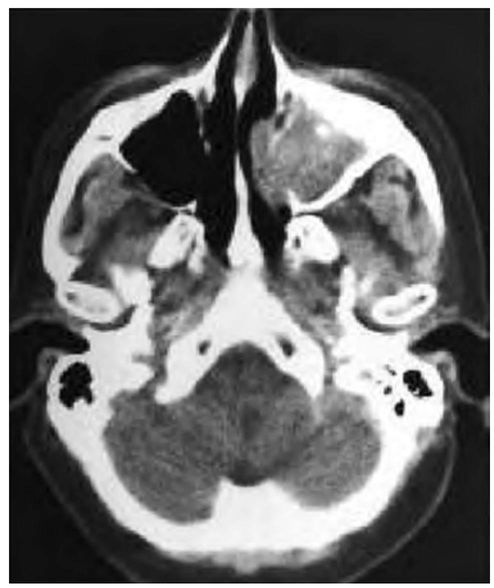

Figure 5.25 Axial view of a contrast-enhanced computed tomography scan of the sinuses showing an inverted papilloma involving the lateral wall of the nasal cavity and left maxillary sinus.

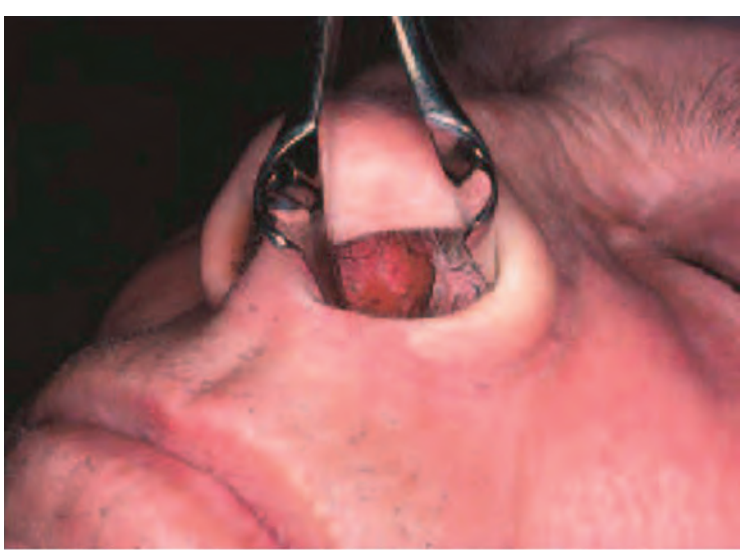

Figure 5.24 Squamous papilloma of the nasal septum.

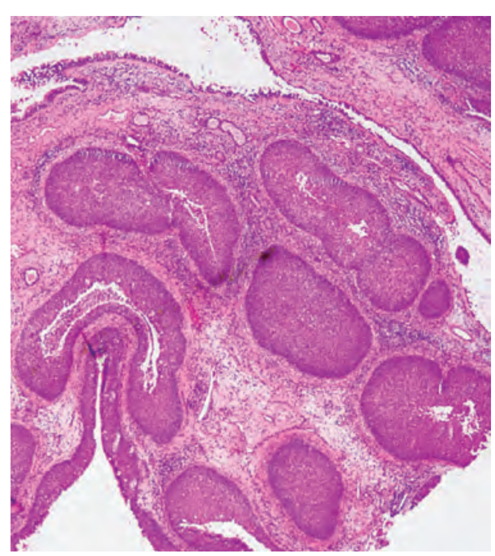

Figure 5.26 The histomicrographic appearance of an inverted papilloma of the lateral nasal wall (hematoxylin and eosin ×40).

location of the tumor. Long-term follow-up is recommended, given the possibility for late failure.

Juvenile nasopharyngeal angiofibromas (JNAs) are tumors that most commonly arise in adolescent boys. A JNA typically arises submucosally in the posterolateral nasal wall, posterior to the sphenopalatine foramen. Although the cell of origin for this neoplasm is still under debate (i.e., whether these tumors are derived from stromal cells or are vascular in origin), data suggest that this complex pathogenesis involves androgenic hormones, angiogenic factors, and the adenomatous polyposis coli/β-catenin pathway. Epidemiologic observations showing spontaneous regression after puberty, combined with empirical and laboratory evidence of responsiveness to estrogen therapy, suggest that JNA may be hormonally regulated. In an age-matched population, JNAs are 25 times more common in patients with familial adenomatous polyposis. These tumors show a propensity toward expansion into adjacent structures, causing local mass effects. Diagnosis usually is made on the basis of patients' age and gender, clinical history of frank epistaxis, nasal endoscopic examination, and imaging studies. Grossly, JNAs are smooth, lobulated or multinodular pink-white masses that may show surface ulceration and distinct vascularization. The corresponding histology demonstrates a collagenous stroma with stellate cells and prominent thin-walled vascular channels that may be "staghorn" in appearance, similar to those seen in hemangiopericytomas (Fig. 5.27). These tumors are highly vascular, and thus biopsy is not recommended because of the risk of significant hemorrhage. The characteristic radiologic features of JNA include signal voids and strong postcontrast enhancement on MRI and CT scans. Surgical treatment is typically recommended with either an endoscopic or an open surgical approach to access the lesion. Preoperative embolization has been shown to decrease intraoperative bleeding. It clearly reduces vascularity of the tumor and minimizes intraoperative bleeding (Fig. 5.28). Radiation therapy has been shown to restrict growth and augment control as an adjuvant to surgery in selected cases. However, it is considered only in situations of massive unresectable tumors, or recurrent tumors in difficult locations, since there is the risk of long-term sequelae of radiation therapy in the young patient.

Other benign tumors of the sinonasal tract include those of epithelial origin (adenomas), mesenchymal origin (hemangiomas, fibromyxomas, and chondromas), and bony origin (osteomas, fibrous dysplasias, and ossifying fibromas). Most of these tumors can be diagnosed accurately on the basis of clinical and radiologic features, with biopsy required only in select situations.

Osteomas are bony lesions covered by mucosa that most commonly arise in the frontoethmoidal region. In general, they show slow and steady growth. Treatment is required only for symptomatic lesions or for a rapidly growing tumor that causes compression of vital structures or facial deformity. Patients with multiple osteomas should be carefully screened for Gardner's syndrome, an autosomal-dominant condition associated with a triad of colonic polyps that degenerate into malignancy, supernumerary teeth, other fibroosseous tumors and skeletal abnormalities.

Fibrous dysplasia primarily occurs in children and typically regresses at puberty. Although fibrous dysplasia can be deforming, it usually is not destructive. Radiologically these lesions are characterized by their "ground glass" appearance. The vast majority of these tumors are monostotic (>75%) but may involve the entire facial skeleton. The polyostotic form is associated with McCune-Albright syndrome, which also includes precocious puberty and café-au-lait spots. In general, because of the high propensity for spontaneous regression, surgical intervention is recommended only for symptomatic cases. Spontaneous regression is characterized by conversion of the classic ground glass

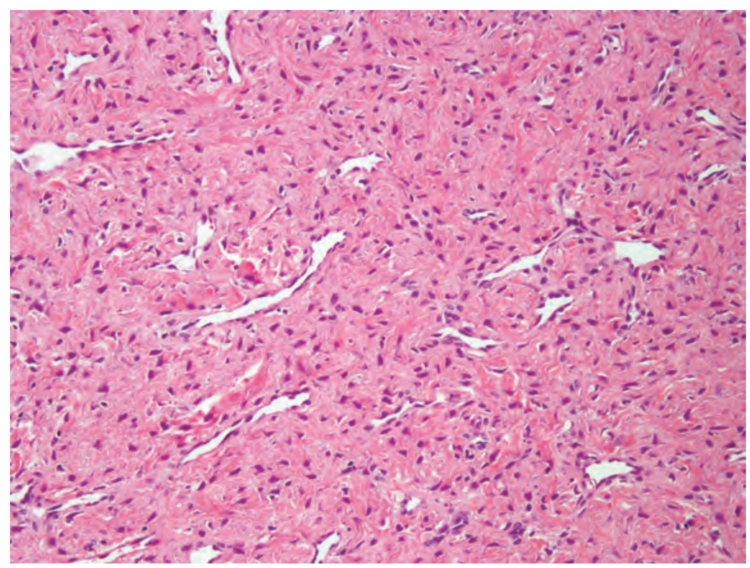

Figure 5.27 A histomicrograph of an angiofibroma composed of stellate tumor cells in a collagenous background containing abundant thin-walled vascular channels.

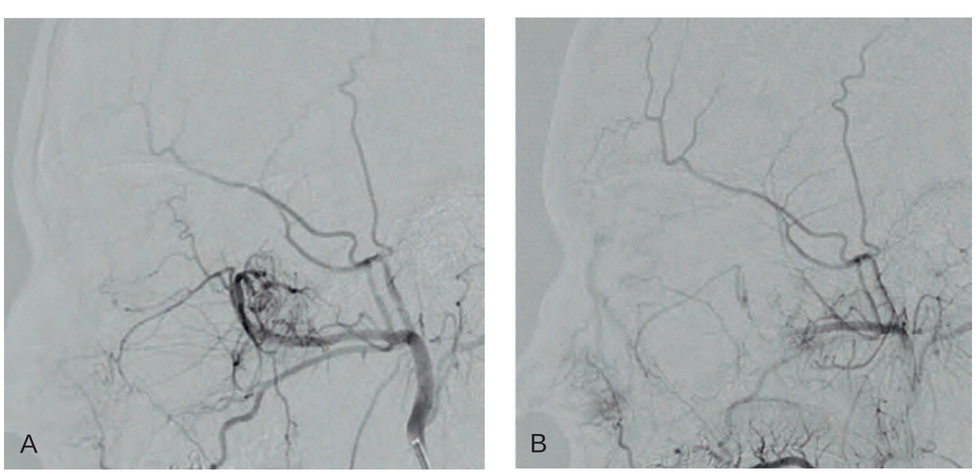

Figure 5.28 Selective external carotid angiogram showing a highly vascular tumor (**A**). Following successful embolization, most of the blood supply of the tumor is cut off (**B**).

radiographic appearance with hazy borders to a cotton wool–like appearance. Malignant degeneration is rare but can occur in the monostotic form. On the other hand, ossifying fibromas present as well-circumscribed lesions having a thin, eggshell-like bony wall and hypodense center. In contrast to other benign bone tumors, ossifying fibromas can be locally destructive, and therefore complete surgical excision is recommended.

MALIGNANT NEOPLASMS

Malignant tumors of the sinonasal region most commonly arise from the maxillary antrum, the lateral wall of the nasal cavity, the septum, and ethmoid air cells. Although primary tumors rarely arise from the sphenoid and frontal sinuses, their involvement, as well as that of the skull base, is not uncommon by contiguous disease extension from other paranasal sinuses. Symptoms such as obstruction, epistaxis, epiphora, headache, and diplopia develop late in the course of the disease, and therefore many patients present with an advanced stage at diagnosis. However, presenting symptoms depend on the anatomic site of the tumor.

Öhngren described an imaginary plane defined by a line joining the medial canthus of the eye to the angle of the mandible. This plane divides the region of the nasal cavity and maxillary antrum into two halves (Fig. 5.29). The anatomic region located anterior and inferior to this plane is called the *infrastructure,* and the region located posterosuperior to this plane is called the *suprastructure.* In patients with lesions arising from the infrastructure, symptoms generally develop early during the course of the disease, and tumors are readily amenable to a satisfactory surgical resection with an excellent chance for local control. On the other hand, in patients with lesions involving the suprastructure, symptoms develop late in the course of the disease. These tumors generally present with advanced disease and are technically difficult to resect because they often extend to the infratemporal fossa, pterygomaxillary fossa, orbit, skull base at the middle cranial fossa, and/or anterior cranial fossa. The potential for cure of these lesions is clearly less likely compared with tumors arising in the infrastructure.

Tumors of the infrastructure of the maxillary antrum may extend through the floor of the antrum into the oral cavity, through its medial wall into the nasal cavity, through its anterior wall to the soft tissues of the cheek, or through its lateral wall into the masticator space (Fig. 5.30). On the other hand, tumors of the suprastructure spread by local extension through the posterior wall of the antrum into the pterygomaxillary space, infratemporal fossa, and the middle cranial fossa; through the roof of the antrum into the orbit; or via the ethmoid air cells to the anterior cranial fossa. Primary malignant tumors of the nasal cavity may invade the hard palate, maxillary antrum, ethmoid air cells, or orbit by local extension (Fig. 5.31). Ethmoid tumors can extend to the sphenoid sinus, anterior cranial fossa, frontal sinus, orbits, nasal cavity, or nasopharynx or into the maxillary antrum (Fig. 5.32). Primary tumors of the frontal and sphenoid sinuses are uncommon and are generally less amenable for curative resection because of more frequent local spread into the cranial cavity with invasion of the dura and brain, cavernous sinus, or clivus (Fig. 5.33). Overall, dissemination to regional lymph nodes is relatively infrequent, occurring in less than 10% of all patients with malignant tumors of the paranasal sinuses.

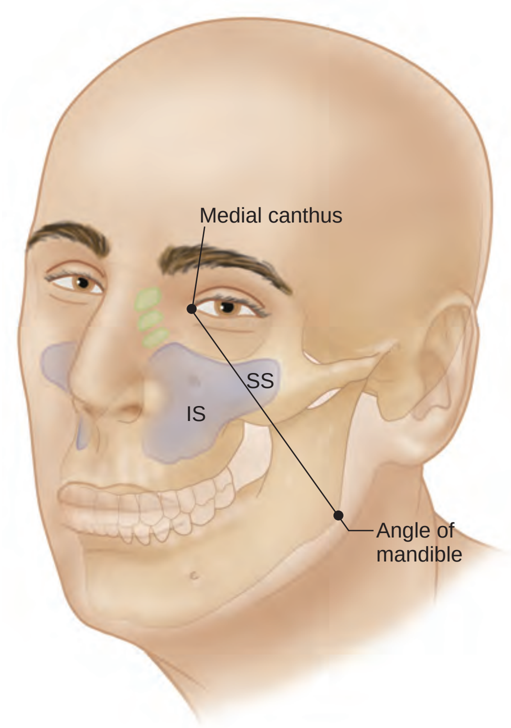

Figure 5.29 The plane described by Öhngren's line divides the region of the nasal cavity and maxillary antrum into infrastructure *(IS)* and suprastructure *(SS).*

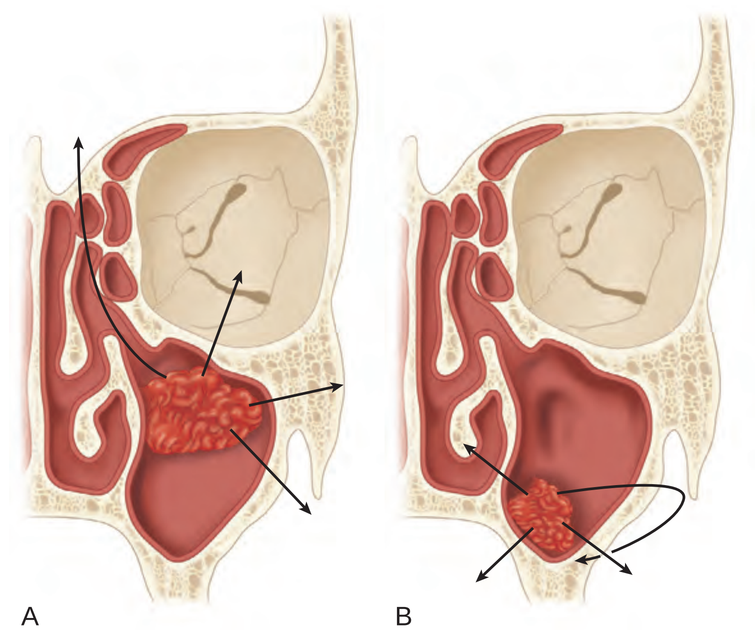

Figure 5.30 Routes of spread of tumors of the maxillary antrum. **A**, Suprastructure. **B**, Infrastructure.

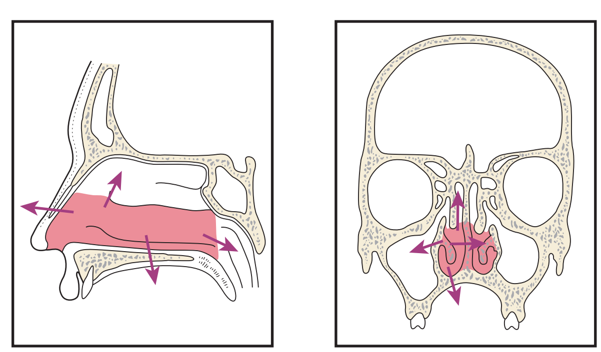

Figure 5.31 Routes of spread of tumors of the nasal cavity.

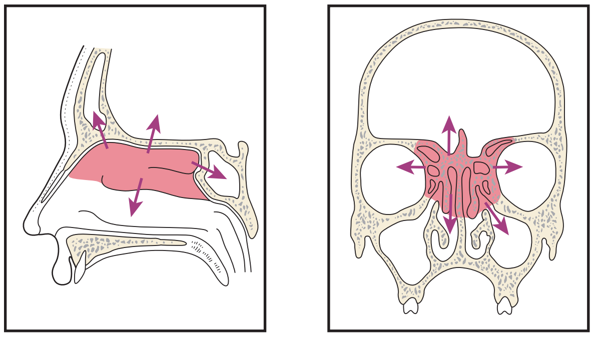

Figure 5.32 Routes of spread of tumors of the ethmoid cavity.

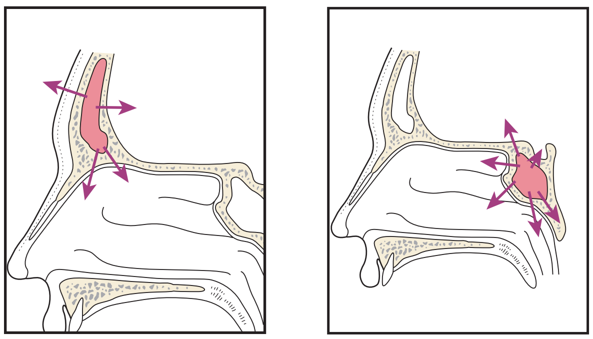

Figure 5.33 Routes of spread of tumors of the frontal and sphenoid sinuses.

Squamous cell carcinoma is the most common malignant neoplasm of the sinonasal region, accounting for more than 80% of cases. The development of these tumors is associated with tobacco use and occupational exposure to compounds that contain nickel.

Nonsquamous malignant tumors of the sinonasal region include, in order of frequency, carcinomas of minor salivary gland origin, sarcomas, esthesioneuroblastomas, lymphomas, sinonasal undifferentiated carcinomas (SNUCs), and melanomas. The most frequent minor salivary gland malignancy of the sinonasal region is adenoid cystic carcinoma, followed by adenocarcinoma, mucoepidermoid carcinoma, clear cell carcinoma, acinic cell carcinoma, and other rare histologies. Adenoid cystic carcinoma characteristically shows slow progression, with high propensity for perineural invasion and pulmonary metastasis. Exposure to wood dust and chemicals used in the leather manufacturing industry is known to increase the risk for development of sinonasal adenocarcinomas.

Esthesioneuroblastoma, also commonly called *olfactory neuroblastoma (ONB),* is a malignant neoplasm derived from olfactory epithelium. In 2005 the World Health Organization adopted Hyams' four-tiered grading system, which is based on lobular architecture, mitosis, necrosis, nuclear pleomorphism, fibrillary matrix, and rosettes. Grades I and II may be placed together as low grade (Fig. 5.34), and grades III and IV are considered high grade. Immunohistochemistry is useful in the evaluation of ONB, with strong synaptophysin and neuron-specific enolase labeling and an absence of cytokeratin and epithelial membrane antigen immunoreactivity. Additionally, S-100 protein immunoreactivity is frequently seen surrounding the nests or lobules, labeling sustentacular cells; however, this feature may be lost in higher grade tumors.

In addition to salivary gland–type adenocarcinomas and metastatic adenocarcinomas, sinonasal adenocarcinomas can be split into intestinal type and nonintestinal type (Fig. 5.35). Low-grade nonintestinal-type sinonasal adenocarcinomas have an excellent prognosis; however, local recurrence may occur in up to 20% to 30% of patients. Sinonasal intestinal-type adenocarcinomas generally are locally aggressive malignancies with a high risk of metastasis to cervical lymph nodes and infrequently to the lung. Local recurrence rates are high, with 5-year cumulative survival at approximately 50%. Mucinous adenocarcinomas, particularly those demonstrating signet ring cells, have the highest mortality.

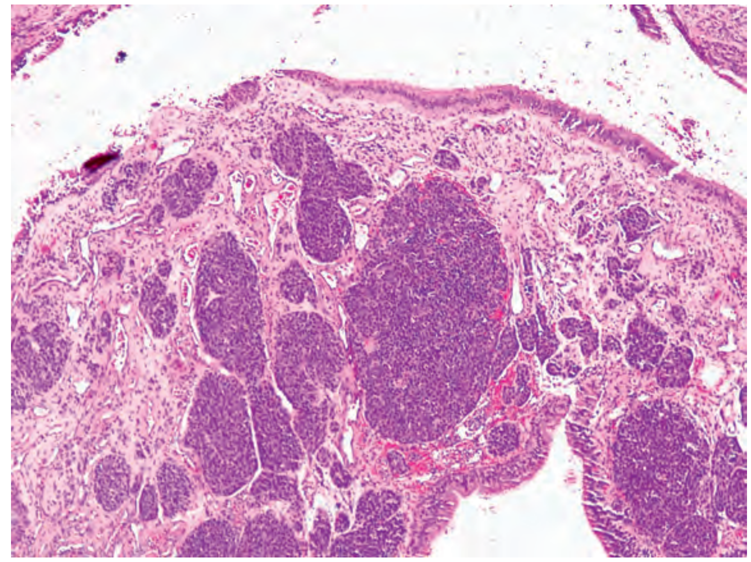

Figure 5.34 A histomicrograph of a low-grade olfactory neuroblastoma showing small round cells proliferating in a lobular, nested pattern beneath intact respiratory epithelium.

Sinonasal undifferentiated carcinoma (SNUC) is defined as a high-grade malignant epithelial neoplasm without light microscopic evidence of squamous or glandular differentiation. Although the histogenesis of these tumors is uncertain, they are thought to arise from the Schneiderian epithelium or nasal ectoderm. Histologically these tumors are composed of solid sheets and nests of high-grade pleomorphic cells with inconspicuous to prominent nucleoli, abundant mitoses, and necrosis (Fig. 5.36). Although immunohistochemistry is neither specific nor pathognomonic, it plays a role in eliminating other diagnostic entities, such as ONB and malignant melanoma. SNUCs react with a variety of cytokeratins but usually lack immunoreactivity for neuroendocrine markers (i.e., chromogranin and synaptophysin). These tumors are usually locally extensive at presentation and show a propensity toward rapid growth. Despite aggressive treatment, SNUCs have high rates of locoregional failure and distant metastases, particularly to the lungs and bone. Multimodality treatment is usually recommended, including surgery, radiation, and chemotherapy, but despite aggressive treatment, prognosis remains poor.

The nasal cavity is the most common site for mucosal melanomas in the head and neck. Mucosal melanomas are less commonly pigmented than are their cutaneous counterparts. Two clinical variants are seen: nodular and mucosal multifocal. The cells of this malignant neoplasm are less cohesive than in a carcinoma. The presence of in situ melanoma is essential to differentiate a primary mucosal melanoma from a metastatic lesion. Another clue to the diagnosis is the presence of the prominent nucleoli within the nuclei (Fig. 5.37).

SELECTION OF TREATMENT

Because of the bony confines of the paranasal sinuses and the proximity of vital structures such as the orbit and brain, external

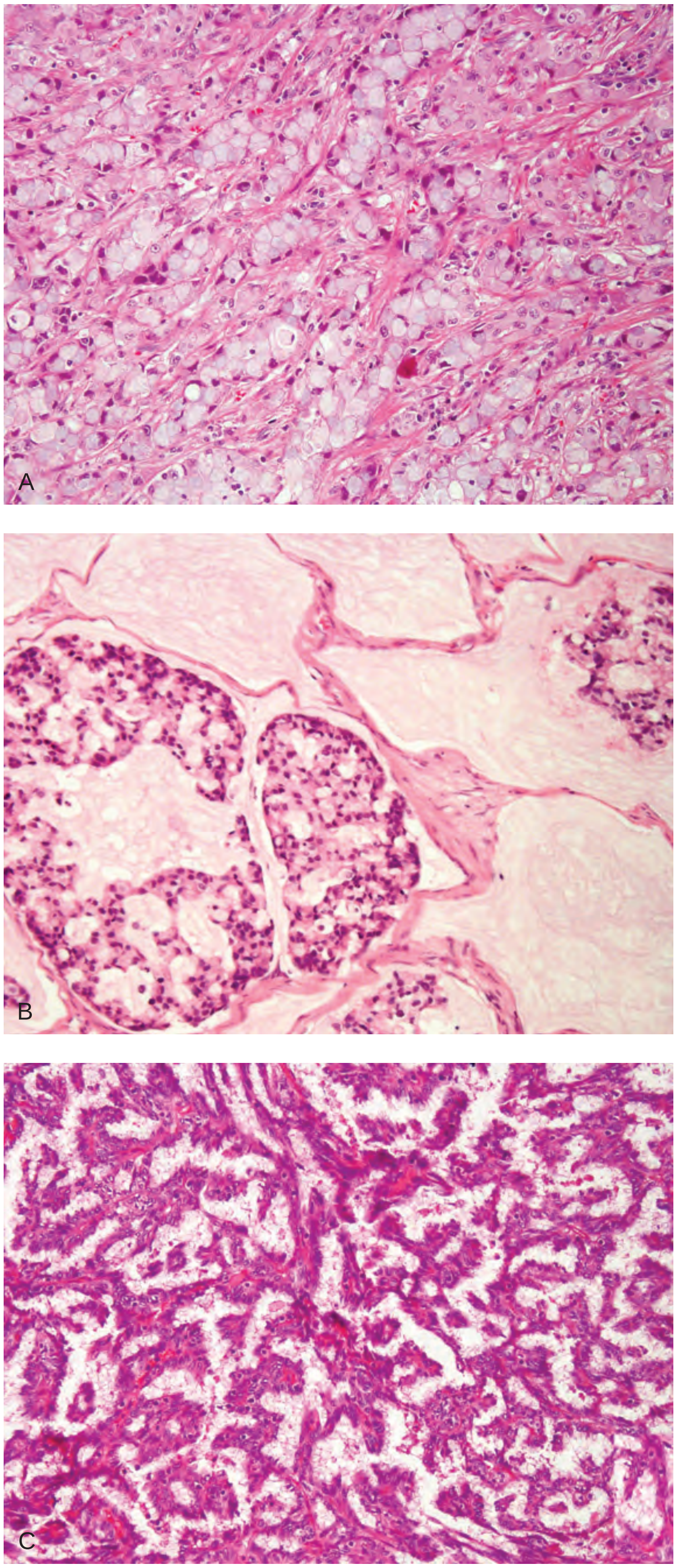

Figure 5.35 Photomicrographs of adenocarcinomas of minor salivary gland origin. **A**, Intestinal-type sinonasal adenocarcinoma with signet ring cells. **B**, Mucinous intestinal-type adenocarcinoma with neoplastic glands floating within pools of mucin. **C,** Nonintestinal sinonasal adenocarcinoma with papillary structures and fibrovascular cores.

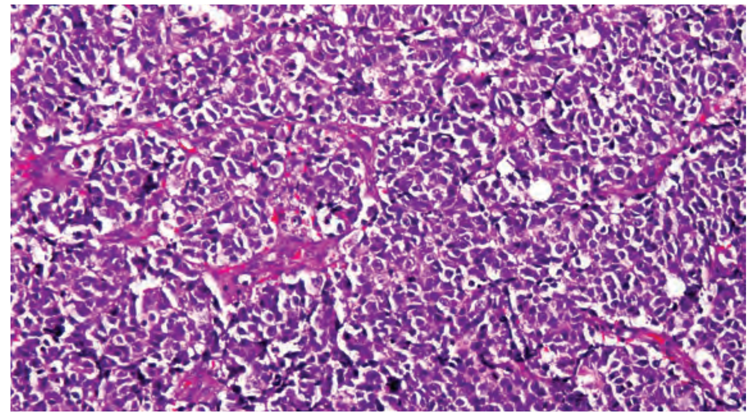

Figure 5.36 A histomicrograph of a sinonasal undifferentiated carcinoma (hematoxylin and eosin ×40).

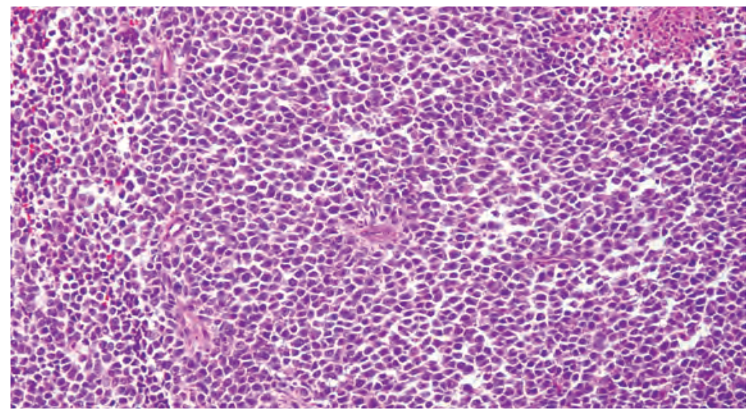

Figure 5.37 A histomicrograph of a mucosal melanoma of the nasal cavity (hematoxylin and eosin ×40).

irradiation is not considered as a preferred definitive treatment modality for primary malignant tumors arising in this region. Surgical resection thus remains the initial treatment of choice for most tumors of the nasal cavity and paranasal sinuses, although induction chemotherapy and concurrent chemoradiation therapy may be considered for very advanced tumors preoperatively and for selected histologies such as SNUC. Lesions staged as T4b are considered unresectable, and radiation with chemotherapy may be employed as definitive treatment. A systematic approach is therefore essential in proper selection of an appropriate surgical procedure, whether endoscopic or open, for adequate resection of early and advanced tumors of the nasal cavity and paranasal sinuses. These considerations involve invasion of the skin, bones (such as frontal, nasal, clivus, maxilla, hard palate), orbit, cavernous sinus, brain, and carotid artery. Surgical treatment alone is considered appropriate for nearly all benign tumors and early staged malignant tumors amenable to a curative surgical resection with negative margins.

A contraindication to surgical intervention for advanced tumors of the nasal cavity and paranasal sinuses includes the presence of trismus resulting from invasion of the pterygoid muscles and soft tissues in the masticator space around the temporomandibular joint and the pterygomaxillary fossa. Invasion of the skull base with bone destruction of the posterosuperior wall and the lateral walls of the sphenoid sinus also is considered a contraindication for surgical intervention. Similarly, significant brain invasion, invasion of the cavernous sinus with cranial nerve paralysis, (CN II, III, IV, V, or VI) and invasion of the carotid artery by a tumor are contraindications to surgical intervention.

NONSURGICAL TREATMENT

The National Comprehensive Cancer Network (NCCN) guidelines recommend that for T1-T4a tumors, surgical resection with or without postoperative radiation or chemoradiotherapy is the standard of care for malignant sinonasal tumors. However, alternative approaches have been shown to be efficacious in selected cases. Concurrent treatment with systemic chemotherapy and radiotherapy (intensity-modulated radiotherapy) has shown promising results for the management of some sinonasal malignancies. The advent of proton beam radiation treatment has enabled the administration of an appropriate target dose to the tumor with a decreased dose to collateral tissue. The use of proton radiation is becoming more steadily adopted in the United States for sinonasal and skull base malignancy. The chemotherapeutic drugs currently being used include a combination of cisplatinum, 5-fluorouracil (5-FU), and Taxotere, in a variety of dosage schedules. Patients who are unable to tolerate cisplatinum are candidates for treatment with carboplatinum. High doses of intraarterial cisplatin given selectively through the vessels feeding the tumor along with an intravenous infusion of a neutralizing agent (sodium thiosulfate) and concomitant radiotherapy have been reported by some authors to be effective in the treatment of advanced sinonasal malignancies. This approach is suggested to decrease systemic toxicity while increasing locoregional control. Targeted therapies with anti–epidermal growth factor receptor and anti–vascular endothelial growth factor agents in combination with or without other cytotoxic agents and radiotherapy are currently under investigation. Similarly, immunotherapeutic agents such as PD 1 and PDL 1 inhibitors are currently being tested in clinical trials.

SURGICAL TREATMENT

Anatomy

The nasal cavity is the inlet to the upper airway, beginning at the anterior nares and ending at the posterior choanae that open into the nasopharynx. It provides a portal of entry that filters, humidifies, and warms incoming air on its way to the lungs. The nasal cavity is divided in the midline by the nasal septum, which is composed of the septal cartilage and the vomer bone, covered on each side by the nasal mucosa. The lateral walls of the nasal cavity are partly cartilaginous and partly bony, and its floor is purely bony. Laterally, the nasal cavity contains the nasal conchae; the inferior concha is part of the nasal cavity, and the superior and middle conchae are composite parts of the ethmoid complex. The mucous membrane that lines the nasal cavity is densely adherent to the underlying periosteum and perichondrium. The majority of the mucous membrane is pseudostratified columnar ciliated epithelium of the Schneiderian type. The lining is highly vascular and contains mucous glands, minor salivary glands, and melanocytes. The olfactory neuroepithelium that is responsible for the sense of smell overlies the cribriform plate in the roof of the nasal cavity and is less vascular compared with the remainder of the mucosa. The lateral nasal wall bears the conchae or turbinates, and the meati or air spaces between them contain the openings of the paranasal sinuses. The inferior meatus is located below and lateral to the inferior concha and receives the opening of the nasolacrimal duct on the anterior portion of its lateral wall. The ostium of the maxillary sinus opens into the ethmoidal infundibulum of the middle meatus, whereas the sphenoid sinus drains into the sphenoethmoidal recess above the uppermost concha. The blood supply to the nasal cavity is from branches of both the external carotid arteries (sphenopalatine branches of the internal maxillary artery and facial artery) and internal carotid arteries (anterior and posterior ethmoid branches of the ophthalmic artery). The veins of the nose arise in the dense venous plexuses that are especially concentrated on the inferior nasal concha, the inferior meatus, and the posterior septum, and the venous drainage parallels the arteries. Lymphatic drainage is primarily to the jugulodigastric nodes and the retropharyngeal nodes.

The nasal cavity is surrounded by bony spaces that are lined with mucosa and contain air, called *paranasal sinuses,* the largest of which are the maxillary sinuses. Ethmoid air cells occupy the superior aspect of the nasal cavity and separate it from the anterior skull base at the level of the cribriform plate. For purposes of staging malignant tumors, the lower half of the nasoethmoid region, including the inferior turbinate and concha, is considered the nasal cavity, whereas the upper half, consisting of the middle and superior turbinates and ethmoid air cells, constitutes the ethmoid region. Superoanteriorly, the frontal sinus contained within the frontal bone forms a biloculated or multiloculated pneumatic space. The sphenoid sinus at the superoposterior part of the nasal cavity is located at the roof of the nasopharynx. The sphenoid sinus is divided by a median septum and may be multiloculated. The anatomic location of the paranasal sinuses and their relationship to each other are shown in Figs. 5.38 and 5.39.

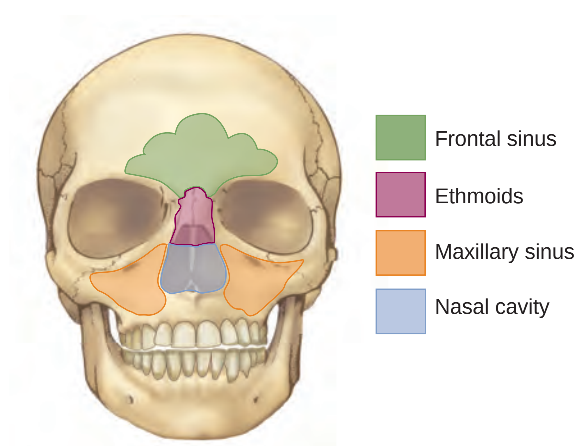

Figure 5.38 The anatomic location of the paranasal sinuses.

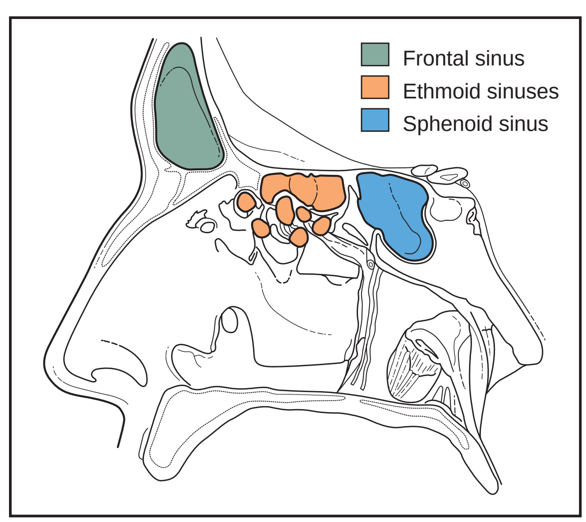

Figure 5.39 The relationship of the paranasal sinuses to each other.

Preoperative Preparation

Preoperative preparation for patients who require surgery for tumors of the nasal cavity and paranasal sinuses largely depends on the extent of the tumor, the nature of the surgical procedure, and the impact of the surgery on the patient's function and appearance. Perioperative antibiotics are recommended for most patients requiring a maxillectomy. In addition to routine presurgical measures, careful preoperative dental evaluation is mandatory. Although grossly septic teeth should be attended to, loose teeth in the tumor-bearing alveolus should not be manipulated. In addition, dental impressions should be taken and used for fabrication of the immediate and final palatal obturator to correct the anticipated surgical defect in the palate, where infrastructure of the maxilla is to be removed. The fabrication of an adequate obturator requires cooperation between the surgeon and the prosthodontist. The surgeon marks the anticipated extent of resection of the palate on the dental cast model, which is the basis for fabrication of the immediate obturator by the prosthodontist. If resection of a portion of the soft palate is anticipated, the obturator should be extended posteriorly to prevent nasal regurgitation. The immediate dental obturator also helps retain the surgical packing in place and aids postoperative recovery by supporting swallowing and clearance of pulmonary secretions. Placement of an immediate dental obturator following palatal resection allows the patient to swallow immediately postoperatively and obviates the need for a feeding tube.

For patients requiring orbital exenteration or extensive resection of the nose or face, facial moulage and clinical photographs should be obtained to facilitate subsequent fabrication of a facial prosthesis. If a large composite defect is anticipated that will require reconstruction with a composite free flap, a plastic and reconstructive surgeon should be consulted. A neurosurgeon should be consulted preoperatively regarding tumors that approach the skull base and require a craniofacial approach to achieve a monobloc resection (see Chapter 6). All patients undergoing surgery for tumors of the nasal cavity or paranasal sinuses must have detailed preoperative imaging studies, but particularly those undergoing endoscopic or cranioendoscopic surgery for malignancy require the appropriate preoperative imaging (CT and/or MRI) with fine axial cuts to be used for image-guided surgery.

Anesthesia and Position

Accurate marking of the incision along facial subunits can become difficult because of the distortion of facial and nasal landmarks that occurs with taping of the endotracheal tube. Therefore the surgical incision on the face should be marked out with a marking pen before induction of anesthesia. The route of intubation, either nasotracheal or orotracheal, is selected on the basis of the surgical approach—for example, oral, transnasal, or transfascial. Patients with trismus may require fiberoptic nasotracheal intubation or a preliminary tracheostomy. Once intubated, the patient is placed in the supine position and the upper half of the body is elevated 30 degrees, with the neck extended and slightly rotated to the ipsilateral side. Satisfactory muscle relaxation is essential for adequate exposure and ease of instrumentation during surgery in the oral cavity. Because the eye on the side where the surgery is being performed may be in the surgical field, either a ceramic corneal shield is used or the eyelids are sutured shut with a fine nylon suture to protect the cornea during surgery. The patient's head is covered with sterile drapes in such a fashion that movement of the head during the operation does not cause contamination of the sterile field (see Chapter 2). A transparent plastic head drape provides isolation of the anesthetic tubing and offers both the surgeon and the anesthesiologist a clear view of the patient's eyes, nose, and endotracheal tube. If intraoperative image guidance using a CT, MRI, or PET/CT is to be used, this is arranged as part of the sterile field. If intraoperative navigation is used, then it is important that the head is fixed in the desired position with neurosurgical pins in the skull. This is crucial, since any movement of the head (intentional or not) will shift the location of the target on the monitor and mislead the surgeon to a wrong location. If a split-thickness skin graft is to be used to cover the surgical defect, it is harvested from a suitable donor site before the surgical procedure is begun.

Surgical Approaches

The surgical approach selected should provide adequate exposure for a safe and satisfactory surgical resection. The surgical approach is dependent on the anatomic location, extent, and histology of the tumor. Transnasal endoscopic resection is an accepted approach for benign and selected malignant tumors. Endoscopic approaches require special instrumentation and considerable expertise and experience and thus should be performed only by surgeons with such special expertise. Surgically resectable lesions (via an open surgical approach) with contraindications for endoscopic resection for nasal cavity and ethmoid tumors include extension to the anterior wall of the maxillary sinus or skin, bony walls of the maxillary sinus, or floor of the nasal cavity; orbital invasion; significant brain invasion; invasion of the clivus; and extension of the tumor lateral to the medial third of the orbital roof.

Malignant tumors of the "infrastructure" of the maxilla, including tumors of the upper gum, hard palate, or floor of the maxillary antrum, can be adequately excised by a transoral partial maxillectomy. A sublabial degloving approach is suitable for larger tumors of the anteroinferior aspect of the nasal cavity and the infrastructure of the maxillary sinus, and particularly when access to the posterosuperior part of the nasal cavity is not satisfactory through the perioral approach. This approach is often used for large benign tumors of the nasopharynx, such as angiofibromas.

More extensive tumors require a facial incision to provide adequate exposure. Small tumors localized to the lower part of the nasal cavity and nasal septum that are inaccessible for endoscopic excision through the nasal vestibule are best approached via a lateral rhinotomy. Although the "classic" Weber-Ferguson-Dieffenbach incision provides excellent exposure for resection of tumors of the maxilla, it leads to an aesthetically unacceptable scar, distortion of facial contour and expression, ectropion, and alteration of the shape of the nasal vestibule (Fig. 5.40). Therefore the Weber-Ferguson incision should be modified to retain facial symmetry, nasal subunits, and aesthetics. A modified Weber-Ferguson incision based on nasal and facial subunits results in superior aesthetic and functional outcomes (Fig. 5.41). The incision divides the upper lip in the midline through the philtrum of the upper lip up to the columella. It then turns laterally and cephalad to enter the floor of the nasal vestibule along the root of the columella and takes a 45-degree turn and exits the floor of the nasal cavity, remaining in the groove of the lateral aspect of the ala, and follows the alar subunit all the way up to the lateral aspect of the nose. At this point,

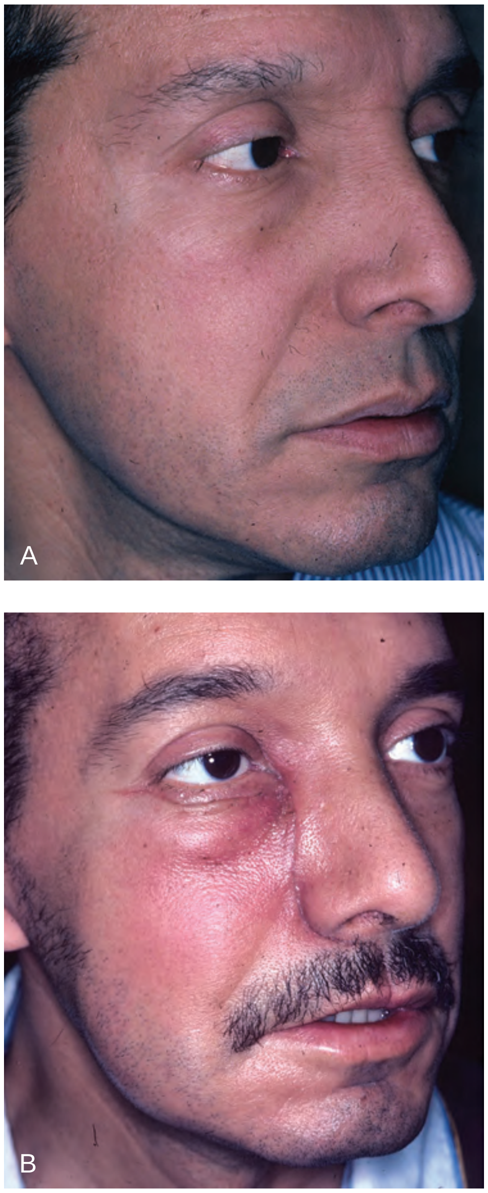

Figure 5.40 The preoperative (**A**) and postoperative (**B**) appearance of a patient who underwent a maxillectomy via a classic Weber-Ferguson incision.

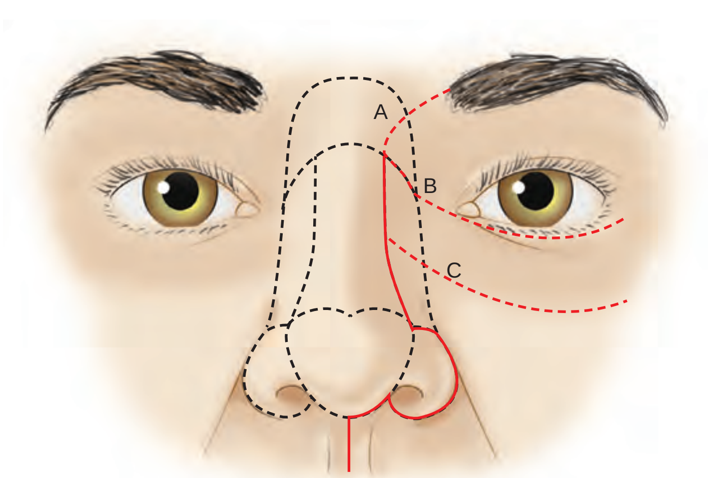

Figure 5.41 The modified Weber-Ferguson incision is designed to conform to the nasal and facial subunits. *A*, lynch extension; *B*, subciliary extension; *C*, infraorbital extension.

the incision proceeds cephalad along the lateral aspect of the dorsal subunit of the nose up to the level of the medial canthus. This extent of incision is adequate for lateral rhinotomy.

The incision can be modified to exclude the splitting of the upper lip for smaller tumors of the lateral wall of the nasal cavity. The incision can be extended with a Lynch or subciliary extension for larger tumors with significant superior or lateral extension. For the Lynch extension, the incision continues cephalad on the lateral aspect of the bridge of the nose up to the medial aspect of the eyebrow (see Fig. 5.41 *A*). A subciliary extension takes a 90-degree turn laterally onto the infraorbital skin and follows the most prominent skin crease of the lower eyelid close to the tarsal margin, toward the zygomatic process (see Fig. 5.41 *B*). However, this causes slight eversion and ectropion of the lower eyelid. This causes significant facial asymmetry. On the other hand, the skin of the infraorbital region is slightly hyperpigmented compared with the skin of the cheek in most individuals. In that setting the lateral or infraorbital extension is made at the junction of the hyperpigmented area and the less pigmented skin of the cheek (see Fig. 5.41 *C*). Some examples of the modified Weber-Ferguson incision and the eventual aesthetic outcome are shown here. The patient shown in Fig. 5.42 underwent resection of a hemangioma of the nasal process of the maxilla, through a modified Weber-Ferguson incision. Another patient with a carcinoma of the infrastructure of the maxilla underwent partial maxillectomy through a modified Weber-Ferguson incision (Fig. 5.43). The aesthetic results following this modification of the Weber-Ferguson incision are clearly superior. The patient shown in Fig. 5.44 underwent subtotal maxillectomy through the modified Weber-Ferguson incision with a lateral infraorbital extension along the line of pigmentation. The postoperative appearance of the face shows a well-healed scar. Tumors of the paranasal sinuses that approach or involve the skull base that are not suitable for endonasal resection require an open craniofacial approach for intracranial exposure of the upper end of the tumor to secure clear margins. Surgical access to tumors that originate or extend into the nasopharynx or retromaxillary space can be difficult and require special considerations. The common clinical entities arising in this location are angiofibromas and nasopharyngeal carcinomas. Limited lesions can be accessed either endonasally or through a transpalatal approach. Larger lesions presenting in the paranasopharyngeal region and retromaxillary space can be accessed via an open medial maxillectomy or endoscopic transmaxillary transpterygoid approach. More laterally situated retromaxillary tumors can be approached through a maxillary swing approach.

Lateral Rhinotomy

A lateral rhinotomy is required for excision of nasal cavity tumors that are not suitable for endoscopic resection because of their location (generally extending anteriorly to nasal bone or soft tissue or the lateral nasal wall).

Open Medial Maxillectomy

A medial maxillectomy is indicated for well-differentiated or low-grade malignant tumors, inverted papillomas, and other tumors of limited extent on the lateral wall of the nasal cavity or the medial wall of the maxillary antrum. The open surgical approach is through a lateral rhinotomy or a modified Weber-Ferguson incision, depending on the extent and location of the tumor. Technically, removing the surgical specimen of a medial maxillectomy in a monobloc fashion is often difficult. Because of the fragile nature of ethmoid air cells, mobilization

Figure 5.42 A patient with a hemangioma with the nasal process of maxilla excised through a modified Weber-Ferguson incision. Axial (**A**) and coronal (**B**) views of the computed tomography scan of the sinuses show a typical honeycomb appearance of the hemangioma. **C**, The skin incision is outlined on the face. **D**, Postoperative appearance of the patient 1 year following surgery.

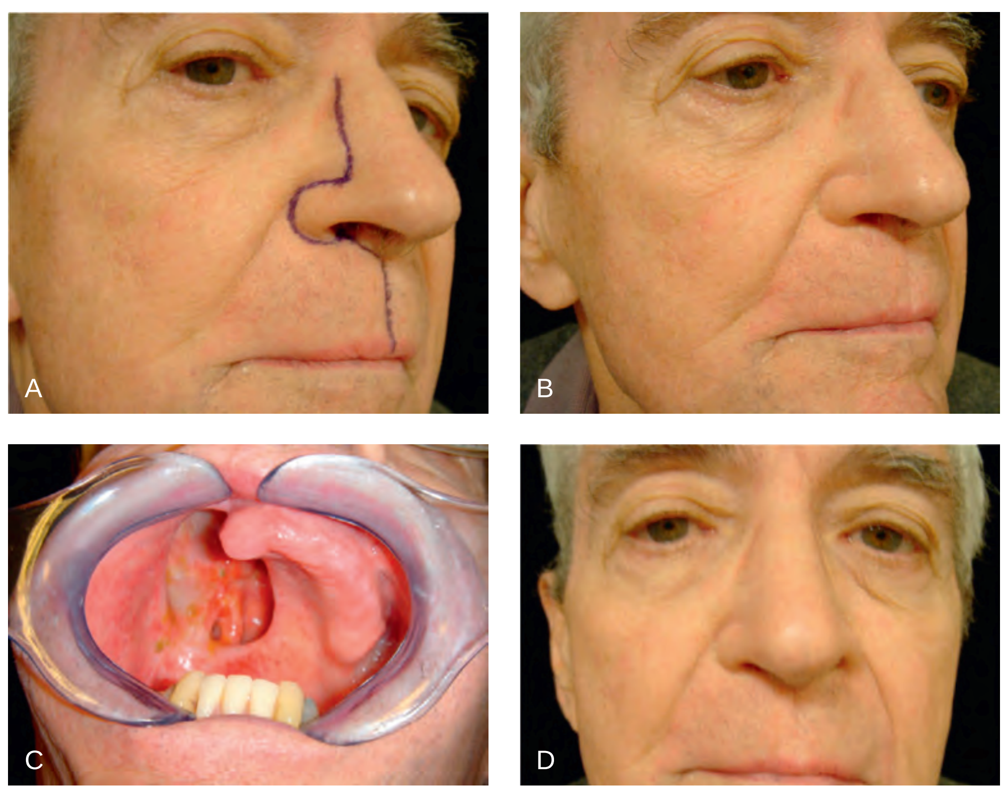

Figure 5.43 **A**, Outline of the modified Weber-Ferguson incision for infrastructure, partial maxillectomy. **B**, Postoperative appearance of the patient 1 year following surgery. **C**, Intraoral maxillectomy defect. **D**, Frontal view of the face showing excellent aesthetic outcome.

of an ethmoid tumor should be performed gently and with extreme care. The bone cuts for a medial maxillectomy are shown on frontal and oblique views of the skull in Figs. 5.45 and 5.46. The extent of bone resection, shown on the lateral wall of the nasal cavity on a skull, includes the inferior and middle turbinates and ethmoid air cells cephalad, and to the floor of the nasal cavity caudad (Fig. 5.47).

A CT scan of the sinuses of the patient shown in this procedure demonstrates a tumor mass arising on the medial wall of the maxillary antrum with extension into the nasal cavity and obstruction of the remaining maxillary antrum. In the axial view, note that the medial wall of the maxilla is destroyed by the tumor, but the lateral and anterior walls are intact (Fig. 5.48). The tumor extends into the nasal cavity in the region

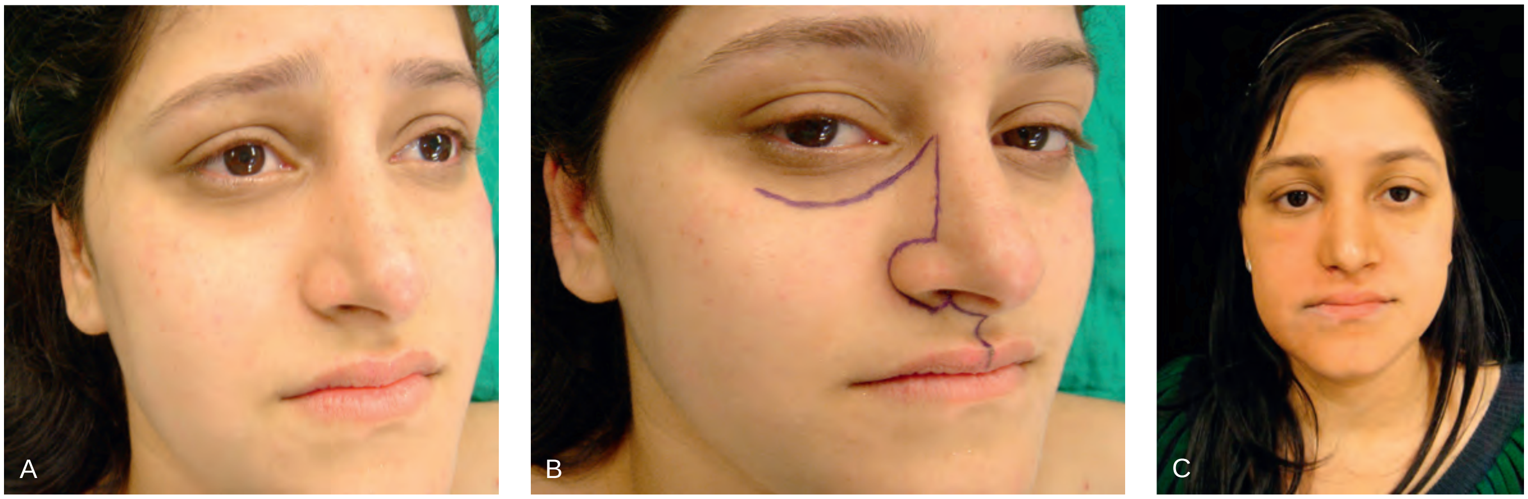

Figure 5.44 **A**, Modified Weber-Ferguson incision with lateral extension along pigmented infraorbital skin. **B**, The skin incision is outlined on the patient. **C**, Postoperative appearance of the patient 1 year following surgery and postoperative radiation therapy.

Figure 5.45 The bone cuts for a medial maxillectomy shown on the frontal view of a skull.

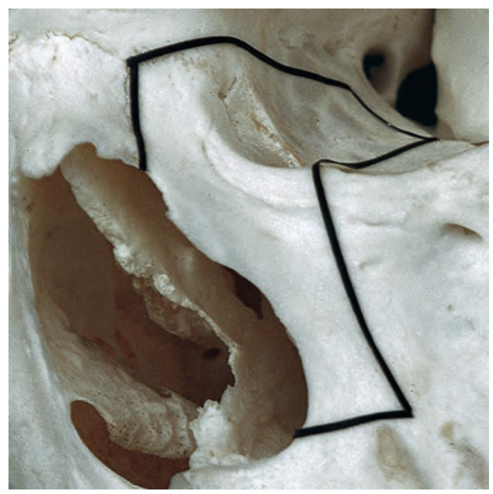

Figure 5.46 The bone cuts for a medial maxillectomy shown on the oblique view of a skull.

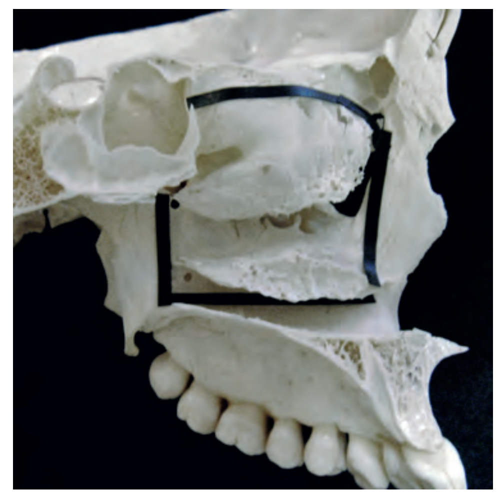

Figure 5.47 The lateral wall of the nasal cavity on a skull shows the extent of bone resection.

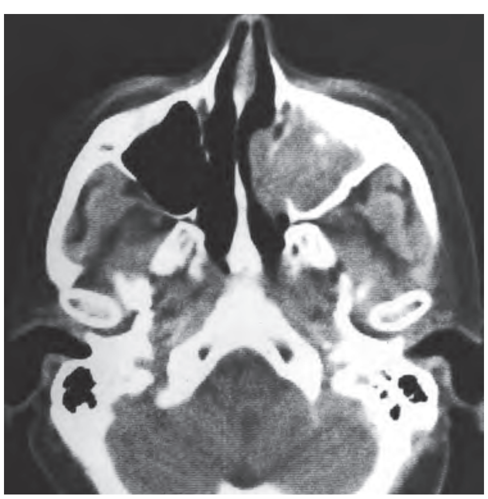

Figure 5.48 The axial view of a computed tomography scan shows that the medial wall of the maxilla is destroyed by the tumor, but the lateral and anterior walls are intact.

Figure 5.49 The coronal view of a computed tomography scan shows that the tumor appears to arise in the region of the medial wall of the maxillary antrum cephalad to the inferior turbinate, but it does not extend into the orbit.

of the middle turbinate. On the coronal view, the tumor appears to arise in the region of the medial wall of the maxillary antrum cephalad to the inferior turbinate, but it does not extend into the orbit (Fig. 5.49). A biopsy done through the nasal cavity showed that this lesion was an inverted papilloma.

The Weber-Ferguson incision is often required to expose tumors arising in the medial wall of the maxillary antrum. A modified Weber-Ferguson incision along the nasal subunits is preferred. For a medial maxillectomy, however, the Lynch extension of this incision is necessary, taking it up to the medial

end of the eyebrow (Fig. 5.50). A ceramic shield is used in this patient to protect the cornea. The skin incision is deepened through the soft tissues and the musculature of the upper lip and cheek up to the anterior bony wall of the maxilla (Fig. 5.51). Superiorly, the incision is extended through the soft tissues up to the bony margin of the orbit. The intended area of resection is the entire medial wall of the maxillary antrum along with the inferior turbinate and ethmoid air cells and the lamina papyracea on that side in a monobloc fashion. As the cheek flap is elevated, the infraorbital nerve near the orbital rim is carefully preserved (Fig. 5.52).

Entry into the maxillary antrum is now made with a high-speed drill and a burr. Use of the high-speed drill permits enlargement of the anterior wall antrotomy in a precise manner. A good portion of the anterior wall of the maxillary antrum is burred out to allow digital access in the maxillary antrum (Fig. 5.53). The interior of the maxillary antrum is carefully examined to assess the extent of the tumor in the antrum.

If a medial maxillectomy is feasible, the periosteum of the medial wall of the orbit is incised and elevated along the medial orbital rim and a periosteal elevator is used to separate it from the lamina papyracea. During this maneuver, the medial canthal ligament is detached and retracted with the orbital periosteum laterally. A silk suture is placed through the detached medial canthal ligament and left long for identification, for subsequent reapproximation to the nasal bone (Fig. 5.54). Meticulous attention is paid to preserve the continuity and contour of the bony rim of the inferior and inferomedial margins of the orbit. A malleable retractor is used to retract the periosteum and the

Figure 5.50 The Lynch extension of the classic Weber-Ferguson incision was used for this patient.

Figure 5.51 The skin incision is deepened through the soft tissues and the musculature of the upper lip and cheek up to the anterior bony wall of the maxilla.

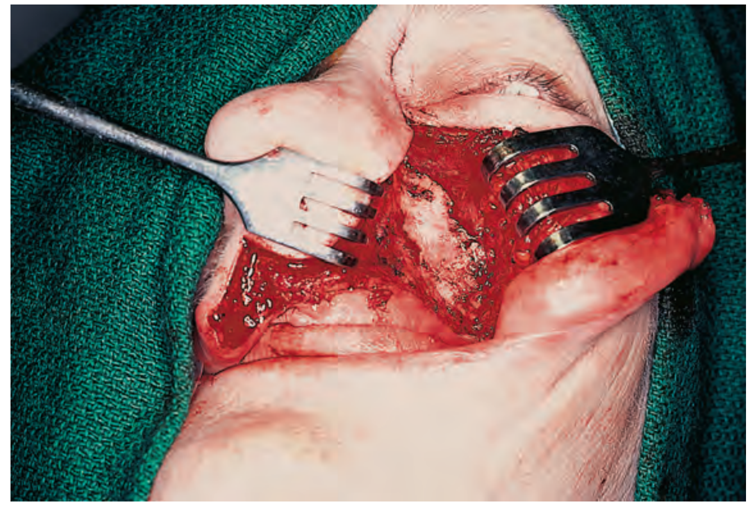

Figure 5.52 As the cheek flap is elevated, the infraorbital nerve near the orbital rim is carefully preserved.

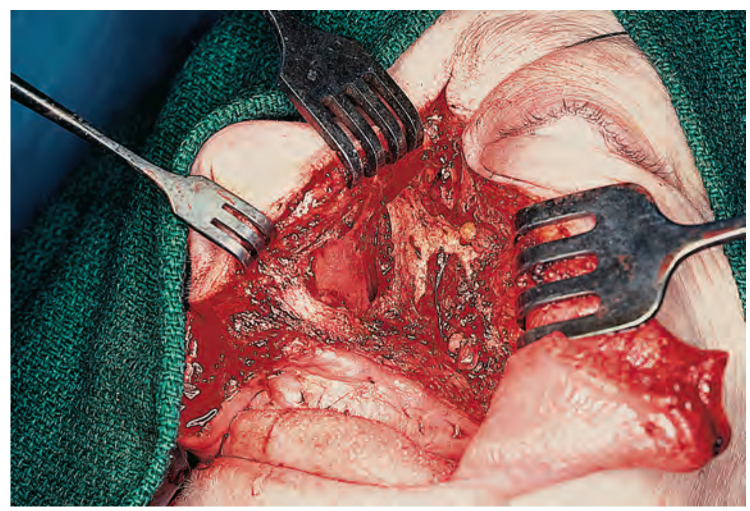

Figure 5.53 A good portion of the anterior wall of the maxillary antrum is burred out to allow digital access in the maxillary antrum.

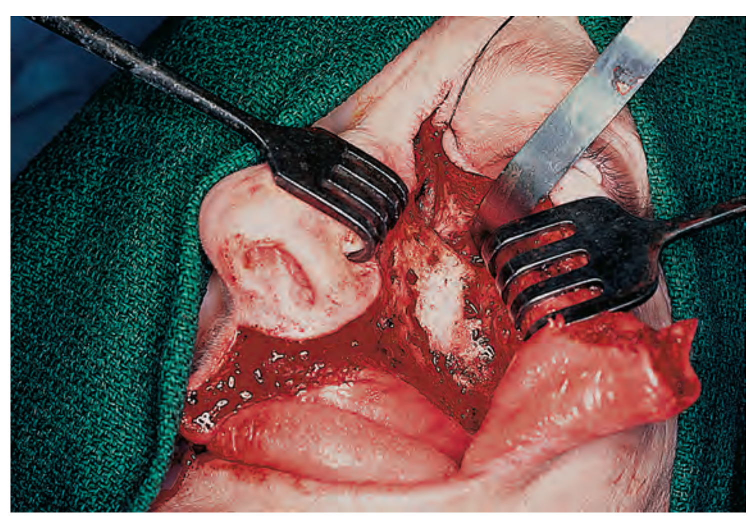

Figure 5.54 A silk suture is placed through the detached medial canthal ligament and left long for identification, for subsequent reapproximation to the nasal bone.

contents of the orbit laterally to aid dissection in the inferomedial quadrant of the orbit. Both the lacrimal sac and duct are elevated from the lacrimal fossa (Fig. 5.55). Use of a fine periosteal elevator facilitates dissection of the lacrimal sac and lacrimal duct from the lacrimal fossa. The lacrimal duct is transected flush with the rim of the orbit. Dissection of the medial orbital periosteum is taken posteriorly as far back as possible. During this maneuver, the anterior and posterior ethmoidal arteries, as they exit from the lamina papyracea, are transected and ligated or electrocoagulated. Once adequate mobilization of the orbital contents is performed in an extraperiosteal plane, a dry piece of gauze is inserted between the orbital contents and the lamina papyracea for hemostasis.

Attention is now focused on dissection of the ala of the nose and its retraction medially, allowing entry into the nasal cavity (Fig. 5.56). A curved osteotome is used to divide the medial wall of the maxillary antrum in a horizontal plane at the floor of the nasal cavity. This procedure is accomplished with gentle strokes using a mallet over the osteotome until the posterior margin of the maxillary antrum is reached, as seen through the anterior wall antrotomy. Similarly, the bone cut of the medial wall is extended cephalad, up to the medial wall of the orbit, with use of the same instruments. In some patients the ipsilateral nasal bone may have to be removed to provide a satisfactory en bloc resection.

Once the medial wall of the maxillary antrum is adequately mobilized, the index finger of one hand is inserted into the maxillary antrum and the index finger of the other hand is inserted into the nasal cavity. This provides bimanual palpation of the surgical specimen, which is gently rocked from side to side. This procedure will facilitate fracture of the superior and posterior ethmoid air cells. An osteotome may be used to fracture the lamina papyracea from the orbital surface of maxilla, the nasal bone, and the orbital surface of the frontal bone.

Finally, angled scissors are used to transect the posterior attachment of the surgical specimen near the posterior choana, and the entire surgical specimen containing the inferior turbinate and the middle turbinate with the lower ethmoid air cells is removed. Hemostasis is secured by electrocoagulation of the bleeding points over the cut bony surfaces. The surgical defect is shown in Fig. 5.57. Sharp bony spicules in the surgical defect are smoothed out with a fine burr.

The wound is now irrigated and a nasolacrimal duct stent is placed through the upper and lower puncta of the medial canthus. The distal ends of the stent in the nasal cavity are tied together. A skin graft usually is not required, because the nasal mucosa reepithelializes satisfactorily. A ribbon roll of Xeroform gauze packing is used to pack the maxillary antrum and the nasal cavity. The packing is brought out through the anterior naris (Fig. 5.58).

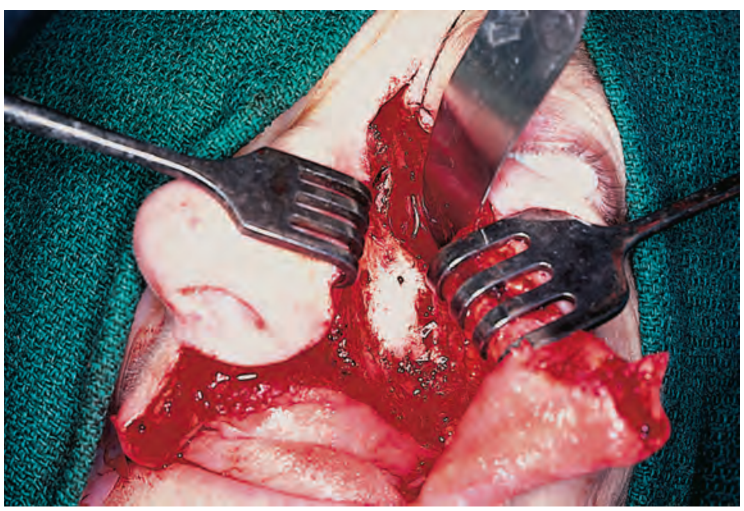

Figure 5.55 Both the lacrimal sac and the duct are elevated from the lacrimal fossa.

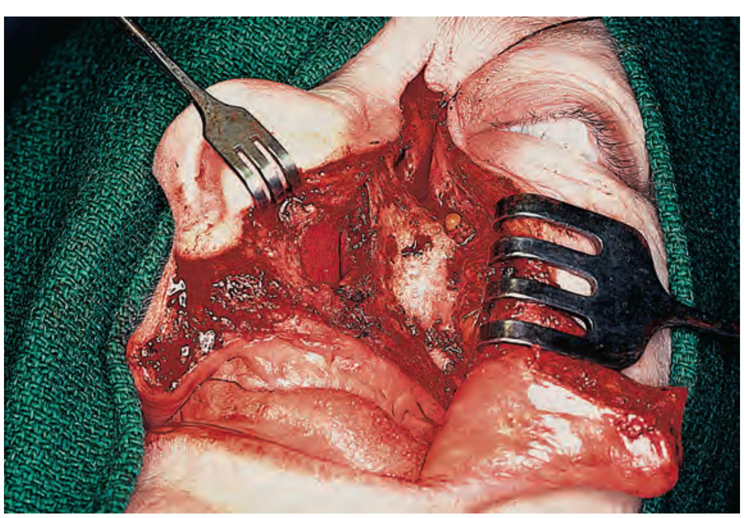

Figure 5.56 The ala of the nose is retracted medially, allowing entry into the nasal cavity.

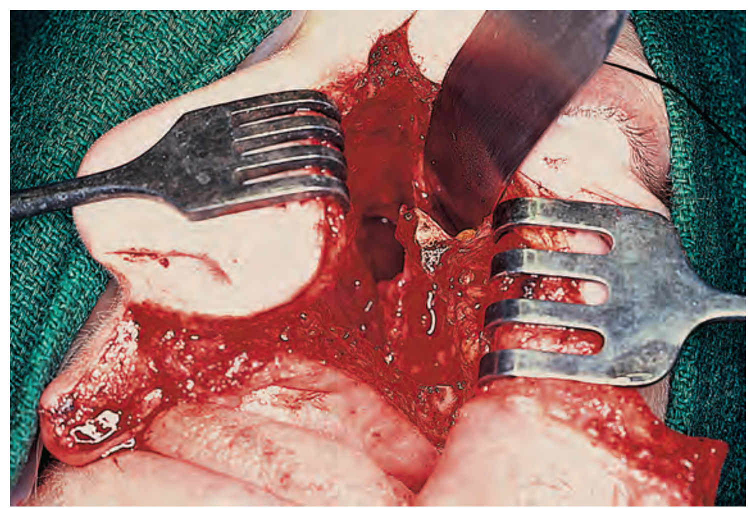

Figure 5.57 The surgical defect.

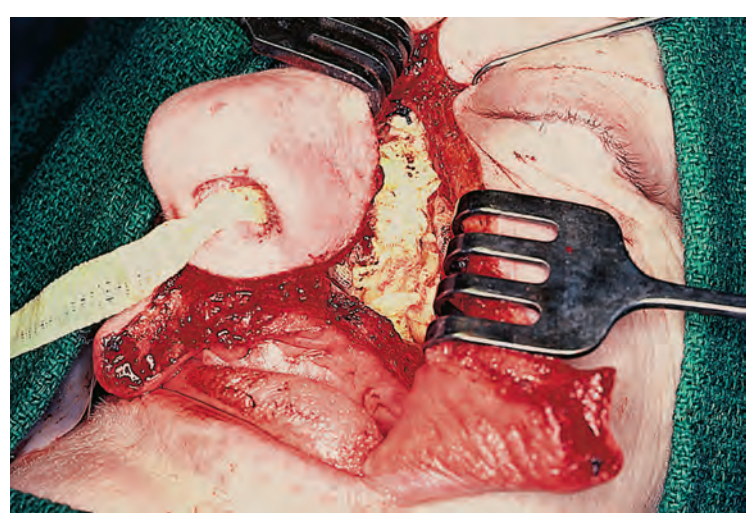

Figure 5.58 Xeroform packing is brought out through the anterior naris.

The medial canthal ligament is sutured back to a drill hole made in the nasal bone using nonabsorbable suture material. The medial canthus is reattached to exactly the same level as the contralateral medial canthus, thus restoring the normal position of the orbital contents. The remaining incision is closed in two layers with absorbable interrupted sutures for the soft tissues and nylon for skin (Fig. 5.59). Blood loss during the procedure is minimal, and blood transfusion usually is not required.

A lateral view of the surgical specimen shows the medial wall of the maxillary antrum with a polypoid tumor that occupied the maxillary sinus. Note the normal mucosa of the remainder of the medial wall of the maxilla (Fig. 5.60). A superior view of the surgical specimen shows the tumor projecting into the maxillary antrum on the right-hand side through the medial wall of the maxilla, along with the inferior turbinate on the left-hand side of the surgical specimen (Fig. 5.61). The tumor straddles the medial wall of the maxilla, presenting in the nasal cavity, but with its bulk filling the maxillary antrum. A medial view of the surgical specimen shows a small portion of the tumor present in the nasal cavity (Fig. 5.62).

Postoperative Care. The nasal packing is removed after 5 to 6 days. Because a skin graft generally is not necessary after a medial maxillectomy, debridement of the defect usually is not required. However, vigorous nasal irrigation and provision of excess humidity are vital to remove clots and crusts until complete epithelialization of the defect is achieved. Because the only access to the maxillary antrum is through the anterior nares, patients are taught nasal irrigation with a catheter. The procedure results in essentially no aesthetic deformity and minimal functional disability, although some patients may experience dry crusting because of a lack of mucus in the nasal cavity, and some patients report loss of a sense of smell. The postoperative appearance of the patient shows a well-healed scar and essentially no functional or aesthetic deformity. The globe is aligned well with the opposite side, and the patient has normal binocular vision (Fig. 5.63).

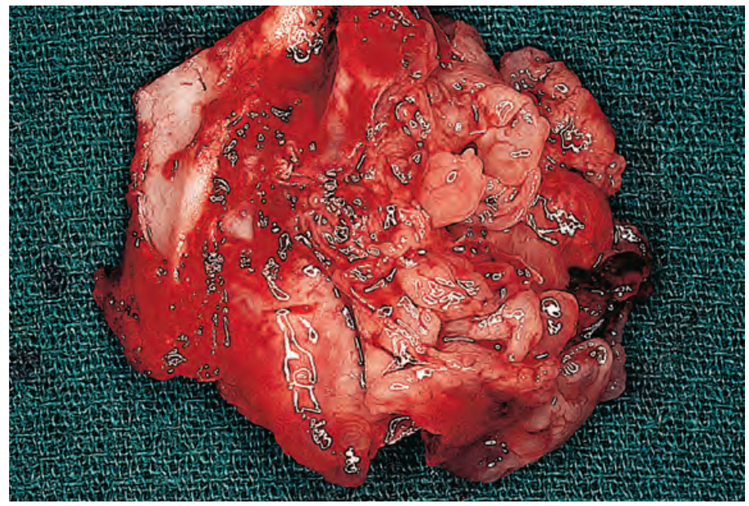

Figure 5.61 The superior view of the surgical specimen.

Figure 5.59 The remaining incision is closed in two layers.

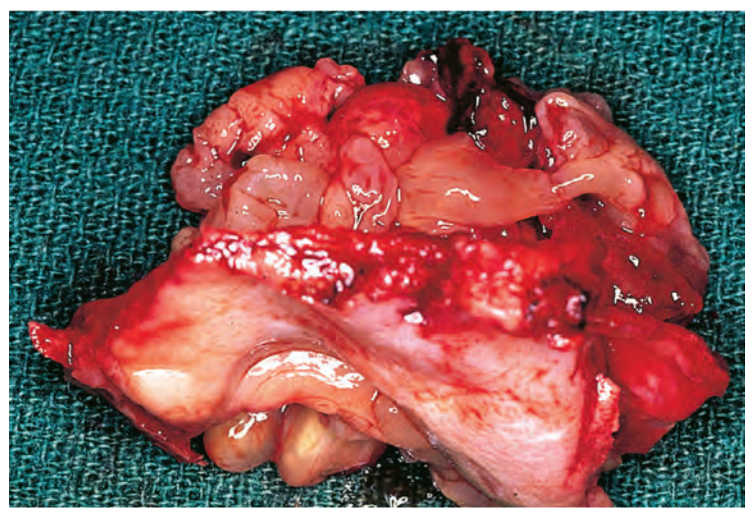

Figure 5.62 The medial view of the surgical specimen.

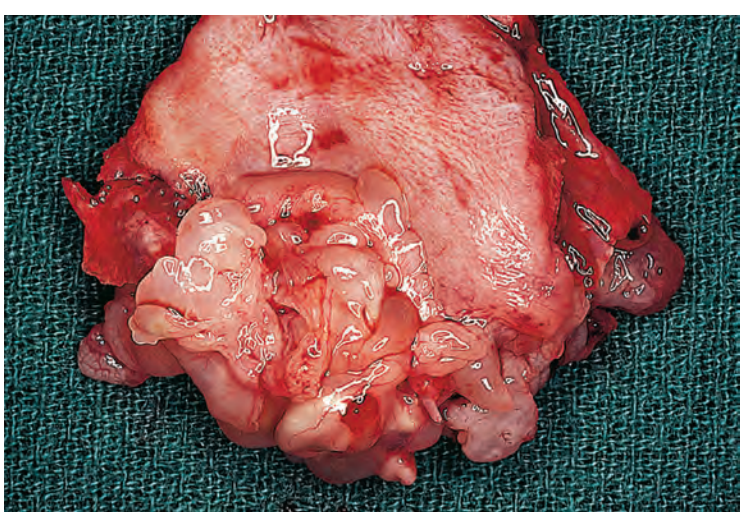

Figure 5.60 A lateral view of the specimen shows a polypoid tumor on the medial wall of the maxilla.

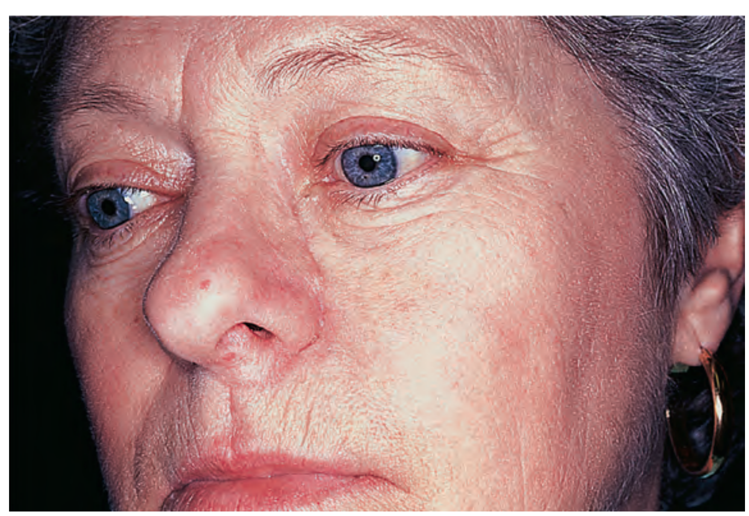

Figure 5.63 The postoperative appearance of the patient 8 months following surgery.

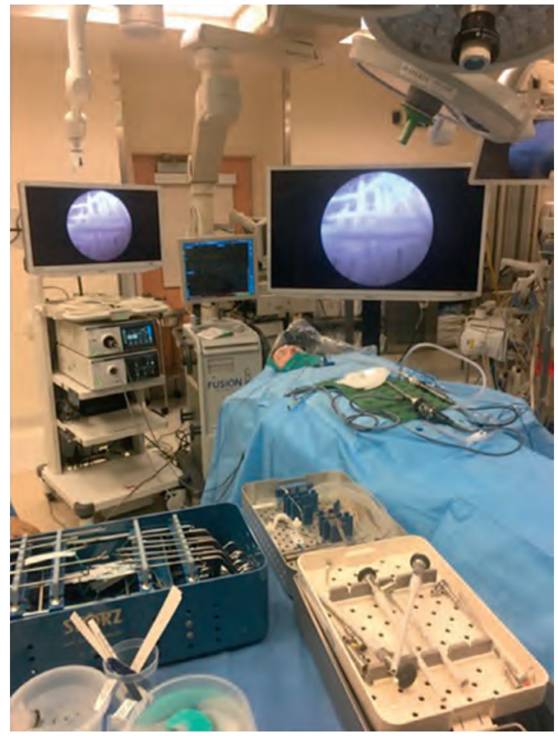

Figure 5.64 Setup for endonasal surgery with intraoperative navigation.

Figure 5.65 Injection of lidocaine with epinephrine at the greater palatine foramen.

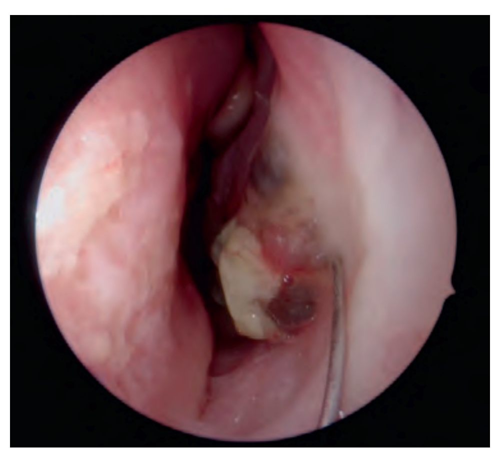

Figure 5.66 Injection of lidocaine with epinephrine in the inferior turbinate.

Endoscopic Medial Maxillectomy

Endoscopic medial maxillectomy has similar indications to the open approach, being used for recalcitrant inflammatory sinus disease as well as for benign and select malignant sinonasal tumors. Endoscopic medial maxillectomy is used for resection of tumors of the inferior turbinate, medial maxillary sinus wall, lateral nasal wall, lacrimal apparatus, and ethmoid sinuses. It is also used for the approach to tumors of the pterygopalatine fossa, infratemporal fossa, pterygoid plates, and nasopharynx. The use of endoscopic technique has the advantage of allowing for high-definition visualization with magnification out of the usual line of site as well as the seamless incorporation of intraoperative image guidance. In addition, the use of endoscopic techniques obviates the need for facial incisions and leads to earlier discharge from the hospital.

Unlike open medial maxillectomy, en bloc excision of tumor is often not possible but can be performed for small and moderate-size legions. As in all surgery, adequate exposure is critical in endoscopic medial maxillectomy. Lack of space to use endoscopic instrumentation can limit the ability to remove the tumor with adequate margins. In addition, in-office debridement and surveillance of the surgical site requires significant exposure. The basic tenet of endoscopic resection of large sinonasal tumors involves initial partial removal of the lesion to better determine the site of attachment or origin of the lesion. After this is determined, a margin of normal tissue is resected around the entirety of the tumor origin to obtain negative surgical margins. A critical aspect of this resection is examination of frozen sections beyond the region removed. The oncologically sound endoscopic extirpation of a medial maxillary sinus wall tumor requires appropriate patient selection. Contraindications include extension of tumor to bony nasal floor, anterior maxillary sinus wall, and intraorbital extension. Preoperative assessment should include CT and MRI scan to assess the bony and soft-tissue elements of the tumor extension. Depending on the extension of the tumor, patients must be prepared for potential endoscopic dacryocystorhinostomy in case of transection of the lacrimal duct.

The patient whose procedure of medial maxillectomy is shown here presented with a history of nasal congestion. Biopsy of a mass lesion involving the inferior turbinate confirmed the diagnosis of mucosal melanoma. Imaging revealed the tumor was confined to the inferior turbinate and the mucosa of the lateral nasal wall. The surgical procedure begins after the patient is placed under general anesthesia with orotracheal intubation and the eyes taped after placement of Lacri-Lube. The image guidance system is registered so intraoperative assessment with CT and/or MRI can be performed. The setup requires placement of high-definition monitors in locations that are ergonomically favorable for either one or two surgeons. This involves the placement of monitors approximately 30 degrees off the midline with the image guidance in the center (Fig. 5.64). After this is complete, the region is assessed, and the nose is decongested with 4% cocaine pledgets. A transoral injection of 1% lidocaine with epinephrine (1 : 100,000) is instilled into the greater palatine foramen adjacent to the second molar tooth (Fig. 5.65). Similarly, the head of the inferior turbinate, the nasal cavity floor, the axillae of middle turbinate, and the lateral nasal wall are injected (Fig. 5.66). The procedure begins by assessing the nasal cavity and medializing or resecting the middle turbinate with curved endoscopic scissors. After this is complete, a portion of the lesion may be removed to better visualize the attachments if necessary. An uncinectomy is performed using a Cottle elevator or backbiting forceps, and it is removed from the skull base using Blakesley forceps. The natural ostium of the maxillary sinus is widened using cutting

forceps and downbiters. Endoscopic sphenoethmoidectomy is performed to have better access and visualization of the tumor (Fig. 5.67). Anterior ethmoidectomy is performed by using a J curette and placing it posterior to the bullae ethmoidalis in the retrobulbar space and dissecting anteriorly. Soft tissue and bone are removed with grasping Blakesley forceps. The basal lamella is then penetrated above its horizontal aspect, and the posterior ethmoid air cells are dissected with cutting and grasping instrumentation. The superior turbinate is identified, and its inferior third is resected with cutting scissors. At this point, the natural sphenoid ostium is identified and enlarged medially and inferiorly with Kerrison rongeurs and mushroom punches. The skull base is then dissected from posterior to anterior, removing air cells under direct visualization (Fig. 5.68). Dissection proceeds from posterior to anterior. This direction of dissection helps prevent unintended skull base violation. After this is complete, the inferior turbinectomy is performed using curved endoscopic scissors, usually leaving about 1 cm anteriorly, if possible, making the cut beyond the inferior nasal meatus to avoid disruption of the lacrimal duct opening (Fig. 5.69). An incision is made with a Colorado tip electrocautery anteriorly and extending to the floor of the nasal cavity, leaving a safe margin around the tumor. The inferior turbinectomy is carried to the region of the crista ethmoidalis and removed flush with the medial maxillary sinus wall. Posteriorly, the blood supply to the inferior turbinate from the sphenopalatine artery is controlled with cautery. At this time, the medial wall of the maxillary sinus is removed. For tumors pedicled at the medial wall, this structure can be removed with margins using a high-speed drill, downbiting or backbiting instrumentation, or osteotomes. In cases where more lateral and anterior exposure is necessary beyond what can be seen with a large antrostomy and an angled endoscope, a septal window can be created with removal of the cartilage of the anterior septum and placement of the endoscope through the contralateral nostril. In addition, a sublabial incision can be used with endoscope placed through an anterior maxillary antrotomy to expand lateral exposure. The interior of the maxillary antrum is checked for any extension of tumor (Fig. 5.70). The tumor attachment is removed en bloc with frozen section margins obtained to ensure the tumor is cleared. After removal of the medial maxillary sinus wall, lateral nasal wall, and nasal cavity floor mucosa, the defect is open with the floor drilled even with the maxillary sinus. In this patient, the specimen was removed in two pieces, the medial maxillary sinus wall and the inferior turbinate, with the tumor removed in a monobloc fashion with negative margins, confirmed by frozen sections from the surgical defect (Fig. 5.71).

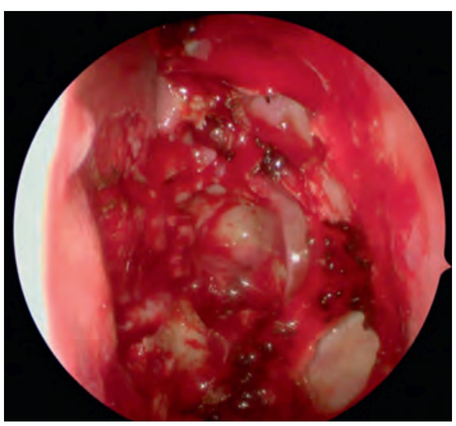

Figure 5.67 A wide sphenoethmoidectomy is performed for better visualization of the tumor.

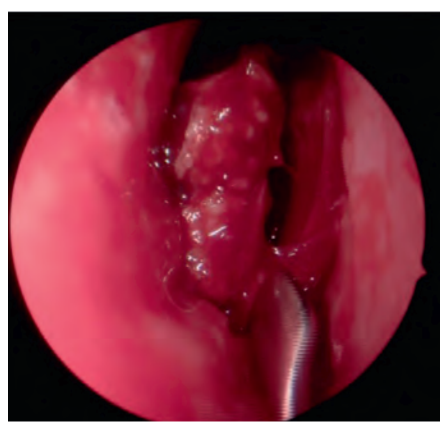

Figure 5.68 The inferior turbinate is dissected back to crista ethmoidalis.

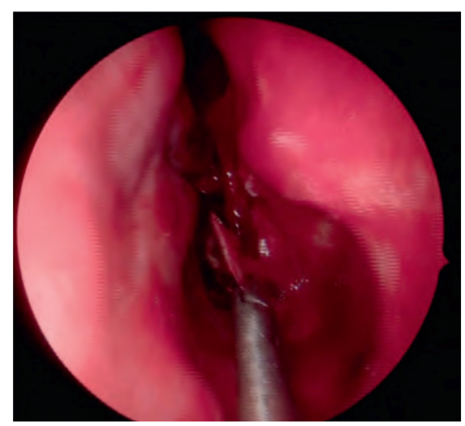

Figure 5.69 The medial wall of the maxillary sinus is dissected and mobilized.

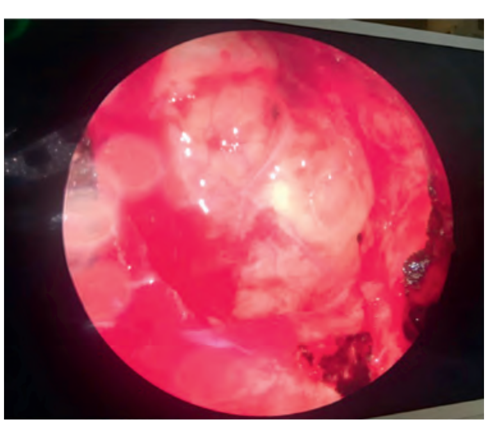

Figure 5.70 Interior view of the maxillary sinus with a 30-degree telescope.

Figure 5.71 Surgical specimen showing the tumor with clear margins.

Postoperative Care. Postoperative management involves a short course of oral antibiotics. Nasal saline irrigation starts in the immediate postoperative period. Frequent debridement in an outpatient or office setting is critical to prevent postoperative synechiae. Crusting is often present for several weeks and longer if the patient has received previous radiation therapy. An endoscopic view of the healed defect in the nasal cavity is shown in Fig. 5.72.

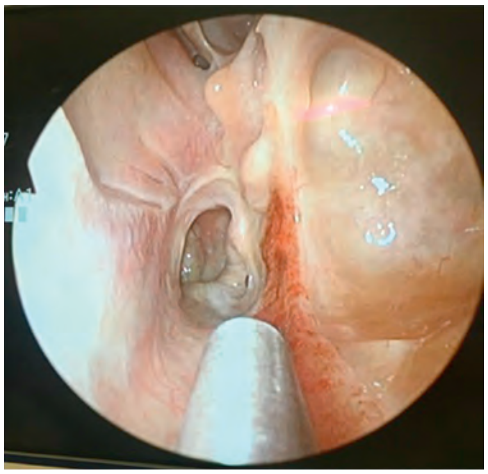

Figure 5.72 Postoperative endoscopic view of the nasal cavity 12 weeks following surgery.

Endonasal Endoscopic Resection of Angiofibroma

Resection of large, benign lesions is feasible through an endoscopic approach. However, careful study of the extent of the lesion and the feasibility of endonasal access and the potential for complete resection should be carefully studied before embarking on the procedure. The patient whose imaging studies are shown in Fig. 5.73 had a highly vascular large angiofibroma extending into the pterygomaxillary space. Due to the vascularity of the lesion, preoperative embolization was carried out. The entire lesion could be resected through an endonasal endoscopic approach. Postoperative follow-up imaging with MRI showed complete removal of the tumor.

Nasal Exenteration and Partial Rhinectomy for Carcinoma of the Nasal Septum

Squamous cell carcinoma of the nasal septum extending to the lateral aspects of the nasal cavity with bone invasion requires exenteration of the nasal cavity. Generally the operation is performed through a lateral rhinotomy, either unilateral or bilateral, depending on the extent of the tumor. However, when the overlying skin is involved by the tumor, a partial rhinectomy is required in addition to nasal exenteration to accomplish a monobloc excision of the tumor. The patient shown in Fig. 5.74 has squamous cell carcinoma of the septum of the nose in its upper half with invasion of the nasal bones and overlying skin. The patient's presenting

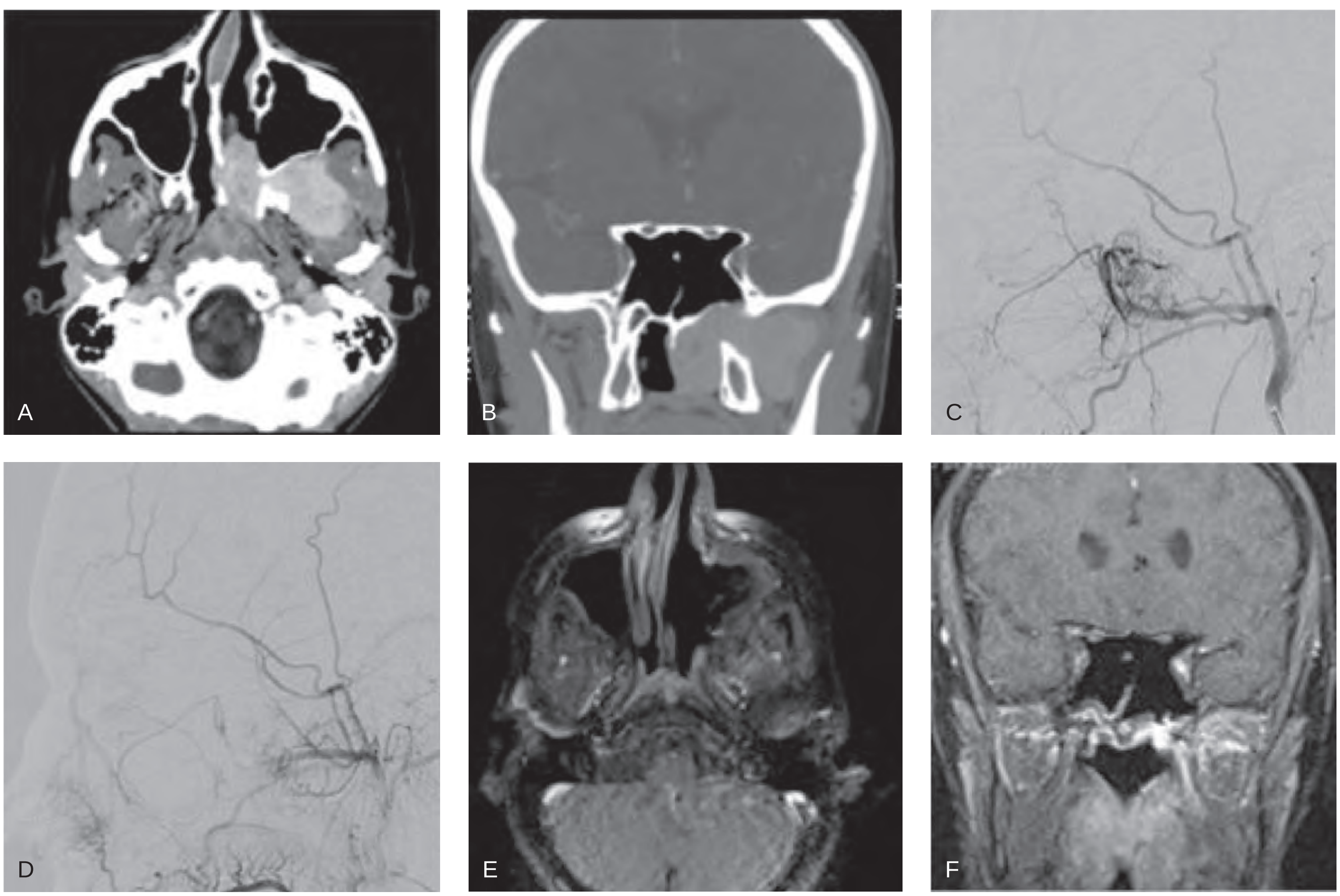

Figure 5.73 Contrast-enhanced computed tomography scan in axial (**A**) and coronal (**B**) views showing an extensive nasopharyngeal angiofibroma. Preoperative selective angiography shows a highly vascular lesion (**C**). Postembolization angiogram shows adequate occlusion of feeding vessels (**D**). Postresection magnetic resonance imaging scan in axial (**E**) and coronal (**F**) views show complete removal of the tumor.

Figure 5.74 A patient with squamous cell carcinoma of the nasal septum.

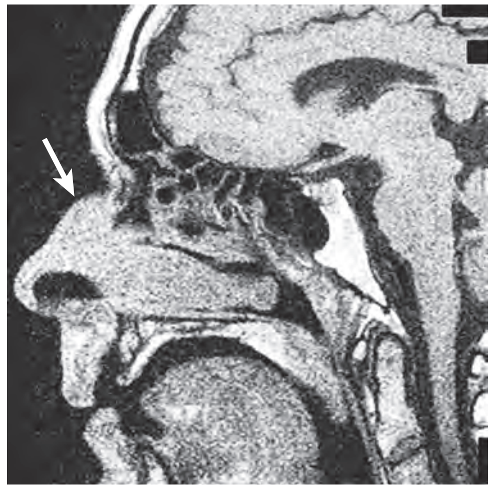

Figure 5.75 A sagittal view of the magnetic resonance imaging scan. Note subcutaneous tissue involvement (*arrow*).

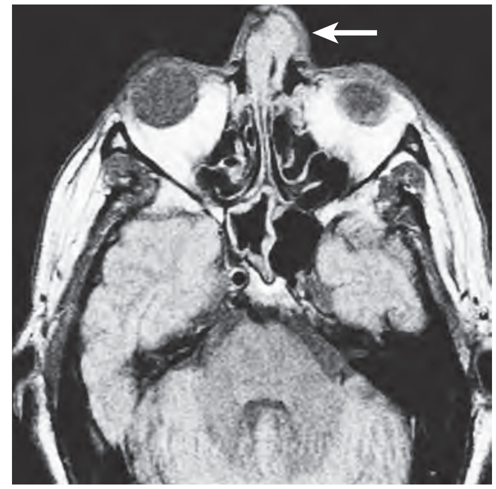

Figure 5.76 An axial view of the magnetic resonance imaging scan. Note subcutaneous tissue involvement (*arrow*).

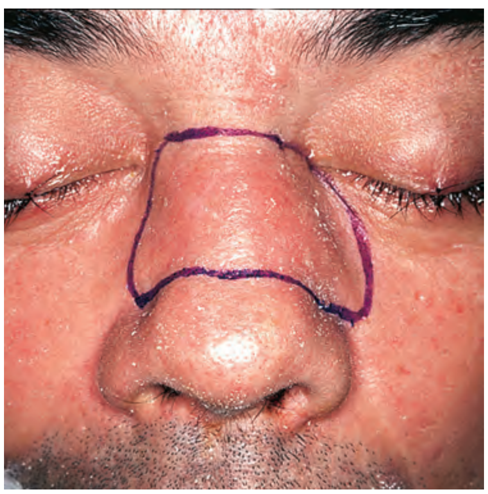

Figure 5.77 The external outline of the extent of the resection.

Figure 5.78 The surgical defect.

symptom was epistaxis and enlargement of the dorsum of the nose.

The radiographic workup of this patient included a CT scan and an MRI scan. A sagittal view of the MRI scan shows that the tumor arises from the nasal septum and extends through the subcutaneous soft tissues up to and involving the overlying skin (Fig. 5.75). An axial view of the MRI scan shows the anteroposterior extent of the tumor (Fig. 5.76). The bulk of the tumor involves the anterior half of the nasal septum and its overlying skin.

Surgical resection of this tumor required through-and-through resection of the upper half of the nose in conjunction with the nasal septum, bilateral ethmoidectomies, and resection of the nasal process of the maxilla bilaterally to obtain adequate soft tissue and bone margins. The extent of the skin to be resected is outlined in Fig. 5.77. The patient is placed under general anesthesia, with orotracheal intubation. The patient's eyelids are sutured shut with 6-0 nylon sutures. The skin incision as outlined is deepened with an electrocautery through the soft tissues up to the underlying bone circumferentially. To gain entry into the nasal cavity, a high-speed power saw is used to divide the nasal process of the maxilla, first on the right-hand side. On the left-hand side a similar bone cut is made, taking a somewhat larger portion of the nasal process of the maxilla and the medial aspect of the orbit. Similarly, the lower half of the nasal bones are divided bilaterally with a power saw to connect the bone cuts on the medial aspect of the orbits bilaterally. At this juncture, small osteotomes are used to fracture through the ethmoid air cells posteriorly up to the nasopharynx. The perpendicular plate of the ethmoid is then divided with gentle strokes using a small, straight osteotome. Heavy straight septal scissors are used to divide the nasal septum at the level of the lower skin incision all the way up to the vomer. The vomer is then fractured with an osteotome. The surgical specimen of the cancer of the nasal septum with bilateral ethmoidectomies and the overlying skin is removed in a monobloc fashion. The surgical defect is shown in Fig. 5.78. Note that the superior surface of the defect is nearly at the cribriform plate and the superior ethmoid air cells. Posteriorly the nasopharynx is seen, and inferiorly the floor of the nasal cavity is readily visualized. On the left-hand side, entry is made into the maxillary antrum; however, on the right-hand side, the antrum is not entered. Frozen sections are obtained from the mucosal edges of the surgical defect to ensure adequacy of the resection.

Repair of a surgical defect of this magnitude requires preoperative treatment planning and appropriate selection of a composite osteocutaneous free flap. A radial forearm osteocutaneous free flap was selected in this patient with a split segment of the lower end of the radius with its overlying skin. The bone is used to provide support to the nose, replacing the nasal septum,

Figure 5.79 The postoperative appearance of the patient 6 months following surgery.

and the skin paddle is divided into two halves, providing an inner lining and external coverage. The blood supply to the flap is reestablished by anastomosis between the radial artery and its accompanying veins to the facial artery and the common facial vein. The appearance of the patient 8 weeks following surgery shows satisfactory healing of the radial forearm flap, restoring the contour of the nose and providing adequate external lining (Fig. 5.79). This patient will need revision of the flap to improve the aesthetic appearance of the reconstructed nose.

Nasal Exenteration and Total Rhinectomy

Massive tumors involving the anterior inferior aspect of the nasal cavity, and particularly the overlying skin, require a rhinectomy and total nasal exenteration. The patient shown in Fig. 5.80 has a massive squamous cell carcinoma involving the anteroinferior aspect of the nasal cavity, including the nasal septum, the floor of the nasal cavity, the premaxilla, the columella, and a portion of the upper lip. The skin and nasal cartilages are also infiltrated by the tumor.

The surgical procedure for a rhinectomy and nasal exenteration is similar to that of bilateral medial maxillectomies with resection of the anterior floor of the nasal cavity and a premaxillectomy. The incision is made around the palpable extent of the tumor on the skin and the nose, extending from the skin of the cheek on one side along the dorsum of the nose to the skin of the cheek on the other side, and it continues on the skin of the upper lip to encompass the tumor. Similarly, a mucosal incision is placed in the gingivolabial sulcus extending from the premolar teeth on the right-hand side up to the premolar teeth on the left-hand side.

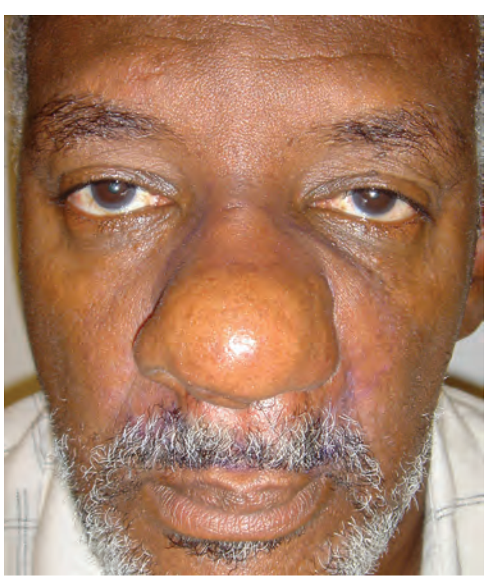

Figure 5.80 The external appearance of a patient with locally advanced carcinoma of the nasal septum and premaxilla.

The skin incision is made with a scalpel and deepened through the soft tissue with electrocautery up to the anterior wall of the maxilla on both sides. Superiorly, the skin incision is deepened through the soft tissues up to the anterior surface of the nasal bones. Inferiorly, the skin incision is deepened through the musculature up to the mucosal incision in the gingivolabial sulcus, dividing the full thickness of the upper lip, sparing the vermilion border.

Initial bone cuts in the anterior wall of the maxilla are made with a power saw. The bone cuts are extended along the nasal process of the maxilla bilaterally and through the lower half of the nasal bones in the midline. In the lower part, a mucosal incision is made in the hard palate, extending from the second premolar tooth on the right-hand side up to the second premolar tooth on the left-hand side to encompass the entire premaxilla. Using a right-angled power saw, the hard palate is transected along this mucosal incision. At this juncture, all soft-tissue attachments of the surgical specimen are completely divided.

A curved osteotome is used to fracture the transected bony structures. The osteotome is used to rock the specimen and free it from the remaining bony attachments. Finally, Mayo scissors are used to divide the remaining soft-tissue attachments at the mucosa of the roof of the mouth and along the gingivobuccal sulcus, and the specimen is removed in a monobloc fashion. Complete hemostasis is secured with the use of electrocautery and bone wax as necessary.

Because only a very small area of bone is exposed, a skin graft is not required except for placement on the raw surface of the transected upper lip to achieve circumferential skin and mucosal coverage. Xeroform gauze is packed snugly into the nasal cavity for hemostasis. The packing is removed in 3 to 4 days, after which intensive hygiene of the surgical defect is instituted using power sprays with half-strength peroxide and saline solution at least two to three times per day. Bacitracin ointment is applied along the skin edge of the surgical defect to minimize crusting. A loose nasal packing with gauze soaked in mineral oil is introduced into the nasal cavity after each irrigation or spray treatment, to minimize crusting. Meticulous care of the surgical defect is required until it has completely epithelialized and crusting has cleared up (Fig. 5.81).

Because the patient underwent postoperative radiation therapy, fabrication of a nasal prosthesis was delayed for 4 months. Nasal exenteration with a rhinectomy and resection of the hard palate create significant aesthetic and functional morbidity. Restoration of aesthetic appearance and speech and swallowing functions is best and most expeditiously achieved with prosthetic rehabilitation. Prosthetic rehabilitation of this patient requires a two-part prosthesis. One part of the prosthesis replaces the hard palate and premaxilla. The other part is a prosthetic nose (Fig. 5.82). The prosthetic nose is attached to the dental prosthesis with magnets (Fig. 5.83). Subsequently this patient had permanent implants placed on the stump of the nasal bones with magnets to hold the prosthetic nose in place (Fig. 5.84).

Figure 5.81 The healed surgical defect shows complete epithelialization and no crusting.

Figure 5.82 The prosthetic nose shows a good color match.

Figure 5.83 The dental prosthesis in place with magnets for attachment of the nasal prosthesis.

Figure 5.84 The external appearance of the patient showing complete prosthetic rehabilitation.

Peroral Partial Maxillectomy (Infrastructure Maxillectomy)

The intraoral view of a patient with squamous cell carcinoma of the upper alveolar ridge extending from the region of the lateral incisor socket up to the region of the second molar socket is shown in Fig. 5.85. The patient is edentulous at this site and presented with a history of an ill-fitting denture. Appropriate radiographic evaluation with CT scans in axial and coronal planes is mandatory for accurate delineation of the extent of the tumor before embarking on a perioral partial maxillectomy.

The procedure is performed under general anesthesia with nasotracheal intubation through the contralateral nasal cavity. The oral cavity is exposed with appropriate cheek retractors. An incision is made in the mucosa of the gingivobuccal sulcus and that of the hard palate with satisfactory mucosal margins around the visible and palpable tumor. If teeth are present, an appropriate tooth is extracted well away from the margin of

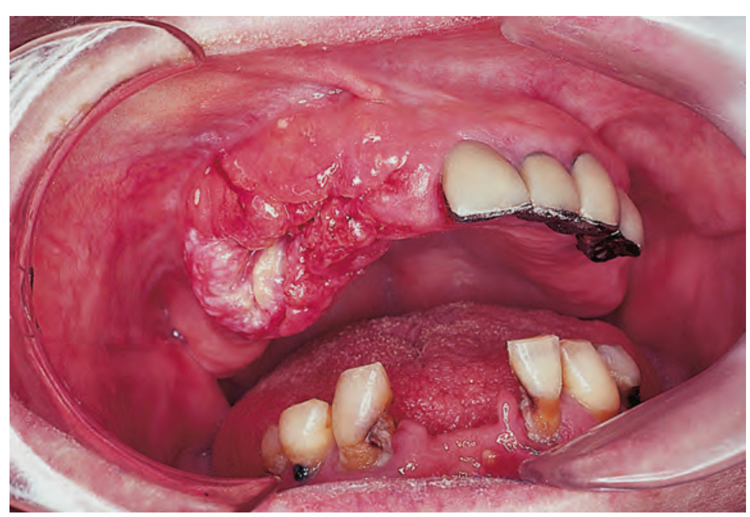

Figure 5.85 Squamous cell carcinoma of the upper gum.

the tumor through the socket of which the bone resection is undertaken to preserve the integrity of the adjacent remaining tooth. The mucosal incision is extended through the soft tissues up to the bony anterior wall of the maxilla and to the hard palate intraorally. This incision is extended through soft tissue circumferentially to divide all the soft-tissue attachments of the hard palate and the lower half of the maxilla before bone division.

A high-speed power saw is used to make bone cuts through the previously outlined mucosal incision, and an osteotome is used to divide the remaining bone attachments and remove the specimen in a monobloc fashion. The anterosuperior view of the surgical specimen shows resection of the lower half of the maxillary antrum with its anterior and lateral wall intact; it was removed in a monobloc fashion with the alveolar process of the maxilla and the adjacent hard palate (Fig. 5.86). A lateral view of the surgical specimen shows satisfactory excision of the tumor of the upper gum with adequate bony, soft tissue, and mucosal margins circumferentially (Fig. 5.87). If the mucosa of the remaining antrum does not show any chronic inflammatory changes, it does not need to be curetted out. In that setting, a skin graft is not required. On the other hand, if the antral mucosa shows chronic inflammatory changes with pseudopolyp formation, it is best curetted out and replaced with a split-thickness skin graft. Whether or not a skin graft is used, Xeroform gauze packing is introduced into the remaining maxillary antrum. A previously fabricated dental obturator is now wired to the remaining teeth to retain the packing in position. If a skin graft is not used, then the packing may be removed in 2 to 3 days, and an interim dental obturator is fabricated until complete epithelialization of the surgical defect is demonstrated. At that point, a permanent removable dental prosthesis is made by maxillofacial prosthodontists.

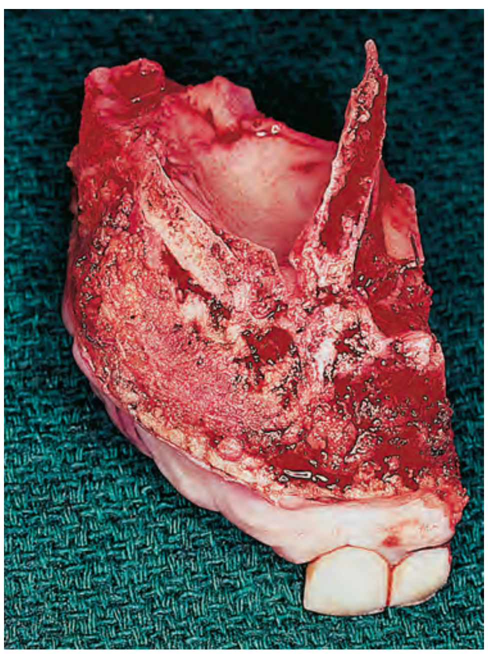

Figure 5.86 An anterosuperior view of the surgical specimen.

Subtotal Maxillectomy

A subtotal maxillectomy essentially removes the entire maxilla except the floor of the orbit and thus includes the infrastructure and suprastructure of the maxilla. If the floor of the orbit is also resected, the operation is termed a *total maxillectomy*. In that setting, it is essential to reconstruct the floor of the orbit to prevent ptosis of the globe. An intraoral view of the palate of a patient with a 3-month history of an enlarging submucosal mass is shown in Fig. 5.88. Although the lesion was painless, the patient experienced discomfort in mastication, and the presence of a mass on the hard palate also caused intraoral discomfort. Radiographic evaluation of the tumor showed that the tumor had caused bone destruction of the floor of the maxillary antrum, confined to the infrastructure of the left maxilla. The clinical presentation and radiographic findings are suggestive of a carcinoma arising from the minor salivary glands of the hard palate with secondary extension into the maxillary antrum through the hard palate. A biopsy of this mass confirmed that it was an intermediate-grade mucoepidermoid carcinoma.

The patient is placed on the operating table under general anesthesia that is maintained through an orotracheal tube. In this patient, a classic Weber-Ferguson incision was used. The skin incision is made with a scalpel for elevation of the cheek flap and electrocautery is used thereafter, which provides excellent hemostasis. The upper lip is divided through its full thickness up to the gingivolabial sulcus (Fig. 5.89). Brisk hemorrhage from the superior labial artery requires ligation of that vessel.

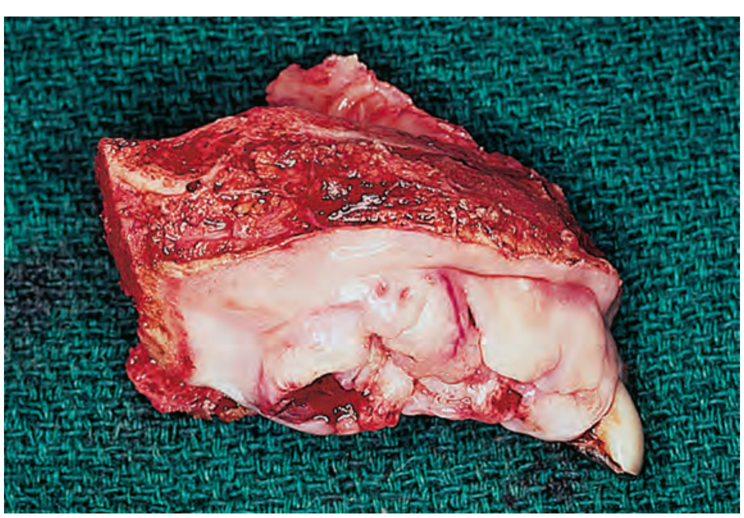

Figure 5.87 A lateral view of the surgical specimen, showing monobloc resection of the tumor with adequate mucosal, soft tissue, and bone margins.

Figure 5.88 An intraoral photograph of the palate of a patient with a 3-month history of an enlarging submucosal mass.

Figure 5.89 The upper lip is divided through its full thickness up to the gingivolabial sulcus.

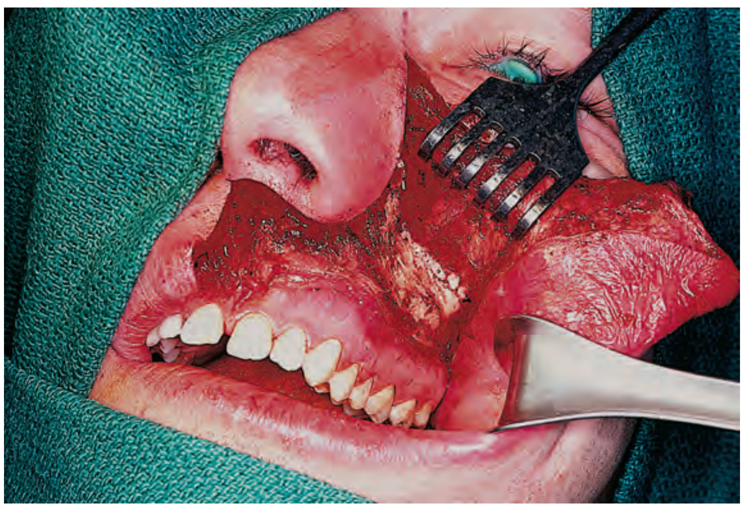

Figure 5.90 Continued elevation of the cheek flap in the infraorbital region exposes the infraorbital nerve and its entry into the soft tissues of the cheek.

To elevate the upper cheek flap, an incision is made in the mucosa of the upper gingivobuccal sulcus, remaining close to the gingiva; it is elevated full thickness, remaining right over the periosteum of the maxilla until its posterolateral aspect is exposed.

Continued elevation of the cheek flap in the infraorbital region exposes the infraorbital nerve and its entry into the soft tissues of the cheek (Fig. 5.90). If only the lower half of the maxilla is to be resected, then the infraorbital nerve should be carefully preserved to retain the cutaneous sensations of the cheek. It is important to elevate the cheek flap as far back as the posterolateral surface of the maxilla, exposing the undersurface of the zygoma to gain access to the pterygomaxillary fissure.

Entry is made into the nasal cavity by dividing the soft tissues along the ala of the nose and through the mucosa of the lateral wall of the nasal cavity (Fig. 5.91). A mouth gag is now introduced on the opposite side and the oral cavity is opened as widely as possible to expose the alveolar process and the hard palate (Fig. 5.92). A high-speed power saw with a very fine blade is used to divide the anterior wall of the maxilla just below the infraorbital foramen. The line of bone division is shown on the lateral view of a skull (Fig. 5.93). The bone cut is extended anteriorly and posteriorly to create the proposed line of resection through the anterior wall of the maxillary antrum and to allow excision of the lower half of the maxilla as the surgical specimen. The line of transection is continued anteriorly through the nasal process of the maxilla and posteriorly up to the zygoma and around the posterolateral surface of the maxilla.

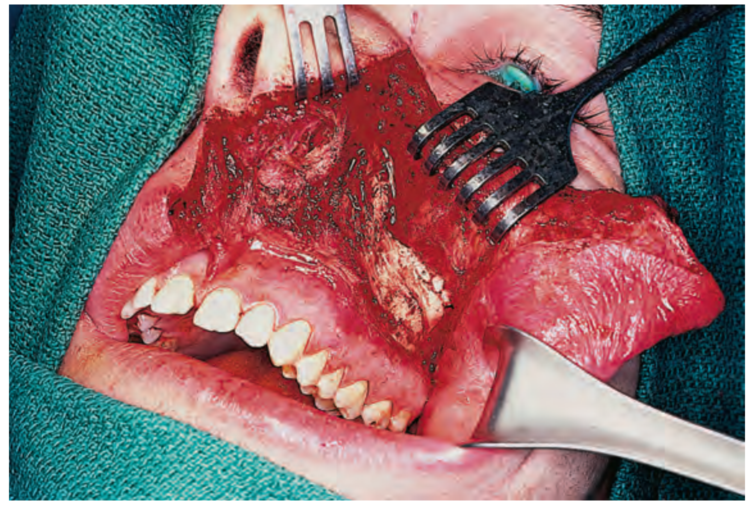

Figure 5.91 Entry is made into the nasal cavity by dividing the soft tissues along the ala of the nose and through the mucosa of the lateral wall of the nasal cavity.

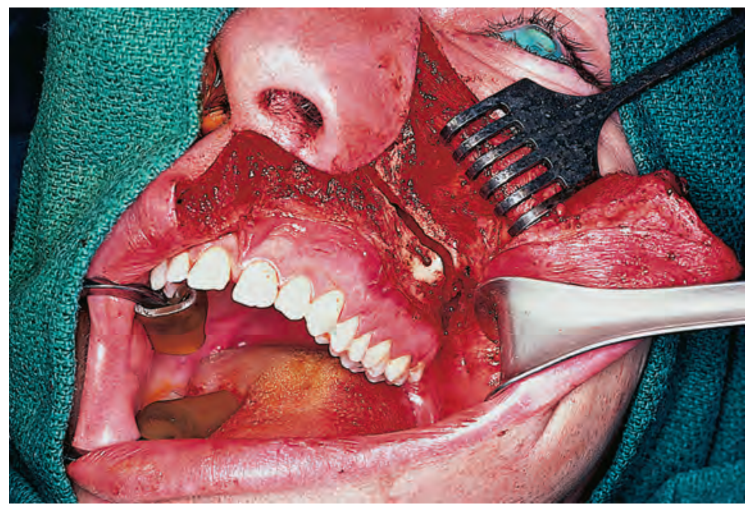

Figure 5.92 The oral cavity is opened as wide as possible to expose the alveolar process and the hard palate.

Figure 5.93 The line of bone division is shown on the lateral view of a skull.

The proposed line of transection through the alveolar process is now examined. If space exists between two teeth, the line of fracture is carried between them. However, if the teeth are intact, it is quite likely that the last tooth on the remaining alveolar process will become loose and may be lost, so it is advisable to extract one tooth at the proposed line of transection of the alveolar process, as was done in this patient. The power saw is used again and the bone cut between the previously created transverse line of transection and the alveolar process is connected. Use of a power saw with a fine blade gives a very precise bone cut at the line of transection through the maxilla for the proposed specimen (Fig. 5.94).

Attention is now focused on the mucosa of the hard palate. With the mouth wide open, a tongue depressor is used to provide adequate exposure. With use of a needle-tip electrocautery, an incision is made in the mucosa of the hard palate around the primary tumor, keeping satisfactory mucosal margins in all directions (Fig. 5.95). The incision begins posteriorly at the maxillary tubercle and then curves anteromedially around the tumor. Anteriorly, the incision is continued behind the alveolar process bearing the incisors and canine teeth of the left-hand side. This mucosal incision meets the socket of the extracted first molar tooth to complete circumferential mobilization of the specimen. The mucosal incision in the hard palate is deepened through the mucoperiosteum up to the bone throughout its length. The proposed bone cut through the hard palate is shown on a skull in Fig. 5.96.

A close-up view of the surgical field shows the incision in the mucosa of the hard palate as well as a portion of the soft palate (Fig. 5.97). The power saw is used to divide the hard palate along the line of mucosal incision. Brisk bleeding during this part of the operation is encountered because of hemorrhage from the palatine vessels and the branches of the internal maxillary artery coming through the posterior wall of the maxilla and the pterygoid fossa. Attempts to control this bleeding are unsuccessful until the surgical specimen is removed, and thus it is essential to expedite this step of the operation.

Once all the bone cuts are made with the power saw, an osteotome is used to connect the fracture lines, permitting the specimen to be rocked over the soft-tissue attachments. With use of either electrocautery or Mayo scissors, the posterior soft-tissue attachments of the specimen (the pterygoid muscles) are divided, and the surgical specimen of the lower half of the maxilla is removed.

Bleeding at this point is usually from the branches of the internal maxillary artery, the sphenopalatine artery, and smaller

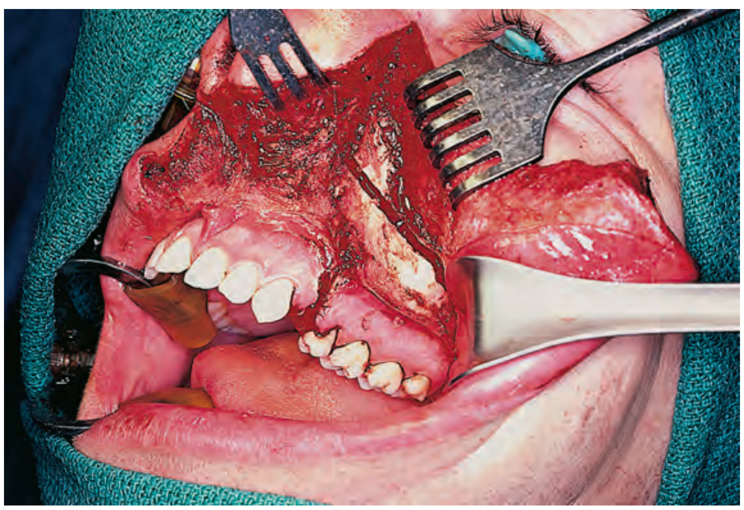

Figure 5.94 A power saw with a fine blade gives a very precise bone cut at the line of transection through the maxilla for the proposed specimen.

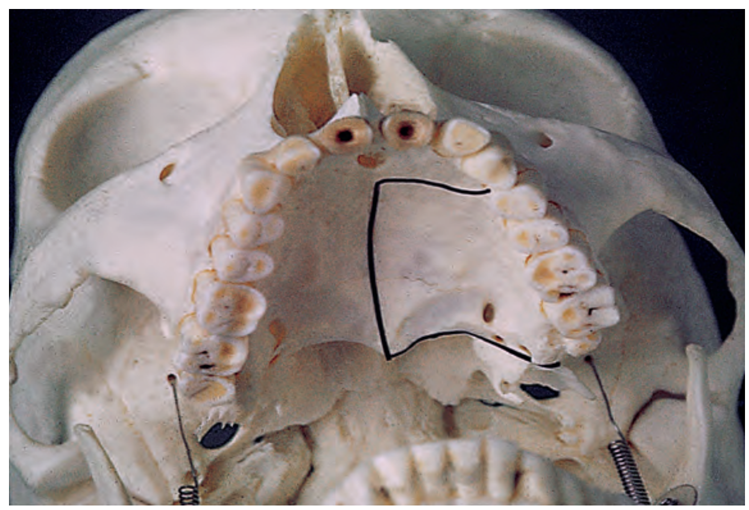

Figure 5.96 The proposed bone cut through the hard palate is shown on a skull.

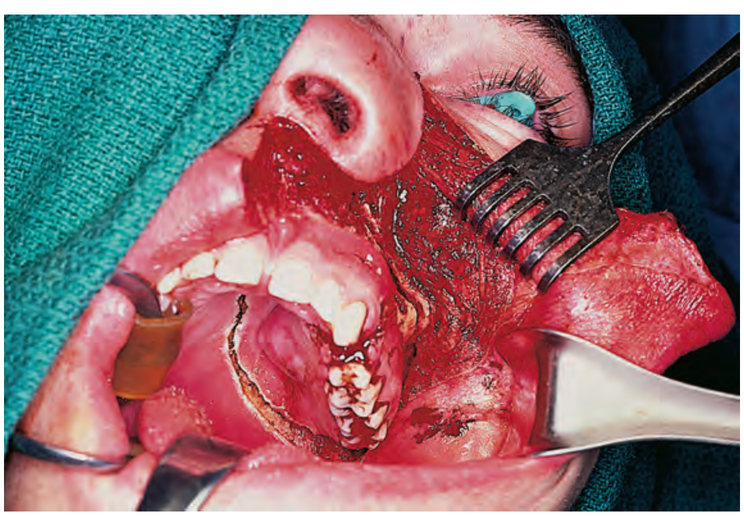

Figure 5.95 An incision is made in the mucosa of the hard palate around the primary tumor, keeping satisfactory mucosal margins in all directions.

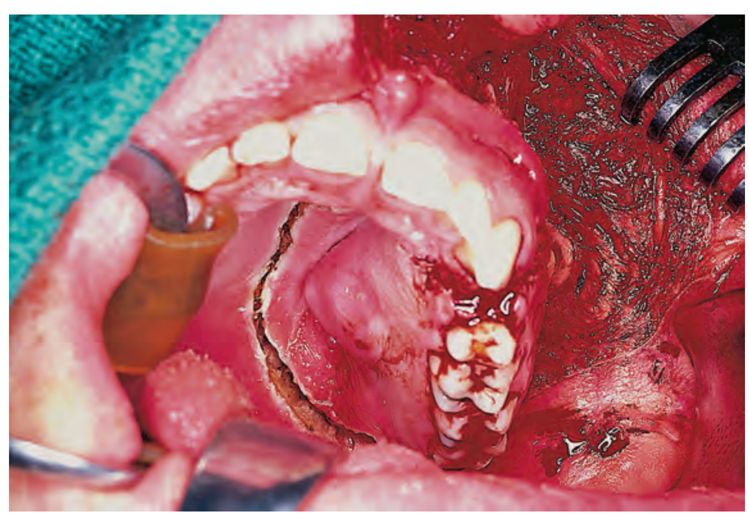

Figure 5.97 A close-up view of the surgical field shows the incision in the mucosa of the hard palate as well as a portion of the soft palate.

blood vessels of the soft palate. Hemorrhage from the internal maxillary artery is controlled by ligation of that vessel or, alternatively, a chromic catgut suture ligature is placed through the stumps of the pterygoid muscles. However, bleeding from the sphenopalatine artery is rarely amenable to control by ligation; the stump of this vessel is usually in a bony crevice, and hemostasis is best achieved by electrocoagulation.

The surgical defect shows the upper half of the maxillary antrum, which is lined by mucus-secreting epithelium (Fig. 5.98). The mucosa of the maxillary antrum should be curetted out completely if it shows chronic inflammatory changes. This procedure will provide a specimen for histologic analysis of the mucosal lining of the maxillary antrum and leave the bony remnant of the antrum clean. If inflamed mucosa is left behind, chronic edema in the mucosa will lead to pseudopolyp formation with excessive amounts of mucus that drains directly into the oral cavity, giving a salty taste. However, if the antral mucosa appears normal and does not show any inflammation, it may be left alone. All sharp spicules on the bony edges are now smoothed out with a burr. The cut edges of the mucosa of the anterior and posterior walls of the soft palate are approximated with interrupted chromic catgut sutures. The wound is irrigated with Bacitracin solution, and blood clots are evacuated.

A split-thickness skin graft is used to line the undersurface of the cheek flap and the bare, bony wall of the remaining maxillary antrum. The graft is sutured to the mucosal edge of the cheek flap with 3-0 chromic catgut interrupted sutures (Fig. 5.99). The skin graft is not sutured but merely applied to the bare, bony surface of the upper half of the antrum and retained in that position with Xeroform gauze packing, which is applied snugly into the maxillary defect. Once the skin graft is sutured and applied appropriately, packing begins from the roof of the antrum with Xeroform gauze that is applied into the defect digitally and retained in that position by gentle digital pressure to conform to the crevices and corners of the maxillary antrum. The remainder of the defect is completely packed to snugly fill the surgical defect (Fig. 5.100). The packing stretches the skin graft and maintains it in contact with the raw areas of the cheek and the maxillary antrum.

The previously fabricated dental obturator is now applied and secured with wires (Fig. 5.101). The obturator is wired to the remaining teeth to replace the excised portion of the hard palate. If the patient is edentulous, the obturator is wired to the remaining alveolus by means of drill holes. After the obturator is applied, additional Xeroform gauze packing may be required to keep the skin graft over the cheek flap in position with a moderate degree of pressure. Installation of the dental obturator replaces the lost portion of the hard palate and allows

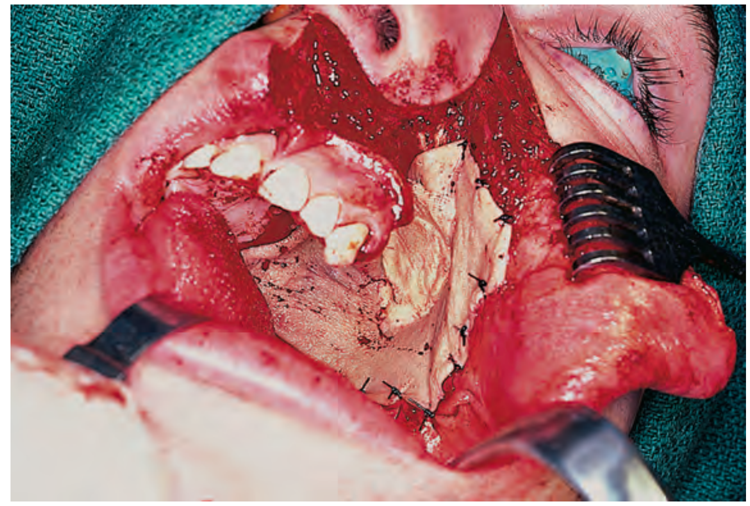

Figure 5.99 The skin graft is sutured to the mucosal edge of the cheek flap.

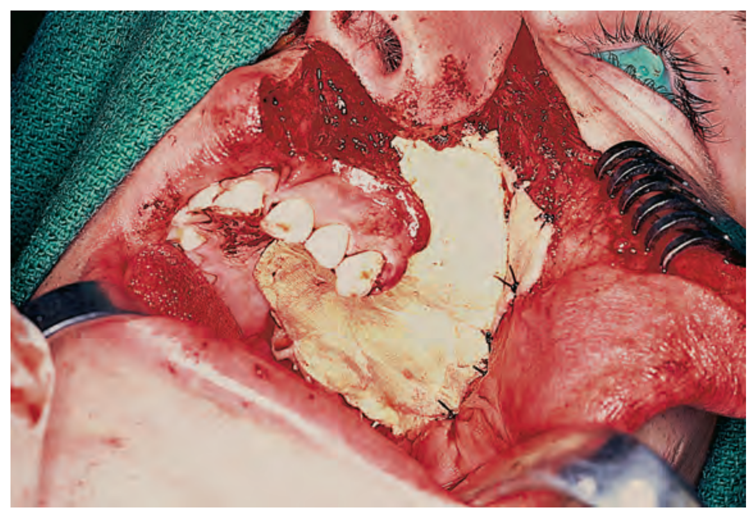

Figure 5.100 Xeroform gauze packing is used to snugly fill the surgical defect and hold the skin graft in position.

Figure 5.98 The surgical defect shows the upper half of the maxillary antrum, which is lined by mucus-secreting epithelium.

Figure 5.101 The previously fabricated dental obturator is applied and secured with wires.

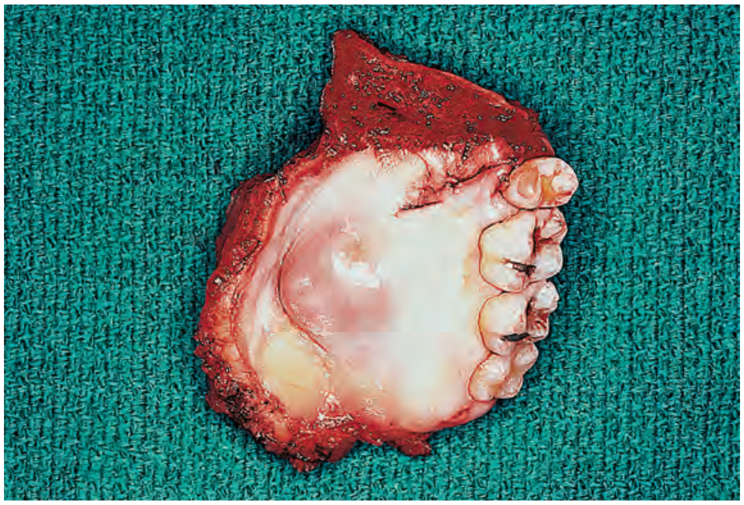

Figure 5.102 The palatal aspect of the surgical specimen.

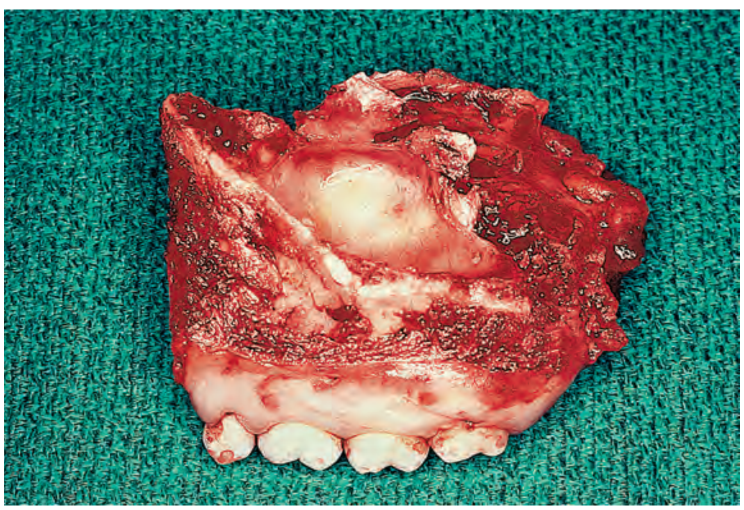

Figure 5.103 A lateral view of the surgical specimen showing the excised lateral wall of the maxilla with a submucosal tumor mass in the floor of the antrum and adequate margins in all directions.

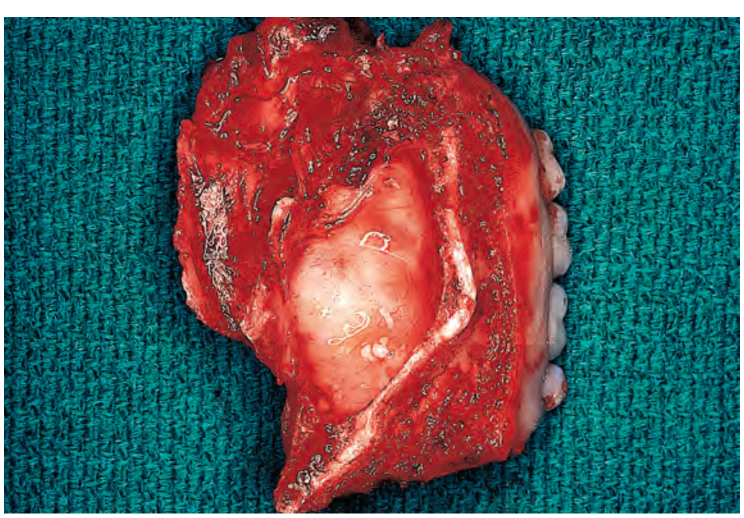

Figure 5.104 A superior view of the surgical specimen showing the nasal process and anterior wall of the maxilla in its lower part with the tumor mass contained well within the maxillary antrum.

the patient to swallow liquids and soft foods immediately after surgery without much difficulty.

The skin incision is closed in two layers with use of chromic catgut interrupted sutures for subcutaneous tissues and nylon for skin. Meticulous attention is paid to accurate approximation of the skin edges to achieve a superior aesthetic result. Accurate realignment of the skin edges near the ala and the floor of the nasal cavity is particularly important in that regard. The corneal shield from the eye is removed, and a fine coating of Bacitracin ointment is applied to the incision. A pressure dressing usually is not necessary. Blood loss during this operation is minimal. The patient is awakened soon, and the endotracheal tube is removed promptly. A moderate degree of swelling of the lower eyelid and cheek is apparent on the first day after surgery, but this swelling is transient and usually resolves within 2 to 3 days without taking any specific measures. Most patients are able to tolerate a soft diet within a day after surgery.

The palatal aspect of the surgical specimen is shown in Fig. 5.102. Note that the submucosal tumor mass is well within the center of the resected portion of the hard palate with adequate mucosal and bony margins in all three dimensions.

The lateral view of the surgical specimen shows the excised lateral wall of the maxilla with a submucosal tumor mass in the floor of the antrum with adequate margins in all directions (Fig. 5.103). A superior view of the surgical specimen shows the nasal process and anterior wall of the maxilla in its lower part with the tumor mass contained well within the resected maxillary antrum (Fig. 5.104).

Postoperative Care

Postoperative care of the patient following partial maxillectomy centers around the maintenance of optimal oral hygiene and care of the facial wound until sutures are removed. Meticulous attention is paid to removal of all clots and crusts over the suture line, because they provide a nidus for infection and may lead to suture line sepsis with occasional wound separation. Occasionally the use of warm compresses over the cheek is necessary in the presence of persistent swelling and/or an inflammatory reaction.

On the second postoperative day, the patient is taught to irrigate and rinse the oral cavity every 3 to 4 hours with a solution of baking soda and salt in warm water to keep the mouth clean of all debris and secretions. Mechanical cleansing of the oral cavity with a power spray of half-strength hydrogen peroxide and saline solution is desirable twice daily.

One week after surgery, the dental obturator is removed by cutting the wires. The packing is gently removed thereafter. The skin graft in the surgical defect is inspected, and any excess shreds of the graft are trimmed off. An interim obturator is now made by the prosthodontist and is retained with clasps on the remaining teeth. Retention of a prosthesis in edentulous patients may be difficult and often unsatisfactory initially. Oral and nasal irrigations are continued until complete healing of the skin graft is seen in the surgical defect. A permanent dental obturator is fabricated approximately 6 to 8 weeks later.

The surgical defect in the oral cavity approximately 3 months after surgery shows a clean maxillary defect with the lost portion of the alveolus and hard palate on the left-hand side (Fig. 5.105). The permanent dental obturator is clasped onto the remaining teeth, providing complete replacement of the excised hard palate and lost dentition (Fig. 5.106). This permanent obturator restores the patient's ability to speak normally and eat all types of foods.

Figure 5.105 The surgical defect in the oral cavity approximately 3 months following surgery.

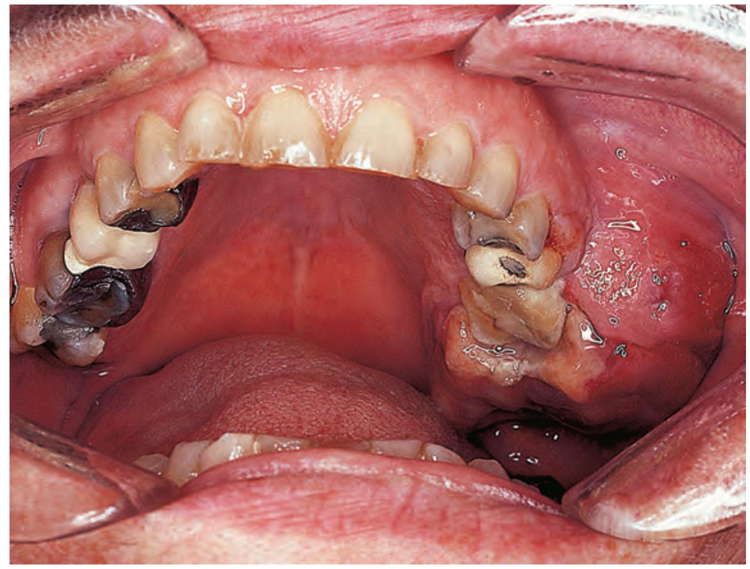

Figure 5.107 An intraoral view of the tumor of a patient with an odontogenic myxoma of the left mandible.

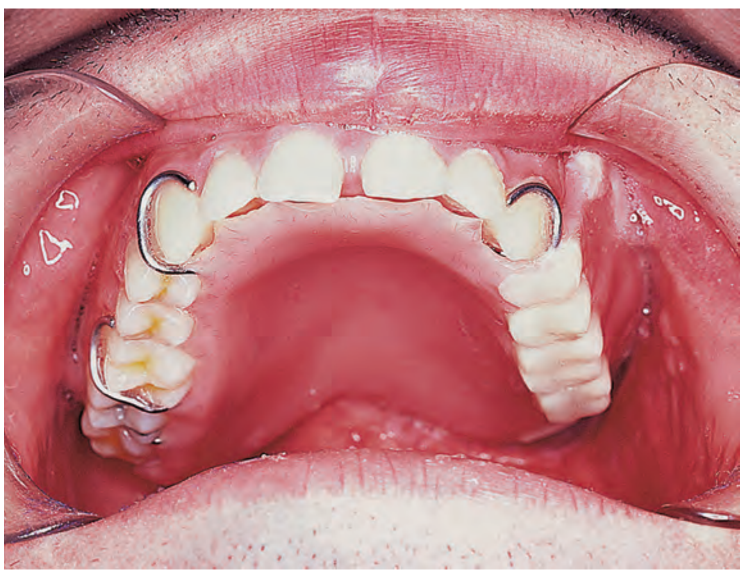

Figure 5.106 The permanent dental obturator is clasped onto the remaining teeth, providing complete replacement of the excised hard palate and lost dentition.

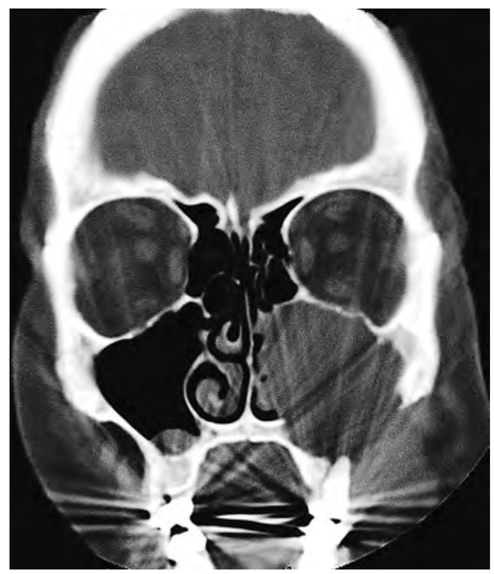

Figure 5.108 The bone window of the computed tomography scan in a coronal plane.

Total Maxillectomy

Complete removal of the maxilla becomes necessary when a primary tumor arising from the surface lining of the maxillary sinus fills up the entire antrum. Primary mesenchymal tumors arising in the maxilla such as soft tissue and bone sarcomas also require total removal of the maxilla to encompass the entire lesion.

Although the surgical approach for total maxillectomy is similar to that used for partial maxillectomy, a much wider exposure is necessary. With proper care and attention to detail, it usually is possible to remove the entire maxilla as a monobloc specimen for total removal of tumors contained within it.

The intraoral view of the tumor of a patient with an odontogenic myxoma of the maxilla is shown in Fig. 5.107. This patient presented with a bleeding lesion in the oral cavity and loose upper teeth on the left-hand side. A CT scan of the paranasal sinuses of this patient in a coronal view shows a soft-tissue tumor filling up the entire left maxillary antrum, which is expanded. The tumor is relatively homogeneous and displaces the medial wall of the maxilla, causing obstruction to the left nasal cavity and expansion of the lateral wall of the maxilla under the zygomatic arch (Fig. 5.108). However, the tumor does not extend into the orbit or the ethmoid region. An axial view on the bone window shows extension of the tumor through the posterolateral wall of the maxilla with expansion of the anterior and medial walls (Fig. 5.109).

The surgical approach for a total maxillectomy requires a Weber-Ferguson incision with subciliary extension along the lower eyelid. A modified Weber-Ferguson incision respecting the nasal subunits is preferred. The incision begins in the midline of the upper lip, dividing the philtrum from the vermilion border up to the root of the columella. At that point, the incision extends into the floor of the nasal cavity for a few millimeters and then returns back outside of the nasal cavity around the ala of the nose to permit accurate realignment of the cheek flap at the time of closure (Fig. 5.110). The skin incision is deepened through the soft tissues and musculature of the upper lip and the left cheek. An upper cheek flap is elevated by a mucosal incision through the upper gingivolabial and upper gingivobuccal sulcus on the left-hand side (Fig. 5.111). The skin incision for the subciliary extension begins at about the level of the medial canthus of the eye and follows the closest skin crease adjacent to the tarsal plate. The skin incision here should be placed very delicately, because the skin of the lower

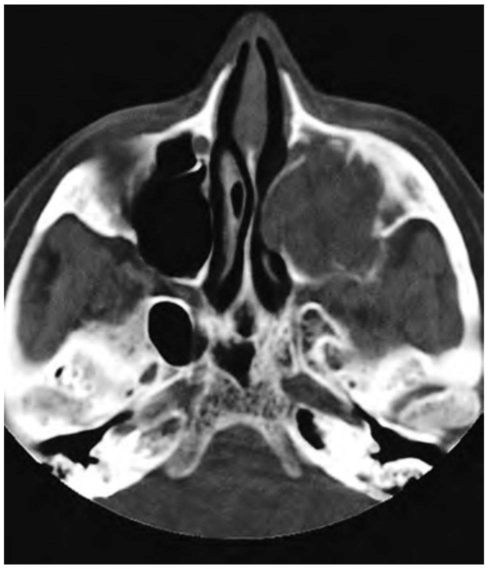

Figure 5.109 The bone window of the computed tomography scan in an axial plane.

eyelid is extremely thin and tears easily. In addition, the skin of the lower eyelid is elevated superficial to the orbicularis oculi muscle to preserve the nerve and blood supply to that muscle to retain function of the eyelids (Fig. 5.112). This delicate elevation of the skin of the lower eyelid and its separation from the orbicularis oculi muscle is best accomplished with a low-voltage electrocautery and a microtip for fine dissection (Fig. 5.113). The upper cheek flap is elevated to approximately 1 cm lateral to the lateral canthus of the eye to provide sufficient exposure of the entire anterior and anterolateral wall of the maxilla (Fig. 5.114). Note that the orbicularis oculi muscle is preserved intact on the eyelid, from whence only the skin has been elevated.

Subperiosteal dissection of the orbital contents in the lower part of the orbit permits excision of the orbital plate of the maxilla, which will be the superior margin of the surgical specimen (Fig. 5.115). The orbicularis oculi muscle is retracted cephalad to expose the inferior orbital rim. An incision is made in the periosteal attachment at the infraorbital rim, and a Freer elevator is used to separate the periosteum from the bony floor of the orbit. Elevation of the periosteum is carried as far posteriorly as possible to

Figure 5.110 The incision extends into the floor of the nasal cavity for a few millimeters and then returns back outside of the nasal cavity around the ala of the nose to permit accurate realignment of the cheek flap at the time of closure.

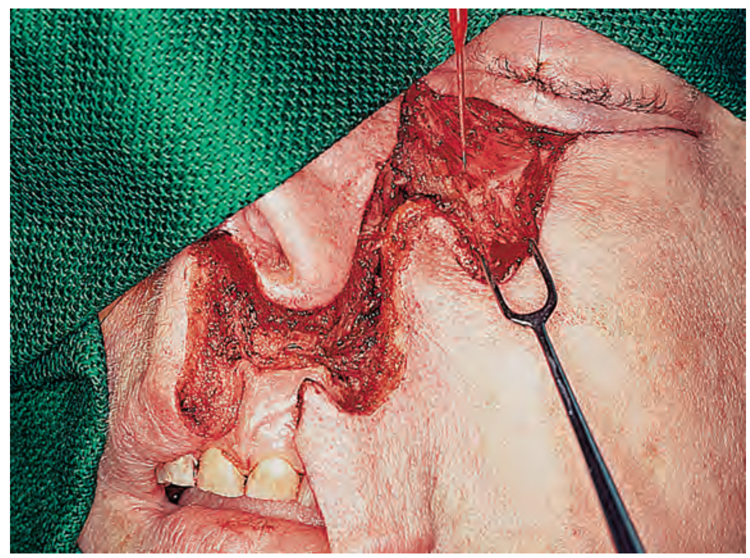

Figure 5.112 The skin of the lower eyelid is elevated superficial to the orbicularis oculi muscle to preserve the nerve and blood supply to that muscle to retain function of the eyelids.

Figure 5.111 The skin incision is deepened through the soft tissues and the upper cheek flap is elevated by a mucosal incision through the upper gingivolabial and upper gingivobuccal sulcus on the left-hand side.

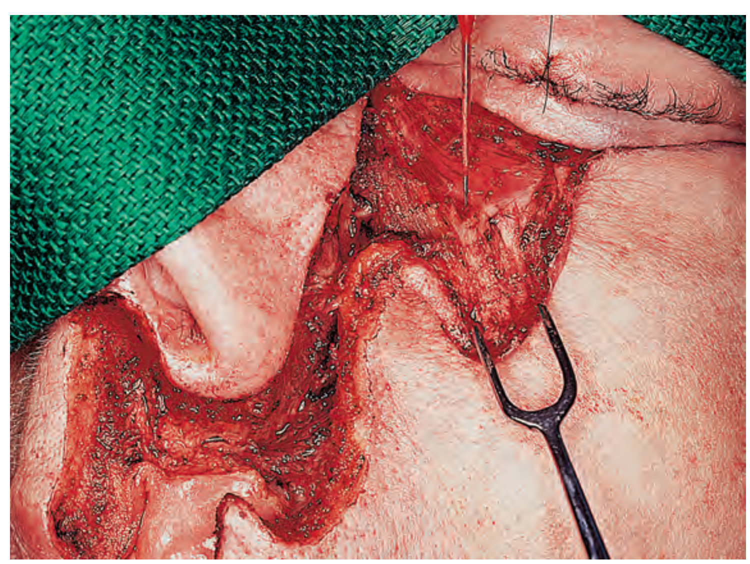

Figure 5.113 This delicate elevation of the skin of the lower eyelid and its separation from the orbicularis oculi muscle is best accomplished with an electrocautery with a low voltage and a microtip for fine dissection.

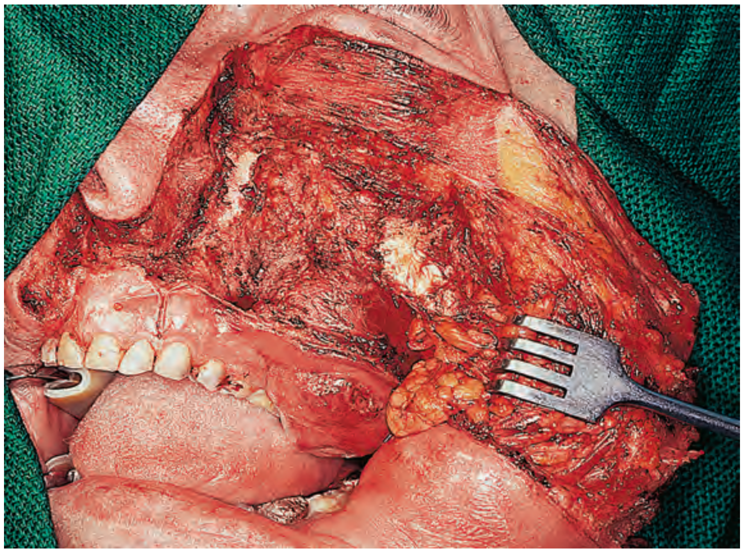

Figure 5.114 The upper cheek flap is elevated approximately 1 cm lateral to the lateral canthus of the eye to provide sufficient exposure of the entire anterior and anterolateral wall of the maxilla.

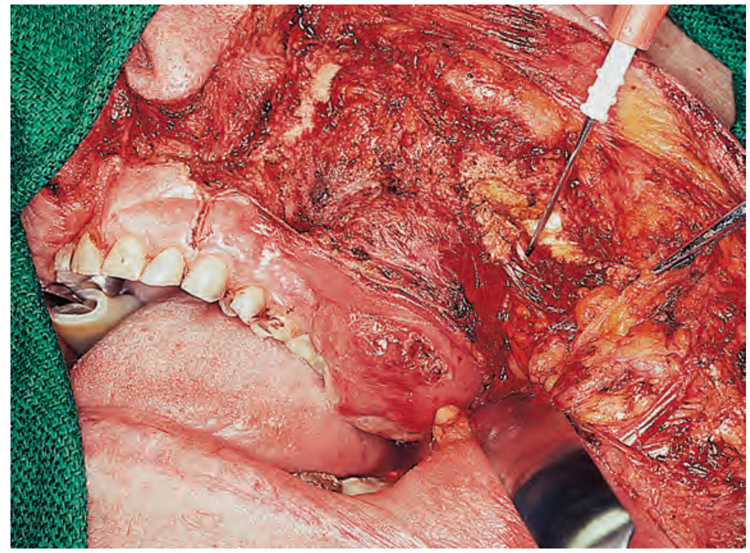

Figure 5.116 Division of the attachment of the masseter muscle on the inferior border of the zygoma.

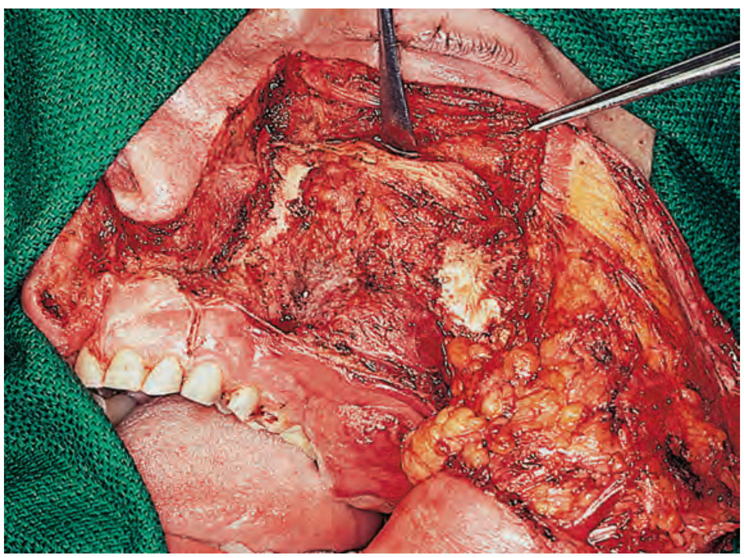

Figure 5.115 Subperiosteal dissection of the orbital contents in the lower part of the orbit permits excision of the orbital plate of the maxilla, which will be the superior margin of the surgical specimen.

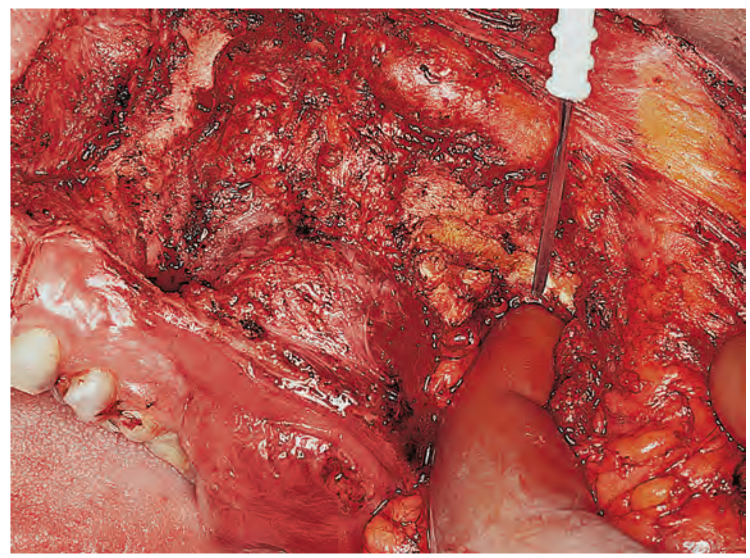

Figure 5.117 Insertion of a finger under the tendon puts it on stretch, allowing it to be divided easily with electrocautery.

expose the entire orbital plate of the maxilla. The attachment of the masseter muscle on the inferior border of the zygoma is divided next with use of an electrocautery (Fig. 5.116). In most patients the masseter muscle is tendinous in this area, and inserting a finger under the tendon puts it on stretch, allowing it to be divided easily with electrocautery (Fig. 5.117).

Attention is now focused on the oral cavity, which is exposed with use of a mouth gag and a tongue depressor. A mucosal incision is placed between the lateral incisor and the canine tooth, which would be the anterior line of resection through the alveolar process of the left maxilla to encompass a total maxillectomy. An incision is now made in the mucosa of the hard palate extending from the canine tooth up to the midline. The incision is extended posteriorly in the midline up to the junction of the hard and soft palate, at which point it turns laterally behind the maxillary tubercle up to the gingivobuccal sulcus (Fig. 5.118). This incision is deepened through the mucoperiosteum of the hard palate. Posteriorly the incision is deepened through the attachments of the medial pterygoid muscle to free up soft-tissue attachments to the left maxilla.

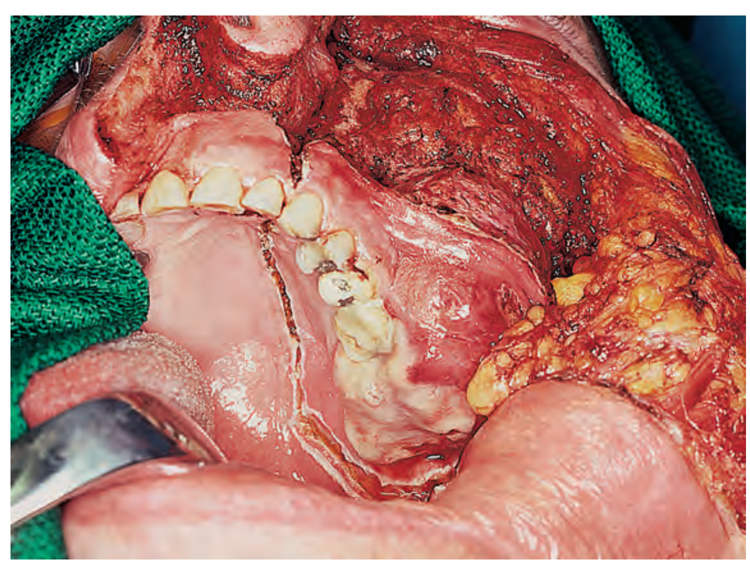

Figure 5.118 The palatal incision is extended posteriorly in the midline up to the junction of the hard and soft palate, at which point it turns laterally behind the maxillary tubercle up to the gingivobuccal sulcus.

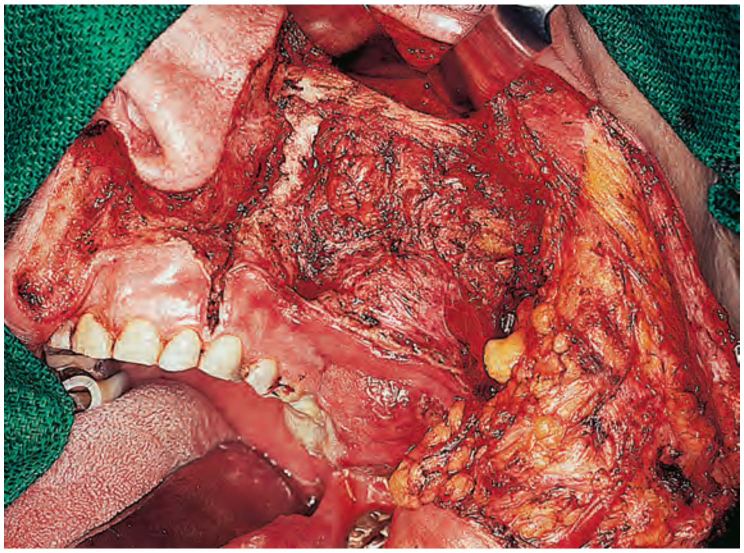

Figure 5.119 Entry is made into the nasal cavity by opening the vestibule of the nasal cavity through the piriform recess to expose the nasal process of the maxilla.

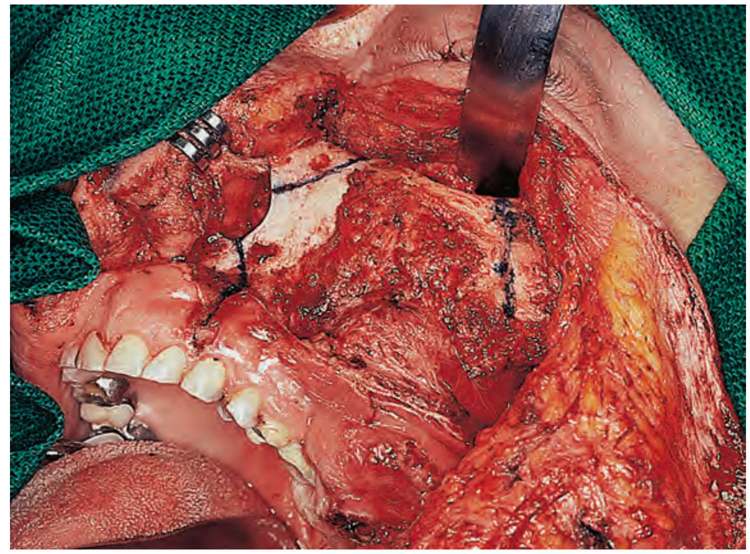

Figure 5.120 The proposed bone cuts for total maxillectomy are marked on the patient with the use of electrocautery.

Figure 5.121 The proposed bone cuts are shown on a skull.

Figure 5.122 A thin strut of the infraorbital rim can be preserved in some patients.

Figure 5.123 The zygoma is divided lateral to the lateral wall of the maxilla.

At this juncture, entry is made into the nasal cavity by opening the vestibule of the nasal cavity through the piriform recess to expose the nasal process of the maxilla (Fig. 5.119). Nearly all the soft-tissue attachments of the maxilla anteriorly, laterally, and in the oral cavity, as well as in the orbit, are divided. The proposed bone cuts for a total maxillectomy are marked out with the use of electrocautery (Fig. 5.120). Superomedially, the nasal process of the maxilla is divided. Superolaterally, the maxilla is separated from the zygomatic arch, and inferiorly the maxilla is divided through its alveolar process between the lateral incisor and canine tooth up to the midline and from there onward through the midline up to its posterior margin. Inferolaterally, the maxilla is separated from the pterygoid plates through its hamulus to provide a monobloc resection. The proposed bone cuts are shown on a skull, demonstrating division of the nasal process of the maxilla, the zygomatic process of the maxilla, and the premaxillary region (Fig. 5.121). The orbital plate of the maxilla is divided. In some patients a thin strut of the infraorbital rim can be preserved, as shown in Fig. 5.122. The zygoma is divided lateral to the lateral wall of the maxilla, as shown in Fig. 5.123. The bone cuts through the hard palate are shown in Fig. 5.124. A malleable retractor is used to retract

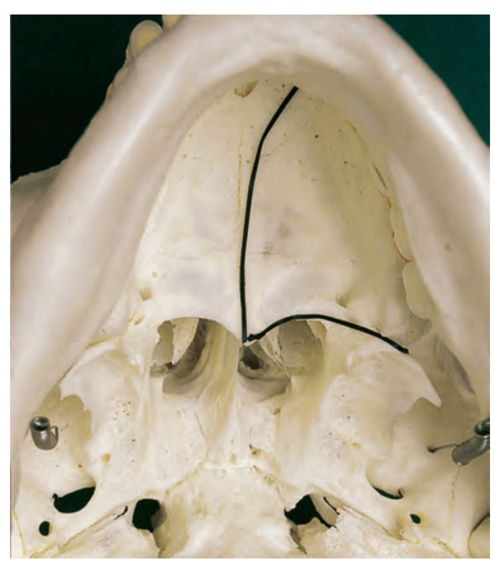

Figure 5.124 Bone cuts through the hard palate.

the orbital contents, and a high-speed power saw is used to accomplish the bone cuts previously outlined (Fig. 5.125). All the bone cuts are completed within a short period to minimize blood loss. Brisk bleeding is expected to occur from each bone cut, and thus it is crucial to conduct the operative procedure expeditiously at this juncture. Once all the bone cuts are completed with the power saw, an osteotome is used to complete the fracture lines and remove the specimen in a monobloc fashion. Soft-tissue and muscular attachments on the posterior aspect of the maxilla are divided with heavy Mayo scissors.

The surgical defect following total maxillectomy is shown in Fig. 5.126. Note that the floor of the orbit is missing, although the periosteum is intact. The nasal cavity, pterygoid fossa, and nasopharynx are seen in the depth of the surgical defect. Complete hemostasis is secured by ligating or electrocoagulating bleeding points. The wound is irrigated with Bacitracin solution at this point.

A previously harvested split-thickness skin graft is now used to line the raw areas in the surgical defect (Fig. 5.127). The skin graft is appropriately applied and retained in place with a roll of Xeroform gauze packing. The skin graft is secured with interrupted chromic catgut sutures to the mucosal edges of the cheek flap, after which it is splayed out over the surgical defect and appropriately positioned while packing is introduced to provide complete coverage of the surgical defect and support to the periosteum of the orbit. The skin incision is closed in two layers with use of interrupted 3-0 chromic catgut sutures for soft tissues and 5-0 nylon for the skin along the nasolabial fold and the upper lip (Fig. 5.128). The skin of the lower eyelid is sutured, but with a subcuticular absorbable suture extending from the medial canthus to the lateral edge of the incision. A prefabricated surgical dental obturator is now wired to the remaining teeth to retain the packing in position for 1 week (Fig. 5.129).

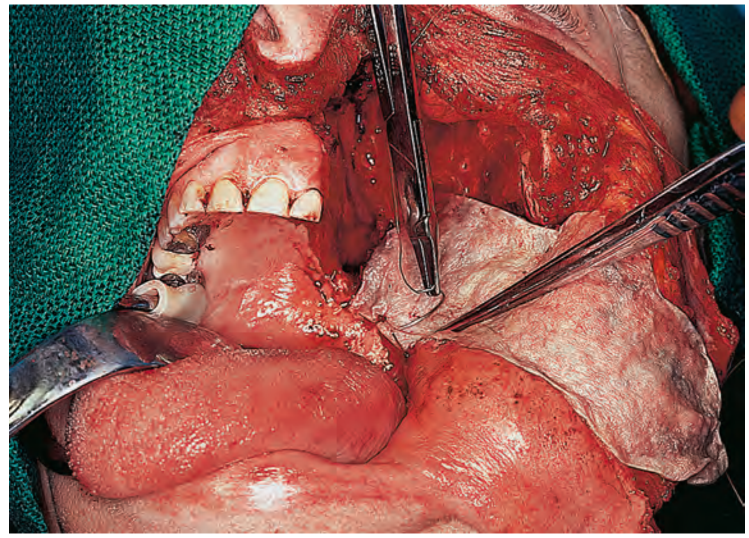

Figure 5.127 A split-thickness skin graft is used to line the raw areas in the surgical defect.

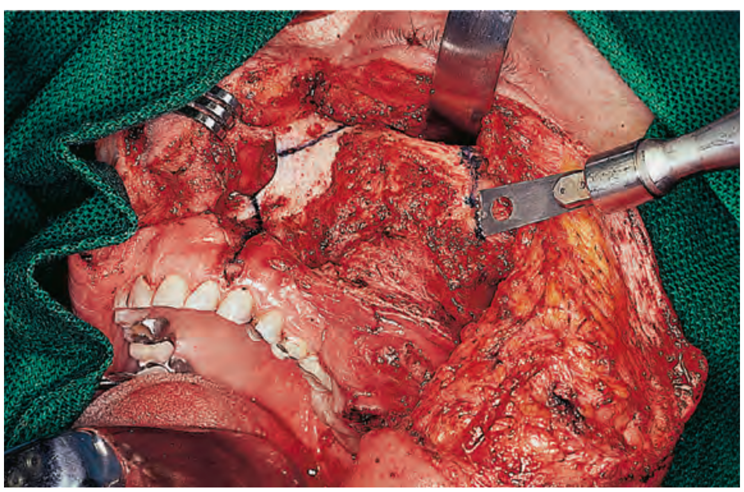

Figure 5.125 A malleable retractor is used to retract the orbital contents, and a high-speed power saw is used to complete the bone cuts.

Figure 5.128 The skin incision is closed in two layers.

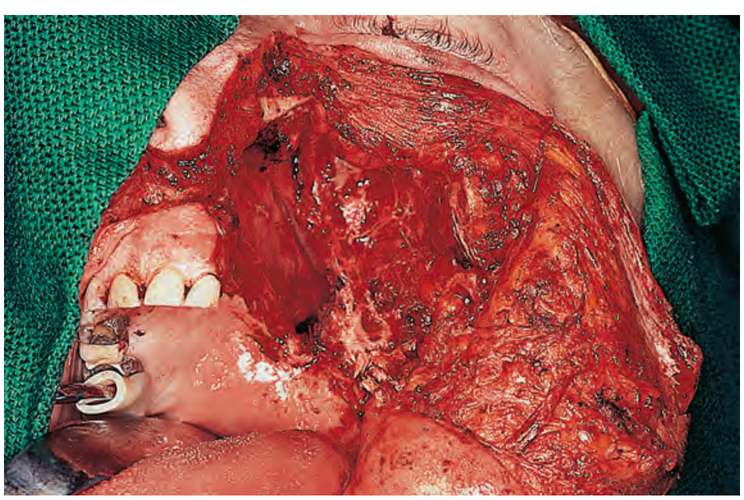

Figure 5.126 The surgical defect following total maxillectomy.

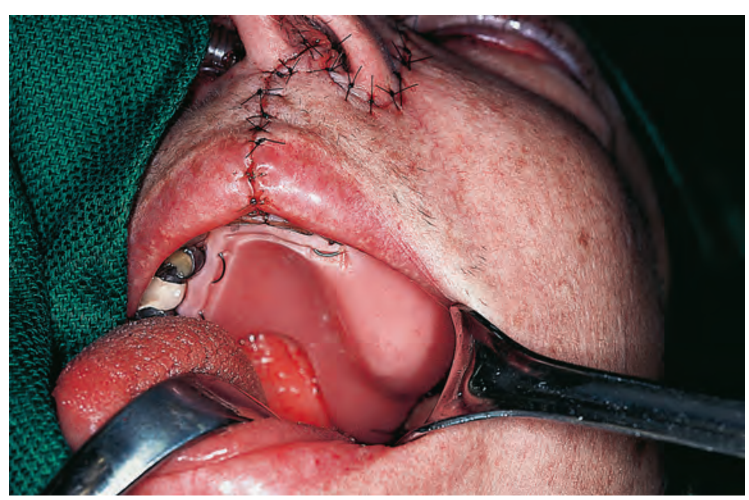

Figure 5.129 A prefabricated surgical dental obturator is wired to the remaining teeth to retain the packing in position for a week.

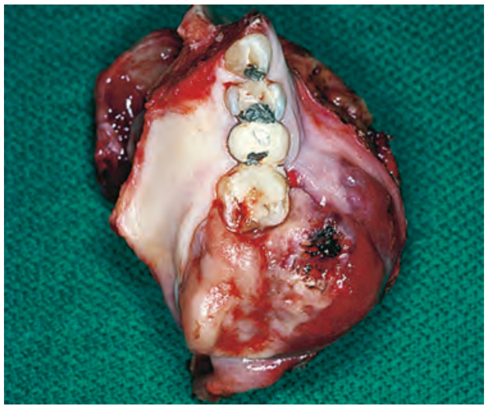

Figure 5.130 A palatal view of the surgical specimen.

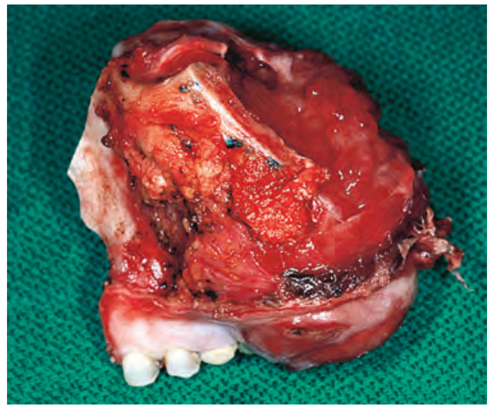

Figure 5.131 A lateral view of the surgical specimen.

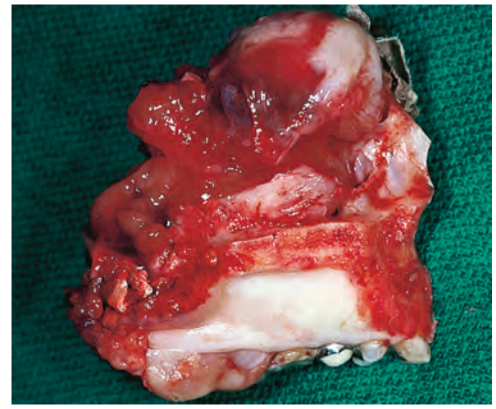

Figure 5.132 A medial view of the surgical specimen.

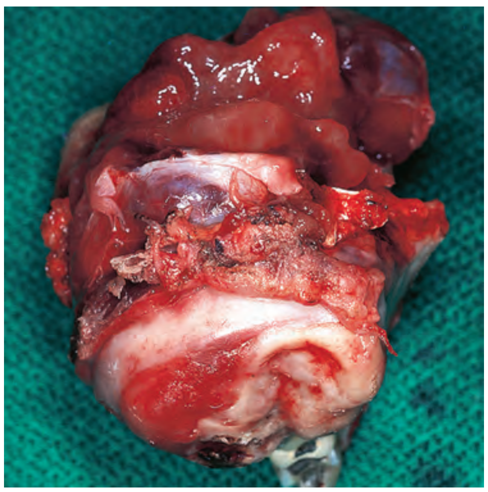

Figure 5.133 A posterior view of the surgical specimen.

Figure 5.134 A superior view of the surgical specimen.

The surgical specimen shown from the palatal view demonstrates the resected hard palate, alveolar process, and the fungating tumor through the region of the molar teeth (Fig. 5.130). The lateral view of the surgical specimen shows the transected zygomatic process of the maxilla and the soft-tissue attachment on the posterolateral wall of the maxilla. Note that the tumor is removed in a monobloc fashion (Fig. 5.131). The medial view of the surgical specimen demonstrates the inferior and middle turbinates in the lateral wall of the nasal cavity with the stumps of the pterygoid muscles on the posterior aspect of the maxilla (Fig. 5.132). The posterior view of the surgical specimen demonstrates complete excision of the posterior wall of the maxilla (Fig. 5.133). The superior view of the surgical specimen demonstrates the nasal process of the maxilla, the zygomatic process of the maxilla, and the tumor contained within the maxillary antrum pushing the lateral wall of the nasal cavity medially and the floor of the antrum superiorly (Fig. 5.134).

Postoperative Care. Postoperative care after a total maxillectomy is similar to that after a partial maxillectomy. Patients are encouraged and trained to perform frequent oral irrigations (particularly after each meal) and exercises of the jaw to prevent trismus and relieve pain resulting from fibrosis. Subsequent management of the patient is similar to that described for a patient who has had a partial maxillectomy. However, certain aspects of the procedure deserve special mention. Minor bleeding from raw areas and granulation tissue in the pterygoid fossa is not uncommon and may require cauterization with silver nitrate. Oral exercises are mandatory for several months to prevent trismus. Fabrication of the definitive dental obturator should take into consideration obliteration of the air space in the surgical defect, which affects the quality of the voice. Satisfactory quality of the voice is achieved by a bolus extension of the dental obturator in the maxillectomy defect.

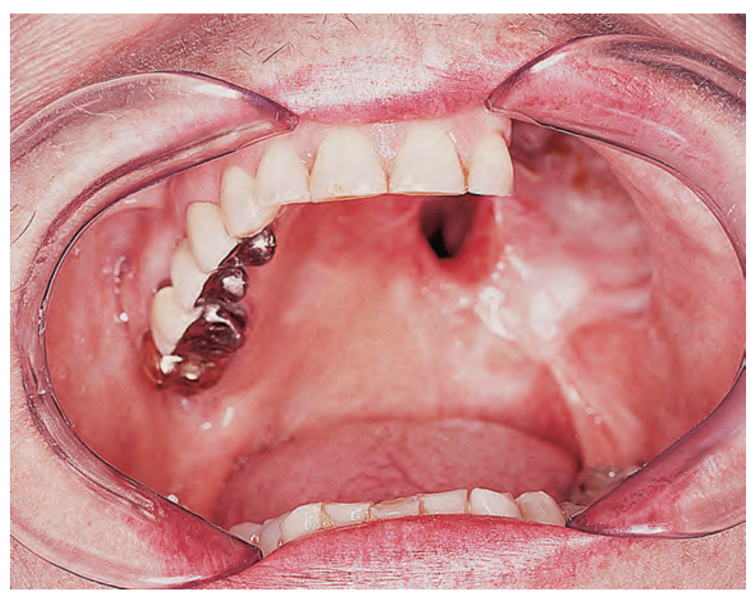

Figure 5.135 An intraoral view 3 months following surgery.

An intraoral view 3 months after surgery shows a well-healed skin graft in the maxillectomy defect (Fig. 5.135). A permanent

dental obturator fabricated by the maxillofacial prosthodontist is shown in Fig. 5.136. The intraoral view of the dental obturator in position shows obliteration of the maxillectomy defect. Restoration of the alveolar process and teeth facilitates speech and mastication (Fig. 5.137). A photograph of the patient 3 months following surgery shows excellent healing of the skin incision, although a soft tissue deficit is seen in the infraorbital region as a result of removal of the left maxilla (Fig. 5.138).

Total Maxillectomy With Orbital Exenteration

A radical maxillectomy with orbital exenteration is indicated when a primary tumor of the nasal cavity or paranasal sinuses extends into the orbit through the orbital periosteum. Orbital exenteration of a functioning eye with normal vision is considered only if the possibility of a curative resection exists. Removal of a functioning eye for a palliative operation is not recommended. The diagnostic workup and preoperative preparation of the patient are similar to that of other patients with tumors of the nasal cavity or paranasal sinuses, as previously discussed.

Figure 5.136 The permanent dental obturator.

A modified Weber-Ferguson incision is required with a subciliary and supraciliary extension circumferentially encompassing the palpebral fissure of the eye. Thus the lateral extensions follow the margin of the lower eyelid as well as that of the upper eyelid up to the lateral canthus. In essence, nearly all of the steps for mobilization of the maxilla are the same as those described for the total maxillectomy procedure. However, several additional steps of the operative procedure to mobilize the orbital contents and exenterate the orbit are described here.

Skin incisions are placed over the lower and upper eyelid extending from the medial to the lateral canthus. Sharp skin hooks are used to elevate the skin of the upper eyelid as a flap, remaining superficial to the orbicularis oculi muscle. The skin of the upper eyelid is elevated all the way up to the superior rim of the orbit. The lower cheek flap is elevated through the subciliary extension of the Weber-Ferguson incision in the usual manner. Once the orbital rim is circumferentially exposed, the attachment of the orbital periosteum to the orbital rim is incised in its superior half. A Freer periosteal elevator is used to separate the orbital periosteum from the bony roof of the orbit all the way up to the apex of the orbit. If the primary tumor arises in the maxillary antrum and extends to the orbit through the roof of the antrum, no attempt is made to mobilize the periosteum in the lower half of the orbit. On the other hand, if the primary tumor arises in the nasal cavity or ethmoid, the orbital periosteum on the medial half of the orbit is left attached to the lamina papyracea and is not elevated. The extraocular muscles at the apex of the orbit are then divided with use of electrocautery. Finally, a right-angled hemostat is used to clamp the optic nerve and its accompanying blood vessels. The remaining extraocular muscles and the optic nerve are then divided with Mayo scissors. Brisk hemorrhage is to be expected and is easily controlled with packing until the surgical specimen is removed.

The remaining steps of the operation are similar to those described in the total maxillectomy procedure except that superior mobilization of the specimen is done around the contents of the orbit, with either the floor of the orbit or the medial wall of the orbit remaining attached to the maxilla, depending on the location of the primary tumor. The surgical defect created by a radical maxillectomy and orbital exenteration

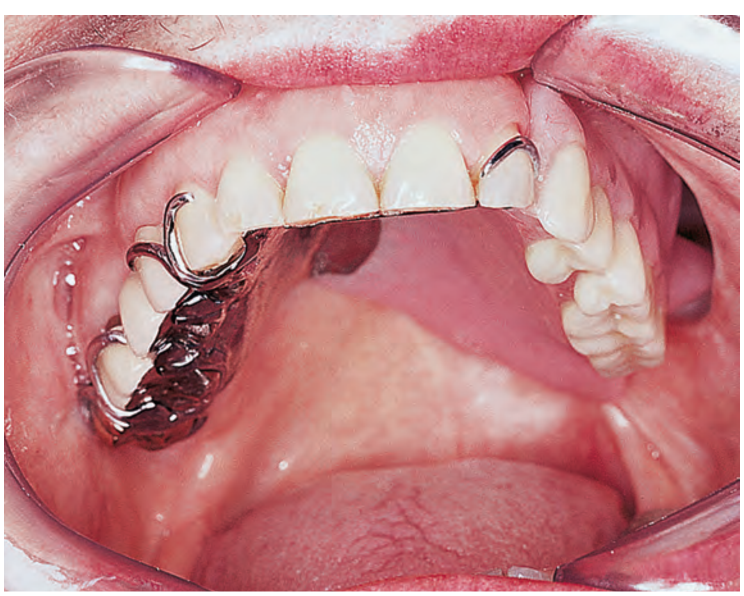

Figure 5.137 An intraoral view of the dental obturator in position.

Figure 5.138 The appearance of the patient 3 months after surgery.

leaves a large, raw area of the bony orbital socket and the maxillectomy defect with exposure of the musculature and soft tissues in the pterygoid fossa communicating with the nasal cavity and nasopharynx. If the hard palate is removed, then the surgical defect communicates with the oral cavity.

Reconstruction of the surgical defect can be accomplished with use of either a split-thickness skin graft and a maxillofacial prosthesis or a microvascular composite free flap. The patient shown in Fig. 5.139 underwent a radical maxillectomy with orbital exenteration for squamous cell carcinoma of the maxillary antrum extending to the orbit. The appearance of the patient several weeks after surgery shows an open orbital socket communicating with the nasal cavity, nasopharynx, and oral cavity. Functional and aesthetic restoration of this debilitating defect is accomplished with use of maxillofacial prostheses. A dental prosthesis is applied to restore the defect in the hard palate. A close-up view of the orbit shows the upper surface of the dental obturator (Fig. 5.140). A facial prosthesis with an artificial eye is then introduced into the orbital socket and retained with glue, restoring the aesthetic appearance of the patient (Fig. 5.141). Alternatively, the orbital facial prosthesis can be retained with osseointegrated implants introduced into the orbital margin of the frontal bone to which it is attached either mechanically or with a magnet.

Total Maxillectomy With Orbital Exenteration and Reconstruction With Free Tissue Transfer

When a radical maxillectomy with orbital exenteration requires sacrifice of the overlying skin of the face, the surgical defect becomes quite complex and difficult to repair without a microvascular free flap. Prosthetic restoration alone, without soft tissue support and skin coverage, leaves a significant functional and aesthetic debility and is not recommended. The patient shown in Fig. 5.142 has a recurrent carcinoma of the right maxilla extending into the right orbit following a previous partial maxillectomy performed for squamous cell carcinoma. The recurrent tumor involves the skin of the cheek extending from the parotid region to the nasolabial fold and from the eyebrow to the level of the upper lip. A radical maxillectomy with orbital exenteration and through-and-through resection of the cheek was performed in this patient. The surgical specimen is shown in Fig. 5.143. The surgical defect shows loss of skin of the face on the right-hand side along with the defect in the orbit and maxilla communicating with the nasal cavity, nasopharynx, and oral cavity (Fig. 5.144). In the lower part of the surgical defect, the exposed lateral aspect of the body of the mandible is seen along with the pterygoid muscles. This complex defect was immediately reconstructed with use of a rectus

Figure 5.139 This patient underwent a radical maxillectomy with orbital exenteration for squamous cell carcinoma of the maxillary antrum extending to the orbit.

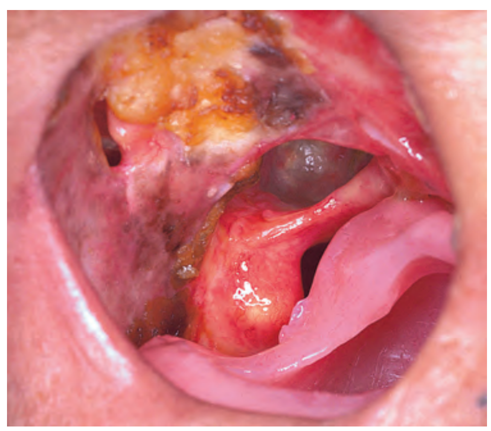

Figure 5.140 The appearance of the orbital socket several weeks after surgery. The upper end of the dental prosthesis is seen in the lower part of the photograph.

Figure 5.141 A second facial prosthesis with an artificial eye is introduced into the orbital socket and retained with glue, restoring the aesthetic appearance of the patient.

Figure 5.142 This patient has a recurrent carcinoma of the right maxilla extending into the right orbit following a previous partial maxillectomy performed to remove a squamous cell carcinoma.

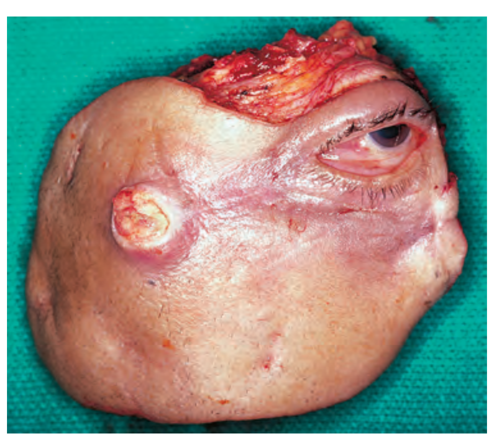

Figure 5.143 The surgical specimen shows monobloc resection of the skin of the cheek, the orbit, and the maxilla.

Figure 5.144 The surgical defect shows loss of skin of the face on the right-hand side along with the defect in the orbit and maxilla communicating with the nasal cavity, nasopharynx, and oral cavity.

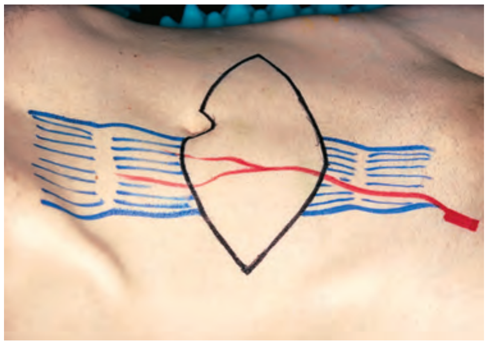

Figure 5.145 The outline of the rectus abdominis myocutaneous free flap.

Figure 5.146 The appearance of the patient approximately 3 months after surgery.

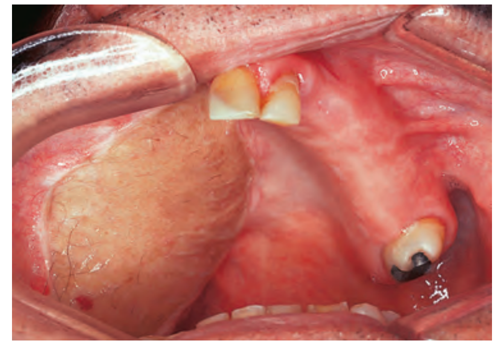

Figure 5.147 An intraoral view showing complete obliteration of the defect in the hard palate.

abdominis myocutaneous free flap. The outline of the flap is shown in Fig. 5.145. The skin paddle was divided into three skin islands, with one island providing coverage of the skin of the cheek, the second island providing closure of the defect in the hard palate, and the third island providing lining in the nasal cavity. The appearance of the patient approximately 3 months after surgery shows satisfactory reconstruction of the skin and soft tissues of the cheek (Fig. 5.146). An intraoral view shows complete obliteration of the defect in the hard palate, eliminating the need for a dental prosthesis (Fig. 5.147). Microvascular free flap reconstruction thus provides an expeditious and immediate means of reconstruction of complex surgical defects where soft tissue replacement and lining in multiple areas are required.

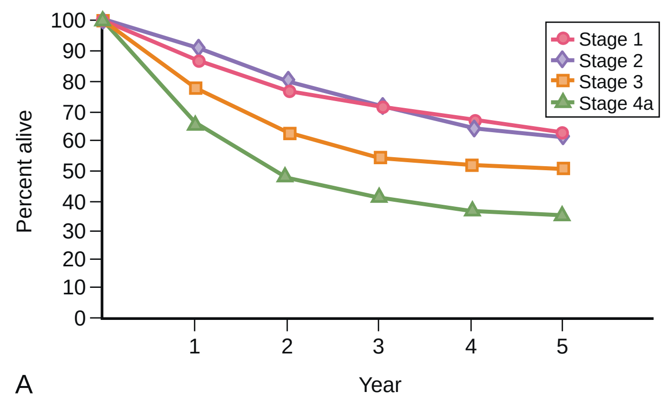

Figure 5.148 Five-year survival rates by stage for squamous carcinoma of the maxilla. *(Data from Memorial Sloan Kettering Cancer Center.)*

RESULTS OF TREATMENT

Many patients with malignant tumors of the nasal cavity and paranasal sinuses present with an advanced stage of disease at the time of diagnosis and treatment. In addition to the stage of disease, cure rates also depend on the histology of the primary tumor. Tumors such as mucosal melanoma, squamous cell carcinoma, sinonasal undifferentiated carcinoma, and high-grade neuroendocrine carcinoma are biologically more aggressive and associated with worse outcomes compared with well-differentiated tumors such as carcinoma arising in an inverted papilloma, esthesioneuroblastoma, and chondrosarcoma. Survival following initial therapy is also dependent on the site of the primary tumor. For squamous cell carcinoma, the nasal cavity has by far the most favorable prognosis, followed by the maxillary antrum. Tumors of the infrastructure of the maxilla have a better prognosis compared with those of the suprastructure. Ethmoid sinus tumors in general carry the worst prognosis, due to the contiguity of vital structures, such as the orbit, dura, and brain, making wide resection with generous margins difficult. Because the maxillary antrum is the most frequent site for squamous cell carcinomas of the paranasal sinuses, survival by stage of disease is presented for this particular site. Stage I squamous cell carcinomas of the maxilla have nearly a 100% survival rate. Stage II tumors have a 5-year survival rate of 86%. However, stage III and stage IV tumors have a poor survival rate of 39% and 25%, respectively (Fig. 5.148).

Treatment failure occurs in over 50% of patients undergoing surgical treatment. Review of patterns of failure indicate that local recurrence is by far the most common site of treatment failure for squamous carcinoma of the maxilla. Failure with regional metastasis is exceedingly rare and occurs in less than 20% of all treated patients. On the other hand, with increasing use of adjuvant radiotherapy, improved local control with an increasing number of patients in whom distant metastasis develops is observed. Distant metastases develop in approximately 20% of patients who fail treatment.

With increasing interest and expertise in endonasal surgery for tumors of the paranasal sinuses, over the past two decades, experience is gathering at major centers of excellence. Early reports from Europe as well as United States show excellent outcomes for carefully selected cases of malignant tumors of the paranasal sinuses undergoing endonasal endoscopic or cranioendoscopic resections. Due to a whole array of histologies and various stages of disease, in patients undergoing endonasal surgery for malignant tumors, it is difficult to define the exact indications for endonasal surgery or compare the outcomes to open craniofacial resections. Clearly, patient selection is crucial for a successful outcome. The long-term outcomes for endonasal surgery for malignant tumors of the paranasal sinuses from two centers of excellence are shown here. The combined experience of the otolaryngology head and neck surgery departments from the Universities of Varese and Brescia in Italy of 659 patients with a variety of histologic entities is shown in Figs. 5.149 through 5.151. Similar experience on 255 patients from the M D Anderson Cancer Center, in Houston, Texas, is shown in Figs. 5.152 through 5.154. Clearly a favorable histology, limited extent of disease, in an accessible location and expertise in endonasal surgery play a crucial role for successful outcome.

Due to the rarity of these tumors, long-term survival data across institutions is not feasible. However, recent comparative analysis of outcomes for sinonasal cancers (SNC) in Europe (EUROCARE database) and the United States (SEER database)

are shown here. Survival in relation to various age groups is shown in Fig. 5.155. Similarly, survival in relation to gender is shown in Fig. 5.156. Overall survival for SNC in the United States was better than all of Europe. However, there are significant differences in outcome in various parts of Europe (Fig. 5.157). Overall, there is modest improvement in survival over the past 20 years (Fig. 5.158). The observations of this report show that sinonasal cancers are more common after the age of 55 years and in men. Age older than 75 years and male gender are poor prognostic factors. Five-year survival rates are higher in the United States in these comparative data sets.

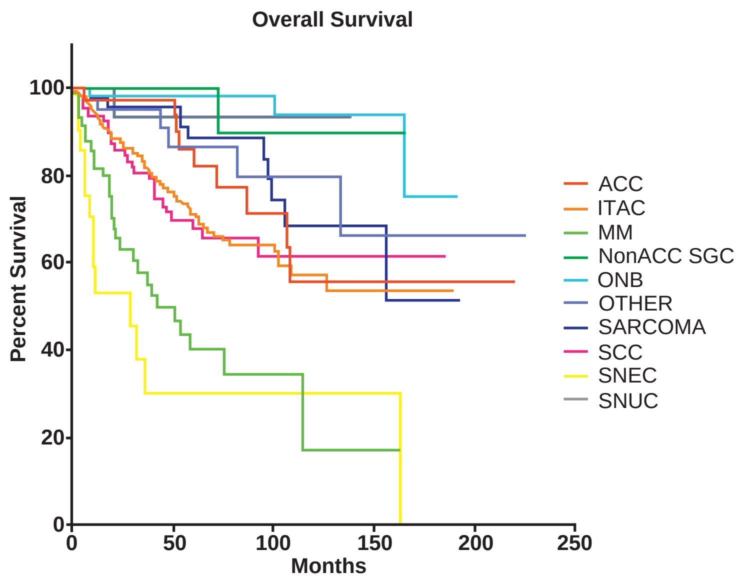

Figure 5.149 Overall survival in 659 patients with sinonasal cancers (by histology) undergoing endonasal surgery with or without transnasal craniectomy or cranioendoscopic resection, at the Departments of Otolaryngology, Head and Neck Surgery, of the Universities of Varese and Brescia, Italy. *(Courtesy Piero Nicolai, MD.)*

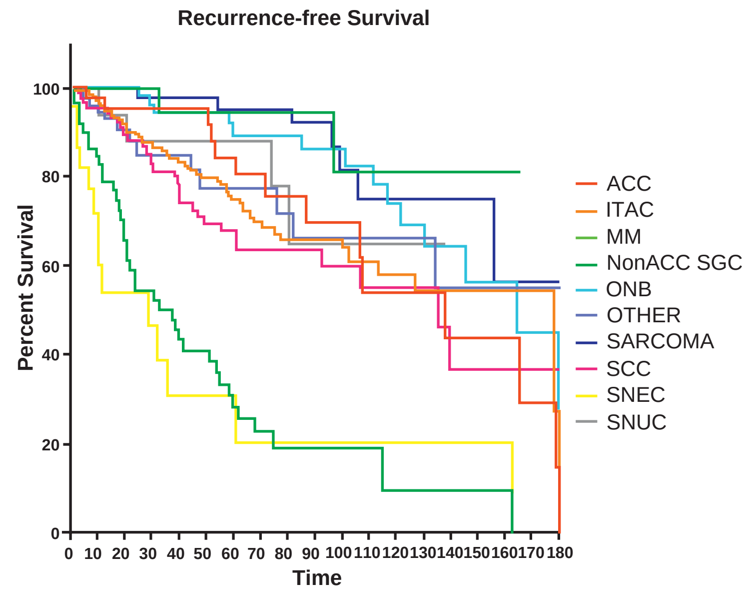

Figure 5.151 Recurrence-free survival in 659 patients with sinonasal cancers (by histology) undergoing endonasal surgery with or without transnasal craniectomy or cranioendoscopic resection, at the Departments of Otolaryngology, Head and Neck Surgery, of the Universities of Varese and Brescia, Italy. *(Courtesy Piero Nicolai, MD.)*

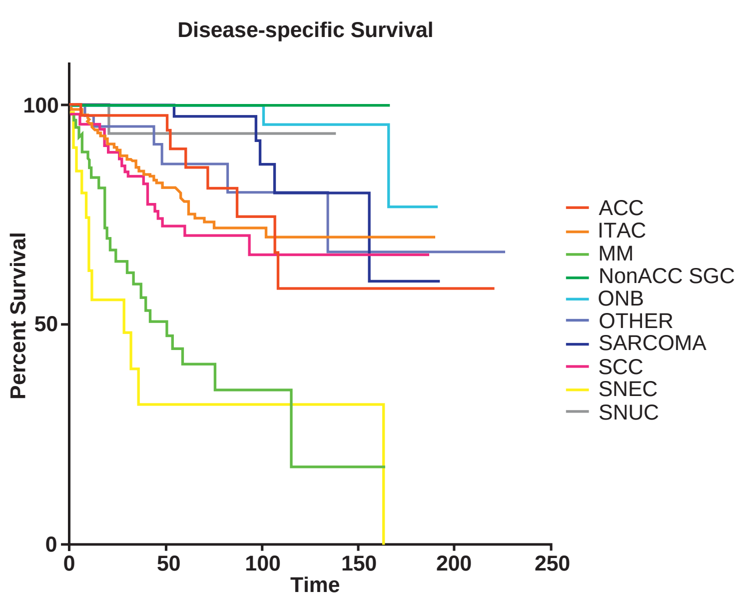

Figure 5.150 Disease-specific survival in 659 patients with sinonasal cancers (by histology) undergoing endonasal surgery with or without transnasal craniectomy or cranioendoscopic resection, at the Departments of Otolaryngology, Head and Neck Surgery, of the Universities of Varese and Brescia, Italy. *(Courtesy Piero Nicolai, MD.)*

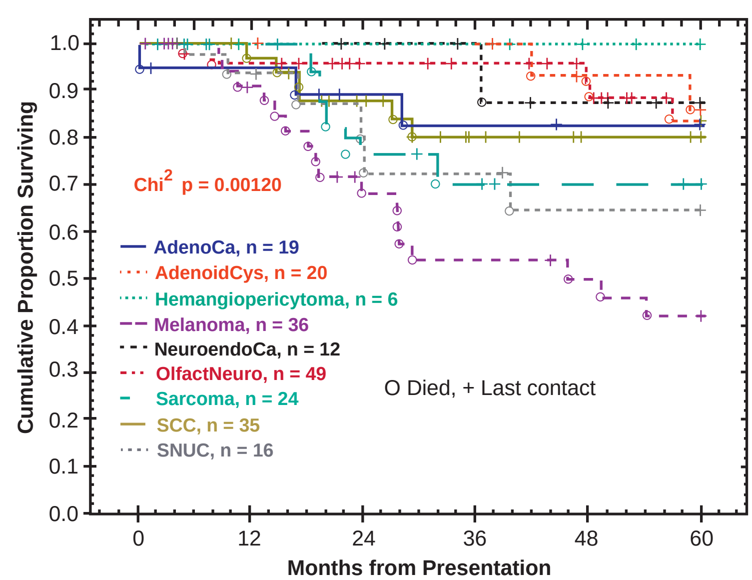

Figure 5.152 Five-year survival in 255 patients with sinonasal cancers (by histology) undergoing endoscopic surgery at M D Anderson Cancer Center in Houston, Texas. *(Courtesy Ehab Hanna, MD.)*

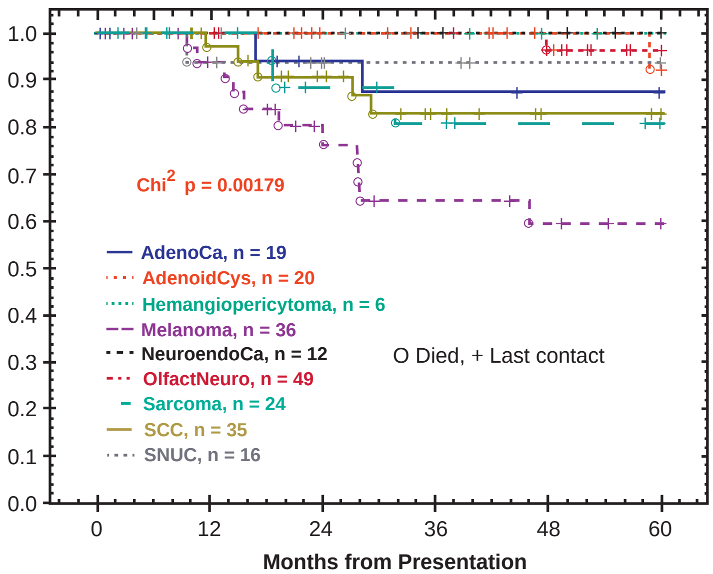

Figure 5.153 Five-year survival in 255 patients with sinonasal cancers (by histology) undergoing endoscopic surgery at M D Anderson Cancer Center in Houston, Texas. *(Courtesy Ehab Hanna, MD.)*

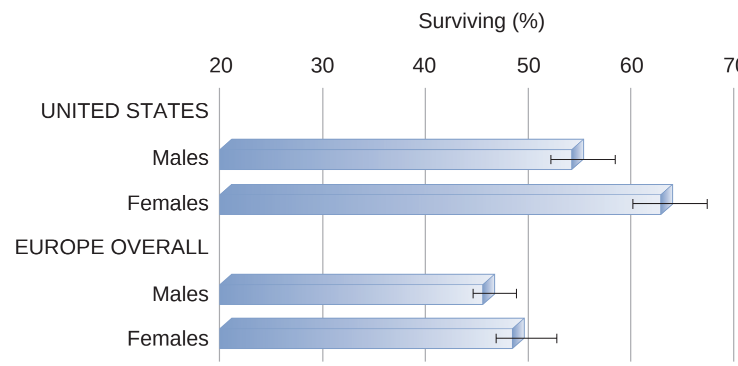

Figure 5.156 Comparative 5-year overall survival data for sinonasal cancer by gender between Europe and the United States.

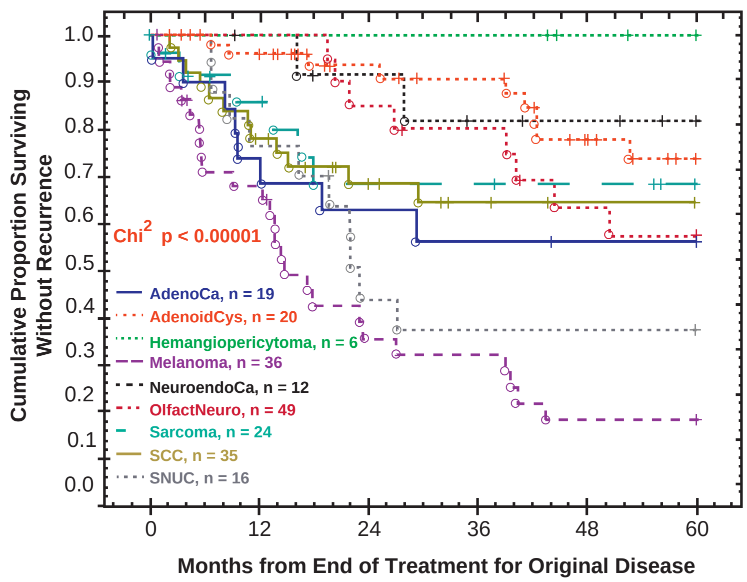

Figure 5.154 Five-year survival in 255 patients with sinonasal cancers (by histology) undergoing endoscopic surgery at M D Anderson Cancer Center in Houston, Texas. *(Courtesy Ehab Hanna, MD.)*

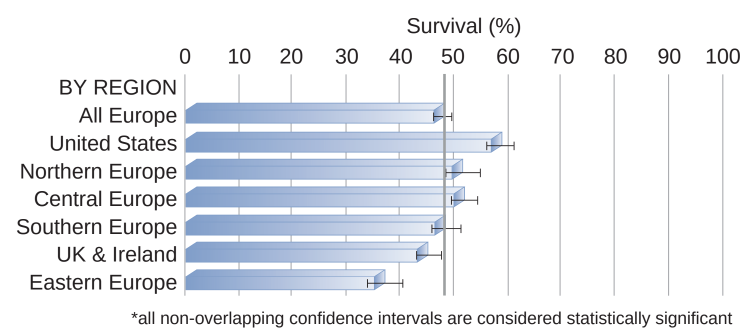

Figure 5.157 Five-year age-adjusted relative survival between United States and various regions of Europe. Vertical line represents aggregate mean survival for all of Europe.

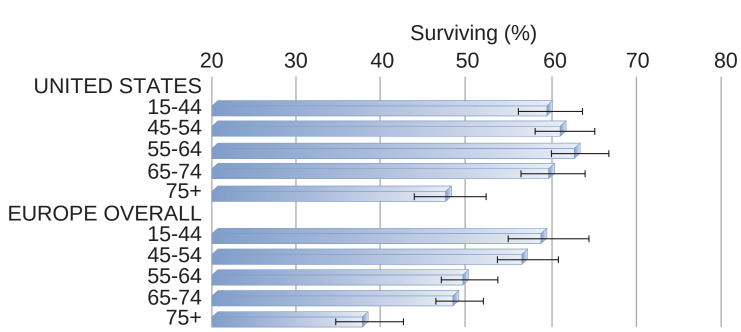

Figure 5.155 Comparative 5-year survival data for sinonasal cancer by age groups between Europe and the United States.

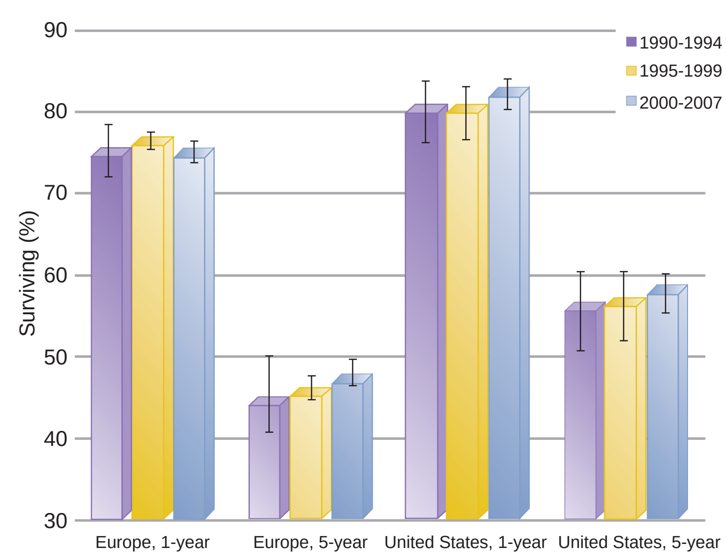

Figure 5.158 Age-adjusted 1- and 5-year relative survival by diagnostic time periods.

CHAPTER 6

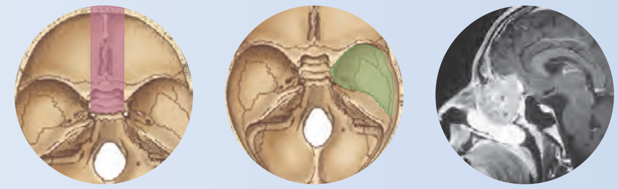

Skull Base

Tumors involving the skull base of the anterior cranial fossa usually arise extracranially with secondary extension to the skull base. Occasionally intracranial tumors such as meningiomas may have extracranial extensions. The site distribution of tumors involving the anterior skull base is shown in Fig. 6.1. The nasal cavity and ethmoid region are by far the most common sites of tumors, with secondary extension through the cribriform plate into the base of the anterior cranial fossa. The remaining group of tumors extending to the anterior cranial base are those arising in the lacrimal glands, frontal sinus, orbit, maxillary sinus, craniofacial skeleton, and soft tissues and skin of the forehead and scalp.

The most frequently encountered benign lesions involving the skull base are angiofibromas, osteomas, chondromas, and neurovascular tumors. The histologic distribution of malignant tumors invading the anterior skull base is shown in Fig. 6.2. Squamous cell carcinomas, carcinomas of minor salivary gland origin, esthesioneuroblastomas, sinonasal undifferentiated carcinomas, neuroendocrine carcinomas, and melanomas are the most frequently encountered epithelial tumors. Somatic soft tissue tumors in this region include leiomyosarcomas, fibrosarcomas, angiosarcomas, and other rare tumors. Chondrosarcomas and osteogenic sarcomas are the most frequently encountered bone tumors. Most patients whose primary malignant tumors involve the central anterior skull base require craniofacial resection with preservation of the orbit. However, when direct extension to the orbit is present, then resection of the lateral anterior skull base along with orbital exenteration is indicated. This scenario is particularly true for malignant tumors arising in the orbit and lacrimal apparatus or those of the ethmoid sinuses with secondary extension to the orbit (Fig. 6.3).

Neoplasms involving the middle cranial fossa are most commonly of neurovascular, soft tissue, or bone origin. The most frequently encountered neurogenic tumors are schwannomas and neurofibromas of the trigeminal nerve. Perineural extension of tumors along the trigeminal nerve is often seen from cutaneous and mucosal squamous cell carcinomas, melanomas, and minor salivary gland tumors such as adenoid cystic carcinomas. Soft tissue and bone sarcomas of the infratemporal fossa may involve the middle cranial fossa by direct extension. Benign and malignant paragangliomas also may extend to the middle cranial fossa through the foramina at the skull base.

Invasion of the temporal bone by primary tumors in the auditory canal or mastoid process requires special consideration. Although malignant tumors of the auditory canal are infrequent, invasion of the temporal bone by carcinomas of the parotid gland is not uncommon. The most frequently encountered neurogenic tumor of the temporal bone is the acoustic neuroma. The infratemporal portion of the facial nerve may be involved by perineural extension from neurotropic tumors of the skin or parotid gland. Neoplasms involving the posterior fossa at the skull base are those that extend through the jugular foramen, such as glomus tumors and chordomas of the clivus.

Open craniofacial resection remains the mainstay of therapy for a significant number of skull base neoplasms. Over the past two decades, there is increasing interest and enthusiasm for endonasal endoscopic resection of tumors involving the anterior central skull base. Although this approach has shown good early results, adherence to strict selection criteria is necessary to achieve similar cure rates as that from open operations. The earliest application of craniofacial surgery was reported by Dandy for a tumor of the orbit. A later report by Smith and Malecki described a craniofacial surgical approach for a tumor of the ethmoid. However, credit goes to Ketcham and colleagues for systematically developing a standardized technique of craniofacial resection for malignant neoplasms involving the nasal cavity and paranasal sinuses. Their early reports demonstrated nearly a doubling of survival time for patients with malignant tumors of the nasal cavity and paranasal sinuses compared with the previously used transfacial approaches alone. During the past 50 years, significant advances have taken place in technical refinements in craniofacial surgery, largely because of advances in imaging with the availability of computed tomography (CT) and magnetic resonance imaging (MRI) scans, development of better instrumentation, sophistication of surgical techniques with development of newer approaches, and availability of intraoperative neuronavigation. At the same time, availability of microvascular free tissue transfer allowed for more extensive resections, because it was now possible to repair major defects at the cranial base. Thus by the end of the 20th century, craniofacial surgery had become safe enough to become the standard of care for skull base lesions with significantly improved oncologic outcomes. However, morbidity and functional outcomes of surgery have remained a problem.

In the past 20 years, increased interest has been demonstrated in minimizing the morbidity of craniofacial surgery in selected patients through the use of endoscopic approaches. Endoscopic endonasal resection of benign lesions and favorable low-grade malignant tumors and small central malignant lesions at the anterior skull base is technically feasible, and safe in the hands of properly trained endoscopic surgeons. Published reports from experts from high-volume centers indicate that in properly selected patients, tumor control is similar to that achieved by open operations. However, the learning curve for achieving expertise in endonasal endoscopic resections for malignant tumors is quite steep, and significant expertise and experience

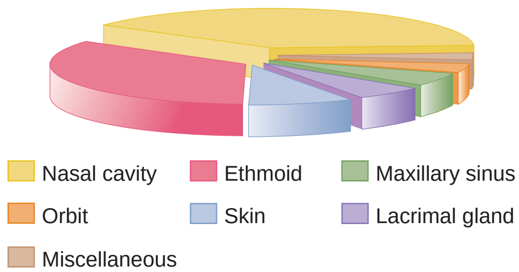

Figure 6.1 Site of origin of tumors involving the anterior skull base. *(Data from Memorial Sloan Kettering Cancer Center.)*

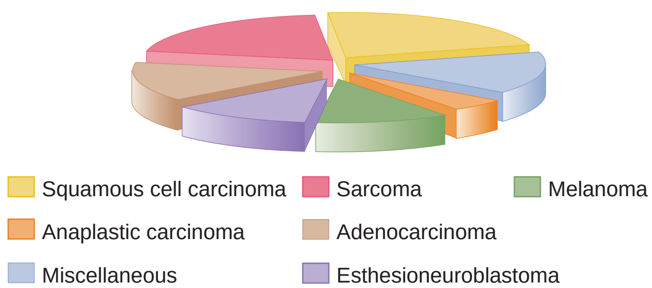

Figure 6.2 Histologic distribution of tumors involving the anterior skull base. *(Data from Memorial Sloan Kettering Cancer Center.)*

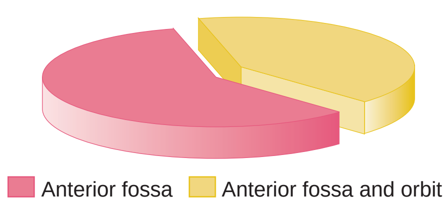

Figure 6.3 Extent of resection of tumors involving the anterior skull base.

in endonasal sinus surgery are essential before a head and neck surgeon, coupled with an equally expert endonasal neurosurgeon, can embark upon such surgical resections. Reported follow-up and outcomes data of patients undergoing such surgical interventions for malignant tumors from expert centers support its validity. Thus endonasal endoscopic skull base surgery in select patients now has an established role in skull base surgery.

EVALUATION

Clinical evaluation and preoperative treatment planning for patients with neoplasms that involve the cranial base or are in proximity to the cranial base require special consideration. For most patients with malignant tumors that involve the anterior skull base, the primary lesions arise in the nasal cavity or paranasal sinuses, orbit, or the skin and soft tissues of the upper face and calvarium. Tumors of the infratemporal fossa and parotid gland and neurovascular tumors at the skull base often involve the floor of the middle cranial fossa. Tumors of the auditory canal may involve the temporal bone, and tumors of the seventh and eighth cranial nerves may involve the petrous apex and the cerebellopontine angle. Thus the workup and evaluation of these lesions are dependent on the site of origin and the histologic diagnosis before surgical intervention.

The routine clinical evaluation of such patients requires assessment of the function of the cranial nerves. Patients with tumors of the ethmoid complex may present with anosmia or an altered sense of smell. Tumors involving the orbit, the apex of the orbit, or the central skull base may present with disturbances of cranial nerves II, III, IV, and VI, manifested by partial or complete loss of vision or altered movements of extraocular muscles. Tumors at the base of the middle cranial fossa and in the infratemporal fossa may present with altered function of cranial nerve V, manifested by loss of sensation, or they may present with pain along the sensory branches of the fifth nerve and altered function of the muscles of mastication. Tumors involving the temporal bone may manifest with alteration of function of the facial nerve, presenting as facial weakness or paralysis, and those at the petrous apex may manifest with diminished hearing or loss of balance as the first sign of involvement of cranial nerve VIII. Symptoms resulting from involvement of the lower cranial nerves manifest as disturbances in swallowing, hoarseness of voice, altered clarity of speech, difficulty with mastication, or drooping of the shoulder. Tumors presenting at the jugular foramen classically involve cranial nerves IX, X, XI, and XII and may present with the classic combination of clinical signs and symptoms described as "jugular foramen syndrome." However, cranial nerve dysfunction may not be readily apparent in patients with slow-growing neoplasms.

In addition to assessment of the cranial nerves, patients should undergo an audiogram, particularly for tumors of cranial nerves VII or VIII, tumors of the auditory canal, or when invasion of the temporal bone is suspected. Assessment of brainstem functions for tumors at the cerebellopontine angle and petrous apex is essential. A careful history regarding cerebrospinal fluid rhinorrhea or otorrhea should be taken, and appropriate testing should be done for confirmation of cerebrospinal fluid (CSF) leakage.

The mainstay of the preoperative workup for patients with tumors that approach or involve the skull base is radiographic imaging with CT and MRI. Direct preoperative angiographic studies and embolization are considered in highly vascular lesions and neurovascular tumors. Finally, balloon occlusion testing may be required in patients for whom circulation of one hemisphere is at risk because of the tumor or surgery.

Tissue diagnosis is essential in all patients except those with highly vascular tumors such as paragangliomas, glomus tumors, acoustic neuromas, and angiofibromas. However, these lesions have a characteristic radiologic appearance that is sufficient for a working diagnosis. A punch biopsy of lesions of the skin or those accessible through the nasal cavity and auditory canal should be performed. A CT-guided needle biopsy should be considered to establish tissue diagnosis of tumors that are not readily accessible.

Radiographic Workup

Some skull base neoplasms such as paragangliomas or schwannomas have classic imaging characteristics that can point to a diagnosis (see Chapter 14). However, the primary reason to perform imaging studies in most patients with skull base tumors is to obtain anatomic information about the extent of the tumor. In certain circumstances, imaging is also necessary to determine the adequacy of circulation and to assess risk of cerebrovascular injury from surgical intervention. Finally, invasive angiography is indicated in select patients, including those who require embolization of their tumor or balloon occlusion testing.

Radiographic imaging of the extent of the tumor and its relationship to anatomic structures at the skull base is pivotal for making decisions regarding treatment and planning surgery. The most important features of a skull base tumor that influence treatment selection and surgical planning include the site and extent of bone involvement, relationship to the orbits, the extent of intracranial extension, and perineural spread. Both

Figure 6.4 A coronal computed tomography scan (bone algorithm) showing early erosion of the cribriform plate (*white arrows*) from an esthesioneuroblastoma of the nasal cavity.

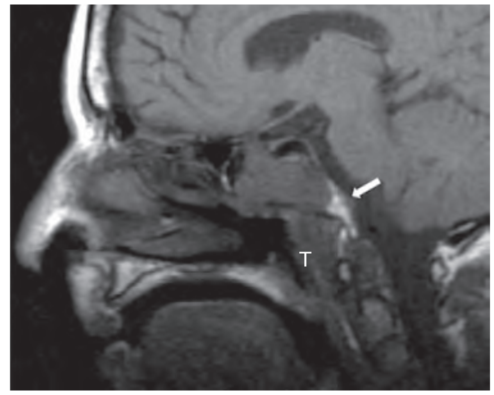

Figure 6.5 A sagittal T1-weighted magnetic resonance imaging scan showing replacement of the fatty marrow (*white arrow*) of the clivus by a sinus carcinoma (*T*).

CT and MRI are excellent imaging modalities for delineating these characteristics, but they each have their specific attributes, which provide different information. Therefore most patients with skull base tumors will benefit from the information gleaned from both CT and MRI.

Bone erosion of the anterior skull base or orbit is generally evident earlier on CT compared with MRI. The coronal reformatted sequence of a sinonasal CT scan best demonstrates potential or actual tumor invasion of the skull base or orbit. Early erosion of the thin bones in this region, such as the cribriform plate/fovea ethmoidalis and lamina papyracea, is easily appreciated on the bone algorithm of the CT scan (Fig. 6.4). MRI is likely to miss early bone involvement because of the thin nature of the bone and minimal fatty marrow medullary space in these bones, which makes evaluation difficult. An exception to this general rule is tumor involvement of the clivus, especially from nasopharyngeal carcinomas, in which case bone invasion is far more easily seen on an MRI scan than on a CT scan (Fig. 6.5). Tumor invasion of the sphenoid and temporal bones can be detected either on CT or MRI scans, but MRI can be helpful in delineating the extent of involvement. CT scans can show cortical bone destruction easily, but the natural contrast of normal adult fatty "white" marrow against "dark" tumor seen on MRI scans is useful in providing an estimate of the extent of bone involvement. Ultrathin-slice CT imaging of the temporal bone in at least two planes is mandatory for evaluation of temporal bone tumors, and it easily shows bone destruction, including ossicular destruction that would be missed on an MRI scan.

Involvement of the soft tissues, orbit, paranasal sinuses, and perineural spread is ideally evaluated by MRI. When evaluating for orbital soft tissue invasion, precontrast axial and coronal imaging is the best sequence to show the contrast of normal "white" fat infiltrated by "dark" tumor. Once contrast material is administered, utilization of the fat-suppression technique becomes necessary so that the enhancing "white" tumor does not blend into the normal orbital fat. The fat-suppression technique causes normal fat to become dark, which makes the enhanced tumor obvious (Fig. 6.6). Precontrast axial T1-weighted images also are excellent for evaluation of extracranial perineural spread, such as in the pterygopalatine fossa (PPF) and along the infraorbital nerve. The "white"-appearing fat that is normally present in the PPF can be used as a natural contrast agent for the darker abnormal nerve affected by a tumor (Fig. 6.7). Because fat in the PPF is easily imaged on a CT scan, perineural spread

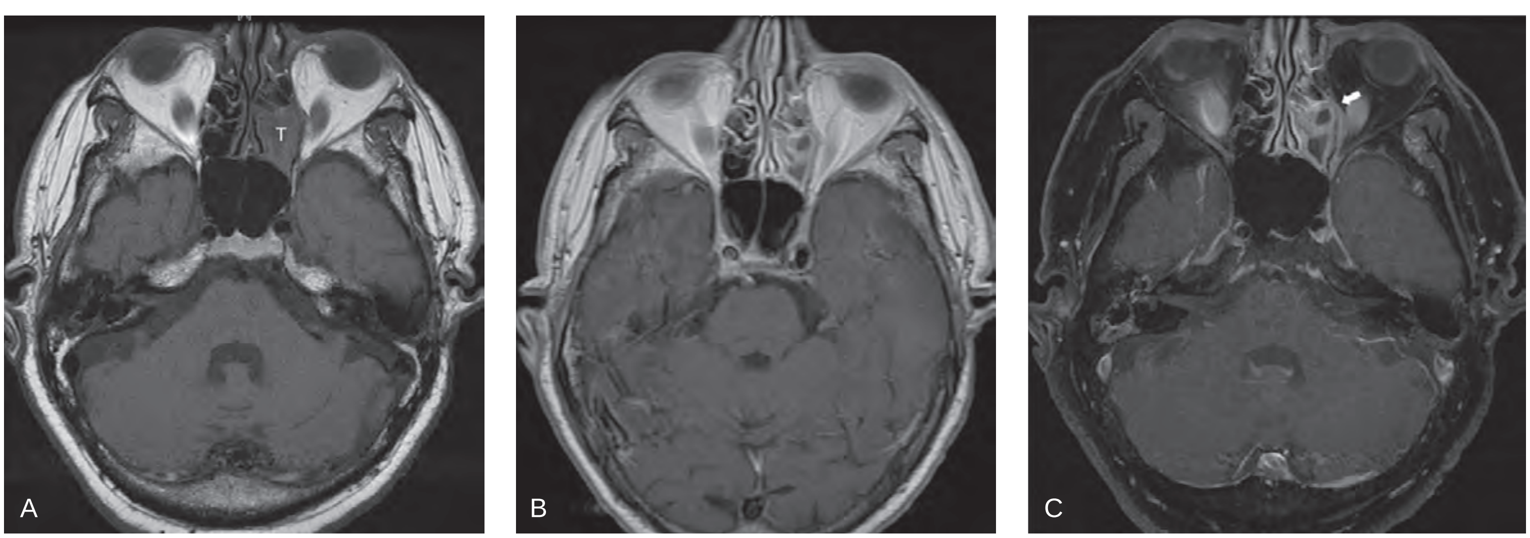

Figure 6.6 The importance of a T1-weighted magnetic resonance imaging (MRI) scan in the evaluation of orbital involvement by sinus cancer. **A**, A precontrast T1-weighted MRI scan showing minor intraorbital extension of left ethmoid carcinoma (T) contrasted against normal adjacent intraorbital fat. **B**, The distinction between tumor and intraorbital fat is lost in the postcontrast T1-weighted MRI scan because of enhancement of the tumor. **C**, Fat suppression allows visualization of the enhancing intraorbital component of the tumor (*white arrow*) because the adjacent normal orbital fat becomes dark.

also can be diagnosed reliably if normal fat in the PPF is seen to be replaced by a tumor. Widening of the bony confines of the PPF provides additional evidence to support the diagnosis of perineural spread (Fig. 6.8). To declare perineural spread of tumor, it is essential to demonstrate abnormal enlargement of the nerve as well as enhancement. If the nerve is in a bony canal, such as the infraorbital nerve, or if it is in a foramen, such as the rotundum or ovale, the canal or foramen is often widened, but the cortical margins remain intact on the CT scan (Fig. 6.9).

Extracranial perineural spread of a tumor along nerve V3 can be diagnosed easily by visualization of an enhanced, enlarged nerve on MRI (Fig. 6.10). Intracranial perineural spread of a tumor into Meckel's cave and the cavernous sinus is best seen on a contrast-enhanced T1-weighted MRI scan. The T2-weighted sequence helps confirm invasion of Meckel's cave where the normally bright CSF is replaced by the dark tumor (Fig. 6.11).

Intracranial extension of the tumor and involvement of the dura or brain are ideally demonstrated by MRI. Contrast-enhanced T1-weighted images in the sagittal or coronal plane are very accurate at detecting dural and/or parenchymal brain invasion, although minor dural involvement may not be easy to detect. Dural involvement is characterized by focal thickening and enhancement, and the scan also should be examined carefully for the extent of dural involvement (Fig. 6.12). A peculiar feature of intracranial extension of esthesioneuroblastomas is the formation of peripheral cysts around the invading tumor (Fig. 6.13). Although it is relatively uncommon with skull base tumors, leptomeningeal involvement by a tumor is an ominous prognostic sign (Fig. 6.14). Once a tumor has invaded the brain

Figure 6.9 Coronal reconstruction of the bone algorithm of a computed tomography scan showing widening of the left foramen rotundum (*arrow*) by perineural spread of a maxillary sinus carcinoma. Note that the integrity of the bony walls of the foramen is preserved.

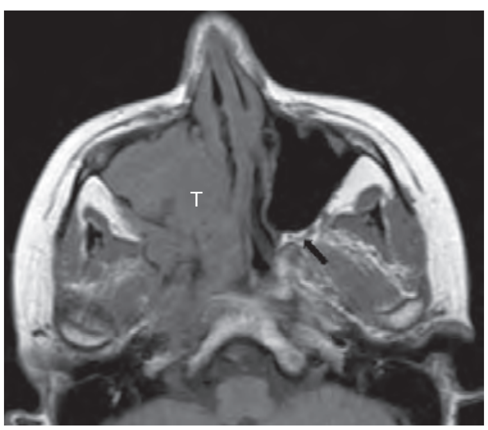

Figure 6.7 A precontrast T1-weighted magnetic resonance imaging (MRI) scan showing invasion of the right pterygopalatine fossa by a right maxillary sinus carcinoma (T). Note the normal appearance of the fat-filled opposite pterygopalatine fossa (*black arrow*).

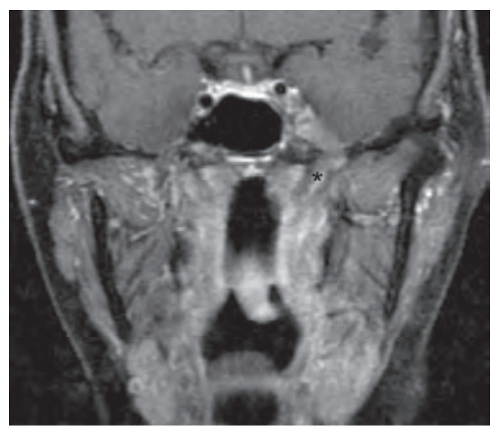

Figure 6.10 Perineural involvement of the left V3 seen as a thickened, enhancing nerve (*) on a contrast-enhanced T1-weighted magnetic resonance imaging scan.

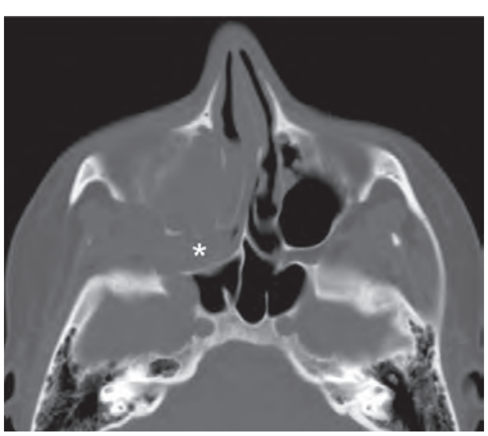

Figure 6.8 An axial computed tomography scan (bone algorithm) showing widening of the right pterygo palatine fossa (*) compared to left.

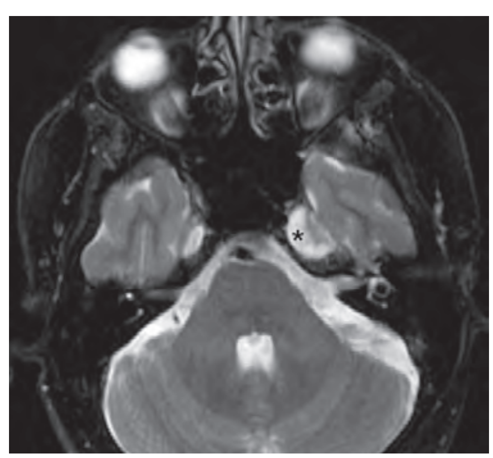

Figure 6.11 The normally bright cerebrospinal fluid (*) on a T2-weighted magnetic resonance imaging scan helps confirm Meckel's cave invasion by the darker appearing perineural tumor spread.

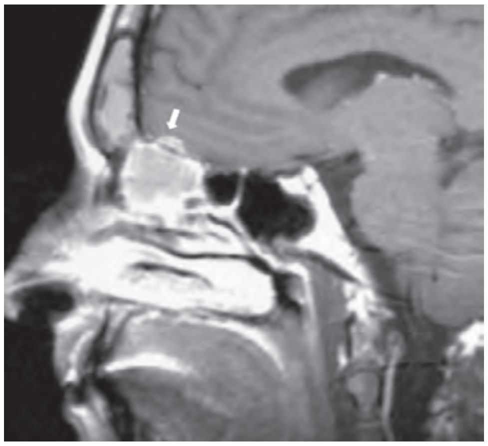

Figure 6.12 A sagittal postcontrast T1-weighted magnetic resonance imaging scan showing dural enhancement (*white arrow*) from invasion by an esthesioneuroblastoma.

parenchyma, the axial T2-weighted and short T1-inversion recovery sequences easily show associated edema, which is the hallmark of brain parenchymal invasion (Fig. 6.15).

Fluorodeoxyglucose–positron emission tomography (FDG-PET) scanning has a limited role in the evaluation of skull base tumors but is a useful modality in posttreatment surveillance for differentiating treatment-related changes from recurrent disease.

Assessment of circulatory patency is indicated when surgical intervention involves resection of or risk of injury to a major artery, such as the internal carotid artery or a major sinus artery. Noninvasive imaging tests such as magnetic resonance angiography (MRA) and CT angiography (CTA) are adequate at demonstrating the anatomic relationship of the tumor to the major blood vessels. However, invasive angiography is required to assess the potential neurologic sequelae of occlusion of a major vessel, such as the carotid artery. Angiography also is

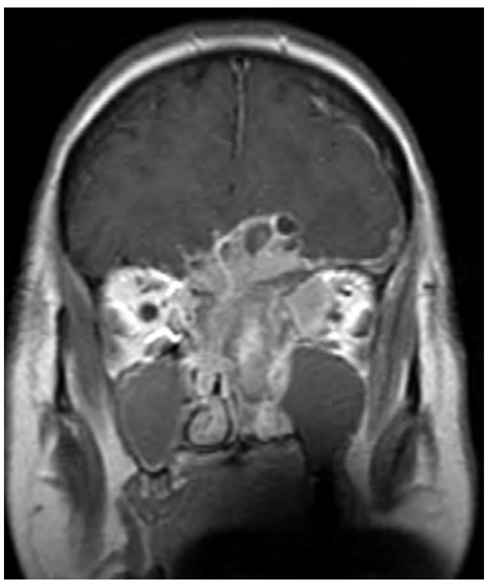

Figure 6.13 Peripheral cysts around an area of brain parenchymal invasion in a patient with an esthesioneuroblastoma.

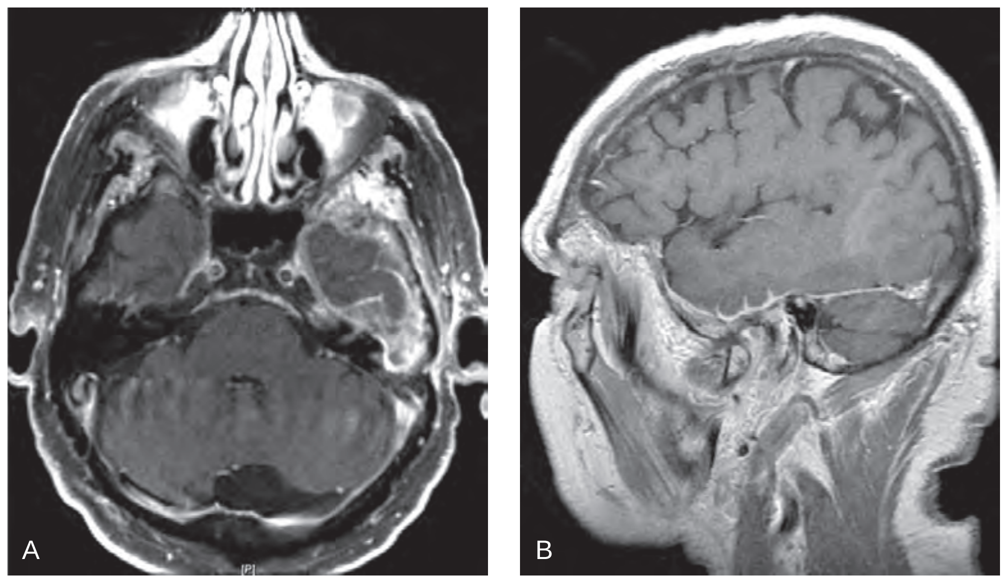

Figure 6.14 Postcontrast axial (**A**) and T1-weighted (**B**) magnetic resonance imaging scans showing leptomeningeal spread along the temporal lobe sulci in a patient with a squamous cell carcinoma of the left temporal bone.

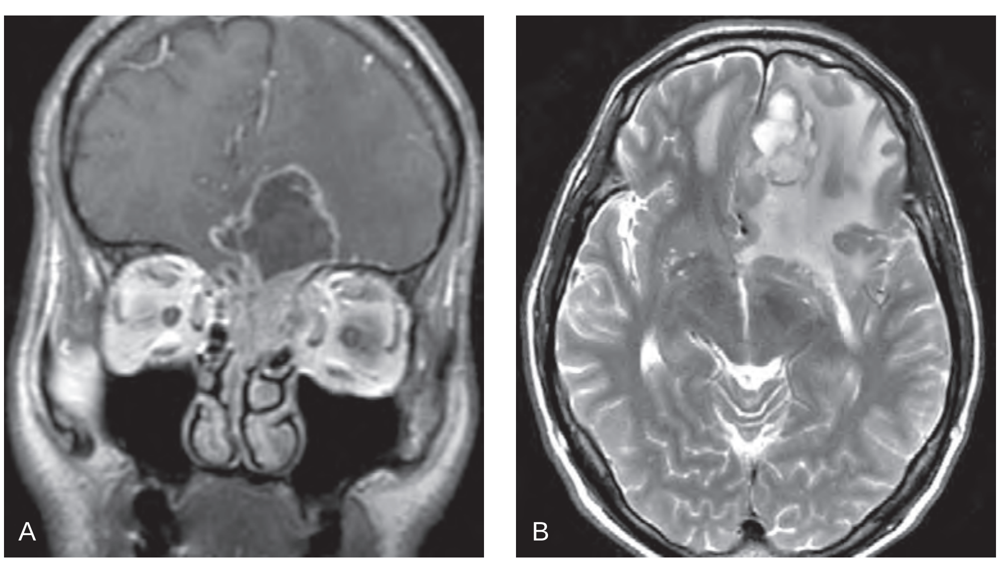

Figure 6.15 **A**, A coronal T1-weighted magnetic resonance imaging (MRI) scan shows intracranial extension of a poorly differentiated carcinoma of the left nasal cavity. **B**, Diffuse edema of the brain parenchyma surrounding the invading tumor on an axial T2-weighted MRI scan confirms the presence of brain invasion.

indicated if preoperative embolization of the tumor is part of the treatment plan, for example, for juvenile nasopharyngeal angiofibromas or meningiomas.

Demonstration of the anatomic patency of the cerebral circulation and its collaterals, however, does not accurately predict the risk of cerebral ischemia if sacrifice of the internal carotid artery is required. Several methods have become available for more precise evaluation of adequate cross-circulation to the brain through the circle of Willis. These methods include transcranial Doppler examination, single-photon emission computed tomography (SPECT) with balloon occlusion of the carotid artery, and angiography and balloon occlusion and ^{99m}Tc-hexamethyl-propyleneamine oxime brain SPECT. Balloon occlusion of the ipsilateral carotid artery and ^{99m}Tc-hexamethyl-propyl-eneamine oxime brain SPECT has the best sensitivity and specificity, but even this test is not entirely reliable in predicting the risk of cerebral ischemia because it does not take into account the adverse impact of other potential intraoperative events such as hypotension and hypoxia. Additionally, a finite risk of stroke exists if the surgical procedure affects other collateral vessels not assessed by balloon occlusion testing or if thromboembolism develops after ligation of the carotid artery. Moreover, to perform these invasive angiographic procedures safely, a multidisciplinary infrastructure is essential, and the tests themselves carry a risk of neurologic complications.

TREATMENT

Initial definitive treatment for most patients with neoplasms that involve the skull base entails surgical resection. In general, most patients with malignant tumors will require adjuvant postoperative radiation therapy because of the proximity of the surgical margins to the vital structure, which limits the ability of the surgeon to secure generous margins. Nonsurgical treatment with radiation and/or chemotherapy is reserved for patients with tumors that technically cannot be resected and for patients who otherwise are not surgical candidates. Some benign tumors such as schwannomas and paragangliomas may be managed expectantly with continued surveillance. Chemotherapy with or without radiation therapy may be used for lymphomas involving the skull base.

SURGICAL TREATMENT

The complex anatomy of the vital structures at the base of the skull make surgical resection of tumors involving this area extremely difficult. Tumors of the nasal cavity, paranasal sinuses, orbit, scalp, and calvarium may extend to the anterior cranial fossa through the base of the skull. Further spread of these tumors can lead to intracranial extension with involvement of the dura or brain. A thorough understanding of the anatomy is therefore essential to master complex surgical techniques for operative procedures in this area.

A complete review of the anatomy of the skull base is beyond the scope of this book; however, to recapitulate the anatomic structures at the base of the skull, several views of the human skull are presented here.

A sagittal section of the skull through the left nasal cavity (Fig. 6.16) shows the position of the floor of the anterior cranial fossa in relation to the sphenoid sinus, the nasal cavity, and the frontal sinus.

The intracranial view of the anterior cranial fossa (Fig. 6.17) shows the anatomic structures located on its floor. The crista galli and cribriform plate, as well as the planum sphenoidale, are important landmarks to be remembered during surgery of the anterior cranial fossa.

The intracranial view of the middle fossa (Fig. 6.18) demonstrates the relative locations of the middle meningeal artery over the dura and the sigmoid sinus adjacent to the petrous portion of the temporal bone. These landmarks are vitally important in surgery of the middle cranial fossa and temporal bone. A skull should be available in the operating room to review the anatomy when surgical procedures are undertaken in these areas. A review of the anatomy of the petrous portion of the temporal bone in relation to the tumor to be surgically resected is vitally important before surgery. Radiographic studies including MRI and CT scans (Figs. 6.19 through 6.21), as well as angiograms of the patient, should be reviewed with the skull in hand.

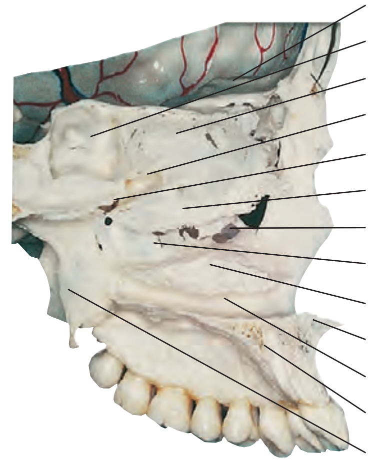

Figure 6.16 Sagittal section of the skull through the left nasal cavity.

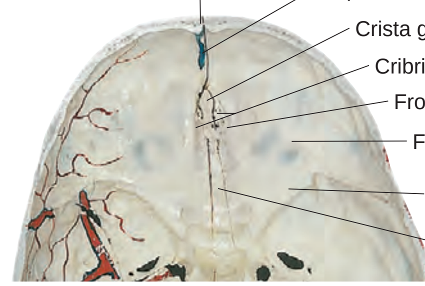

Figure 6.17 Intracranial view of the floor of the anterior cranial fossa.

Figure 6.18 Intracranial view of the middle fossa.

Figure 6.19 An axial view of a computed tomography scan at the level of the optic canal.

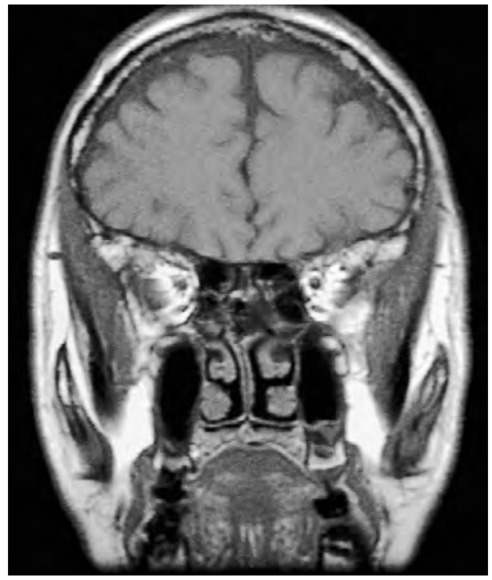

Figure 6.20 A coronal view of a computed tomography scan at the level of the optic foramen.

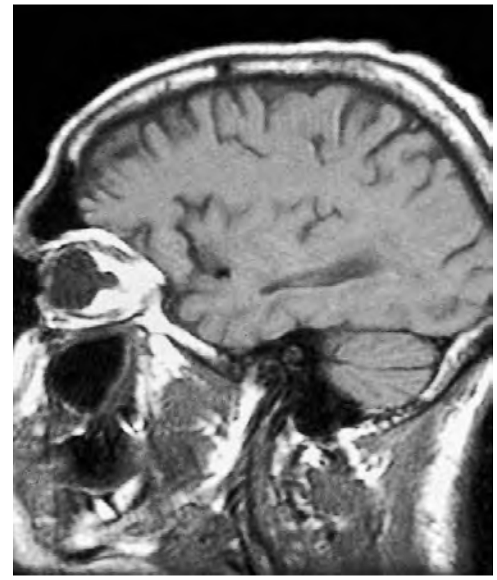

Figure 6.21 A sagittal view of a computed tomography scan at the level of the optic canal.

Figure 6.22 An oblique view of the extracranial aspect of the base of the skull at the middle fossa.

An oblique view of the extracranial aspect of the base of the skull at the middle fossa (Fig. 6.22) demonstrates the area of the pterygomaxillary region and the infratemporal fossa. Tumors presenting in this region require special attention for exposure and resection, and the complex anatomy in these areas must be reviewed before undertaking surgical resection.

The fundamental problem in tumors involving the skull base is that access to these tumors is difficult. Use of the facial approach alone to address these tumors without adequate exposure and control of the intracranial component is likely to result in inadequate resection, CSF leakage, hemorrhage, and infection and its grave sequelae. One must adhere to the following principles when embarking upon craniofacial surgery:

1. Thorough review of imaging studies and tissue diagnosis is crucial to decide upon the surgical approach to be undertaken. Tumors with favorable histology and of limited extent without invasion of the orbit, frontal sinus, or intracranial extension may be considered for endonasal endoscopic resection.
2. If an open craniofacial resection is planned, then adequate exposure of the area of surgical resection must be obtained.
3. Brain retraction should be avoided whenever possible.

The brain can be slackened with use of either continuous spinal drainage or mannitol-induced diuresis. If the dura is injured or resected, a watertight dural repair must be undertaken, and the repaired area should be adequately covered with either a galeal-pericranial flap or a microvascular free flap.

A skin graft is sometimes used to provide an additional layer of support to the resected skull base. Use of a bone graft to repair skull base defects is seldom necessary. The clear-cut advantages of open craniofacial surgery are (1) a clear assessment of the resectability of the tumor can be achieved, (2) vital structures are protected, and (3) en bloc resection can be achieved. In addition, if the dura is involved it can be resected and repaired, and the surgical defect can be appropriately reconstructed to support the brain.

For the purpose of classifying operative procedures in various areas of the skull base, a scheme of division of different regions of the skull base is recommended. The skull base is divided into three regions anteroposteriorly; these are the anterior, middle, and posterior fossae, which are subdivided into several subsites. Midline structures in the floor, such as the crista galli, cribriform plate, and planum sphenoidale, constitute the anterior fossa cribriform plate region. Laterally, the floor of the anterior cranial fossa in the region of the roof of the orbit is called the *anterior fossa orbit region* (Fig. 6.23). The squamous part of the temporal bone, the greater wing of the sphenoid bone, and the lower part of the parietal bone comprise the middle fossa skull base region (Fig. 6.24). The auditory canal, mastoid process, and petrous portion of the temporal bone are described as the temporal bone region (Fig. 6.25). Tumors that secondarily involve the petrous part of the temporal bone or present posterior to it and involve the clivus are classified in the posterior fossa/clivus region (Fig. 6.26). Tumors that involve the cerebellopontine angle also can present in this location and involve the clivus.

Indications and Contraindications for Open Craniofacial Resection

When patients present with a benign or malignant tumor with extension to the anterior skull base and the clinical and radiographic extent of the tumor makes a potentially curative operation technically feasible, craniofacial surgery should be

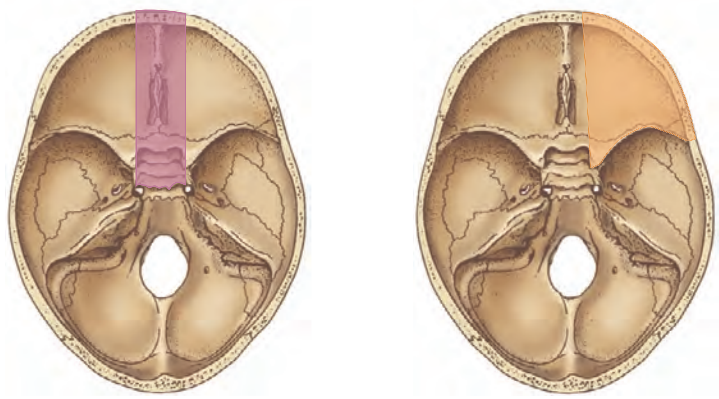

Figure 6.23 Anterior fossa cribriform plate region (*left*); anterior fossa orbit region (*right*).

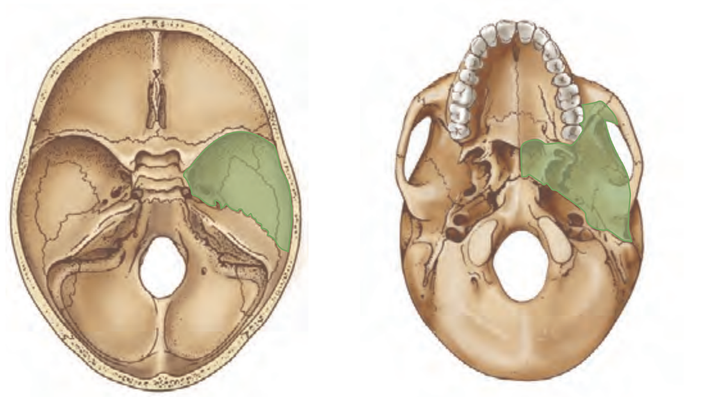

Figure 6.24 Middle fossa: skull base region.

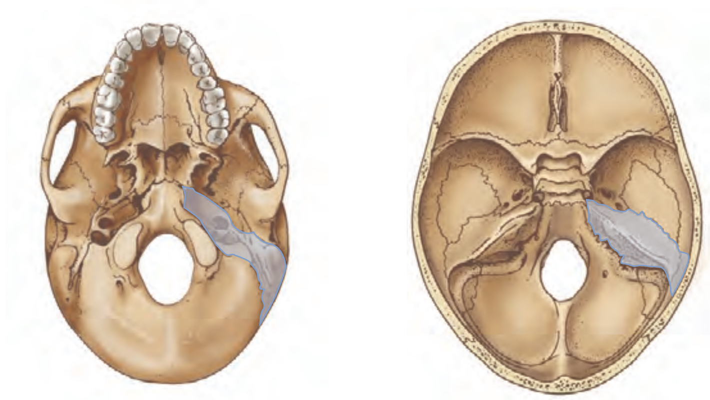

Figure 6.25 Temporal bone region.

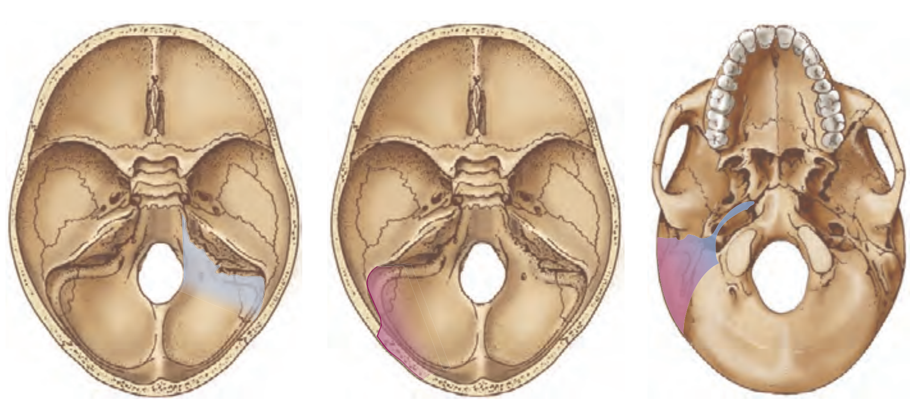

Figure 6.26 Posterior fossa: clivus region.

undertaken. Craniofacial surgery is a team effort requiring the expertise of a multidisciplinary surgical team that consists of a head and neck surgeon, neurosurgeon, microvascular reconstructive surgeon, maxillofacial prosthodontist, diagnostic neuroradiologist, radiation oncologist, and a psychosocial-vocational rehabilitation team consisting of psychiatrists, occupational therapists, physiotherapists, and social workers. Furthermore, an expert operating room team and perioperative nursing support are essential for the successful outcome of craniofacial surgery. Successful skull base surgery is unlikely to be achieved in the absence of a well-established multidisciplinary team.

Increasing experience at multiple centers have revealed the limitations of skull base surgery for malignant disease. Thus the following contraindications for craniofacial approaches in the surgical treatment of patients with malignant disease have been defined:

- Gross invasion of the brain
- Invasion of both orbits
- Encasement of the internal carotid artery (relative contraindication)
- Invasion of the cavernous sinus (relative contraindication)
- Advanced age of the patient (elderly patients are not suited physically, emotionally, and physiologically for such major surgical interventions)
- Massive high-grade tumors (e.g., melanomas and poorly differentiated carcinomas and high-grade sarcomas) with dural invasion (relative contraindication)
- Recurrent disease with invasion of the skull base following previous radiotherapy or chemoradiotherapy (relative contraindication)

Preoperative Preparation

All patients requiring craniofacial surgery should receive appropriate preoperative counseling regarding the nature and extent of the surgical procedure, the postoperative recovery and sequelae of treatment, and potential complications. Bacterial cultures from the nasal cavity should be obtained for patients undergoing resection of the floor of the anterior cranial fossa where direct communication will occur between the nasal cavity and the cranial cavity at the time of surgery. Preoperative antibiotics should be administered intravenously during the induction of anesthesia before an incision is made to provide broad-spectrum coverage. The antibiotic regimen should provide prophylaxis against gram-positive and gram-negative bacteria, as well as bacteroides. Our current preference is a combination of ceftazidime, vancomycin, and metronidazole. Intravenous antibiotic coverage is continued throughout the postoperative period as long as the nasal packing is in place (6–8 days).

Surgical Approaches

For the purpose of describing various surgical approaches, the skull base is divided into four anatomic regions:

1. The floor of the anterior cranial fossa covering the roof of the orbit, the cribriform plate, and the planum sphenoidale is called the anterior skull base. This region also covers the posterior wall of the frontal sinus, the frontal crest, the crista galli, and the anterior clinoid processes up to the ridge of the lesser wing of the sphenoid. Thus the floor of the anterior cranial fossa is composed of the frontal bone, the ethmoid bone, and two parts of the sphenoid bone (the body and lesser wing) posteriorly.
2. The skull base of the middle cranial fossa consists of parts of the sphenoid and temporal bones. The fissures and foramen traveling through the middle cranial fossa are important from a surgical standpoint because several pathologic conditions involve these structures. The superior orbital fissure, foramen rotundum, foramen ovale, and foramen lacerum pass through the floor of the middle cranial fossa. The posterior limit of the skull base of the middle cranial fossa is the superior ridge of the petrous temporal bone.
3. The temporal bone, particularly its petrous part, requires a separate anatomic designation because surgical approaches and the pathologic entities arising in the temporal bone are distinct.
4. Finally, the skull base of the posterior cranial fossa begins posterior to the temporal bone and is composed largely of the occipital bone, the jugular fossa and foramen, the hypoglossal canal, and the foramen magnum, which are all important structures from a surgical standpoint. Special consideration is also required for the undersurface of the middle cranial fossa, known as the infratemporal fossa, where significant pathologic entities arise that require specific surgical management considerations.

The most common pathologic conditions that require surgical intervention by the head and neck surgeon involve the skull base at the anterior and middle cranial fossae as well as the temporal bone. Lesions that arise from or involve the anterior cranial fossa generally are approached via a bifrontal craniotomy to get a wide exposure of the floor of the anterior cranial fossa and via a facial approach through a modified Weber-Ferguson incision. This approach also is suitable for tumors that involve or arise from the orbit and require orbital exenteration and resection of the roof of the orbit. However, this approach is not suitable for lesions that involve or arise from the floor of the middle cranial fossa. Some lesions of the central part of the floor of the anterior cranial fossa near the cribriform plate can be accessed through a subfrontal craniotomy. Selected central lesions of the anterior skull base can be accessed easily through an endonasal approach without the need for a facial incision.

The cranioorbito-zygomatic (COZ) approach is best suited for access to the floor of the middle cranial fossa and the infratemporal fossa. Disassembly of the zygomatic arch may be required to gain access to the deep temporal space. Other lesions at the floor of the middle cranial fossa, such as neurogenic tumors arising from the fifth cranial nerve or soft tissue tumors involving the floor of the middle cranial fossa, require surgical exposure via a pterional craniotomy to gain intracranial exposure. Transfacial access to these tumors can be obtained through a maxillary swing via a modified Weber-Ferguson incision or a mandibulotomy through a lower lip–splitting incision. Tumors arising in the lateral aspect of the infratemporal fossa are best accessed via a mandibulotomy, whereas tumors arising in the retromaxillary region, in the medial aspect of the infratemporal fossa, and in the nasopharynx are best approached via a maxillary swing procedure.

Tumors of the auditory canal and temporal bone require a temporal craniotomy for lateral subtotal or total temporal bone resection. Finally, a temporal or occipitotemporal craniotomy is required for adequate exposure and access to tumors arising in the posterior fossa (the far lateral approach described by Fisch). This access is required for neurovascular tumors, chordomas arising in the clivus or the craniocervical junction, and meningiomas arising at the cerebellopontine angle.

Surgical Procedures

Surgical Techniques for Tumors Involving the Skull Base of the Anterior Cranial Fossa

A variety of technical approaches are available for craniofacial resection for tumors involving the anterior skull base. The individual technique used varies with each surgeon and his or her personal preference. However, the standard surgical approach for resection of the anterior central skull base for a malignant tumor of the ethmoid is described here, followed by several technical variations.

Craniofacial Resection for an Esthesioneuroblastoma. The patient undergoing this procedure has an esthesioneuroblastoma that is arising from the region of the cribriform plate and is filling up the left nasal cavity. This patient presented with symptoms of nasal obstruction and epistaxis. A CT scan in a coronal view shows a bone-destructive lesion arising from the ethmoid region with extension caudad to involve the lower part of the nasal cavity and pushing the lamina papyracea of the left orbit laterally. A further posterior cut of the coronal view shows tumor extension in the sphenoid sinus through its floor. The tumor obstructs the osteomeatal complex of the maxillary antrum but does not extend into the maxillary sinus. Similarly, the tumor approximates the perpendicular plate of the ethmoid bone and the nasal septum but does not perforate through to extend to the opposite side of the nasal cavity. Although there is no intracranial extension of the tumor, it approximates the cribriform plate at the floor of the anterior cranial fossa (Fig. 6.27). An endoscopic view of the tumor is shown in Fig. 6.28.

An artist's rendering of the extent of the tumor as seen on the coronal section of the CT scan is shown in Fig. 6.29. Note that the surgical resection will include the cribriform plate and thus the central part of the anterior cranial base.

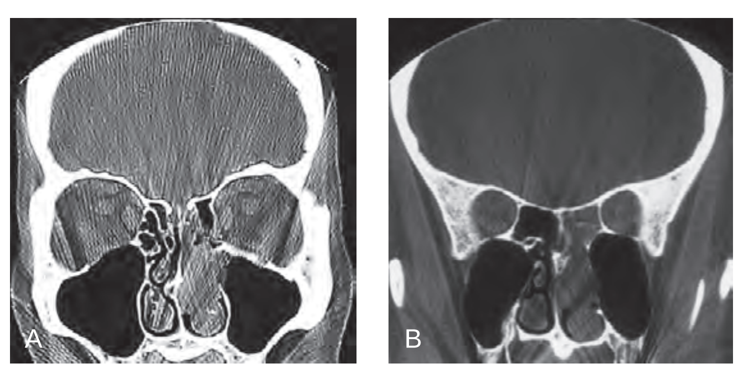

Figure 6.27 Coronal views of a computed tomography scan. **A**, Through cribriform plate. **B**, Through sphenoid sinus.

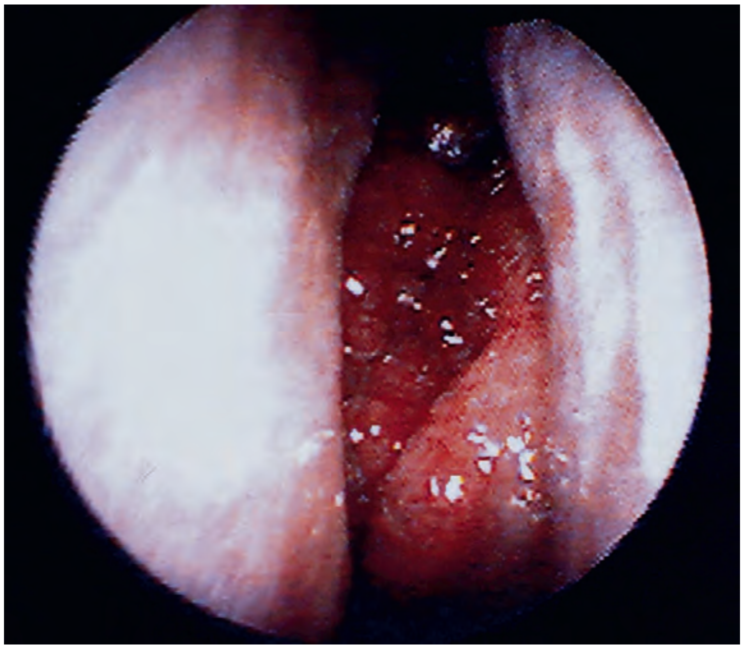

Figure 6.28 An endoscopic view showing the granular tumor in the nasal vault.

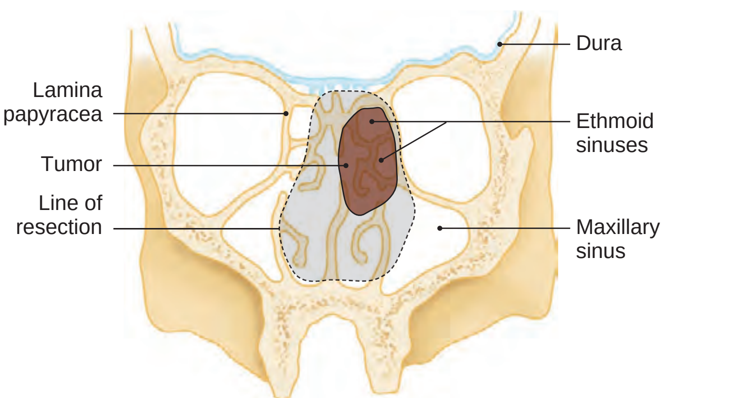

Figure 6.29 An artist's rendering of the extent of the tumor (*brown*) and the extent of surgical resection (*light gray*) as seen on the coronal section of the computed tomography scan.

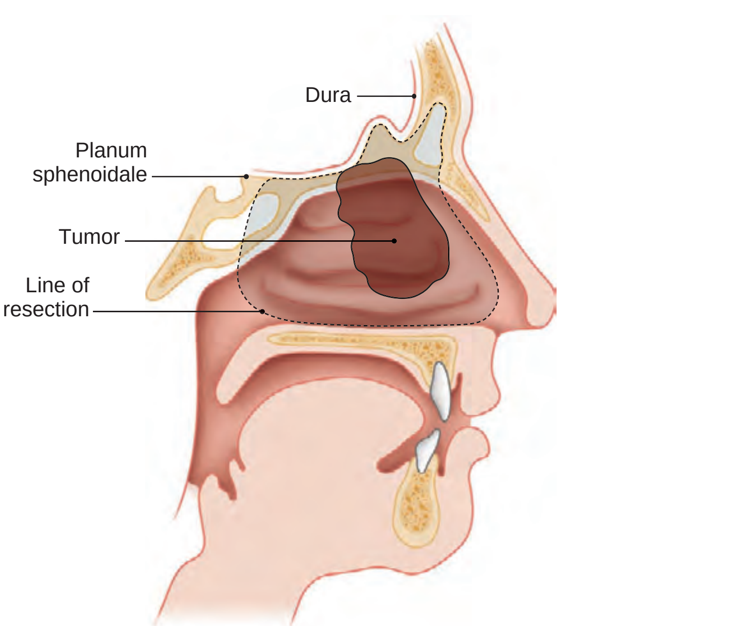

Figure 6.30 The extent of the tumor and the proposed surgical resection are shown in a sagittal plane.

The extent of the tumor and the proposed surgical resection are shown in a sagittal plane in Fig. 6.30. The anterior wall and the floor of the sphenoid sinus will be removed in conjunction with the tumor and the contents of the nasal cavity on the left-hand side.

If a split-thickness skin graft is to be used for repair, it is harvested before beginning the surgical procedure for resection of the tumor. The anterolateral aspect of the thigh is the most suitable donor site. However, because the surgical defect in this patient will be small, it does not require a skin graft. On the other hand, if a free flap is to be used, then the appropriate donor site is isolated for simultaneous harvest of the flap.

The patient is then placed in the lateral position and a lumbar puncture is performed (Fig. 6.31). An indwelling spinal catheter is introduced through the lumbar puncture needle for continuous spinal drainage and monitoring of the CSF pressure during the procedure and in the immediate postoperative period. The spinal catheter is appropriately positioned and connected to a closed circuit drainage system with a 50-mL syringe. The patient's head is appropriately positioned on the operating table on a head rest and maintained in a neutral position with slight flexion at the atlanto-occipital joint (Fig. 6.32).

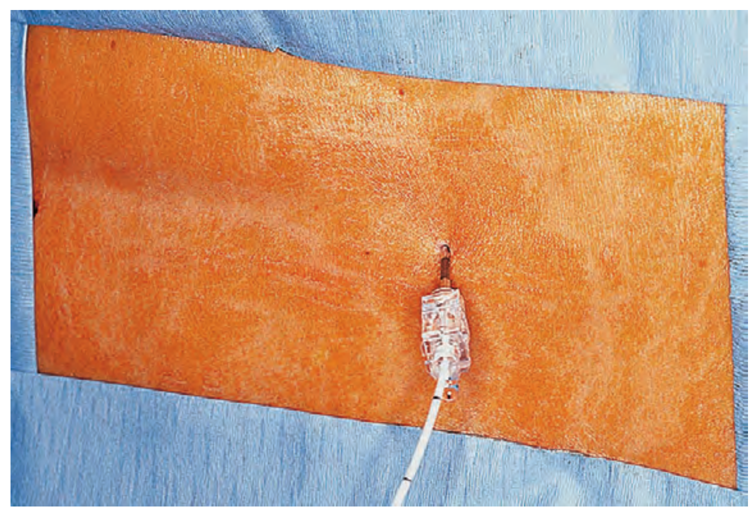

Figure 6.31 The patient is placed in the lateral position and an indwelling spinal catheter is inserted.

Figure 6.32 The patient's head is appropriately positioned on the operating table on a doughnut cusion and may be stabilized with neurosurgical pins.

General anesthetic is administered through an endotracheal tube that is brought out through the commissure of the oral cavity on the right-hand side and isolated by sterile drapes. The eyelids are sutured shut with 6-0 nylon sutures through the skin of the upper and lower eyelids to protect the cornea during the surgical procedure. The scalp is shaved in the area of the craniotomy incision. Cloth drape towels are sutured to the skin with silk sutures to maintain strict asepsis and isolation of the field. The skin of the face and scalp is prepared with Betadine solution. The proposed lines of incisions are shown in Fig. 6.33. A bicoronal incision is planned posterior to the hairline extending from the tragus of one ear to that of the other to provide a wide exposure for the anterior fossa craniotomy (Fig. 6.34). The facial exposure is usually obtained through a modified Weber-Ferguson incision, respecting the nasal subunits (Fig. 6.35). If exposure of the lower half of the nasal cavity, hard palate, or maxilla is required, then the incision is extended to split the upper lip in the midline. The incision then follows the nasal subunits along the nasolabial fold and extends up to the medial end of the eyebrow. Two potential extensions of the incision can be used, depending on the required exposure. A glabellar extension up to the opposite eyebrow can be used if facial disassembly of the nasal bones is planned to gain the necessary exposure. On the other hand, if a total maxillectomy or a maxillectomy with orbital exenteration is required, then a subciliary extension up to the lateral canthus is used, as shown with the dotted line in Fig. 6.35. The scalp is incised through its subcutaneous tissue up to a plane superficial to the galea aponeurotica and the pericranium (Fig. 6.36). The plane between the subcutaneous tissue and galea is tedious to dissect, under the posterior scalp flap. The posterior scalp flap is elevated several centimeters posteriorly to expose the pericranium. Hemostasis on the cut edges of the scalp can be secured with use of Raney clips. These hemostatic clips are applied on both edges of the cut incision as shown in Fig. 6.37.

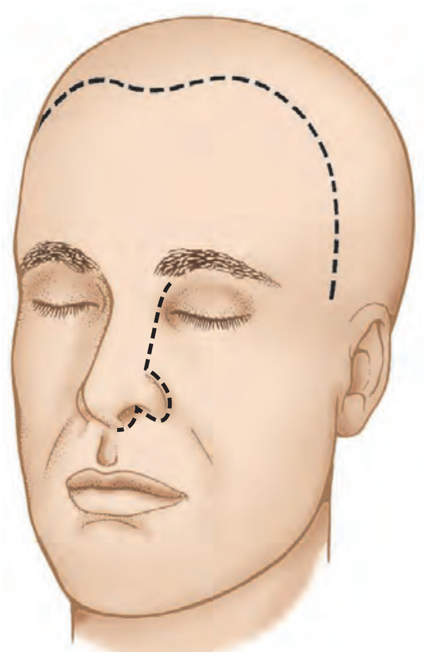

Figure 6.33 The proposed lines of incisions.

Figure 6.34 A bicoronal incision is planned posterior to the hairline extending from the tragus of one ear to that of the other to provide a wide exposure for the bifrontal craniotomy.

Figure 6.35 The facial exposure is usually obtained through a modified Weber-Ferguson incision, respecting the nasal subunits.

Figure 6.36 The scalp flap is elevated in a plane superficial to the galea aponeurotica and the pericranium.

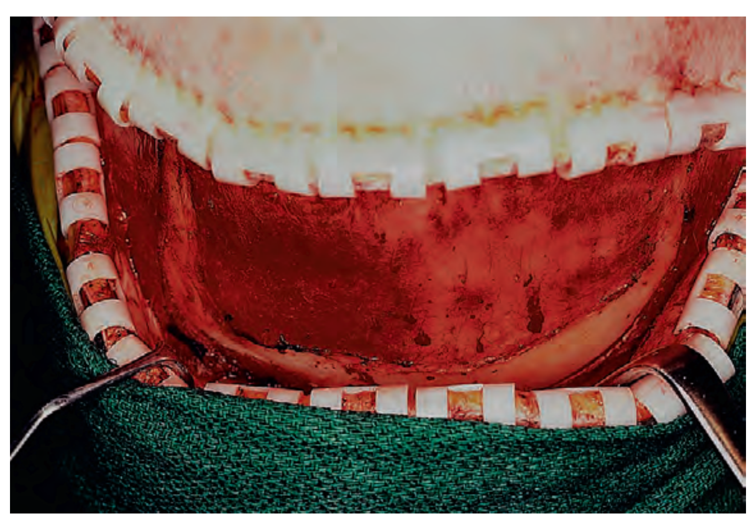

Figure 6.37 The posterior scalp flap is retracted significantly to obtain a generous portion of the galea and pericranium for the pedicled flap.

The proposed line of incision in the pericranium for the elevation of a pedicled galeal pericranial flap for subsequent use during repair of the skull base defect is shown in Fig. 6.38. The incision in the pericranium has been made as previously described. Note that the posterior scalp flap is retracted significantly to obtain a generous length of the pedicled galeal pericranial flap. With use of a periosteal elevator, the pericranium is then elevated very carefully over the calvarium all the way up to the supraorbital ridges. Extreme care should be exercised to avoid injury to the pericranium, causing "button holes." The anterior scalp flap is elevated in a similar fashion but remaining superficial to the galea aponeurotica up to the supraorbital ridge. Careful elevation of the galeal pericranial flap requires sharp dissection with a scalpel between the subcutaneous tissue and the galea, as shown in Fig. 6.39. The blood supply to the galeal pericranial flap comes from the supraorbital and supratrochlear vessels. Extreme care should be exercised as elevation of the galea approaches the supraorbital ridge to avoid any injury to the supratrochlear and supraorbital vessels. A long and robust flap is thus available for reconstruction of the skull base defect (Fig. 6.40). Complete elevation of the flap over the calvarium thus exposes the underlying frontal bone (Fig. 6.41). The pedicled galeal pericranial flap is shown elevated and lifted to reveal its available dimensions for repair of the surgical defect.

Elevation of the anterior scalp flap is carried out as far down as possible to expose the glabellar region and the upper half of the nasal bones. A retractor placed in the center of the field shows the exposed upper part of the nasal bones and the supraorbital ridges bilaterally (Fig. 6.42). The proposed line of bone cut is marked out on the anterior wall of the frontal sinus and the frontal bone (Fig. 6.43). A limited craniotomy of this

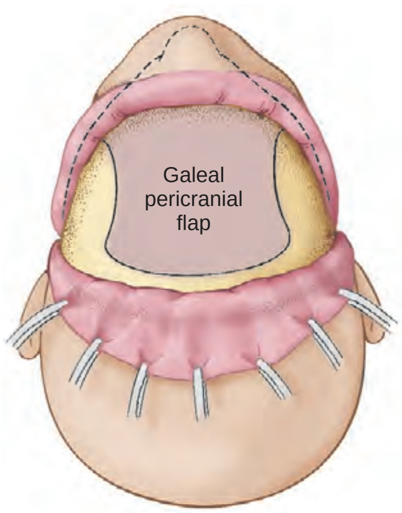

Figure 6.38 The proposed line of incision (U-shaped) in the pericranium for the elevation of a pedicled galeal-pericranial flap for subsequent use during repair of the skull base.

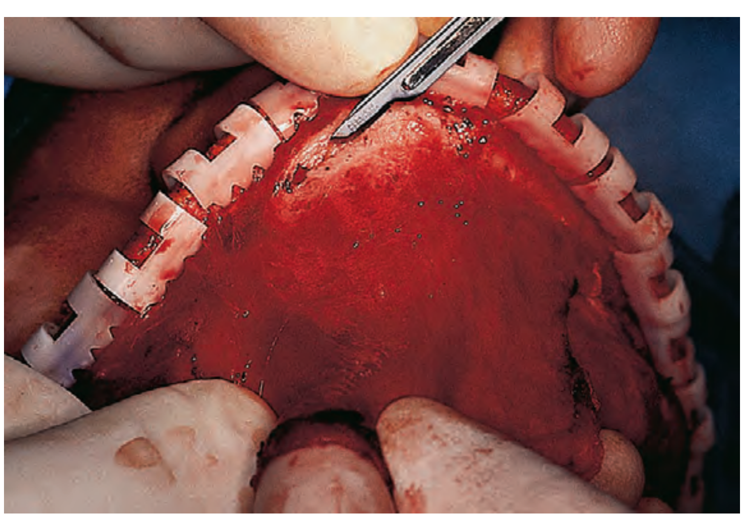

Figure 6.39 Elevation of the galeal pericranial flap requires careful sharp dissection with a scalpel between the subcutaneous tissue and the galea.

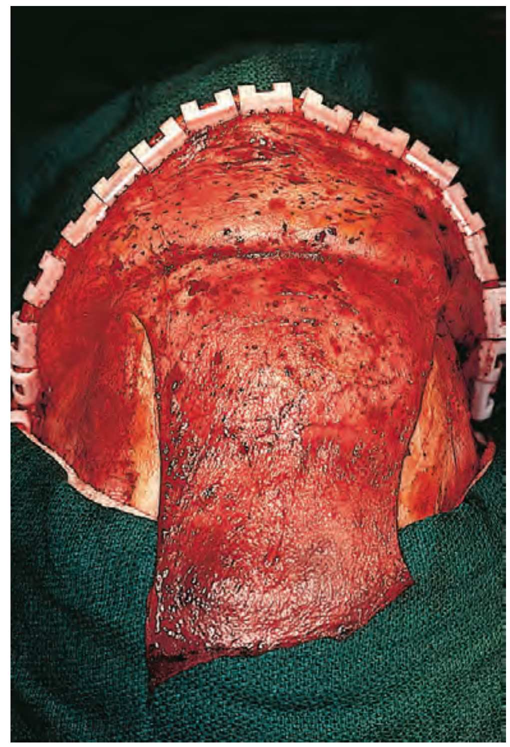

Figure 6.40 The galeal pericranial flap is a robust flap of sufficient length to allow for reconstruction of the skull base defect.

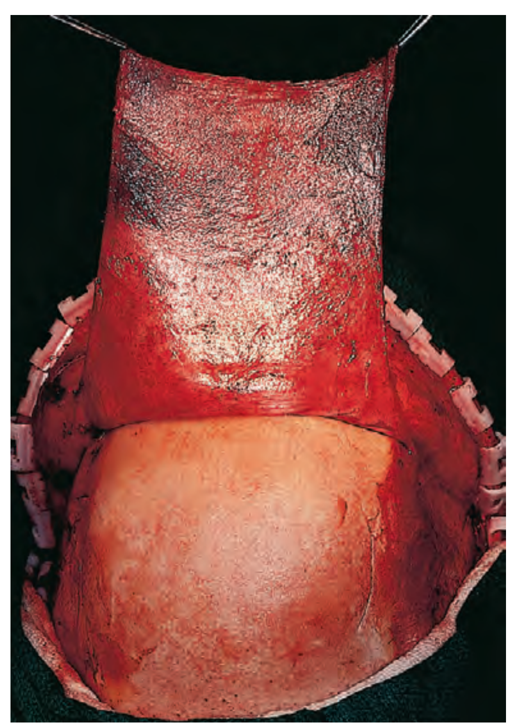

Figure 6.41 Complete elevation of the flap over the calvarium exposes the underlying frontal bone.

dimension is satisfactory to get the necessary exposure for a subcranial approach to the cribriform plate.

A craniotome is used to make a single burr hole in the midline. Dural elevators are used to elevate the dura adjacent to the burr hole on both sides to permit introduction of the side-cutting Midas Rex saw to complete the craniotomy (Fig. 6.44). A circumferential bone cut is made at the proposed line of the craniotomy (Fig. 6.45). Inferiorly only the anterior wall of the frontal sinus is cut with the side-cutting saw to complete the craniotomy (Fig. 6.46). An osteotome is used to elevate the bone flap. The septum in the frontal sinus is fractured, and the bone flap is carefully elevated without injury to the underlying dura. Removal of the bone flap exposes the dura over the frontal lobes as well as the frontal sinus (Fig. 6.47). The bony septa in the frontal sinus are removed with a rongeur and forceps. All the sharp bony spicules are smoothed out with a high-speed burr. The mucosa of the sinus is completely curetted out, and its posterior wall is removed to cranialize the frontal sinus (Fig. 6.48). The openings of the nasofrontal ducts are plugged with Gelfoam.

Attention is now directed to elevation of the dura from the floor of the anterior cranial fossa (Fig. 6.49). Attachments of the dura to the crista galli require sharp division. The dural sleeves along the olfactory nerves are individually divided and ligated. The exposed crista galli, after elevation of the dura, is excised with a rongeur. Meticulous attention should be paid to avoid inadvertent tears in the dura during removal of the crista galli. Any tears that occur are immediately repaired with 4-0 Nurolon sutures. Attention is now directed to the dural sleeves that contain the olfactory nerves traversing the cribriform plate. Each dural sleeve is individually identified, dissected, divided, and ligated. Immediate ligation of the dural sleeves is desirable to avoid contamination of the brain during subsequent phases of the operation. However, if part of the tumor is seen perforating through the cribriform plate at this juncture, then the dura is opened and the entire segment of dura overlying the cribriform plate, along with the dural sleeves of the olfactory nerves, are resected with the tumor. This procedure creates a dural defect at the anterior cranial base that is repaired with use of a free graft of pericranium in a watertight fashion. The patient described here has no extension of tumor through the cribriform plate.

All the dural sleeves have been divided and ligated, as shown in Fig. 6.50. Approximately 10 to 15 mL of cerebrospinal fluid is removed through the spinal catheter at this juncture to allow slackening of the brain. A retractor is used along the midline over the sagittal sinus to expose the posterior part of

Figure 6.42 A retractor placed in the center of the field shows the exposed upper part of the nasal bones and the supraorbital ridges bilaterally.

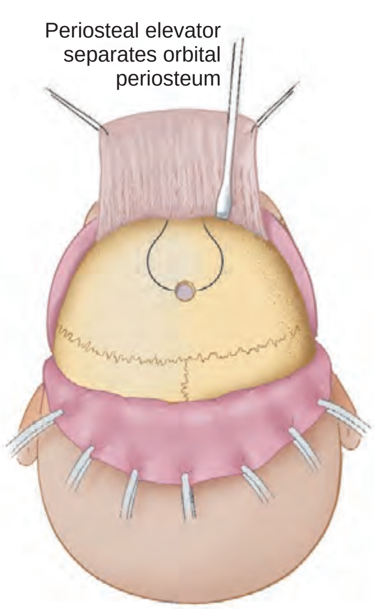

Figure 6.43 The proposed line of the bone cut is marked on the anterior wall of the frontal sinus and the frontal bone.

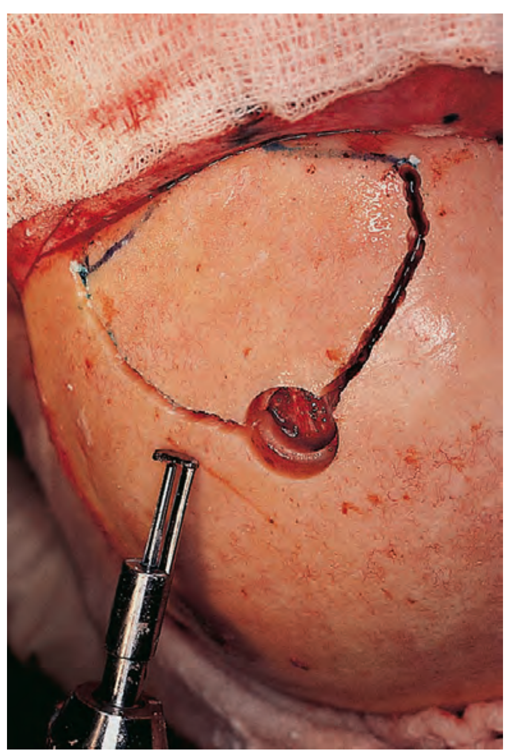

Figure 6.44 A single burr hole is made in the midline and dural elevators are used to elevate the dura adjacent to the burr hole on both sides to permit introduction of the side-cutting Midas Rex saw.

Figure 6.45 A circumferential bone cut is made at the proposed line of the craniotomy.

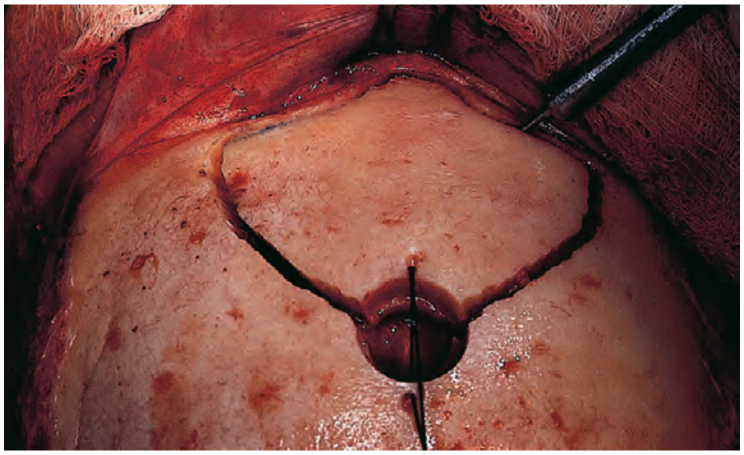

Figure 6.46 Inferiorly only, the anterior wall of the frontal sinus is cut with the side-cutting saw to complete the craniotomy.

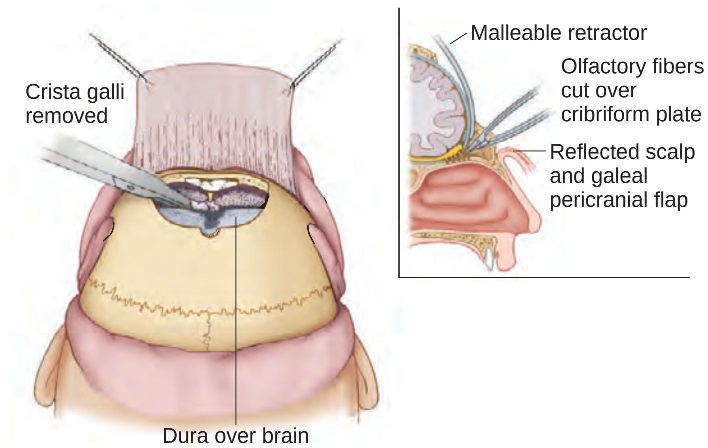

Figure 6.49 Attention is now directed to the elevation of the dura from the floor of the anterior cranial fossa.

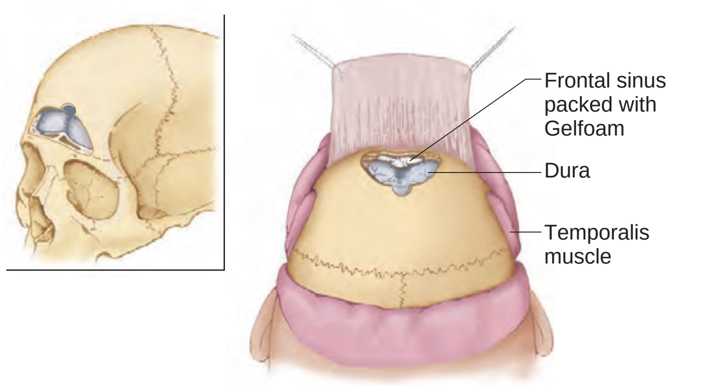

Figure 6.47 Removal of the bone flap exposes the dura over the frontal lobes as well as the frontal sinus.

Figure 6.50 The dural sleeves have been divided and ligated.

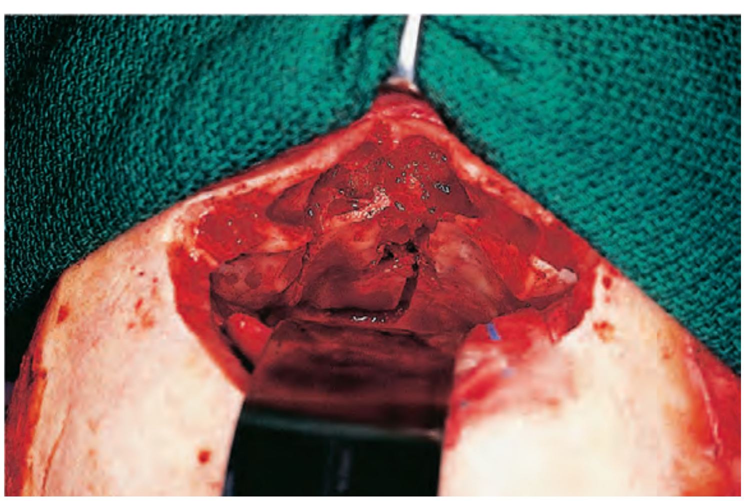

Figure 6.48 The mucosa of the frontal sinus is completely curetted out, and its posterior wall is removed to cranialize the sinus.

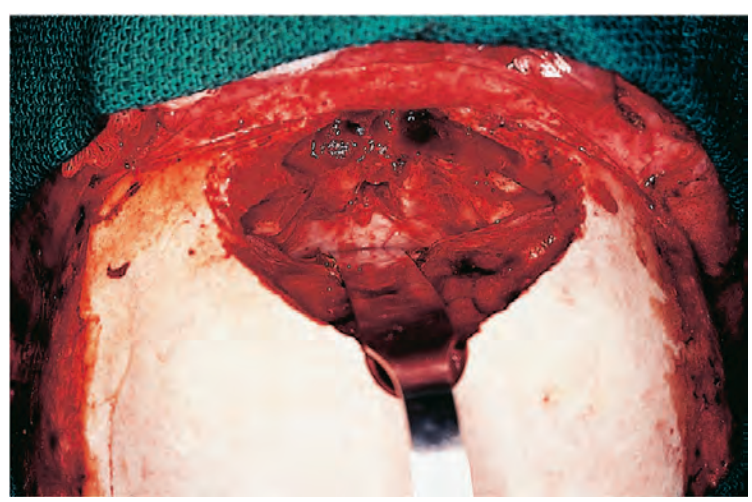

Figure 6.51 A retractor placed along the midline over the sagittal sinus exposes the posterior part of the cribriform plate and the planum sphenoidale.

the cribriform plate and the planum sphenoidale (Fig. 6.51). To ensure a complete seal of the sutured dural sleeves and any dural repairs, fibrin glue is used to attain an additional protective layer of watertight closure (Fig. 6.52). The gel formed by mixing the fibrin glue components is shown in Fig. 6.53.

After adequate slackening of the brain is achieved, a wide malleable retractor is used to protect the frontal lobes in the midline posteriorly to gain wide exposure of the planum sphenoidale and the cribriform plate. A high-speed drill with a fine burr is now used to make the bone cuts through the floor of the anterior cranial fossa (Fig. 6.54). The circumferential bone cut around the cribriform plate is completed. Note that the bone cut goes through the roof of the left orbit, remaining lateral to the lamina papyracea on the left side, through the sphenoid sinus posteriorly, and through the cribriform plate, remaining medial to the lamina papyracea on the right-hand

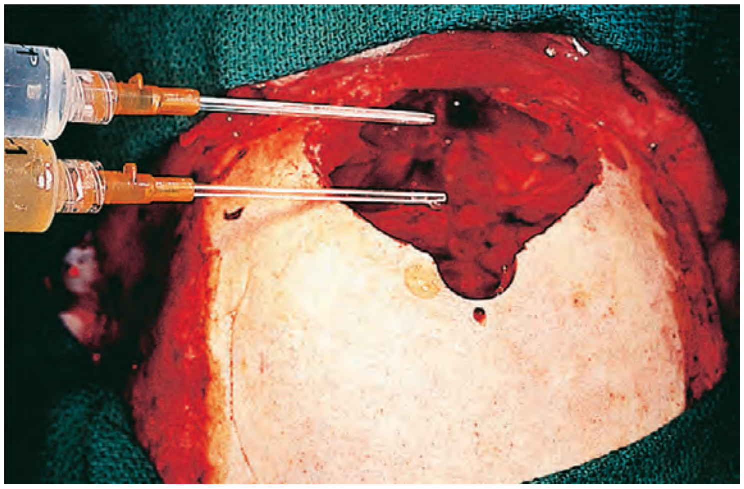

Figure 6.52 Fibrin glue is used to attain an additional protective layer of water-tight closure over the sutured dural sleeves.

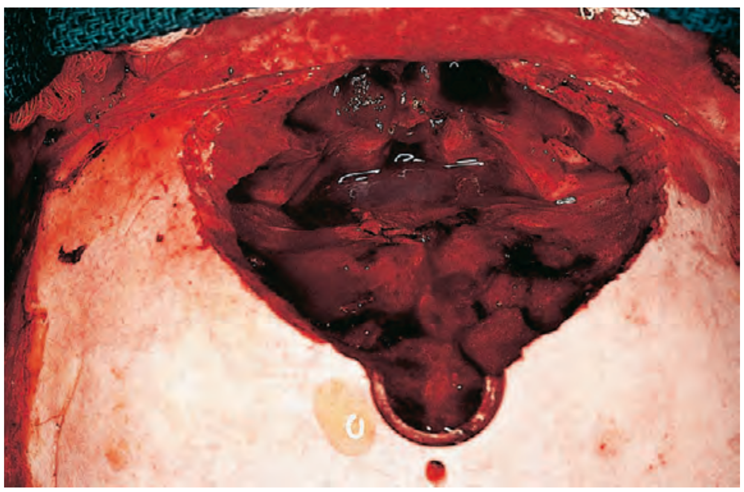

Figure 6.53 The gel formed by mixing the fibrin glue components.

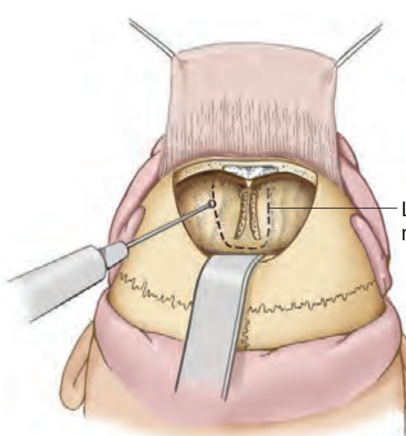

Figure 6.54 A high-speed drill with a fine burr is used to make the bone cuts through the floor of the anterior cranial fossa.

side and through the frontal sinus anteriorly to encompass the superior aspect of the surgical specimen. At this juncture, the first phase of the operative procedure through the craniotomy is complete.

The facial approach begins with a modified Weber-Ferguson incision that is extended up to the medial aspect of the eyebrow on the left-hand side (Fig. 6.55). The skin incision goes through the full thickness of the soft tissues and musculature of the nasolabial region.

Figure 6.55 The facial approach begins with a modified Weber-Ferguson incision that is extended up to the medial aspect of the eyebrow on the left-hand side.

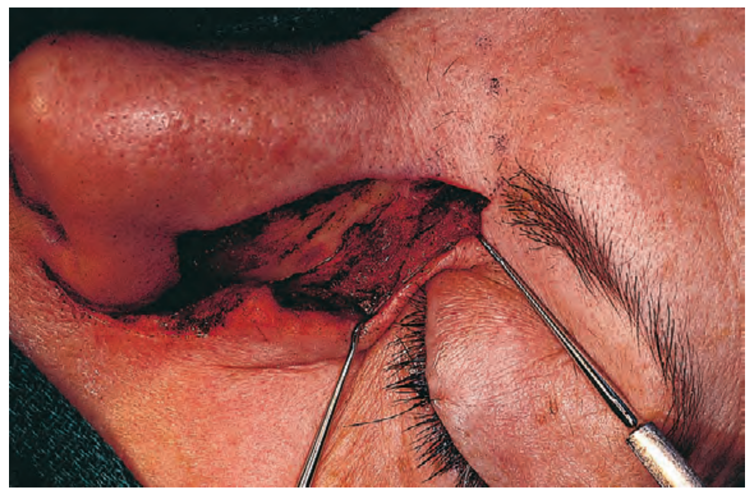

Figure 6.56 The attachment of the medial canthal ligament is identified.

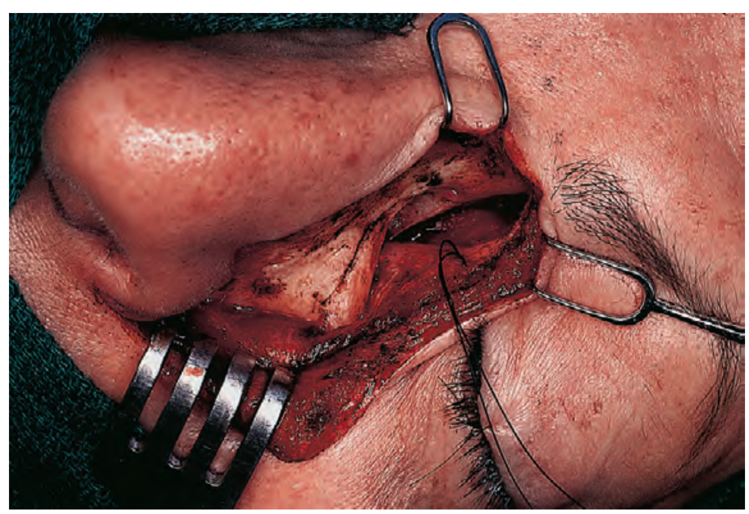

Figure 6.57 The medial canthal ligament is detached and retracted with a 4-0 Nurolon suture that will be used subsequently for its fixation to the nasal bone during closure.

The periosteum of the medial wall of the orbit is elevated to keep the contents of the orbit within its periosteal envelope. Attachment of the medial canthal ligament is identified (Fig. 6.56). The medial canthal ligament is detached and retracted with a 4-0 Nurolon suture, which subsequently will be used for its fixation to the nasal bone during closure (Fig. 6.57). The

nasolacrimal duct is dissected out of its fossa with use of fine periosteal elevators (Fig. 6.58), and a scalpel is used to divide the duct flush with the rim of the orbit. The cheek flap is elevated directly over the anterior bony wall of the maxilla, carefully preserving the infraorbital nerve as it exits from the infraorbital foramen (Fig. 6.59). The orbital periosteum is elevated from the bony orbit in its medial half. A malleable retractor is introduced into the orbit, and the globe is retracted laterally. As the periosteum of the medial half of the orbit is elevated from the lamina papyracea, the anterior and posterior ethmoid vessels are encountered, coming from the orbital periosteum and perforating through the lamina papyracea. These vessels are carefully identified and electrocoagulated with a bipolar cautery. The mucosa of the nasal cavity is now incised through its lateral wall at the vestibule along the anteromedial wall of the maxilla (Fig. 6.60), which provides exposure of the interior of the nasal cavity.

The anterior wall of the maxillary antrum is opened with use of a high-speed drill and a burr (Fig. 6.61). The opening is enlarged enough to permit easy insertion of an index finger in the maxillary antrum (Fig. 6.62). Careful inspection of the interior of the antrum is made to see if any tumor is present. No tumor could be seen in this patient. The skin and soft tissues of the nose are elevated over the nasal bones to gain further exposure of the region of the upper half of the nasal cavity. Bone cuts are now made through the nasal process of maxilla and through the lacrimal fossa and the anterior aspect of the lamina papyracea within the orbit on the left-hand side (Fig. 6.63), which permits mobilization of the bony attachments

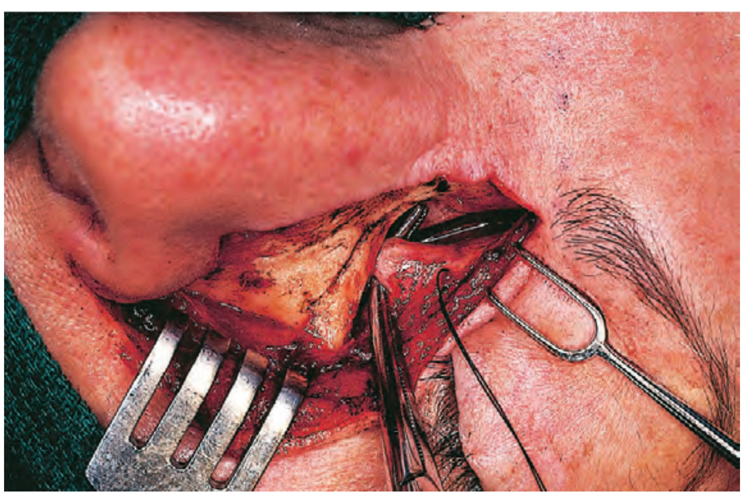

Figure 6.58 The nasolacrimal duct is dissected out of its fossa with use of fine periosteal elevators.

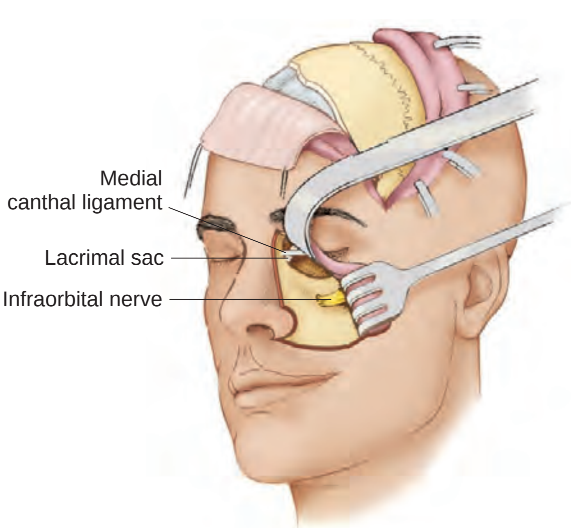

Figure 6.59 The cheek flap is elevated directly over the anterior bony wall of the maxilla, carefully preserving the intraorbital nerve as it exits from the infraorbital foramen.

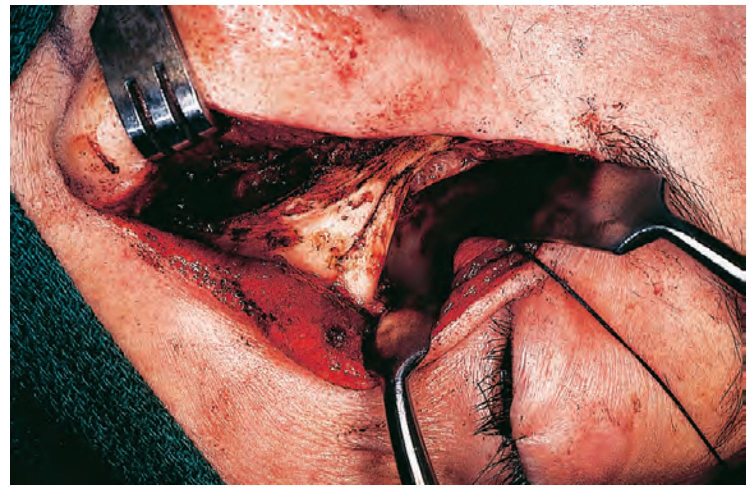

Figure 6.60 The mucosa of the naval cavity is now incised through its lateral wall at the vestibule along the anteromedial wall of the maxilla.

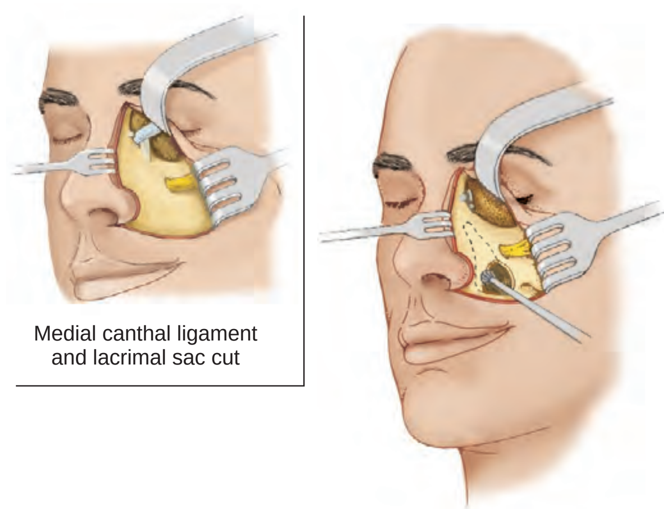

Figure 6.61 The anterior wall of the maxillary antrum is opened with use of a high-speed drill and a burr.

Figure 6.62 The opening is enlarged enough to permit easy insertion of an index finger in the maxillary antrum.

of the lamina papyracea. These bone cuts are made with fine osteotomes and a high-speed drill with a fine burr. The medial wall of the maxilla in its lower part is divided with an osteotome through the floor of the nasal cavity as far back as posteriorly as possible.

An incision is made in the nasal septum to complete medial mobilization of the surgical specimen and totally remove the contents of the nasal cavity. The incision in the nasal septum is made with an electrocautery, remaining approximately 8 mm posterior to the columella. The septal incision is completed through the floor of the nasal cavity all the way up to and including the vomer bone. This incision is accomplished with either an osteotome or heavy serrated scissors. Similarly, the incision in the nasal septum is carried cephalad along the bridge of the nose and the nasal bone, leaving a strip of the nasal strut to support the nasal framework in the lower half of the nasal cavity. Right-angled scissors are used to cut through the posterior aspect of the lateral wall of the nasal cavity (Fig. 6.64). The scissors are introduced through the nostril and guided with a finger from the antrum to direct the cut cephalad. To remove the specimen safely, cranial exposure of the skull base is now necessary.

The intracranial aspect of the surgical field is now exposed. Under digital and visual guidance provided by the head and neck surgeon from the facial aspect, the specimen is removed. Straight osteotomes are used from the cranial cavity to separate the specimen laterally through the medial aspect of the left orbit and through the ethmoid air cells on the right-hand side as well as through the sphenoid sinus posteriorly (Fig. 6.65). Gentle strokes with a mallet on the osteotome are necessary to complete the fracture of the remaining bony attachments to allow removal of the specimen.

The surgical defect from the facial aspect shows complete exenteration of the nasal cavity and removal of its left lateral wall (Fig. 6.66). The silk suture tagged to the medial canthal ligament overlies the upper eyelid. It must be resutured to the remaining nasal bone for repositioning of the medial canthus in its normal position. The medial canthal ligament is sutured through a drill hole to the left nasal bone with the 4-0 Nurolon suture. The point of fixation is matched to the opposite medial canthus. The surgical defect seen from the cranial cavity demonstrates a through-and-through resection of the bony floor of the anterior cranial fossa in the region of the cribriform plate (Fig. 6.67).

The previously elevated galeal pericranial flap is now brought into the field to cover the bony defect in the anterior skull base. Several drill holes are made in the posterior edges of the bony defect in the floor of the anterior cranial fossa. This procedure involves making drill holes through the roof of the orbit on the left-hand side, through the shelf of the bone along the right ethmoid air cells, and through the planum sphenoidale posteriorly.

A diagrammatic representation of how the galeal pericranial pedicled flap is swung down to cover the bony defect in the skull base is shown in Fig. 6.68. The flap is sutured to the bony

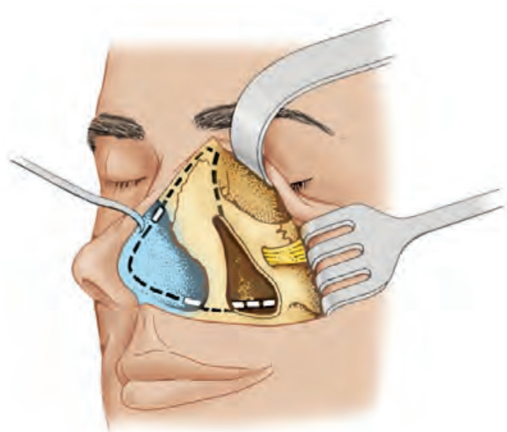

Figure 6.63 Bone cuts are now made through the nasal process of the maxilla and through the lacrimal fossa and the anterior aspect of the lamina papyracea within the orbit on the left-hand side.

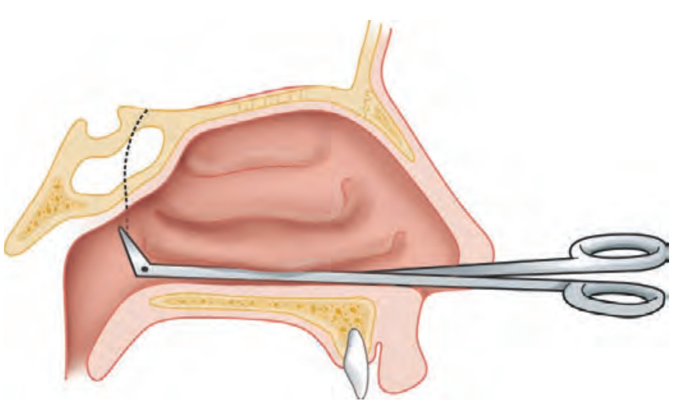

Figure 6.64 Right-angled scissors are used to cut through the posterior aspect of the lateral wall of the nasal cavity.

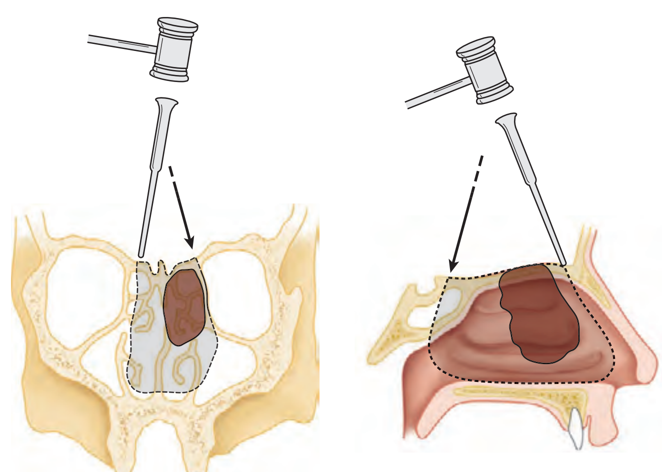

Figure 6.65 The specimen is removed under digital and visual guidance through the cranial and facial exposures.

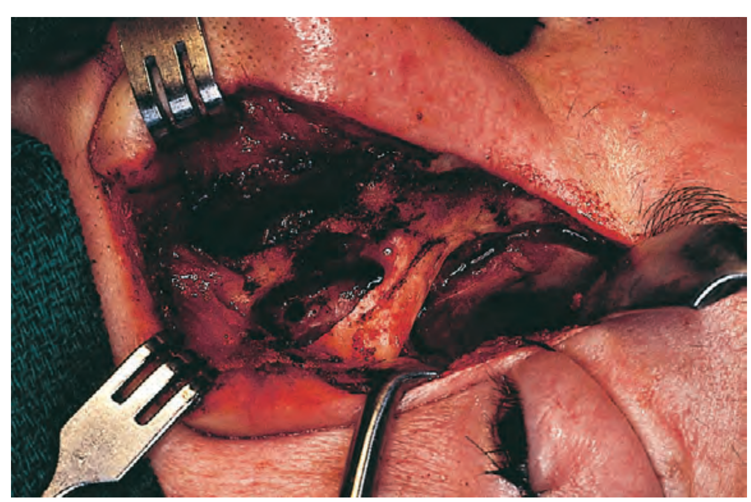

Figure 6.66 The surgical defect seen from the facial aspect.

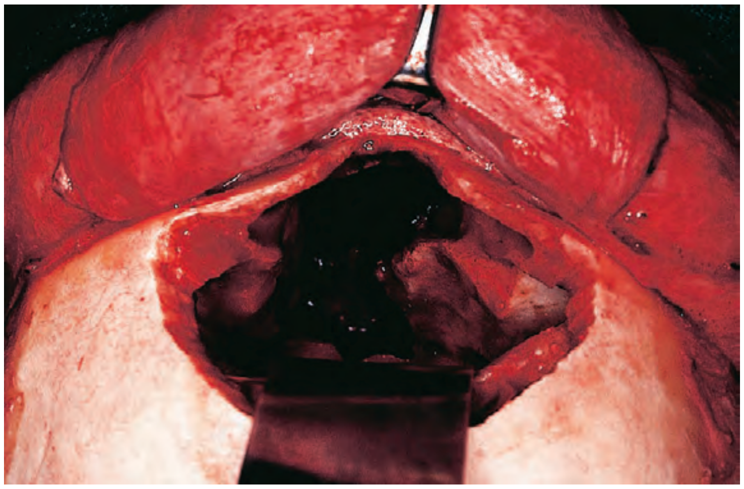

Figure 6.67 The surgical defect seen from the cranial aspect.

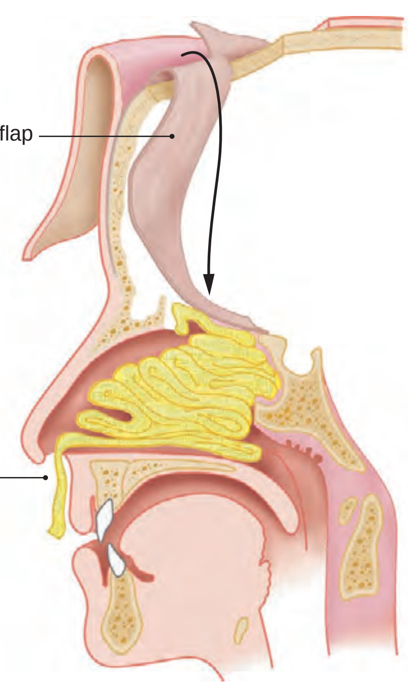

Figure 6.68 A diagrammatic representation of how the galeal pericranial pedicled flap is swung down to cover the bony defect in the skull base.

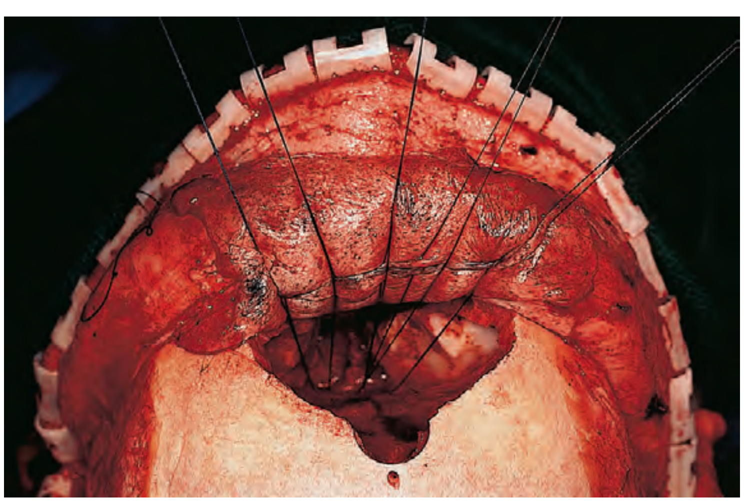

Figure 6.69 Several interrupted sutures are taken between the galeal pericranial flap and the drill holes through the floor of the anterior cranial fossa.

skull base, providing complete closure of the bony defect in the skull. Several interrupted sutures are taken between the galeal pericranial flap and the drill holes through the floor of the anterior cranial fossa (Fig. 6.69). A secure closure and adequate support to the cranial base defect are thus achieved (Fig. 6.70). The craniotomy is then closed with appropriate miniplates. A suction drain is placed through the burr hole in the extradural space, deep to the bone flap (Fig. 6.71). The scalp incision is closed in the usual fashion.

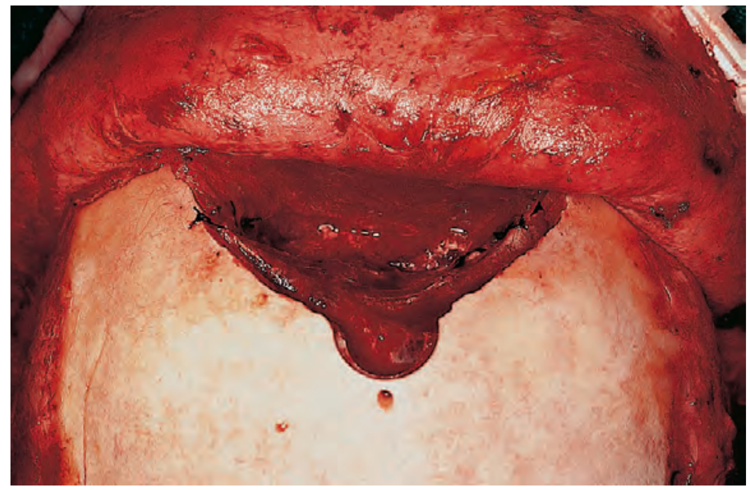

Figure 6.70 The galeal pericranial flap is sutured to the bony skull base, providing complete closure of the bony defect in the skull.

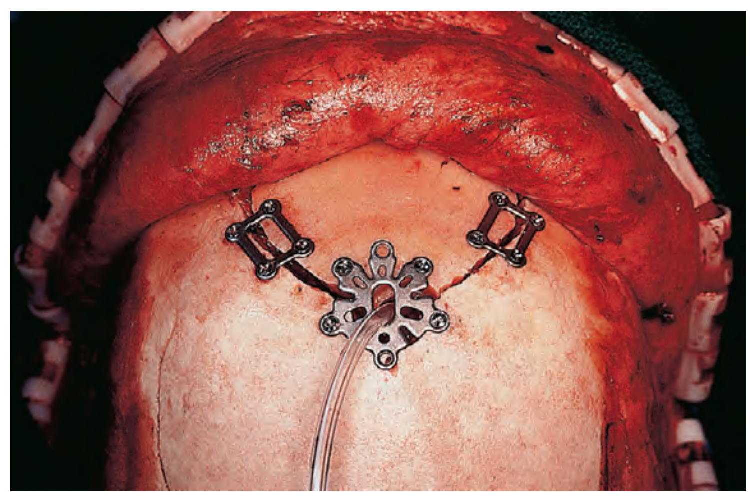

Figure 6.71 The craniotomy is closed with appropriate miniplates. A suction drain is placed through the burr hole in the extradural space, deep to the bone flap.

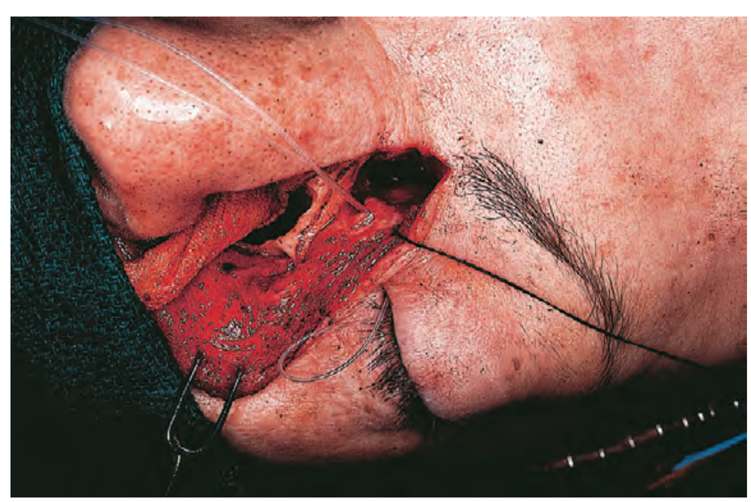

Figure 6.72 The nasolacrimal duct is cannulated with a Silastic stent and Xeroform roller gauze is packed into the nasal cavity.

On the facial aspect, the puncta of the nasolacrimal duct are cannulated with a Silastic stent (see Fig. 6.72), the ends of which are knotted in place within the nasal cavity (see Chapter 4 for details). Xeroform roller gauze packing is introduced into the nasal cavity to provide support to the galeal pericranial flap from the nasal aspect. The packing is introduced snugly to fill up the entire nasal cavity and support the galeal pericranial flap cephalad and the periosteum of the orbit on the left lateral side. The packing is brought out through the nostril. The skin incision on the face is closed in two layers (Fig. 6.73). The packing in the nose is retained for approximately 1 week.

Figure 6.73 The facial incision is closed in the usual fashion.

The appearance of the patient approximately 8 weeks after surgery shows well-healed incisions (Fig. 6.74). The external facial deformity is minimal, the patient has binocular vision, and the position of the globe on the left-hand side is essentially normal.

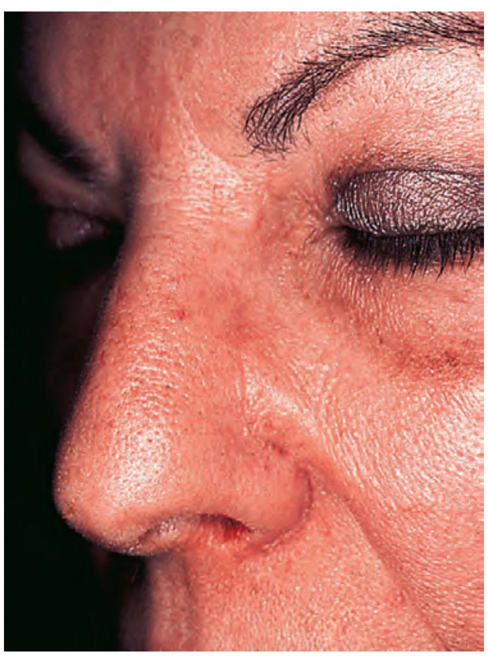

Figure 6.74 Postoperative appearance of the patient 8 weeks following surgery.

Postoperative MRI scans in axial and coronal views show total exenteration of the nasal cavity and the ethmoid complex up to and including the cribriform plate. The ethmoid tumor is thus completely resected (Figs. 6.75 and 6.76).

Figure 6.75 An axial view of the postoperative magnetic resonance imaging scan.

Figure 6.76 A coronal view of the postoperative magnetic resonance imaging scan.

Technical Variations in Craniofacial Resection for Tumors Involving the Anterior Skull Base. Several technical variations in the operative procedure can be used, depending on the individual situation and the preference of the surgeon. The evolution of craniofacial surgery during the past 50 years has led to the development of refinements in surgical techniques for better access, ease of resection, and reduction in morbidity and sequelae of the surgical procedure. These refinements largely have been able to be developed because of the availability of newer instruments and increasing cooperative efforts between multidisciplinary surgery teams to bring about an expeditious and successful execution of the operative procedure. In addition, long-term follow-up data for several patients who underwent operations during the course of the past 40 years are now available, which has provided the opportunity to observe the aesthetic and functional sequelae of craniofacial surgery. Several technical modifications now enable us to reduce the long-term sequelae of craniofacial surgery. These technical variations are described for each stage of the operative procedure.

Incisions. The standard incisions required for anterior craniofacial resection requires a bifrontal coronal incision for craniotomy and a Weber-Ferguson incision. However, several variations in this standard approach can be used, depending on the individual situation. A unilateral supraorbital incision can be used for a limited frontal craniotomy when a primary tumor of one orbit involves the orbital roof, requiring limited resection. An upper lip–splitting modified Weber-Ferguson incision is the standard approach. However, for limited exposure, a lateral rhinotomy is often satisfactory. Alternatively, the facial incision can be avoided altogether, and nasoendoscopic assistance is often satisfactory for a complete resection.

Craniotomy. In the past the usual approach to obtain satisfactory exposure with a craniotomy was to use multiple burr holes and connect these burr holes for a wide bifrontal craniotomy. The current standard approach for exposure of the skull base of the anterior cranial fossa is to perform a single midline burr

hole, and with use of the side-cutting Midas Rex saw, a bifrontal craniotomy is completed with a linear bone cut to elevate the bone flap, as seen in Fig. 6.46. Alternatively, an anterior subcranial approach may be undertaken to get a similar exposure.

Craniofacial Resection with Craniectomy. When any portion of the calvarium is resected, no repair may be undertaken, particularly if the bone defect is small and is under the hair-bearing scalp. On the other hand, larger bone defects, regardless of location, require reconstruction to protect the brain. Calvarial defects on the forehead require reconstruction to avoid aesthetic deformity.

The patient shown in Fig. 6.77 has squamous cell carcinoma of the frontal sinus perforating through the anterior wall of the sinus into the subcutaneous soft tissues. The outline of the frontal sinus and the radiographic extent of the tumor are shown in Fig. 6.78. An axial view of the postcontrast T1-weighted MRI scan shows the tumor in the frontal sinus extending to the subcutaneous soft tissues with obstructive changes in the right frontal sinus (Fig. 6.79). The sagittal view of the MRI scan shows that the tumor is contained in the frontal sinus without any brain edema (Fig. 6.80). An axial view of the CT scan (Fig. 6.81) demonstrates that the posterior wall of the frontal sinus is intact. Surgical resection of this tumor was undertaken through a frontal sinus craniectomy, remaining cephalad and lateral to the radiographic extent of the tumor. A bicoronal scalp flap is elevated, leaving the frontalis muscle and subcutaneous soft tissue on the surgical specimen (Fig. 6.82). A circumferential craniotomy is performed with a side-cutting burr around the outlined area of frontal bone resection (Fig. 6.83). The dura of the frontal lobes is elevated from the cranial surface of the posterior wall of the frontal sinus. With gentle use of osteotomes, the nasofrontal junction is fractured and the surgical specimen is removed (Fig. 6.84). A monobloc excision is performed with the tumor contained in an intact frontal sinus with its anterior and posterior walls and the floor intact (Fig. 6.85). The surgical defect shown in Fig. 6.86 demonstrates an intact dura with complete excision of the tumor. Reconstruction of this large bony defect in the frontal bone is accomplished with use of a calvarial graft harvested from the parieto-occipital region of the calvarium (Fig. 6.87). The graft is anchored to the margins of the frontal bone defect with miniplates and screws. The donor site in the calvarium is repaired with a flexible Porex prosthesis. The axial view of a postoperative CT scan shows excellent restoration of the contour of the forehead by the bone graft (Fig. 6.88). The appearance of the patient 4 months after completion of postoperative radiation therapy is shown in Fig. 6.89.

Figure 6.77 The lateral profile of the patient showing a diffuse bulge of the central part of the forehead.

Figure 6.78 The frontal sinus and the radiographic extent of the tumor are outlined on the patient.

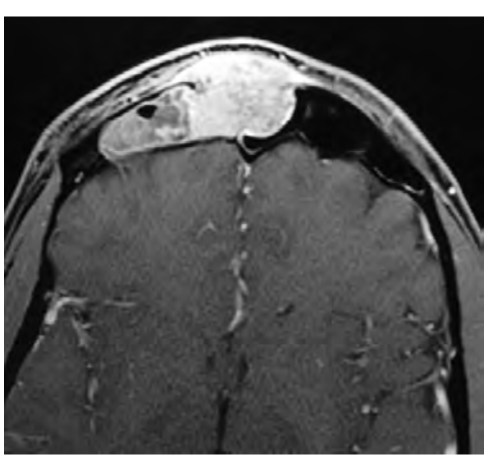

Figure 6.79 An axial view of the postcontrast T1-weighted magnetic resonance imaging scan shows a tumor of the frontal sinus extending into the subcutaneous soft tissues with fluid collection in the right frontal sinus.

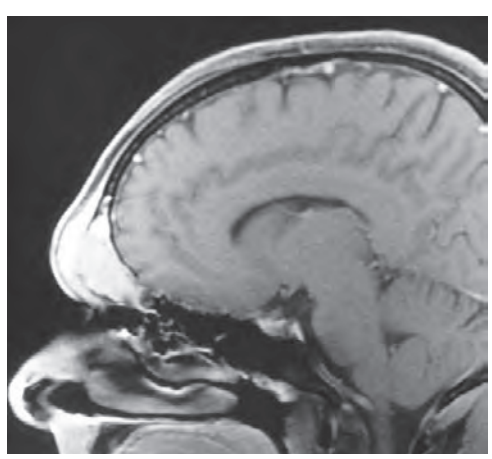

Figure 6.80 A sagittal view of the T1-weighted postcontrast magnetic resonance imaging scan shows that the tumor is confined to the frontal sinus without any brain edema.

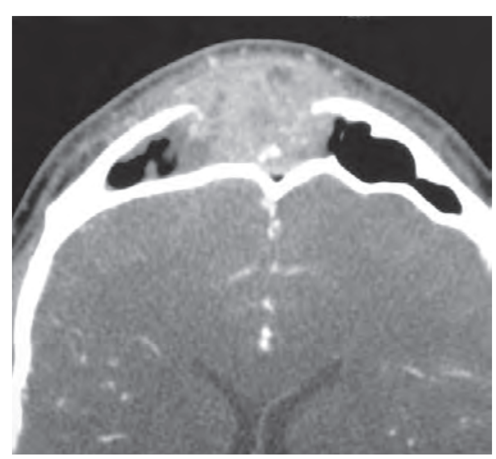

Figure 6.81 An axial view of the computed tomography scan of the head shows the intact posterior wall of the frontal sinus.

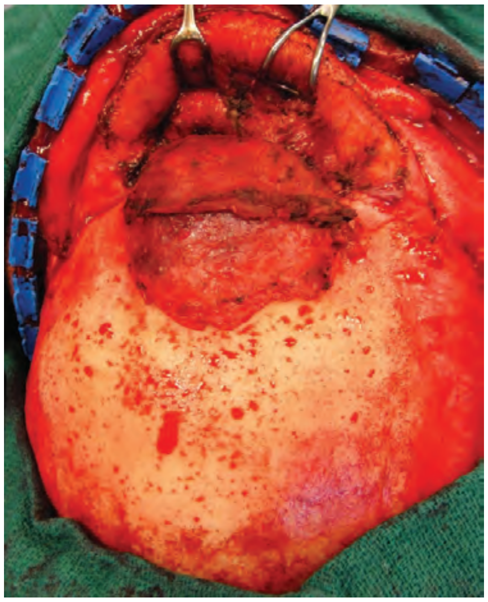

Figure 6.82 A bicoronal scalp flap is elevated, leaving the frontalis muscle and subcutaneous soft tissue as the anterior margin of the specimen.

Figure 6.83 A circumferential craniotomy is performed with a side-cutting burr through the frontal sinus around the outlined area of the frontal bone resection.

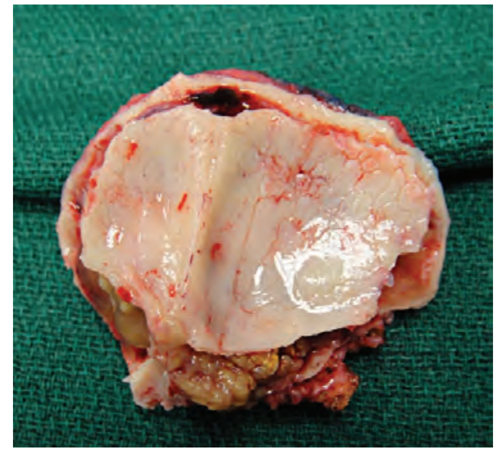

Figure 6.84 The surgical specimen showing the intact posterior wall of the frontal sinus.

Figure 6.85 A lateral view of the surgical specimen shows the tumor contained within the intact frontal sinus removed in a monobloc fashion.

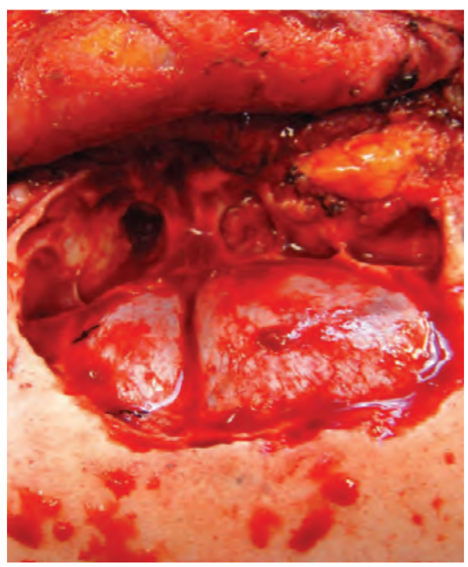

Figure 6.86 The surgical field showing a large defect in the frontal bone with an intact dura.

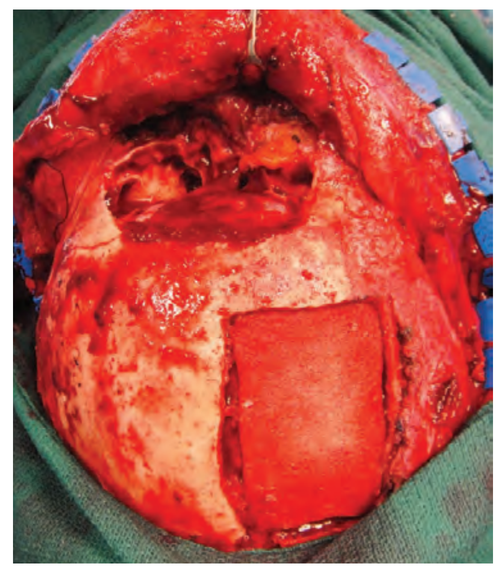

Figure 6.87 A calvarial graft for reconstruction of the surgical defect is harvested from the parietal region.

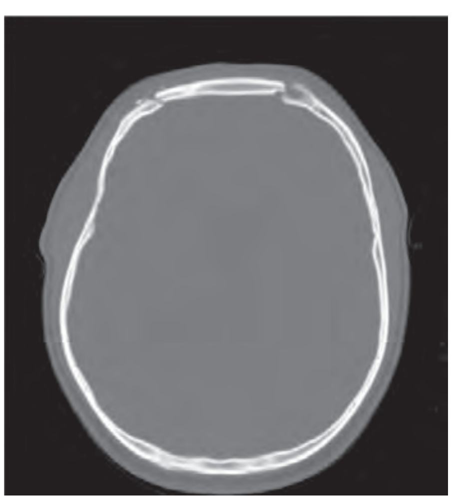

Figure 6.88 A postoperative axial view of the computed tomography scan of the head showing restoration of the contour of the forehead with the bone graft.

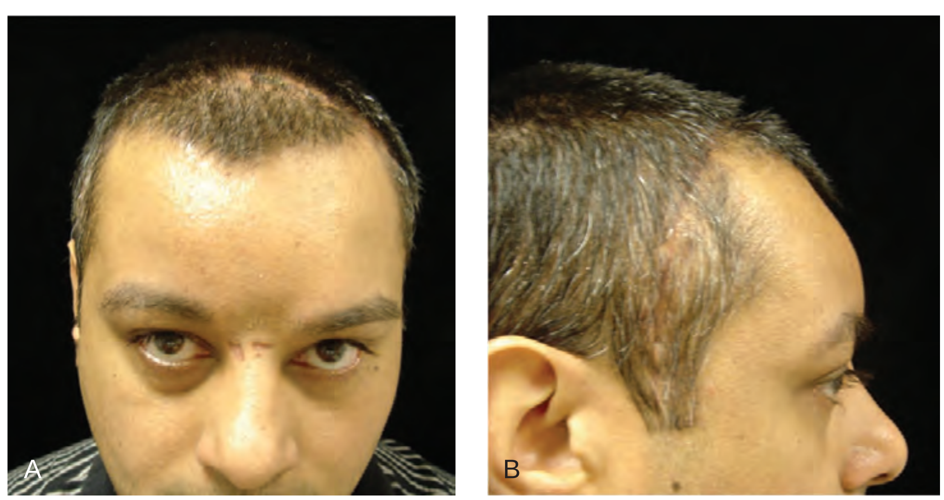

Figure 6.89 The postoperative appearance of the patient showing satisfactory reconstruction of the surgical defect. **A**, Frontal view. **B**, Lateral view.

The patient shown in Fig. 6.90 has an ossifying fibroma of the nasal cavity that extends through the frontal sinus and involves the frontal bone. Sagittal and coronal views of the MRI scan clearly demonstrate the radiographic extent of the tumor (Figs. 6.91 and 6.92). Craniofacial resection for this tumor required resection of a portion of the frontal bone (Fig. 6.93). A split calvarial graft is harvested from the parietal bone posterior to the bifrontal craniotomy site (Fig. 6.94). This bone graft is appropriately fashioned to fill the surgical defect (Fig. 6.95). The graft is secured in position with miniplates and screws (Fig. 6.96). The postoperative MRI scans of the patient are shown in Figs. 6.97 and 6.98. The postoperative appearance of the patient shows essentially no aesthetic deformity as a result of reconstruction of the resected frontal bone with a split calvarial graft (Fig. 6.99).

If reconstruction is not undertaken, then a prosthesis must be fabricated for aesthetic rehabilitation. The patient shown in Fig. 6.100 has locally advanced carcinoma of the frontal sinus with invasion of the orbit requiring craniofacial resection with a frontal craniectomy and orbital exenteration (Fig. 6.101). A postoperative CT scan shows the bone defect in the forehead

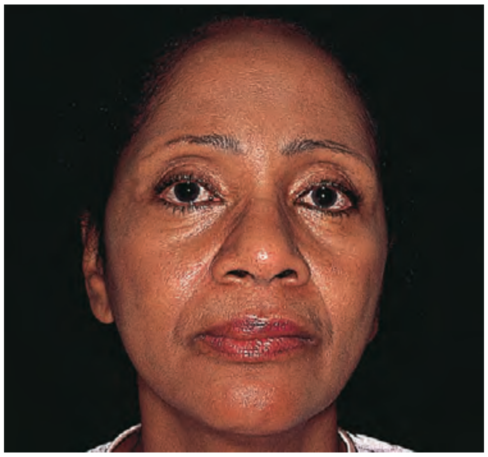

Figure 6.90 A patient with an ossifying fibroma of the nasal cavity extending through the frontal sinus to involve the frontal bone.

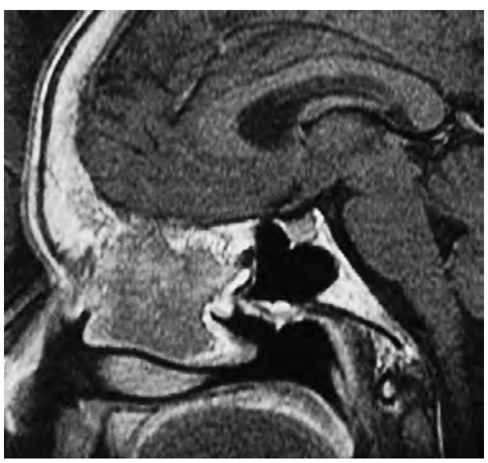

Figure 6.91 A sagittal view of the preoperative magnetic resonance imaging scan.

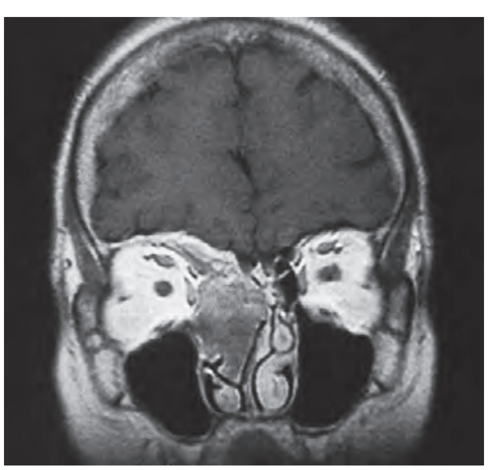

Figure 6.92 A coronal view of the preoperative magnetic resonance imaging scan.

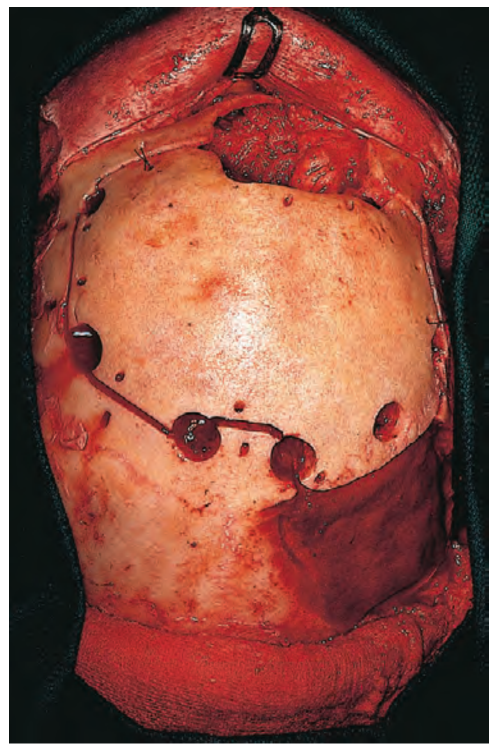

Figure 6.93 Craniofacial resection for this tumor required resection of a portion of the frontal bone.

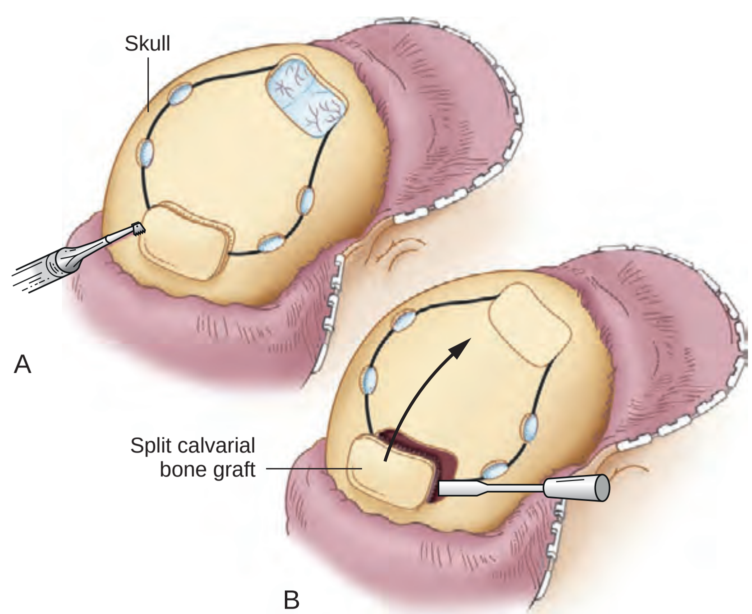

Figure 6.94 Schematic representation of the harvest of a split calvarial bone graft.

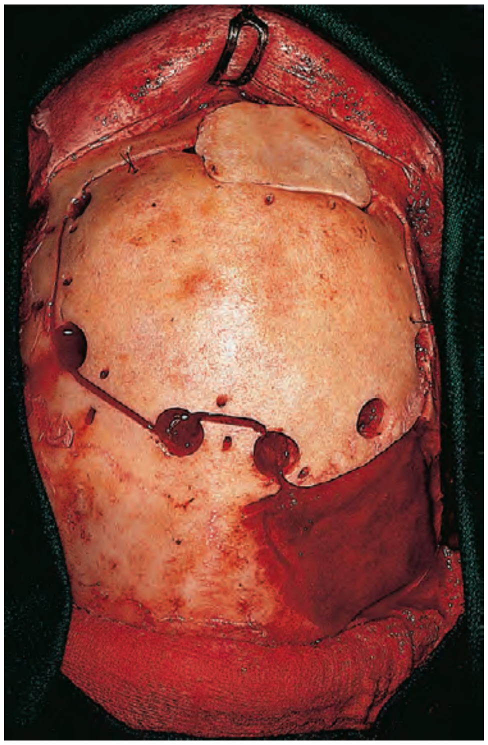

Figure 6.95 A split calvarial graft harvested from the right parietal region is shaped to fit the defect.

Figure 6.96 The graft is secured in position with miniplates and screws.

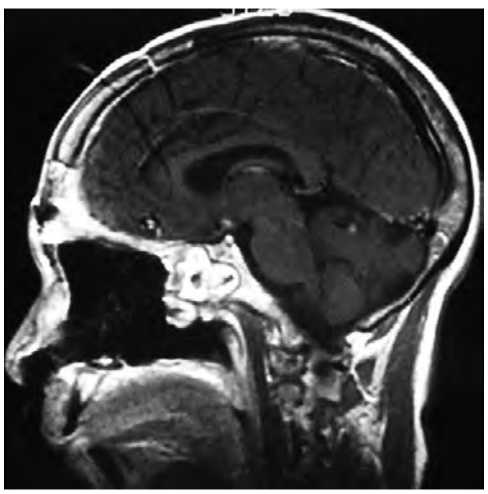

Figure 6.97 A sagittal view of the postoperative magnetic resonance imaging scan shows the surgical defect and reconstructed calvarium.

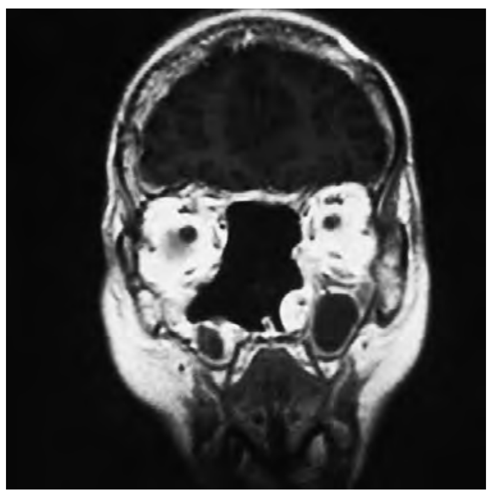

Figure 6.98 A coronal view of the postoperative magnetic resonance imaging scan shows complete excision of the tumor.

Figure 6.99 The postoperative appearance of the patient 1 year following surgery.

(Fig. 6.102). A postoperative photograph shows an aesthetically unacceptable deformity (Fig. 6.103). A surgical defect of this nature is best rehabilitated with use of either a facial prosthesis (Fig. 6.104) or a composite free flap.

Dura. Whenever any tear or minor deficit in the dura is created during the surgical procedure, it should be repaired immediately to secure a watertight closure. If a minor leak through a repaired suture line is observed, it can be handled with a soft tissue bolster of a piece of muscle or fascia. On the other hand, use of fibrin glue in that setting provides an effective seal. However, when deliberate resection of a segment of the dura is undertaken, reconstruction of the dura is mandatory to provide a watertight closure of the dural defect. The dural defect can be repaired with use of a free graft of the pericranium or fascia lata. The patient shown in Fig. 6.105 had a chondrosarcoma of the orbit extending through the bony skull base in the anterior cranial fossa. Her computerized tomogram showed extensive tumor involving the orbit, nasal cavity, and ethmoid complex. The surgical specimen demonstrates a monobloc resection of the tumor (Fig. 6.106). A facial view of the surgical field demonstrates the dural defect with exposed brain communicating with the orbital and nasal defect after removal of the surgical specimen (Fig. 6.107). The defect in the dura is repaired with a free graft of pericranium harvested from the parietal region of the skull (Fig. 6.108). Several interrupted Nurolon sutures are placed to secure a watertight closure. The suture line is further sealed with fibrin glue. A pedicled pericranial flap is rotated to provide a second layer of support to the dural repair at the skull base (Fig. 6.109). A surgical defect of this magnitude is best repaired with a microvascular composite free flap.

Figure 6.100 Locally advanced carcinoma of the frontal sinus requiring craniofacial resection with a frontal craniectomy and orbital exenteration.

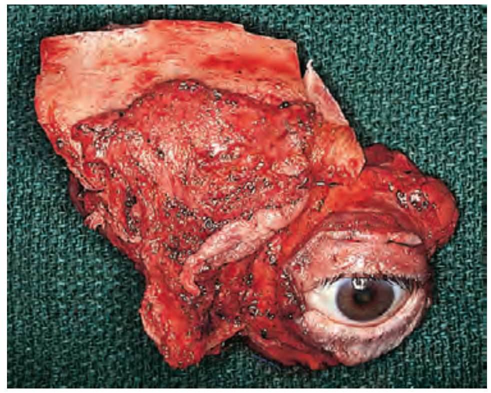

Figure 6.101 The surgical specimen.

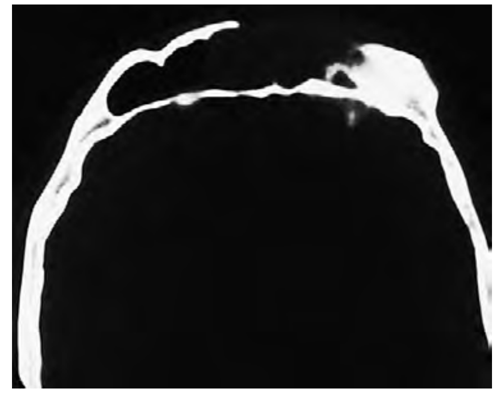

Figure 6.102 A postoperative computed tomography scan showing the craniectomy defect.

Figure 6.103 A postoperative photograph showing the surgical defect.

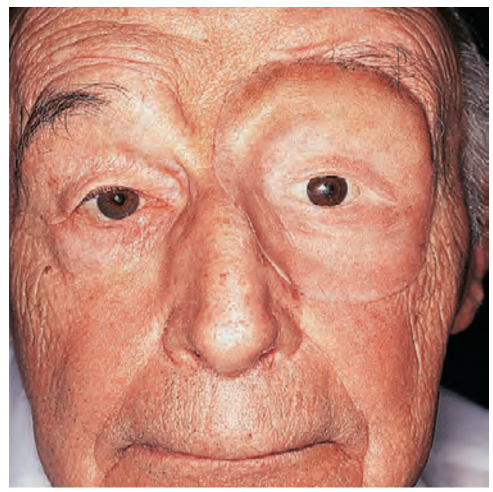

Figure 6.104 A surgical defect of this nature is best rehabilitated with use of a facial prosthesis.

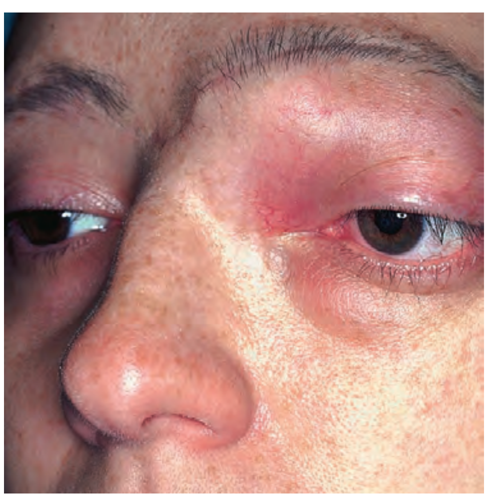

Figure 6.105 A patient with a chondrosarcoma of the orbit extending through the bony skull base to the anterior cranial fossa.

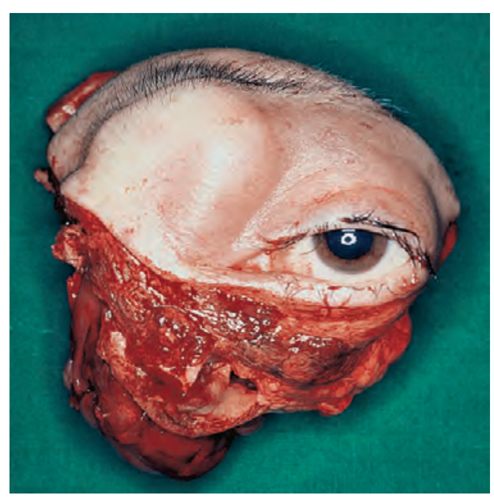

Figure 6.106 A facial view of the surgical specimen demonstrates a monobloc resection of the tumor.

Total Ethmoidectomy Through an Intracranial or Endonasal Approach Alone. Limited tumors of the superior aspect of the ethmoid can be adequately excised through intracranial exposure alone. Small esthesioneuroblastomas are ideally suited for this approach. Coronal and sagittal views of the MRI scan of a patient with a small esthesioneuroblastoma involving the superior aspect of the ethmoid are shown in Figs. 6.110 and 6.111. The entire lesion could be adequately excised through the craniotomy without the need for exposure through the face. This lesion is ideally suited for excision through the anterior subcranial approach as well.

Transnasal endoscopic assistance during intracranial exposure alone and excision of the tumor as previously described are quite valuable in select circumstances. They also may permit mobilization of the lower extent of the surgical specimen, because mucosal incisions can be placed under direct vision through the endoscope.

Figure 6.107 The surgical field showing a large defect in the dura requiring watertight repair.

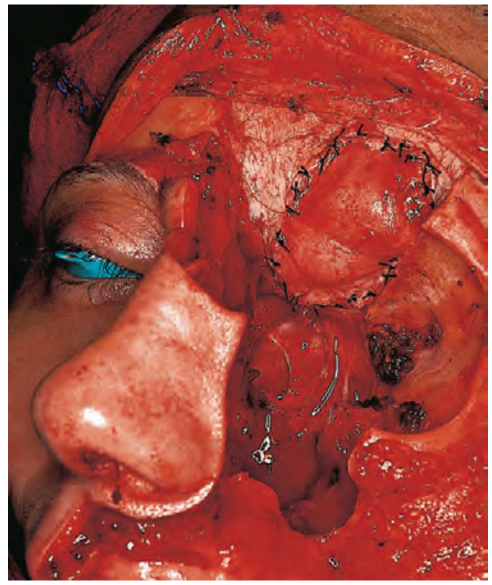

Figure 6.108 The defect in the dura is repaired with a free graft of pericranium harvested from the parietal region of the skull.

Figure 6.109 A pedicled pericranial flap is rotated to provide a second layer of support to the dural repair at the skull base.

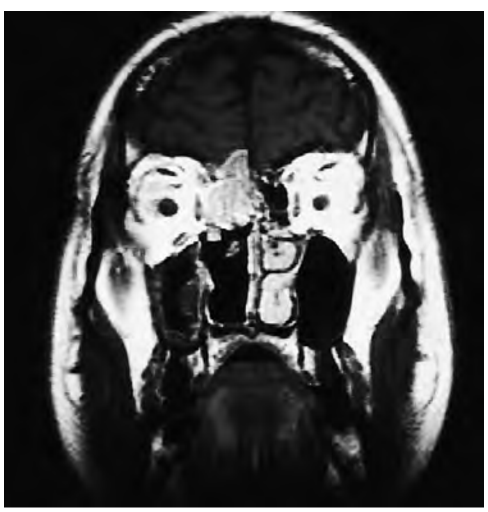

Figure 6.110 A coronal view of a magnetic resonance imaging scan of a patient with a small esthesioneuroblastoma.

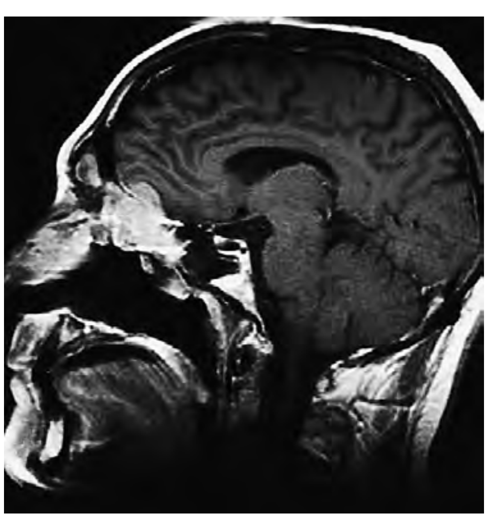

Figure 6.111 A sagittal view of a magnetic resonance imaging scan showing the tumor perforating through the cribriform plate.

Endonasal, Endoscopic Resection of Tumor of the Anterior Skull Base

Selected tumors of limited extent and favorable histology can be removed totally through an endonasal endoscopic approach. However, significant expertise and experience are required on the part of the head and neck surgeon and the neurosurgeon, and they must work as a team to bring about an successful outcome. The MRI scans of a patient with an esthesioneuroblastoma of the ethmoid are shown in Fig. 6.112. The tumor arises in the ethmoid complex and reaches the cribriform plate without any intracranial extension. It extends into the left maxillary antrum and the anterior wall of the sphenoid sinus. The tumor approaches the nasofrontal duct but does not involve the frontal sinus. The tumor perforates through the nasal septum to present in both sides of the nasal cavity. Endoscopic view of the tumor shows its lower extent at the level of the middle turbinate on both sides of the nasal cavity (Fig. 6.113). After thorough endoscopic evaluation, the procedure generally begins by submucosal injection of lidocaine with epinephrine for elevation of the nasoseptal flap. However, in this patient, nasoseptal flap will not be used because of its involvement by tumor. Similarly, lidocaine with epinephrine is injected on the middle turbinate. The tumor is found to be medial to the turbinate. Tumor debulking now begins to identify the site of origin of the tumor at the cribriform plate (Fig. 6.114). Further, debulking of the tumor shows that the lamina papyracea is uninvolved (Fig. 6.115). A centripetal sub periosteal dissection is now undertaken at the level of the nasal vault (Fig. 6.116). Sub periosteal dissection is undertaken at the cribriform plate to expose the olfactory phyla (Fig. 6.117). Circumferential dissection continues in the subperiosteal plane along the nasal cavity (Fig. 6.118). A frontal sinusotomy is performed with a high power drill and a septectomy and Draf III procedure are performed (Fig. 6.119). The anterior ethmoidal artery is coagulated and divided (Fig. 6.120). Circumferential mobilization of the tumor at the cribriform plate is performed, and the crista galli is removed (Fig. 6.121). The dura is now opened and a segment of the dura is removed as superior margin over the tumor, exposing the olfactory bulbs and creating a pocket for the extradural

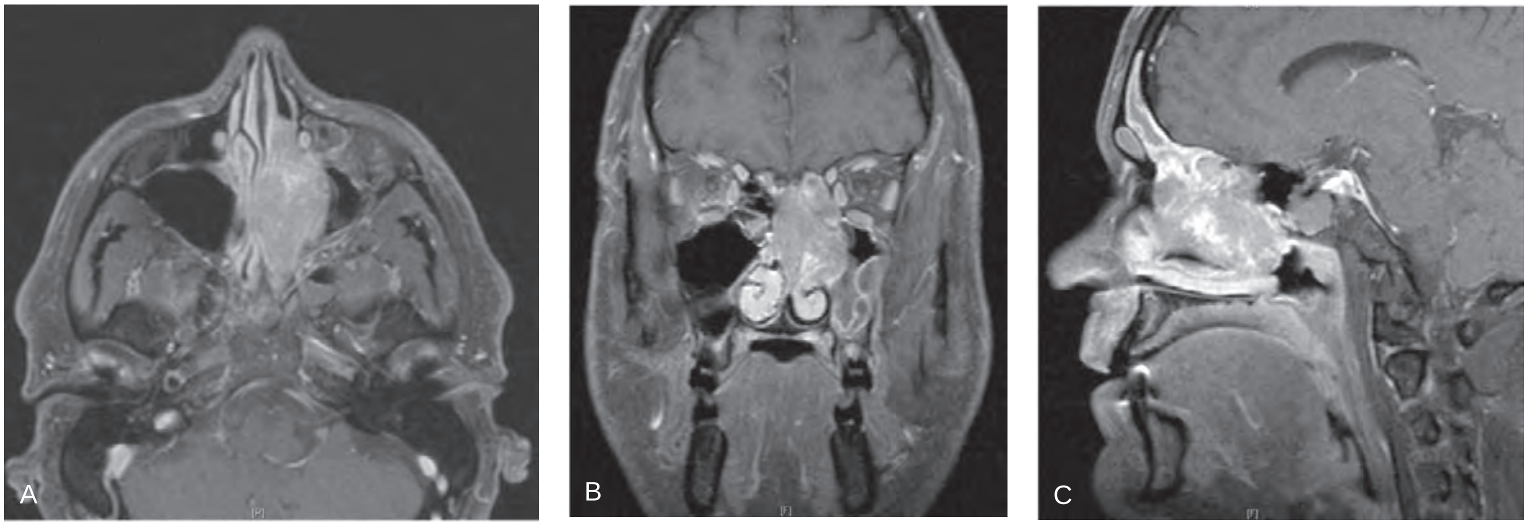

Figure 6.112 Axial (**A**), coronal (**B**), and sagittal (**C**) views of the magnetic resonance imaging scan of a patient with esthesioneuroblastoma.

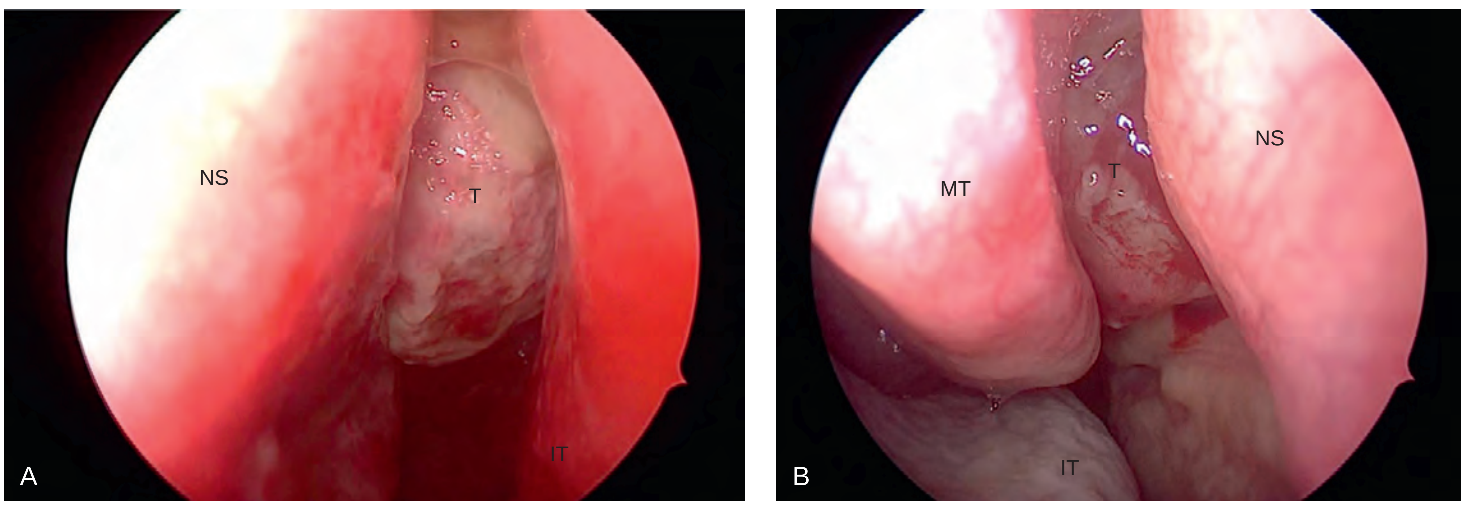

Figure 6.113 **A**, Lesion involving the left nasal fossa. *NS*, nasal septum; *T*, tumor; *IT*, inferior turbinate. *(Courtesy of Piero Nicolai, MD.)* **B**, Tumor extension in the right nasal fossa through the nasal septum. *NS*, nasal septum; *T*, tumor; *MT*, middle turbinate; *IT*, inferior turbinate. *(Courtesy of Piero Nicolai, MD.)*

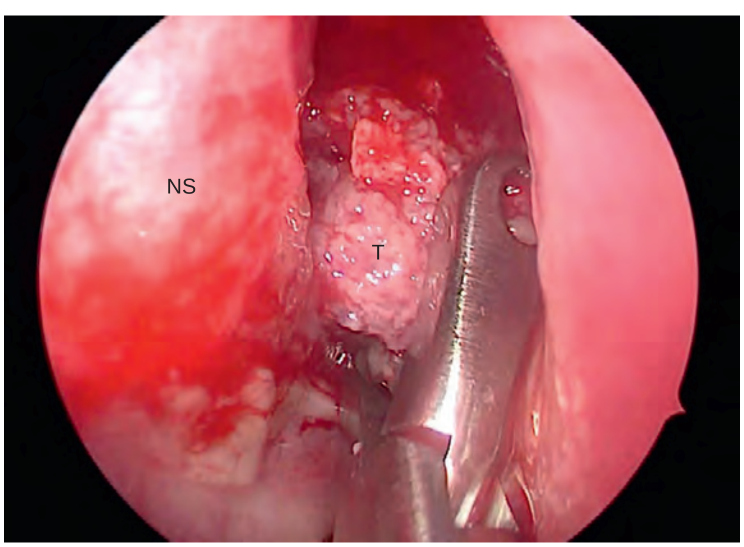

Figure 6.114 Initial debulking of the tumor. *NS*, nasal septum; *T*, tumor. *(Courtesy of Piero Nicolai, MD.)*

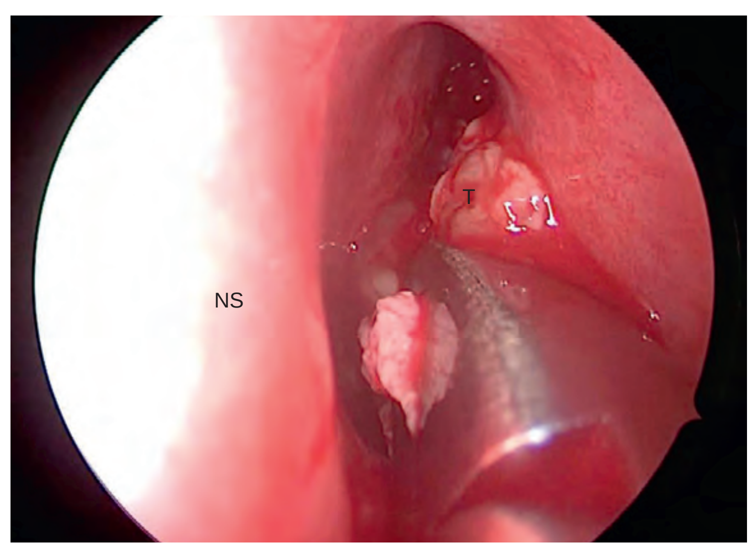

Figure 6.115 Further debulking of the tumor. *NS*, nasal septum; *T*, tumor. *(Courtesy of Piero Nicolai, MD.)*

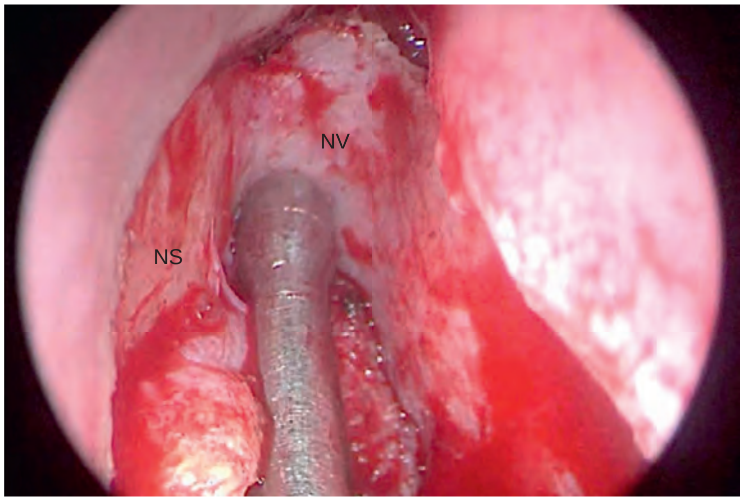

Figure 6.116 Centripetal subperiosteal dissection at the level of the nasal vault. *NS*, nasal septum; *NV*, nasal vault. *(Courtesy of Piero Nicolai, MD.)*

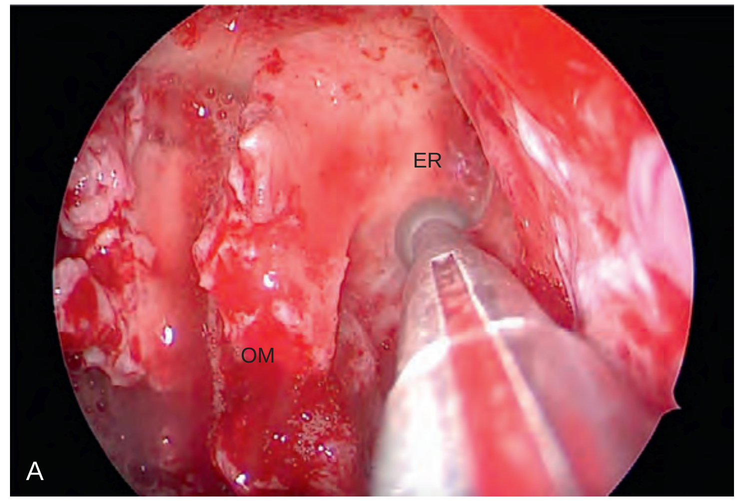

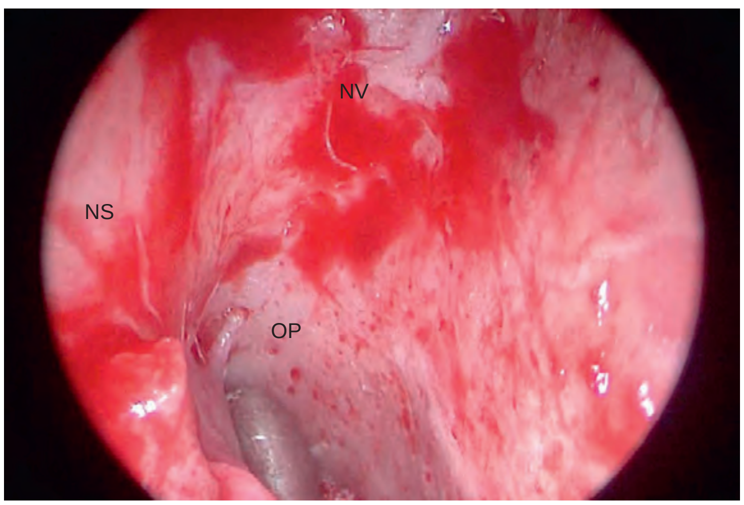

Figure 6.117 Exposure of the olfactory fila. *OF*, olfactory fila; *NV*, nasal vault; *NS*, nasal suptum. *(Courtesy of Piero Nicolai, MD.)*

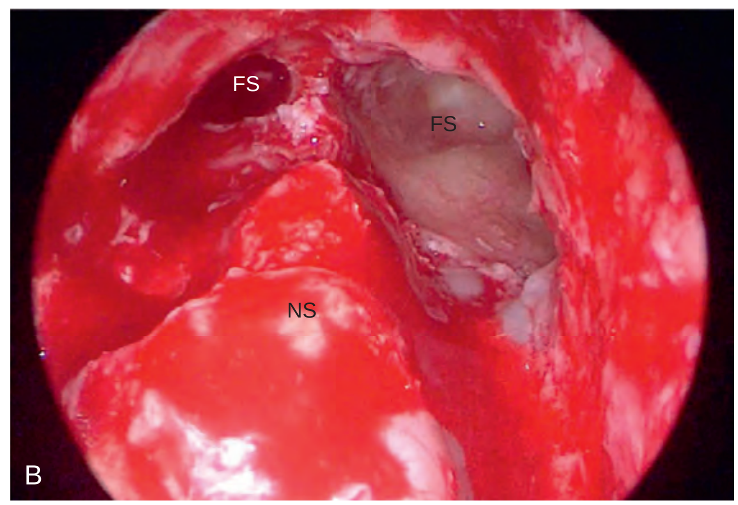

Figure 6.119 **A**, Drilling of the skull base at the ethmoidal roof with exposure of the dura. *ER*, ethmoidal roof; *OM*, olfactory mucosa. **B**, Septectomy and Draf III procedure. *FS*, frontal sinus; *NS*, nasal septum. *(Courtesy of Piero Nicolai, MD.)*

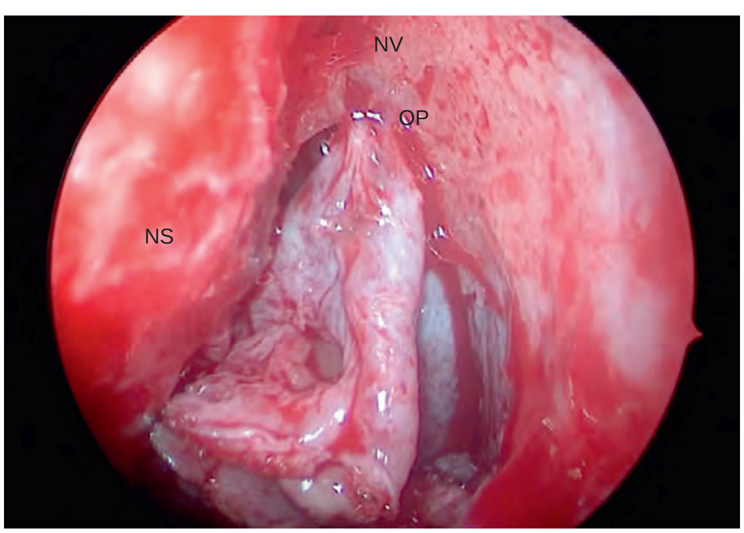

Figure 6.118 Completion of subperiosteal dissection at the nasal vault. *OF*, olfactory fila; *NV*, nasal vault; *NS*, nasal septum. *(Courtesy of Piero Nicolai, MD.)*

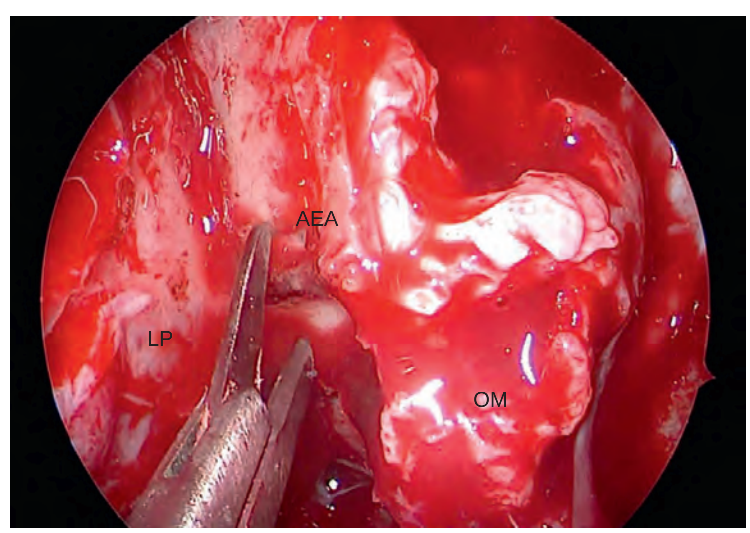

Figure 6.120 Coagulation and division of the anterior ethmoidal artery. *LP*, lamina paperacea; *AEA*, anterior ethmoidal artery; *OM*, olfactory mucosa. *(Courtesy of Piero Nicolai, MD.)*

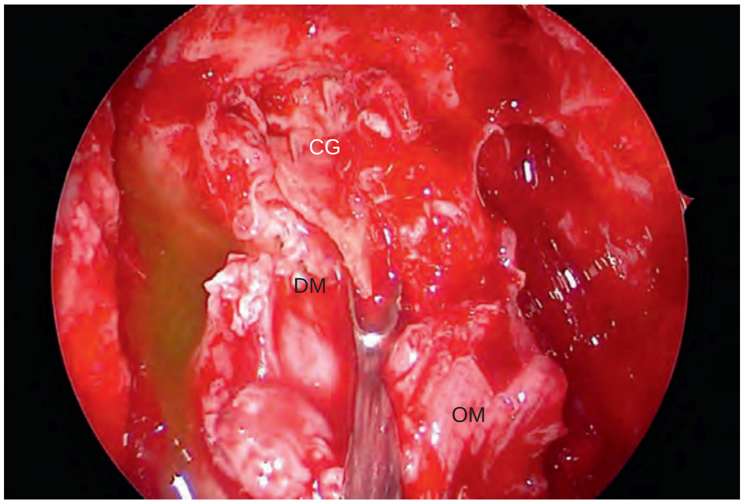

Figure 6.121 Dissection and removal of the crista galli. *CG*, crista galli; *DM*, dura matter; *OM*, olfactory mucosa. *(Courtesy of Piero Nicolai, MD.)*

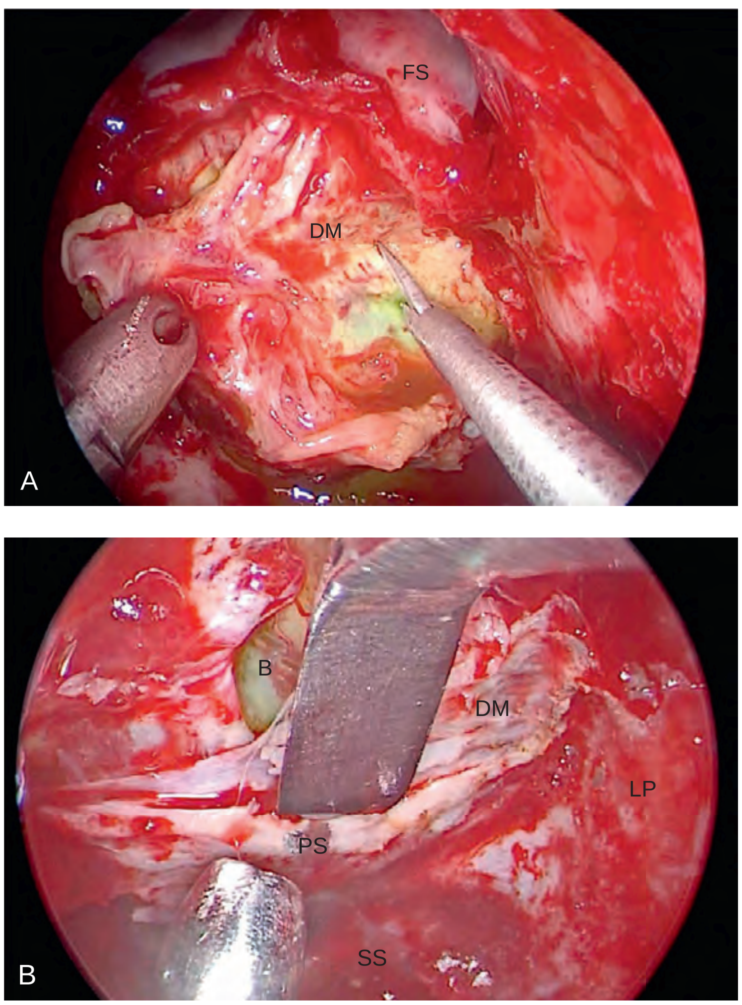

Figure 6.122 **A,** Incision and resection of the dura. *DM*, dura matter; *FS*, frontal sinus. **B,** Dissection of the dura matter and creation of a pocket in the extra dural space for reconstruction. *LP*, lamina paperacea; *PS*, planum sphenoidale; *B*, brain; *DM*, dura matter; *SS*, sphenoid sinus. *(Courtesy of Piero Nicolai, MD.)*

layer of reconstruction (Fig. 6.122). The surgical defect exposing the brain is shown in Fig. 6.123A. Complete homeostasis is secured before beginning the repair. The defect at the anterior skull base, including that of the dura, is repaired in three layers. An underlay of fascia lata or ilio tibial tract is performed first

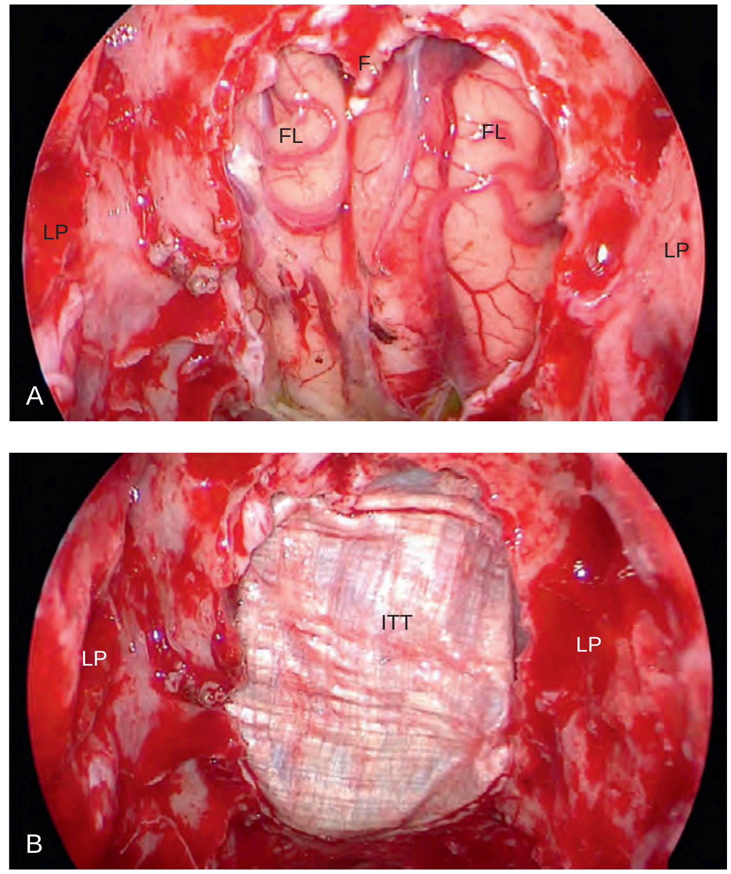

Figure 6.123 **A,** Surgical defect with exposure of the frontal lobels. *LP*, lamina paperacea; *F*, falx; *FL*, frontal lobe. **B,** Three layer reconstruction of the skull base. First layer shown here with ileotibial tract for intradural layer. *LP*, lamina paperacea; *ITT*, ilotibial tract. *(Courtesy of Piero Nicolai, MD.)*

(Fig. 6.123B). Bovine pericardium (Dura Guard) is used as the second layer. Fibrin glue is used next, followed by a single layer of Surgicel. If a nasoseptal flap is available (not in this case), then this previously elevated vascularized flap is rotated as the final layer of closure (Fig. 6.124).

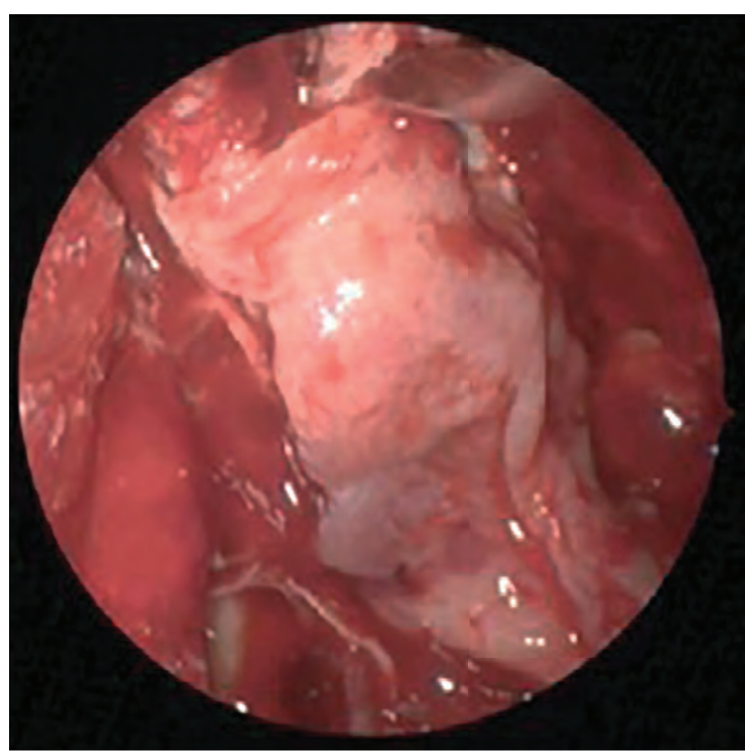

Figure 6.124 Vascularized nasoseptal flap in position.

Figure 6.125 Clinical appearance (**A**) and axial (**B**) and coronal (**C**) views of a patient with extensive carcinoma of the ethmoid. Note exophthalmos and displacement of the globe in **A**. The tumor extends into the right periorbita as seen in **B** and breaks through the cribriform plate to the floor of the anterior cranial fossa **C**.

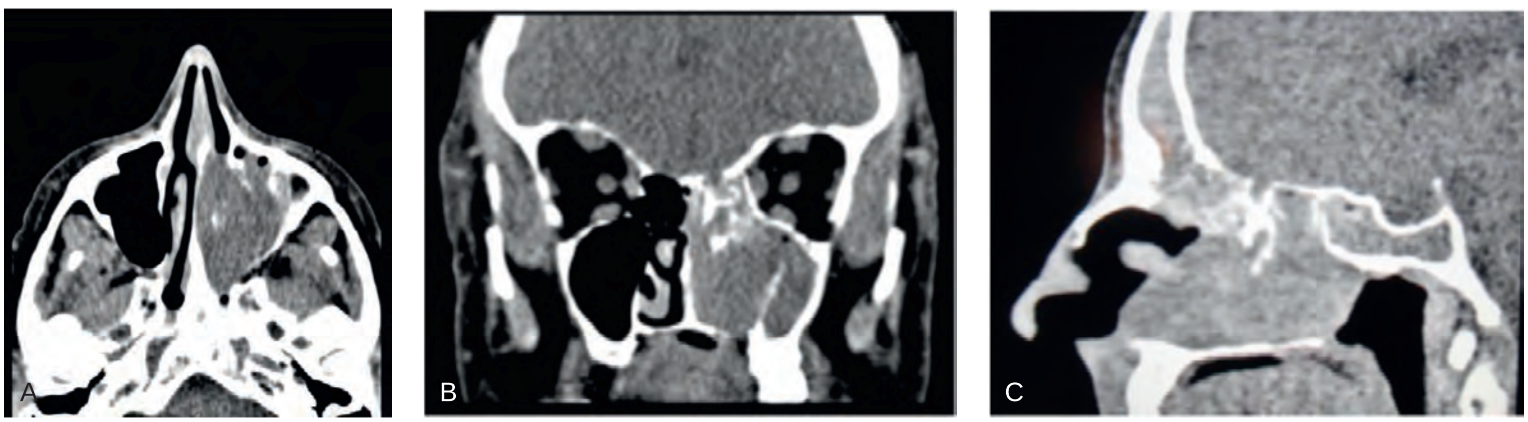

Figure 6.126 Locally advanced carcinoma of the ethmoid. **A**, Axial view of the computed tomography scan showing tumor filling up the nasal cavity with destruction of the lateral nasal wall and extension in the left maxillary antrum. **B**, On coronal view, the tumor destroys the ethmoid and breaks through the cribriform plate. **C**, On sagittal view, the tumor infiltrates through the floor of the frontal sinus into the frontal bone.

The endonasal endoscopic resection of properly selected patients offers equally good results, in terms of local tumor control and disease-specific survival. The need for adjuvant postoperative radiotherapy is determined based on several factors, including completeness of resection, status of margins, tumor histology, and extent of the tumor. There are several contraindications to endonasal endoscopic surgery for malignant tumors, and they are listed here:

1. Lateral extension involving the orbit (Fig. 6.125)
2. Anterior extension involving the frontal sinus (Fig. 6.126)
3. Brain invasion
4. Lateral extension of a malignant tumor to the pterygoid fossa or infratemporal fossa
5. Posterior or lateral extension involving the cavernous sinus
6. Bone-destructive lesion involving the maxilla, nasal bones, or hard palate
7. Extensive high-grade malignant tumors (e.g., undifferentiated carcinomas or high-grade sarcomas)
8. Invasion of the calvarium or skin
9. Inexperienced surgeon in endonasal tumor surgery
10. Unavailability of neurosurgical, navigation, and operating room support

Facial Disassembly

Tumors of the nasal cavity, paranasal sinuses, orbit, or skull base that require generous exposure often entail excision of relatively uninvolved portions of the normal facial skeleton, which results in significant functional and aesthetic morbidity. The technical development of facial disassembly procedures provides adequate exposure to secure a satisfactory surgical resection but avoids disfigurement resulting from the loss of normal skeletal support. Facial disassembly requires very meticulous and delicate removal of uninvolved portions of facial skeleton to expose the site of the tumor and replacement of the removed facial skeleton with rigid fixation to restore the bony architecture. The patient whose MRI scans are shown in Figs. 6.127 and 6.128 has an adenocarcinoma of the ethmoid cavity extending through the cribriform plate into the anterior skull base. The tumor extends anteriorly up to the posterior surface of the nasal bones, as seen on both axial and sagittal scans, although the nasal bones themselves are not involved. Surgical exposure to remove this tumor required a bifrontal craniotomy and a lateral rhinotomy with glabellar extension to expose the nasal bones (Fig. 6.129). The assembly of nasal bones on both sides is meticulously removed with an ultrafine saw to gain exposure of the ethmoid region (Fig. 6.130). The surgical specimen shows an intact nasal septum with the ethmoid tumor removed in a monobloc fashion through the facial disassembly exposure (Fig. 6.131). The surgical defect following removal of the specimen shows total exenteration of the upper part of the nasal cavity (Fig. 6.132). The disassembled portion of the nasal bones is replaced and secured with miniplates and screws in

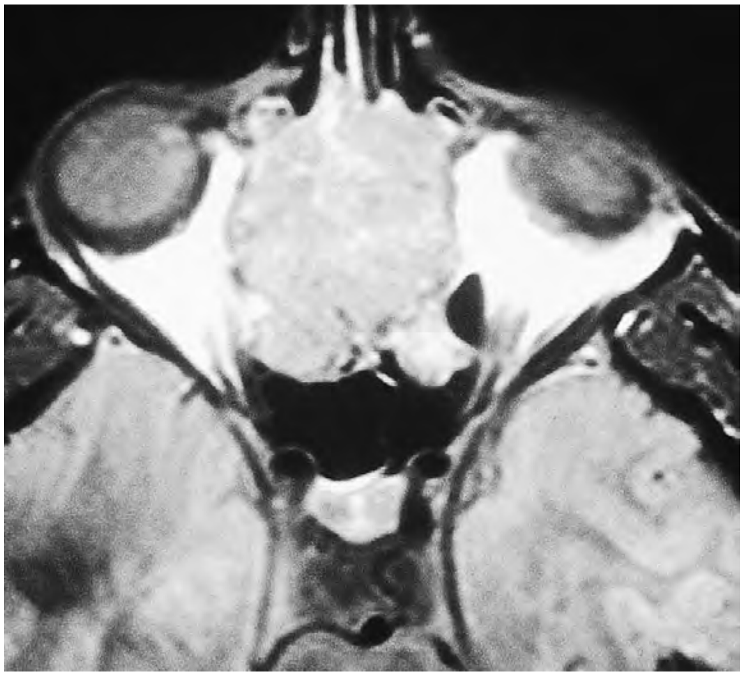

Figure 6.127 An axial view of a magnetic resonance imaging scan of a patient with an adenocarcinoma of the ethmoid cavity.

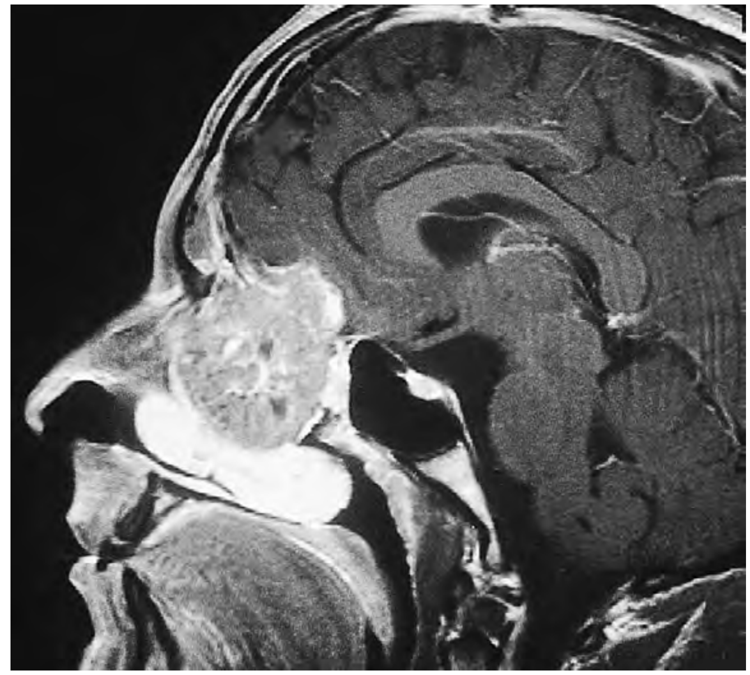

Figure 6.128 A sagittal view of a magnetic resonance imaging scan shows the tumor extending through the cribriform plate to the anterior cranial fossa.

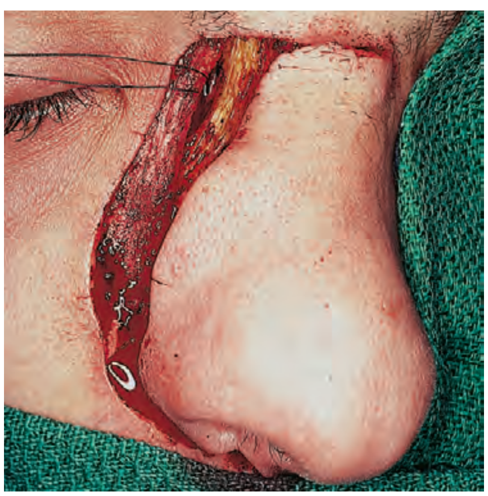

Figure 6.129 Surgical exposure required a bifrontal craniotomy and a lateral rhinotomy with glabellar extension to expose the nasal bones.

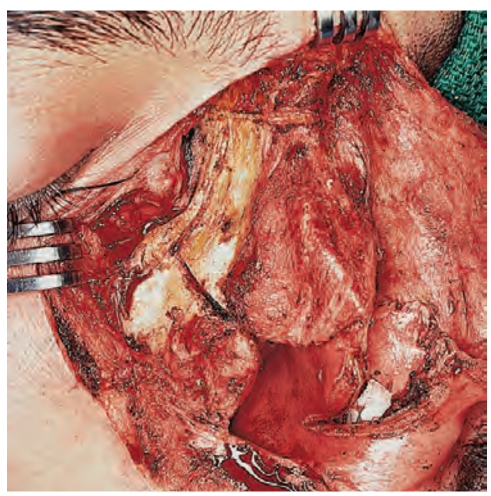

Figure 6.130 The assembly of nasal bones on both sides is meticulously excised with an ultrafine saw to gain exposure to the ethmoid region.

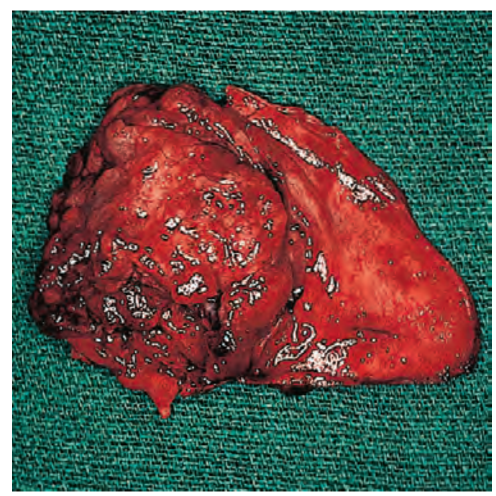

Figure 6.131 The surgical specimen.

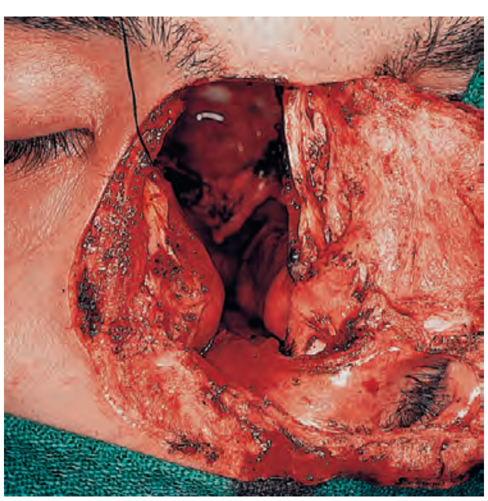

Figure 6.132 An anterior view of the surgical defect.

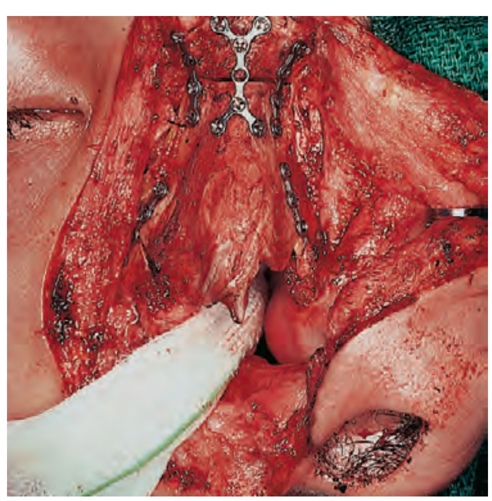

Figure 6.133 The disassembled portion of the nasal bones is replaced and secured with miniplates and screws in the normal position.

Figure 6.134 Postoperative appearance of the patient 1 month following surgery.

the normal position (Fig. 6.133). The appearance of the patient approximately 1 month after surgery shows complete restoration of the facial contour without any aesthetic deformity (Fig. 6.134).

Skull Base Defect Reconstruction

Reconstruction of the bony defect in the skull base following resection of a tumor rarely requires rigid support, and thus bone grafts are seldom necessary. Alloplastic material can be used to reconstruct defects of the calvarium, but it is not suitable for skull base defects because of the high risk of infection resulting from contamination of the cranial cavity from the nasal cavity. In most circumstances, closure of the skull base defect with use of a pedicled pericranial flap or a pedicled galeal pericranial flap is satisfactory. The pericranial flap is relatively thin, and its blood supply is somewhat tenuous (Fig. 6.135). On the other hand, a galeal pericranial flap is more sturdy, and its vascularity is superior (Fig. 6.136). Elevation of the galeal pericranial flap is somewhat tedious, because its separation from the scalp during elevation of the scalp flap is through the subcutaneous plane. A well-defined tissue plane does not exist, and therefore meticulous attention is required to remain superficial to the galea during elevation of the scalp flap. If the galeal pericranial flap is believed to be unsatisfactory for coverage of a large defect, then a microvascular composite free flap should be used to provide adequate coverage of the surgical defect and avoid brain herniation.

Reconstruction With Composite Free Flaps. Reconstruction of composite surgical defects after major transcranial transfacial resection often warrants the need for immediate reconstruction. However, the decision to embark upon immediate reconstructive surgery depends on the biology of the tumor, the risk of recurrence of the tumor, and the potential need for future multiple surgical procedures to excise recurrent disease. Thus a major reconstructive effort using microvascular free tissue transfer should be avoided in patients who have a high risk of local recurrence with the possibility of successful salvage surgical procedures. Such large surgical defects are best managed with the help of dental or maxillofacial prostheses, as exemplified in a case here.

This is a 60-year-old female with a high-grade mucoepidermoid carcinoma of the lacrimal fossa with invasion of the orbit and frontal bone (Fig. 6.137). A craniofacial resection with orbital exenteration and superomedial orbitectomy with excision of

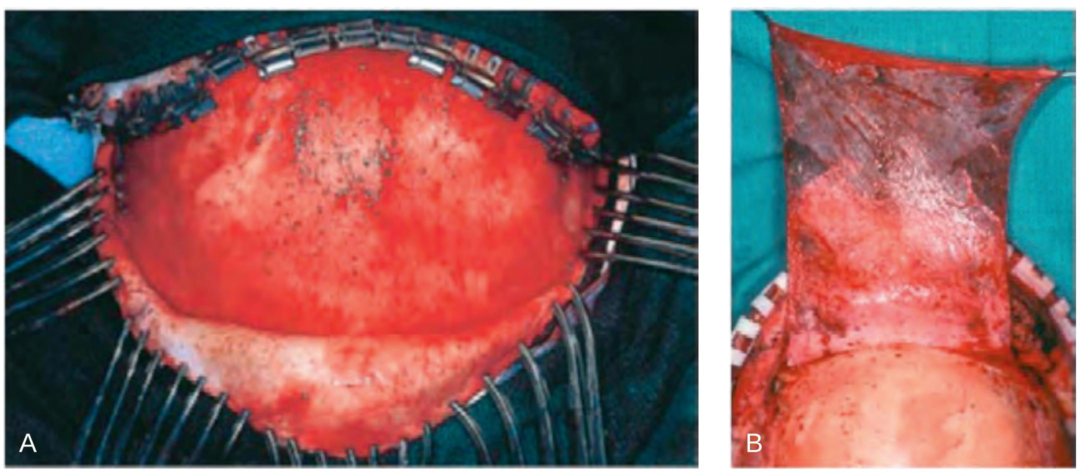

Figure 6.135 **A**, For the pericranial flap, the scalp is elevated superficial to the pericranium. **B**, The pericranial flap is relatively thin, and blood supply to its distal part is unreliable.

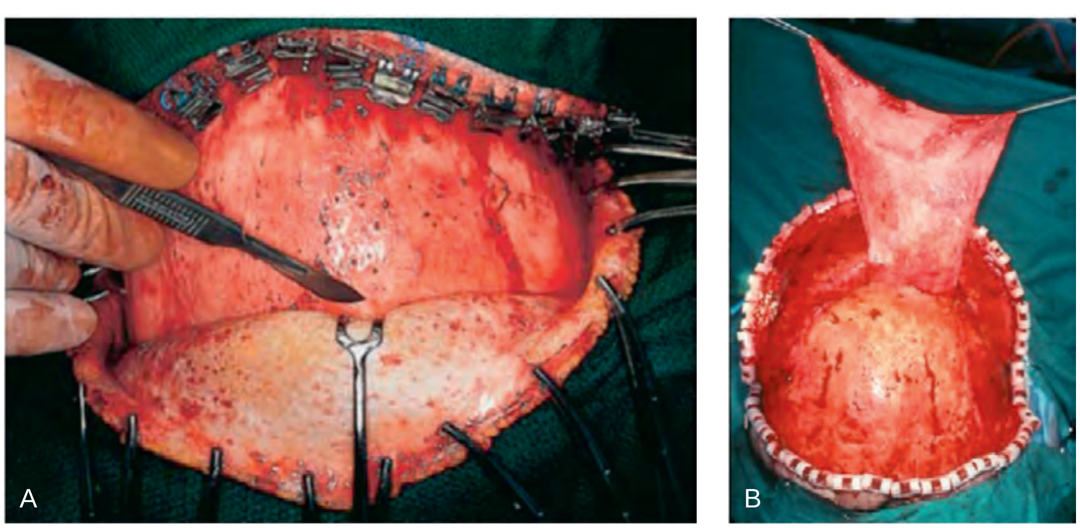

Figure 6.136 **A**, For the galeal pericranial flap, the scalp is elevated superficial to the galea. **B**, The galeal pericranial flap is robust with better vascularity than the pericranial flap.

part of the frontal bone was accomplished in a monobloc fashion (Fig. 6.138). In spite of the negative margins and postoperative radiation therapy, her risk of local recurrence was high (Fig. 6.139). Therefore an orbital prosthesis was fabricated, which would allow easy inspection of the surgical site (Fig. 6.140). Sixteen months following surgery, she did develop local recurrence, which after adequate radiologic studies was felt to be resectable (Fig. 6.141). The surgical procedure at this time required resection of the roof of the orbit and underlying dura and reconstruction with a dural graft and a rotated scalp flap (Fig. 6.142). The patient continued to use orbital prosthesis for aesthetic appearance.

Figure 6.137 Preoperative appearance of a patient with locally advanced high-grade mucoepidermoid carcinoma of the lacrimal sac.

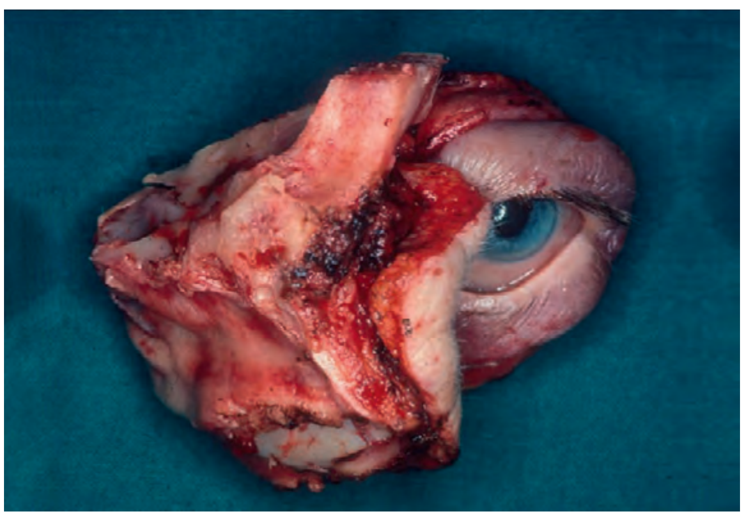

Figure 6.138 Surgical specimen showing monobloc excision of the tumor with orbital exenteration and excision of superomedial left orbit including nasal bone, frontal bone, roof of the orbit, left ethmoids, and perpendicular plate of the ethmoid bone.

Figure 6.139 Surgical defect 6 months following surgery and completion of postoperative radiation therapy.

Figure 6.140 Orbital prosthesis covering the surgical defect.

Figure 6.141 Local recurrence in the roof of the orbit 16 months following initial surgery.

Figure 6.142 Postoperative appearance of the left orbital defect following second surgical resection.

On the other hand, reconstruction with use of a microvascular composite free flap is essential for composite transcranial facial defects where there is risk for brain herniation, where there is a large dural defect repaired with a nonvascularized fascial graft, or for high-grade tumors when combined modality treatment, including radiotherapy, is needed in the postoperative period. The patient shown in Fig. 6.143 has a malignant fibrous histiocytoma involving the left orbit. The coronal view of her MRI scan shows the tumor, which involves the upper outer quadrant of the left orbit with invasion of the skull base and extension

Figure 6.143 A malignant fibrous histiocytoma involving the left orbit.

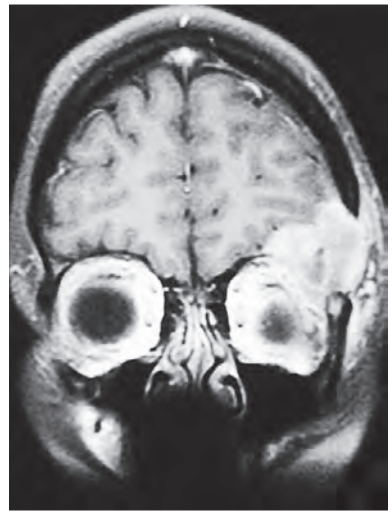

Figure 6.144 A coronal view of the magnetic resonance imaging scan.

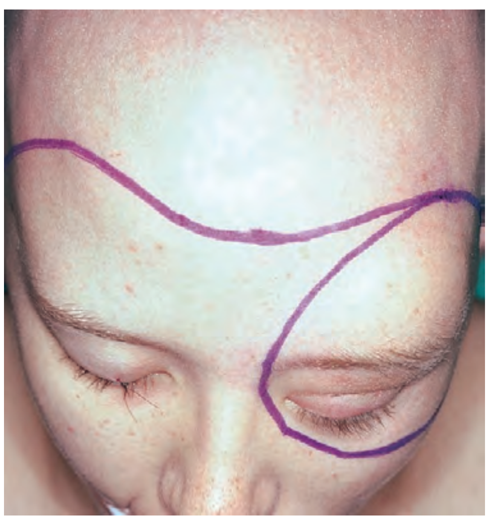

Figure 6.145 The surgical procedure required a bifrontal craniotomy with resection of generous portion of the skin of the forehead and the frontal and temporal bones as well as orbital exenteration.

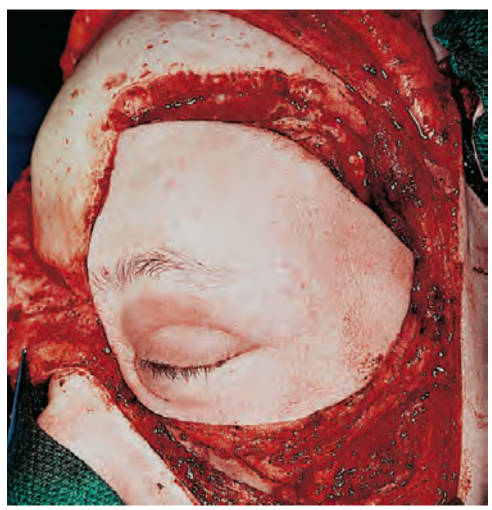

Figure 6.146 Monobloc excision of the tumor required resection of a portion of the frontal bone, an orbitectomy, and resection of the squamous part of the temporal bone, the zygoma, and the upper part of the maxilla.

Figure 6.147 The surgical specimen shows monobloc excision of the tumor with adequate soft tissue and bony margins.

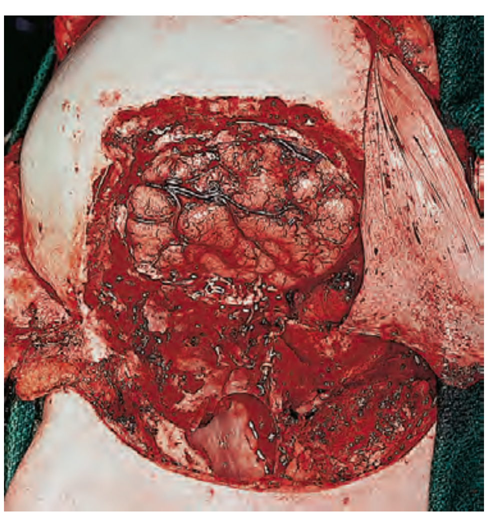

Figure 6.148 The surgical defect showing the sacrifice of a large segment of the dura with exposure of the underlying brain.

Figure 6.149 The defect of the dura is repaired with use of a pericranial graft to secure a watertight closure.

Figure 6.150 A microvascular free rectus abdominis myocutaneous flap provided sufficient soft tissue to fill the surgical defect and provide skin coverage.

Figure 6.151 An extensive carcinoma of the right maxilla extending to the skull base, orbit, facial skin, and hard palate.

Figure 6.152 A coronal view of the computed tomography scan.

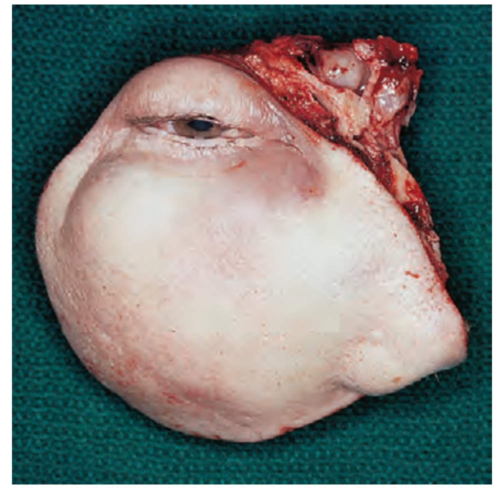

Figure 6.153 The surgical specimen.

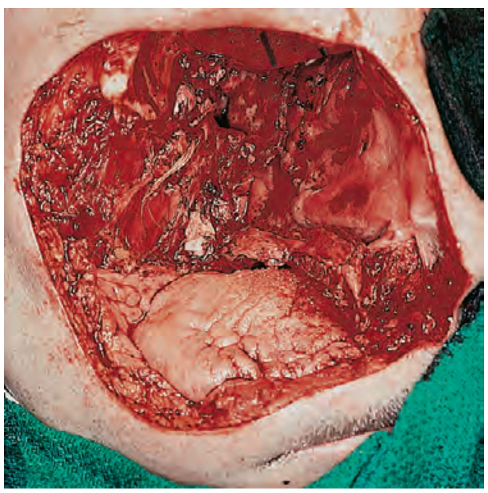

Figure 6.154 The surgical defect.

Figure 6.155 The postoperative appearance of the patient.

Figure 6.156 The postoperative intraoral view, showing repair of the palatal defect with the flap.

into the frontal fossa and the calvarium (Fig. 6.144). The surgical procedure required a bifrontal craniotomy with resection of a generous portion of the skin of the forehead and the frontal and temporal bones as well as orbital exenteration (Fig. 6.145). Monobloc excision of the tumor included resection of a portion of the frontal bone, an orbitectomy, and resection of the squamous part of the temporal bone, the zygoma, and the upper part of the maxilla (Fig. 6.146). The surgical specimen shows monobloc excision of the tumor with adequate soft tissue and bone margins (Fig. 6.147). The deep margin of the tumor required sacrifice of a large segment of the dura with exposure of the underlying brain (Fig. 6.148). The defect of the dura was repaired with use of a pericranial graft to secure a watertight closure (Fig. 6.149). A microvascular free rectus abdominis myocutaneous flap provided sufficient soft tissue to fill the surgical defect and provide support to the brain and skin coverage of the orbital defect (Fig. 6.150). Primary healing of the reconstructed area permitted institution of postoperative radiation therapy within 3 weeks.

The patient shown in Fig. 6.151 has an extensive carcinoma of the right maxilla extending to the skull base, orbit, facial skin, and hard palate. The coronal view of the CT scan demonstrates the radiographic extent of the tumor (Fig. 6.152). The surgical specimen shows monobloc excision of the tumor through a bifrontal craniotomy and a radical total maxillectomy with exenteration of the orbit and resection of the soft tissues and skin of the face with partial amputation of the nose (Fig. 6.153). The surgical field demonstrates the bony defect in the anterior skull base, exenteration of the orbit and nasal cavity, and a total maxillectomy with resection of the hard palate on the right-hand side, exposing the oral tongue (Fig. 6.154). Reconstruction of a surgical defect of this magnitude requires a generous amount of soft tissue to provide support at the skull base to prevent brain herniation; it also requires skin lining in the nasal cavity, in the oral cavity, and for facial skin. A rectus abdominis microvascular myocutaneous free flap with three islands of skin provided the necessary tissues to reconstruct this surgical defect in one stage. The postoperative appearance of the patient demonstrates adequate coverage of the facial skin (Fig. 6.155). An intraoral view demonstrates a second island of skin of the same flap replacing the hard palate and obliterating the defect created by the total maxillectomy (Fig. 6.156).

The availability and applicability of composite microvascular free flaps have opened up new vistas in the ability of the craniofacial surgeon to resect any part of the facial and cranial anatomy with confidence regarding the ability to reconstruct the surgical defect without the fear of cerebrospinal fluid leakage, brain herniation, infection, or significant dysfunction.

Craniofacial Resection for Locally Advanced Skin Cancer

The patient shown in Fig. 6.157 has an extensive, neglected basal cell carcinoma of the scalp that has been present for several years. The tumor involves the full thickness of the scalp and the underlying bone and extends to involve the glabellar region of the nose and the superior quadrant of the right orbit. An MRI scan with gadolinium contrast in the coronal plane shows the extensive infiltrative nature of the tumor, with extension into the anterior cranial fossa and displacement of the right frontal lobe. The tumor has not invaded the brain, although it appears to invade the dura (Fig. 6.158). An extensive frontoparietal craniectomy along with cranioorbital resection via a craniofacial approach was performed in a monobloc fashion. The surgical specimen from the external view is shown in Fig. 6.159. A through-and-through resection of the tumor along with the adjacent rim of normal scalp and the underlying calvarium, as well as the dura, was performed to achieve a monobloc resection. The intracranial view of the surgical specimen in Fig. 6.160 shows that the tumor displaces the resected portion of the dura but does not perforate through it to involve the brain. A generous margin of dura was resected along with the overlying calvarium for this extensive tumor.

Fig. 6.161 shows the exposed frontal and parietal lobes of the brain with a large dural defect, along with a defect of the calvarium, scalp, and skin of the face and the defect resulting from orbital exenteration and ethmoidectomy. The dura was repaired with use of a bovine pericardial graft to secure a watertight closure (Fig. 6.162). The remainder of the massive soft tissue and skin defect was repaired with use of a large rectus abdominis myocutaneous free flap. The postoperative appearance of the patient approximately 6 weeks after surgery is shown in Fig. 6.163. The patient subsequently had a facial prosthesis fabricated for restoration of the facial appearance. Thus massive soft tissue and skin defects can be repaired readily with a rectus abdominis or latissimus dorsi myocutaneous free flap.

Figure 6.157 Extensive basal cell carcinoma of the scalp.

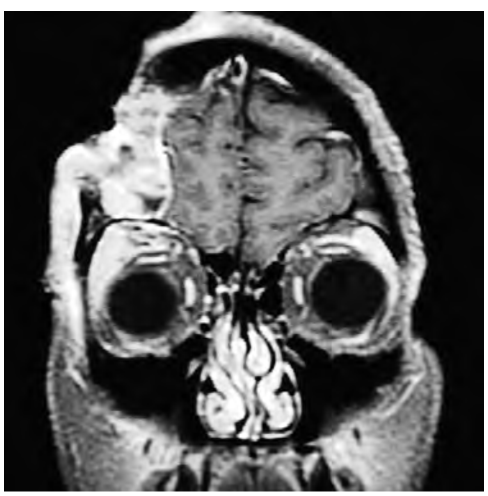

Figure 6.158 A coronal view of the magnetic resonance imaging scan.

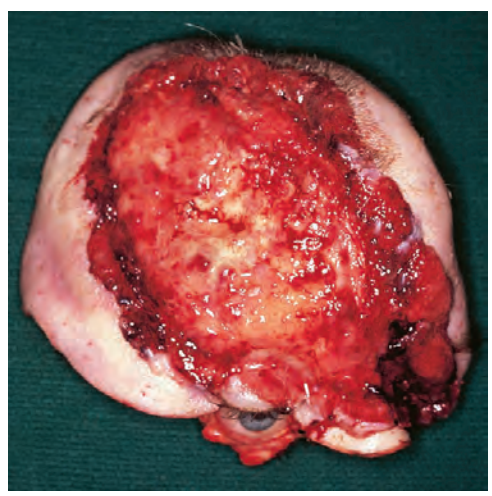

Figure 6.159 An external view of the surgical specimen.

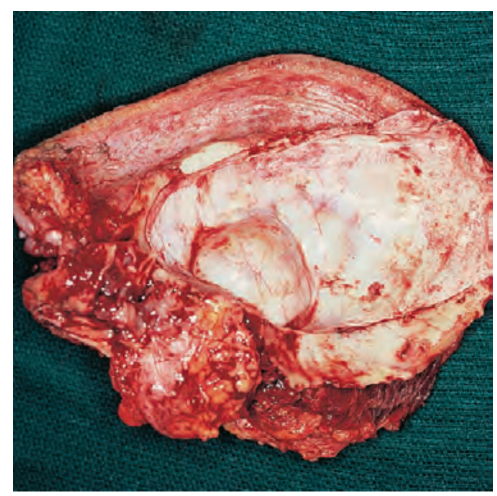

Figure 6.160 An intracranial view of the surgical specimen.

Figure 6.161 The surgical defect viewed from the cranial aspect.

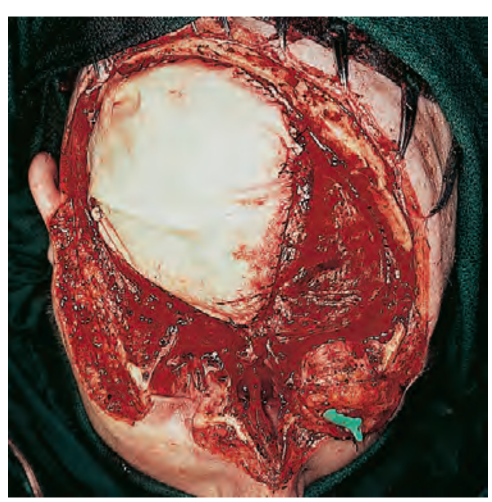

Figure 6.162 A bovine pericardial graft is used to repair the dura.

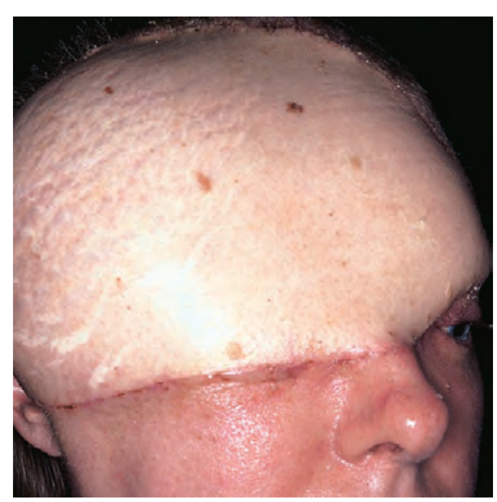

Figure 6.163 Postoperative appearance of the patient 6 weeks following surgery.

Resection of Tumors Involving the Skull Base of the Middle Cranial Fossa

The Infratemporal Fossa

Maxillary Swing for Tumors of the Infratemporal Fossa. Tumors of the infratemporal fossa presenting in the pterygomaxillary region can be approached via a maxillary swing procedure. This surgical approach is most suitable for lesions that are located on the medial aspect of the infratemporal fossa in the pterygomaxillary region or in the lateral wall of the nasopharynx. The operative procedure is most suitable for neurogenic tumors arising from the trigeminal nerve, such as schwannomas of the second and third division of the nerve and tumors of the nasopharynx.

The maxilla derives its blood supply from the internal maxillary, sphenopalatine, and facial arteries. This blood supply is provided through soft-tissue and muscular attachments on various external surfaces of the maxilla. The maxillary swing procedure is intended to preserve the entire maxilla intact. However, quite often the posterior surface of the maxilla is so thinned out, like an egg shell, that it fractures easily during the maxillary swing and is difficult to preserve. Sometimes the posterior wall is involved by the tumor, and therefore its removal is required. However, the alveolar process, the anterior wall, and the anterolateral wall of the maxilla are able to be preserved, thus retaining the facial contour and the ability to chew. The maxillary bone is pedicled on its anterior and lateral soft-tissue attachments, preserving its blood supply. Therefore it is crucial to carefully preserve these soft-tissue attachments when a maxillary swing procedure is performed.

An MRI scan of a patient with a schwannoma of the second division of the trigeminal nerve presenting on the medial aspect of the infratemporal fossa is shown in Fig. 6.164. These T2-weighted images of the MRI in axial, coronal, and sagittal planes clearly demonstrate a well-circumscribed tumor arising from the second division of the trigeminal nerve and extending through the foramen rotundum into the middle cranial fossa and occupying the pterygomaxillary region, displacing the posterolateral wall of the maxilla. The tumor is well circumscribed and shows areas of necrosis with a high-intensity signal on the T2-weighted images, a characteristic feature for schwannomas. The tumor extends through the foramen rotundum into the floor of the middle cranial fossa and therefore will require an intracranial exposure of the superior end of the tumor for transection of the second division of the trigeminal nerve proximal to the upper end of the tumor intracranially. The remaining tumor will be removed in a monobloc fashion via a maxillary swing.

A pterional craniotomy is planned through a hemicoronal incision, just posterior to the hairline (Fig. 6.165). The incision extends from the midline on the scalp up to the tragus of the ear. A standard pterional craniotomy is performed in an extradural fashion. The dura of the temporal lobe is elevated from the floor of the middle cranial fossa medially all the way up to the trigeminal ganglion. Meticulous hemostasis is maintained at all stages of the operation. The upper end of the tumor is readily visualized at the floor of the middle cranial fossa through a grossly expanded foramen rotundum. The root of the second division of the trigeminal nerve, coming off the trigeminal ganglion, is carefully transected just above the upper end of the tumor (Fig. 6.166). Two large hemoclips are placed on the stump of the nerve above the tumor for identification of the superior end of the tumor. The intracranial component of the tumor is extradural, and it is carefully mobilized circumferentially up to the edge of the expanded foramen rotundum. A green rubber dam is placed over the upper end of the tumor to isolate and protect the dura of the floor of the middle cranial fossa and for identification of the floor of the middle cranial fossa during the maxillary swing procedure (Fig. 6.167). This rubber dam is removed following removal of the tumor, ensuring complete excision of the tumor. The craniotomy is closed in the usual fashion.

A modified Weber-Ferguson incision that respects the nasal subunits and a subciliary extension along a skin crease in the infraorbital region are planned. The incision is marked while the patient is awake to identify the appropriate skin creases and the midline of the upper lip before induction of general anesthesia and endotracheal intubation (Fig. 6.168). The skin incision is deepened through the full thickness of the musculature of the upper lip to expose the alveolar process of the maxilla in the midline (Fig. 6.169). The incision extends along the ala of the nose and the nasolabial region to expose the underlying nasal process of the maxilla. Extreme care should be exercised to elevate full-thickness soft tissues and skin of the cheek in a minimal fashion, just enough to expose the underlying anterior bony wall of the maxilla. Excessive

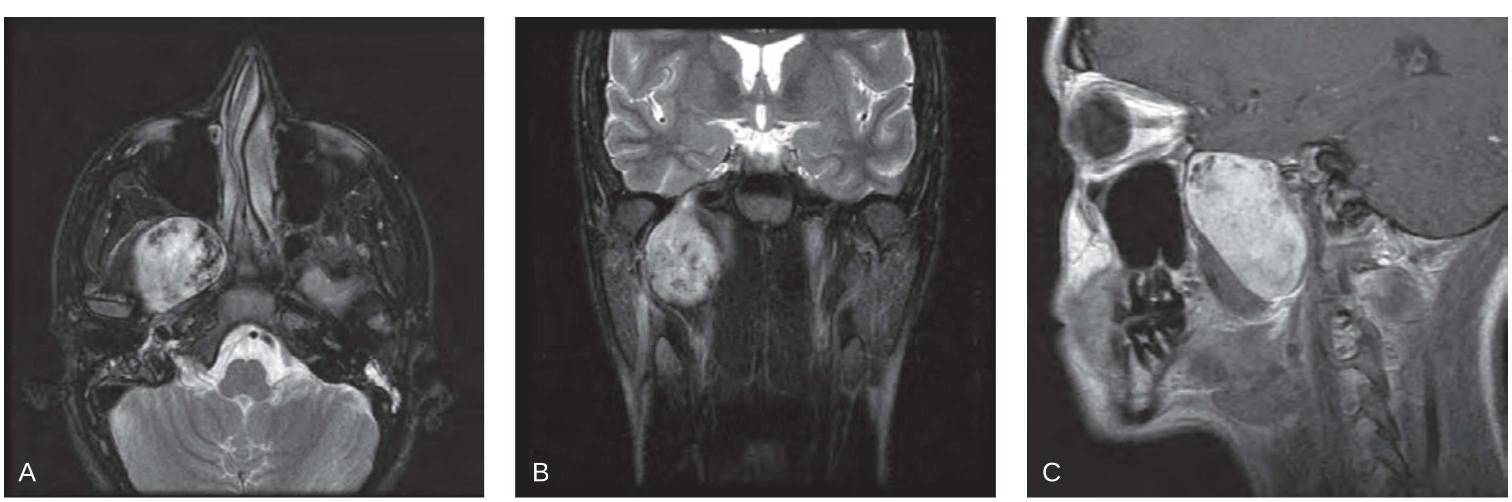

Figure 6.164 A magnetic resonance imaging scan in axial (**A**), coronal (**B**), and sagittal (**C**) planes showing a schwannoma of the right trigeminal nerve.

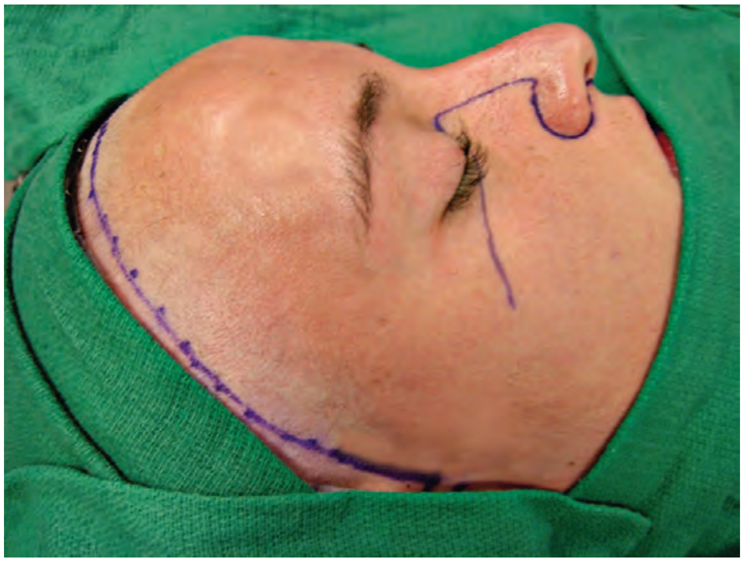

Figure 6.165 A hemicoronal incision is outlined for a pterional craniotomy.

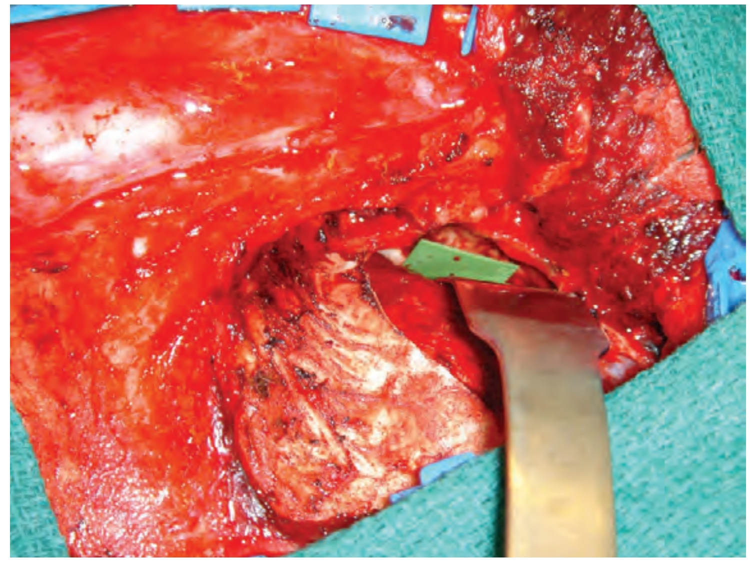

Figure 6.167 A green rubber dam is placed to separate the upper border of the tumor from the cranial cavity.

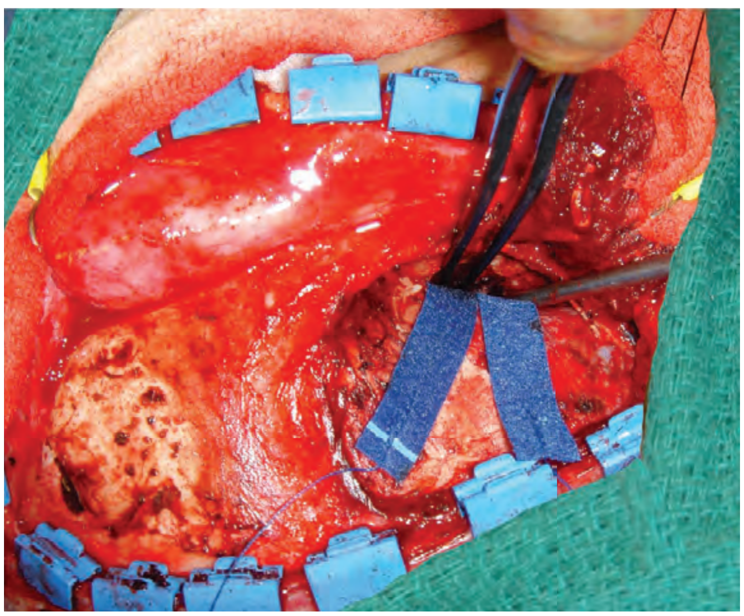

Figure 6.166 Bipolar electrocoagulation facilitates sharp division of V2.

mobilization of the anterior soft tissues of the cheek will compromise the blood supply to the maxilla, and therefore it should be avoided. A skin incision is now made along the previously outlined marking in the subciliary region. The skin of the infraorbital region is dissected off the orbicularis oculi muscle. This skin is very thin, and therefore meticulous attention should be paid to very careful elevation of the skin over the muscle to avoid tearing or perforating it. This portion of the skin of the cheek is reflected downward to expose the orbicularis oculi muscle (Fig. 6.170). The orbicularis oculi muscle is then elevated from the anterior wall of the maxilla to expose the inferior orbital rim from the nasolabial region medially up to the zygomatic bone laterally. Soft tissues over the anterior surface of the zygomatic bone are then elevated to expose the anterior bony surface of the zygoma. At this juncture, the four sites for osteotomies of the anterior wall of the maxilla are exposed enough, preserving the soft-tissue attachments on the maxilla. These sites are (1) the alveolar process at the anterior midline between the two central incisor teeth, (2) the nasal process of the maxilla, (3) the inferior orbital rim, and (4) the anterior surface of the zygomatic bone (Fig. 6.171).

Attention is now focused in the oral cavity, where mucosal incisions are made on the hard palate to expose the midline of the bony hard palate, from the central incisor teeth up to the posterior edge of the hard palate. The mucosal incision begins at the posterior surface of the alveolar process in the midline. This incision continues along the palatal surface of the alveolar process up to the medial aspect of the maxillary tubercle just posterior to the last molar tooth. At that point, the incision is taken medially up to the midline of the soft palate (Fig. 6.172). Even though the proposed line of osteotomy of the palate will be in the midline, the mucosal incision is placed on the side of the maxillary swing along the alveolar process, such that the suture line of the mucosa of the hard palate will not superimpose on the line of division of the hard palate. This approach avoids the development of a midline oronasal fistula if the mucosal incision is placed in the midline directly overlying the site of division of the hard palate. The mucosal incision is deepened through the underlying mucoperiosteum, up to the underlying bone. It is carefully elevated over the bone with a Freer elevator medially beyond the midline toward the left side of the hard palate (Fig. 6.173). Extreme care should be exercised in elevating the mucoperiosteum of the hard palate so as not to tear it, because the integrity of this mucoperiosteal flap is essential for repair of the palatal defect. Blood supply to this mucoperiosteal flap of the hard palate is derived from the contralateral sphenopalatine and the superior alveolar arteries. At this point, all the proposed sites of the osteotomies are exposed and soft-tissue attachments are elevated to facilitate expeditious performance of the appropriate osteotomies to minimize bleeding.

In performing these osteotomies, extreme care should be exercised to prevent inadvertent fracture of segments of the maxilla, which are difficult to repair. The first osteotomy is between the central incisor teeth through the alveolar process in the anterior midline up to the floor of the nasal cavity. A second osteotomy is performed between the nasal vestibule and the nasal process of the maxilla up to within 5 mm of the

Figure 6.168 A modified Weber-Ferguson incision respecting the nasal subunits is planned.

Figure 6.169 The skin incision is deepened up to the bone with minimal elevation of soft tissues on the maxilla.

Figure 6.170 The orbicularis oculi muscle is exposed.

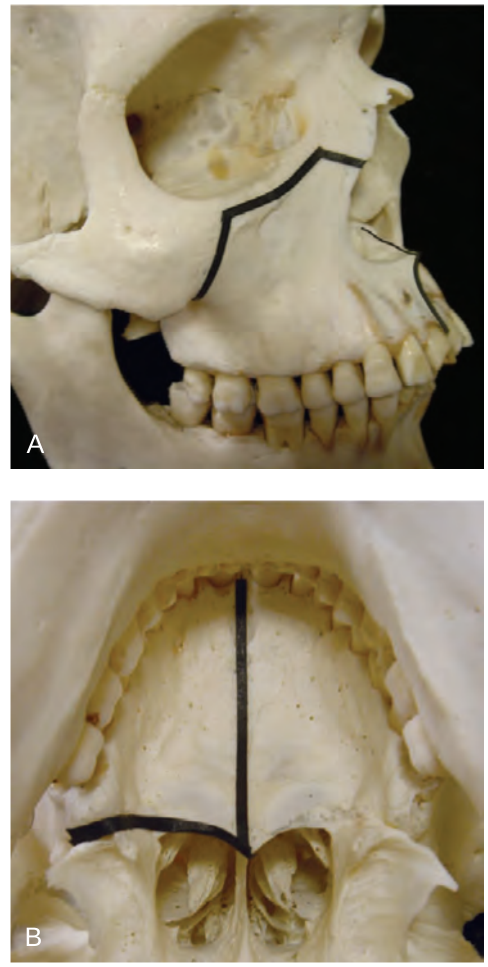

Figure 6.171 **A** The planned external osteotomies of the maxilla are shown on a skull; **B** The planned intraoral osteotomy is shown on a skull."

Figure 6.172 The mucosal incision on the hard and soft palates is outlined.

infraorbital rim. A third osteotomy is made on the anterior surface of the maxilla approximately 5 mm below the orbital rim, connecting to the osteotomy of the nasal process of the maxilla medially. Thus this osteotomy extends from the upper end of the osteotomy on the nasal process of the maxilla and laterally up to the zygoma. A fourth osteotomy is made from the lateral end of the infraorbital osteotomy through the full thickness of the zygoma. The next osteotomy is made intraorally, dividing the hard palate in the midline and connecting the previous osteotomy through the alveolar process all the way

up to the posterior edge of the hard palate (see Fig. 6.173). At this juncture, all the planned osteotomies of the anterior and medial wall of the maxilla have been completed. A curved osteotome is now used to make the final osteotomy between the posterior wall of the maxilla and the pterygoid plates at the hamulus of the pterygoid. The osteotome is placed just posterior to the maxillary tubercle in the pterygomaxillary notch, and by means of gentle strokes with a mallet, this part of the maxillary bone is fractured. Once this procedure is completed, gentle rocking of the maxilla and leverage of the posterior attachments of the maxilla with an osteotome permit maxillary swing laterally (Fig. 6.174). Complete hemostasis is secured by ligating or coagulating all bleeding points. The laterally swung part of the maxilla shows the maxillary antrum, the right half of the hard palate; the alveolar process; and all the anterior, lateral, and posterior soft-tissue attachments on the maxilla carefully preserved (Fig. 6.175). This close-up view after maxillary swing shows the infratemporal fossa in the pterygomaxillary region.

Dissection of the soft tissues now begins at this juncture by division of the pterygoid muscles. First the medial pterygoid and then the lateral pterygoid muscle is divided near the pterygoid plates. At each step of the operative procedure, absolute hemostasis must be maintained to keep the surgical field dry and clean and avoid undue hemorrhage. As dissection proceeds further cephalad, the lower end of the tumor is visible (Fig. 6.176). By alternate blunt and sharp dissection, the tumor is mobilized circumferentially in the infratemporal fossa. Soft-tissue attachments around the tumor are carefully divided and meticulous hemostasis with the bipolar cautery is achieved as the mobilization progresses cephalad toward the base of the skull. Finally, by careful circumferential dissection, the tumor is delivered in a monobloc fashion. Extreme care should be exercised to ensure that the hemoclips applied to the stump of the second division of the trigeminal nerve intracranially proximal to the tumor are removed and are present at the upper end of the surgical specimen. This step ensures complete removal of the tumor.

The surgical field following removal of the tumor shows the green rubber dam at the floor of the middle cranial fossa, protecting the underlying dura (Fig. 6.177). The surgical field is checked for leakage of cerebrospinal fluid and to ensure complete hemostasis. Minor venous bleeding from the stumps of the pterygoid muscles and the soft tissues in the infratemporal fossa is easily controlled with the bipolar cautery and by placement of a piece of Surgicel near the base of the skull and in the pterygoid fossa. After ensuring complete hemostasis, the laterally swung maxilla is brought back in its normal anatomic position and secured to the facial skeleton with miniplates and screws. A three-point fixation is required, with use of one miniplate for the zygoma, one at the nasal process of the maxilla, and one on the alveolar process at the anterior midline just above the roots of the central incisor teeth (Fig. 6.178). The mucosal incision in the palate is closed with interrupted Vicryl sutures extending from the midline anteriorly up to the junction of the soft and hard palate posteriorly and from the midline of the soft palate medially up to the lateral aspect of the mucosa posterior to the maxillary tubercle. A previously fabricated dental obturator is wired to the teeth on both sides of the upper alveolar ridge to ensure accurate alignment of the upper alveolar arch and maintain proper occlusion. The soft tissue

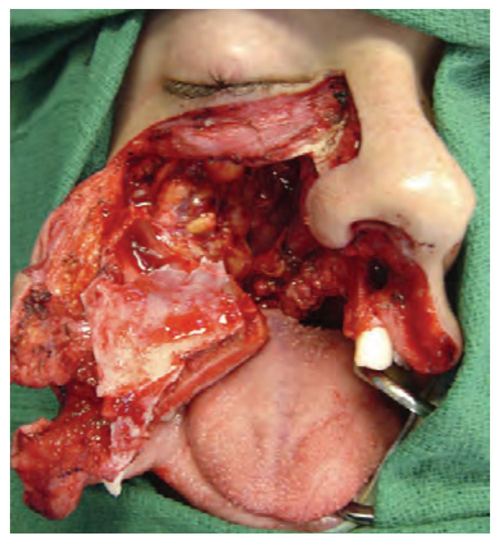

Figure 6.174 The maxilla is swung laterally with the anterior soft tissues of the cheek attached.

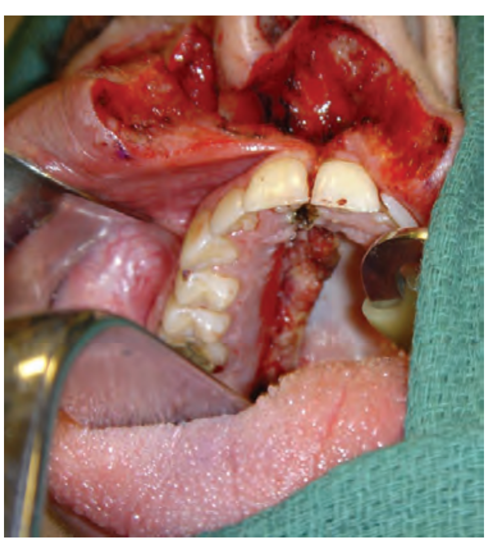

Figure 6.173 The mucoperiosteal flap of the hard palate is elevated beyond the midline.

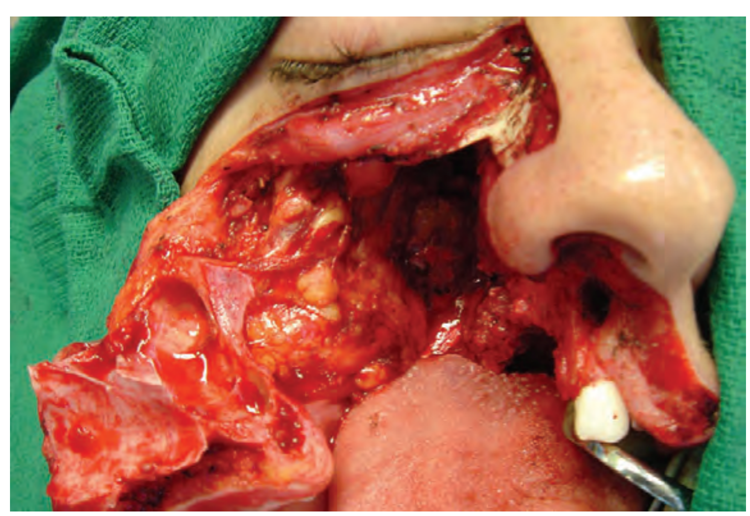

Figure 6.175 A close-up view shows the maxillary antrum, hard palate, and soft-tissue attachments on the maxilla.

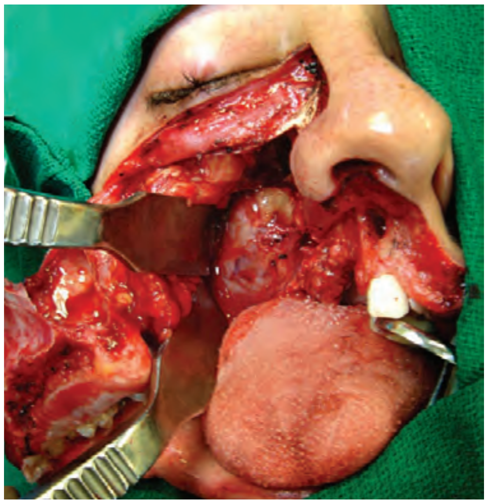

Figure 6.176 The lower end of the tumor is exposed.

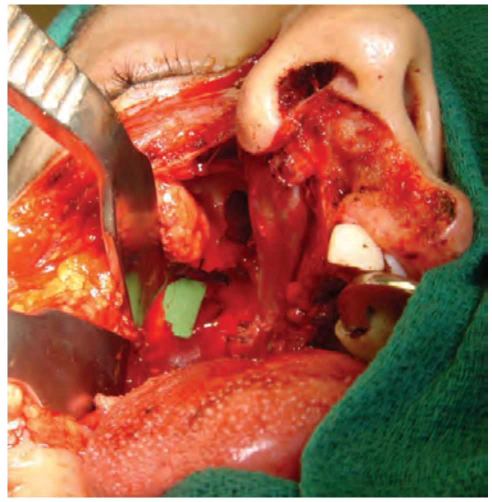

Figure 6.177 After removal of the tumor, the green rubber dam is seen protecting the dura.

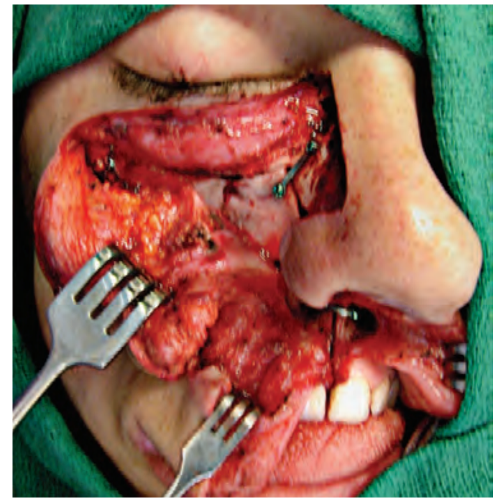

Figure 6.178 Miniplates and screws are used for three-point fixation of the maxilla.

Figure 6.179 The skin incision is closed in layers.

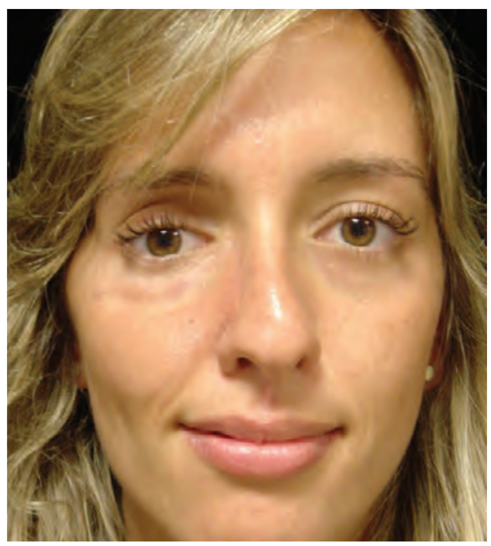

Figure 6.180 The external appearance of the patient 1 year after surgery.

Figure 6.181 An intraoral view shows perfect healing of the palate with alignment of teeth.

and skin incisions are closed in layers, accurately aligning the nasal subunits (Fig. 6.179).

The patient is permitted to ingest clear liquids and pureed foods within 24 to 48 hours after surgery. The dental obturator is retained for approximately 6 to 8 weeks to allow primary healing of the soft tissues at the site of the maxillary osteotomies. The wired palatal obturator is removed at 6 to 8 weeks and is replaced with a removable hard palate obturator that is clasped

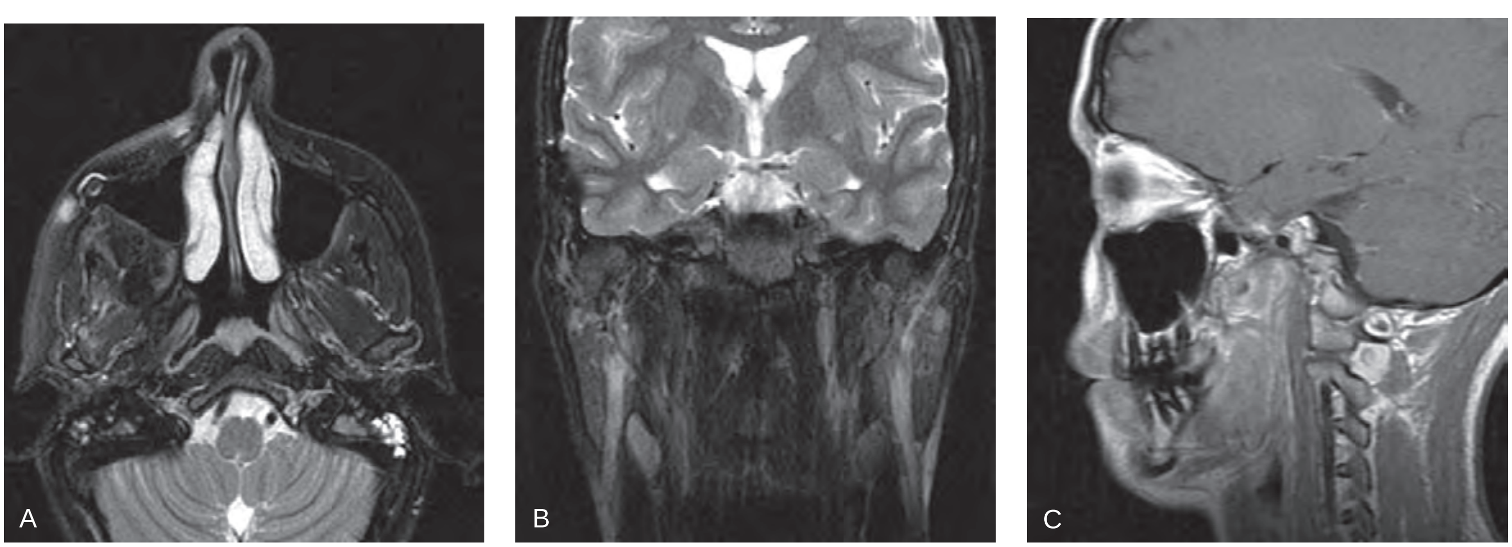

Figure 6.182 A magnetic resonance imaging scan in axial (**A**), coronal (**B**), and sagittal (**C**) planes 1 year following surgery.

to the upper teeth on both sides of the palate. The patient is advised to wear the hard palate obturator for approximately 6 months after surgery.

The appearance of the patient 1 year after surgery shows complete healing of the skin incision with minimal aesthetic impact on her facial appearance (Fig. 6.180). The intraoral view shows complete healing of the mucosal incision on the hard palate with accurate alignment of the upper teeth, maintaining normal occlusion (Fig. 6.181). An MRI scan 1 year after surgery shows complete removal of the tumor (Fig. 6.182).

The maxillary swing is a well-conceived surgical approach for tumors located on the medial aspect of the infratemporal fossa at the pterygomaxillary fissure or in the paranasopharyngeal space. However, this approach does not provide satisfactory exposure for tumors located in the lateral aspect of the infratemporal fossa medial to the ascending ramus of the mandible. For such tumors, a mandibulotomy approach is more satisfactory.

Maxillary Swing for a Chondrosarcoma of the Infratemporal Fossa. The maxillary swing operation previously described is also applicable to benign and malignant soft tissue or bone tumors in the medial aspect of the pterygomaxillary region of the infratemporal fossa. Axial and coronal views of the CT scan of a patient with a chondrosarcoma of the retromaxillary region and the medial aspect of the infratemporal fossa are shown in Fig. 6.183. Chondrosarcomas generally grow by displacing adjacent tissues rather than by invading through infiltration. It is easy to see that the soft tissues are displaced by this multilobulated solid tumor of the posteromedial wall of the maxilla and the paranasopharyngeal and retromaxillary region. A maxillary swing procedure through a modified Weber-Ferguson incision with a lateral extension along a skin crease in the infraorbital region is planned (Fig. 6.184). Complete excision of the tumor is achieved in this patient with preservation of the aesthetics of the face and integrity of the upper alveolar arch. The appearance of the patient 1 year after surgery shows excellent healing

Figure 6.183 Axial (**A**) and coronal (**B**) views of a computed tomography scan showing a chondrosarcoma of the left infratemporal fossa.

Figure 6.184 The skin incision is outlined for a maxillary swing procedure.

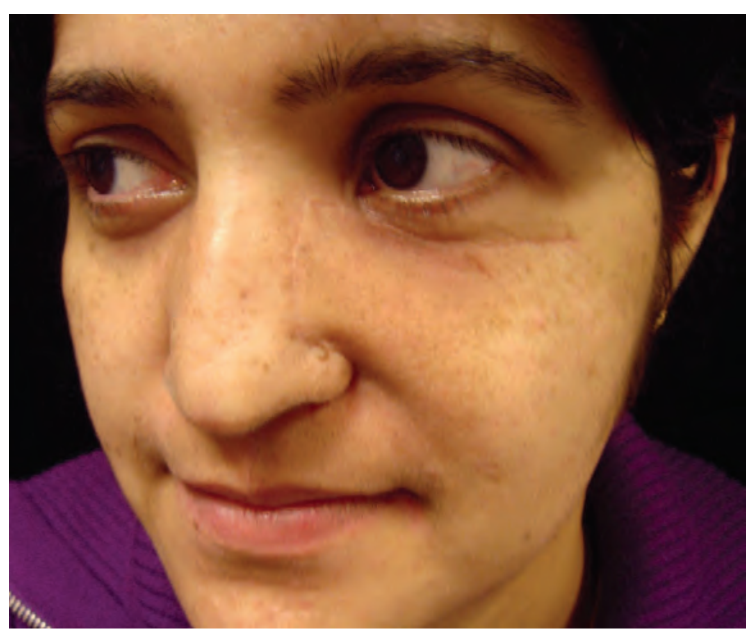

Figure 6.185 Postoperative appearance of the patient 1 year following surgery.

of the skin incision, restoring facial appearance and function (Fig. 6.185).

Mandibulotomy Approach to the Infratemporal Fossa. Tumors presenting in the lateral aspect of the infratemporal fossa between the lateral pterygoid plate and the mandible or under the zygomatic arch are not suitable for resection through a maxillary swing approach. Such lesions may be reached via a mandibulotomy approach or facial disassembly of the zygomatic arch in conjunction with a craniotomy.

The patient presented here has an extracranial and intracranial meningioma involving the floor of the middle cranial fossa with extension through the greater wing of the sphenoid bone into the infratemporal fossa. The procedure in this patient was accomplished in two stages, with the intracranial component of the tumor resected via a middle fossa craniotomy in the first stage. A watertight closure of the dural defect was accomplished with a fascial graft. Several weeks after recovery from this surgery, the patient was brought back to the operating room for the second stage of the operative procedure.

Preoperative MRI scans of the patient in the axial, coronal, and sagittal planes clearly demonstrate the dumbbell-shaped tumor transgressing the floor of the middle cranial fossa. In the axial view (Fig. 6.186), the tumor is well demonstrated in the infratemporal fossa on the right-hand side. The tumor is situated medial to the condyloid process of the mandible and the mandibular notch. In the coronal plane (Fig. 6.187), the tumor resembles an hourglass involving the dura of the floor of the middle cranial fossa with the larger component of the tumor appearing in the infratemporal fossa. The dural component in the floor of the middle cranial fossa is well demonstrated on the sagittal view, as seen in Fig. 6.188.

General anesthesia is induced through a nasotracheal tube, and the head and neck area is isolated in the usual fashion. A midline lower lip–splitting incision begins at the vermilion border of the lower lip and extends up to the level of the hyoid bone in the midline (Fig. 6.189). The incision then extends laterally along an upper neck skin crease up to the anterior border of the sternomastoid muscle. Intraorally, the incision extends on the mucosal surface of the lower lip up to the reflection of the gingivo-labial sulcus, at which point the incision

Figure 6.189 The outline of the midline lower lip–splitting incision.

extends laterally on the right-hand side up to the space between the lateral incisor and canine teeth. A mandibulotomy would be performed at that site. The incision then extends along the floor of the mouth, remaining medial to the attached gingiva up to the retromolar trigone. At that point the incision extends laterally into the upper gingivobuccal sulcus, as shown in Fig. 6.190. The exposure gained through this approach provides lateral rotation of the right half of the mandible, giving wide exposure of the infratemporal fossa.

The lower lip has been split and the incision completed, elevating short cheek flaps on both sides and remaining medial to the mental foramen bilaterally so as not to disturb the mental nerves. The cheek flap on the right-hand side is elevated enough to expose the space between the lateral incisor and the canine tooth. The flap is elevated directly over the outer cortex of the mandible (Fig. 6.191). The outline of the proposed angled mandibulotomy is marked out as shown in Fig. 6.192. A sagittal

Figure 6.186 An axial view of the magnetic resonance imaging scan of a patient with extracranial and intracranial meningioma.

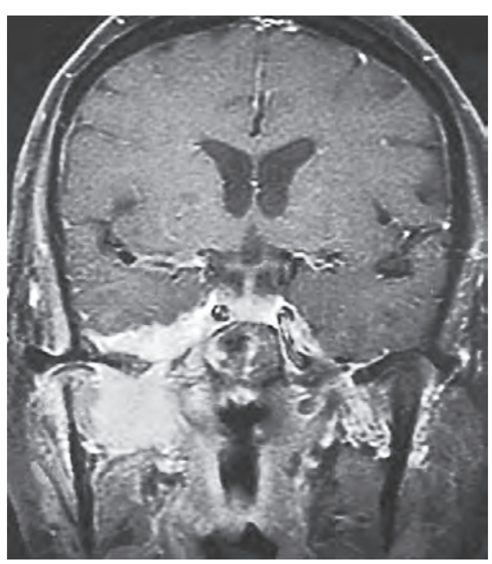

Figure 6.187 A coronal view of the magnetic resonance imaging scan.

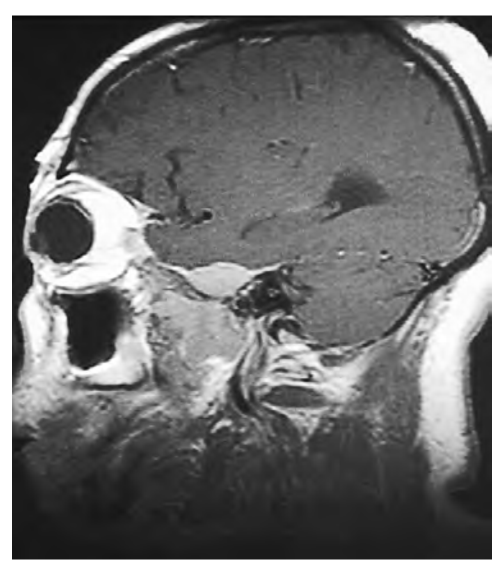

Figure 6.188 A sagittal view of the magnetic resonance imaging scan.

saw is used to complete the mandibulotomy. Brisk bleeding from the cut ends of the mandible is controlled with bone wax.

Retraction of the two halves of the mandible provides exposure of the floor of the mouth. An incision is now placed in the mucosa of the floor of the mouth from the mandibulotomy site up to the retromolar gingiva, leaving approximately a centimeter of mucosa of the floor of the mouth on the lingual gingiva. Further retraction of the two halves of the mandible following this incision exposes the mylohyoid muscle (Fig. 6.193). The mylohyoid muscle is divided, which provides further exposure of the pterygomaxillary space. The mucosal incision is now extended along the retromolar gingiva, curving laterally and extending anteriorly in the upper gingivobuccal sulcus. The incision is deepened through the soft tissues, providing further retraction of the two halves of the mandible (Fig. 6.194). This provides exposure of the medial pterygoid muscle (Fig. 6.195). Exposure of the medial pterygoid muscle (Fig. 6.194). A close-up view of the surgical field shows the musculotendinous fibers of the medial pterygoid muscle (Fig. 6.196). Brisk hemorrhage from branches of the internal maxillary artery is to be expected. This bleeding is carefully controlled, and absolute hemostasis is secured. The lateral pterygoid muscle is now exposed. The lateral pterygoid muscle is divided, exposing the tumor in the infratemporal fossa. A close-up view of the surgical field clearly demonstrates the lower border of the tumor in the infratemporal fossa (Fig. 6.197). Careful and meticulous dissection of the tumor is now undertaken. Bleeding from the venous plexus in the infratemporal fossa and the pterygoid veins is often tedious and troublesome and requires that absolute hemostasis be maintained during the entire phase of mobilization of the tumor. With meticulous and careful dissection, the remaining tumor is removed in toto until the repaired portion of the dura is exposed, ensuring gross total tumor resection (Fig. 6.198). Continued minor oozing from the tumor bed and the surgical field is to be expected and is adequately controlled with the use of either Gelfoam or Surgicel. After ensuring total tumor resection and after achieving satisfactory hemostasis, closure of the surgical field begins. A Penrose drain is inserted into the dead space in the infratemporal fossa and is brought out through the cervical incision medial to the ascending ramus of the mandible. The incision is then closed in a single layer

Figure 6.191 The cheek flap is elevated directly over the outer cortex of the mandible.

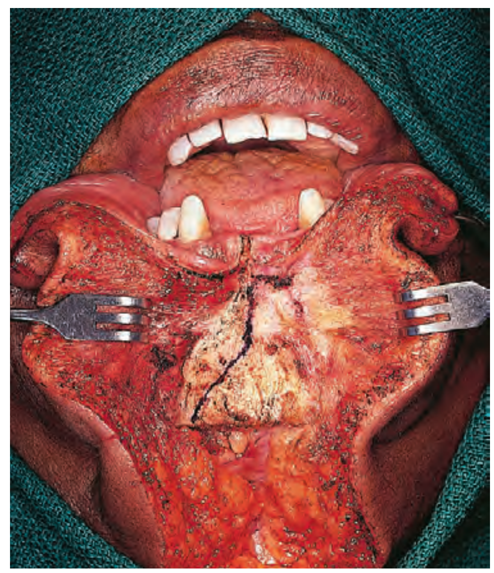

Figure 6.192 The outline of the proposed angled mandibulotomy.

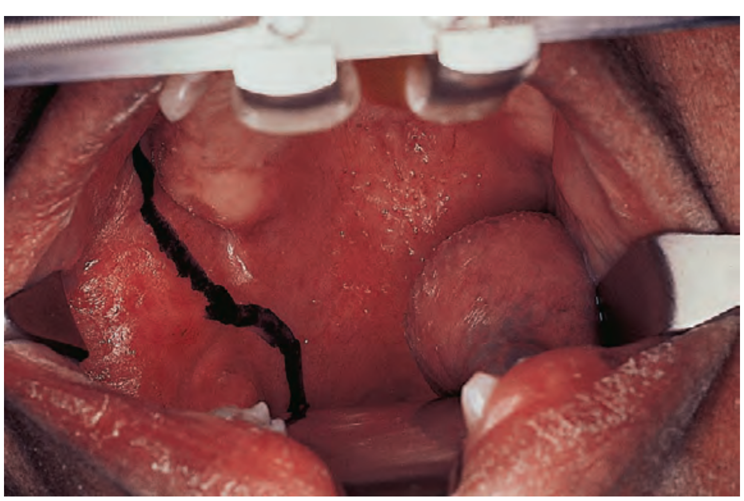

Figure 6.190 The mucosal incision extends laterally into the upper gingivobuccal sulcus.

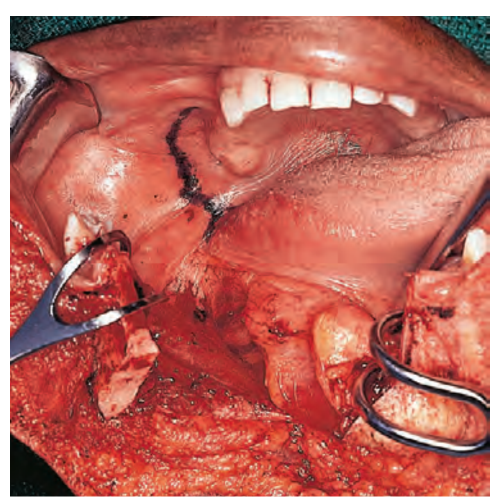

Figure 6.193 Retraction of the halves of the mandible exposes the mylohyoid muscle.

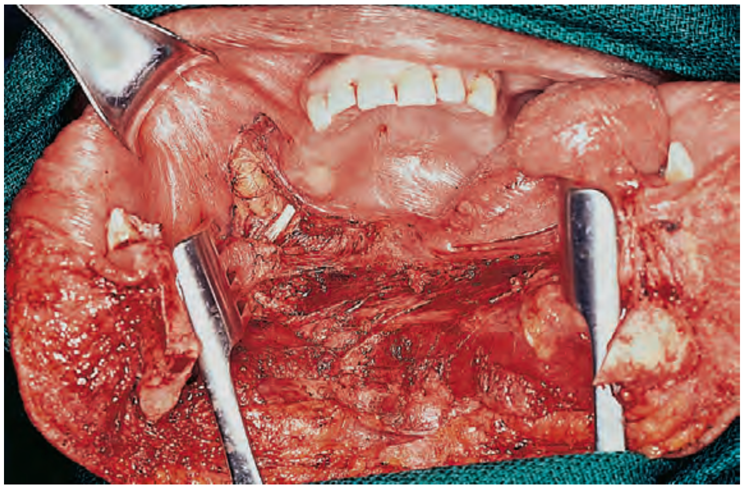

Figure 6.194 The medial pterygoid muscle is exposed on further retraction of the halves of the divided mandible.

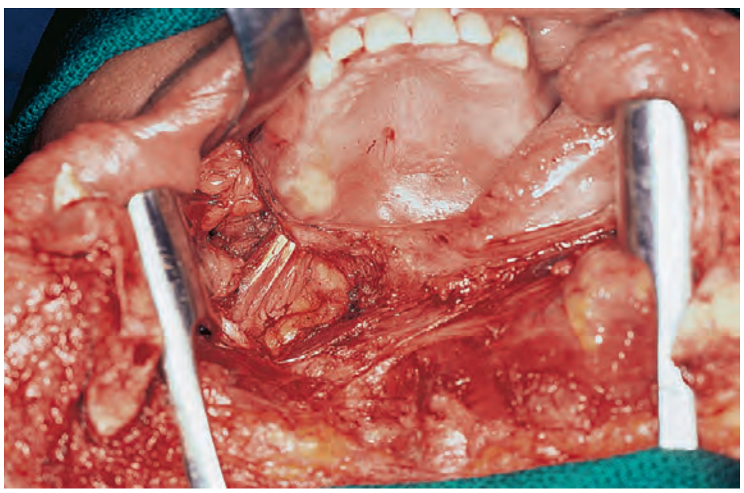

Figure 6.195 The lateral pterygoid muscle is now exposed.

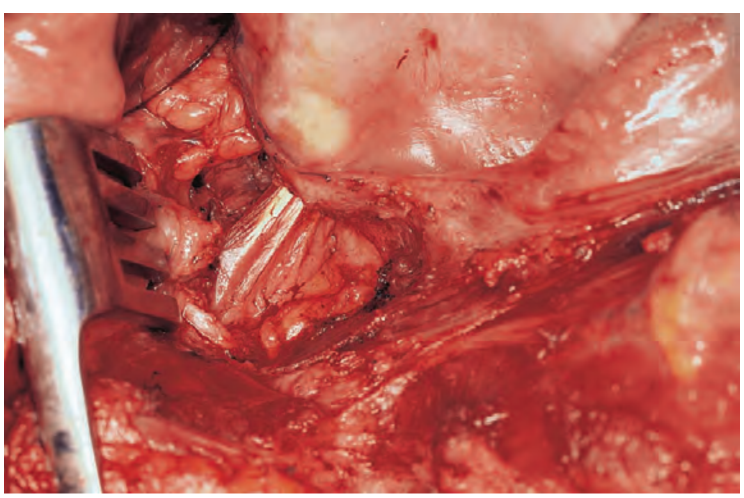

Figure 6.196 Division of the lateral pterygoid muscle exposes the tumor in the infratemporal fossa.

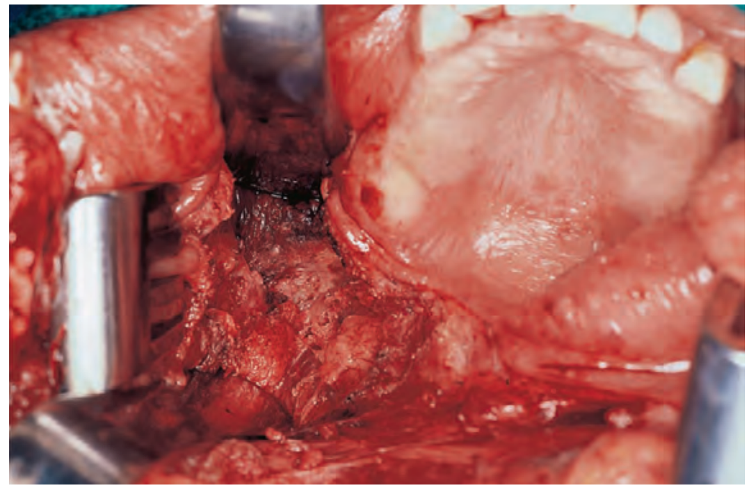

Figure 6.197 A close-up view of the surgical field shows the lower border of the tumor.

Figure 6.198 A close-up view of the tumor bed after gross total tumor resection showing the rubber dam at the site of dural repair.

with interrupted 2-0 chromic catgut sutures extending from the upper gingivobuccal sulcus, the retromolar region, and the floor of the mouth. The mandibulotomy is repaired with four-hole miniplates and screws. Two plates are used, one on the lateral cortex of the mandible and one on the inferior border of the mandible in the usual fashion. For details of the mandibulotomy repair, please refer to Chapter 9. The remaining incision is closed in the usual fashion.

Resection of a benign tumor with intracranial extension require a simultaneous craniotomy and mandibulotomy exposure for a one-stage resection. For benign lesions, a staged procedure with excision of the intracranial component in the first stage and removal of the remaining tumor in the second stage also can be accomplished as shown here.

Technical Variations in Surgery of the Skull Base at the Middle Cranial Fossa

The technical aspects of exposure of the skull base at the middle cranial fossa require a middle fossa craniotomy and either a maxillary swing, maxillectomy, or mandibulotomy as described previously. On the other hand, tumors in the vicinity of the temporal bone may not need any of those procedures. The technical details of each operative procedure will vary depending on the anatomic extent, location, and the histology of the tumor under consideration. Oncologically sound and satisfactory surgical resection for extensive malignant tumors that involve the skull base at the middle cranial fossa is not only technically demanding but often unsatisfactory. On the other hand, a very gratifying surgical resection can be accomplished for histologically benign but locally aggressive tumors. An example of such a tumor is shown here.

Resection of a Chondroblastic Tumor of the Temporomandibular Joint Involving the Middle Cranial Fossa. An axial view of the CT scan of a patient with a chondroblastoma involving the condyloid process of the mandible with extension to the adjacent skull base is shown in Fig. 6.199. A sagittal view of the MRI scan in its most lateral aspect shows a well-defined tumor involving the skull base in the middle cranial fossa just anterior to the auditory canal (Fig. 6.200). The operative procedure required a temporal craniotomy performed through a C-shaped incision that was continued through the preauricular skin crease up to the retromandibular region and then into the anterior aspect of the upper part of the neck (Fig. 6.201). The location and extent of the tumor and the incision are shown on the patient in Fig. 6.202. The temporalis muscle is resected after elevation of the scalp flap to expose the calvarium (Fig. 6.203). A temporal craniotomy is performed, and the middle cranial fossa is explored. A subtemporal craniectomy is performed with a high-speed drill and a burr, whereupon the greater wing of the sphenoid and the skull base of the middle cranial fossa are drilled out (Fig. 6.204). Because the dura is uninvolved, it is left intact. The greater wing of the sphenoid is drilled out up to the lateral wall of the carotid canal and the foramen ovale medially.

At this point the remaining skin incision is completed and a subtotal parotidectomy is performed, preserving the main trunk and the peripheral branches of the facial nerve (Fig. 6.205). In the upper part of the neck, the region of the jugular foramen is exposed, and the hypoglossal and the vagus nerves are carefully preserved. The masseter muscle is then divided over the lateral

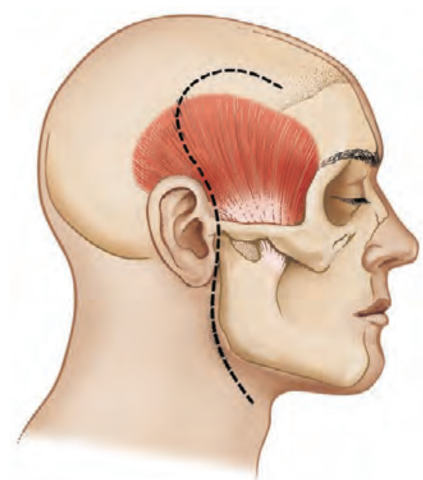

Figure 6.201 The skin incision provides exposure for a temporal craniotomy, a parotidectomy, and access to the upper part of the neck.

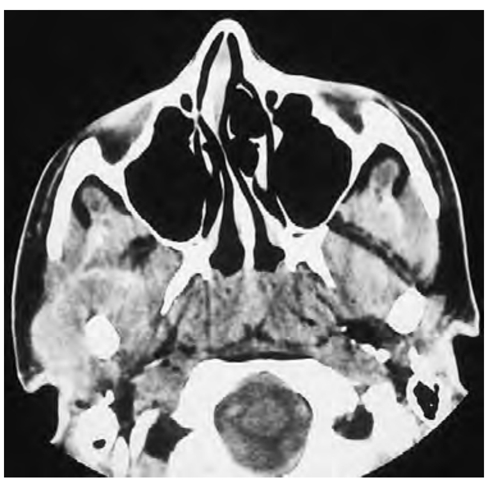

Figure 6.199 An axial view of the computed tomography scan of a patient with a chondroblastoma involving the condyloid process of the mandible with extension to the adjacent skull base.

Figure 6.202 The location and extent of the tumor, as well as the incision, are marked.

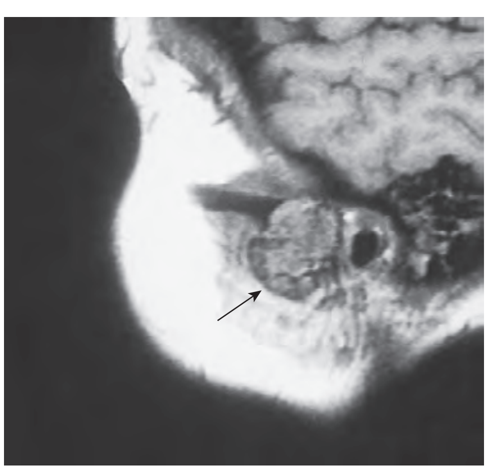

Figure 6.200 A sagittal view of the magnetic resonance imaging scan in its most lateral aspect shows the tumor located anterior to the auditory canal (*arrow*).

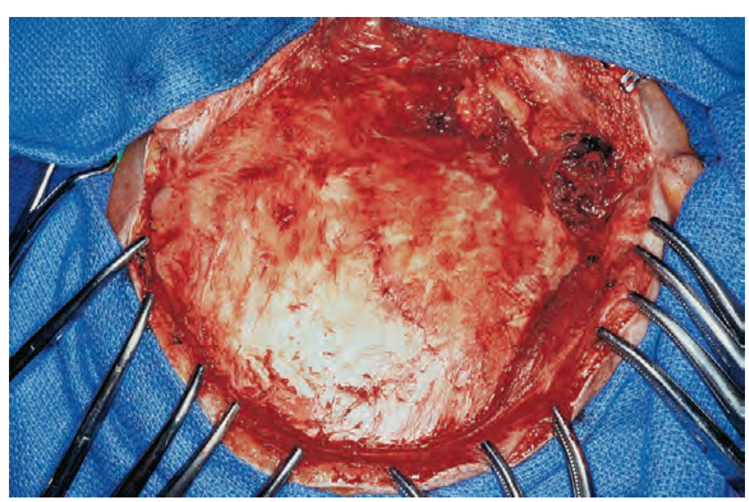

Figure 6.203 The temporalis muscle is resected after elevation of the scalp flap to expose the calvarium.

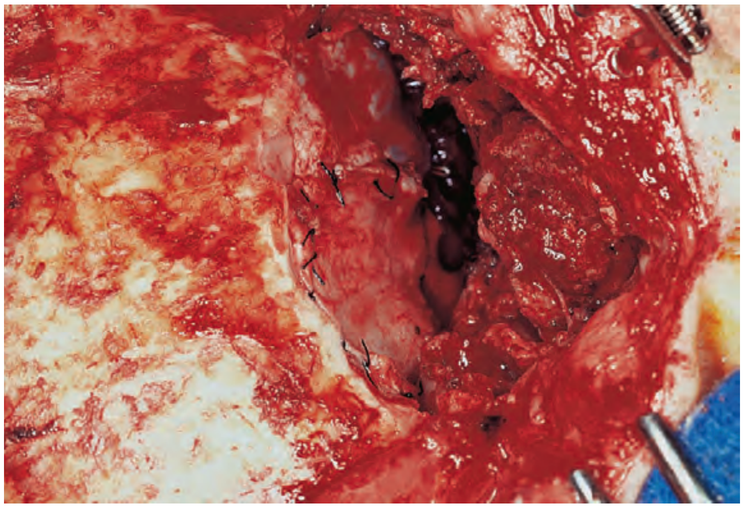

Figure 6.204 A subtemporal craniectomy is performed with a high-speed drill and a burr, whereupon the greater wing of the sphenoid and the skull base of the middle cranial fossa are drilled out.

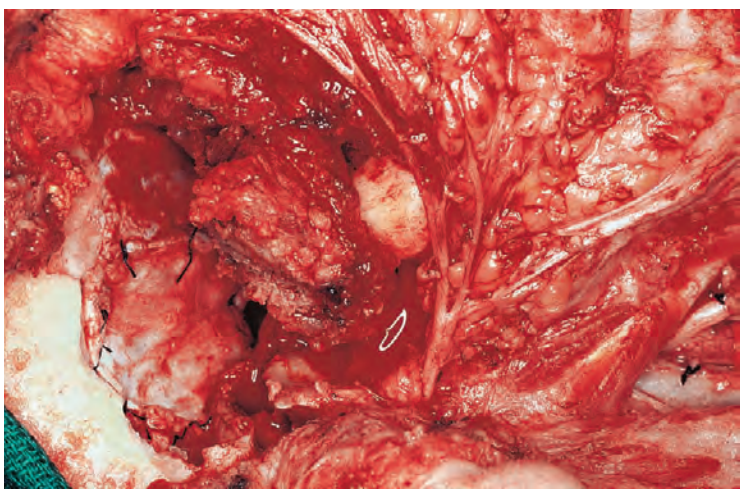

Figure 6.205 The remaining skin incision is completed and a subtotal parotidectomy is performed, preserving the main trunk and the peripheral branches of the facial nerve.

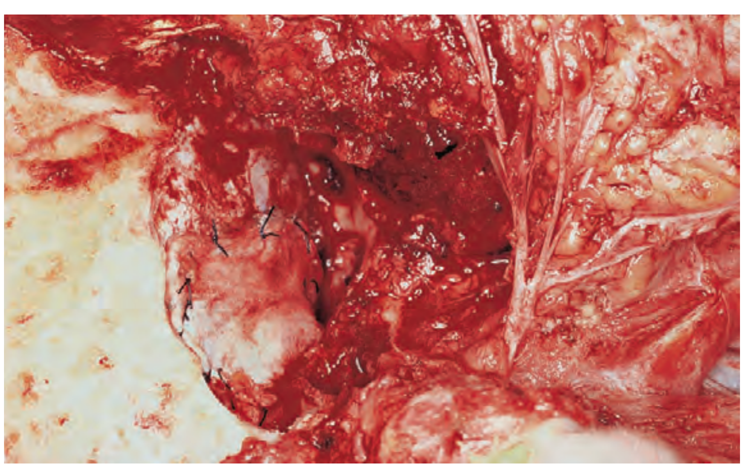

Figure 6.206 The surgical field following removal of the tumor.

cortex of the ascending ramus of the mandible below the main trunk of the facial nerve. A high-speed power saw is used to divide the ascending ramus of the mandible just below the mandibular notch. The tumor mass arising from the condyloid process of the mandible is then resected in a monobloc fashion with the bony remnants of the glenoid fossa and the involved portion of the greater wing of the sphenoid bone. To achieve this resection, the pterygoid muscles are detached from the medial aspect of the tumor. The surgical field following removal of the tumor is shown in Fig. 6.206. A photograph of the patient approximately 3 months after surgery shows complete preservation of the function of the facial nerve and minimal aesthetic deformity as a result of the loss of the temporalis muscle on the right-hand side (Fig. 6.207).

Figure 6.207 Postoperative appearance of the patient 3 months following surgery.

Temporal Bone Resection

Excision of tumors arising in the auditory canal, either in the cartilaginous or bony part, require a temporal bone resection. Although external radiotherapy can be used as definitive treatment for squamous carcinoma of the auditory canal, the results of surgical treatment with temporal bone resection are significantly better. Tumors presenting in the cartilaginous portion of the auditory canal or the lateral portion of the bony canal are amenable to satisfactory monobloc surgical resection with significant improvement in disease control and survival.

The patient shown in Fig. 6.208 has carcinoma of the auditory canal fungating through the external ear in the retroauricular skin crease. Although the patient does not have grossly palpable cervical lymph nodes, significant induration is present in the retromandibular region at the angle of the mandible. A biopsy of the lesion from the auditory canal confirmed the diagnosis of squamous cell carcinoma.

Adequate radiographic evaluation of this tumor requires soft tissue and bone windows of the CT scan in the axial and coronal views. A representative axial view of the CT scan through the temporal bone is shown in Fig. 6.209, demonstrating bone destruction at the tip of the mastoid process by the tumor. However, the medial aspect of the petrous temporal bone is not involved. The coronal view of the CT scan through the mastoid process shown in Fig. 6.210 demonstrates bone destruction of the mastoid tip. The inner ear, however, is uninvolved by

Figure 6.208 A carcinoma of the auditory canal fungating through its posterior wall with involvement of the adjacent skin.

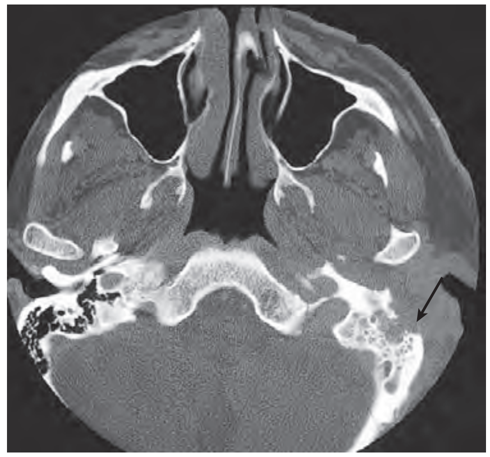

Figure 6.209 The bone window of an axial view of the computed tomography scan shows destruction of the lateral aspect of the temporal bone (*arrow*).

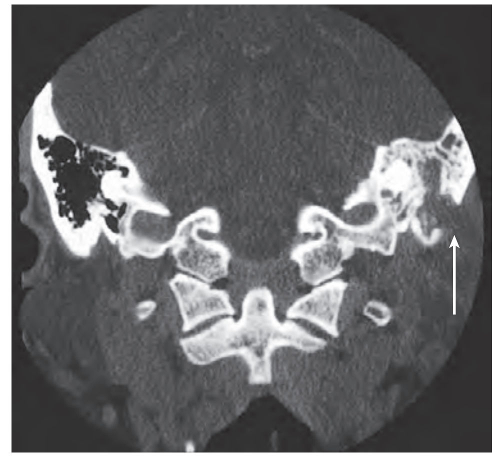

Figure 6.210 The bone window of a coronal view of the computed tomography scan shows destruction of the tip of the mastoid process by the tumor (*arrow*).

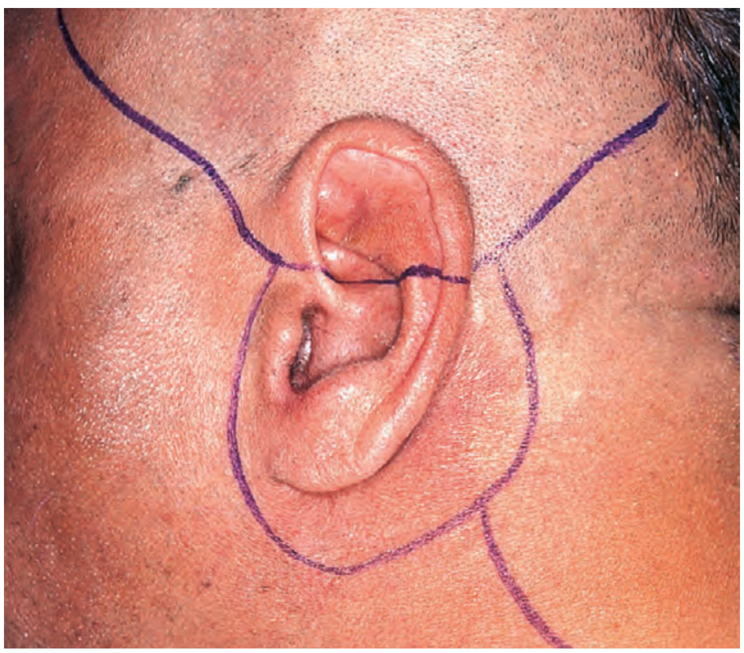

Figure 6.211 The incisions outlined show sacrifice of the lower two-thirds of the external ear with adjacent skin.

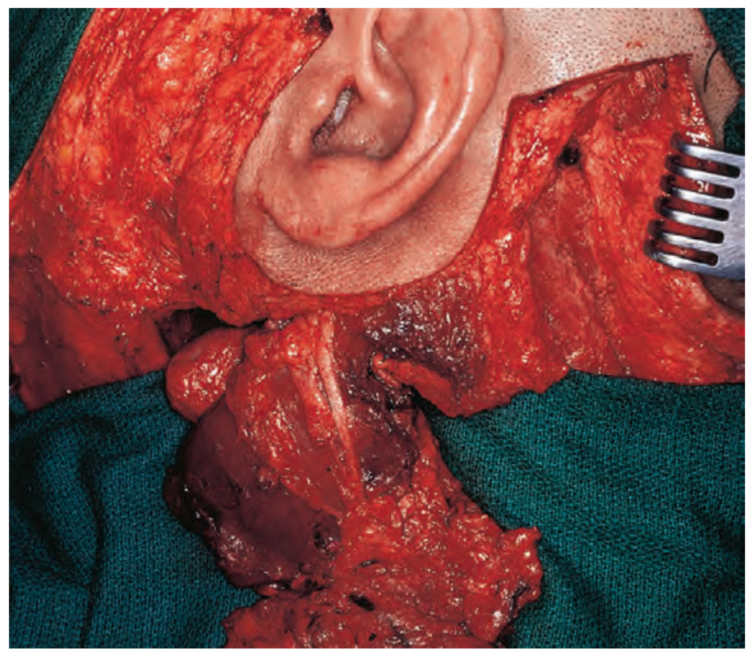

Figure 6.212 A modified radical neck dissection is completed, keeping the specimen attached to the primary tumor at the tail of the parotid gland and the mastoid process.

cancer. Therefore this patient is considered a suitable candidate for subtotal temporal bone resection in conjunction with a parotidectomy and left-sided neck dissection.

The surgical incisions are outlined in Fig. 6.211. Amputation of the lower two-thirds of the pinna with adjacent skin overlying the mastoid process is planned in continuity with temporal bone resection, a total parotidectomy, and left modified radical neck dissection. The upper third of the external ear is preserved to provide support for eyeglasses. A vertical incision along the anterior border of the trapezius muscle curving anteriorly toward the sternoclavicular joint is planned for neck dissection. Reconstruction of the surgical defect in this patient is planned with a posterior vertical trapezius myocutaneous flap. Alternatively, a rectus abdominis myocutaneous free flap or an anterolateral thigh (ALT) free flap can be used to reconstruct this defect. General endotracheal anesthesia is induced, and the patient is placed in the right lateral position on the operating table. An indwelling spinal catheter is introduced for monitoring CSF pressure.

A modified radical neck dissection preserving the accessory nerve is completed first. The surgical specimen of dissected neck nodes is kept attached to the tail of the parotid gland and the mastoid process to remain in continuity with the resection of the primary tumor (Fig. 6.212). The anterior skin flap is then further elevated and retracted medially to accomplish a total parotidectomy with sacrifice of the underlying masseter muscle, which is elevated directly over the lateral cortex of the ascending ramus of the mandible. The masseter muscle is detached from the zygomatic arch. The lateral aspect of the ascending ramus of the mandible is thus exposed. The condyloid process of the mandible is now divided to facilitate removal of the temporo mandibular joint and the temporal bone in a monobloc fashion. The planned circumferential incision around the tumor is now completed. The temporal scalp is elevated directly over the squamous part of the temporal bone, remaining deep to the temporalis muscle. The lower part of the temporalis muscle is transected just above the zygomatic arch. With use of a periosteal elevator, the pericranium overlying the squamous part of the temporal bone is elevated to provide adequate exposure of the bone (Fig. 6.213).

A craniotome is now used and three burr holes are made to perform a temporal craniotomy (Fig. 6.214). The burr holes are connected with a side-cutting drill, with the underlying dura

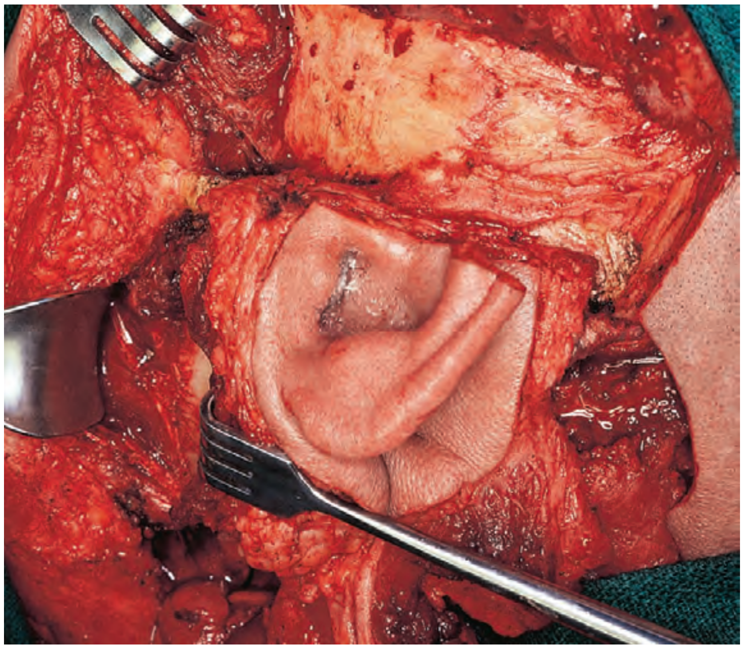

Figure 6.213 The circumferential incision around the auditory canal is completed and the temporal scalp is elevated, including the temporalis muscle, to expose the calvarium.

being carefully protected. Fine dural elevators are used to separate the dura from the undersurface of the temporal bone. With use of appropriate rongeurs and a high-speed burr, the squamous temporal bone is removed to expose the dura of the middle cranial fossa. Approximately 20 mL of cerebrospinal fluid is removed from the spinal catheter at this time. The dura of the middle cranial fossa is gently stripped away from the floor of the middle cranial fossa, the mastoid process, and the posterior fossa, up to the attachment of the sigmoid sinus.

A variable-speed drill with a burr and suction irrigator is now used to perform a mastoidectomy. The goal at this point is to expose the superior aspect of the sigmoid sinus, skirting the temporal bone posteriorly. Meticulous attention should be paid to leaving a thin shell of bone over the sigmoid sinus to prevent hemorrhage. This dissection is tedious and slow, but it can be expedited with use of the variable-speed drill with a fine burr. As the sigmoid sinus is approached, a thin shell of bone is left over it, beneath which one can see the bluish discoloration of the sinus. Elevation of the dura over the petrous part of the temporal bone continues medially (Fig. 6.215). Meticulous dissection is now undertaken with fine dural elevators to elevate the sigmoid sinus from its bed, exposing the posterior part of the petrous temporal bone. Bleeding from the superior petrosal sinus is usually encountered at this point and can be controlled easily with Gelfoam or bone wax.

The zygomatic process is now divided with use of a power saw. The line of transection on the petrous part of the temporal bone remaining just lateral to the internal acoustic meatus is demarcated with use of the high-speed drill and a fine burr. Similarly, using the drill, a kerf is made over the floor of the middle cranial fossa through the squamous part of the temporal bone just anterior to the auditory canal and the petrous temporal bone up to the temporal craniotomy. This kerf of the bone is deepened as much as possible with the high-speed drill and the fine burr. At this point, all the vascular connections of the temporal bone are carefully dissected off, including the sigmoid sinus from its posterior aspect. The bone cut through the medial aspect of the temporal bone is deepened further with use of the fine burr. At this juncture, the specimen is nearly completely

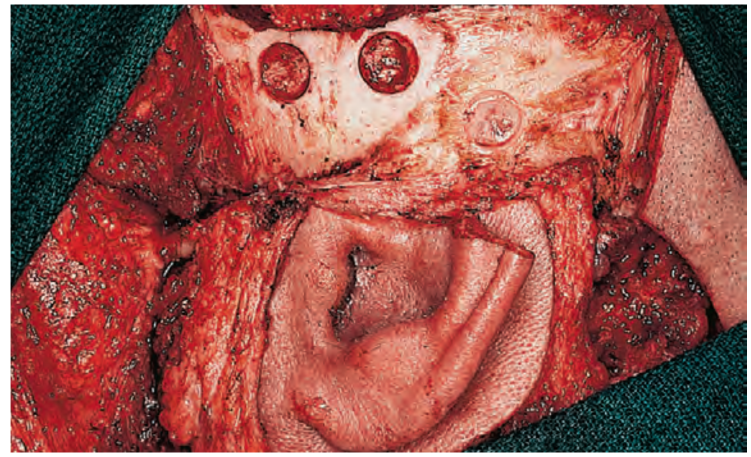

Figure 6.214 A craniotome is used and three burr holes are made to perform a temporal craniotomy.

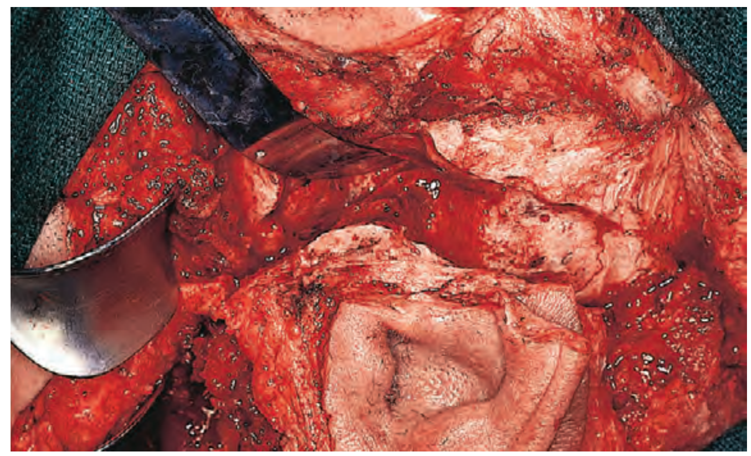

Figure 6.215 A mastoidectomy is completed, leaving a thin shell of bone over the sigmoid sinus, thus permitting further medial elevation of the dura over the petrous temporal bone.

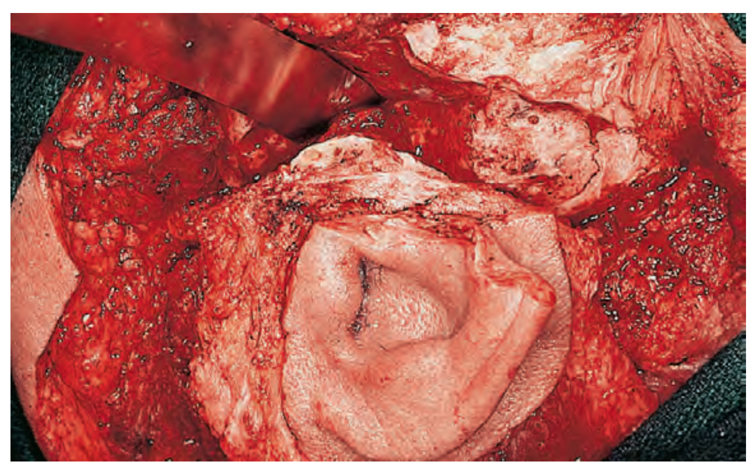

Figure 6.216 A curved osteotome is placed in the kerf over the temporal bone lateral to the internal acoustic meatus.

mobilized from all its attachments except medially at the petrous apex (Fig. 6.216). Using a curved osteotome, the petrous temporal bone is fractured through the kerf previously made by the burr. Similarly, the osteotome is used to fracture the anterior part of the petrous temporal bone through the line of previously demarcated bone kerf made with the burr. Once this fracture is completed, the specimen can be mobilized laterally and anteriorly to divide the lateral pterygoid muscle that is attached to the condyloid process of the mandible. The remaining soft-tissue attachments are divided and the specimen is removed.

Once the specimen is removed, the stump of the jugular vein at the jugular foramen along with the adjacent cranial nerves come into view (Fig. 6.217). The soft-tissue attachments must be divided meticulously and carefully to preserve the vagus and hypoglossal nerves exiting from the skull base. The internal carotid artery remains medial as it enters the carotid canal and is also carefully isolated and preserved. The lateral wall of the jugular foramen may have to be excised with the surgical specimen, depending on the extent of the tumor. A monobloc resection of the temporal bone extending from the lateral lip of the internal acoustic meatus and including the lateral wall of the jugular foramen all the way up to the external ear is thus completed.

The surgical specimen shows the lower half of the external ear with the auditory canal, periauricular skin, temporal bone, parotid gland, masseter muscle, and the contents of the dissected neck removed in a monobloc fashion (Fig. 6.218). The resection of the external ear and periauricular skin with the temporal bone results in the loss of a large portion of skin, underlying soft tissues, and bone, leaving a huge dead space with exposed dura. If any CSF leakage occurs at the time of surgery, its source should be meticulously repaired to prevent continued leakage and subsequent meningitis. Coverage of this surgical defect requires a regional myocutaneous flap or a microvascular composite musculocutaneous free flap. In this patient, a vertical posterior trapezius myocutaneous flap is used to repair the surgical defect (Fig. 6.219). After elevation of the flap with meticulous attention to preservation of its vascular pedicle, the flap is rotated cephalad and appropriately trimmed to fill the surgical defect and provide soft-tissue replacement and skin coverage (Fig. 6.220). Alternatively, a rectus abdominis myocutaneous free flap or ALT free flap may be used to repair this surgical defect. Because of the resection of the temporal bone, complete facial paralysis is to be expected. A gold weight implant is placed in the upper eyelid at a later date to achieve dynamic rehabilitation of the paralyzed eyelid.

The procedure is generally well tolerated by most patients, although complete loss of hearing and facial paralysis are to be expected. Loss of balance is transient and lasts from 2 to 3 weeks. Most patients are ambulatory by the third postoperative day.

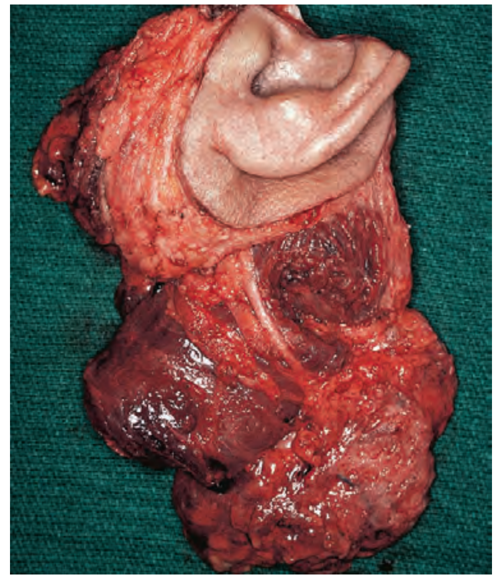

Figure 6.218 The surgical specimen of the temporal bone, external ear, parotid gland, and neck dissection removed in a monobloc fashion.

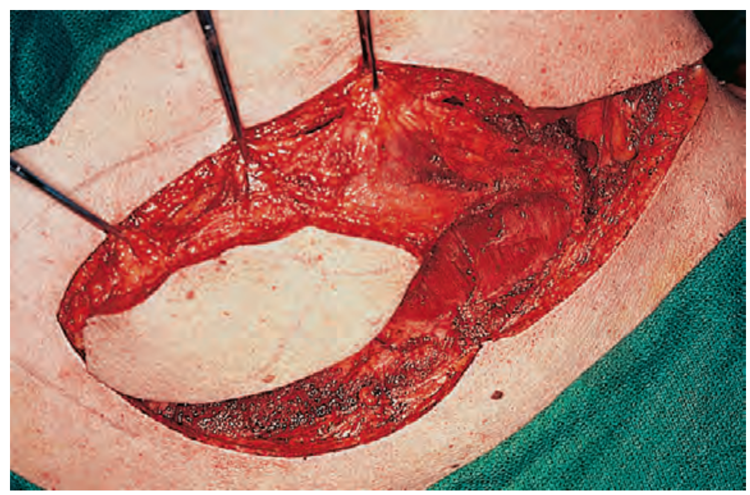

Figure 6.219 A vertical posterior trapezius myocutaneous flap is elevated for repair of the surgical defect.

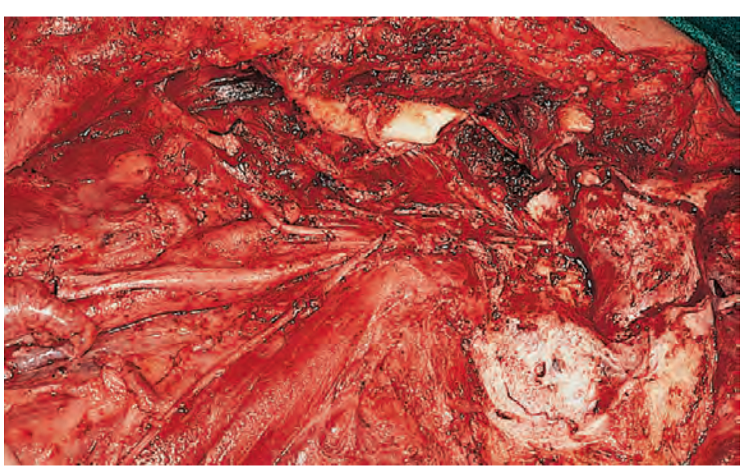

Figure 6.217 The surgical defect following removal of the specimen shows the anatomic structures adjacent to the jugular foramen.

Figure 6.220 Completed closure of skin incisions and repair of the surgical defect with a trapezius myocutaneous flap.

Resection of a Glomus Jugulare Tumor

The infratemporal fossa approach is an excellent surgical procedure for tumors in the vicinity of the petrous portion of the temporal bone. It also provides a very good approach for extensive tumors of the jugular foramen, extending to the clivus and parasellar region. The operative procedure requires anterior transposition of the facial nerve, obliteration of the pneumatic spaces of the temporal bone via a mastoidectomy, and permanent occlusion of the eustachian tube. The external auditory canal is closed like a blind sac, which prevents postoperative infection and permits primary wound healing, but the function of the inner ear is preserved by this approach.

The patient described here presented with tinnitus and dizziness and was found to have a glomus jugulare tumor on the left-hand side. Her CT scans show the presence of a large bone-destructive tumor in the region of the apex of the petrous temporal bone, presenting posteriorly, adjacent to the clivus (Fig. 6.221). Lower down, the CT scan showed the tumor extending up to the lateral lip of foramen magnum, although the margin of the foramen magnum was intact (Fig. 6.222). The CT scan in a coronal plane shows significant enlargement of the jugular foramen compared with the opposite side (Fig. 6.223). Carotid angiography showed that this tumor was a vascular lesion. During the arterial phase of the angiographic study, a tumor blush could not be appreciated (Fig. 6.224). During the venous phase, however, a large lesion was seen involving the region of the jugular bulb and medial aspect of the sigmoid sinus (Fig. 6.225).

The patient is positioned supine on the operating table with an indwelling spinal catheter for drainage of CSF. The head is turned to the right-hand side and a postauricular incision is planned, extending into the upper part of the neck inferiorly and over the temporoparietal scalp anteriorly (Fig. 6.226).

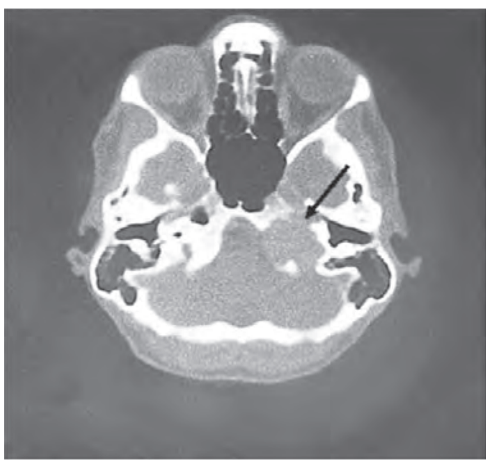

Figure 6.221 An axial view of a computed tomography scan shows a large tumor in the region of the apex of the petrous temporal bone adjacent to the clivus (*arrow*).

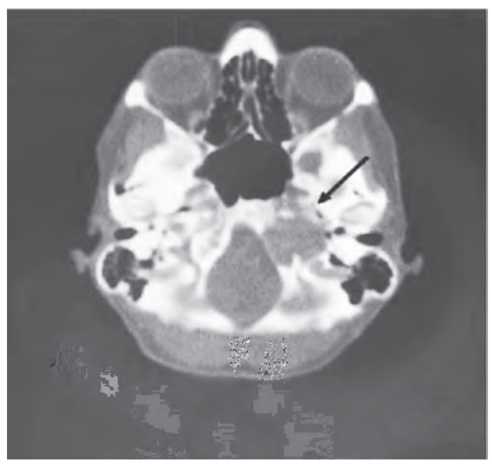

Figure 6.222 A computed tomography scan lower down showing the tumor extending up to the lateral lip of the foramen magnum (*arrow*).

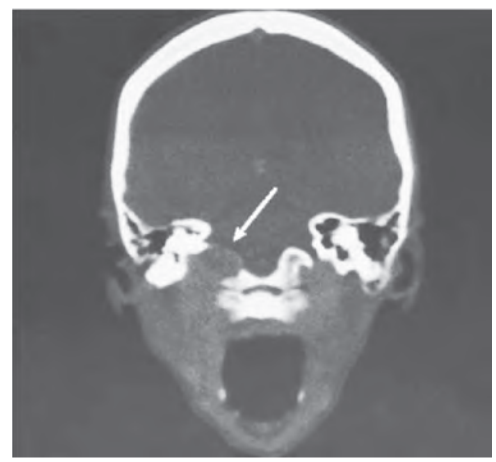

Figure 6.223 A computed tomography scan in a coronal plane shows the tumor with expansion of the jugular foramen (*arrow*).

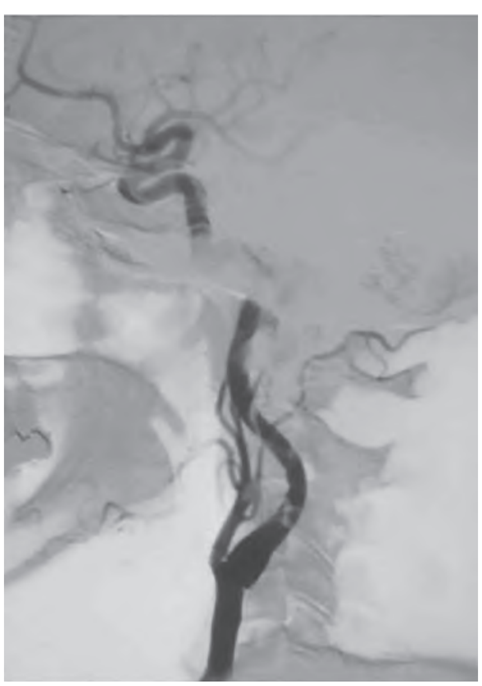

Figure 6.224 The arterial phase of the angiographic study (lateral view).

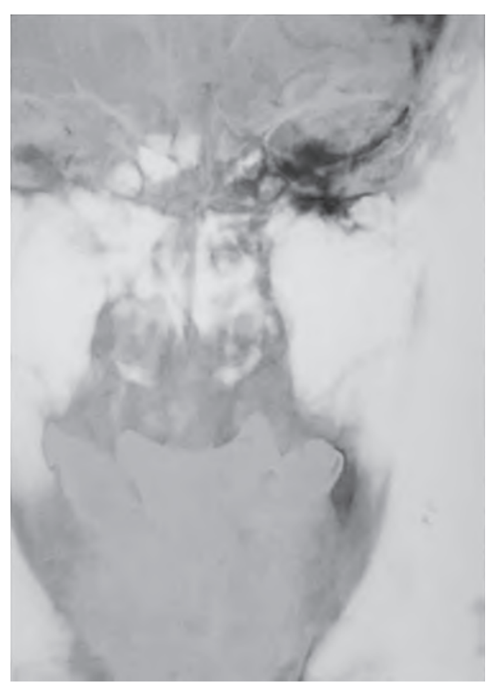

Figure 6.225 The venous phase of the angiographic study (anterior view).

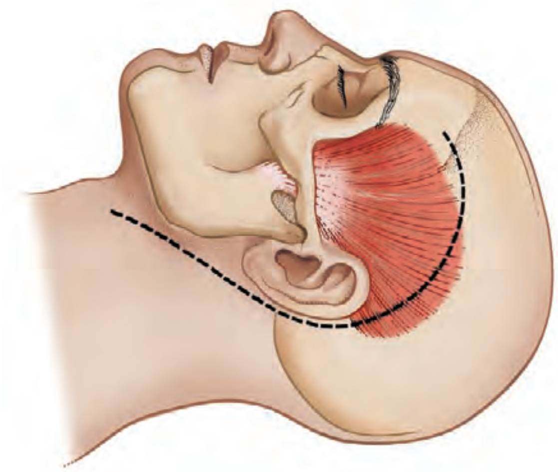

Figure 6.226 The incision provides exposure for a temporal craniotomy, and it also provides exposure of the petrous temporal bone and upper part of the neck.

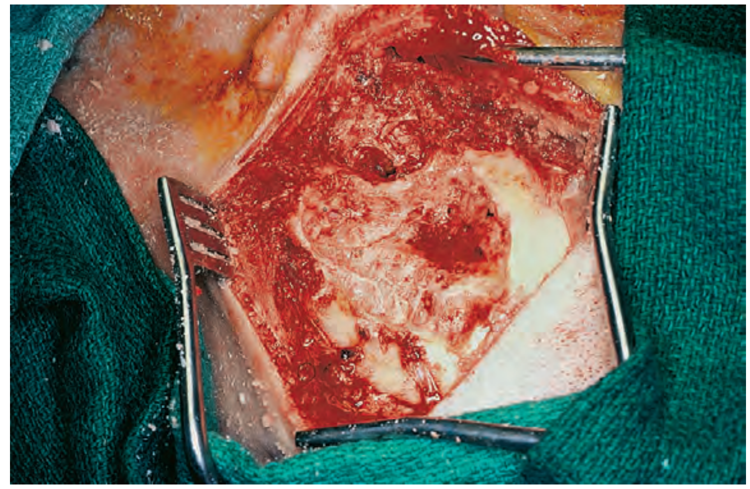

Figure 6.229 The temporal bone is drilled as far back as 1 cm posterior to the sigmoid sinus, inferiorly up to the tip of the mastoid process, and anteriorly, as far as the root of the zygoma.

The incision on the postauricular skin has been taken and deepened through the soft-tissue attachments to expose the mastoid process (Fig. 6.227). The cartilaginous portion of the auditory canal is retracted with the external ear anteriorly (Fig. 6.228). Elevation of the posterior scalp flap is taken up to the mastoid emissary vein.

Figure 6.227 The skin incision is deepened through the soft tissues to expose the mastoid process.

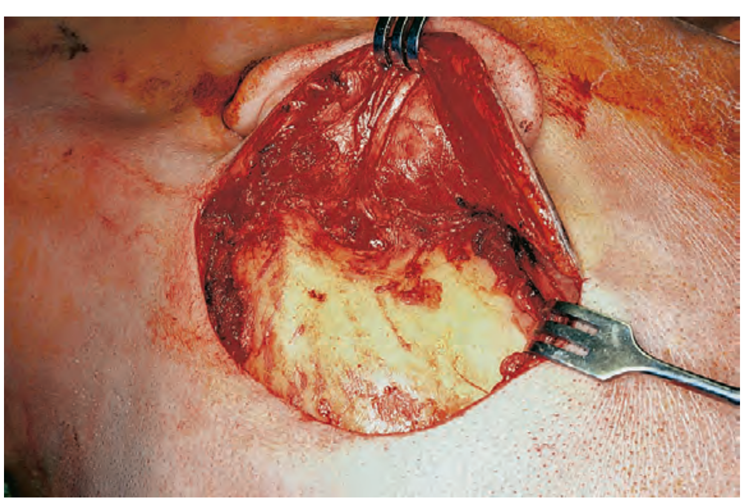

Figure 6.228 The cartilaginous portion of the auditory canal is retracted with the external ear anteriorly.

Self-retaining retractors are now placed and a mastoidectomy is performed, using a high-speed drill with a fine burr and suction irrigator equipment. The cortex of the temporal bone in this area is first drilled as far back as approximately 1 cm posterior to the sigmoid sinus, inferiorly up to the tip of the mastoid process, and anteriorly as far as the root of the zygoma (Fig. 6.229). Medially the drilling is first directed toward the antrum, which is identified, as is the horizontal semicircular canal.

At this point, the edges of the mastoidectomy cavity are saucerized with a high-speed drill, and the mastoidectomy is carried further to expose the sigmoid sinus along its entire length down to the level of the jugular bulb (Fig. 6.230). The facial nerve is still protected in its canal and is not visualized. The landmarks identified at this point are the short process of the incus and the digastric ridge inferiorly. The posterior fossa is also exposed along the sigmoid sinus up to the level of the posterior semicircular canal. However, a thin shell of bone is left over the semicircular canal and the entire length of the sigmoid sinus. The area of the jugular bulb is now identified, and no tumor can be seen as yet at that level (Fig. 6.231).

At this stage, the intracranial portion of the operative procedure is held and the C-shaped incision is extended into the upper part of the neck. The anterior and posterior skin flaps are elevated. The anterior border of the sternomastoid muscle is identified and is retracted posteriorly to expose the carotid bulb; the internal jugular vein; and the hypoglossal, vagus, superior laryngeal, and glossopharyngeal nerves (Fig. 6.232). Rubber tapes are placed around each of these structures, with particular attention being paid to achieving control of the left internal jugular vein. Note that the white rubber tapes are around the hypoglossal, vagus, and accessory nerves; the blue tape is around the internal jugular vein; and the red tape is around the internal carotid artery. Upon palpation of the jugular vein near the jugular foramen, a firm tumor could be felt in its lumen. Because this patient has a history of breast cancer, it was mandatory to establish a tissue diagnosis before proceeding further with the surgical procedure for removal of the “glomus tumor.” A vascular clamp is therefore applied on the jugular vein at the jugular foramen, and a vessel loop is placed lower down in the neck around the vein.

The vein is then opened, showing the tumor in the lumen of the jugular vein (Fig. 6.233). A small wedge from the tumor

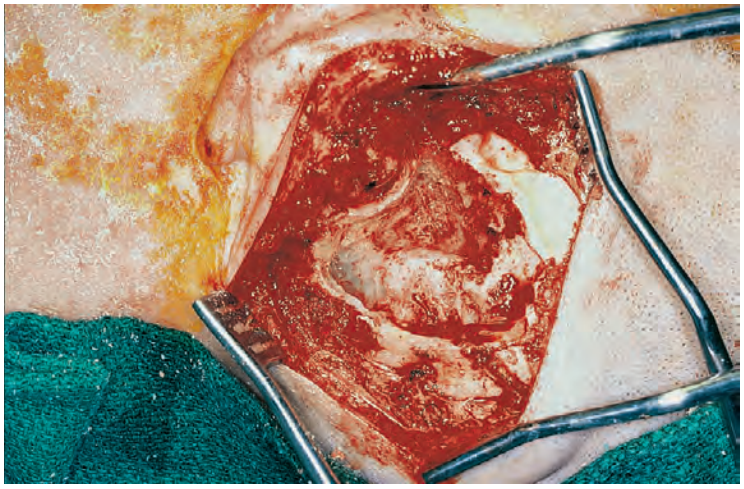

Figure 6.230 The edges of the mastoidectomy cavity are saucerized with a high-speed drill and the mastoidectomy is carried further to expose the sigmoid sinus along its entire length down to the level of the jugular bulb.

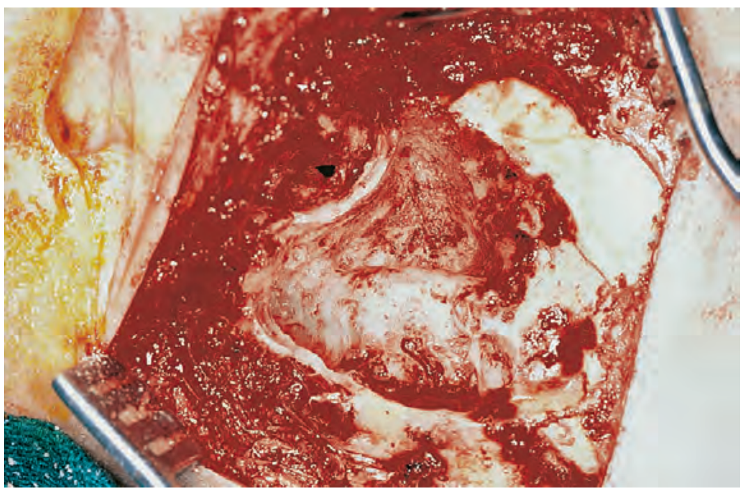

Figure 6.231 The area of the jugular bulb is identified, and no tumor can be seen as yet at that level.

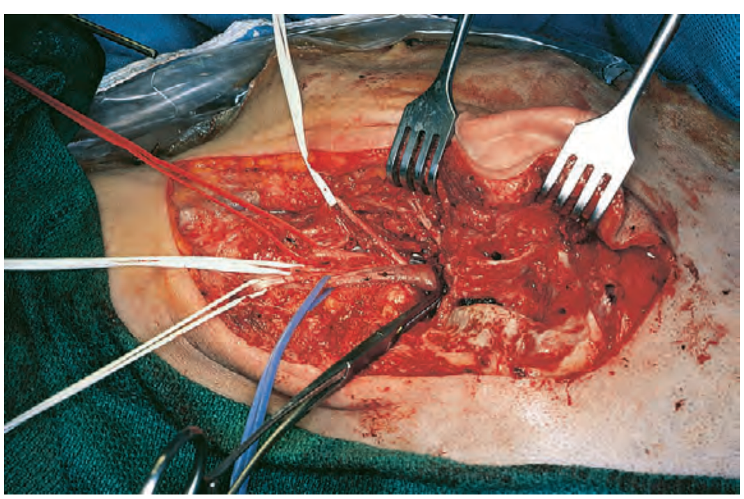

Figure 6.232 The anterior border of the sternomastoid muscle is identified and is retracted posteriorly to expose the carotid bulb; the internal jugular vein; and the hypoglossal, vagus, superior laryngeal, and glossopharyngeal nerves.

was removed and sent for frozen-section examination. The diagnosis of a paraganglioma was confirmed. The vein is therefore ligated below the presenting tumor and divided, and the vascular clamp is removed. A superficial parotidectomy is then performed and the main trunk and peripheral branches of the facial nerve

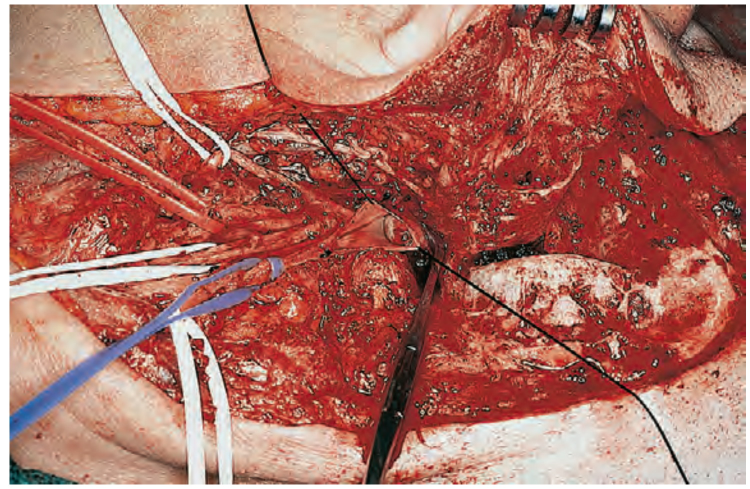

Figure 6.233 The tumor is clearly seen as it presents itself in the lumen of the jugular vein.

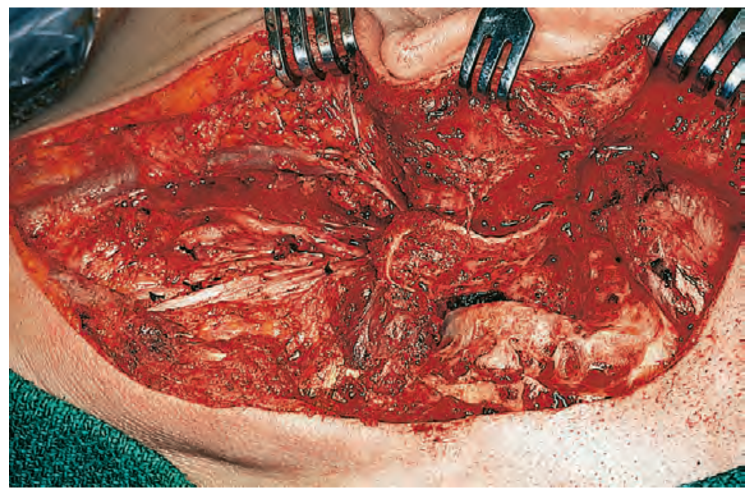

Figure 6.234 A superficial parotidectomy is performed and the main trunk and peripheral branches of the facial nerve are identified and dissected to expose the main trunk at the stylomastoid foramen.

are identified and dissected to expose the entry of the main trunk into the stylomastoid foramen (Fig. 6.234).

Attention is now directed back to the intracranial portion of the operative procedure. The cartilaginous ear canal is transected and reflected anteriorly, and the posterior canal wall is removed. The tympanic membrane is dissected off the malleus. The incusostapedial joint is dislocated and the incus is freed from its junction with the malleus and removed, after which the malleus is also removed with use of a cup forceps. All of this is done to prevent transmission of vibrations through the ossicles to the inner ear. The facial nerve is then identified along its entire course after drilling the bone around the facial canal to identify it from the geniculate ganglion superiorly and down to its exit through the stylomastoid foramen inferiorly. With use of a diamond burr all around the facial canal, the bone is removed from nearly 270 degrees around the canal, leaving a very thin covering that is removed with use of curettes and hooks. The nerve is thus dissected through its full length, and the deep branch of the chorda tympani and the stapedius branches are cut. The nerve is carefully elevated from its exit through the stylomastoid foramen and from the surrounding structures using sharp dissection to minimize traction, and it is carefully removed from its fallopian canal with use of blunt and sharp dissection where necessary. The entire dissection of the facial nerve requires the use of the operating microscope, a high-speed drill with a diamond burr, and a suction irrigator.

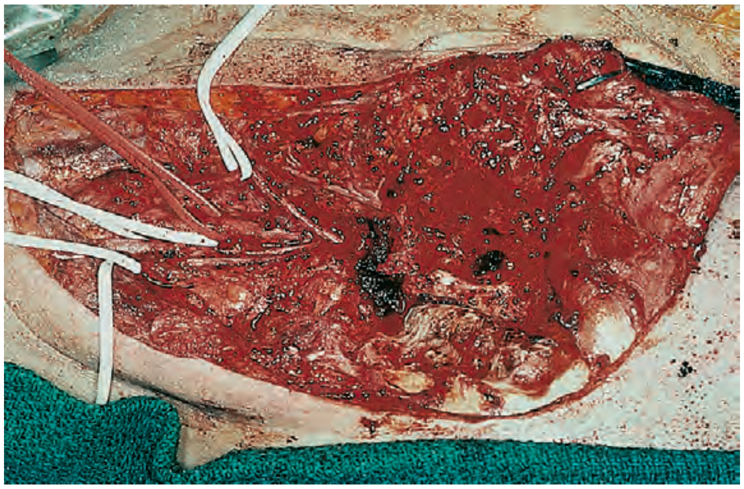

Figure 6.235 The nerve is rerouted both anteriorly and superiorly, leaving no nerve structure in the bone between the mastoid, the hypotympanum, and the jugular foramen.

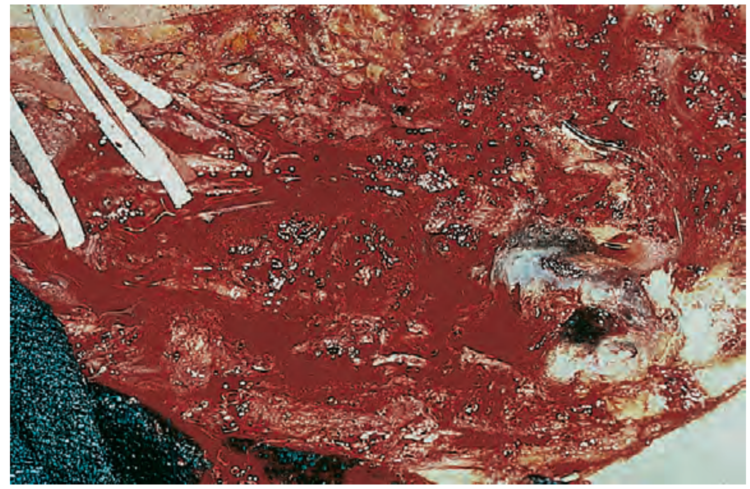

Figure 6.237 The tumor is dissected off from the carotid artery and also from all the nerves that leave the skull through the jugular foramen.

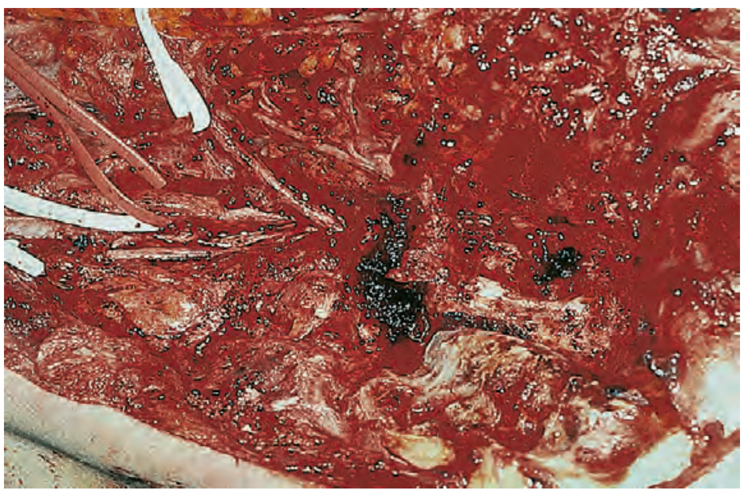

Figure 6.236 Dissection of the stump of the jugular vein along with the contents of the sigmoid sinus, including the intravascular tumor, is undertaken.

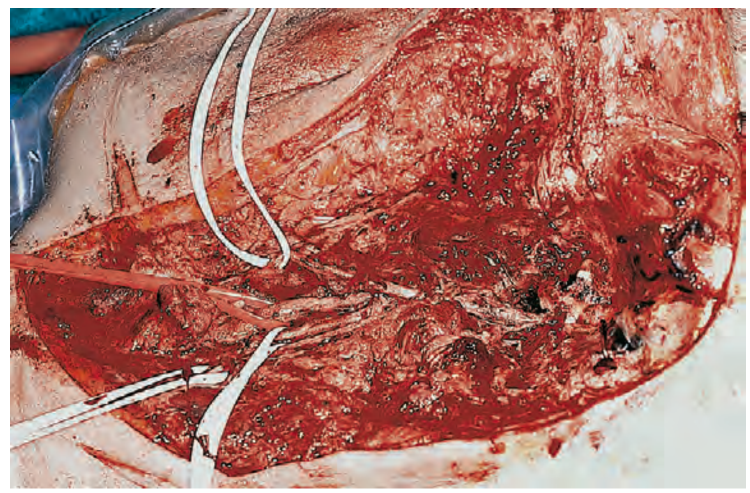

Figure 6.238 Cranial nerves exiting from the jugular foramen are carefully preserved.

Dissection and removal of the nerve continue up to the geniculate ganglion.

Following this maneuver, the nerve is rerouted both anteriorly and superiorly, leaving no nerve structure in the bone between the mastoid, the hypotympanum, and the jugular foramen (Fig. 6.235). After identification of the posterior semicircular canal, the bone is drilled out from that level to the area of the jugular foramen, and the mastoid tip is taken out with use of rongeurs. The lateral lip of the carotid canal is also removed with use of Kerrison forceps. At this point, distal but not proximal control of the jugular vein is secured. Therefore the thin shell of the bone over the sigmoid sinus is drilled out and peeled off the sigmoid sinus. Incisions in the dura are made on each side of the sigmoid sinus, a blunt needle is passed along the medial surface of the sinus, and a large vascular clip is applied through the dural holes. The dural openings are sutured with 4-0 Nurolon sutures. The lateral wall of the sigmoid sinus is then opened and followed to the area of the jugular bulb. Some bleeding is encountered at this time, but the sinus is packed distally with Gelfoam.

Dissection of the stump of the jugular vein along with the contents of the sigmoid sinus, including the intravascular tumor, is then undertaken (Fig. 6.236). When the sigmoid sinus is opened, some bleeding is to be expected from the inferior petrosal sinus, which is packed with muscle. In this patient, tumor extension was found beyond the vein in the area anterior and medial to the jugular bulb. The tumor is then dissected off from the carotid artery and also from all the nerves that leave the skull through the jugular foramen (Fig. 6.237).

Gross total removal of the tumor is thus accomplished. The surgical field shows the open area of the excised sigmoid sinus and the jugular foramen with its lateral lip missing. Cranial nerves exiting from the jugular foramen are carefully preserved (Fig. 6.238). The proximal part of the sigmoid sinus, which has been clipped, is also seen. The wound is reinspected for bleeding and then irrigated.

Figure 6.239 A suction drain is placed through a separate stab incision, and the skin incision is closed in layers.

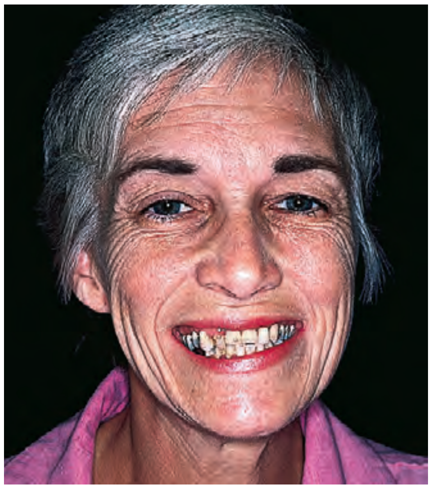

Figure 6.240 Postoperative appearance of the patient 5 months following surgery.

Figure 6.241 A malignant schwannoma arising in the suboccipital region with extension to the base of the posterior cranial fossa.

The rerouted facial nerve is placed over the zygomatic bone, and the incision is closed. The posterior aspect of the auditory canal is closed with a suture in the soft tissues to create a blind sac of the auditory canal. All the vessel loops around the identified nerves and vessels are removed. A suction drain is placed through a separate stab incision, and the skin incision is closed in layers (Fig. 6.239).

The appearance of the patient 5 months following surgery shows complete recovery of the facial nerve function, which was transiently paretic (Fig. 6.240).

Excision of glomus jugulare tumor is a complex surgical procedure demanding a high degree of technical expertise and great familiarity with the anatomy of this area. Radiographic findings of a CT scan should be correlated with the skull before the surgical procedure, and a skull should always be available in the operating room for orientation during surgery if necessary. The intracranial part of the operative procedure should be undertaken by a neurosurgeon or a neurootologist.

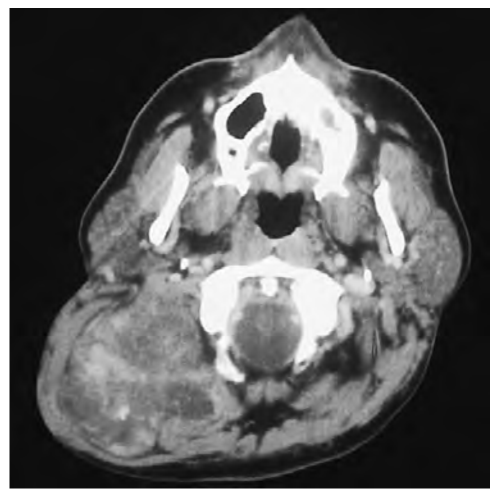

Figure 6.242 An axial view of the computed tomography scan at the level of the upper alveolus.

Resection of a Neurogenic Tumor Involving the Base of the Posterior Cranial Fossa

Extracranial tumors that extend to involve the base of the posterior cranial fossa are exceedingly rare. The patient shown in Fig. 6.241 has a malignant schwannoma arising in the suboccipital region with extension to the base of the posterior cranial fossa. The axial view of the CT scan at the level of the upper alveolus shows a massive soft tissue tumor in the apex of the posterior triangle of the neck adjacent to the vertebral column (Fig. 6.242). A coronal view of the CT scan demonstrates invasion of the skull base posterior to the mastoid process (Fig. 6.243). The surgical approach for resection of this massive soft-tissue tumor requires a posterior fossa craniotomy with meticulous dissection through the musculature in the posterior aspect of the neck to achieve a monobloc resection. Because of two previous skin incisions for biopsy purposes performed elsewhere, a generous portion of the overlying skin had to be sacrificed in this patient, as outlined in Fig. 6.244. A reverse U-shaped incision is then extended from the tip of the mastoid process up to the midline of the occiput to provide exposure for a posterior fossa craniotomy.

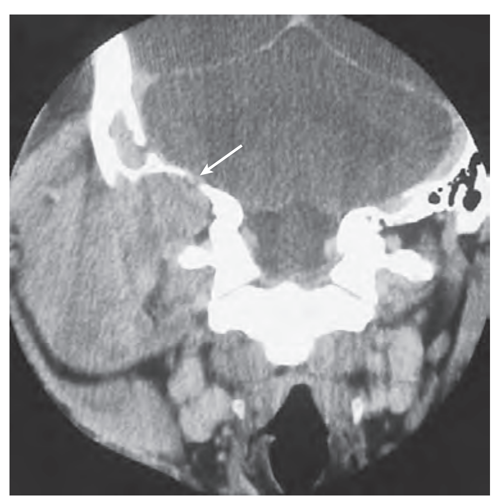

Figure 6.243 A coronal view of the computed tomography scan shows invasion of the skull base posteroinferior to the mastoid process.

The craniotomy is performed first by elevation of the posterior scalp flap and with multiple burr holes, which are connected with a high-speed side-cutting drill. Because the tumor had involved the bone, a craniectomy was performed by careful elevation of the underlying dura. At one point, intracranial extension of the tumor through the lateral aspect of the occipital bone was encountered, and therefore a portion of the dura overlying this tumor was resected (Fig. 6.245). A close-up view of the site of resection of the dura demonstrates a dural defect, which is repaired with use of a free pericranial graft (Fig. 6.246).

Figure 6.244 A generous portion of the overlying skin is sacrificed as a result of previous biopsy incisions.

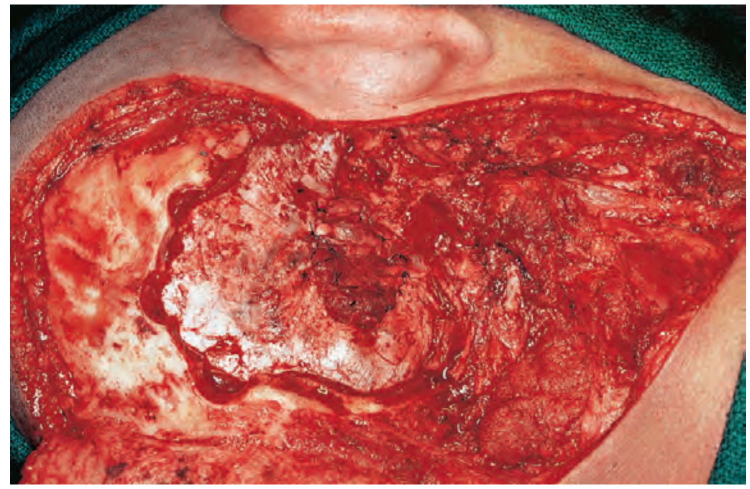

Figure 6.245 A portion of the dura overlying this tumor is resected.

Following complete circumferential division of the calvarium, all the other soft-tissue attachments around the tumor are divided with use of an electrocautery up to the lateral and posterior aspects of the vertebral column. Because no important neurovascular structures are located in the posterior triangle of the neck, this dissection proceeds rather expeditiously. The surgical specimen demonstrates a monobloc resection of the tumor, including the overlying skin, the adjacent musculature, and the underlying calvarium (Fig. 6.247). The intracranial surface of the surgical specimen shows a tumor nodule perforating through the calvarium to involve the dura (Fig. 6.248). The surgical defect in this patient was repaired with use of a posterior vertical trapezius myocutaneous flap. The appearance of the patient 6 weeks following surgery is shown in Fig. 6.249.

Monobloc resection of tumors involving the skull base in the posterior fossa can be safely accomplished by a two-team surgical approach consisting of a neurosurgeon and a head and neck surgeon. Depending on the extent and location of the surgical defect, a microvascular free flap of skin and soft tissue may be required to repair the site of resection.

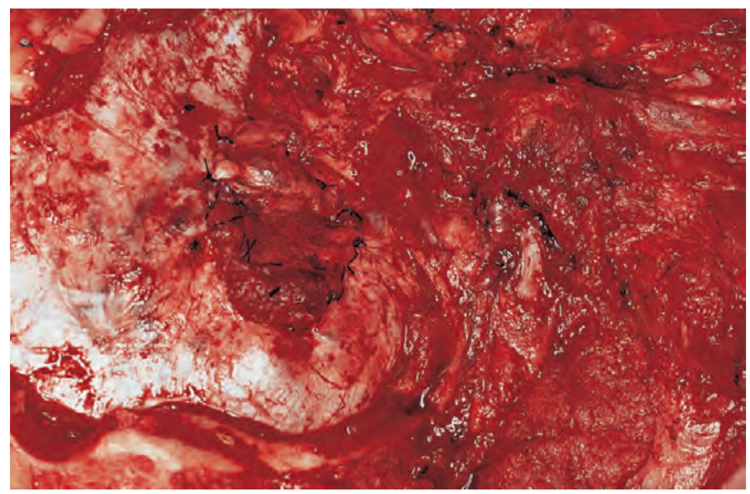

Figure 6.246 A close-up view of the site of resection of the dura, which is repaired with a pericranial graft.

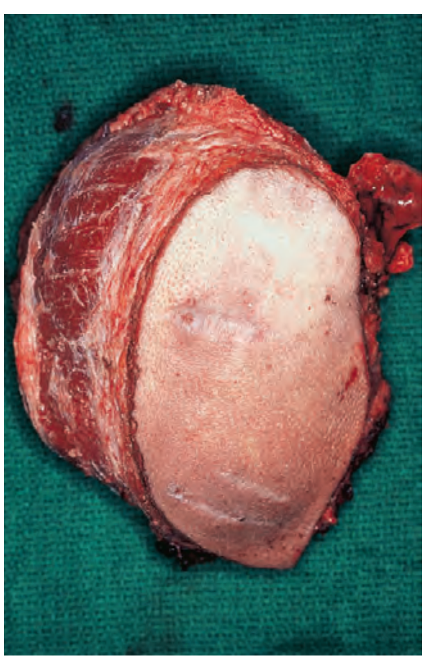

Figure 6.247 The surgical specimen is removed in a monobloc fashion.

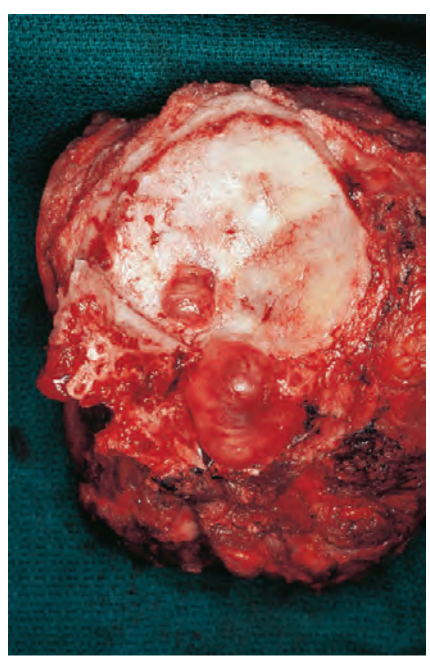

Figure 6.248 The intracranial surface of the surgical specimen showing dural invasion by a tumor.

Figure 6.249 The postoperative appearance of the patient showing repair of the surgical defect with a posterior trapezius myocutaneous flap.

POSTOPERATIVE CARE

Neuromonitoring

The postoperative care for patients undergoing resection of tumors at the skull base requires a combination of criteria used for patients undergoing craniotomy and those applied to patients undergoing major head and neck surgery. The fluid management approach during surgery continues in the immediate postoperative period, keeping the patient on the "dry" side to avoid an overload of fluids. Once the patient wakes up from anesthesia, neuromonitoring is important in immediate postoperative care. During the first few days, the patient is maintained on strict vigilance in a neurosurgical intensive care unit, if one is available. In the absence of such a unit, patients are monitored with vigilant nursing care, and neurologic parameters such as level of consciousness; orientation to time, space, and events; size of pupils; reflexes and movement of extremities are monitored. If an indwelling spinal drain is used, the drainage is connected to a gravity drainage system with controlled drainage of the CSF to maintain acceptable levels of intracranial pressure and avoid headache. To this end, patients are kept in a 180-degree recumbent position for the first 48 hours, and thereafter the head is gradually elevated to 15 degrees, 30 degrees, and 45 degrees for several hours at each level of elevation before allowing the patient to sit up. In many patients the indwelling spinal catheter can be removed at the end of the surgical procedure. However, in patients in whom the indwelling spinal drain is retained, it is usually removed in approximately 48 hours. Headache manifested by increased intracranial pressure requires retention of the indwelling spinal drain for a longer period, and it is appropriately monitored to make a decision regarding the optimal time for removal of the drain. Corticosteroids are used to reduce brain edema intraoperatively and are tapered off over several days in the postoperative period.

Antibiotics

The choice of antibiotics in the perioperative period is dictated by the nature of the surgical procedure. For patients in whom contamination of the cranial cavity with secretions from the upper aerodigestive tract is likely to take place, wide-spectrum antibiotic coverage is necessary. The authors have found the combination of vancomycin, ceftazidime, and metronidazole to be optimal based on a retrospective review of wound cultures and significant reduction in wound sepsis following use of this combination. This combination has been used as a prophylactic regimen for patients undergoing craniofacial surgery since 1996 at Memorial Sloan Kettering Cancer Center in New York. Administration of the antibiotics is started at the beginning of the operation, and use of the antibiotics is maintained as long as the risk of contamination of the cranial cavity from the nasal air passages is present. In patients who have nasal packing, we prefer to continue the antibiotic regimen until the packing is removed. In general, antibiotic coverage is continued for at least 7 days.

Nasolacrimal Drainage

For patients who have disruption of the nasolacrimal drainage system, appropriate eye care is necessary. Epiphora leading to dryness of the cornea and conjunctival irritation poses a risk for corneal damage. Instillation of eyedrops of methyl cellulose solution during the day and of a similar ointment during the night maintains moisture in the conjunctival sac, reducing the risk of corneal dryness and injury. When the nasolacrimal duct is resected, an indwelling nasolacrimal stent is placed at the time of surgery to retain a natural draining passage for tears and to reestablish epithelialization of a neonasolacrimal duct tract.

Wound Care

Patients undergoing surgery for tumors in the nasal cavity or paranasal sinuses often will be breathing through the oral cavity and thus will experience significant dryness and crusting of the nasal cavity. Whether or not a packing is used in the nasal cavity, crusting after surgery is an expected sequela of procedures in the nasal cavity and paranasal sinuses. Therefore extensive humidification of the air is necessary to reduce dryness, crusting, and bleeding. Humidity in the inhaled air is provided with a facial tent or a mask connected to a nebulizer for humidification. Similarly, irrigations with saline solution in the nasal cavity or oral power sprays of saline solution and mechanical hydrodebridement of the suture line in the oral cavity are crucial to maintaining optimal hygiene at the site of the wound in the oral cavity or nasal cavity. Care of the suture line in the oral cavity or the operated side in the nasal cavity minimizes the risk of suture line sepsis and promotes primary healing.

Airway

Most patients undergoing craniofacial surgery have an intact orotracheal airway. However, a tracheostomy may be necessary to prevent pneumocranium (free air in the cranial cavity), which may occur if the patient strains, sneezes, or has violent coughing in the postoperative period.

Other Postoperative Care

Pulmonary care for prevention of pneumonia and routine prophylaxis for deep vein thrombosis are used while the patient is still confined to bed and early ambulation is not feasible. Once the patient is able to sit up, gradual progressive ambulation is encouraged, with the goal of having the patient fully ambulatory by the fifth to seventh postoperative day.

When the surgical intervention involves the masticator space or temporomandibular joint, the development of trismus is a risk. Initially trismus develops because of spasm of the muscles of mastication resulting from postoperative pain and discomfort, and later, trismus occurs as a result of fibrosis around the temporomandibular joint and the masticator group of muscles. Therefore exercises of the jaw are initiated in the early postoperative period, and the patient is instructed to self-execute jaw exercises during the recovery phase. Mechanical devices for prevention and/or improvement of trismus are available and should be used when indicated.

OUTCOMES

The development of open craniofacial surgery for management of malignant diseases of the nasal cavity and paranasal sinuses approaching or involving the skull base has significantly improved the prognosis of patients with such tumors. Because a variety of malignant tumors arise in this region with varying natural histories, a meaningful reporting of survival or disease control is difficult. No one individual or single institution has a sufficient number of patients at each site and in each histologic

group to have meaningful data. Therefore an International Collaborative study from 17 contributing centers was undertaken to provide a large database of more than 1500 patients. The outcomes presented here are from that study. An overall 5-year survival of approximately 60% is observed for patients undergoing open craniofacial resections for malignant tumors of all histologies and all stages involving the anterior skull base (Fig. 6.250). Survival is directly affected by the extent of disease and the histologic type and grade of the tumor. Patients with low-grade tumors experience excellent disease control and survival, whereas patients with high-grade tumors have an unfavorable prognosis. Excellent cure rates are observed in patients with esthesioneuroblastomas and localized adenoid cystic carcinomas. On the other hand, undifferentiated carcinomas and mucosal melanomas have a poor prognosis. Squamous carcinomas, minor salivary gland carcinomas, and high-grade sarcomas have an intermediate prognosis, with 5-year survival in approximately 50% of patients (Fig. 6.251). Patients whose tumors involve the dura have an unfavorable prognosis compared with those in whom no dural invasion is identified (Fig. 6.252). Complete surgical resection with negative surgical margins is a favorable prognostic indicator (Fig. 6.253). Independent predictors of prognosis in patients undergoing craniofacial resection are listed in Table 6.1.

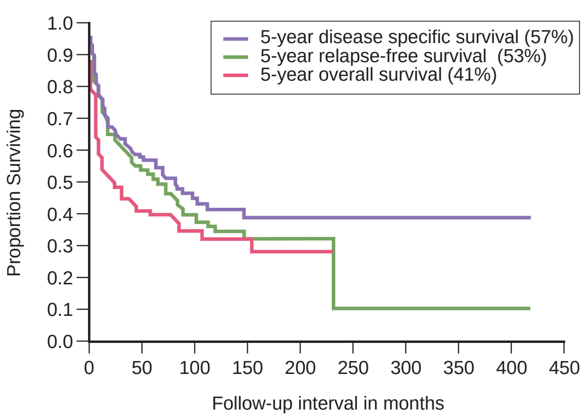

Figure 6.250 Overall survival rates for persons with malignant tumors involving the anterior skull base who undergo craniofacial resection.

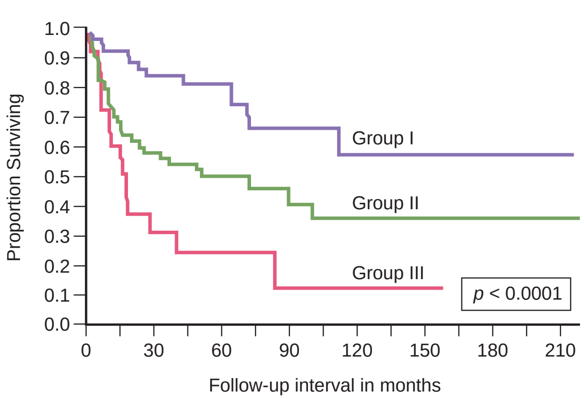

Figure 6.251 Survival by histologic group. Group I: Esthesioneuroblastomas, localized adenoid cystic carcinomas, and low-grade sarcomas. Group II: Squamous cell carcinomas, adenocarcinomas, high-grade sarcomas, and minor salivary gland carcinomas. Group III: Undifferentiated carcinomas and mucosal melanomas.

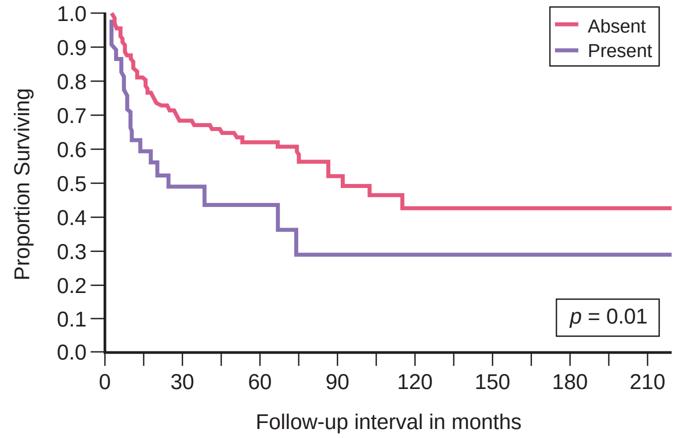

Figure 6.252 The impact of dural invasion on the survival of patients who undergo a craniofacial resection.

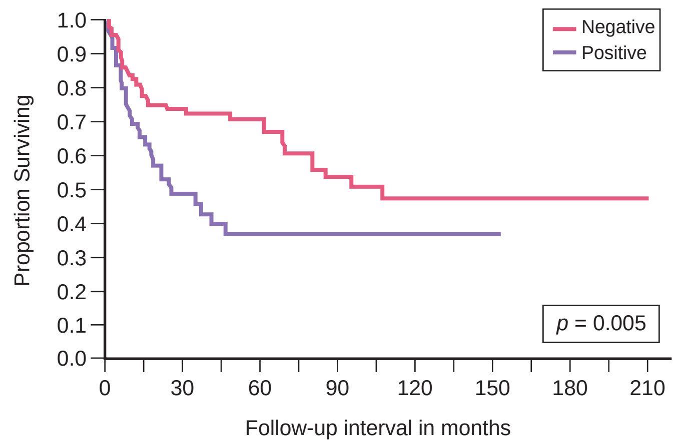

Figure 6.253 The impact of surgical margin status on survival.

Table 6.1 Independent Predictors of Prognosis in Patients Who Undergo Open Craniofacial Resection

FACTOR	*P* VALUE
Surgical margins	0.04
Dural invasion	0.04
Histology of primary tumor	0.001
Intraorbital extension	0.05

During the past two decades, increasing interest and development in endonasal endoscopic resections of tumors of the anterior skull base has led to the development of centers of excellence, where significant experience and expertise is available. A large experience at these centers is reported on endonasal surgery for benign tumors and tumors of the nasal cavity. However, even in these centers of excellence, experience with malignant tumors is limited. With properly selected patients, technically-adequate surgical resection is feasible, and emerging data is available to show tumor control rates comparable to open surgical procedures in similar cases. The crucial factors for successful outcome for endonasal endoscopic resections are stringent case selection, favorable histology, limited extent of disease, accessible locations, the ability to secure negative margins, and technical expertise in endoscopic surgery are the factors that impact upon successful outcome.

CHAPTER 7

Lips

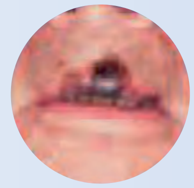

The lips, which are located at the entrance to the alimentary tract, are essential for a variety of complex tasks, including articulation of speech, facial expression, and the oral phase of deglutition. The anatomic structure of the lips is complex; they consist of skin, mucosa, minor salivary glands, muscles, and neurovascular structures. Accordingly, a variety of neoplasms can arise in the lips from these structures. Because sun exposure is the most prominent risk factor, epithelial neoplasms are by far the most common cancers involving the lips. Therefore fair-skinned persons and those living in the sun belt have the highest risk for lip cancers. This risk can be as high as 13.5 per 100,000 people. Although lip cancers develop in men more frequently than women, changing behaviors with regard to sun exposure have resulted in an increase in the proportion of women with lip cancer in many parts of the world.

The lower lip is the most frequent site for cancers. Only 7% of lip cancers arise in the upper lip, and 4% arise at the oral commissure (Fig. 7.1). Most cancers occur in the lower lip because compared with the upper lip, the projecting vermilion border of the lower lip receives more sun exposure. Other factors that contribute to the risk of lip cancer include alcohol and tobacco use, especially when direct contact with tobacco is present, as with pipe and cigar smoking.

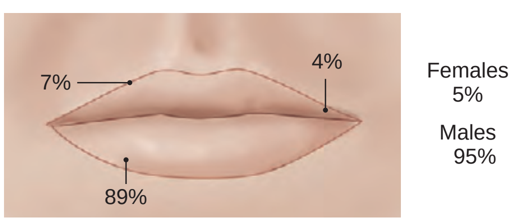

Figure 7.1 Site and gender distribution for squamous cell carcinoma of the lips.

Squamous cell carcinoma is the most common malignant tumor of the lips (95%). The site allocation and staging criteria for lip cancers have been recently revised. In the past the lips were included as one of the primary sites in the oral cavity; however, the clinical behavior of most lip cancers is closer to that of skin cancers than it is to that of the oral mucosa. Therefore in the most recent revision of the American Joint Committee on Cancer (AJCC) and the International Union Against Cancer (UICC) staging system (eighth edition), the lips are divided in two separate regions (Fig. 7.2). The visible vermilion border covered by keratinizing squamous epithelium, or the "dry vermilion," is staged according to the criteria for skin cancers. The lip mucosa that is in contact with each other (the lower and upper lip) and extending further on the labial mucosa, also called the "wet vermilion," or mucusola lips containing minor salivary glands is staged as one of the sites in the oral cavity (Fig. 7.3). Basal cell carcinomas, melanomas, and minor salivary gland cancers represent the next most common primary neoplasms of the lip. Soft tissue sarcomas are exceedingly rare.

EVALUATION

Clinically, epithelial cancers of the visible vermilion border of the lip have a characteristic exophytic cauliflower-like or ulcerated, endophytic nodular appearance. They have varying degrees

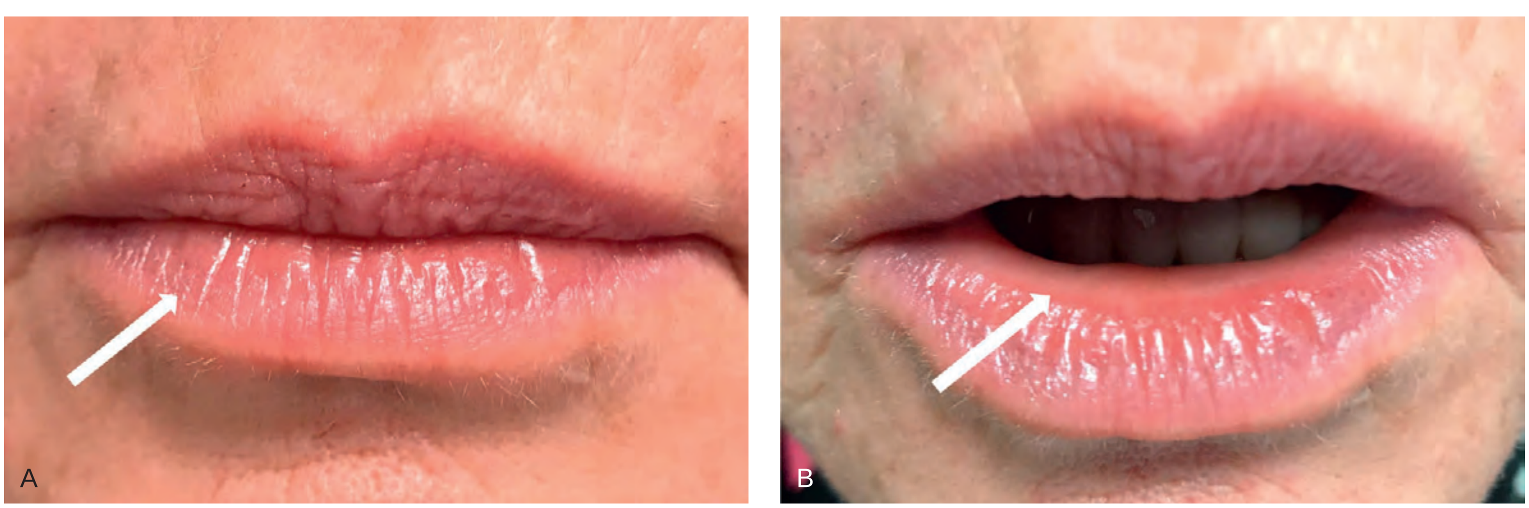

Figure 7.2 Demarcation between (**A**) vermilion (dry vermilion, *arrow*) and (**B**) mucosal lip (wet vermilion, *arrow*).

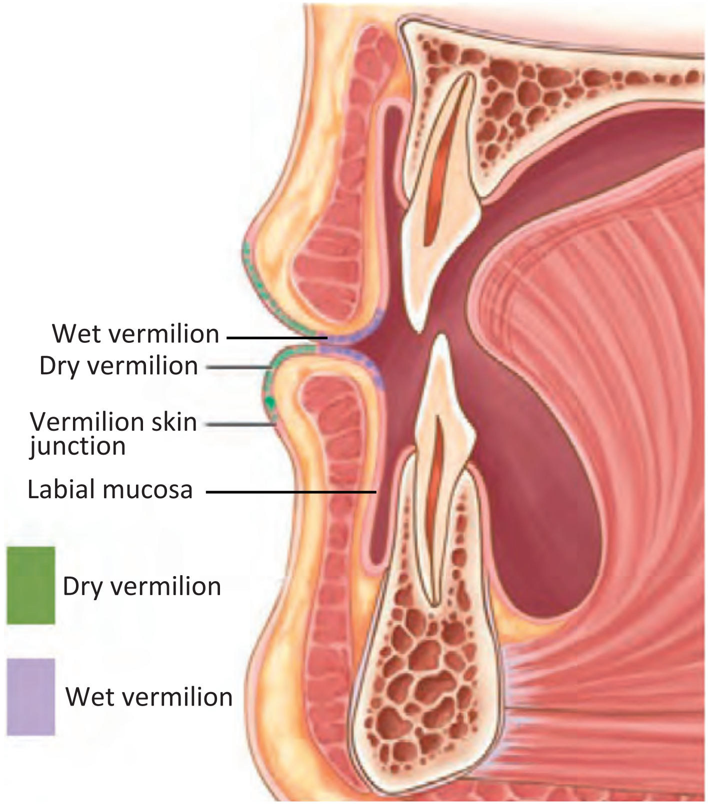

Figure 7.3 Sagittal section of the lips showing vermilion border (dry vermilion) and mucosal lip (wet vermilion).

Figure 7.4 Early stage (T1) squamous cell carcinoma of the lower lip.

Figure 7.5 A minor salivary gland adenocarcinoma of the upper lip.

Figure 7.6 A lymphangioma of the upper lip.

Figure 7.7 A malignant melanoma of the lower lip.

of infiltration of the underlying musculature and invasion of the overlying skin and/or labial mucosa (Fig. 7.4). Minor salivary gland tumors of the lip present as slow-growing nodular masses that may be subcutaneous or submucosal (Fig. 7.5). Soft tissue tumors also present as a subcutaneous or submucosal mass of varying consistency. Hemangiomas and lymphangiomas are characteristically soft and spongy in nature and usually manifest at an early age (Fig. 7.6). Melanomas of the vermilion border or mucosa of the lips are usually pigmented but also may be amelanotic (Fig. 7.7).

The lesion may involve a portion of the lower lip, the entire lower lip, the commissure of the oral cavity, or both the upper and lower lips (Figs. 7.8 through 7.11). Many well-differentiated squamous carcinomas are associated with varying degrees of hyperkeratosis and leukoplakia of the vermilion border. These pathologic changes also should be considered part of the lesion in surgical treatment planning.

The recently revised staging criteria for primary cancer of the external/visible/dry vermilion border of the lip are similar to those for skin cancers, and those for the nonvisible/wet vermilion and labial mucosa are similar to those for mucosal

Figure 7.8 An advanced carcinoma of the lower lip with deep infiltration of soft tissues and skin.

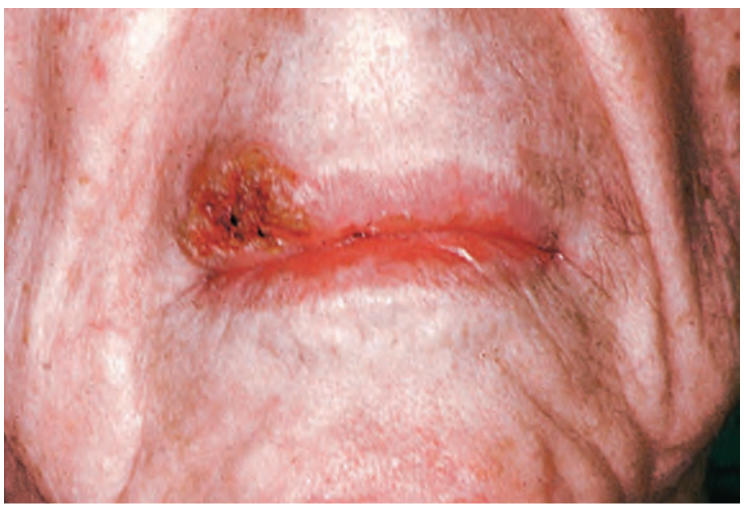

Figure 7.9 A squamous cell carcinoma of the upper lip adjacent to the commissure.

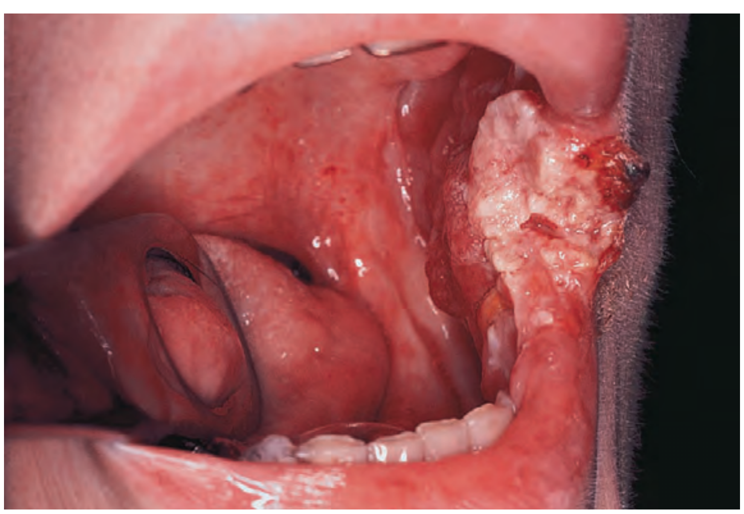

Figure 7.10 An exophytic, cauliflower-like carcinoma of the oral commissure.

cancers of the oral cavity (AJCC/UICC eighth edition Staging Manual). Most patients present with early-stage tumors. Only 10% of patients present with clinically palpable cervical lymph node metastasis. The stage distribution of patients with carcinoma of the lip at diagnosis is shown in Fig. 7.12.

Figure 7.11 A keratinizing squamous cell carcinoma of the oral commissure with extension to the upper and lower lips.

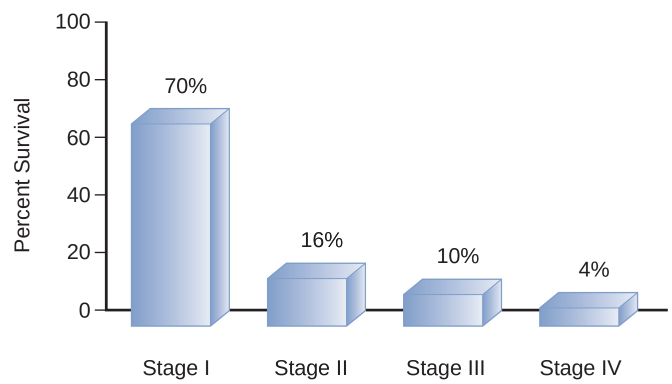

Figure 7.12 Stage distribution of squamous cell carcinoma of the lips. (Memorial Sloan Kettering Cancer Center data.)

Imaging

Radiographic workup of early-stage tumors of the lips is usually not required. However, advanced tumors of the lips, particularly those that are adherent to the adjacent bone, require radiographic evaluation to assess the extent of bone invasion. A high index of suspicion for invasion of the inferior alveolar nerve should be maintained for patients with numbness of the skin of the chin and lower lip. This phenomenon is most common in persons with neurotropic tumors, including adenoid cystic carcinoma, melanoma, and squamous carcinoma (Fig. 7.13). Therefore detailed radiographic evaluation of the mandible is vitally important in treatment planning. Panoramic radiographs of the mandible provide a good initial assessment of the bone and mandibular canal (Fig. 7.14). However, more detailed studies require a computed tomography (CT) scan or magnetic resonance imaging (MRI) for accurate delineation of the extent of bone invasion and for evaluation of invasion of the inferior alveolar canal or for demonstration of perineural invasion (Fig. 7.15). MRI is particularly helpful in assessing bone invasion through alteration in the bone marrow signal, whereby the normal fatty signal is replaced by grayish tumor infiltration (Fig. 7.16). Perineural invasion is demonstrated by enhancement of the inferior alveolar nerve on T2-weighted images. It also may show tumor extension through the foramen ovale into the middle cranial fossa.

TREATMENT

The obvious goal of therapy is long-term control of cancer with preservation of competency of the oral cavity and

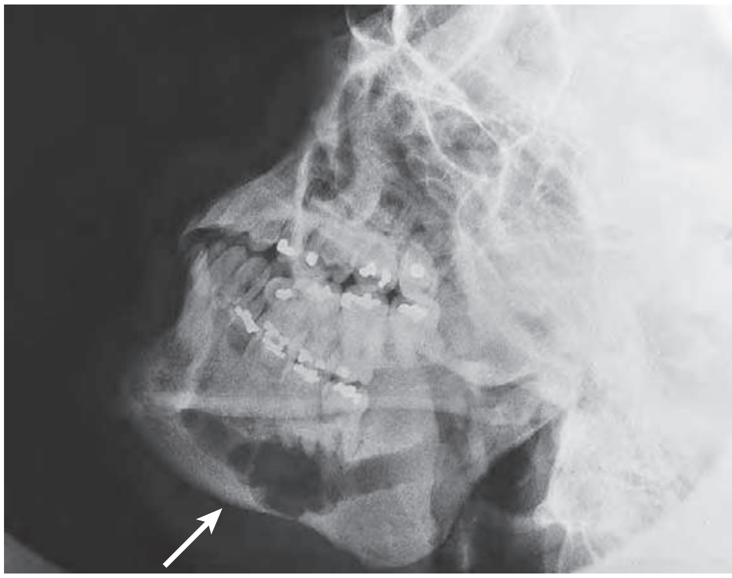

Figure 7.13 Invasion of the mandibular canal (*arrow*) seen on an oblique plain radiograph of the mandible.

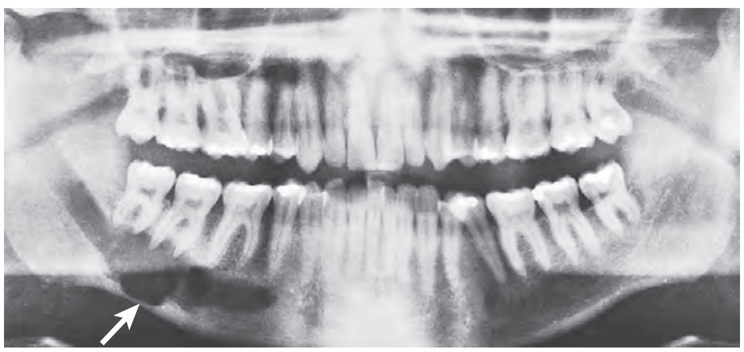

Figure 7.14 A panoramic radiograph of the mandible of the same patient in Fig. 7.13 shows invasion of the inferior alveolar nerve in the mandibular canal (*arrow*).

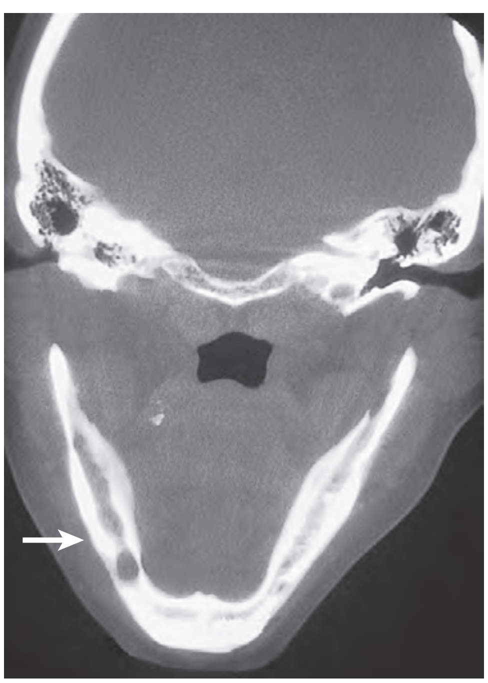

Figure 7.15 A computed tomography scan of the mandible of the same patient in Figs. 7.13 and 7.14 shows invasion of the inferior alveolar canal (*arrow*) by cancer.

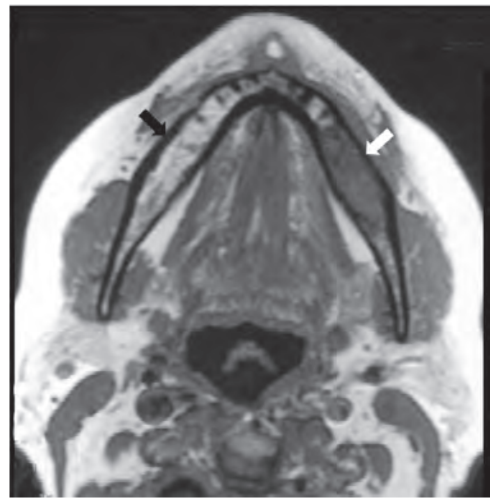

Figure 7.16 Magnetic resonance imaging showing bone marrow invasion by tumor. *Black arrow,* normal fat in bone marrow; *white arrow,* tumor in bone marrow.

Box 7.1 Factors Affecting Choice of Therapy

Tumor factors
- Size (T-stage) of the primary tumor
- Histology of the tumor
- Extent of lip resection necessary
- Availability of local tissues for reconstruction
- Anticipated aesthetic and functional outcome of reconstructive surgery

Patient factors
- Age
- General medical condition
- Compliance by the patient
- Cost and convenience of treatment

maintenance of aesthetic appearance of the lips. Small primary tumors of the lower or upper lip are very well controlled by either surgical excision or irradiation. Surgical excision for a small lesion is expeditious and leaves essentially no aesthetic or functional debility, even in the long term. In contrast, long-term sequelae of radiotherapy to the lip include atrophy of the skin and underlying musculature, resulting in indentation at the site of the primary tumor. Larger lesions require planned surgical resection with reconstruction, keeping in mind the aesthetics, function, and preservation of the nerve and blood supply to the remaining musculature of the lips to maintain facial expression. Although the lips have a rich lymphatic drainage to regional lymph nodes, metastatic dissemination is uncommon in early-stage tumors. Therefore elective treatment of regional lymph nodes is considered for only very advanced primary tumors.

Factors Affecting Choice of Treatment

The factors that affect the selection of initial therapy are related to the tumor and the patient (Box 7.1). Tumor factors include the T stage (particularly bone invasion in T4 tumors), histology, extent of dysplastic vermilion surface, depth of infiltration of the labial musculature, and involvement of the oral commissure.

In planning surgical treatment, preservation or restoration of oral competency and the size of the mouth opening as well as aesthetic appearance are crucial factors. These factors affect

the ability to eat, clarity of speech, and facial expression. Small superficial lesions are easily managed by a simple wedge excision with primary repair, with excellent preservation of lip function and aesthetic appearance. Larger lesions of the lip can pose a reconstructive challenge. In general, local flaps from adjacent skin and soft tissues and the opposite lip often provide sufficient tissue for an excellent functional and aesthetic outcome. More extensive lesions that involve a large volume of lip or invasion of the underlying bone often require a composite resection with reconstruction using a composite free flap.

Patient-related factors include the general medical condition of the patient with regard to the safety of anesthesia and surgery, particularly when a major composite resection with free flap reconstruction is required. The age of the patient is an important factor in considering surgical treatment. Unlike young patients, older patients generally have lax lips, which permit primary closure or reconstruction with local flaps.

RADIATION THERAPY

Definitive radiotherapy is equally effective as surgery in local control of early-stage epithelial malignancies of the lips such as basal cell and squamous cell carcinomas. However, radiotherapy is not effective in the treatment of melanoma, minor salivary gland carcinomas, and soft tissue tumors. In planning radiotherapy as definitive treatment, the status of adjacent dentition and the age of the patient are important considerations.

External beam radiation therapy with electrons generally is used for lesions confined to the skin and soft tissues of the lips. A therapeutic dose of 6600 cGy is delivered in conventional fractionation of 200 cGy per day in 33 treatments. Elective irradiation of regional lymph nodes is not recommended in early-stage tumors (T1 and T2). On the other hand, interstitial irradiation alone with iridium-192 implant also has been shown to be equally effective in local control of tumors of limited extent (Figs. 7.17 through 7.19). In spite of excellent local control, irradiation is generally not recommended as the preferred treatment because of the long-term sequelae of radiotherapy. Skin dryness, soft tissue atrophy, and indentation of the vermilion border at the site of the primary tumor often result in a suboptimal long-term outcome. Therefore radiotherapy is recommended only in select situations.

SURGICAL TREATMENT

Surgical Anatomy

The upper lip is formed by the fusion of lateral maxillary processes and a central nasofrontal process. This embryonic fusion leads to the presence of a central midline mass with two lateral larger segments. Because of the separation of the lateral segments, contralateral neck metastasis from upper lip cancer is exceedingly rare. On the other hand, the lower lip is formed by the fusion of two lateral mandibular processes in the midline, which puts lower lip cancers at increased risk of contralateral neck metastasis. Blood supply to the lips is provided by the superior and inferior labial arteries and branches of the facial artery on each side. The labial arteries form an arcade around the oral cavity in such a way that lesions in the lateral aspect of the lip receive blood supply both from its medial and lateral regions. Sensory supply to the skin and the vermilion border of the upper and lower lips is provided by the maxillary and mandibular divisions of the trigeminal nerve, respectively. Oral competency is the primary function of the orbicularis oris muscle, which also works in concert with the levators and depressors of the commissures to provide facial expression in addition to their contribution to oral competency. In surgical treatment planning, restoration of the purse-string function of the orbicularis oris muscle is crucial for maintaining oral competency. Muscular control of the orbicularis oris, the levators, and the depressors of the oral commissure is provided by the facial nerve. Lymphatic drainage of the lips is well defined and follows a predictable pattern for metastatic dissemination. Lesions of the lateral aspect of the upper lip first drain to buccal, periparotid, and prevascular facial lymph nodes overlying the body of the mandible. Lymph node metastasis occurs at level I in the submandibular triangle and then into the deep jugular chain. Lymphatics of the lower lip initially drain to lymph nodes at level I in the submental (Ia) and submandibular (Ib) regions and to the prevascular facial lymph nodes overlying the body of the mandible. Lymphatics of the lower lip often cross the midline and drain to the contralateral lymph nodes. Therefore bilateral metastasis to level I lymph nodes is not uncommon. Subsequent dissemination of metastatic disease occurs to deep jugular lymph nodes at levels II and III. Metastatic dissemination to level IV and level V is exceedingly rare.

Figure 7.17 A nodular squamous cell carcinoma of the lower lip with invasion of the skin.

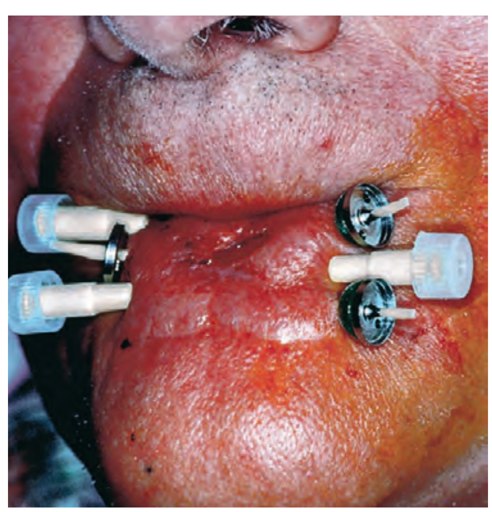

Figure 7.18 Treatment with iridium-192 after-loading interstitial implants.

Figure 7.19 Posttreatment result 1 year after therapy.

Surgical Approaches

The approaches for surgical resection of neoplasms of the lips are categorized by the methods used to restore the surgical defect. Thus they are (1) resection and primary closure, (2) resection and reconstruction with local flaps, and (3) resection and reconstruction with free tissue transfer. Limited lesions (T1 and T2) of the upper or lower lip are easily treated with a wedge resection and repaired with primary closure, particularly in older patients. Early stage lesions of the oral commissure require special consideration in reconstruction to avoid a rounded commissure. Lesions that create a surgical defect not suitable for primary closure by virtue of size or location require reconstruction with local flaps from adjacent skin and soft tissues or the opposing lip. Larger defects of the upper lip, lower lip, or commissure and composite defects, including the underlying mandible or maxilla, require complex reconstruction with composite free tissue transfer.

Procedures

Lower Lip

V Excision of the Lower Lip. Small superficial lesions involving the vermilion border and the underlying musculature of the lip are easily amenable to an elliptical excision that can be performed under local anesthesia with very gratifying aesthetic and functional results. It is important to remember that the natural skin creases on the vermilion border are in a radial direction along the circumference of the mouth (Fig. 7.20). Excision is therefore planned accordingly. The resulting scar virtually merges with the natural skin lines, resulting in a very pleasing aesthetic result. The patient shown in Fig. 7.21 has a squamous carcinoma involving the cutaneous surface of the lower lip with deep infiltration of the underlying musculature extending up to the submucosal plane on the labial aspect of the lower lip. A simple through-and-through V excision of the lower lip is planned to excise the lesion in a three-dimensional fashion (Fig. 7.22). The skin incision is performed with a scalpel to maintain sharp cut edges of the skin for accurate reapproximation of the vermilion border to acheive an acceptable aesthetic result. The remainder of the operation is completed with use of an electrocautery to minimize blood loss. The inferior labial artery must be carefully identified during excision and ligated. A through-and-through surgical defect is thus created (Fig. 7.23). Reapproximation of the surgical defect requires meticulous alignment of the vermilion border. A 5-0 nylon suture is placed initially at the mucocutaneous junction of the vermilion border, accurately aligning the vermilion edge. With traction on this suture, 3-0 chromic catgut interrupted sutures are placed in the subcutaneous tissue and muscular layer to approximate the orbicularis oris muscle and subcutaneous soft tissues. After this reapproximation, mucosal closure with interrupted 3-0 chromic catgut sutures starting from the gingivolabial sulcus up to the vermilion edge is performed. Finally, 5-0 nylon interrupted sutures are taken for the skin and the vermilion border. Accurate alignment of the vermilion edge results in a very pleasing aesthetic appearance (Fig. 7.24).

Lip Shave. The most important indications for a lip shave operation are areas of leukoplakia with keratosis and in situ or superficially invasive carcinomas. The entire vermilion surface of the lip may require excision for these entities. The operative procedure is likely to be successful if the diseased areas of the lip are confined to the wet and dry vermilion surfaces of the lip

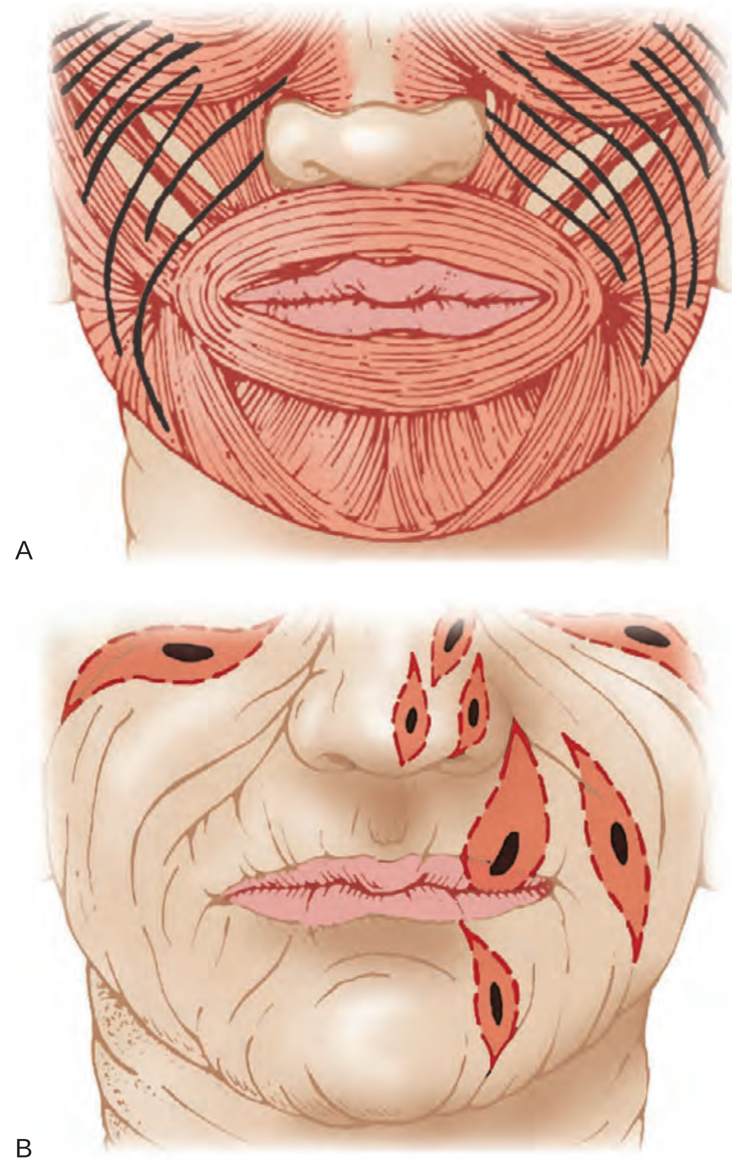

Figure 7.20 Natural skin creases around the mouth. **A**, The facial skin lines are at right angles to the underlying muscles of facial expression. **B**, Elliptical incisions along the skin lines produce optimal cosmetic results.

Figure 7.21 A squamous cell carcinoma of the skin involving the lower lip.

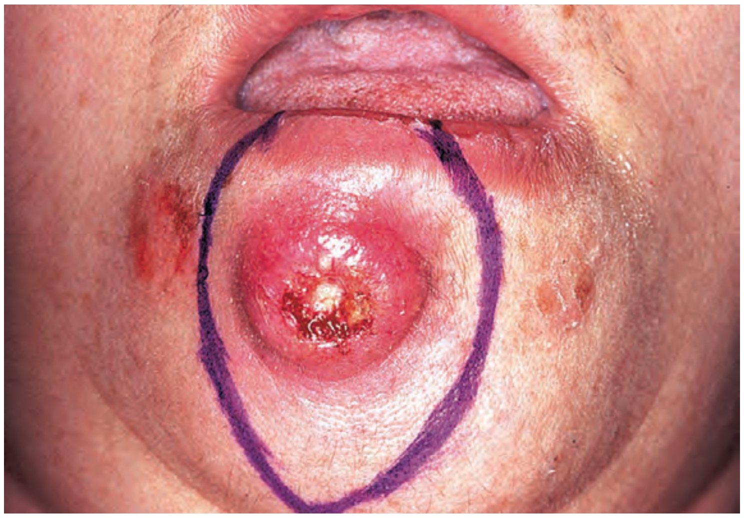

Figure 7.22 A simple V excision is outlined.

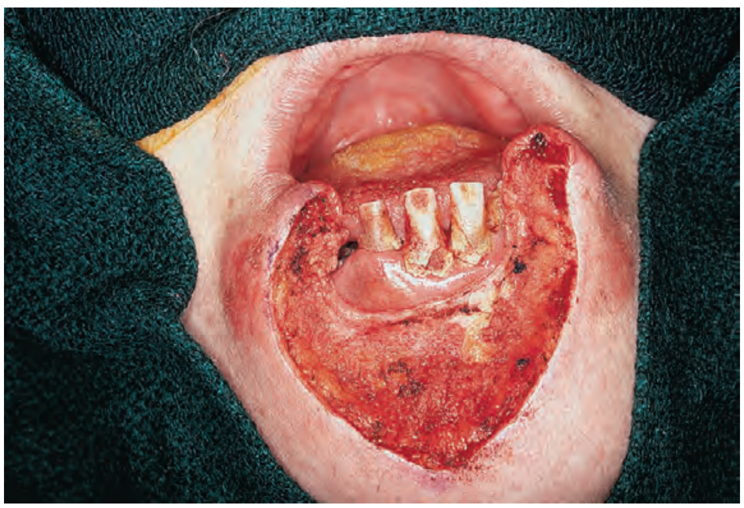

Figure 7.23 The through-and-through surgical defect.

Figure 7.24 Primary closure with accurate alignment of the vermilion edge.

on the vermilion border and are not of an infiltrating nature. Small and superficial limited regions of the vermilion mucosa can be excised by a lip shave procedure under local anesthesia. However, extensive lip shave procedures require administration of a general anesthetic to accomplish a satisfactory surgical resection with appropriate reconstruction using a bipedicled labial mucosal flap for restoration of the vermilion border. The patient

Figure 7.25 A hyperkeratotic superficially infiltrating squamous cell carcinoma of the lower lip.

Figure 7.26 The surgical defect.

shown in Fig. 7.25 presented with a hyperkeratotic superficial infiltrating squamous cell carcinoma involving nearly 80% of the vermilion border of the lower lip. Palpation revealed that the lesion had essentially no infiltrative component in the underlying musculature. An extensive lip shave procedure with resection of only a small amount of lip musculature is planned. The surgical procedure is performed under general anesthesia through a nasotracheal tube. Adequate excision of the vermilion border is performed through an extensive lip shave procedure in a monobloc fashion. The margins of the surgical defect must be checked by frozen section analysis to ensure adequate resection.

The surgical defect is shown in Fig. 7.26. The mucosa of the lower lip is now mobilized all the way up to the attached gingivolabial sulcus, keeping its blood supply intact through its lateral pedicles (Fig. 7.27). Thus the entire labial mucosa is mobilized throughout the extent of the lower lip in a bipedicled flap fashion. A horizontal relaxing incision is now placed in the gingivolabial sulcus. This bipedicled mucosal flap is now advanced anteriorly and externally to cover the surgical defect appropriately. Interrupted nonabsorbable sutures are used to approximate the labial mucosa to the cutaneous margin of the surgical defect. Accurate alignment of the mucosa to the remaining vermilion border is vitally important to restore the anatomic configuration of the reconstructed lower lip (Fig. 7.28). The mucosal defect in the gingivolabial sulcus created by advancement of the bipedicled flap is left open to heal by secondary intention. The appearance of the patient approximately 3 months after surgery shows quite satisfactory primary healing of the lower lip with restoration of the aesthetic appearance and

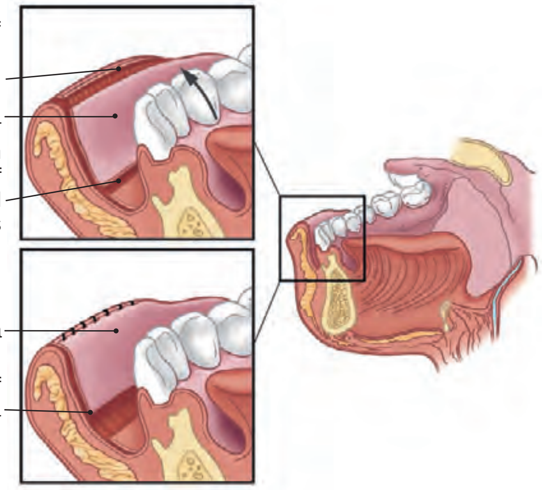

Figure 7.27 Mobilization of the bipedicled labial mucosal flap.

Figure 7.30 A nodular infiltrating squamous cell carcinoma of the lower lip.

Figure 7.28 Accurate alignment of the bipedicled mucosal flap to the skin.

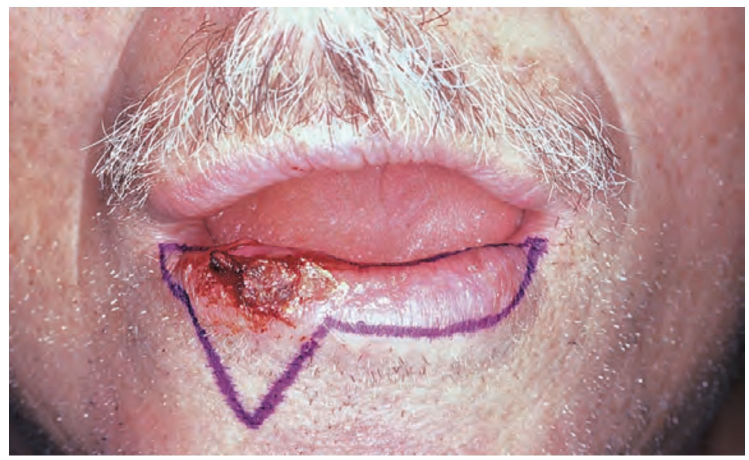

Figure 7.31 The outline of the incision.

Figure 7.29 The appearance of the patient 3 months after surgery.

preservation of the functional competency of the lower lip and the oral cavity (Fig. 7.29).

Lip Shave Operation With V Excision for Carcinoma of the Lower Lip. The patient shown in Fig. 7.30 has a nodular infiltrating squamous cell carcinoma of the vermilion border of the lower lip on the right-hand side measuring approximately 1.5 cm on its surface. He also has diffuse areas of leukoplakia involving the vermilion border of most of the lower lip. Except for the palpable nodule at the site of the infiltrating cancer, the remaining lesion is very superficial.

Surgical excision of this lesion will require a V excision at the site of the palpable nodule in conjunction with a lip shave procedure for excision of the vermilion border of the lower lip. The outline of the incision is shown in Fig. 7.31. The operation can be performed under local or general anesthesia. If a local anesthetic is used, the entire lower lip is infiltrated with 1% lidocaine with epinephrine (adrenaline) 1:100,000 solution. If, however, local anesthesia is used, then the surgical incision must be marked with a skin marking pen before infiltration of the local anesthetic. On the other hand general anesthetic is usually preferred, because it allows more satisfactory control of the operative procedure and avoids any distortion in the configuration of the mucocutaneous junction of the lip. The operation begins with the lip shave part of the procedure first. A skin incision is made at the mucocutaneous junction of the lower lip beginning on the left-hand side of the patient and up to the edge of the proposed V excision. A similar incision is made on the mucosal aspect of the lower lip following the outline previously marked. Brisk bleeding from this area should be expected, and therefore use of suction with a Frazier suction tip is preferable for a dry field. A toothed Adson forceps is then used to grasp the tip of the surgical specimen on the left side, and the remainder of the dissection proceeds with the use of fine needle tip electrocautery with coagulating current (Fig. 7.32). Dissection now proceeds in a relatively superficial plane, taking as little of the underlying musculature as possible, but ensuring that no "buttonholes" are made through the mucosa of the surgical specimen.

As the specimen is mobilized toward the right-hand side, dissection continues, keeping uniform thickness of the excised specimen until the edge of the V excision is reached (Fig. 7.33).

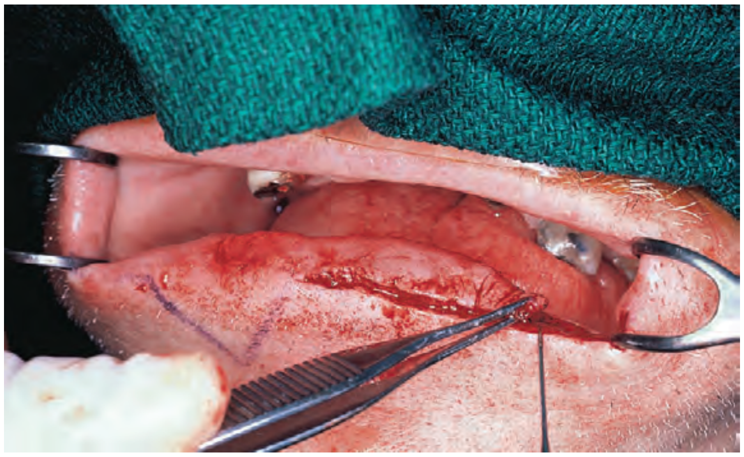

Figure 7.32 The excision begins with a lip shave.

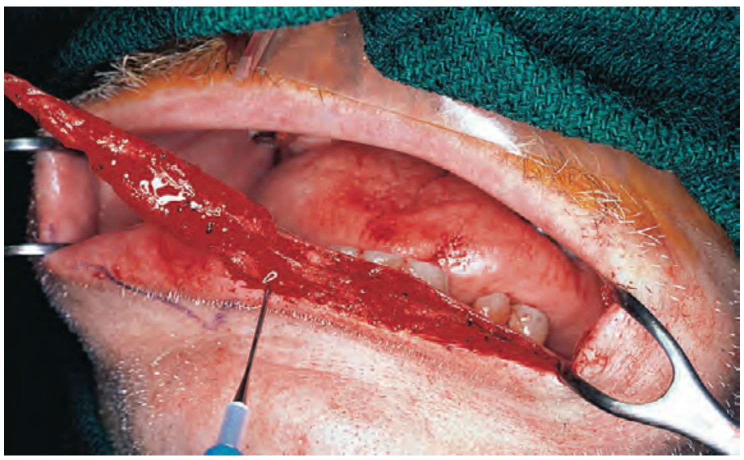

Figure 7.33 Dissection continues in a submucosal plane.

Figure 7.34 The procedure continues with a V excision.

Complete hemostasis is secured at this stage of the operation by electrocoagulating the bleeding points, which usually are from the dermal and the mucosal edges of the surgical defect.

At this point a skin incision is made with a number 15 scalpel along the previously marked V and is carried across to the right-hand side near the commissure of the mouth, completing the entire length of the incision on the labial mucosa posteriorly (Fig. 7.34). The remainder of the surgical excision is then completed, again using electrocautery. At the site of the V, a through-and-through wedge of the lower lip is excised, with the underlying musculature and the overlying mucosa posteriorly. Usually the labial artery can be easily identified, clamped, divided, and ligated to minimize brisk hemorrhage from the vessel. Pulling on the specimen must be avoided, because if it is pulled too hard during the dissection, unnecessary amounts of the labial musculature will be resected, resulting in a notched deformity at the site of the surgical excision.

Figure 7.35 The surgical defect.

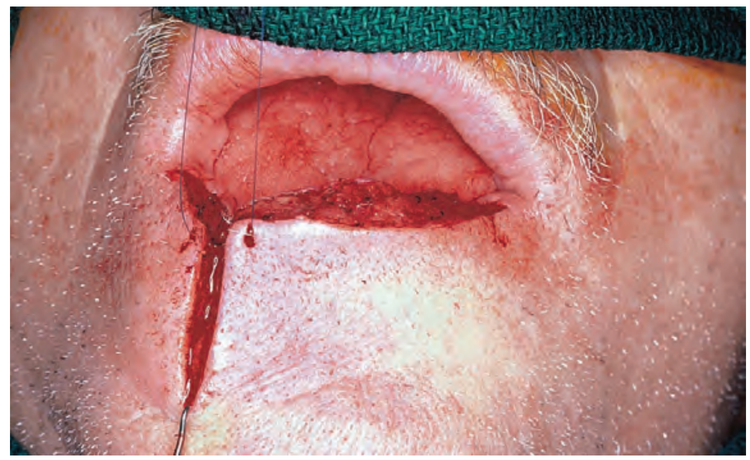

Figure 7.36 The muscular layer is accurately reapproximated.

The surgical defect resulting from this excision is shown in Fig. 7.35. The labial artery requires ligation at both ends of the defect of the V excision. The adequacy of the surgical excision is confirmed by frozen section examination of the margins. Meticulous attention should be given to absolute hemostasis; otherwise, bleeding and a hematoma will develop in the postoperative period.

Closure of the surgical defect begins with a fine nylon suture taken through the vermilion edge of the skin defect at both ends of the V excision defect of the lower lip. The suture is placed and held tight, but it is not tied. This process will allow accurate approximation of the vermilion edges to avoid a notched deformity or inaccurate approximation of the vermilion border of the reconstructed lower lip. Traction is now applied to the ends of this skin suture to allow both sides of the surgical defect to collapse to permit accurate placement of the muscular sutures. Once the muscular layer is closed, dynamic reconstruction for maintenance of competency of the oral cavity is accomplished (Fig. 7.36).

Attention is now focused on mobilization of the labial mucosa, which will be used to reconstruct the new vermilion surface (Fig. 7.37). The oral cavity is opened generously, and large Richardson retractors are placed at the oral commissure on both sides to expose the gingivolabial sulcus. Electrocautery is used to place a relaxing incision in the gingivolabial sulcus as shown. The labial mucosa is placed under tension by retracting

it, while the incision in the gingivolabial sulcus is made with electrocautery to allow easy separation of the mucosa covering the gum and the lower lip.

An Adson forceps is now used to grasp the upper edge of the labial mucosa, and submucosal dissection of this bipedicled, labial mucosal flap is undertaken with use of electrocautery (Fig. 7.38). The dissection technique in the submucosal plane requires meticulous attention; otherwise, buttonholes will occur in the mucosa if the flap is too thin, or unnecessary musculature of the lower lip will be taken if the flap is too thick. The accurate plane of dissection is such that some minor salivary gland tissue remains on the mucosal flap while the musculature remains intact (Fig. 7.39). The entire flap is mobilized through the length of the incision in the mucosa of the gingivolabial sulcus; thus this becomes a bipedicled, labial, mucosal flap of the lower lip.

Adequate mobilization allows the labial mucosa to be retracted superiorly and everted out to restore the vermilion border (Fig. 7.40). If excessive tension is present, then further mobilization is necessary on both sides near the commissure of the mouth to provide satisfactory eversion of the mucosa. Complete hemostasis must be ensured before closure of the mucosa to the skin edge of the surgical defect. The labial mucosal flap is sutured to the skin of the lower lip in a single layer with nonabsorbable sutures (Fig. 7.41). Extreme care must be exercised for accurate approximation between the mucosal and the skin edges to restore a new mucocutaneous junction of the vermilion surface. Some trimming of the mucosa may be necessary at the two lateral edges of the surgical defect.

The entire vermilion border is thus restored with the mucosa of the lower lip. Finally, the skin closure at the site of the V excision is completed with interrupted, nonabsorbable sutures. The intraoral mucosal defect at the gingivolabial sulcus is left open to heal by secondary intention.

The surgical specimen in Fig. 7.42 shows complete stripping of the mucosa of the lower lip in conjunction with a V excision at the site of the infiltrating cancer. The appearance of the patient approximately 8 weeks following surgery shows complete restoration of the normal configuration of the lips and commissure with the mouth closed (Fig. 7.43). At the site of the V

Figure 7.39 The accurate plane of dissection is superficial to the muscular layer.

Figure 7.37 Mobilization of the labial mucosa with a relaxing incision in the gingivolabial sulcus.

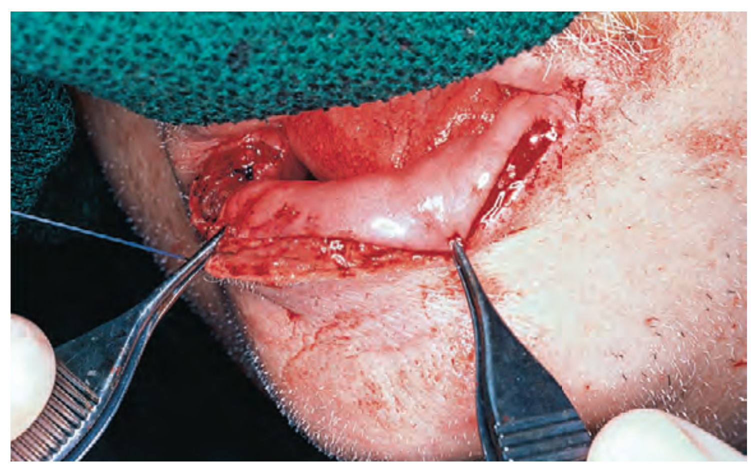

Figure 7.40 Adequate mobilization of the bipedicled mucosal flap provides coverage of the vermilion surface.

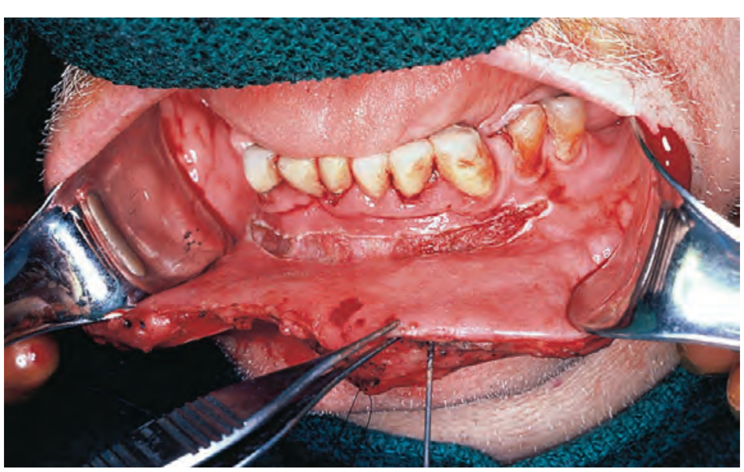

Figure 7.38 Submucosal dissection is undertaken.

Figure 7.41 Skin and mucocutaneous closure is completed.

Figure 7.42 The surgical specimen.

Figure 7.43 The postoperative appearance of the patient after 8 weeks.

excision only a linear, vertical scar is noticeable. With the mouth open, the mucocutaneous suture line becomes apparent (Fig. 7.44). The substance of the lower lip is preserved, and a satisfactory vermilion border is restored. Accurate approximation of the musculature of the lower lip prevents any notching at the site of repair of the V excision defect, and competency of the oral commissure has remained intact.

Lower Lip Resection and Reconstruction With an Abbe-Estlander Flap. When more than 30% of the width of either the lower or the upper lip is resected, reconstruction of the lip requires mobilization of a flap from the opposite lip (Fig. 7.45). When approximately two-thirds of the lower lip has been excised, it can be reconstructed by borrowing tissue equivalent to half the surgical defect from the upper lip. The technique was popularized by Abbe for reconstruction of the upper lip and by Estlander for reconstruction of the lower lip.

Figure 7.44 The mucocutaneous suture line demonstrates the new vermilion surface.

The patient shown in Fig. 7.46 has a large squamous cell carcinoma that involves more than 40% of the vermilion surface and the adjacent skin of the lower lip. The plan of excision is a full-thickness resection of the vermilion border, adjacent skin, and the underlying musculature and mucosa of the lower lip. The plan of reconstruction is to use an Abbe-Estlander flap from the upper lip pedicled on the superior labial artery on the right-hand side. The incision for the flap goes through the full thickness of the vermilion border on the left-hand side but stops short at the mucocutaneous junction to protect the superior labial artery in the pedicle (Fig. 7.47). The flap will be rotated caudad to repair the surgical defect. Surgical excision of the lesion is performed with full-thickness resection of the lower lip. Frozen sections are obtained from the lateral

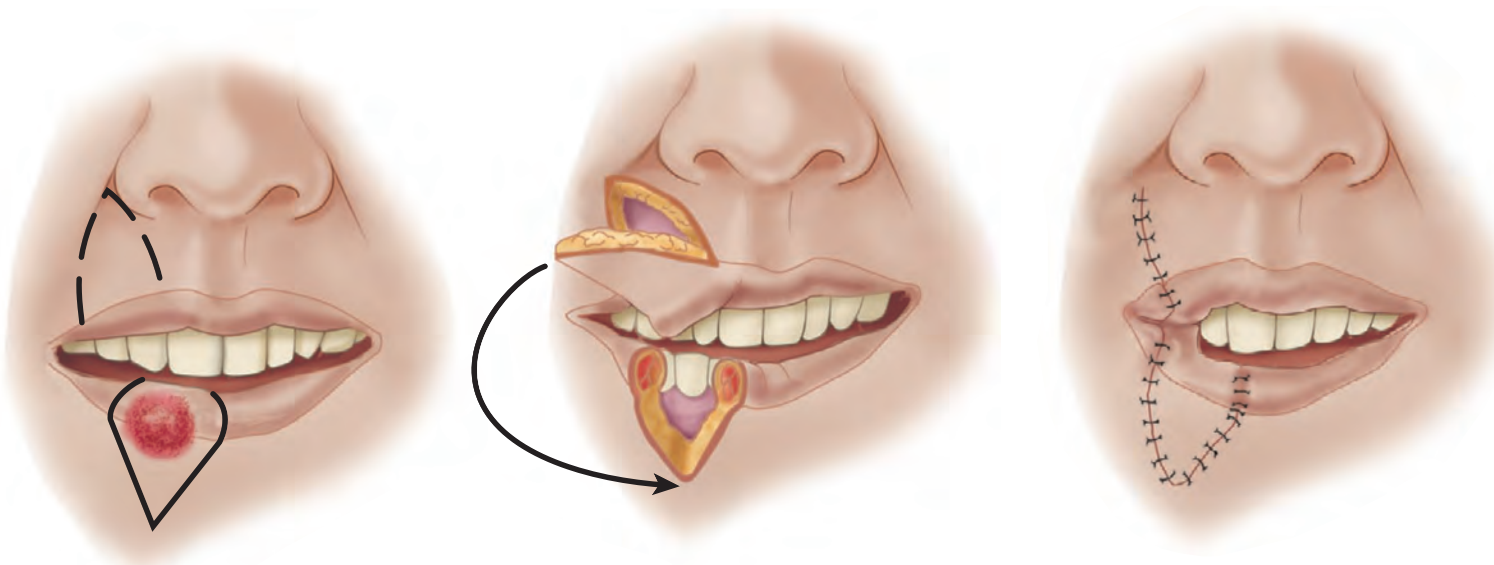

Figure 7.45 A schematic diagram of reconstruction of a lower lip defect with an Abbe-Estlander flap.

Figure 7.46 Outline of the incision around a large squamous cell carcinoma that involves more than 40% of the vermilion surface and the adjacent skin of the lower lip.

Figure 7.47 An Abbe-Estlander flap from the upper lip pedicled on the superior labial artery will be rotated caudad to repair the surgical defect.

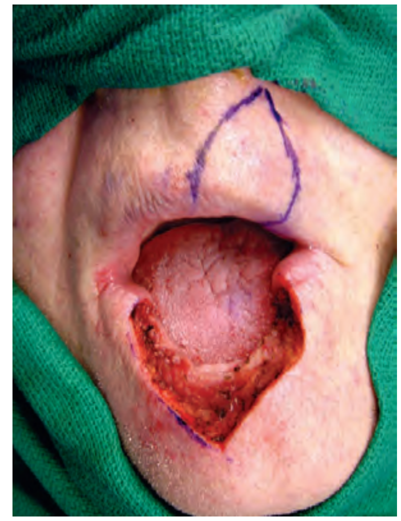

Figure 7.48 The surgical defect.

Figure 7.49 The superior labial artery is carefully preserved at the right-hand side of the flap near the vermilion border.

Figure 7.50 A three-layered closure is completed.

Figure 7.51 The appearance of the patient approximately 2 weeks following surgery shows a healing flap with the pedicle attached to the upper lip.

Figure 7.52 The postoperative appearance of the patient approximately 1 year following surgery.

margins of the surgical defect to ensure adequacy of excision. The surgical defect is shown in Fig. 7.48. An Abbe-Estlander flap is designed from the left side of the upper lip pedicled on the superior labial artery medially. Extreme care should be exercised in dissecting the vascular pedicle of this flap at the lower medial end near the vermilion border to preserve the integrity of the superior labial artery (Fig. 7.49). The flap is designed to be somewhat smaller than the surgical defect to minimize the deficiency at the donor site and still achieve the goal of repairing the large surgical defect of the lower lip. Repair of the surgical site begins with primary closure of the apex of the wedge-shaped defect at its lower end. The flap is then inset, taking care to accurately align the edges of the vermilion border. A three-layered closure is performed with mucosal, muscular, and skin layers, as shown in Fig. 7.50. The vascular pedicle of the flap remains attached to the upper lip. The appearance of the patient approximately 2 weeks following surgery shows excellent vascularity of the flap, which derives its blood supply from the pedicle from the upper lip and neovasculature from the healed edges of the surgical defect

(Fig. 7.51). The bridged pedicle is divided approximately 3 to 4 weeks following surgery, and appropriate revisions are made at the vermilion border to achieve an aesthetic closure. The postoperative appearance of the patient approximately 1 year after following surgery shows excellent aesthetic and functional outcome, preserving the dimensions of the oral opening and achieving a full-thickness reconstruction at the site of the large surgical defect (Fig. 7.52).

Lower Lip Resection at the Commissure and Reconstruction With an Abbe-Estlander Flap. The patient shown in Fig. 7.53 is an elderly man with a deeply infiltrating squamous cell carcinoma of the lower lip involving the underlying musculature and the adjacent vermilion border, warranting excision of nearly half of the lower lip. When the mouth is open, the lesion appears to be clear of the oral commissure on the right-hand side, and therefore no specific measures are necessary for restoration of the commissure (Fig. 7.54).

The proposed line of excision of the lower lip is marked (Fig. 7.55). Note that the long axis of the V excision is planned in such a fashion that a generous portion of the area of tumor involvement is excised while there is some sacrifice of the skin and the underlying musculature. A 1-cm margin at each end is desirable for deeply infiltrating tumors. A through-and-through excision is performed so that a triangular portion of mucosa, similar to the triangular portion of skin, is excised with the specimen. The principle of Abbe-Estlander flap repair is such that the width of the base of the triangular flap is half that of the width of the base of the triangular surgical defect. By doing this the recipient and the donor lip “share” the surgical defect and maintain relatively equal width to maintain balance between the upper and lower lips. The flap is marked on the upper lip on the same side; however, it also can be obtained from the opposite side of the upper lip if that is felt to be more appropriate at the time of surgery. The long axis at the site of closure is kept along the radial skin lines around the oral cavity. The incision at the site of the surgical excision is made with a number 15 scalpel through both skin and mucosa. The remaining excision is completed with electrocautery. A through-and-through wedge excision including the underlying musculature is completed. While the specimen is being mobilized, it should not be grasped and pulled too hard; otherwise an undue amount of muscle of the lower lip will be excised as a result of stretching and pulling, leading to a notched deformity at the site of repair.

The surgical specimen shows a through-and-through resection of the lower lip (Fig. 7.56). The adequacy of resection is confirmed by frozen section examination of the margins of the surgical defect.

A skin incision is now made at the previously marked outline of the Abbe-Estlander flap on the lateral aspect of the upper lip. The lateral incision is deepened through both the musculature and the mucosa, extending from the vermilion border up to the

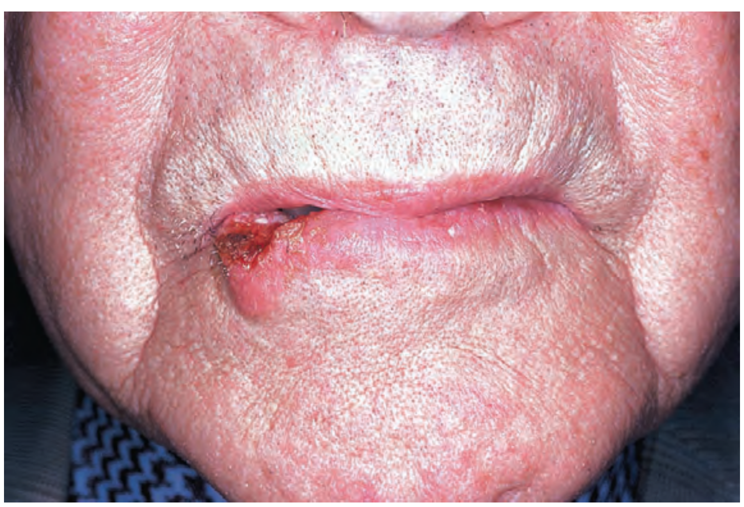

Figure 7.53 An elderly man with a deeply infiltrating squamous cell carcinoma of the lower lip.

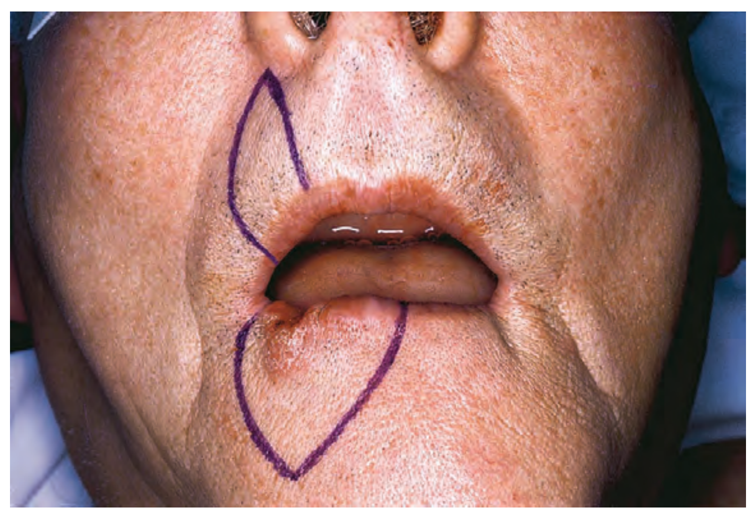

Figure 7.55 The proposed lines of incision for resection of the tumor and elevation of the flap with the pedicle on the left-hand side.

Figure 7.54 The lesion is close to the oral commissure on the right-hand side.

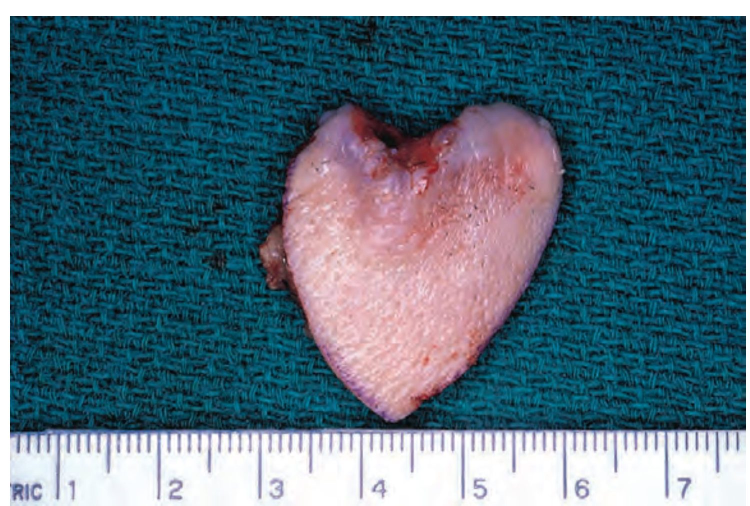

Figure 7.56 The surgical specimen.

apex of the flap (Fig. 7.57). Incision on the medial margin of the flap is done with extreme caution and care, beginning at the apex of the triangular flap and working toward its base, the vermilion border, to avoid injury to the labial artery. As mobilization of the flap toward the vermilion border proceeds, it is desirable to separate the musculature of the upper lip with a hemostat and divide small segments of the muscle fibers with scissors a little bit at a time. Once the labial artery is identified, the other attachments of the musculature of the upper lip around the labial artery are divided under direct vision, still keeping the mucosa of the vermilion border intact. Thus the contents of the pedicle of the flap are the labial artery, its accompanying vein, and the musculature between the artery and the vermilion border as well as the mucosa of the vermilion border. The labial mucosa on the medial aspect of the flap is also divided, from the apex of the flap up to the vermilion border.

The Abbe-Estlander flap, thus mobilized, derives its blood supply from the thin pedicle that remains attached to the upper lip (Fig. 7.58). The flap is rotated 180 degrees to fill the surgical defect in the lower lip. Setting and approximation of the flap into the defect of the lower lip begin by accurate approximation of the vermilion edges of the flap and the lower lip. A fine nylon suture is taken through the vermilion edges between the Abbe-Estlander flap and the surgical defect in the lower lip (Fig. 7.59), held tight, and retracted to allow accurate placement of the flap in the surgical defect. The muscular layer of the flap and the lower lip is now sutured together with interrupted 3-0 chromic catgut sutures. Extreme care must be exercised in placing the catgut suture between the right-hand side of the edge of the flap and the musculature of the lower lip near the commissure of the mouth to avoid injury to the labial artery in the pedicle of the flap.

After approximation of the muscular layer in the lower lip, closure of the donor site defect in the upper lip is undertaken (Fig. 7.60). The mucosal layer is closed with interrupted chromic catgut sutures followed by a muscular layer of interrupted 3-0 chromic catgut sutures. Accurate approximation of the vermilion border of the upper lip is not possible because of the still-attached pedicle of the flap. However, skin closure is completed in as accurate a manner as possible to avoid any discrepancy between the commissure and the vermilion border of the upper lip.

Closure of the skin incisions of the upper and lower lip is performed with 5-0 nylon interrupted sutures (Fig. 7.61). Chromic catgut interrupted sutures are used for closure of the mucosa of the flap and the labial mucosa of the lower lip. The flap thus remains attached to the upper lip through its pedicle, leaving a

Figure 7.57 The full-thickness flap is elevated with its pedicle on the labial artery medially.

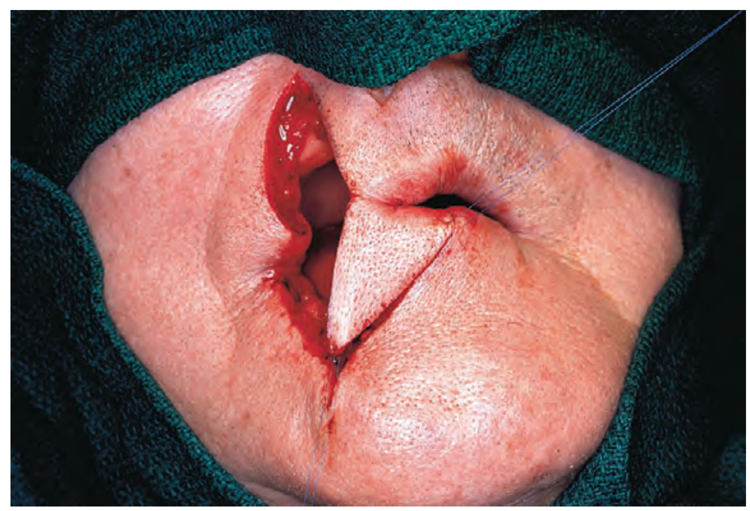

Figure 7.59 A fine nylon suture is taken through the vermilion edges for accurate alignment.

Figure 7.58 The Abbe–Estlander flap is rotated to fill the surgical defect.

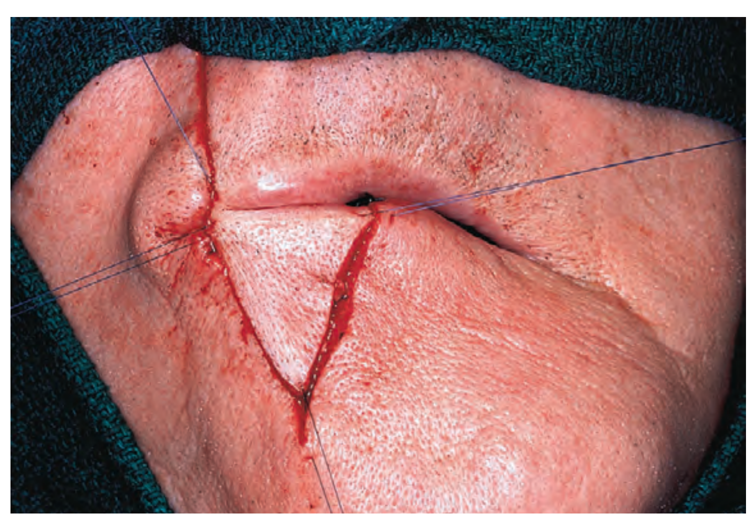

Figure 7.60 The muscular layers between the flap and lower lip are repaired, along with the donor site.

Figure 7.61 Closure of the skin incisions.

Figure 7.63 The bridged pedicle of the Abbe-Estlander flap.

Figure 7.62 The appearance of the patient 3 weeks after surgery.

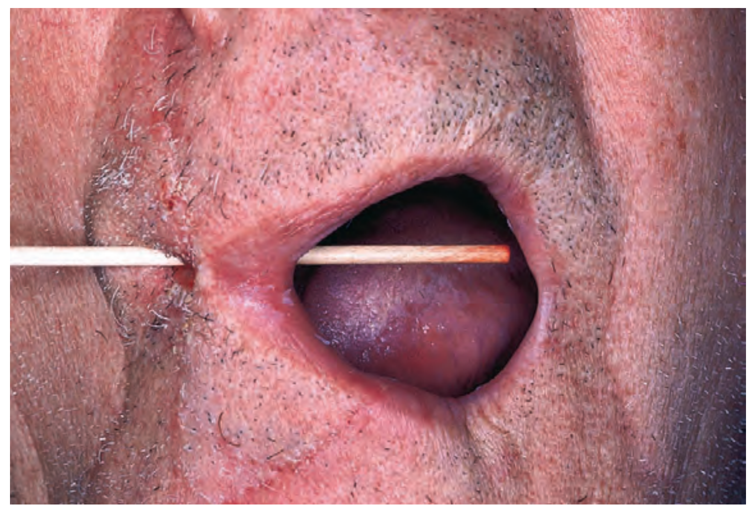

Figure 7.64 The bridged pedicle providing blood supply from the upper lip.

bridged pedicle between the upper and the lower lips. The patient must be warned preoperatively about this bridge so that in the immediate postoperative period he or she does not inadvertently traumatize, disrupt, or tear the pedicle of the flap. Because of the compromised size of the mouth, the patient can only ingest liquid and pureed foods. Skin sutures may be removed at approximately 1 week. In the immediate postoperative period the flap may look bluish and dusky, usually because of venous congestion. However, as long as capillary filling is present, the flap will survive and remain viable in its entirety. The appearance of the patient at approximately 3 weeks following surgery is shown in Fig. 7.62. Note that the skin incision at the donor site in the upper lip has healed very well with an almost imperceptible scar. The flap is set well and has filled the defect very adequately, restoring the continuity of the lower lip and the configuration of the mouth. When the patient opens his mouth, the bridged pedicle of the Abbe-Estlander flap becomes evident, demonstrating continuity of the mucosa of the vermilion border between the flap and the upper lip (Fig. 7.63).

A wooden stick is passed through the opening between the oral commissure and the bridge of the pedicle of the flap, demonstrating the vascular pedicle derived from the upper lip (Fig. 7.64). In approximately 3 weeks, the circulation of the flap by neovascularization is established sufficiently to allow division of the bridged pedicle. However, before undertaking the division, the vascularity of the flap must be checked by applying compression on the bridged pedicle with either a hemostat or a rubber band. If the flap turns blue, then division of the pedicle should be delayed. Slight discoloration of the flap is expected upon compression of the pedicle; however, if capillary blanching is present, it is safe to divide the pedicle.

Division of the bridged pedicle is relatively simple and can be performed under local anesthesia. A hemostat is introduced through the lateral opening of the oral cavity under the bridge (Fig. 7.65). A scalpel is used to transect the pedicle, thus releasing the upper lip from the attachment to the lower lip. The only bleeding in this maneuver is from the labial artery, which is clamped and ligated. Small wedge excisions are performed to match and revise the raw areas at the site of the divided pedicle to facilitate primary closure (Fig. 7.66). Accurate approximation of the vermilion edges of both the upper and lower lips is vital for achieving an optimal aesthetic result (Fig. 7.67). Although the size of the mouth is reduced somewhat, symmetry is maintained and excellent functional and aesthetic reconstruction of the lip is achieved with the use of this flap.

When the oral commissure must be sacrificed along with excision of the lower lip tumor, a nonbridged Estlander flap

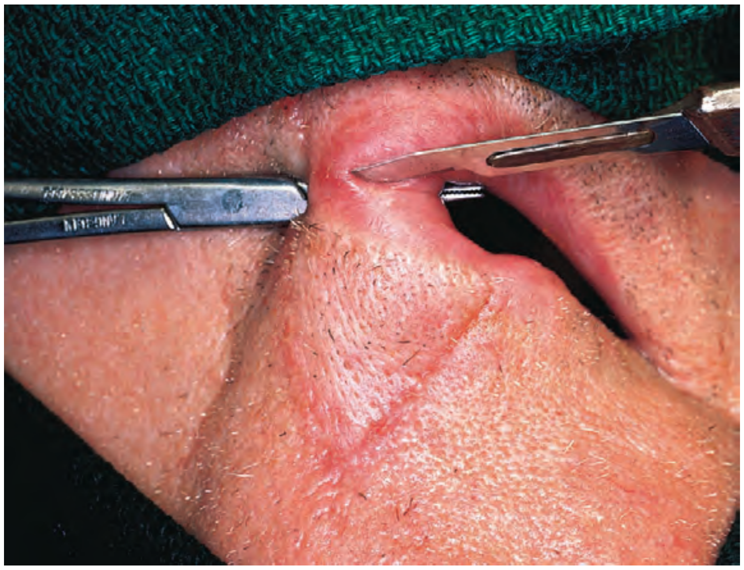

Figure 7.65 The bridged pedicle is divided.

Figure 7.66 Small wedge excisions are performed at the site of the divided pedicle.

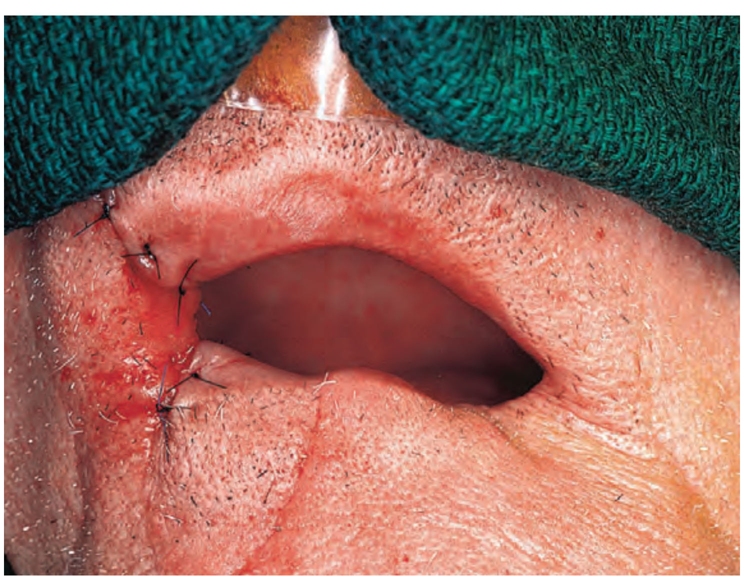

Figure 7.67 Accurate approximation of the vermilion edges is crucial for a superior aesthetic result.

can be used. However, this procedure will result in rounding of the commissure, which requires a secondary revision. The Abbe-Estlander flap can be used in reverse when a lesion of the upper lip is excised, whereupon the flap is elevated from the lower lip.

Karapandzic Flap Repair. Karapandzic flap repair for reconstruction of defects of the lower lip is ideally suited in situations in which 80% or more of the lower lip is resected in its central part, leaving the lateral ends near the commissures intact. A schematic diagram of the Karapandzic flap is shown in Fig. 7.68. The principle of Karapandzic flap reconstruction is mobilization and utility of the skin, muscle, and mucosa of the lower portion of the nasolabial region, which are shifted medially, preserving the nerve and blood supply to the orbicularis oris muscle, which is rotated medially. Thus the incisions for elevation of this flap require mobilization of the skin and subcutaneous tissues superficial to the orbicularis oris muscle and the mucosa deep to the orbicularis oris muscle, keeping the muscle itself intact with its nerve and blood supply preserved. The skin incision is placed approximately 2 cm inferior to the vermilion border to encompass the full width of the orbicularis oris muscle. The mucosal incision is placed at the gingivolabial sulcus.

The patient shown in Fig. 7.69 has a large invasive squamous cell carcinoma of the lower lip in its central two-thirds, with extension laterally on the vermilion border within a few millimeters of the commissure on both sides. The surgical defect created by excision of this tumor results in a through-and-through defect of the lower lip from the vermilion border up to the gingivolabial sulcus, involving approximately 80% of the central component of the lower lip.

The incisions for resection of the lower lip and reconstruction by Karapandzic flap repair are shown in Fig. 7.70. The lateral incisions for elevation of the flaps follow the nasolabial skin crease and must be modified in each patient, depending on the location of the skin crease in the nasolabial region.

Resection of the lower lip lesion is performed in the usual three-dimensional fashion. Adequacy of the resection is confirmed by frozen section examination of margins of the surgical defect. The skin incisions for elevation of the Karapandzic flaps are made with a scalpel (Fig. 7.71). Mobilization of the subcutaneous soft tissues and the skin component of the flap is meticulously undertaken with an electrocautery, remaining superficial to the orbicularis oris muscle (Fig. 7.72). It is crucial to avoid inadvertent division of the muscle fibers, to maintain the

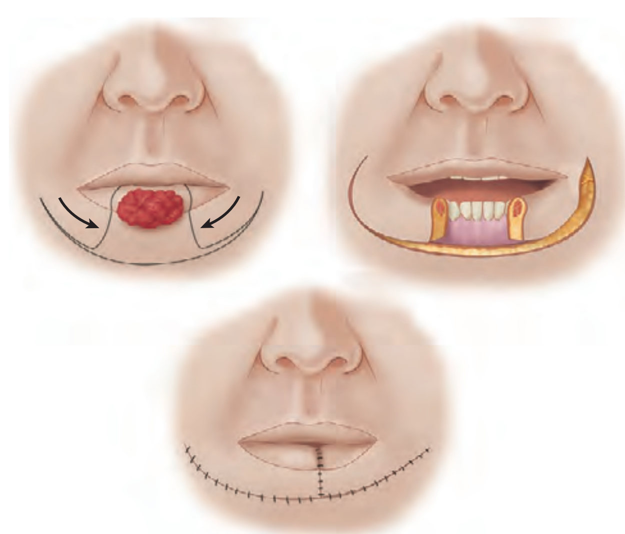

Figure 7.68 A schematic diagram of Karapandzic flap reconstruction.

Figure 7.69 A large invasive squamous cell carcinoma of the lower lip.

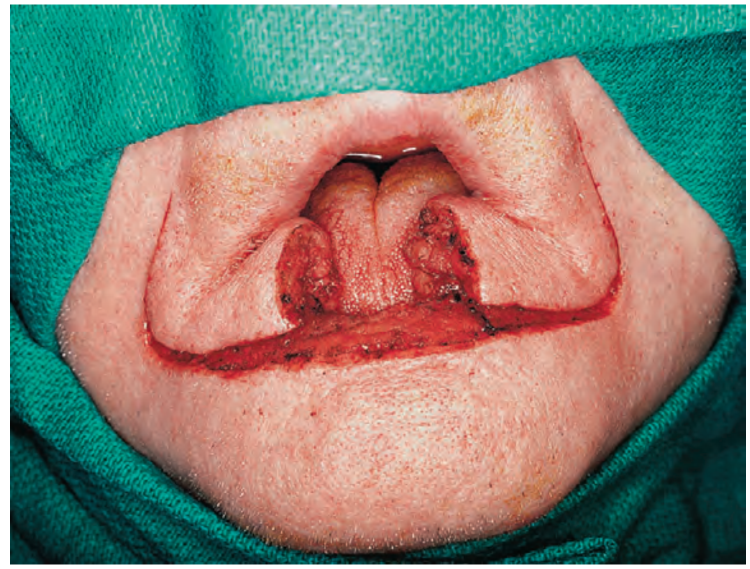

Figure 7.71 The tumor is resected and skin incisions for the Karapandzic flap are placed.

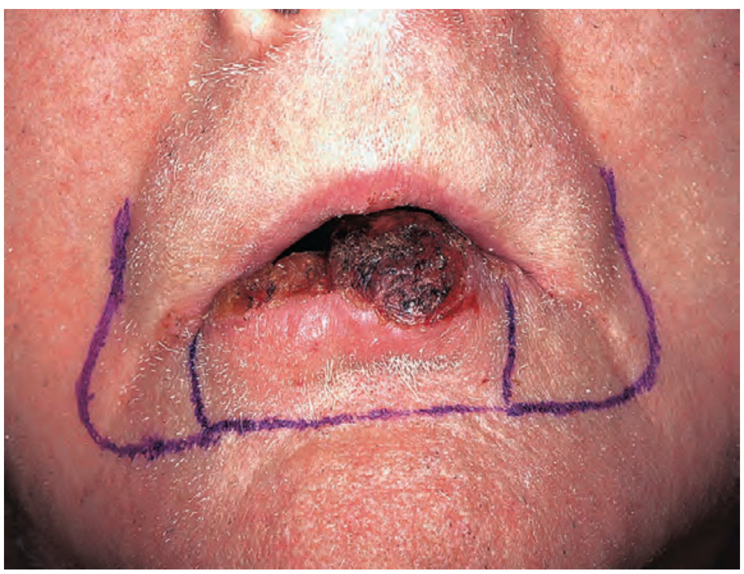

Figure 7.70 The incisions for resection and reconstruction of the lower lip with a Karapandzic flap are outlined.

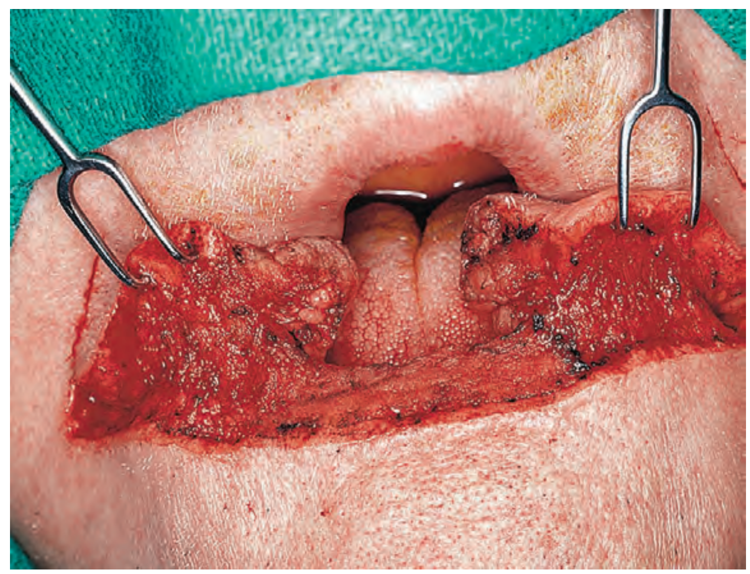

Figure 7.72 The flap is elevated in a subcutaneous plane remaining superficial to the orbicularis oris.

neuromuscular control of the orbicularis oris muscle and thus retain competency of the oral cavity. After adequate mobilization of the skin and subcutaneous tissues of the flap on both sides, incisions are placed in the mucosa of the gingivolabial sulcus on each side, again carefully preserving the anatomic continuity of the orbicularis oris muscle (Fig. 7.73). Sufficient length of the mucosal incisions must be performed to permit medial mobilization of both the flaps for a midline closure. Repair of the surgical defect then begins with vertical midline closure of the transected edges of the lower lip with accurate approximation of the vermilion border by a 5-0 nylon suture first. This suture is held and used for retraction, permitting approximation of the muscular layer of the two ends of the Karapandzic flaps. Following approximation of the muscular layer, the cutaneous and mucosal closures on both sides of the reconstructed lower lip are completed (Fig. 7.74). After this procedure, reapproximation of the suture line between the cutaneous margin of the flaps and the cutaneous margin of the chin and the nasolabial region is undertaken, accurately aligning the two sides and preserving the aesthetic continuity of the nasolabial folds (Fig.

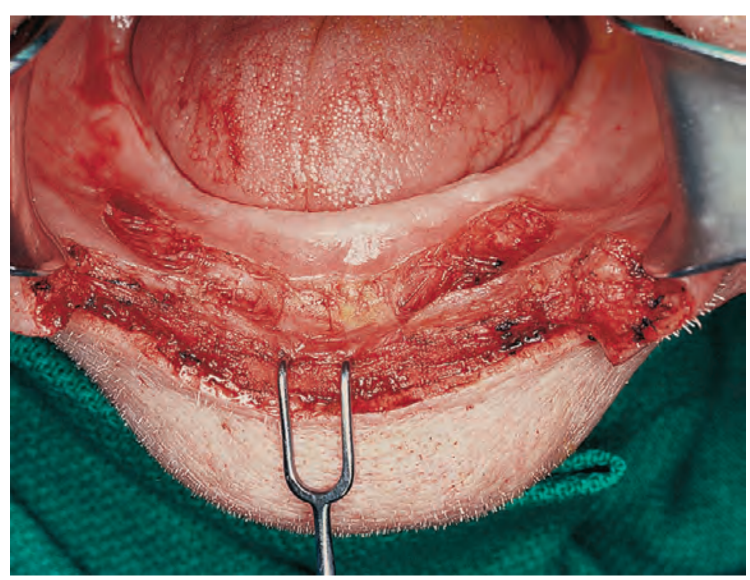

Figure 7.73 Mucosal incisions are placed in the gingivolabial sulcus on each side.

7.75). The postoperative result at approximately 3 months following surgery shows accurate restoration and reconstruction of the large defect of the lower lip with minimal aesthetic deformity but with adequate restoration of the competency of the oral cavity (Fig. 7.76).

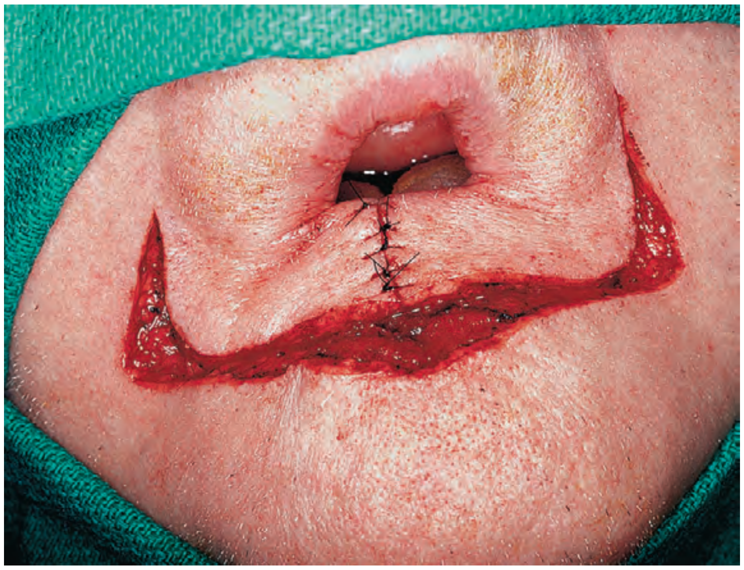

Figure 7.74 Mucosal, muscular, and cutaneous closure of the lower lip is completed.

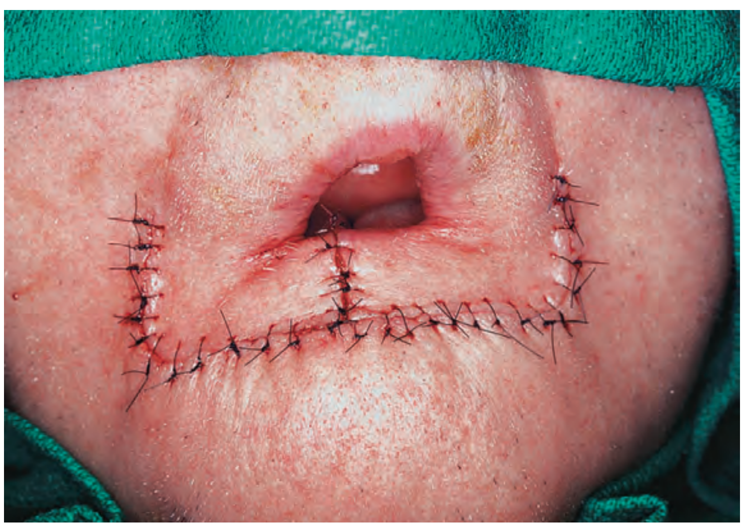

Figure 7.75 The donor site defects are repaired in two layers.

Figure 7.76 The appearance of the patient 3 months following surgery.

Bernard Reconstruction of the Lower Lip. Bernard reconstruction of the lower lip is designed for tumors that are too extensive for reconstruction with the Abbe-Estlander or Karapandzic flaps. The lower lip may be excised in its entirety along with soft tissues and skin of the chin, with the resulting defect closed by lateral cheek flaps to form a new lower lip. To set back the commissures and to prevent a fish-mouth deformity, triangles of skin are excised from both sides of the upper lip, preserving the mucous membrane, to help form a new vermilion border (Fig. 7.77). The distinct advantage of this operation is its ability to reconstruct nearly the entire lower lip in a single-stage procedure and retain or restore competency of the oral cavity. An obvious disadvantage is reduction in the size of the orifice of the oral cavity and a "permanent smile" deformity of the lips, particularly in edentulous patients.

The patient shown in Fig. 7.78 has a large primary squamous cell carcinoma involving the entire thickness of the lower lip with extension to involve the skin and soft tissues of the upper part of the chin. The area of excision is outlined along with the intended wedges of the skin to be excised from the upper lip near the nasolabial skin crease to facilitate advancement of the Bernard flaps for reconstruction of the lower lip (Fig. 7.79). Resection of the tumor is performed in the usual fashion. Adequacy of the tumor resection is confirmed by frozen section examination of the margins of the surgical defect.

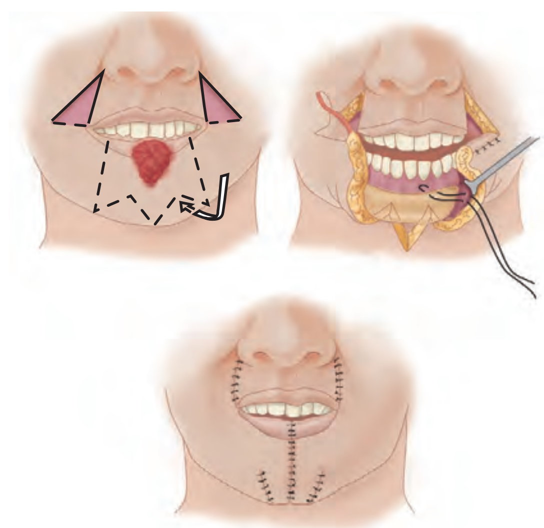

Figure 7.77 The plan of excision and reconstruction.

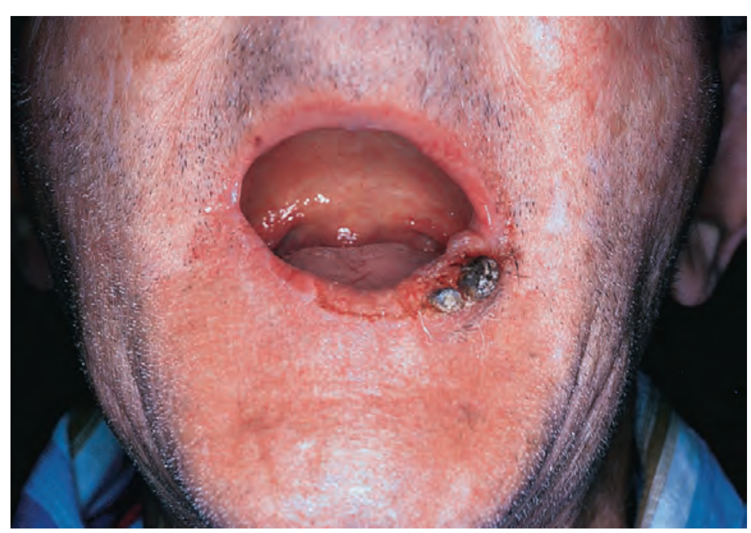

Figure 7.78 A large primary squamous cell carcinoma involving the entire lower lip.

The surgical defect shows a through-and-through resection of nearly seven-eighths of the lower lip (Fig. 7.80). Note that the surgical excision on the labial surface goes right up to the gingivolabial sulcus. A generous portion of the skin of the chin and the underlying soft tissues also is resected en bloc with the primary tumor.

When a significant portion of the skin of the chin is excised, it is important to plan the lower incision on the chin in such a way that the advancement flaps will allow satisfactory closure. Generally, a rectangular-shaped excision is preferred to facilitate closure. However, varieties of other surgical incisions are available, including double triangles, to aid reapproximation of the lateral cheek flaps and repair the chin.

Triangular wedges of the skin and subcutaneous tissue are now excised from the nasolabial crease on both sides. The base of the triangle extends from the commissure of the mouth up to the nasolabial crease, depending on the width of the cheek flap to be mobilized medially. After excision of the triangular wedges of the skin in this way, the mucosa from the inner aspect of these triangular wedges is incised and the triangular flaps of mucosa of the upper lip that are retrieved from these locations are shifted medially along with the flaps. Now an incision is made in the lower gingivolabial sulcus on both sides and both cheek flaps are mobilized medially. In the center of the surgical defect, the apex of the triangular part of the skin of the chin is mobilized by appropriate wedge excisions on the chin to provide a satisfactory closure. Closure of the musculature of the lip on both sides is performed with interrupted chromic catgut sutures. The triangular wedges of the mucosa from the upper lip are everted and rolled inferiorly to provide the new vermilion surface. Mucosal closure is completed inferiorly in the gingivolabial sulcus. The full-thickness wedges created in the skin of the upper lip at the commissure are closed in three layers on each side. The completed closure is shown in Fig. 7.81.

The appearance of the patient approximately 3 months following surgery shows the reconstructed lower lip with restoration of both the size of the oral orifice and the vermilion border (Fig. 7.82).

Figure 7.79 The outline of excision and reconstruction.

Figure 7.81 The completed closure.

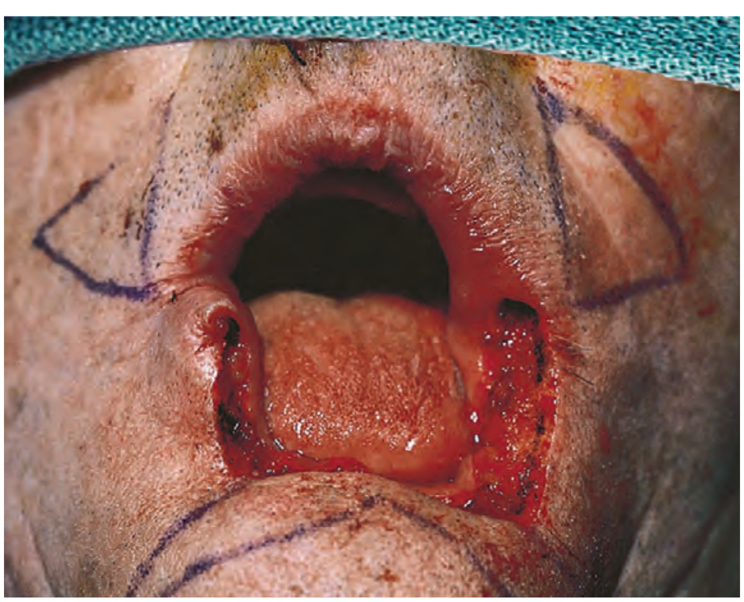

Figure 7.80 The surgical defect.

Figure 7.82 The patient's appearance 3 months following surgery.

Composite Resection of the Lower Lip, Chin, and Anterior Arch of the Mandible With Free Flap Reconstruction. Massive primary or recurrent carcinomas of the lower lip with invasion of the overlying skin of the chin and the underlying mandible require a through-and-through composite resection with immediate reconstruction of the mandible, the overlying soft tissues, and the skin of the chin as well as the lower lip to restore facial contour and oral competency. The patient shown in Fig. 7.83 has recurrent carcinoma of the lower lip with invasion of the skin of the chin and the underlying arch of the mandible. Through-and-through resection of the entire lower lip with the skin of the chin and anterior arch of the mandible in conjunction with bilateral supraomohyoid neck dissections is required to encompass the recurrent tumor and regional lymph nodes. This patient had palpable metastatic lymph nodes at level I in the prevascular facial lymph nodes on the left-hand side; however, because the recurrent tumor invaded the entire lower lip, bilateral supraomohyoid neck dissections were performed. The surgical defect of this patient demonstrates the stumps of the mandible on both sides, as well as soft tissue and skin deficits created by surgical resection of the tumor (Fig. 7.84). The surgical specimen seen from the anterior aspect shows wide excision of the skin of the chin and the entire lower lip performed in continuity with bilateral supraomohyoid neck dissections, including submental lymph nodes (Fig. 7.85). The posterior view of the surgical specimen shows the arch of the mandible resected in a monobloc fashion with the tumor of the lower lip, including soft tissues of the submental triangle (Fig. 7.86).

A microvascular composite osteocutaneous flap from the forearm is ideal for reconstruction of a short segment of the mandible and provides an excellent supple and soft skin flap for reconstruction of the skin of the chin and the lower lip. The bony component of this composite flap consists of a split portion of the lower half of the radius bone, which provides sufficient bone to reconstruct the surgical defect in this edentulous patient. Two osteotomies are performed in this bone; however, the osteotomized segments are not quite stable enough to provide a sturdy bone repair, and therefore these bone segments are stabilized over a titanium AO plate to reconstruct the arch of the mandible. The cutaneous component of the flap provides coverage of the skin of the chin and has adequate soft tissue to restore the contour of the chin. The skin flap is folded over itself to create the lower lip, and the edges of the

Figure 7.83 A recurrent carcinoma of the lower lip involving the mandible.

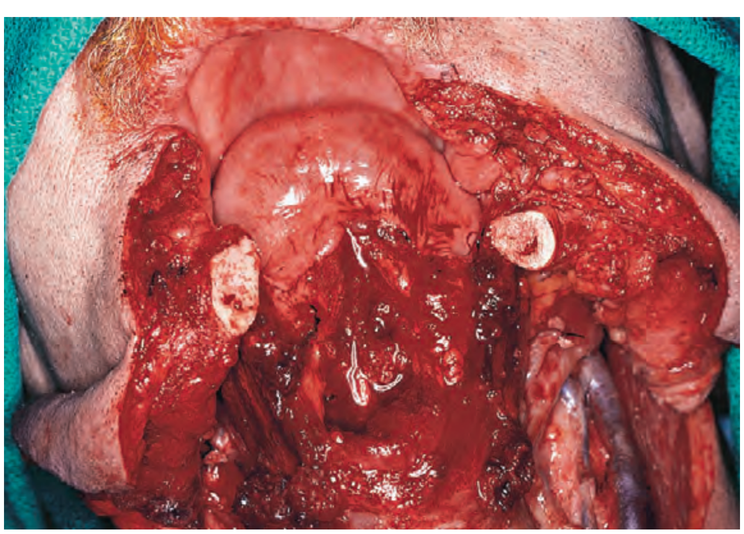

Figure 7.84 The surgical defect.

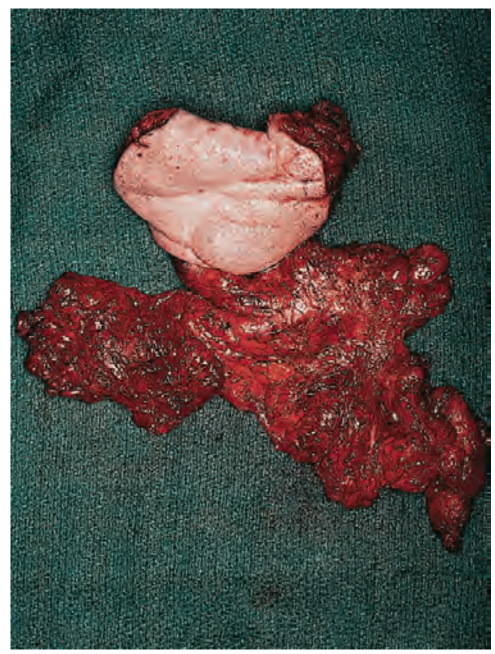

Figure 7.85 The surgical specimen, seen from the anterior aspect.

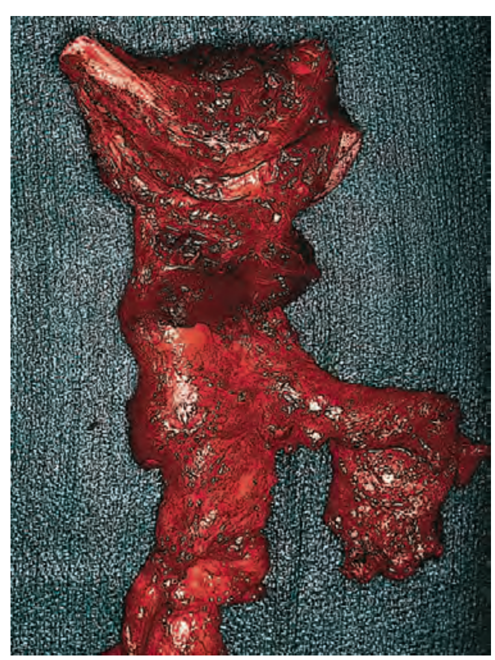

Figure 7.86 A posterior view of the surgical specimen.

skin flap are sutured to the commissure of the residual upper lip. Alternatively, two microvascular free flaps may be used, a scapula or fibula free flap for bone and a radial forearm free flap for skin. The appearance of the patient approximately 2 months following surgery shows satisfactory reconstruction of the contour of the chin, providing an excellent repair of the lower lip (Fig. 7.87). The lateral view of the face of the patient shows satisfactory restoration of the protrusion of the chin for this through-and-through defect of the lower lip and anterior arch of the mandible (Fig. 7.88). Complex reconstructions such as this one require detailed preoperative planning of the reconstructive procedure to achieve a satisfactory postoperative result.

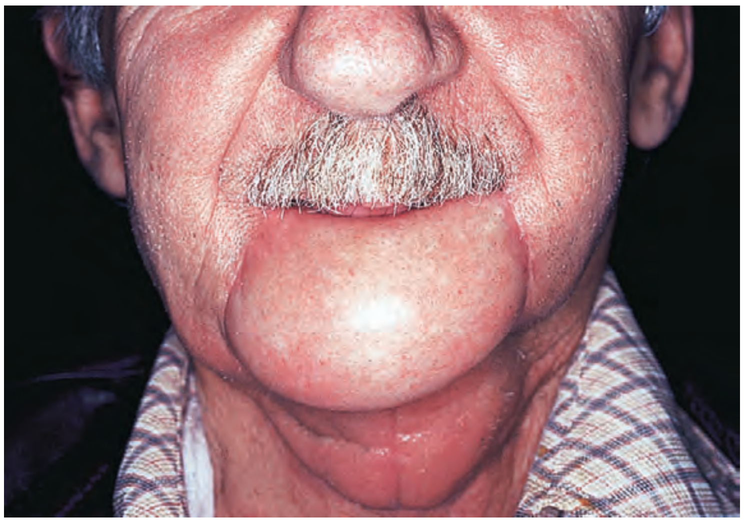

Figure 7.87 The appearance of the patient 2 months following surgery.

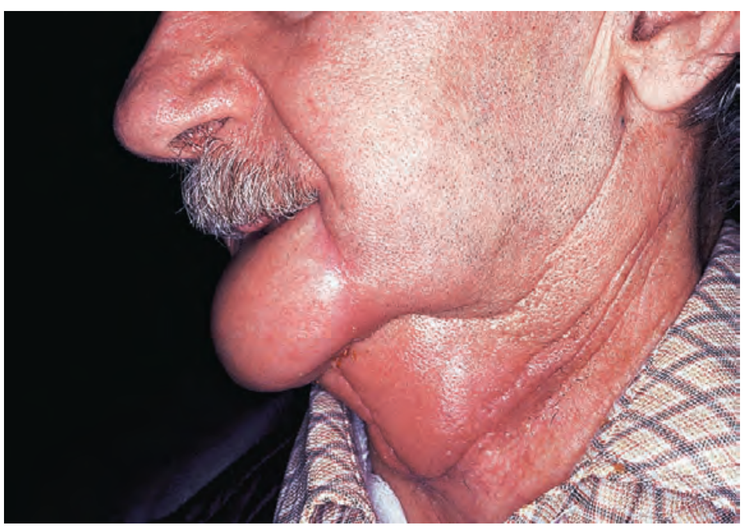

Figure 7.88 A lateral view of the face of the patient.

Composite Resection of the Lower Lip With Segmental Mandibulectomy and Free Flap Reconstruction. Certain malignant tumors of the lower lip manifest neurotropism with extension of tumor along the mental nerve into the alveolar canal. Squamous cell carcinomas and melanomas are the most common epithelial malignant tumors manifesting this behavior. Adenoid cystic carcinomas, among minor salivary gland tumors, have a specific proclivity for neurotropic spread. Thus for patients with advanced tumors of the lip, or those presenting with anesthesia of the skin of the chin, appropriate radiographic evaluation should be performed to assess the presence of neurotropic extension along the inferior alveolar canal. The absence of radiographic abnormalities does not rule out tumor extension, but its presence confirms it and facilitates surgical treatment planning.

The patient shown in Fig. 7.89 had squamous cell carcinoma of the mucosal surface of the lower lip on the right-hand side, perforating through the full thickness of the lip and the overlying skin. This patient reported anesthesia of the skin of the chin on the right-hand side. A CT scan of the oral cavity and mandible clearly shows soft tissue disease overlying the lateral cortex of the mandible with invasion of the overlying skin (Fig. 7.90). The bone window of the CT scan shows expansion of the mental foramen and extension of tumor along the inferior alveolar canal in the cancellous part of the mandible on the right-hand side (Fig. 7.91). The plan of surgical excision required a through-and-through resection of the lower lip, a generous portion of the overlying skin of the chin, and segmental mandibulectomy (Fig. 7.92). The extent of mandible resection required includes the entire intraosseous course of the inferior alveolar nerve. Thus the mandible is divided, remaining anterior to the mental foramen, and posteriorly it is divided through the midascending ramus, above the inferior alveolar canal. The inferior alveolar

Figure 7.89 A squamous cell carcinoma of the mucosal surface of the lower lip on the right-hand side that is perforating through the full thickness of the lip and the overlying skin.

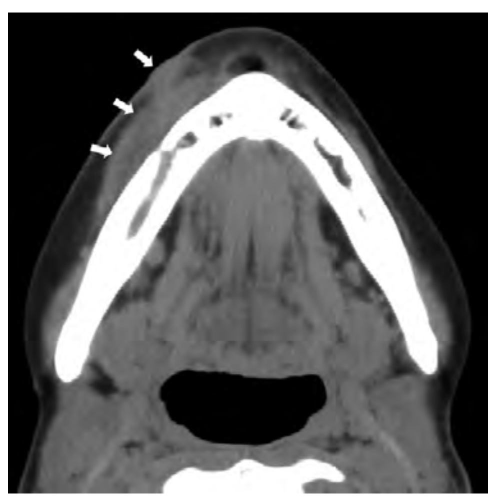

Figure 7.90 A computed tomography scan of the oral cavity and mandible shows soft tissue disease overlying the lateral cortex of the mandible with invasion of the overlying skin (*arrows*).

Figure 7.91 The bone window of the computed tomography scan shows expansion of the mental foramen and extension of the tumor along the inferior alveolar canal (*arrows*) in the cancellous part of the mandible on the right-hand side.

Figure 7.92 The outline of the incision for resection of the lower lip and skin of the chin with modified neck dissection.

nerve is resected immediately after separation of the lingual nerve from the third division of the trigeminal nerve. The surgical specimen seen from the lateral aspect shows the right side of the mandible with a generous portion of soft tissues and skin overlying the mental foramen (Fig. 7.93). The surgical specimen is bisected in a sagittal plane to show the expanded mandibular canal, demonstrating neurotropic infiltration and extension of tumor along the inferior alveolar nerve (Fig. 7.94).

Reconstruction of this complex surgical defect is accomplished with use of a composite fibula free flap. This patient underwent postoperative radiotherapy. The appearance of the patient approximately 2 years following surgery shows an excellent aesthetic and functional outcome (Fig. 7.95).

Upper Lip

Nasolabial Flap Repair for the Upper Lip. Defects of the skin and underlying soft tissues of the upper lip are most amenable to reconstruction with an inferiorly based nasolabial flap. This axial skin flap is highly reliable and provides skin coverage and enough soft tissue replacement for the excised portion of the upper lip. However, one distinct disadvantage of this flap is that it does not restore the muscular action of the upper lip, and thus a functional deficit persists. However, the aesthetic result is excellent. Thus nasolabial flap repair would be unsatisfactory for full-thickness resection of upper lip defects.

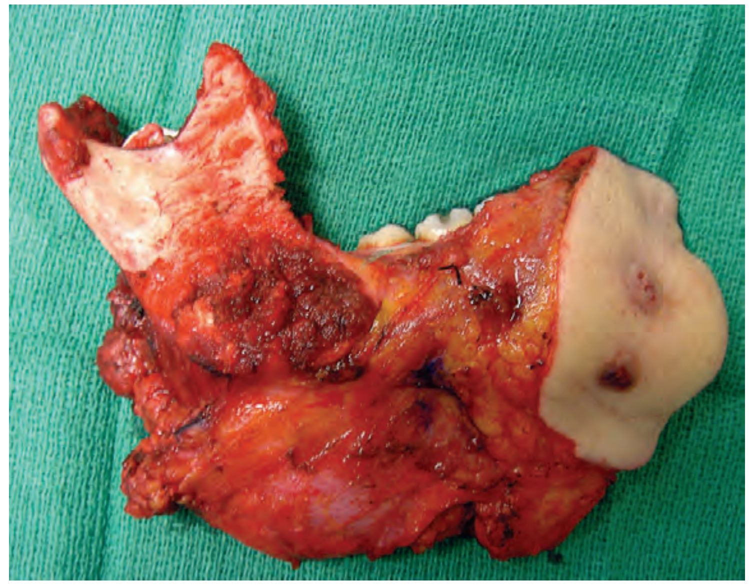

Figure 7.93 A lateral view of the surgical specimen.

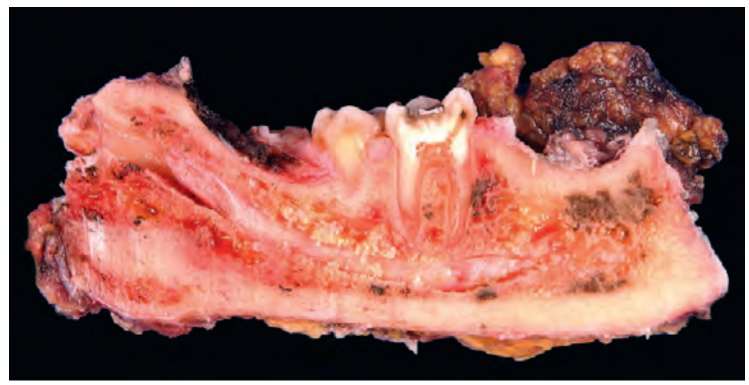

Figure 7.94 The surgical specimen is bisected in a sagittal plane to show neurotropic infiltration and extension of the tumor along the inferior alveolar nerve in an expanded mandibular canal.

Figure 7.95 The appearance of the patient approximately 2 years following surgery.

The patient shown in Fig. 7.96 has a recurrent basal cell carcinoma of the skin of the upper lip on its lateral aspect. This lesion was treated previously with electrodesiccation and

curettage. The lesion involves underlying soft tissues but does not infiltrate through the musculature of the upper lip. The inferior margin of the lesion approaches the vermilion border, and the lesion reaches the alar groove superomedially.

The incisions for resection and reconstruction are outlined in Fig. 7.97. The nasolabial flap is elevated longer than its measured required length so the repair can be accomplished without tension and the donor site defect can be closed with very little distortion of the facial features.

The surgical defect following excision of this lesion shows the orbicularis oris muscle of the upper lip in the depth of the defect (Fig. 7.98). The nasolabial flap is rotated inferiorly and medially to fill the surgical defect. The donor site defect is primarily closed by mobilization of the skin of the cheek. A two-layered closure is performed with use of 3-0 chromic catgut interrupted sutures for subcutaneous tissues and 5-0 nylon for skin (Fig. 7.99). The same patient's appearance approximately 1 year following surgery (Fig. 7.100) shows a very gratifying result with use of the nasolabial flap for repair of the skin defect of the upper lip. The donor site defect is very nicely healed. A minor revision may be necessary to revise the lateral scar and remove

Figure 7.98 The surgical defect and the elevated nasolabial flap.

Figure 7.96 A recurrent basal cell carcinoma of the skin of the upper lip.

Figure 7.99 A two-layered closure is completed.

Figure 7.97 The incisions are outlined.

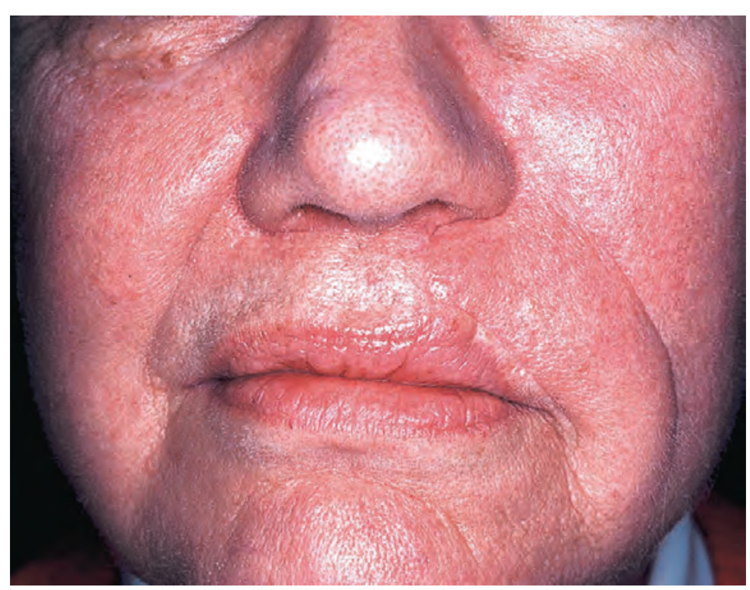

Figure 7.100 Postoperative appearance of the patient 1 year following surgery.

some fat to get a perfect result. The contour of the reconstructed lip and vermilion border appears essentially normal.

Resection and Reconstruction of the Upper Lip With Unilateral Burrows Triangle Repair. The patient shown in Fig. 7.101 has a sweat gland carcinoma involving the vermilion border of the left-hand side of the upper lip and the adjacent skin with involvement of the underlying soft tissues. Surgical resection of this tumor requires a through-and-through resection of the upper lip extending from the right-hand side of the midline up to within 1 cm of the oral commissure on the left-hand side. The surgical defect following excision of this tumor is shown in Fig. 7.102. Frozen section examination of the margins of the surgical defect is performed to ensure the adequacy of resection. A Burrows triangle is marked along the nasolabial skin crease and the alar groove on the left-hand side, with an incision marked for advancement of the skin of the cheek for reconstruction of the upper lip. Skin and soft tissues from the Burrows triangle are excised and the skin incision on the left cheek has been placed with mobilization of the subcutaneous soft tissues, remaining superficial to the orbicularis oris muscle (Fig. 7.103). Medial advancement of the residual upper lip of the left-hand side and the mobilized soft tissues of the left cheek provides satisfactory closure of the surgical defect (Fig. 7.104). The vermilion border is accurately aligned first and then mucosal, muscular, and skin closure of the upper lip is completed. Finally, the skin along the alar groove and the advancement incision on the left cheek are closed meticulously in two layers (Fig. 7.105). The appearance of the patient approximately 3 months after surgery shows a very satisfactory reconstruction of the resected portion of the upper lip with the unilateral Burrows triangle technique (Fig. 7.106).

Bilateral Burrows Triangle Repair of the Upper Lip. Full-thickness resection of the upper lip, up to one-third of its width,

Figure 7.101 A sweat gland carcinoma of the upper lip.

Figure 7.102 The surgical defect.

Figure 7.103 Skin and soft tissues from the Burrows triangle are excised, and an advancement incision is placed on the skin of the cheek.

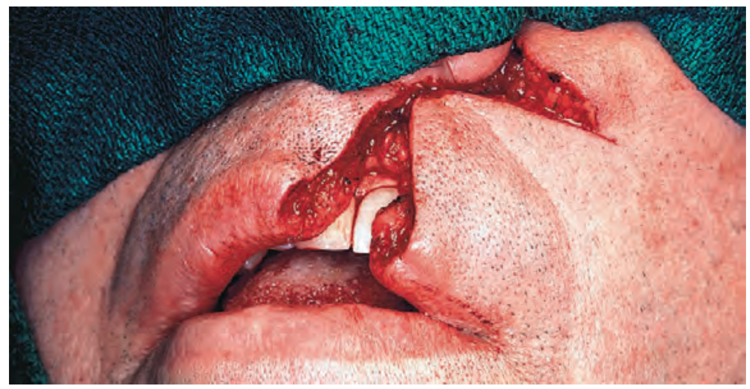

Figure 7.104 Medial advancement of the residual upper lip of the left-hand side.

Figure 7.105 Three-layered closure of mucosa, muscle, and skin is completed.

Figure 7.106 Postoperative appearance of the patient 3 months following surgery.

is easily amenable to repair by direct primary closure similar to the V excision of the lower lip. However, when a larger portion of the upper lip is resected, use of the Burrows technique is very satisfactory for its reconstruction. The principles of reconstruction are similar to the Bernard triangle repair. Triangular wedges of skin between the alar groove and the nasolabial crease are excised, permitting lateral upper lip–cheek flaps to be mobilized medially to accomplish the repair.

A patient with a primary infiltrating squamous cell carcinoma of the skin and vermilion border of the upper lip in the region of the philtrum is shown in Fig. 7.107. The tumor infiltrates the underlying musculature but does not perforate through the labial mucosa.

The plan of surgical excision, outlined in Fig. 7.108, shows a through-and-through resection of the upper lip, with proposed triangular wedges of skin to be excised from the nasolabial creases bilaterally, adjacent to the nasal ala. The arrows indicate the extent of mobilization and medial advancement of the residual upper lip on both sides. The surgical defect following excision of the tumor shows a through-and-through resection of the central part of the upper lip. Note that the mucosal incision goes right up to the gingivolabial sulcus (Fig. 7.109).

After excision of the triangular wedges of the skin, the lateral cheek flap and residual upper lip are advanced medially, and a three-layered closure is performed with use of interrupted chromic catgut sutures for mucosa and muscles and 5-0 nylon for skin (Fig. 7.110). If the triangular wedges are accurately placed along the side of the ala, the scar of the closure goes right along the groove of the ala and minimizes aesthetic deformity. However, the size of the oral orifice is reduced, and some tension on the upper lip is to be expected.

The postoperative appearance 3 months following surgery (Fig. 7.111) shows excellent healing and reconstruction of the upper lip, which is now distinctly smaller in length than before, causing backward pull and recession in this edentulous patient. Note that the midline scar at the philtrum is well healed, so there is minimal aesthetic deformity and an imperceptible scar along the nasal ala on both sides.

The same patient's appearance 8 months later after fabrication of an upper denture to push the upper lip out and restore the

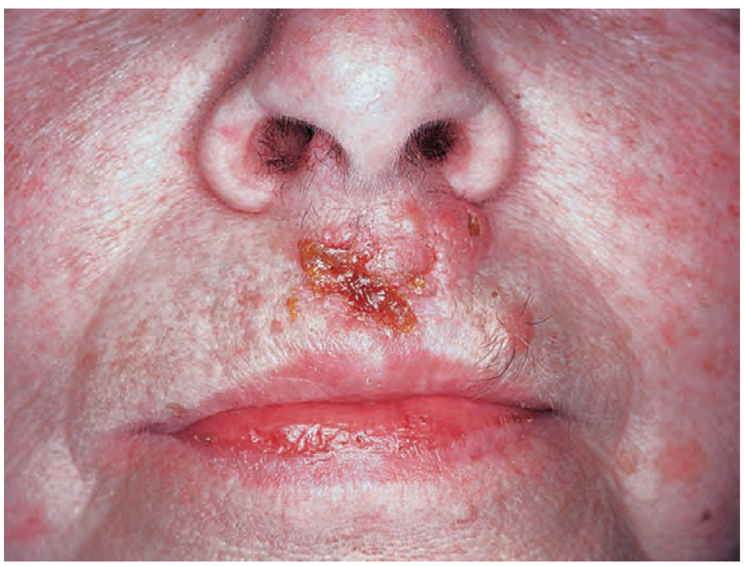

Figure 7.107 A patient with a primary infiltrating squamous cell carcinoma of the skin of the upper lip.

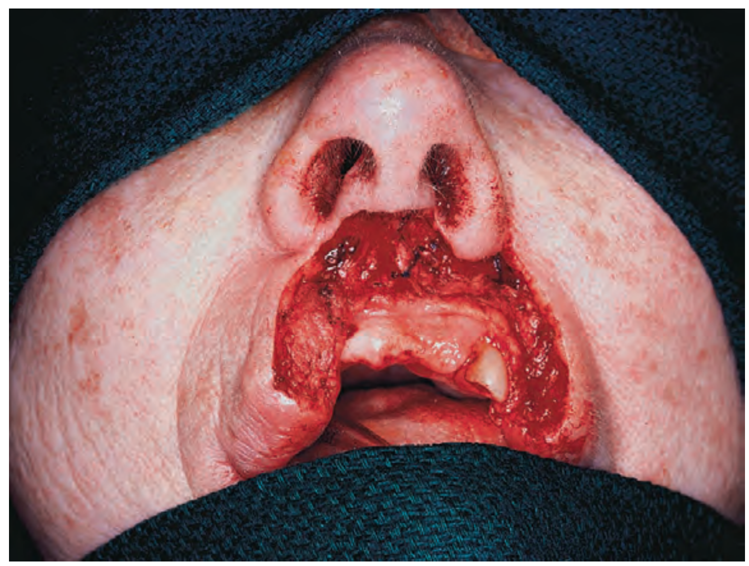

Figure 7.109 The surgical defect.

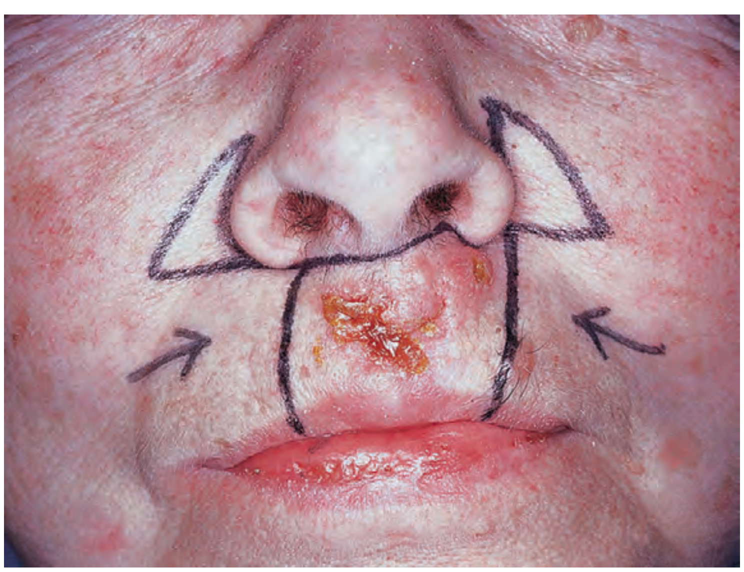

Figure 7.108 The plan of surgical excision is outlined.

Figure 7.110 The lateral cheek flap and residual upper lip are mobilized medially after excision of Burrows triangles.

Figure 7.111 The postoperative appearance 3 months following surgery.

Figure 7.113 The incisions for an Estlander flap and its insertion into the reconstructed left cheek are marked.

Figure 7.112 The same patient's appearance 8 months following surgery.

Figure 7.114 The Estlander flap is elevated in the usual fashion.

configuration of the lip is shown in Fig. 7.112. A very gratifying result of reconstruction was achieved after resection of a sizable tumor of the upper lip.

Oral Commissure

Secondary Reconstruction of the Oral Commissure. Full-thickness resection of the cheek, including the oral commissure, presents a significant functional and aesthetic deformity for the patient. A variety of reconstructive techniques are available for restoration of the full thickness of the cheek, including a folded forehead flap, a pectoralis myocutaneous flap with a skin graft, or a microvascular radial forearm free flap. None of these reconstructive methods, however, restore the competency of the oral commissure, and drooling remains a problem because of lack of competency of the oral cavity. However, a modification of the Estlander flap, described by Converse as the "over-and-out technique," can be used to reconstruct the commissure and restore oral competency.

The patient shown in Fig. 7.113 had recurrent carcinoma of the cheek mucosa, which radiation therapy had failed to heal. A through-and-through resection of the cheek, including the oral commissure, was performed, and the cheek was reconstructed with use of a folded forehead flap, which provided inner lining as well as external skin coverage. The patient's appearance approximately 3 months after forehead flap reconstruction shows restoration of the cheek and closure of the surgical defect but lack of oral competency because of the absence of the oral commissure. One can anticipate a similar situation after reconstruction of a through-and-through cheek defect with a folded radial forearm flap.

The proposed outlines for both the Estlander flap and excision of the skin in the reconstructed left cheek to create a space for insertion of the Estlander flap are marked. The Estlander flap is elevated in the usual fashion, keeping its pedicle on the left-hand side (Fig. 7.114). The blood supply is derived from the superior labial artery. It is a full-thickness through-and-through flap providing coverage of the skin as well as the mucosa and vermilion surface. The flap is rotated 180 degrees, demonstrating its very thin pedicle (Fig. 7.115), and then it is further rotated 90 degrees to a total rotation of 270 degrees (Fig. 7.116),

and it is inserted in the space created between the two layers of the reconstructed left cheek by excising the skin edge. The Estlander flap is now sutured in two layers, leaving a transient bridge between the upper lip and the commissure on the left side. The surgical defect in the upper lip at the donor site of the Estlander flap is visible in Fig. 7.116. A wooden stick is inserted through the opening in the upper lip between the bridge of the Estlander flap and the reconstructed commissure, demonstrating the pedicle of the flap.

The final closure of the surgical defect at the donor site demonstrates the immediate appearance of the patient on the operating table (Fig. 7.117). The bridge of the pedicle divides the oral cavity into two separate openings.

The same patient's appearance approximately 3 weeks following this operative procedure shows the small bridged flap still attached through its pedicle to the upper lip (Fig. 7.118). The pedicle of the flap is divided, and the configuration of the commissure is achieved by suturing the apex of the mucosa of the Estlander flap to the inner lining of the cheek, as in a V-Y plasty, pulling the mucosa and creating a horizontal crease in the flap.

After restoration of the commissure is completed, the patient's appearance with the open oral cavity is shown. The mouth is of an acceptable size and competency of the reconstructed commissure is complete (Fig. 7.119).

The same patient is shown in Fig. 7.120 with the mouth closed, giving an acceptable aesthetic appearance with reconstruction of the commissure and restoration of full competency of the oral cavity.

Paralysis of the Lip

Reconstruction of the Paralyzed Lip. Facial paralysis can be a devastating condition, particularly when all muscles of facial expression are involved. In the case of most head and neck cancer patients, paralysis affecting the lip is usually due to tumor involving those branches of the facial nerve that require surgical sacrifice. The impact on the lip is mainly aesthetic but can also be functional. Involvement of the buccal and

Figure 7.115 The flap is rotated 180 degrees.

Figure 7.117 The final closure of the surgical defect at the donor site.

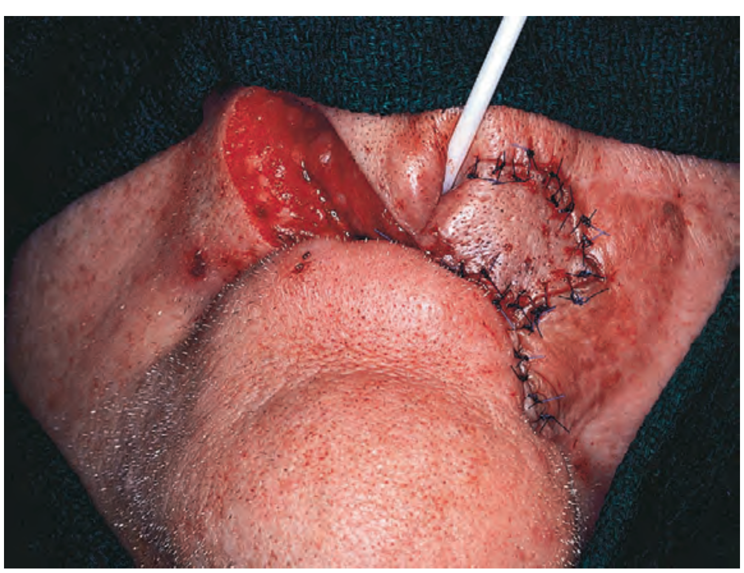

Figure 7.116 The flap is further rotated 90 degrees to a total rotation of 270 degrees and is inserted in the left cheek to recreate the oral commissure. The surgical defect at the donor site is seen in the upper lip.

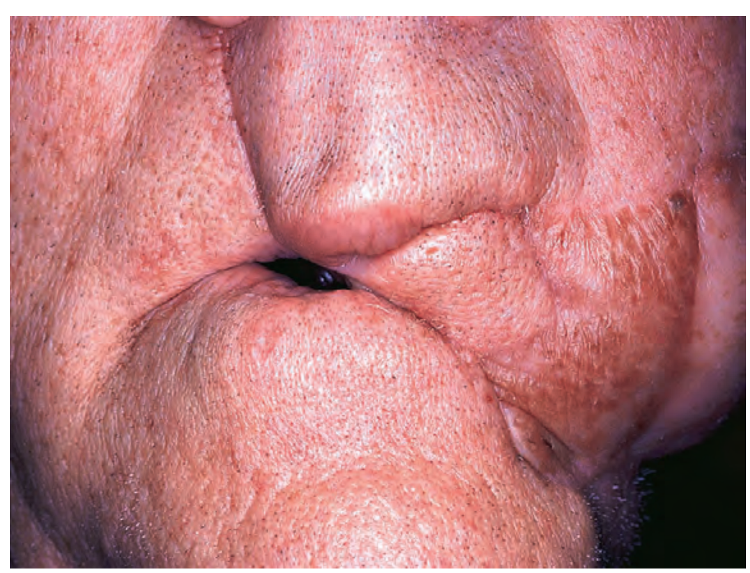

Figure 7.118 The patient's appearance approximately 3 weeks following surgery.

Figure 7.119 The patient's appearance with an open oral cavity.

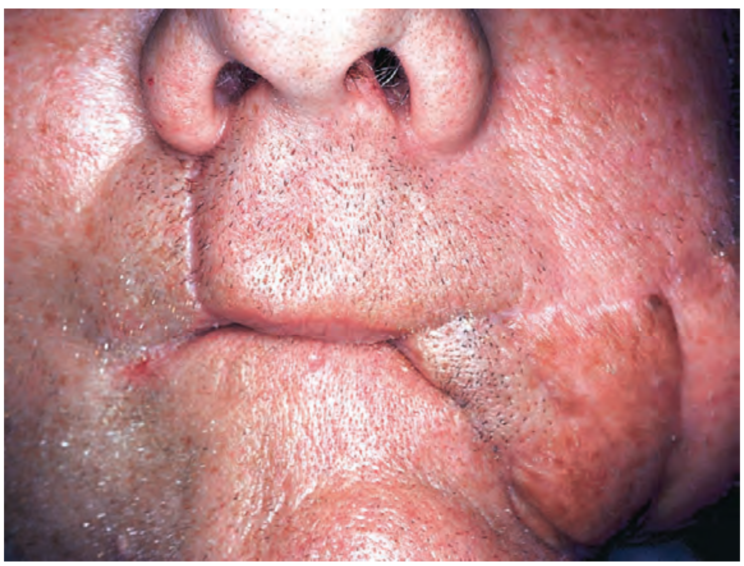

Figure 7.120 The patient's appearance with the mouth closed shows the reconstructed oral commissure.

mandibular branches of the facial nerve can lead to significant asymmetry of the lip, with functional loss of the depressor anguli oris, zygomaticus minor, and depressor anguli oris on one side of the face, resulting in asymmetry of the mouth and lips, in resting as well as animated positions. This leads to significant aesthetic deformity and functional morbidity. If only the depressor anguli oris is impacted due to loss of the marginal branch, nonsurgical approaches to improve symmetry can be very effective. Thus the contralateral marginal mandibular branch can either be surgically transected or paralyzed using botulinum toxin in order to achieve symmetry. There are multiple buccal branches to the muscles of facial expression that lift the corner of the mouth. Surgical correction is indicated only when most or all of the branches to the commissure are resected. As the cheek and the corner of the mouth sag over time, particularly in the older patient, the aesthetic deficit can become quite significant. In some cases, if the commissure droops significantly, then patients can have functional problems such as drooling. The usual complaints are facial asymmetry at rest and the inability to smile. Surgical management should be tailored to the patient's main concerns.

Static Reconstruction. If asymmetry at rest is the primary problem, then a static sling can be used to suspend the corner of the mouth and the cheek in order to improve symmetry. Although prosthetic materials, such as Gore-Tex, can be utilized, it is preferable to use autologous tissue, which offers better incorporation and lower rejection rates. The tensor fascia lata is easy to harvest and can be used to suspend the commissure and nasolabial fold. This fascia, or any static sling, can be sutured to the dermis in an incision made within the nasolabial fold and around the modiolus. This procedure is usually combined with an ipsilateral facelift where the skin of the face is elevated to the facelift plane through a preauricular incision. Once the skin is elevated, the proximal end of the sling is sutured to the deep tissues of the submuscular aponeurotic system (SMAS) overlying the zygomatic arch. The vector of pull is adjusted to maximize the correct position of the nasolabial fold and the lateral corner of the mouth. It is desirable to overcorrect the deficit since these tissues will tend to sag with time. Overcorrection can be performed to the point of achieving canine show. Acellular dermal matrix can also be used as a sling; it tends to relax very quickly over time. Therefore this type of tissue matrix is felt to be not rigid enough to maintain good position of the commissure. For most elderly patients, as well as patients who do not wish to undergo extensive procedures, the static sling combined with the facelift procedure is sufficient to achieve correction of the deficit. The procedure provides symmetry at rest and also improves function in patients who are extremely symptomatic, with drooling.

Dynamic Reconstruction. If the patient wishes to have symmetry at rest as well as an active smile, a temporalis transfer can be an effective procedure. The skin of the cheek is elevated in the facelift plane, and an incision is made in the nasolabial crease in order to inset the temporalis fascia. A temporal or coronal incision is used in order to expose the temporalis muscle. It is important to leave the temporalis fascia as well as the periosteum connected to the muscle so that this can be elevated and used to create the sling. In many cases it is not necessary to use the entire temporalis muscle. It is possible to divide fascia and muscle into anterior and posterior segments. The anterior segment is turned down as a sling, and the posterior segment is mobilized anteriorly in order to fill the temporal depression. On the other hand, if the entire temporalis muscle is used, the temporal defect can be recontoured with a prosthetic implant. The sling/muscle should be inset with significant overcorrection to show the canine tooth, because this will also tend to relax over time. In order to achieve dynamic function, the patient should be trained to bite down in order to achieve movement of the temporalis. However, this procedure quite often winds up working as a static sling instead of a dynamic repair. Theoretically, it should provide some function and does work as such in some patients. The masseter muscle can also be transferred in a similar fashion to achieve dynamic function.

Active function can also be restored with a neurotized flap with gracilis or serratus anterior muscles. This procedure usually involves two stages. A cross-facial nerve graft is first performed by anastomosing a buccal branch from the unaffected side to the nerve graft and transferring the nerve in the subcutaneous tissues over the upper lip. In 6 to 9 months, the nerve will grow through the graft to the ipsilateral side. Once the Tinel sign has reached the appropriate position on the affected side, the patient is ready for muscle transfer. Through a facelift exposure, a gracilis or serratus neurotized muscle flap is

transferred to the face with its vascular pedicle anatomized to the facial vessels. The muscle is inset under the appropriate tension and vector. The nerve to the muscle is anastomosed to the cross-facial nerve graft. Depending on the extent of the deficit and the required lift, a portion of the gracilis muscle is transferred. Successful muscle transfer and recovery of reinnervation should result in the patient achieving spontaneous smile. In general, patients with malignant tumors of the parotid gland often undergo surgery and postoperative radiation therapy, resulting in significant fibrosis and stiff soft tissues. Therefore, in an oncologic setting, such multistaged reconstructive procedures do not result in the anticipated outcome and are not preferred. Static slings can be quite effective to create symmetry with less morbidity and less extensive surgery.

OUTCOMES

Because a majority of patients with cancer of the lip present at an early stage for diagnosis and treatment, excellent results are achieved with appropriate initial therapy. Survival by stage of disease is shown in Fig. 7.121. Overall, 85% 5-year survival is achieved for cancer of the lip following surgical treatment. Ninety-four percent of patients with stage I disease are cured at 5 years. Even with stage IV disease, a 50% survival rate is achieved.

Initial therapy fails for approximately 15% of patients. The patterns of failure are shown in Fig. 7.122. Local recurrence and regional lymph node metastasis are the most common sites of treatment failure. Salvage treatment is often successful and should be aggressively undertaken for tumors of the lip. The potential for a long-term cure is excellent with salvage treatment.

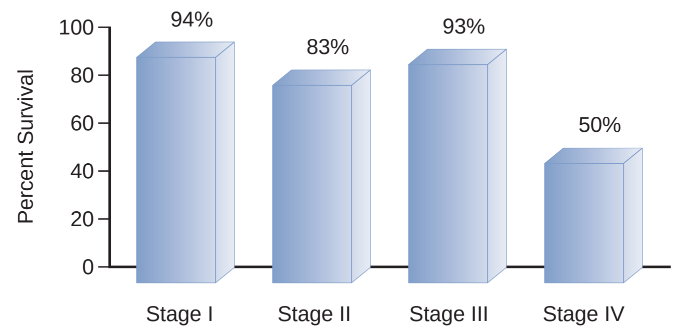

Figure 7.121 Survival by stage of squamous cell carcinoma of the lips.

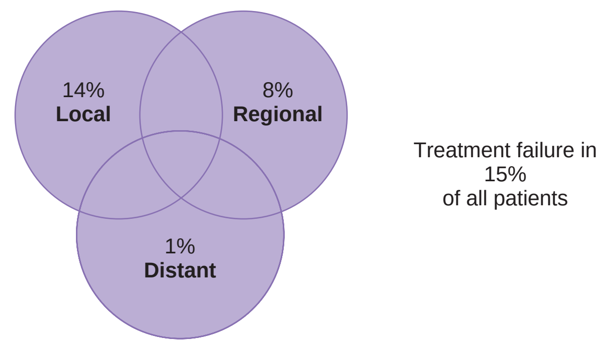

Figure 7.122 Patterns of failure of treatment of squamous cell carcinoma of lips.

CHAPTER 8

Oral Cavity

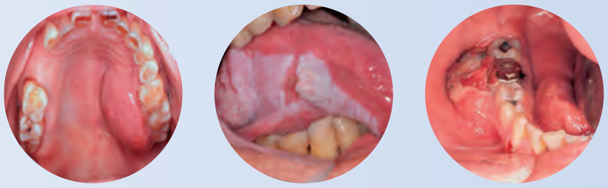

The oral cavity represents the entrance to the upper aerodigestive tract, which begins at the lips and ends at the anterior surface of the faucial arch. It is lined by squamous epithelium with interspersed minor salivary glands. The oral cavity also contains the dentoalveolar structures with the upper and lower dentition. The oral cavity is continuously exposed to inhaled and ingested carcinogens, and thus it is the most common site for the origin of malignant epithelial neoplasms in the head and neck region. Known carcinogens for oral cavity carcinoma include those present in tobacco, alcohol, and betel nuts. The association of human papilloma virus with oral cancer is not as well established as in oropharyngeal cancers.

Primary tumors of the oral cavity may arise from the surface epithelium, minor salivary glands, or submucosal soft tissues. Lesions of dentoalveolar origin represent a unique group of neoplasms and cysts (discussed in Chapter 16). The various anatomic sites within the oral cavity as described by the American Joint Committee on Cancer (AJCC) and International Union Against Cancer (UICC) staging system are shown in Fig. 8.1. More than 90% of malignant tumors in the oral cavity are squamous cell carcinomas, and the remainder are minor salivary gland carcinomas and other rare tumors. The worldwide incidence and mortality of oral cancers in men and women is shown in Figs. 8.2 and 8.3. Most patients with cancer in the oral cavity are men, although the incidence of tongue cancer in women in the United States has progressively increased over the past several decades. In the Western world, the tongue and floor of the mouth are the most common sites of origin for primary squamous cell carcinomas in the oral cavity. However, the retromolar trigone and buccal mucosa are the most frequently encountered primary sites in areas of the world where chewing of tobacco and/or betel nuts is common. The site distribution of various primary cancers in the oral cavity in the United States is shown in Fig. 8.4.

EVALUATION

The clinical features of the primary tumors arising from the mucosal surface of the oral cavity are variable. The tumor may be ulcerative, exophytic, or endophytic. The gross characteristics of the lesion are usually sufficient to raise the index of suspicion regarding the need for a biopsy to establish tissue diagnosis. Ulcerative lesions usually are accompanied by an irregular edge and induration of the underlying soft tissues (Fig. 8.5). On the other hand, exophytic lesions may present either as a cauliflower-like irregular growth or as flat, pink to pinkish-white proliferative lesions (Figs. 8.6 and 8.7). Occasionally, a red to pink velvety flat lesion is the only manifestation of superficially invasive or in situ carcinoma (Fig. 8.8). Squamous

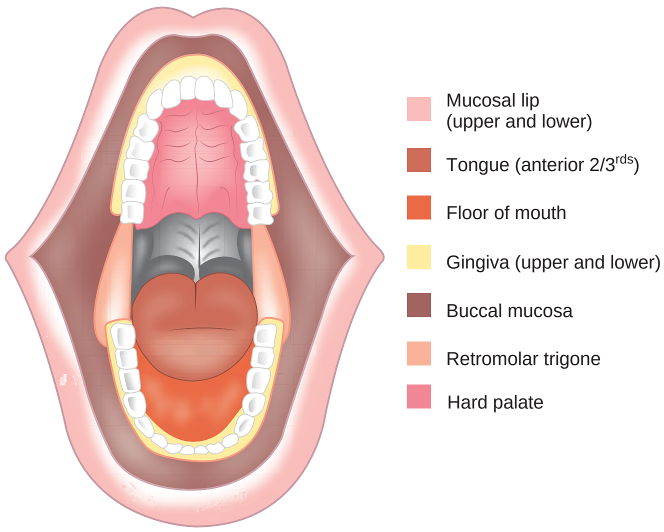

Figure 8.1 Anatomic sites within the oral cavity.

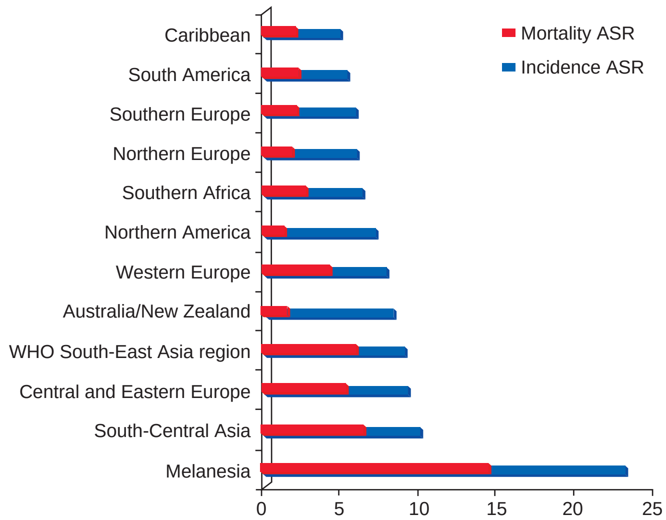

Figure 8.2 Geographic regions with the highest age-standardized incidence and mortality rates for lip and oral cancer per 100,000 in men. *(From Ferlay J, Soerjomataram I, Ervik M, Dikshit R, Eser S, Mathers C, Rebelo M, Parkin DM, Forman D, Bray F. GLOBOCAN 2012 v1.0, Cancer Incidence and Mortality Worldwide: IARC CancerBase No. 11. Lyon, France, International Agency for Research on Cancer, 2013. Available from* http://gco.iarc.fr/today/home.*)*

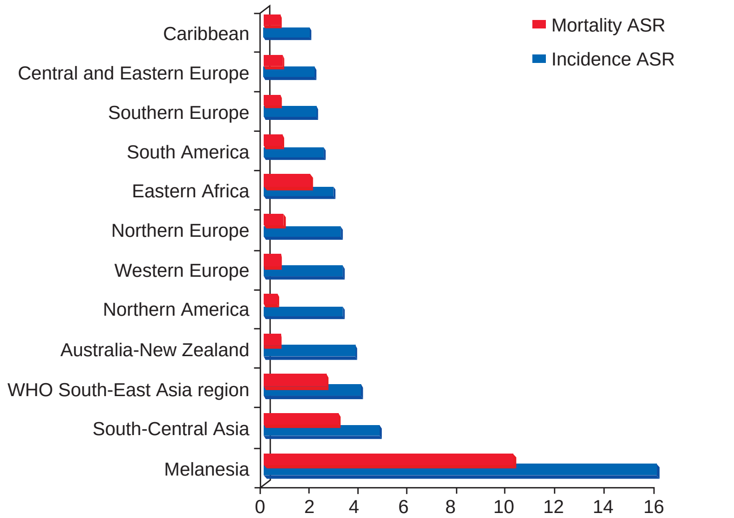

Figure 8.3 Geographic regions with the highest age-standardized incidence and mortality rates for lip and oral cancer per 100,000 in women. *(From Ferlay J, Soerjomataram I, Ervik M, Dikshit R, Eser S, Mathers C, Rebelo M, Parkin DM, Forman D, Bray F. GLOBOCAN 2012 v1.0, Cancer Incidence and Mortality Worldwide: IARC CancerBase No. 11. Lyon, France, International Agency for Research on Cancer, 2013. Available from* http://gco.iarc.fr/today/home.*)*

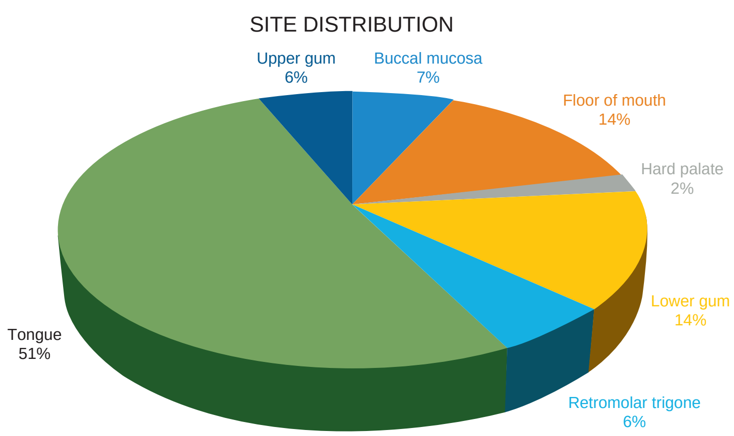

Figure 8.4 The site distribution of primary cancers in the oral cavity (MSK data 1985–2015; *all patients re-staged according to AJCC 8th edition criteria).*

Figure 8.5 An ulcerative squamous cell carcinoma of the undersurface of the tongue.

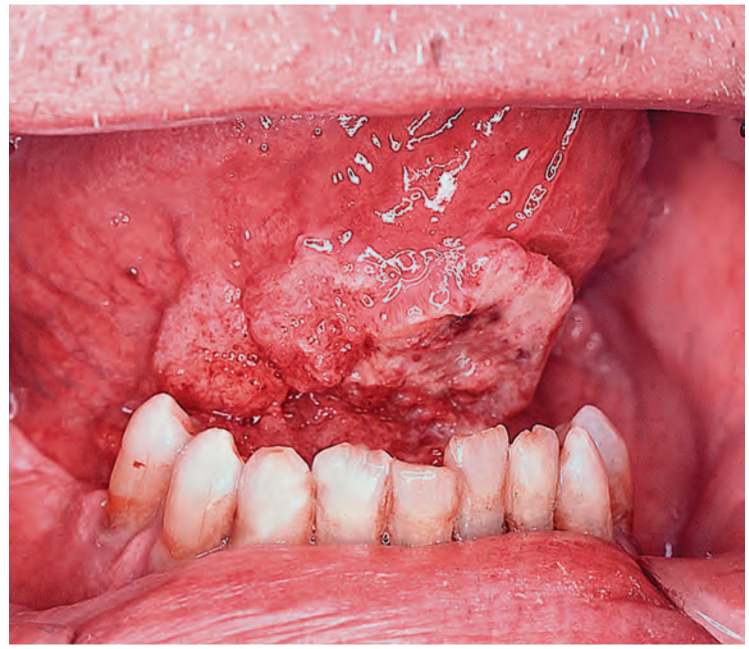

Figure 8.6 A deeply infiltrating and exophytic carcinoma of the floor of the mouth.

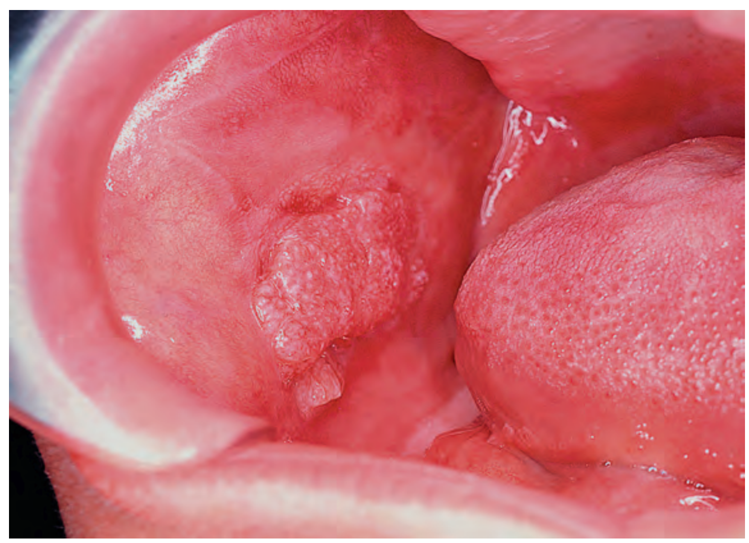

Figure 8.7 An exophytic papillary squamous cell carcinoma of the buccal mucosa.

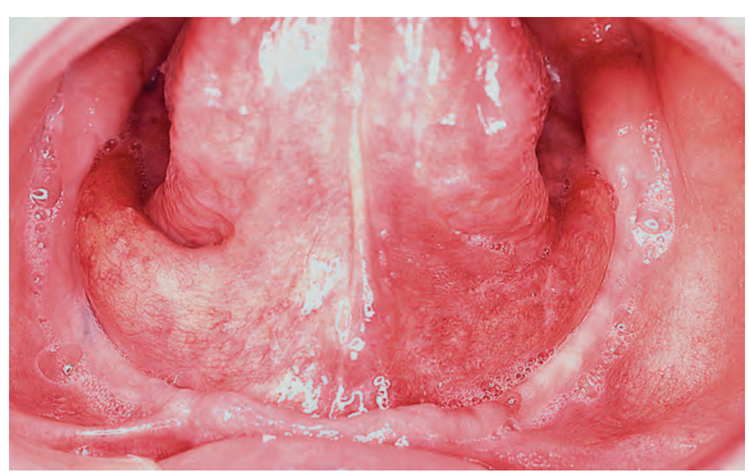

Figure 8.8 A red to pink velvety flat in situ carcinoma of the floor of the mouth.

cell carcinomas with excessive keratin production and verrucous carcinomas present as white heaped-up keratotic lesions with varying degrees of keratin debris on the surface (Figs. 8.9 through 8.11). Papillary projections often are seen in lesions that are accompanied or preceded by a squamous papilloma (Figs. 8.12 and 8.13). Compare the appearance of a papilloma to papillary polypoid squamous cell carcinoma, shown in Fig. 8.14. Bleeding from the surface of the lesion is a characteristic of malignancy and immediately raises suspicion for a neoplastic process. Endophytic lesions have a very small surface component but a substantial amount of soft-tissue involvement beneath the surface (Fig. 8.15).

Figure 8.9 Squamous cell carcinoma of the tongue associated with hyperkeratosis.

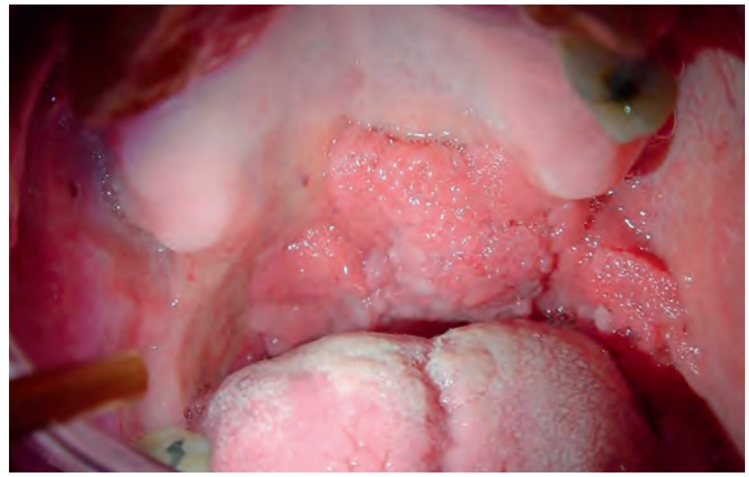

Figure 8.12 Squamous papilloma of the palate and buccal mucosa.

Figure 8.10 An exophytic squamous cell carcinoma of cheek mucosa with white keratin debris.

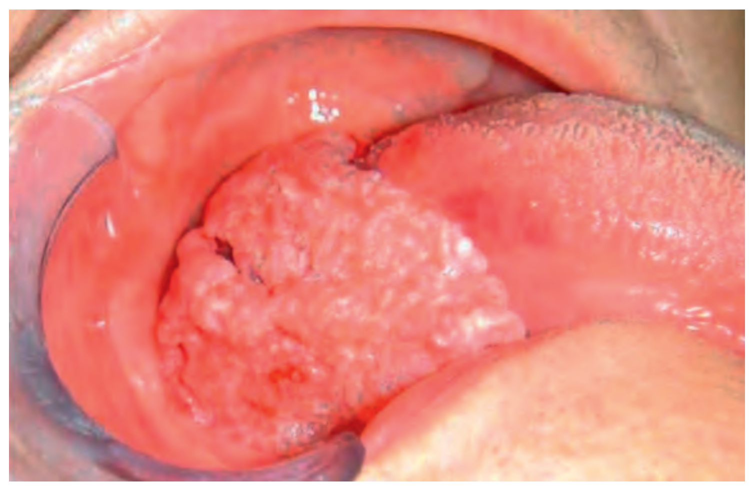

Figure 8.13 Squamous papilloma of the lateral border of the tongue.

Figure 8.11 A verrucous carcinoma of the tongue.

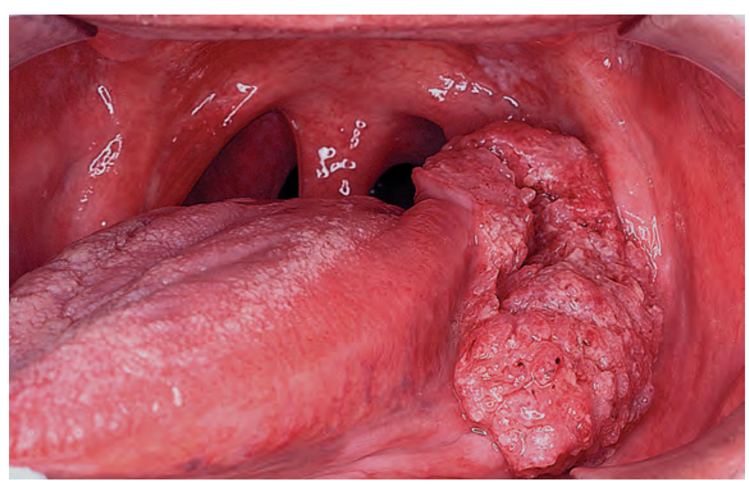

Figure 8.14 An exophytic papillary polypoid squamous cell carcinoma of the retromolar gingiva.

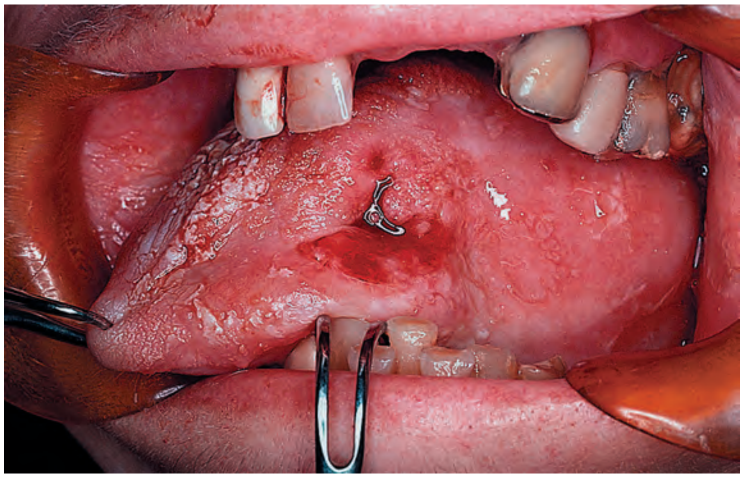

Figure 8.15 A deeply invasive endophytic squamous cell carcinoma of the tongue.

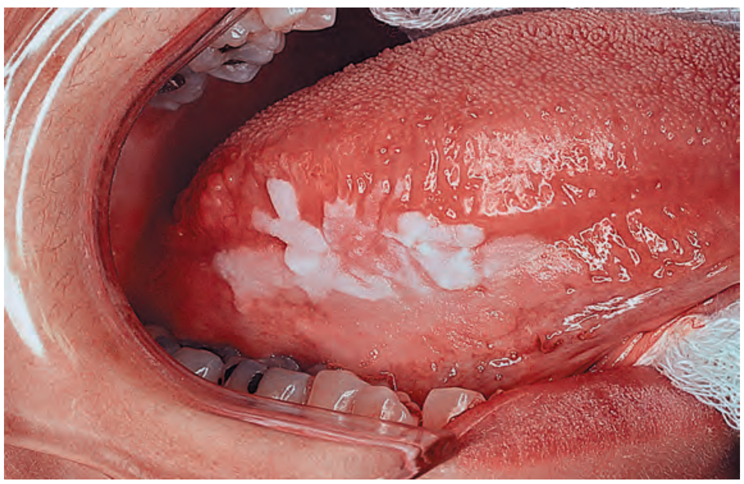

Figure 8.16 Leukoplakia (hyperkeratosis) of the oral tongue.

Figure 8.17 Discoid leukoplakia with hyperkeratosis of the undersurface of the tongue.

Figure 8.18 Verrucoid hyperkeratosis of the lateral border of the tongue.

Figure 8.19 Papillary hyperkeratosis with squamous papilloma of the commissure of the mouth.

Diagnosis of precancerous lesions or early cancer can be difficult. Leukoplakia and erythroplakia are precancerous lesions that have a varying risk of progression to malignancy. Conversion from leukoplakia to carcinoma is reported in up to 5% to 7% of patients observed over several years. Keratoses of a variety of degrees manifest as leukoplakia (Figs. 8.16 through 8.20). Erythroplakia usually manifests as a pinkish, velvety flat discoloration without any papillary projections (Fig. 8.21). The risk of development of malignancy in erythroplakia approaches 30%. Speckled leukoplakia has a particularly high incidence of malignant transformation, similar to erythroplakia (Fig. 8.22). Synchronous multiple primary cancers occur in approximately 4% of patients with oral cancers (Figs. 8.23 through 8.25). Therefore a thorough examination of the upper aerodigestive tract mucosa should be performed in every case. Mucosal melanomas usually present as characteristic pigmented lesions, although they can be amelanotic (Figs. 8.26 and 8.27). Tumors of minor salivary origin present as submucosal masses (Figs. 8.28 through 8.31). Metastatic tumors also may present as submucosal masses (Fig. 8.32). A variety of benign conditions can have an appearance that resembles malignant neoplasms (Figs. 8.33 and 8.34). A high index of suspicion is crucial to early diagnosis of cancer, especially in high-risk individuals. Biopsy and histopathologic examination represent the standard of care for diagnosis, but noninvasive in vivo imaging techniques such as reflectance confocal microscopy (RCM) are showing

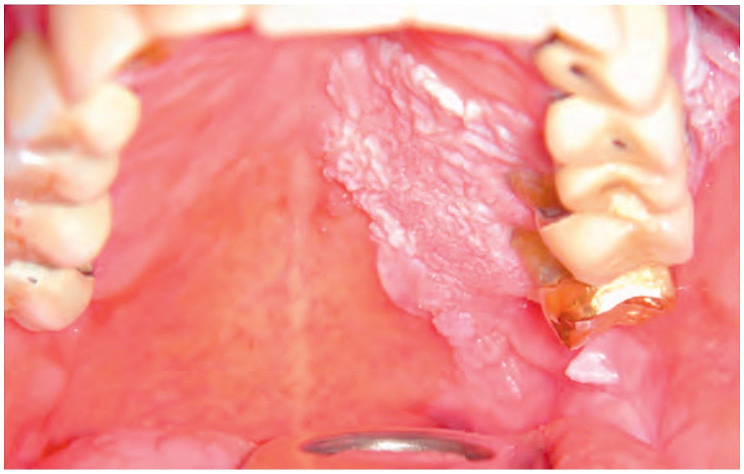

Figure 8.20 Hyperkeratosis of the hard palate and upper gingiva.

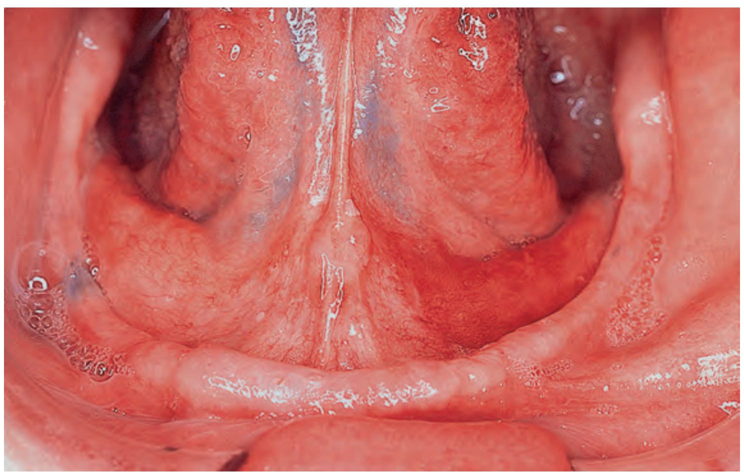

Figure 8.21 Erythroplakia of the left floor of the mouth.

Figure 8.22 Speckled leukoplakia of the oral tongue.

Figure 8.23 Two separate foci of squamous cell carcinoma of the tongue.

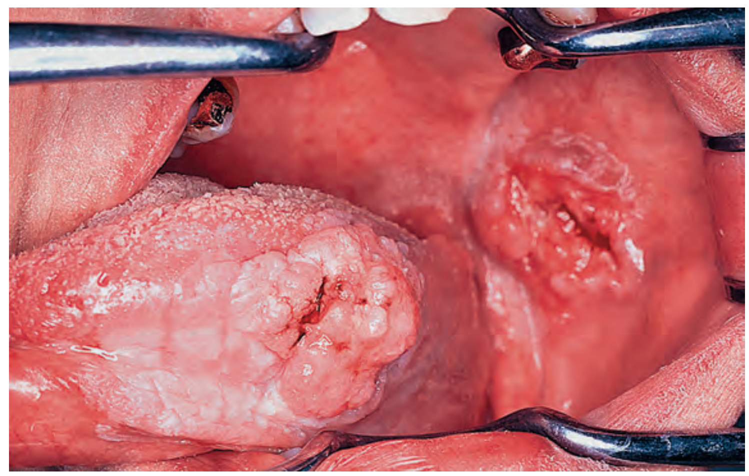

Figure 8.24 Synchronous squamous cell carcinomas of the tongue and cheek mucosa.

Figure 8.25 Synchronous primary carcinomas of the upper and lower alveolar ridges.

promise (Figs. 8.35 and 8.36). The RCM can be performed with a handheld probe in an outpatient setting, without the need for anesthesia.

Tissue diagnosis is usually confirmed by a wedge or punch biopsy obtained from the lesion with adequate volume of viable tissue. A biopsy specimen taken from necrotic areas of the tumor is not adequate, and therefore attention must be given to obtaining a vascularized, viable tumor specimen. Superficial biopsy specimens from highly keratinizing squamous cell carcinomas and verrucous carcinomas often do not provide satisfactory representative tissue, and thus the diagnosis of invasive carcinoma can be missed. Therefore in situations in which an excessive deposit of keratin is seen on the surface of an exophytic lesion, the biopsy should be obtained from the

Figure 8.26 A mucosal melanoma of the upper gum.

Figure 8.27 Extensive mucosal melanoma of the hard palate and upper gum.

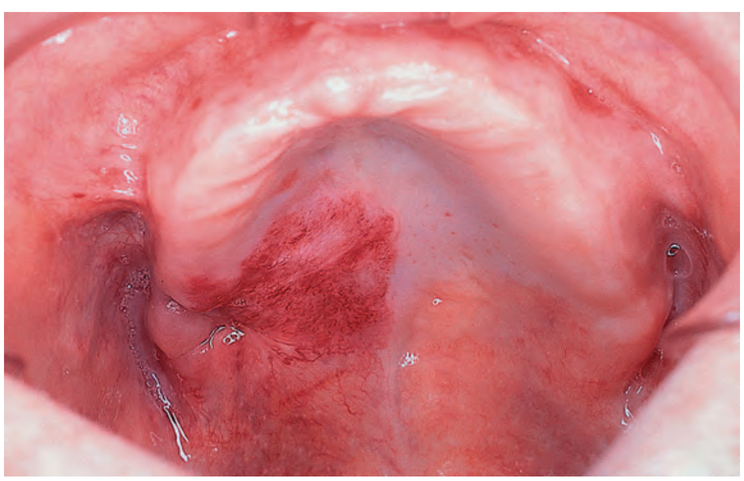

Figure 8.28 Ill-defined submucosal mucoepidermoid carcinoma of the hard palate.

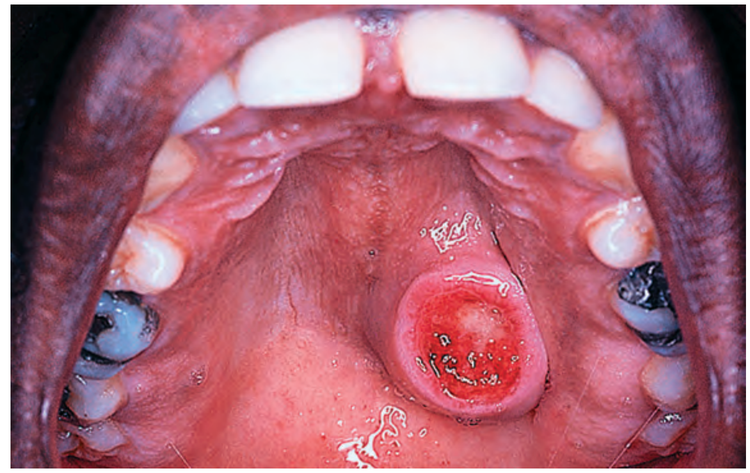

Figure 8.29 Ulcerated adenoid cystic carcinoma of the hard palate.

Figure 8.30 Mucoepidermoid carcinoma of the hard palate.

Figure 8.31 An adenocarcinoma of the hard palate.

adjacent invasive zone or from the depth of the lesion rather than from the surface. If a biopsy does not show carcinoma in a lesion that clinically shows signs of malignancy, then the biopsy should be repeated.

The staging of primary tumors of the oral cavity as published by the AJCC and UICC is widely accepted. In its most recent revision (eighth edition of the AJCC Staging Manual), depth of invasion (DOI) is added to the surface dimensions and local extent of the tumor as the required parameters for primary tumor staging in the oral cavity (Fig. 8.37). Accurate assessment of DOI by clinical examination is not possible. However, the staging system stratifies DOI by 5 mm increments, and thus clinical estimates of DOI can be categorized into thin (<5 mm), thick (5-10 mm), and very thick (>10 mm) by palpation to assign clinical T stage (Fig. 8.38). The stage distribution of patients with squamous cell carcinoma of the oral cavity at the Memorial Sloan Kettering Cancer Center in New York is shown in Fig. 8.39.

Figure 8.32 A metastatic lung carcinoma in the tongue.

Figure 8.34 "Brown tumor" of primary hyperparathyroidism involving the left lower gum.

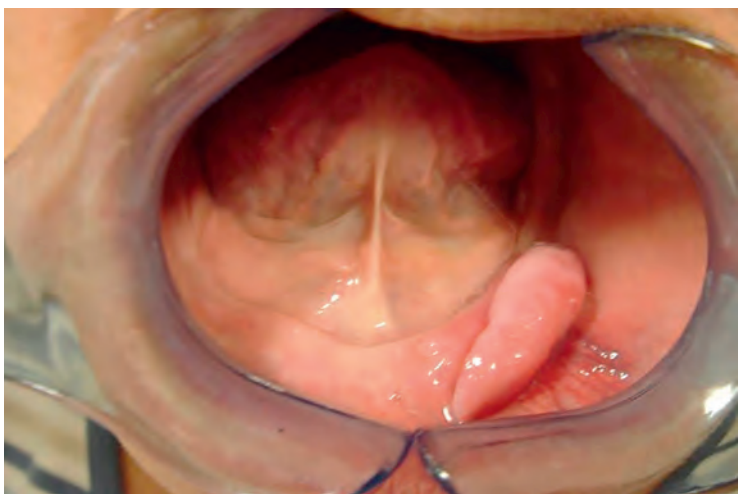

Figure 8.33 Epulis fissuratum of the left lower gum.

Figure 8.35 Reflectance confocal microscopy performed with a handheld probe directly applied on the surface of the lesion.

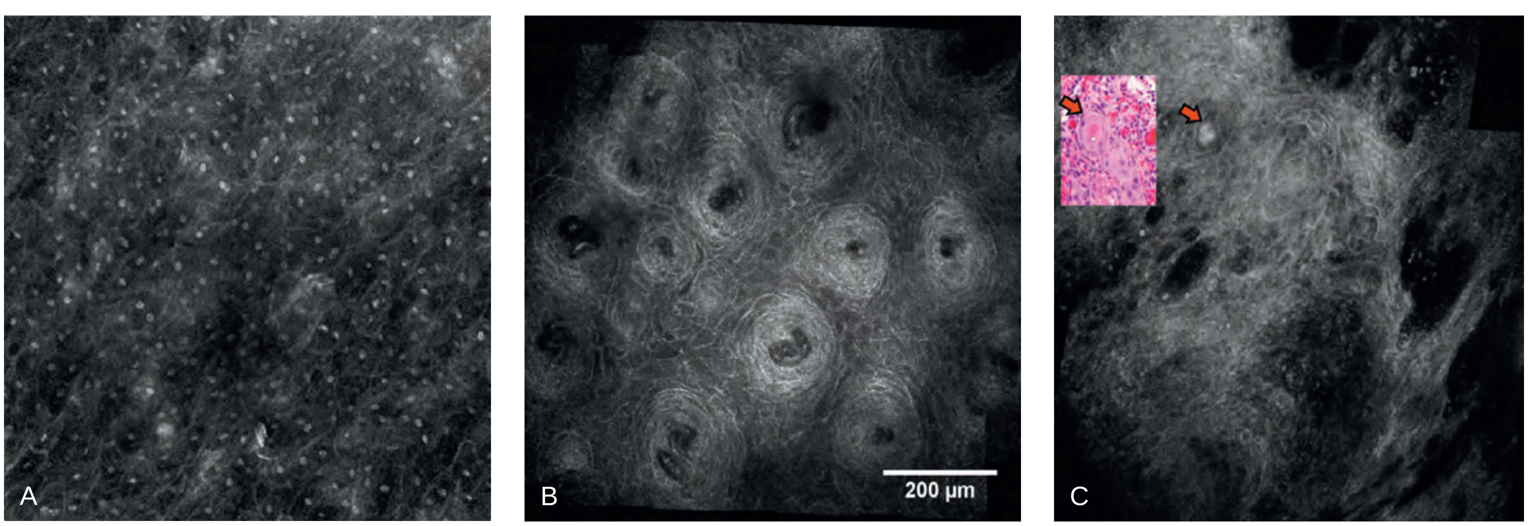

Figure 8.36 Reflectance confocal microscopy (RCM) showing normal buccal mucosa. **A**, Superficial epithelial layer showing a monomorphic cellular pattern with highly reflective chromatin. **B**, Deeper layer showing perpendicularly cut, regularly distributed blood vessels. **C**, RCM of oral squamous cell carcinoma showing keratin pearl (*arrow*) on RCM and H&E image (*inset*).

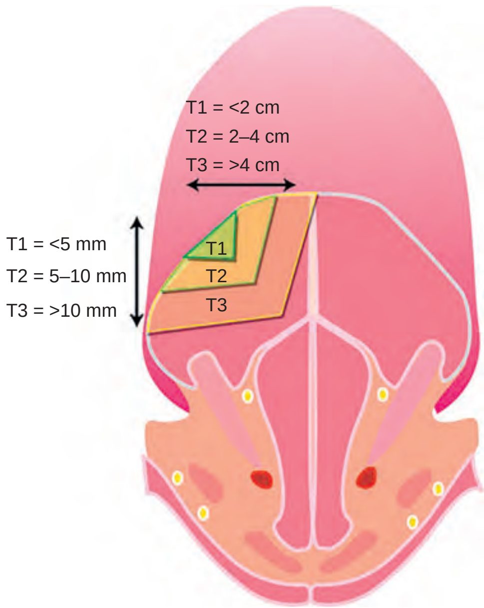

Figure 8.37 Depth of invasion and surface dimensions are the parameters required for T staging of oral cancer.

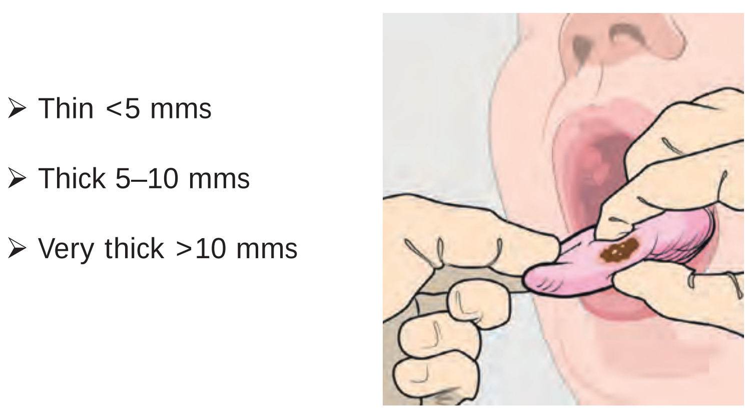

Figure 8.38 Primary tumors of the oral cavity are categorized as thin, thick, and very thick by palpation.

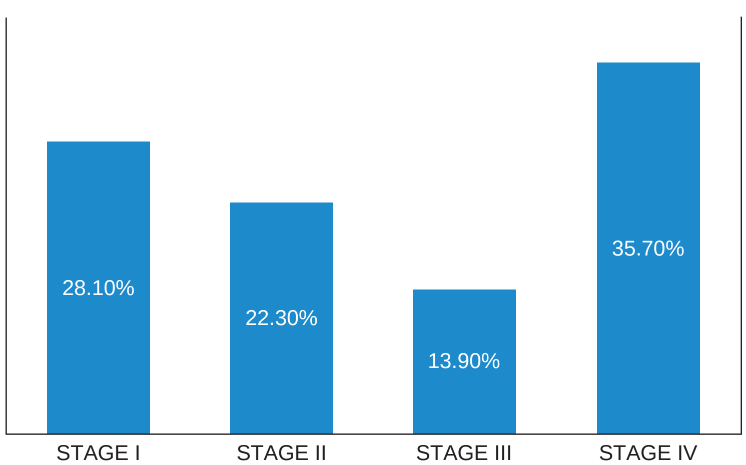

Figure 8.39 Stage distribution for squamous cell carcinoma of the oral cavity (MSK data 1985–2015; *all patients re-staged according to AJCC 8th edition criteria*).

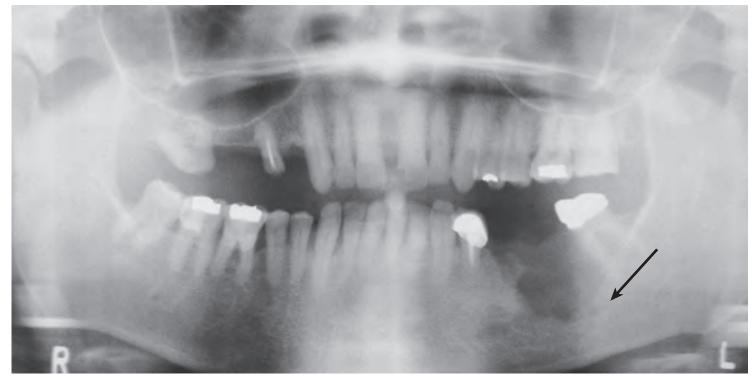

Figure 8.40 A panoramic radiograph of the mandible showing bone invasion (*arrow* points to lesion).

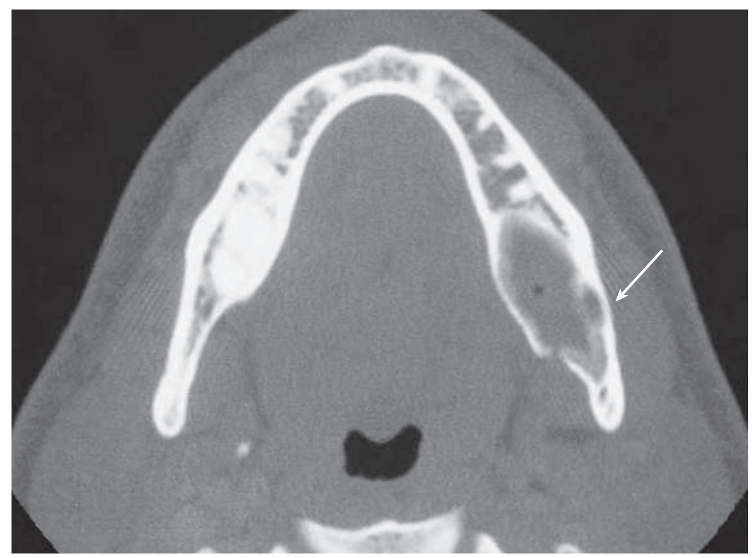

Figure 8.41 A computerized tomogram of the mandible showing an intraosseous cystic lesion (*arrow* points to lesion).

Imaging

The proximity or direct extension of a primary tumor of the oral cavity to the mandible requires appropriate radiologic studies to establish the presence and extent of bone involvement. Although the absence of radiographic findings does not rule out bone invasion, bone destruction as seen on the radiograph confirms tumor invasion.

Plain radiographs of the mandible in the anteroposterior and oblique views are not satisfactory as a routine screening test to establish or rule out bone destruction. A panoramic view of the mandible (an orthopantomogram) is helpful to assess the general architecture of the mandible in relation to the dentoalveolar structures and invasion by the tumor (Fig. 8.40). However, for technical reasons, the midline of the mandible near the symphysis is not adequately evaluated by a panoramic x-ray. In addition, early invasion of the lingual cortex of the mandible cannot be assessed on a panoramic view. A computerized tomogram of the oral cavity and neck is the standard initial radiographic study for assessment of locoregional extent of the tumor. It allows comprehensive evaluation of neck nodes and also the relationship of the primary tumor to adjoining bone, especially in situations such as primary tumors of the mandible and lesions where soft-tissue extension from tumors involving the ascending ramus of the mandible is suspected (Fig. 8.41).

In addition, three-dimensional reconstructions of CT images provide an excellent overview of the mandible or maxilla from any desired angle. Three-dimensional reconstructions of the mandible of a patient with an ossifying fibroma of the body of the mandible on the left-hand side causing expansion and involving the lingual cortex are shown in Figs. 8.42 and 8.43. A three-dimensional CT scan and computer-assisted design and computer-assisted model (CAD-CAM) planning is of great value

Figure 8.42 Three-dimensional reconstruction of the computed tomography scan in a lateral view showing the expansile lesion of the body of the mandible.

Figure 8.43 Three-dimensional reconstruction of an oblique caudal view of the body of the mandible showing an expansile lesion involving the lingual cortex.

to the surgeon for mandible reconstruction with a microvascular free flap. This process is a significant advance in reconstruction of mandibular defects and dental implant planning (see Chapters 17 and 18). Invasion of the maxilla by primary tumors of the oral cavity, such as those arising from the palate or upper alveolus, is best assessed by a CT scan. It is important to obtain coronal cuts of the computerized scans with soft tissue and bone windows to adequately assess the extent of tumor involving the hard palate and alveolus.

Magnetic resonance imaging (MRI) is superior in defining soft-tissue detail, evaluating bone marrow invasion of the mandible and hard palate, and assessing for perineural invasion. A sagittal MRI scan of a patient with an endophytic tongue carcinoma vividly demonstrates its intramural extent (Fig. 8.44), as seen in the bisected specimen (Figs. 8.45 and 8.46). Also, in situations in which extensive soft-tissue invasion in the parapharyngeal space is suspected, an MRI scan is desirable. However, bony details are not very well delineated on MRI, and a CT scan is preferred in these situations. Regardless of the presence or absence of invasion of the mandible or maxilla by a tumor, if any bone resection or osteotomy is to be undertaken for surgical treatment of a primary tumor of the oral cavity or oropharynx, appropriate radiographic studies of the bone under consideration must be obtained before the surgical procedure to avoid any "surprises" on the operating table. Early invasion of the mandible is difficult to detect even on a CT scan, but

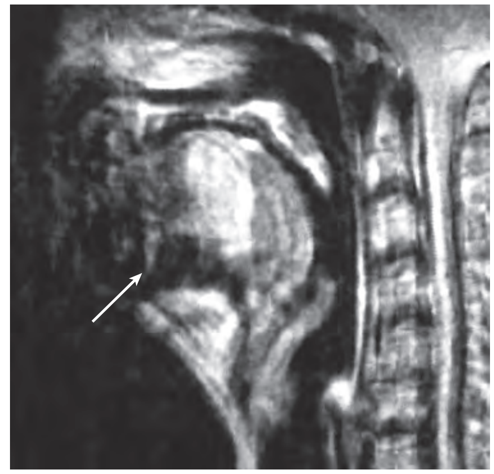

Figure 8.44 A sagittal view of a magnetic resonance imaging scan of the oral cavity showing a large endophytic tumor of the tongue (*arrow* points to lesion).

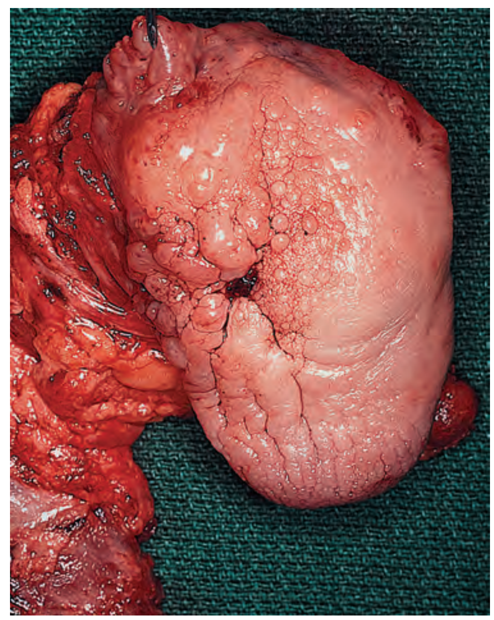

Figure 8.45 The surgical specimen of a total glossectomy shows minimal surface ulceration.

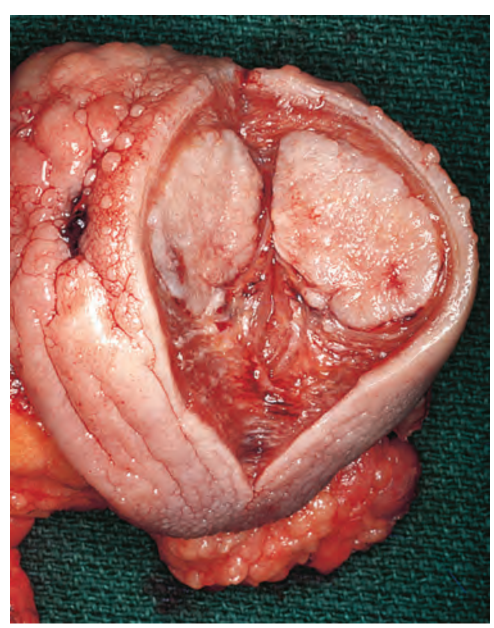

Figure 8.46 The bisected specimen of the tongue shows a large endophytic tumor.

on a practical basis, tumors that are in close proximity to the mandible without demonstrable radiographic bone invasion are adequately treated with a marginal mandibulectomy (Fig. 8.47). When assessing patients who have no obvious bone invasion on a CT scan, it is important to examine the coronal views to image the relationship of the tumor to the craniocaudal height of the mandible. Marginal resection may not be safe even in the absence of bone invasion if the tumor extends along the entire height of the mandible (Fig. 8.48). In the presence of gross invasion of the mandible, CT provides useful information on the extent of bone that needs resection (Fig. 8.49). Extent of bone marrow involvement is best evaluated on T1-weighted MRI, which nicely demonstrates replacement of adult fatty marrow (Fig. 8.50).

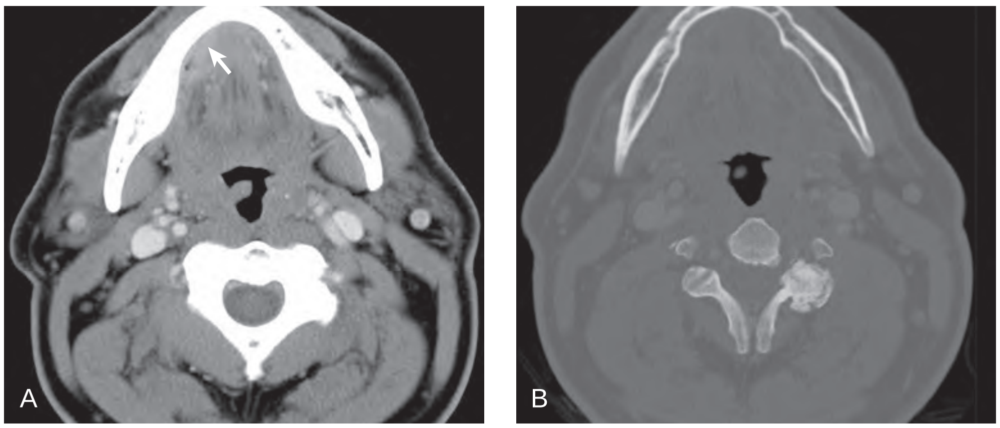

Figure 8.47 An axial view of a computed tomography scan of the oral cavity showing (**A**) an enhanced tumor of the right floor of the mouth in close proximity to the lingual plate of the mandible and (**B**) no obvious bone invasion on the bone algorithm (*arrow* points to lesion in **A**).

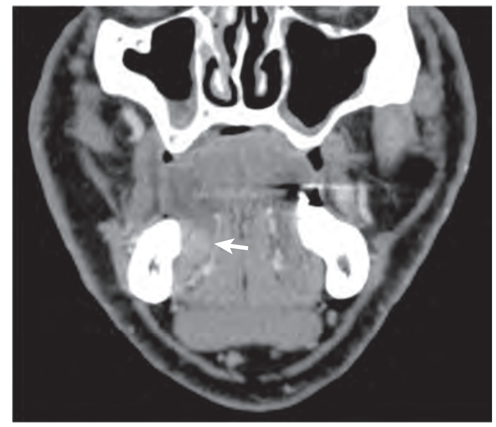

Figure 8.48 A coronal view of a computed tomography scan of the oral cavity demonstrating the relationship of the tumor in the right floor of the mouth to the vertical height of the uninvolved right mandible (*arrow* points to lesion).

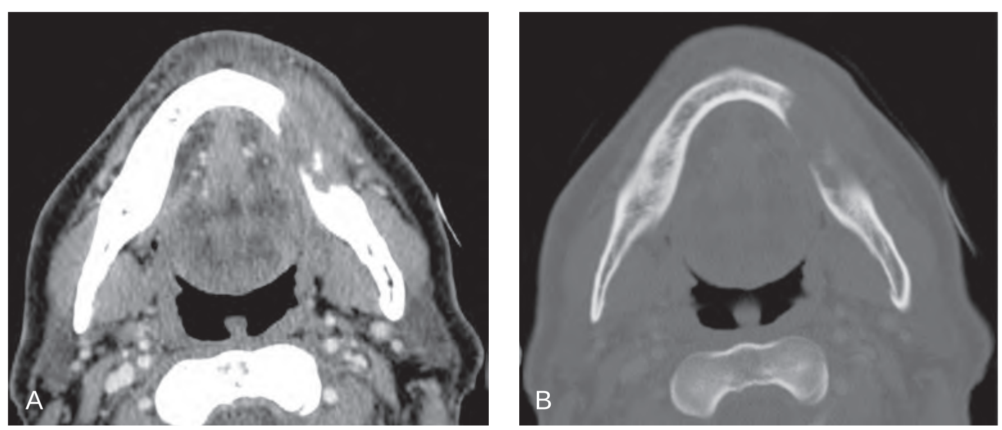

Figure 8.49 A computed tomography scan of the oral cavity. **A**, Soft tissue algorithm. **B**, Bone algorithm showing the extent of mandible involvement.

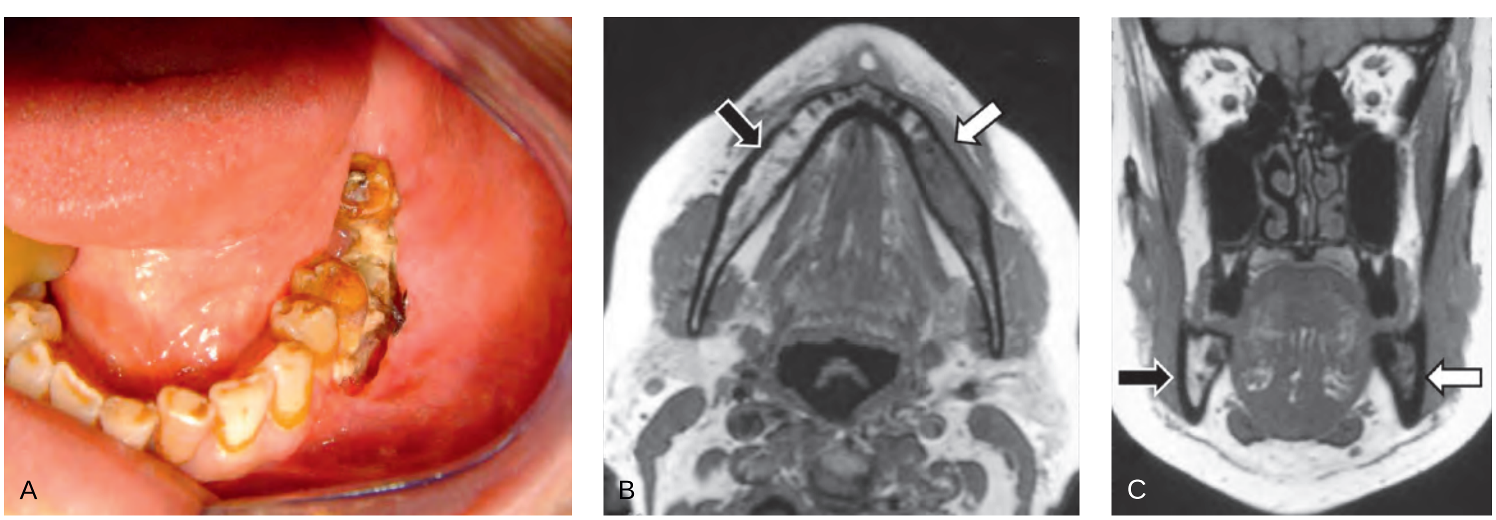

Figure 8.50 Squamous cell carcinoma of the lower gum (**A**). Axial (**B**) and coronal (**C**) views of T1-weighted magnetic resonance imaging shows normal fatty bone marrow (*black arrows*) and bone marrow involved by tumor (*white arrows*).

Pathology

Most lesions of squamous cell origin have a varying degree of histologic progression from in situ to invasive carcinoma. The histologic grade of the lesion generally reflects the aggressiveness of the tumor. Squamous cell carcinoma may range from well differentiated to poorly differentiated as well as undifferentiated and sarcomatoid, as defined by the extent to which a tumor demonstrates nuclear pleomorphism, cytologic atypia, and morphologic resemblance to benign squamous mucosa. The histologic grade reflects the aggressiveness of the tumor. Tumors that are undifferentiated or sarcomatoid are the most aggressive.

The most important histologic feature of the primary tumor that affects selection of treatment and eventual prognosis is its DOI. Thin and superficially invasive lesions have a lower risk of regional lymph node metastasis, are highly curable, and offer an excellent prognosis. On the other hand, thicker lesions that deeply infiltrate the underlying soft tissues have a significantly increased incidence of regional lymph node metastasis and an adverse impact on prognosis. The risk of lymph node metastasis and survival rates in relation to the DOI of the primary lesion for T1 and T2 squamous carcinomas of the oral tongue and floor of mouth are shown in Fig. 8.51. Although it would be ideal to know the exact DOI of the lesion before surgical intervention, having that information before surgical excision and histopathologic examination of the primary tumor is not possible. In general, however, estimate of DOI by assessing thickness of the lesion as appreciated by palpation is a reasonably good indicator of deeply invasive lesions versus superficial lesions to estimate the extent of soft tissue and/or bone resection for the primary lesion and to decide on the need for elective dissection of the regional lymph nodes at risk in a clinically negative neck. Several retrospective studies have identified DOI of the primary tumor as an important determinant of prognosis. Thus DOI is now included in T staging of primary tumors of the oral cavity. The presence of perineural invasion and the presence of lymphovascular tumor emboli are other prognostic indicators for tumor control and survival. Local control of the primary tumor is also affected by the pattern of tumor infiltration, with single cell infiltration more unfavorable than a broad, "pushing" border. As one would expect, negative margins are another key factor in locoregional control. In reporting pathologic analysis of resected oral cancer specimen, tumor clearance from the closest margin should be reported. Traditionally, the presence of invasive carcinoma within 5 mm is felt to be associated with a significant risk of local recurrence. However, some studies report that the risk of recurrence in oral tongue squamous cell carcinoma starts to increase when the tumor is within 2 mm rather than 5 mm from the margin. Histologic features of the primary tumor that have an impact on therapeutic outcomes are shown in Box 8.1.

TREATMENT

The goals of treatment of cancer of the oral cavity are (1) cure of the cancer; (2) preservation or restoration of speech, mastication, swallowing, and external appearance; (3) minimization of the sequelae of treatment such as dental decay, osteonecrosis of the mandible, and trismus; and (4) selecting options with the awareness of the risk of subsequent primary tumors and their management. Factors that influence the choice of initial treatment are related to the characteristics of the primary tumor (tumor factors), the patient (patient factors), and the treatment team (physician factors).

In general, small and superficial tumors of the oral cavity are equally amenable to being cured by surgical resection or radiotherapy. Therefore use of a single modality is preferred as the definitive treatment in early stage (T1 and T2) tumors of the oral cavity. When the end point of treatment, that is, cure of cancer, is comparable, other factors must play a role in the selection of initial treatment. These factors include complications, cost, convenience, compliance, and long-term sequelae of treatment (Fig. 8.52). Considering these factors, surgery is the preferred treatment for T1 and T2 tumors of the oral cavity.

Box 8.1 Pathologic Features That Affect the Prognosis of Oral Cancer

Degree of differentiation
Size of tumor
Depth of invasion
Endophytic versus exophytic growth
Lymphovascular invasion
Perineural invasion
Invasive front
Margins
Bone invasion

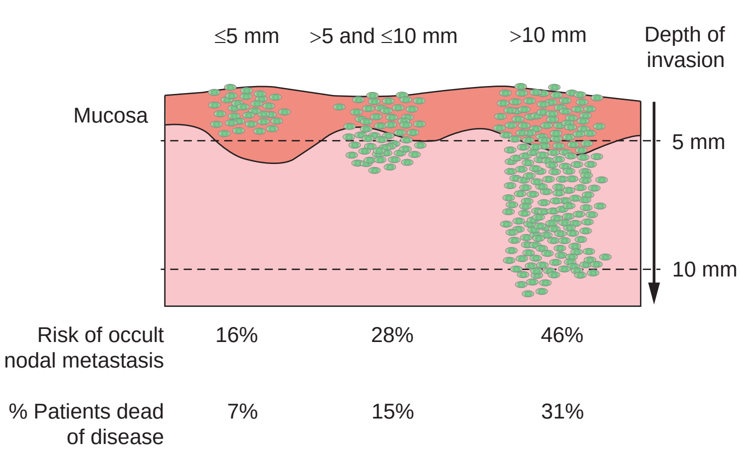

Figure 8.51 The incidence of occult nodal metastasis in the clinically negative neck for patients and disease-specific survival for patients with T1 and T2 oral carcinoma in relation to depth of invasion (DOI). (Memorial Sloan Kettering Cancer Center data, 1985–2015).

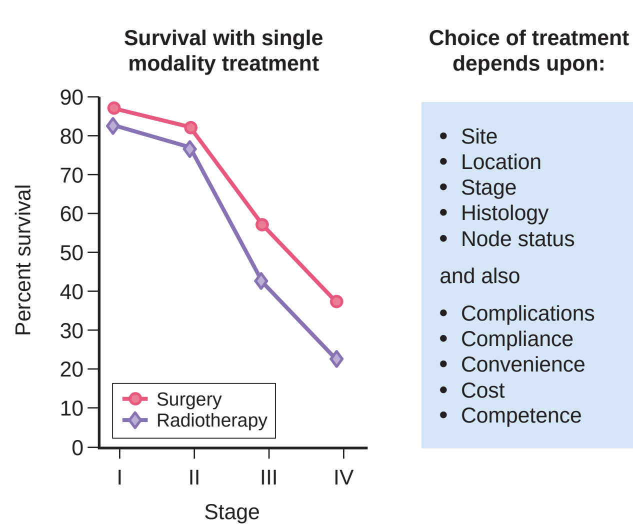

Figure 8.52 Factors that play a role in the selection of initial treatment.

Single modality treatment with either surgery or radiotherapy in advanced stage (T3 and T4) oral cancer offers poor locoregional control and survival. Combining adjuvant postoperative radiotherapy offers improved locoregional control but has not improved survival. Two independent, prospective, randomized trials of adding concurrent chemotherapy to postoperative radiotherapy (Radiation Therapy Oncology Group [#22931] and European Organization for Research and Treatment of Cancer [#9501]) in patients with advanced stage (III and IV) squamous cell carcinomas of the head and neck with high-risk features show improved locoregional control and survival compared with postoperative radiation alone. Further analysis of the data from these trials suggests that the most important high-risk features are positive margins and extranodal spread of metastatic cancer. Relative high-risk factors include multiple positive nodes, perineural or vascular invasion, and metastasis to lymph nodes at level 4 or 5. Adding chemotherapy to postoperative radiation has helped to improve local control compared with radiation alone, but the acute high-grade toxicity and significant long-term morbidity associated with postoperative chemoradiotherapy remain significant problems. More importantly, only about a quarter of patients in these two trials had primary oral cancer, of which only a small percentage received adjuvant treatment solely for positive margin status. Further research in defining the optimal treatment for advanced stage oral cancer is essential.

Although studies suggest that brachytherapy results in good disease control rates for cancers of the tongue, it usually requires placement of a tracheostomy and can result in worse functional outcomes compared with primary surgical treatment.

Oral cavity cancers typically do not respond well to radiotherapy; therefore surgery is the preferred treatment modality. In select cases, tumors of the tongue, the floor of the mouth, and the buccal mucosa classified as T1 and select cases of early T2 tumors can be treated with radiation alone—either external beam radiotherapy, brachytherapy, or both. If a combination of external beam radiotherapy and an interstitial implant is considered for oral tongue lesions, use of an adequate interstitial implant dose is important, because according to several reports, the dose is correlated with local control.

SURGICAL TREATMENT

Management of cancer of the oral cavity is a multidisciplinary team effort, and technical capabilities and support services from various disciplines are essential for a successful outcome. A comprehensive head and neck surgery team includes not only the head and neck surgeon but also other surgical specialties, including plastic and reconstructive surgeons with expertise in microsurgery, dental and maxillofacial prosthodontists, and rehabilitation specialists.

Factors that influence the choice of surgical treatment for a primary tumor of the oral cavity are tumor factors such as the size and site of the primary tumor (i.e., anterior versus posterior location), its depth of invasion, and the proximity of the tumor to the mandible or maxilla. Therefore thorough clinical assessment of the primary tumor is mandatory to ensure that the appropriate surgical procedure is selected. Examination under anesthesia often is indicated to accomplish this goal. The proximity of the tumor to the maxilla or mandible mandates the need for adequate clinical and radiographic assessment to rule out the possibility of bone involvement. In addition, radiographic evaluation provides information regarding the extent of soft-tissue involvement and the status of the dentition.

The histologic characteristics of the primary tumor (i.e., type, grade, and depth of invasion) and the status of cervical lymph nodes are other important features that influence the surgical approach.

The natural history of primary tumors at different sites in the oral cavity is variable. Primary cancer of the vermilion border of the lip has a biologic behavior similar to that of skin cancer, with an excellent potential for cure and thus a very favorable prognosis. Squamous cell carcinomas of the hard palate and upper gum have an intermediate risk of regional lymph node metastases. On the other hand, cancers of the tongue, floor of the mouth, and lower gum have a higher risk of regional lymph node metastases with an adverse impact on prognosis.

The size of the primary tumor clearly has a heavy significant impact on the decision regarding choice of initial treatment. Small and superficial primary tumors of the oral cavity are easily accessible for surgical resection through the open mouth. On the other hand, larger and/or posteriorly located tumors require more extensive surgical approaches for exposure and excision. With increasing size and depth of invasion of the primary lesion, the risk of regional lymph node metastasis increases, bringing into consideration the need for elective treatment of the neck. In general, primary tumors located in the posterior part of the oral cavity have a higher risk for dissemination to regional lymph nodes compared with similarly staged lesions in the anterior oral cavity. Thus, more posteriorly located lesions require consideration of elective treatment of the clinically negative neck.

Adequate assessment of the mandible for invasion by a tumor is essential for appropriate surgical treatment planning. The mandible is considered at risk when the primary tumor is adherent to or adjacent to the mandible. In addition to careful examination under anesthesia by bimanual palpation, radiographic evaluation of the mandible is essential for surgical treatment planning. To determine the need for and extent of mandible resection, it is essential to understand the pathway by which oral cancers invade the mandible. Primary carcinomas of the mucosal lip, buccal mucosa, tongue, and floor of the mouth extend along the surface mucosa and the submucosal soft tissues to approach the attached labial, buccal, or lingual gingiva. From this point, the tumor does not extend directly through intact periosteum and cortical bone toward the cancellous part of the mandible because the periosteum acts as a significant protective barrier. Instead, the tumor advances from the attached gingiva toward the alveolus. In patients with teeth, the tumor extends through the dental socket into the cancellous part of the bone and invades the mandible via that route (Fig. 8.53). In edentulous patients, the tumor extends up to the alveolar process and then infiltrates the dental pores in the alveolar ridge and extends to the cancellous part of the mandible (Fig. 8.54). Thus in patients with tumors approaching the mandible without infiltration of the tooth sockets, a marginal mandibulectomy is feasible. In edentulous patients, however, the feasibility of marginal mandibulectomy depends on the vertical height of the body of the mandible. With aging, the alveolar process recedes and the mandibular canal comes closer to the surface of the alveolar process. As shown in Fig. 8.55, resorption of the alveolar process eventually leads to a "pipestem" mandible in elderly patients (Fig. 8.56). It is almost impossible to perform a marginal mandibulectomy in such patients because the probability of iatrogenic fracture or postsurgical spontaneous fracture of the remaining portion of the mandible is very high. Similarly, in patients who have received previous

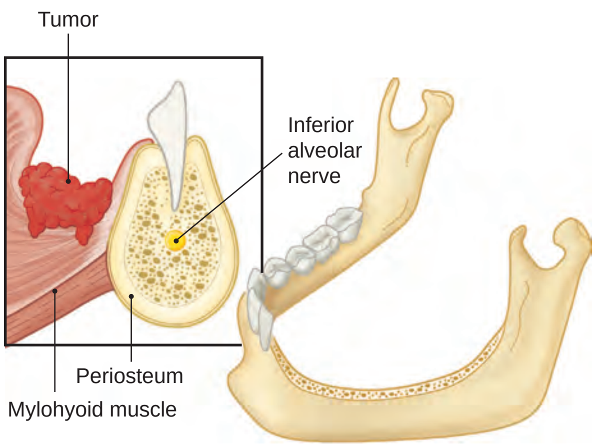

Figure 8.53 Tumor invasion of the dentate mandible occurs through the dental socket to the cancellous bone and then to the alveolar canal.

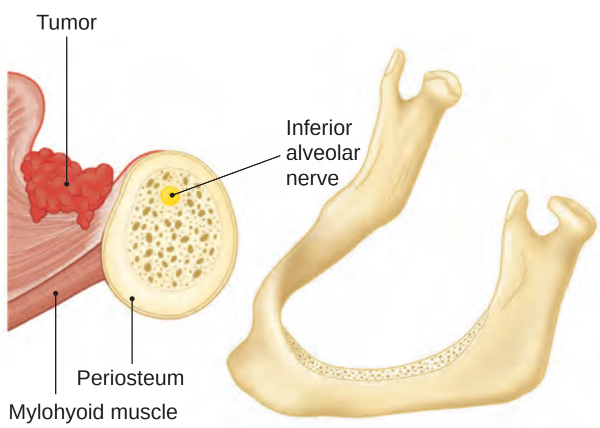

Figure 8.54 Tumor invasion of the edentulous mandible occurs through the dental pores on the alveolar process to the cancellous bone and then to the alveolar canal.

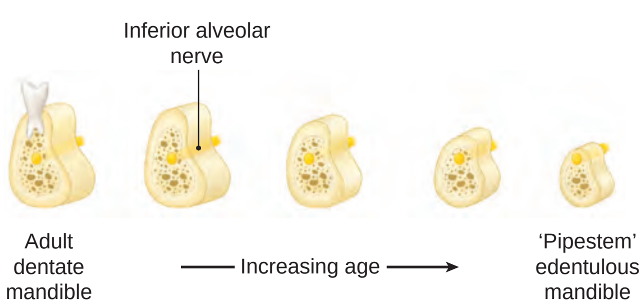

Figure 8.55 Vertical height and location of the alveolar canal in dentate and edentulous mandibles.

Figure 8.56 Panoramic x-ray of a "pipestem" mandible.

radiotherapy, a marginal mandibulectomy should be performed with extreme caution. The probability of pathologic fracture at the site of the marginal mandibulectomy in such patients is very high.

Another important issue about marginal mandibulectomy is the ultimate goal for dental rehabilitation. Implant-based dental rehabilitation is not possible in the molar region of the mandible, due to lack of sufficient bone height above the mandibular canal after marginal mandibulectomy. Therefore, if optimal dental rehabilitation is the goal, then marginal mandibulectomy should not be done in the body of the mandible posterior to the mental foramen. For those patients, segmental mandibulectomy and fibula free flap reconstruction with immediate placement of dental implants would be indicated.

When the tumor extends to involve the cancellous part of the mandible, a segmental mandibulectomy must be performed. A segmental mandibulectomy also may be required in patients with massive primary tumors with significant soft-tissue disease in the proximity of the mandible. Sacrifice of the normal mandible to gain access to the primary tumors of the oral cavity or to accomplish an in-continuity composite resection should be avoided. The concept of the "commando operation" has been revised because no lymphatic channels pass through the mandible, and thus the need for an in-continuity "composite resection" of the uninvolved mandible is not warranted. The current indications for a segmental mandibulectomy include (1) gross invasion by oral cancer; (2) invasion of inferior alveolar nerve or canal by the tumor; (3) massive soft-tissue disease adjacent to the mandible; (4) a primary malignant tumor of the mandible; and (5) a tumor that has metastasized to the mandible.

As with other sites in the head and neck, patient factors such as age, general medical condition, tolerance of surgical treatment, occupation, acceptance, compliance, lifestyle (smoking/drinking), and socioeconomic status are important in the selection of the initial treatment of oral cancer. In addition, specific patient factors that need to be considered in the selection of treatment of oral cancer include status of dentition, the presence of submucous fibrosis or trismus, and continued use of chewing tobacco products. In general, older age is not considered to be a contraindication for implementation of adequate initial surgical treatment for oral carcinoma. However, advancing age, intercurrent disease, and debility due to associated cardiopulmonary conditions increases the risk of morbidity and mortality after extensive surgery. Previous treatment for other lesions in the same area also influences decisions regarding the selection of treatment; for example, radiation therapy previously delivered to the same area for a different lesion may not be available to treat a second tumor in the same area.

Preoperative Preparation

Many patients with primary carcinomas of the oral cavity have poor oral hygiene and poor dentition, often harboring gross infection. It is very important that a preoperative dental evaluation and appropriate dental care is provided to achieve optimal hygiene in the oral cavity before a surgical procedure is performed. All grossly septic teeth should be adequately assessed for consideration of extraction, either preoperatively or intraoperatively if indicated. However, teeth (whether loose or immobile within the tumor or in its vicinity) should *not* be extracted before the definitive surgical procedure. Extraction of teeth near a tumor opens up dental sockets, which increases

the risk of implantation of tumor into the mandibular canal. The feasibility of a marginal mandibulectomy is seriously compromised under these circumstances. Deposits of tartar must be removed and appropriate scaling of the dentition must be undertaken to avoid dental complications and prevent sepsis in the oral cavity after surgery. However, any restorative dental work should be postponed until adequate surgical treatment of the primary oral cancer is completed.

If the contemplated surgical procedure requires resection of any part of the mandible or maxilla, appropriate dental consultation should be obtained for consideration of intraoperative placement of dental implants in the reconstructed mandible with a fibula free flap, or for fabrication of either a palatal obturator, mandibular splint, or intermaxillary fixation. If any postoperative splints, obturators, or dental prostheses are desired, it is imperative that dental impressions be obtained before surgery.

If the patient has undergone radiation therapy or will undergo postoperative radiotherapy, dental consultation becomes even more imperative. Before starting radiation therapy, it is important that the patient receive comprehensive dental evaluation and prophylaxis, including extraction and/or treatment of septic teeth, restoration of salvageable teeth, and fluoride treatment for prevention of caries of remaining viable teeth.

Anesthesia and Position

Although excision of small primary lesions in the oral cavity can be accomplished under local anesthesia, most surgical procedures for primary cancers of the oral cavity require general endotracheal anesthesia with adequate relaxation. A nasotracheal intubation is desirable for ease of access to the oral cavity and instrumentation during surgery. However, it is essential that skin incisions be marked before endotracheal intubation and taping of the tube to avoid distortion of facial skin lines, leading to improperly placed incisions. To minimize the risk of postoperative infection, broad-spectrum antibiotics should be administered before making the skin incision. The patient is positioned supine on the operating table, with the upper half of the body at 45 degrees.

Surgical Anatomy

The mucosa of the oral cavity is separated from the skin by the vermilion border at the margins of the lips. The mucosa of the cheek is adherent to the underlying buccinator muscle and Stensen's duct opens into it on the parotid papilla adjacent to the maxillary second molar tooth. The pterygomandibular raphe is located under the mucosa of the retromolar region. The buccinator and the superior constrictor muscles are attached to the pterygomandibular raphe, and tumors of the retromolar trigone have easy access to both muscles if they infiltrate deeply. The lingual and inferior alveolar nerves are also related to the mucosa of the retromolar trigone and lie medial to the anterior border of the ramus of the mandible. The buccal branch of the maxillary artery provides blood to the cheek mucosa, and nerves are supplied from the maxillary and mandibular branches of the trigeminal nerve.

The mucosa of the horseshoe-shaped floor of the mouth is supported by the mylohyoid muscles, which constitute the muscular diaphragm that separates the oral cavity from the neck. In the anterior midline, the submandibular salivary ducts (Wharton's ducts) open into the sublingual caruncle at the lingual frenulum. The submandibular ducts and sublingual salivary glands are located on either side of the sublingual caruncle and separate the mucosa of the floor of the mouth from the mylohyoid muscle. The mylohyoid muscle is attached to the mylohyoid line on the mandible and interdigitates with fibers from the opposite side in a median raphe. If the raphe is deficient, the sublingual gland may protrude into the neck.

The mucosa of the hard palate is densely adherent to the underlying periosteum of the maxilla. The neurovascular bundle of the hard palate runs in the submucosa of its lateral aspects. The submucosa of the posterior half of the hard palate contains minor salivary glands that are mainly the mucus-secreting type. The glands may open into paired paramedian depressions located at the posterior border of the hard palate. These fovea are a useful landmark to separate the hard from the soft palate. The blood supply to the palate is from the greater palatine artery, which is a branch of the internal maxillary artery. The artery descends in the palatine canal to the greater palatine foramen adjacent to the second maxillary molar tooth. It then runs forward to the incisive canal in a curved groove along the alveolar border of the palate. In the incisive canal, it anastomoses with the septal branches of the nasopalatine artery. Preservation of the integrity of the greater palatine artery is crucial in the maxillary swing procedure. The greater and lesser palatine nerves, which are branches of the second division of the trigeminal nerve (V2), provide sensory supply to the palate. These nerves are susceptible to invasion by hard-palate tumors. Perineural spread can occur along these nerves to the pterygopalatine ganglion located in the pterygopalatine fossa and the maxillary (V2) and vidian nerves.

The oral part of the tongue (the anterior two-thirds) lies anterior to the sulcus terminalis that begins at the foramen cecum and runs laterally along the circumvallate papillae toward the palatoglossal arches. The mucosa of the dorsum of the tongue is covered by the filiform, fungiform, and circumvallate papillae, whereas the mucosa of the ventral surface is smooth, which continues to the floor of the mouth. On the anterior ventral surface of the tongue, the lingual frenulum connects the mucosa to the anterior floor of the mouth. The deep lingual vein lies lateral to the frenulum. The intrinsic muscles (bilateral superior and inferior longitudinal, transverse, and vertical) interdigitate and have no tissue spaces, which allows invasive cancers to spread easily. On the other hand, infiltration of the extrinsic muscles of the tongue (genioglossus, hyoglossus, styloglossus, and palatoglossus) is a feature of locally advanced cancer. The arterial supply to the tongue and floor of the mouth is from the dorsal lingual, sublingual, and deep lingual branches of the lingual artery. The venous drainage of the tongue is into the lingual veins, which drain into the facial and retromandibular veins, which join to form the common facial vein. The hypoglossal nerve provides motor innervations to all muscles of the tongue except the palatoglossus, which is supplied by the pharyngeal plexus. The lingual nerve is the sensory nerve to the anterior two-thirds of the tongue, the floor of the mouth, and the lower gum, while taste sensation is carried along the chorda tympani branch of the facial nerve.

The dental sockets on the alveolar process of the mandible and maxilla are covered by attached buccal mucosa that is reflected from the lips, the floor of the mouth, and the hard palate. The nerve supply to the lower gum and dentition is from the inferior alveolar nerve (the mandibular branch of the trigeminal nerve [V3]). The nerve enters the mandibular canal on the medial aspect of the ascending ramus of the mandible

and exits at the mental foramen on the lateral surface of the body of the mandible. The blood supply to the lower gum and teeth is from the inferior alveolar branch of the internal maxillary artery and is the sole endosteal blood supply to the body of the mandible. The mandibular periosteum provides blood to the cortical bone.

The first echelon lymph nodes of the tongue and floor of mouth are located in the supraomohyoid triangle (levels I to III). The lymphatic channels accompany the veins, and their density increases from the anterior to the posterior third of the tongue. Similarly, lymphatic drainage to bilateral cervical lymph nodes also becomes more frequent in posteriorly based tumors. Lymphatic metastases generally occur in a predictable fashion, but lymph nodes at level IV may be involved directly without involvement of level II nodes. The central portions of the tongue toward the midline may drain bilaterally.

SURGICAL APPROACHES

A variety of surgical approaches are available for resection of primary tumors of the oral cavity. The choice of a particular approach will depend on factors such as the size and site (anterior versus posterior) of the primary tumor as well as its depth of invasion and proximity to the mandible or maxilla. Factors such as dentition, size of the oral aperture, trismus, and the size and mobility of the tongue also influence selection of the surgical approach. The various surgical approaches such as peroral, mandibulotomy, lower cheek flap approach, visor flap approach, and upper cheek flap approach are shown in Fig. 8.57. The transoral approach has wider applications with technologic advances using lasers (transoral laser microsurgery [TLM]) and robotics (transoral robotic surgery [TORS]).

The peroral approach can be safely used for small, anteriorly located, and easily accessible tumors of the oral tongue, floor of mouth, gum, cheek mucosa, and hard or soft palate. Small but deeply infiltrating tumors may not be adequately resectable through the open mouth. Proximity of the tumor to the mandible or maxilla may influence the surgical approach even for small tumors.

When the peroral approach does not offer adequate exposure, the visor flap or cheek flap approaches (upper or lower) become necessary. The visor flap approach provides sufficient exposure for anteriorly located lesions but is not satisfactory for tumors located in the posterior oral cavity. The benefit of this approach is that it avoids a lower lip–splitting incision but produces permanent numbness of the chin because the mental nerves need to be transected for adequate mobilization of the flap. It also may cause sagging of the lower lip and drooling because of a loss of support and sensation. Thus its utility is limited. The lower cheek flap approach requires a midline lip–splitting incision that is continued laterally into the neck for exposure and neck dissection. This approach provides excellent exposure for nearly all tumors of the oral cavity except those of the upper gum and hard palate. Mandible resection (marginal or segmental) and reconstruction require the lower cheek flap approach in most instances. The lower cheek flap approach is required for marginal or segmental mandibulectomy of tumors adjacent to the body of the mandible. The upper cheek flap approach (the Weber-Ferguson incision and its modifications; see Chapter 5) is required for resection of larger tumors of the hard palate and upper alveolus, particularly if they are posteriorly located.

Access to larger tumors of the tongue, particularly those closer to the base of the tongue where the mandible is not

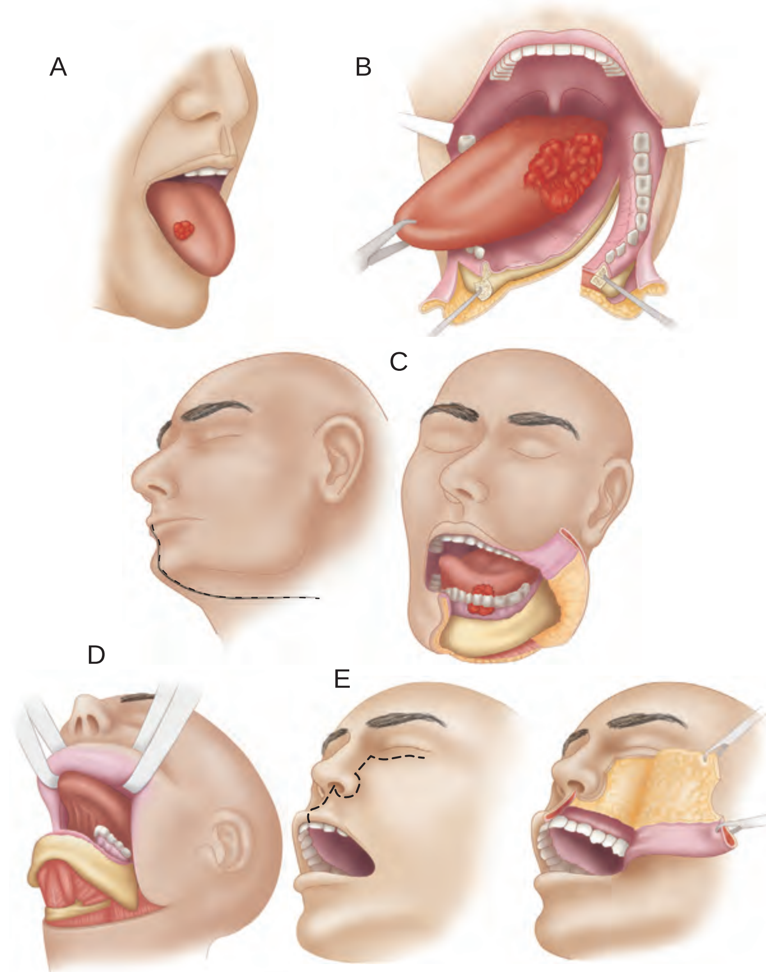

Figure 8.57 Various surgical approaches. **A**, Peroral. **B**, Mandibulotomy. **C**, Lower cheek flap. **D**, Visor flap. **E**, Upper cheek flap.

involved, requires wider exposure for resection. A mandibulotomy or mandibular osteotomy is an excellent mandible-sparing surgical approach designed to gain access to the oral cavity or oropharynx for resection of primary tumors otherwise not accessible through the open mouth or by the lower cheek flap approach (Fig. 8.58). The mandibulotomy can be performed in one of three locations: (1) lateral (through the body or angle of the mandible); (2) midline; or (3) paramedian.

A lateral mandibulotomy has several disadvantages. First, the muscular pull on the two segments of the mandible is unequal, putting the mandibulotomy site under significant stress and causing a delay in healing. For this reason, intermaxillary fixation may be required. Second, the ability to gain access to the suture line to maintain cleanliness following surgery in the oral cavity is hampered as a result of intermaxillary fixation, leading to poor oral hygiene and the potential risk for sepsis of the suture line. In addition, a lateral mandibulotomy poses several anatomic disadvantages including denervation of the teeth distal to the mandibulotomy site and the skin of the chin as a result of transection of the inferior alveolar nerve. A lateral mandibulotomy also causes devascularization of the distal teeth and the distal segment of the mandible from its endosteal blood supply. The exposure provided by a lateral mandibulotomy is limited, and if the patient needs postoperative radiation therapy, delayed healing can lead to complications at the site of the mandibulotomy. For these reasons, a lateral mandibulotomy is not recommended.

By placing the mandibulotomy in the anterior midline, all the disadvantages of a lateral mandibulotomy are avoided.

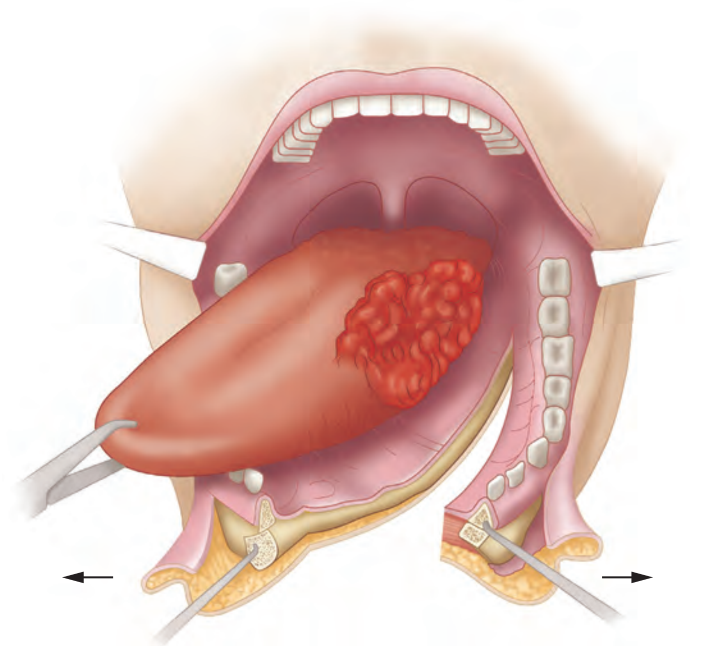

Figure 8.58 A mandibulotomy is an excellent mandible-sparing surgical approach to gain access to bulky tumors of the oral cavity or oropharynx.

However, splitting the mandible in the midline requires extraction of one central incisor tooth to avoid exposure of the roots of both central incisor teeth, which are at risk of extrusion. Extraction of one central incisor tooth alters the aesthetic appearance of the lower dentition. In addition, a midline mandibulotomy requires division of muscles arising from the genial tubercle, that is, the geniohyoid and genioglossus, leading to a delayed recovery of the functions of mastication and swallowing. Therefore a median mandibulotomy also is not preferred for these reasons.

A paramedian mandibulotomy, on the other hand, avoids all the disadvantages of a lateral mandibulotomy and the sequelae of a midline mandibulotomy. It offers significant advantages, such as wide exposure and preservation of the geniohyoid and genioglossus muscles, leading to preservation of the hyomandibular complex. The only muscle requiring division is the mylohyoid muscle, which leads to minimal swallowing difficulties. A paramedian mandibulotomy does not cause denervation or devascularization of the skin of the chin or the teeth and mandible. Fixation at the mandibulotomy site is easy, and the site of the mandibulotomy is able to withstand radiation therapy if the patient needs postoperative treatment. Thus at present a paramedian mandibulotomy remains an optimal surgical approach for access to posteriorly located larger lesions of the oral cavity and tumors of the oropharynx and parapharyngeal space. Alternatively, posteriorly located lesions of the tongue and those of the oropharynx can be approached transorally with robotic instrumentation, without mandibulotomy, and thus avoid its morbidity.

Transoral Robotic Surgery

Transoral robotic-assisted surgical resection is now commonly employed in lieu of mandibulotomy for surgical resection of patients with primary tumors arising from the base of the tongue. TORS may be used for accessing the posterior limit of a posteriorly located oral tongue tumor that extends into the base of the tongue in combination with peroral excision with the goal of avoiding a mandibulotomy. However, this is difficult in practice, because the angulation and excursion of the robotic arms often does not allow adequate visualization and access to the dorsal surface of the posterior oral tongue. Moreover, even if surgical excision is accomplished, the plastic surgeon may not be able to adequately access the surgical defect for suturing a microvascular free flap. For these reasons, TORS should be used in very selected instances only by very experienced surgical teams that are not just familiar with resection techniques but also facile with suturing using the surgical robot.

Peroral Laser Excision of Leukoplakia

Premalignant lesions of the mucosa of the oral cavity such as hyperkeratosis, keratosis with dysplasia, and even carcinoma in situ can be treated by a relatively conservative peroral excision. Surgical excision of these lesions is advisable if they are focal and limited in surface extent. However, if the lesions are diffuse or multifocal and involve a large surface area, then surgical excision is impractical. Laser vaporization appears to be an effective method of treatment of such lesions, particularly if they are strictly limited to the mucosa and have been confirmed to be not invasive carcinoma by representative biopsies from the most suspicious-looking areas. The laser may be used with a microscope (TLM) or with a hand-held probe. A patient with leukoplakia involving a large area of the soft palate with punctate changes is shown in Fig. 8.59. To encompass the entire area involved, a large surface of the mucosa of the soft and hard palate needs to be treated.

The patient is placed under general anesthesia with nasotracheal intubation, and adequate relaxation is obtained with the use of muscle relaxants. A Dingman self-retaining oral retractor is used to expose the lesion and the area to be treated (Fig. 8.60). The skin of the face in the field is shielded with wet towels to protect against accidental injury by the laser beam. The posterior pharyngeal wall is similarly protected with a wet roll of gauze as a packing that also covers and protects the nasotracheal tube in the oropharynx.

A carbon dioxide laser with a handheld piece is now brought into the field, and the laser beam is focused over the area of desired tissue destruction (Fig. 8.61). The desired depth of tissue destruction for leukoplakia is approximately 1 to 2 mm in thickness. This level of tissue destruction is safely obtained with the laser set at approximately 15 watts in continuous mode. Tissue destruction is performed in segments, with intermittent irrigation of the oral cavity with saline solution. The smoke generated by tissue destruction is constantly suctioned out with suction tip held adjacent to the laser beam.

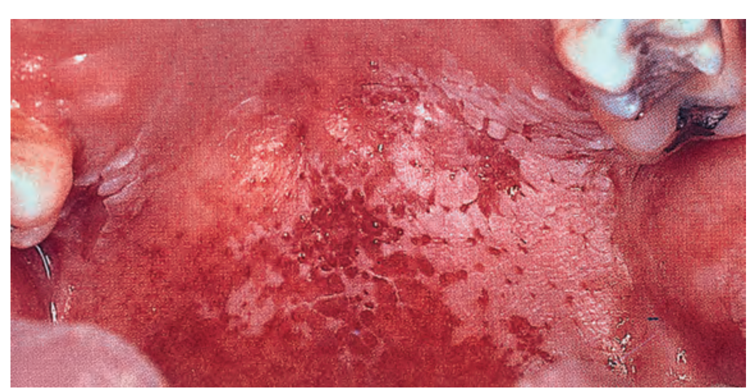

Figure 8.59 A patient with leukoplakia of a large area of the soft palate.

Figure 8.60 The oral cavity is exposed with a Dingman self-retaining oral retractor.

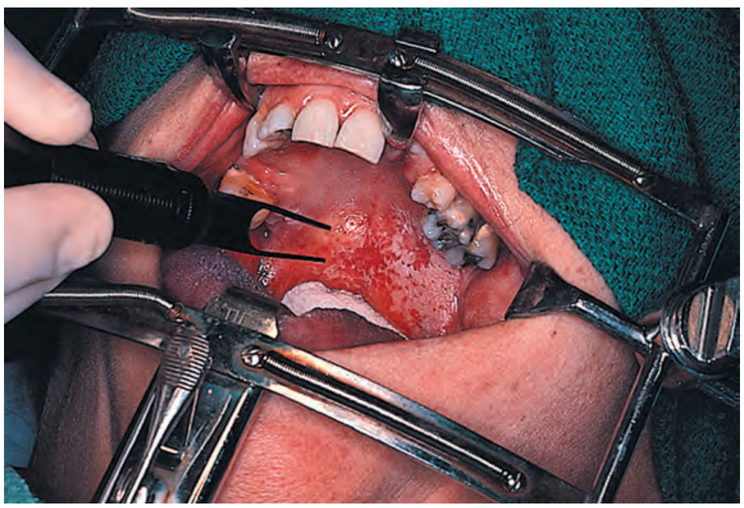

Figure 8.61 The carbon dioxide laser beam is focused over the area of desired tissue destruction.

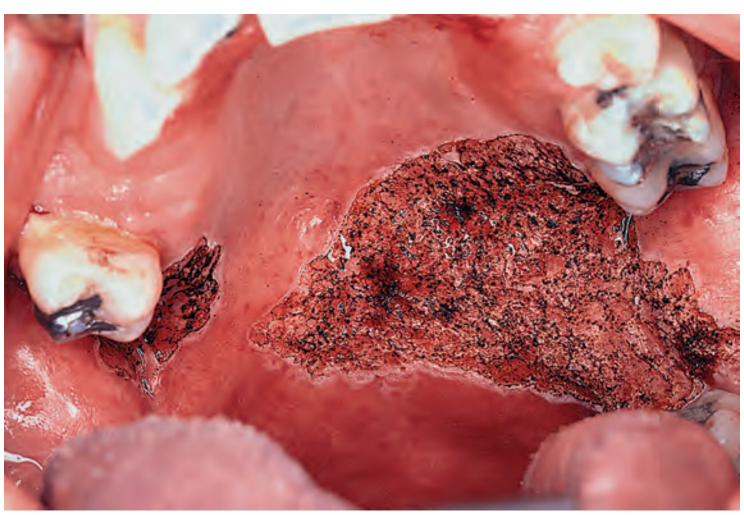

Figure 8.62 The area of laser vaporization.

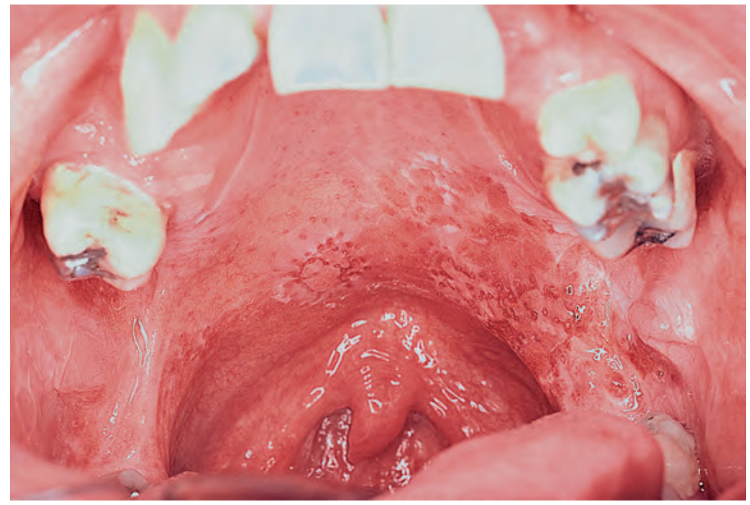

Figure 8.63 The appearance of the oral cavity 1 week following surgery.

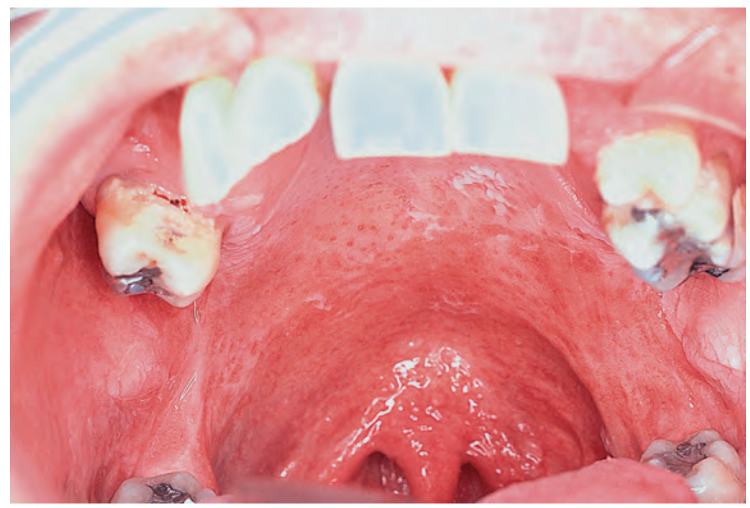

Figure 8.64 The appearance of the oral cavity 1 month following surgery.

In Fig. 8.62, the area of laser vaporization is shown at the conclusion of the procedure. Complete hemostasis is obtained by controlling focal bleeding points by defocusing the laser beam. To control hemorrhage, the handheld piece is brought away from the target area to diffuse the focus, which provides maximum hemostasis. The surgical field at this stage shows adequate tissue destruction in the desired area. The patient is allowed to take liquids by mouth the same day, and instructions are given for maintenance of optimal oral hygiene by frequent oral irrigations and rinses using a solution of warm water with baking soda and salt. One quart of warm water with a teaspoon of salt and a teaspoon of baking soda is recommended for oral rinses and irrigations.

The postoperative view of the oral cavity 1 week after laser vaporization is shown in Fig. 8.63. Superficial granulation tissue is seen in focal areas at the site of tissue destruction. Minimal inflammatory reaction and growth of normal-appearing mucosa can be seen in some areas.

The appearance of the oral cavity 1 month after laser vaporization for leukoplakia is shown in Fig. 8.64. Complete restoration of the normal epithelium is now seen. Palpation of this area shows completely normal soft tissues with no scar formation or fibrosis beneath.

Superficial in situ carcinomas of the oral cavity and diffuse areas of leukoplakia (such as hyperkeratosis and dysplasia) are suitable for treatment by laser vaporization. However, laser vaporization as definitive treatment is inadequate for infiltrating carcinomas of the mucosa of the oral cavity.

Partial Glossectomy

Nearly all T1 and most T2 lesions of the oral tongue, that is, the anterior two-thirds of the tongue, are suitable for a peroral partial glossectomy. The patient shown in Fig. 8.65 has an ulcerated, endophytic, 2.5-cm carcinoma involving the lateral border of the anterior and middle one-third of the tongue on the right-hand side. Mobility of the tongue is not restricted, and the tumor does not extend to involve the adjacent floor of the mouth. The tumor also does not extend across the midline to involve the opposite side of the tongue.

The patient is placed under general anesthesia with nasotracheal intubation, and the oral cavity is isolated. For bulky tumors involving the lateral aspect of the oral tongue, it is preferable to perform a wedge excision oriented in a transverse rather than a longitudinal fashion. A longitudinally oriented excision of a large tumor will result in an elongated narrow tongue that often impairs speech and interferes with mastication. On the other hand, transversely oriented wedge excisions foreshorten the length of the tongue and result in a functionally better tongue that appears normal visually (Fig. 8.66). The area of excision is marked as shown in Fig. 8.67, with a generous portion of the mucosa adjacent to the tumor and the full complement of the thickness of the musculature of the tongue surrounding the palpable tumor.

Surgical excision is performed preferably with an electrocautery, with use of the cutting current to incise the mucosa of the tongue both on its superior and inferior aspects. After the mucosal incision, coagulating current is used to perform resection of the underlying musculature of the tongue. Minor bleeding points in the musculature of the tongue are electrocoagulated, while major branches of the lingual artery are ligated with chromic catgut. The surgical defect shows satisfactory excision of the primary tumor of the oral tongue (Fig. 8.68). Frozen sections are now obtained from the mucosal margins and from the depth of the surgical defect to ensure that an adequate excision of the primary tumor is accomplished.

After negative margins are confirmed by frozen section and hemostasis is secured, repair of the surgical defect begins. A two-layered repair is performed with use of 3-0 chromic catgut or 3-0 Vicryl interrupted sutures to approximate the musculature, and the same suture material is used for approximation of the mucosa on the superior and inferior aspects of the tongue. A skin hook is used to retract the apex of the wedge-shaped surgical defect for transverse orientation of the closure. Interrupted sutures are used throughout. Blood loss during the procedure is negligible.

The surgical specimen shown in Fig. 8.69 demonstrates full-thickness, three-dimensional resection of the tumor of the oral tongue with adequate mucosal and soft-tissue margins. The postoperative appearance of the tongue approximately 3 months after the partial glossectomy is shown in Fig. 8.70. Note the transverse scar at the suture line, giving a normal configuration of the oral tongue. The patient has no speech impairment, has normal mastication, and is able to tolerate all types of food by mouth.

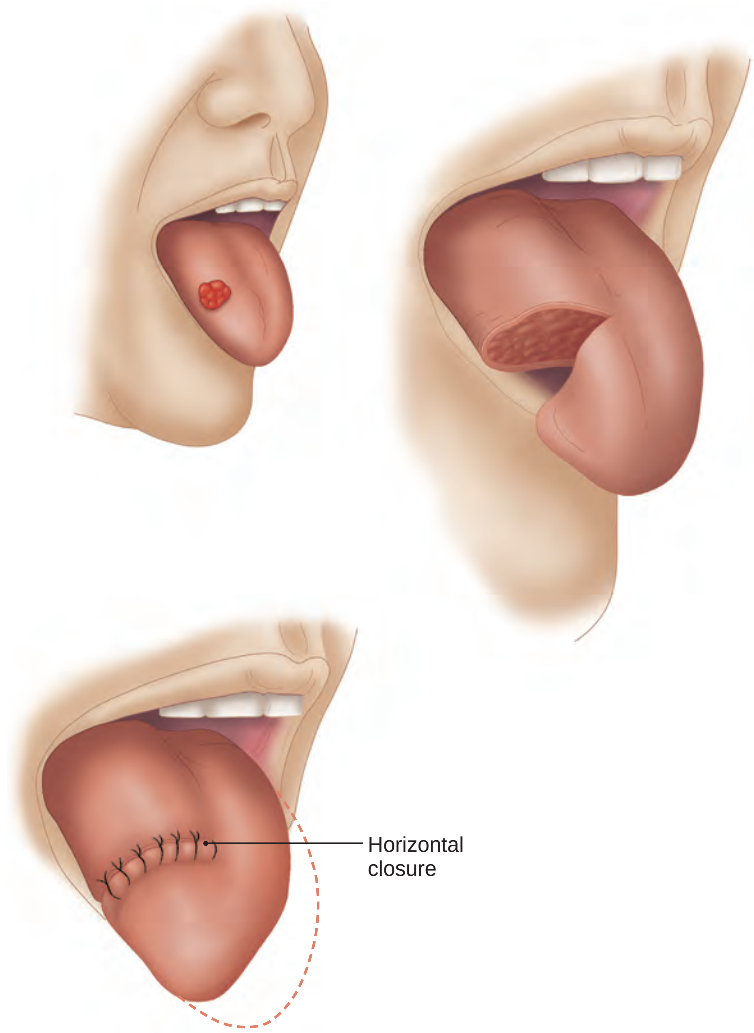

Figure 8.66 Small primary tumors of the oral cavity are suitable for peroral excision.

Figure 8.65 An ulcerated, endophytic carcinoma of the oral tongue.

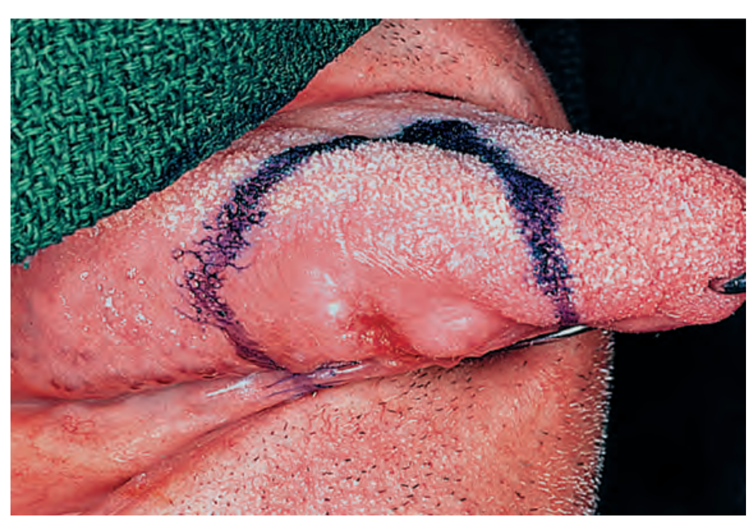

Figure 8.67 The area of excision is outlined.

Figure 8.68 The surgical defect.

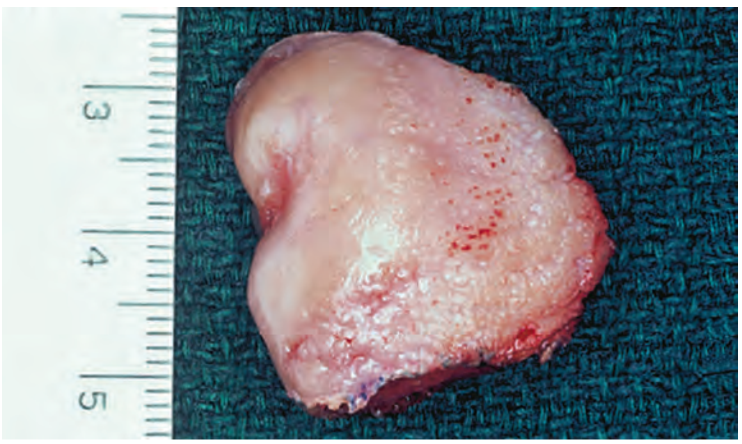

Figure 8.69 The surgical specimen.

Figure 8.70 The appearance of the tongue 3 months following partial glossectomy.

Near Total Peroral Glossectomy

Larger lesions of the oral tongue (anterior two-thirds) can also be resected through the open mouth as long as the tumor is confined to the tongue and does not extend to the floor of the mouth, the lower gingiva, or the posterior third of the tongue. The patient shown in Fig. 8.71 has an extensive carcinoma involving nearly the entire anterior two-thirds of the tongue. Mobility of the tongue is normal. An anterior two-thirds glossectomy was done through the open mouth. The surgical specimen shows the entire tumor resected in a monobloc fashion (Fig. 8.72). Reconstruction of this defect was performed with a radial forearm free flap. The postoperative appearance of the oral cavity 3 months following surgery shows excellent healing with optimal bulk of the flap to replace the resected portion of the tongue and facilitate speech and swallowing (Fig. 8.73).

Figure 8.71 Locally extensive carcinoma of the anterior two-thirds of the tongue with deep muscle invasion.

Figure 8.72 Surgical specimen of subtotal glossectomy (anterior two-thirds of the tongue).

Figure 8.73 Postoperative appearance of the oral cavity 6 months following subtotal glossectomy and reconstruction with a radial forearm free flap.

Excision of a Tumor of the Floor of the Mouth and Reconstruction With a Full-Thickness Skin Graft

Peroral excision for superficial lesions of the floor of the mouth, cheek mucosa, or soft palate can be performed with the surgical defect safely left open to granulate and heal by secondary intention. However, when such an excision is performed in certain critical areas where mobility is essential or when the depth of the excision includes the underlying musculature, then secondary healing leads to fibrosis and contracture, resulting in impairment of function. Immediate coverage of such surgical defects by a skin graft is desirable. A primary carcinoma of the floor of the mouth involving the frenulum and the openings of Wharton's ducts on both sides with involvement of the adjacent mucosa is shown in Fig. 8.74. The lesion does not involve the lingual gingiva and does not infiltrate deeply to involve the underlying muscular diaphragm of the floor of the mouth.

The patient is placed under general anesthesia with nasotracheal intubation, and the oral cavity is isolated and exposed with self-retaining mouth retractors. With use of an electrocautery, the proposed area of surgical excision with satisfactory mucosal margins is marked (Fig. 8.75). Note that the line of excision goes through the lingual gingiva anteriorly and through the undersurface of the tongue posteriorly.

A three-dimensional resection of the primary tumor is undertaken with use of the electrocautery. As the underlying soft tissues are mobilized and divided, Wharton's ducts become visible, as shown in Fig. 8.76. Portions of sublingual salivary glands form the deep margin of the surgical specimen. Wharton's ducts are transected and their stumps are held by 4-0 chromic catgut sutures.

The openings of the transected Wharton's ducts are transposed posteriorly. The ducts are transected obliquely to provide a larger circumference at its opening. The posterior half of its circumference is approximated to the mucosa of the floor of the mouth with interrupted 4-0 chromic catgut sutures, as shown in Fig. 8.77. The remaining surgical defect reveals the musculature of the undersurface of the tongue and the floor of the mouth.

A full-thickness skin graft is harvested from the supraclavicular area of the neck. The skin graft is appropriately trimmed and sutured to the mucosal edges of the surgical defect with use of 3-0 chromic catgut interrupted sutures (Fig. 8.78). The anterior half of the circumference of the stump of Wharton's duct is approximated to the edge of the skin graft with interrupted 4-0 chromic catgut sutures. After the graft is sutured in place, several stab incisions are made in the skin graft to permit drainage of blood and/or serum that may accumulate beneath the graft.

A Xeroform gauze bolster is made to fit the area of the skin graft and is anchored in position with 2-0 silk tie-over sutures, as shown in Fig. 8.79. A nasogastric feeding tube is inserted to maintain nutritional intake in the postoperative period. The patient is not allowed to take anything by mouth for approximately 1 week, and intense oral irrigations and rinses are encouraged to maintain optimal oral hygiene. At the end of 1 week, the bolster dressing is removed and the patient is asked to continue oral irrigations until the graft has satisfactorily

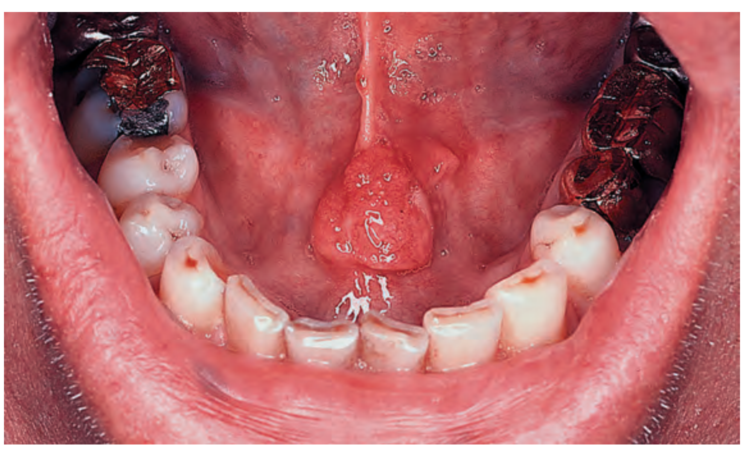

Figure 8.74 A carcinoma of the floor of the mouth involving the frenulum and openings of Wharton's ducts.

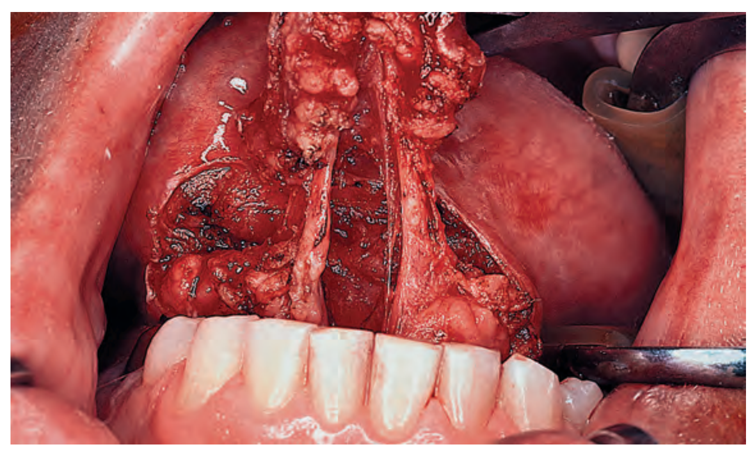

Figure 8.76 Wharton's ducts are dissected.

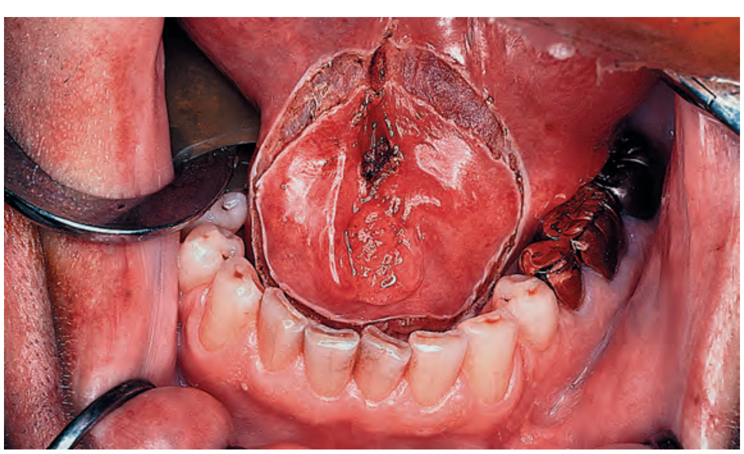

Figure 8.75 The proposed area of surgical excision is outlined by mucosal incision.

Figure 8.77 The stumps of Wharton's ducts are transposed to the posterior mucosal edge.

healed. The patient can now ingest clear liquids and puréed foods by mouth.

The appearance of the skin graft at approximately 8 weeks after surgery is shown in Fig. 8.80. The graft has healed well, normal mobility of the tongue has been retained, and the functions of mastication and speech are also practically normal. In many cases, skin grafts in the oral cavity are not completely successful, although in those instances they do serve an important function of providing a biological dressing on the surgical defect in the immediate postoperative period. Even when the skin graft is not totally successful and some parts of it slough off, the other areas do adhere, and eventually good epithelialization takes place. Split-thickness or full-thickness skin grafts provide excellent coverage of intermediate-depth defects in the oral cavity. Alternatively, a cadaveric acellular collagen matrix (AlloDerm) can be used instead of a skin graft. It works as an excellent biological dressing until mucosal epithelization takes place.

Figure 8.78 The skin graft is trimmed and sutured to the mucosal edges of the surgical defect.

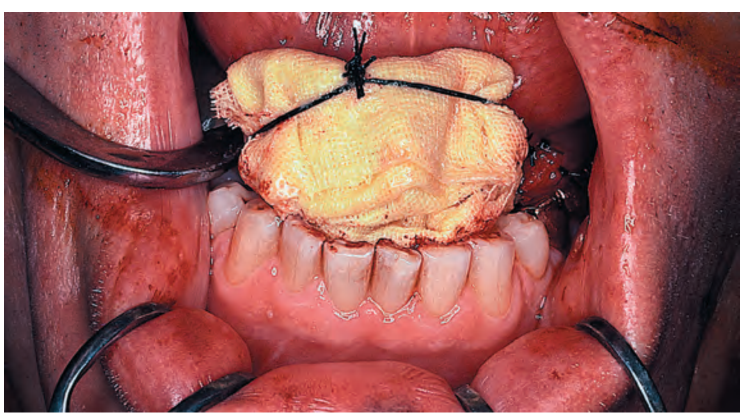

Figure 8.79 The Xeroform gauze bolster is anchored in position.

Paramedian Mandibulotomy for Resection of Cancer of the Tongue

The patient shown in Fig. 8.81 has a primary carcinoma of the middle third of the oral tongue. The tumor is staged as T2, N0, stage II invasive squamous cell carcinoma of the oral tongue. However, this deeply infiltrating tumor involves a significant portion of the underlying musculature, and thus an elective supraomohyoid neck dissection is performed for pathologic staging of regional lymph nodes.

In any patient requiring a mandibulotomy, radiographic assessment of the mandible must be performed before surgery. A panoramic view of the mandible is usually satisfactory. A mandibulotomy through an area of septic teeth should be avoided. When any other pathology is present at the proposed site of the mandibulotomy, radiographic studies help tremendously in selecting the appropriate location for the mandibulotomy. The site of the mandibulotomy is selected based on the disposition of the dental sockets of the incisor and canine teeth. The roots of the lateral incisor and canine teeth usually diverge, creating a space between the two. Therefore a paramedian mandibulotomy between the lateral incisor and canine teeth is preferred. The angled cut of the mandibulotomy should be fashioned in such a way that it does not amputate the roots of the adjacent teeth. Similarly, the straight vertical cut should be exactly between the roots of the adjacent teeth to avoid undue exposure of their roots (Fig. 8.82).

The patient is placed under general anesthesia with nasotracheal intubation on the operating table, and adequate relaxation is obtained. The best opportunity to satisfactorily examine the extent of the tumor is under anesthesia, and such an examination should be performed routinely. An incision is marked as shown, splitting the lower lip in the midline with extension of the incision up to the hyoid bone, at which point the incision is extended on the side of the neck dissection along an upper neck skin crease (Fig. 8.83). Extension of the incision to the lateral aspect of the upper neck provides adequate exposure to carry out the supraomohyoid neck dissection. Initially, only the transverse part of the neck incision is made and the supraomohyoid neck dissection is completed (Fig. 8.84).

The skin incision is now extended in the midline, dividing the chin and the lower lip through its full thickness up to the reflection of the mucosa at the gingivolabial sulcus.

Figure 8.80 The appearance of the skin graft 8 weeks following surgery.

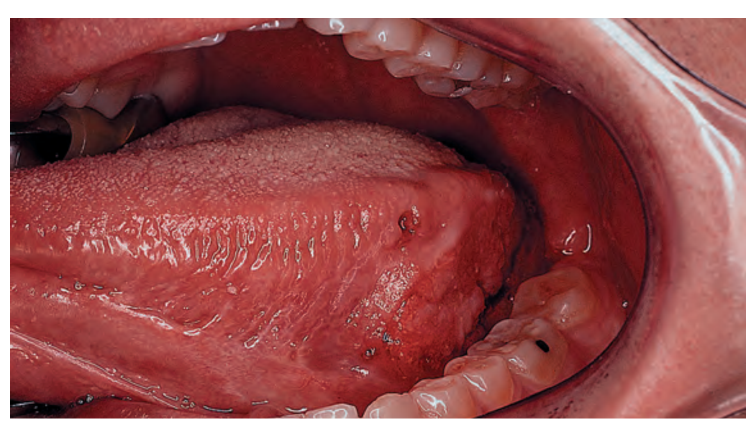

Figure 8.81 A patient with a carcinoma of the middle third of the oral tongue.

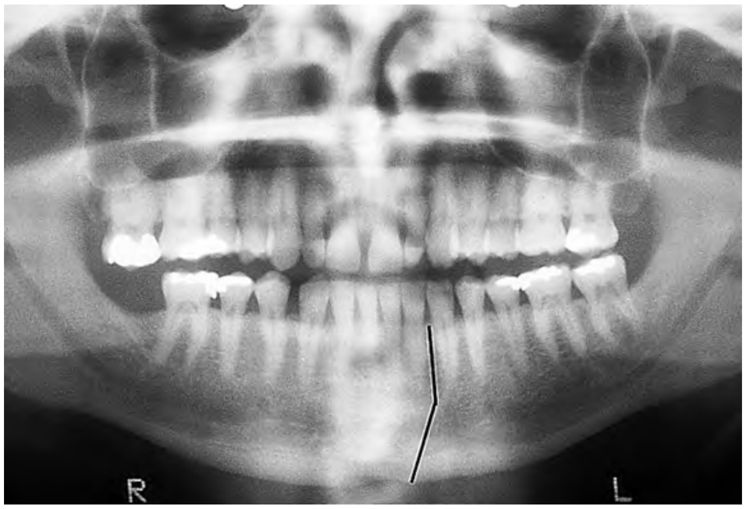

Figure 8.82 A panoramic radiograph showing the site and type of mandibulotomy.

Figure 8.83 The incision for a mandibulotomy and supraomohyoid neck dissection.

Figure 8.84 The supraomohyoid neck dissection is completed.

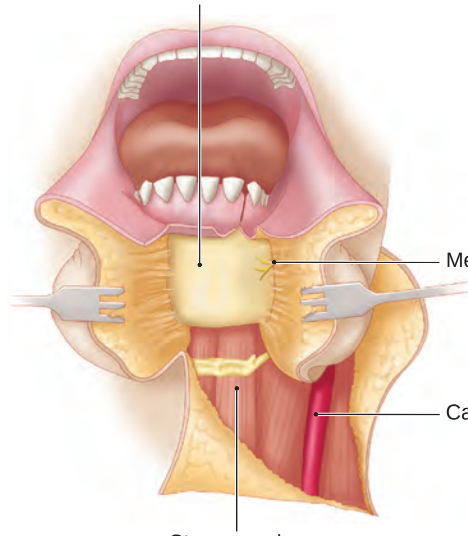

Figure 8.85 A schematic diagram of a paramedian mandibulotomy through a lower lip–splitting incision.

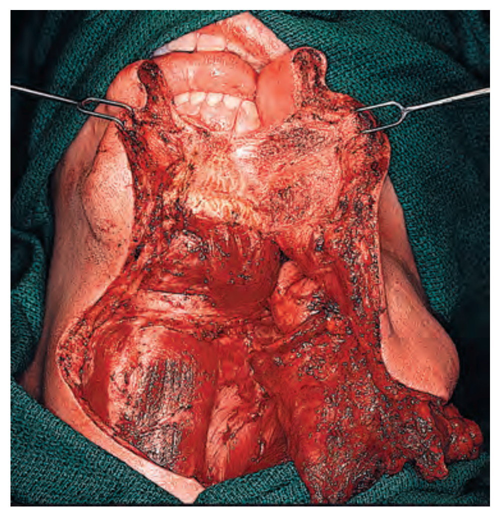

Figure 8.86 The mandibulotomy site is exposed.

Approximately 5 mm of labial mucosa at the gingivolabial sulcus is left attached to the mandible to facilitate closure. At that point, an incision is made in the labial mucosa on the left-hand side of the midline for a distance of approximately 2 cm, and a short cheek flap is elevated (Fig. 8.85). All the soft-tissue attachments of the chin are elevated from the anterior aspect of the mandible to a distance of approximately 2 to 3 cm from the midline on the left-hand side, exposing the mandibulotomy site (Fig. 8.86). Elevation of the cheek flap should be only up to the mental foramen; otherwise the mental nerve is exposed to injury, resulting in loss of sensations of the skin of the chin. Elevation of the left-sided short cheek flap exposes the lateral cortex and the inferior border of the mandible at the mandibulotomy site.

An osteotomy may be performed in a variety of different ways to accomplish a mandibulotomy. The classic Trotter's approach divides the mandible through the midline in a single straight vertical cut. This approach clearly is not desirable because immobilization of the mandible would be extremely difficult as a result of significant motion at the site of the mandibulotomy, causing delayed union or malunion. Alternatively, the mandible may be divided in a stepladder fashion to avoid upward and downward displacement. However, anteroposterior displacement would still be a problem with that approach. In addition, the transverse cut of a stepladder osteotomy may amputate the roots of teeth at that site and devitalize them. A paramedian mandibulotomy is therefore preferred. The mandibulotomy is performed in an angled fashion, dividing the alveolar process between the lateral incisor and canine teeth in a vertical plane for a distance of approximately 10 mm, at which point the

mandibulotomy incision in the bone is angled medially. The angulation in the osteotomy is below the level of the roots of adjacent teeth. The angled cut provides a more stable osteotomy for fixation. A high-speed power saw with an ultrathin blade is used to make the mandibular cuts. Before dividing the bone, appropriate drill holes are placed for fixation of the mandibulotomy site with titanium miniplates. These drill holes are placed before dividing the bone to ensure accurate alignment of the mandibulotomy site at the time of the closure to avoid malocclusion. Two-plane fixation is desirable. A four-hole miniplate is placed on the outer cortex of the mandible over the mandibulotomy site below the level of the roots of the adjacent teeth. With use of benders, the plate is appropriately molded and shaped to fit snugly over the mandibular surface. Four drill holes are now made through the plate holes in the mandible. Another similar plate is shaped to fit over the lower border of the mandible, and four drill holes are made in a vertical plane through the holes in the plate but avoiding entry into adjacent tooth sockets (Fig. 8.87). These plates are then removed and saved for use later in the operation for repair of the osteotomy site. Placement of the drill holes before the osteotomy is performed allows accurate reapproximation of the two ends of the mandible during closure, thus preserving the occlusal surfaces of the upper and lower dentition in perfect alignment. Accurate placement of both miniplates is vitally important to avoid injury to the roots of the adjacent teeth. The mandible is divided exactly as planned with use of a high-speed power saw. Overriding of the bone cuts at the angulation should be avoided to prevent iatrogenic fracture at the mandibulotomy site.

Once the mandible is divided, its two segments are retracted laterally with sharp hooks (Fig. 8.88). Brisk hemorrhage from the cut surface of the mandible is to be expected but can be controlled easily with electrocautery or bone wax. Electrocautery is now used to divide the soft tissue and muscular attachments on the two sides of the mandible. As the two sides of the mandible are retracted, a mucosal incision is made in the floor of the mouth, leaving a cuff of approximately 1 cm of mucosa at the gingiva (Fig. 8.89). This procedure is essential to facilitate closure of the floor of the mouth.

The mucosal incision in the floor of the mouth extends from the mandibulotomy site all the way up to the anterior pillar of the soft palate. If the incision needs to be extended further posteriorly, it will require division of the lingual nerve that crosses the surgical field as it exits from the mandible to enter the lateral aspect of the tongue. The tongue is retracted medially in the oral cavity as the mandibular segment is retracted laterally, providing the necessary exposure.

The soft-tissue attachments on the medial aspect of the mandible, including the sublingual salivary gland, are shown divided, and the two halves of the mandible are retracted with loop retractors (Fig. 8.90). Note that the mucosal incision in the floor of the mouth has retained a cuff of mucosa along the gingiva to facilitate closure. The mylohyoid muscle attached to the mandible is now exposed. It will need to be divided to permit mandibular “swing” and further exposure. The mylohyoid muscle is divided in its center with an electrocautery, leaving its lateral half attached to the mandible. Complete division of the mylohyoid muscle will permit sufficient swing of the mandible to provide exposure of the tongue in the surgical field (Fig. 8.91). Adequate exposure of the lesion is now readily available in the surgical field, allowing satisfactory three-dimensional resection of the primary tumor in continuity with the sublingual and submandibular salivary gland and the adjacent soft tissues and lymph nodes in a monobloc fashion (Fig. 8.92). The proposed line of resection is now marked to guide primary tumor resection (Fig. 8.93). A full-thickness, through-and-through three-dimensional resection of the tumor is now performed with use of an electrocautery with coagulating current. Note that the wedge-shaped resection is oriented transversely to permit repair of the surgical defect by primary closure. Brisk hemorrhage from the lingual artery and/or its branches is to be expected during resection of the tongue but is easily controlled with appropriate hemostasis.

Surgical resection is extended from the dorsum of the tongue through its undersurface to include a full complement of the underlying musculature, providing a true three-dimensional excision as seen in the specimen (Fig. 8.94). Thus a monobloc, in-continuity resection of the primary tumor with the contents of the supraomohyoid triangle is performed to achieve an oncologically sound locoregional excision of the primary tumor and its first echelon lymph nodes and intervening lymphatic channels. The surgical defect in the middle third of the tongue is shown in Fig. 8.95. At this point, frozen sections are obtained from the lateral mucosal margins and the deep soft-tissue margin of the surgical defect to ensure adequacy of the resection. Once satisfactory resection is confirmed, repair of the defect begins

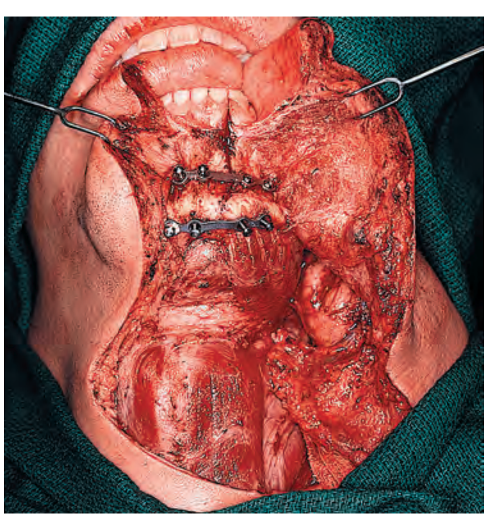

Figure 8.87 Four drill holes are made before bone division.

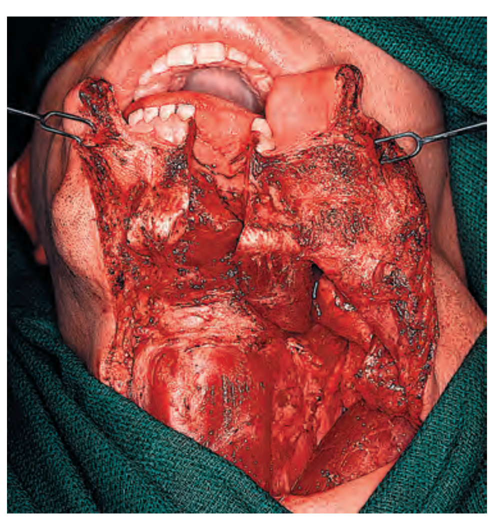

Figure 8.88 The mandible is divided and its two segments are retracted laterally.

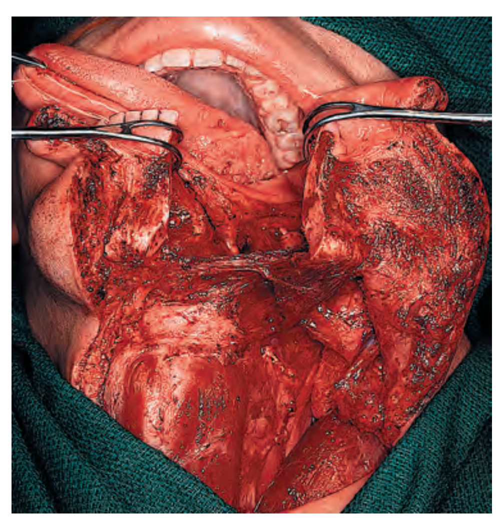

Figure 8.89 An incision is made in the floor of the mouth.

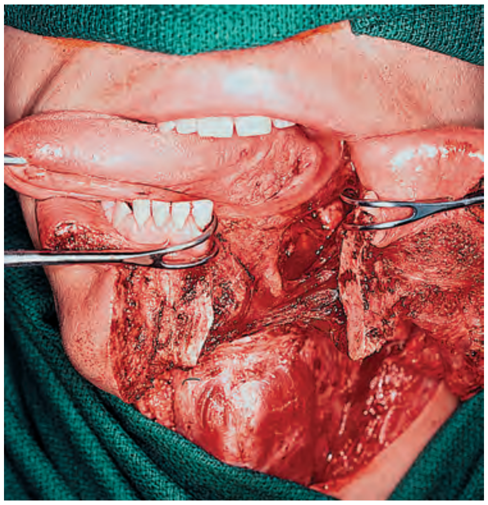

Figure 8.90 The mucosa and submucosal soft tissues are divided and the mandible is retracted to expose the mylohyoid muscle.

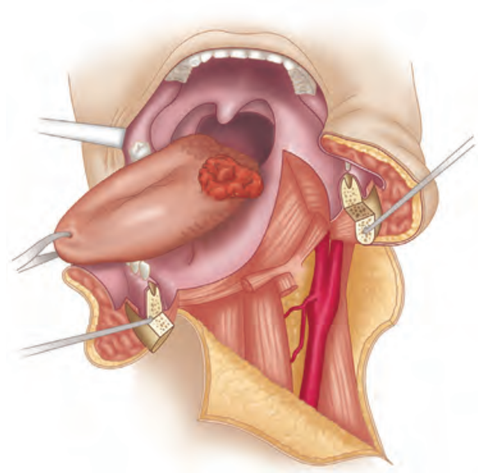

Figure 8.91 A schematic diagram showing exposure of the tumor.

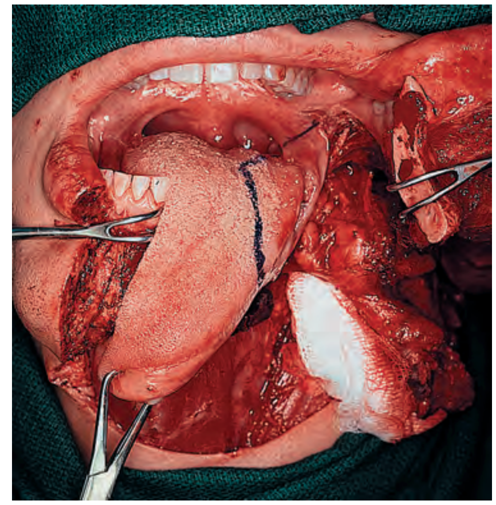

Figure 8.92 Adequate exposure permits three-dimensional resection of the primary tumor with lymph nodes in a monobloc fashion.

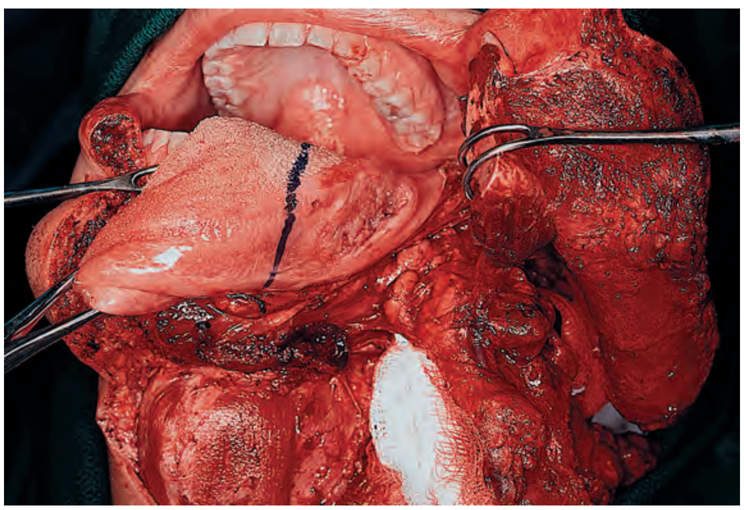

Figure 8.93 The proposed site of resection is marked.

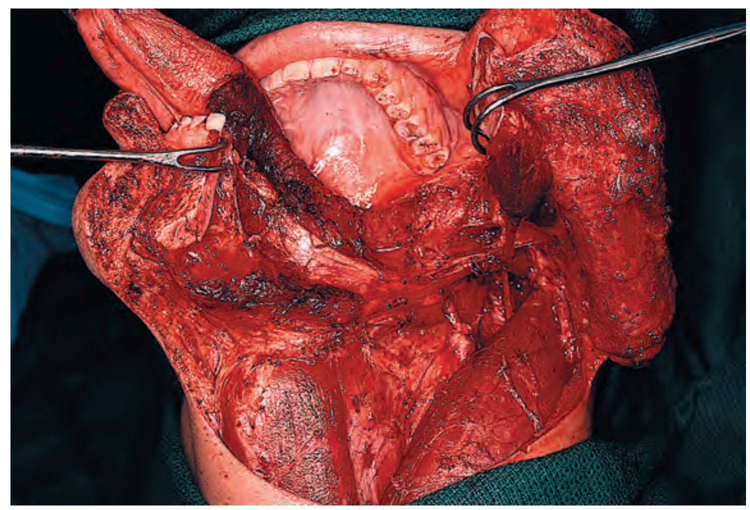

Figure 8.95 The surgical defect in the middle third of the tongue.

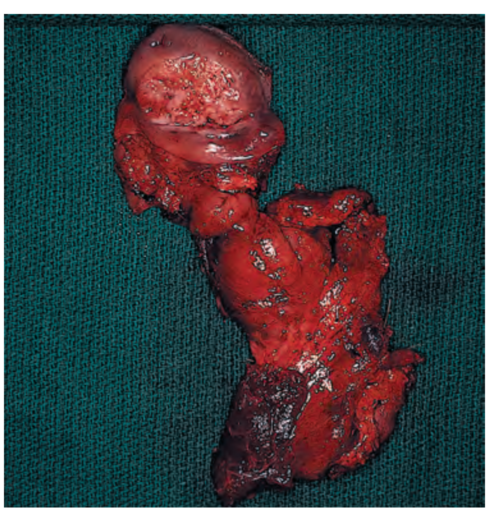

Figure 8.94 The surgical specimen showing three-dimensional excision.

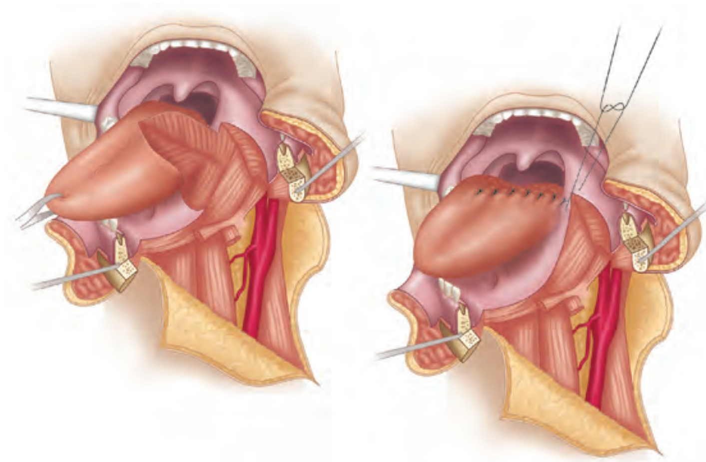

Figure 8.96 Primary closure of the transverse wedge-shaped defect.

(Fig. 8.96). A nasogastric feeding tube is inserted before beginning the closure. It is important to introduce the feeding tube at this point, because if it is difficult to place the tube after the wound is closed and digital manipulation is necessary, it may disrupt the suture line. A skin hook is placed at the apex of the wedge-shaped surgical defect on the dorsum of the tongue, and traction is applied toward the right-hand side. This procedure allows the front of the tongue to draw posteriorly, providing easy approximation of the raw areas. Closure is performed with use of interrupted 2-0 chromic catgut sutures for the muscular layer.

Closure of the tongue is completed with 2-0 chromic catgut interrupted sutures, which also are used for the mucosa of the tongue. Following repair of the tongue, the retracted left half of the mandible is allowed to fall back in its normal position.

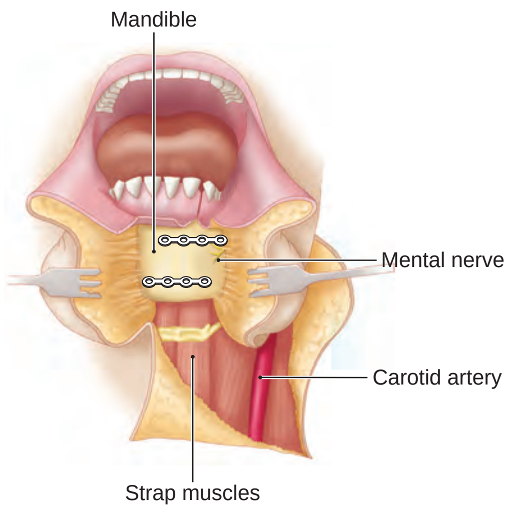

Figure 8.97 Repair of the mandibulotomy with miniplates and screws.

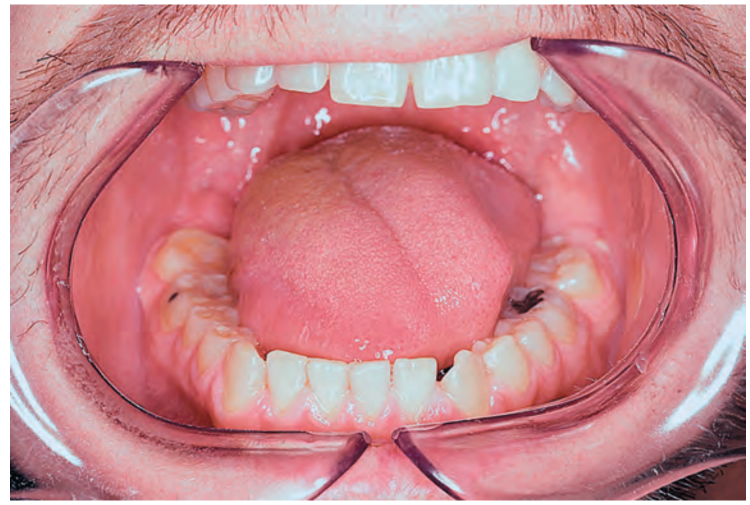

Figure 8.99 An intraoral view 3 months following surgery shows excellent healing of the tongue.

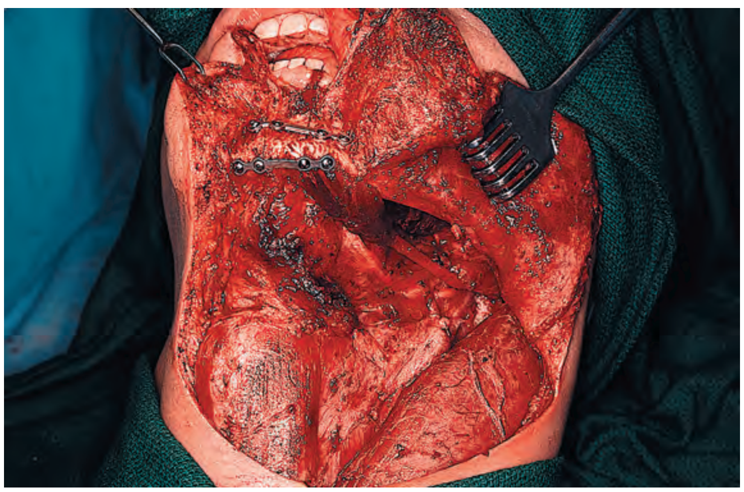

Figure 8.98 Mandibular fixation is completed with titanium miniplates and screws.

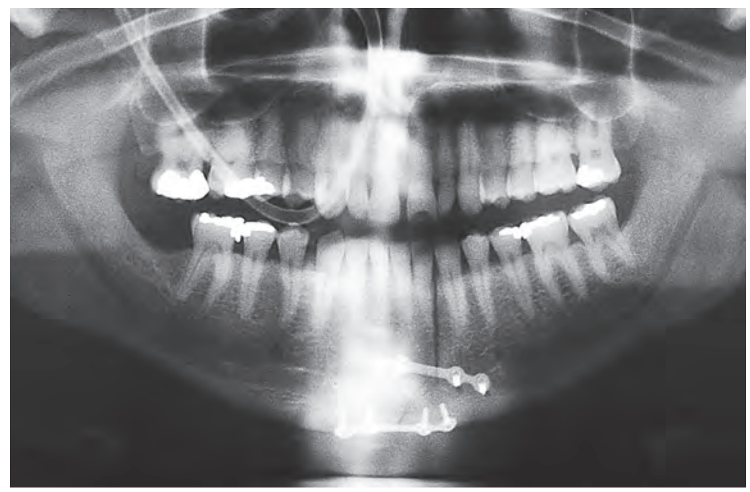

Figure 8.100 Postoperative panoramic x-ray shows excellent alignment of the mandibular segments with miniplates and screws.

Closure of the mucosa of the lateral aspect of the tongue to the mucosa of the floor of the mouth on the gingiva continues with interrupted chromic catgut sutures. As the closure proceeds anteriorly, the mandible draws closer and closer to the mandibulotomy site until complete mucosal closure of the floor of the mouth is accomplished. At this point, the mandibulotomy is repaired with fixation with use of the previously shaped miniplates (Fig. 8.97).

A depth gauge is used to select the length of the screws to be used for the miniplates. The screws should be long enough to go through both cortices of the mandible for the lateral plate. However, they should not project through the lingual cortex of the mandible into the soft tissues of the oral cavity. Similarly, the miniplate on the lower border of the mandible is fixed with relatively short screws to avoid injury to the roots of the adjacent teeth. Every attempt is made to secure perfect alignment of the two ends of the mandible to restore normal occlusion. The screws are tightened snugly but not too tightly; otherwise, the heads of the titanium screws will break (Fig. 8.98).

Mucosal closure now begins by reapproximation of the cut edge of the labial mucosa to the cuff of the mucosa at the gingivolabial sulcus on the alveolar process. This closure is accomplished with use of 3-0 chromic catgut interrupted sutures. Chromic catgut sutures are used for the muscular and the mucosal layers of the lip, and nylon sutures are used for the skin and vermilion border. For perfect closure of the midline lip-splitting incision, a fine nylon suture is first placed, accurately aligning the vermilion border.

This suture is held as a retractor, and closure of the labial mucosa progresses in a retrograde fashion from the vermilion border up to the gingivolabial reflection. Interrupted sutures to approximate the muscular layer are applied in a similar fashion. Accurate reapproximation of the skin of the lip and chin is essential to obtain an aesthetically acceptable scar. The stumps of the divided mylohyoid muscle are reapproximated using interrupted chromic catgut sutures. Although this reapproximation is seldom accurate, it permits reduction of the dead space in the submandibular region.

A suction drain is placed in the wound and brought out through a separate stab incision. The neck incision is closed in two layers in a routine fashion.

In the postoperative period, the patient receives nasogastric tube feedings for approximately 1 week. At that time, a trial with puréed food is conducted to see whether swallowing is successful. If the patient is able to tolerate puréed food, he or she is gradually advanced to a soft diet during the next few days. The intraoral view shows excellent healing of the tongue (Fig. 8.99). The postoperative panoramic radiograph shows perfect alignment and accurate approximation of the two segments of the mandible, maintaining essentially a normal occlusion (Fig. 8.100). Postoperative appearance of the patient 3 months following surgery shows a well-healed midline scar

Figure 8.101 Postoperative appearance of the patient 3 months following surgery.

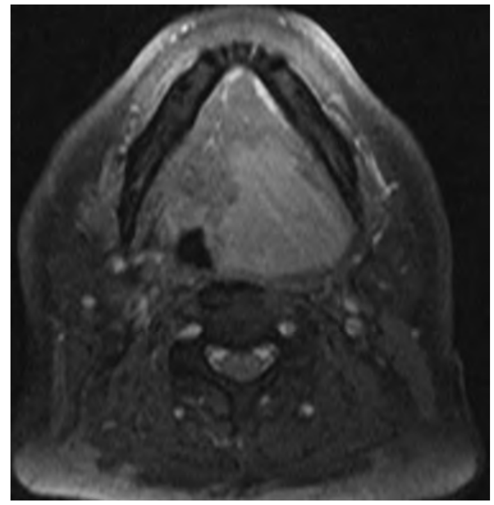

Figure 8.103 An axial view of a magnetic resonance imaging scan showing a multilobulated tumor crossing the midline.

Figure 8.102 A "zigzag" incision in the submental region avoids a vertical band of scar.

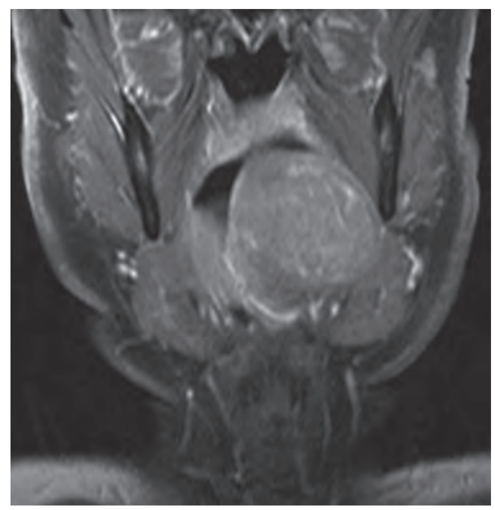

Figure 8.104 A coronal view of a magnetic resonance imaging scan showing a massive tumor in the base of the tongue.

and an aesthetically acceptable external appearance (Fig. 8.101). Note the vertical band of scar in the submental region due to the straight midline incision. To avoid this the vertical component of the incision can be modified. That part of the incision between the undersurface of the chin and up to the hyoid bone is made in a zigzag fashion, like multiple "Z" plasties (Fig. 8.102). This avoids the vertical band of scar.

Median Labiomandibular Glossotomy (Trotter's Operation)

Tumors located in the midline of the oropharynx and the craniocervical junction can be approached optimally with a mandibulotomy and median glossotomy. Splitting the tongue in the midline through a relatively avascular plane permits preservation of the lateral neurovascular bundles to both halves of the tongue and leaves the patient with very little functional deficit.

The procedure described here is that performed on a patient who had a large benign rhabdomyoma of the base of the tongue. A contrast-enhanced MRI scan in the axial view clearly shows an extensive tumor arising from the left side of the base of the tongue and extending across the midline (Fig. 8.103). The tumor is well circumscribed and multilobulated. The coronal view of the MRI again demonstrates a massive tumor involving the base of the tongue (Fig. 8.104). Endoscopic assessment of the tumor showed that it did not involve the supraglottic larynx and did not ulcerate through the mucosa of the base of the tongue. A core biopsy was performed before the surgical procedure that confirmed the diagnosis of a benign rhabdomyoma.

The patient is put under general anesthesia through nasotracheal intubation, and the head and neck area is prepared with antiseptic solution in the usual manner. A midline lip–splitting incision is planned, extending from the vermilion border of the lower lip up to the hyoid bone (Fig. 8.105). The skin incision is deepened through the musculature of the lip and the mucosa of the labial surface of the lip up to the gingivolabial sulcus. The incision is extended laterally up to the canine tooth on both sides, carefully preserving the mental nerve to retain skin sensation in the chin and lower lip. An angled, mandibular osteotomy is performed between the central incisor teeth in the usual fashion with the vertical division of the mandible up to midway through its vertical height, and at that point it is angled laterally to provide vertical stability at the mandibulotomy site (Fig. 8.106). By remaining in the midline,

Figure 8.105 A lower lip–splitting midline incision is marked.

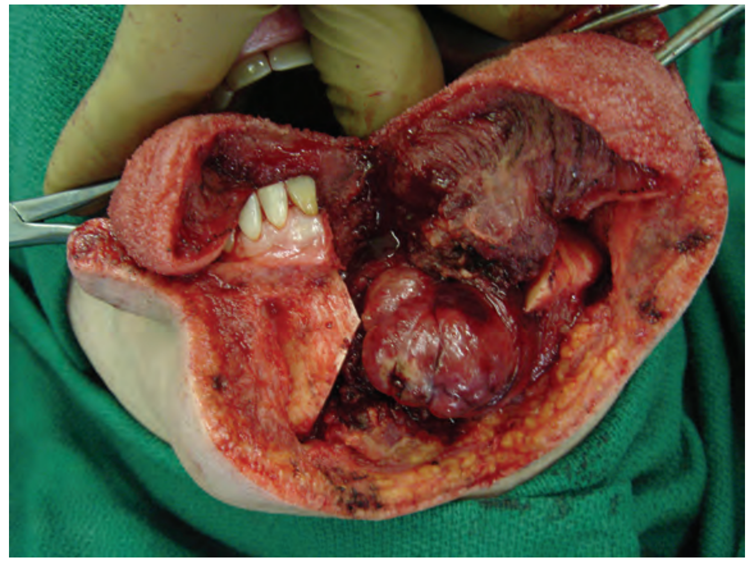

Figure 8.107 The tumor is exposed through a midline glossotomy.

Figure 8.106 An angled midline mandibulotomy is performed.

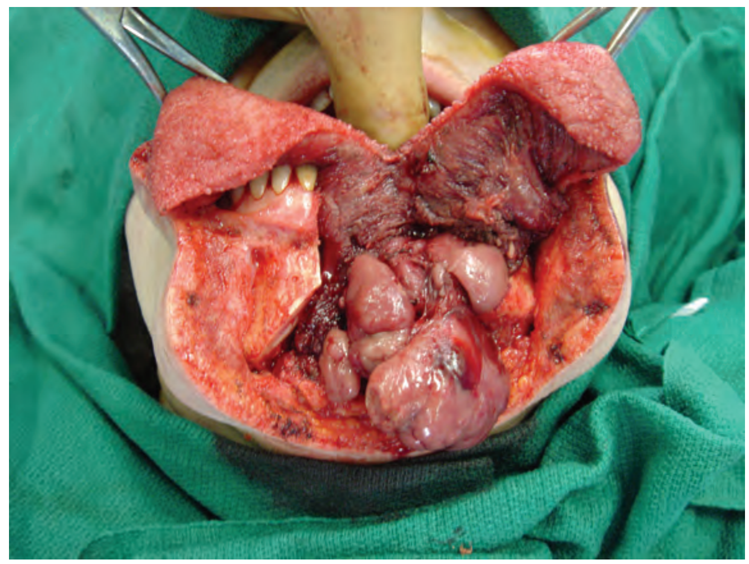

Figure 8.108 All lobulations of the tumor are meticulously dissected.

all the neurovascular structures of the skin of the chin, lip, mandible, and tongue are preserved, because they all come from the lateral aspect of the oral cavity.

The divided halves of the mandible are retracted laterally. A mucosal incision from the midline of the attached gingiva is extended through the floor of the mouth, remaining between the openings of Wharton's ducts, carefully preserving their integrity. The incision is then extended along the undersurface of the midline of the tongue up to the tip of the tongue and then extended farther posteriorly on the dorsum of the tongue along its midline. Electrocautery is used to divide the tongue in the midline through the median raphe, which permits retraction of the two halves of the tongue laterally. The very anterior surface of the tumor is now readily visible at the base of the tongue in the suprahyoid region, embedded within the hyoglossus muscle. With the index finger of the operating surgeon pushing the dorsum of the base of the tongue anteriorly, the tumor easily protrudes out through the glossotomy (Fig. 8.107).

Meticulous dissection is now performed around the multilobulated benign tumor, working through the interdigitating fibers of the deep muscles of the tongue. Careful attention should be given to removing each of the lobules of the tumor so no remnants are left behind, thereby risking local recurrence. Nearly all of the tumor has been dissected and delivered into the wound at this point (Fig. 8.108). The tumor is then completely excised and removed. Meticulous hemostasis is achieved with the use of electrocautery and ligation of larger vessels as necessary. The surgical defect shows normal musculature of the tongue on both sides of its base with a potential space remaining because of removal of the tumor (Fig. 8.109). Deep sutures with 2-0 chromic catgut are placed to reapproximate the musculature of each half of the base of the tongue to obliterate the potential space. Two-layered closure of the tongue is then performed with approximation of the deep intrinsic muscles and mucosa. Accurate approximation of the two sides is performed without overlapping and aligning the tip. The mandibulotomy is reconstructed in the usual fashion with two miniplates. One miniplate is applied on the lateral aspect of the cortex of the mandible, and one is applied on the inferior border of the mandible to achieve two-plane fixation. The skin incision of the lip, chin, and submental region is closed in the usual fashion and a Penrose drain is placed, which is removed within 48 hours.

The appearance of the patient approximately 1 year after surgery shows perfect alignment and healing of the labiomandibular glossotomy with a barely perceptible scar on the lip

and chin (Fig. 8.110). The mandible is aligned in a perfectly normal position with accurate approximation and occlusion of the central incisor teeth. The tongue maintains its normal shape, sensations, and mobility with normal articulation and mastication (Fig. 8.111).

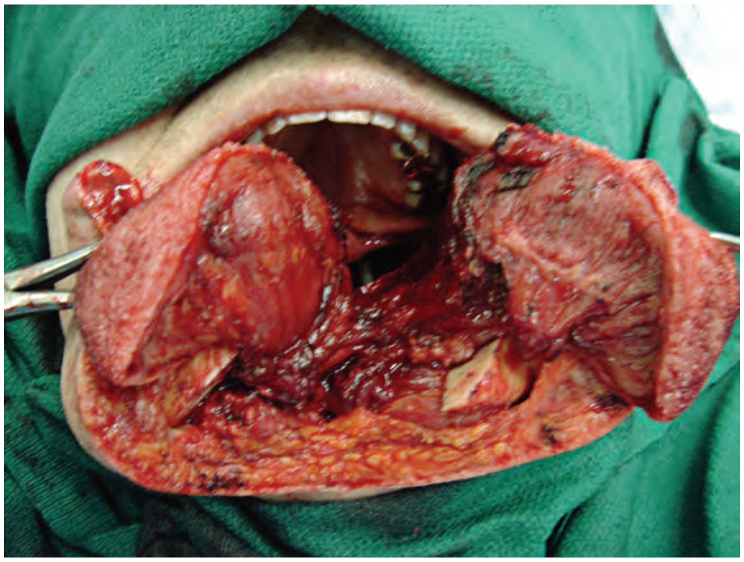

Figure 8.109 The surgical defect following excision of the tumor.

Figure 8.110 The appearance of the patient 1 year after surgery.

Figure 8.111 Mobility of the tongue is preserved.

A median labiomandibular glossotomy thus provides excellent exposure for selected tumors of the base of the tongue, posterior pharyngeal wall, and craniocervical junction. (See Chapter 15 for a description of a mandibulotomy for a chordoma.)

Mandible Resection in the Management of Oral Cancer

Surgical resection of the mandible becomes necessary when a primary malignant tumor of the oral cavity involves the mandible or directly extends to the gingiva over the alveolar process or infiltrates into the mandible. If the tumor extends directly from the alveolar process to the cancellous part of the mandible or if contiguous tumor infiltration to the lingual or lateral cortex of the mandible is present, a segmental mandibulectomy becomes necessary (Fig. 8.112).

A marginal mandibulectomy can be performed to resect the alveolar process, the lingual cortex of the mandible, or both for tumors of the oral cavity (Fig. 8.113). A marginal mandibulectomy can also be performed for lesions adjacent to the retromolar trigone, whereupon the anterior aspect of the ascending ramus of the mandible, including the coronoid process

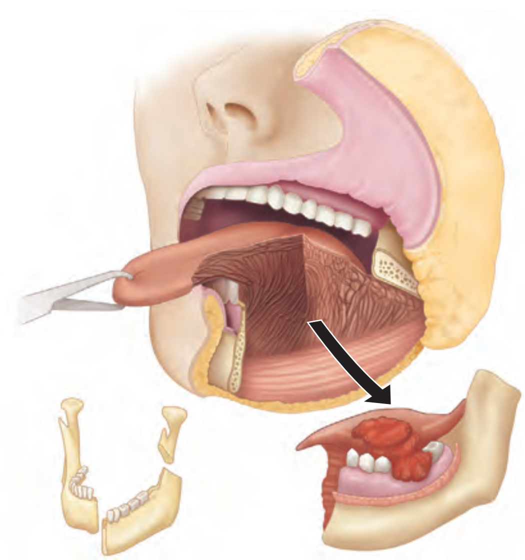

Figure 8.112 A segmental mandibulectomy.

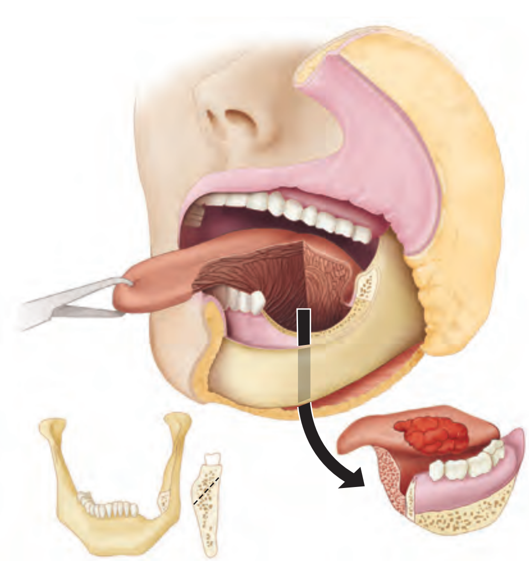

Figure 8.113 A schematic diagram of a marginal mandibulectomy for cancer of the floor of the mouth through a lower cheek flap approach.

Figure 8.114 A marginal mandibulectomy of the symphysis of the mandible.

Figure 8.115 A marginal mandibulectomy of the body of the mandible.

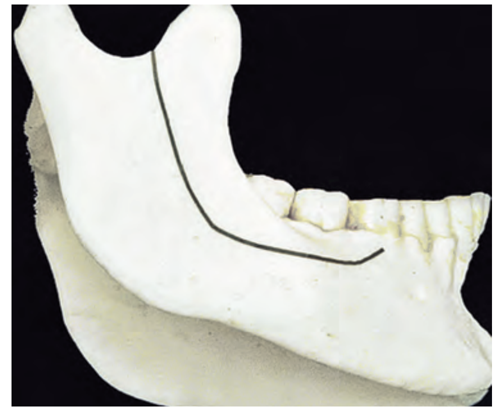

Figure 8.116 A marginal mandibulectomy of the retromolar trigone and coronoid process of the mandible.

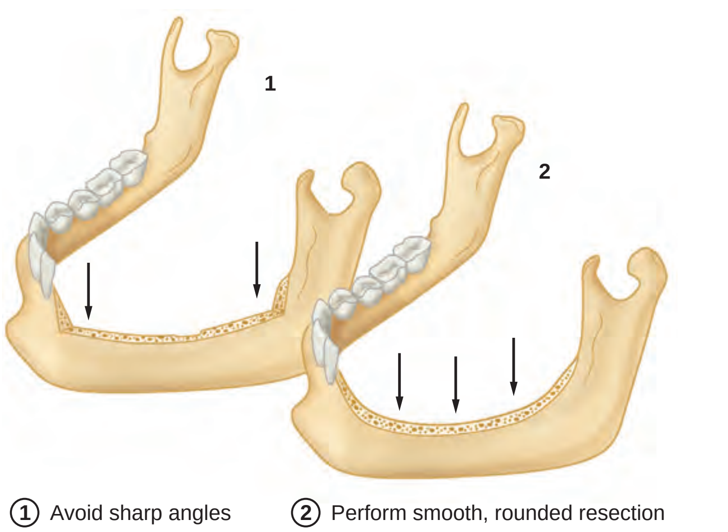

Figure 8.117 The marginal mandibulectomy is performed in a smooth curve to evenly distribute the stress at the site of resection.

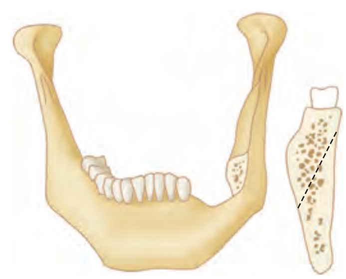

Figure 8.118 A marginal mandibulectomy removing the lingual cortex and the alveolar process of the mandible.

and the adjacent alveolar process of the body of the mandible, are resected (Figs. 8.114 through 8.116). A reverse marginal mandibulectomy is indicated in patients who have soft-tissue disease such as fixation of prevascular facial lymph nodes to the lower cortex of the mandible.

In performing a marginal mandibulectomy, right-angled cuts at the site of the marginal mandibulectomy should be avoided, because they lead to points of excessive stress, which leads to the risk of spontaneous fracture. Therefore the marginal mandibulectomy should be performed in a smooth curve to evenly distribute the stress at the site of resection (Fig. 8.117). The exposed bone following a marginal mandibulectomy is covered by primary closure between the mucosa of the tongue or floor of the mouth to the mucosa of the cheek, a split-thickness skin graft, or a radial forearm free flap. However, it must be remembered that primary closure will eliminate the lingual or the buccal sulcus, rendering fabrication of a removable denture exceedingly difficult. Alternatively, a skin graft can be applied directly over the marginally resected mandible, which would permit retention of the sulci and the ability of the patient to wear a partial denture that can be clasped to the remaining teeth. In edentulous patients, wearing a denture over a marginally resected mandible is nearly impossible. In general, however, even in patients with remaining teeth, a partial denture clasped to the remaining teeth for dental rehabilitation at the site of marginal mandibulectomy is not satisfactory, because it is not stable, and it often moves during mastication. Ideally, therefore, an implant-based permanent or removable denture that provides better stability and permits mastication would be desirable. Unfortunately, there are limitations in implant placement after marginal mandibulectomy because of insufficient bone height between the alveolar crest and the mandibular canal. A minimum of 8 mm of bone height is necessary to even consider short implants. That much bone height is not available after marginal mandibulectomy. Therefore implant-based dental rehabilitation is not possible in the lateral segment (premolar and molar) of the mandible. On the other hand, implant-based denture can be easily performed in the anterior segment of the mandible (between the mental foramina) where sufficient bone height is available to consider even the standard 10 mm high implants. Therefore, if optimal dental rehabilitation is the ultimate goal in patients who are suitable for marginal mandibulectomy, then consideration should be given to segmental mandibulectomy and fibula free flap reconstruction with immediate placement of dental implants in the fibula. When significant soft tissue and mucosal loss has occurred after oral cancer resection, a radial forearm free flap should be planned for soft tissue and lining for reconstruction.

On the other hand, if a primary tumor of the oral cavity approximates the alveolar process or the lingual surface of the mandible, then resection of the alveolar process or the lingual cortex of the mandible, preserving the mandibular arch, is possible (Fig. 8.118). The routes of spread of intraoral tumors in proximity to the mandible are such that marginal resection is feasible even in edentulous patients, as long as sufficient bone height is available above the mandibular canal. Mandible reconstruction is not necessary following a marginal mandibulectomy, since the mandibular arch is preserved, and thus its

aesthetic impact is minimal. However, satisfactory dental and functional rehabilitation remains an issue.

On the other hand, following a segmental mandibulectomy, immediate mandible reconstruction must be considered, unless there are medical contraindications to a long free flap procedure.

Peroral Marginal Mandibulectomy and Primary Closure

Small primary tumors of the anterior aspect of the lower gum are suitable for excision through the open mouth, including the alveolar process, regardless of the presence or absence of teeth. Such a resection requires a marginal mandibulectomy. This operation is also indicated for lesions of the floor of the mouth or cheek mucosa approaching the lower alveolus.

A marginal mandibulectomy can be performed safely through the open mouth for small lesions, particularly in the anterior aspect of the oral cavity. The patient shown in Fig. 8.119 has a 1-cm, ulcerated, superficial carcinoma involving the alveolus of the edentulous mandible adjacent to her remaining central incisor tooth. Radiographic imaging studies did not show any evidence of bone invasion. This tumor therefore is suitable for a marginal mandibulectomy.

The surgical specimen removed through the open mouth is shown in Fig. 8.120. Note that satisfactory mucosal and soft-tissue margins are secured, as seen in the surface view of the specimen. In the side view, as seen in Fig. 8.121, the height of the surgical specimen is shown, with an ample deep bone margin for this superficial ulcerated carcinoma. The surgical defect is repaired by primary closure of the mucosa of the floor of the mouth to the mucosa of the lower lip. Although the sulci at the site of the resected mandible in the floor of the mouth and the gingivolabial region are eliminated, the functional impairment in the immediate postoperative period is minimal.

The postoperative appearance of the mouth at approximately 1 year following surgery shows a well-healed suture line (Fig. 8.122). Note the absence of gingivolabial sulcus as well as flattening of the mucosa of the floor of the mouth. This patient is a suitable candidate for dental implants for a fixed denture, which will provide not only lip support but would significantly improve oral aesthetics. If wider exposure is necessary for access to the primary tumor and its satisfactory resection, then a lower cheek flap approach is recommended. In most instances, the lower cheek flap approach provides satisfactory exposure and permits resection of the primary tumor and ipsilateral cervical lymph nodes in continuity in a monobloc fashion (Fig. 8.123).

The lower cheek flap approach involves splitting the lower lip and the chin in the midline through its full thickness up to the symphysis of the mandible. The incision continues in the midline up to the thyrohyoid membrane, where it turns toward the ipsilateral neck along an upper neck skin crease. This transverse component of the incision should be at least two finger breadths below the body of the mandible to prevent inadvertent injury to the mandibular branch of the facial nerve during elevation of the cheek flap.

Figure 8.119 An ulcerated superficial carcinoma of the lower gum.

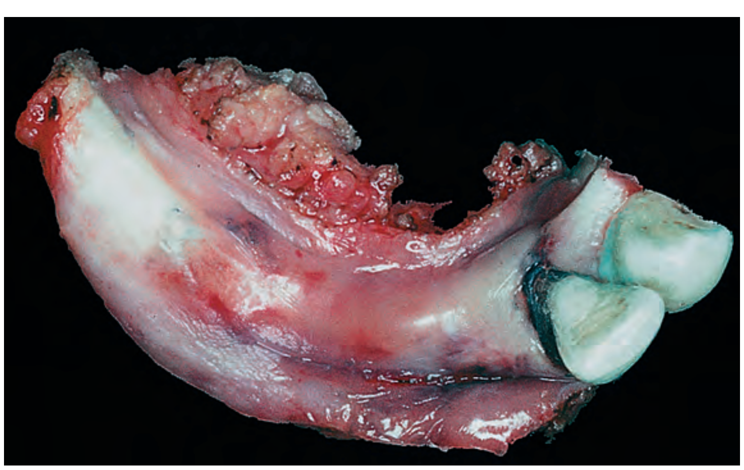

Figure 8.120 The surgical specimen (surface view).

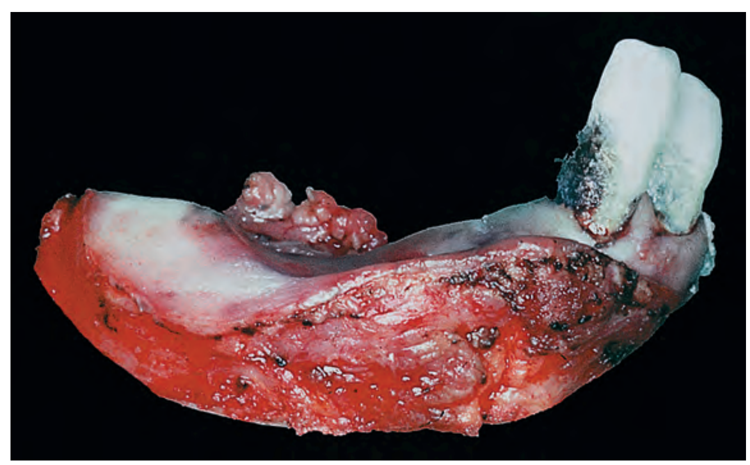

Figure 8.121 The surgical specimen (side view).

Figure 8.122 The appearance of the mouth 1 year postoperatively.

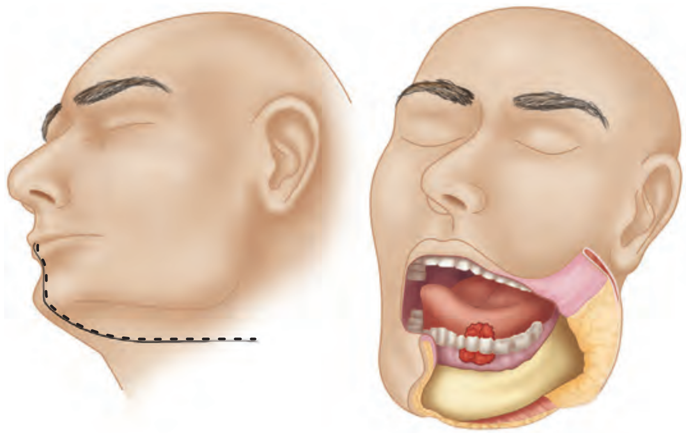

Figure 8.123 The lower cheek flap approach.

Marginal Mandibulectomy and Skin Graft Reconstruction

An intraoral photograph of a patient with carcinoma of the lower alveolus adjacent to her remaining teeth is shown in Fig. 8.124. The primary lesion is exophytic and relatively superficial, involving the alveolar process and attached gingiva of the adjacent teeth. A panoramic radiograph of the mandible fails to show any evidence of bone destruction (Fig. 8.125). A marginal mandibulectomy is performed through a lip-splitting lower cheek flap approach. A high-speed sagittal power saw is used to perform a marginal mandibulectomy in a smooth curved fashion to evenly distribute the stress at the site of the bone resection. The surgical specimen in Fig. 8.126 shows a satisfactory three-dimensional resection of the primary tumor. The surgical defect shown in Fig. 8.127 demonstrates a smooth curved marginal resection of the mandible with sufficient cortical bone remaining to provide stability to the mandible and to preserve the continuity of its arch. The surgical defect in this patient is repaired with a split-thickness skin graft. The skin graft usually heals satisfactorily and provides excellent coverage of the exposed bone (Fig. 8.128). Because the patient has remaining teeth in the lower dentition, a removable denture is fabricated that can be clasped to the teeth to restore the lower dentition (Fig. 8.129).

If adequate vertical height of the remaining body of the mandible following a marginal mandibulectomy is available, then osseointegrated implants can be inserted at the time of the marginal mandibulectomy or later. However, if the osseointegrated implants are inserted primarily, satisfactory coverage over the mandible should be secured to avoid exposure and loss of the implants. A radial forearm free flap would be ideal in that setting.

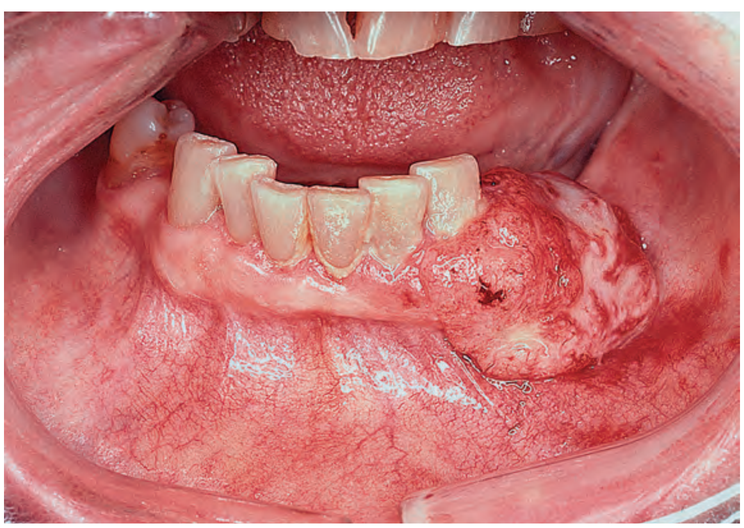

Figure 8.124 A carcinoma of the lower alveolus.

Figure 8.126 The surgical specimen.

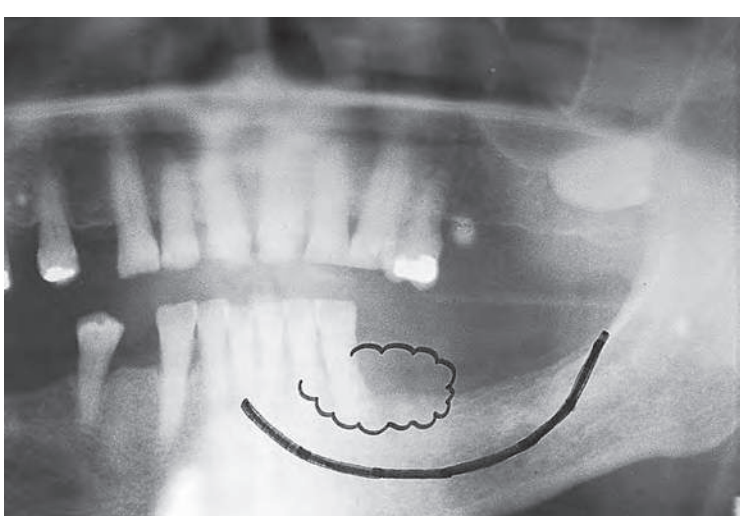

Figure 8.125 A panoramic radiograph of the mandible.

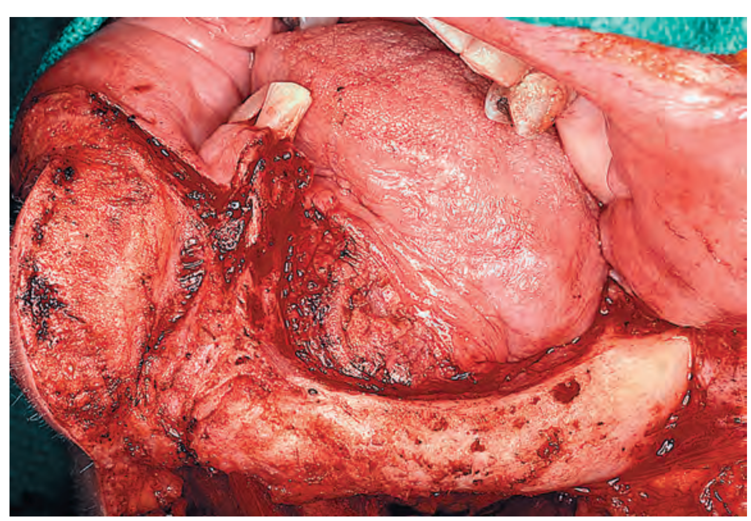

Figure 8.127 The surgical defect.

Figure 8.128 The healed skin graft.

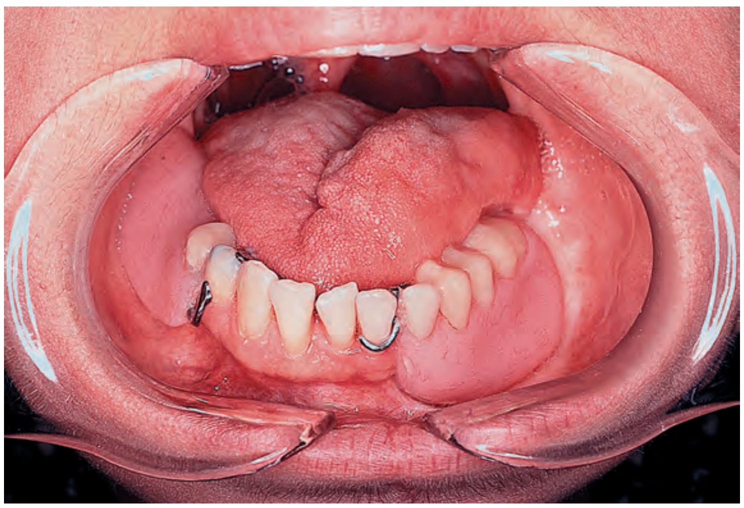

Figure 8.129 A removable denture.

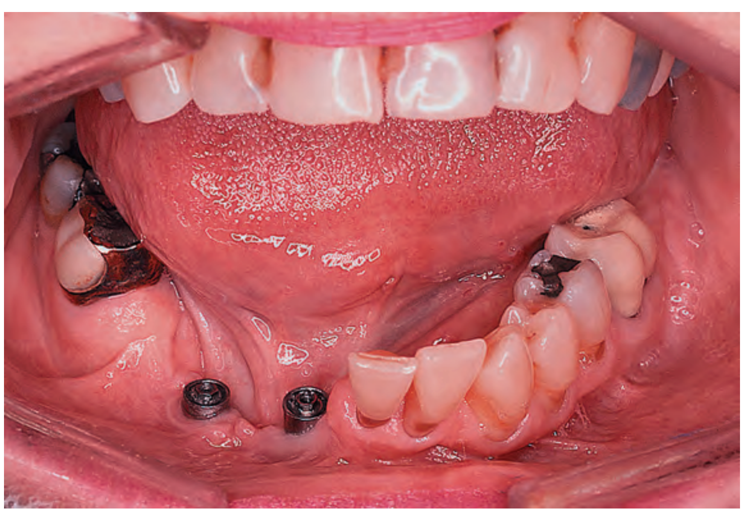

Figure 8.130 A patient with osseointegrated implants at the site of a marginal mandibulectomy.

Another patient shown in Fig. 8.130 had osseointegrated implants placed at the site of marginal mandibulectomy with a permanent fixed denture in place. A panoramic radiograph shown in Fig. 8.131 demonstrates the satisfactory position of the implants in the area of the mandible where the marginal mandibulectomy was performed. An intraoral view of the permanent fixed denture is shown in Fig. 8.132. Thus, when feasible, particularly in the anterior segment of the mandible, osseointegrated implants should be considered for complete dental rehabilitation following a marginal mandibulectomy.

Figure 8.131 A panoramic radiograph showing implants with a fixed denture in place.

Figure 8.132 An intraoral view of a permanent fixed denture.

Marginal Mandibulectomy and Primary Vestibuloplasty With a Skin Graft

After marginal resection of a part of the mandible, patients who have remaining teeth in the lower dentition can be considered for immediate vestibuloplasty to restore the sulci. They can wear an intermediate dental prosthesis as soon as the skin graft of the vestibuloplasty has healed.

An intraoral photograph of a patient with a primary carcinoma of the right-hand side of the floor of the mouth, approaching the lingual gingiva, is shown in Fig. 8.133. He also has clinically palpable cervical lymph nodes at level I, requiring a right neck dissection. A panoramic view of the mandible fails to show any evidence of bone destruction by the tumor (Fig. 8.134). The surgical specimen of the resection of the floor of the mouth with a marginal mandibulectomy and in-continuity right neck dissection is shown in Fig. 8.135. Resection of the alveolar process and most of the lingual plate of the mandible has been accomplished in a monobloc fashion, in continuity with the contents of the dissected right side of the neck. The surgical field shows a through-and-through defect in the floor of the mouth with the preserved arch of the mandible (Fig. 8.136).

Figure 8.133 An intraoral photograph of a carcinoma of the right side of the floor of the mouth.

Figure 8.134 A panoramic radiograph of the mandible.

Figure 8.135 The surgical specimen.

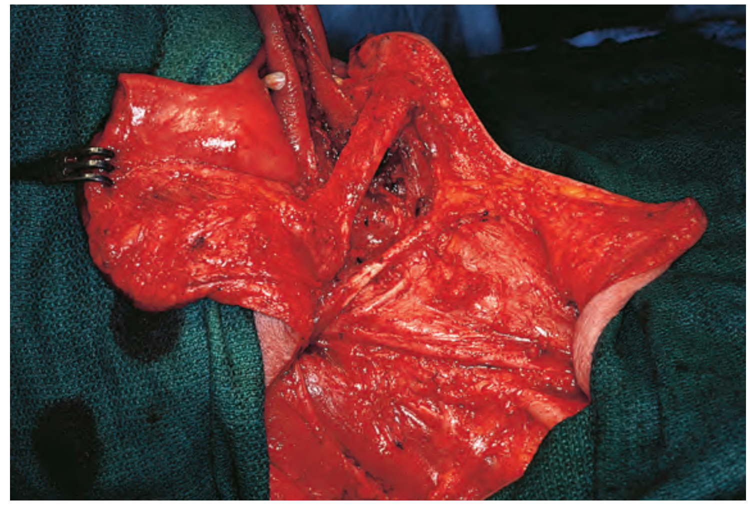

Figure 8.136 The surgical field.

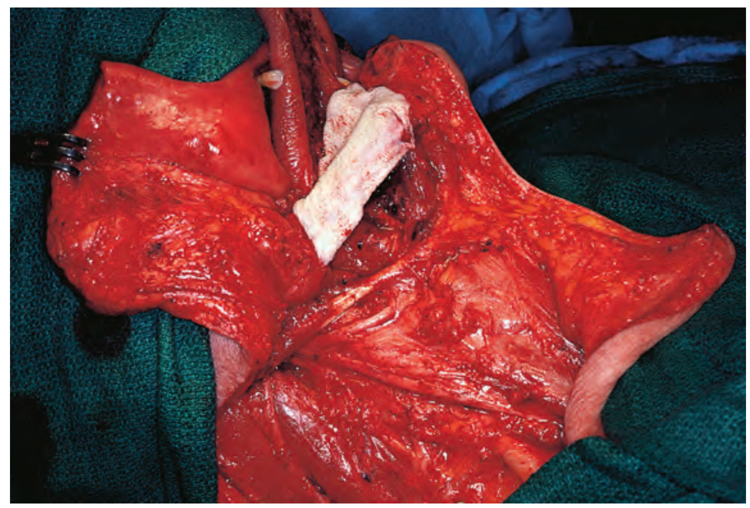

Figure 8.137 The skin graft is draped over the marginally resected mandible.

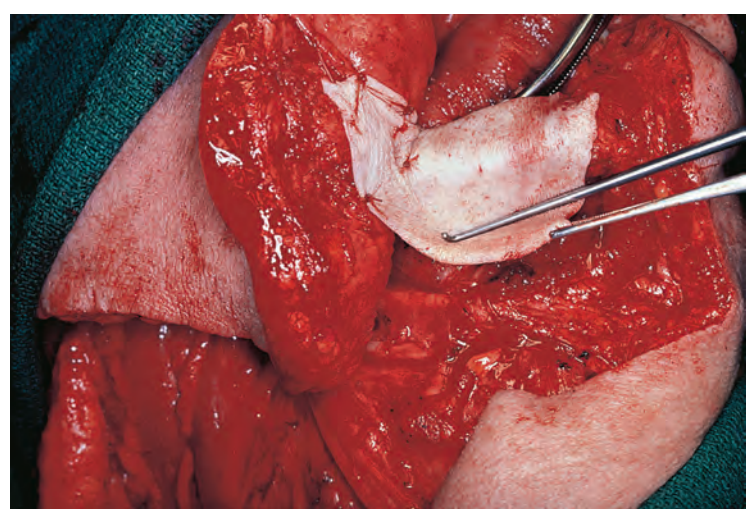

Figure 8.138 A gingivobuccal sulcus and lingual sulcus in the floor of the mouth are created.

Note in particular the exposed muscles of the undersurface of the tongue, which is retracted cephalad.

A split-thickness skin graft is harvested from the lateral aspect of the thigh. It must be quite thick, because it will be applied directly over the marginally resected mandible, which will support the lower denture. A very thin skin graft is likely to ulcerate and produce denture sores because of a lack of supporting soft tissues over the mandible. The skin graft is draped over the marginally resected mandible, as shown in Fig. 8.137. The rectangular skin graft is placed over the marginally resected mandible, beginning at the retromolar area and extending to the anterior edge of the bony defect. The skin graft is appropriately trimmed and positioned to create a gingivobuccal sulcus as well as a lingual sulcus in the floor of the mouth (Fig. 8.138).

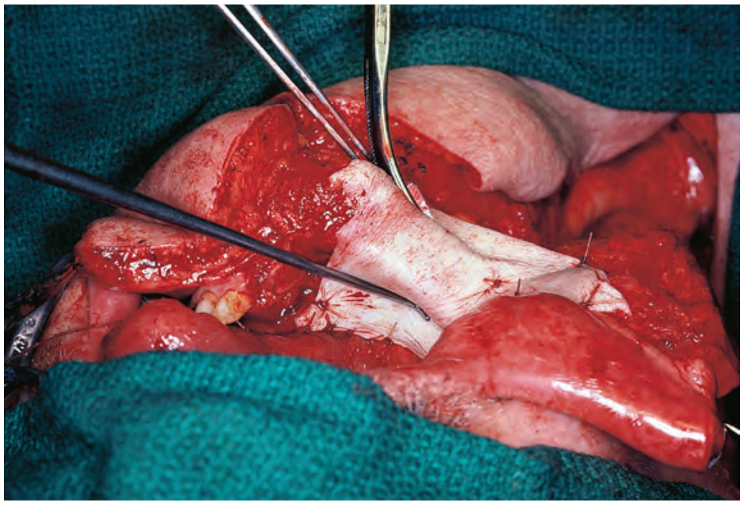

Figure 8.139 Circummandibular absorbable sutures are used to hold the skin graft in place.

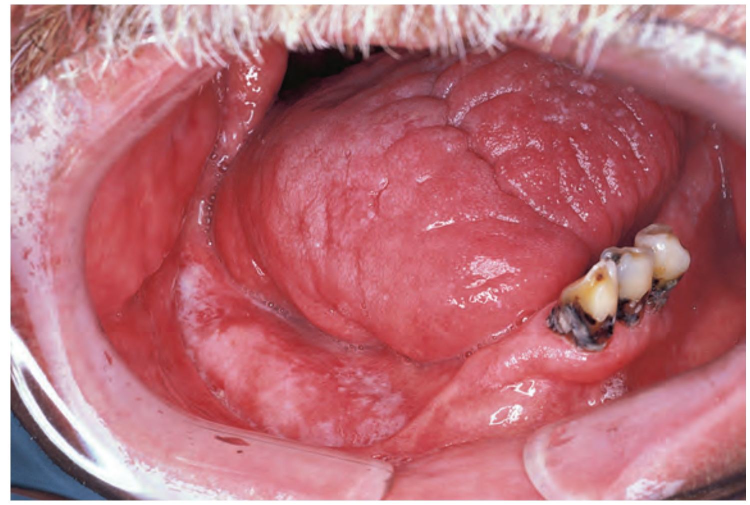

Figure 8.141 A photograph of the oral cavity 8 months after surgery.

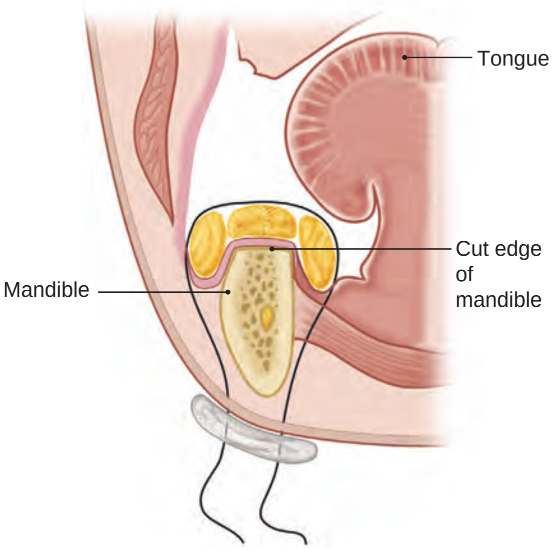

Figure 8.140 A schematic diagram showing a circummandibular silk suture holding the bolsters in place over, medial, and lateral to the skin graft.

Circummandibular chromic catgut sutures will hold the skin graft in place. These sutures begin from the lower border of the mandible on the buccal aspect and end at the lower border of the mandible on the lingual aspect (Fig. 8.139).

Once the graft is appropriately positioned, closure of the surgical defect begins, approximating the lateral edge of the skin graft to the mucosa of the cheek and lower lip using interrupted chromic catgut sutures. The medial edge of the skin graft is sutured to the mucosa of the undersurface of the tongue, also using interrupted chromic catgut sutures. Following complete closure of the mucosal defect, the newly created sulci on two sides of the mandible are maintained, using either bolsters of Xeroform gauze or, preferably, short segments of soft rubber tubing. Size 24 or 26 soft rubber tubing is preferable. Appropriate lengths of the tubing are cut to fit the gingivobuccal sulcus and the lingual sulcus medial to the mandible.

The cut segments of the tubing are then placed in the newly created sulci and are retained there with circummandibular sutures using No. 2 silk (Fig. 8.140). The suture begins on the tube in the gingivobuccal sulcus and goes through the tubing and the soft tissues and skin of the cheek, lateral to the mandible, where it comes out. The same suture continues, reentering the skin of the submental region medial to the mandible, and then traverses the rubber tube in the floor of the mouth, where it exits. Three such sutures are placed and tied over the marginally resected mandible covered with the skin graft. The remaining incisions are closed in the usual fashion. Alternatively a Xeroform gauze bolster can be used and retained there in a similar fashion (see Fig. 8.140).

Meticulous oral hygiene must be maintained in the postoperative period for the skin graft to take and heal over the marginally resected mandible. The bolsters of Xeroform gauze or rubber tubing used to recreate the sulci are kept in place for 1 week. In most cases, the skin graft will take well and effectively create the desired sulci. Immediately upon removal of the bolsters or the rubber tubing, the patient must be seen by a prosthodontist for fabrication of an immediate temporary lower denture, with buccal and lingual flanges, which will fit over the mandible into the new sulci. This step is absolutely mandatory; otherwise, the skin graft will flatten out and the newly created sulci will be lost. The final denture should not be made until approximately 6 to 8 weeks after surgery.

A photograph of the oral cavity approximately 8 months after a marginal mandibulectomy and an immediate vestibuloplasty shows well-created lingual and buccal sulci (Fig. 8.141). The skin graft has lost its keratinizing layer and is "mucosalized." An immediate vestibuloplasty with a skin graft is therefore indicated in patients who have remaining lower dentition following a marginal mandibulectomy for resection of intraoral cancer. This reconstructive effort is simple and restores sulci effectively to permit satisfactory use of a partial lower denture clasped to the remaining teeth. Patients such as this are not candidates for dental implants, due to the lack of adequate vertical height of the mandible over the mandibular canal.

Marginal Mandibulectomy in an Edentulous Patient

When a marginal mandibulectomy is performed in an edentulous patient, extreme caution must be exercised regarding maintenance of the structural stability of the remaining mandible; otherwise the possibility of a fracture exists at that site. If the risk is thought to be with fracture, then the remaining mandible should be supported by a metallic plate as a buttress to prevent spontaneous fracture.

The patient shown in Fig. 8.142 has carcinoma of the retromolar region and the adjacent lower gingiva on the left-hand side with invasion of the underlying cortical bone. A panoramic

Figure 8.142 Carcinoma of the left retromolar trigone.

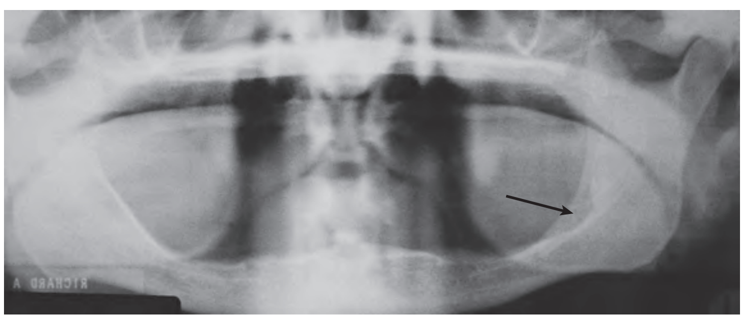

Figure 8.143 A panoramic radiograph of the edentulous mandible showing cortical erosion at the left retromolar trigone (*arrow*).

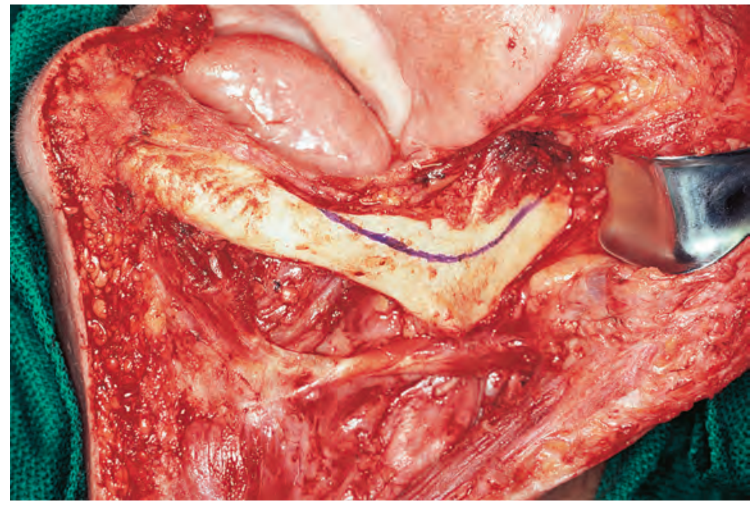

Figure 8.144 The extent of bone resection is outlined on the mandible.

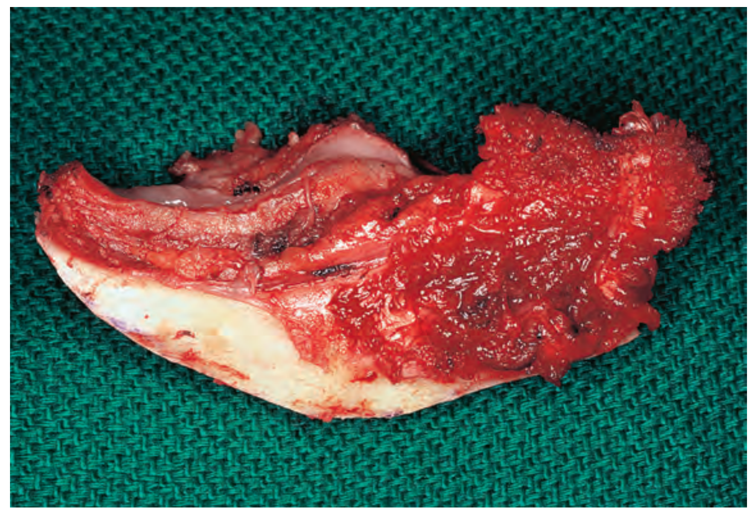

Figure 8.145 The surgical specimen (lateral aspect).

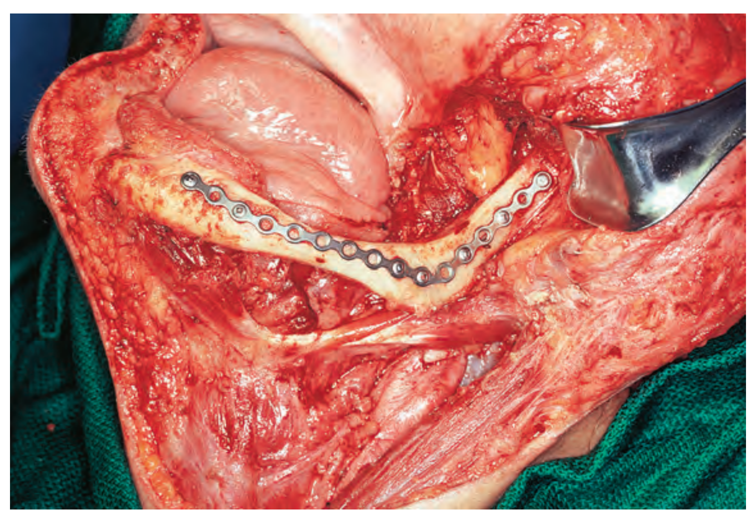

Figure 8.146 The miniplate is shaped to fit the lateral cortex of the mandible.

radiograph of the edentulous mandible (Fig. 8.143) demonstrates cortical erosion of the mandible at the retromolar trigone requiring a marginal mandibulectomy. A supraomohyoid neck dissection was performed in conjunction with a marginal mandibulectomy. The surgical field shows the lower cheek flap elevated in the usual fashion, remaining lateral to the outer cortex of the mandible from the symphysis up to the mandibular notch posteriorly (Fig. 8.144). The extent of bone resection is marked on the mandible to resect the alveolar process of the posterior part of the body of the mandible and the anterior part of the ascending ramus of the mandible.

Appropriate three-dimensional resection is then undertaken with use of a high-speed power saw. The surgical specimen as viewed from the lateral aspect is shown in Fig. 8.145. Note that a three-dimensional resection has been accomplished with a satisfactory deep margin to excise the alveolar process of the mandible in a monobloc fashion. Bony spicules at the surgical defect in the mandible are smoothed out. Because the remaining mandible is very thin and tenuous, it is at risk of spontaneous fracture, and thus a long miniplate is used to support the remaining mandible to prevent a fracture (Fig. 8.146). The miniplate is appropriately shaped to fit the lateral cortex of the mandible, extending from the upper end of the ascending ramus up to the anterior aspect of the body of the mandible. Several screws are used to hold the miniplate in position. The point of maximum stress is at the angle of the mandible, and by application of the plate, support is provided at that site to prevent a spontaneous fracture. A miniplate support in this totally edentulous patient is satisfactory, since she is not likely to exert pressure and stress at this site during mastication. In

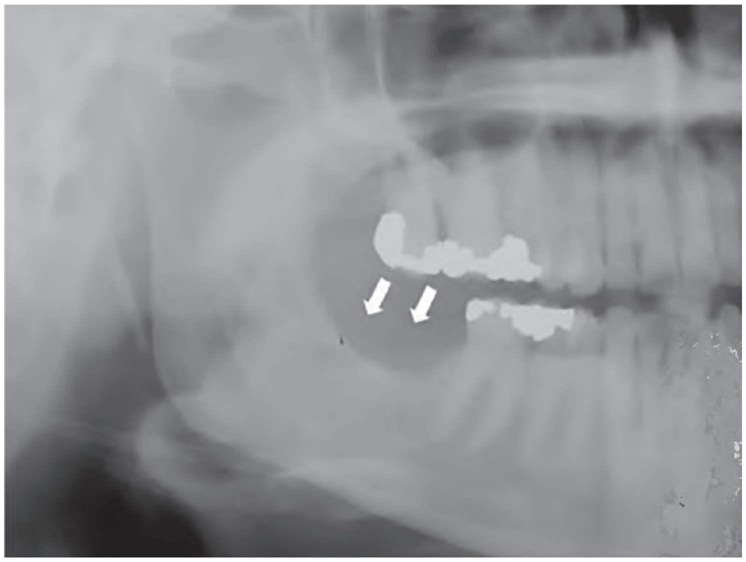
Figure 8.147 Panoramic x-ray of the mandible in a patient with carcinoma of the retromolar gingiva (*arrows* show the site of tumor).

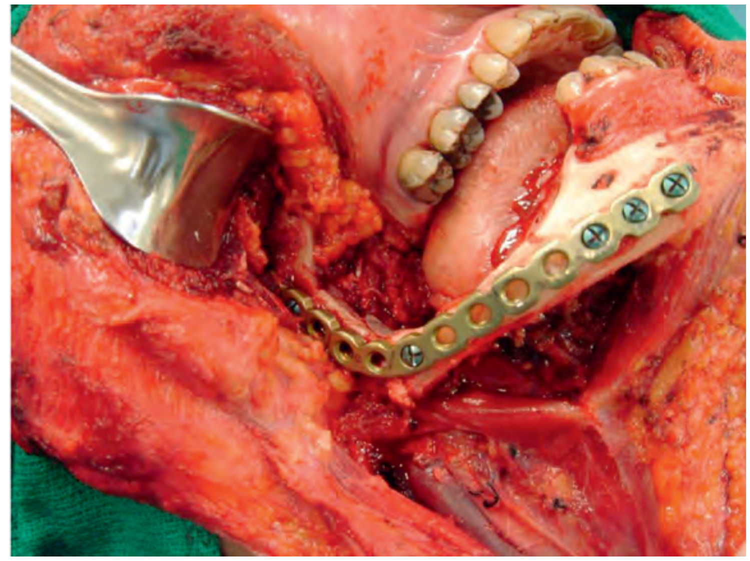
Figure 8.149 Marginal mandibulectomy site supported by AO reconstruction plate.

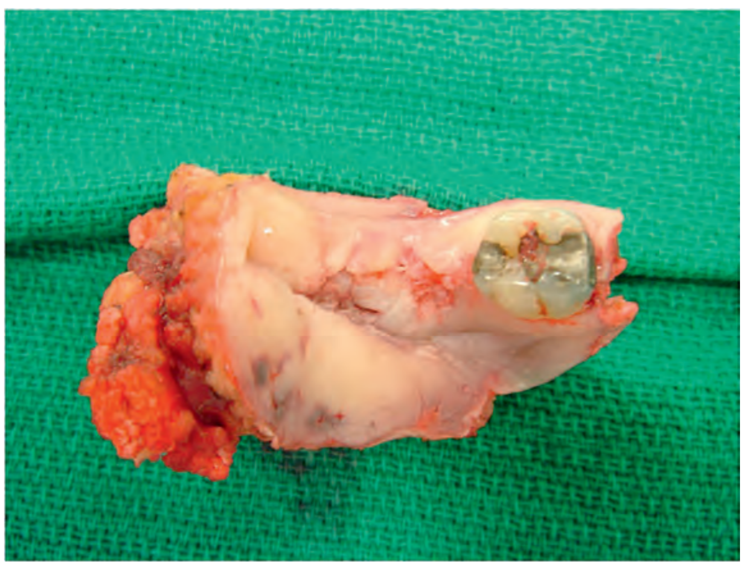
Figure 8.148 Surgical specimen of marginal mandibulectomy for carcinoma of the retromolar gingiva.


Figure 8.150 Surgical specimen of carcinoma of the buccal mucosa with marginal mandibulectomy and upper alveolectomy (horseshoe resection).

this patient a primary closure could be achieved easily between the mucosa of the floor of the mouth and the buccal mucosa.

Marginal Mandibulectomy of the Retromolar Area in a Dentate Patient

Another patient with a full set of teeth had a carcinoma of the right retromolar trigone (Fig. 8.147). She underwent marginal mandibulectomy. The surgical specimen shows satisfactory resection of the tumor (Fig. 8.148). The remaining mandibular arch in her is at a significant risk of spontaneous fracture due to the stress and strain created at that site during mastication with her remaining teeth. Therefore she needs a stronger support to prevent such fracture. An AO reconstruction plate is used to support her marginally resected mandible, and provide the necessary strength (Fig. 8.149). Because of this larger plate and a large soft tissue and mucosal defect, she will require a radial forearm flap to cover the defect.

Marginal mandibulectomy with an upper alveolectomy (horseshoe resection) is required in some patients who have buccal mucosa cancer approaching the upper and lower gingivobuccal sulci. The surgical specimen of such a patient with carcinoma of the right buccal mucosa is shown in Fig. 8.150. Note a three-dimensional resection accomplished to excise the tumor with satisfactory margins. This patient will require a radial forearm fasciocutaneous flap to reconstruct the surgical defect.

Segmental Mandibulectomy

When resection of a segment of the mandible is indicated for carcinoma of the oral cavity, immediate reconstruction of the resected mandible should be considered. Resection of the body of the mandible produces one of the most significant aesthetic and functional deformities in surgery for oral cancer. The aesthetic appearance of the patient is unacceptable, and the functions of speech and mastication are seriously compromised.

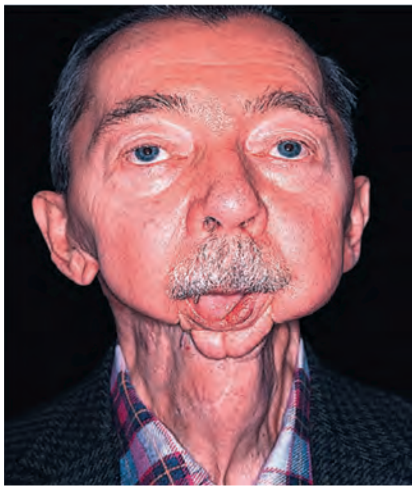

Figure 8.151 This patient had arch resection without immediate reconstruction.

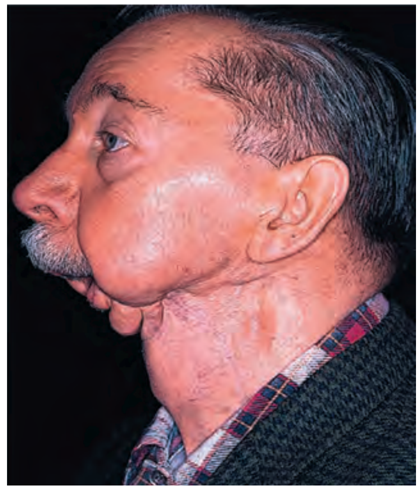

Figure 8.152 The lateral profile following resection of the arch of the mandible.

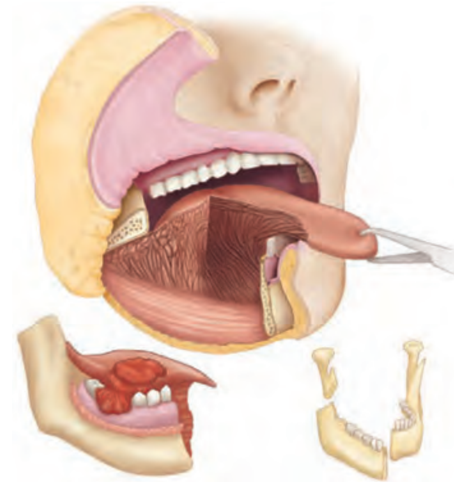

Figure 8.153 A segmental mandibulectomy.

The impact of resection of the anterior arch is even more devastating. The patient shown in Figs. 8.151 and 8.152 had arch resection without immediate reconstruction. Many patients drool saliva after resection of the anterior arch of the mandible and have significant swallowing difficulties. The optimal method of reconstruction of the resected mandible at the present time is with a fibula free flap.

Segmental Mandibulectomy With Neck Dissection (Commando Operation)

A composite resection—also called a *commando operation*—is a surgical procedure recommended in patients with oral cancer requiring a segmental mandibulectomy in continuity with neck dissection for primary tumors that extend to involve the mandible (Fig. 8.153). On occasion, a composite resection may be indicated for patients whose primary tumor has extensive soft-tissue disease around the mandible, even if the bone is not involved by cancer, thus requiring the need to sacrifice an intervening segment of mandible to accomplish an in-continuity resection of the primary tumor in conjunction with neck dissection. Thus a commando operation or a composite resection entails excision of the intraoral primary tumor along with a segment of the intervening mandible performed in conjunction with ipsilateral neck dissection as a monobloc surgical resection.

Figure 8.154 A deeply infiltrating locally advanced tumor of the right side of the oral tongue.

Figure 8.155 The patient has a clinically palpable lymph node at level II in the ipsilateral neck.

The patient shown in Fig. 8.154 has primary squamous cell carcinoma of the oral tongue with extension to the adjacent floor of the mouth and the lingual gingiva. The primary tumor is a deeply infiltrating lesion occupying literally the right half of the oral tongue with infiltration of its musculature and causing restriction in the mobility of the tongue. Radiologic studies did not demonstrate any bone destruction of the mandible, but extensive soft-tissue disease is plastered against the lingual surface of the mandible on the right-hand side. In addition, the patient has clinically palpable cervical lymph node metastasis at level II, as shown in Fig. 8.155.

The incision for the operation is a trifurcate incision for neck dissection beginning at the tip of the mastoid process and curving anteriorly, remaining at least two finger breadths below the body of the mandible along an upper neck skin crease up to the midline of the neck at the level of the hyoid bone (Fig. 8.156). At that point the incision turns cephalad, dividing the skin and soft tissues of the submental region, chin, and lower lip in the midline. A vertical curvaceous component of the incision begins at the region of the posterior border of the sternocleidomastoid muscle on the transverse incision and extends down to the clavicle up to the midclavicular point. Because the clinically palpable cervical lymph nodes did not

Figure 8.156 The outline of the skin incision.

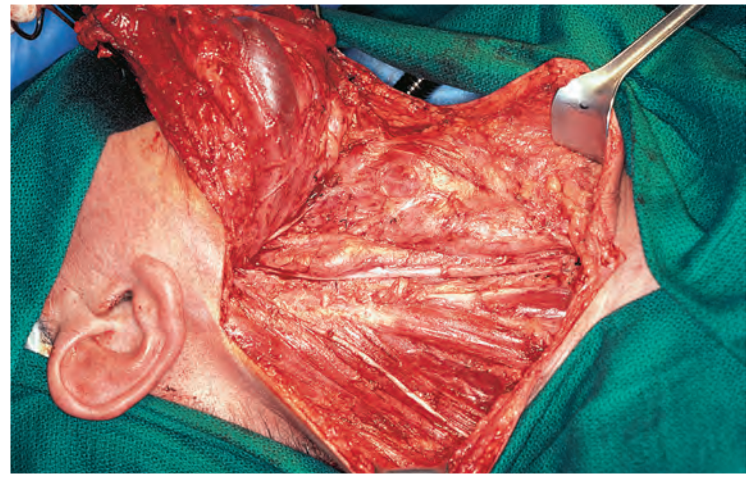

Figure 8.158 The internal jugular vein is divided, and levels II, III, and IV are dissected.

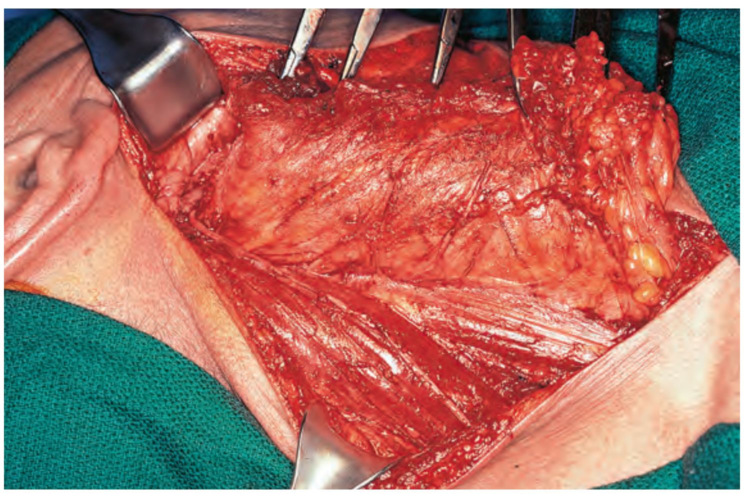

Figure 8.157 The posterior skin flap is elevated and the contents of the posterior triangle are dissected.

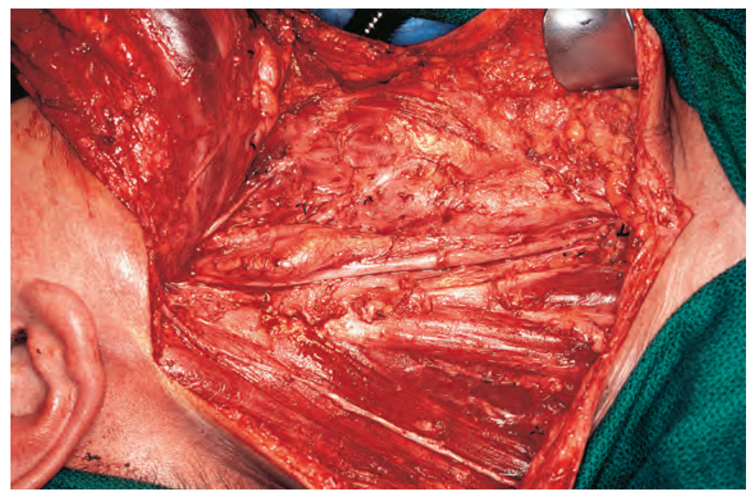

Figure 8.159 A close-up view of the completed dissection showing the digastric muscle and hypoglossal nerve.

have gross extranodal extension along the course of the spinal accessory nerve, a modified neck dissection type I preserving the accessory nerve is planned. The sequential steps of modified neck dissection type I are described in Chapter 11. However, the operation begins with dissection of the posterior triangle of the neck by elevation of the posterior skin flap (Fig. 8.157). The posterior triangle dissection is completed, carefully preserving the accessory nerve, the phrenic nerve, and the brachial plexus. The cutaneous roots of the cervical plexus are divided, and dissection from the posterior triangle extends up to the lateral aspect of the carotid sheath.

The anterior skin flap is elevated next. The lower end of the sternocleidomastoid muscle is detached from the clavicle and the manubrium to expose the carotid sheath. The internal jugular vein is divided (Fig. 8.158). Dissection now proceeds cephalad along the carotid sheath up to the digastric muscle. A close-up view shows completed dissection of levels II, III, IV, and V with exposure of the digastric muscle and hypoglossal nerve, with the specimen reflected cephalad (Fig. 8.159). As the operation proceeds cephalad toward level I, no attempt is made to dissect the contents of the submandibular triangle, which remains attached through the floor of the mouth and the soft tissues medial to the mandible to the primary site. All the soft-tissue attachments of the deeper lymphatics and vessels are divided to expose the entire inferior surface of the digastric muscle. The tail of the parotid gland may need to be divided to clear the retromandibular lymph nodes. Several pharyngeal veins traversing over the digastric tendon and medial to the posterior belly of the digastric muscle are divided and ligated. At this juncture, the upper end of the internal jugular vein is divided and its stump is doubly ligated at the jugular foramen.

The neck incision is now extended cephalad in the midline, dividing the skin of the chin and the lower lip through its full thickness (Fig. 8.160). The upper skin flap of the neck dissection is now elevated, remaining deep to the platysma, which is retained on the flap. Meticulous dissection should be undertaken at this point to identify and carefully preserve the marginal branch of the facial nerve to maintain the function of the lower lip and the competency of the oral cavity. The upper skin flap is elevated up to the lower border of the mandible, extending from the midline of the chin all the way up to the angle of the mandible. Division of the upper lip in the midline through its full thickness is now completed up to the lateral cortex of the mandible at the symphysis.

A mucosal incision is now placed in the gingivobuccal sulcus, remaining close to the attached gingiva. The lower cheek flap is elevated, remaining right over the lateral cortex of the mandible from the midline all the way up to the angle of the mandible, keeping all the musculature and soft tissues in

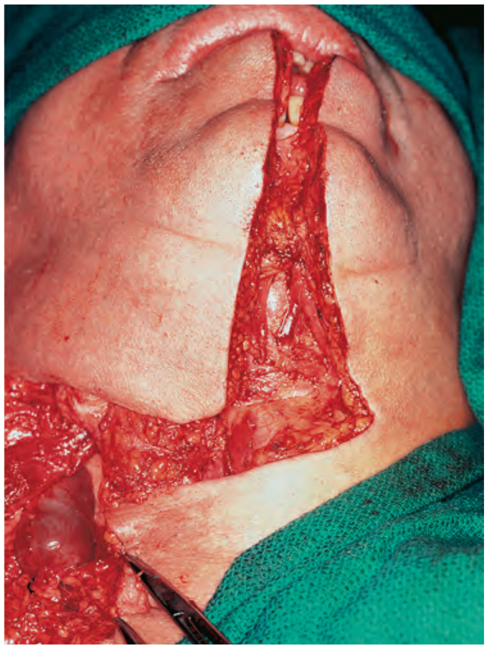

Figure 8.160 The skin of the chin and lower lip is divided in the midline.

Figure 8.161 The lower cheek flap is elevated up to the angle of the mandible, keeping all the musculature in the cheek flap.

the cheek flap (Fig. 8.161). Using electrocautery, the masseter muscle is now detached from the lateral cortex of the ascending ramus of the mandible up to the mandibular notch. This maneuver provides exposure of the entire lateral aspect of the mandible from the mandibular notch up to the midline at the symphysis menti (Fig. 8.162). A close-up view of the surgical field shows the primary tumor with the exposed segment of the mandible to be resected to achieve a monobloc composite resection of the primary tumor, intervening soft tissues in the floor of the mouth at level I, along with a segment of the mandible and the contents of the dissected neck on the right-hand side (Fig. 8.163). Because the bone has not been invaded, an appropriate segment of the mandible is sacrificed to encompass the contiguous oral cancer. A hemimandibulectomy in this situation is not necessary. The ascending ramus of the mandible can be safely preserved and used for reconstruction of the mandible with a fibula free flap. Thus the segment of the mandible to be resected in this patient extends from the angle of the mandible posteriorly up to the lateral incisor tooth anteriorly.

Figure 8.162 The entire lateral cortex of the mandible is exposed from the mandibular notch up to the midline at the symphysis menti.

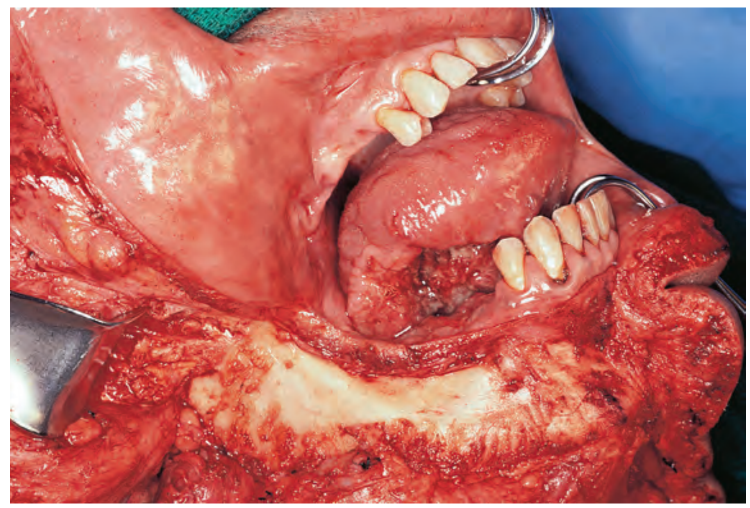

Figure 8.163 The exposed segment of the mandible with the primary tumor, intervening soft tissues in the floor of the mouth, and the contents of the dissected neck on the right-hand side.

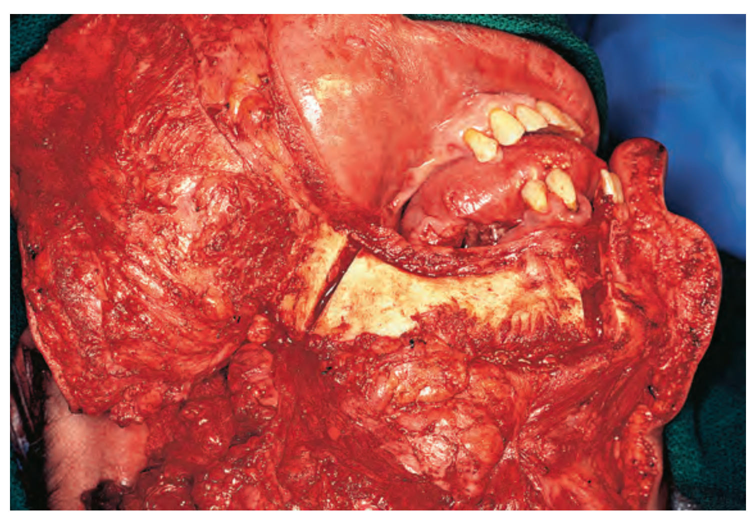

Figure 8.164 A sagittal power saw is now used to divide the mandible.

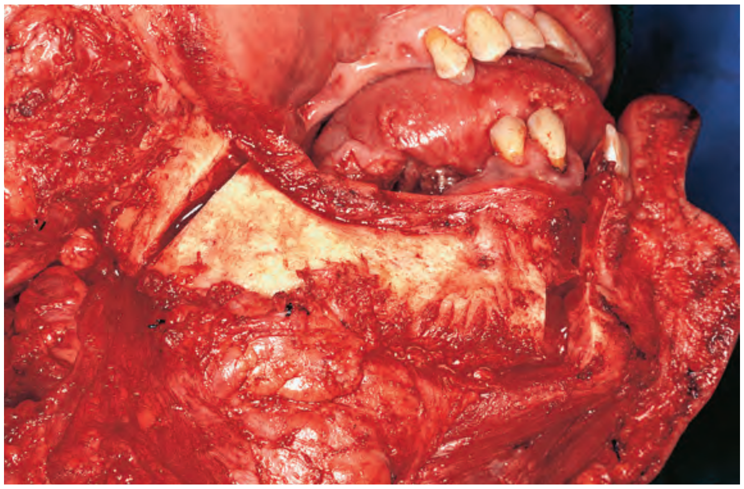

Figure 8.165 A close-up view of the surgical field demonstrates the divided ends of the mandible with the segment to be resected along with the primary tumor.

Figure 8.166 The surgical field at the completion of resection.

A sagittal power saw is used to divide the mandible at the designated locations (Fig. 8.164). Brisk hemorrhage should be expected following division of the mandible from its cut ends. Bone wax is used to control the bleeding. Extreme caution should be exercised not to allow the power saw to cut through the soft tissues medial to the mandible; otherwise excessive hemorrhage will result from laceration of the pterygoid muscle posteriorly and the musculature of the floor of the mouth anteriorly. A close-up view of the surgical field shown in Fig. 8.165 demonstrates the divided ends of the mandible with the segment to be resected along with the primary tumor. The mandible is divided at both places with straight cuts to facilitate introduction of a vascularized free graft of fibula to achieve a satisfactory reconstruction.

Once the mandible is divided, the primary tumor can be delivered easily into the surgical field. An Adair clamp is used to grasp the tip of the tongue and move the tongue out into the surgical field. Electrocautery is used to place a mucosal incision around the surface extent of the primary tumor with a generous cuff of normal mucosa and soft tissues to secure satisfactory margins. Electrocautery is used to perform a three-dimensional resection of the primary tumor along with the underlying soft tissues and musculature of the tongue and floor of mouth, remaining in continuity with the mandible and the contents of the dissected neck. In this patient, it will entail division of the tongue from its tip up to the circumvallate papillae in the midline, where the incision turns laterally up to the soft palate. The hyoglossus and genioglossus muscles are divided. Brisk hemorrhage from the lingual artery is to be expected and is appropriately controlled. Finally, the mylohyoid muscle is detached from the hyoid bone and the remaining soft-tissue attachments of the specimen are divided to deliver the specimen. The extent of mucosal and soft-tissue resection clearly depends on the surface extent and invasive nature of the primary tumor and the involvement of the underlying musculature, soft tissues, and neurovascular bundles.

Once the specimen is removed, appropriate hemostasis is secured in the surgical field. A monobloc resection of the primary tumor in conjunction with the contents of the dissected neck and the intervening soft tissues, lymphatics, and mandible is thus accomplished (Fig. 8.166). Note that a hemiglossectomy has been performed on the right-hand side, showing the cut surface of the tongue through its midline, demonstrating the genioglossus and hyoglossus muscles.

The tongue is retracted anteroinferiorly to demonstrate the mucosal surface of its remaining half in the surgical field (Fig. 8.167). Frozen sections are obtained from appropriate areas of the surgical defect, depending on the extent of the primary tumor and the judgment of the surgeon regarding the proximity of the tumor to the surgical margins.

The surgical specimen shows the primary tumor in conjunction with a segment of the body of the mandible and the contents of the dissected neck on the right-hand side removed in a monobloc fashion (Fig. 8.168). A close-up view of the surgical specimen shows the surface extent of the primary tumor and the preserved continuity between the primary tumor, the floor of the mouth, a segment of the mandible, and soft tissues and lymphatics in the floor of the mouth and lymph nodes at level I (Fig. 8.169).

Immediate reconstruction of the mandible and the resected portion of the tongue is accomplished with a composite fibula free flap with its attached musculature and overlying skin to restore the continuity of the resected portion of the mandible and reconstruct the right half of the tongue.

The harvest of the composite free flap generally begins simultaneously during the course of the composite resection. The fabrication of the fibula free flap to reconstruct the mandible is guided by preoperative CAD-CAM planning. This makes the harvest and design of the fibula accurate and expeditious. Appropriate osteotomies are made in the fibula according to the CAD-CAM guide planes to achieve the desired shape, contour, and curvature of the graft to match the mandibular defect. This is done at the donor site on the leg. If immediate dental implants are planned, then the implants are inserted in the fibula free flap at this juncture. The exact location for placement of the implants is again guided by the CAD-CAM plan. Appropriate shaping and trimming of the soft tissue and skin component of the flap are undertaken at the recipient site to reconstruct the resected portion of the tongue. Microvascular anastomoses are completed, and thus a composite reconstruction is achieved in a single-stage operative procedure.

A nasogastric feeding tube is inserted. The remaining mandibular teeth on the left-hand side are placed in intermaxillary fixation with arch bars and wires to maintain occlusion and position of the reconstructed fibular graft. The incisions are then closed in the usual fashion, with suction drains placed in the neck. Special attention should be given to closure of the lower lip for perfect alignment of the vermilion border. The

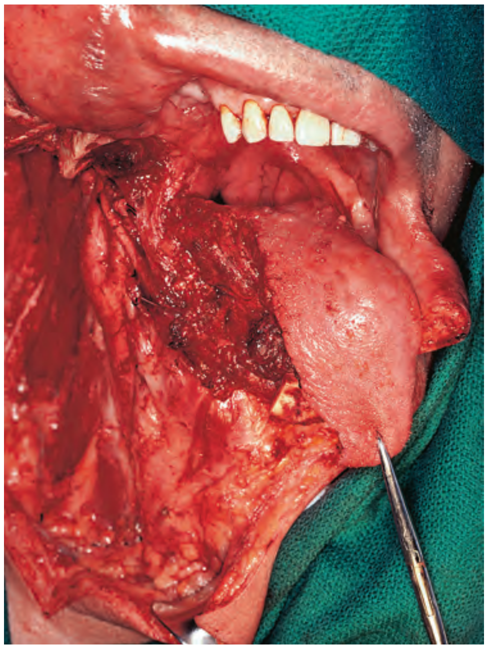

Figure 8.167 The extent of resection of soft tissue of the tongue.

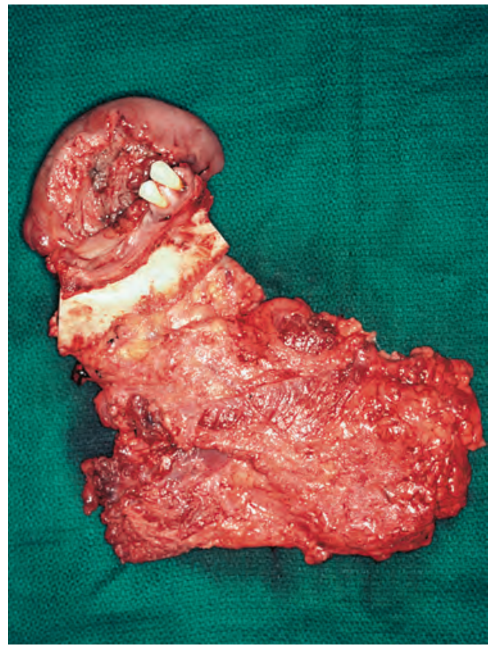

Figure 8.168 The surgical specimen demonstrating monobloc excision.

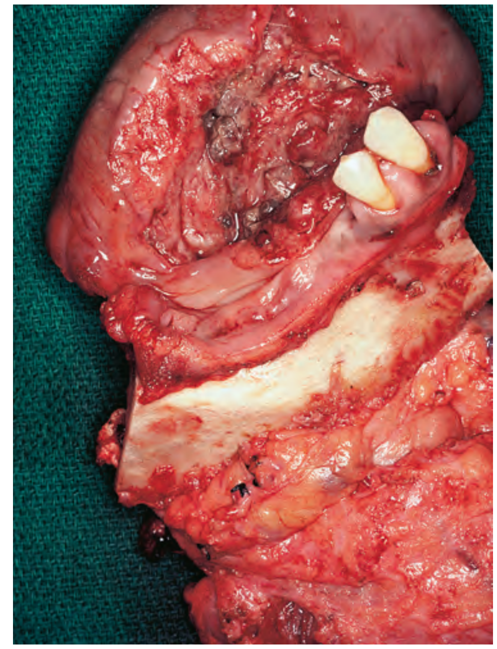

Figure 8.169 A close-up view of the specimen.

mucocutaneous junction of the vermilion border is accurately aligned with a nylon suture and retrograde closure of the mucosal aspect of the lip incision is performed, first beginning at the vermilion border and proceeding up to the gingivolabial sulcus. Accurate alignment of the musculature of the lip is performed next, followed by accurate closure of the skin of the lower lip and chin to achieve a perfectly aligned skin closure.

A tracheostomy is performed at the conclusion of the operation to facilitate clearance of pulmonary secretions postoperatively and for provision of a satisfactory airway to facilitate smooth postoperative recovery. Blood loss during this procedure is minimal, and a blood transfusion is seldom necessary. If there is no tension on the suture line of the mucosa in the oral cavity, then primary healing should be expected within 1 to 2 weeks. At that point puréed foods are permitted by mouth and the patient gradually advances to a soft diet. A postoperative panoramic view of the reconstructed mandible shows the fibula free flap in perfect position, achieving a satisfactory mandibular reconstruction (Fig. 8.170). The external appearance of the patient approximately 6 months after surgery shows accurate restoration of the facial contour and restored arch of the mandible (Fig. 8.171). An intraoral view demonstrates the skin component of the composite fibula free flap used for reconstruction of the right half of the tongue (Fig. 8.172). Within 6 weeks after surgery, if the healing

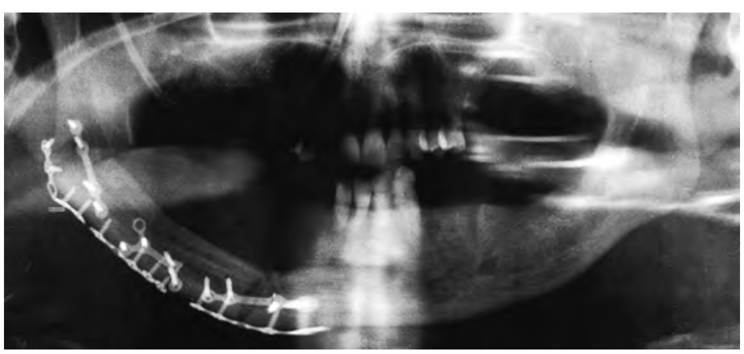

Figure 8.170 A postoperative orthopantomogram showing the fibula free flap.

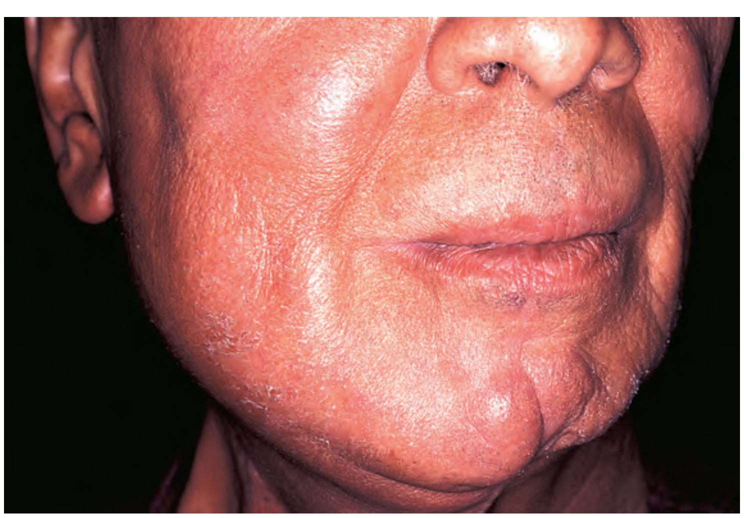

Figure 8.171 Postoperative appearance of the patient 6 months following surgery.

Figure 8.172 A postoperative intraoral view showing the well-healed skin component of the fibula free flap.

is complete, the patient is ready to start postoperative radiation therapy. Anatomic, aesthetic, and functional reconstruction of the composite resection defect is thus achieved in a single operative procedure.

Segmental Mandibulectomy and Reconstruction With a Fibula Free Flap

The goal of modern day reconstructive surgery of the mandible is to achieve exactly the same form and function as the patient had preoperatively. Availability of the CAD-CAM technology allows this to be achieved accurately and expeditiously. The patient in Fig. 8.173, whose preoperative profile demonstrates normal facial contour, has carcinoma of the lower gum involving the retromolar trigone and the body of the mandible (Fig. 8.174). Significant induration is present because of infiltration of the adjacent musculature of the floor of the mouth, mandating resection of the floor of the mouth with the body of the mandible. The surgical specimen of the resected tumor with satisfactory mucosal, soft tissue, and bony margins is shown in Fig. 8.175. The surgical defect thus created (Fig. 8.176) requires replacement of the bone and soft tissues in the floor of the mouth along with the mucosal lining in the oral cavity.

A composite microvascular free graft of a segment of fibula, guided by the CAD-CAM modeling, is created at the donor site with its attached muscles and overlying skin to reconstruct the

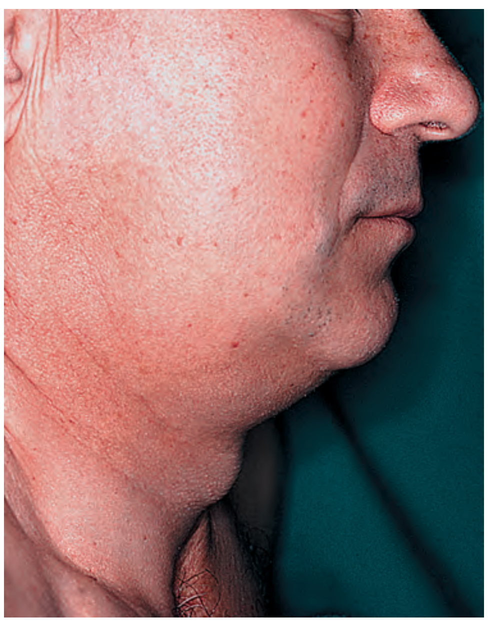

Figure 8.173 The preoperative profile of a patient with a carcinoma of the right lower gum.

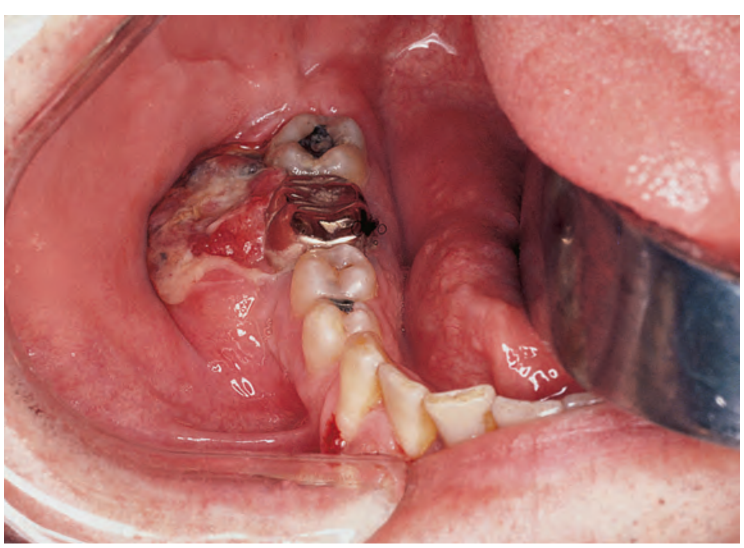

Figure 8.174 An intraoral view of the primary tumor.

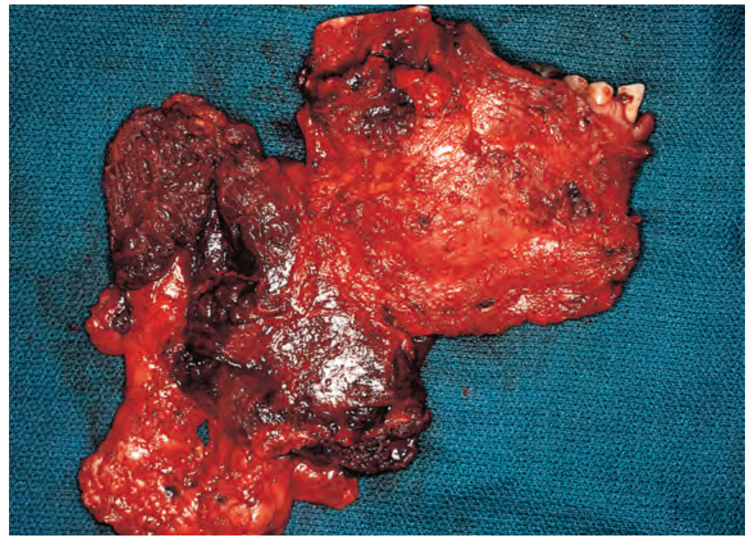

Figure 8.175 The surgical specimen of a composite resection.

Figure 8.176 The surgical defect.

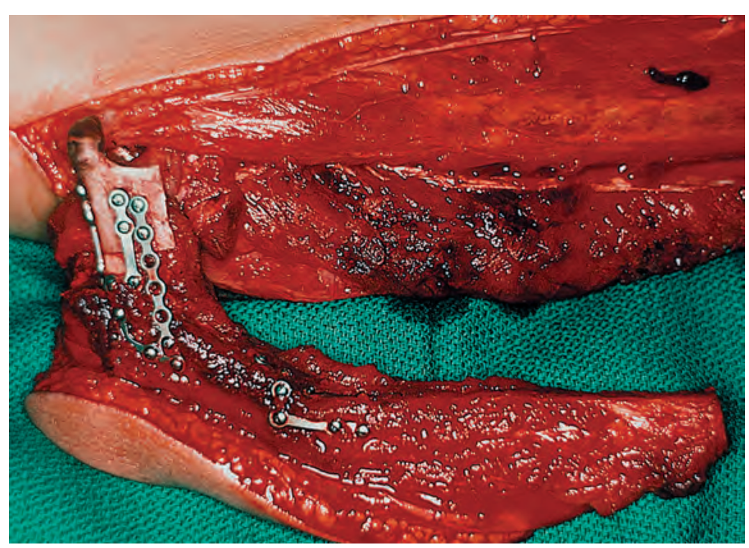

Figure 8.177 A composite fibula free flap.

Figure 8.178 A postoperative panoramic radiograph of the mandible.

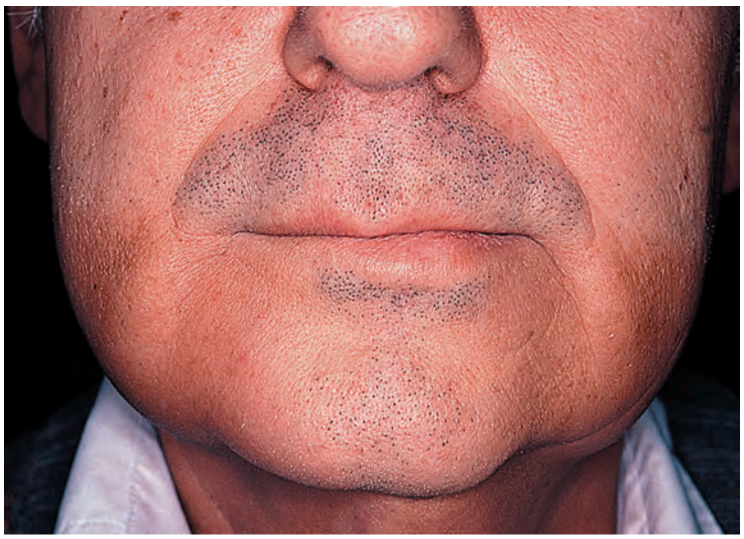

Figure 8.179 Postoperative appearance of the patient 8 months following surgery showing restoration of normal contour of the face.

surgical defect in this patient (Fig. 8.177). The fibula free flap is fabricated into a neomandible by multiple osteotomies directed by the guide planes to match the curvature, angulation, and shape of the resected mandible. The technical details of the use of CAD-CAM technology and fibula free flap reconstruction are described in Chapter 17. The postoperative panoramic view of the mandible shows the fibula free flap in position attached to the stumps of the mandible (Fig. 8.178). The postoperative appearance of the patient 8 months following surgery shows excellent restoration of the contour of the face (Fig. 8.179).

Microvascular composite free tissue transfer is the state of the art in reconstruction of major composite defects following resection for advanced carcinomas of the oral cavity. However, caution must be exercised in selecting patients who are candidates for such a major reconstructive effort. The selection of patients should take into account the age and medical condition of the patient, the size of the surgical defect, resultant disability from ablative surgery, disability at the donor site, and the overall prognosis.

Dental Implants in the Reconstructed Mandible

Complete anatomic and physiologic restoration and rehabilitation of the oral cavity following cancer ablation and reconstruction of the mandible requires either a satisfactory removable lower denture clasped to remaining teeth or osseointegrated implants to facilitate a permanent fixed denture. If osseointegrated dental implants are planned, they may be performed primarily at the time of mandible reconstruction or secondarily

Figure 8.180 A patient with a central salivary carcinoma of the lower gum.

Figure 8.181 Coronal view with bone windows of the CT scan of the mandible shows an expansile lesion on the left-hand side.

Figure 8.182 A radiograph of the specimen.

after satisfactory healing of the bone. Various factors that influence the decision for and the timing of the implants is discussed in detail in Chapter-18.

The patient whose intraoral photograph is shown in Fig. 8.180 has a central salivary carcinoma of the lower gum. His

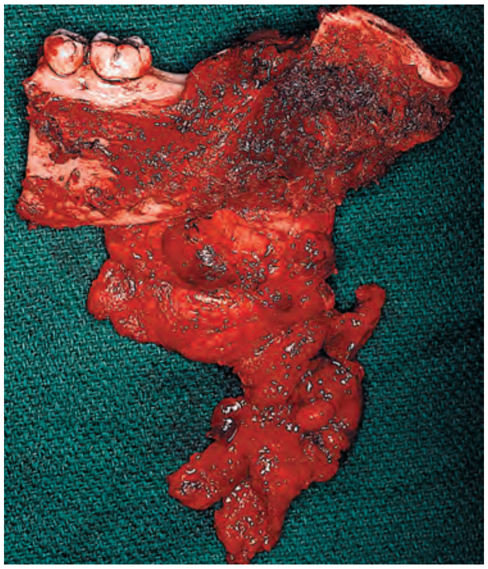

Figure 8.183 The surgical specimen.

Figure 8.185 The permanent fixed denture in place over dental implants.

Figure 8.184 An intraoral view showing the healed site of the surgery.

preoperative CT scan shows expansion of the involved mandible by the tumor (Fig. 8.181). He underwent segmental mandibulectomy. The specimen is shown in Fig. 8.182. A radiograph of the specimen shows the extent of bone invasion (Fig. 8.183). The mandible was reconstructed with a microvascular free flap of fibula. The postoperative intraoral picture shows satisfactory mucosal healing (Fig. 8.184).

If secondary dental implants are planned, then a minimum of 12 months should elapse before osseointegrated implants are considered to allow satisfactory healing of the fibula free flap. Radiologic studies of the reconstructed mandible should show satisfactory bony union between the fibula and the mandible and satisfactory bony healing of the osteotomies in the free flap. If metallic titanium plates and screws used for reconstruction of the mandible are in the way at the site where the implants are to be placed, then they are removed to clear that area to receive the implants.

The location and number of implants to be placed are best assessed by the oral surgeon or prosthodontist, who will assume the responsibility of placement of the implants and their subsequent exposure and the eventual fabrication of the permanent fixed denture. The satisfactorily integrated implants are exposed

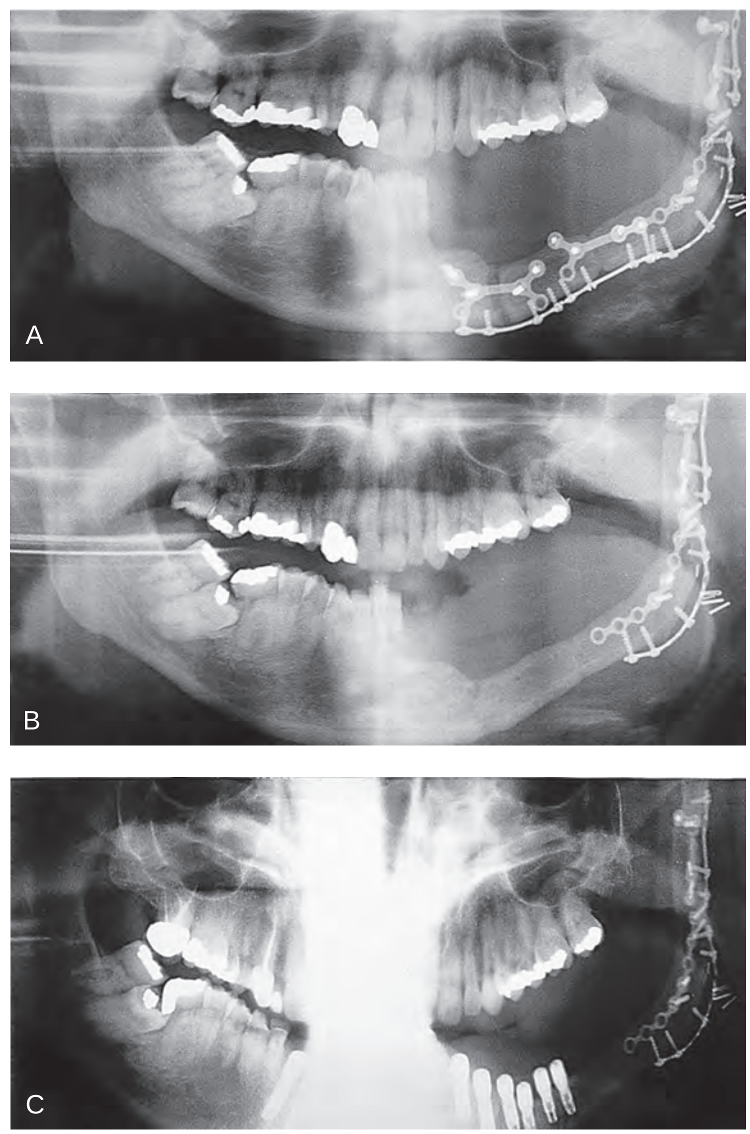

Figure 8.186 Serial panoramic radiographs of the mandible showing a reconstructed mandible immediately postoperatively (**A**), after bone healing and removal of miniplates and screws (**B**), and after dental implants (**C**).

Figure 8.187 The patient's external appearance 2 years after mandible reconstruction.

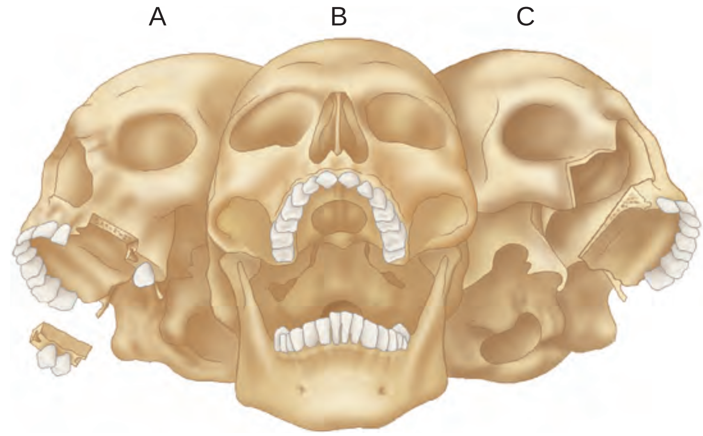

Figure 8.188 Types of maxillary resections. **A**, Alveolectomy. **B**, Central palatectomy. **C**, Infrastructure partial maxillectomy.

Figure 8.189 T1 squamous cell carcinoma of the upper gum.

4 to 6 months following placement. The finished permanent fixed denture is shown in Fig. 8.185. Serial panoramic views of the mandible show the immediate postoperative appearance of the reconstructed mandible, after removal of plates and screws and after placement of implants (Fig. 8.186). At this time, the patient is considered fully rehabilitated following ablative cancer surgery and reconstruction to restore form and function. The patient's external appearance is shown in Fig. 8.187.

Certain trends in the surgical management of oral cancer have become apparent during the past 15 years, particularly with regard to management of the mandible. Because of increased understanding of the biological behavior of oral cancer as it progresses, fewer and fewer patients are undergoing the commando operation with resection of normal intervening mandible to access large primary tumors of the oral cavity. Instead, an increasing number of patients undergo a marginal mandibulectomy or a mandibulotomy to provide access to these tumors. On the other hand, if total dental rehabilitation is the ultimate goal, then patients suitable for marginal mandibulectomy of the posterior segment of the mandible should be considered for segmental mandibulectomy, with fibula free flap reconstruction of the mandible, and immediate placement of dental implants in the fibula. The current trend is to offer immediate dental implants to patients undergoing fibula free flap reconstruction after segmental mandibulectomy.

Peroral Partial Maxillectomy

Primary epithelial tumors of the oral cavity arising on the hard palate, upper alveolus, upper gingivobuccal sulcus, and anterior aspect of the soft palate require consideration of resection of the maxilla in surgical treatment planning. If the primary tumor involves the underlying hard palate or the upper gum, then resection of the maxilla becomes mandatory (Fig. 8.188). Even when a tumor is adherent to or in direct contiguity with the maxilla, maxillary resection should be considered. The resection may be just an alveolectomy (see Fig. 8.188A), central palatectomy (see Fig. 8.188B), or an infrastructure partial maxillectomy (see Fig. 8.188C), depending on the extent of involvement of the maxilla. Radiographic evaluation for assessment of bone invasion is mandatory, but it must be remembered that early invasion of bone may not be seen on radiographic studies.

Preoperative dental evaluation is vitally important to assess the status of dentition in the vicinity of the primary tumor. If any dental care is necessary, it should be undertaken either preoperatively or intraoperatively with appropriate assistance from a dental surgeon. If any part of the upper gum or hard palate is to be resected, leading to communication between the oral cavity and the nasal cavity or the maxillary antrum, then appropriate impressions of the upper alveolus and hard palate must be obtained preoperatively. These impressions will be used to make dental cast models, which will facilitate fabrication of an immediate hard palate surgical obturator to be used intraoperatively for restoration of the surgical defect and subsequently for fabrication of a removable palatal or maxillary prosthesis.

Small lesions that are easily accessible through the open mouth can be resected in conjunction with a limited partial maxillectomy via the peroral approach. The patient shown in Fig. 8.189 has a squamous cell carcinoma of the upper gum presenting on the labial surface of the upper gum adjacent to the canine and premolar teeth. A CT scan of the patient demonstrates that the tumor involves the soft tissues of the upper gum with only minor cortical erosion of the underlying bone (Fig. 8.190). A peroral partial maxillectomy could be performed easily, thus securing a satisfactory surgical resection with negative mucosal soft tissue and bone margins (Fig. 8.191). The small surgical defect in this patient is best left open to be rehabilitated

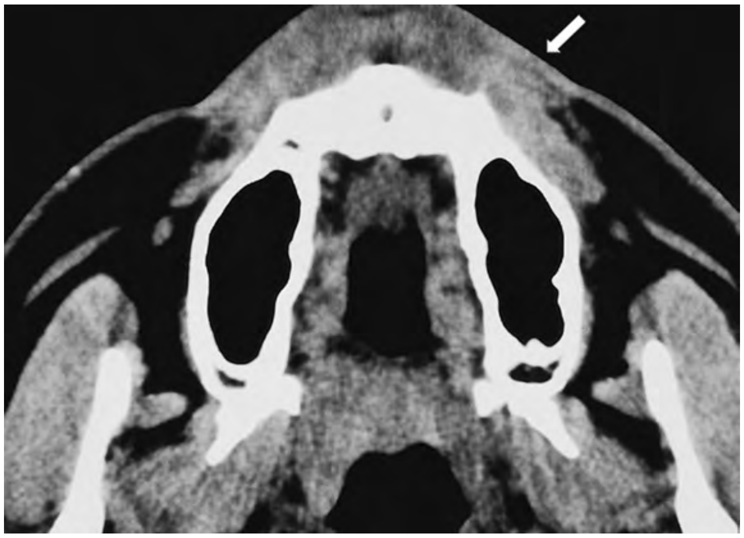

Figure 8.190 An axial view of the computed tomography scan shows soft tissue disease with minor bone erosion (*arrow* points to lesion).

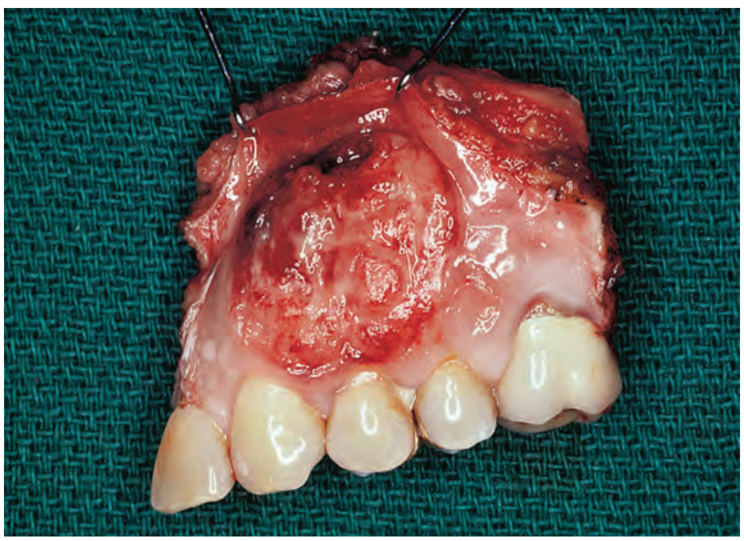

Figure 8.191 The surgical specimen after a peroral partial maxillectomy.

Figure 8.192 An intraoral photograph 3 months following surgery showing complete epithelialization of the surgical defect.

with a dental obturator. Absolute hemostasis is secured with the use of electrocautery. Sharp edges at the margins of the cut ends of the bone are smoothed out with a fine burr. Xeroform packing is introduced into the surgical defect, and an immediate dental obturator is placed over the defect and retained in position

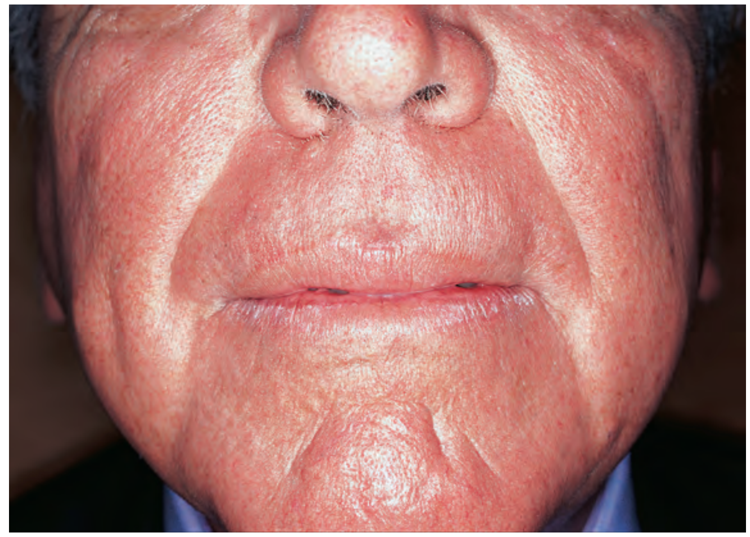

Figure 8.193 The external appearance of the patient with a permanent dental obturator in place.

by wiring it to the remaining teeth. Approximately 1 week following surgery, the packing is removed and the defect is allowed to granulate. In approximately 3 to 4 weeks, adequate epithelialization at the surgical defect occurs (Fig. 8.192). At this point, a permanent dental obturator is fabricated with teeth to restore the dental/alveolar/palatal defect. The obturator restores the patient's ability to speak and eat normally and also restores the external appearance of the face (Fig. 8.193).

Partial Maxillectomy Through an Upper Cheek Flap Approach

For larger tumors of the upper gum and hard palate, or for those located posteriorly, adequate exposure for resection is not feasible through a peroral approach. In these patients an upper cheek flap approach is indicated (Fig. 8.194). This approach requires a modified Weber-Ferguson incision with either a Lynch or a subciliary extension, depending on the location of the primary tumor and the exposure necessary. In most instances, if only the hard palate or the upper gum (infrastructure) is to be resected, then neither the Lynch nor the subciliary extension is necessary.

The design of the modified Weber-Ferguson incision is very important for preservation of the aesthetics of the face. The philtrum of the upper lip is divided exactly in the midline from the vermilion border up to the columella, where the incision turns laterally along the columella into the floor of the nasal

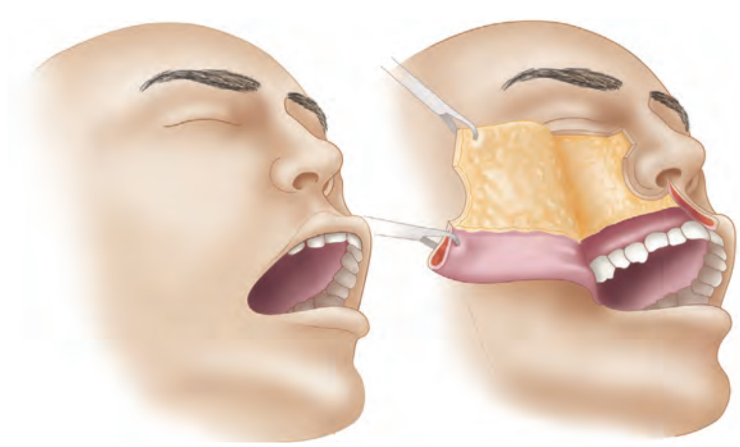

Figure 8.194 The upper cheek flap approach.

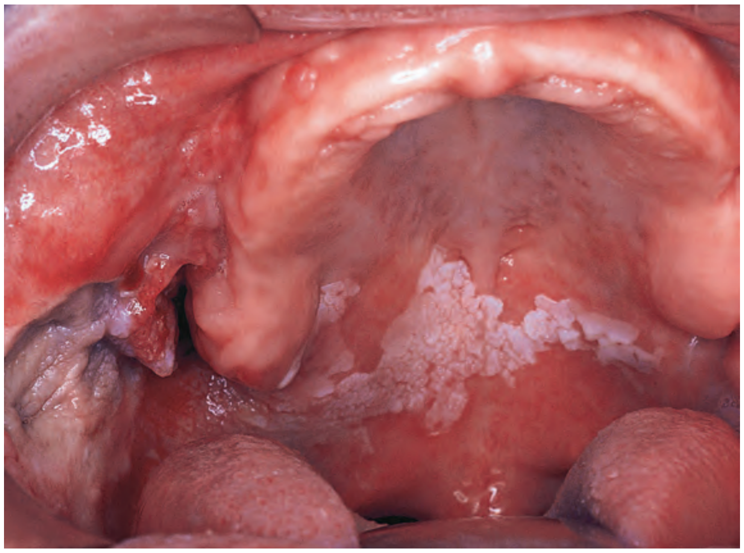

Figure 8.195 A carcinoma of the right upper gingivobuccal sulcus.

Figure 8.196 A Weber-Ferguson incision is marked.

vestibule. It then exits the nasal vestibule and follows the ala of the nostril and the lateral aspect of the nose, respecting the nasal subunits. (For details see Chapter 5.)

The patient described here presented initially with a long-standing history of multifocal areas of hyperkeratoses and in situ carcinomas in the oral cavity. As seen in her intraoral photograph, she had undergone excision of a superficial squamous cell carcinoma of the mucosa of the right cheek with skin graft coverage several years ago (Fig. 8.195). At this time a new primary carcinoma developed involving the right upper gingivobuccal sulcus with extension of the tumor up to the margin of the previously placed skin graft. The lesion involves the maxillary tubercle of the upper alveolus on the right-hand side. The tumor measures 2.5 cm on its surface and appears to be deeply infiltrating the soft tissues. The patient also has a diffuse area of keratosis involving the junction of the hard and soft palate that clinically appears to be benign. Imaging studies showed only minor erosion of the lateral aspect of the alveolar process.

The surgical procedure for resection of this tumor requires an infrastructure partial maxillectomy excising the alveolar process and hard palate on the right side, in conjunction with soft tissues of the cheek and the adjacent mucosa and the lower half of the right maxilla. General anesthesia is administered with the airway secured via an endotracheal tube introduced through the oral cavity. After satisfactory relaxation is obtained, the head and neck area is isolated as usual. The endotracheal tube is positioned at the left oral commissure and is secured in place with appropriate taping. A ceramic corneal shield is introduced into the right conjunctival sac to protect the cornea. A standard Weber-Ferguson incision is marked (Fig. 8.196) before the induction of anesthesia and endotracheal intubation.

The skin incision is made with a scalpel, but afterward an electrocautery is used to divide the remainder of the thickness of the right upper cheek flap. The orbicularis oris and the musculature around the ala of the right nostril are divided with the electrocautery up to the anterior surface of the maxilla (Fig. 8.197). Bleeding is usually controlled with electrocoagulation; however, major branches of the facial artery require ligation.

A mucosal incision is now made in the upper gingivolabial and gingivobuccal sulcus, leaving an appropriate cuff of mucosa

Figure 8.197 The orbicularis oris and the musculature around the ala of the right nostril are divided.

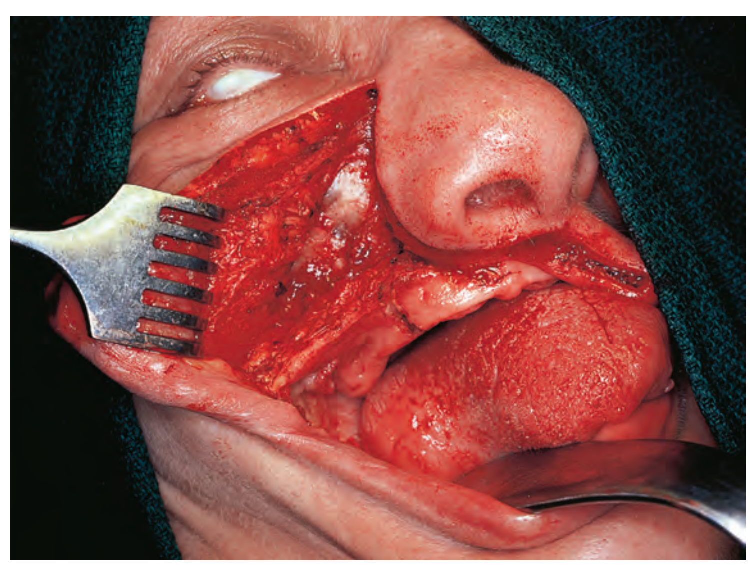

Figure 8.198 A mucosal incision is made in the upper gingivolabial and gingivobuccal sulcus.

and soft tissues attached to the hard palate as a margin around the periphery of the tumor (Fig. 8.198). A 5 mm cuff of mucosa is left attached to that part of the gum which is to be used for reapproximation of the cheek to the gum. Soft tissues of the cheek are then elevated, remaining directly over the anterior aspect of the bony wall of the maxillary antrum. As the cheek flap is elevated laterally and superiorly, the infraorbital nerve exiting from the intraorbital foramen comes into view. Care should be taken to preserve this nerve if possible, because sacrificing it will result in permanent anesthesia of the skin of the cheek.

A close-up view of the exposure obtained thus far shows the tumor freed up anteriorly and laterally (Fig. 8.199). Using electrocautery, an incision is now made in the mucosa of the upper gum and the hard palate to encompass the primary tumor circumferentially. The incision is deepened through the mucoperiosteum up to the underlying bone of the alveolar process and the hard palate. A power saw is then used to divide the alveolar process and the hard palate through the line of mucosal incision. Similarly, the anterior wall of maxilla is divided with the saw. After all the bone cuts are made with the power saw, a small curved osteotome is used to fracture the remaining bony attachments to remove the specimen. Final soft-tissue attachments of the specimen are divided with use of Mayo scissors.

The surgical specimen shows complete removal of the primary tumor with a generous cuff of normal mucosa on all its margins and the alveolar process as its medial margin (Fig. 8.200). The surgical defect following removal of the specimen shows absence of the lower half of the maxilla and the posterior part of the alveolar process, creating a direct communication between the oral cavity and the maxillary antrum (Fig. 8.201). The surgical field is irrigated with Bacitracin solution. If the mucosa of the maxillary antrum is edematous, it is curetted out to prevent any pseudopolyp formation, but if it appears to be normal, it is best left alone. If the antral mucosa is retained, a skin graft is not necessary.

Sharp spicules of bone are smoothed out by using a power drill with a fine burr. A split-thickness skin graft is used in this patient for lining of the denuded bone in the maxillary antrum. The skin graft will facilitate speedy healing of the defect and provide a smooth lining over the raw areas.

The skin graft is sutured to the mucosal edges of the defect and draped over the maxillary antrum, where it is retained in position with a snug packing of Xeroform gauze. The packing

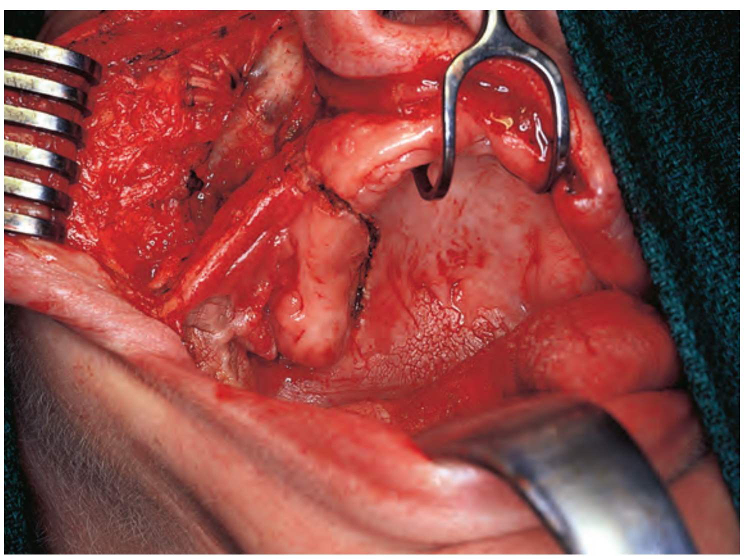

Figure 8.199 A close-up view of the exposure.

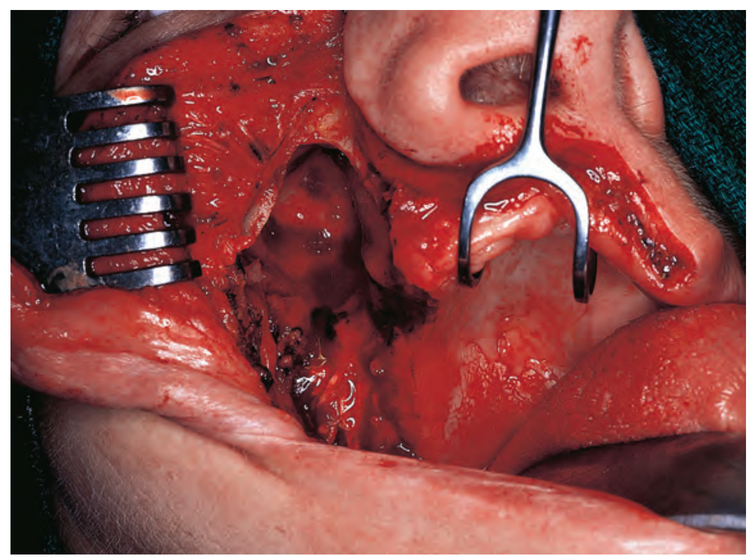

Figure 8.201 The surgical defect.

Figure 8.200 The surgical specimen.

Figure 8.202 The dental obturator is wired to the alveolar process.

is placed tight enough to stretch the graft out entirely over the raw surfaces of the surgical defect.

A previously fabricated surgical dental obturator is now wired to the alveolar process (Fig. 8.202). Because this patient does not have teeth, multiple drill holes are made in the remaining alveolar process through which wires are threaded to anchor the obturator. When teeth are present, the obturator is wired to the remaining teeth to keep it in position. The obturator satisfactorily covers the surgical defect, holds the packing in position, and allows the patient to begin oral alimentation postoperatively.

The incision is then closed in two layers. Chromic catgut interrupted sutures are used for approximation of the soft tissues and muscles. With interrupted sutures, the mucosa of the cheek is reapproximated to the cuff of mucosa that is left over the remaining alveolus. Meticulous attention must be given to accurate reapproximation of the vermilion border of the upper lip, the philtrum, and the skin edges around the ala of the nose.

The skin incision is closed with 5-0 nylon interrupted sutures (Fig. 8.203). Dressings are not necessary, but Bacitracin ointment is applied over the suture line. During the postoperative period the patient is exposed to extra humidity with a vaporizer and mask to prevent dryness of the oral cavity. Clear liquids are permitted by mouth the day after surgery, and the patient proceeds to a puréed diet during the next 24 hours. The patient is instructed to use frequent oral irrigations to keep the maxillectomy defect clean. Irrigations of the oral cavity and the surgical site are necessary, particularly after every meal. Occasional minor bleeding may occur from granulation tissue in the immediate postoperative period while the skin graft is healing. However, once satisfactory healing is achieved, the defect remains clean. A photograph of the oral cavity 3 months after surgery shows a well-healed skin graft (Fig. 8.204).

A final dental prosthesis with teeth is fabricated approximately 3 months after surgery (Fig. 8.205). This dental prosthesis effectively plugs the surgical defect and also incorporates the remaining denture. When inserted in the oral cavity, it stays in place well, as seen in the patient's mouth (Fig. 8.206). The prosthesis provides satisfactory restoration of speech and mastication. A frontal view of the patient's postoperative appearance with the dental obturator in place shows a well-healed skin incision and an acceptable aesthetic result (Fig. 8.207). It is important to reemphasize that in any type of surgery for primary tumors of the oral cavity where removal of the alveolar process or hard palate is indicated, continuous communication between the surgeon and the prosthodontist is essential for the satisfactory outcome of functional and aesthetic rehabilitation.

Figure 8.203 The skin incision is closed.

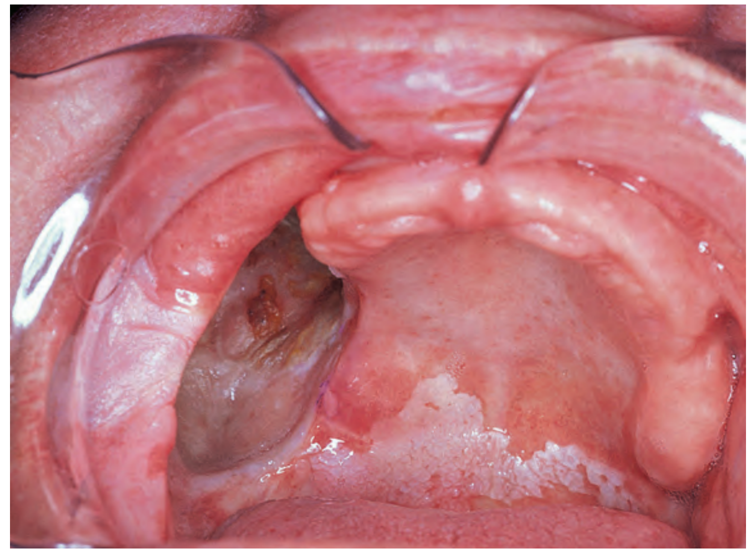

Figure 8.204 A photograph of the oral cavity 3 months following surgery shows a healed skin graft.

Figure 8.205 The permanent dental prosthesis.

Figure 8.206 The permanent prosthesis in the oral cavity.

Figure 8.207 Postoperative appearance of the patient 1 year following surgery.

Immediate Reconstruction of the Maxillectomy Defect

Patients with good long-term prognosis are considered for complex reconstruction with a free flap to eliminate the communication between the oral cavity and maxillary antrum and nasal cavity. Edentulous patients with an atrophic alveolar process and elderly patients unable to take care of the maxillectomy defect are best reconstructed with a composite soft-tissue flap only, such as the rectus abdominis free flap or anterolateral thigh flap. Even dentate patients with good remaining teeth can be reconstructed with a free flap of only soft tissue and skin (Fig. 8.208). Their dental rehabilitation is completed with a removable denture, clasped to the remaining teeth (Fig. 8.209).

The postoperative appearance of the same patient 6 months following surgery shows excellent aesthetic outcome from a modified Weber-Fergusson incision (Fig. 8.210).

Patients requiring total maxillectomy need a complex reconstructive surgery plan with a composite flap of bone, soft tissue, and skin. Accurate restoration of such large defects is significantly aided by using the CAD-CAM technology (see Chapter 17).

POSTOPERATIVE CARE

Patients undergoing surgery for tumors of the oral cavity require rigorous oral hygiene in the postoperative period. Oral irrigations and mechanical cleansing with power sprays of dilute hydrogen peroxide and saline solution should start on the day after surgery. Over the course of the next few days, the patient is taught self-care with oral irrigations that should continue until complete healing of the oral suture lines has been achieved. Similarly, the skin incision is cleared of all crusts and clots on a daily basis. Humidified air delivered through a face tent is recommended to minimize drying of the oral cavity.

Perioperative antibiotic coverage with cephalosporin and metronidazole is continued for 24 hours. The efficacy of the extended use of postoperative antibiotics to prevent postoperative sepsis remains controversial. However, under select circumstances, such as in the presence of a bolster or packing, antibiotics may be continued for a longer period.

A tracheostomy is required in patients with extensive resections, particularly in the posterior oral cavity, or when significant postoperative edema is anticipated. Routine tracheostomy care is mandatory. Once the patient is able to swallow saliva and fluids without major aspiration, the tracheostomy tube is removed.

Oral alimentation with clear liquids may be started within 24 hours in patients who have undergone a relatively minor peroral resection. Diet is progressively advanced to puréed, soft, and then regular food during the next 10 days. Nutrition is maintained through a nasogastric feeding tube in most patients

Figure 8.208 Intraoral view 1 year following partial maxillectomy for minor salivary gland carcinoma and reconstruction with an anterolateral thigh flap.

Figure 8.209 Dental rehabilitation achieved with a removable partial denture clasped to remaining teeth.

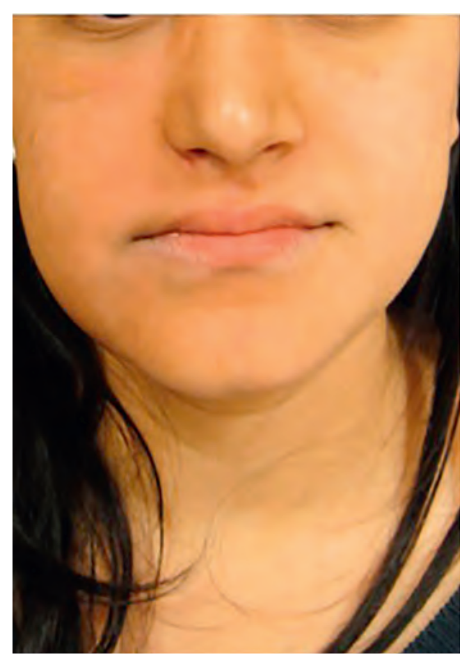

Figure 8.210 Postoperative appearance of the patient 1 year following surgery.

in whom normal swallowing is compromised as a result of surgery or when oral alimentation may compromise the intraoral suture line or skin graft.

Trismus can develop in patients whose surgical procedure involves the retromolar region or the masticator space. Preventive jaw exercises are initiated as soon as the oral suture line has healed. The assistance of mechanical devices such as a "corkscrew" or commercially available appliances is indicated in patients who manifest the development of trismus.

OUTCOMES

The single most important factor that affects long-term results following treatment for carcinoma of the oral cavity is the stage of disease at the time of presentation. For early-stage tumors, excellent cure rates are anticipated. However, once regional lymph node metastases become apparent, a significant drop in overall and disease-specific survival rates is observed (Fig. 8.211). The proportion of patients with advanced stage oral cancer treated at Memorial Sloan Kettering Cancer Center from 1985 to 2015 has remained essentially the same. Consequently, significant improvement in overall and disease-specific survival is not observed. The 5-year disease-specific survival has ranged between 77% to 81% (Fig. 8.212). Disease-specific survival rates in oral cancer vary with the anatomic site of the primary tumor (Fig. 8.213). The overall survival, disease-specific survival, and the impact of T stage and surgical margin status in patients treated between 1985 and 2015 are shown in Figs. 8.214 through 8.217. The significant drop between disease-specific survival and overall survival is attributed to comorbid conditions and other causes of death.

With the use of adjuvant postoperative radiation therapy and chemoradiotherapy (in patients with positive margins and extranodal spread), significant improvement in locoregional control and modest improvement in survival for patients with advanced-stage oral carcinoma has been observed compared with single modality treatment. In approximately one-third of the patients, multiple primary tumors develop either in the upper aerodigestive tract, lung, or other sites. Long-term prognosis in these patients depends on the stage and extent of multiple primary lesions.

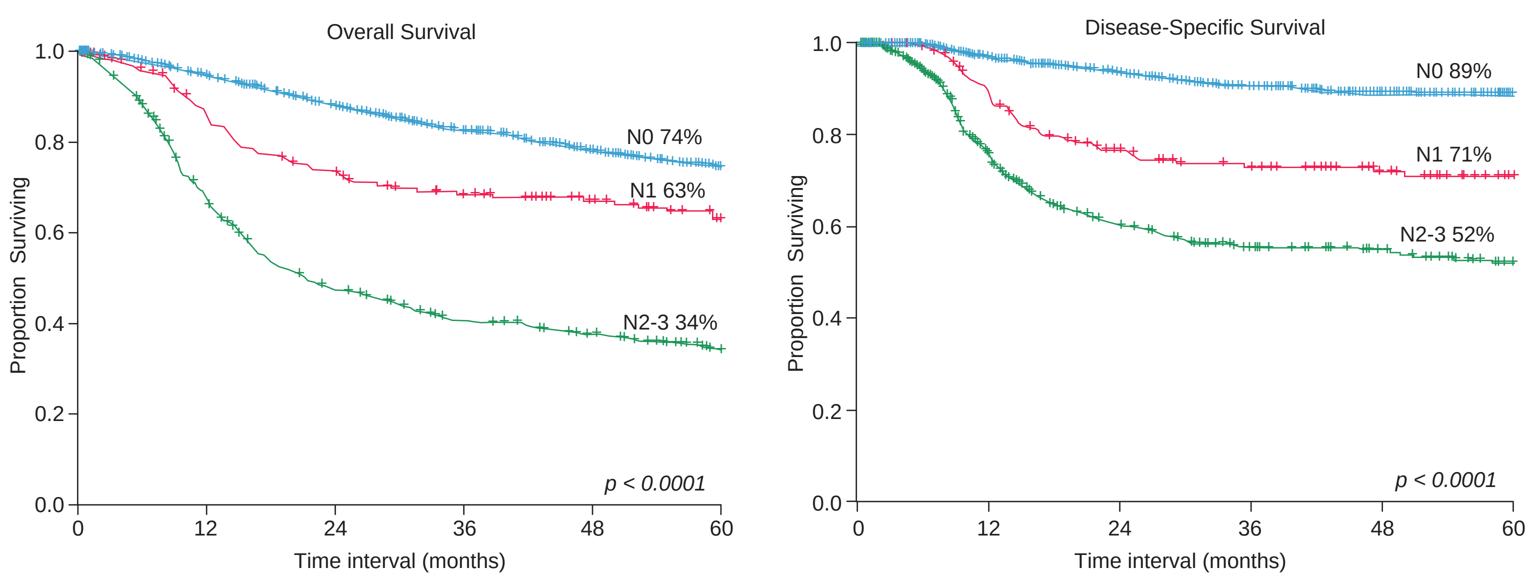

Figure 8.211 Overall and disease-specific survival is significantly reduced by the presence of lymph node metastases (American Joint Committee on Cancer eighth edition N staging.) (Memorial Sloan Kettering Cancer Center data, 1985–2015.)

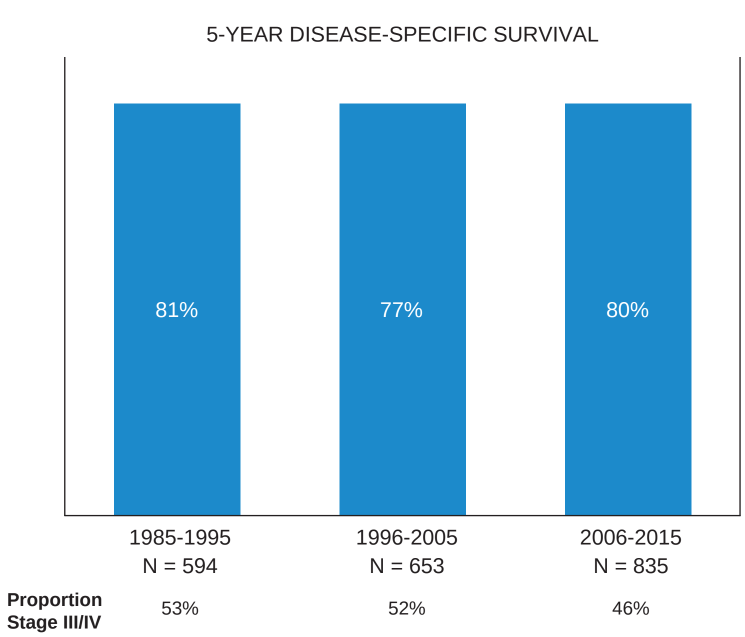

Figure 8.212 Proportion of patients with advanced stage disease and 5-year disease-specific survival for all stages of oral cancer at Memorial Sloan Kettering Cancer Center (1985–2015).

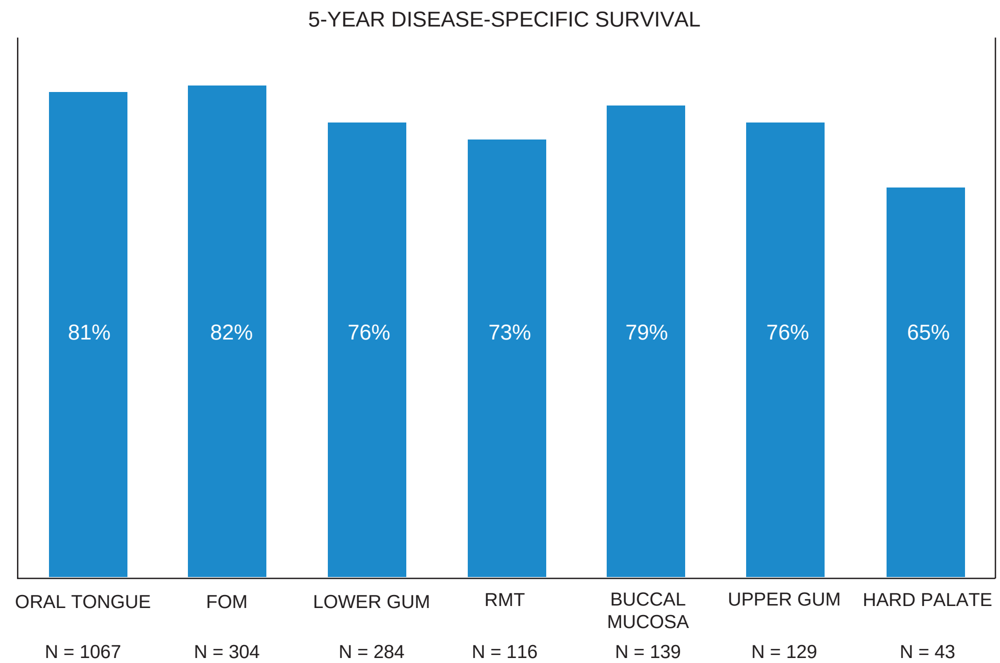

Figure 8.213 Survival outcomes by primary site (all stages). (Memorial Sloan Kettering Cancer Center data, 1985–2015.) *FOM,* Floor of mouth; *RMT,* retromolar trigone.

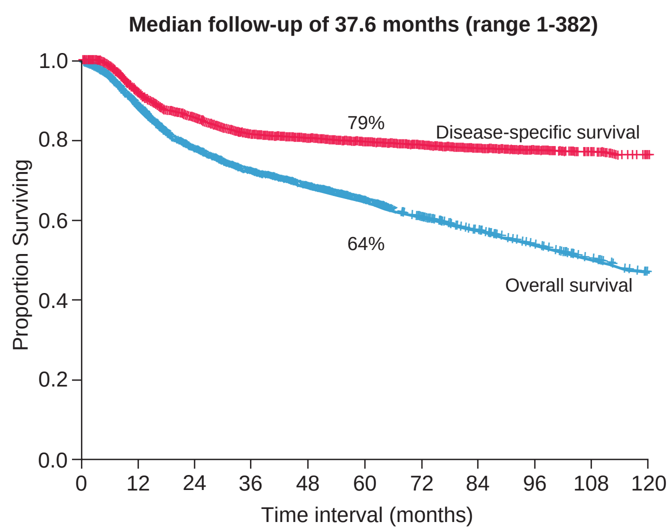

Figure 8.214 Five-year disease-specific and overall survival rates for oral cancer, all stages. (Memorial Sloan Kettering Cancer Center data, 1985–2015.)

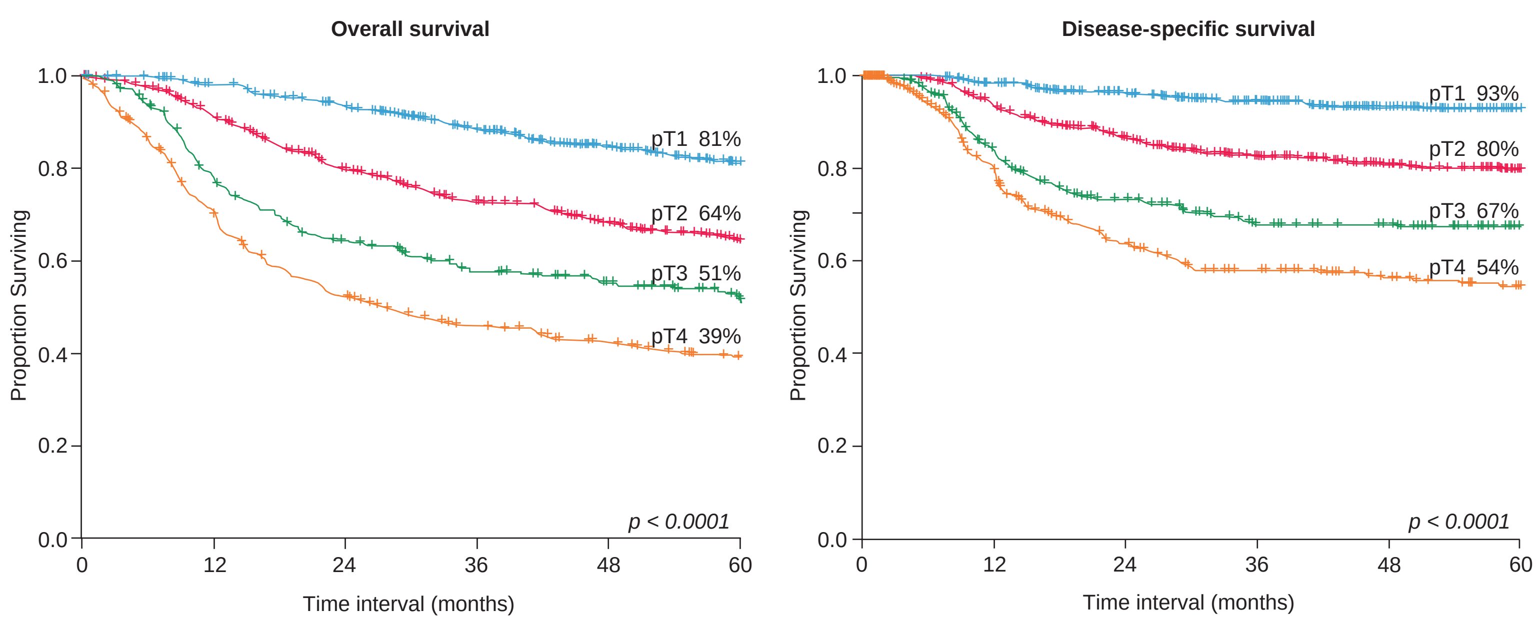

Figure 8.215 The pathologic T stage (American Joint Committee on Cancer eighth edition T staging) of the tumor is a significant predictor of survival. (Memorial Sloan Kettering Cancer Center data, 1985–2015.)

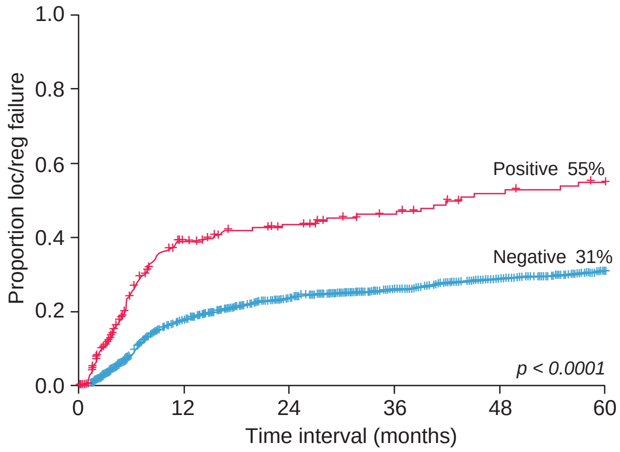

Figure 8.216 The status of the surgical margins is a powerful predictor of locoregional failure. (Memorial Sloan Kettering Cancer Center data, 1985–2015.)

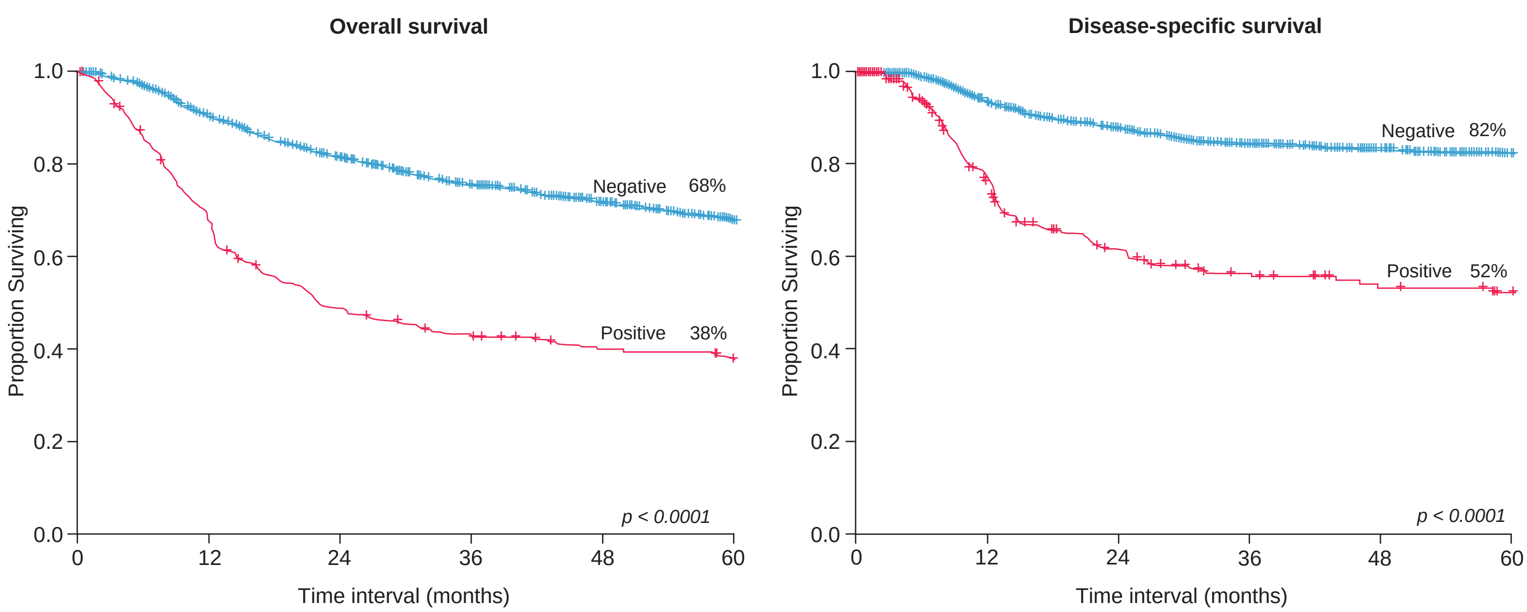

Figure 8.217 Patients with positive surgical margins have significantly worse survival. (Memorial Sloan Kettering Cancer Center data, 1985–2015.)

CHAPTER 9

Pharynx and Esophagus

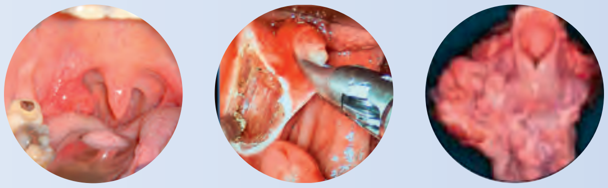

The pharynx is the intermediate part of the upper aerodigestive tract in the head and neck region, connecting the nasal cavity to the lower airway thru the larynx and the oral cavity to the esophagus. It is divided into three contiguous anatomic regions: the nasopharynx, oropharynx, and hypopharynx (Fig. 9.1). Each of these three divisions has distinct anatomic features and physiologic functions. The most frequently encountered neoplasm in the pharynx is squamous cell carcinoma. Although tobacco and alcohol consumption remain the most important etiologic factors, viral exposure (such as Epstein-Barr virus [EBV] for the nasopharynx and human papilloma virus [HPV]) for the oropharynx) frequently is associated with these tumors. These and other factors may account for geographic variations in the incidence of pharyngeal carcinomas. The worldwide incidence rates for cancer of the nasopharynx and other pharyngeal cancers are shown in Fig. 9.2. In the United States the American Cancer Society estimates that approximately 17,000 new cases of cancer of the pharynx were diagnosed in 2017. Death-rate estimates vary depending on the stage of the tumor. However, overall, 3050 cause-specific deaths were estimated for 2017 (Fig. 9.3).

The nasopharynx begins at the posterior choana of the nasal cavity and extends up to the level of the free edge of the soft palate. Various sites within the nasopharynx include the vault, the lateral walls, and the posterior wall. The lateral wall includes the fossa of Rosenmüller and the mucosa overlying the opening of the eustachian tube (torus tubarius). The posterior surface of the soft palate forms the floor of the nasopharynx. The mucosa of the pharynx is composed of squamous cells with varying degrees of keratinization and is interspersed with minor salivary glands in the submucosa. Primary neoplasms of the nasopharynx are squamous cell carcinomas; rarely, minor salivary gland tumors, chordomas, soft tissue tumors, and bone tumors may arise in the nasopharynx. Waldeyer's ring (which is composed of the lingual and pharyngeal tonsils, the adenoids, and mucosa covering the nasopharynx and oropharynx) has a rich lymphoid network. Waldeyer's ring also is a common site for involvement by lymphoma (particularly B-cell lymphoma); the tonsils and the base of the tongue are involved most frequently. Exposure to EBV (a gamma herpes virus) is frequently associated with nasopharyngeal carcinoma (NPC). EBV-associated NPC tumors have a unique histopathologic composition; they are undifferentiated carcinomas with a prominent lymphocytic infiltrate, and historically they were called "lymphoepitheliomas." The interaction between cancer cells and lymphocytes is thought to contribute to the propagation of malignancy. Geographic variation in the incidence of NPC is observed, with the highest incidence in Southeast Asia and Africa. The precise reason for this geographic variation remains to be elucidated, but environmental factors, inherited genetic susceptibility, and EBV exposure may be contributory. Serologic screening for EBV-specific antibody titers are used for early diagnosis and to monitor response to therapy in select high-risk populations. Genetic predisposition also is suggested by the high incidence of NPC in Chinese men (especially Cantonese men) regardless of where they live. Environmental cofactors, such as consumption of salted fish, also may contribute to geographic variations in incidence.

The oropharynx begins at the anterior aspect of the faucial arch and extends posteriorly. It includes the soft palate and tonsillar fossae on each side, as well as the posterior pharyngeal wall and the posterior third of the tongue (the base of the tongue). Historically, the base of the tongue was the most frequent site of primary tumors in the oropharynx, followed by the tonsils and soft palate. However, during the past two decades in the United States, the tonsils are observed to be the most predominant site of primary carcinomas in the oropharynx. This shift in site distribution is attributed to the steep rise in the incidence of HPV-associated squamous cell carcinomas in the oropharynx. Tobacco and alcohol consumption as etiologic factors for cancers in the oropharynx is declining, whereas HPV-associated squamous cell carcinoma in the nonsmoking

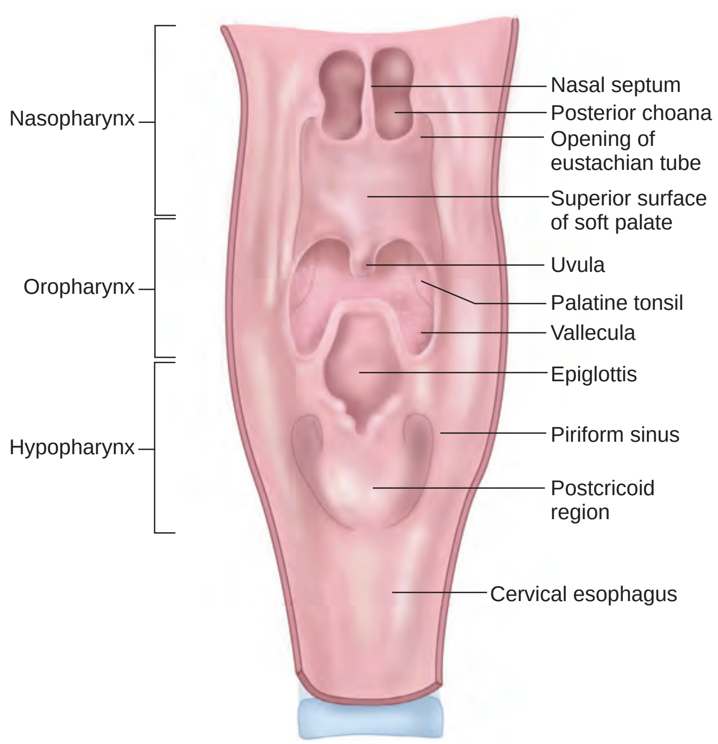

Figure 9.1 Anatomic regions of the pharynx.

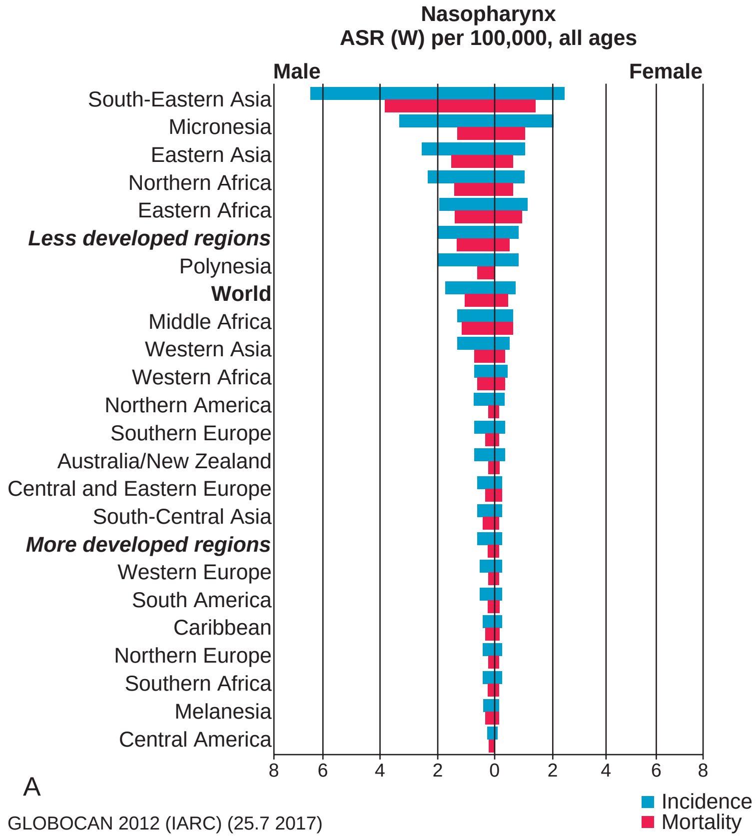

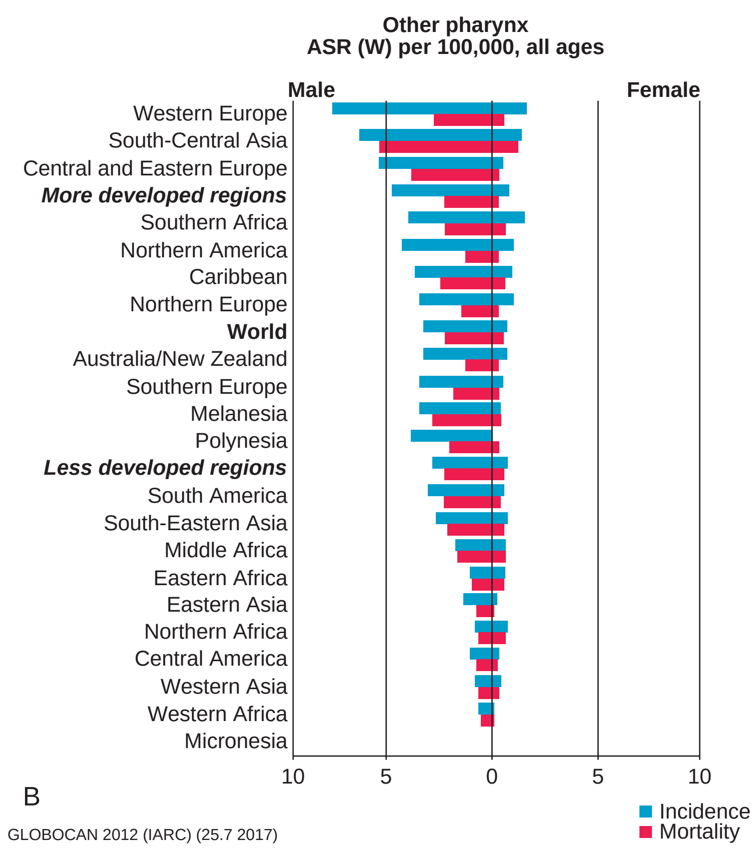

Figure 9.2 Worldwide incidence and mortality rates in males and females for cancer of the nasopharynx (**A**) and other pharynx sites (**B**). *(From Ferlay J, Soerjomataram I, Ervik M, Dikshit R, Eser S, Mathers C, Rebelo M, Parkin DM, Forman D, Bray F. GLOBOCAN 2012 v1.0, Cancer Incidence and Mortality Worldwide: IARC CancerBase No. 11. Lyon, France, International Agency for Research on Cancer, 2013. Available from http://gco.iarc.fr/today/home.)*

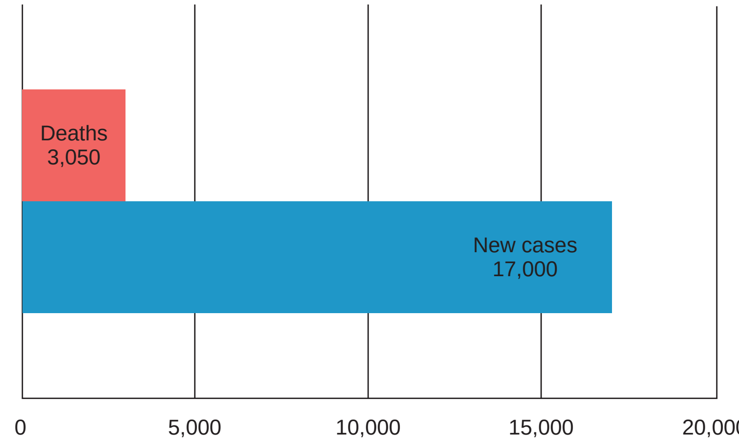

Figure 9.3 American Cancer Society estimates of new cases and deaths for cancer of the pharynx in the United States in 2017.

younger population is continuing to rise. The carcinogenic role of HPV in cancer pathogenesis is well established based on studies of cervical carcinomas in women. Although similar, the precise role of HPV infection in the pathogenesis of head and neck cancer is not analogous to cervical cancer, because infection appears to be neither necessary nor sufficient for development of these tumors. Epidemiologic and molecular studies have, however, identified HPV as a causative agent of oropharyngeal carcinoma. Moreover, lending further support to their being distinct clinical entities, the clinical course of HPV-positive oropharyngeal carcinomas appears to be different from that of HPV-negative tobacco- or alcohol-related tumors. Demographically, HPV-associated oropharyngeal cancer occurs more often in younger males with little or no tobacco exposure. Clinically, the primary tumor is often small and the presenting symptom is lymphadenopathy. HPV-associated oropharyngeal cancer is highly responsive to treatment and carries an excellent prognosis, in contrast to its HPV-negative counterpart. The impact of these improved outcomes has generated debate on selection of treatment for oropharynx cancer, with a focus on de-escalation to reduce treatment-related morbidities. Several clinical trials of de-escalation of treatment programs are currently under way. The site distribution for primary tumors of the oropharynx observed at Memorial Sloan Kettering Cancer Center is shown in Fig. 9.4. Although squamous cell carcinomas are the most frequently encountered primary tumors of epithelial origin in the oropharynx, lymphomas often are seen because of the abundance of lymphoid tissue in the oropharynx, which is a significant component of Waldeyer's ring. A primary lymphoma of the tonsil, pharyngeal wall, or base of the tongue therefore can present as a surface lesion with ulceration because of rapid proliferation. Physiologically, the oropharynx is important as an entry portal to the pharyngoesophageal region during the pharyngeal phase of deglutition. Transport of the food bolus from the oral cavity to the hypopharynx requires that the velopharyngeal sphincter be competent, preventing regurgitation of the bolus into the nasopharynx and nasal cavity. Similarly, elevation of the larynx during the pharyngeal phase of deglutition requires that the muscles of the tongue and the hyomandibular complex be intact. Disturbance in any of these well-coordinated muscular functions will produce swallowing dysfunction, including nasal regurgitation and aspiration.

The hypopharynx is the lowermost part of the pharynx, beginning at the level of the tip of the epiglottis and ending at the level of the lower border of the cricoid cartilage. At that point the upper aerodigestive tract continues into the

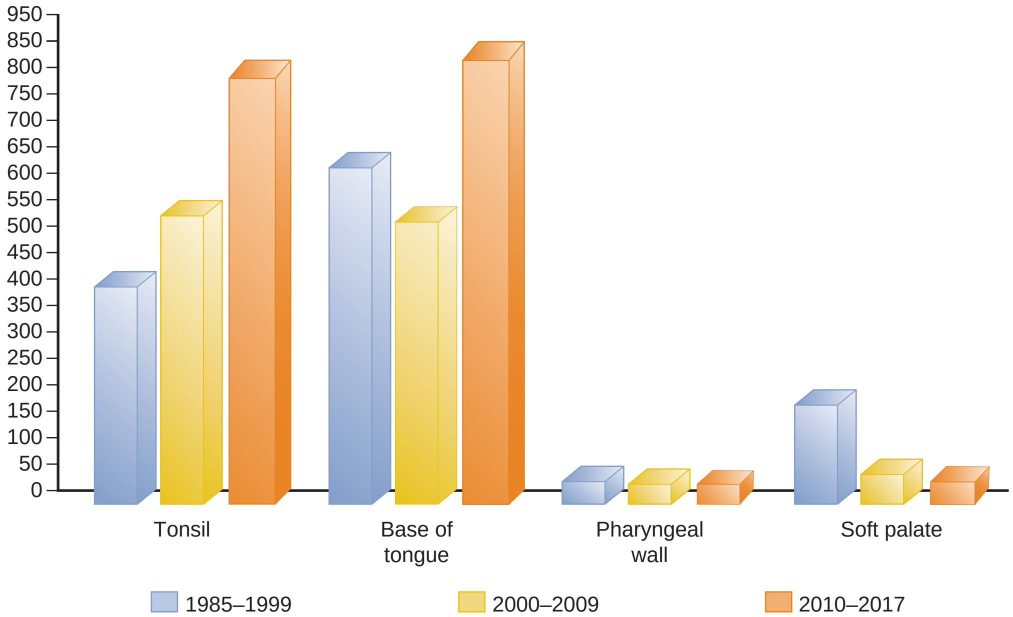

Figure 9.4 Site distribution of primary carcinoma of the oropharynx at Memorial Sloan Kettering Cancer Center, 1985 to 1999, 2000 to 2009, and 2010 to 2017.

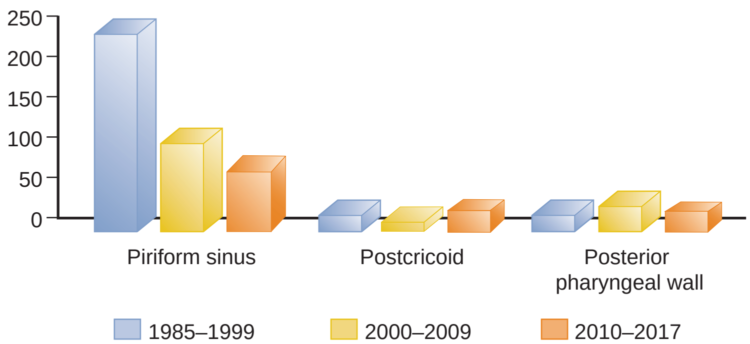

Figure 9.5 Site distribution of primary carcinoma of the hypopharynx at Memorial Sloan Kettering Cancer Center, 1985 to 1999, 2000 to 2009, and 2010 to 2017.

cervical esophagus. The pyriform sinuses on each side, the posterior pharyngeal wall, and the postcricoid region form the three designated anatomic sites within the hypopharynx. However, their boundaries overlap because their demarcation is somewhat arbitrary. The site distribution of primary squamous cell carcinomas of the hypopharynx is shown in Fig. 9.5. Physiologically, the hypopharynx is a critically important anatomic site because it is a component of the upper aerodigestive tract, contiguous with the supraglottic larynx. The pharyngeal phase of deglutition requires a well-coordinated process controlled by the glossopharyngeal, vagus, and hypoglossal nerves. Normal mucosal sensations of the oropharynx, supraglottic larynx, and hypopharynx are essential in initiating the swallowing reflex. Similarly, coordinated action of muscles of the tongue, pharynx, and intrinsic muscles of the larynx is required for successful passage of the food bolus into the cervical esophagus without aspiration into the airway. Thus surgical treatment of any tumor arising in the hypopharynx will, by necessity, produce disturbance in swallowing, with risk of aspiration into the respiratory tract. In the Western world, primary malignant tumors within the hypopharynx are seen most frequently in the pyriform sinuses, followed by the posterior pharyngeal wall. The least frequent site is the postcricoid region. In other parts of the world, distribution of primary tumors of the hypopharynx is somewhat different.

The cervical esophagus begins where the hypopharynx ends, at the level of the lower border of the cricoid cartilage. The exact lower extent of the cervical esophagus is somewhat arbitrary. It is generally accepted that the cervical esophagus ends at the thoracic inlet. The most common site of origin for primary cancers of the esophagus is in its lower third, followed by the middle third, and last in the cervical esophagus. Although primary tumors of the cervical esophagus are infrequent, direct extension of postcricoid or pharyngeal wall tumors to the cervical esophagus is quite common. Because of its contiguity to the postcricoid region cephalad and to the larynx and proximal trachea anteriorly, surgical treatment of cancer of the cervical esophagus requires consideration of management of the larynx and proximal trachea along with the primary tumor. The most frequently seen malignant tumor in the hypopharynx and cervical esophagus is squamous cell carcinoma, although adenocarcinoma of minor salivary gland origin does occur infrequently. Melanomas, soft tissue tumors, and occasionally metastatic tumors also may be seen.

STAGING

Staging for primary nasopharynx cancer (NPC) depends on local extension to the adjacent soft tissues (parapharyngeal space) and bone (skull base). Tumors of the nasopharynx commonly invade adjacent muscles, including medial pterygoid, lateral pterygoid, and prevertebral muscles. In contrast to oral cavity cancers, these are still considered in early T stages in the AJCC/UICC staging system. In addition, because of the rich lymphatic network of the nasopharynx, regional lymph node metastases occur early and often, and a neck mass may be the presenting symptom in many patients. Nodal metastases occur in a predictable fashion with involvement of retropharyngeal and parapharyngeal lymph nodes, the deep jugular chain, and posterior triangle lymph nodes, in that order. Bilateral metastases are common.

The most recent revision of the American Joint Committee on Cancer (AJCC)/International Union Against Cancer (UICC) staging system (eighth edition) has introduced separate staging for "high-risk HPV (p16-positive)"–associated oropharynx cancer (OPC) from the "non-HPV (p16-negative)—," tobacco-, and alcohol- associated OPC due to the distinctly improved prognosis for HPV-positive cancers. T classification in both HPV-positive and HPV-negative oropharyngeal cancer remains the same and is staged on the basis of the surface dimensions of the primary

tumor. On the other hand, the impact of regional lymph node metastases in HPV-positive tumors is not the same. Regional lymph node metastases are quite common and may be the first manifestation of the disease. Nodal metastases occur in a predictable and sequential manner, with lymph nodes in the anterior triangle of the neck (levels I to IV) being at highest risk. Nodal staging for HPV-negative oropharynx cancer remains the same as that for other sites. Extranodal extension is an adverse risk feature that upstages N staging for all mucosal squamous cell carcinomas, including HPV-negative oropharynx tumors. This finding has not been found to be prognostic in HPV-positive cancer and therefore is not included in the N staging. Laterality and size of metastatic nodes are the only factors included in the N staging for HPV-positive OPC (see Chapter 11). These changes will more accurately classify HPV-positive oropharynx cancers, improve prognostication, and enhance stratification for clinical trials and outcome reporting.

Staging of primary tumors of the hypopharynx is not dependent on the surface dimensions of the tumor but is related to local extent and invasion of various sites within the hypopharynx or to adjacent regions such as the oropharynx and larynx. Fixation of the vocal cord implies deep invasion into the musculature of the larynx, putting it in an advanced stage category. Because of its anatomic location, a small primary tumor of the hypopharynx is seldom symptomatic and is diagnosed infrequently. The majority of symptomatic tumors, therefore, have an advanced T stage at presentation. In addition, the lymphatic network of the hypopharynx is quite rich, and dissemination of the primary lesion to the regional lymph nodes occurs often and early in the course of the disease. The T stage distribution of hypopharyngeal tumors at diagnosis is shown in Fig. 9.6. Nearly two-thirds of patients present with clinically apparent cervical lymph node metastases (Fig. 9.7).

EVALUATION

Patients with lesions of the nasopharynx present with symptoms of nasal obstruction, epistaxis, otalgia, unilateral or bilateral middle ear effusion, or cranial neuropathy as a result of the location and extent of the primary tumor. On the other hand, cervical lymph node metastases may be the first and occasionally the only clinical manifestation in patients with carcinoma of the nasopharynx. Clinical diagnosis requires adequate evaluation of the primary tumor through flexible or rigid nasal endoscopy and/or examination of the nasopharynx through the oral cavity with a 30-degree and 70-degree rigid telescope if the nasopharynx is obstructed. The surface appearance of the lesion often provides a clue to the diagnosis. Smooth, submucosal lesions such as a retention cyst (Thornwaldt cyst), meningocele, craniopharyngioma, or minor salivary gland tumor have normal overlying mucosa. Several examples of lesions in the nasopharynx are shown in Figs. 9.8 through 9.10. On the other hand, mucosal lesions have a characteristic appearance with irregular, cauliflower-like growth. These lesions should be differentiated from enlarged adenoids, which can be seen in patients with human immunodeficiency virus (Figs. 9.11 through 9.14). Tissue diagnosis of exophytic mucosal lesions can be established easily by a transnasal or peroral biopsy under topical anesthesia. However, a biopsy of submucosal and highly vascular lesions should not be performed before appropriate radiographic imaging and only under controlled circumstances in the operating room. Radiologic imaging of the nasopharynx and neck with computed tomography (CT) and magnetic resonance imaging (MRI) is essential for accurate assessment of the extent of the lesion and staging of malignant tumors.

Tumors of the oropharynx are readily assessed by clinical examination through the oral cavity and by flexible fiberoptic

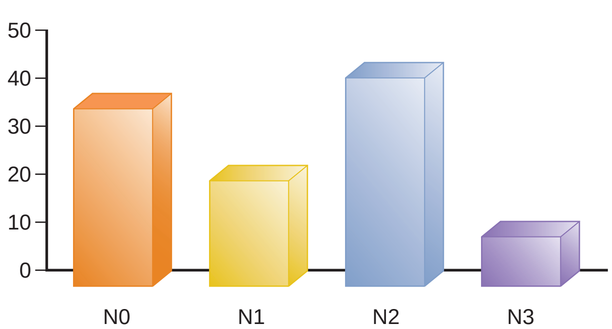

Figure 9.7 Incidence of nodal metastases at presentation for squamous cell carcinoma of the hypopharynx (MSKCC data).

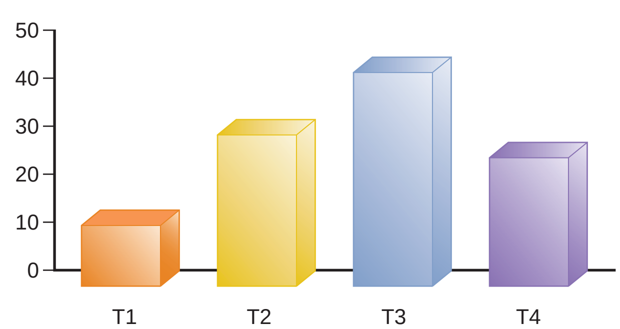

Figure 9.6 Clinical T stage distribution at presentation of squamous cell carcinoma of the hypopharynx (MSKCC data).

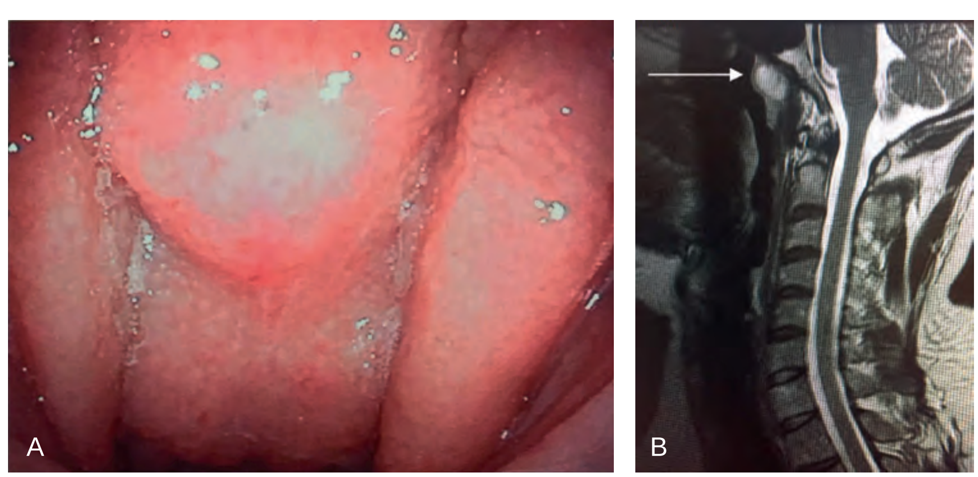

Figure 9.8 A Thornwaldt cyst of the nasopharynx, nasal endoscopic view **(A)** and T2 weighted sagittal MRI showing the cyst in the posterior wall of the nasopharynx **(B)**.

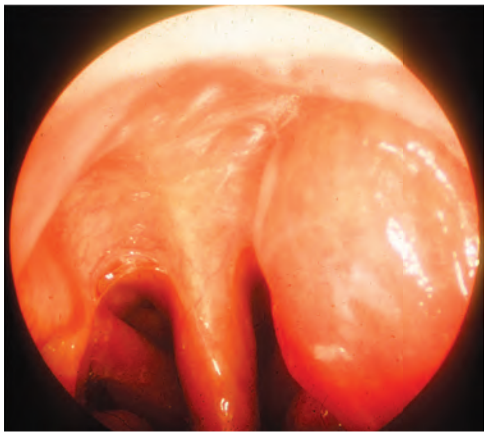

Figure 9.9 A hemangioma of the nasopharynx.

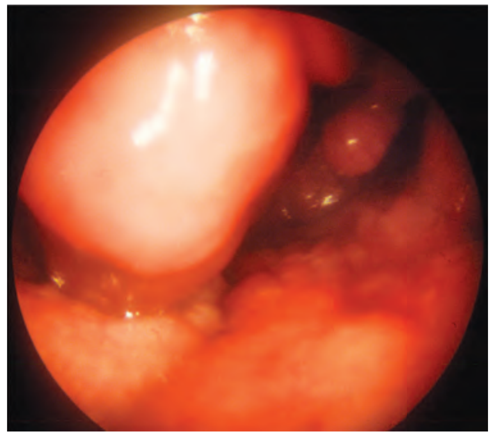

Figure 9.10 A plasmacytoma of the nasopharynx.

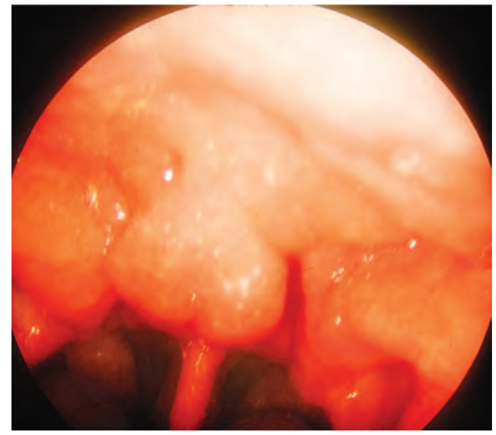

Figure 9.11 A hypertrophic adenoid in the nasopharynx.

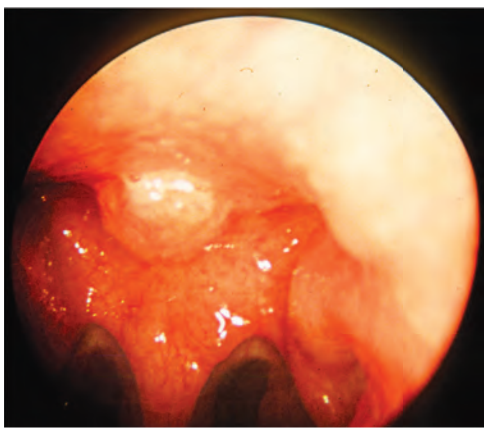

Figure 9.12 A squamous cell carcinoma of the roof of the nasopharynx.

Figure 9.13 A squamous cell carcinoma of the lateral wall of the nasopharynx.

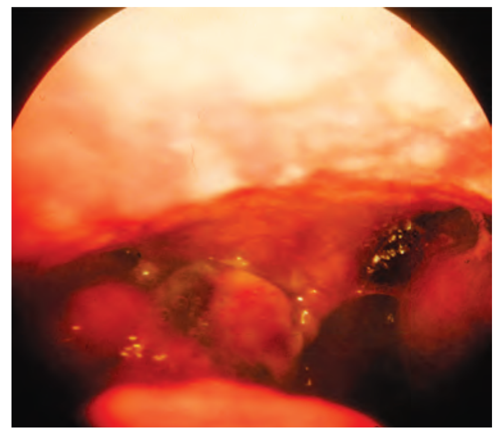

Figure 9.14 A melanoma of the nasopharynx.

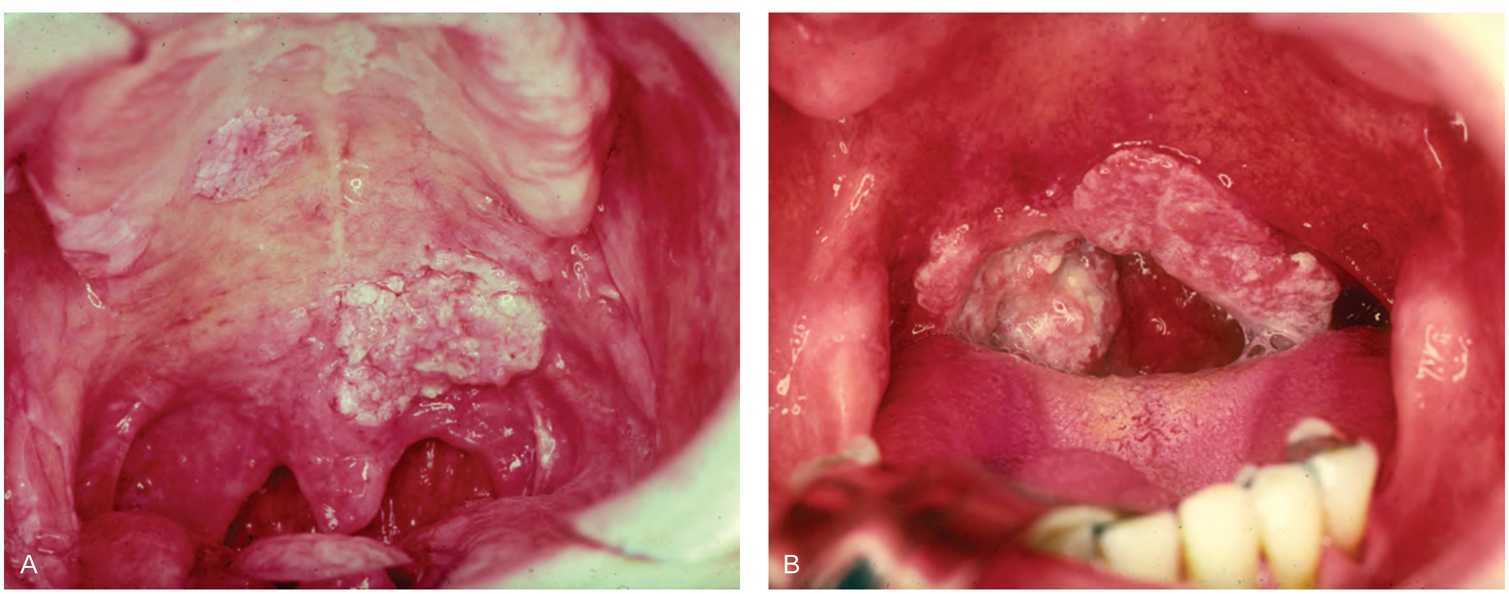

Figure 9.15 Squamous cell carcinomas of the soft palate. **A**, Early stage. Two separate lesions of the hard and soft palate. **B**, Advanced stage.

nasolaryngoscopy under topical anesthesia in the office setting. Some examples of peroral view of tumors of the oropharynx are shown in Figs. 9.15 through 9.18. Cervical lymph node metastases occur often in patients with oropharyngeal primary tumors. It is not uncommon to see a small primary tumor with bulky lymph node metastases (Fig. 9.19). This is particularly true in patients with HPV-positive oropharynx cancers. It is the volume and extent of nodal metastases that will determine the treatment approach. For example, a patient with a small primary and bulky nodal metastases is likely to be treated with chemoradiotherapy, in contrast to a patient with a small primary and low-volume neck metastases (Fig. 9.20). Metastatic lymph nodes from primary carcinomas of the tonsil often have cystic degeneration and may be misinterpreted clinically and radiologically as a branchial cleft cyst. Radiologic imaging with CT and MRI is necessary for assessment of these features and regional lymph nodes. Flexible fiberoptic laryngoscopy provides excellent visual assessment of the surface extent of the tumor, but digital

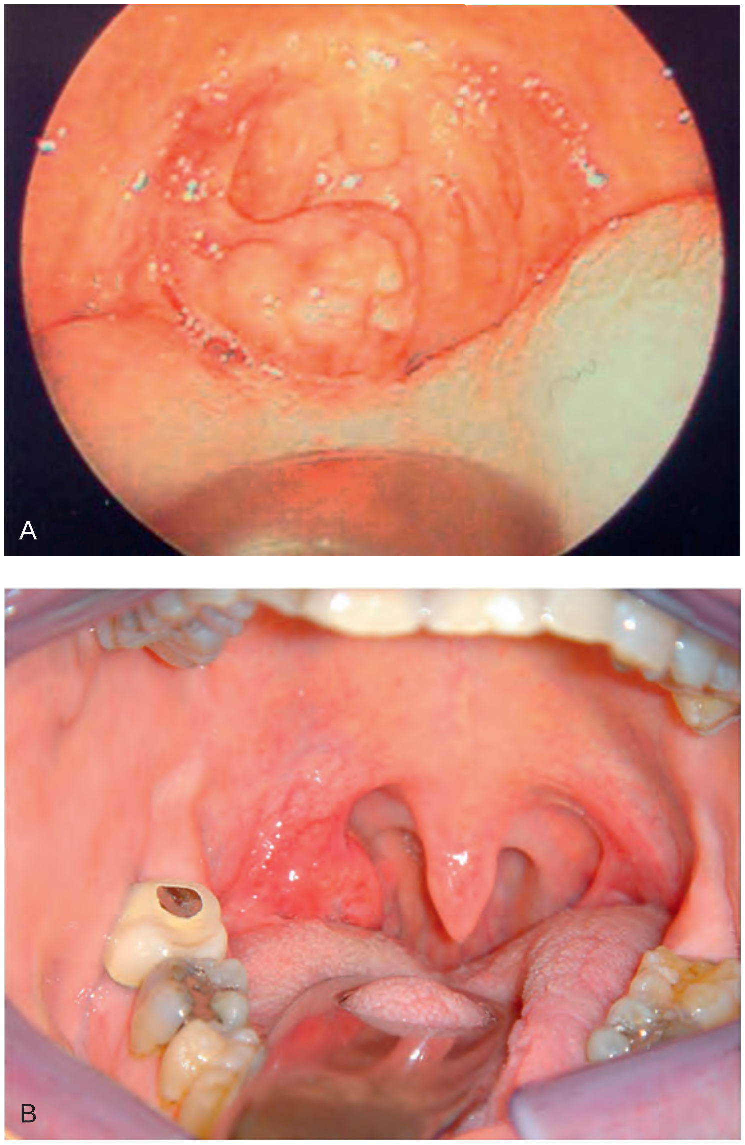

Figure 9.16 Squamous cell carcinomas of the tonsil. **A**, An exophytic lesion of the left tonsil. **B**, A submucosal lesion of the right tonsil.

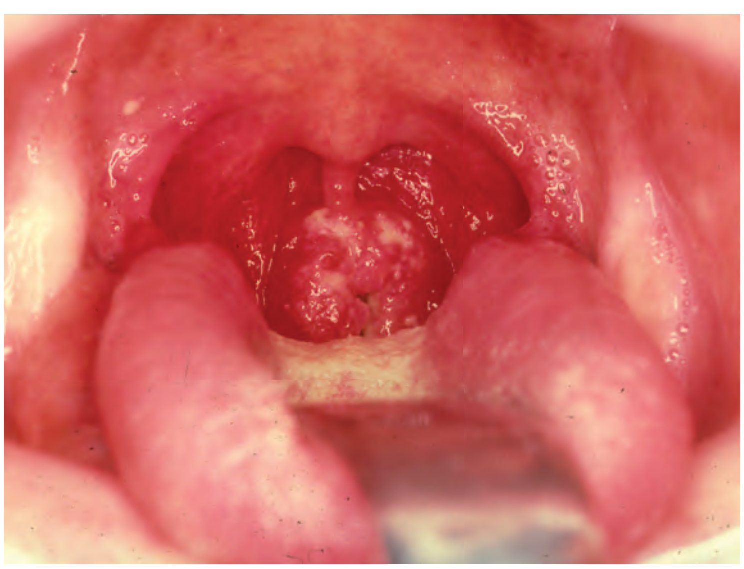

Figure 9.17 A carcinoma of the posterior pharyngeal wall.

Figure 9.18 Ulcerated endophytic carcinoma of the base of the tongue **(A)**. Exophytic carcinoma of the base of the tongue; lateral **(B)** and midline **(C)**.

palpation is essential to estimate the depth of infiltration in the pharyngeal wall and deep muscles of the base of the tongue. Some examples of endoscopic views of lesions of the base of the tongue are shown in Fig. 9.21. Clinical differentiation between a hypertrophic lingual tonsil, exophytic squamous cell carcinoma, and lymphoma can sometimes be difficult. For primary tumors of the tonsil, extension to the nasopharynx, soft palate, and base of the tongue are crucial determinants in accurate staging and treatment planning. On the other hand, for primary tumors of the base of the tongue, assessment of extension to the supraglottic larynx and deep infiltration into the extrinsic musculature of the tongue is necessary for accurate staging. Endoscopy, palpation, and biopsy under general anesthesia are usually required for accurate assessment of tumors of the base of the tongue.

Patients with primary tumors of the hypopharynx usually present with the complaints of discomfort in the throat, dysphagia, odynophagia, sensation of something stuck in the throat, otalgia (referred pain in the ipsilateral ear), hemoptysis, hoarseness of voice, or shortness of breath. A significant proportion of patients have clinically palpable cervical lymph nodes at presentation. In most instances, diagnosis is made by a thorough clinical examination, which would include mirror examination of the hypopharynx and larynx as well as either rigid telescopic or flexible fiber-optic nasolaryngopharyngoscopic examination for adequate clinical assessment of the primary tumor. Several examples of the presenting features of primary tumors of the hypopharynx are shown in Figs. 9.22 through 9.27. Although clinical examination permits the establishment of the diagnosis of a primary tumor of the hypopharynx, direct laryngoscopy and esophagoscopy under general anesthesia are essential for accurate assessment of the extent of the tumor and to obtain a biopsy specimen for histologic diagnosis to facilitate treatment planning. The important features to be assessed during endoscopic examination under anesthesia include the site of origin of the primary tumor and its local extension to the other sites within the hypopharynx and adjacent regions, including the larynx, oropharynx, and cervical esophagus. For a primary tumor of the pyriform sinus, it is essential to assess its lateral and cephalocaudad extents, particularly as they relate to the apex of the pyriform sinus (Fig. 9.28).


Figure 9.19 Bulky lymph node metastases to the neck from a small primary cancer of the right tonsil.


Figure 9.20 Carcinoma of the right tonsil (T1) with low volume (N1) nodal metastases.

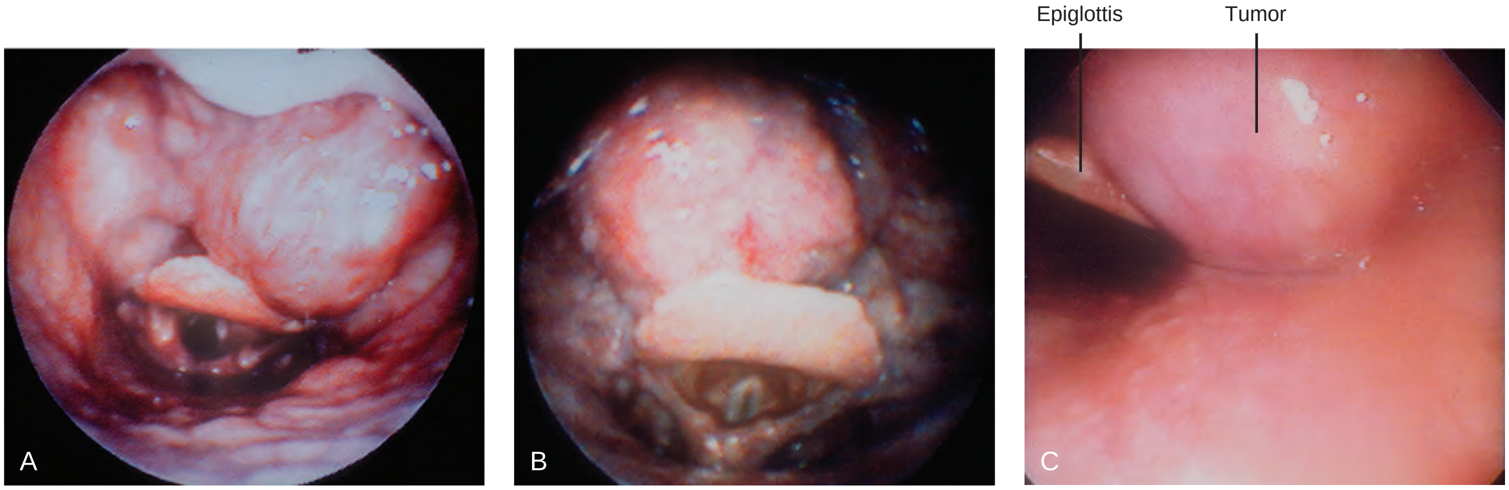

Figure 9.21 Endoscopic view of lesions of the base of the tongue. **A**, Hypertrophic lingual tonsil. **B**, Squamous cell carcinoma. **C**, Adenocarcinoma.

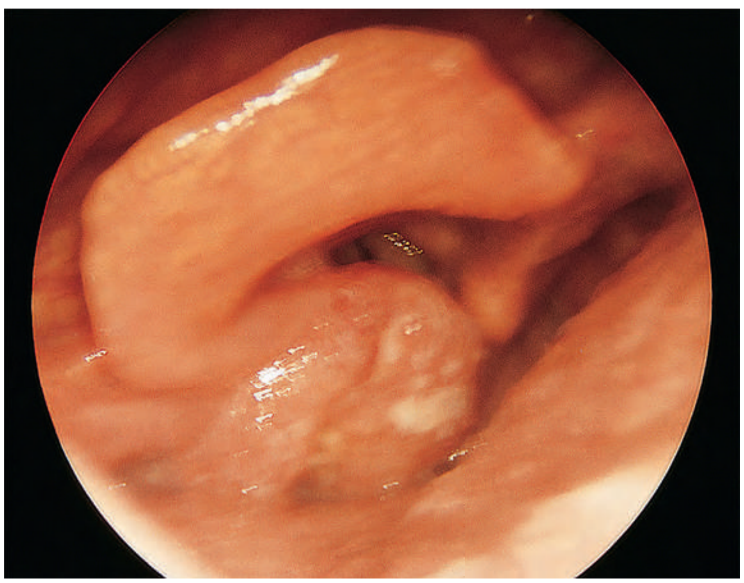

Figure 9.22 A carcinoma of the medial wall of the left pyriform sinus with extension to the arytenoid.

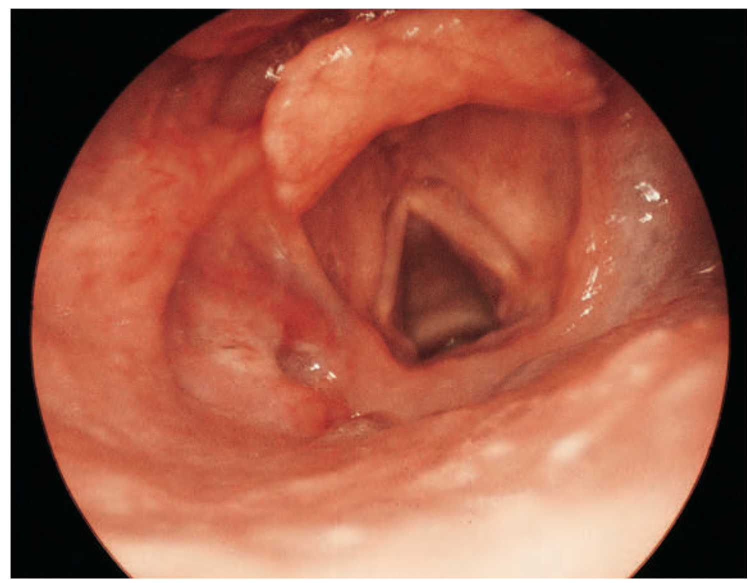

Figure 9.24 A carcinoma of the left pyriform sinus extending to its apex.

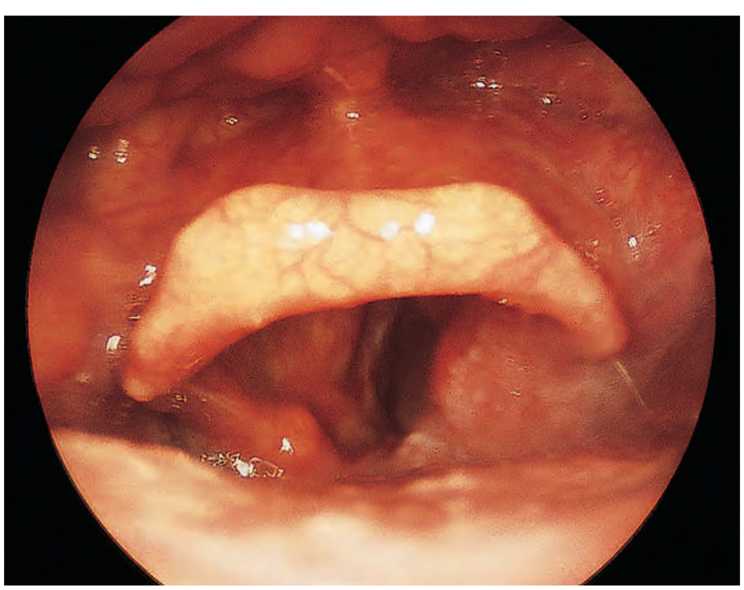

Figure 9.23 An advanced carcinoma of the right pyriform sinus with transglottic invasion.

Figure 9.25 An advanced carcinoma of the right pyriform sinus with extension to the larynx.

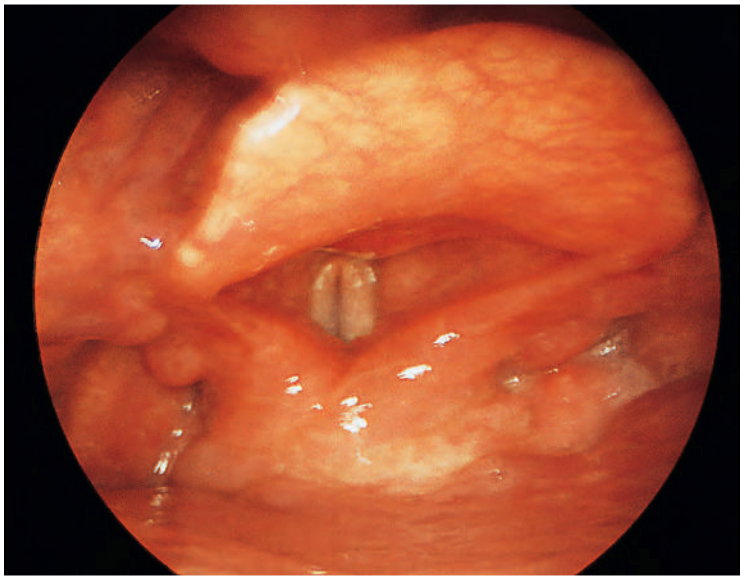

Figure 9.26 A postcricoid carcinoma.

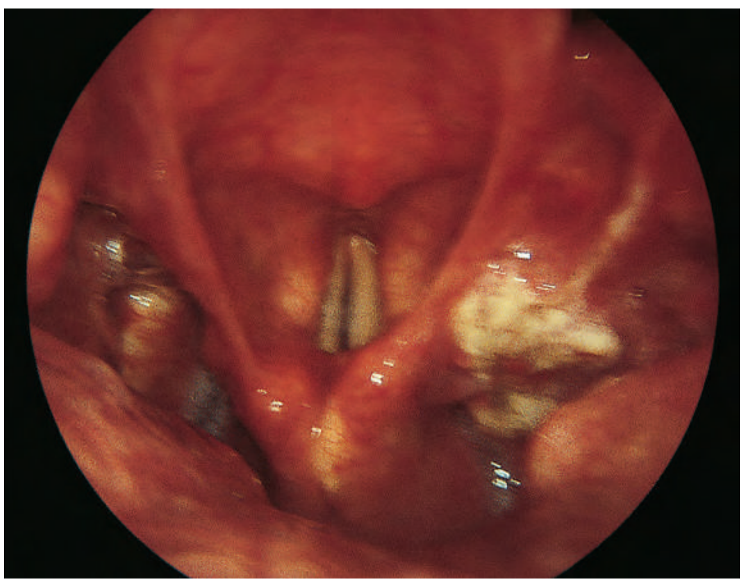

Figure 9.27 A localized tumor of the medial wall of the right pyriform sinus.

Figure 9.28 Surgical specimen of locally advanced carcinoma of the pyriform sinus extending into cervical esophagus.

Radiographic Evaluation

The lining of the upper aerodigestive tract, including the nasopharynx, oropharynx, and hypopharynx, is radiographically termed the *pharyngeal mucosal space*. Radiographic imaging is crucial for delineating the third dimension of the primary tumor and the extent of its local invasion, whereas clinical examination is more reliable for assessment of its surface extent. Although MRI is superior for assessment of the soft tissue extent of the tumor, its utility is limited by motion artifact if the patient cannot control swallowing during the examination because of a bulky tumor at the base of the tongue or hypopharynx. In contrast, new generation CT scanners allow rapid acquisition of data that can be reconstructed in coronal and sagittal planes, which is particularly useful in patients who are unable to tolerate an adequate MRI examination.

When evaluating the nasopharynx, MRI is the modality of choice. Although CT is excellent for assessment of cortical bone and foramina at the skull base, nasopharyngeal tumors have a tendency to invade the medullary space of the clivus, and bone involvement therefore is detected earlier on MRI than on CT. Benign lesions of the nasopharynx such as a Thornwaldt cyst and retention cysts have characteristic imaging features that are helpful in making a diagnosis. Thornwaldt cysts arise from the notochord remnant and are located submucosally in the midline. They are very well defined and generally are bright on T2-weighted MRI (Fig. 9.29). Retention cysts, generally located paramedian or laterally, are also bright on T2-weighted MRI and do not enhance with contrast (Fig. 9.30).

The presence of an asymmetric mass in the nasopharynx is an obvious feature that should raise suspicion for a tumor in adults, especially if unilateral opacification of the ipsilateral mastoid air cells is noted. However, adenoidal tissue can be a source of confusion, especially in children. The presence of certain other features such as skull base invasion can point to the diagnosis of malignancy in these situations. Invasion of the skull base is seen frequently in patients with NPC, because the pharyngobasilar fascia acts as a barrier to lateral spread and funnels the tumor cephalad toward the central skull base. Early clival invasion is nicely seen on precontrast T1-weighted MRI, because normal bright adult fatty marrow provides contrast for grayish tumor infiltration. The tumor generally has a high signal on T2-weighted MRI and enhances on postcontrast images (Fig. 9.31). Another feature of NPC is infiltration of the petroclival fissure, which is best demonstrated on bone windows of a CT scan (Fig. 9.32). Gross extension into the parapharyngeal space occurs with breach of the pharyngobasilar fascia (Fig. 9.33). The tumor can directly involve the lower cranial nerves, or perineural spread of tumor can occur along the branches of the trigeminal nerve. A tumor also can extend into the pterygopalatine fossa, gaining access to the vidian nerve and V2 (Fig. 9.34), and it can involve the muscles of mastication in the masticator space (Fig. 9.35), although this happens rarely.

Small and superficial tumors of the base of the tongue can be difficult to differentiate from lingual tonsillar tissue. The diagnosis of malignancy is obvious if infiltration into the base

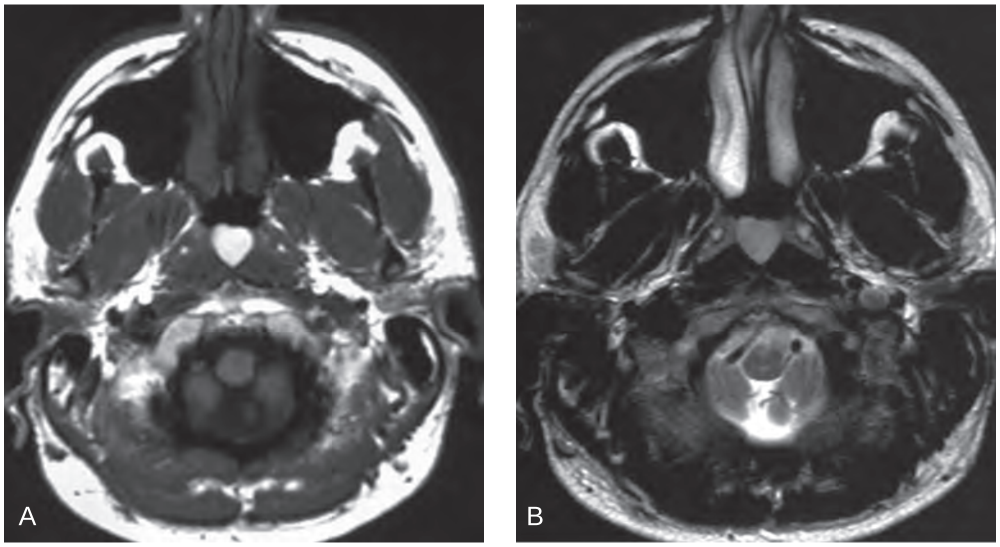

Figure 9.29 A Thornwaldt cyst of the nasopharynx. **A**, A T1-weighted magnetic resonance imaging scan showing a well-defined midline submucosal lesion of the nasopharynx located between the longus colli muscles. The lesion is T1 bright because of its high protein content. **B**, This lesion has an intermediate signal on T2-weighted MRI, but the signal can vary depending on the protein content of the lesion.

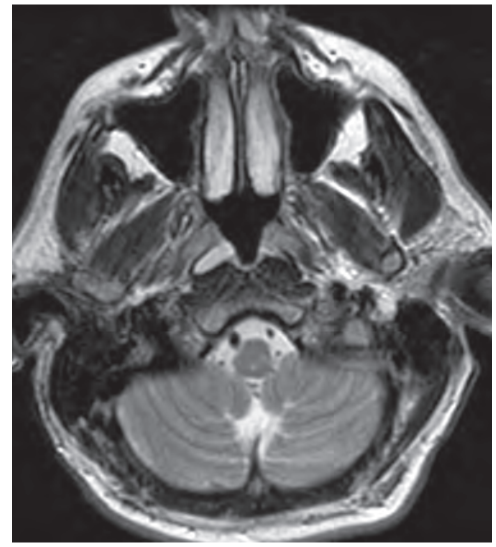

Figure 9.30 A T2-weighted magnetic resonance imaging scan showing a well-defined hyperintense retention cyst in the right fossa of Rosenmüller.

Figure 9.31 Invasion of the clivus by a nasopharyngeal carcinoma seen on a magnetic resonance imaging (MRI) scan. **A**, An axial precontrast T1-weighted MRI scan showing a grayish tumor infiltrating normal bright adult fatty marrow. **B**, The tumor has a high signal on T2-weighted MRI. **C**, The tumor enhances on a postcontrast T1-weighted MRI scan.

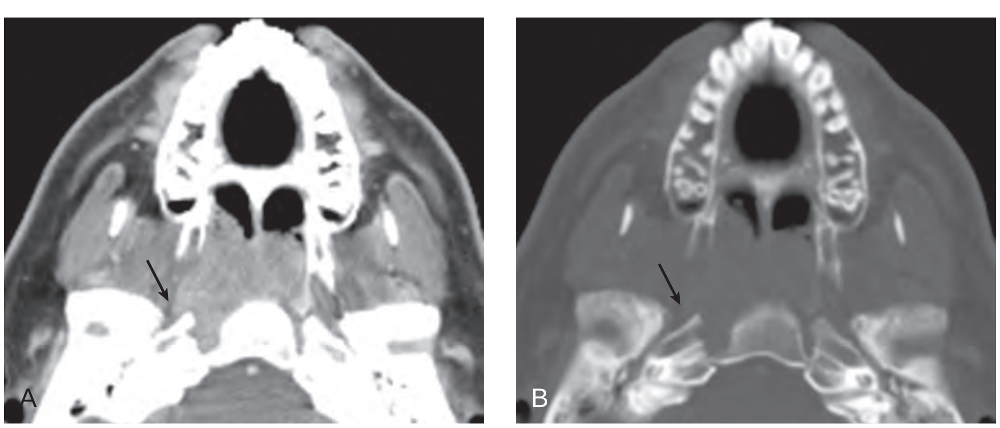

Figure 9.32 A computed tomography scan. **A**, Soft tissue. **B**, Bone window showing widening of the petroclival fissure by a nasopharyngeal carcinoma (*arrow*).

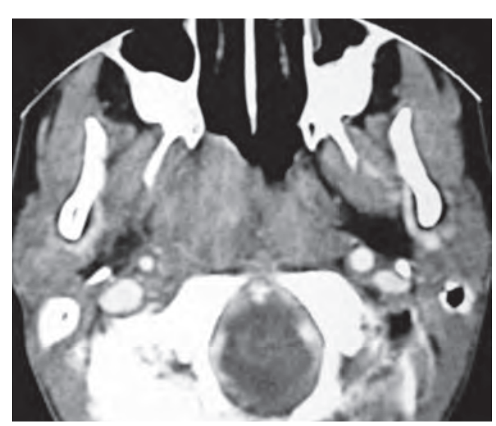

Figure 9.33 An axial postcontrast computed tomography scan showing invasion of the right parapharyngeal space by a nasopharyngeal carcinoma.

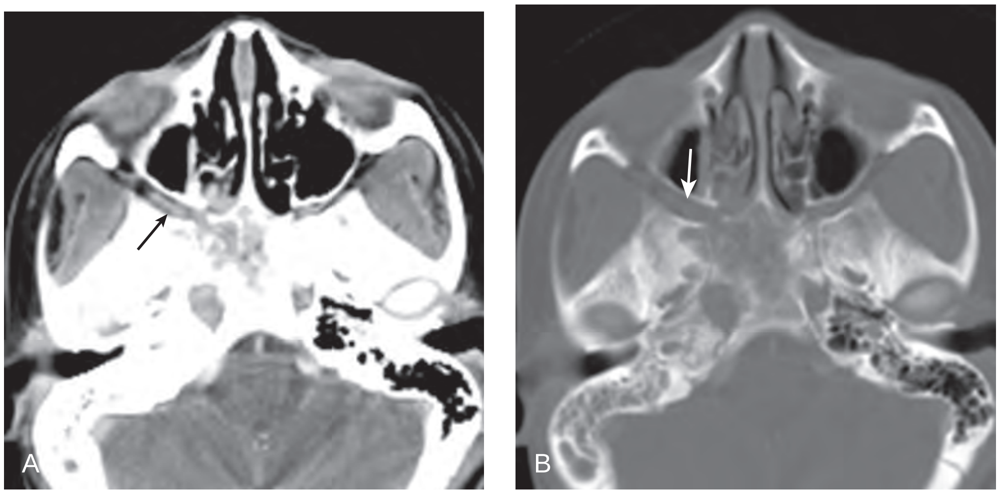

Figure 9.34 An axial postcontrast computed tomography scan. **A**, Arrow shows abnormal soft tissue in the right pterygopalatine fossa on the soft-tissue window. **B**, Arrow shows widening of the bony right pterygopalatine fossa on the bone window.

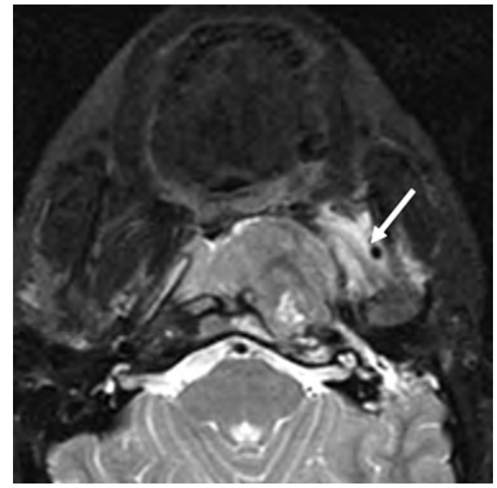

Figure 9.35 A T2-weighted magnetic resonance imaging scan showing involvement of the left masticator space by a nasopharyngeal carcinoma. Arrow indicates tumor extension.

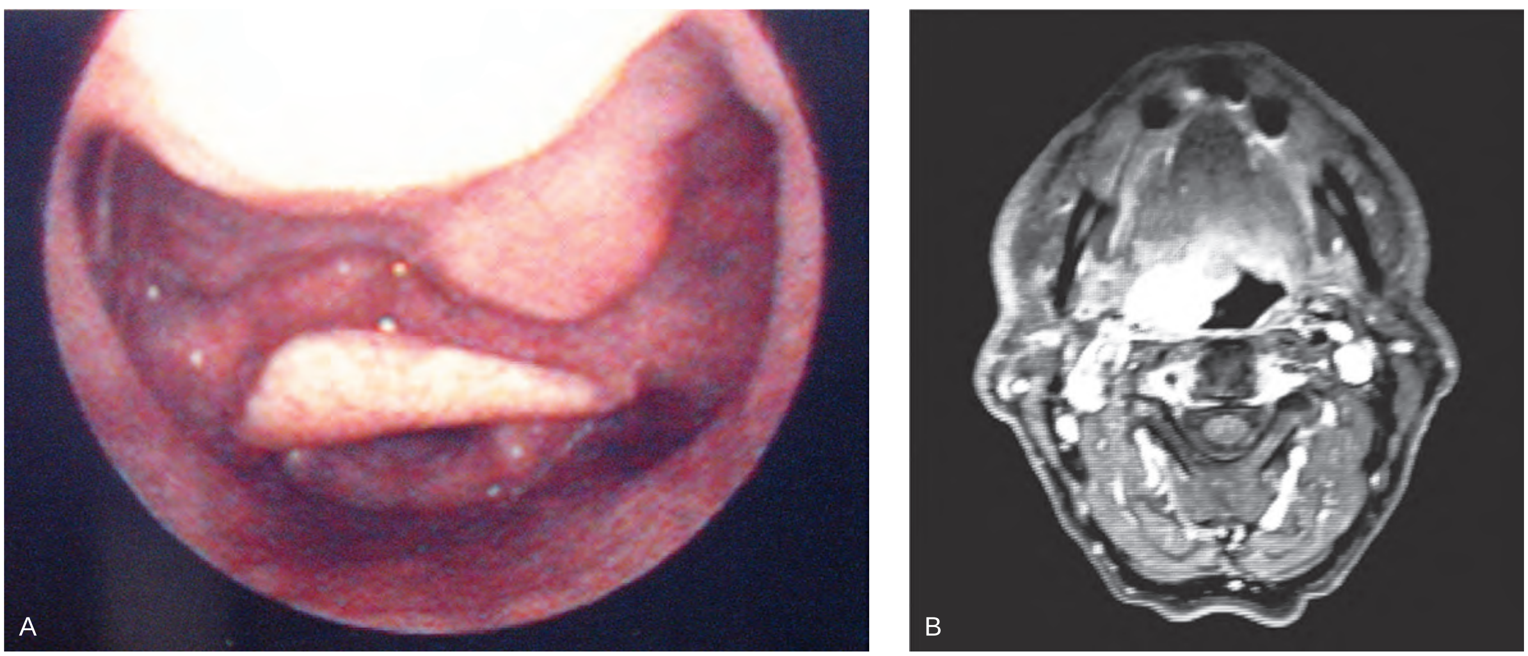

Figure 9.36 A minor salivary gland tumor of the right base of the tongue. **A**, Endoscopic view. **B**, Postcontrast, T1-weighted magnetic resonance imaging scan shows contrast-enhancing tumor of the right base of the tongue.

of tongue musculature is seen, but tumors of minor salivary gland origin can be well defined and difficult to differentiate from benign lesions (Fig. 9.36). Imaging for lesions of the base of the tongue can be helpful in delineating the relationship of the tumor to the neurovascular bundles and for assessment of submucosal spread to the tonsillar fossa, soft palate, and pharyngeal wall (Fig. 9.37). Sagittal T1-weighted precontrast MRI is useful for assessment of preepiglottic space invasion by a base of tongue tumor. Tumors of the tonsil also can spread submucosally to the base of the tongue via the glossotonsillar fold or to the soft palate (Fig. 9.38). More advanced tumors can extend into the masticator space, involve the mandible, or encase the internal carotid artery.

Early staged carcinomas of the hypopharynx are rare but are evident on CT scans as an area of thickened, enhancing mucosa (Fig. 9.39). Tumors of the medial wall of the pyriform sinus can extend into the paraglottic space and cause vocal cord fixation (Fig. 9.40). Laterally, the thyroid cartilage is located immediately beneath the pyriform mucosa and is at risk for invasion by cancer. Involvement of the apex of the pyriform sinus places the cricoid cartilage at risk for invasion, and the adjacent recurrent laryngeal nerve can be directly invaded by tumor in the upper tracheoesophageal groove (Fig. 9.41). Early carcinomas of the posterior pharyngeal wall appear as an area of subtle thickening with enhancement on contrast-enhanced CT, but more advanced tumors are readily apparent because of asymmetry (Fig. 9.42). Imaging can be useful in delineating the relationship of these tumors to the prevertebral musculature if obvious infiltration is present, but early invasion often is difficult to define. Postcricoid tumors can spread submucosally to involve the circumference of the hypopharynx and often extend caudally into the cervical esophagus (Fig. 9.43). Involvement of the cervical esophagus appears as asymmetric thickening of its wall, which is more easily seen on T2-weighted MRI. Extraluminal spread is indicated by obliteration of fat in the upper tracheoesophageal groove.

Radiographic imaging with CT or MRI is especially important in the evaluation of the regional lymph nodes in patients with cancer of the pharynx, because retropharyngeal lymph nodes are not amenable to clinical evaluation or ultrasound

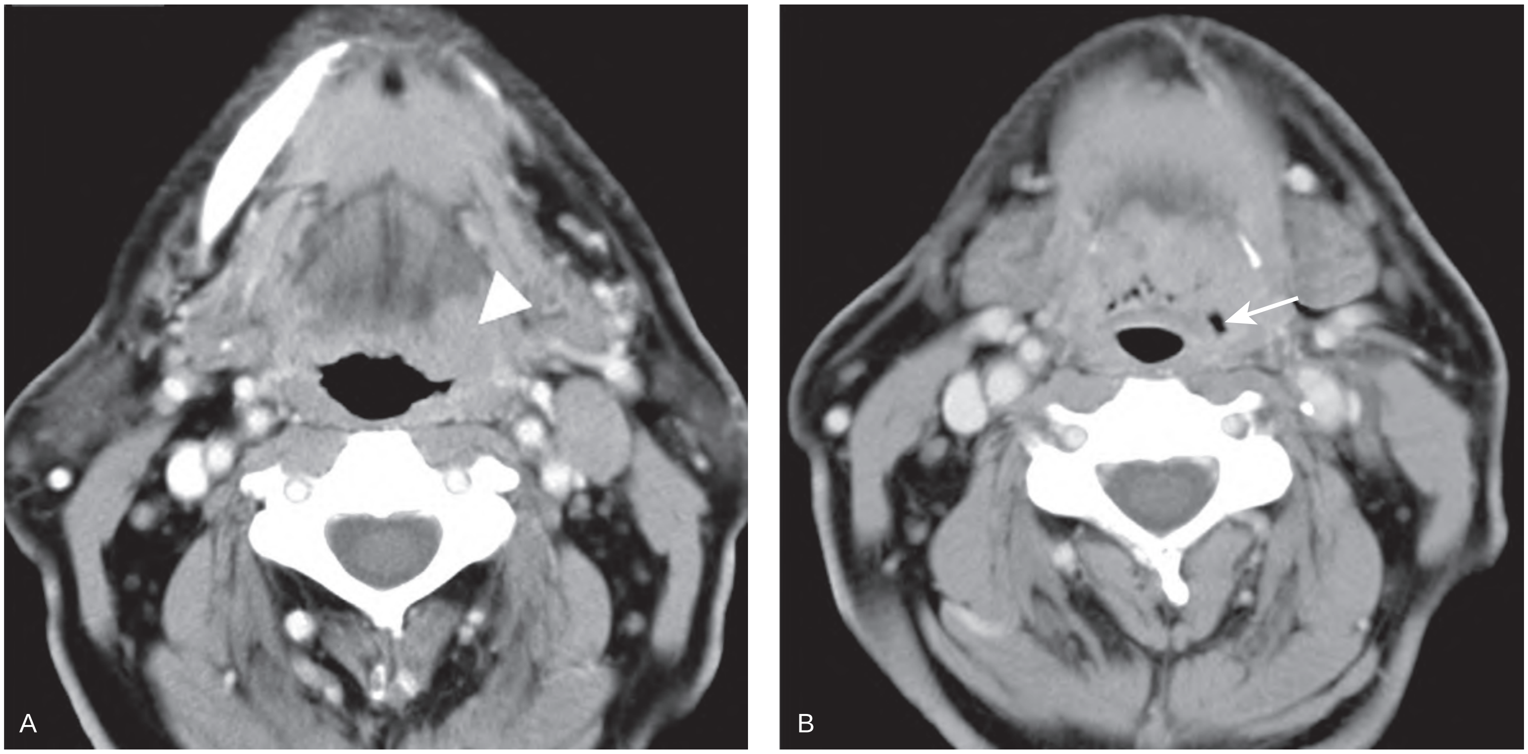

Figure 9.37 A contrast-enhanced computed tomography scan showing spread of a tumor (**A**) at the left base of the tongue (*arrowhead*) and (**B**) laterally to the lateral pharyngeal wall (*arrow*).

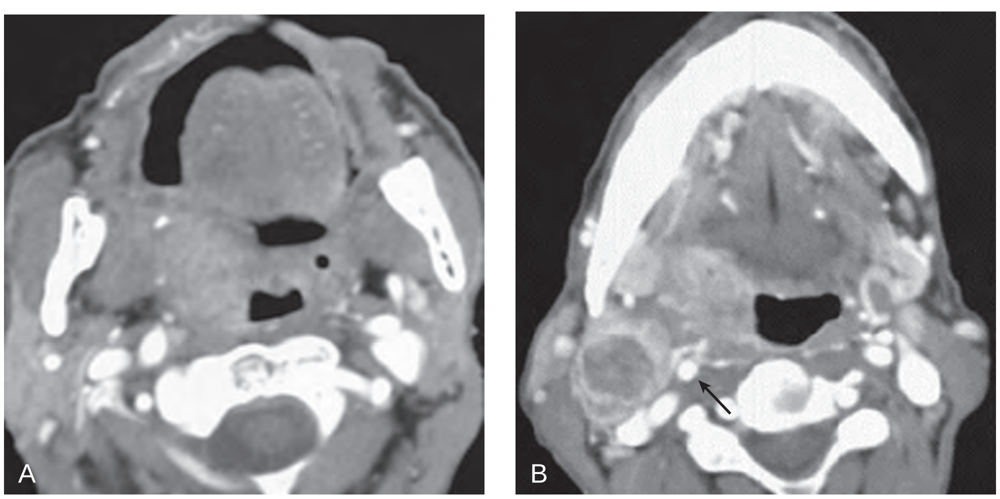

Figure 9.38 Patterns of spread of a tonsillar carcinoma shown on a computed tomography scan. **A**, Invasion of the right soft palate. **B**, Involvement of the base of the tongue. Note the location of the right internal carotid artery shown by the arrow between the primary tumor and the necrotic right level II lymph node. The artery is at risk for encasement or involvement by advanced tonsil cancer.

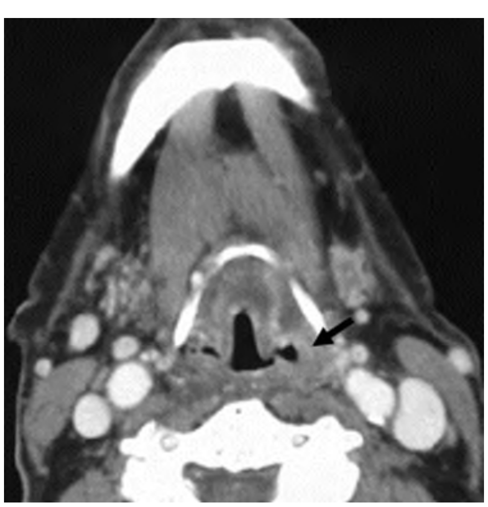

Figure 9.39 A contrast-enhanced axial computed tomography scan showing thickened, enhancing reverse-C–shaped lesion of the left pyriform sinus (*arrow*). Note the pencil-thin mucosa of the normal contralateral pyriform sinus for comparison.

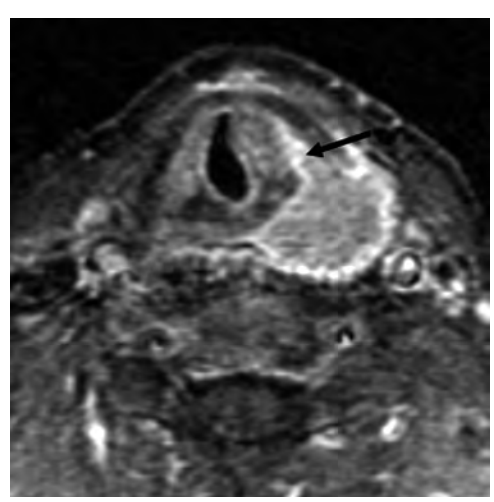

Figure 9.40 A postcontrast T1-weighted fat-saturated magnetic resonance imaging scan showing extension of a left pyriform sinus tumor into the left paraglottic space (*arrow*).

Figure 9.41 A contrast-enhanced computed tomography scan showing (**A**) a locally advanced tumor of the right pyriform sinus that has (**B**) destroyed the posterior aspect of the lamina of the right thyroid cartilage and (**C**) the right half of the cricoid cartilage with obvious extralaryngeal soft-tissue extension.

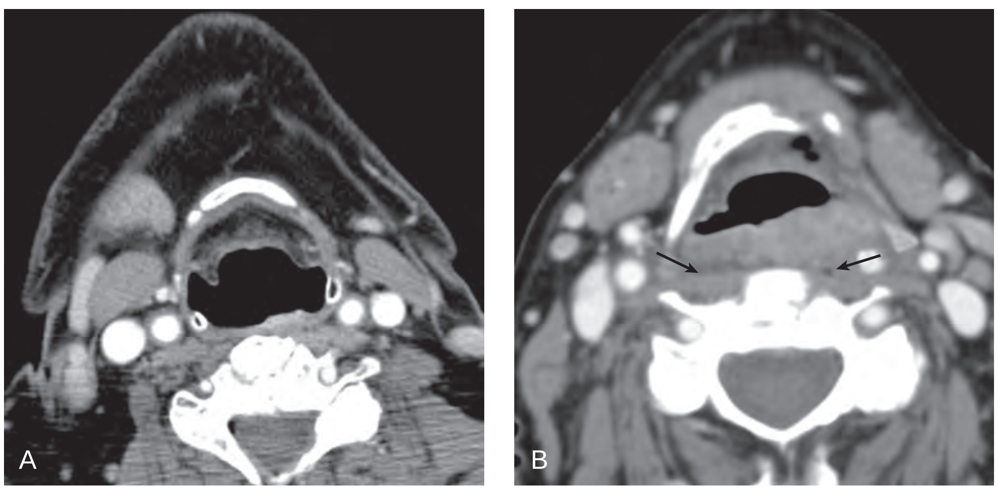

Figure 9.42 A carcinoma of the posterior pharyngeal wall seen on a contrast-enhanced computed tomography scan. **A**, Early tumor of the left posterior pharyngeal wall. **B**, Obvious abnormal thickening and enhancement of the posterior pharyngeal wall in a more advanced tumor. Note the presence of a fat plane (*arrows*) overlying the prevertebral musculature.

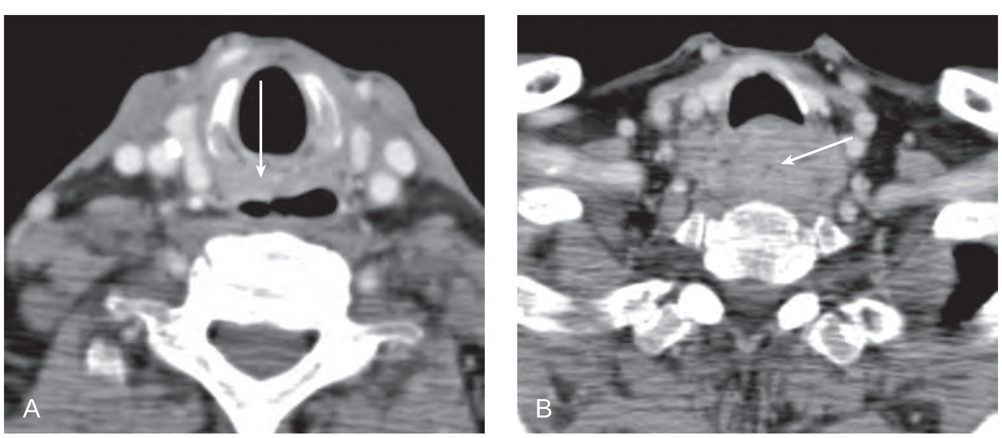

Figure 9.43 A contrast-enhanced computed tomography scan showing (**A**) abnormal soft tissue thickening of the postcricoid hypopharynx (*arrow*) and (**B**) circumferential extension caudad into the cervical esophagus (*arrow* shows esophageal lumen).

examination. The lateral retropharyngeal lymph nodes (which have a normal size of less than 8 mm in adults) are located between the prevertebral musculature (longus colli and capitis muscles) and the internal carotid artery. These lymph nodes are at risk for involvement by tumors of the nasopharynx and tonsil (Fig. 9.44). Cystic cervical nodal metastases are a hallmark of primary cancer of Waldeyer's ring and should not be confused with "branchial cleft cyst." A cystic neck mass in an adult always should be considered indicative of metastatic disease unless proven otherwise. Branchial cleft cysts have homogeneous content and a thin and smooth wall that does not enhance unless the cyst is infected. Cystic metastases, on the other hand, usually have a thick wall with rim enhancement, may be multiple, and are most often associated with a demonstrable primary tumor (Fig. 9.45).

Positron emission tomography (PET) scanning has become essential in pretreatment assessment of the extent of primary tumor and regional lymph node metastases (Fig. 9.46). It is

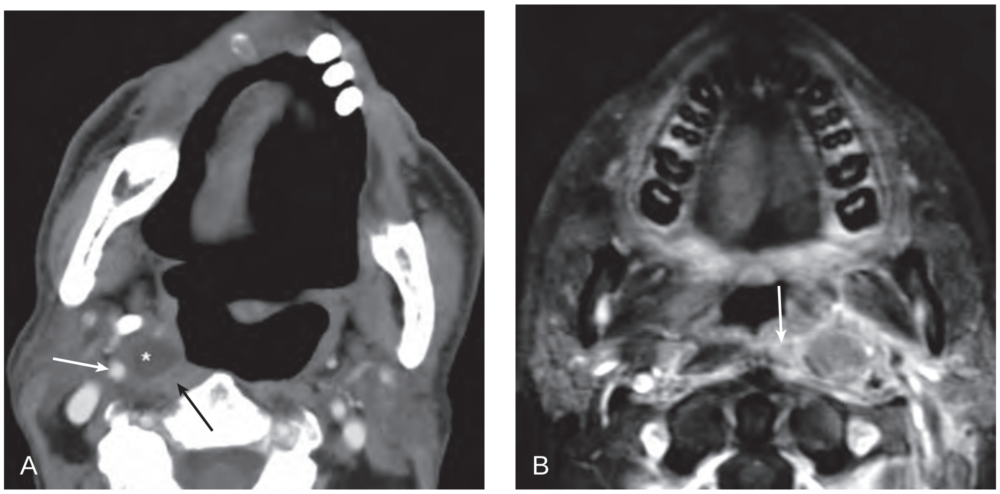

Figure 9.44 Lateral retropharyngeal lymphadenopathy. **A**, Contrast-enhanced computed tomography scan showing a cystic right lateral retropharyngeal lymph node from a primary tonsil squamous cell carcinoma. Note the location of the lymph node (*) between the prevertebral musculature (*black arrow*) and the internal carotid artery (*white arrow*). **B**, A postcontrast axial T1-weighted fat-saturated magnetic resonance imaging scan showing a metastatic left retropharyngeal node from a nasopharyngeal primary tumor. The prevertebral musculature (*white arrow*) is infiltrated by extracapsular spread from the retropharyngeal lymph node.

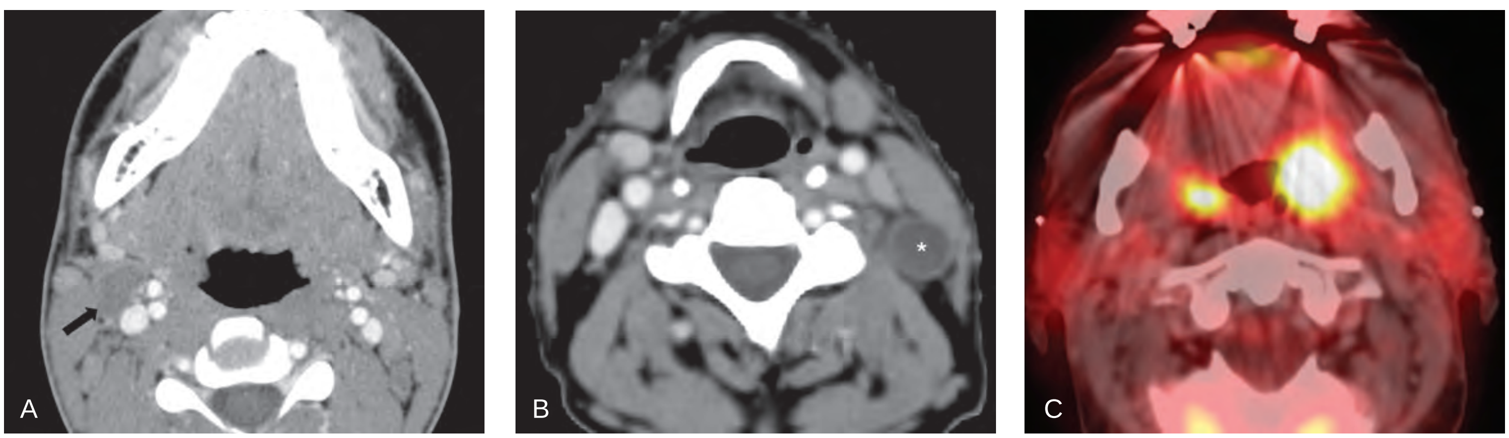

Figure 9.45 **A**, A contrast-enhanced computed tomography scan showing a cystic homogeneous mass with a thin nonenhancing rim (*arrow*) in a young male patient indicative of a branchial cleft cyst of the right neck. **B**, A computed tomography simulation film showing a cystic mass with an enhancing rim (*) in the left side of the neck consistent with cystic nodal metastasis. This patient had bilateral cystic nodal metastases from a primary carcinoma of the left tonsil evident on a positron emission tomography scan (**C**).

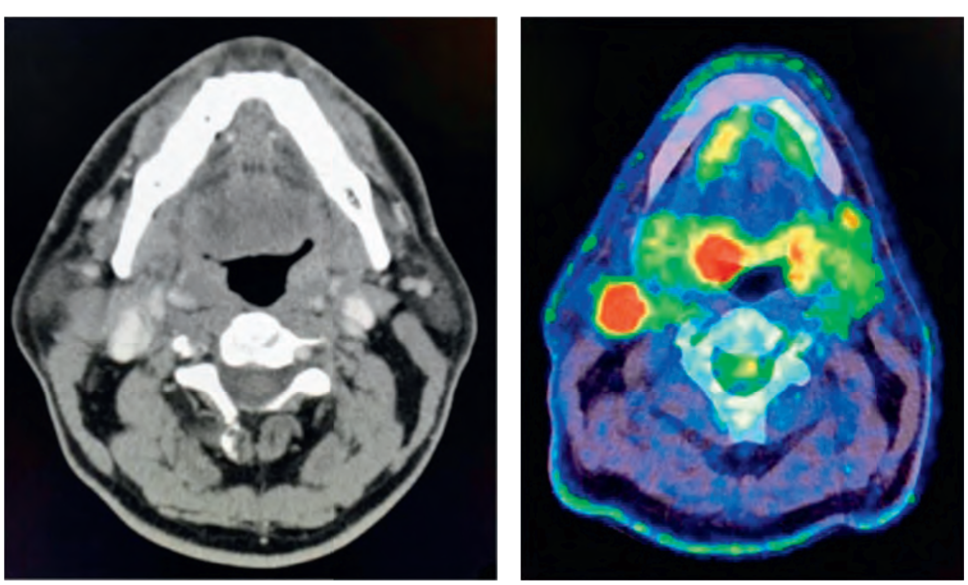

Figure 9.46 Pretreatment imaging with a contrast-enhanced CT scan and a PET scan for carcinoma of the tonsil.

regularly used for radiation treatment planning and is an essential imaging study for evaluating response to therapy in cancers of the oropharynx and other sites treated by chemoradiotherapy. Generally, PET scan assessment should be done at least 3 months following completion of treatment.

Pathologic Evaluation

Nasopharynx

Nasopharyngeal squamous cell carcinoma is classified by the World Health Organization into keratinizing, nonkeratinizing, and undifferentiated types (Table 9.1). Nonkeratinizing carcinoma is further subclassified into differentiated and undifferentiated subtypes. The undifferentiated subtype of nonkeratinizing carcinoma is particularly common in southeast Asia, where it represents 15% to 20% of all cancers and is thought to be associated with EBV infection. EBV can be detected in the tumor cells of almost all nonkeratinizing carcinoma but rarely in keratinizing NPC (Fig. 9.47).

Differentiated nonkeratinizing nasopharyngeal carcinomas display a stratified appearance and distinct cell margins. By contrast, undifferentiated tumors exhibit clusters of poorly delineated or syncytial cells bearing large vesicular oval nuclei and scant eosinophilic cytoplasm. The undifferentiated variant often features a conspicuous lymphoid infiltrate, accounting for the obsolete (and misleading) term “lymphoepithelioma” (Fig. 9.48). Both subtypes are immunoreactive with cytokeratin. The epithelial nature of this tumor is underscored by the fact that tumor cells express cytokeratin but no hematologic or lymphoid markers.

Oropharynx

Worldwide, up to 25% of head and neck squamous cell carcinomas are associated with high-risk HPV, the great majority of which are HPV 16. However, HPV serotypes 18, 31, 33, and 35 also have been associated with oropharyngeal squamous cell carcinoma. The HPV oncoproteins (E6 and E7) transform oral squamous epithelial cells. These proteins bind with p53 and Rb,

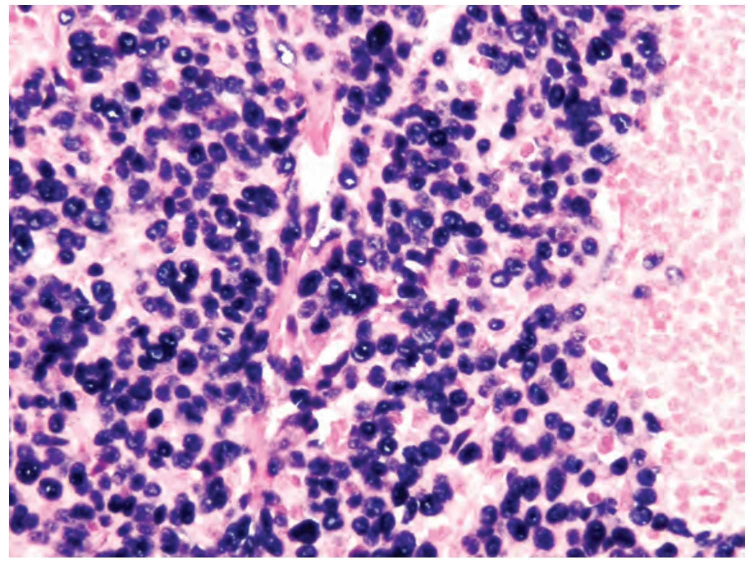

Figure 9.47 Epstein-Barr virus–encoded ribonucleic acid in situ hybridization showing strong nuclear labeling of tumor for Epstein-Barr virus in nasopharyngeal carcinoma.

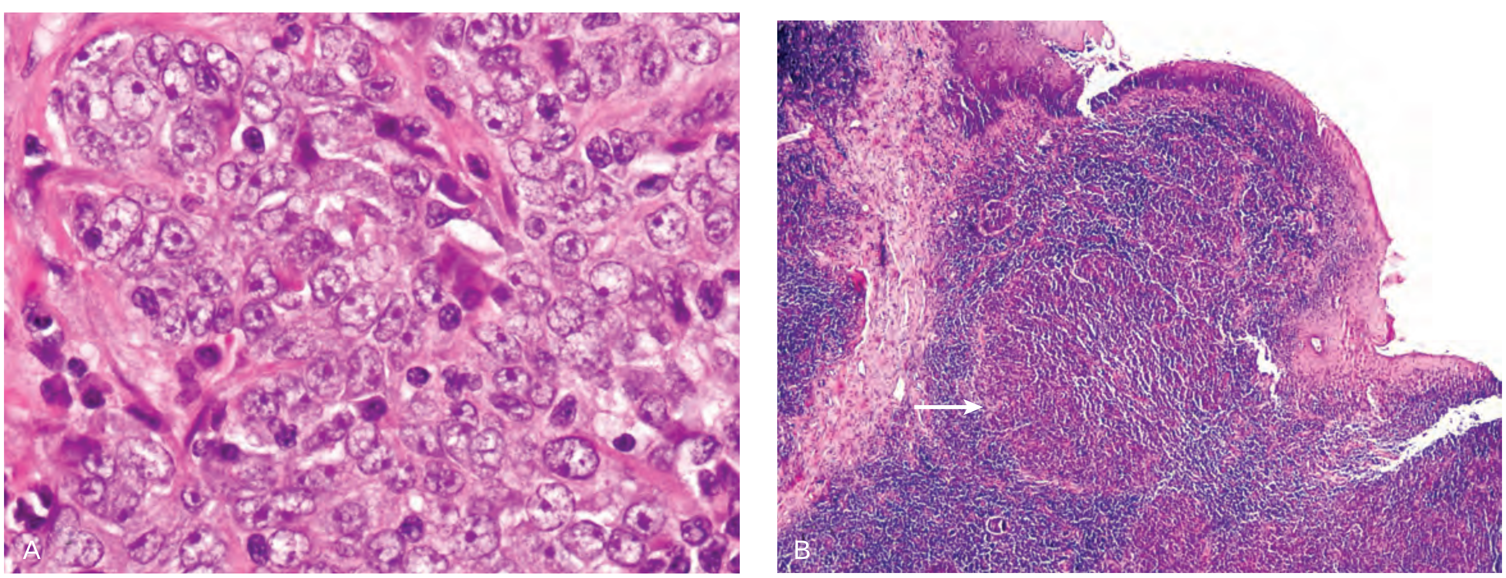

Figure 9.48 Undifferentiated nasopharyngeal carcinoma. **A**, Tumor cells growing in a nested, syncytial pattern with indistinct cell borders, open chromatin, and prominent nucleoli. (Hematoxylin-eosin stain; ×400.) **B**, Abundant lymphoid infiltrate that obscures nests of tumor cells (*arrow*). (Hematoxylin-eosin stain; ×100.)

Table 9.1 The World Health Organization (WHO) Classification of Nasopharyngeal Carcinoma (2005)

WHO 1978	WHO 1991	WHO 2005
I. Squamous cell carcinoma	I. Squamous cell carcinoma	Keratinizing squamous cell carcinoma
II. Nonkeratinizing carcinoma	II. Nonkeratinizing carcinoma a. Differentiated nonkeratinizing carcinoma	Nonkeratinizing carcinoma Differentiated
III. Undifferentiated carcinoma	b. Undifferentiated carcinoma	Undifferentiated
		Basaloid squamous cell carcinoma

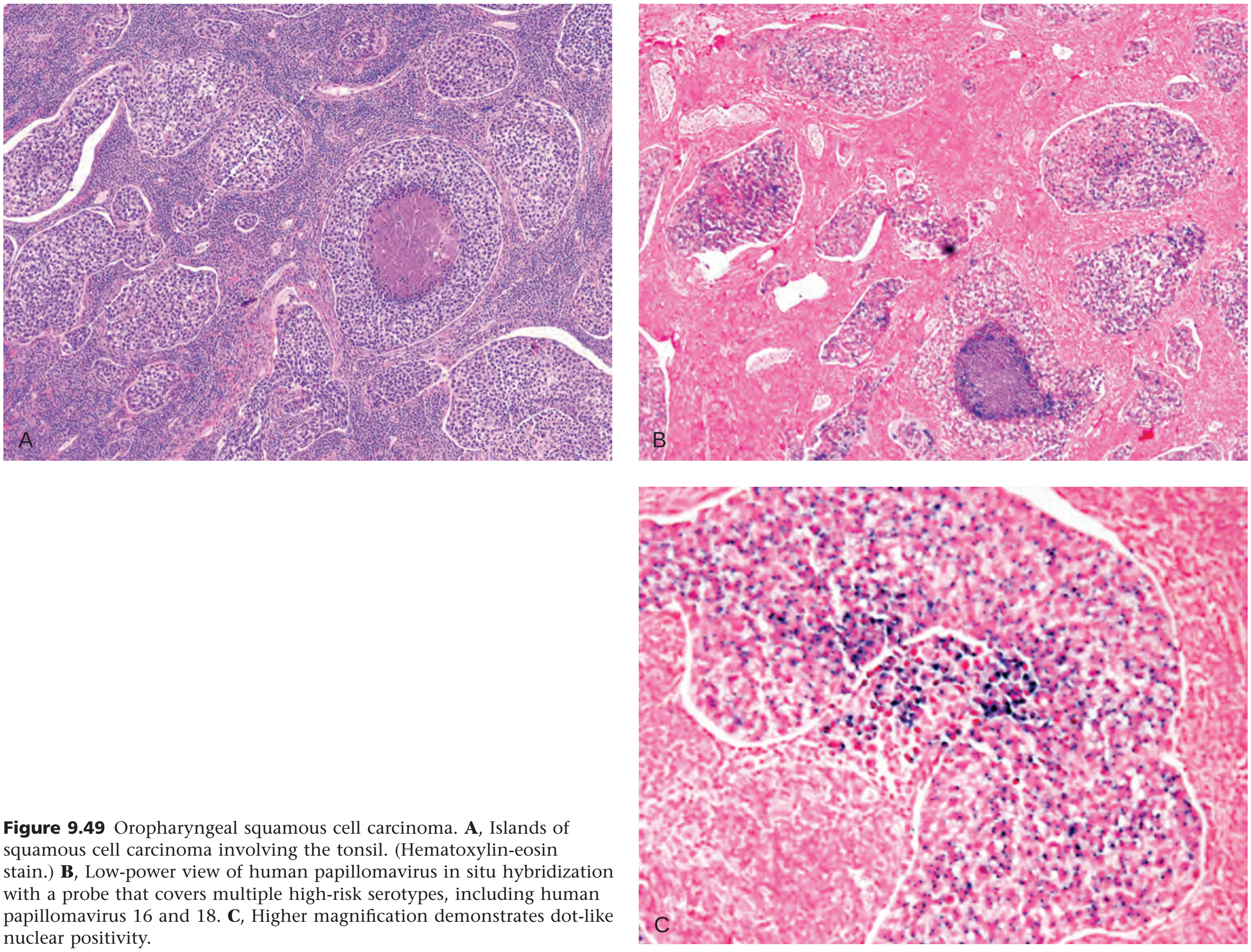

Figure 9.49 Oropharyngeal squamous cell carcinoma. **A**, Islands of squamous cell carcinoma involving the tonsil. (Hematoxylin-eosin stain.) **B**, Low-power view of human papillomavirus in situ hybridization with a probe that covers multiple high-risk serotypes, including human papillomavirus 16 and 18. **C**, Higher magnification demonstrates dot-like nuclear positivity.

respectively, interfering with their tumor suppressor functions and leading to cell cycle dysregulation and genetic instability. Immunohistochemistry for p16 is commonly used as a surrogate marker to identify HPV infection. Diffuse (>70%) and strong nuclear and cytoplasmic immunoreactivity is required to label a tumor as positive for that marker. In situ hybridization for HPV DNA (Fig. 9.49) and RNA are now available. The latter has high sensitivity and specificity and localizes to the nucleus and cytoplasm.

In the United States approximately 80% of oropharyngeal squamous cell carcinomas are associated with high-risk HPV. The tonsil is the most frequent site for these tumors, which have a basaloid morphologic appearance, are usually moderately to poorly differentiated, and have minimal to no associated keratin production. HPV-associated carcinomas in general carry a better prognosis than do their non-HPV–related counterparts. The histologic distinction between these tumors and the classic basaloid squamous cell carcinoma is not clear.

HPV-positive oropharyngeal squamous cell carcinomas are seen in a younger patient population, two to three decades earlier than the usual head and neck squamous cell carcinoma population. Patients usually do not have a history of smoking or heavy alcohol consumption. These patients have a better response to treatment with superior outcomes. On the other hand, heavy smokers and drinkers who also are HPV positive do not have the same favorable outcomes.

Hypopharynx

The majority of patients with hypopharyngeal squamous cell carcinoma have a history of tobacco and alcohol consumption. The risk is especially increased in patients with heavy alcohol consumption, as is observed in southern Europe. Historically, nutritional deficiency and anemia were said to be associated with postcricoid carcinoma, as reported from Scandinavia (Plummer-Vinson syndrome). Histologically, these tumors are moderate to poorly differentiated carcinomas with significant proclivity for submucosal spread, especially distally (Fig. 9.50). Skip areas of tumor spread with additional lesions often are seen in the cervical esophagus. The hypopharynx is the most frequent site for synchronous primary tumors in the upper aerodigestive tract. Lymphatic drainage of the hypopharynx to the regional lymph nodes is profuse, and lymph node metastasis is a common feature at presentation. Consequently, management of cervical lymph nodes is integral in treatment planning.

TREATMENT

Nasopharyngeal squamous cell carcinomas, by virtue of their anatomic location and relative inaccessibility for a curative surgical resection, are generally managed by nonsurgical treatment. In addition, these tumors are highly responsive to radiotherapy and chemotherapy. Thus a combination of

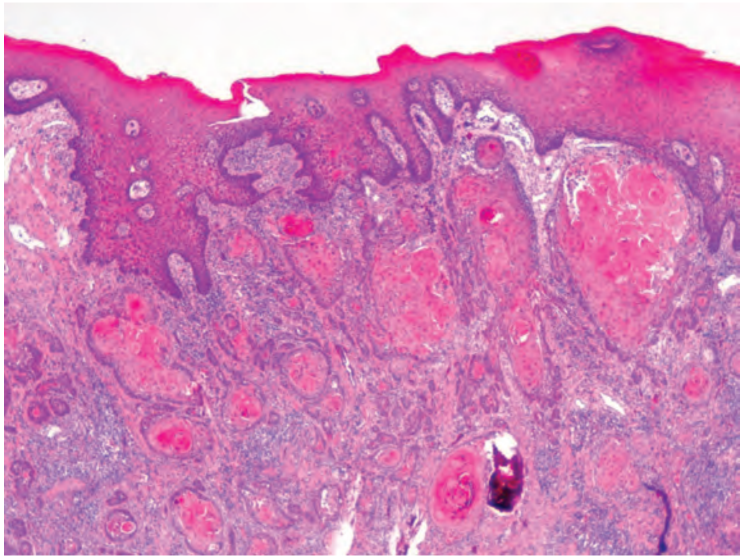

Figure 9.50 Submucosal extension of tumor in a hypopharyngeal squamous cell carcinoma (hematoxylin-eosin stain).

chemotherapy and radiotherapy remains the choice of initial definitive treatment (see Chapter 19 for details). Surgical intervention may be considered in a select group of patients for whom previous chemoradiation therapy has failed and who have a localized, well-defined, residual or recurrent cancer (confined to the mucosa and underlying soft tissues only). Similarly, neck dissection for regional metastases is considered only in the setting of residual or recurrent nodal metastases that have failed to respond to chemoradiotherapy. However, minor salivary gland tumors, angiofibromas, and other benign and malignant lesions of the nasopharynx do require surgical intervention with or without postoperative radiation therapy.

Treatment of oropharyngeal cancer is evolving with improved understanding of tumor biology, technical advances in instrumentation, and emerging data from retrospective studies and clinical trials. In general, oropharyngeal squamous cell carcinomas are responsive to primary radiation approaches with the addition of concurrent chemotherapy for advanced stage tumors. There has also been a renewed interest in surgery as a definitive treatment with or without postoperative radiation therapy with technologic advancements in transoral robotic surgery (TORS) and transoral laser microsurgery (TOLM). Traditional open approaches via mandibulotomy are reserved for recurrent disease, advanced tumors in patients who are not candidates for chemoradiation therapy, minor salivary gland tumors, and other neoplasms that are not sensitive to primary radiation approaches.

The ultimate goal for the treatment of tumors of the hypopharynx is control of the cancer. However, when feasible, preservation of the functions of speech and normal swallowing and avoidance of a tracheostomy are other desirable goals. Small and superficial lesions of the hypopharynx can be managed by external radiation therapy or endoscopic resection as definitive treatment. In select patients requiring a laryngectomy for advanced pharyngeal cancers, nonsurgical means of treatment with the aim of preservation of the larynx, using a multimodal treatment program consisting of chemotherapy and radiation therapy, should be considered. In the past two decades, an increasing number of patients with hypopharyngeal cancers requiring total laryngectomy are being treated with a larynx preservation treatment program of neoadjuvant or concurrent chemoradiotherapy, except for those with gross thyroid cartilage destruction by cancer (see Chapter 20 for details).

For patients presenting with advanced disease for whom a pharyngolaryngectomy is essential, the goals of treatment are directed at reestablishing the anatomic continuity of the alimentary tract with restoration of the patient's ability to swallow by mouth as soon as possible. However, in patients in whom the larynx is uninvolved but the extent of pharyngeal resection requires the need for immediate reconstruction, significant clinical judgment needs to be exercised for the successful outcome of such an undertaking, because postoperative aspiration becomes a major problem. In patients requiring a circumferential pharyngolaryngectomy, restoration of the continuity of the alimentary tract becomes an integral part of initial surgical treatment planning. Most patients with advanced primary tumors require multimodality treatment to enhance the chances of control of the cancer. Because of the aggressive nature of this tumor and its increased proclivity to early involvement of regional lymph nodes by metastatic disease, a combined treatment program of surgical excision of the primary tumor with or without neck dissection followed by postoperative radiation therapy with or without chemotherapy for the primary site and regional lymphatics is currently considered the standard of care.

Factors Affecting Choice of Treatment

The anticipated response to chemoradiation therapy is a key factor in the selection of initial definitive treatment. In general, early staged pharyngeal squamous cell carcinomas are responsive to radiation, with only a small proportion of patients requiring salvage surgery. Therefore most of these cancers, and particularly those where the larynx is at risk, are currently treated with radiation or chemoradiation therapy. This approach is supported by several prospective trials (see Chapter 20) and has become the standard of care.

Current treatment guidelines for oropharynx squamous cell carcinoma are in a state of evolution in light of the favorable prognostic influence of HPV status and with the goal of reducing treatment-related morbidity. Quantifying risk in this patient population has affected the choice of treatment. Specifically, risk stratification studies have attempted to identify "low-risk" patients who may be candidates for de-escalation of treatment. In the Radiation Therapy and Oncology Group trial (RTOG–0129), HPV-positive patients who were nonsmokers or with a smoking history of less than 10 pack-years and/or N0–N2a were considered "low risk" with a 3-year overall survival rate of 93%. T1-T3N0-N2b HPV-positive patients were identified as having a very low risk of distant metastases and therefore could be possible candidates for radiation alone. Surgery as a de-escalation strategy is also under evaluation. In 2009 the US Food and Drug Administration approved transoral robotic surgery for the treatment of T1–T2 oropharyngeal carcinoma. Proponents of surgery argue that TORS may achieve better functional outcomes compared with primary radiation approaches by reducing radiotherapy doses or eliminating chemotherapy. This is being tested in a randomized controlled trial at this time. TORS represents an attractive option in highly selected patients in whom surgery as a single modality of treatment may be all that is required for disease control. On the other hand, utilizing primary surgery as a deintensifying approach may be counterproductive if adjuvant radiation with possible concurrent chemotherapy is required based on the pathologic results of the resected primary tumor and neck nodes. This may be the case with a positive margin resection or if metastatic lymph nodes are found to have extranodal spread. Several de-escalation

strategies are currently being evaluated in ongoing clinical trials, and they will need to show long-term better functional outcomes and at least equally good tumor control rates. Although concurrent chemoradiation is recommend for advanced stage tumors, selected deeply infiltrating endophytic tumors have a lower probability of complete response to chemoradiation and may be better treated with initial surgical resection. Very advanced tumors of the oropharynx with invasion of the mandible also are best treated with initial surgery. The factors that influence the choice of treatment for squamous cell carcinoma of the hypopharynx are related to the tumor, the patient, and the treatment team. Primary site, T stage, local extension, circumferential extent, cephalo-caudad extent, multifocality, extent of laryngeal invasion, histology, and involvement of regional lymph nodes are important tumor factors that would influence the decision regarding initial treatment. Invasion of the larynx with fixation of the vocal cords clearly puts the larynx in jeopardy. Early staged tumors of the hypopharynx may be treated by external beam radiation therapy alone or endoscopic laser resection with or without neck dissection and postoperative radiation therapy. Lesions that are not suitable for endoscopic resection where the larynx is not involved may be candidates for a partial laryngopharyngectomy. Patients in whom a laryngectomy is required for resection of a hypopharyngeal carcinoma are candidates for organ preservation treatment with chemoradiation given sequentially or concurrently. Very advanced tumors of the hypopharynx with invasion of the thyroid or cricoid cartilage require a pharyngolaryngectomy with appropriate reconstruction and postoperative adjuvant treatment. Tumors of the postcricoid region or lesions of the pharyngeal wall with circumferential involvement have a high risk of development of stricture following chemoradiation and should be considered for initial surgery.

With regard to patient factors, general status of health, airway compromise, and pulmonary function are vitally important. Patients with chronic obstructive pulmonary disease are poor candidates for consideration of an endoscopic or open partial laryngopharyngectomy because their ability to handle resulting postoperative aspiration is poor. Thus the possibility of extended pharyngeal resections with a partial laryngectomy is exceedingly small in patients who have poor pulmonary reserve. Similarly, the choice of reconstructive procedures for restoration of the anatomic continuity of the alimentary tract depends on various patient factors. These factors include availability of regional cutaneous and myocutaneous flaps, the status of peripheral vessels to permit the use of microvascular composite free flaps, and the availability of the stomach in patients who require a pharyngolaryngoesophagectomy for large tumors with extension to the cervical esophagus. In addition, a patient's habits, lifestyle, compliance, and preference are other factors to be considered.

Availability of a multidisciplinary surgical and comprehensive head and neck oncology team is the most important physician-related factor that influences the successful outcome of a comprehensive treatment program. These factors include surgical skills, especially endoscopic diagnostic capabilities; skills in laser resection and robotic surgery; experience in open conservation surgery; and experience in contemporary reconstructive techniques, including microvascular surgery as well as the availability of a postoperative swallowing and speech rehabilitation team. On the other hand, for nonsurgical organ preservation treatments, excellence in multidisciplinary management, including expertise in medical oncology and radiation oncology and availability of a speech and swallowing rehabilitation team, is essential for a successful outcome.

SURGICAL TREATMENT

During the past two decades, the role of initial definitive surgery in the management of oropharyngeal and hypopharyngeal carcinomas has diminished considerably. Primary surgery is reserved for highly selected patients as mentioned previously. However, surgery remains the only effective option for salvage of patients who do not respond to initial nonsurgical treatment. The management of these patients is challenging, both from the perspective of the cancer and the patient. Tumors that are resistant to chemotherapy and radiation are biologically more aggressive than those that respond, leading to higher rates of recurrence even after complete surgical resection. In addition, chemoradiated tissues heal poorly, leading to increased risk for surgical complications. Accordingly, surgical treatment planning in these patients should include the judicious use of nonirradiated vascularized regional or free flaps for reconstruction and to promote healing of radiated mucosal suture lines.

In preparing the patient for surgical resection, preoperative evaluation to assess the anatomic extent of the tumor and the functional integrity of the upper aerodigestive tract is crucial. Velopharyngeal competence and mobility of the vocal cords are best assessed by careful clinical examination and flexible nasolaryngoscopy. However, to assess the anatomic extent of the tumor; detailed radiographic imaging; examination under anesthesia; and nasopharyngoscopy, laryngoscopy, and esophagoscopy are required. Palpation of the base of the tongue and pharyngeal wall for lesions of the oropharynx provides valuable information regarding the third dimension of the tumor. Similarly, evaluation of the apex of the pyriform sinus and pharyngoesophageal junction is crucial in planning surgical resection for hypopharyngeal tumors.

Surgical Anatomy

The nasopharynx begins at the posterior choana of the nasal cavity and extends up to the free border of the soft palate. The oropharynx extends from the plane of the superior surface of the soft palate to the plane of the superior surface of the hyoid bone. The hypopharynx extends from the plane of the superior surface of the hyoid bone to the plane corresponding to the lower border of the cricoid cartilage (C6 vertebra), where it continues into the cervical esophagus. The musculature of the pharynx consists of the pharyngeal constrictors and the pharyngeal elevators. The three pharyngeal constrictor muscles are oriented in a "cup within a cup" fashion, and their fibers insert posteriorly into a midline fibrous raphe, which is attached superiorly to the pharyngeal tubercle of the occipital bone. The pharyngeal mucosa immediately superior to the level of the superior constrictor muscle is in direct contact with and is supported by a thickened pharyngobasilar fascia. This fascia is attached at the skull base to the basilar portion of the occipital bone, the petrous temporal bone along the medial border of the pharyngotympanic tube, and the posterior border of the medial pterygoid plate and pterygomandibular raphe. The pharyngeal elevators attach to the skull base and help elevate the pharynx during swallowing and breathing.

The branches of the external carotid artery provide blood supply to the pharynx via the ascending pharyngeal artery, the ascending palatine and tonsillar branches of the facial artery, the greater palatine and pharyngeal branches of the maxillary artery, and the dorsal lingual branches of the lingual artery. The pharyngeal veins drain into the internal jugular vein and lymphatics drain into the retropharyngeal and parapharyngeal

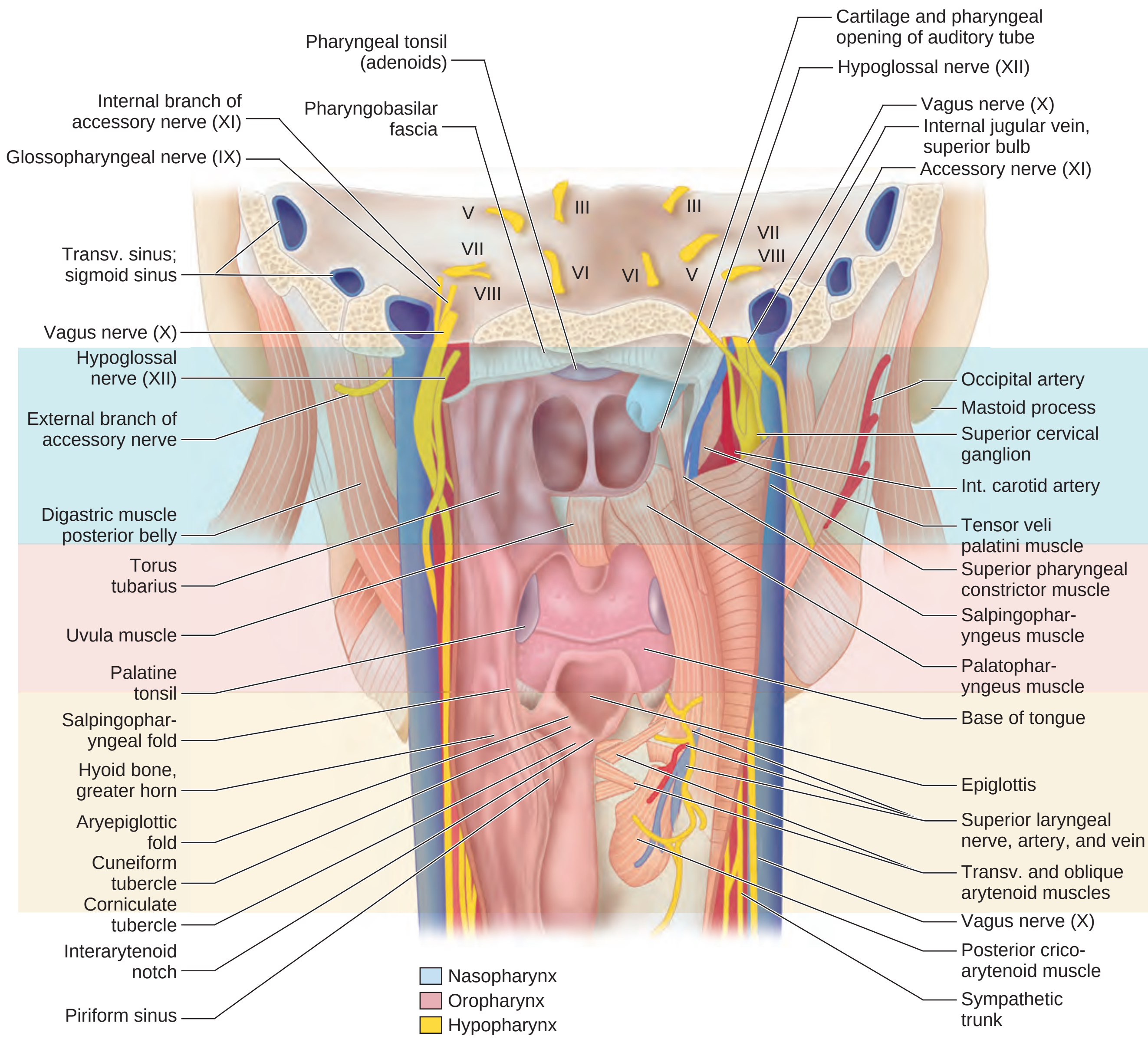

Figure 9.51 Anatomic relation of the major nerves and blood vessels to the pharynx.

nodes and the nodes at levels II, III, and IV in the neck. The branches of the pharyngeal plexus (from the IX and X cranial nerves) provide sensory and motor innervation to the pharynx. The anatomic location of the major nerves and blood vessels in relation to the pharynx is shown in Fig. 9.51.

Nasopharynx

The mucosal surface of the nasopharynx can be divided into its roof, the posterior wall, and two lateral walls. The dome-shaped roof consists of the mucosa that overlies the body of the sphenoid bone and the basilar part of the occipital bone up to the pharyngeal tubercle (clivus). Inferiorly, the mucosa of the posterior wall covers the pharyngobasilar fascia and the anterior arch of the atlas. The nasopharyngeal tonsil or adenoid is a midline lymphoid mass that is located in the roof of the nasopharynx as it curves into the posterior wall. The adenoid is relatively large at birth and generally atrophies by preadolescence. However, the adenoid may persist even as late as the seventh decade of life and can cause confusion with a nasopharyngeal tumor. The eustachian (pharyngotympanic) tube connects the tympanic cavity of the ear to the nasopharynx and serves the important function of equilibrating pressure in the middle ear. The trumpet-shaped bony part of the tube arises from the anterior tympanic wall and narrows down to the junction of the squamous and petrous parts of the temporal bone, where it lies medial to the carotid canal. The cartilaginous portion arises at this isthmus and flares out to open onto the lateral wall of the nasopharynx through a triangular opening that lies immediately anterior to the small mound of lymphoid tissue (torus tubarius) and the pharyngeal recess (fossa of Rosenmüller). The petrous portion of the temporal bone and the levator veli palatini muscle are located posteromedial, while the salpingopharyngeus muscle is attached to the inferior lip of the tube underlying the mucosal fold that bounds the tubal opening. The tensor veli palatini muscle separates the eustachian tube anterolaterally from the otic ganglion, V3 and its branches, the middle meningeal artery, and the chorda tympani. The superior surface of the soft palate constitutes the floor of the nasopharynx, which is deficient posteriorly as it continues into the oropharynx. The lateral wall of the nasopharynx is in close anatomic proximity to the lower cranial nerves (IX–XII), which are at risk for involvement not only by tumor but also from long-term sequelae of radiation.

Oropharynx

The soft palate is a musculoaponeurotic curtain that hangs down from the posterior border of the hard palate and maintains velopharyngeal competence during speech and swallowing. The

midline uvula is located on the free inferior border, and the sides blend into the faucial arches that attach to the lateral pharyngeal walls. The mucosa of the soft palate is of the stratified squamous type, and the submucosa contains minor salivary glands that mainly secrete mucus. The muscles of the soft palate include the palatopharyngeus, palatoglossus, tensor veli palatini, levator veli palatini, and musculus uvulae. Resection of the musculature of the soft palate often will lead to dysfunction of the eustachian tube and middle ear effusion, requiring placement of ventilation tubes. Passavant's ridge, which is formed by contraction of the fibers of the superior constrictor muscle, often compensates for the loss of the soft palate and provides velopharyngeal competence. The pterygomandibular raphe provides attachment to the superior constrictor and buccinator muscles. It extends from the pterygoid hamulus, which is located immediately posterior and medial to the upper alveolar process, to the posterior end of the mylohyoid line on the lingual aspect of the mandible. The inferior alveolar nerve lies underneath the mucosal fold formed by the raphe and is at risk for involvement by tumors.

The pharyngeal tonsils are located in the tonsillar fossae, which are bounded by the anterior and posterior tonsillar pillars and contain the palatoglossus and palatopharyngeus muscles, respectively. The pharyngeal tonsils blend inferiorly into the lingual tonsils at the base of the tongue. These tonsils, together with nasopharyngeal adenoid tissue, form Waldeyer's ring. The deep or lateral boundary of the tonsillar fossa is composed of the superior constrictor and stylopharyngeus muscles, and the tonsil is separated from the pharyngeal wall by loose areolar tissue. The arterial supply to the tonsils is provided primarily by the superior and inferior tonsillar arteries, which are branches of the facial and palatine arteries. The pharyngeal tonsils are lined by squamous mucosa that forms crypts within aggregations of lymphoid tissue. These crypts can harbor a "clinically occult" primary squamous cell carcinoma that may be asymptomatic. Larger tumors extend beyond the tonsil and may involve the pharyngeal wall, base of the tongue, larynx, or parapharyngeal space.

The base of the tongue is demarcated by the circumvallate papillae anteriorly and the valleculae (pharyngoepiglottic folds) posteriorly and is bounded laterally by the tonsillar fossae. The muscles of the base of the tongue consist of the extrinsic muscles (hyoglossus, styloglossus, and genioglossus) and the intrinsic muscles. Minor salivary glands and aggregates of lymphoid tissue (lingual tonsil) are dispersed throughout its submucosa. The base of the tongue, along with other suprahyoid muscles, have an important function in laryngeal elevation during the pharyngeal phase of deglutition. Therefore resection of any part of the base of the tongue has the potential to alter swallowing. The sensory supply of the base of the tongue is from the glossopharyngeal nerve. Reconstruction of surgical defects of the base of tongue therefore ideally is accomplished with primary closure, because insensate flaps may increase the risk for aspiration.

Hypopharynx

The paired pyriform sinuses, the postcricoid region, and the posterior pharyngeal wall compose the hypopharynx. The hypopharynx is indented anteriorly by the larynx so that the paired pyriform sinuses lie lateral to the larynx on each side. The lateral wall of the pyriform sinus is bounded by the lamina of the thyroid cartilage and the thyrohyoid membrane, while its apex is in close relationship to the upper border of the cricoid cartilage. The internal branch of the superior laryngeal nerve enters the larynx through the thyrohyoid membrane and lies under the mucosa of the superior aspect of the pyriform sinus, while the recurrent laryngeal nerve lies in close anatomic proximity to the apex of the pyriform sinus. The lateral walls of the pyriform sinus continue into the posterior pharyngeal wall, and therefore circumferential spread of tumors is not uncommon. The postcricoid region of the hypopharynx lies on the posterior wall of the larynx immediately inferior to the arytenoids and extends up to the lower border of the cricoid cartilage. Sensory supply to the mucosa of the pyriform sinus is provided by the superior laryngeal and glossopharyngeal nerves. The pyriform sinuses have a rich lymphatic network primarily draining to ipsilateral levels II and III lymph nodes. Contralateral metastases from invasion of the medial wall of the pyriform sinus are not uncommon.

SURGICAL APPROACHES

Nasopharynx

The surgical approach to lesions of the nasopharynx is difficult and inadequate because of the location of the nasopharynx, which complicates access. Small superficial and well-demarcated lesions can be approached endoscopically. Larger lesions, malignant tumors, and recurrent squamous cell carcinomas require open access for wider exposure and satisfactory resection. The surgical approaches to the nasopharynx are listed in Box 9.1.

The choice of a particular approach is dictated by the extent and location of the tumor. The endonasal endoscopic approach is suitable for small superficial and localized malignant tumors, without bone invasion, and larger benign lesions, such as angiofibromas. The peroral transpalatal approach may be used for small angiofibromas and other benign lesions. The exposure provided by the sublabial, LeFort osteotomy, and medial maxillectomy approaches is limited and often unsatisfactory. For lesions of the nasopharynx extending to the lateral wall and pterygopalatine fossa, the maxillary swing approach provides excellent exposure for a satisfactory and safe resection (for details see Chapter 6). Tumors of the lower part of the nasopharynx with lateral extension to the infratemporal fossa require a mandibulotomy approach. Massive tumors of the nasopharynx with extension to the paranasal sinuses, such as chondrosarcomas, may require a maxillectomy approach with consideration of immediate reconstruction of the surgical defect with a free flap.

Oropharynx

In contrast to the nasopharynx, small superficial and well-circumscribed tumors of the tonsil, soft palate, and pharyngeal wall can be approached satisfactorily through the open mouth.

Box 9.1 Surgical Approaches to the Nasopharynx

- Endonasal endoscopic
- Endoscope-assisted transcranial
- Peroral-transpalatal
- Sublabial-transnasal
- LeFort osteotomy
- Medial maxillectomy
- Maxillary swing
- Mandibulotomy
- Maxillectomy

Surgical excision may be performed with the use of a head light and electrocautery, the robot (TORS), or a CO_2 laser either with a handpiece or the microscope (TOLM). Larger lesions of the tonsil, pharyngeal wall, and base of the tongue may be considered for TORS or TOLM if the equipment and expertise is available. Alternatively, large tumors of the base of tongue not involving the mandible can be resected through a mandibulotomy approach. A transhyoid or lateral pharyngotomy is rarely used because it provides limited exposure and incurs significant postoperative functional morbidity. Advanced tumors with invasion of the mandible require a composite resection with a segmental mandibulectomy. Similarly advanced tumors of the base of the tongue with invasion of the larynx require a laryngectomy with appropriate reconstruction.

Hypopharynx

A small, relatively superficial primary tumor of the posterior pharyngeal wall can be excised perorally by TORS or TOLM or through a transhyoid pharyngotomy. The surgical defect may simply be left open to granulate by secondary intention, or a split-thickness skin graft may be used in such a situation. However, when the full-thickness defect of the posterior pharyngeal wall is of a substantial dimension, the need for immediate reconstruction becomes obvious. The choices of reconstruction lie between a regional myocutaneous flap or a microvascular free flap. Although a pectoralis major myocutaneous flap can be used in this setting, it is often too bulky and is detrimental in the subsequent restoration of the patient's ability to swallow by mouth. On the other hand, a microvascular composite anterolateral thigh (ALT) or radial forearm fasciocutaneous flap (RFFF) is an ideal method of reconstructing full-thickness defects of the posterior pharyngeal wall of large dimensions.

Patients with primary tumors of the pyriform sinus with limited extension to adjacent sites or the larynx are candidates for consideration of TOLM or an open partial laryngopharyngectomy as long as their pulmonary functions are satisfactory. For the successful performance of a partial laryngopharyngectomy, the primary tumor of the pyriform sinus should be limited to that site without extension to the apex of the pyriform sinus. The tumor may involve the adjacent supraglottic larynx and in select patients may even cause fixation of the vocal cord as long as the lesion does not cross the midline. However, due to the potential of significant swallowing dysfunction and aspiration, patients with such extensive tumors are generally treated nonsurgically with chemoradiotherapy, keeping surgery in reserve for salvage by total laryngopharyngectomy. Invasion of the thyroid cartilage in general is considered a contraindication for a partial laryngopharyngectomy as well as larynx-preserving chemoradiotherapy program. Invasion of the postcricoid region is an obvious contraindication to larynx-preserving surgery. Similarly, deep invasion into the musculature of the base of the tongue is also a contraindication for a partial laryngopharyngectomy. In general, young and vigorous patients with good pulmonary function are considered suitable candidates.

Advanced tumors of the pyriform sinus or pharyngeal wall or primary postcricoid tumors require a pharyngectomy with a total laryngectomy. The need for a circumferential pharyngectomy depends on the surface extent of the primary tumor. Patients with primary tumors of the cervical esophagus and lesions of the hypopharynx with significant extension into the cervical esophagus require a pharyngolaryngoesophagectomy with immediate appropriate reconstruction (Fig. 9.52). Patients with synchronous multifocal lesions also are candidates for a pharyngolaryngoesophagectomy.

Figure 9.52 Surgical specimen of carcinoma of the right pyriform sinus with circumferential involvement and extension to cervical esophagus.

The need for reconstructive surgery and the choice of the technique selected depend on the size and extent of the surgical defect. Small superficial defects may be left open to granulate and epithelialize. Small full-thickness defects can be repaired with skin grafts. For larger partial pharyngeal defects, the choice of reconstruction is between a regional myocutaneous flap and ALT or RFFF free flaps. However, for circumferential repair, the choices for reconstruction include a tubed RFFF or ALT free flap, a free jejunum graft, or gastric transposition with a pharyngogastrostomy. Multistaged reconstructive procedures employed in the past are no longer used. Obviously, free tissue transfer of a segment of the jejunum, fasciocutaneous flap, or gastric transposition provides immediate reconstruction for circumferential defects in a single-stage operation. The pectoralis myocutaneous flap, radial forearm flap, or anterolateral thigh free flap are most satisfactory for partial pharyngeal repair. Partial pharyngeal repair can also be performed with a free mucosal flap using either split jejunum or the gastric wall.

OPEN SURGICAL PROCEDURES FOR THE NASOPHARYNX

Surgical access to the nasopharyngeal and retromaxillary region is dictated by the size and location of the tumor. Small, centrally located tumors can be approached through the palate. Larger and lateral lesions may require a medial maxillectomy or maxillary swing approach. The procedures illustrated here for angiofibromas can also be used for resection of malignant tumors of a similar size and location. The maxillary swing procedure is described in detail in Chapter 6.

Transpalatal Excision of a Nasopharyngeal Angiofibroma

Nasopharyngeal angiofibromas are highly vascular fibroangiomatous tumors that are most common in men during the second

decade of life. Nasal obstruction or epistaxis is the usual presenting symptom. Small tumors in critical locations may produce early symptoms, or some tumors may achieve massive proportions before symptoms develop. Large angiofibromas may extend from the nasal cavity and nasopharynx to the pterygoid fossa, infratemporal fossa, and sphenoid sinus, or they may even have intracranial extension. Adequate radiographic evaluation of the lesion requires assessment with a CT scan or an MRI scan, and occasionally angiography is recommended to delineate the vascular supply to the lesion and for consideration of preoperative embolization.

The patient whose CT scan is shown in Fig. 9.53 has a small angiofibroma in the nasopharynx presenting superolateral to the soft palate on the left-hand side. A coronal view of the MRI scan demonstrates the presence of the tumor at the posterior choana and the lateral nasopharyngeal wall on the left-hand side (Fig. 9.54). A sagittal view of the MRI scan shown in Fig. 9.55 demonstrates the cephalocaudad location of the tumor between the superior margin of the posterior choana and up to the upper surface of the soft palate. Limited tumors of this nature can be excised by endoscopic endonasal technique or through a transpalatal approach without an external incision. General anesthesia is induced through an orotracheal tube. A Dingman self-retaining retractor is used to expose the hard palate and the roof of the oral cavity. An inverted U-shaped incision is outlined, extending from one maxillary tubercle to the other (Fig. 9.56). The mucosal incision is deepened through the mucoperiosteum up to the underlying bone of the hard palate. Using a periosteal elevator, the posteriorly based bipedicled mucoperiosteal palatal flap is elevated (Fig. 9.57). The blood supply to the bipedicled flap is derived from the palatine arteries on each side, which are carefully preserved as the elevation of

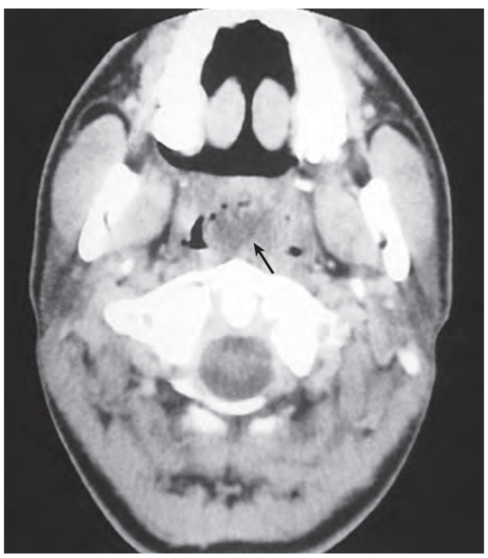

Figure 9.53 An axial view of the computed tomography scan of a patient with a small angiofibroma in the nasopharynx. Arrow shows the tumor.

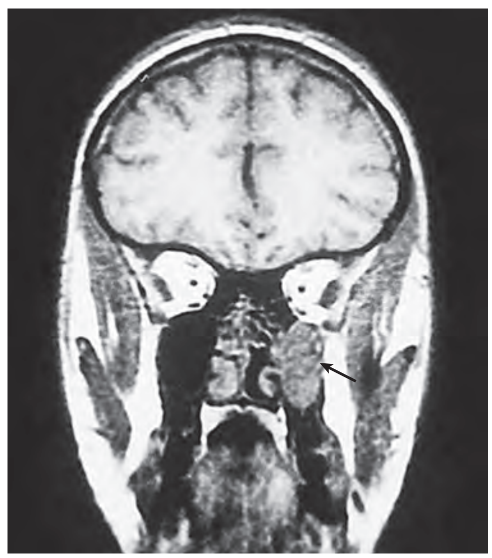

Figure 9.54 A coronal view of a magnetic resonance imaging scan showing a localized tumor at the posterior choana. Arrow shows the tumor.

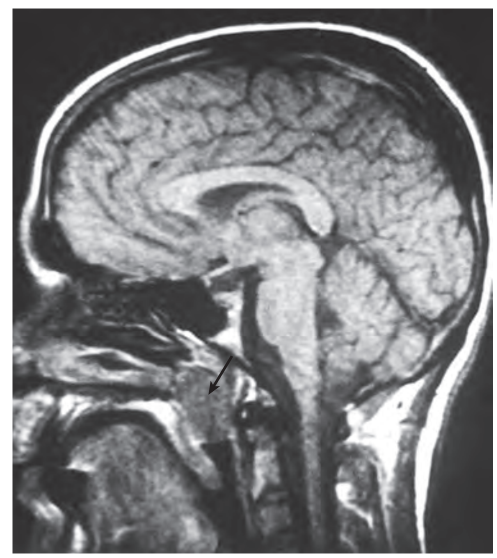

Figure 9.55 A sagittal view of a magnetic resonance imaging scan of the same patient as in Box 9.1 showing a small tumor confined to the nasopharynx. Arrow shows the tumor.

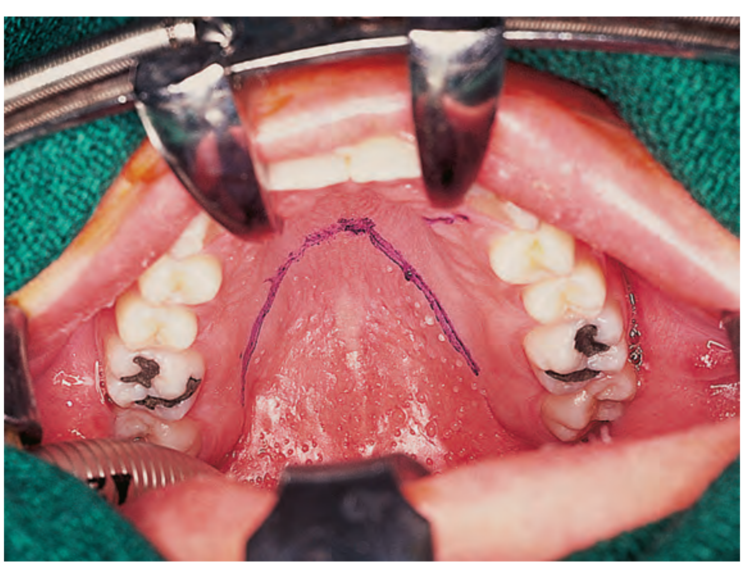

Figure 9.56 A Dingman self-retaining retractor is used to expose the hard palate and the roof of the oral cavity. An inverted U-shaped incision extending from one maxillary tubercle to the other is outlined.

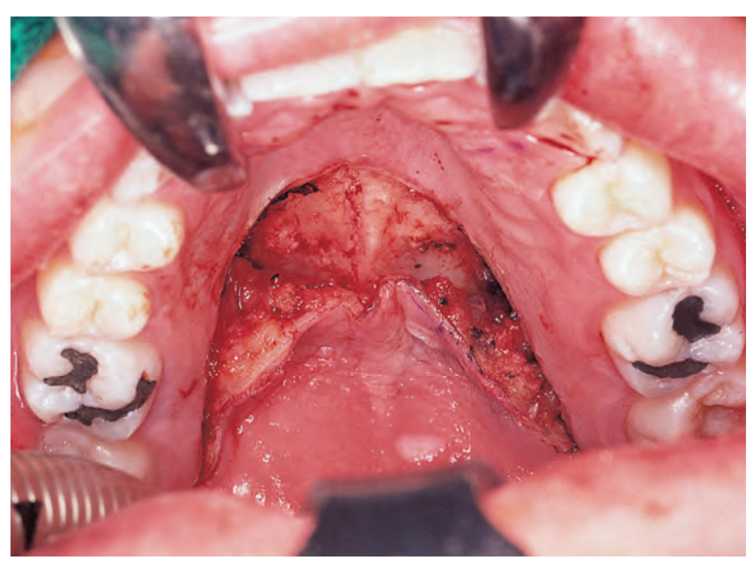

Figure 9.57 The posteriorly based bipedicled mucoperiosteal flap of the palate is elevated using a periosteal elevator.

the flap approaches the soft palate. With use of an osteotome or a high-speed drill with a burr, the posterior margin of the hard palate is excised to gain access to the region of the posterior choana on the left-hand side (Fig. 9.58). The mucoperiosteal flap is now retracted caudad with a tongue depressor to gain adequate exposure of the posterior choana and nasopharynx (Fig. 9.59). A close-up view of the exposure thus far shows the lower border of the tumor presenting from the nasopharynx on the left-hand side (Fig. 9.60). A heavy silk suture is placed through the tumor and used as a retractor to permit mobilization of the tumor (Fig. 9.61). With use of careful and diligent alternate blunt and sharp dissection with the electrocautery or a curved scissors, the tumor is mobilized from its various soft tissue attachments and dislodged from its bed in the nasopharynx (Fig. 9.62). Brisk hemorrhage from its feeding blood vessels is to be expected; however, this bleeding can be controlled easily with electrocautery or with sutures as appropriate. The blood supply usually is derived from the sphenopalatine artery, which is electrocoagulated for hemostasis. The surgical defect shown in Fig. 9.63 demonstrates the empty space created by excision of the tumor at the posterior aspect of the left nasal cavity communicating with the nasopharynx. After the wound is irrigated, the mucosal defect in the nasopharynx is left open to epithelialize by secondary intention. The mucoperiosteal bipedicled palatal flap is now returned to its position and sutured to the mucoperiosteal edge of the anterior aspect of the hard palate mucosa with interrupted Vicryl sutures (Fig. 9.64). The surgical specimen shown in Fig. 9.65 demonstrates a monobloc excision of the bilobed tumor. The cut surface shows a yellowish-white compact fibromatous tumor (Fig. 9.66).

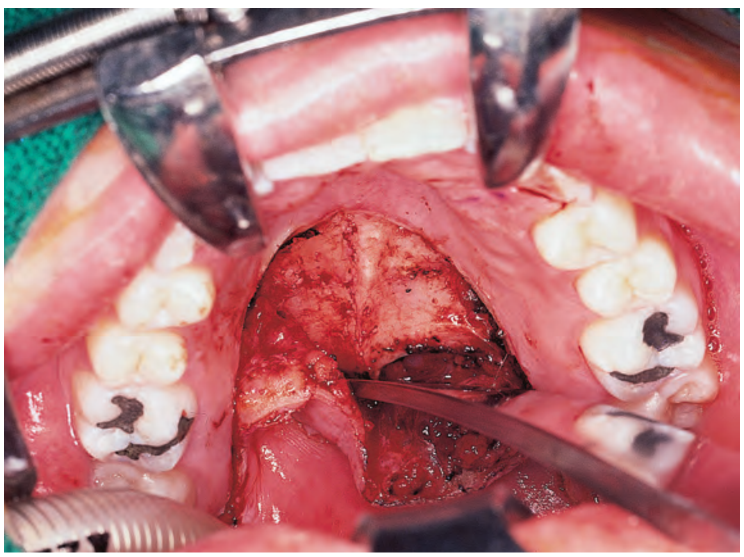

Figure 9.58 The posterior margin of the hard palate bone is excised to gain access to the region of the posterior choana on the left-hand side.

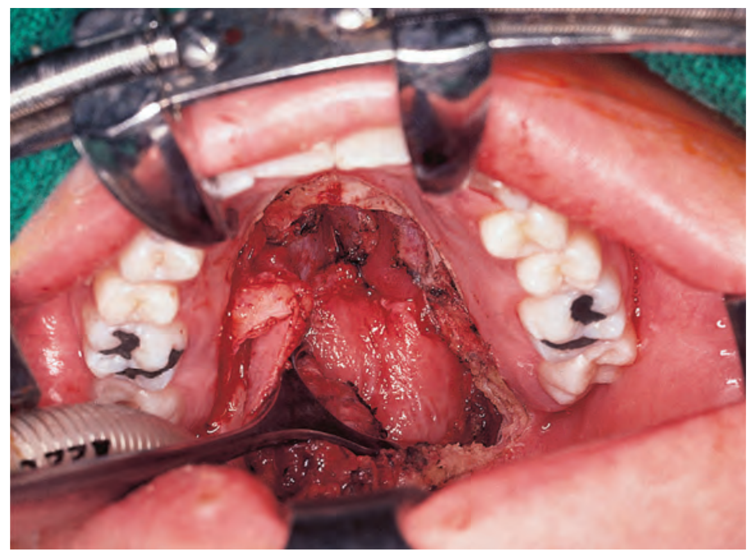

Figure 9.60 Close-up view of the exposure thus far shows the lower border of the tumor presenting from the nasopharynx on the left- hand side.

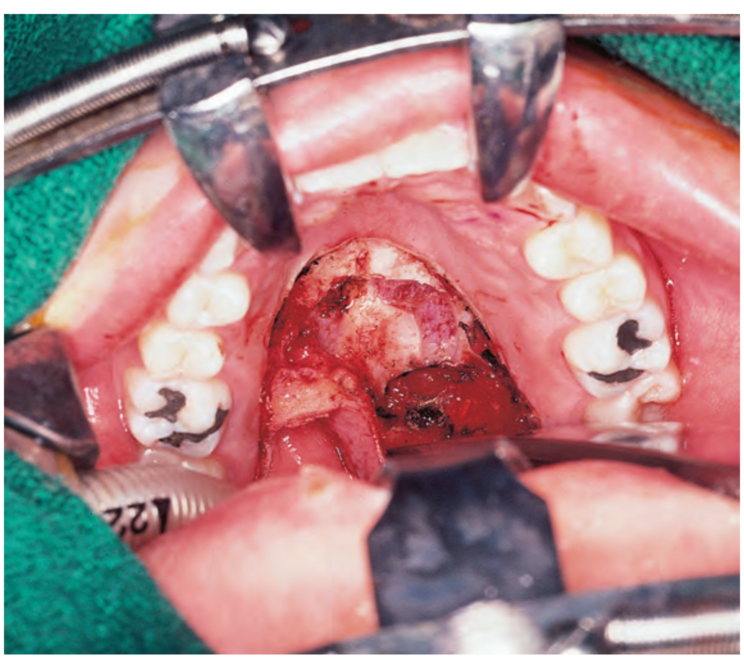

Figure 9.59 The mucoperiosteal flap is retracted caudad with a tongue depressor to gain adequate exposure of the posterior choana and nasopharynx.

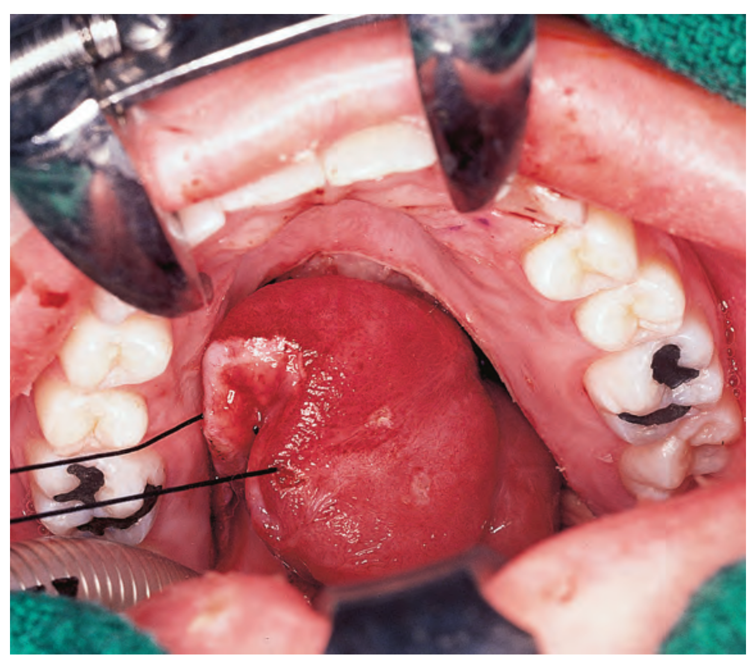

Figure 9.61 A heavy silk suture is placed through the tumor and used as a retractor to permit mobilization of the tumor.

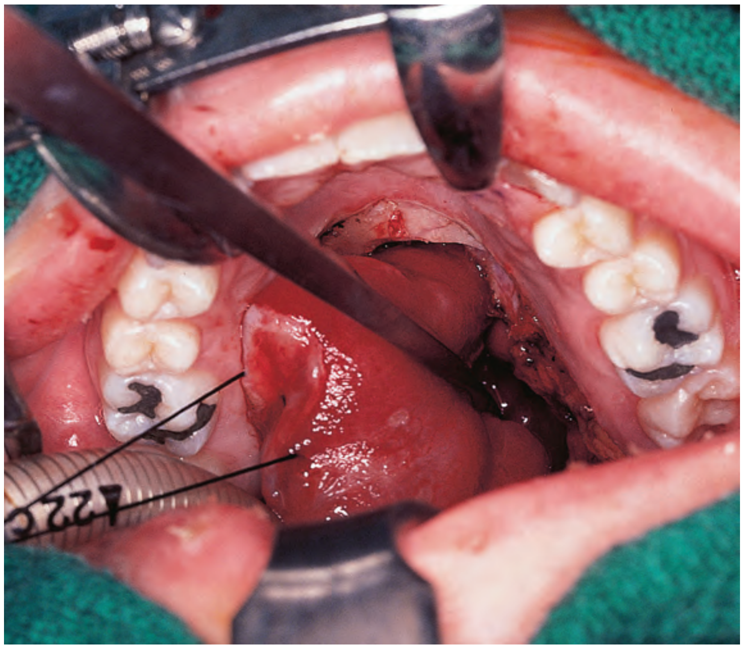

Figure 9.62 The tumor is mobilized from its various soft tissue attachments and dislodged from its bed in the nasopharynx.

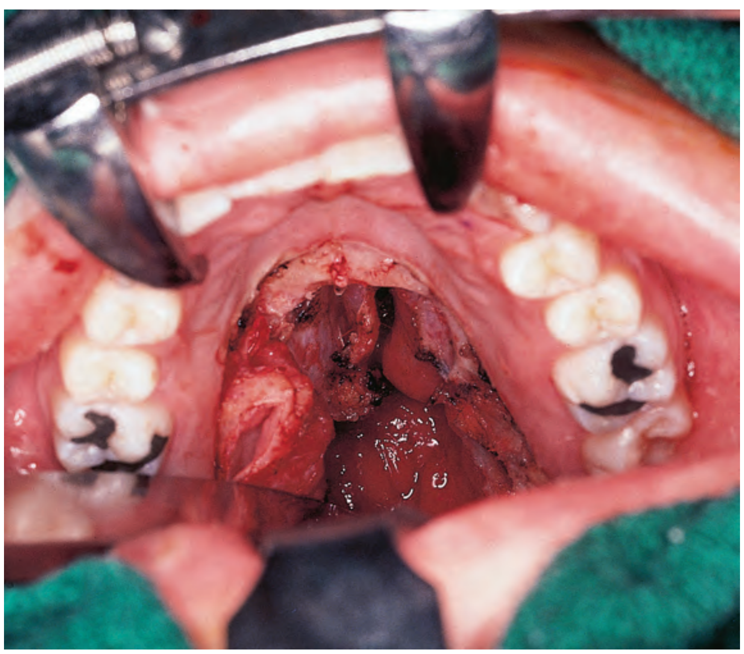

Figure 9.63 The surgical defect showing a raw area in the nasopharynx and parapharyngeal space.

Postoperative Care

Postoperative care requires intense humidification to avoid crusting and drying of clots in the nasal cavity. Oral irrigations are begun on the first postoperative day, and the patient is allowed to take liquids by mouth approximately 48 hours after surgery. A palatal obturator clasped to the upper teeth to protect the suture line may be fabricated. This protects the suture line and promotes primary healing. Irrigations in the nasal cavity are started beginning the first postoperative day and are continued until full epithelialization of the mucosa in the raw areas in the nasopharynx is demonstrated. Postoperative aesthetic and functional results of this surgical procedure are excellent with no disability in swallowing, speech, or breathing.

Figure 9.64 The mucoperiosteal bipedicled palatal flap is returned to its position and sutured to the mucoperiosteal edge of the anterior aspect of the hard palate.

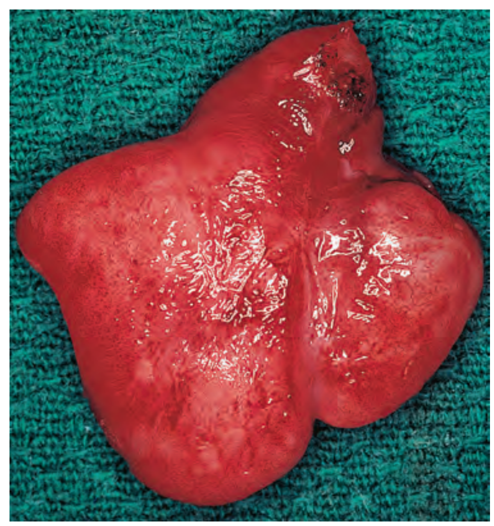

Figure 9.65 The surgical specimen shows a smooth, multilobulated tumor excised in a monobloc fashion.

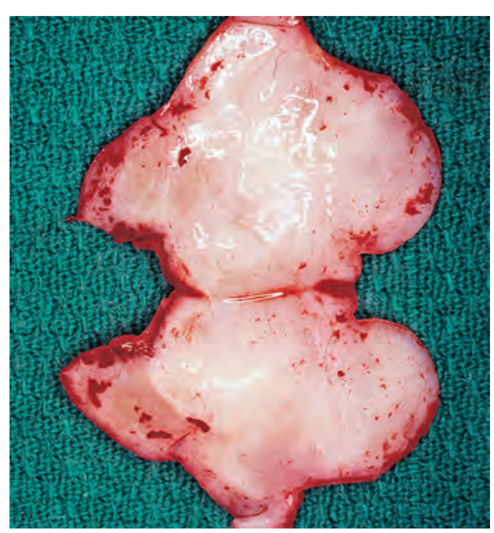

Figure 9.66 The cut surface of the surgical specimen shows a yellowish-white compact fibromatous tumor.

Transpalatal Resection of a Nasopharyngeal Tumor

Tumors and cystic lesions in the nasopharynx can be approached through a transpalatal approach to achieve wide exposure of the lesion and permit a monobloc and complete resection. The patient whose endoscopic photograph is seen in Fig. 9.67 has a submucosal mass arising from the lateral wall of the nasopharynx on the right-hand side. On endoscopic assessment, the lesion was sessile, and it was firm on palpation. MRI of the nasopharynx shows a well-circumscribed mass arising from the lateral wall of the nasopharynx on the coronal view (Fig. 9.68). The lesion appears to be adjacent to the medial pterygoid plate. On a sagittal view of the MRI, the lesion is well clear of the vault of the nasopharynx and appears to extend from the superior surface of the soft palate to the posterior wall of the nasopharynx (Fig. 9.69). This lesion can also be excised by endonasal endoscopic surgery, or by a transpalatal approach as described previously.

Excision of a Large Nasopharyngeal Angiofibroma Through a Medial Maxillectomy Approach

Larger angiofibromas extending from the nasal cavity and nasopharynx into the maxillary, ethmoid, or sphenoid sinuses require a wider exposure through a modified Weber-Ferguson incision or via a sublabial degloving approach. The patient shown in Fig. 9.70 presented with a history of nasal obstruction and epistaxis of 6 months' duration. Examination of the nasopharynx through the oral cavity with a 90-degree telescope showed a tumor projecting from the left posterior choana into the nasopharynx (Fig. 9.71). However, the posterior choana on the right-hand side is within normal limits. The CT scan in a coronal plane shows the tumor filling up the entire nasal cavity with extension into the nasopharynx and breaking through the medial wall of the maxilla into the left maxillary antrum (Fig. 9.72). Carotid angiography shows that this lesion is a vascular tumor deriving its blood supply mostly from the

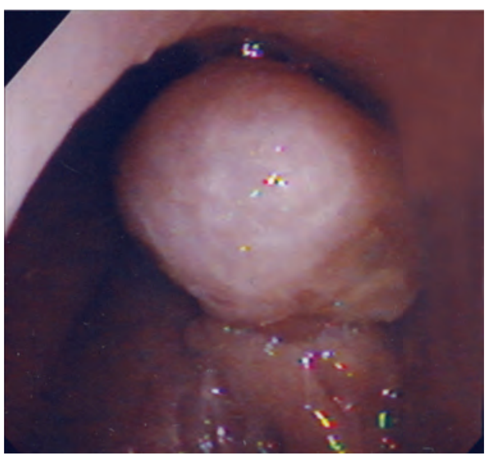

Figure 9.67 A transnasal endoscopic view showing a submucosal lesion of the lateral wall of the nasopharynx.

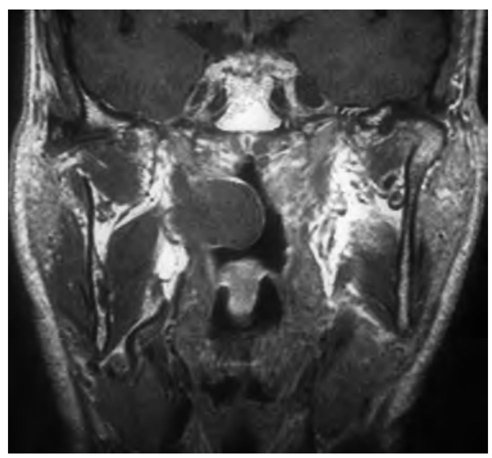

Figure 9.68 A coronal view of the magnetic resonance imaging scan shows a well-circumscribed lesion arising from the lateral wall of the nasopharynx.

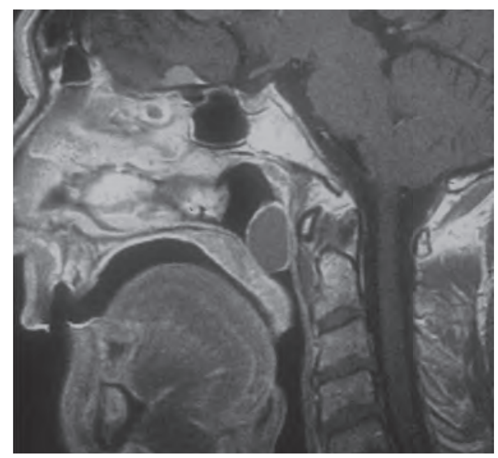

Figure 9.69 A sagittal view of the magnetic resonance imaging scan shows the lesion above the soft palate in the nasopharynx.

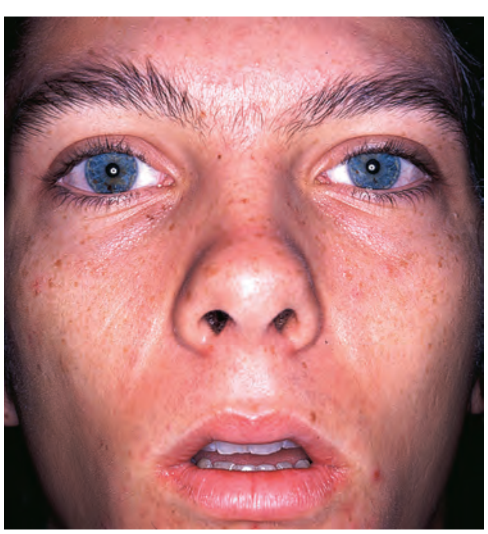

Figure 9.70 This patient presented with a history of nasal obstruction and epistaxis.

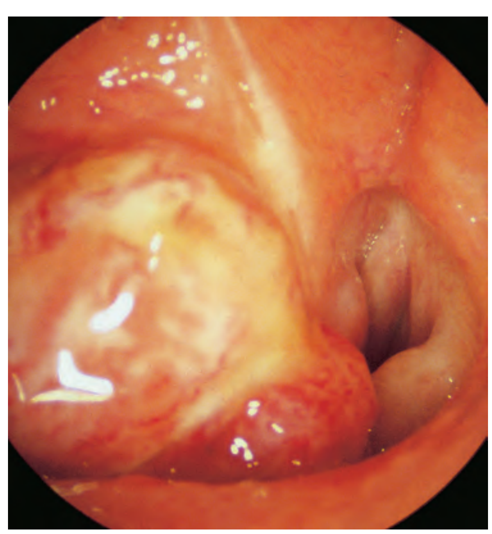

Figure 9.71 A tumor projecting from the left posterior choana into the nasopharynx.

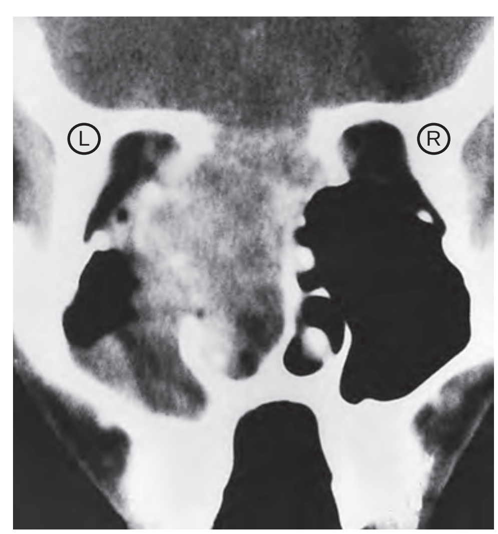

Figure 9.72 A computed tomography scan in the coronal plane shows contrast-enhancing tumor extending up to the cribriform plate.

branches of the external carotid artery through the internal maxillary and sphenopalatine vessels (Fig. 9.73). During the venous phase of the angiogram, a highly vascular lesion is demonstrated (Fig. 9.74). Selective embolization of the feeding vessels is recommended when the angiogram is performed.

The surgical approach for a nasopharyngeal angiofibroma of this extent is via a medial maxillectomy. The eye is protected with a corneal shield. A modified Weber-Ferguson incision with a Lynch extension is preferred. The incision is extended through the soft tissues of the cheek to expose the anterior wall of the maxilla (Fig. 9.75). A generous anterior wall antrotomy is made using a high-speed drill with a burr (Fig. 9.76). The opening in the anterior wall of the maxilla is made wide enough to provide good digital access to the antrum. Care is taken, however, to prevent injury to the infraorbital nerve, which is carefully preserved. The opening in the anterior wall is extended up to the nasal process of the maxilla.

In a close-up view of the exposure obtained thus far, the nodular tumor is seen presenting into the maxillary antrum from the nasal cavity (Fig. 9.77). Entry is now made into the nasal cavity by retracting the ala of the nostril to the right-hand side. Because this tumor is benign and has a rubbery consistency, it can be mobilized easily by digital maneuvers through the antrum and the nasal cavity and by palpation and mobilization of the tumor through the nasopharynx with a finger behind the soft palate into the nasopharynx. The nasal process of the maxilla is excised to create a large opening between the nasal cavity and the maxilla to facilitate delivery of the tumor. With use of appropriate digital maneuvers as previously described, the angiofibroma is removed. Meticulous attention should be given to gradual, smooth, complete removal of all the lobulations of the tumor, because it is easy to fracture the tumor and leave parts of it behind. Brisk hemorrhage is to be anticipated during mobilization and removal of the specimen. However, preoperative embolization minimizes blood loss. As soon as the specimen is delivered, all bleeding points can be controlled with electrocoagulation.

The surgical defect shows a large, hollow space in the nasal cavity, nasopharynx, and maxillary antrum (Fig. 9.78). All sharp, bony spicules are smoothed out from the edges of the surgical

Figure 9.73 The arterial phase of a carotid angiogram in the lateral view shows large feeding vessels from the external carotid artery.

Figure 9.74 The venous phase of the angiogram in the lateral view shows tumor blush, which is indicative of a highly vascular lesion.

Figure 9.75 A medial maxillectomy approach through a Weber-Ferguson incision with a Lynch extension is used.

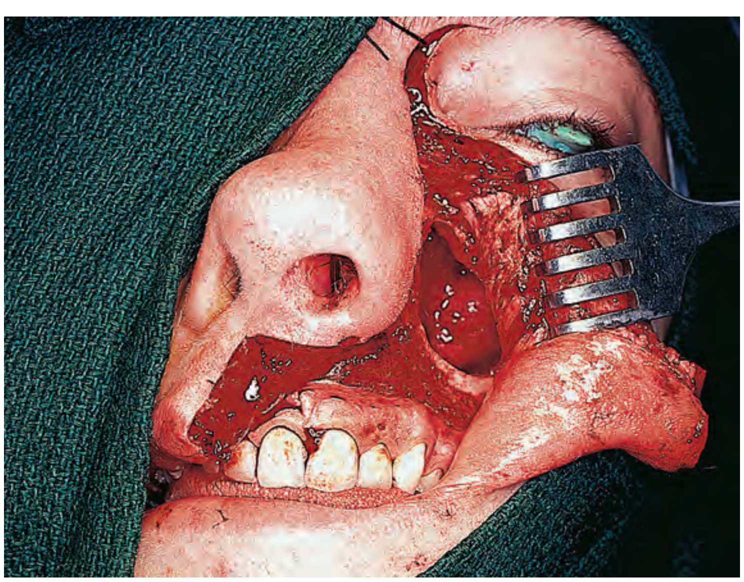

Figure 9.76 A generous anterior wall antrostomy is made using a high-speed drill with a burr.

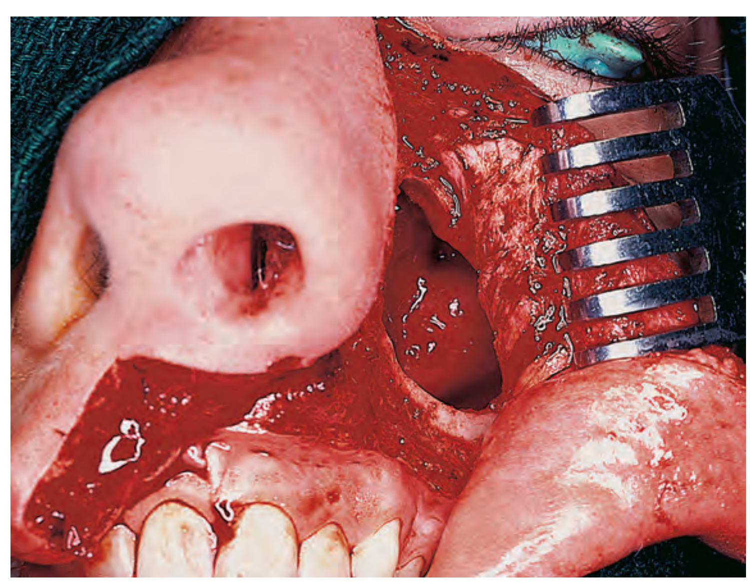

Figure 9.77 A close-up view showing the nodular tumor presenting into the maxillary antrum from the nasal cavity.

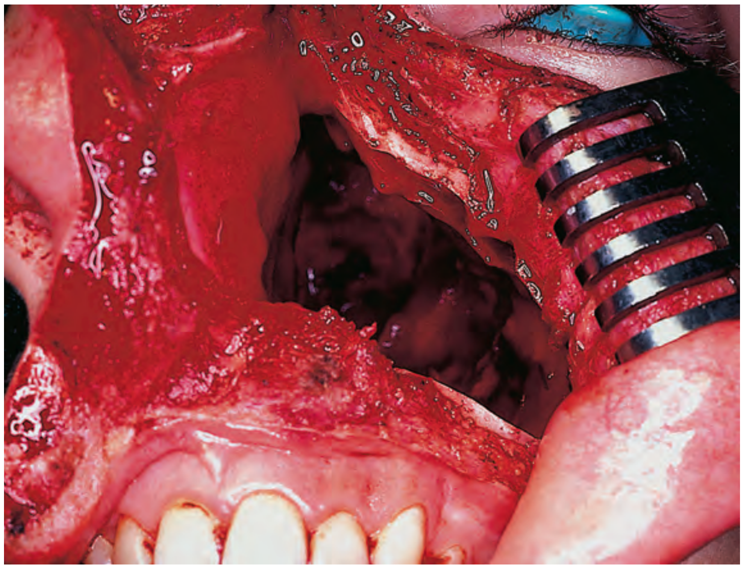

Figure 9.78 The surgical defect showing the nasopharynx through the medial maxillectomy defect.

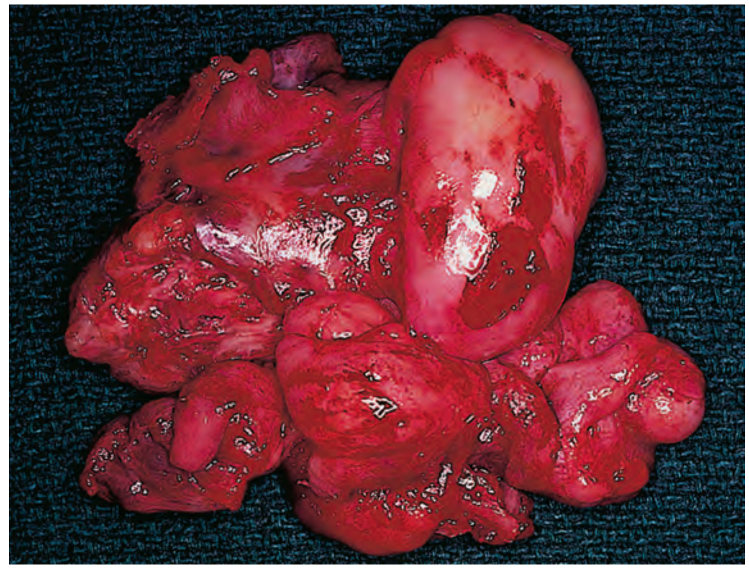

Figure 9.80 The surgical specimen shows a multilobulated tumor.

Figure 9.79 The skin incision is closed in two layers.

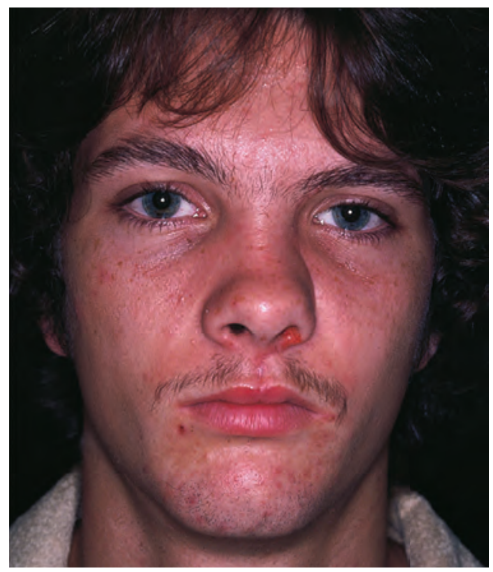

Figure 9.81 The appearance of the patient 3 months after surgery.

defect. The wound is irrigated with Bacitracin solution, and Xeroform packing is used in the surgical defect, which is brought out through the left nostril. The skin incision is closed in the usual fashion in two layers using 3-0 chromic catgut interrupted sutures for subcutaneous tissues and 5-0 nylon for skin (Fig. 9.79).

The surgical specimen shows a multilobulated nasopharyngeal angiofibroma removed from the sphenoid sinus, nasopharynx, nasal cavity, and left maxillary antrum (Fig. 9.80).

Postoperative care requires frequent irrigations of the nasal cavity and intranasal wound after the packing is removed in 5 to 7 days. Irrigations are continued until all crusting has cleared up and the nasal mucosa has epithelialized. Extra humidity is provided in the postoperative period to prevent crusting and bleeding from the nasal cavity.

The postoperative photograph of the patient approximately 3 months after surgery shows a well-healed, aesthetically acceptable scar (Fig. 9.81). An endoscopic view of the nasopharynx shows total removal of tumor with clear choana and a well-epithelialized mucosal surface (Fig. 9.82).

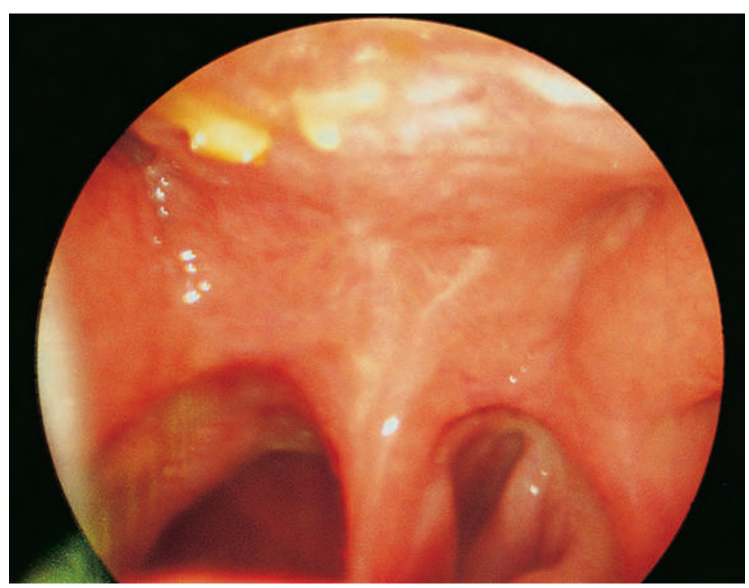

Figure 9.82 A postoperative endoscopic view showing well-healed mucosa of the nasopharynx.

Maxillary Swing for Excision of a Nasopharyngeal Carcinoma

Surgical resection is advocated for select patients with a nasopharyngeal carcinoma that recurs after radiotherapy or chemoradiation. The selection is based on the extent of the tumor, which must be limited to the mucosa and soft tissues without significant paranasopharyngeal extension or invasion of the bony skull base or cranial nerves. The steps of the surgical approach via a maxillary swing are described in Chapter 6. The essential steps remain similar with displacement (swing) of the maxilla laterally to provide wide exposure. An MRI scan of a patient with a recurrent NPC is shown in Fig. 9.83. In this instance a maxillary swing is performed with the entire maxilla rotated laterally based on its anterior and lateral soft-tissue attachments (Fig. 9.84). The recurrent tumor is widely exposed for adequate excision. The line of resection is outlined on an MRI scan in Fig. 9.85. The surgical defect may be left open to granulate or, alternatively, a split-thickness skin graft or a radial forearm free flap may be used for reconstruction. Following resection of the tumor, the maxilla is replaced in its normal position with fixation using miniplates or wire sutures across the osteotomies (Fig. 9.86). For details of the steps for a maxillary swing procedure, see Chapter 6.

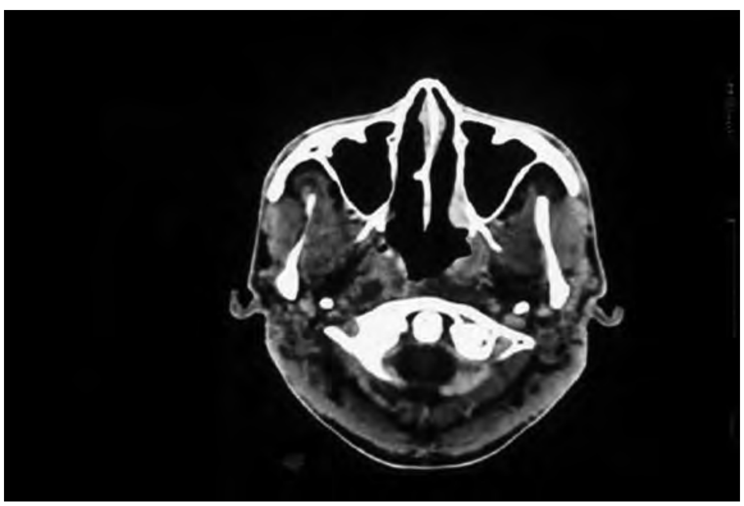

Figure 9.83 A CT scan showing a recurrent nasopharyngeal carcinoma. *(Courtesy William Wei, MD.)*

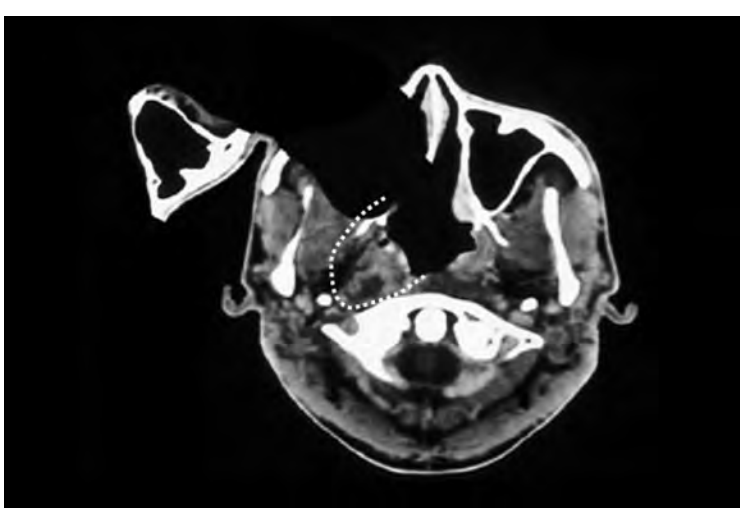

Figure 9.84 A CT scan depiction of the lateral rotation of the maxilla based on its anterior and lateral soft-tissue attachments. The resection of the tumor is outlined. *(Courtesy William Wei, MD.)*

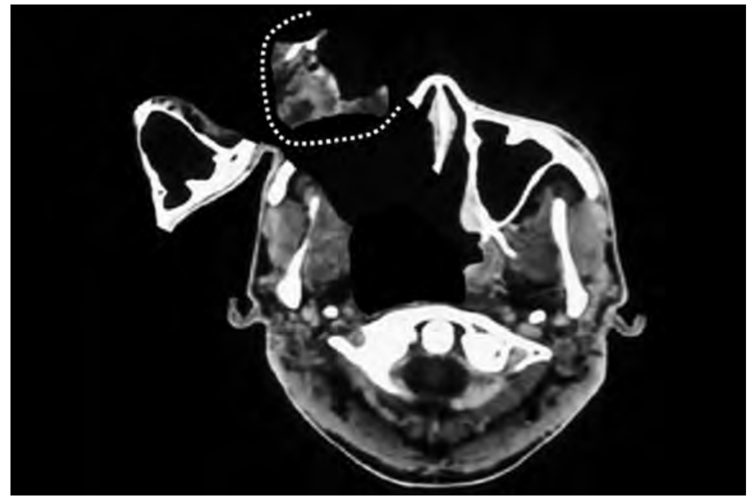

Figure 9.85 The surgical specimen is removed on a schematic of a CT scan. *(Courtesy William Wei, MD.)*

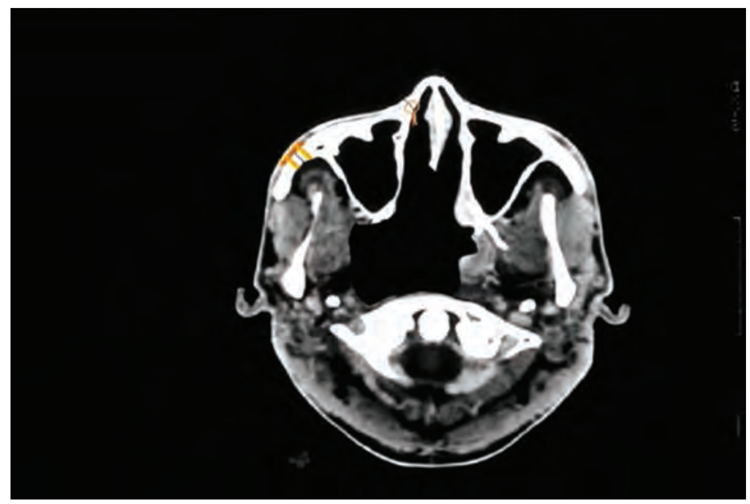

Figure 9.86 A CT scan schematic to show that fixation miniplates or wire sutures across the osteotomies secure the maxilla in its normal position after resection of the tumor. *(Courtesy William Wei, MD.)*

SURGICAL PROCEDURES FOR THE OROPHARYNX

Excision of a Benign Mixed Tumor of the Minor Salivary Glands of the Soft Palate

Tumors of minor salivary gland origin arise anywhere in the mucosa of the upper aerodigestive tract: in the nasal cavity, paranasal sinuses, nasopharynx, oral cavity, oropharynx, hypopharynx, larynx, esophagus, or trachea. Most tumors of minor salivary gland origin are malignant; however, benign tumors arise occasionally. Most benign tumors of minor salivary origin occur in the hard or soft palate. The patient shown in Fig. 9.87 was unaware of the presence of a tumor in his oral cavity until his dentist indicated a bulge on the right side of his soft palate.

A CT scan through the area of the tumor shown in Fig. 9.88 demonstrates a well-encapsulated tumor mass involving the soft palate but not extending to involve the pterygoid musculature or the parapharyngeal space. The patient had an open biopsy of this tumor performed through the mouth elsewhere, and the diagnosis of a benign mixed tumor was established.

The patient is placed under general anesthesia with nasotracheal intubation, and adequate relaxation is obtained with the use of muscle relaxants. The oral cavity is exposed with the use of a Dingman self-retaining retractor (Fig. 9.89). The entire

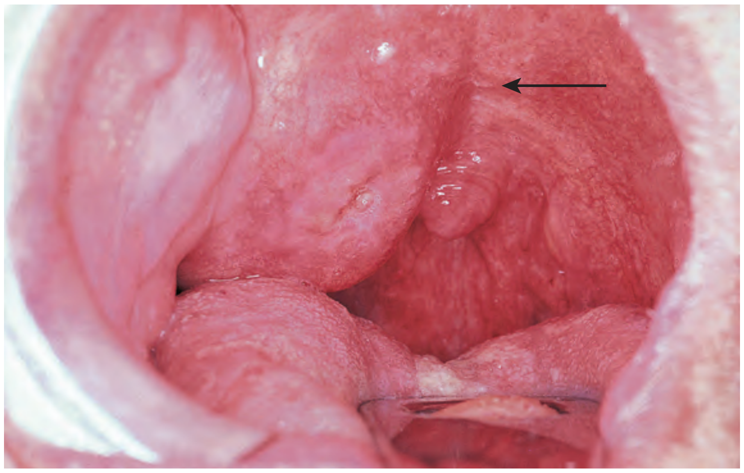

Figure 9.87 A benign mixed tumor of the soft palate on the right hand side (*arrow*).

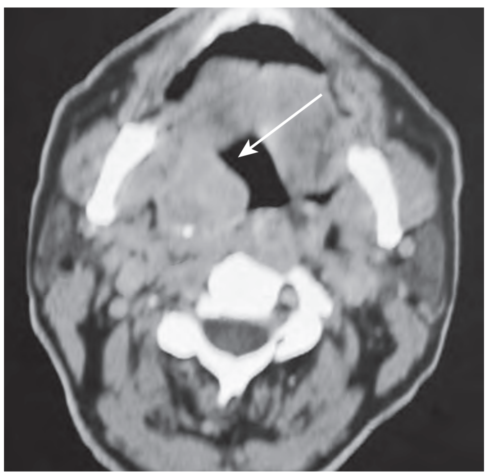

Figure 9.88 An axial view of the computed tomography scan showing a minor salivary gland tumor of the soft palate without extension to the parapharyngeal space (*arrow*).

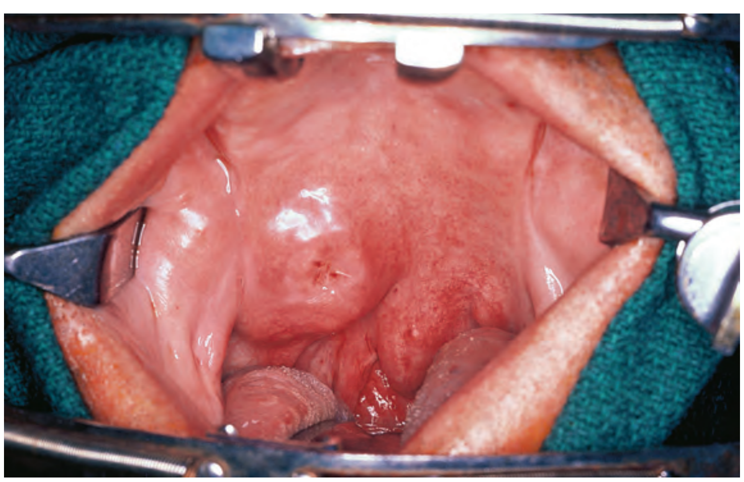

Figure 9.89 The patient is placed under general anesthesia with nasotracheal intubation. A Dingman retractor is used to expose the oral cavity.

surface of the tumor is now exposed, and upon palpation, the tumor is felt to be mobile over the deeper soft tissues. With use of electrocautery, an incision is made in the intact mucosa of the anterior aspect of the soft palate. The incision is deepened through the submucous soft tissues until the pseudocapsule of the tumor is reached (Fig. 9.90).

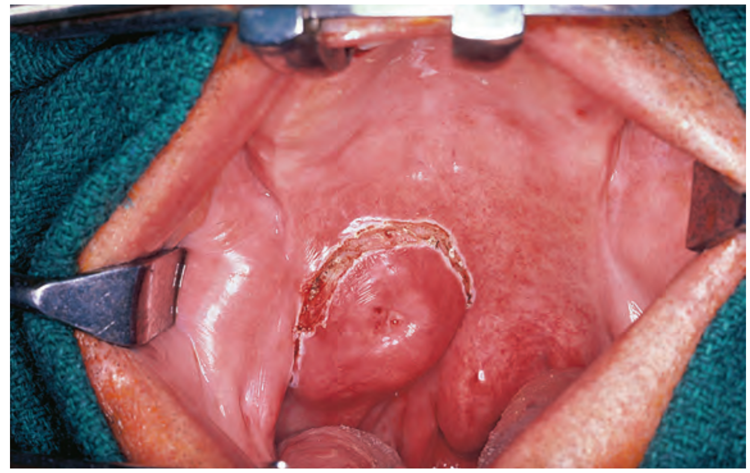

Figure 9.90 A circular incision is placed and is deepened up to the pseudocapsule of the tumor.

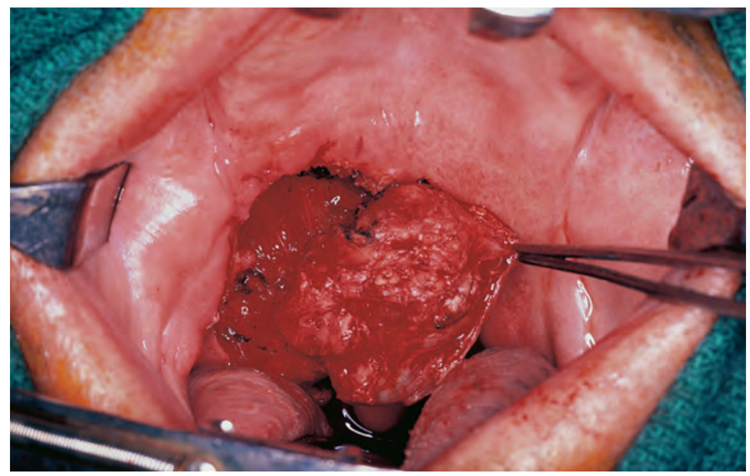

Figure 9.91 Dissection around the pseudocapsule of the tumor continues.

Dissection around the pseudocapsule of the tumor continues, with gentle traction on the tumor, which is extracted by retracting the edges of the surgical defect (Fig. 9.91). Circumferential mobilization of the tumor proceeds in this way with blunt and sharp dissection. Mobilization of the tumor around its entire circumference is now complete, as shown in Fig. 9.92. Deeper attachments containing blood supply to the tumor are clamped and divided, and the tumor is removed in a monobloc fashion.

The surgical defect resulting from excision of the tumor is shown in Fig. 9.93. Note the superficial aspects of the surgical defect, which show minor salivary gland tissue, while the depth of the defect shows musculature of the soft palate. Complete hemostasis is ascertained. No attempt is made to close this surgical defect, which will be allowed to heal by secondary intention. Any attempt at closure would result in distortion of the faucial arch with impairment of velopharyngeal competence, leading to distortion of the quality of voice and nasal regurgitation during swallowing. A nasogastric feeding tube is inserted, and the patient is not permitted to eat by mouth for approximately 1 week. During this time, optimal oral hygiene is maintained with frequent oral irrigations and rinses and power sprays of the surgical defect, using half-strength hydrogen peroxide solution to provide mechanical cleaning of the defect.

The surgical specimen (Fig. 9.94) shows that the tumor measures approximately 4 cm in diameter. Note the attachment of adjacent soft tissues on the pseudocapsule of the tumor, ensuring its complete removal. Upon bisecting the specimen, the rubbery

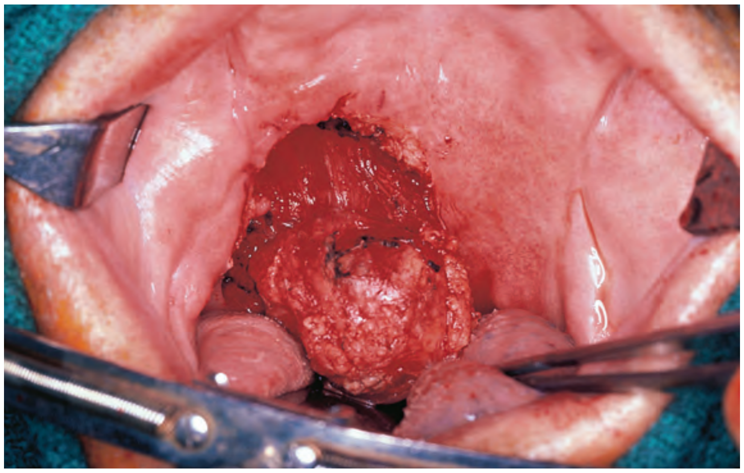

Figure 9.92 Complete mobilization of the tumor.

Figure 9.95 The bisected specimen.

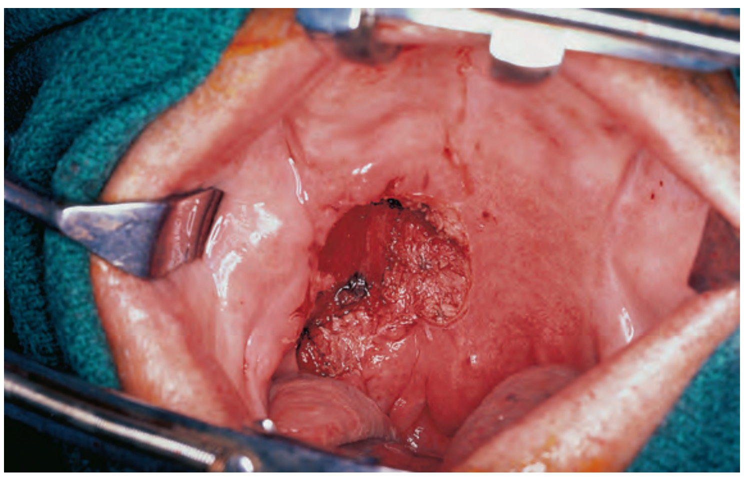

Figure 9.93 The surgical defect.

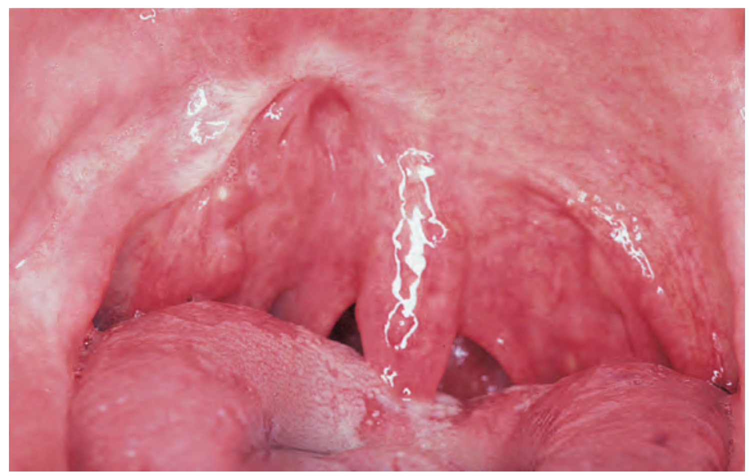

Figure 9.96 The surgical site 1 month following excision of the tumor.

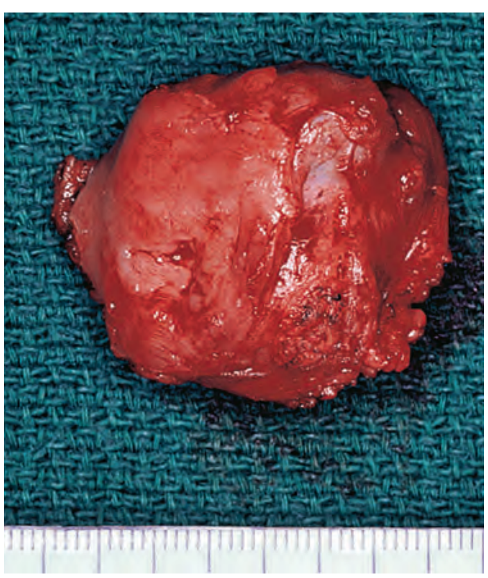

Figure 9.94 The surgical specimen.

consistency of the nodular fleshy, firm, and tightly packed benign mixed tumor becomes apparent, as seen in Fig. 9.95.

The appearance of the surgical site approximately 1 month after excision of the tumor shows complete healing of the large surgical defect, which has filled in with cicatrix and has epithelialized spontaneously (Fig. 9.96). Note that the faucial arch is only minimally distorted. The patient has no impairment of speech or swallowing and is able to open his mouth normally.

Thus the excision of benign minor salivary gland tumors arising in the soft palate can be safely accomplished through the open mouth. However, benign mixed tumors of the deep lobe of the parotid gland that produce a bulge of the soft palate are not accessible through the open mouth, and resection should not be attempted in this way. Such an undertaking would not only be hazardous but, because of inadequate exposure, it would result in piecemeal or incomplete removal of the tumor with occasional uncontrolled hemorrhage and significant risk of injury to the facial nerve.

Resection for Carcinoma of the Tonsil

Small superficial (T1) lesions confined to the tonsil can be managed simply by a peroral monobloc tonsillectomy, securing adequate margins in all three dimensions. Larger lesions (T2 or bigger) may require either TORS or TOLM to include the underlying pharyngeal wall and/or the adjacent base of the tongue to secure clear margins. Much larger lesions (some T3 and nearly all T4 tumors) can be approached through a lower cheek flap approach with either a marginal or segmental mandibulectomy. The surgical defect in this instance will require reconstruction, generally with a free flap or a regional myocutaneous flap.

Transoral Robotic Surgery (TORS) Tonsillectomy

When selecting a primary surgical approach for early-stage tonsil or base of tongue carcinomas, tumor and patient factors should

be carefully considered to avoid the need for trimodality treatments (surgery, radiotherapy, and chemotherapy). Tumor characteristics such as whether the tumor is exophytic or endophytic, T status, ability to secure negative margins, the pathologic nodal status and likelihood of gross extranodal spread by clinical and radiologic assessment, the proximity of the tonsillar fossa resection in relation to the carotid artery and ensuring that the patient has adequate mouth opening to expose the tumor should be carefully studied to avoid the addition of chemotherapy as a result of positive margin of resection at the primary site or gross extranodal extension of metastatic disease. After appropriate patient selection, TORS was selected as a primary treatment in this HPV-positive T1 oropharyngeal tonsil cancer. Transoral robotic surgery is performed with the patient under general anesthesia with nasotracheal intubation using a wire–reinforced endotracheal tube. Examination under general anesthesia should be performed before docking the robot. Palpation of the lesion to appreciate the deep third dimension should be done. Use of a laryngoscope to visualize the entire lateral pharyngeal wall down to the pyriform sinus helps to identify the inferior extent of the tumor. Once the tumor has been defined by inspection and palpation, the oropharynx is exposed using a retraction suture placed in the tongue and the oropharynx is exposed with a Crowe-Davis mouth gag, and a suspension device is attached. It is important throughout the procedure to periodically release the retraction suture on the tongue and the mouth gag to prevent ischemia of the tongue. Once the patient is appropriately positioned the surgeon is seated at the console while the assistant is positioned at head of the operating table (Fig. 9.97). The assistant at the operating table provides smoke evacuation and countertraction using a Yankauer suction. The assistant is also responsible for hemostasis with the use of suction cautery or for application of vascular clips for major vessels. Once the oropharynx is exposed the robot is docked. The 0-degree telescope is placed in the center with the spatula cautery and a Maryland forceps positioned on either side. For this right-sided lesion, the Maryland forceps is positioned on the left to provide retraction medially and the cautery arm is on the right (Fig. 9.98).

Figure 9.97 The position of the surgeon for transoral robotic surgery (TORS).

The operation begins with a mucosal incision parallel to the pterygomandibular raphe along the anterior pillar (Fig. 9.99). Superiorly the incision extends up to the maxillary tubercle and inferiorly to the most posterior floor of mouth (Fig. 9.100). The superior constrictor muscle is located at the most superolateral portion of the resection. If the tonsillar tumor is freely mobile over the constrictor muscle, then the dissection proceeds superficial to the muscle through the loose areolar tissue (Fig. 9.101). Remaining in this plane, dissection continues from inferior to superior pole of the tonsil, and the tonsil is removed (Fig. 9.102). Now, the constrictor muscle is excised as a separate deep margin of resection. The muscle is grasped and pulled medially for excision (Fig. 9.103). On the other hand, if the deep aspect of the tumor is adherent to the constrictor muscle, then it is incised and represents the deep plane of the dissection. The Maryland forceps grasps the superior constrictor and retracts this medially. Using blunt dissection the pharyngeal fat is pushed laterally. The medial pterygoid muscle is identified at the superior lateral edge of the dissection. The styloglossus and stylopharyngeus are divided. The styloglossus is encountered first, is positioned more superficially, and crosses the parapharyngeal dissection in a lateral to medial fashion. After the muscle is

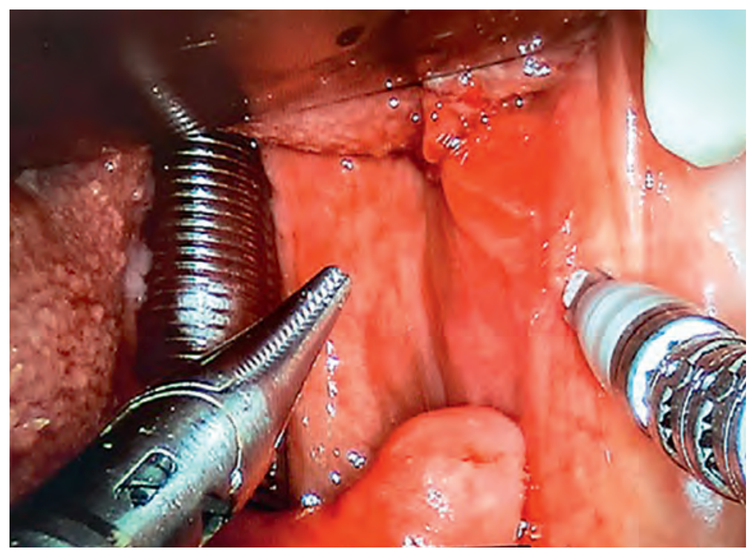

Figure 9.98 Exposure of the tonsil with self-retaining retractor and position of the robotic arms.

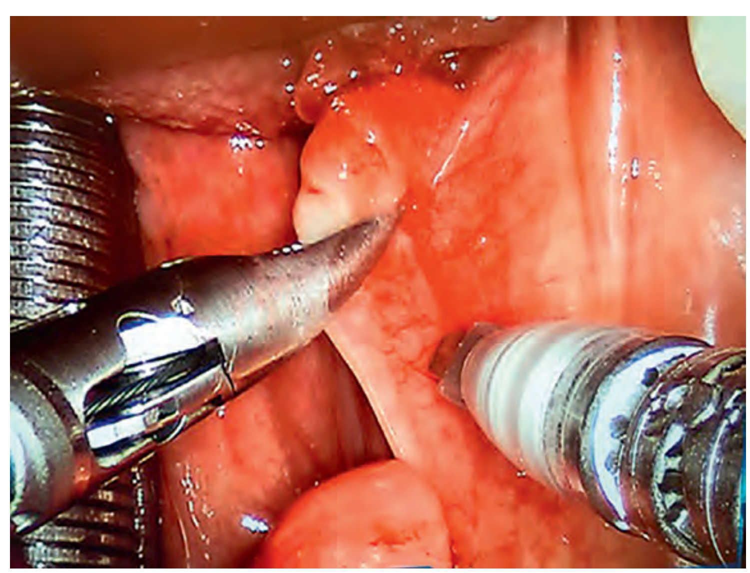

Figure 9.99 Initial incision on the anterior pillar of the soft palate.

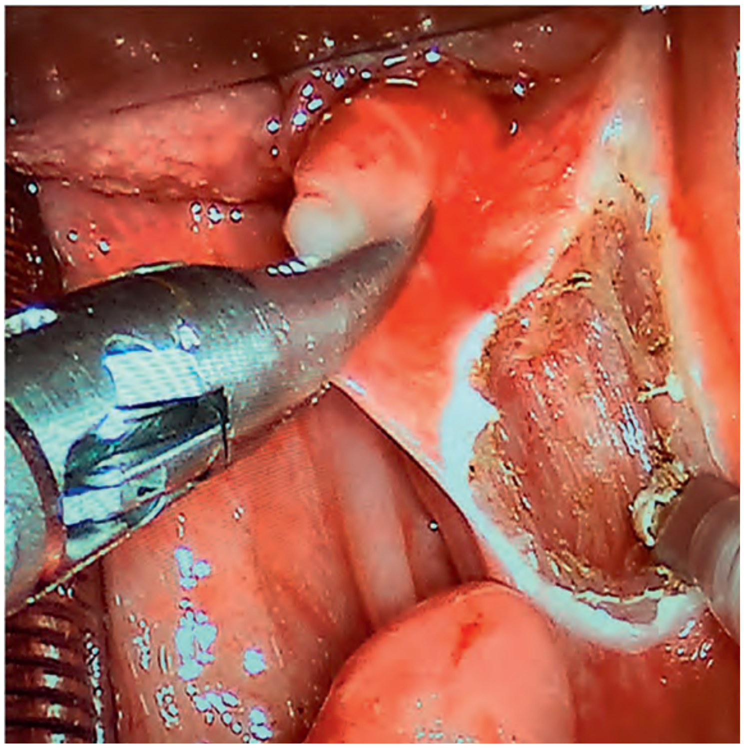

Figure 9.100 The incision is extended up to the maxillary tubercle.

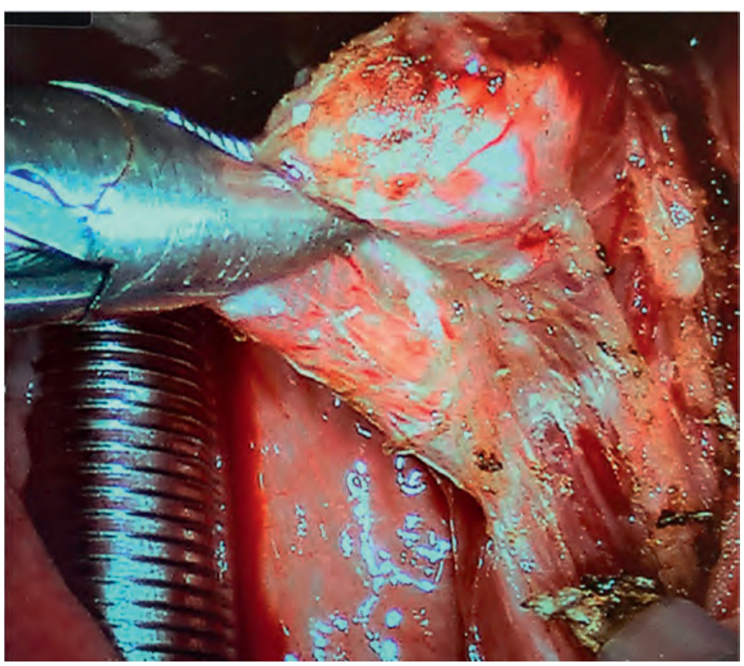

Figure 9.101 Dissection of the tonsil over the superior constrictor muscle.

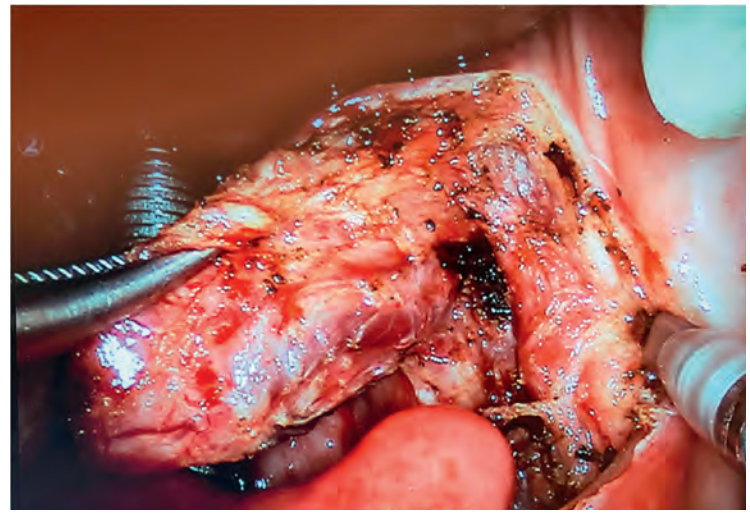

Figure 9.102 Tonsil tumor completely dissected off the superior constrictor muscle.

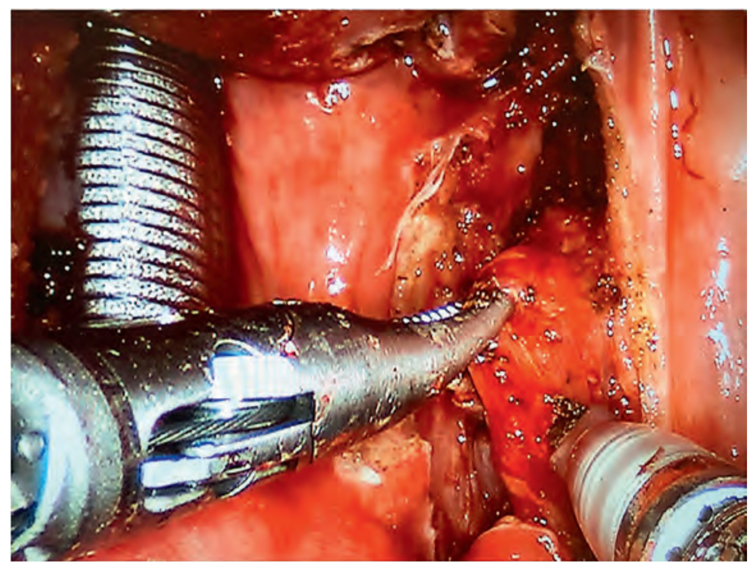

Figure 9.103 Superior constrictor muscle excised separately as deep margin of resection.

identified and circumferentially skeletonized, it is grasped with the Maryland forceps adjacent to the constrictor muscle and divided under direct vision. Posterior and medial to the styloglossus, the stylopharyngeus is identified coursing through the parapharyngeal dissection in a more vertical plane. Incising this muscle parallel to the superior constrictor after circumferential dissection frees the specimen from the lateral attachments of the parapharyngeal space. Veins of the pharyngeal plexus and the tonsillar branch of the facial artery may be encountered during this lateral dissection and should be controlled with the use of hemoclips. Attention is then turned inferiorly for resection of the base of the tongue. The extent of base of tongue resection is dictated by the location of the primary tumor. Inferiorly based tonsil tumors require a more extensive base of tongue resection. An incision is made across the posterior floor of the mouth onto the lateral tongue base mucosa. The lingual artery should be identified and controlled with hemoclips. The dissection extends up to the vallecula and is then carried further onto the posterior pharyngeal wall. A vertical incision on the posterolateral pharyngeal wall is extended superiorly up to the level of the soft palate. This represents the posterior limit of the resection. Superiorly, perpendicular cuts are made through the palatoglossus (anterior pillar) and palatopharyngeus muscle (posterior pillar). The dissection through this incision is taken to the level of the prevertebral fascia and brought into continuity with the posterior pharyngeal wall cut. At this point the specimen has been circumferentially mobilized. The tumor is then removed in a lateral to medial fashion by transecting the constrictor muscle at the most medial deep portion of the resection. The specimen is removed from the oral cavity by the assistant while carefully keeping orientation. The surgeon then examines, orients, and inks the specimen with the pathologist for proper margin study. The parapharyngeal fat and soft tissues are exposed in the surgical defect (Fig. 9.104). Absolute hemostasis is secured,

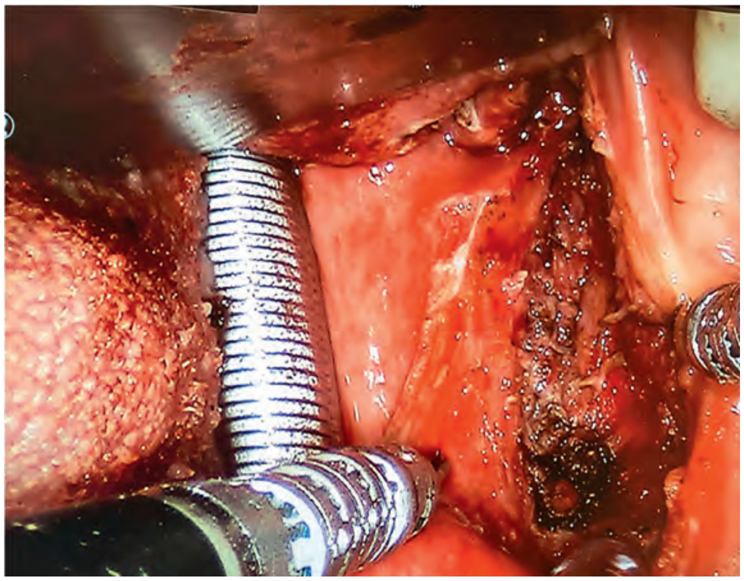

Figure 9.104 Parapharyngeal fat and soft tissues exposed in the surgical defect.

and the defect of resection is left open to heal by secondary intention. A nasogastric feeding tube may be inserted and retained for the first 24 to 48 hours. If extensive dissection in the parapharyngeal space is not performed, then the feeding tube is not necessary, and the patient is permitted liquids by mouth on the day of surgery.

Composite Resection for Recurrent Tonsil Carcinoma

The patient whose panoramic radiograph is shown in Fig. 9.105 underwent composite resection of the tonsillar fossa, adjacent soft palate, base of the tongue, and floor of the mouth for squamous cell carcinoma of the tonsil that had failed to respond to radiation therapy. A satisfactory monobloc three-dimensional resection of the tonsil tumor required a marginal mandibulectomy of the coronoid process of the mandible along with the anterior half of the ascending ramus of the mandible and the alveolar process of the posterior part of the body of the mandible. However, the posterior and inferior cortex of the mandible could be preserved along with an intact temporomandibular joint. The previously irradiated remaining mandible would be at a very high risk for spontaneous fracture. Therefore an A-0 plate is used to support the mandible near the angle and provide the necessary strength to avoid a spontaneous fracture.

The surgical defect in this patient was repaired with a radial forearm free flap to provide replacement of the soft tissue defect and mucosal coverage. The postoperative intraoperative photograph 4 months following surgery shows a well-healed radial forearm free flap replacing the soft palate, tonsillar fossa, posterior pharyngeal wall, retromolar region, and the adjacent base of the tongue (Fig. 9.106). Achieving a complete closure of the mucosal defect is crucial to avoid sepsis and exposure of the A-0 plate. Infection and exposure mandate removal of the plate and pose the risk of osteoradionecrosis and spontaneous fracture of the previously irradiated and now infected residual weakened mandible. In a setting such as that, it would be best to proceed with segmental resection of the mandible and consider reconstruction with a fibula free flap. The postoperative external appearance of the patient shows excellent retention of the contour of the face with maintenance of the continuity of the arch of the mandible and thus a very desirable functional and aesthetic result (Fig. 9.107).

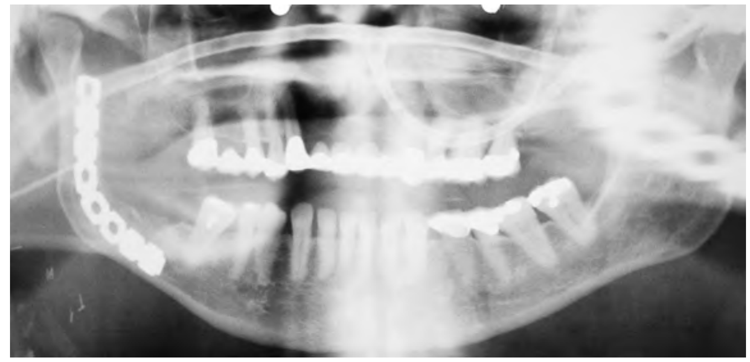

Figure 9.105 Miniplate stabilization of a thin, remnant mandible after marginal resection.

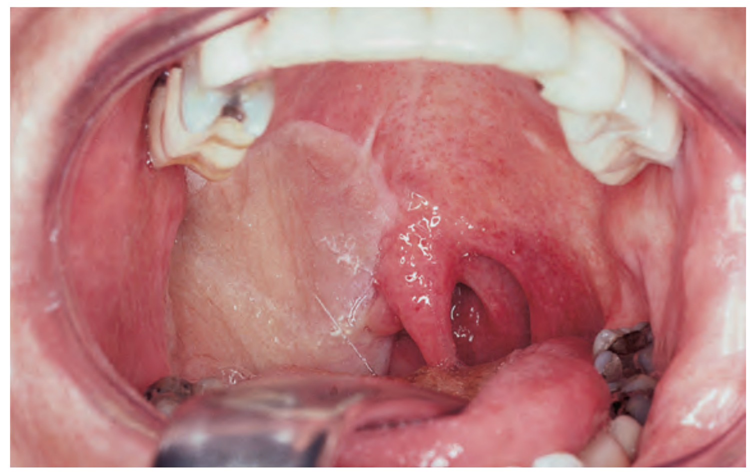

Figure 9.106 A postoperative intraoral view showing a well-healed radial forearm flap.

Figure 9.107 The external appearance of the patient.

Resection of the Base of the Tongue via Mandibulotomy

Primary neoplasms of the base of the tongue are difficult to access through the oral cavity, particularly if they have a significant infiltrative component into the musculature of the tongue base. Small superficial and well-defined lesions are amenable to transoral resection with a laser, TOLM, or with a robot (TORS) if appropriate facilities and expertise are available. In the absence of such technologic support and expertise, tumors of the base of the tongue can be approached via a mandibulotomy. The selection of the site of a mandibulotomy is discussed in Chapter 8. A

paramedian mandibulotomy causes minimal disruption of normal anatomic structures and thus leads to minimal postoperative morbidity for mastication, swallowing, and speech. In patients with intact lower dentition, the mandibulotomy site is preferred between the lateral incisor and canine teeth, because the roots of these two adjacent teeth diverge from each other, giving satisfactory space for the mandibular osteotomy.

The patient whose endoscopic picture shows an exophytic cauliflower-like lesion in Fig. 9.108 has an adenoid cystic carcinoma arising from minor salivary glands of the base of the tongue. The tumor does not extend to the supraglottic larynx, nor does it extend laterally to involve the tonsillar fossa or lateral pharyngeal wall. An MRI scan in the axial view shows that although the bulk of the tumor is exophytic, it does have an infiltrative component into the deep muscles of the tongue (Fig. 9.109). A coronal view of the MRI shows a large tumor occupying the base of the tongue and oropharyngeal airway, causing partial airway compromise at the level of the laryngeal vestibule (Fig. 9.110).

A preoperative panoramic view of the mandible shows that this patient is edentulous in his lower dentition but has several dental implants inserted for restoration of his teeth (Fig. 9.111). Therefore the mandibulotomy site is selected between two dental implants so as not to expose the implants. The osteotomy is performed in an angled fashion to prevent cephalocaudad movement of the two segments of the mandible at the site of the mandibulotomy. A biplane fixation is required with miniplates on the lateral cortex of the mandible and on the inferior border of the mandible to achieve adequate immobilization.

A vertical midline incision is outlined on the lower lip that extends through the chin into the submental region up to the hyoid bone. At that point the incision may be extended laterally along an upper neck skin crease to proceed with a neck dissection if indicated. Neck dissection was not performed in this patient with an adenocystic carcinoma because clinical and radiologic findings of the neck were negative. Anatomically, a midline lip-splitting incision is the most sound location for placement of an incision, and if it is repaired accurately, it provides the most aesthetically acceptable scar (Fig. 9.112). The skin incision is placed with a scalpel, and then it is deepened through the soft tissues and muscles of the lower lip and chin with electrocautery up to the outer cortex of the mandible. Short cheek flaps are elevated, remaining anterior to the mental foramen

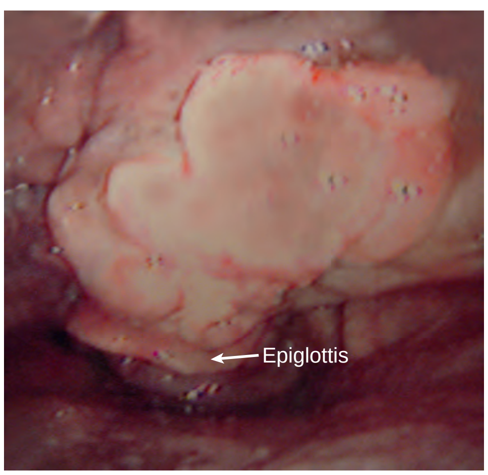

Figure 9.108 An endoscopic view of an exophytic tumor of the right base of the tongue.

Figure 9.110 A coronal view of the magnetic resonance imaging scan showing the exophytic component of the tumor.

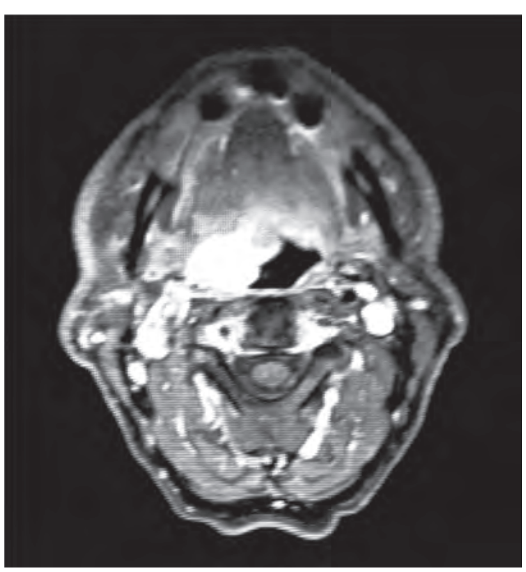

Figure 9.109 An axial view of the magnetic resonance imaging scan showing the extent of infiltration into the right base of the tongue.

Figure 9.111 A preoperative panoramic radiograph shows the planned site of mandibular osteotomy relative to the dental implants.

Figure 9.112 A midline lip-splitting incision is outlined.

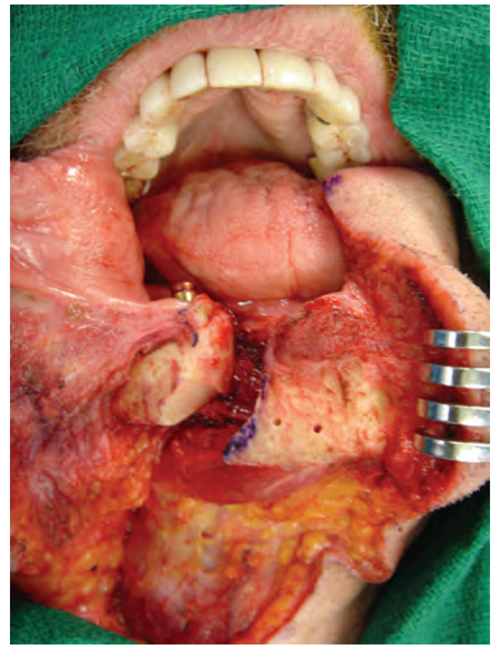

Figure 9.114 The mandibular osteotomy is completed after the holes for the miniplate screws are predrilled.

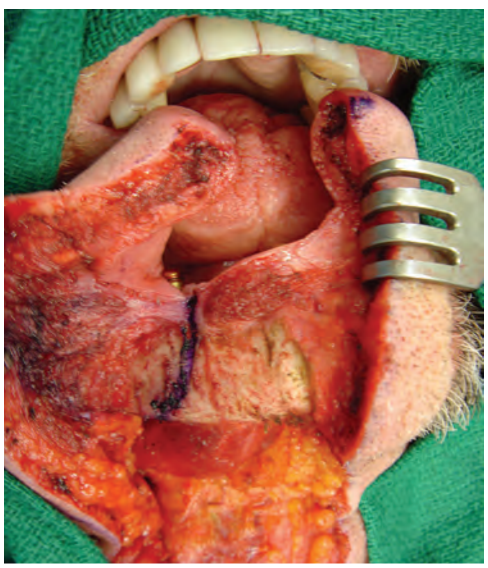

Figure 9.113 The mandibular osteotomy is outlined.

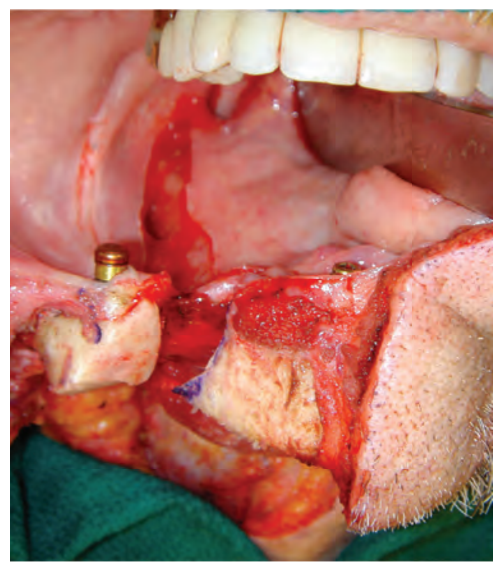

Figure 9.115 The mucosal incision in the floor of the mouth extends up to the anterior pillar of the tonsil.

on both sides to preserve the mental nerves. On the left-hand side the cheek flap extends approximately 1 cm lateral to the midline. A short cuff of attached gingival mucosa is preserved on the alveolar process to facilitate mucosal closure between the labial mucosa and the lower gum after resection. The mandibulotomy site is outlined with a marking pen, remaining between the two dental implants, carefully preserving enough cortical bone around each implant (Fig. 9.113).

Two miniplates with four screw holes are contoured to the shape of the mandible and applied at the mandibulotomy site, and the screw holes are predrilled, avoiding the adjacent implants or dental roots. This maneuver retains optimal occlusion of the upper and lower dentition. A power saw with an ultrafine blade is used to complete the mandibular osteotomy in an angled fashion. Bone wax is used to control bleeding from the cut ends of the bone (Fig. 9.114). Once the two segments of the mandible are divided, they are retracted laterally to expose the underlying mylohyoid muscle and the mucosa of the floor of the mouth. A mucosal incision is placed in the floor of the mouth on the right-hand side approximately 1 cm medial to the attached gingiva, extending from the mandibulotomy site up to the anterior pillar of the soft palate (Fig. 9.115). This mucosal incision is deepened through the underlying sublingual gland, which is retracted medially to expose the mylohyoid muscle (Fig. 9.116). The two mandibular segments are now retracted, further laterally stretching the mylohyoid muscle. The muscle is now divided exactly halfway through its attachment between the mandible and the hyoid bone, as shown by a nerve hook in Fig. 9.117. This step is important so as to leave sufficient stumps of the mylohyoid muscles at both ends, which should be available for reapproximation to support the mucosal suture line during closure. Once the mylohyoid muscle is divided, the right-hand segment of the mandible can be retracted even farther out (mandibular swing), providing exposure of the

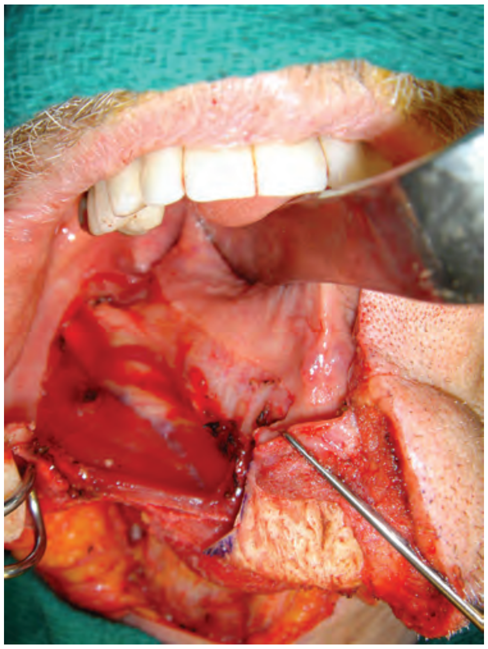

Figure 9.116 The divided segments of the mandible are retracted to expose the mylohyoid muscle.

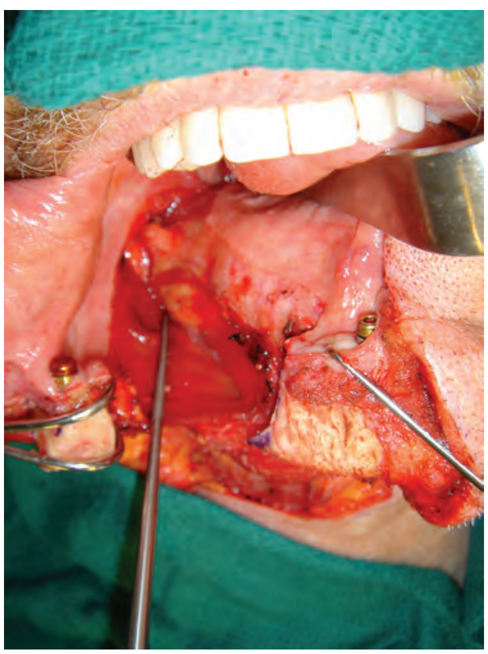

Figure 9.117 The mylohyoid muscle is divided in the middle at the level depicted by the nerve hook.

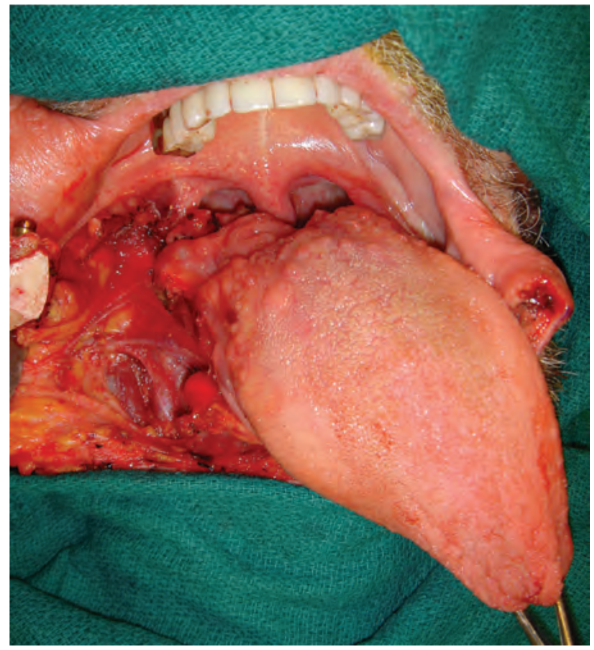

Figure 9.118 Division of the mylohyoid muscle allows lateral retraction of the mandible.

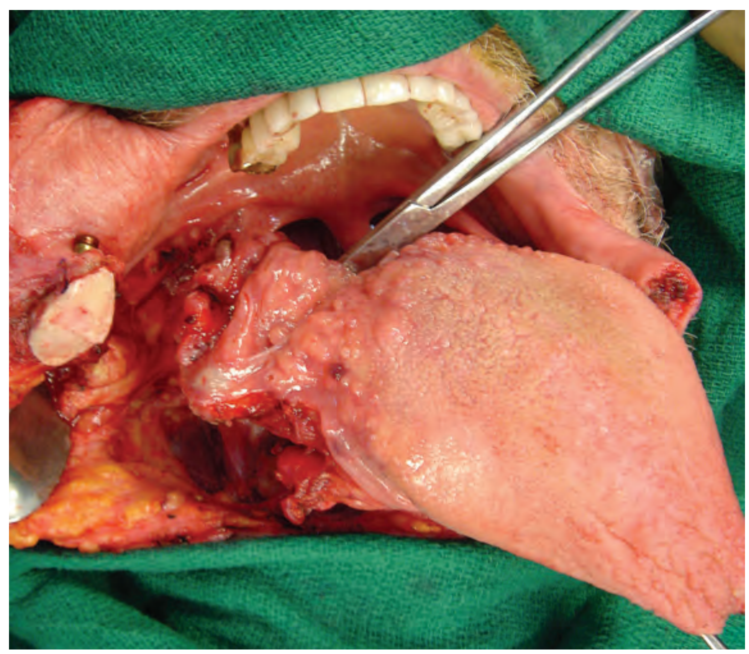

Figure 9.119 The tumor is exposed into the surgical field.

oropharynx and the tumor at the base of the tongue (Fig. 9.118). The exophytic component of the tumor in the base of the tongue on the right-hand side is shown with a hemostat as it is delivered into the wound by retraction of the mandible (Fig. 9.119). A transverse wedge resection of the base of the tongue is planned, securing adequate margins in all three dimensions around the tumor. The site of incision in the mucosa of the tongue base is outlined, keeping the apex of the transverse wedge across the midline extending into the contralateral base of the tongue (Fig. 9.120). Resection of the tumor now begins with electrocautery. The resection is done in a systematic and careful manner, securing hemostasis at each step of the way. The anterior aspect of the surgical resection is completed first, followed by the posterior incision, which begins at the apex of the transverse wedge and ends at the lateral aspect of the vallecula. This mobilization delivers the tumor out into the wound, keeping only its deep margin at the muscles of the tongue attached (Fig. 9.121). A wide three-dimensional resection is performed, keeping adequate lateral mucosal margins and a generous cuff of deep muscular margin. The surgical defect following resection of the tumor shows the lingual surface of the epiglottis posteriorly and a large defect between the middle third of the tongue and the supraglottic larynx (Fig. 9.122).

Closure of the surgical defect begins with interrupted 2-0 Vicryl sutures in at least two layers. A deep layer approximates the deep muscles of the tongue to the suprahyoid soft tissues

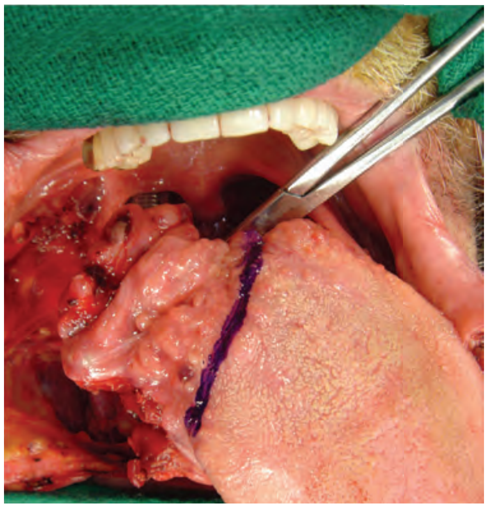

Figure 9.120 The transverse wedge resection is outlined.

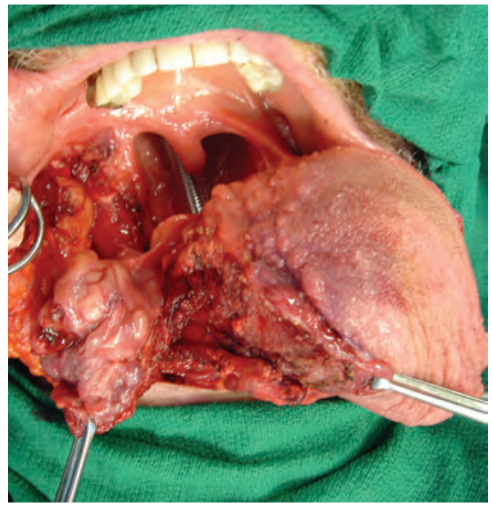

Figure 9.121 Resection of the anterior aspect of the tumor is completed.

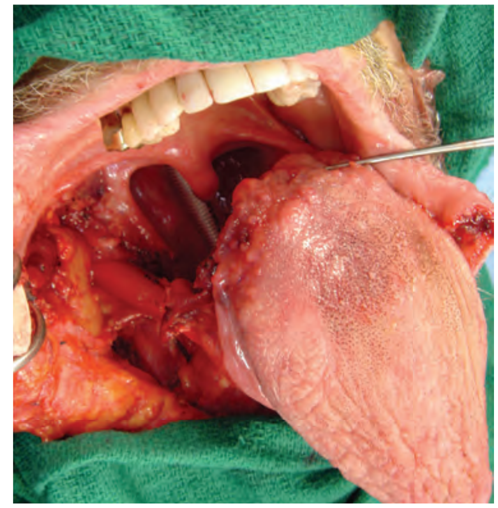

Figure 9.122 The surgical defect.

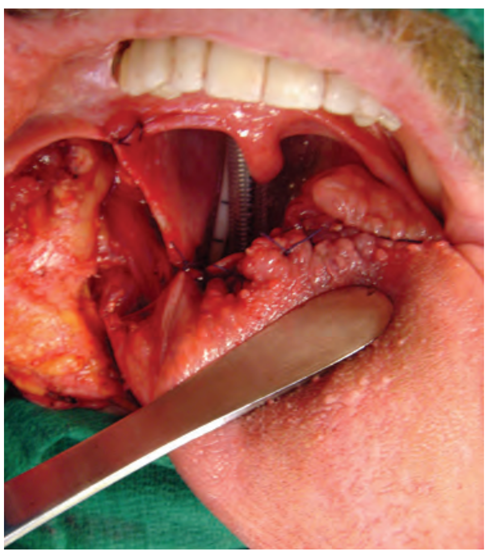

Figure 9.123 Transverse closure of the base of the tongue is completed.

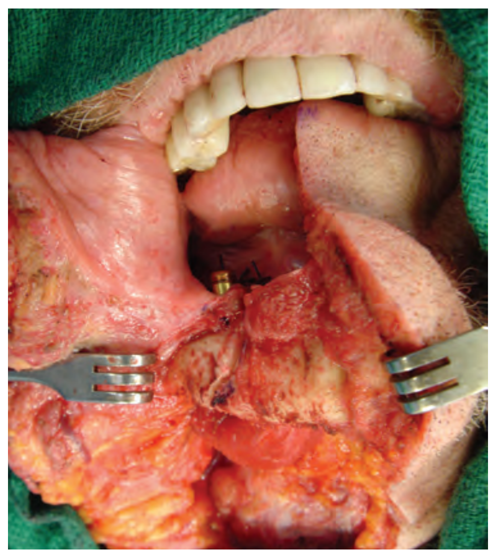

Figure 9.124 Closure of the floor of the mouth realigns the mandible.

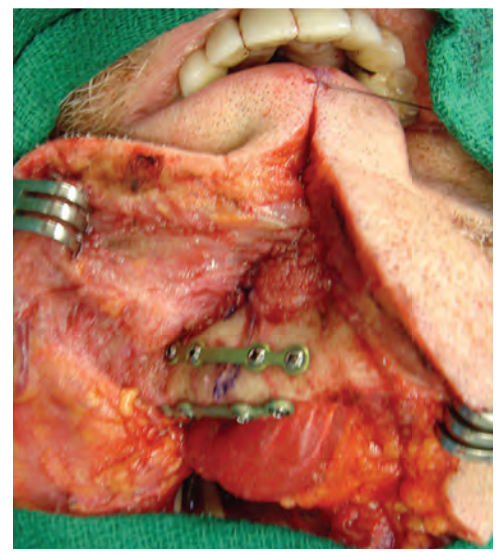

Figure 9.125 Miniplates are used to immobilize the mandibular osteotomy.

at the lingual surface of the epiglottis. The mucosa is approximated with interrupted sutures between the middle third of the tongue and the lingual surface of the epiglottis, continuing on to the anterior wall of the right pyriform sinus (Fig. 9.123). Complete closure of the surgical defect can be accomplished easily in this manner with a transverse suture line, which extends from the lower border of the right tonsillar fossa to the contralateral base of the tongue. Vertical closure of the incision at the anterior pillar of the soft palate now begins at the upper pole of the tonsil and is carried anteriorly along the floor of the mouth. Interrupted Vicryl sutures are used for this mucosal closure. As the closure proceeds anteriorly, the right half of the mandible swung laterally is brought back toward the midline, allowing easy approximation between the mucosa of the undersurface of the tongue and the attached gingiva with interrupted Vicryl sutures. Retraction of the mandible at this juncture should be avoided; otherwise the suture line will be disrupted. Complete mucosal closure in a watertight fashion is achieved in this manner, bringing the retracted mandible back toward the midline and aligned at the mandibulotomy site with the contralateral half of the mandible (Fig. 9.124).

The mandibular osteotomy is now repaired with two four-hole miniplates, and 7-mm screws are placed in the predrilled holes to immobilize the mandibulotomy site. One plate is applied on the lateral/anterior cortex of the mandible, keeping the mandibulotomy site exactly in the middle of the miniplate while a similar four-hole miniplate is applied at the lower border of the mandible, again keeping the mandibulotomy site in the center of the miniplate. Thus a biplane fixation of the mandibulotomy is secured (Fig. 9.125). After application and tightening of the screws, the two segments of the mandible are tested to see if any mobility is present. If motion occurs between the two segments of the mandible, additional fixation will be required. Very rarely, intermaxillary fixation may be necessary in patients with intact dentition. The stumps of the mylohyoid muscle are reapproximated using interrupted absorbable sutures, which provides a second layer of support to the mucosal suture line in the floor of the mouth. Closure of the wound now proceeds in a meticulous fashion in two layers, accurately reapproximating the vermilion border of the lower lip and the soft tissues and the skin of the chin along the natural skin creases to accurately realign the two sides of the incision. This patient will require

Figure 9.126 The surgical specimen.

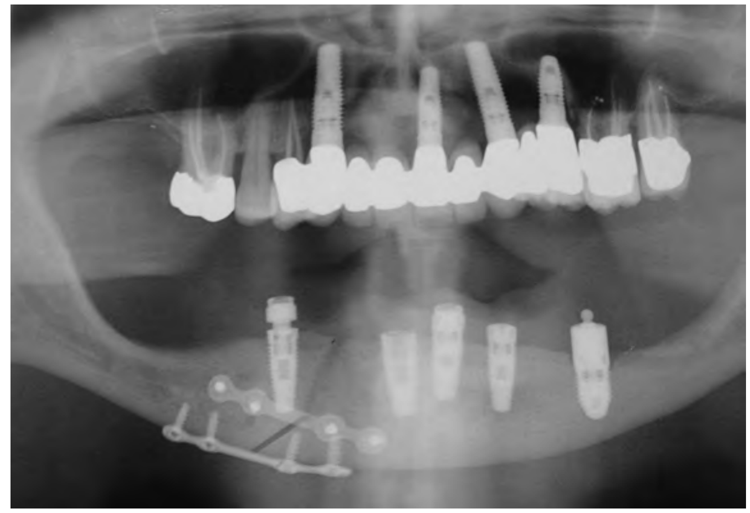

Figure 9.127 A postoperative panoramic radiograph shows accurate restoration of mandibular continuity.

Figure 9.128 The postoperative appearance of the healed incision.

Figure 9.129 The patient is able to protrude the tongue (**A**) and has excellent dental occlusion (**B**).

a tracheostomy for management of the airway and pulmonary secretions and a nasogastric feeding tube for nutrition in the postoperative period.

The surgical specimen shown in Fig. 9.126 shows a three-dimensional resection of adenoid cystic carcinoma of minor salivary gland origin of the right base of the tongue. A postoperative panoramic radiograph of the mandible shows that the miniplates have achieved excellent immobilization at the site of the mandibulotomy and the screws used for fixation of miniplates do not interfere with the preexisting dental implants in the mandible (Fig. 9.127).

Routine measures for maintenance of optimal oral hygiene are instituted in the postoperative period. The patient is encouraged to practice swallowing his or her own saliva by the third or fourth postoperative day, and generally by the end of the first postoperative week, the patient is able to swallow puréed foods without aspiration. If satisfactory mucosal healing is seen by the fifth to seventh postoperative day, oral alimentation is begun. The tracheostomy tube is removed as soon as the patient is able to tolerate fluids and food by mouth without aspiration. By the third postoperative week, nearly all patients are able to handle a regular diet. The appearance of the patient 6 months after surgery shows a well-healed scar with minimal aesthetic morbidity (Fig. 9.128). The patient has excellent mobility of the tongue and dental occlusion, as seen in Fig. 9.129.

Mandibulotomy for Resection of the Base of the Tongue With a Supraglottic Partial Laryngectomy

Patients with primary tumors that arise in the base of the tongue with secondary extension to involve the supraglottic larynx or primary tumors of the epiglottis with significant extension to the base of the tongue require a mandibulotomy to provide access for satisfactory resection of the tongue base. If involvement of the base of the tongue is minimal, then resection of the base of the tongue in conjunction with the supraglottic larynx can be performed via the conventional transhyoid approach utilized for a standard supraglottic partial laryngectomy. On the other hand, if there is extensive involvement of the base of the tongue, then satisfactory exposure through a transhyoid approach is not obtained, and a mandibulotomy approach is preferred. A diagrammatic representation of the exposure necessary for resection of the base of the tongue, in conjunction with supraglottic partial laryngectomy, is shown in Fig. 9.130.

The patient shown in Fig. 9.131 has a primary carcinoma of the base of the tongue with extension to the supraglottic larynx that requires resection of the base of the tongue in conjunction with a supraglottic partial laryngectomy. Clinical findings of both sides of the neck are negative, and therefore elective neck dissection is not performed at the time of resection of the primary tumor. However, the entire neck on both sides

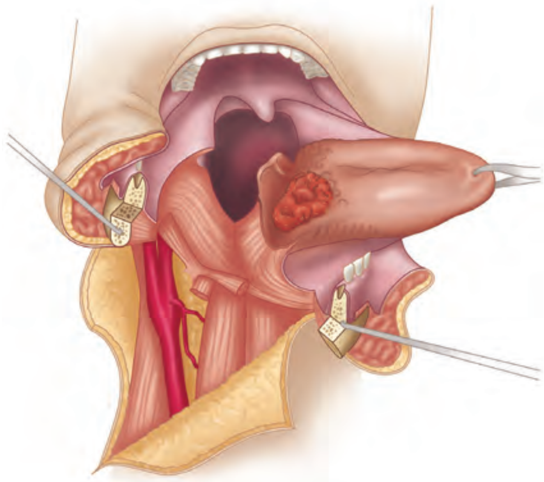

Figure 9.130 Diagrammatic representation of the exposure obtained through a mandibulotomy.

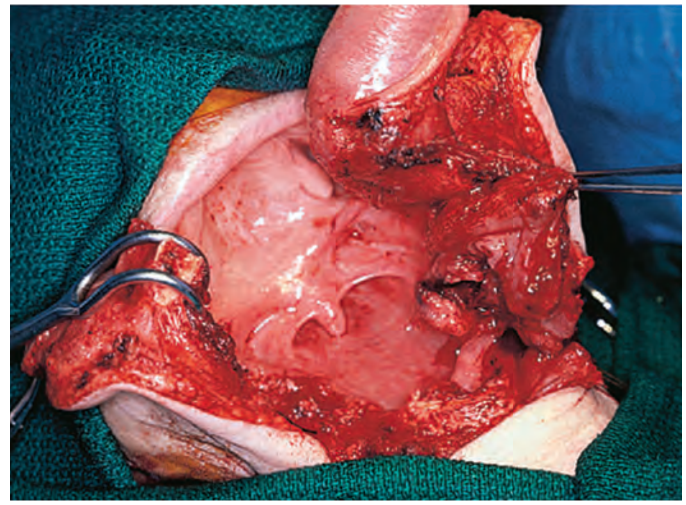

Figure 9.132 Exposure of the tumor through a mandibulotomy.

Figure 9.131 The skin incision is outlined.

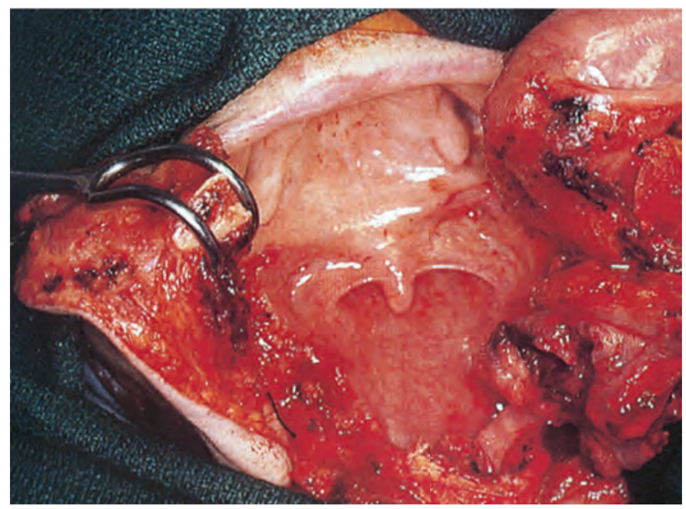

Figure 9.133 The surgical specimen is mobilized by division of the right base of the tongue and right aryepiglottic fold.

will be treated with elective postoperative radiation, because both sides of the neck remain at risk for metastatic disease.

A preliminary tracheostomy is performed under local anesthesia, after which general anesthesia is induced. Examination under anesthesia and direct laryngoscopy are performed at this point to adequately assess the extent of the tumor to facilitate a satisfactory resection. The incision outlined is like a reverse letter T (see Fig. 9.131).

Exposure of the surgical field following a mandibulotomy with paralingual extension and mandibular swing of the right half of the mandible is shown in Fig. 9.132. An incision is made in the base of the tongue anterior to the palpable tumor. The base of the tongue on the left side is retracted to the left, while the anterior margin of the base of the tongue on the right side, which is to be resected with the supraglottic larynx, is held with a toothed forceps. Note the bulky cauliflower-like tumor arising from the lingual surface of the epiglottis with extension to the base of the tongue in the center of the surgical field. A very generous exposure is obtained by this approach, which permits satisfactory resection of the tumor with adequate margins.

A somewhat anterior view with anterior retraction of the surgical specimen shows the aryepiglottic fold on the right-hand side that is now divided, showing the inferior margin of the surgical specimen to be resected (Fig. 9.133). Approximately 3 to 4 mm of the superior edge of the thyroid cartilage on both sides, as well as the central third of the hyoid bone, is resected along with the tongue base to permit a monobloc resection of the preepiglottic space. Division of the thyroid cartilage is performed with use of a power saw with an ultrafine blade, while the hyoid bone is divided just lateral to the lesser cornua on both sides with use of a bone cutter. Once the cartilage cuts are made, the remainder of the resection of the specimen is performed with use of electrocautery. Bleeding from the branches of the superior laryngeal artery on both sides is to be expected, and these vessels are suture ligated with 3-0 chromic catgut.

The surgical defect following removal of the specimen shows a through-and-through resection of the base of the tongue along with the supraglottic larynx, preserving the hypoglossal nerve on the left-hand side (Fig. 9.134). The remaining attachments of the neurovascular bundle of the tongue on the left-hand side are seen here. The tongue remains viable with its blood supply from the left lingual artery, while motion of the tongue on the left side is retained because of preservation of the left hypoglossal nerve. The transected edges of the thyroid cartilage, as well as the arytenoids on both sides, are seen at the lower part of the surgical field.

Frozen sections are now obtained from the mucosal margins of the false vocal cords on both sides as well as the pharyngeal margins on the left and right sides and the anterior margin of the mucosa and musculature of the base of the tongue. A massive resection of the base of the tongue in conjunction with the supraglottic larynx is thus satisfactorily performed via this approach.

A nasogastric feeding tube is inserted before closure. Repair of the surgical defect requires careful attention to detail, because anatomic continuity of the upper alimentary tract is important, as is restoration of the physiologic function of deglutition. Therefore the larynx must be resuspended back to the base of the tongue to simulate the normal anatomy and physiology during the pharyngeal phase of deglutition. A high-speed drill is used to make several drill holes through the upper edge of the transected thyroid cartilage on each side. Approximately four to five drill holes are made on each side of the thyroid lamina. The larynx is approximated back to the musculature of the base of the tongue using 0 chromic catgut or 00 Vicryl sutures (Fig. 9.135). This closure is similar to the procedure following a standard supraglottic partial laryngectomy. No attempt is made to obtain mucosal closure between the cut edge of the mucosa of the base of the tongue and the cut edge of the mucosa of the supraglottic larynx. On the other hand, these heavy sutures are used to approximate the transected stump of the musculature of the base of the tongue to the transected thyroid cartilage, as shown here. All sutures are appropriately placed first and then tied sequentially. Note that these sutures traverse through the stump of the musculature of the base of the tongue, while the mucosal edge is left free to epithelialize spontaneously.

The remaining closure of the mandibulotomy has been described previously. The floor of the mouth mucosa is approximated to the mucosa of the lingual gingiva by interrupted 2-0 chromic catgut sutures. The mandibulotomy is repaired with miniplates and screws. Mylohyoid muscle is resutured, and the remainder of the incision of the neck is closed in layers.

The posterior view of the specimen shows the remnant of the epiglottis destroyed by the tumor (Fig. 9.136). Note that the inferior margin of the surgical specimen is clear of the tumor. The larynx is transected at about the level of the upper border of the false vocal cords on both sides. At the upper border of the specimen, the anterior margin of the transected base of the tongue is seen, clear of tumor.

The caudal view of the specimen is shown in Fig. 9.137. Note the resected superior rim of the thyroid cartilage at the lower part of the specimen. The mucosa and soft tissues of the petiole of the epiglottis form the inferior soft-tissue margin of the specimen. Thus an oncologically sound surgical resection of the tumor is performed via the mandibulotomy approach.

Rehabilitation of the patient in terms of the ability to handle secretions and restore the act of swallowing requires much training and time. Once the patient is able to handle his or her secretions, a trial is given with puréed foods. Patients undergoing surgery of this nature initially will be unable to take liquids by mouth. If the patient is able to handle puréed foods, then he or she is advanced to a soft diet and can take clear liquids last. Swallowing rehabilitation following a resection of this magnitude can take as long as 3 months. However, the eventual functional and aesthetic result is very satisfactory. The endoscopic view approximately 1 year after surgery shows approximation of the remaining tongue to the remaining larynx (Fig. 9.138). A well-healed external incision is shown in Fig. 9.139.

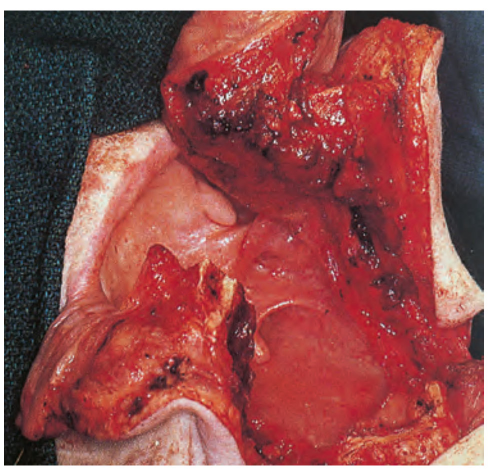

Figure 9.134 The surgical defect showing the remaining larynx and tongue with an intact neurovascular pedicle from the left side.

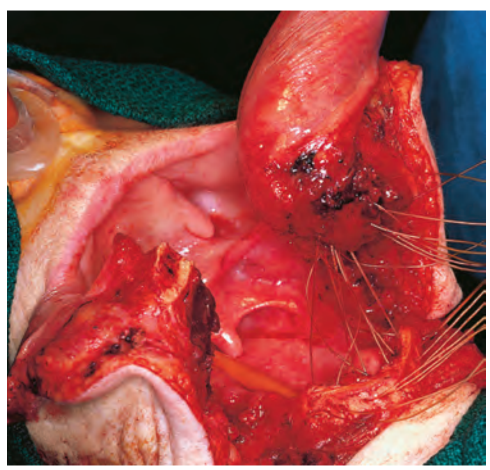

Figure 9.135 The larynx is approximated back to the musculature of the base of the tongue.

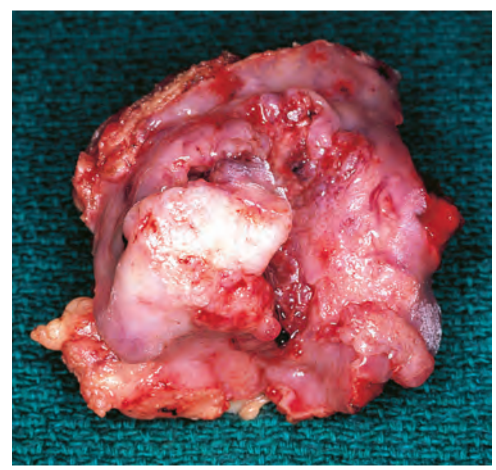

Figure 9.136 The posterior view of the specimen.

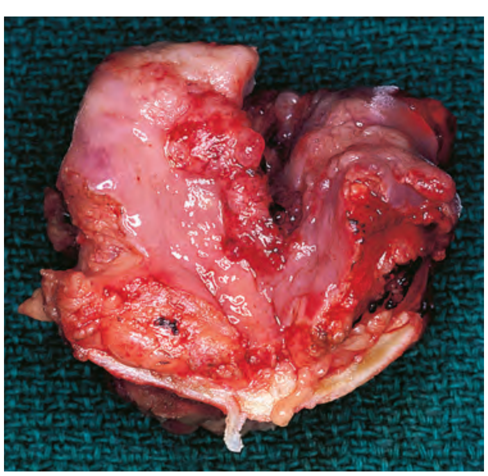

Figure 9.137 The caudal view of the specimen.

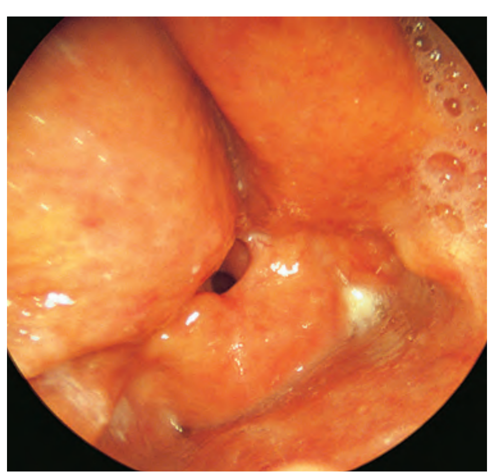

Figure 9.138 An endoscopic view 1 year after surgery.

Figure 9.139 A postoperative photograph showing a well-healed incision.

SURGICAL PROCEDURES FOR THE HYPOPHARYNX

Transhyoid Partial Pharyngectomy

Primary carcinomas of the posterior pharyngeal wall of limited extent are suitable for excision via several approaches, depending on the location and extent of the tumor, its surface dimension, and its depth of infiltration into the musculature of the posterior pharyngeal wall. Small superficial tumors of the posterior pharyngeal wall in its upper part, particularly those that extend into the oropharynx, can be excised through the open mouth. Any of the previously described techniques, such as TOLM or TORS, can be used. The surgical defect in this clinical situation may be left open to granulate and epithelialize. However, when such a procedure is undertaken, it is important to remember that the mucosal edges of the surgical defect should be tacked down to the prevertebral fascia with interrupted chromic catgut sutures. This step is necessary to prevent retraction of the pharyngeal wall and also to prevent dissection of sepsis into the prevertebral plane.

If, however, the lesion requires full-thickness resection of the posterior pharyngeal wall, then a split-thickness skin graft can be used to cover the surgical defect. To retain the skin graft in snug contact with the prevertebral fascia, several quilting sutures of chromic catgut are used to tack the skin graft down to the prevertebral fascia in addition to its fixation to the mucosa of the pharyngeal defect circumferentially.

Limited lesions of the lower part of the posterior pharyngeal wall also can be excised in a similar fashion, but to gain exposure a transhyoid pharyngotomy may be necessary (Fig. 9.140 and 9.141). A transhyoid pharyngotomy is performed via a transverse incision in a skin crease at the level of the hyoid bone to expose the suprahyoid musculature. The skin incision is deepened through the platysma, and upper and lower skin flaps are elevated (Fig. 9.142). The suprahyoid musculature is detached from the superior surface of the hyoid bone with use of electrocautery (Fig. 9.143). All the suprahyoid muscles should be detached to gain wide exposure through the anterior pharyngotomy in this

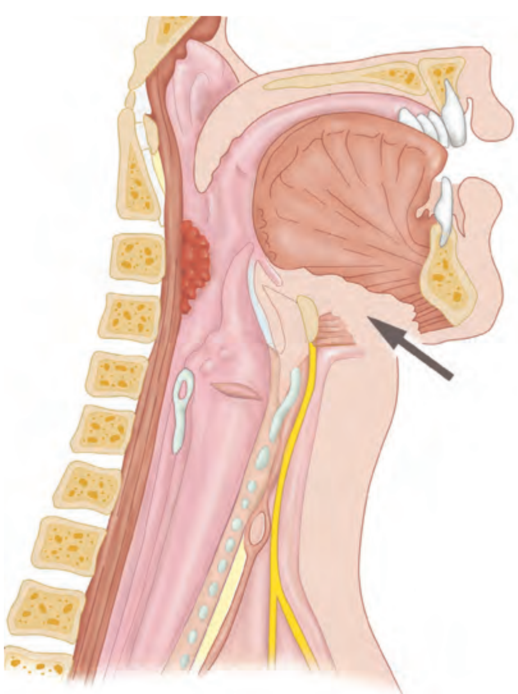

Figure 9.140 Transhyoid pharyngotomy. Arrow indicates direction of exposure.

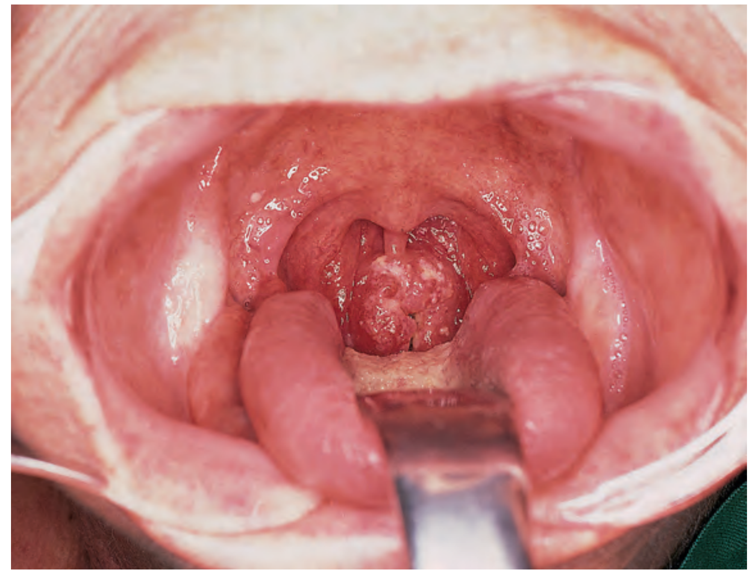

Figure 9.141 A carcinoma of the posterior pharyngeal wall that is accessible with a transhyoid pharyngotomy.

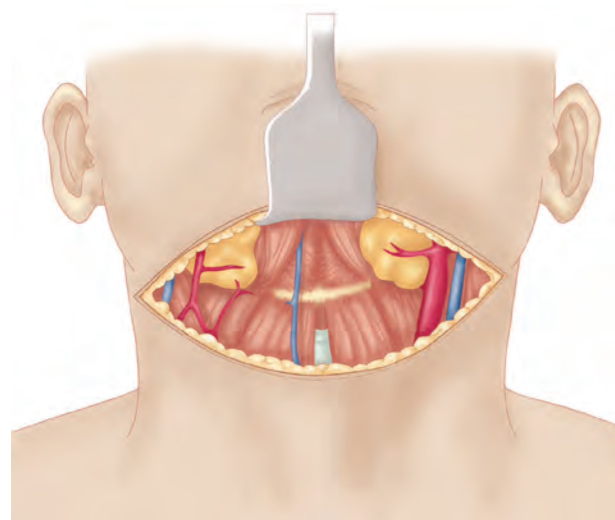

Figure 9.142 The upper and lower skin flaps are elevated.

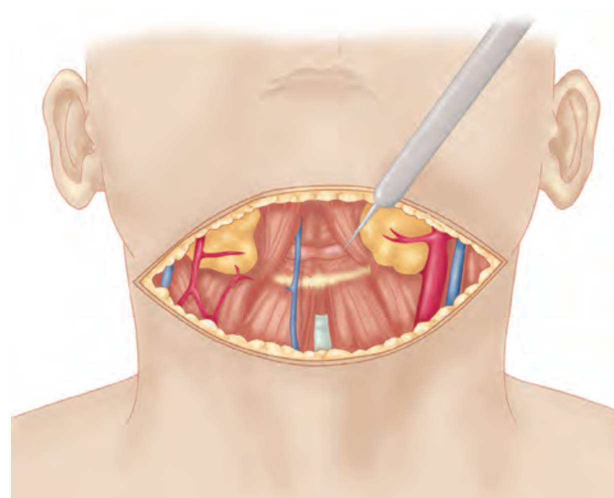

Figure 9.143 Detachment of the suprahyoid musculature.

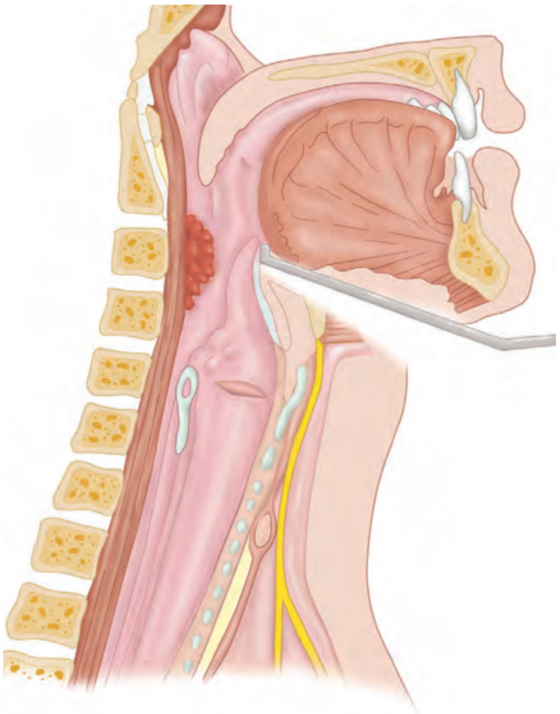

Figure 9.144 Exposure of the posterior pharyngeal wall.

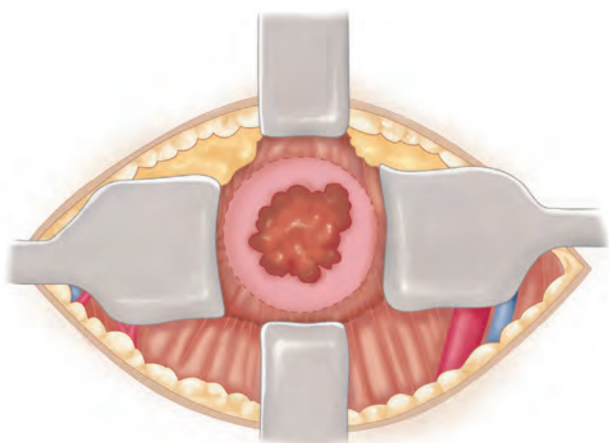

Figure 9.145 Excision of the posterior pharyngeal wall tumor.

fashion. Entry is made into the hypopharynx by incision through the mucosa of the vallecula on one side and across the glossoepiglottic fold to the vallecula on the opposite site. Generous exposure of the posterior pharyngeal wall can be obtained in this fashion (Fig. 9.144). The posterior pharyngeal wall tumor is thus exposed, providing direct access for excision with satisfactory peripheral margins (Fig. 9.145). As discussed earlier, the surgical defect may either be left open to heal by secondary intention or it can be covered with a split-thickness skin graft, fixed in position with quilting sutures (Fig. 9.146). In either event, the mucosal edges of the pharyngeal wall defect are tacked down to the prevertebral fascia with use of interrupted chromic catgut sutures.

Closure of the pharyngotomy is performed with heavy absorbable sutures such as 0 chromic catgut interrupted sutures. These sutures are taken with a deep bite through the musculature of the base of the tongue and around the hyoid bone, through the thyrohyoid membrane, to reapproximate the musculature to the hyoid bone. Extreme care should be exercised during closure of the lateral aspect of the pharyngotomy, because the lingual artery and the hypoglossal nerve in the base of the tongue are in the vicinity of the lateral edge of the greater cornua of the hyoid bone cephalad. Similarly, care should be exercised to protect the internal laryngeal branch of the superior laryngeal nerve, which enters the thyrohyoid membrane just caudad to the lateral end of the greater cornua of the hyoid bone. Several interrupted sutures are taken to resuspend the larynx back to the tongue. The remaining incision is closed in the usual fashion. No attempt is made to close the mucosa of the base of the tongue to the mucosa of the glossoepiglottic fold and the anterior wall of the pyriform sinus. Simple resuspension of the hyoid bone to the musculature of the base of the tongue provides satisfactory closure, and the mucosal incision heals without difficulty. A nasogastric feeding tube and tracheostomy are essential until the patient is able to swallow by mouth without aspiration.

Figure 9.146 A postoperative photograph showing a healed skin graft.

Partial Pharyngectomy and Reconstruction With a Radial Forearm Free Flap

Larger defects of the posterior pharyngeal wall require a more elaborate reconstructive effort. One can easily excise the entire posterior pharyngeal wall extending from the oropharynx down to the cervical esophagus cephalocaudad and from the lateral wall of the pyriform sinus on one side to that on the opposite side and still be able to preserve the larynx. However, for such large defects, vascularized free flaps with skin lining are essential to achieve primary healing. A pectoralis major myocutaneous flap can be used in this clinical setting and may be satisfactory in thin patients, but in patients with a substantial bulk of pectoral muscle or in women, excessive bulk of the flap makes the reconstruction technically difficult and functionally suboptimal. In that setting, a fasciocutaneous radial forearm free flap or an ALT flap is ideal to achieve watertight mucosal closure and restore satisfactory function of swallowing.

Most patients requiring excision of lesions of this magnitude either will have clinically apparent cervical lymph node metastases that require a neck dissection or will need an elective dissection of regional lymph nodes involving levels II, III, and IV on one or both sides because of the high risk of micrometastasis in a clinically negative neck. Therefore the surgical procedure of bilateral jugular lymph node dissection (levels II, III, and IV) with posterior wall pharyngectomy is considered

optimal for patients with carcinoma of the posterior pharyngeal wall and negative clinical findings of the neck. The surgical procedure can be accomplished through a single transverse incision that extends from the anterior border of the trapezius muscle on one side of the neck to that on the other side of the neck at the level of the thyrohyoid membrane. The patient is given general anesthesia after a preliminary tracheostomy is performed under local anesthesia to avoid any trauma to the region of the primary tumor as a result of orotracheal intubation. After adequate assessment of the lesion has been performed by appropriate endoscopy, the surgical procedure begins.

The patient described here has a carcinoma of the posterior pharyngeal wall with negative clinical findings of the neck. A CT scan at the level of the supraglottic larynx shows a centrally necrotic lesion of the posterior pharyngeal wall with negative radiographic findings of the neck on both sides (Fig. 9.147). The operative procedure begins with a transverse skin incision as previously described that is deepened through the platysma. The upper and lower skin flaps are elevated in the usual fashion, exposing the suprahyoid musculature cephalad and up to the lower border of the cricoid cartilage caudad. Jugular node dissection on both sides is completed in the usual fashion (see Chapter 11 for the technique of jugular lymph node dissection). Jugular node dissection requires satisfactory clearance of lymph nodes at levels II, III, and IV and excision of deep jugular lymph nodes anterior, medial, and lateral to the internal jugular vein, thus exposing the cutaneous roots of the cervical plexus in the posterior triangle.

After the specimen of the jugular node dissection is removed, attention is focused on the exposed inferior constrictor muscle on the side where there is no extension of the posterior pharyngeal wall tumor (Fig. 9.148). Note complete clearance of jugular nodes in this patient on the left side of the neck. At the upper end of the internal jugular vein, the submandibular salivary gland is seen anterior to it. The sternomastoid muscle is retracted posteriorly to show the carotid sheath and roots of the cervical plexus. The exposed inferior constrictor muscle attached to the posterior margin of the thyroid cartilage is seen anterior to the carotid sheath. Using electrocautery, the inferior constrictor muscle is incised throughout its cephalocaudad extent to expose the mucosa of the apex of the pyriform sinus. Entry is made in the pharynx through the apex of the pyriform sinus, and the mucosal incision is extended cephalad and caudad to expose the hypopharynx (Fig. 9.149). Adequate exposure of the posterior pharyngeal wall tumor is achieved in this fashion.

Using a Richardson retractor, the larynx and the base of the tongue are retracted anteriorly to provide wider exposure and to create space to mobilize the posterior pharyngeal wall for resection of the tumor. The entire thickness of the posterior pharyngeal wall is dissected from the prevertebral fascia, and traction is applied to the lateral aspect of the specimen, permitting delivery of the tumor out of the hypopharynx into the wound (Fig. 9.150). Then, under direct vision and securing adequate circumferential mucosal margins, full-thickness resection of the posterior pharyngeal wall is accomplished to remove the tumor in a monobloc fashion (Fig. 9.151). Hemostasis is secured by electrocoagulation of bleeding from the mucosal edges and by

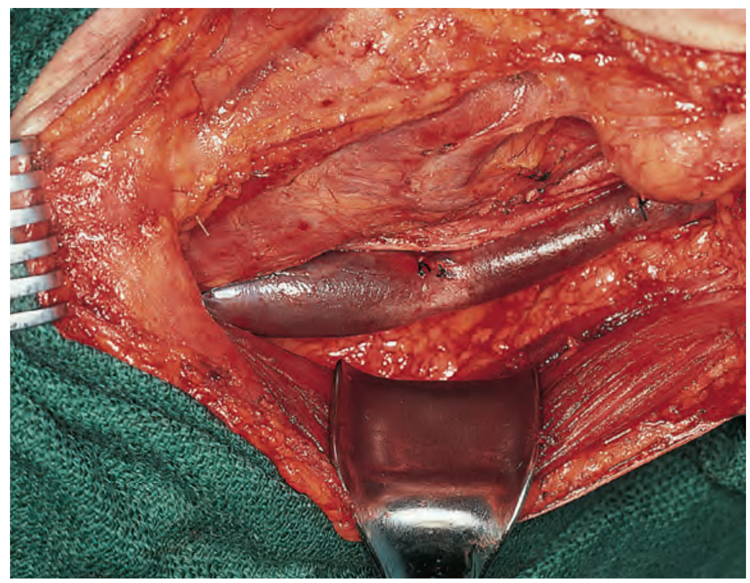

Figure 9.148 Jugular node dissection on the left-hand side is completed and the inferior constrictor muscle is exposed.

Figure 9.147 A computed tomography scan of the neck at the level of the supraglottic larynx showing a tumor of the posterior pharyngeal wall (*arrow*).

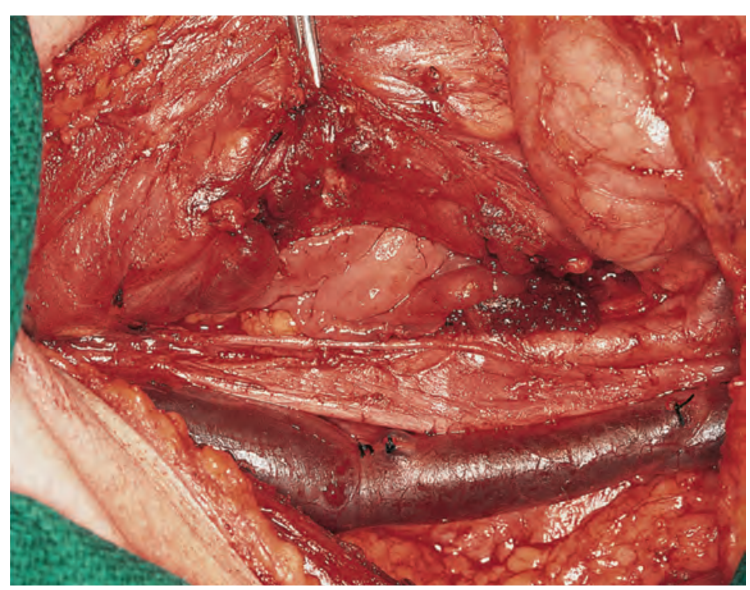

Figure 9.149 The pharynx is entered through a mucosal incision at the apex of the left pyriform sinus, and the tumor is exposed.

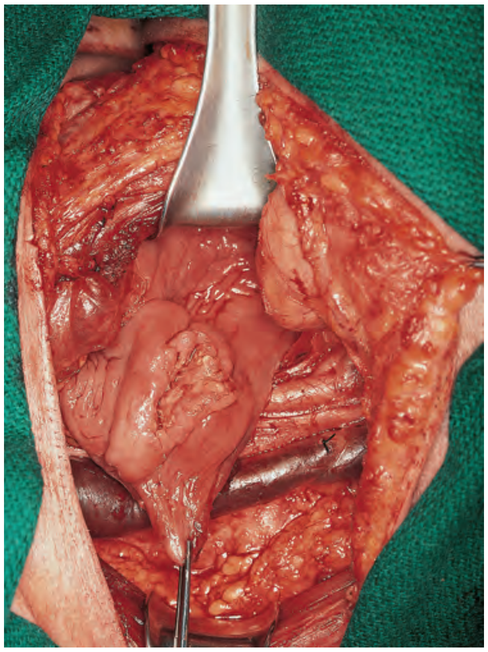

Figure 9.150 Traction is applied to the lateral margin of the pharyngeal wall to facilitate excision of the tumor.

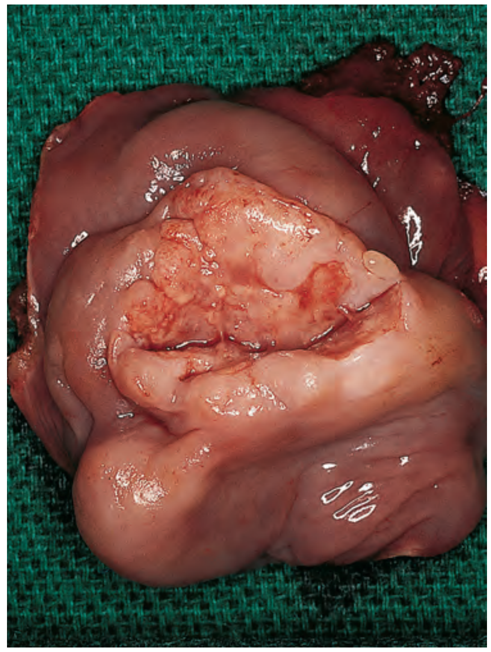

Figure 9.151 Full-thickness resection of the posterior pharyngeal wall tumor.

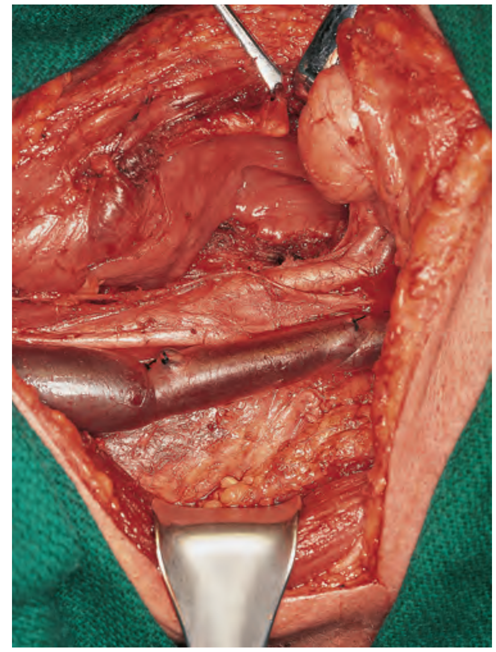

Figure 9.152 The surgical defect.

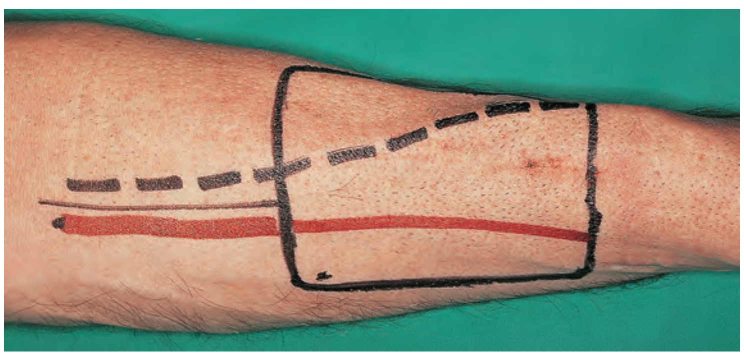

Figure 9.153 A radial forearm fasciocutaneous flap of appropriate dimensions is outlined on the left forearm.

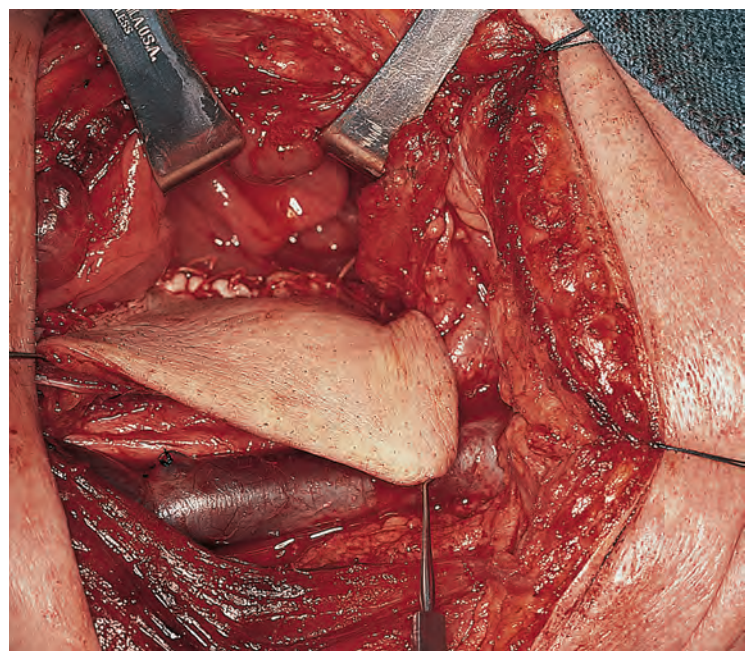

Figure 9.154 The radial forearm flap is inset, showing closure of the defect in progress.

ligating larger pharyngeal vessels. Frozen sections are obtained from the margins of the surgical defect to ensure adequacy of resection. The surgical defect created in this patient extends from the medial wall of the left pyriform sinus to the lateral wall of the contralateral pyriform sinus. Superoinferiorly it extends from the oropharynx cephalad to the lower border of the cricoid cartilage caudad (Fig. 9.152). At this point, appropriate measurements of the surgical defect are taken to design a radial forearm free flap of comparable dimensions (Fig. 9.153).

The technique used to harvest a radial forearm fasciocutaneous free flap is beyond the scope of this chapter. The reader is referred to many excellent works on microvascular surgery for technical details of harvesting a radial forearm free flap and microvascular anastomosis.

After the flap is appropriately harvested, it is transferred to the neck, and the vascular anastomoses are completed. Alternatively, one may place the flap in a satisfactory fashion and complete three-quarters of the circumferential closure before vascular anastomoses are complete (Fig. 9.154). Absolute diligence in the placement of sutures must be exercised to secure a watertight closure; otherwise the risk of leakage and a pharyngocutaneous fistula exists. The closure is accomplished with use of interrupted absorbable sutures. Extreme care should be exercised at the lower margin of the closure between the posterior wall of the cervical esophagus and the lower border of the free flap to avoid stenosis by stricture formation. It may be desirable to split the esophagus vertically in the posterior midline to insert a wedge of the skin flap in it to avoid stricture formation.

Patients with excessive hair on the forearm will transfer hair-bearing skin on the radial forearm free flap. However, if the patient is to receive postoperative radiation therapy, the hair follicles will be epilated and the skin of the forearm flap will not pose any problem. On the other hand, if surgery is undertaken for patients who have had previous radiation therapy or for whom radiation therapy is not to be used, a hairy skin flap is likely to produce difficulty with irritation and tickle in

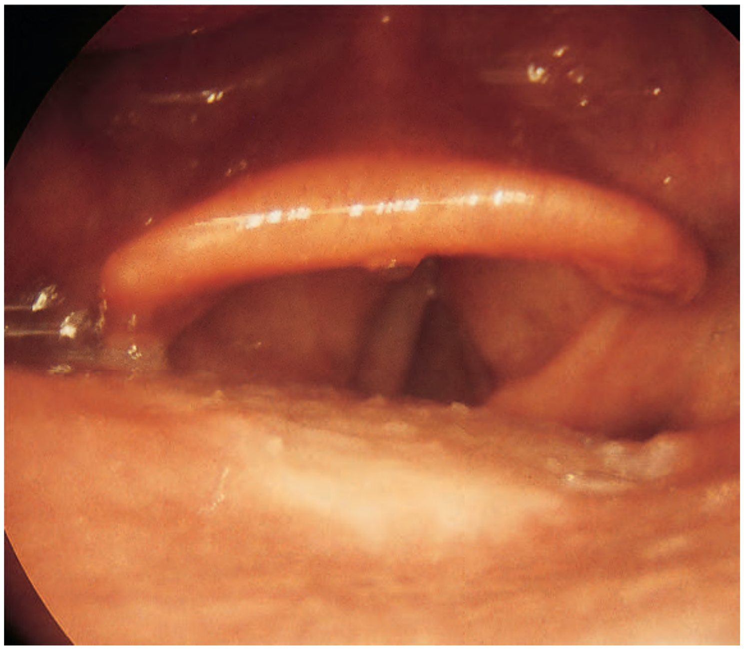

Figure 9.155 The postoperative appearance of the reconstructed posterior pharyngeal wall.

the pharynx. Under those circumstances, the radial forearm flap should be deepithelialized to eradicate the hair follicles.

Use of a nasogastric feeding tube and tracheostomy is essential. Primary healing should be expected in every instance because the transferred flap is well vascularized and seldom creates ischemic necrosis. Oral feedings may be attempted approximately 2 to 3 weeks after surgery. Most patients will require a gradual increment in oral feedings under supervision and with guidance from a speech and swallowing therapist. The postoperative endoscopic view of the reconstructed posterior pharyngeal wall shows primary healing of the skin flap to the mucosa of the pharyngeal wall with a smooth, flat reconstruction and no obstruction to the laryngeal introitus (Fig. 9.155). The radial forearm free flap provides an ideal method of reconstruction of large full-thickness defects of the posterior pharyngeal wall. The ALT flap in a thin patient will serve equally well and avoid the need for a skin graft and the resultant deformity at the donor site.

Partial Laryngopharyngectomy

The following important criteria must be met for the successful performance of a partial laryngopharyngectomy for pyriform sinus or pharyngeal wall primary cancer:

1. The primary tumor must be confined only to the anatomic site of origin within the hypopharynx, that is, either the pyriform sinus or pharyngeal wall.
2. The tumor must not extend up to the apex of the pyriform sinus.
3. The tumor must be limited to the pyriform sinus with no significant extension to the base of the tongue.
4. The ipsilateral hemilarynx must be mobile.
5. The tumor may extend to involve the supraglottic larynx but should not extend in a transglottic fashion.

The surgical approach for a partial laryngopharyngectomy is generally similar to the approach for a supraglottic partial laryngectomy. Technical steps for the transhyoid approach to the supraglottic larynx are described in Chapter 10.

The patient described here has a primary carcinoma involving the medial wall of the right pyriform sinus with minimal extension to the adjacent vallecula (Fig. 9.156). The tumor does not reach the apex of the pyriform sinus, and the ipsilateral hemilarynx is mobile. The patient is a 46-year-old, otherwise healthy man who had undergone radical neck dissection 3 years earlier for metastatic squamous cell carcinoma from an unknown primary source. The primary tumor of the right pyriform sinus was detected during a routine follow-up examination and is felt to be the primary source for the previously treated neck metastases.

The patient is placed under general anesthesia with an endotracheal tube. After adequate endoscopic assessment, a tracheostomy is performed first, the airway is switched over to the tracheostomy tube, and the endotracheal tube is removed. The head and neck area is then prepped and draped as usual. A transverse incision is taken at the level of the thyrohyoid membrane, extending from the anterior border of the sternomastoid muscle on one side to that on the opposite side. The skin incision is deepened through the platysma, and the upper and lower skin flaps are elevated to expose the hyoid bone and the upper half of the thyroid cartilage.

The strap muscles are detached from the undersurface of the hyoid bone and are retracted laterally for subsequent closure. Musculature of the base of the tongue on the ipsilateral side of the hyoid bone is detached with an electrocautery to bare the superior surface of the hyoid bone on that side. The hyoid bone is divided in the midline with a bone cutter.

Using a power sagittal saw, the upper end of the thyroid cartilage on the ipsilateral side is divided from the midline up to its posterior margin. Approximately 3 to 5 mm of the upper edge of the thyroid cartilage is resected. At this point, entry is made into the oropharynx via the mucosa of the glossoepiglottic fold in the midline. The tip of the epiglottis is visualized through this opening in the oropharynx. The epiglottis is grasped with a toothed forceps, and using an electrocautery with a needle tip, it is divided through its full thickness in the midline from its tip down to its infrahyoid portion.

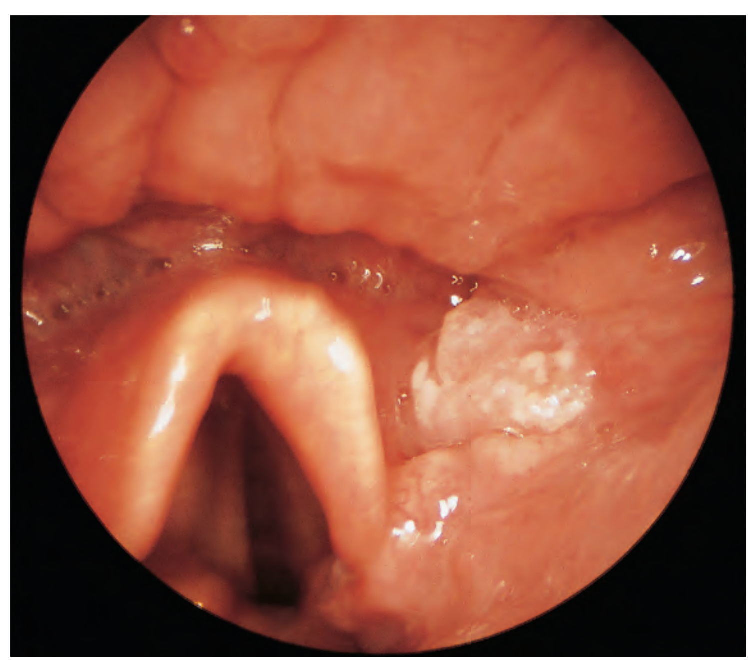

Figure 9.156 A primary carcinoma involving the medial wall of the right pyriform sinus.

The cut in the epiglottic cartilage now meets with the cut through the thyroid notch. The vertical cut in the midline is connected to the transverse cut of the thyroid cartilage on the right-hand side. This step will permit rotation of the surgical specimen to the right-hand side, providing a view of the primary tumor of the pyriform sinus. With use of an electrocautery or angled scissors, the surgical specimen of the right half of the supraglottic larynx, in conjunction with the pyriform sinus, is resected with adequate mucosal and soft-tissue margins around the primary tumor, obtained under direct vision. Brisk hemorrhage from the branches of the superior laryngeal artery is to be expected but is easily controlled with appropriate hemostasis.

The surgical defect following removal of the specimen shows the remaining left side of the larynx, including the left half of the epiglottis, the aryepiglottic fold, and the glottic larynx (Fig. 9.157). A large raw area remains at the right lateral pharyngeal wall from where the primary tumor is removed. Frozen sections are obtained from the margins of the surgical defect to ensure satisfactory resection of the tumor. No attempt is made to obtain mucosal closure of this surgical defect, which is allowed to granulate.

A nasogastric feeding tube is inserted and pharyngeal closure is performed, with reapproximation of the musculature of the left base of the tongue to the left half of the hyoid bone if any muscles were detached in that area. The musculature of the base of the tongue of the right-hand side (ipsilateral side) is sutured to the detached strap muscles of the right side with interrupted chromic catgut sutures. No mucosal or skin flaps are necessary to provide lining to the lateral pharyngeal wall. The raw area will spontaneously epithelialize during the next few weeks. After adequate muscular closure is obtained, a Penrose drain is inserted, and the remaining incision is closed with 3-0 chromic catgut sutures for platysma and 5-0 nylon for skin.

The surgical specimen, viewed from the posterior aspect, shows the right half of the supraglottic larynx with the right half of the epiglottis and aryepiglottic fold as well as the right false cord (Fig. 9.158). The primary tumor of the medial wall of the pyriform sinus is resected with satisfactory mucosal and soft tissue margins. The patient will require nasogastric feedings for approximately 2 weeks, and then semisolid foods may be tried. Aspiration of saliva and clear liquids is anticipated for several weeks, but liquids can be handled as time progresses. The nasogastric feeding tube and the tracheostomy tube eventually are removed in almost every patient. Alternatively, if prolonged swallowing difficulties are anticipated, a percutaneous gastrostomy may be performed for nutritional support. This procedure avoids the need for a nasogastric feeding tube and also avoids putting pressure on the patient to make rapid progress in swallowing without aspiration so as to permit removal of the nasogastric tube. Some patients are frustrated because it simply takes time to overcome aspiration. A percutaneous endoscopic gastrostomy is most desirable in such patients.

A postoperative view of the larynx and hypopharynx approximately 1 year after the partial laryngopharyngectomy in the same patient is shown in Fig. 9.159. Note that the glottis is

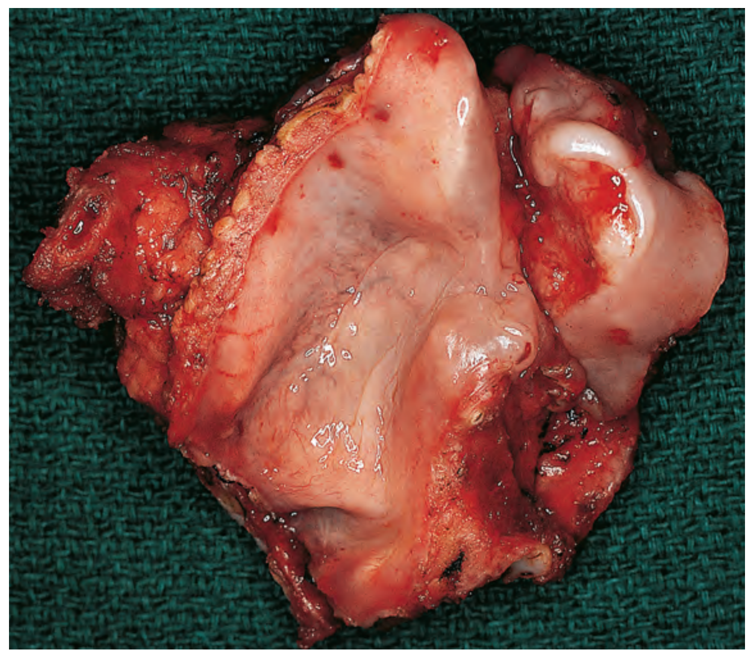

Figure 9.158 The surgical specimen.

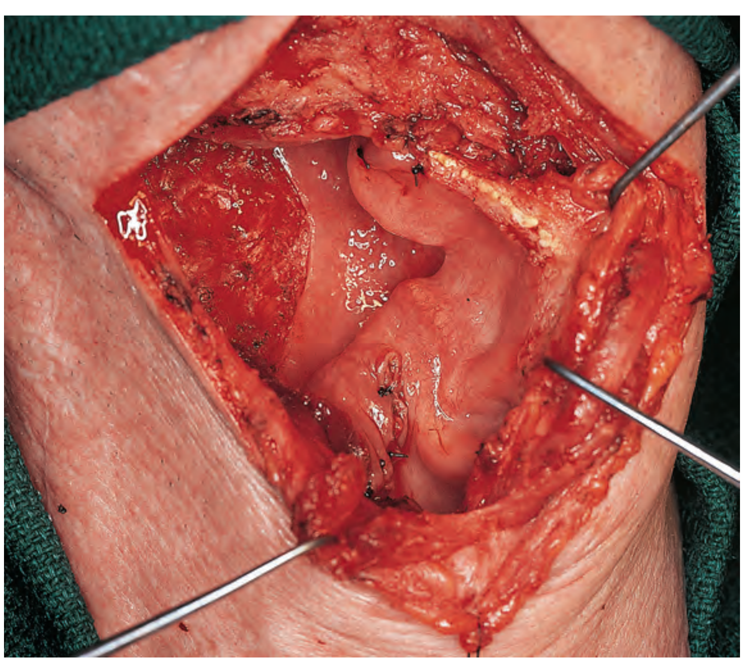

Figure 9.157 The surgical defect shows the remaining left half of the supraglottic larynx.

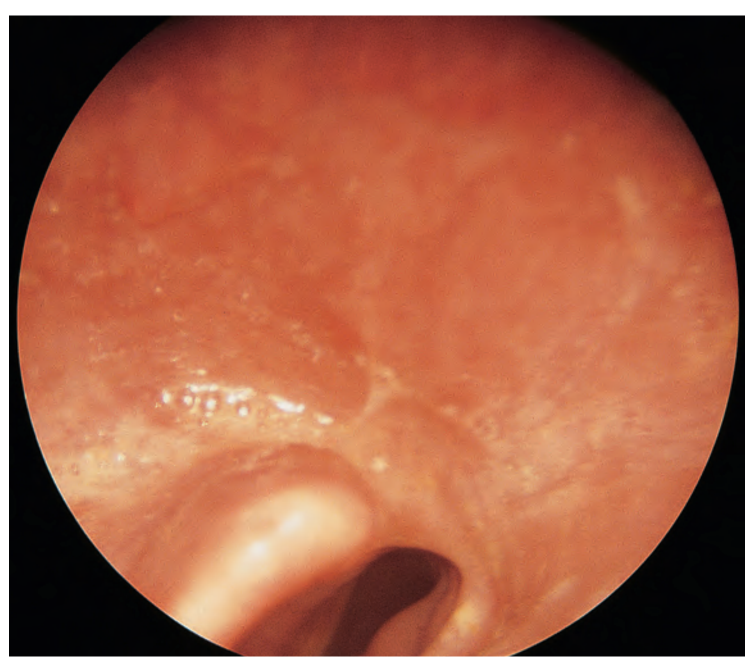

Figure 9.159 A postoperative view of the larynx and hypopharynx.

adequate, competent, and intact. A band of scar tissue is evident on the right side where the aryepiglottic fold and pyriform sinus were resected. However, the arytenoid is intact, maintaining competence of the larynx. Partial laryngopharyngectomy is a very satisfactory operation in highly selected patients with limited lesions of the hypopharynx. Appropriate radiographic and endoscopic assessment is essential, in addition to exercising good judgment in patient selection for the successful outcome of these highly sophisticated surgical procedures.

Pharyngolaryngectomy and Reconstruction With Pectoralis Major Myocutaneous Flap

Locally advanced carcinomas of the hypopharynx with extension to the larynx or the base of the tongue require a wide-field total laryngectomy with partial pharyngectomy. On the other hand, primary carcinomas of the larynx with extension to the pyriform sinus, postcricoid area, or lateral pharyngeal wall also require a pharyngolaryngectomy with immediate appropriate reconstruction of the gullet.

In addition to the clinical examination and radiographic studies, endoscopic evaluation of the primary tumor is mandatory before surgical resection. If the airway is adequate, then endotracheal intubation is safe, but it should be performed very carefully to avoid any trauma at the site of the primary tumor. Bleeding from the tumor jeopardizes accurate endoscopic assessment of the primary lesion. If the tumor impinges on the airway and the patency of the airway is in question, a preliminary tracheostomy should be performed under local anesthesia to establish a safe airway before general anesthesia is induced.

Endoscopic assessment should include evaluation of local extension of the tumor to the base of the tongue, the apex of the pyriform sinus, and in the interior of the larynx as well as to the postcricoid area and cervical esophagus. Digital palpation of the base of the tongue and the lateral pharyngeal wall is mandatory to assess deep infiltration of the underlying soft tissues. At this point, the operating surgeon is well equipped with information regarding the extent of the primary tumor and the presence or the potential risk of involvement of adjacent structures. This information will help the surgeon plan the extent of the anticipated surgical resection and the need for and the type of immediate reconstructive effort.

The patient described here had undergone an open biopsy of a cervical lymph node elsewhere before presentation for surgical treatment of his locally advanced carcinoma of the right pyriform sinus. The histologic diagnosis of metastatic squamous cell carcinoma in a lymph node from a primary tumor of the right pyriform sinus was confirmed. Endoscopic assessment revealed that the tumor had involved the right hemilarynx and at least one-third of the circumference of the hypopharynx.

The surgical procedure therefore will include a right neck dissection in conjunction with a total laryngectomy and a subtotal pharyngectomy. It is anticipated that only a small portion of the posterolateral pharyngeal wall on the left-hand side of the pharynx will remain after resection. This extent of surgical resection was reconstructed immediately with a pectoralis major myocutaneous flap. The proposed incisions for the neck dissection and the pectoralis major myocutaneous flap are outlined (Fig. 9.160). The proposed site of a permanent tracheostome in the suprasternal notch is also outlined on the skin before the operative procedure begins. The scar of the previous lymph node biopsy will be excised and incorporated in the transverse component of the incision for neck dissection.

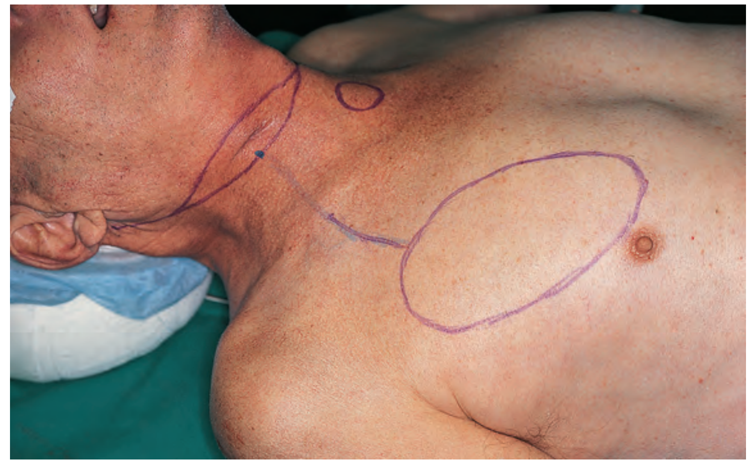

Figure 9.160 Incisions for a pharyngolaryngectomy, radical neck dissection, and pectoralis major myocutaneous flap reconstruction are outlined.

The technical details of a neck dissection are discussed in Chapter 11. The contents of the posterior triangle of the neck are dissected and mobilized medially. The sternomastoid muscle is detached from its lower and upper insertion and dissection of the submandibular triangle is completed, leaving the neck dissection specimen attached medially to the larynx and hypopharynx. A circular disc of skin is now excised at the site of the proposed permanent tracheostome. The strap muscles in front of the thyroid gland are divided low in the neck and allowed to retract cephalad. The isthmus of the thyroid gland is divided and the (contralateral) left thyroid lobe (with its blood supply intact) and the parathyroid glands are separated from the trachea and the tracheoesophageal groove and retracted laterally. This will ensure preservation of at least the two left viable parathyroid glands.

The trachea is transected at an appropriate level in a beveled fashion, and its stump is sutured to the skin edges of the tracheostome with interrupted nylon sutures. Dissection now proceeds in the suprahyoid region. All the suprahyoid muscles are detached from the superior surface of the hyoid bone with use of electrocautery. Entry is made in the pharynx by incising the mucosa of the left vallecula. A finger is introduced through this area in the (contralateral) left pyriform sinus, and the pharyngeal musculature, including the inferior constrictor muscle, is divided with electrocautery. The mucosa of the medial wall of the left pyriform sinus is also incised to permit rotation of the larynx and the hypopharynx to the right-hand side, as shown in Fig. 9.161. Note the extensive tumor of the right pyriform sinus, with direct encroachment upon the right hemilarynx and extension cephalad into the lateral pharyngeal wall and caudad up to the apex of the pyriform sinus.

Posteriorly, the tumor extends up to the midline of the posterior pharyngeal wall. At this point, under direct vision, the mucosa of the cervical esophagus, proximal to the site of the transection of the trachea, is incised with electrocautery, leaving a generous margin around the primary tumor. Full-thickness resection of the esophageal and pharyngeal wall, around the tumor with adequate margins, is then undertaken with electrocautery.

A similar incision is made in the mucosa of the posterior pharyngeal wall all around the visible extent of the primary tumor with a margin of normal mucosa and underlying soft tissues. Through-and-through resection of the posterior pharyngeal wall is then undertaken. The superior laryngeal vessels on the right

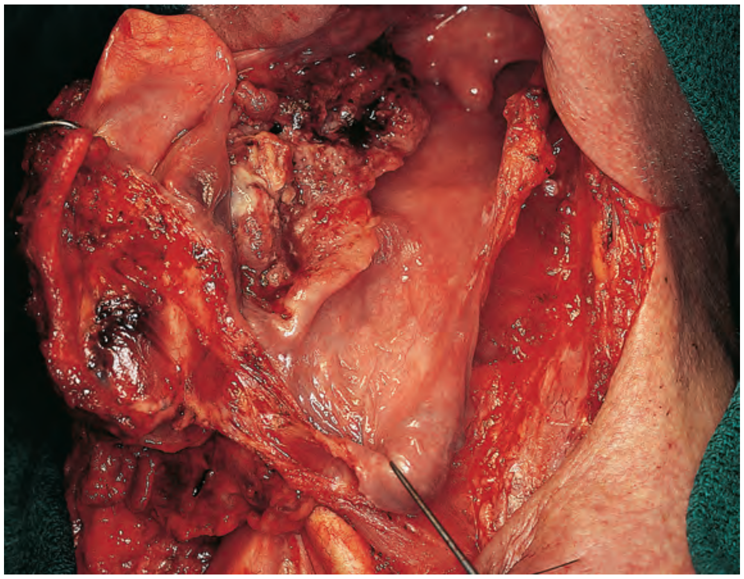

Figure 9.161 The pharynx is entered through the left pyriform sinus and the larynx is rotated toward the right-hand side, exposing the tumor.

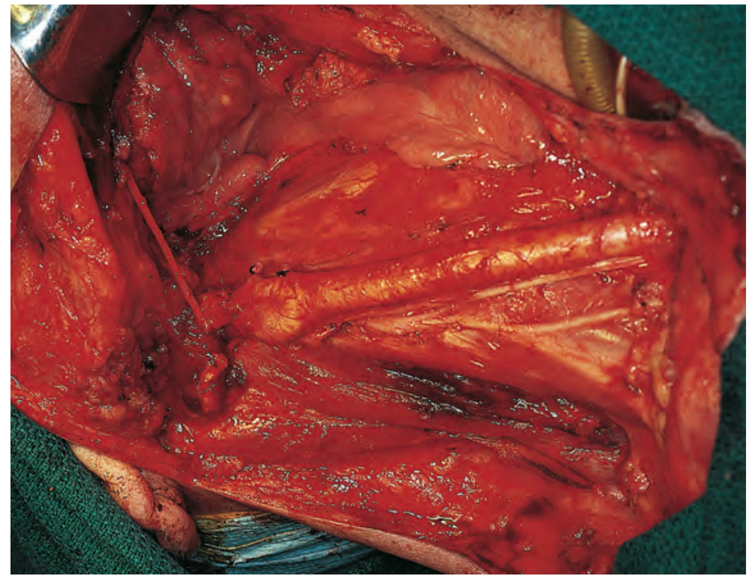

Figure 9.163 The surgical defect following radical neck dissection, a total laryngectomy, and a partial pharyngectomy.

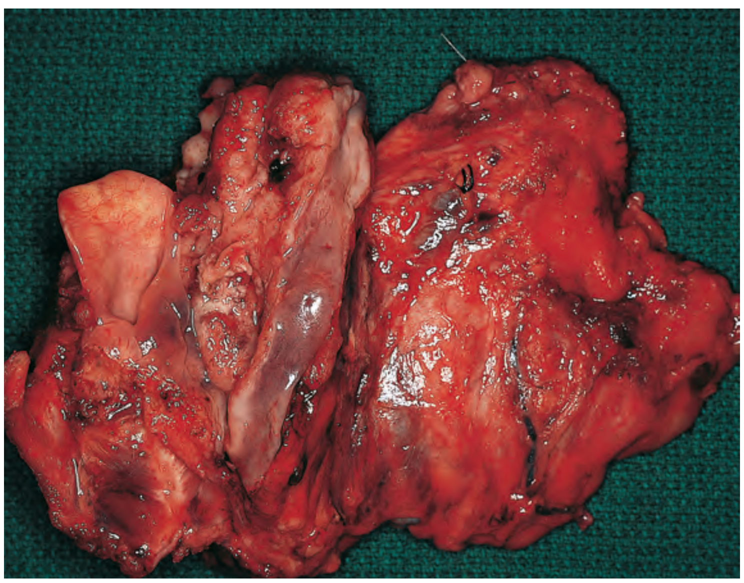

Figure 9.162 The surgical specimen shows the larynx, pharynx, and dissected contents of the right side of the neck.

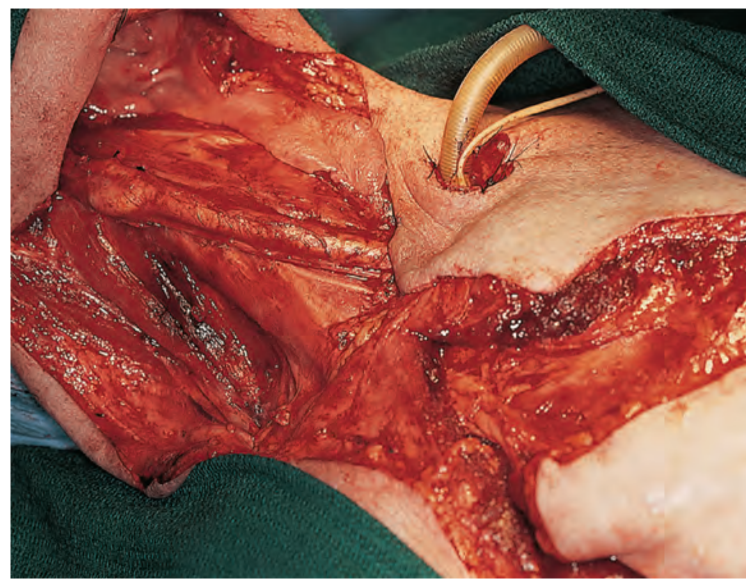

Figure 9.164 The pectoralis major myocutaneous flap is elevated and its vascular pedicle is skeletonized.

side and other terminal branches of the external carotid artery that provide blood supply to the pharyngeal wall and tonsillar bed are divided and ligated. This step will enable removal of the surgical specimen, which shows the larynx, adjacent pharynx, and the cervical lymph nodes from neck dissection on the right-hand side removed in a monobloc fashion (Fig. 9.162). The surgical specimen should be carefully examined in the operating room to assess the adequacy of margins around the primary tumor.

Complete hemostasis is obtained in the surgical field. At this point, the wound is irrigated with Bacitracin solution. Frozen sections are obtained from the margins of the surgical defect to ensure complete removal of the primary tumor with negative margins (Fig. 9.163). Note the remaining wall of the pharynx on the left-hand side connecting the oropharynx to the cervical esophagus. The width of the remaining pharyngeal wall clearly is not sufficient for primary closure. However, the remaining pharyngeal wall is wide enough not to be resected in toto and thrown away. This patient thus requires a partial pharyngeal repair to recreate the neopharynx. The dimensions of the pharyngeal defect are measured again, and the previously outlined markings of the proposed pectoralis major myocutaneous flap are compared. If any adjustment is necessary in the dimensions of the flap or the length of its pedicle, they are corrected at this point.

The pectoralis major myocutaneous flap is elevated in the usual manner (Fig. 9.164). The technical details of the elevation of the pectoralis major myocutaneous island flap are described in Chapter 17. After the flap is completely elevated and its vascular pedicle is appropriately isolated, it is flipped 180 degrees to bring the skin side in, which will direct the blood flow in its vascular pedicle from its natural caudad direction to its new position cephalad.

The rotated myocutaneous flap is now allowed to rest in the neck. Closure of the pharyngeal defect begins with approximation of the right lateral edge of the remaining pharyngeal wall with the left lateral edge of the myocutaneous flap using interrupted 2-0 chromic catgut sutures (Fig. 9.165). The closure starts at the lowermost part of the defect near the cervical esophagus. A circular suture line at the lower end should be avoided. Every

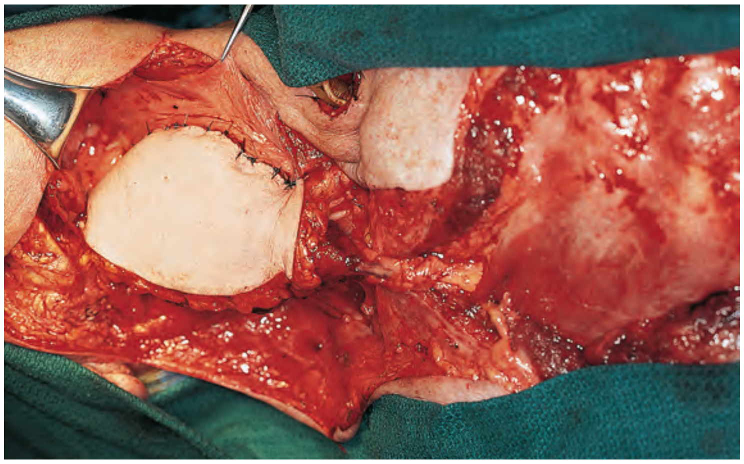

Figure 9.165 Closure of the pharyngeal defect with interrupted sutures between the flap and the pharyngeal wall.

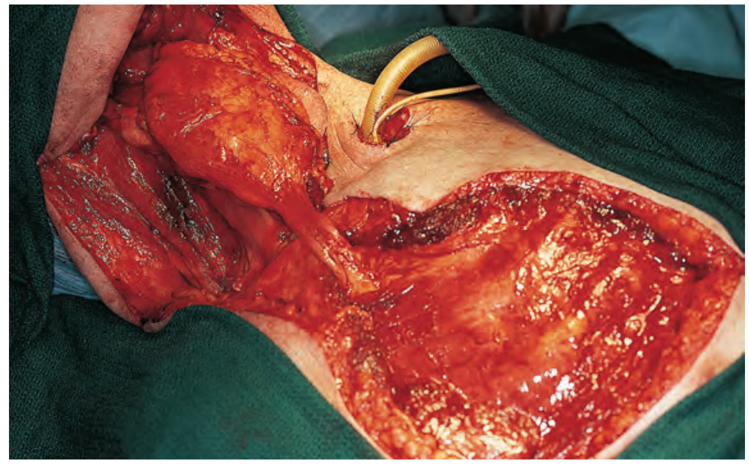

Figure 9.166 The completed pharyngeal repair showing the pectoralis major muscle with its vascular pedicle.

attempt should be made to form the pharyngoesophageal defect in the shape of a racquet. The apex of the myocutaneous flap is then inserted into the narrow angle of the racquet-shaped pharyngeal defect to avoid concentric stricture formation. The right lateral vertical suture line is continued until the upper end of the flap reaches the upper end of the posterior pharyngeal wall defect. The suture line between the superior margin of the posterior pharyngeal wall defect and the upper end of the skin flap continues until the right-hand margin of the distal part of the myocutaneous flap approximates the base of the tongue on the right side. At this point the flap is turned over and the suture line continues with interrupted chromic catgut sutures between the mucosa of the base of the tongue and the distal cutaneous margin of the myocutaneous flap.

As the suture line progresses toward the left side, the flap starts turning over itself. Eventually the suture line between the base of the tongue and the right lateral aspect of the flap meets with the anterior wall or the left lateral edge of the remaining pharyngeal wall. The vertical suture line between the left lateral edge of the remaining pharynx and the right lateral wall of the myocutaneous flap continues caudad until the entire pharynx is fully reconstructed. A nasogastric feeding tube is inserted and passed into the distal esophagus before complete closure of the pharyngeal defect.

The pharyngeal repair is now complete, demonstrating the muscular part of the pectoralis major myocutaneous flap seen in the neck, with its vascular pedicle coming from the subclavian artery and vein from below the clavicle (Fig. 9.166). Tension on the vascular pedicle should be avoided by measuring the length of the flap and the pedicle before its elevation and rotation. The neck wound is irrigated again with Bacitracin solution. The skin incisions are closed with suction drains on the anterior chest wall as well as in the neck. The vascular pedicle of the myocutaneous flap lies immediately beneath the skin overlying the clavicle and is easily available for monitoring by palpation in the postoperative period.

Nasogastric tube feedings can be started 24 hours postoperatively and should continue until satisfactory healing of the neck wound is seen. The suction drains are removed when drainage from the neck and chest wounds is minimal. If the neck flaps remain well healed and there is no evidence of salivary leakage, clear liquids are given by mouth approximately 7 to 10 days after surgery. If these liquids are well tolerated, the nasogastric feeding tube is removed, and the patient is allowed to progress to a puréed diet.

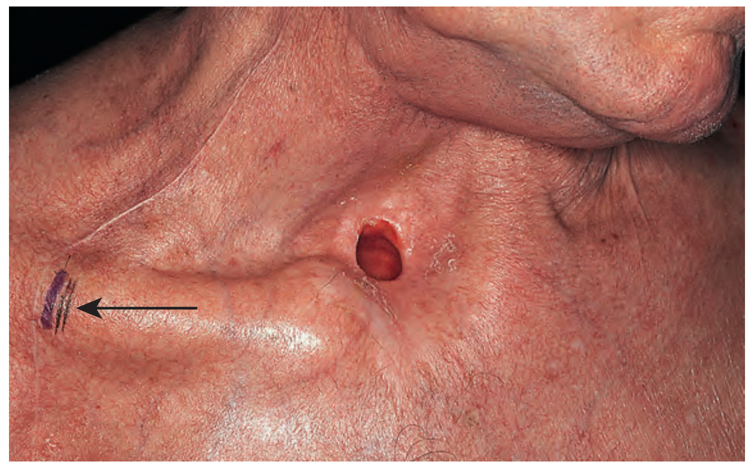

Figure 9.167 The healed neck incision. *Arrow* points to the vascular pedicle under the skin.

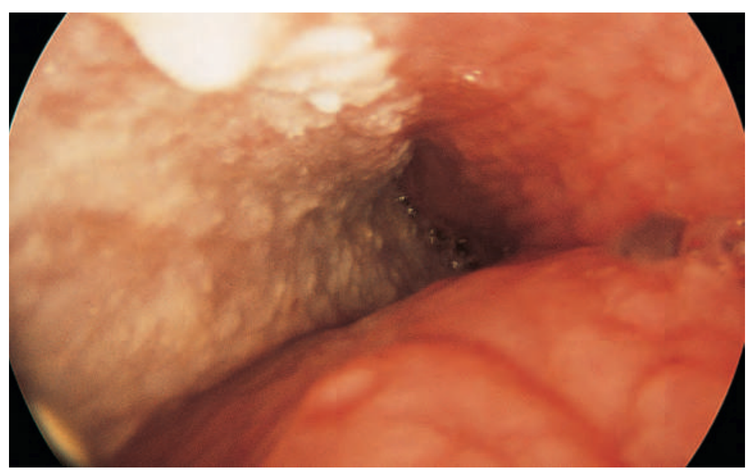

Figure 9.168 An endoscopic view of the reconstructed pharynx 3 months after surgery.

The healed neck incision is shown in Fig. 9.167. The location of the vascular pedicle of the myocutaneous flap can be seen overlying the clavicle. The aesthetic deformity as a result of elevation and use of the pectoralis major myocutaneous island flap is minimal. Excessive bulk is not seen overlying the clavicle, because this is an island flap created by skeletonizing the vascular pedicle by trimming off excess muscle.

Fig. 9.168 shows an endoscopic view of the reconstructed pharynx approximately 3 months after surgery. Note that the myocutaneous flap has effectively reconstructed the pharynx, providing an adequate lumen for the consumption of a regular

diet. The pectoralis major myocutaneous flap reconstruction is an excellent technique for the repair of partial pharyngeal defects to restore the continuity of the gullet. The flap is reliable and highly successful and thus an excellent choice in the repair of partial pharyngeal defects.

Total Pharyngolaryngectomy and Reconstruction With a Jejunal Free Flap

Circumferential defects of the pharynx and cervical esophagus are readily amenable to one-stage reconstruction with a vascularized segment of the intestinal tract. The surgical procedure is simple but requires a high degree of technical skill and expertise in microvascular surgery. Therefore, to ensure a successful outcome, it is essential that the operating surgeon has technical expertise in microvascular surgery. Alternatively, a microvascular surgeon should be available to work with the head and neck surgeon for the reconstructive effort. Ideally, a head and neck surgical team and a microvascular reconstructive team should work simultaneously in a two-team effort to bring about an expeditious and successful completion of the surgical procedure.

Careful and detailed head and neck examination as well as endoscopic assessment of the primary tumor are essential before embarking on this surgical procedure. Adequate radiographic studies of the site of the primary tumor also are necessary. A barium swallow usually will suffice in delineating the extent of a lesion of the cervical esophagus and particularly its lower border, but this study must be complemented by satisfactory endoscopic examination under general anesthesia. A CT scan with contrast enhancement should be obtained to assess cervical lymph nodes.

Patients with significant peripheral vascular disease and particularly those with small vessel disease are not ideal candidates for composite free tissue transfer with microvascular anastomosis.

The barium swallow of a patient with a carcinoma of the postcricoid region shown in Fig. 9.169 demonstrates a filling defect in the hypopharynx. The lower end of the filling defect extends into the upper part of the cervical esophagus. In spite of a bulky primary tumor, the regional cervical lymph nodes were not palpable. Because of the midline location of the tumor, the risk of regional lymph node metastasis is nearly equal on both sides. Therefore this patient underwent bilateral jugular lymph node dissection (levels II, III, and IV) in conjunction with a circumferential pharyngolaryngectomy. The details of a pharyngolaryngectomy have been previously described, and the technique of jugular node dissection is described in Chapter 11.

Because of the nature of the reconstructive procedure planned, it is important to dissect and isolate a donor vessel from the branches of the external carotid artery and a recipient vein in its vicinity. These vessels will be used for vascular anastomosis, with the pedicle of the jejunal free flap. The facial artery, superior thyroid artery, lingual artery, or transverse cervical artery is best suited as the donor vessel. The common facial vein, external jugular vein, or even internal jugular vein may be used as the recipient vein.

The surgical specimen shows a large obstructing postcricoid carcinoma resected in a monobloc fashion with the larynx (Fig. 9.170). Note the infiltrating nature of the tumor with deep excavation in the postcricoid region.

A diagrammatic representation of the surgical field after removal of the specimen shows the stump of the oropharynx with the base of the tongue anteriorly and the transected edge of the lateral and posterior pharyngeal wall (Fig. 9.171). At the lower end of the diagram, the stump of the distal esophagus is seen posterior to the stump of the trachea. The superior thyroid artery and vein on the right-hand side are shown in the center of the surgical defect and are dissected for anastomosis with the vascular pedicle of the graft.

The surgical defect in the patient is shown in Fig. 9.172. Note the transected stump of the posterior pharyngeal wall at the upper end of the surgical field. The tracheostome is completed with anastomosis between the mucosa of the stump of the trachea to the skin of the suprasternal region. The superior thyroid artery and a branch of the internal jugular vein are isolated and prepared for anastomosis to the arterial stump of the jejunal graft. The stump of the esophagus posterior to the tracheostome is identified by black silk sutures. Complete hemostasis in the surgical field must be secured before the reconstructive procedure begins.

Figure 9.169 A barium swallow showing a lesion of the postcricoid region.

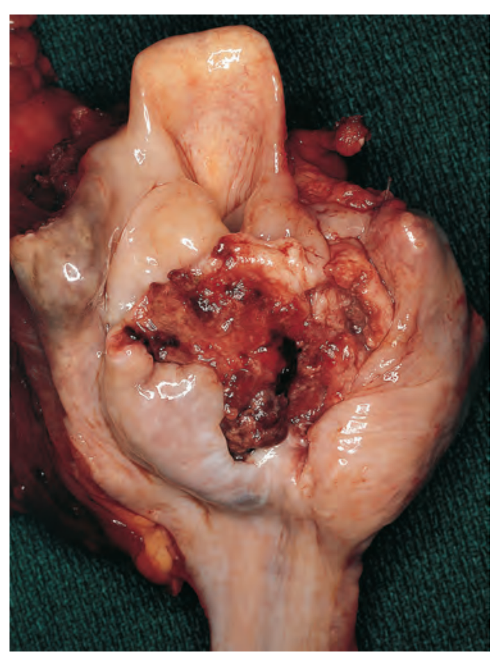

Figure 9.170 The surgical specimen.

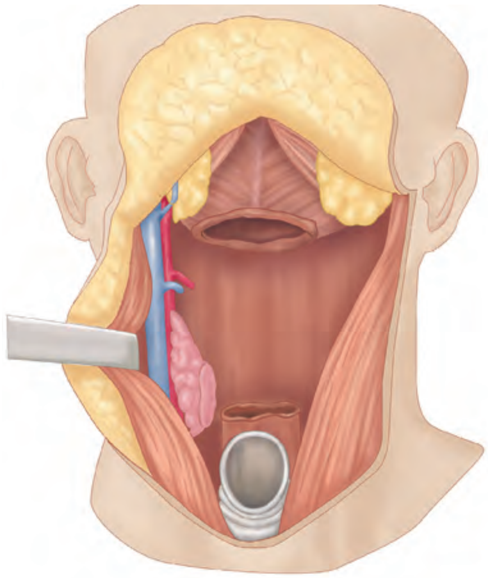

Figure 9.171 A diagrammatic representation of the surgical field.

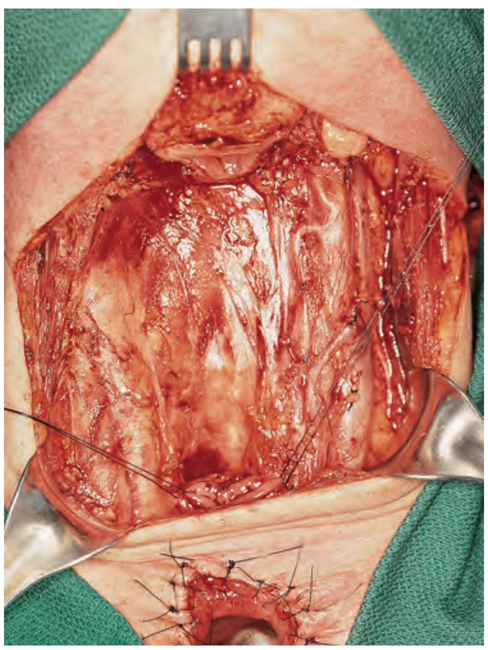

Figure 9.172 The surgical defect.

Attention is focused on the abdomen, where an upper abdominal midline laparotomy is performed. Alternatively, the jejunal graft may be harvested by laparoscopic techniques. If harvesting of the graft is to be done by the same surgical team, then the entire team should rescrub. On the other hand, it is ideal to have two surgical teams, with the reconstructive team starting the laparotomy simultaneously with the ablative procedure in the neck. Following exploration of the abdomen, a satisfactory loop of intestine is selected as a donor graft. Ideally, proximal jejunum is preferable because of its rich vascular arcades (Fig. 9.173). The jejunum is also ideal for end-to-end anastomosis with the esophagus but should be beveled at the proximal end to create a larger circumference for anastomosis with the oropharynx. An appropriate segment of the jejunum is selected with a satisfactory vascular arcade leading to a single artery and a vein at the root of its mesentery (Fig. 9.174). The vascular pedicle of the mesentery leading to this segment of the jejunum should not be divided until just before transfer of the graft. The segment of the jejunum is divided with the use of a gastrointestinal stapler.

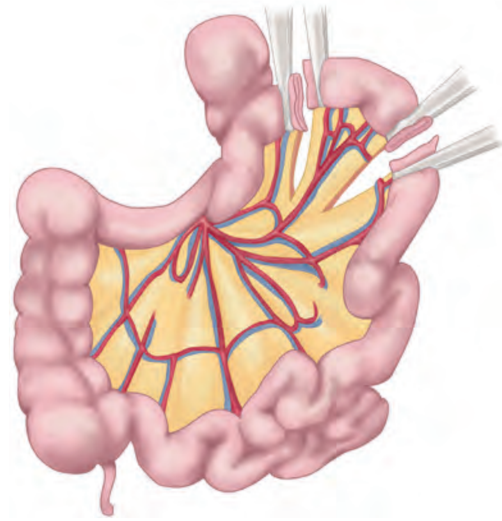

Figure 9.173 A segment of jejunum is used as a donor graft.

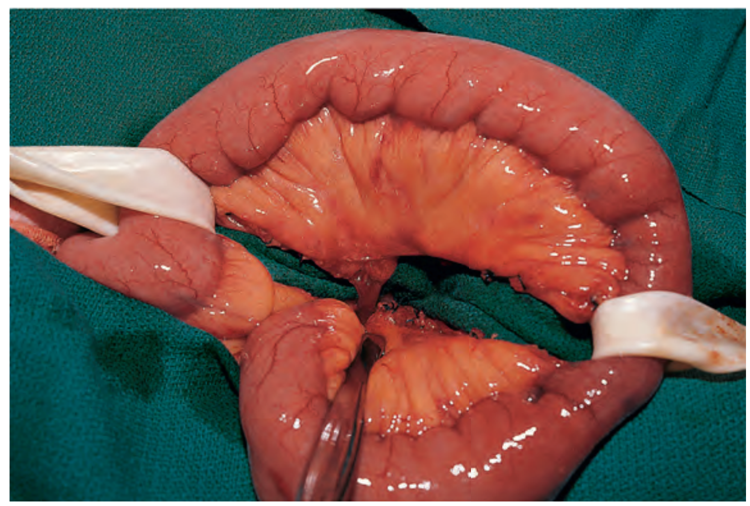

Figure 9.174 The jejunal graft is isolated.

The anastomosis between the proximal and distal ends of the jejunum is completed in the abdomen in the usual fashion to reestablish continuity of the intestinal tract. Following completion of the anastomosis of the jejunum, the vascular pedicle of the graft is dissected to isolate its artery and vein. Microvascular clamps are applied on the graft side of the isolated vascular pedicle, and hemostats are applied to the proximal part of the vascular pedicle, individually clamping the artery and vein. The vascular pedicle is now divided, and the stumps of the vessels of the mesentery are suture ligated. The defect in the mesentery is closed with interrupted 3-0 chromic catgut sutures. Complete hemostasis is secured in the abdomen and the anterior abdominal wall is closed in layers in the usual fashion.

The harvested graft with its vascular pedicle dissected is shown in Fig. 9.175. Note a black silk suture on the right-hand side of the graft, which identifies its proximal end to facilitate its placement in the neck in an isoperistaltic fashion. A diagrammatic representation of the reconstructed surgical defect shows the reestablishment of the continuity of the alimentary tract (Fig. 9.176). The anastomosis between the pharynx and the jejunal graft and the graft and the distal esophagus at the lower end is completed in a single layer of interrupted inverting chromic catgut sutures. The vascular anastomoses are completed

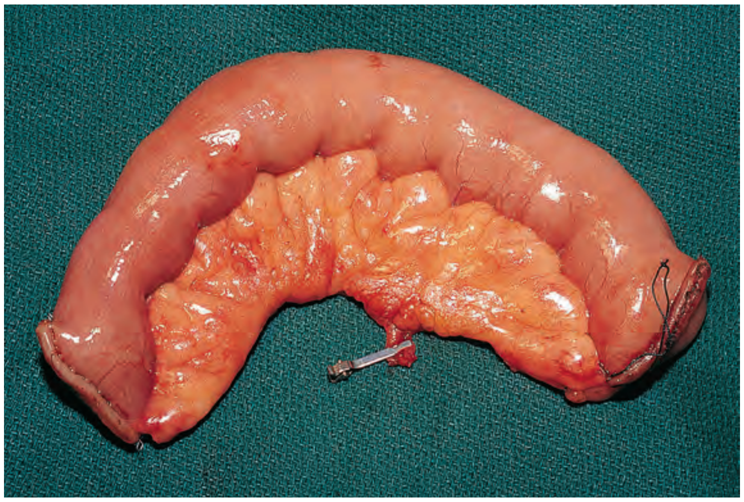

Figure 9.175 A jejunal free flap with its vascular pedicle.

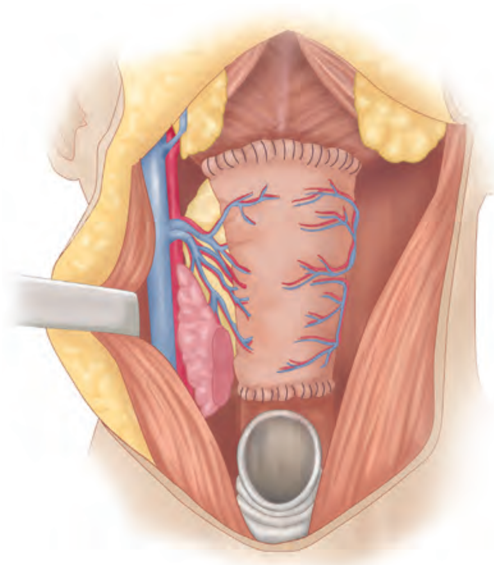

Figure 9.176 A diagram of completed reconstruction showing vascular, pharyngojejunal, and jejunoesophageal anastomoses.

similarly between the superior thyroid artery and the mesenteric artery to the graft and between the mesenteric vein and the recipient vein. Generally, the graft is inset and the pharyngojejunal and jejunoesophageal anastomoses are performed first to secure the graft in proper position. The vascular anastomoses are undertaken thereafter with use of the operating microscope. The vascular anastomoses are accomplished by using the microvascular suture technique with 9-0 or 10-0 Ethilon interrupted sutures.

A description of the details of the technique of microvascular anastomoses is beyond the scope of this book. However, a word of caution is essential: Occasional microvascular surgery performed by a head and neck surgeon is hazardous and should be discouraged. The success of the microvascular anastomosis and the viability of the graft depend on the technical abilities and experience of the microvascular surgeon, who should be involved in this field on a regular basis.

It is vitally important that the placement of the graft be decided upon before the vascular anastomoses are undertaken. Inlay of the graft in the neck should be performed in an isoperistaltic fashion to facilitate swallowing. An excessive length of the jejunal graft causes redundancy and a delay in swallowing. A nasogastric tube is inserted before completion of

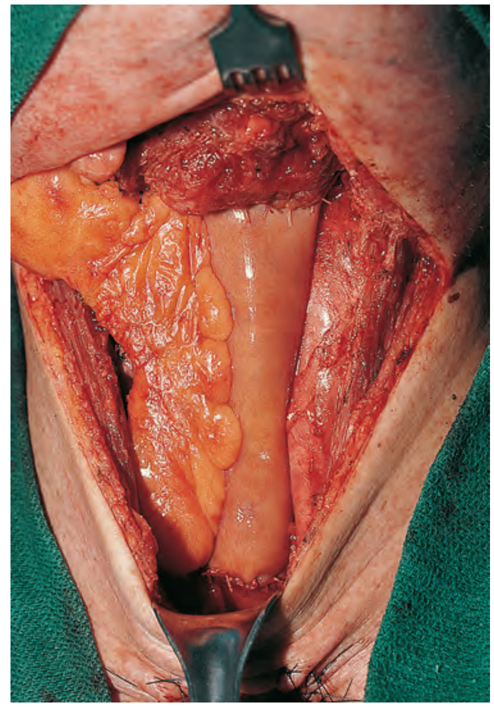

Figure 9.177 All anastomoses for the jejunal free flap are completed, and the continuity of the alimentary tract is restored.

all anastomoses. The distal end of the nasogastric tube is placed in the stomach initially for evacuating the gastric contents until peristalsis reappears. Subsequent to that time, the nasogastric tube is used for nutritional support until the patient is allowed to take fluids by mouth.

Completed visceral and vascular anastomoses in the patient are shown in Fig. 9.177. Several points regarding pharyngojejunal anastomosis and jejunoesophageal anastomosis require reemphasis. The proximal end of the jejunal graft is beveled to obtain a wider circumference to match the circumference of the oropharynx. It is important to note that the stump of the esophagus must be readily available in the neck for jejunoesophageal anastomosis. If esophageal resection requires its transection in the superior mediastinum, then anastomosis between the jejunal graft and the distal esophagus is unlikely to be technically satisfactory, and alternative methods of reconstruction of the alimentary tract must be considered.

Patency of the vascular anastomosis is either monitored with a percutaneous Doppler scanner or the color of the jejunal mucosa is observed through a fiber-optic nasopharyngoscope. Alternatively, a small segment of the jejunum from one end of the graft can be isolated and exteriorized from the neck incision with its vascular pedicle as a monitor. It is trimmed off after a week. The nasogastric tube is connected to a suction apparatus until peristalsis reappears in the abdomen. Nasogastric feedings may then begin. If the healing process in the neck is progressing well, clear liquids may be given by mouth 7 to 10 days after surgery.

An endoscopic view of the jejunal graft at the pharyngojejunal anastomosis several weeks after surgery is shown in Fig. 9.178. Note the healthy pink color of the jejunal graft and a well-healed anastomosis. Edema of the jejunal mucosa causing partial functional obstruction of solid food is not uncommon. Several weeks may pass before the edema subsides and the patient is able to swallow solids. A barium swallow performed 2 weeks after surgery shows a well-healed jejunal graft reconstructing the cervical esophagus and showing free passage of barium

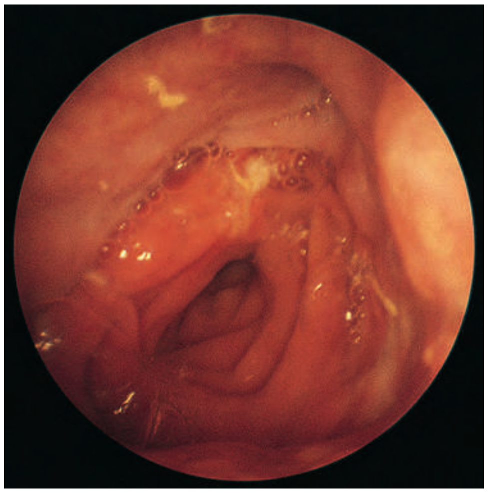

Figure 9.178 An endoscopic view of the jejunal graft several weeks after surgery.

Figure 9.179 A barium swallow 2 weeks after surgery.

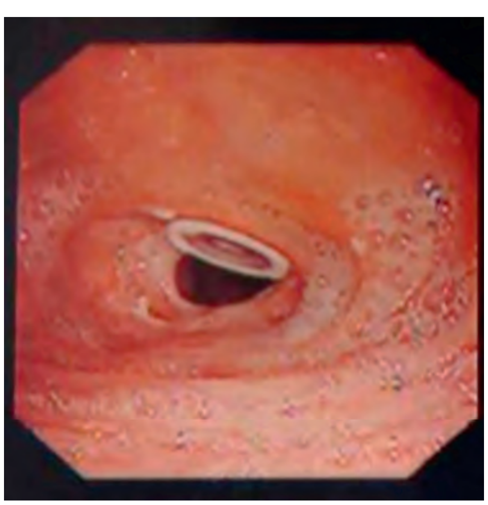

Figure 9.180 The inner flange of provox prosthesis seen in the jejunum.

from the oropharynx to the thoracic esophagus without leakage (Fig. 9.179). Reconstruction with a microvascular jejunal graft is an ideal method for repairing circumferential pharyngoesophageal defect in the neck. If the patient requires postoperative radiation therapy, it can begin 4 to 6 weeks following surgery, and after all wounds have healed well. Speech rehabilitation is also possible in patients who have undergone jejunal free flap reconstruction. If possible the trachea-esophageal puncture (TEP) is made below the pharyngoesophageal suture line. However, if the anastomosis between the jejunum and esophagus is below the level of the tracheostome, then the TEP can be performed through the jejunum. An endoscopic view of the inner flange of a provox prosthesis projecting into the jejunum is shown in Fig. 9.180.

Pharyngolaryngoesophagectomy and Reconstruction With Gastric Transposition

When primary carcinomas of the hypopharynx, particularly in the postcricoid region, circumferentially involve the pharynx and extend to the cervical esophagus, there is an obvious need

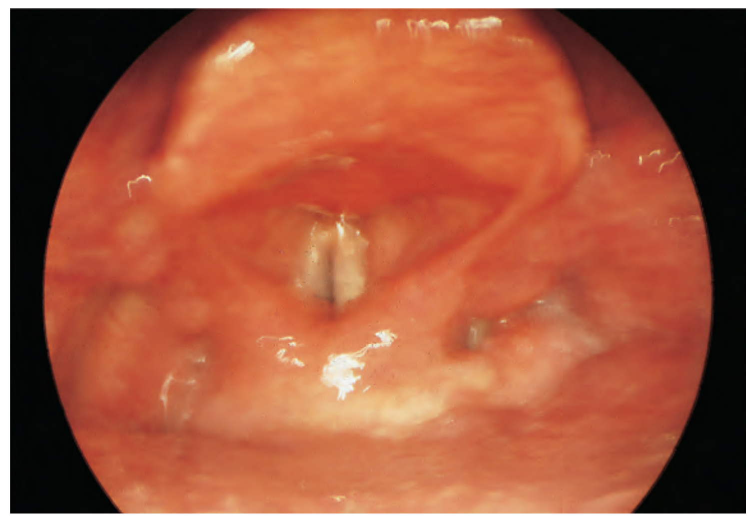

Figure 9.181 An endoscopic view of the laryngopharynx showing carcinoma of the postcricoid region.

for a total circumferential pharyngolaryngectomy. The rationale for performing a total esophagectomy in such situations is debatable. Advocates of a total esophagectomy believe that patients with such lesions have skip areas within the submucosal plane of the esophagus with involvement of cancer, requiring a total esophagectomy. In some patients, clinically apparent multiple primary cancers demand a total esophagectomy. However, when the primary tumor arises in the cervical esophagus and when the distal margin of resection of the cervical esophagus extends behind the manubrium sterni, a total esophagectomy must be performed. On the other hand, if the capabilities for microvascular reconstruction with a free segment of jejunum to replace the cervical esophagus are not available, then pharyngolaryngoesophagectomy with gastric transposition may also be considered for reconstruction of circumferential defects of the pharynx and cervical esophagus.

The endoscopic view of the laryngopharynx of a patient with a primary carcinoma of the cervical esophagus extending into the postcricoid region is shown in Fig. 9.181. There is pooling of saliva in the postcricoid region, with the upper margin of the tumor seen at the apex of the right pyriform sinus. Although the mobility of both vocal cords is within normal limits, the patient clearly requires a total laryngectomy

because of the extensive involvement of the proximal cervical esophagus and postcricoid region.

A barium swallow examination shows a filling defect in the cervical esophagus with a concentric obstruction (Fig. 9.182). It is imperative that the entire upper aerodigestive tract be adequately studied radiographically to assess the remaining esophagus and the status of the stomach to rule out any other pathology. The remaining esophagus as seen in the upper part of the barium swallow is normal.

The upper gastrointestinal series with air contrast shows a normal stomach with no intraluminal pathology (Fig. 9.183). If any radiographic abnormality is detected in the stomach, it is advisable to establish its nature before proceeding with the gastric pull-up operation. If the stomach is unsuitable or unavailable for transposition, then alternate methods of reconstruction of the pharyngoesophageal defect such as colon interposition should be considered.

The surgical procedure is ideally performed with two surgical teams working simultaneously. The collaboration of a head and neck surgical team and a thoracic surgical team helps the operation proceed expeditiously and offers the capabilities of handling with ease any intraoperative technical difficulties that may ensue during surgery.

Figure 9.182 A barium swallow examination showing a filling defect in the cervical esophagus.

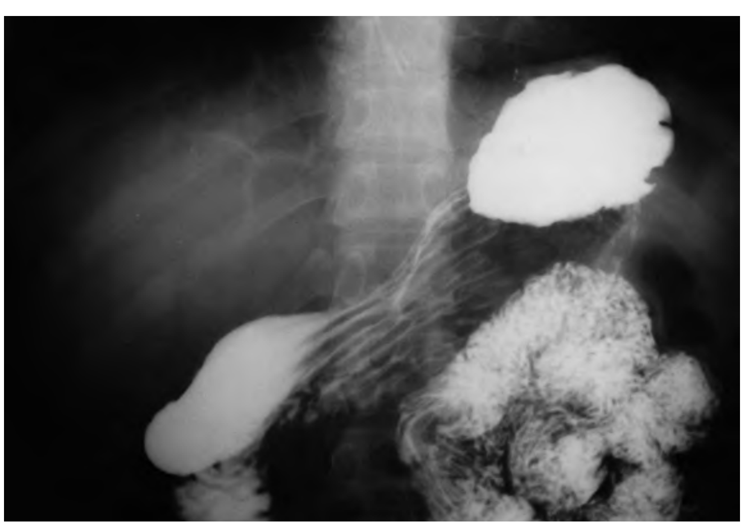

Figure 9.183 An upper gastrointestinal series showing a normal stomach with no intraluminal pathology.

The operative procedure is performed with the patient in the supine position on the operating table with the neck extended. The head and neck surgeon should work from the left-hand side of the patient and the abdominal surgeon should work from the right-hand side of the patient, avoiding unnecessary crowding on the same side of the operating table. However, this plan may change if dissection of the right side of the neck is required in conjunction with resection of the primary tumor.

A U-shaped incision is planned for a pharyngolaryngectomy in the neck in this patient, with creation of a permanent tracheostome in the suprasternal notch (Fig. 9.184). Alternatively, the procedure can be performed with a single transverse incision in a lower neck skin crease, with the tracheostome created through a separate circular incision. If this is to be done, the upper end of the tracheostome incision should be at least 2 cm away from the transverse skin incision for the operation. The abdomen is explored via an upper abdominal midline incision. Two separate sets of instruments and scrub nurses are needed to perform the two aspects of the operative procedure simultaneously and smoothly. If the resectability of the tumor is not certain, then the head and neck procedure begins first to assess resectability before the abdomen is opened.

The patient is placed in the supine position on the operating table with extension of the neck. The surgical field for exploration of the neck is isolated with sterile drapes. A U-shaped incision overlying the anterior border of the sternomastoid muscle on both sides of the neck is marked and the permanent tracheostome is incorporated in it, outlined in the suprasternal notch (Fig. 9.185). A possible extension of this incision in the midline of the anterior chest wall overlying the manubrium sterni is shown with dotted lines. Occasionally this extension is necessary, particularly when resection of the manubrium sterni is required. This maneuver may be necessary in patients in whom the primary

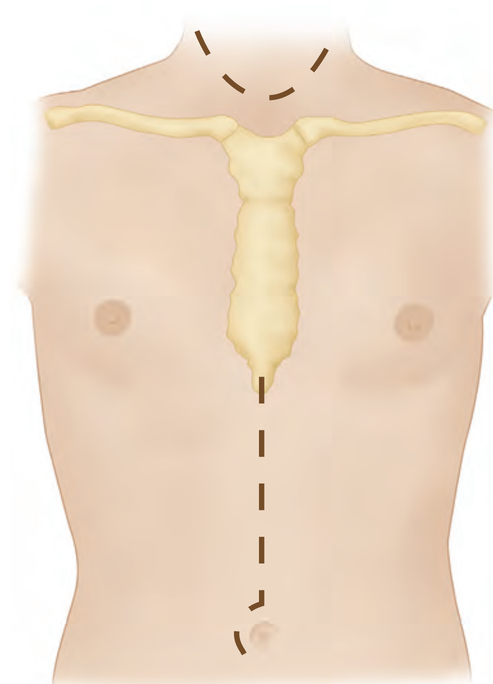

Figure 9.184 The cervical and abdominal incisions are outlined.

Figure 9.185 The cervical incision is outlined on the patient, incorporating the permanent tracheostome.

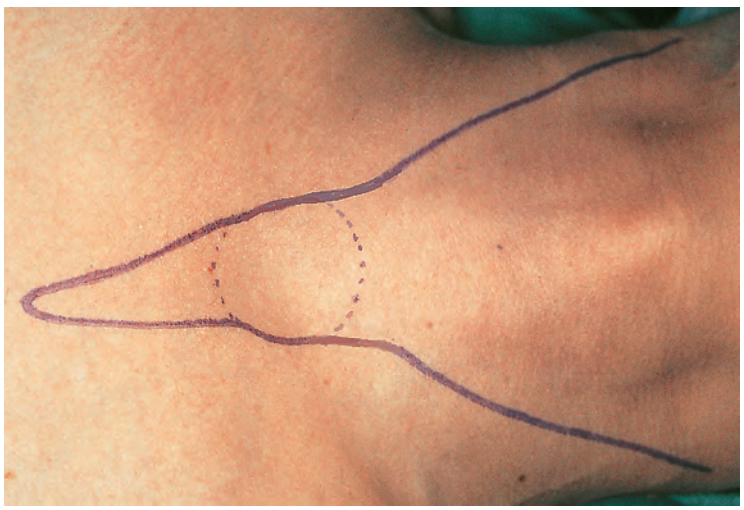

Figure 9.186 Modification of the cervical skin incision to incorporate a "tail" of skin for reconstruction of the membranous trachea.

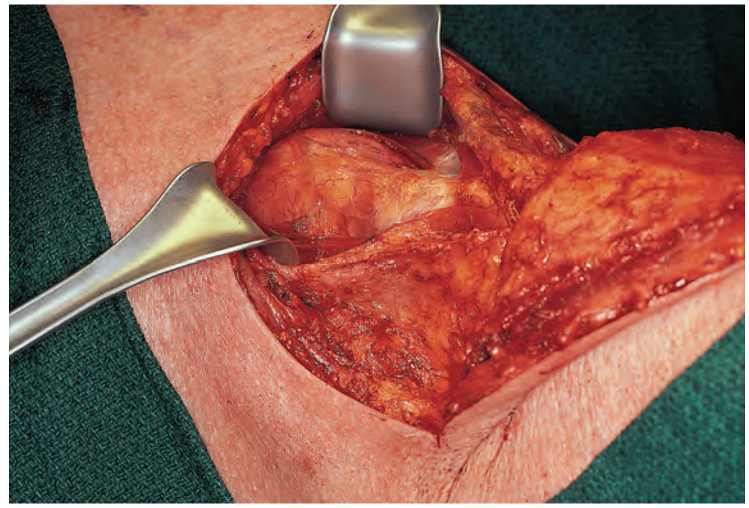

Figure 9.187 The skin flaps are elevated and the sternomastoid muscles are retracted laterally.

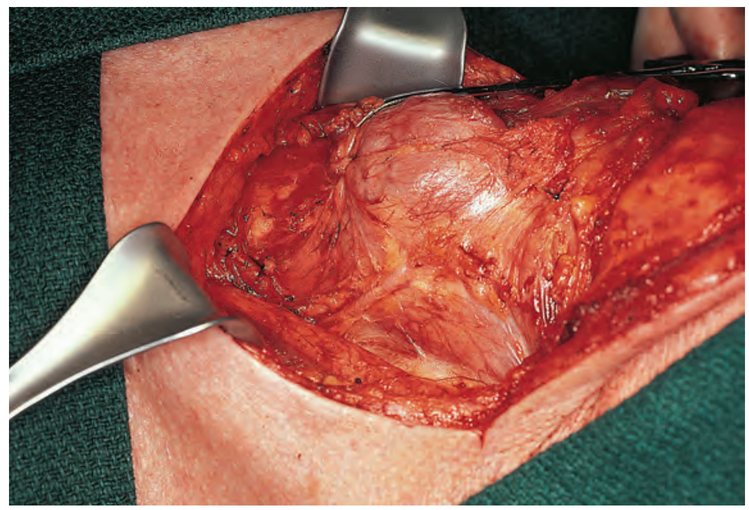

Figure 9.188 The strap muscles are divided, and the isthmus of the thyroid gland is exposed.

tumor is at the thoracic inlet with invasion of the trachea when resection of the trachea may be warranted in the superior mediastinum. On the other hand, in some obese patients, sufficient space is not available for transposition of the stomach through the thoracic inlet. In such situations, resection of the manubrium may need to be considered to create enough space for transposition of the stomach. The neck incision is also modified as shown in Fig. 9.186, with a long tail of the cervical skin flap from the skin overlying the manubrium in patients where the membranous trachea requires resection as a result of invasion by or adherence to the tumor of the esophagus. This tail of skin is then used to reconstruct the membranous trachea at the end of the operation.

The skin incision is deepened through the platysma, and the upper and lower skin flaps are elevated. The upper skin flap is elevated cephalad until the superior surface of the hyoid bone is exposed. The fascia at the anterior border of the sternomastoid muscle on the left side is incised to expose the strap muscles, which are divided low in the neck to expose the thyroid gland (Fig. 9.187). The middle thyroid vein on the left side is divided and ligated, which will permit exposure of the tracheoesophageal groove and access to the prevertebral plane. Assessment of resectability of the tumor now can be made easily by exploring the prevertebral plane behind the cervical esophagus and the postcricoid region. Similarly, the prevertebral plane in the superior mediastinum can be explored easily for assessment of resectability. Once the tumor is considered resectable, the operative procedure begins with the abdominal team starting simultaneously.

The isthmus of the thyroid gland is exposed (Fig. 9.188). By alternate blunt and sharp dissection, the isthmus is mobilized from the pretracheal plane and divided between straight Kocher clamps. The stump of the isthmus on the right hand side (opposite side) is suture ligated with 3-0 chromic catgut interlocking sutures for hemostasis. The right thyroid lobe is preserved in this patient to keep thyroid and parathyroid function, but the left lobe of the thyroid gland is sacrificed with the primary tumor (which is left sided) to obtain better exposure and clearance of the tracheoesophageal groove lymph nodes on the left-hand side.

The right lobe is now dissected from the trachea and the tracheoesophageal groove with the use of electrocautery. Meticulous attention should be given to avoid any injury to the posterior capsule of the right lobe and injury to the parathyroid glands. Small vessels present on the ligament of Berry near the cricothyroid membrane are individually clamped, divided, and ligated. Once the thyroid lobe is separated from the tracheoesophageal groove, it is retracted with the use of a

Richardson retractor behind the right sternomastoid muscle. Note that the left lobe of the thyroid gland remains attached to the tracheoesophageal groove and the cricothyroid membrane on the left side. The strap muscles have been divided, and they are seen retracted cephalad to the left thyroid lobe (Fig. 9.189).

Attention is now focused on clearance of the lower margin of the trachea and creation of the permanent tracheostome. The trachea is divided at a suitable level, remaining lower to the lower border of the palpable tumor. If the lower border of the primary tumor is at the lower border of the cricoid, then the trachea may be divided through the third ring. However, if the primary tumor lies in the cervical esophagus, then the trachea may need to be divided lower down to obtain a sufficient soft tissue margin in the tracheoesophageal plane.

The trachea is transected in a bevel-shaped fashion for creation of the permanent tracheostome. The orotracheal tube is now removed, and the anesthesia tube is transferred to distal trachea with use of a flexible reinforced endotracheal tube (Fig. 9.190). Dissection continues in the tracheoesophageal plane in the superior mediastinum, and the membranous trachea is separated from the anterior aspect of the upper thoracic esophagus (Fig. 9.191). Rough handling of the membranous trachea must be avoided to prevent a tear in the mucosa. If possible the largest-bore endotracheal tube should be used without inflation of its balloon, which will avoid stretching the membranous trachea, with the potential risk of injury during mobilization.

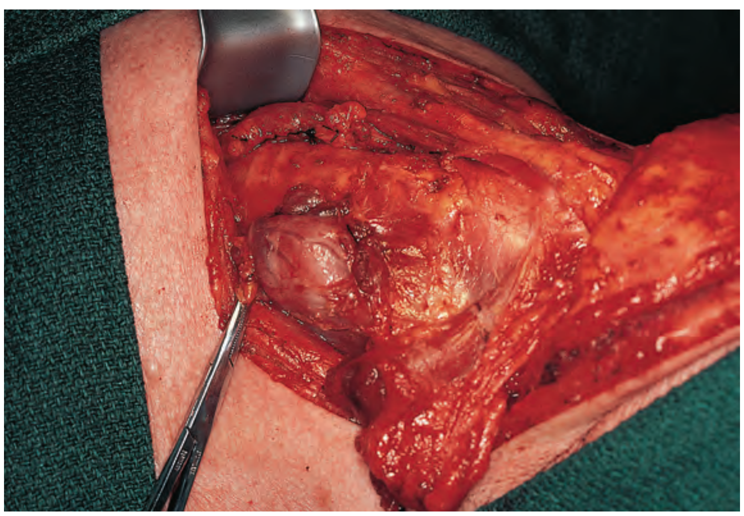

Figure 9.189 The isthmus of the thyroid is divided, and the right lobe is dissected off the trachea and preserved.

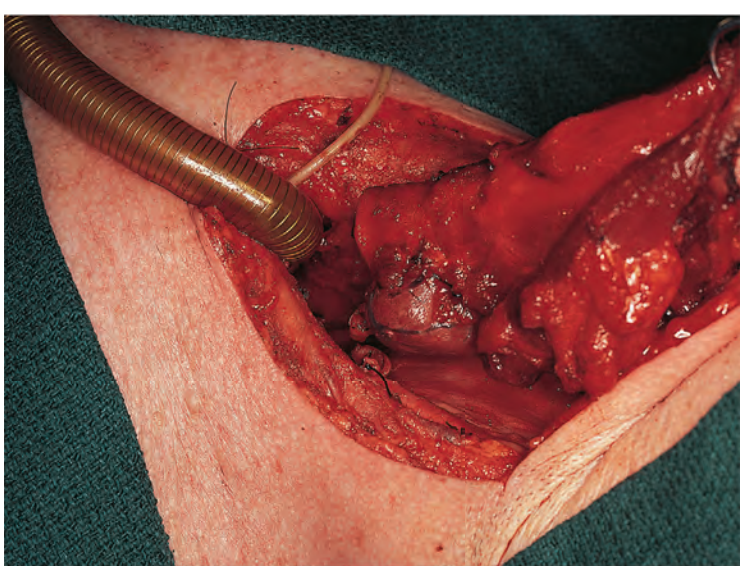

Figure 9.190 The orotracheal tube is removed after the trachea is divided and the method of inducing anesthesia is switched to direct tracheal intubation with use of a reinforced endotracheal tube.

Attention is now focused on the hyoid bone. All the suprahyoid muscles are detached from the upper surface of the hyoid with an electrocautery, and entry is made into the pharynx through the contralateral vallecula. The mucosa of the glossoepiglottic fold and the ipsilateral vallecula is incised, permitting entry in the pharynx. Under direct vision, the remaining circumference of the pharynx is divided, staying well above the superior border of the primary tumor. This procedure is best accomplished by digital dissection, mobilizing the hypopharynx over the prevertebral fascia and allowing the index finger of the left hand to remain behind the posterior pharyngeal wall while the pharynx is circumferentially transected. Electrocautery will achieve transection of the pharynx with minimal blood loss.

Bleeding is to be expected from the superior laryngeal vessels and the pharyngeal vessels, which are clamped and ligated before division. Once the pharynx is circumferentially transected, the upper part of the specimen, composed of the larynx, pharynx, and cervical esophagus, is now available for providing traction to the upper thoracic esophagus during its mobilization in the superior mediastinum (Fig. 9.192).

Mobilization of the upper thoracic esophagus is achieved under direct vision with the use of long instruments and intermittent digital dissection. The use of vascular clips (hemoclips) will facilitate this dissection and expedite the process of securing hemostasis. During digital mobilization in the tracheoesophageal plane, extreme care must be exercised to avoid rough dissection over the membranous trachea; otherwise, tears will occur in the membranous trachea, resulting in significant postoperative morbidity and management problems.

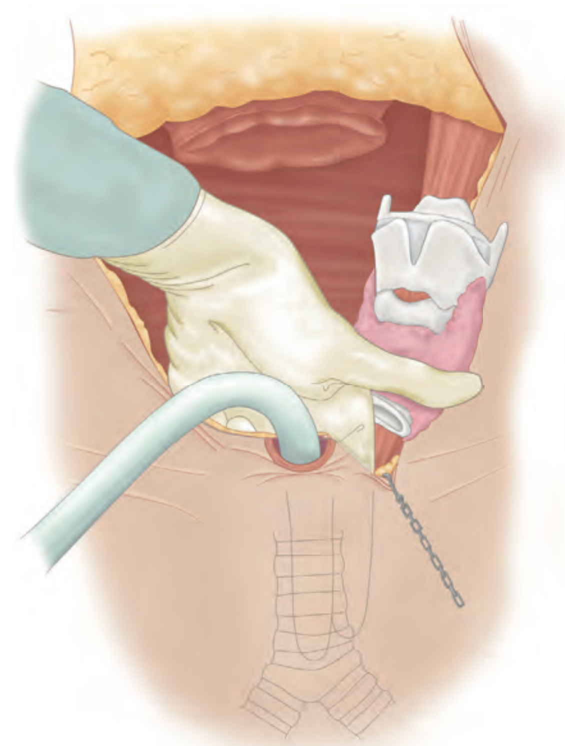

Figure 9.191 The upper thoracic esophagus in the superior mediastinum is mobilized by digital dissection.

The specimen of the larynx and esophagus is moved from side to side and anteroposteriorly to provide circumferential mobilization of the upper thoracic esophagus. The major blood supply to this part of the esophagus is segmental through the branches of the intercostal vessels and prevertebral vessels, which are clamped with hemoclips and divided as mobilization proceeds caudad. A narrow Deaver retractor permits anterior retraction of the distal trachea, providing a direct view of the mobilized upper thoracic esophagus as far down as the carina.

Similar mobilization of the esophagus is accomplished on both lateral aspects as well as posteriorly in the prevertebral plane. If the plane of dissection remains close to the esophagus, then entry into the pleura is unlikely. However, inadvertent entry into the pleural space often can occur and should be immediately recognized. When it occurs the anesthesiologist should be alerted to keep the patient on positive pressure respiratory support.

The upper thoracic esophagus is thus completely mobilized from the neck all the way up to the carina. It must be reemphasized that this mobilization is not achieved by blind digital dissection but is done under direct vision with long DeBakey forceps and Metzenbaum scissors. Hemoclips are used as necessary. During this time, the lower thoracic esophagus is being mobilized by the abdominal team. If the two surgical teams start working simultaneously, mobilization of the upper and lower thoracic esophagus is accomplished at about the same time.

The abdomen is shaved and prepared with antiseptic solution and isolated from the xiphisternum to the pubis. The xyphoid process and the costal margins are marked for orientation (Fig. 9.193). A sufficient length of the anterior abdominal wall should be exposed in the isolated field to extend the incision around the umbilicus if necessary. A midline skin incision is taken in the upper abdomen, exposing the rectus sheath (Fig. 9.194). The xyphoid cartilage often protrudes downward and may require excision to gain access to the esophageal hiatus in the diaphragm. After the peritoneum is opened, the abdomen is explored to rule out the presence of intraabdominal metastatic disease or any other pathology. A self-retaining retractor is used to expose the abdomen (Fig. 9.195). Note the left lobe of the liver and the transverse colon in the field obscuring the view of the stomach. The triangular ligament of the left lobe of the liver is divided and the left lobe is retracted toward the right-hand side, bringing the anterior aspect of the stomach into view (Fig. 9.196).

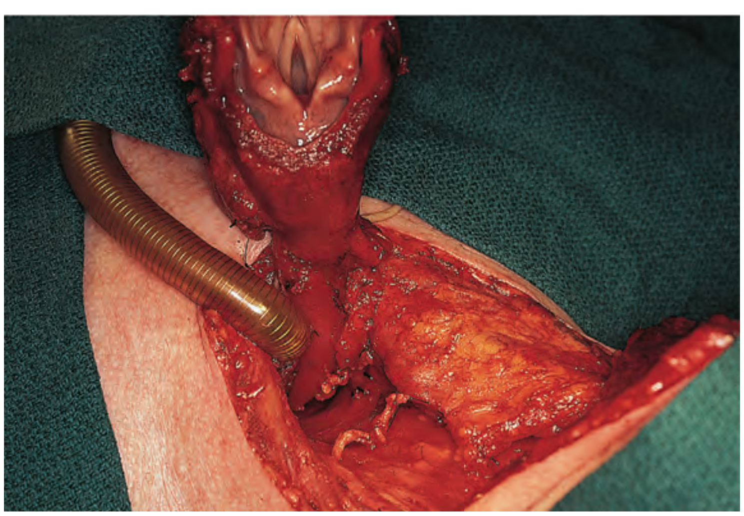

Figure 9.192 The pharynx is circumferentially divided at the level of the hyoid bone. The mobilized larynx permits traction on the cervical esophagus.

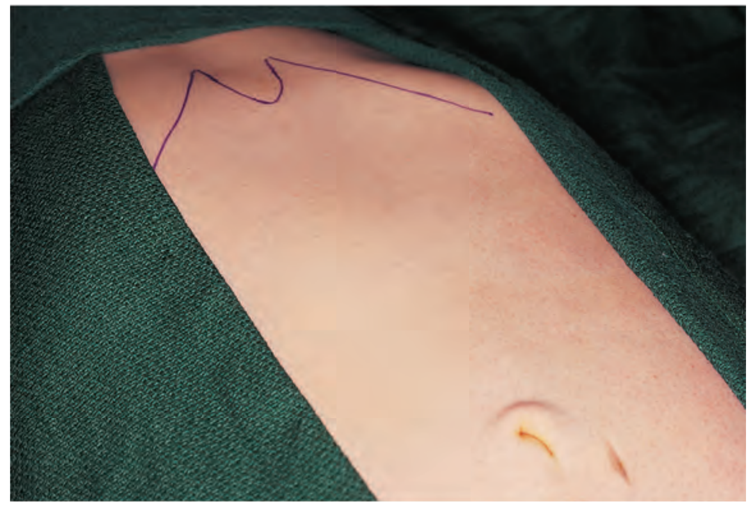

Figure 9.193 The xyphoid process and the costal margins are marked for orientation.

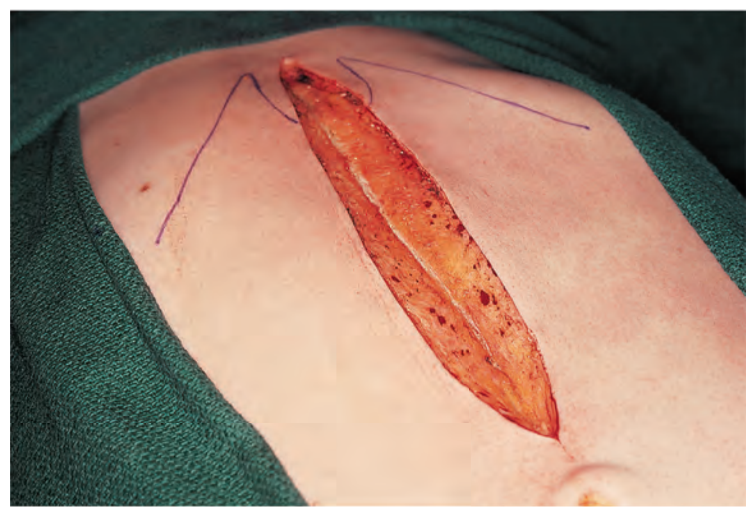

Figure 9.194 The rectus sheath is exposed through a midline incision.

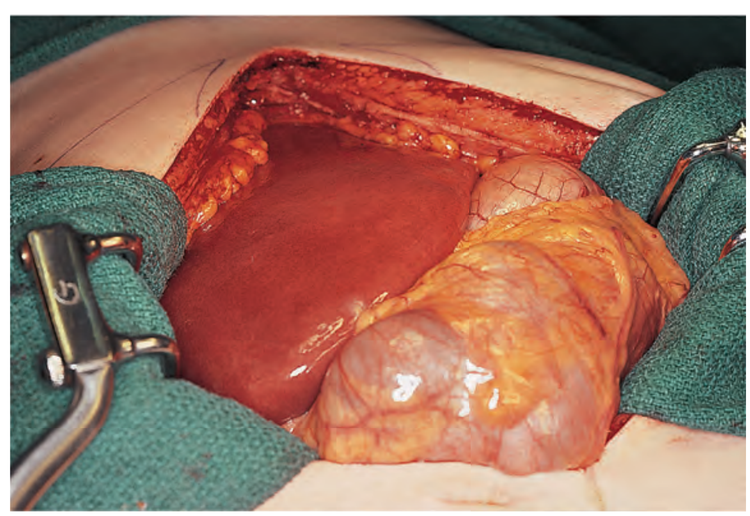

Figure 9.195 A self-retaining retractor is used to expose the abdomen.

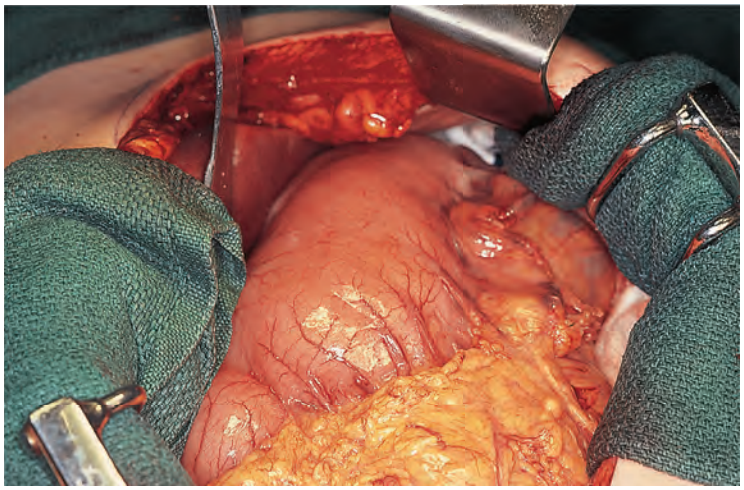

Figure 9.196 The left lobe of the liver is mobilized to expose the anterior aspect of the stomach.

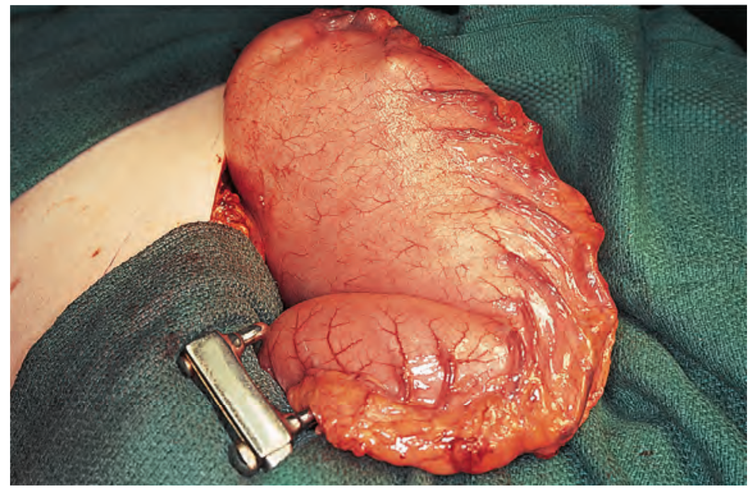

Figure 9.198 The completely mobilized stomach is delivered from the abdominal wound.

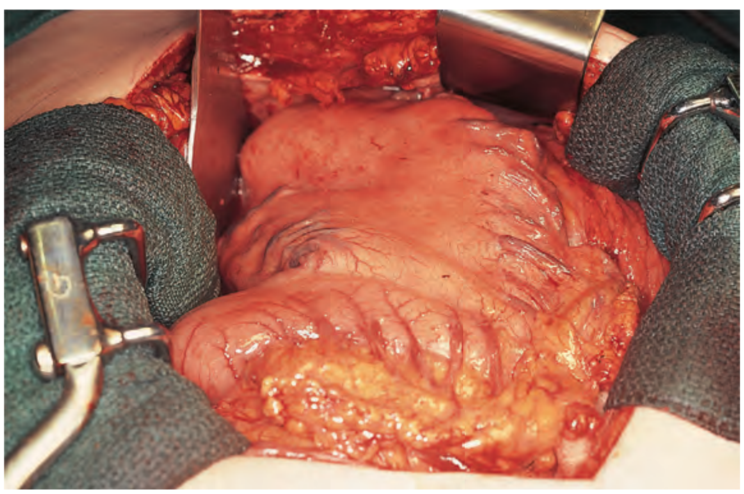

Figure 9.197 Isolation and ligation of the branches leading to the gastrocolic ligament from the gastroepiploic vessels.

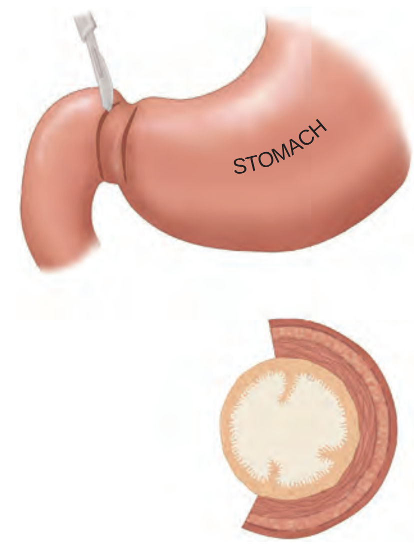

Figure 9.199 A pyloromyectomy.

Mobilization of the stomach now begins by dividing the gastrocolic and gastrosplenic ligaments. This procedure is done very carefully to avoid injury to the right gastric and right gastroepiploic vessels. This mobilization requires the isolation and individual ligation of each of the branches leading to the gastrocolic ligament from the gastroepiploic vessels (Fig. 9.197). The left gastric vessels, the short gastric vessels, and the left gastroepiploic vessels are divided and ligated. The completely mobilized stomach delivered from the abdominal wound is shown in Fig. 9.198. The stomach is still attached to the cardioesophageal junction at the diaphragmatic hiatus and is continuous with the duodenum distally. Its blood supply comes from the right gastric and right gastroepiploic vessels, which are preserved.

Because the patient will have a total esophagectomy, he also will have a bilateral vagectomy, requiring a drainage procedure through the pylorus. Therefore a pyloroplasty, pyloromyotomy, or pyloromyectomy is performed to provide adequate drainage of the stomach. A pyloromyectomy is considered to be the best procedure because it provides adequate drainage without constricting the lumen at the gastroduodenal junction (Fig. 9.199). Inadvertent injury to the mucosa and entry into the stomach must be avoided during the pyloromyectomy. The procedure in progress shows the prolapse of pyloric mucosa in the wound of the pyloromyectomy (Fig. 9.200). Meticulous hemostasis at the site of the pyloromyectomy must be achieved before proceeding with further mobilization of the stomach and the distal esophagus.

The cardiac end of the stomach is now retracted with use of a Penrose drain passed around the cardioesophageal junction, allowing exposure of the hiatus in the diaphragm. With electrocautery, a semicircular incision is made on the anterior aspect of the esophageal hiatus to provide entry into the posterior mediastinum. The hiatus is dilated by digital dissection, which usually gives satisfactory exposure for dissection of the distal esophagus. Occasionally, the right or left crus of the diaphragm may need to be divided to gain exposure. Under direct vision, the distal part of the esophagus is mobilized circumferentially (Fig. 9.201). This procedure requires long instruments and adequate lighting. A flexible fiber-optic light source and a pistol-grip type of a single arm hemoclip applier are most useful. After the hiatus of the diaphragm is enlarged, a Harrington retractor is introduced into the posterior mediastinum to provide anterior retraction of the heart (Fig. 9.202). During this retraction, the

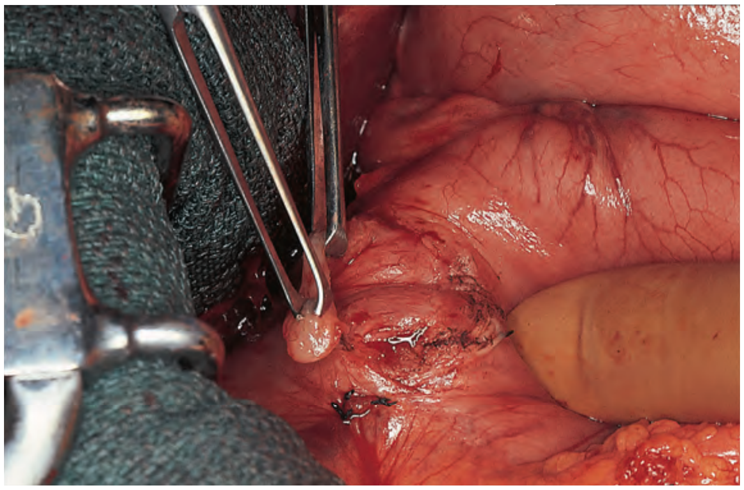

Figure 9.200 Prolapse of pyloric mucosa at the site of the pyloromyectomy.

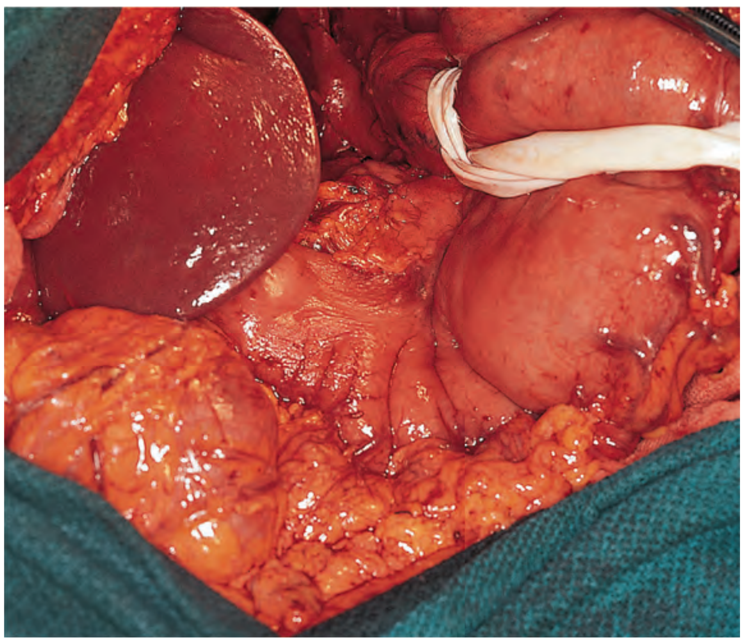

Figure 9.201 The distal part of the esophagus is mobilized circumferentially.

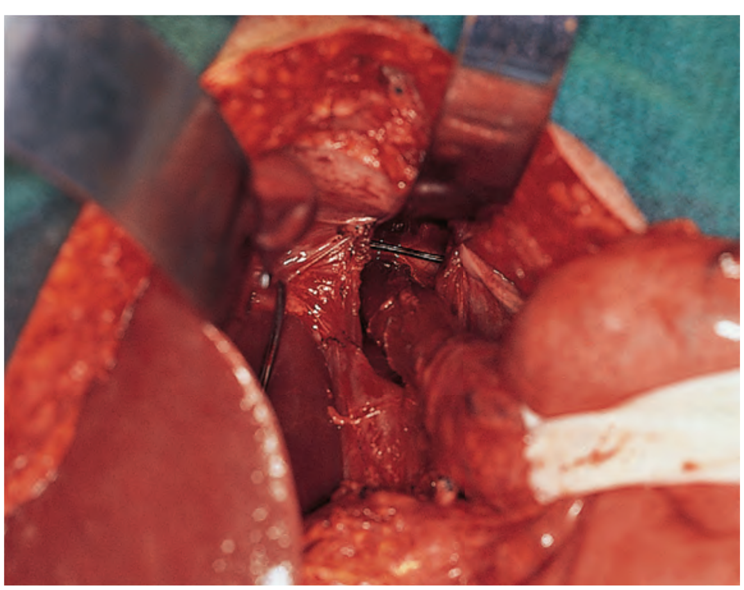

Figure 9.202 The heart is retracted anteriorly with a Harrington retractor to permit dissection of the distal thoracic esophagus.

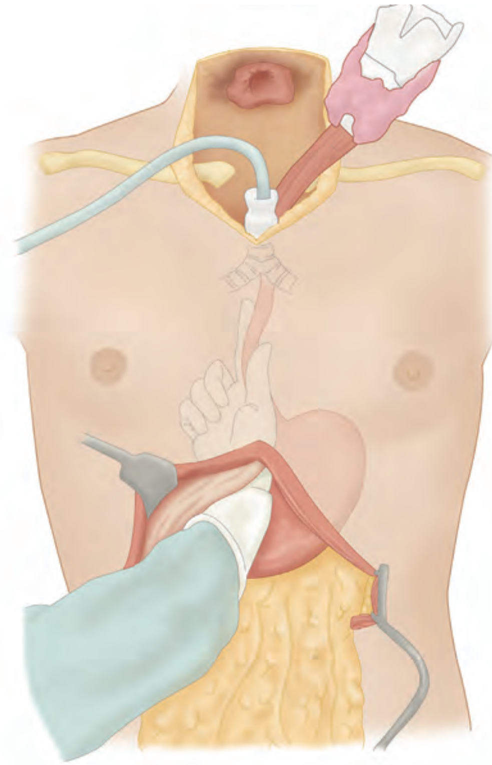

Figure 9.203 The carina is reached in the posterior mediastinum.

anesthesiologist must be alerted, because the patient's blood pressure may drop while the heart is retracted anteriorly. This procedure should be done very gently and only intermittently to avoid any intraoperative episodes of prolonged hypotension.

Digital and sharp mobilization of the distal thoracic esophagus continues until the carina is reached in the posterior mediastinum (Fig. 9.203). To facilitate complete and circumferential mobilization of the entire thoracic esophagus, it is often helpful to railroad the esophagus back and forth from the neck into the abdomen and from the abdomen into the neck, which will allow retraction of the esophagus up or down to permit division of the final few attachments safely under vision. Once the esophagus is totally mobilized with digital confirmation by the two operating surgeons in the posterior mediastinum, the stomach is ready for transposition into the neck.

Gentle traction is applied to the surgical specimen of the larynx and the upper thoracic esophagus while the distal esophagus and the stomach are gently fed through the posterior mediastinum into the upper part of the chest. As the pull on the esophagus continues, the thoracic esophagus is delivered into the neck, bringing along with it the cardiac end of the stomach. Once the cardiac end of the stomach is seen in the neck, a Babcock clamp is used to deliver the fundus of the stomach from the superior mediastinum into the neck. An adequate length of the fundus is brought in the neck to permit a tension-free anastomosis between the stump of the pharynx and the upper border of the fundus of the stomach.

The cardioesophageal junction is divided with use of a gastrointestinal stapler. Alternatively, it may be divided with a scalpel and the transected cardiac end of the stomach may be oversewn with interrupted inverting chromic catgut sutures and a second layer of interrupted serosal sutures with 3-0 silk. After the cardiac end of the stomach is closed, a gastrotomy is made at the convex upper end of the fundus of the stomach that should be wide enough to allow at least three fingers through the gastrotomy site.

Meticulous hemostasis is achieved by either ligating or coagulating all the bleeding points from the mucosal edges of the gastrotomy. Occasionally, the stomach at this point may look rather blue because of venous congestion. However, arterial perfusion is maintained as long as the right gastric and the right gastroepiploic vessels remain intact.

Anastomosis between the stomach and the pharynx is undertaken with a single layer of 2-0 chromic catgut interrupted inverting sutures (Fig. 9.204). The posterior layer includes the prevertebral fascia in every suture to anchor the stomach in the neck, avoiding any pull on the suture line. Before the anastomosis is completed, a nasogastric feeding tube is passed through the stomach into the proximal part of the duodenum. Its location in the proximal part of the duodenum is confirmed by palpation in the abdomen before abdominal closure begins.

After completion of the anastomosis, the wound in the neck is irrigated with Bacitracin solution. Two Hemovac drains are inserted, and the neck incision is closed in two layers using 3-0 chromic catgut interrupted sutures for platysma and 5-0 nylon sutures for skin. A skin disc of at least 2.5 cm in diameter is excised to facilitate the creation of a satisfactory tracheostome. The permanent tracheostome is created by suturing the stump of the trachea to the skin edges at the site of the proposed tracheostome with interrupted nylon sutures. If membranous trachea is resected from the tracheal stump, then appropriate trimming of the skin edges is performed at the trifurcation to create a permanent tracheostome.

The abdominal wound is closed after irrigation in the usual fashion. Immediate postoperative chest radiographs are performed to rule out pneumothorax on either side. The pleural cavity is drained with a chest tube and an underwater seal drainage system if a pneumothorax is documented. If entry is made in both sides of the pleura, then both chest cavities require drainage.

The specimen shows a locally advanced primary carcinoma of the cervical esophagus extending into the postcricoid region (Fig. 9.205). Note that the tumor encompasses nearly the entire circumference of the postcricoid region with deep infiltration into the musculature of the pharynx and cervical esophagus.

The postoperative care of a patient with a pharyngolaryngoesophagectomy and gastric transposition is relatively simple. The nasogastric tube is attached to suction drainage until peristalsis returns. Chest tubes are connected to the underwater seal with suction attached. Periodic chest radiographs are performed to confirm expansion of the lungs. When drainage from the pleural spaces is minimal and the lungs remain expanded, the chest tubes are removed.

Once peristalsis has returned, feeding begins through the nasogastric tube. Hemovac drains in the neck are attached to suction drain systems. When the drainage from the neck wound is minimal, the drainage tubes are removed. A laryngectomy tube usually is not necessary in most patients. However, in some patients the membranous trachea is pushed anteriorly because of a prolapsing stomach wall. In these patients, a laryngectomy tube is desirable to maintain patency of the upper airway in the immediate postoperative period.

If the neck wound is healing well, with the skin flaps remaining down and well healed, then oral alimentation is started by the seventh to tenth postoperative day. The patient is instructed to eat small quantities of food several times a day and is advised to remain in an upright position for at least 30 minutes, after eating to avoid regurgitation of food as a result of the absence of a cricopharyngeal sphincter. Initially the symptoms of dumping are seen in some patients, but within a few weeks these symptoms spontaneously disappear. Some patients occasionally experience diarrhea, but this symptom is also transient.

An endoscopic view of the pharyngogastric anastomosis shows a well-healed suture line with rugae of the stomach in the center of the field (Fig. 9.206). A barium swallow performed postoperatively shows free flow of barium from the pharynx through the transposed stomach into the first part of the duodenum (Fig. 9.207).

The postoperative photograph of the patient shows a well-healed neck incision and a satisfactory tracheostome (Fig. 9.208).

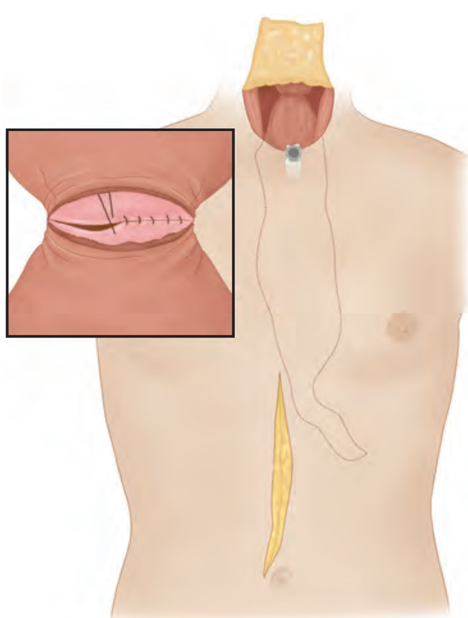

Figure 9.204 Anastomosis between the stomach and the pharynx.

Figure 9.205 A locally advanced carcinoma of the cervical esophagus extending up to the postcricoid region.

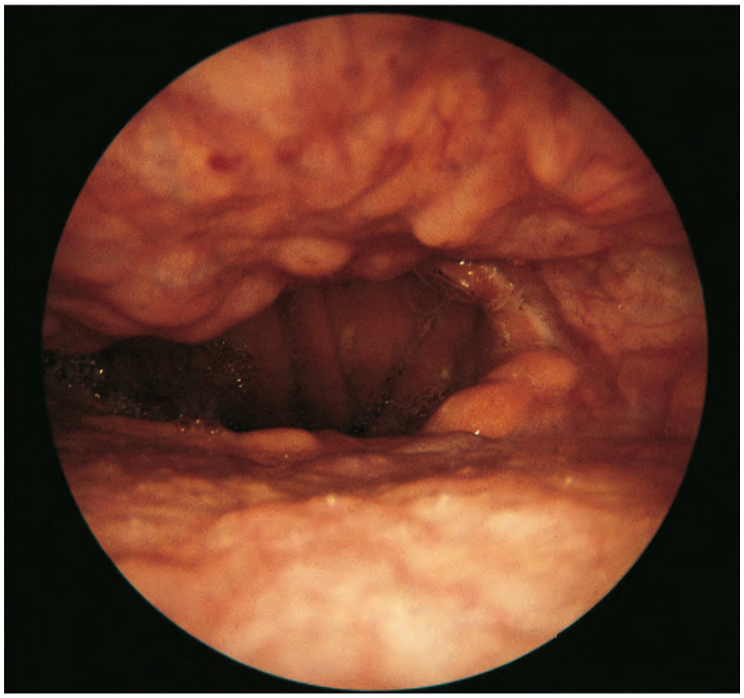

Figure 9.206 An endoscopic view of the pharyngogastric anastomosis.

Figure 9.207 A postoperative barium swallow.

Most patients are not able to produce esophageal speech and must use an electrolarynx. However, some patients produce "gastric speech" that is quite intelligible, although its quality is not optimal.

Pharyngolaryngoesophagectomy with transthoracic gastric transposition and pharyngogastrostomy is a safe operative procedure that accomplishes resection of the primary tumor of the pharynx and esophagus with restoration of the continuity of the alimentary tract in one stage. The average operating time for a simultaneous two-team effort is approximately 3 to 6 hours: Operative blood loss is usually minimal, and most patients do not require a blood transfusion. Swallowing, on average, will take approximately 7 to 10 days, and hospitalization for recovery will take from 2 to 3 weeks.

Figure 9.208 The postoperative appearance of the tracheostome.

If the primary tumor of the esophagus involves the trachea and perforates through the membranous trachea into the tracheal lumen, then resection of a portion of the trachea is necessary. An axial view of the MRI scan of a patient who has a recurrent carcinoma of the cervical esophagus following treatment with chemoradiotherapy is shown in Fig. 9.209. Upon endoscopy, the tumor was noted to involve the membranous trachea (see Fig. 9.210), and adequate clearance would require en bloc resection of the membranous trachea along with the esophagus (see Fig. 9.211). A total laryngo-pharyngo-esophagectomy was performed along with resection of the upper membranous trachea through which the tumor had perforated (see Fig. 9.212). Involvement of the membranous trachea is clearly visible in Fig. 9.213. The pharyngo-esophageal defect was reconstructed with a gastric pull-up, while the tail of the cervical skin flap was used to reconstruct the resected portion of membranous trachea (see Fig. 9.214). The appearance of the patient's tracheostome 3 months after reconstruction is shown in Figure Fig. 9.215.

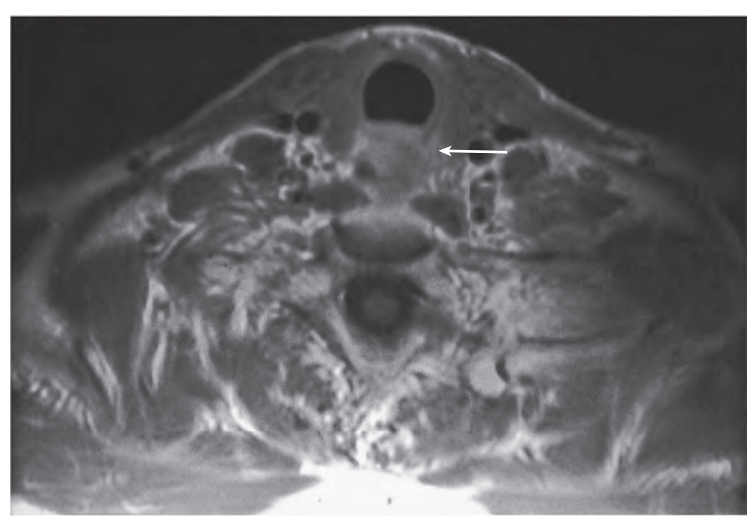

Figure 9.209 An axial view of a magnetic resonance scan showing a cervical esophageal tumor extending anteriorly to involve the membranous trachea (*arrow*).

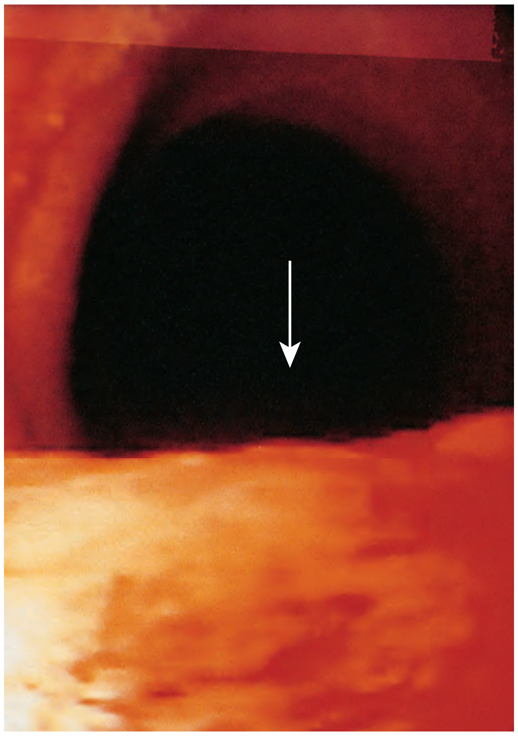

Figure 9.210 An endoscopic view showing involvement of the membranous trachea (*arrow*).

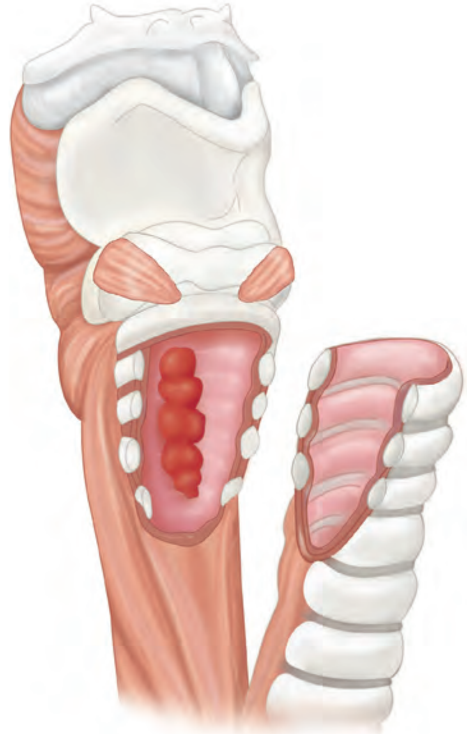

Figure 9.211 En bloc resection of the tumor, including the membranous tracheal wall.

Figure 9.212 A surgical specimen showing the surface extent of the tumor in the esophagus.

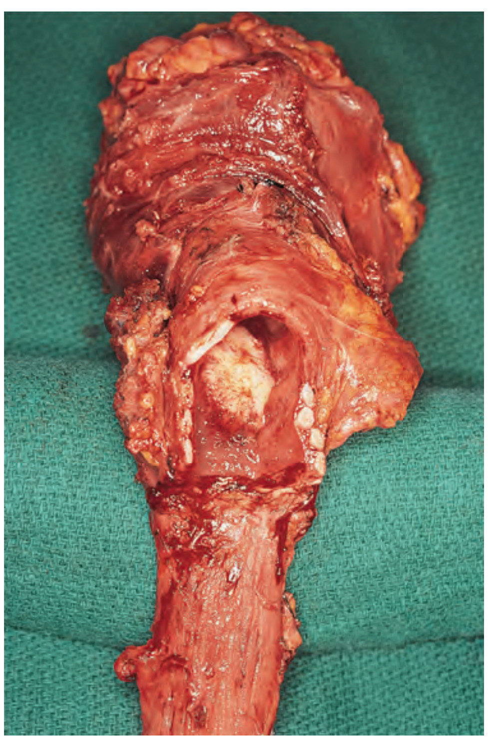

Figure 9.213 A close-up view of the specimen demonstrating invasion of the membranous tracheal wall.

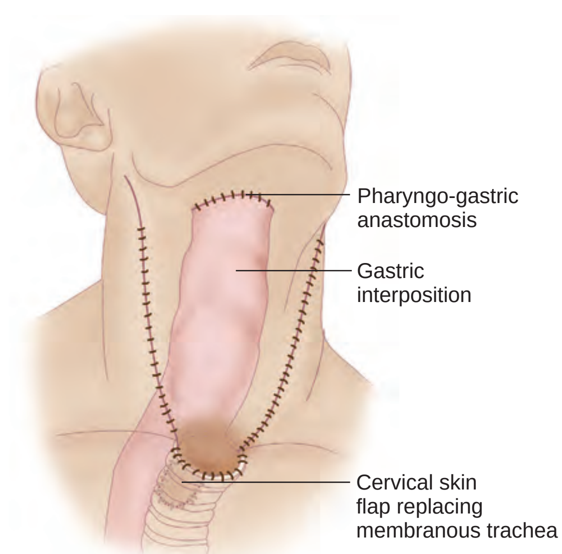

Figure 9.214 The tail of the cervical skin flap is used to reconstruct the membranous tracheal defect.

Figure 9.215 The appearance of the tracheostome 3 months after reconstruction.

Resection of Zenker's Diverticulum

Zenker's diverticulum is an outpouching resulting from mucosal prolapse through weakness in the musculature of the inferior constrictor muscle. The diverticulum itself may be asymptomatic and discovered through radiographic studies performed for other symptoms. On the other hand, it often becomes large enough to produce symptoms warranting its surgical treatment. Barium swallow examination is probably the only radiographic study necessary to establish diagnosis. The pictures shown in Fig. 9.216 demonstrate a large diverticulum presenting in the posterior midline in the neck. Endoscopy is performed with extreme caution. It may be hazardous if proper care is not taken to maneuver the endoscope in the region of the neck of the diverticulum. Select patients with Zenker's diverticulae can be managed endoscopically when adequate surgical expertise and instrumentation such as endoscopic stapling devices and/or laser are available.

Surgical exposure of the cervical esophagus and postcricoid region for resection of a Zenker's diverticulum is best obtained via an anterior cervical approach. The patient is placed on the operating table under general endotracheal anesthesia with the neck extended and rotated to the opposite side. A transverse midcervical incision is placed through a skin crease. The patient shown in Fig. 9.217 had previously undergone a modified neck dissection, and therefore the vertical component of the trifurcate neck dissection incision was used for the necessary exposure. The skin incision is deepened through the platysma. The fascia over the anterior border of the sternomastoid muscle is incised, and a space is created to permit insertion of a retractor (Fig. 9.218). The omohyoid muscle and the middle thyroid vein are divided, and midline structures, including the strap muscles, trachea, larynx, and thyroid gland, are retracted medially (Fig. 9.219).

Attention is now directed to the prevertebral plane, where the diverticulum presents itself. By alternate blunt and sharp dissection, the diverticulum is carefully mobilized from the prevertebral plane. The ipsilateral thyroid lobe, particularly its upper pole, often overlies the region of the diverticulum and will require mobilization and traction medially. Occasionally division of the superior thyroid artery may need to be considered to permit satisfactory retraction of the thyroid lobe medially to provide satisfactory exposure. If this division must be done, extreme caution must be exercised to carefully dissect the superior thyroid artery and vein, but carefully preserving the external laryngeal branch of the superior laryngeal nerve. As dissection proceeds in the prevertebral plane cephalad and caudad, more of the sac of the diverticulum becomes visible. A Babcock clamp is applied for traction to the fundus of the diverticulum, which is now delivered in the wound. Alternatively, traction sutures may be applied at the fundus of the diverticulum as shown (Fig. 9.220). Attention should be focused to avoid undue pulling on the diverticulum, because that may result in tenting of the esophageal wall, leading to resection of excessive esophageal wall, which may cause stricture formation. Identifying and demonstrating the distal esophagus are essential before embarking on resection of the diverticulum.

A sharp scalpel is now used to make an incision through the muscular layer of the diverticulum approximately at a midpoint between its fundus and its neck (Fig. 9.221). Meticulous dissection of the muscular wall of the diverticulum is now taken all the way up to its neck. Every attempt must be made to avoid inadvertent entry into the mucosal layer of the diverticulum. The mucosa is isolated up to the neck of the diverticulum circumferentially. At this point, a No. 28 Foley catheter is passed through the patient's mouth into the cervical esophagus, with its balloon remaining distal to the neck of the diverticulum. Five millimeters of saline solution are introduced into the balloon of the Foley catheter, and the catheter is

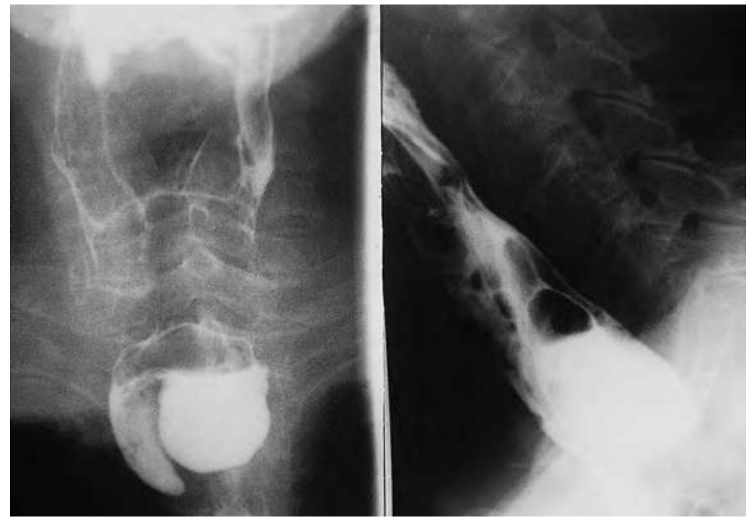

Figure 9.216 A large diverticulum presents in the posterior midline in the neck.

Figure 9.217 The skin incision is outlined.

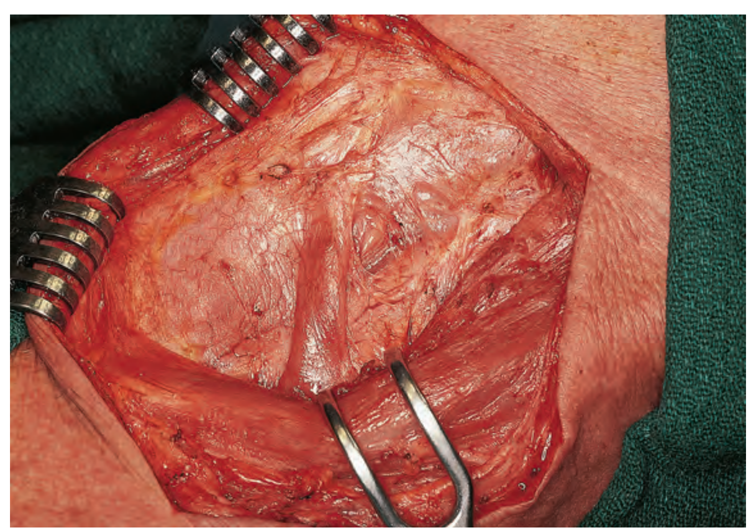

Figure 9.218 Incision of the fascia over the anterior border of the sternomastoid muscle permits its retraction laterally.

withdrawn until the balloon appears in the region of the neck of the diverticulum. This step will ensure that sufficient circumference of esophageal mucosa is preserved at the level of the diverticulum to prevent stricture formation. The neck of the diverticulum is now divided with sharp scissors, leaving sufficient esophageal mucosa around the balloon of the Foley catheter for closure (Fig. 9.222).

After delivery of the specimen, closure of the esophageal mucosa begins with interrupted chromic catgut inverting sutures. The Foley catheter is deflated and withdrawn at this point. The mucosa is closed in a watertight fashion. After this procedure, excess musculature of the esophageal wall is trimmed off and the muscular layer also is repaired in a single layer with interrupted 3-0 chromic catgut sutures (Fig. 9.223).

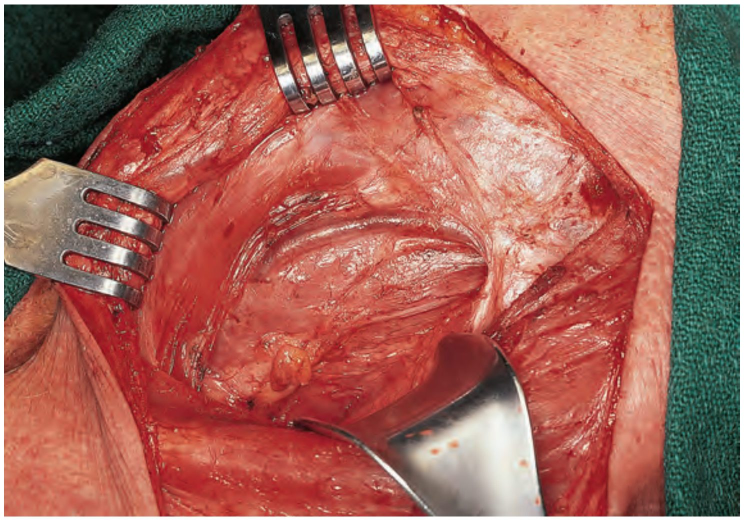

Figure 9.219 The omohyoid muscle and the middle thyroid vein are divided.

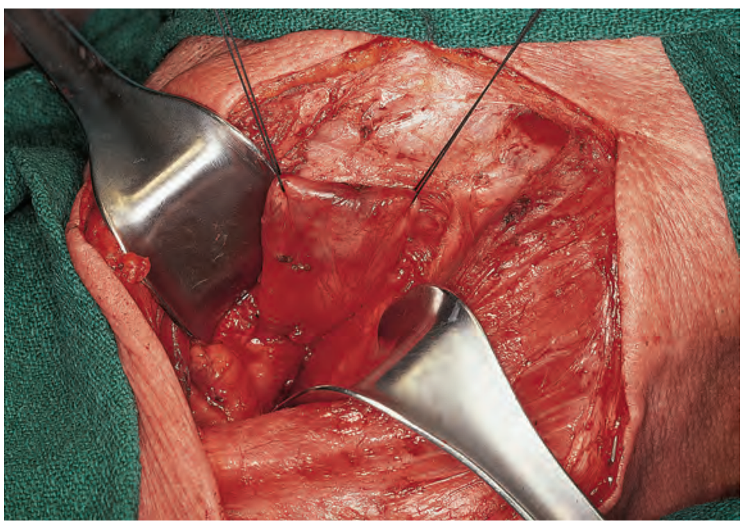

Figure 9.220 Traction sutures are applied to the fundus of the diverticulum.

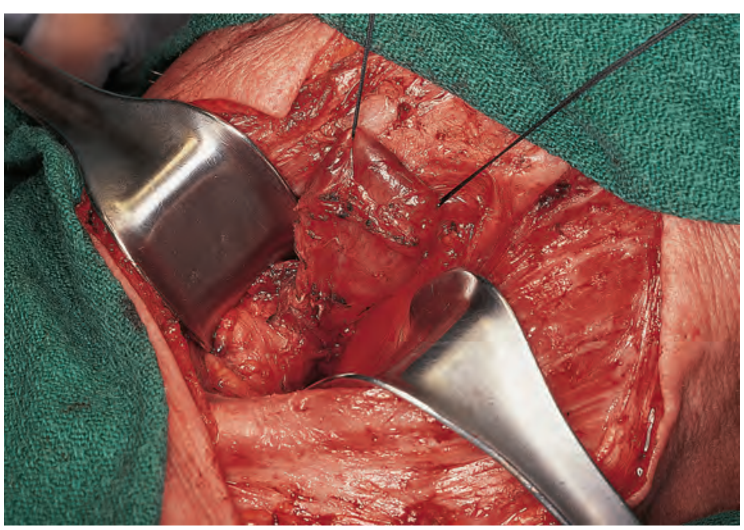

Figure 9.221 An incision is made through the muscular layer of the diverticulum.

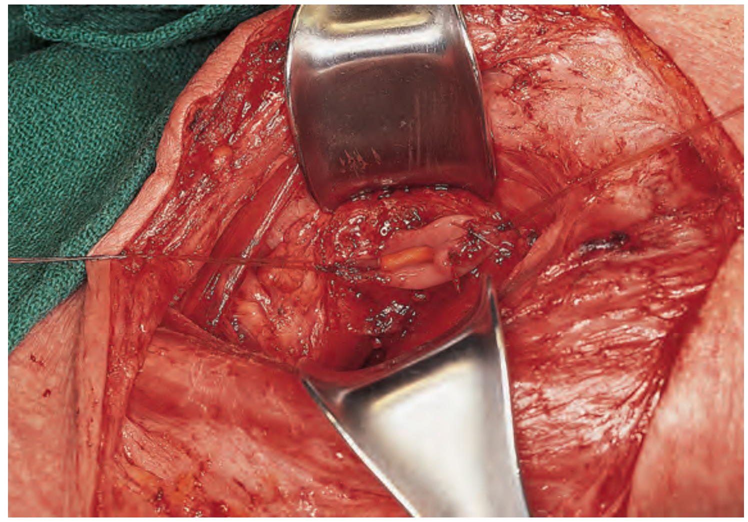

Figure 9.222 Division of the neck of the diverticulum.

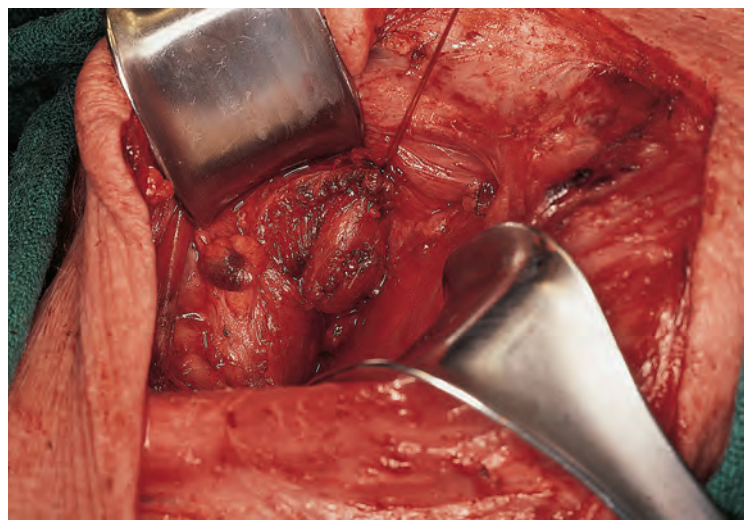

Figure 9.223 Repair of the muscular layer.

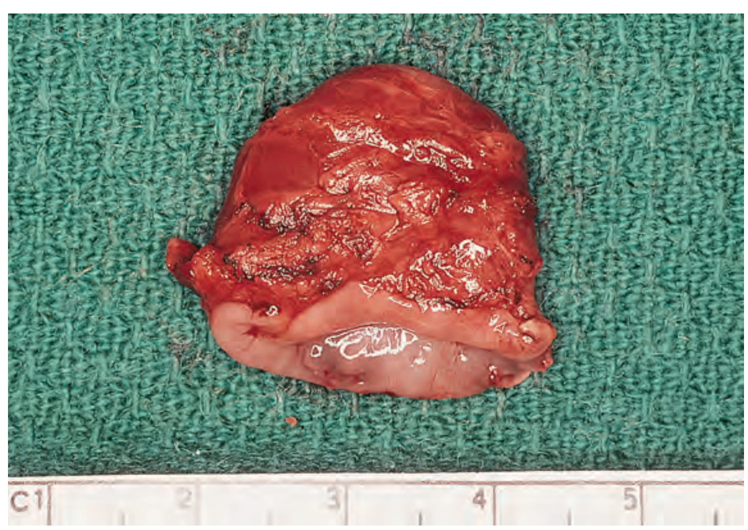

Figure 9.224 The surgical specimen of excised Zenker's diverticulum.

The wound is irrigated. A small suction drain is inserted and brought out through a separate stab incision. The remainder of the wound is closed in two layers using interrupted 3-0 chromic catgut sutures to reapproximate platysma and interrupted nylon sutures for skin. Light dressings are applied. A soft Silastic nasogastric feeding tube is inserted for maintenance of nutritional intake. The surgical specimen shows the distal two-thirds of the diverticulum with its mucosal lining and full-thickness muscular wall (Fig. 9.224).

Postoperative care is simple. Nasogastric tube feedings are begun on the day after surgery, and the drain is removed when serosanguineous drainage is minimal. Clear liquids are permitted by mouth approximately 7 days after surgery, and the patient is advanced to a regular diet during the following week. Recurrence of the diverticulum is rare unless excess mucosa is left behind, leaving a pseudopouch. If excessive mucosa is resected, stricture formation at the site of the resected Zenker's diverticulum is not uncommon. However, this complication is avoidable if appropriate care and attention are given to details at the time of surgical excision.

RESULTS OF TREATMENT FOR CANCER OF THE PHARYNX

The steep rise in HPV-associated oropharynx cancer over the past two decades has completely changed the landscape of epidemiology, incidence, workup, and treatment strategies for cancers of the oropharynx. P16 positivity serves as a surrogate marker for HPV status. The outcomes of p16 positive patients with cancers of the oropharynx has been shown to be remarkably well compared with p16-negative patients with all treatment strategies employed. In addition to the positive impact of outcome in relation to HPV status, smoking as a negative predictor of outcome has also been reported in numerous studies. The progression-free survival results for p16-positive and p16-negative oropharynx cancers are shown in Fig. 9.225. So profound is the impact of HPV positivity on outcome that the criteria used for staging HPV-negative and tobacco-associated oropharynx cancers is not considered valid anymore. Therefore the AJCC/UICC has developed a separate staging system for HPV-associated oropharynx cancers (eighth edition). According to this new staging system, stage IV is assigned only to patients with distant metastases. The survival curves for stages I to III are shown in Fig. 9.226. Due to the positive impact of HPV status on outcome, the current focus of clinical research is on reduction of treatment-related morbidity in this favorable group. Several clinical trials are currently underway to define the optimal treatment for HPV-positive oropharynx cancer with minimum sequela of treatment in the long term.

Cancer of the hypopharynx and cervical esophagus carry by far the worst prognosis among all primary sites in the upper aerodigestive tract, largely because of the high incidence of regional lymph node metastasis and advanced stage of disease at the time of diagnosis and treatment. More than 75% of all patients with hypopharyngeal cancer will have involvement of regional lymph nodes during the course of the disease. Sixty-six percent of the patients treated at Memorial Sloan Kettering Cancer Center presented with regional lymph node metastasis. Of the patients with negative clinical findings of the neck who underwent elective neck dissection, 41% were found to have micrometastasis in the N0 neck. Of patients whose N0 neck was not treated electively, subsequent metastases developed in 25%. Thus survival in these patients is, as expected, stage dependent. However, several patients die because of intercurrent disease and not directly as a result of recurrent cancer.

The survival among various sites within the hypopharynx is not very different. The 5-year overall survival ranges from 28% to 40% within various sites of hypopharynx. Disease-free 5-year survival ranges from 42% to 50% (Fig. 9.227). The few patients who present with early-stage disease have a 45% to 50% probability of 5-year overall survival. However, disease-free survival is 68% for stage I and 52% for stage II. Even with stage III disease, approximately 50% of patients are expected to survive for 5 years disease-free. Patients with advanced stage disease, particularly those with multiple regional lymph node involvement, have a very poor 5-year survival record that does not exceed 20% (Fig. 9.228). The patterns of failure indicate that the incidence of failure at the primary site, regional lymph nodes, and distant sites is almost equal (Fig. 9.229). Fifty-eight percent of patients treated at Memorial Sloan Kettering Cancer

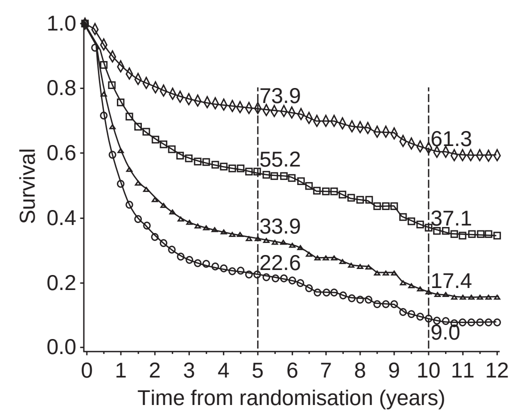

At risk

p16-positive Never	86	76	70	60	34	10	8
p16-positive Former or current	252	170	145	126	78	38	34
p16-negative Never	21	10	9	9	3	3	1
p16-negative Former or current	290	99	68	55	30	14	12

Figure 9.225 Progression-free survival curves in relation to P16 status and smoking status. *(Reproduced with permission from Lassen P et al. Prognostic impact of HPV-associated p16-expression and smoking status on outcomes following radiotherapy for oropharyngeal cancer: The MARCH-HPV project. Radiotherapy and Oncology, 2017. doi: 10.1016/j.radonc.2017.10.018.)*

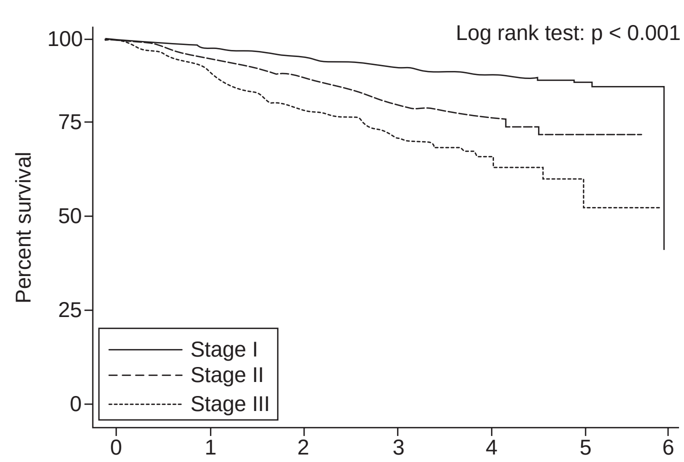

Number at risk

Stage I	3198	2932	2187	1227	556	124	0
Stage II	795	712	507	252	96	20	0
Stage III	450	392	260	137	52	12	0

Figure 9.226 Survival curves stratified by AJCC eighth edition staging system for HPV-positive oropharynx cancers (NCDB data).

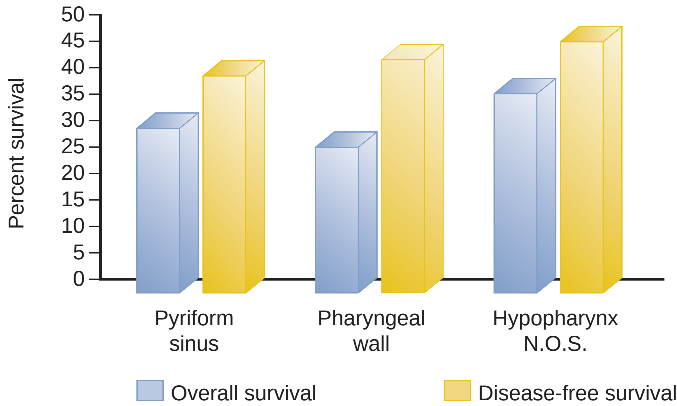

Figure 9.227 Overall and disease-free 5-year survival rates for cancer of the hypopharynx by primary site (MSKCC data). *N.O.S.,* Not otherwise specified.

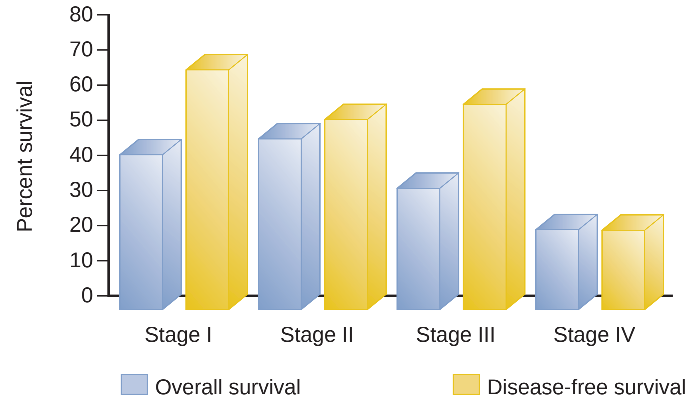

Figure 9.228 Overall and disease-free 5-year survival rates for cancer of the hypopharynx by stage of disease (MSKCC data).

Center between 1975 and 1985 did not respond to treatment. The median survival time in these patients was 24 months. With the use of a combination of surgery and postoperative radiation therapy, improvement in local and regional control is expected. However, prevention of distant metastasis requires availability of effective adjuvant systemic chemotherapy. The overall survival for advanced stage hypopharyngeal carcinoma has remained stable over the past several decades, in spite of evolution in treatment strategies and larynx preservation strategies with chemoradiotherapy.

The consideration of quality of life in these patients is therefore vitally important in initial treatment planning. Multidisciplinary nonsurgical treatment programs of chemotherapy and radiotherapy aimed at preservation of the larynx are successful in select patients. Tumors that manifest complete response to induction chemotherapy have an excellent chance of responding to radiotherapy with preservation of the larynx without compromising survival. However, nonresponders carry a dismal prognosis. For patients who require a pharyngolaryngectomy, the focus of surgery is on immediate reconstruction of the alimentary tract to restore swallowing as soon as possible. Contemporary methods of reconstruction include the use of the pectoralis major myocutaneous flap or the use of a radial forearm or ALT free flap for repair of partial pharyngeal defects. These flaps provide an ideal method for one-stage reconstruction.

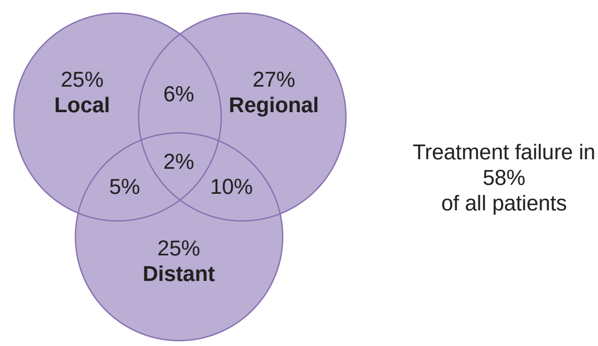

Figure 9.229 Patterns of treatment failure for cancer of the hypopharynx (MSKCC data).

However, for circumferential defects of the pharynx, regional cutaneous or myocutaneous flaps are not quite satisfactory. For short circumferential defects of the pharyngoesophageal region in the neck, a tubed RFFF, ALT flap, or free jejunal graft is ideal. In most patients, the ability to swallow is restored in less than 2 weeks. On the other hand, for patients who require a total pharyngectomy and a total esophagectomy, gastric transposition remains the reconstructive method of choice. For the majority of the patients, swallowing by mouth will be restored in less than 2 weeks.

CHAPTER 10

Larynx and Trachea

The larynx plays a central role in coordinating the functions of the upper aerodigestive tract, including respiration, speech, and swallowing. The larynx is the second most common site for squamous cell carcinoma in the head and neck, which is causally related to tobacco and alcohol exposure. The larynx is divided into supraglottic, glottic, and subglottic regions (Fig. 10.1). These anatomic divisions are based on embryologic development and have important clinical implications. Lymphatic drainage of the supraglottic larynx is very rich compared with the scanty lymphatic network in the submucosal plane of the true vocal cords. The patterns of regional spread of laryngeal cancer therefore depend on the site of origin and the local extent of the primary tumor. Each of the three regions of the larynx is divided into various sites (Fig. 10.2). The sites in the supraglottic region are the laryngeal surface of the epiglottis, the aryepiglottic folds, the arytenoids, the ventricular bands or false vocal cords, and the ventricles, which are potential spaces between the false and true vocal cords. In the glottic larynx, the right and left vocal cords and anterior commissure represent the three designated sites. The subglottic region is generally considered as one site and is divided into its right and left lateral walls.

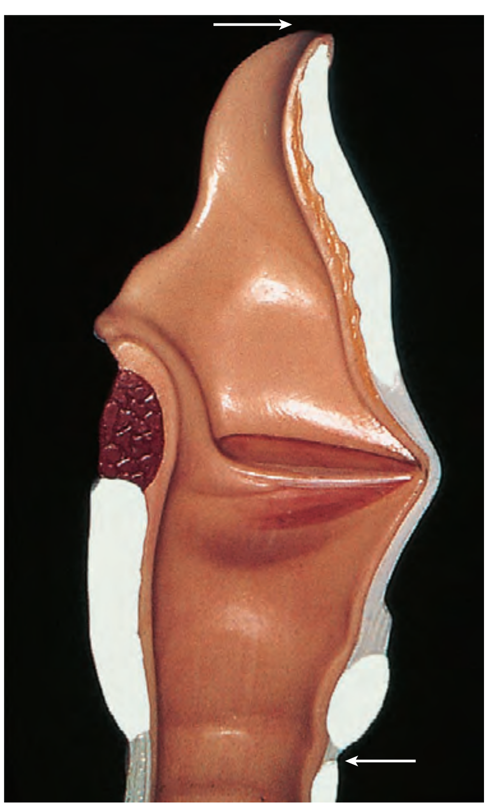

Figure 10.1 The anatomic limits of the larynx. Upper arrow, Tip of epiglottis. Lower arrow, Lower border of cricoid cartilage.

Squamous cell carcinomas constitute more than 95% of primary malignant tumors of the larynx. The remaining tumors are those arising from the minor salivary glands, neuroepithelial tumors, soft tissue tumors, and, rarely, the cartilaginous laryngeal framework. In 2018, the American Cancer Society estimated that approximately 13,150 new cases of cancer of the larynx would be diagnosed in the United States, which represents 0.8% of all new cancers. Death rate estimates vary, depending on the site and stage of the primary tumor. Overall, 3,710 cause-specific deaths for cancer of the larynx were estimated for 2018 in the United States. Worldwide, the incidence of laryngeal cancer varies in different countries (Fig. 10.3). Southern Europe has by far the highest incidence of laryngeal cancer in men in the world. The geographic variation in the incidence rates and anatomic site distribution may be a reflection of lifestyle and habits of the patient population in different parts of the world, as well as other environmental factors.

The site distribution of larynx cancer is shown in Fig. 10.4. The glottic region is by far the most common site for primary malignant tumors in the larynx. The stage distribution of patients with supraglottic carcinoma and glottic carcinoma at the time of presentation at Memorial Sloan Kettering Cancer Center is shown in Figs. 10.5 and 10.6. Nearly 75% of patients with glottic carcinoma have localized disease at the time of diagnosis, in contrast to nearly 70% of patients with supraglottic carcinoma who have advanced disease at presentation.

The age distribution of larynx cancer cases from the SEER (Surveillance, Epidemiology, and End Results) database in the

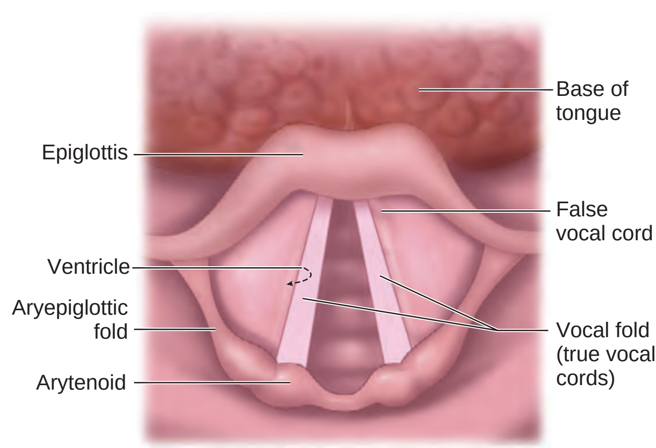

Figure 10.2 The anatomic regions and sites of the larynx.

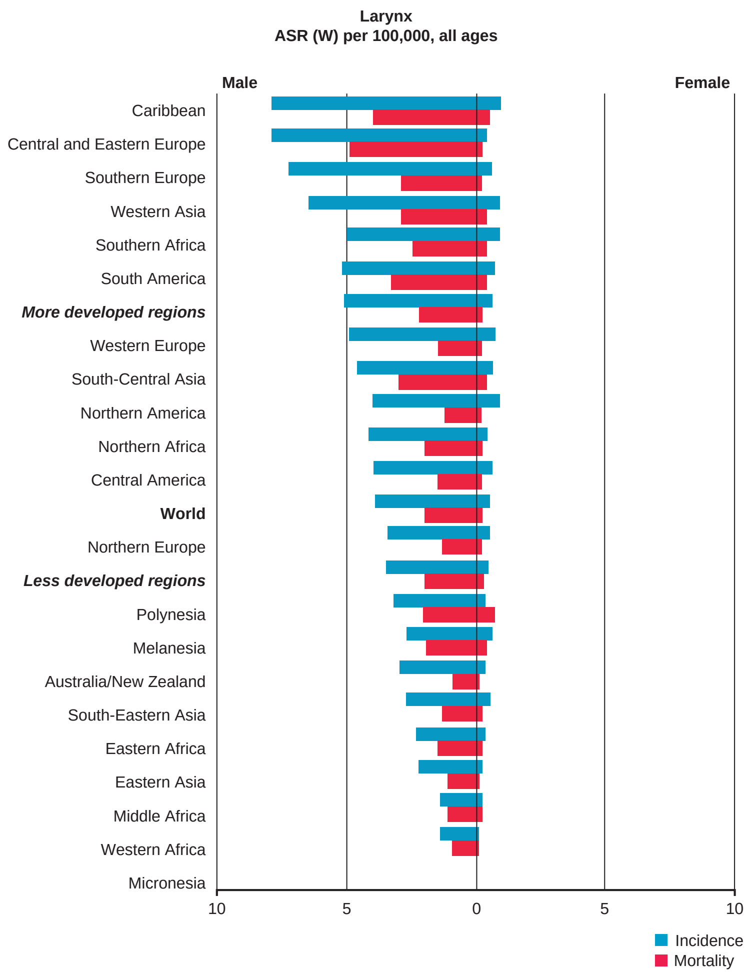

Figure 10.3 World incidence of cancer of the larynx (incidence per 100,000 population) in males and females. *ASR*, Age-standardized rate. *(From Ferlay J, Soerjomataram I, Ervik M, Dikshit R, Eser S, Mathers C, Rebelo M, Parkin DM, Forman D, Bray F. GLOBOCAN 2012 v1.0, Cancer Incidence and Mortality Worldwide: IARC CancerBase No. 11. Lyon, France, International Agency for Research on Cancer, 2013. Available from http://gco.iarc.fr/today/home.)*

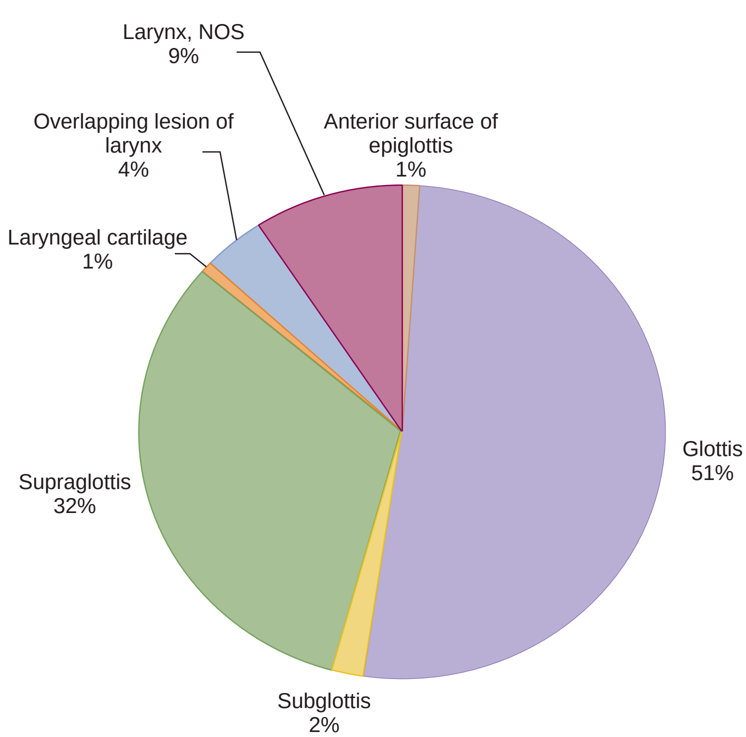

Figure 10.4 Site distribution of squamous cell carcinoma of the larynx in the United States (NCDB data).

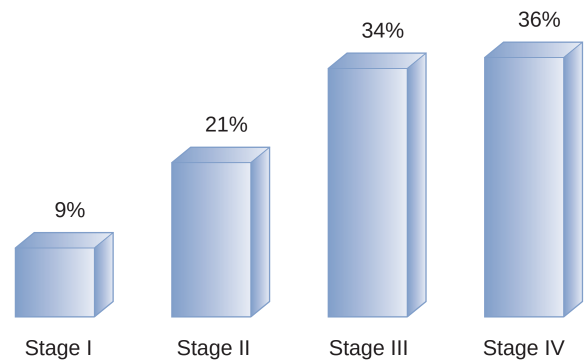

Figure 10.5 The stage distribution of patients with supraglottic carcinoma at initial presentation (MSKCC data).

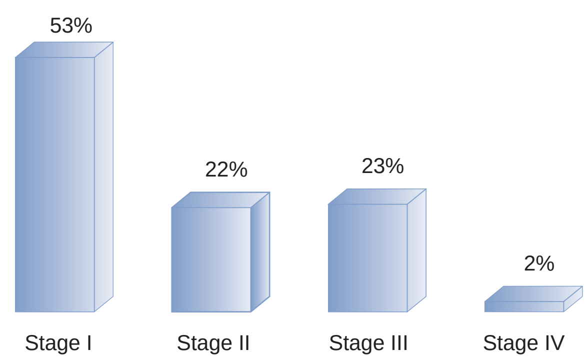

Figure 10.6 The stage distribution of patients with glottic carcinoma at initial presentation (MSKCC data).

United States from 2010-2014 shows peak age between the 5th to 7th decade of life (Fig. 10.7). The trend in incidence, mortality, and 5-year relative survival are shown in Fig. 10.8. Since 1975 the incidence of larynx cancer has declined, and this has been associated with a progressive decline in mortality from larynx cancer. However, the 5-year relative survival has not improved over this time period. The 5-year relative survival for cases diagnosed from 1975 to 1977 was 66%, for cases diagnosed 1987 to 1989 was 66%, but for cases diagnosed 2006 to 2012 was 62%. This may account for other causes of death, including treatment-related morbidity and mortality as a result of increasing use of nonsurgical larynx preservation treatment programs.

EVALUATION

Patients with primary tumors of the larynx usually present with complaints of hoarseness, discomfort in the throat, dysphagia, odynophagia, the sensation of something stuck in the throat, occasional respiratory obstruction, hemoptysis, or referred pain to the ipsilateral ear. The diagnosis in most instances is made by a thorough clinical examination using a rigid telescope or flexible fiber-optic laryngoscope, which allows adequate assessment of the surface extent of the primary tumor and mobility of the vocal cords. When lesions of the larynx are described, it is advisable to document them by a photograph or to depict them on a drawing to precisely demarcate the site and the local extent of the lesion. It is vitally important to specifically designate the site of origin of the primary lesion with its local extension to adjacent sites within the same region of the larynx or from one region to another region. Bulky lesions may extend beyond the larynx into the adjacent base of the tongue, pyriform sinus, or postcricoid region. This initial documentation is important not only for surgical treatment planning, but more so if the patient is to be treated by a nonsurgical larynx preservation

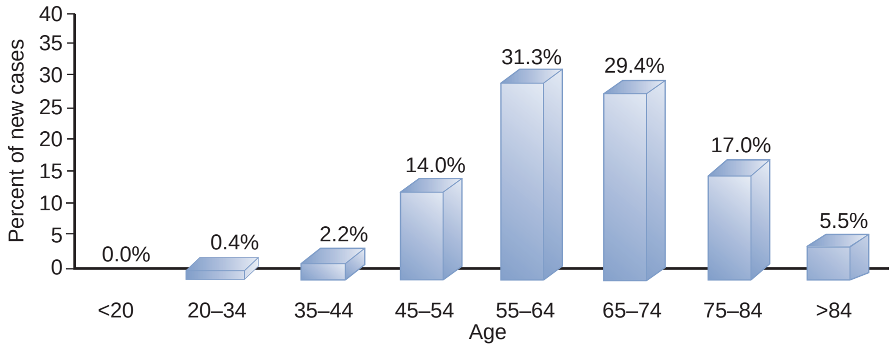

Figure 10.7 Percent of larynx cancer cases by age group (SEER 18, 2010-2014, all ages, both sexes).

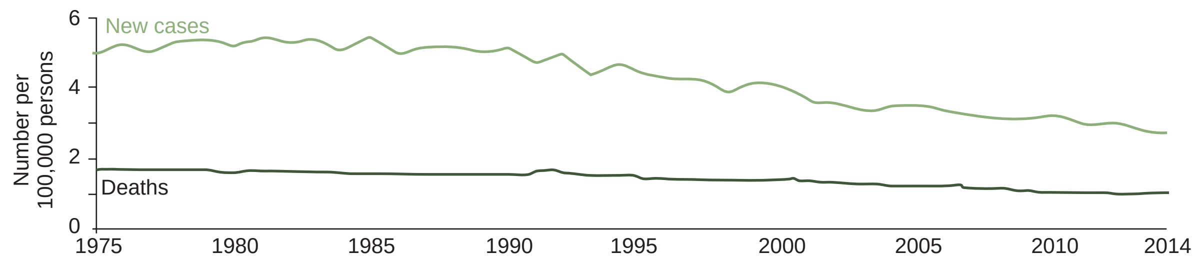

Year	1975	1980	1985	1990	1995	2000	2005	2009
5–year relative survival	63.2%	66.5%	67.4%	64.6%	66.1%	63.3%	65.7%	63.9%

Figure 10.8 New cases, deaths, and 5-year relative survival for cancer of the larynx (SEER 9, incidence and mortality, 1975-2014).

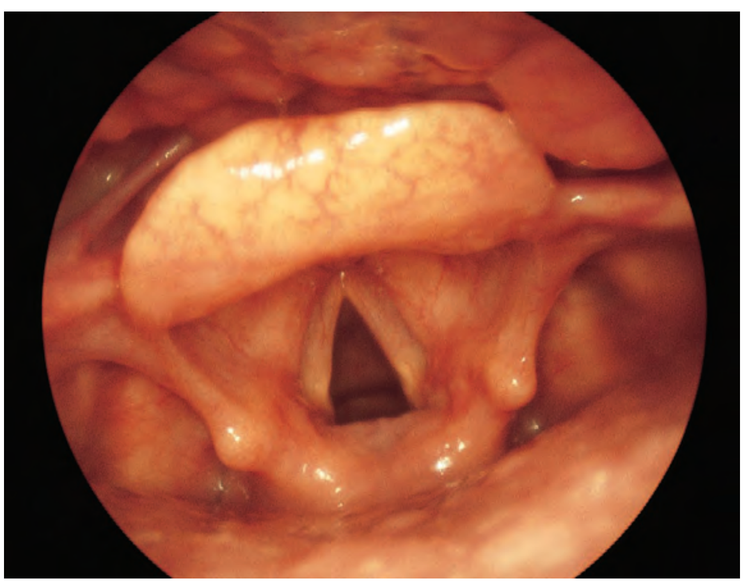

Figure 10.9 Endoscopic view of the normal larynx.

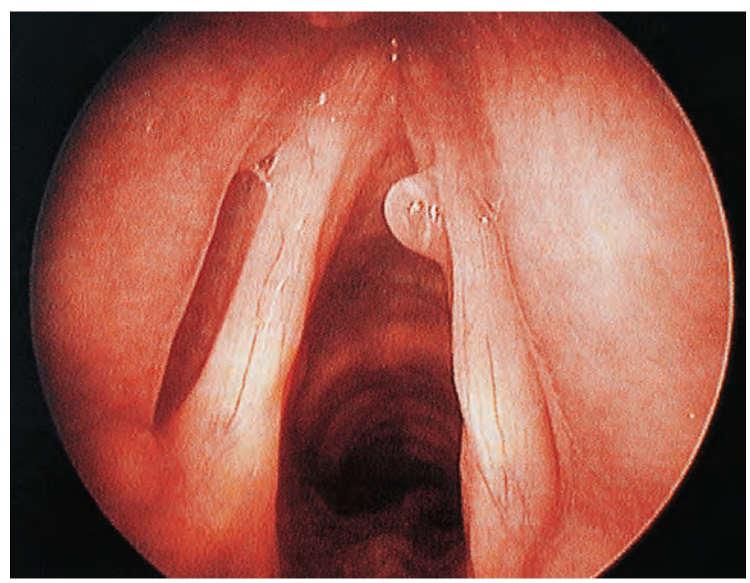

Figure 10.10 Benign mucosal polyp on the free edge of the anterior third of the right vocal cord.

program with chemoradiotherapy to assess response to therapy and for subsequent comparison during follow up.

The endoscopic appearance of a normal larynx is shown in Fig. 10.9. Benign polyps have a smooth, glistening appearance with varying degrees of mucosal vascularity. They may be sessile or pedunculated and usually present on the true vocal folds (Figs. 10.10 and 10.11). Reinke's edema presents as pseudopolyps and often is bilateral (Fig. 10.12). Postintubation granulomas and benign inflammatory conditions also may present as polypoid lesions (Figs. 10.13 through 10.15). Granulomas of the vocal cord also can occur as a foreign body reaction resulting from injection of Teflon for medialization of a paralyzed vocal cord (Fig. 10.16). Squamous papillomas may have an appearance that is similar to that of a carcinoma (Fig. 10.17). Epithelial neoplasms often present as whitish or erythematous, flat or exophytic lesions. These lesions may represent benign keratoses, premalignancy, or invasive cancer (Figs. 10.18 through 10.28). Other submucosal lesions have a characteristic appearance with an intact overlying mucosa, such as a hemangioma (Fig. 10.29). Subglottic lesions may be sometimes visible by indirect laryngoscopy with a flexible laryngoscope in the outpatient setting (Fig. 10.30). However, accurate assessment of the true extent of the lesion requires laryngoscopy under anesthesia. Direct laryngoscopy with the use of rigid telescopes (0, 30, 70, and 120 degrees) or an operating microscope provides an excellent and detailed view of the lesion (Fig. 10.31). For supraglottic lesions, extension of the tumor beyond the larynx into the adjacent base of the tongue, pyriform sinuses, or postcricoid

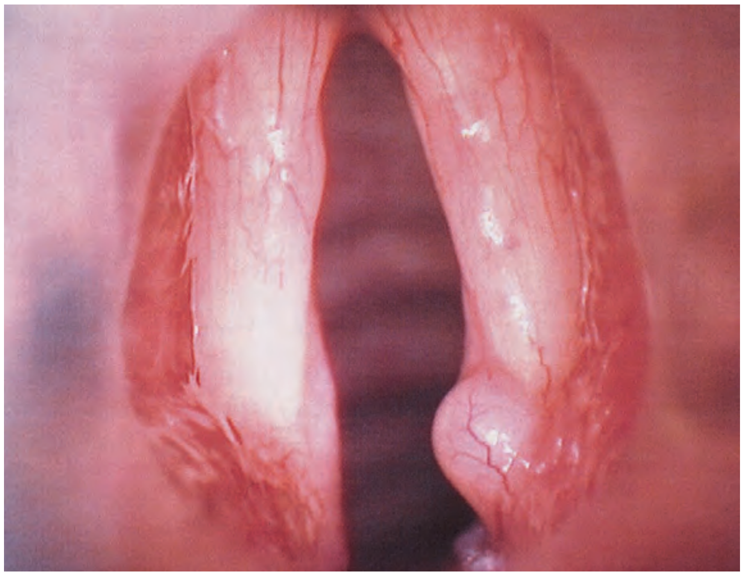

Figure 10.11 Benign mucosal polyp near the vocal process on the right vocal cord.

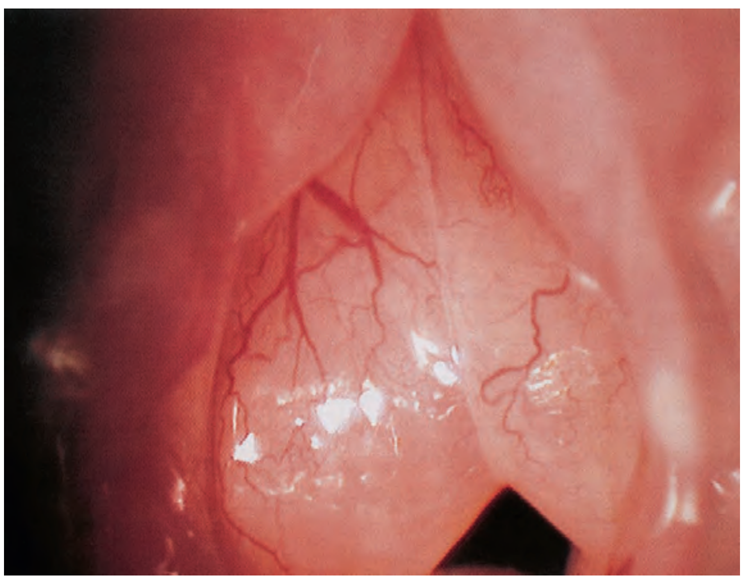

Figure 10.12 Reinke's edema of the vocal cords.

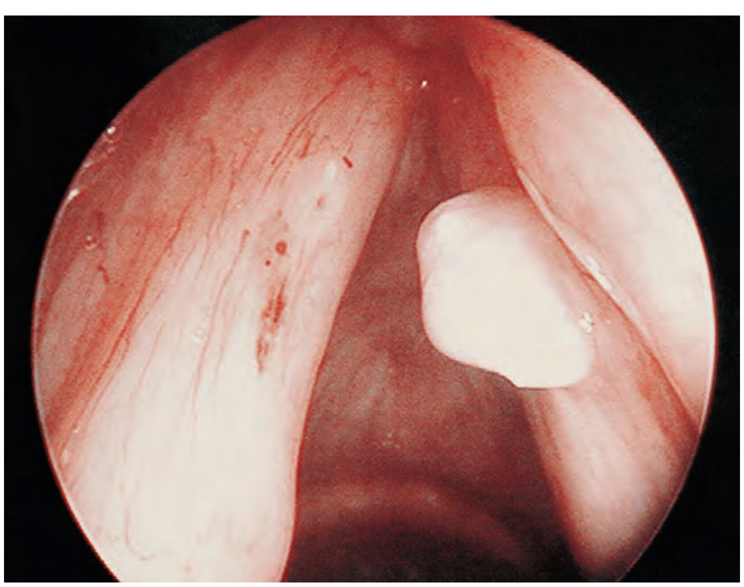

Figure 10.13 Fibrous polyp of the right vocal cord.

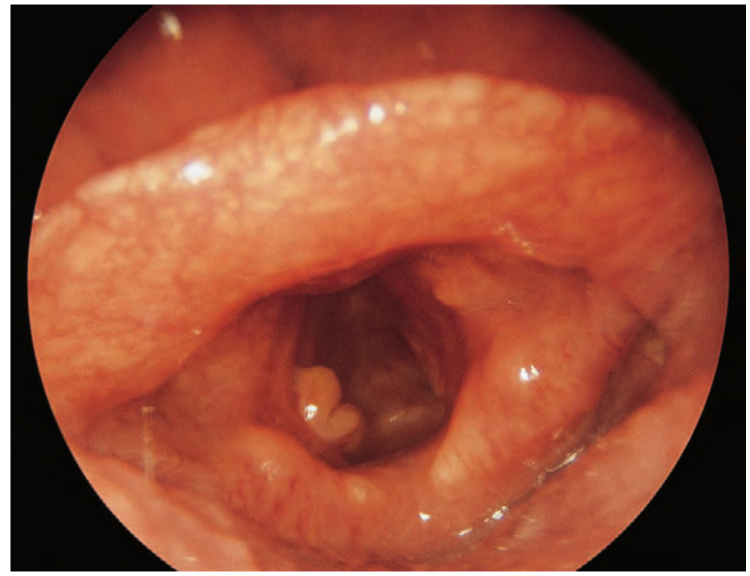

Figure 10.14 Postintubation granuloma of the posterior third of the left vocal cord.

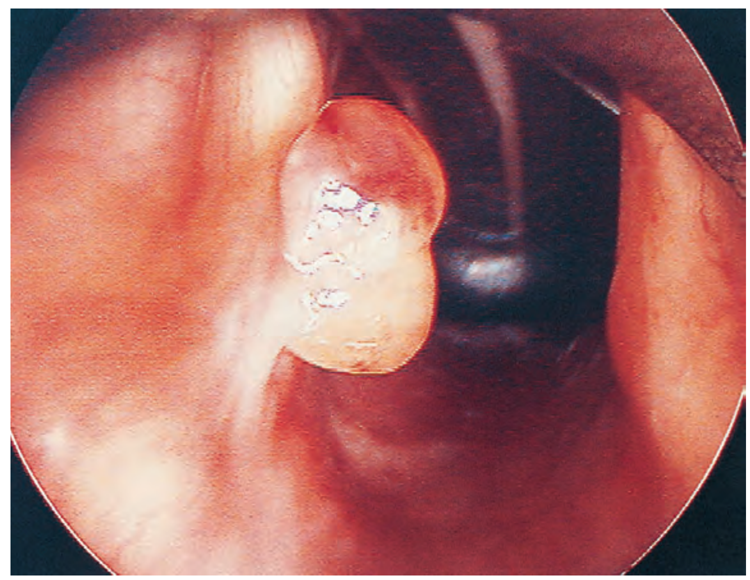

Figure 10.15 Granuloma of the left vocal cord seen through the operating microscope.

Figure 10.16 Teflon granuloma of the right vocal cord postinjection of Teflon paste for paralyzed vocal cord.

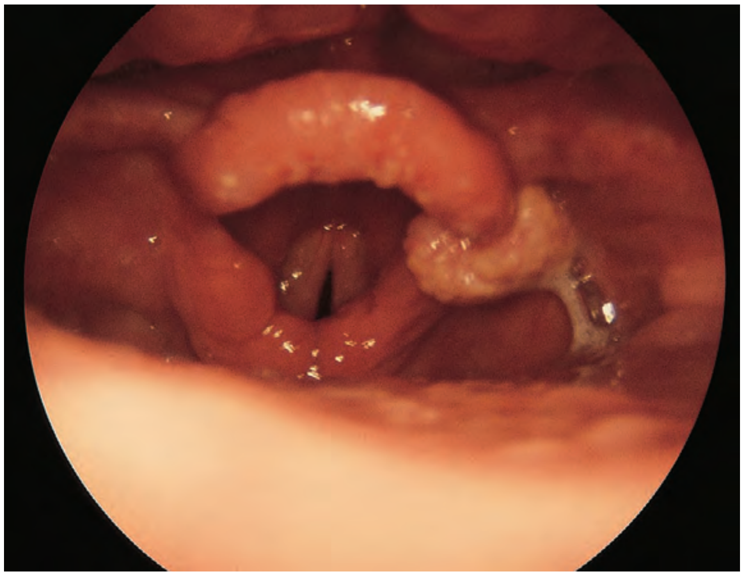

Figure 10.17 Squamous papilloma of the right aryepiglottic fold.

Figure 10.18 Hyperkeratosis of the right vocal cord.

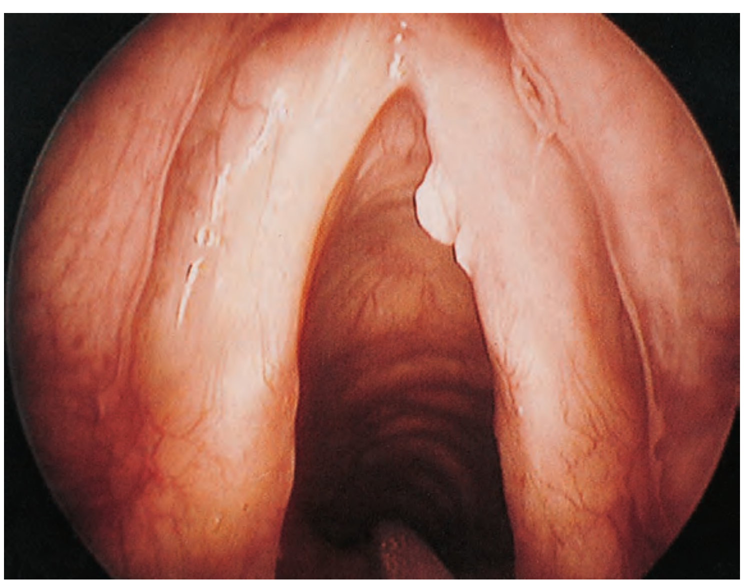

Figure 10.19 Carcinoma in situ presenting as a keratotic nodule of the right vocal cord.

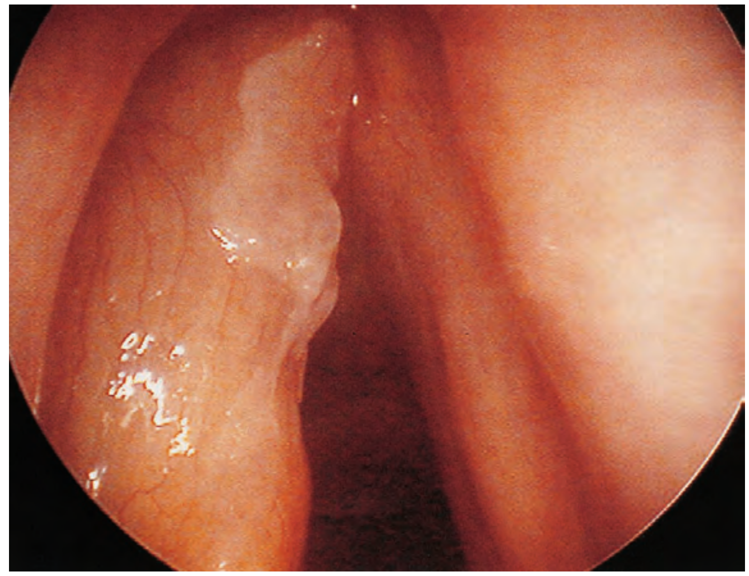

Figure 10.20 Superficial carcinosarcoma of the left true vocal cord.

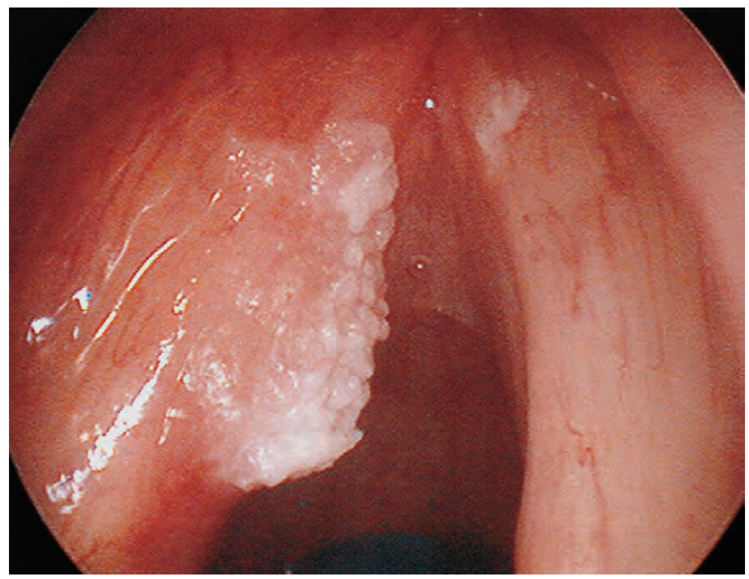

Figure 10.21 Papillary squamous carcinoma of the left true vocal cord.

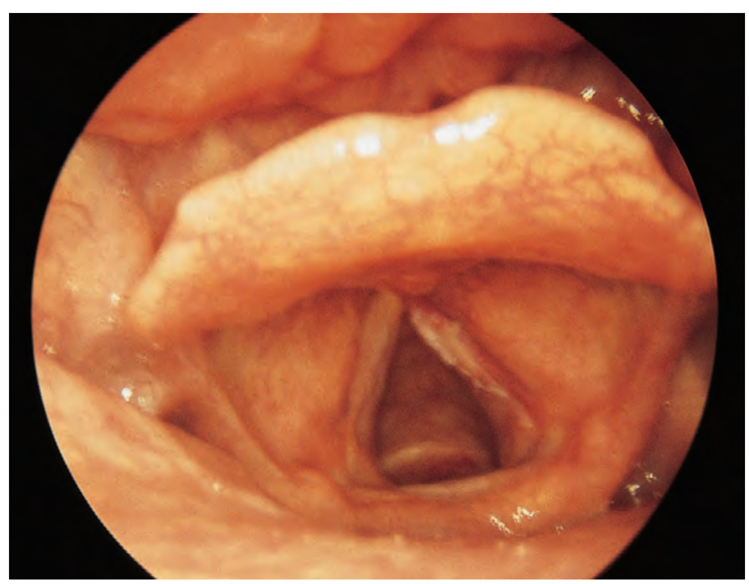

Figure 10.22 Ulcerated squamous cell carcinoma of the right vocal cord, viewed during quiet breathing.

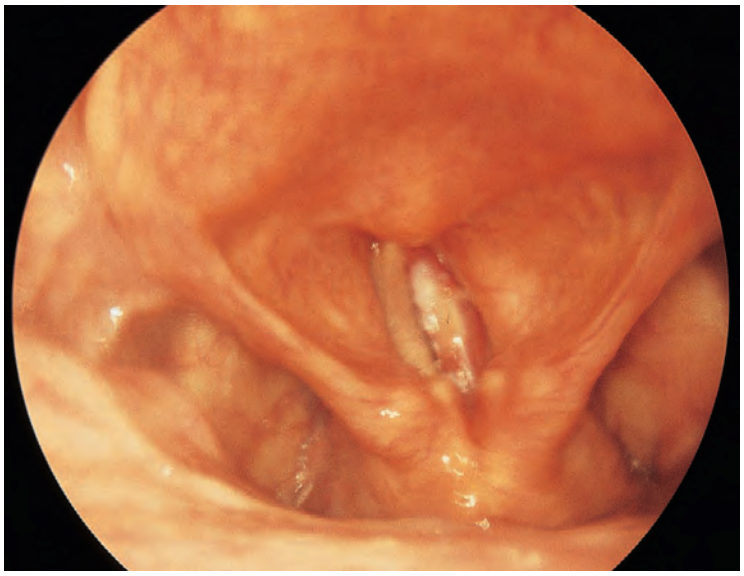

Figure 10.23 Ulcerated carcinoma of the right vocal cord, viewed during phonation.

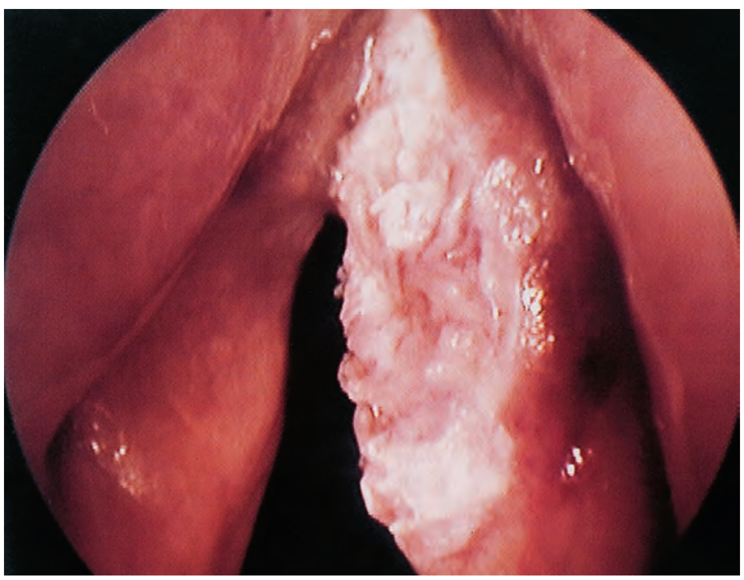

Figure 10.24 Ulcerated exophytic keratotic squamous carcinoma of the right vocal cord.

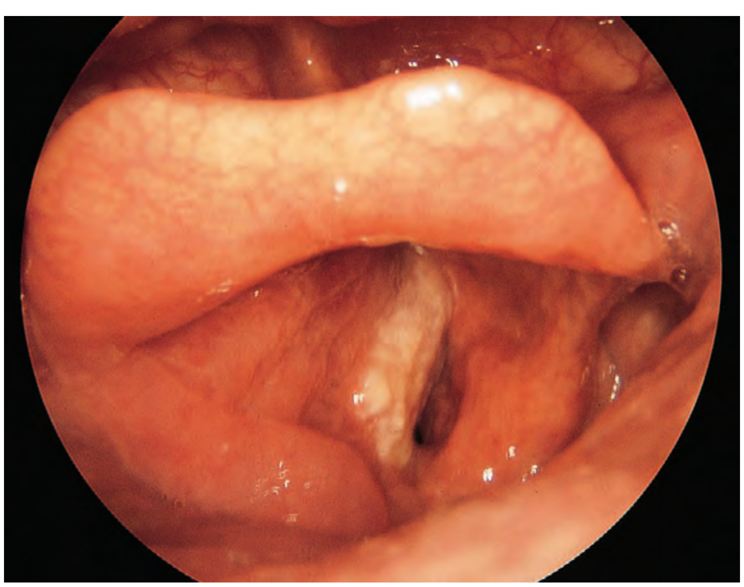

Figure 10.25 Squamous carcinoma of the left vocal cord with fixation.

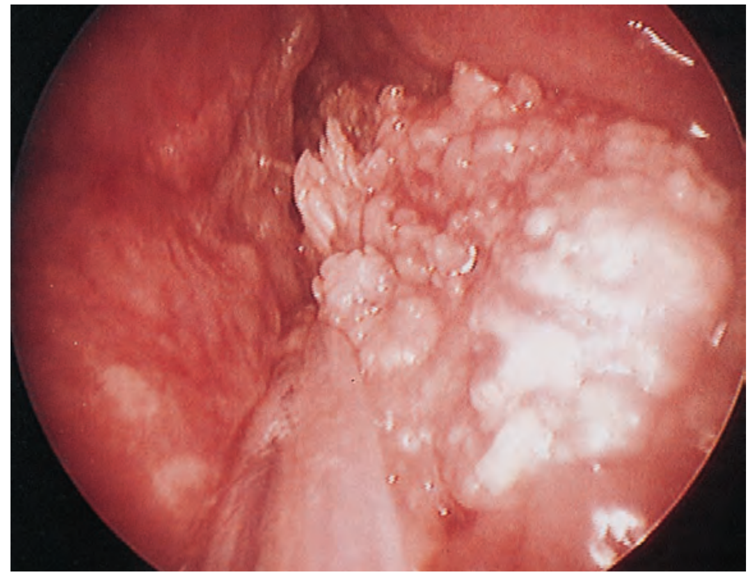

Figure 10.26 Papillary verrucous carcinoma of the right arytenoid.

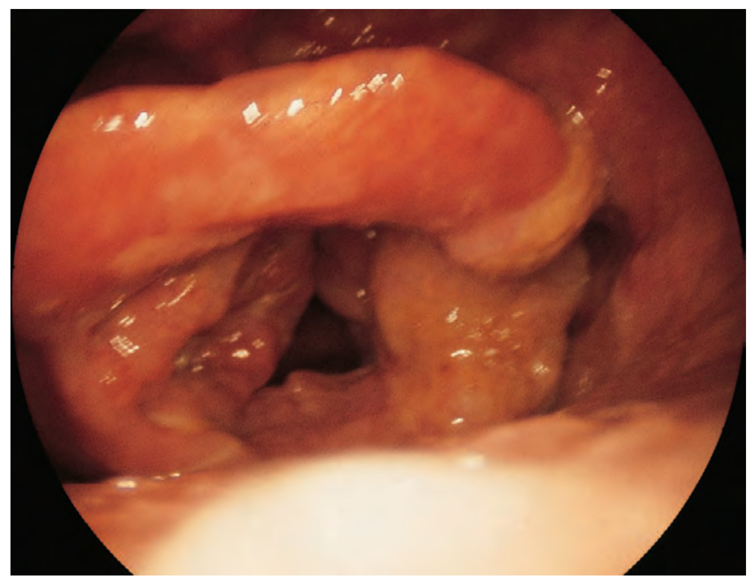

Figure 10.27 Squamous carcinoma of the right aryepiglottic fold.

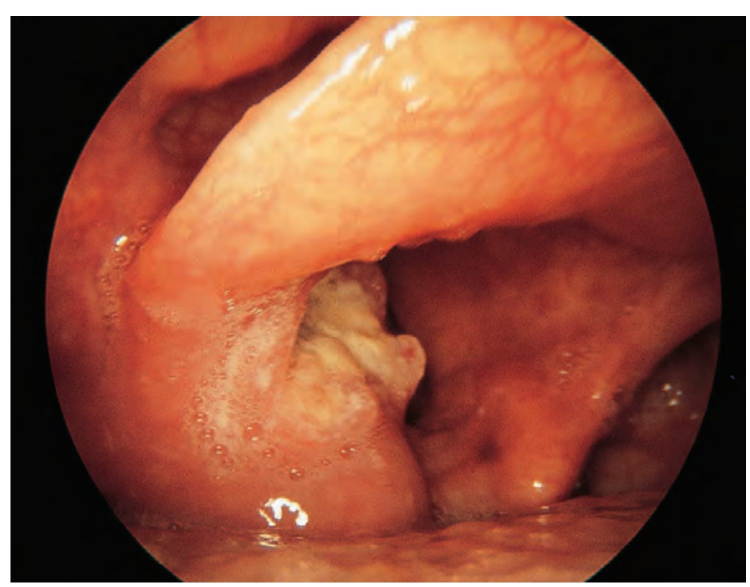

Figure 10.28 Squamous carcinoma of the left arytenoid.

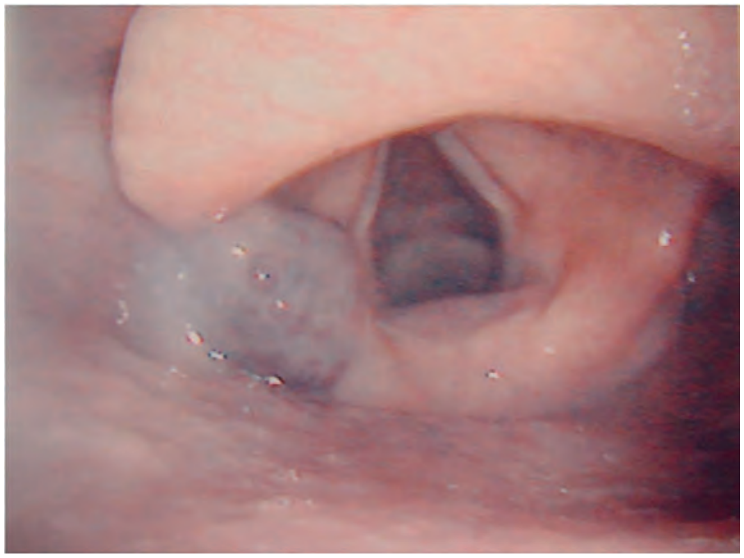

Figure 10.29 Hemangioma of the left pyriform sinus.

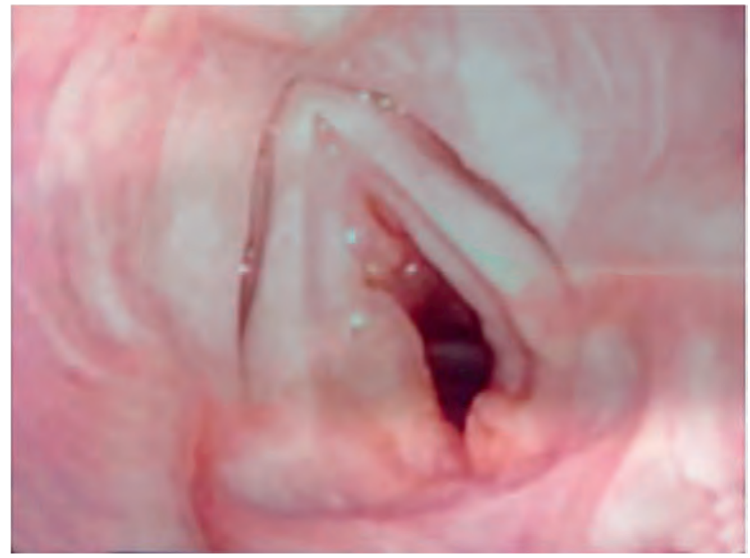

Figure 10.30 Carcinoma of the subglottic larynx.

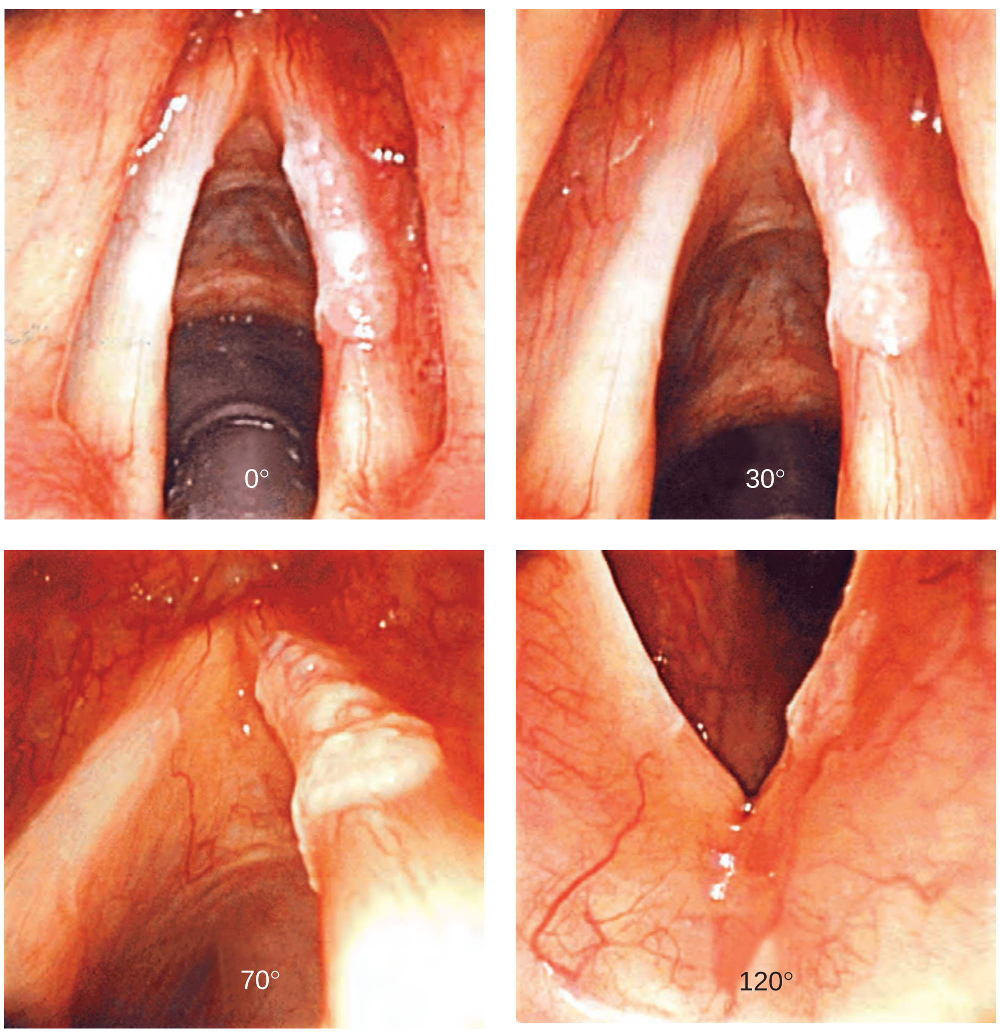

Figure 10.31 Examination under anesthesia with rigid telescopes showing extent of early stage vocal cord carcinoma.

region should be assessed. For lesions involving the laryngeal surface of the epiglottis, its inferior extent in relation to the anterior commissure is very important. Subglottic extension of glottis or transglottic cancers is crucial to accurately stage the tumor and plan definitive treatment. Accurate evaluation of the primary tumor in this manner prior to initiating treatment is vitally important, especially if any voice-sparing surgical procedure is a consideration. Finally, the precise nature of the lesion requires a representative biopsy for histologic diagnosis.

Imaging

Radiographic assessment of the larynx is vitally important for delineating the extent of a tumor, particularly the third

dimension, because it may influence staging and treatment selection. A computed tomography (CT) scan with intravenous contrast is usually the first and often the only radiographic study required to assess a laryngeal tumor. A CT scan with thin slices is quite accurate in assessment of laryngeal lesions, particularly with reference to tumor extension in the paraglottic space and invasion of cartilages and adjacent soft tissues. In addition, a CT scan provides the benefit of radiographic evaluation of cervical lymph nodes. Magnetic resonance imaging (MRI) of the larynx has an added ability to provide three-dimensional images in axial, coronal, and sagittal planes to further demonstrate local extension of a laryngeal lesion. This capability is of particular value in assessing the subglottic extent of the tumor.

The MRI scans of a patient who previously had undergone radiation therapy for vocal cord cancer and now presented with a recurrent tumor are shown in Figs. 10.32 through 10.34. The axial view shows a tumor of the right vocal cord with subglottic extension partially compromising the airway. In a coronal view of the MRI scan, an exophytic lesion obstructing the subglottic airway is seen clearly. Further vivid demonstration of the subglottic tumor can be seen in the sagittal MRI view, which shows a significant obstruction produced by the recurrent tumor. The surgical specimen of the same patient who underwent a hemilaryngectomy shows the extent of subglottic disease from recurrent carcinoma of the right true vocal cord (Fig. 10.35).

An axial view of the CT scan through the subglottic region of a patient with partial airway compromise from a chondrosarcoma of the larynx shows the tumor arising from the right side of the cricoid cartilage and projecting into the subglottic airway (Fig. 10.36). The surgical specimen following total laryngectomy shows a bulky submucosal tumor arising from the right side of the subglottic region and extending across the anterior midline to the left-hand side (Fig. 10.37). Note the degree of airway compromise due to the bulk of the lesion on both sides of the midline.

Another patient with a chondrosarcoma of the cricoid cartilage presented with significant respiratory obstruction. A CT scan in the axial view without contrast shows a cartilaginous tumor arising from the cricoid cartilage and presenting anteriorly, causing compromise of the airway (Fig. 10.38). An endoscopic view of the same patient under general anesthesia shows a bulky submucosal multilobulated tumor arising from the cricoid

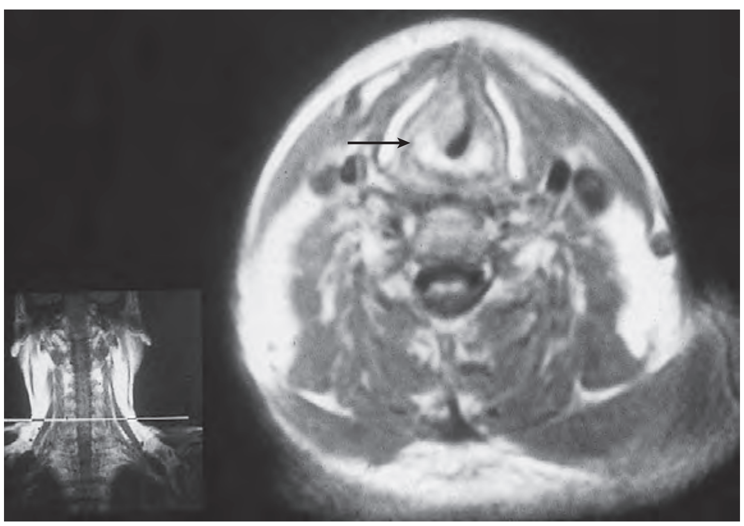

Figure 10.32 MRI scan in axial view shows tumor of the right vocal cord (*arrow*).

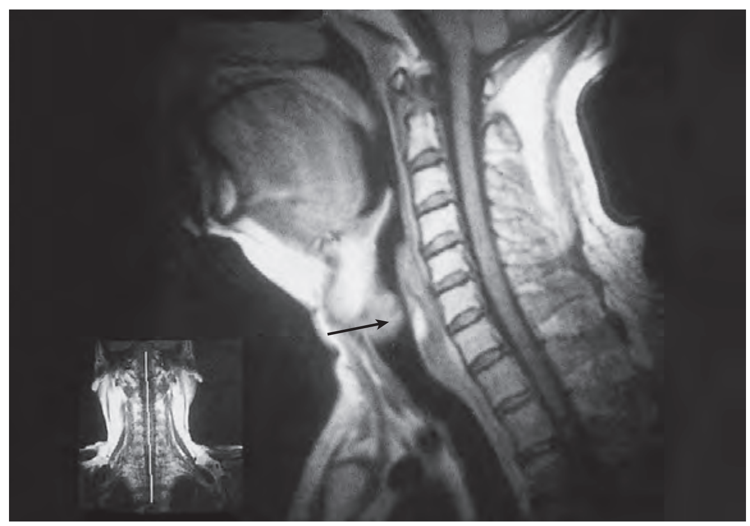

Figure 10.34 Sagittal view of the MRI scan shows transglottic tumor (*arrow*).

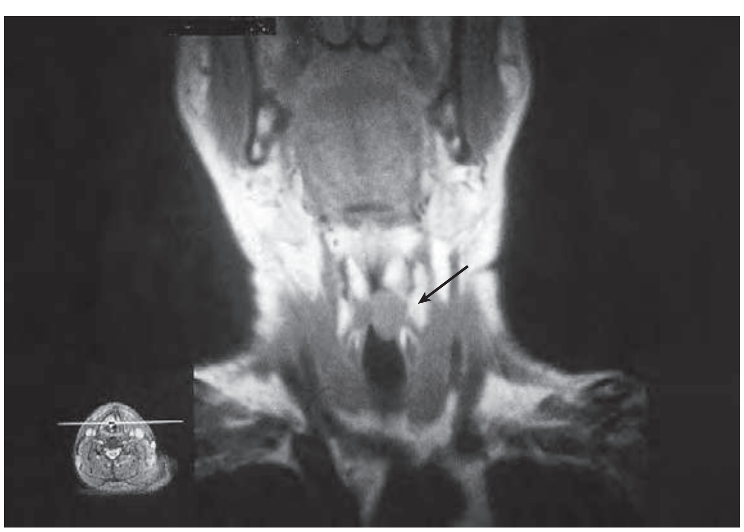

Figure 10.33 Coronal view of the MRI scan shows subglottic extension of vocal cord tumor (*arrow*).

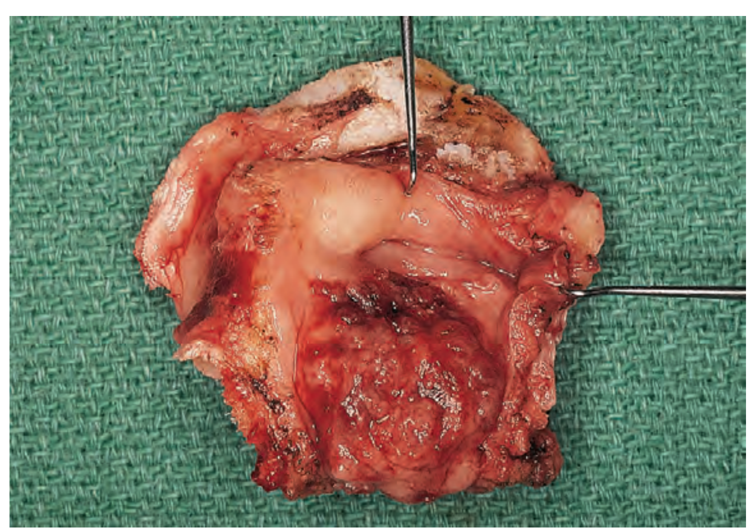

Figure 10.35 The surgical specimen of hemilaryngectomy showing transglottic tumor.

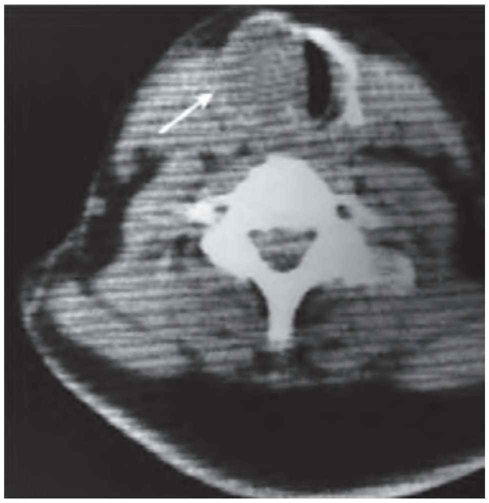

Figure 10.36 Axial view of CT scan of the larynx showing a tumor of the cricoid cartilage (*arrow*).

Figure 10.37 The surgical specimen of total laryngectomy done for chondrosarcoma of the cricoid cartilage, shown on the CT scan in Fig. 10.36.

Figure 10.38 CT scan in the axial view showing a chondrosarcoma of the cricoid cartilage encroaching upon the airway.

Figure 10.39 Endoscopic view of the tumor shown in Fig. 10.36.

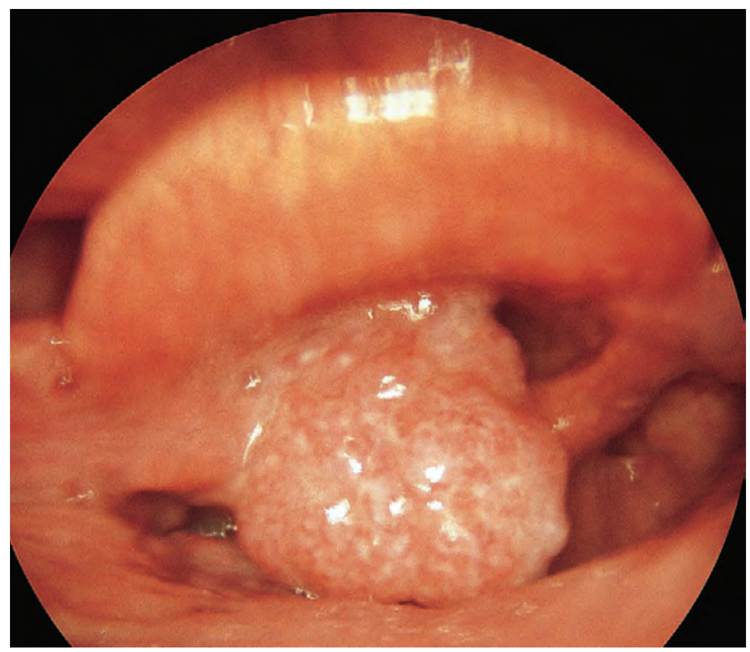

Figure 10.40 Telescopic view of the larynx showing a tumor of the aryepiglottic fold.

cartilage and the region of the cricoarytenoid joint on the left-hand side with compromise of the airway (Fig. 10.39).

Occasionally a CT scan will detect an unsuspected second primary tumor or, more importantly, enlarged cervical lymph nodes that are not palpable clinically. An example of this finding is shown in a patient whose telescopic view of the larynx is shown in Fig. 10.40. A primary tumor is seen arising from the left aryepiglottic fold, and both pyriform sinuses open well and appear to be clear. However, the same patient's CT scan at the level of the thyrohyoid membrane shows the presence of one lesion on the aryepiglottic fold with what appears to be a second lesion on the lateral wall of the pyriform sinus (Fig. 10.41). The surgical specimen of the same patient after a supraglottic partial laryngopharyngectomy shows two separate primary lesions: one on the aryepiglottic fold and a second lesion on the lateral wall of the pyriform sinus that clinically was not appreciated (Fig. 10.42). Thus CT scans of the larynx are recommended for initial assessment of laryngeal cancer,

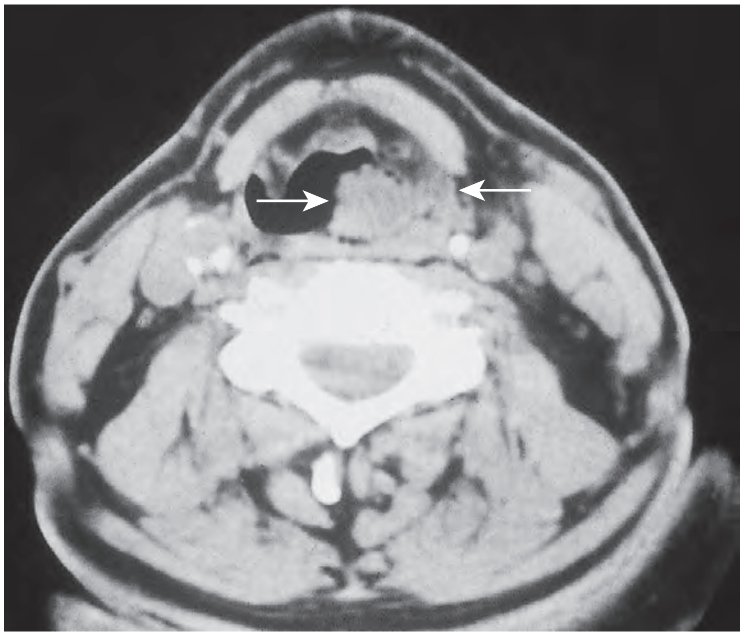

Figure 10.41 CT scan showing one lesion on the aryepiglottic fold (*left arrow*) and a second lesion on the lateral wall of the pyriform sinus (*right arrow*).

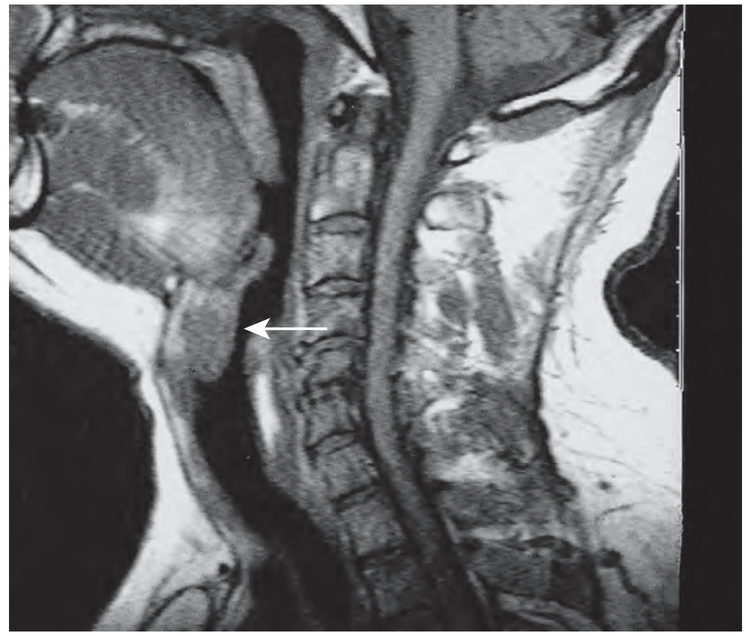

Figure 10.43 Sagittal view of the MRI scan showing a submucosal lesion of the infrahyoid portion of the epiglottis (*arrow*).

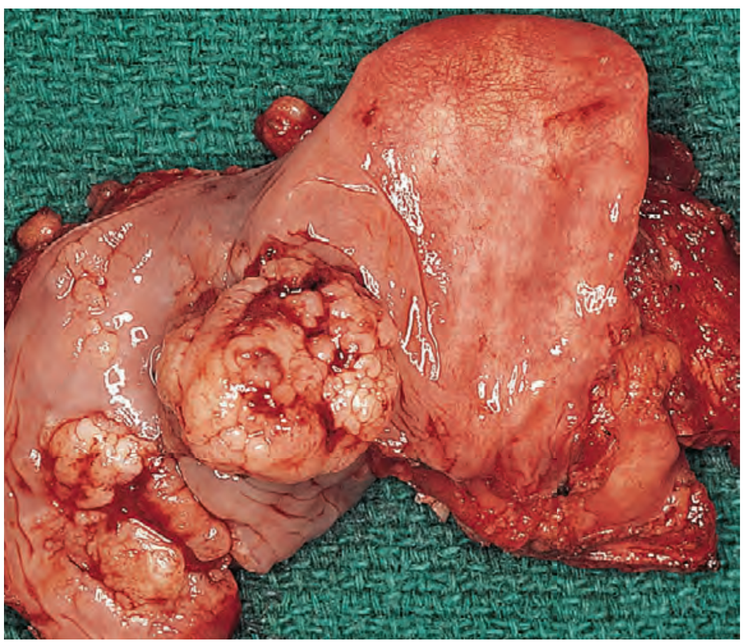

Figure 10.42 The surgical specimen of the tumors shown in Fig. 10.41.

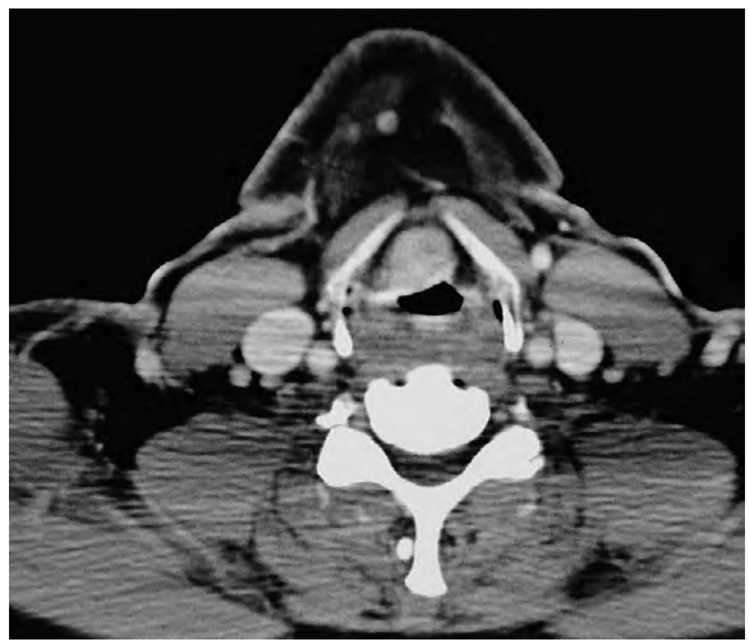

Figure 10.44 Axial view of the MRI showing extension into the preepiglottic space.

regardless of the treatment plan for the tumor. An MRI scan of another patient with a submucosal lesion of the infrahyoid portion of the laryngeal surface of the epiglottis is shown in Fig. 10.43. Note the extension of the tumor into the preepiglottic space and its cephalocaudad extension, as well as the posterior projection of the tumor, which is causing compromise of the airway. An axial view of the MRI scan of the same patient shown in Fig. 10.44 demonstrates the extension of the tumor into the preepiglottic space at the level of the superior border of the thyroid cartilage. An endoscopic view of this patient under general anesthesia shows the multilobulated submucosal tumor of the laryngeal surface of the epiglottis (Fig. 10.45). A biopsy of this tumor confirmed that it was an adenoid cystic carcinoma.

Another patient with a submucosal lesion of the suprahyoid portion of the laryngeal surface of the epiglottis is shown in Fig. 10.46. This sagittal view of the MRI shows a submucosal

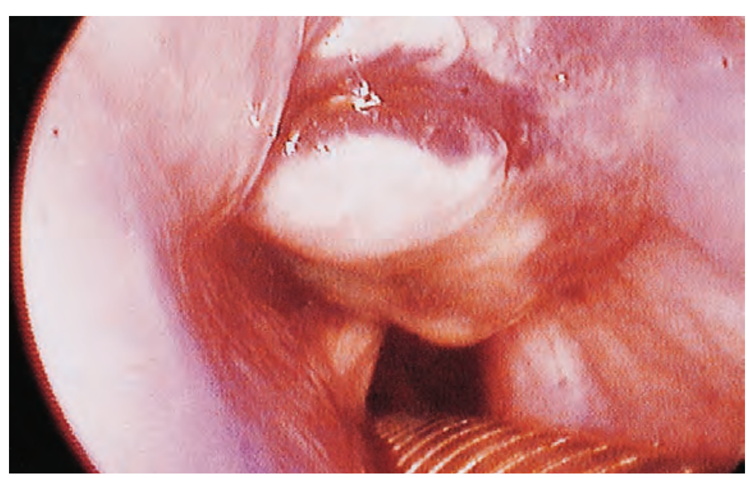

Figure 10.45 Endoscopy demonstrates the multilobulated submucosal tumor of the laryngeal surface of the epiglottis.

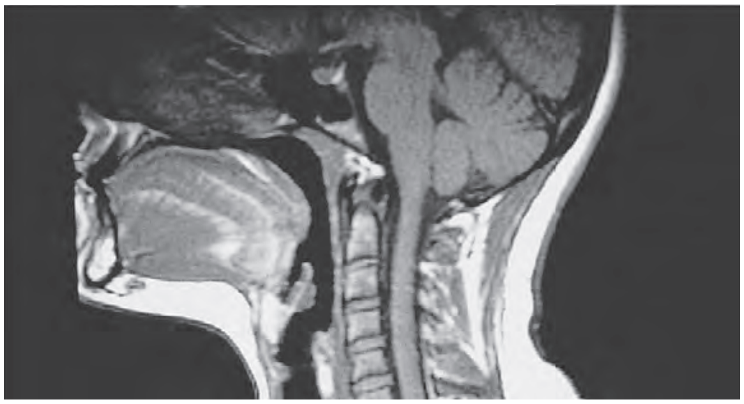

Figure 10.46 Sagittal view of the MRI scan showing a submucosal lesion of the suprahyoid epiglottis.

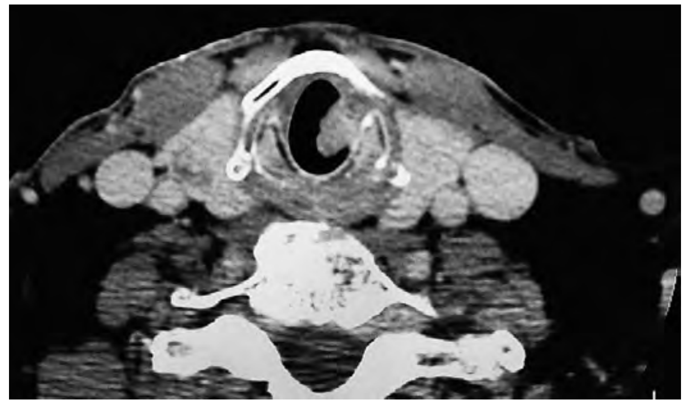

Figure 10.48 Axial view of the CT scan of a patient showing tumor in the subglottic region.

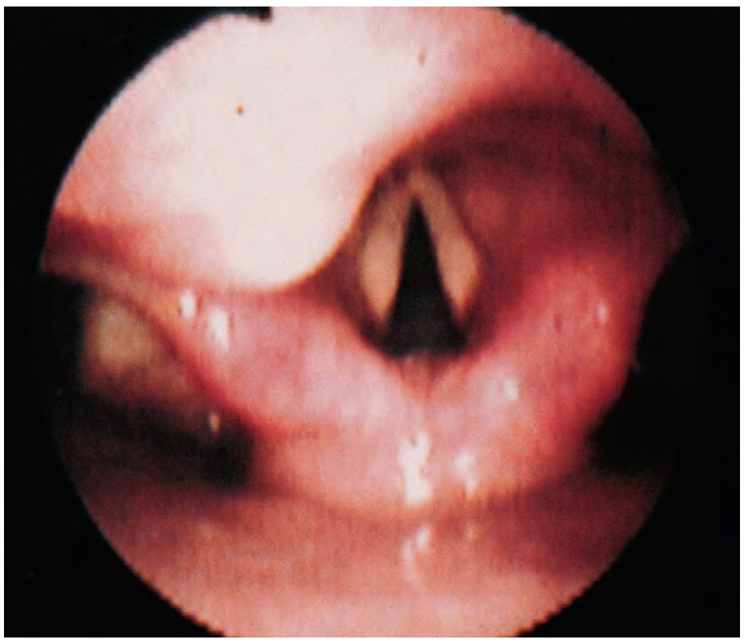

Figure 10.47 Endoscopic examination revealed a smooth submucosal lesion involving the laryngeal surface of the epiglottis.

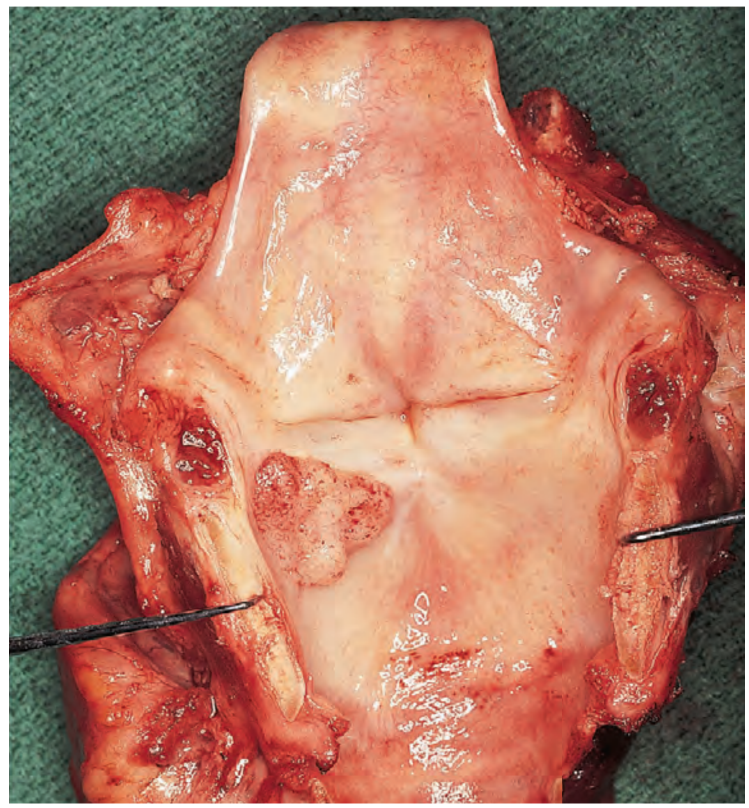

Figure 10.49 Total laryngectomy specimen of the patient shown in Fig. 10.47.

lesion of limited extent involving only the suprahyoid portion of the epiglottis without any extension to the preepiglottic space. Endoscopic examination of the patient shows the lesion to be a smooth submucosal lesion involving the laryngeal surface of the epiglottis (Fig. 10.47). This lesion was adequately resected endoscopically and proved to be a schwannoma of the epiglottis.

Fig. 10.48 shows an axial CT scan of a patient who previously had undergone endoscopic excision followed by external radiotherapy for a left glottic carcinoma. The radiologic extent of recurrent tumor in the left subglottic region was indicative of the actual extent of tumor found in the total laryngectomy specimen (Fig. 10.49).

Both CT and MRI scans have the added advantage of providing assessment of regional lymphatics of the neck, particularly for patients in whom regional lymph nodes are not palpable clinically.

TREATMENT

The primary goal for the treatment of cancer of the larynx is clearly control of the disease. In considering treatment approaches, preservation of speech and swallowing and avoidance of a tracheostome are desirable secondary goals. Traditionally the treatment of laryngeal carcinoma has been either radiation therapy or surgery or a combination of both. In the past, early-stage cancers were treated with external radiation therapy, keeping surgery in reserve for salvage. On the other hand, advanced cancers of the supraglottis and glottic cancers were treated with a total laryngectomy, followed by postoperative radiation therapy. However, over the course of the past 25 years, advances in technology and instrumentation have offered another option for initial treatment of early-stage tumors. Similarly, experience with larynx preservation with chemoradiation therapy has accumulated, with data, clearly defining the indications for and the efficacy with concurrent or sequential chemoradiotherapy. Thus this approach has now become the standard of care for most advanced-stage tumors. The treatment of laryngeal cancer continues to evolve with

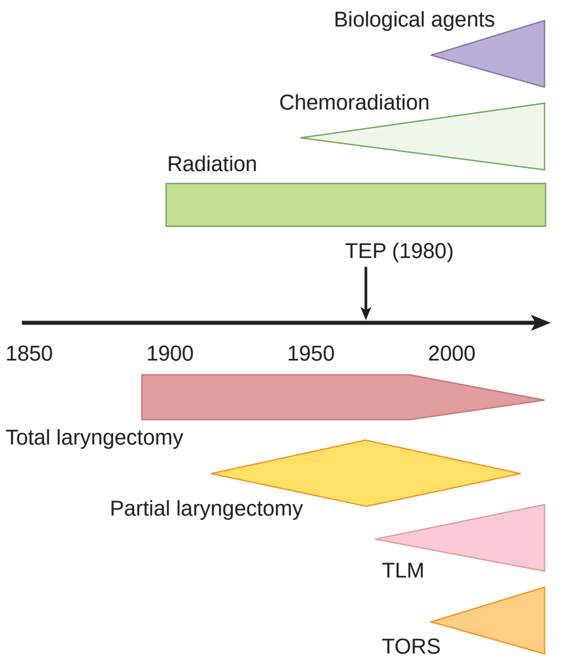

Figure 10.50 A timeline showing evolution in the treatment of cancer of the larynx. *TEP,* Tracheoesophageal prothesis; *TLM,* transoral laser microsurgery; *TORS,* transoral robotic surgery.

the availability of newer modalities such as biological agents, transoral laser microsurgery (TOLM), and transoral robotic surgery (TORS) (Fig. 10.50).

Factors Affecting Choice of Treatment

Surgical and nonsurgical approaches have shown equivalent efficacy in survival outcomes for treatment of laryngeal cancer. However, the functional sequelae of each treatment approach must be considered in selecting the most appropriate treatment program for the individual patient. Treatment selection in patients with laryngeal cancers is also influenced by tumor, patient, and physician factors.

Expertise and knowledge on the part of the physician and the treatment team about the biological behavior of laryngeal cancer and the anticipated response to therapy influence treatment selection. Technical expertise and access to state-of-the-art equipment are equally important factors influencing treatment selection. For early-stage tumors, endoscopic laser resection should be offered to patients if the equipment, and expertise and experience of the surgical team are available. Similarly, effective tumor control and minimization of sequelae of therapy require expertise in contemporary radiation techniques such as intensity-modulated radiotherapy and in selected cases unilateral laryngeal RT. Coordinated multidisciplinary management teams are essential for the successful outcome of chemoradiation therapy for organ-preserving treatment of advanced laryngeal carcinoma. Additional support from speech and swallowing therapists, nutritionists, psychiatrists, and social services, along with expert nursing care, are equally important. Therefore such treatment programs are best delivered at tertiary care centers.

In selecting treatment for an individual patient, several anatomic, physiologic, geographic, and vocational factors play a role. Patients with significant medical comorbidity and/or poor pulmonary reserve are not candidates for conservation laryngeal surgery, even if it is done endoscopically. Similarly, patients with unfavorable anatomy for endoscopic exposure of the larynx (e.g., a short neck, cervical osteoarthritis, trismus, or prominent upper incisor teeth) may not be candidates for transoral laser surgery. Radiation therapy may not be a viable option for patients who are not able to travel to the treatment facility. This factor is particularly applicable to persons with very early vocal cord cancers for whom endoscopic laser excision provides equally good disease control and an acceptable quality of voice compared with external radiation therapy, which takes approximately 6 to 7 weeks to complete. If the quality of voice is a critically important issue for the patient, then radiotherapy may be chosen as the initial treatment. On the other hand, patients who are unable to receive or comply with radiotherapy may prefer endoscopic laser resection, even if the quality of voice may be inferior.

The most important parameters influencing treatment selection are the location and extent of the primary tumor and the status of the regional lymph nodes. In general, carcinomas of the supraglottic larynx have a higher risk of regional nodal metastases compared with glottic carcinomas, and these are often bilateral. Management of the neck thus becomes an integral part of the overall treatment plan for supraglottic cancer. Treatment of the ipsilateral neck with negative clinical findings is indicated for well-lateralized supraglottic cancers, and both sides need to be addressed when tumors approach or involve the midline. Early-stage supraglottic cancers can be treated effectively with either external radiation therapy or endoscopic resection. Exophytic tumors in particular are highly radioresponsive. The advantage of radiation therapy is that it can treat the regional lymph nodes electively along with the primary tumor. On the other hand, if the primary tumor is treated surgically, unilateral or bilateral elective dissection of first-echelon lymph nodes is recommended in most patients. The morbidity of elective neck dissection is minimal. However, if metastatic disease is confirmed, then postoperative radiation therapy may be indicated and is associated with significantly increased morbidity in this setting.

Early-stage carcinomas of the glottic larynx can be treated effectively by single-modality treatment consisting of either endoscopic resection or radiotherapy. Endoscopic resection is ideally suited for most T1 lesions that are confined to the mucosa of one vocal cord without involvement of the anterior commissure. Bilateral involvement (T1b) generally is not considered suitable for endoscopic resection. Although endoscopic resection is expeditious and cost-effective, the quality of voice may not be as good as with radiotherapy. On the other hand, radiation therapy is ideally suited for lesions with bilateral involvement, involvement of the anterior commissure, and infiltration into the underlying vocalis muscle. Vocal cord carcinomas staged as T2 represent a spectrum of diseases with diverse behavior. Tumors that are staged T2B by virtue of reduced vocal cord mobility are better treated with radiation therapy, whereas endoscopic laser resection may be an option for exophytic tumors (T2A) that do not compromise vocal cord function. Open voice-preserving partial laryngeal surgery, which once was popular for early-staged laryngeal carcinoma, is now considered only in select circumstances. Patients suitable for endoscopic resection avoid an open operation and the tracheostomy that traditionally is required after an open partial laryngectomy. At present, an open partial laryngectomy for supraglottic or glottic cancer is considered in patients not suitable for endoscopic resection and for those with persistent or recurrent tumors after previous radiation therapy. Involvement of the

regional lymph nodes is exceedingly rare in early-stage glottic carcinoma. Therefore elective treatment of regional lymph nodes is not indicated.

More advanced lesions of the larynx (T3 and T4a) require multidisciplinary treatment. Initial surgery often requires a total laryngectomy by virtue of tumor extent or the anticipated functional status of the residual organ after an extended partial laryngectomy. On the other hand, radiation therapy alone offers lower local control rates, requiring a total laryngectomy for salvage in a large proportion of patients. Although a total laryngectomy followed by postoperative radiation therapy was considered the standard of care, the posttreatment quality of life of patients was significantly influenced by the loss of the larynx. During the course of the past 25 years, the management of advanced laryngeal carcinomas has been profoundly influenced by results from organ preservation trials. Results of a prospective randomized trial from the Department of Veterans Affairs Laryngeal Cancer Study Group (VA Trial), conducted in the 1980s, first demonstrated that the use of neoadjuvant chemotherapy followed by radiation therapy achieved survival outcomes similar to those of a total laryngectomy followed by postoperative radiation therapy but with the advantage of preserving the larynx in two-thirds of patients. A subsequent radiation therapy oncology group head and neck intergroup study (RTOG 91-11) showed that concomitant chemoradiation treatment was superior to sequential treatment for locoregional control and larynx preservation. Therefore concomitant chemoradiation has become the standard of care for most patients with advanced laryngeal carcinomas. More recently, further intensification in treatment with multiple drugs and the addition of neoadjuvant chemotherapy to concomitant chemoradiation therapy has been suggested to enhance outcomes. However, the latter two treatment strategies are accompanied by increased acute toxicity and long-term sequelae in a significant number of patients. Further research is required to develop an optimal multimodal regimen that is less toxic and more effective for larynx preservation. At present, patients with significant medical comorbidities who are unable to complete a larynx preservation treatment program are considered candidates for primary total laryngectomy. Similarly, patients with very advanced laryngeal tumors with destruction of the thyroid or cricoid cartilage are best treated by an initial total laryngectomy followed by postoperative radiotherapy or chemoradiotherapy. Organ preservation strategies with concurrent chemoradiotherapy in these patients have high failure rates, with a significant number of patients requiring a salvage total laryngectomy. For details on nonsurgical larynx preservation programs, see Chapters 19 and 20.

SURGICAL TREATMENT

The role of surgery in the management of laryngeal carcinomas has evolved during the past few decades. Transoral endoscopic laser surgery has gained popularity compared with open partial laryngectomy as initial definitive treatment for early-stage laryngeal carcinomas.

Transoral laser surgery avoids an open operation and a tracheostomy in most patients. In addition, postoperative functional recovery of swallowing is quicker than for open procedures. The treatment outcomes after endoscopic approaches are comparable with those after open conservation surgery of the larynx. Nonetheless, open conservation laryngeal surgery still has a role in the management of highly selected patients as a primary modality and for salvage surgery after failure of radiation therapy in selected patients. A total laryngectomy is indicated as initial therapy only in a very select population of patients with very advanced cancers. Salvage surgery after failure of organ preservation treatment requires a total laryngectomy, which is often associated with significant postoperative complications because of poor wound healing.

Surgical Anatomy

Anatomically, the larynx begins at the tip of the epiglottis and ends at the lower border of the cricoid cartilage (Fig. 10.51). Its lower border is continuous with the cervical trachea (Fig. 10.52). It is in juxtaposition to the base of the tongue anterosuperiorly and to the hypopharynx and cervical esophagus posterolaterally (Fig. 10.53). The laryngeal cartilages include the thyroid, cricoid, epiglottic, arytenoid, cuneiform, and corniculate cartilages. The location of the anterior commissure in relation to the height of the anterior midline of the thyroid cartilage is variable. In general, the anterior commissure is located at or above the midpoint of the anterior midline of the thyroid cartilage in women, and it is located below the midpoint in men. Although the hyoid bone, attached to the thyroid cartilage through the thyrohyoid membrane, is not a part of the laryngeal framework, it plays an important role in the swallowing function of the upper aerodigestive tract. Calcification of the laryngeal cartilages is variable and may present diagnostic difficulties in the radiographic interpretation of tumor invasion.

The surface mucosa of the larynx consists of squamous epithelium with interspersed mucous glands. The true vocal cords are lined by stratified squamous epithelium. The sensory nerve supply to the supraglottic larynx is provided by the internal branch of the superior laryngeal nerve, which enters the larynx through the thyrohyoid membrane. The mucosa of the true vocal cords derives dual sensory nerve supply from the superior laryngeal and recurrent laryngeal nerves, whereas the subglottic

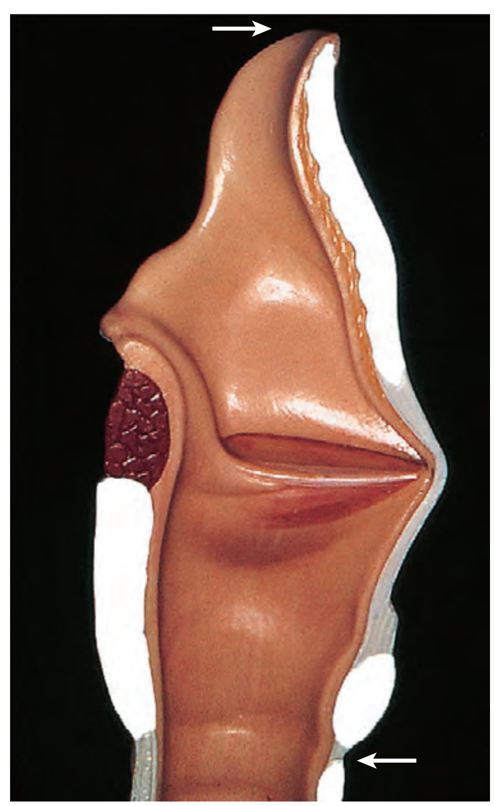

Figure 10.51 The anatomic limits of the larynx. *Upper arrow*, tip of the epiglottis; *lower arrow*, lower border of cricoid.

larynx derives sensory supply from the recurrent laryngeal nerve. The intrinsic musculature of the larynx derives its innervation from the recurrent laryngeal nerve except for the cricothyroid muscle, which is innervated by the external laryngeal branch of the superior laryngeal nerve. The larynx derives its blood supply from branches of the superior and inferior thyroid arteries. These vessels enter the larynx accompanied by the superior and recurrent laryngeal nerves. The supraglottic larynx has a rich lymphatic network draining through the thyrohyoid membrane into first-echelon lymph nodes at levels II and III. The lymphatic network of the glottic larynx is very sparse, especially the free edge of the true vocal cord, which is devoid of lymphatics. The lymphatic drainage of the subglottic larynx exits through the cricothyroid membrane to drain into the paratracheal and deep jugular lymph nodes. The perithyroid and Delphian lymph nodes also receive lymphatic drainage from the larynx.

Figure 10.52 The anatomic relationships of the larynx.

Preoperative Preparation

All patients undergoing surgery for laryngeal cancer should undergo assessment of preoperative pulmonary function. This assessment is particularly important for persons who have a history of chronic obstructive pulmonary disease and are being considered for conservation surgery. Preoperative counseling regarding cessation of smoking is crucial. Patients dependant on smoking tobacco consumption are counseled and put on a nicotine withdrawal program. Similarly, preoperative counseling regarding postoperative pulmonary care and breathing exercises is vitally important. Consultation and counseling from a speech pathologist is essential for patients for whom a total laryngectomy is planned. Alternatives regarding speech rehabilitation are discussed at this meeting. A preoperative visit reduces the patient's anxiety and apprehension regarding loss of speech and results in improved understanding of voice rehabilitation after surgery.

Direct Laryngoscopy and Suspension Microlaryngoscopy

The need to accurately assess the extent of a primary tumor of the larynx before selection of treatment cannot be overemphasized. The accuracy of diagnosis and selection of treatment

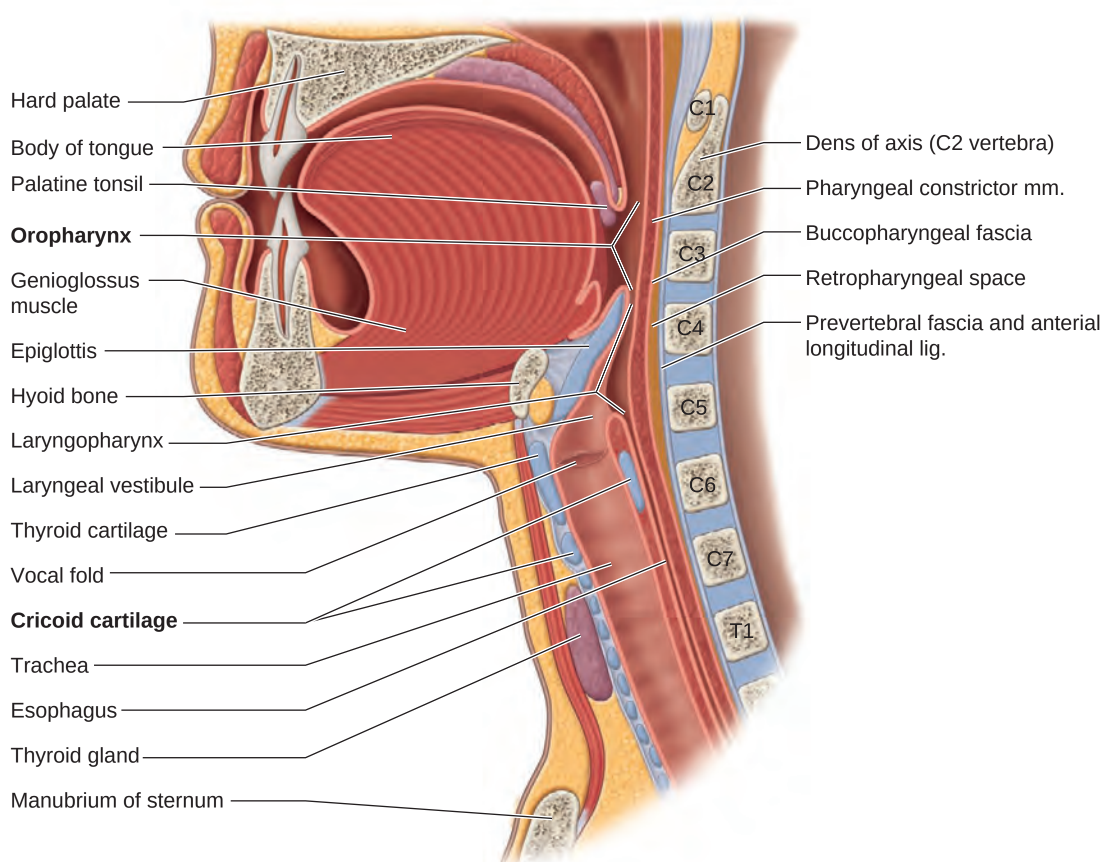

Figure 10.53 Anatomic diagram showing sagittal section of the oral cavity, pharynx, and larynx.

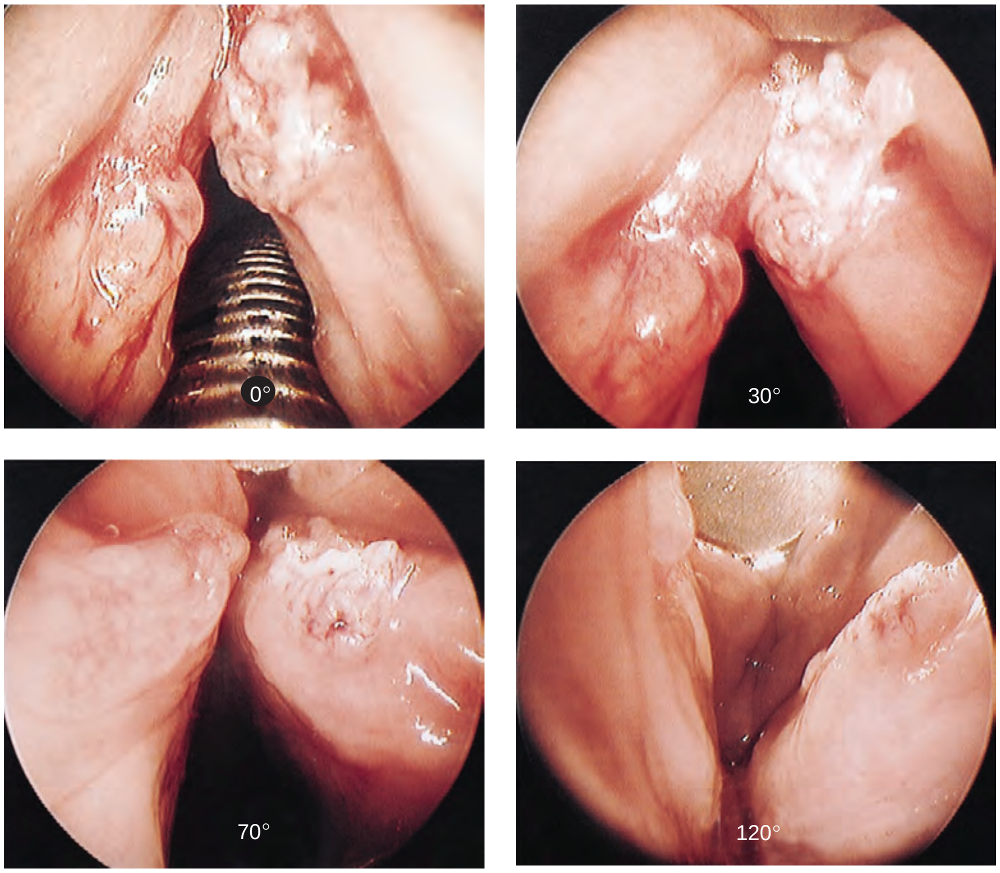

Figure 10.54 The endoscopic view of a recurrent squamous cell carcinoma of the right vocal cord with an edematous left vocal cord through 0-degree, 30-degree, 70-degree, and 120-degree telescopes.

directly depend on the extent of the primary tumor. Direct laryngoscopy is best done under general anesthesia, either with a small endotracheal tube or with jet ventilation, and requires complete relaxation to permit adequate assessment of the larynx and hypopharynx. The appropriate choice of laryngoscopes should be available in the operating room to meet the demands of varying configurations of larynges and locations of lesions. For diagnostic purposes and biopsy, a Dedo or Jako laryngoscope allows a binocular view of the larynx. A bivalved laryngoscope offers a comprehensive view of the supraglottic region and hypopharynx and is preferred for endoscopic laser resection.

Detailed endoscopic evaluation of the larynx requires the use of telescopes (0, 30, 70, and 120 degrees) to accurately evaluate the anterior commissure, the ventricles, and the subglottic region. The details of the views obtained through telescopes of various angles are shown in Fig. 10.54, in a patient with glottic carcinoma involving both vocal cords. Such detailed evaluation of a laryngeal lesion is crucial, regardless of the treatment selected. If the patient is suitable for endoscopic surgery, the procedure begins after photo documentation of the lesion. On the other hand, if the patient is to have other treatment (e.g., radiotherapy or chemotherapy/radiotherapy), then after adequate photo documentation and biopsy the procedure is terminated.

Endolaryngeal Microsurgery—Excision of a Vocal Cord Polyp

For endoscopic laryngeal surgery, the patient is placed under general anesthesia with a small endotracheal tube or on jet ventilation, and the larynx is suspended with appropriate laryngoscope and suspension equipment. An endoscopic view of the larynx as seen through the operating microscope with a 40× magnification shows a mucosal polyp involving the middle third of the left true vocal cord (Fig. 10.55). The remaining larynx is unremarkable. The polyp is grasped with an angled biopsy forceps as shown in Fig. 10.56, and with the use of angled scissors with its tip to the right, the mucosal polyp is excised in toto. No attempt should be made to excise any part of the underlying musculature since this is a lesion of only the mucosa; otherwise, the voice quality could be adversely affected. Excision of the polyp in progress is shown in Fig. 10.57. Every attempt must be made to remove the entire specimen in one piece. The whole specimen should be fixed in a paraffin block for accurate histologic processing after its orientation by the operating surgeon for the pathologist regarding its anterior,

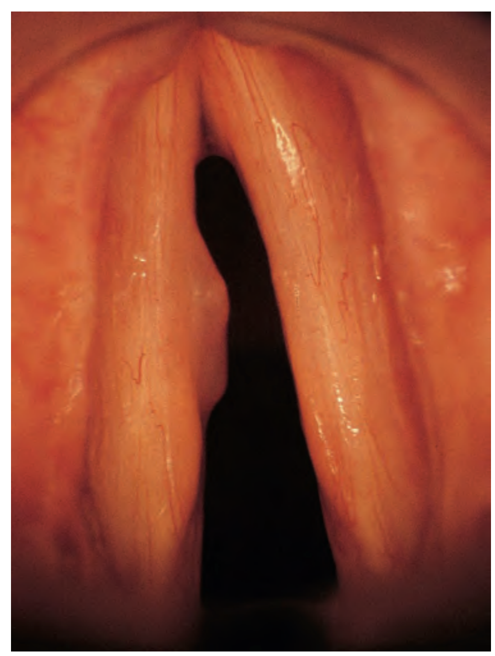

Figure 10.55 An endoscopic view of the larynx showing a mucosal polyp on the free edge of the left vocal cord.

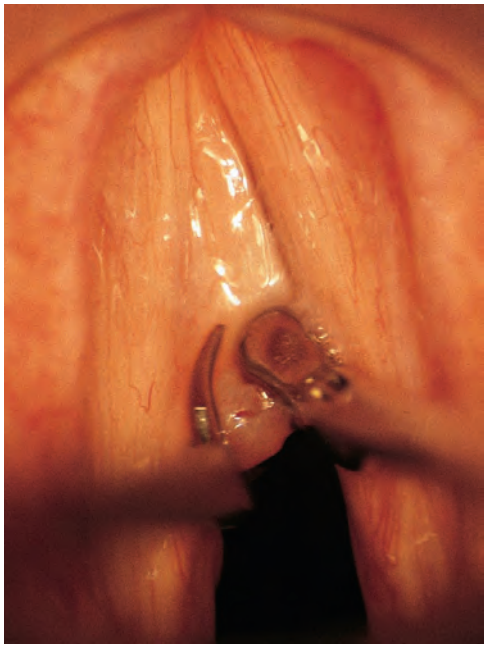

Figure 10.56 The mucosal polyp is grasped with a biopsy forceps and excised with a curved scissors.

Figure 10.57 Only the mucosa is excised, without any underlying muscle.

Figure 10.58 Hemostasis with a cotton pledget.

Figure 10.59 The surgical defect.

posterior, superior, and inferior margins. Hemostasis is obtained by gentle pressure with a cotton pledget soaked in adrenaline diluted in saline solution (Fig. 10.58). Bleeding from tiny vessels is usually controlled in this manner (Fig. 10.59). Hemostasis of minor bleeding can be secured by cauterization with silver nitrate or with the use of a low-power carbon dioxide laser.

During endoscopic laryngeal surgery, 4 mg of dexamethasone is administered, which is continued every 6 hours and is tapered off during the next 48 hours. The purpose of administering steroids is to reduce laryngeal edema and occasional respiratory difficulty in the immediate postoperative period. A regular diet is permitted by mouth, but the patient is advised to remain on voice rest until satisfactory epithelialization of the vocal cords takes place. In general, voice rest is recommended for approximately 1 week after vocal cord surgery.

Various other benign and early malignant lesions of the larynx are considered suitable for management through endoscopic microlaryngeal surgical techniques. Use of the carbon dioxide laser may be considered appropriate under select circumstances for benign lesions and for some patients with malignant disease.

Endolaryngeal Microsurgery—Excision of Keratosis of the Vocal Cord With the Hydrodissection Technique

Mucosal lesions of the true vocal cord that are relatively flat require special attention during microlaryngeal surgery. Because these lesions do not have an exophytic component, they are difficult to grasp and lift away from the underlying submucosa of the true vocal cord. Thus if the lesion is grasped and excision is performed in the usual manner, the probability of lacerating and fragmenting the specimen or of sacrifice of the underlying vocalis muscle is high. Lesions such as these therefore are excised endoscopically with use of the hydrodissection technique. The patient shown in Fig. 10.60 has superficial

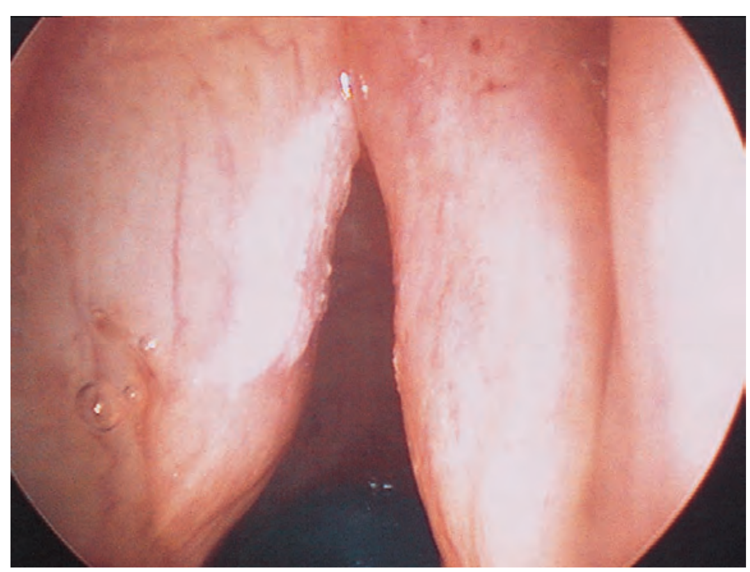

Figure 10.60 An endoscopic view of the larynx showing superficial keratosis of the anterior third of the left vocal cord.

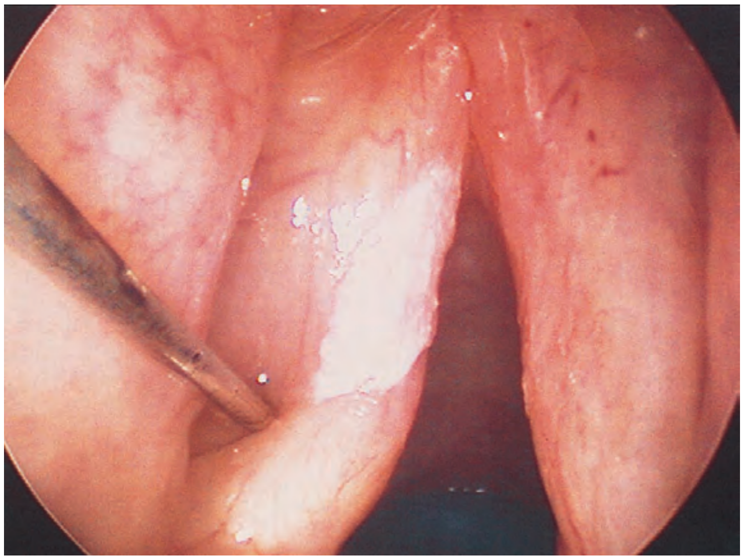

Figure 10.61 A long mediastinal needle is used to inject saline solution.

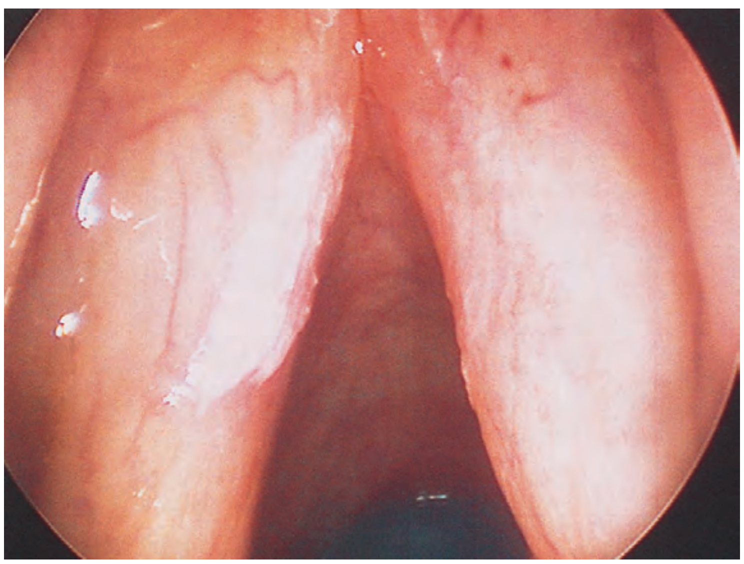

Figure 10.62 Adequate injection of saline solution into the submucosal plane lifts up the lesion from the underlying vocalis muscle.

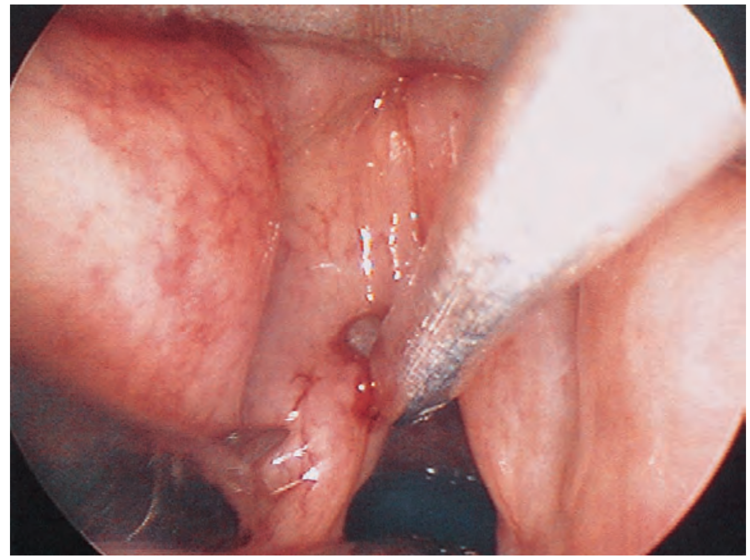

Figure 10.63 The lesion is excised in a monobloc fashion.

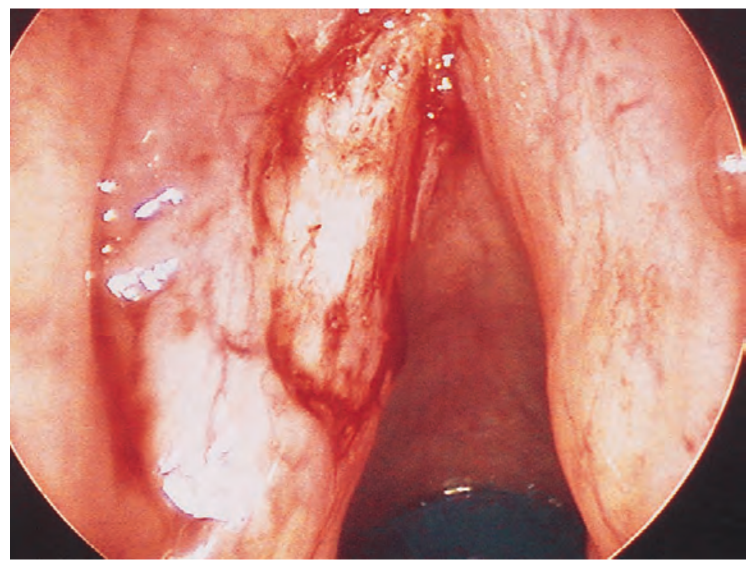

Figure 10.64 The surgical defect.

keratosis of the left true vocal cord in its anterior third. The lesion is flat and has minimal exophytic component. To lift the lesion from the underlying vocalis muscle, normal saline solution with epinephrine (adrenaline) is injected in the submucosal plane. A long mediastinal 25-gauge needle is attached to a 5-mL syringe. One milliliter of epinephrine (1:50,000) is mixed with 5 mL of normal saline solution. The needle is introduced through the laryngoscope, and the saline solution is injected in the submucosal plane of the anterior half of the left true vocal cord (Fig. 10.61). The injected amount should be just sufficient to elevate the lesion. Overinjection should be avoided; otherwise, it will distort the anatomy. Note that the lesion is now lifted from the underlying vocalis muscle and is easy to grasp and excise without sacrifice of normal tissue (Fig. 10.62).

The lesion is grasped with a small biopsy forceps and retracted toward the midline. Curved scissors with the tip to the right are used to excise the lesion in a monobloc fashion (Fig. 10.63). Every attempt must be made to excise the lesion in one piece. The surgical defect following excision of the lesion is seen in Fig. 10.64. Hemostasis for minor bleeding points is controlled with cotton pledgets soaked in epinephrine diluted in saline solution. If further bleeding is encountered, it may be controlled with silver nitrate cauterization, electrocautery, or a carbon dioxide laser.

Another patient with carcinoma in situ of the right true vocal cord with the lesion confined strictly to the mucosa of the vocal cord, suitable for endoscopic excision with the hydrodissection technique, is shown here. The endoscopic view of the larynx with 0-degree, 30-degree, 70-degree, and 120-degree telescopes show that the lesion is confined to the mucosa of the free edge of the vocal cord (Fig. 10.65). Endoscopic view of the larynx after excision shows only loss of the mucosa of the vocal cord, which will spontaneously epithelize, with return of normal voice (Fig. 10.66).

Transoral Endoscopic Laser Surgery for Larynx Cancer

For early stage laryngeal cancer, options of treatment include radiation, transoral endoscopic laser microsurgery (TLM), or open partial laryngectomy. In glottic cancer, the treatment of

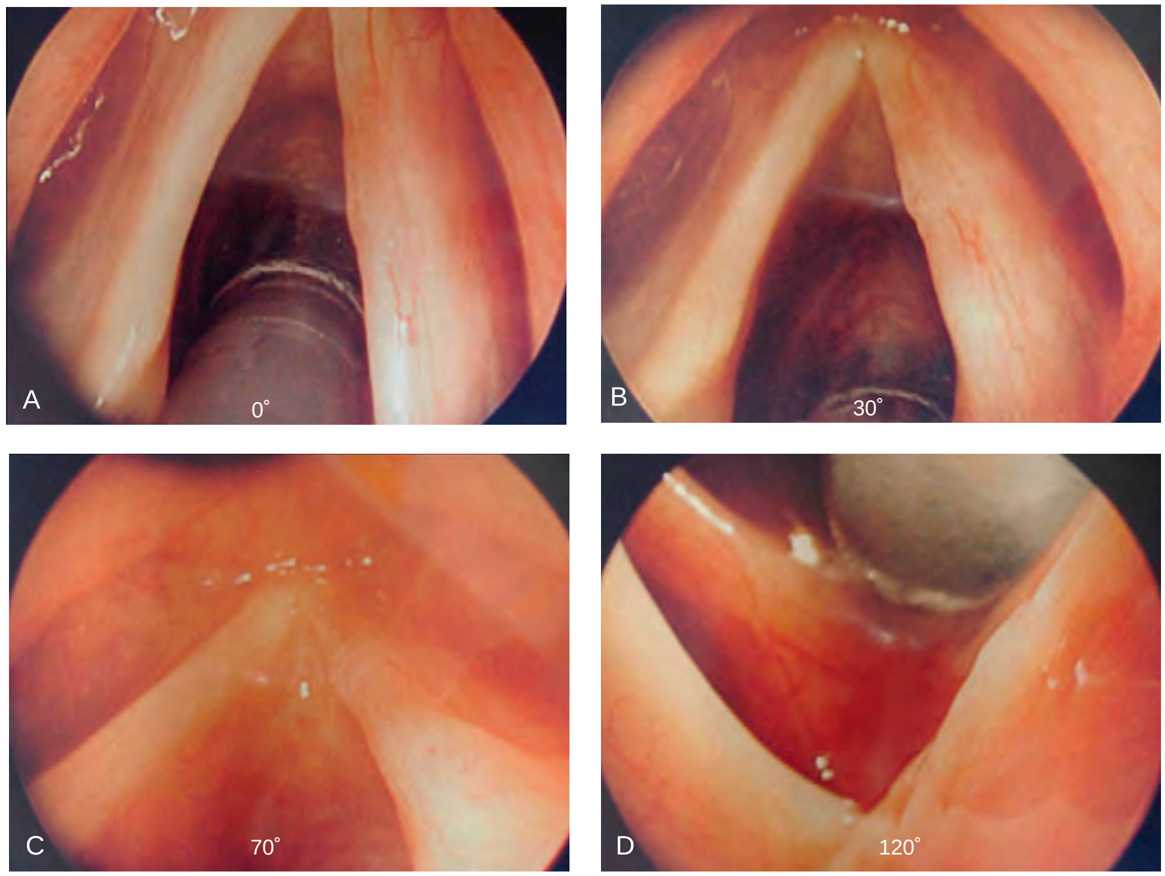

Figure 10.65 Carcinoma in situ of the right vocal cord seen through 0-degree (**A**), 30-degree (**B**), 70-degree (**C**), and 120-degree (**D**) telescopes.

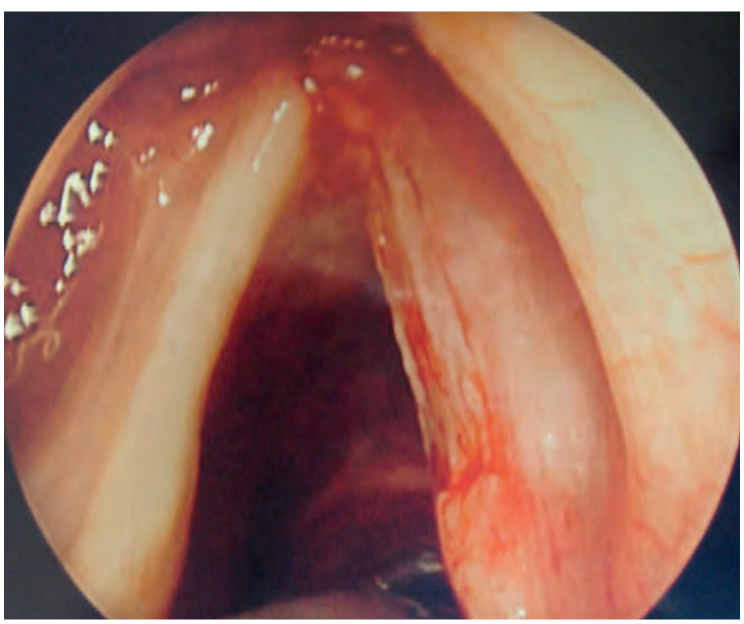

Figure 10.66 Appearance of the vocal cord following microlaryngeal excision of carcinoma in situ of the mucosa.

only the primary tumor is necessary. In contrast, in supraglottic laryngeal cancer, treatment of both necks with selective neck dissection or with radiation is required due to the high incidence of occult metastases, estimated to be up to 20% to 30%.

The two most common lasers used are the KTP (potassium titanyl phosphate) laser and the CO_2 laser. The CO_2 laser has a wavelength of 10.6 μm and is in the infrared (invisible) region of the light spectrum. A built-in He-Ne coaxial laser is therefore required. The CO_2 laser has several advantages, including minimal scatter, minimal reflection, and strong absorption by water. The area of surrounding necrosis is less than 0.5 μm with an absorption depth of 0.2 mm.

Typically a laser-safe double-cuff endotracheal tube is used, with the cuffs inflated with saline solution. The laryngeal structures are exposed with use of an operating laryngoscope that has a smoke evacuator channel, including adjustable bivalved laryngoscopes when appropriate. Surgery is generally performed with use of a CO_2 laser coupled to an operating microscope, and the laser beam is manipulated with use of a micromanipulator. The use of 0-, 30-, and 70-degree laryngeal telescopes and fiber-optic laser delivery systems also may be helpful. Microlaryngeal instruments with electrocautery and suction are essential for the success of the technique.

The principle of laser surgery is still complete oncologic removal, but unlike open surgery, access to the tumor does not require disrupting the laryngeal framework or sacrificing normal neurovascular pedicles. Resection involves following the individual spread of tumor, and therefore the resection is personalized to each individual patient. Due to the small operative field, it is often required to transect the tumor in order to assess depth of invasion and to create the necessary visualization for sequential tumor resection, as illustrated in Fig. 10.67.

The en bloc technique is ideal for localized superficial lesions of the true vocal cord, as shown in Fig. 10.68. This patient had a subtle mucosal lesion on the ventral surface of the right true vocal fold. A previous biopsy was reported to show superficially invasive squamous cell carcinoma. After exposure of the lesion, the carbon dioxide laser is used to incise the mucosa around the lesion (Fig. 10.69). The carbon dioxide laser allows precise incision up to the lamina propria, and dissection is then continued in this plane, using the suction coagulator to retract the specimen (Fig. 10.70). For lesions of the vocal cord, the CO_2 laser typically is used in the continuous mode at a low (3 to 5 W) power setting. The surgical defect after excision of the lesion is shown in Fig. 10.71. The suction coagulator is used for hemostasis, but the defocused CO_2 laser also is an effective

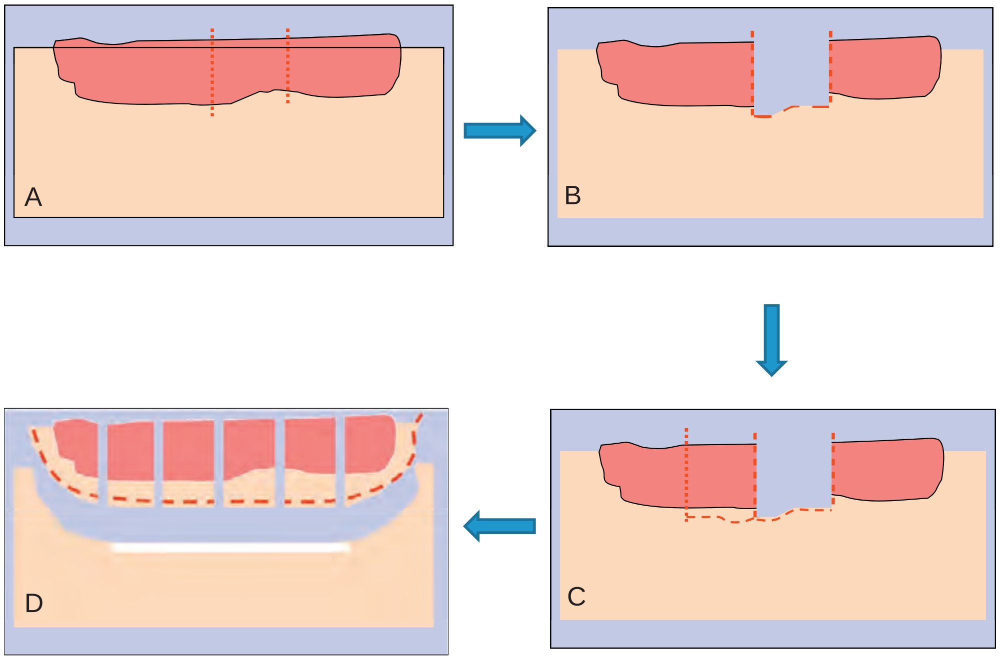

Figure 10.67 Technique for transoral endoscopic resection by sequential transection and excision of laryngeal cancer. **A**, Initial parallel vertical cuts through tumor to assess depth of invasion. **B**, Resect a small piece and identify the deep margin of tumor. **C**, Follow the deep margin of the tumor and systematically resect in pieces. **D**, Accurate orientation of the specimen is crucial.

Figure 10.68 An endoscopic view showing a superficial carcinoma in situ of the right true vocal fold.

Figure 10.69 A carbon dioxide laser is used to incise the mucosa around the lesion.

Figure 10.70 The plane of dissection is maintained in the lamina propria.

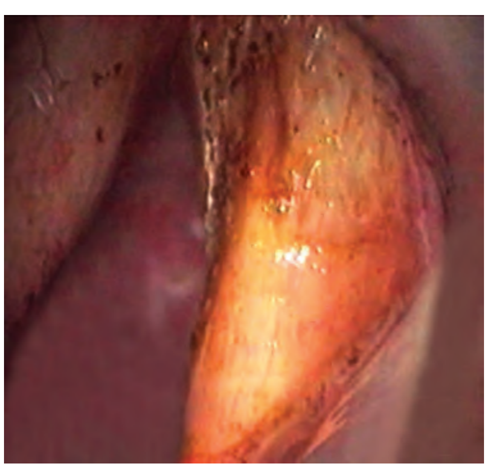

Figure 10.71 The surgical defect.

Figure 10.72 An endoscopic view of the larynx 6 months after surgery.

option. The surgical defect heals by secondary intention, and vocal cord function can be preserved if the excision is relatively superficial (Fig. 10.72).

The European Laryngological Society has classified endoscopic resections into types I to VI for glottic cancer resections and types I to IV for supraglottic cancer resections. The vocal cord is divided into different layers (Fig. 10.73), and the classification for glottic cancer resection is determined by which layer is removed. Type I describes subepithelial resection, type II subligamental resection, type III transmuscular resection, and type IV total muscular resection. More extended surgical procedures are classified as type V, and resections of the anterior commissure

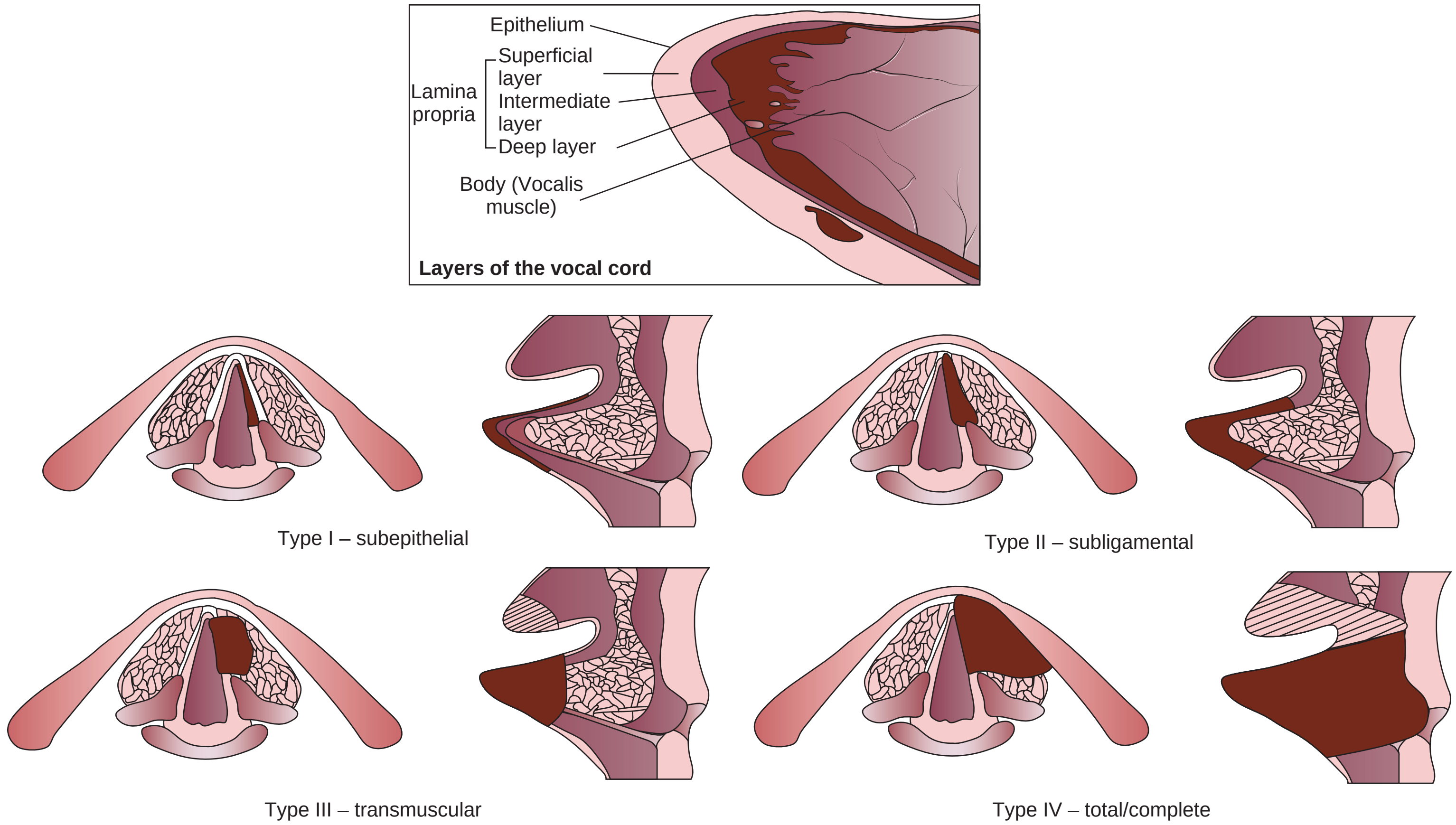

Figure 10.73 European Laryngological Society classification of endoscopic cordectomy for glottic cancer (type I-IV).

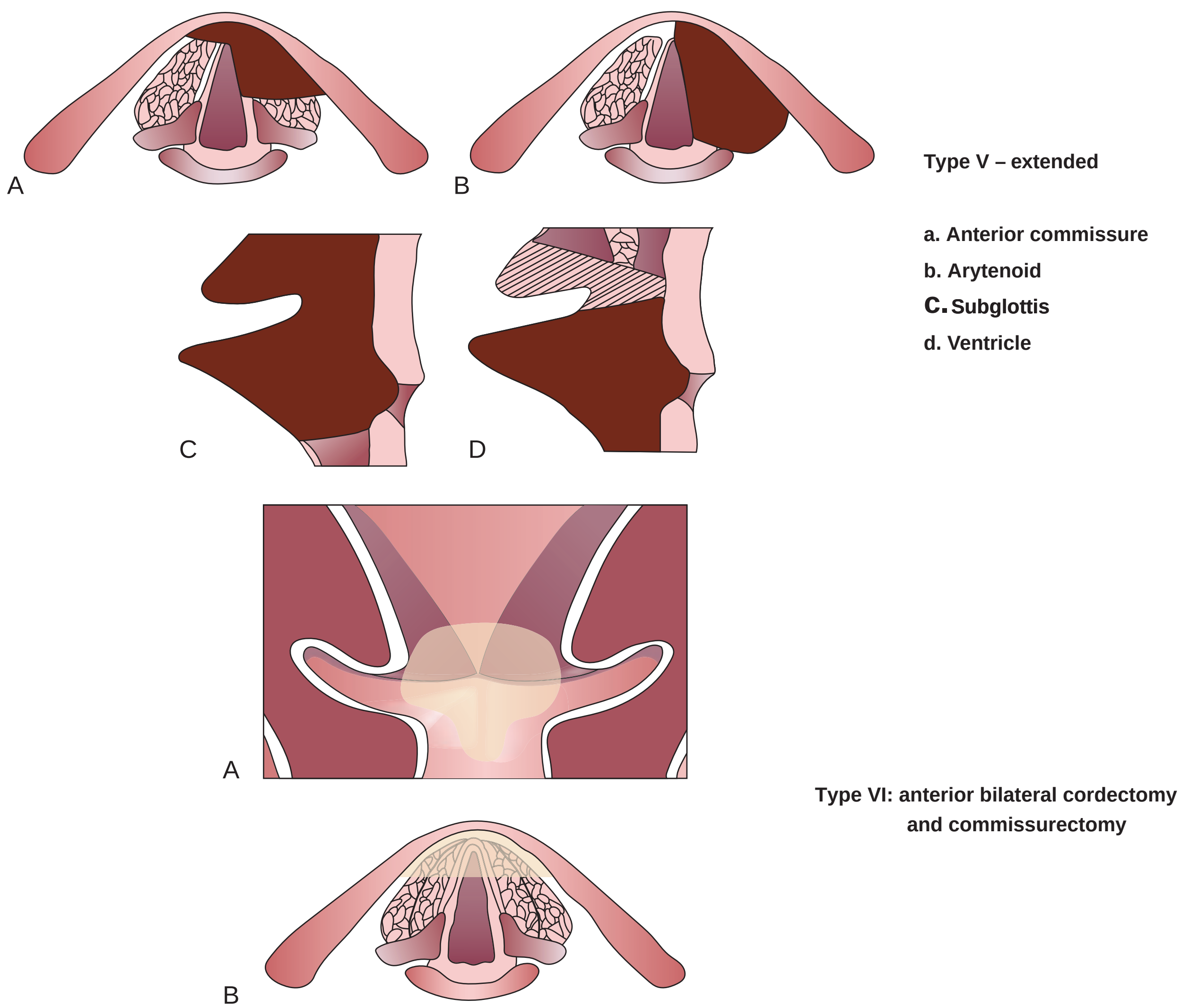

Figure 10.74 European Laryngological Society classification of endoscopic cordectomy for extended dissections for glottic cancer (type V and VI).

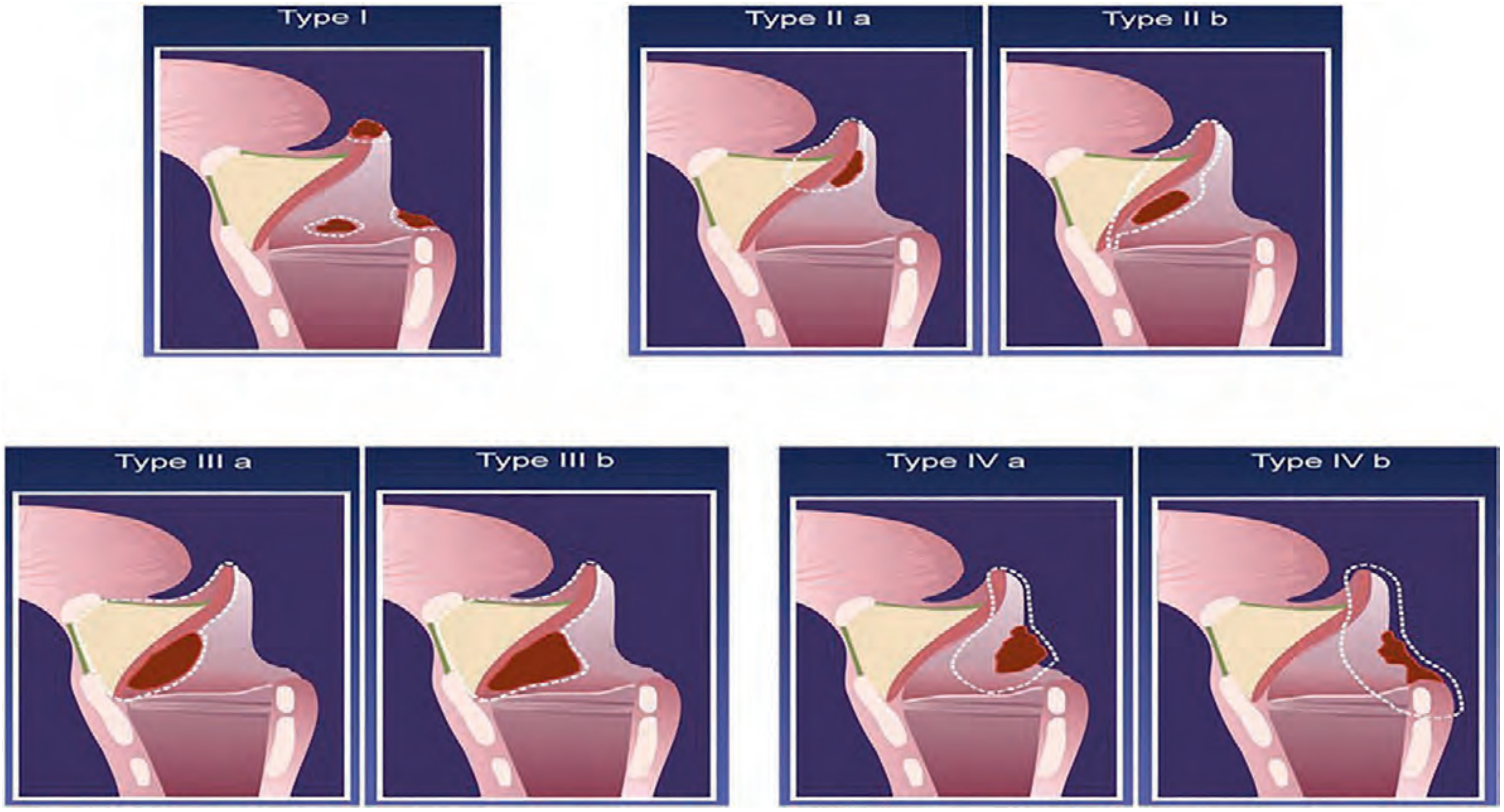

Figure 10.75 European Laryngological Society classification of endoscopic resection of supraglottic cancer. *(Courtesy of the European Laryngological Society.)*

are classified as type VI (Fig. 10.74). For supraglottic cancer (Fig. 10.75), type I describes limited resection of small superficial lesions, and type II is superior hemiepiglottectomy or total epiglottectomy, without resection of the preepiglottic space. Type III describes medial supraglottic laryngectomy with resection of the preepiglottic space, and type IV describes lateral supraglottic laryngectomy.

Choice of patients for endoscopic laser surgery has been prone to selection bias, which ultimately makes any comparison with other treatments such as radiation and open partial laryngectomy difficult. The factors that influence the selection process are related to the patient, physician, tumor, and institutional preferences, which determine whether a patient will be selected for laser surgery (Fig. 10.76). Important patient factors include the ability for exposure of the larynx under laryngoscopy. The most optimum position for laser surgery is the same as that for endotracheal intubation. This so called “sniffing position” is illustrated in Fig. 10.77. Patients with trismus, prominent teeth, and prior neck radiation will be unable to achieve this optimum position. The Mallampati class is an easy method for assessing the ability to intubate a patient and carry out laser surgery. Patients with class I or II are likely to be suitable, whereas patients with class III or IV are not (Fig. 10.78). Tumor factors important in patient selection include the location of the tumor and whether it is exophytic or endophytic. Tumors located in the anterior commissure must be carefully selected, because there is little deep margin available for resection at this site. This means recurrence rates for anterior commissure tumors are higher and functional outcomes not as good due to anterior web formation. The patient shown in Fig. 10.79 has a right vocal cord tumor extending to the anterior commissure but with little contralateral cord involvement. This patient was deemed suitable for endoscopic laser resection and obtained an excellent outcome. In contrast, a patient with diffuse

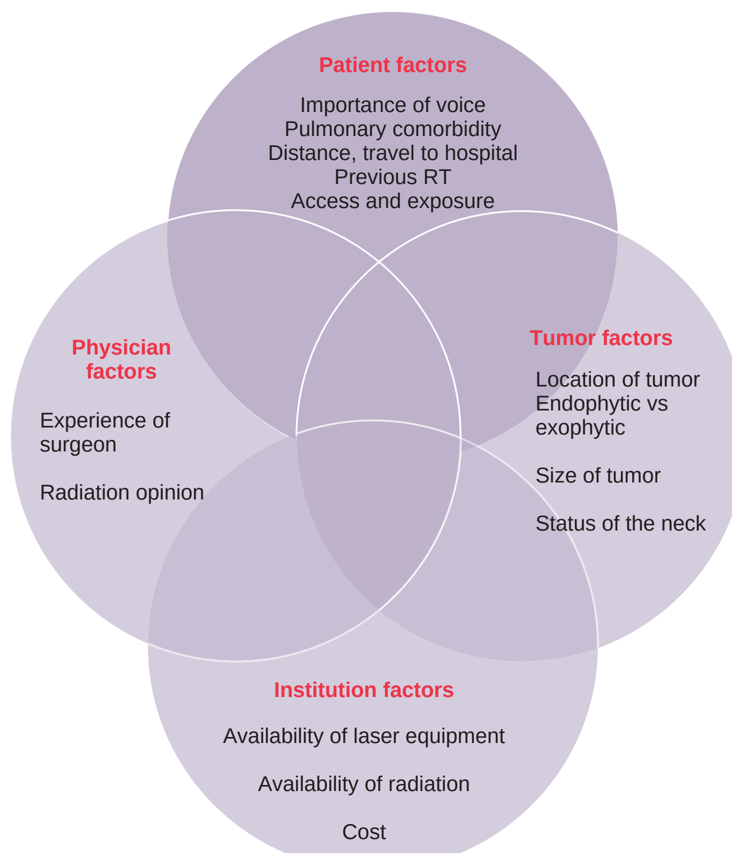

Figure 10.76 Factors which influence patient selection for transoral endoscopic laser microsurgery.

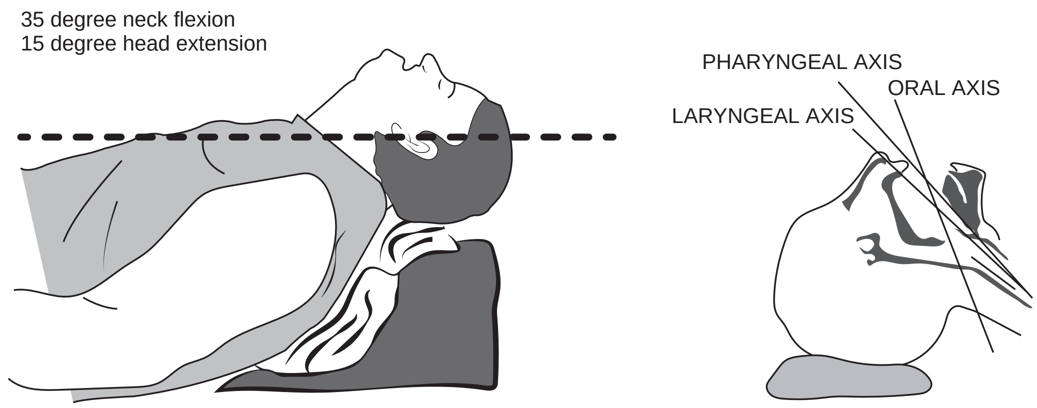

Figure 10.77 The optimum position for laser surgery. The neck is flexed (on a pillow) and the head extended, aligning the axes of the oral cavity, pharynx, and trachea.

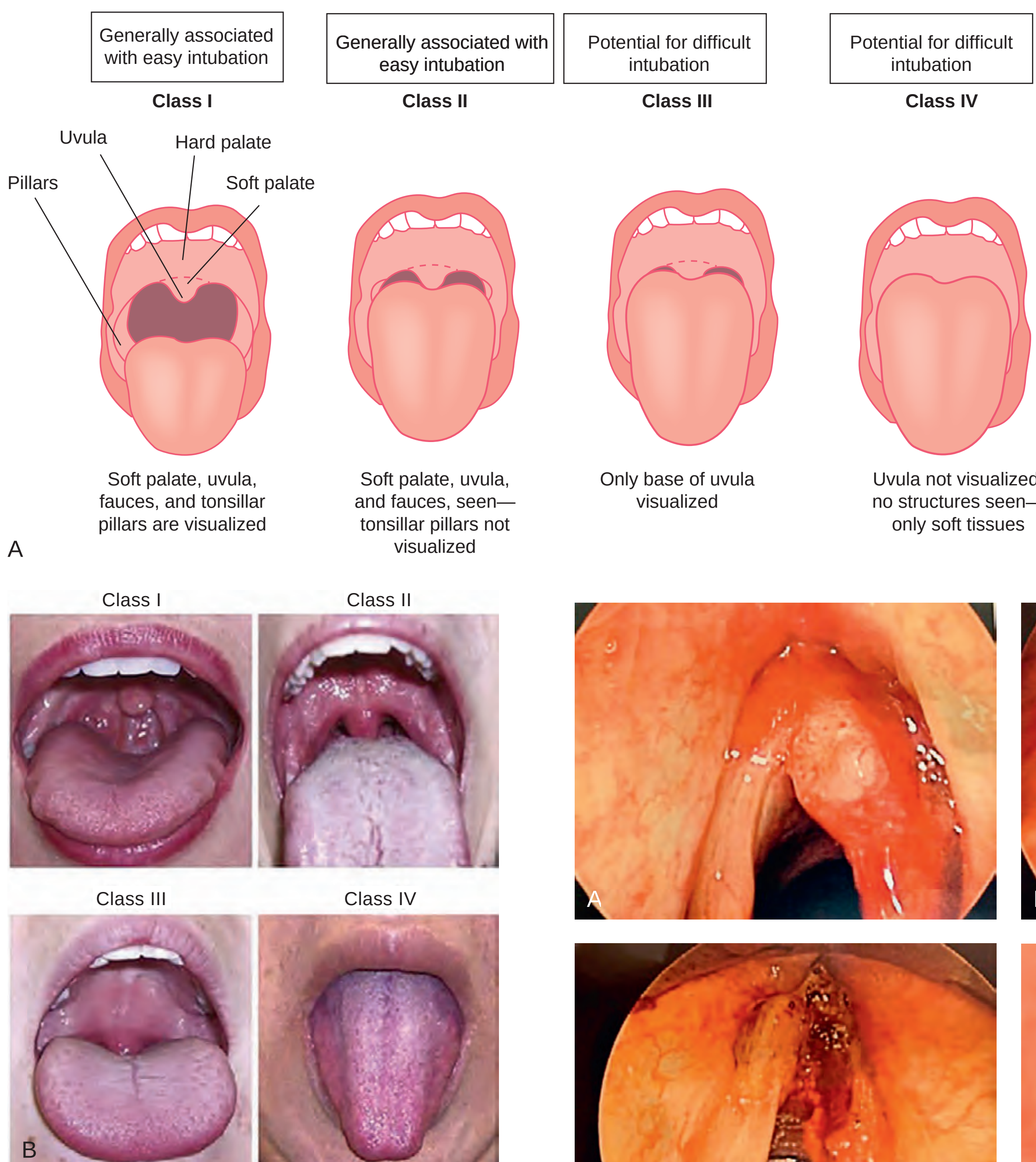

Figure 10.78 Diagrammatic representation of Mallampati classification **(A)**. Patient examples showing Mallampati classification **(B)**.

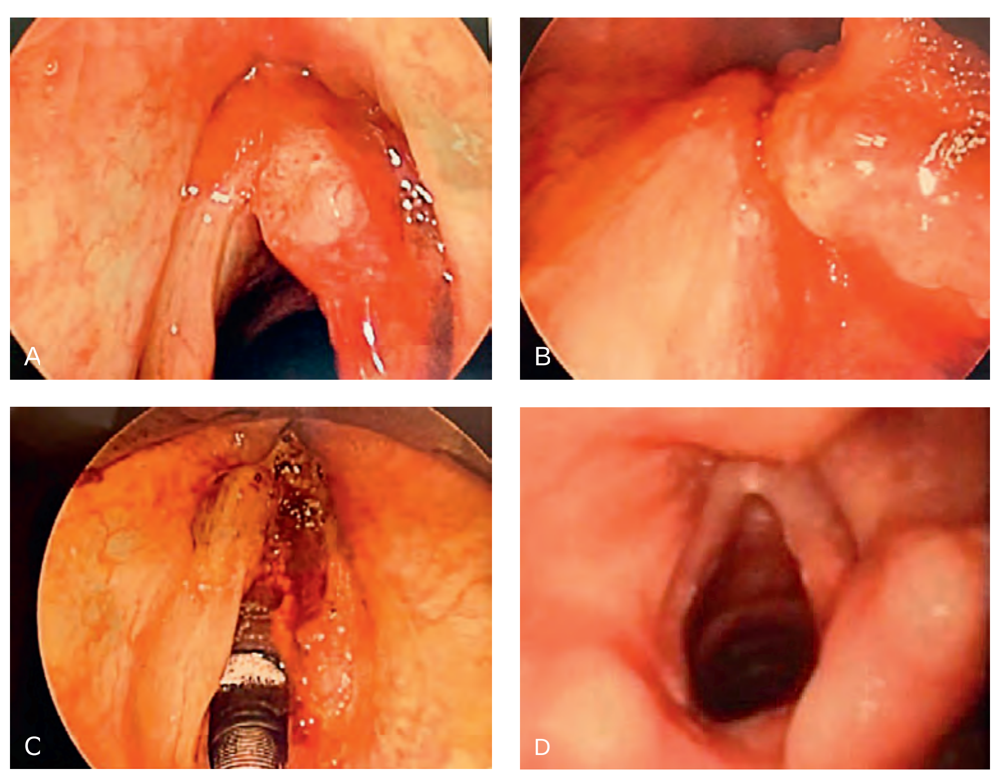

Figure 10.79 Endoscopic photographs of resection of squamous cell cancer right vocal cord with extension to anterior commissure. Endoscopic view with a 0-degree telescope (**A**), with a 30-degree telescope (**B**), postexcision (**C**), and endoscopic view 6 weeks following surgery (**D**).

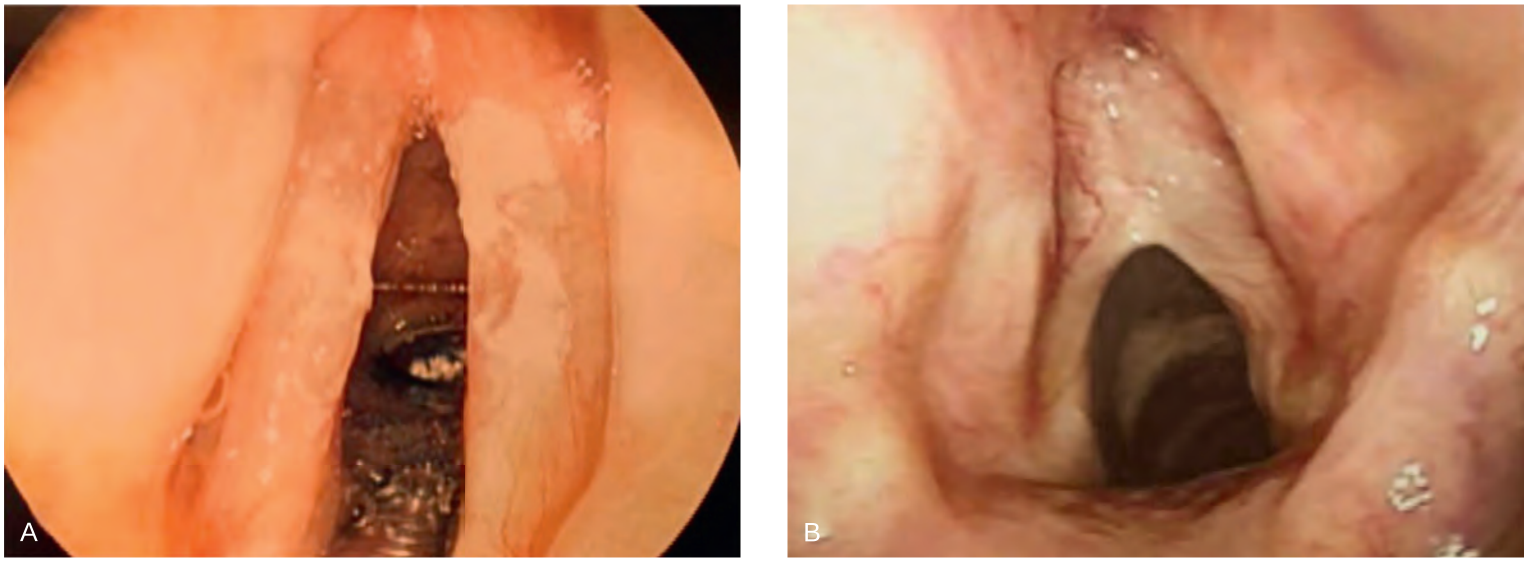

Figure 10.80 **A**, Endoscopic view of glottic larynx showing (T1B) squamous carcinoma involving both vocal cords. **B**, Postoperative endoscopic view 6 months following surgery showing an anterior web.

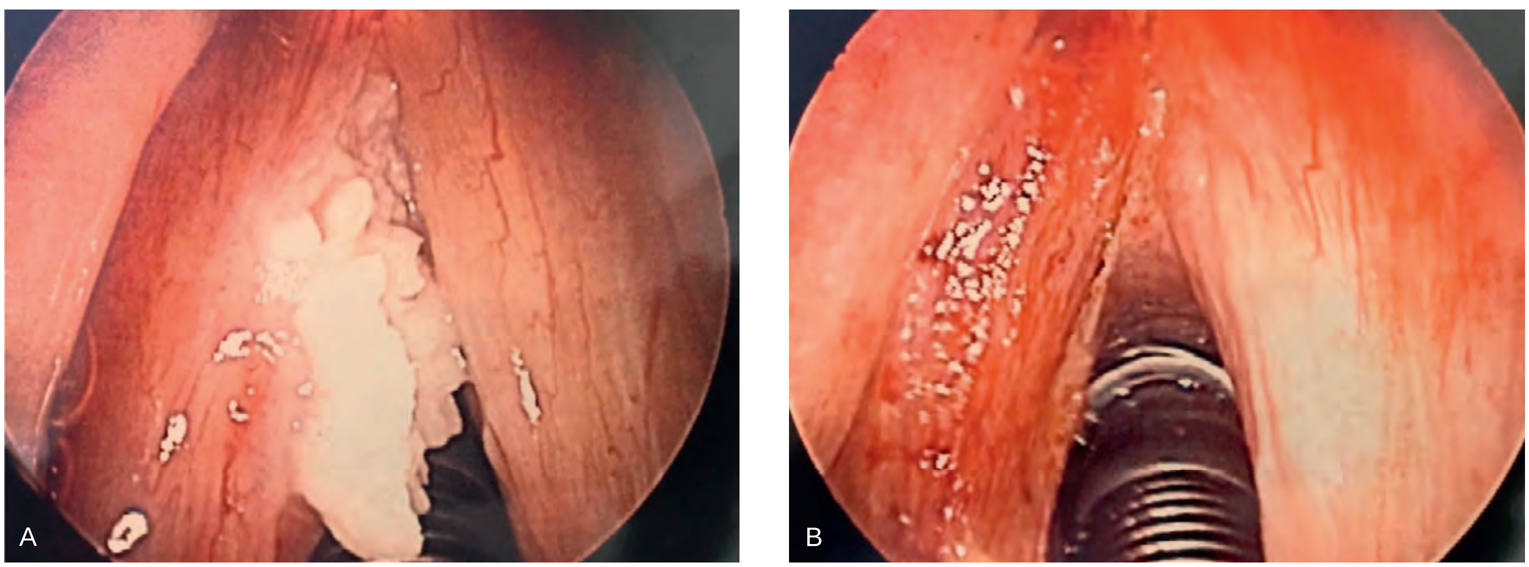

Figure 10.81 **A**, An exophytic tumor of the left vocal cord suitable for endoscopic laser resection. **B**, Post excision view of the larynx.

involvement of both vocal cords including the anterior commissure developed an anterior web after endoscopic laser excision (Fig. 10.80). Exophytic tumors of the vocal cord are highly suitable for laser surgery, as often a type II or type III resection will be possible. A type II cordectomy could be performed on a patient with an exophytic tumor of the left vocal cord (Fig. 10.81). In contrast, endophytic tumors will require deeper resections with removal of more vocalis muscle resulting in poor quality voice and a glottic gap and aspiration. Such a tumor in a patient with a poorly defined endophytic tumor of the left vocal cord, seen in Fig. 10.82, is not suitable for endoscopic laser resection.

Recurrence outcomes of transoral laser surgery are comparable to those of radiation. In a meta-anaysis of pooled cases, a trend is observed favoring TLM for improved overall-survival. However, there is no clear difference in oncologic outcomes between TLM and RT. On the other hand, a trend toward improved post-treatment voice quality is observed with RT. Patients who have failed RT often require total laryngectomy because there is a higher incidence of multi-focal recurrence. It is important to appreciate, however, that these are not outcomes of a prospective randomized trial comparing similar T1 patients.

Figure 10.82 Endophytic tumor of the left vocal cord not suitable for laser resection.

Clearly there is a selection bias in patients who underwent laser surgery.

Open Conservation Surgery for Glottic Cancer

A vertical partial laryngectomy is indicated for primary tumors of the vocal cords that extend to involve the supraglottic larynx or the anterior commissure or that have significant subglottic extension. Patients with reduced mobility of the involved vocal cord, those who have failed to respond to previous radiation therapy for a locally advanced lesion that still remains confined to one side of the larynx, and select patients with fixed vocal cord lesions also are considered for a vertical partial laryngectomy. Certain criteria pertaining to the tumor however, must be met before a patient is considered suitable for a vertical partial laryngectomy. These criteria, shown in Fig. 10.83, are general guidelines in the selection of a lesion suitable for a vertical partial laryngectomy. However, these criteria are not absolute, and the indications for a partial laryngectomy may be extended. Some technical variations of vertical partial laryngectomy are described in this chapter.

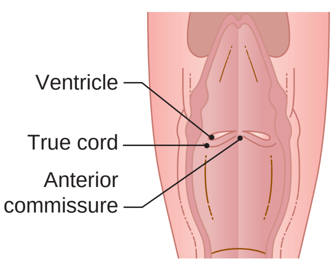

1. Lesion of mobile cord extending to anterior commissure.
2. Lesion of mobile cord involving vocal process and antero-superior portion of arytenoid.
3. Subglottic extension should not be more than 5 mm.
4. Select patients with fixed vocal cord lesion not extending across the midline.
5. A unilateral transglottic lesion not violating the above criteria.
6. True cord/anterior commissure lesion not involving more than anterior third of opposite cord.

Figure 10.83 Criteria for the selection of a lesion suitable for a vertical partial laryngectomy.

Vertical (Anterolateral) Partial Laryngectomy (Hemilaryngectomy) for Recurrent Carcinoma of the Vocal Cord

A carcinoma of the mobile vocal cord with extension to the false cord can be treated definitively by external irradiation. In some patients, however, radiation therapy fails to control the tumor and surgical treatment is necessary. The patient whose preradiation endoscopic picture of the larynx is shown in Fig. 10.84 had a primary carcinoma of the right true vocal cord that extended from the anterior commissure to the vocal process and involved the right ventricle and false vocal cord. The mobility of the vocal cord was unaffected, as seen in Fig. 10.85, where complete adduction is demonstrated during phonation. External irradiation initially was used as definitive treatment in this patient with apparent control of his cancer. However, approximately 11 months after completion of radiotherapy, local recurrence developed, manifesting in the anterior half of the right vocal cord (Fig. 10.86). At this point, surgical resection is the only viable option. Although the recurrent tumor is still suitable for a conservation procedure on the larynx, it must be emphasized that the extent of surgical resection in this clinical setting should conform to the initial extent of the tumor prior to external irradiation.

A preliminary tracheostomy is performed under local anesthesia. General anesthesia is then induced, and adequate endoscopic assessment of the lesion is performed to accurately delineate the extent of the recurrent tumor. The skin of the neck is prepared with antiseptic solution and isolated with sterile drapes (Fig. 10.87). The surface markings of the hyoid bone, the superior border of the thyroid cartilage, and the cricoid cartilage are shown. The incision for a partial laryngectomy is placed approximately at the middle of the vertical height of the thyroid cartilage through a skin crease in the neck. The skin incision is deepened through the platysma (Fig. 10.88). The upper and lower skin flaps are elevated deep to the platysma to expose the prelaryngeal strap muscles from the thyrohyoid membrane to the cricothyroid membrane (Fig. 10.89). The fascia in the midline between the strap muscles is now incised with an electrocautery until the plane of the thyroid cartilage is reached (Fig. 10.90).

The strap muscles on both sides are retracted to expose the midline of the thyroid cartilage (Fig. 10.91). The blood supply

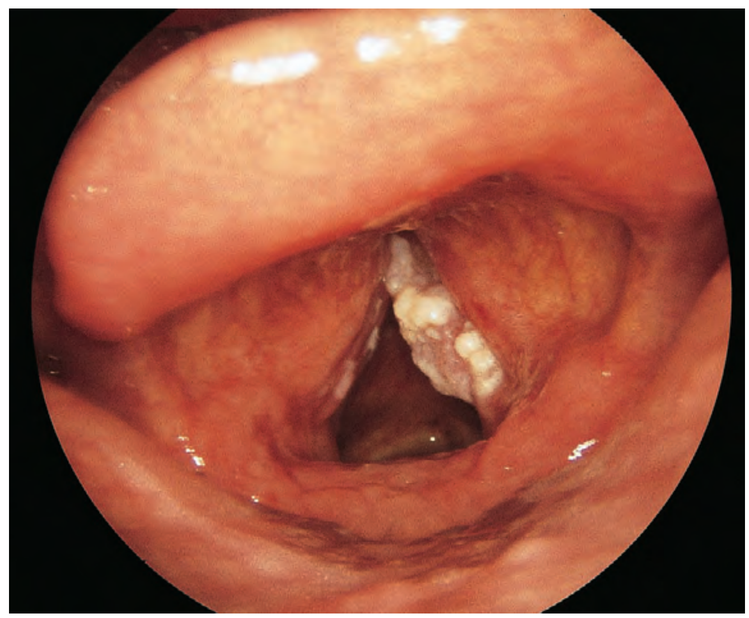

Figure 10.84 A telescopic view of a primary carcinoma of the right true vocal cord.

Figure 10.85 The vocal cord during phonation.

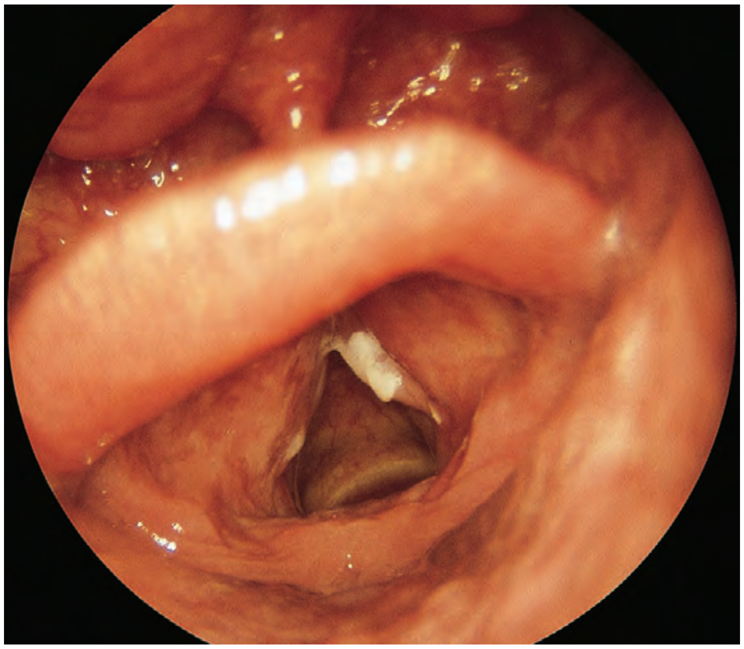

Figure 10.86 Recurrence in the anterior half of the right vocal cord after radiotherapy was used as the initial treatment.

Figure 10.87 Surface markings of the hyoid bone, thyroid, and cricoid cartilages and the outline of the skin incision.

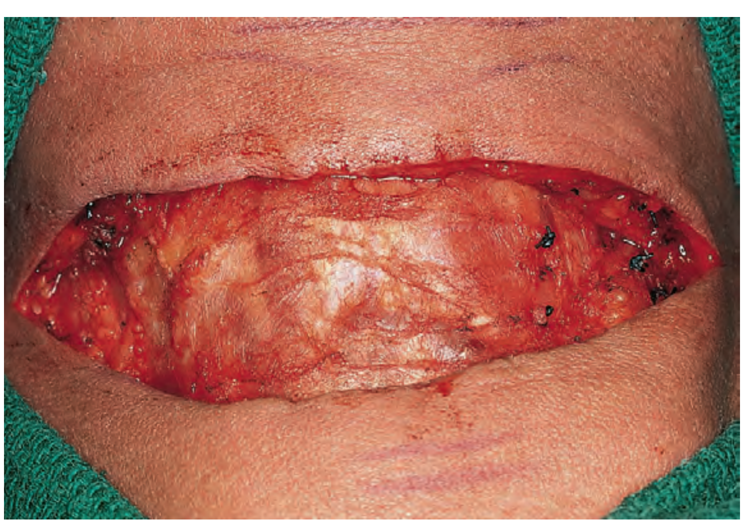

Figure 10.88 The skin incision is deepened through the platysma.

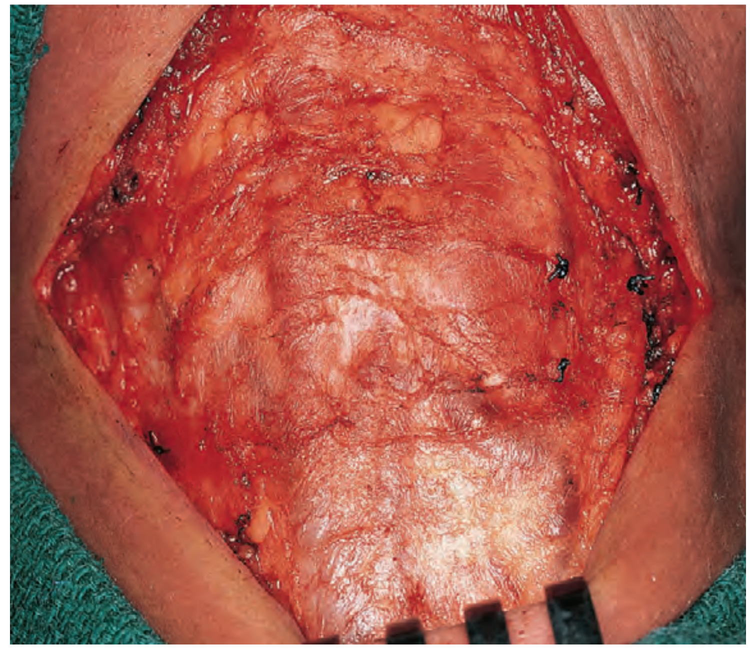

Figure 10.89 Elevation of the upper and lower skin flaps.

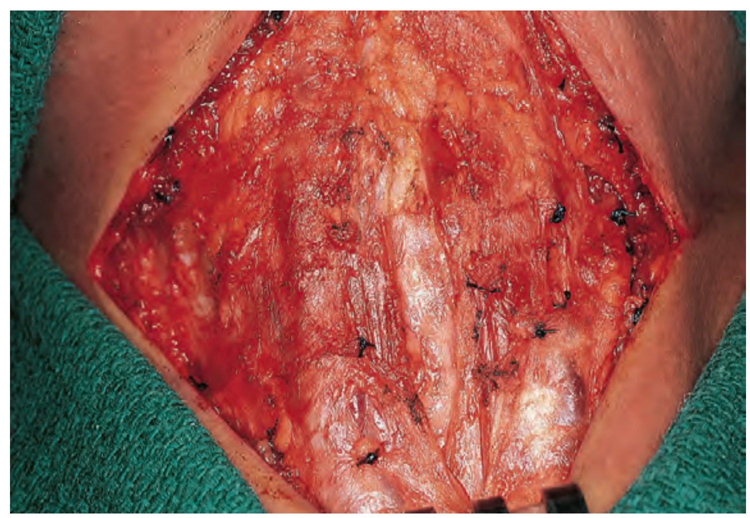

Figure 10.90 The fascia in the midline is incised.

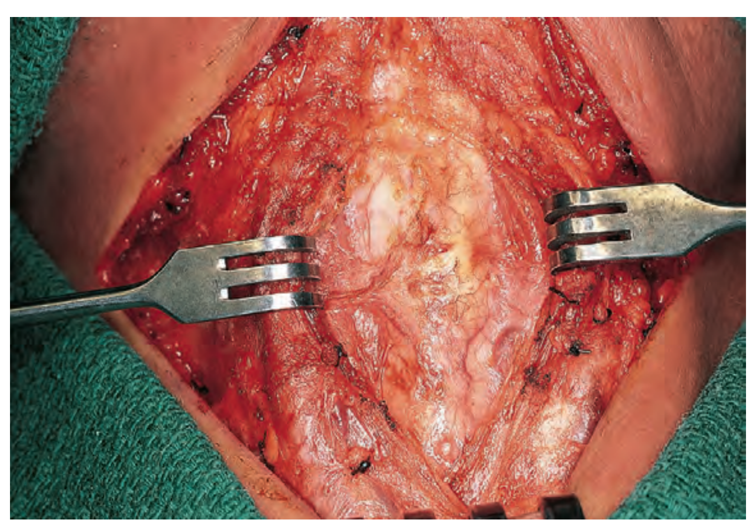

Figure 10.91 The strap muscles are retracted laterally.

to the thyroid cartilage is provided by the blood vessels in the perichondrium. Unnecessary elevation of the perichondrium therefore should be avoided to reduce the risk of necrosis of the remaining radiated larynx after surgery. An electrocautery with a fine needle tip is used to make an incision in the perichondrium of the thyroid cartilage in the anterior midline extending from the thyroid notch to the cricothyroid membrane (Fig. 10.92). Using a fine periosteal elevator, the perichondrium of the right ala of the thyroid cartilage is elevated up to the posterior margin of the thyroid cartilage (Fig. 10.93). To accomplish this maneuver, the perichondrium must be detached superiorly from the upper border of the thyroid cartilage and inferiorly from the cricothyroid membrane.

Chromic catgut tagging sutures are now applied to the upper and lower edges of the elevated perichondrium, and these sutures are left long for retraction (Fig. 10.94). A sagittal power saw with a right-angled blade is now used to perform laryngofissure through the anterior midline, as shown in the model (Fig. 10.95). The thyroid cartilage is divided from its notch up to the cricothyroid membrane with the saw, sparing the underlying soft tissues and mucosa (Fig. 10.96). As soon as the full thickness of the cartilage is divided, a give is felt and use of the saw should then cease (Fig. 10.97). Right-angled double hooks are

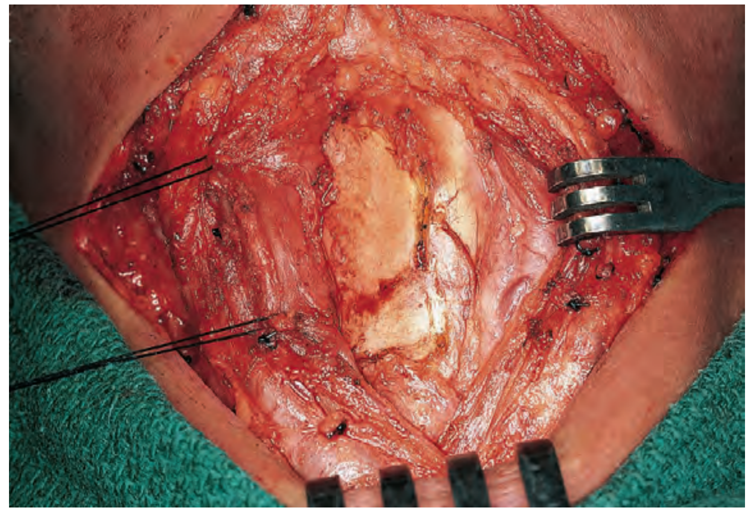

Figure 10.94 The perichondrium is tagged with sutures and retracted laterally.

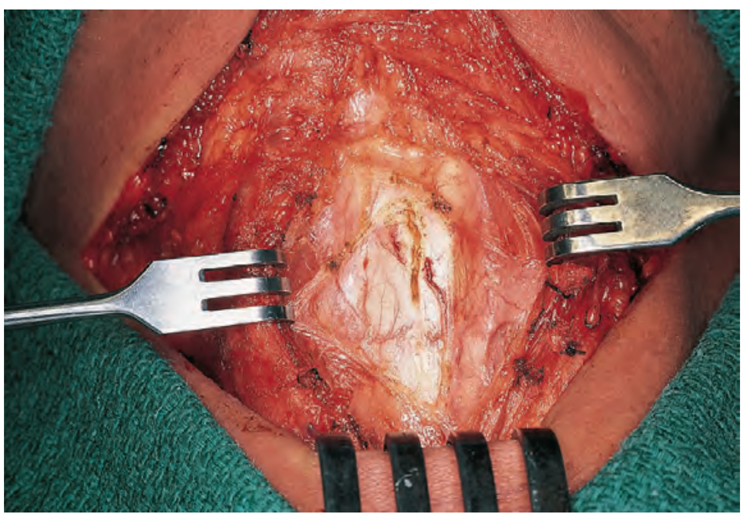

Figure 10.92 The perichondrium of the thyroid cartilage is incised in the midline.

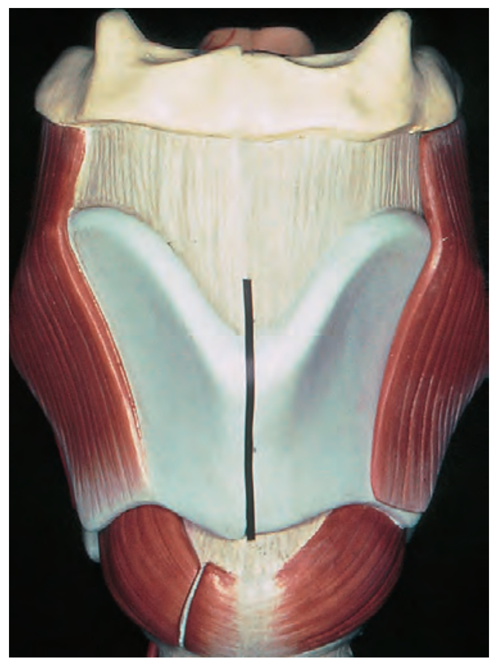

Figure 10.95 Model showing a midline thyrotomy.

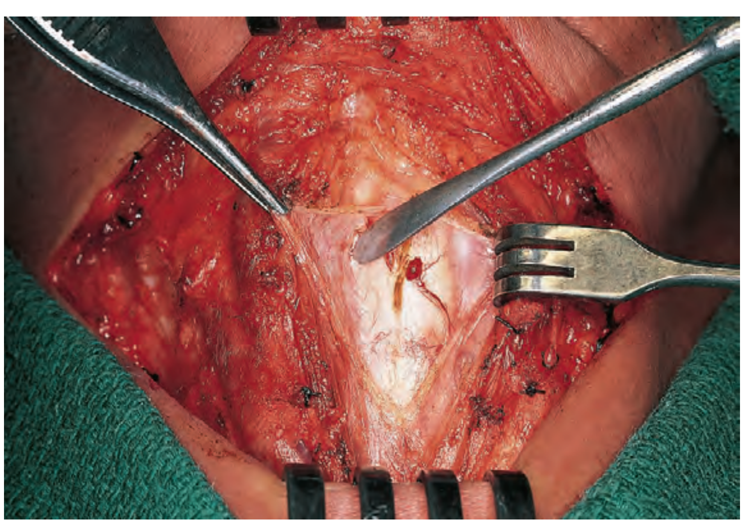

Figure 10.93 The perichondrium of the right ala of the thyroid cartilage is elevated up to its posterior border.

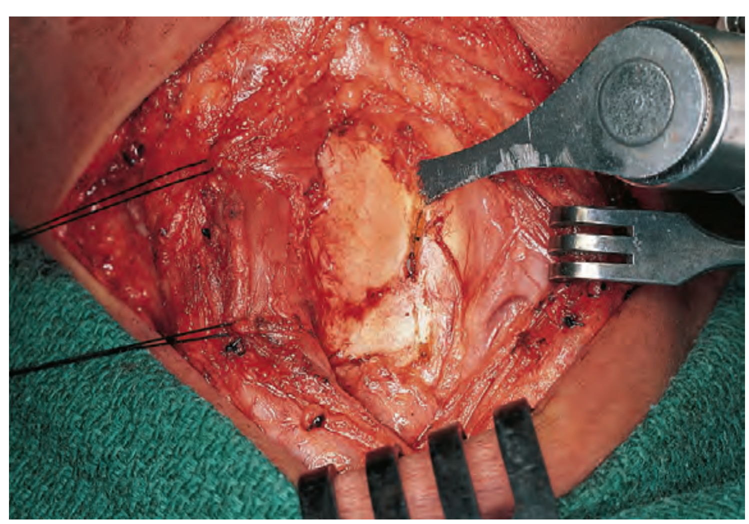

Figure 10.96 Division of the thyroid cartilage with a power saw.

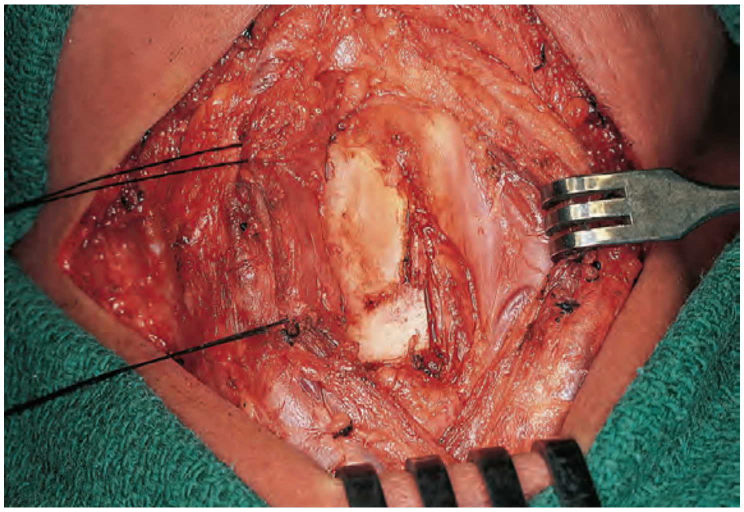

Figure 10.97 The full thickness of the cartilage is divided.

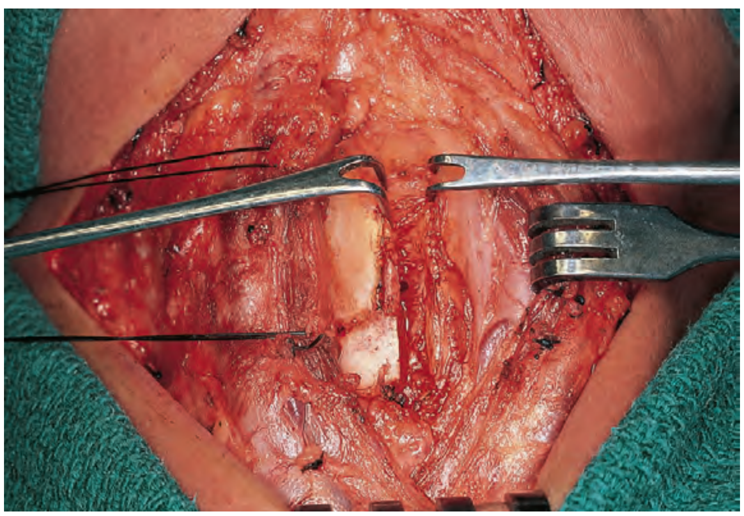

Figure 10.98 The divided thyroid cartilage is retracted laterally.

now used to retract the divided thyroid cartilage on each side, exposing the underlying soft tissues (Fig. 10.98). As the divided cartilage is retracted laterally, a deficiency in the mucosa of the subglottic region becomes apparent. An electrocautery with a needle tip is now used to enlarge the opening in the subglottic mucosa (Fig. 10.99). A hemostat is inserted through this opening. The opened hemostat is used as a guide for division of the remaining soft tissues and mucosa of the larynx in the anterior midline (Fig. 10.100). The double hooks are used again to retract each half of the larynx further (Fig. 10.101), providing a view of the interior of the larynx. Note the recurrent tumor, which is mostly submucosal with a bulky vocal cord on the right side. A close-up view of the surgical field shows that the tumor ulceration at the superior surface of the true vocal cord is posterior to the line of division of the mucosa at the anterior commissure (Fig. 10.102).

A deep right-angled retractor is now introduced through the laryngotomy site, and the supraglottic larynx is retracted cephalad (Fig. 10.103). Using the electrocautery, the cricothyroid membrane is now divided along the lower border of the thyroid cartilage (Fig. 10.104). Under direct vision, the mucosa of the subglottic larynx also is incised along the cricothyroid membrane up to the posterior midline (Fig. 10.105). Soft-tissue attachments at the upper border of the thyroid cartilage on the right side are divided next (Fig. 10.106).

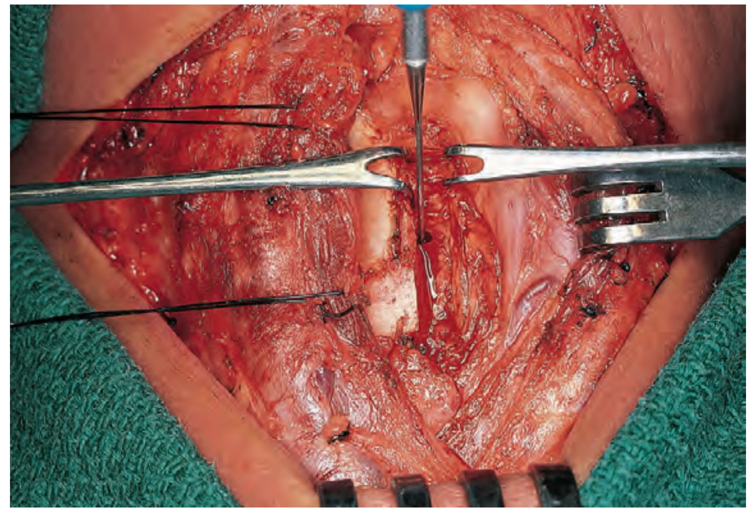

Figure 10.99 The opening in the subglottic mucosa is enlarged with an electrocautery.

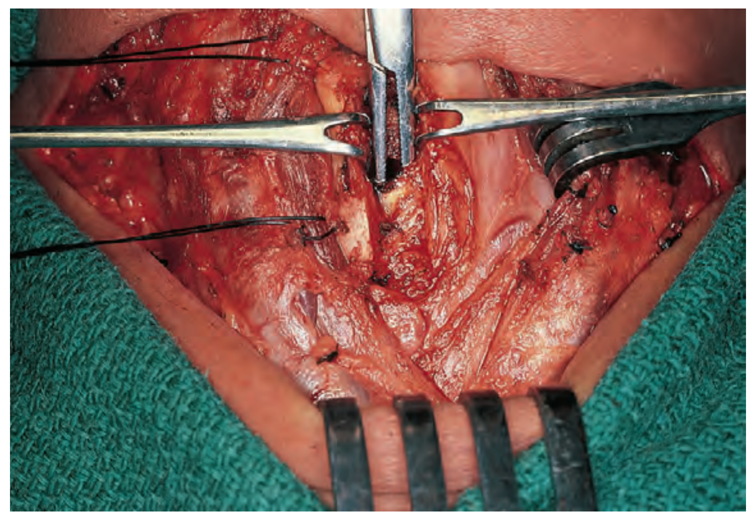

Figure 10.100 A hemostat is used to facilitate the division of the laryngeal mucosa.

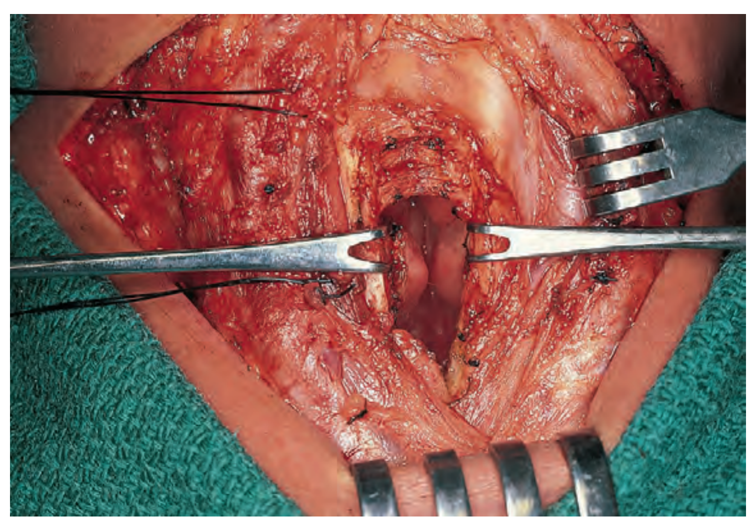

Figure 10.101 The interior of the larynx is exposed.

A mucosal incision in the right hemilarynx encompassing the tumor with adequate margins is shown in the model (Fig. 10.107). An electrocautery is used to make this incision on the false vocal cord, the right arytenoid, and the posterior edge of the right vocal cord at the midline connecting the mucosal incision in the subglottic region (Fig. 10.108). Finally, serrated

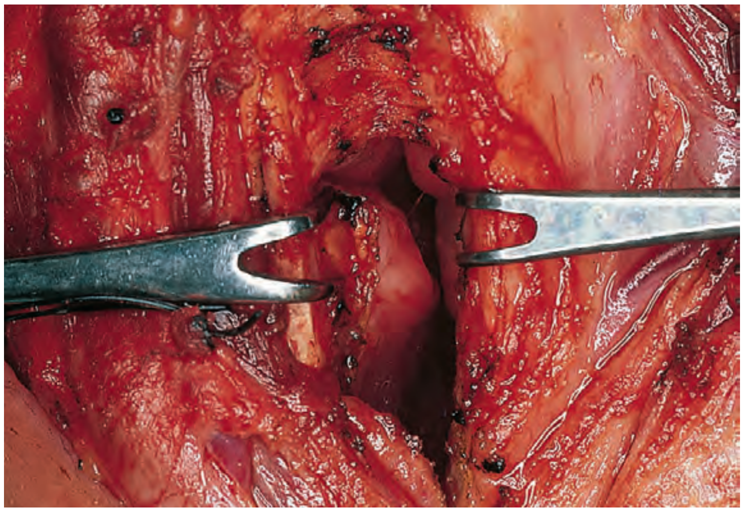
Figure 10.102 A close-up view of the surgical field.

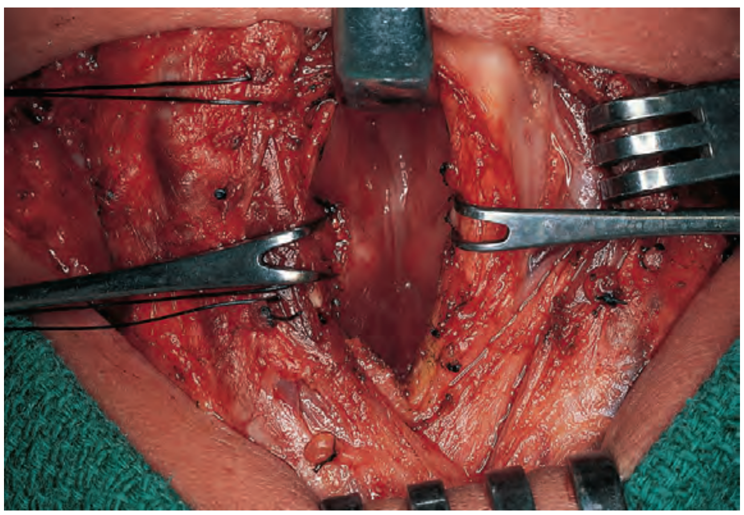
Figure 10.103 The supraglottic larynx is retracted cephalad with a right-angled retractor.

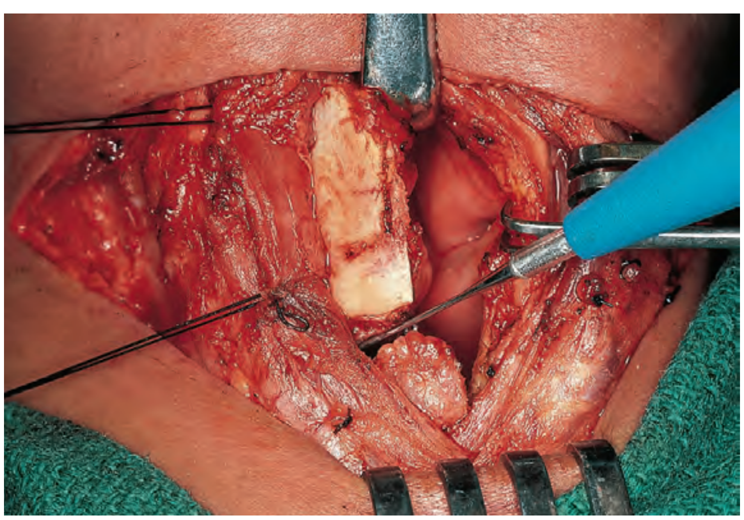
Figure 10.104 The cricothyroid membrane is divided to mobilize the lower border of the specimen.

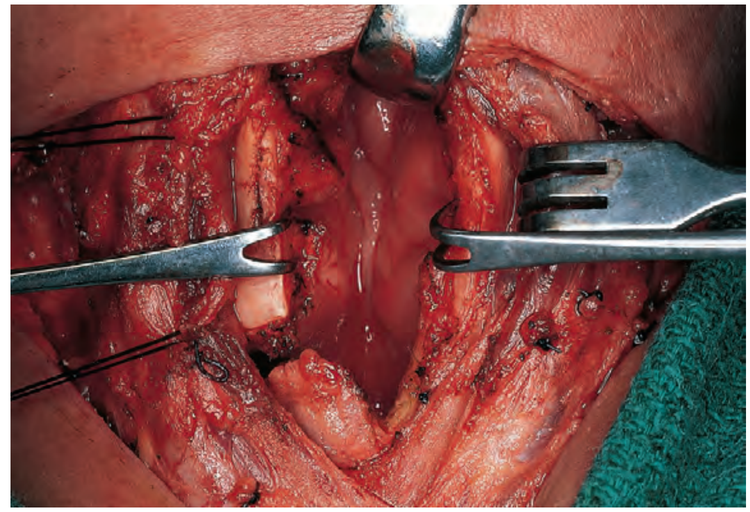
Figure 10.105 Incision of the mucosa of the subglottic larynx.

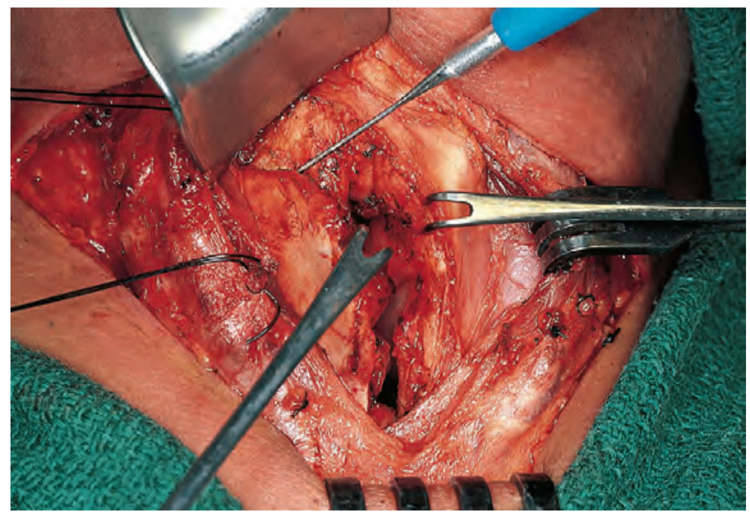
Figure 10.106 Division of soft-tissue attachments at the upper border of the thyroid lamina.


Figure 10.107 A model showing the mucosal incision.

scissors with an angle on the flat side are used to excise the surgical specimen of the right hemilarynx, encompassing the entire ala of the thyroid cartilage on the right-hand side, along with all the soft tissues of the paraglottic space and the overlying mucosa (Fig. 10.109). The superior horn of the thyroid cartilage must be divided for removal of the thyroid ala (Fig. 10.110). The extent of thyroid cartilage resection is shown in the model (Fig. 10.111). Serrated scissors are used again for excision through the cricoarytenoid junction and the remaining muscular attachments of the inferior constrictor muscle at the posterior edge of the thyroid ala (Fig. 10.112). Brisk hemorrhage from the branches of the superior laryngeal artery is encountered but is easily controlled once the specimen is removed. The surgical defect following excision of the right hemilarynx extending

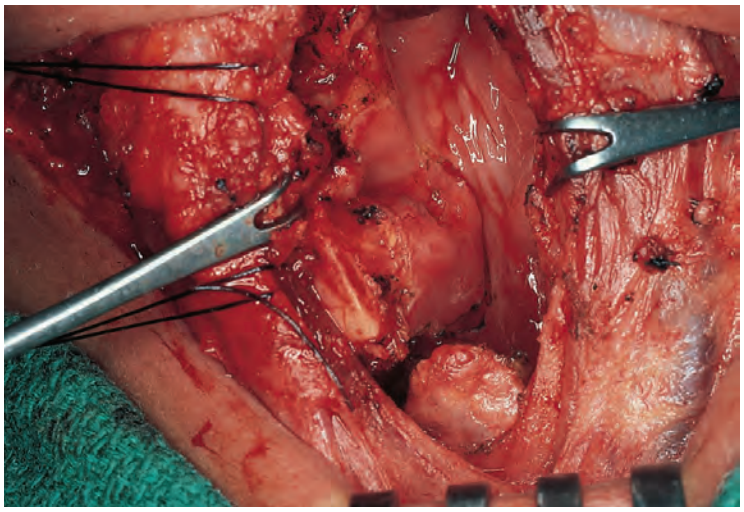

Figure 10.108 The mucosal incision on the false vocal cord.

Figure 10.111 A model showing the extent of thyroid cartilage resection.

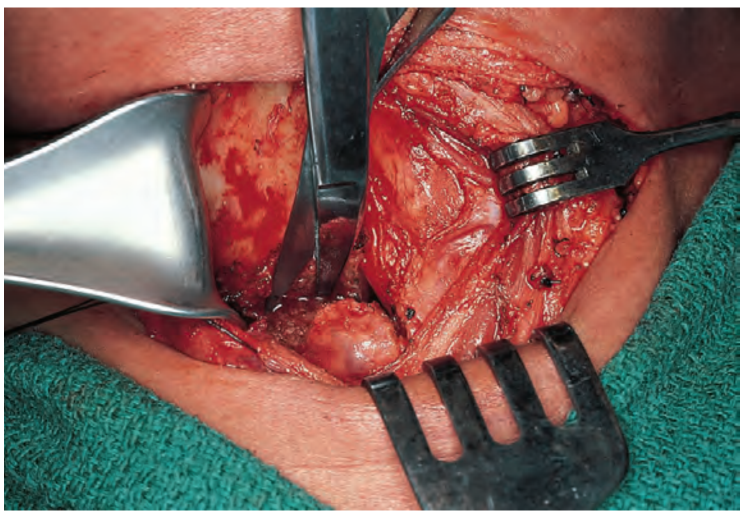

Figure 10.109 The posterior attachments of the specimen are divided with scissors.

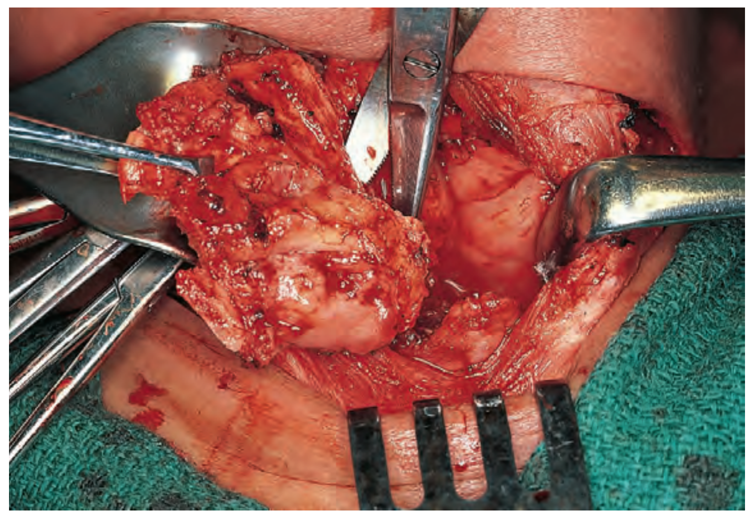

Figure 10.112 Excision through the cricoarytenoid junction.

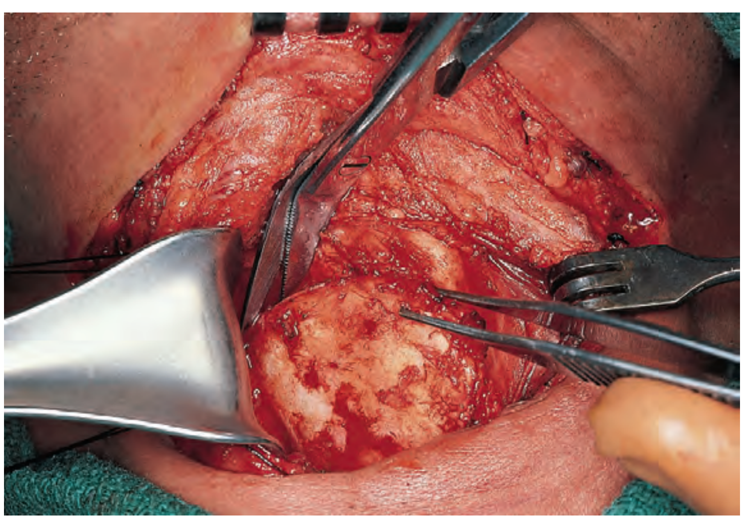

Figure 10.110 The superior horn of the thyroid cartilage also is divided with scissors.

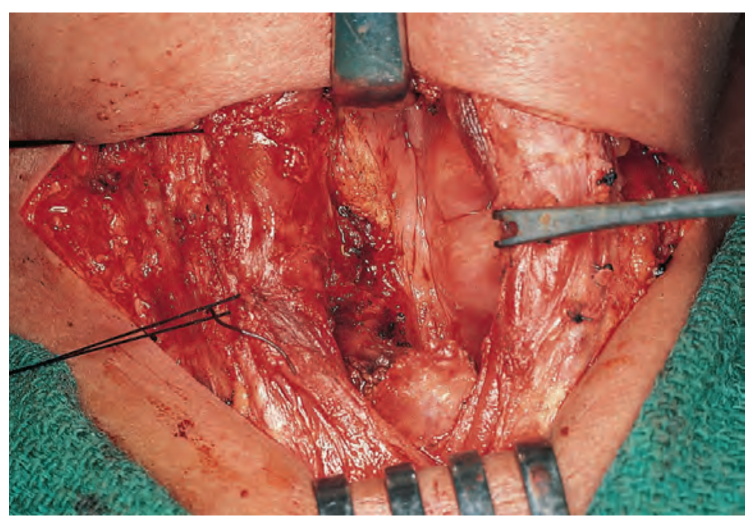

Figure 10.113 The surgical defect following excision of the right hemilarynx.

from the right aryepiglottic fold cephalad up to the superior border of the cricoid cartilage caudad is shown in Fig. 10.113.

A close-up view of the surgical field with the left ala of the thyroid cartilage retracted shows the normal left vocal cord, ventricle, and false cord (Fig. 10.114). On the other side, the surgical defect shows stumps of the laryngeal muscles attached to the cricoid cartilage as well as the stump of the right inferior constrictor muscle (Fig. 10.115). No attempt is made to obtain mucosal closure of the surgical defect. The raw area granulates and spontaneously epithelializes satisfactorily in every instance,

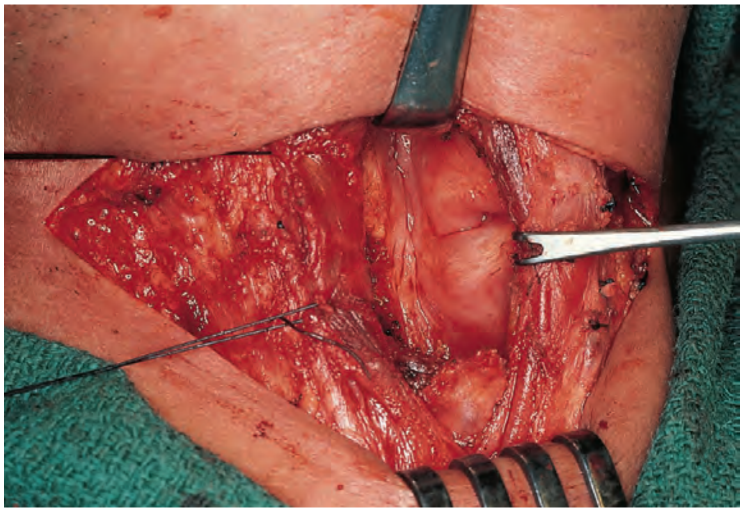

Figure 10.114 A close-up view of the surgical field shows the normal left hemilarynx.

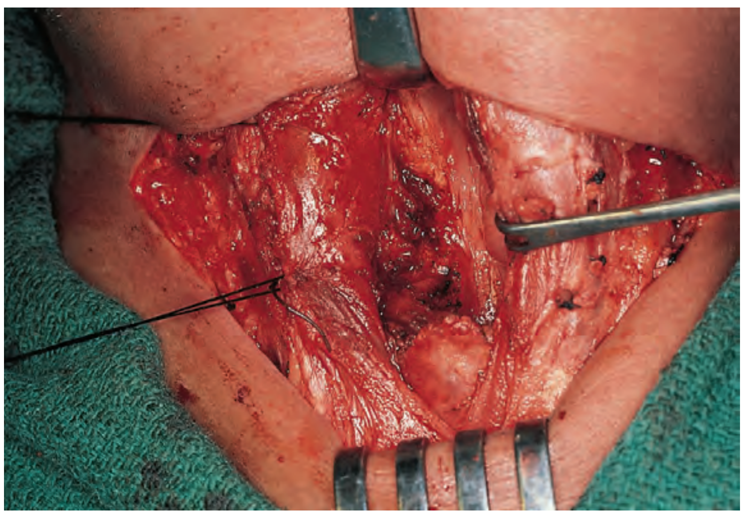

Figure 10.115 The detached inferior constrictor muscle is seen in the surgical defect.

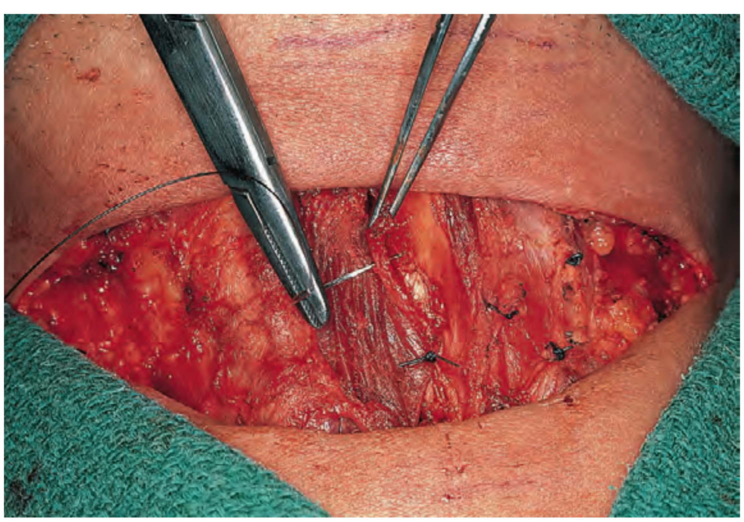

Figure 10.116 Reapproximation of the perichondrium.

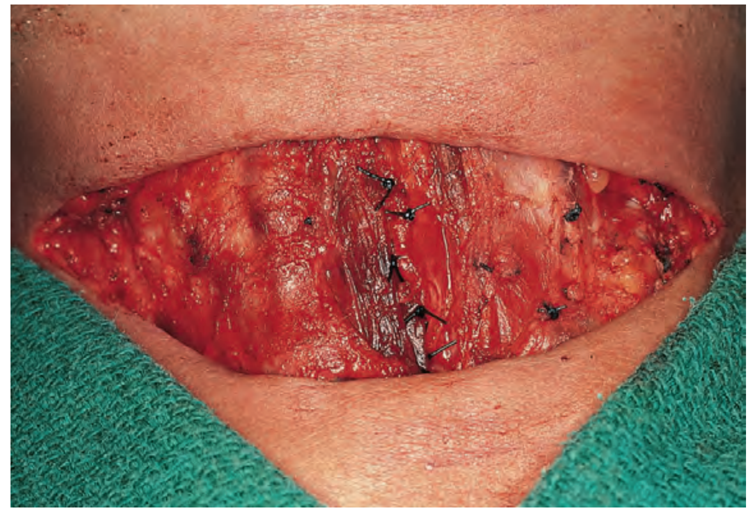

Figure 10.117 Watertight perichondrial closure.

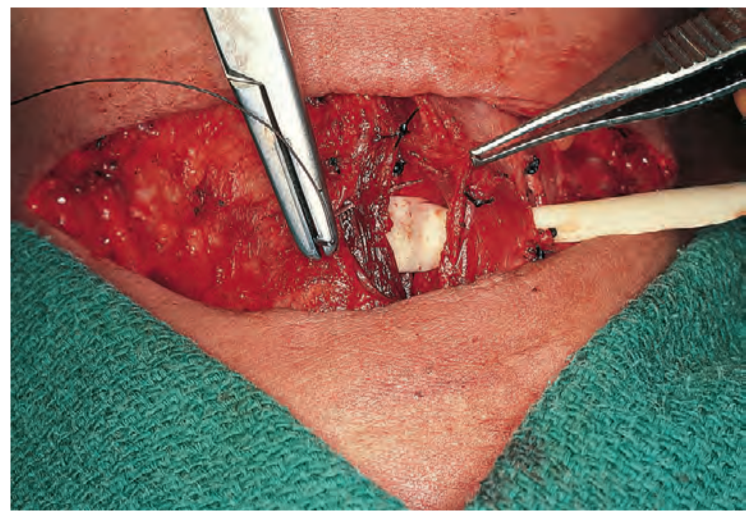

Figure 10.118 One Penrose drain is placed deep to the strap muscles.

Figure 10.119 Another drain is placed deep to the platysma.

although this process may take longer in patients who have undergone previous radiation therapy. A nasogastric feeding tube is introduced prior to the closure of the incision.

Closure begins with reapproximation of the perichondrium from the right-hand side to the perichondrium of the left-hand side (Fig. 10.116). Several interrupted chromic catgut sutures are placed to obtain a watertight perichondrial closure (Fig. 10.117).

The strap muscles are reapproximated next in the midline. A Penrose drain is placed deep to the strap muscles and brought out on the left side as seen in Fig. 10.118. A second Penrose drain is placed superficial to the strap muscles and brought out at the other end of the incision. The platysma is closed with interrupted chromic catgut sutures (Fig. 10.119). The skin incision is closed with interrupted nylon sutures (Fig. 10.120).

Figure 10.120 Closure of the skin incision.

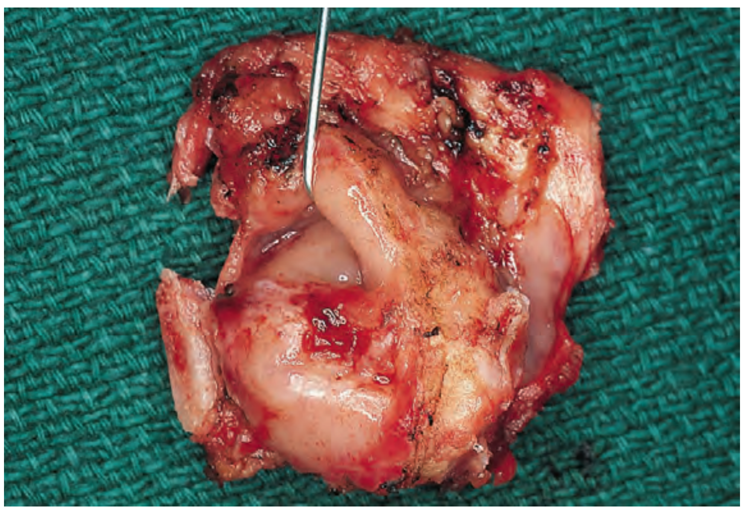

Figure 10.121 The surgical specimen.

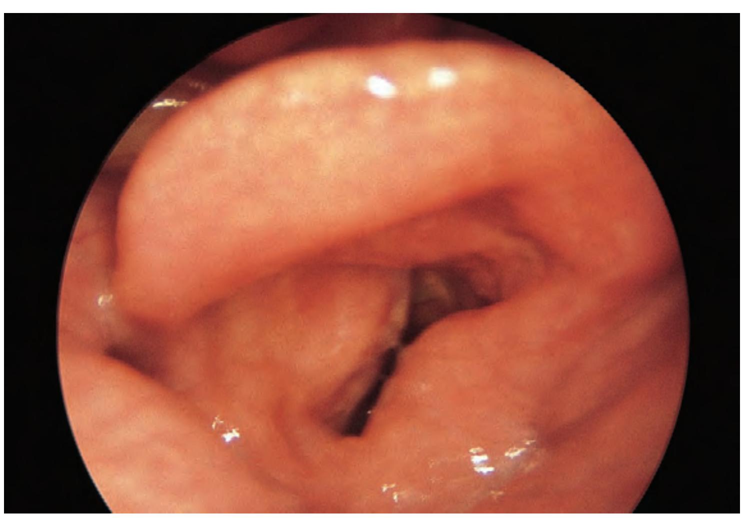

Figure 10.122 An endoscopic view of the larynx 3 months after surgery.

The surgical specimen of the right hemilaryngectomy with removal of the entire lamina of the thyroid cartilage is shown in Fig. 10.121. Note the right vocal cord tumor with significant subglottic extension, which has been excised with satisfactory mucosal margins. A metallic hook retracting the right false vocal cord shows that the bulk of the tumor is occupying the ventricle in a submucosal fashion.

In the postoperative period, nutrition is maintained through the nasogastric feeding tube. Clearance of pulmonary secretions is maintained through the tracheostomy. A moderate degree of serosanguinous drainage is to be expected from the drains, and the patient may expectorate blood-stained secretions for the first 48 hours because of oozing from the raw area. Most patients will be able to swallow semi-solid and liquid food by the end of 1 week, when the nasogastric feeding tube is removed. The tracheostomy tube may be removed soon thereafter. A satisfactory laryngeal air passage should be confirmed by fiberoptic laryngoscopic examination before removal of the tracheostomy tube.

A postoperative endoscopic view of the larynx 3 months following surgery shows satisfactory healing of the surgical defect on the right-hand side (Fig. 10.122). Note the prolapse of the mucosa of the right arytenoid toward the glottis as a result of the resection of the arytenoid. The prolapsed mucosa may create compromise of the airway in some patients, requiring its excision to improve the airway.

Vertical Partial Laryngectomy (Anterior) for an Anterior Commissure Lesion

A primary carcinoma of the glottic larynx arising at the anterior commissure or a carcinoma of the true vocal cord with extension to the anterior commissure requires resection of the anterior commissure in conjunction with the involved true vocal cord. The endoscopic picture of the larynx of a patient with a primary carcinoma arising at the anterior commissure is shown in Fig. 10.123. Note that the tumor extends to involve the anterior thirds of the left and right true vocal cords. Accurate endoscopic assessment of this tumor requires an operating microscope and angled telescopes. A tracheostomy under local anesthesia is performed first, and general anesthesia is induced thereafter. The surface markings of the thyroid notch and the cricoid cartilage are shown in Fig. 10.124, with the incision along an upper neck skin crease. The skin incision is deepened through the platysma, and the upper and lower skin flaps are elevated (Fig. 10.125).

The larynx is exposed from the thyrohyoid membrane down to the cricothyroid membrane. The fascia in the midline between the strap muscles is incised (Fig. 10.126). A plane is now

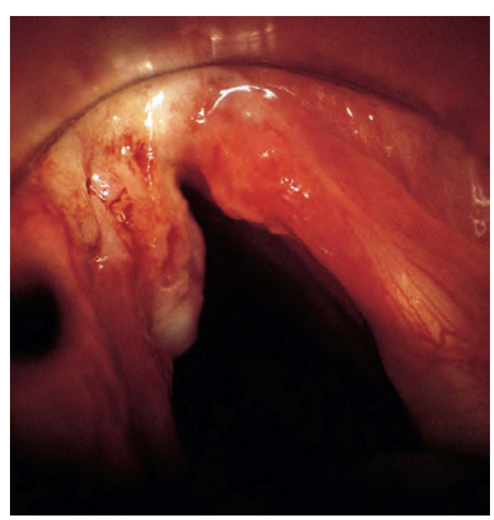

Figure 10.123 An endoscopic picture of the larynx showing carcinoma of the anterior commissure.

Figure 10.124 The surface markings of the thyroid notch and the cricoid cartilage and an outline of the skin incision.

Figure 10.125 The upper and lower skin flaps are elevated.

Figure 10.126 The fascia is incised in the midline.

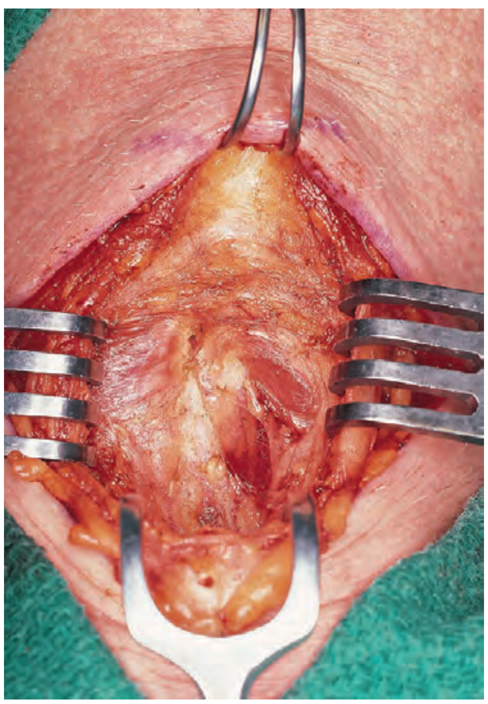

Figure 10.127 The strap muscles are retracted laterally.

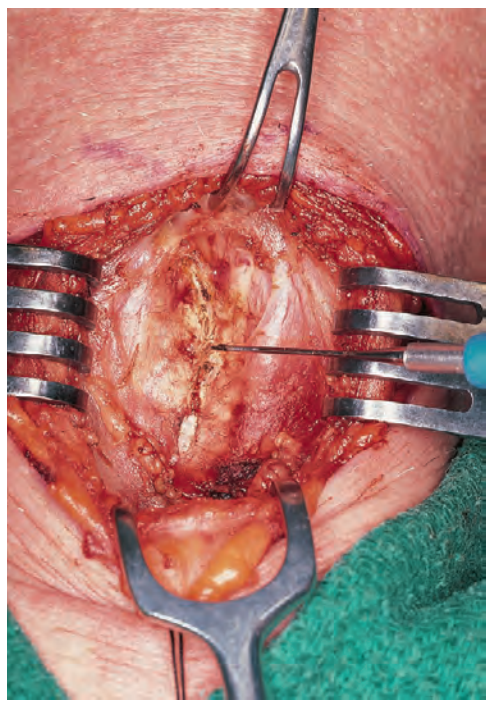

Figure 10.128 The perichondrium is incised in the midline.

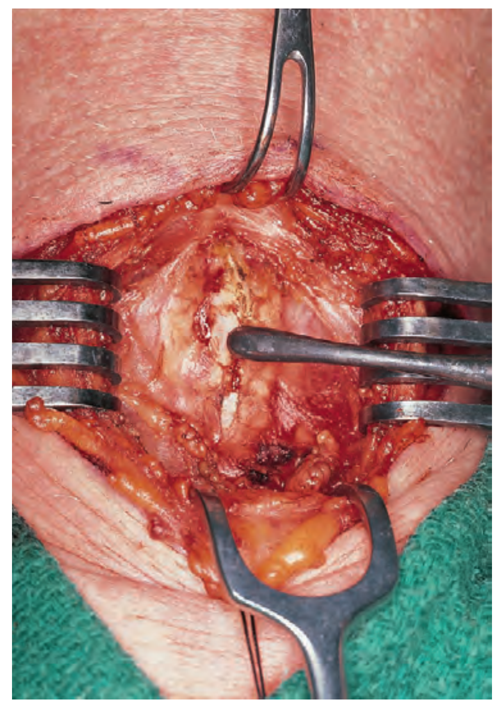

Figure 10.129 Elevation of the perichondrium.

developed between the thyroid cartilage and the strap muscles, permitting them to be retracted laterally (Fig. 10.127). The perichondrium is incised in the midline with an electrocautery (Fig. 10.128). It is then elevated with a fine periosteal elevator to expose approximately 6 mm of the ala of the thyroid cartilage on the right-hand side (Fig. 10.129). A suture is taken through the edge of the elevated perichondrium as a tag for subsequent identification during repair of the larynx (Fig. 10.130). On the left side, the perichondrium is elevated farther back to expose the anterior half of the ala of the thyroid cartilage. The cartilage cuts, based on the endoscopic assessment of the tumor, are shown on the model in Fig. 10.131. Using the electrocautery, vertical lines are marked on the thyroid cartilage at the proposed site of division (Fig. 10.132). These lines are drawn based on the endoscopic assessment of the extent of the tumor and its lateral extension on each vocal cord. More cartilage will have to be resected on the left side because of involvement of the anterior half of the left vocal cord. A lesser width of the cartilage needs to be excised on the right-hand side because of a lesser extent of involvement of the right vocal cord.

A power sagittal saw is now used, and the thyroid cartilage is divided through the previously marked lines from its superior border up to the cricothyroid membrane (Fig. 10.133). Every attempt must be made to avoid laceration of the soft tissues and mucosa of the interior of the larynx with the power saw. As soon as the cartilage division is complete, a give is felt in the soft tissues. A similar cut is made on the left side. A double hook is used to retract the lower border of the cartilaginous component of the surgical specimen cephalad, and entry is made in the subglottic region of the larynx through the

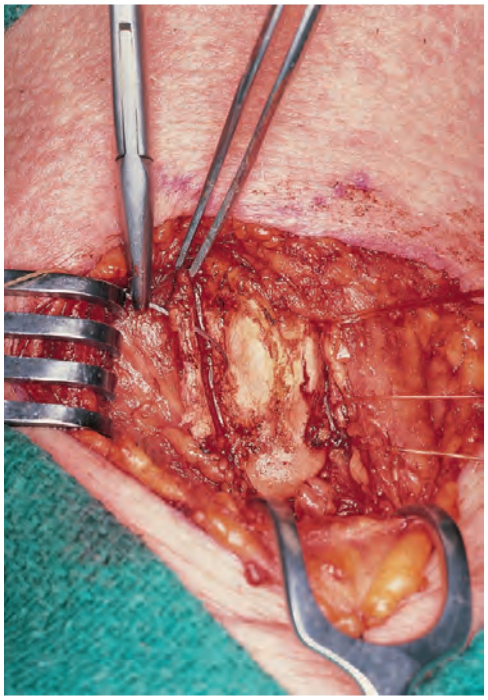

Figure 10.130 A suture is taken through the edge of the elevated perichondrium.

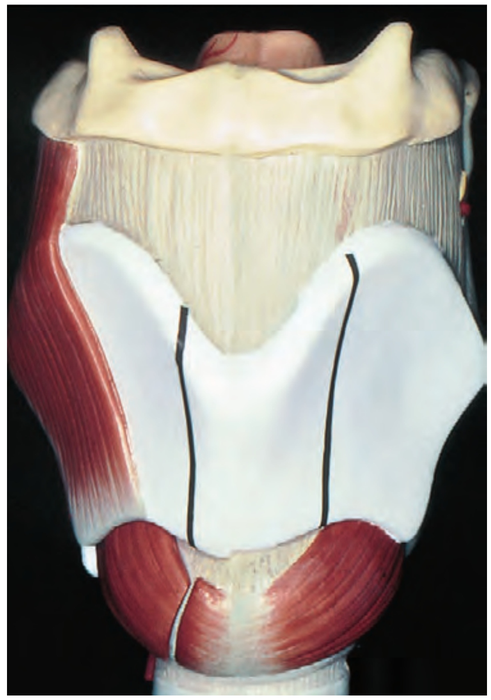

Figure 10.131 The proposed cartilage cuts outlined on a model.

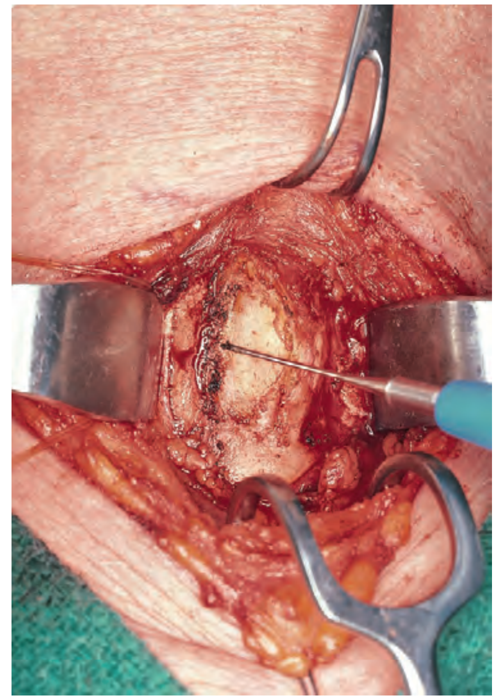

Figure 10.132 Vertical lines of division are marked on the thyroid cartilage.

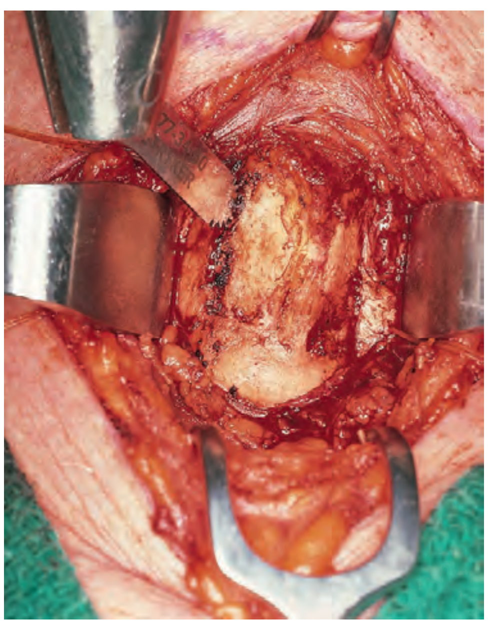

Figure 10.133 Division of the thyroid cartilage with a power saw.

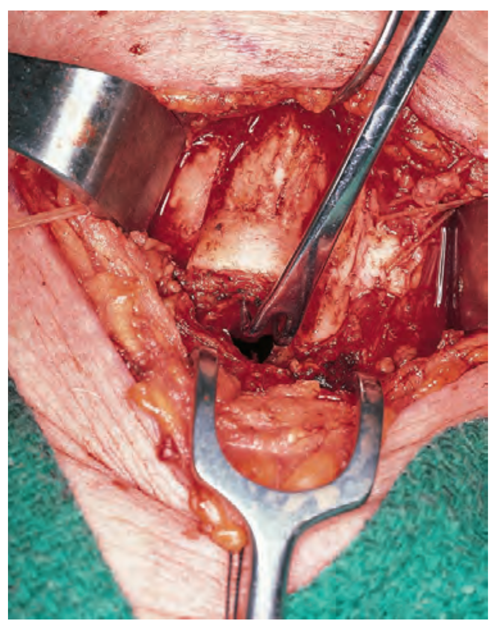

Figure 10.134 Cephalad retraction of the lower border of the surgical specimen.

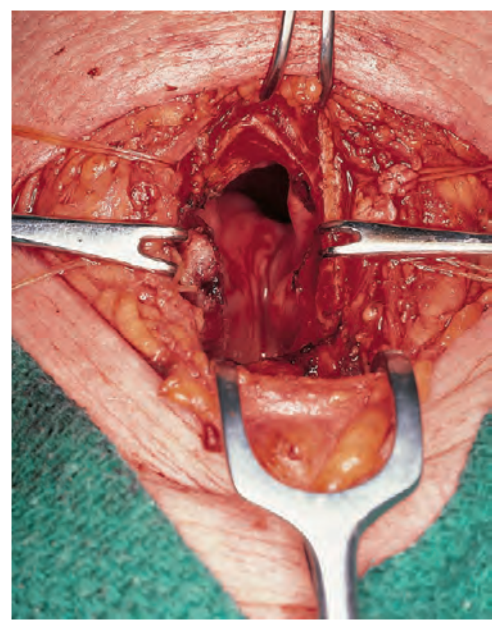

Figure 10.135 Mucosal incisions on the vocal cords are made with the specimen retracted cephalad.

cricothyroid membrane (Fig. 10.134). With continued retraction cephalad, a further view of the interior of the larynx is obtained. Under direct vision, mucosal incisions are placed on the vocal cords, securing adequate margins (Fig. 10.135). Serrated angled scissors are now used to divide the musculature of the vocal cords on both sides, and the specimen is removed (Fig. 10.136). The surgical defect shown in Fig. 10.137 demonstrates the stumps of the vocal cords on both sides and the interarytenoid mucosa. A close-up examination of the larynx shows that approximately half of the right vocal cord and one-third of the left vocal cord remain (Fig. 10.138). Note that both arytenoids and the remaining supraglottic larynx are intact.

To ensure adequate function of the remaining vocal cords, it is essential to restore their bow string configuration. A drill hole is made through the remaining ala of the thyroid cartilage on each side at the level of the vocal cords. A 4-0 Vicryl suture is now taken through this hole and through the full thickness of the stump of the vocal cord. When this suture is tied, it approximates the stump of the vocal cord to the cut end of the thyroid cartilage, making it taut (Fig. 10.139). Similar tightening of the vocal cord is performed on the opposite side.

To reconstruct the anterior commissure and prevent an anterior web, a laryngeal keel is used. A Silastic keel as shown in Fig. 10.140 is used for restoration of the anterior commissure. The keel is placed between the cut edges of the thyroid cartilage and is retained in position by anchoring it to the remaining ala on each side with 2-0 chromic catgut. Sutures are passed through the horizontal flange of the keel and then the ala of

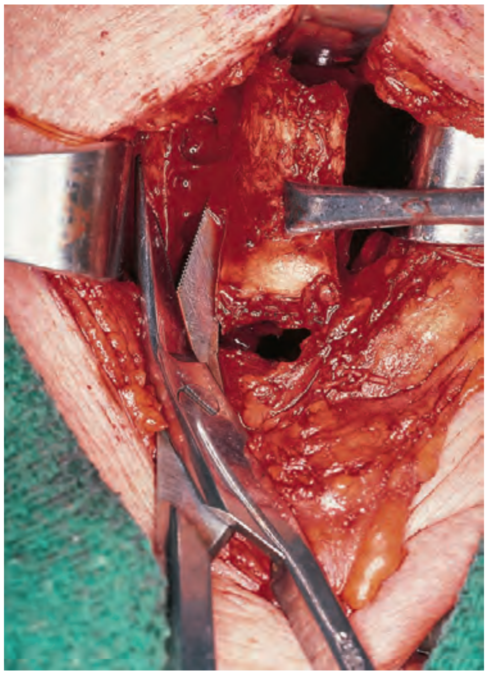

Figure 10.136 The specimen is removed by division of the remaining attachments.

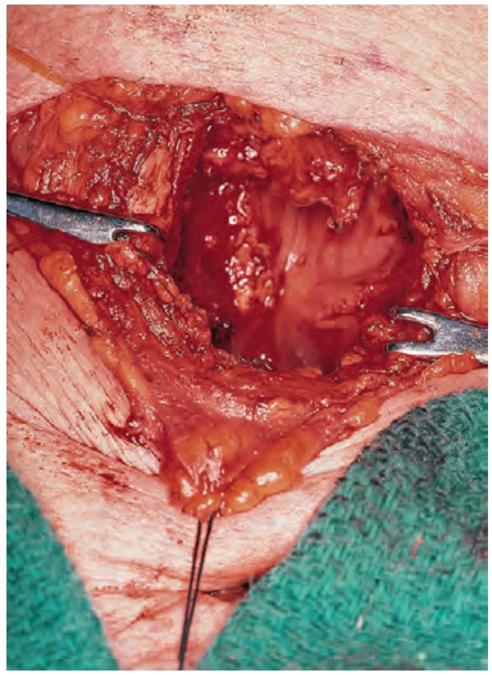

Figure 10.137 The surgical defect.

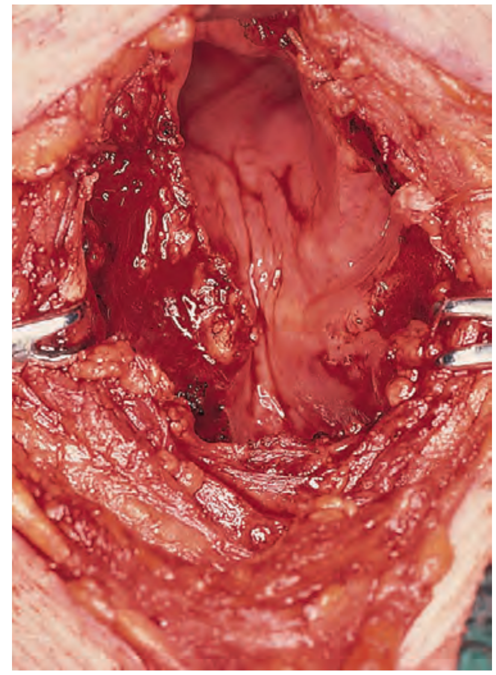

Figure 10.138 A close-up view of the remaining larynx.

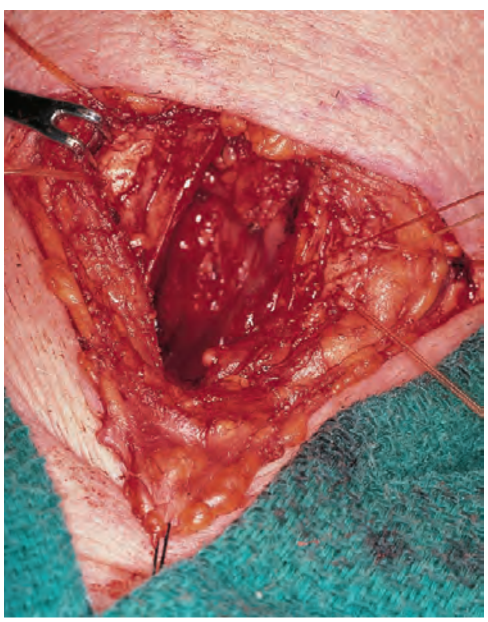

Figure 10.139 The stump of the left vocal cord is anchored to the thyroid cartilage.

Figure 10.140 A Silastic keel.

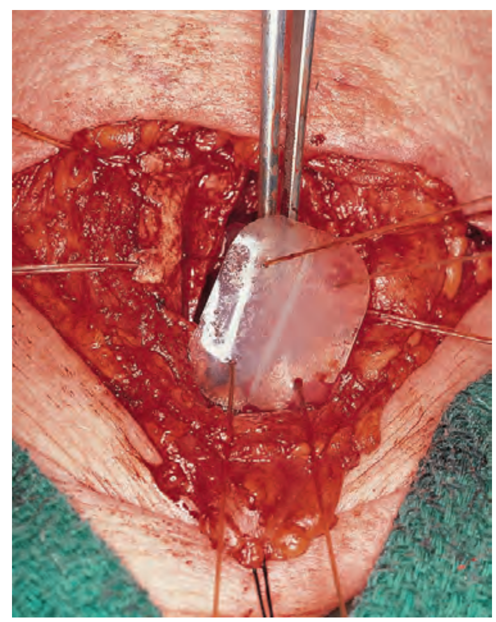

Figure 10.141 The Silastic keel is fixed to the thyroid laminae with an absorbable suture.

the thyroid cartilage on one side; they are then passed through the vertical flange of the keel and out through the other side of the thyroid cartilage and the keel, as shown in Fig. 10.141. The vertical flange of the keel remains between the two reconstructed stumps of the vocal cords and the two cut ends of the thyroid cartilage (Fig. 10.142). The catgut sutures are tied over the flat surface of the keel. A heavy nylon suture is passed from one end of the flat surface of the keel through its vertical flange and out from the other side of the flat surface. The ends of this nylon suture are kept long and brought out through the skin incision (Fig. 10.143). Placing a nylon suture in the keel in this fashion facilitates its easy removal under local anesthesia as an outpatient procedure. Alternatively, the keel may be removed endoscopically, in which case the nylon suture is unnecessary, but general anesthesia is required for direct laryngoscopy and removal of the keel.

Following insertion of the keel, the perichondrium is sutured over the keel with interrupted chromic catgut sutures. The strap muscles are reapproximated in the midline as shown in Fig. 10.144. Note the long ends of the nylon suture from the keel, which are brought out through the midline closure. The platysma is closed with interrupted chromic catgut sutures. A Penrose drain is placed deep to the platysma and is brought out through the skin incision, which is closed with fine nylon sutures (Fig. 10.145). An anterior view of the surgical specimen shows the external aspect of the thyroid cartilage in the midline, which forms the deep margin of the tumor (Fig. 10.146). The tumor is not seen from this view. A posterior view of the specimen

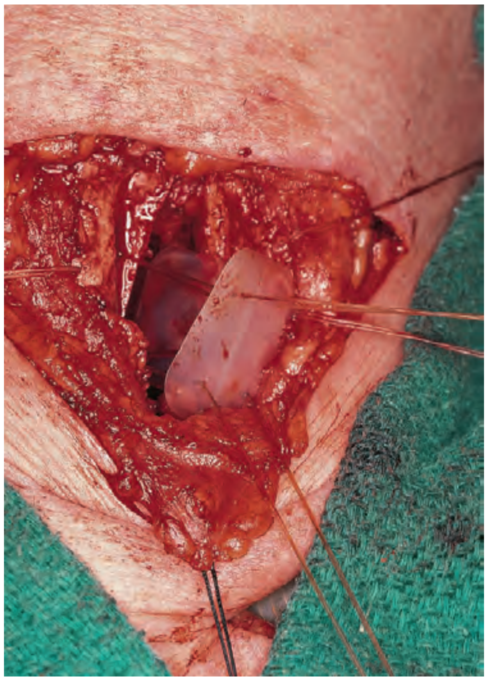

Figure 10.142 The vertical flange of the keel remains between the anterior ends of the vocal cords.

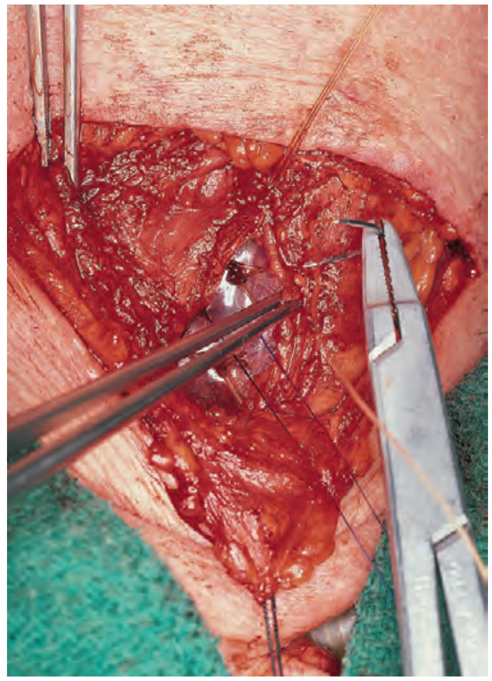

Figure 10.143 The ends of the nylon suture applied to the keel are kept long.

Figure 10.144 The strap muscles are reapproximated in the midline.

Figure 10.145 A Penrose drain is placed and the incision is closed.

Figure 10.146 The anterior view of the surgical specimen.

Figure 10.147 The posterior view of the surgical specimen.

shows the exophytic polypoid tumor of the anterior commissure in the center with the stumps of the left and right vocal cords, which are clear of the tumor (Fig. 10.147). The tumor appears to be arising from the superior surface of the anterior commissure and the true vocal cords.

Postoperatively, the tracheostomy tube is retained until the keel is removed. Clear liquids and a soft diet are permitted approximately 48 hours after surgery. If satisfactory healing is observed by fiberoptic laryngoscopy, then the keel is removed at approximately 3 to 4 weeks. Under local anesthesia, the center of the incision is reopened. The nylon suture anchored to the keel is followed up to the keel by blunt dissection with a hemostat. A gentle pull on the nylon suture dislodges the keel, which is delivered outside. The skin incision is then closed in two layers. Alternatively, if the nylon suture is not used, the keel may be removed endoscopically. A postoperative view of the reconstructed larynx 6 months following resection of the anterior commissure is seen during quiet breathing in Fig. 10.148. Although the anteroposterior dimension of the glottis is foreshortened, the airway is quite adequate. During phonation, satisfactory adduction of the vocal cords is seen with a well-constructed anterior commissure (Fig. 10.149). The quality of

Figure 10.148 An endoscopic view of the larynx during breathing, 6 months after surgery.

Figure 10.149 An endoscopic view of the larynx during phonation.

voice in this patient is quite good. The use of the laryngeal keel prevented formation of an anterior web between the vocal cords.

Supracricoid Subtotal Laryngectomy With Cricohyoidoepiglottopexy

Invasive carcinomas of the true vocal cord, which extend across the midline through the anterior commissure to the opposite vocal cord, sometimes are not suitable for a conventional anterolateral vertical partial laryngectomy. These tumors are best managed by a conservation surgical procedure that comprehensively removes the entire glottic region on both sides in a monobloc fashion. The surgical procedure encompasses the entire thyroid cartilage bilaterally along with both true vocal cords and both false vocal cords and may include one arytenoid. The patient whose endoscopic photograph of the larynx is shown in Fig. 10.150 had received external irradiation as definitive treatment for invasive carcinoma of the glottic larynx involving both vocal cords. Both vocal cords were mobile, although minimal subglottic disease was appreciated on the left-hand side and in the anterior midline. The extent of the patient's recurrent cancer could be encompassed easily with a supracricoid subtotal laryngectomy with a cricohyoidoepiglottopexy (CHEP). If, however, the laryngeal tumor extends to involve the infrahyoid portion of the epiglottis or false vocal cords, then the epiglottis cannot be preserved and the operation required is a supracricoid subtotal laryngectomy with a cricohyoidopexy (CHP).

The operative procedure is performed under general endotracheal anesthesia. Detailed endoscopic evaluation is performed to assess the feasibility of the operation. A transverse incision is placed at the level of the cricothyroid membrane, and the skin incision is deepened through the platysma (Fig. 10.151). Upper and lower skin flaps are elevated deep to the platysma

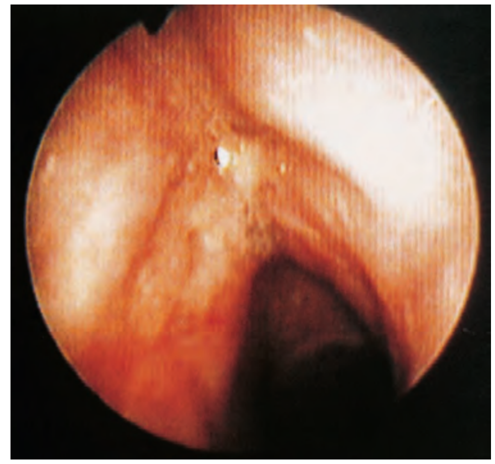

Figure 10.150 The endoscopic appearance of a recurrent carcinoma involving both vocal cords following radiotherapy.

Figure 10.151 A transverse incision is made at the level of the cricothyroid membrane.

to expose the strap muscles in the midline. The upper skin flap is elevated to expose the hyoid bone and the lower skin flap is elevated to expose the isthmus of the thyroid gland and the proximal trachea (Fig. 10.152). The midline fascia is incised and the strap muscles are retracted laterally to expose the thyroid cartilage and the cricoid cartilage (Fig. 10.153). The isthmus of the thyroid gland is divided in the midline to expose the proximal trachea, and a low tracheostomy through the third or fourth tracheal ring is performed in the operative field. The orotracheal tube is removed, and anesthesia is switched over to an endotracheal tube through the tracheostomy. The sternohyoid muscles on both sides are detached from the hyoid and are retracted laterally (Fig. 10.154).

Sharp double hooks are used to retract the thyroid cartilage to the patient's right-hand side to expose the posterior edge of the left thyroid lamina (Fig. 10.155). The inferior constrictor muscle along the oblique line of the thyroid cartilage is transected all the way up to the superior horn of the thyroid cartilage. A similar procedure is repeated on the opposite side. The superior laryngeal neurovascular pedicle is identified and the superior laryngeal artery and vein are divided and ligated, carefully preserving the superior laryngeal nerve (Fig. 10.156). The cricothyroid muscles are then carefully transected anteriorly to

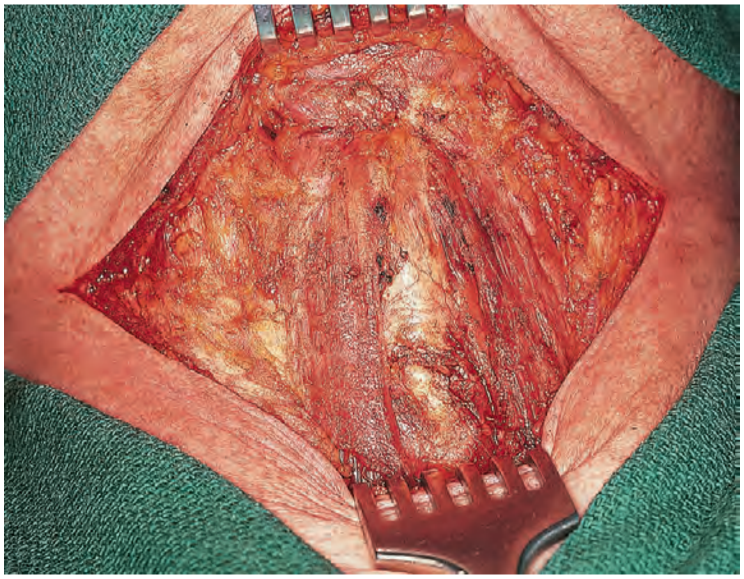

Figure 10.152 Upper and lower skin flaps are elevated.

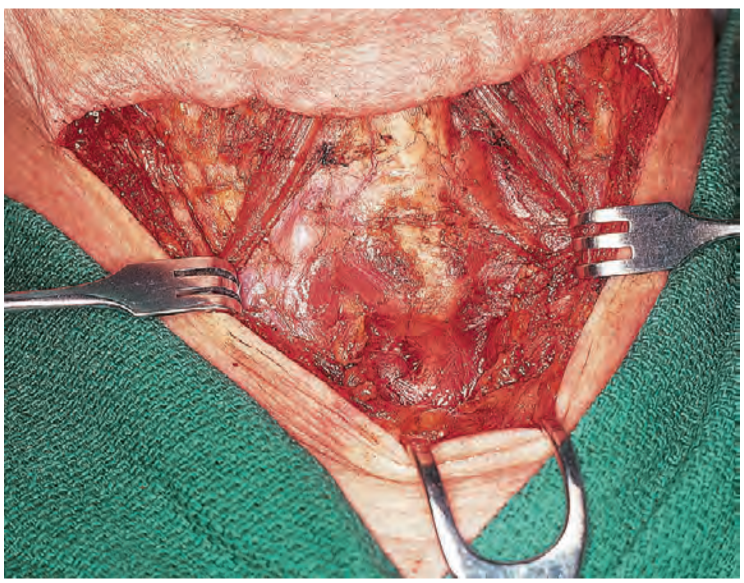

Figure 10.153 The strap muscles are separated in the midline and retracted laterally.

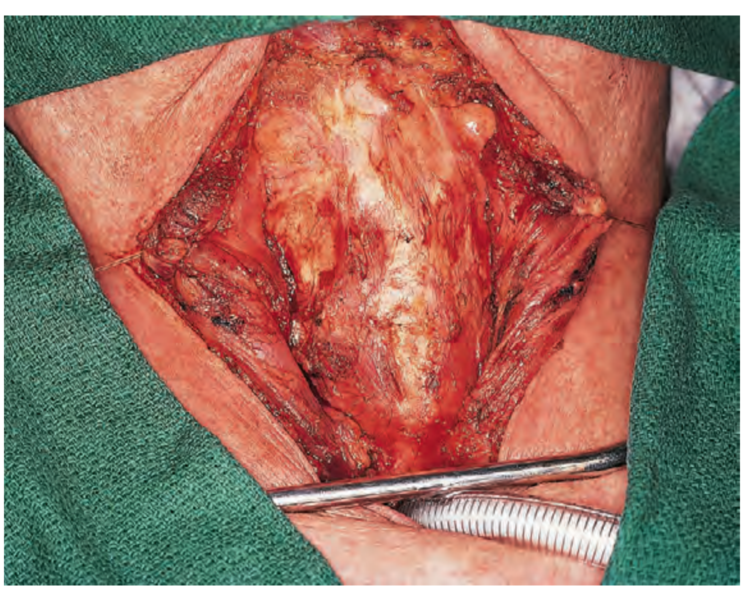

Figure 10.154 The isthmus of the thyroid gland is divided, and a low tracheostomy is performed.

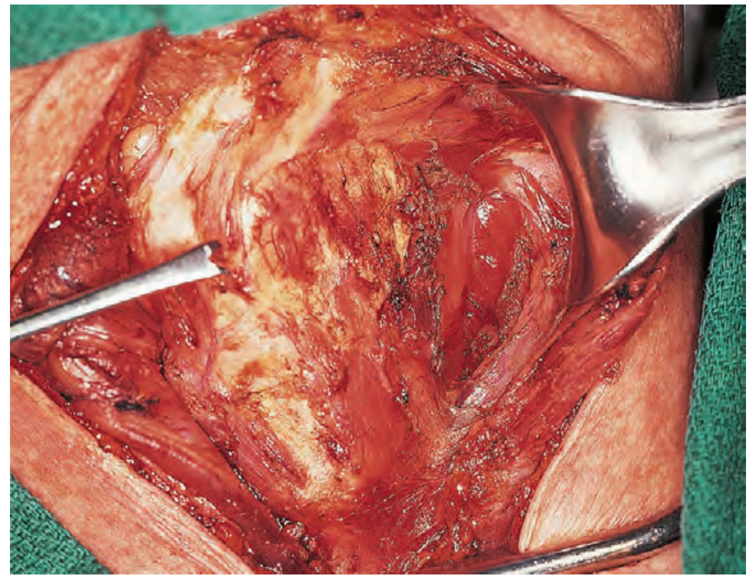

Figure 10.155 The inferior constrictor muscle on the left side is detached from the thyroid cartilage.

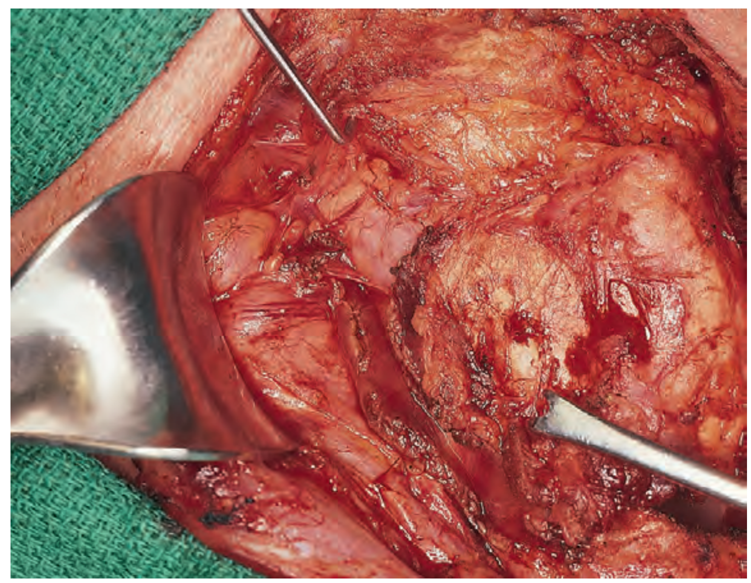

Figure 10.156 The superior laryngeal artery and vein are divided, but the nerve is preserved.

expose the cricothyroid membrane, which is incised to gain entry into the subglottic region of the larynx (Fig. 10.157). The entire thyroid cartilage is removed, including its superior horns, but the inferior horns are preserved to protect the recurrent laryngeal nerves (Fig. 10.158). The inferior cornu of the thyroid cartilage is transected on the side opposite the tumor to avoid injury to the recurrent laryngeal nerve during excision of the thyroid cartilage. On the other hand, the inferior cornu on the side of the bulkier component of the tumor is disarticulated to allow the paraglottic space to be completely removed. The mucosa of the subglottic region may be elevated on the more involved side to obtain a wider margin.

The thyrohyoid membrane is incised next and divided to gain entry into the supraglottic region. The epiglottis is transected at its base near the petiole. The larynx is thus entered into just superior to the false vocal cords (Fig. 10.159). Under direct vision a mucosal incision now is placed just anterior to the arytenoid, preserving the vocal process. This incision is continued inferiorly up to the superior border of the cricoid cartilage. The mucosal incision is shown on the model in Fig. 10.160. The lateral

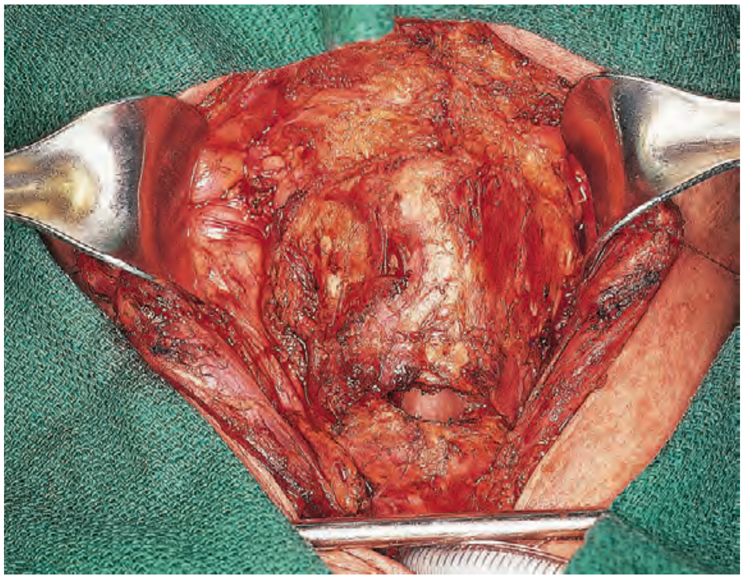

Figure 10.157 The cricothyroid muscle is divided to gain entry into the larynx through the cricothyroid membrane.

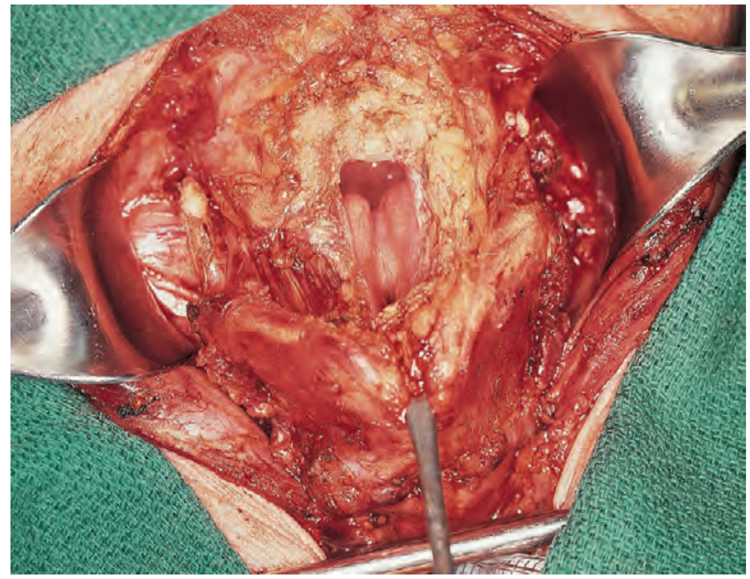

Figure 10.159 The epiglottis is divided above the false vocal cords to gain entry into the supraglottic region.

Figure 10.158 Cartilage cuts shown on a model to demonstrate that the superior laryngeal vascular pedicle is divided, protecting the nerve.

Figure 10.160 Mucosal incisions are made to excise the entire thyroid cartilage, preserving its inferior horns and the cricoid cartilage.

cricoarytenoid muscle can be spared on the side opposite to the tumor to retain anterior motion of the remaining arytenoid. On the dominant side, a mucosal incision may be made directly over the arytenoid, conserving the posterior mucosa. Both these vertical incisions are then carried anteriorly to meet with the incision in the cricothyroid membrane by a right-angled turn from the medial to the lateral aspect of the incision. In this patient, however, the tumor involved only the anterior two-thirds of both the vocal cords, and therefore both arytenoids could be preserved (Fig. 10.161). The mucosal incisions are then connected and a full-thickness resection of the entire thyroid cartilage with the glottic larynx is performed in a monobloc fashion. The surgical field following removal of the specimen is shown in Fig. 10.162. At this juncture, the pyriform sinuses should be checked to ensure that no accidental perforations are present. The redundant mucosa overlying the arytenoid is used to cover the denuded cricoid cartilage, particularly on the side of arytenoid resection if such a resection is performed. Frozen sections are obtained from the margins of the surgical defect to ensure the adequacy of the resection.

Repair of the surgical defect is simple. The larynx is closed with three No. 0 Vicryl sutures. These stitches encircle the cricoid and traverse through the preepiglottic space encircling the hyoid bone. An anterior midline suture is placed, and one lateral suture on each side is applied (Fig. 10.163). Attention should be given to carefully avoiding the lateral sutures encircling the superior laryngeal nerves. Once these sutures are tied, the cricoid comes into contact with the hyoid (Fig. 10.164). The tracheostomy site has automatically moved cephalad as a result of this closure. The strap muscles are reapproximated in the midline and to the

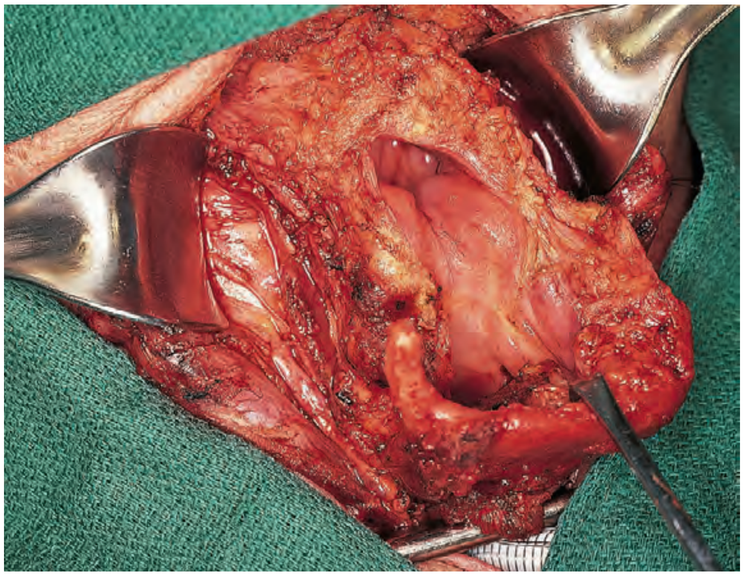

Figure 10.161 Mucosal incisions are made anterior to the arytenoids up to the cricothyroid membrane.

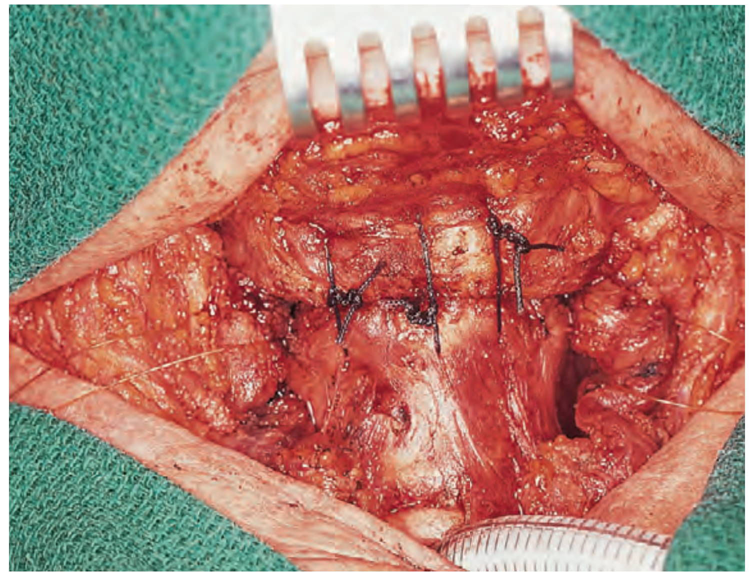

Figure 10.164 The cricohyoidoepiglottopexy is completed.

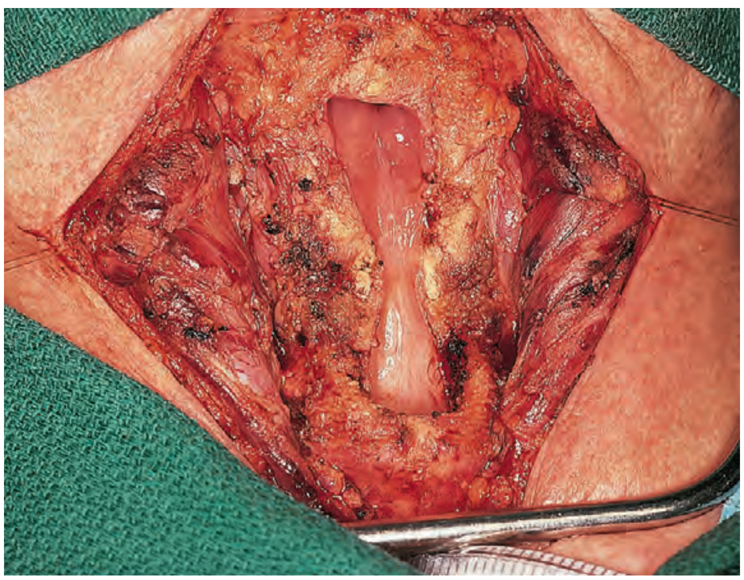

Figure 10.162 The surgical defect after removal of the tumor.

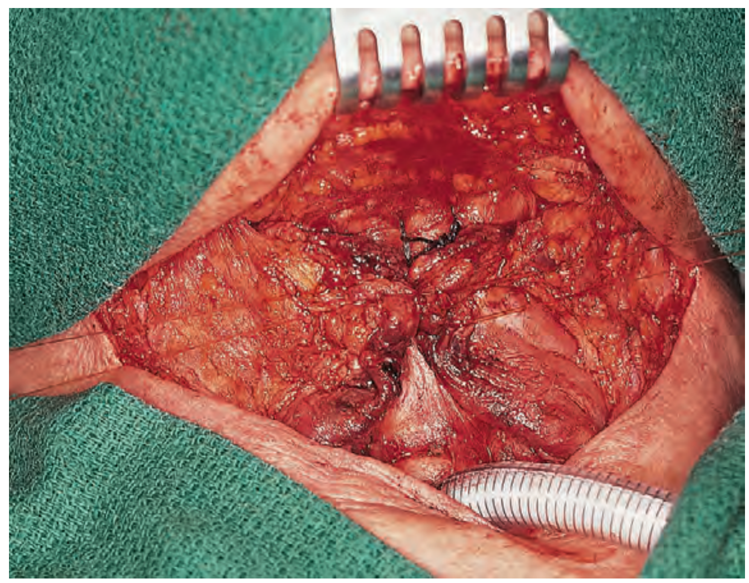

Figure 10.165 The strap muscles are reapproximated in the midline.

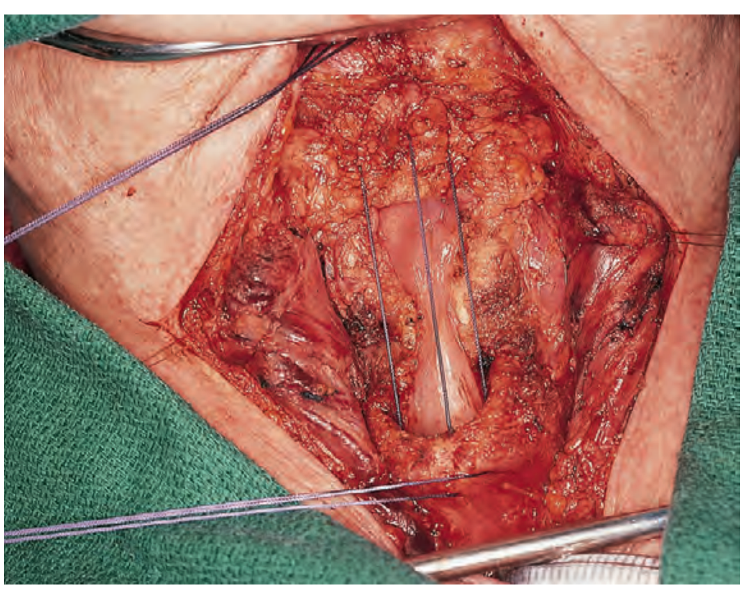

Figure 10.163 Closure is performed with three Vicryl sutures between the hyoid and the cricoid.

hyoid bone (Fig. 10.165). The tracheostomy is now switched over through a separate incision through the lower skin flap to isolate the tracheostomy wound from the operative incision (Fig. 10.166). The remaining incision is closed in two layers with a small Penrose drain in the subcutaneous plane.

An external view of the surgical specimen shows complete excision of the entire thyroid cartilage in a monobloc fashion (Fig. 10.167). The posterior view of the surgical specimen with the vocal cords retracted shows complete monobloc excision of the glottic carcinoma invading both vocal cords with subglottic extension. The entire paraglottic space on both sides is resected in a monobloc fashion with adequate superior and inferior mucosal and soft tissue margins (Fig. 10.168).

Postoperative care of the patient requires the use of a nasogastric feeding tube to maintain nutrition. The tracheostomy is retained to facilitate clearance of pulmonary secretions until the patient is able to manage his or her own saliva and secretions. Once the patient is able to breathe through the natural passages, the tracheostomy tube is plugged. If the patient can tolerate having the tracheostomy tube plugged without any respiratory

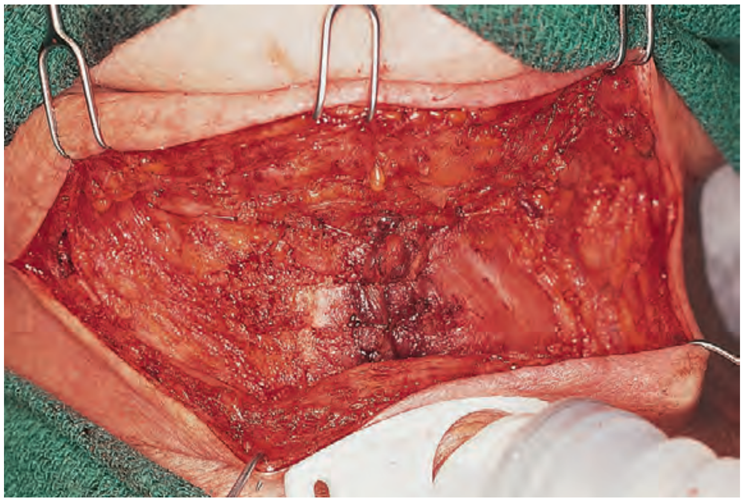

Figure 10.166 The tracheostomy is transferred to a separate incision in the lower neck.

Figure 10.167 The anterior view of the surgical specimen.

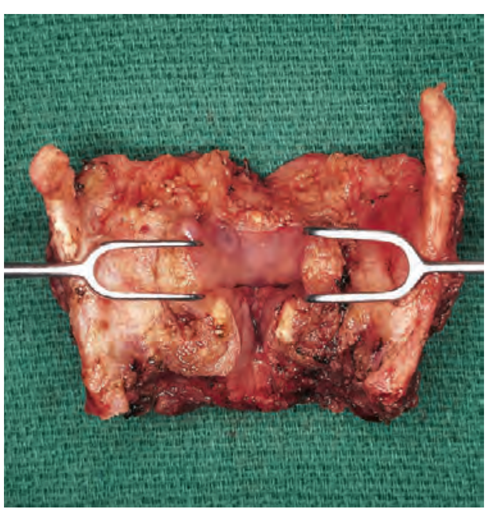

Figure 10.168 The posterior view of the surgical specimen.

difficulties, the tube is removed. Oral alimentation is begun once the patient is able to swallow his or her saliva without aspiration. Usually within 3 to 4 weeks, the patient is able to tolerate a soft diet. During the next few weeks, the patient is able to advance to a regular diet and all types of fluids.

A postoperative endoscopic view of the reconstructed larynx during quiet breathing is shown in Fig. 10.169. Note that the

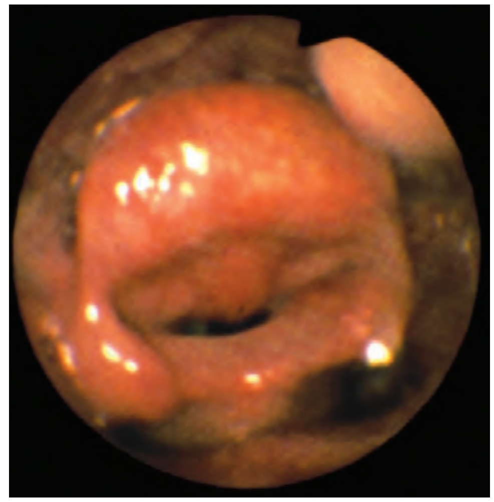

Figure 10.169 A postoperative endoscopic view of the larynx during breathing.

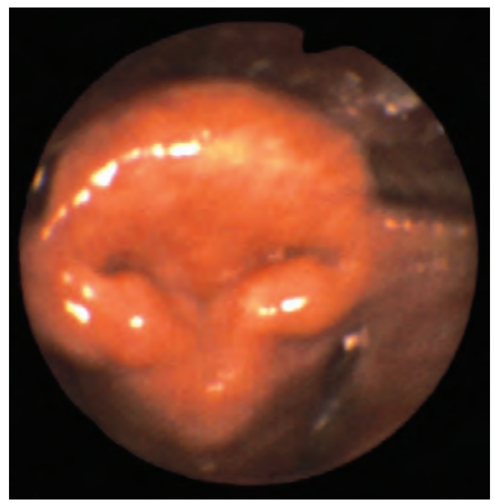

Figure 10.170 A postoperative endoscopic view of the larynx during phonation.

laryngeal airway is now transversely oriented. During phonation, the arytenoids adduct, permitting closure of the airway to produce sound and prevent aspiration (Fig. 10.170). A supracricoid subtotal laryngectomy with a cricohyoidoepiglottopexy is an oncologically sound surgical procedure permitting monobloc resection of the entire glottic larynx for lesions that involve both vocal cords and manifest paraglottic extension.

Open Conservation Surgery for Supraglottic Cancer

Primary tumors of the supraglottic larynx produce minimal symptoms initially such as soreness or a sensation of discomfort in the throat. Changes in the quality of voice are late to occur and result from extension of the tumor to the glottic larynx. Bulky supraglottic tumors may cause stridor due to respiratory obstruction, or occasionally they may cause difficulty in swallowing. Most early staged (T1 and T2) lesions are suitable for endoscopic laser resection. However, patients who have trismus, projecting teeth, inadequate mouth opening, or cervical spine disease with fixed deformity whose neck cannot be extended are not suitable candidates for endoscopic laser resection. External irradiation as definitive treatment for a supraglottic lesion is not as successful as for early lesions of the vocal cords. Radiation portals by necessity are large, resulting in postirradiation dryness, which is a somewhat disabling sequela of treatment. Follow-up

1. At least 5 mm margin at anterior commissure.
2. True vocal cords must be mobile.
3. Only one arytenoid may be removed.
4. No cartilage invasion by tumor.
5. Tongue mobility should be normal.
6. No extension to interarytenoid or post-cricoid area.
7. Apex of pyriform sinus should be free.
8. Generally, lesions < 3 cm.

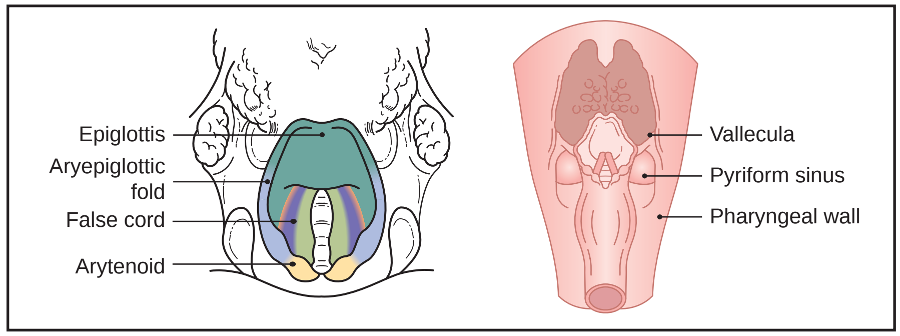

Figure 10.171 Criteria for the selection of a lesion suitable for a supraglottic partial laryngectomy.

evaluation of the larynx in some patients is difficult because of persistent laryngeal edema.

On the other hand, surgical treatment of tumors of the supraglottic larynx creates a significant physiologic disturbance in the act of deglutition. Almost every patient aspirates to a varying degree after a supraglottic partial laryngectomy. Most patients, however, handle this physiologic disturbance with little difficulty and are able to tolerate most types of foods without significant pulmonary complications. Aspiration of saliva to a varying degree is almost uniform but is tolerated well within the pulmonary reserve of most patients. Patients with poor pulmonary functions, those with an advanced degree of emphysema, and those of advanced age are poor candidates for a supraglottic partial laryngectomy. Likewise, patients who are poorly motivated and unable to understand the complexity of their problem and the rigorous efforts necessary for postoperative recovery are not ideal candidates for this surgical procedure. Patient participation and effort are essential in rehabilitation after a supraglottic partial laryngectomy for a successful outcome.

Several criteria related to tumor factors must be met by patients who otherwise are considered suitable candidates for a supraglottic partial laryngectomy. These criteria are described in Fig. 10.171. Although these criteria provide good general guidelines regarding the selection of patients whose tumors are suitable for a supraglottic partial laryngectomy, the indications for the operation expand as the experience of the surgeon performing the operation increases. A supraglottic partial laryngectomy also may be necessary for surgical treatment of highly selected patients with primary tumors of the base of the tongue with secondary extension to the supraglottic larynx and tumors of the pyriform sinus involving its medial wall.

Supraglottic (Horizontal) Partial Laryngectomy

The operative procedure described here is in a patient with a primary squamous cell carcinoma of the aryepiglottic fold. An endoscopic view of the supraglottic larynx shows the tumor arising from the tip of the epiglottis with extension to the left aryepiglottic fold, with the glottis open during quiet breathing (Fig. 10.172). During phonation, however, as shown in Fig. 10.173, the glottis closes well and brings into view both vocal cords, which are clear of tumor and maintain normal mobility. The lower extent of the tumor on the laryngeal surface of the epiglottis is better appreciated during phonation.

An axial view of the CT scan of the larynx at the level of the suprahyoid region shows that the tumor involves the entire thickness of the epiglottis with infiltration of its cartilage (Fig. 10.174).

As mentioned earlier in this chapter, endoscopic evaluation of the lesion immediately prior to surgery is mandatory for an

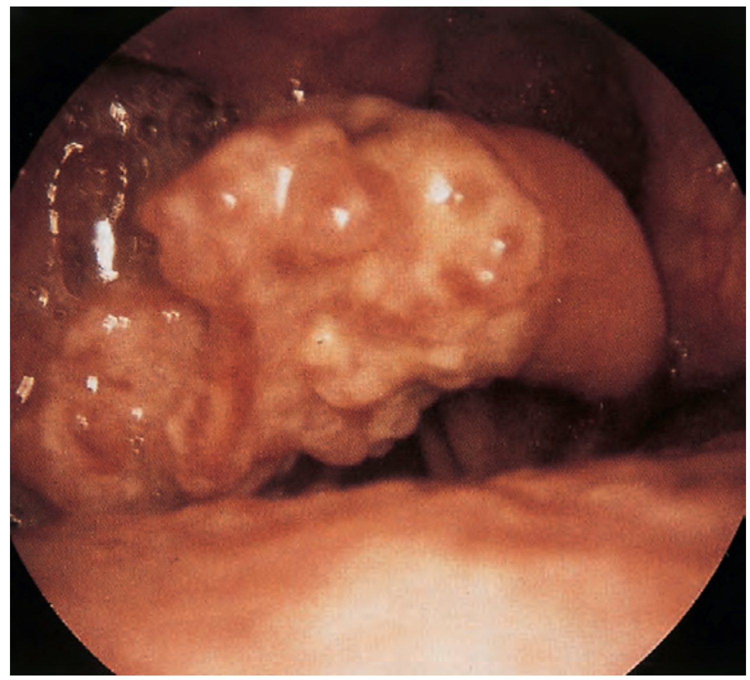

Figure 10.172 A telescopic view of the supraglottic larynx during breathing.

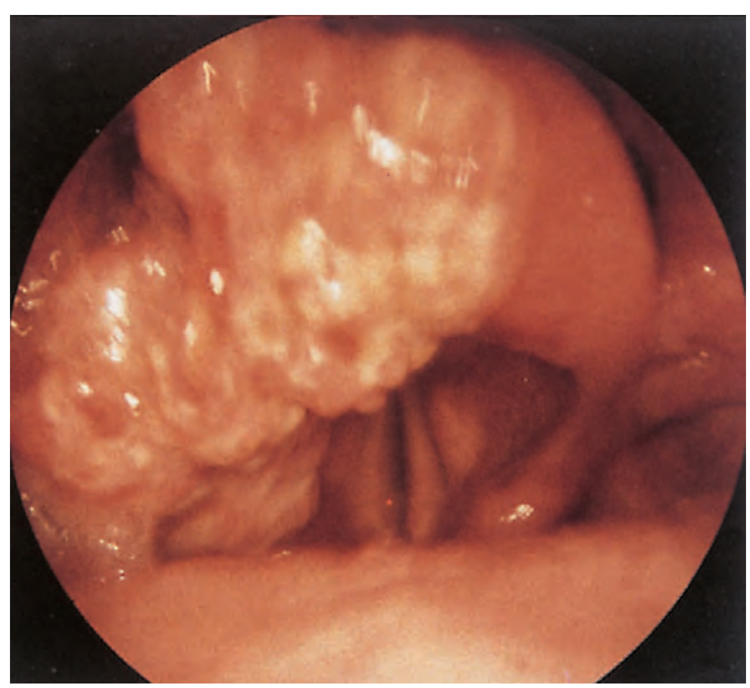

Figure 10.173 A telescopic view of the larynx of the patient from Fig. 10.172 during phonation.

accurate assessment of the extent of the lesion. A preliminary tracheostomy is performed under local anesthesia and an endotracheal tube is introduced into the distal trachea. After adequate relaxation is obtained under general anesthesia, endoscopy is performed to examine the tumor and its extensions to various sites within the larynx and adjacent regions. The skin of the neck is then prepared with antiseptic solution and isolated with sterile drapes. The surface markings of the hyoid bone and the thyroid notch are shown (Fig. 10.175). The skin incision is taken through an upper neck skin crease at the level of the thyrohyoid membrane as shown by the dotted line extending from the anterior border of the sternomastoid muscle on one side to the anterior border of the sternomastoid muscle on the other side. The skin incision is deepened through the platysma to expose the strap muscles (Fig. 10.176). The upper skin flap is elevated to expose the hyoid bone and the attachments of the suprahyoid muscles (Fig. 10.177). The lower skin flap is sufficiently elevated to expose the thyroid cartilage. Elevation of the skin flaps to this extent exposes the medial aspect of the carotid sheath on both sides.

Attention is now focused on the region of the thyrohyoid membrane. The strap muscles are detached from the hyoid bone on both sides to expose the thyrohyoid membrane (Fig. 10.178). The stumps of the strap muscles are tagged with a

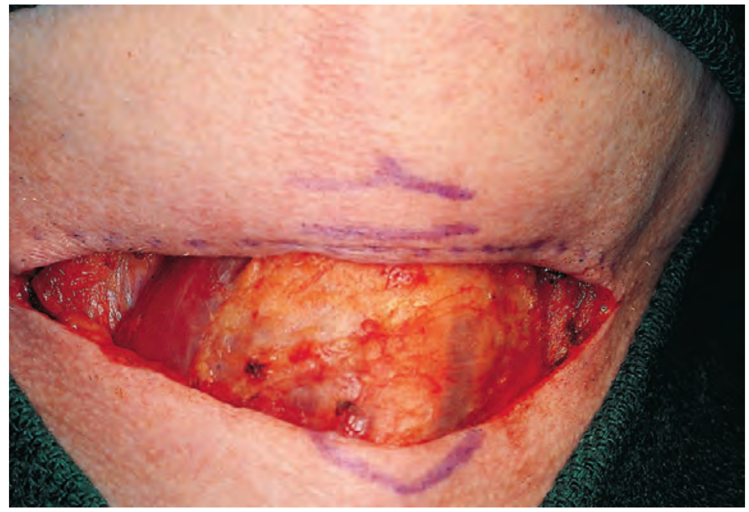

Figure 10.176 The skin incision is deepened through the platysma.

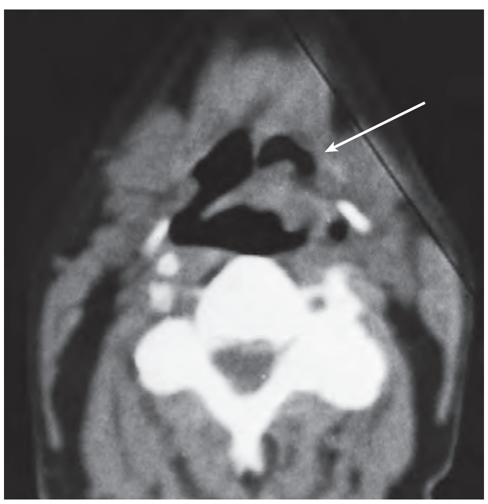

Figure 10.174 A computed tomography scan of the larynx showing a tumor of the left aryepiglottic fold (*arrow*).

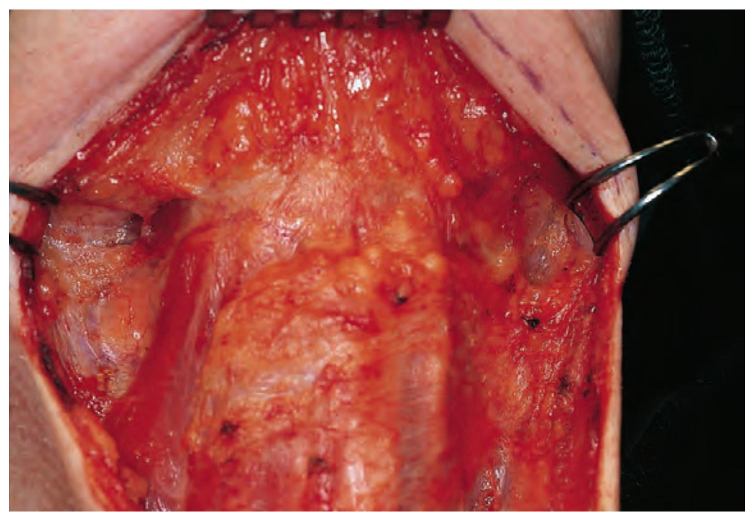

Figure 10.177 The upper and lower skin flaps are elevated.

Figure 10.175 Surface markings of the hyoid bone and the thyroid notch with the incision outlined.

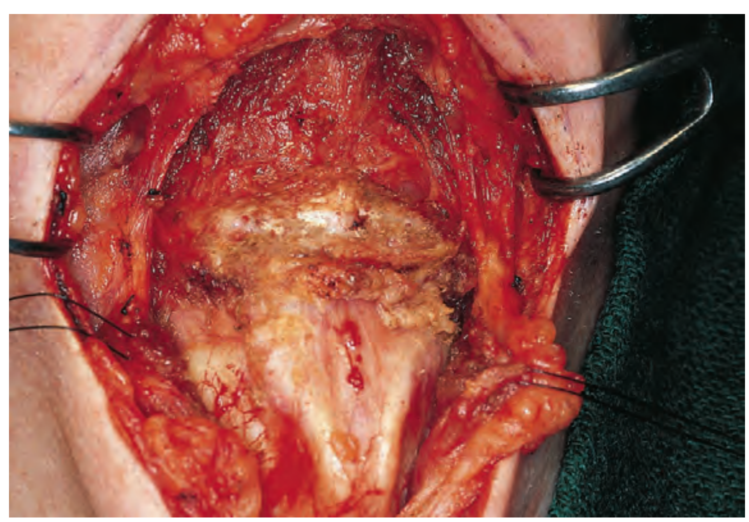

Figure 10.178 The strap muscles are detached from the hyoid bone.

chromic catgut suture and retracted laterally, exposing the thyrohyoid membrane and the upper border of the thyroid cartilage. In Fig. 10.179, two hemostats are used to demonstrate the vertical height of the thyroid cartilage. One hemostat is placed at the thyroid notch and the other at the cricothyroid membrane. The anterior commissure is located exactly at the midpoint of the vertical height of the anterior midline of the thyroid cartilage. Excision of the upper third of the ala of the cartilage on each side therefore can be performed safely without risk of inadvertent injury to the anterior commissure. An incision in the perichondrium of the thyroid cartilage is made along the proposed line of division of the thyroid cartilage with an electrocautery, using a needle tip. Note that while the incision is progressing posteriorly, it curves cephalad to reach the superior border of the thyroid cartilage (Fig. 10.180).

The suprahyoid muscles are detached from the upper border of the central third of the hyoid bone to denude it completely. The detachment of the suprahyoid muscles extends laterally over the hyoid bone up to the lesser cornua on each side. The central third of the hyoid bone will be resected to accomplish a monobloc excision of the preepiglottic space. Therefore, using an electrocautery, the proposed line of division of the hyoid bone is marked out, remaining just lateral to the lesser cornua on each side, as shown in the model (Fig. 10.181).

If the primary tumor of the supraglottic larynx extends well posteriorly along the aryepiglottic fold up to the arytenoids, then the resection of the hyoid bone on that side should be taken further posteriorly, even up to and including the whole greater cornua if indicated (Fig. 10.182). In that setting, the ipsilateral superior laryngeal nerve is sacrificed, resulting in a somewhat increased postoperative morbidity because of aspiration. In this patient the lesion is relatively central and therefore both superior laryngeal nerves can be spared. It is important to reiterate that the superior laryngeal nerves enter the larynx through the thyrohyoid membrane at an angle. The course of the superior laryngeal nerve extends from the superior aspect of the carotid sheath running medially and caudad to enter the thyrohyoid membrane.

Before division of the thyroid cartilage, multiple drill holes are made near the upper border of the thyroid cartilage that will remain in the larynx (Fig. 10.183). A right-angled drill with a very fine drill bit is best suited for this procedure. Approximately four to five drill holes are made on each side of the midline (Fig. 10.184). The holes are used for resuspension of the remaining larynx to the base of the tongue to restore the anatomic and physiologic relationship of the base of the tongue to the larynx. A right-angled saw is used next to divide the

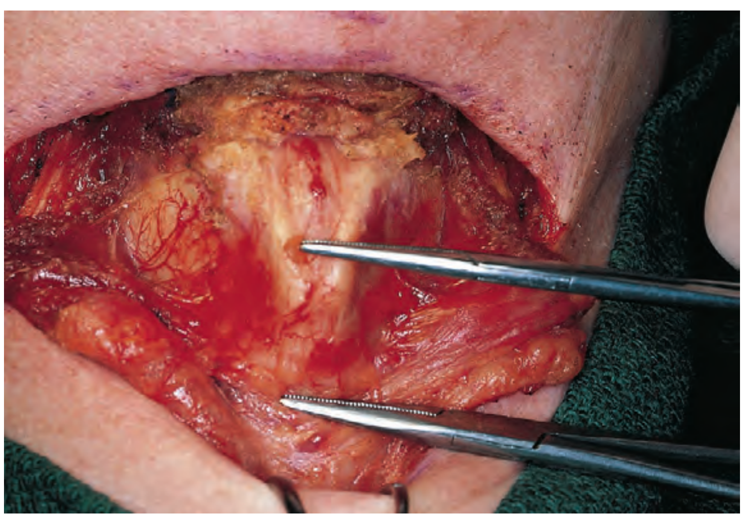

Figure 10.179 Hemostats are used to demonstrate the vertical height of the thyroid cartilage.

Figure 10.181 The line of transection of the thyroid cartilage and hyoid bone are shown on the model.

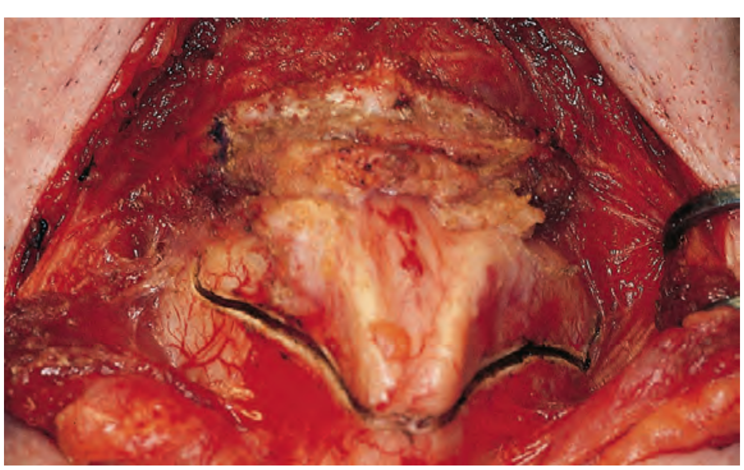

Figure 10.180 The incision in the thyroid cartilage curves cephalad to reach the superior border of the thyroid cartilage.

Figure 10.182 On the side of invasion of the aryepiglottic fold, the hyoid bone may be excised up to its posterior border.

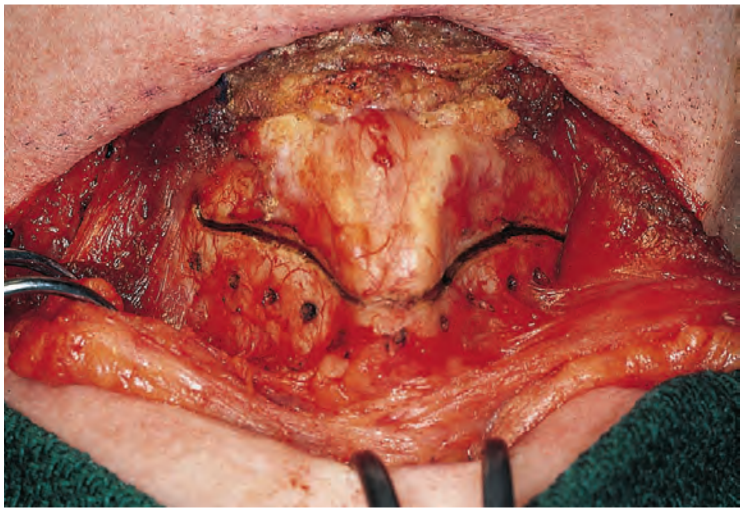

Figure 10.183 Drill holes on each side of the midline on the remaining thyroid cartilage are marked.

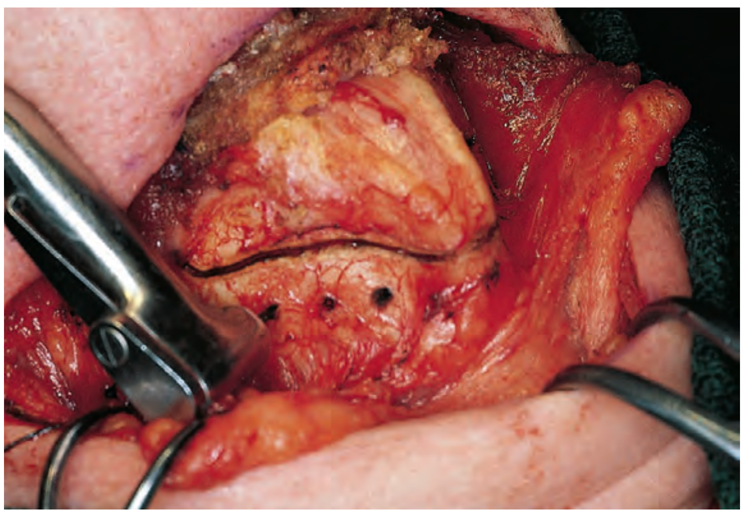

Figure 10.184 Multiple drill holes are made for resuspension of the larynx.

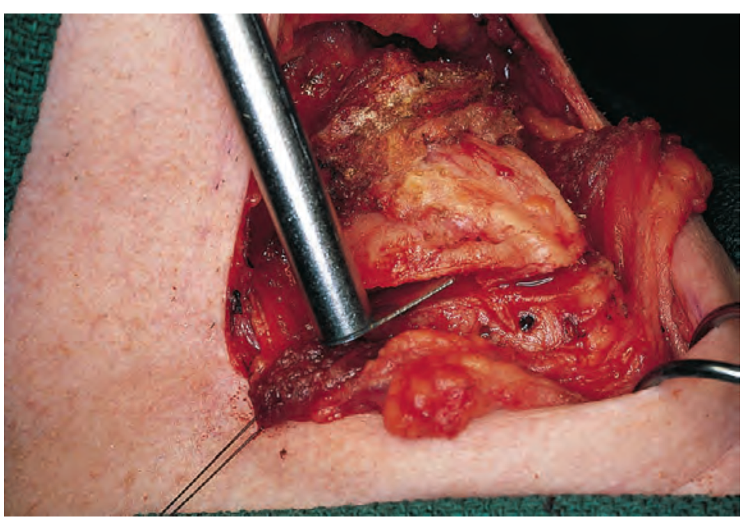

Figure 10.185 Division of the thyroid cartilage with a saw.

thyroid cartilage through the proposed line of transection (Fig. 10.185). Extreme care should be taken so that only the cartilage is divided and the internal soft tissues and mucosa are not lacerated. As soon as the thyroid cartilage is divided, a give is felt and the sawing should then cease.

After division of the thyroid cartilage on both sides is completed, a bone cutter is used to divide the hyoid bone through the previously marked sites of division (Fig. 10.186). Division of the framework of the larynx to excise the surgical specimen is now complete. Note that up to this point division of the hyoid bone and thyroid cartilage is done without having the tumor under direct vision. Accurate preoperative endoscopic assessment of the extent of the tumor is therefore essential before surgery begins.

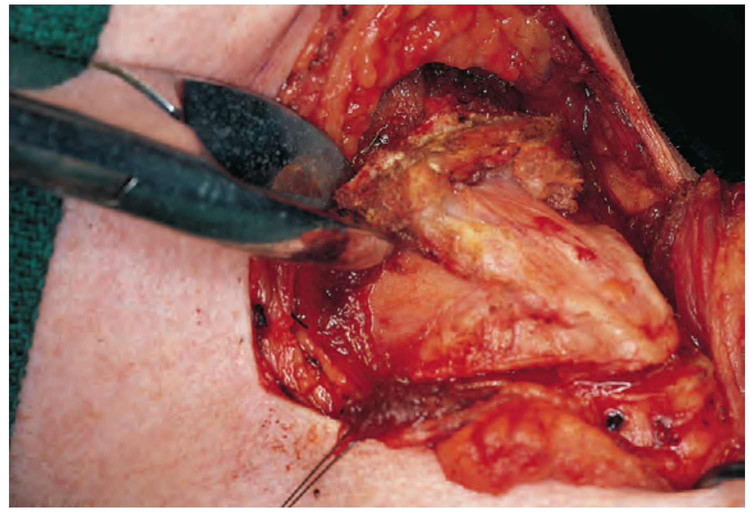

Figure 10.186 Division of the hyoid bone with a bone cutter.

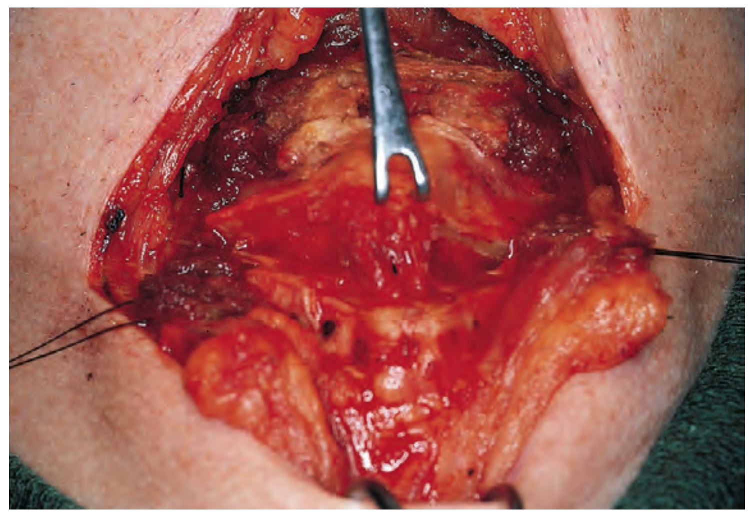

Figure 10.187 The upper part of the thyroid cartilage is retracted cephalad to expose the soft tissues.

Using a right-angled double hook, the divided upper part of the thyroid cartilage is retracted cephalad to put the internal soft tissues on a stretch (Fig. 10.187). An electrocautery with a needle tip is used to incise the intralaryngeal soft tissues and mucosa to gain access to the interior of the larynx (Fig. 10.188). Division of the mucosa of the false vocal cords now continues posteriorly (Fig. 10.189). As the mucosal incision and soft tissue division progress posteriorly with gentle traction, the specimen becomes mobilized cephalad. A right-angled retractor will facilitate gentle traction on the specimen. An Adair clamp also may be used to grasp the divided portion of the central third of the hyoid bone to provide traction. Further division of the thyrohyoid membrane and the soft tissue attachments at the level of the divided hyoid bone continues cephalad on the contralateral side as shown in Fig. 10.190. The plane of transection for supraglottic resection is shown in the model in Fig. 10.191.

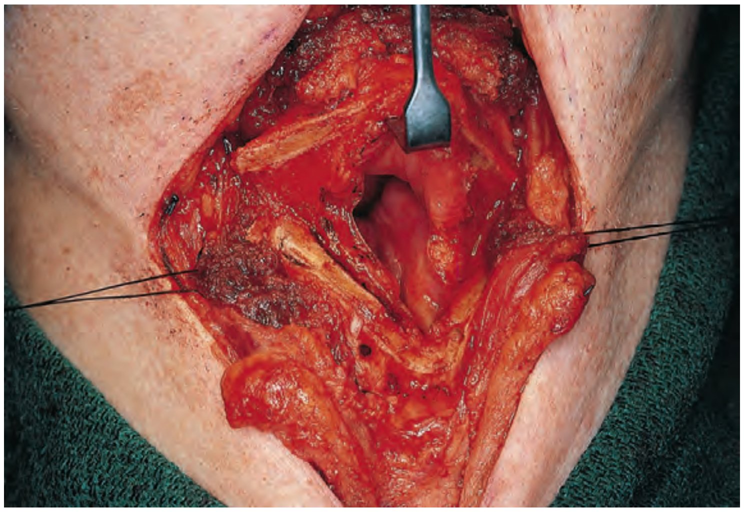

Figure 10.188 The intralaryngeal soft tissues and mucosa are incised to gain entry into the larynx.

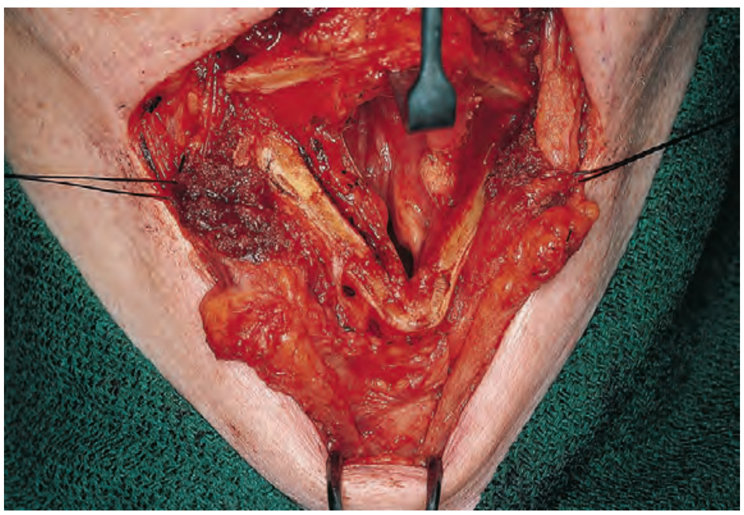

Figure 10.189 Division of the mucosa of the false vocal cords to separate the lower border of the specimen.

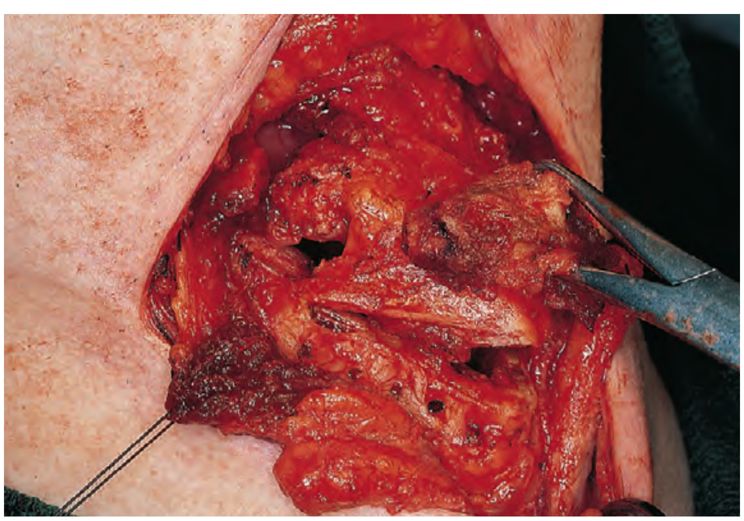

Figure 10.190 The thyrohyoid membrane is divided up to the vallecula.

The oropharynx is entered by dividing the mucosa of the right vallecula. At this point, the mucosal incision through the right false vocal cord is completed by connecting it with the incision in the right vallecula, allowing rotation of the specimen toward the left side (Fig. 10.192). Rotation of the

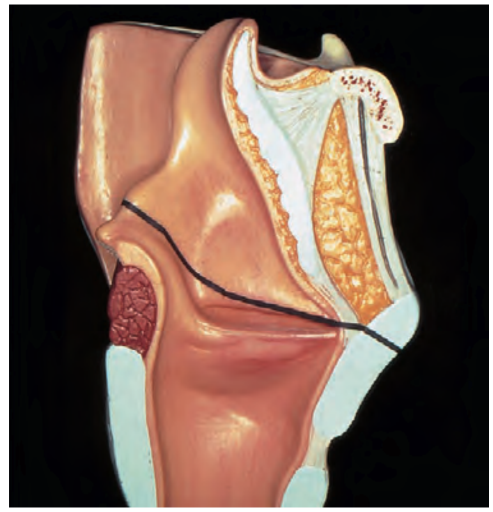

Figure 10.191 A model showing the plane of transection for a supraglottic partial laryngectomy.

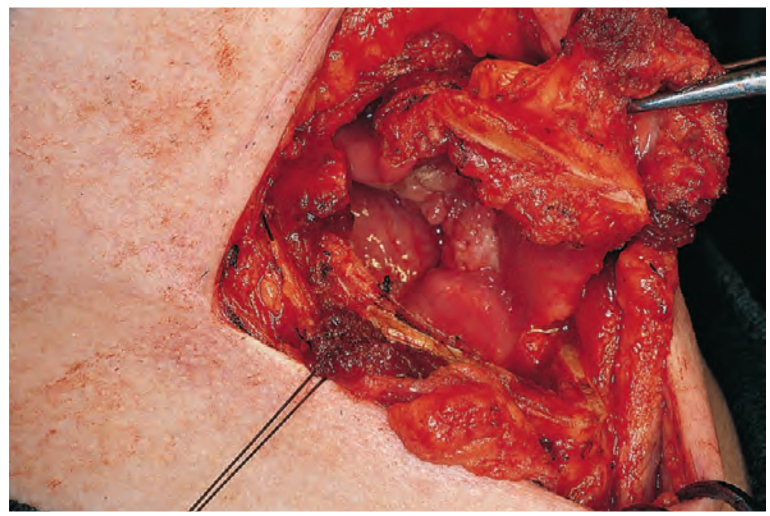

Figure 10.192 A mucosal incision in the vallecula is connected to the mucosal incision on the false vocal cord.

specimen brings the primary tumor into view. A close-up view of the rotated specimen shows the interior of the larynx and the oropharynx, demonstrating the surface extent of the tumor on the laryngeal surface of the epiglottis and the left aryepiglottic fold (Fig. 10.193). A Richardson retractor is now used to retract the base of the tongue cephalad, stretching the glossoepiglottic fold, which facilitates its division toward the left side. This maneuver will free up the tip of the epiglottis, which is now delivered in the wound, aiding further mobilization of the specimen (Fig. 10.194).

Now, under direct vision, an electrocautery with a needle tip is used to place a mucosal incision around the visible tumor with adequate margins on the left side of the larynx. Remaining soft-tissue attachments to the thyrohyoid membrane and the left vallecula are divided, and the surgical specimen is removed. Brisk hemorrhage from branches of the superior laryngeal artery is to be expected during division of the thyrohyoid membrane. These branches are promptly clamped and ligated. The surgical defect following removal of the specimen is shown in Fig. 10.195. The transected false cords on both sides show their superior surfaces, denuded of mucosa, but the mucosa over both arytenoids remains intact. If the larynx is viewed further down by anterior traction on the thyroid cartilage, the true vocal cords

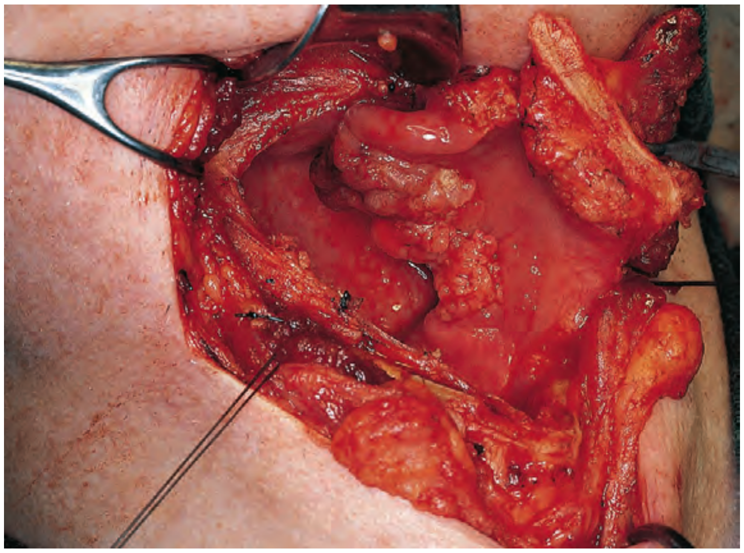

Figure 10.193 A close-up view of the rotated specimen shows the tumor on the left aryepiglottic fold.

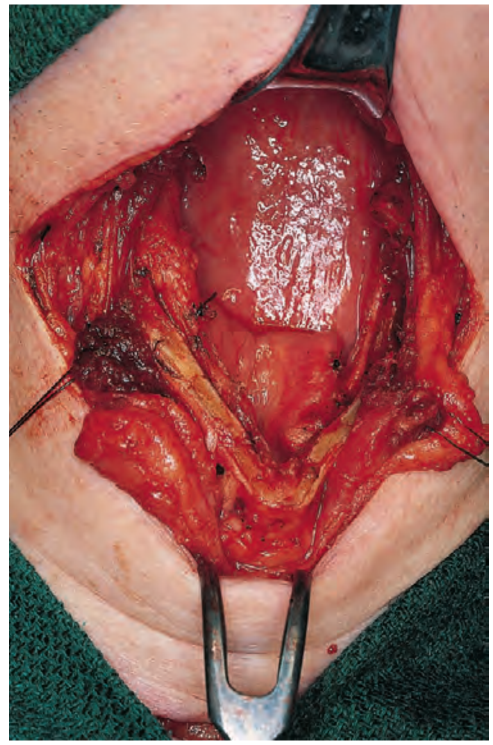

Figure 10.195 The surgical defect showing the arytenoids.

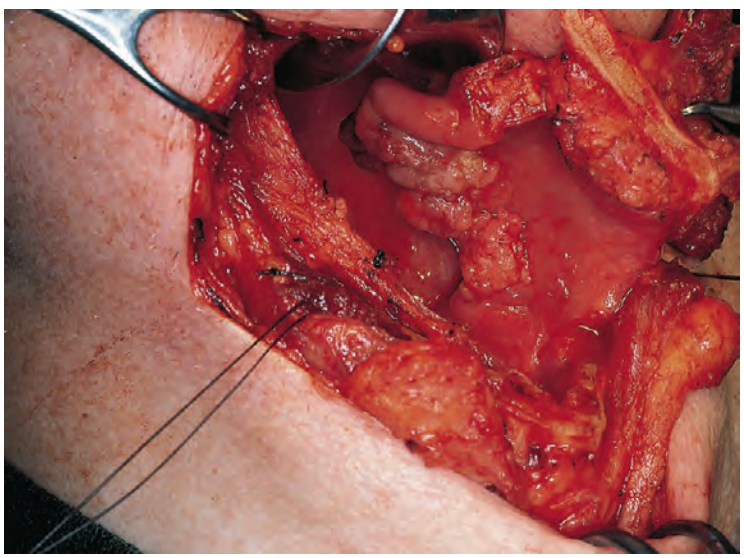

Figure 10.194 The epiglottis is delivered in the wound to facilitate resection of the tumor under vision.

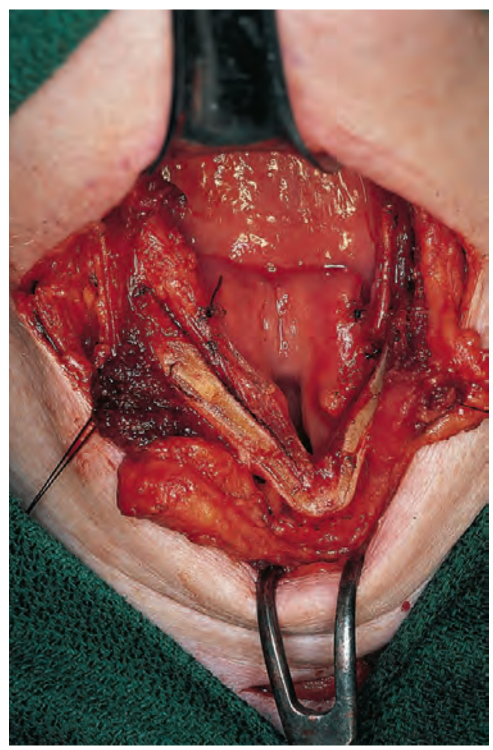

Figure 10.196 The true vocal cords and transected false vocal cords are seen.

become visible (Fig. 10.196). Note that a generous margin of normal mucosa still remains above the vocal cords following removal of the specimen.

Closure of the surgical defect begins by approximation of the mucosal edge of the medial wall of the pyriform sinus to the remaining mucosa of the false vocal cord (Fig. 10.197). Interrupted sutures with 4-0 chromic catgut are taken to approximate these mucosal edges. Coverage of the denuded false cords in their posterior half is easily accomplished, but the anterior half is left open to granulate. The completed suture line of the false cords is shown in Fig. 10.198. A nasogastric feeding tube is now inserted. Mucosal closure of the remainder of the surgical defect is not possible and is unnecessary. The only area where mucosal closure may be attempted is at the lateral edges of the surgical defect near the stumps of the hyoid bone. Perhaps two or three interrupted sutures between the cut edges of the lateral pharyngeal wall may be taken on each side. No attempt is made to approximate the mucosa of the base of the tongue to the mucosa of the larynx.

Closure of the remaining defect is done with No. 0 chromic catgut interrupted sutures beginning at the lower end through the previously drilled holes in the thyroid cartilage (Fig. 10.199). At the upper end, the sutures pass through the musculature of the base of the tongue. Approximating the stumps of the

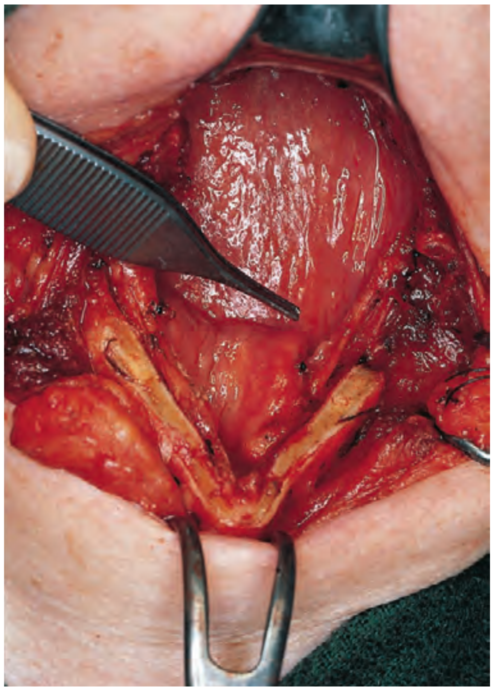

Figure 10.197 The mucosa of the pyriform sinus is sutured to the mucosa of the false vocal cord.

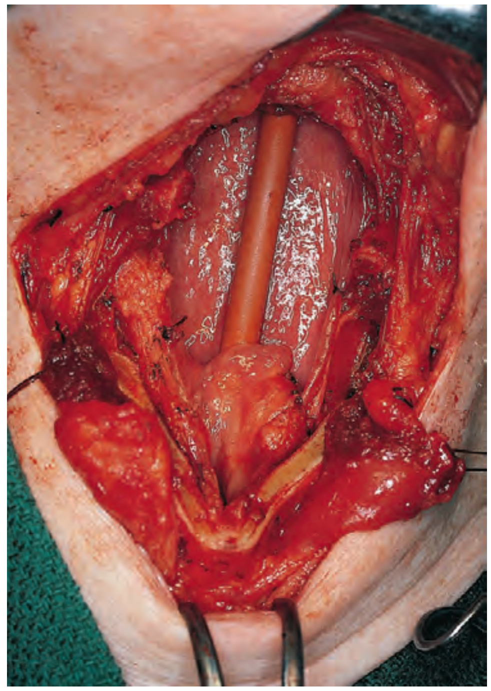

Figure 10.198 The completed suture line of the false cords.

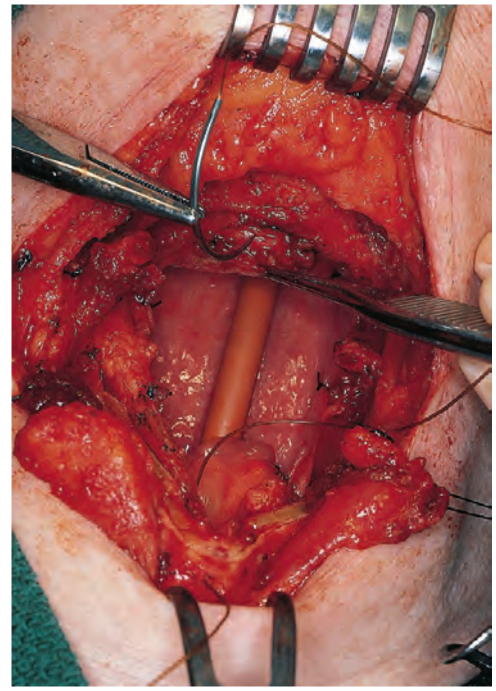

Figure 10.199 A suture between the thyroid cartilage and the muscles of the base of the tongue.

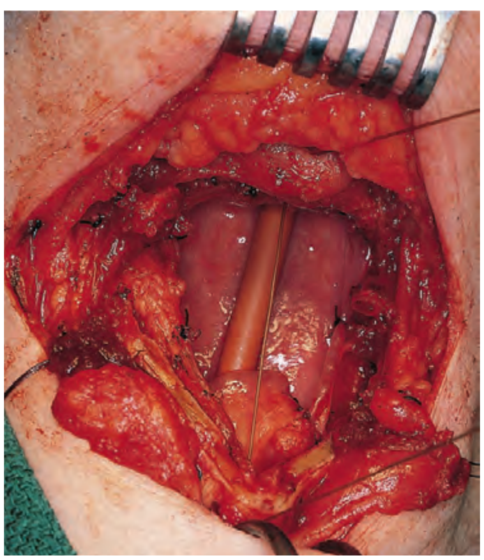

Figure 10.200 A completed suture.

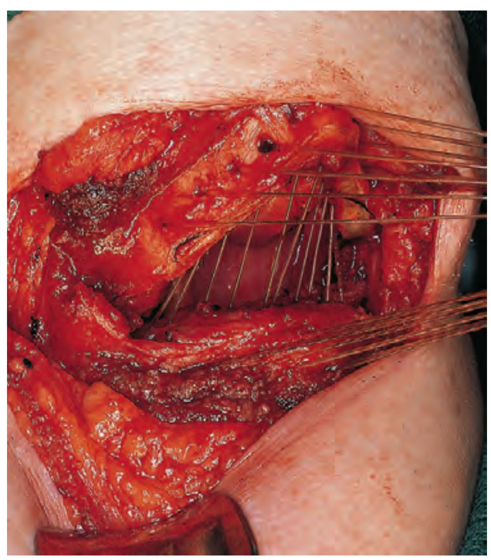

Figure 10.201 All sutures are placed first and then tied sequentially.

Figure 10.202 Completed closure.

musculature of the base of the tongue to the remaining thyroid cartilage produces a shelf of overhanging muscles of the base of the tongue with its covering mucosa on the anterior part of the glottis. This shelf effect provides protection to the glottis during deglutition. Note the completed suture in Fig. 10.200 showing the placement of the suture through the muscles of the base of the tongue.

All sutures are taken in a similar fashion through each of the drill holes in the thyroid cartilage and the base of the tongue. They are not tied at this point but are held long until all of them are placed, and then they are tied sequentially (Fig. 10.201). The interior of the larynx is irrigated once again and hemostasis is reconfirmed. All the suspension sutures held until now are tied, starting from one end to the other. As this closure progresses, the larynx gets reattached to the base of the tongue, restoring its anatomic relationship of suspension from the tongue for satisfactory physiologic function during the act of swallowing.

In Fig. 10.202 all sutures are seen tied in place, with suspension of the larynx to the base of the tongue completed. The sternohyoid and sternothyroid muscles detached from the central third of the hyoid bone are now sutured to the detached mylohyoid muscle with interrupted catgut sutures (Fig. 10.203). This second layer of muscular closure also restores the anatomic attachments of the strap muscles to the base of the tongue at the site of the resected hyoid bone (Fig. 10.204). A Penrose drain inserted in a plane between the strap muscles and the larynx is brought out through one lateral end of the skin incision (Fig. 10.205). A second Penrose drain is placed superficial to the strap muscles but deep to the platysma and is brought out

Figure 10.203 The sternohyoid and sternothyroid muscles are sutured to the detached mylohyoid muscle.

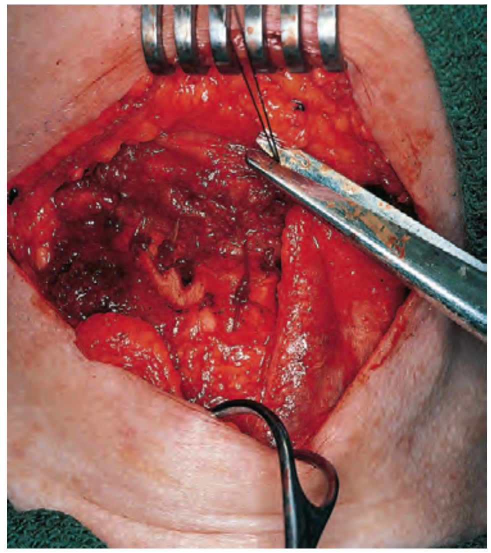

Figure 10.204 The anatomic attachments of the strap muscles are restored to the base of the tongue.

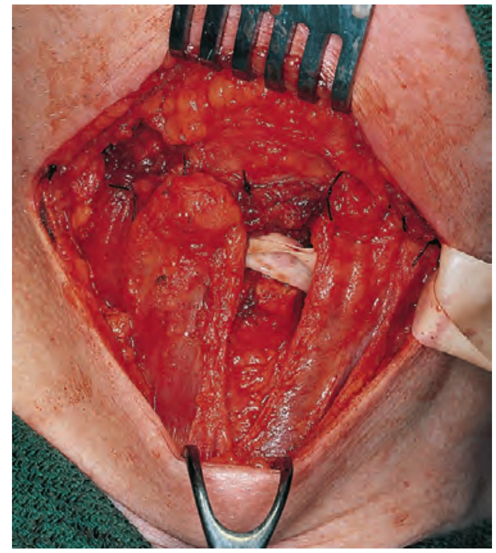

Figure 10.205 A Penrose drain is placed deep to the strap muscles.

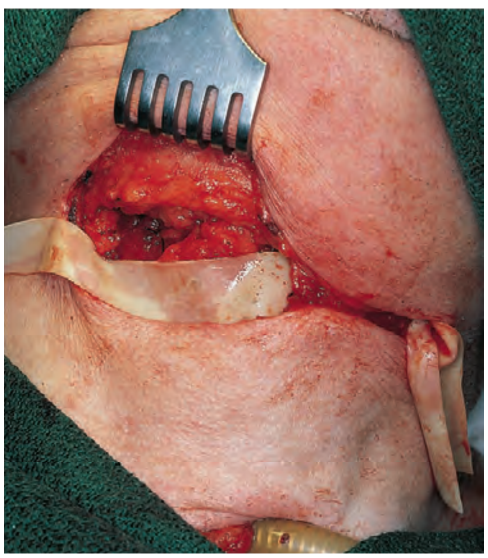

Figure 10.206 A second Penrose drain is placed under the platysma.

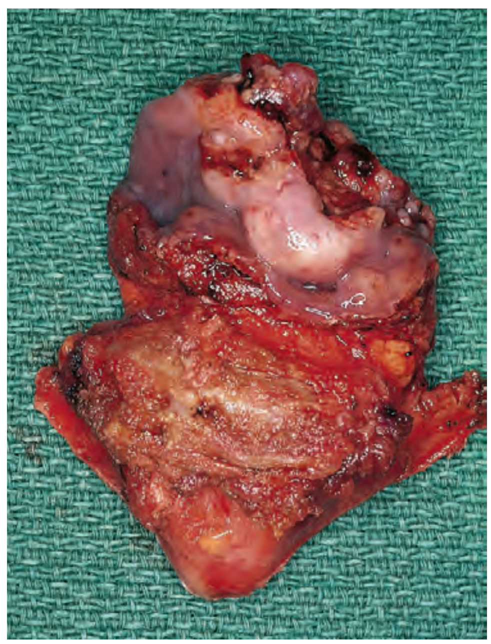

Figure 10.207 The anterior view of the surgical specimen shows the lingual surface of the epiglottis.

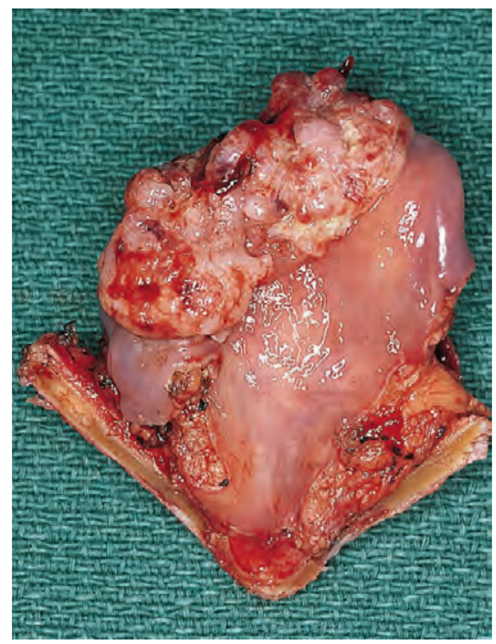

Figure 10.208 The primary tumor on the posterior surface of the epiglottis.

through the opposite end of the skin incision (Fig. 10.206). The platysma is closed with interrupted chromic catgut sutures and the skin is closed with nylon sutures.

The specimen demonstrates the primary tumor of the tip of the epiglottis and left aryepiglottic fold seen from an anterior view (Fig. 10.207). Note a monobloc resection of the supraglottic larynx and the preepiglottic space with the hyoid bone as its anterior margin and the resected portion of the thyroid cartilage at its inferior margin. Thus a satisfactory soft tissue resection of the preepiglottic space is achieved. On the posterior surface of the epiglottis, the bulk of the primary tumor is seen occupying the left aryepiglottic fold and the laryngeal surface of the epiglottis with a generous inferior mucosal margin and generous soft tissue and mucosal margins laterally (Fig. 10.208).

Intensive pulmonary care is essential after surgery, because in the immediate postoperative period the patient will aspirate his or her own secretions. Frequent suctioning through the tracheostomy tube is indicated to evacuate pulmonary secretions. However, nasogastric tube feedings may begin as early as 24 hours after surgery. As healing progresses, most patients begin to swallow their own saliva with minimal aspiration by the end of the first week. At this point, the tracheostomy tube may be either corked or removed to assist with further progress in swallowing. It is preferable to keep the tracheostomy tube in place with a cork, allowing access to the tracheobronchial tree in the event of massive aspiration once the patient starts taking food by mouth.

Initially the patient is given puréed and semisolid food. Clear liquids are not permitted until later, because aspiration in the early postoperative period is almost uniform. Once the patient masters ingestion of semisolid food, he or she gradually advances to liquids by mouth. Most patients will be able to swallow most types of foods by the end of the third

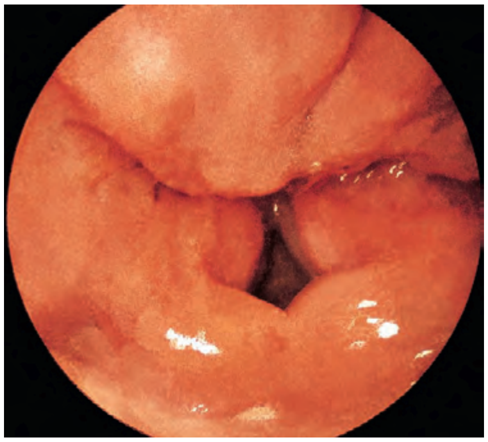

Figure 10.209 A postoperative endoscopic view of the larynx during breathing.

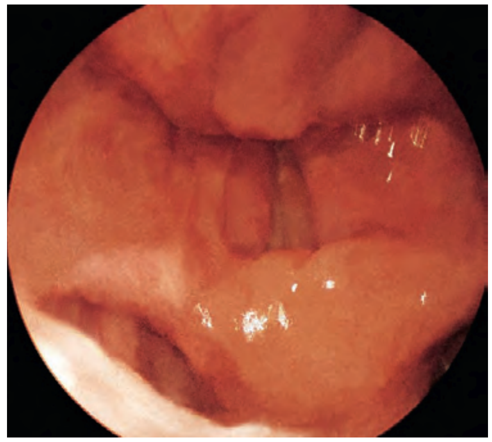

Figure 10.210 An endoscopic view of the larynx during phonation.

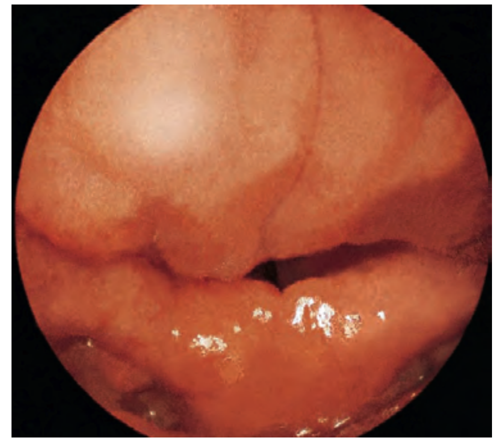

Figure 10.211 The base of the tongue moves posteriorly as the larynx is lifted up, exaggerating the shelf effect to protect the glottis during swallowing.

week after surgery. The nasogastric feeding tube now may be removed. Nearly all patients with a supraglottic partial laryngectomy aspirate their own saliva in varying amounts. Most patients, however, handle this degree of aspiration within the physiologic limits of their pulmonary reserve without any symptoms.

A postoperative endoscopic view of the larynx during quiet breathing is shown in Fig. 10.209. Note the relationship between the base of the tongue and the remaining larynx. The mucosal continuity between the base of the tongue and the anterior part of the glottis is not seen because of the shelf effect of the musculature of the base of the tongue that overhangs the anterior aspect of the glottis. During phonation, both vocal cords adduct normally with satisfactory closure of the glottis (Fig. 10.210). During the act of swallowing, the base of the tongue overhanging the glottis moves posteriorly as the larynx is elevated, exaggerating the shelf effect to protect the glottis and thus prevent aspiration (Fig. 10.211). This particular result can be achieved if meticulous attention to detail is given to placement of the sutures from the thyroid laminae to the musculature of the base of the tongue at the time of closure of the surgical defect.

A supraglottic (horizontal) partial laryngectomy is thus a technically simple operative procedure that provides an oncologically sound surgical resection for tumors of the supraglottic larynx. It allows a satisfactory restoration of the anatomic continuity of the upper aerodigestive tract combined with restoration of the physiologic aspects of the pharyngeal phase of deglutition.

A supraglottic partial laryngectomy also is feasible in select patients who previously have failed to respond to external irradiation used as initial definitive treatment for limited lesions of the supraglottic larynx. An endoscopic view of the supraglottic larynx of such a patient shows an ulcerated, mostly endophytic lesion of the laryngeal surface of the epiglottis (Fig. 10.212). This lesion has recurred within 6 months after completion of external irradiation. In such situations, if patient selection is appropriate and other criteria for selection of the operative procedure are followed, then a satisfactory operation can be performed with a predictably successful outcome. The specimen of the supraglottic larynx of the same patient is shown in Fig. 10.213, demonstrating adequate resection with negative mucosal and soft tissue margins.

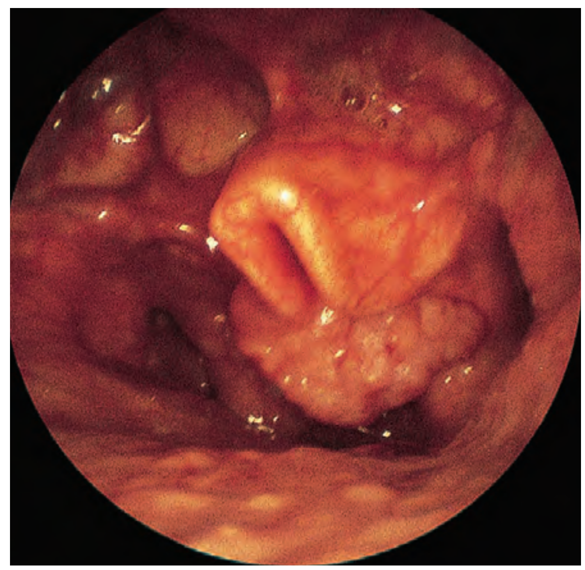

Figure 10.212 An endoscopic view of the larynx showing carcinoma of minor salivary glands of the epiglottis.

Figure 10.213 The surgical specimen of a supraglottic partial laryngectomy.

Wide-Field Total Laryngectomy

A total laryngectomy is indicated as the initial definitive treatment for patients with (1) advanced cancers of the larynx or hypopharynx with invasion of the thyroid or cricoid cartilage and extralaryngeal soft tissues (T4a), (2) tumors that have failed to respond to the larynx preservation treatment program of radiotherapy or chemoradiotherapy, and (3) extensive tumors of minor salivary origin and other histologic entities not suitable for a partial laryngectomy or radiation therapy. Examples of patients requiring a total laryngectomy either as initial definitive treatment or for salvage after failure to respond to radiation are shown in Figs. 10.214 through 10.217.

Whenever a total laryngectomy is considered for a primary carcinoma of the larynx, the operation of choice is a wide-field total laryngectomy. This procedure encompasses the entire larynx with its attached prelaryngeal strap muscles and the lymph nodes in the jugular chain (levels II, III, and IV) on the ipsilateral side as well as the lymph nodes in the tracheoesophageal groove on the same side. For lesions that involve the glottic larynx with significant subglottic extension, ipsilateral thyroid lobectomy should be performed to facilitate adequate clearance of the ipsilateral tracheoesophageal groove lymph nodes. If the laryngeal lesion requiring total laryngectomy extends on both sides of the midline, then bilateral jugular node dissection (levels II, III, and IV) should be performed. If clinically palpable metastatic nodes are present, then a more comprehensive modified neck dissection that preserves only the accessory nerve may have to be considered.

The operative procedure described here is performed on a patient with a large tumor of the right vocal cord with fixation of the right hemilarynx. Significant submucosal extension of disease was present that invaded the medial wall of the right pyriform sinus. A CT scan of the larynx showed thyroid cartilage invasion. At endoscopy, the tumor was found to involve the anterior commissure with significant subglottic disease. No cervical lymph nodes were clinically palpable.

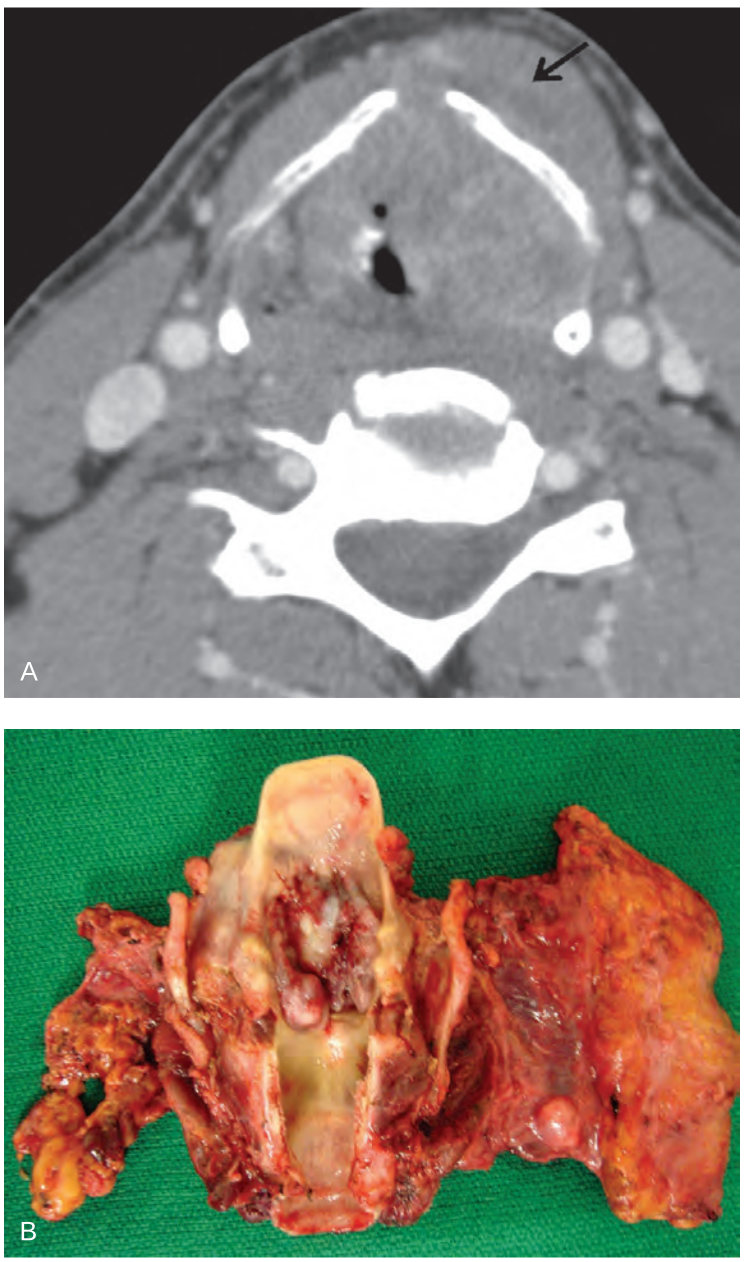

Figure 10.214 **A**, A computed tomography scan showing extralaryngeal spread of the tumor through thyroid cartilage (*arrow*). **B**, The surgical specimen of a total laryngectomy, with bilateral modified neck dissections.

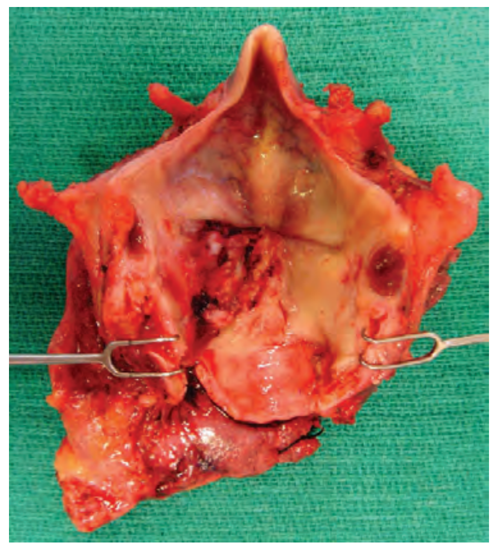

Figure 10.215 The surgical specimen of a total laryngectomy for salvage of a glottic carcinoma with subglottic extension that had recurred after radiation therapy.

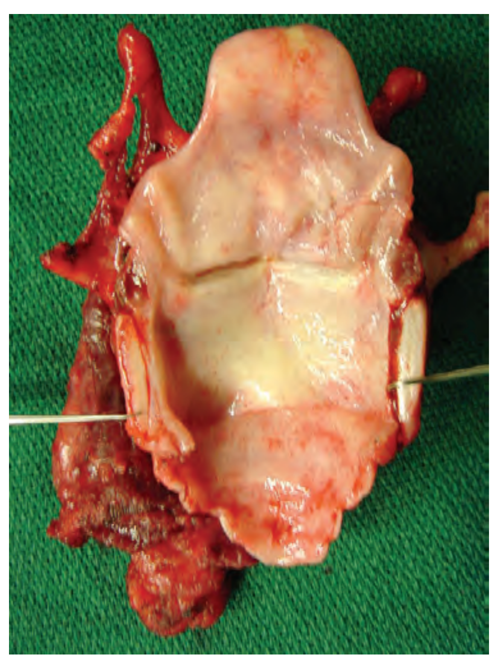

Figure 10.216 The surgical specimen of a total laryngectomy for a recurrent adenoid cystic carcinoma of minor salivary origin of the right hemilarynx after previous neutron beam radiation therapy.

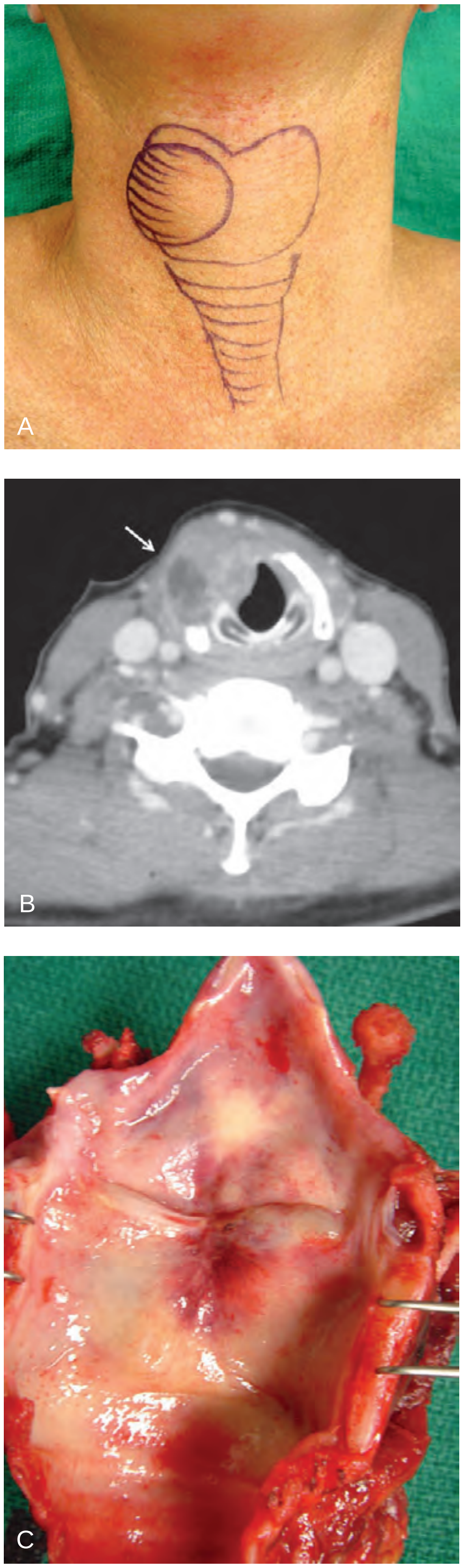

Figure 10.217 Recurrent carcinoma of the larynx. **A**, Clinical examination showed a palpable mass on the right thyroid cartilage. **B**, An axial view of a contrast-enhanced computed tomography scan showing a massive tumor with destruction of thyroid cartilage and a soft tissue tumor in the subcutaneous plane (*arrow*). **C**, The surgical specimen showing transglottic submucosal tumor recurrence.

Figure 10.218 A transverse incision placed over upper neck skin crease. The tracheostome is outlined.

The patient is placed on the operating table, under general endotracheal anesthesia through an orotracheal tube, and the head and neck area is isolated in the usual fashion. A transverse incision placed over an upper neck skin crease approximately at the level of the thyrohyoid membrane is most suitable for the necessary exposure (Fig. 10.218). The incision extends from the anterior border of the trapezius muscle on one side to the anterior border of the trapezius muscle on the opposite side. A circular disc of skin approximately 2.5 cm in diameter is marked in the suprasternal notch at the site of the proposed permanent tracheostome. The skin incision is deepened through the platysma to expose the prelaryngeal strap muscles in the central compartment. The upper neck flap is elevated cephalad to expose the hyoid bone and the attached suprahyoid muscles. The lower skin flap is elevated up to the suprasternal notch (Fig. 10.219). The anterior jugular veins encountered during elevation of the skin flaps are divided and ligated.

Mobilization of the larynx begins superiorly by detaching the muscles attached to the upper surface of the hyoid bone (Fig. 10.220). The hyoid is grasped with an Adair clamp and, with use of an electrocautery, all the suprahyoid muscles are detached from the midline up to the tip of the greater cornua on both sides. Note the lingual artery on the right side, which is exposed to the risk of inadvertent injury if sufficient care is not taken during this part of the operative procedure.

Dissection now proceeds to isolate the right superior thyroid artery and its superior laryngeal branch as it enters the thyrohyoid membrane. The hemostat shown in Fig. 10.221 is holding the fascia over the superior thyroid artery near its superior laryngeal branch. This vessel is identified, carefully dissected, divided between clamps, and ligated. Most of the blood supply to the larynx is derived from the superior laryngeal arteries. Early identification, division, and ligation of these vessels therefore will minimize hemorrhage during mobilization of the larynx.

Because this patient requires a right thyroid lobectomy, the superior thyroid artery is divided near its origin and ligated (Fig. 10.222). The hemostat still remains applied to the distal stump of the superior thyroid artery, which is now retracted with the specimen. The sternomastoid muscle is retracted laterally to expose the carotid sheath near the carotid bulb. Deep jugular

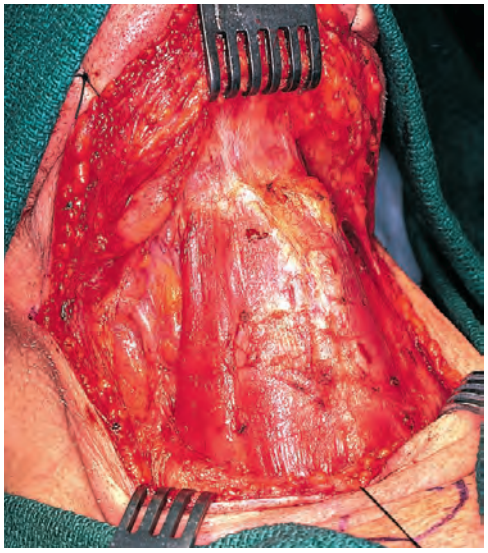

Figure 10.219 The upper and lower skin flaps are elevated to get exposure from the hyoid to the suprasternal notch.

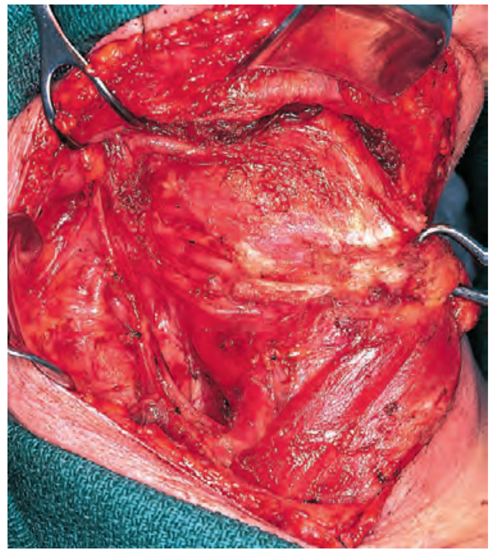

Figure 10.220 Mobilization of the larynx begins by detaching the suprahyoid muscles.

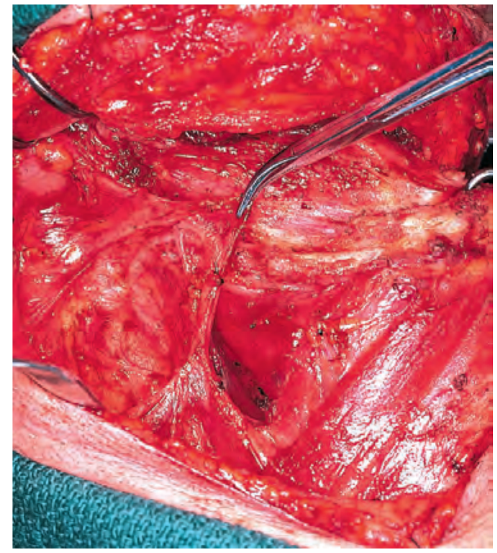

Figure 10.221 The superior thyroid artery near its superior laryngeal branch is shown by a hemostat.

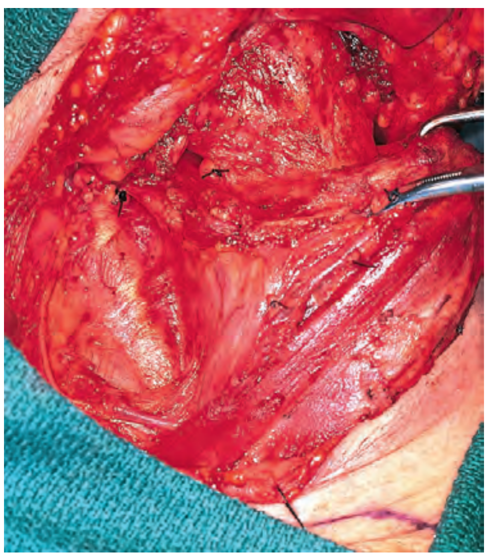

Figure 10.222 The superior thyroid artery is divided near its origin and ligated.

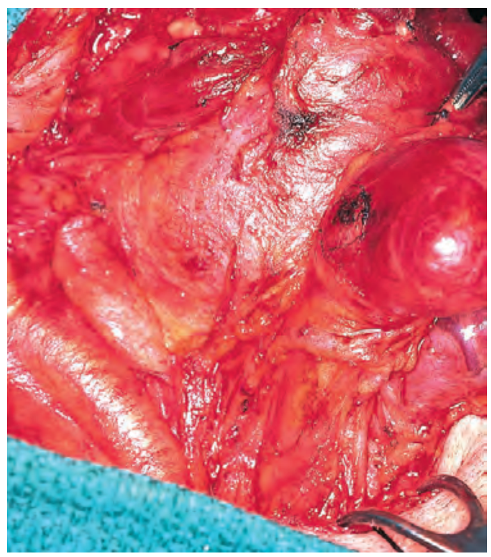

Figure 10.223 A close-up view of the surgical field showing the mobilized right thyroid lobe.

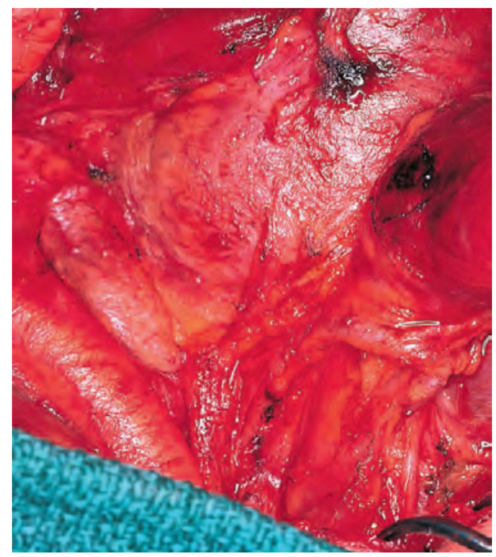

Figure 10.224 The strap muscles are divided low in the neck.

lymph nodes at levels II, III, and IV are dissected and mobilized toward the specimen. The superior belly of the omohyoid muscle in the lower part of the exposed surgical field is divided to gain further access to the cricothyroid region and the tracheoesophageal groove on the right side. A close-up view of the surgical field at this point demonstrates the right thyroid lobe mobilized medially with clearance of the lymph nodes at levels III and IV, exposing the right common carotid artery (Fig. 10.223).

As dissection proceeds toward the suprasternal notch, the sternomastoid muscle is retracted laterally and the sternohyoid and sternothyroid muscles are divided as low in the neck as possible. The surgical field now shows the strap muscles of both sides divided low in the neck (Fig. 10.224). Their stumps retract cephalad immediately upon division. Gentle traction is applied to the larynx toward the chin with an Adair clamp holding the hyoid bone. The inferior thyroid artery on the right-hand side is now divided and ligated. All the capsular vessels of the right thyroid lobe are divided and ligated. Finally, the isthmus of the thyroid gland is separated from the trachea by blunt dissection. Two Kocher clamps are applied to the isthmus, and it is divided in between the clamps. The stump of the left lobe of the thyroid gland is suture ligated with continuous interlocking 3-0 chromic catgut suture, which will provide adequate hemostasis from the cut surface of the isthmus.

Division of the isthmus of the thyroid gland exposes the cervical trachea (Fig. 10.225). The strap muscles on the left side are separated from the anterior surface of the left lobe up to the thyrohyoid membrane. The left lobe is then separated from the trachea, preserving the superior thyroid vessels. Several small vessels on the posterior capsule of the left lobe require ligation. The separated left lobe is now retracted laterally. Superior laryngeal vessels and nerves on the left side are divided and ligated as described previously. The inferior constrictor muscle is detached from the posterior edge of the thyroid cartilage bilaterally with the electrocautery.

The outlined disc of skin in the suprasternal notch is now excised. The circular skin incision is taken with a scalpel and the center of the skin disc is grasped with a hemostat and pulled. Using an electrocautery, the subcutaneous tissues and underlying platysma are divided and the skin disc is removed. Adequate hemostasis is achieved at the cut edge of the skin. An incision is made in the anterior tracheal wall at a

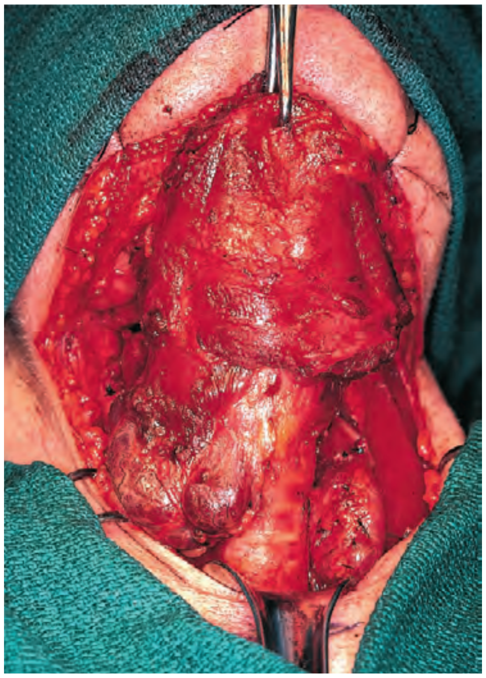

Figure 10.225 The cervical trachea is exposed by division of the thyroid isthmus.

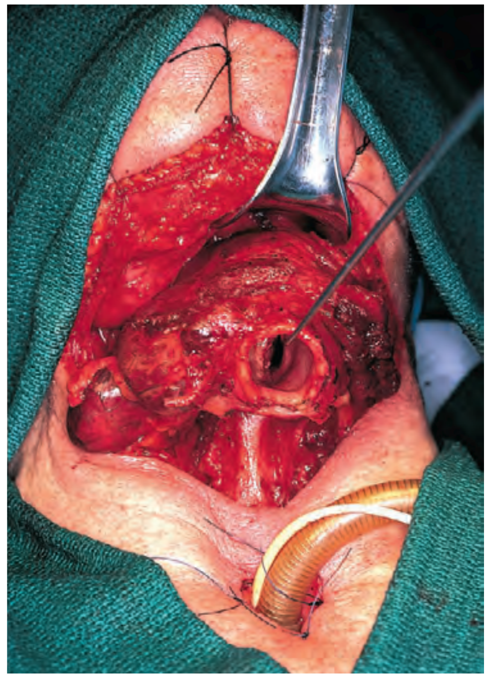

Figure 10.226 The stump of the trachea attached to the larynx is retracted cephalad.

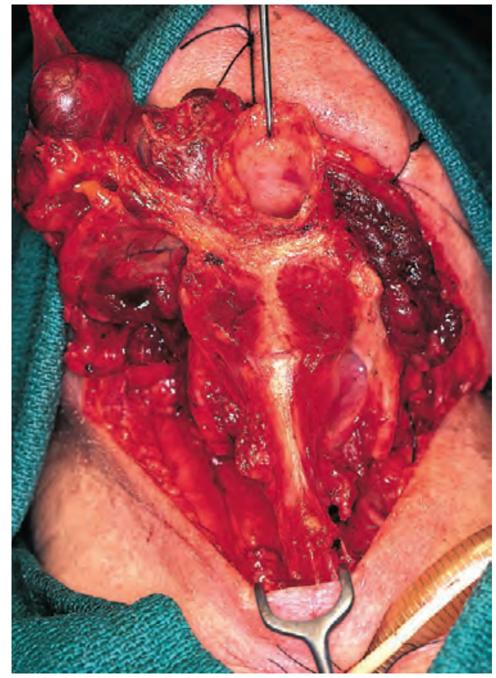

Figure 10.227 Mobilization of the larynx in the postcricoid region continues cephalad.

desired level, depending on the lower extent of the tumor in the larynx. The trachea is divided obliquely, leaving a short anterior wall and a long posterior wall. This bevel-shaped stump of the trachea provides a larger circumference for the permanent tracheostome. The stump of the trachea attached to the larynx is retracted cephalad with a hook (Fig. 10.226). The distal trachea is sutured to the skin edges of the permanent tracheostome with interrupted nylon sutures. Maintenance of anesthesia is now transferred from the orotracheal tube to a direct endotracheal tube introduced through the permanent tracheostome. Because of the beveled nature of the tracheal stump, the permanent tracheostome becomes oval in shape. The retracted upper part of the transected trachea gives an intraluminal view that demonstrates subglottic extension of tumor on the patient's right-hand side. The proximal trachea and larynx are dissected from the cervical esophagus by sharp dissection that is facilitated by cephalad traction on the tracheal stump. This dissection is best done with an electrocautery to minimize blood loss.

Further mobilization of the larynx in the postcricoid region continues cephalad (Fig. 10.227). By applying continuous moderate traction on the stump of the trachea, the plane between the larynx and the esophageal mucosa easily separates with use of the electrocautery. Note that entry is not yet made in the pharynx, because mobilization of the larynx from all its external attachments should be done before the pharynx is entered. Finally, entry is made in the pharynx either through the vallecula or the postcricoid region, depending on the location of the primary tumor for which the total laryngectomy is undertaken. If the primary tumor is completely endolaryngeal, then entry in the pharynx is made through the vallecula. On the other hand, if the primary tumor is supraglottic in nature with involvement of the aryepiglottic fold or the tip of the epiglottis, then entry in the pharynx is best made through the postcricoid region.

After opening the mucosa to enter the pharynx, the mucosal incision is continued along the periphery of the larynx until the opening is large enough to permit introduction of a retractor in the pharynx. Subsequent removal of the larynx by division of its mucosal attachments is completed under direct vision. The surgical field with a defect in the anterior wall of the pharynx as a result of removal of the larynx is shown in Fig. 10.228. If any of the mucosal margins appear to be close to the primary tumor, they must be examined histologically to rule out the microscopic spread of tumor. A nasogastric feeding tube is inserted at this time.

If an immediate tracheoesophageal puncture (TEP) is planned, it is performed at this time. It is important to avoid unnecessary dissection in the tracheoesophageal plane, posterior to the tracheostome between the membranous trachea and esophagus. A right-angled hemostat (a Mixter clamp) is introduced through the pharyngeal defect into the cervical esophagus. Its tip is pushed through the anterior esophageal wall behind the tracheostome to point through the membranous trachea in the tracheostome at the 12 o'clock position, approximately 8 mm from the tracheocutaneous suture line. With a No. 15 scalpel, the membranous trachea is incised and the tip of the clamp is pushed through. The clamp is opened approximately 3 to 4 mm to enlarge the opening. A No. 14 red rubber catheter is introduced through this opening and passed into the distal esophagus. The outer end of the catheter is secured with a silk suture to the skin of the subclavicular region. The red rubber catheter is replaced by a voice prosthesis 7 to 10 days after surgery. This allows the TEP to "mature" before insertion of the voice prosthesis. Alternatively, the voice prosthesis may be introduced immediately, with the use of the special kits for TEP available for immediate insertion of the voice prosthesis.

A pharyngeal defect of these dimensions is quite suitable for primary closure. The pharynx preferably should be closed in a transverse fashion. Closure begins with a 2-0 chromic catgut suture taken through the mucosa and muscle of the midline of the base of the tongue and the mucosa of the anterior wall of the cervical esophagus. An anterior pull on this suture, which is still untied, divides the pharyngeal defect into equal halves on each

Figure 10.228 The circular defect in the anterior pharyngeal wall after removal of the larynx.

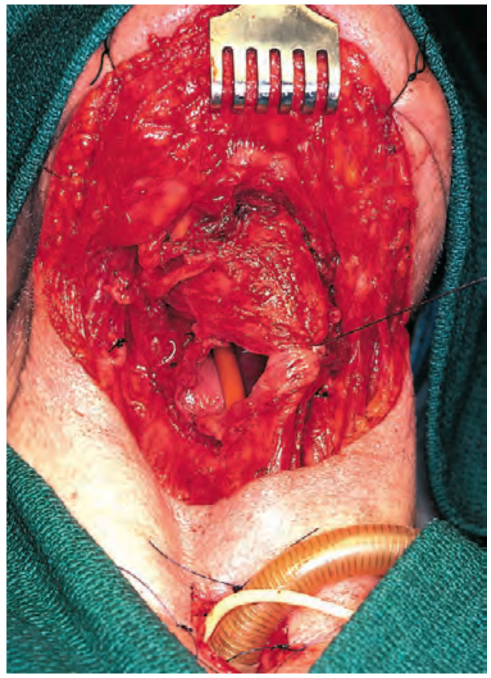

Figure 10.229 The circular pharyngeal defect is converted to two elliptical defects by the application of a suture between the midline of the base of the tongue and the anterior esophageal wall.

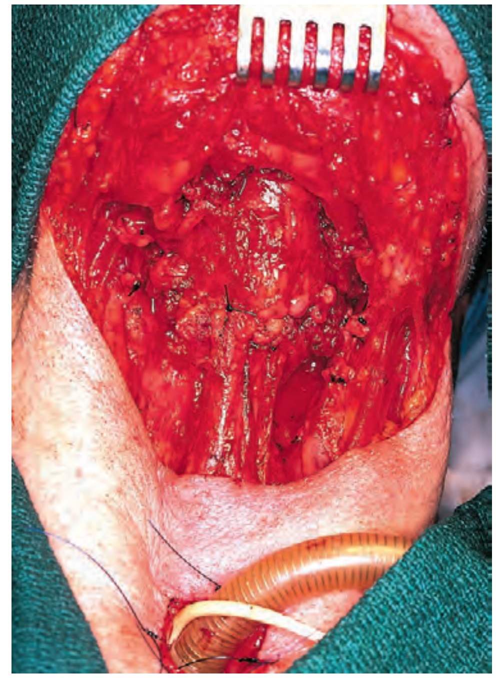

Figure 10.230 The pharyngeal closure is completed.

side. Note that the circular pharyngeal defect seen in Fig. 10.228 is now converted to two elliptical defects by the application of the midline inverting suture (Fig. 10.229). The pharyngeal defect on each side of this midline suture is closed with 2-0 chromic catgut interrupted inverting sutures. The closure should begin at the lateral edges of the defect, and it should proceed toward the midline. Careful attention should be given to inverting the mucosal edges as each suture is tied during this closure. Mucosal prolapse through the suture line may cause delayed healing and a potential for fistula formation. While tying the knots, meticulous attention is required to ensure that the edges of the mucosa do get inverted and buried under the suture.

The pharyngeal closure is thus completed (Fig. 10.230). Note that the closure has no tension. After closure of the pharynx, the surgical field is irrigated with Bacitracin solution. Suction drains are placed lateral to the pharynx and are brought out through separate stab incisions in the skin. The platysma is closed with interrupted chromic catgut sutures, and the skin is closed with interrupted nylon sutures.

The surgical specimen demonstrates a transglottic tumor of the right hemilarynx with significant submucosal extension in the supraglottic larynx, paraglottic space, and medial wall of the right pyriform sinus (Fig. 10.231). The specimen is divided in the posterior midline, showing the interior of the larynx as well as invasion of the thyroid cartilage. Note the significant expansion of the right hemilarynx and subglottic extension of the tumor on the right-hand side.

Postoperative care after a total laryngectomy requires nasogastric tube feedings that may begin within 24 hours. Suction drains are removed when they cease to function. If the neck flaps and skin incision are well healed, oral fluids and a puréed diet may be started in 7 to 8 days. Sutures on the tracheostome are removed at 2 weeks. Esophageal speech training may begin as early as 3 weeks after surgery. If an immediate TEP is performed and a red rubber catheter is introduced, then it is removed on the tenth day and replaced with a voice prosthesis. TEP speech training may begin as early as 3 weeks after surgery.

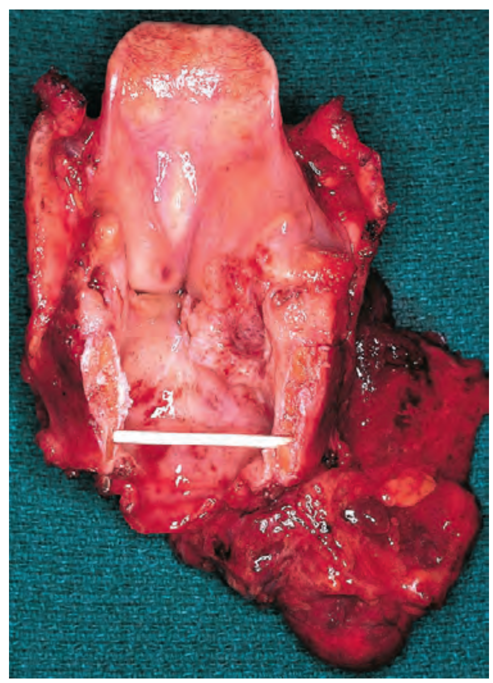

Figure 10.231 The surgical specimen.

Figure 10.232 The appearance of the tracheostome 3 months after surgery.

The appearance of the patient approximately 3 months after surgery shows a well-healed scar in the central compartment of the neck. The tracheostome is of a very satisfactory size and shape and is properly placed in the suprasternal notch (Fig. 10.232). It is preferable not to use any laryngectomy tube in the tracheostome, except for the immediate postoperative period, until the sutures are removed. If the permanent tracheostome is large enough, then a laryngectomy tube is unnecessary.

Salvage Total Laryngectomy

In general, advanced stage III/IV laryngeal cancer is treated with organ-preserving radiation or chemoradiation. The RTOG 91-11 randomized clinical trial randomized 520 patients to either radiation alone, induction chemotherapy followed by chemoradiation (CTRT), or concomitant CTRT. The 10-year follow-up results of this study were published in 2013 and reported that locoregional control was superior with concomitant CTRT, followed by induction CTRT and then radiotherapy alone. The laryngeal preservation rate was 82% with concomitant CTRT, 68% for induction CTRT, and 63% for RT alone. Overall, 20% to 30% of patients having CTRT will require a salvage total laryngectomy. Salvage total laryngectomy is associated with a very high incidence of local complications occurring in 40% to 50% of patients. The most common local complication is pharyngocutaneous fistula occurring in 30% to 40% of patients. Because of this high local complication rate, primary closure of the pharyngeal defect is now rarely done. A metaanalysis showed that the use of vascularized flaps reduced the rate of pharyngocutaneous fistula by 30%. There are several options for reconstruction of the pharyngeal defect following salvage total laryngectomy. If the posterior pharyngeal wall is retained the pharynx can be reconstructed with a myocutaneous pedicled flap (Fig. 10.233), free radial forearm flap (Fig. 10.234), or free anterolateral thigh flap. For circumferential defects in which a total laryngopharyngectomy is required the defect can be repaired with a free jejunum flap (Fig. 10.235), tubed free radial forearm flap, or tubed free anterolateral thigh flap. Despite a successful salvage operation, the overall survival of patients who require salvage laryngectomy is quite low (40%) compared with those who have a complete response to CTRT (60% to 70%).

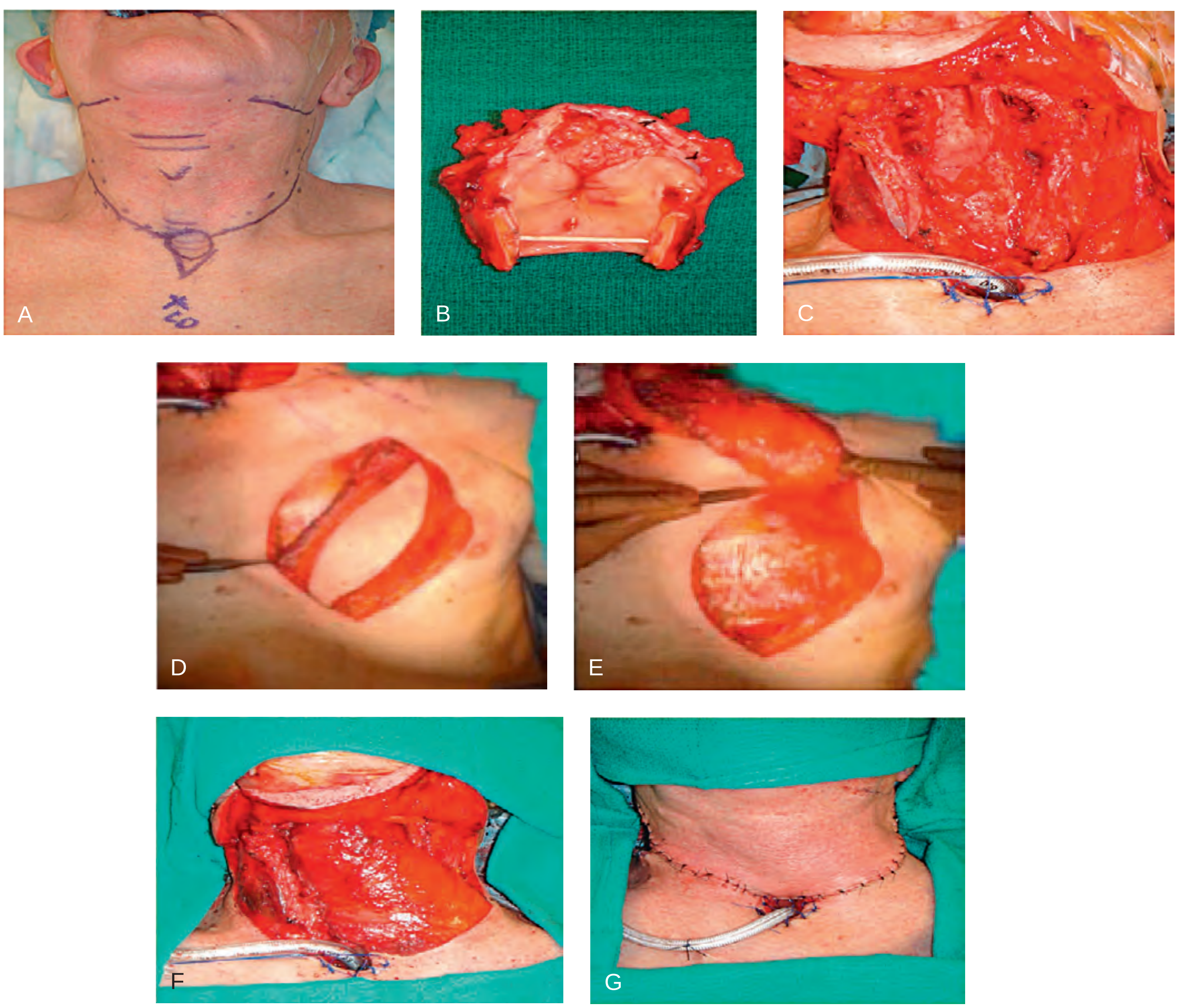

Figure 10.233 **A**, Skin incisions for laryngectomy and permanent tracheostome. **B**, Surgical specimen of total laryngectomy for carcinoma of the supraglottic larynx. **C**, Surgical field showing defect of the anterior pharyngeal wall. **D**, Evaluation of left-sided pectoralis major myocutaneous flap. **E**, Rotation of the flap with skin island for repair of anterior pharyngeal wall. **F**, Closure of the pharyngeal defect. **G**, Final closure of skin flaps.

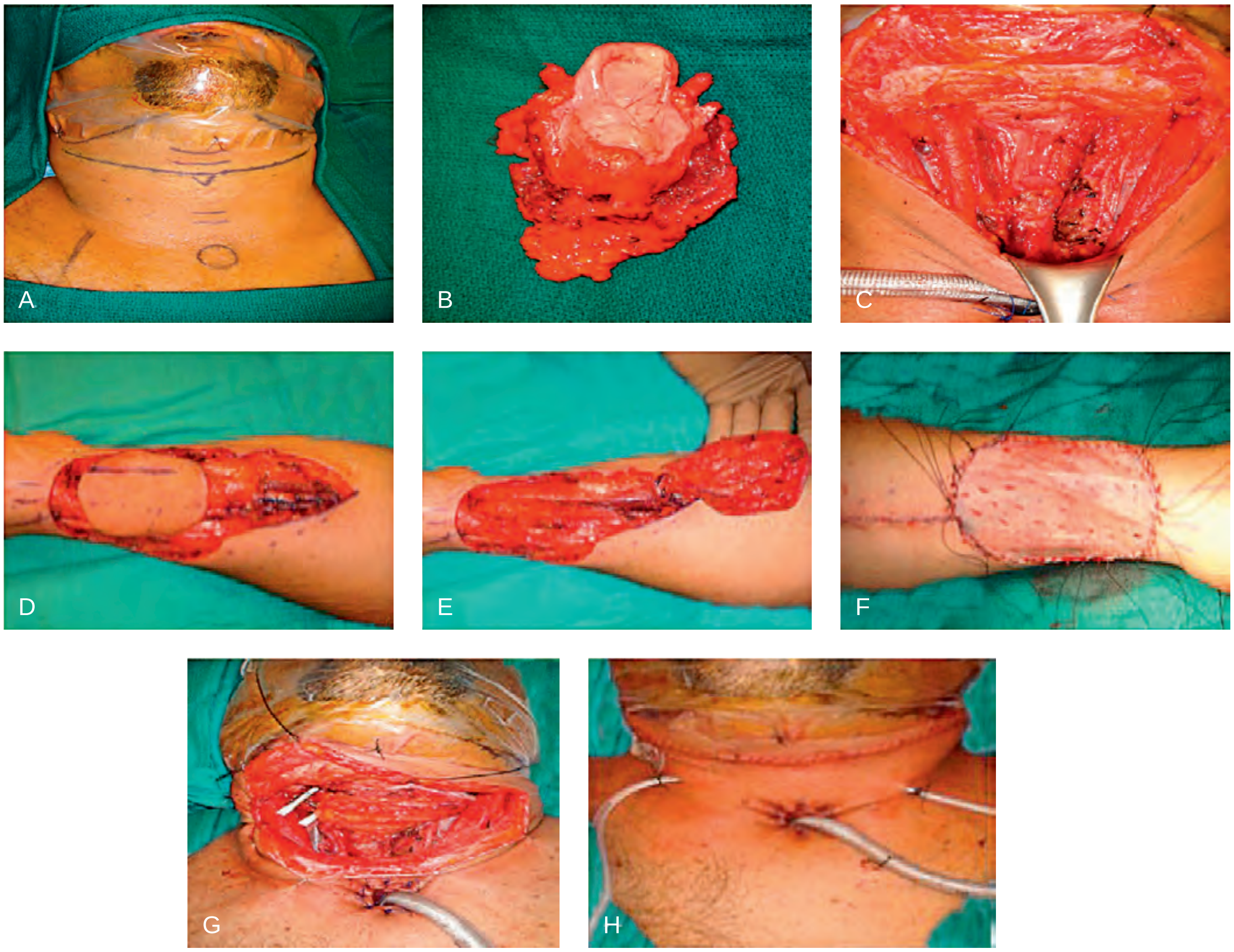

Figure 10.234 **A**, Skin incision for laryngectomy and tracheostome. **B**, Surgical specimen of transglottic carcinoma. **C**, Surgical field showing defect of the anterior pharyngeal wall. **D**, Elevation of radial forearm free flap. **E**, Radial forearm free flap rotated 180 degrees. **F**, Split-thickness skin graft on donor site in the arm. **G**, Radial forearm free flap showing closure of the pharyngeal defect. **H**, Final closure of skin of the neck.

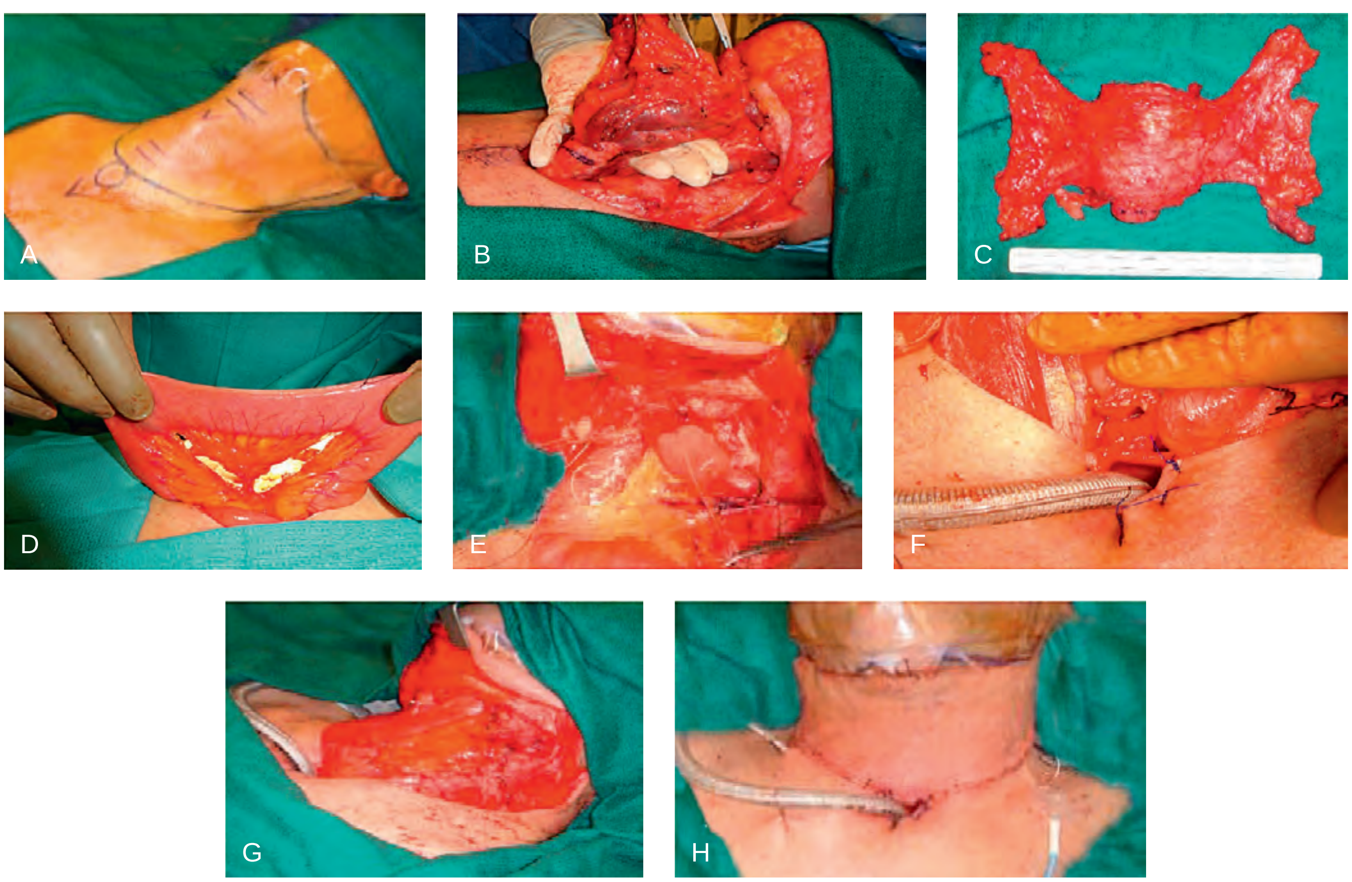

Figure 10.235 **A**, Skin incision for pharyngolaryngectomy and bilateral neck dissections. **B**, Circumferentially mobilized larynx and pharynx. **C**, Surgical specimen of total pharyngolaryngectomy and bilateral neck dissections. **D**, Harvest of jejunum and isolation of its vascular pedicle. **E**, Anastomosis between jejunum, base of tongue, and pharyngeal wall. **F**, Distal anastomosis between jejunum and esophagus. **G**, Reconstructed pharynx with microvascular anastomosis. **H**, Final skin closure.

Surgery for Subglottic Stenosis

Subglottic stenosis resulting from any etiology is a surgical problem, and a variety of different surgical techniques are available for its repair, including endoscopic maneuvers and open operative procedures. The operation described here is one method of excision and repair of the stenosed area.

The patient shown here had undergone repeated endotracheal intubations for bronchoscopic examinations as well as ventilatory support with prolonged intubations during episodes of respiratory difficulties. At the time of this presentation, he had significant respiratory stridor because of an area of concentric stenosis that could be seen easily in the subglottic region. The endoscopic view of the larynx is shown in Fig. 10.236. Attempts at management of this stenotic area by endoscopic laser excision had failed on two previous occasions.

A coronal tomogram of the larynx shows a concentric stricture approximately at the level of the lower border of the cricoid cartilage (Fig. 10.237). An endoscopic examination under general anesthesia with a 0-degree telescope passed through the glottis into the subglottic region shows a concentric stenotic area with a dense scar forming its edges (Fig. 10.238). Normal tracheal rings are seen distal to the stenosed area. The surgical procedure consists of excision of the concentric stricture and adjacent normal mucosa and repair of the denuded area with a mucosal graft supported by a T-tube stent.

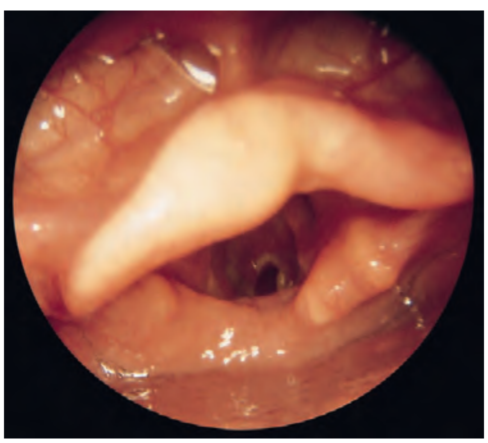

Figure 10.236 An endoscopic view of the larynx showing subglottic stenosis.

The patient is placed under general endotracheal anesthesia with a very small endotracheal tube placed distal to the stenosed subglottic region. The surface markings of the thyroid cartilage, cricoid cartilage, and the suprasternal notch are shown with the line of proposed incision for exposure of the subglottic region (Fig. 10.239). The skin incision is deepened through the platysma, and the upper and lower skin flaps are elevated. The strap muscles are separated in the midline and retracted laterally to expose the isthmus of the thyroid gland (Fig. 10.240).

A close-up view of the surgical field with retraction of the strap muscles on each side shows the isthmus of the thyroid overlying the region of the cricoid cartilage and the first two tracheal rings (Fig. 10.241). Note the relationship of the cricothyroid muscle just cephalad to the isthmus of the thyroid gland. The isthmus is mobilized from the trachea, doubly clamped, and divided. The stumps of the isthmus on each side are sutured with continuous interlocking 3-0 chromic catgut sutures for hemostasis. Retraction of the right and left thyroid lobes laterally provides exposure of the lower border of the cricoid and the first four tracheal rings.

The thyroid lobes are further dissected from the trachea on each side to obtain additional exposure (Fig. 10.242). During this dissection, extreme care should be taken not to continue mobilization up to the tracheoesophageal groove. Excessive lateral mobilization of the thyroid lobes poses the risk of inadvertent injury to the recurrent laryngeal nerves in the tracheoesophageal grooves. Therefore excessive lateral mobilization of the thyroid lobes should be avoided. Exposure of the anterior third of the circumference of the tracheal wall is sufficient for the surgical procedure to be performed.

The thyroid lobes are now retracted laterally (Fig. 10.243). In this close-up view, the area of narrowing between the cricoid and the second tracheal ring is shown. A tracheostomy is now performed low in the trachea at approximately the level of the

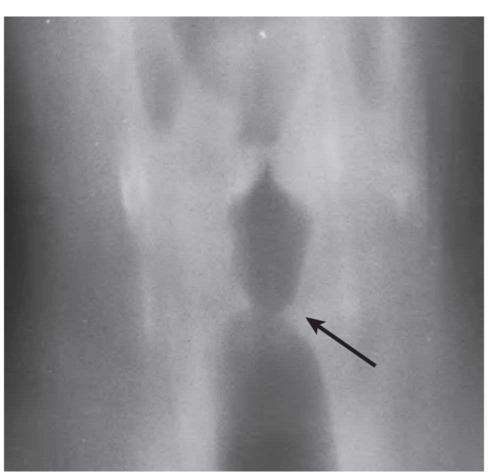

Figure 10.237 A coronal tomogram of the larynx showing a concentric stricture (*arrow*).

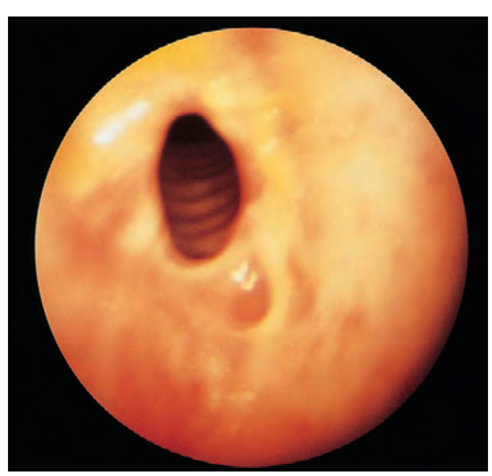

Figure 10.238 An endoscopic view of the stricture through a 0-degree telescope.

Figure 10.239 The surface markings of the thyroid cartilage, cricoid cartilage, and the suprasternal notch, with the line of proposed incision for exposure of the subglottic region.

Figure 10.240 The strap muscles are separated in the midline and retracted laterally.

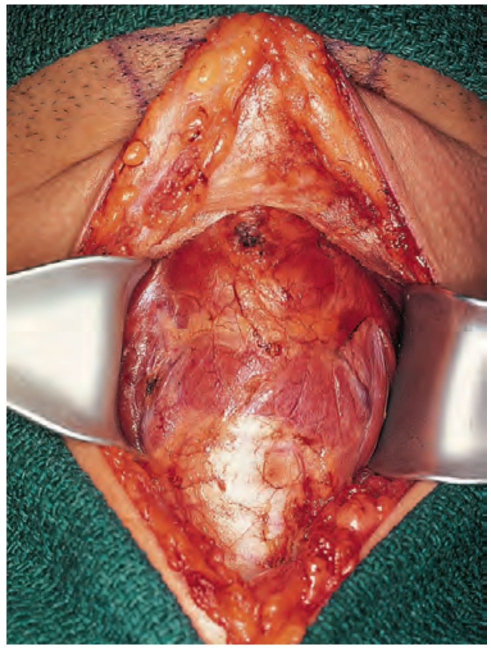

Figure 10.241 A close-up view of the surgical field showing the isthmus of the thyroid gland.

Figure 10.242 The thyroid lobes are dissected from the trachea on each side.

Figure 10.243 The thyroid lobes are retracted laterally to expose the trachea.

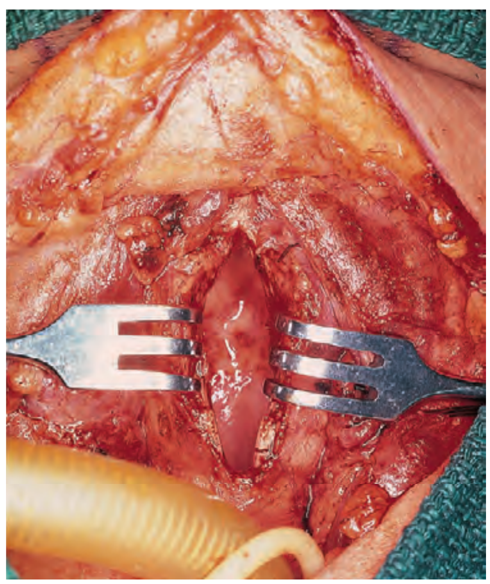

Figure 10.244 The trachea is opened in the anterior midline by a vertical incision.

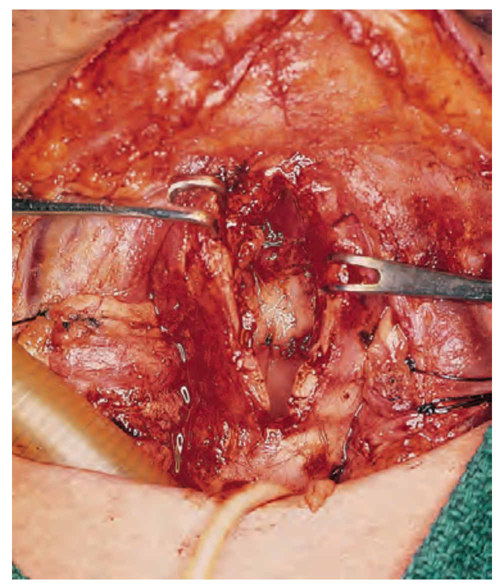

Figure 10.245 A mucosal graft is sutured to the edges of the tracheal mucosa and the mucosa of the subglottic larynx.

sixth or seventh ring, and maintenance of the anesthesia is transferred to an endotracheal tube placed in the distal trachea. The orotracheal tube is removed. The trachea is opened in the anterior midline by a vertical incision that begins at the level of the cricothyroid membrane, dividing the anterior ring of the cricoid cartilage and also dividing the first four rings of the trachea (Fig. 10.244). Retraction of the cricoid cartilage and the tracheal wall on each side clearly demonstrates the area of stricture at the junction of the cricoid cartilage and the first two rings of the trachea.

Using an electrocautery, incisions are made circumferentially in the tracheal mucosa below and above the stenotic area. A Freer elevator is used to elevate the area of stenosis submucosally, and it is completely excised. Several minor bleeding points are encountered from the tracheal wall during this procedure, but they are easily controlled with electrocoagulation.

The surgical defect that has been created is repaired with a free mucosal graft obtained from the cheek mucosa. Alternatively, a mucosal graft can be obtained from the nasal septum. In this patient, the graft was harvested from the mucosa of the cheek. The graft is shown sutured to the edges of the tracheal mucosa and the mucosa of the subglottic larynx with interrupted 4-0 chromic catgut sutures (Fig. 10.245). Circumferential closure of the denuded area should be obtained with the mucosal graft. A close-up view of the surgical field clearly shows satisfactory repair of the surgical defect with the mucosal graft (Fig. 10.246). At this point, the endotracheal tube is removed from the tracheostomy site and is replaced by a Montgomery T tube (Fig. 10.247). The vertical arm of the T tube remains in the subglottic region and distal trachea, while the horizontal arm comes out through the tracheostomy site.

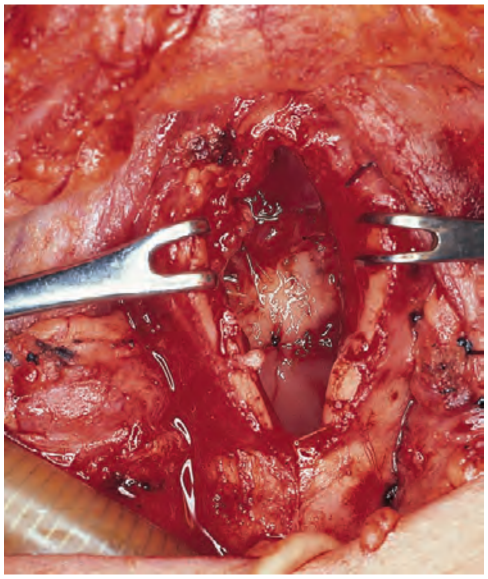

Figure 10.246 A close-up view of the surgical field showing adequate coverage of the defect with a mucosal graft.

Figure 10.247 A Montgomery T tube.

After the tube is positioned, the trachea is closed with 3-0 Prolene interrupted sutures. The isthmus of the thyroid is replaced back in the midline, but no attempt is made to suture the two sides of the thyroid gland. The strap muscles are reapproximated in the midline with interrupted chromic catgut sutures, and the skin incision is closed in two layers using 3-0 chromic catgut for platysma and 5-0 nylon for skin.

The postoperative care is similar to that for any laryngeal surgery. No special precautions are necessary for management of the T tube. During suctioning of the tracheostomy, it is important to remember that the horizontal arm of the T tube may have to be tilted cephalad to permit introduction of a suction catheter. If this is not done, the catheter will not negotiate the right-angled curve of the T tube. The T tube is retained for approximately 3 weeks, and then it is removed and replaced with a regular tracheostomy tube. Following this procedure, the patient is weaned from the tracheostomy gradually by progressive corking of the tracheostomy tube. The tracheostomy tube can be removed in approximately 4 to 5 weeks.

An endoscopic telescopic view of the larynx 6 months after surgery is shown in Fig. 10.248. This translaryngeal view of the subglottic region shows the area of repaired stricture with a wide-open airway. Excision and repair of the submucosal stenosis with a free mucosal graft and T-tube stent are very satisfactory methods of repair of small areas of strictures in the subglottic region. The mucosal graft usually heals well, and most patients do not require any further surgical intervention.

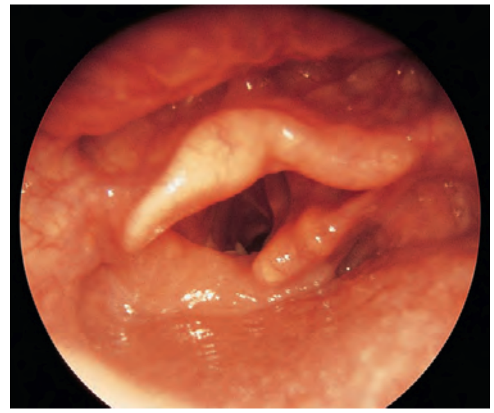

Figure 10.248 A telescopic view of the larynx 6 months after surgery.

Tracheal Tumors

Primary tumors in the trachea may arise from the mucosa, such as squamous carcinoma or minor salivary gland tumors, or from the cartilage or neurovascular structures in the tracheal wall. On the other hand, invasion of the larynx and trachea from cancer of the thyroid gland occurs much more often and may need laryngeal or tracheal resection. (See further details about thyroid cancer and airway invasion in Chapter 12.) Vascular lesions such as hemangiomas involving the airway are quite common in infancy and childhood. Management of these lesions requires thorough consideration of a variety of factors including the extent of the lesion, symptoms of the patient, potential risks of airway obstruction, and hemorrhage.

An axial view of a postcontrast T1-weighted MRI of an 18-month-old infant shows an obstructing lesion in the cervical trachea at the level of the thyroid gland (Fig. 10.249A). This child presented with respiratory stridor but was not in acute respiratory distress. A sagittal view of the MRI shows the lesion to be of limited cephalocaudad extent, but it significantly compromised the airway (Fig. 10.249B). At endoscopy, the lesion was found to be covered by hypervascular but smooth mucosa (Fig. 10.250). The clinical and radiologic diagnosis of a hemangioma was made. Vascular lesions in infants rarely need surgery and often undergo spontaneous regression. However, this obstructing lesion had a significant risk of respiratory compromise and required urgent treatment.

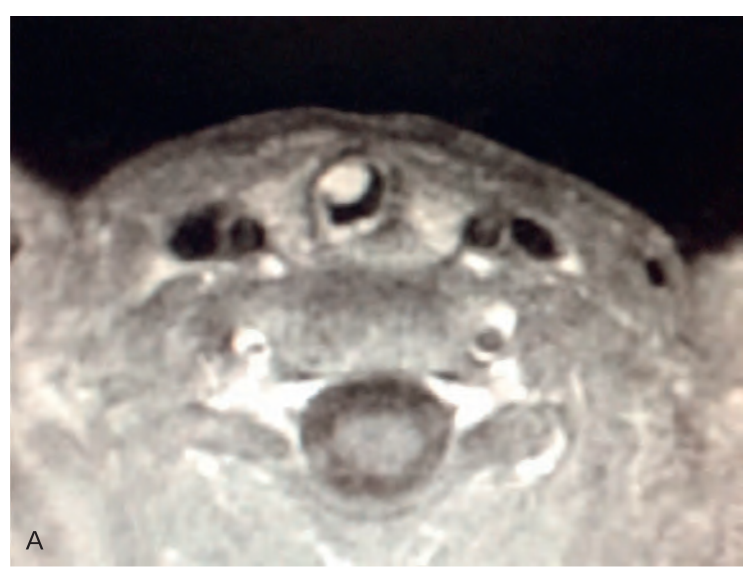

Figure 10.249 **A**, Axial view of T1-weighted magnetic resonance imaging (MRI) showing an obstructing lesion in the trachea.

Figure 10.249, cont'd B, Sagittal view of the MRI showing the cephalocaudad extent of the tumor (*arrow*).

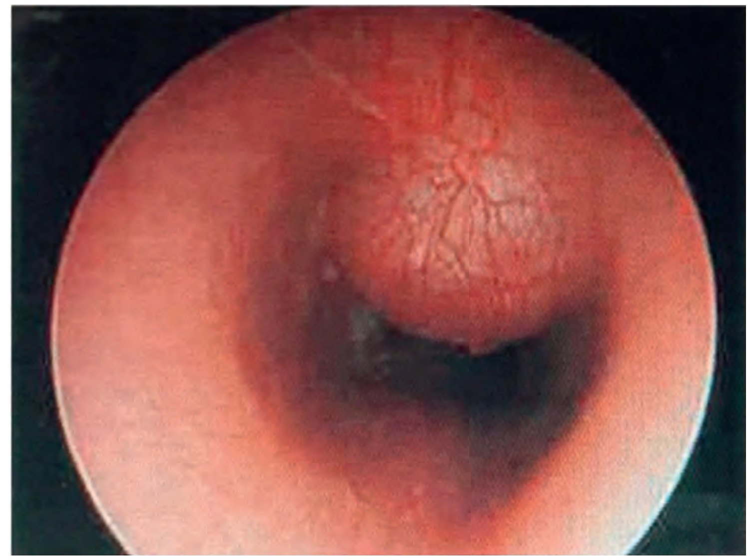

Figure 10.250 Endoscopic view of the lesion in the trachea.

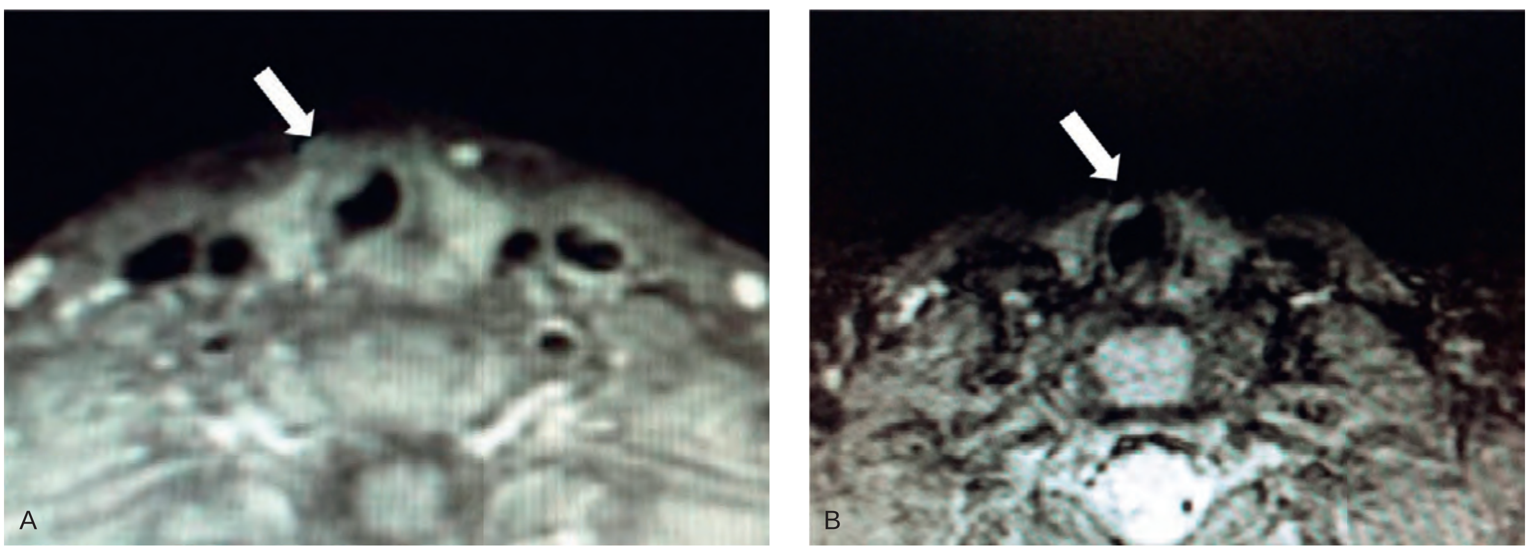

Figure 10.251 Posttreatment magnetic resonance imaging at 3 months (**A**) and 6 months (**B**) showing near-complete resolution of the tumor (*arrows*).

These vascular lesions respond quite well to systemic treatment with propranolol. The child was started on propranolol and showed significant clinical improvement in 3 weeks. Follow-up MRIs done at 3 months and 6 months show near complete resolution of the lesion (Fig. 10.251).

Tracheal Resection for Tumors

The most common primary tumors of the trachea are adenoid cystic carcinoma and squamous cell carcinoma. Patients with tracheal tumors present with increasing respiratory difficulty, wheezing, and sometimes hemoptysis. Tumors of the trachea involving short segments are best managed by surgical resection. The patient whose CT scan is shown in Fig. 10.252 had persistent wheezing with mild respiratory distress for nearly 4 years. She had been under the care of an internist for "wheezing due to asthma," although no imaging studies were obtained to assess the upper airway. Eventually the patient was seen by an otolaryngologist, who noted respiratory stridor and obtained a CT scan, which showed an obstructing lesion of the trachea requiring further workup and treatment (see Fig. 10.252).

Endoscopic assessment requires induction of general anesthesia with jet ventilation and tracheoscopy for tissue diagnosis, as well as to measure the vertical dimension of the tumor, which is necessary to plan the extent of tracheal resection and reconstruction (Fig. 10.253). A biopsy of the lesion showed adenoid cystic carcinoma of minor salivary gland origin. Up to six to seven rings of the trachea can be safely excised with primary anastomosis to restore the airway. After adequate laryngotracheoscopy, endotracheal intubation is performed with the balloon of the endotracheal tube well distal to the lower border of the tumor. The neck is entered through a transverse incision at the level of the cricoid cartilage, and the central compartment is explored from the hyoid up to the suprasternal notch. The strap muscles are retracted laterally, and the thyroid gland is exposed. Because of the direct involvement of the thyroid gland, as seen in the preoperative CT scan (see Fig. 10.252), a total thyroidectomy was planned in this patient (Fig. 10.254).

Careful dissection of the tracheoesophageal grooves is performed on both sides to preserve the recurrent laryngeal nerves and the parathyroid glands (Fig. 10.255). A plane is created

between the trachea and esophagus and a Penrose drain is passed to lift the trachea into the wound. At this juncture, the trachea is opened below the lower border of the tumor to gain access to its lumen. This maneuver permits monobloc sleeve resection of the trachea, securing satisfactory margins at the upper and lower ends (Fig. 10.256). Circumferential sleeve resection of the trachea with a total thyroidectomy is performed in this patient. Release of the suprahyoid muscles from the hyoid bone allows the larynx to advance approximately 2 to 2.5 cm caudad. Mobilization of the distal trachea should be avoided to prevent devascularization of the tracheal stump. A single-layer anastomosis is performed in a watertight fashion with Vicryl sutures (Fig. 10.257). The surgical specimen shows complete excision of the tumor with satisfactory margins in all three dimensions (Fig. 10.258). The anastomotic suture line must be maintained without tension, and therefore a chin-to-chest suture is applied to keep the neck in flexion for 3 weeks (Fig. 10.259). An endoscopic view 3 months after surgery shows a healed suture line between the lower border of the cricoid cartilage and the trachea (Fig. 10.260).

Figure 10.254 The central compartment is exposed, showing the thyroid gland overlying the tracheal tumor.

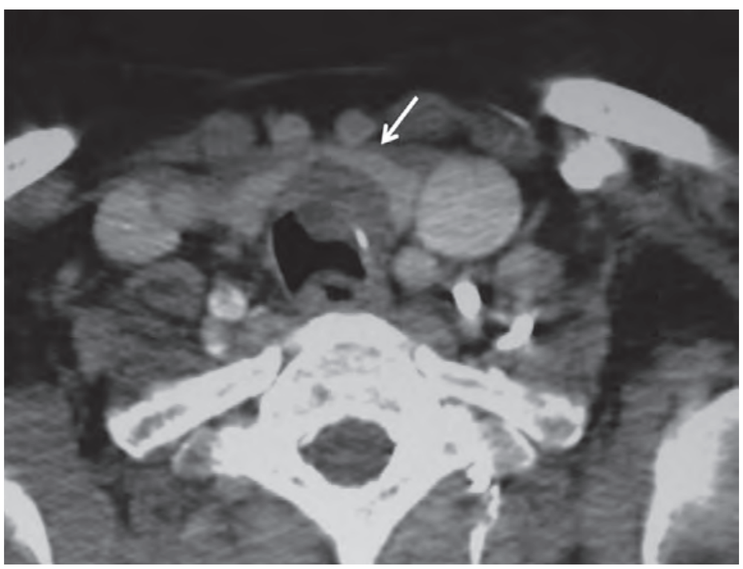

Figure 10.252 An axial view of a contrast-enhanced computed tomography scan shows a tracheal tumor invading the thyroid gland (*arrow*).

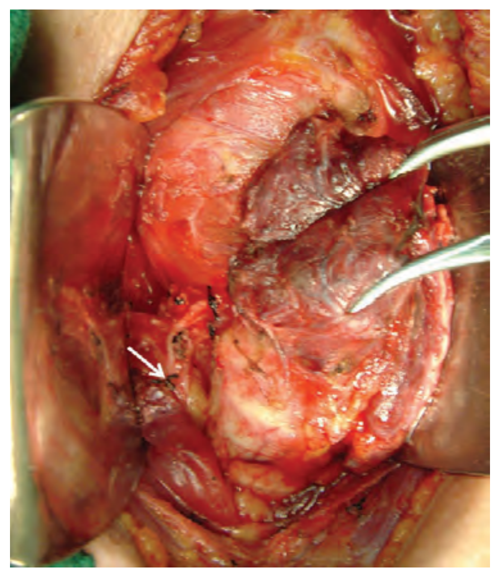

Figure 10.255 Paratracheal dissection showing the right recurrent laryngeal nerve (*arrow*) and inferior parathyroid gland.

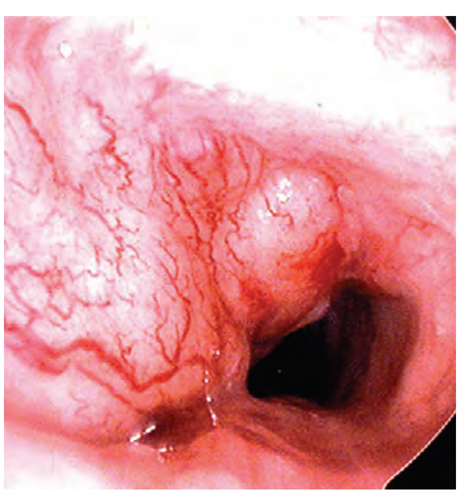

Figure 10.253 An endoscopic view of the trachea shows a nodular tumor partially obstructing the tracheal lumen.

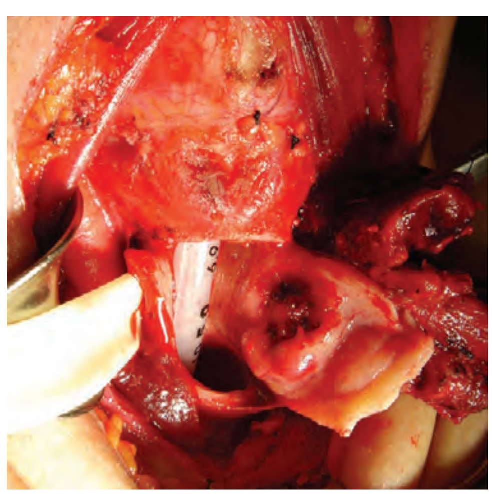

Figure 10.256 The trachea is opened to facilitate resection of the tumor with adequate margins.

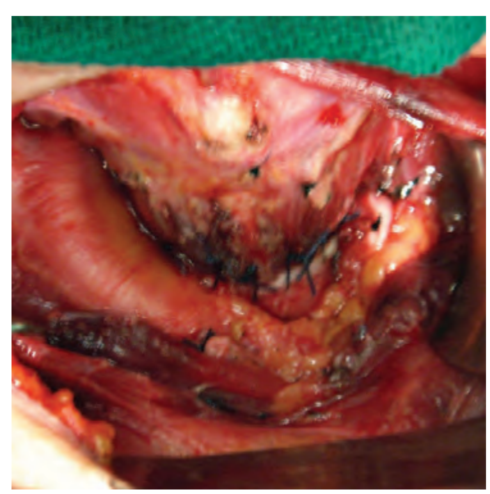

Figure 10.257 Tracheal anastomosis is performed in a single layer.

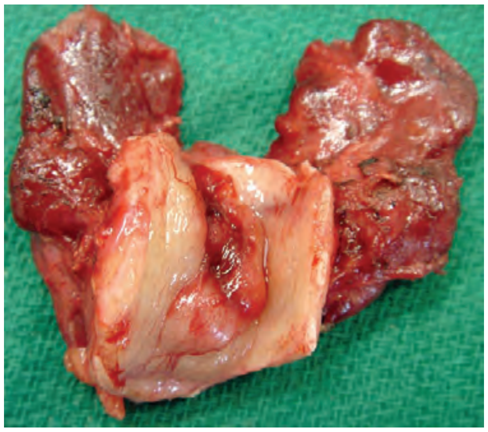

Figure 10.258 The surgical specimen showing monobloc resection of the tracheal tumor with the thyroid gland.

Figure 10.259 A chin-to-chest suture.

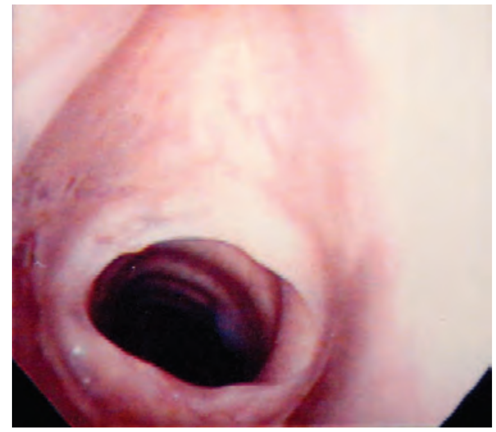

Figure 10.260 A postoperative endoscopic view of the anastomosis between the larynx and the trachea.

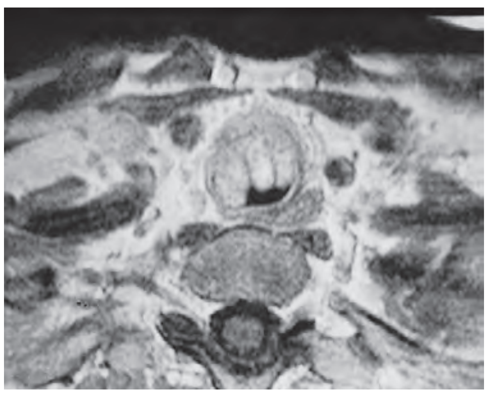

Figure 10.261 An axial view of the magnetic resonance imaging scan showing squamous cell carcinoma of the trachea.

Figure 10.262 A sagittal view of the magnetic resonance imaging scan demonstrates the length of tracheal involvement.

Figure 10.263 An endoscopic view through a 0-degree telescope.

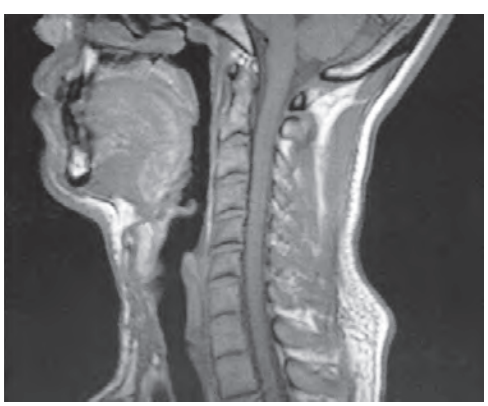

Figure 10.264 A postoperative magnetic resonance imaging scan in the sagittal view demonstrates restoration of the airway.

Primary squamous cell carcinomas of the trachea are infrequent. The axial view of the MRI scan of a patient with squamous cell carcinoma of the trachea is shown in Fig. 10.261. Note that the tumor has reduced the airway to approximately 10% of normal. A sagittal view of the MRI scan shows the tumor involving approximately six rings of trachea (Fig. 10.262). Induction of general anesthesia for endoscopy and surgical resection required jet ventilation. The jet ventilation catheter was passed posterior to the tumor and its tip was placed distal to the tumor. An endoscopic view of the tumor with a 0-degree telescope shows the tumor presenting like a horseshoe, occupying the anterior three quarters of the circumference of the trachea, as seen on the preoperative MRI scan (Fig. 10.263). A sleeve resection of the trachea and primary anastomosis was performed for this patient. A postoperative MRI scan shows a restored normal airway (Fig. 10.264).

Resection of Parastomal Recurrence

Parastomal recurrence of a carcinoma following a total laryngectomy is most frequently seen as a result of recurrent disease developing in tracheoesophageal groove/paratracheal lymph nodes presenting under the skin. The parastomal recurrence may manifest as a small mobile tumor mass in the superior or lateral aspect of the tracheostome, or it may manifest in the lower half of the tracheostome with direct extension of disease to the mediastinal lymph nodes.

Figure 10.265 A patient with a parastomal recurrence involving the superolateral aspect of the left-hand side of the tracheostome.

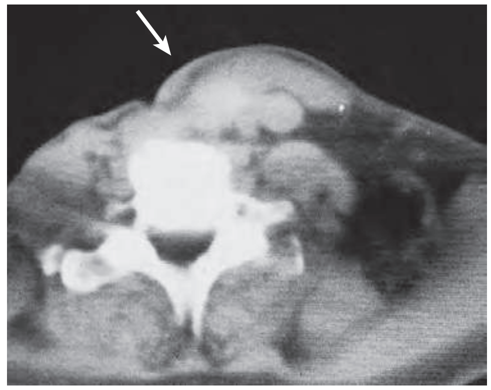

Figure 10.266 A computed tomography scan of the lower part of the neck, showing parastomal recurrence (*arrow*).

Figure 10.267 The extent of skin resection and the sternoclavicular joints are outlined.

From a strictly surgical standpoint, the parastomal recurrence that presents adjacent to the upper half of the circumference of the tracheostome is relatively easy to manage and has a higher potential for control of disease. On the other hand, lesions that present at the lower half of the circumference of the tracheostome have reduced mobility because of direct extension of disease in the mediastinum and are less likely to be amenable to a satisfactory surgical resection.

The patient shown in Fig. 10.265 has a parastomal recurrence involving the superolateral aspect of the left-hand side of the tracheostome. The tumor mass measures 3.5 cm in diameter and is mobile over the deeper soft tissues. A CT scan of the lower part of the neck shows the tumor clearly presenting as a distinct mass under the medial head of the sternomastoid muscle at the level of the tracheostome, with extension of disease outside the capsule of the metastatic node to involve the adjacent soft tissues (Fig. 10.266). The mass is adherent to the sternoclavicular joint inferiorly.

Surgical resection of this tumor requires wide excision of a generous portion of skin around the tracheostome, including the mucocutaneous junction of the tracheostome and the stump of the distal trachea, as outlined in Fig. 10.267. Note the surface markings of the manubrium and the sternoclavicular joints on both sides in relation to the extent of the skin excision.

The surgical resection entails a through-and-through resection of the skin, underlying soft tissues, distal trachea, and all the gross disease en bloc with the medial third of the left clavicle and the manubrium sterni. A circular skin incision is made at the site of the proposed excision of skin over the parastomal recurrence. A second midline vertical incision is made from the lower border of the circular skin incision over the manubrium sterni. The lower skin flaps are elevated first, and then the muscular attachments over the medial half of the clavicle are detached. The sternomastoid muscle is detached from its superior surface and the subclavius muscle is detached from its undersurface.

A periosteal elevator is then used to elevate the periosteum of the medial third of the clavicle, and a Doyen's rib raspatory is used to elevate the periosteum of the clavicle circumferentially. The clavicle is divided with a power saw. The sternal attachments of the pectoralis major muscle are then elevated to expose the manubrium, and a sternal power saw is used to divide the sternum at the desired level of resection. Alternatively, a power drill and an olive-shaped burr may be used to create a trench along the right sternocostal and inferior manubriosternal joints. This trench is created through the outer cortex and the cancellous part of the manubrium up to its posterior cortex. A Lebsche knife is then used to divide the manubrium along this trench.

Division of the manubrium and the clavicle as described will now permit mobilization of the surgical specimen and entry into the superior mediastinum. By alternate blunt and sharp dissection and particularly by delicate sharp dissection behind the sternoclavicular joint and at the junction of the clavicle and the first rib, the bony component of the specimen is mobilized. During this dissection, meticulous attention is required to avoid inadvertent injury to the subclavian and innominate veins. Careful dissection of these veins from the posterior aspect of the sternoclavicular joint is undertaken first and, using a malleable retractor, these delicate great veins are protected during this phase of the operation.

Finally the specimen is rotated to the right-hand side and cephalad to dissect all the mediastinal lymph nodes and soft tissues. The specimen now remains attached only through the trachea, which is divided last, distal to the visible and palpable recurrent tumor. The endotracheal tube is removed, the trachea is transected to deliver the specimen, and the endotracheal tube is reintroduced into the distal trachea.

After removal of the specimen, the surgical field shows adequate clearance of the superior mediastinum (Fig. 10.268). The confluence of the internal jugular and subclavian veins forming the left innominate vein is seen clearly in the field. A close-up view of the upper part of the surgical field demonstrates the lower end of the carotid sheath with the left common carotid artery and the internal jugular vein as well as the esophagus (Fig. 10.269). In a close-up view of the superior mediastinum, the innominate vein and the stump of the trachea are seen clearly (Fig. 10.270).

The specimen shows a generous portion of skin with the mucocutaneous junction and distal trachea resected en bloc with the manubrium and the medial half of the left clavicle (Fig. 10.271). The posterior aspect of the specimen shows all

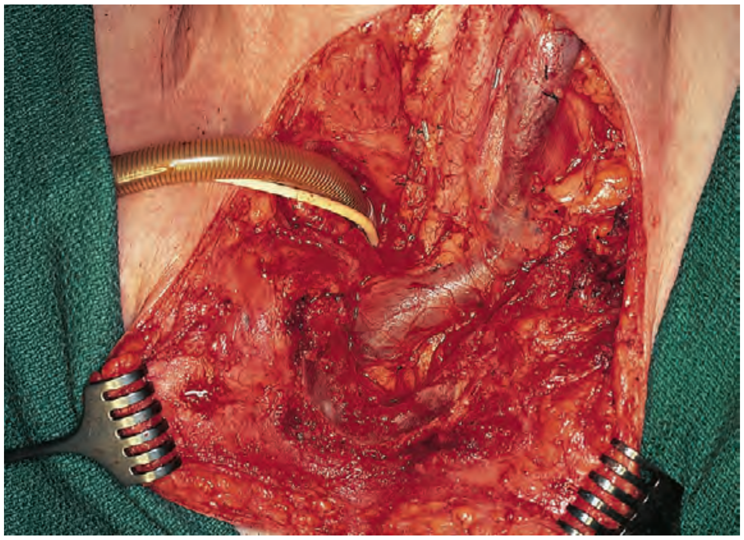

Figure 10.268 The surgical field following resection of the tumor.

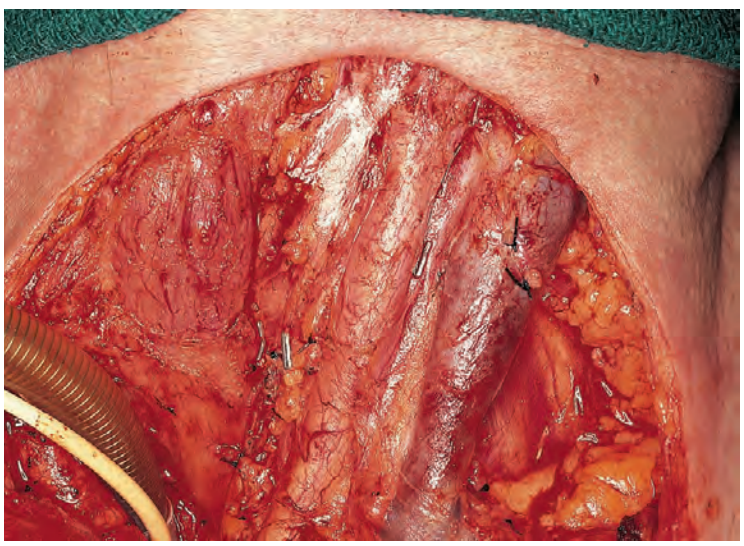

Figure 10.269 A close-up view of the upper part of the surgical field shows the carotid artery and internal jugular vein.

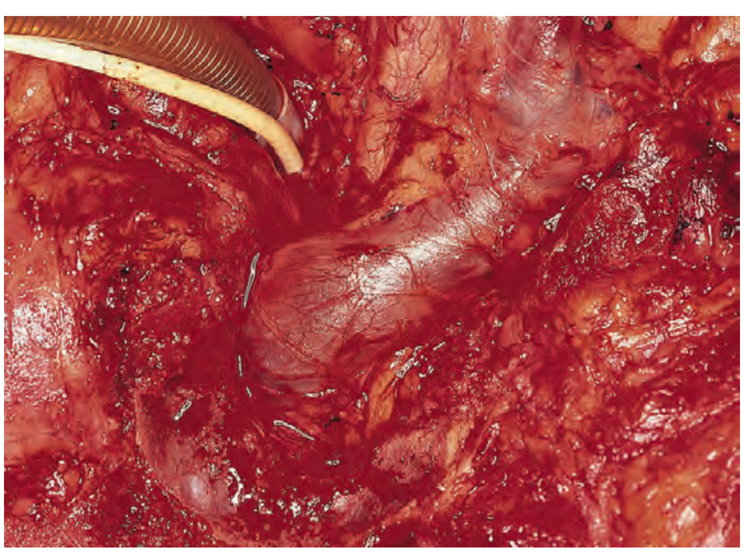

Figure 10.270 A close-up view of the superior mediastinum shows the left innominate vein and the stump of the trachea.

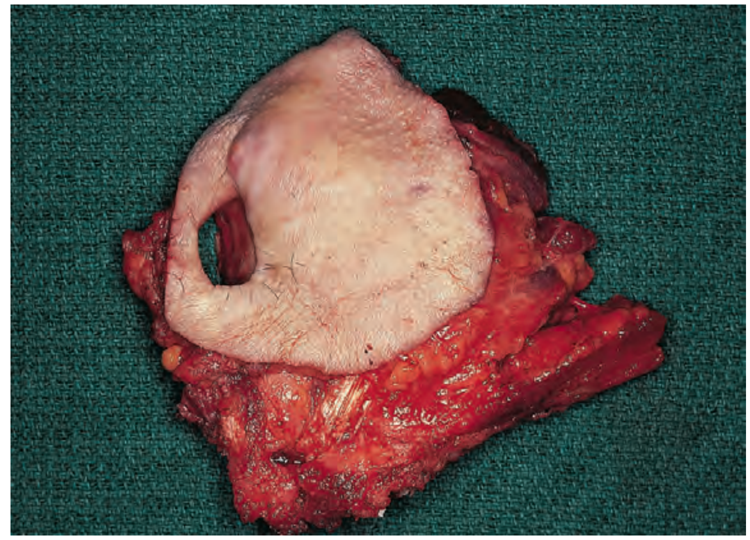

Figure 10.271 The anterior view of the surgical specimen.

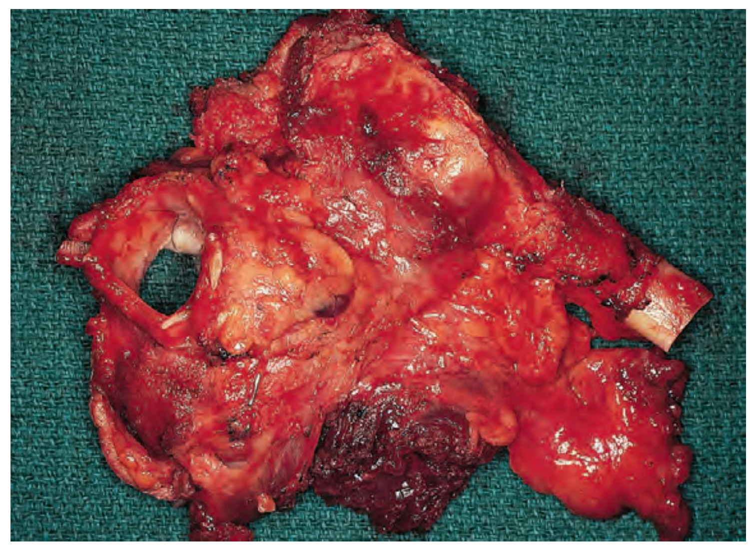

Figure 10.272 The posterior aspect of the specimen.

the excised superior mediastinal lymph nodes along with the stump of the trachea, the posterior surface of the sternoclavicular joint, and the stump of the attached sternomastoid muscle (Fig. 10.272).

The surgical defect created by resection of this parastomal recurrence requires coverage of a large area of skin loss and soft tissue to fill the dead space beneath. A variety of flaps are available to accomplish this objective. From the simplest to the more complex, they are (1) a deltopectoral flap, (2) a pectoralis major myocutaneous flap, and (3) a rectus abdominis or anterolateral thigh (ALT) free flap. In this patient, a medially based deltopectoral flap is elevated from the left side and rotated cephalad and medially to cover the surgical defect. The tip of the deltopectoral flap is first brought to the surgical defect and sutured to the stump of the tracheostome. The flap rotates easily into the space created by resection of the clavicle and the sternum and helps fill the dead space.

The donor site defect of the deltopectoral flap on the anterior chest wall is closed primarily by mobilizing the upper and lower skin flaps. Completed closure of the surgical defect is shown in Fig. 10.273.

Figure 10.273 Completed closure of the surgical defect with a deltopectoral flap.

Figure 10.275 The preoperative appearance of a patient with an extensive parastomal recurrence.

Figure 10.274 The appearance of the patient 6 months after surgery.

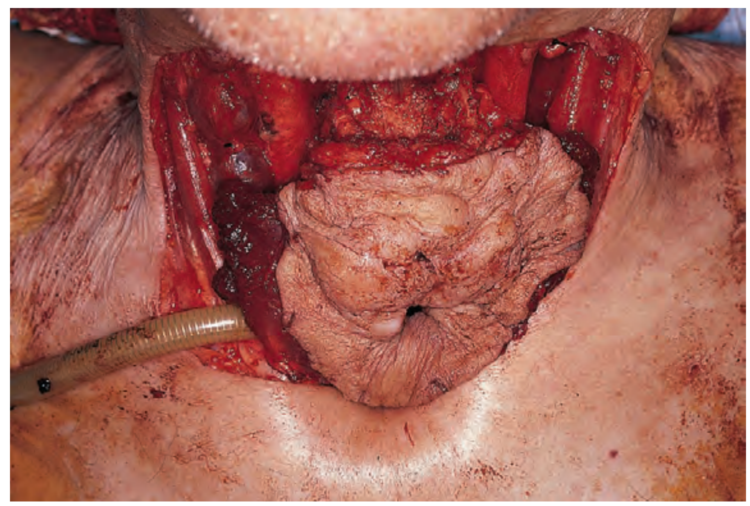

Figure 10.276 A generous portion of the skin is excised along with the tumor and viscera of the central compartment.

The appearance of the patient 6 months following surgery shows well-healed scars (Fig. 10.274). The deltopectoral flap has provided satisfactory closure of the skin defect in the mediastinum and has helped to bring a mediastinal tracheostome to the surface.

A parastomal recurrence of modest dimensions at the upper half of the circumference of the tracheostome as described in the preceding procedure is suitable for a relatively conservative surgical resection. The surgical defect usually can be closed with rotated regional flaps. The potential for cure in this clinical setting is reasonably good, and the surgical procedure is worthy of consideration.

Resection of Extensive Parastomal Recurrence With a Total Pharyngoesophagectomy

Patients with a parastomal recurrence that involves the upper half of the margin of the tracheostome and extensively invades the adjacent skin, soft tissues, and the underlying pharynx or esophagus are considered suitable candidates for a curative resection as long as the disease does not invade the carotid sheath on either side. The patient shown in Fig. 10.275 has an extensive parastomal recurrence, with a tumor fungating through the skin of the central compartment of the neck and invading the underlying pharyngoesophageal junction. However, the tumor does not invade the carotid sheath or extend into the mediastinum. The plan of surgical resection is to excise a generous portion of the skin of the neck in conjunction with through-and-through resection of the soft tissues of the central compartment of the neck, including the pharynx, esophagus, distal trachea, and all the soft tissues and lymph nodes in the superior mediastinum (Fig. 10.276). Clearance of the neck will include all the tissues from carotid sheath to carotid sheath.

Mobilization of the surgical specimen in the neck has been completed with adequate clearance of the tumor (Fig. 10.277). The upper thoracic esophagus has been mobilized from this exposure up to the carina. A laparotomy is performed to mobilize the stomach and the distal thoracic esophagus. Once the esophagus is completely mobilized, it is pulled out of the thoracic cavity, bringing the stomach in to the neck. The gastroesophageal junction is divided and the specimen is removed.

A pharyngogastrostomy is completed between the fundus of the stomach and the lower end of the stump of the pharynx. The skin and soft tissue defect in the neck is reconstructed with a pectoralis major myocutaneous flap. The appearance of the patient 3 months following surgery (Fig. 10.278) shows satisfactory coverage of the soft tissue and skin defect with the tracheostome created low in the suprasternal notch.

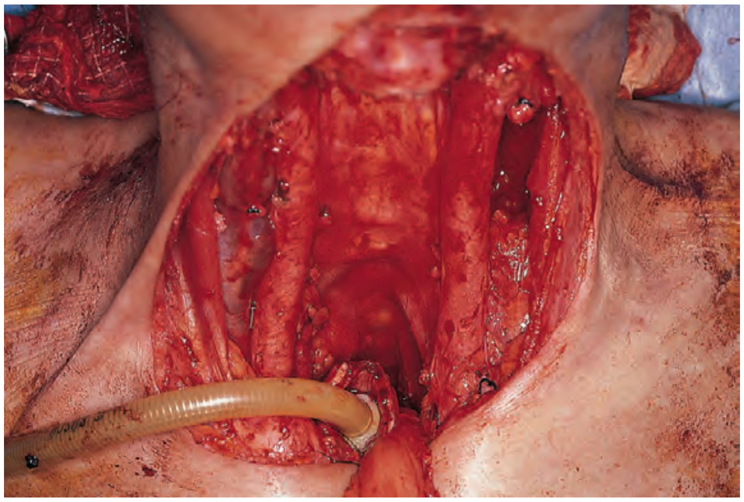

Figure 10.277 The surgical defect showing clearance of all tissue from one carotid sheath to the other.

Figure 10.278 The appearance of the patient 3 months after surgery.

If a total esophagectomy is not believed to be necessary, the pharyngoesophageal junction can be reconstructed with a jejunal free flap or a tubed radial forearm or ALT flap, and coverage for the skin can be provided by a deltopectoral flap or a pectoralis myocutaneous flap. Resections of this magnitude are still believed to be curative in some patients but prove to be palliative in most situations.

Rehabilitation of a Paralyzed Vocal Cord

Vocal cord paralysis may result from primary carcinomas of the larynx or other conditions such as cerebrovascular stroke, central neurologic lesions, involvement of the vagus nerve by tumor or surgery, invasion of the recurrent laryngeal nerve from thyroid cancer and mediastinal disease, or iatrogenic injury to the vagus or recurrent laryngeal nerve. Paralysis of the vocal cord caused by any reason other than a primary carcinoma of the larynx should be considered for rehabilitation. Hoarseness and aspiration are sequelae resulting from a paralyzed vocal cord. Hoarseness occurs because of a glottal gap as a result of fixation of the vocal cord in the paramedian or lateral (abducted) position and atrophy of the paralyzed vocalis muscle. The resultant glottic incompetence leads to aspiration of saliva and fluids, posing the risk for pneumonia. Some patients regain glottic competence as a result of adequate compensation from

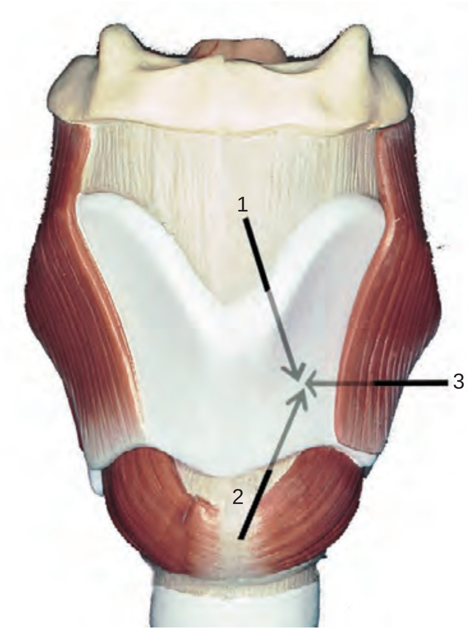

Figure 10.279 Routes of injection for vocal cord medialization: *1*, thyrohyoid membrane; *2*, cricothyroid membrane; *3*, thyroid cartilage.

the contralateral functioning vocal cord, thus achieving reasonable glottic closure. When a persistent glottal gap exists, restoration of glottic competency can be achieved by medialization of the paralyzed vocal cord.

Predictable improvement in the quality of voice can be expected for patients with unilateral paralysis of the vocal cord when medialization procedures are used. Medialization of the paralyzed vocal cord can be accomplished by introduction of inert substances in the paraglottic space. The materials available for medialization are injectable or solid. Injectable materials offer medialization for varying lengths of time, ranging from a few weeks to a couple of years. Temporary medialization can be achieved with injection of liquid Gelfoam, which usually is recommended if return of function of the paralyzed vocal cord is anticipated. On the other hand, a permanently paralyzed vocal cord can be medialized with injectable materials such as hydroxyapatite paste, acellular dermis, and Teflon paste. The risk of granuloma formation resulting from exposure to the injected material is high with Teflon paste, and therefore it generally is not the material of choice for vocal cord medialization. Permanent medialization requires placement of an inert, solid shim made of soft Silastic material or polytetrafluoroethylene (Gore-Tex) ribbon.

Injection for Vocal Cord Medialization

The technique for injection of an inert substance for medialization of the vocal cord is simple and can be done in an ambulatory setting. The equipment required consists of a flexible fiberoptic nasolaryngoscope with video display, a disposable syringe with a 21-gauge needle, and the material selected for injection. The patient is positioned upright in a chair, and the nasal cavity and pharynx are topically anesthetized with 1% lidocaine spray. The nasolaryngoscope is positioned to give a panoramic view of the interior of the larynx.

Injection may be performed through one of three routes: (1) through the thyrohyoid membrane, (2) through the cricothyroid membrane, or (3) through the thyroid cartilage (Fig. 10.279). The thyrohyoid membrane route is preferred, because the thyroid cartilage often is difficult to negotiate with a fine-bore needle.

The needle is inserted through the thyrohyoid membrane and directed toward the paraglottic space along the inner surface of the thyroid cartilage. Under direct visualization through the nasolaryngoscope, the tip of the needle is positioned in the paraglottic space just below the plane of the free edge of the true vocal fold. The injection material is deposited in two locations to achieve adequate medialization for accurate apposition by the contralateral vocal cord. The patient is asked to phonate during the injection to minimize overinjection and airway compromise. The amount of material necessary to achieve satisfactory medialization in most patients is less than 1 mL. Injection directly under the mucosa should be avoided to prevent extrusion of the material. The procedure is terminated when satisfactory voice quality is achieved without compromise of the airway.

Laryngoplasty for Vocal Cord Medialization

The laryngoplasty procedure is recommended in patients in whom unilateral paralysis of the vocal cord has taken place for any reason and for whom life expectancy is reasonably good. A laryngoplasty effectively attains medial shift of the paralyzed vocal cord, allowing adequate apposition by the mobile contralateral vocal cord and thus improving the voice quality.

The operative procedure usually is performed under local anesthesia with mild sedation. A topical anesthetic is applied to the mucosa of the supraglottic larynx either by a spray or by direct instillation of a topical anesthetic agent in the valleculae and pyriform sinuses and in the vestibule of the larynx. In addition, a bilateral superior laryngeal nerve block is performed by injecting approximately 5 mL of 1% lidocaine (lignocaine) with epinephrine on the lateral aspect of the thyrohyoid membrane where the surface marking for the entry of the superior laryngeal nerve into the supraglottic larynx is fairly constant. This process is depicted on the model in Fig. 10.280, where the superior laryngeal nerve is shown entering the thyrohyoid membrane near the lateral end of the greater cornua of the hyoid. After adequate topical anesthesia is achieved and a superior laryngeal nerve block is performed, 1% lidocaine is injected through the skin and subcutaneous tissues up to the lamina of the thyroid cartilage on the side where the surgery is to be performed. An area of skin and soft tissues overlying the ala of the thyroid cartilage from the midline up to the posterior border of the thyroid lamina is anesthetized.

A transverse incision approximately 3 cm in length is made, extending from the midline of the thyroid cartilage up to its posterior edge approximately 5 to 7 mm superior to the lower border of the thyroid cartilage (Fig. 10.281). The skin incision is deepened through the platysma to expose the strap muscles (Fig. 10.282). The fascia in the midline is incised (Fig. 10.283). Similarly, the perichondrium also is incised in the midline to expose the underlying thyroid cartilage. The perichondrium is elevated with a fine periosteal elevator to expose the anterior half of the lamina of the thyroid cartilage. A Richardson retractor is used to retract the strap muscles and the perichondrium to expose the thyroid lamina (Fig. 10.284). A rectangular window in the thyroid cartilage is now made with a variable-speed electric drill with an ultrafine burr (Fig. 10.285). The position of this rectangular window is critically important. The rectangle is horizontally oriented, with its anterior border beginning approximately 5 mm posterior to the midline of the thyroid cartilage (Fig. 10.286). The lower border of the rectangular window is approximately 5 mm from the lower border of the thyroid cartilage, as shown in the model. The high-speed drill

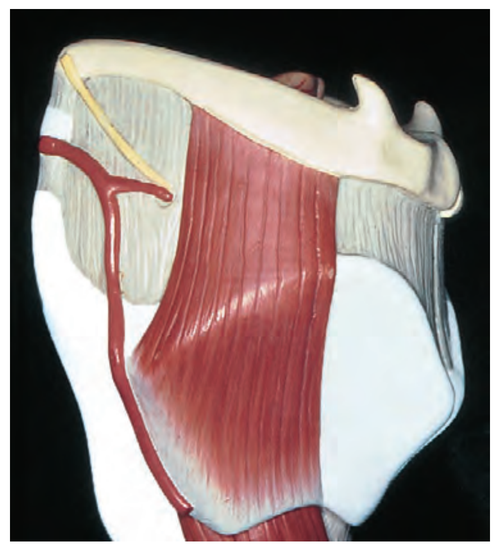

Figure 10.280 Model showing the superior laryngeal nerve entering the thyrohyoid membrane near the lateral end of the greater cornua of the hyoid.

Figure 10.281 The outlines of the thyroid and cricoid cartilages are shown in relation to the skin incision.

Figure 10.282 The skin incision is deepened through the platysma.

Figure 10.283 The fascia in the midline is incised longitudinally along its long axis.

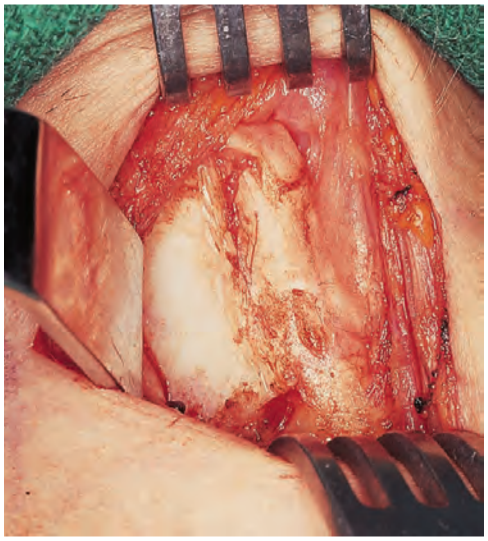

Figure 10.284 The strap muscles and the perichondrium are retracted to expose the thyroid lamina.

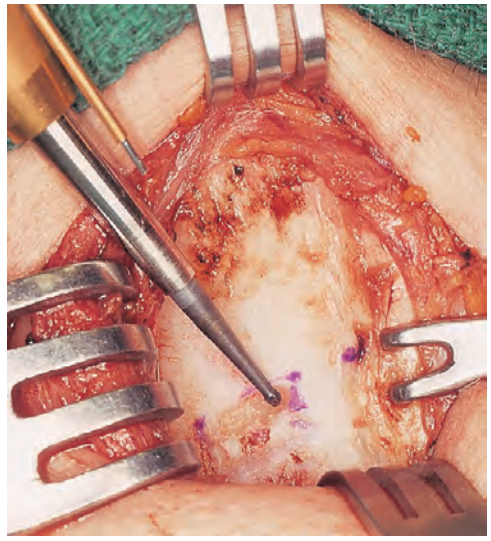

Figure 10.285 A rectangular window in the thyroid cartilage is made with a drill and a fine burr.

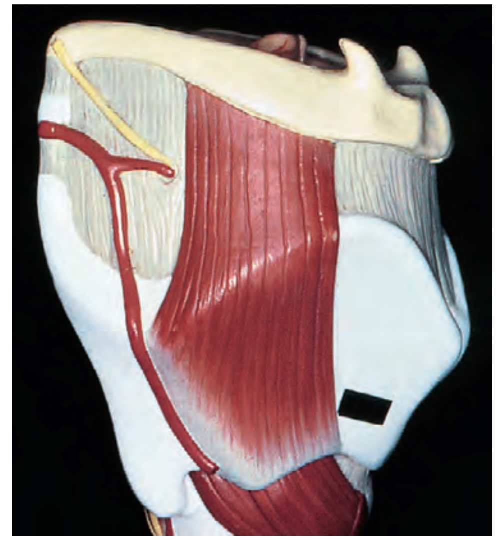

Figure 10.286 The location of the rectangular window in the thyroid cartilage.

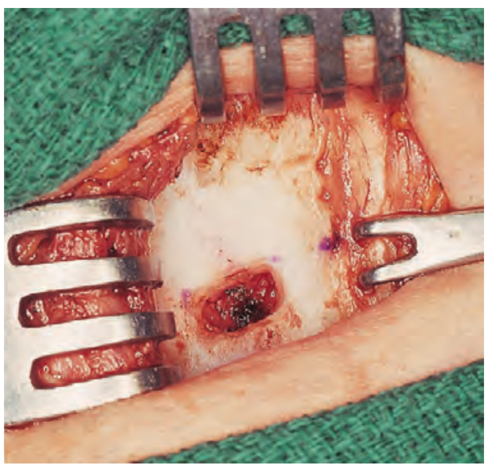

Figure 10.287 The cartilage window extends up to the inner perichondrium.

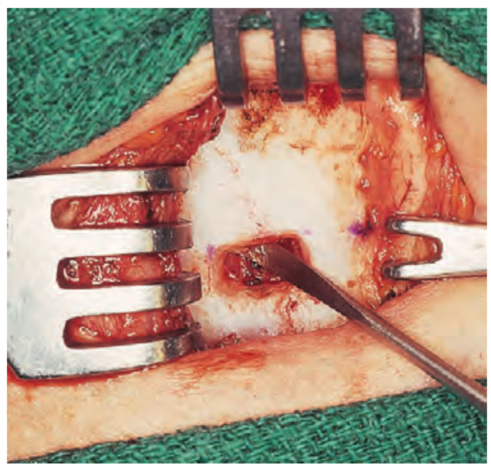

Figure 10.288 A Penfield dural elevator is used to elevate the inner perichondrium and the underlying soft tissues of the interior of the larynx.

Figure 10.289 A solid block of soft Silastic material is now used to fabricate the wedge-shaped Silastic shim.

is used with extreme caution to avoid laceration of the inner perichondrium or the soft tissues in the interior of the larynx; otherwise, a hematoma invariably will occur and significantly jeopardize the operative procedure (Fig. 10.287). Once the cartilage window is created with the drill, a Penfield dural elevator is used to elevate the inner perichondrium and the underlying soft tissues of the interior of the larynx in all four directions (Fig. 10.288). A Freer periosteal elevator is now used to assess the degree of medial displacement of the vocal cord necessary to achieve the desired quality of voice. The periosteal elevator is introduced through the rectangular window pointing posteriorly, the soft tissues of the interior of the larynx are shifted medially, and the patient is asked to phonate. When the desired quality of voice is achieved, an estimate is made regarding the size of the Silastic wedge necessary to create such displacement of the vocal cord and to maintain it in that position. A solid block of soft Silastic material is used to fabricate the wedge-shaped Silastic shim necessary for medial displacement of the vocal cord (Fig. 10.289). Alternatively, a Dacron (Gore-Tex) ribbon may be used (Fig. 10.290). The advantage of the ribbon is that it enables the surgeon to customize the quality of voice desired by introducing only the necessary length of the ribbon to achieve the desired result (Fig. 10.291). The pitch of the voice can be tested with varying lengths of the ribbon until the exact length necessary to achieve the desired voice quality is found.

With use of nontoothed fine DeBakey forceps, the shim is grasped with its handle, and its posterior portion (the base of the triangular wedge) is first introduced through the rectangular window toward the posterior part of the larynx. The anterior part of the shim then is introduced by compressing the shim and easing it into the paraglottic space (Fig. 10.292). Once the shim is in position, its handle is used to adjust its permanent position. The patient is now asked to phonate again to assess the voice quality. If the voice is still too hollow, the shim is too small and a bigger shim is necessary. On the other hand, if the voice is too shrill or the patient experiences difficulty with breathing, causing stridor, then the shim is too big and needs to be trimmed. With experience, a shim of an appropriate size is fabricated to reach the desired quality of voice without compromise of the airway (Fig. 10.293). Once the shim is properly positioned, the strap muscles are allowed to return to their normal position and are reapproximated with interrupted

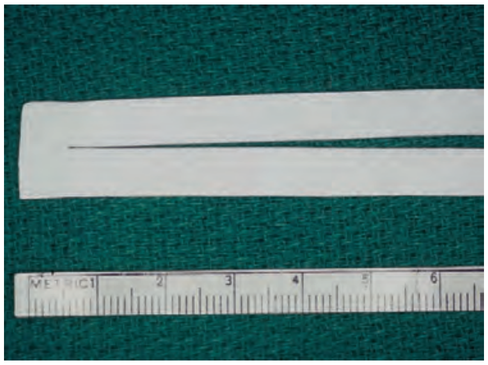

Figure 10.290 Gore-Tex ribbon.

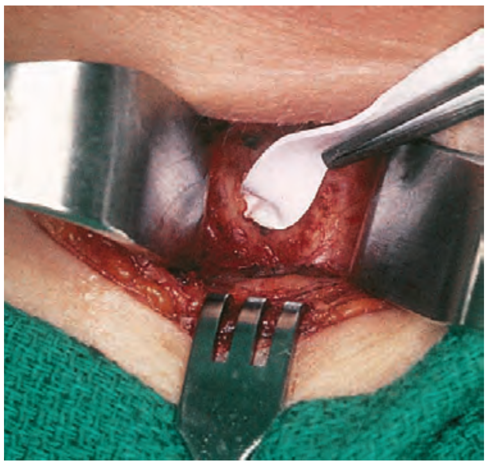

Figure 10.291 A Gore-Tex thyroplasty.

Figure 10.292 The posterior part of the shim is introduced by compressing the shim and easing it into the paraglottic space.

chromic catgut sutures. The platysma is closed with interrupted chromic catgut sutures, and the skin is closed in the usual fashion with interrupted 5-0 nylon sutures.

Minimal postoperative care is necessary after this procedure. However, the patient should be observed carefully for several hours for the possibility of respiratory distress. Occasionally a hematoma may occur, leading to progressive respiratory difficulty. After this operative procedure, significant laryngeal edema may develop in patients who previously have undergone irradiation, and they may need to be observed carefully for respiratory compromise. Significant improvement in the voice quality should be expected in most patients who undergo a laryngoplasty.

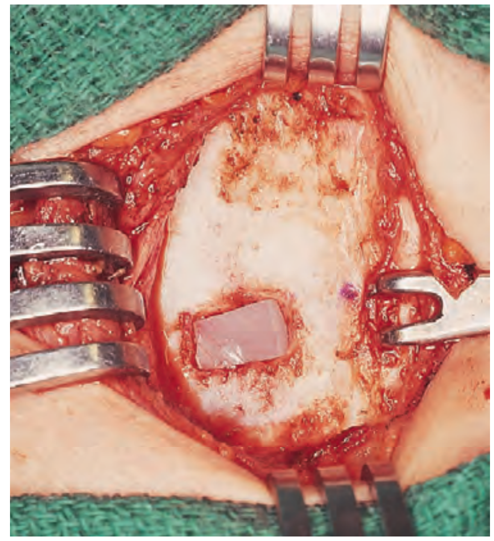

Figure 10.293 An appropriate size of the shim is fabricated to reach the desired quality of voice without compromise of the airway.

Voice Rehabilitation After Total Laryngectomy

Restoration of voice after a total laryngectomy can be achieved by (1) esophageal speech, (2) an electrolarynx, and (3) TEP and voice prosthesis. Esophageal speech requires intense training, a motivated patient, and prolonged practice to achieve serviceable speech. Only a minority of patients are able to develop good esophageal speech, and even in these patients, the quality of speech is suboptimal and the length of words produced per charge of regurgitated air is limited. Use of an electrolarynx does not require swallowing and regurgitation of air; it produces sound by mechanical resonance of the pharyngeal air column. An electrolarynx also requires prolonged training and practice to produce understandable speech. The quality of speech produced sounds mechanical and thus is suboptimal in many patients. Tracheoesophageal puncture, and voice prosthesis on the other hand, provides lung-powered speech by driving air from the lungs into the pharynx through the prosthetic valve, and thus the voice has a stronger, sustained, and more intelligible quality. Delivery of the pulmonary air into the pharynx is controlled by a duckbill type of prosthesis that has a one-way valve that prevents regurgitation of saliva and food into the trachea but permits delivery of air into the esophagus freely. The currently available prosthetic devices include the Blom-Singer and the Provox prosthesis, which is a significant improvement over the duckbill valve because it can be retained in place up to 6 months without a change. TEP can be performed primarily at the time of total laryngectomy and is preferred if local tissue quality and pharyngeal closure are satisfactory (see the details provided in the description of the wide-field total laryngectomy procedure). On the other hand, in patients who previously have undergone irradiation and in patients who have a high risk for wound complications, TEP is best delayed to a secondary setting after complete healing of the pharyngoesophageal suture line.

Secondary Tracheoesophageal Puncture

The secondary TEP operative procedure can be performed either under general anesthesia or under local anesthesia with mild sedation. For satisfactory performance of the tracheoesophageal puncture, an adequate tracheostome is essential (Fig. 10.294). Ideally the tracheostome should be of an oval shape with direct access to the membranous trachea and its mucocutaneous junction in the posterior wall of the tracheostome. The location of

Figure 10.294 An adequate tracheostome is essential.

Figure 10.295 The instruments required for a tracheoesophageal puncture.

the tracheoesophageal puncture is approximately 5 mm below the mucocutaneous junction. The instruments required for the procedure are shown in Fig. 10.295. This is a commercially available kit for performing a TEP and introduction of the voice prosthesis. The kit consists of a curved introducer with a removable trocar to fit in the introducer. It has a semirigid flexible guidewire with a hole at its tip. Any commercially available voice prosthesis (Blom-Singer or Provox) can be used with the kit. The kit also has a couple of microhemostats. The currently available voice prostheses do not require change for at least 6 months (Fig. 10.296). The short Jesberg esophagoscope with the light source at its tip is the ideal instrument for the procedure, because it has a wide oval-shaped mouth with a protective anterior lip at the tip (Fig. 10.297). The Jesberg esophagoscope is introduced through the oral cavity in the esophagus and advanced up to the level of the tracheostome (Fig. 10.298). It is now rotated 180 degrees to have its "mouth" face the membranous trachea at the upper end of the tracheostome The light at the distal end of the esophagoscope readily shows illumination through the membranous trachea, showing the position of the tip of the esophagoscope (Fig. 10.299). The trocar with the introducer threaded over it is used to make a puncture through the membranous trachea at the desired location (Fig. 10.300). By looking through the esophagoscope, the tip of the trocar is seen projecting in the lumen of the esophagoscope. The posterior lip of the esophagoscope readily protects the anterior wall of the esophagus from inadvertent injury by the

Figure 10.296 Currently used voice prostheses.

Figure 10.297 The distal tip of the Jesberg esophagoscope.

Figure 10.298 A Jesberg esophagoscope is introduced through the oral cavity.

trocar. The curvature of the trocar directs the puncture and the trocar tip cephalad, and within the lumen of the esophagoscope. The trocar is now withdrawn, leaving the introducer in position. The guidewire is now threaded through the introducer into the lumen of the esophagoscope until its distal tip is brought out of the esophagoscope. The esophagoscope is now withdrawn, leaving the guidewire in position (Fig. 10.301). The long flange of the voice prosthesis is now threaded through the hole in the distal end of the guidewire (Fig. 10.302). The introducer is now withdrawn from the tracheostome, and the guidewire is pulled out of the puncture site along with the threaded voice prosthesis, until its long flange is pulled out of the trocar hole in membranous

Figure 10.299 The light at the distal end of the esophagoscope locates its position.

Figure 10.300 A puncture is made through the membranous trachea into the esophagus with the trocar and the introducer.

Figure 10.301 A guidewire is threaded through the introducer and brought out of the esophagoscope in the oral cavity.

trachea (Fig. 10.303). A fine hemostat is now used to grasp and ease out the outer flange of the prosthesis through the trocar hole into the tracheostome. The long flange on the prosthesis is cut, and the prosthesis rotated in its proper position (Fig. 10.304). Finally, the esophagoscope is introduced again in the esophagus

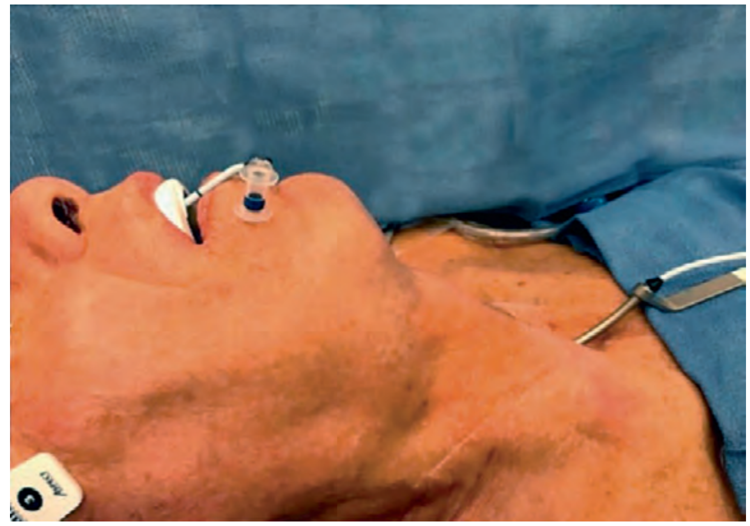

Figure 10.302 The long flange of the voice prothesis is threaded onto the guidewire.

Figure 10.303 The guidewire and the voice prosthesis are pulled out of the tracheoesophageal puncture.

Figure 10.304 The accurate positioning of the voice prosthesis in the tracheostome.

to check the position of the inner flange of the prosthesis in the lumen of the esophagus. It should be sitting snug against the inner wall of the esophagus (Fig. 10.305). Postoperatively the patient receives instruction regarding production of tracheo-esophageal speech and maintenance of the prosthesis from a

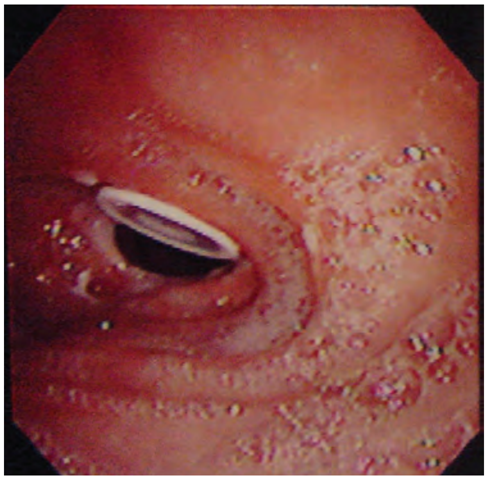

Figure 10.305 An endoscopic view showing the inner flange of the voice prosthesis in the cervical esophagus.

Figure 10.306 A stoma valve facilitates hands-free tracheoesophageal speech.

speech therapist. Significantly improved quality of speech is expected in most patients undergoing tracheoesophageal puncture and placement of a voice prosthesis.

To produce speech, the patient must direct air from the trachea to the esophagus, which requires occlusion of the tracheostome during phonation. This process requires the use of a thumb or a finger to occlude the stoma while the patient is speaking. Most patients get along well with this technique. However, if the patient finds use of the finger to be cumbersome, one-way tracheostome valves are available that are applied to the tracheostome for spontaneous production of speech. These valves are glued to the skin adjacent to the tracheostome and carry a one-way flip valve that permits inhalation of air through the valve into the tracheobronchial tree, but during exhalation the valve closes itself and directs the air into the esophagus through the tracheoesophageal prosthesis (Fig. 10.306). The valve is calibrated in such a way that during quiet breathing, air passage through the valve takes place in both directions; however, during phonation, higher intrathoracic pressure is created, which forces the valve to close and directs the air into the esophagus. The currently available tracheostome valves are serviceable but not optimal, and further technical research into their development is required.

POSTOPERATIVE CARE

Postoperative care of patients undergoing laryngeal surgery is directed by whether the surgical procedure is transoral endoscopic or open. Most patients who have undergone endoscopic surgery will not have a tracheostomy. The immediate postoperative care therefore centers around careful observation of the airway and monitoring for bleeding. In general, administration of steroids is recommended to minimize postoperative edema and airway compromise. Antibiotics are given depending on the extent of endoscopic resection and the exposed raw area. Resection for glottic tumors generally does not require antibiotic coverage. On the other hand, patients undergoing larger resections for tumors of the supraglottic larynx, hypopharynx, and oropharynx should receive broad-spectrum antibiotic coverage, especially if they previously have undergone radiation therapy. Antireflux medication is also found to be beneficial in these patients. Humidification of the inspired air is crucial to prevent desiccation of secretions and exudate in the airway, and it improves healing by minimizing crusting of the raw area. Oral alimentation is begun as soon as the patient is able to swallow salivary secretions. Use of a nasogastric feeding tube may be necessary if spontaneous swallowing is delayed because of pain or aspiration.

Patients undergoing open partial laryngeal surgery usually will have a tracheostomy. Therefore intensive tracheostomy care for clearance of pulmonary secretions is crucial to prevent pneumonia. Management of the tracheostomy and suctioning of pulmonary secretions should be provided initially by nursing support. Self-care should be taught to the patient during hospitalization if prolonged use of a tracheostomy is anticipated. Patients undergoing surgery for supraglottic and hypopharyngeal tumors require a temporary nasogastric feeding tube. However, if delayed recovery of swallowing is anticipated, then a percutaneous gastrostomy should be considered for nutritional support.

Patients undergoing a total laryngectomy have a permanent tracheostome. Humidification of inspired air is mandatory in these patients to prevent drying of secretions, crusting, and bleeding from the trachea. Nutrition is maintained through a nasogastric feeding tube during the initial postoperative period. Commencement of oral alimentation depends on several factors: (1) satisfactory healing of the skin wound must occur without significant induration; (2) the patient must be afebrile without a significantly elevated white cell count; and (3) the patient must be able to spontaneously swallow salivary secretions. In general, most patients are able to initiate an oral liquid diet by 7 to 10 days postoperatively.

Although no special wound care is required for patients undergoing a total laryngectomy, these patients are at risk for pharyngeal suture line dehiscence with a resultant pharyngocutaneous fistula. The incidence of fistula formation is dependent on (1) tension on the pharyngeal suture line, (2) configuration of the pharyngeal closure ("T" closure instead of horizontal closure), (3) previous radiation or chemoradiation therapy, (4) nutritional status of the patient, and (5) medical comorbidity such as anemia and diabetes. Certain precautionary measures are helpful to reduce the risk of this serious and morbid complication. The patient should be in an optimal nutritional state and medically fit for the operation. The presence of heavily irradiated and edematous, fibrotic tissue increases the risk of a fistula because of poor wound healing. In such patients, a plan should be made for reconstruction of the surgical defect with nonirradiated regional or distant flaps. Support of the pharyngeal suture line with a pectoralis muscle flap is an additional measure that may reduce the risk and severity of pharyngocutaneous fistulae. If the residual pharynx after a pharyngolaryngectomy is marginal in dimensions or vascularity, it is desirable to complete a circumferential pharyngectomy and use

free tissue transfer for reconstruction. In spite of these measures, a pharyngocutaneous fistula develops in up to 15% to 20% of patients undergoing a laryngectomy, and the incidence increases to 25% to 35% for patients undergoing a salvage laryngectomy after chemoradiation treatment. The development of a fistula in patients who also undergo a neck dissection along with laryngectomy incurs the additional risk of carotid exposure and rupture. Special immediate and definitive measures for prevention of carotid rupture are discussed in Chapter 11. In the absence of massive tissue necrosis or carotid exposure, most fistulae can be managed conservatively with intensive wound care and heal spontaneously. Secondary reconstruction for persistent fistulae should be delayed until inflammatory changes and induration in the neck have subsided.

The potential long-term sequelae of patients undergoing partial laryngeal surgery include alteration of speech, swallowing dysfunction, and compromised airway protection. Alteration of the normal sensorimotor function of the pharyngeal phase of swallowing leads to aspiration and risk of pneumonia. Services of a speech pathologist for instruction in techniques of swallowing are crucial to overcome this functional deficit.

Olfactory dysfunction occurs in the majority of patients undergoing a laryngectomy, because patients no longer have air passing through the nasal cavity. However, some patients regain the sense of smell by developing compensatory techniques. Moreover, gustatory function in these patients is also influenced by olfactory dysfunction. Speech and swallowing dysfunction after a laryngectomy are exacerbated as a result of xerostomia, fibrosis, and neuromuscular dysfunction if the patient has undergone previous radiation or chemoradiation therapy. Finally, the quality of life in patients undergoing a total laryngectomy can be affected because of loss of self-esteem, depression, and social isolation, and thus these patients require appropriate psychosocial support and counseling.

OUTCOMES

The results of treatment for cancer of the larynx are directly dependent on the site of origin of the primary tumor in the larynx and the stage of disease at the time of diagnosis and treatment. Survival for larynx cancer in the United States has modestly declined over the course of the past three decades (Fig. 10.307). There are many reasons that can be hypothesized to explain this decline. These declining trends happened during the years where larynx preservation became an important therapeutic strategy for advanced laryngeal cancers (Fig. 10.308). Whether the increasing use of nonsurgical larynx preservation programs of chemoradiotherapy and declining use of initial surgery for advanced stage laryngeal cancers can be attributed to the decline in survival is an issue which needs further investigation. Overall, for patients from 1994 to 1996 in the United States (NCDB data), the best survival was observed in patients who had initial surgery alone or surgery followed by postoperative radiation therapy (Fig. 10.309). On the other hand, taking an example of T3N0 stage III glottic cancer, the

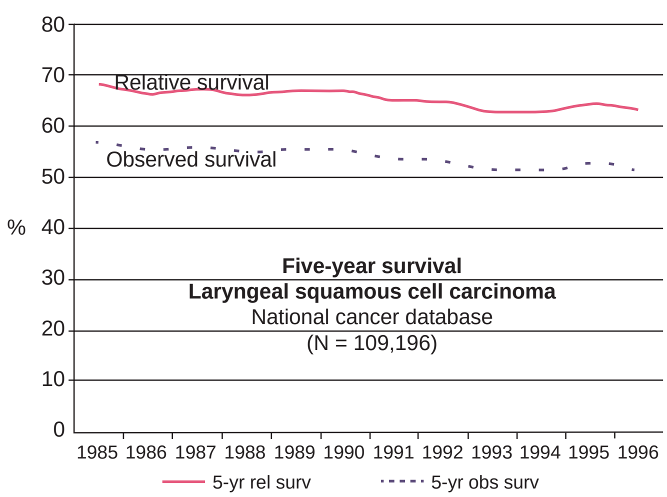

Figure 10.307 Survival for patients with laryngeal squamous cell carcinoma in the United States (NCDB 1985-1996, N = 109, 106 patients).

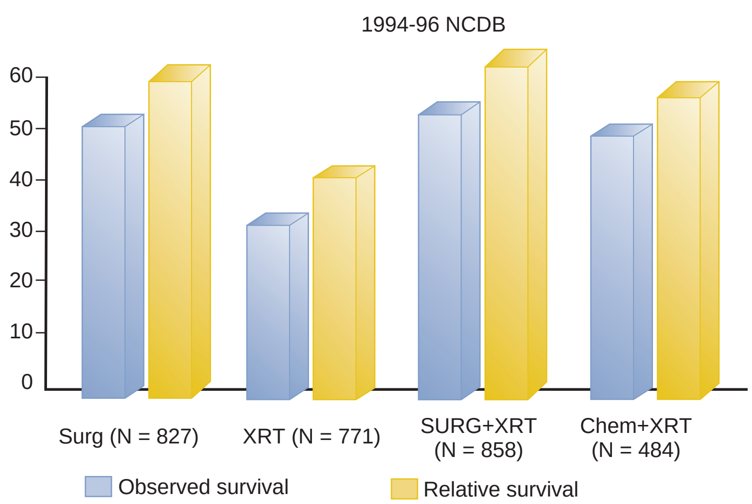

Figure 10.309 The 5-year survival for T3 N0 squamous cell carcinoma of the larynx (all sites) in relation to type of initial treatment (NCDB 1994-1996).

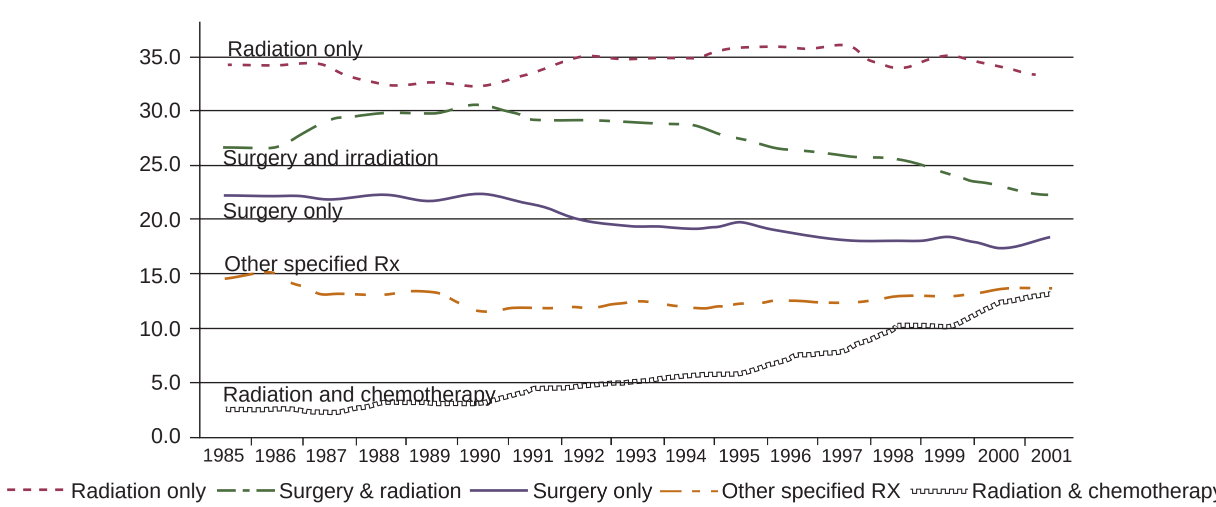

Figure 10.308 Trends in treatment for laryngeal carcinoma in the United States (NCDB 1985-2001, N = 158,426 patients).

survival of these patients is comparable to initial surgery in one reported dataset (Fig. 10.310). Thus the overall impact of initial treatment on advanced stage laryngeal cancers is an area of active investigation, although general trends of disease-specific survival by stage of disease has not shown any significant change over the years (see Fig. 10.8).

The overall 5-year survival rates following treatment for each region of the larynx in patients treated between 1984 and 1998 at Memorial Sloan Kettering Cancer Center are shown in Fig. 10.311. Eighty-one percent of patients with a glottic carcinoma, 77% with a subglottic carcinoma, and 51% with a supraglottic carcinoma survive 5 years. The 5-year disease-free survival of

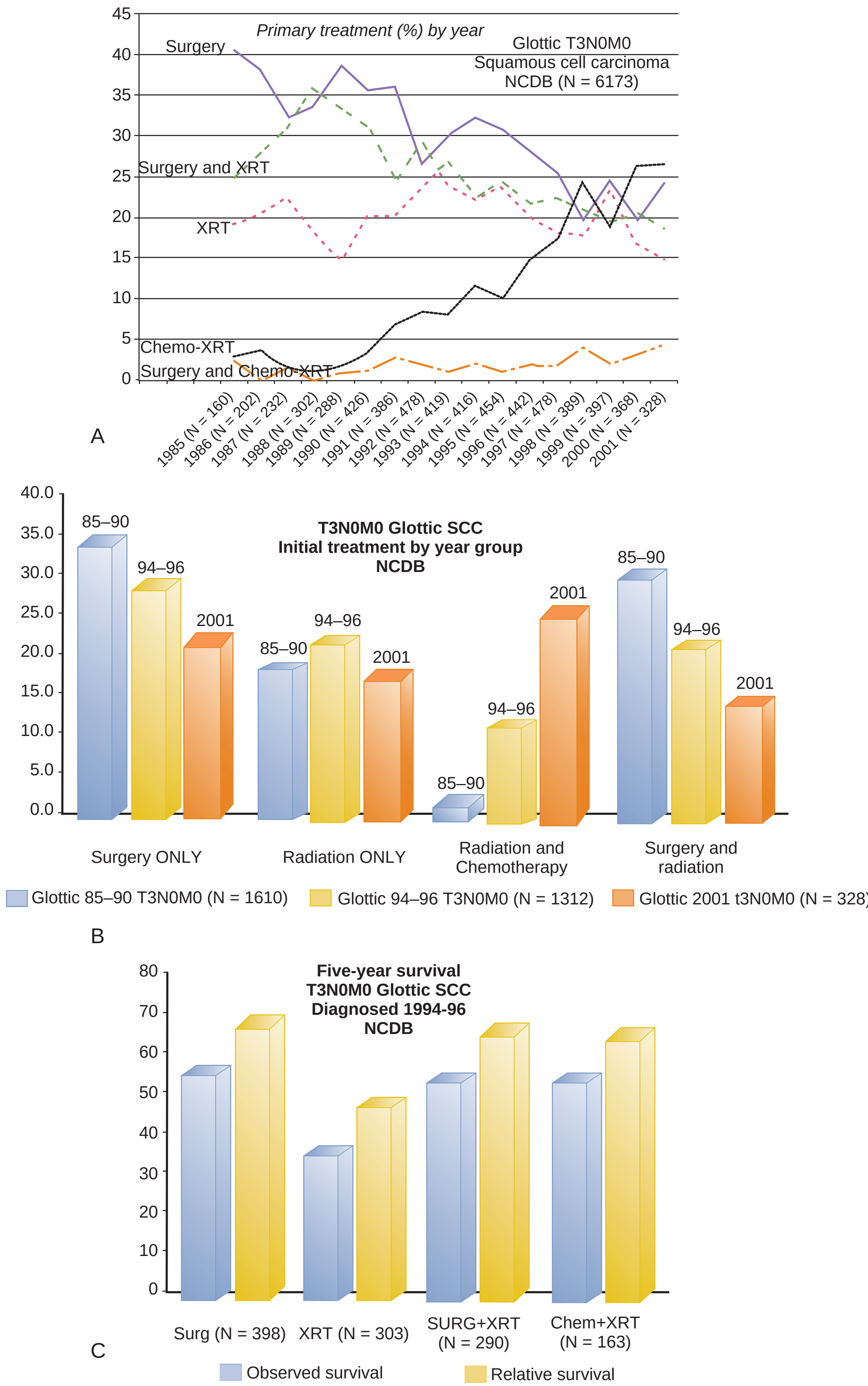

Figure 10.310 Trends in initial treatment and survival for T3 N0 squamous cell carcinoma of the glottic larynx in the United States (NCDB 1985-2001, N = 6,173 patients). **A**, Chemoradiation became the most common initial treatment in 1999. **B**, Comparative treatment preferences by three time periods. **C**, Five-year relative survival rates in relation to type of initial treatment.

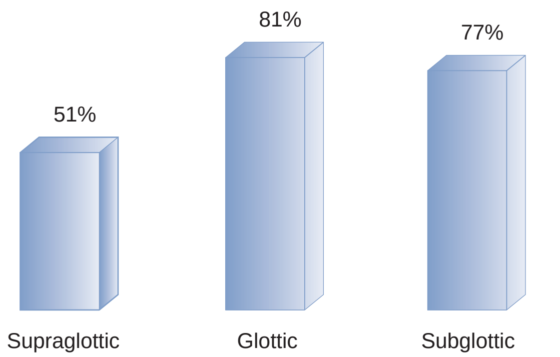

Figure 10.311 The overall 5-year survival after treatment for each region of the larynx.

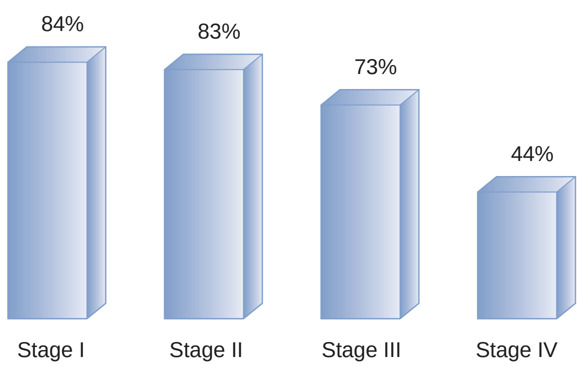

Figure 10.312 The 5-year disease-free survival of patients with supraglottic cancer by stage.

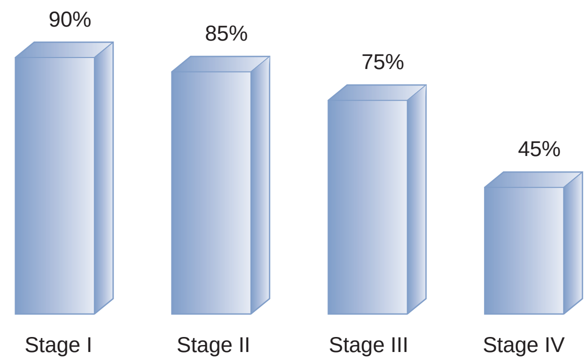

Figure 10.313 The 5-year disease-free survival of patients with glottic cancer by stage.

patients with supraglottic cancer by stage is shown in Fig. 10.312. Eighty-four percent of patients with stage I disease, 83% with stage II disease, and 73% with stage III disease survive 5 years. In contrast, patients with stage IV disease have a 44% probability of 5-year survival. Patients with a carcinoma of the glottic larynx have an excellent long-term prognosis. Ninety percent of patients with stage I tumors and 85% with stage II tumors survive for 5 years (Fig. 10.313). Even with stage III disease, 75% of the patients survive 5 years. The 5-year survival for stage IV disease, however, is only 45%. Data for subglottic carcinoma are not presented by stage because of the small number of patients with a carcinoma in this region.

CHAPTER 11

Cervical Lymph Nodes

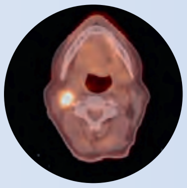

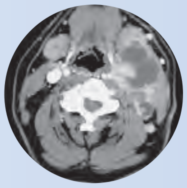

One of the most important factors affecting prognosis for patients with squamous cell carcinoma of the upper aerodigestive tract is the status of cervical lymph nodes at the time of presentation. The presence of nodal metastasis reduces survival by nearly 50% in nearly all squamous cell carcinomas of the upper aerodigestive tract (Fig. 11.1). The exceptions to this are cancers of the nasopharynx and human papillomavirus (HPV)–associated oropharynx cancer, in which presence of ipsilateral lymph node metastasis does not have the same negative prognostic value. In spite of the progress in early detection and advances in imaging techniques during the past few decades, a significant number of patients still present with disease at an advanced stage. Reports from the American Cancer Society indicate that, in the United States, more than 40% of the patients with squamous cell carcinomas of the oral cavity and pharynx present with regional dissemination of disease at the time of initial diagnosis (Fig. 11.2). In other parts of the world, such as South Asia and Latin America, a larger proportion of patients with cancer of the upper aerodigestive tract present with advanced stage disease. Therefore the management of cervical lymph nodes becomes a vitally important component in the overall treatment strategy for patients with cancers of the head and neck. Regional lymphatic drainage from the scalp and skin of the head and neck region, the mucosa of the upper aerodigestive tract, the paranasal sinuses, the salivary glands, and the thyroid gland is well defined, and metastasis from cancers in these locations occurs in a sequential and predictable manner to specific regional lymph nodes. As such, understanding the risk and patterns of metastasis for each primary site is essential in planning treatment.

LYMPHATICS OF THE HEAD AND NECK

The lymphatic network of the head and neck area is located in two layers separated by the deep cervical fascia. The superficial lymphatics drain into suboccipital, preauricular and postauricular, prevascular facial, and external jugular lymph nodes. These lymph nodes eventually drain into the deep jugular lymph nodes. The major lymph node groups of the head and neck region are shown in Fig. 11.3. The preauricular, periparotid, and intraparotid lymph nodes are the first-echelon lymph nodes for the anterior half of the scalp, the skin of the forehead, and the upper part of the face. The postauricular and suboccipital groups of lymph nodes provide drainage from the posterior half of the scalp and the posterior aspect of the external ear. Deep cervical lymph nodes in the lateral aspect of the neck primarily drain from the mucosa of the upper aerodigestive tract. These lymph nodes include the submental, prevascular facial, and submandibular group located in the submental and submandibular triangles of the neck. Deep jugular lymph nodes include the jugulodigastric, juguloomohyoid, and supraclavicular group of lymph nodes adjacent to the internal jugular vein. Lymph nodes in the posterior triangle of the neck include the accessory chain located along the spinal accessory nerve and the transverse cervical chain in the floor of the posterior triangle

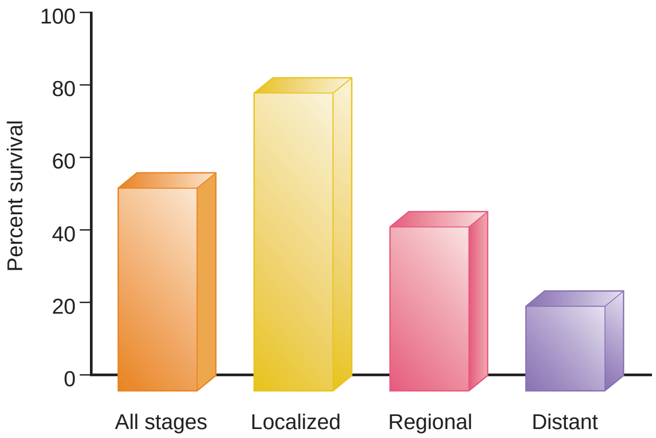

Figure 11.1 Five-year survival rates in patients with squamous cell carcinoma of the upper aerodigestive tract in relation to the extent of disease.

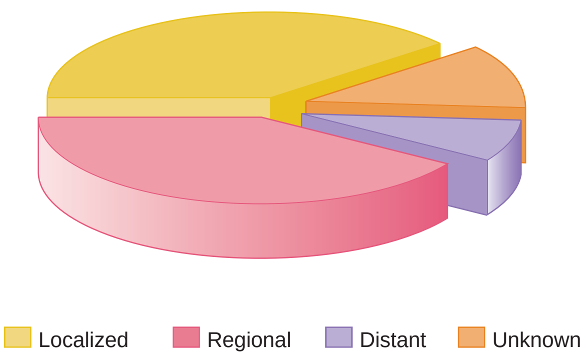

Figure 11.2 The distribution of patients with squamous cell carcinomas of the oral cavity and pharynx in relation to the extent of disease at the time of initial diagnosis.

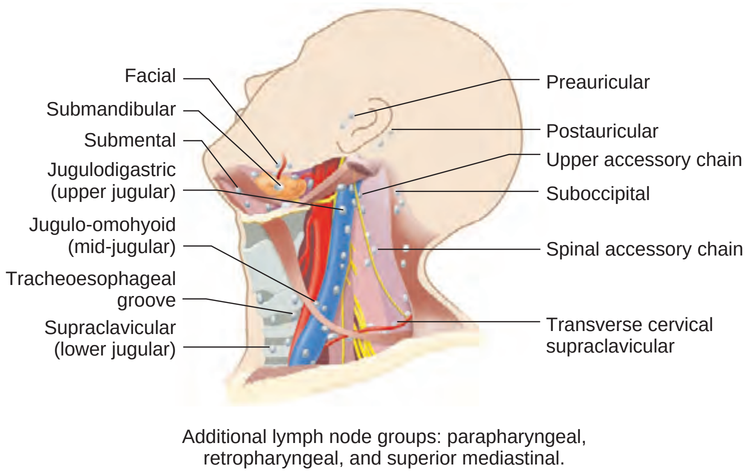

Figure 11.3 The regional lymph nodes of the head and neck region. *(Courtesy Memorial Sloan Kettering Cancer Center.)*

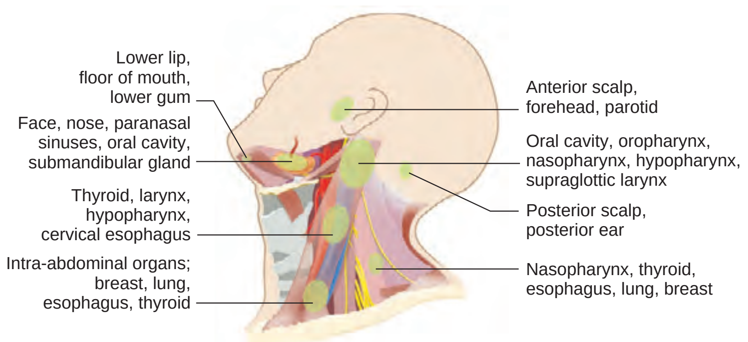

Figure 11.4 The regional lymph node groups draining a specific primary site as first-echelon lymph nodes. *(Courtesy Memorial Sloan Kettering Cancer Center.)*

of the neck. Lymphatics of the pharynx also drain into the parapharyngeal and retropharyngeal lymph nodes.

The central compartment of the neck includes the Delphian lymph node overlying the thyroid cartilage in the midline, which drains from the larynx and thyroid gland, and the perithyroid lymph nodes, as well as the pretracheal, paratracheal, and paraesophageal lymph nodes. Lymphatics of the thyroid gland, hypopharynx, subglottic larynx, and cervical esophagus drain into the paratracheal lymph nodes. Lymph nodes in the anterosuperior mediastinum provide drainage from the thyroid gland and the cervical esophagus and serve as a secondary lymphatic basin for central compartment viscera. Each previously described anatomic subgroup of lymph nodes serve as primary-echelon lymph nodes that drain from a specific site in the head and neck region. Thus the location of a palpable metastatic lymph node often may indicate the potential site of a primary tumor (Fig. 11.4).

The conventional description of regional nodes is based on the leveling system first proposed from the Head and Neck Service at Memorial Sloan Kettering Cancer Center in New York nearly a century ago (Fig. 11.5). This system divides the lymph nodes in the lateral aspect of the neck into five nodal groups or levels. In addition, lymph nodes in the central compartment of the neck are assigned level VI, and those in the anterosuperior mediastinum are assigned level VII.

The American Academy of Otolaryngology-Head and Neck Surgery has modified the above system by subdividing levels I, II, and V into A and B categories for each of these levels (Fig. 11.6).

Level I

The submental group or level I (IA) includes the lymph nodes between the anterior bellies of the digastric muscles from the lower border of the symphysis of the mandible cephalad to the hyoid bone caudad. The submandibular group or level I (IB) includes lymph nodes in the triangular area bounded by the anterior and posterior bellies of the digastric muscle and the inferior border of the body of the mandible. The lymph nodes adjacent to the submandibular salivary gland and along the facial artery (prevascular facial) are included in this group.

Level II

Level II is the upper jugular group, which includes lymph nodes around the upper third of the internal jugular vein and the upper part of the spinal accessory nerve, extending from the base of the skull up to the bifurcation of the carotid artery or to the level of the hyoid bone. The posterior limit for this level is the posterior border of the sternocleidomastoid muscle, and the anterior limit is the lateral border of the sternohyoid muscle. Lymph nodes anterior to the spinal accessory nerve are designated level IIA, and those posterior to it are designated level IIB.

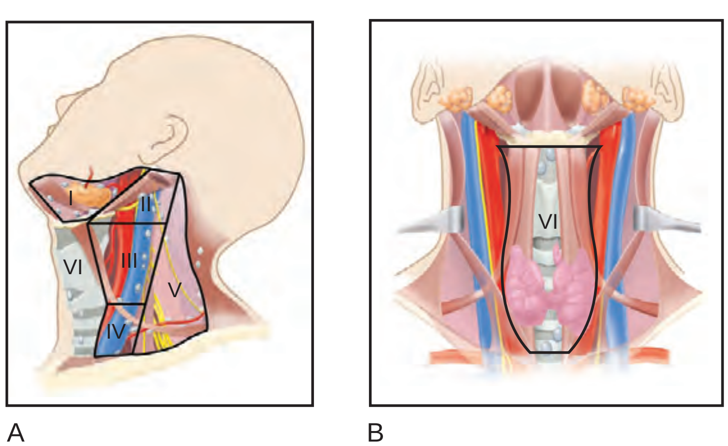

Figure 11.5 The Memorial Sloan Kettering Cancer Center system of assigning levels to cervical lymph nodes. **A**, The lateral side of the neck. **B**, The central compartment and superior mediastinum. *(Courtesy Memorial Sloan Kettering Cancer Center.)*

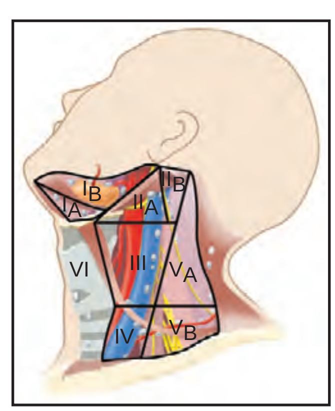

Figure 11.6 The American Academy of Otolaryngology-Head and Neck Surgery modification of the system of assigning levels for cervical lymph nodes. *(Courtesy Memorial Sloan Kettering Cancer Center.)*

Level III

Level III is the midjugular group, which includes lymph nodes around the middle third of the internal jugular vein from the hyoid bone up to the inferior border of cricoid cartilage. The anterior and posterior borders are the same as those for level II.

Level IV

Level IV is the lower jugular group, which includes lymph nodes around the lower third of the internal jugular vein from the inferior border of cricoid cartilage up to the clavicle. The anterior and posterior borders are the same as those for levels II and III.

Level V

Level V is the posterior triangle group, which includes lymph nodes around the lower portion of the spinal accessory nerve and along the transverse cervical vessels. It is bounded by the triangle formed by the clavicle, the posterior border of the sternocleidomastoid muscle, and the anterior border of the trapezius muscle. Level V is divided into two levels by a plane at the level of the inferior border of the cricoid cartilage. Level VA is superior to this plane, and level VB is inferior to it. Generally, level VA includes accessory chain lymph nodes and level VB includes transverse cervical chain and supraclavicular lymph nodes.

Level VI

Level VI is the central compartment group, which includes lymph nodes in the prelaryngeal, (Delphian), pretracheal, paratracheal, and tracheoesophageal groove. The boundaries are the hyoid bone cephalad to the suprasternal notch caudad and between the medial borders of the carotid sheaths.

Level VII

Level VII is the anterosuperior mediastinal group, which includes lymph nodes in the anterosuperior mediastinum and tracheo-esophageal grooves, extending from the suprasternal notch to the innominate artery.

PATTERNS OF NECK METASTASIS

Dissemination of metastatic cancer to regional lymph nodes from primary sites in the upper aerodigestive tract occurs in a predictable and sequential fashion. Thus only a select group of lymph nodes are at risk of initial metastases from a given primary site. Understanding the sequential patterns of neck metastasis greatly facilitates surgical management of regional lymph nodes in the clinically negative neck (N0), but if the lymph nodes are at risk of harboring micrometastasis.

For primary tumors in the oral cavity, the regional lymph nodes at highest risk for early dissemination by metastatic cancer are limited to levels I, II, and III (Fig. 11.7). Anatomically, this translates into regional lymph node groups contained within the supraomohyoid triangle of the neck bounded superiorly by the lower border of the mandible, posteriorly by the posterior border of the sternocleidomastoid muscle, and anteriorly by the superior belly of the omohyoid muscle, and which includes the submental triangle. The following lymph node groups are

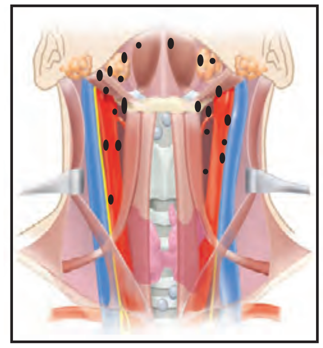

Figure 11.7 The first-echelon lymph nodes at highest risk for early dissemination by metastatic cancer from primary tumors in the oral cavity.

contained in the supraomohyoid triangle: submental, submandibular, prevascular facial, jugulodigastric, upper deep jugular, superior spinal accessory chain of lymph nodes, and midjugular lymph nodes. Skip metastasis to levels IV and V in the absence of metastatic disease at levels I, II, or III is exceedingly rare. Therefore if findings of the neck are clinically negative, level IV and V lymph nodes generally are not at risk of harboring micrometastasis from primary squamous cell carcinomas of the oral cavity. Primary carcinomas of the lateral border of the tongue has a somewhat higher risk of involvement of lymph nodes at level IV, particularly if there is already metastatic disease present at levels II or III.

For tumors of the lateral aspect of oropharynx, hypopharynx, and larynx, the first-echelon lymph nodes at highest risk of harboring micrometastasis in the clinically negative neck are the deep jugular lymph nodes at levels II, III, and IV on the ipsilateral side (Fig. 11.8). Contiguous lymph nodes lateral to the internal jugular vein overlying the cutaneous roots of the cervical plexus usually are considered a component of levels II, III, and IV. In patients with primary carcinomas of the oropharynx, hypopharynx, and larynx who have clinically negative neck, the risk of micrometastasis to levels I and V is exceedingly small. Skip metastasis to levels I and V in the absence of disease at levels II, III, or IV usually is not seen. Primary tumors that involve both sides of the midline in these primary sites have a potential risk of microscopic dissemination of metastatic disease to jugular lymph nodes on both sides of the neck. Similarly, tumors of the medial wall of the pyriform sinus are reported to have an increased risk of contralateral neck metastases.

Regional lymph node metastases from primary differentiated carcinomas of the thyroid gland occur in an occult manner in a high proportion of patients (approximately 50%), although clinically gross metastases at initial presentation are infrequent. The first-echelon lymph nodes at highest risk for metastases from a primary differentiated carcinoma of the thyroid gland are those adjacent to the thyroid gland, the so-called perithyroid lymph nodes, and those in the tracheoesophageal groove and superior mediastinum (Fig. 11.9). Metastatic disease sequentially progresses from the central compartment lymph nodes to lower, middle, and upper jugular lymph nodes. Lymph nodes in the posterior triangle of the neck are involved infrequently unless there is gross metastatic disease at level IV, where contiguous metastatic spread to level VB is not uncommon. Metastatic disease from a primary carcinoma of the thyroid to level I is exceedingly rare.

Regional lymph node metastasis develops in only 20% to 25% of patients with a carcinoma of the parotid gland. The

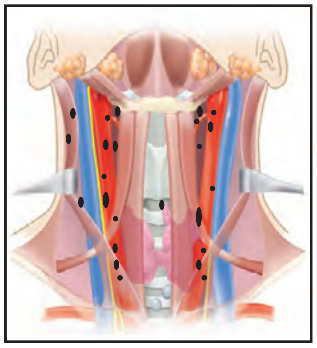

Figure 11.8 The first-echelon lymph nodes at highest risk for micrometastasis in a neck with clinically negative findings from primary tumors of the hypopharynx and larynx.

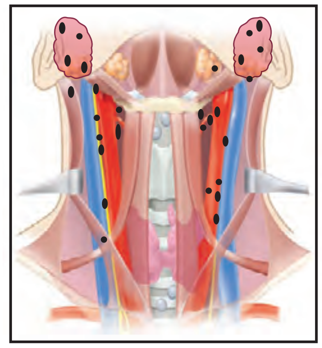

Figure 11.10 The first-echelon lymph nodes at highest risk for dissemination of metastatic cancer from a carcinoma of the parotid gland are in the periparotid and upper cervical region.

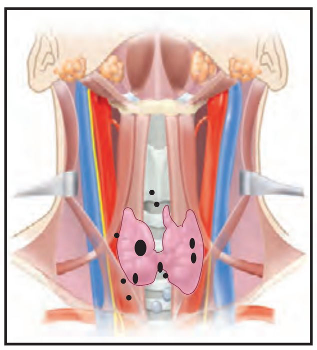

Figure 11.9 The first-echelon lymph nodes at highest risk for micrometastasis in a neck with clinically negative findings from a primary carcinoma of the thyroid gland.

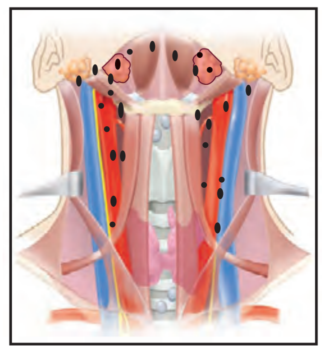

Figure 11.11 The initial dissemination of metastatic cancer from primary malignant tumors of the submandibular and sublingual salivary glands occurs at lymph nodes in the supraomohyoid triangle.

lymph node groups at highest risk for metastases from a primary carcinoma of the parotid gland are those in the preauricular, periparotid, and intraparotid regions, as well as lymph nodes in the upper deep jugular chain and those in the upper spinal accessory chain in the posterior triangle of the neck (Fig. 11.10). Initial dissemination of metastatic cancer from primary malignant tumors of the submandibular salivary gland occurs to lymph nodes in the supraomohyoid triangle (Fig. 11.11).

Cutaneous malignant tumors of the scalp also spread to regional lymph nodes in a predictable fashion. A line joining the helix of one ear to the helix of the opposite ear in a coronal plane separates the watershed areas of the scalp. Tumors located anterior to this line in general metastasize to preauricular, periparotid, and anterior cervical lymph nodes (levels I to IV) and seldom metastasize to the posterior triangle of the neck. On the other hand, primary tumors of the scalp posterior to this line metastasize to the suboccipital and postauricular group of lymph nodes as well as those in the posterior triangle of the neck and the deep jugular chain (levels II to V).

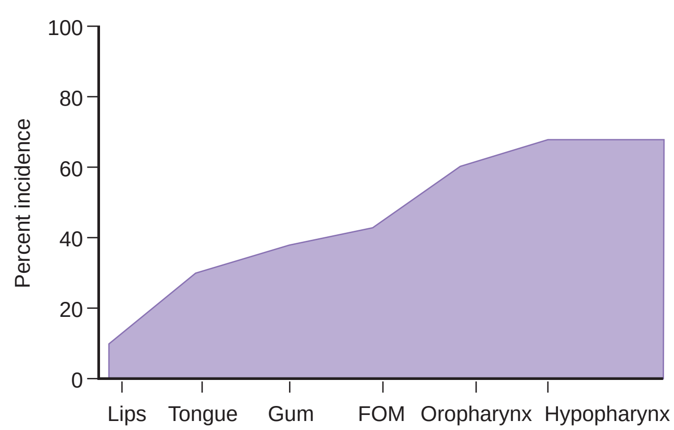

Figure 11.12 The risk of nodal metastasis increases in relation to the location of primary squamous cell carcinomas of the upper aerodigestive tract. *FOM,* Floor of mouth.

RISK FOR REGIONAL METASTASIS

The risk for metastasis to regional lymphatics from primary squamous cell carcinomas of the upper aerodigestive tract depends on the primary site, T stage, and histomorphologic features of the primary tumor. In general, the risk of nodal metastasis increases from the anterior to posterior aspect of the upper aerodigestive tract, that is, the lips, oral cavity, oropharynx, and hypopharynx (Fig. 11.12). For tumors of the larynx and pharynx, the risk of nodal metastasis increases with progression from the center of the upper aerodigestive tract (the vocal cords) to the periphery (the lateral pharyngeal wall). For example, the risk of regional lymph node metastasis from a carcinoma of the true vocal cords is exceedingly small. However, the risk increases with progression from the vocal cords to the false vocal cords, aryepiglottic fold, pyriform sinus, and pharyngeal wall. Nearly two-thirds of patients with primary carcinomas of the hypopharynx present with clinically palpable regional lymph node metastasis.

The T stage usually reflects tumor burden or invasiveness and is correlated with risk for nodal metastasis for any given primary site. Overall, the risk for metastasis is less than 15%

for T1, 15% to 30% for T2, 30% to 50% for T3, and up to 75% for T4 head and neck primary squamous cell carcinomas. Certain histomorphologic features of the primary tumor also increase the risk of nodal metastasis. The risk of nodal metastases from HPV-positive oropharynx cancer is disproportionately high, even with a low T stage of the primary tumor. Endophytic tumors have a higher risk for metastasis compared with exophytic tumors. This is particularly true for primary carcinomas of the oral cavity (tongue and floor of mouth), where there is increasing risk of nodal metastases, with increasing depth of invasion (DOI). The AJCC and UICC have therefore revised the T staging of primary squamous cell carcinomas of the oral cavity, where each 5 mm increase in DOI will upstage the tumor by one T stage. Poorly differentiated carcinomas have a higher risk of nodal metastases compared with well-differentiated lesions. The pattern of invasion also has been shown to affect risk for metastasis. However, the influence of these parameters is not independent of T stage based on multivariate analysis. Only DOI has been shown to be an independent predictor of the risk for nodal metastases for cancers of the tongue and floor of the mouth. Metastatic spread from primary carcinomas of salivary origin is generally low (approximately 20%). The risk depends on the histology, grade, and stage of the primary tumor. Similarly, most head and neck sarcomas have a very low risk for regional metastasis with the exception of rhabdomyosarcoma, epithelioid sarcoma, synovial sarcoma, and angiosarcoma. Unlike other head and neck malignancies, even though the risk for dissemination to regional lymph nodes from differentiated carcinomas of the thyroid (papillary) is quite high (approximately 50% of occult metastases), elective dissection of regional lymph nodes is not recommended because it does not have an adverse impact on prognosis in a majority of patients who fall into the low-risk group stratification.

Risk of nodal metastases from cutaneous malignancies is relatively low. Basal cell carcinomas have a very low risk for metastasis (<1%), whereas the risk can be as high as 10% for cutaneous squamous cell carcinomas. Larger cutaneous squamous cell carcinomas (>2 cm) and those with adverse pathologic features (i.e., poor differentiation, DOI of >6 mm, and perineural invasion) have a higher risk for metastases. Once metastases develop from a cutaneous malignancy, the probability of survival decreases by up to 90%. On the other hand, cutaneous tumors of neuroendocrine origin (e.g., Merkel cell carcinoma and malignant melanoma) have a much higher risk for regional metastasis. For Merkel cell carcinomas larger than 1 cm, the risk of nodal metastases is 20% or more. The risk for nodal metastasis for cutaneous melanomas is related to tumor thickness and is higher for tumors thicker than 1 mm (Fig. 11.13). Adnexal tumors of the skin rarely metastasize with the exception of sebaceous and eccrine gland carcinomas.

CLINICAL STAGING OF CERVICAL LYMPH NODES (CN STAGING)

The American Joint Committee on Cancer and the International Union Against Cancer have agreed upon a uniform staging system for cervical lymph nodes. The site, number, size, and extranodal extension (ENE) are the most important factors considered in nodal staging of most squamous cell carcinomas of the head and neck. The presence of clinical evidence of ENE has such an important negative prognostic impact that any lymph node with clinical or radiologic evidence of ENE gets upstaged to N3B category. ENE can be diagnosed clinically by

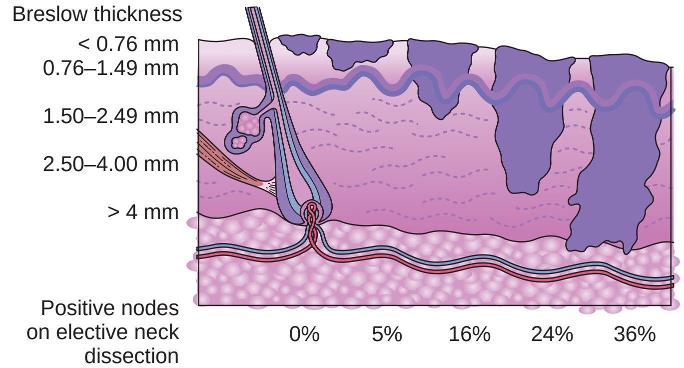

Figure 11.13 The risk of occult nodal metastasis in a cutaneous melanoma relative to the depth of the primary lesion.

the presence of a matted mass of nodes fixed to the overlying skin or adjacent soft tissue or clinical signs of cranial nerve invasion. Radiologic signs of ENE include amorphous, spiculated margins of a metastatic node and stranding of the perinodal soft tissue in previously untreated patients. The exact description of each clinical N stage of lymph node metastases from squamous cell carcinomas of the head and neck (oral cavity, HPV-negative oropharynx, hypopharynx, larynx, paranasal sinuses, salivary glands, and nonmelanoma skin cancers of the head and neck) is shown in Fig. 11.14 and Table 11.1. Squamous cell carcinomas of the nasopharynx, HPV-positive cancers of the oropharynx (OPC), and well-differentiated thyroid carcinomas have a different biology, and cervical metastases from these tumors are assigned different staging systems. The natural history and response to treatment of cervical nodal metastases from nasopharynx and HPV-positive oropharynx primary sites are different in terms of their impact on prognosis, so they justify a different N classification scheme. For the nasopharynx, the size and location of the metastatic node(s) are important parameters (Table 11.2). For HPV-positive OPC only the size of the metastatic nodes are considered in staging (Table 11.3). Regional node metastases from well-differentiated thyroid cancer do not significantly affect the ultimate prognosis in a majority of patients (approximately 80%) who fall in the low-risk group category and therefore also justify a unique staging system. Staging for

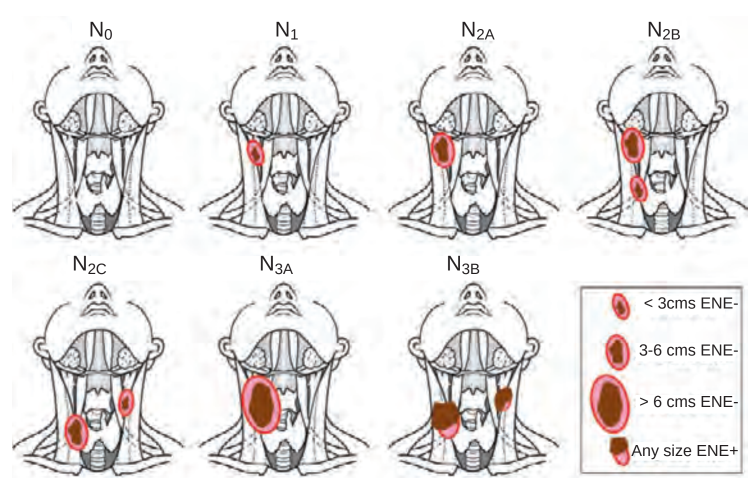

Figure 11.14 Clinical N staging (cN) of lymph node metastases from squamous cell carcinoma of the head and neck except for nasopharynx, human papillomavirus–positive oropharynx, and differentiated thyroid cancer. *(Used with the permission of the American Joint Committee on Cancer (AJCC), Chicago, Illinois. The original source for this material is the AJCC Cancer Staging Manual, 8th edition, Springer Science and Business Media LLC, 2016. www.springer.com.)*

Table 11.1 Clinical Staging (cN) for Squamous Cell Carcinoma of the Head and Neck

N CATEGORY	N CRITERIA
NX	Regional lymph nodes cannot be assessed
N0	No regional lymph node metastasis
N1	Metastasis in a single ipsilateral lymph node, 3 cm or smaller in greatest dimension ENE(–)
N2	Metastasis in a single ipsilateral node larger than 3 cm but not larger than 6 cm in greatest dimension and ENE(–); *or* metastases in multiple ipsilateral lymph nodes, none larger than 6 cm in greatest dimension and ENE(–); *or* in bilateral or contralateral lymph nodes, none larger than 6 cm in greatest dimension, and ENE(–)
N2a	Metastases in a single ipsilateral node larger than 3 cm but not larger than 6 cm in greatest dimension, and ENE(–)
N2b	Metastasis in multiple ipsilateral nodes, none larger than 6 cm in greatest dimension, and ENE(–)
N2c	Metastasis in bilateral or contralateral lymph nodes, none larger than 6 cm in greatest dimension, and ENE(–)
N3	Metastasis in a lymph node larger than 6 cm in greatest dimension and ENE(–); *or* metastasis in any node(s) and clinically overt ENE(+)
N3a	Metastasis in a lymph node larger than 6 cm in greatest dimension and ENE(–)
N3b	Metastasis in any node(s) and clinically overt ENE(+)

Note: A designation of "U" or "L" may be used for any N category to indicate metastasis above the lower border of the cricoid (U) or below the lower border of the cricoid (L) Similarly, clinical and pathologic extranodal extension (*ENE*) should be recorded as ENE(–) or ENE(+).

(Used with the permission of the American Joint Committee on Cancer [AJCC], Chicago, Illinois. The original source for this material is the AJCC Cancer Staging Manual, 8th ed. Springer Science and Business Media LLC, 2016, www.springer.com.)

Table 11.2 N Staging for Nasopharyngeal Carcinoma

N CATEGORY	N CRITERIA
NX	Regional lymph nodes cannot be assessed
N0	No regional lymph node metastasis
N1	Unilateral metastasis in cervical lymph node(s) and/or unilateral or bilateral metastasis in retropharyngeal lymph node(s), 6 cm or smaller in greatest dimension, above the caudal border of cricoid cartilage
N2	Bilateral metastasis in cervical lymph node(s), 6 cm or smaller in greatest dimension, above the caudal border of cricoid cartilage
N3	Unilateral or bilateral metastasis in cervical lymph node(s), larger than 6 cm in greatest dimension, and/or extension below the caudal border of cricoid cartilage

(Used with the permission of the American Joint Committee on Cancer [AJCC], Chicago, Illinois. The original source for this material is the AJCC Cancer Staging Manual, 8th ed. Springer Science and Business Media LLC, 2016, www.springer.com.)

nodal metastases from differentiated thyroid carcinoma is largely based on the location of the metastases (Table 11.4).

PATHOLOGIC STAGING OF CERVICAL LYMPH NODES (PN STAGING)

The American Joint Committee on Cancer and the International Union Against Cancer have developed a separate pathologic staging (pN) for those tumors primarily treated surgically, and

Table 11.3 Clinical Staging (cN) for Human Papilloma Virus–Positive (HPV-positive, p16+) Oropharynx Carcinoma

N CATEGORY	N CRITERIA
NX	Regional lymph nodes cannot be assessed
N0	No regional lymph node metastasis
N1	One or more ipsilateral lymph nodes, none larger than 6 cm
N2	Contralateral or bilateral lymph nodes, none larger than 6 cm
N3	Lymph node(s) larger than 6 cm

(Used with the permission of the American Joint Committee on Cancer [AJCC], Chicago, Illinois. The original source for this material is the AJCC Cancer Staging Manual, 8th ed. Springer Science and Business Media LLC, 2016, www.springer.com.)

Table 11.4 N Staging for Differentiated Thyroid Carcinoma

N CATEGORY	N CRITERIA
NX	Regional lymph nodes cannot be assessed
N0	No evidence of locoregional lymph node metastasis
N0a	One or more cytologically or histologically confirmed benign lymph nodes
N0b	No radiologic or clinical evidence of locoregional lymph node metastasis
N1	Metastasis to regional nodes
N1a	Metastasis to level VI or VII (pretracheal, paratracheal, or prelaryngeal/Delphian, or upper mediastinal) lymph nodes; this can be unilateral or bilateral disease
N1b	Metastasis to unilateral, bilateral, or contralateral lateral neck lymph nodes (levels I, II, III, IV, or V) or retropharyngeal lymph nodes

(Used with the permission of the American Joint Committee on Cancer [AJCC], Chicago, Illinois. The original source for this material is the AJCC Cancer Staging Manual, 8th ed. Springer Science and Business Media LLC, 2016, www.springer.com.)

where a pathologic specimen is available for accurate assessment of the extent of nodal metastases. For example even microscopic ENE (<2 mm) is considered as ENE(+), and thus entered into upstaging N category. This nodal staging is different than cN staging and offers more accurate information for overall pN staging of these cancers. Thus pN staging is often used for adjuvant treatment planning as well as for more accurate assessment of prognosis. The pN staging for oral cavity, HPV-negative oropharynx, hypopharynx, larynx, paranasal sinuses, salivary glands, and nonmelanoma skin cancers of the head and neck is shown in Table 11.5. The pN staging for HPV-positive oropharynx cancers is shown in Table 11.6. There is no pN staging developed for cancers of the nasopharynx and differentiated cancers of the thyroid gland.

OTHER NODAL FACTORS AFFECTING PROGNOSIS

The pattern of the lymphatic drainage varies for different anatomic sites. However, the location of the lymph node metastases has prognostic significance in patients with squamous cell carcinoma of the head and neck. Survival is significantly worse when metastases involve lymph nodes beyond the first echelon of lymphatic drainage and, particularly, lymph nodes in the lower parts of the neck, i.e., level IV and level VB (supraclavicular region). Therefore the AJCC recommends that each N staging category be recorded on the staging forms to show whether the nodes involved are located in the upper (U) or lower (L) regions of the neck, depending on their location above or below the lower border of the cricoid cartilage.

When enlarged lymph nodes are detected, the actual size of the nodal mass(es) should be measured. It is recognized that most masses over 3 cm in diameter are not single nodes but are confluent nodes or tumor in soft tissues of the neck. Careful clinical examination; radiologic assessment; and, in surgically treated patients, detailed pathologic examination is necessary for documentation of tumor extent in terms of the location or level of the lymph node(s) involved, the number of nodes that contain metastases, and the presence or absence of ENE.

Involvement of lower cervical lymph nodes (levels IV and VB) by metastatic cancer usually is ominous. Lymph node density, which reflects tumor factors (number of positive lymph nodes), treatment factors (number of lymph nodes removed during neck dissection), and staging factors (completeness of the sampling procedure, including those related to the surgeon and pathologist) has been found to stratify risk of local regional recurrence and survival. Lymphovascular invasion (LVI) and perineural invasion (PNI) by a tumor, as well as the presence of tumor emboli in regional lymphatics, also has an adverse impact on prognosis. Therefore these factors must be considered when developing a treatment strategy for patients in whom regional lymph nodes are involved by metastatic disease, particularly for planning adjuvant therapy and in the assessment of prognosis.

Table 11.5 Pathologic Staging (pN) for Lymph Node Metastases From Squamous Cell Carcinoma of the Head and Neck Except for Nasopharynx, Human Papillomavirus–Positive Oropharynx, and Differentiated Thyroid Cancer

N CATEGORY	N CRITERIA
NX	Regional lymph nodes cannot be assessed.
N0	No regional lymph node metastasis
N1	Metastasis in a single ipsilateral lymph node, 3 cm or smaller in greatest dimension and ENE(–)
N2	Metastasis in a single ipsilateral lymph node, 3 cm or smaller in greatest dimension and ENE(+); *or* larger than 3 cm but not larger than 6 cm in greatest dimension and ENE(–); *or* metastasis in multiple ipsilateral lymph nodes, none larger than 6 cm in greatest dimension, ENE(–)
N2a	Metastasis in a single ipsilateral or contralateral node 3 cm or smaller in greatest dimension and ENE(+); *or* a single ipsilateral node larger than 3 cm but not larger than 6 cm in greatest dimension and ENE(–)
N2b	Metastasis in multiple ipsilateral nodes, none larger than 6 cm in greatest dimension and ENE(–)
N2c	Metastasis in bilateral or contralateral lymph nodes, none larger than 6 cm in greatest dimension and ENE(–)
N3	Metastasis in a lymph node larger than 6 cm in greatest dimension and ENE(–); *or* in a single ipsilateral node larger than 3 cm in greatest dimension and ENE(+); *or* multiple ipsilateral, contralateral, or bilateral nodes any with ENE(+)
N3a	Metastasis in a lymph node larger than 6 cm in greatest dimension and ENE(–)
N3b	Metastasis in a single ipsilateral node larger than 3 cm in greatest dimension and ENE(+); *or* multiple ipsilateral, contralateral, or bilateral nodes any with ENE(+)

Note: A designation of "U" or "L" may be used for any N category to indicate metastasis above the lower border of the cricoid (U) or below the lower border of the cricoid (L). Similarly, clinical and pathological ENE should be recorded as ENE(–) or ENE(+).
ENE, Extranodal extension.
(Used with the permission of the American Joint Committee on Cancer [AJCC], Chicago, Illinois. The original source for this material is the AJCC Cancer Staging Manual, 8th ed. Springer Science and Business Media LLC, 2016, www.springer.com.)

Table 11.6 Pathologic Staging (pN) for Human Papilloma Virus–Positive Oropharyngeal Carcinoma

N CATEGORY	N CRITERIA
NX	Regional lymph nodes cannot be assessed
pN0	No regional lymph nodes metastasis
pN1	Metastasis in 4 or fewer lymph nodes
pN2	Metastasis in more than 4 lymph nodes

(Used with the permission of the American Joint Committee on Cancer [AJCC], Chicago, Illinois. The original source for this material is the AJCC Cancer Staging Manual, 8th ed. Springer Science and Business Media LLC, 2016, www.springer.com.)

EVALUATION

Assessment and management of patients with head and neck primary tumors presenting with regional lymphatic metastasis can be divided into those with clinically detectable metastasis and those at risk of harboring occult metastasis. The approach to management of these two clinical scenarios is defined by patterns and risk of regional spread.

Clinically Evident Metastasis With a Known Primary Tumor

"A clinically palpable, firm, enlarged lymph node(s) in an adult should be considered metastatic until proven otherwise." This was a statement made by Hayes Martin over six decades ago, and it still holds true. The clinically enlarged lymph node may be present at any of the previously described anatomic locations in the head and neck region. The location of a palpable lymph node may point to the potential site of a primary tumor (Fig. 11.15). Important features to note during examination of the neck for cervical lymph nodes are the location, size, consistency, and number of palpable lymph nodes as well as clinical signs of ENE such as invasion of the overlying skin, fixation to deeper soft tissues, or paralysis of cranial nerves (Fig. 11.16).

A thorough clinical examination of the head and neck should be performed, including careful evaluation of the scalp, external auditory canals, and the skin. This examination is followed by careful clinical evaluation of the oral cavity, oropharynx, hypopharynx, and larynx, including digital palpation of the tonsillar fossae and the base of the tongue. After this evaluation, flexible

Figure 11.15 Clinically palpable 3-cm size mobile metastatic lymph node at level II with no clinical signs of extranodal extension (N1).

Figure 11.16 Conglomerate mass of multiple metastatic lymph nodes with reduced mobility and adherence of overlying skin, signifying extra nodal extension (ENE+ [N3b]).

fiberoptic nasolaryngoscopy is performed to assess the nasal cavity, nasopharynx, oropharynx, (particularly the base of the tongue) hypopharynx, and larynx for identification of the primary tumor. Erythema and mucosal hypervascularity should raise suspicion for a primary tumor. In the vast majority of cases, the primary tumor will be identified with a thorough clinical examination. Management of the neck in these patients is dictated by the site and stage of the primary tumor. However, approximately 10% of patients with a clinically palpable metastatic lymph node will not have a clinically obvious primary tumor. Many small primary tumors that may be missed on mirror examination are readily visible with the use of a fiber-optic nasolaryngoscope. If the primary tumor is identified, then further management is directed by the site and stage of the primary tumor.

Histologic diagnosis of metastatic carcinoma is usually established by fine-needle aspiration biopsy and cytologic examination of the smears. In addition to cytology, immunohistochemistry for p16 staining should be requested. An open biopsy is rarely indicated, usually only if the cytology is suspicious for lymphoma. If an open biopsy is planned, the incision should be made in such a location that it can be incorporated in the incision for a subsequent neck dissection if required.

Clinically Evident Metastasis With an Occult Primary Tumor

Approximately 10% of patients with metastatic squamous cell carcinoma to cervical lymph nodes do not have a clinically identifiable primary tumor. If a primary tumor is not evident after a thorough clinical examination, including fiberoptic nasolaryngoscopy, then the next step in the evaluation of the patient is the cytologic diagnosis of the neck mass by fine-needle aspiration biopsy. Further workup and management depend on the cytologic diagnosis. The algorithm for further management of cytologically confirmed metastatic carcinoma from an unknown primary source is shown in Fig. 11.17. If the diagnosis of squamous cell carcinoma (SCC) or any of the variants of SCC is confirmed, then a p16 staining should be requested, to see if the cancer is HPV related. Further workup for the tumor requires imaging studies, including a contrast-enhanced computed tomography (CT) scan and a positron emission tomography (PET) scan to evaluate the head and neck region and also to rule out distant metastases. The PET scan may identify an occult primary tumor in a small percentage of patients. It is particularly important to perform the PET scan before any invasive intervention such as random biopsies in the search for a primary tumor. A contrast-enhanced CT scan, on the other hand, provides information about the size, extent, and number of lymph nodes as well as ENE from the metastatic lymph node. Cystic nodal metastases are seen commonly in patients with primary squamous cell carcinoma of the HPV-associated oropharynx cancer and papillary carcinoma of the thyroid gland. The presence of cystic metastasis in the upper neck often is confused with the diagnosis of a branchial cleft cyst. Although a branchiogenic carcinoma can occur, a primary carcinoma arising in a branchial cleft cyst is exceedingly rare.

At this juncture, further management of the patient requires examination and endoscopy under general anesthesia to search for the primary tumor. Evaluation under anesthesia allows palpation of areas that are not accessible during clinical examination in the office. These include the base of the tongue and tonsillar fossae, as well as the nasopharynx, which should be palpated from behind the soft palate. Suspicion of a primary tumor is raised by firm nodularity, submucosal induration, or surface bleeding upon palpation. Directed biopsy specimens are taken from areas that look suspicious for a primary site. The practice of performing multiple "random biopsies" is strongly discouraged, because it rarely identifies an occult primary tumor. If a primary tumor is not identified by routine evaluation, then bilateral tonsillectomies should be considered, particularly if the metastatic node is p16 positive, because a primary tumor can be hidden in the tonsillar crypts. Further management of the cervical lymph node metastases is deferred until after the final pathology report becomes available.

The vast majority of metastatic lymph nodes from an occult primary source are squamous cell or poorly differentiated or undifferentiated carcinomas, or basaloid squamous cell carcinomas, followed by adenocarcinoma, melanoma, and lymphoma. Metastatic adenocarcinoma in the upper neck usually originates from a primary tumor of salivary origin, whereas those in the lower neck represent systemic metastasis if thyroid carcinoma is ruled out. Immunohistochemical studies for thyroglobulin and calcitonin are helpful to rule out thyroid origin. A thorough examination of the skin of the entire body is required if the cytology of the neck node shows metastatic melanoma. Finally, a core or open biopsy of the neck node may be necessary for histologic diagnosis if cytologic examination raises suspicion for a lymphoma.

Clinically Negative Neck With a Known Primary Tumor

Management of the neck in patients who have an identified primary cancer but no clinically or radiographically demonstrable cervical lymph node metastasis depends on the risk of occult or microscopic metastases in regional lymph nodes. A varying number of patients whose cancer is staged N0 clinically will have occult metastases in the neck. Clinical and pathologic factors associated with increasing risk for lymphatic metastasis are discussed in the respective chapters and in general include anatomic site and stage, as well as histomorphologic features of the primary tumor. Radiologic studies, including CT, magnetic

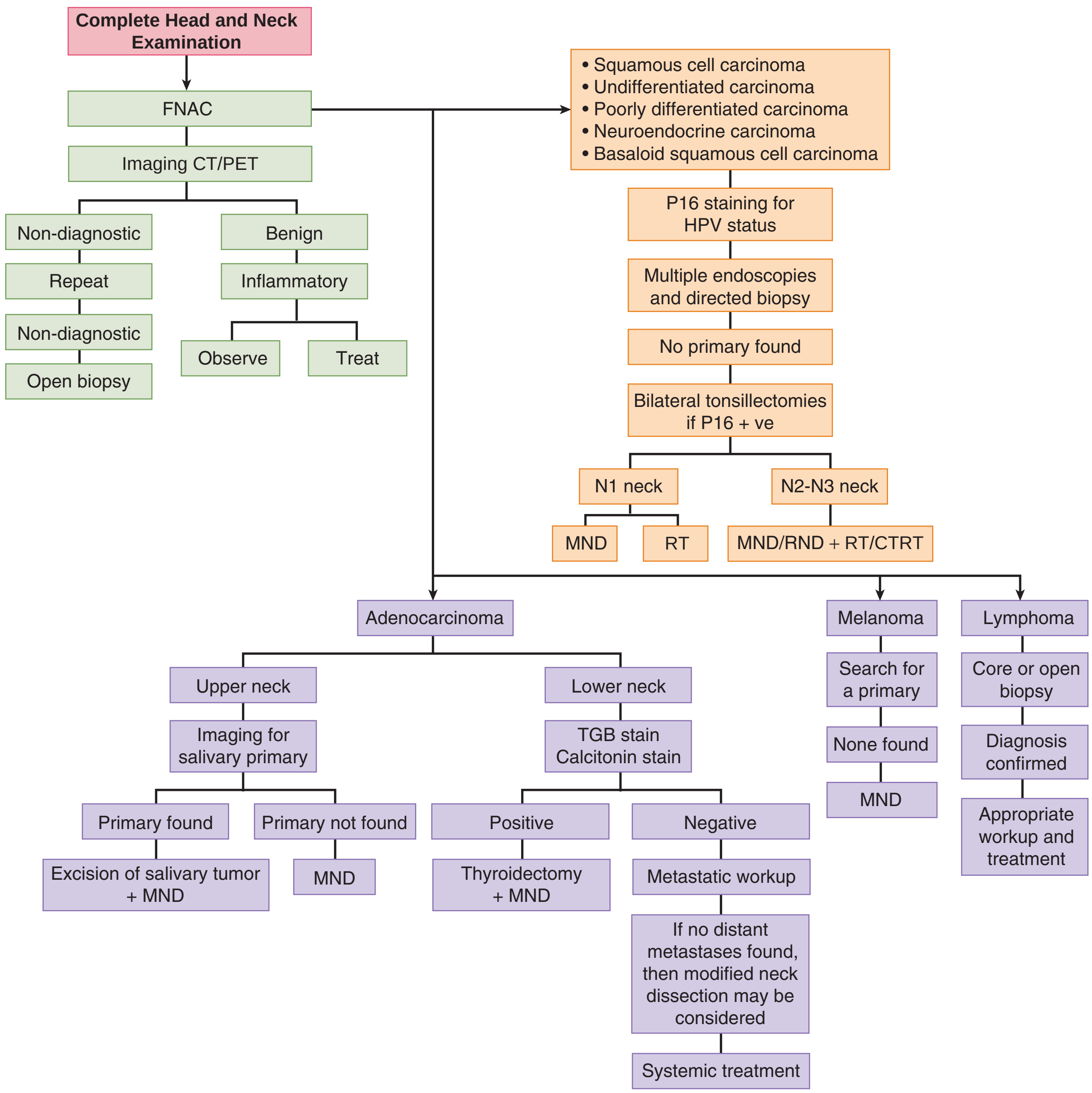

Figure 11.17 Algorithm for workup and management of a patient with a metastatic neck node from an unknown primary source. *CT,* Computed tomography; *FNAC,* fine-needle aspiration cytology; *MND,* modified neck dissection; *RND,* radical neck dissection; *RT,* radiation therapy; *PET,* positron emission tomography; *TGB,* thyroglobulin.

resonance imaging (MRI), ultrasound (US), and PET scanning may identify metastatic lymph nodes that clinically are not palpable in a significant number of patients. US-guided fine-needle aspiration biopsy has a high accuracy rate for detection of minute nodal metastases in expert hands, but none of the imaging studies that are currently available have the resolution to detect microscopic metastatic deposits. Sentinel lymph node biopsy for early stage, node-negative disease has been shown to accurately predict pathologically negative necks in the hands of experienced surgeons and in prospective trials. Novel agents designed to improve lymphatic mapping such as Lymphoseek and Cdot nanoparticles represent promising advancements in staging nodal basins. The use of molecular studies to determine occult metastasis from mucosal squamous cell carcinoma remains investigational. Overall, even with the use of supplemental studies, current methods cannot accurately identify microscopic nodal metastasis, and histologic analysis of the first echelon nodes at risk is the only accurate method to establish a definitive diagnosis. Accordingly, the threshold for elective treatment of the clinically negative neck (stage N0) is an arbitrary decision based on the assumed risk that 15% to 20% of patients will harbor occult metastasis. Prospective randomized trials have demonstrated overall survival benefit in patients with early stage, node-negative, oral cavity cancer who undergo elective neck dissection versus subsequent therapeutic neck dissection.

Management of the Post–Chemoradiation Therapy Neck

During the course of the past three decades, an increasing number of patients have received varying combinations of chemotherapy and radiation therapy for advanced stage squamous cell carcinomas of the pharynx and larynx. Initial neck dissection is seldom performed in these patients who have clinically evident neck metastases. However, a significant number of patients need surgical intervention for persistent or recurrent metastatic disease in the neck. To address this issue, planned dissection of the neck after chemoradiation therapy had been

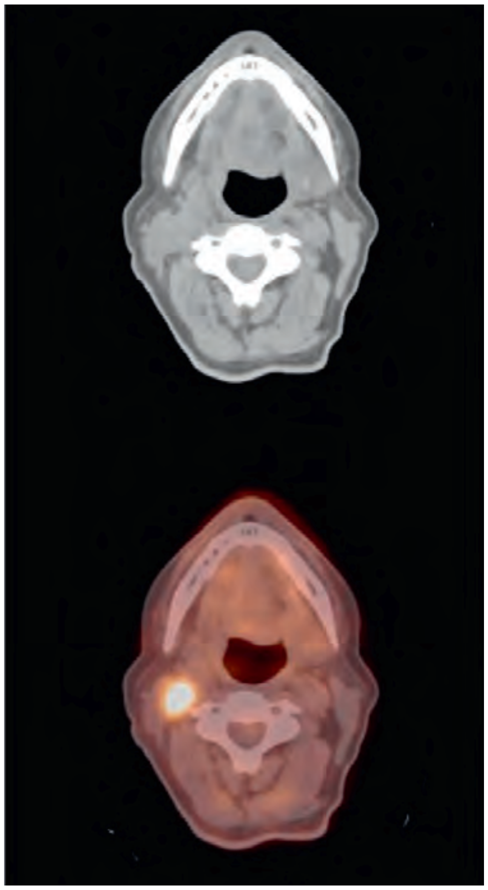

Figure 11.18 18F-fluorodeoxyglucose (FDG) PET scan 1 week following completion of concurrent chemoradiation therapy for carcinoma of the base of the tongue with right neck node metastases showing persistent FDG-avid nodal mass at level II.

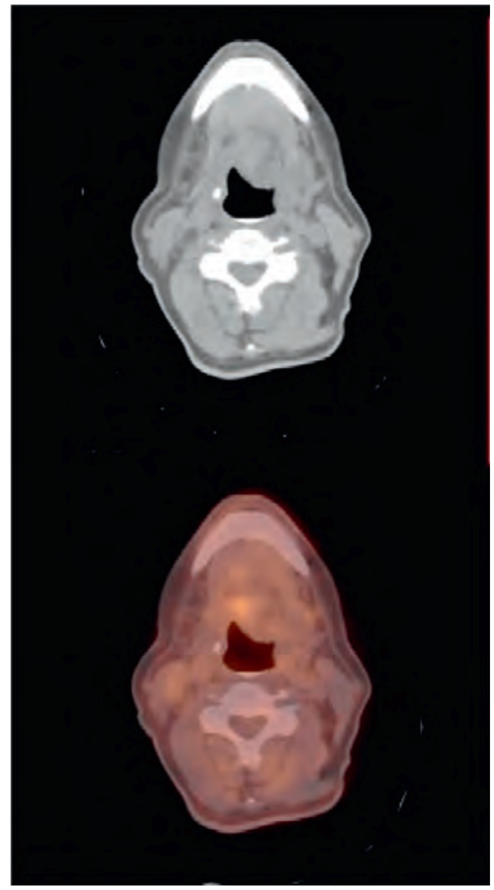

Figure 11.19 18F-fluorodeoxyglucose (FDG) PET scan 3 months following completion of concurrent chemoradiation therapy for carcinoma of the base of the tongue with right neck node metastases showing a complete resolution of FDG activity in the nodal metastases at level II. Mild activity is noted at the base of the tongue due to postradiation ulceration at the primary site.

advocated in the past. However, a majority of patients undergoing planned neck dissection had histologically negative lymph nodes. Therefore planned neck dissection after chemoradiation therapy is no longer recommended. Neck dissection should be considered only in patients who have proven persistent viable disease or a high probability of residual metastatic cancer. Evaluation of the neck following chemoradiation therapy for persistence of metastatic disease is challenging. Grossly palpable or radiographically demonstrable metastatic lymph nodes are an obvious indication for salvage neck dissection. The use of PET/CT in the standard posttreatment clinical evaluation of response following chemoradiation has emerged as a very reliable indicator of viable tumor. However, the PET scan should not be performed earlier than 3 months after completion of treatment (Fig. 11.18). In general, a period of at least 3 months is required for the PET scan to be accurate to show absence of any metabolic activity (Fig. 11.19). A negative PET scan has allowed for the observation of initially N-positive necks who have achieved a complete clinical response. The algorithm for evaluation and management of the neck in patients treated with chemoradiation therapy is shown in Fig. 11.20.

RADIOGRAPHIC EVALUATION

Identification of metastatic lymphadenopathy in the neck upon clinical examination obviously depends on the experience of the clinician, but factors such as the size of the node, the location in the neck, and the body habitus of the patient may render palpation of low-volume disease difficult. Other factors such as prior history of surgery or radiation to the neck may hamper the clinical detection of early metastatic disease. Therefore radiographic examination is of significant value in accurate assessment of the neck. Our ability to detect clinically occult metastasis has improved with the availability of anatomic imaging modalities such as US, contrast-enhanced CT, and MRI. Lymph nodes as small as 3 to 4 mm can be identified on CT or MRI. However, it is not easy to differentiate reactive from metastatic nodes. The role of 18F-fluorodeoxyglucose (FDG) PET for evaluation of a neck with cancer staged as cN0 is debatable, and the utility of this technique may be limited by its suboptimal resolution in detecting small metastases. However, PET scan may identify additional lymph nodes not clinically appreciated, as well as may show unsuspected distant metastatic sites, or occasionally a second primary tumor. In patients who do not have an obvious primary tumor identified on clinical examination or CT/MRI, PET scan may sometimes identify an occult primary tumor. While PET scan will show FDG avidity in metastatic tumor deposits, it is often negative in patients with cystic metastasis (Fig. 11.21).

In addition to the nodal size and shape, structural changes within the metastatic nodes should be studied for accurate imaging diagnosis of the metastatic cervical nodes. The radiographic features for diagnosis of a metastatic node are size, rim enhancement, central necrosis, and ENE (Figs. 11.22 and 11.23). Even in patients who have clinically evident metastasis, radiographic evaluation is desirable to assess the extent of the nodal

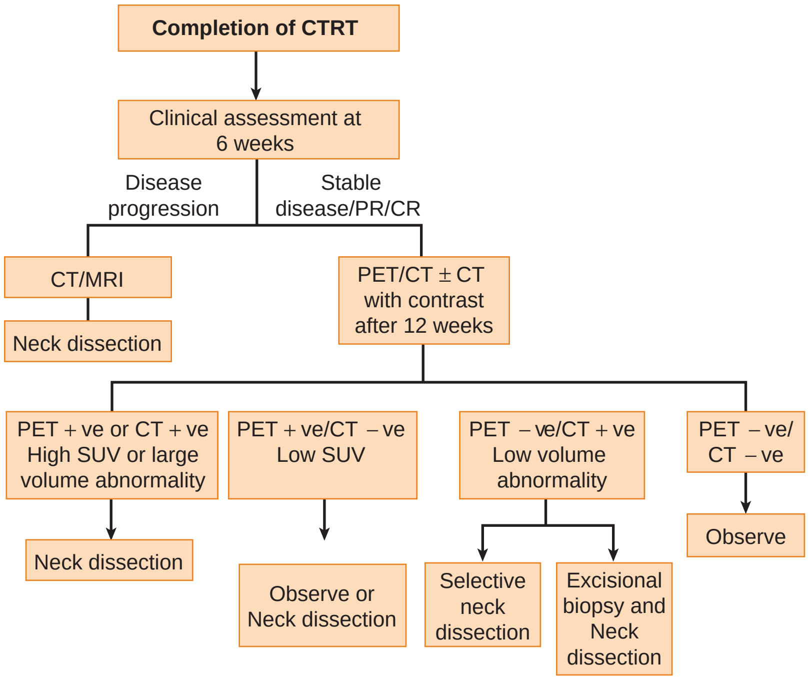

Figure 11.20 Algorithm for evaluation and management of the neck of a patient who has had chemoradiation therapy. *CR,* Complete response; *CT,* computed tomography; *CTRT,* chemotherapy and radiation therapy; *MRI,* magnetic resonance imaging; *PET,* positron emission tomography; *PR,* partial response; *SUV,* standardized uptake value; + ve, positive; – ve, negative.

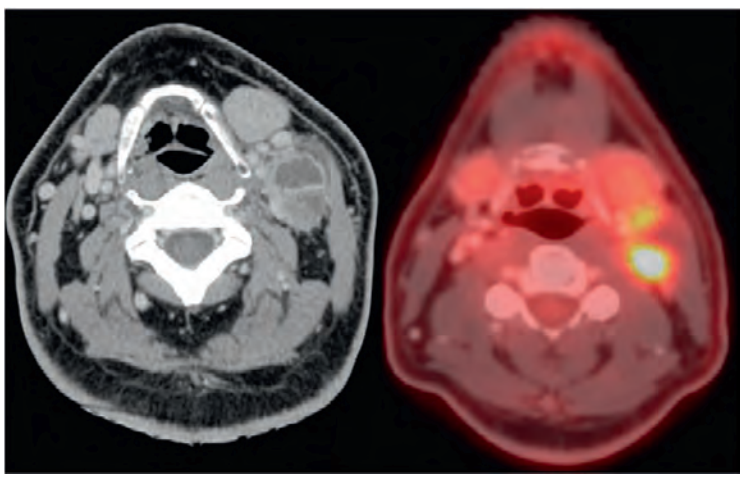

Figure 11.21 A contrast-enhanced computed tomography scan and an 18F-fluorodeoxyglucose (FDG) PET scan of a patient with partially cystic metastasis from squamous cell carcinoma of the tonsil. Note that the cystic component of the tumor shows no FDG activity, while the solid component shows intense FDG avidity.

disease, such as number of nodes and location of nodes as well as extranodal extension and relationship of the nodes to the carotid artery, the skull base, and the parapharyngeal space on the ipsilateral side as well as to evaluate the clinically negative contralateral side of the neck. Several lymph node groups that are not accessible to clinical examination, such as those in the superior mediastinal, parapharyngeal, and retropharyngeal areas, are best assessed by a CT scan or an MRI scan.

US-guided or CT scan–guided fine-needle aspiration biopsy is an excellent option for establishing accurate tissue diagnosis in a small lymph node that is detected radiographically but is not evident clinically. Although US-guided fine-needle aspiration biopsy is adequate for most cervical lymph nodes, a CT-guided biopsy becomes necessary in certain situations such as retropharyngeal and superior mediastinal lymph nodes.

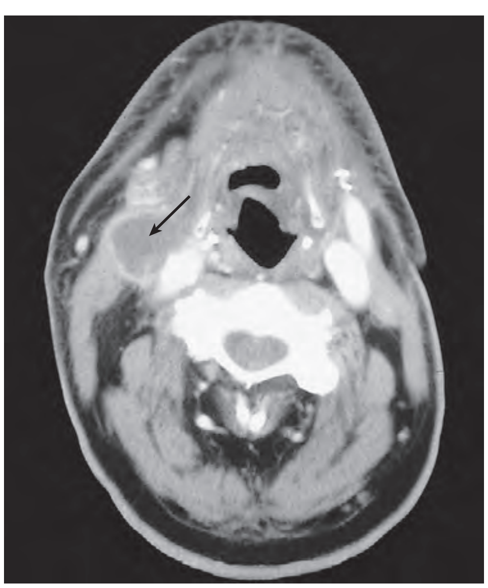

Figure 11.22 The radiographic features for diagnosis of a partly cystic metastatic lymph node (*arrow*) on a computed tomography scan of the neck.

Figure 11.23 An axial view of the computed tomography scan of a patient with N3 metastasis showing extranodal extension with carotid artery invasion.

PATHOLOGIC EVALUATION

It is desirable to have a standard protocol for submission of neck dissection specimen to the pathology laboratory for routine analysis. To maintain anatomic accuracy following en bloc neck dissection, the surgical specimen is oriented on a card board with the levels of the dissected nodes identified, or each level is separated by the operating surgeon in the operating room and submitted separately in multiple containers designated by level and laterality. Upon gross evaluation and prosection of the neck dissection specimen performed by the pathologist, all lymph nodes must be submitted for histopathologic evaluation.

Evaluation of a sentinel node biopsy specimen for melanoma involves serial stepwise tests. Therefore generally the excised node is not sent for frozen section examination. Adequate assessment of the sentinel node requires subserial sections. If multiple hematoxylin and eosin serial sections are negative, immunohistochemistry is performed for a panel of melanoma markers. If this panel is negative, reverse transcriptase-polymerase chain reaction for tyrosinase messenger ribonucleic acid is performed. Similarly, examination of a sentinel node for squamous cell carcinoma may show isolated micrometastases (<2 mm) on hematoxylin and eosin serial sections, or isolated tumor cells may stain for cytokeratin. Although our ability to detect tumor cells has increased compared with the recent past, the precise implications of these findings in terms of selection of treatment and prognosis require continued investigation.

TREATMENT

Clearly the goal of treatment for cervical lymph node metastasis is improved survival and regional control of neck disease. Management of the neck must be considered on the basis of the plan for overall treatment of the primary tumor. The extent of the nodal metastasis also influences management.

Elective treatment of occult metastases in the neck with clinically negative findings intuitively would seem to offer improved survival, but prospective studies have failed to confirm this hypothesis. However, elective treatment of regional nodes has been shown to improve disease-free survival. Moreover, patients who are at risk of having micrometastasis do not progress to clinically or radiographically evident metastasis in a consistent and predictable manner (Fig. 11.24). Most patients who are observed for a cancer in the neck that clinically is staged as N0 have nodal disease that is stage N2 or higher at the time of subsequent detection, even with close follow-up (Figs. 11.25 and 11.26). Micrometastases are reported to show comparable control rates with elective neck dissection or radiation therapy. However, elective neck dissection has the advantage of assessing prognosis and identifies patients who may require adjuvant treatment. Patients whose primary tumors are treated with radiation therapy are best treated with elective irradiation of the neck. On the other hand, if the primary tumor is treated surgically, then elective neck dissection will provide information to select only those patients who need adjuvant radiation therapy and avoid unnecessary radiation in the remainder.

Similarly, management of clinically evident nodal metastasis also is influenced by the treatment selected for the primary tumor. For example, patients with laryngopharyngeal carcinomas who are undergoing definitive chemoradiation therapy require neck dissection only for salvage of persistent or recurrent neck metastasis. For patients undergoing surgical management of the primary tumor (i.e., an oral cavity tumor), neck dissection is an integral part of the surgical plan. Following neck dissection, regional recurrence in the dissected neck is dependent on the volume and extent of neck metastasis at the time of neck dissection. Regional failure rates with surgical treatment alone are very high for patients with multiple positive lymph nodes in the neck. Other ominous findings that increase the risk for local recurrence include lymphovascular or perineural invasion by the tumor, tumor emboli in the lymphatics, and ENE of the tumor. Postoperative radiation therapy has been shown to significantly improve locoregional control in these settings. In addition, prospective clinical trials suggest that regional control may be further enhanced in selected patients, such as those with ENE when treated with postoperative chemoradiation, compared with patients treated with postoperative radiation alone.

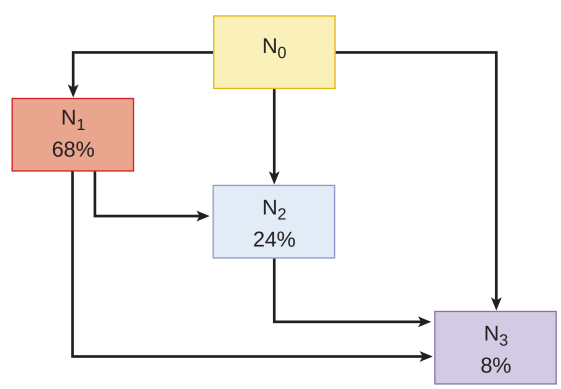

Figure 11.25 Clinical findings in a consecutive series of patients who had cancer staged as N0 in the neck were observed initially and subsequently underwent therapeutic neck dissection.

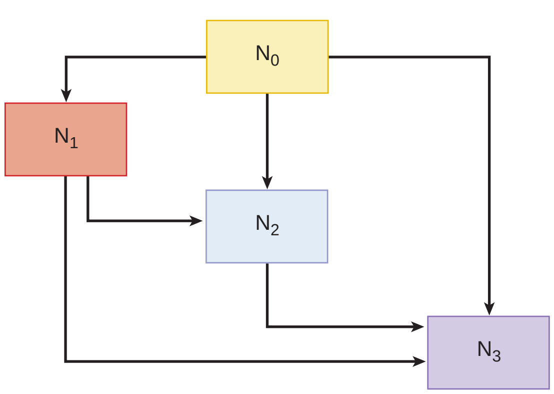

Figure 11.24 Not all patients with cancer staged as N0 in the neck who are at risk of having micrometastasis present for therapeutic neck dissection with N1 disease.

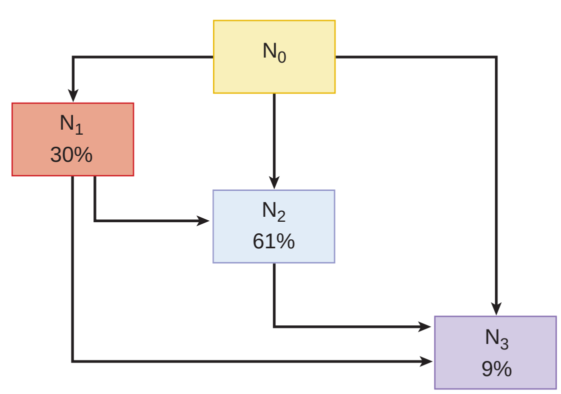

Figure 11.26 Pathologic findings in a consecutive series of patients who had cancer staged as N0 in the neck, were observed initially, and underwent subsequent therapeutic neck dissection.

In patients with clinically evident nodal metastasis and an occult primary site, treatment decisions are based on the location and extent of nodal disease in the neck. Patients with low-volume metastatic disease in the neck can be treated equally well with neck dissection or radiation therapy alone. The need for adjuvant radiation therapy in patients undergoing neck dissection depends on the location and extent of nodal metastases. Similarly, the need to include potential primary sites within the radiation portals is dependent on the location of the metastatic nodes in the neck. For example, metastatic lymph nodes confined to level VA would indicate a potential primary tumor in the nasopharynx that would be included in the radiation portal.

SURGICAL TREATMENT

The surgical treatment of regional lymph nodes for carcinoma of the head and neck region is based on the understanding of the anatomy of the regional lymphatics, the risk of nodal metastasis and the patterns of regional lymph node metastasis, depending on the characteristics of the primary tumor. When regional metastases are clinically palpable, comprehensive clearance of all regional lymph nodes at risk is recommended. The classic radical neck dissection traditionally has been the "gold standard" for the management of neck in patients with head and neck cancer. Although oncologically sound, the classic radical neck dissection is associated with significant cosmetic deformity and functional morbidity. Chronic pain resulting from shoulder disability secondary to accessory nerve sacrifice is common. In addition, atrophy of the trapezius muscle causing shoulder droop and winging of scapula is also a debilitating sequelae. Improved understanding of the biology of metastatic spread of head and neck cancer, and understanding of the patterns of neck metastases, has allowed modifications in the surgical management of cervical lymph nodes to reduce morbidity without compromising regional control or disease-specific survival. Preservation of the spinal accessory nerve significantly reduces the morbidity of neck dissection. Thus if the spinal accessory nerve is not involved by metastatic cancer, it should be routinely preserved even in patients with clinically evident metastatic lymph nodes. In spite of anatomic preservation of the accessory nerve, up to a third of the patients experience varying degrees of shoulder disability. This is due to ischemic injury to the nerve, which has been dissected circumferentially. Preservation of the sternocleidomastoid muscle or internal jugular vein in patients with gross cervical lymph node metastasis results in high regional failure rates but may be considered for low-volume disease.

When an elective neck dissection is undertaken to excise cervical lymph nodes at risk of harboring micrometastasis (occult metastasis), it is seldom necessary to perform a comprehensive neck dissection of all five neck nodal levels. The patterns of cervical lymph node metastasis from mucosal squamous cell carcinomas of the head and neck are predictable and occur in a predictable and sequential fashion. Thus an elective neck dissection can safely include the lymph node groups at highest risk of micrometastasis. Such a limited or "selective" dissection of lymph nodes is usually considered a "staging procedure." The histologic information derived from the study of the excised lymph nodes facilitates selection of adjuvant therapy in patients who are at increased risk of neck failure and spares the need for a more comprehensive and morbid operation or adjuvant radiotherapy in others who are at reduced risk. Thus an elective operation for primary tumors of the oral cavity with a clinically N0 neck requires dissection of lymph nodes at levels I, II, and III and occasionally level IV (for lateral tongue lesions). For primary tumors of the pharynx and larynx, dissection of lymph nodes at levels II, III, and IV is recommended. If the primary tumor crosses the midline, bilateral clearance of levels II, III, and IV should be undertaken.

Classification of Neck Dissections

The understanding of the biological progression of metastatic disease from primary sites in the head and neck region to cervical lymph nodes has allowed the development of several modifications of neck dissection to reduce morbidity while maintaining therapeutic efficacy. To standardize the terminology of various types of neck dissections, several classification systems have been developed. A broad classification between comprehensive and selective neck dissection has been used for the past two decades. However, a more practical and synoptic recording of dissected nodes may be more practical and useful in the future.

Comprehensive Neck Dissection

The term "comprehensive neck dissection" is applied to all surgical procedures in the lateral part of the neck that comprehensively remove cervical lymph nodes from levels I to V. The world "radical" is used only for the description of classical radical neck dissection. It has been removed from all other types of modified, comprehensive operations. The following operative procedures are included under this broad category:

- Classic radical neck dissection
- Extended radical neck dissection (i.e., resection of additional regional lymph nodes or sacrifice of other structures such as cranial nerves, muscles, or skin)
- Modified neck dissection type I (MND-I), which selectively preserves one structure, the spinal accessory nerve
- Modified neck dissection type II (MND-II), which preserves two anatomic structures, the spinal accessory nerve and the sternocleidomastoid muscle, but sacrifices the internal jugular vein
- Modified neck dissection type III (MND-III), which preserves three anatomic structures, the spinal accessory nerve, internal jugular vein, and sternocleidomastoid muscle

Selective Neck Dissection

Selective neck dissection operations remove only select groups of lymph nodes at risk of micrometastasis in the clinically N0 neck. These operations include the following:

- Supraomohyoid neck dissection, which encompasses dissection of lymph nodes at levels I, II, and III for primary tumors of the oral cavity (an extended supraomohyoid neck dissection encompassing levels I, II, III, and IV is recommended for primary cancers of the lateral border of the oral tongue)
- Jugular node dissection, which encompasses dissection of lymph nodes at levels II, III, and IV for primary tumors of the hypopharynx and larynx
- Anterolateral neck dissection, which encompasses dissection of lymph nodes at levels I, II, III, and IV for primary tumors of the oral cavity and oropharynx; this operation is employed as an elective operation as mentioned previously but is also possible for low-volume metastatic nodes at only levels I and II, as a therapeutic operation
- Posterolateral neck dissection, which encompasses lymph nodes in the suboccipital triangle, posterior triangle of the neck, level V, and the deep jugular chain of lymph nodes at

levels II, III, and IV for melanomas and squamous carcinomas of the posterior scalp

- Central compartment neck dissection, which encompasses clearance of lymph nodes at level VI in the central compartment of the neck adjacent to the thyroid gland and in the tracheoesophageal groove for thyroid cancer

Because of variations in nomenclature of neck dissection modifications, whether selective or comprehensive, the term does reflect what a surgeon actually has done during a modified neck dissection. In addition, the term "modified neck dissection" has been used broadly to cover a large variety of different operations. For these reasons, the American Head and Neck Society recommends that after a neck dissection operation, the surgeon should accurately record the levels of lymph nodes removed as well as other nonlymphatic structures resected in each case. This type of synoptic recording conveys what was actually removed during the procedure and what was preserved. The general scheme of synoptic recording is as follows:

- The symbol "ND" should be used to represent the term *neck dissection* and applied as the first component of the description. A prefix should be included to denote the side of the neck upon which the dissection has been performed using the abbreviation L for left, and R for right. If bilateral, both sides must be classified independently.
- The second component of the description should be the neck levels and/or sublevels removed, each designated by the Roman numerals I through VII, in ascending order.
- The third component of the description should be the nonlymphatic structures removed, each identified through the use of specified acronyms (symbols), all of which have been universally accepted. The synoptic designations of various operations and their current names in use are shown in Table 11.7.

Table 11.7 Synoptic Recording of Various Types of Neck Dissections and Their Equivalent Terminology

PROPOSED NOMENCLATURE	AAO-HNS/AHNS NOMENCLATURE
ND (I–V, SCM, IJV, CNXI)	Radical neck dissection
ND (II–IV)	Selective neck dissection (II–IV)
ND (I–III)	Selective neck dissection (I–III)
ND (I–V, SCM, IJV)	Modified radical neck dissection with preservation of the SAN
ND (I–V, SCM, IJV, CNXI and XII)	Extended neck dissection with removal of the hypoglossal nerve
ND (II, III)	Selective neck dissection (II, III)
ND (II–IV, SCM)	NA
ND (I–III, SCM, IJV, CNXI)	NA
ND (II–IV, VI)	NA
ND (VI)	Central compartment neck dissection or selective neck dissection (VI)
ND (VI, VII)	Selective neck dissection (VI, VII)

Preoperative Preparation

No specific preoperative preparation is required for patients undergoing neck dissection other than planning of the incisions for neck dissection, particularly if the primary tumor is to be resected simultaneously. In addition, planning of the neck dissection incisions must take into consideration any reconstructive effort required to repair the surgical defect created after excision of the primary tumor. In the past, a variety of incisions were practiced for selective, comprehensive, unilateral, or bilateral neck dissections. Several such incisions created subsequent problems for reconstructive surgery or additional surgical procedures. In addition, such incisions resulted in aesthetically unacceptable scars.

Currently the preferred incision for any type of neck dissection is a transverse incision along a skin crease in the neck. Vertical extensions of the incision are rarely required. The placement of the transverse incision will vary depending on the type of neck dissection and the site of the primary tumor. Examples of variations in the transverse incision for various types of neck dissections are shown in Fig. 11.27. An upper neck skin crease below the hairline in men is usually chosen for placement of the transverse incision. Patients who require clearance of submental lymph nodes should have the transverse incision extended across the midline rather than placement of a vertical extension toward the chin. Similarly, if posterolateral neck dissection is required, the transverse incision is extended posteriorly along the same skin crease. Patients requiring comprehensive neck dissection with a thyroidectomy or those with long necks have the transverse incision placed in a lower neck skin crease at the level of the cricoid cartilage.

PROCEDURES

Sentinel Node Mapping

Sentinel node mapping uses one or all of the following three techniques: (1) radioisotope scan imaging; (2) injection of blue dye; and (3) use of a handheld isotope tracer probe for localization. It has been shown that the combination of all three techniques increases the accuracy and the yield of sentinel lymph node identification. A preoperative technetium scan is obtained first, which requires injection of a radioactive technetium 99m–labeled sulfur colloid. In general, 0.05 mCi of the isotope is injected in four quadrants around the primary lesion, and a gamma camera is used to obtain visual images at 3 minutes and 15 minutes and a delayed image at 1 hour (Fig. 11.28). Usually the first lymph node identified by the technetium scan is considered the sentinel lymph node. In some patients, more than one sentinel lymph node is identified. The addition of single photon emission computed tomography with CT (SPECT-CT) has been shown to visualize more sentinel lymph nodes than the technetium scan alone and also provides information about their anatomic location, and therefore it is now routinely used in head and neck sentinel node biopsy procedures (Fig. 11.29). A handheld gamma probe is used before placing the incision to localize the lymph node seen on the preoperative scan (Fig. 11.30). The background activity is averaged from measurements in four quadrants of the neck, and any node that has an in vivo 10-second count more than three times that of the background is considered "hot." Correlation is made with the preoperative scan, and this area is marked with a marking pen on the skin.

Further localization of sentinel nodes can be done by injection of a blue dye. This is optional but may be useful to the surgeon for visual localization of the sentinel node. Immediately prior to the surgical procedure, isosulfan blue dye 1% (Lymphazurin) is injected similarly in four quadrants around the primary tumor (Fig. 11.31). No more than 0.5 mL of the dye is injected in the

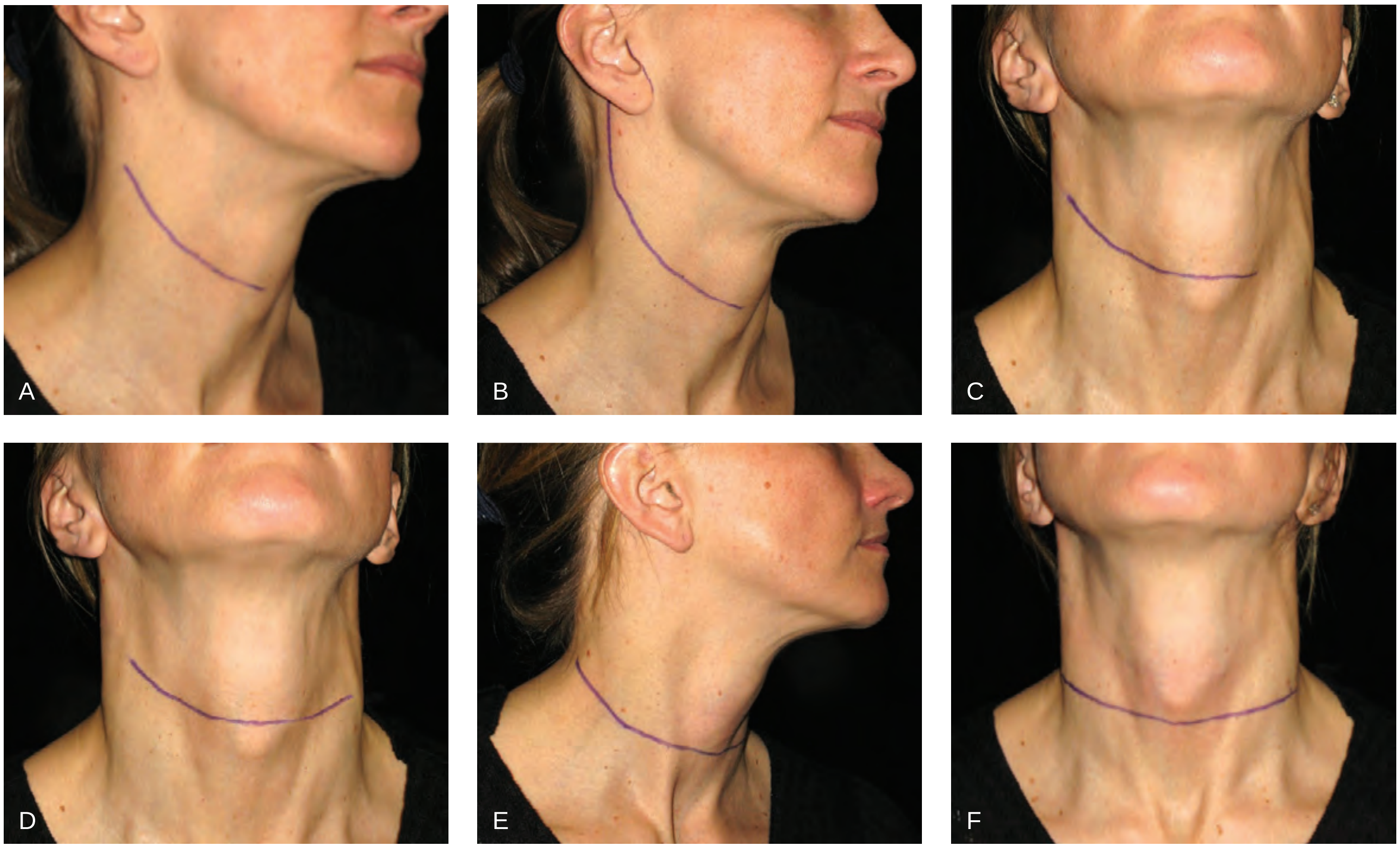

Figure 11.27 Variations in transverse incisions for several types of neck dissections. **A**, Supraomohyoid neck dissection. **B**, Supraomohyoid neck dissection with a parotidectomy. **C**, Supraomohyoid neck dissection with extension for submental dissection. **D**, Jugular node dissection. **E**, Comprehensive neck dissection. **F**, Comprehensive neck dissection with a thyroidectomy.

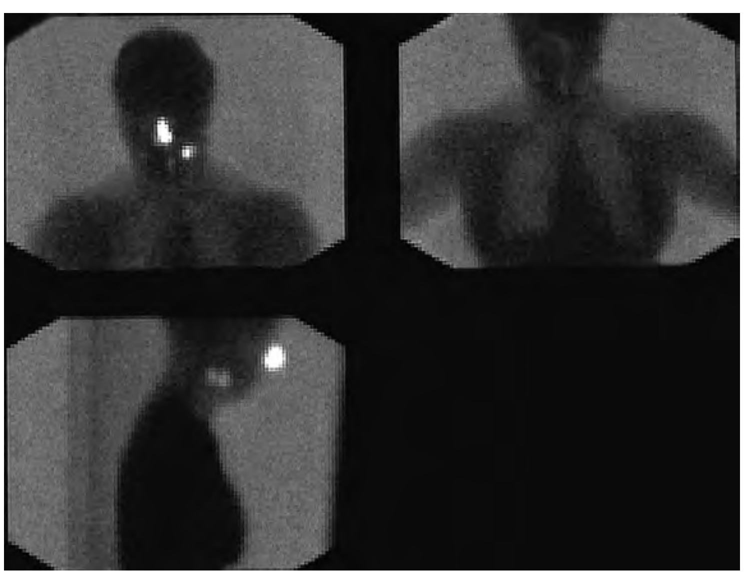

Figure 11.28 A preoperative technetium 99m–labeled sulfur colloid scan showing a sentinel node in the left lower neck from a primary on the skin of the nose.

subdermal plane around the tumor. The operative procedure then is carried out within 30 minutes of the injection.

An incision is placed directly overlying the localized sentinel lymph node, and by careful alternate blunt and sharp dissection, the visually identified "blue node" is localized (Fig. 11.32). The handheld probe is again used to measure the count of highest radiotracer activity. If the blue node corresponds to the area of highest radiotracer activity, then the lymph node is excised and sent for histopathologic analysis. After excision of

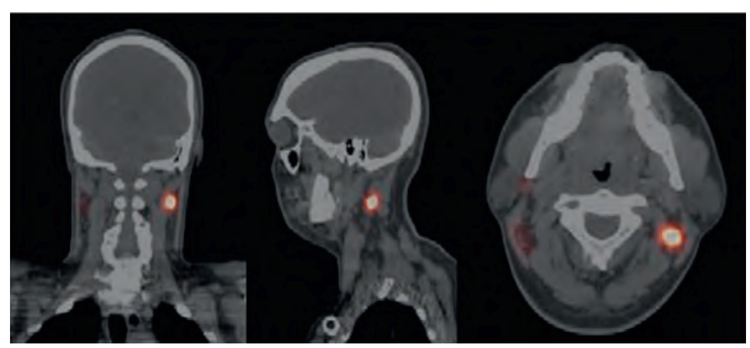

Figure 11.29 Single photon emission computed tomography images of a patient with a melanoma of the frontal scalp showing a sentinel node at level II.

the lymph node, the surgical bed is tested with the handheld probe to show that the radiotracer activity is now reduced to that observed in the adjacent background area, confirming that the true "sentinel lymph node" has been excised and sent for pathologic analysis. If the residual radioactivity in the basin is more than 10% of the ex vivo count of the hottest node in the basin, further exploration to find more sentinel nodes is warranted. Similarly, after the node is excised, the radiotracer activity is measured with a handheld probe from the lymph node ex vivo to demonstrate that the lymph node itself has a count at least 10 times that of an adjacent nonsentinel node. This step ensures that the excised lymph node is indeed a true sentinel lymph node. Because of the special processing required by subserial sectioning of the lymph node to identify occult metastasis, some investigators prefer not to send the lymph

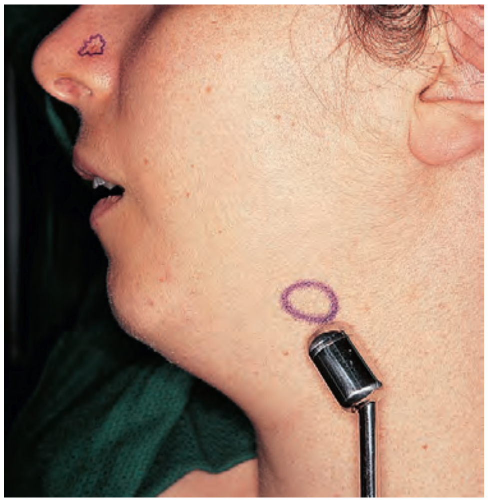

Figure 11.30 A handheld gamma probe.

Figure 11.31 Injection of isosulfan blue dye around the primary lesion.

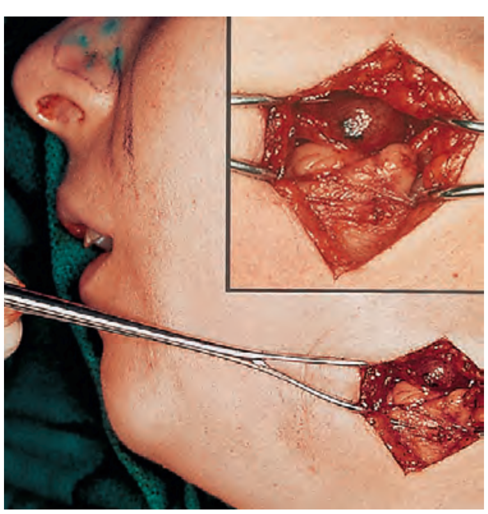

Figure 11.32 The blue-colored sentinel node that also had a high radioactive count.

node for frozen section and wait for "paraffin sections." Further surgical management of regional lymph nodes then depends on the pathologic analysis of the excised sentinel lymph node.

SELECTIVE NECK DISSECTIONS

Supraomohyoid Neck Dissection

Supraomohyoid neck dissection may be performed in conjunction with excision of the primary tumor from the oral cavity, either in continuity where the primary tumor and lymph nodes

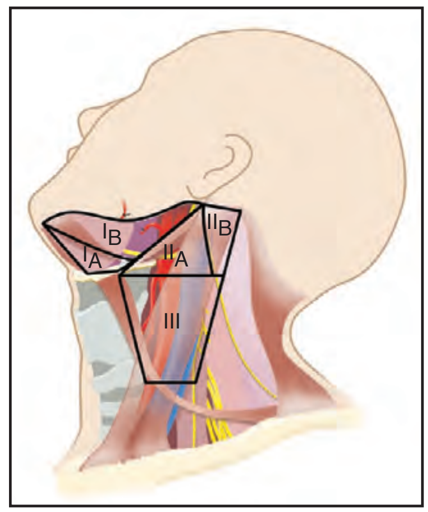

Lymph nodes dissected

- Level I
- Level II
- Level III

Other structures excised

- Submandibular salivary gland

Figure 11.33 Lymph node levels and structures excised in supraomohyoid neck dissection. *(Courtesy Memorial Sloan Kettering Cancer Center.)*

at levels I, II, and III are removed in a monobloc fashion or as a discontinuous procedure in which the primary tumor in the oral cavity may be excised through a peroral approach and the supraomohyoid neck dissection is done through a separate transverse incision in the upper part of the neck (Fig. 11.33). The incision is placed in an upper neck skin crease extending from the posterior border of the sternocleidomastoid muscle toward the hyoid bone up to the midline. The incision should be at least two fingerbreadths below the angle of the mandible. If the primary tumor is to be resected perorally, this incision should be satisfactory. On the other hand, if the primary tumor is not accessible through the open mouth or if the primary tumor of the oral cavity is to be excised en bloc with the contents of the supraomohyoid triangle of the neck, then a lower cheek flap approach will be required. The skin incision therefore is extended cephalad in the midline to divide the lower lip in the midline.

The skin incision is outlined in Fig. 11.34, with an alternate extension in the midline shown by the dotted line. The patient's neck is extended and rotated to the opposite side to put the skin at the site of surgery under tension.

The skin incision is deepened through the platysma throughout its length (Fig. 11.35). Because the incision is quite low in

Figure 11.34 The outlined skin incision.

Figure 11.35 The skin incision is deepened through the platysma.

the neck, use of electrocautery to divide the platysma has no risk of injury to the mandibular branch of the facial nerve. However, in the posterior aspect of the skin incision, attention is required to avoid injury to the greater auricular nerve, which can be preserved. Similarly, the external jugular vein should be preserved carefully if a microvascular free flap is to be used for reconstructive surgery because it is an excellent recipient vein.

The upper skin flap is elevated first, remaining close to the platysma, and the marginal branch of the facial nerve is identified with care. Posteriorly the greater auricular nerve and the external jugular vein overlying the sternomastoid muscle come into view as elevation of the flap continues. The greater auricular nerve and the external jugular vein should be identified carefully and preserved (Fig. 11.36). The nerve is demonstrated here with a hook.

Attention is now focused on careful identification, dissection, and preservation of the mandibular branch of the facial nerve that directly overlies the submandibular salivary gland (Fig. 11.37). This dissection should be performed sharply, using either a scalpel or scissors, because use of electrocautery in the vicinity of the mandibular branch can produce temporary paralysis of this nerve. In identifying and preserving the mandibular branch of the nerve, it may become necessary to sacrifice the cervical branch of the facial nerve.

Once the nerve is identified and dissected along its course, it is retracted cephalad along with the upper skin flap by shifting

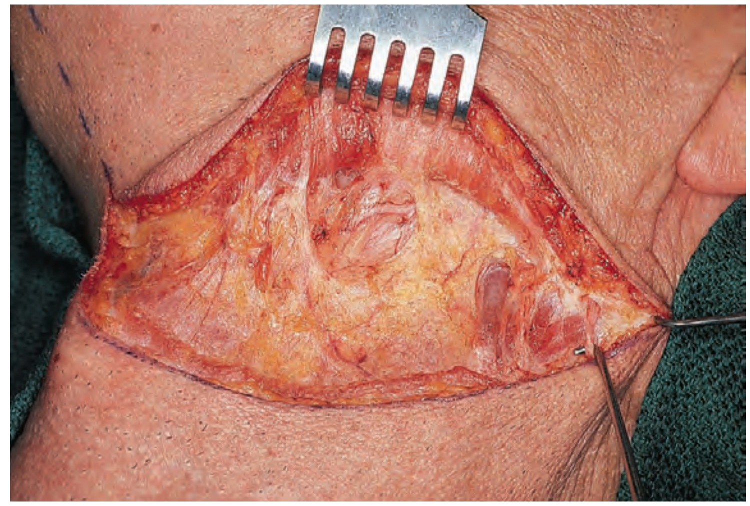

Figure 11.36 The greater auricular nerve and the external jugular vein should be identified carefully and preserved.

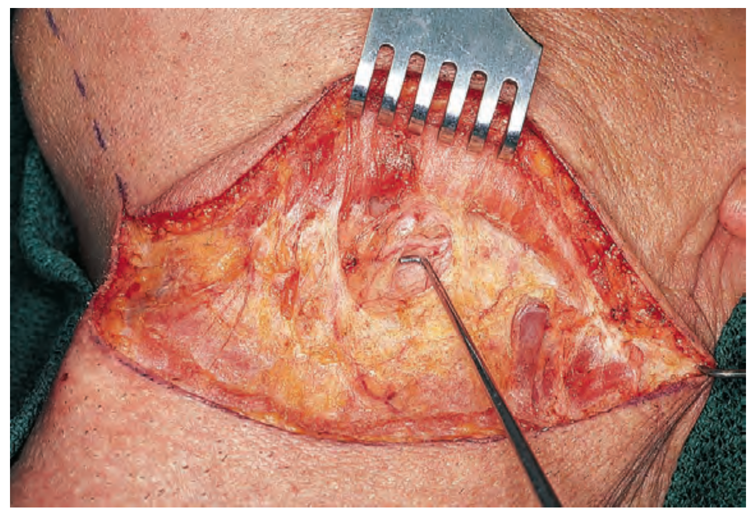

Figure 11.37 The mandibular branch of the facial nerve is carefully identified, dissected, and preserved.

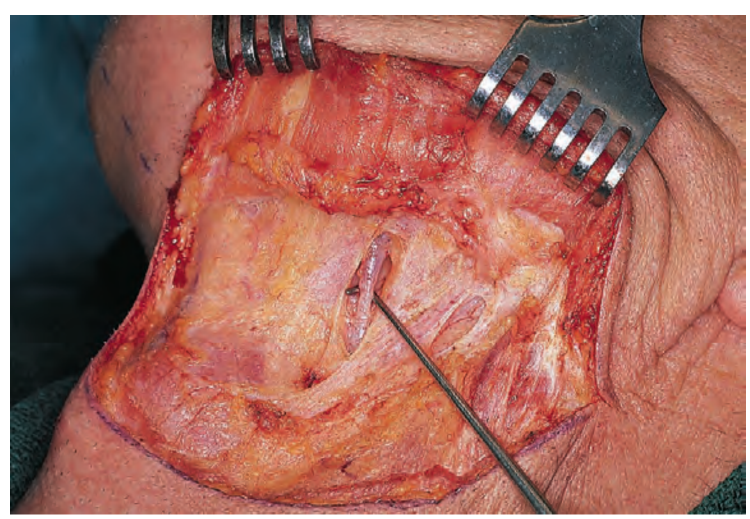

Figure 11.38 The posterior facial vein may be divided and its stump used to retract the mandibular branch of facial nerve.

the nerve with the flap. Alternatively, a suture is placed between soft tissues caudad to the nerve and those of the upper cheek flap cephalad to the nerve to form an envelope to protect the nerve. Similarly, the posterior facial vein may be identified first, as shown in Fig. 11.38.

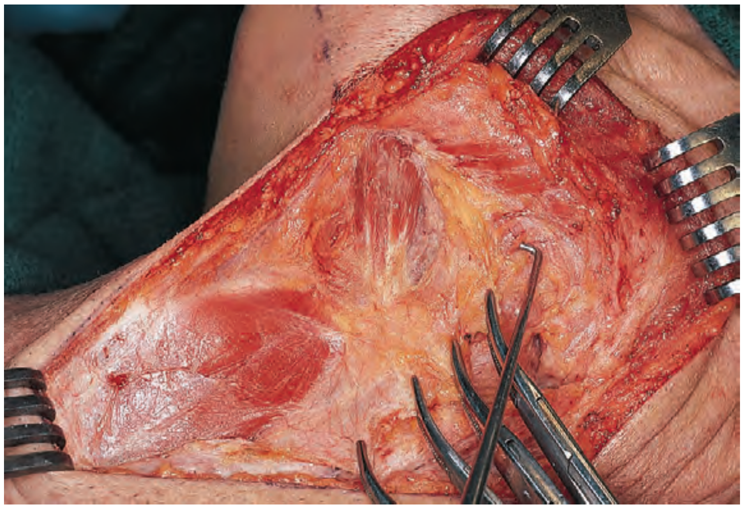

Figure 11.39 Mobilization of soft tissues along the lower border of the body of the mandible exposes the prevascular facial lymph nodes.

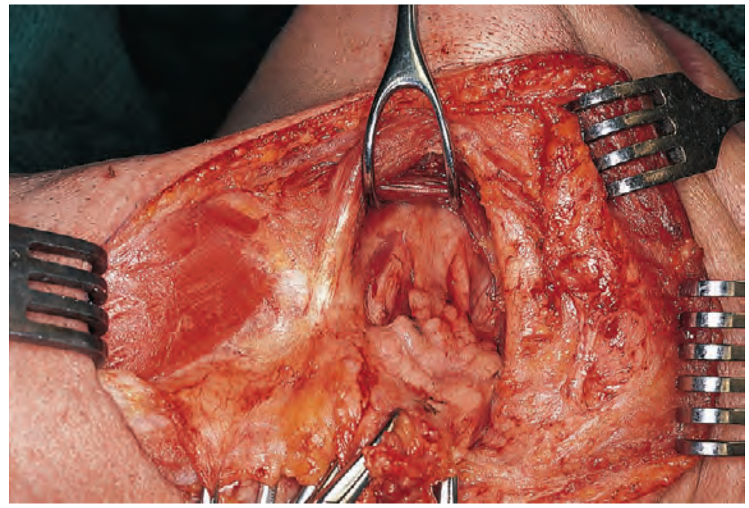

Figure 11.42 The mylohyoid muscle is retracted medially toward the chin of the patient.

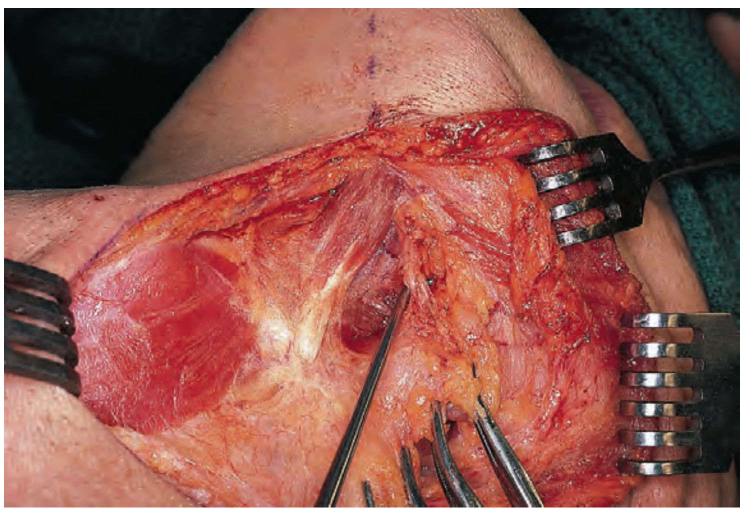

Figure 11.40 The neurovascular bundle to the mylohyoid muscle is identified, clamped, divided, and ligated.

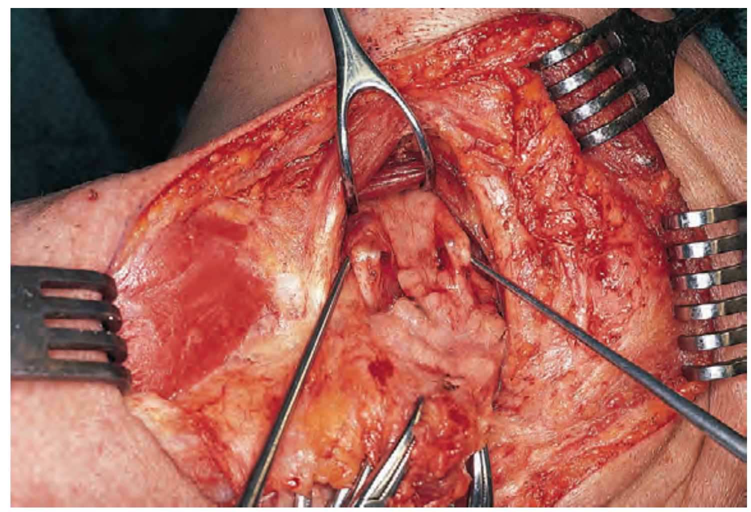

Figure 11.43 The lingual and the hypoglossal nerves are shown, with Wharton's duct in the middle.

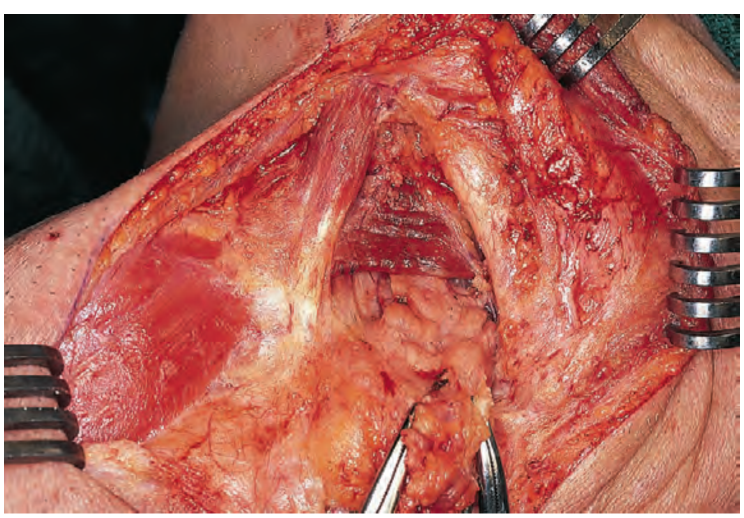

Figure 11.41 The lateral border of the mylohyoid muscle is exposed.

The vein is divided and its stump is ligated with a suture at its upper end, with the platysma on the upper skin flap carefully preserving the marginal branch of the facial nerve between the stump of the vein and the platysma muscle. Dissection now proceeds along the lower border of the body of the mandible. The fascial attachments between the sternomastoid muscle and the angle of the mandible are divided. Mobilization of soft tissues along the lower border of the body of the mandible exposes the prevascular facial lymph nodes (Fig. 11.39). These nodes are meticulously dissected and maintained in continuity with the remainder of the specimen. The facial artery and its accompanying veins adjacent to these nodes are divided between clamps and ligated.

Dissection now continues anteriorly along the lower border of the body of the mandible up to the attachment of the anterior belly of the digastric muscle. Soft tissues between the mandible and anterior belly of the digastric muscle are separated. At this point, brisk hemorrhage is likely to be encountered from several vessels that provide blood supply to the anterior belly of the digastric muscle and the mylohyoid muscle. The nerve and vessels to the mylohyoid muscle, however, enter parallel to each other in a fascial envelope that is identified, clamped, divided, and ligated (Fig. 11.40). Once all the nerve filaments and vessels along the free border of the mylohyoid muscle are divided, the muscle will come into full view.

Gentle traction on the submandibular salivary gland with several hemostats allows mobilization and delivery of the submandibular gland from its bed (Fig. 11.41). A loop retractor is now placed along the lateral border of the mylohyoid muscle, and it is retracted medially toward the chin of the patient (Fig.

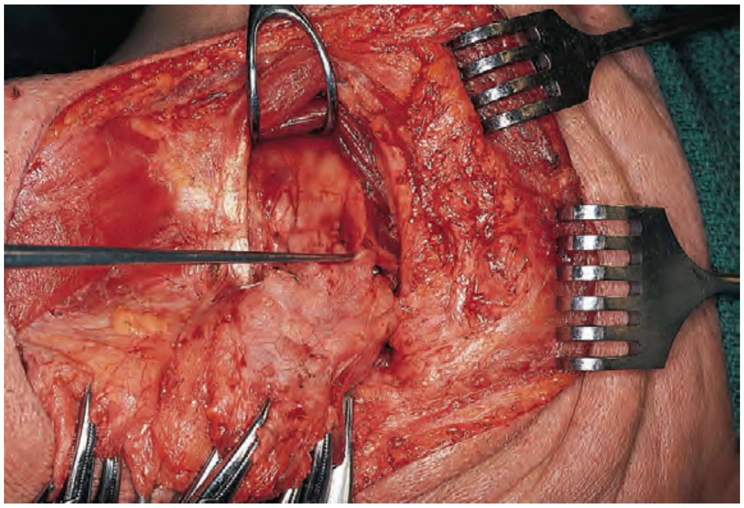

Figure 11.44 The secretomotor fibers to the submandibular gland shown here are divided.

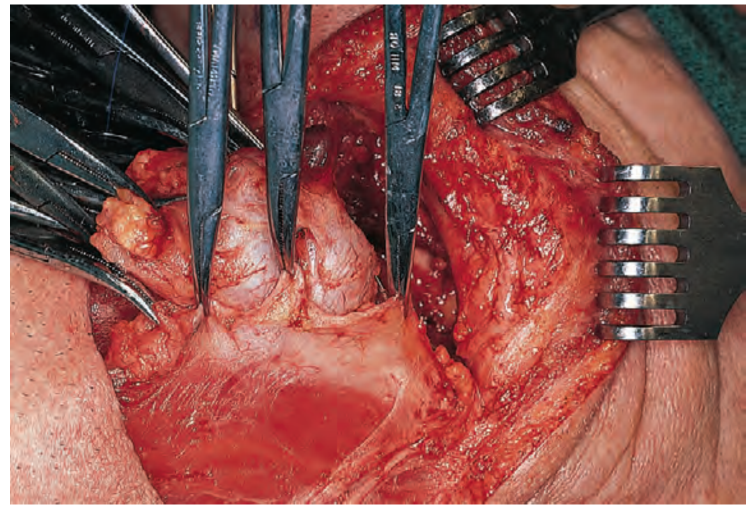

Figure 11.46 The fascia along the anterior border of the sternomastoid muscle is retracted medially to provide traction along its anterior border.

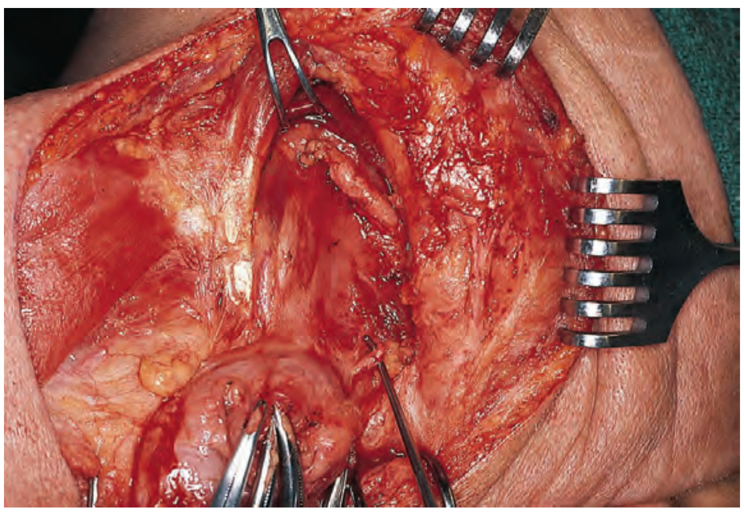

Figure 11.45 The proximal part of the facial artery cephalad to the digastric tendon is divided.

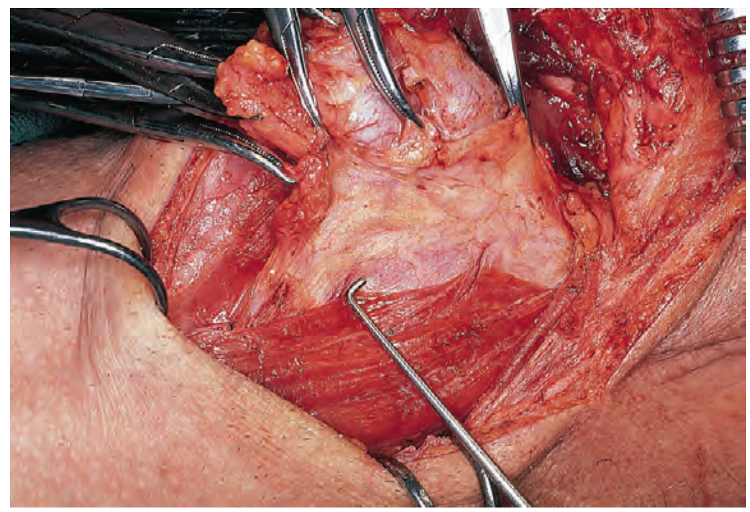

Figure 11.47 The carotid sheath is exposed.

11.42). This maneuver provides exposure of the undersurface of the floor of the mouth and brings the secretomotor fibers to the submandibular salivary gland into view as they come off the lingual nerve, along with Wharton's duct with accessory salivary tissue along the duct. At this juncture, alternate blunt and sharp dissection is necessary to clearly identify Wharton's duct and the lingual and hypoglossal nerves in the floor of the mouth as they enter the tongue.

The lingual and the hypoglossal nerves are shown in Fig. 11.43. Wharton's duct is in the middle and shows small amounts of salivary gland tissue along its length. Once the lingual nerve is clearly identified, the secretomotor fibers to the submandibular gland are divided. The latter are shown in Fig. 11.44 as they come off the lingual nerve. A small blood vessel usually accompanies this nerve; it is divided between clamps and ligated. Similarly, Wharton's duct is divided between clamps and its distal stump is ligated. The entire submandibular gland is now retracted posteroinferiorly, and loose areolar tissue between the salivary gland and the digastric muscle is divided. As the posterior belly of the digastric muscle is approached, the proximal part of the facial artery is exposed as it enters the submandibular salivary gland (Fig. 11.45). It is divided between clamps and ligated. The entire contents of the submandibular triangle are now dissected and retracted inferiorly.

Attention is now focused on the region of the tail of the parotid gland and the anterior border of the upper part of the sternomastoid muscle. The fascia along the anterior border of the sternomastoid muscle is grasped with several hemostats and retracted medially to provide traction along its anterior border (Fig. 11.46). With use of electrocautery, the anterior border of the sternomastoid muscle is cleared off its facial attachments. Several tiny vessels entering the upper part of the sternomastoid muscle (branches from the occipital and superior thyroid arteries) are divided with the electrocautery. Further medial retraction of the specimen exposes the carotid sheath, as shown in Fig. 11.47. This sheath is incised and dissection now proceeds cephalad toward the base of the skull.

A hemostat is used to separate the fascia of the carotid sheath, which is divided and retracted medially (Fig. 11.48). This dissection continues cephalad up to the posterior belly of the digastric muscle, which is retracted cephalad to expose the upper end of the jugular vein entering the jugular foramen. Several pharyngeal veins and tributaries to the common facial vein may need to be divided to mobilize the specimen.

One of the pharyngeal veins that will be divided to facilitate mobilization of the specimen is shown in Fig. 11.49. The sternomastoid muscle is now retracted further posteriorly, exposing the jugular vein in its entirety. The latter is still covered by a fascial envelope containing upper deep jugular and jugulodigastric

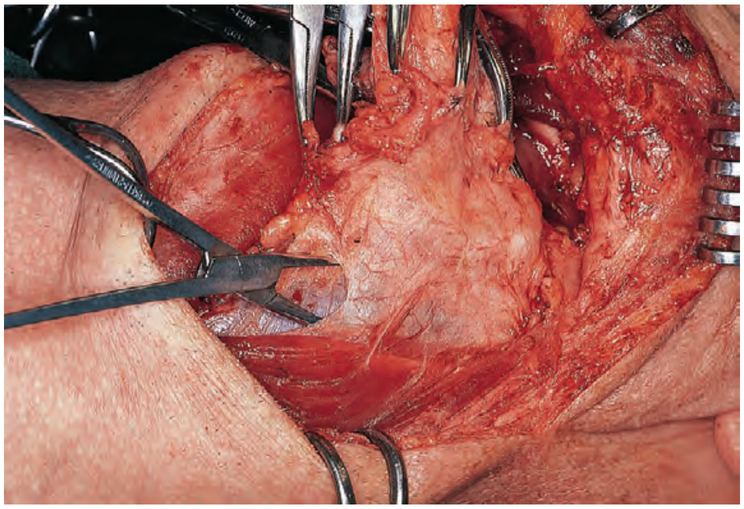

Figure 11.48 The fascia of the carotid sheath is divided and retracted medially.

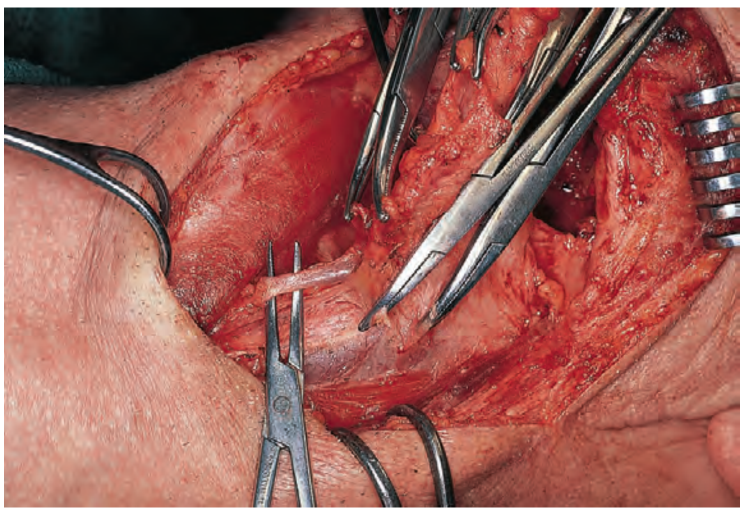

Figure 11.49 One or more of the pharyngeal veins are divided to facilitate mobilization of the specimen.

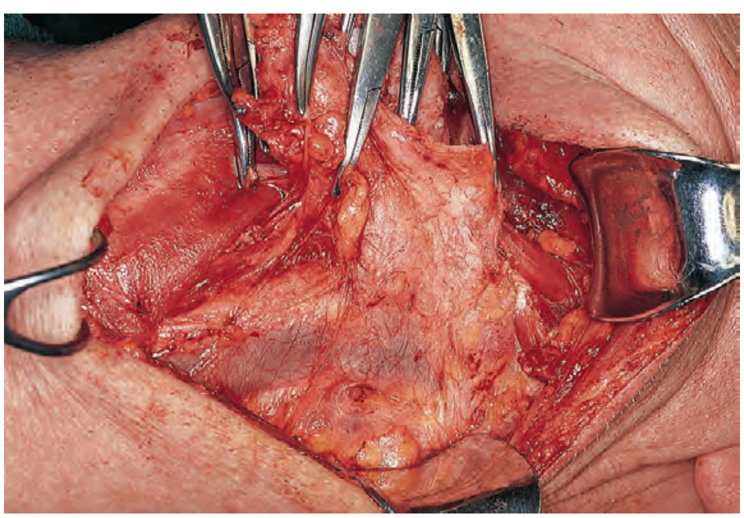

Figure 11.50 The jugular vein is still covered by a fascial envelope containing upper deep jugular and jugulodigastric lymph nodes.

lymph nodes (Fig. 11.50). The sternomastoid muscle is retracted posteriorly to expose lymph nodes in the accessory chain at the apex of the posterior triangle; these nodes are meticulously dissected and retracted anteriorly with the remainder of the surgical specimen.

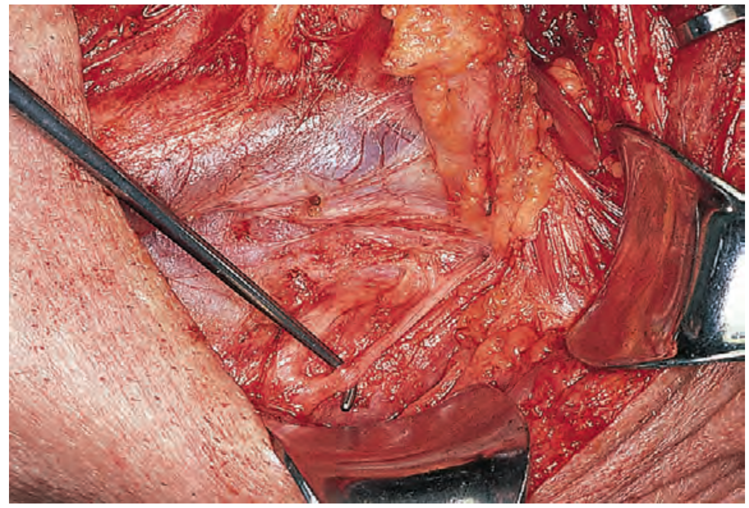

Figure 11.51 The accessory nerve and the cutaneous and muscular branches of the cervical plexus should be identified and preserved carefully.

While dissecting the lymph nodes at the apex of the posterior triangle of the neck, extreme care should be exercised to identify and carefully preserve the spinal accessory nerve as well as the cutaneous and muscular branches of the cervical plexus (Fig. 11.51). Once the spinal accessory nerve is identified, the lymph nodes posterolateral to it are dissected and passed beneath the nerve anteriorly to remain in continuity with the remainder of the specimen. The upper end of the jugular vein is now nearly fully cleared of deep jugular, jugulodigastric, and upper accessory chain lymph nodes.

Dissection of the apex of the posterior triangle clearly shows the upper end of the internal jugular vein and the overlying occipital artery crossing it at right angles.

The highest root of the cervical plexus is exposed with further dissection of the eleventh nerve and removal of lymph nodes in the jugulodigastric region. The posterior limit of the supraomohyoid neck dissection in this area is rather arbitrary, because no specific anatomic landmarks exist to define the extent of the posterior triangle lymph node dissection, and thus clinical judgment must be exercised to decide on the extent of their removal.

Dissection of the accessory chain lymph nodes posterior to the internal jugular vein at the apex of the posterior triangle is now complete (Fig. 11.52). The entire jugular vein is exposed, with the posterior belly of the digastric muscle retracted cephalad. The specimen is now reflected anteriorly, and the common facial vein is divided as it enters the internal jugular vein and is ligated (Fig. 11.53). Dissection continues anteriorly, with careful identification and preservation of the hypoglossal nerve and the descendens hypoglossi, the nerve supply to the strap muscles.

The descendens hypoglossi is shown in Fig. 11.54 as it comes off the hypoglossal nerve and runs anteroinferiorly. Dissection also continues along the medial aspect of the carotid sheath, exposing the carotid bulb. The surgical specimen mobilized thus far consists of the contents of the submandibular triangle, lymph nodes from the jugulodigastric region and the apex of the posterior triangle of the neck, and the upper deep jugular lymph nodes.

Dissection is now continued caudad toward the apex of the supraomohyoid triangle, the junction where the superior belly of the omohyoid muscle crosses the sternomastoid muscle. A loop retractor is placed to expose the lower part of the carotid sheath, from where midjugular lymph nodes are dissected and

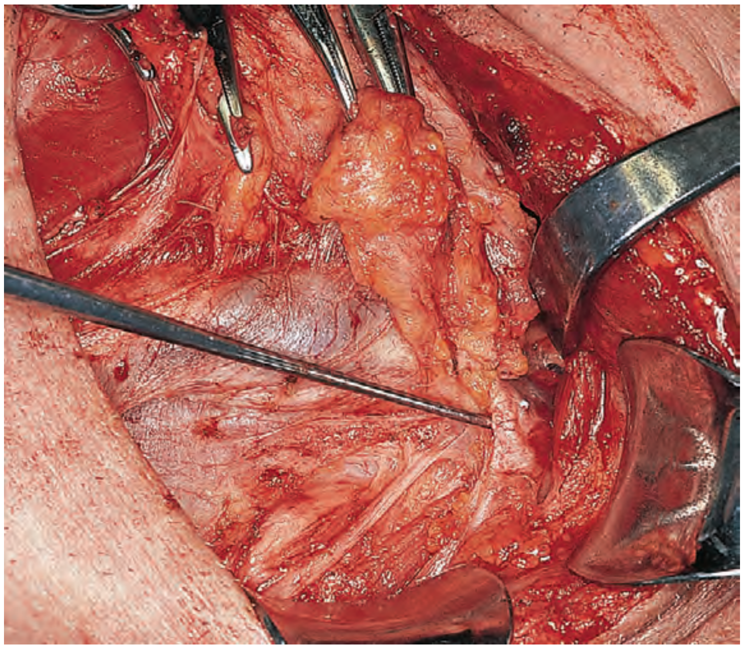

Figure 11.52 The completed dissection of the accessory chain lymph nodes posterior to the internal jugular vein at the apex of the posterior triangle exposes the occipital artery.

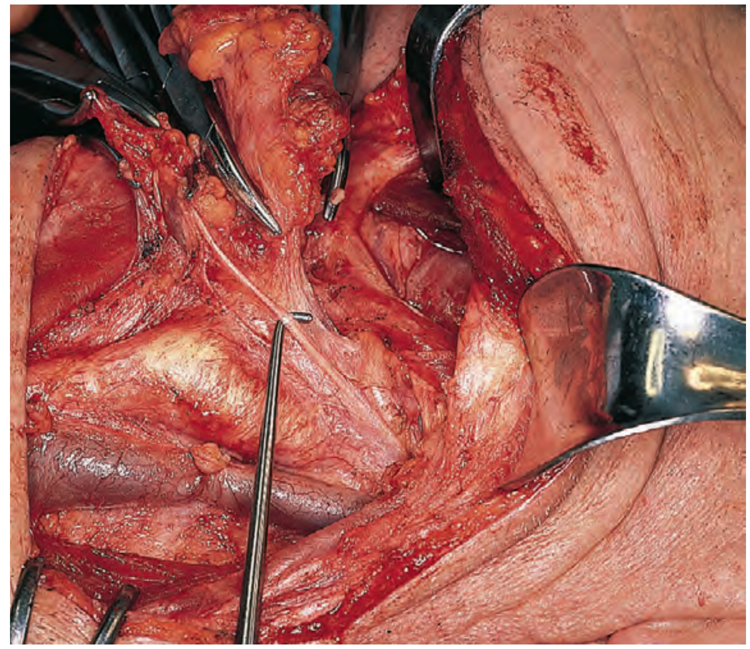

Figure 11.54 The descendens hypoglossi.

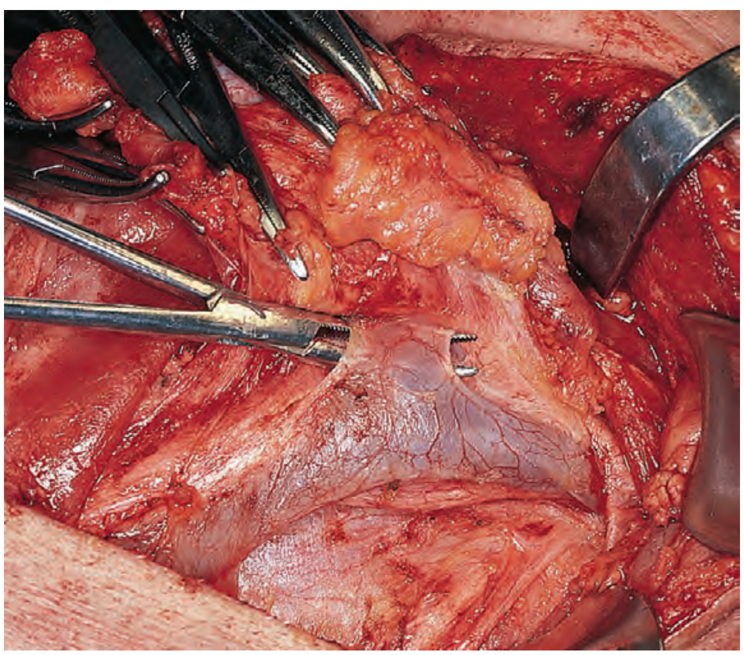

Figure 11.53 The specimen is reflected anteriorly and the common facial vein is divided and ligated.

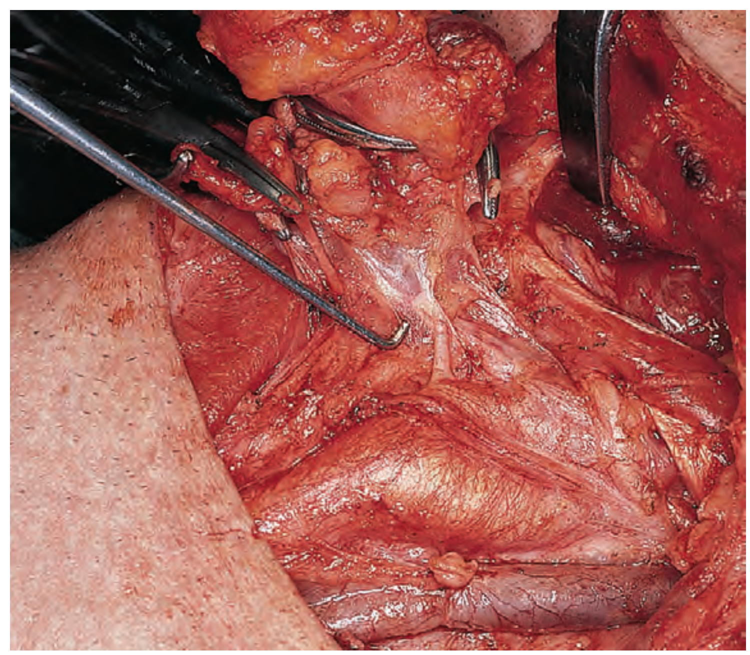

Figure 11.55 Dissection is continued caudad toward the apex of the supraomohyoid triangle.

reflected cephalad. Dissection continues further medially, exposing the origin of the superior thyroid artery, which is preserved, but the superior thyroid vein must be sacrificed, because it previously was divided from the internal jugular vein (Fig. 11.55). The final attachments of the specimen in the region of the thyrohyoid membrane and the insertion of the strap muscles over the hyoid bone are divided with electrocautery.

After removal of the specimen, the surgical field shows complete clearance of the supraomohyoid triangle (Fig. 11.56). The anatomic structures demonstrated here are the anterior and posterior bellies of the digastric and mylohyoid muscles. The lingual and hypoglossal nerves and the marginal branch of the facial nerve also are seen in the submandibular triangle. The superior belly of the omohyoid, sternohyoid, and stylohyoid muscles, as well as the bifurcation of the carotid artery, also are in clear view. Note that the lymph nodes from levels II and III along the internal jugular vein are all dissected off with the specimen. The posterior and inferior views of the surgical field demonstrate the spinal accessory nerve and branches of the cervical plexus, along with the lower end of the supraomohyoid triangle where the sternomastoid and the omohyoid muscles cross each other (Fig. 11.57).

The wound is now irrigated with Bacitracin solution. A single suction drain is inserted through a separate stab incision and is placed parallel to the anterior border of the sternomastoid muscle up to the submandibular triangle (Fig. 11.58). The drain is secured in place with a silk suture to the skin at the site of entry, and the incision is closed in two layers using 3-0 chromic

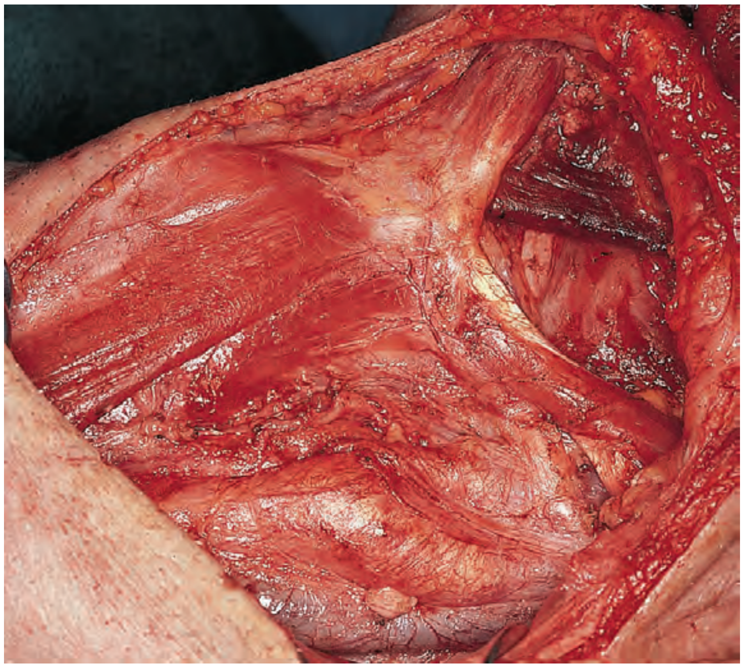

Figure 11.56 The surgical field after removal of the specimen.

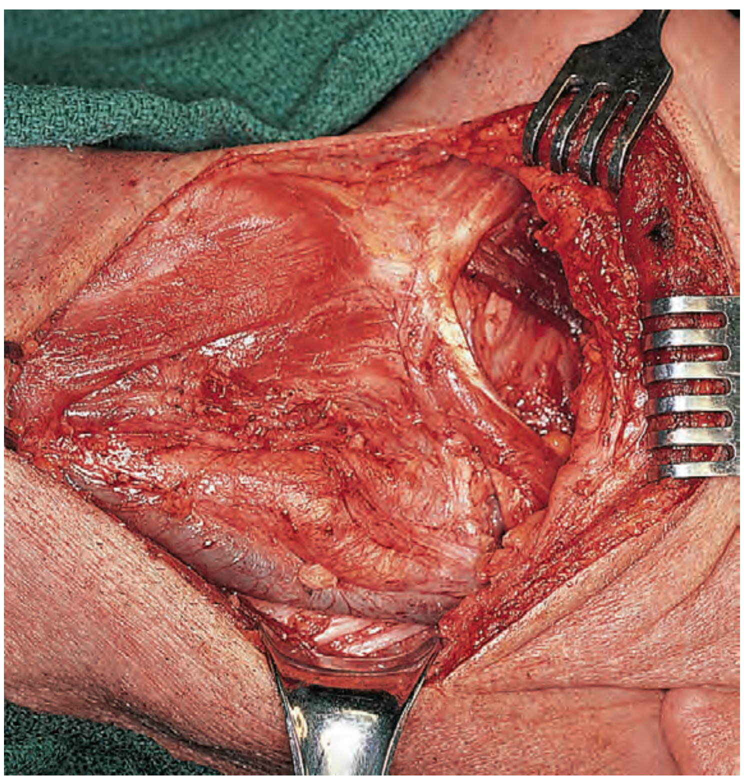

Figure 11.57 Posterior and inferior views of the surgical field.

catgut interrupted sutures for platysma and 5-0 nylon interrupted sutures for skin (Fig. 11.59). Blood loss during this operative procedure should be minimal. The postoperative appearance of the patient demonstrates that there is essentially no aesthetic or functional deformity after this operation (Fig. 11.60).

By placement of the transverse incision along a skin crease, the aesthetic morbidity of supraomohyoid neck dissection is minimal if any, as seen in another patient in Fig. 11.61. If access is necessary to level IA, then the incision should not be curved along the submental region but should be extended along the same crease across the midline to the opposite side of the neck (Fig. 11.62). Aesthetically that is a much more acceptable incision than a vertical incision in the submental region in the midline.

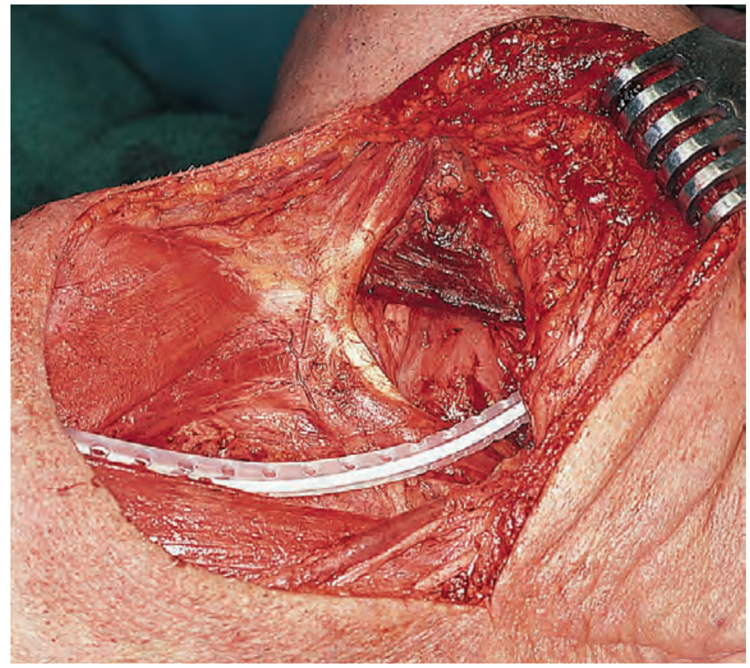

Figure 11.58 A single suction drain is inserted through a separate stab incision.

Figure 11.59 The drain is secured in place, and the incision is closed in layers.

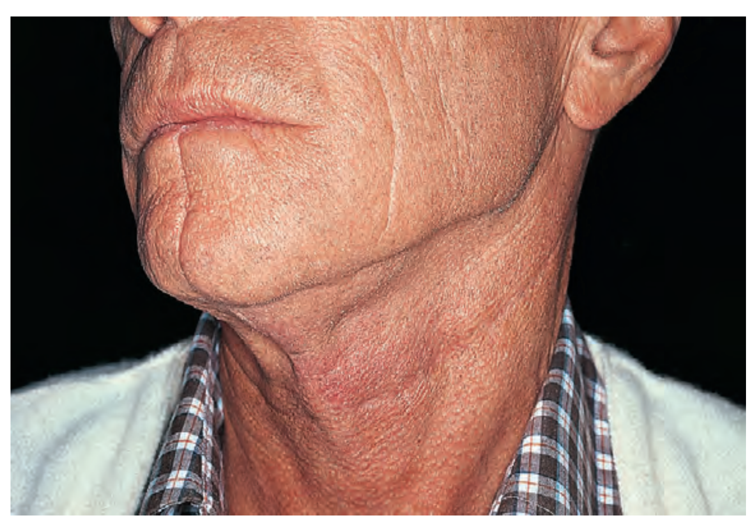

Figure 11.60 The postoperative appearance of the patient 6 months following surgery.

Figure 11.61 Postoperative scar 1 year after supraomohyoid neck dissection.

Figure 11.62 The postoperative scar 1 year after surgery of an incision that extended across the midline for supraomohyoid neck dissection, to include level IA.

Extended Supraomohyoid Neck Dissection

Patients with primary carcinoma of the lateral border of the oral tongue have a small risk of having skip metastasis to level IV of the ipsilateral neck. Therefore an elective operation being undertaken for primary carcinomas of the oral tongue should include level IV in addition to the standard supraomohyoid neck dissection. This extended supraomohyoid neck dissection is an operative procedure very similar to the standard supraomohyoid neck dissection (Fig. 11.63).

During the course of dissection of level III lymph nodes, the lower skin flap is retracted caudad, and the tendon of the omohyoid muscle crossing the lower half of the internal jugular vein is divided. This procedure permits further retraction of the lower skin flap toward the clavicle. Dissection is now continued along the lower half of the internal jugular vein to include the lymph nodes at level IV. In this part of the dissection, meticulous attention is required to carefully identify the lymphatic channels at the root of the neck. These channels should be clamped individually, divided, and ligated. In the left side of the neck, the thoracic duct should be sought out, identified,

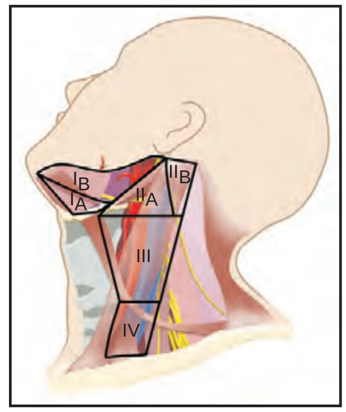

Figure 11.63 Extended supraomohyoid neck dissection. *(Courtesy Memorial Sloan Kettering Cancer Center.)*

and ligated with care. Dissection of lymph nodes at level IV therefore includes the lymph nodes medial and anterior to the internal jugular vein and lateral to the internal jugular vein in the region of the lymphatic channels/thoracic duct, and the origin of the transverse cervical artery. These lymph nodes then should be brought over to remain in continuity with the specimen of other deep jugular lymph nodes from levels II and III. The extended supraomohyoid neck dissection therefore will include all the lymph nodes in the anterolateral triangle of the neck, including levels I, II, III, and IV. The only lymph nodes that are not resected with this operation are the ones along the lower spinal accessory chain and transverse cervical chain in the posterior triangle of the neck.

Jugular Node Dissection

A jugular neck dissection usually is performed in conjunction with resection of the primary tumor of the larynx or hypopharynx. Jugular node dissection may be performed on the ipsilateral side for lesions that are unilateral in its mucosal extent, or it may be performed bilaterally for lesions that cross the midline to involve both sides of the laryngopharyngeal mucosa. The operative procedure is performed through the same incision used for resection of the primary tumor, which is usually a transverse incision along an upper neck skin crease in the region of the thyrohyoid membrane extending from the posterior border of sternocleidomastoid muscle on one side of the neck to that on the other side of the neck (Fig. 11.64).

After an incision is made in the skin, the platysma is divided throughout the entire length of the incision and upper and lower skin flaps are elevated in the usual fashion, exposing the anterior border of the sternocleidomastoid muscle in its entirety from the region of the posterior belly of the digastric muscle cephalad to the insertion of the sternal head caudad. There is no particular advantage in performing jugular node dissection in continuity with resection of the primary tumor unless a total pharyngolaryngectomy is being performed. Inasmuch as all internal jugular lymph nodes at levels II, III, and IV are excised in a monobloc fashion, the oncologic purpose of this operation is served. The extent of the nodal tissue to be cleared is shown in Fig. 11.65. The internal jugular group of lymph nodes, which lie anterior, lateral, and posterior to the internal jugular vein, are excised in a monobloc fashion. This procedure by necessity will require clearance of lymph nodes of the internal jugular chain at least up to the posterior border of the sternocleidomastoid muscle.

The operative procedure begins by incising the fascia along the anterior border of the sternocleidomastoid muscle, which is

Figure 11.64 The outline of a skin incision for a jugular neck dissection.

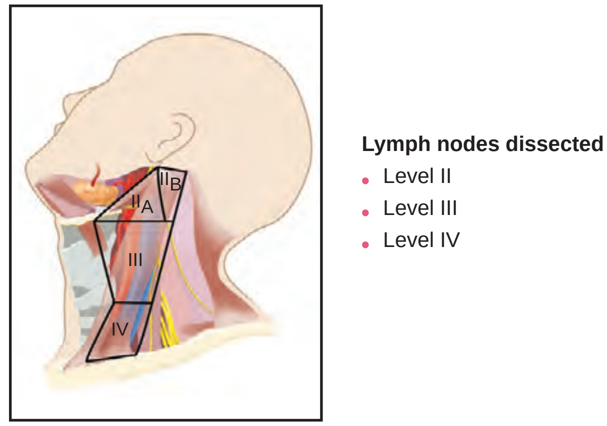

Figure 11.65 Jugular neck dissection. *(Courtesy Memorial Sloan Kettering Cancer Center.)*

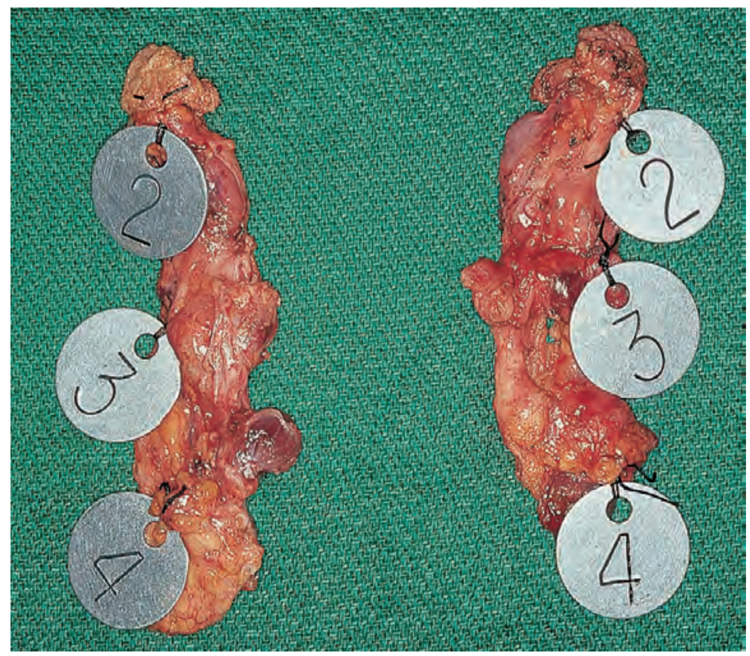

Figure 11.66 The surgical specimen.

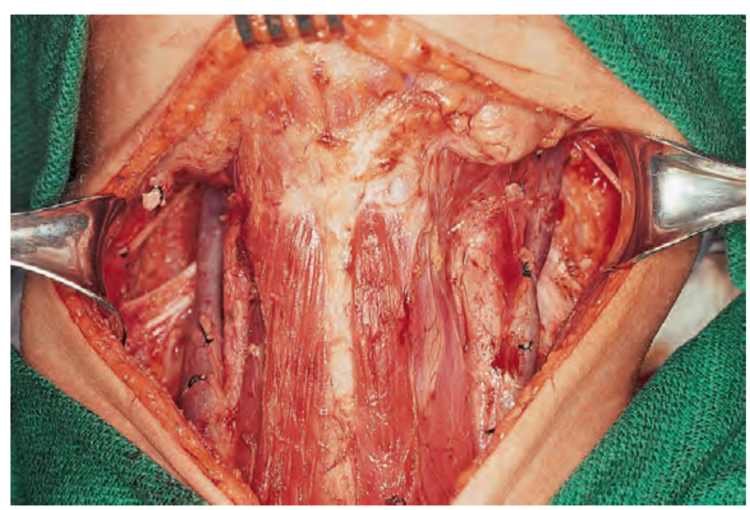

Figure 11.67 The surgical field after bilateral jugular node dissections.

grasped with hemostats to permit retraction of the sternomastoid muscle posteriorly. This dissection continues on the undersurface of the sternocleidomastoid muscle all the way up to its posterior border. During the course of this part of the operation, the blood supply to the sternocleidomastoid muscle from branches of the occipital artery and superior thyroid artery will be encountered. These vessels are divided and ligated carefully. Once this step is accomplished, the entire sternocleidomastoid muscle can be retracted with Richardson retractors posteriorly, totally exposing the internal jugular lymph nodes from the jugulodigastric region cephalad to the supraclavicular region caudad.

Dissection begins at the upper end, clearing the lymph nodes that are posterior to the spinal accessory nerve as it exits from the jugular foramen. These lymph nodes are covered by the upper end of the sternocleidomastoid muscle and lie over the splenius capitis and levator scapulae muscles in the floor of the posterior triangle of the neck. Meticulous dissection of these lymph nodes allows delivery from beneath the accessory nerve anteriorly to remain in continuity with the jugulodigastric group of lymph nodes. Similarly, dissection of lymph nodes overlying the sensory roots of the cervical plexus is undertaken, exposing the sensory roots, and the dissection is continued with care up to the lateral border of the internal jugular vein to keep these lymph nodes in continuity with the deep jugular lymph nodes. Clearance of the accessory chain of lymph nodes and exposure of all the cervical roots are essential to provide satisfactory clearance of contiguous lymph nodes in the posterior triangle.

At this juncture, dissection continues anterolateral to the internal jugular vein, clearing off all the lymph nodes and freeing up the internal jugular vein in its entirety from the jugular foramen cephalad and to the supraclavicular region caudad. In so doing, the tendon of the omohyoid muscle is divided. No attempt is made to continue the dissection of lymph nodes in the submandibular triangle, and thus the submandibular salivary gland is left intact. However, several pharyngeal branches of the internal jugular vein and the common facial vein must be divided and ligated to facilitate dissection of the upper jugular lymph nodes. By meticulous alternate blunt and sharp dissection, the hypoglossal nerve, the descendens hypoglossi, and the branches of the superior thyroid artery are identified and carefully preserved, and the specimen is removed.

The specimen shown in Fig. 11.66 demonstrates monobloc excision of the bilateral internal jugular group of lymph nodes from levels II, III, and IV. To facilitate accurate description of the excised lymph nodes, it is important to apply numerical tags to the lymph nodes depicting levels II, III, and IV. This step facilitates proper analysis of the surgical specimen to render an accurate histopathologic report. Alternatively, the specimen should be divided into separate levels and submitted in separate containers for pathologic analysis.

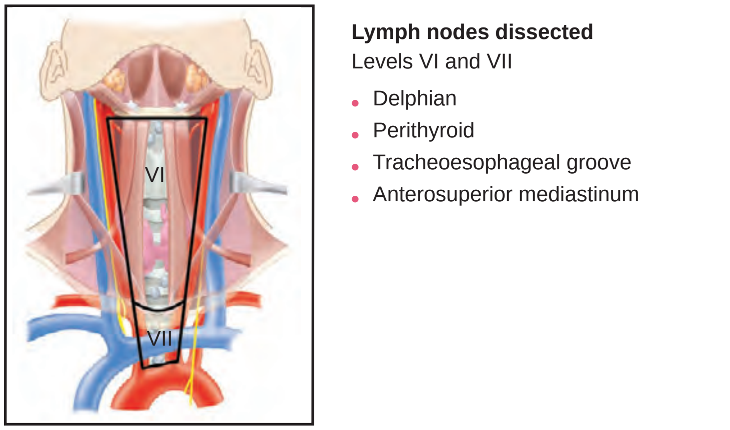

Figure 11.68 Level VI and VII lymph nodes (N1a) are included in a central compartment node dissection. *(Courtesy Memorial Sloan Kettering Cancer Center.)*

Fig. 11.67 shows the surgical field after bilateral jugular lymph node dissections were performed in this patient, who had a carcinoma of the posterior pharyngeal wall. Note the complete clearance of the internal jugular lymph nodes, which exposes the internal jugular vein in its entirety. The roots of the cervical plexus in the posterior triangle also are exposed. The submandibular salivary glands are seen cephalad. Suction drains are placed appropriately, and the incision is closed in layers in the usual manner. This surgical procedure essentially has no functional and aesthetic impact. However, the histologic information derived from analysis of the surgical specimen allows accurate pathologic staging of the primary tumor to select patients who require adjuvant postoperative radiation therapy.

Central Compartment Node Dissection

A therapeutic central compartment node dissection is undertaken for dissection of regional lymph nodes involved by metastases from primary differentiated carcinomas of the thyroid gland. Elective central compartment node dissection is considered when the primary tumor is extensive, with invasion of the capsule of the thyroid gland or with extension beyond the capsule of the thyroid gland, to secure satisfactory clearance of local and regional disease from the central compartment of the neck. If the primary tumor is of significant dimensions or involves both sides of the thyroid gland, then bilateral tracheoesophageal groove lymph node dissection is undertaken. When minimal enlargement of the central compartment lymph nodes is observed during the course of thyroidectomy, as long as findings of the lateral part of the neck are grossly negative, a central compartment node dissection of the neck is considered adequate (Fig. 11.68).

The operative procedure usually begins with a thyroidectomy. A transverse incision in a natural skin crease at the level of the cricoid cartilage is placed (Fig. 11.69). After exploration of the thyroid gland and the central compartment, if any enlarged lymph nodes are found, then a decision is made to proceed with a central compartment lymph node dissection. The first step in the operative procedure is careful identification and preservation of the parathyroid glands with their blood supply intact. This step usually is accomplished by incising the fascia over the lateral border of the thyroid gland. This fascia is carefully elevated from the posterior border of the thyroid gland, and several terminal branches of the superior and inferior thyroid arteries distal to the parathyroid glands are then encountered. These branches are clamped individually, divided, and ligated.

Figure 11.69 Incision for thyroidectomy and central compartment lymph node dissection (N1a).

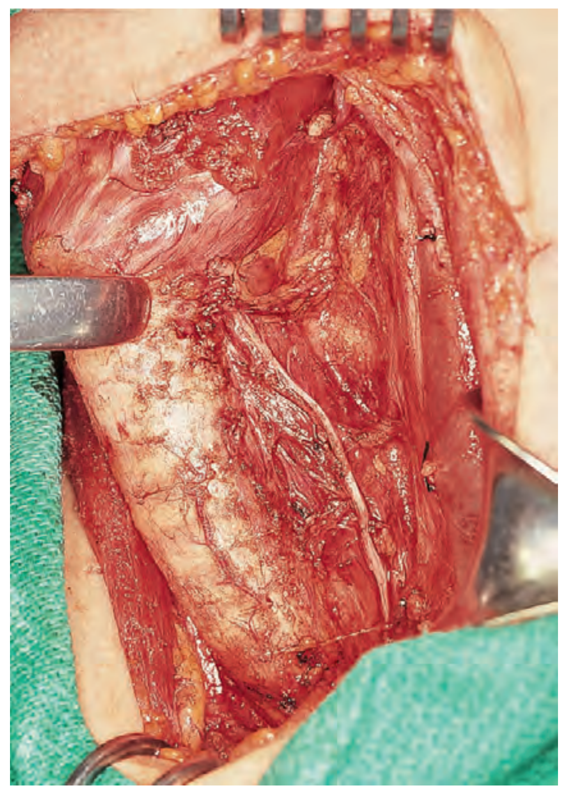

Figure 11.70 The surgical field after a total thyroidectomy and tracheoesophageal groove lymph node dissection.

Once the parathyroid glands are safely dissected off the thyroid gland, the recurrent laryngeal nerve is identified and exposed throughout its course in the central compartment of the neck to facilitate clearance of the tracheoesophageal groove lymph nodes. After identification and dissection of the recurrent laryngeal nerve, all the fibrofatty tissue and lymph nodes in the central compartment of the neck are excised, extending from the carotid sheath laterally to the tracheoesophageal groove medially and extending from the level of the hyoid bone superiorly to the superior mediastinum inferiorly. The lower limit of the tracheoesophageal groove node dissection is somewhat arbitrary and ends at the level of the innominate artery in the superior mediastinum. Often the tracheoesophageal groove node dissection is not able to be accomplished in a monobloc fashion. This situation is particularly true if the parathyroid glands are to be dissected and preserved with their blood supply

intact. Sacrifice of the strap muscles often facilitates exposure and dissection of the central compartment lymph nodes.

Fig. 11.70 shows the surgical field after clearance of bilateral tracheoesophageal groove lymph nodes and the central compartment of the neck in a patient who underwent a total thyroidectomy for a papillary carcinoma of the thyroid gland that diffusely involved both lobes. If the parathyroid glands are inadvertently injured or dissected off during the course of tracheoesophageal groove node dissection, they should be implanted in one of the muscles of the lateral side of the neck.

Posterolateral Neck Dissection

Posterolateral neck dissection is recommended for clearance of regional lymph nodes from the suboccipital triangle and the posterior triangle of the neck at level V in conjunction with deep jugular lymph nodes at levels II, III, and IV (Fig. 11.71). The operative procedure may be performed in continuity with excision of the primary skin carcinoma or melanoma of the posterior scalp, or it may be performed discontinuously using a hockey-stick–type incision with posterior extension at the upper end to expose the occipital region (Fig. 11.72). The skin flaps are elevated in the usual fashion. To accomplish dissection of the suboccipital lymph nodes, the trapezius muscle is detached from the occipital bone and reflected posteriorly to expose the suboccipital triangle. Suboccipital lymph nodes and the lymph nodes deep to the trapezius muscle then are dissected off from the underlying muscles and reflected anteriorly to remain in continuity with lymph nodes of the posterior triangle of the neck (Fig. 11.73). During dissection of the lymph nodes in the posterior triangle of the neck, the accessory nerve is preserved if it is not grossly involved by metastatic disease or if it does not compromise satisfactory clearance of grossly enlarged metastatic lymph nodes. Dissection of the deep jugular lymph nodes is undertaken by retracting the sternocleidomastoid muscle anteriorly, exposing the internal jugular vein and permitting clearance of lymph nodes at levels II, III, and IV in continuity with lymph nodes in the posterior triangle of the neck. The postoperative appearance of the patient shows a well-healed, aesthetically acceptable scar (Fig. 11.74). The surgical defect at the primary site is covered with a skin graft.

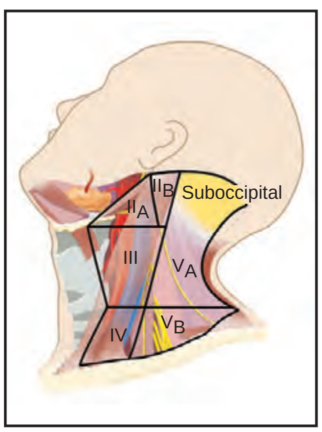

Lymph nodes dissected
- Level II
- Level III
- Level IV
- Level V
- Suboccipital triangle

Figure 11.71 Posterolateral neck dissection. *(Courtesy Memorial Sloan Kettering Cancer Center.)*

Figure 11.72 Wide excision of a melanoma of the postauricular region in continuity with posterolateral neck dissection.

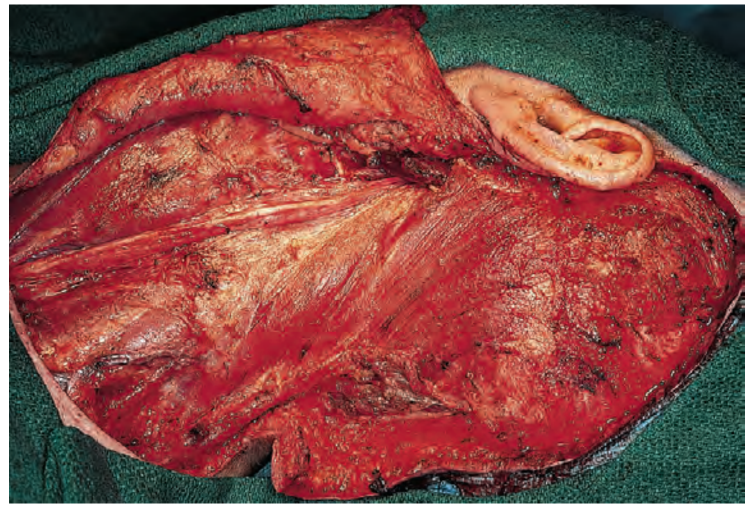

Figure 11.73 Suboccipital lymph nodes and the lymph nodes deep to the trapezius muscle are dissected off from the underlying muscles, with clearance of levels II to V in the lateral part of the neck.

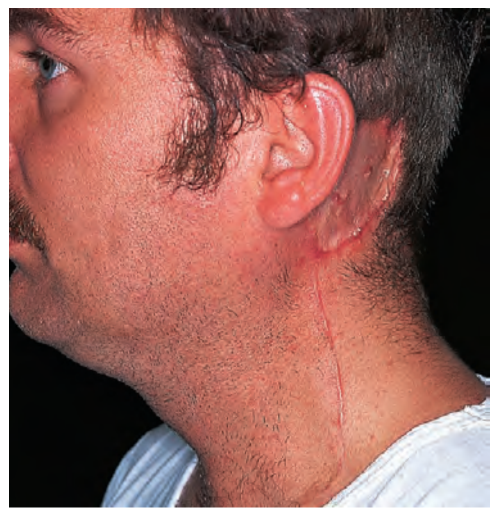

Figure 11.74 The postoperative appearance of the patient.

COMPREHENSIVE NECK DISSECTIONS

Modified Neck Dissection Type I

A modified neck dissection type I (MND-I) provides comprehensive clearance of cervical lymph nodes at all five levels in the neck but selectively preserves only one anatomic structure: the spinal accessory nerve (Fig. 11.75). The patient described here has a metastatic lymph node at level II in the right side of the neck. The location of the lymph node is shown in relation

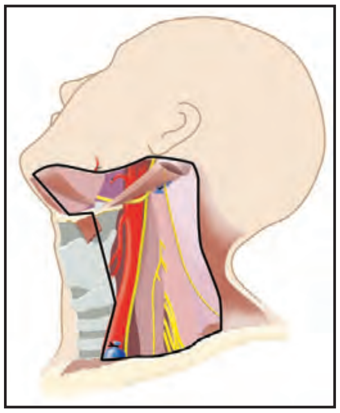

Lymph nodes dissected
- Level I
- Level II
- Level III
- Level IV
- Level V

Other structures excised
- Sternocleidomastoid muscle
- Internal jugular vein
- Submandibular salivary gland

Structures preserved
- Spinal accessory nerve

Figure 11.75 Lymph node levels and structures excised in a modified neck dissection type I. *(Courtesy Memorial Sloan Kettering Cancer Center.)*

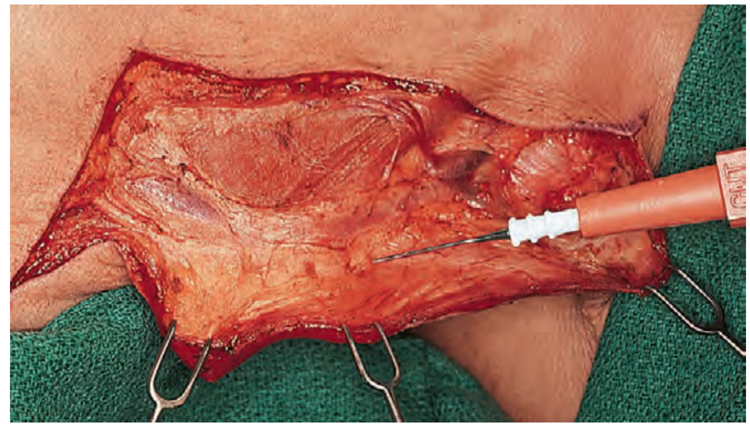

Figure 11.78 The posterior skin flap is elevated first, keeping the platysma on the skin flap.

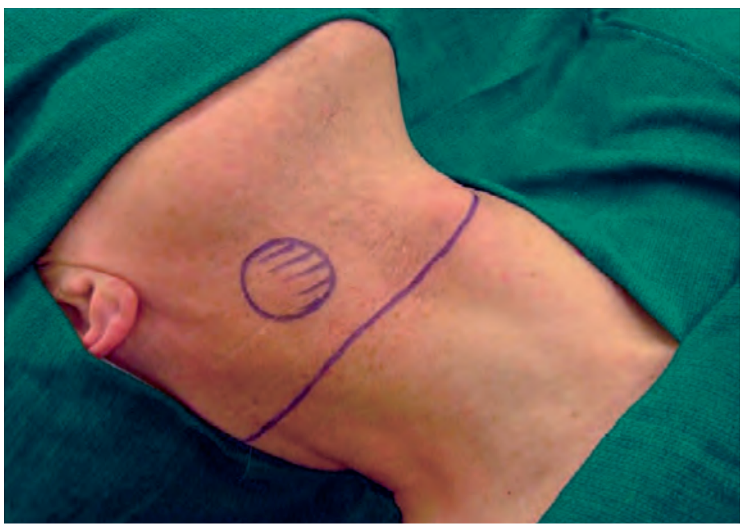

Figure 11.76 A transverse incision along a midcervical skin crease is preferred for neck dissection.

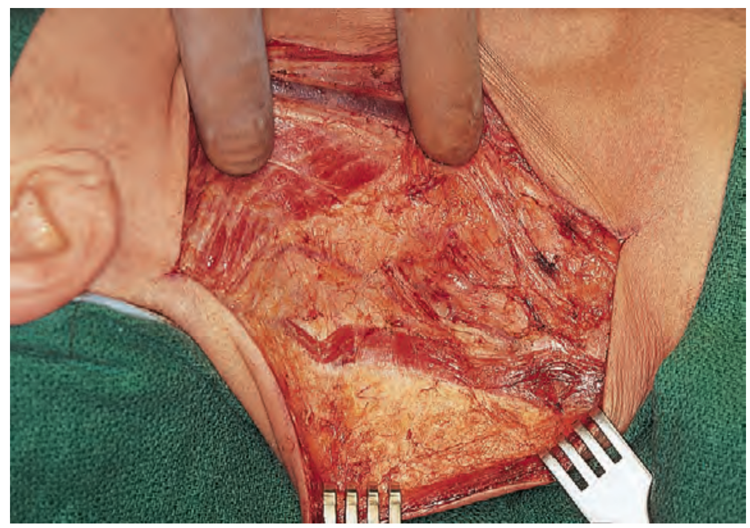

Figure 11.79 The posterior skin flap is elevated until the anterior border of the trapezius muscle is exposed.

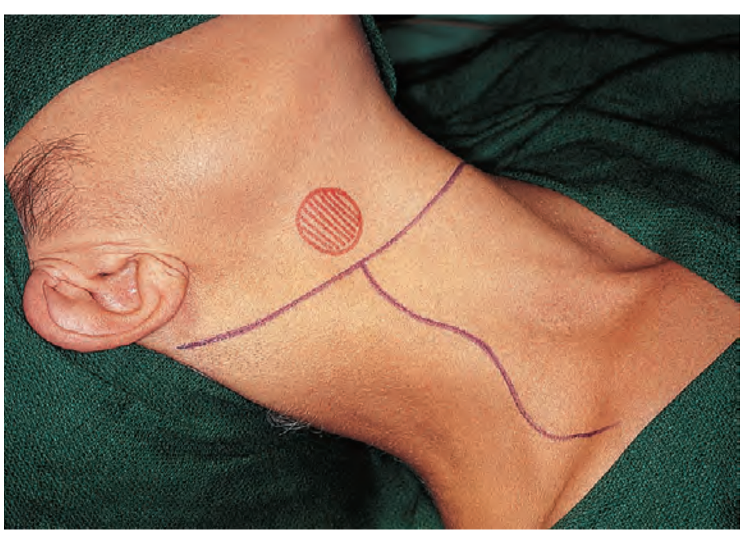

Figure 11.77 The location of the palpable lymph node and a single trifurcate incision is outlined on the patient.

to the skin incision for this operation (Fig. 11.76). A single transverse incision in a natural skin crease is the preferred incision for all types of neck dissections. The incision is at least two fingerbreadths below the angle of the mandible, preferably in a midcervical skin crease below the hairline in men. In this patient, however, a single trifurcate incision was used with a curvaceous vertical limb marked, beginning at a point posterior to the carotid artery (Fig. 11.77).

The operation begins with elevation of the posterior skin flap first, remaining just on the undersurface of the platysma (Fig. 11.78). Meticulous attention is required as elevation of the lateral aspect of the skin flap approaches the anterior border of the trapezius muscle in the lower part of the neck, because the accessory nerve enters the muscle in this region. The posterior flap is elevated well over the anterior border of the trapezius muscle to expose at least 1 cm of its anterolateral surface (Fig. 11.79). At this point, the spinal accessory nerve is identified as it enters the trapezius muscle medial to its anterior border. A tissue-spreading technique with an Adson clamp (long hemostat) is used to dissect the fascia and soft tissue over the nerve to prevent any injury to it (Fig. 11.80). The nerve is traced up to its exit from the posterior border of the sternocleidomastoid muscle. No further dissection of the accessory nerve is performed at this point.

Dissection of the soft tissue and lymph nodes of the posterior triangle of the neck in the upper part now proceeds, remaining superficial to the posterior compartment muscles, that is, the splenius capitis and levator scapulae (Fig. 11.81). The upper end of the sternocleidomastoid muscle is now detached from the mastoid process. The spinal accessory nerve in its lower part is dissected free of the remainder of the specimen with use of a Martin forceps and sharp scissors to skeletonize the nerve (Fig. 11.82). Further dissection of the nerve requires

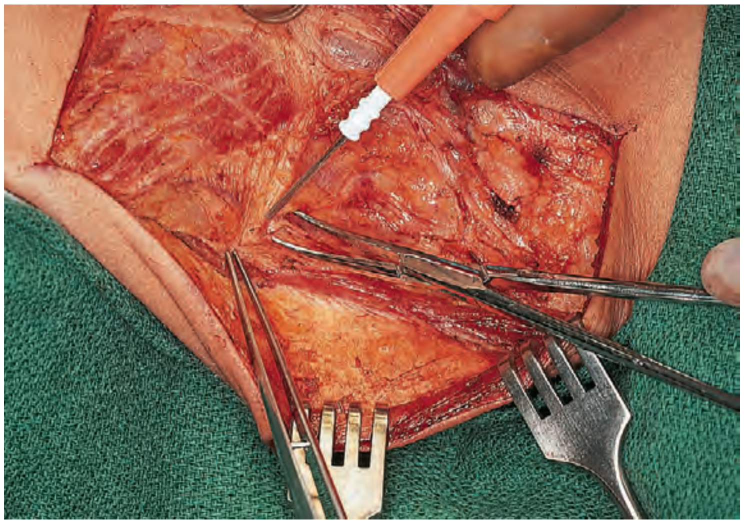

Figure 11.80 The spinal accessory nerve is identified at its point of entry in the trapezius muscle.

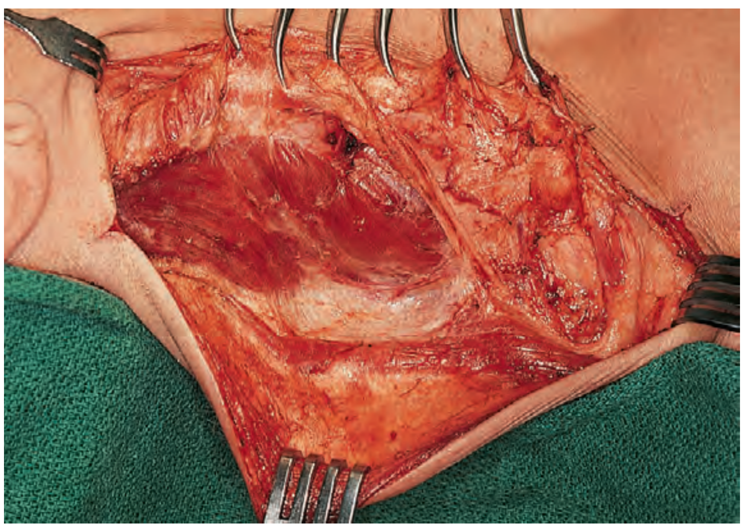

Figure 11.81 Dissection of the upper part of the posterior triangle lymph nodes is carefully completed, preserving the spinal accessory nerve.

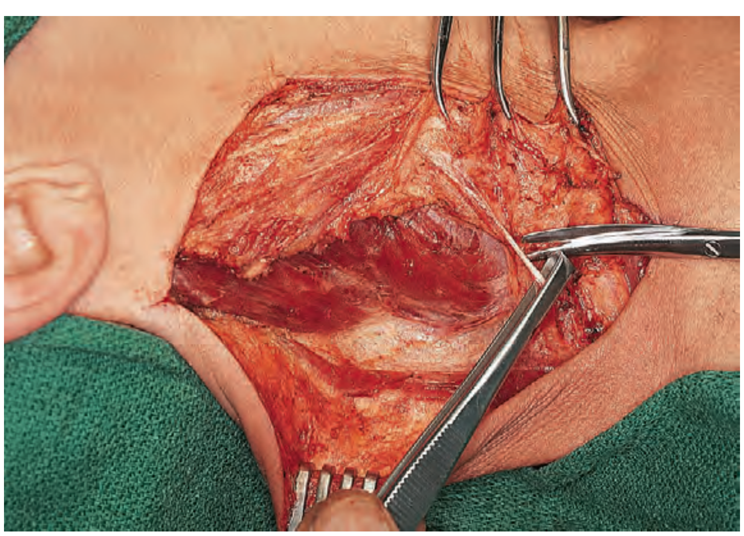

Figure 11.82 The spinal accessory nerve is lifted off the specimen and meticulously dissected from the lymph nodes in the lower part of the posterior triangle of the neck.

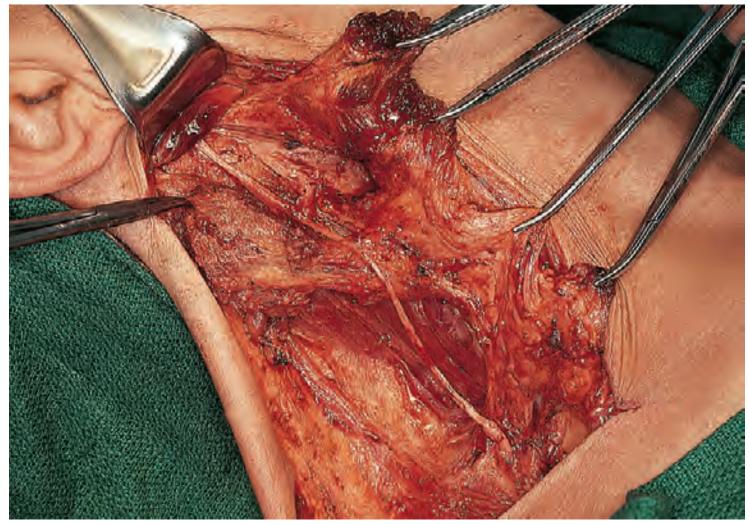

Figure 11.83 Dissection of the posterior triangle of the neck is complete with preservation of the accessory nerve.

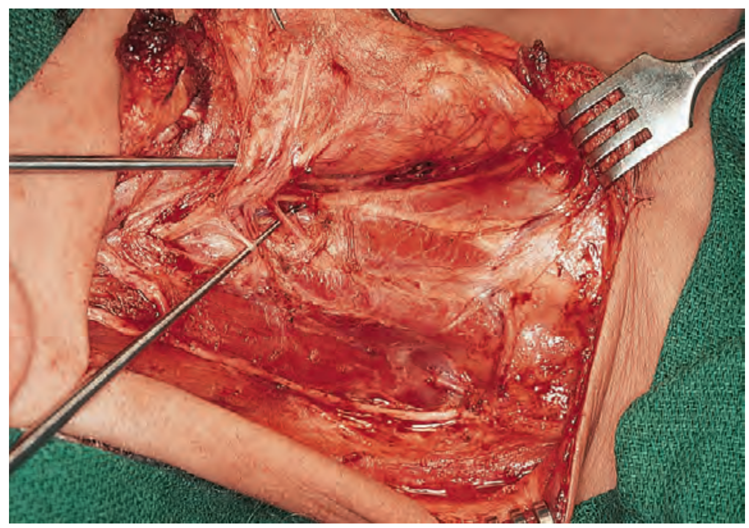

Figure 11.84 Cutaneous roots of the cervical plexus are divided, but contributions to the phrenic nerve and the nerve supply to the scalene muscles are preserved.

splitting of the sternocleidomastoid muscle in its upper half, keeping the nerve under constant view at all times.

The sternocleidomastoid muscle is divided up to the posterior belly of digastric muscle to expose the spinal accessory nerve in its entirety, from the jugular foramen cephalad until its entry into the trapezius muscle caudad (Fig. 11.83). The nerve is now completely dissected free circumferentially throughout its length. The dissected portion of the specimen of the contents of the posterior triangle is now passed underneath the nerve and retracted medially.

Dissection now proceeds along the medial border of the levator scapulae and scalene muscles, exposing the roots of the cervical plexus (Fig. 11.84). The cervical roots have three components. Nerve supply to the posterior compartment muscles is preserved carefully, as shown in Fig. 11.85. The descending fibers contributing to the phrenic nerve also are preserved carefully; however, the cutaneous branches of the cervical plexus are divided. The stumps of the cutaneous roots are ligated because small blood vessels accompany these nerve roots. Further

Figure 11.85 Medial retraction of the specimen exposes the internal jugular vein.

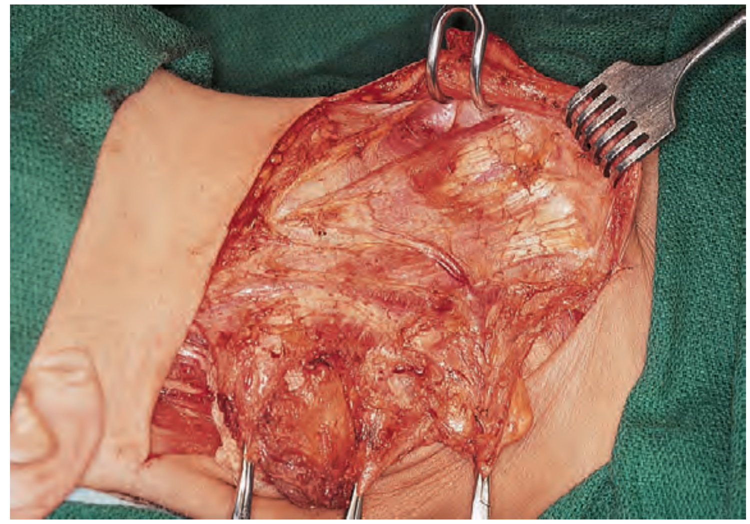

Figure 11.86 The medial skin flap is elevated to expose the lower end of the sternocleidomastoid muscle.

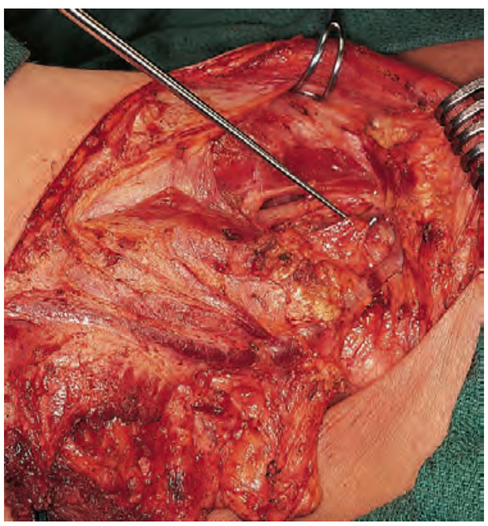

Figure 11.87 The lymphatic ducts at the root of the neck are divided and ligated with care.

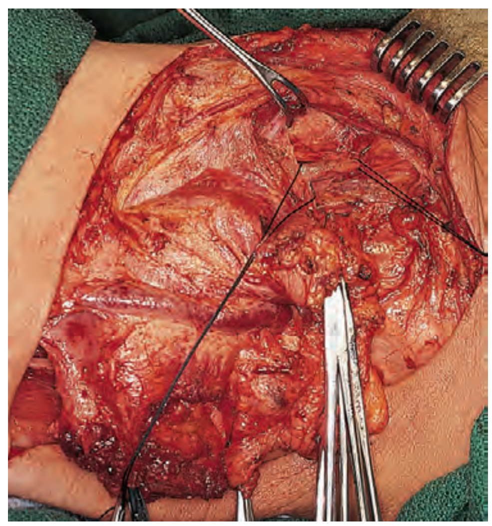

Figure 11.88 The lower end of the internal jugular vein is divided and ligated.

Figure 11.89 Further dissection cephalad along the carotid sheath exposes the hypoglossal nerve and descendens hypoglossi.

mobilization of the specimen provides exposure of the internal jugular vein from the posterior belly of the digastric muscle cephalad, up to the root of the neck caudad (see Fig. 11.85).

The surgical specimen is now flipped laterally and the medial skin flap is elevated to expose the lower insertion of the sternocleidomastoid muscle. The skin flap is elevated to provide exposure of the entire medial border of the sternomastoid muscle, as shown in Fig. 11.86. With use of the electrocautery, the sternal as well as the clavicular heads of the sternocleidomastoid muscle are divided just near their insertion. A layer of fibrofatty tissue is present between the undersurface of the sternocleidomastoid muscle and the carotid sheath. At this juncture, the lymphatic ducts between the deep jugular lymph nodes at the lateral aspect of the lower end of the internal jugular vein are identified, divided, and ligated with care (Fig. 11.87). The transverse cervical artery and its accompanying vein also are divided and ligated. By alternate blunt and sharp dissection, the lower end of the jugular vein is circumferentially dissected and freed, while carefully protecting the common carotid artery, the vagus nerve, the sympathetic chain, and the phrenic nerve (Fig. 11.88). The vein is doubly ligated and divided, and its stump is ligated with a suture.

Dissection now proceeds along the carotid sheath cephalad all the way up to the lower border of the digastric muscle, where the hypoglossal nerve with its descendens hypoglossi branch is visible (Fig. 11.89). Medially the dissection proceeds along the superior belly of the omohyoid muscle up to the hyoid bone, from which it is detached. The superior thyroid artery is preserved carefully, but the superior thyroid vein is divided and ligated. Several minor bleeding points along the branches of the descendens hypoglossi are divided and electrocoagulated. At this juncture, the dissection of the lower part of the neck is completed.

The surgical specimen is now allowed to rest over the lower part of the neck and the upper skin flap is elevated carefully, identifying and preserving the mandibular branch of the facial nerve (Fig. 11.90). The skin flap is elevated up to the lower border of the body of the mandible to permit dissection of the prevascular facial group of lymph nodes. The anterior belly of the digastric muscle is identified next, and the submental group of lymph nodes is dissected from the midline and brought toward the right-hand side. The nerve and blood supply to the mylohyoid muscle is divided and ligated. This maneuver permits retraction of the

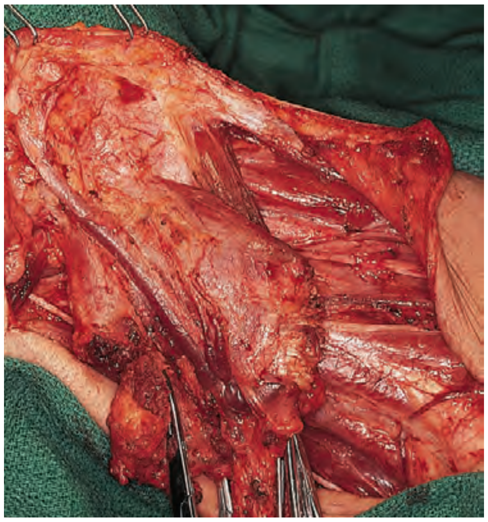

Figure 11.90 The upper skin flap is elevated, carefully preserving the mandibular branch of the facial nerve.

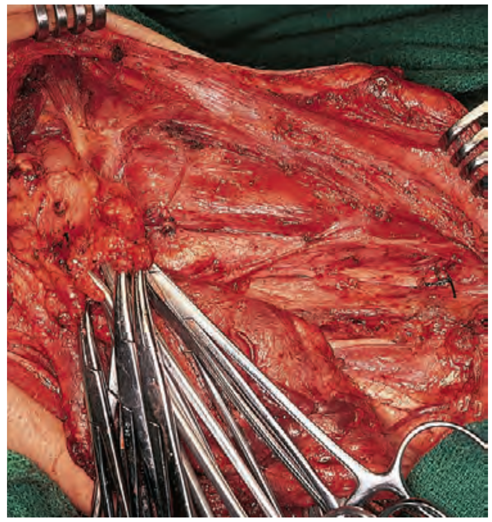

Figure 11.91 The facial artery and vein are divided and ligated near the lower border of the mandible.

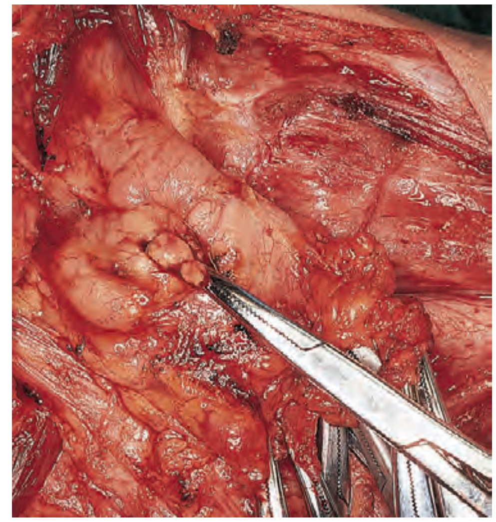

Figure 11.92 The secretomotor fibers to the submandibular salivary gland are divided.

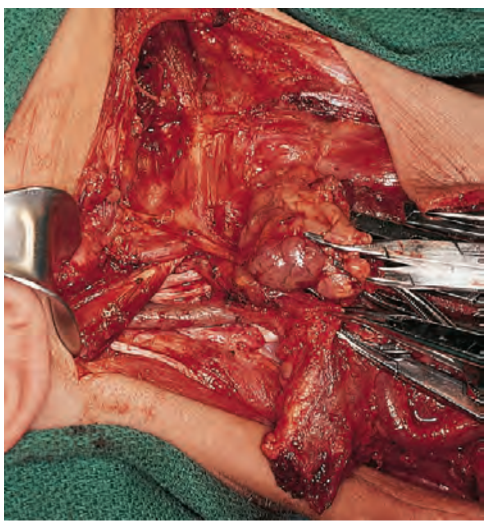

Figure 11.93 The facial artery entering the submandibular salivary gland and the upper end of the internal jugular vein are exposed.

Figure 11.94 The surgical field after removal of the specimen.

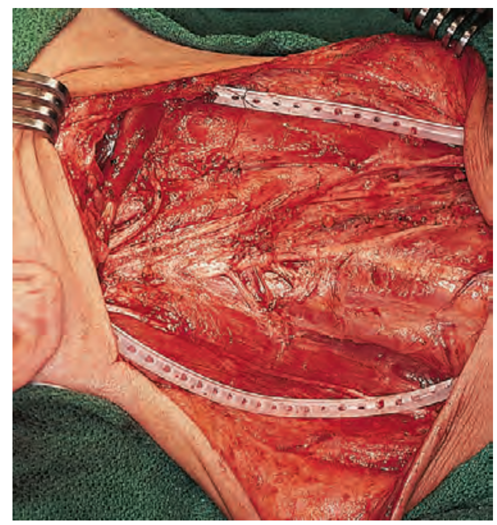

Figure 11.95 Two suction drains are placed in the surgical field.

submandibular salivary gland, which is freed up by dividing the facial artery and vein at the lower border of the body of the mandible (Fig. 11.91).

A large loop retractor is now used to retract the mylohyoid muscle cephalad to expose Wharton's duct, the lingual nerve, and the secretomotor fibers to the submandibular salivary gland. The secretomotor fibers are divided and ligated (Fig. 11.92). Division of Wharton's duct between clamps permits the dissection and delivery of the submandibular salivary gland from the submandibular triangle. The remaining attachment of the submandibular gland is now through the proximal stump of the facial artery, as shown in Fig. 11.93. The facial artery is divided and ligated. Finally, the only remaining attachment of the specimen to the patient is at the upper end of the internal jugular vein, which is doubly ligated and divided, and its stump is ligated with a suture (see Fig. 11.93). The surgical field following removal of the specimen is shown in Fig. 11.94. Absolute hemostasis is secured.

Two suction drains are introduced through separate stab incisions. The posterior drain is allowed to rest along the anterior border of the trapezius muscle, and the anterior drain is placed parallel to the strap muscles (Fig. 11.95). The drains are secured

Figure 11.96 The skin incision is closed in layers.

in position with loose loops of chromic catgut sutures through the underlying muscles to prevent their displacement. The skin incision then is closed in two layers using 3-0 chromic catgut interrupted sutures for platysma and 5-0 nylon sutures or staples for skin (Fig. 11.96).

Preservation of the spinal accessory nerve significantly minimizes aesthetic and functional morbidity. Shoulder function is preserved even after bilateral MND-I without atrophy of the trapezius muscle (Fig. 11.97). Note the absence of dropped shoulders. The trapezius muscle mass is preserved, which demonstrates that the nerve supply to the muscle is intact, thus preserving shoulder function. The patient is able to raise his or her shoulders all the way up. The only aesthetic debility results from the loss of the sternomastoid muscle and soft tissues. Even though most patients maintain near-normal shoulder function in the early postoperative period, about a third manifest some long-term shoulder weakness, especially if they are treated with postoperative radiation therapy.

The functional debility following MND-I as previously described occurs as a result of circumferential mobilization and dissection of the spinal accessory nerve, which compromises its blood supply, leading to ischemic injury and loss of function in some patients. Therefore when MRND-I is performed, a further modification is recommended to preserve the vascularity of the accessory nerve. The superior part of the posterior triangle of the neck cephalad to the spinal accessory nerve generally is devoid of any lymph nodes and seldom if ever has metastatic lymphadenopathy (Fig. 11.98). Circumferential dissection of the spinal accessory nerve is only necessary when gross metastatic disease is present along the course of the nerve, especially at levels IIB and III (see Fig. 11.83). Avoiding dissection of the fatty tissue in this area and allowing the nerve to remain in its anatomic bed preserve its vascularity and prevent ischemic injury (Fig. 11.99). This MRND-I modification prevents postoperative deficit in shoulder function that is observed with circumferential dissection of the accessory nerve and does not increase the risk of regional failure in the neck.

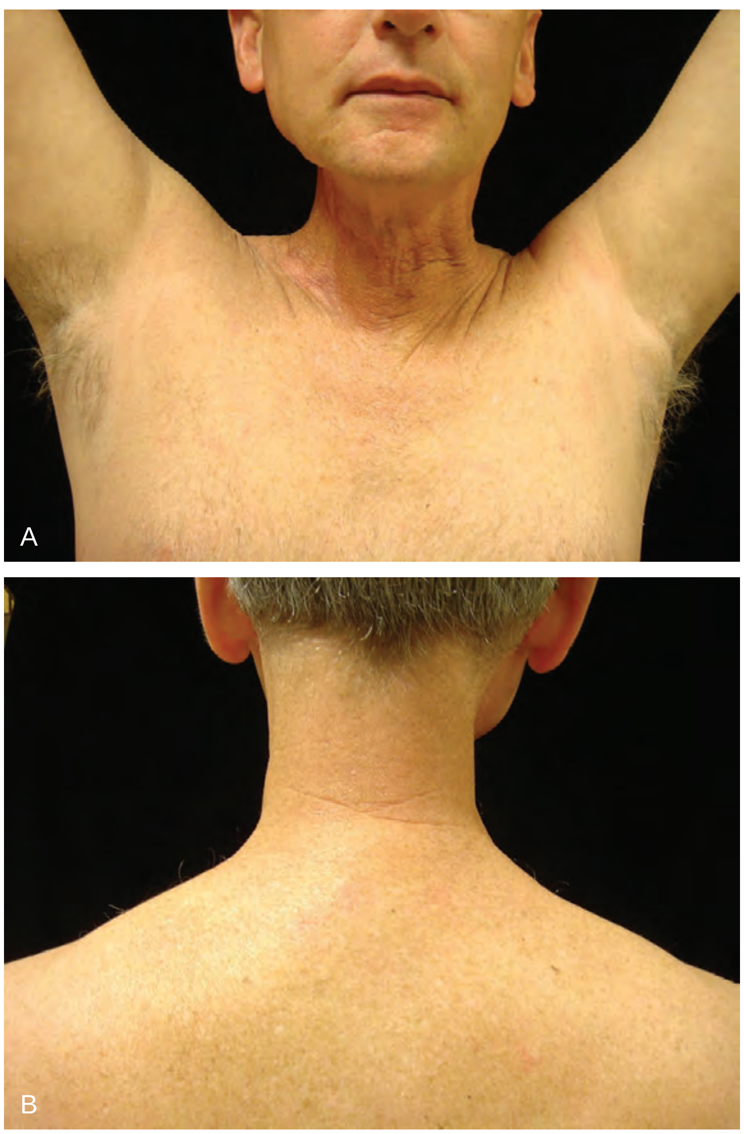

Figure 11.97 Shoulder function after bilateral modified neck dissections type I. **A**, Elevation of both shoulders is preserved. **B**, Trapezius muscle mass is maintained.

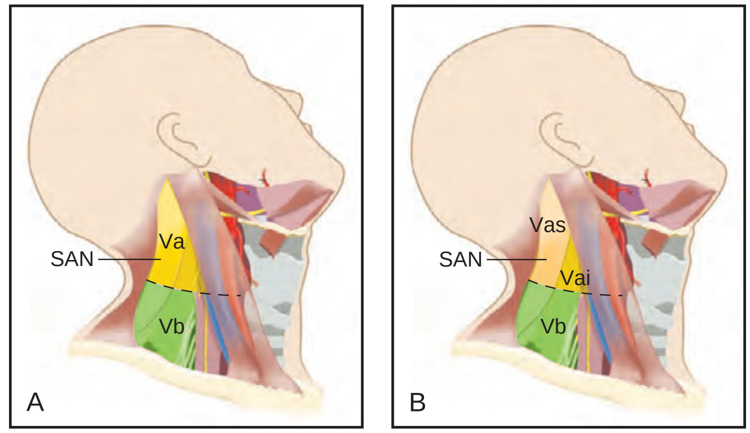

Figure 11.98 **A**, Existing classification of level V according to the *AJCC Cancer Staging Manual,* eighth edition. **B**, Subdivision of level VA into level VAs (superior), which is usually devoid of lymph nodes, and level VAi (inferior), which contains spinal accessory chain lymph nodes.

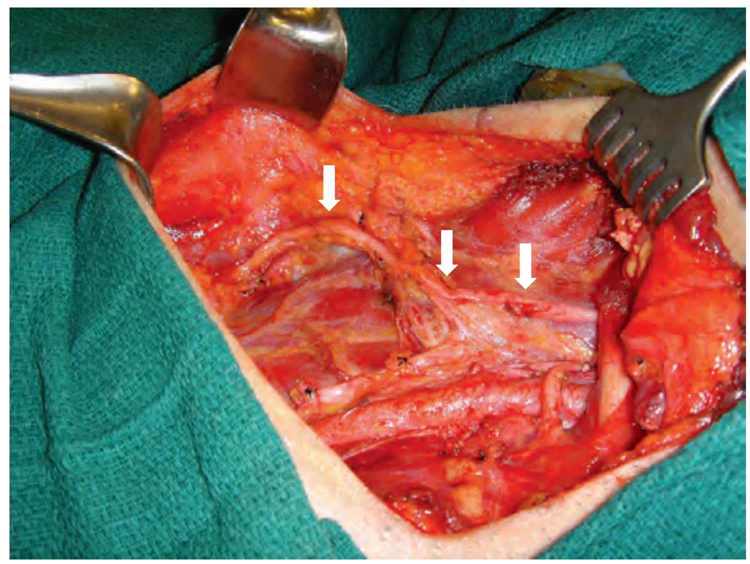
Figure 11.99 The surgical field following a right modified neck dissection type I without circumferential dissection of the spinal accessory nerve. Note that the nerve is preserved in its soft tissue bed with blood supply coming through fascial attachments preserved (*arrows*).

MND-I Through a Single Transverse Incision

Comprehensive neck dissection of all five levels of lymph nodes in the neck has been done in the past with a variety of different incisions to gain exposure and access to lymphatic regions from level IA to VB. However, the aesthetic appearance after previously used incisions has been less than satisfactory. By making a transverse incision at the midcervical region, adequate exposure is obtained to dissect all five levels of the neck. If additional exposure is necessary, the same transverse incision is extended across the midline to the opposite side and further posteriorly over the trapezius muscle. In men, this transverse incision should

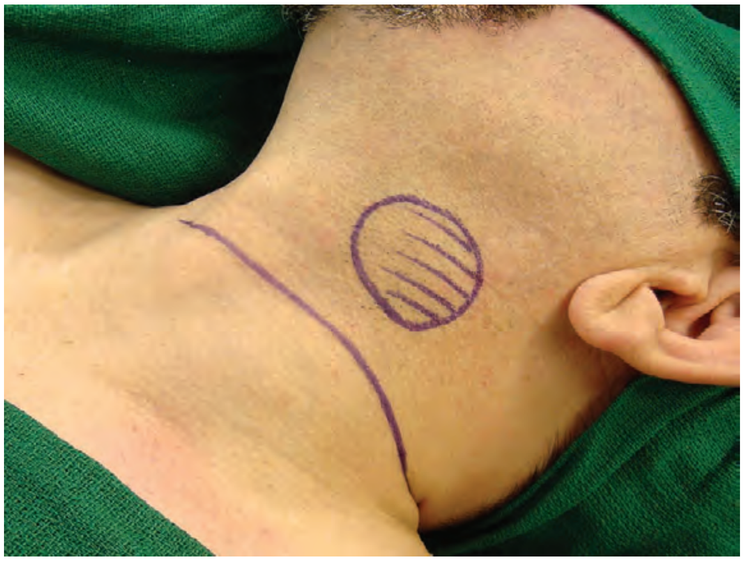

Figure 11.100 A transverse incision is marked in a midcervical skin crease below the hairline.

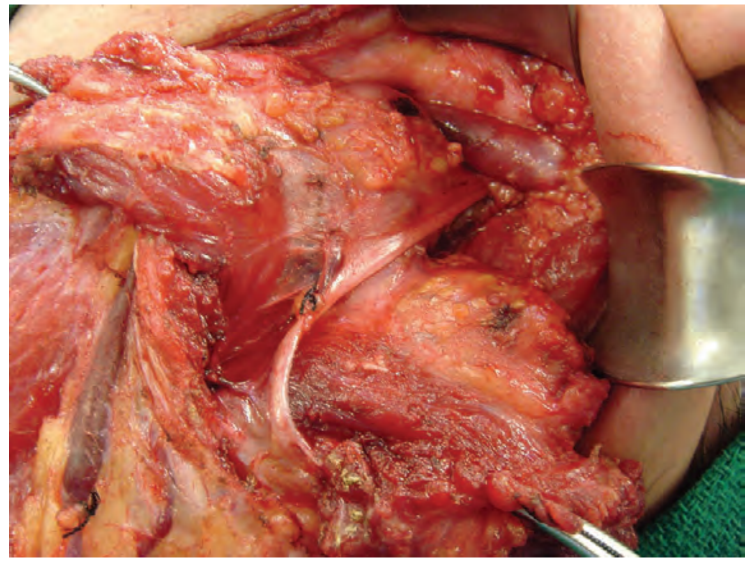

Figure 11.102 The upper end of the spinal accessory nerve is dissected.

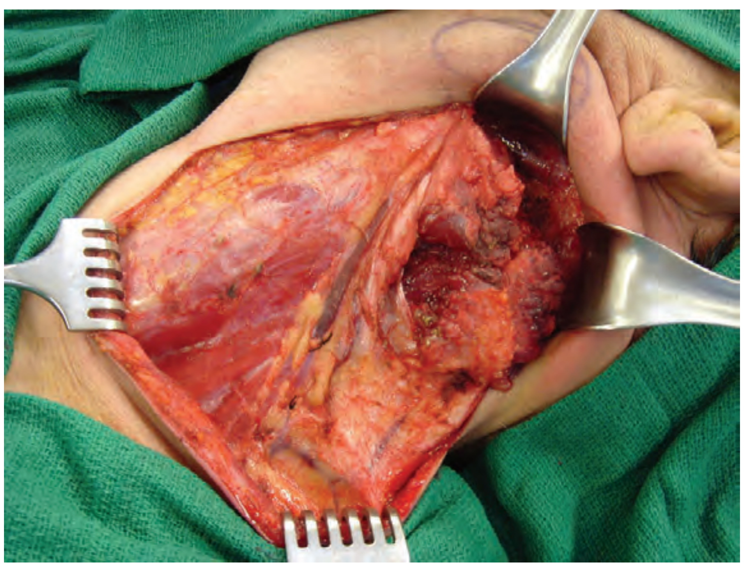

Figure 11.101 Sternocleidomastoid muscle is detached from the mastoid process and its fibers are divided along the course of the spinal accessory nerve.

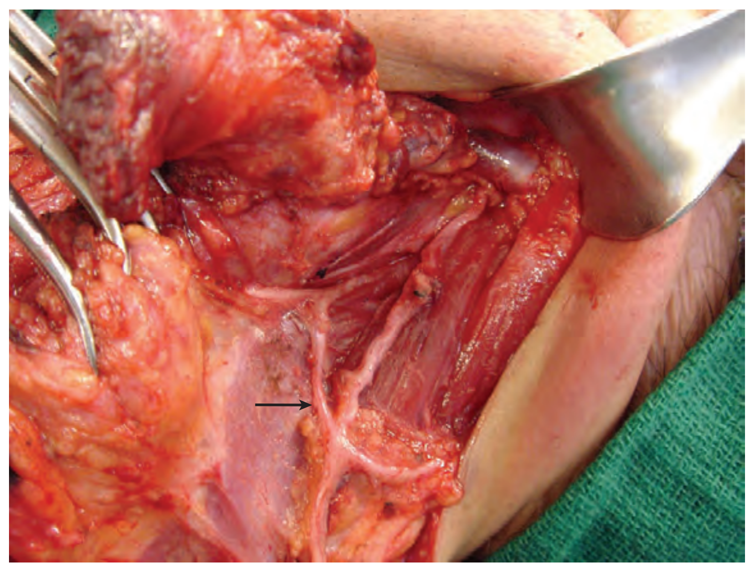

Figure 11.103 Contribution from C2 (*arrow*) to the spinal accessory nerve is preserved.

be made below the hairline of the beard. In general, the single transverse incision for a comprehensive neck dissection is placed at the level of the cricoid thyroid membrane, which provides adequate exposure.

The patient described here has a mass of matted metastatic lymph nodes at level II in the left side of the neck from an unknown primary source. The skin incision is outlined along the skin crease in the midcervical region below the hairline (Fig. 11.100). Both the upper and lower skin flaps are elevated in the subplatysmal plane, inferiorly up to the clavicle, superiorly up to the tail of the parotid gland and the angle of the mandible posteriorly, and up to the suprahyoid and submental region anteriorly. Dissection may begin by identifying the spinal accessory nerve in the floor of the posterior triangle of the neck at level VB, or the sternocleidomastoid muscle may be detached from the mastoid process and the nerve may be identified as it exits from the jugular foramen under the posterior belly of the digastric muscle (Fig. 11.101). In this patient the nerve was identified at the upper end first and followed caudad for its preservation (Fig. 11.102).

Dissection proceeds in the posterior triangle of the neck along the course of the accessory nerve. The divided lateral portion of the upper end of the sternocleidomastoid muscle and lymph nodes at levels VA and IIB posterior and lateral to the accessory nerve are dissected off the prevertebral muscles and passed medially underneath the nerve, maintaining continuity with the main specimen. Dissection in the posterior triangle of the neck continues caudad. In this patient a significant contribution is present from the second cervical root to the accessory nerve (Fig. 11.103). Every effort should be made to preserve such a contribution when it is found, because in some patients it may have a significant motor component that contributes to the nerve supply to the trapezius muscle. However, the distal branches of the cervical roots lateral to the accessory nerve are cutaneous sensory branches, and they may be divided.

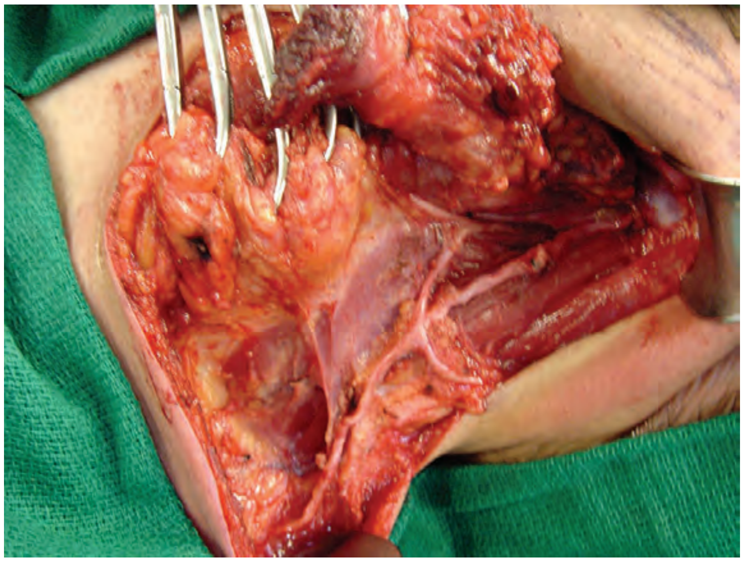

Figure 11.104 The spinal accessory nerve is preserved in its entire course up to its entry into the trapezius muscle.

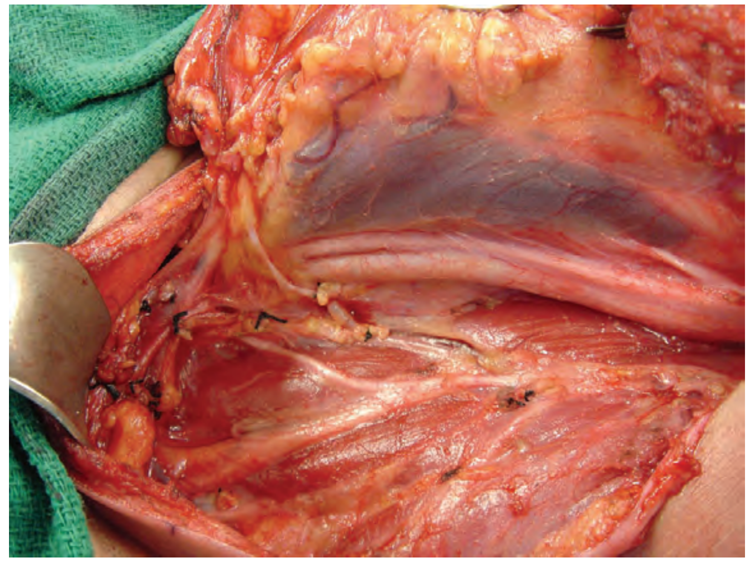

Figure 11.106 The phrenic nerve is dissected and preserved.

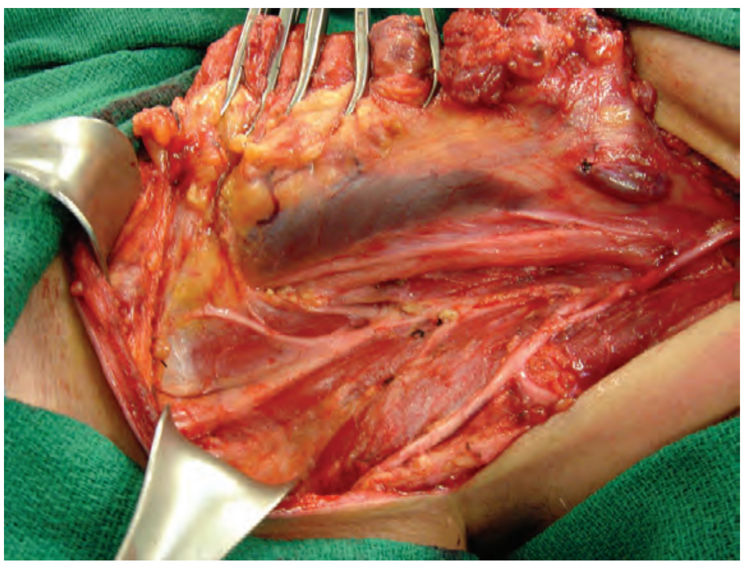

Figure 11.105 The cutaneous branches of the cervical plexus are divided.

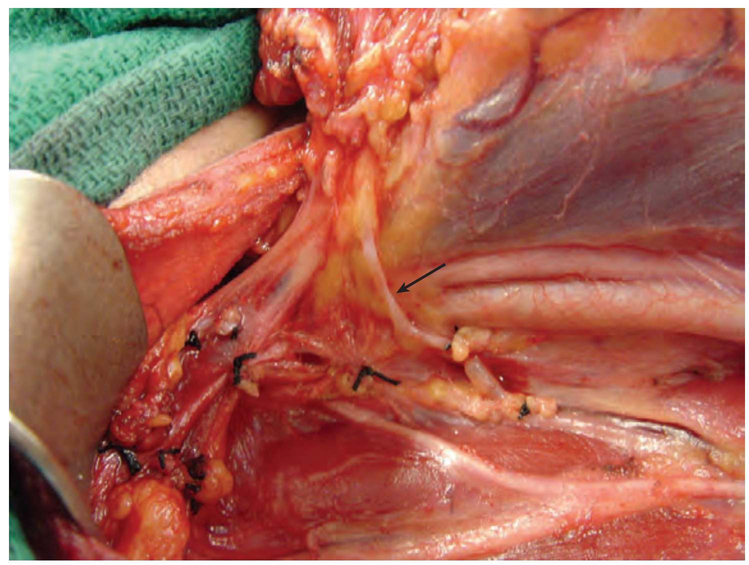

Figure 11.107 Lymphatic channels (*arrow*) entering the thoracic duct are divided and ligated.

The nerve is traced all the way up to its entry into the trapezius muscle (Fig. 11.104). Once the nerve is dissected completely, the surgical specimen is mobilized medially. Dissection proceeds along the floor of the posterior triangle of the neck, lifting off the fibrofatty tissue and lymph nodes of the posterior triangle from the prevertebral muscles and carefully identifying and dividing the cutaneous branches of the cervical roots (Fig. 11.105). The phrenic nerve is dissected at the root of the neck posterolateral to the carotid sheath at level IV (Fig. 11.106). At this juncture, meticulous attention is required to identify the lymphatic channels entering the thoracic duct. These lymphatic channels should be divided and ligated with care. Neglecting the transected lymphatic ducts leads to development of a chyle fistula. A close-up view of the lower part of level IV at the root of the neck clearly shows the lymphatic ducts from the cervical lymph nodes in the surgical specimen draining into the thoracic duct (Fig. 11.107). Once the lymphatic channels are controlled, dissection of lymph nodes at level IV near the lower end of the carotid sheath is undertaken. The internal jugular vein is divided carefully and ligated with a suture. Dissection now proceeds cephalad along the carotid sheath up to the hypoglossal nerve (Fig. 11.108). The superior thyroid artery is identified and preserved, and the minor venous tributaries to the internal jugular vein are divided and ligated. The hypoglossal nerve should be preserved with care as it exits from the hypoglossal canal and enters the muscles of the tongue under the digastric muscle.

Attention is now focused on dissection of level I. The upper skin flap is retracted and meticulous dissection proceeds along the fascia over the submandibular gland. The marginal branch of the facial nerve is identified with care and preserved. Some patients have multiple branches, and they should be identified, dissected, and retracted cephalad with care (Fig. 11.109). Once that step is done, dissection of the submandibular triangle is completed in the usual fashion, with delivery of the specimen of levels I to V in a comprehensive manner and preservation of the spinal accessory nerve (Fig. 11.110). Suction drains are placed, and the wound is closed in the usual fashion. The postoperative appearance of the patient shows an excellent aesthetic outcome (Fig. 11.111).

Figure 11.108 Deep jugular lymph nodes are dissected off the carotid sheath up to the hypoglossal nerve.

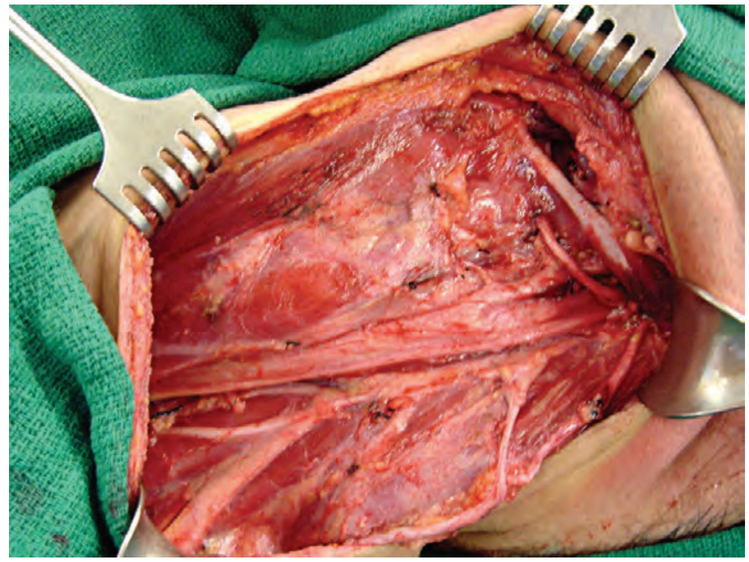

Figure 11.110 The surgical field after removal of the specimen.

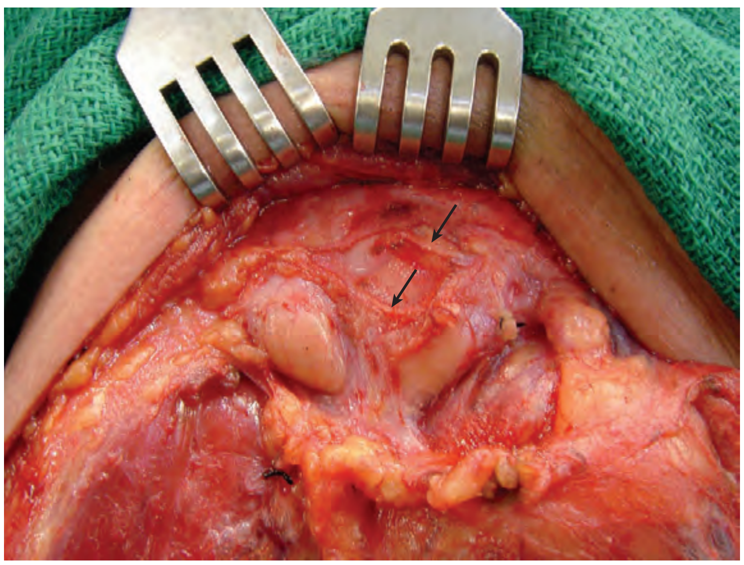

Figure 11.109 The marginal mandibular branches of the facial nerve (*arrows*) are preserved.

Figure 11.111 The appearance of the neck 6 months after completion of postoperative radiation therapy.

Modified Neck Dissection Type II

The MND-II is similar to the MND-III in that it preserves the sternocleidomastoid muscle and the spinal accessory nerve but selectively sacrifices the internal jugular vein (Fig. 11.112). The indications for this operation are massive metastatic disease from a differentiated carcinoma of the thyroid gland grossly involving the internal jugular vein or from a metastatic squamous cell carcinoma selectively invading the internal jugular vein in the midcervical or lower cervical region. All the steps of the operative procedure are otherwise essentially similar to those described for the MND-III procedure.

Massive metastatic lymph nodes from a differentiated carcinoma of the thyroid gland often involve the strap muscles at the lower part of the neck, requiring that they be sacrificed. Under those circumstances, a thyroidectomy and MND-II are performed in a monobloc fashion. To accomplish such an operative procedure with technical ease, the sternocleidomastoid muscle is retracted laterally to expose soft tissues at level VB and laterally up to the spinal accessory nerve. The accessory nerve is protected in its fascial envelope all the way up to the posterior belly of the digastric muscle.

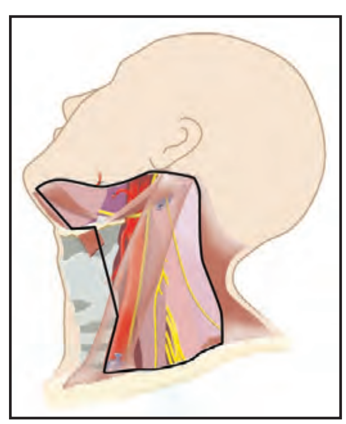

Figure 11.112 Lymph node levels and structures excised in a modified neck dissection type II. *(Courtesy Memorial Sloan Kettering Cancer Center.)*

The posterior triangle lymph nodes and deep jugular chain lymph nodes surrounding the internal jugular vein are removed in a monobloc fashion, with the primary lesion in the thyroid gland. The internal jugular vein in these situations often is adherent to, invaded by, or occluded by metastatic lymph nodes. Particular attention should be paid to metastatic lymph nodes, posterior to the carotid sheath, and multiple lymphatic channels draining into the thoracic duct.

Modified Neck Dissection Type III

The MND-III operation comprehensively clears lymph nodes from all five levels in the lateral neck while preserving the sternocleidomastoid muscle, the spinal accessory nerve, and the internal jugular vein (Fig. 11.113). This procedure usually is indicated in patients with metastatic lymph nodes from differentiated carcinomas of the thyroid gland. It is not a satisfactory operation for a metastatic squamous cell carcinoma or a metastatic adenocarcinoma of salivary gland origin. The operation usually is performed in conjunction with a thyroidectomy for clinically palpable neck metastases and is done through a single transverse incision of the level of the cricoid cartilage. The incision extends from the anterior border of the trapezius muscle on one side to that on the other. The upper skin flap is elevated all the way up to the mastoid process laterally and above the hyoid bone in the midline. The neck dissection specimen may be removed in two segments: (1) the primary tumor of the thyroid gland with central compartment lymph nodes and lymph nodes from the anterior triangle of the neck on the ipsilateral side and (2) the lymph nodes from the posterior triangle of the neck on the ipsilateral side. If bilateral neck dissections are done simultaneously, then the specimen of posterior triangle lymph nodes from the contralateral neck is removed separately.

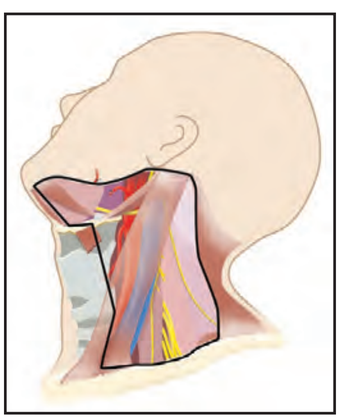

Lymph nodes dissected
- Level I
- Level II
- Level III
- Level IV
- Level V

Other structures excised
- Submandibular salivary gland

Structures preserved
- Internal jugular vein
- Sternocleidomastoid muscle
- Spinal accessory nerve

Figure 11.113 Lymph node levels and structures excised in a modified neck dissection type III. *(Courtesy Memorial Sloan Kettering Cancer Center.)*

The surgical field of a patient who has undergone a total thyroidectomy and a comprehensive MND-III for a metastatic papillary carcinoma of the thyroid is shown in Fig. 11.114. The technical details of the steps of the operation are similar to those described for other neck dissections. The anterior view of the surgical field shows clearance of the central compartment of the neck after a radical total thyroidectomy. Complete dissection of the tracheoesophageal groove lymph nodes on both sides is accomplished in this patient, preserving the right lower parathyroid gland with its vascular pedicle. Both carotid sheaths are opened, and the deep jugular nodes in the central compartment of the neck on the right-hand side also are cleared. The

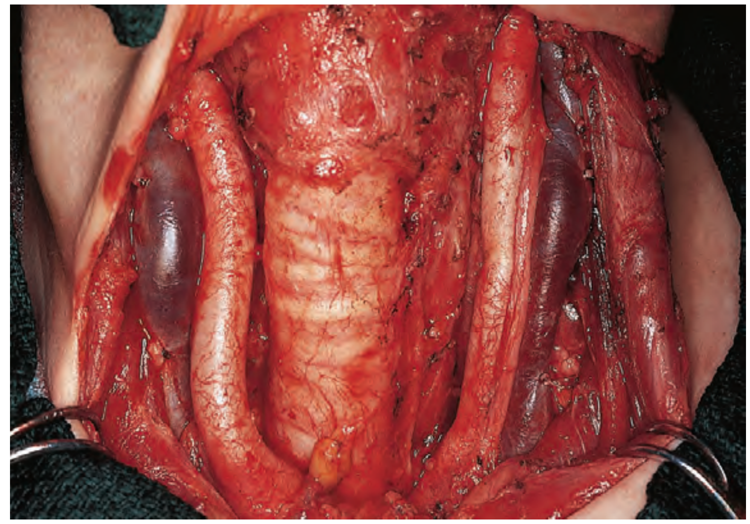

Figure 11.114 The anterior view of the surgical field after a total thyroidectomy, central compartment node dissection, and left modified neck dissection type III.

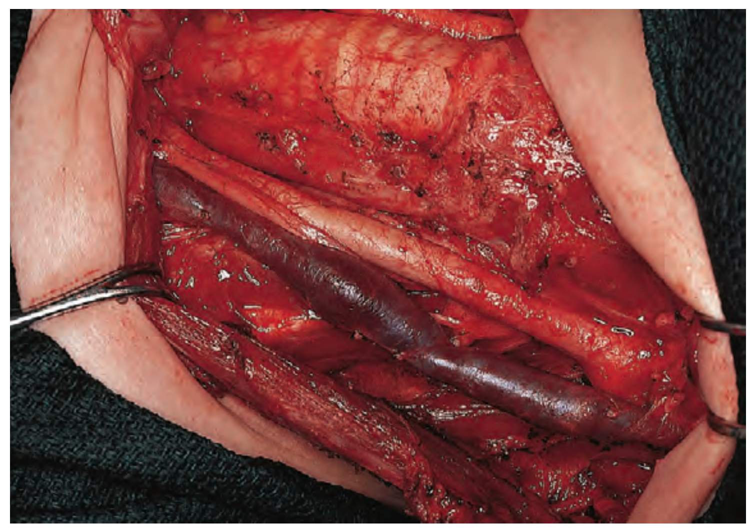

Figure 11.115 The lateral view of the surgical field with the sternomastoid retracted laterally shows clearance of the tracheoesophageal groove and the deep jugular chain of lymph nodes.

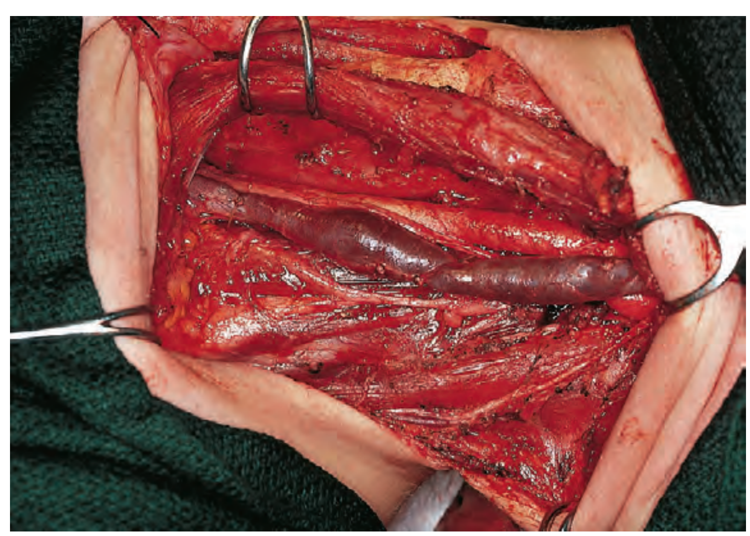

Figure 11.116 The lateral view of the surgical field with the sternomastoid retracted medially shows clearance of the deep jugular chain of lymph nodes and posterior triangle of the neck.

sternomastoid muscle on the left side is retracted laterally, showing clearance of the cervical lymph nodes at level IV in the supraclavicular region.

The lateral view of the surgical field from the patient's left-hand side, with the sternomastoid muscle retracted posteriorly, shows complete clearance of the tracheoesophageal groove lymph nodes. The recurrent laryngeal nerve is preserved. Lymph nodes in the central compartment and jugular chain are excised en bloc with the primary lesion. The laterally retracted sternomastoid muscle exposes the contents of the carotid sheath, demonstrating total clearance of lymph nodes from the anterior triangle of the neck (Fig. 11.115).

The lateral view of the surgical field with the sternomastoid muscle now retracted anteriorly demonstrates the carotid sheath with its contents clearly dissected (Fig. 11.116). All the lymph nodes lateral to the carotid sheath and from the posterior triangle of the neck are completely removed. Note that the vagus, phrenic, and accessory nerves in the lower part of the surgical field overlying the trapezius muscle are preserved carefully.

Because this operation must be performed with the sternomastoid muscle intact, it often is difficult to keep the surgical specimen in continuity as a monobloc resection. The contents of the anterior triangle of the neck and the primary tumor may be resected en bloc, while lymph nodes from the posterior triangle may be removed as a separate specimen. Wound closure with suction drains is similar to previously described surgical procedures on the neck.

The appearance of the patient approximately 6 months after a bilateral MND-III with a total thyroidectomy for a papillary carcinoma of the thyroid with bilateral neck node metastasis is shown in Fig. 11.117. Although soft tissue has been lost, the contour of the neck and shoulder function are preserved, giving an excellent aesthetic result.

Figure 11.117 The appearance of the patient 6 months after surgery.

Classical Radical Neck Dissection

The classical radical neck dissection has been the gold standard for surgical treatment of clinically apparent, metastatic cervical lymph nodes. This procedure comprehensively clears lymph nodes from levels I, II, III, IV, and V; however, it also requires sacrifice of the sternocleidomastoid muscle, spinal accessory nerve, internal jugular vein, and the submandibular salivary gland (Fig. 11.118). Because of significant postoperative aesthetic deformity and functional disability, the operation currently is recommended only when appropriate indications are present. These indications include N3 disease, extensive soft-tissue disease either appreciated clinically or demonstrated radiologically (Fig. 11.119), invasion of the spinal accessory nerve by tumor, or recurrent disease in the upper neck after previous radiotherapy or chemoradiotherapy.

A variety of incisions have been described for radical neck dissection. As previously discussed, even classic radical neck dissection can be performed through a single transverse incision placed in a midcervical skin crease. However, a single trifurcate T-shaped incision is used in this patient (Fig. 11.120). The transverse limb of the T begins at the mastoid process and follows an upper neck skin crease, remaining at least two fingerbreadths below the angle of the mandible. The incision extends across the midline up to the anterior border of the opposite sternomastoid muscle. At about the midpoint of the transverse incision near the posterior border of the sternomastoid muscle, the vertical limb of the T incision is begun. This vertical limb is curvaceous and ends at the midclavicular point. The incision provides adequate exposure for completion of a radical neck dissection. It is suitable both for bilateral radical neck dissections with a similar incision on the opposite side of the neck and for a pectoralis major myocutaneous flap reconstruction, because the vertical limb can be safely extended down on the anterior chest wall for elevation of the myocutaneous flap. Because the blood supply to the three skin flaps resulting from this incision is not disturbed, marginal necrosis at the trifurcation of the skin incision is rarely seen. The trifurcation of the incision is shown marked on the skin here in relation to the carotid artery. The trifurcation point should be kept posterior to the carotid artery when feasible. This incision provides the necessary exposure by elevation of the posterior, anterior, and superior skin flaps.

The dissection begins with elevation of the posterior skin flap first. The incision begins with the posterior half of the transverse incision at the mastoid process and continues with the vertical incision at the trifurcation point (Fig. 11.121). The anterior and superior skin flaps are not elevated at this time. The skin incision is made with a scalpel, but the remainder of the dissection is carried out with electrocautery. The skin incision is deepened through the platysma, but if grossly enlarged lymph nodes are present and extension of disease is suspected beyond the capsule of the lymph nodes, then the flap is elevated superficial to the platysma muscle, which is sacrificed. Electrocautery aids rapid elevation of the posterior skin flap. Several skin hooks are used to retract the posterior skin flap, while

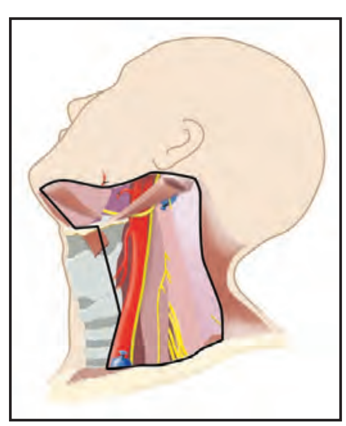

Lymph nodes dissected
- Level I
- Level II
- Level III
- Level IV
- Level V

Other structures excised
- Sternocleidomastoid muscle
- Internal jugular vein
- Spinal accessory nerve
- Submandibular salivary gland

Figure 11.118 Lymph node levels and structures excised in a classic radical neck dissection. *(Courtesy Memorial Sloan Kettering Cancer Center.)*

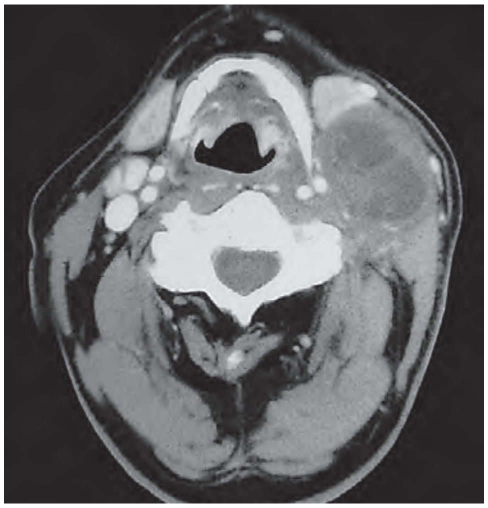

Figure 11.119 An axial view of the computed tomography scan of a patient with N3 nodal metastasis from a squamous cell carcinoma of the tonsil.

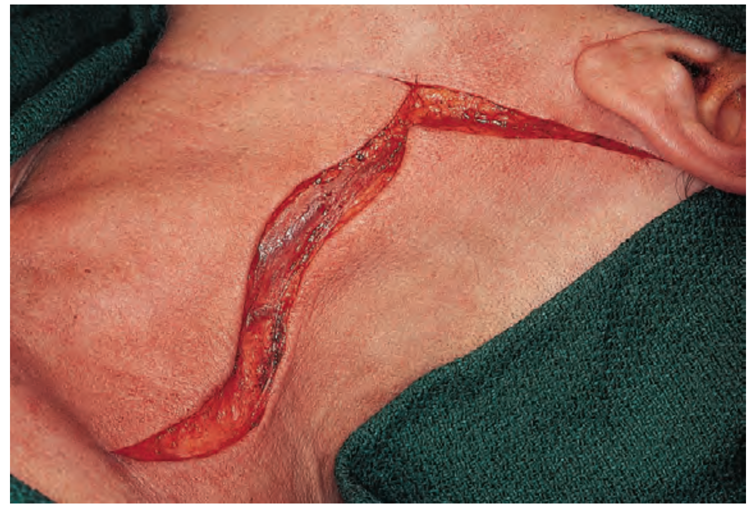

Figure 11.121 The incision begins with the posterior half of the transverse incision at the mastoid process and continues with the vertical incision up to the clavicle.

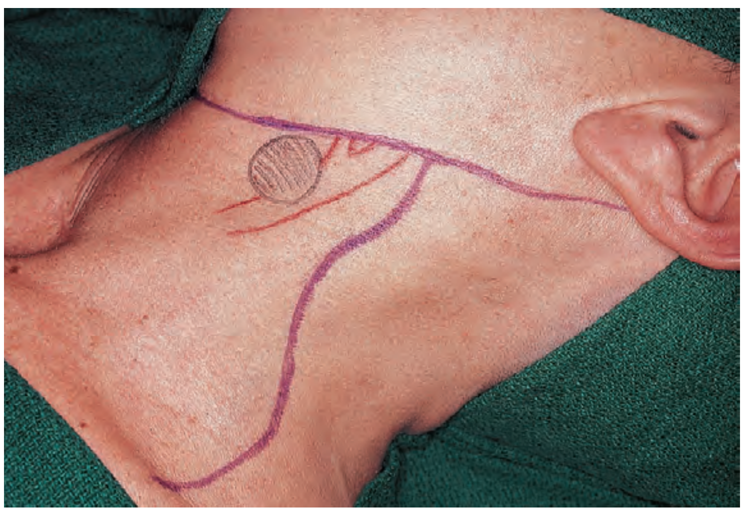

Figure 11.120 A single trifurcate T-shaped incision.

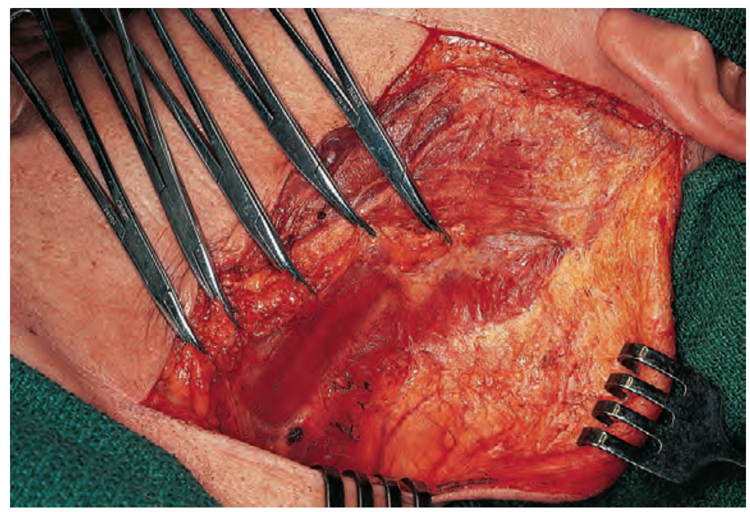

Figure 11.122 Dissection of the posterior triangle begins at the anterior border of the trapezius muscle.

countertraction is provided by the second assistant over the soft tissues in the neck. The plane of dissection is along the undersurface of the platysma muscle. The posterior skin flap is elevated until the anterior border of the trapezius muscle is identified, and it is exposed all the way from the mastoid process down to the clavicle. It is important to remember that platysma is not present all the way up to the trapezius muscle, and therefore meticulous attention is required to remain in the proper subcutaneous plane beyond the platysma to maintain uniform thickness of the skin flap.

Sharp rake retractors are now used to retract the posterior skin flap (Fig. 11.122). Soft tissues anterior to the trapezius muscle are now grasped with several hemostats that are used to provide traction on the surgical specimen. Dissection proceeds along the floor of the posterior triangle of the neck, exposing each succeeding muscle with anterior elevation of the specimen. The superior attachment of the sternomastoid muscle is detached from the mastoid process and retracted anteriorly. The plane of dissection continues just anterior to the anterior border of each succeeding muscle in the posterior triangle of the neck. The splenius capitis and levator scapulae muscles are then exposed. Several small veins must be divided and ligated as this dissection proceeds anteriorly.

In the lower part of the neck, the transverse cervical artery and its accompanying vein are identified, divided between clamps, and ligated. Likewise, the inferior belly of the omohyoid muscle is divided in the floor of the posterior triangle of the neck, and its anterior stump is retracted medially. Dissection continues medially, exposing the posterior scalene muscle. The lower end of the external jugular vein is divided between clamps near the clavicle and its stump is ligated.

As the scalene muscles are exposed, the roots of the cervical plexus come into view (Fig. 11.123). However, these roots are left intact until the phrenic nerve is identified lying on the anterior aspect of the scalenus anticus muscle. Similarly, motor branches of the cervical plexus providing nerve supply to the posterior compartment muscles should be preserved carefully. The cutaneous branches of the cervical plexus, however, are transected, leaving short stumps to prevent injury to the phrenic nerve. The cutaneous branches of the cervical roots carry with them small blood vessels, and therefore these stumps should be ligated. In the lower part of the posterior triangle of the neck, the brachial plexus comes into view. Dissection over the brachial plexus is easy because a plane of loose areolar tissue between the cervical lymph nodes and the supraclavicular fat pad is contained within the deep cervical fascia.

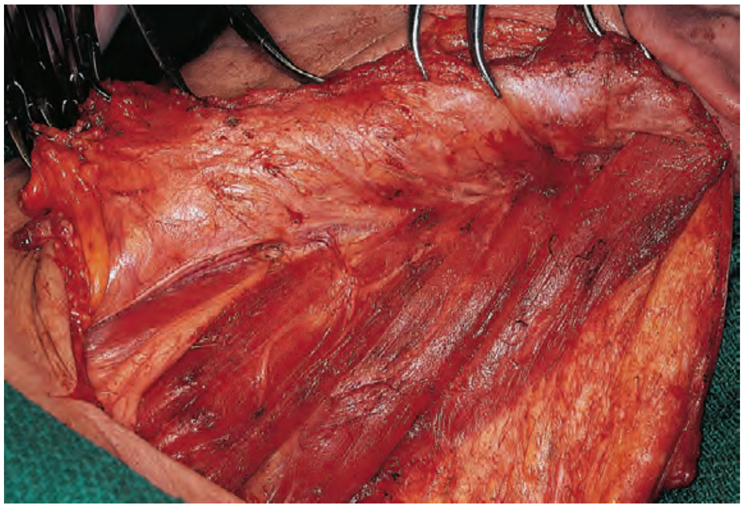

Figure 11.123 Dissection of the posterior triangle medially leads to exposure of the brachial plexus, the phrenic nerve, and the cutaneous roots of the cervical plexus.

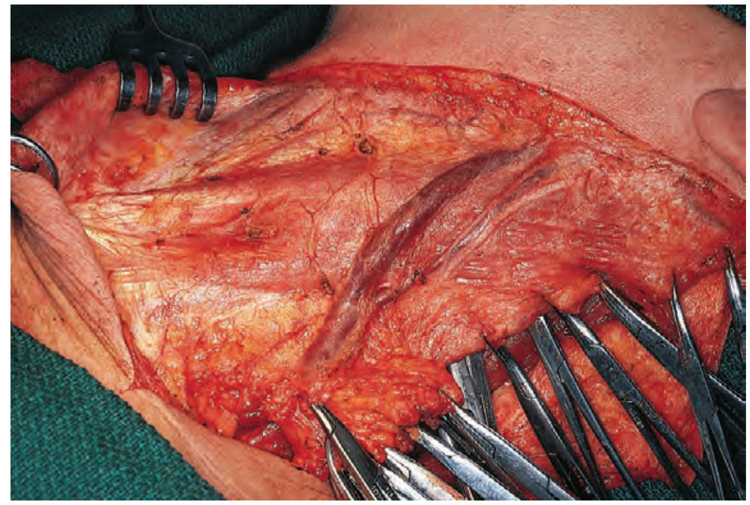

Figure 11.124 The specimen is reflected posteriorly, and the anterior flap is elevated to expose the sternal head of the sternocleidomastoid muscle.

Dissection of the posterior triangle of the neck is now complete. The specimen mobilized thus far is now allowed to rest over the posterior triangle (Fig. 11.124). A dry gauze pad is placed on the musculature of the posterior triangle of the neck, over which the surgical specimen is allowed to rest.

Attention is now focused on the anterior skin flap. The transverse skin incision is completed by extending it from the trifurcation point up to the medial end, deepening it through the platysma. The anterior skin flap is retracted medially with use of skin hooks and rake retractors. The use of electrocautery permits rapid elevation of this skin flap through the loose plane of areolar tissue lying deep to the platysma muscle. Several cutaneous vessels are encountered during elevation and are electrocoagulated. The skin flap is elevated up to the medial border of the omohyoid muscle superiorly and up to the medial border of the sternocleidomastoid muscle at its attachment to the manubrium sterni inferiorly.

A large loop retractor is now used to expose the sternal head of the sternomastoid muscle, which facilitates complete elevation of the anterior skin flap. The cutting current of the electrocautery is used to divide the tendon of the sternomastoid muscle from the sternal end, and the remainder of the muscular attachment on the manubrium and the clavicle is divided with use of the coagulating current of the electrocautery. A plane of loose areolar tissue containing fat is present between the carotid sheath and the posterior aspect of the sternomastoid muscle, and thus the latter can be safely divided with electrocautery.

Several small vessels enter the anterior skin flap as it is elevated near the clavicle. These vessels are branches from the first perforating branch of the internal mammary artery, which provide blood supply to the lower skin flap. They are preserved carefully. Once the sternomastoid muscle is detached from both its sternal and clavicular heads, it is grasped with hemostats and retracted cephalad. A scalpel is used to incise the fascia between the carotid sheath and the strap muscles. A small loop retractor is used to retract the strap muscles medially to expose the common carotid artery and the vagus nerve. By alternate blunt and sharp dissection, the areolar tissue of the carotid sheath is divided circumferentially around the internal jugular vein (Fig. 11.125).

At this juncture, the proximal end of the transverse cervical artery and vein are identified, divided, and ligated. Lymphatic

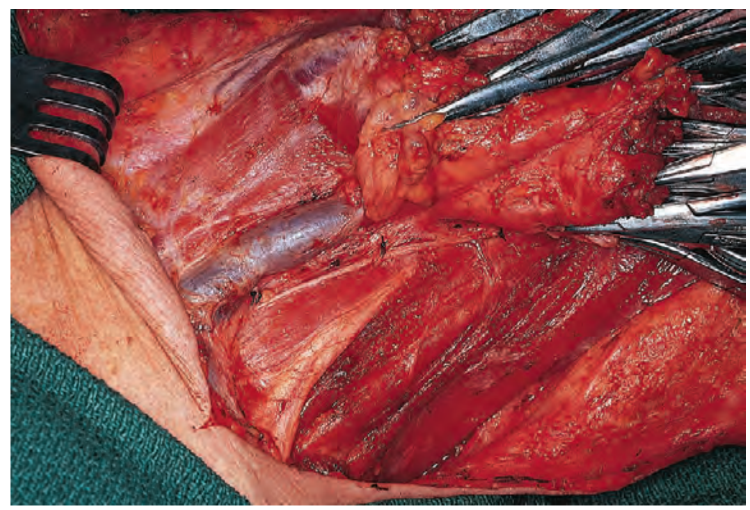

Figure 11.125 The sternomastoid muscle is detached from the sternum and clavicle and retracted cephalad to expose the carotid sheath.

vessels present in the vicinity of the jugular vein are identified, divided, and ligated with care. On the left-hand side of the neck, the thoracic duct requires special attention. It should be identified meticulously, dissected with care, divided, and ligated to prevent chyle leak and a fistula. Lymph nodes contained in loose areolar tissue behind the internal jugular vein are dissected and pulled out at this time to remain in continuity with the remainder of the specimen. During this dissection, the phrenic nerve should be protected carefully and kept out of harm's way.

The small loop retractor placed on the strap muscles is now pulled to expose the common carotid artery and the vagus nerve (Fig. 11.126). The internal jugular vein should not be ligated until after both the carotid artery and the vagus nerve are identified and retracted medially. The vein is doubly ligated and divided in between, and its proximal stump is ligated with a suture.

The middle thyroid vein, which usually is seen at this point entering the medial aspect of the internal jugular vein, is divided and ligated. Dissection now proceeds along the lateral border of the carotid sheath, remaining posterior to the vein but anterolateral to the vagus nerve. This plane is relatively avascular, and the carotid sheath can be divided safely along this plane

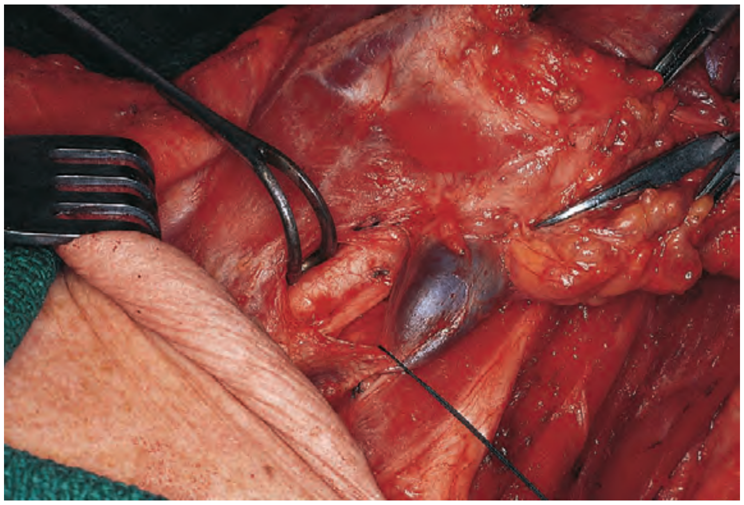

Figure 11.126 The internal jugular vein is ligated and divided after the common carotid artery and the vagus nerve are exposed and retracted medially.

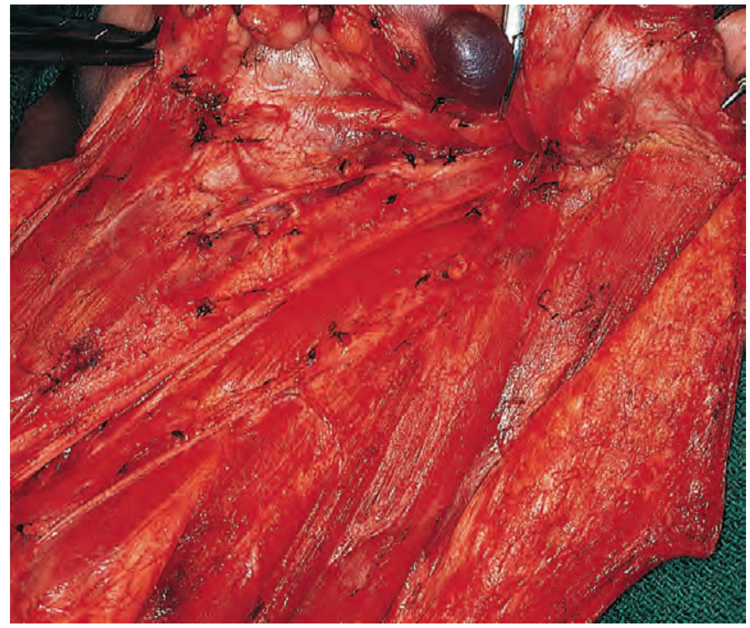

Figure 11.127 Dissection proceeds cephalad along the carotid sheath up to the base of the skull.

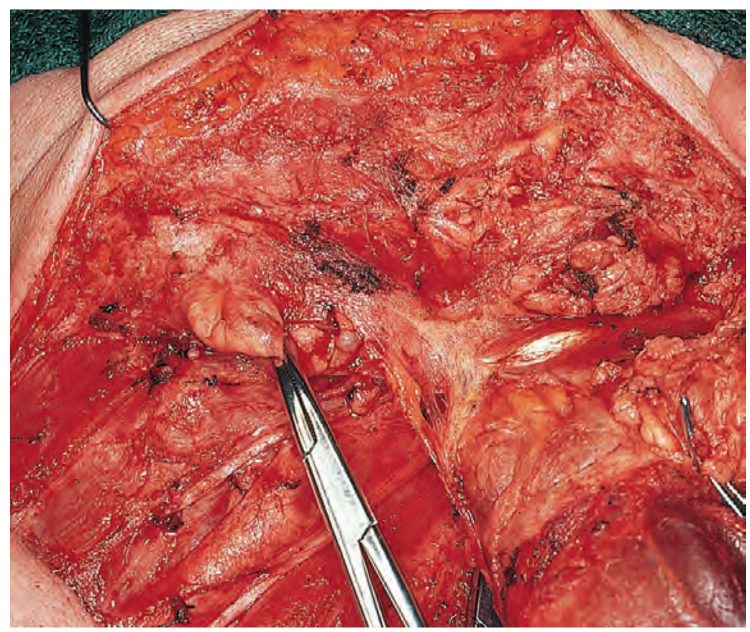

Figure 11.128 The upper skin flap is now elevated, preserving the mandibular branch of the facial nerve.

all the way up to the base of the skull. As dissection proceeds cephalad, minor vessels in the carotid sheath may cause bleeding, which is easily controlled with electrocoagulation (Fig. 11.127).

Dissection of the lateral aspect of the carotid sheath in the upper part of the neck brings the hypoglossal nerve into view. On the medial aspect of the carotid sheath, the dissection is carried cephalad along the medial border of the superior belly of the omohyoid muscle up to the hyoid bone, from which it is detached. Small blood vessels running along the descendens hypoglossi are divided and ligated. The superior thyroid artery is preserved, but the superior thyroid vein must be divided and ligated. A dry gauze pad is now placed on the surgical field and the entire specimen is allowed to rest over the gauze pad.

The superior skin flap is now elevated in the usual fashion, remaining close to the platysma. The mandibular branch of the facial nerve is located in the fascia over the submandibular salivary gland approximately two fingerbreadths below and two fingerbreadths anterior to the angle of the mandible. The nerve is carefully identified, dissected off the fascia, and retracted cephalad with the skin flap. The facial vessels are divided and ligated (Fig. 11.128). The contents of the submandibular triangle are dissected off by dividing the secretomotor fibers to the submandibular salivary gland and Wharton's duct but preserving the lingual and hypoglossal nerves. The submandibular gland and level I lymph nodes thus are reflected caudad to remain in continuity with the remainder of the specimen. Several pharyngeal veins along the digastric tendon and posterior belly of the digastric muscle are divided and ligated. At this juncture the hypoglossal nerve should be dissected carefully, protected, and preserved. Finally, the tail of the parotid gland is separated or transected along the superior border of the posterior belly of the digastric muscle. In dividing the tail of the parotid gland, the posterior facial vein and several arterial branches of the occipital artery must be divided and ligated.

The posterior belly of the digastric muscle is now retracted cephalad with a deep, right-angled retractor, bringing into view the occipital artery, which runs across the internal jugular vein anteriorly at right angles to it. If the occipital artery is high behind the digastric muscle, it may be left alone, but if it is quite low it will have to be divided and ligated. The adipose tissue and lymph nodes lateral to the internal jugular vein under the sternomastoid muscle are dissected out, which is easily accomplished once the tendon of the sternomastoid muscle is detached from the mastoid process.

The accessory nerve is divided near the jugular foramen and its proximal stump is ligated because a small vessel runs with the nerve. Finally, the upper end of the internal jugular vein is skeletonized and the vein is doubly ligated and divided. The surgical specimen is now removed.

The surgical field after radical neck dissection shows clearance of all five levels of lymph nodes as previously described, along with loss of the sternomastoid muscle, internal jugular vein, spinal accessory nerve, and the submandibular salivary gland (Fig. 11.129). The wound is now irrigated with Bacitracin solution. Meticulous hemostasis must be ensured prior to closure of the wound. Two suction drains are inserted through separate stab incisions (Fig. 11.130). One drain overlies the anterior border of the trapezius muscle in the posterior triangle and is

Figure 11.129 The surgical field after radical neck dissection.

Figure 11.130 Two suction drains are inserted through separate stab incisions.

Figure 11.131 The skin wound is closed in two layers.

Figure 11.132 The appearance of the patient 6 months after surgery.

retained there through a loop of chromic catgut suture between the skin flap and the trapezius muscle. Another drain is maintained over the strap muscles anteriorly and is retained by a loop of catgut suture. The remainder of the wound is closed in two layers using 3-0 chromic catgut interrupted sutures for platysma and 5-0 nylon sutures for skin (Fig. 11.131). It is vital for the suction drains to be on continuous suction while the wound is being closed.

As soon as the last skin sutures are applied, the wound should be made airtight, allowing the skin flaps to remain completely down and snug to the deeper tissues by suction through the drains. If suction in this manner is not maintained, minor venous oozing will allow the flaps to lift, causing a collection of hematoma and clotting of blood in drainage tubes that will, in turn, initiate new venous oozing, leading to a larger hematoma. The suction drains are retained until the volume of serous drainage is minimal.

The appearance of the patient approximately 6 months after surgery shows a well-healed scar with aesthetic deformity because of the loss of the sternomastoid muscle (Fig. 11.132). The functional disability due to the sacrifice of the spinal accessory nerve results in the inability to abduct the shoulder beyond 90 degrees cephalad. This functional disability is due to the loss of function of the trapezius muscle. In addition, the imbalance of shoulder musculature due to the paralyzed trapezius muscle causes drooping of the shoulder and winging of the scapula (Fig. 11.133).

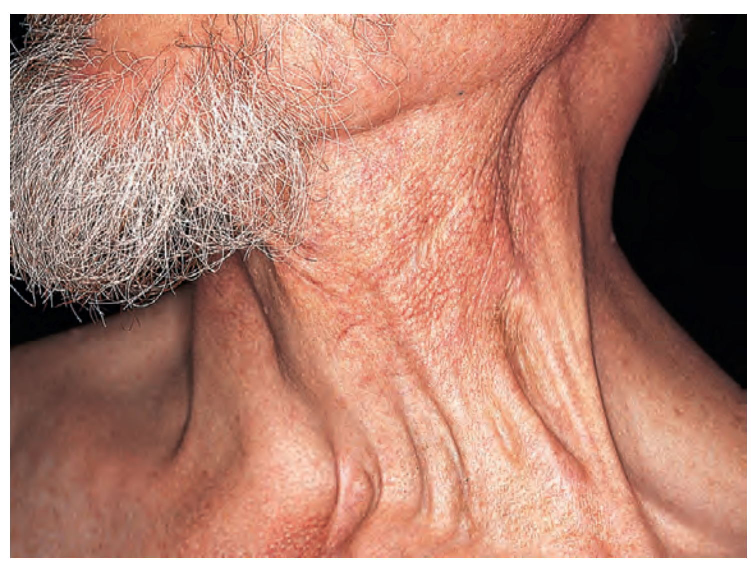

Figure 11.133 Aesthetic deformity and functional disability due to a paralyzed trapezius muscle causes drooping of the shoulder, muscle atrophy, and winging of the scapula after radical neck dissection.

Figure 11.134 Chronic lymphedema of the face with thickening of the subdermal plane and cutaneous telangiectasia after bilateral radical neck dissections.

Figure 11.135 Massive venous and lymphatic edema of the face following simultaneous bilateral radial neck dissections and laryngectomy.

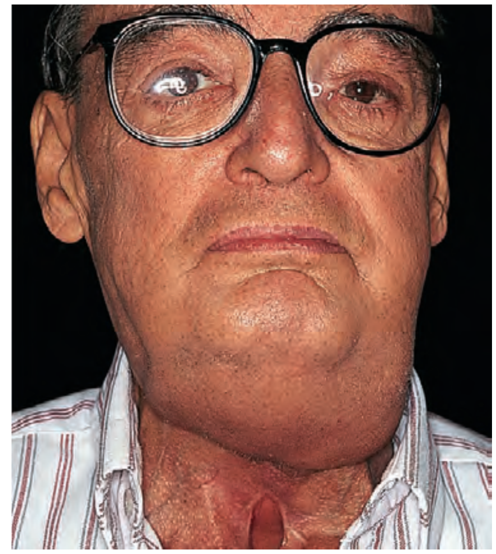

Figure 11.136 Resolution of facial edema through prevertebral venous collaterals 3 months after surgery.

When bilateral radical neck dissections are performed with sacrifice of the internal jugular vein on both sides for a tumor of the oral cavity or oropharynx, chronic lymphedema of the face and swelling takes place. Although venous drainage initially is compromised, within a few weeks collateral venous drainage through the pharyngeal veins restores venous drainage as long as the anatomy of the central compartment is not disturbed. However, chronic lymphedema of the face with thickening of the subdermal plane and cutaneous telangiectasia remains (Fig. 11.134). On the other hand, when simultaneous bilateral radical neck dissections are performed in conjunction with a laryngectomy, acute obstruction of intracranial and extracranial venous drainage takes place. This obstruction leads to the development of massive venous and lymphatic edema of the face in the postoperative period (Fig. 11.135). However, with the passage of time, collateral venous drainage is established through the Batson prevertebral venous plexus, and the extent of venous and lymphatic edema diminishes (Fig. 11.136). In addition, operative mortality of such a massive resection is significant, and therefore, when feasible, bilateral radical neck dissections in conjunction with pharyngolaryngectomy as a single stage procedure should be avoided. Patients undergoing classical radical neck dissection require an intensive program of postoperative physiotherapy for rehabilitation of shoulder function and to avoid a painful and stiff shoulder syndrome.

Extended Radical Neck Dissections

An extended radical neck dissection is an operation in which all five nodal levels are dissected and additional nodes, tissues, or structures are excised (Fig. 11.137). Thus an extended radical neck dissection may include removal of additional lymph nodes from the parapharyngeal and retropharyngeal areas, from the superior mediastinum, and from the apex of the axilla, or nonlymphatic structures may be resected, such as skin, cranial nerves, the carotid artery, or musculature of the floor of the posterior triangle of the neck.

Extensions of neck dissections are required in patients with a locally advanced metastatic carcinoma in regional cervical lymph nodes. The patient shown in Fig. 11.138 has massive matted metastatic lymph nodes at levels IV and V that are fungating through the skin. A large area of skin is involved by the tumor mass; however, the mass is mobile over the deeper soft tissues and prevertebral muscles. A contrast-enhanced CT scan seen in Fig. 11.139 demonstrates obliteration of the internal jugular vein and invasion of the skin.

A hockey-stick–type incision is made in the neck beginning at the tip of the mastoid process and heading down along the anterior border of the trapezius muscle, encompassing the area of the skin to be sacrificed in an elliptical manner and ending at the right sternoclavicular joint. A pectoralis myocutaneous flap of appropriate dimensions is outlined on the anterior chest wall on the right-hand side (Fig. 11.140). The pectoralis myocutaneous flap will be used to fill the soft tissue defect and resurface the skin defect in the dissected neck. The surgical defect following extended comprehensive neck dissection is shown in Fig. 11.141. Note that portions of the prevertebral muscles had to be resected, although the brachial plexus was able to be preserved. A pectoralis major myocutaneous island flap is developed to reconstruct the surgical defect in the neck (Fig. 11.142). The flap is rotated 180 degrees and positioned in the surgical defect without causing undue tension on its vascular pedicle (Fig. 11.143). The skin closure is completed, providing complete resurfacing of the skin and the soft-tissue defect in the neck (Fig. 11.144).

The appearance of the patient approximately 1 month after surgery shows primary healing at the surgical site (Fig. 11.145). This patient will undergo a course of postoperative chemoradiotherapy with the intent of improving local regional control of metastatic cancer in the neck.

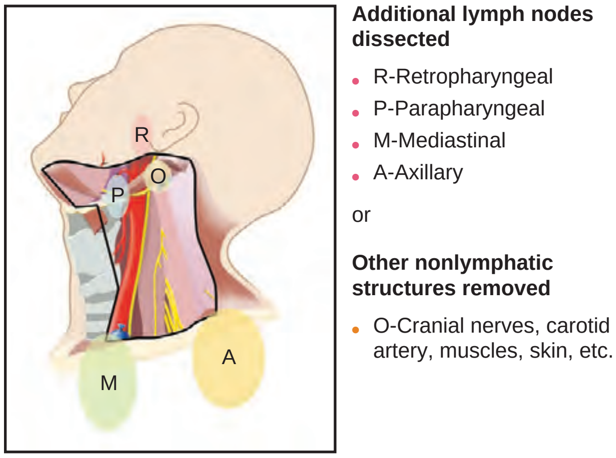

Figure 11.137 Additional lymph node levels or other structures excised in extended radical neck dissections. *(Courtesy Memorial Sloan Kettering Cancer Center.)*

Figure 11.138 A fungating metastatic lymph node mass with infiltration of the skin.

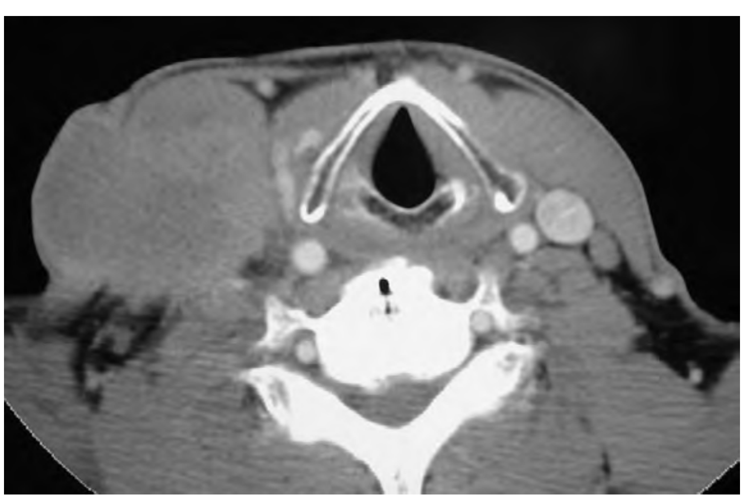

Figure 11.139 A contrast-enhanced axial computed tomography scan showing skin invasion and obliteration of the right internal jugular vein by metastatic lymph nodes.

Figure 11.140 The skin incision is outlined, encompassing the area of skin to be resected. Skin incision for pectoralis myocutaneous flap is also outlined.

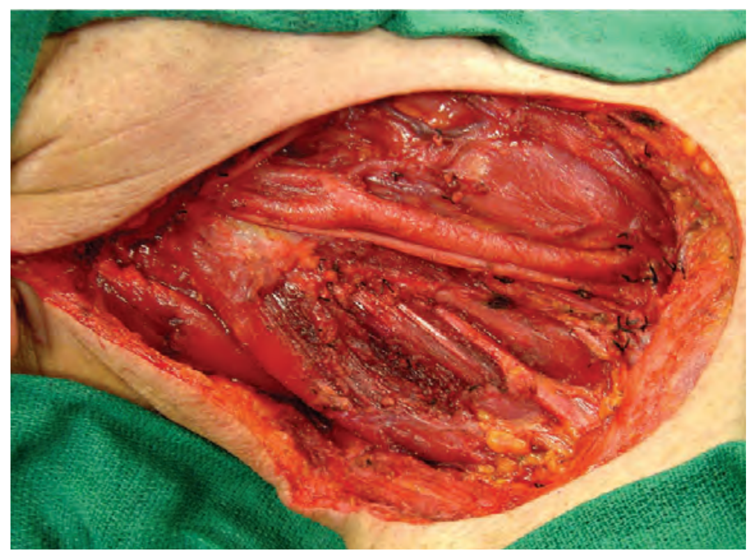

Figure 11.141 The surgical defect showing the floor of the posterior triangle with an intact brachial plexus, carotid artery, and vagus nerve.

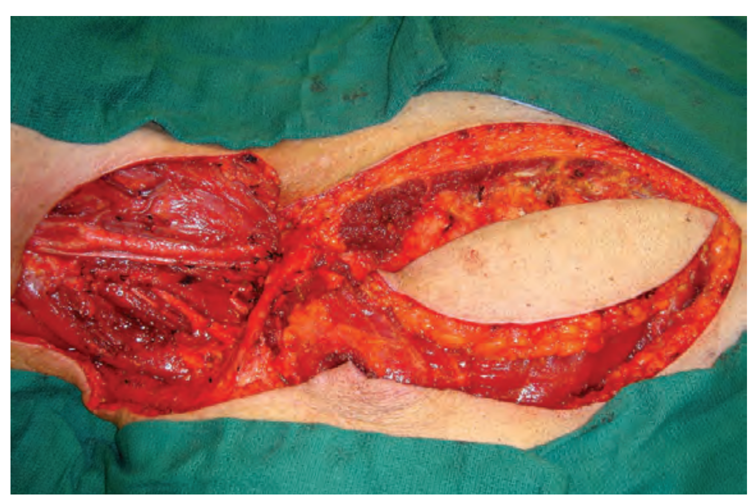

Figure 11.142 A pectoralis major myocutaneous island flap is developed.

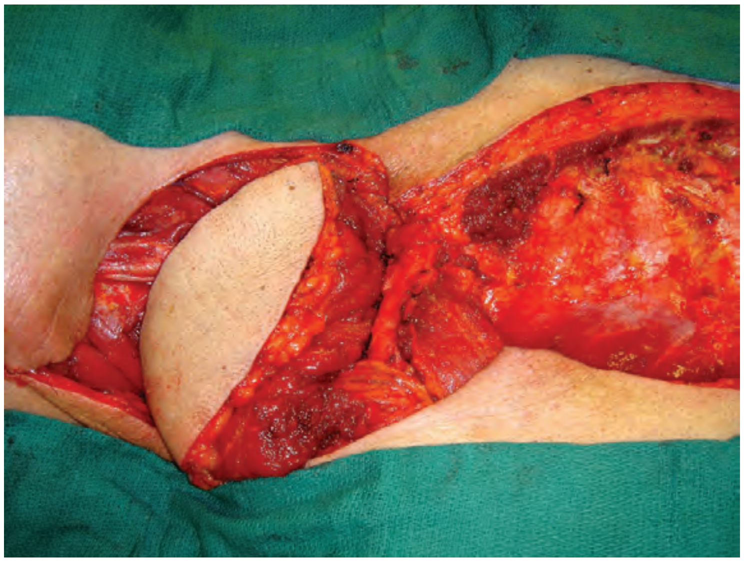

Figure 11.143 The flap is rotated 180 degrees and positioned in the surgical defect.

Extended Radical Neck Dissection With Mediastinal Lymph Node Dissection

The clinical presence of lymph node metastases in the lower part of the neck with contiguous involvement of superior mediastinal lymph nodes often requires combined cervical and mediastinal lymph node dissection. Such operative procedures may be necessary in patients presenting either with a thyroid carcinoma or occasionally with a melanoma. The patient described here had a primary melanoma of the skin of the lower part of the neck with clinically apparent cervical lymph node metastasis in the supraclavicular region and extension of metastatic disease to the superior mediastinal lymph nodes.

The CT scan of the patient through the superior mediastinum at the level of the arch of the aorta shows a large, centrally necrotic metastatic mass on the right-hand side of the superior mediastinum (Fig. 11.146).

The surgical procedure includes dissection of the right side of the neck with sacrifice of a large area of skin at the site of the primary tumor in continuity with superior mediastinal node dissection. The skin incision for neck dissection begins at the mastoid process and descends along the trapezius muscle to connect with the outline of an area of wide excision of the skin in the supraclavicular region. The skin incision then continues medially to the suprasternal notch, where a straight vertical limb is extended caudad over the manubrium up to the xiphoid process (Fig. 11.147).

Figure 11.144 The surgical defect is reconstructed.

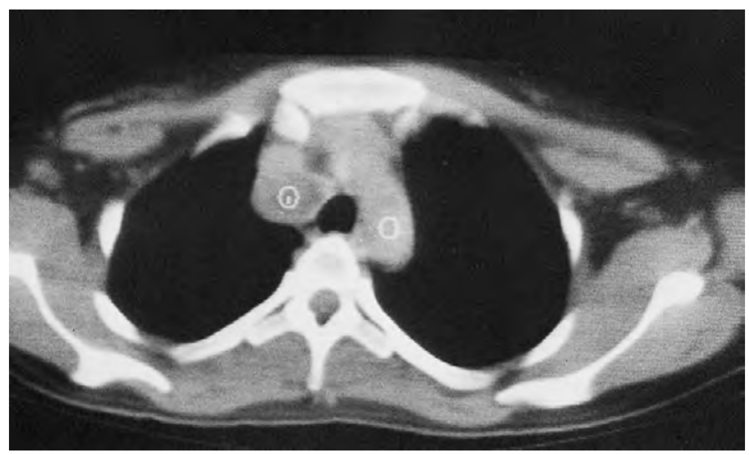

Figure 11.146 A computed tomography scan through the superior mediastinum.

Figure 11.145 The appearance of the patient approximately 1 month after surgery.

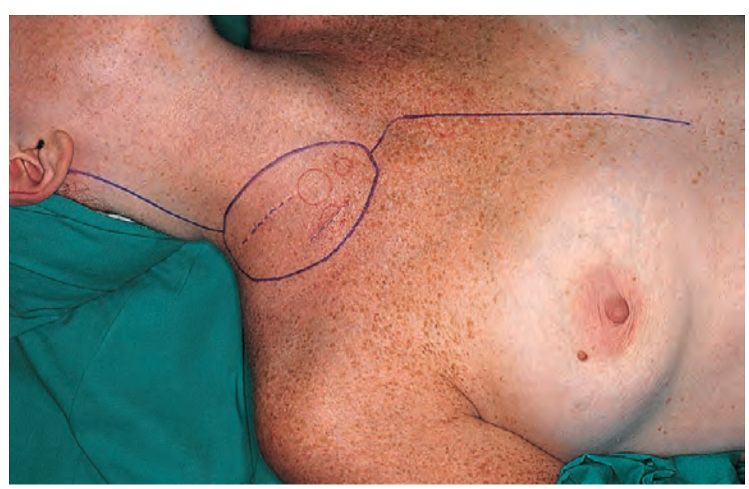

Figure 11.147 The skin incision for a radical neck dissection and median sternotomy incorporates wide excision of the primary site.

A median sternotomy for mediastinal node dissection is performed first (Fig. 11.148). The skin incision from the suprasternal notch to the xiphoid process is deepened through the subcutaneous tissue up to the anterior surface of the sternum. Using digital blunt dissection in the suprasternal notch, a space is created in the superior mediastinum behind the manubrium sterni by detaching the strap muscles from the posterior aspect of the manubrium (Fig. 11.149). Digital dissection posterior to the manubrium creates a space for insertion of the sternal saw, which is used to divide the sternum (Fig. 11.150). The median sternotomy extends from the suprasternal notch to the xiphoid process. The sternum is lifted up with the distal lip of the sternal saw during its division to prevent injury to the mediastinal structures beneath. Brisk hemorrhage occurs from the cut ends of the sternum but is easily controlled with bone wax applied to the cut edges of the sternum (Fig. 11.151).

A self-retaining sternal retractor is now used to expose the mediastinum (Fig. 11.152). Careful and meticulous dissection of the mediastinal fat and lymph nodes is undertaken, denuding the innominate veins and the superior vena cava. The complete mass of fibrofatty tissue and lymph nodes is dissected and swept toward the right-hand side. Dissection of the mediastinal lymph nodes begins with identification of the left innominate vein (Fig. 11.153). Lymph nodes from the region of the superior vena cava are mobilized and dissected toward the right-hand side. This dissection is tedious and should be carefully undertaken to prevent inadvertent injury to the innominate veins. Both innominate veins and the superior vena cava are cleared of the lymph nodes. Note that all the tissues are dissected and reflected superiorly toward the right-hand side (Fig. 11.154).

At this point, dissection continues to mobilize the large mass of lymph node metastases present between the innominate artery and right innominate vein (Fig. 11.155). A cuff of the parietal pleura of the right-hand side is removed because the mass is adherent to the pleura. Once this step is accomplished, superior mobilization of the metastatic nodes is possible along the innominate artery.

The view of the surgical field from the opposite side (the left-hand side of the patient) shows the mass of metastatic lymph nodes overlying the innominate artery in the superior mediastinum (Fig. 11.156). At this point, excision of the primary site is completed in continuity with the right radical neck dissection. However, the specimen remains attached at the root of the neck to the mediastinal nodes, near the origin of the common carotid artery from the innominate artery. Further dissection along the innominate artery at its bifurcation shows the takeoff of the common carotid artery and the subclavian artery (Fig. 11.157). Note the defect in the parietal pleura on the right-hand side showing the lung in the right pleural cavity. The big mass of metastatic nodes lying inferior to the

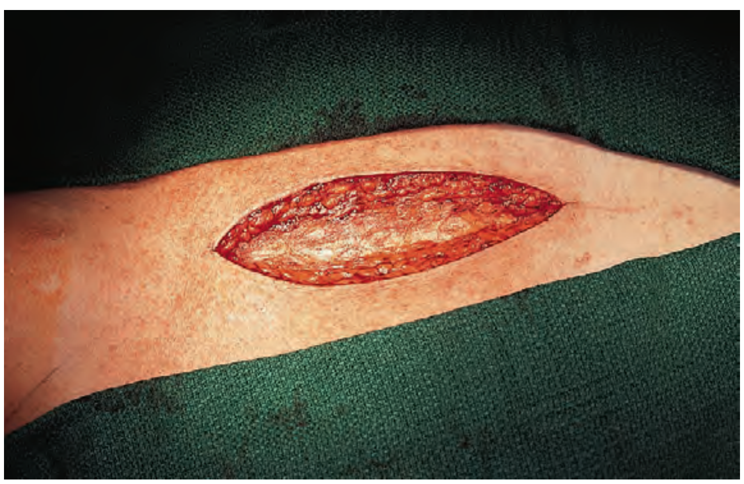

Figure 11.148 The operation begins with a median sternotomy for mediastinal node dissection.

Figure 11.150 A sternal saw is used to divide the sternum from the suprasternal notch up to the xiphoid process.

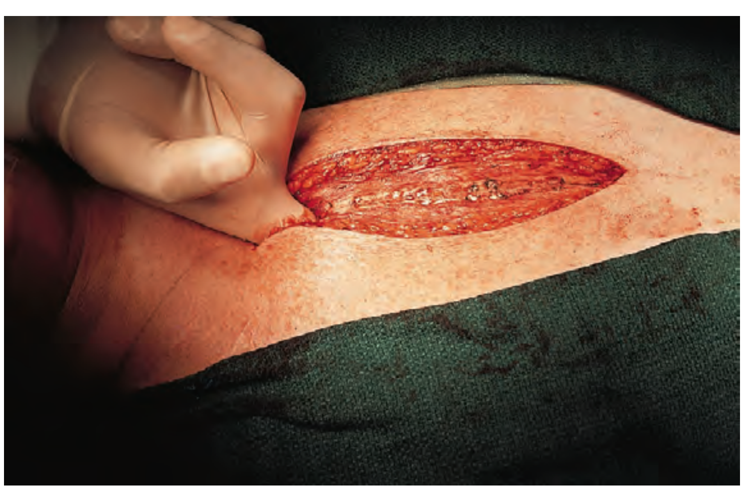

Figure 11.149 The strap muscles are detached from the posterior aspect of the manubrium, and digital dissection is performed to free up the posterior surface of the sternum.

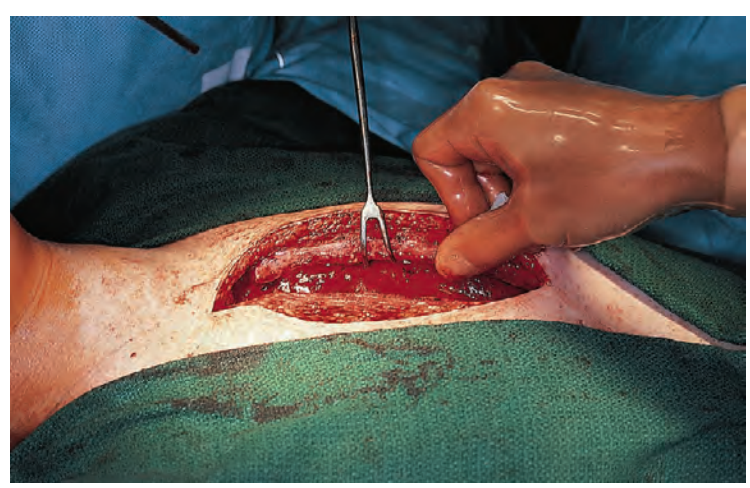

Figure 11.151 Hemorrhage is easily controlled with bone wax applied to the cut edges of the sternum.

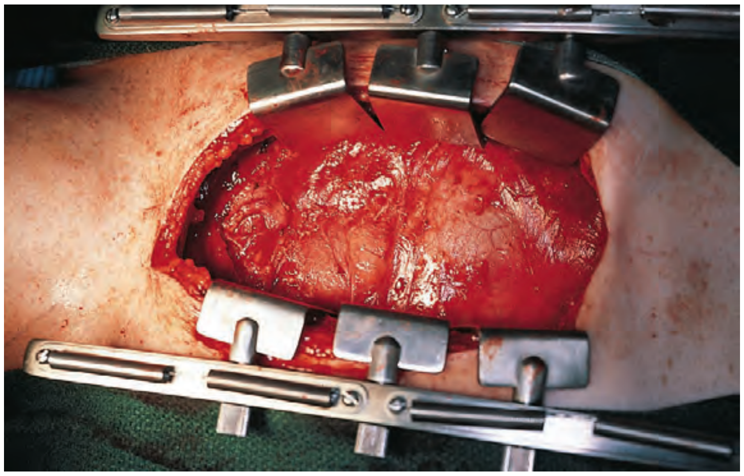

Figure 11.152 The mediastinum is exposed with a self-retaining retractor.

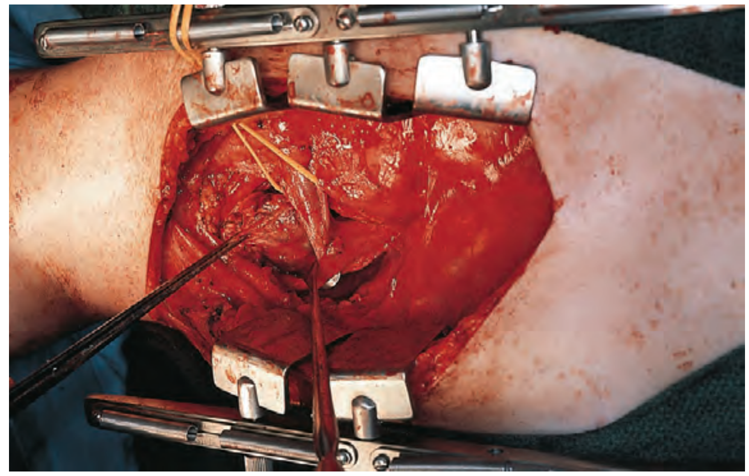

Figure 11.155 Dissection continues to mobilize the large mass of lymph node metastases present between the innominate artery and right innominate vein.

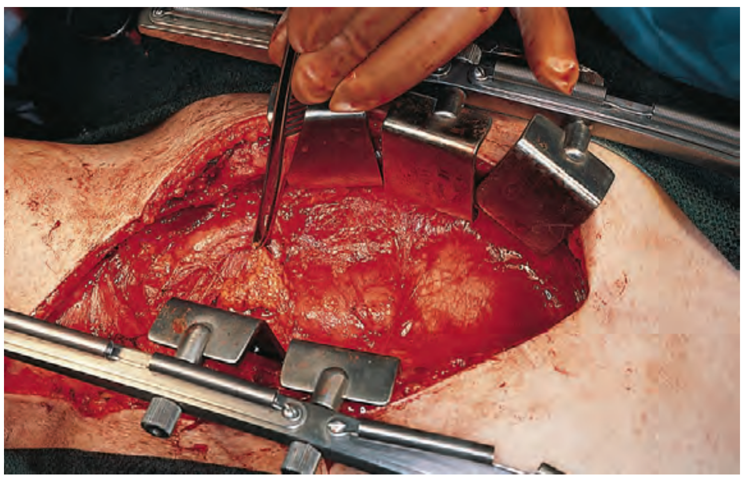

Figure 11.153 Dissection begins from the left-hand side with identification of the left innominate vein.

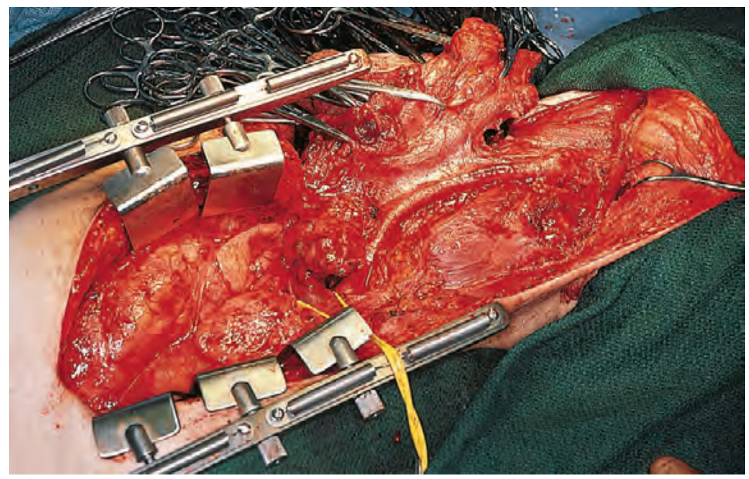

Figure 11.156 The view of the surgical field from the left-hand side of the patient.

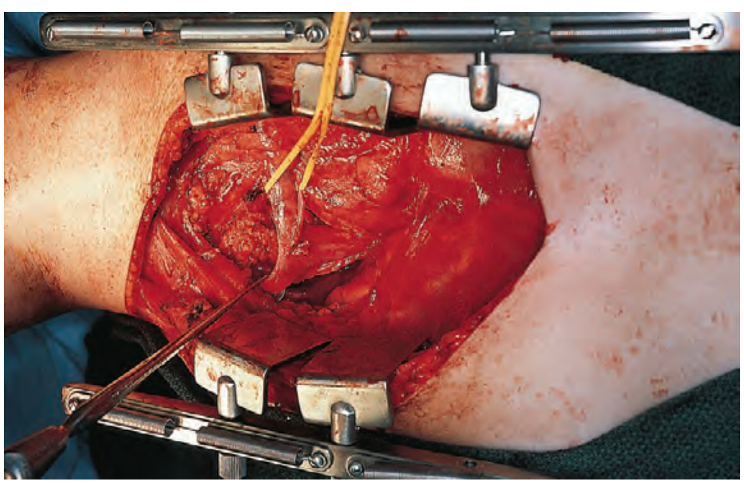

Figure 11.154 All tissues over the innominate veins are dissected and reflected superiorly toward the right-hand side.

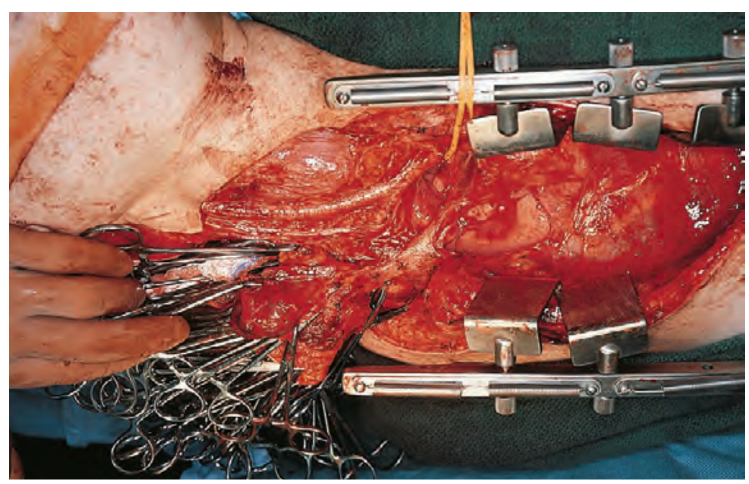

Figure 11.157 The takeoff of the common carotid artery and the subclavian artery at the root of the neck.

innominate artery and posterior to the right innominate vein is now dissected out and reflected cephalad toward the neck. As dissection proceeds toward the root of the neck, the vagus nerve comes into view with its recurrent laryngeal branch as it winds around the subclavian artery to return into the neck (Fig. 11.158). Remaining attachments of the surgical specimen in this area are divided carefully, avoiding any injury to the vagus or recurrent laryngeal nerves.

The surgical field following radical neck dissection in continuity with superior mediastinal lymph node dissection is shown in Fig. 11.159. Note the intact great vessels of the mediastinum, which include the left and right innominate veins and superior

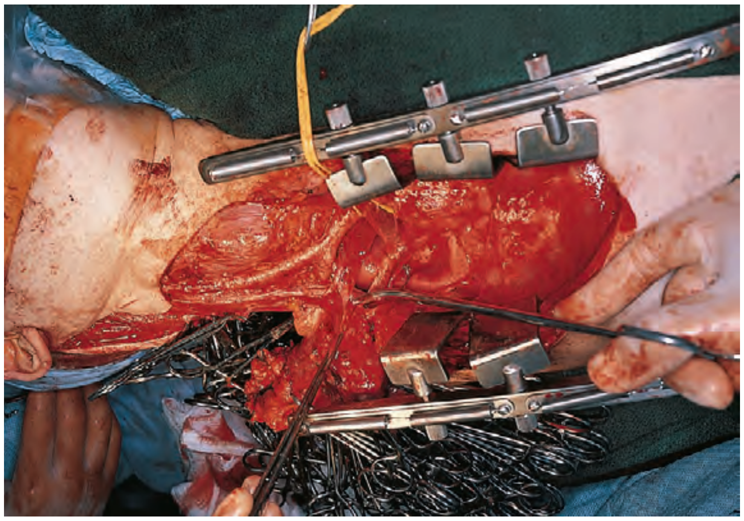

Figure 11.158 The recurrent laryngeal branch of the right vagus nerve winds around the subclavian artery to return into the neck.

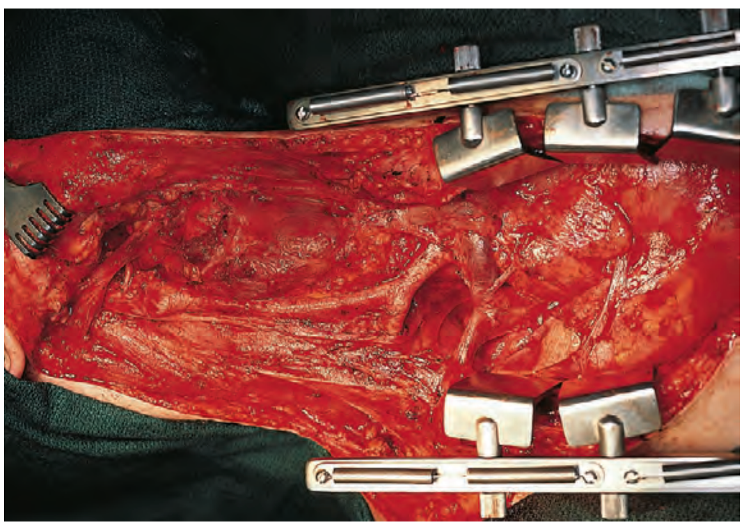

Figure 11.159 The surgical field after removal of the specimen.

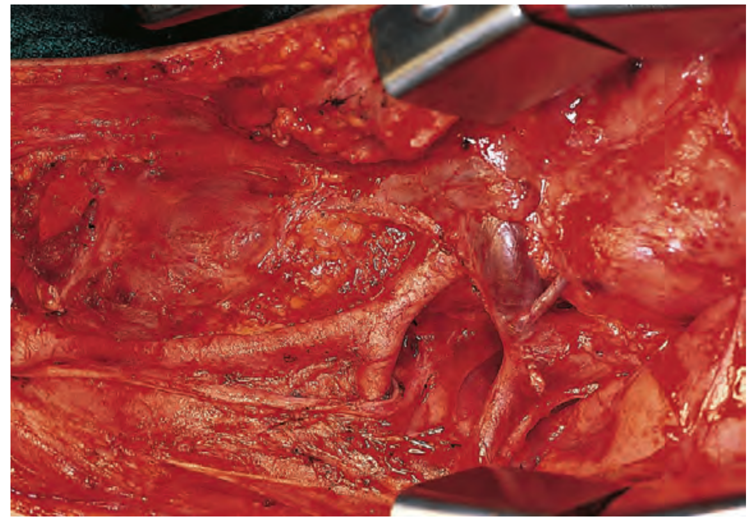

Figure 11.160 A close-up view of the surgical field showing the location of the metastatic mass.

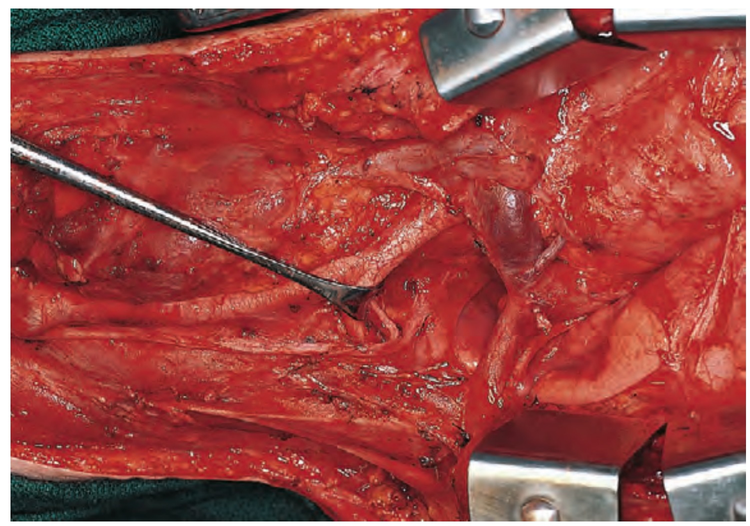

Figure 11.161 The recurrent laryngeal branch of the right vagus nerve turning cephalad behind the subclavian artery.

vena cava, and the innominate artery with its common carotid and subclavian branches. A close-up view of the surgical field shows that the mass of metastatic lymph nodes was located inferior to both the innominate and subclavian arteries and superior and posterior to the right innominate vein and superior vena cava (Fig. 11.160). Retraction of the subclavian artery clearly shows the recurrent laryngeal branch of the right vagus nerve turning cephalad behind the artery (Fig. 11.161). The surgical specimen shows a large area of skin at the site of the primary melanoma resected in continuity with right radical neck dissection and superior mediastinal lymph node dissection (Fig. 11.162).

The surgical defect is irrigated with Bacitracin solution. Drainage with a right thoracostomy tube with an underwater seal is established. The pleural defect is repaired with primary closure. The median sternotomy is repaired with peristernal heavy silver wires. The skin incision in the chest is closed in layers. The surgical defect in the neck requires coverage with a rotation advancement flap obtained from the anterior chest wall. The incision for the flap begins at the lateral aspect of the skin defect in the neck and is taken down along the deltopectoral groove. The flap is elevated superficial to the pectoralis major muscle and is advanced cephalad and rotated medially to cover the surgical defect. The appearance of the patient

Figure 11.162 The surgical specimen of a melanoma of the skin of the neck in continuity with a radical neck dissection and mediastinal node dissection.

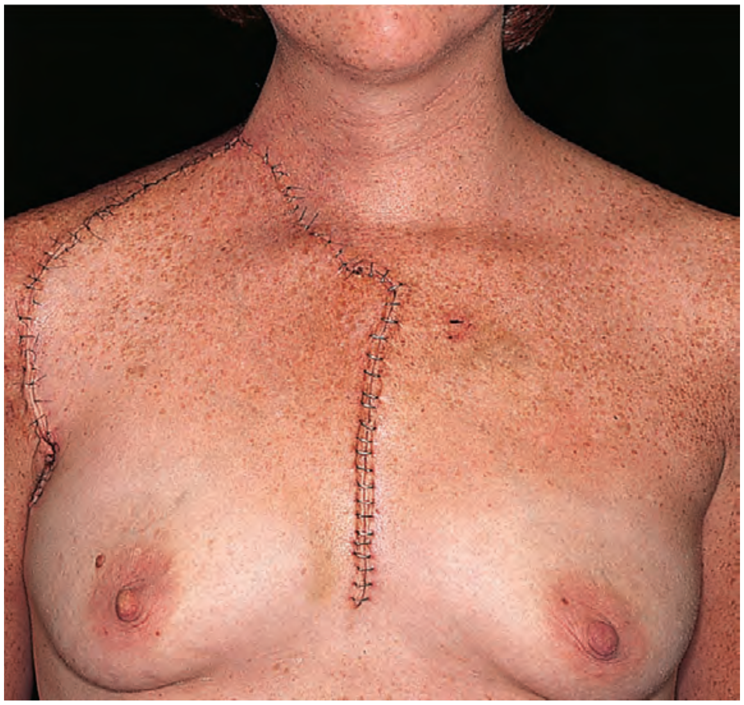

Figure 11.163 The appearance of the patient approximately 1 week after surgery.

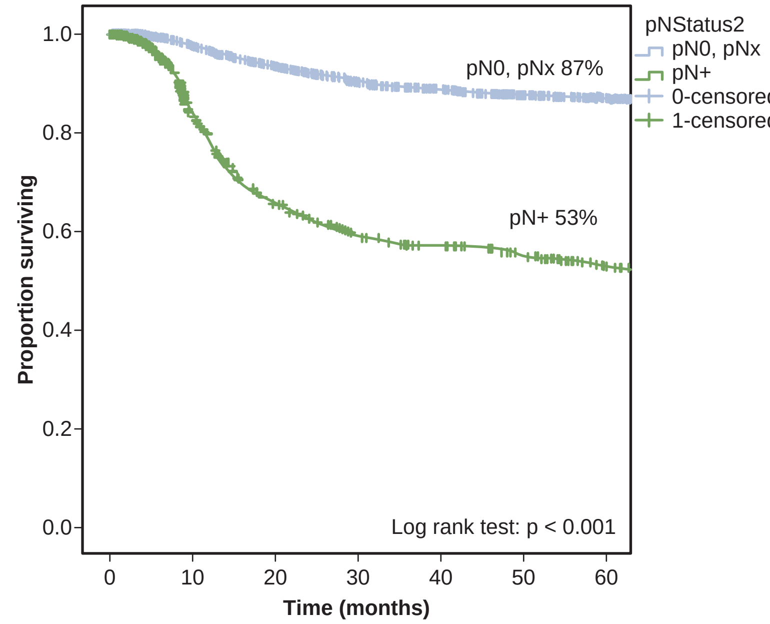

Figure 11.164 The impact of nodal metastasis on disease-specific survival in patients with oral cancer. *(Courtesy Memorial Sloan Kettering Cancer Center data, 1985–2012.)*

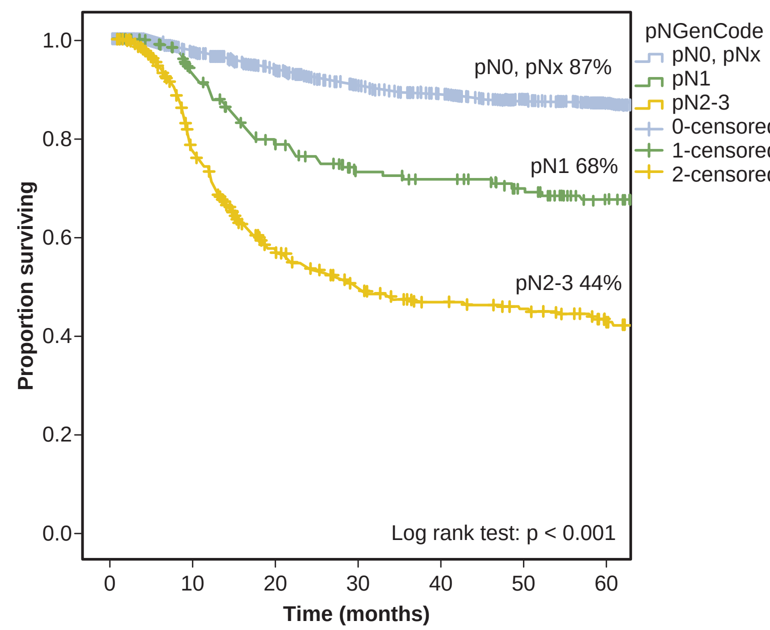

Figure 11.165 The impact of N stage on disease-specific survival in patients with oral cancer. *(Courtesy Memorial Sloan Kettering Cancer Center data, 1985–2012.)*

approximately 1 week after surgery shows primary healing of the incisions (Fig. 11.163).

RESULTS OF TREATMENT

One of the most important factors in prognosis for squamous cell carcinoma of the head and neck is the presence or absence of cervical lymph node metastasis at initial diagnosis. Cure rates for patients who present with cervical lymph node metastasis are substantially lower than for those who present with tumors localized at the primary site (Fig. 11.164). The extent of nodal metastases in the neck clearly has an impact on prognosis, even in patients who have an unknown or occult primary tumor. Patients with N1 disease in the neck have a better prognosis compared with those with N2 or N3 disease (Fig. 11.165). In addition, the presence of capsular rupture and ENE also has an adverse impact on prognosis (Fig. 11.166). At present, the oral cavity is probably the most common primary site in the upper aerodigestive tract where patients undergo neck dissection first before any other modality of treatment is used. Prognostic information related to the status of the regional lymph nodes and their surgical management is most accurately assessed in patients with oral cancer. Therefore the data shown here are for patients undergoing neck dissection for primary oral squamous cell carcinomas.

Patients undergoing neck dissection for potential occult microscopic metastases who are staged as N0 have the lowest risk of recurrence in the neck compared with those with N1, N2, or N3 disease (Fig. 11.167). Thus the risk for regional failure in the dissected neck depends on the extent of nodal disease. Patients with multiple-level involvement experience recurrence in the dissected neck twice as often as those with single-level involvement. Patients with high-risk features in the neck dissection specimen, such as high N stage, ENE, increased nodal density, and other ominous pathologic findings have an increased risk of regional failure after neck dissection. These patients are candidates for postoperative adjuvant treatment with radiation therapy with or without chemotherapy. Adjuvant postoperative radiation therapy significantly improves regional control in persons who have undergone a neck dissection and brings the outcome closer to that of patients treated with neck dissection alone who did not require adjuvant treatment (Fig. 11.168). Further improvement in regional control is reported with the

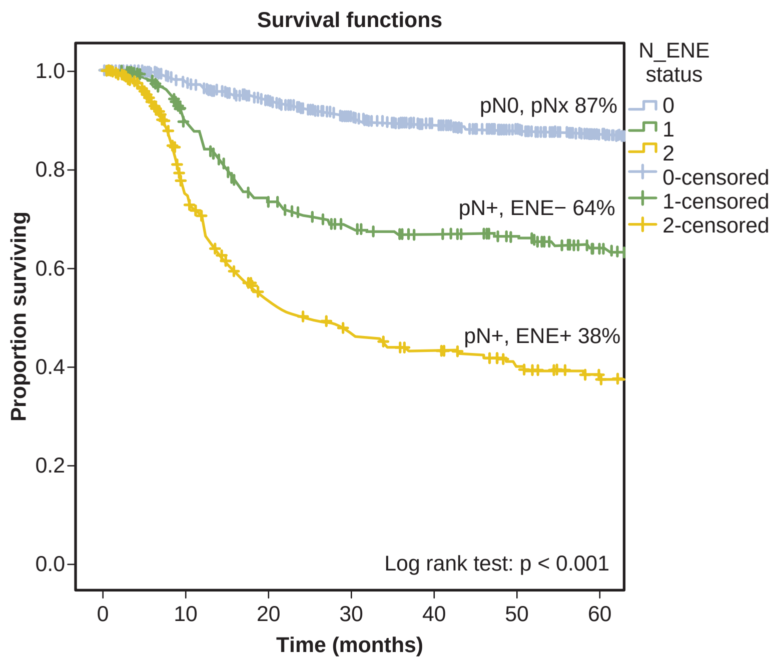

Figure 11.166 The impact of extranodal extension on disease-specific survival in patients with oral cancer. *ECS,* Extranodal extension; *pN,* pathologic node status; *RR,* relative risk. *(Courtesy Memorial Sloan Kettering Cancer Center data, 1985–2012.)*

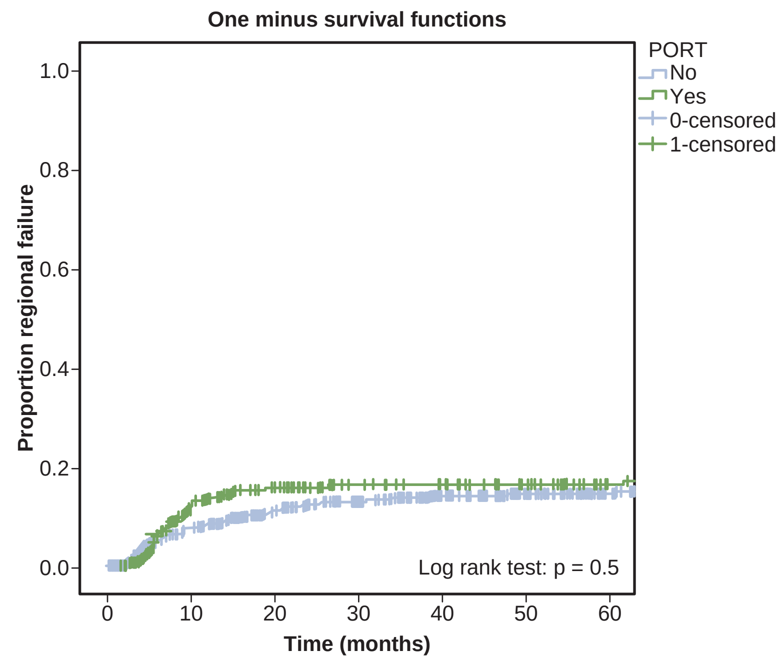

Figure 11.168 The impact of postoperative radiotherapy on regional control in patients undergoing neck dissection. *RT,* Radiation therapy. *(Courtesy Memorial Sloan Kettering Cancer Center data, 1985–2012.)*

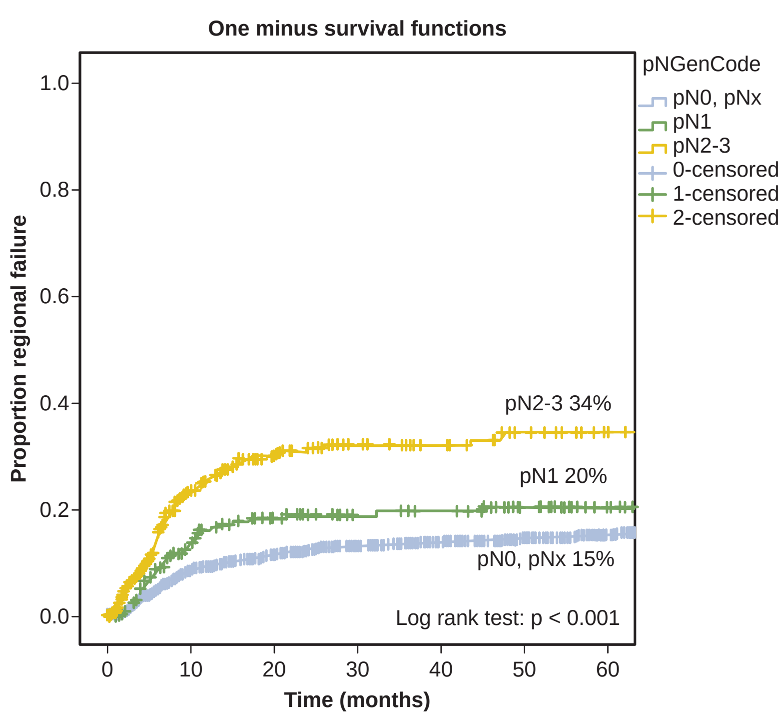

Figure 11.167 The impact of N stage on failure in the neck in patients with oral cancer. *(Courtesy Memorial Sloan Kettering Cancer Center data, 1985–2012.)*

addition of chemotherapy to postoperative radiation in patients with ENE, but this improvement is accompanied by high-grade toxicity in a significant number of patients.

Severe functional and aesthetic morbidity following classic radical neck dissection has warranted the need to modify the operation to reduce morbidity without compromising regional control or survival. Five-year survival rates, regional failure rates, and the patterns of recurrence have been observed to be comparable for patients undergoing classic radical neck dissection and MND-I. The trend therefore has shifted from classic radical neck dissection to MND-I in patients with nodal metastases without gross ENE, in whom the spinal accessory nerve is not involved by cancer. Appreciation of the patterns of neck metastasis has further allowed function-preserving selective neck dissections in patients with N0 or low-volume N+ disease in the neck without compromising regional control rates and survival. However, careful selection of patients with a clinically positive neck with low-volume upper neck disease is crucial to a successful outcome after a therapeutic selective neck dissection. For patients with oral cancer, careful selection implies low-volume disease limited to level I or IIA.

CHAPTER 12

Thyroid and Parathyroid Glands

Palpable nodularity in the thyroid gland is common, especially in women and older persons. The incidence of palpable nodularity in the thyroid gland in the United States is reported to be 4% to 7% of the adult population. However, sonographic or other imaging studies indicate that thyroid nodules may be present in as many as 50% of the adult population. The vast majority of clinically detectable thyroid nodules are benign. The incidence of occult cancer in the thyroid gland ranges from 4% to 35% in adults based on autopsy studies and increases significantly with advancing age.

During the past two decades, a steep rise in the incidence of differentiated carcinoma of the thyroid gland has been observed worldwide. According to the American Cancer Society, the annual estimate for thyroid cancer has risen from 18,400 new cases in the year 2000 to 56,000 new cases in 2017 (Fig. 12.1). Similar trends are reported in Europe and elsewhere in the world. However, the number of deaths attributed to thyroid cancer has not changed much during this time period, with an estimate of approximately 2000 deaths annually in the United States in the past few years. Moreover, most (nearly 90%) of the thyroid cancers that account for the observed increase in incidence are less than 2 cm, and in approximately 50% of patients they are less than 1 cm. These findings suggest that the apparent increase in the incidence of thyroid cancer likely represents detection of clinically occult, micropapillary carcinomas. Often, these tumors are detected on routine imaging studies done for other reasons, such as computed tomography (CT) scan; magnetic resonance imaging (MRI); positron emission tomography (PET) scan; or, more commonly, ultrasound of the neck done for study of the carotid arteries, breast examination, and sometimes as a simple screening test. Routine use of ultrasound as a cancer screening test, commonly practiced in South Korea, has resulted in a 15-fold rise in the detection of clinically occult micropapillary carcinomas.

Most of these tumors are well differentiated and indolent in behavior. The histologic distribution of primary carcinomas in the thyroid gland is shown in Fig. 12.2. Most thyroid cancers are of follicular cell origin, but they also may arise from parafollicular cells (C cells). Follicular cell–derived thyroid cancers represent a spectrum of diseases, ranging from the indolent papillary and follicular carcinoma to the more aggressive variants such as tall cell and insular carcinomas, poorly differentiated carcinomas, and anaplastic carcinoma, which is almost universally fatal. Well-differentiated thyroid carcinomas can transform into more aggressive variants in a small proportion of patients, especially those with multiple recurrences. However, this transition occurs over decades in most instances. Evidence for such transition is the presence of focal areas of differentiated carcinoma in patients with poorly differentiated/undifferentiated or anaplastic carcinomas. A review of serial pathologic specimens in patients with multiple recurrences of papillary carcinoma often shows progression to an undifferentiated carcinoma. Thus, tumor heterogeneity at initial presentation and progressive anaplasia with multiple recurrences are in direct evidence that a tumor progression model exists in thyroid cancer. This tumor progression model is depicted in Fig. 12.3.

BENIGN THYROID NODULES

A nodular goiter is one of the most common structural abnormalities of the thyroid gland. Goiters may present as a diffuse enlargement of the thyroid gland, as a single nodule, or as multiple nodules. The most common cause of goiters is dietary iodine deficiency. Thus goiters are more common in some parts of the world, where common salt used in dietary preparations is not routinely iodized. The other common cause for a diffuse goiter is an autoimmune disease such as Hashimoto thyroiditis or Graves' disease, which can be identified through clinical features or laboratory studies. Lithium, used in the treatment of some psychiatric disorders, also promotes the development of goiters. Goiters can get quite large but rarely become symptomatic unless the airway is compressed by the mass. Benign neoplasms of the thyroid gland primarily include follicular and Hürthle cell adenomas, and they must be differentiated from their malignant counterparts.

NEOPLASMS OF FOLLICULAR CELL ORIGIN

Collectively grouped as differentiated thyroid cancers, papillary and follicular carcinomas constitute more than 90% of all malignant neoplasms of the thyroid gland. These tumors are most common in young adults, with a 2:1 predilection for women compared with men (Fig. 12.4). In the last two decades, there has been a shift in age distribution in newly diagnosed patients with papillary carcinoma. The peak incidence in the past was in the fourth decade of life. However, in the past 20 years, the peak incidence is now in the fifth decade of life. Epidemiologic evidence suggests that papillary thyroid cancer may be inherited in up to 5% of patients. Although the precise genes involved have yet to be identified, the mode of transmission is thought to be autosomal dominant, with incomplete penetrance and variable expression. Several susceptibility loci have been identified, including those at 19p13.2, 14q, 1p13.2-1q22, and 2q21. A germline mutation in the *TTF1* gene is suggested to account for at least a subset of these patients. None of these genetic mutations, however, are in routine clinical use since their role

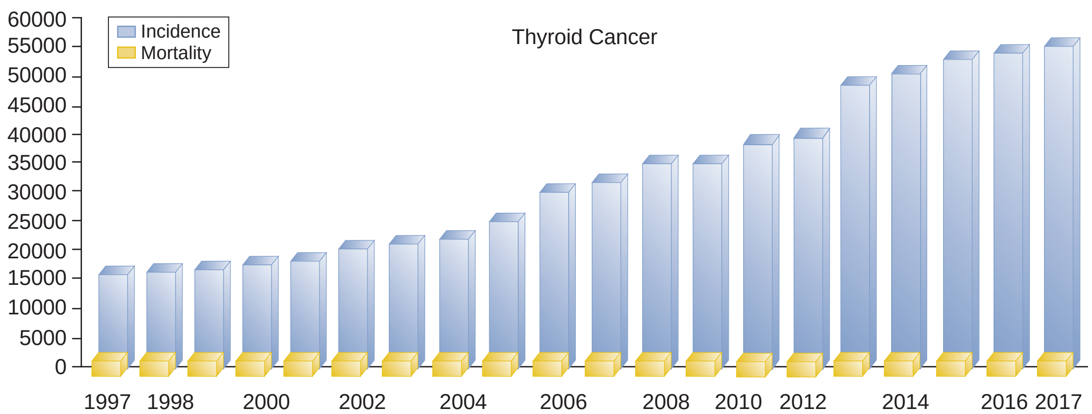

Figure 12.1 The rising incidence of cancer of the thyroid in the United States (1997–2017).

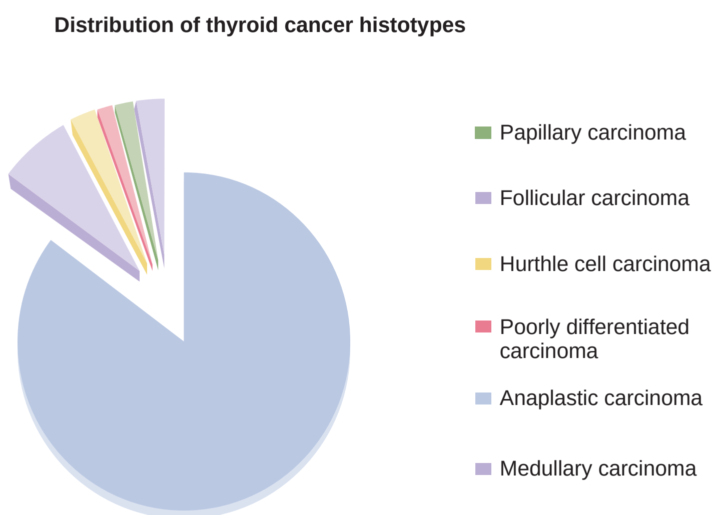

Figure 12.2 The histologic distribution of primary carcinomas in the thyroid gland.

in the genesis of carcinoma is not uniformly reproducible. Nevertheless, the risk of thyroid cancer in affected families is more than five times higher than in the general population. These patients have a predilection for multifocal disease and a more aggressive clinical course. Thyroid cancers also can occur as part of established genetic syndromes including Cowden disease, familial adenomatous polyposis (cribriform-morular variant), and Carney complex.

Childhood exposure to radiation increases the risk for thyroid cancer by up to twentyfold. The highest incidence is observed in children exposed to radiation fallout from the Chernobyl nuclear accident and the atomic bomb explosions in Japan. Increased incidence of thyroid cancer is observed in adults who were exposed to low-dose radiation during childhood for the treatment of acne, a common practice until the 1960s. Similarly, increased incidence of thyroid cancer is observed in adults who were treated for lymphoma in childhood with mantle port radiation. Although the development of thyroid malignancy appeared to have a latency period of 20 years or more in patients treated with radiation during childhood, it is considerably shorter for children exposed to nuclear fallout. This, however, may be a reflection of the huge number of children exposed to the fallout showing the early age of the latency curve and increased awareness about the carcinogenic effect on the thyroid gland. Thyroid cancer rates also are reported to be higher in iodine-deficient areas, which suggests that iodine deficiency may be a predisposing factor. The presence of autoimmune thyroiditis may increase the risk for the development of lymphoma in the thyroid but does not appear to affect the incidence of thyroid carcinoma.

As stated previously, thyroid cancer presents a spectrum of histologic entities with diverse clinical behavior. A great majority of follicular cell–derived carcinomas have an indolent behavior and are curable. A small percentage of thyroid cancers of follicular cell origin (~10%–15%) have a more aggressive behavior and can be a threat to life.

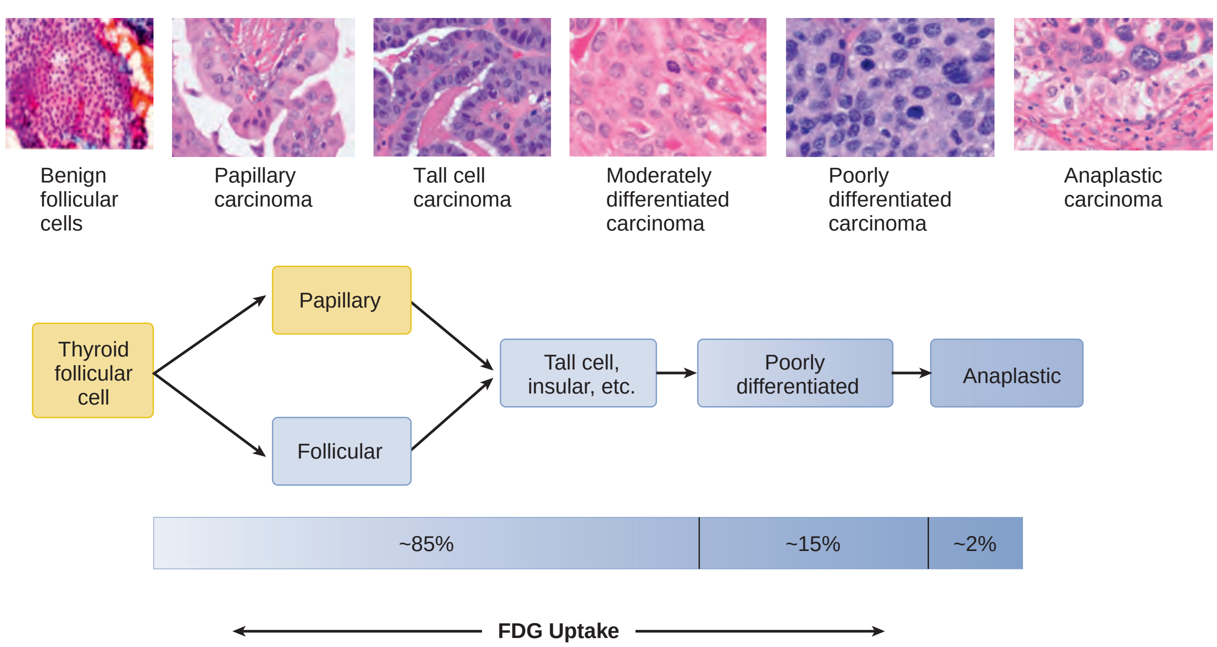

Figure 12.3 Tumor progression of thyroid cancer from differentiated to anaplastic carcinoma, incidence, and 5-year survival.

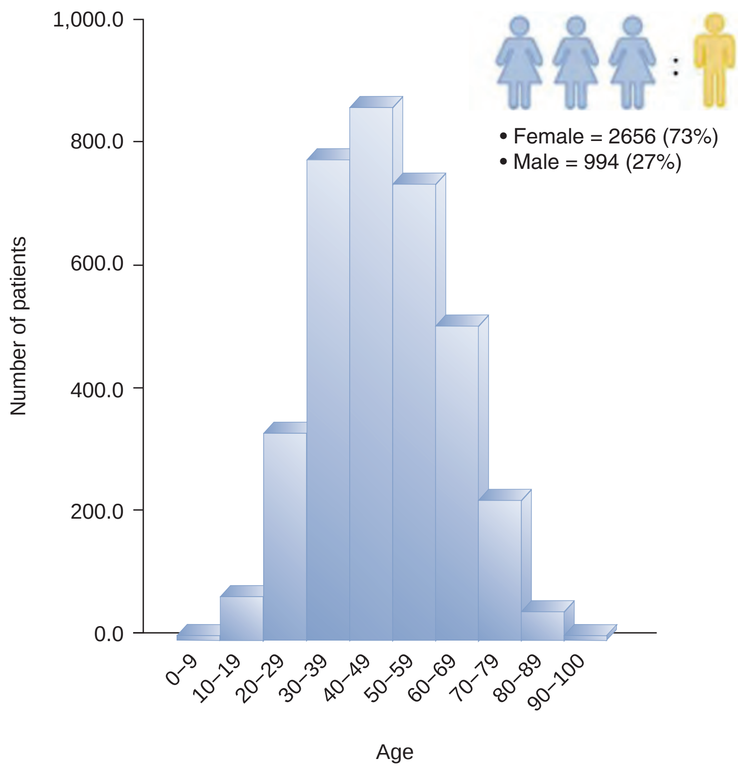

Figure 12.4 Age and sex distribution in 3,650 patients with differentiated carcinoma of the thyroid gland (Memorial Sloan Kettering Cancer Center, 1986–2010).

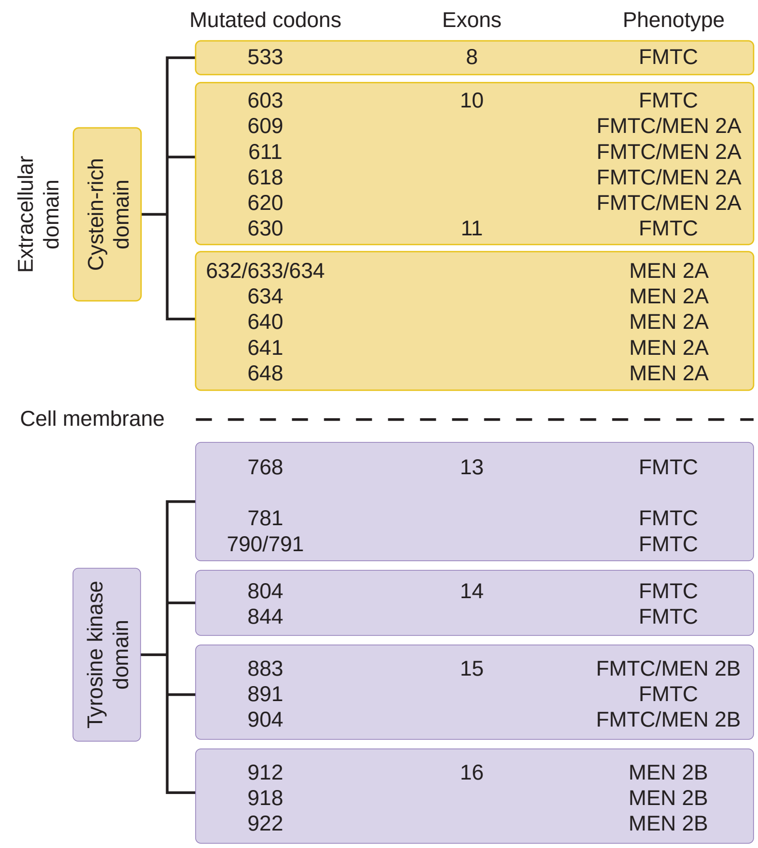

Figure 12.5 Location of mutations in the *RET* protooncogene in patients with medullary carcinoma of the thyroid. *FMTC,* Familial medullary thyroid cancer; *MEN,* multiple endocrine neoplasia.

MEDULLARY THYROID CARCINOMA

Medullary carcinoma of the thyroid (MTC) accounts for approximately 4% of all malignant tumors of the thyroid gland. MTC can occur sporadically (in 75%–80% of all cases) or as part of an inherited cancer syndrome (in 20%–25% of cases). Inherited MTC results from mutation in the *RET* protooncogene; however, this gene also is mutated in up to 50% of sporadic cases. This is a somatic mutation and is only present within the tumor. On the other hand, RAS mutations are found in a significant number of patients without RET somatic mutation. MTC can occur as part of multiple endocrine neoplasia (MEN) syndromes (MEN 2A and 2B) as well as familial MTC (FMTC). MEN 2A is the most common inherited MTC, accounting for 80% of cases, whereas MEN 2B accounts for 5% to 10%, and FMTC accounts for the remainder of cases. MTC typically presents in the third to fourth decade of life in patients with MEN 2A, and these patients also are prone to the development of pheochromocytoma and primary hyperparathyroidism. According to 2015 American Thyroid Association (ATA) guidelines, MEN2A has been categorized into four categories: (1) classic MEN2A, of which 95% of patients have RET mutations; (2) MEN2A with cutaneous lichenoid amyloidosis (CLA); (3) MEN2A and Hirschsprung's disease (HD); and (4) familial medullary thyroid carcinoma (FMTC). FMTC is thought to be a variant of MEN 2A in which only MTC develops. MTC becomes manifest later in life (in the fourth decade) in patients with FMTC and tends to have a less aggressive course relative to patients with MEN 2A.

The onset of MTC is earlier in patients with MEN 2B (<30 years), and the disease typically is more aggressive in these patients. The characteristic features of MEN 2B include musculoskeletal abnormalities (i.e., marfanoid habitus), mucosal neuromas (on the lips, tongue, and conjunctiva), and urinary and intestinal ganglioneuromatosis. Although patients with MEN 2B are at risk for the development of pheochromocytoma, in contrast to patients with MEN 2A, hyperparathyroidism does not develop in these patients.

Each inherited MTC syndrome is associated with specific mutations in the *RET* gene (Fig. 12.5). The location of the mutation affects the oncogenic potency of the *RET* gene. Mutations in the tyrosine kinase domain result in higher oncogenic potential and are associated with MEN 2B (912, 918, and 922), whereas those in the extracellular domain are less frequent, have lower virulence, and are associated with FMTC or MEN 2A.

EVALUATION: WORK UP AND STAGING

Neoplasms of Follicular Cell Origin

Tumors of the thyroid gland most frequently present as asymptomatic nodules. With more widespread use of ultrasound, MRI, CT, and 18F-fluorodeoxyglucose (FDG) PET scanning, small, subclinical thyroid nodules are increasingly being detected. Fortunately, the vast majority of thyroid nodules are benign, but 5% to 10% of nodules prove to be primary thyroid cancer.

Initial evaluation of any thyroid nodule begins with a complete history and physical examination that focuses on the

thyroid gland and surrounding cervical lymph nodes. Clinical features such as a history of childhood radiation, a family history of thyroid cancer, a genetic syndrome that could include thyroid cancer (e.g., Cowden syndrome, familial adenomatosis polyposis, Carney complex, multiple endocrine neoplasia syndrome, or Werner syndrome), rapid nodule growth, palpable cervical lymphadenopathy, or hoarseness of voice due to vocal cord paralysis all increase the likelihood of thyroid malignancy.

Following a complete history and physical examination, the next step in evaluation of a thyroid nodule is measurement of the serum thyroid-stimulating hormone (TSH) level. Even though thyroid function tests, including TSH, are almost always normal in the setting of primary thyroid cancers, a suppressed TSH would raise the possibility of an autonomously functioning nodule. Such nodules can be identified by radionuclide scanning and carry an extremely low risk of malignancy; therefore they do not require further workup, such as fine-needle aspiration biopsy. Depending on the degree of hyperthyroidism, observation or therapy may be indicated to treat the autonomous hyperfunctioning thyroid nodule. While not a clinically useful discriminator, several studies have shown that the risk of thyroid malignancy is positively correlated with the degree of TSH elevation, even if within the normal reference range; that is, the higher the TSH at presentation, the greater the chance that a nodule harbors malignancy.

Serum thyroglobulin values are not helpful in the evaluation of thyroid nodules, as benign nodules can also produce thyroglobulin values significantly above the normal range. There continues to be controversy about whether serum calcitonin values should be measured in all patients with clinically significant thyroid nodules. Based on the available evidence, the ATA guidelines do not have a specific recommendation for or against measurement of serum calcitonin in the workup of thyroid nodules. Since many patients with benign disease have mildly elevated calcitonin values, the concern is that these false-positive calcitonin values would lead to more surgeries than necessary. Conversely, several studies have shown that routine use of calcitonin in the evaluation of thyroid nodules does increase the sensitivity for detecting medullary thyroid cancer. Therefore further studies are needed to address this issue.

The ATA 2015 guidelines provide a rational and risk-adapted approach to the evaluation and management of thyroid nodules. After a complete history and physical, and confirmation of a nonsuppressed TSH, the next step in evaluation of a thyroid nodule is neck ultrasonography. Neck ultrasounds should routinely provide a description of the sonographic features of the nodule(s) to enable malignancy risk stratification (as discussed below) and evaluate cervical lymph nodes in the central and lateral neck (Fig. 12.6).

If very suspicious cervical lymph nodes are seen, then fine-needle aspiration of those lymph nodes can establish a diagnosis and lead to appropriate additional workup and treatment. If there are no suspicious lymph nodes identified, then the management algorithm for thyroid nodules relies on (1) sonographic features that define the risk of malignancy within the nodule and (2) the size of the nodule. This differs from previous approaches, where the size of the nodule was the primary factor influencing the decision to perform fine-needle aspiration biopsy (Table 12.1).

As shown in Table 12.1, nodules with sonographic patterns showing high suspicion features carry a risk of malignancy in over 70% to 90% of patients, while nodules with intermediate suspicious features carry a risk of malignancy of 10% to 20%, low suspicion features have a risk of 5% to 10%, and very low suspicion characteristics have a risk of malignancy in less than 3% of patients. Once these nodules have been risk stratified based on sonographic pattern, then the size of the nodule is used to recommend cutoff points for routine use of fine-needle aspiration biopsy (Fig. 12.6). When multiple nodules are present, fine-needle aspiration should be preferentially directed toward the nodule with the highest risk of malignancy based on sonographic pattern and nodule size. In previous iterations of the ATA guidelines, essentially every nodule greater than 5 mm was considered for biopsy. However, in the 2015 edition of the ATA guidelines, nodules with low or very low suspicion are candidates for biopsy only if they are larger than 1.5 to 2 cm. Moreover, it is recommended that nodules with an intermediate- or high-suspicion pattern are considered for biopsy only if they are greater than 1 cm in size. This risk-stratified approach results in a significant number of sonographically detected thyroid nodules where routine use of fine-needle aspiration biopsy is not recommended. Using the same risk-stratified approach, thyroid nodules with a high suspicion pattern that are less than 1 cm can be followed with observation with repeat neck ultrasound in 6 to 12 months. Nodules with low to intermediate suspicion can be followed with repeat neck ultrasound in 12 to 24 months. Nodules greater than 2 cm with very low suspicion should have follow-up ultrasound no sooner than 24 months. Finally, nodules less than 1 cm with very-low-suspicion ultrasound pattern do not require routine sonographic follow-up.

These recommendations allow for observation rather than immediate fine-needle aspiration and surgery for highly suspicious subcentimeter nodules. This approach indirectly endorses an active surveillance management of such potentially malignant low-risk microcarcinomas. As noted in the ATA 2015 guidelines, while thyroid surgery is usually recommended for primary papillary thyroid cancer, active surveillance is now a reasonable alternative to immediate surgery, based largely on the experience published by Drs. Ito and Miyauchi from Kuma Clinic in Kobe Japan. Since cytologic confirmation of disease is not required for active surveillance, both the observation of biopsy-proven papillary thyroid cancer and observation of subcentimeter nodules that are highly suspicious for papillary thyroid cancer are appropriate within an active surveillance paradigm. Therefore an active surveillance option can be offered to patients with subcentimeter thyroid nodules, which are suspicious for or proven to be papillary thyroid carcinoma. However, this approach is recommended in a systematic active surveillance program with well-defined criteria and follow-up strategies. The usual observational approach includes a detailed neck ultrasound every 6 months for the first 2 years. The change in tumor size and volume during the first 2 years is used to establish the doubling time of the tumor. This doubling time is then used to plan the frequency of follow-up ultrasounds and the need for intervention. It is important to recognize that not every subcentimeter suspicious nodule is appropriate for observation. If the suspicious nodule has documented rapid growth, if there is evidence of metastatic disease outside the thyroid, if there is evidence of extrathyroidal extension, or if the tumor is sitting in a location where even minor extrathyroidal extension would be associated with neurovascular or tracheal compromise, then cytologic confirmation followed by surgery is usually recommended.

When fine-needle aspiration is indicated, the Bethesda classification system for cytology is very valuable in helping to risk stratify the various cytologic patterns into a risk of malignancy

ATA THYROID NODULE/DTC GUIDELINES

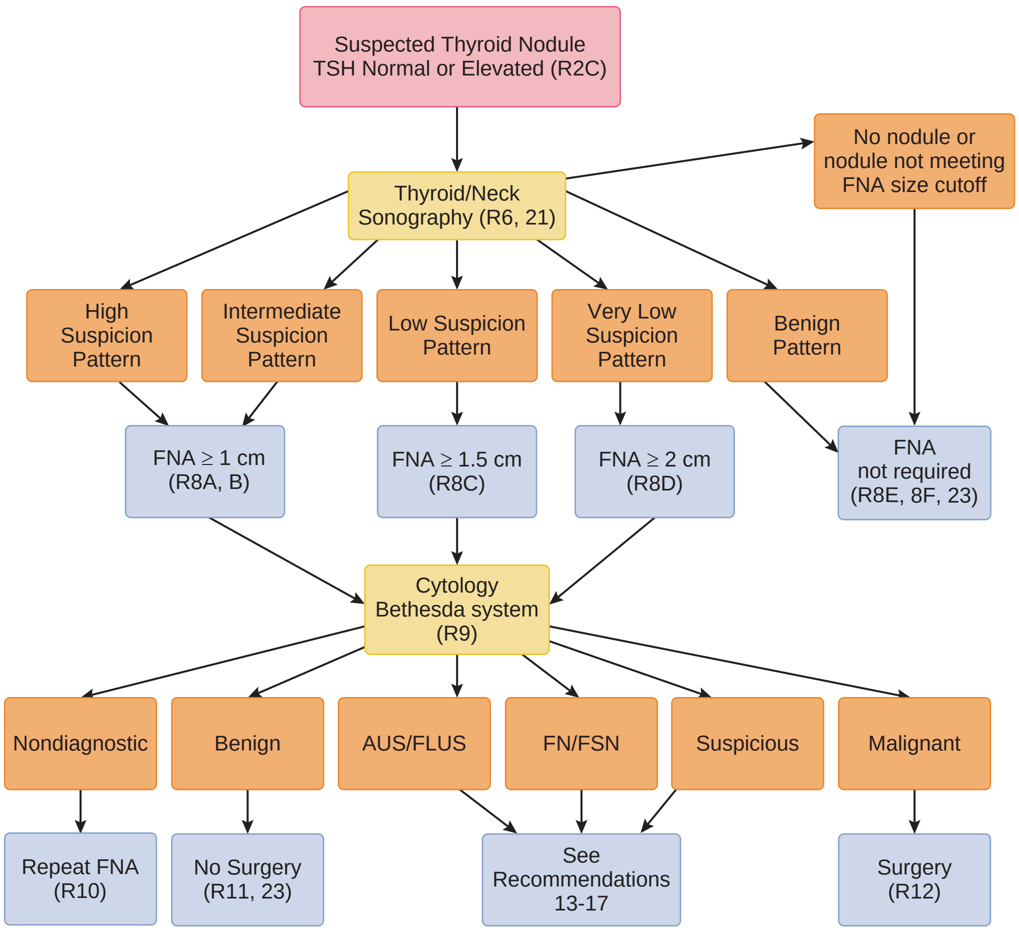

Figure 12.6 Risk-based algorithm for workup of a thyroid nodule. *(2015 American Thyroid Association guidelines.)*

Table 12.1 Sonographic Patterns and Risk of Malignancy in Thyroid Nodules

SONOGRAPHIC PATTERN	ULTRASOUND FEATURES	ESTIMATED RISK OF MALIGNANCY, %	FINE-NEEDLE ASPIRATION SIZE CUTOFF (LARGEST DIMENSION)
High suspicion	Solid hypoechoic nodule or solid hypoechoic component of a partially cystic nodule with one or more of the following features: irregular margins (infiltrative, microlobulated), microcalcifications, taller than wide shape, rim calcifications with small extrusive soft-tissue component, evidence of ETE	>70-90a	Recommend FNA at ≥1 cm
Intermediate suspicion	Hypoechoic solid nodule with smoother margins without microcalcifications, ETE, or taller than wide shape	10-20	Recommend FNA at ≥1 cm
Low suspicion	Isoechoic or hyperechoic solid nodule or partially cystic nodule with eccentric solid areas, without microcalcification, irregular margin or ETE, or taller than wide shape	5-10	Recommend FNA at ≥1.5 cm
Very low suspicion	Spongiform or partially cystic nodules without any of the sonographic features described in low-, intermediate-, or high-suspicion patterns.	<3	Consider FNA at ≥2 cm. Observation without FNA is also a reasonable option.
Benign	Purely cystic nodules (no solid component)	<1	No biopsy

ETE, Extrathyroidal extension; *FNA,* fine-needle aspiration. *(2015 American Thyroid Association guidelines.)*

(Box 12.1). If the cytology is nondiagnostic, a repeat fine-needle aspiration is usually warranted. For benign cytology, in the absence of other worrisome clinical features, a follow-up ultrasound done at an interval consistent with the overall suspicion of the nodule is appropriate. When appropriate nodules are biopsied, a malignant cytology (i.e., Bethesda VI) almost always leads to surgery. Likewise, cytologically suspicious nodules (i.e., Bethesda V lesions) usually require surgical resection for definitive diagnosis and therapy.

Despite many advances in the molecular biology of thyroid nodules, the cytologic classification of AUS/FLUS (atypia of undetermined significance or follicular lesion of undetermined

Box 12.1 Bethesda Classification of Fine-Needle Aspiration Cytology of Thyroid Nodules

I. Nondiagnostic or unsatisfactory
II. Benign
III. Atypia of undetermined significance (AUS) or follicular lesion of undetermined significance (FLUS)
IV. Follicular neoplasm or suspicious for a follicular neoplasm
V. Suspicious for malignancy
VI. Malignant

significance) and FN/FSN (follicular neoplasm or suspicious for follicular neoplasm), Bethesda category III and IV, remain problematic and carry a risk of malignancy that approximates 5% to 15% and 15% to 30%, respectively. Multiple molecular markers have been developed for clinical use to further delineate the risk of malignancy of an indeterminate lesion. Therefore, depending on the clinical risk factors, sonographic features, availability of molecular testing, and patient preference, these molecular profiles may be useful in clinical decision-making.

Following the recommendations of the ATA 2015 guidelines, the interval for repeat ultrasonography following establishment of benign cytology is based on the sonographic pattern of the nodule. Even after a benign fine-needle aspiration, nodules that have a high-suspicion pattern on the ultrasound should probably have a repeat neck ultrasound and fine-needle aspiration within 12 months. However, nodules with low to intermediate suspicion can have a repeat neck ultrasound at 12 to 24 months, reserving a repeat biopsy for those nodules that exhibit evidence of growth of at least 2 to 3 mm, or more than 50% change in volume, or the development of new suspicious sonographic features. Overall, appropriate risk stratification for the management and follow up of thyroid nodules requires accurate initial characterization of the sonographic features of the nodule, proper selection of nodules to undergo fine-needle aspiration versus observation, and standardized communication of cytology results using Bethesda classification.

With regards to medical therapy for benign nodules, routine TSH suppressive therapy is not recommended. Although TSH suppression may lead to a modest deceleration of nodule growth, the potential adverse effects of long-term TSH suppression are thought to outweigh this minor treatment benefit. Iodine status should be assessed, and iodine deficiency should be treated with 150 µg of supplemental iodine daily.

Medullary Thyroid Cancer

Patients with MTC may present with a palpable mass in the thyroid or with cervical lymphadenopathy. In some patients, thyroid workup is undertaken because of the family history of medullary carcinoma, and in that setting, a clinically occult primary tumor may be identified. FNAC is usually sufficient to establish tissue diagnosis, but immunocytochemistry to determine the presence of calcitonin or serum calcitonin level may be helpful if the diagnosis is unclear. In addition to serum calcitonin, serum CEA is also a necessary part of the workup. All patients with a diagnosis of MTC should be counseled and tested for the presence of *RET* mutation, because absence of a family history is not sufficient to rule out inherited disease. Up to 7% of patients with apparently sporadic MTC harbor a germline mutation. This finding is especially true in persons with MEN 2B, for whom de novo germline *RET* mutation is seen in 50% of cases. Germline mutations are seen more commonly in younger patients or in those with multifocal disease, but they also may occur in older patients or in patients who present with a single thyroid nodule. Testing of all first-degree relative family members is recommended if the patient has a germline *RET* mutation. Additional workup includes contrast-enhanced CT scan of the neck and mediastinum to assess the presence and extent of regional lymph node metastasis to facilitate surgical planning. A whole-body FDG PET scan may be used to rule out distant metastases.

Staging

The American Joint Committee on Cancer (AJCC) and International Union Against Cancer (UICC), have jointly developed a uniform staging system, published in the eighth edition of the AJCC staging manual in 2016. For full details on the staging for all thyroid cancers, one should review the eighth edition staging manual published by the AJCC. However, the major changes in the recent revision mentioned here incorporate the biological behavior of differentiated thyroid cancer. In this revised staging system, patient's age is an important criterion distinguishing between high- and low-risk groups. This age cutoff is now advanced to 55 from the previous 45 years. In addition, other important changes include removal of microscopic extrathyroid extension to upstage a tumor to T3. For a tumor to be staged as T3, it should have gross minor (anterior) extrathyroid extension to strap muscles or perithyroid soft tissues. All gross major (posterior) extrathyroid extension would upstage the tumor to T4a. Further, lymph nodes at level VI and VII are now combined and included under the category N1a, and all lateral neck nodes are staged as N1b.

RADIOGRAPHIC EVALUATION

Currently used imaging techniques for the thyroid gland include ultrasonography, a CT scan, an MRI scan, a Technetium-99 or iodine-131 thyroid scan, and FDG-PET scanning. Ultrasonography is the most widely used imaging modality for initial evaluation of the thyroid gland and regional lymph nodes as has been described in detail previously. In most instances, no other specific radiographic studies are required when planning a surgical procedure on the thyroid gland. A CT scan of the neck is necessary when planning surgical treatment for patients whose primary tumors have extrathyroid extension to involve the central compartment structures like larynx or trachea. It is essential that the CT scan be performed with contrast enhancement for accurate assessment of the primary tumor as well as regional lymph nodes. CT and MRI scans also are useful in evaluating the retropharyngeal lymph nodes, which are not accessible for ultrasound examination. A thyroid scan provides functional evaluation of the thyroid gland, but this information generally is not useful in treatment planning. FDG-PET scanning is useful in selected patients, especially older patients with poorly differentiated tumors that are not expected to concentrate radioactive iodine.

Ultrasound is the first and often the only radiologic study required. It is more accurate than any other imaging study for small nodules and low-volume nodal metastases, particularly in the central compartment of the neck. It clearly differentiates between a solid, cystic, or a mixed echostructure nodule. Several sonographic features of the nodule increase the index of suspicion for malignancy. These are extrathyroid extension, irregular

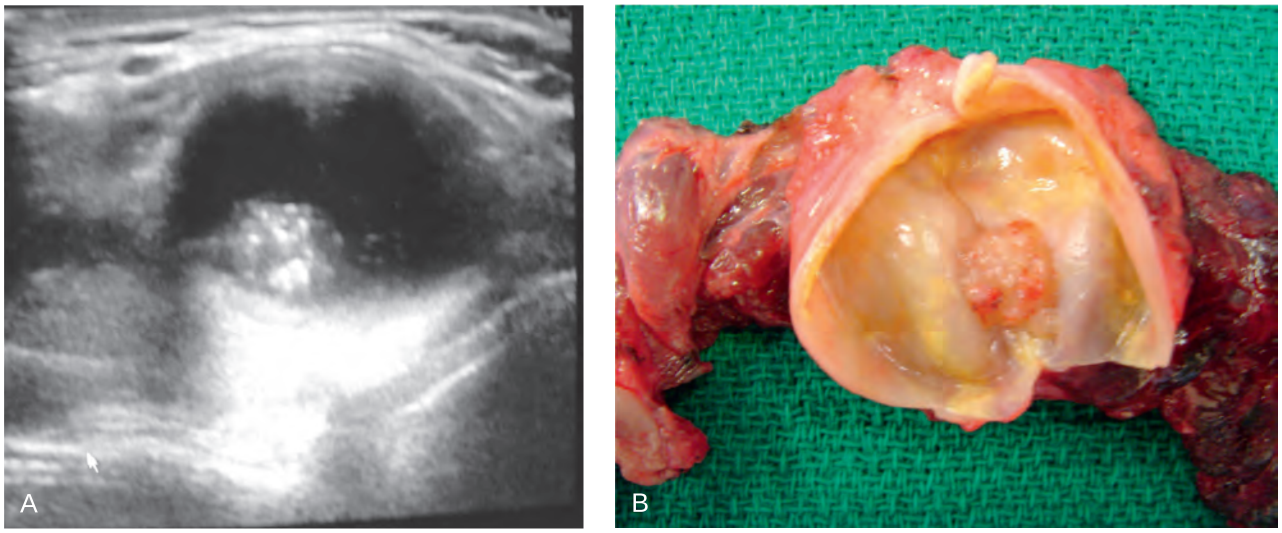

Figure 12.7 **A**, Sagittal view of the ultrasound of a cystic nodule showing an intracystic lesion with microcalcifications. **B**, Surgical specimen of the thyroid gland shown in **A** demonstrating an intracystic papillary carcinoma.

margins, microcalcification in the nodule, internal hypervascularity, and hypoechoic pattern. In addition, intracystic solid lesions particularly with microcalcifications within the nodule raise the suspicion for cancer. An example of a small intracystic papillary carcinoma suspected on an ultrasound and confirmed by surgical resection is shown in Fig. 12.7. Similarly, large cystic lesions with an intracystic growth with papillary fronds is highly suspicious for carcinoma, as can be seen on a CT scan in Fig. 12.8. The sonographic features with increasing index of suspicion for cancer to warrant the need for fine-needle aspiration biopsy are described in Table 12.1. In addition, ultrasound is a cost-effective and convenient way for imaging follow up after surgery, particularly in the office setting. On the other hand, CT scan is the most accurate structural study for the thyroid gland, the central compartment, lateral neck, and the mediastinum. In the past, it was felt that a contrast-enhanced CT scan should not be performed as initial imaging since iodinated intravenous contrast would interfere with radioactive iodine uptake and can compromise timing of postoperative adjuvant radioiodine treatment. However, it is now understood that delay in the administration of radioactive iodine by a few weeks does not have a negative impact in the overall outcome of patients with thyroid cancer. On the other hand, if extrathyroid extension of a thyroid tumor is suspected, or if lymph node metastases are identified clinically, good-quality cross-sectional imaging can provide crucial information regarding the relationship of the tumor to the central compartment viscera and the carotid artery and provide more comprehensive mapping of regional lymph nodes in the neck and mediastinum. Thus a contrast-enhanced CT scan is an important study in these patients for optimal assessment.

The patient shown in Fig. 12.9 has a 4- by 6-cm mass involving the upper pole of the right lobe of the thyroid gland that is adherent to the thyroid cartilage. The CT scan of the same patient (Fig. 12.10) shows invasion of the strap muscles with fixation of the tumor to the ala of the thyroid cartilage on the right-hand side. This patient requires resection of the thyroid ala for adequate excision of the thyroid cancer.

The patient shown in Fig. 12.11 has extensive recurrent carcinoma of the thyroid gland extending from the root of the

Figure 12.8 Coronal view of a contrast-enhanced computed tomography scan showing a large cystic lesion of the left lobe of thyroid with intracystic papillary carcinoma.

Figure 12.9 A patient with a tumor in the upper pole of the right lobe of the thyroid gland.

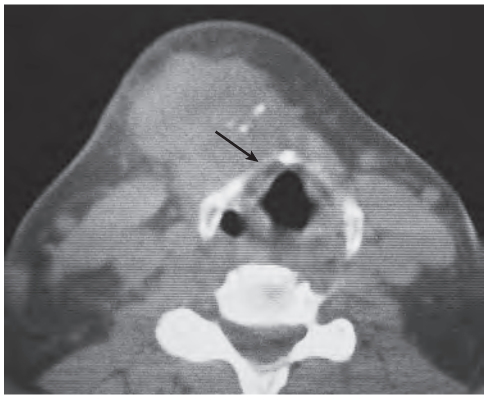

Figure 12.10 A computed tomography scan of the patient shown in Fig. 12.9.

neck into the superior mediastinum with encasement of the common carotid artery. A contrast-enhanced CT scan of the same patient (Fig. 12.12) clearly shows the common carotid artery completely surrounded by the recurrent tumor mass. This information greatly facilitates planning of surgical treatment, which in this patient required resection of the common carotid artery and replacement with a bypass graft.

MRI also provides anatomic information about the relationship of the tumor to the central compartment viscera and has the advantage of not interfering with radioactive iodine administration. It is also a study of choice for patients who have allergy to iodine contrast dye. However, the study takes considerably longer time to acquire compared with a CT scan and may be difficult to obtain in patients who are unable to lie flat or have difficulty swallowing with pooling of saliva. An axial image of the MRI scan of a patient with thyroid cancer demonstrates a locally advanced carcinoma with extension through the anterior tracheal wall into the lumen of the trachea and the subglottic larynx (Fig. 12.13). A sagittal view of the MRI scan of the same patient clearly demonstrates extension of tumor through the cricoid cartilage into the distal part of the subglottic larynx and proximal trachea (Fig. 12.14). An axial view of the MRI scan of another patient demonstrates a large recurrent mass of thyroid cancer extending up to the prevertebral space and displacing the trachea and esophagus with invasion of the muscular wall of the esophagus (Fig. 12.15). A sagittal view of the MRI scan of the same patient clearly shows the presence of the tumor between the trachea and the esophagus, causing anterior displacement of the membranous trachea with partial compromise of the air column (Fig. 12.16).

The greatest value of an MRI scan is in the assessment of a retrosternal goiter, particularly with respect to its relation to the great vessels in the mediastinum. An axial plane MRI scan of a patient with a large retrosternal goiter shows the location of the goiter in the mediastinum in relation to the great vessels

Figure 12.11 A patient with extensive recurrence of carcinoma of the thyroid gland.

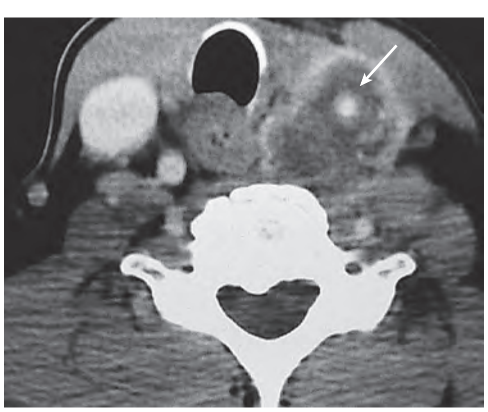

Figure 12.12 A computed tomography scan of the patient in Fig. 12.11 showing encasement of the carotid artery (*arrow*).

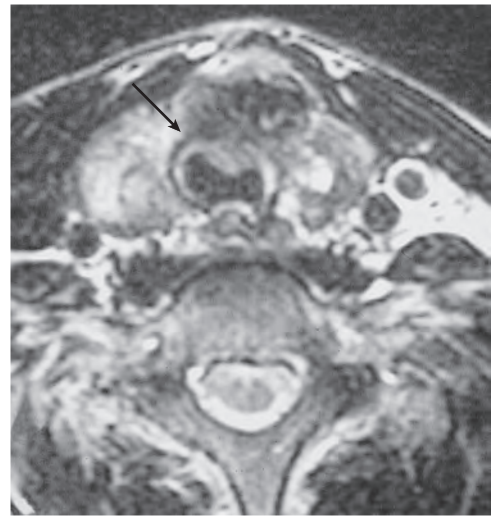

Figure 12.13 An axial view of a magnetic resonance imaging scan of a patient showing invasion of the anterior tracheal wall by thyroid cancer (*arrow*).

Figure 12.14 A sagittal view of the magnetic resonance imaging scan of the same patient shown in Fig. 12.13.

Figure 12.15 An axial view of a magnetic resonance imaging of a patient with recurrent thyroid cancer extending to the prevertebral space (*arrow*).

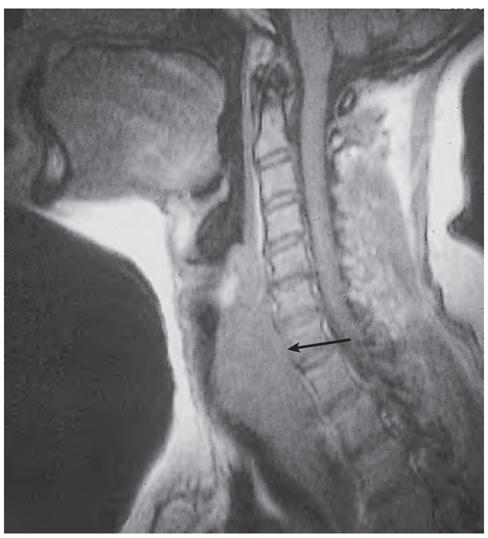

Figure 12.16 A sagittal view of a magnetic resonance imaging scan of the same patient shown in Fig. 12.15.

(Fig. 12.17). A coronal MRI scan of the same patient shows a 10- by 17-cm mass lateral to the trachea and just above the mainstem bronchus on the right-hand side in the mediastinum (Fig. 12.18). The sagittal section of the MRI scan clearly shows this massive retrosternal goiter in the anterosuperior mediastinum (Fig. 12.19).

MRI is also quite informative in demonstrating parathyroid abnormalities.

FDG-PET scanning relies on the demonstration of tumor-bearing tissue with increased glucose metabolism. This technique has been of immense value in identifying tumor deposits not seen on radioactive iodine scans or on routine imaging with CT or MRI. It is of value in patients with thyroid cancer that does not concentrate radioactive iodine (poorly differentiated carcinoma) and in patients with medullary carcinoma. It is well known that a direct relationship exists between the degree of differentiation of the tumor and its ability to concentrate radioactive iodine. In general, FDG-avid tumors are poorly differentiated, do not concentrate radioactive iodine, and have a worse prognosis compared with radioactive iodine–avid well-differentiated tumors that generally show low FDG avidity. Thus, with progressive anaplasia from well differentiated papillary carcinoma to poorly differentiated carcinoma and anaplastic

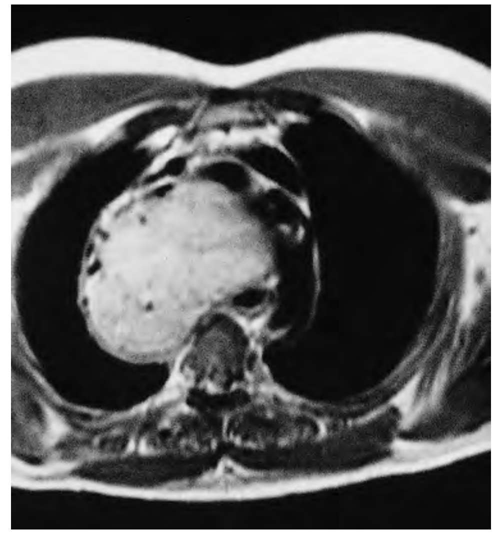

Figure 12.17 An axial view of a magnetic resonance imaging scan showing a large retrosternal goiter in relation to the great vessels.

Figure 12.18 A coronal view of the magnetic resonance imaging scan of the same patient shown in Fig. 12.17.

Figure 12.19 A sagittal view of the magnetic resonance imaging scan of the same patient shown in Figs. 12.17 and 12.18.

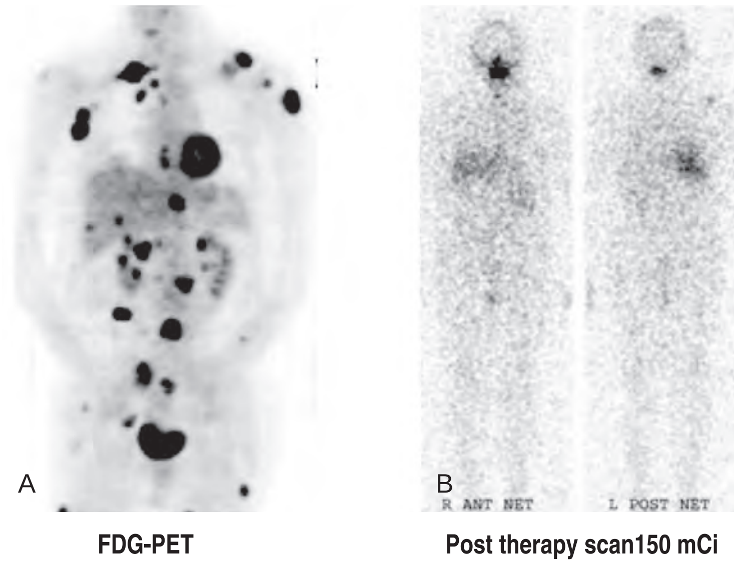

Figure 12.20 A positron emission tomography (PET) scan demonstrating extensive metastatic disease **(A)** that did not concentrate radioactive iodine **(B)**. *FDG-PET,* Fluorodeoxyglucose positron emission tomography.

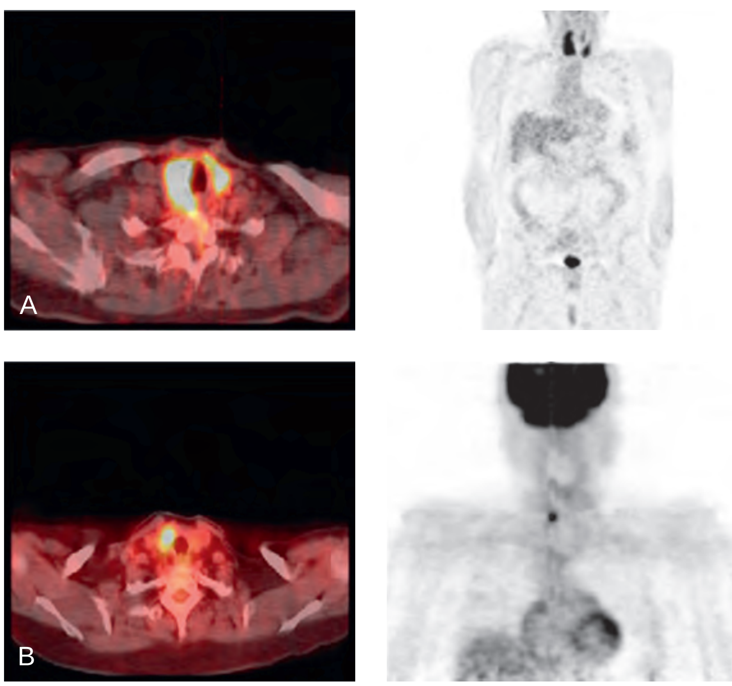

Figure 12.21 18-Fluorodeoxyglucose positron emission tomography scan showing diffuse uptake (**A**) in a patient with Hashimoto's thyroiditis and focal uptake (**B**) in a patient with papillary carcinoma of thyroid gland.

carcinoma, one can anticipate increasing FDG avidity (see Fig. 12.3). An example is a patient with extensive metastatic disease whose posttherapy radioactive iodine-131 scan showed very little presence of metastatic disease, but a whole-body PET scan shows extensive metastatic disease (Fig. 12.20). In addition, PET scan often detects clinically occult thyroid cancer. For example, PET scans done for other cancers often identify an incidental FDG-avid lesion in the thyroid gland. While diffuse uptake in the thyroid gland is often present in patients with Hashimoto's thyroiditis, focal uptake in a single lesion with the remaining thyroid gland not showing any FDG avidity demands further work up (Fig. 12.21). The risk of such a focal FDG-avid lesion being a primary thyroid carcinoma is nearly 60%. PET scanning also may be of value for localizing metastases in patients with medullary carcinoma with persistently high calcitonin levels after thyroidectomy.

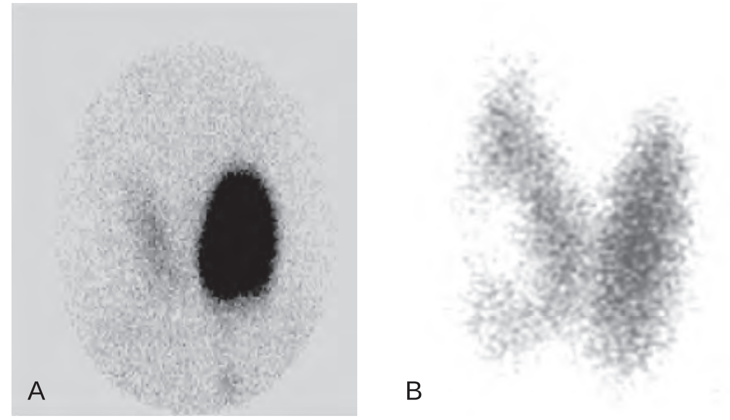

Figure 12.22 I-131 scans showing (**A**) a hot nodule and (**B**) a cold nodule.

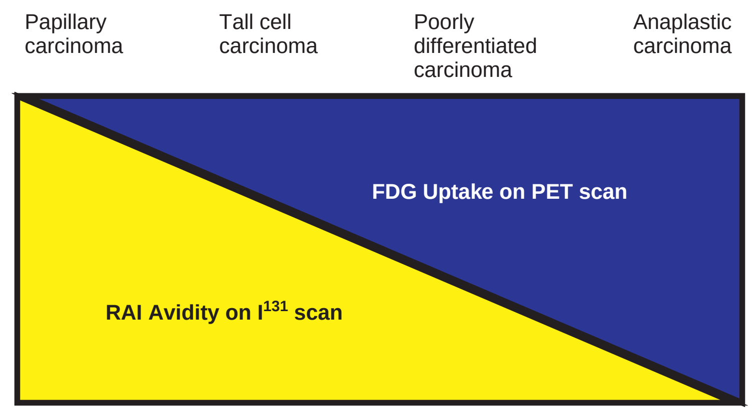

Figure 12.23 Iodine avidity declines, and fluorodeoxyglucose (FDG) uptake increases as the tumor progresses from well differentiated to poorly differentiated and anaplastic carcinoma.

Radioactive iodine (RAI) scanning was popular in the past for initial diagnostic workup imaging for thyroid nodules, but ultrasound has replaced it as the initial imaging study. However, occasionally, RAI scans may be done for initial workup. Four patterns can be seen on RAI scanning: (1) hot nodule, (2) cold nodule, (3) diffuse increased uptake, and (4) multinodular goiter (Fig. 12.22). Hot nodules are rarely malignant (3%–5%). Most cold nodules are benign. Diffuse increased uptake represents hyperthyroidism, and multinodular goiter is manifested by a mixed picture of cold and warm nodules. Currently, RAI scanning is used under three circumstances: (1) postsurgical assessment of residual functioning thyroid tissue, (2) post–RAI therapy whole body scan for demonstration of iodine avid disease, and (3) follow-up of iodine-avid residual, recurrent, or metastatic disease. However, it should be remembered that iodine avidity is essential for disease to be seen on an RAI scan. Generally, iodine avidity diminishes as the histologic differentiation of thyroid cancer progresses toward poorly differentiated and anaplastic carcinoma. Conversely, FDG avidity on PET scan increases as the tumor becomes less well-differentiated and metabolically more active (Fig. 12.23).

PATHOLOGY

Papillary carcinoma is the most common histologic type of thyroid cancer. The histologic spectrum comprises the classic papillary carcinoma and other variants such as tall cell variant, which are thought to have a more aggressive clinical behavior. The most recent World Health Organization classification of

Table 12.2 World Health Organization Classification of Thyroid Tumors

Follicular adenoma	8330/0
Hyalinizing trabecular tumor	8336/1
Other encapsulated follicular-patterned thyroid tumors	
Follicular tumor of uncertain malignant potential	8335/1
Well-differentiated tumor of uncertain malignant potential	8348/1
Noninvasive follicular thyroid neoplasm with papillary-like nuclear features (NIFTP)	8349/1
Papillary thyroid carcinoma (PTC)	
Papillary carcinoma	8260/3
Follicular variant of PTC	8340/3
Encapsulated variant of PTC	8343/3
Papillary microcarcinoma	8341/3
Columnar cell variant of PTC	8344/3
Oncocytic variant of PTC	8342/3
Follicular thyroid carcinoma (FTC), NOS	8330/3
FTC, minimally invasive	8335/3
FTC, encapsulated angioinvasive	8339/3
FTC, widely invasive	8330/3
Hürthle (oncocytic) cell tumors	
Hürthle cell adenoma	8290/0
Hürthle cell carcinoma	8290/3
Poorly differentiated thyroid carcinoma	8337/3
Anaplastic thyroid carcinoma	8020/3
Squamous cell carcinoma	8070/3
Medullary thyroid carcinoma	8345/3
Mixed medullary and follicular thyroid carcinoma	8346/3
Mucoepidermoid carcinoma	8430/3
Sclerosing mucoepidermoid carcinoma with eosinophilia	8430/3
Mucinous carcinoma	8480/3

NOS, Not otherwise specified.

thyroid tumors is shown in Table 12.2. An important and common variant is the follicular variant of papillary thyroid carcinoma, which is defined by the presence of follicles lined by cells having the nuclear features of papillary carcinoma. The follicular variant can be separated into completely encapsulated/well defined and infiltrative (either partially or not encapsulated). The encapsulated follicular variant without invasion has been shown to be very indolent, behaving like a follicular adenoma. It was therefore renamed noninvasive follicular thyroid neoplasm with papillary-like nuclear features (NIFTP). This diagnosis avoids overtreatment with aggressive surgery and/or radioactive iodine therapy.

Papillary carcinomas can be solid, cystic, or mixed cystic and solid on gross examination. They may be encapsulated and exhibit calcification on cut sections. The thyroid gland sometimes presents as a completely black gland, the so-called "black thyroid." This presentation occurs in patients who have undergone long-term therapy with tetracycline and particularly minocycline. The surgical specimen of a patient with multifocal papillary carcinoma in a black thyroid is shown in Fig. 12.24.

The differential diagnosis of follicular and Hürthle cell carcinomas from their adenoma counterparts is based on the demonstration of vascular and/or capsular invasion. This diagnosis is not feasible with cytologic evaluation and requires histologic evaluation of the thyroid nodule. Hürthle cell carcinomas tend to be more aggressive than follicular carcinomas and are now considered as a separate entity from follicular

Figure 12.24 Multifocal papillary carcinomas in a "black thyroid" in a patient who had received long-term treatment with minocycline.

carcinomas. Poorly differentiated carcinomas are at the histologic and behavior level intermediate between well-differentiated thyroid carcinoma and anaplastic thyroid carcinomas. Anaplastic thyroid carcinomas are characterized by pleomorphic cells (often spindle in shape), marked mitotic activity, tumor necrosis, and a lack of organoid formation (follicles, papillae, nests). These carcinomas have considerable genomic instability and a highly complex genome. Well-differentiated thyroid carcinomas exhibit immunoreactivity for thyroglobulin, PAX8 and thyroid transcription factor 1 (TTF-1), and the expression of these markers progressively diminishes with poorer differentiation. As the progression from a well-differentiated papillary carcinoma to anaplastic carcinoma takes place, there is progressive anaplasia with decreased RAI avidity and increased FDG avidity on a PET scan (see Figs. 12.3 and 12.23).

Medullary thyroid carcinomas are encountered more frequently in the middle third or upper half of the gland, and this distribution is thought to be due to the greater concentration of C cells in this region. The presence of amyloid is a characteristic histologic feature. Immunohistochemical diagnosis is very reliable and depends on demonstrating reactivity to calcitonin and carcinoembryonic antigen (CEA). Other neuroendocrine markers such as neuron-specific enolase (NSE) and chromogranins also may be positive.

TREATMENT

Surgery is the mainstay of treatment for nearly all thyroid neoplasms and symptomatic goiters as well as other conditions, such as thyroglossal duct cysts. The ultimate goal in the treatment of cancer of the thyroid gland is cure of cancer with minimal or no impact on the quality of life. Surgery plays a central role in the management of all types of thyroid cancers, with RAI-131 therapy used as adjuvant treatment. Administration of RAI is indicated for treatment of residual local or regional disease and for distant metastases and also for ablation of any remnant thyroid tissue left behind after surgery. However, RAI is beneficial only in patients who have iodine-avid differentiated cancer of the thyroid gland. Unfortunately, poorly differentiated and undifferentiated carcinomas that are clinically more

aggressive do not concentrate iodine, and therefore radioactive iodine is of little value in these patients. Nonetheless, RAI often is administered even in these patients, because many poorly differentiated tumors manifest heterogeneity and may have well-differentiated areas within the tumor that are RAI avid. Hürthle cell carcinomas also tend to take up RAI less often (in ~25% of cases). Treatment with RAI is not recommended in persons with anaplastic carcinomas, because these tumors do not concentrate iodine. Postoperative RAI therapy should follow a period of a low-iodine diet and a hypothyroid state induced by either thyroxine withdrawal or by administration of recombinant human (rh) TSH.

The role of external beam radiation therapy in the management of thyroid carcinoma remains controversial. However, it may be used in selected patients who have a high risk for failure in the central compartment. External beam radiation therapy is the mainstay of treatment for anaplastic carcinoma in combination with cytotoxic chemotherapy. The recent availability of targeted agents such kinase inhibitors that target the *RET* gene, vascular endothelial growth factor (VEGF) inhibitors, epidermal growth factor receptor (EGFR) inhibitors, and BRAF V600E inhibitors have opened a whole new landscape of systemic therapies in patients with metastatic disease and RAI refractory tumors. Clinical trials and early but limited data show effectiveness of drugs such as Vandetanib, Sorafenib, Lenvatinib, Selumetinib, Pazopanib, Cabozantinib in selected patients.

Treatment for MTC consists of surgery for the primary tumor and regional lymph nodes and occasionally for distant metastasis. External beam radiation therapy has a limited role and generally is used in an adjunctive or in a palliative setting. Similarly, systemic treatments have a role in the setting of a clinical trial or for palliation of symptoms.

SURGICAL TREATMENT

Neoplasms of Follicular Cell Origin

Benign adenomas confined to one lobe of the gland without any abnormality in the contralateral lobe are cured by an ipsilateral lobectomy. A total thyroidectomy is indicated for bilateral involvement. Patients with retrosternal extension require appropriate surgical intervention with a curative intent.

Management of patients with carcinomas of follicular cell origin is dictated by risk group stratification based on prognostic factors related to patient and tumor characteristics. The prognostic importance of age (≤55 versus >55 years), the size of the tumor (≤4 versus >4 cm), the extent of the tumor (i.e., the presence or absence of gross extrathyroid extension), the histologic differentiation (well versus poorly differentiated), and distant metastasis (present or absent) have been reported in several classification systems (Table 12.3). Based on these prognostic factors, risk groups can be identified to facilitate selection of therapy (Fig. 12.25). The intermediate-risk group consists of young patients with high-risk tumors or older patients with low-risk tumors.

All surgical procedures for the treatment of thyroid carcinoma or for tumors suspected to be cancers should be extracapsular operations leaving no residual thyroid tissue in the surgical bed. Procedures commonly described as a "subtotal" and "near-total" thyroidectomy are incomplete operations for malignant disease and are discouraged. In performing a true extracapsular thyroidectomy, particular attention should be paid to the pyramidal lobe, the upper pole, and the region of the Berry's ligament, where no thyroid tissue should be left behind. Following a "true extracapsular" total thyroidectomy, patients should not have any measurable serum Thyroglobulin (usually <1), thus avoiding the need for RAI ablation for "potential residual thyroid tissue (thyroid remnant)."

Low-risk patients with a unifocal, intrathyroidal tumor and a sonographically normal opposite lobe need an ipsilateral extracapsular lobectomy (including patients with tumors staged T1 and T2). Inasmuch as the primary tumor is intrathyroidal, the size difference between 1 cm and 4 cm has little impact on local control, regional lymph node metastasis, distant metastasis, or survival. An ipsilateral lobectomy is an adequate operation for definitive treatment in this setting. A total thyroidectomy should be considered for patients with bilateral nodularity (either clinically or sonographically identified thyroid abnormalities),

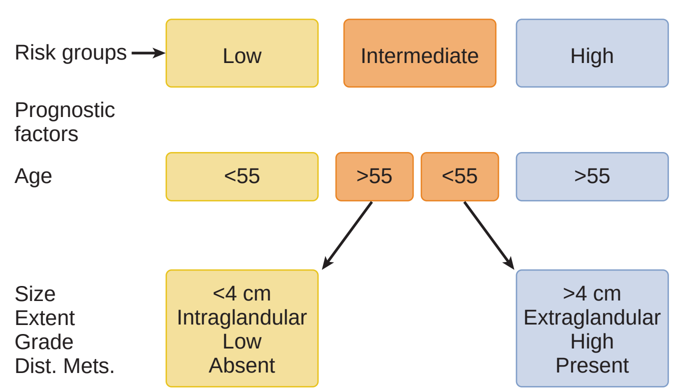

Figure 12.25 Risk group categories. *Dist. Mets.*, Distant metastases.

Table 12.3 The Prognostic Importance of Age and Gender of the Patient and the Size, Local Extent, Histologic Grade, and Deoxyribonucleic Acid Ploidy of the Primary Tumor, as Well as the Presence or Absence of Distant Metastasis, Have Been Reported in Several Major Studies.

MSKCC	MAYO CLINIC, 1987	MAYO CLINIC, 1993	LAHEY CLINIC	KAROLINSKA INSTITUTE
GAMES	**AGES**	**MACIS**	**AMES**	**DAMES**
Grade	Age	Distant Metastases	Age	DNA
Age	Grade Age	Age	Metastases	Age
Metastases	Extension	Completeness of Resection	Extension	Metastases
Extension	Size	Invasion	Size	Extension
Size		Size		Size

(Courtesy Memorial Sloan Kettering Cancer Center.)

regardless of the size of the primary cancer. Other indications for considering a total thyroidectomy in low-risk patients include a high-risk ipsilateral tumor with gross extrathyroidal extension, a history of radiation exposure, a strong family history of thyroid cancer, and extensive regional nodal metastases.

For high-risk patients, an extracapsular total thyroidectomy is the recommended surgical procedure. Minor extrathyroid extension (ETE) is no longer considered to upstage a tumor to T3. For a tumor to be staged T3, it has to be larger than 4 cm (T3a) or may have gross extrathyroid extension involving strap muscles (T3b). This degree of ETE is easily encompassed in a properly done total thyroidectomy with resection of the strap muscles, easily achieving an R0 resection. On the other hand, major or gross ETE to the posterior aspect of the thyroid gland is staged T4a with involvement of either the trachea, larynx, esophagus, or recurrent laryngeal nerve. These extensive tumors require adequate preoperative imaging for detailed assessment of the extent of the tumor to facilitate surgical treatment planning for complete resection. Preoperative CT scan with contrast is quite helpful in evaluating the extent of disease. An MRI may be complementary to give added information in a three-dimensional manner. The aim of surgical resection should be to achieve gross total clearance of all demonstrable disease (R0 resection). However, a primary total laryngectomy is required only rarely and is performed in highly selected patients based on histology and the probability of lack of iodine avidity of the cancer.

Patients in the intermediate-risk group require individualized treatment selection. Older patients with a low-risk, unifocal intrathyroidal tumor are equally well treated with a lobectomy. On the other hand, younger patients with high-risk tumors may require not only a total thyroidectomy but also more extensive operations based on the extent of their disease. Decisions about the extent of thyroidectomy are best made based on initial extent of disease, prognostic factors, risk group stratification, and anticipated need of RAI.

Completion total thyroidectomy is required in some patients who have undergone inadequate initial surgery, such as those who had an open biopsy or less than a lobectomy when a total thyroidectomy would have been indicated as the initial surgical procedure. Other indications for completion of a total thyroidectomy are patients who have undergone a lobectomy and (1) have indications for postoperative RAI, (2) have gross residual tumor that is resectable, or (3) have contralateral gross nodular disease that is suspicious for multifocal thyroid carcinoma.

Recurrent thyroid carcinoma poses specific challenges regarding preservation of the larynx and its function, the parathyroid glands, and the integrity of the esophagus and adjacent neurovascular structures. Historically, in the past the most common cause of mortality from carcinoma of the thyroid was uncontrolled local/regional disease leading to asphyxia, hemorrhage, and inanition. However, in the past three decades that scenario has changed due to appropriate selection of cases and aggressive initial surgical procedures achieving an R0 resection. Thus control of disease in the central compartment is of paramount importance because it improves longevity in many patients and quality of life in nearly all. The issues to be considered in resection include (1) the goal of surgical intervention (i.e., curative treatment versus symptomatic palliation), (2) the feasibility of (R0) gross total resection, (3) the availability and efficacy of alternate means of treatment, and (4) the sequelae of surgery.

Anaplastic thyroid carcinoma poses unique challenges for the surgeon. The role of the surgeon is generally to establish tissue diagnosis and management of the airway. In rare circumstances, anaplastic carcinoma may be surgically resectable, as in the case of anaplastic carcinoma developing in a preexisting nodular goiter and confined to the goiter or as a small component of a poorly differentiated resectable carcinoma. An elective tracheostomy for prevention of airway distress in most patients with an anaplastic carcinoma requires careful consideration of the overall treatment plan and prognosis and is rarely indicated unless the patient is in impending airway distress. Multidisciplinary discussion is required to inform the patient and the family of the dismal prognosis and the anticipated course of events. If a decision is made to perform a tracheostomy, it should be done after endotracheal intubation under general anesthesia in the operating room with all available support. Technically, tracheostomy may be very difficult due to the presence of gross disease in front of the trachea, and also, the potential of the tumor which may grow through the tracheostomy. Therefore, if possible, placing the tracheostomy in the usual suprasternal location should be avoided. It is desirable to perform a cricothyrotomy and use a long tracheostomy tube to provide a safe airway into the distal trachea.

Regional lymph node dissection is recommended for clinically palpable or radiologically identified metastatic lymph nodes on imaging studies (ultrasound or CT scan) before thyroidectomy. Routine elective dissection for removal of possible micrometastases in regional lymph nodes is not recommended, because it offers no benefit to the patient and may increase morbidity. Elective dissection of central compartment lymph nodes may be considered in patients undergoing thyroidectomy for advanced primary tumors. The surgical procedure for excision of gross metastases should be a systematic compartmental dissection of regional lymph node groups. Excision of isolated lymph nodes ("berry-picking") is not recommended. The presence of lymph node metastases in the central compartment (N1a) requires a systematic dissection of lymph nodes from the hyoid bone cephalad to the innominate artery caudad, and between the two carotid sheaths (levels VI and VII). Lateral neck metastases (N1b) require a systematic dissection of lymph nodes from levels IIA to V. Metastatic disease at level I and level IIB is rare, and dissection of these regions is recommended only if contiguous gross nodal metastases are present. Involvement of mediastinal lymph nodes below the innominate artery is infrequent, and surgical resection should be considered carefully in the context of the overall status of the disease and the patient. On the other hand, dissection of anterosuperior mediastinal lymph nodes (level VII) is feasible through the cervical approach and should be included in central compartment node dissection. However, massive metastases or metastatic disease inferior to the innominate artery may require a sternotomy.

Medullary Thyroid Carcinoma

Surgery is the only effective treatment for MTC, and thus comprehensive surgical resection of the primary tumor and involved lymph nodes is crucial to achieve local/regional control and improve survival. Lobectomy for a small unifocal intrathyroidal primary tumor in a patient with sporadic MTC is acceptable. On the other hand, a total thyroidectomy with central compartment lymph node dissection is the recommended surgical procedure for most patients whose diagnosis is confirmed preoperatively. Elective dissection of lymph node groups at risk in the lateral neck is controversial. However, if metastatic disease is identified clinically or radiologically, a comprehensive systematic compartmental neck dissection is required. The decision

about elective lateral neck dissection is also made based on the size of the primary tumor, presence of central compartment nodal metastases, and preoperative calcitonin level. Surgery on the thyroid gland and regional lymph nodes is recommended even in the presence of distant metastases, because control of disease in the neck directly affects the quality of life of these patients. When the diagnosis of MTC is made as an incidental finding in a thyroidectomy specimen, the patient should undergo studies for calcitonin levels, ultrasound of the neck, and *RET* mutation. If findings of these studies are normal, further surgery is not necessary.

Genetic testing is indicated in family members of a patient who tests positive for *RET* mutation. The timing of genetic testing and the treatment of family members is based on the type of mutation present in the patient. The ATA has classified mutations into four risk groups. Level A mutations include 768, 790, 791, and 891. Persons with these mutations generally have indolent, late-onset MTC. Testing for *RET* mutation in children of these patients is recommended at 3 to 5 years of age, and prophylactic surgical treatment may be deferred until an older age (>5 years) as long as thyroid ultrasound and serum calcitonin levels are normal. The rationale to delay treatment is to minimize the risk of permanent hypoparathyroidism in infants. ATA level B mutations include 609, 611, 618, 620, and 630. Patients with these mutations have slightly earlier onset of MTC, and a prophylactic thyroidectomy is recommended for their children before age 5 years who have the *RET* mutation. ATA level C includes patients with mutation 634. Elective thyroidectomy is recommended in children harboring this mutation before the age of 5 years, because MTC develops earlier and clinically is more aggressive. Finally, the ATA level D risk group, which includes mutations 883 and 918, is associated with very early onset of medullary thyroid cancer that often is aggressive. Elective treatment of children who test positive for these mutations is recommended as soon as possible, even before age 1 year.

SURGICAL ANATOMY

The thyroid gland descends from the foramen cecum of the base of the tongue to the lower part of the neck during embryonic development. During this descent, the normal thyroid remnant or the entire thyroid may remain at the foramen cecum (lingual thyroid) or along the thyroglossal tract. The presence and extent of thyroid tissue along the thyroglossal tract determines the presence or absence of the pyramidal lobe. In some instances, thyroid tissue gets sequestered along the thyroglossal tract and may present as a thyroglossal duct cyst. Occasionally, sequestered thyroid tissue may be found in the mediastinum below the normal position of the gland in the neck.

The blood supply to the thyroid gland is derived from the branches of the superior and inferior thyroid arteries. Occasionally, a midline thyroidea ima provides blood supply to the isthmus directly from the innominate artery. Numerous venous tributaries drain into the internal jugular and innominate veins. The primary lymphatic drainage of the thyroid gland is to the perithyroid and paratracheal lymph nodes. Anteriorly, it may drain into the Delphian lymph node. Secondary drainage occurs into lymph nodes in the anterosuperior mediastinum and deep jugular nodes.

The laryngeal nerves lie in close juxtaposition to the thyroid gland and hence are important in thyroid surgery. The superior laryngeal nerve arises from the vagus and traverses posteromedial to the superior thyroid artery. It divides into an internal branch, which enters the larynx through the thyrohyoid membrane, and an external laryngeal branch which descends with the superior thyroid artery and turns medially over the cricothyroid muscle, for which it is the motor nerve. Usually it is located just cephalad to the superior pole of the thyroid lobe. The terminal branches of the superior laryngeal nerve have a variable relationship with the distal branches of the superior thyroid artery, the cricothyroid muscle, and the superior pole of the thyroid gland (Fig. 12.26). The recurrent (inferior) laryngeal nerves arise from the vagus in the mediastinum and return to the neck around the arch of the aorta on the left-hand side and around the innominate artery on the right-hand side. Thus the left recurrent laryngeal nerve ascends parallel to the trachea while the right nerve travels from lateral to medial as it ascends in the neck. Normally the inferior thyroid artery is located anterior to the recurrent laryngeal nerve, but numerous variations are seen in this relationship (Fig. 12.27). The recurrent laryngeal

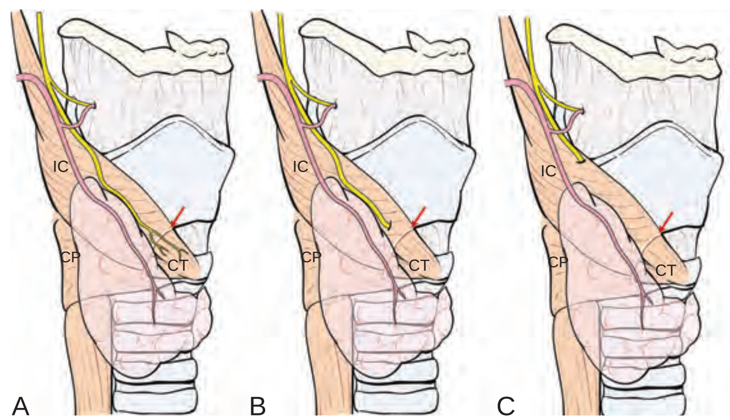

Figure 12.26 Variations in anatomic relations of the external branch of the superior laryngeal nerve (ESLN). **A**, The ELSN is superficial to the inferior constrictor (IC) muscle and runs along superior thyroid vessels so that it is visible in its entire course up to the cricothyroid (CT) muscle. **B**, The ESLN pierces the IC muscle approximately 1 cm above the cricothyroid membrane (*red arrow*) so that only its upper portion is at risk for injury. **C**, The entire ESLN runs deep to the IC muscle and therefore is protected from unintended injury during dissection of the superior thyroid pole. *(Courtesy Memorial Sloan Kettering Cancer Center.)*

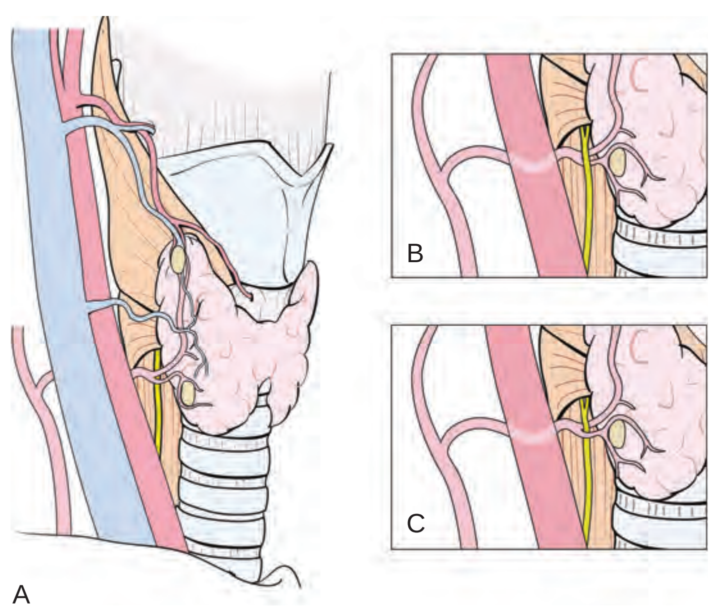

Figure 12.27 Anatomic relationships of the recurrent laryngeal nerve to the inferior thyroid artery. **A**, Posterior. **B**, Anterior. **C**, Between branches of the inferior thyroid artery. *(Courtesy Memorial Sloan Kettering Cancer Center.)*

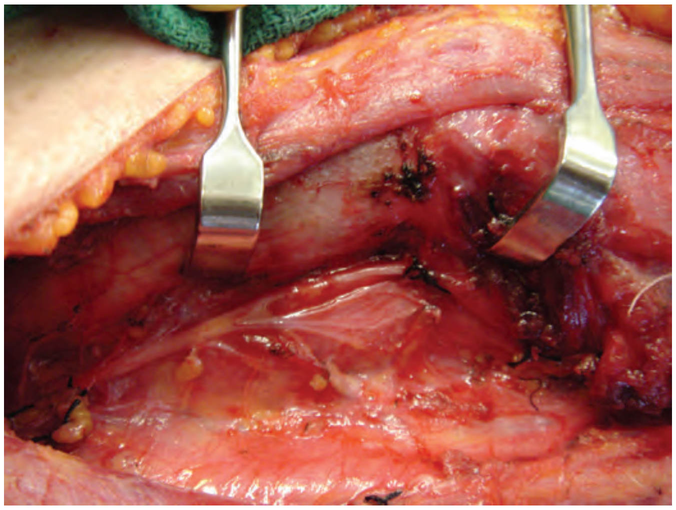

Figure 12.28 The recurrent laryngeal nerve may divide into several branches before entering the larynx.

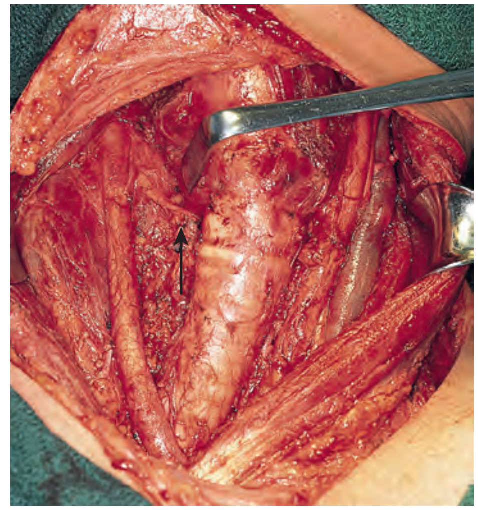

Figure 12.30 Nonrecurrent (inferior laryngeal) nerve, entering the cricothyroid membrane (*arrow*).

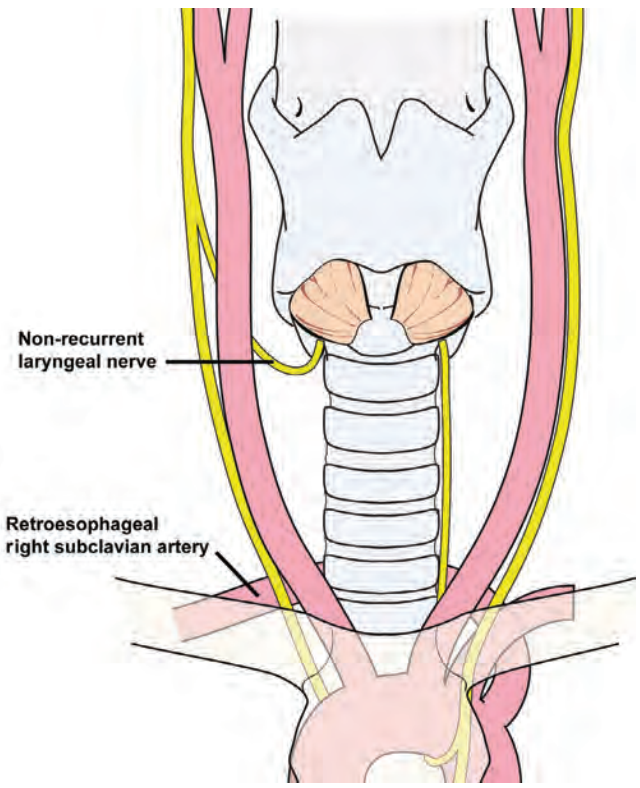

Figure 12.29 Nonrecurrent right inferior laryngeal nerve. *(Courtesy Memorial Sloan Kettering Cancer Center.)*

nerve may divide into several branches before entering the larynx (Fig. 12.28). In such instances it is vital that each of these branches be carefully preserved during thyroid surgery, because it is impossible to predict which particular branch will have the major role in function of the vocal cord. Occasionally the right recurrent laryngeal nerve does not ascend from the mediastinum but arises from the vagus nerve in the neck to directly enter the larynx (nonrecurrent right inferior laryngeal nerve) (Fig. 12.29). An example is shown in Fig. 12.30.

Blood supply to the parathyroid glands is derived from the inferior and superior thyroid arteries. Careful dissection of the parathyroid glands with their blood supply intact is crucial during thyroidectomy. While the major blood supply to both parathyroid glands comes from the inferior thyroid artery, several small collateral arterial branches from the superior thyroid artery also provide blood supply to the superior thyroid glands.

PROCEDURES

Minimally Invasive, Endoscopic/Video-Assisted, and Remote Access/Robotic Techniques of Thyroidectomy

Over the course of the past two decades, there has been increasing interest in employing minimally invasive or remote access techniques for thyroidectomy to avoid a scar in the neck resulting from a "conventional thyroidectomy." The explicit purpose for using these approaches is to minimize the length of the scar in the neck or to avoid an incision in the neck altogether for thyroid lobectomy or total thyroidectomy. These techniques have gained popularity among some surgeons largely because of the availability of endoscopic and robotic instrumentation and are fueled by technologic developments and industry. In general, the concept of minimally invasive surgery is gaining popularity in all specialties, largely because of the reduction of surgical morbidity associated with conventional open operations and improved aesthetic appeal of smaller scars or no visible scars as a result of incisions in remote locations. This is particularly true for surgical procedures in the abdomen and in the thorax. When resections of neoplasms, particularly malignant neoplasms, are dealt with, however, strict criteria for using minimally invasive procedures must be adhered to so as not to compromise an oncologically complete and safe surgical procedure. Clearly, thyroid surgery is no exception to these general guidelines. With increasing concern on the part of patients undergoing thyroid surgery, with reference to the aesthetic result of the surgical scar in the neck, thyroid surgeons have become sensitive to these concerns of the patients and have used smaller and smaller incisions, placed in natural skin creases, where appropriate, for thyroidectomy.

Minimally Invasive Thyroidectomy

In general, most patients with relatively small lesions (nodules or tumors) are suitable for using smaller incisions (2–2.5 cm) for performing a thyroid lobectomy or total thyroidectomy. It is crucial, however, that the incision be placed in a natural skin crease, closer to the cricoid cartilage. Thus progressively smaller incisions have been used over the course of the past several years. Not all patients, however, are suitable for surgery through small incisions, and strict criteria must be met to perform a satisfactory, safe, and oncologically uncompromised surgical

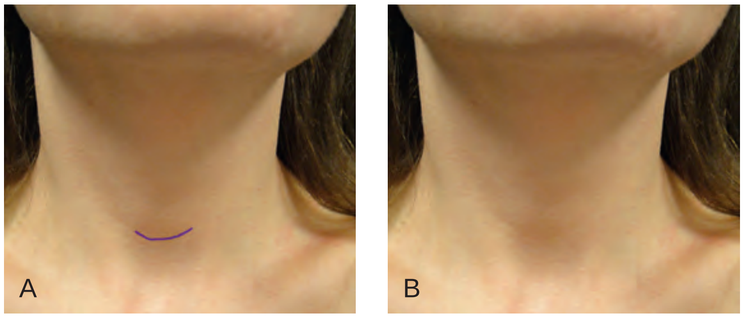

Figure 12.31 **A**, Planned incision for minimally invasive thyroidectomy in a natural skin crease close to the cricoid cartilage. **B**, Healed scar 1 year after surgery.

procedure. Therefore the following are indications for minimally invasive thyroidectomy (using a small incision):

1. The thyroid nodule is benign.
2. The cancer is intrathyroidal.
3. The nodule or tumor is small (<3 cm in diameter).
4. The thyroid gland is small (5–6 cm).
5. There is no need for regional lymph node dissection.
6. The patient does not have Hashimoto's thyroiditis.
7. The patient is not obese.
8. There is no previous surgery in the neck or superior mediastinum.

If these criteria are met, then minimally invasive thyroidectomy can be safely performed, either with or without the need for endoscopic or video-assisted techniques. Most patients undergoing a minimally invasive thyroidectomy do not need a drainage tube from the surgical field and can have a simple primary closure of the incision. An example of such a small incision and eventual aesthetic outcome from a minimally invasive thyroidectomy without endoscopic or video assistance is shown in Fig. 12.31.

Minimally Invasive Endoscopic or Video-Assisted Thyroidectomy

All the criteria mentioned previously for minimally invasive thyroidectomy must be met, even when endoscopic assistance is used. In some patients, exposing the thyroid gland through a small incision (approximately 2 cm) provides a limited exposure for open access operations. Technologic advances with the development of instrumentation for better vision (telescopes, cameras, and video monitors) and minimal access/endoscopic instrumentation for dissection and for homeostasis (bipolar electrocautery, vascular clips, ultrasonically activated shears, and electrothermal bipolar sealing systems) have permitted the development of safe endoscopic or video-assisted minimally invasive thyroidectomy. Clearly, the view obtained by the telescopes on a video monitor is magnified severalfold and is superior to open-eye view. However, the familiarity and ease of using endoscopic instrumentation require training and practice to develop the necessary expertise. The procedure requires two assistants in addition to the operating surgeon for smooth conduct of the operation. A disadvantage of this technique is that the skin edges of the incision are significantly traumatized because of excessive stretching from retraction and may be inadvertently torn or traumatized by the instruments because of severe retraction. These traumatized skin edges often require trimming before closure. Sometimes, this results in an aesthetically unacceptable and hypertrophic scar, although it may be small in length.

Remote Access Robotic Thyroidectomy

In certain parts of the world, young female patients have preferred to have thyroidectomy, avoiding an incision in the neck altogether. To address this issue, thyroid surgeons have developed remote access robotic techniques, approaching the thyroid gland from remote locations. These techniques are (1) through a postauricular incision below the hairline in the neck, (2) through an axillary incision either unilaterally or bilaterally, and (3) through a periareolar incision on the breast or an incision on the anterior chest wall for introducing the camera arm of the robot. Although these techniques avoid the placement of a small incision in the neck, they require much larger incisions at the site of entry of the robotic arms and require a tremendous amount of soft tissue dissection and mobilization of flaps through an extended area to approach the thyroid gland and thus cause significant tissue trauma. In addition, if total thyroidectomy is necessary, a bilateral approach may be required. The operating time is clearly much longer, and significant technical expertise is required in accomplishing a robotic thyroidectomy. The cost of the procedure to the patient thus increases severalfold.

As mentioned previously, a variety of minimally invasive endoscopic and remote-access thyroid surgery approaches are reported in the recent literature. The value of these approaches remains debatable, largely due to excessive tissue trauma, as a result of dissection from remote sites simply to avoid a cervical incision. These include transaxillary robotic, transoral, and endoscopic through small incision over the thyroid gland or through a hairline suboccipital incision. However, whether they are truly minimally invasive or simply "minimal access" remains a subject of controversy. Clearly adequate exposure to conduct a proper "cancer operation" should be the first consideration in any operative procedure planned for thyroid cancer. In addition, the cost of these procedures and the additional time involved is also of great concern. The average time required for endoscopic or remote access surgical procedures is almost twice as much compared with a regular cervical approach. The only major advantage of these approaches is to avoid a scar in the neck. However, most patients are quite happy and comfortable with a well-placed scar of just the required length in a natural skin crease in the neck. Avoidance of excessive stretch of skin flaps through a small incision and meticulous skin closure results in a very acceptable and almost invisible scar in a natural skin crease.

The endoscopic approaches can be divided into cervical and extracervical approaches. The cervical approach is to make a small incision in the neck and perform dissection with the assistance of a video telescope. This approach has not gained much popularity outside a few centers. The extracervical approach includes a variety of techniques, including transaxillary robotic surgery, a bilateral breast and axillary approach, or an inframammary or periareolar approach. All these approaches have their pros and cons, including making an incision on the breast. The long-term effects of the incision on the breast and dissection through and around the breast remain unclear. Whether this has any direct impact on the long-term mammographic changes has also not been reported yet. Further, long-term cancer-related outcomes remain to be seen.

There appears to be some interest in a postauricular facelift approach. Again, there are several limitations of this approach, including difficulties in central compartment dissection, difficulties in evaluating the extrathyroid extension of the disease, and the trauma produced by extensive tunneling and dissection.

What remains somewhat unclear at this stage is what happens to these individuals when they develop recurrent disease either in the thyroid bed or in the cervical lymph nodes, and how easy or difficult is the "reoperation." A majority of the thyroid surgeries performed in the United States are primarily for proven thyroid cancer or for a nodule suspicious for cancer. Whether these approaches are most appropriate for suspected thyroid cancer remain unclear. The goal in the management of thyroid cancer should be the best oncologic procedure the first time. Apart from avoiding a scar in the neck, there does not appear to be any definite benefit of these surgical approaches, which obviously have a long learning curve and high incidence of major complications. Recently there appears to be considerable interest in natural orifice thyroid surgery. There appears to be special interest in the transoral or sublabial approach. However, similar issues and comments made previously for other endoscopic procedures apply for transoral thyroidectomy. The gold standard of thyroid surgery still is transcervical standard cervical approach.

Although the currently available and technologically supported minimally invasive thyroidectomy techniques may be appealing to some surgeons and patients for a variety of reasons, these techniques must be offered to patients selectively by appropriately trained surgeons who have the experience and the requisite infrastructure. Clearly, however, it must be remembered that these techniques are applicable only to relatively small tumors in patients with small thyroid glands and in patients who meet all the criteria mentioned previously for minimally invasive thyroidectomy. For most patients who require thyroidectomy, in the hands of a well-trained surgeon, a relatively small incision (2.5–3 cm), placed in a natural skin crease, closer to the cricoid cartilage, results in a perfectly acceptable scar.

Excision of the Thyroglossal Duct Cyst

A thyroglossal duct cyst is a developmental anomaly that may manifest clinically as a cystic mass. It generally presents at a young age, but the appearance of a thyroglossal duct cyst in adults is not uncommon. In an adult, it usually is preceded by an episode of upper respiratory tract infection. The thyroglossal duct cyst may arise anywhere along the thyroglossal tract, which extends from the foramen cecum (on the dorsum of the tongue at the junction of its posterior and middle third) to the isthmus of the thyroid gland. The thyroglossal tract is invaginated during development by the hyoid bone, and therefore it curves behind the hyoid bone along its course. This location has specific surgical significance, because if a segment of the patent tract is left behind the hyoid, local recurrence of the cyst will take place. Therefore a segment of the central third of the hyoid bone should be excised to totally resect the entire thyroglossal tract (referred to as a *Sistrunk operation*). An example of a thyroglossal duct cyst extending into the preepiglottic space posterior to the hyoid bone is shown in Fig. 12.32. The surgical field demonstrating extension into the preepiglottic space and the specimen after a Sistrunk operation are shown in Fig. 12.33.

The cyst usually presents in the midline, but occasionally it may have a paramedian location. Most thyroglossal cysts do not have connections with a patent tract. The patient whose CT scan is shown in Fig. 12.34 has a 5-cm mass in the infrahyoid region overlying the thyrohyoid membrane. This patient also had a multinodular thyroid gland for which a total thyroidectomy was deemed appropriate. Patients whose thyroid glands are clinically and radiologically normal do not need a thyroidectomy, even in the presence of a well-differentiated carcinoma that is confined to the cyst.

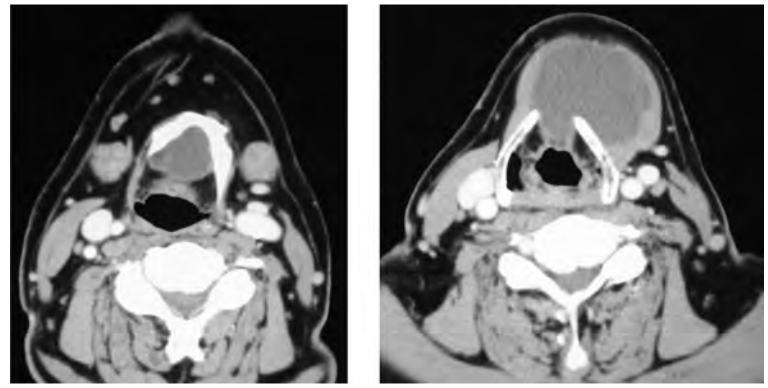

Figure 12.32 An axial view of a contrast-enhanced computed tomography scan showing extension of the thyroglossal duct cyst into the posthyoid preepiglottic space.

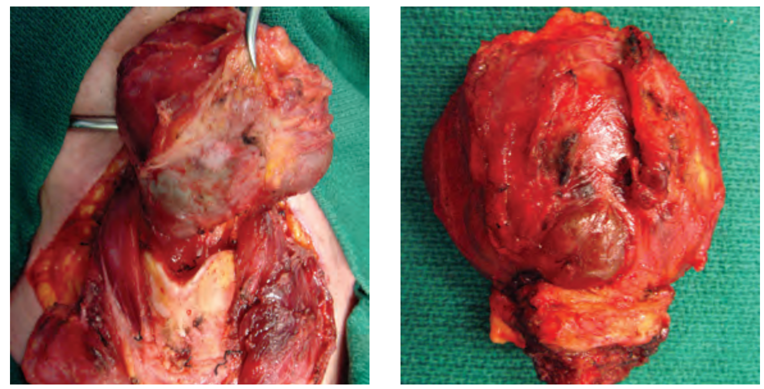

Figure 12.33 The surgical field showing extension into the preepiglottic space and the specimen.

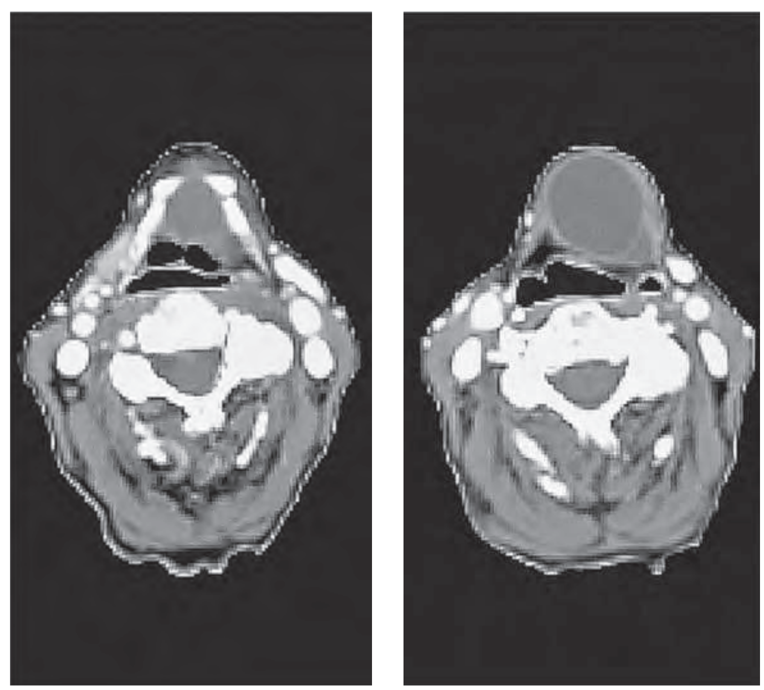

Figure 12.34 An axial view of a computed tomography scan at the level of the thyrohyoid membrane showing the bilobulated mass.

The operative procedure is performed under general endotracheal anesthesia. The patient is placed in supine position on the operating table with the neck extended. The incision is outlined in relation to the location of the palpable mass along an upper neck skin crease. The incision should be placed

Figure 12.35 Outline of the incision and the clinically palpable mass overlying the thyrohyoid membrane.

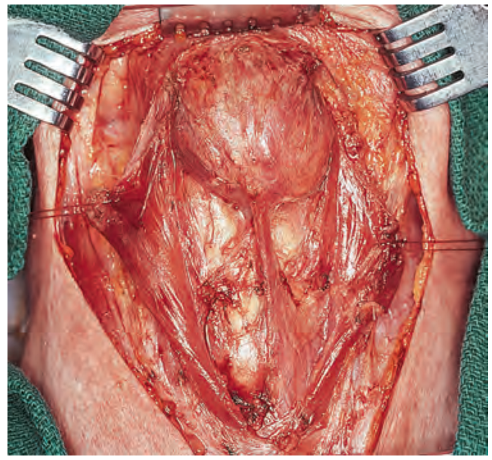

Figure 12.36 The soft tissues surrounding the cyst are carefully dissected.

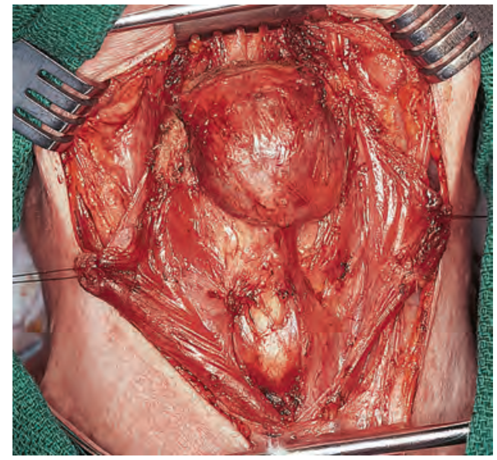

Figure 12.37 The infrahyoid strap muscles are divided.

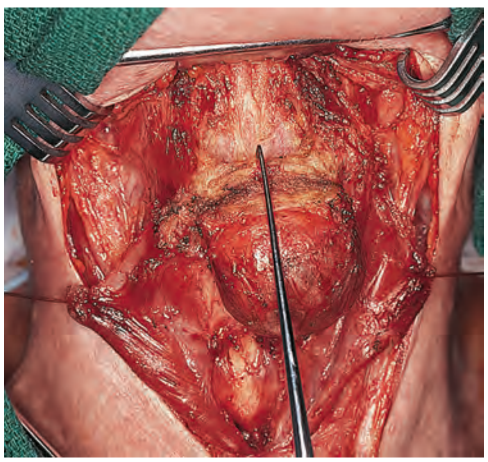

Figure 12.38 The mylohyoid and hyoglossus muscles are detached from the central third of the hyoid bone.

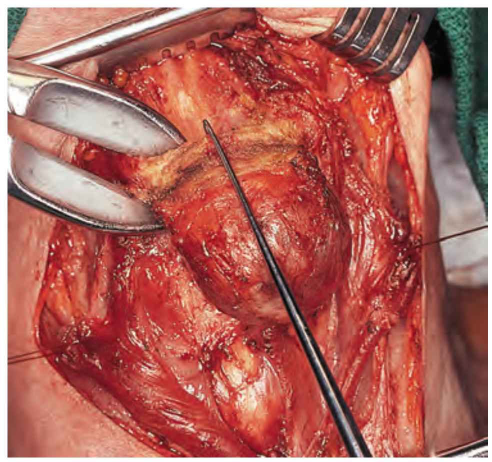

Figure 12.39 The hyoid bone is divided on both sides.

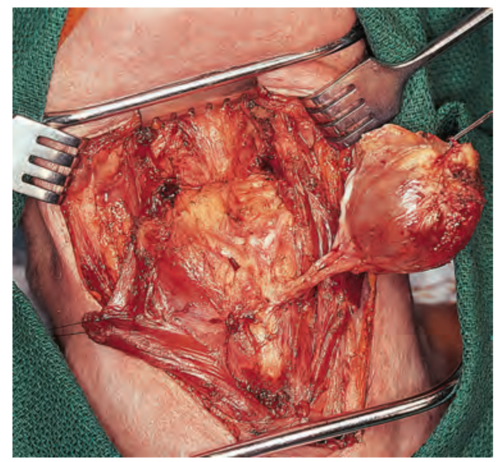

Figure 12.40 The cyst is retracted caudad.

so it is adequate for excision of the cyst; it also should provide access to the hyoid bone.

The clinically palpable mass is shown in Fig. 12.35. An incision is made over the mass at the level of the thyrohyoid membrane. It is deepened through the platysma, and the upper and lower skin flaps are elevated with an electrocautery. In the left side of the exposed field, the cyst is located beneath the deep cervical fascia. The soft tissues surrounding the thyroglossal cyst are dissected with extreme care to avoid rupture of the cyst (Fig. 12.36).

Large cysts have a thin wall and are particularly vulnerable to rupture during mobilization. Division of the infrahyoid strap muscles facilitates exposure (Fig. 12.37). The hyoid bone adjacent to the cyst is denuded of its musculature, which is detached with the electrocautery (Fig. 12.38). The central third of the hyoid bone is divided with a bone cutter, remaining medial to the lesser cornua on each side (Fig. 12.39). The thyroglossal tract usually runs in the midline on the posterior aspect of the hyoid bone, as seen in the preoperative CT scan. After the hyoid is divided on both sides, it is grasped with an Ellis clamp and gently retracted to give a pull to the underlying soft-tissue attachments of the cystic mass.

At this point a meticulous search for the thyroglossal duct tract should be undertaken, and it should be followed cephalad as far as it can be traced (Fig. 12.40). After separation of the deeper soft-tissue attachments in the lower part, the specimen is retracted caudad, and the thyroglossal tract is followed further

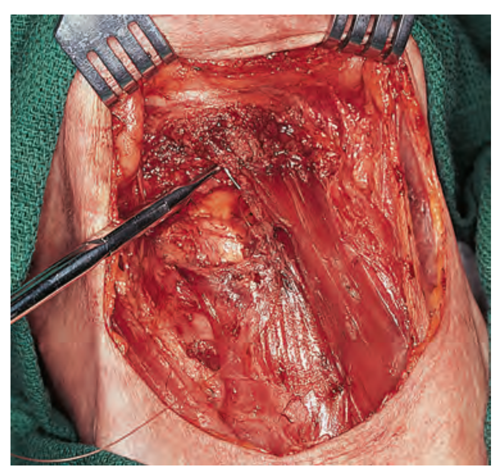

Figure 12.41 The surgical field after excision of the cyst.

cephalad in the musculature of the base of the tongue if it continues toward the foramen cecum.

Fig. 12.41 shows the surgical field after removal of the thyroglossal cyst, demonstrating the thyrohyoid membrane and the central part of the preepiglottic space, which are exposed because of the removal of the central segment of the hyoid bone. The wound is now irrigated with Bacitracin solution. A small Penrose drain placed in the field is brought out to the edge of the incision. Alternatively, a small, closed suction drain

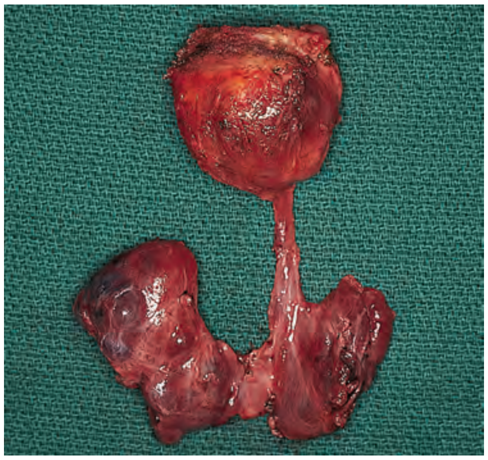

Figure 12.42 The surgical specimen consists of the thyroglossal cyst, the central third of the hyoid bone, and the entire thyroid gland. A total thyroidectomy usually is not indicated but was performed in this patient because of the presence of a multinodular goiter.

may be used. The incision is then closed in two layers using 3-0 chromic catgut interrupted sutures for platysma and 5-0 nylon for skin. The surgical specimen shows the intact cyst excised with the central third of the hyoid bone and the remnant of the thyroglossal tract (Fig. 12.42).

Postoperative care is minimal. The Penrose drain is removed when serosanguineous drainage is scanty. Primary wound healing should be expected, and the skin sutures may be removed at the end of 1 week. Recurrence of a thyroglossal duct cyst is rare and occurs only if a portion of the patent thyroglossal tract or a part of the cyst wall is left behind at the time of surgery.

Thyroid Lobectomy

A total extracapsular thyroid lobectomy is the operation performed most frequently on the thyroid gland for patients presenting with a solitary nodule. Often these are unifocal intrathyroidal papillary carcinomas. Solitary mass lesions of the thyroid gland that are confined to one lobe and are possibly neoplastic are best treated with a diagnostic as well as therapeutic thyroid lobectomy. The specimen that is removed contains the entire lesion, which provides accurate diagnosis and, in most instances, adequate treatment, if it proves to be a well-differentiated cancer and the opposite lobe is normal.

The patient shown in Fig. 12.43 has a 3-cm, smooth, fleshy lesion confined to the right lobe of the thyroid gland. The left lobe has no palpable abnormalities and preoperatively showed no abnormalities in the opposite lobe. The patient is placed under general endotracheal anesthesia in the supine position on the operating table with the neck extended. The palpable thyroid mass is shown. The skin incision should be placed in a natural skin crease. We generally prefer a smaller incision in a skin crease near the cricoid cartilage. Such an incision heals beautifully, with barely perceptible scar. However, in this patient the incision is lower and longer than usual for demonstration of surgical anatomy. In women with heavy breasts, the incision should be placed higher than usual, because in an upright position, the weight of the breasts results in a pull on the scar resulting in a hypertrophic scar. The skin incision is made with a scalpel, and the rest of the procedure is done with an electrocautery. The platysma is divided, and the upper and lower skin flaps are elevated, exposing the fascia over the strap muscles (Fig. 12.44). The upper and lower skin flaps are shown retracted

Figure 12.43 A patient with a solitary lesion confined to the right lobe of the thyroid gland.

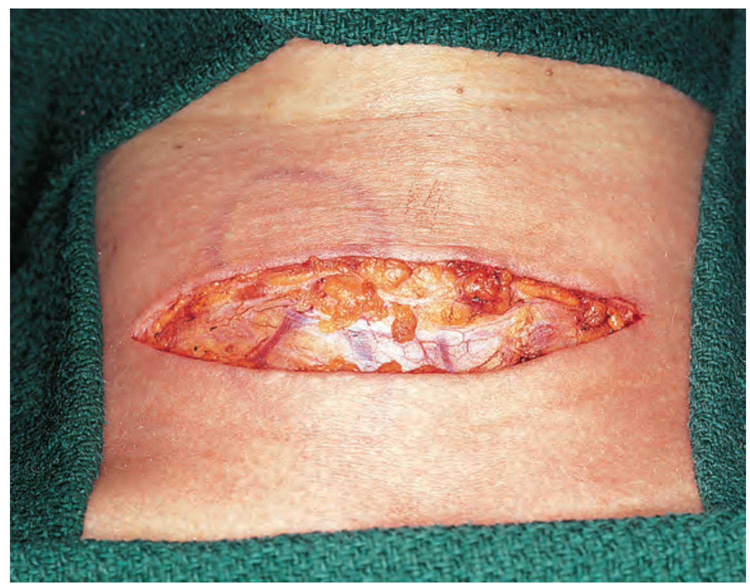

Figure 12.44 The skin incision.

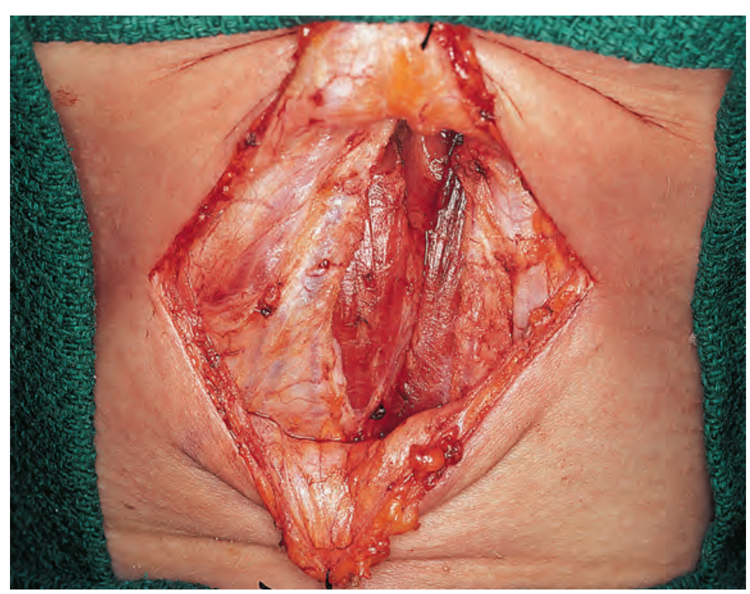

Figure 12.45 The strap muscles covering the thyroid gland are exposed.

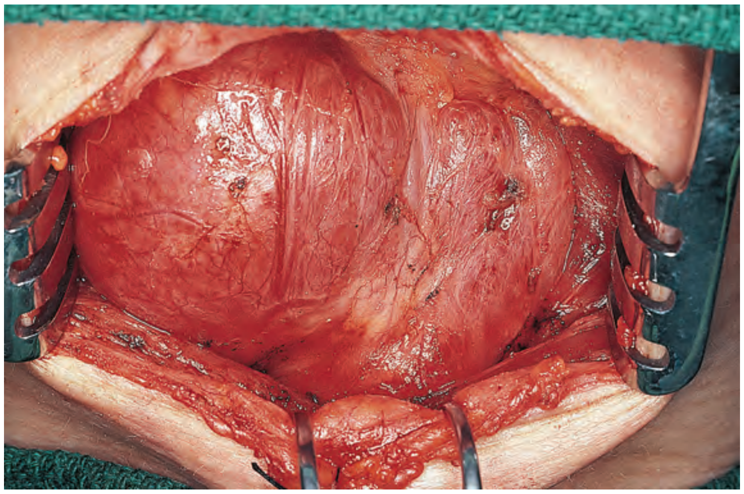

Figure 12.46 The anterior surface of the thyroid gland is exposed.

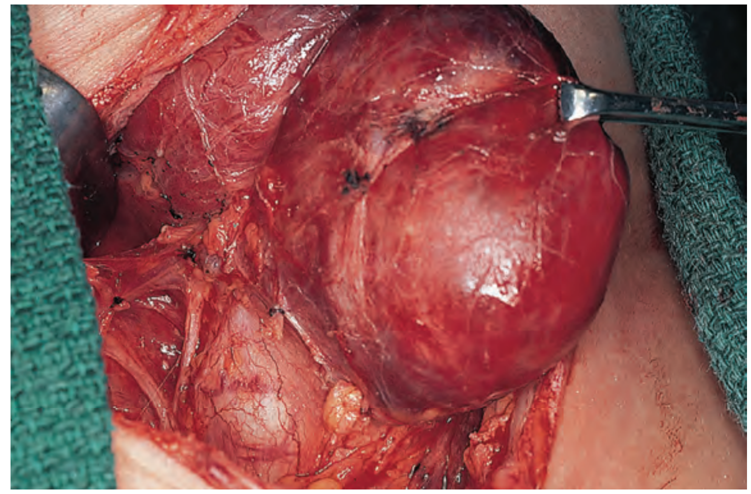

Figure 12.47 The recurrent laryngeal nerve is traced cephalad until it enters the cricothyroid membrane.

to expose the strap muscles covering the thyroid gland (Fig. 12.45). The fascia over the strap muscles is incised in the midline, and the sternohyoid muscles are carefully dissected and retracted laterally to expose the underlying sternothyroid muscles and anterior surface of the thyroid gland (Fig. 12.46).

The entire thyroid gland and the central compartment is explored and examined by inspection and palpation before any decision is made regarding the extent of a thyroidectomy. Once the decision is made to proceed with ipsilateral lobectomy, the sternothyroid muscle is divided near its upper end to gain exposure of the upper pole of the thyroid lobe. The middle thyroid vein is divided and ligated first. The capsular vessels on the anterior surface of the thyroid gland at its upper pole are then individually dissected, divided, and ligated. Each of the branches of the superior thyroid artery is individually clamped and divided as close to the capsule of the upper pole as possible to avoid injury to the external laryngeal branch of the superior laryngeal nerve. The nerve is located posteromedial to the superior thyroid artery and curves medially to enter the cricothyroid muscle near the upper pole of the thyroid gland. Therefore the terminal branches of the superior thyroid artery should be divided as close to the upper pole as possible without leaving remnants of upper pole thyroid tissue behind. Mass ligature of the vascular pedicle at the upper pole is hazardous and should not be undertaken. Thus the upper pole is mobilized in an extracapsular plane. The upper pole is now rotated medially, exposing its posterior surface, where the superior parathyroid gland is located. The parathyroid is carefully dissected off the thyroid capsule by blunt and sharp dissection, preserving its blood supply. The dissection now proceeds caudad, over the posterior capsule of the thyroid gland, toward its lower pole. The next step in the operation is to find the lower parathyroid gland. Meticulous dissection should be undertaken to preserve the integrity of both the parathyroid glands and their blood supply coming from the inferior thyroid artery. Ligation of the inferior thyroid artery should never be done at its main trunk, since that will devascularize the parathyroid glands. Only the terminal branches of the inferior thyroid artery entering the thyroid gland, distal to the blood supply to the parathyroid glands, are divided and ligated. The blood supply to the parathyroid glands is through very delicate branches of the inferior thyroid artery. Rough handling and inadvertent clamping during this dissection can traumatize these vessels and jeopardize the vascularity of the parathyroid glands and their function.

The veins emanating from the lower pole of the thyroid gland are carefully divided and ligated, permitting its medial rotation.

The dissection now proceeds medially toward the tracheoesophageal groove to identify the recurrent laryngeal nerve. Once identified, it is traced cephalad until it enters the cricothyroid membrane (Fig. 12.47).

There are three areas of possible injury to the recurrent laryngeal nerve in the tracheoesophageal groove. In the lower portion of the tracheoesophageal groove, the nerve can be easily found medial to the carotid artery. If there is bulky nodal disease, with the nerve intertwined between the nodes, it is likely to be traumatized during its separation from the nodes. The next area of risk of injury to the nerve is where it crosses the inferior thyroid artery. Generally, the nerve is located posterior to the inferior thyroid artery. However, in approximately 25% of patients, its relation to the inferior thyroid artery is at a variance. It may be anterior to the inferior thyroid artery or traversing between the branches of the inferior thyroid artery. In addition, the nerve may be branching, in which case all the branches of the nerve should be carefully preserved. The anterior-most branch is the motor branch and the most crucial one, since any injury to this branch will lead to vocal cord paresis. The third most common area where the nerve is at risk of injury is the region of the ligament of Berry. This is the region where the thyroid gland is intimately adherent to the trachea, and its separation may be quite difficult due to close proximity of the nerve to the ligament of Berry and the posterior portion of the tuberculum Zuckerkandl. Invariably, there are tiny vessels traversing the ligament of Berry, which may be traumatized, causing minor but sometimes tedious bleeding. The control of this bleeding, even with bipolar cautery, can cause thermal injury to the recurrent laryngeal nerve. The most common injuries to the recurrent nerve are traction injury or thermal injury, rather than true transection of the nerve.

After dissection of the parathyroid glands, keeping their blood supply intact, all the terminal branches of the inferior thyroid artery are divided. As the branches are divided, the recurrent laryngeal nerve is kept in view at all times. Dissection of the right lobe continues cephalad over the pretracheal plane toward the cricothyroid membrane, where it is densely adherent through its fascial attachment, the ligament of Berry. This dense fascial attachment is carefully divided under direct vision, preferably with a sharp scalpel. Use of electrocautery should be avoided here to prevent inadvertent thermal injury to the recurrent

laryngeal nerve. Several small vessels traversing the ligament of Berry in front of and behind the recurrent laryngeal nerve are individually clamped, divided, and ligated.

The thyroid lobe is nearly completely mobilized except for its attachment through the isthmus to the opposite lobe. The isthmus is separated from the trachea, doubly clamped, and divided. The cut surface of the left lobe is ligated, with a continuous interlocking 3-0 chromic catgut suture for hemostasis.

The specimen of the right lobe and isthmus of the thyroid gland with its capsule intact is shown in Fig. 12.48. The bisected specimen shows a solid, fleshy, well-circumscribed tumor mass occupying the lower pole (Fig. 12.49). Upon frozen-section examination, the partly cystic and centrally necrotic tumor was diagnosed as a follicular lesion. After removal of the right lobe of the thyroid gland, the surgical field shows a suture ligature on the isthmus of the thyroid gland. The intact recurrent laryngeal nerve and the parathyroid glands are demonstrated in Fig. 12.50. The wound is irrigated with Bacitracin solution. In general a drainage tube after thyroid surgery is not required, unless the operation is for a big goiter, leaving a large dead space, or when an extensive central compartment lymph node dissection is performed. A Penrose drain is placed in this patient in the bed of the right lobe of the thyroid gland and is brought out through the midline of the skin incision. The strap muscles are reapproximated with interrupted 3-0 chromic catgut sutures (Fig. 12.51). The platysma is reapproximated in a similar fashion, and the skin is sutured with fine nylon (Fig. 12.52).

If an intrathyroidal tumor is excised by a lobectomy then a frozen section is not necessary. Pathologists are unable to differentiate a benign follicular adenoma from a well-differentiated carcinoma on frozen section. In addition, even if the diagnosis

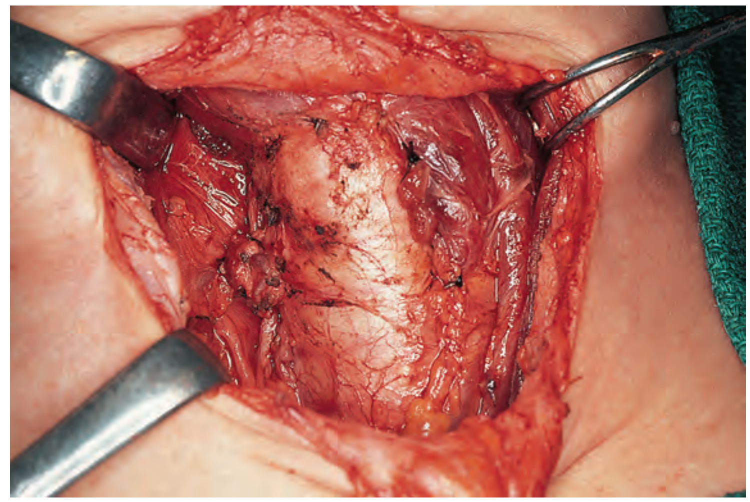

Figure 12.50 The intact recurrent laryngeal nerve and the parathyroid glands.

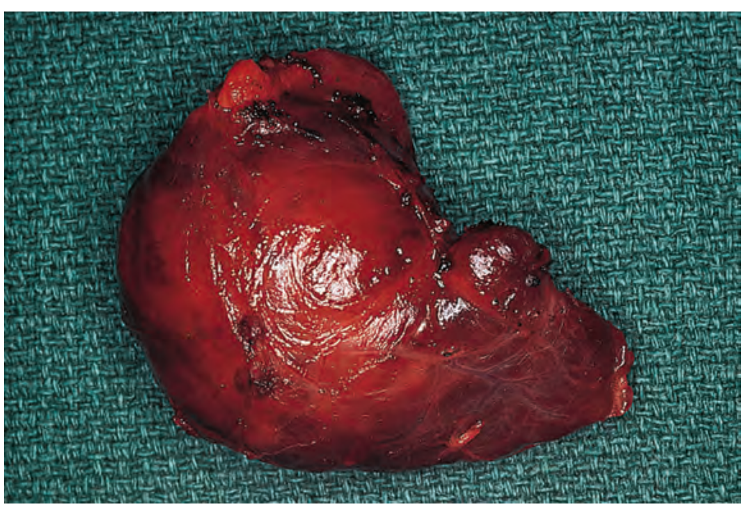

Figure 12.48 The surgical specimen of the right lobe and isthmus.

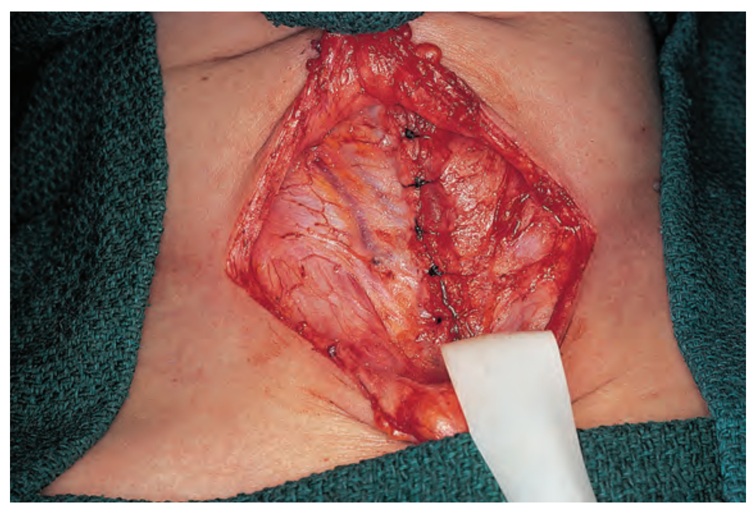

Figure 12.51 The strap muscles are reapproximated in the midline after a Penrose drain is placed in the thyroid bed.

Figure 12.49 The bisected specimen.

Figure 12.52 The incision is closed in layers with the Penrose drain brought out through the center of the incision.

is of a well-differentiated carcinoma, then a lobectomy is adequate surgical treatment for an intrathyroidal tumor. Before closure of the incision, the tracheoesophageal grooves on both sides should be carefully inspected and palpated to rule out gross metastases. If any suspicious lymph nodes are palpated, then frozen section should be obtained from the most suspicious-looking lymph node, and upon confirmation of metastatic disease, central compartment node dissection should be completed. This procedure avoids the need to return to the surgical bed of a previous lobectomy should the patient require a regional lymph node dissection for metastases in the future.

Often it is impossible to secure a monobloc specimen of tracheoesophageal lymph nodes because of the scanty amount of fat in this area and loose areolar tissue interconnecting the lymph nodes. Node dissection in the tracheoesophageal groove poses the risk of injury to the blood supply of the parathyroid glands. Therefore it is important to emphasize that meticulous care is necessary during this dissection to avoid rough handling of the parathyroid glands; otherwise, they can be devascularized easily. If a parathyroid gland is inadvertently devascularized, it is minced into tiny slices and implanted in the sternocleidomastoid muscle. Frozen section confirmation of the small piece of parathyroid tissue should be undertaken before autotransplantation.

Postoperative care is simple. The drainage tube is removed when the serosanguineous drainage is scanty, and the skin sutures may be removed at the end of 1 week. The patient now can perform neck exercises to alleviate local discomfort.

Resection of a Large Goiter With Tracheal Compression

Extensive multinodular goiters often can cause compression of the trachea and respiratory compromise. The axial view of an MRI scan with gadolinium contrast enhancement of a patient with a massive retrosternal goiter shows that the tracheal lumen is reduced to a narrow sliver, with significant displacement of the esophagus and extension of goiter into the anterior superior mediastinum (Fig. 12.53). The coronal view of the MRI scan (Fig. 12.54) demonstrates compromise of the tracheal air column to approximately 10% of normal. The extent of the goiter and compression of the trachea are depicted in Fig. 12.55. The trachea is displaced laterally almost behind the left sternoclavicular joint and in the left side of the neck. An intraoperative view after resection of the goiter shows indentation into the tracheal wall resulting from the goiter (Fig. 12.56). The commonly feared

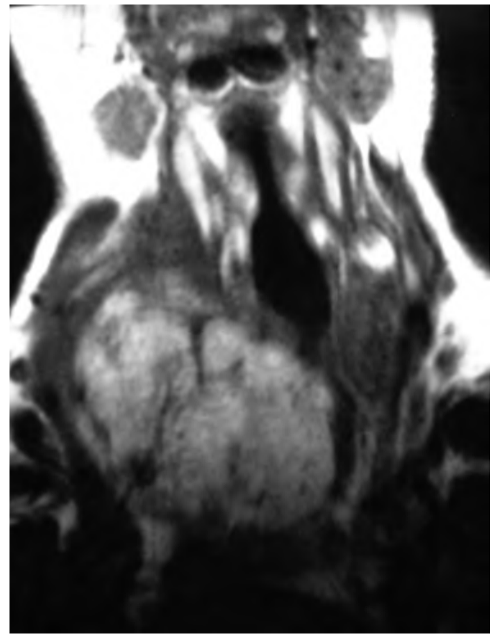

Figure 12.54 A coronal view of the magnetic resonance imaging scan showing displacement of the trachea to the left.

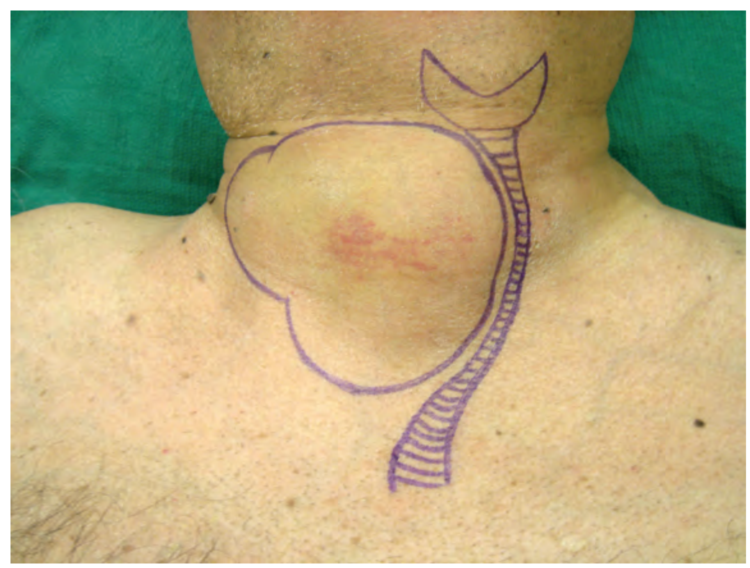

Figure 12.55 Dimensions of the goiter and displacement of the trachea.

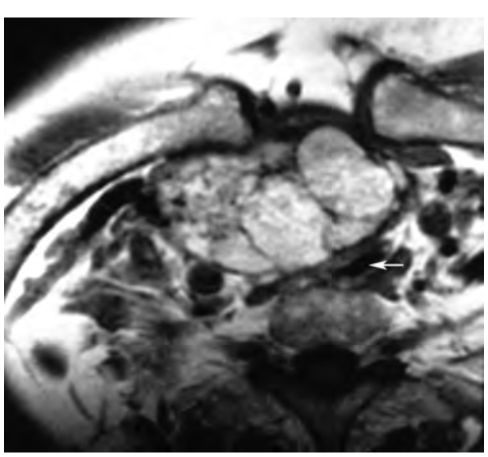

Figure 12.53 An axial view of the magnetic resonance imaging scan showing tracheal compression (*arrow*).

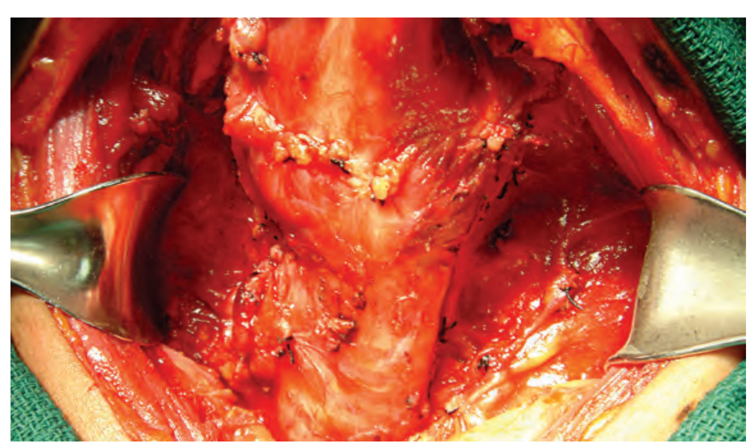

Figure 12.56 The surgical field after removal of the goiter showing indentation on the trachea.

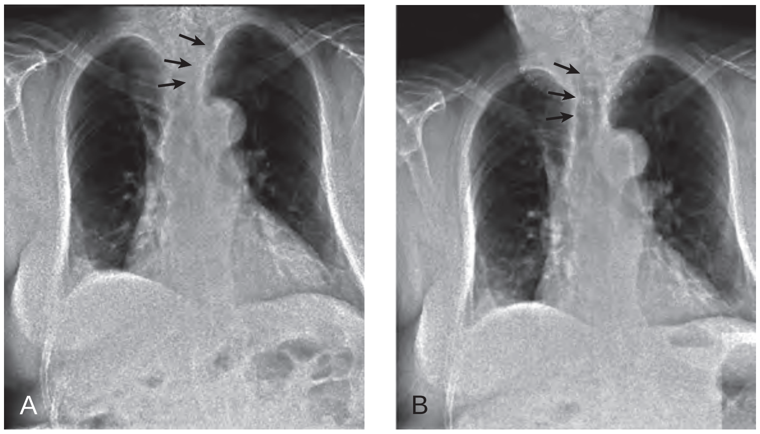

Figure 12.57 Posteroanterior views of chest radiographs. **A**, The preoperative view showing compression of tracheal air column. **B**, The postoperative view showing restoration of the tracheal air column.

postoperative complication of tracheomalacia is rarely seen. Once the compressing goiter has been removed, the trachea rapidly assumes its normal dimensions during the next several days (Fig. 12.57).

Resection of a Retrosternal Goiter

Enlargement of the thyroid gland may extend into the superior mediastinum. This presentation often may be the result of a nontoxic nodular goiter, or it may be a neoplasm involving the lower pole of the thyroid lobe with direct extension into the superior mediastinum. Most patients with small masses in the superior mediastinum remain asymptomatic and the condition is not detected. However, with progressive increase in the size of the thyroid mass, local symptoms develop because of compression of the trachea, esophagus, and the great vessels at the thoracic inlet, causing shortness of breath, difficulty in swallowing, or symptoms of venous congestion in the head and neck area as a result of compression of the innominate veins.

The patient described here had shortness of breath with exertion for several months. An anteroposterior projection of the chest radiograph shows the presence of a soft-tissue mass causing extrinsic compression of the trachea in the superior mediastinum (Fig. 12.58). A CT scan obtained through the superior mediastinum shows a hypodense thyroid mass on the right-hand side with displacement of the trachea to the left (Fig. 12.59).

Figure 12.58 A chest radiograph of a patient with a retrosternal goiter showing tracheal deviation and compression.

Most retrosternal goiters can be excised via a cervical approach. A sternotomy is rarely indicated for untreated benign retrosternal goiters. On the other hand, for recurrent goiters in the mediastinum and for thyroid cancer in the retrosternal location, one should be prepared to perform a sternotomy. A thyroid mass of the dimensions shown here is approached via a low cervical incision, which will provide adequate exposure of the lower part of the neck and the superior mediastinum.

The estimated size of the goiter along with the displaced trachea are drawn on the patient (Fig. 12.60). The patient is placed under general anesthesia with a small endotracheal tube passed distal to the site of tracheal compression. The surgical exposure obtained by a low collar incision is usually adequate (Fig. 12.61). The skin incision is deepened through the platysma, and the upper and lower skin flaps are elevated to obtain wide exposure of the central compartment of the neck. The strap muscles are dissected from the capsule of the thyroid gland and a Richardson retractor is inserted underneath to retract them laterally (Fig. 12.62). In this patient, the left lobe has no palpable abnormalities. Similarly, the sternohyoid muscle on the right side is elevated and retracted to the right-hand side. The sternothyroid muscle is divided, exposing the anterior surface of the right lobe of the thyroid gland. No other palpable abnormalities are noted in the right thyroid lobe except the large mass at its lower pole.

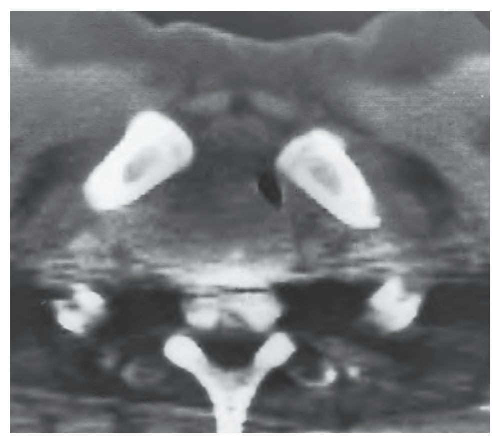

Figure 12.59 An axial view of the computed tomography scan through the superior mediastinum showing the retrosternal goiter.

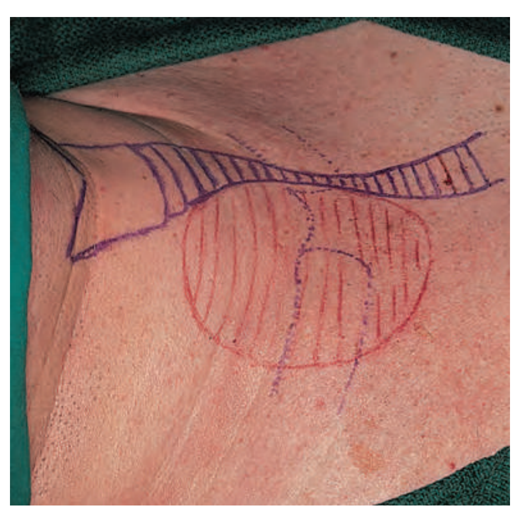

Figure 12.60 The estimated size of the goiter and the displaced trachea is drawn on the patient.

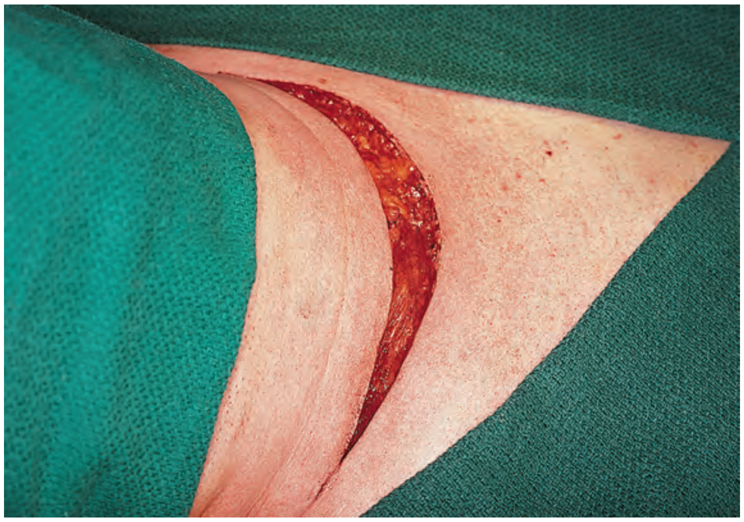

Figure 12.61 A generous low collar incision is made.

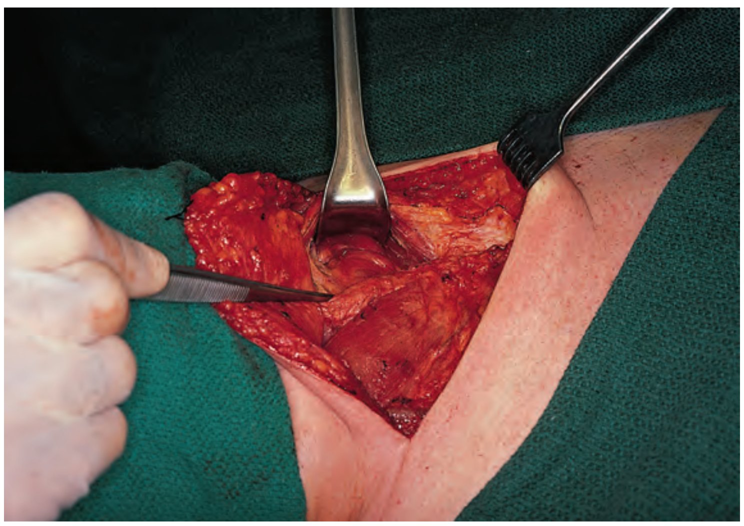

Figure 12.62 The left lobe of the thyroid gland is exposed and inspected first.

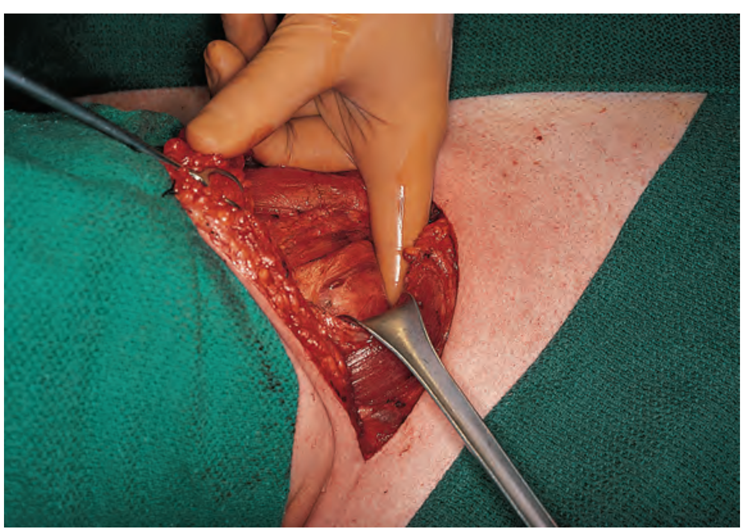

Figure 12.63 Gentle digital dissection is carried out over the capsule of the right lobe mass.

The right middle thyroid vein is divided first and ligated. This maneuver will free the lateral edge of the right thyroid lobe. Gentle digital dissection is carried out over the anterior surface of the right lobe to assess the intrathoracic component of the goiter (Fig. 12.63). If the digital dissection is performed

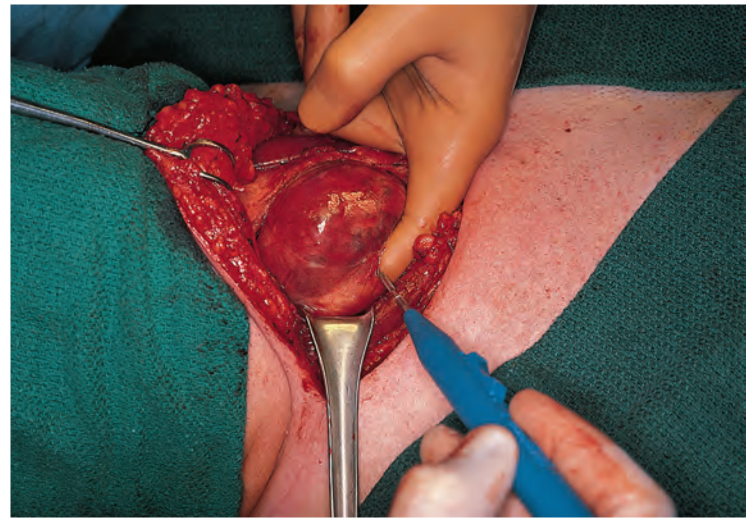

Figure 12.64 Several fascial bands forming a pseudocapsule around the goiter are carefully dissected and divided.

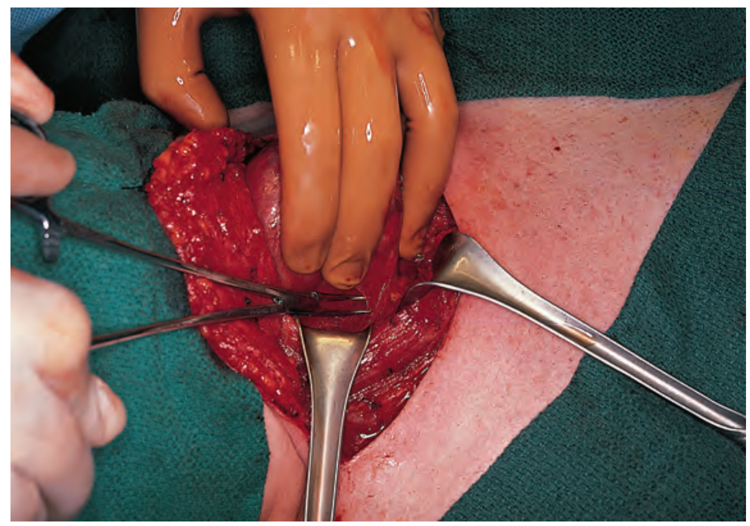

Figure 12.65 Large capsular veins identified during the course of this dissection are individually clamped, divided, and ligated.

easily, it is continued so as to mobilize the anterior surface of the retrosternal goiter. By gentle digital dissection of the right lobe and its mediastinal extension, it may be possible to deliver the retrosternal component out of the superior mediastinum. However, extreme care must be taken to avoid rough or forceful dissection of the mediastinal component of the goiter, because it may tear capsular vessels and produce significant hemorrhage. Several fascial bands that form a pseudocapsule around the goiter usually are encountered (Fig. 12.64) and are carefully divided with electrocautery until the correct plane of the capsule of the goiter is reached. Large capsular veins identified during the course of this dissection are individually clamped, divided, and ligated (Fig. 12.65). The goiter, thus mobilized, is ready for delivery out of the superior mediastinum into the neck.

Dissection now begins in the tracheoesophageal groove by retracting the right lobe toward the left side. A meticulous search now should be undertaken to identify the recurrent laryngeal nerve and the parathyroid glands. With a goiter of this size they may be displaced to abnormal locations, and a thorough search should be undertaken to locate them before the inferior thyroid artery is divided. However, the parathyroid glands often are difficult to identify during delivery and resection of a large retrosternal goiter. At this point the upper pole vessels

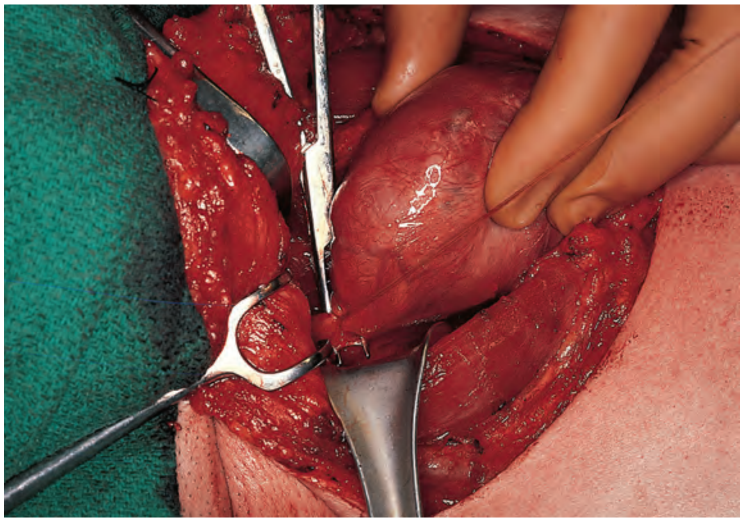

Figure 12.66 The upper pole vessels of the right lobe of the thyroid gland are dissected, clamped, divided, and ligated.

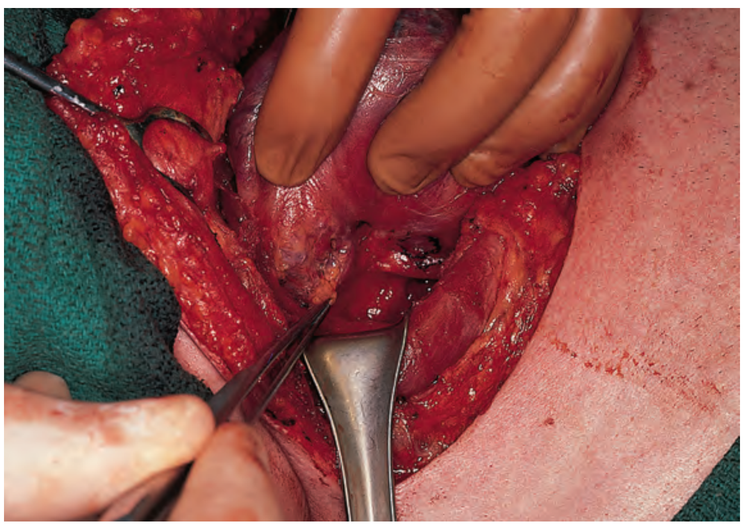

Figure 12.67 The right lower parathyroid gland is identified.

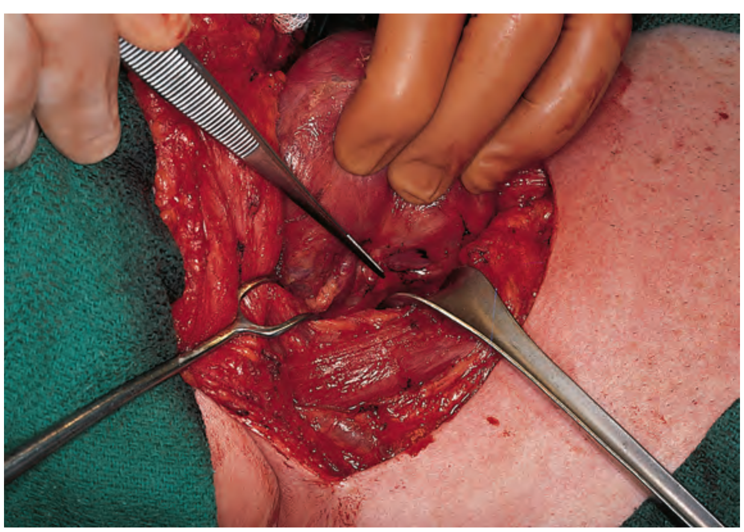

Figure 12.68 The right recurrent laryngeal nerve is isolated.

of the right lobe of the thyroid gland are dissected, clamped, divided, and ligated (Fig. 12.66).

With the additional exposure obtained, the search for and identification of the parathyroid glands should continue. The right lower parathyroid gland is identified at this time (Fig. 12.67). Further dissection in this area continues until the right

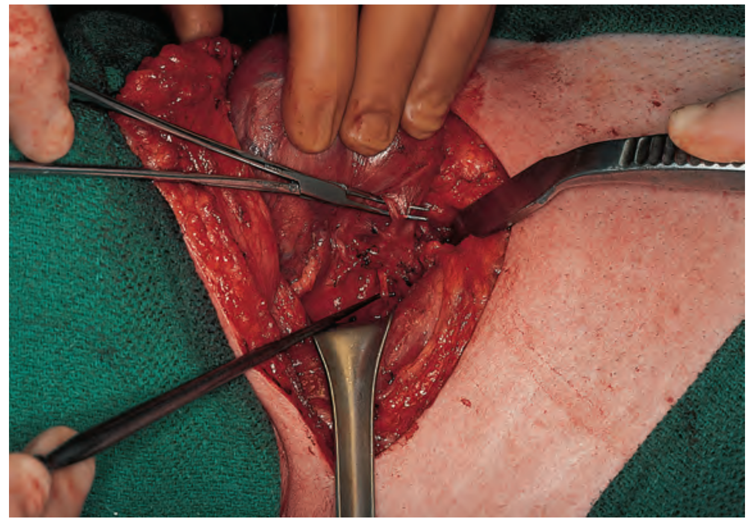

Figure 12.69 The inferior thyroid artery distal to its parathyroid branch is divided and ligated.

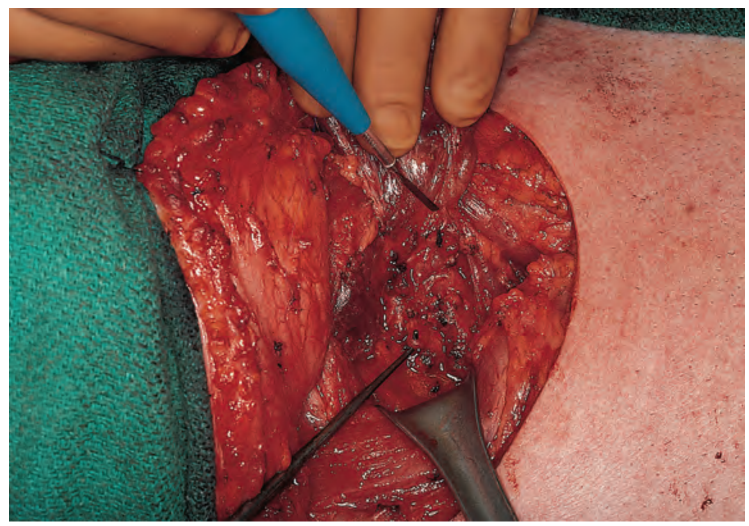

Figure 12.70 The goiter is mobilized and rotated medially over the trachea.

recurrent laryngeal nerve is isolated (Fig. 12.68). The nerve is traced cephalad as far as its entry into the larynx through the cricothyroid membrane.

The inferior thyroid vessels are now ready to be divided. A hemostat is passed underneath the inferior thyroid artery distal to its parathyroid branch, where it is divided and ligated (Fig. 12.69). The goiter is thus further mobilized and rotated medially over the trachea (Fig. 12.70). Using an electrocautery, the isthmus of the thyroid gland is separated from the trachea. Small identifiable vessels along the ligament of Berry should be individually clamped, divided, and ligated to minimize bleeding.

The isthmus now can be mobilized from the trachea up to the left lobe of the thyroid gland. The isthmus is doubly clamped near the left lobe and divided, and the specimen is removed (Fig. 12.71). The stump of the isthmus at the left lobe is sutured with a 3-0 chromic catgut continuous interlocking suture for hemostasis. The wound is irrigated, and hemostasis is reconfirmed.

Before closure, the surgical field shows complete clearance of the right thyroid bed where the large goiter was removed. The trachea is bared in the midline. Occasionally the trachea may feel quite flaccid after removal of a long-standing large goiter that had caused extrinsic compression. However, airway compromise due to tracheal flaccidity is seldom observed. The

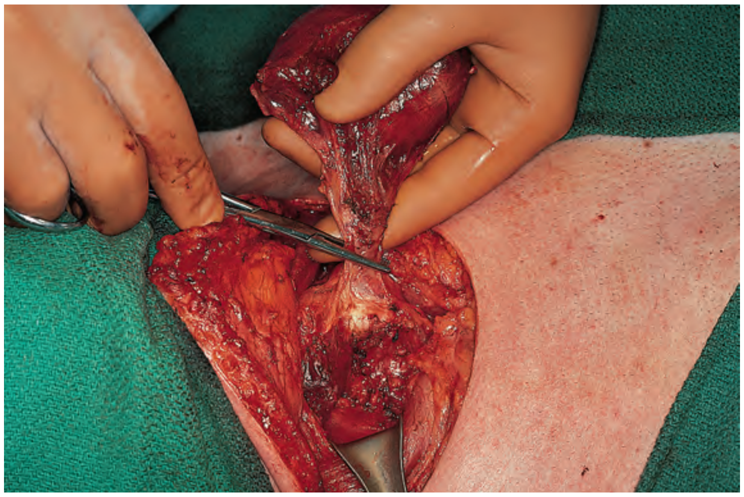

Figure 12.71 The specimen is delivered.

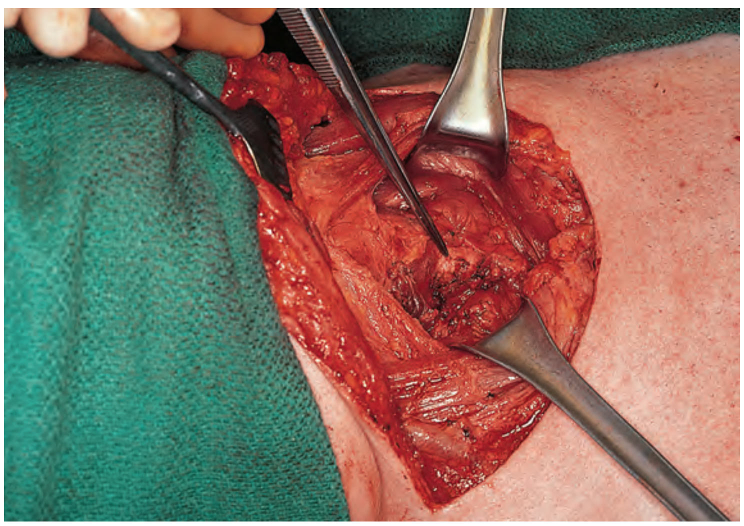

Figure 12.72 The trachea looks and feels normal after the specimen is removed.

Figure 12.73 A Penrose drain is placed in the thyroid bed and brought out through the midline of the incision.

trachea in this patient is normal in its configuration and consistency (Fig. 12.72).

A Penrose drain is placed in the thyroid bed and brought out through the midline of the incision and the incision is closed in layers (Fig. 12.73).

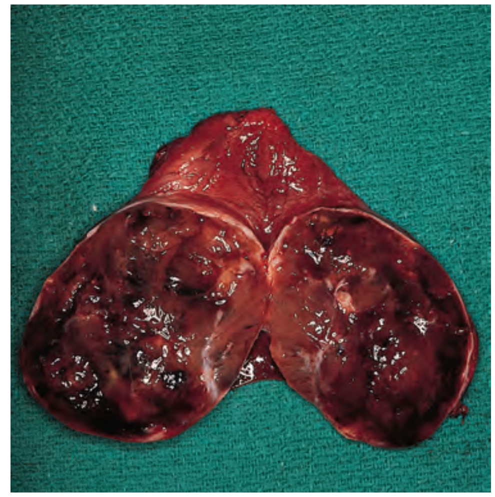

Figure 12.74 The bisected specimen.

The surgical specimen shows a mass at the lower pole of the right lobe of the thyroid gland measuring 6 by 8 cm. On the bisected specimen, the appearance of this lesion suggests a colloid adenoma with cystic changes and a densely fibrosed, partially calcified capsule (Fig. 12.74).

Resection of a Massive Retrosternal Goiter

Massive goiters with retrosternal extension often extend up to the innominate artery or even further caudad into the mediastinum up to the arch of the aorta (Fig. 12.75). It is possible, however, in most instances to excise these goiters through the transcervical approach. The only exceptions are excessive adhesions due to malignant transformation in a retrosternal goiter or a recurrent retrosternal goiter, where digital manipulation can produce excessive bleeding or fracture of the tumor with fragmentation requiring piecemeal removal.

The patient whose MRI scans are shown in Figs. 12.17 through 12.19 has a 17- by 10-cm retrosternal goiter extending well below the level of the innominate artery. The surgical approach requires a generous transverse low cervical incision with a "T" extension overlying the manubrium sterni. After elevation of the skin flaps, the sternohyoid and sternothyroid muscles are excised. Gentle digital dissection then proceeds around the goiter in the superior mediastinum, which allows delivery of

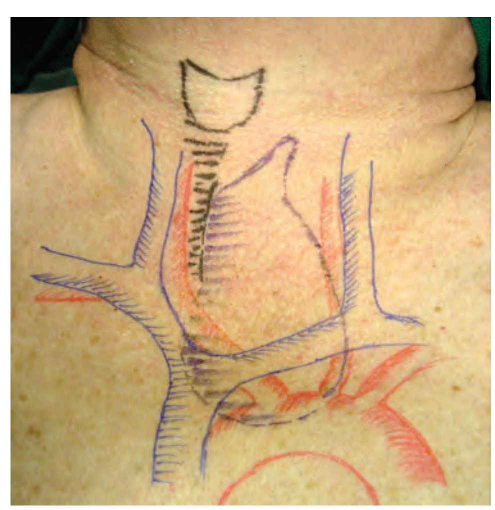

Figure 12.75 Retrosternal extension of a massive goiter is depicted on a patient to show extension into the mediastinum.

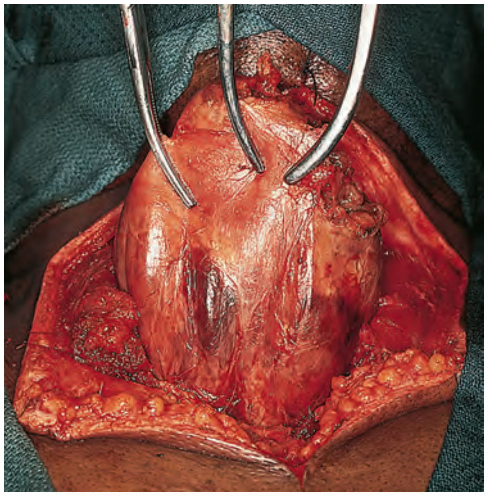

Figure 12.76 Gentle traction with Kocher clamps allows delivery of the goiter into the neck.

Figure 12.77 Completed dissection showing the entire goiter delivered from its retrosternal location.

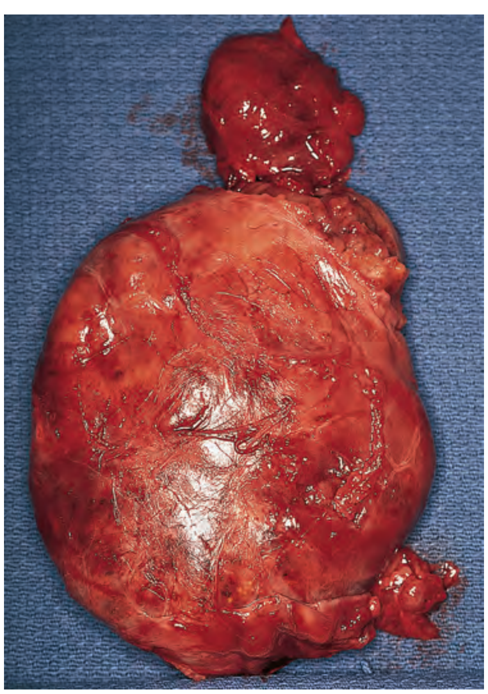

Figure 12.78 The surgical specimen.

the upper pole of the goiter in the neck. Several Kocher clamps are applied to the goiter, and gentle traction is applied (Fig. 12.76). With the tumor under traction, meticulous gentle digital dissection continues, carefully ligating capsular vessels and facilitating progressive delivery of the goiter in the neck (Fig. 12.77). The surgical specimen shows the massive goiter excised through a cervical approach in an intact manner (Fig. 12.78). Inadvertent entry into the pleural cavity may occur during this dissection and may require insertion of a chest tube.

Regional Lymph Node Dissection

The incidence of clinically occult lymph node metastases in patients with a differentiated carcinoma of the thyroid gland is well over 50%, but fewer than 10% present with palpable lymphadenopathy. The most common locations for early involvement of metastatic lymph nodes is in the central compartment of the neck (level VI and VII, N1a). Most of such lymph nodes are clinically not detectable but may be seen on preoperative ultrasound or detected during surgery. Clinically palpable metastatic lymph nodes in the lateral neck from thyroid cancer are most often seen at levels III and IV. It is exceedingly rare to find metastatic disease at level I. The patterns of regional lymph node metastasis from thyroid carcinoma are predictable, and a select group of lymph nodes are initially involved (Fig. 12.79). Although central compartment nodes are the first echelon lymph nodes, occasionally patients may present with a clinically palpable lateral neck lymph node as the first or the only manifestation of metastatic disease. In spite of a high incidence of occult metastases in patients with differentiated carcinoma, elective dissection of regional lymph nodes is not recommended in low-risk patients, since it has very little impact on long-term

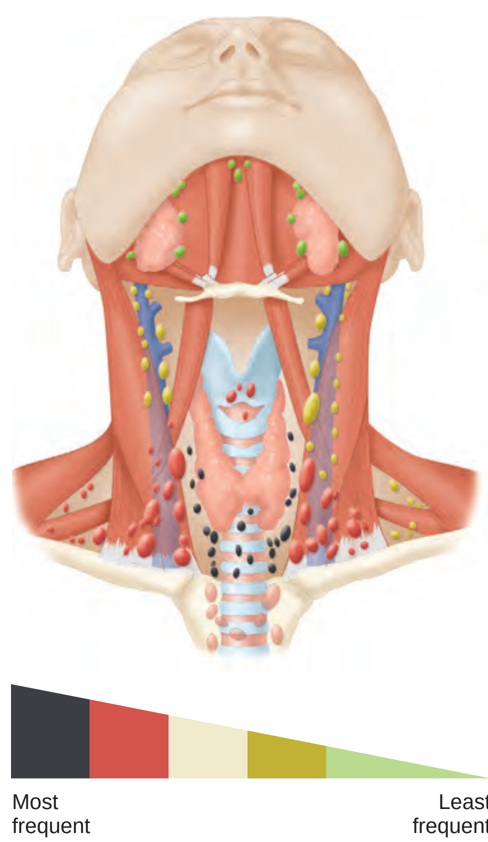

Figure 12.79 Patterns of lymph node metastases from cancer of the thyroid gland. The risk of involvement is highest for level VI (*black*), intermediate for levels IV and VII (*red*), and lowest for levels V, III, and II (*yellow*).

prognosis. On the other hand, elective dissection of central compartment lymph nodes should be considered in patients with advanced primary cancers with gross extrathyroid extension, poorly differentiated histology, and selected patients who fall into the high-risk category.

Central Compartment Node Dissection

The central compartment of the neck is defined by its superior boundary at the undersurface of the hyoid bone and its inferior boundary at the suprasternal notch. It is bounded laterally by the carotid sheaths. It contains lymph nodes at level VI. However, the separation between levels VI and VII is somewhat arbitrary, since there is no fixed landmark separating the two levels. The level of suprasternal notch varies, depending upon whether the neck is flexed or extended. Therefore, to do away with this arbitrary division between levels VI and VII, in the revised staging of nodal metastases (AJCC/UICC eighth edition), all the lymph nodes at level VI and VII are now considered under nodal staging, N1a. Therefore we may need to redefine the boundaries of the central compartment to extend from the hyoid bone cephalad to the innominate artery caudad (Fig. 12.80). This space contains the prelaryngeal, Delphian, pretracheal, paratracheal, and perithyroid lymph nodes as well as lymph nodes in the tracheoesophageal grooves and paraesophageal lymph nodes up to the superior border of the innominate artery.

This procedure is performed electively in the clinical N0 setting only in patients with large primary cancers of the thyroid gland (T4a), which usually involve gross extrathyroid extension in the neck, and where the risk of nodal metastases is very high, and also to facilitate a better resection of the primary tumor. If grossly enlarged lymph nodes are encountered in the central compartment during the course of thyroidectomy, central compartment dissection should be undertaken bilaterally to clear all lymph nodes at risk in level VI and VII. This operation is believed to be adequate for clearance of regional lymphatic spread if the lateral neck nodes are not grossly enlarged. Unilateral clearance of paratracheal lymph nodes in the central compartment may be considered for low-risk papillary carcinomas, where incidentally pathologic but small nodes are encountered during the course of a thyroid lobectomy. It is imperative however, that the contralateral and the entire central compartment is explored thoroughly, visually and by palpation, before a decision is made regarding the limited extent of ipsilateral tracheoesophageal groove node dissection. The surgical specimen of a patient with a low-risk thyroid cancer who underwent a lobectomy and ipsilateral tracheoesophageal groove lymph node dissection is shown in Fig. 12.81. Meticulous attention is required to carefully preserve the parathyroid glands with their blood supply intact as well as the recurrent laryngeal nerves. The surgical field shows preserved parathyroid glands and a recurrent laryngeal nerve with complete clearance of the central compartment on the ipsilateral side (Fig. 12.82). If the parathyroid glands are devascularized, they should be reimplanted in the lateral neck muscles.

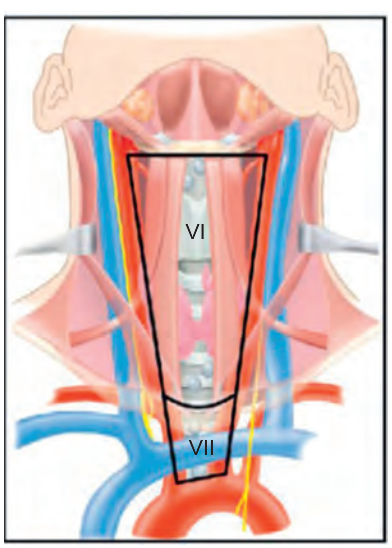

Figure 12.80 Lymph nodes of the central compartment: levels VI and VII (N1a).

Figure 12.81 The surgical specimen of left thyroid lobectomy and ipsilateral paratracheal lymph node dissection. Note the thymus at the lower end of the specimen.

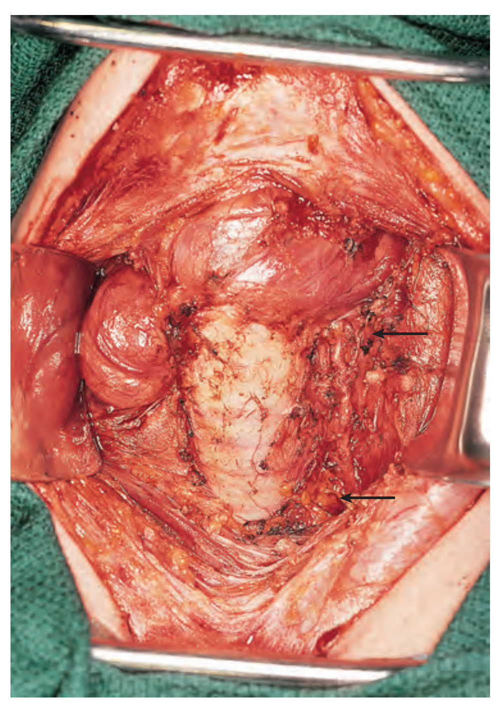

Figure 12.82 The surgical bed shows preserved parathyroid glands (*arrows*) and the recurrent laryngeal nerve on the left-hand side.

Total Thyroidectomy With Comprehensive Modified Neck Dissection Type III

Regional lymph node metastases from differentiated carcinomas of the thyroid occur most frequently in the central compartment lymph nodes (level VI) as well as in those in the superior mediastinum (level VII), now staged as N1a. The lateral spread of metastatic disease usually involves the midjugular and low jugular lymph nodes first and then those in the posterior triangle of the neck and upper jugular nodes (levels II, III, IV, and V). These nodes are clinically staged as N1b. The presence of metastatic lymph nodes in the submandibular triangle (level I) from differentiated thyroid cancer is very rare. Thus the submandibular triangle can be spared during neck dissection for metastatic thyroid cancer, particularly if gross metastases are not present in the middle or upper jugular lymph nodes. On the other hand, it is quite common to see metastatic nodes, posterior to the carotid sheath at level IV. Therefore particular attention should be paid to explore this area, adjacent to the lymphatic ducts, and posterior to the internal jugular vein and carotid artery to remove all gross disease. Because of the biologically indolent nature of differentiated thyroid cancer, local invasion of the soft tissues of the neck from metastatic nodes is unusual. A modified but comprehensive compartmental neck dissection preserving the sternocleidomastoid muscle, the internal jugular vein, and the accessory nerve therefore is considered a satisfactory operation for clearance of regional lymph nodes in the lateral part of the neck.

Serial axial and coronal views of a noncontrast CT scan of a patient with papillary carcinoma of the left thyroid lobe (with calcification), and several calcified metastatic nodes in the central as well as lateral compartments of the neck are shown in Figs. 12.83 and 12.84. A coronal view of the reconstructed CT scan shows the calcified primary lesion and multiple calcified paratracheal, superior mediastinal, and left lateral cervical lymph nodes (Fig. 12.85). The surgical procedure in this patient requires complete clearance of the central compartment of the neck from the hyoid up to the innominate artery to clear all N1a lymph nodes with a total thyroidectomy. In addition, comprehensive neck dissection of bilateral levels II to V is performed to encompass all demonstrable disease. The entire surgical procedure is performed through a single transverse incision at the level of the cricoid cartilage extending from the anterior border of the trapezius muscle on one side of the neck to that of the other (Fig. 12.86). The location of radiologically demonstrable lymph nodes is depicted on the patient.

The skin flaps are elevated in a subplatysmal plane sufficient to expose the entire surgical field required for completion of the operation. Thus the superior skin flap is elevated to a level above the hyoid bone to expose the lower border of the submandibular salivary glands on both sides (Fig. 12.87). Inferiorly, the lower skin flap is elevated to expose the suprasternal notch and the clavicles bilaterally.

Dissection begins by incising the fascia over the anterior border of the sternocleidomastoid muscle on the left-hand side for dissection of left lateral cervical lymph nodes (Fig. 12.88). This dissection is accomplished very safely and in a bloodless manner with an electrocautery using coagulating current. Meticulous dissection of all the visible and palpable lymph nodes is undertaken, carefully preserving the neurovascular structures of the carotid sheath. Lateral retraction of the sternocleidomastoid muscle demonstrates the omohyoid muscle arising from the lower border of the hyoid bone and extending inferolaterally to cross the carotid sheath (Fig. 12.89). The soft

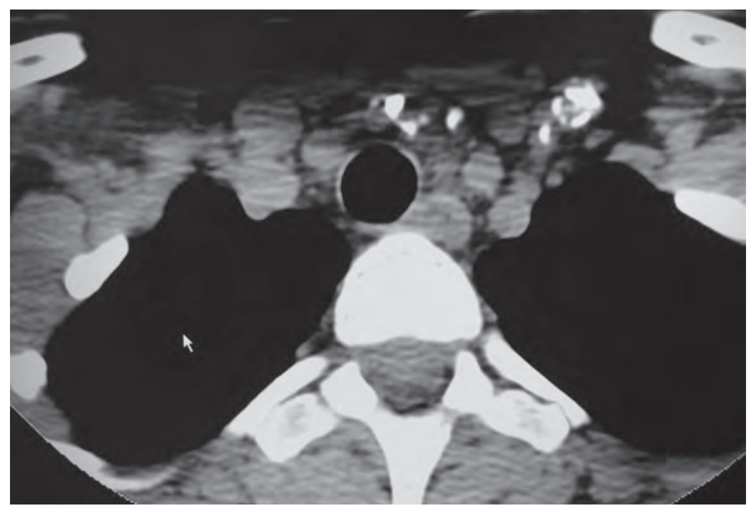

Figure 12.84 An axial view of a computed tomography scan shows multiple calcified lymph nodes in the pretracheal and paratracheal regions.

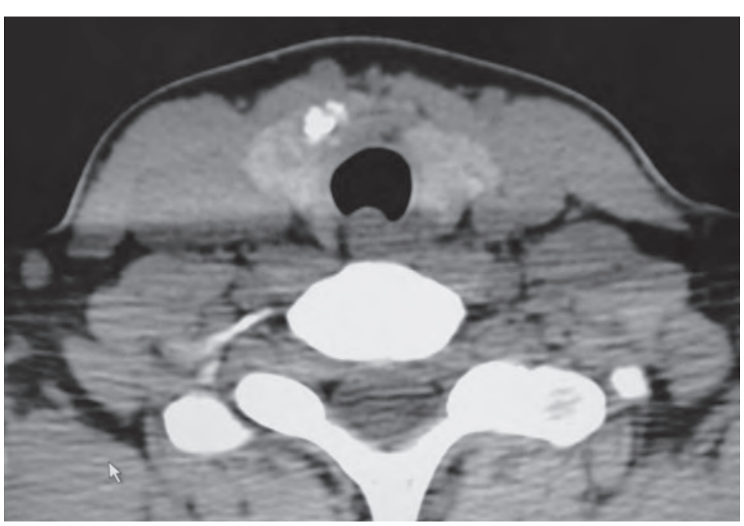

Figure 12.83 An axial view of a noncontrast computed tomography scan shows a calcified mass in the right thyroid lobe, raising the suspicion of a papillary carcinoma.

Figure 12.85 A coronal view of the computed tomography scan shows multiple calcified lesions in the thyroid gland and adjacent lymph nodes.

Figure 12.86 A transverse incision is marked at the level of the cricoid cartilage.

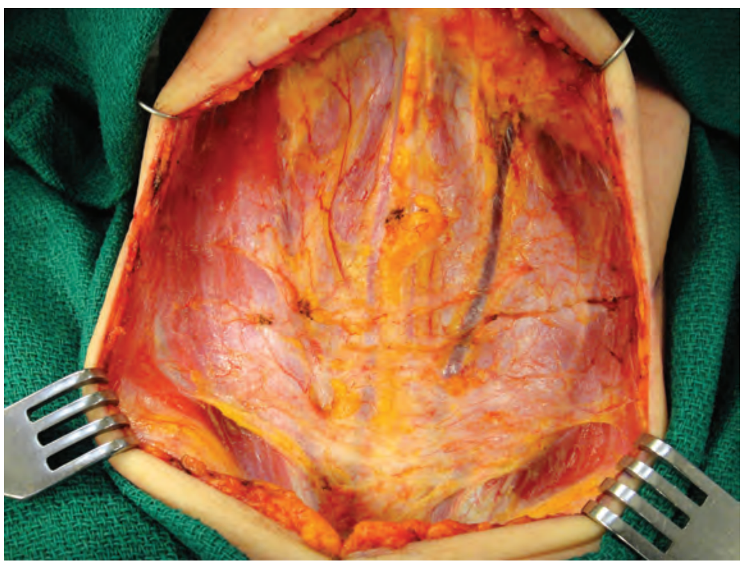

Figure 12.87 Upper and lower skin flaps are elevated.

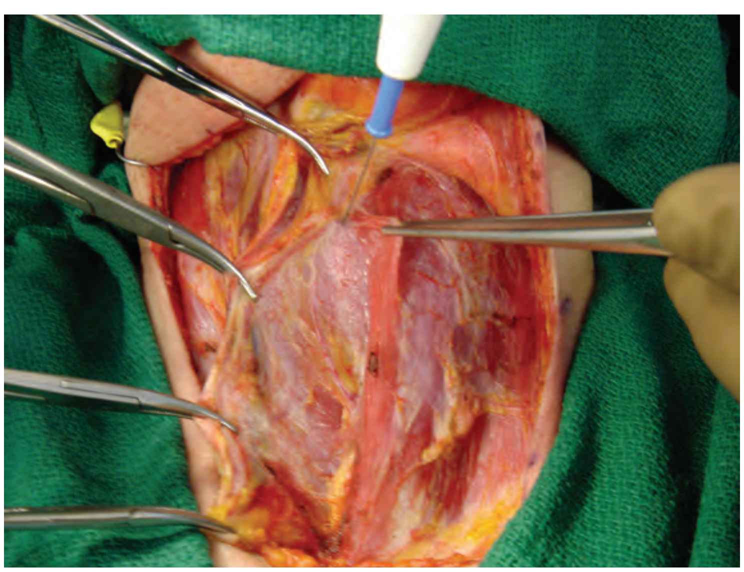

Figure 12.88 Dissection begins at the anterior border of the sternocleidomastoid muscle.

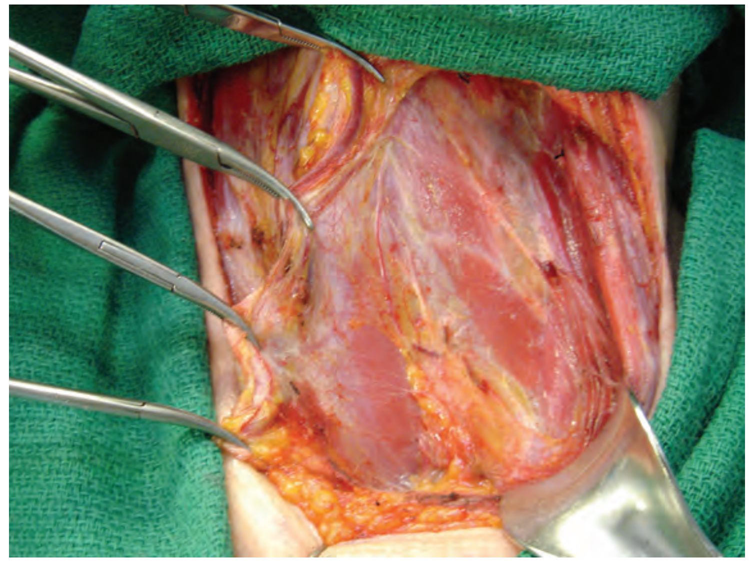

Figure 12.89 The omohyoid muscle is seen crossing the carotid sheath.

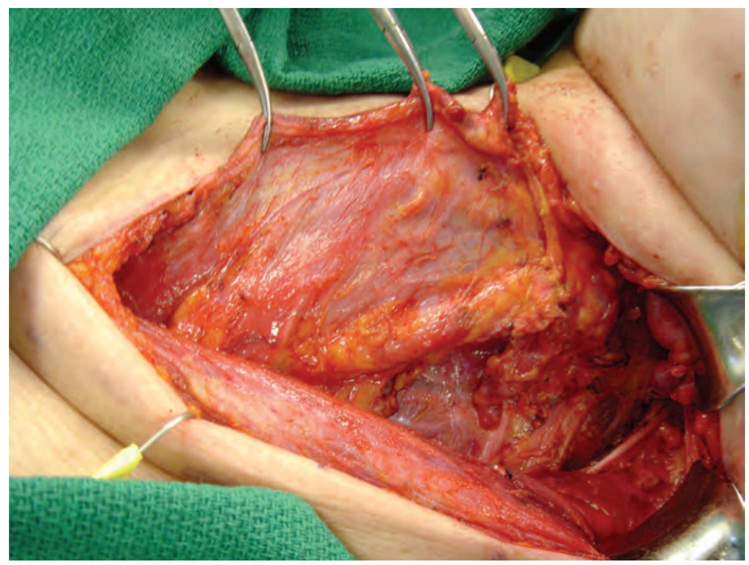

Figure 12.90 Dissection of lymph nodes in the posterior triangle begins over the cervical plexus.

tissue on the undersurface of the sternomastoid muscle is dissected off the muscle as far back as possible to expose the anterior border of the trapezius muscle inferiorly and the floor of the posterior triangle of the neck superiorly.

Dissection now begins with mobilization of lymph nodes lateral to the internal jugular vein overlying the cutaneous roots of the cervical plexus. These lymph nodes are meticulously dissected and separated off from the anterior surface of the cervical plexus. At the upper end of the surgical field, the spinal accessory nerve is identified. Lymph nodes are dissected from level IIA. If, however, gross disease is present at level IIA, then every effort should be made to clear all the lymph nodes from level IIB also. The superior border for clearance of lymph nodes is the posterior belly of the digastric muscle. Meticulous hemostasis must be maintained throughout the surgical field while the posterior triangle is being cleared (Fig. 12.90).

Once the lymph nodes from the posterior triangle are dissected, the surgical procedure progresses medially to expose the lateral aspect of the carotid sheath (Fig. 12.91). All the lymphatic tissue lateral to the carotid artery is dissected and

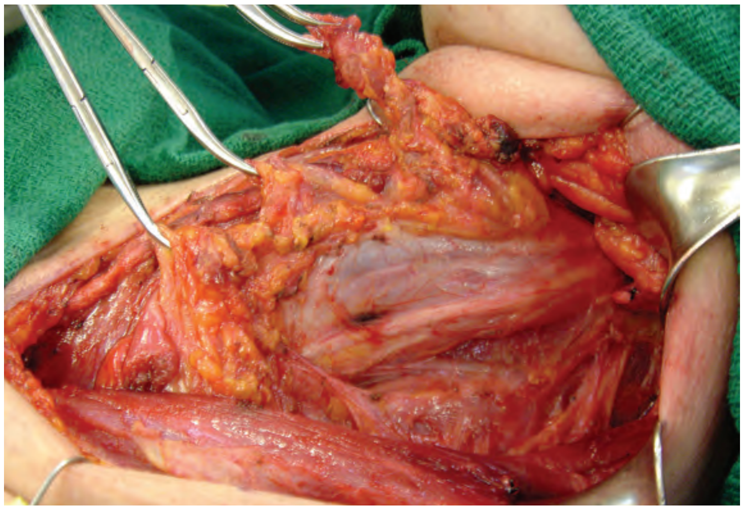

Figure 12.91 Posterior triangle lymph nodes lateral to the carotid sheath are dissected.

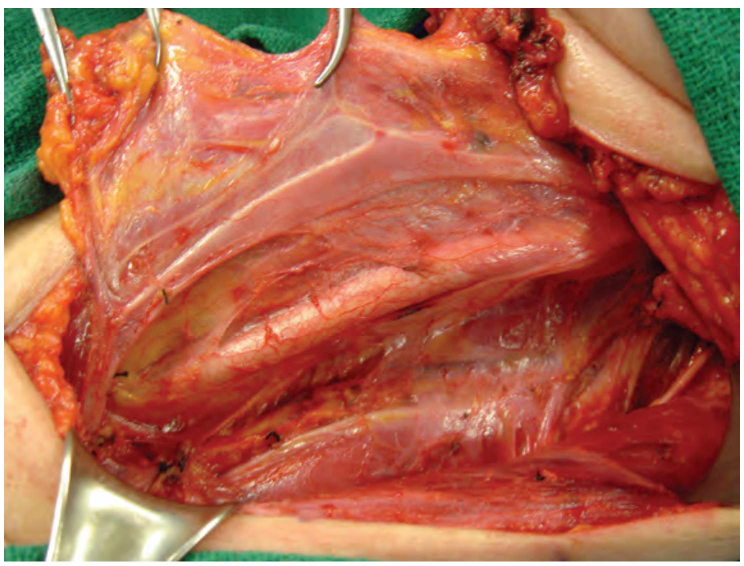

Figure 12.92 Lymphatics in the lower neck are divided and ligated.

meticulously reflected medially to expose the vagus nerve, the internal and common carotid arteries, and the lateral aspect of the internal jugular vein. At the lower end of the surgical field, communicating lymphatic vessels to the thoracic duct are identified and carefully divided and ligated (Fig. 12.92). Once all the lymphatic tissue lateral to the carotid sheath is divided and separated, the entire surgical specimen is rotated medially, exposing the internal jugular vein and the common carotid artery. The medial aspect of the internal jugular vein is freed from the surgical specimen, dividing the tributaries to the internal jugular vein, which are ligated with care. Particular attention should be paid at this point to explore the space posterior to the carotid sheath, where often one can find a cluster of metastatic nodes intimately associated with collateral lymphatic channels. All these nodes should be meticulously dissected. The surgical field after completion of the lateral neck dissection clearing levels II, III, IV, and V is shown in Fig. 12.93. Note the spinal accessory nerve cephalad, the roots of the cervical plexus posteriorly, and the carotid sheath medially. The strap muscles are seen medial to the carotid sheath.

Dissection now begins for the central compartment of the neck, and total thyroidectomy is performed. To accomplish this part of the surgical procedure in a comprehensive monobloc manner, the strap muscles are sacrificed. The sternohyoid and

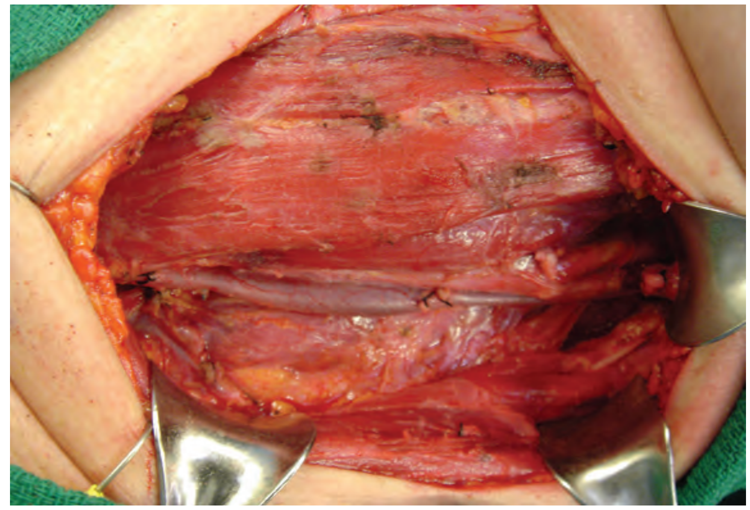

Figure 12.93 The surgical field following dissection of the left side of the neck.

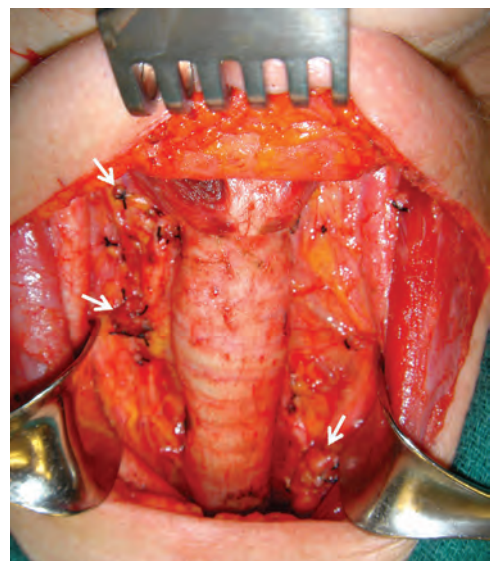

Figure 12.94 The surgical field after a total thyroidectomy and central compartment node dissection. Note the three parathyroid glands that were preserved (*arrows*).

sternothyroid muscles are detached from the undersurface of the hyoid bone, the thyroid cartilage, and posterior to the sternoclavicular joints bilaterally at their lower ends. Meticulous dissection of the pretracheal and paratracheal lymph nodes medial to the carotid artery is undertaken bilaterally with the dissection proceeding farther caudad to complete a total thyroidectomy, carefully preserving the parathyroid glands with their blood supply intact.

When a thorough central compartment neck dissection is undertaken, it is often difficult to preserve the vascularity of the parathyroid glands, particularly the inferior parathyroid glands. If it appears that the parathyroid gland is turning brownish in color because of lack of perfusion, it is advisable to send a small sliver for frozen-section analysis for confirmation of parathyroid tissue and then reimplant that parathyroid gland in the muscles of the lateral part of the neck.

Dissection then proceeds along the lower part of the central compartment of the neck. The recurrent laryngeal nerves are carefully identified and preserved to clear the thyroid bed, and the parathyroid glands are preserved. In this patient three glands could be preserved (Fig. 12.94). Complete clearance of prelaryngeal, pretracheal, perithyroid, and paratracheal lymph nodes

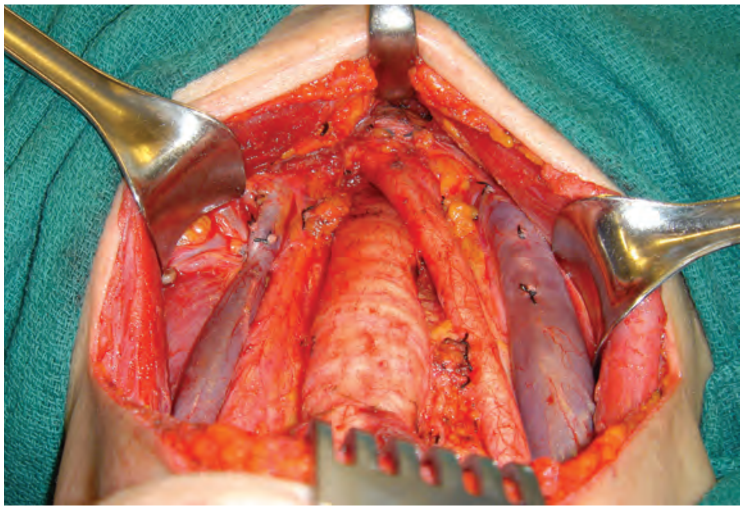

Figure 12.95 Paratracheal lymph nodes are dissected up to the innominate artery in the superior mediastinum.

Figure 12.97 The surgical specimen of a total thyroidectomy with lymph nodes at levels VI and VII and bilateral levels II to V.

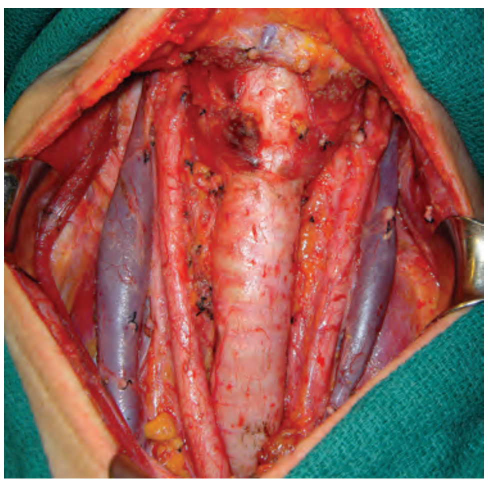

Figure 12.96 The surgical field showing complete clearance of regional lymph nodes from the hyoid bone to the innominate artery and bilateral levels II to V.

Figure 12.98 Postoperative appearance of the patient 1 month following surgery.

in the central compartment is completed at this stage. Dissection further continues into the superior mediastinum along the carotid sheath bilaterally to clear the pretracheal and paratracheal lymph nodes up to the innominate artery.

The surgical field after completion of the pretracheal and paratracheal dissection in the superior mediastinum is shown in Fig. 12.95. The origins of both common carotid arteries are shown in the surgical field. After completion of the surgical procedure the entire surgical field displays the contents of the carotid sheath bilaterally with the larynx, trachea, recurrent laryngeal nerves, and three parathyroid glands preserved (Fig. 12.96). The surgical specimen shown in Fig. 12.97 demonstrates three separate parts, including a total thyroidectomy with central compartment nodes and bilateral levels II to V. Many of the lymph nodes appear to be black, which is due to the cystic nature of metastases that often contain old hemorrhagic fluid.

The functional and aesthetic impact of this operative procedure is transient and relatively minor. The postoperative appearance of the patient 1 month following surgery shows that the scar is healing well, although there is still some edema of the upper skin flap. With passage of time, in the long term, this scar will appear to be a fine line along a skin crease in the lower part of the neck (Fig. 12.98). The patient is able to maintain normal range of motion of both shoulders and has very little anesthesia of the skin of the lower part of the neck.

Mediastinal Node Dissection

Massive primary papillary carcinomas of the thyroid gland with retrosternal extension or massive metastatic disease in the anterior superior mediastinum may require a sternotomy for complete excision. Serial sections of a contrast-enhanced CT scan of a patient with an extensive papillary carcinoma of the thyroid gland with massive cystic metastasis extending in the retrosternal region displacing the carotid sheath posterolaterally is shown in Figs. 12.99 through 12.102. Note the partial compromise of the tracheal air column with massive cystic metastases displacing the carotid artery and jugular vein posteriorly. The cystic metastases are seen contiguous with the primary tumor in the mediastinum extending up to the level of the arch of the aorta.

A papillary carcinoma with massive extension into the retrosternal region can cause superior vena cava syndrome with hypervascularity of the skin and subcutaneous soft tissues with collateral venous channels, easily seen on clinical examination (Fig. 12.103). The surgical approach for resection of this tumor requires a standard collar incision for a thyroidectomy and appropriate lateral neck dissection and a vertical midline incision extending caudad from the transverse cervical incision up to the level of the xiphisternum.

A midline sternotomy is performed, and meticulous mediastinal dissection is undertaken in conjunction with a total

Figure 12.99 An axial view of a contrast-enhanced computed tomography scan of the neck showing a massive goiter with calcification.

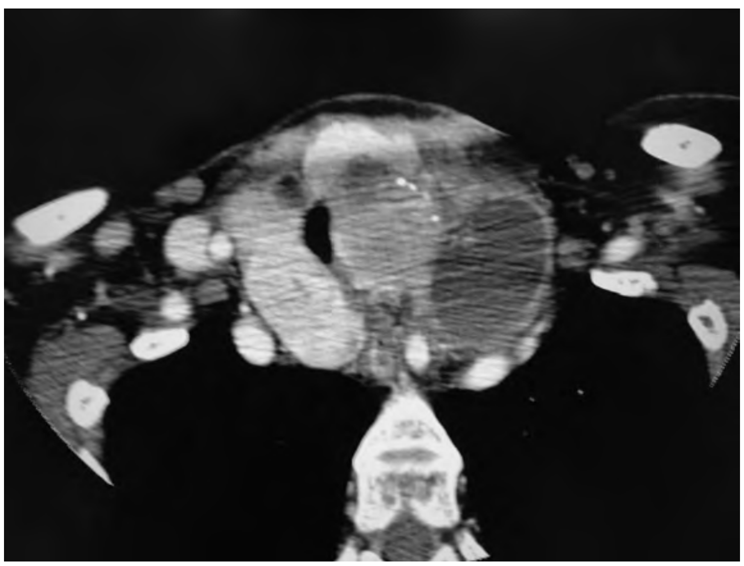

Figure 12.100 Cystic metastases causing compression of the trachea.

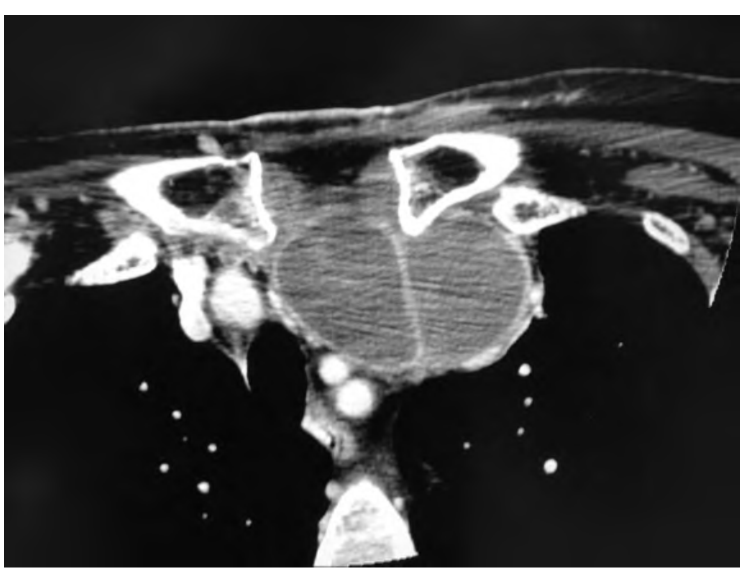

Figure 12.101 Retrosternal extension of cystic metastases.

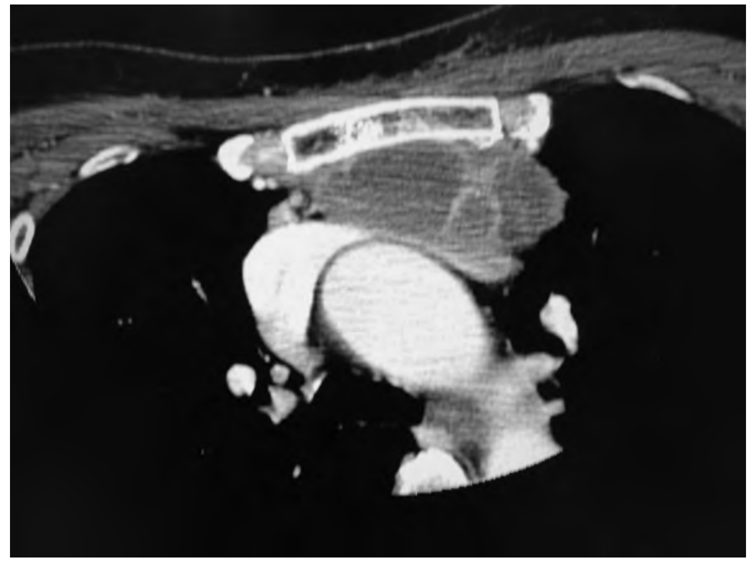

Figure 12.102 Cystic metastases in the anterior mediastinum extending up to the arch of the aorta.

Figure 12.103 A skin incision is outlined for a thyroidectomy, neck dissection, sternotomy, and mediastinal node dissection.

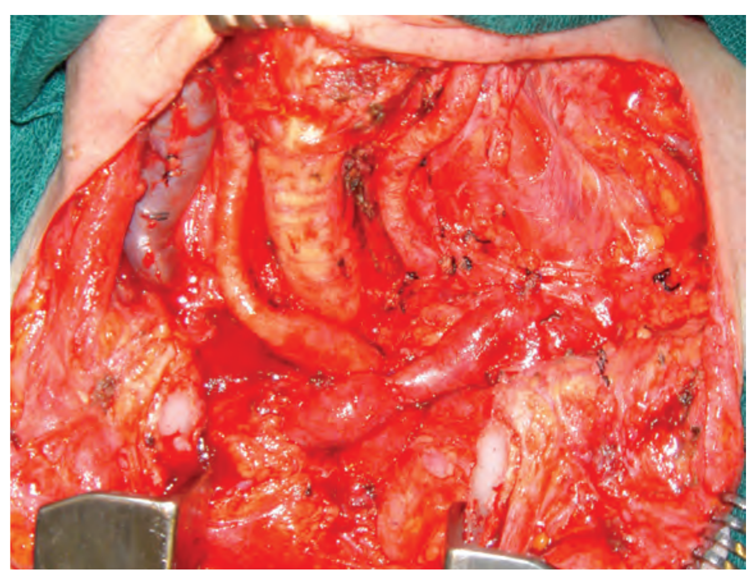

Figure 12.104 The surgical field after total thyroidectomy, left modified neck dissection, central compartment (level VI and VII), and mediastinal node dissection.

thyroidectomy, central compartment lymph node dissection, and left comprehensive modified neck dissection. The surgical field following resection of all gross tumor is shown in Fig. 12.104. Note the clearance of all disease from the level of the hyoid bone superiorly to the arch of the aorta inferiorly and from the lateral aspect of the right carotid sheath to the anterior border of the left trapezius muscle, sacrificing the left internal jugular vein, which was involved by cancer, but preserving the spinal accessory nerve. The recurrent laryngeal nerves are preserved if they are not directly infiltrated by cancer. Similarly, every attempt should be made to preserve the parathyroid glands if possible. If the vascularity of one or more parathyroid glands appears compromised and if the glands are not involved by cancer, they should be reimplanted into adjacent muscles after confirmation of histology by frozen section.

Surgery for Locally Advanced Thyroid Cancer

Locally advanced thyroid cancers are staged T3 and T4a/b by clinical and radiographic criteria. Minor extrathyroid extension or anterior extension with invasion of strap muscles (T3) is easily managed by en bloc resection of the involved strap muscles with total thyroidectomy. However, T4 tumors (gross posterior extension) require detailed preoperative workup with cross-sectional anatomic imaging, including contrast-enhanced CT scans or MRI to assess resectability. The CT scan is a very important evaluation in patients presenting with locally advanced thyroid cancer, fixed thyroid tumor, recurrent laryngeal nerve palsy, invasion of the surrounding structures, or clinically apparent nodal metastasis in the lateral neck. These patients undergo thorough evaluation of the extent of the disease, including superior mediastinal and parapharyngeal lymph nodes. The CT scan should be performed with contrast. The ATA's recent guidelines (2015) strongly endorse the use of preoperative CT scan with contrast. The voice evaluation before surgery either with mirror examination or better with fiberoptic laryngoscopy is important to evaluate the vocal cord function both preoperatively and postoperatively. Tumors involving the recurrent laryngeal nerve, larynx, trachea, or esophagus generally are surgically resectable and therefore staged as T4a. Tumors with invasion of the prevertebral fascia, encasement of the carotid artery, or mediastinal large vessels are staged T4b. Surgery may be feasible in some patients with T4b disease, but a high degree of selectivity is necessary to justify an operation.

Invasion of the Recurrent Laryngeal Nerve

Invasion of the recurrent laryngeal nerve may occur by infiltration or encasement by the primary tumor or by a cluster of matted metastatic lymph nodes along the course of the nerve from the mediastinum until its entry into the cricothyroid membrane (Fig. 12.105). Clearly, if the ipsilateral vocal cord is paralyzed, the involved nerve should be sacrificed to achieve a monobloc resection of the tumor. On the other hand, the need to sacrifice a functioning recurrent nerve should be assessed very carefully intraoperatively based on (1) the status of the contralateral nerve, (2) the feasibility of gross total tumor excision, (3) the need to sacrifice other adjacent structures, (4) the potential efficacy of adjuvant treatment for residual disease, (5) the patient's ability to tolerate the functional sequelae of a paralyzed vocal cord, and (6) the overall prognosis of the patient. Invasion of both recurrent laryngeal nerves requiring their sacrifice mandates the need for a tracheostomy. After sacrificing a functioning ipsilateral nerve, due consideration should be given to reconstruction of the recurrent laryngeal nerve, either with an interposition nerve graft or by anastomosing the distal stump of the nerve to the ansa hypoglossi. This will improve tone of the paralyzed vocalis muscle and strengthen vocal cord function, but the vocal cord mobility is not regained.

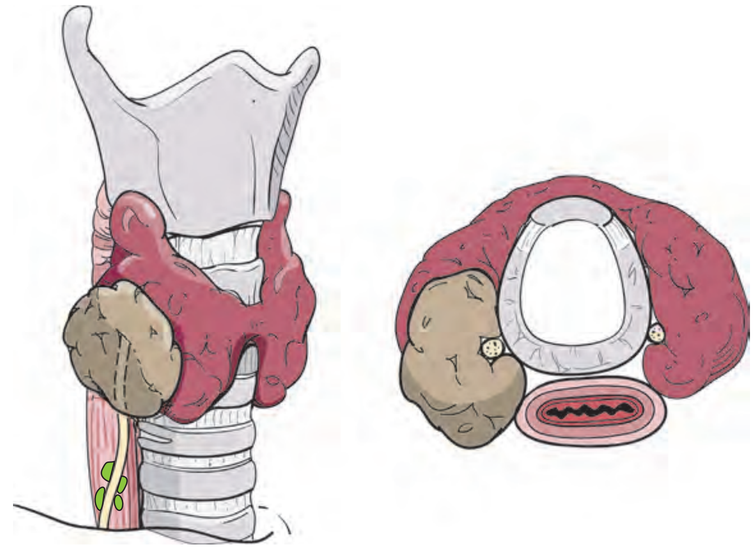

Figure 12.105 A schematic depiction of invasion of the recurrent laryngeal nerve by primary carcinoma of the thyroid gland near the cricothyroid membrane and/or by metastatic lymph nodes around the nerve. *(Courtesy Memorial Sloan Kettering Cancer Center.)*

Invasion of the Larynx

Locally invasive thyroid cancer may involve the underlying larynx or trachea by direct infiltration through the anterior or lateral wall of the laryngotracheal complex. Infiltration of the thyroid cartilage, subglottic larynx, cricothyroid membrane, anterior ring of cricoid, or tracheal wall is a common route of local invasion by extensive carcinomas of the thyroid gland with extrathyroid extension. In the absence of metastatic disease elsewhere, an aggressive surgical approach is recommended, which may include resection of parts of the larynx and trachea or portions of the esophagus. Infiltration of the laryngeal framework by locally aggressive thyroid cancer requires preoperative assessment not only by anatomic imaging but by functional assessment regarding the competency of the larynx, the status of the airway, and pulmonary function. If the functional integrity of the larynx is preserved but there is tumor extension to the laryngeal framework, then a partial laryngectomy is considered.

The patient shown in Fig. 12.106 had a mass fixed to the thyroid cartilage with an open biopsy done elsewhere, confirming the diagnosis of papillary carcinoma. She also had gross lymph node metastases at levels II and III in the right side of the neck. After a comprehensive modified neck dissection, type 1, that preserved only the accessory nerve, the surgical field shows tumor infiltration into the thyroid lamina, requiring its resection (Fig. 12.107). Excision of the thyroid cartilage is planned with an adequate margin around the grossly infiltrated lamina, which is achieved with a fine burr. A Freer elevator is used to separate the inner perichondrium from the thyroid lamina without violating

Figure 12.106 The outline of a locally advanced thyroid carcinoma invading the thyroid cartilage.

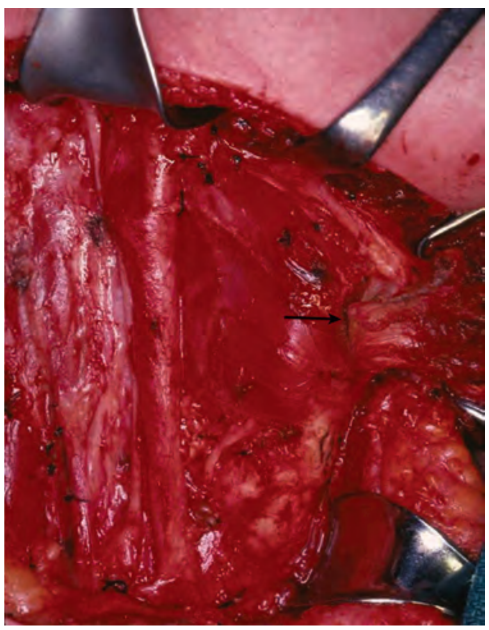

Figure 12.107 The surgical field after neck dissection showing infiltration of the tumor into the right thyroid lamina (*arrow*).

the paraglottic space. The entire thyroid lamina is resected in a monobloc fashion, preserving the mucosal integrity of the larynx (Fig. 12.108). This procedure has minimal if any functional sequelae while achieving gross total tumor resection.

Extension of primary or recurrent tumor to the anterior part of the subglottis larynx is amenable to a partial laryngectomy with preservation of a functioning larynx, and without a tracheostomy. However, a very careful radiographic and endoscopic assessment of the tumor extent is essential to carry out a successful surgical procedure. The anterior part of the subglottic larynx is functionally "relatively silent," since no important neuromuscular components of the larynx are present there. A patient with recurrent papillary carcinoma of the thyroid had previously undergone total thyroidectomy followed by RAI therapy. In the preceding 2 years before presentation, she had experienced increased respiratory discomfort with labored breathing. Her contrast-enhanced CT scan at the level of the cricoid cartilage shows recurrent tumor with destruction of the anterior aspect of the cricoid (Fig. 12.109). Endoscopic evaluation of the larynx with suspension laryngoscopy clearly shows the presence of recurrent tumor in the subglottic larynx at the anterior commissure, below the vocal cords (Fig. 12.110). Both vocal cords were mobile. Further assessment of the subglottic larynx shows the tumor confined to the anterior aspect of the subglottic larynx, extending up to the first tracheal ring (Fig. 12.111). The plan of surgical excision required resection of the subglottic larynx with anterior third of the cricoid ring and reconstruction of the larynx with an anterior tracheal flap.

The central compartment of the neck is explored in the usual fashion, and both recurrent laryngeal nerves are carefully identified, dissected, and preserved (Fig. 12.112). Based on the endoscopic assessment the area of the laryngocricotracheal resection is marked out (Fig. 12.113). The trachea is opened first between the first and second tracheal rings and is circumferentially separated from the larynx, carefully preserving the

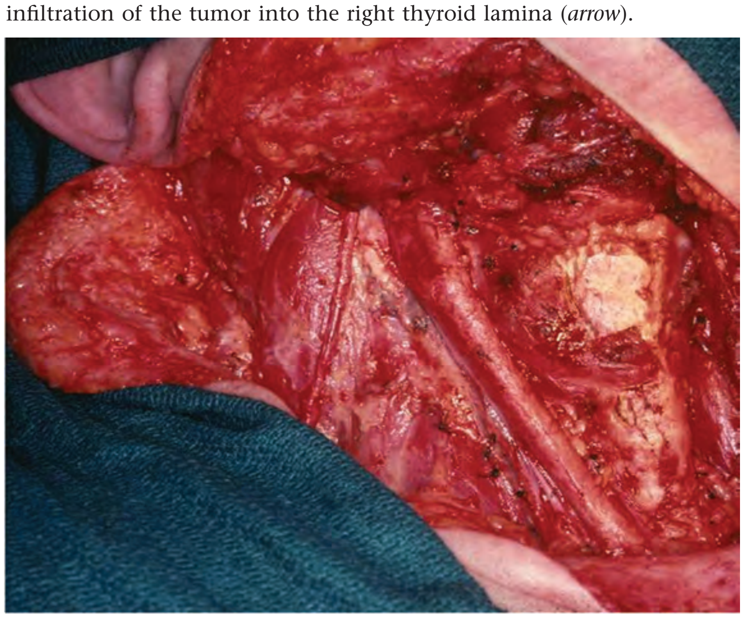

Figure 12.108 The surgical field after removal of the specimen showing preservation of the inner perichondrium and mucosal integrity of the larynx.

Figure 12.109 Axial view of a contrast-enhanced computed tomography scan showing recurrent cancer involving the cricoid cartilage (*arrow*).

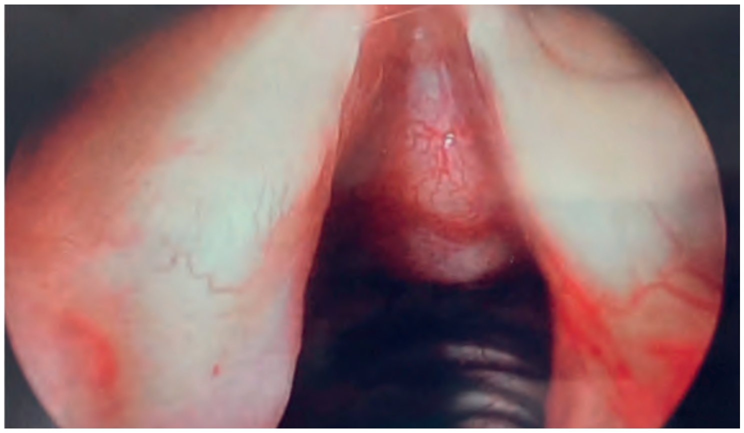

Figure 12.110 Endoscopic view at the level of the vocal cords showing subglottic tumor in the anterior midline.

Figure 12.111 Endoscopic view of the subglottic larynx showing the lower extent of the tumor up to the first ring of trachea.

recurrent laryngeal nerves (Fig. 12.114). The cricoid cartilage is then divided with a fine power saw, lateral to the recurrent tumor, with a safe margin on both sides. The detached cricoid segment is now retracted cephalad, to bring the tumor into view. Under direct vision, the thyroid cartilage is excised around the tumor bilaterally, and up to the anterior commissure cephalad. The surgical field following removal of the tumor is shown in Fig. 12.115A. Frozen sections are obtained from the margins of the surgical defect to ensure an R0 resection. The surgical specimen shows complete tumor resection (Fig. 12.115B).

Reconstruction is accomplished with a tracheal flap of its anterior wall. The posterolateral portions of the upper end of trachea are trimmed off to create a tongue-shaped flap of anterior tracheal wall (Fig. 12.116). This flap easily reaches the upper border of the defect in the thyroid cartilage. A single-layer watertight closure is performed with interrupted Prolene sutures (Fig. 12.117). The reconstructed larynx has a normal airway, and bilateral vocal cord function is preserved. No tracheostomy is necessary. The patient could be extubated a few hours after surgery. Thus many innovative function-preserving procedures can be performed on the laryngotracheal complex for locally advanced thyroid cancers. Postoperative view of the reconstructed larynx 2 years following surgery shows excellent restoration of airway and bilaterally mobile vocal cords (Fig. 12.118A). Sagittal view of a CT scan shows a reconstructed larynx by the tracheal flap with restoration of a normal airway (Fig. 12.118B).

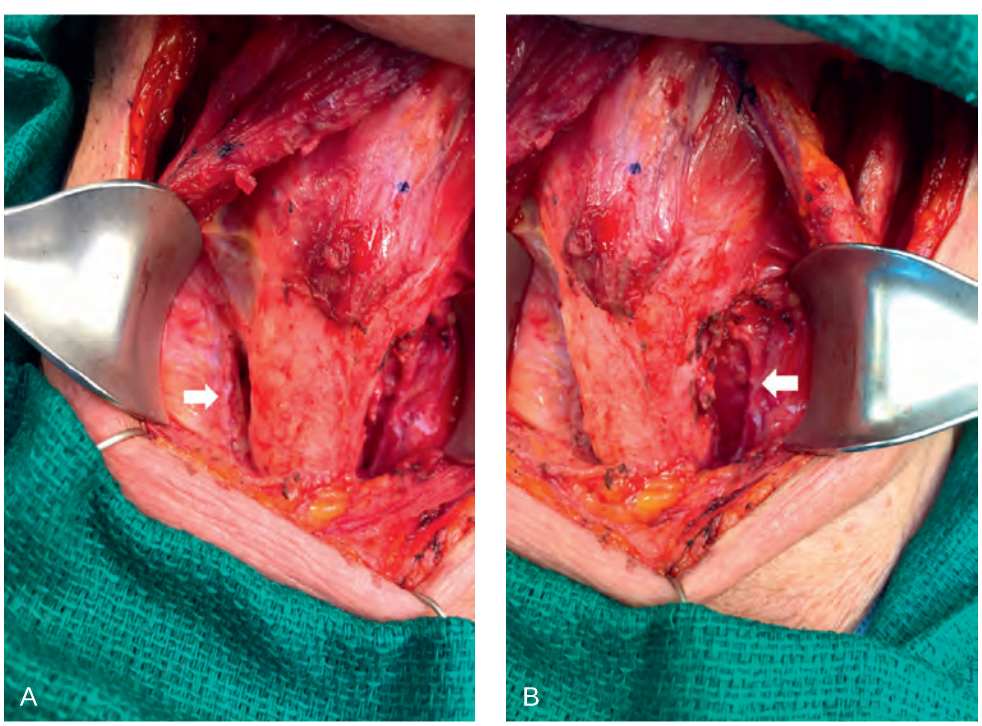

Figure 12.112 Surgical field showing the right (**A**) and left (**B**) recurrent laryngeal nerves *(arrows)*.

Figure 12.113 Outline of the extent of surgical resection to include portions of thyroid cartilage, cricoid cartilage, and the first ring of the trachea.

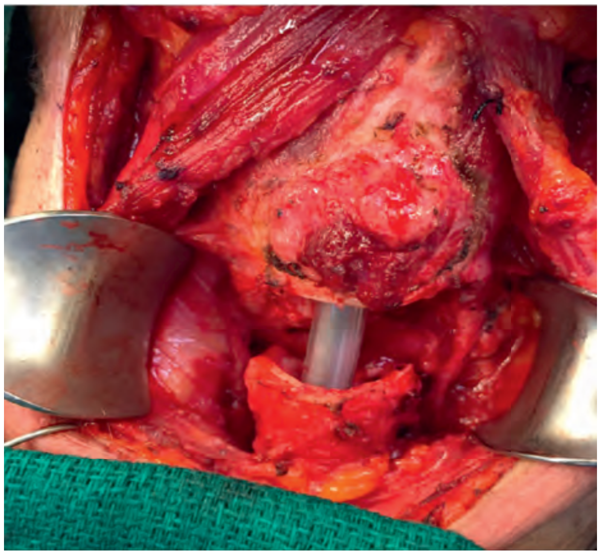

Figure 12.114 Circumferential transaction of distal trachea.

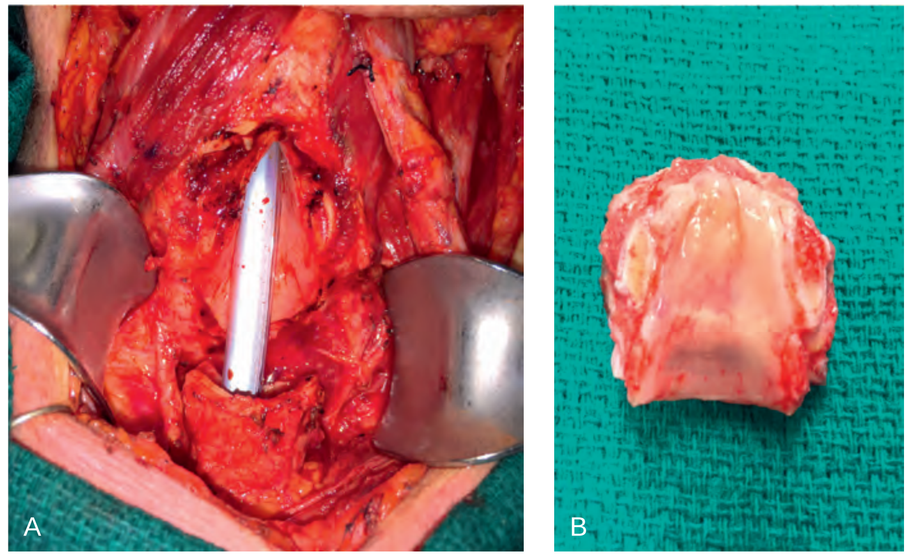

Figure 12.115 Surgical defect following resection of tumor showing the undersurface of both vocal cords and stumps of the cricoid cartilage (**A**), and the surgical specimen showing recurrent tumor in the subglottic larynx (**B**).

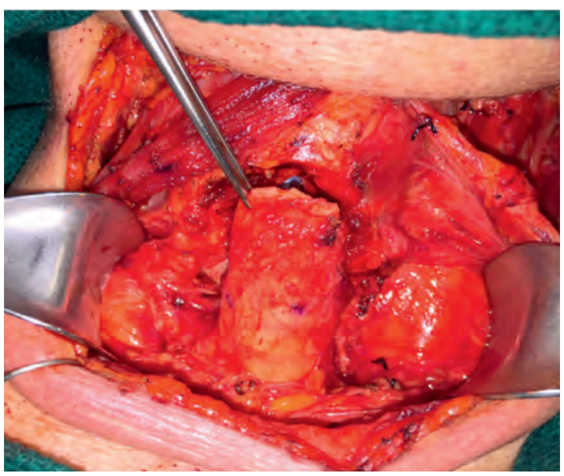

Figure 12.116 Advancement of distal trachea to reconstruct the surgical defect.

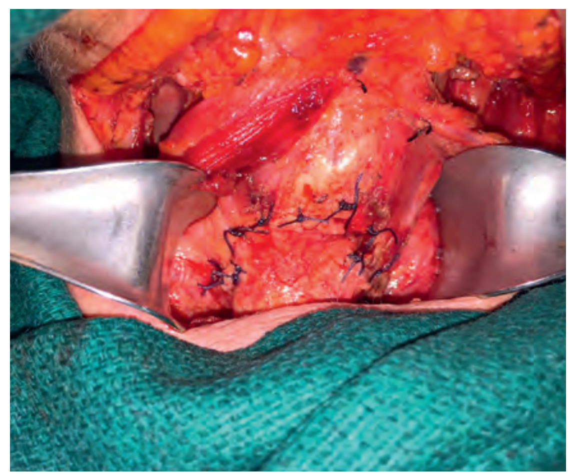

Figure 12.117 Single layer, watertight closure between the trachea and larynx.

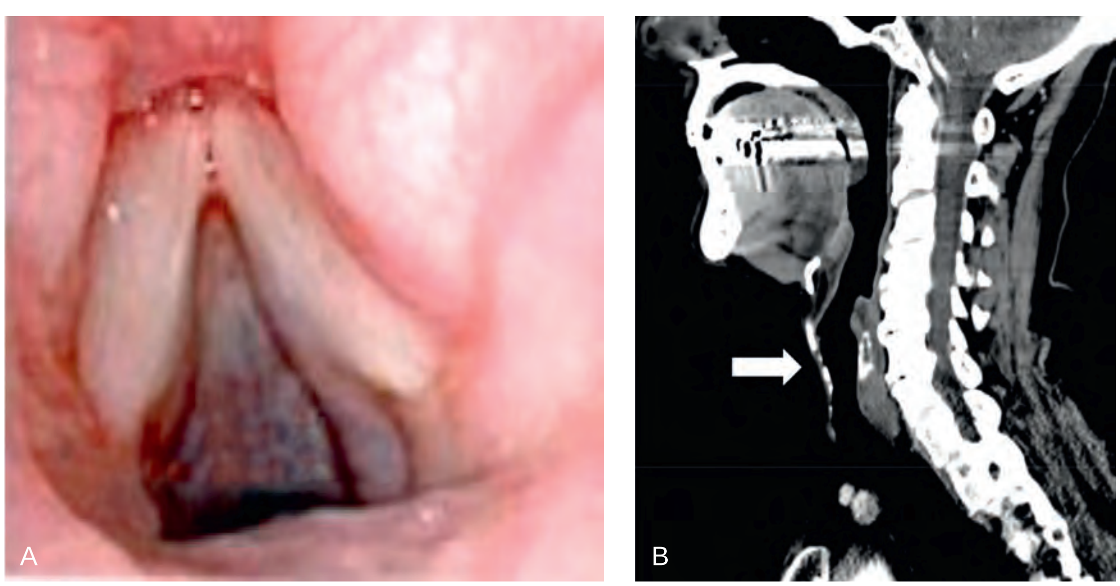

Figure 12.118 Postoperative view of the larynx 2 years following surgery showing the reconstructed subglottic larynx with the tracheal flap (**A**), and sagittal view of the computed tomography scan showing normal laryngotracheal airway reconstructed by an anterior tracheal wall flap (*arrow*) (**B**).

If the primary tumor, however, involves both thyroid laminae, the paraglottic space, or the lateral subglottic region or if it perforates through the mucosa of the larynx, then a total laryngectomy becomes necessary (Figs. 12.119 and 12.120). In a majority of instances, such locally aggressive tumors, especially in older patients, often are poorly differentiated carcinomas that usually are not amenable to radioiodine therapy. Preoperative assessment with a PET scan is helpful in such circumstances. Extremely FDG-avid lesions with a high standard uptake value (SUV) generally are nonresponsive to radioiodine therapy. In such instances, an initial total laryngectomy offers the best chance for local control of disease and possible cure. Examples of extensive thyroid carcinoma with invasion of the larynx requiring a total laryngectomy are shown in Figs. 12.121 and 12.122. Conversely, tumors with a low SUV on an FDG-PET scan generally are well differentiated papillary carcinomas with a higher probability of response to radioiodine treatment. Subtotal removal of the tumor, thus preserving a functionally intact remnant larynx, may be considered in such highly selected patients. Occasionally, a functioning larynx may be able to be preserved for long periods of time with control of cancer, although some may need a delayed total laryngectomy.

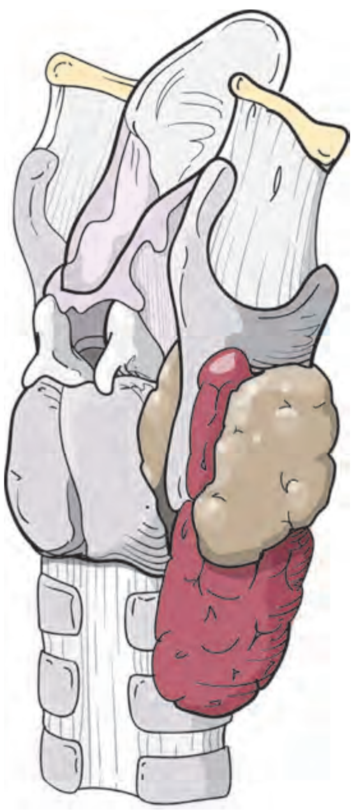

Figure 12.119 A schematic diagram showing invasion of the larynx through the cartilage by thyroid cancer. *(Courtesy Memorial Sloan Kettering Cancer Center.)*

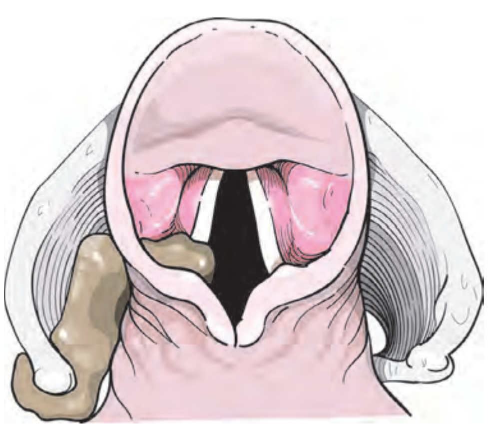

Figure 12.120 A schematic diagram showing the presence of cancer in the paraglottic space. *(Courtesy Memorial Sloan Kettering Cancer Center.)*

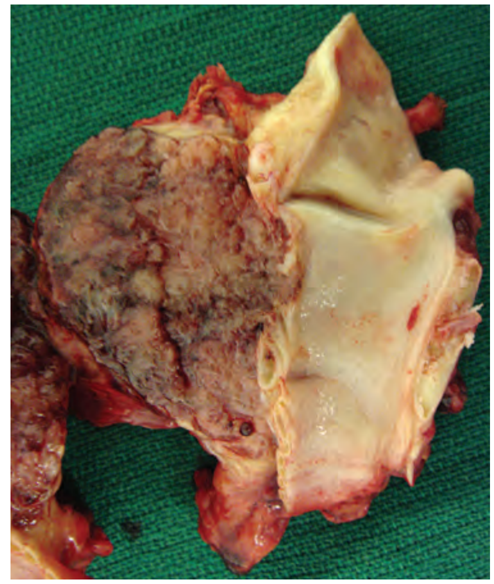

Figure 12.121 The surgical specimen of a total thyroidectomy and laryngectomy showing extensive invasion of the laryngeal framework.

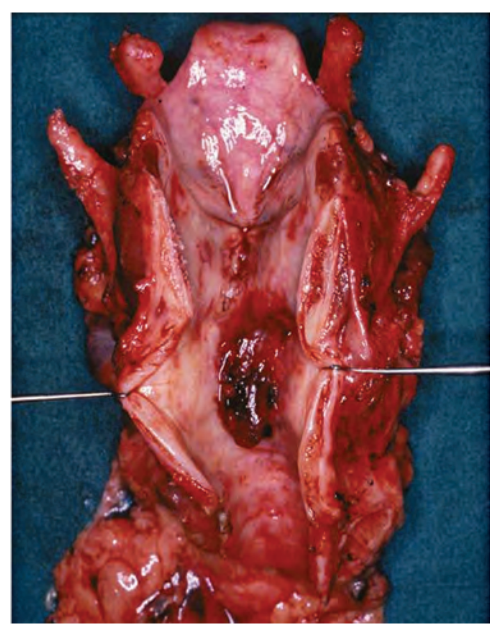

Figure 12.122 The surgical specimen of a total laryngectomy with a thyroidectomy showing the tumor in the subglottic larynx causing airway compromise.

Invasion of Cricotracheal Region

The patient described here presented with palpable cervical lymph node metastasis in the lower part of the neck on the left-hand side with diffuse enlargement of the thyroid gland from a primary differentiated carcinoma of the thyroid gland extending to the subglottic region and the proximal trachea. An MRI scan of this patient in the axial plane at the level of

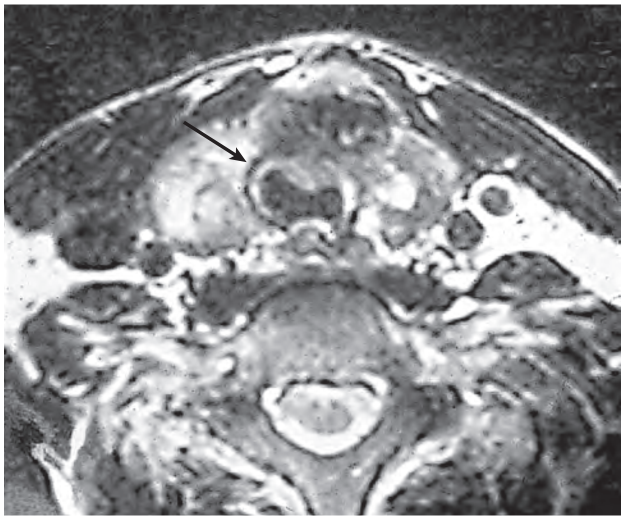

Figure 12.123 An axial view of a magnetic resonance imaging scan showing tracheal invasion by cancer of the thyroid gland *(arrow)*.

Figure 12.124 A sagittal view of a magnetic resonance imaging scan showing the tumor in the subglottic larynx and proximal trachea (*arrow*).

Figure 12.125 An endoscopic view of the proximal trachea showing a submucosal tumor in the anterior tracheal wall.

the first ring of the trachea clearly demonstrates extension of the tumor into the tracheal lumen from a massive tumor of the thyroid in the central compartment of the neck (Fig. 12.123). A sagittal view of the MRI clearly demonstrates extension of tumor through the cricoid into the subglottic region and through the first three rings of the trachea intraluminally (Fig. 12.124). In spite of this extensive invasion of the larynx and trachea, mobility of both vocal cords is within normal limits. An endoscopic view of the proximal trachea with a fiberoptic bronchoscope demonstrates submucosal extension of the tumor through the anterior tracheal wall (Fig. 12.125).

The surgical procedure consists of a comprehensive left modified neck dissection in conjunction with a total thyroidectomy and resection of the anterior portion of the cricoid ring and anterior wall of the proximal trachea, excising approximately 50% of the circumference of the trachea (Fig. 12.126). Thus all of the anterior and the left lateral wall of the trachea is resected. The operative field (Fig. 12.127) demonstrates the surgical defect in the trachea with an endotracheal tube in the lumen. A total thyroidectomy has been completed with clearance of central compartment lymph nodes but with preservation of the right recurrent laryngeal nerve and the parathyroid glands on the right-hand side. The left recurrent laryngeal nerve was encased by tumor and is therefore resected. The surgical defect demonstrates the resected portion of the cricoid in the subglottic region and the deficit on the anterolateral tracheal wall on the left-hand side. To repair this defect in the laryngotracheal junction and restore the continuity of the airway, the following reconstructive technique is utilized.

The connection between the larynx and trachea is completely separated, allowing the remnant of the lateral tracheal wall on the right-hand side to be freed up from the larynx. This result is clearly seen in Fig. 12.128. This remnant is accurately trimmed and fashioned in a shape appropriate to match the defect in the cricoid ring. The cervical portion of the trachea is now circumferentially mobilized. A 90-degree axial rotation of the trachea permits the appropriately fashioned right lateral wall remnant to be brought anteriorly to fit the surgical defect in the cricoid region (Fig. 12.129). After appropriate trimming of the edges of the trachea to allow laryngotracheal anastomosis in an end-to-end fashion, closure of the airway begins, which is accomplished with a single layer of interrupted 3-0 Prolene sutures. A watertight closure is secured to prevent air leak from the suture line (Fig. 12.130).

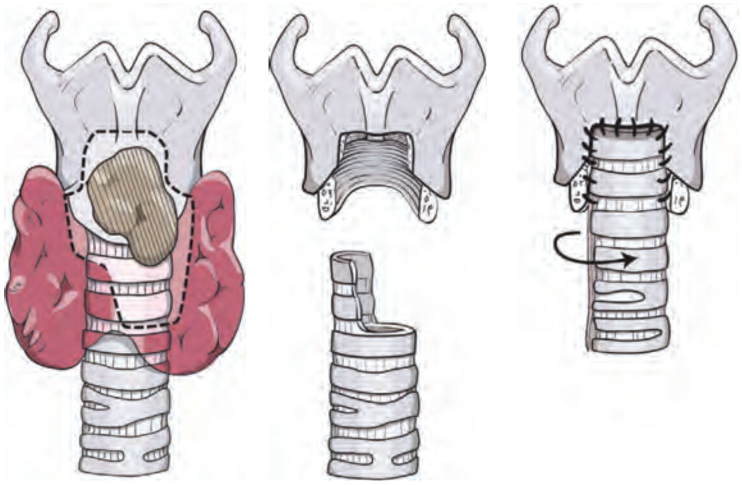

Figure 12.126 A schematic diagram showing the technique of cricotracheal reconstruction by axial rotation of trachea. *(Courtesy Memorial Sloan Kettering Cancer Center.)*

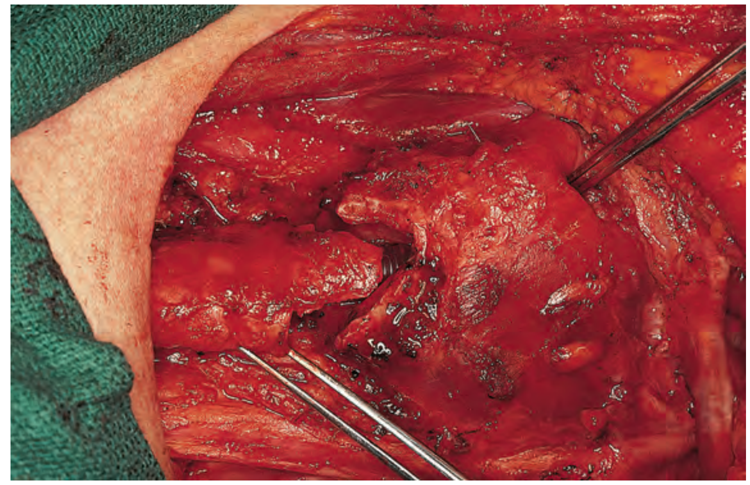

Figure 12.129 The remnant of the lateral tracheal wall on the right-hand side is trimmed to fit the defect in the cricoid cartilage.

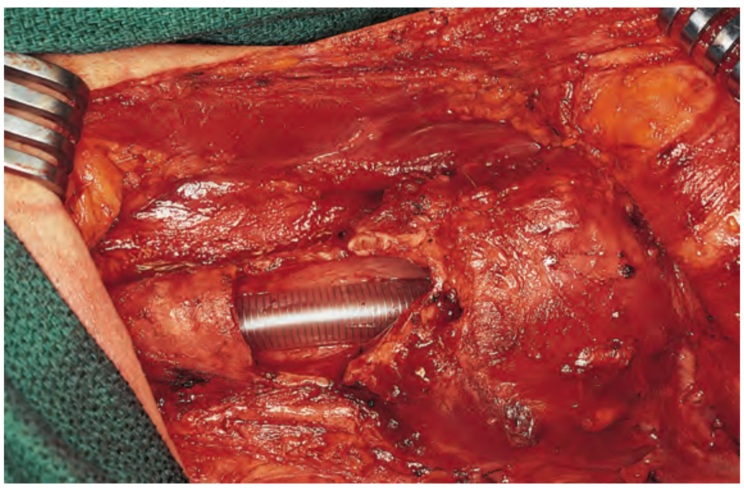

Figure 12.127 The operative field following a total thyroidectomy with resection of anterior aspects of the cricoid and proximal trachea.

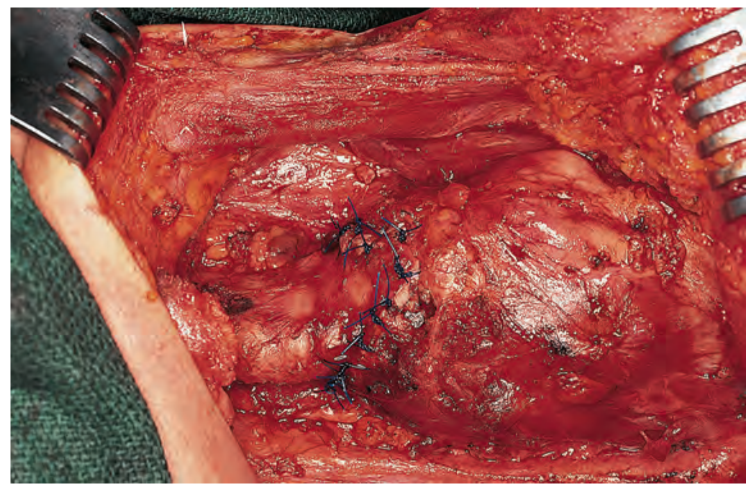

Figure 12.130 Watertight closure between the trachea and cricoid.

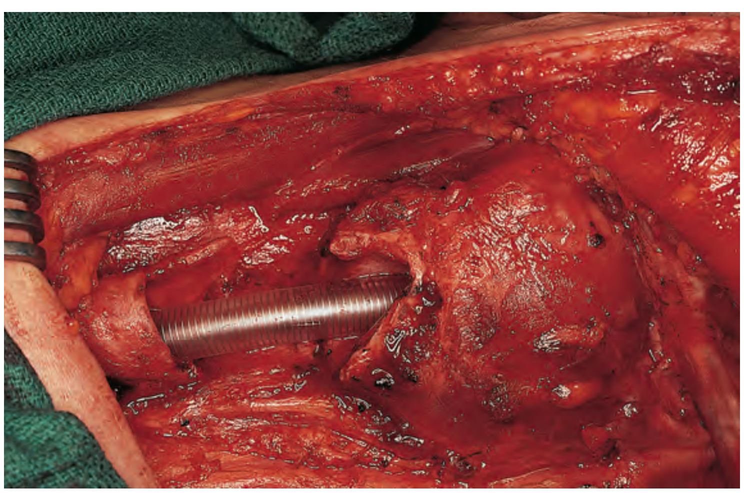

Figure 12.128 The trachea is completely freed from the cricoid.

Figure 12.131 A postoperative sagittal view of a magnetic resonance imaging scan showing a satisfactory reconstruction of the airway.

The endotracheal tube is retained for 24 hours. A tracheostomy is not necessary. The neck of the patient is kept in flexion with either a halo splint or a heavy silk suture between the chin and the anterior chest wall. Liquids are permitted by mouth in approximately 48 hours, and a soft diet is advanced over the course of the next 3 days. Extension of the neck is permitted at the end of 2 weeks if primary healing of the neck wound is manifested. A postoperative MRI scan in a sagittal plane demonstrates adequate airway (Fig. 12.131).

Invasion of the Trachea

A locally invasive but histologically well-differentiated carcinoma of the thyroid sometimes extensively involves the trachea. The extent of tracheal invasion is classified into (I) adherence to the external tracheal wall, (II) cartilage invasion, (III) infiltration through the cartilage into the submucosal plane, or (IV) frank tumor in the tracheal lumen (Figs. 12.132 and 12.133). The rationale for aggressive surgical resection in this clinical setting

is supported by significant long-term local control with its positive impact on survival.

The patient presented here was unaware that he had a mass in his thyroid gland. An episode of massive hemoptysis suddenly developed, requiring urgent hospitalization. Preoperative radiographic workup included a CT scan, which showed the presence of a mass in the left lobe of the thyroid gland with extension into the tracheal lumen and focal calcification (Fig. 12.134). Sagittal and axial MRI scans confirmed the presence of an intraluminal tumor in the proximal trachea beginning at the level of the second tracheal ring (Figs. 12.135 and 12.136). Clinical examination confirmed the presence of a palpable hard mass in the left thyroid lobe with palpable metastatic lymph nodes in the lower jugular chain on the left-hand side. Bronchoscopy demonstrated the presence of a fungating ulcerated lesion in the tracheal lumen, coming from its anterolateral wall on the left-hand side (Fig. 12.137). The tumor involved a segment of the trachea approximately 3.5 to 4 cm in length. Sleeve resection of the trachea with primary end-to-end anastomosis can be accomplished for defects up to 5 to 6 cm in length with use of a variety of maneuvers (Fig. 12.138).

The surgical procedure requires a total thyroidectomy in conjunction with sleeve resection of the trachea and a left modified radical neck dissection. The patient is put under general endotracheal anesthesia with a No. 6 endotracheal tube. The balloon of the endotracheal tube is passed distal to

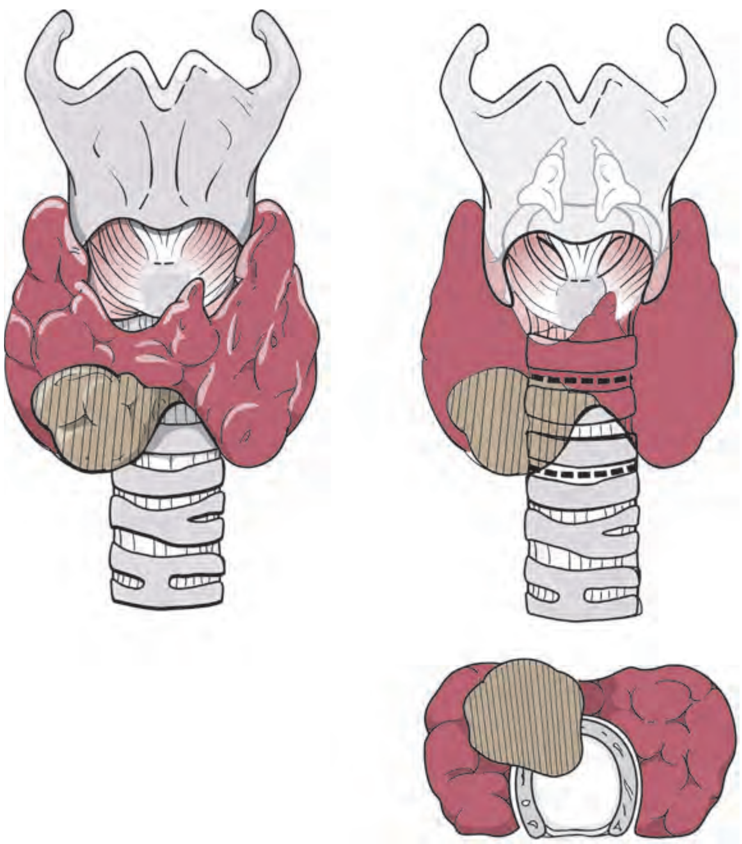

Figure 12.132 A schematic diagram showing direct infiltration of the trachea by thyroid cancer. *(Courtesy Memorial Sloan Kettering Cancer Center.)*

Figure 12.134 An axial view of a computed tomography scan showing a massive tumor of the thyroid gland with calcification and invasion of the anterolateral wall of the trachea on the left-hand side.

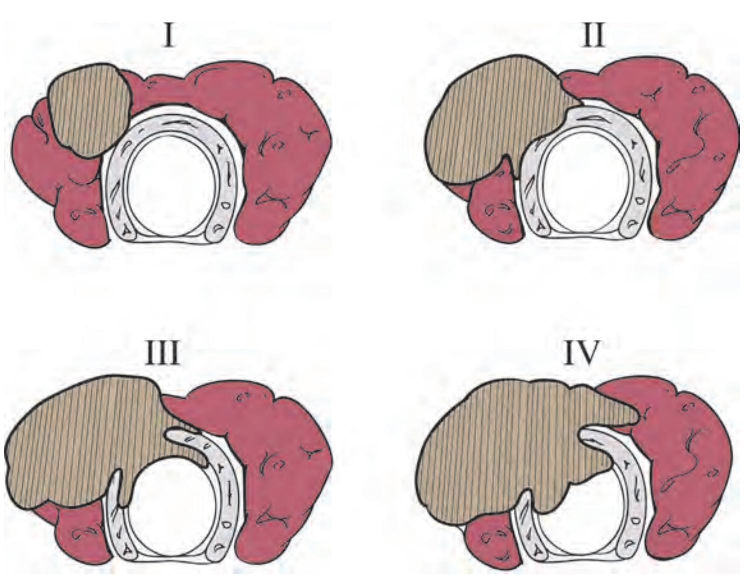

Figure 12.133 Classification of the extent of tracheal invasion by thyroid cancer. *(Courtesy Memorial Sloan Kettering Cancer Center.)*

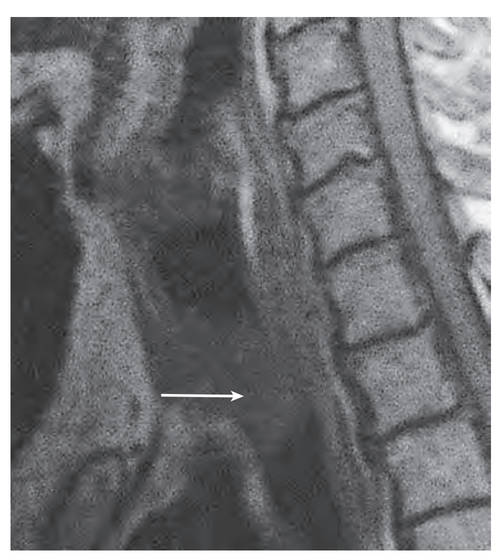

Figure 12.135 A sagittal view of a magnetic resonance imaging scan showing the tumor in the proximal trachea (*arrow*).

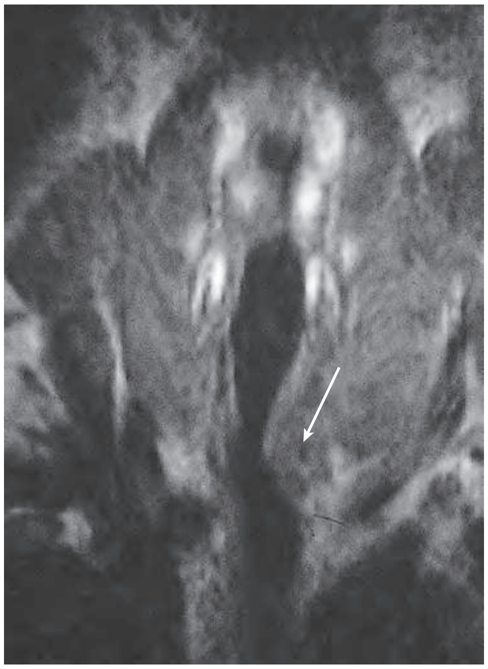

Figure 12.136 A coronal view of the magnetic resonance imaging scan showing invasion of the trachea through its lateral wall with the tumor presenting within its lumen (*arrow*).

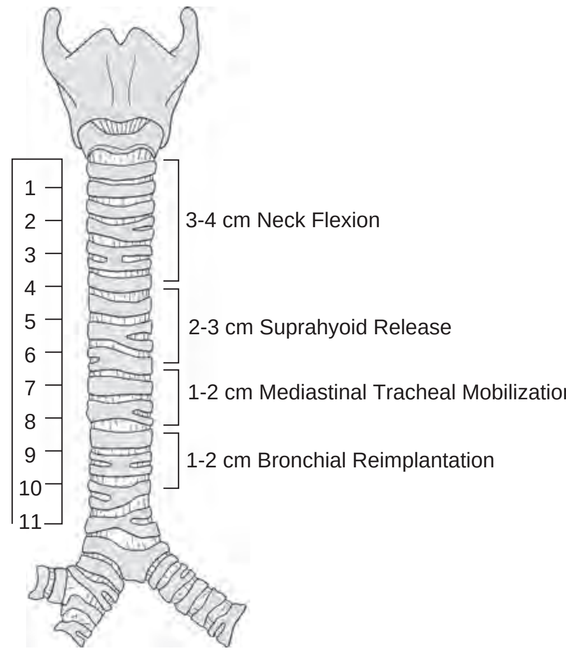

Figure 12.138 Techniques of mobilization of the trachea for end-to-end anastomosis after sleeve resection. *(Courtesy Memorial Sloan Kettering Cancer Center.)*

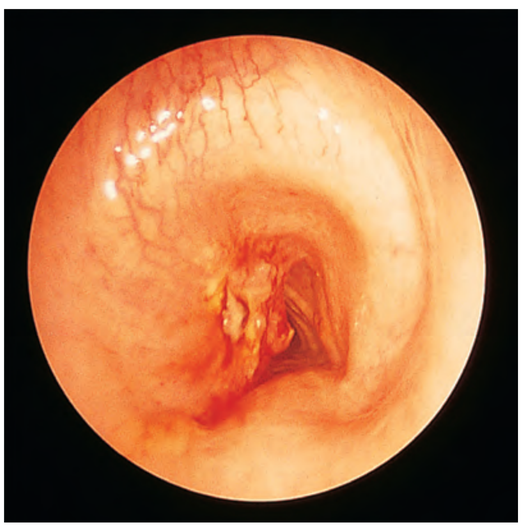

Figure 12.137 An endoscopic view of the trachea showing the tumor fungating through its left anterolateral wall.

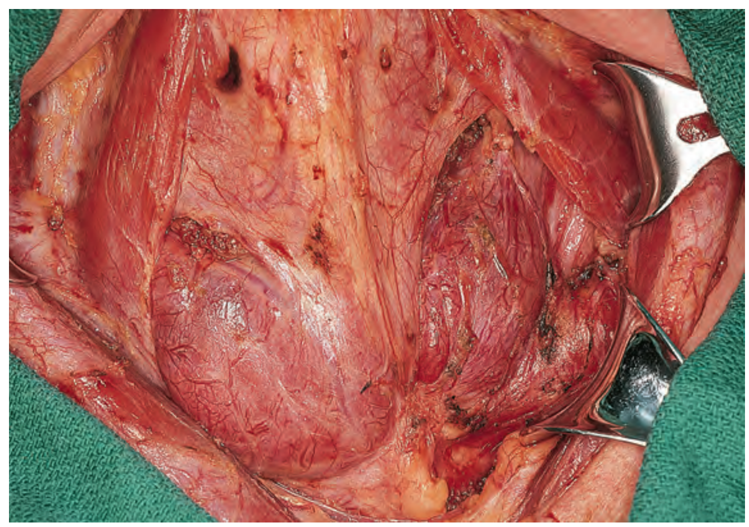

Figure 12.139 The strap muscles are excised to expose the anterior surface of the thyroid gland.

the lower border of the tumor and is inflated. A transverse lower cervical incision is made approximately two fingerbreadths above the clavicle, extending from the lateral border of the right sternocleidomastoid muscle up to the anterior border of the left trapezius muscle. Upper and lower skin flaps are elevated in the usual fashion. The left modified neck dissection is completed in the usual fashion, keeping the specimen attached to the left thyroid lobe. The sternohyoid and sternothyroid muscles are excised to facilitate adequate exposure of the central compartment and the anterior surface of the thyroid gland (Fig. 12.139).

Dissection of the thyroid gland begins with mobilization of the right lobe, carefully preserving the right upper and lower parathyroid glands (Fig. 12.140). As the tumor is mobilized toward the left side, it becomes apparent that it is perforating through the anterior wall of the trachea. At this juncture, the right recurrent laryngeal nerve is carefully dissected and traced until its entry into the larynx through the cricothyroid membrane (Fig. 12.141). The nerve is retracted away from the tracheoesophageal groove to develop a plane between the trachea and the esophagus. A similar plane is created on the left-hand side to circumferentially mobilize the trachea distal to the region of tumor invasion. A Penrose drain is inserted between the tracheoesophageal plane, and the trachea is retracted anteriorly to permit mobilization of the left thyroid lobe and dissection in the left tracheoesophageal groove.

Dissection of the left thyroid lobe is much more tedious because of extensive tumor infiltration in the soft tissues. No attempt is made to identify the parathyroid glands on the left-hand side. Further mobilization of the left thyroid lobe on its posterior surface demonstrated that the tumor had invaded the muscular wall of the esophagus, requiring that it be sacrificed (Fig. 12.142). In a close-up view of the surgical field, the prolapsed mucosa of the esophagus at the site of resection of its muscular wall is demonstrated (Fig. 12.143). Because of extensive invasion by the tumor in the tracheoesophageal wall on the left-hand side, the left recurrent laryngeal nerve is sacrificed. The left superior and inferior thyroid arteries and veins are divided and

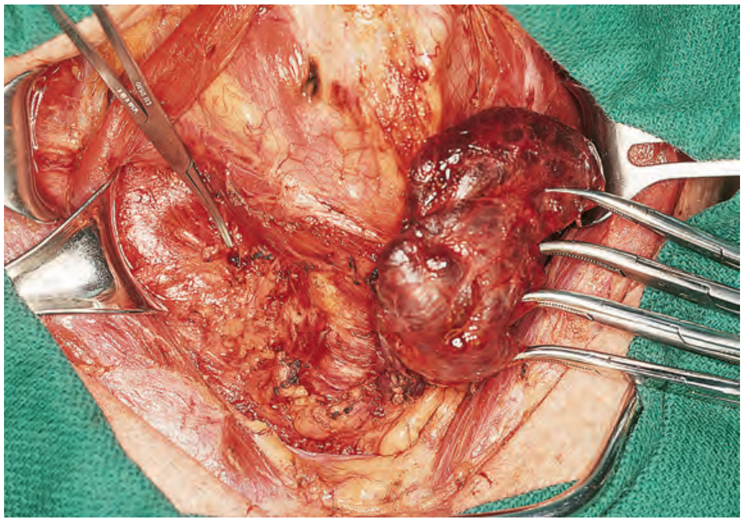

Figure 12.140 The right thyroid lobe is dissected from its bed, carefully preserving the parathyroid glands.

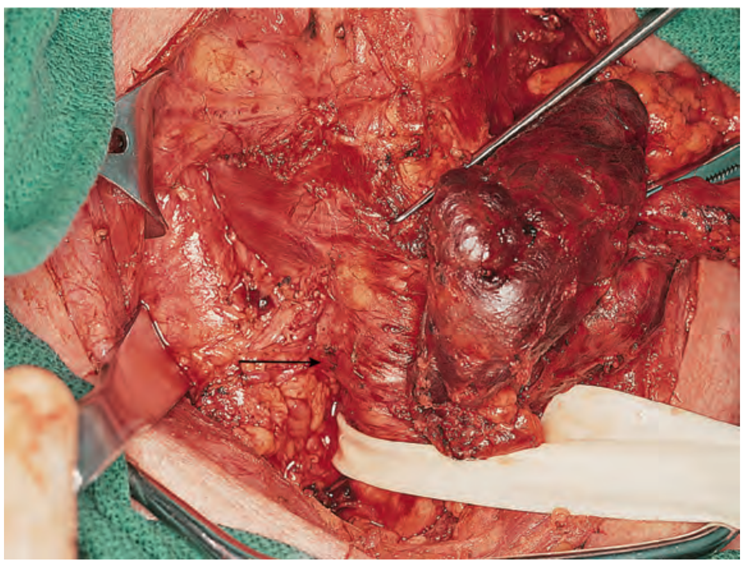

Figure 12.141 The right recurrent laryngeal nerve is preserved (*arrow*), and the trachea is circumferentially mobilized and retracted with a Penrose drain.

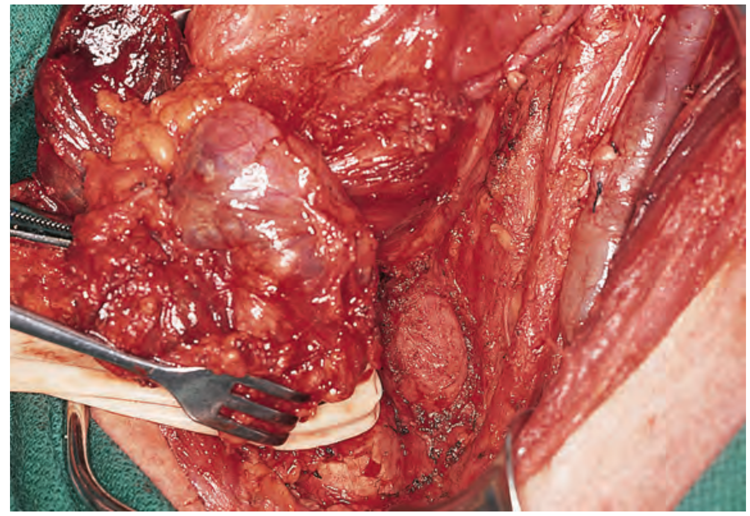

Figure 12.142 Dissection of the left thyroid lobe demonstrates invasion of the muscular wall of the esophagus, which is resected.

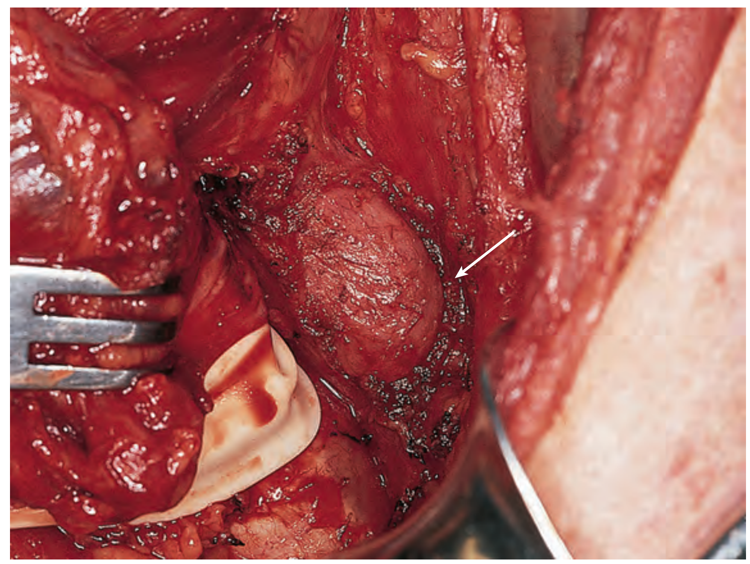

Figure 12.143 Prolapsed mucosa of the cervical esophagus is seen at the site of excision of esophageal musculature (*arrow*).

ligated. The specimen is now nearly completely mobilized circumferentially except for its attachment to the trachea.

Entry is made into the tracheal lumen through the first tracheal ring on the right-hand side of the midline to inspect the lumen. Under direct vision, circumferential transection of the trachea through the first tracheal ring is accomplished, remaining above the visible level of the tumor. Similarly, under direct vision, the trachea is transected inferiorly through the seventh tracheal ring as shown in Fig. 12.144. The surgical specimen is now completely free and can be removed. The balloon on the endotracheal tube is deflated and the endotracheal tube is withdrawn in the larynx to permit removal of the specimen. The endotracheal tube is then readvanced, and its balloon is inserted in the distal stump of the trachea and reinflated (Fig. 12.145). The defect in the trachea measures approximately 4 cm. A tracheal defect of this length can be reconstructed easily by primary anastomosis between the first and the seventh tracheal rings. To accomplish the tracheal anastomosis without tension on the suture line, a suprahyoid release of the larynx is performed, which requires detachment of the tongue muscles attached on the superior surface of the hyoid bone. Using an electrocautery, the mylohyoid, hyoglossus, and geniohyoid muscles are detached from the superior surface of the hyoid bone, which is denuded between the two lesser corneae of the hyoid. The patient's neck is then positioned in extreme flexion to permit approximation of the larynx to the stump of the trachea (Fig. 12.146). Primary anastomosis between the first and the seventh tracheal rings is then performed using interrupted 3-0 Prolene sutures.

The closure begins at the midline of the membranous trachea, keeping the knots of the sutures outside the lumen. This closure is brought up to the lateral wall of the trachea on one side. Similar closure begins from the midline of the membranous trachea, keeping the knots on the outside, up to the lateral wall of the trachea on that side. Simple interrupted sutures are then taken for the anterior tracheal wall, securing a watertight closure. The adequacy of the anastomosis is confirmed by covering the anastomotic site with saline solution and asking the anesthesiologist to release the balloon on the endotracheal tube and give positive pressure breathing. If air bubbles through the suture line are identified, additional sutures are placed to secure a watertight closure (Fig. 12.147). Suction drains are avoided, but

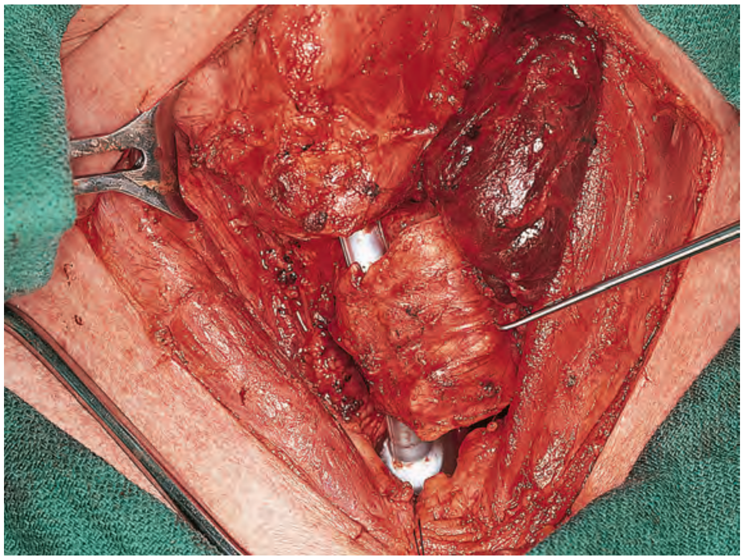

Figure 12.144 The trachea is circumferentially transected above and below the level of tumor invasion.

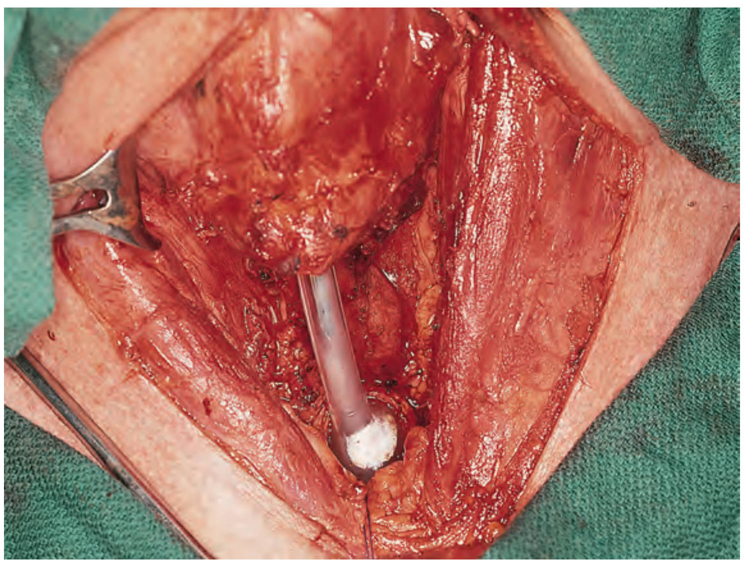

Figure 12.145 The extent of the surgical defect in the trachea is demonstrated by the endotracheal tube between the larynx and the distal stump of the trachea.

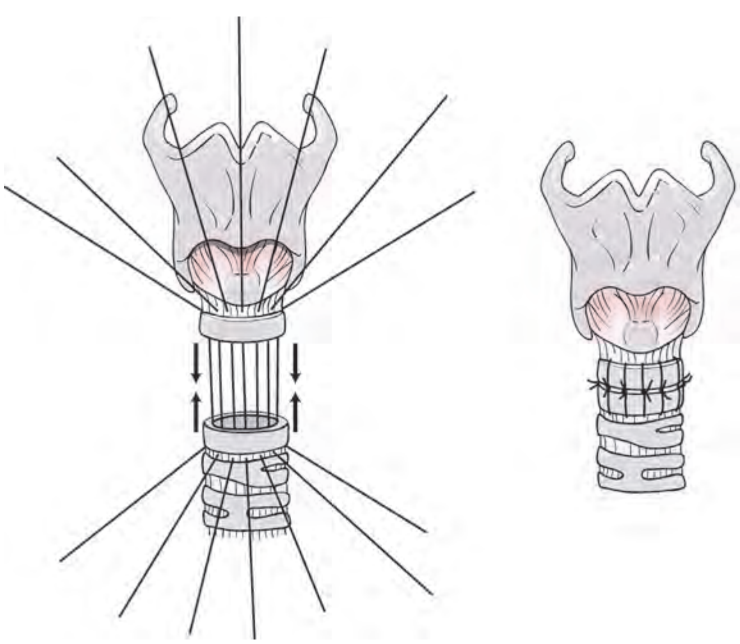

Figure 12.146 The technique of end-to-end anastomosis. *(Courtesy Memorial Sloan Kettering Cancer Center.)*

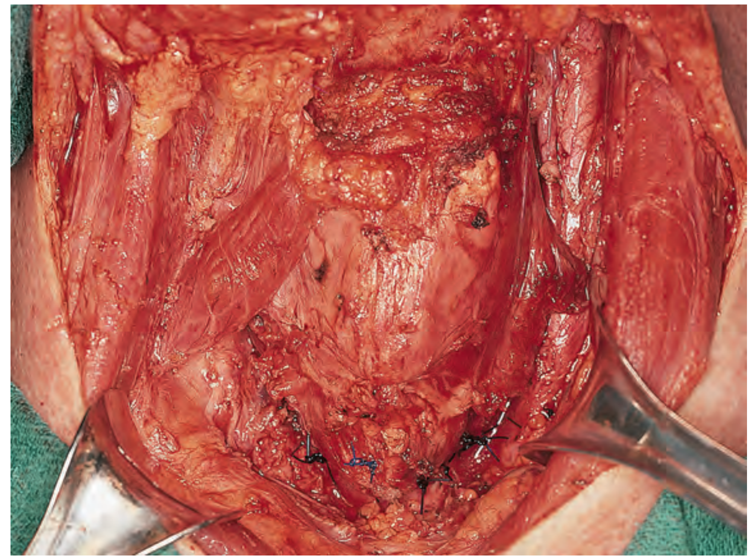

Figure 12.147 Primary anastomosis between the larynx and distal trachea is completed after suprahyoid release of the larynx.

Figure 12.148 A heavy nylon suture between the chin and the presternal region maintains flexion of the neck in the postoperative period.

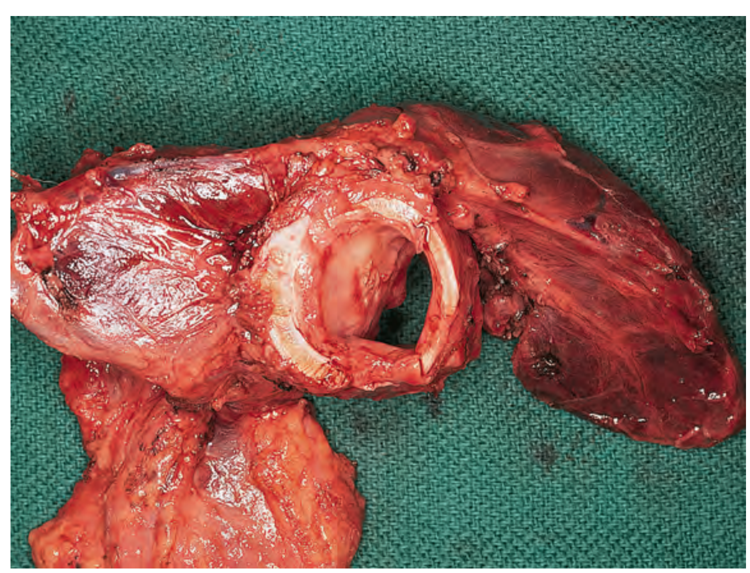

Figure 12.149 An end-on view of the surgical specimen shows cancer of the thyroid perforating through the tracheal wall into its lumen.

Penrose drains are inserted, and the incision is closed in layers using 3-0 chromic catgut interrupted sutures for platysma and 5-0 nylon for skin. The neck is maintained in extreme flexion with use of either a halo splint or simply a No. 1 heavy nylon suture between the skin and soft tissues of the submental region and the skin and soft tissues of the presternal region (Fig. 12.148). This suture is retained for approximately 2 weeks. The surgical specimen shown in Fig. 12.149 demonstrates an end-on view of the trachea showing tumor infiltration from the left lobe of the thyroid gland into the lumen of the trachea.

Postoperative care requires maintenance of the patient's head in the fully flexed chin-to-chest position assisted by the suture. Intensive care and pulmonary support are essential for clearance of pulmonary secretions. The cough reflex and ability to expectorate are compromised because of the extremely flexed position of the neck. However, the patient is able to swallow by mouth within 2 to 3 days after surgery. The chin-to-chest suture is removed at 2 weeks, at which time the patient is asked to gradually extend the neck and resume normal activities. Postoperative monitoring of serum calcium levels and supplements as necessary is required until the calcium level has stabilized. Intravenous or oral calcium supplements may be required for transient hypocalcemia.

A tracheostomy after sleeve resection of the trachea is to be avoided, because the adequacy of the airway is clearly far superior in the postoperative period than it was preoperatively. In addition, sepsis at the suture line is likely to occur if a tracheostomy is performed, leading to dehiscence of the anastomosis and a long-term complication of tracheal stenosis at the anastomotic site. Sleeve resection with primary reconstruction of the trachea is a simple one-stage procedure that adequately addresses the problem of tracheal invasion by thyroid cancer.

Invasion of the Pharynx and Esophagus

Invasion of the inferior constrictor muscle and muscular wall of the cervical esophagus adjacent to the cricotracheal junction occurs frequently in aggressive cancers with gross extrathyroid extension (Fig. 12.150). Although muscle infiltration by a tumor is common, the mucosa of the esophagus is seldom involved. It is exceedingly rare to see thyroid cancer perforating through the mucosa into the lumen of the esophagus. Excision of the involved segment of pharyngoesophageal musculature up to the submucosal plane is technically feasible and oncologically safe (Fig. 12.151). The mucosa of the esophagus can be preserved with meticulous dissection to maintain the continuity and patency of the alimentary tract (Fig. 12.152). The contrast-enhanced CT scan of a patient with a recurrent carcinoma of the thyroid gland with invasion of soft tissues in the right tracheoesophageal groove is shown in Fig. 12.153. All gross

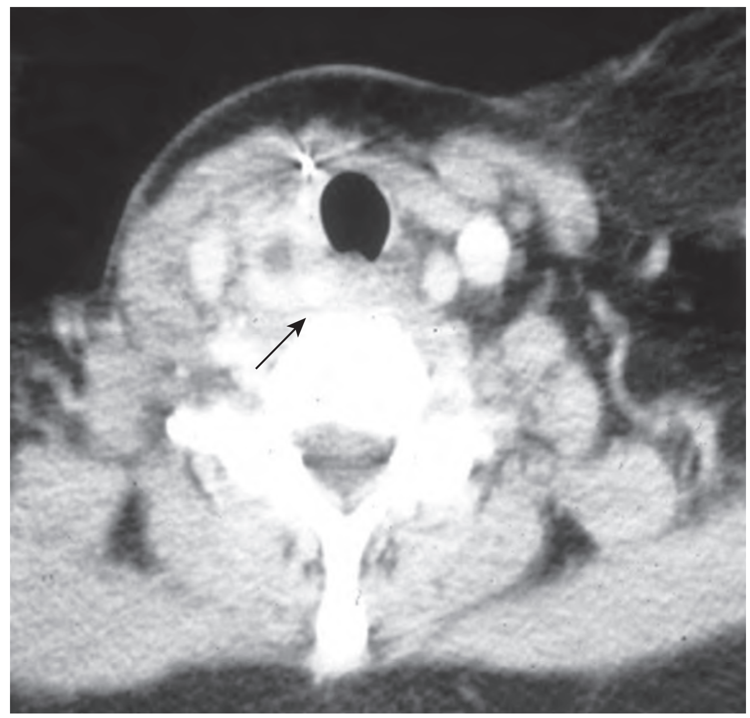

Figure 12.153 An axial view of a contrast-enhanced computed tomography scan of the neck showing a recurrent carcinoma of the thyroid invading the esophageal wall (*arrow*).

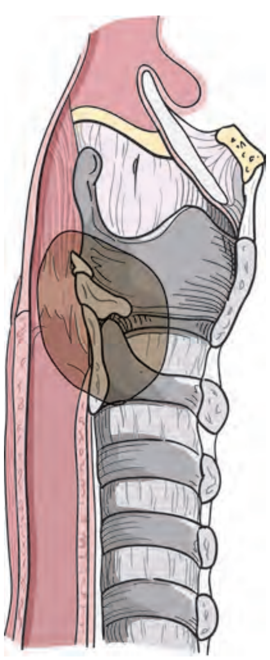

Figure 12.150 A schematic diagram showing invasion of pharyngoesophageal junction by thyroid cancer. *(Courtesy Memorial Sloan Kettering Cancer Center.)*

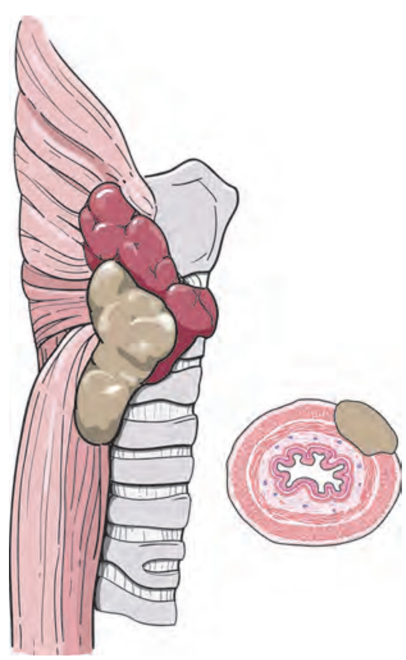

Figure 12.151 A schematic diagram showing invasion of the muscular wall of the esophagus without invasion of the mucosa. *(Courtesy Memorial Sloan Kettering Cancer Center.)*

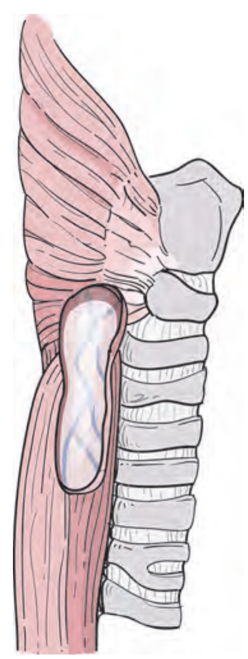

Figure 12.152 A schematic diagram showing excision of the tumor with the muscular wall of the esophagus, preserving the mucosa. *(Courtesy Memorial Sloan Kettering Cancer Center.)*

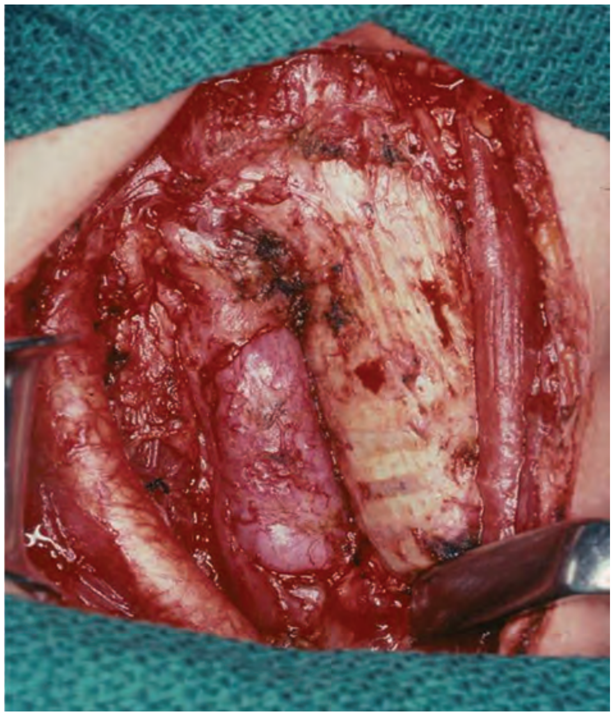

Figure 12.154 The surgical defect after excision of the tumor with the muscular wall of the esophagus and preservation of the esophageal mucosa.

tumor is excised with resection of the muscular wall of the esophagus, preserving its mucosa (Fig. 12.154).

Invasion of the Carotid Artery

Extensive invasion of the larynx, trachea, and esophagus occasionally is seen in locally advanced thyroid cancers that remain confined to the central compartment of the neck. Such patients may benefit from an aggressive surgical approach with total thyroidectomy and pharyngolaryngectomy with appropriate reconstruction of the pharyngoesophageal junction. Improved local control of the disease can be achieved with such aggressive surgical resection in the appropriate setting.

Differentiated carcinomas of the thyroid gland occasionally recur locally after previous thyroid surgery. The clinical behavior of recurrent thyroid cancer is similar to that of a locally aggressive untreated papillary carcinoma. Therefore when local recurrence invades adjacent tissues in the neck, radical surgical resection should be considered. Although invasion of the carotid artery by thyroid cancer generally is considered to be stage T4b (surgically unresectable), in some situations limited invasion of the common carotid artery makes it suitable for resection and reconstruction.

The patient described here had undergone a total thyroidectomy for a multifocal papillary carcinoma of the thyroid gland 7 years before presentation. After undergoing a total thyroidectomy, she was treated with radioactive iodine therapy. At the time of this presentation, she had a recurrent tumor mass with reduced mobility in the lower part of the neck from the tumor mass that extended behind the left sternoclavicular joint into the superior mediastinum. She had paralysis of the left vocal cord and Horner's syndrome on the left-hand side. The palpable extent of the mass and its intrathoracic extension are depicted in Fig. 12.155, demonstrating encasement of the common carotid artery by the mass. A contrast-enhanced CT scan of the neck clearly showed the presence of the left common carotid artery within the center of the recurrent tumor mass (Fig. 12.156). Angiography performed through the ascending aorta showed encasement of the common carotid artery with partial compromise of its lumen (Fig. 12.157).

Balloon occlusion testing of the left common carotid artery demonstrated that the patient had satisfactory contralateral intracranial circulation to maintain perfusion of the left hemisphere in the event of the need to sacrifice and ligate the left

Figure 12.155 A recurrent carcinoma of the thyroid with invasion of the carotid artery.

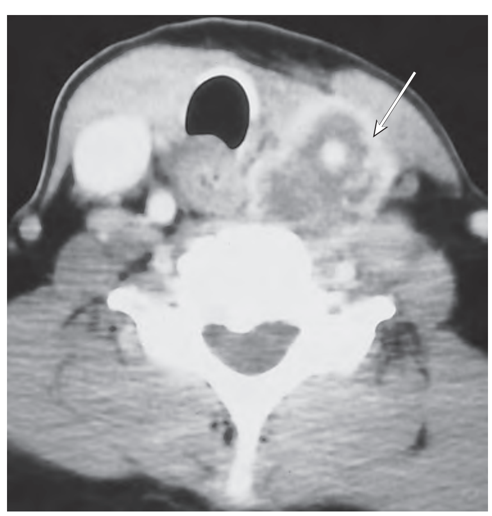

Figure 12.156 A computed tomography scan of the neck showing encasement of the left common carotid artery by the tumor (*arrow*).

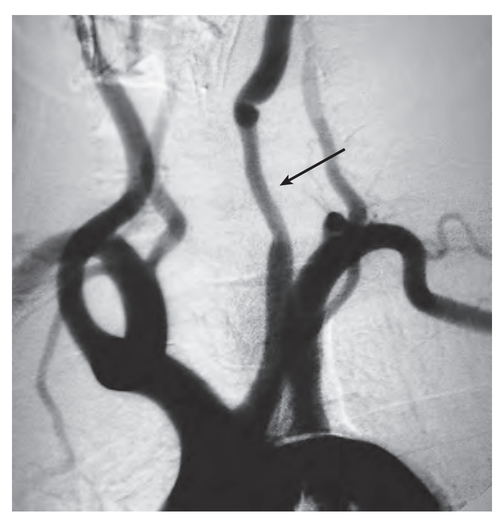

Figure 12.157 This arch aortogram shows a narrowing of the left common carotid artery (*arrow*).

internal carotid artery. The planned surgical procedure required two surgical teams (a head and neck team and a thoracic team) for resection of the tumor through a cervical-mediastinotomy approach with total resection of the tumor in conjunction with resection of the common carotid artery and reconstruction of the resected artery with an interposition saphenous vein graft. In Fig. 12.158, the patient is shown on the operating table under general endotracheal anesthesia; she is in the supine position and the incision is outlined. A transverse low neck incision was made that excised the scar of her previous thyroidectomy. A vertical incision was made at the midpoint of the transverse cervical incision over the sternum curving to the left inframammary fold to facilitate a median sternotomy to expose the anterior aspect of the mediastinum.

The operative procedure begins with a left neck dissection, sacrificing the vagus nerve and the sympathetic chain in the upper part of the neck at the level of the carotid bifurcation and carefully preserving the superior laryngeal nerve to maintain sensations of the interior of the larynx. The tumor mass was mobilized from the larynx and trachea medially and at its upper end (Fig. 12.159). Note the distal common carotid artery emanating from the tumor mass. At this point a median sternotomy is performed, splitting the sternum from the suprasternal notch to the xyphoid process. After retraction of the two sides of the anterior chest wall, dissection of the anterior mediastinum is carefully undertaken to meticulously identify each of the great vessels and isolate them with vessel loops (Fig. 12.160). The origin of the left common carotid artery from the arch of the aorta and the origin of the innominate artery are carefully dissected, freeing the tumor mass from these vessels. To facilitate dissection of the left subclavian artery and the subclavian vein, the medial third of the left clavicle and the left sternoclavicular joint are resected. This maneuver provides immediate direct exposure of the confluence of the internal jugular vein and the subclavian vein behind the sternoclavicular joint at the root of the neck (Fig. 12.161).

Lateral mobilization of the mass after division and ligation of the internal jugular vein from the subclavian vein is accomplished, freeing the mass from the brachial plexus and the prevertebral soft tissues (Fig. 12.162). The mass is then mobilized medially from the tracheoesophageal groove and the prevertebral fascia, carefully retracting the trachea and the esophagus toward the right-hand side (Fig. 12.163). Division of the remaining attachment of the tumor mass from the prevertebral fascia over the scalene muscles and the anterior aspect of the vertebral bodies is next undertaken to circumferentially mobilize the mass, which now is able to be retracted medially (Fig. 12.164).

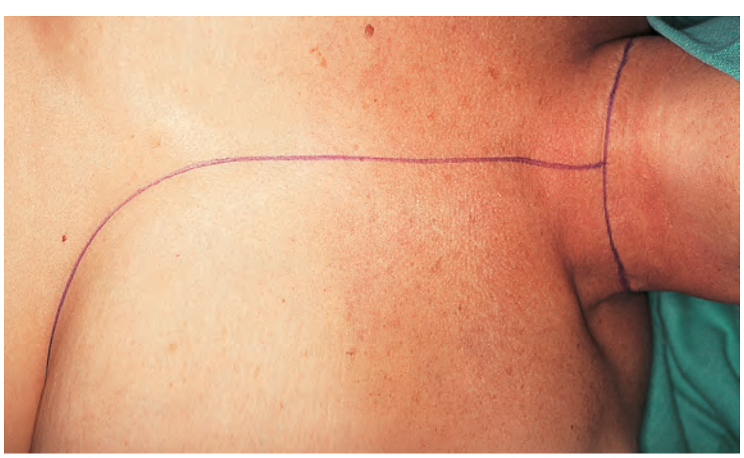

Figure 12.158 The incision is outlined for cervicothoracic exploration.

With a vessel loop on the proximal aspect of the common carotid artery and a well-dissected distal segment of the common carotid artery, the entire mass is free to be resected with a segment of the common carotid artery (Fig. 12.165).

At this juncture a bypass is established between the innominate artery and the distal common carotid artery, after which

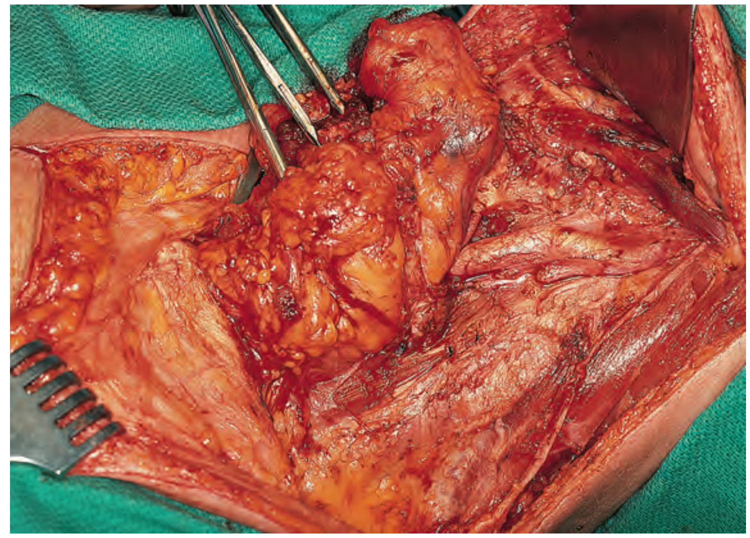

Figure 12.159 The tumor mass is mobilized at its upper end in the neck.

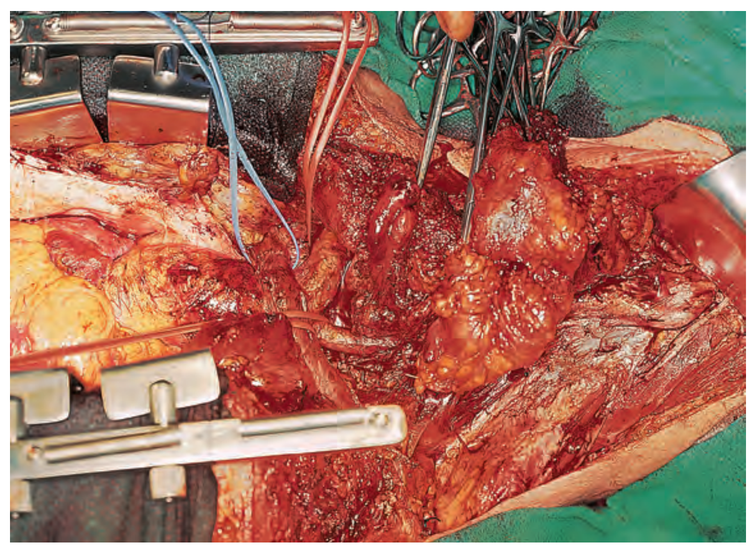

Figure 12.160 A median sternotomy is performed, and the great vessels are isolated.

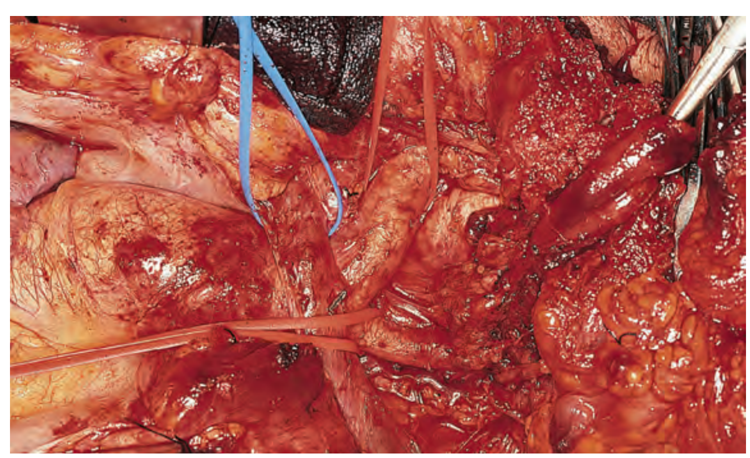

Figure 12.161 The sternoclavicular joint is resected to expose the subclavian and internal jugular veins.

Figure 12.162 The mass is dissected laterally off the brachial plexus.

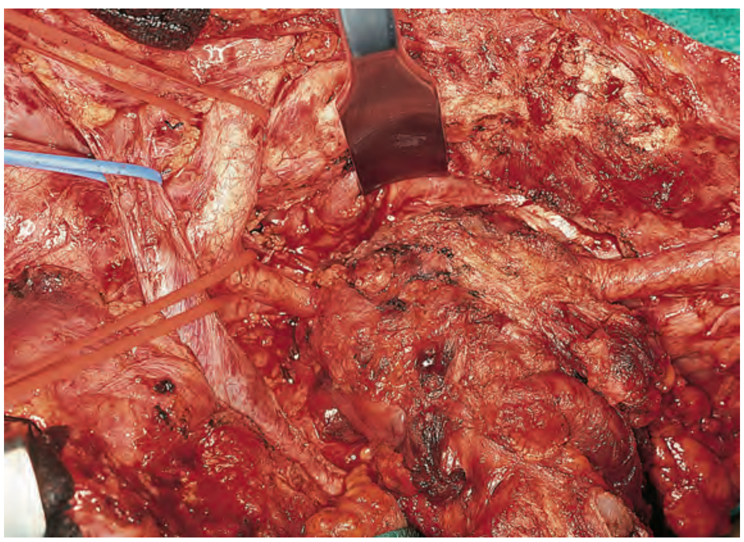

Figure 12.163 The mass is dissected medially off the trachea and esophagus.

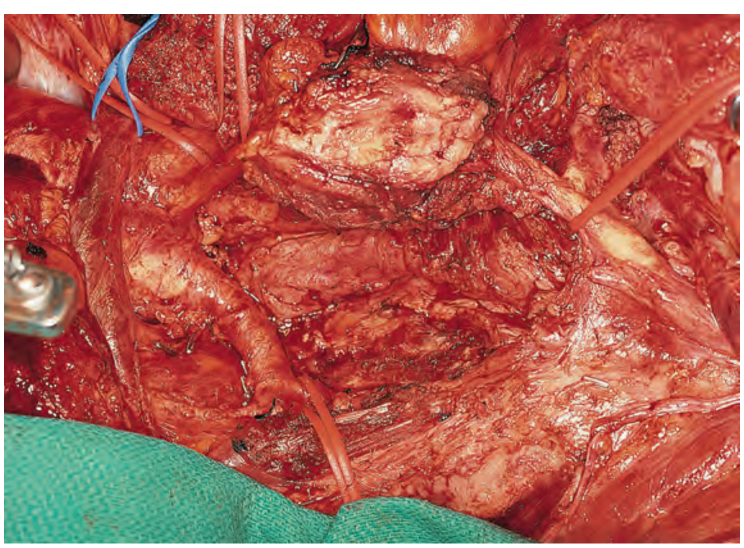

Figure 12.164 The mass is retracted medially after its separation from the prevertebral fascia.

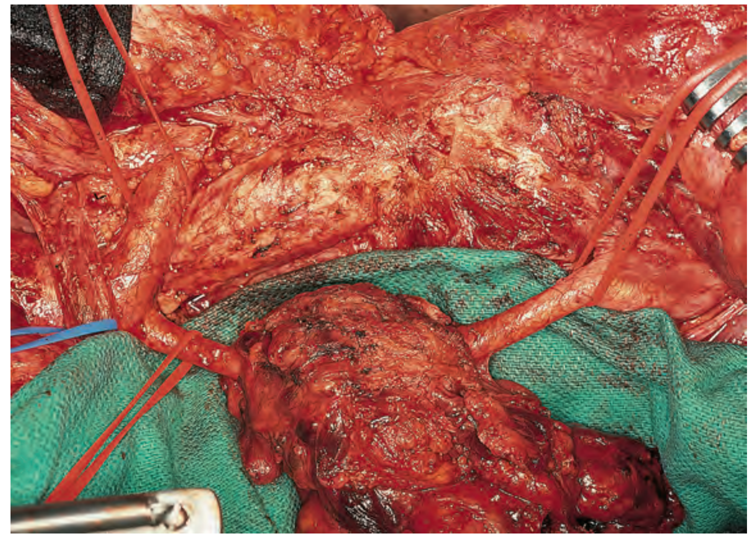

Figure 12.165 The recurrent tumor mass is free to be resected with a segment of the common carotid artery.

Figure 12.166 The common carotid artery is repaired with a saphenous vein graft.

the tumor is resected and an end-to-end anastomosis is created between the proximal and distal stumps of the common carotid artery with a saphenous vein bypass graft (Fig. 12.166). This anastomosis reestablishes the blood flow through the carotid system to the left hemisphere of the brain and the left side of the head. The dead space created by resection of the sternoclavicular joint and the tumor mass is obliterated with use of a pectoralis muscle pedicled flap rotated superomedially (Fig. 12.167). The sternotomy is repaired with use of heavy wire sutures, suction drains are placed through separate stab incisions, and the skin incision is closed in the usual fashion (Fig. 12.168). The post-operative magnetic resonance angiogram clearly demonstrates patent reconstruction of the common carotid artery for resection of locally extensive recurrent papillary carcinoma of the thyroid gland that was not responsive to radioactive iodine therapy (Fig. 12.169).

Gross extrathyroid extension to central compartment viscera occurs infrequently. In the Memorial Sloan Kettering Cancer Center (SKCC) series of 3664 patients (1986–2010), 4.1% of patients (153 of 3664) had gross extrathyroid extension staged as T4a. The role of appropriate surgical intervention to extirpate all demonstrable tumor in patients with T4a disease cannot be overemphasized. Historically, the most common cause of death

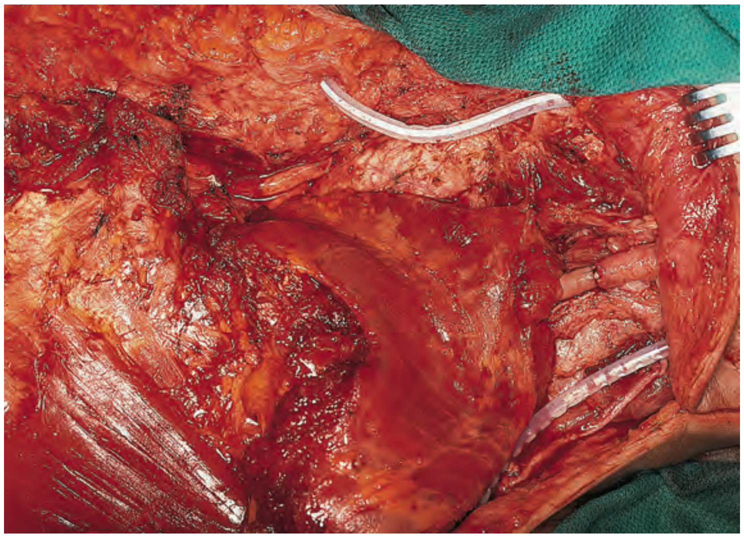

Figure 12.167 A pectoralis muscle pedicled flap is used to fill the dead space.

Figure 12.168 The sternotomy and skin incisions are closed.

Figure 12.169 A postoperative magnetic resonance angiogram demonstrating a patent saphenous vein graft (*arrow*).

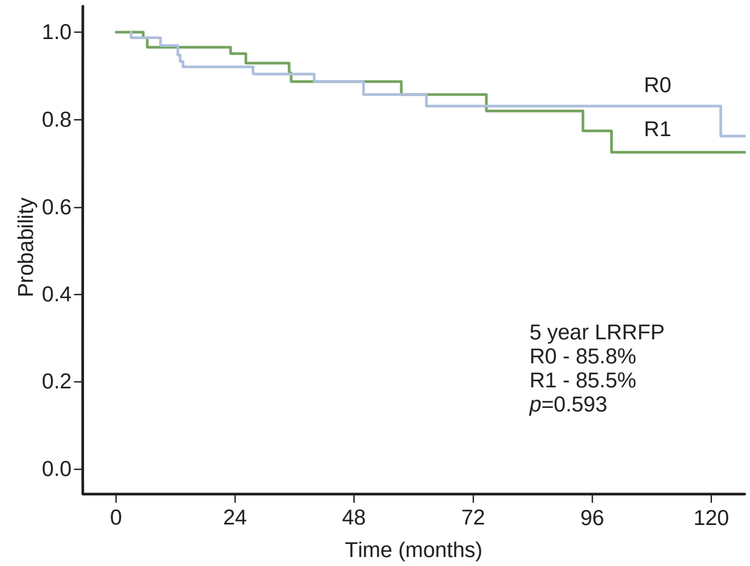

Figure 12.170 Locoregional recurrence-free survival in relation to the completeness of resection (R stage) for locally advanced cancer of the thyroid gland. (Memorial Sloan Kettering Cancer Center data 1986–2010, 153 patients.)

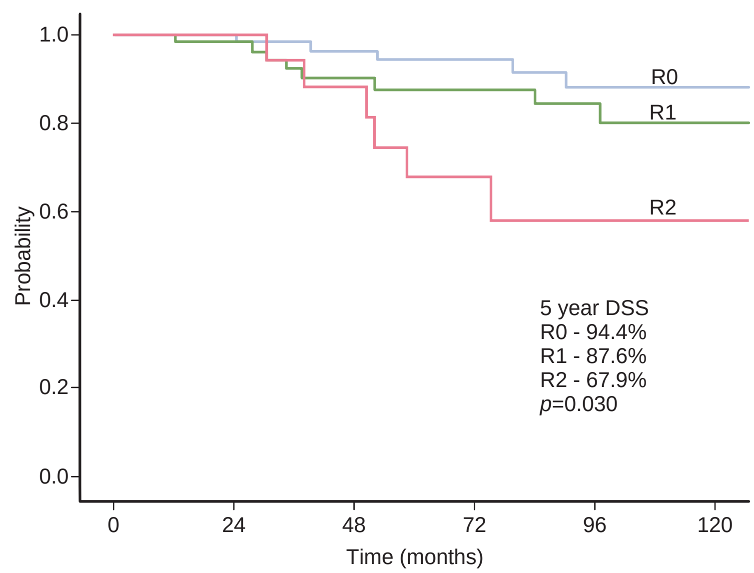

Figure 12.171 Disease-specific survival in relation to the completion of resection (R stage) for locally advanced cancer of the thyroid gland. (Memorial Sloan Kettering Cancer Center data 1986–2010, 153 patients.)

in patients with thyroid carcinoma was uncontrolled locoregional recurrence, leading to hemorrhage, asphyxia, dysphagia, and inanition. The implementation of advanced surgical techniques and achieving R0 resection, where possible, has changed the natural history of advanced thyroid cancer (Figs. 12.170 and 12.171). In the past three decades, locoregional failure is observed to be a rare cause of death.

2015 AMERICAN THYROID ASSOCIATION (ATA) GUIDELINES AND SHIFTING PARADIGMS

The ATA has published guidelines for management of thyroid cancer in the past and have revised them periodically (2006, 2009, and 2015). The most recent version was published in January 2016. These guidelines are used extensively both by endocrinologists and surgeons around the world. Similar guidelines are

published by other nations also, such as the British Thyroid Association (BTA), with some variations. The ATA guidelines describe state of the art management of thyroid cancer with more than 100 recommendations with appropriate supporting evidence where available from the literature. The most recent guidelines reflect incorporation of the biological behavior of thyroid cancer, with generous descriptions about the extent of thyroidectomy and use of radioactive iodine ablation. For example, the former practice of routine subtotal thyroidectomy and postoperative RAI remnant ablation in all patients is no longer recommended. The practice of lobectomy for unifocal intrathyroidal cancers up to 4 cm is now acceptable, and more specific indications for postoperative RAI ablation are defined. Similarly, the role of and indications for completion and total thyroidectomy are also well described. The guidelines have also endorsed the observation approach for papillary microcarcinomas. The guidelines have also strongly recommended the use of contrast-enhanced CT scan in preoperative surgical evaluation for the first time.

Postoperative Surveillance and Adjuvant Therapy for Cancer of the Thyroid

Risk stratification is a dynamic and interactive process that forms the cornerstone of postoperative surveillance and adjuvant therapy recommendations. Risk stratification begins before the diagnosis of cancer and continues throughout follow-up. This process is depicted in Fig. 12.172. First, clinical features and sonographic characteristics of a nodule (including size) are used to estimate its risk of malignancy, guiding the decision to biopsy or observe the lesion. Once diagnosed as malignancy,

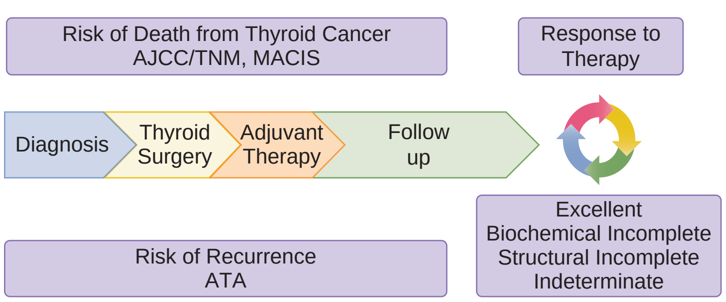

Figure 12.172 Risk stratification for death (cause specific) and recurrence in thyroid cancer.

risk stratification guides recommendations for surgical management, including the extent of initial surgery and need for cervical lymph node dissection. Next, clinicians must employ all preoperative, intraoperative, and postoperative data to guide management decisions on adjuvant therapy and follow up. For example, initial and dynamic risk stratification helps determine a patient's TSH target and need for radioactive iodine ablation or therapy. Moreover, it aids in deciding the intensity and type of long-term follow-up needed to establish disease remission and to detect clinically significant disease recurrence. Critical factors such as the extent of gross extrathyroidal extension, the completeness of surgical resection, and the presence of potential distant metastasis on imaging cannot be adequately ascertained by simply reviewing the pathology report of the thyroid specimen. Knowledge of the surgeon's intraoperative findings and any postoperative imaging that is performed may also significantly impact risk stratification. Therefore communication between all members of the patient's care team is paramount.

With regard to decisions on adjuvant therapy and follow-up, the AJCC/TNM system (or the MACIS system from the Mayo Clinic) provides valuable initial risk estimates of disease-related mortality, based on all the information available in the first few months postoperatively. Recently the eighth edition of the AJCC staging system was published and included several significant changes compared with the seventh edition. The three major changes include (1) the age cut off for staging changed from 45 to 55 years of age at diagnosis, (2) lymph node metastasis (N1) no longer constitutes stage III disease, (3) minor extrathyroidal extension seen only on histopathologic examination was removed from T3 disease and no longer upstages the patient to stage III, and (4) the importance of gross extrathyroidal extension is further emphasized by requiring the clinician and tumor registry personnel to understand the specific structures that were grossly invaded in order to be able to provide accurate AJCC staging (i.e., T3b versus T4 disease).

From a practical standpoint, the primary variables that determine AJCC stage are age at diagnosis, presence or absence of distant metastasis, presence or absence of gross extrathyroidal extension, tumor size, and lymph node status. As can be seen in Table 12.4, the first major break point is age, with patients younger than 55 years of age classified as stage I if there are no distant metastases and stage II if there are distant metastases. Therefore in patients younger than 55 years of age, the other

Table 12.4 Clinical Parameters Used for AJCC/UICC Staging for Differentiated Thyroid Cancer

	DISTANT METASTASIS	GROSS EXTRATHYROIDAL EXTENSION PRESENT?	STRUCTURES INVOLVED WITH GROSS EXTRATHYROIDAL EXTENSION	T CATEGORY	N CATEGORY	STAGE
<55 years	No	Yes or No	Any or none	Any	Any	I
	Yes	Yes or No	Any or none	Any	Any	II
≥55 years	No	No	None	≤4 cm (T1-T2)	N0/Nx	I
					N1a/N1b	II
				>4 cm (T3a)	N0/Nx/N1a/N1b	II
		Yes	Only strap muscle (T3b)	Any	Any	II
			Subcutaneous, larynx, trachea, esophagus, recurrent laryngeal nerve (T4a)	Any	Any	III
			Prevertebral fascia, encasing major vessels (T4b)	Any	Any	IVA
	Yes	Yes or no	Any or none	Any	Any	IVB

From Tuttle RM, Haugen B, Perrier D. Updated American Joint Committee on Cancer/Tumor-Node-Metastasis staging system for differentiated and anaplastic thyroid cancer (eighth edition): what changed and why. Thyroid. 2017;27(6):751-756.

variables do not enter the actual stage classification but can be used to modify an individual patient's expected outcome.

In patients 55 years of age or older at diagnosis, if there are no distant metastases, the primary determinant of poor outcome is the presence or absence of gross extrathyroidal extension. In the absence of gross extrathyroidal extension, tumors less than 4 cm confined to the thyroid are stage I, while tumors greater than 4 cm or those associated with lymph node metastasis are stage II. If gross extrathyroidal extension is present, then the specific structures involved determine the stage. Stage II (minor extrathyroid extension) represents involvement only of the strap muscles. Stage III (major extrathyroid extension) represents involvement of the subcutaneous tissue, larynx, trachea, esophagus, or recurrent laryngeal nerve. Stage IVa represents involvement of the prevertebral fascia or tumor encasing major vessels. The presence of distant metastasis warrants a stage IVb classification regardless of other features.

The changes in the eighth edition staging system result in a significant downstaging of many patients into more appropriate low-risk categories despite lymph node metastases, minor extrathyroidal extension, or age between 45 and 55 years of age at diagnosis. Recent studies have confirmed the expected 10-year, disease-specific survival for patients younger than 55 years old with stage I or II disease is 98% to 100% and 85% to 95%, respectively. For patients 55 years of age or older, the expected 10-year, disease-specific survival for stage I, II, III, and IV disease is 98% to 100%, 85% to 95%, 60% to 70%, and less than 50%, respectively.

While the eighth edition has appropriately downstaged most low-risk patients younger than 55 years of age into AJCC stage I, this category will now include patients with a wide range of clinical outcomes, including a few higher risk patients. For example, a 50-year-old patient with papillary microcarcinoma of little clinical significance and a 50-year-old patient with poorly differentiated thyroid carcinoma with gross extrathyroidal extension are both considered stage I. The vast majority of stage I patients are low risk, and therefore, the overall survival of stage I patients is expected to remain excellent despite the recent stage migration of a significant number of patients. However, a small number of higher risk patients will enter stage I; these patients will not do as well as others in stage I, and thus require more aggressive therapy and follow up. To properly address these patients, appropriate risk stratification requires augmenting AJCC staging with other clinical data. We recommend the joint use of both the AJCC staging system and the ATA risk of recurrence staging system to better understand the expected clinical outcomes for an individual patient and to guide management recommendations.

While the AJCC staging system provides valuable information with regard to disease-specific mortality, it was not designed to predict the risk of recurrent or persistent disease. To address this need, the ATA has endorsed a validated, three-tiered initial risk stratification scheme that predicts the risk of recurrent or persistent disease. This three-tiered system reliably predicts a risk of structural disease recurrence of 2% to 3% in ATA low-risk patients, 20% in intermediate-risk patients, and 50% to 75% in high-risk patients. The ATA 2015 guidelines expanded the definition of low-risk tumors to include lymph node micrometastasis and several other low-risk tumor types (Table 12.5).

However, the guidelines also recognize that the risk of structural disease recurrence associated with various histologies and histopathologic features of differentiated thyroid cancer is best viewed as a continuum and not as three discrete risk categories, which is reflected in Fig. 12.173.

Table 12.5 American Thyroid Association 2009 Risk-Stratification System With Proposed Modifications

Low risk	Papillary thyroid cancer (with all of the following): No local or distant metastases All macroscopic tumor has been resected No tumor invasion of locoregional tissues or structures The tumor does not have aggressive histology (e.g., tall cell, hobnail variant, columnar cell carcinoma) No vascular invasion Clinical N0 or ≤5 pathologic N1 micrometastases (<0.2 cm in largest dimension)* If 131I is given, there are no RAI-avid metastatic foci outside the thyroid bed on the first posttreatment whole-body RAI scan Intrathyroidal, encapsulated follicular variant of papillary thyroid cancer* Intrathyroidal, well-differentiated follicular thyroid cancer with only capsular invasion* Intrathyroidal, well-differentiated follicular thyroid with minor vascular invasion* Intrathyroidal, papillary microcarcinoma, unifocal or multifocal, including V600E BRAF mutated (if known)*
ATA intermediate risk	Microscopic invasion of tumor into the perithyroidal soft tissues Clinical N1 or >5 pathologic N1 with all involved lymph nodes <3 cm in largest dimension* RAI-avid metastatic foci in the neck on the first posttreatment whole-body RAI scan Aggressive histology (e.g., tall cell, hobnail variant, columnar cell carcinoma) Papillary thyroid cancer with vascular invasion Intrathyroid, papillary thyroid cancer, primary tumor 1-4 cm, V600E BRAF mutated (if known)* Multifocal papillary microcarcinoma with extrathyroidal extension and V600E BRAF mutated (if known)*
ATA high risk	Macroscopic invasion of tumor into the perithyroidal soft tissues (gross extrathyroidal extension) Incomplete tumor resection Distant metastases Pathologic N1 with any metastatic lymph node ≥3 in largest dimension* Postoperative serum thyroglobulin suggestive of distant metastases Follicular thyroid cancer with extensive vascular invasion (>4 foci of vascular invasion)*

ATA, American Thyroid Association; *RAI,* radioactive iodine.
From Haugen BR, Alexander EK, Bible KC, et al. 2015 American Thyroid Association management guidelines for adult patients with thyroid nodules and differentiated thyroid cancer: the American Thyroid Association guidelines task force on thyroid nodules and differentiated thyroid cancer. Thyroid. 2016;26(1):1-133.
**Proposed modifications, not present in the original 2009 initial risk-stratification system. See sections [B19]-[B23] and Recommendation 48B.*

Therefore initial risk stratification should be based on the patient's risk of dying from thyroid cancer, utilizing the AJCC/TNM system (or MACIS system), in conjunction with the risk of recurrent or persistent disease, using the ATA risk-stratification system (or similar three-tiered risk-stratification systems endorsed by other thyroid associations). Clinicians can individualize initial adjuvant therapy recommendations based on these initial risk assessments. For example, patients with both a low risk of dying from thyroid cancer and a low risk of recurrence do not require radioactive iodine ablation or adjuvant therapy and do not require TSH suppression. A simple follow-up paradigm that includes periodic physical examinations and maintenance of

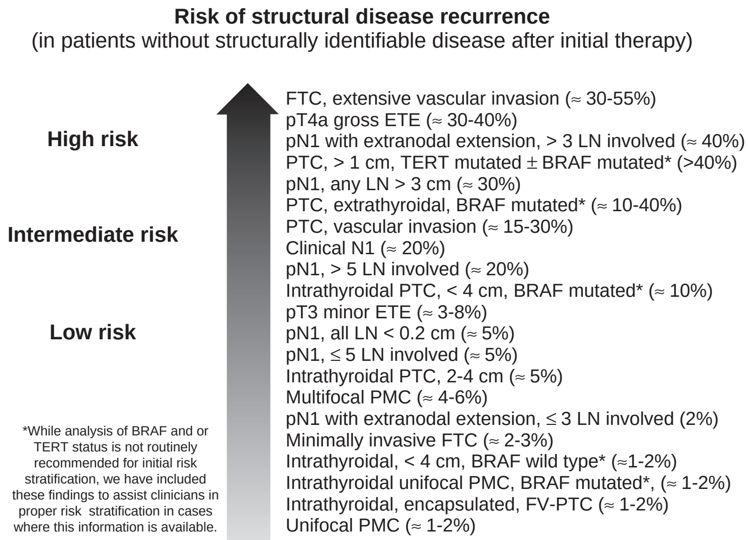

Figure 12.173 American Thyroid Association (ATA) risk stratification for structural recurrence (2015). *FTC,* Follicular thyroid cancer; *FV,* follicular variant; *LN,* lymph node; *PTC,* papillary thyroid cancer; *PTMC,* papillary thyroid microcarcinoma.

TSH in the low-normal range is adequate. In these patients, routine use of neck ultrasonography may result in significantly more false positive findings than identification of real disease. Conversely, patients with a high risk of recurrence and a high risk of dying from thyroid cancer would likely benefit from more aggressive adjuvant therapy such as radioactive iodine and TSH suppression.

There continues to be significant controversy regarding a large cohort of thyroid cancer patients, namely, the intermediate-risk patients, who are at low risk of dying from thyroid cancer but an intermediate risk of recurrent disease. While many authors recommend routine use of radioactive iodine for all patients with lymph node metastasis, minor extrathyroidal extension, or primary tumor size greater than 2 cm, our approach has been much more selective. We utilize a postoperative thyroglobulin level with thyroglobulin antibodies, performed 6 weeks after surgery, as an initial response to therapy and to assess the presence of persistent disease or residual thyroid tissue. Intermediate-risk patients with a postoperative nonstimulated thyroglobulin less than 1 are often followed without routine radioactive iodine ablation or adjuvant therapy. There are some clinical scenarios in which radioactive iodine scanning or ablation may be preferred. For instance, radioactive iodine ablation may be necessary to complete initial staging in the setting of nonspecific imaging findings that could represent metastatic thyroid cancer (e.g., nonspecific pulmonary nodules). It may also be helpful in the presence of high-level antithyroglobulin antibodies, which make thyroglobulin measurements unreliable. Radioactive iodine remnant ablation may also be undertaken due to patient preference. In general, if more than five lymph nodes were involved, and all lymph nodes were smaller than 1 cm in size, radioactive iodine adjuvant therapy is not recommended. Conversely, if more than 10 lymph nodes were involved, if the lymph nodes were larger than 1 to 2 cm, or if there were a host of other worrisome features, then radioactive iodine adjuvant therapy is considered in these intermediate-risk patients. Therefore our adjuvant therapy approach aligns with the selective use approach promoted by the ATA guidelines.

Successful use of radioactive iodine requires proper preparation. A low-iodine diet is recommended for 7 to 10 days before radioactive iodine scanning or therapy. The requisite TSH elevation can be accomplished either by several weeks of thyroid hormone withdrawal or by using recombinant human TSH injections when radioactive iodine is used for scanning, remnant ablation, or adjuvant therapy. Recombinant human TSH is not approved for preparation of patients with known distant metastasis. However, several groups have published retrospective studies suggesting the efficacy of recombinant human TSH in this setting. Moreover, the ATA guidelines allow for the use of recombinant human TSH in patients with known distant metastasis if there are medical contraindications to thyroid hormone withdrawal.

FDG PET scanning is not routinely used as part of initial risk stratification for patients with low- to intermediate-risk thyroid cancer. However, high-risk patients, particularly those likely to have non–radioiodine-avid disease, may benefit from upfront FDG PET scanning for staging and prognostic purposes. For example, FDG PET scanning is often done for poorly differentiated or Hürthle cell cancers that have gross extrathyroidal extension into major structures in the neck, in patients at high risk of having persistent disease after initial surgery, or in patients at high risk of distant metastasis that may not be identifiable on radioactive iodine scanning. FDG PET scanning is also considered when the postoperative serum thyroglobulin is elevated beyond what would be expected based on initial presentation or the radioactive iodine scan.

Initial TSH targets are also based on initial risk stratification and are 1 to 2 mU/L in low-risk patients, 0.5 to 1.5 mU/L in intermediate-risk patients, and about 0.1 mU/L in high-risk patients. As described later, these TSH targets evolve over time depending on a patient's response to therapy.

Adjuvant therapy with external beam radiation is considered in older patients who present with significant gross extrathyroidal extension, particularly if the tumor is unlikely to be responsive to radioactive iodine or if a subsequent recurrence is unlikely to be amenable to salvage therapy.

Our standard follow-up algorithm following initial surgery involves evaluation of the patient every 6 to 12 months for the first 2 years depending on their initial risk assessment. Low-risk patients are followed with suppressed thyroglobulin and thyroid function tests at 6 months and a neck ultrasound at 12 to 24 months. Ongoing follow-up is then based on dynamic risk stratification. Intermediate- and high-risk patients are usually seen every 6 months for the first 2 years with suppressed thyroglobulin, thyroid function tests, and serial ultrasound. They may also require other cross-sectional or functional imaging depending on their risk assessment, trend in thyroglobulin, presence of thyroglobulin antibodies, and underlying histology.

While initial risk stratification provides guidance for early management decisions postoperatively, long-term management recommendations must be based on an evolving understanding of the patient's risk of recurrence or disease-related death, based on the biological behavior of a patient's disease and their response to previous therapies. In order to facilitate application of this long-standing philosophy, the ATA has endorsed a nomenclature that describes both the clinical and structural status of patients at any point during follow-up.

The response to therapy definitions provided in Table 12.6 refer to patients treated with total thyroidectomy and radioactive iodine ablation. By simply modifying the thyroglobulin value cut points, the same category names can be used for patients treated with total thyroidectomy without radioactive iodine ablation, or even with lobectomy alone. For example, in patients with total thyroidectomy without radioactive iodine ablation, excellent response is still defined as a nonstimulated

Table 12.6 Clinical Implications of Response to Therapy Reclassification in Differentiated Thyroid Cancer Patients Treated With Total Thyroidectomy and Radioactive Iodine Remnant Ablation

CATEGORY	DEFINITIONS	CLINICAL OUTCOMES	MANAGEMENT IMPLICATIONS
Excellent response	Negative imaging and either Suppressed Tg <0.2 ng/mL or TSH-stimulated Tg <1 ng/mL	1%-4% recurrence <1% disease-specific death	An excellent response to therapy should lead to an early decrease in the intensity and frequency of follow-up and the degree of TSH suppression.
Biochemical incomplete response	Negative imaging and Suppressed Tg >1 ng/mL or Stimulated Tg >10 ng/mL or Rising anti-Tg Ab levels	At least 30% spontaneously evolve to NED 20% achieve NED after additional therapy 20% develop structural disease <1% disease-specific death	If associated with stable or declining serum Tg values, a biochemical incomplete response should lead to continued observation with ongoing TSH suppression in most patients. Rising Tg or Tg antibody values should prompt additional investigations and potentially additional therapies.
Structural incomplete response	Structural or functional evidence of disease with any Tg level +/– Tg Ab	50%-85% continue to have persistent disease despite additional therapy. Disease-specific death rates as high as 11% with locoregional metastases and 50% with structural distant metastases.	A structural incomplete response may lead to additional treatments or ongoing observation depending on multiple clinicopathologic factors including the size, location, rate of growth, RAI avidity, FDG avidity, and specific pathology of the structural lesions.
Indeterminate response	Nonspecific findings on imaging studies Faint uptake in thyroid bed on RAI scanning Nonstimulated Tg detectable, but less than 1 ng/mL Stimulated Tg detectable, but less than 10 ng/mL or Tg antibodies stable or declining in the absence of structural or functional disease	15%-20% will have structural disease identified during follow-up In the remainder, the nonspecific changes are either stable or resolve; <1% disease-specific death	An indeterminate response should lead to continued observation with appropriate serial imaging of the nonspecific lesions and serum Tg monitoring. Nonspecific findings that become suspicious over time can be further evaluated with additional imaging or biopsy.

FDG, Fluorodeoxyglucose; *NED,* no evidence of disease; *TSH,* thyroid-stimulating hormone.

thyroglobulin less than 2 ng/mL, but the biochemical incomplete response requires a stimulated thyroglobulin greater than 5. Similarly, in lobectomy patients, a nonstimulated thyroglobulin value less than 30 would be considered an excellent response, and values over 30 would be considered a biochemical incomplete response. These changes in thyroglobulin cut points simply reflect the amount of thyroglobulin that a clinician should expect following the initial surgery, be it a total thyroidectomy or lobectomy without radioactive iodine.

Patients demonstrating an excellent response to therapy have recurrence rates in the 1% to 4% range, and a risk of dying of thyroid cancer less than 1%. Therefore these patients should have decreased intensity and frequency of both follow-up and TSH suppression. Patients with a biochemical incomplete response have abnormal thyroglobulin values but no structural evidence of recurrent disease. Interestingly, the thyroglobulin value often declines spontaneously in these patients over years, and they may never require additional therapy. However, rising thyroglobulin values or rising antithyroglobulin antibody values indicate a need for additional imaging, as these patients will likely transition into a structural incomplete response. Therefore assessment of the thyroglobulin doubling time as a precise measurement of the trend in thyroglobulin values provides important information that can guide patient follow-up. A thyroglobulin that trends down over time is usually followed with observation, while a thyroglobulin that is increasing exponentially would indicate the need for additional cross-sectional and/or functional imaging to identify the metastatic foci. A structural incomplete response defines those patients with suspected or proven recurrent or persistent structural disease. Some of these patients may be followed with observation, while others require therapy. The final category is indeterminate response, in which the patient cannot be confidently classified into one of the other three categories. It is hoped over time, as more information becomes available, that a patient with indeterminate response can be moved into one of the other three categories. Unlike the AJCC/TNM system and the ATA risk system, the response to therapy classification can change over time, and in fact these changes should trigger changes in the intensity, type, and frequency of follow-up.

While most patients with an excellent response, biochemical incomplete response, or indeterminate response can be followed for years without evidence of structural disease recurrence, patients with a structural incomplete response to therapy present a significant clinical challenge. Due to high-sensitivity thyroglobulin assays and high-resolution neck ultrasonography, we are now able to identify very small volume disease at an earlier time in the course of a patient's disease. Given the asymptomatic and often slow growing nature of such disease, these patients may be better served with an observational, active surveillance approach rather than immediate intervention. Conversely, the identification of rapidly changing, structurally progressive disease would be an indication for intervention. When slow-growing, small volume, structural disease persistence or recurrence is identified in patients with well-differentiated tumors, it is reasonable to consider additional radioactive iodine therapy. Conversely, for tumors that are more rapidly growing, larger than 1 cm, positive on FDG PET scanning, or exhibit histology that is not likely to concentrate radioactive iodine, consideration is given to either a localized therapy (such as surgery or external

beam radiation) or a systemic therapy if there is progression of multiple foci. In each case, a careful consideration of both the risks and benefits of intervention and the natural history of disease without intervention is necessary in order to determine the best course of action.

From a practical standpoint, our decision making with regard to structural incomplete response is dependent on the size of the recurrent or metastatic lesion (expressed as volume), the rate of change of the metastatic lesion (expressed as the tumor doubling time), and the location of the lesion (whether it is near important neurovascular or airway structures). Structural disease progression in the neck is preferentially treated by surgery. Isolated distant metastases are usually treated by localized therapy such as surgery or external beam radiation. Diffuse, distant metastases that are structurally progressive or symptomatic are considered for one of the approved multitargeted kinase inhibitors (such as Sorafenib or Lenvatinib), which have been shown in randomized phase 3 clinical trials to improve progression-free survival. These multitargeted kinase inhibitors can have a significant deleterious effect on quality of life, which often requires dose modifications or dose interruptions, and require aggressive management of the expected side effects. Therefore these agents are best used by clinicians with experience in assessing their risks and benefits and the appropriate infrastructure to properly monitor and manage their adverse effects.

OUTCOMES

Cancer of the thyroid gland presents a spectrum of diseases with prognoses ranging from outstanding to uniformly fatal. Nearly all low-risk patients with differentiated carcinoma of the thyroid gland enjoy normal quality and length of life. In contrast, patients with anaplastic carcinoma have a dismal prognosis with a median survival time of approximately 12 months.

Results from multivariate analyses of a consecutive series of over 3600 patients treated between 1986 and 2010 at Memorial Sloan Kettering Cancer Center are shown here. Each of the independent factors affecting long-term disease-specific survival is presented here. Patients' age at diagnosis is by far the most important prognostic factor in differentiated carcinoma of the thyroid gland. Patients younger than 55 years have an outstanding long-term outcome compared with those older than 55 years (Fig. 12.174). Overall, females have a better outcome in the long term compared with males (Fig. 12.175). Among well-differentiated carcinomas, papillary carcinoma by far has the best outcome, followed by follicular carcinoma and Hürthle cell carcinoma (Fig. 12.176). With increasing size of the tumor, prognosis worsens. However, up to 4 cm, the differences are relatively minor. Long-term survival for patients with tumors smaller than 4 cm and larger than 4 cm are shown in Fig. 12.177. Gross extrathyroid extension has a significant negative impact on long-term tumor control. However, microscopic extrathyroid extension does not seem to have the same negative impact on long-term outcome (Fig. 12.178). Nearly one-third of patients in this cohort had regional lymph node metastases documented during the study period. Lymph node metastases do have a small but significant negative impact on long-term outcome (Fig. 12.179). Although presence of lymph node metastases has a negative impact on outcome, it is only observed in the older age group of patients (>55 years). In the younger age group (<55 years), nodal metastasis has essentially no impact on long-term survival (Fig. 12.180). Distant metastasis clearly has a very significant impact on long-term survival (Fig. 12.181).

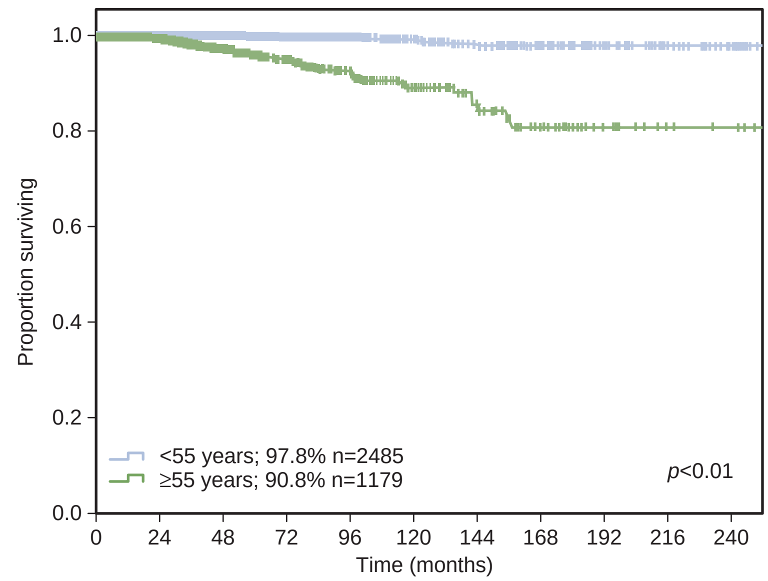

Figure 12.174 Long-term disease-specific survival in relation to age at diagnosis.

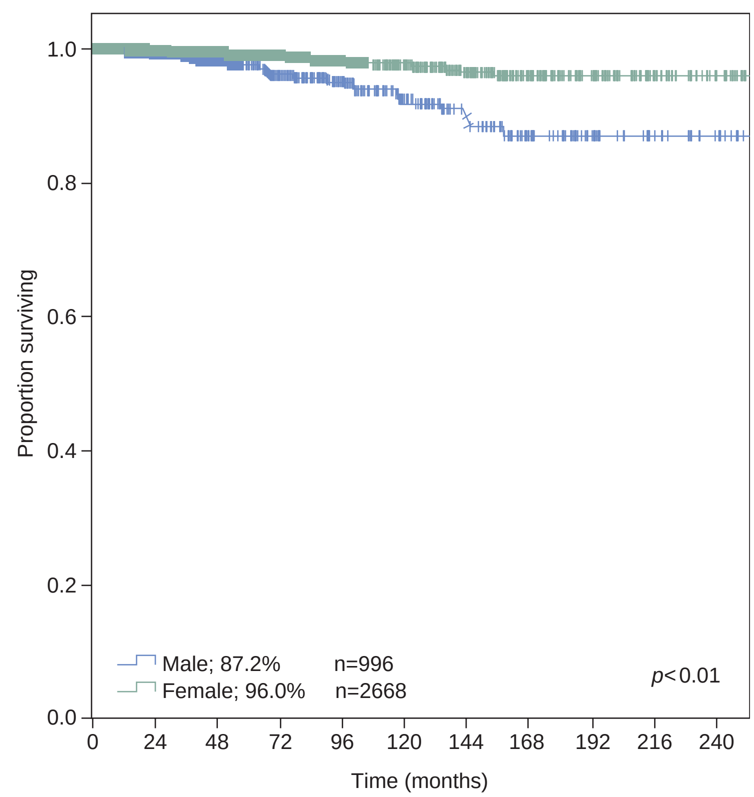

Figure 12.175 Long-term disease-specific survival in relation to sex.

Patients who presented with distant metastases or developed metastases during the study period had only 31% long-term survival.

In general, low-risk patients fall into the AJCC/UICC stage I category, and a majority of patients fall into this group. The disease-specific survival in these patients is excellent. The stage distribution and 10-year disease-specific survival in all patients by stage of disease is shown in Fig. 12.182. For patients younger than 55 years of age, there are only two stage groupings, since there is no stage III or stage IV in these patients. All patients without distant metastases are stage I, and those who present

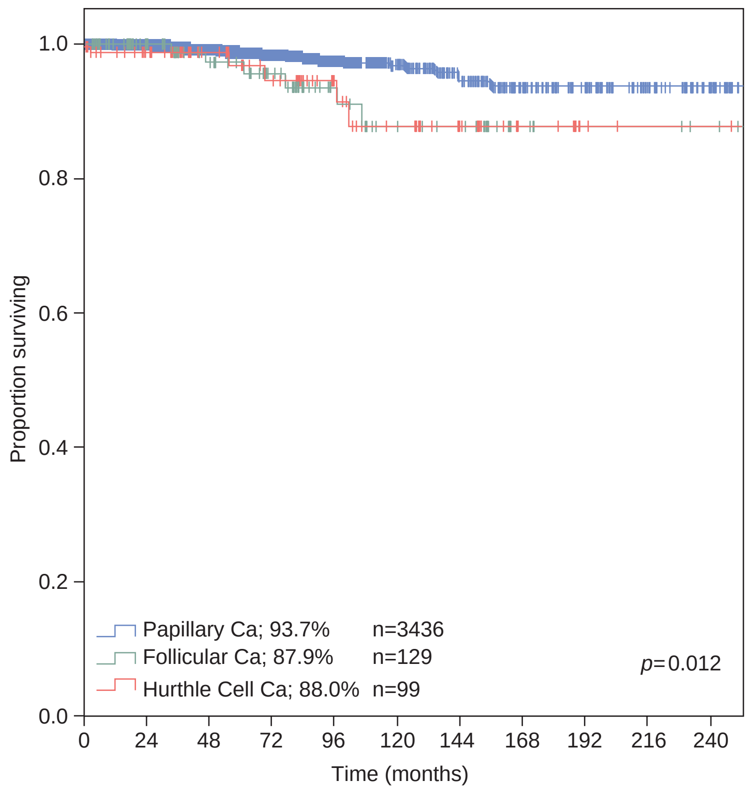

Figure 12.176 Long-term disease-specific survival in relation to histologic subtype among differentiated carcinoma of the thyroid gland.

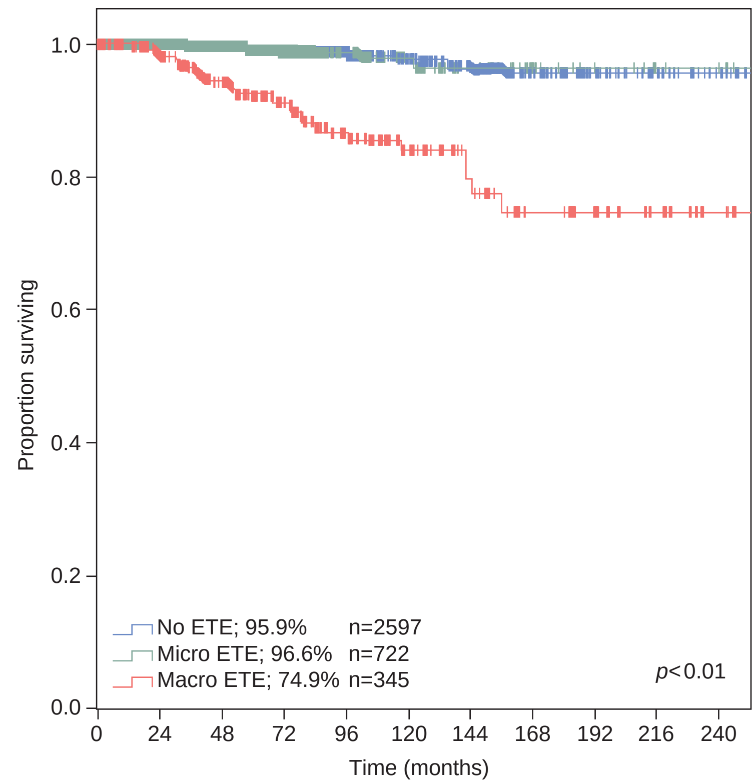

Figure 12.178 Long-term disease-specific survival in relation to extrathyroid extension. Note, only gross extra thyroid extension has a negative impact on outcome.

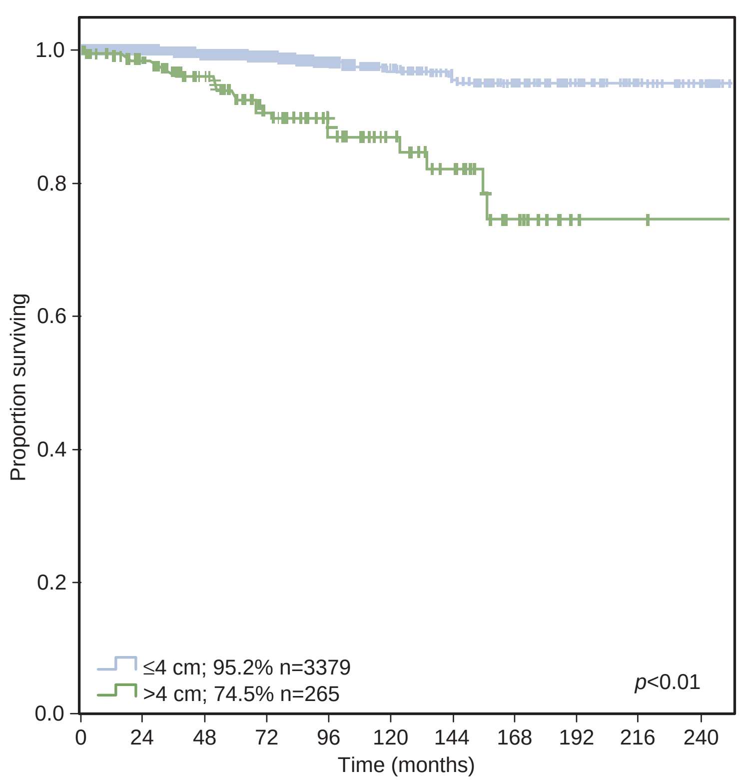

Figure 12.177 Long-term disease-specific survival in relation to size of the primary tumor.

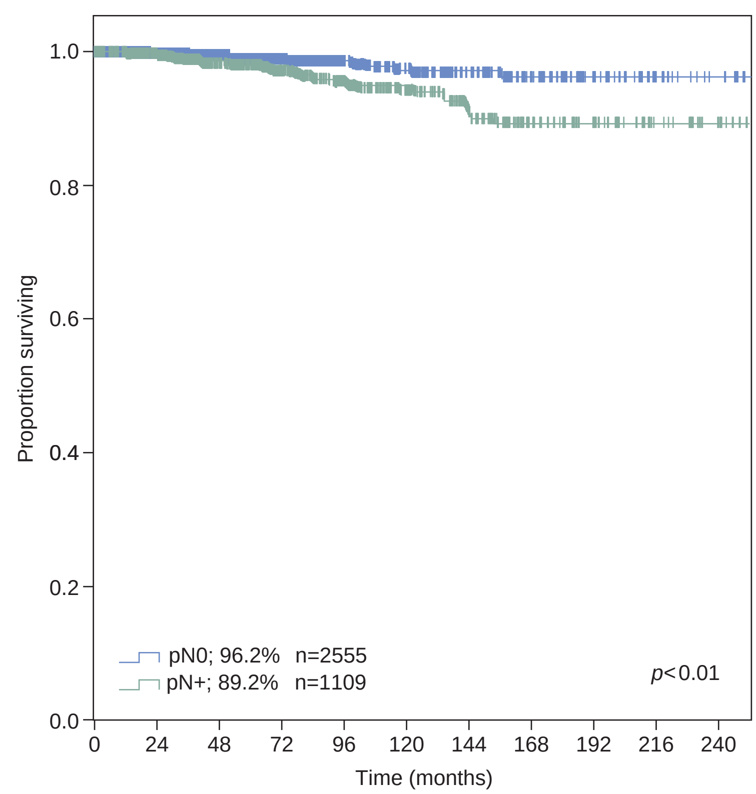

Figure 12.179 Long-term disease-specific survival in relation to regional lymph node metastases.

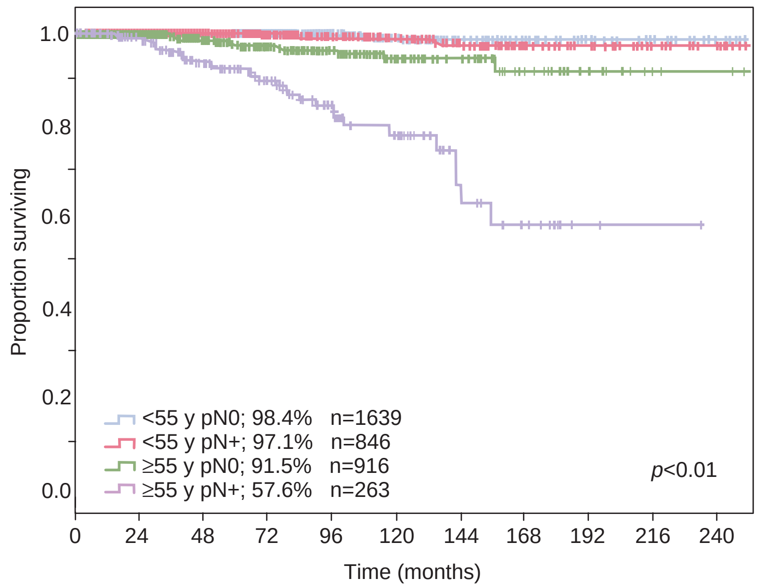

Figure 12.180 Long-term disease-specific survival in relation to regional lymph node metastases and age at initial treatment.

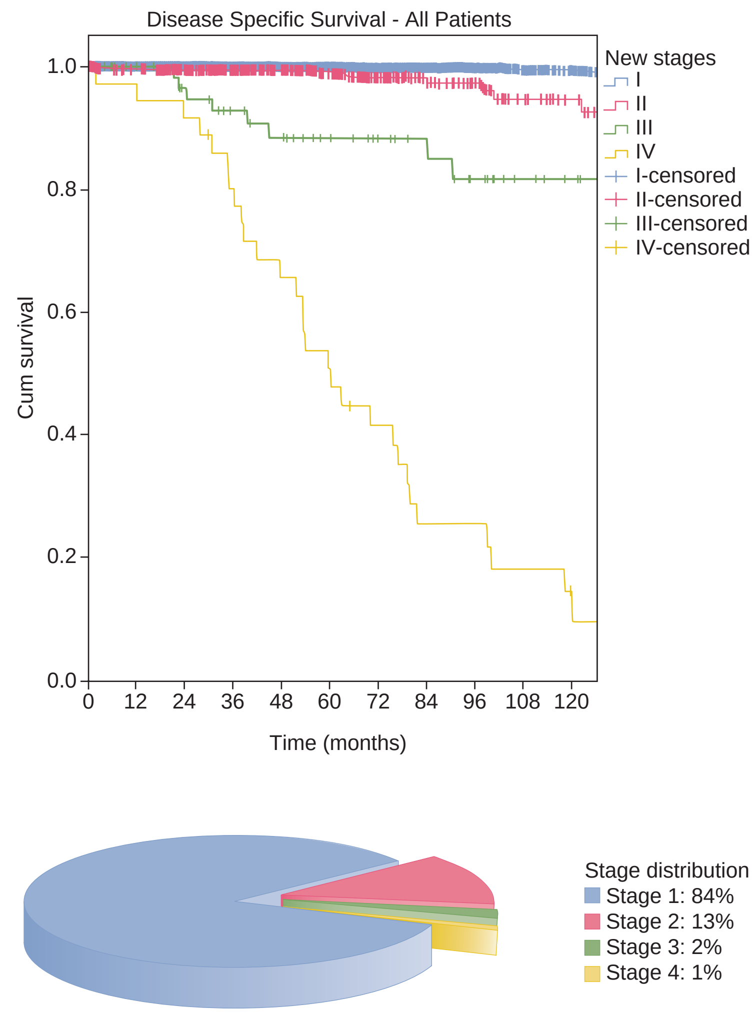

Figure 12.182 Stage distribution and 10-year disease-specific survival in all patients by American Joint Committee on Cancer (AJCC) and International Union Against Cancer (UICC) (eighth edition) clinical stage.

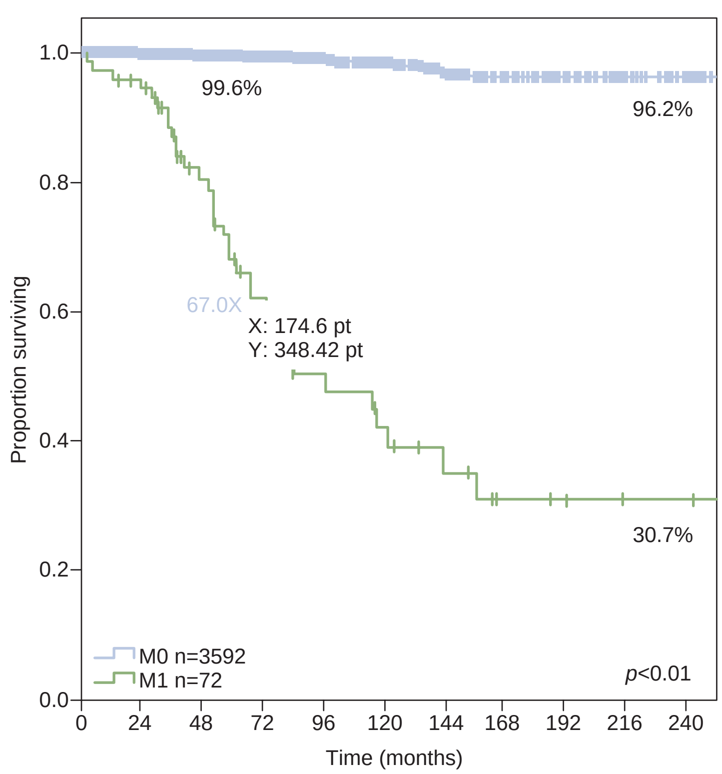

Figure 12.181 Long-term disease-specific survival in relation to distant metastases.

with distant metastases are stage II (36 of 2475, or 1.5%). In stage I disease, the 10-year disease-specific survival is nearly 100%. However, there were 5 deaths in the 36 patients with stage II disease, giving a 10-year survival of 86% (Fig. 12.183). For patients older than 55 years of age, the 10-year disease-specific survival by stage of disease is shown in Fig. 12.184. Note that in stage II disease (T1-T3 and any N), there were only 5 deaths out of 406 patients, giving a 10-year survival of 98.8%. However, in this high-risk group, more cause-specific deaths are expected with longer follow-up. Stage III disease implies locally advanced primary tumor (T4a with any N) but no distant metastases, and stage IVa is assigned to those with very advanced primary tumor (T4b with any N), while stage IVb is assigned to those with distant metastases. As can be seen from these survival curves, the survival progressively declines with advancing stage.

The previously mentioned independent factors affecting outcome allow for risk group stratification, which impacts upon selection of initial treatment, the need for adjuvant therapy, and the intensity of follow-up surveillance strategies. A majority of patients fall into the low- and intermediate-risk group categories with excellent long-term survival (see Fig. 12.185). Only 22% of patients fell into the high-risk category, requiring intensive initial treatment and adjuvant therapies, as well as rigorous follow-up surveillance. At 5 years, 94% of the patients in the high-risk group were alive, but continued attrition in survival is observed in this group over the years, resulting in only 77% surviving at 20 years (Fig. 12.186). The patterns of treatment failure are also dependent on risk group stratification, as shown in Fig. 12.187. In the low-risk group, the most frequent site of treatment failure is regional lymph node metastases, which, however, has little impact on long-term survival. On the other hand, in the high-risk group, regional and distant failure are more common, which impact upon long-term survival. Overall, patients in the low-risk category and even those in the intermediate-risk group category have an excellent long-term disease-specific survival, and it is only those in the high-risk group where there is continued mortality to thyroid cancer in the long term.

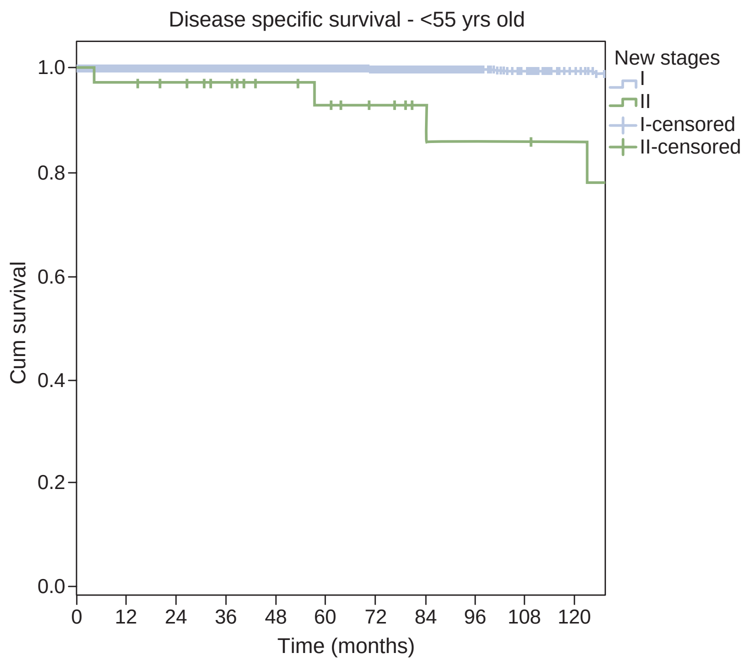

Case processing summary

New stages_T123N2 moved to II - T4a III- M1 IV T2N0-1	Total N	N of events	Censored	
			N	Percent
I	2439	5	2434	99.8%
II	36	5	31	86.1%
Overall	2475	10	2465	99.6%

Figure 12.183 Ten-year disease-specific survival in patients younger than 55 years by American Joint Committee on Cancer (AJCC) and International Union Against Cancer (UICC) (eighth edition) clinical stage.

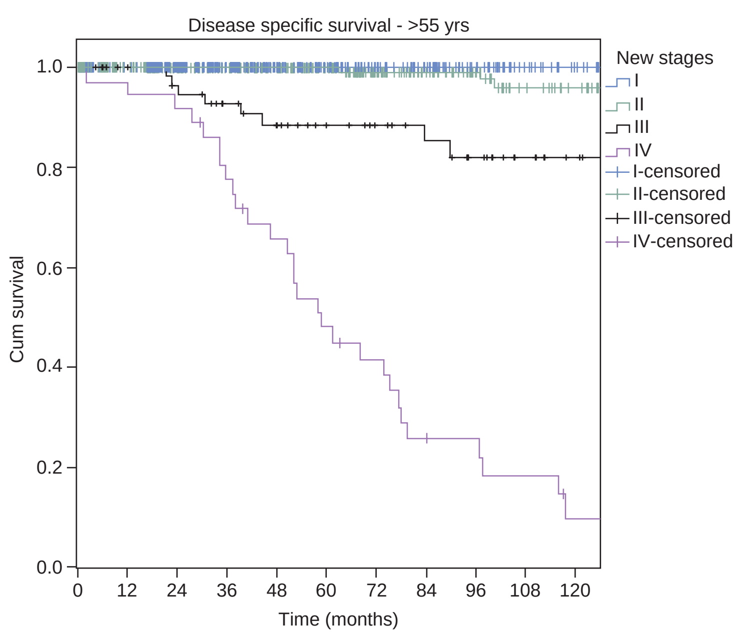

Case processing summary

New stages_T123N2 moved to II - T4a III- M1 IV T2N0-1	Total N	N of events	Censored	
			N	Percent
I	625	0	625	100.0%
II	406	5	401	98.8%
III	66	12	54	81.8%
IV	36	30	6	16.7%
Overall	1133	47	1086	95.9%

Figure 12.184 Ten-year disease-specific survival in patients older than 55 years by American Joint Committee on Cancer (AJCC) and International Union Against Cancer (UICC) (eighth edition) clinical stage.

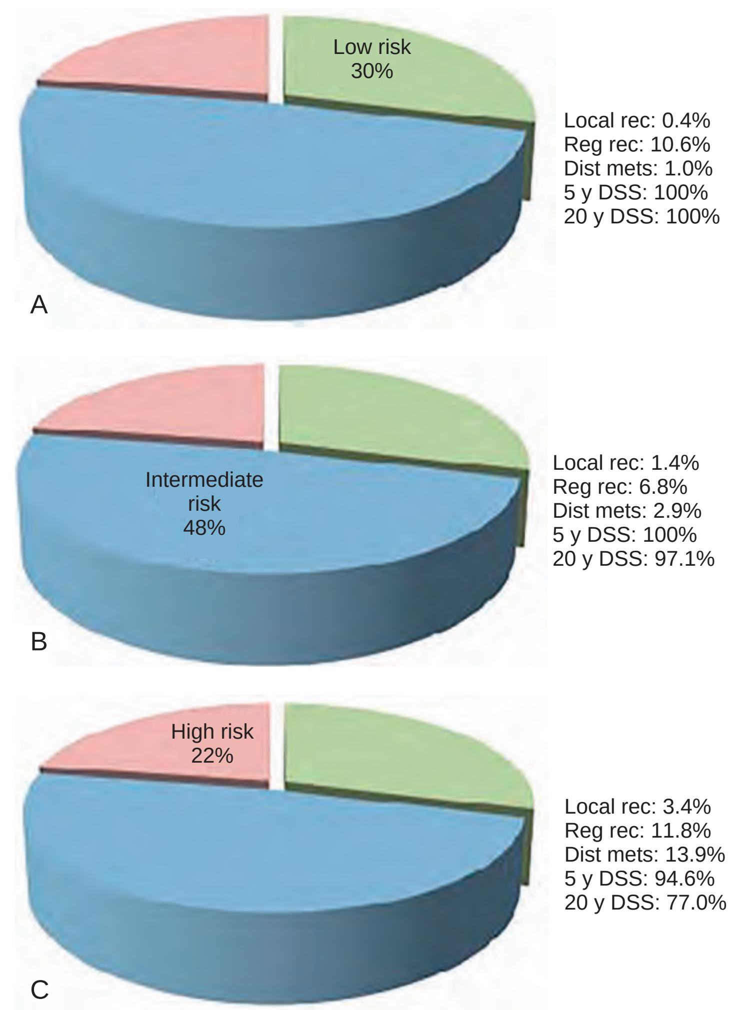

Figure 12.185 Patterns of treatment failure in relation to risk-group stratification.

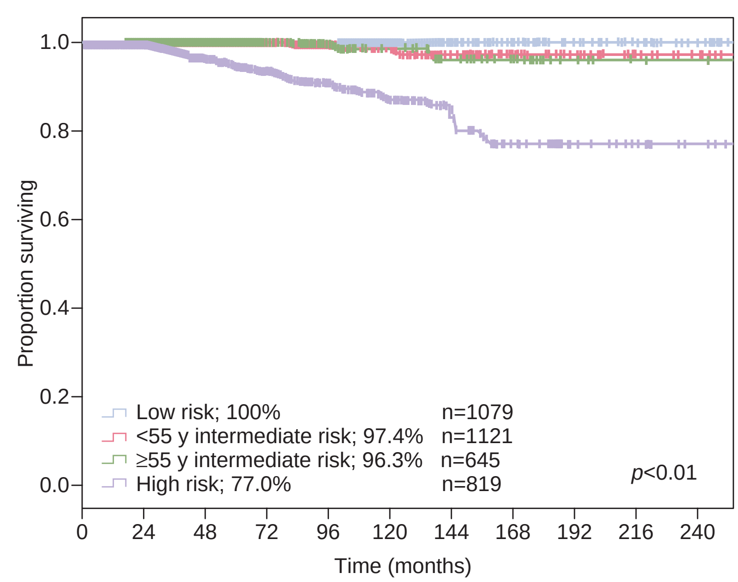

Figure 12.186 Long-term disease-specific survival in relation to risk-group stratification.

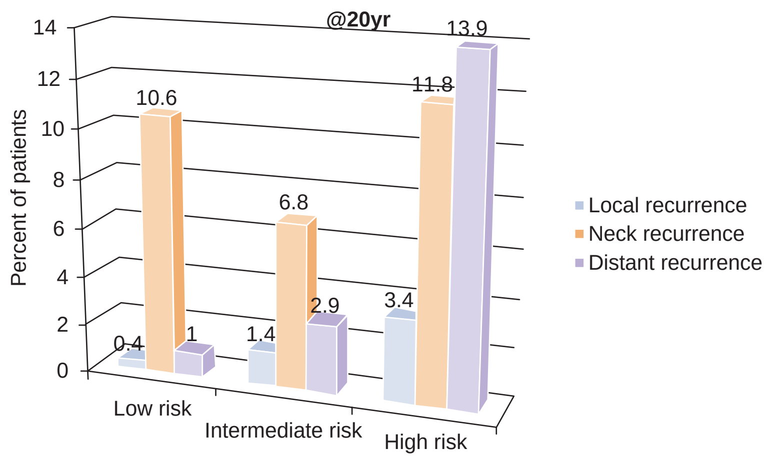

Figure 12.187 Patterns of treatment failure in relation to risk-group stratification.

Medullary Carcinoma

Survival from medullary carcinoma of the thyroid gland is expected to be approximately 50% for all patients (Fig. 12.188). Prognosis in medullary carcinoma of the thyroid gland is dependent on the extent of disease at the time of presentation; this includes the extent of the primary tumor and the extent of regional lymph node metastasis and the presence of distant metastases. Thus in patients without distant metastases, meticulous clearance of all disease at the primary site and regional lymph nodes is essential to enhance prognosis (Fig. 12.189).

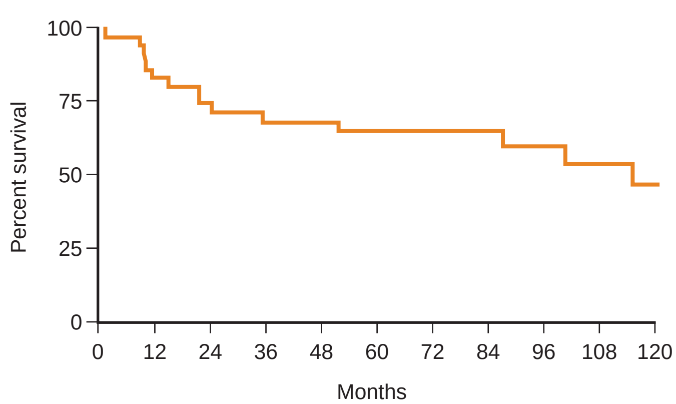

Figure 12.188 Survival in patients with medullary carcinoma of the thyroid.

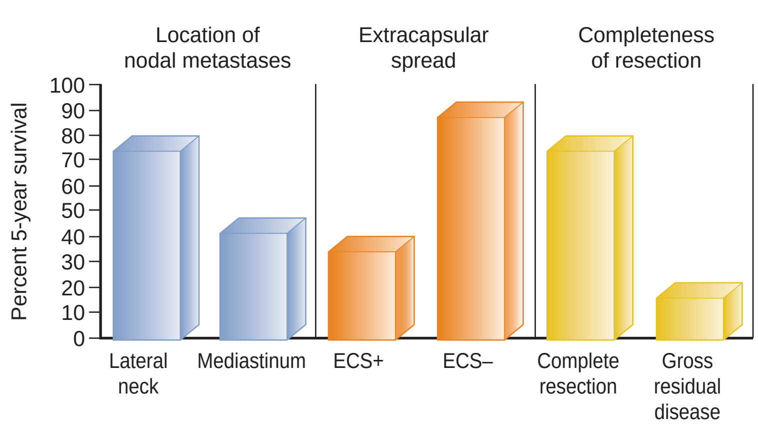

Figure 12.189 Impact of nodal metastases on 5-year survival in patients with medullary carcinoma of the thyroid. *ECS,* Extracapsular spread.

The Parathyroid Glands

The parathyroid glands produce parathormone (PTH), which controls calcium homeostasis. Hyperparathyroidism results from overproduction of PTH from the parathyroid glands. The classic symptom complex of "bones, groans, abdominal moans, and psychic overtones" is rarely seen in modern times. Patients with primary hyperparathyroidism present with hypercalcemia, hypophosphatemia, hypercalciuria, and elevated PTH levels. Most patients with primary hyperparathyroidism have a single adenoma (85%), and multiple adenomas or multigland hyperplasia comprise the remaining 15% of cases. The genetic drivers of primary hyperparathyroidism are diverse but most commonly result from somatic mutations in the MEN1 gene. Secondary hyperparathyroidism occurs in patients with renal failure (renal hyperparathyroidism), resulting in hypocalcemia, and causes hyperplasia of all parathyroid tissue. Primary carcinomas of the parathyroid gland are rare and are associated with extreme hypercalcemia. Parathyroid carcinomas are locally aggressive, with a high rate of metastasis to regional lymph nodes.

EVALUATION

The diagnosis of hyperparathyroidism is made through evaluation of the PTH-calcium balance detected in the serum. Patients with osteoporosis, fragility fractures, and kidney stones are typically evaluated with calcium and PTH levels. Those with renal insufficiency are closely monitored in order to medically manage manifestations of renal hyperparathyroidism. Increasingly, asymptomatic primary hyperparathyroidism has been identified on routine serum tests or for workup of other conditions. Appropriate workup and confirmation of diagnosis requires assessment of serum calcium, PTH, and 25-hydroxyvitamin D as well as urine analysis for hypercalciuria. Other causes of hypercalcemia must be ruled out before proceeding with additional workup for primary hyperparathyroidism. Symptomatic patients should undergo parathyroidectomy. For asymptomatic patients, parathyroidectomy should be performed for high calcium levels (> 1 mg/dL above normal), osteoporosis as defined on bone mineral density testing (T score < –2.5 at lumbar spine, total hip, distal radius, or femoral neck), and those with elevated risks of kidney stones as determined by radiograph or CT scan or biochemical stone risk or urine calcium levels (>400 mg/d). Once a diagnosis of hyperparathyroidism has been made and a decision made to proceed with parathyroidectomy, imaging studies should be performed to localize the hyperfunctioning parathyroid glands. Imaging studies include ultrasound of the neck, technetium-99m sestamibi scan, sestamibi single-photon emission computed tomography (SPECT), and four-dimensional (4D) CT scan.

Radiographic Imaging (Localization)

The choice of preoperative imaging for hyperparathyroidism is controversial, as substantial variation exists across surgical practices due to access to imaging facilities and experience in interpreting results. In general, ultrasound, sestamibi scanning, and 4D CT are the mainstays of preoperative imaging. While some surgeons advocate at least two studies before surgical exploration, others suggest that a single study is sufficient, and surgeon experience is paramount. Importantly, patients with a biochemical diagnosis of primary hyperparathyroidism and

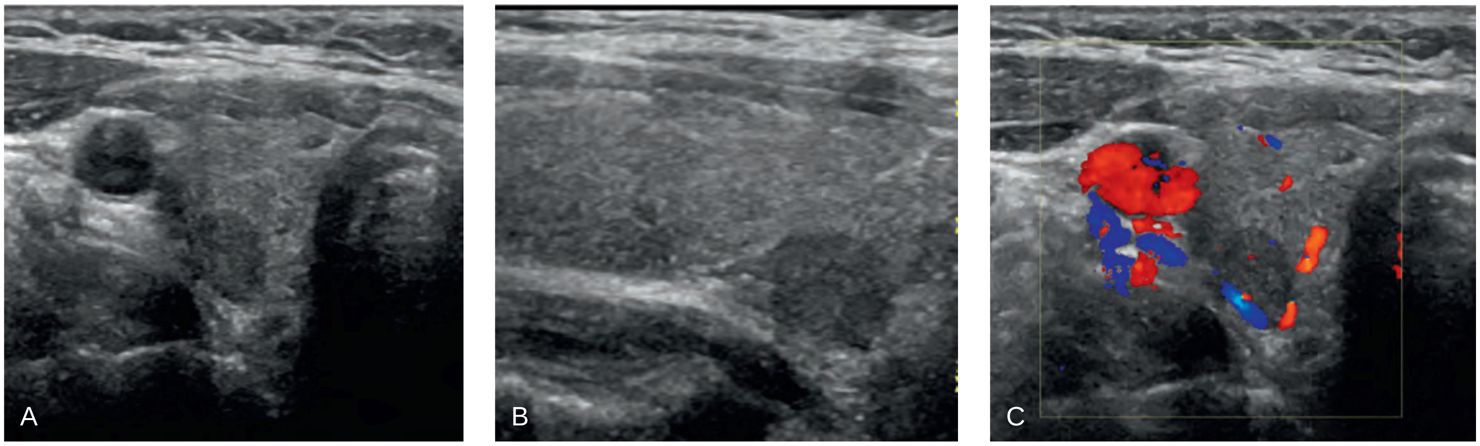

Figure 12.190 Ultrasound examination showing right lower parathyroid adenoma. **A**, Axial view. **B**, Sagittal view. **C**, Doppler study.

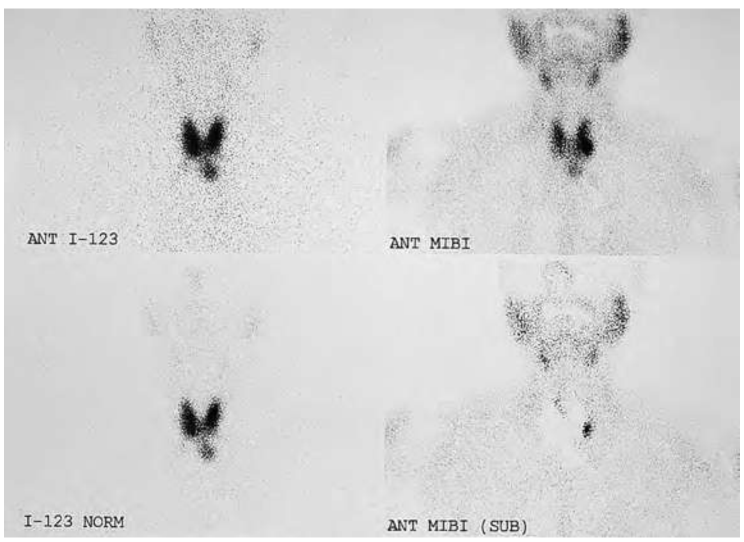

Figure 12.191 An iodine-131–^{99m}Tc-sestamibi subtraction scan demonstrating a left lower parathyroid adenoma. *ANT I-123,* Anterior iodine 123 scan; *ANT MIBI (SUB),* anterior MIBI subtraction scan; *I-123 NORM,* anterior iodine normal scan.

negative imaging studies should be offered four-gland surgical exploration, as these patients will often have an abnormal gland or glands identified at surgery.

Abnormal parathyroid glands can be identified by ultrasound, as they are hypoechoic compared with thyroid parenchyma (Fig. 12.190). False negatives can result from poor imaging quality due to shadowing by the trachea, but movement of the neck can facilitate visualization of adenomas in the tracheoesophageal groove and in a retroesophageal location. False positives can occur with enlarged lymph nodes and thyroid nodules. If a thyroid nodule is noted, fine-needle aspiration biopsy should be considered in accordance with ATA guidelines.

A ^{99m}Tc-sestamibi scan is the most commonly used initial localizing study after an ultrasound. It is generally successful in localizing a parathyroid adenoma. The scan is performed in conjunction with an iodine-131 scan, and the subtraction images clearly demonstrate the location of the adenoma (Fig. 12.191). SPECT imaging provides a more accurate and three-dimensional anatomic localization of the adenoma compared with a ^{99m}Tc-sestamibi scan alone (Fig. 12.192). Since sestamibi scanning evaluates the neck and chest, ectopic glands can be visualized that may not be seen by ultrasound. However, not all parathyroid tumors can be visualized with sestamibi, as patients with small glands and multigland disease have greater numbers of false-negative results.

4D CT scans take advantage of enhancement characteristics of parathyroid tumors. They are particularly useful for patients with persistent disease or to identify ectopic glands. Some surgeons use this modality in combination with ultrasound or sestamibi. Comparative accuracy and anatomic localization of a superior parathyroid adenoma by ultrasound, sestamibi scan, sestamibi SPECT and 4D CT scan is shown in Fig. 12.193. No matter which imaging modalities are employed, experience and familiarity with interpretation of the images are critical to successful localization.

TREATMENT

Surgery is the only curative treatment for primary hyperparathyroidism. An image-localized, single adenoma can be removed with a small cervical incision of a 2 to 3 cm (minimally invasive) parathyroidectomy. Success of the operation can be confirmed intraoperatively by frozen-section analysis of the specimen and intraoperative PTH assay after removal of the adenoma. Typically, two baseline measurements of PTH are obtained, one at induction of anesthesia, and another at the time of gland identification. After tumor excision, two additional samples are drawn for PTH, one at 5 minutes and another at 10 minutes. If a 50% or greater drop in the PTH level occurs and levels return to the normal range, the procedure is terminated. In some patients, drop in PTH levels may take longer than 10 minutes, and therefore, a third sample at 20 minutes following removal of the adenoma should be sent. Surgeons should be aware of high normal PTH values even if a 50% drop has occurred, as some of these patients may have persistent disease. If the PTH levels do not drop appropriately, then systematic exploration of the remaining parathyroid glands should be performed.

Patients with multiple adenomas, the absence of localization of a single adenoma, or secondary hyperparathyroidism require exploration of all four parathyroid glands. In patients with primary hyperparathyroidism and multigland hyperplasia, excision of all enlarged parathyroid glands is recommended, removing three and a half glands and leaving a 50 to 100 mg viable remnant. If total parathyroidectomy is required (secondary hyperparathyroidism), then autotransplantation into the forearm should be performed selectively, as these patients are at a higher

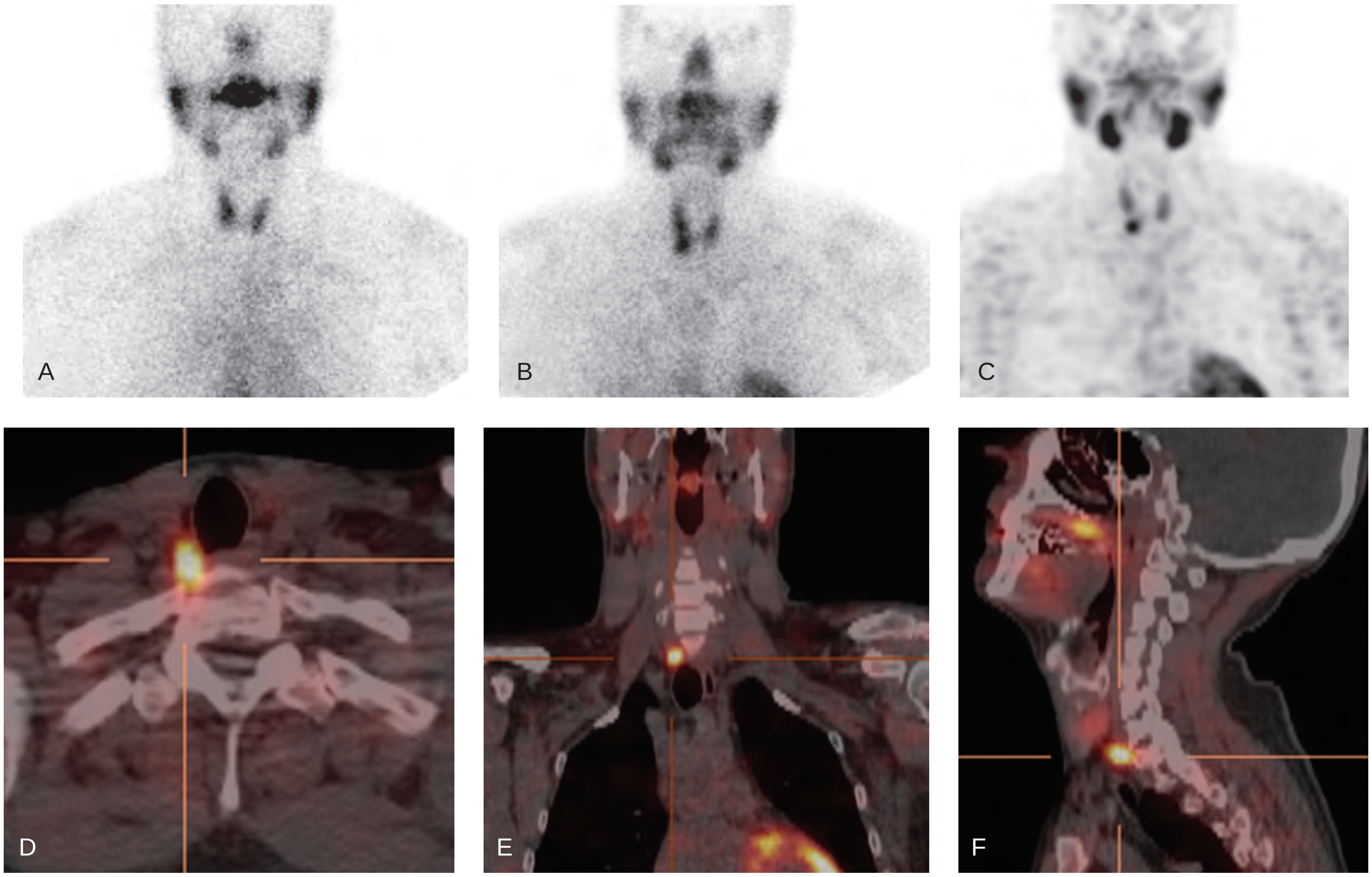

Figure 12.192 A ^{99m}Tc-sestamibi and single-photon emission computed tomography (SPECT) scan showing a right lower parathyroid adenoma. **A**, A ^{99m}Tc scan. **B**, A ^{99m}Tc with sestamibi scan. **C**, Maximum intensity projection of a ^{99m}Tc-sestamibi scan. **D**, An axial view of a SPECT scan. **E**, A coronal view of a SPECT scan. **F**, A sagittal view of a SPECT scan.

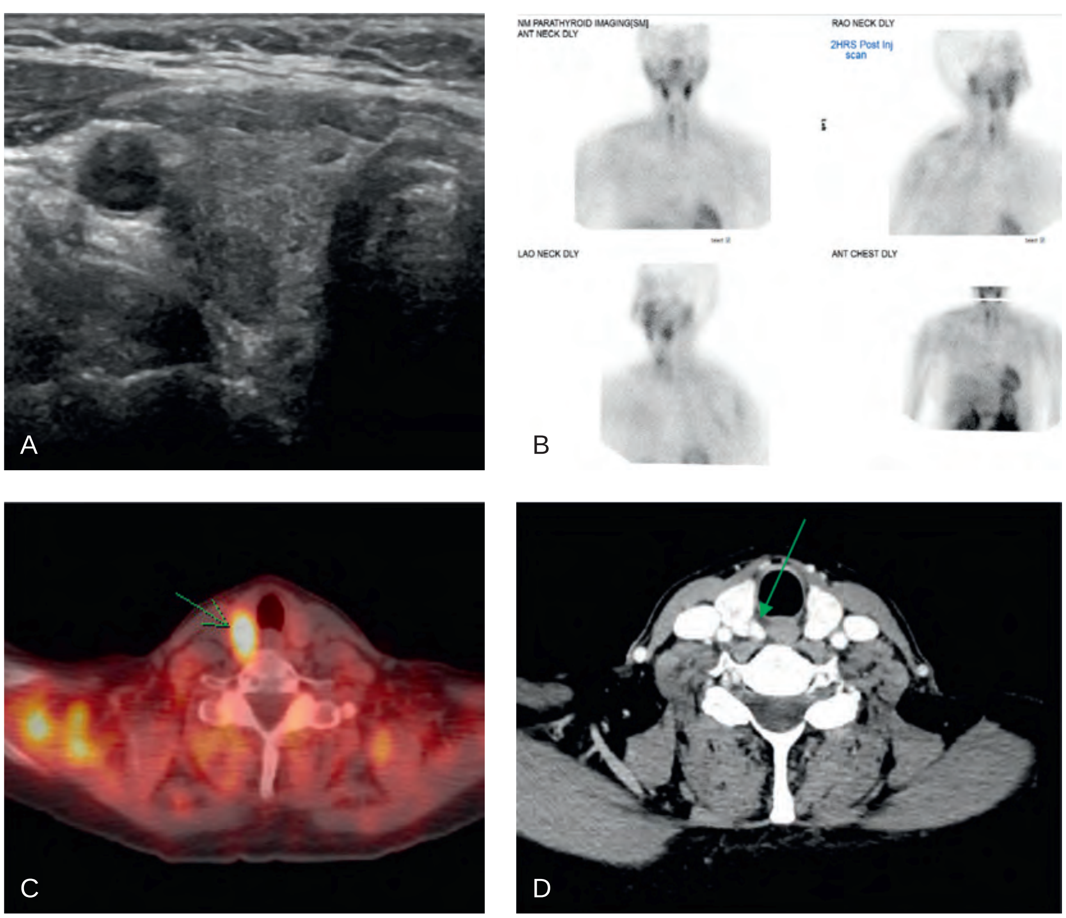

Figure 12.193 Anatomic localization of a right upper parathyroid adenoma by (**A**) ultrasound, (**B**) sestamibi scan, (**C**) sestimbi single-photon emission computed tomography *(arrow)*, and (**D**) four-dimensional computed tomography scan at 60 seconds *(arrow)*.

risk of permanent hypoparathyroidism, compared with three and half gland excision. In this setting, forearm grafts can facilitate relatively easy excision of subsequent hyperplastic parathyroid tissue without requiring reexploration of the neck.

SURGICAL ANATOMY

The normal parathyroid glands measure 5 to 6 mm in their largest dimension and weigh about 50 mg. They are yellowish-brown or caramel colored and flat in cross section. Differentiating between lobules of fat, a normal parathyroid gland, and a slightly enlarged hyperplastic paratracheal lymph node is often difficult during surgery. The fat lobules are clearly yellow, the lymph nodes have pinkish discoloration, and the parathyroid glands have a typical caramel color distinct from the other two (Fig. 12.194).

Normally the four parathyroid glands are located on the posterior surface of the thyroid gland. On rare occasions, patients may have more or less than four parathyroid glands. During embryonic development, the lower parathyroid glands descend along with the thymus from the third pharyngeal pouch, while the upper parathyroid glands descend with the thyroid gland from the fourth pharyngeal pouch. The superior parathyroid glands are located dorsally, and the inferior parathyroid glands are located ventrally in relation to the recurrent laryngeal nerve. Occasionally the parathyroid glands may be found in unusual locations such as the superior mediastinum, the lateral aspect of the central compartment of the neck, in the prevertebral space, rarely in the carotid sheath, or as high as the thyrohyoid membrane (Fig. 12.195). The presence of parathyroid glands within the capsule of the thyroid gland is exceedingly rare (Fig. 12.196). The parathyroid glands derive their blood supply from the inferior thyroid artery, but the superior parathyroid glands in addition may derive their blood supply also from the superior thyroid artery.

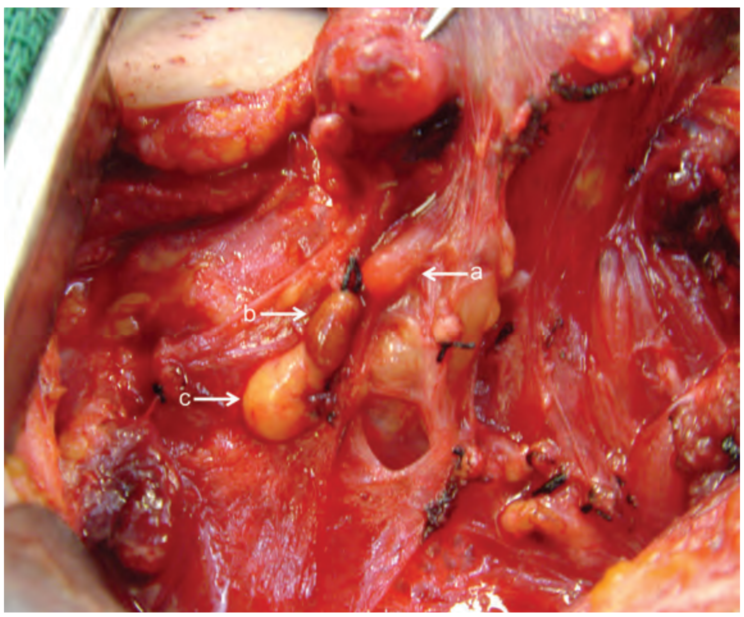

Figure 12.194 Gross appearance of (*a*) a lymph node, (*b*) a parathyroid gland, and (*c*) a fat lobule in a surgical field.

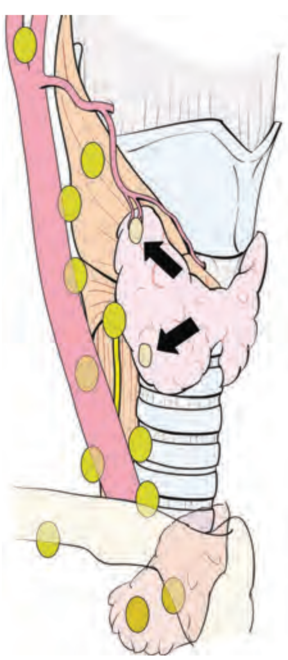

Figure 12.195 Variations in location of parathyroid glands (*arrows* point to the normal location of the parathyroid glands on the posterior surface of the thyroid). *(Courtesy Memorial Sloan Kettering Cancer Center.)*

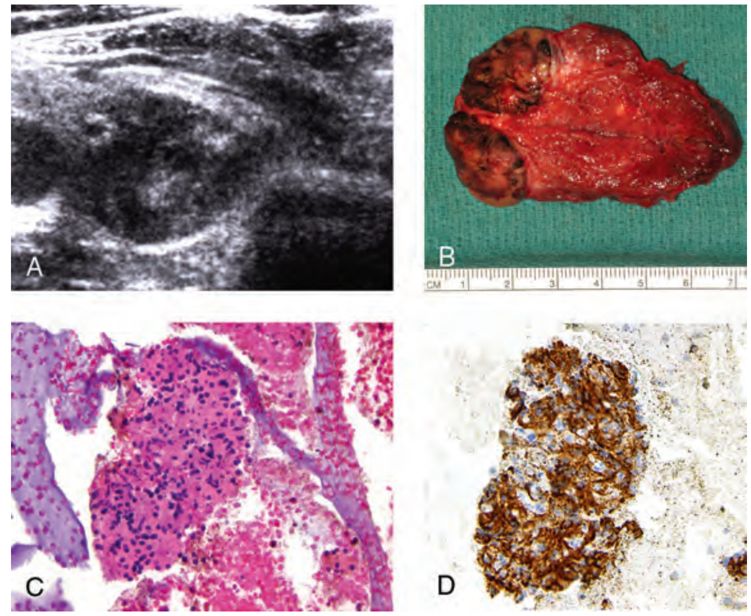

Figure 12.196 Intrathyroid parathyroid gland. **A**, Ultrasound image. **B**, Surgical specimen. **C**, Hematoxylin and eosin stain. **D**, Parathormone immunohistochemistry.

Minimally Invasive or Focused Parathyroidectomy

When a single parathyroid adenoma is localized by imaging studies, a minimally invasive or focused parathyroidectomy is feasible. It is not necessary to explore all four parathyroid glands in this setting as long as intraoperative frozen section diagnosis of the specimen and appropriate drop in the PTH levels confirms a successful parathyroidectomy. A sestamibi scan of a patient shown in Fig. 12.197 demonstrates a single adenoma in the left lower parathyroid location. A minimally invasive parathyroidectomy can be performed for this adenoma through either a small midline cervical incision or an incision (1.5–2 cm) between the anterior border of the sternocleidomastoid muscle and the midline inferior to the lower border of the cricoid cartilage (Fig. 12.198). The skin incision is deepened through the platysma to expose the anterior border of the sternocleidomastoid muscle and the sternohyoid muscle. Dissection then proceeds lateral to the thyroid lobe, creating a plane between the sternocleidomastoid muscle and the lateral border of the sternohyoid and sternothyroid muscles (Fig. 12.199). The parathyroid adenoma is identified by alternate blunt and sharp

Figure 12.197 A ^{99m}Tc-sestamibi scan showing a left lower parathyroid adenoma.

Figure 12.198 The skin incision is marked along a lower neck skin crease.

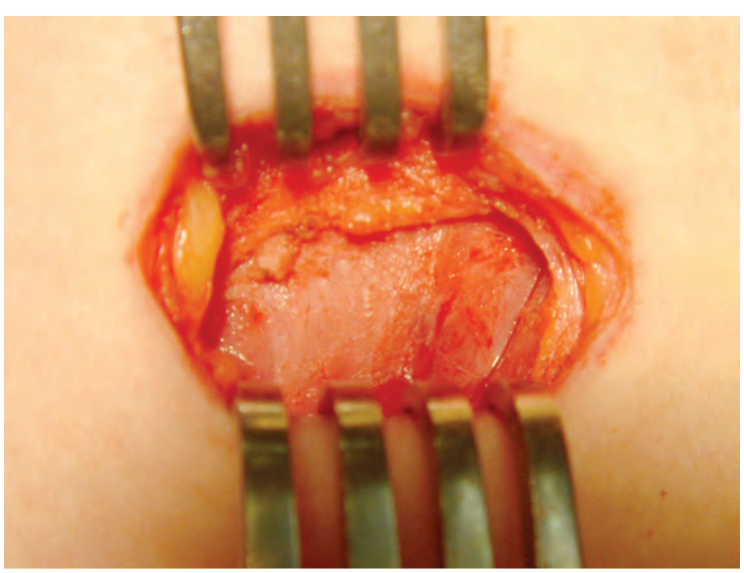

Figure 12.199 The plane of dissection is created between the sternomastoid and sternohyoid muscles.

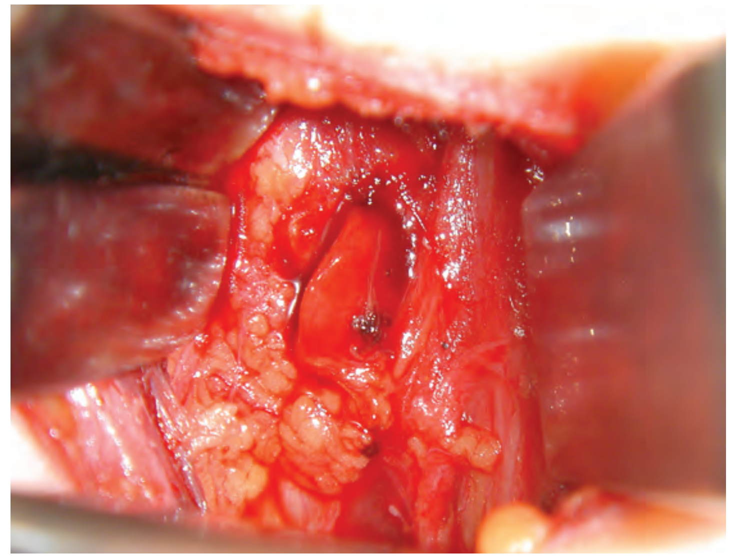

Figure 12.200 The parathyroid adenoma is identified on the posterior surface of the left thyroid lobe.

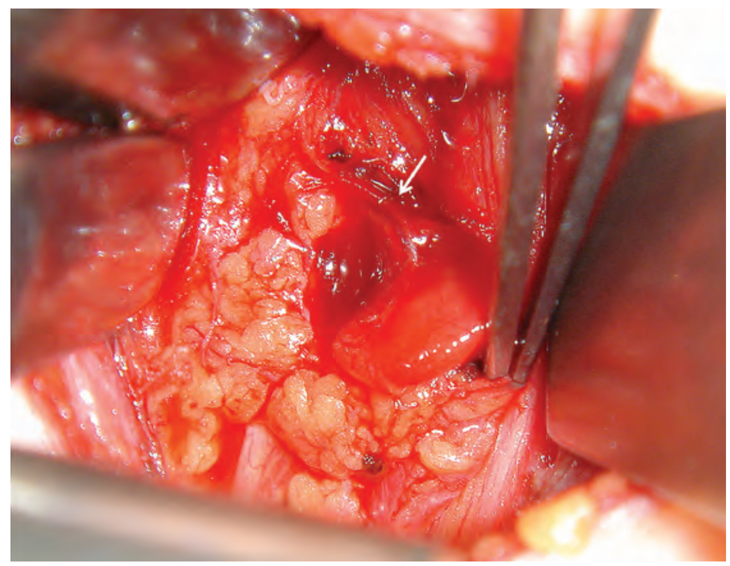

Figure 12.201 The vascular pedicle of the adenoma (*arrow*) is divided and ligated.

Figure 12.202 The surgical specimen showing an intact adenoma.

dissection, retracting the thyroid lobe medially in a plane between the common carotid artery and the tracheoesophageal groove (Fig. 12.200). The adenoma must be handled delicately to ensure that the tumor does not fragment. Usually the parathyroid adenoma is supplied by a vascular pedicle containing a single vascular bundle; this is divided, and its stump is ligated (Fig. 12.201). The surgical specimen shows an intact 1.5- by 3-cm parathyroid adenoma (Fig. 12.202). The diagnosis of a parathyroid adenoma should be confirmed by frozen section to ensure that the excised tissue is indeed of parathyroid origin. Success of the procedure is confirmed by intraoperative assessment of intact PTH.

Surgical Excision of a Parathyroid Adenoma: Four-Gland Exploration

Primary hyperparathyroidism of any etiology requires surgical exploration of the parathyroid glands and appropriate parathyroidectomy. The diagnosis of adenoma versus hyperplasia occasionally is not established before surgical exploration. The patient described here presented with asymptomatic hypercalcemia that was discovered upon routine biochemical testing. Increased levels of PTH confirmed the diagnosis of primary hyperparathyroidism. Preoperative imaging studies did not localize a single adenoma. The operation demonstrated here is that of surgical exploration of four glands for hyperparathyroidism.

The incision for parathyroid exploration should be long enough to provide exposure of the thyroid bed on both sides, and this can typically be established with a 2- to 3-cm incision depending on the size of the neck. The skin incision is deepened through the platysma, and the upper and lower skin flaps are elevated. It is imperative that absolute hemostasis be maintained during the operative procedure of parathyroid exploration. If excess oozing or bleeding occurs, the surgical field will not be clear enough to facilitate identification of the parathyroid glands.

Dissection begins by dividing the middle thyroid vein and capsular veins, allowing elevation and medial rotation of the thyroid lobe. The posterior capsule of the thyroid gland is very delicately preserved, and all branches of the inferior thyroid artery are diligently preserved. The following is an example of four-gland exploration through a conventional thyroidectomy incision. The right thyroid lobe shown in Fig. 12.203 has been mobilized, carefully preserving the parathyroid glands. Note the normal right upper parathyroid gland clearly visible on its posterior capsule. The lower parathyroid gland is located quite low, as indicated with a hemostat in Fig. 12.204.

To locate the parathyroid glands, dissection and identification of the recurrent laryngeal nerve and the inferior thyroid artery with its branches should be performed in a systematic and meticulous fashion to prevent inadvertent trauma to the glands. When an anatomic structure resembling a parathyroid gland is identified, it is handled with extreme care until all four glands are located. Sometimes a hyperplastic lymph node or a lymph node containing a metastatic papillary carcinoma looks like a parathyroid gland; therefore histologic confirmation of the identified structure is essential if any doubt exists.

Having identified two normal parathyroid glands on the right-hand side, attention is focused on exploration of the left parathyroid glands. The left lobe of the thyroid is mobilized medially in a similar fashion, exposing a large adenoma in the upper parathyroid location (Fig. 12.205). A close-up view of the surgical field clearly demonstrates an adenoma of the upper

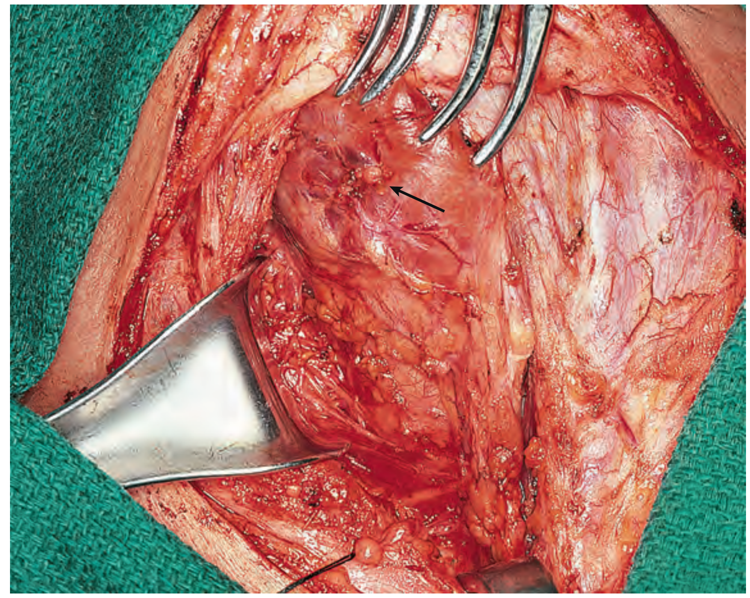

Figure 12.203 The right thyroid lobe is mobilized first, showing a normal upper parathyroid gland (*arrow*).

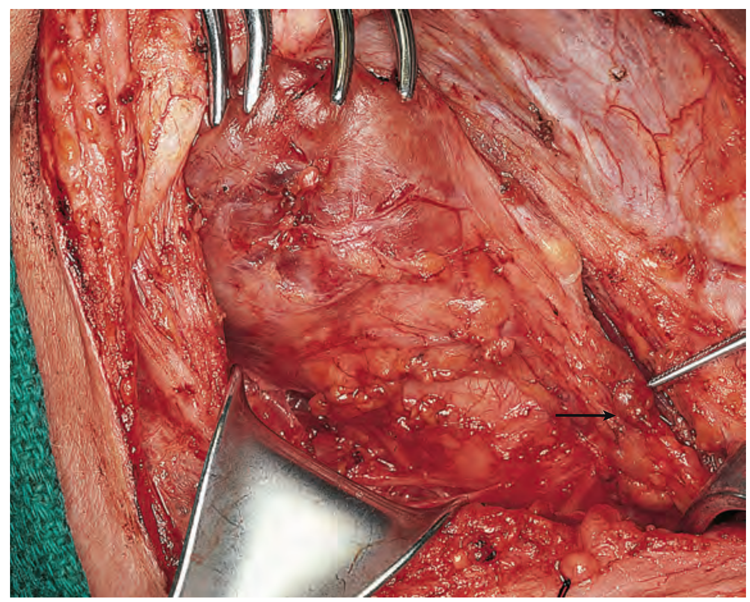

Figure 12.204 The right lower normal parathyroid gland is found quite low (*arrow*).

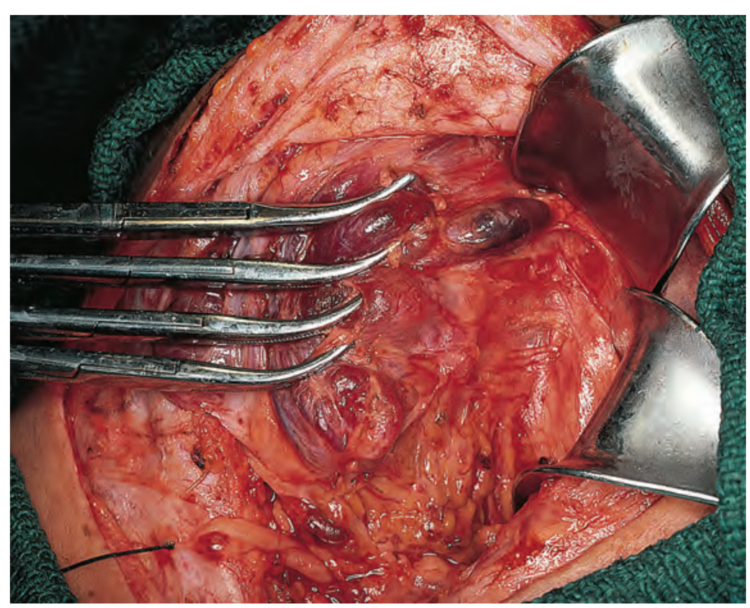

Figure 12.205 An adenoma is identified in left upper parathyroid location.

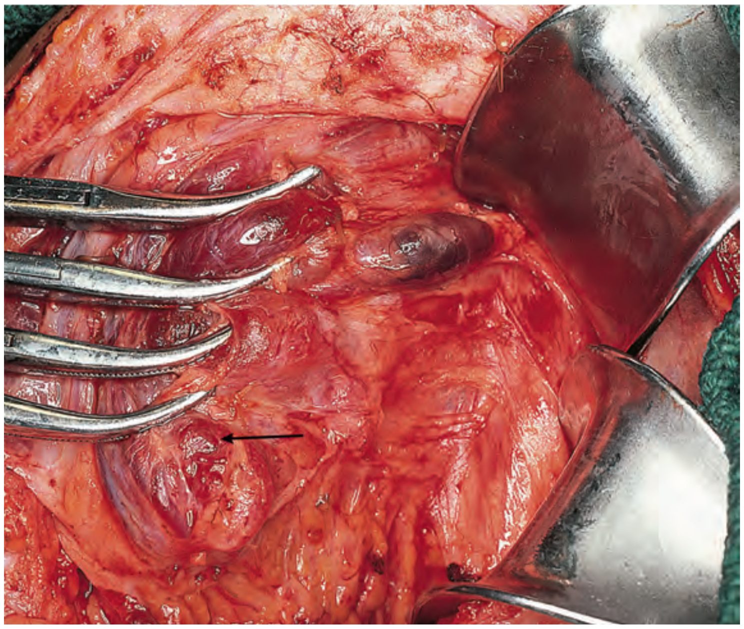

Figure 12.206 This close-up view shows an upper left parathyroid adenoma and a normal left lower parathyroid gland (*arrow*).

Figure 12.207 The surgical specimen of a parathyroid adenoma.

parathyroid gland (Fig. 12.206). The lower parathyroid gland is of normal size and shape. The adenoma is excised and sent for frozen-section examination to confirm its diagnosis (Fig. 12.207). If an adenoma is identified and the remaining three parathyroid glands are located and are found to be of normal size and configuration, then the operative procedure is terminated. However, even in this setting, intraoperative PTH assay should be performed to ensure appropriate drop in PTH value and thus a successful operative procedure. Postoperative care consists of routine management of the wound and monitoring of the patient's serum calcium levels.

Reexploration for Persistent Hyperparathyroidism

Reexploration of the neck for persistent hyperparathyroidism is a much more challenging and demanding operation. Postoperative fibrosis and a disturbed anatomic relationship of the explored parathyroid bed from previous surgery significantly jeopardizes the operative procedure for locating a parathyroid adenoma. Therefore it is advisable to obtain appropriate radiographic studies preoperatively for localization of a missed adenoma. We typically perform 4D CT scans in all patients with persistent hyperparathyroidism.

In Fig. 12.208 a technetium-99 scan of the thyroid region of a patient who had previously undergone parathyroid exploration is shown. She had persistent postoperative hypercalcemia requiring reexploration for treatment of her persistent hyperparathyroidism. The technetium-99 scan shows retained radionuclide in the right thyroid lobe and the submandibular salivary glands on both sides. A subtraction scan after injection of radioactive thallium clearly shows a parathyroid adenoma in the upper right location (Fig. 12.209). Such preoperative localization of the adenoma would help the operating surgeon considerably in carrying out a safe, expeditious, and successful operation. Unnecessary surgical exploration to look for an adenoma is therefore avoided.

Surgical exposure through the previous scar demonstrates a large parathyroid adenoma posterior to the thyroid gland near the cricothyroid membrane (Fig. 12.210). The adenoma is located in a deep tissue plane near the tracheoesophageal groove. Extreme care should be taken during dissection to excise the adenoma with its capsule intact. Fracturing of the adenoma or leaving residual parathyroid tissue behind increases the risk for development of recurrent hyperparathyroidism, requiring a

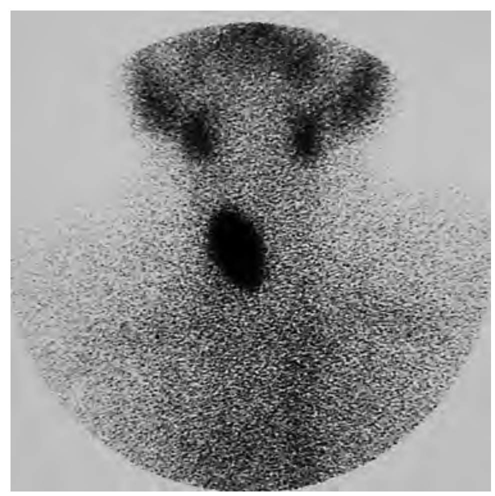

Figure 12.208 A technetium-99 scan of the thyroid region.

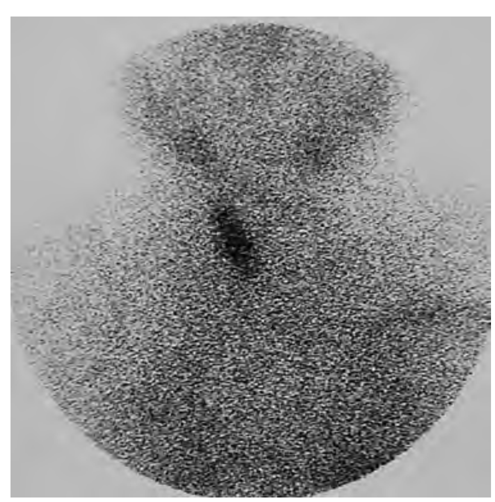

Figure 12.209 A thallium–technetium-99 subtraction scan.

further and more tedious surgical procedure in the future. The specimen shown in Fig. 12.211 clearly demonstrates a large adenoma excised in toto at reexploration. Following confirmation of the histologic diagnosis of a parathyroid adenoma, and after appropriate drop in the intact PTH level, the surgical procedure is terminated.

Occasionally, localization studies are not quite as helpful, in which case the entire central compartment should be meticulously reexplored to search for the missed adenoma. If exploration of the central compartment of the neck is unrewarding, then the lateral compartments of the neck, the upper part of the neck, the carotid sheath, and the superior mediastinum should be meticulously and systematically explored to identify, confirm, and excise the retained adenoma. Rarely a parathyroid adenoma may be within the thymus. Therefore, if thorough exploration does not identify the missing adenoma, then a thymectomy should be performed, and the thymus serially sectioned to locate the hidden adenoma.

Parathyroidectomy for Multiple Endocrine Neoplasia Syndrome

Patients with MEN syndrome often present with multiple parathyroid adenomas. The patient described here had MEN 1 syndrome with a pituitary tumor, multiple parathyroid adenomas, and a tumor of the pancreas. The surgical procedure for parathyroid adenomas in patients with MEN syndrome must include exploration and excision of all adenomas. Every attempt must be made to demonstrate all four parathyroid glands and remove all enlarged parathyroid glands, keeping a reasonable volume of viable parathyroid tissue to prevent permanent hypoparathyroidism.

This patient had four-gland disease with large adenomas on both sides. Two large adenomas on the right-hand side are shown in Fig. 12.212. Similarly, two large adenomas are shown on the left-hand side in Fig. 12.213. Excision of three adenomas and three-quarters of the fourth adenoma was performed on this patient, leaving a viable vascularized portion of the lower

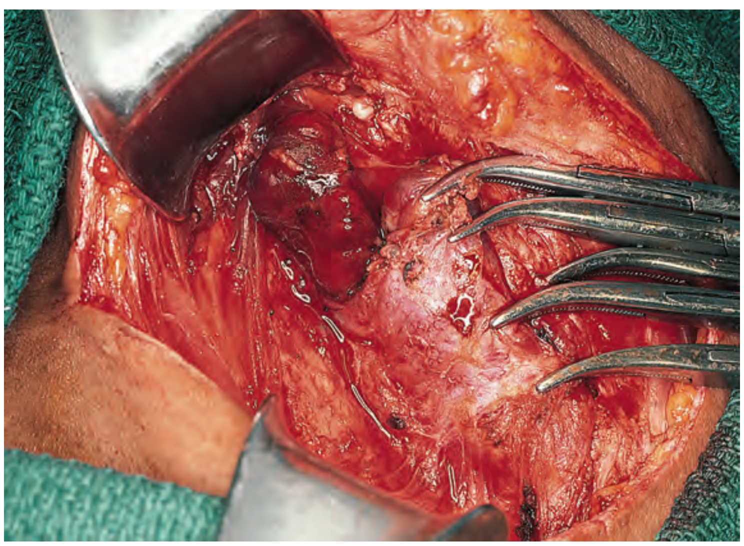

Figure 12.210 A large parathyroid adenoma near the cricothyroid membrane.

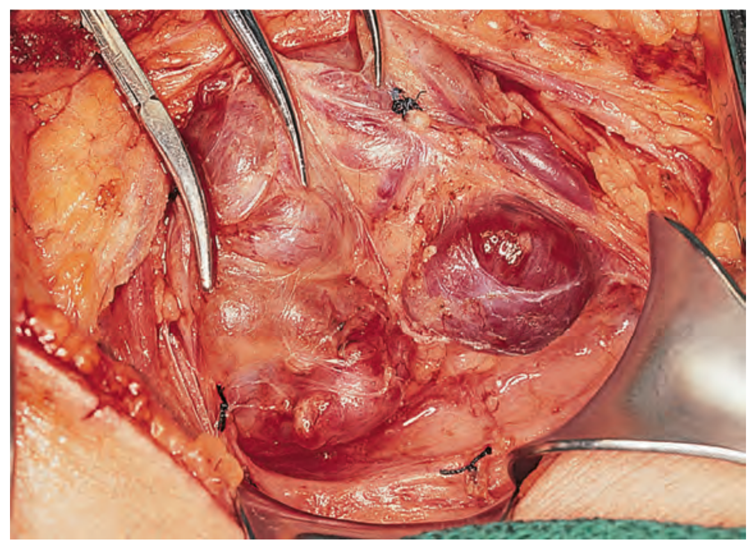

Figure 12.212 Two parathyroid adenomas on the right-hand side.

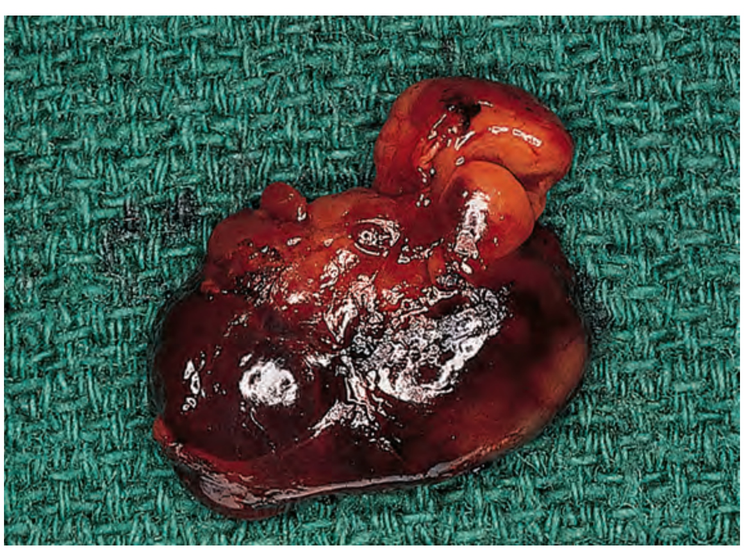

Figure 12.211 The surgical specimen.

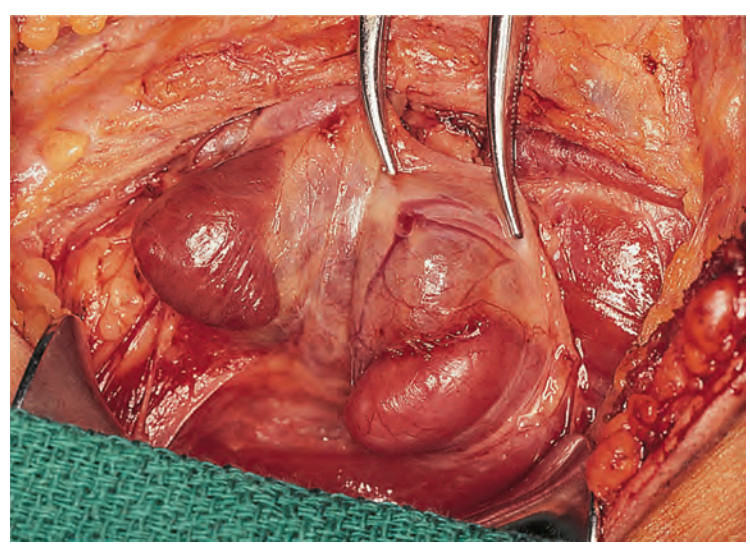

Figure 12.213 The patient also had two large adenomas on the left-hand side.

left parathyroid gland to maintain normal parathormone production and normocalcemia. In addition to parathyroidectomy, a cervical thymectomy is recommended to remove any supernumerary or ectopic parathyroid glands.

Resection of a Parathyroid Carcinoma

The diagnosis of parathyroid carcinoma is usually made by the severity of hypercalcemia, extremely high levels of parathormone, local invasiveness of the tumor, or the presence of regional lymph node metastases or distant metastases. The cardinal features of malignancy at the histopathologic level are infiltration of adjacent tissues (such as thyroid), vascular invasion, or perineural invasion. These microscopic features can be difficult to identify and subject to interobserver variability. Therefore it is often difficult to differentiate only histologically between a parathyroid adenoma and a parathyroid carcinoma. However, the combination of clinical and biochemical features as well as operative findings and histomorphologic findings are all essential to make a conclusive diagnosis of parathyroid carcinoma.

The patient shown in Fig. 12.214 reported to his family physician with the generalized complaints of lassitude and weakness. Physical examination showed the presence of a 2.5-cm, firm, palpable mass adherent to the laryngotracheal complex on the right-hand side, as shown in the diagram. Routine blood work showed a serum calcium level of 14.7 mg/mL. The physical findings and an extremely high serum calcium level raised the suspicion for a parathyroid carcinoma. Serum parathormone level was 1024 pg/mL. These values were essentially confirmatory of the diagnosis of a parathyroid carcinoma. A preoperative MRI scan in an axial plane showed the presence of a contrast-enhancing lesion involving the right tracheoesophageal groove with extension in a submucosal plane protruding through the membranous trachea in the tracheal lumen (Fig. 12.215). Coronal view of the MRI scan clearly demonstrates a well-circumscribed mass in the right tracheoesophageal region protruding into the lumen of the trachea (Fig. 12.216).

Surgical exploration for excision of the parathyroid carcinoma is similar to that undertaken for a parathyroid adenoma. A transverse lower cervical incision is made, and the skin flaps are elevated in the usual fashion. The strap muscles are retracted laterally to expose the anterior surface of the thyroid gland. Exploration of the left parathyroid glands demonstrated that they were of normal configuration. Mobilization of the right thyroid lobe is then performed, demonstrating the anatomic relationship between the inferior thyroid artery and the recurrent laryngeal nerve on the posterior surface of the right thyroid lobe (Fig. 12.217). The tumor is located posteromedial to the

Figure 12.215 An axial view of the computed tomography scan shows the tumor of the tracheoesophageal groove projecting in the tracheal lumen.

Figure 12.216 A coronal view of the magnetic resonance imaging scan demonstrates a tumor of the right tracheoesophageal groove projecting into the tracheal lumen.

Figure 12.214 A firm mass adherent to the trachea could be palpated in the region of the right thyroid lobe.

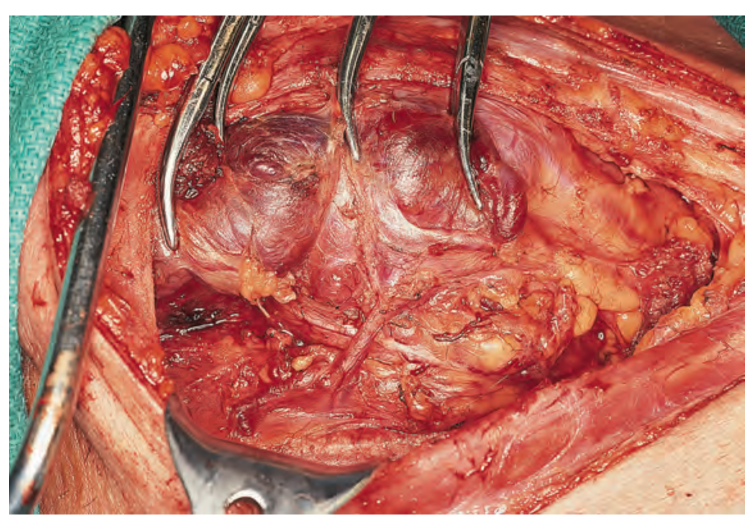

Figure 12.217 Anatomic relationships between the inferior thyroid artery, recurrent laryngeal nerve, and the parathyroid tumor on the posterior surface of the right thyroid lobe.

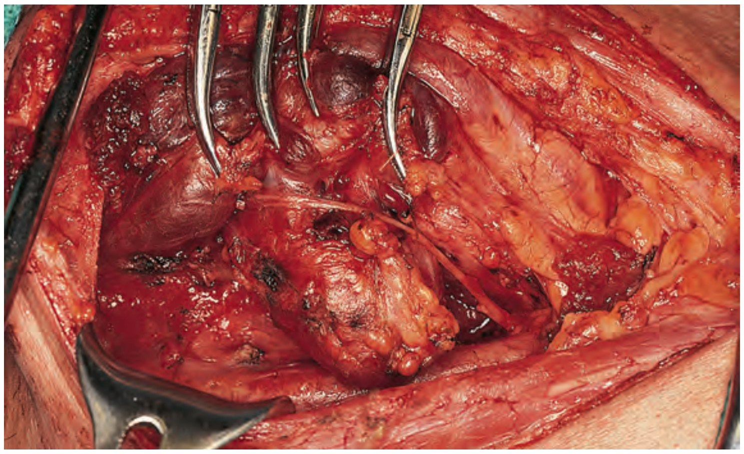

Figure 12.218 The tumor is located posterior to the recurrent laryngeal nerve in the tracheoesophageal groove.

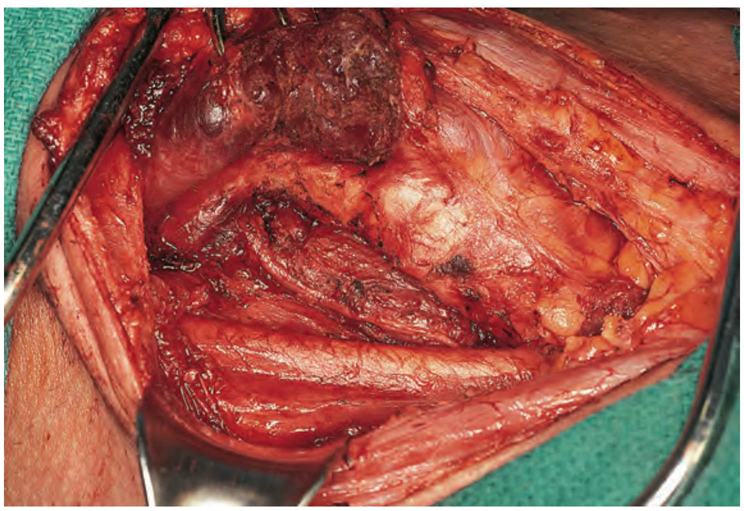

Figure 12.219 The surgical field demonstrating an intact recurrent laryngeal nerve and the tumor bed in the tracheoesophageal groove.

recurrent laryngeal nerve, indenting into the tracheal lumen. The inferior thyroid artery is divided and ligated and the recurrent laryngeal nerve is carefully dissected and retracted anteriorly, exposing the tumor that is deeply indenting the trachea and esophagus in a submucosal fashion (Fig. 12.218). By meticulous dissection around the capsule of the tumor, it is delivered from the deep tracheoesophageal plane without injury to the membranous trachea or the esophagus. The surgical field following excision of the tumor is shown in Fig. 12.219. It is vitally important to remove the parathyroid carcinoma in an intact monobloc fashion. Rupture of the tumor can lead to implantation of the tumor cells, leading to multifocal recurrence and recurrent hypercalcemia. Similarly, a diligent search should be undertaken to identify any enlarged lymph nodes, which are suspicious for metastasis. If enlarged lymph nodes are found, a comprehensive clearance of regional lymph nodes at risk should be undertaken immediately. The surgical specimen shown in Fig. 12.220 shows a parathyroid carcinoma removed intact in a monobloc fashion. The surgical incision is closed in layers with a Penrose drain in the usual fashion.

Postoperative care of this patient is relatively simple. The serum calcium level and the parathormone levels promptly

Figure 12.220 The surgical specimen demonstrates monobloc excision of a parathyroid carcinoma.

return to normal. Persistent hypercalcemia or persistent high levels of parathormone raise the possibility of metastatic parathyroid carcinoma to regional lymph nodes or other sites. Appropriate additional workup and surgical treatment should be undertaken to correct that problem.

POSTOPERATIVE CARE AND COMPLICATIONS

A hematoma can develop in up to 1% of patients undergoing surgery for thyroid or parathyroid glands. Although smaller, nonexpanding hematomas can be managed conservatively, larger or expanding hematomas need urgent attention because they can compromise the airway. In severe cases, the neck wound should be opened at the bedside to decompress the central compartment and relieve pressure on the airway. Surgical management consists of exploration of the wound with evacuation of the hematoma, irrigation of the surgical wound, and control of hemorrhage, to secure complete hemostasis. The most common complications of thyroid surgery are hypoparathyroidism and injury to the recurrent or superior laryngeal nerves. Although temporary parathyroid dysfunction is not uncommon (it occurs in up to 25% of cases), this dysfunction resolves in 4 to 6 weeks in nearly all patients. Postoperatively these patients require calcium supplementation with or without vitamin D, which can be tapered over a 6-week period.

Clinical manifestation of injury to the superior laryngeal nerve tends to be subtle, with the patient complaining of loss of vocal pitch and strength. Risk of injury to the nerve is minimized by individual ligation of terminal branches of the superior thyroid vessels on the surface of the gland, avoiding mass ligature of the vascular pedicle. Permanent injury to the recurrent laryngeal nerve is uncommon, occurring in 1% to 2% of cases. Patients with recurrent nerve dysfunction in whom the nerve has been preserved should be observed, because the majority of patients recover spontaneously. Prolonged significant dysfunction or permanent paralysis due to injury or deliberate sacrifice of the recurrent nerve can be treated with vocal cord medialization procedures (see Chapter 10).

CHAPTER 13

Salivary Glands

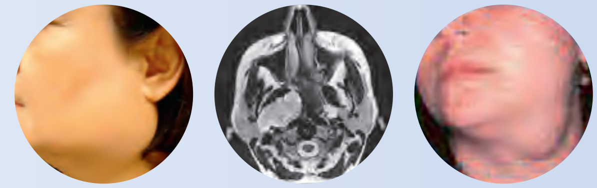

Salivary glands are divided into major (parotid, submandibular, and sublingual) and minor salivary glands. Major salivary glands are paired structures, and minor glands exist in a submucosal location throughout the upper aerodigestive tract starting from the nasal cavity and lips down to the esophagus and trachea. Embryologically, the salivary glands are tubuloacinar structures arising from invaginations of the somatoderm (ectodermal) and foregut (endodermal). The salivary gland network is composed of secretory elements that produce saliva upon stimulation by mastication or sensory/autonomous nervous system stimuli (i.e., smell, taste, and thought).

The composition of saliva depends on the site of the salivary gland producing it. For example, a larger concentration of serous glands is found in the parotid and mucous glands in the hard palate. Saliva produced by these glands facilitates digestion, provides lubrication and protection of mucous membrane and dentition, and provides clearance of foreign materials. In addition, saliva contains enzymes (e.g., amylases, lipases, other enzymes) that initiate the digestive process, primarily of materials that contain starch. Saliva also plays an essential role in preventing dental caries and infection by direct cleansing of foreign materials and antibacterial activity that is mediated through multiple factors (i.e., immunoglobulin A and leukotrienes).

Neoplasms of the salivary glands are rare and account for approximately 3% to 6% of all tumors of the head and neck region. Cancers of the salivary gland occur with an incidence of approximately 2.5 to 3.0 cases per 100,000 per year in the United States. Factors that predispose to neoplastic processes in the major salivary glands include a history of exposure to low-dose radiation. In addition, chronic exposure to wood dust (especially soft wood) and chemicals used in the leather tanning industry also may increase the risk for minor salivary gland cancers in the sinonasal tract (especially adenocarcinomas). An increased incidence of adenocarcinoma of minor salivary origin of the nasal cavity and ethmoid region is reported from Europe, in contrast to the United States, where squamous cell carcinoma is most common in these sites. Although no known links exist, a higher rate of malignant oncocytomas in Alaskan natives suggests that other unidentified environmental and/or inherited factors also may contribute to salivary carcinogenesis.

The risk for malignancy and the histopathologic distribution of malignant tumors differs between major and minor salivary glands. The incidence of malignancy in the parotid, submandibular, and minor salivary glands is 25%, 50%, and 80%, respectively (Fig. 13.1). Overall, 65% of salivary gland cancers arise in the parotid gland, 8% arise in the submandibular gland, and 27% arise in the minor salivary glands (Fig. 13.2). The mucosa of the hard palate is the most frequent site of origin of minor salivary gland tumors, followed by other sites in the oral cavity and paranasal sinuses (Fig. 13.3). The histologic classification of salivary tumors is shown in Table 13.1.

The most common benign tumor of salivary gland origin is the pleomorphic adenoma (mixed tumor). The parotid gland is the most common site of origin, followed by the submandibular gland and then by minor salivary glands. These tumors most frequently arise in the fifth to sixth decades of life and have a slight predilection for women. In general, pleomorphic adenomas tend to be asymptomatic and grow slowly; rapid growth raises concern for malignant transformation. Warthin's tumor is the next most common benign salivary neoplasm, which occurs most frequently in the tail of the parotid gland. An association with tobacco use has been suggested, because smokers have a fivefold to tenfold increased risk for these tumors. These tumors have a predilection for older white men and can be bilateral in up to 10% of cases.

Oncocytomas typically occur in older persons and are relatively rare. These tumors are characterized by a high mitochondrial content, which accounts for fluorodeoxyglucose avidity on positron emission tomography scans, similar to Warthin's tumors. Lymphoepithelial lesions are relatively rare but can occur in increased frequency in patients with human immunodeficiency virus infection, in whom they are often bilateral. *Monomorphic adenoma* is a term that was used in the past to describe a less heterogeneous group of tumors than pleomorphic adenoma that includes basal cell adenoma, canalicular adenoma, and myoepithelioma. Of these, basal cell adenoma is the most common and typically occurs in the parotid gland of older persons. Although canalicular adenomas also occur in older persons, they typically originate from the minor salivary gland of the upper lip and buccal mucosa.

The distribution of various types of malignant tumors of the salivary glands is shown in Fig. 13.4. Mucoepidermoid carcinomas are found most commonly in the parotid gland, whereas adenoid cystic carcinomas are seen most frequently in submandibular and minor salivary glands. Histologic differentiation is crucial in predicting the biological behavior of salivary neoplasms. Low-grade malignant tumors have an indolent course and have an excellent prognosis. On the other hand, high-grade tumors behave aggressively, with increased risk of regional and distant metastasis, and are associated with poor prognosis.

Mucoepidermoid carcinoma is the most common malignant salivary gland tumor. Based on their histologic features, these tumors are further subdivided into low-grade, intermediate-grade, and high-grade tumors. Although low-grade and intermediate-grade tumors are slow growing, they can be locally aggressive; however, they rarely metastasize. In contrast, high-grade

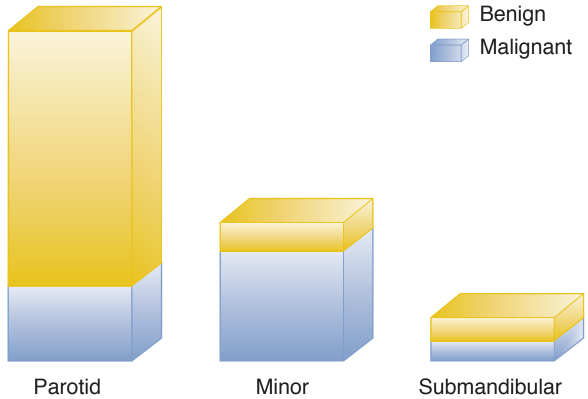

Figure 13.1 The incidence of malignant tumors among salivary glands.

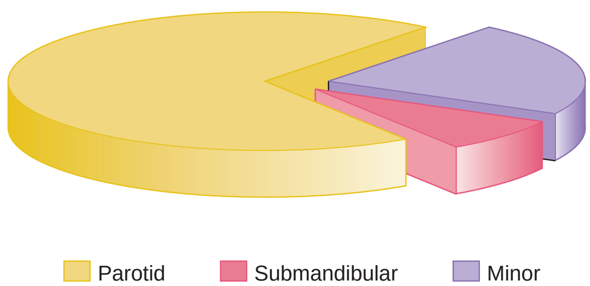

Figure 13.2 The distribution of salivary tumors among major and minor salivary glands.

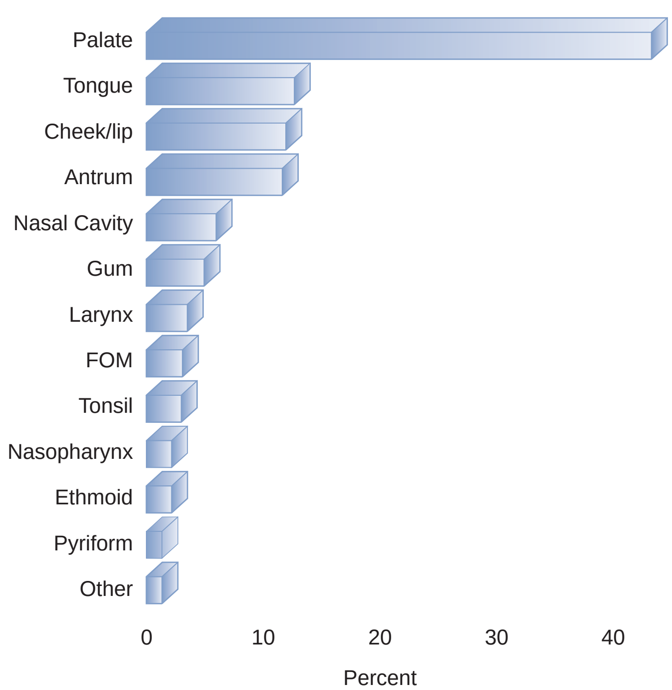

Figure 13.3 The distribution of the anatomic sites of origin for minor salivary gland tumors. *FOM,* Floor of mouth.

mucoepidermoid carcinomas have an aggressive clinical course with local invasion and increased risk of regional nodal metastasis.

Mucoepidermoid carcinomas can arise not only in minor salivary glands but also in salivary nests within the mandible (i.e., a "central salivary carcinoma") and in ectopic salivary tissue in the parapharyngeal space.

Adenoid cystic carcinoma is the most common malignant tumor of the submandibular and minor salivary glands. Although grading systems have been proposed for these tumors, tumor grading does not seem to influence the behavior of adenoid cystic carcinomas. These tumors have a high degree of neurotropism, leading to the propensity for perineural spread. Although the overall outcome of adenoid cystic carcinomas is poor, the disease course typically is protracted, with survival measuring in decades, even in the presence of distant metastases. Although regional

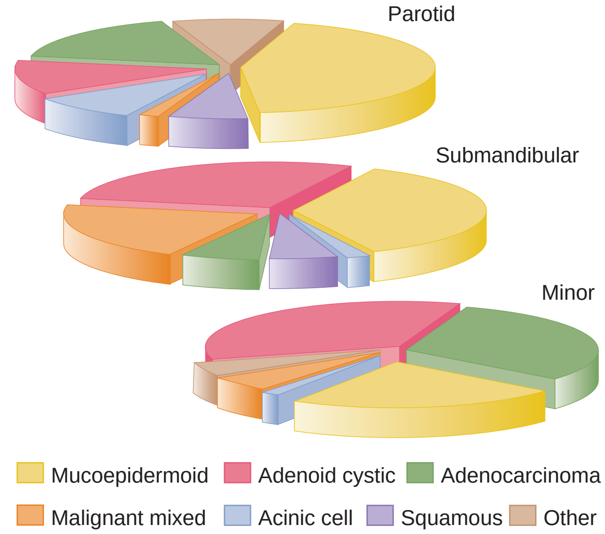

Figure 13.4 The histologic distribution of malignant tumors of the salivary glands.

Table 13.1 The World Health Organization Histologic Classification of Salivary Gland Tumors

Nonneoplastic epithelial lesions	Sclerosing polycystic adenosis Nodular oncocytic hyperplasia Lymphoepithelial sialadenitis Intercalated duct hyperplasia
Benign tumors	Pleomorphic adenoma Myoepithelioma Basal cell adenoma Warthin's tumor Oncocytoma Lymphadenoma Cystadenoma Sialadenoma papilliferum Ductal papillomas Sebaceous adenoma Canalicular adenoma and other ductal adenomas
Uncertain malignant potential	Sialoblastoma
Malignant tumors	Acinic cell carcinoma Secretory carcinoma Mucoepidermoid carcinoma Adenoid cystic carcinoma Polymorphous adenocarcinoma Epithelial myoepithelial carcinoma Clear cell carcinoma Basal cell adenocarcinoma Sebaceous adenocarcinoma Intraductal carcinoma Cystadenocarcinoma Adenocarcinoma not otherwise specified (NOS) Salivary duct carcinoma Myoepithelial carcinoma Carcinoma ex pleomorphic adenoma Carcinosarcoma Poorly differentiated carcinoma (undifferentiated carcinoma, large cell neuroendocrine carcinoma, and small cell carcinoma) Lymphoepithelial carcinoma Squamous cell carcinoma Oncocytic carcinoma

lymph node metastases are uncommon, pulmonary metastases occur frequently.

Polymorphous adenocarcinomas occur mainly in minor salivary glands and typically have an indolent course. These tumors most commonly arise in the oral cavity, with the hard palate being the principal site of origin. The "adenocarcinoma not otherwise specified (NOS)" category includes a heterogenous group of neoplasms that lacks any of the histologic features that characterize the other defined types of salivary tumors. Among other malignant tumors are acinic cell carcinomas, mammary analog secretory carcinoma, salivary duct carcinoma, myoepithelial carcinoma, and carcinoma ex pleomorphic adenoma. About 10% of malignant neoplasms of salivary origin are acinic cell carcinomas, and they most commonly arise from the parotid gland. These tumors tend to be indolent but have the capacity of high-grade tumors.

Primary squamous cell carcinoma of the parotid gland is extremely rare and needs to be differentiated from squamous cell carcinoma that has metastasized to an intraparotid lymph node from a synchronous or previously treated skin cancer.

EVALUATION

Tumors of salivary gland origin usually present as an asymptomatic mass. The majority of parotid tumors arise in the superficial lobe and present as a rubbery nodular mass, generally located anterior to the lobule of the ear in the region of the tail of the parotid gland (Figs. 13.5 through 13.7). Most mixed tumors are asymptomatic. Facial paralysis does not occur with mixed tumors regardless of the size of the tumor. Enlarged ipsilateral cervical lymph nodes or the presence of facial nerve dysfunction or invasion of the overlying skin almost invariably are suggestive of a malignant tumor (Figs. 13.8 through 13.11). Tumors in the deep lobe of the parotid gland usually present with diffuse enlargement and fullness in the retromandibular region.

Figure 13.5 A large benign mixed tumor of the right parotid gland. Note stretched skin over the tumor.

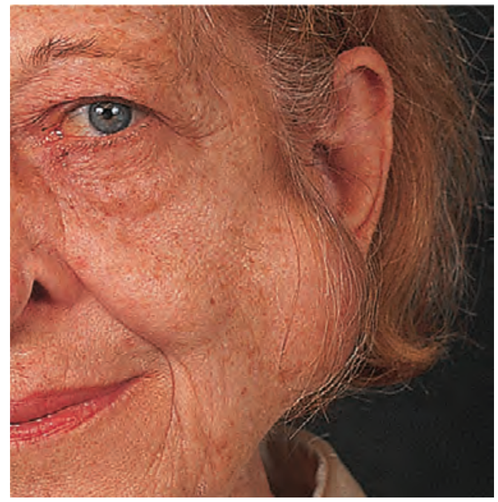

Figure 13.6 The anterior view of a patient with a benign mixed tumor of the left parotid gland.

Figure 13.7 A large parotid tumor of the left parotid gland.

Figure 13.8 Involvement of a periparotid or cervical lymph node by metastasis is almost diagnostic of a malignant parotid tumor.

Figure 13.9 Invasion of the overlying skin is highly suggestive of a malignant tumor.

Figure 13.10 The lateral view of a patient with a carcinoma of the parotid gland.

Figure 13.11 Facial nerve paralysis is diagnostic of a malignant tumor of the parotid gland.

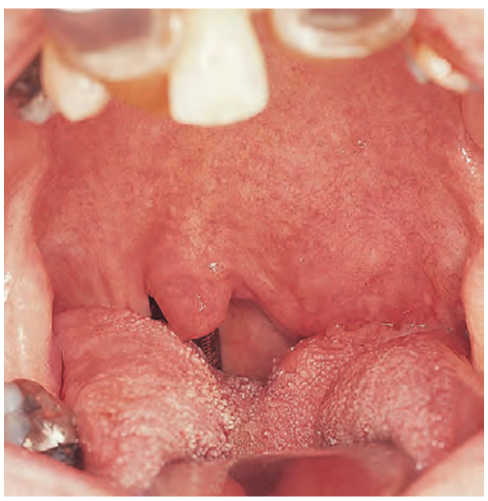

Figure 13.12 A deep lobe parotid tumor presenting as a parapharyngeal mass.

Figure 13.13 An accessory parotid tumor.

Radiographic studies are essential to accurately delineate the location and extent of the deep lobe tumor. Tumors of the deep lobe of the parotid gland, extending into the parapharyngeal space, may cause medial displacement of the soft palate, tonsil, and/or lateral pharyngeal wall (Fig. 13.12). They may or may not be associated with a palpable parotid mass. Occasionally tumors may arise in accessory parotid tissue along the course of the Stensen duct and present as a mass in the soft tissues of the midportion of the cheek (Fig. 13.13). Metastatic tumors to the parotid gland from primary cutaneous malignant lesions of the scalp and forehead such as squamous cell carcinomas and melanomas also are important differential diagnostic entities. Diffuse enlargement of the entire parotid gland may be seen in patients with lymphoma, Sjogren's syndrome, and those with extensive eosinophilic infiltrate, as seen in patients with Kim-Kimura's disease (Fig. 13.14).

A painless swelling in the submandibular triangle is the usual presenting symptom for a tumor of the submandibular gland (Fig. 13.15). The presence of pain signifies an obstructive and/or inflammatory phenomenon and may prove to be sialadenitis of the submandibular salivary gland. Bimanual palpation of the mass through the floor of the mouth confirms the location of the tumor in the submandibular gland

Figure 13.14 Diffuse enlargement of the entire parotid gland with a firm to hard mass (Kim-Kimura disease).

Figure 13.15 A mixed tumor of the submandibular salivary gland.

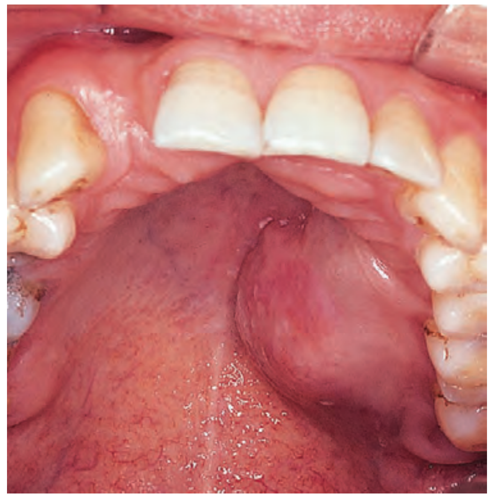

Figure 13.16 An adenoid cystic carcinoma of the hard palate.

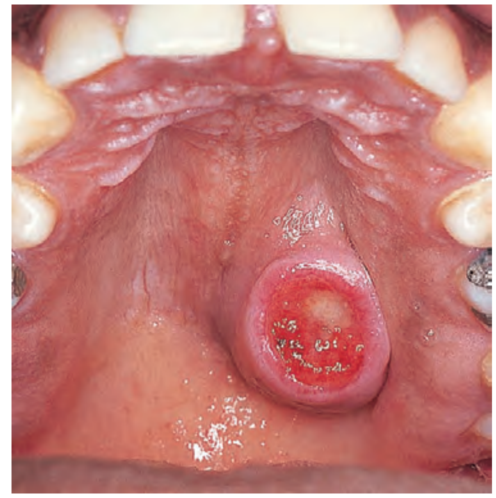

Figure 13.17 A malignant mixed tumor of the hard palate.

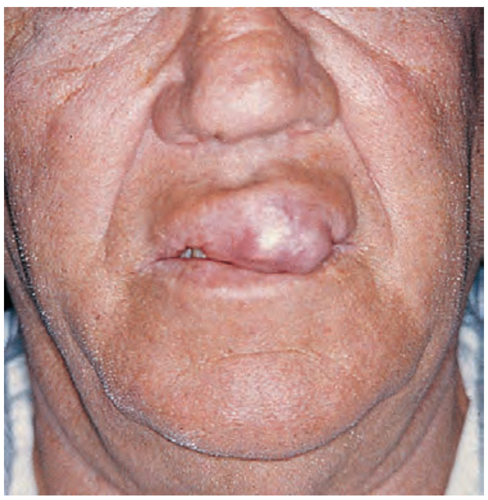

Figure 13.18 An adenocarcinoma of the upper lip.

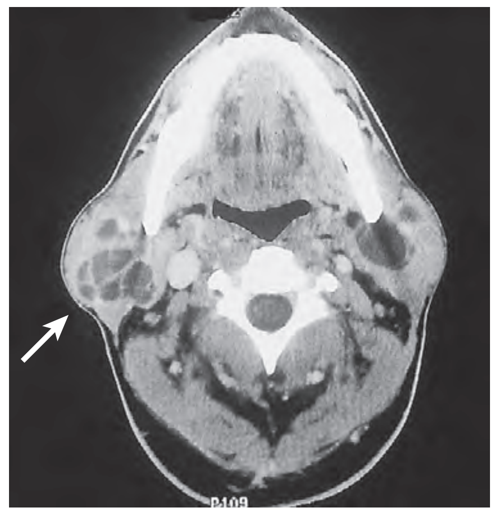

Figure 13.19 A computed tomography scan showing bilateral Warthin's tumors, which are multiloculated on the right-hand side (*arrow*) and uniloculated on the left-hand side.

and differentiates this entity from adjacent enlarged cervical lymph nodes.

Tumors of minor salivary gland origin usually present as a submucosal mass that may be ulcerated (Figs. 13.16 and 13.17). The majority of tumors of minor salivary gland origin are malignant. Minor salivary tumors of the lip often mimic a mucocele or a mucous cyst (Fig. 13.18). The presence of a soft-to-firm rubbery submucosal mass should raise the index of suspicion regarding the possibility of a minor salivary gland tumor.

Radiographic Evaluation

Diagnostic imaging studies are necessary if clinical examination does not provide accurate delineation of the location and extent of the tumor. Thus imaging is essential in the evaluation of a deep-seated or a fixed lesion for which invasion into adjacent anatomic structures is a concern. Plain radiographs, sialography, nuclear scans, and ultrasonography add very little to the desired diagnostic information and are seldom indicated. On the other hand, computerized tomography (CT) and magnetic resonance imaging (MRI) permit better visualization of masses of the salivary glands.

CT and MRI are equally satisfactory in differentiating cystic from solid lesions and allow evaluation of the relationship of the mass to the major salivary gland or adjacent structures, including soft tissues and bones (Figs. 13.19 through 13.21). For minor salivary lesions, CT provides valuable information that assists in treatment planning; in particular, it shows the relationship of the tumor to surrounding structures and demonstrates

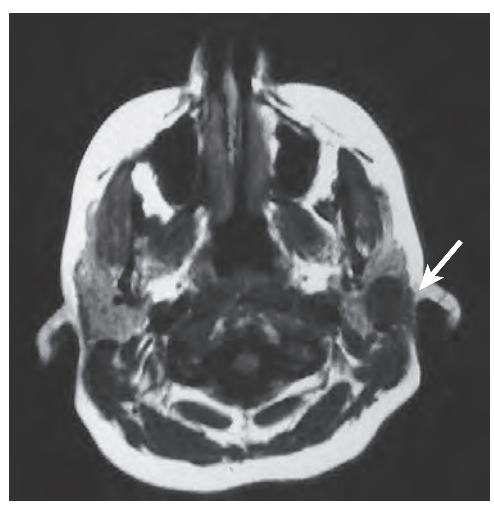

Figure 13.20 A T1-weighted magnetic resonance imaging scan showing a benign mixed tumor in the superficial lobe of the left parotid gland (*arrow*).

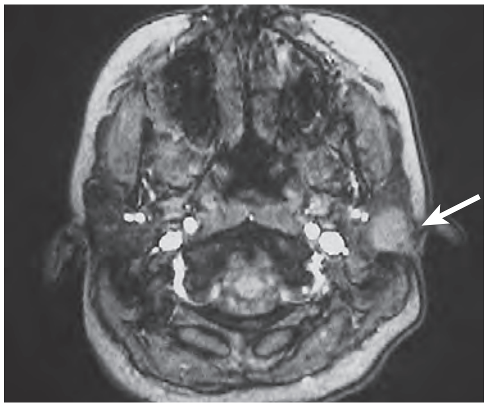

Figure 13.21 A T2-weighted magnetic resonance imaging scan showing a benign mixed tumor in the superficial lobe of the left parotid gland (*arrow*).

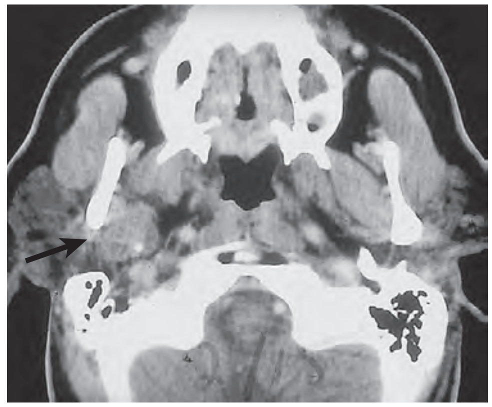

Figure 13.22 An axial view of a computed tomography scan showing a deep lobe parotid tumor (*arrow*).

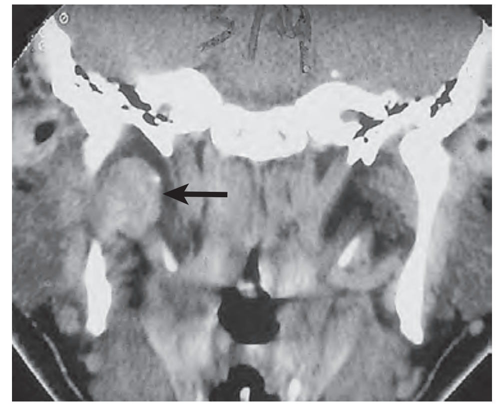

Figure 13.23 A coronal view of the computed tomography scan of the same patient as in Fig. 13.20 showing the deep lobe parotid tumor (*arrow*).

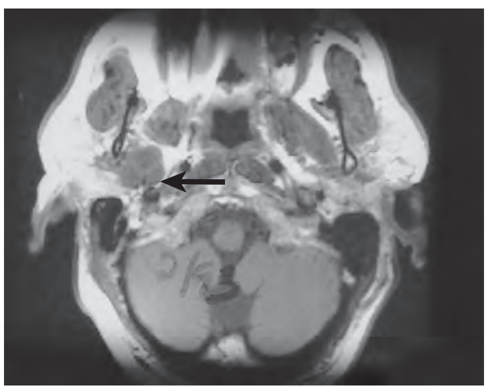

Figure 13.24 An axial view of a magnetic resonance imaging scan of the same patient as in Fig. 13.20 showing the deep lobe parotid tumor (*arrow*).

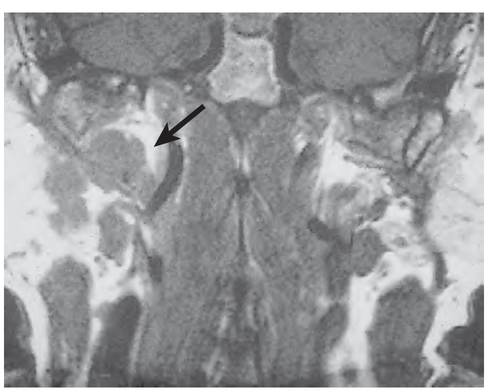

Figure 13.25 A coronal view of the magnetic resonance imaging scan of the same patient as in Fig. 13.20 showing the deep lobe parotid tumor (*arrow*).

tumor extension, permitting assessment of the resectability of advanced lesions. CT scans are invaluable in the evaluation of deep lobe parotid tumors and assist in differentiating them from tumors arising in the parapharyngeal space (Figs. 13.22 through 13.25). MRI is equally valuable in the assessment of deep lobe parotid tumors and in differentiating them from tumors of ectopic or minor salivary gland origin (Fig. 13.26). CT scans are particularly of value in the assessment of bone erosion, whereas MRI is of particular value in demonstrating tumor extension along cranial nerves.

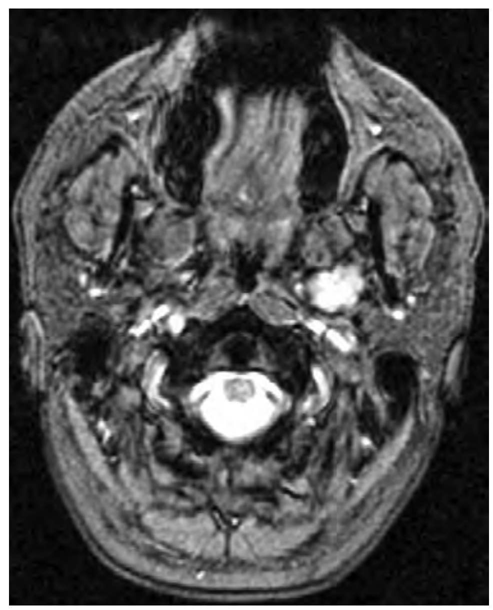

Figure 13.26 An axial view of a contrast-enhanced T2-weighted magnetic resonance imaging scan showing a left parapharyngeal space tumor of ectopic salivary tissue. Note fat separating the tumor from adjacent deep lobe parotid tissue.

PATHOLOGY

Histologically, major and minor salivary glands consist of the secretory acinus and related ducts and myoepithelial cells. Acini may be serous, mucous, or mixed serous and mucinous. The cytoplasm of serous cells contains zymogen granules, and their principle secretion is amylase. The cytoplasm of mucinous cells is clear and contains mucin. Secretions from the acini empty into smaller duct systems that lead to branching larger duct systems and eventually into the main excretory duct (Fig. 13.27). Myoepithelial cells surround the acinar and ductal cells.

In most patients presenting with the clinical features of a discrete parotid tumor, tissue diagnosis is seldom required before surgical exploration. However, if clinical suspicion of a malignant tumor is high, then cytologic diagnosis of a malignant tumor can be established by a fine-needle aspiration biopsy. Aspiration with a 21-gauge needle is usually satisfactory in securing tissue for diagnosis or as a screening tool to triage the

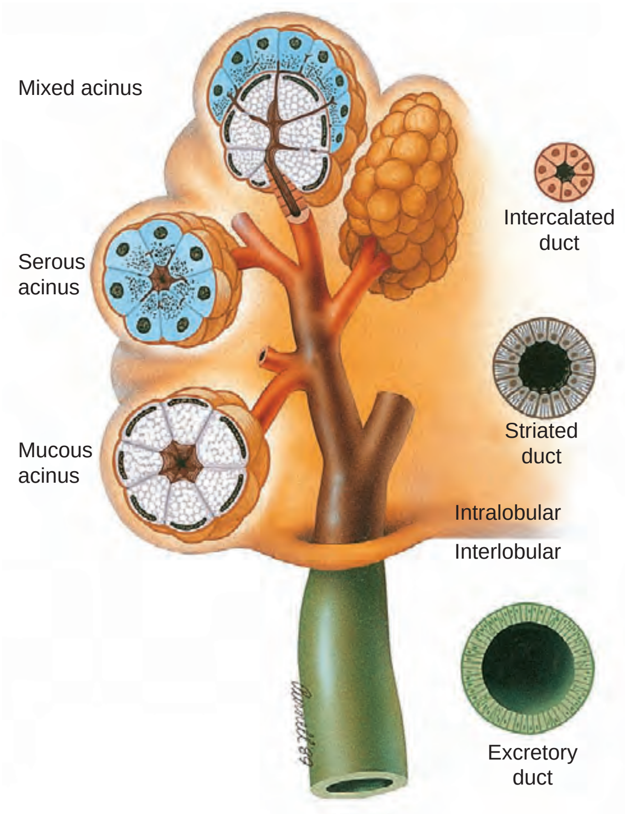

Figure 13.27 The histologic structure of the normal salivary gland.

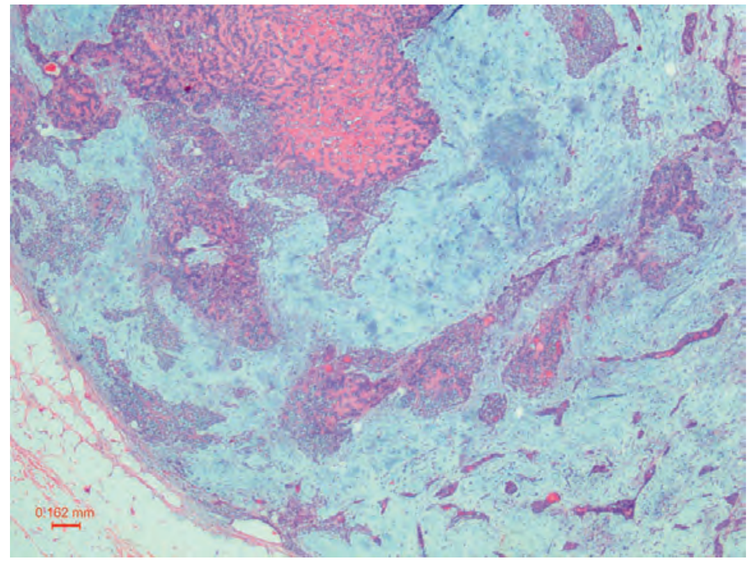

Figure 13.28 Pleomorphic adenoma demonstrating abundant myxochondroid matrix and myoepithelial cells (25× H&E stain).

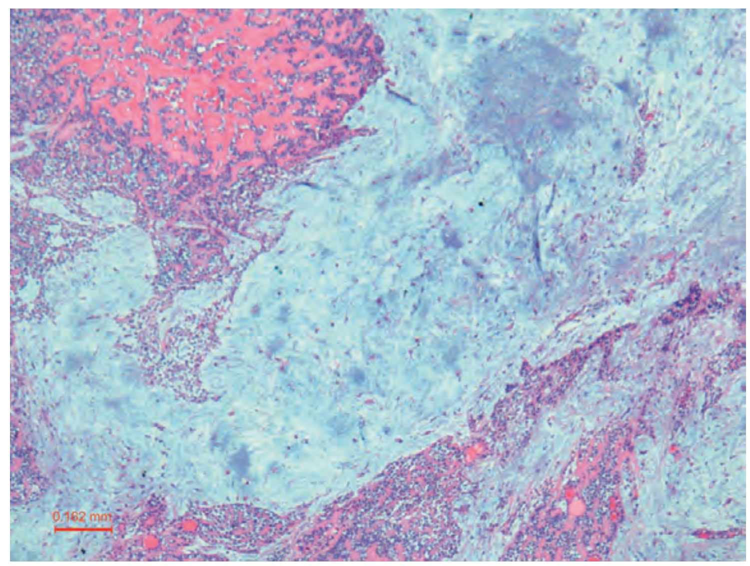

Figure 13.29 Pleomorphic adenoma demonstrating abundant myxochondroid matrix and myoepithelial cells (50× H&E stain).

patients to different treatment. The rate of correctly establishing the diagnosis as benign or malignant range from 81% to 98%; however, a specific diagnosis can be made in only 60% to 75%. Inadequate sampling appears to be the most frequent cause of false negatives.

Pleomorphic Adenoma (Mixed Tumor)

Pleomorphic adenoma is a benign neoplasm characterized by an admixture of epithelial, myoepithelial, and stromal elements with architectural pleomorphism. This neoplasm represents two-thirds of all tumors of the major salivary glands and less than half of those in the minor salivary glands, with the greatest frequency of occurrence in the superficial lobe of the parotid gland.

Grossly, pleomorphic adenoma is generally white and firm, with a smooth outer and cut surface. The tumor may be vaguely lobulated and nodular, with "podocytes," which are more commonly noted microscopically. Microscopically, pleomorphic adenomas demonstrate an admixture of epithelial and mesenchymal elements, with ductal and myoepithelial cell types intermingled with myxoid, mucoid, or chondroid stroma (Figs. 13.28 and 13.29). Most pleomorphic adenomas are encapsulated, especially in the major salivary gland, with a variable amount of capsule thickness. Irregular peripheral borders and local extension of fingerlike processes into the capsule might be seen. Pleomorphic adenomas are characterized by a remarkable degree of morphologic diversity between individual tumors or within a single tumor. Therefore a definite diagnosis might not be possible on a representative frozen section or on a small amount of fine-needle aspiration material. Recurrence of pleomorphic adenomas generally represents local regrowth and not necessarily malignancy, and further surgery becomes technically demanding with reference to the safety of the facial nerve. Many recurrent pleomorphic adenomas are multifocal, and some can be so widely distributed that surgical control becomes impossible.

Carcinoma ex pleomorphic adenoma is a malignant neoplasm that arises in association with pleomorphic adenoma. Typically, these tumors are high grade and show similar histology to their de novo counterparts. The malignant tumor component is most frequently salivary duct carcinoma, followed by myoepithelial carcinoma. However, any histologic subtype of salivary gland carcinoma can arise in association with pleomorphic adenoma. Carcinoma ex pleomorphic adenoma is classified based on the degree of tumor invasion through the preexistent pleomorphic adenoma capsule into the surrounding tissue as intracapsular, minimally invasive, and invasive. The extent of invasion has been found to correlate with the clinical outcome. A very low rate of local recurrence and regional metastases are noted in patients with intracapsular minimally invasive tumors, while the risk of local recurrence, metastases, and fatal outcome is higher in patients with invasive tumors. At the molecular level, rearrangements of *PLAG1* (pleomorphic adenoma gene 1) on 8q12 and *HMGA2* on 12q14-15 are the most frequent genetic alterations in both pleomorphic adenoma and carcinoma ex pleomorphic adenoma.

Warthin's Tumor (Papillary Cystadenoma Lymphomatosum)

Warthin's tumors are benign salivary gland neoplasia that usually arise in the parotid gland and are composed of eosinophilic glandular epithelium, lined by basaloid cells, with papillary cystic spaces, embedded in dense lymphoid tissue (Fig. 13.30).

Oncocytoma

Oncocytoma, also known as oxyphil adenoma or oncocytic adenoma, is a benign salivary gland neoplasm composed of oncocytes that are benign epithelial cells packed with mitochondria, imparting a granular appearance to the cytoplasm (Fig. 13.31).

Mucoepidermoid Carcinoma

Mucoepidermoid carcinoma is the most common malignant salivary gland tumor in both adults and children. More than half of these tumors occur in the parotid gland; when they arise in the minor salivary glands, they are most frequently in the palate.

Histologically, this tumor is composed of varying proportions of epidermoid (squamoid), mucous, and intermediate cells, arranged in cystic or glandular structures or in a solid growth pattern. Mucicarmine stain highlights intracytoplasmic mucin. CK5/6 and p63 immunohistochemical stains will stain the epidermoid and intermediate cells. S100 and myoepithelial markers (Calponin and smooth muscle actin) are usually negative in mucoepidermoid carcinoma. Variable histologic parameters such as perineural invasion and vascular invasion have been reported to correlate with the patients' clinical outcome. However, prognosis seems to be largely dependent on tumor grade. Several grading systems exist for mucoepidermoid carcinomas, but they are graded by most pathologists, using three tiers (based on tumor cytologic and proliferative features and architecture): low, intermediate, and high grade (Fig. 13.32 and Fig. 13.33). At the molecular level, a chromosomal translocation (11,19), resulting in *MECT1/MAML2* fusion genes, has been

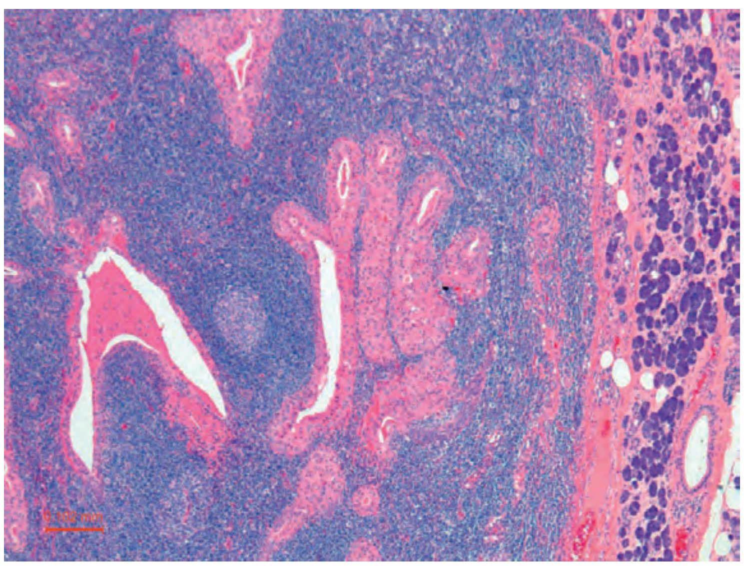

Figure 13.30 Warthin's tumor with adjacent normal parotid gland parenchyma on the right (50× H&E stain).

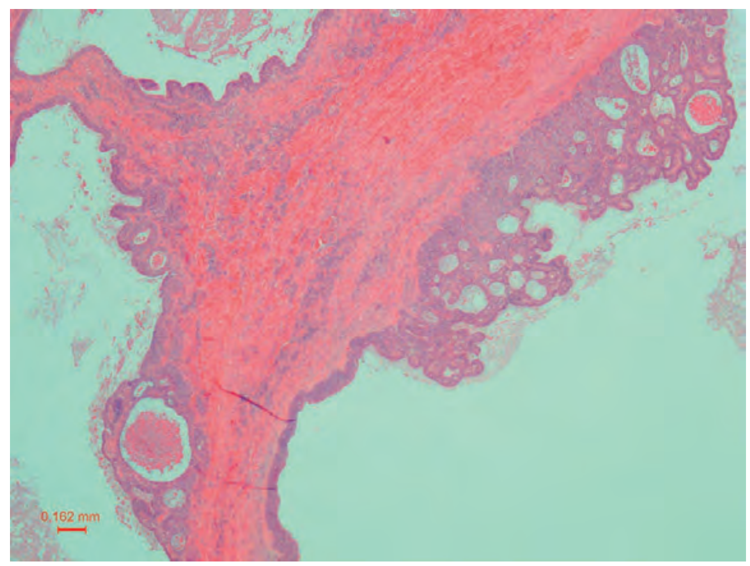

Figure 13.32 Low-grade mucoepidermoid carcinoma with more than 20% of the tumor represented by cystic spaces lined by squamoid epithelial cells (25× H&E stain).

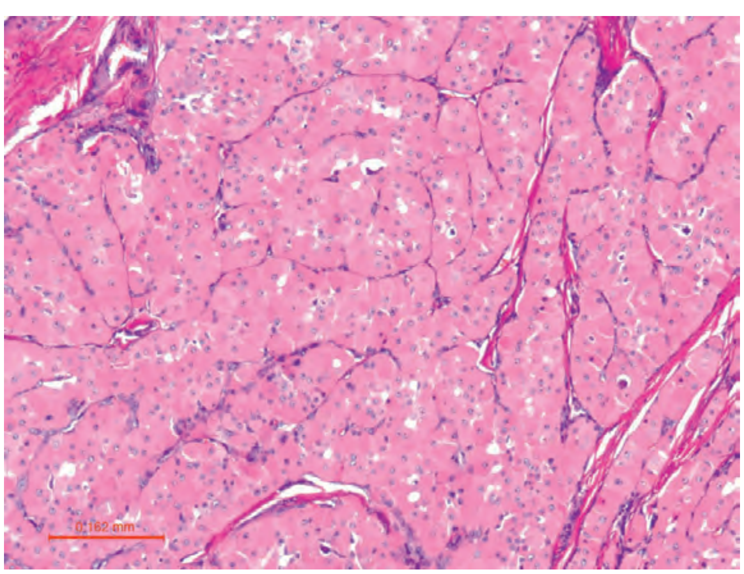

Figure 13.31 Abundant eosinophilic cells of oncocytoma separated by thin fibrovascular septae (100× H&E stain).

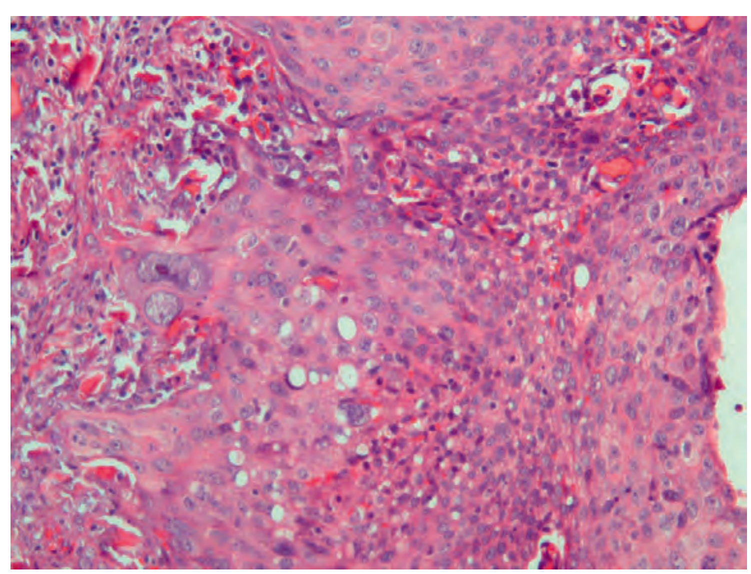

Figure 13.33 High-grade mucoepidermoid carcinoma demonstrating marked nuclear pleomorphism and areas of single-cell necrosis (200× H&E stain).

identified in 40% to 80% of mucoepidermoid carcinomas. The translocation has been suggested to be associated with more indolent clinical behavior.

Adenoid Cystic Carcinoma

Adenoid cystic carcinoma is a slowly growing, insidious salivary gland malignancy, occurring in both minor and major glands, notorious for its tendency for perineural invasion, as well as local invasion and recurrence after surgical resection. These tumors may arise in the major salivary glands and also in the oral cavity, nasopharynx, nasal cavity, paranasal sinuses, lacrimal glands, and lower respiratory tract. Adenoid cystic carcinoma grows as solid, white to gray, scirrhous, infiltrative masses that tend to be hard and fixed and may tether overlying skin.

Histologically, adenoid cystic carcinoma is composed of ductal and myoepithelial cells and shows hyalinized or myxoid matrix (Fig. 13.34). The tumor demonstrates three main growth patterns: cribriform, tubular, and solid (Fig. 13.35). Perineural invasion is commonly seen in adenoid cystic carcinoma (Fig. 13.36).

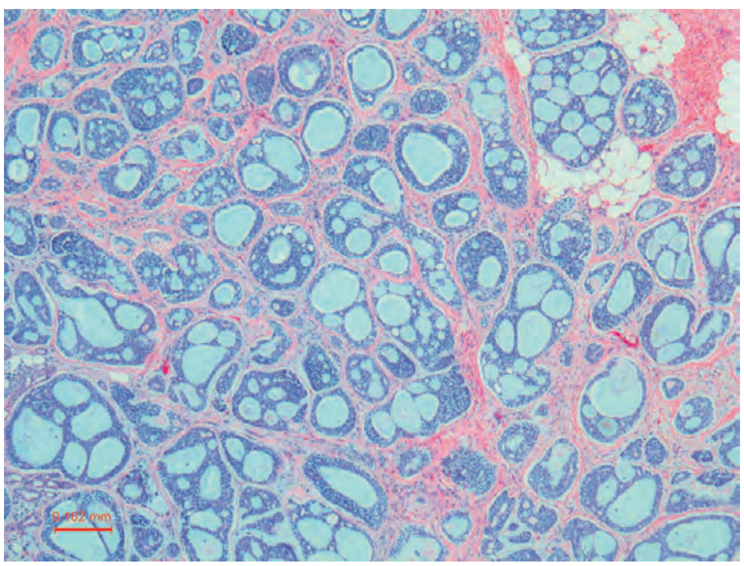

Figure 13.34 Adenoid cystic carcinoma of the parotid gland demonstrating a predominantly cribriform architectural pattern (50× H&E stain).

Unlike mucoepidermoid carcinoma, grading of adenoid cystic carcinoma does not seem to be significant in the prediction of the behavior of this malignancy. The presence of solid tumor growth seems to correlate with more aggressive behavior and poor survival. It is infrequent to see lymph node metastases; rather, one is more likely to see distant spread to the lungs and solid organs such as the kidney, with as much as a 15-year latency period.

The MYB protooncogene occurs in the majority of adenoid cystic carcinomas, with a translocation (6,9) resulting in fusion of the *MYB* and *NFIB* genes being the most common mechanism. The 6,9 translocation has been described in about 65% of adenoid cystic carcinomas of the head and neck and various anatomic sites, including the breast and lung.

Polymorphous Low-Grade Adenocarcinoma

Polymorphous low-grade adenocarcinoma (PLGA), now shortened to polymorphous adenocarcinoma (PAC), occurs mainly in minor salivary glands, with the hard palate being the most common location. It is important to differentiate PAC from adenoid cystic carcinoma since it typically has an indolent course. These tumors show one cell type with cytologic uniformity and various growth patterns. Perineural invasion may be seen. A cribriform variant, which is considered a separate entity by some authors, has been reported to have a greater capacity for regional metastasis. Activation of *PRKD1* point mutation has been recently reported in about 73% of PLGA.

Epithelial-Myoepithelial Carcinoma

Epithelial-myoepithelial carcinoma is another typically indolent salivary gland tumor that is characterized by a multinodular pattern and biphasic or bilayered arrangement of inner ductal cells and outer myoepithelial cells, with classically clear cytoplasm.

Acinic Cell Carcinoma

Acinic cell carcinomas account for approximately 10% of all malignant salivary gland carcinomas and arise almost exclusively

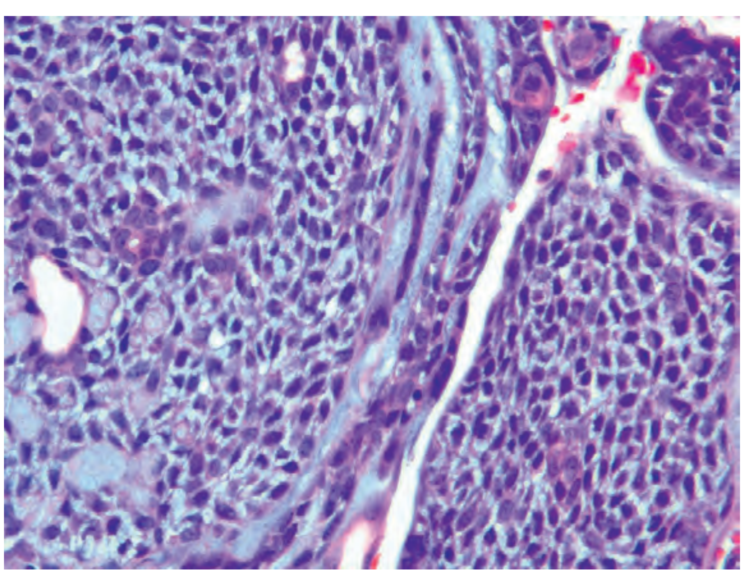

Figure 13.35 Area of solid growth in adenoid cystic carcinoma, with rare ductal cells and a predominance of myoepithelial cells (400× H&E stain).

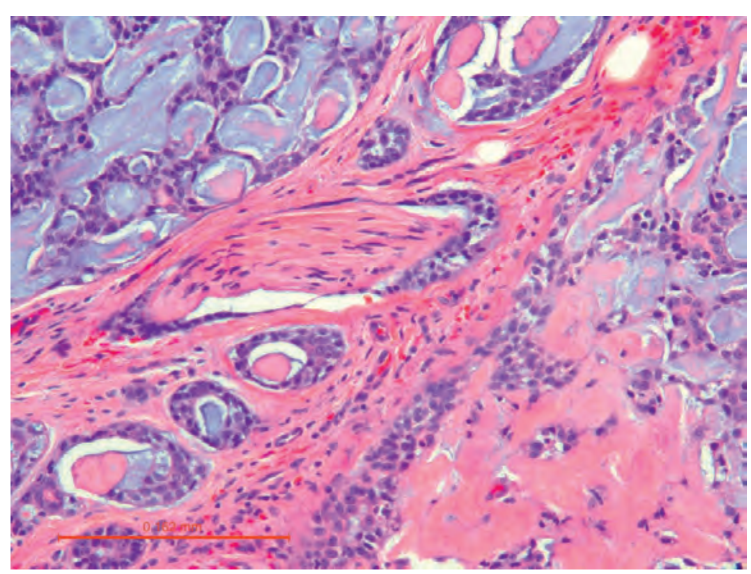

Figure 13.36 Perineural invasion is present centrally within this adenoid cystic carcinoma (400× H&E stain).

in the parotid. These tumors are characterized by serous acinar cell differentiation with zymogen-type cytoplasmic granules. They tend to be indolent and low grade but have the capacity to present as high-grade tumors.

Secretory Carcinoma

Mammary analog secretory carcinoma (MASC) is a recently described salivary gland tumor that was likely classified as acinic cell carcinoma in the past. The tumor has striking histologic and molecular similarities to secretory carcinoma of the breast. The official terminology of this entity is now "secretory carcinoma." At the histologic level, tumor cells have eosinophilic or clear bubbly cytoplasm, and they may grow as tubules or microcysts, papillae, or macrocysts. Secretions are almost always present in the microcysts and/or macrocysts. MASC characteristically harbors a balanced chromosomal translocation (12, 15), resulting in the formation of the *ETV6–NTRK3* fusion genes.

Salivary Duct Carcinoma

Salivary duct carcinoma is an aggressive, high-grade carcinoma that resembles high-grade breast ductal carcinoma. Typically the tumor is composed of ductal cells arranging in tubules, as solid and cribriform growth with central necrosis (Fig. 13.37). Androgen receptor (AR) expression by immunohistochemistry is identified in the vast majority of salivary duct carcinoma. In addition to AR, immunohistochemical overexpression of human epidermal growth factor receptor 2 *(HER2)* has been reported in a good percentage of salivary duct carcinoma with or without amplification of the gene by fluorescence in situ hybridization. Targeted therapeutic modalities, including anti-ERBB2 antibodies and androgen deprivation therapy, are characterized by variable results. Additionally, various genetic alterations have been reported in salivary duct carcinoma, including *TP53, PTEN, EGFR,* and phosphoinositide 3-kinase *(PIK3CA)* pathway.

Myoepithelial Carcinoma

Myoepithelial carcinoma is a rare salivary gland tumor that is composed almost exclusively of myoepithelial cells. The tumor seems to be locally aggressive with diverse clinical outcome.

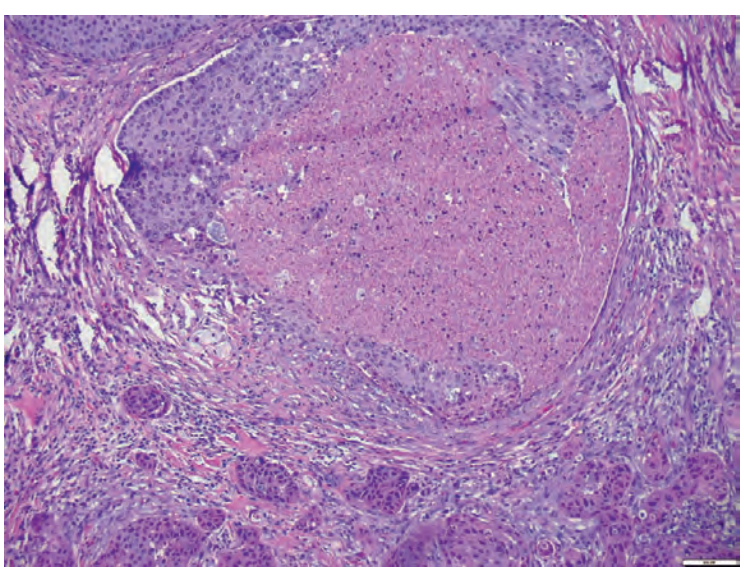

Figure 13.37 Salivary duct carcinoma.

Both myoepithelial carcinoma and salivary duct carcinoma may arise de novo or in association with pleomorphic adenoma (carcinoma ex pleomorphic adenoma).

TREATMENT

The primary goal for treatment of patients with benign or malignant tumors of the salivary glands is gross total removal of the tumor for accurate diagnosis and local control. Because the majority of salivary tumors are benign and occur with the highest frequency in the parotid gland, the goal of therapy is to achieve complete excision of the tumor to reduce the risk of local recurrence. The same principles of treatment apply for benign tumors arising from the submandibular, sublingual, and minor salivary glands.

Preservation of function, particularly of the facial nerve and its branches, is an important goal in surgery for parotid and submandibular gland tumors. Similarly, the goal for treatment of malignant tumors of salivary origin is control of cancer with preservation of function when feasible. Regardless of the histology, if a parotid tumor is confined to the superficial lobe of the parotid gland and the facial nerve is not directly infiltrated by the tumor, a superficial parotidectomy with dissection and preservation of the facial nerve is indicated. Sacrifice of a functioning, uninvolved facial nerve is rarely necessary for resection of malignant tumors of the parotid gland. Deliberate sacrifice of the facial nerve can be justified if an invasive tumor directly extends into the facial nerve or when resection of the facial nerve would facilitate monobloc excision of a malignant tumor. Whenever the facial nerve is resected, rehabilitation of the paralyzed face becomes an important priority. Rehabilitation may be accomplished by primary nerve grafting to reconstruct the excised facial nerve or by secondary means of restoration of function or appearance. For cancers of the submandibular salivary gland, wider resection of adjacent soft tissues in the submandibular triangle, including a limited neck dissection, may be necessary to improve local control. Surgery remains the mainstay of initial therapy for malignant tumors of the salivary glands.

Although generous surgical resection with adequate soft-tissue margins remains the fundamental principle in surgical oncology, it may not be feasible in malignant tumors of the parotid gland, where a functioning facial nerve is contiguous to the tumor. Thus close margins and/or microscopically positive margins in the vicinity of the facial nerve are acceptable, because adjuvant radiation therapy offers respectable local control rates. Radiotherapy as definitive treatment is rarely indicated for salivary tumors other than in a palliative setting. On the other hand, it is of great value as adjuvant treatment after surgery for improvement of local and regional control for advanced malignant tumors of the major and minor salivary glands.

Advanced unresectable tumors generally are treated by radiotherapy with a palliative intent. Although treatment with neutrons is considered preferential, no high-level evidence exists to support its superiority over photons. In addition, its long-term sequelae with extensive fibrosis is a major and significant drawback. Currently, interest is increasing in the use of protons to limit irradiation to adjacent vital structures and to deliver an effective target dose. Data on long-term outcomes and sequelae of proton therapy for salivary tumors are not available at this time. In addition, no chemotherapeutic agents with predictable efficacy are available for routine use in the treatment of salivary gland tumors at present. Thus systemic chemotherapy

currently is used only in a palliative setting. The role of targeted agents against EGFR, estrogen receptor, and human epidermal growth factor receptor 2/neu–positive salivary gland tumors remains investigational.

Factors Affecting Choice of Treatment

The factors that affect the choice of initial therapy are related to the tumor and the patient. The size of the primary tumor and its histologic grade are vitally important tumor factors that influence choice of initial therapy. Low-grade, low-stage malignant tumors confined to the superficial lobe of the parotid gland are easily treatable with a superficial parotidectomy. Surgery alone in this clinical setting is adequate treatment. On the other hand, high-grade, high-staged tumors may require a total parotidectomy or even an extended radical parotidectomy with or without sacrifice of the facial nerve and with or without neck dissection.

Advanced tumors occasionally may require excision of the auditory canal, the ascending ramus of the mandible, or even temporal bone resection. Sacrifice of the facial nerve leads to significant functional and aesthetic morbidity in all age groups. Therefore facial nerve grafting should be considered when appropriate. If a facial nerve graft is not feasible, then rehabilitative measures for facial nerve paralysis should be instituted. These measures include a lateral tarsorrhaphy, a lateral canthoplasty, and a gold weight implant in the upper eyelid as well as static or dynamic reconstruction of the oral commissure.

Similar principles can be applied to malignant tumors of the submandibular salivary gland and those of minor salivary origin. Loss of the hypoglossal and lingual nerves and the marginal branch of the facial nerve is not as debilitating as the loss of the entire facial nerve. Therefore special rehabilitative measures are seldom indicated for radical operations for submandibular salivary gland tumors.

SURGICAL TREATMENT

Surgical Anatomy

The three paired major salivary glands are associated with cranial nerves V, VII, and XII and the peripheral branches of the cervical plexus (Fig. 13.38). Because of the proximity of these nerves, appreciation of surgical anatomy is crucial in salivary gland surgery.

The parotid glands lie in the retromandibular fossae posterior to the ascending ramus of the mandible and in the area anteroinferior to the external auditory canal. The parotid gland is a unilobular structure traversed by the extracranial portion of the facial nerve and its branches. The facial nerve divides the gland into superficial and deep portions. Nearly 80% of the parotid gland is lateral to the facial nerve and is called the "superficial lobe." The remaining portion of the gland lying medial to the facial nerve consists of approximately 20% of parotid tissue and is considered the "deep lobe." The parotid gland drains its secretions through the Stensen duct, which lies on the lateral surface of the anterior aspect of the masseter muscle, traverses through the buccinator muscle, and opens into the oral cavity on the cheek mucosa at the occlusal dental line adjacent to the second upper premolar tooth.

Three important nerves are related to the parotid gland: the facial nerve, the greater auricular nerve, and the auriculotemporal nerve. The greater auricular nerve lies on the tail of the parotid gland and divides into anterior and posterior branches. It provides sensations to the skin of the face near the tragus and the earlobe. The auriculotemporal nerve is a branch of the mandibular division of the fifth cranial nerve. It contains the parasympathetic fibers to the parotid gland by the otic ganglia. The facial nerve exits from the stylomastoid foramen lateral to the styloid process and is located cephalad to the posterior belly of the digastric muscle and anteroinferior to the external auditory canal, where it enters the substance of the parotid gland. The anatomic landmarks for the main trunk of the facial nerve, which measures anywhere from 5 to 15 mm, are at a point where the tip of the mastoid process, cartilaginous auditory canal, and superior border of the posterior belly of the digastric muscle meet (Fig. 13.39). The main trunk usually branches into the zygomaticotemporal and cervicofacial divisions. Significant anatomic variations in the intraglandular branching of the facial nerve exist, some examples of which are shown in Figs. 13.40 through 13.55.

The anatomic relationship of the deep portion of the parotid gland to other structures in the parapharyngeal space is shown in Fig. 13.56. Although tumors arising in the deep lobe of the parotid gland are rare, they are the most common neoplasms

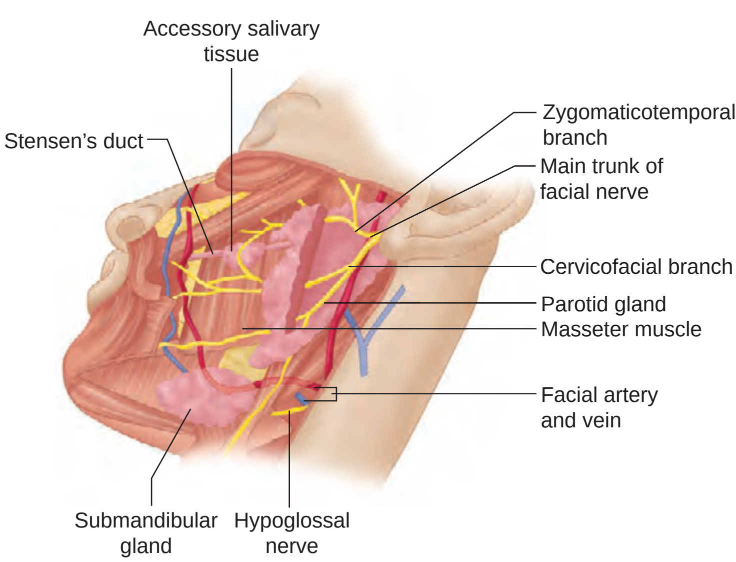

Figure 13.38 The anatomic relationships of the parotid and submandibular salivary glands to adjacent cranial nerves.

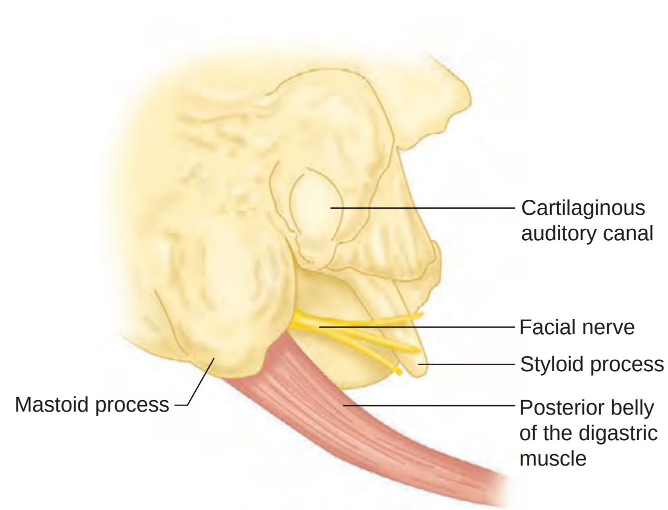

Figure 13.39 Anatomic landmarks for intraoperative identification of the facial nerve.

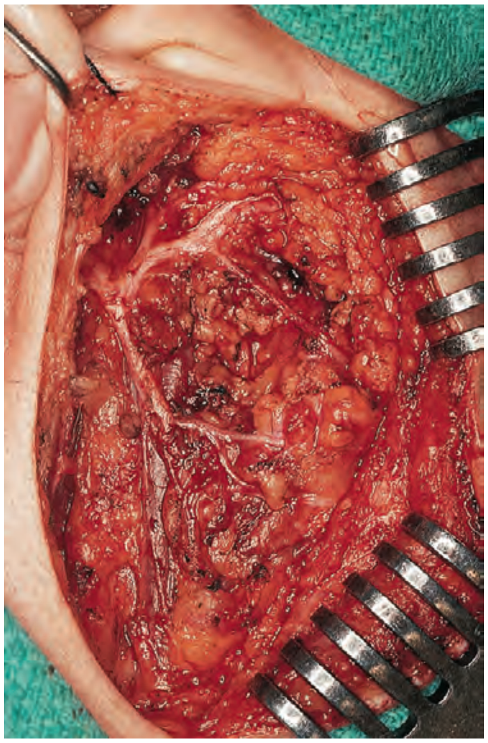
Figure 13.40 Anatomic variation in the intraglandular branching of the extracranial facial nerve.


Figure 13.41 Anatomic variation in the intraglandular branching of the extracranial facial nerve.

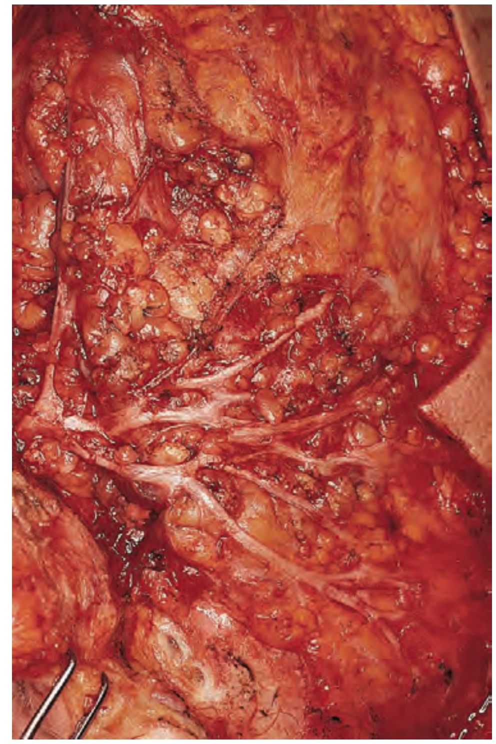
Figure 13.42 Anatomic variation in the intraglandular branching of the extracranial facial nerve.

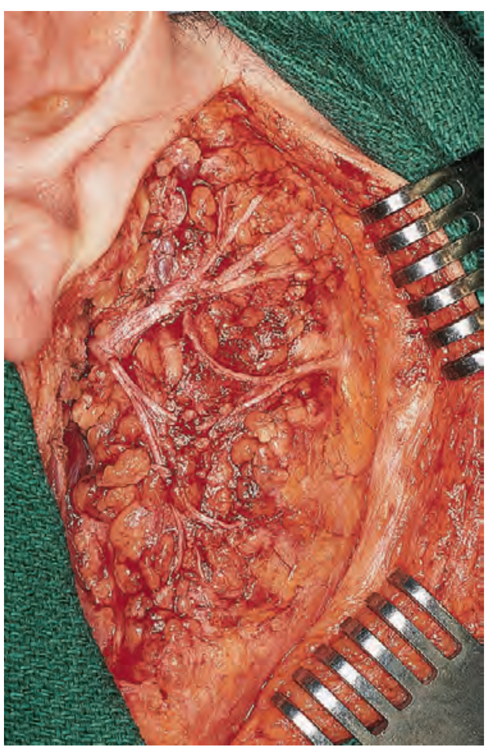
Figure 13.43 Anatomic variation in the intraglandular branching of the extracranial facial nerve.

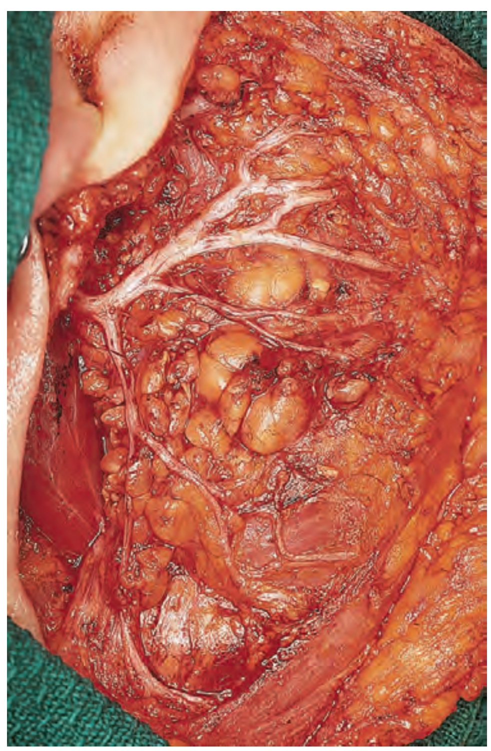
Figure 13.44 Anatomic variation in the intraglandular branching of the extracranial facial nerve.

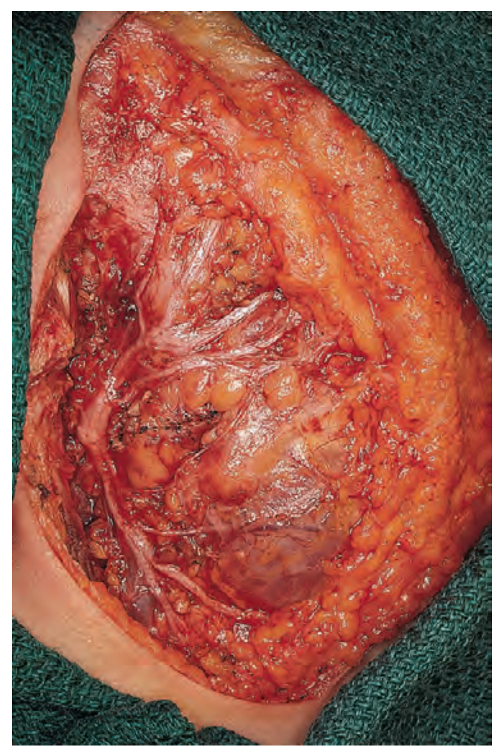
Figure 13.45 Anatomic variation in the intraglandular branching of the extracranial facial nerve.

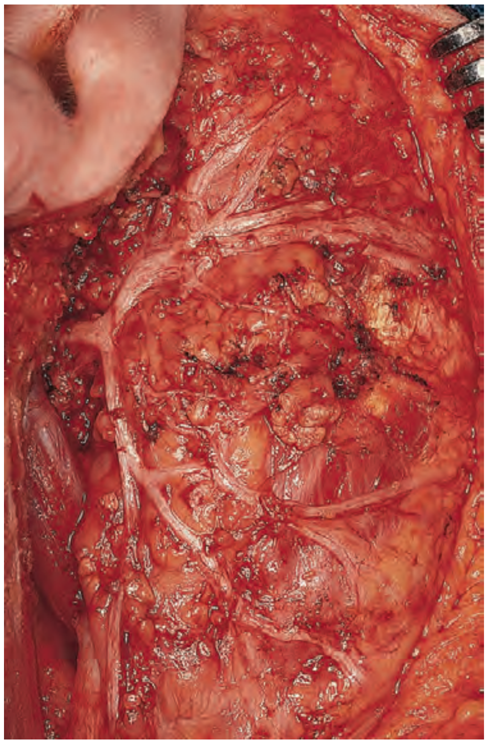

Figure 13.46 Anatomic variation in the intraglandular branching of the extracranial facial nerve.

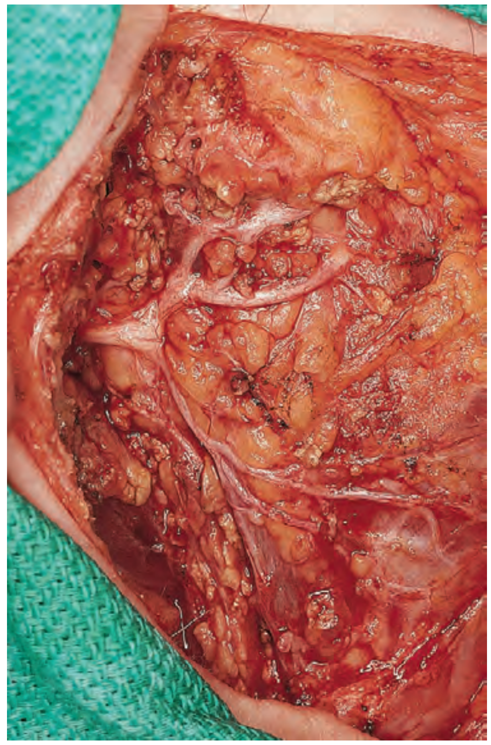

Figure 13.47 Anatomic variation in the intraglandular branching of the extracranial facial nerve.

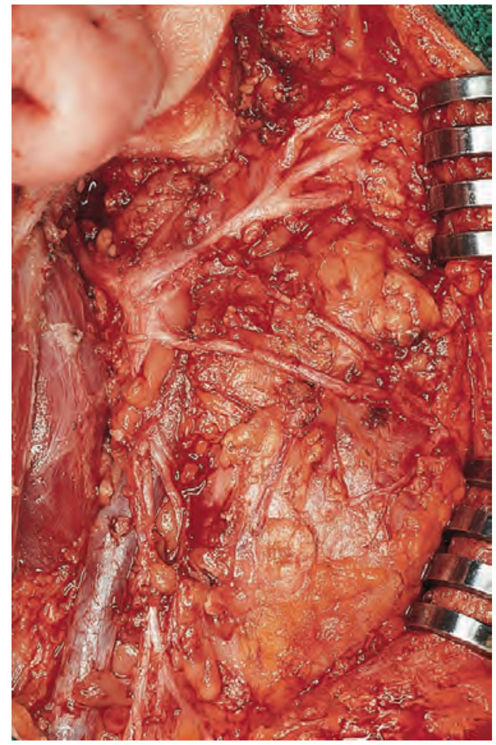

Figure 13.48 Anatomic variation in the intraglandular branching of the extracranial facial nerve.

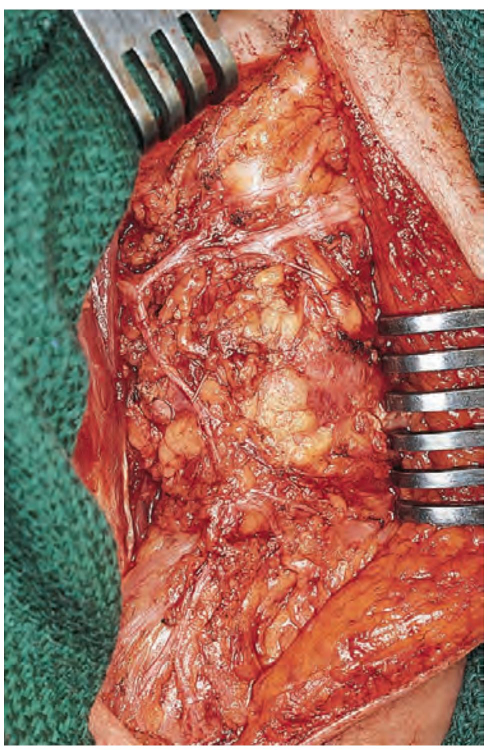

Figure 13.49 Anatomic variation in the intraglandular branching of the extracranial facial nerve.

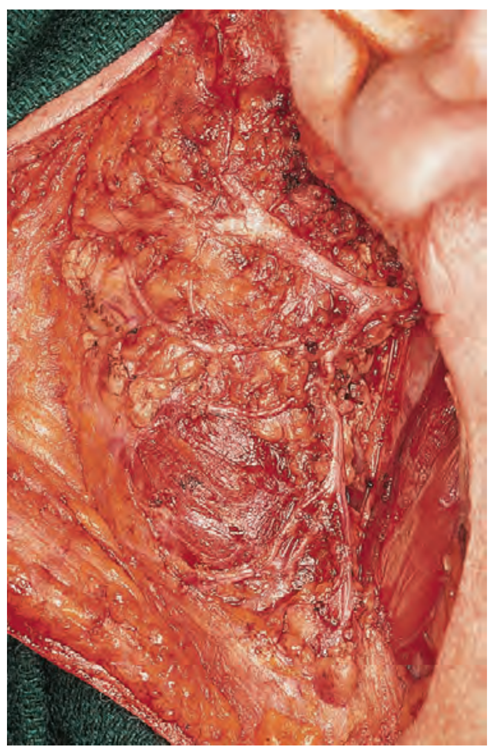

Figure 13.50 Anatomic variation in the intraglandular branching of the extracranial facial nerve.

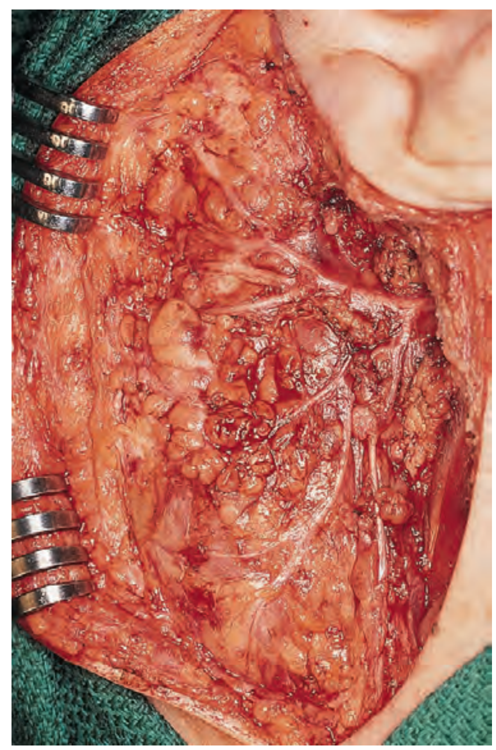

Figure 13.51 Anatomic variation in the intraglandular branching of the extracranial facial nerve.

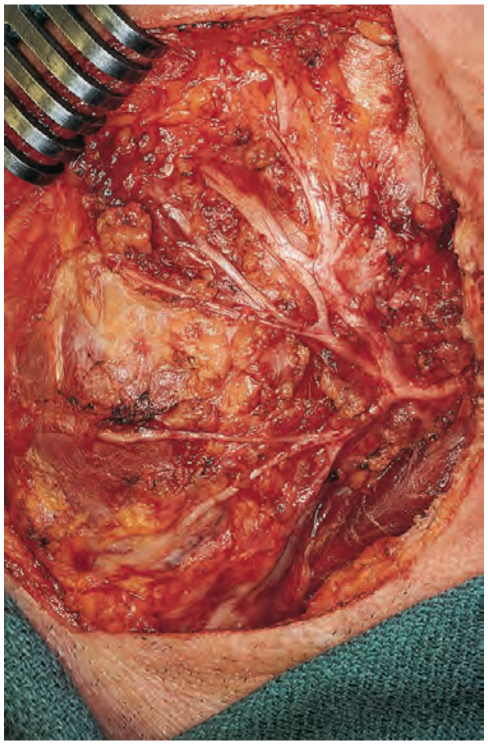

Figure 13.52 Anatomic variation in the intraglandular branching of the extracranial facial nerve.

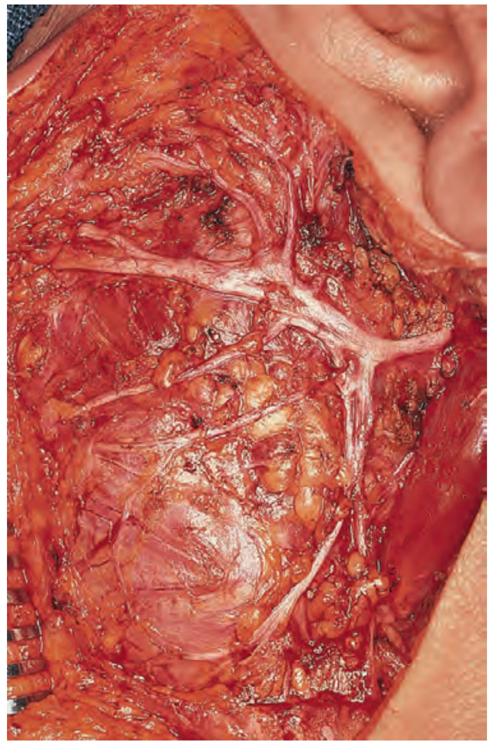

Figure 13.53 Anatomic variation in the intraglandular branching of the extracranial facial nerve.

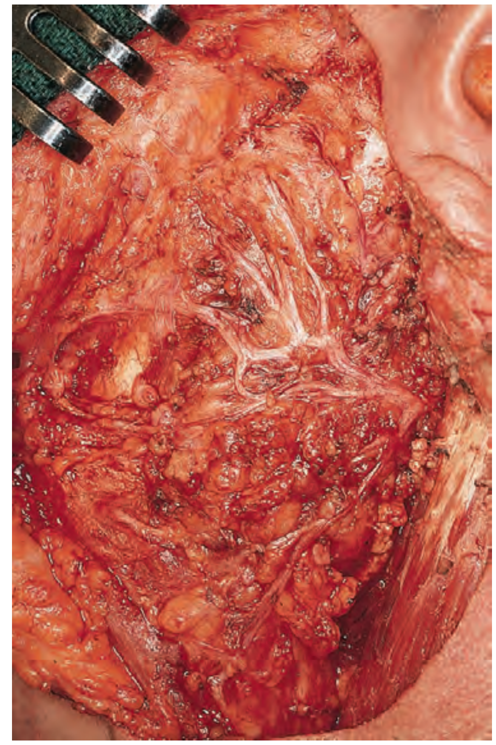

Figure 13.54 Anatomic variation in the intraglandular branching of the extracranial facial nerve.

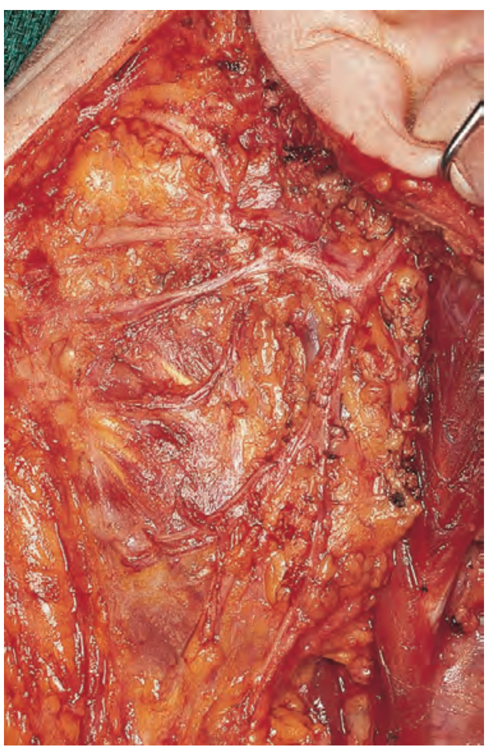

Figure 13.55 Anatomic variation in the intraglandular branching of the extracranial facial nerve.

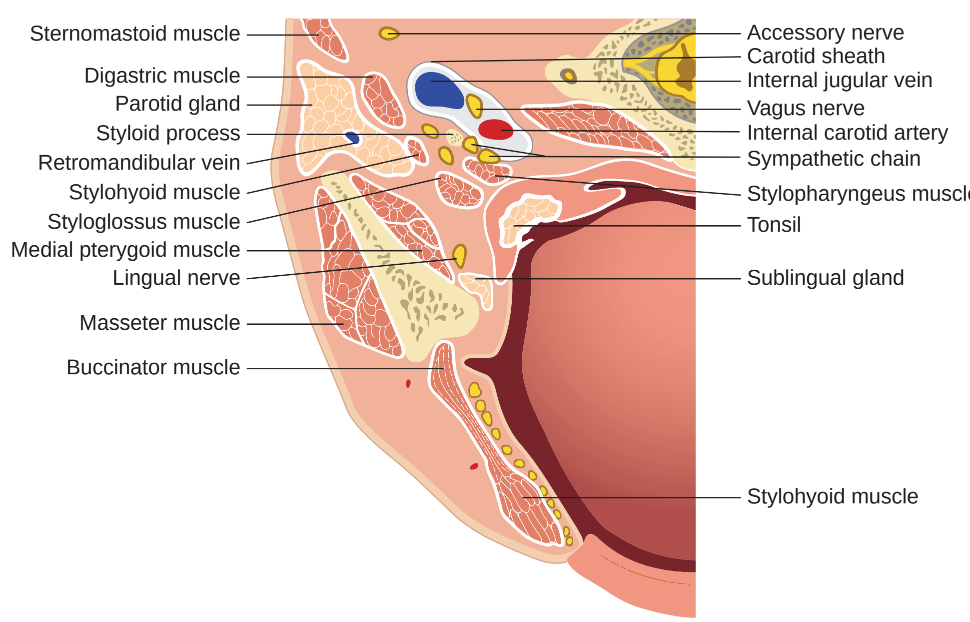

Figure 13.56 The anatomic relationships of the deep lobe of the parotid gland.

encountered in the prestyloid compartment of the parapharyngeal space (masticator space). Tumors of the deep lobe of the parotid gland, by definition, arise in parotid tissue lying medial to the facial nerve. They may present in the retromandibular location or in the parapharyngeal location. From a surgical standpoint, it is important to understand the anatomic relationships of structures in the parapharyngeal space with the deep lobe parotid tissue. Salivary tumors in the parapharyngeal space also arise from ectopic salivary tissue and occasionally from minor salivary glands of the lateral pharyngeal wall.

The submandibular glands, also called the *submaxillary glands,* reside in the submandibular space within the digastric triangle and beneath and anterior to the angle of the mandible. They overlie the mylohyoid muscle and extend around its free border

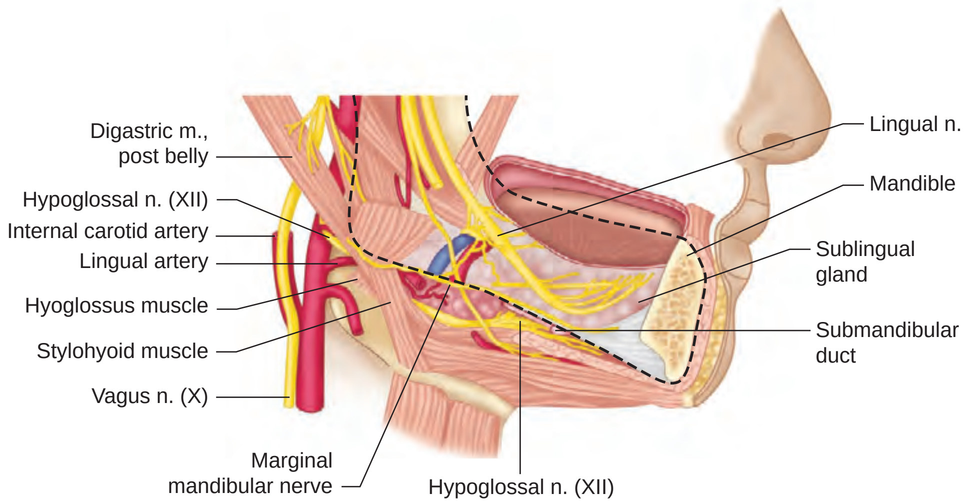

Figure 13.57 The anatomic relationships of the submandibular salivary gland. *M,* muscle; *n,* nerve.

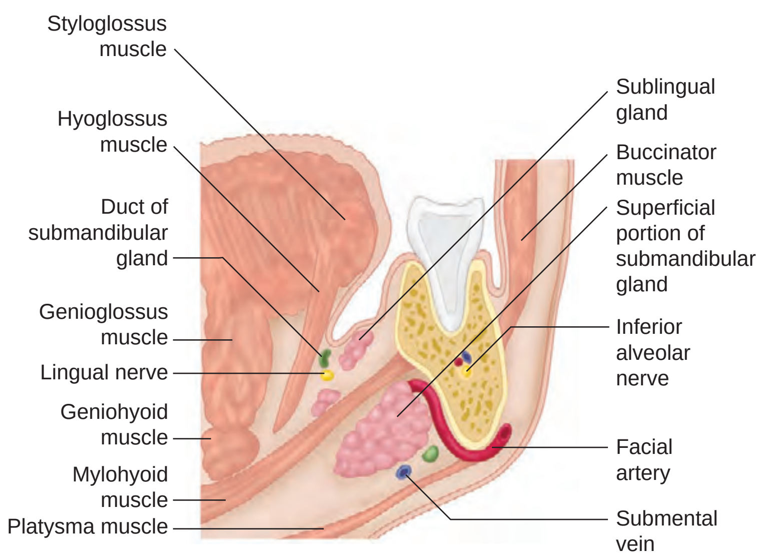

Figure 13.58 The anatomic relationships of the sublingual and submandibular salivary glands to the oral cavity.

in the floor of the mouth along the course of Wharton's duct. The gland lies on the hyoglossus muscle and is in direct contact with the stylomandibular ligament posteriorly. Three important nerves are in direct contiguity to the gland: the marginal branch of the facial nerve, the hypoglossal nerve, and the lingual nerve (Fig. 13.57). Submandibular glands drain into the anterior floor of the mouth through Wharton's duct, the papilla of which opens just lateral to the frenulum of the tongue.

The smallest of the major salivary glands are the sublingual glands, which are located just beneath the mucous membrane of the floor of the mouth and rest on the mylohyoid muscle (Fig. 13.58). They are poorly encapsulated and drain by way of several small ducts directly into the oral cavity or into the submandibular duct.

Preoperative Preparation

All patients undergoing parotid surgery should be counseled about potential transient or permanent loss of facial nerve function. If facial nerve sacrifice is anticipated, then preoperative counseling regarding rehabilitative measures should be discussed with the patient.

Although parotid gland surgery opens salivary ducts into the surgical field, the operation is essentially clean, and use of perioperative antibiotics usually is not necessary. Preoperative preparation for surgical treatment of a malignant tumor of minor salivary origin is essentially the same as it would be for any epithelial lesion in a similar location of the upper aerodigestive tract.

Excision of the Submandibular Salivary Gland for Infection, Calculus, or Tumor

Chronic inflammatory disease occurs more frequently in the submandibular salivary gland than in the parotid gland. Repeated attacks of the inflammatory process eventually may develop into calculus disease, producing chronic intermittent obstruction with painful enlargement of the gland. If the calculus lodged in Wharton's duct presents in the oral cavity and is easily palpable, then the stone may be extracted intraorally by a direct mucosal incision over Wharton's duct. This extraction of the calculus preferably should be performed under general anesthesia in the operating room. If this conservative procedure does not resolve the chronic inflammatory process, then it is advisable to proceed with excision of the entire submandibular gland to alleviate the persistent problem.

The patient shown in Fig. 13.59 has a 4-cm enlargement of the right submandibular salivary gland. The mass is firm, discrete, mobile, and somewhat sensitive, although not very tender. No calculi could be palpated in Wharton's duct by bimanual palpation of the floor of the mouth. The clinical diagnosis of a chronic sialadenitis was entertained based on the patient's history of fluctuation in the size of this mass, but the possibility of a primary tumor could not be ruled out. Such uncertainty in clinical diagnosis is common.

The patient is placed on the operating table under general endotracheal anesthesia. The patient is in a supine position with the neck turned to the opposite side. The palpable mass is outlined in red. The surface marking of the angle of the mandible and the proposed line of incision also are shown in Fig. 13.59. The skin incision is made on an upper neck skin crease at least two fingerbreadths below the angle of the mandible to protect the mandibular branch of the facial nerve. The surface marking for the mandibular branch of the facial nerve is at a point two fingerbreadths below the angle of the mandible and two fingerbreadths anterior to the angle of the mandible, where it lies

Figure 13.59 A patient with enlargement of the right submandibular salivary gland. The surface markings indicate the angle of the mandible and the proposed line of incision.

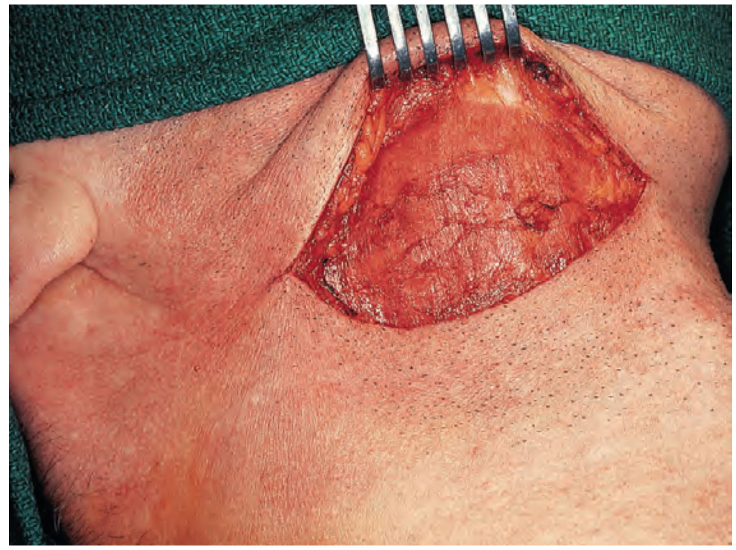

Figure 13.61 The upper skin flap is elevated superficial to the platysma.

Figure 13.60 The skin incision is made through subcutaneous tissue up to the platysma.

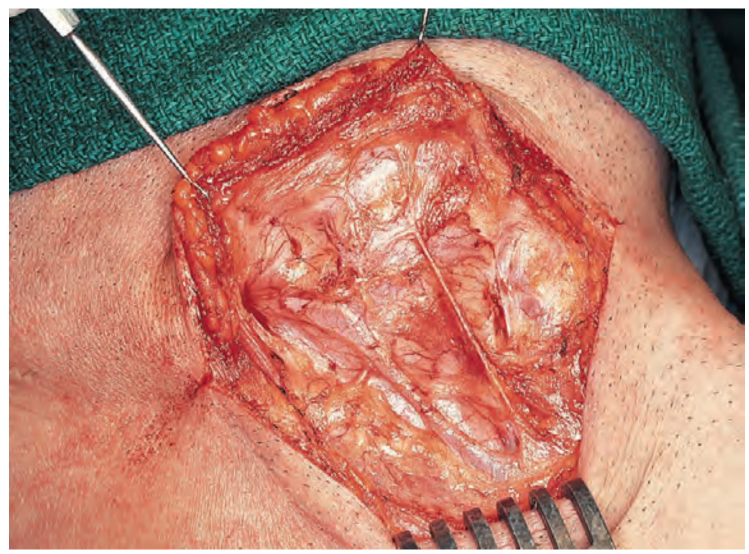

Figure 13.62 The mandibular and cervical branches of the facial nerve are seen anterior to the facial vein.

over the surface of the submandibular salivary gland. The skin incision is completed, remaining superficial to the platysma (Fig. 13.60). The upper skin flap is elevated first with an electrocautery, remaining superficial to the platysma (Fig. 13.61).

The mandibular branch of the facial nerve is now carefully identified, dissected, and protected in the following manner: The platysma is incised with a scalpel in a small area at a point two fingerbreadths below and two fingerbreadths anterior to the angle of the mandible. The remaining platysma along the length of the incision is then divided after blunt dissection underneath with a hemostat, spreading the hemostat open and protecting the underlying soft tissues over the capsule of the submandibular gland. The mandibular branch of the facial nerve rests on this fascia. If the nerve is not located during division of the platysma, a meticulous search is now undertaken so it can be identified.

The mandibular branch and the cervical branch are shown descending down in the neck in Fig. 13.62. Note also the posterior facial vein running almost parallel to the cervical branch. Both of these structures are divided to facilitate retraction of the mandibular branch cephalad along with the upper skin flap. It is important to note that the posterior facial vein lies deep to the mandibular branch. Thus dividing the posterior facial vein low and retracting its upper stump cephalad will protect the dissected and mobilized mandibular branch of the facial nerve on the upper skin flap.

In Fig. 13.63, the upper skin flap is shown retracted with rake retractors, thus protecting the mandibular branch underneath them. With use of an electrocautery, the soft tissues overlying the submandibular salivary gland are now dissected. The anterior belly of the digastric muscle is identified anteriorly in the submental region. During this dissection, small blood vessels overlying the anterior belly of the digastric and the mylohyoid muscles are divided. This procedure enables mobilization of the submandibular gland, which is retracted caudad as shown in Fig. 13.64, exposing the anterior belly and the tendon of the digastric muscle further. More traction on the gland in the caudad direction exposes the underlying mylohyoid muscle.

The nerve and vessels to the mylohyoid muscle located over its surface are individually clamped, divided, and ligated. The

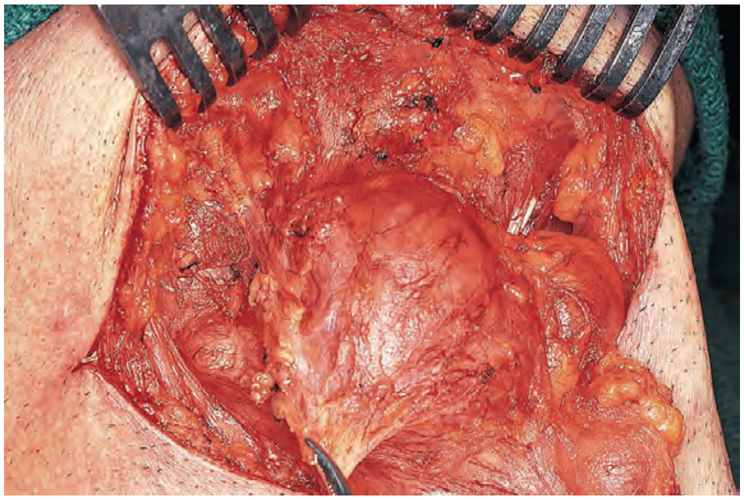

Figure 13.63 The gland is now retracted caudad, exposing the anterior belly of the digastric muscle.

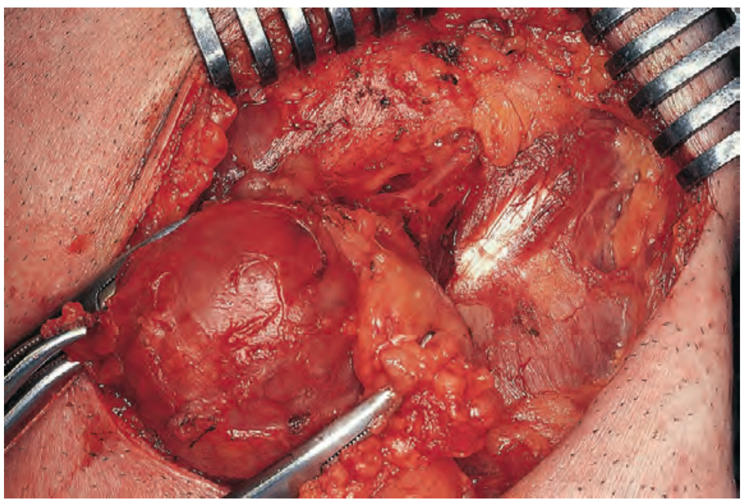

Figure 13.64 Further retraction of the submandibular gland exposes the anterior belly and tendon of the digastric muscle.

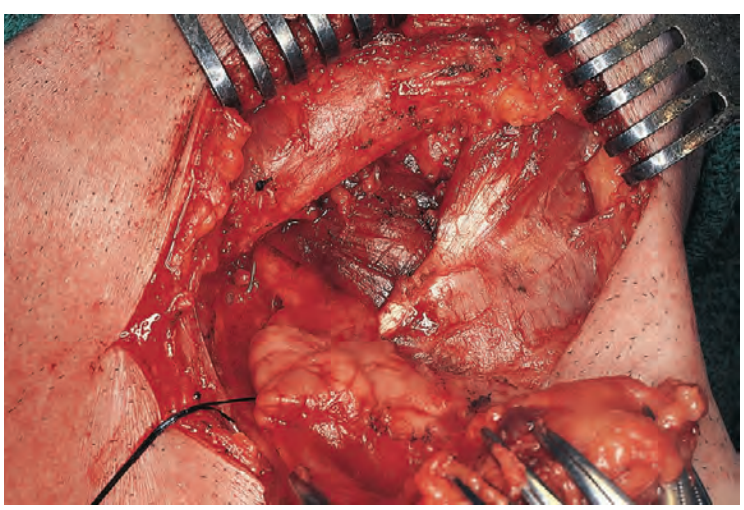

Figure 13.65 The mylohyoid muscle is dissected up to its lateral border.

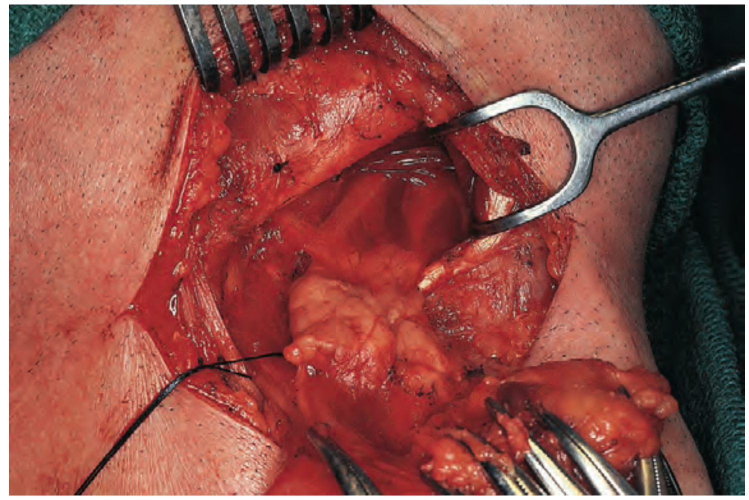

Figure 13.66 The submandibular ganglion and the secretomotor fibers are clamped, divided, and ligated.

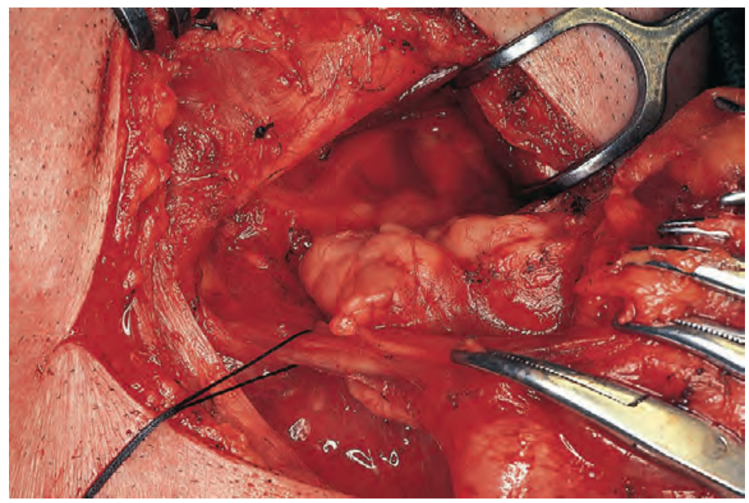

Figure 13.67 Wharton's duct is divided, and its stump is ligated.

facial artery and vein on the posterior aspect of the gland proceeding toward the body of the mandible are dissected next. They are individually clamped, divided, and ligated. Minor branches of the facial nerve crossing this area are carefully protected. Division of the facial vessels permits caudad retraction of the submandibular gland, fully exposing the underlying mylohyoid muscle (Fig. 13.65). A large loop retractor is now used to retract the mylohyoid muscle toward the chin, exposing the underlying lingual nerve and the secretomotor branches to the submandibular gland. The submandibular ganglion and the secretomotor fibers are clamped, divided, and ligated (Fig. 13.66). The remaining attachments of the submandibular gland are Wharton's duct and the vessels running along with it and the proximal part of the facial artery and vein.

Wharton's duct is divided as close to the floor of the mouth as possible (Fig. 13.67). The duct is isolated by dissecting the underlying soft tissues with a hemostat. During this dissection, the hypoglossal nerve is seen in a plane deep to Wharton's duct. It should be carefully protected. Division of Wharton's duct close to the floor of the mouth is particularly important in operations for chronic inflammatory disease with calculi either in the gland or in the duct. Further caudad traction on the gland exposes the proximal part of the facial artery deep to the posterior belly of the digastric muscle. It is carefully dissected, clamped, and divided. This artery often is accompanied by its vena comitantes, and if these are present, they also are divided and ligated.

Fig. 13.68 shows the surgical field after removal of the specimen. The hemostat is on the stump of the facial artery, which is to be ligated. The hypoglossal nerve is adjacent to the tendon of the digastric muscle overlying the hyoglossus, and the lingual nerve is just cephalad to it, with the stump of the secretomotor

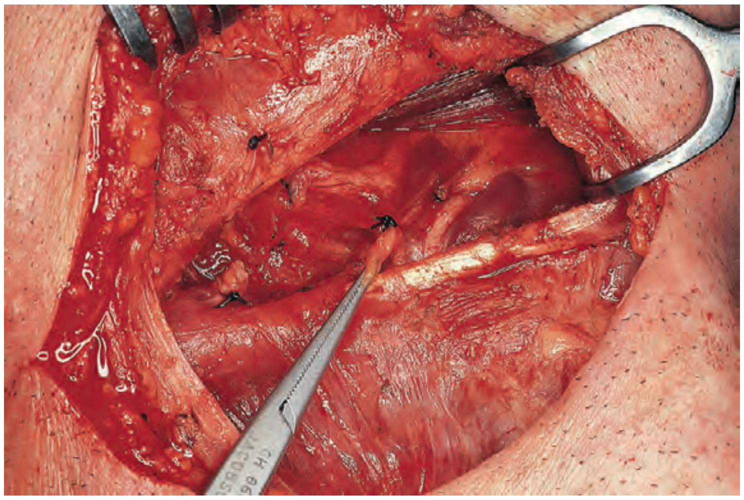

Figure 13.68 The surgical field after removal of the specimen.

Figure 13.70 The surgical specimen of the submandibular gland showing several impacted calculi in Wharton's duct.

Figure 13.69 The wound is closed in layers after placement of a Penrose drain.

Figure 13.71 Postoperative appearance of the patient 3 months following surgery.

fibers ligated. The wound is now irrigated with Bacitracin solution. A Penrose drain is inserted, and the wound is closed in layers (Fig. 13.69).

The specimen shows a chronically inflamed, somewhat enlarged, submandibular salivary gland with a large calculus at the origin of Wharton's duct and several small calculi that produced intermittent obstruction causing chronic sialadenitis (Fig. 13.70).

Postoperative care after excision of the submandibular salivary gland is simple. Most patients should be able to swallow clear liquids and a puréed diet within 24 hours of surgery and proceed to a regular diet within the next 24 hours. The Penrose drain is removed as soon as the drainage becomes scanty. Sutures may be removed when satisfactory healing of the skin is observed.

The postoperative appearance of the patient shows a well-healed, aesthetically acceptable scar in the neck with the function of the mandibular branch of the facial nerve remaining intact, as seen in the bilaterally symmetric corners of the mouth (Fig. 13.71).

If the operation on the submandibular salivary gland is performed for a possible tumor, then the gland is removed along with the adjacent lymph nodes as a monobloc specimen. If the diagnosis of a malignant tumor is established, a more comprehensive operative procedure should be considered. If the primary tumor is small and confined within the capsule of the submandibular salivary gland, then en bloc excision of the submandibular gland along with its adjacent lymph nodes in the suprahyoid triangle is considered adequate.

On the other hand, if the primary tumor is large, or if it has transgressed the capsule of the submandibular salivary gland or has involved adjacent lymph nodes by metastases, then a more radical operation may need to be considered. Such an operation may require sacrifice of both the anterior and posterior bellies of the digastric muscle; a portion of the mylohyoid muscle; and even the hypoglossal nerve, lingual nerve, and mandibular branch of the facial nerve, particularly if the primary tumor is an adenoid cystic carcinoma. A comprehensive neck dissection is performed if neck node metastases are confirmed.

Excision of a Lipoma of the Parotid Gland

Benign tumors such as a lipoma, hemangioma, or lymphangioma are occasionally seen in and around the parotid gland. It is crucial to carefully review the imaging studies for accurate evaluation of the nature and location of the tumor for appropriate surgical intervention. An axial view of the contrast-enhanced CT scan of a patient with a mass in the parotid region shows

Figure 13.72 Contrast-enhanced CT scan in an axial view shows a bland homogeneous nonenhancing lipoma in the parotid gland.

a homogeneous, nonenhancing, bland fatty tumor consistent with a lipoma in the left parotid gland (Fig. 13.72). Surgical excision of this tumor requires a standard parotidectomy incision and identification of the main trunk of the facial nerve. Subsequent dissection of the peripheral branches of the facial nerve is generally not required. Dissection of the tumor in a pericapsular plane permits easy and safe excision of the tumor in a monobloc fashion (Fig. 13.73). The surgical field after removal of the tumor shows the main trunk of the facial nerve (Fig. 13.74). The entire parotid gland is left intact.

Superficial Parotidectomy for a Benign Mixed Tumor

A benign mixed tumor may arise anywhere in the parotid gland, but the most common location is the tail of the superficial lobe of the parotid gland. Occasionally, however, it may arise in the parotid tissue deep to the plane of the facial nerve. In this instance the tumor may present in the retromandibular location or in the parapharyngeal space medial to the ascending ramus of the mandible. Occasionally parotid tumors may arise

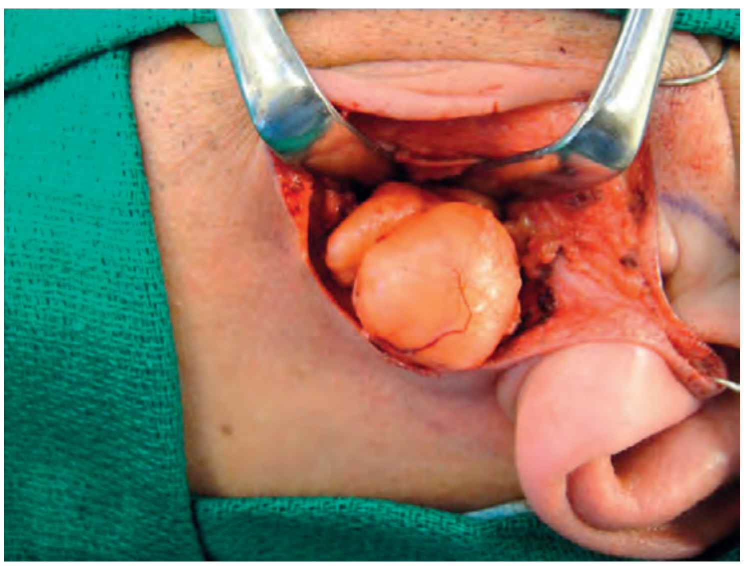

Figure 13.73 Extracapsular dissection of the lipoma after identification of the main trunk of the facial nerve.

Figure 13.75 Surface marking of the tumor in the right parotid gland.

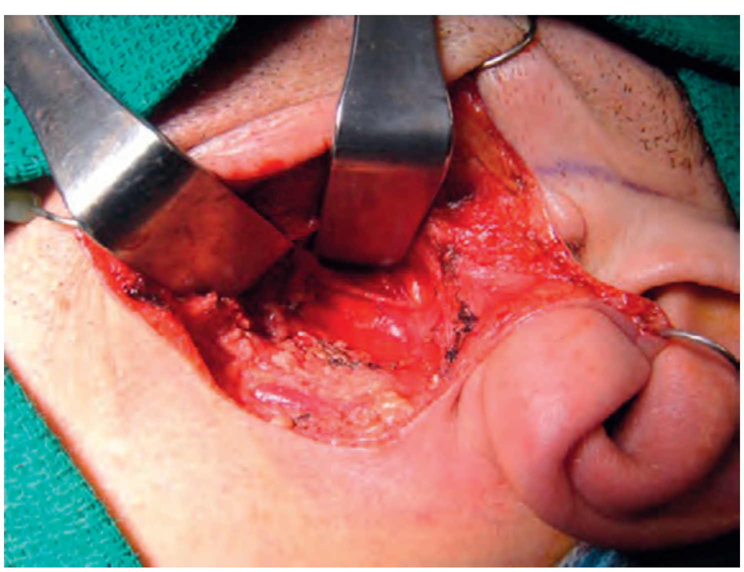

Figure 13.74 Surgical field following the removal of the tumor shows an intact facial nerve.

in the accessory parotid tissue along the Stensen duct. The patient shown in Fig. 13.75 has a 1.5-cm mass in the lower part of the superficial lobe of the parotid gland adjacent to the lobule of the ear. The clinical diagnosis of a mixed tumor is made based on the patient's history and physical findings. An MRI scan of the parotid gland shows a well-circumscribed tumor within the superficial lobe of the parotid gland, consistent with the radiologic diagnosis of a benign mixed tumor (Fig. 13.76). The operation indicated for removal of this tumor is a superficial parotid lobectomy with dissection and preservation of the facial nerve.

A standard parotidectomy incision begins in the preauricular skin crease and curves around the lobule of the ear anteriorly along an upper neck skin crease. Nearly all elderly patients do have a preauricular skin crease. Depending on the location of the tumor, the incision may be appropriately modified. A horizontal extension of the incision along the zygomatic arch may be required for tumors in the preauricular region or for accessory parotid tumors. In very young patients in whom a preauricular skin crease is not present or is not obvious, the

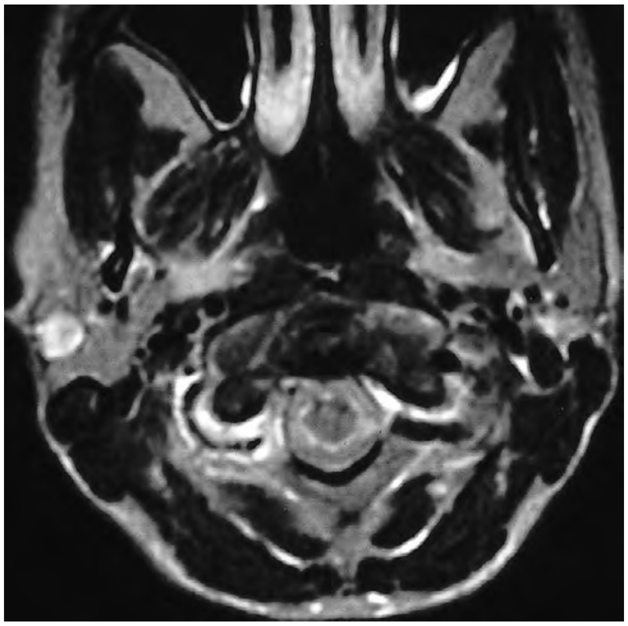

Figure 13.76 An axial view of the magnetic resonance imaging scan showing a well-circumscribed tumor within the superficial lobe of the right parotid gland.

incision is modified as shown in this patient (the tragal incision). The incision is placed on the free edge of the tragus. It curves around the lobule of the ear, turning posteriorly toward the mastoid process. It then follows an upper neck skin crease (Fig. 13.77).

By placing the incision along the free edge of the tragus and along the attachment of the lobule, the eventual scar is inconspicuous. The posterior extension of the incision is hidden behind the lobule of the ear, and the only visible component of the incision is along the upper neck skin crease in the retromandibular area. The skin incision is completed, remaining superficial to the platysma (Fig. 13.78). Extreme care should be exercised in elevating the skin over the tragal cartilage to avoid perforation. A No. 15 scalpel is used, oriented sideways, after the skin incision to elevate this thin skin flap, avoiding injury to the tragal cartilage. Approximately 1 cm of the skin flap over the tragus is elevated with the scalpel. Thereafter the anterior skin flap may be elevated with electrocautery, as long as the plane of dissection remains superficial to the platysma. All the subcutaneous fat is retained on the skin flap, which is elevated directly over the parotid fascia.

Figure 13.77 The modified tragal incision is outlined.

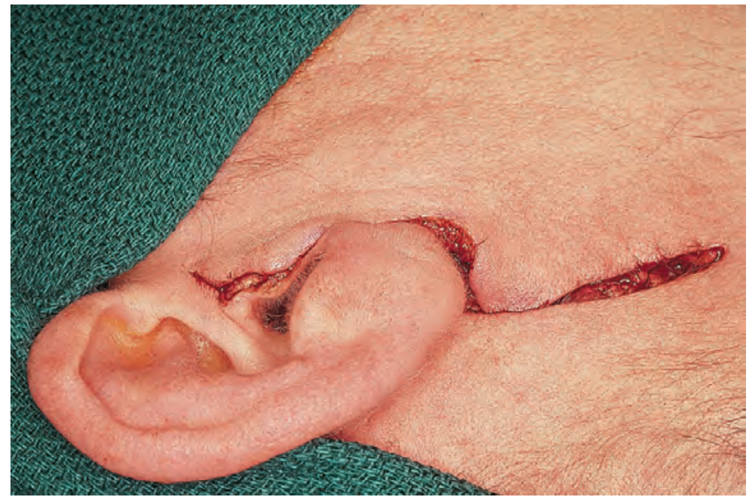

Figure 13.78 The skin incision is deepened through the subcutaneous tissues.

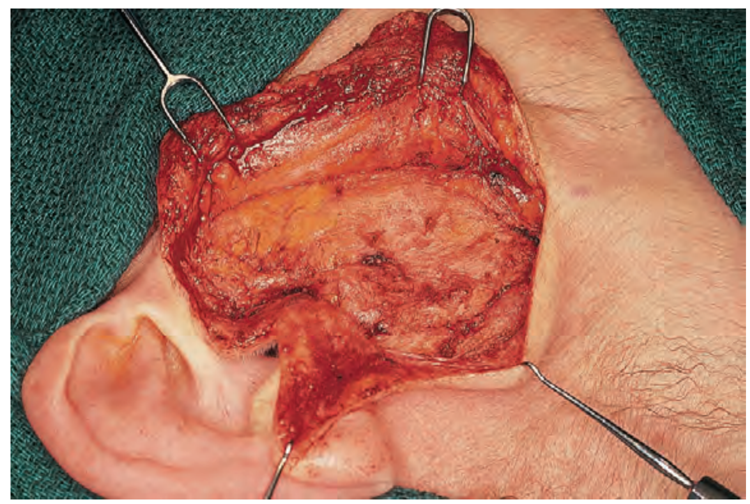

Figure 13.79 The anterior skin flap is elevated superficial to the platysma.

A clear tissue plane exists between the subcutaneous tissue and the parotid fascia (Fig. 13.79). However, if the platysma is elevated and preserved on the anterior skin flap, the incidence of the development of Frey syndrome is significantly reduced. In that case, extreme care should be exercised to avoid injury to the peripheral branches of the facial nerve as they exit from the parotid gland. The posterior skin flap is similarly elevated, exposing the cartilaginous portion of the auditory canal, the tip of the mastoid process, and the anterior border of the sternomastoid muscle. The posterior flap, however, requires minimal elevation, just enough to see the anterior border of the sternocleidomastoid muscle.

The fascia over the anterior border of the sternomastoid muscle is incised, and dissection starts in a plane deep to the tail of the parotid gland, which is retracted anteriorly with several hemostats, as shown in Fig. 13.80. During this part of the operation the greater auricular nerve, which courses over the sternomastoid muscle, is encountered. In most instances the nerve presents as a single trunk, traversing directly from the superficial surface of the sternocleidomastoid muscle to the superficial aspect of the parotid gland. In that instance the nerve must be divided. On occasion, however, instead of a single trunk, the nerve presents with several branches. In that

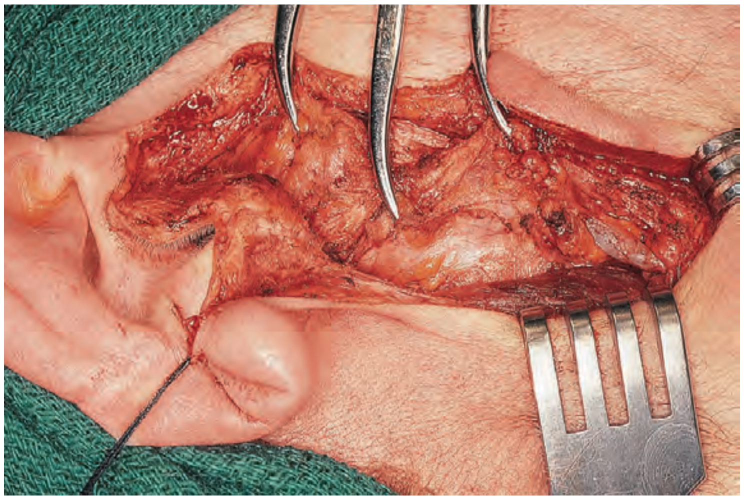

Figure 13.80 The parotid gland is retracted anteriorly.

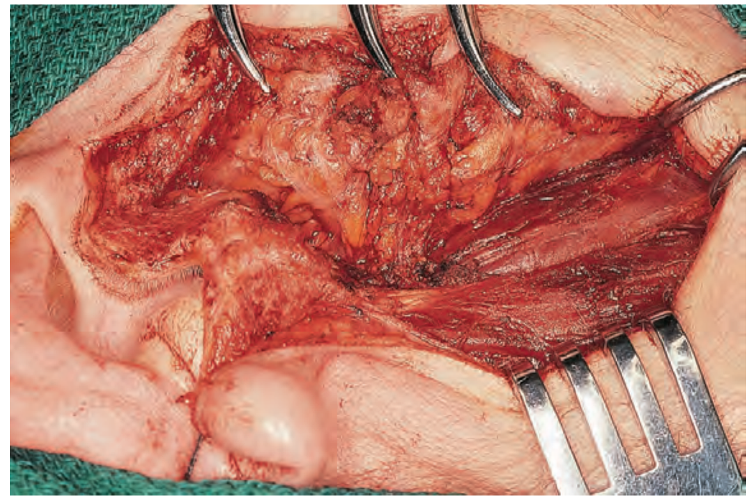

Figure 13.82 Exposure of the posterior belly of the digastric muscle continues up to the digastric groove.

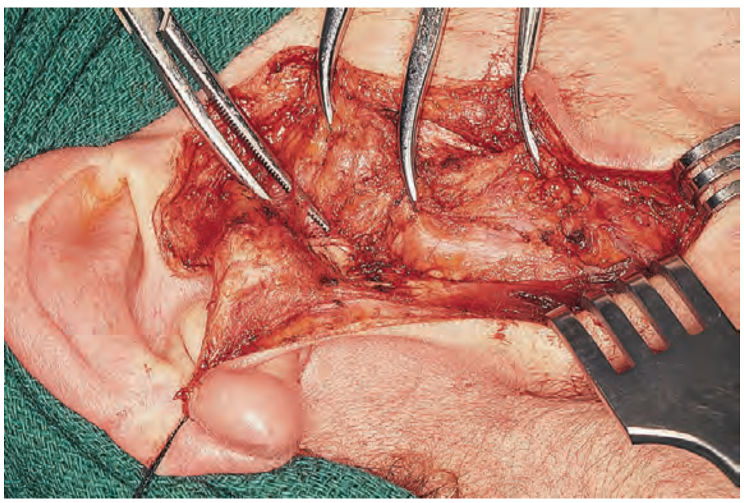

Figure 13.81 The posterior border of the superficial lobe is separated from the auditory canal and retracted anteriorly.

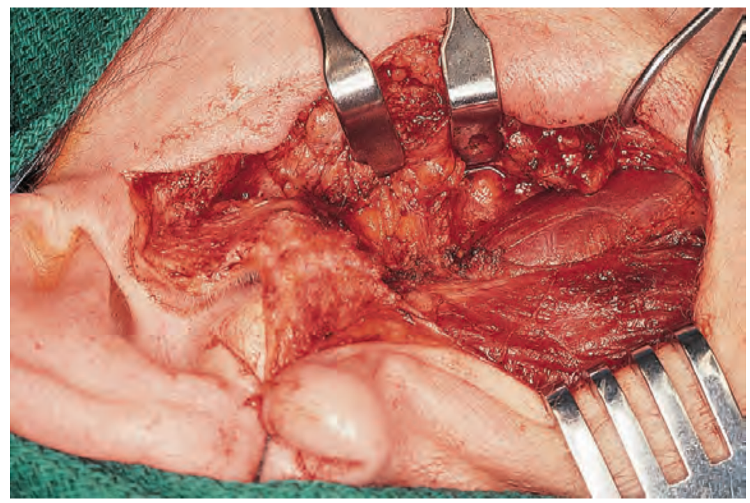

Figure 13.83 Deep right-angled retractors are used to facilitate exposure.

case, the posterior branch going toward the external ear can be preserved, thereby keeping the sensations of the external ear intact. As much of the length of the greater auricular nerve as is available should be preserved; this is particularly important in case a nerve graft is needed. If the facial nerve needs to be sacrificed and a nerve graft is required for its repair, then the greater auricular nerve with its branches is readily available in the same surgical field.

Dissection now proceeds anteriorly, lifting off the parotid gland by separating it from the sternomastoid muscle until the posterior belly of the digastric muscle is exposed. From this point, absolute hemostasis should be maintained to facilitate identification and dissection of the facial nerve. A bipolar electrocautery is essential to conduct this operation safely. The posterior border of the superficial lobe is separated from the auditory canal and retracted anteriorly (Fig. 13.81). This step of the operation is performed with a long hemostat that is used to separate the auditory canal from the parotid substance progressively, putting the fibrous tissue on stretch and dividing it under direct vision in a step-by-step fashion. Exposure of the posterior belly of the digastric muscle continues toward its insertion on the digastric groove near the mastoid process (Fig. 13.82). A blunt rake retractor is used to retract the sternocleidomastoid muscle, exposing the posterior belly of the digastric muscle at its insertion on the digastric groove.

Dissection of the parotid gland now proceeds toward the mastoid process along the superior border of the posterior belly of the digastric muscle. It is inadvisable to use the monopolar electrocautery from here on near the facial nerve. Fine hemostats are used to separate the salivary tissue from the cartilaginous auditory canal and the tympanomastoid sulcus to expose the main trunk of the facial nerve emerging from the stylomastoid foramen.

As dissection proceeds further, absolute hemostasis must be secured to facilitate the remainder of the operation. Deep right-angled retractors are used to retract the mobilized superficial lobe of the parotid gland anteriorly. The residual parotid tissue superficial to the facial nerve is put on stretch by these deep right-angled retractors, facilitating dissection of the main trunk of the facial nerve (Fig. 13.83). The salivary tissue and fibrous tissue are separated step by step with careful use of a hemostat and the bipolar electrocautery, thus exposing the main trunk of the facial nerve at a point where the mastoid process, the cartilaginous portion of the auditory canal, and the superior border of the posterior belly of the digastric muscle meet (Fig. 13.84). In nearly all patients an unnamed branch of the posterior auricular artery is found just superficial to the main trunk of the facial nerve. This vessel should be carefully identified, clamped, and ligated. It is important to remember the anatomic landmarks mentioned previously, because they positively aid the surgeon

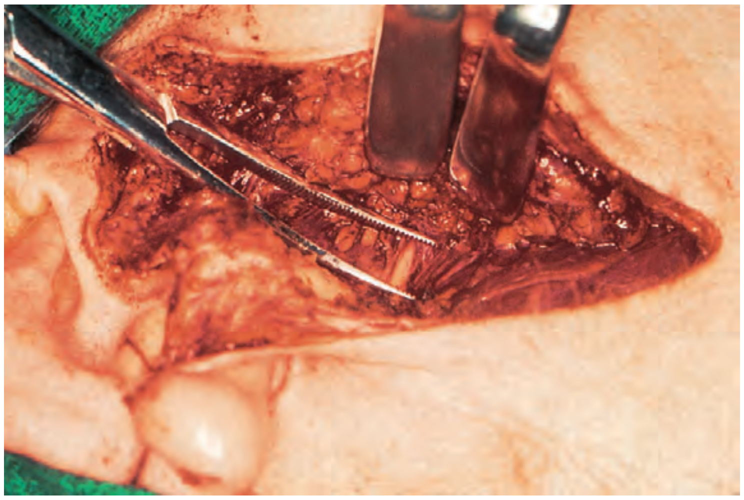

Figure 13.84 The main trunk of the facial nerve is identified.

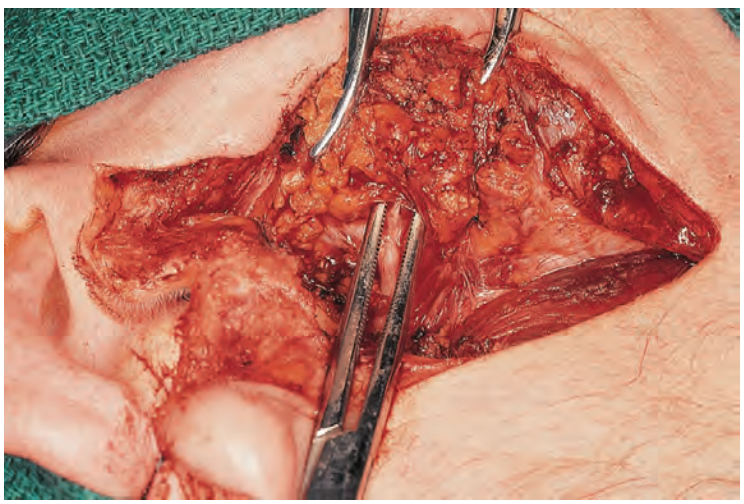

Figure 13.85 Dissection proceeds in a plane superficial to the facial nerve and its branches.

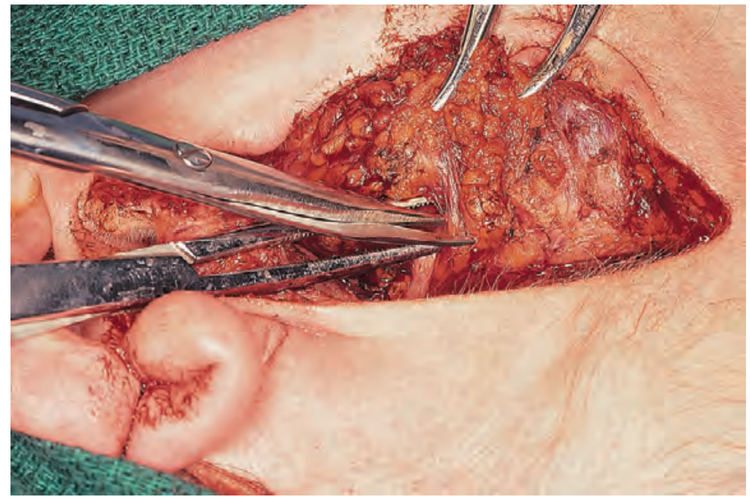

Figure 13.86 Parotid tissue is spread out over a curved hemostat and divided sharply with Reynold scissors.

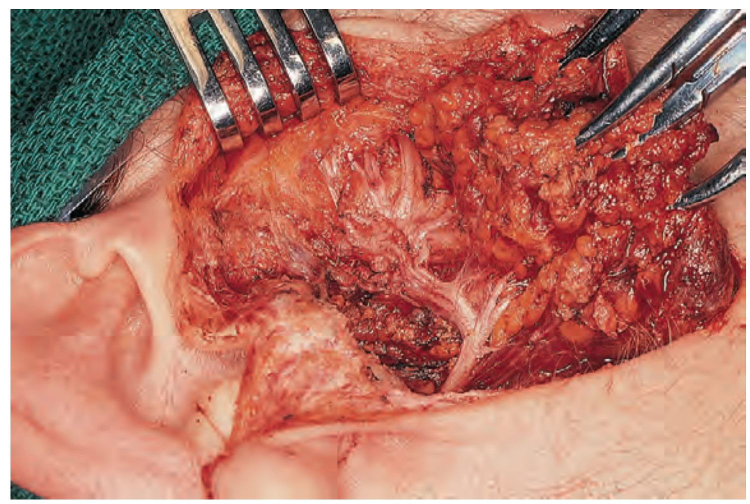

Figure 13.87 Dissection of the upper division of the facial nerve is in progress.

in locating the main trunk of the facial nerve safely without any inadvertent injury. The fixed point of the superior surface of the posterior belly of the digastric muscle, the tip of the mastoid process, and the anteroinferior surface of the auditory canal are shown in the diagram in Fig. 13.39 to illustrate the point.

Once the main trunk of the facial nerve is identified, dissection proceeds in a plane superficial to the nerve toward the periphery of the gland. A curved hemostat is used to spread the parotid tissue immediately superficial to the nerve, keeping it under constant vision between the two ends of the hemostat while the salivary tissue is electrocoagulated with a bipolar cautery and divided (Fig. 13.85).

The main trunk of the facial nerve may vary in length, ranging from 5 to 15 mm. However, it may stretch to several centimeters, depending on the size and location of the tumor. Thus the bifurcation of the upper and lower divisions of the facial nerve may be at a varying distance from the stylomastoid foramen. Fig. 13.86 demonstrates the technique of spreading the salivary tissue superficial to the nerve, keeping the nerve under vision, and dividing the spread salivary tissue on a stretch with Reynold scissors. It is important to reemphasize that while the facial nerve is being dissected, absolute hemostasis is required in the operative field. Bipolar cautery should be used judiciously to coagulate fine bleeding points. Bigger vessels are best ligated with 4-0 chromic catgut.

Dissection continues along the peripheral branches of the facial nerve. If the tumor is located in the lower half of the parotid gland, dissection of the upper division of the facial nerve is undertaken first, as shown in Fig. 13.87. The salivary tissue adjacent to the auditory canal and in the zygomatic region may be divided safely and retracted anteriorly as the facial nerve, which is in a deeper plane, remains under constant view. The superficial temporal artery and vein course through the substance of the parotid gland and may need to be divided and ligated. The technique of dissection of the facial nerve with use of a hemostat to expose a segment of the nerve by spreading the salivary tissue just superficial to it continues to be used throughout the dissection of the nerve and each of its branches. The open hemostat is retained in position, keeping the exposed nerve underneath in view while the stretched salivary tissue is being electrocoagulated and divided with scissors.

Dissection of the upper division of the facial nerve is now completed, exposing each of its peripheral branches. The upper half of the superficial lobe of the parotid gland is reflected caudad and held with hemostats. As the buccal branch of the facial nerve is approached, extra attention is required because of the presence of the Stensen duct in the central part of the

Figure 13.88 The surgical field after removal of the specimen.

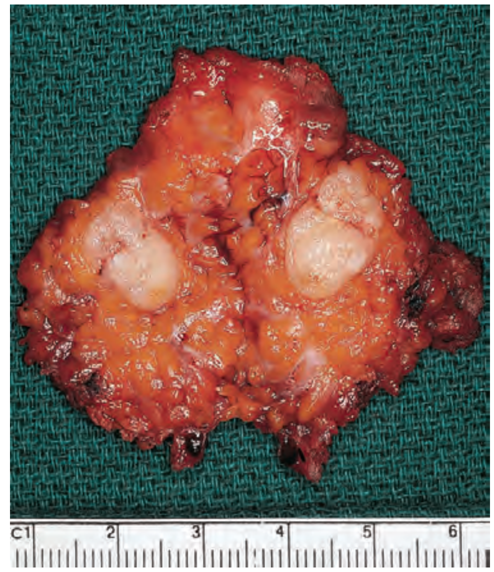

Figure 13.90 The surgical specimen.

Figure 13.89 Closure of the incision.

Figure 13.91 The postoperative appearance of the patient.

gland, which is in close association with the buccal branch in many instances. Extra attention is required while dissecting the buccal branch of the facial nerve, which is usually tenuous and runs parallel to the Stensen duct. After isolation and careful dissection of the buccal branch, the Stensen duct is divided. Its stump, which may be tied, needs no further attention.

Dissection of the lower division of the facial nerve continues in a similar fashion, leading to complete removal of the superficial lobe of the parotid gland that contains the tumor. Fig. 13.88 shows the surgical field after removal of the superficial lobe of the parotid gland. Note that the dissected facial nerve is completely preserved, with each of its peripheral branches remaining intact. The retromandibular vein is seen lying directly beneath the lower division of the facial nerve, entering the deep lobe of the parotid gland. Absolute hemostasis must be confirmed before closure of the wound begins. A Penrose drain is inserted and brought out through the center of the incision behind the lobule of the ear. Alternatively, suction drains may be used, but the drain should be positioned carefully to avoid placement next to the nerve. The incision is closed in two layers, and light dressings are applied (Fig. 13.89). The specimen shown in Fig. 13.90 demonstrates the tumor arising in the superficial lobe of the parotid gland with a good rim of normal parotid tissue around the tumor. The final histologic diagnosis of the tumor was a pleomorphic adenoma.

Postoperative care is relatively simple. The Penrose drain is removed when the drainage becomes scant. It is extremely unusual to find salivary leakage, because the bulk of the parotid gland is removed with a superficial lobectomy. The remaining salivary tissue in the deep lobe undergoes atrophy and fibrosis. On the other hand, a salivary fistula is more likely to occur after local excision of a parotid tumor, leaving the superficial lobe behind. A fistula occurs because a large component of functioning salivary tissue is left behind, with some of its collecting ducts transected. Facial nerve function remains intact, but the patient will experience numbness in the area of the lobule of the ear because of division of the greater auricular nerve. A superficial parotidectomy should be performed with attention to detail, meticulous gentle dissection, and avoidance of direct trauma or stretch to the nerve to prevent facial weakness. The postoperative appearance of the patient 1 year after surgery is shown in Fig. 13.91. Several examples of aesthetic outcomes after a parotidectomy using the tragal incision are shown in Fig. 13.92.

Figure 13.92 Aesthetic outcome of tragal modification of a standard parotidectomy incision. **A**, Incision outline. **B**, Postoperative appearance.

Figure 13.93 A 3-cm tumor palpable in the superficial lobe of the left parotid gland.

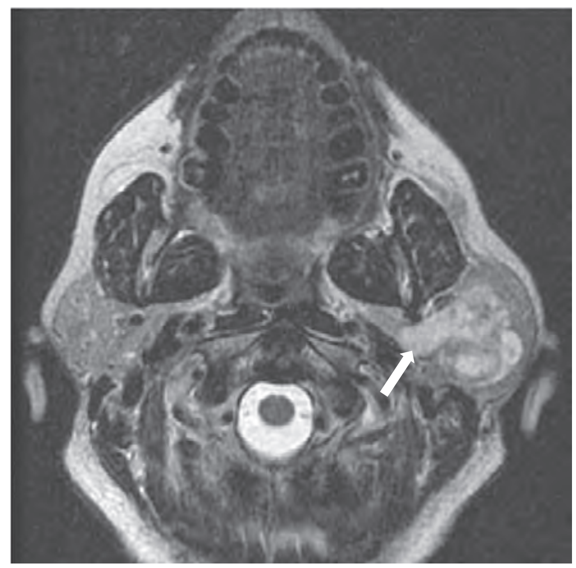

Figure 13.94 T2-weighted MRI scan showing extension of a superficial lobe tumor in the retromandibular region (*arrow*).

Excision of a Superficial Lobe Parotid Tumor With Extension to the Deep Lobe

In some patients a predominantly superficial lobe tumor may extend to the deep lobe (parotid tissue, deep to the facial nerve), either below or above the main trunk of the nerve, or sometimes between the upper and lower divisions of the facial nerve. The patient shown in Fig. 13.93 has a tumor easily palpable in the superficial lobe of the parotid gland. An axial view of his T2-weighted MRI scan shows a heterogenous hyperintense tumor located in the superficial lobe with retromandibular extension to the deep part of the parotid gland (Fig. 13.94). Intraoperatively, the main trunk of the facial nerve is identified in the normal location, but the tumor seems to extend to the deep parotid tissue between the upper and lower divisions of the facial nerve (Fig. 13.95). Meticulous and delicate dissection of the nerve branches is undertaken to deliver the tumor out from the deep lobe tissue, without undue stretch on the nerve. The surgical field after removal of the tumor shows complete preservation of all the branches of the facial nerve (Fig. 13.96). The surgical

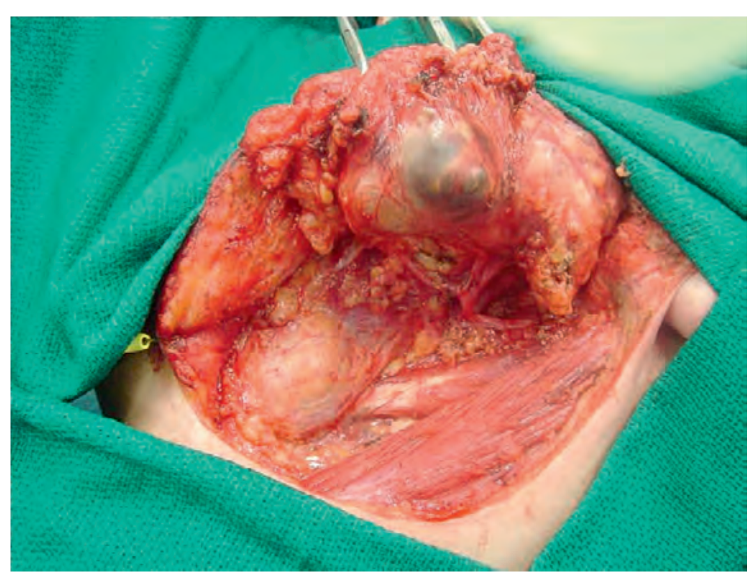

Figure 13.95 Extension of a superficial lobe tumor to the deep parotid tissue between the upper and lower divisions of the facial nerve.

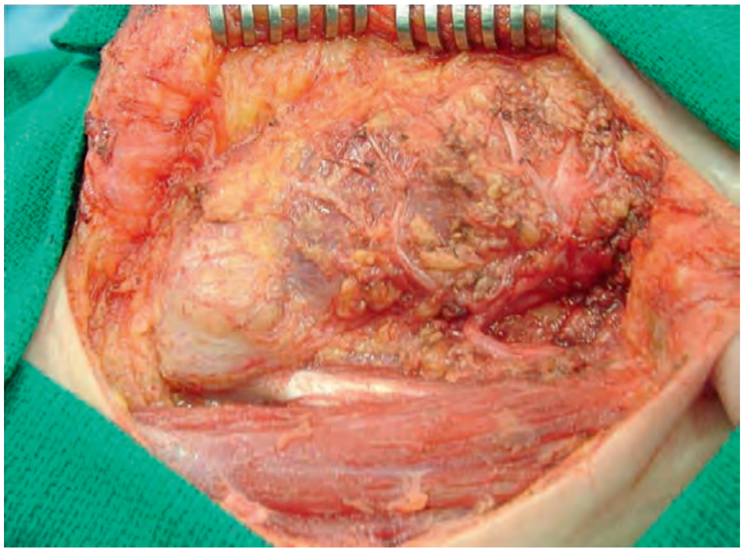

Figure 13.96 The surgical field following the removal of the tumor shows intact facial nerve.

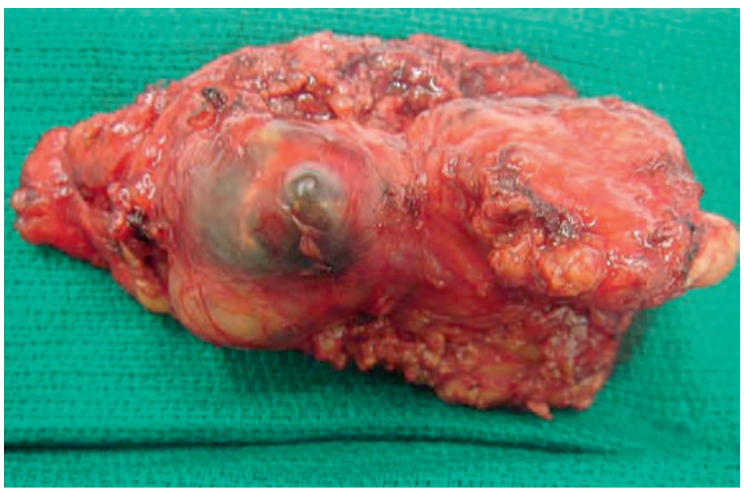

Figure 13.97 The surgical specimen shows a bilobed tumor with indentation created by the bifurcation of the facial nerve.

Figure 13.98 The outline of a rubbery nodular tumor just anteroinferior to the lobule of the ear.

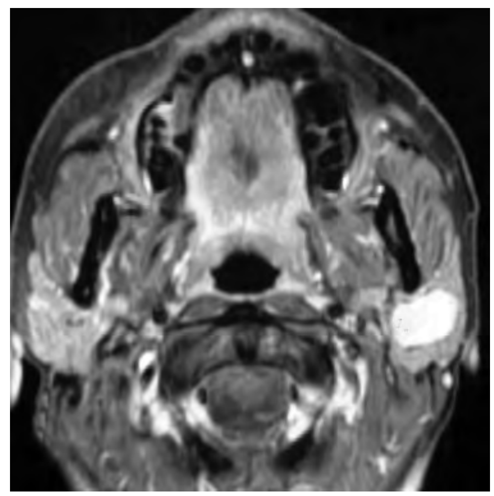

Figure 13.99 An axial view of a magnetic resonance imaging scan shows a well-demarcated tumor in the retromandibular region.

specimen shows the tumor removed intact in a monobloc fashion (Fig. 13.97). Note the indentation in this bilobed tumor created by the bifurcation of the facial nerve.

Excision of a Mixed Tumor Deep to the Facial Nerve

Mixed tumors of the deep lobe of the parotid gland presenting in the retromandibular region often have clinical features and even radiologic features similar to a tumor of the superficial lobe of the parotid gland. The patient shown in Fig. 13.98 has a 2.5- by 3-cm rubbery nodular tumor just anteroinferior to the lobule of the ear. The overlying skin is not involved by the tumor, and the tumor is freely mobile over the deeper soft tissues. The clinical diagnosis of a mixed tumor of the superficial lobe of the parotid gland was made. An MRI scan in an axial view shows a well-demarcated tumor within the superficial lobe of the parotid gland, although the tumor does extend into the retromandibular region (Fig. 13.99). Retromandibular extension of the tumor should alert one to the possibility that this tumor could be deep to the facial nerve and that the facial nerve may be displaced laterally (superficially) by the tumor. Therefore extreme caution must be exercised during dissection to locate the main trunk of the facial nerve, which may be stretched and found superficial to the tumor.

A tragal incision is used along the free edge of the tragus up to the lobule of the ear, and the incision then follows the crease of the lobule in the retroauricular region overlying the mastoid process, curving downward along an upper neck skin crease. The incision is outlined on the skin of the patient (Fig. 13.100). Elevation of the skin flap begins with incision of the skin over the tragus first, with meticulous and gentle dissection of the skin with a scalpel, remaining in a plane between the skin and the cartilage. This skin is extremely thin and can be perforated easily by rough handling or with the use of electrocautery. Approximately 1 cm of skin needs to be elevated in this fashion with a scalpel to avoid injury to the tragal cartilage. The subsequent skin flap can be elevated easily with electrocautery (Fig. 13.101).

The rest of the skin flap is elevated expeditiously, remaining directly over the parotid fascia and keeping all the subcutaneous fat on the skin flap. The anterior skin flap is elevated up to the anterior margin of the superficial lobe of the parotid gland. Posteriorly the gland is separated from the anterior surface of the auditory canal superiorly and from the tip of the mastoid process and the anterior border of the sternocleidomastoid muscle inferiorly (Fig. 13.102). This elevation can be safely accomplished with monopolar electrocautery. At this juncture, the three landmarks that are essential in locating the main

Figure 13.100 The skin incision is outlined on the patient.

Figure 13.101 Skin elevation over the tragal cartilage.

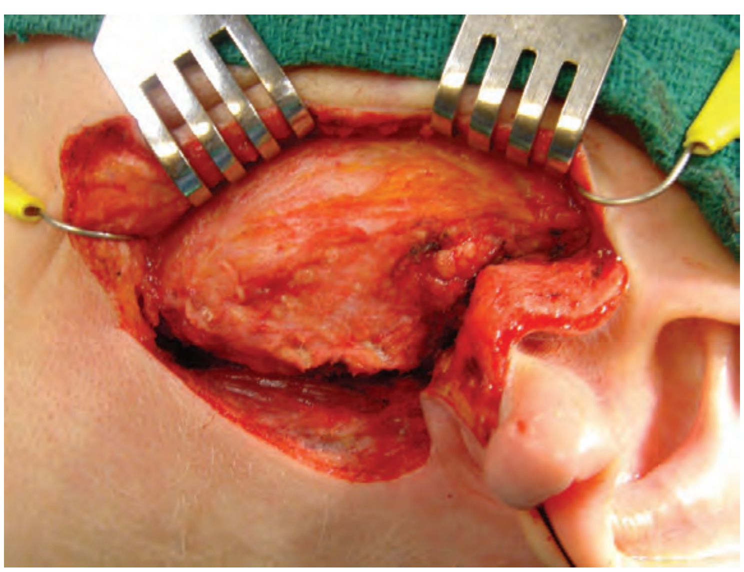

Figure 13.102 The parotid gland is separated from the ear canal and mastoid process.

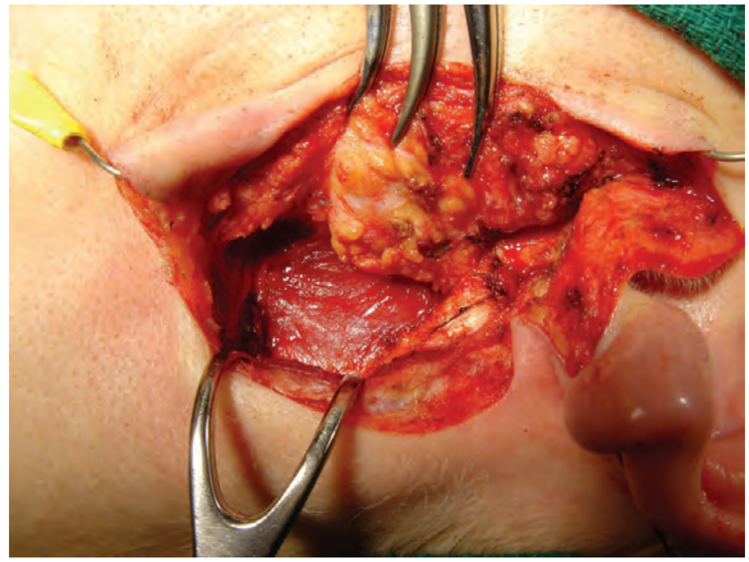

Figure 13.103 The posterior belly of the digastric muscle is exposed.

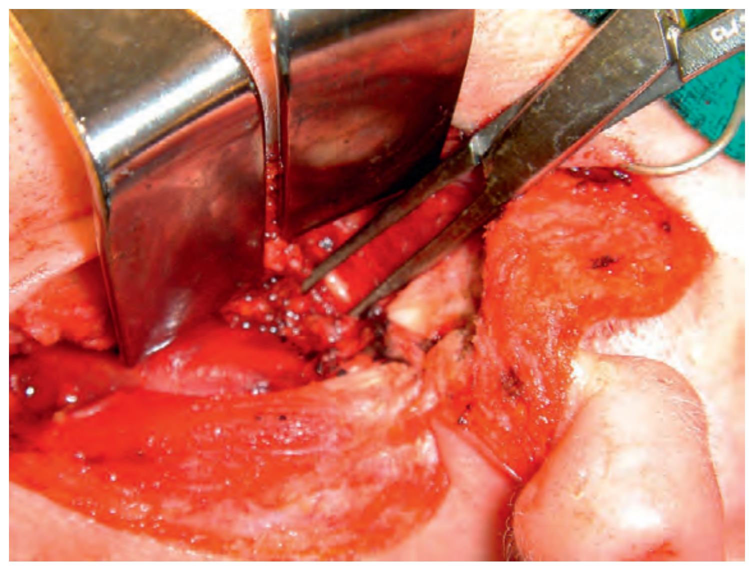

Figure 13.104 The main trunk of the facial nerve is identified.

trunk of the facial nerve must be identified. These landmarks are the superior surface of the posterior belly of the digastric muscle, the tip of the mastoid process, and the anteroinferior surface of the auditory canal. The sternomastoid muscle is retracted laterally, and the superficial lobe of the parotid gland is retracted medially to expose the posterior belly of digastric muscle (Fig. 13.103). By alternate blunt and sharp dissection, a plane is created between the undersurface of the parotid gland and the superior surface of the posterior belly of the digastric muscle. Once this area is exposed, the three essential landmarks to identify the main trunk of the facial nerve are in view.

At this point, all further dissection should be done sharply with either a scalpel or fine scissors and bipolar cautery. Use of a monopolar cautery should be avoided at this point to prevent thermal injury to the facial nerve. By alternate blunt and sharp dissection in this region through the attached parotid tissue, the main trunk of the facial nerve is identified (Fig. 13.104). However, it should be borne in mind that before the main trunk of the facial nerve comes into view, a branch from the posterior auricular artery consistently crosses the surgical field along the same direction as the main trunk of the facial

nerve. This artery is a good pointer, indicating that the surgeon is in the vicinity of the facial nerve. This artery is carefully dissected, divided, and ligated.

Once the main trunk of the facial nerve is identified, dissection proceeds along its upper and lower divisions. At this juncture it becomes apparent that the tumor is located deep to the facial nerve, and its upper and lower divisions are stretched over the surface of the tumor. Therefore mobilization of the superficial lobe of the parotid gland continues peripherally along the course of each of the peripheral branches of the facial nerve, which are dissected carefully and preserved intact. Once the entire superficial lobe is freed, the tumor comes into view, completely wrapped around by the branches of the upper and lower division of the facial nerve (Fig. 13.105).

Meticulous dissection is undertaken at this point to elevate the branches of the facial nerve from the pseudocapsule of the tumor by sharp dissection. This dissection can be accomplished either with a scalpel or with tenotomy scissors. During this dissection, excessive traction on the facial nerve with a nerve hook should be avoided to prevent neuropraxia. With use of gentle dissection, the facial nerve is carefully preserved, and the entire tumor is delivered in a monobloc fashion. After removal of the tumor, the surgical field shows an intact facial nerve, with each of the peripheral branches of its upper and lower division preserved (Fig. 13.106). After securing complete hemostasis, the wound is closed in the usual fashion in two layers.

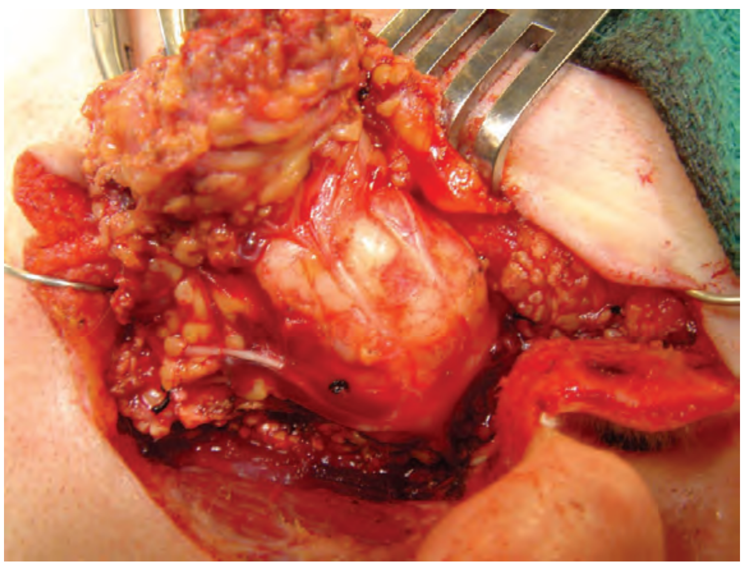

Figure 13.105 The branches of the facial nerve are stretched like a rubber band over the tumor.

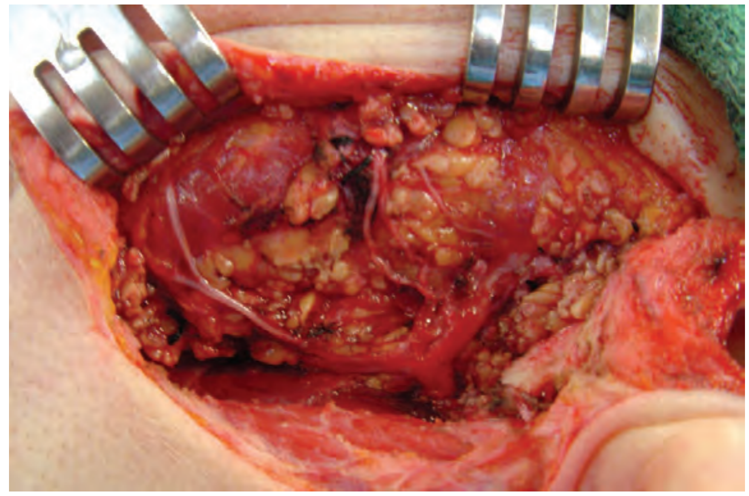

Figure 13.106 The surgical field showing the preserved facial nerve.

Occasionally a tumor from the deep parotid tissue grows around the branches of the facial nerve. In this situation it is extremely hazardous to embark upon blunt dissection of the tumor in the deep parotid tissue without complete exposure of the entire facial nerve with each of its branches under vision. A contrast-enhanced CT scan of a patient with a tumor arising in the deep part of the parotid gland is shown in Fig. 13.107. Note that the tumor is nearly all medial to the mandible but does not extend into the parapharyngeal space. At surgical exploration significant tumor growth is noted both above and below the main trunk of the facial nerve, with its peripheral branches splayed out over the tumor (Fig. 13.108). Facial nerve dissection in these situations is quite tedious and hazardous if extreme caution is not exercised to avoid stretching the nerve branches.

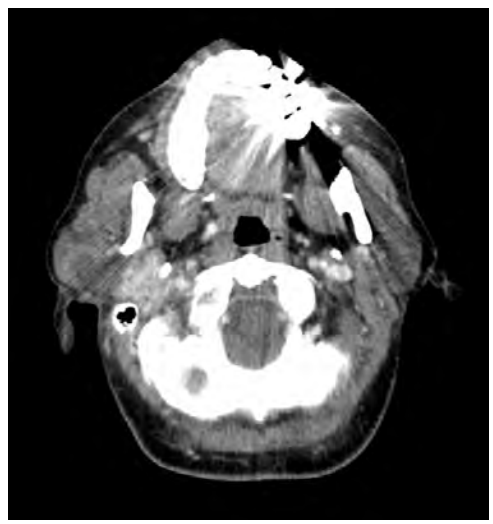

Figure 13.107 A contrast-enhanced computed tomography scan shows a lobulated tumor in the deep parotid tissue medial to the mandible.

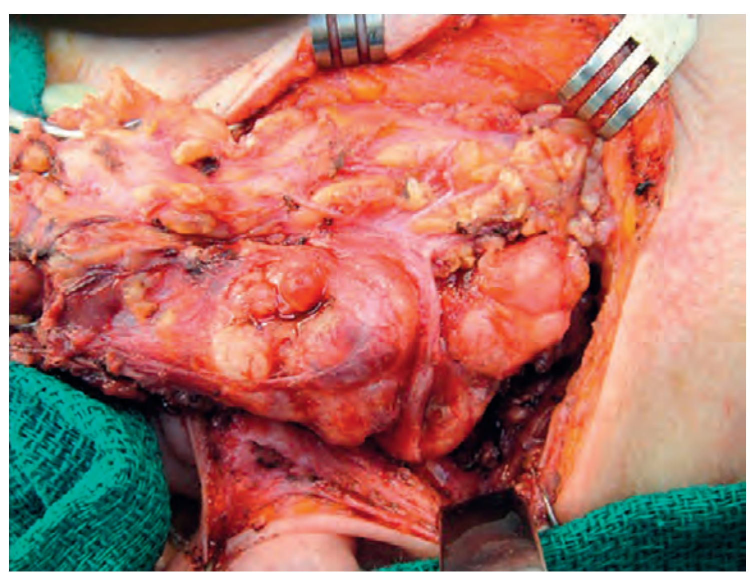

Figure 13.108 Intraoperative view showing nodular tumor growing from the deep parotid tissue into the superficial lobe both below and above the main trunk of the facial nerve.

Excision of a Deep Lobe Parotid Tumor

Most tumors arising in the salivary tissue medial to the facial nerve (deep lobe) are histologically benign. Deep lobe tumors may present in the retromandibular location or in the parapharyngeal location. To safely conduct the operative procedure for excision of a deep lobe parotid tumor, careful dissection of the facial nerve in its entirety is vitally important. The patient shown in Fig. 13.109 has an ill-defined firm rubbery mass in the retromandibular region of the right parotid gland. A CT scan performed after sialography of the left parotid gland shows a well-circumscribed tumor in the deep lobe, extending posterior to the ascending ramus of the mandible (Fig. 13.110).

The surgical approach for excision of a deep lobe tumor is similar to that for a tumor located in the superficial lobe of the parotid gland. The curvilinear incision begins in the preauricular skin crease and extends along an upper neck skin crease. The anterior skin flap is elevated to expose the lateral surface of the parotid gland. The posterior skin flap is elevated to expose the anterior border of the sternomastoid muscle (Fig. 13.111). After meticulous and careful dissection, the main trunk of the facial nerve is identified and a superficial parotidectomy is undertaken, as previously discussed. As the superficial lobe becomes elevated, the tumor situated deep to the facial nerve comes into view (Fig. 13.112). The superficial lobe is excised as a separate specimen, demonstrating the fully dissected facial nerve with all of its peripheral branches and the deep lobe tumor situated medial to the nerve, which is stretched tight because of the presence of the bulky tumor (Fig. 13.113).

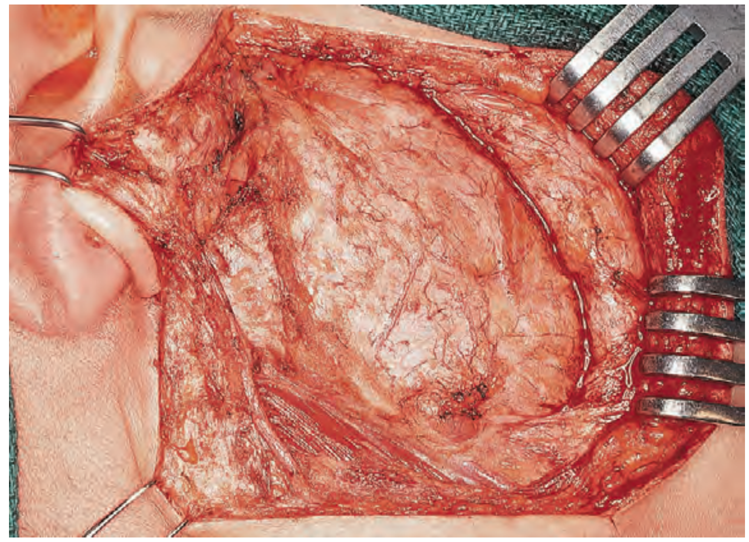

Figure 13.111 Skin flaps are elevated to expose the superficial lobe of the parotid gland.

Figure 13.109 A patient with an ill-defined, firm, retromandibular mass.

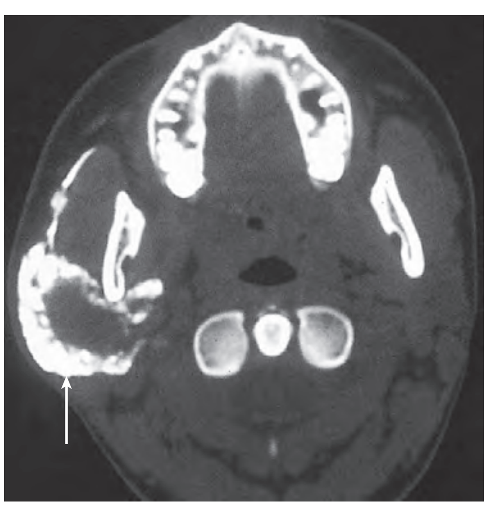

Figure 13.110 An axial view of a computed tomography scan after sialography shows a well-circumscribed tumor in the deep lobe of the right parotid gland (*arrow*).

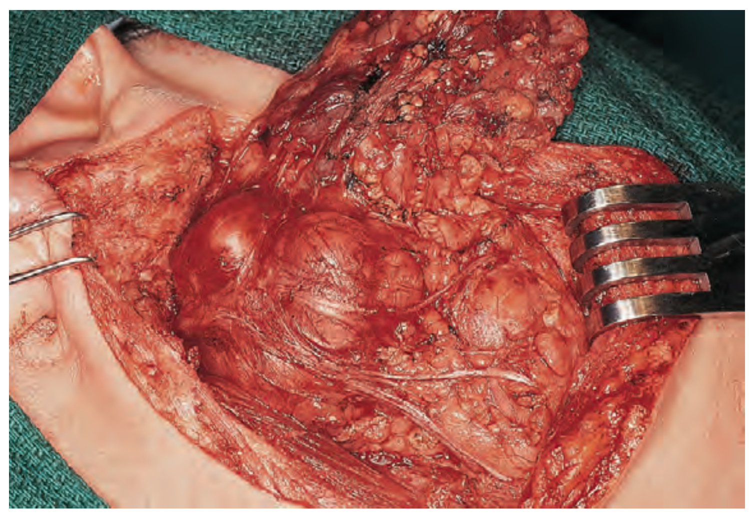

Figure 13.112 The main trunk of the facial nerve is identified, and its major divisions are dissected.

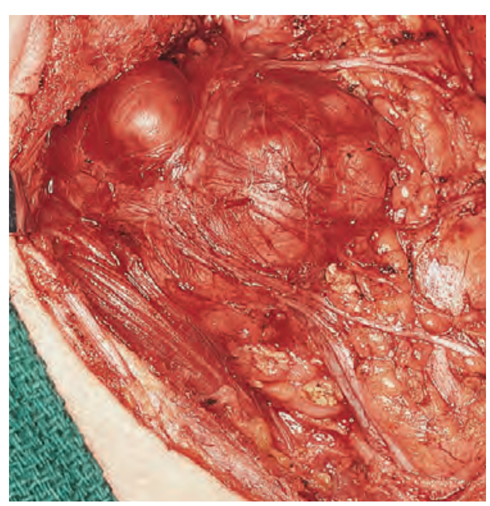

Figure 13.113 The superficial lobe of the parotid gland is removed to expose the deep lobe tumor medial to the facial nerve.

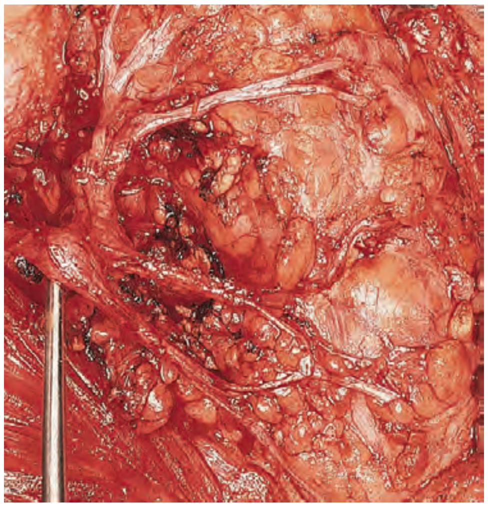

Figure 13.114 The deep lobe tumor is removed, and the facial nerve is preserved intact.

Figure 13.115 The surgical specimen shows a multilobulated rubbery tumor of the deep lobe.

Extremely delicate and meticulous dissection of the main trunk of the facial nerve and each of its peripheral branches is now undertaken, lifting the nerve off the tumor to permit adequate and safe mobilization of the underlying tumor mass. After each of the branches is completely freed from the tumor, nerve hooks are used to lift the nerve off the tumor, which is mobilized by digital dissection as well as sharp and blunt dissection throughout its circumference.

After removal of the tumor, the surgical field shows the entire facial nerve preserved intact. Because of the stretch caused by the tumor, the facial nerve is now quite lax; it is shown in Fig. 13.114 with its main trunk lifted by a nerve hook. The surgical specimen shown in Fig. 13.115 demonstrates a multilobulated rubbery tumor arising from the deep lobe, removed in a monobloc fashion.

Excision of a Deep Lobe Parotid Tumor in the Parapharyngeal Space

The tumor encountered most frequently in the deep lobe of the parotid gland is a mixed tumor. This tumor may present intraorally as a smooth submucosal mass displacing the lateral pharyngeal wall, tonsil, and soft palate anteromedially. The intraoral view of a patient with a deep lobe parotid tumor is shown in Fig. 13.116. Note the anteromedial displacement of the left side of the soft palate.

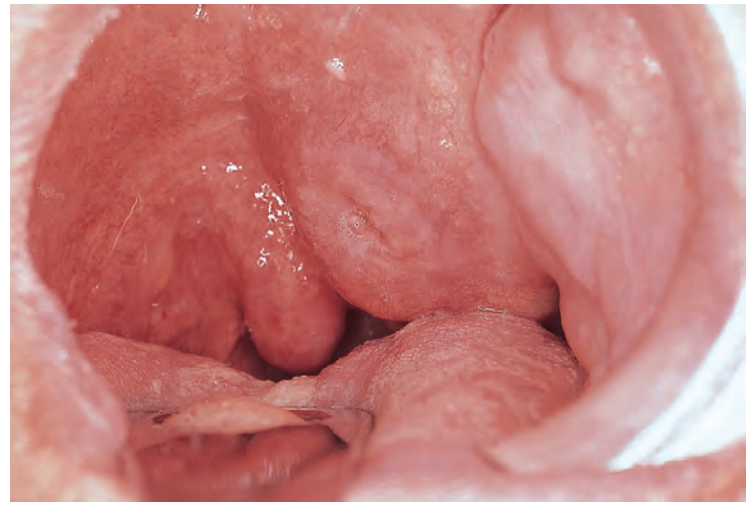

Figure 13.116 An intraoral view of a deep lobe parotid tumor presenting behind the soft palate.

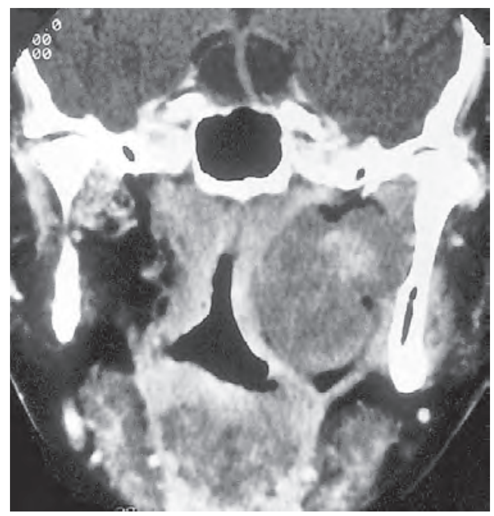

Figure 13.117 A coronal view of a computed tomography scan shows the tumor medial to the mandible.

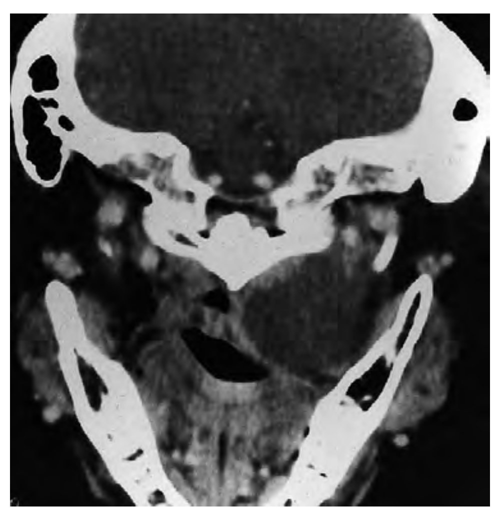

Figure 13.118 A coronal view of a computed tomography scan shows the tumor located medial to the styloid process and adjacent to the skull base.

A CT scan of the head in a coronal plane demonstrates a large tumor medial to the ascending ramus of the mandible displacing the lateral pharyngeal wall (Fig. 13.117). The tumor

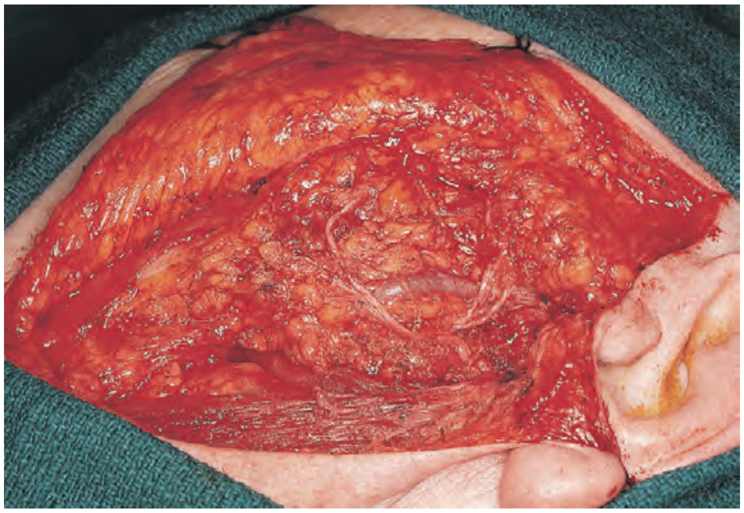

Figure 13.119 The superficial parotid lobectomy has been completed with dissection of the facial nerve.

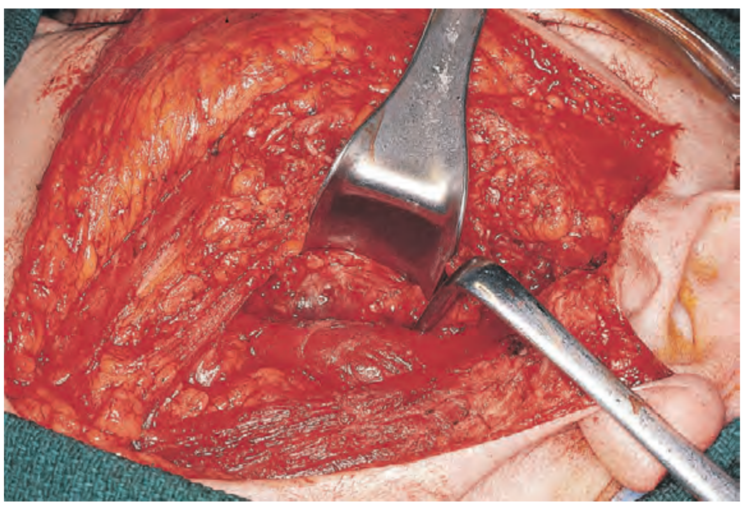

Figure 13.120 The main trunk of the facial nerve and its lower division are gently retracted cephalad over the angle of the mandible to expose the retromandibular region.

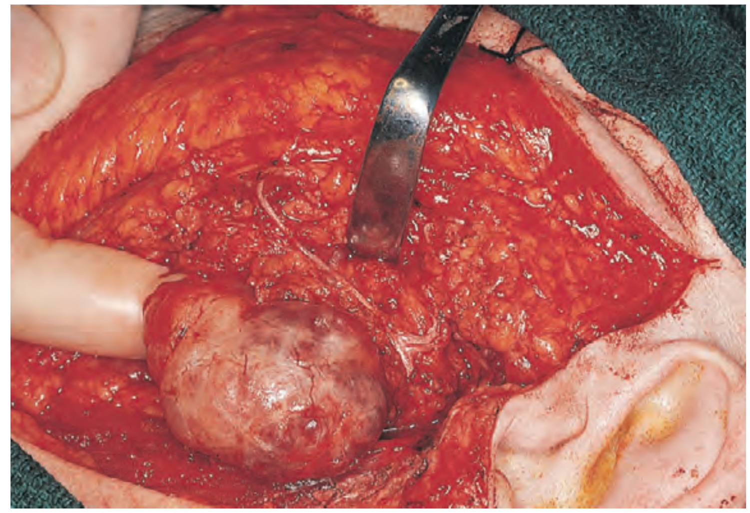

Figure 13.121 The tumor is mobilized circumferentially and is delivered through the retromandibular space.

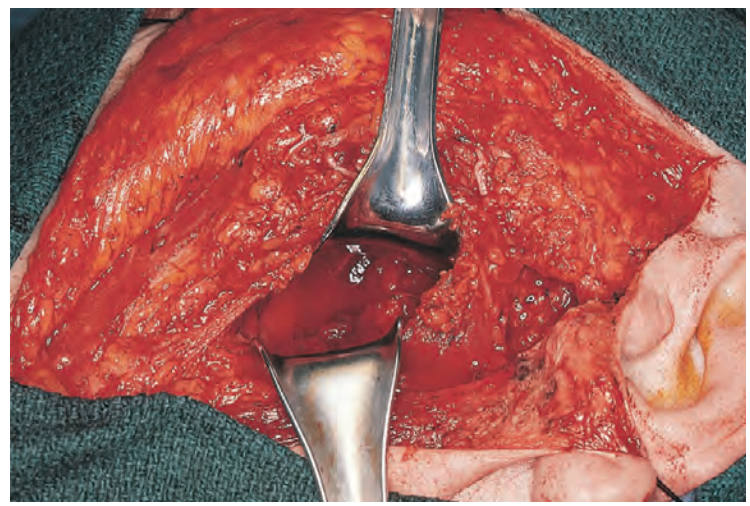

Figure 13.122 The bed of the tumor in the parapharyngeal space.

has a smooth outline but is inhomogeneous. A layer of fat is present between the tumor and the pharyngeal wall, signifying that the lesion is a deep lobe parotid tumor rather than a primary parapharyngeal tumor of neurovascular origin. A somewhat posterior cut of the CT scan shows that the tumor is adjacent to the base of the skull and medial to the styloid process (Fig. 13.118).

Most deep lobe tumors of the parotid gland can be removed via the external approach after a superficial lobectomy that is performed to identify, dissect, and carefully preserve the facial nerve. In Fig. 13.119, a superficial parotidectomy has been completed with dissection of all the branches of the facial nerve. It is now safe to proceed with removal of the deep lobe tumor, because the facial nerve, which is constantly under vision, remains protected.

With the use of a Richardson retractor, the main trunk of the facial nerve and its lower division are gently retracted cephalad over the angle of the mandible to expose the retromandibular region (Fig. 13.120). A right-angled retractor is used to retract the posterior belly of the digastric muscle caudad, providing exposure of the parapharyngeal space. Soft tissue and fibrous adhesions in this area are divided. The space created will permit digital dissection of the deep lobe tumor. Extreme care must be exercised, however, during digital dissection of this

Figure 13.123 The multilobulated rubbery mixed tumor of the deep lobe.

tumor in the parapharyngeal space, because rough handling may cause rupture of the tumor and spillage in the surgical field. Any tight bands of tissue around the tumor are sharply divided with scissors as digital dissection continues through the loose areolar plane in the parapharyngeal space around the tumor.

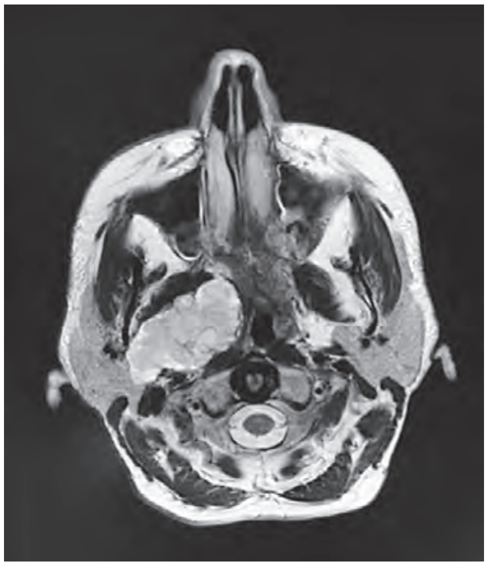

Figure 13.124 A T2-weighted magnetic resonance imaging scan shows a large multilobulated deep lobe parotid tumor in the parapharyngeal space.

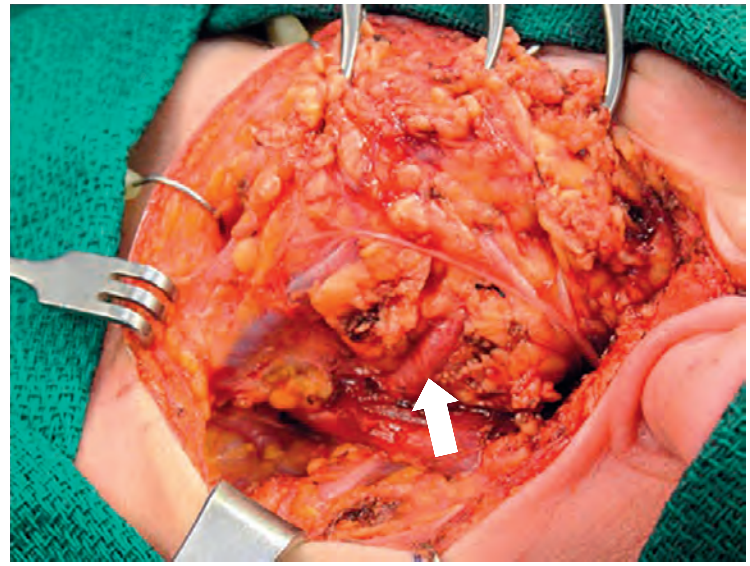

Figure 13.125 The external carotid artery (*arrow*) is tightly bound on the surface of the tumor.

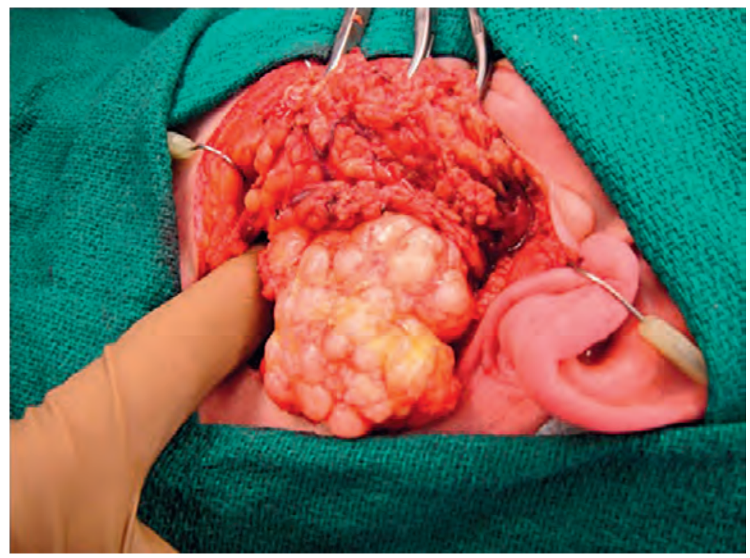

Figure 13.126 Gentle digital dissection in the parapharyngeal space allows delivery of all the nodules of the tumor intact.

Eventually the tumor is mobilized circumferentially and is delivered through the retromandibular space, as shown in Fig. 13.121. Meticulous attention is required for complete removal with delivery of an intact tumor; otherwise, local recurrence is assured. In Fig. 13.122, two Richardson retractors are used to demonstrate the bed of the tumor in the parapharyngeal space after its removal. Absolute hemostasis must be secured before closure. The wound is irrigated with Bacitracin solution. A Penrose drain is inserted, and the wound is closed in the usual fashion in two layers. The specimen of the excised tumor is shown in Fig. 13.123. Note the lobulated, firm, rubbery tumor removed intact via the external approach.

Even massive mixed tumors of the deep lobe of the parotid gland in the parapharyngeal space can be removed through this parotid/cervical approach. A T2-weighted MRI scan of a patient with a large tumor of the parapharyngeal space is shown in Fig. 13.124. Such large tumors displace the neurovascular structure in the parapharyngeal space as they grow bigger. The commonest among these is the external carotid artery, which is often stretched like a rubber band on the inferolateral part of the tumor cephalad to the posterior belly of the digastric muscle. An intraoperative view of the surgical field after dissection of the main trunk and buccal and lower divisions of the facial nerve clearly shows the stretched external carotid artery over the tumor (Fig. 13.125). The artery needs to be doubly clamped, divided, and ligated. It is essential to remember that, as the superior part of the tumor is being delivered, the distal part of the external carotid artery emerging from the upper end of the tumor will also need to be divided again, and its distal end ligated. This maneuver allows for easy mobilization of the tumor and minimizes blood loss. Once the proximal part of the external carotid artery is divided, mobilization of the tumor in the parapharyngeal space by gentle digital dissection continues. The loose areolar tissue in the parapharyngeal space permits easy dissection. However, this must be a very careful and gentle dissection, without rupturing a cystic tumor or fracturing a multinodular solid tumor. After complete mobilization, the tumor is delivered from the retromandibular space (Fig. 13.126). In this patient a complete superficial parotidectomy was not necessary, since the important divisions of the facial nerve were dissected and were in constant view during mobilization and delivery of the deep lobe tumor. The surgical field after removal of the tumor shows the open space in the parapharyngeal region occupied by the tumor (Fig. 13.127). Note that all the dissected branches of the facial nerve are intact. The elevated portion of the superficial lobe of the parotid will be returned to its normal position and anchored to the posterior belly of the digastric muscle and preauricular soft tissues with a few interrupted absorbable sutures. A Penrose drain is inserted in the deep parotid space, and the wound is closed in layers. Complete removal of the tumor is accomplished in a monobloc fashion (Fig. 13.128). Note that all of the nodules of this multilobulated tumor are removed carefully in a monobloc fashion. Removal of the deep lobe tumor via the external approach is not possible in some patients because of the size of the tumor or dense adhesions, particularly in patients with a recurrent or malignant tumor or when a previous attempt has been made at removal or biopsy through a peroral approach. In that setting, a mandibulotomy with paralingual extension should be considered to gain access

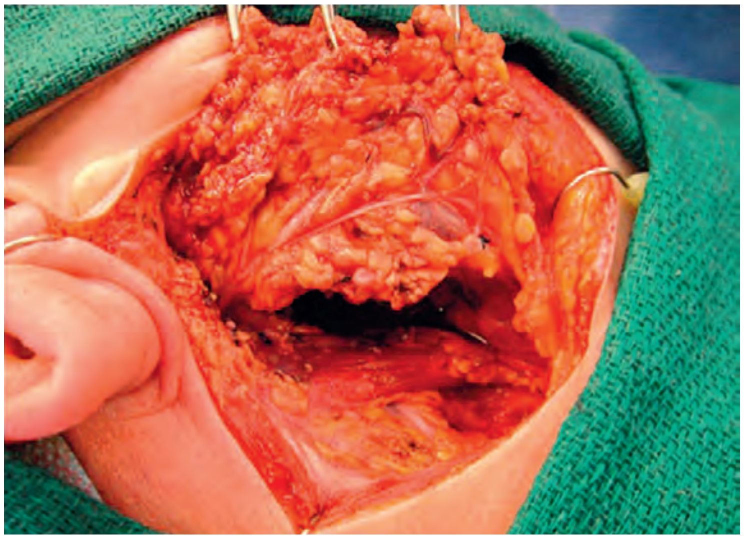

Figure 13.127 Surgical field following the removal of the tumor shows the space occupied by the tumor in the parapharyngeal area, intact lower division of the facial nerve, and superficial lobe of the parotid gland.

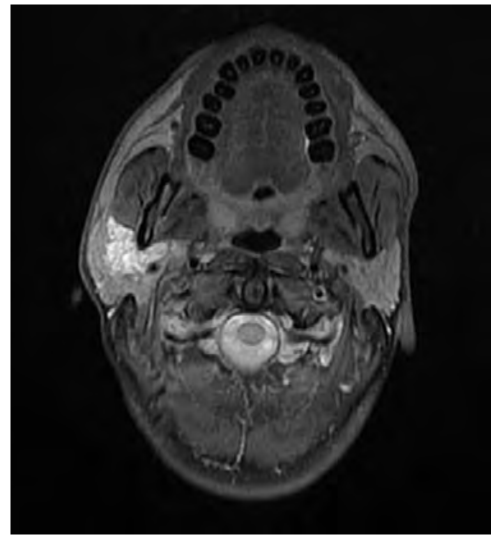

Figure 13.129 A T2-weighted magnetic resonance imaging scan shows a vascular lesion in the deep parotid region with a honeycomb appearance.

Figure 13.128 Surgical specimen shows monobloc removal of the multilobulated nodular deep lobe tumor.

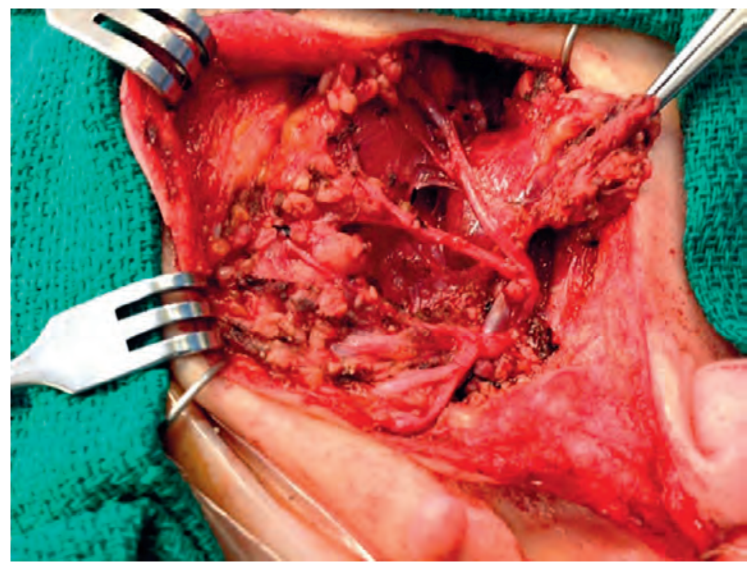

Figure 13.130 Hemangioma of the deep lobe being delivered from under the upper division of the facial nerve.

to and exposure of the parapharyngeal space for delivery of the intact tumor.

Excision of Hemangioma of the Deep Lobe of the Parotid

Occasionally nonsalivary tumors of lymphovascular origin arise in the parotid gland. A T2-weighted MRI of a patient with a hemangioma in the deep lobe of the parotid is shown in Fig. 13.129. Note the honeycomb appearance of the tumor, which is characteristic of a multiloculated vascular lesion. The principles of parotid gland surgery remain the same even in these highly vascular lesions. Meticulous hemostasis, gentle dissection, and identification and preservation of the facial nerve without any stretch neuropraxia are the hallmarks of safe surgery. The tumor in this patient was located in the upper half of the deep lobe of the parotid gland. An intraoperative view of the surgical field shows complete dissection of the facial nerve, with the tumor of the deep lobe remaining attached to the superficial parotid lobe and being delivered from above the main trunk of the nerve (Fig. 13.130). The surgical field after removal of

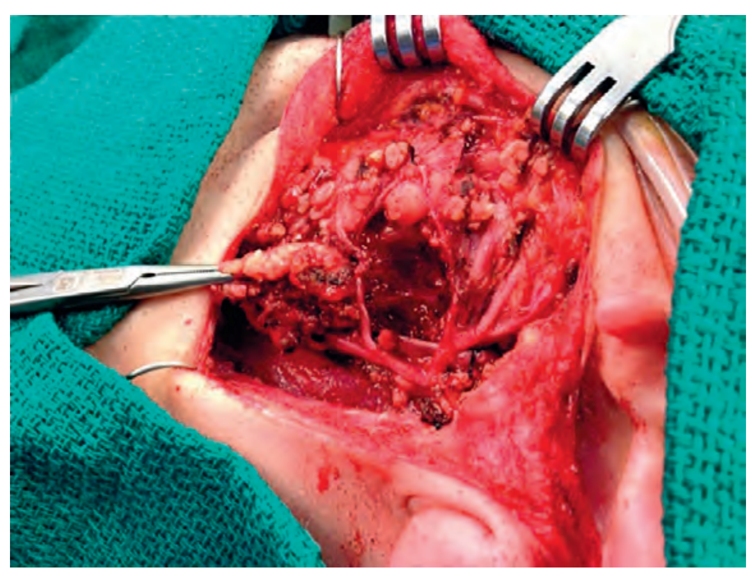

Figure 13.131 Surgical field following removal of the tumor shows the dead space occupied by the tumor in the deep parotid tissue with intact facial nerve.

the tumor shows all branches of the facial nerve intact and the dead space in the deep parotid region after removal of the tumor (Fig. 13.131).

Excision of an Accessory Parotid Tumor

Occasionally, primary tumors may arise in the accessory salivary tissue located along the course of the Stensen's duct in the soft tissues of the cheek. These tumors therefore should be included in the differential diagnosis of masses of the soft tissues of the cheek. The patient shown in Fig. 13.132 has a 2.5-cm, firm, rubbery, nodular, mobile mass in the cheek. Facial nerve function is intact. Although dissection of the facial nerve before excision of the accessory parotid tumor is a safe approach, occasionally a small accessory parotid tumor can be removed without a formal superficial parotidectomy.

An MRI scan in the axial and coronal planes shows a well-circumscribed mass in the soft tissues of the cheek just anterior to the anterior border of the parotid gland overlying the masseter muscle (Figs. 13.133 and 13.134).

In general it is a sound policy to proceed with a superficial parotidectomy first in order to dissect and protect the facial nerve and then excise the tumor. A superficial parotidectomy is clearly indicated if the tumor arises from the anterior aspect of the superficial lobe parotid tissue. The outline of the proposed incision is shown in Fig. 13.135. Note that the incision is much longer than a routine superficial parotidectomy, because exposure of the anterior soft tissues of the cheek is necessary. Thus anterior extension cephalad and inferior extension caudad of the standard parotid incision are necessary. After elevation of the anterior skin flap, diligent dissection for identification of the peripheral ends of the zygomatic and buccal branches is undertaken before excision of the tumor.

In Fig. 13.136, a superficial parotidectomy with excision of the tumor is completed. The surgical field shows the facial nerve with all its branches. Note particularly the zygomatic and buccal branches of the facial nerve traced all the way to their entry into the facial muscles. The tendon of the masseter muscle that forms the bed of the tumor is exposed. The zygomatic and buccal branches of the facial nerve were in the immediate vicinity of the tumor. The specimen shown in Fig. 13.137 demonstrates a small primary tumor of the accessory parotid tissue with the remaining superficial lobe grossly normal.

Figure 13.132 A patient with a firm, rubbery, nodular, mobile mass in the cheek.

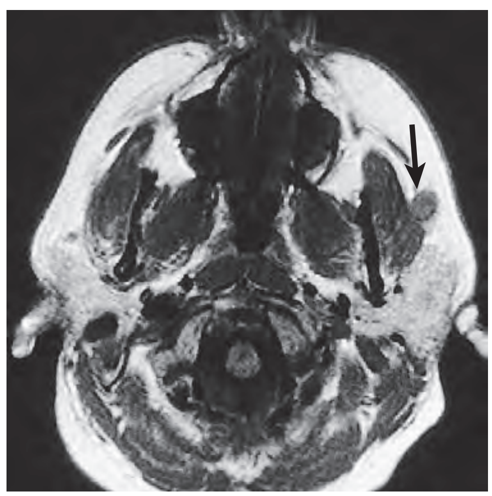

Figure 13.133 An axial view of a magnetic resonance imaging scan shows the tumor anterior to the parotid gland along the course of the Stensen duct (*arrow*).

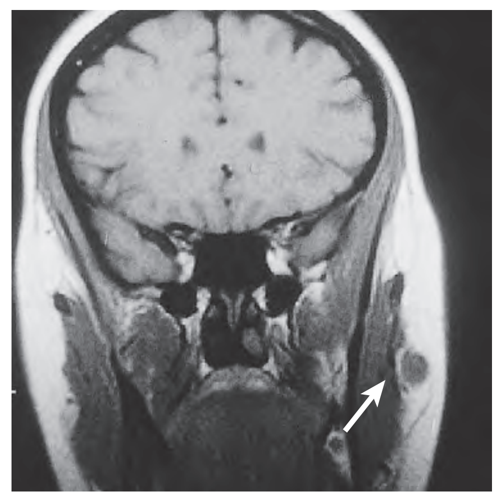

Figure 13.134 A coronal view of the magnetic resonance imaging scan shows the tumor overlying the masseter muscle (*arrow*).

Figure 13.135 The outline of the proposed incision.

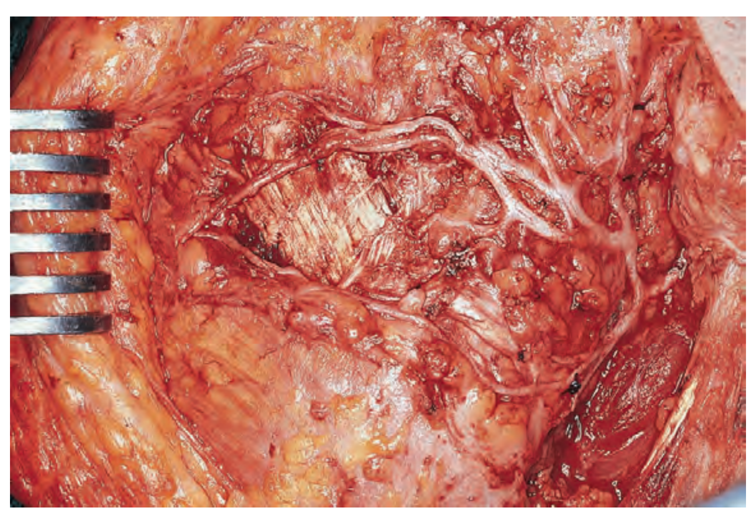

Figure 13.136 The excision of the tumor is completed with a superficial parotidectomy.

Figure 13.137 The surgical specimen of an accessory parotid tumor.

Excision of Accessory Parotid Tumor Without Superficial Parotidectomy

It is not always necessary to perform a superficial parotidectomy for an accessory parotid tumor. If the accessory tumor is discrete and separate from the substance of the superficial lobe of the parotid gland, then a formal superficial parotidectomy can be avoided. The CT scan with contrast of a patient with an accessory parotid tumor is shown in Fig. 13.138. Note that the tumor is discrete and completely detached from the main mass of the parotid gland. In such a situation the tumor can be excised without a formal superficial parotidectomy. However, it must be emphasized that meticulous and diligent dissection should be undertaken to identify and carefully preserve the buccal and zygomatic branches of the facial nerve in their distal part as they emerge from the anterior border of the parotid gland. The surgical field in this patient demonstrates that the anterior skin flap is elevated beyond the anterior border of the superficial lobe, and the zygomatic and buccal branches of the facial nerve emerging from the parotid gland are identified and dissected to separate them from the small accessory parotid tumor that is mobilized and being delivered (Fig. 13.139). The tumor is located between two branches of the facial nerve as well as directly overlying the Stensen's duct. In most instances the Stensen's duct is able to be preserved. The surgical field after removal of the tumor shows the preserved facial nerve branches and the Stensen's duct between them (Fig. 13.140).

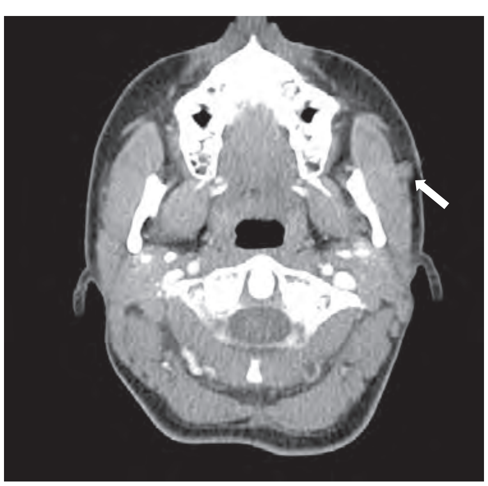

Figure 13.138 Contrast-enhanced computed tomography scan shows a well-demarcated tumor in the soft tissues of the cheek (*arrow*) in the location of the accessory parotid tissue. Note there is no continuity of the tumor to the superficial lobe of the parotid gland.

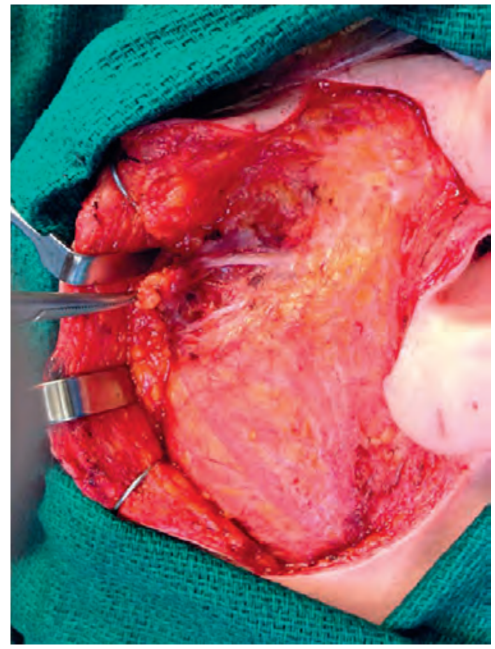

Figure 13.139 The surgical field shows dissection of the zygomatic and buccal branches of the facial nerve at the periphery of the parotid gland and delivery of the tumor from between these two branches.

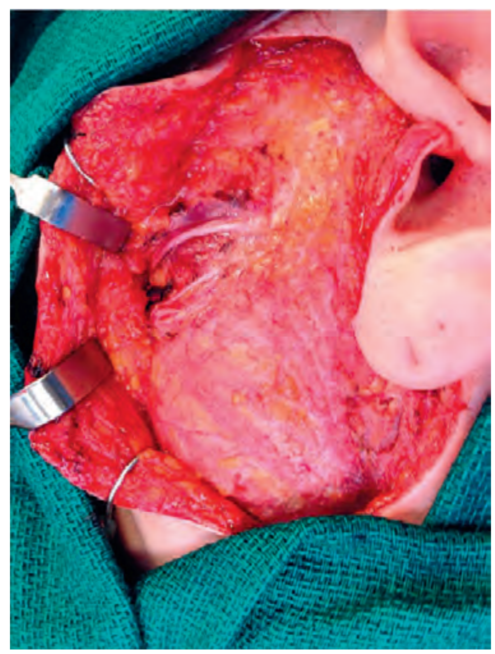

Figure 13.140 The surgical field following removal of the tumor showing intact zygomatic and buccal branches of the facial nerve and the Stenson's duct in between.

Excision of a Warthin's Tumor of the Parotid Gland

A Warthin's tumor (papillary cystadenoma lymphomatosum) is a benign lesion of the parotid gland that usually is found in young men adjacent to the tail of the parotid gland and its periphery. Approximately 10% of Warthin's tumors occur in women. If the lesion is small and at the very periphery of the parotid gland, adequate excision of the tumor can be accomplished without the need for a formal superficial parotid lobectomy with dissection of the facial nerve. However, for larger lesions, as seen in the patient in Fig. 13.141, a superficial parotidectomy with dissection of the facial nerve is considered appropriate.

The CT scan of the patient (Fig. 13.142) shows a well-circumscribed mass involving the region of the tail of the parotid

Figure 13.141 A large, soft, cystic mass near the tail of the parotid gland.

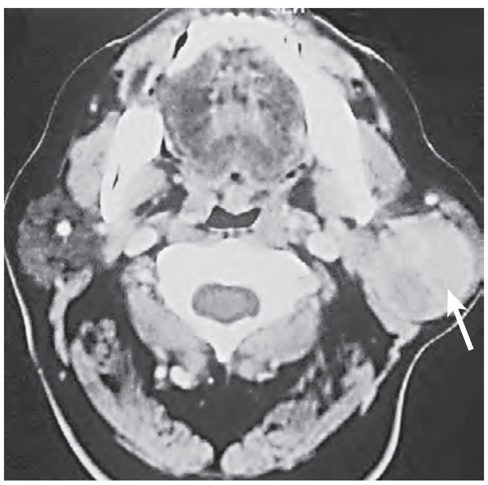

Figure 13.142 A computed tomography scan shows a centrally necrotic hypodense mass (*arrow*).

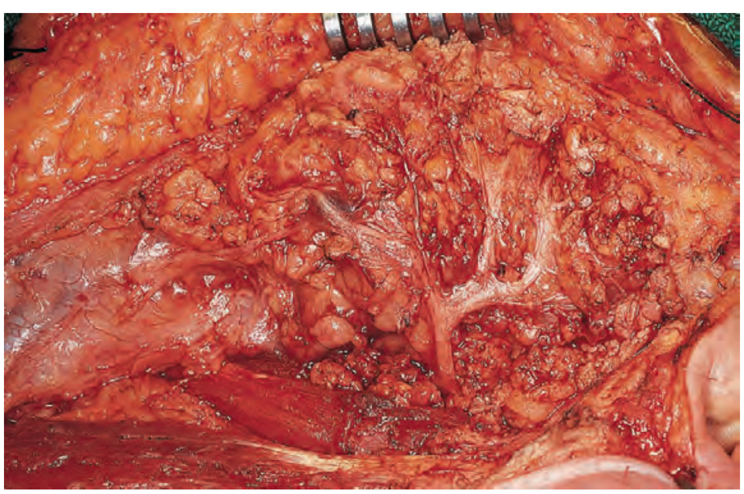

Figure 13.143 Superficial parotidectomy.

gland in the superficial lobe with a hypodense area in the center, signifying the presence of fluid or necrotic material. A superficial parotidectomy is performed in the usual fashion with resection and preservation of the facial nerve (Fig. 13.143). The surgical specimen, which was removed in a monobloc fashion with the intact cystic lesion, is shown in Fig. 13.144. Upon bisecting the specimen, thick cheesy fluid is found in the cystic lesion (Fig. 13.145). The cystic lesion on occasion can be multiloculated. Approximately 10% of Warthin's tumors

Figure 13.144 The intact surgical specimen.

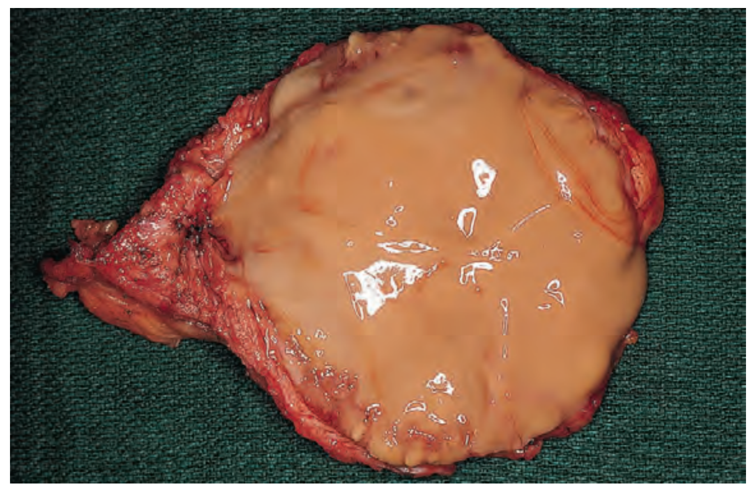

Figure 13.145 The bisected specimen shows cheesy material.

are bilateral, and very rarely they involve the deep lobe of the parotid gland.

Surgery for Chronic Cystic Parotitis

Patients with recurrent episodes of infection in the parotid gland have an increased risk of further episodes of recurrent parotitis with formation of loculi or cysts in a manner similar to that observed in patients with bronchiectasis. These patients have chronic cystic spaces that are sanctuaries of infected secretions, cellular debris, and nondraining salivary pockets that lead to recurrent episodes of infection and abscess formation. The patient whose CT scan is shown in Fig. 13.146 had recurrent episodes of parotitis for 3 years that were treated conservatively with antibiotics without resolution of her symptoms. The frequency and the intensity of her recurrent episodes of parotitis increased during the past year, and hence a decision was made to proceed with a parotidectomy.

If a parotidectomy is to be undertaken for recurrent parotitis, it should be done at an optimal time when no signs of acute inflammation are present (i.e., all induration, tenderness, and inflammatory response has subsided; the patient's total white blood cell count is normal; and clinically no tender spots are present). The patient had several palpable nodules in the superficial lobe of the parotid gland, each signifying a loculated cystic space from previous episodes of parotitis (Fig. 13.147). The surgical procedure of parotidectomy in patients with

Figure 13.146 An axial view of a contrast-enhanced computed tomography scan showing a multiloculated cystic mass in the left parotid gland.

Figure 13.147 Multiple palpable nodules in the left parotid gland.

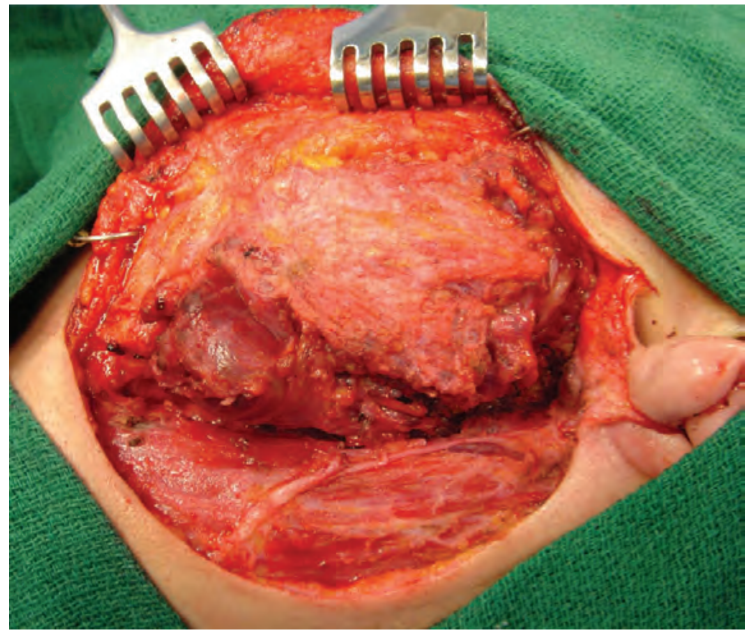

Figure 13.148 The bifurcated greater auricular nerve allowing preservation of its posterior branch.

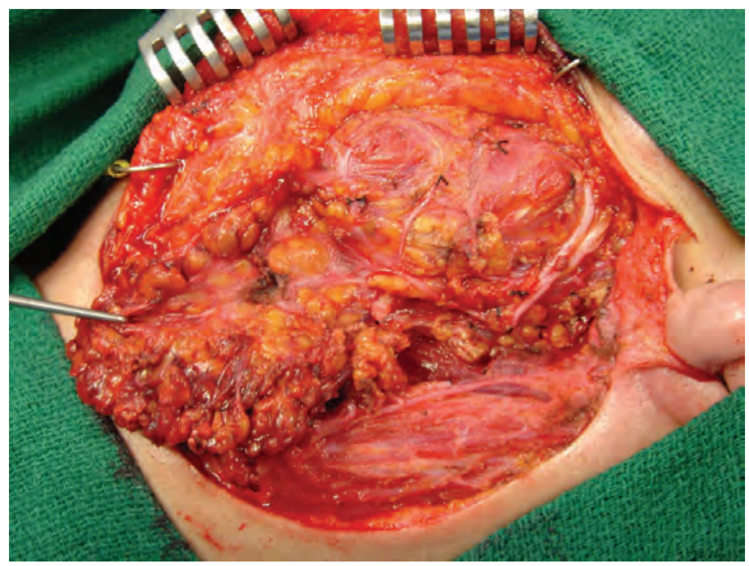

Figure 13.149 Dissection and preservation of the facial nerve are completed.

recurrent parotitis is a much more hazardous, tedious, and difficult procedure because of the inflammatory response and intense fibrosis. Therefore extreme caution should be exercised in identifying, dissecting, and preserving the facial nerve. Facial nerve monitoring may be a useful adjunct in such situations.

The surgical exposure is undertaken in the usual fashion with a tragal incision and postauricular upper cervical extension. Note that the greater auricular nerve in this patient had a bifurcation allowing preservation of its posterior branch, which would retain sensation to the external ear (Fig. 13.148). All possible loculi of the cystic spaces should be excised, and therefore it should be a "complete" parotidectomy, leaving essentially no parotid tissue behind. The facial nerve in its upper division has been identified and preserved, lifting off all the parotid tissue, bringing it caudad toward the most prominent area of multiple cystic nodules in the superficial lobe of the left parotid gland (Fig. 13.149). The surgical field following removal of all parotid tissue shows a preserved facial nerve with the masseter muscle underneath, clearing the entire parotid bed of all infected parotid tissue and cystic spaces (Fig. 13.150).

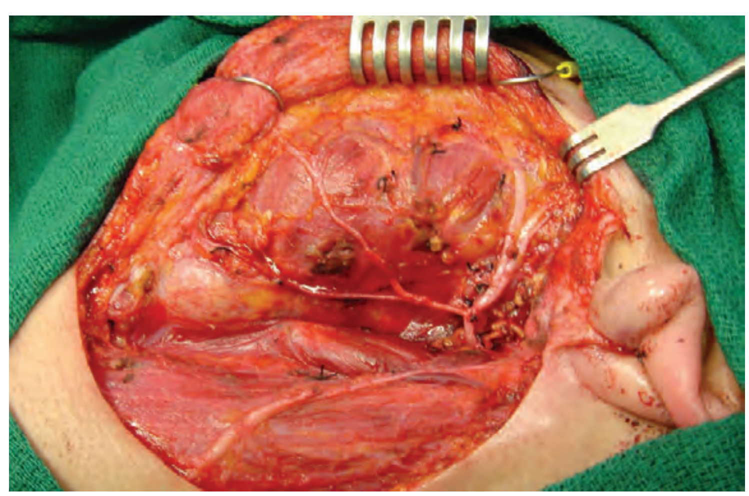

Figure 13.150 The surgical field after resection of all parotid tissue.

Figure 13.151 The surgical specimen showing multiple cystic spaces.

This degree of diligence is essential if future episodes of recurrent parotitis are to be avoided.

The bisected surgical specimen shows multiple cystic spaces and granulomatous lesions throughout the parotid substance, consistent with a classic picture of chronic cystic parotitis (Fig. 13.151).

Excision of a Recurrent Mixed Tumor (Pleomorphic Adenoma) of the Parotid Gland

Local recurrence of a mixed tumor of the parotid gland is rare if the initial operation is a complete superficial parotidectomy. However, local recurrence is seen quite frequently when the initial operation is enucleation or only a local excision. Local recurrence of a mixed tumor may occur in a unifocal or a multifocal fashion. Unifocal recurrence is usually seen in patients who previously have undergone enucleation of a benign mixed tumor in the superficial lobe or a local excision without a formal superficial parotidectomy (Fig. 13.152). On the other hand, multifocal recurrence, with tumor nodules even involving the overlying skin, is usually the case in patients who have undergone a previous superficial parotidectomy. The operative procedure for excision of a recurrent benign mixed tumor is relatively easy if the previous operation was only a local excision of the tumor. On the other hand, multifocal recurrence after a superficial parotidectomy is indeed a technically demanding and difficult operative procedure with significant risk of injury to the facial nerve.

Figure 13.152 Multinodular unifocal recurrent benign mixed tumor following enucleation of the tumor previously.

Figure 13.153 This patient had previously undergone two operative procedures for the excision of benign mixed tumors.

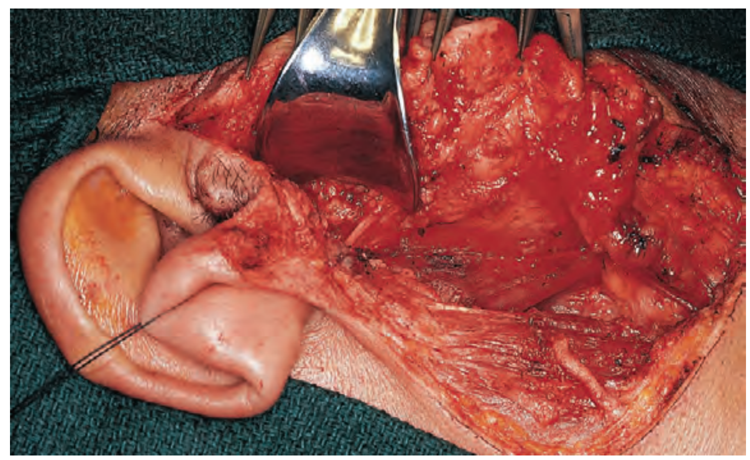

Figure 13.154 The main trunk of the facial nerve is identified.

The patient shown in Fig. 13.153 had previously undergone two operative procedures. The initial operation was a local excision of a benign mixed tumor and the second procedure was also a local excision for a recurrent tumor. At the time of presentation, the patient had multifocal recurrence of his tumor involving the preauricular skin and the remaining parotid gland. Adherence of the tumor nodules to the preauricular skin mandates its sacrifice along with excision of all previous scars.

The area of skin to be excised is outlined along with a posteriorly based cervical flap that will be rotated cephalad to repair the skin defect. The operative procedure progresses in the standard fashion with the posterior skin incision taken through the preauricular skin crease and separating the lower border of the surgical specimen from the superior border of the cervical flap. After identification of the anterior border of the sternomastoid muscle, the posterior belly of the digastric muscle, the mastoid process, and the auditory canal, the main trunk of the facial nerve could be identified easily (Fig. 13.154). It soon became apparent that the facial nerve in this patient was never dissected during the course of his previous operations.

The remainder of the operation proceeds in the usual way, with careful identification of the peripheral branches of the facial nerve. After removal of the specimen, the surgical field shows a completely intact facial nerve with all its peripheral

branches meticulously dissected (Fig. 13.155). The specimen shown in Fig. 13.156 demonstrates multiple recurrent tumor nodules involving the subcutaneous tissue and the underlying superficial lobe of the parotid gland. The postoperative appearance of the patient shows an aesthetically acceptable well-healed scar and normal function of the facial nerve on the right-hand side (Fig. 13.157).

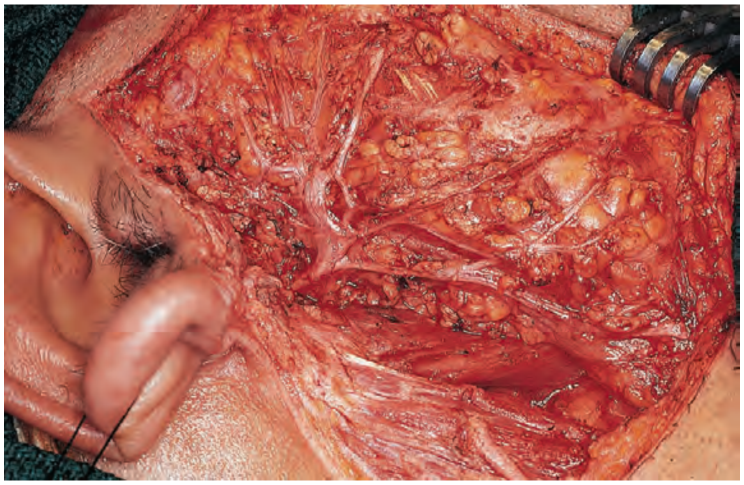

Figure 13.155 The surgical field after removal of the specimen.

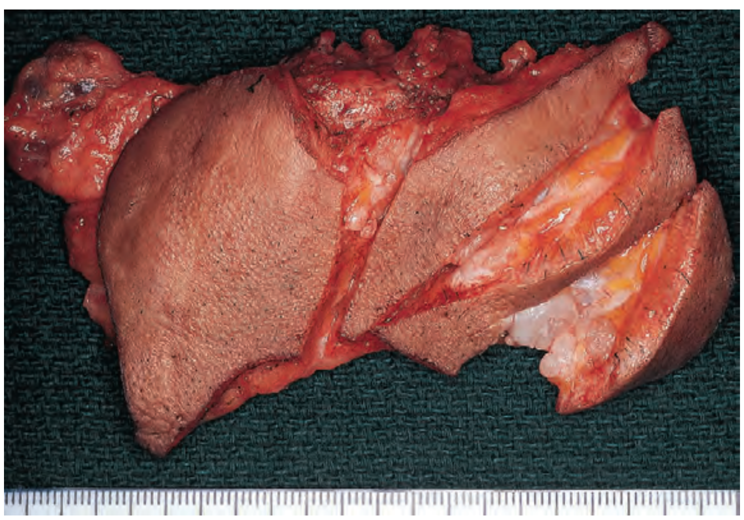

Figure 13.156 The surgical specimen showing a multifocal, recurrent, benign mixed tumor.

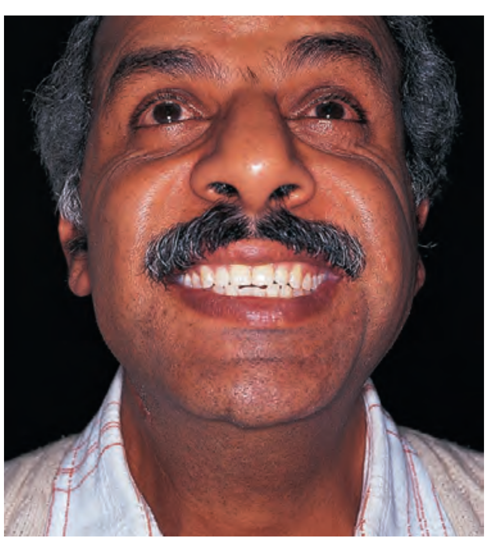

Figure 13.157 The postoperative appearance of the patient.

Total Parotidectomy for Multifocal Recurrent Pleomorphic Adenoma Involving Both Superficial and Deep Lobes of the Parotid Gland

The patient shown in Fig. 13.158 had undergone two previous operations, requiring superficial parotidectomy each time. Within 3 years of her last operation, she noted appearance of new tumor nodules. Clinical examination showed multiple firm tumor nodules throughout the parotid space extending from the zygoma to the midcervical region. Her facial nerve function was intact with only minor weakness in the mandibular branch of the nerve. Her T2-weighted MRI scan showed multiple tumor nodules involving both the superficial and deep parotid lobes and into the parapharyngeal space (Fig. 13.159). Situations like these are extremely difficult cases, and thorough preoperative discussion with the patient is essential for an informed consent, particularly with reference to the function of the facial nerve. The patient should also be counseled regarding the need for postoperative radiotherapy to reduce the risk of further recurrence.

Figure 13.158 Third recurrence of benign mixed tumor with multiple firm nodules extending from the zygoma to the midcervical region.

Figure 13.159 Coronal view T2-weighted MRI shows multiple tumor nodules occupying the superficial as well as the deep lobe of the parotid gland.

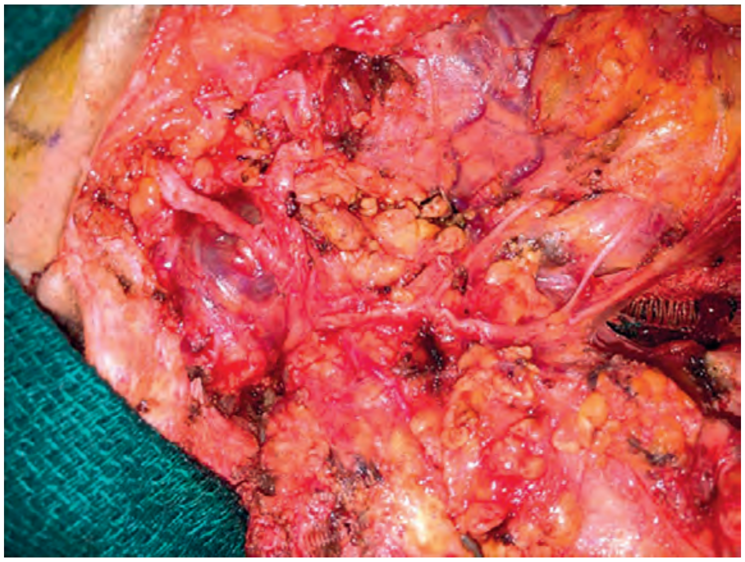

Figure 13.160 Intraoperative view showing dissection of the facial nerve and mobilization of recurrent tumor nodules of the superficial lobe caudad with the plan to remove deep lobe nodules from under the facial nerve.

The operation in this case requires a meticulous and thorough dissection of all tumor nodules as well as all remaining parotid tissue. In addition, nerve monitoring in situations like this is crucial and must be at hand. Locating the facial nerve and preserving each of its branches will be an arduous task. Operation in this patient begins in the usual fashion to identify the main trunk of the facial nerve and trace each of its branches peripherally (Fig. 13.160). As the nerve branches are being identified and dissected peripherally, all the surrounding parotid tissue is removed systematically, encompassing all recurrent tumor nodules. The dissection proceeds in a cephalocaudad fashion, beginning at the zygomatic process and mobilizing the specimen caudad, as facial nerve dissection proceeds from branch to branch. It is not possible to remove all tumor nodules in this patient in a monobloc fashion and still preserve the facial nerve. Therefore a superficial parotidectomy is done first. Once the facial nerve is dissected and preserved, systematic dissection of all recurrent tumor nodules and parotid tissue in the deep lobe is undertaken. The surgical field at the conclusion of the operation shows complete preservation of all branches of the facial nerve with gross removal of all tumor nodules (Fig. 13.161). This patient will need postoperative radiation therapy to reduce the risk of further recurrence.

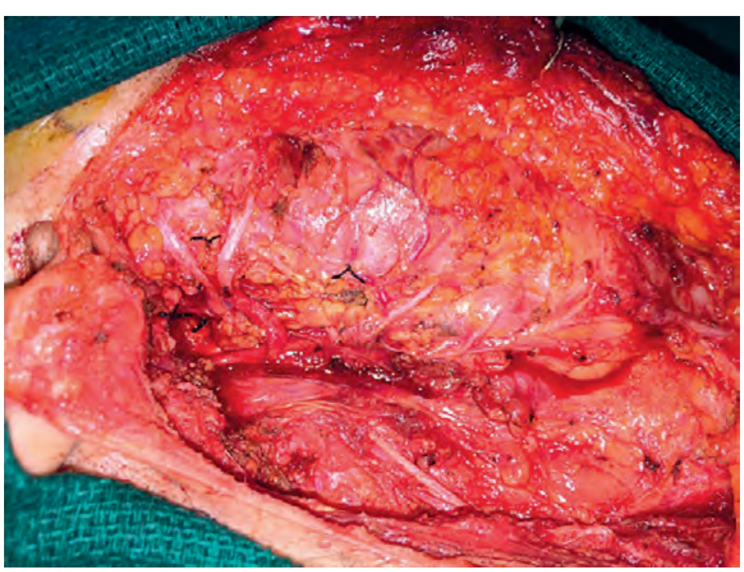

Figure 13.161 The surgical field following removal of all tumor nodules showing an intact facial nerve and all its branches.

Radical Parotidectomy With Resection of the Facial Nerve and Nerve Graft

Malignant tumors of the parotid gland require radical resection with adequate soft-tissue margins. Sacrifice of the facial nerve, however, requires several considerations. If the primary malignant tumor is located in the superficial lobe of the parotid gland, is small, and is contained within the salivary tissue with no gross extension to the facial nerve, then sacrifice of the facial nerve cannot be justified. On the other hand, if the facial nerve is preoperatively paralyzed, then no reason exists to preserve it when an operation is undertaken for a malignant tumor. If the facial nerve function is intact preoperatively but the primary malignant tumor of the parotid gland grossly involves the nerve, then sacrifice of the facial nerve is mandatory. Consideration should be given to grafting of the facial nerve with a nerve graft if, after resection of a segment of the facial nerve, the proximal and distal stumps are available for anastomosis and are histologically confirmed as being uninvolved by tumor.

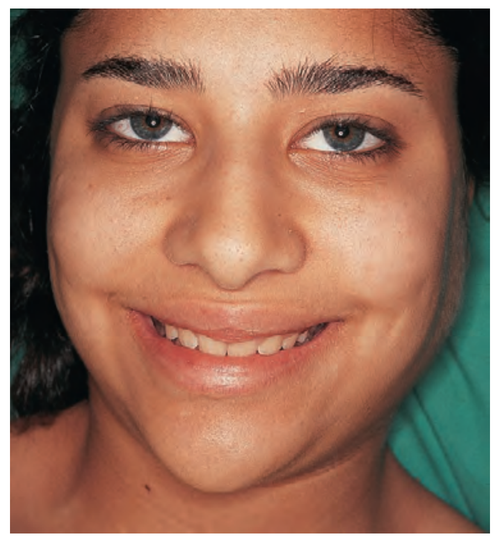

Figure 13.162 A preoperative photograph of the patient with an adenoid cystic carcinoma of the left parotid gland.

The patient shown in Fig. 13.162 had an adenoid cystic carcinoma that had been diagnosed erroneously as a benign mixed tumor. An attempt at a superficial parotidectomy was undertaken. However, because of the extensive infiltrative nature of the tumor, an open biopsy was performed and the operative procedure was terminated. The palpable extent of the tumor with the scar of her previous attempted parotidectomy is shown in Fig. 13.163. The tumor measured approximately 6 by 5 cm on palpation and had slightly reduced mobility.

The operative procedure begins with the standard curvilinear incision for a parotidectomy, with excision of the scar of her previous operative procedure. The anterior skin flap is elevated superficial to the platysma to expose the tumor. Meticulous dissection is undertaken to identify the main trunk of the facial nerve at its exit from the stylomastoid foramen, just anteroinferior to the auditory canal and adjacent to the superior border of the posterior belly of the digastric muscle. The upper division of the facial nerve could be dissected easily with preservation of the zygomatic and temporal divisions and their

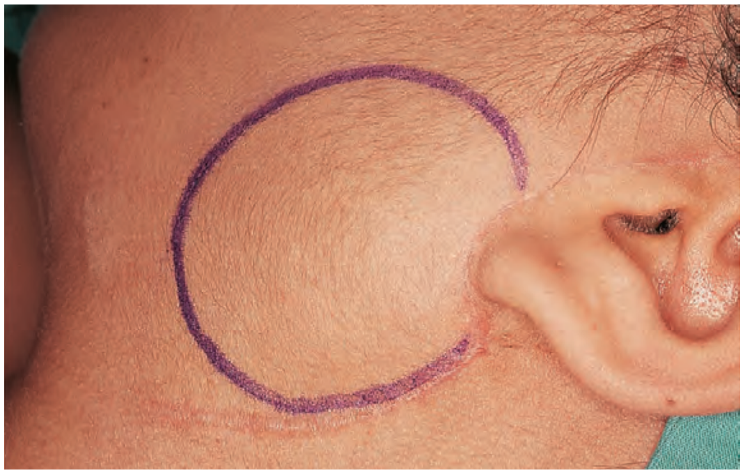

Figure 13.163 The tumor of the patient shown in Fig. 13.162 measured 5 by 6 cm.

peripheral branches (Fig. 13.164). At this juncture, it becomes evident that the lower division of the facial nerve is totally encased by the tumor, which has infiltrated the superficial fibers of the masseter muscle. Therefore a decision is made to sacrifice the lower division of the facial nerve, including the mandibular and cervical branches.

The lower division of the facial nerve is transected proximal to the tumor, and a margin is examined by frozen section to rule out invasion by adenoid cystic carcinoma. Peripheral ends of the buccal, mandibular, and cervical branches are identified and appropriately tagged with fine silk sutures, and the tumor is then resected in a monobloc fashion with the lower division of the facial nerve. The surgical field after removal of the tumor is shown in Fig. 13.165. Note that the posterior aspect of the masseter muscle has been excised, exposing the lateral cortex of the mandible near its angle. Gross total resection of the tumor is thus accomplished.

After ensuring that the proximal and the distal ends of the transected nerve are histologically free of carcinoma, a nerve graft procedure is undertaken. The donor nerve may be harvested from the peripheral cutaneous branches of the cervical plexus. The most readily available segment of the nerve is the greater auricular nerve with its adjacent cutaneous branches. If that segment is not believed to be suitable, then a graft is harvested from the sural nerve.

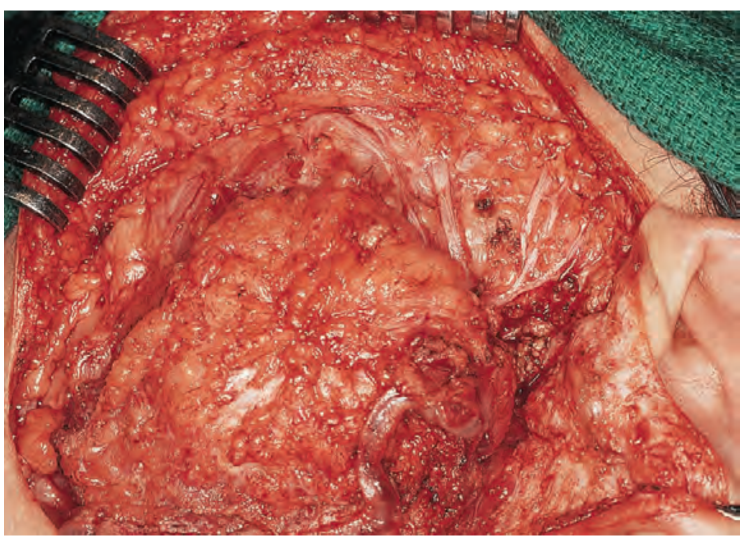

Figure 13.164 The upper division of the facial nerve could be dissected and preserved.

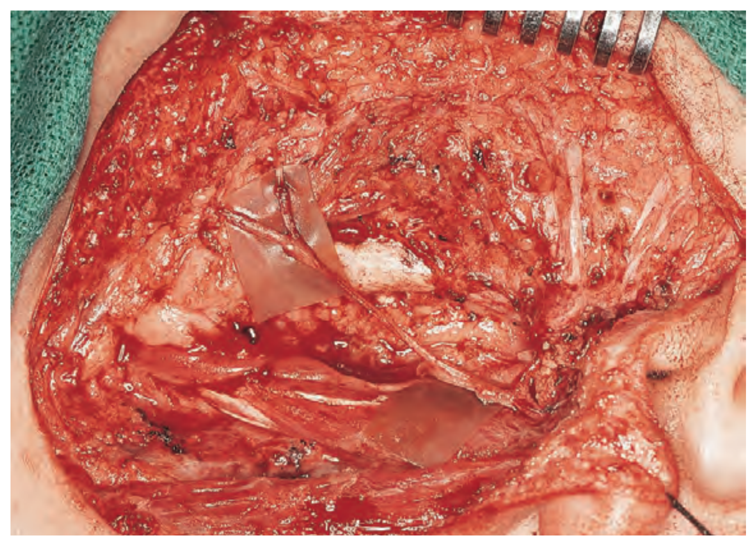

Figure 13.166 Reconstruction of the lower division of the facial nerve with a sural nerve graft.

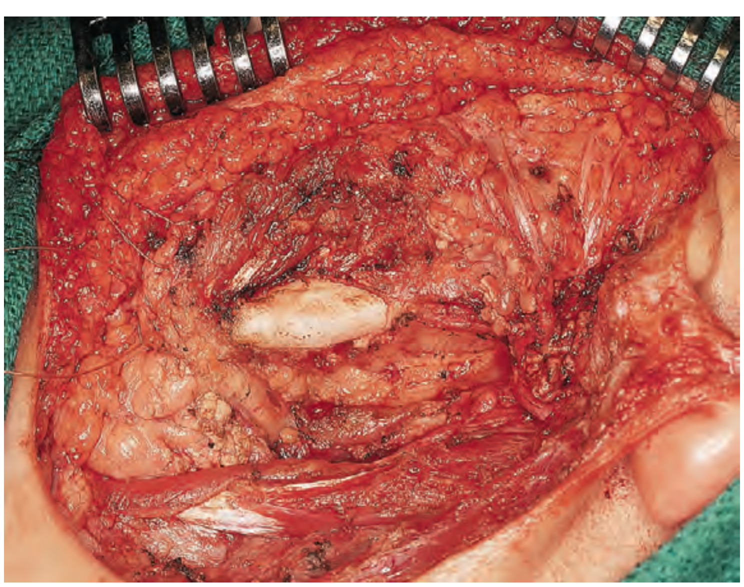

Figure 13.165 The surgical field after removal of the tumor with sacrifice of the lower division of the facial nerve and the masseter muscle.

Microsurgical techniques are used to perform an accurate nerve graft with microneural suture for anastomosis. Accurate alignment of the nerve bundles should be achieved as far as possible. Several 9-0 or 10-0 Ethilon sutures are used for the neural anastomosis. The completed nerve graft is shown in Fig. 13.166. Note that a natural branching nerve graft has been harvested to replace the lower division of the facial nerve with distal anastomosis between the buccal and mandibular branches. The wound is irrigated with Bacitracin solution. A Penrose drain is inserted, and routine wound closure is performed.

The appearance of the patient approximately 9 months after surgery shows nearly complete restoration of the function of the facial nerve with a normal, balanced appearance (Fig. 13.167). Restoration of the function of the facial nerve is demonstrated in Figs. 13.168 and 13.169.

In spite of the most meticulous and accurate neural anastomosis, varying degrees of dyskinesia are to be expected. However, in more than 80% of patients, restoration of facial nerve function is quite satisfactory.

Figure 13.167 The appearance of the patient 9 months after surgery.

Figure 13.168 The postoperative appearance of the patient showing return of function of the buccal and mandibular branches of the left facial nerve.

Figure 13.169 Function of the zygomatic and temporal branches remains intact.

Radical Resection for Adenoid Cystic Carcinoma of the Parotid Gland

In the patient shown in Fig. 13.170, a firm mass developed in the preauricular subzygomatic region over a period of 6 months. Upon clinical examination, the mass extended deep to the zygomatic arch and presented in the temporal region, as shown in the diagram. The mass was somewhat immobile, and the patient had weakness of the zygomatic branch of the facial nerve. An axial view of the MRI scan shows extensive diffuse tumor infiltration in the superficial part of the parotid gland, extending into the subzygomatic region and into the masticator space anterior and medial to the condyloid process of the mandible (Fig. 13.171). Coronal views of the MRI clearly show the tumor surrounding the zygomatic arch (Fig. 13.172).

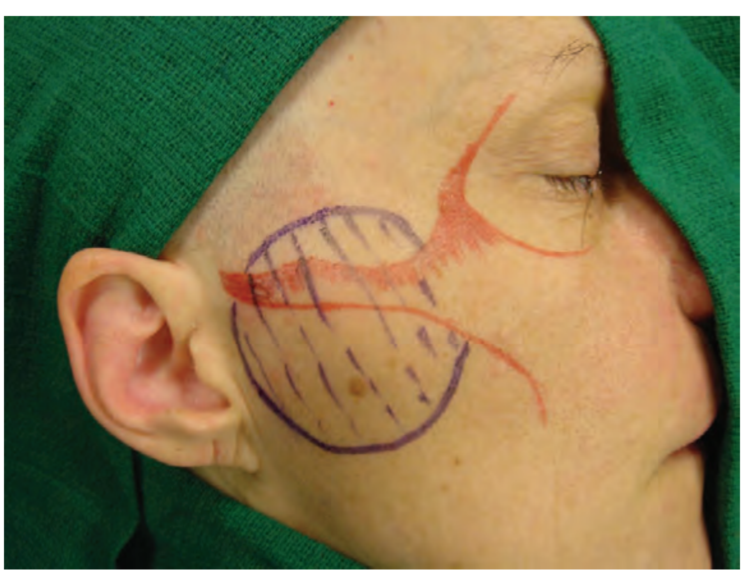

Figure 13.170 The extent of tumor in relation to the zygoma is outlined on the patient.

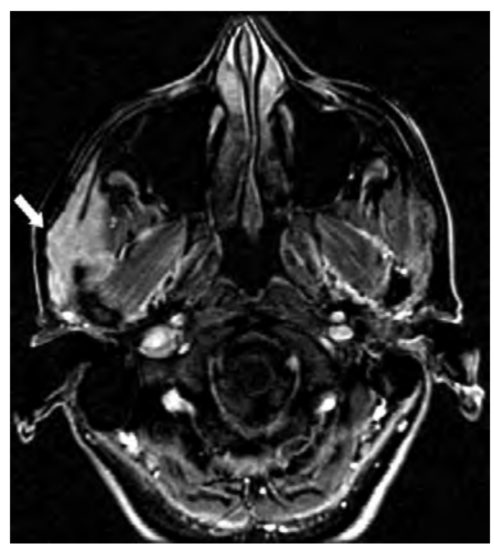

Figure 13.171 An axial view of a magnetic resonance imaging scan showing a right parotid tumor involving the zygomatic arch and temporomandibular joint (*arrow*).

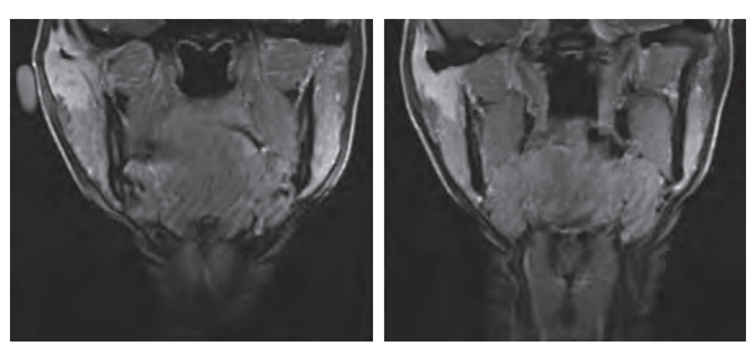

Figure 13.172 Coronal views of the magnetic resonance imaging scan show the tumor surrounding the zygomatic arch.

Adenoid cystic carcinoma has a significant proclivity for perineural invasion. However, if the nerve in question is clinically functioning and grossly not involved, then deliberate sacrifice of the functioning nerve is not indicated. In this patient, upper division of the facial nerve already manifested weakness and therefore was sacrificed. A generous preauricular incision is outlined to gain exposure of the parotid gland, the zygomatic arch, and the temporal region (Fig. 13.173). The incision begins along the hairline on the lateral aspect of the forehead and follows the hairline up to the preauricular skin crease and then continues along a skin crease in the upper part of the neck. The skin incision is deepened through the subcutaneous tissue, and an anterior skin flap is elevated. Dissection initially begins with identification of the main trunk of the facial nerve in its usual location. At this juncture it becomes apparent that the lower division of the facial nerve is uninvolved and could be spared safely. Therefore the cervical, marginal, and buccal branches coming from the lower division of the facial nerve were dissected and preserved.

Figure 13.173 The outline of the skin incision.

The surgical resection encompassed the parotid gland, the upper division of the facial nerve, the zygomatic arch, the temporomandibular joint, and surrounding soft tissues. The surgical specimen consists of the entire parotid gland, a portion of the zygomatic bone and zygomatic arch, the temporomandibular joint and condyloid process of the mandible, and portions of the lateral and medial pterygoid muscles as well as a portion of the temporalis muscle and the coronoid process of the mandible. The surgical defect after removal of the specimen is shown in Fig. 13.174. Note that the lower division of the facial nerve has been preserved. The surgical defect shows the stump of the condyloid process of the mandible, the stump of the zygomatic process, and the cortical defect of the lateral temporal bone.

This patient's wound is reconstructed with use of a rectus muscle free flap to provide soft tissue to fill the surgical defect. Rehabilitation of the paralyzed eyelid is accomplished with a gold weight implant. This patient underwent postoperative proton beam radiation therapy and remains free of recurrent disease at 5 years after surgery.

Radical Parotidectomy With Neck Dissection for a High-Grade Carcinoma

The risk of regional lymph node metastases is directly related to the histologic grade and clinical stage of the tumor. Thus high-grade and high-stage tumors have a very high risk of nodal metastases. If cervical lymph node metastases are not already present at initial diagnosis, they have a very high risk of harboring occult metastases in the clinically and radiologically negative neck. The patient shown in Fig. 13.175 has a high-grade mucoepidermoid carcinoma with invasion of the overlying skin and palpable lymph node metastases at level II. Her contrast-enhanced CT scan shows an extensive primary tumor involving the overlying skin and extension to the deep lobe. In spite of this extensive tumor, her facial nerve function was intact (Fig. 13.176).

The principles of parotid surgery for malignant tumors require understanding the biology of the disease, the morbidity of surgery, and the role of adjuvant postoperative radiotherapy. In general a functioning facial nerve is not sacrificed if the primary tumor can be removed intact in a monobloc fashion

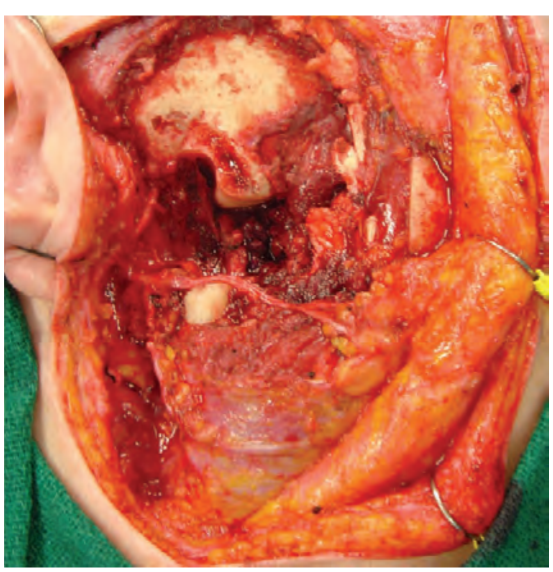

Figure 13.174 The surgical defect after removal of the specimen showing preservation of the lower division of the facial nerve.

Figure 13.175 High-grade mucoepidermal carcinoma with invasion of the overlying skin.

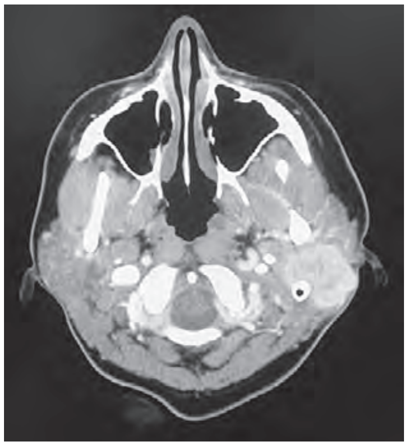

Figure 13.176 Axial view of a contrast-enhanced computed tomography scan shows an extensive tumor of the superficial lobe extending in the retromandibular region and involving the overlying skin.

Figure 13.178 Surgical specimen showing monobloc resection of the tumor with overlying skin and neck dissection done in continuity.

Figure 13.177 Plan of surgical excision requiring sacrifice of a large area of skin overlying the tumor.

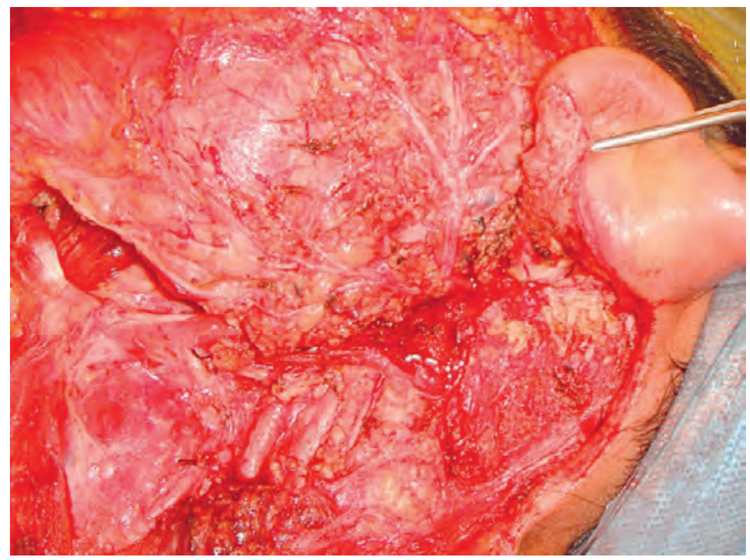

Figure 13.179 Surgical field following removal of the specimen shows a large soft tissue and skin defect in the parotid region and upper part of the neck.

without leaving any gross tumor behind. Proximity or contiguity of the facial nerve to the tumor is not an indication to sacrifice a functioning nerve. Similarly the possibility of a microscopic positive margin is also not an indication to sacrifice a functioning facial nerve.

The surgical plan in this patient required sacrifice of a large area of skin overlying the tumor, en bloc with parotidectomy and neck dissection. The surgical incision is shown in Fig. 13.177. The surgical procedure begins with neck dissection working from the supraclavicular region toward the parotid gland. The neck dissection proceeds in the usual fashion. (For details on the steps of neck dissection, refer to Chapter 11.) Once the neck dissection specimen is mobilized up to the digastric muscle, attention is focused on identification of the main trunk of the facial nerve. In spite of a large and invasive tumor, her facial nerve was not directly infiltrated by tumor. Therefore meticulous dissection of all facial nerve branches was undertaken. The posterior belly of the digastric muscle and a portion of the upper end of the sternocleidomastoid muscle had to be sacrificed to achieve a monobloc total resection of the tumor. The surgical specimen shows monobloc excision of the primary tumor in continuity with the neck dissection specimen (Fig. 13.178).

Figure 13.180 Primary closure of the surgical defect by advancement of the skin of the neck and face.

The surgical field following removal of the specimen shows an intact facial nerve and a large defect in the parotid and upper cervical region (Fig. 13.179). Repair of the defect required advancement of the facial and cervical skin to accomplish a primary closure (Fig. 13.180).

Retrograde Dissection of the Facial Nerve

In some patients the primary tumor of the parotid gland either arises or is located in the region of the stylomastoid foramen, making dissection and identification of the main trunk of the facial nerve difficult during the early part of the operation. This scenario is particularly true if the tumor happens to be a malignant tumor, and the main trunk of the facial nerve can easily or inadvertently be injured or transected before it is identified. In such patients, retrograde dissection of the facial nerve is recommended.

The patient described here had undergone two previous operations for partial excision of a parotid tumor over a period of 6 years. A formal superficial parotidectomy was never carried out, and each time the tumor was said to be a "benign tumor." An MRI scan clearly shows an irregular, ill-defined tumor involving the superficial, retromandibular, and deep parts of the parotid gland (Fig. 13.181).

Dissection initially begins in the usual manner, with identification of the sternocleidomastoid muscle, the posterior belly of the digastric muscle, and the auditory canal. However, it soon becomes apparent that gross tumor is present immediately lateral to the main trunk of the facial nerve, and therefore at that point antegrade dissection is stopped at that site and the anterior skin flap is elevated beyond the periphery of the superficial lobe of the parotid gland. The peripheral branches of the facial nerve are identified and dissected toward their exit from the parotid gland (Fig. 13.182). In identifying and dissecting the peripheral branches, it is always easy to identify the buccal branches of the facial nerve first, because they are in a constant location along the Stensen's duct and are of sufficient dimension to be identified and traced proximally. Zygomatic division is the next division to dissect and preserve. Dissection is continued in this manner, and thus if a portion of the main trunk or the main divisions of the facial nerve must be sacrificed and facial nerve grafting is planned, then the peripheral branches are already identified, dissected, and tagged and would be readily available for neural anastomosis.

As dissection proceeds further in this patient, the upper and lower division of the facial nerve are identified, lifting off the superficial lobe from the masseter muscle. Note that both the upper and lower divisions of the facial nerve appear quite "thick" and reddish with hyperemia and irregular in shape, raising a strong suspicion of tumor infiltration into the nerve (Fig. 13.183). Further dissection of the main trunk of the facial nerve makes it readily apparent that it is completely surrounded by the tumor, making it impossible to preserve its integrity (Fig. 13.184).

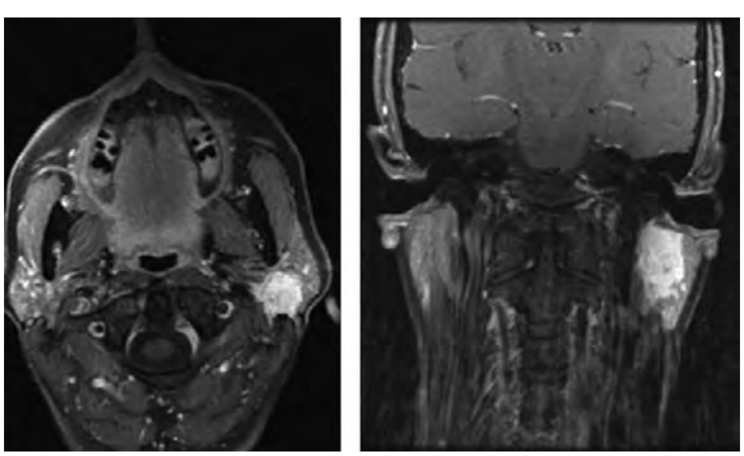

Figure 13.181 Axial and coronal views of a T1-weighted magnetic resonance imaging scan show an irregular ill-defined tumor involving the superficial and deep parts of the parotid gland.

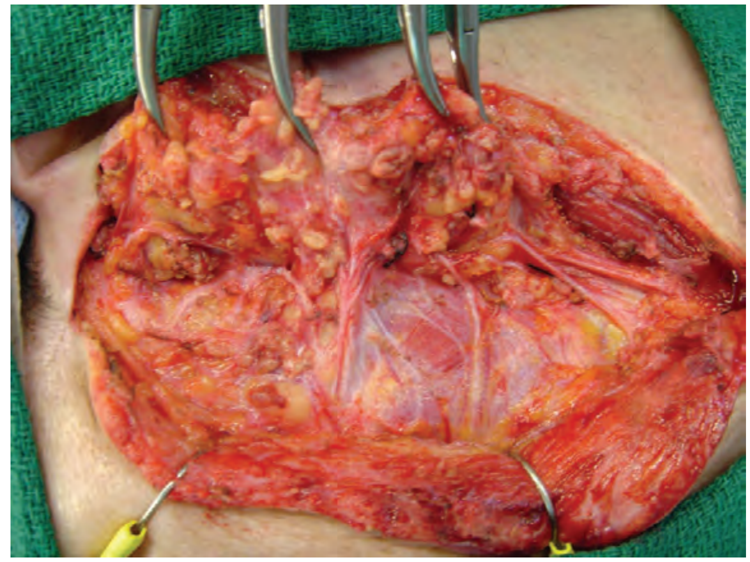

Figure 13.182 Peripheral branches of the facial nerve are dissected.

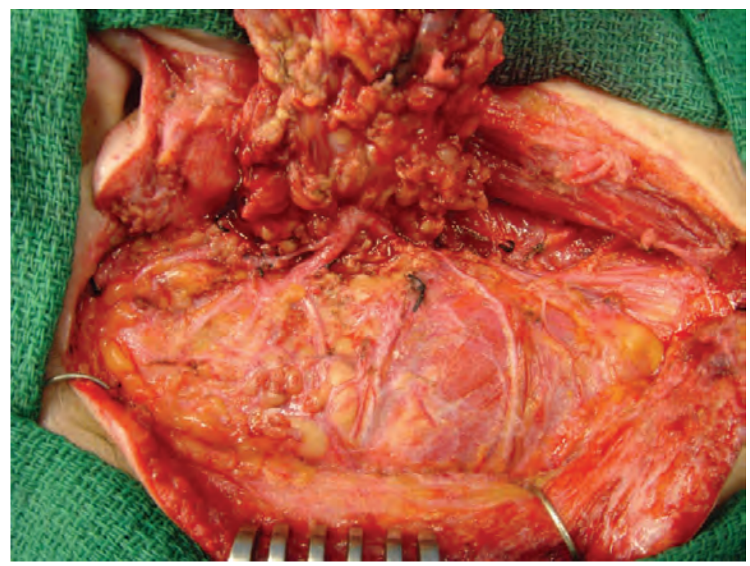

Figure 13.183 The upper and lower divisions of the facial nerve are thickened.

Figure 13.184 Complete encasement of the facial nerve by the tumor.

At this juncture, a monobloc resection of the tumor with the parotid gland and the involved part of the facial nerve is undertaken. Frozen sections are obtained from the transected edges of the facial nerve to ensure the absence of microscopic tumor infiltration. If the proximal and distal ends of the facial nerve are identified as being histologically free of tumor, then facial nerve grafting may be considered. On the other hand, if clear margins cannot be obtained, then no nerve grafting is undertaken, and the patient will require secondary efforts at rehabilitation of the paralyzed face.

Radical Resection for a Recurrent Carcinoma of the Parotid Gland With Sleeve Resection of the Auditory Canal and a Radical Mastoidectomy

A primary or recurrent carcinoma of the parotid gland that is intimately adherent to or invading the cartilage of the auditory canal requires a locally aggressive surgical resection with excision of the cartilaginous auditory canal. If the tumor does not involve the external ear, the pinna can be safely preserved with sleeve resection of the auditory canal, which is reconstructed with a skin graft. The patient presented here has a recurrent carcinoma of the parotid gland with invasion of the auditory canal. This patient had previously undergone a superficial parotidectomy for carcinoma, followed by postoperative radiation therapy. Local recurrence has produced facial paralysis and discomfort in the parotid region. Diffuse induration could be palpated in the retromandibular region.

The CT scan shown in Fig. 13.185 demonstrates a contrast-enhancing tumor mass involving the residual parotid tissue with adherence to the posterior margin of the ascending ramus of the mandible. The tumor is in close proximity to the styloid process and also is adherent to the overlying skin. The incisions for the operation are outlined in Fig. 13.186. A generous portion of the preauricular skin, which was elevated at the time of the previous superficial parotidectomy, should be sacrificed. In addition, a radical parotidectomy in conjunction with resection of the ascending ramus of the mandible, a radical mastoidectomy, and a sleeve resection of the cartilaginous auditory canal will be performed in a monobloc fashion. Although metastatic lymph nodes are not palpated, a neck dissection should be performed, because no adjunctive postoperative radiation therapy is possible in this patient. The external ear can be preserved by detaching it from the external auditory canal, but it remains attached to the scalp, from which it will derive its blood supply.

The operation begins with the radical neck dissection. The specimen from the posterior triangle and the supraclavicular fossa is mobilized cephalad. The dissection continues up to the mastoid process, where the specimen remains attached. The body of the mandible just anterior to the retromolar trigone is divided in an extramucosal fashion. The ascending ramus of the mandible is now rotated laterally to expose the medial and lateral pterygoid muscles, which are divided with an electrocautery. The zygomatic arch is then divided. The temporalis muscle is divided next, leaving its tendon attached to the coronoid process of the mandible. The skin incision is now extended along the preauricular skin crease, around the lobule of the ear, and posterior to the ear canal. The cartilaginous ear canal of the external ear is divided, and the pinna is reflected cephalad.

The operation continues with a radical mastoidectomy to gain further exposure of the remaining cartilaginous canal up to its junction with the bony canal. This procedure is best done with a variable-speed power drill and a suction irrigator. Meticulous slow dissection should occur during this stage of the operation to avoid any injury to the sigmoid sinus. The internal jugular vein is now divided and ligated near the jugular foramen. Using an osteotome, the most lateral aspect of the bony auditory canal is transected. Finally, the temporomandibular joint is opened and the mandible is disarticulated, delivering the specimen.

The surgical field following removal of the specimen is shown in Fig. 13.187. The remaining mastoid air cells and the tympanic membrane in the bony auditory canal are seen. Also evident

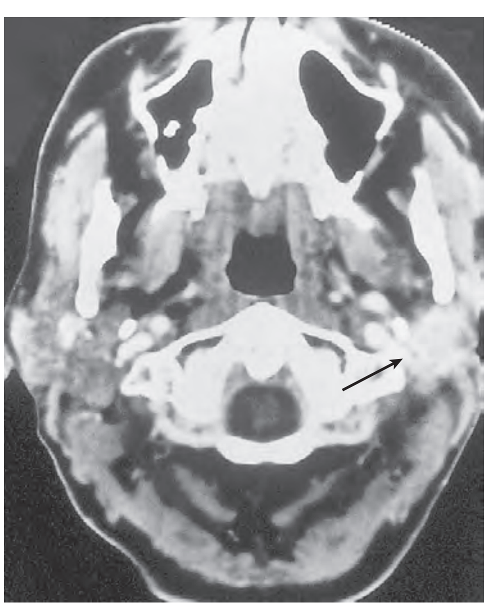

Figure 13.185 A computed tomography scan shows the recurrent tumor in the retromandibular region (*arrow*).

Figure 13.186 The outline of the incisions.

Figure 13.187 The surgical field after removal of the specimen.

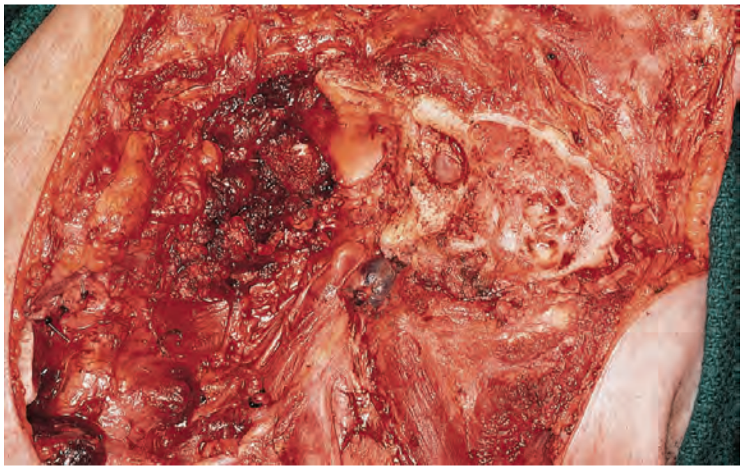

Figure 13.188 A close-up view of the surgical defect.

Figure 13.190 The external ear is reapproximated to the bony ear canal.

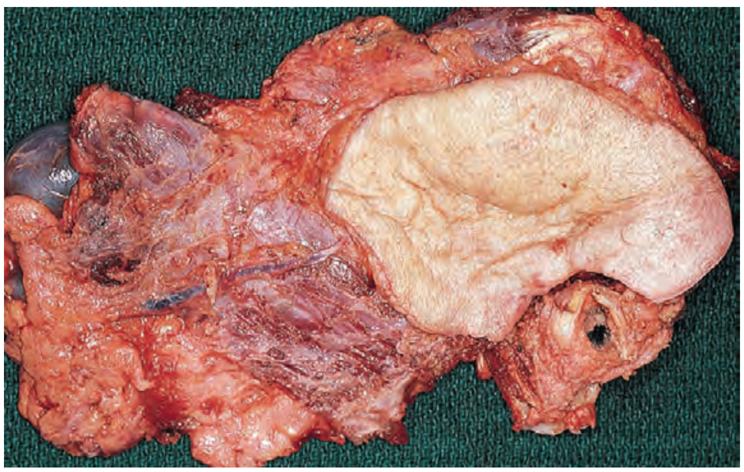

Figure 13.189 The surgical specimen.

Figure 13.191 The surgical defect is repaired with a pectoralis major myocutaneous flap.

in the field are the glenoid fossa of the temporomandibular joint, the pterygoid muscles, and the stump of the mandible. A close-up view of the surgical defect in the region of the jugular foramen shows the stump of the ligated internal jugular vein with the tortuous part of the internal carotid artery just before its entry in the carotid canal (Fig. 13.188). The intact tympanic membrane in the auditory canal is clearly seen.

The specimen of the radical neck dissection, radical parotidectomy, and sleeve resection of the ear canal is shown in Fig. 13.189. The tumor can be seen perforating through the cartilage into the external auditory canal. The resected ear canal is repaired by reapproximating the skin edges of the external ear with the skin edges of the bony auditory canal. Several nonabsorbable sutures are taken between these edges (Fig. 13.190). The ear canal is packed tight with Xeroform gauze. The soft tissue and skin defect in the parotid region are repaired with use of a pectoralis major myocutaneous flap.

The repaired surgical defect is shown in Fig. 13.191 with the myocutaneous flap covering the soft tissue and skin loss in the preauricular region. The ear canal is foreshortened because of the loss of its cartilaginous portion, but the function of hearing is preserved. A sleeve resection of the auditory canal for parotid cancer is applicable in highly selected situations. Very accurate clinical and radiographic assessment of the tumor is essential for such selection. If bone destruction is manifest, then this operation is unsuitable and a temporal bone resection in conjunction with a radical parotidectomy should be considered.

Radical Parotidectomy With Temporal Bone Resection and Amputation of the External Ear

Extensive malignant tumors of the parotid gland with invasion of the middle ear, mastoid process, or temporal bone require a radical parotidectomy with temporal bone resection. The patient shown in Fig. 13.192 has an extensive high-grade carcinoma of the left parotid gland. Her CT scan shows a massive

Figure 13.192 A locally advanced high-grade carcinoma of the left parotid gland.

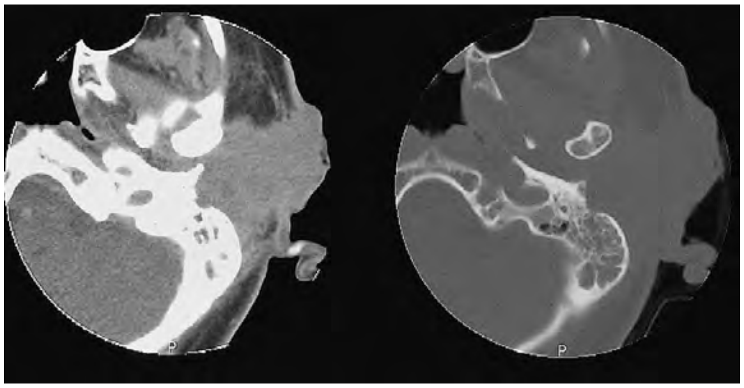

Figure 13.193 A computed tomography scan demonstrates involvement of the lateral temporal bone.

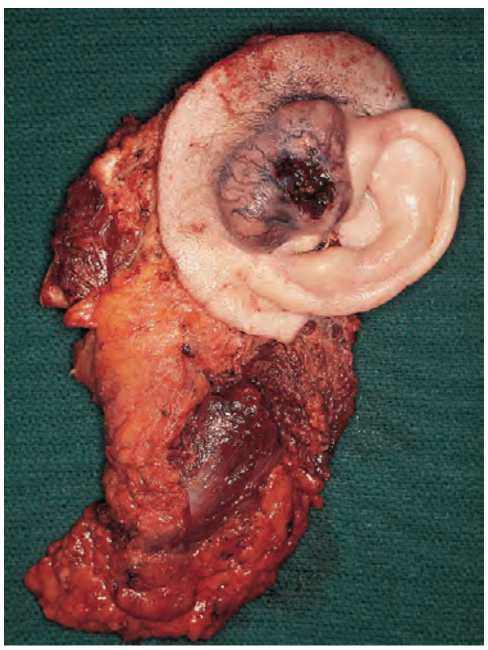

Figure 13.194 The surgical specimen showing monobloc excision of the tumor.

tumor with invasion of the lateral temporal bone (Fig. 13.193). The operative procedure consisted of a modified comprehensive neck dissection with preservation of the spinal accessory nerve in conjunction with a radical total parotidectomy with sacrifice of the facial nerve and overlying skin and amputation of the external ear with temporal bone resection. The surgical specimen shows monobloc excision of the tumor with gross total clearance of the tumor (Fig. 13.194). The surgical defect shows the stump of the petrous temporal bone, dura covering the temporal lobe, the ascending ramus of the mandible, and the surgical field of the neck dissection (Fig. 13.195).

Repair of this surgical defect requires a composite free flap to provide soft tissue and skin coverage. A rectus abdominis free flap provides an excellent immediate means of reconstruction (Fig. 13.196). Her paralyzed eyelid will be rehabilitated by a gold weight implant in 3 to 4 weeks. The paralyzed lips will require a fascial sling procedure several months later, after completion of postoperative radiotherapy.

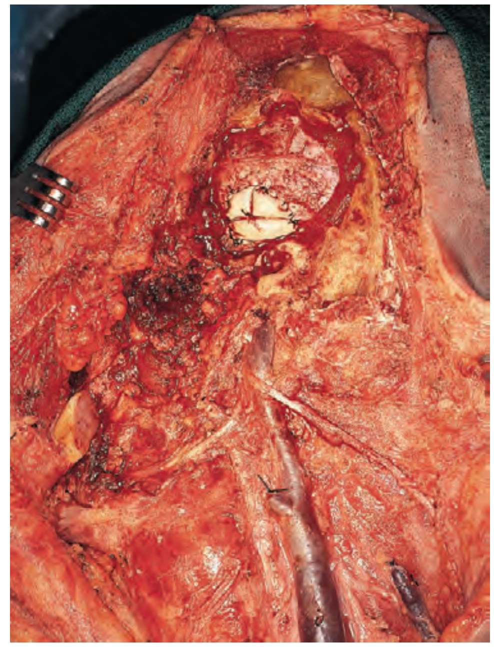

Figure 13.195 The surgical defect.

Figure 13.196 A rectus abdominis free flap is used to reconstruct the defect.

Rehabilitation of the Paralyzed Face

Dynamic panfacial reanimation is the preferred goal even in cases with locally advanced disease requiring adjuvant radiotherapy. Current trends in improving quality of life have moved away from static procedures and into the creative realm of combining nerve transfers and nerve grafting at the time of tumor ablation. Facial nerve grafting is always preferred as it restores spontaneous motion to the face. However, extensive defects that leave a very proximal facial nerve trunk can be challenging, as nerve grafting all of the branches may lead to potentially disabling synkinesis. Preference is typically given to targeting distal facial nerve branches responsible for smile and lower eyelid motion. The zygomatic branch running alongside the transverse facial artery is consistently responsible for this motion. Static procedures to support the lower eyelid and a platinum or gold weight can be used, although patients

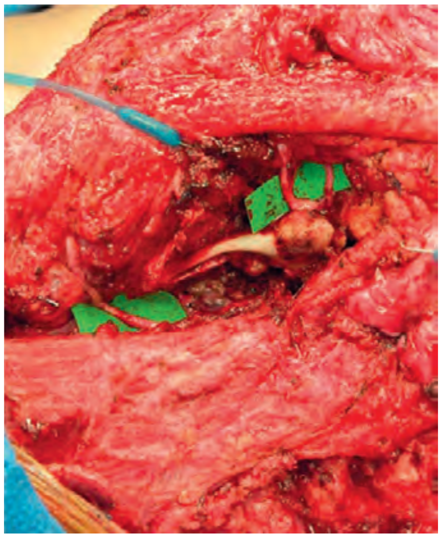

Figure 13.197 Nerve-to-masseter and mini hypoglossal nerve transfers targeting the upper divisions and the lower divisions of the facial nerve, respectively.

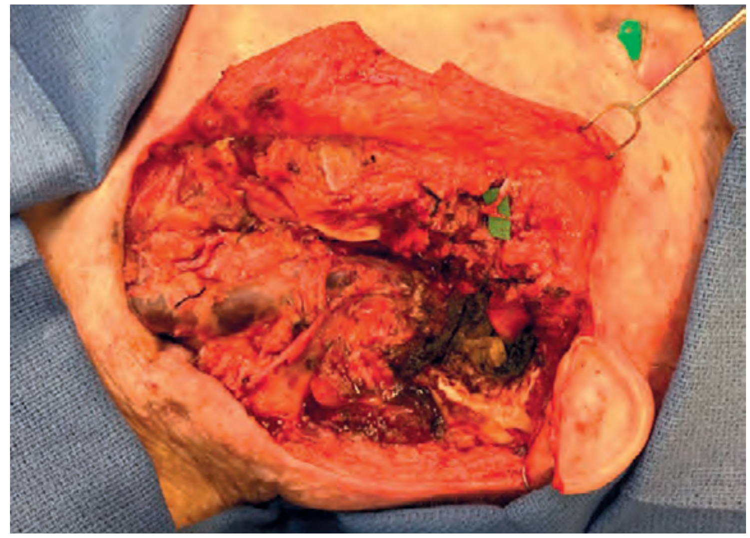

Figure 13.198 Nerve-to-masseter transfer in an 84-year-old gentleman at the time of radical parotidectomy and subtotal auriculectomy.

may still experience chronic epiphora. Alternatively, additional nerve donors can be used to supplement facial nerve function such as a nerve-to-masseter transfer for lower eyelid motion or eye sphincter closure (Fig. 13.197). This will lead to blinking during mastication but can be modulated by the patient with rehabilitation and often eliminates the need for eyedrops. Additionally, a mini hypoglossal nerve transfer can be used to reanimate the lower face by end-to-side coaptation of the marginal mandibular nerve. An epineurial window is created on the superior surface of the hypoglossal nerve with longitudinal axotomies performed through the cranial 30% of the nerve. Neurorrhaphy is performed with 10-0 or 11-0 nylon sutures. This approach of targeting specific distal facial nerve branches with different nerve donors allows the surgeon to minimize dyskinetic facial motion and also increases the reliability in recovering panfacial motion. An upper eyelid weight is not necessarily required in these cases and can be delayed unless the patient does not have a Bell's reflex and is at high risk for vision compromise. At present, gold weight implant in the upper eyelid is considered the best means for rehabilitation of the upper eyelid and achieving harmonious closure and protect the cornea (see Chapter 4 for details).

Cases in which a proximal nerve trunk is not available or there is a positive tumor margin are well suited for dual nerve transfers using a nerve to masseter for smile and possibly blink, and a mini hypoglossal nerve transfer for lower facial motion.

Figure 13.199 Anterolateral thigh free flap reconstruction of the auriculectomy defect.

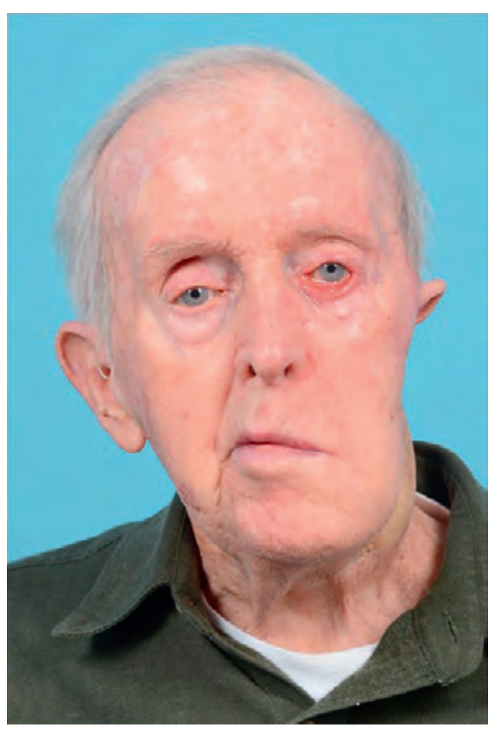

Figure 13.200 Early postoperative result before reinnervation.

Figure 13.201 Twelve-month postoperative result demonstrating smile and near-complete resolution of the ectropion due to nerve-to-masseter transfer.

The nerve to masseter is highly reliable, and facial motion is often evident within 3 months even in the setting of adjuvant radiotherapy. The nerve to masseter is also reliable in older patients. Satisfactory recovery can be expected, even in elderly patients. In this case a radical parotidectomy and subtotal resection of the auricle were performed without a reliable proximal facial nerve stump available. A nerve-to-masseter transfer to zygomatic branches targeting smile and eye closure were performed at the time of ablation (Fig. 13.198). An anterolateral thigh free flap was used to cover the soft tissue and skin defect (Fig. 13.199). Early postoperative pictures demonstrate complete left facial paralysis with profound paralytic ectropion (Fig. 13.200). The patient regained smile within 4 months. At 12 months postoperatively, his ectropion is mostly resolved, his eyes close without an eyelid weight, and he only occasionally requires eye drops (Fig. 13.201).

An alternate approach to dynamic smile is the Labbé procedure involving temporalis transfer to the oral commissure. This has the benefit of providing an immediate smile but does not provide any significant recovery to the eye. Reinnervation to even part of the eye sphincter is worthwhile if feasible to mitigate long-term disability in this area.

Finally, addressing brow ptosis and facial volume loss are also important considerations in rehabilitating the face. Brow ptosis can be addressed with a variety of approaches from direct browlift to endoscopic techniques. In parotid resections resulting in significant volume loss and anticipated radiotherapy, an anterolateral thigh free flap is a reliable tool. Even if skin replacement is not required, we routinely bury a deepithelialized or thinned flap to fill the ablative defect, provide reliable vascularized coverage over the nerve repairs, and minimize the effects of radiotherapy. Because there is no muscle component, the volume of the alanine transaminase (ALT) remains constant. The ALT donor site also provides an excellent source of nerve graft as motor branches to the nerve to vastus lateralis muscle are harvested for this purpose.

RESULTS OF TREATMENT

Surgery remains the mainstay of definitive treatment of salivary gland cancers. However, radiation plays a significant role as adjuvant treatment in advanced-stage disease. Adjuvant radiotherapy has improved local and regional control and has a favorable impact on long-term prognosis. Although 5-year survival is considered a yardstick for evaluation of the success of treatment, long-term follow-up is essential for salivary gland cancers, because recurrence of disease can occur several years after initial therapy, leading to continued attrition over the years.

The overall survival of patients with malignant tumors of the major and minor salivary glands is shown in Fig. 13.202. Parotid carcinomas have the best prognosis by far.

Factors Predictive of Outcome

The clinical stage of the disease and histologic grade of the primary tumor are two of the most reliable prognostic indicators for salivary cancers. The impact of stage of disease and histologic grade of the primary tumor on long-term prognosis is shown in Figs. 13.203 and 13.204. The histologic type of the primary tumor also influences prognosis, as seen in Fig. 13.205, where three broad groups can be identified. Acinic cell carcinoma and low-grade mucoepidermoid carcinoma carry the most favorable prognoses, and squamous carcinoma and anaplastic carcinoma carry the worst prognoses. All other histologic variants have intermediate prognoses. The favorable impact of adjuvant postoperative radiotherapy is observed in advanced stage disease but not in early stage disease (Fig. 13.206). Thus patients with advanced-stage disease and high-grade histology should be considered for postoperative radiation therapy after appropriate surgical resection with the expectation of improvement in locoregional control and overall survival.

In cancers of the major salivary glands the main clinical factors that predict for poor cancer-specific survival (CSS) include

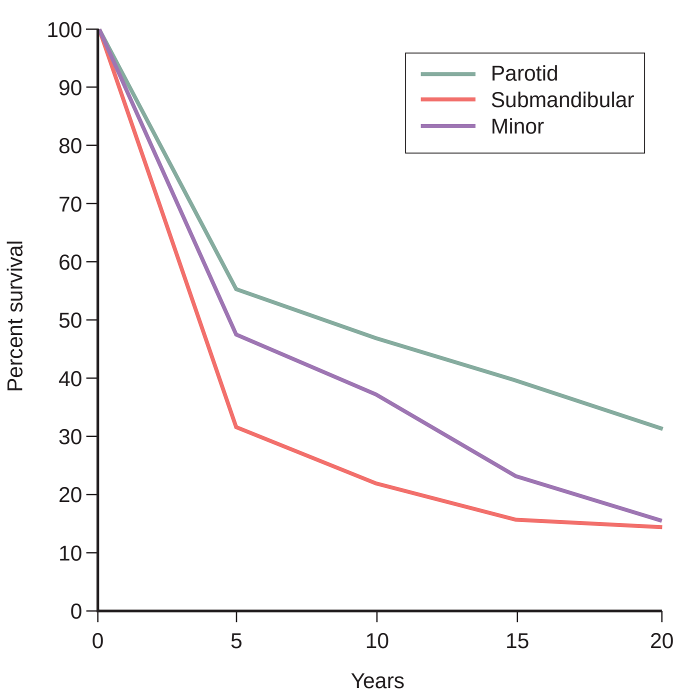

Figure 13.202 The overall survival of patients with malignant tumors of the major and minor salivary glands.

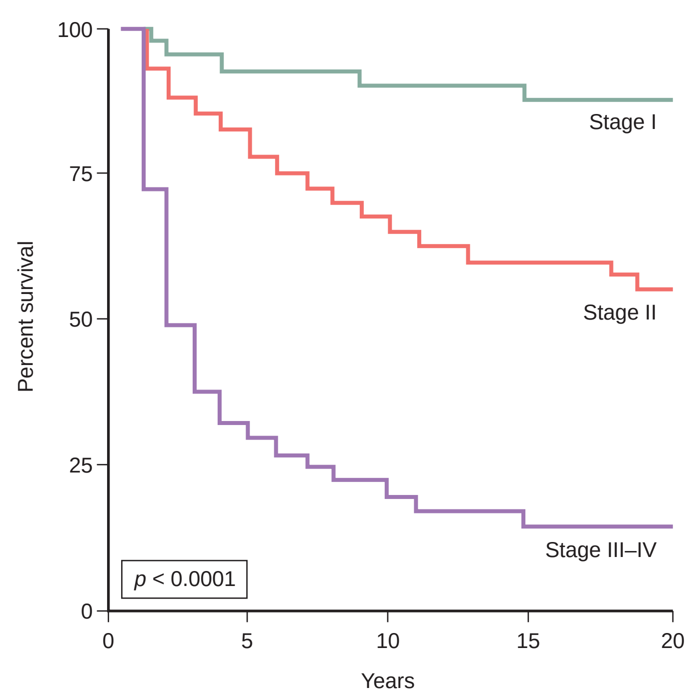

Figure 13.203 The impact of stage of disease on long-term prognosis.

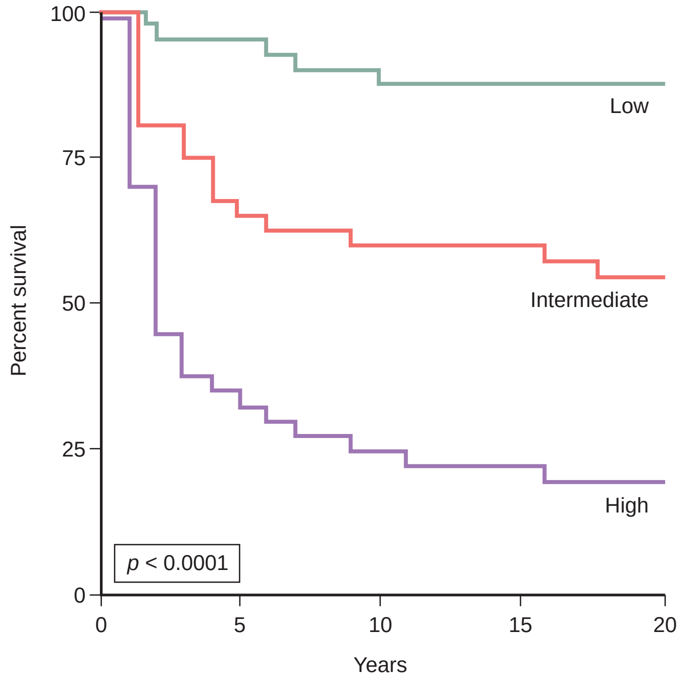

Figure 13.204 The impact of histologic grade on survival.

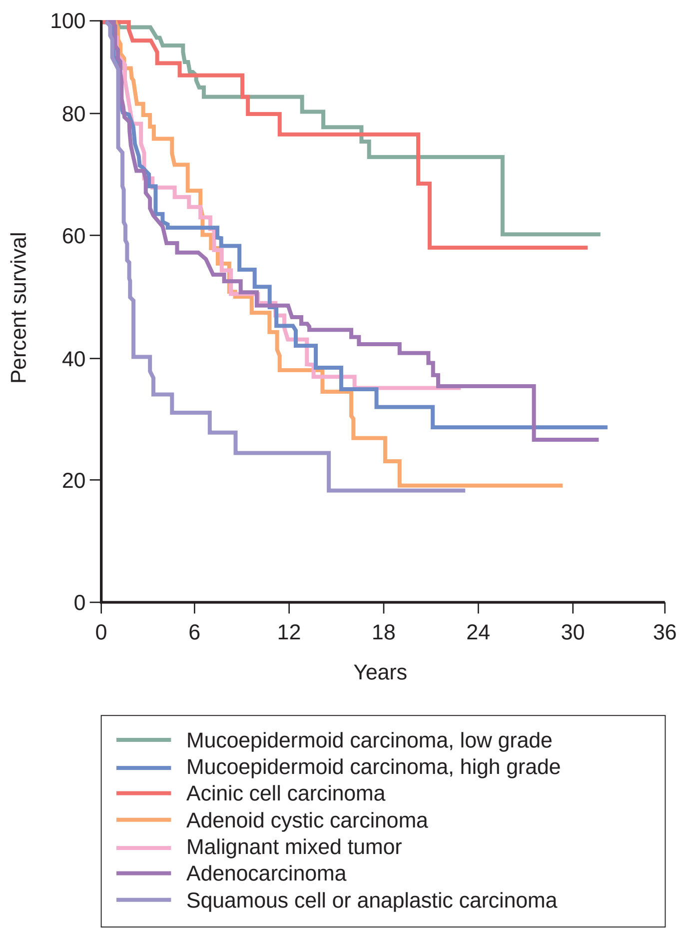

Figure 13.205 Survival in relation to the histologic type of the primary tumor.

overall clinical stage (5 year-CSS: stage IV 26% vs stage I 97%, p <0.001), facial nerve involvement (5-year CSS 25% vs 78%, p <0.001), skin involvement (5-year CSS 30% vs 71%, p <0.001), advanced T stage (5-year CSS T4 22% vs T1 97%, p <0.001), and positive parotid or lateral neck nodes (5-year CSS N+ 32% vs N0 87%, p <0.001).

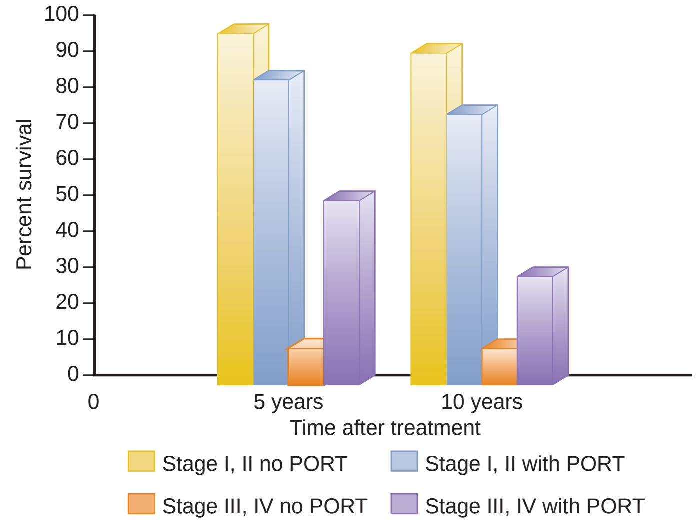

Figure 13.206 The favorable impact of adjuvant postoperative radiotherapy (PORT) is observed in advanced stage disease but not in early stage disease.

Table 13.2 Incidence of Distant Metastases According to Histology of the Primary Tumor

HISTOLOGY GROUP	TOTAL COUNT	DISTANT RECURRENCE	%
Salivary duct carcinoma	17	9	53%
Adenocarcinoma	33	14	42%
High grade carcinoma	13	3	23%
Carcinoma ex pleomorphic adenoma	59	12	20%
Acinic cell carcinoma	37	6	16%
Adenoid cystic carcinoma	28	4	14%
Mucoepidermoid carcinoma	94	7	7%
Myoepithelial carcinoma	17	1	6%
Other	3	0	0%

Pathologic factors that predict for poor cancer-specific survival include perineural invasion (5-year CSS 48% vs 90%, p <0.001), vascular invasion (5-year CSS 41% vs 89%, p <0.001), close/positive margins (5-year CSS 64% vs 88% for negative margins, p <0.001), histologic grade (5-year CSS high grade 44% vs low grade 100%, p <0.001).

These same factors also predict for recurrence. In general, distant recurrence is more common than local or regional recurrence. In an analysis of 301 patients with major salivary gland cancers treated at Memorial Sloan Kettering Cancer Center from 1985 to 2009, 56 had distant recurrence compared with 12 local recurrences and 18 regional recurrences.

The two histologic subtypes in which distant metastasis was most likely to develop were salivary duct carcinoma (53%) and adenocarcinoma (42%). The remaining five histologies and the percentage of patients in each who experienced distant metastases were adenoid cystic carcinoma (14%), acinic cell carcinoma (16%), carcinoma ex pleomorphic adenoma (20%), mucoepidermoid carcinoma (7%), myoepithelial carcinoma (6%), and high-grade carcinoma (23%) (Table 13.2).

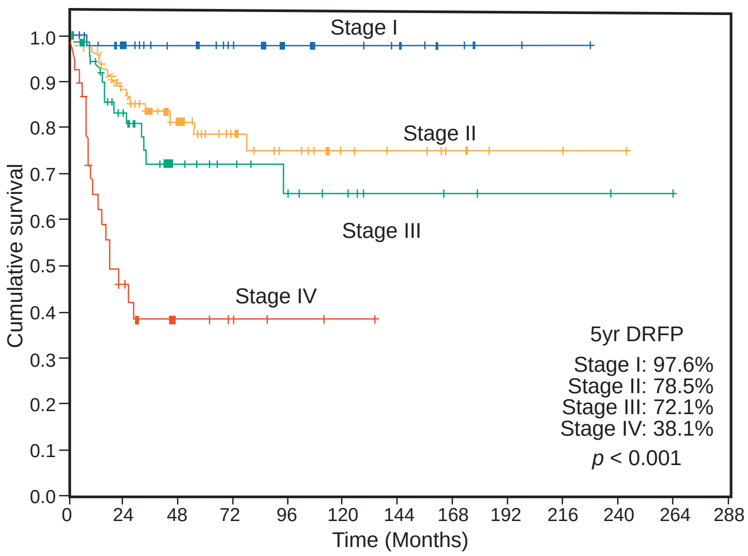

Figure 13.207 Long-term survival rates by stage of disease in a recent group of patients treated at Memorial Sloan Kettering Cancer Center (1985–2009).

Distant recurrence is most likely to occur in stage IV tumors compared with stage I tumors, as shown in the Kaplan Meir plot (Fig. 13.207). The distant recurrence-free survival for a stage IV patient is 38% compared with 98% for stage I patients.

Nomograms Predictive of Outcome

The current system used to assess prognosis in patients with salivary gland cancer is the TNM staging system. This system has been widely used to plan treatment, evaluate treatment results, and compare outcomes between institutions around the world. Despite this popularity, the TNM staging system does not accommodate other patient and tumor-related variables that are known to predict outcome. This is particularly the case with cancers of the major salivary glands, which include multiple different histologies with a varied clinical behavior. Statistical tools such as nomograms have the ability to take into account many variables to predict outcomes, allowing individual risk prediction and stage grouping while balancing complexity with user friendliness. They rely on the statistical methodology of the Cox proportional hazards regression model or competing risks regression. Nomograms for overall survival, disease-specific survival, and risk of recurrence for major salivary gland cancers have now been developed.

The nomogram for overall survival utilizes five variables: age, cT4, grade, perineural invasion, and tumor size (Fig. 13.208). This nomogram had a high concordance index of 0.81.

The nomogram for cancer-specific survival utilizes five variables: grade, perineural invasion, cT4 stage, positive nodal status, and margins (Fig. 13.209). This also has a high concordance index of 0.86.

Finally, the nomogram for recurrence utilizes age, grade, vascular invasion, perineural invasion, and nodal metastasis (Fig. 13.210). This has a high concordance index (CI) of 0.85.

To illustrate the utility of the nomogram we can consider two hypothetical patients. A 30-year-old man with a T1N0 low-grade mucoepidermoid carcinoma has a recurrence-free survival probability of 95% (Fig. 13.211). In contrast, a 60-year-old woman

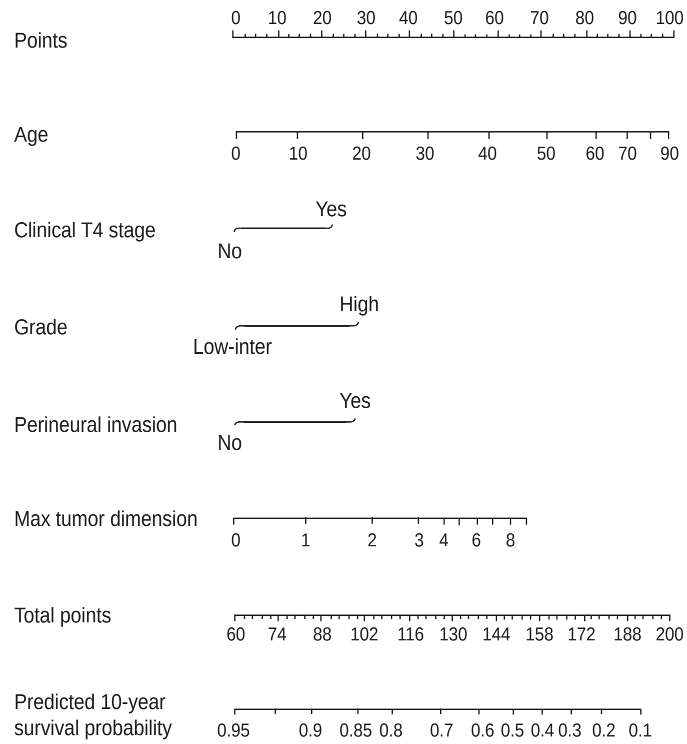

Figure 13.208 Prognostic nomogram for overall survival for salivary gland cancers.

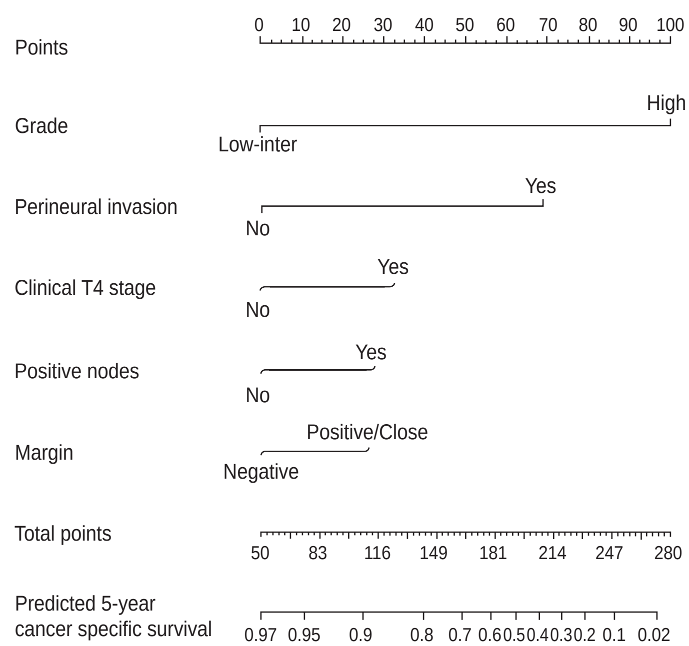

Figure 13.209 Prognostic nomogram for cancer-specific survival for salivary gland cancers.

with T4N1 high-grade salivary duct cancer has a recurrence-free survival probability of only 9% (Fig. 13.212).

By identifying patients at higher risk of recurrence, we can personalize treatment by providing more aggressive treatments to those at high risk and reserve less aggressive treatment for those with low risk of recurrence. The nomogram can also be used to tailor the frequency and extent of imaging, such as CT, MRI and PET, in the follow-up of patients to identify recurrence early in those patients at high risk.

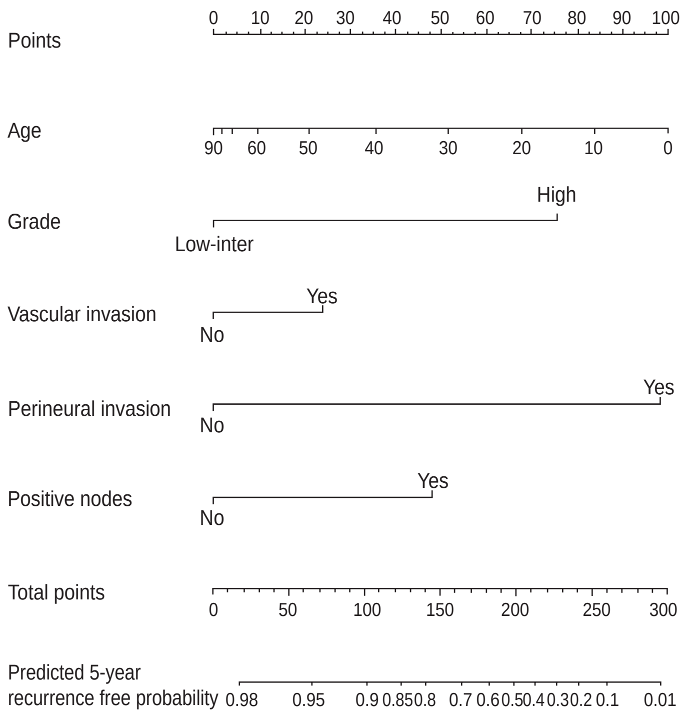

Figure 13.210 Prognostic nomogram for recurrence of salivary gland cancers.

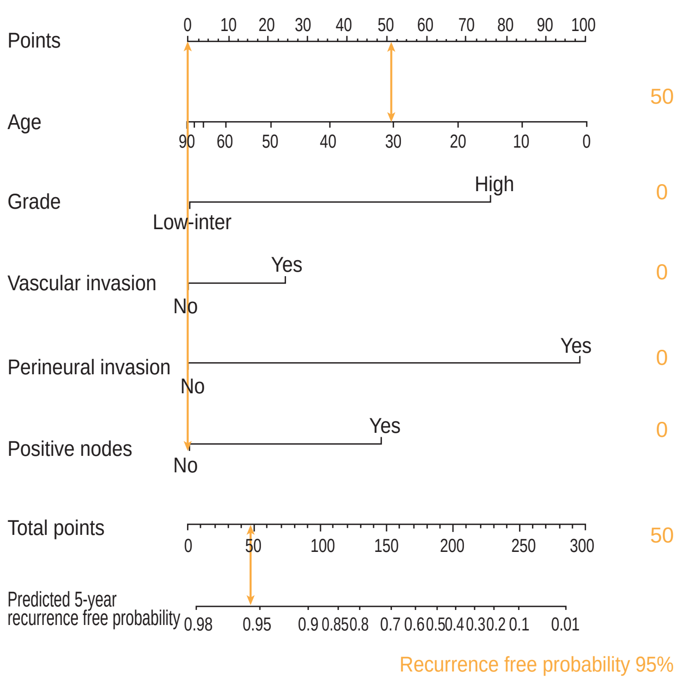

Figure 13.211 Prognostic nomogram showing a 95% recurrence-free survival probability in a 30-year-old male with a low-grade mucoepidermoid carcinoma.

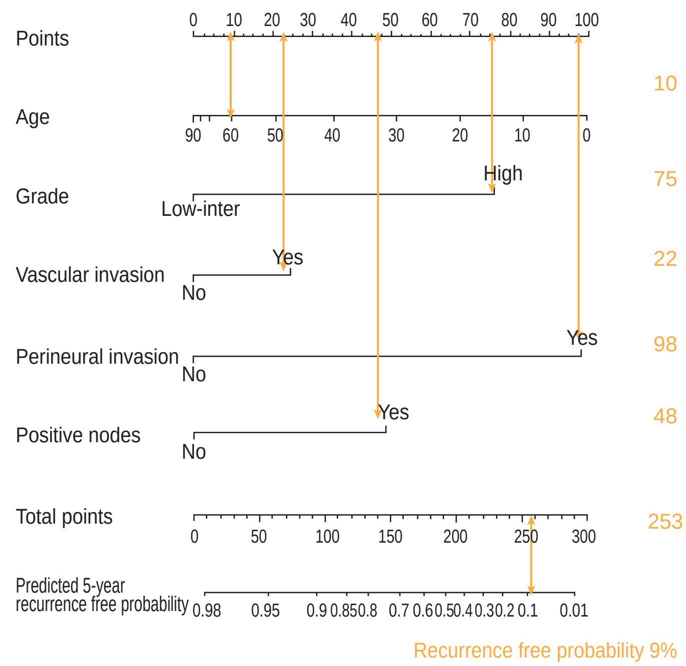

Figure 13.212 Prognostic nomogram showing a 9% recurrence-free survival probability in a 60-year-old female with a high-grade salivary duct cancer staged T4N1.

CHAPTER 14

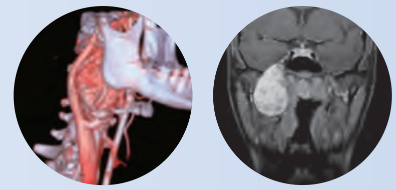

Neurogenic Tumors and Paragangliomas

Neurogenic tumors and paragangliomas form a very small percentage of all neoplastic lesions of the head and neck region. Although these tumors are considered under the major heading of "soft tissue tumors," the unique presentation and systematic workup and imaging studies necessary for accurate diagnosis to facilitate selection of management strategy warrant their consideration as a separate entity.

Most paragangliomas and neurogenic tumors arise from or in the vicinity of the lower cranial nerves, carotid artery, internal jugular vein, and sympathetic chain in the upper part of the neck. Characteristically, these tumors are located in the parapharyngeal space (PPS) (Fig. 14.1). The PPS is a potential space in the shape of an inverted cone with its base at the base of the skull and its apex at the level of the tip of the hyoid bone. The lateral pharyngeal wall and tonsillar fossa form its medial wall, and the pterygoid muscles, parotid gland, and prevertebral muscles form its posterolateral boundary. For clinical purposes, the PPS is divided into two components

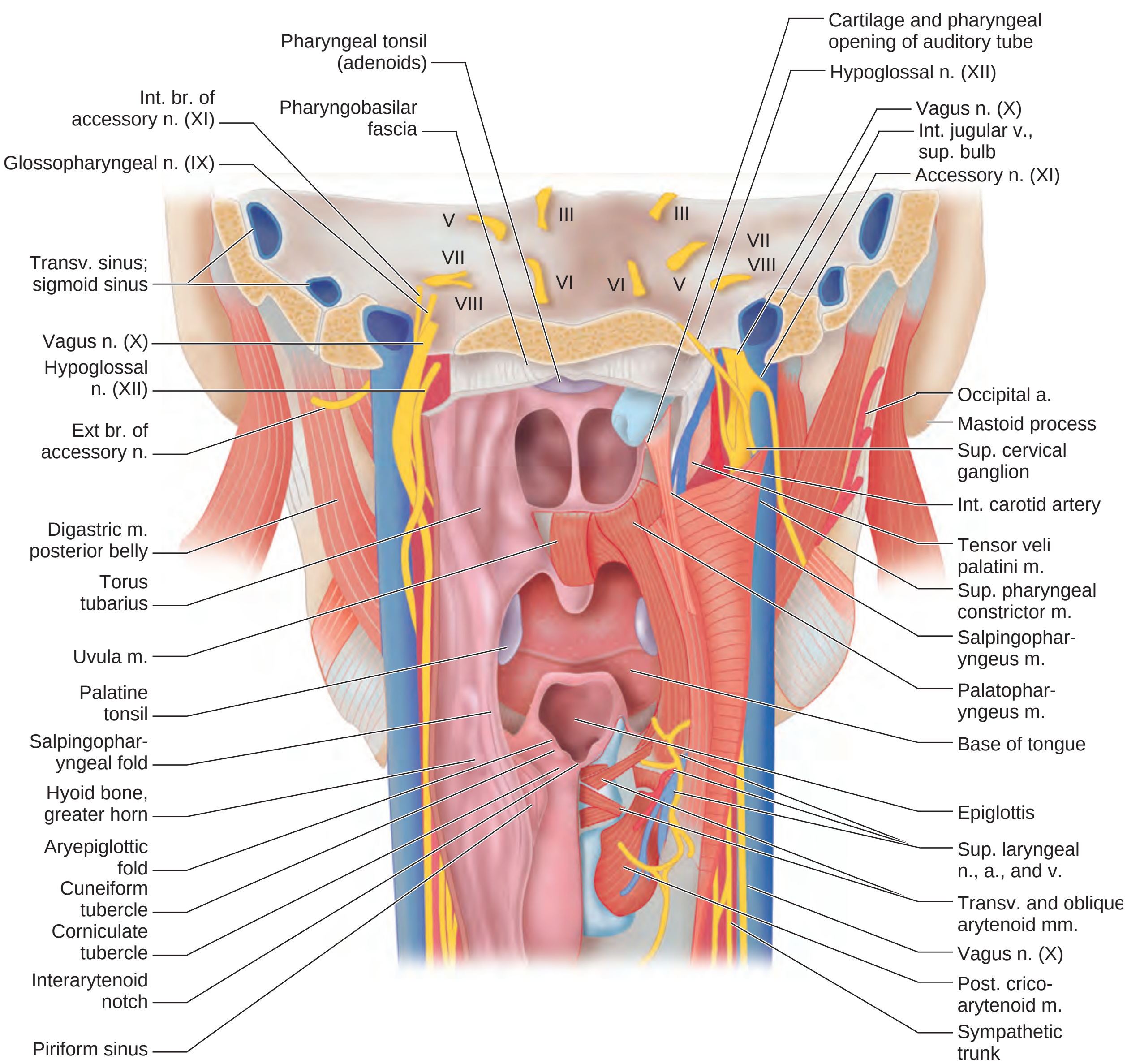

Figure 14.1 Anatomy of the parapharyngeal space. *a,* Artery; *Int. br.,* internal branch; *n,* nerve; *m,* muscle; *mm,* muscles; *sup.,* superior; *v,* vein.

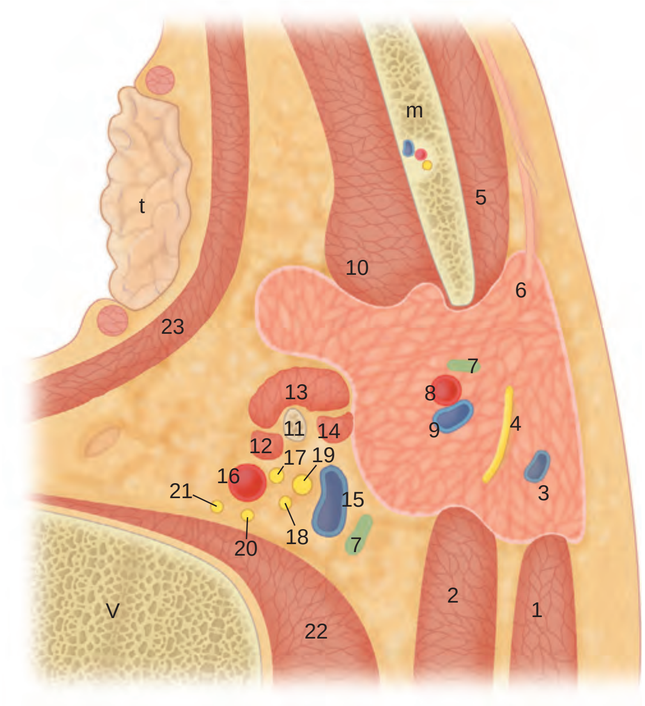

m = mandible	11 = styloid process
t = palatine tonsil	12 = stylopharyngeus
v = vertebral body	13 = styloglossus
1 = sternocleidomastoid muscle	14 = stylohyoid muscle
2 = posterior belly of digastric muscle	15 = internal jugular vein
3 = external jugular vein	16 = internal carotid artery
4 = facial nerve	17 = glossopharyngeal nerve
5 = masseter muscle	18 = spinal accessory nerve
6 = parotid duct	19 = vagus
7 = intraparotid lymph nodes	20 = cervical sympathetic chain
8 = external carotid artery	21 = hypoglossal nerve
9 = retromandibular vein (or external carotid vein)	22 = prevertebral muscles
10 = medial pterygoid muscle	23 = superior constrictor muscle of the pharynx

Figure 14.2 A cross section of the upper part of the neck at the level of the tonsil showing cross-sectional anatomy and the relationship of neurovascular structures in the parapharyngeal space.

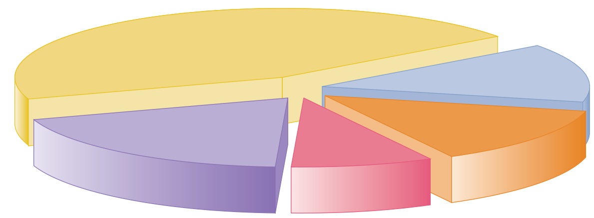

Figure 14.3 The location of benign peripheral nerve tumors.

Table 14.1 Benign and Malignant Tumors of Neural Origin

Benign	Malignant
Reactive	Malignant peripheral nerve sheath tumors (MPNST)
Traumatic neuroma	(malignant schwannoma, neurofibrosarcoma) – Epithelioid MPNST – Pigmented (melanotic) MPNST – Peripheral primitive neuroectodermal tumor (Askin tumor)
Hamartoma: mucosal neuromas (MEN IIB, Gorlin's syndrome)	Autonomic nerve tumor (plexosarcoma)
Schwannoma (neurilemmoma)	Malignant melanoma of soft tissues (clear cell sarcoma)
Neurofibroma: solitary, multiple, diffuse, plexiform (NF-1)	
Perineurioma (storiform perineurial fibroma)	
Dermal nerve sheath myxoma	
Granular cell tumor	

MEN, Multiple endocrine neoplasia; *MPNST,* malignant peripheral nerve sheath tumor; *NF,* neurofibromatosis.

separated by the styloid process and its attached muscles (Fig. 14.2).

The space anterolateral to the styloid process is also called the *true PPS* or *the masticator space*; it contains loose areolar tissue, the deep lobe of the parotid gland, the retropharyngeal lymph nodes, blood vessels, and fat. The most common neoplasm occurring in this space is of salivary origin, arising either from the deep lobe of the parotid gland, from minor salivary glands in the lateral pharyngeal wall, or from salivary rests in the parapharyngeal space. The parapharyngeal region posteromedial to the styloid process is called the *carotid space,* and it contains the carotid artery, internal jugular vein, lower cranial nerves (IX, X, XI, and XII), and the sympathetic chain. The most common neoplasms in this space are paragangliomas and neurogenic tumors arising from the lower cranial nerves.

NEUROGENIC TUMORS

The head and neck region is by far the most common location for benign peripheral nerve tumors (Fig. 14.3). Neurogenic tumors of the cervical region are divided into those arising in either the medial or lateral compartment of the neck. Neurogenic tumors of the medial compartment arise from the lower cranial nerves or the sympathetic chain. Neurogenic tumors of the lateral compartment of the neck arise from the cutaneous or muscular branches of the cervical plexus or the brachial plexus. Occasionally these tumors arise at the spinal foramina with an intraspinal and extraspinal component presenting as a "dumbbell tumor." The various types of benign and malignant tumors of neural origin are listed in Table 14.1.

Schwannomas originate from the neuroectodermal sheath surrounding peripheral nerves. They can arise in any part of the head and neck region, including the face, scalp, cranial cavity, orbit, middle ear, nasal cavity, oral cavity, larynx, and neck. Schwannomas also frequently arise from cranial nerves V, VII, VIII, and X and the sympathetic chain. On rare occasions schwannomas can be seen in the glossopharyngeal or hypoglossal nerves and even less commonly in other cranial nerves. Schwannomas are usually solitary neoplasms. Multifocal presentation raises the suspicion for neurofibromatosis type 2 (NF2), which results from inherited mutations in the *NF2* suppressor gene. The formation of nonfamilial schwannomas also has been attributed to somatic alterations of the *NF2* gene. Histologically, schwannomas show pallisading nuclei from Verocay bodies in the cellular Antoni A areas. They are strongly and diffusely immunoreactive to S-100 protein (Figs. 14.4 and 14.5).

Neurofibromas are benign, unencapsulated tumors that may be localized, diffuse, or plexiform and are either familial or sporadic. The presence of a plexiform neurofibroma is virtually pathognomonic of familial neurofibromatosis (NF1). Neurofibromas

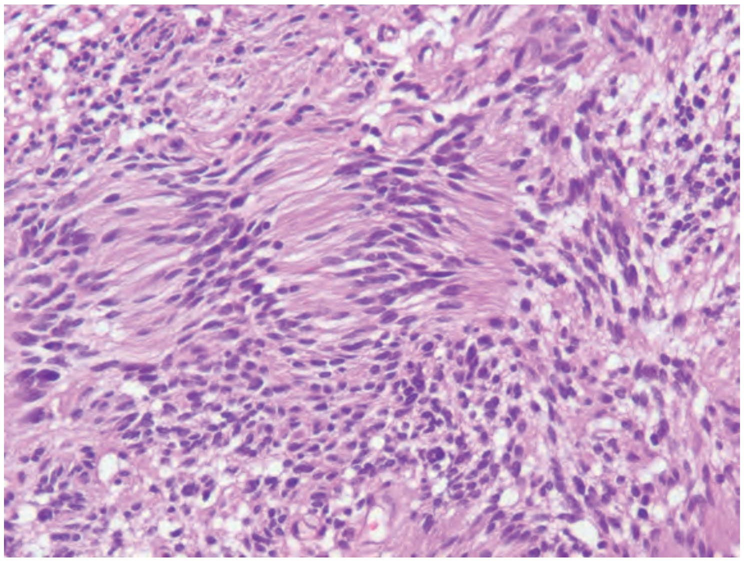

Figure 14.4 The histologic appearance of a schwannoma (hematoxylin and eosin stain). Palisading nuclei form Verocay bodies in the cellular Antoni A areas. The looser, myxoid areas are referred to as Antoni B areas. Prominent thick-walled blood vessels are another common histologic feature.

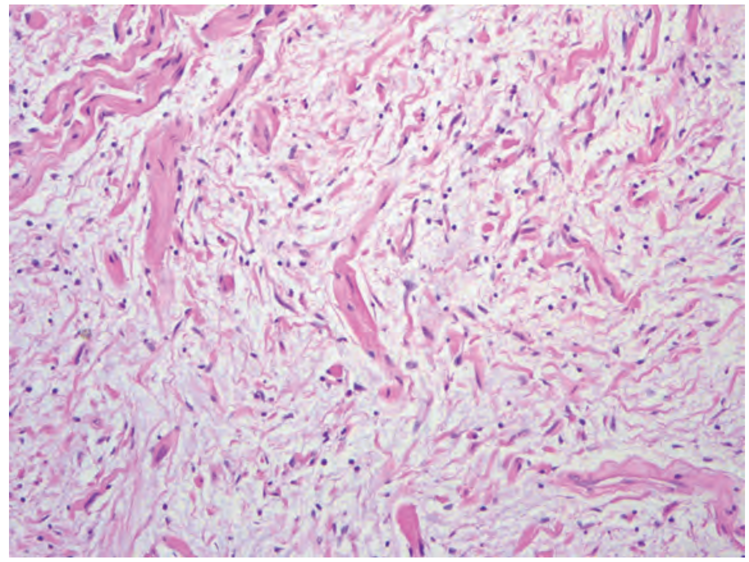

Figure 14.6 The histologic appearance of a neurofibroma (hematoxylin and eosin stain). Histologically, a neurofibroma will have a loosely arranged background of collagen fibrils, which have been likened to “shredded carrots,” with small, uniform nuclei. These tumors are positive for S-100 protein, although not as strongly and diffusely as are schwannomas.

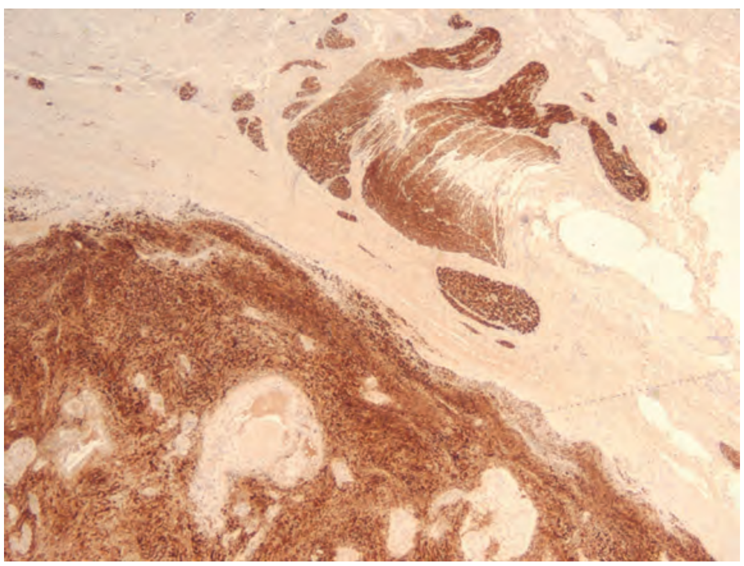

Figure 14.5 An immunohistochemical stain for S-100 protein. Like their normal counterparts, schwannomas are strongly and diffusely immunoreactive for S-100 protein.

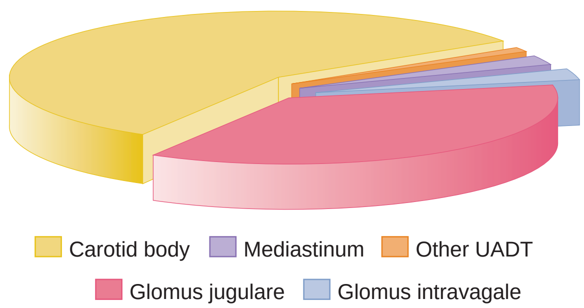

Figure 14.7 Distribution of paragangliomas of the head and neck region. *UADT,* Upper aerodigestive tract.

typically present as ill-defined lesions in the scalp and skin of the head and neck. They occasionally may be seen from terminal branches of the trigeminal nerve in the sinonasal tract or in the larynx. Cutaneous neurofibromas have a raised, plaquelike appearance and are slow-growing, painless lesions that may be located in the dermis or in the subcutaneous fibroadipose tissue. Their borders can be indistinct, contributing to the high rates of incomplete excision and subsequent recurrence. Histologically, neurofibromas show loosely arranged collagen fibrils with small uniform nuclei. They are also positive for S-100 protein, although not as strongly as schwannomas (Fig. 14.6).

Malignant peripheral nerve sheath tumors (MPNSTs) are of Schwann or perineurial cell origin and arise either de novo or from a preexisting neurofibroma (NF1). At least two-thirds of MPNSTs are derived from neurofibromas in patients with NF1, and approximately 10% are induced by radiation. De novo MPNSTs most commonly occur in the fourth decade of life. When seen in conjunction with NF1, MPNSTs occur in younger patients and have a male predominance. In the sinonasal tract and nasopharynx, MPNSTs commonly arise from the ophthalmic and maxillary branches of the trigeminal nerve, but these tumors can arise from any cranial nerve. Quite rarely these tumors occur in the larynx, where they may cause mucosal ulceration. Operative findings of a thick pseudocapsule and firm adherence to surrounding soft tissue are harbingers of malignancy, and inspection of the cut surface of an MPNST often reveals hemorrhage and necrosis. Histologically, MPNSTs may be spindled or epithelioid. MPNSTs demonstrate immunoreactivity for the S-100 protein, but not to the same extent or intensity as a schwannoma. The local recurrence rate is quite high, and distant metastases can occur to the lungs, bone, and liver.

Paragangliomas

Paraganglia are neural cell aggregates of the sympathetic or parasympathetic nervous system and they typically reside in the adventitia of blood vessels and nerves. Whereas sympathetic paragangliomas secrete catecholamine and most commonly occur in the adrenal medulla, those of parasympathetic origin typically do not secrete catecholamines and primarily occur in the head and neck region. The distribution of paragangliomas of the head and neck region is shown in Fig. 14.7. Most paragangliomas in the head and neck region arise in the carotid body jugulotympanic region, vagal body, superior and inferior

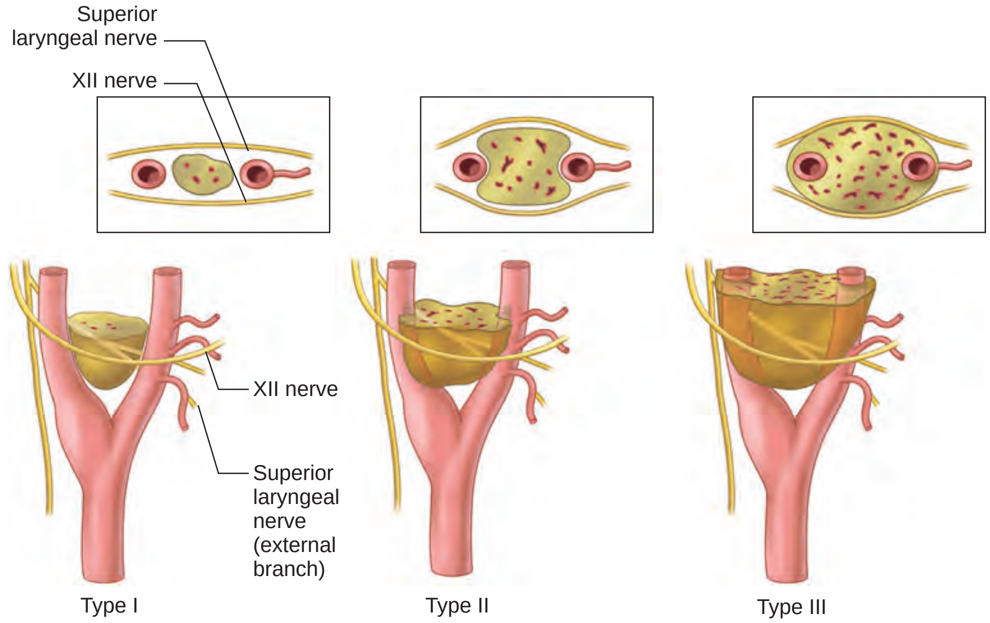

Figure 14.8 Shamblin's classification of carotid body tumors.

laryngeal paraganglionic tissue, nasal cavity, or the orbit, reflecting the distribution of parasympathetic ganglia.

Paragangliomas typically occur in older persons, are unifocal, and are histologically benign. However, approximately 10% of head and neck paragangliomas can be malignant, 10% are bilateral or multiple, and 10% occur in patients with a family history of paragangliomas. Rarely, paragangliomas are functioning, and in those instances, patients present with a history of episodic flushing of the face and hypertension. In such patients, appropriate systemic imaging studies to rule out other paragangliomas should be undertaken, and serum and urinary catecholamine levels should be measured to establish an accurate diagnosis.

Carotid body tumors (also known as chemodectomas or nonchromaffin paragangliomas) are by far the most common of all paragangliomas in the neck and are more common in persons residing at high altitudes. Carotid body tumors arise from the chemoreceptor cells in the carotid sheath, which most commonly are located at the bifurcation of the carotid artery. These tumors are slow growing, are highly vascular, and are histologically benign in most instances. The characteristic location is in the upper part of the neck, where it may present as an external mass, or it may appear as a parapharyngeal mass pushing the lateral pharyngeal wall medially in the oropharynx. In either location, the mass usually has palpable pulsations. If the clinical diagnosis of a carotid body tumor is suspected, appropriate radiographic studies must be performed before deciding on a management plan. Shamblin classified carotid body tumors into three categories, based on the relationship of the carotid arteries and the adjoining nerves to the tumor (Fig. 14.8). In type I, the external and internal carotid arteries are simply displaced by the tumor, and the hypoglossal and superior laryngeal nerves lie on the surface of the tumor. In type II, the tumor is indented by the external and internal carotid arteries, making a deep groove within the tumor, and the hypoglossal and superior laryngeal nerves are on the tumor's surface. In type III, the arteries are encased by the tumor.

Although they are rare, malignant paragangliomas have a significant potential for local invasion, cranial nerve paralysis, and regional or distant metastases. Histologically, paragangliomas have a characteristic nested or "Zellballen" appearance. Immunohistochemical staining shows positivity for S-100 protein, and a chromogranin stain for the cytoplasm of chief cells shows neurosecretory granules (Figs. 14.9 through 14.11). Benign paragangliomas and malignant paragangliomas have a similar histologic picture, and often it is difficult for pathologists to differentiate between the two. Therefore the diagnosis of a malignant paraganglioma is made on the basis of the following features: (1) local invasion, cranial nerve paralysis, invasion of the carotid artery, or infiltration of the soft tissues in the parapharyngeal space or bone destruction at the skull base; (2) the presence of regional lymph node metastasis; or (3) distant metastasis. Clinically, adherence of the tumor with reduced mobility or cranial nerve paralysis suggests malignancy. Upon radiologic imaging, the presence of regional lymph node metastasis and evidence of invasion and infiltration into adjacent structures would raise suspicion of the tumor being malignant.

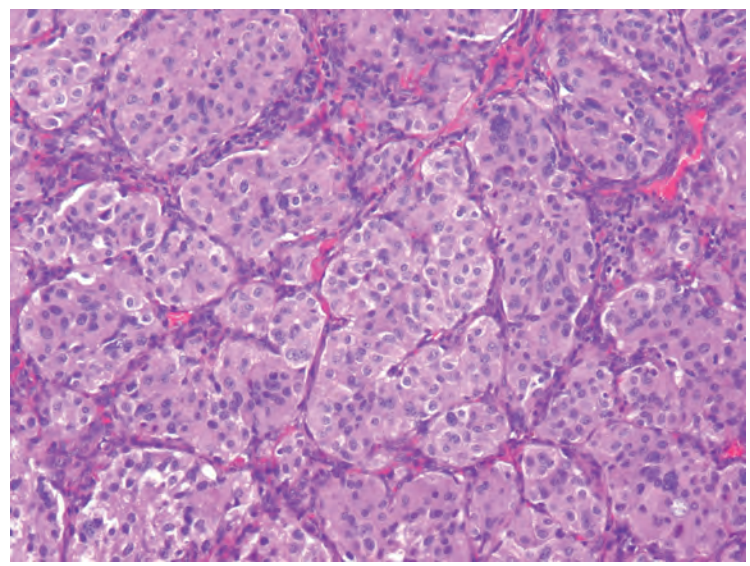

Figure 14.9 A paraganglioma (hematoxylin and eosin stain). Paragangliomas have a characteristic nested, or Zellballen, appearance.

Paragangliomas that appear in younger patients and/or present in multiple locations raise concern for a genetic predisposition. Linkage analysis has identified four possible loci, termed "paraganglioma loci 1 to 4" (PGL 1, PGL 2, PGL 3, and PGL 4). Although the gene in PGL 2 remains to be identified, PGL 1,

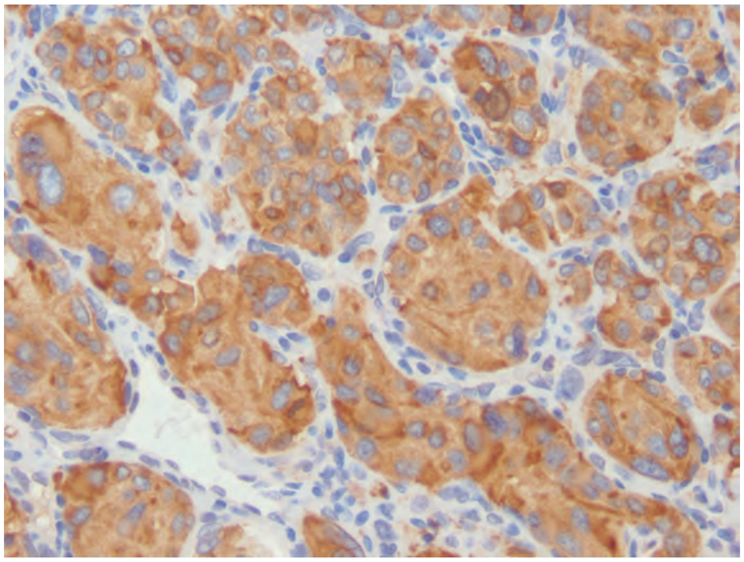

Figure 14.10 Immunohistochemistry for S-100 protein highlights peripheral sustentacular cells in a paraganglioma.

Table 14.2 Significance of Genetic Abnormalities in Head and Neck Paragangliomas

	SDHB (PGL4)	SDHC (PGL3)	SDHD (PGL1)
Chromosomal locus	1p35-36	1q21	11q23
Inheritance	Monogenic, autosomal dominant	Monogenic, autosomal dominant	Monogenic, autosomal dominant with paternal imprinting
Penetrance	>75%	>75%	?
Pheochromocytoma	+	–	+
Percent with head and neck tumors	15%-50%	50%-100%	50%-100%
Frequency	5%-10% of cases	<5%	80%-90% of cases
Malignancy	+ (5%-35%)	–	–
Multicentricity	15%-50%	~10%	50%-90%

PGL, Paraganglioma locus; *SDH,* succinate dehydrogenase.

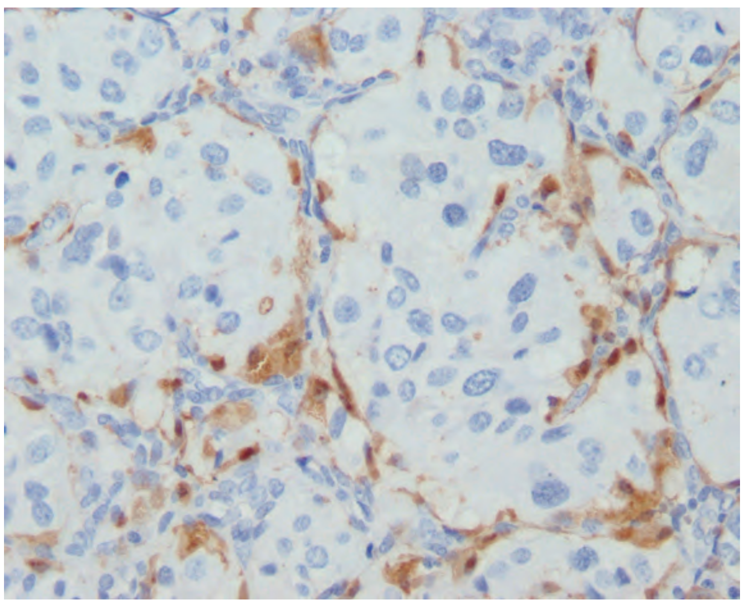

Figure 14.11 Chromogranin labels the cytoplasm of the chief cells, reflecting the presence of neurosecretory granules. Similarly, synaptophysin also will be positive. Cytokeratin, carcinoembryonic antigen (CEA), and calcitonin are negative.

PGL 3, and PGL 4 have been identified as succinate dehydrogenases (SDHs), including *SDHD, SDHC,* and *SDHB,* respectively. These genes encode for components of the four-subunit mitochondrial complex II (also known as the *succinate ubiquinone oxidoreductase*) that is involved in electron transport and the Krebs tricarboxylic acid cycle. The mitochondrial complex II is one of five complexes in the mitochondrial electron transport chain; it catalyzes conversion of succinate to fulminate and is essential for normal development. Homozygous defects in the mitochondrial complex II result in Leigh syndrome (associated with severe neurologic impairment), whereas heterozygous defects result in paraganglioma and pheochromocytoma development. The wild-type allele often is inactivated in paragangliomas (Table 14.2).

PGL 2, *SDHB,* and *SDHC* are inherited as autosomal dominant traits. The *SDHD* gene is imprinted from the paternal line, and thus the phenotype is only inherited from the father. Penetrance is variable but is relatively high overall. Patients usually present by the first decade of life; fewer than 5% of paragangliomas are familial in patients older than 50 years. Although paragangliomas are common to all subtypes, pheochromocytomas also can develop in patients with PGL 1 and PGL 4.

Genetic testing is advocated for patients presenting with multiple paragangliomas or a suggestive family history. In addition, testing should be considered in patients with extraadrenal sympathetic paragangliomas or in younger patients, because germline mutations can be detected in *SDHB* or *SDHD* in up to 20% of the cases. The management of familial paraganglioma is a matter of debate. Retrospective studies suggest that intervention may do little to affect the long-term outcome, and observation may be warranted in most cases. Surgery should be considered in patients with carotid body tumors and tumors with rapid growth or significant symptoms.

CLINICAL FEATURES AND DIAGNOSIS

The majority of patients with neurogenic tumors and paragangliomas in the head and neck region are asymptomatic. Presentation with a mass that is accidentally discovered in the neck or is consequent to an incidental finding on an imaging study, such as a computed tomography (CT) or magnetic resonance imaging (MRI) scan performed for other reasons, is common. Tumors arising from the lower cranial nerves usually present in the retromandibular region of the upper part of the neck with ill-defined fullness, and they can be pulsatile. The pulsatile nature of the mass reflects increased vascularity or, more commonly, transmitted pulsations from the carotid vessels. On the other hand, schwannomas and neurofibromas arising in the lateral aspect of the neck present as firm, discrete lesions without pulsations. These tumors usually are mobile in an axis perpendicular to the long axis of the nerve.

In the great majority of cases, the nerve of origin of schwannomas or neurofibromas retains its function. Presentation with paralysis of the involved cranial nerve is rare and should raise concern for malignancy. Neurogenic tumors and paragangliomas in the PPS often present as a submucosal mass in the lateral pharyngeal wall, pushing the tonsil and soft palate medially.

Neurofibromas arising from sensory nerves occasionally are painful to touch and pressure.

Diagnosis of these tumors is usually made through clinical assessment and radiologic imaging. Biopsy and tissue diagnosis is seldom required and indeed may be hazardous. Fine-needle aspiration biopsy may establish the diagnosis of neurogenic tumor but is not helpful for paragangliomas. An open biopsy of a paraganglioma causes significant hemorrhage and should be avoided. A transoral open biopsy of a parapharyngeal mass should not be performed.

RADIOGRAPHIC EVALUATION

Modern radiologic imaging has revolutionized the diagnosis and management of neurovascular lesions in the head and neck region. In the past, direct angiography was the only confirmatory radiographic test for a carotid body tumor or paraganglioma. However, with the advent of CT and MRI scanning, direct angiography is seldom performed today unless preoperative embolization of the tumor is required. CT angiography and MRA also provide a noninvasive means of angiography and three-dimensional reconstruction. As such, these imaging studies play an essential role in aiding preoperative diagnosis, surgical planning, or monitoring growth if a decision is made to observe these tumors.

Most neurogenic and vascular tumors of the suprahyoid neck arise from within the carotid space (CS). The CS spans the entire neck from the skull base to the aortic arch. Its contents include the carotid artery, internal jugular vein, cranial nerves IX to XII, and the sympathetic chain. The X nerve lies posterior and lateral to the carotid artery, whereas the sympathetic chain lies posterior and medial to the artery. Although it is a continuous space, the CS is further subdivided into the suprahyoid and infrahyoid portions, with the suprahyoid portion anatomically related to the PPS and the most common site of origin of neurovascular tumors in the head and neck. The suprahyoid CS is located posterior to the PPS and extends superiorly into the carotid canal and jugular foramen at the skull base (Fig. 14.12).

When assessing the imaging, it is important to examine contiguous slices on CT or MRI to avoid confusing anatomic variations such as a dominant jugular vein or tortuous carotid artery. In general, the distinction between suprahyoid CS and PPS tumors can be made simply by assessing the direction of displacement of the fat in the PPS (Fig. 14.13). Tumors originating in the CS characteristically displace the PPS fat and internal carotid artery anteriorly and the internal jugular vein laterally. In contrast, tumors of the PPS result in posterior displacement of these structures.

The two most common tumors in the suprahyoid CS, paragangliomas and nerve sheath tumors, can be distinguished radiographically, because paragangliomas are very vascular tumors. Paragangliomas enhance intensely on CT and MRI and have flow voids on MRI (Fig. 14.14). Although flow voids are diagnostic of paragangliomas, they may not be readily apparent if the tumor is less than 2 cm in diameter. A contrast-enhanced CT scan can help make the diagnosis in these situations, because paragangliomas become intensely enhanced compared with nerve sheath tumors that may or may not become enhanced. Paragangliomas on the CT scan show enhancement and have a characteristic spindle-shaped appearance on the coronal or sagittal views (Fig. 14.15). MRI, on the other hand, characteristically shows the flow voids and also demonstrates the spindle-shaped nature of the tumor giving a "rat tail" appearance on coronal and sagittal sections (Fig. 14.16).

The classic carotid body tumor is located within the carotid bifurcation in the infrahyoid neck and therefore is not in immediate proximity to the PPS. It tends to splay the internal

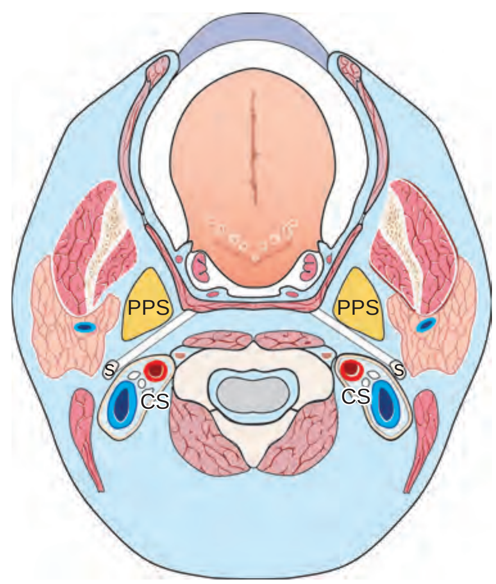

Figure 14.12 Schematic diagram of the normal anatomy of the parapharyngeal space (*PPS*) for correlation with radiographic imaging. The prestyloid space is separated from the poststyloid compartment or carotid space (*CS*) by the tensor-vascular-styloid fascia (*white line*) that extends medially from the styloid process (*S*) to the pharynx and overlies the tensor veli palatini muscle. *(Courtesy Memorial Sloan Kettering Cancer Center.)*

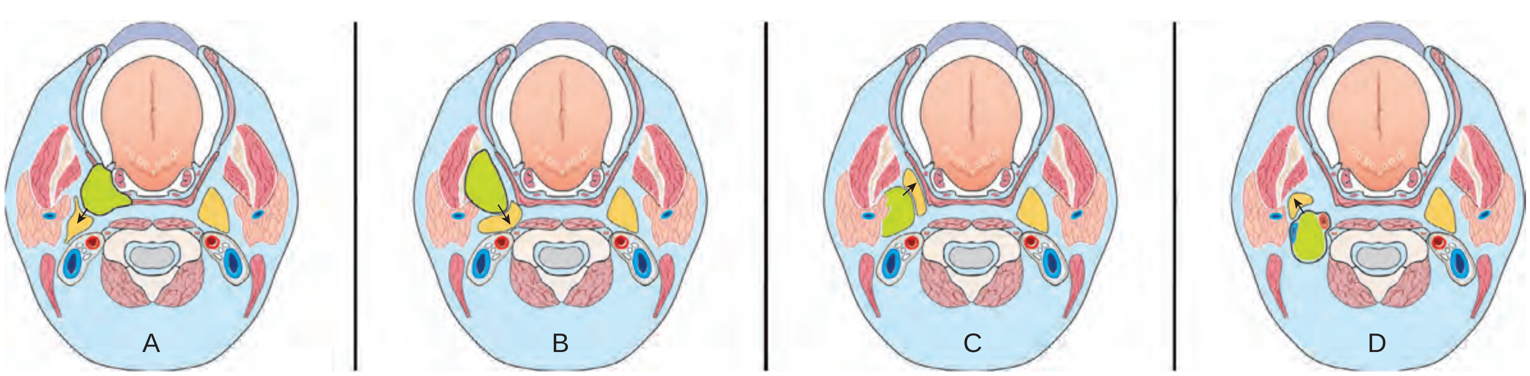

Figure 14.13 The pattern of displacement of parapharyngeal space (PPS) fat by tumors of the surrounding spaces allows identification of the origin of tumors in relation to the PPS. **A**, Pharyngeal mucosal space (PMS). **B**, Masticator space (MS). **C**, Parotid space (PS). **D**, Carotid space (CS). *(Courtesy Memorial Sloan Kettering Cancer Center.)*

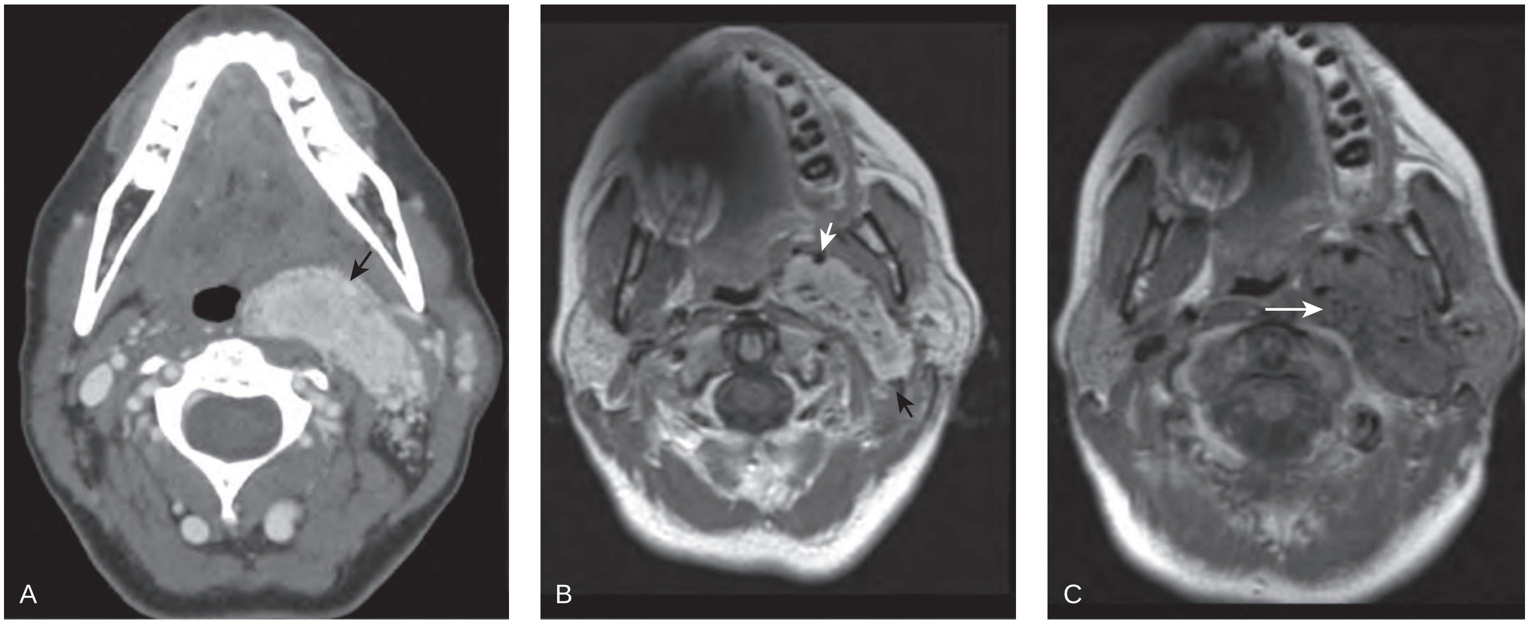

Figure 14.14 **A**, A contrast-enhanced axial CT scan shows a densely enhancing mass in the left carotid space that displaces the internal carotid artery (*arrow*) anteromedially. The internal jugular vein is not visible on this section, because it is effaced by the lesion. **B**, An axial postcontrast T1-weighted magnetic resonance imaging scan shows intense enhancement of the mass. The mass displaces the internal jugular vein posterolaterally (*black arrow*) and the internal carotid artery anteromedially (*white arrow*). **C**, Multiple low-signal flow voids (*white arrow*) on T1-weighted magnetic resonance imaging are a typical characteristic of a paraganglioma. *(From Stambuk HE, Patel SG. Imaging of the parapharyngeal space. Otolaryngol Clin North Am 41[1]:77–101, vi, 2008.)*

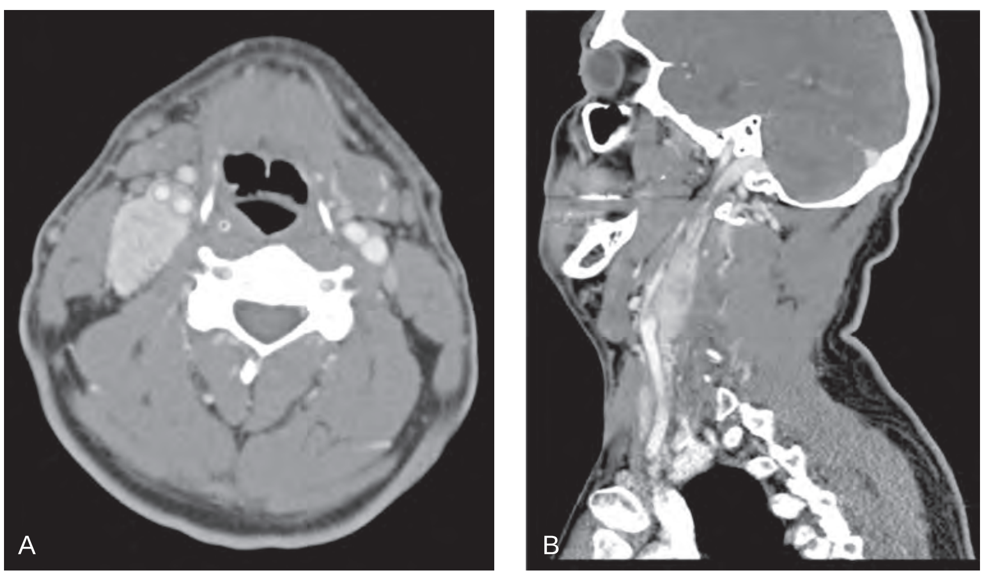

Figure 14.15 Contrast-enhanced computed tomography scan of a patient with vagal paraganglioma in axial (**A**) and sagittal (**B**) views. Note the contrast enhancement and the location of the tumor posterior to the carotid artery and jugular vein on the axial view and a spindle-shaped tumor posterior to the carotid sheath in the sagittal view.

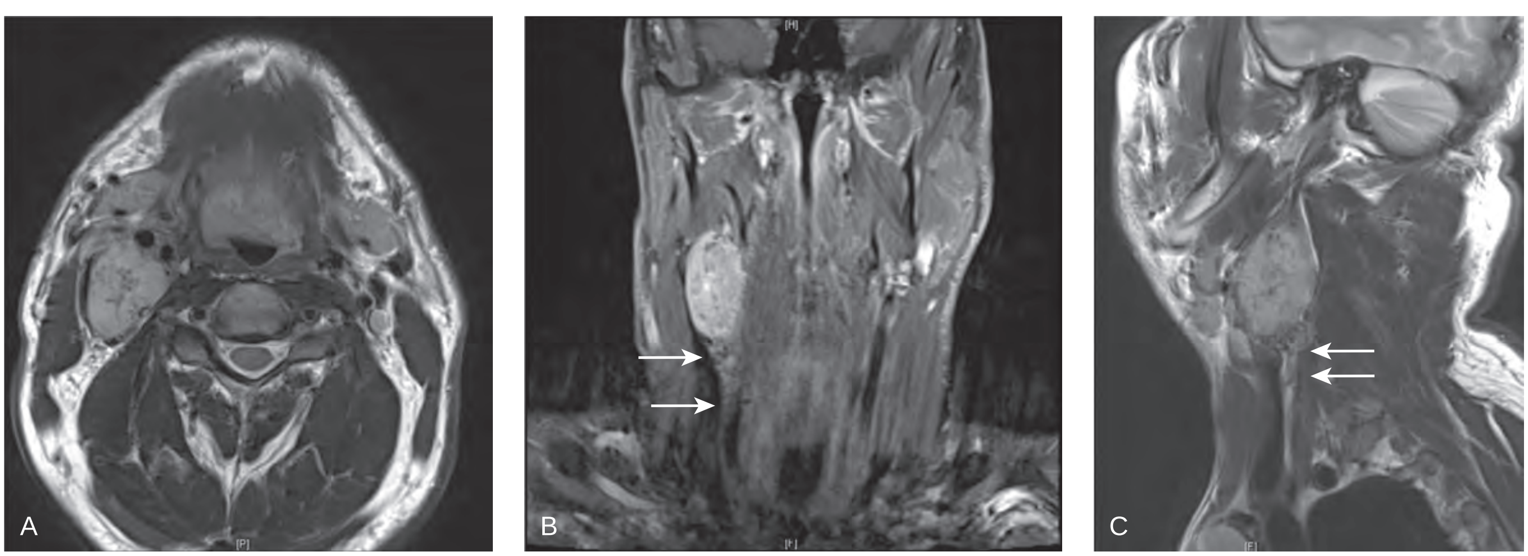

Figure 14.16 Magnetic resonance imaging scans in T2-weighted axial view (**A**), postcontrast T1-weighted coronal view (**B**), and postcontrast T1-weighted sagittal view (**C**) showing a vagal paraganglioma. Note contrast enhancement and flow voids, as well as "rat tail" appearance on coronal and sagittal views, characteristic of a paraganglioma of lower cranial nerves (*arrows*).

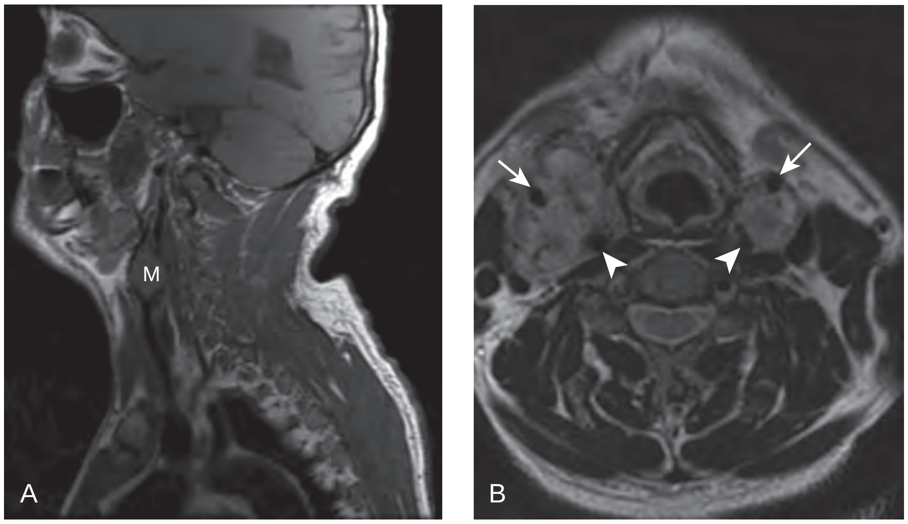

Figure 14.17 Sagittal precontrast T1-weighted magnetic resonance imaging (MRI) shows a mass (M) located in the carotid bifurcation splaying the internal carotid artery posteriorly and the external carotid artery anteriorly (**A**). A T2-weighted MRI scan of the same patient demonstrates bilateral carotid body tumors splaying the internal carotid artery (*arrowheads*) posteriorly and the external carotid artery (*arrows*) anteriorly (**B**). *(From Stambuk HE, Patel SG. Imaging of the parapharyngeal space. Otolaryngol Clin North Am 41[1]:77–101, vi, 2008.)*

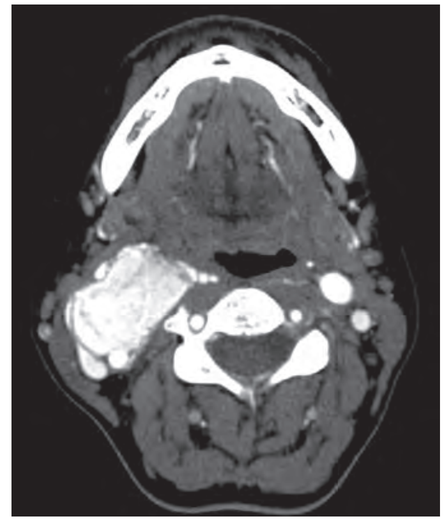

Figure 14.18 An axial view of a contrast-enhanced computed tomography scan of the neck showing a Shamblin type 1 carotid body tumor on the right-hand side.

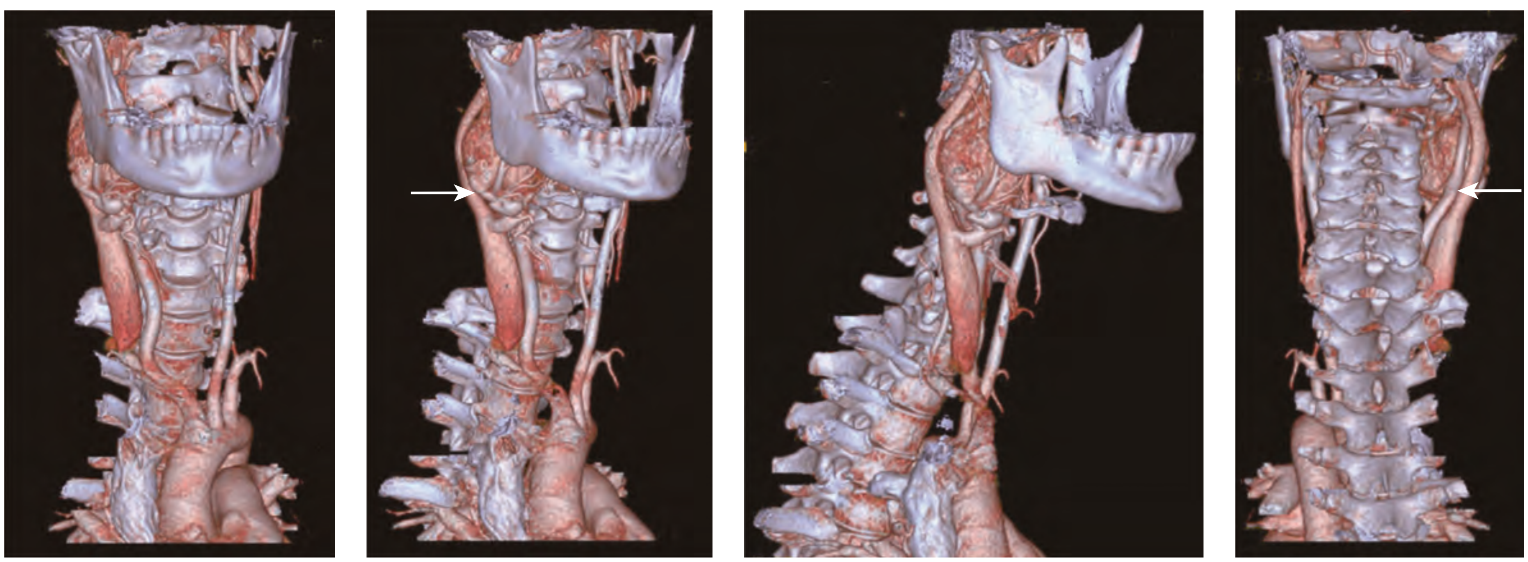

Figure 14.19 Three-dimensional reconstructions of computed tomography angiograms showing a shambling type 1 carotid body tumor on the right-hand side in anterior, lateral, and posterior view showing the relationship of external and internal carotid arteries to the tumor (*arrows*).

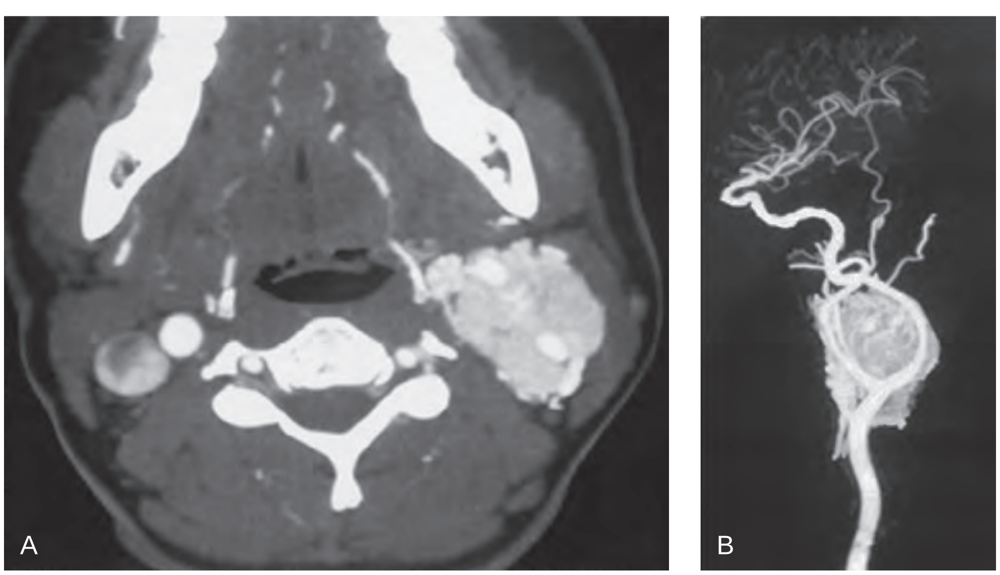

Figure 14.20 An axial view of a contrast-enhanced computed tomography (CT) scan (**A**) showing a Shamblin type 2 carotid body tumor. CT angiography (**B**) clearly shows the location and relationship of the carotid arteries to the tumor.

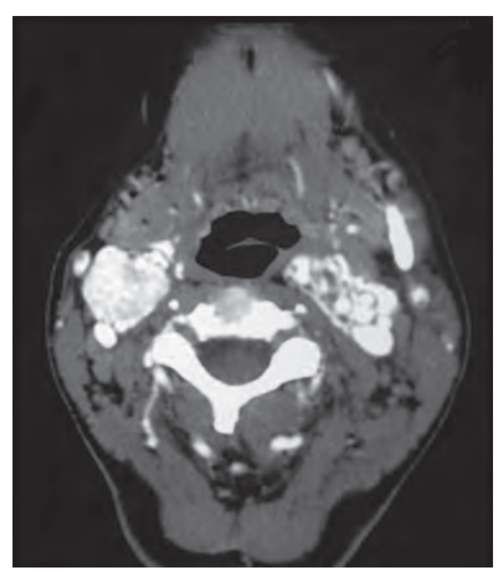

Figure 14.21 An axial view of a contrast-enhanced computed tomography scan of the neck showing bilateral carotid body tumors.

carotid artery and the external carotid artery at the carotid bifurcation (Fig. 14.17). Carotid body tumors enhance intensely on a contrast-enhanced CT scan (Fig. 14.18). The location of the external and internal carotid artery in relation to the tumor is crucial in surgical treatment planning. The carotid vessels may be superficial to the tumor, indenting into the tumor, or encased by the tumor. To assess these relationships, it is often necessary to obtain a contrast-enhanced CT scan with three-dimensional reconstructions, as well as a contrast-enhanced MRI for detailed assessment of the location and extent of the tumor and its relation to the carotid arteries (Fig. 14.19). Three-dimensional reconstructions are also helpful in differentiating various types of carotid body tumors in relation to the carotid arteries (Fig. 14.20). Complete evaluation of the imaging studies is necessary, since some patients may present with multiple paragangliomas on the same side of the neck or bilaterally (Fig. 14.21). In contrast to a carotid body tumor, a glomus vagale tends to displace the carotid artery anteriorly (Fig. 14.22). Unlike

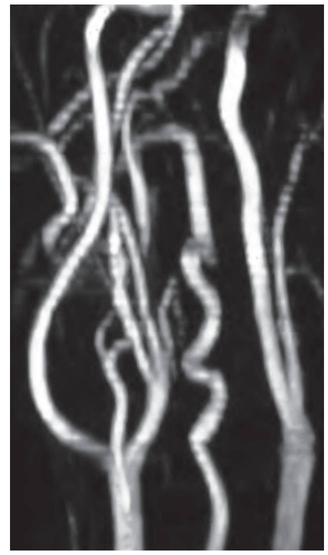

Figure 14.23 Magnetic resonance angiogram of a patient with a carotid body tumor.

Figure 14.24 A direct angiogram through the right common carotid artery shows feeding blood vessels to a vagal paraganglioma.

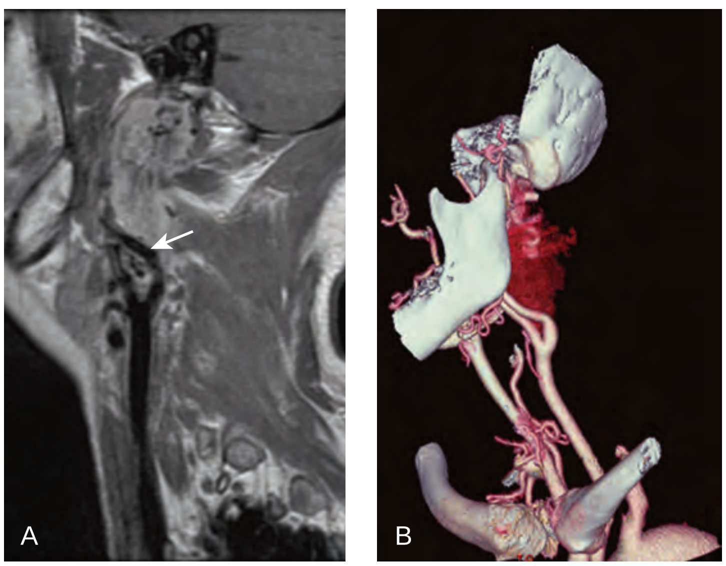

Figure 14.22 A sagittal postcontrast T1-weighted magnetic resonance imaging scan shows a heterogeneously enhancing carotid space mass displacing both the internal carotid artery (*arrow*) and external carotid artery anteriorly and with cephalad extension into the jugular foramen (*arrow*) (**A**). An oblique computed tomography angiogram three-dimensional reconstruction nicely illustrates the relationship to the surrounding structures (**B**). *(From Stambuk HE, Patel SG. Imaging of the parapharyngeal space. Otolaryngol Clin North Am 41[1]:77–101, vi, 2008.)*

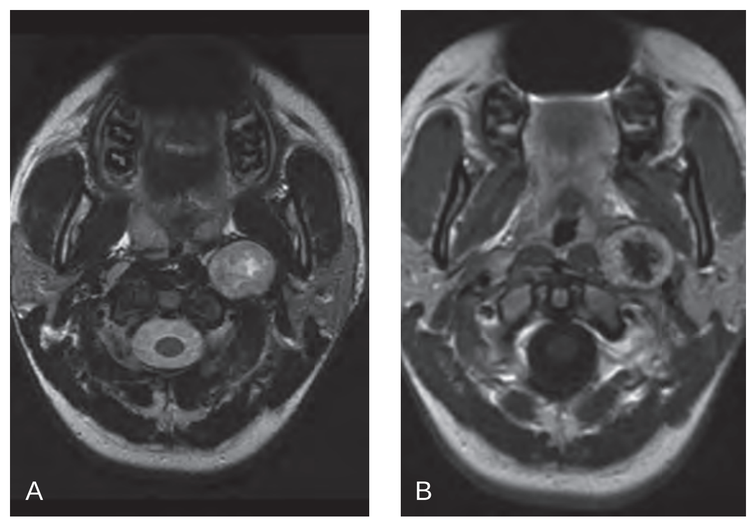

Figure 14.25 An axial T2-weighted magnetic resonance imaging (MRI) scan shows a heterogeneous high-signal mass in the left carotid space without flow voids (**A**). The mass enhances heterogeneously on a postcontrast T1-weighted MRI scan, which is the typical appearance of a schwannoma (**B**). *(From Stambuk HE, Patel SG. Imaging of the parapharyngeal space. Otolaryngol Clin North Am 41[1]:77–101, vi, 2008.)*

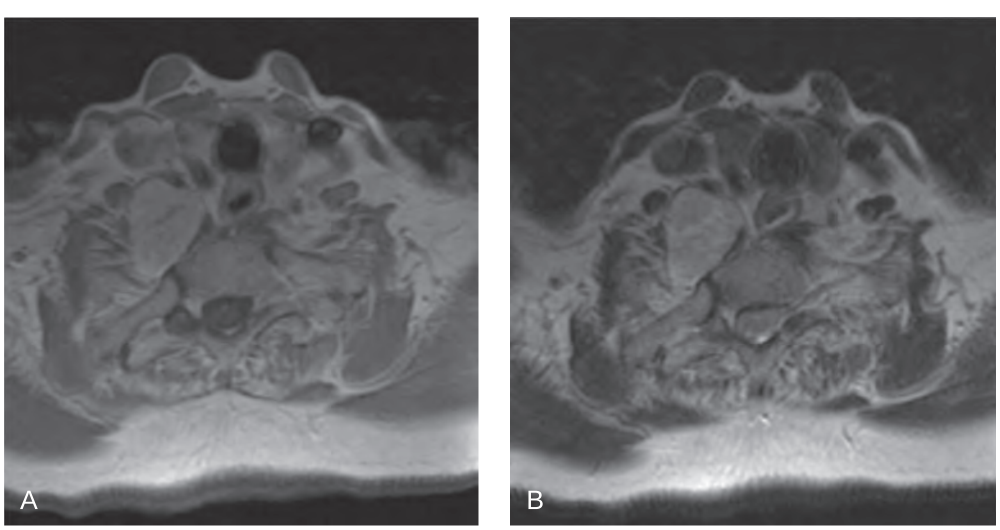

Figure 14.26 A postcontrast T1-weighted axial view of magnetic resonance imaging scan (**A**) showing a contrast enhancing schwannoma posterior to the carotid sheath in the lower part of the neck. On T2-weighted sequence, it is bright (**B**).

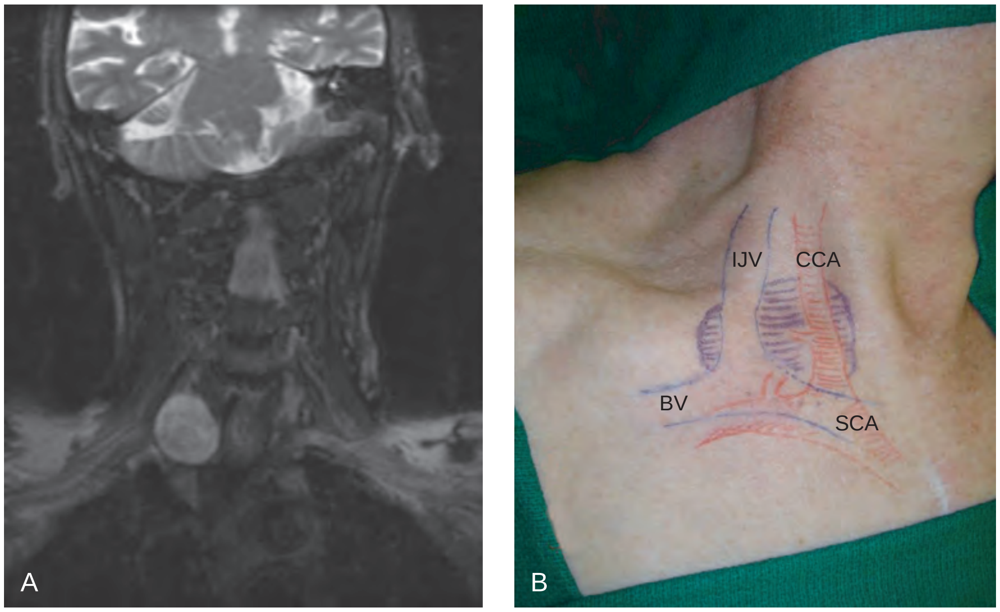

Figure 14.27 **A**, Coronal view of the magnetic resonance image of the tumor shown in Fig. 14.28 demonstrates a well-circumscribed "round" tumor in the lower part of the neck. **B**, Outline of the relationship of the tumor to great vessels in the lower part of the neck. *BV,* Brachial vein; *CCA,* common carotid artery; *IJV,* internal jugular vein; *SCA,* subclavian artery.

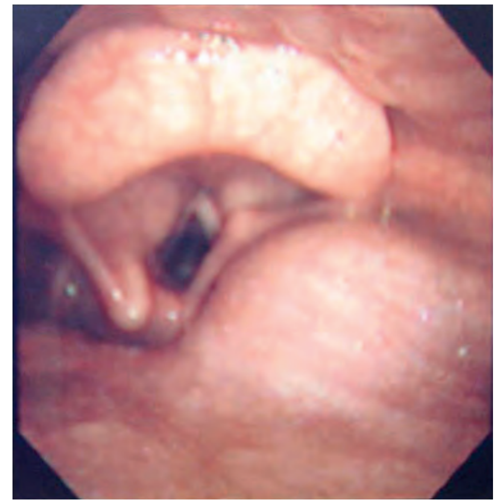

Figure 14.28 Endoscopic view of the hypopharynx showing a submucosal tumor mass of the prevertebral space projecting into the pharynx.

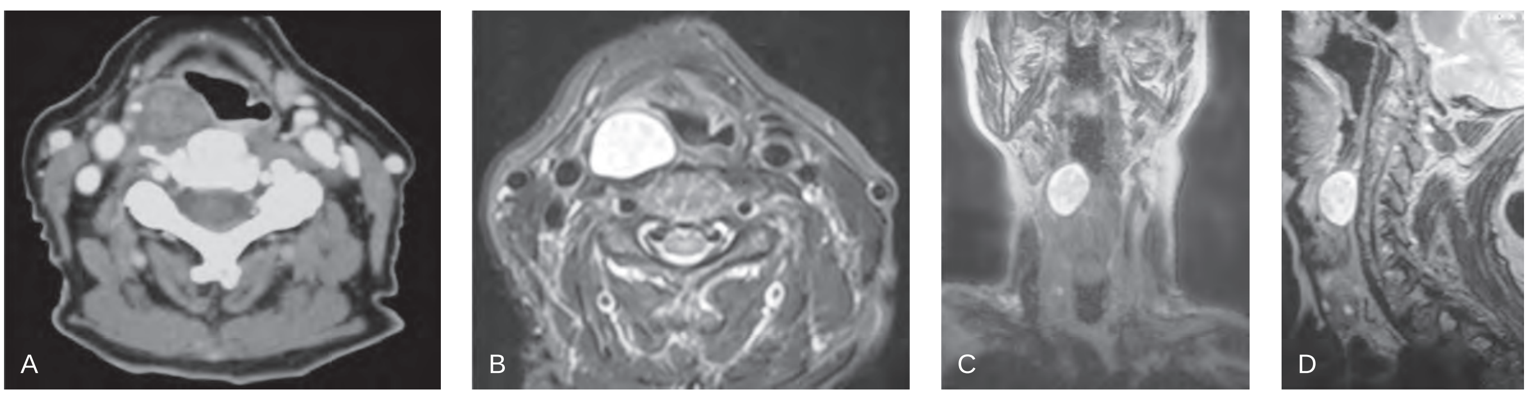

Figure 14.29 Imaging studies of the tumor shown in Fig. 14.28. A contrast-enhanced computed tomography scan (**A**) showing a nonenhancing tumor in the prevertebral space. T2-weighted magnetic resonance imaging scans in axial (**B**), coronal (**C**), and sagittal (**D**) views show a well-demarcated "bright" tumor in the prevertebral space.

carotid body tumors, other paragangliomas often have demonstrable feeder vessels that most commonly arise from the ascending pharyngeal artery. It is important to point out that these feeder vessels are not readily apparent on noninvasive vascular imaging such as computed tomographic angiography (CTA) or magnetic resonance angiography (MRA) (Fig. 14.23). Conventional angiography would be needed to demonstrate the feeder vessels and is recommended only if embolization is part of the treatment plan (Fig. 14.24).

Radiographic differentiation of a schwannoma from a neurofibroma is not straightforward. Heterogeneity within the lesion is more commonly seen in schwannomas because of a cystic change or hemorrhage. Schwannomas are well-encapsulated tumors that appear as round or ovoid masses. On MRI they are isointense to muscle on T1 and hyperintense on T2, and they become enhanced after administration of contrast (Fig. 14.25). These imaging characteristics are by no means unique to schwannomas; paragangliomas can have similar imaging characteristics. However, as previously described, schwannomas do not have flow voids, even when they are large (Fig. 14.26 and Fig. 14.27). The endoscopic view of a schwannoma of the retropharyngeal space projecting through the right posterolateral pharyngeal wall is shown in Fig. 14.28. Typically, schwannomas do not show contrast enhancement on CT scan but are characteristically bright on T2-weighted MRI scan (Fig. 14.29). In addition, schwannomas at the skull base generally cause regressive remodeling of bone, whereas permeative changes are seen more classically with paragangliomas.

MRI also is of significant help in demonstrating neurogenic tumors with intraspinal and extraspinal extension (i.e., dumbbell tumors). A myelogram generally is not used unless MRI is contraindicated, because an MRI scan provides superior information with appropriate contrast enhancement (Fig. 14.30). Noninvasive imaging generally does not provide functional information on the adequacy of cerebral circulation, and dedicated tests should be performed if carotid artery resection is a surgical possibility. These tests include balloon occlusion testing and/or radioactive xenon perfusion imaging.

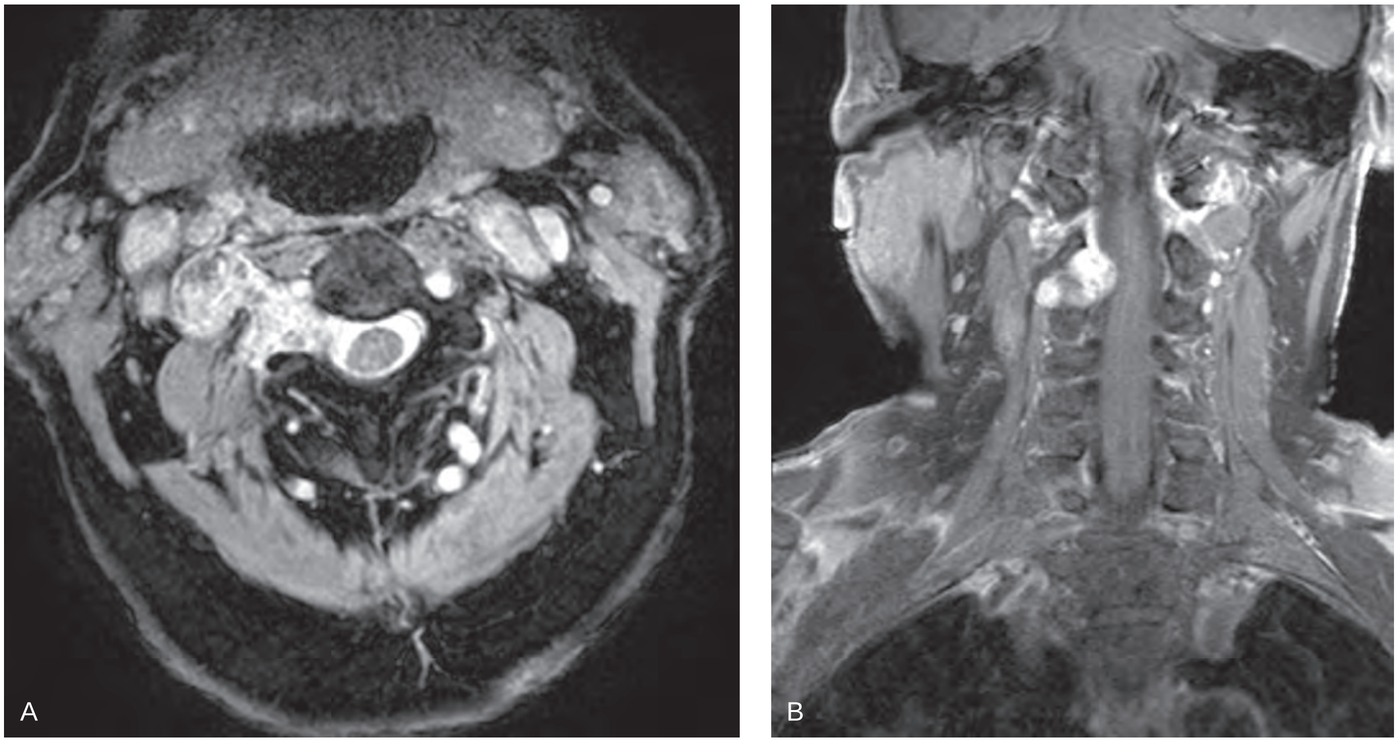

Figure 14.30 An axial T2-weighted magnetic resonance imaging (MRI) scan shows a dumbbell tumor of neurogenic origin with intraspinal extension (**A**). A coronal view of a postcontrast T1-weighted MRI scan clearly shows the intraspinal extension (**B**).

TREATMENT

The management of neurogenic or neurovascular tumors in the head and neck has evolved considerably during the past three decades, along with a better understanding of the natural history of these tumors. Because surgery for carotid body tumors generally does not cause cranial nerve injury or deficit, most patients with carotid body tumors up to 6 to 7 cm without extension to the skull base are treated surgically. On the other hand, surgery for paragangliomas arising from the lower cranial nerves inflicts considerable morbidity. In the past, disability resulting from compromise of function of multiple cranial nerves as a result of a potential increase in the size of the tumor was considered an indication for early surgical intervention. Longitudinal population-based studies in the Netherlands have shown that these tumors grow very slowly (approximately 1 mm per year on average) and that surgical intervention often is associated with more detrimental effects than would be encountered with natural progression of the disease. These findings support the philosophy of observation as the definitive management in most patients. Accordingly, surgery is now used selectively, and the role of radiation in the management of these tumors under select circumstances is increasing.

Treatment selection is based on the size and location of the tumor, surgical risk, age and profession of the patient, and the potential risk of cranial nerve deficits resulting from surgery versus the potential benefit of nonsurgical treatment approaches. In general, younger patients with isolated tumors in whom the risk is limited to one cranial nerve are the best surgical candidates. Older patients who have larger tumors and a high risk for the injury of multiple cranial nerves should be treated nonsurgically. An algorithm for treatment selection for paragangliomas and schwannomas of the lower cranial nerves is shown in Fig. 14.31.

NONSURGICAL TREATMENT

Observation

Once the diagnosis is established, observation of paragangliomas or schwannomas of the lower cranial nerves should be considered for most patients. A thorough and informed discussion with the patient and the family should take place. The pros and cons of surgery, observation, and radiotherapy should be discussed in detail. The possibility of future intervention should be discussed. Most importantly, the need for continued clinical and imaging surveillance should be emphasized. Close observation with serial radiographic imaging either with a CT or MRI is recommended. An annual MRI with contrast enhancement is adequate for surveillance for the first few years. If the tumor is relatively stable, the imaging may be extended to every 2 years. Development of symptoms or rapid tumor growth warrants consideration for intervention.

Radiotherapy

Accumulating evidence suggests that radiation therapy is effective in the treatment of schwannomas and paragangliomas. Radiation therapy does not eradicate the tumor, but it can arrest further growth, and thus on subsequent posttreatment imaging studies the tumor remains stable. Radiation delivery techniques, including conventional fractionated external beam radiotherapy, stereotactic radiosurgery, and gamma knife radiosurgery, have been shown to be safe. More recently, use of intensity-modulated radiation therapy has been increasing. The 10-year local progression-free rates range from 92% to 100% with radiation doses of 45 to 54 Gy. Although transient cranial nerve palsies have been observed, particularly with stereotactic radiosurgery, no permanent neuropathy has been reported. In selecting patients for treatment, the risk for a radiation-induced second

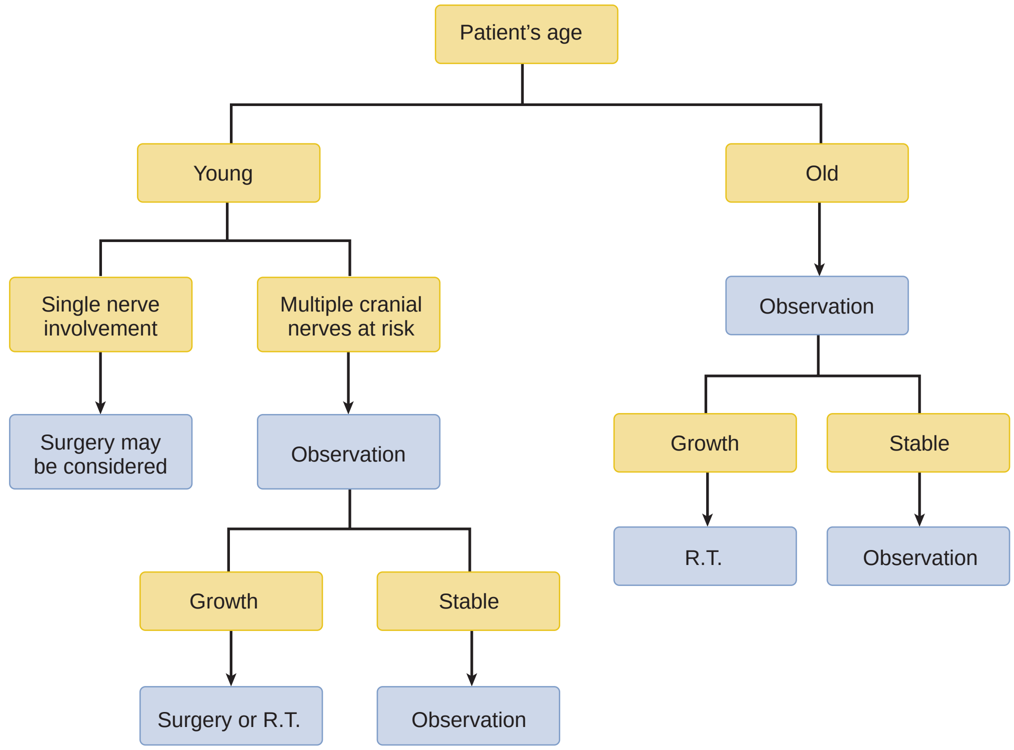

Figure 14.31 An age-related algorithm for selection of therapy of paragangliomas and schwannomas of the lower cranial nerves. *R.T.,* Radiation therapy.

malignancy needs to be balanced against the immediate and permanent risk of cranial neuropathies caused by surgical intervention. Based on this assessment, radiation therapy is generally not recommended for younger patients.

Medical Management

Patients with functioning paragangliomas present with a history of flushing and episodic hypertension. Appropriate medical management requires control of hypertension with alpha blockade. For young patients with large paragangliomas located high in the parapharyngeal space, surgical intervention poses the risk of multiple cranial nerve injuries. If the tumor in a young patient shows progressive growth, then intervention is required for tumor control. Because radiotherapy in young patients poses the danger of radiation-induced tumors at a later age, experimental treatment approaches are considered in these patients. In such patients, a metaiodobenzylguanidine scan is performed, and if the scan is positive at the site of the tumor, such patients are candidates for consideration of treatment with somatostatin analog inhibitors. Response with shrinkage of tumor is observed in approximately 15% of patients who undergo this treatment.

SURGICAL TREATMENT

Indications for surgery are related to tumor and patient factors. Tumor factors include malignancy, rapid growth, or local pressure effects. Patient factors are related to the severity of symptoms and level of apprehension. Because most patients have unifocal lesions, surgical excision may be considered in younger patients if the risk of loss of function of only a single cranial nerve is anticipated. Small paragangliomas usually involve only one cranial nerve, but as the tumor enlarges, involvement of multiple cranial nerves becomes a cause for concern.

On the other hand, when a patient has a relatively stable tumor that is under observation and the cranial nerves are functioning, justification of surgical intervention is difficult. Rapid growth, cervical lymph node metastasis, or radiologic features of local invasion indicate a malignant tumor, warranting consideration for surgery.

Schwannomas and Neurofibromas

Management of neurogenic tumors of lateral and central compartments of the neck require different considerations. Schwannomas and neurofibromas of the lateral compartment (i.e., the cervical plexus and brachial plexus) can be treated with early surgical intervention, because the resultant neurological deficit generally is not significant. The potential risk of a cervical root neurofibroma extending into the spinal canal as a dumbbell tumor warrants the need for surgical intervention. Similarly, a schwannoma of the brachial plexus should be treated surgically to avoid invasion of additional adjacent nerves and thus produce additional neurologic deficit. However, schwannomas of the medial compartment (i.e., cranial nerves VII, IX, X, XII, and the sympathetic chain) require significant consideration of the tumor and the patient before making a decision regarding surgical intervention. The involved nerve rarely retains function after surgical excision, even if the tumor is enucleated with preservation of the surrounding fibers of the nerve. Therefore, if the affected cranial nerve is functioning and the tumor is not observed to be growing in size, simple clinical surveillance with periodic imaging studies to monitor the growth of the tumor is advisable. If significant growth in the lesion is observed, then surgical intervention is warranted. In general, a neurologic deficit occurs only in the nerve of origin of the tumor.

Paragangliomas

Management of paragangliomas is more difficult and requires consideration of the patient's age and occupation and the tumor size, location, and site of origin. In general, carotid body tumors are treated by early surgical intervention if the patient is a safe surgical candidate. Permanent neurologic deficit of lower

cranial nerves is rare, although temporary paralysis may occur in one or more lower cranial nerves, due to manipulation during dissection and removal of the tumor. Paragangliomas arising in the vagus, hypoglossal, and glossopharyngeal nerves or the sympathetic chain are more complicated. Excision of small paragangliomas generally will result in paralysis of the affected nerve alone, whereas surgery for larger paragangliomas located high in the neck at the skull base may result in multiple cranial nerve deficits, often permanently, leaving the patient with a significantly morbid postoperative course. Therefore the indications for surgical intervention are (1) malignant paraganglioma as diagnosed by radiologic features, or with the presence of cervical lymph node metastasis or distant metastasis; and (2) significant growth in the lesion over a short period or a small (<4 cm) paraganglioma in a young patient in the cervical region not approaching the skull base. All other patients with larger paragangliomas or those located at the base of the skull are candidates for nonsurgical management with continued surveillance.

Figure 14.32 Surface markings of the tumor in relation to the common, external, and carotid arteries in the patient.

Preoperative Preparation

All patients undergoing surgical resection for neurogenic tumors and paragangliomas must have an understanding of the nature of the surgery, the intraoperative risks involved, and proper preoperative counseling regarding the potential nerve deficits that may result after surgery. If the lesion is large and highly vascular, then preoperative angiographic studies should be performed to demonstrate the feeding vessels, and consideration should be given to preoperative embolization, which ideally should be performed within 24 hours of the planned surgical procedure. Although blood transfusions are seldom required, blood should be available on demand in the event of unexpected hemorrhage.

For larger lesions where integrity of the internal carotid artery is at risk, appropriate balloon occlusion studies of the carotid arteries should be performed to demonstrate satisfactory intracranial crossover circulation. Thus a balloon occlusion test of the ipsilateral carotid artery and cross-perfusion from the contralateral carotid artery to the ipsilateral cerebral hemisphere should be demonstrated. Anatomic demonstration of cross perfusion and a patent circle of Willis does not guarantee preservation of neurologic function. However, absence of cross perfusion significantly raises the potential for a stroke and should enter into the decision regarding surgical intervention. Thus the preoperative risk of a neurologic deficit must be discussed and the patient informed of such a risk if ligation of the carotid artery becomes necessary during the course of the operation. Similarly, a vascular surgeon should be available in the event of the need for resection of a segment of the internal carotid artery and its reconstruction.

Although it occurs rarely, patients with functioning paragangliomas and episodic facial flushing and hypertension may require preoperative management of hypertension with alpha blockade. Thus careful intraoperative monitoring of blood pressure during mobilization of the tumor is necessary.

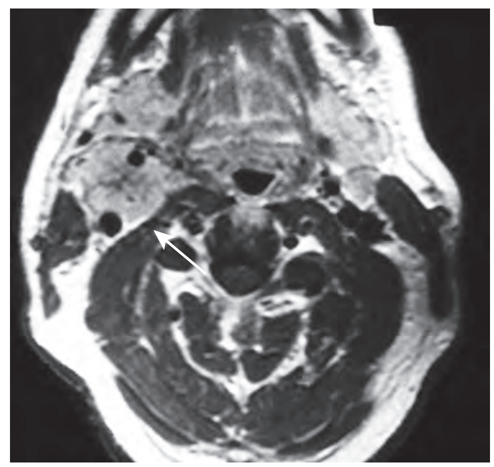

Figure 14.33 An axial view of a magnetic resonance imaging scan showing a carotid body tumor separating the internal and external carotid arteries (*arrow*).

Excision of a Carotid Body Tumor (Shamblin Type II)

The patient described in this procedure has a 6-cm pulsatile mass in the upper part of the neck on the right-hand side (Fig. 14.32). An axial view of the MRI scan shown in Fig. 14.33 demonstrates a tumor mass separating the internal and external carotid arteries, which indent the substance of the tumor. This tumor is a Shamblin type II tumor. An MR angiogram demonstrates splaying of the external and internal carotid arteries by the tumor on the right-hand side (Fig. 14.34).

The operative procedure is performed after induction of general endotracheal anesthesia. A bipolar cautery is essential and must be available for safe performance of the operation. Vascular instruments such as vascular clamps, vessel loops, and Fogarty catheters also should be readily available.

The patient is placed in a supine position on the operating table with the neck extended and rotated to the opposite side. The incision is placed along an upper neck skin crease, providing generous exposure of the structures in the upper part of the neck. Upper and lower skin flaps are elevated in the usual fashion. Because the plane of dissection is deep to the sternocleidomastoid muscle, the greater auricular nerve overlying this muscle can be preserved safely. Meticulous dissection of the skin flaps with electrocautery is recommended to minimize blood loss. Because of the high vascularity of this tumor, rough handling or dissection in an inappropriate plane will cause significant blood loss. However, if gentle and careful dissection is undertaken, the entire operative procedure can be accomplished safely without the need for a blood transfusion.

Several hyperplastic lymph nodes often are encountered overlying the carotid body tumor in the upper part of the neck

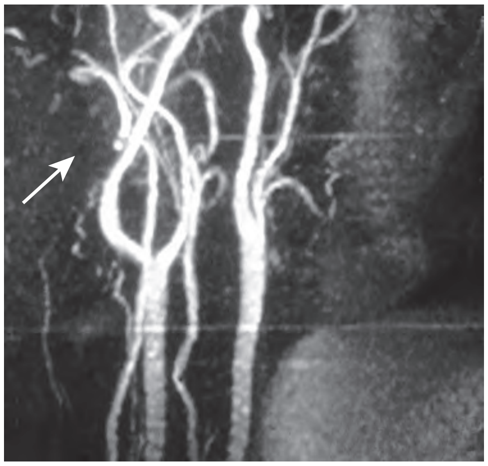

Figure 14.34 A magnetic resonance angiogram demonstrates that the carotid arteries are splayed by the tumor on the right-hand side (*arrow*).

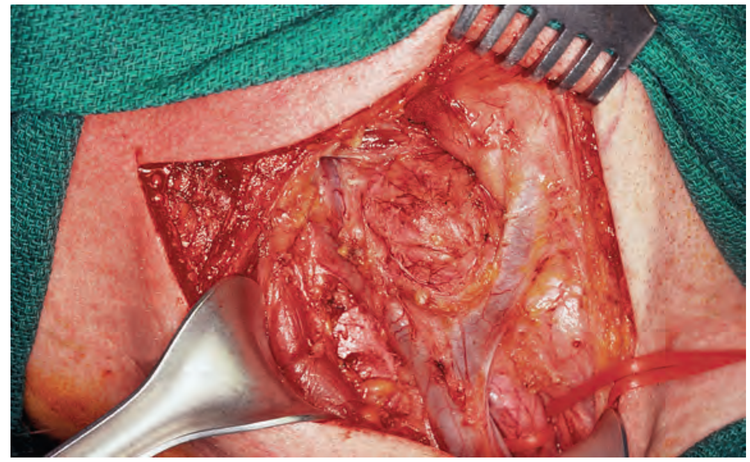

Figure 14.36 A carotid body tumor encasing the carotid bifurcation.

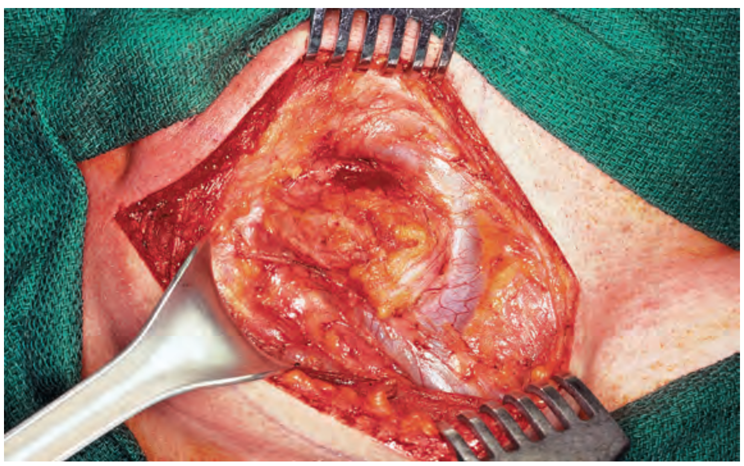

Figure 14.35 Hyperplastic lymph nodes overlying the tumor are excised first.

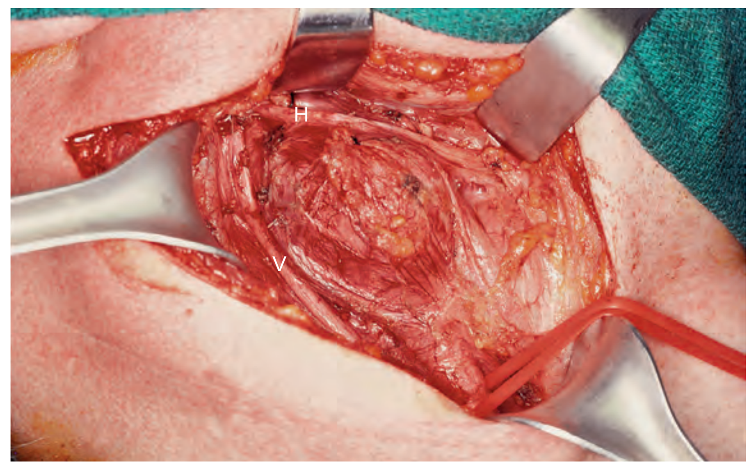

Figure 14.37 The vagus (*V*) and hypoglossal (*H*) nerves are dissected and preserved.

(Fig. 14.35). These hyperplastic lymph nodes are best excised at the outset to provide adequate exposure of the underlying major blood vessels and the tumor. After excision of overlying hyperplastic lymph nodes, the underlying carotid body tumor comes into view (Fig. 14.36). Note the internal jugular vein skirting the posterior surface of the tumor and the common facial vein skirting its lower border.

The initial step in the operative procedure at this juncture is dissection of the common carotid artery proximal to the tumor. The fascia on the anterior border of the sternomastoid muscle is incised, and the muscle is retracted laterally to expose the carotid sheath. The carotid sheath is opened in the lower part of the neck and the common carotid artery is exposed, dissected circumferentially, and isolated with a vessel loop.

Once proximal control of the common carotid artery is secured, dissection of the tumor begins. The incision in the fascia overlying the sternomastoid muscle is extended cephalad up to the tail of the parotid gland. The sternomastoid muscle is now retracted laterally to expose and isolate the lateral border of the tumor (Fig. 14.37). At this juncture, it is imperative that the vagus and the hypoglossal nerves be identified carefully and dissected to preserve their integrity.

Dissection now proceeds along the common carotid artery in a subadventitial plane until its bifurcation. This is a very tedious, slow, and meticulous dissection, and absolute hemostasis must be maintained throughout the process. The usual technique is to use the bipolar cautery to electrodesiccate the adventitia of the carotid artery that is bearing the abnormal hypervascular tissue and sharply divide the coagulated tissue with fine tenotomy scissors. Every minor bleeding point should be electrodesiccated with the bipolar cautery as dissection proceeds to minimize hemorrhage. In most instances, the carotid artery and its bifurcation are partially embedded, producing indentation in the tumor rather than circumferential encasement (Shamblin type II tumor).

Further dissection of the common carotid artery provides exposure of the carotid bifurcation. At this juncture the tumor is lifted off the carotid artery and retracted cephalad. Use of sharp and blunt dural dissectors (Penfield) greatly facilitates subadventitial dissection. It is important to remember that nearly all the blood supply to this tumor is derived from the branches of the external carotid artery and the vasa vasorum of the walls of carotid arteries. However, dissection of the internal carotid artery is undertaken first to protect it from injury. The artery is completely isolated before further mobilization of the tumor is undertaken. Liberal use of monopolar electrocautery for dissection and bipolar electrocautery for hemostasis is recommended.

During the course of dissection, near the carotid bifurcation, bradycardia and hypotension may occur as a result of stimulation of the baroreceptors at the carotid bifurcation. Infiltration of 1% lidocaine in the subadventitial plane of the carotid bulb will reverse the bradycardia and hypotension promptly.

As dissection of the tumor proceeds cephalad, its blood supply coming from the adventitial vessels of the carotid arteries is cut off. This loss of blood supply causes shrinkage in the size of the tumor, which also feels softer and makes subsequent

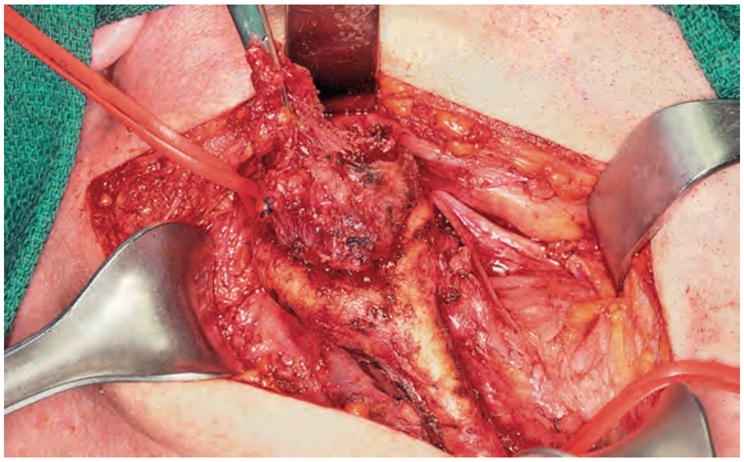

Figure 14.38 The tumor is lifted off the carotid bifurcation.

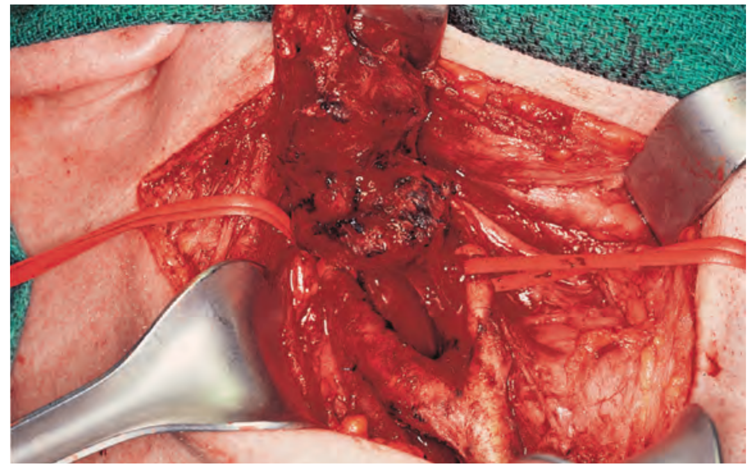

Figure 14.39 The internal and external carotid arteries are dissected away from the tumor.

dissection progressively easier (Fig. 14.38). Finally, dissection of the external carotid artery from the tumor is undertaken. At this point, if it appears that the external carotid artery is inseparable from the tumor, it may be safely cross clamped, divided, and ligated distal to the carotid bulb. However, in most instances, the external carotid artery with its branches can be separated from the tumor. Each feeding vessel to the tumor from the branches of the external carotid artery is dissected and ligated or coagulated.

It is always desirable to have a vessel loop passed around the distal part of the internal carotid artery and the external carotid artery to provide retraction and immediate control of bleeding should any unexpected hemorrhage ensue (Fig. 14.39). Occasionally, feeding blood vessels from the wall of the carotid artery are so short that ligation may not be feasible, and repair of the bleeding from the carotid artery may require a figure of eight fine vascular suture.

Finally, the specimen is removed without undue hemorrhage if all the aforementioned precautions are undertaken. After removal of the tumor the surgical field demonstrates the carotid bifurcation with an intact internal and external carotid artery with its branches as well as the preserved hypoglossal and vagus nerves and internal jugular vein (Fig. 14.40).

The specimen removed from this patient is shown in Fig. 14.41. Note that the tumor appears almost bilobulated with a deep indentation in the substance of the tumor created at the carotid bifurcation by the external and internal carotid arteries.

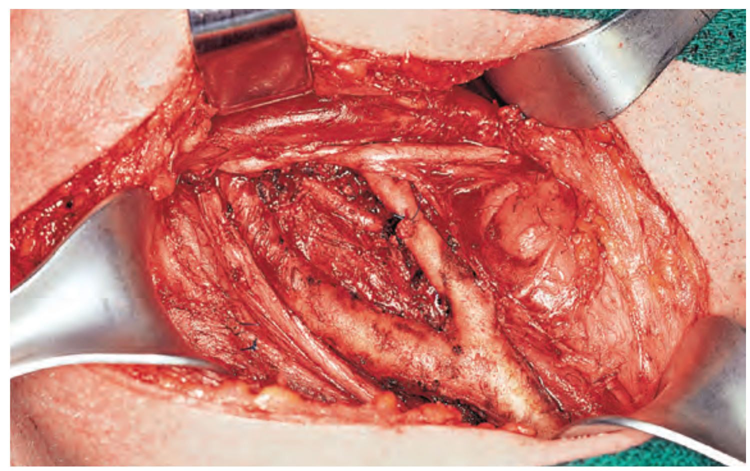

Figure 14.40 After removal of the tumor, the surgical field shows intact carotid bifurcation and adjacent cranial nerves.

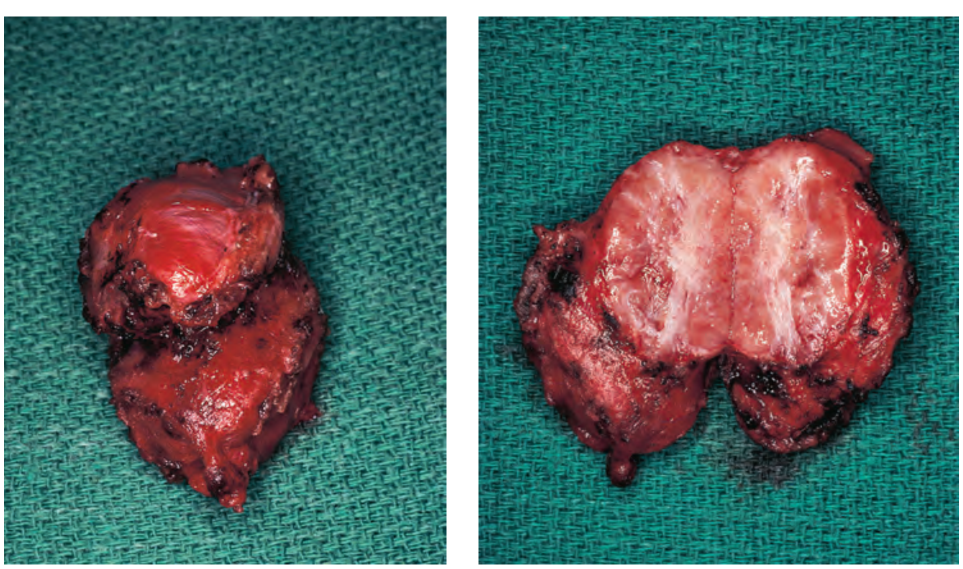

Figure 14.41 The external appearance of the tumor shows a bilobulated tumor indicating indentation as a result of encasement of the carotid arteries.

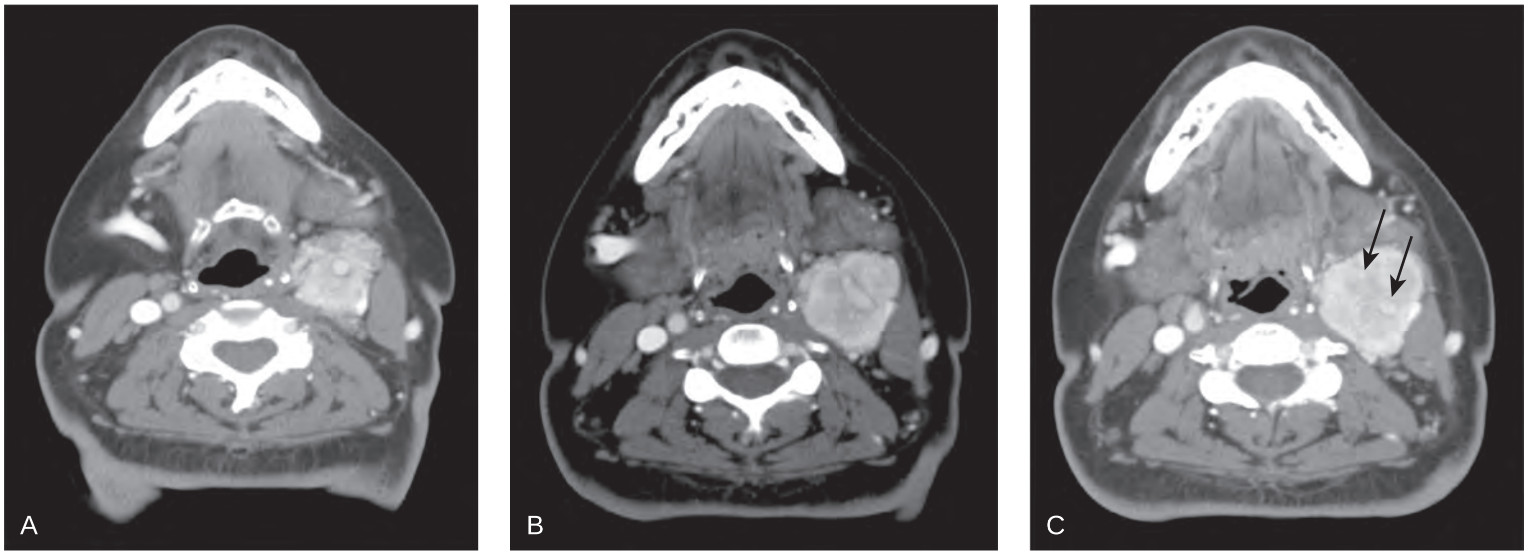

Figure 14.42 Axial views of a contrast-enhanced computed tomography scan of the neck in a patient with Shamblin type III tumor showing encasement of the distal common carotid artery (**A**), carotid bulb (**B**), and proximal external and internal carotid arteries (**C**) (*arrows*).

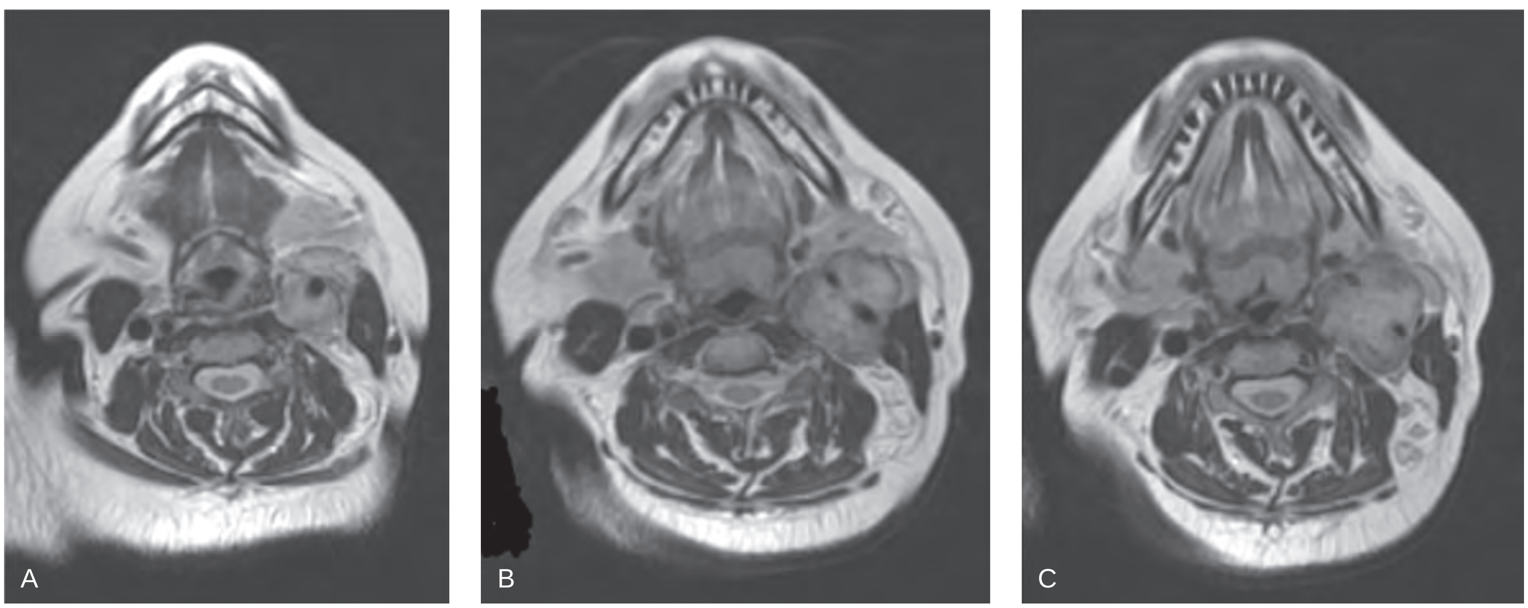

Figure 14.43 Axial views of a T2-weighted magnetic resonance imaging scan of the neck in a patient with Shamblin type III tumor showing encasement of the distal common carotid artery (**A**), carotid bulb (**B**), and proximal external and internal carotid arteries (**C**).

This tumor is a classic Shamblin type II tumor. The cut surface of the tumor is homogeneous and fleshy, consistent with areas of focal hemorrhages.

Excision of a Carotid Body Tumor (Shamblin Type III)

Occasionally, the carotid body tumor surrounds the common carotid artery and its bifurcation (carotid bulb), as well as the proximal external and internal carotid arteries, and the tumor may need to be incised and bisected to dissect out the artery. If this is the case, absolute hemostasis must be secured with the electrocautery during division of the tumor to facilitate a bloodless procedure and the safety of the remainder of the operation. In rare instances, resection of the carotid artery may be required if the tumor is densely adherent and not separable from the carotid bulb.

Preoperative imaging studies of a patient with a Shamblin type III tumor clearly showed encasement of the distal common carotid artery, carotid bulb, and proximal external and internal carotid arteries by the tumor (Fig. 14.42). Axial views of T2-weighted MRI scans show similar disposition of the carotid vessels in relation to the tumor (Fig. 14.43). Sagittal and coronal views of the MRI show the internal carotid artery embedded and emerging from the upper end of the tumor (Fig. 14.44). Three-dimensional reconstruction of the MRI clearly shows encasement of the carotid bifurcation and both vessels emerging out of the tumor at its upper end (Fig. 14.45). Outline of the tumor and the carotid arteries is shown on the patient before surgery (Fig. 14.46).

Preoperative balloon occlusion testing showed excellent cross perfusion from the right carotid artery and a patent circle of Willis. The surgical field showing the common carotid artery encased by the tumor with the carotid bulb and bifurcation embedded in the tumor is shown in (Fig. 14.47). During surgery, the tumor was found to be infiltrating the distal common carotid artery and the carotid bulb and could not be separated. Therefore

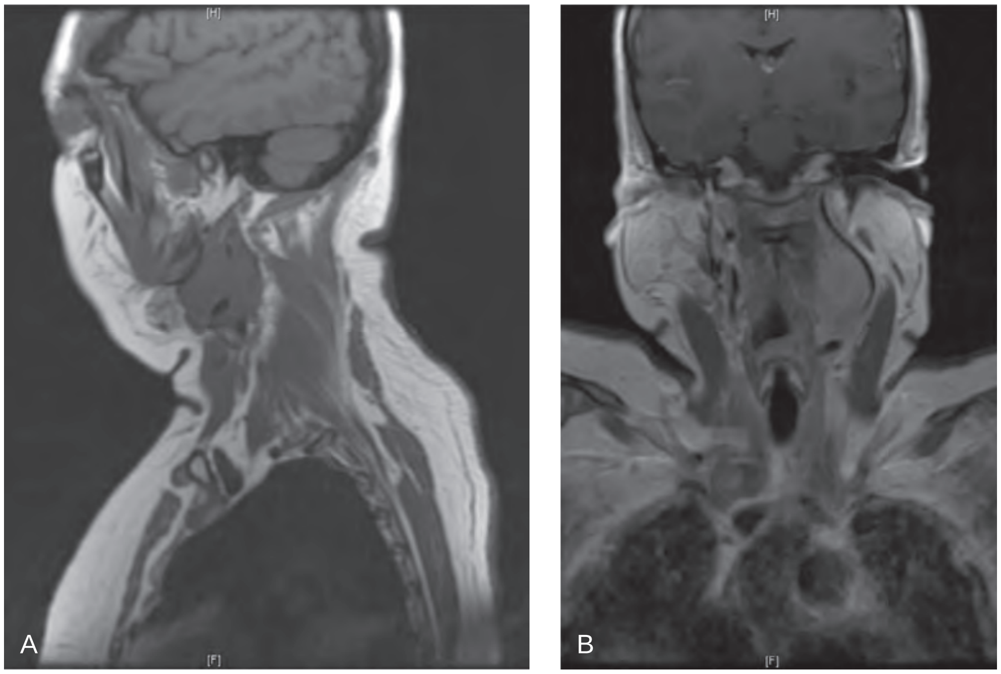

Figure 14.44 Sagittal view of the magnetic resonance imaging scan showing the internal carotid artery embedded in the tumor (**A**) and a coronal view showing the internal carotid artery emerging out of the tumor (**B**).

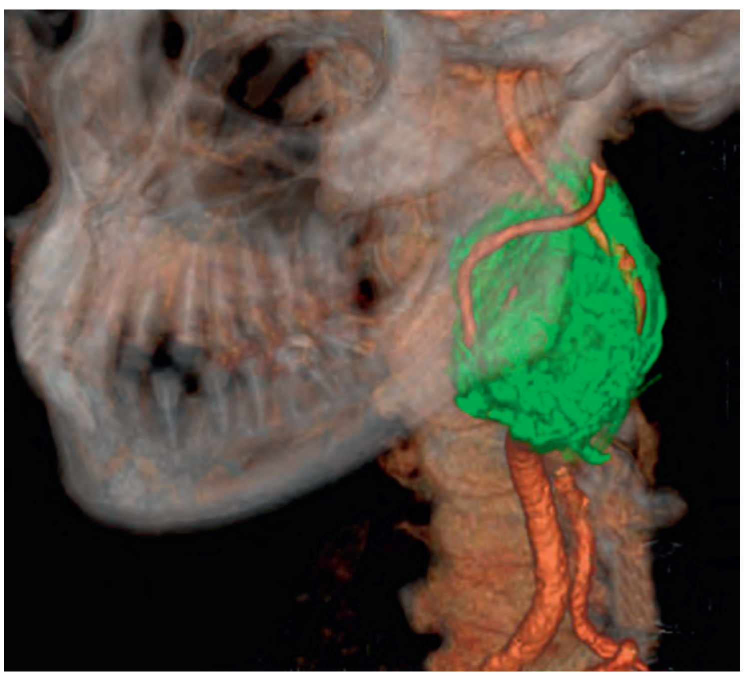

Figure 14.45 Three-dimensional reconstruction of the magnetic resonance imaging scan showing the tumor with encasement of the carotid bifurcation and the vessels emerging out of the tumor at its upper end.

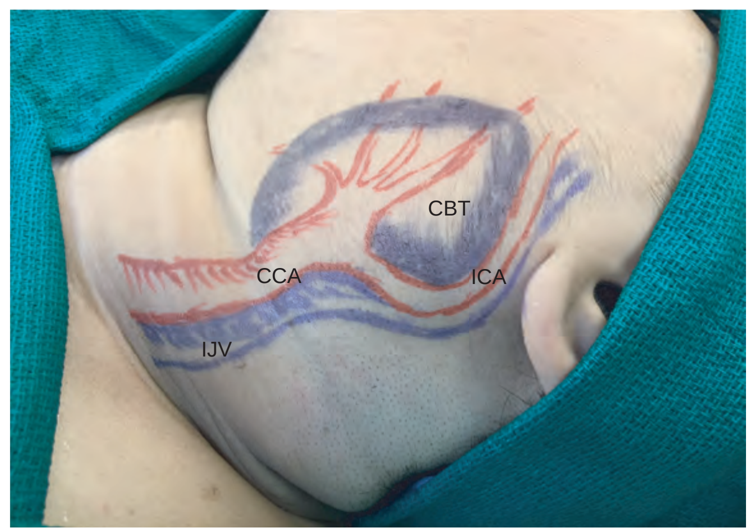

Figure 14.46 Outline of the tumor and carotid arteries depicted on the patient. *CBT,* Carotid body tumor; *CCA,* common carotid artery; *ICA,* internal carotid artery; *IJV,* internal jugular vein.

resection of the carotid bulb, distal common carotid artery, and external and internal carotid arteries was performed. The surgical specimen shows a tumor thrombus in the lumen of the carotid bulb (Fig. 14.48). The internal carotid artery was ligated, and her blood pressure maintained slightly above her normal range to ensure adequate perfusion of the left hemisphere. The patient did not have any permanent neurologic sequela from the procedure.

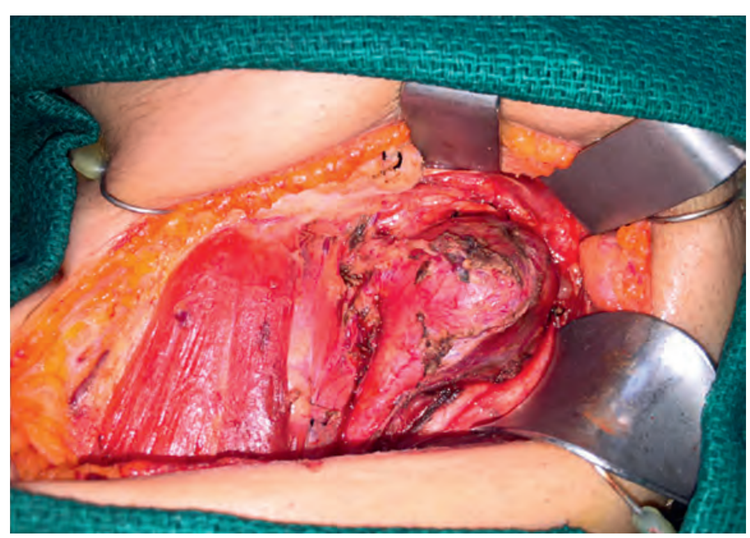

Figure 14.47 The surgical field showing the common carotid artery encased by the tumor with the carotid bulb and bifurcation embedded in the tumor.

Excision of a Malignant Carotid Body Tumor

The procedure described here is on a 45-year-old man with a 6-year history of a slowly enlarging mass in the upper part of the neck on the right-hand side. He had episodes of syncope

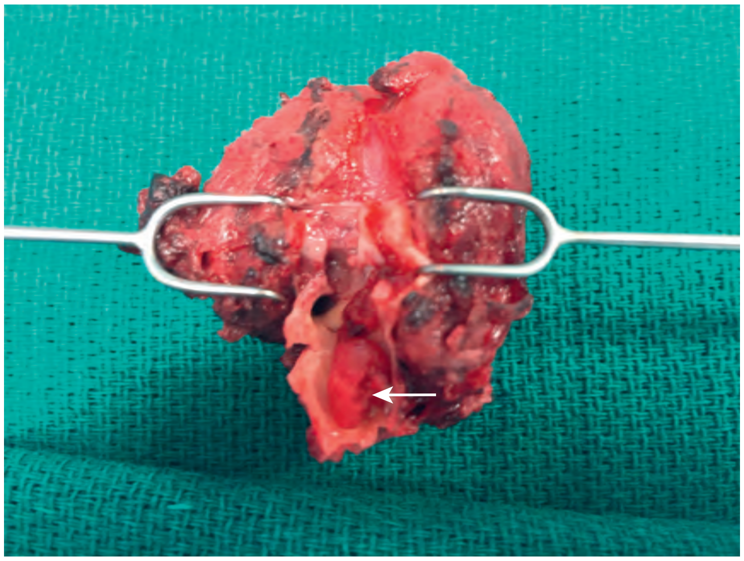

Figure 14.48 Surgical specimen showing the resected carotid bulb in the tumor with a tumor thrombus in its lumen (*arrow*).

for 6 months before presentation. A contrast-enhanced CT scan of the neck at the level of the tip of the epiglottis shows that the tumor splays the external and internal carotid arteries and appears to be intimately adherent to the anteromedial wall of the internal carotid artery (Fig. 14.49). In addition, a metastatic lymph node is appreciated just lateral to the submandibular salivary gland.

Coronal reconstruction of a CT angiogram demonstrates the infiltration of the tumor into the internal carotid artery, causing constriction of its lumen distal to the bifurcation of the common carotid artery (Fig. 14.50). Preoperative preparation of this patient included direct angiography with carotid artery occlusion to test cross circulation in the right cerebral hemisphere through the circle of Willis from the left carotid artery and the vertebral arteries. The patient had a successful balloon occlusion test before surgery. With invasion of the carotid artery, the patient

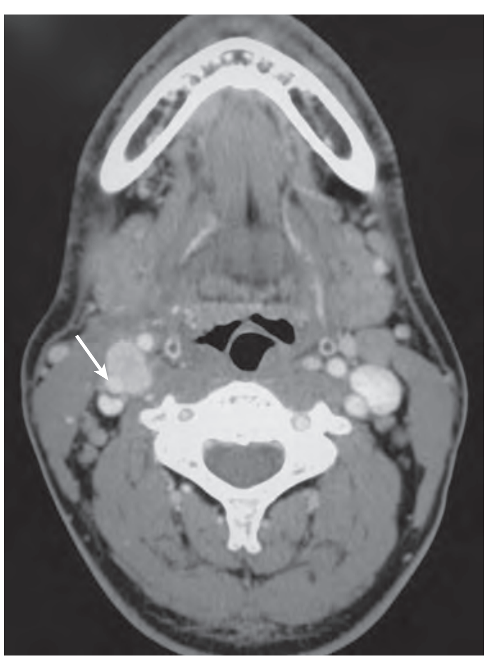

Figure 14.49 An axial view of a contrast-enhanced computed tomography scan of the neck at the level of the tip of the epiglottis shows a highly vascular tumor splaying the carotid arteries and invading the medial wall of the internal carotid artery (*arrow*).

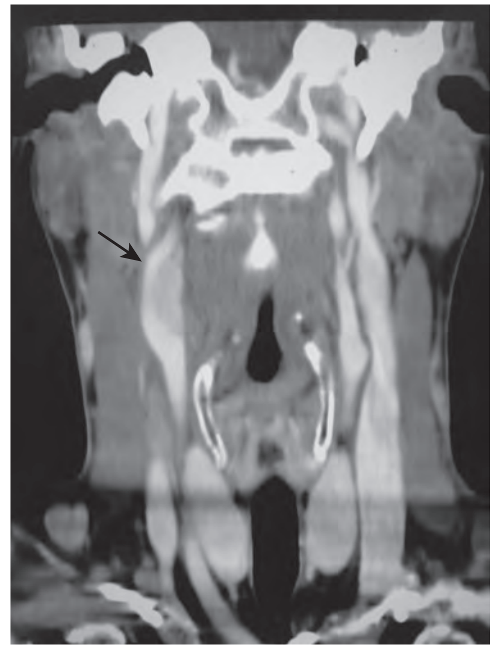

Figure 14.50 A coronal reconstruction of a computed tomography angiogram shows invasion of the medial wall of the right internal carotid artery (*arrow*).

Figure 14.51 The location of the tumor in relation to the carotid arteries and internal jugular vein.

should be informed of the potential risks of cerebrovascular injury, stroke, and even death. The surgeon in this setting should be prepared to resect and reconstruct the internal carotid artery with the assistance of a vascular surgeon.

A depiction of the location of the tumor in relation to the carotid arteries and internal jugular vein is shown with the patient on the operating table (Fig. 14.51). The drawing on the patient's skin shows the anticipated area of tumor infiltration into the internal carotid artery.

The surgical procedure begins with a transverse incision along an upper neck skin crease. Upper and lower skin flaps are elevated. A modified neck dissection is accomplished in light of the fact that the patient already has cervical lymph node metastasis from the malignant paraganglioma. The surgical specimen of neck dissection is reflected medially with dissection and isolation of the common carotid artery and the distal internal carotid artery (Fig. 14.52). Note that the vessel loops provide

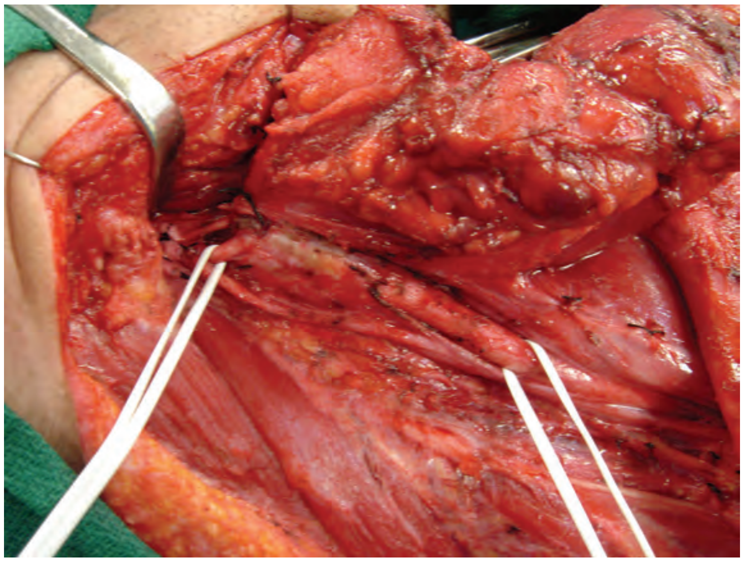

Figure 14.52 The specimen of a neck dissection is rotated medially, showing invasion of the carotid artery, which is mobilized and isolated with vessel loops proximally and distally.

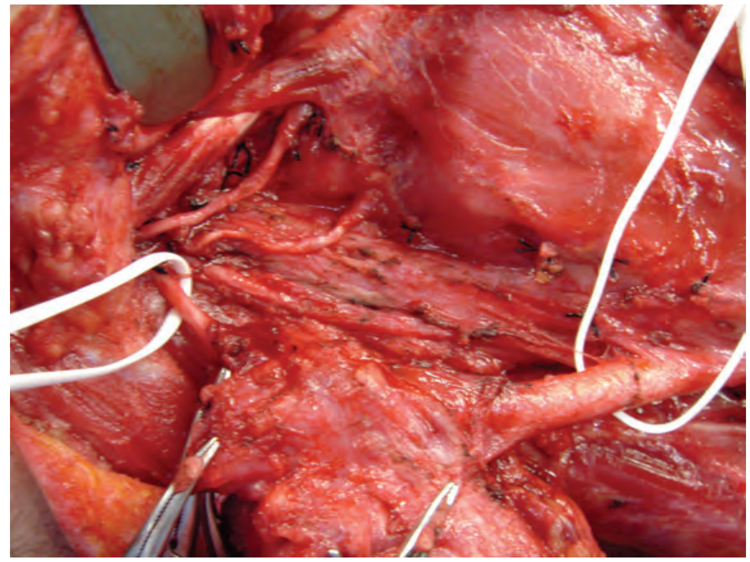

Figure 14.54 The tumor is dissected off medially from the hypoglossal and superior laryngeal nerves, and the specimen is retracted laterally.

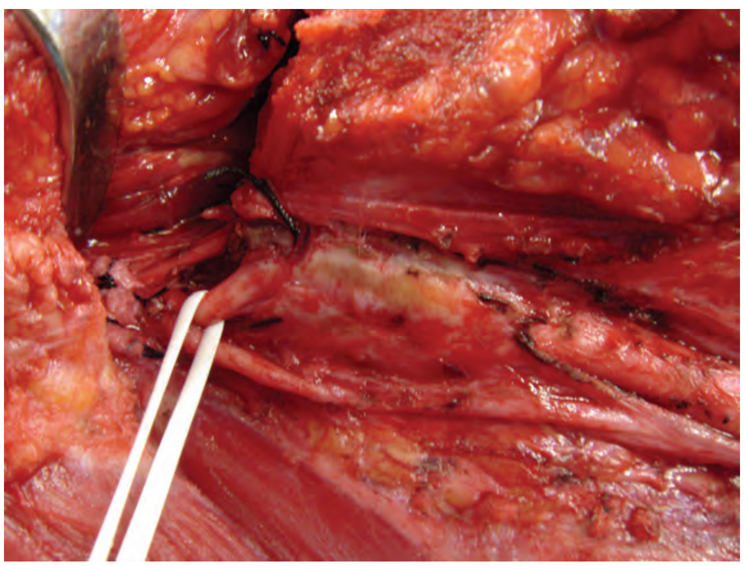

Figure 14.53 A close-up view of the surgical field shows circumferential invasion of the internal carotid artery. The distal stump is free of tumor.

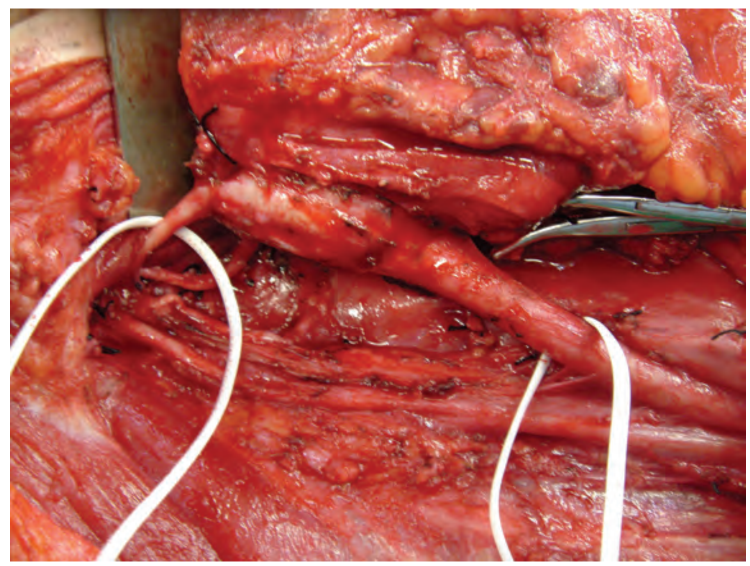

Figure 14.55 Complete mobilization of the tumor with the involved segment of the carotid artery. The common carotid artery and distal internal carotid artery are uninvolved.

retraction and proximal and distal control of the common carotid and the internal carotid arteries. The vagus nerve is separated from the tumor and is preserved.

A close-up view of the surgical field at this stage of the operation clearly shows circumferential invasion of the proximal internal carotid artery, with the distal stump free of tumor (Fig. 14.53). Dissection of the tumor at this juncture continues further medially, freeing the tumor from the hypoglossal nerve and the superior laryngeal nerve cephalad (Fig. 14.54). Distal branches of the external carotid artery are divided and ligated, because the carotid bifurcation (including the proximal internal carotid artery and external carotid artery with the proximal stumps off its peripheral branches) will be resected in a monoblock fashion with the tumor (Fig. 14.55). After complete mobilization of the tumor in a circumferential fashion, the common carotid artery and the internal carotid artery are cross clamped and divided, and the surgical specimen is removed. Before cross clamping, the patient's blood pressure should be maintained slightly above baseline.

A saphenous vein graft is used to reconstruct the internal carotid artery, connecting the stump of the common carotid artery to the distal stump of the internal carotid artery (Fig. 14.56). Anticoagulation is maintained during the procedure and in the immediate postoperative period. The surgical field is irrigated with saline solution. Suction drains are placed, and the wound is closed in two layers in the usual fashion.

The surgical specimen consists of monoblock resection of the malignant paraganglioma with the bifurcation of the carotid artery and regional cervical lymph nodes removed through a modified neck dissection (Fig. 14.57). Gross total excision of the tumor and the regional lymph nodes has been achieved. Dissection of the specimen with the carotid artery bifurcation opened shows infiltration of the tumor into the intima of the internal carotid artery, which is a characteristic feature of tumor infiltration by a malignant carotid body tumor (Fig. 14.58).

Patients with malignant paragangliomas invariably will need adjuvant postoperative radiation therapy to enhance local and regional control. Postoperative radiotherapy is delivered to the

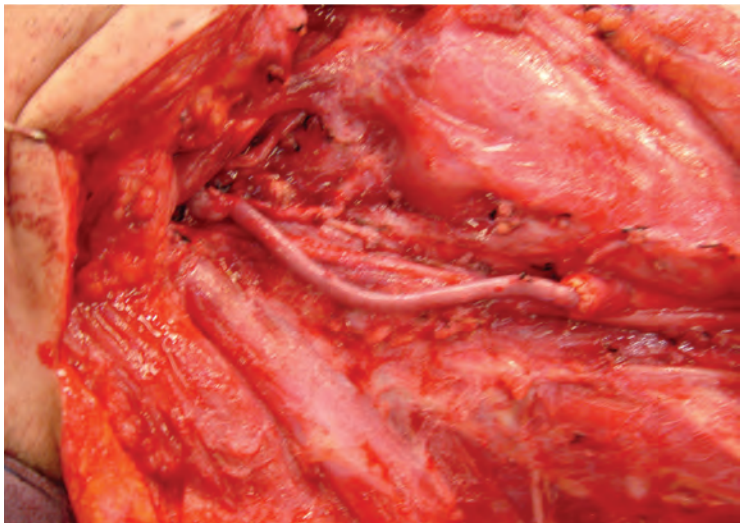

Figure 14.56 A saphenous vein graft is used to reconstruct the internal carotid artery.

ipsilateral neck with photons and intensity-modulated radiation therapy in conventional fractionation.

Excision of a Paraganglioma of the Vagus Nerve (Glomus Intravagale)

The patient described here presented with a history of a mass in the upper cervical region and local discomfort because of pressure from the mass. Palpation revealed a well-defined retromandibular mass, the lower border of which could be palpated easily in the upper part of the neck, although its upper half could not be palpated because of its location in the retromandibular space. An MRI scan in the sagittal and coronal planes vividly demonstrates the anatomic location and the dimensions of the tumor, which are approximately 4 by 7 cm (Figs. 14.59 and 14.60). The tumor is located along the carotid sheath, displacing both the external and internal carotid arteries anteromedially and the internal jugular vein posterolaterally.

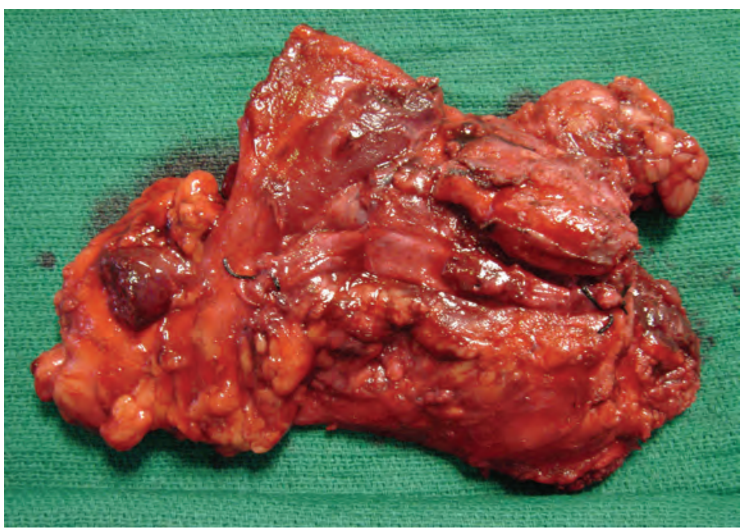

Figure 14.57 The surgical specimen of a modified radical neck dissection and malignant carotid body tumor.

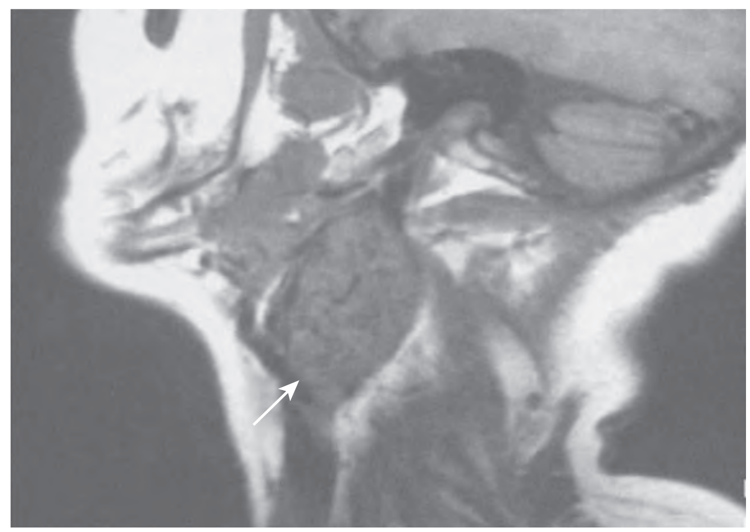

Figure 14.59 The sagittal view of the magnetic resonance imaging scan shows the location and flow voids in the tumor (*arrow*).

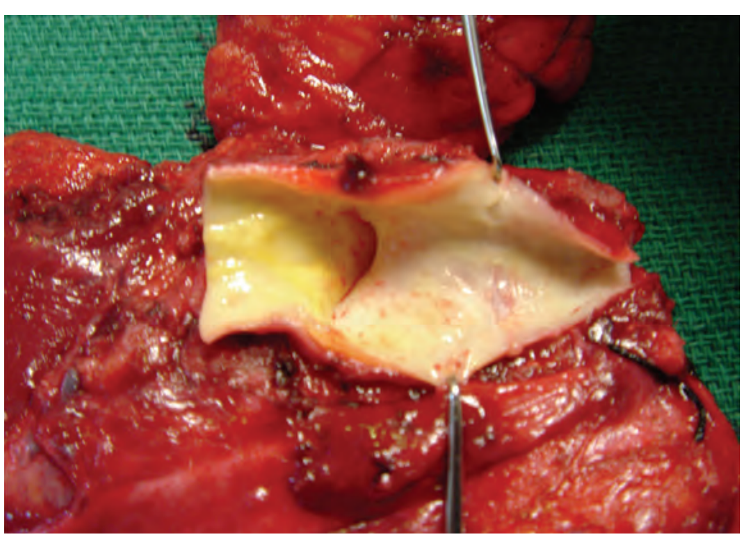

Figure 14.58 The resected segment of the carotid artery at its bifurcation is opened to show infiltration of the intima of the carotid artery by tumor.

Figure 14.60 A coronal view of the magnetic resonance imaging scan shows the location of the tumor and flow voids in the tumor (*arrow*).

Figure 14.61 The palpable tumor and the incision are outlined.

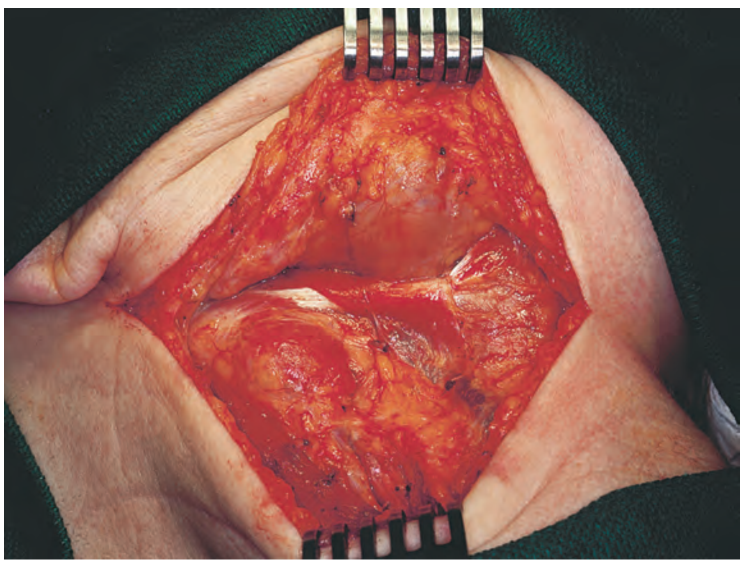

Figure 14.62 Hyperplastic deep jugular lymph nodes are seen overlying the tumor.

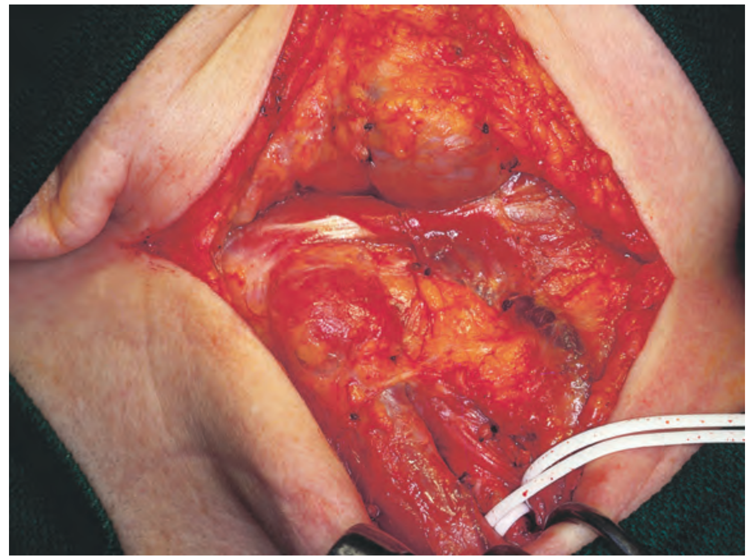

Figure 14.63 The internal jugular vein is found to be displaced posteriorly by the tumor.

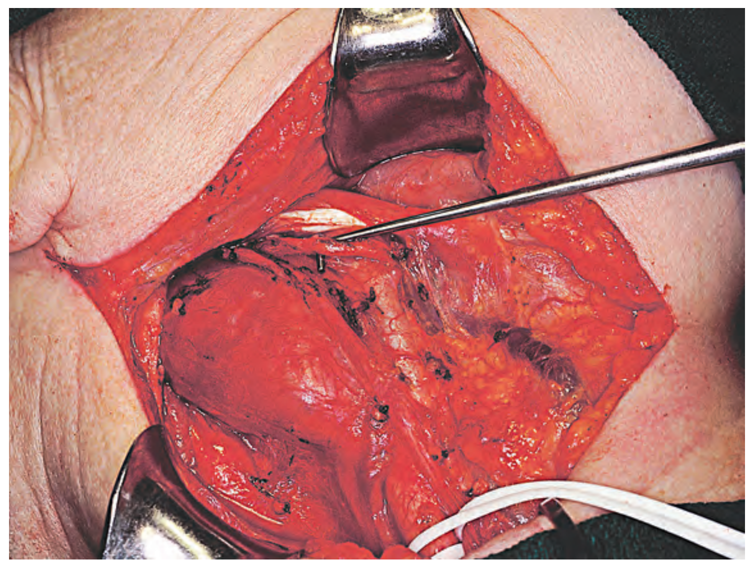

Figure 14.64 The hypoglossal nerve is demonstrated in this close-up view.

Surgical exposure for this lesion requires an incision beginning at the tip of the mastoid process and curving along an upper neck skin crease anteriorly up to the midline of the neck in the submental region (Fig. 14.61). The skin incision is deepened through the platysma, and upper and lower cervical flaps are developed to expose the tumor. Several hyperplastic deep jugular lymph nodes are encountered overlying the palpable tumor mass and caudad to the digastric muscle, obscuring the view and the site of origin of the tumor (Fig. 14.62). These hyperplastic lymph nodes are excised to demonstrate the anatomy of the carotid sheath and the location of the tumor. After excision of these nodes, the common carotid artery is identified, and a vessel loop is passed around it for orientation and proximal control of the carotid artery (Fig. 14.63). The internal jugular vein, displaced posteriorly by the tumor, is identified adjacent to the common carotid artery. The hypoglossal nerve is carefully identified and retracted cephalad out of harm's way (Fig. 14.64).

Meticulous dissection is now undertaken in the carotid sheath, carefully freeing up the internal jugular vein, which is retracted posteriorly, and the common, external, and internal carotid arteries, which are retracted anteriorly (Fig. 14.65). Further dissection of the internal carotid artery requires exposure of the upper part of the neck medial to the posterior belly of the digastric muscle at the jugular foramen and the carotid canal.

At this juncture, it becomes obvious that the tumor arises from the vagus nerve. Other anatomic structures in the carotid sheath are identified and dissected free from the tumor. The carotid vessels are retracted anteriorly, and the internal jugular vein is passed behind the tumor medially to permit mobilization of the distal aspect of the vagus nerve. The tumor is now grasped carefully, and its dissection continues cephalad at the jugular foramen under direct vision, with absolute hemostasis secured every step of the way. By alternate blunt and sharp dissection, the tumor is delivered in a monobloc fashion, leaving a large dead space between the carotid vessels anteromedially, the internal jugular vein posterolaterally, and the sympathetic chain posteromedially (Fig. 14.66). After absolute hemostasis is secured, the wound is irrigated, a Penrose drain is inserted, and the incision is closed in two layers (Fig. 14.67).

The tumor grossly measures 6 by 4 cm and has a fusiform shape (Figs. 14.68 and 14.69). The cut surface shows a fleshy tumor with numerous vascular spaces. This appearance is characteristic

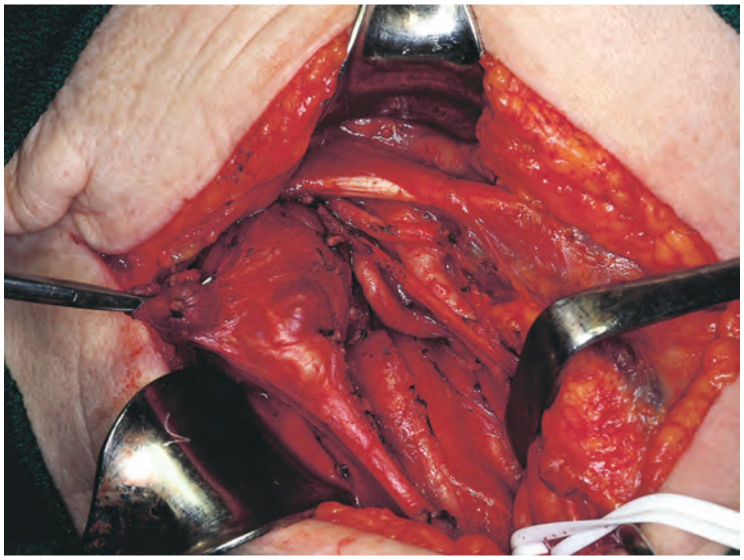

Figure 14.65 The internal jugular vein is displaced medially to facilitate dissection of the distal aspect of the vagus nerve.

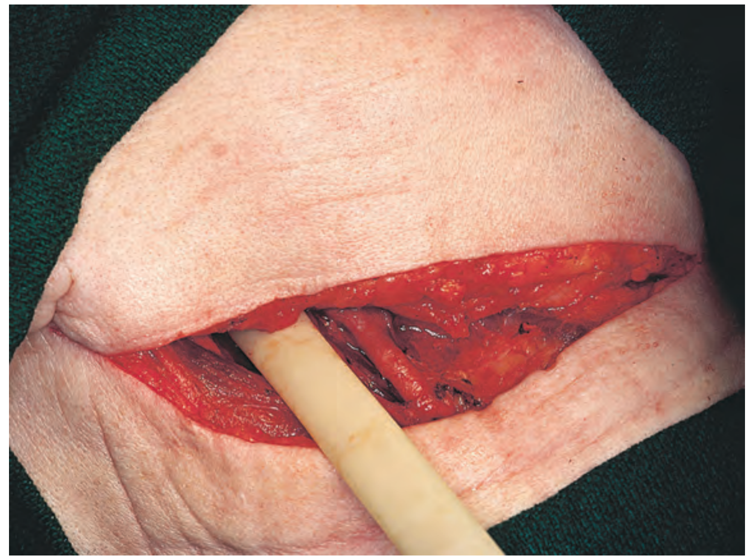

Figure 14.67 A Penrose drain is inserted.

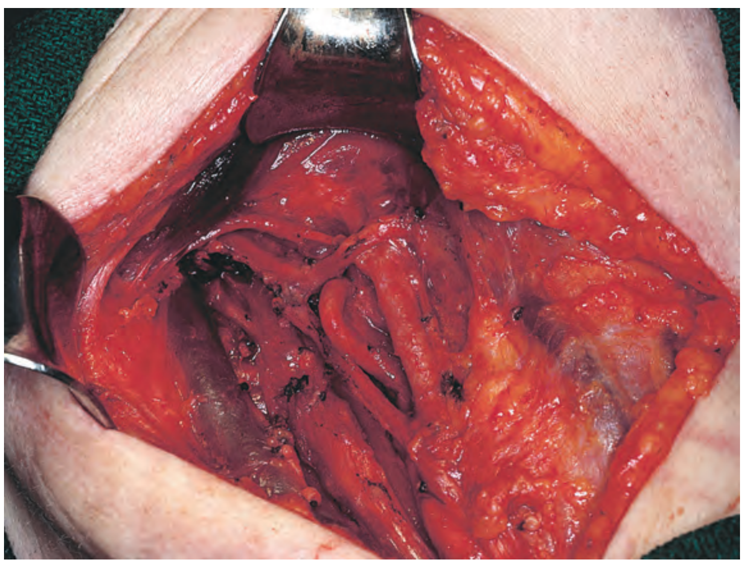

Figure 14.66 The surgical field after removal of the tumor.

Figure 14.68 The gross appearance of the tumor.

Figure 14.69 The cut surface of the tumor.

for a glomus intravagale tumor. The postoperative sequelae of this surgical procedure result from paralysis of the right vagus nerve, leading to hoarseness of voice and aspiration of fluids and saliva because of a lack of sensation in the supraglottic larynx on the right-hand side. Most patients are able to compensate for this deficit without significant functional debility. The quality of the voice can be improved by using a vocal cord medialization procedure with laryngoplasty techniques. Such medialization procedures also restore competency of the larynx and reduce aspiration pneumonia.

Excision of a Paraganglioma of the Superior Mediastinum

The patient shown here had multiple paragangliomas in the head and neck region. He presented with a family history of glomus jugulare and glomus tympanicum tumors, and he had bilateral carotid body tumors as well as right-sided glomus intravagale and a superior mediastinal paraganglioma. He previously had undergone sequential excision of bilateral carotid body tumors and glomus intravagale on the right-hand side. In the present surgical procedure, the paraganglioma located in the superior mediastinum posterior to the innominate artery is being resected.

The CT scan of the patient through the lower part of the neck and the superior mediastinum shows the presence of a highly vascular lesion posterior to the common carotid and innominate arteries on the right-hand side (Fig. 14.70). An MRI scan vividly demonstrates the position of the innominate artery just anterior to the tumor mass, which is wedged between the trachea medially and the innominate artery anteriorly (Fig. 14.71).

The surgical approach to a superior mediastinal paraganglioma requires cervicothoracic exposure to gain access to the great vessels in the superior mediastinum as well as to provide distal control of the carotid and subclavian arteries at the root of the neck. The location of the tumor and the position of the great vessels are shown on the patient in relation to the exposure that is necessary, outlined by the incision (Fig. 14.72).

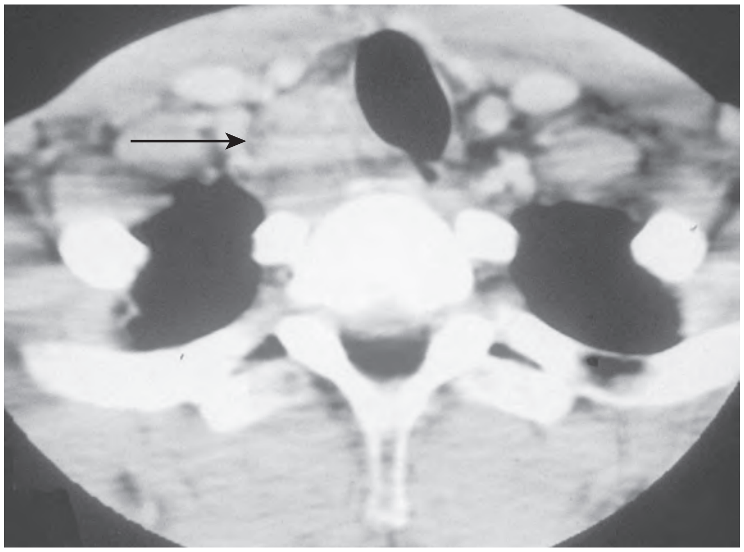

Figure 14.70 A computed tomography scan at the level of the suprasternal notch, showing the tumor (*arrow*).

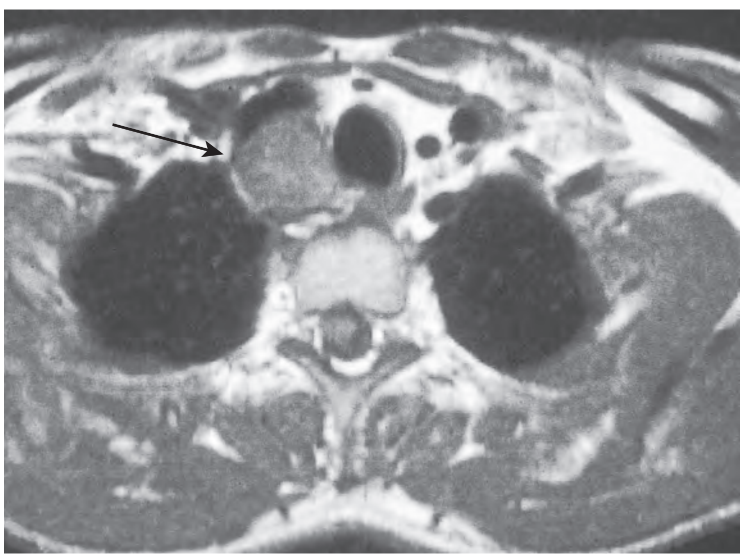

Figure 14.71 A magnetic resonance imaging scan at the level of the suprasternal notch, showing the tumor (*arrow*).

A transverse cervical incision is made in the supraclavicular region beginning at the anterior border of the trapezius muscle and curving anteriorly to the midline in the suprasternal notch. At this point, the incision is continued vertically caudad in the midline up to the third intercostal space. The skin incision is deepened through the platysma, and the sternocleidomastoid muscle is detached from the sternoclavicular insertion. A median sternotomy is performed with use of a sternal saw to divide the manubrium in the midline up to the manubrial-sternal junction. At that point the incision in the sternum is taken laterally through the third interspace to permit opening of the superior mediastinum in a "clamshell" fashion. To gain further exposure, it may be necessary to divide the clavicle at the junction of its middle and medial third (Fig. 14.73). A self-retaining sternotomy retractor is used to provide exposure of the anterosuperior mediastinum. Meticulous dissection of the great vessels now begins, with careful identification of the innominate artery at its takeoff from the ascending aorta and its distal branches (that is, the common carotid artery, the subclavian artery, and the vertebral artery). It may be necessary to identify, divide, and ligate the internal mammary artery to facilitate further exposure.

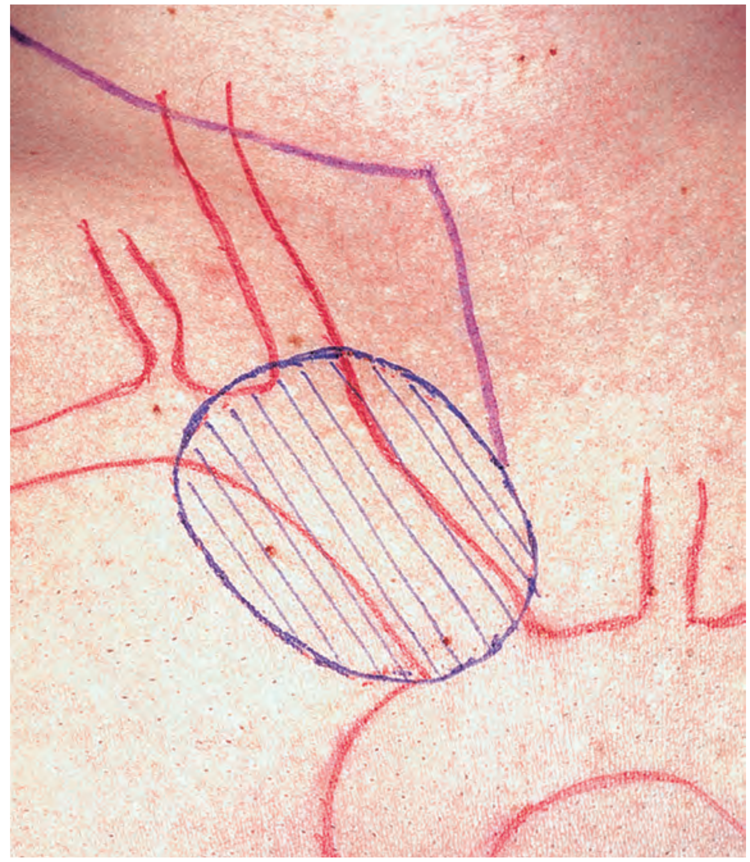

Figure 14.72 The location of the tumor in relation to the great vessels is outlined on the patient. The skin incision is shown in purple.

At this point it becomes evident that the tumor is located posterior and inferior to the innominate artery. Meticulous dissection along the subadventitial plane of the innominate artery is undertaken, with careful coagulation of all the bleeding points while mobilizing the tumor. The right recurrent laryngeal nerve, which crosses the innominate artery and curves upward, is identified. However, this patient had previously undergone resection of a glomus intravagale tumor on the same side, and thus the integrity of the recurrent laryngeal nerve was not of significant importance, because paralysis of the right vocal cord already existed. Vessel loops are passed around the innominate artery, the common carotid artery, and the subclavian artery. With alternate medial and lateral traction using the vessel loops, the anterior attachments of the tumor to the posterior aspect of the innominate artery are divided (Fig. 14.74).

Further mobilization of the tumor continues in a careful and delicate fashion, freeing all the small blood vessels from the loose areolar attachments around the pseudocapsule of the tumor. Digital dissection often facilitates mobilization of the tumor, keeping the need for absolute hemostasis in mind at all times. Once the anterior aspect of the tumor is adequately mobilized, the tumor is grasped with a Kelly clamp and its mobilization begins in the prevertebral plane (Fig. 14.75). After circumferential mobilization and dissection of the tumor, it is delivered in a monobloc fashion with its pseudocapsule intact. A close-up view of the surgical field shows the tumor bed between the innominate and subclavian arteries medially and the subclavian vein superiorly (Fig. 14.76). After securing absolute hemostasis, wound closure begins with use of an A-O plate and screws to realign the clavicle and stainless steel wires to reapproximate the divided sternum. The wound is then closed in two layers after a suction drain is appropriately positioned (Fig. 14.77). The

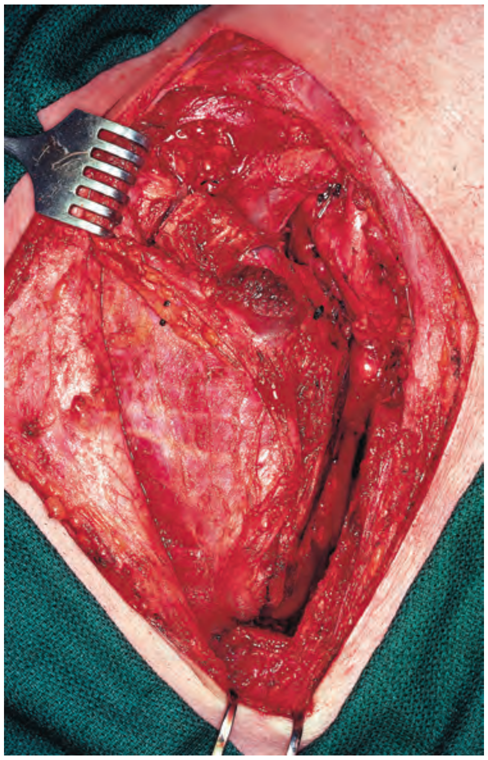

Figure 14.73 A median sternotomy is completed and the site of division of the clavicle is outlined.

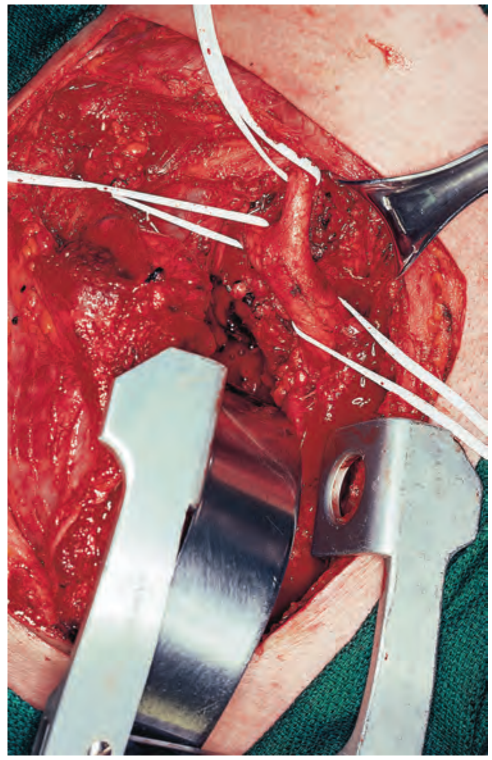

Figure 14.74 The innominate, common carotid, and subclavian arteries are dissected and isolated.

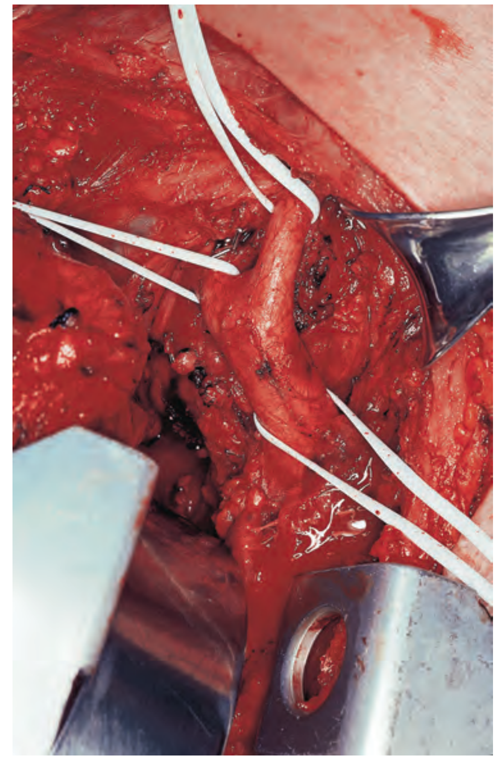

Figure 14.75 A close-up view of the surgical field shows the tumor located posterior to the great vessels.

Figure 14.76 A close-up view of the surgical field after removal of the tumor.

Figure 14.77 Closure of the wound.

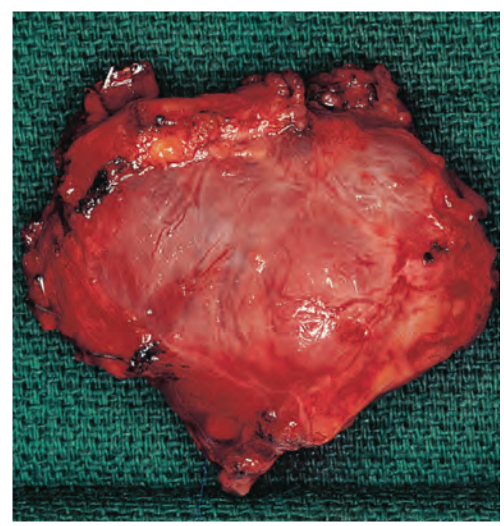

Figure 14.78 The gross appearance of the tumor.

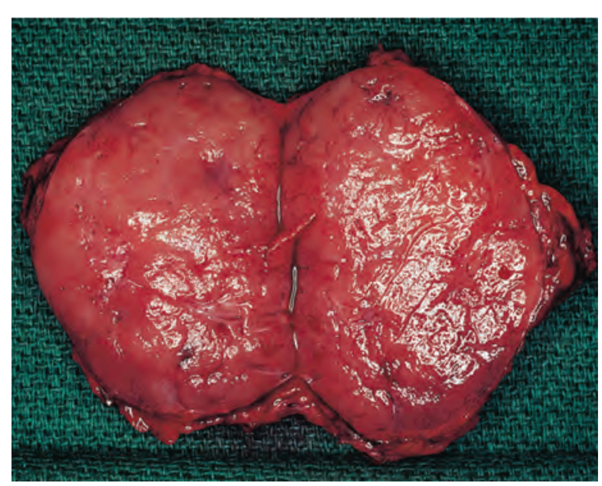

Figure 14.79 A cross section of the tumor.

external appearance of the tumor, which measures 5 by 4 cm in diameter, is shown in Fig. 14.78. On cross section it appears fleshy and is full of vascular spaces, which is the characteristic appearance of a paraganglioma (Fig. 14.79).

Excision of a Schwannoma of the Inferior Alveolar Nerve

Intraosseous schwannomas of the inferior alveolar nerve in the mandibular canal are extremely rare. Usually they present as small intraosseous lesions within the canal and are managed by relatively conservative surgical procedures, with preservation of the remaining fibers of the inferior alveolar nerve if possible. The patient described here with an extensive schwannoma of the entire inferior alveolar nerve presented with sensations of tingling and numbness of the skin of the chin. Findings of a physical examination were entirely negative, except for anesthesia in the distribution of the inferior alveolar nerve. A panoramic radiograph of the mandible shows significant expansion of the inferior alveolar canal on the left-hand side, with a beaded appearance of the shape of the canal extending from the mental foramen inferiorly up to the entry of the inferior alveolar nerve through the lingual plate of the ascending ramus of the mandible (Fig. 14.80). A CT scan with bone windows showed that the entire lesion was completely intraosseous without extension of tumor through the lingual or lateral cortex of the mandible into the soft tissues. Slight soft-tissue swelling overlying the region of the masseter muscle is observed (Fig. 14.81).

The initial plan for surgical excision of this lesion was through decortication of the lingual plate of the mandible via a paramedian mandibulotomy. However, during the course of the procedure it became apparent that the tumor was indeed involving the bony inferior alveolar canal and could not be delivered with the mandible remaining intact. Thus the operative procedure was converted to a segmental mandibulectomy with fibula free flap reconstruction. With tumors such as this it is important to obtain a consent from the patient for a segmental mandibulectomy if required and to be prepared to proceed with immediate mandible reconstruction.

A transverse incision is placed along an upper neck skin crease on the left-hand side, extending from the posterior border of the sternocleidomastoid muscle laterally and across the midline anteriorly. The skin flaps are elevated in a subplatysmal plane. The submandibular gland is excised to provide adequate exposure and access to the mandible (Fig. 14.82). The upper flap is elevated to expose the lateral cortex of the mandible. An incision is placed in the gingivobuccal mucosa from the retromolar trigone up to the midline, and the lower cheek flap then is elevated in the "visor flap" fashion. The mental nerve is divided as it exits from the mental foramen to provide further exposure of the anterior end of the mandible.

The masseter muscle is detached from the lateral aspect of the mandible all the way up to the mandibular notch (Fig. 14.83). The mandible is next divided anterior to the mental foramen vertically between the canine and the first premolar teeth. The divided lateral segment of the mandible is now retracted laterally (Fig. 14.84). The mylohyoid muscle is divided close to the mandible, and further lateral rotation of the mandible is accomplished to expose the lower attachment of the medial pterygoid muscle (Fig. 14.85). The medial pterygoid muscle is carefully detached from the lingual aspect of the

Figure 14.80 A panoramic radiograph of the mandible showing expansion of left inferior alveolar canal.

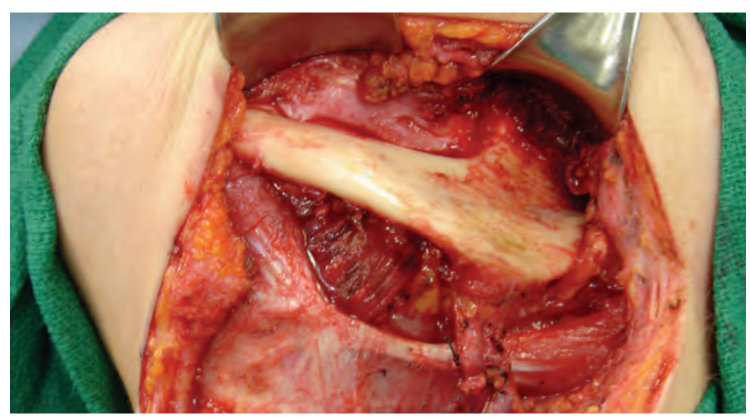

Figure 14.82 The lateral cortex of the mandible is exposed via an upper neck incision.

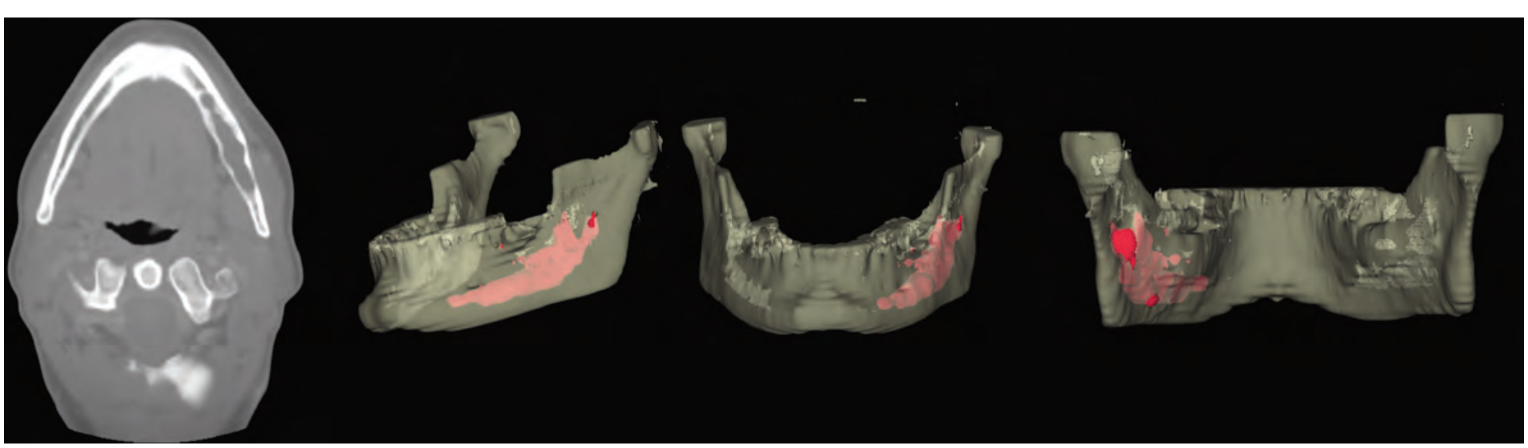

Figure 14.81 An axial view of a computed tomography scan with bone windows and three-dimensional reconstructions shows expansion of the alveolar canal and the completely intraosseous nature of the tumor.

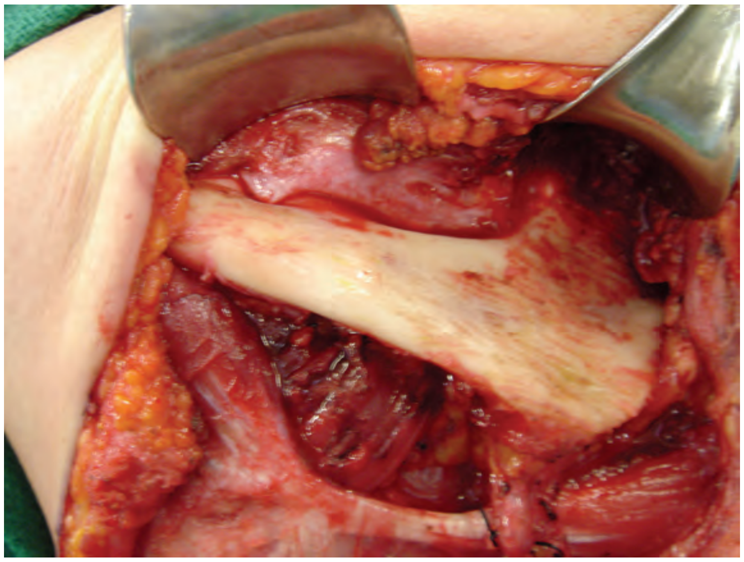

Figure 14.83 A close-up view of the mandible after detachment of the masseter muscle from the ascending ramus.

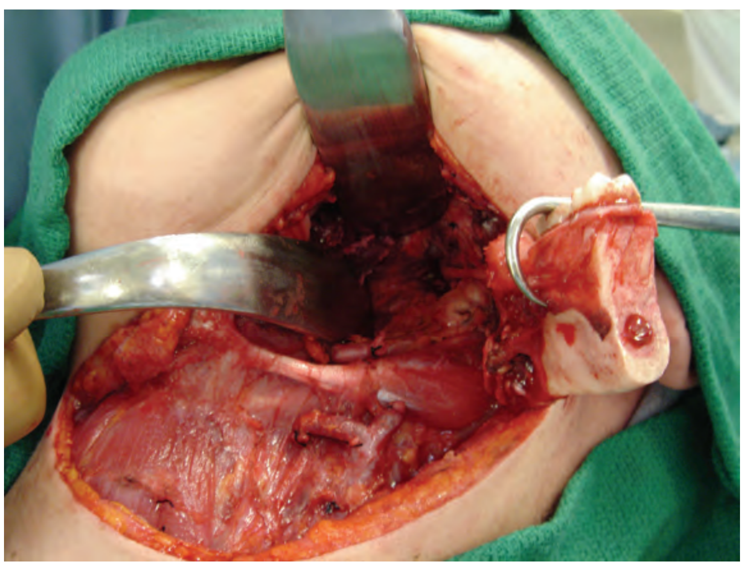

Figure 14.84 The mandible is divided anterior to the tumor and retracted laterally.

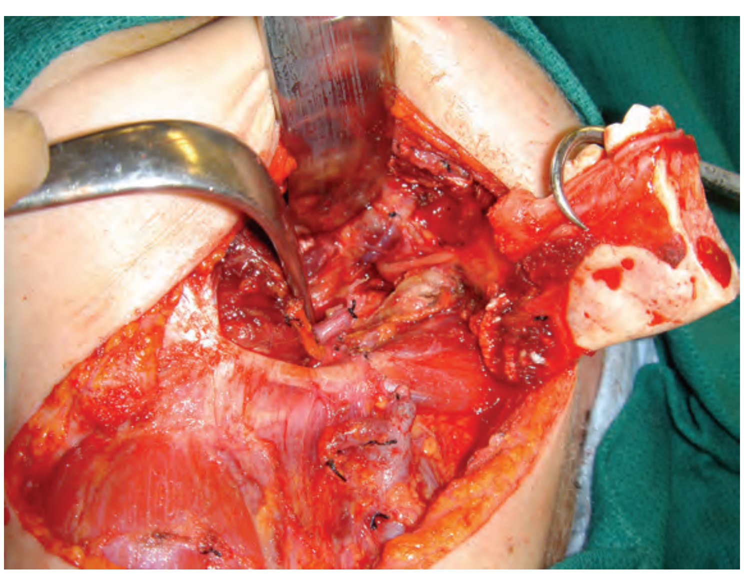

Figure 14.85 Further lateral retraction of the mandible exposes the medial pterygoid muscle.

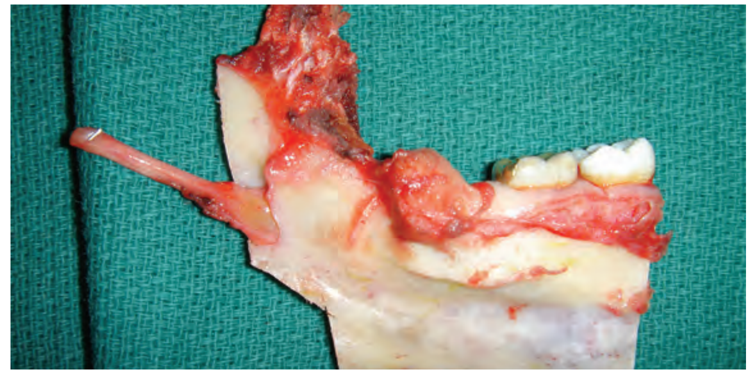

Figure 14.86 A medial view of the resected segment of the mandible and the proximal stump of the inferior alveolar nerve.

Figure 14.87 Removal of the medial wall of the inferior alveolar canal shows the tumor in situ in the inferior alveolar canal.

Figure 14.88 A postoperative panoramic radiograph shows the reconstructed mandible with a fibula free flap.

ascending ramus of the mandible to expose the entry of the inferior alveolar nerve in the mandible.

The inferior alveolar nerve is dissected proximally up to its origin from the third division of the trigeminal nerve. If the main trunk of the third division of the trigeminal nerve is not involved by tumor grossly, and if the lingual nerve also is uninvolved, it can be preserved safely, as was done in this patient. The inferior alveolar nerve is then transected at its origin from the third division of the trigeminal nerve. The proximal stump of the inferior alveolar nerve is checked by frozen section for the presence of tumor. Appropriate osteotomies of the ascending ramus of the mandible then are performed to encompass the entire inferior alveolar nerve in the inferior alveolar canal in the segment of the mandible (Fig. 14.86). The

Figure 14.89 The facial appearance of the patient 1 year following surgery.

lingual cortex of the mandible is removed in the specimen to demonstrate the entire tumor intact, extending from the proximal part of the inferior alveolar nerve all the way up to the mental foramen (Fig. 14.87).

After complete hemostasis is achieved, fibula free flap reconstruction of the resected part of the mandible is performed. (Technical details of reconstruction of the mandible with a fibula free flap are provided in Chapter 17.) A postoperative panoramic view of the mandible shows restoration of the continuity and the contour of the mandible (Fig. 14.88). A photograph of the patient 1 year after surgery shows essentially a normal appearance of the face with no visible features indicating segmental mandibulectomy and fibula free flap reconstruction (Fig. 14.89). This patient is a candidate for osseointegrated dental implants in the fibula free flap, which may be performed primarily, or deferred until complete healing of the fibula with the native mandible occurs, which usually takes 12 to 18 months. In the interim, the patient is able to use a removable partial denture.

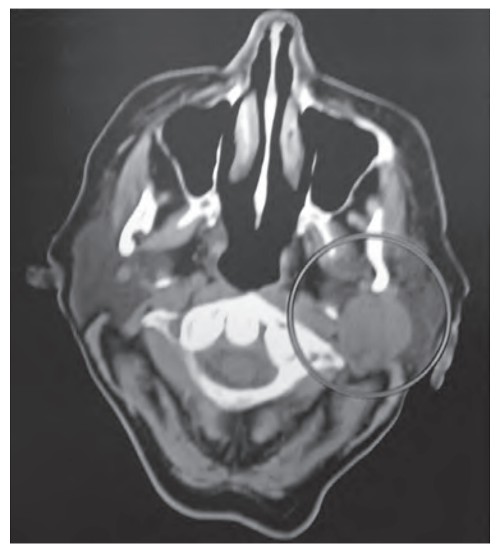

Figure 14.90 An axial view of a contrast-enhanced computed tomography scan shows the tumor in the retromandibular location on the left-hand side.

Excision of a Schwannoma of the Facial Nerve

Schwannomas of the facial nerve are rare neoplasms. They usually present as a mass in the parotid region and often are mistaken for a parotid tumor. The patient presented here gave a 6-year history of a slowly enlarging mass in the left parotid region. She had no other symptoms. The function of the facial nerve was intact until 6 months before presentation, at which time weakness of the marginal branch of the facial nerve became apparent. A contrast-enhanced CT scan of the parotid gland demonstrates a well-circumscribed tumor in the retromandibular region of the left parotid gland (Fig. 14.90). The tumor is well encapsulated and shows some areas of necrosis. However, it is literally impossible to differentiate between a facial nerve schwannoma and a mixed tumor of the parotid gland on the CT scan. An MRI scan on a T2-weighted image shows a bright image of the tumor, indicating the possibility of a schwannoma of the facial nerve, and extension of tumor along the stylomastoid foramen into the temporal bone suggests a facial nerve schwannoma (Fig. 14.91).

The surgical approach to facial nerve schwannomas in the extracranial facial nerve is similar to that for excision of a parotid tumor. On the other hand, extension of tumor through the stylomastoid foramen into the facial canal requires a mastoidectomy and exposure of the vertical segment of the facial nerve to accomplish total removal of the tumor.

The surgical procedure begins with the usual parotidectomy incision in the preauricular skin crease, curving around the lobule of the ear into an upper neck skin crease in the submandibular region. The anterior and posterior skin flaps are elevated, and the usual landmarks for identification of the main trunk of the facial nerve are exposed. These landmarks include the anterior border of the sternocleidomastoid muscle, the posterior belly of the digastric muscle, the tip of the mastoid process, and the anteroinferior surface of the cartilaginous portion of the auditory canal (Fig. 14.92).

By alternate blunt and sharp dissection and retraction of the superficial lobe of the parotid gland anteriorly, the surgical procedure proceeds, while carefully looking for the main trunk of the facial nerve. In patients with facial nerve schwannoma, it is particularly important to see if the proximal end of the extracranial portion of the facial nerve is free of tumor and can be isolated and exposed. If such is the case, then every effort is

Figure 14.91 An axial view of a T2-weighted magnetic resonance imaging scan shows a bright image of the tumor and extension of the tumor through the stylomastoid foramen in the temporal bone on the left side.

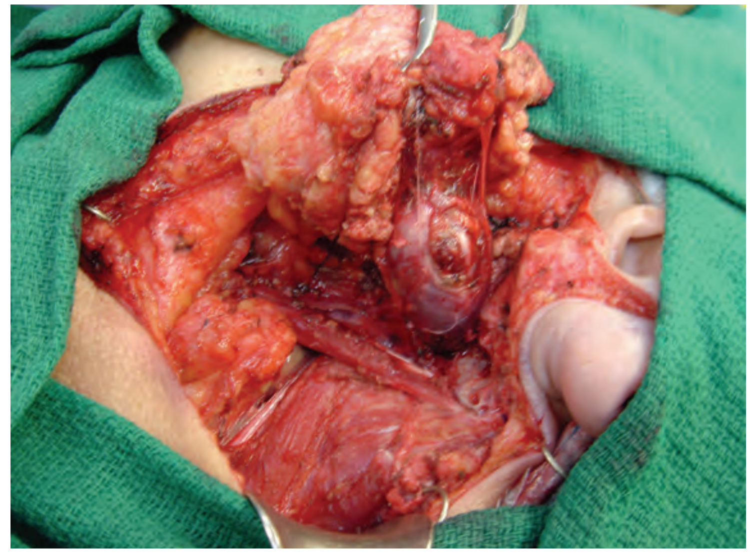

Figure 14.93 A schwannoma of the main trunk of the facial nerve extending into the stylomastoid foramen.

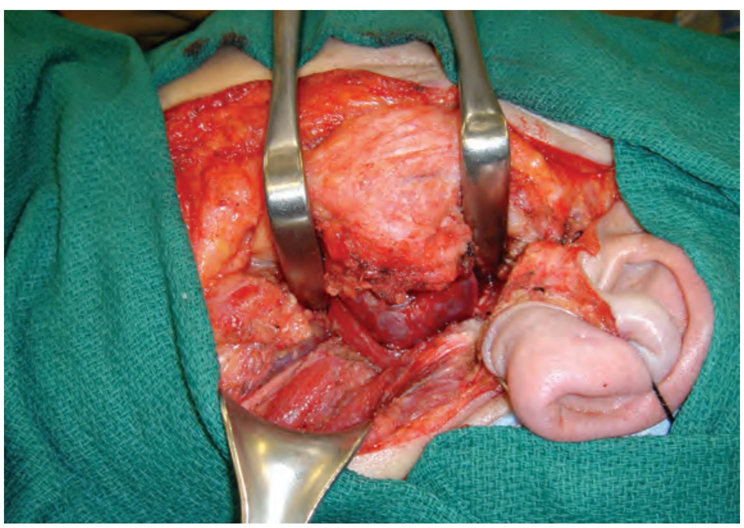

Figure 14.92 Dissection of the superficial lobe of the parotid gland through a standard parotidectomy incision to expose the main trunk of the facial nerve.

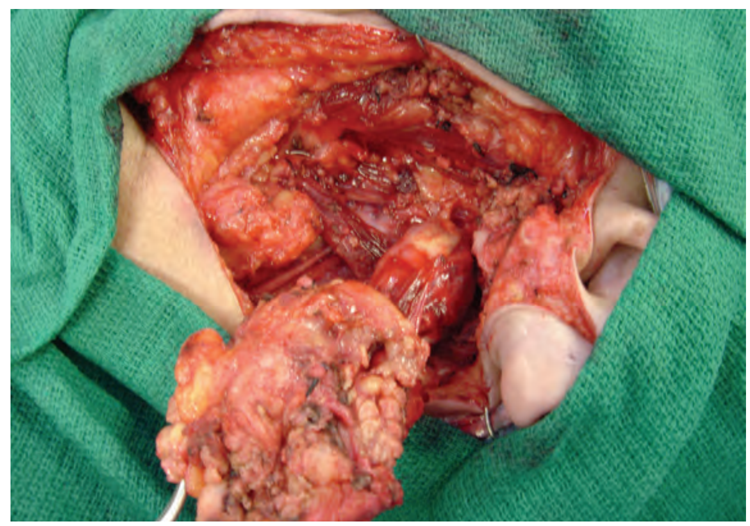

Figure 14.94 Circumferential mobilization of the tumor demonstrates its extension into the stylomastoid foramen.

made to dissect, identify, and preserve a stump of the main trunk of the facial nerve proximal to the tumor for consideration of facial nerve grafting. On the other hand, if the main trunk of the facial nerve is involved by the tumor with extension of the tumor into the temporal bone through the stylomastoid foramen, then the operative procedure at this juncture is extended to include a mastoidectomy and exposure of the facial nerve in the vertical segment of the facial canal. In this patient, the tumor extended right up to the stylomastoid foramen, which was only slightly enlarged. The tumor, which completely replaced the facial nerve and extended into the stylomastoid foramen, is seen during the early part of the operation (Fig. 14.93).

Further dissection of the tumor toward the stylomastoid foramen demonstrates that the tumor is well circumscribed and is located deep to the superficial lobe of the parotid gland and extends directly into the stylomastoid foramen (Fig. 14.94). Circumferential mobilization of the tumor is undertaken through the parotid tissue in the deep lobe medial to the tumor. The only attachment of the surgical specimen to the patient at this point remains at the proximal end of the facial nerve at the stylomastoid foramen.

A mastoidectomy is performed to expose the proximal stump of the facial nerve within the vertical portion of the facial canal. Details of the mastoidectomy are not shown. A sural nerve graft was used to suture the facial nerve proximally in the temporal bone and to its peripheral branches beyond the parotid gland. In a significant number of patients undergoing facial nerve grafting, dyskinesia will develop with unintentional nonsynchronous movement of facial muscles supplied by various divisions of the facial nerve. It is therefore preferable to graft only the lower division of the facial nerve, replacing the buccal and mandibular branches and rehabilitating the zygomatic division (the orbicularis oculi muscle) with placement of a gold weight in the upper eyelid, which restores harmonious movement of the upper eyelid synchronous with the opposite eyelid much more effectively than a nerve graft.

The surgical specimen shows monobloc excision of the tumor with the parotid gland, along with the schwannoma, which was completely excised in a monobloc fashion (Fig. 14.95).

Figure 14.95 The surgical specimen showing the superficial lobe of the parotid gland and a schwannoma of the main trunk of the facial nerve with extension along its upper and lower divisions.

Excision of a Facial Nerve Schwannoma With Nerve Repair

Large tumors in the parotid gland where there is uncertainty about its cell of origin should undergo fine-needle aspiration biopsy. The confusion sometimes arises between a pleomorphic adenoma and schwannoma of the facial nerve. Imaging studies can assist in arriving at a diagnosis, but cytologic confirmation is mandatory to facilitate treatment planning. Before considering surgical resection of a facial nerve schwannoma with a functioning facial nerve, several points should be considered. The duration of the tumor, tumor size, rate of growth, patient symptoms, the feasibility of facial nerve reconstruction or rehabilitation, and finally the age of the patient. These factors will enable a safe surgical procedure and satisfactory rehabilitation of the paralyzed face. To achieve this goal, careful evaluation of the imaging studies should be performed to assess the extensions of tumor in the temporal bone. The patient shown in Fig. 14.96 had previously undergone surgical exploration of a large parotid mass elsewhere, but the surgical procedure was terminated after a biopsy confirmation of facial nerve schwannoma. Her MRI scans show a large intraparotid tumor (Fig. 14.97). Careful assessment of the temporal bone was performed with thin-sliced CT scans, which showed no extension of tumor into the temporal bone.

The plan of surgery was to proceed with exploration of the parotid gland and facial nerve in the usual fashion through the previously employed parotidectomy incision (Fig. 14.98). Dissection and identification of the main trunk of the facial nerve at the stylomastoid foramen was impossible due to the size of the tumor tightly packed in the stylomastoid region (Fig. 14.99). Therefore retrograde dissection of the facial nerve was performed, identifying each of its branches emanating from the tumor, indicating that the tumor arose from the main trunk and the lower division of the facial nerve (Fig. 14.100). A decision was made at this point to proceed with excision of the tumor and reanastomose the peripheral branches of the facial nerve to the main trunk of the facial nerve in the temporal bone. Therefore the uninvolved facial nerve was divided to release it from the tumor (Fig. 14.101). The surgical specimen shows monobloc excision of the tumor with the superficial lobe of the parotid gland (Fig. 14.102). A mastoidectomy is performed at this point, and the facial nerve is dissected out of the facial canal in the temporal bone (Fig. 14.103). Anastomoses between the intratemporal facial nerve and the peripheral branches of the facial nerve is completed with microsutures (Fig. 14.104). The wound is closed in the usual fashion.

The patient had complete facial paralysis in the postoperative period. She was managed with facial muscle exercises and electrical stimulation of facial muscles to maintain the tone of the muscles while waiting for nerve recovery. The postoperative appearance of the patient 18 months following surgery shows near-complete return of facial nerve function (Fig. 14.105).

Excision of Schwannomas of Lower Cranial Nerves

The principles of surgery for schwannomas of the lower cranial nerves are similar to those applied at any other site. An attempt is made to preserve the uninvolved fibers of the nerve of origin if possible. Several examples of schwannomas of lower cranial nerves and the sympathetic chain are shown here.

Figure 14.96 Preoperative appearance of the patient showing a large parotid mass with intact facial nerve function.

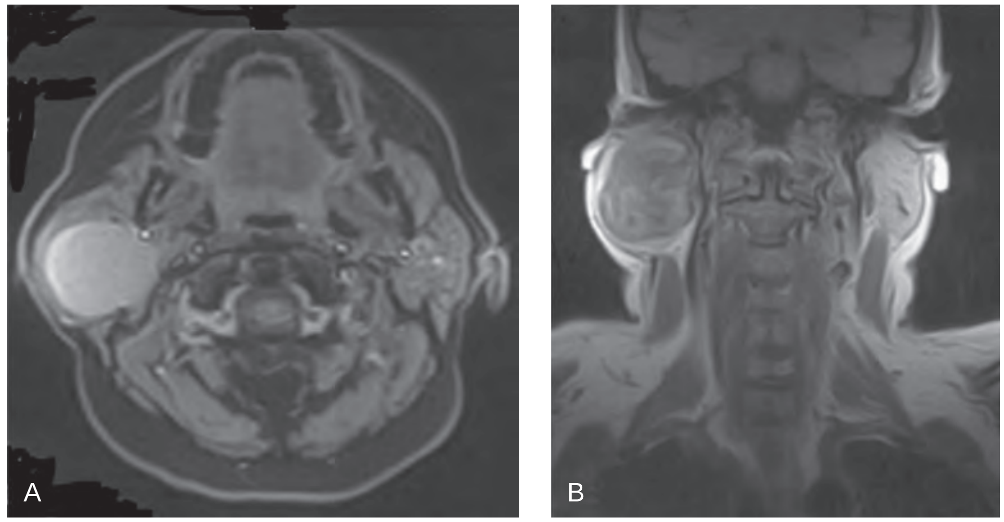

Figure 14.97 Axial (**A**) and coronal (**B**) views of T1-weighted magnetic resonance imaging scans show a large tumor involving the right parotid gland, which is well demarcated.

Figure 14.98 Plan of surgery through the scar of previous parotidectomy incision and retroauricular extension for mastoidectomy and exposure of facial nerve in the temporal bone.

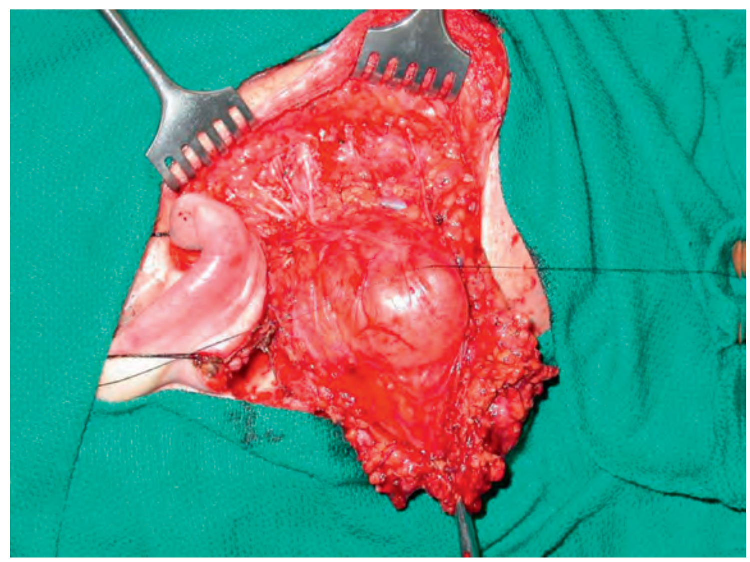

Figure 14.100 Retrograde dissection of the facial nerve demonstrating origin of the schwannoma from the main trunk and lower division of the facial nerve.

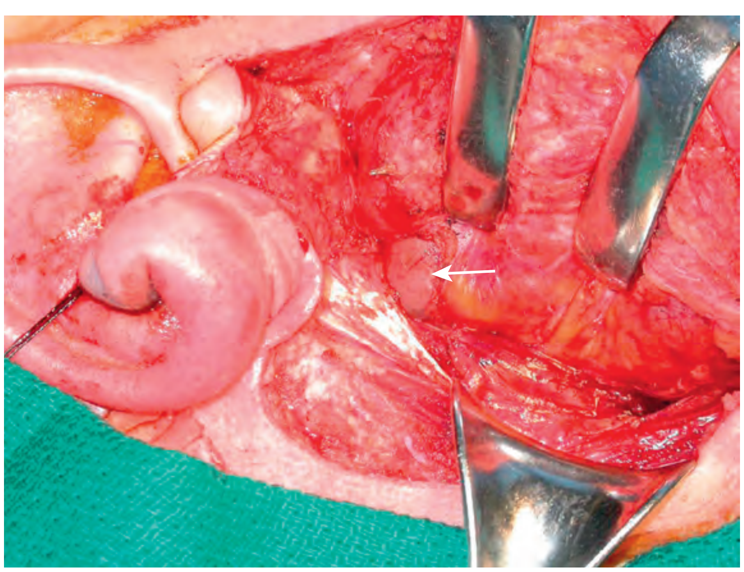

Figure 14.99 Exploration of the parotid gland showed a tightly packed tumor obscuring the view of the main trunk of the facial nerve (*arrow*).

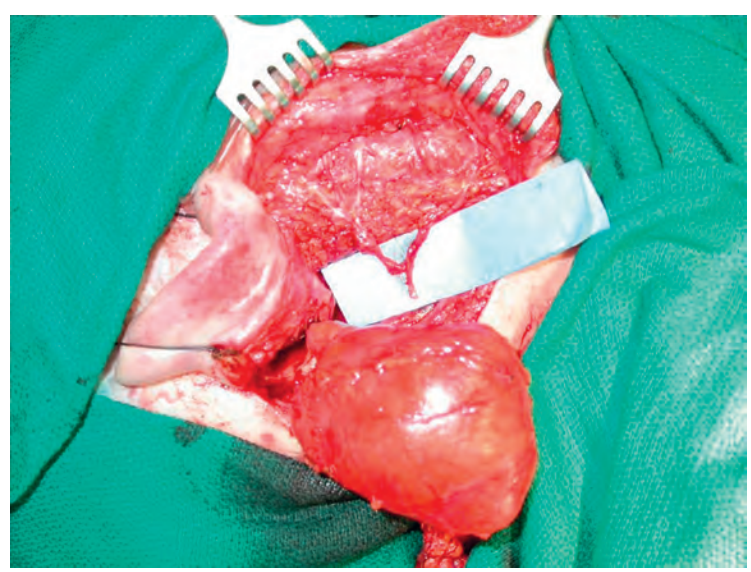

Figure 14.101 Peripheral branches of the facial nerve are separated from the tumor.

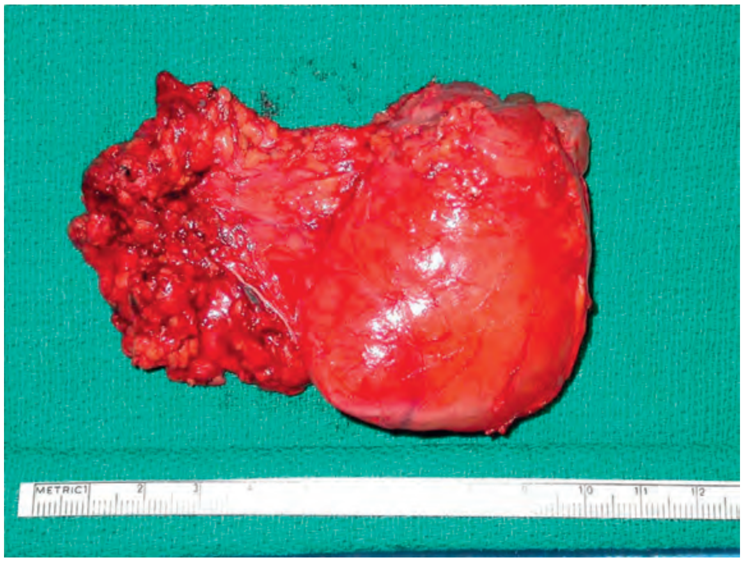

Figure 14.102 Surgical specimen showing monobloc excision of the tumor.

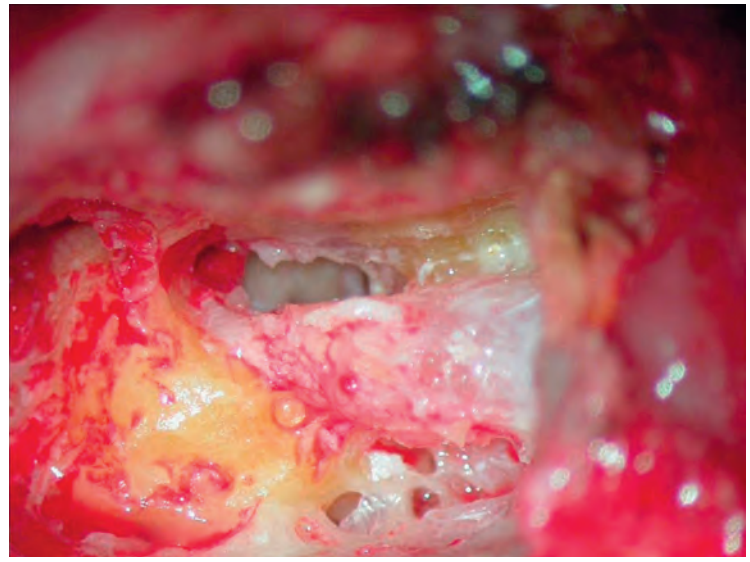

Figure 14.103 Facial nerve dissected out of the facial canal in the temporal bone.

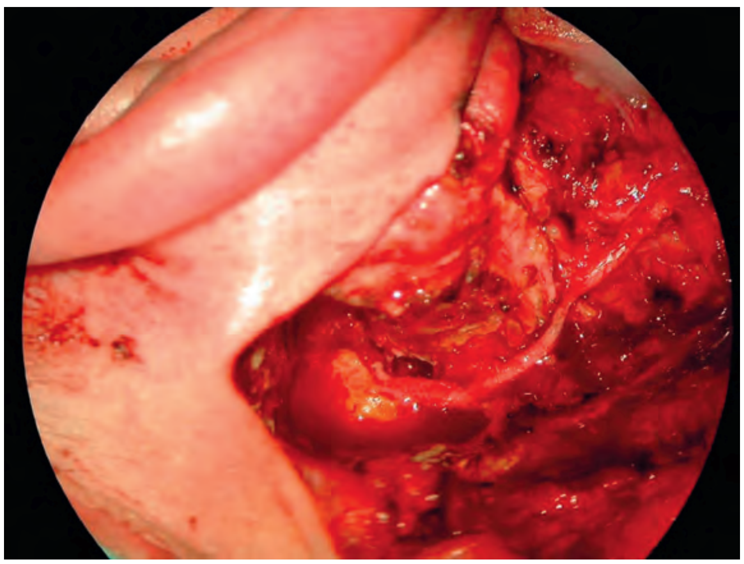

Figure 14.104 Nerve anastomoses between the intratemporal facial nerve and peripheral branches of the facial nerve is completed.

Schwannoma of the Glossopharyngeal Nerve

An endoscopic view of the oropharynx with a fiberoptic laryngoscope showing a lobulated submucosal mass from the base of the tongue on the right-hand side is shown in Fig. 14.106. Imaging studies with a CT scan and MRI scan show the tumor localized in the base of the tongue (Fig. 14.107). A CT-guided fine-needle aspiration biopsy confirmed the diagnosis of a schwannoma. Surgical exploration through the upper part of the neck and exposure of the tumor in the hyoglossus muscle was undertaken (Fig. 14.108). The tumor is delivered intact, and the defect in the hyoglossus muscle is repaired in two layers.

Excision of a Schwannoma of the Vagus Nerve

The patient shown here has a lesion in the parapharyngeal space seen on a CT scan. The postcontrast CT scan shows a well-circumscribed nonenhancing mass in the carotid space on the right-hand side that is displacing the external carotid artery

Figure 14.105 Postoperative appearance of the patient 18 months following surgery shows near-complete recovery of facial nerve function.

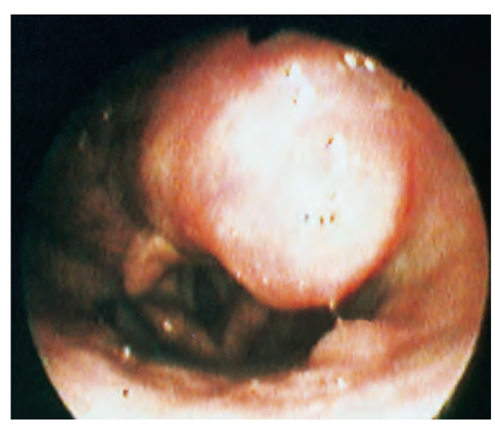

Figure 14.106 A discrete lobulated submucosal lesion of the base of the tongue is seen obscuring the view of the larynx and pharynx.

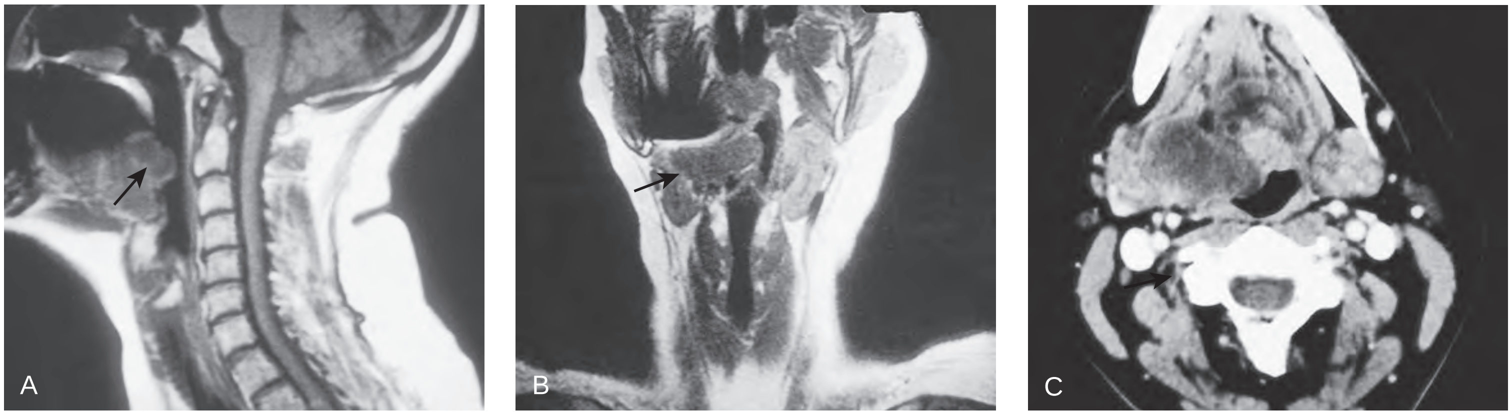

Figure 14.107 **A**, An axial view of a contrast-enhanced computed tomography scan showing an encapsulated tumor of the base of the tongue (*arrow*). **B**, A coronal view of the magnetic resonance imaging (MRI) scan showing the tumor (*arrow*). **C**, A sagittal view of the MRI scan showing the tumor (*arrow*).

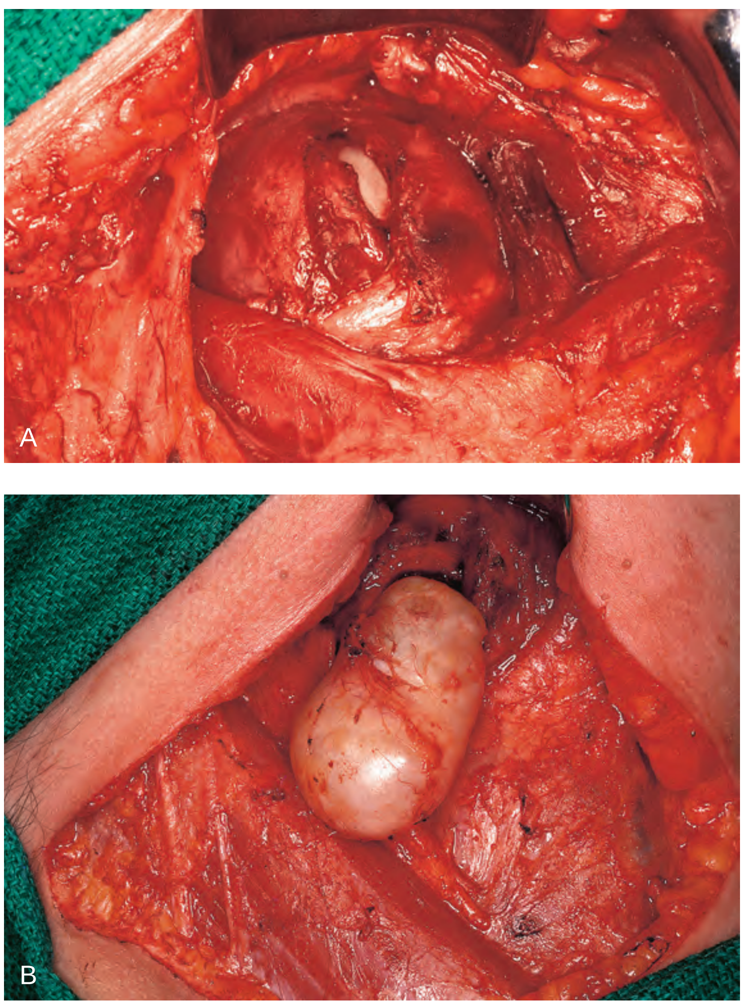

Figure 14.108 **A**, The muscle fibers of the hyoglossus are split to expose the pseudocapsule of the tumor. **B**, The bilobed tumor is delivered intact.

Figure 14.109 An axial view of a postcontrast computed tomography scan at the level of the nasopharynx shows displacement of the external and internal carotid arteries by the tumor on the right-hand side.

anteriorly and medially, while the internal carotid artery and jugular vein remain in their normal locations (Fig. 14.109).

Surgical exploration of the upper neck clearly shows the tumor at the upper end of the vagus nerve. The hypoglossal nerve is seen coursing from lateral to medial over the tumor and carotid artery (Fig. 14.110).

The surgical specimen demonstrates a well-encapsulated, firm, glistening, nodular tumor completely excised with the stump of the vagus nerve (Fig. 14.111). After removal of the tumor, the surgical field shows the intact hypoglossal nerve, the internal jugular vein, the common carotid artery with its bifurcation, and the sympathetic chain posteriorly (Fig. 14.112).

Postoperative sequelae of paralysis of the vagus nerve leads to hoarseness of voice and aspiration of fluids to a varying degree in nearly all patients. Some patients will compensate adequately if

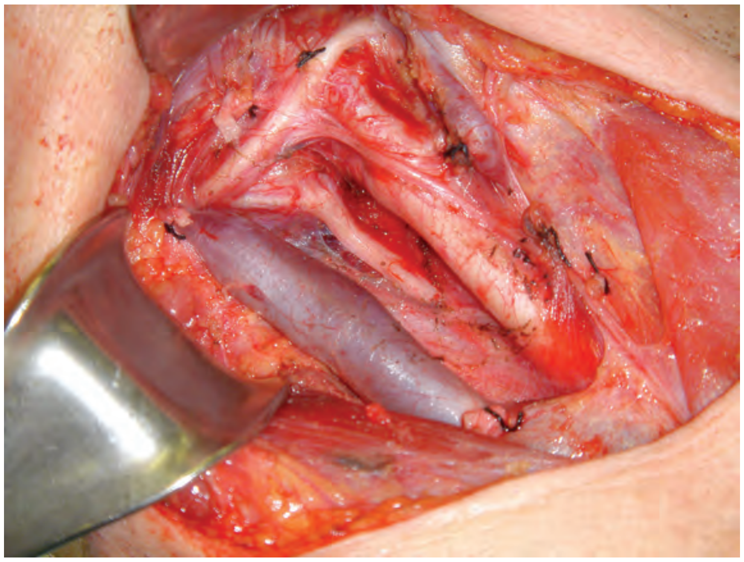

Figure 14.110 The surgical field showing the common carotid artery, internal jugular vein, hypoglossal nerve, and lower part of the vagus nerve below the tumor.

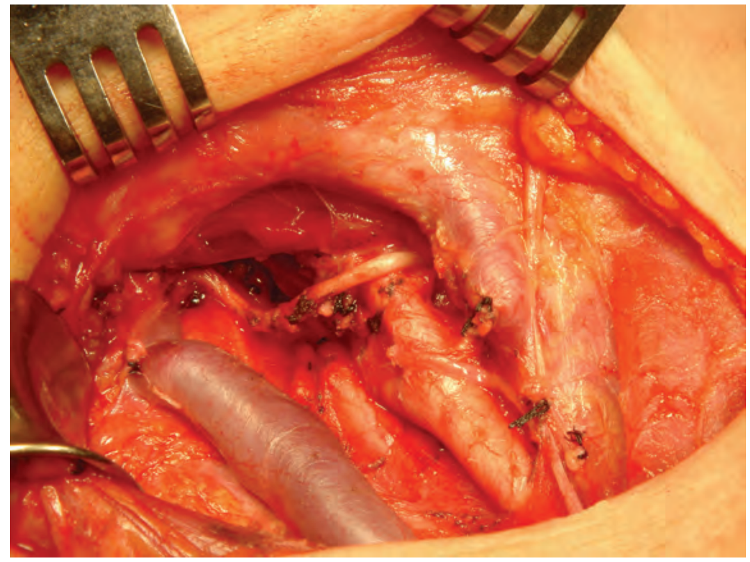

Figure 14.112 The surgical field after removal of the tumor shows an intact hypoglossal nerve, internal jugular vein, and external and internal carotid arteries.

Figure 14.111 An external view of the tumor with a stump of the vagus nerve shows an encapsulated tumor removed intact.

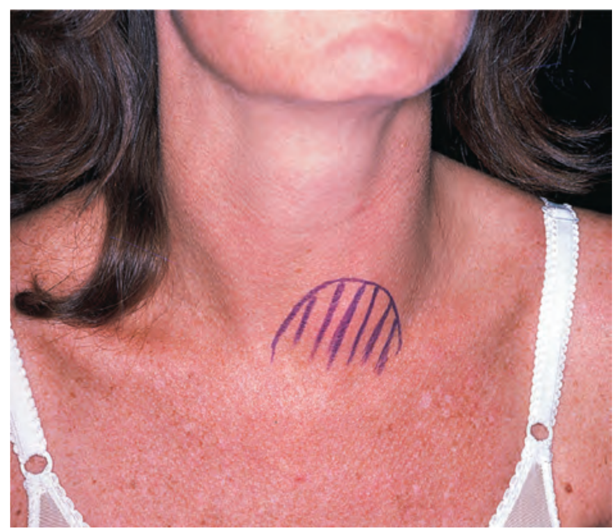

Figure 14.113 A patient with an asymptomatic mass at the suprasternal notch. A chest radiograph showed a superior mediastinal mass with displacement of the trachea.

the vocal cord is paralyzed in adduction, with reasonable quality of voice and minimal aspiration. Other patients will require vocal cord medialization for restoration of competency of the glottis and improvement of the voice, as well as to minimize aspiration.

Excision of Schwannoma of the Vagus Nerve in the Cervicothoracic Region

The patient shown in Fig. 14.113 had a mass in the suprasternal region causing local pressure symptoms of tightness in the lower part of the neck.

A CT scan through the superior mediastinum demonstrates an inhomogeneous tumor that is well circumscribed, measuring 7 by 10 cm (Fig. 14.114). Dissection of a tumor extending into the superior mediastinum through a cervical approach requires special attention to detail, because it relates to other neurovascular and lymphatic structures at the root of the neck. On the left-hand side of the neck, particular attention is required to meticulously identify all the lymphatic channels and ligate them individually to avoid a chyle fistula in the neck or a chylothorax. Similarly, excessive dissection in the prevertebral plane posterior to the carotid sheath easily can produce trauma to the sympathetic chain and the stellate ganglion, producing Horner's syndrome. The fascia overlying the sternomastoid muscle is incised on the left-hand side, and the muscle is retracted laterally to expose the carotid sheath. Upon retraction, the left lobe of the thyroid and the common carotid artery are exposed. The carotid artery is dissected and isolated first, separating it from the tumor in the neck and down in the superior mediastinum (Fig. 14.115). A vessel loop is passed around the carotid artery, which permits its retraction medially. Mobilization of the cervical component of the tumor now begins by dissection lateral to it and by separating it posteriorly from the sympathetic chain. Blunt dissection is continued posterior to the tumor in the superior mediastinum, permitting its delivery in the neck. The dissection continues in a circumferential fashion around the tumor. The fully mobilized tumor now can be pulled cephalad from the mediastinum for total excision (Fig. 14.116). The lower

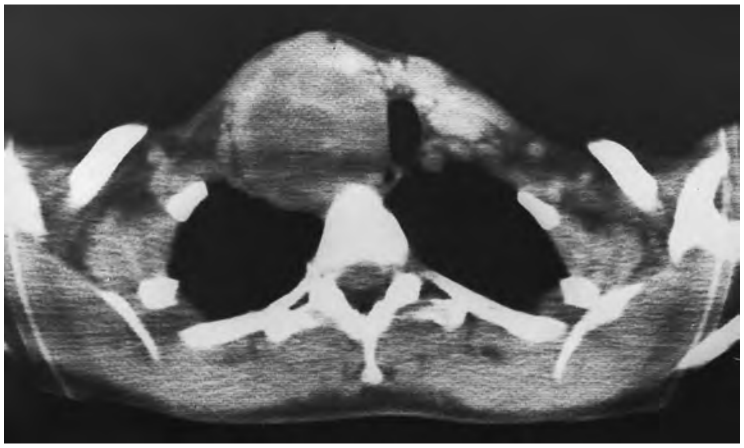

Figure 14.114 A computed tomography scan with contrast at the level of the thoracic inlet showing a heterogeneous but well-defined mass.

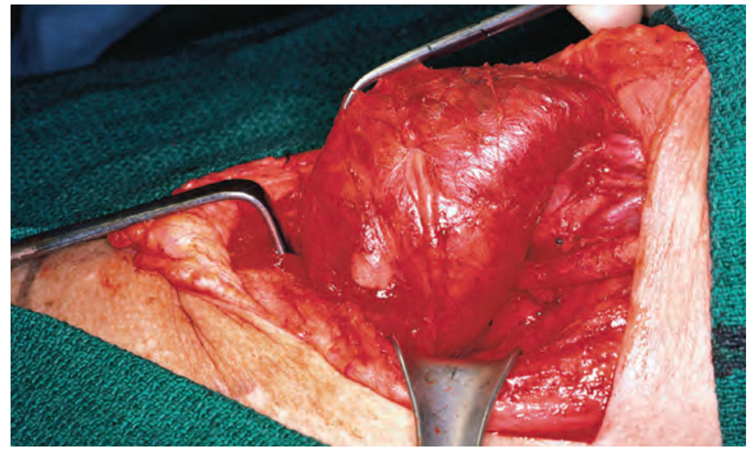

Figure 14.116 Mobilization of the tumor.

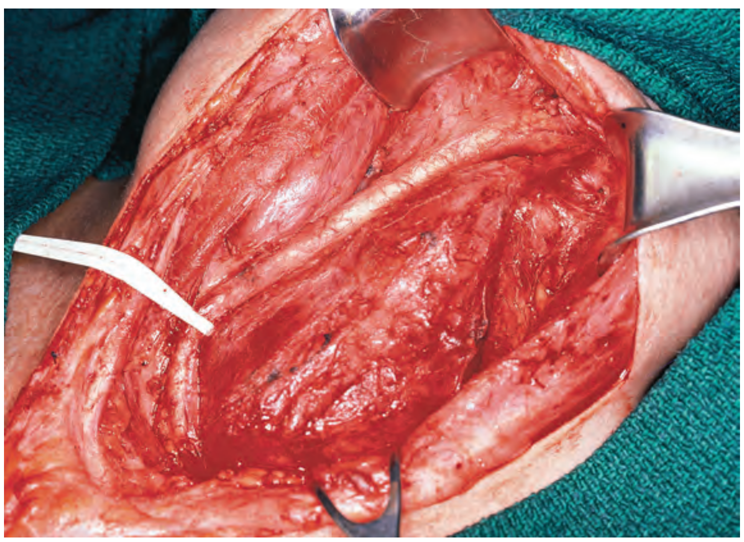

Figure 14.115 The common carotid artery is dissected free from the tumor and retracted medially with a vessel loop.

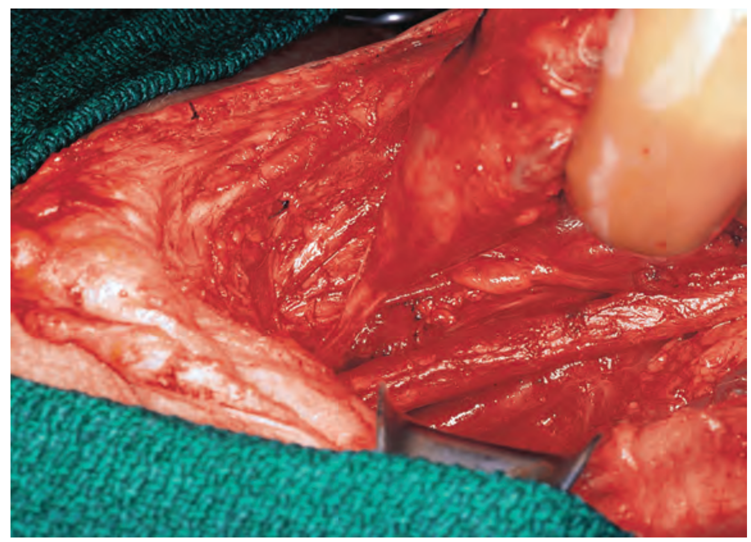

Figure 14.117 The mediastinal component of the tumor is mobilized by blunt digital dissection and pulled into the neck.

part of the tumor is seen at the thoracic inlet from the left side as it is being pulled out of the mediastinum (Fig. 14.117).

The specimen demonstrates the intact tumor (Fig. 14.118), which measures 7 by 12 cm. The paralyzed vocal cord may need medialization to improve voice quality.

Excision of a Schwannoma of the Hypoglossal Nerve

Clinically a schwannoma of the hypoglossal nerve is difficult to differentiate from other neurogenic tumors in the upper part of the neck. The patient described here presented with an incidentally identified mass in the neck. An MRI shows a well-circumscribed homogeneous bright mass on a T2-weighted image in the upper part of the neck with displacement of the carotid vessels anteromedially and the internal jugular vein posterolaterally (Fig. 14.119).

Surgical exploration of the tumor is accomplished through a transverse incision along an upper neck skin crease. Note the transverse orientation of the mass just inferior to the posterior belly of the digastric muscle. At this juncture it becomes apparent that the tumor is arising from the hypoglossal nerve with the

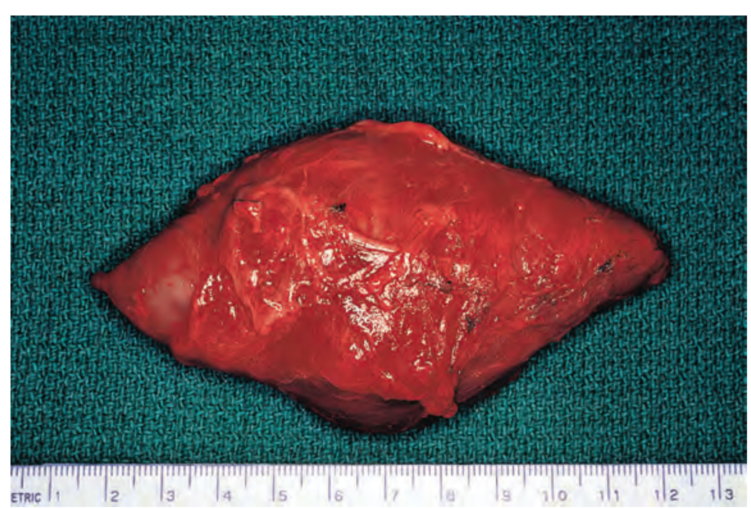

Figure 14.118 The external surface of the specimen.

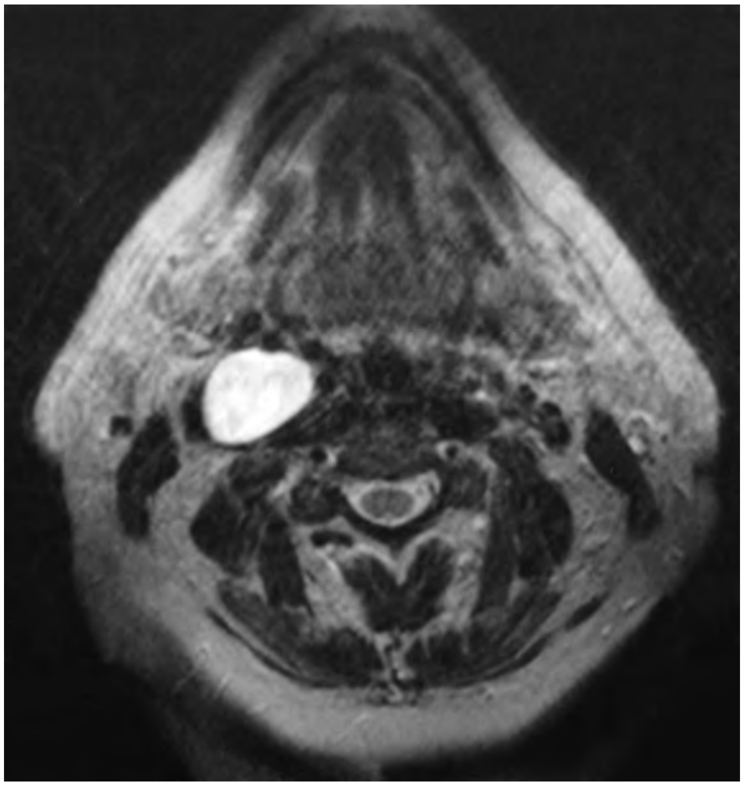

Figure 14.119 An axial view of a T2-weighted magnetic resonance imaging scan of the upper part of the neck.

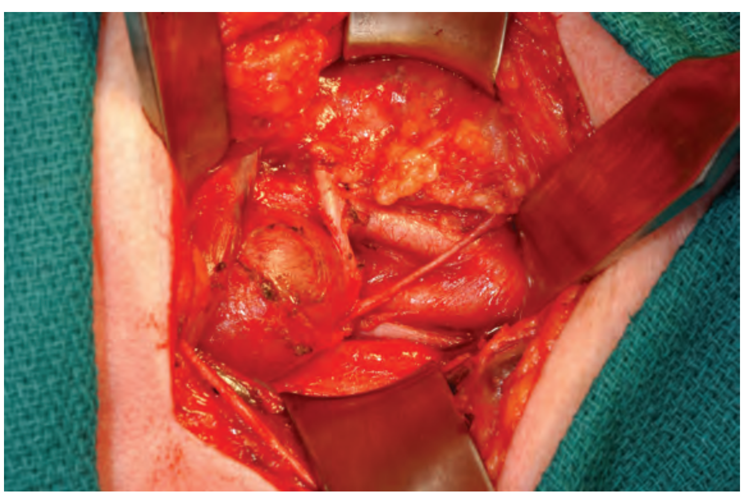

Figure 14.120 The distal end of the hypoglossal nerve and descendens hypoglossi are seen emerging from the lower end of the tumor.

descendens hypoglossi and the distal end of the hypoglossal nerve emerging from the tumor (Fig. 14.120).

The surgical specimen clearly shows the schwannoma arising from the hypoglossal nerve with its upper and lower end showing normal dimensions of the nerve as well as the stump of the descendens hypoglossi nerve (Fig. 14.121). The cut surface of the surgical specimen shows a smooth, glistening, uniform hypovascular lesion characteristic of a schwannoma.

Excision of a Schwannoma of the Sympathetic Chain

The incidence of schwannomas of the sympathetic chain is almost equal to that of schwannomas of the vagus nerve. The

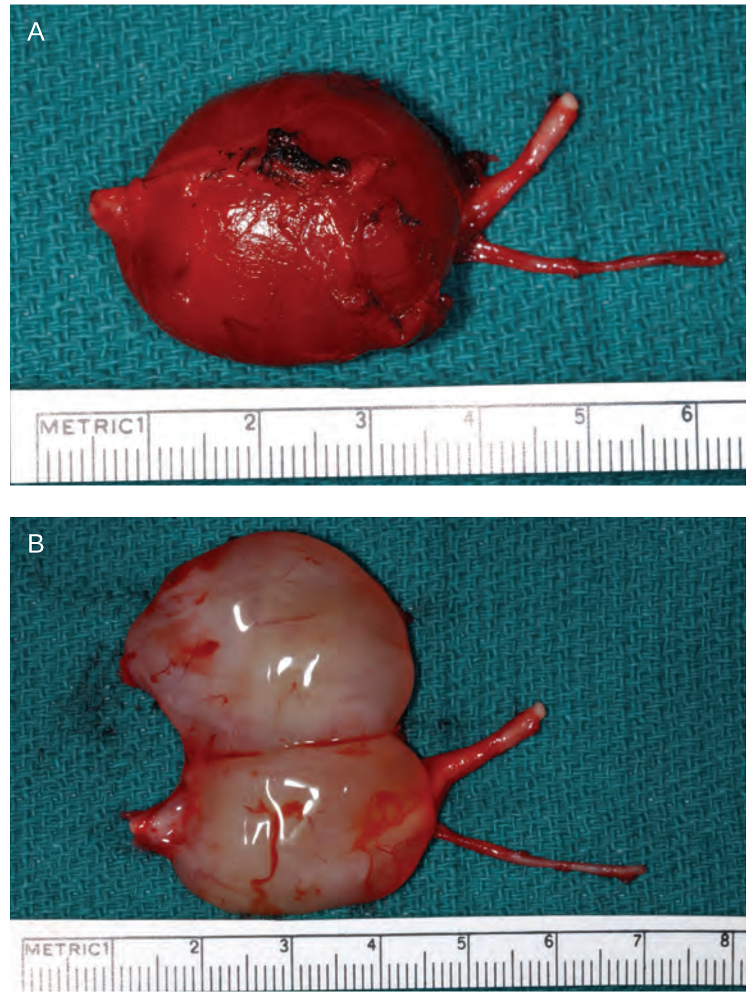

Figure 14.121 The specimen of the intact tumor showing the proximal and distal ends of the hypoglossal nerve and the descendens hypoglossi emerging from the tumor (**A**) and the bisected tumor shows a glistening, hypovascular, well-circumscribed tumor (**B**).

patient described here had an ill-defined, firm to fleshy, nonpulsatile mass in the upper part of the neck in the retromandibular area. A T2-weighted MRI scan in the axial, coronal, and sagittal planes clearly demonstrates a well-demarcated, bright lesion in the upper part of the neck reaching the jugular foramen (Fig. 14.122).

Surgical exposure for excision of this lesion requires an incision in the upper neck skin crease. The surgical field after dissection of the neurovascular structures demonstrates the completely dissected hypoglossal nerve, common carotid artery, internal carotid artery, superior laryngeal nerve, the vagus nerve, and the internal jugular vein (Fig. 14.123).

The carotid artery and vagus nerve are retracted anteriorly and the tumor is mobilized circumferentially up to the jugular foramen cephalad, and the upper end of the sympathetic fibers are divided. The tumor is removed after division of the distal sympathetic chain in the lower part of the neck.

The fusiform tumor has a tail-like component extending caudad in the sympathetic chain. On its cut surface, a typical fleshy tumor is identified, demonstrating the characteristic appearance of a neurogenic tumor (Fig. 14.124). The postoperative sequela of this operation is the development of Horner syndrome.

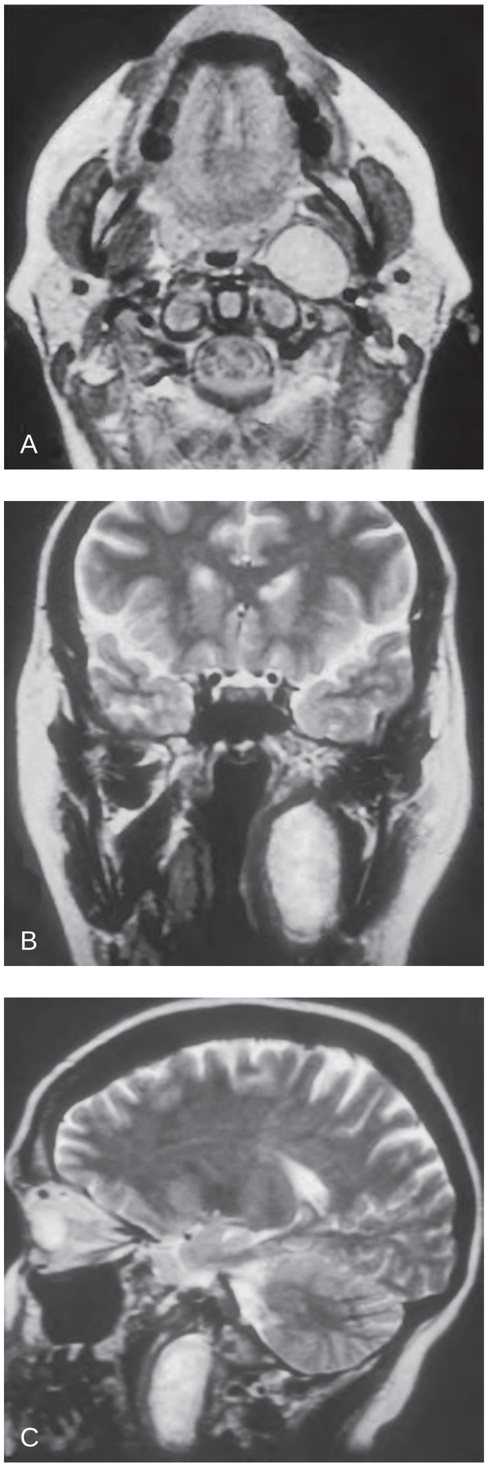

Figure 14.122 Axial (**A**), coronal (**B**), and sagittal (**C**) views of T2-weighted magnetic resonance imaging scans showing a bright white tumor. Note the absence of flow voids.

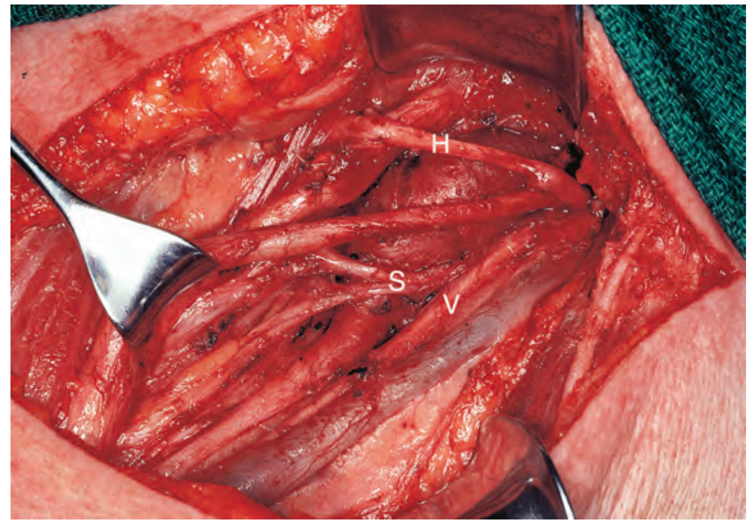

Figure 14.123 The tumor lies deep to the internal carotid artery and the hypoglossal (*H*) and superior (*S*) laryngeal nerves and medial to the vagus (*V*) nerve and internal jugular vein.

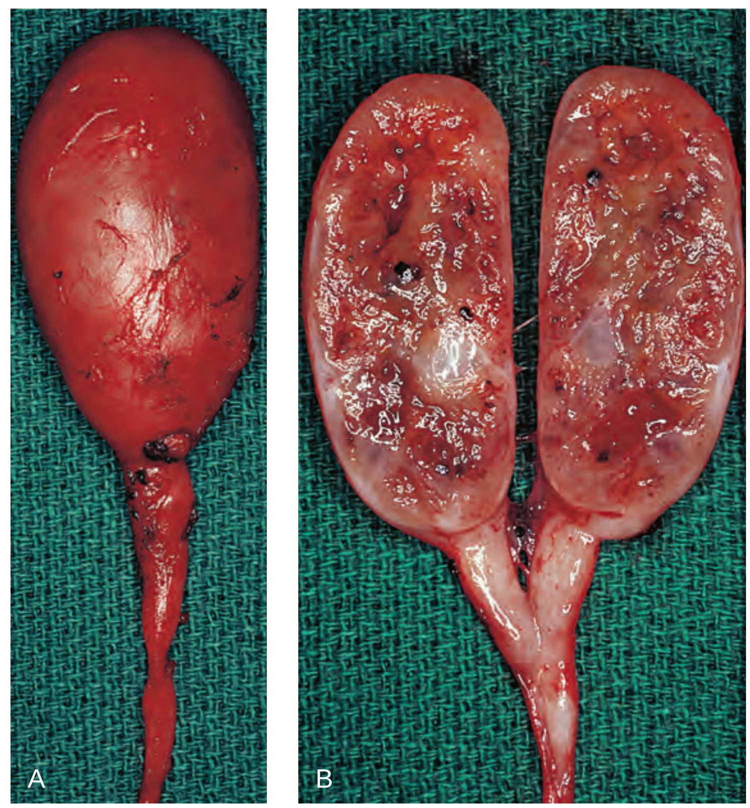

Figure 14.124 **A**, External appearance of the intact fusiform tumor. Note the thickened distal sympathetic chain below the gross tumor. **B**, The cut surface of the tumor shows a well-encapsulated tumor with additional tumor nodules in the distal part of the sympathetic chain.

Multiple Neurofibromas of the Cranial Nerves

Neurofibromas and paragangliomas often are multifocal. They may present as multiple tumors in the same nerve or as multiple tumors involving several cranial nerves. The surgical field on the right-hand side of the neck of a patient with multiple neurofibromas of the cranial nerves shows multiple neurofibromas (Fig. 14.125). For orientation, the patient's head is toward the left side of the picture. Several neurogenic tumors involving the vagus nerve and the sympathetic chain are seen.

A close-up view of the field shows two large neurofibromas, one involving the vagus nerve and the other involving the sympathetic chain (Fig. 14.126). In addition, the patient has other multiple small tumors involving both the vagus nerve and the sympathetic chain lower down. Four neurofibromas were enucleated from the vagus, three were enucleated from the sympathetic chain, and one was enucleated from the cervical plexus. The surgical specimens are shown in Fig. 14.127. The neurofibromas of the vagus are shown in the upper part of the photograph, the three neurofibromas excised from the sympathetic chain are shown in the middle, and the one from the cervical plexus is shown at the bottom. If very meticulous and careful dissection is performed for enucleation of these tumors, then the patient should not have vocal cord paralysis or Horner's syndrome. Optical magnification should be used to spread and separate nerve fibers during enucleation of the tumor to avoid

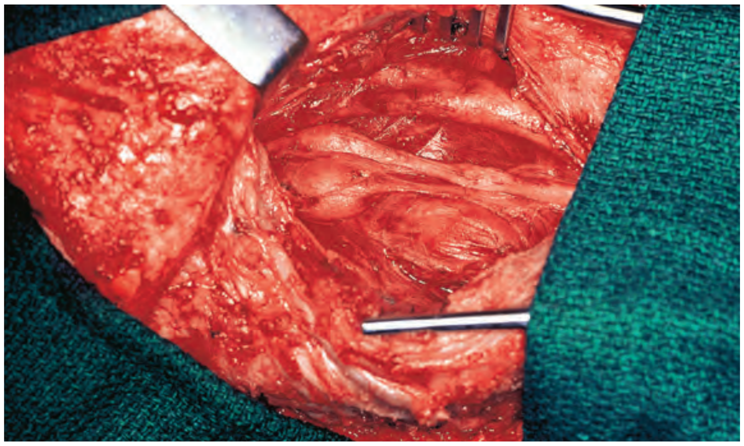

Figure 14.125 Multiple neurogenic tumors of the cervical region.

Figure 14.127 The surgical specimen of multiple neurofibromas.

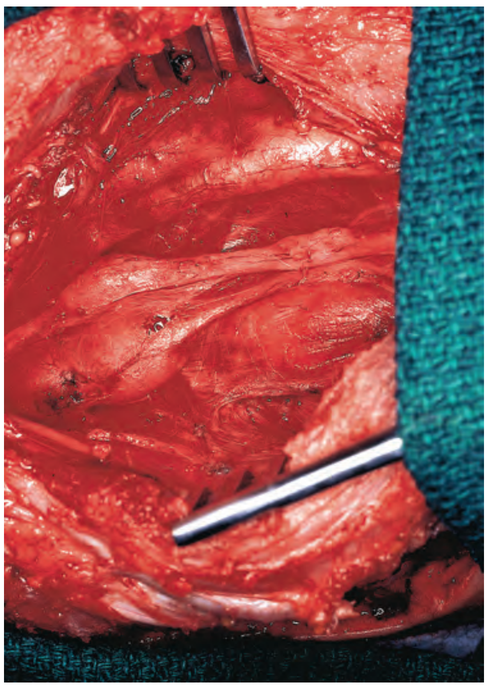

Figure 14.126 A close-up view showing two neurofibromas, one of the vagus nerve and one of the sympathetic chain.

inadvertent injury or division of the normal nerve bundles. Thus small neurogenic lesions such as these can be safely excised with preservation of the function of the involved nerve.

Excision of a Dumbbell Neurofibroma of the Cervical Region

The surgical procedure of a patient with a dumbbell neurofibroma involving the craniocervical junction is described here. A T2-weighted MRI scan at the level of C1 and C2 in an axial plane shows a bright multilobulated tumor with a paraspinal extension of the tumor abutting the spinal cord (Fig. 14.128). The surgical approach for this patient is through a vertical incision from the inion to C4 and a transverse incision from the mastoid process up to the midline (Fig. 14.129). A cervical laminectomy is performed with resection of the left half of the posterior arch of C1 to gain exposure of the root of C1 in the region of its dural sleeve (Fig. 14.130).

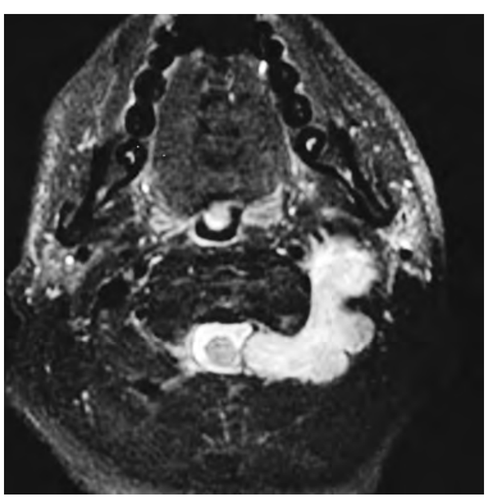

Figure 14.128 An axial view of the T2-weighted magnetic resonance imaging scan showing a bright white dumbbell-shaped tumor of the C1 nerve root abutting the spinal cord.

Figure 14.129 The outline of the T-shaped incision.

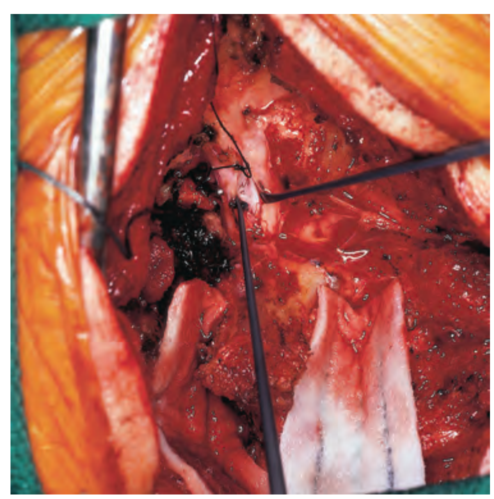

Figure 14.130 Exposure of the C1 root through a cervical laminectomy.

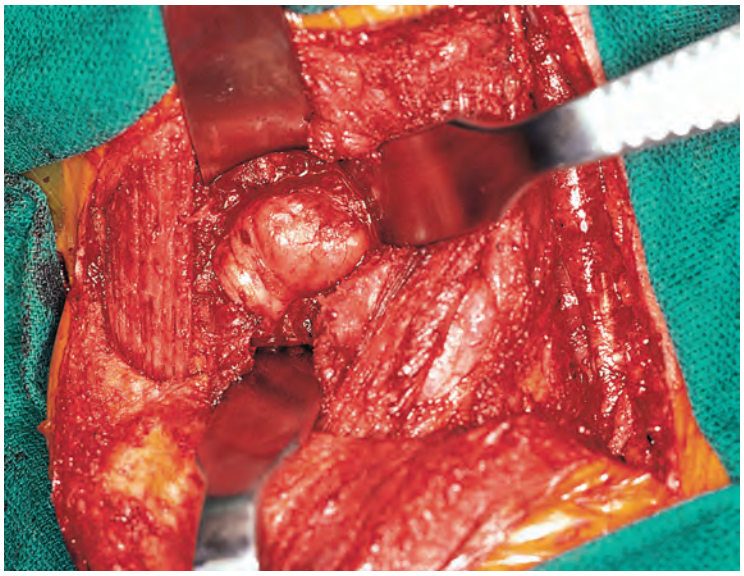

Figure 14.131 The posterior compartment musculature is divided to mobilize the cervical component of the tumor.

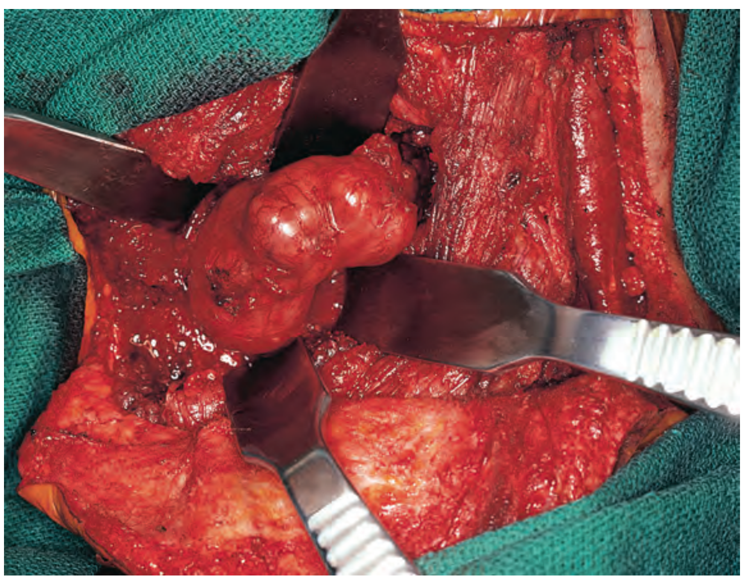

Figure 14.132 The tumor is delivered by circumferential dissection from the surrounding soft tissue.

In this patient a normal nerve root could be demonstrated medial to the tumor, and therefore the dura did not need to be opened. The nerve root is transected and its stump is ligated with a silk suture to prevent cerebrospinal fluid leakage. Mobilization of the cervical component of the tumor begins next through the posterior compartment musculature (Fig. 14.131). Meticulous dissection of the entire tumor permits a monobloc resection of the multilobulated tumor (Fig. 14.132). The surgical specimen shows complete excision of the dumbbell neurofibroma with paraspinal extension at the level of C1 (Fig. 14.133). Excision of a dumbbell neurofibroma of the cervical region requires close cooperation between the neurosurgeon and the head and neck surgeon for safe monobloc removal of the tumor and smooth postoperative recovery.

Figure 14.133 The surgical specimen demonstrates the bilobulated "dumbbell" tumor.

POSTOPERATIVE CARE

In the immediate postoperative period, along with delivery of standard postoperative care, patients undergoing resection of carotid space tumors need to be monitored for cranial neuropathies. Speech and swallowing must be assessed critically, with specific confirmation that the patient is not aspirating.

Most transient neuropathies should resolve if the involved cranial nerve has not been transected. In cases of permanent injury, rehabilitation of palatal insufficiency can be treated effectively with a palatal augmentation prosthesis and vocal cord paralysis with medialization. Speech and swallowing therapy should be considered for all of these patients.

CHAPTER 15

Soft Tissue Tumors

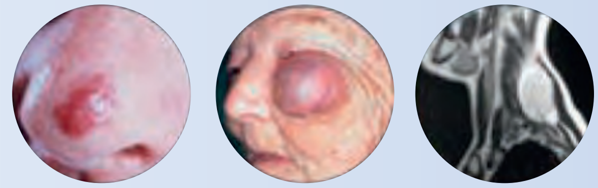

Tumors of the soft somatic tissues form a very small component in the spectrum of tumors requiring surgical treatment in the head and neck region. These tumors may arise from the musculofascial compartment or the visceral compartment in the head and neck region. The histologic variants of benign and malignant soft tissue tumors are listed in Table 15.1. The latest classification of soft-tissue tumors from the WHO in 2013 has resulted in a change of nomenclature of a number of tumors, and these changes are important for the oncologist to be aware of to avoid confusion in management.

The most frequently encountered benign tumors in the head and neck region are lipomas, hemangiomas, lymphangiomas, and neurofibromas. Hemangiomas and lymphangiomas are quite common in children. Only 4.3% of soft-tissue sarcomas in adults arise in the head and neck region (Fig. 15.1). The site distribution of adult soft-tissue sarcomas in the head and neck region is shown in Fig. 15.2. Soft-tissue sarcomas can arise from almost any part of the anatomy in the head and neck area, although the parotid glands, neck, face, forehead, and scalp are the sites encountered most frequently. The most common mode of presentation is a mass lesion or symptoms resulting from pressure on contiguous neurovascular structures or the viscera. The diagnosis of a soft-tissue tumor is made easily by clinical examination, although for surgical treatment planning,

Table 15.1 The Histologic Classification of Benign and Malignant Soft Tissue Tumors

TISSUE OF ORIGIN	BENIGN	INTERMEDIATE*	MALIGNANT
Fat	Lipoma	Atypical lipomatous tumor	Liposarcoma
Fibrous tissue/ myofibroblastic	Fibroma	Desmoid type fibromatosis Dermatofibrosarcoma, solitary fibrous tumor	Fibrosarcoma, myxofibrosarcoma, low-grade fibromyxoid sarcoma, malignant fibrous histiocytoma/ undifferentiated pleomorphic sarcoma
Blood vessels	Hemangioma	Kaposiform hemangioendothelioma	Angiosarcoma, epithelioid hemangioendothelioma
Lymph vessels	Lymphangioma		Lymphangiosarcoma
Smooth muscle	Leiomyoma		Leiomyosarcoma
Skeletal muscle	Rhabdomyoma		Embryonal rhabdomyosarcoma, alveolar rhabdomyosarcoma, pleomorphic rhabdomyosarcoma
Nerve sheath tumors	Schwannoma, neurofibroma, granular cell tumor		MPNST, epithelioid MPNST, malignant granular cell tumor
Tumors of uncertain differentiation	Fibromyxoma, myxoma	Atypical fibroxanthoma, myoepithelioma, phosphaturic mesenchymal tumor	Synovial sarcoma, epithelioid sarcoma, alveolar soft part sarcoma, extraskeletal Ewing sarcoma, undifferentiated/unclassified sarcomas
Miscellaneous/other	Extraskeletal meningioma	Chordoma	

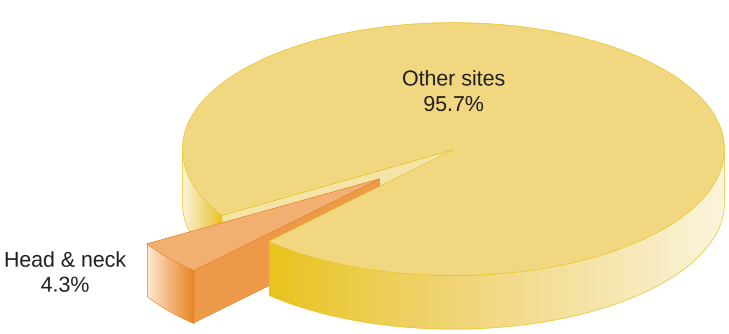

Figure 15.1 The distribution of soft-tissue sarcomas in adults (MSKCC data).

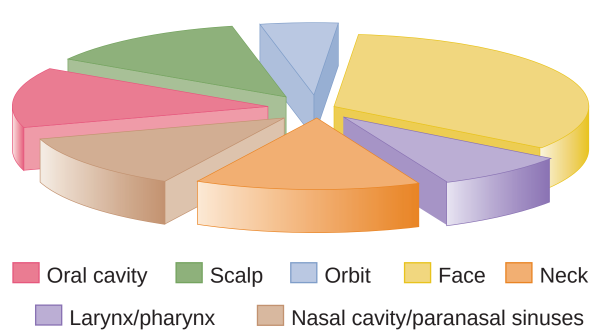

Figure 15.2 The site distribution of soft-tissue sarcomas in the head and neck region in adults (MSKCC data).

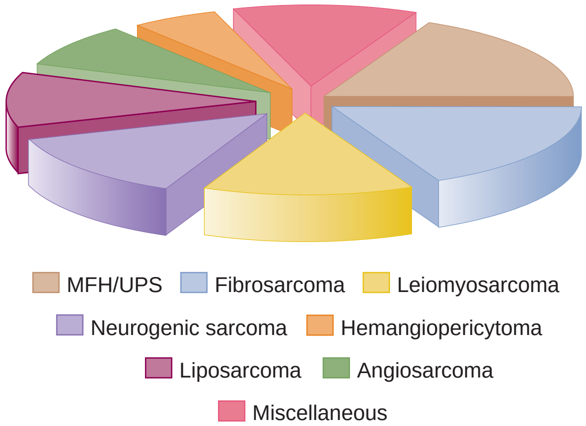

Figure 15.3 The histologic distribution of soft-tissue sarcomas in adults in the head and neck region (MSKCC data). *MFH,* Malignant fibrous histiocytoma; *UPS,* undifferentiated pleomorphic sarcoma.

Figure 15.4 Large lipoma of the suboccipital region.

additional workup is essential. This workup usually consists of radiographic evaluation and establishment of accurate tissue diagnosis. The histologic distribution of soft-tissue sarcomas in the head and neck region in adults is shown in Fig. 15.3.

EVALUATION

Most patients present with the complaint of a mass lesion, with or without any local pressure symptoms. Masses on the face, neck, or scalp show a visual deformity, and those in the oral cavity, pharynx, or larynx may have symptoms of obstruction to the upper aerodigestive tract. Clinical evaluation requires a detailed physical examination of the presenting mass lesion. The location, dimensions, consistency, and fixation to deeper structures are important parameters to arrive at a clinical diagnosis. Lipomas generally present with a mass that is soft in consistency and is mobile over the deeper soft tissues (Fig. 15.4). On the other hand, hemangiomas and lymphangiomas are also soft in consistency and may give the impression of a compressible or even cystic lesion. Deep-seated and intramuscular hemangiomas present with a diffuse ill-defined soft mass and need radiographic assessment to define the dimensions and location of the tumor. In contrast, tumors of fibrous tissue or neural origin present as firm to hard solid lesions. The degree of mobility or fixation to surrounding or deep structures raise the index of suspicion for malignancy. Bimanual palpation

Figure 15.5 Fibrous soft-tissue tumor in the right cheek.

often will give enough information about the nature of the lesion (Fig. 15.5). Lesions of vascular origin involving the skin such as an angiosarcoma may have a characteristic appearance with discoloration like ecchymosis, and nodular lesions of vascular origin involving this skin have discoloration ranging from cherry red to purple. Clinical evaluation should particularly assess fixation to overlying skin or underlying soft tissues, muscle, or bone. For lesions of the pharynx and larynx, adequate endoscopic evaluation is necessary to define the exact location and extent of the tumor.

RADIOGRAPHIC EVALUATION

Accurate assessment of the anatomic extent of a soft-tissue tumor of the head and neck region requires that it be evaluated in all three dimensions. Computed tomography (CT) and magnetic resonance imaging (MRI) scans are most valuable in demonstrating the anatomic extent of the lesion and its relationship to vital structures. For tumors that are highly vascular or are of neurovascular origin, magnetic resonance (MR) angiography or a direct arteriography may be indicated. If direct angiography demonstrates large feeding vessels and a highly vascular lesion, then serious consideration should be given to preoperative embolization of the tumor to minimize blood loss during surgery.

As an example, a CT scan of a patient with a large lipoma in the posterior compartment of the neck is shown in Fig. 15.6. Note the presence of a uniform, well-delineated, hypodense mass displacing the anatomic structures in the left side of the neck medially and occupying the entire posterior compartment of the left side of the neck. Lesions that are in proximity to or involving the underlying bone require bone windows on a CT scan to accurately assess the extent of bone invasion. In contrast to CT scans, an MRI scan has the capability of providing images in the axial, coronal, and sagittal planes to more accurately define the anatomic extent of the lesion. MRI scans in a postcontrast T1-weighted images in a patient with a hemangioma of the tongue in axial, coronal, and sagittal planes clearly demonstrate the anatomic extent of this lesion (Figs. 15.7 through 15.9). An accurate assessment of the size and extent of the lesion within the tongue musculature is demonstrated.

Figure 15.6 An axial view of a computed tomography scan showing a large lipoma (*arrow*) in the posterior compartment of the neck.

In addition to obtaining CT and MRI with contrast, the ability to obtain three-dimensional reconstructions of the CT images allows accurate three-dimensional assessment of the location and extent of the tumor for appropriate surgical planning for complete resection and reconstruction. The patient shown in Fig. 15.10 has a solitary fibrous tumor of the masticator space. His CT and MRI scans in axial, coronal, and sagittal planes are shown in Figs. 15.11 through 15.13. Three-dimensional reconstruction of his CT scan and CT angiogram vividly shows the anatomic location and extent of the tumor with displacement and involvement of the mandible, orbital floor, and skull base, as well as the blood supply to the tumor (Fig. 15.14).

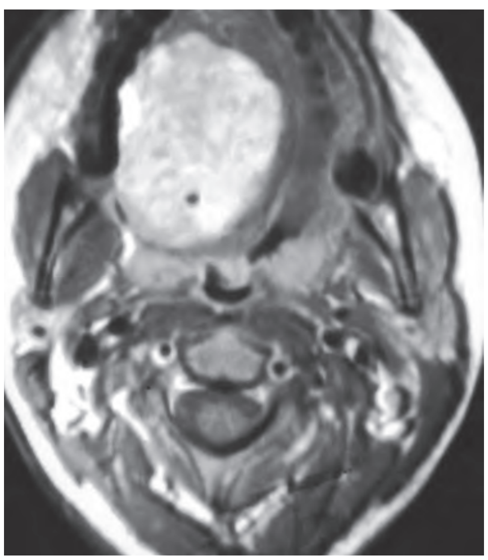

Figure 15.7 An axial view of the magnetic resonance imaging scan with a T1-weighted postcontrast image showing a well-circumscribed hemangioma of the tongue.

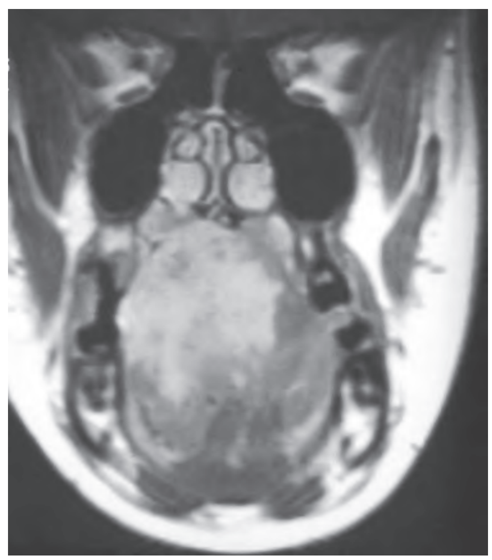

Figure 15.8 A coronal view of the T1-weighted postcontrast magnetic resonance imaging scan of the same patient depicted in Fig. 15.5 showing the hemangioma extending beyond the midline.

Figure 15.9 A sagittal view of a T1-weighted postcontrast magnetic resonance imaging scan of the patient seen in Figs. 15.7 and 15.8 with a hemangioma of the tongue.

Figure 15.10 External appearance of a patient with a large soft-tissue tumor in the masticator space.

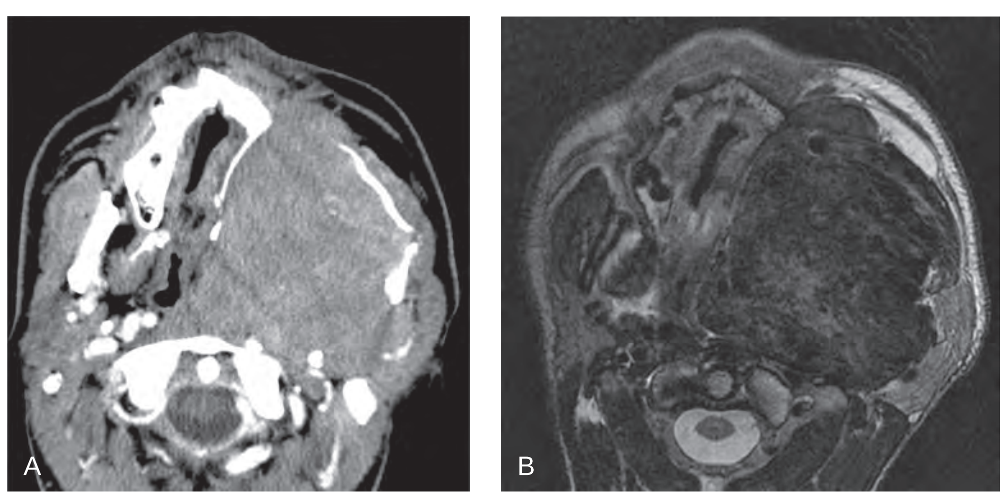

Figure 15.11 A, A contrast-enhanced computed tomography scan in the axial view showing a large tumor that has regressively remodeled the left maxillary bony walls and pterygoid plates. **B**, Corresponding axial T2-weighted magnetic resonance imaging clearly shows the encapsulated, pushing tumor in relation to the left upper alveolus, soft tissues and fat of the cheek, the prevertebral fascia, the deep aspect of the left parotid gland, and the retromandibular vein.

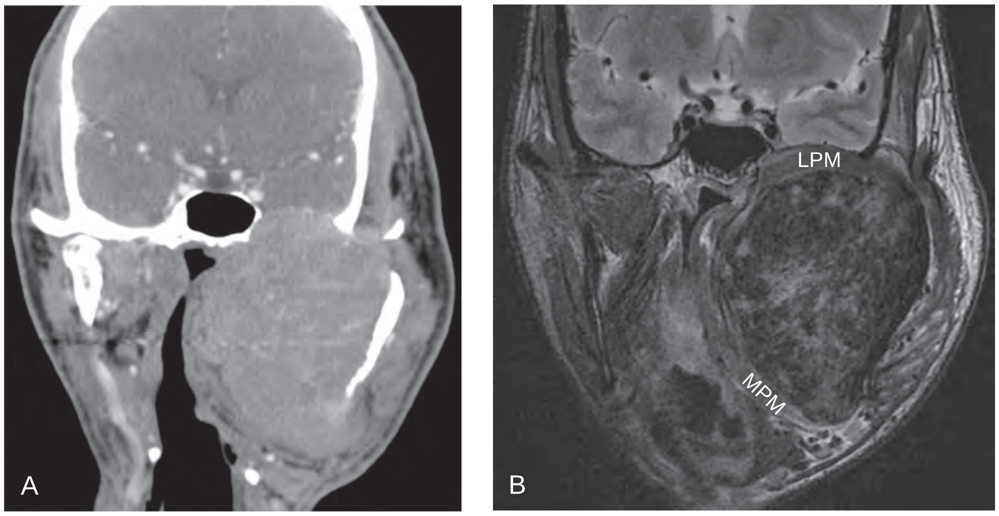

Figure 15.12 **A**, A contrast-enhanced computed tomography scan of the neck in the coronal view demonstrates wide attenuation of the bony skull base, but there is a clear demarcation at the superior interface of the tumor with the dura and brain without signs of invasion. **B**, Corresponding T2-weighted magnetic resonance imaging in the coronal view shows that the tumor is separated from the bony skull base by the superiorly displaced left lateral pterygoid muscle (*LPM*). The medial pterygoid muscle (*MPM*) is draped over the medial aspect of the tumor between the pterygoid plates and the mandible.

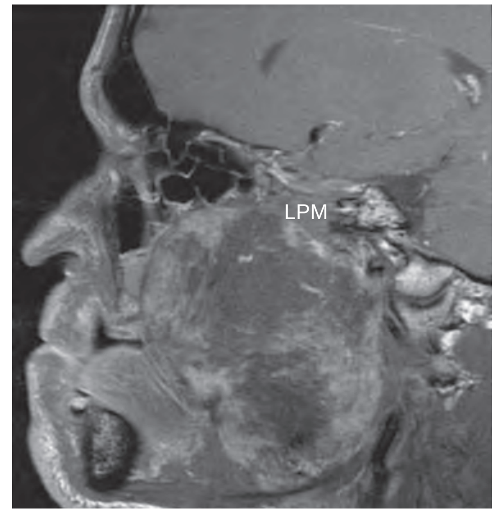

Figure 15.13 Sagittal view of postcontrast T1-weighted magnetic resonance imaging shows the heterogeneously enhancing tumor with the lateral pterygoid muscle (*LPM*) separating it from the skull base.

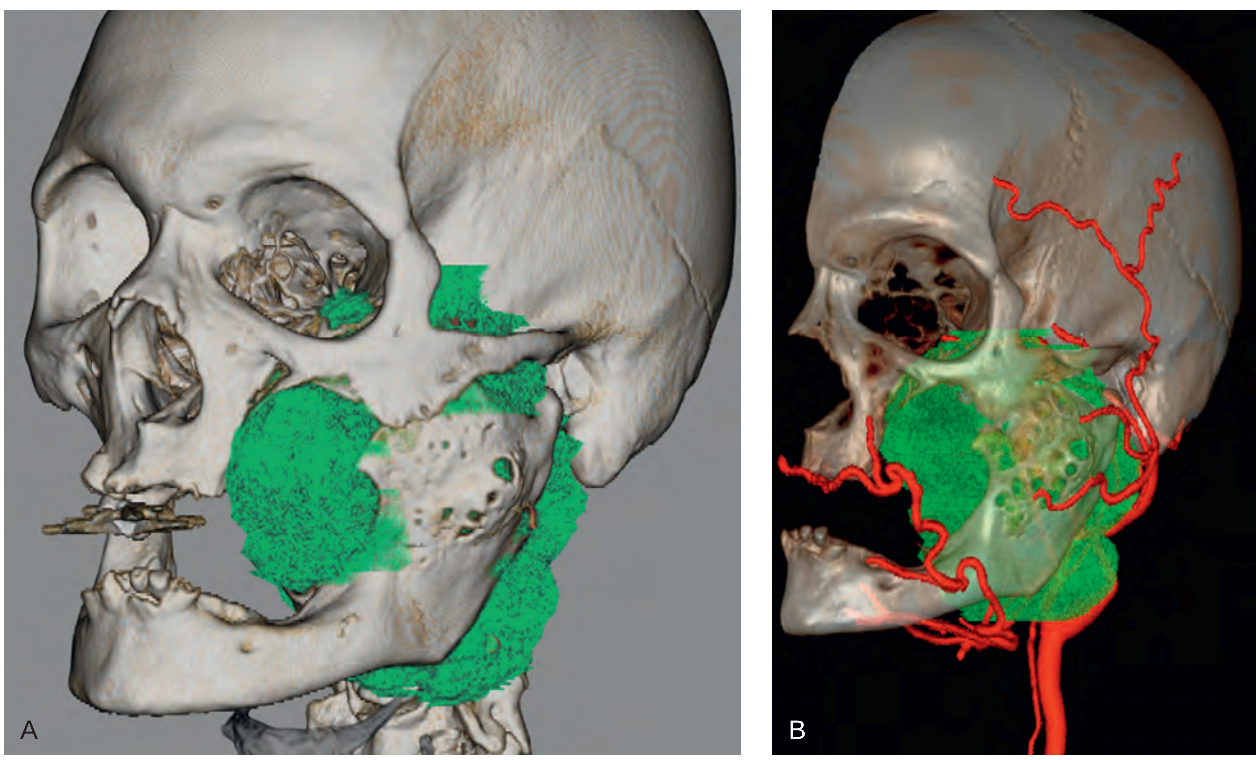

Figure 15.14 Three-dimensional reconstruction of computed tomography (CT) scan (**A**), and CT angiography showing the extent of the tumor in relation to its bony surroundings and the relationship of the arterial vasculature (**B**).

BIOPSY

It is vitally important that accurate tissue diagnosis be established before definitive surgical intervention, particularly in patients whose soft-tissue tumors are suspected to be malignant upon clinical examination. Biopsy techniques are shown in Fig. 15.15. Although fine-needle aspiration cytology may be informative in some patients, for accurate morphologic classification of the soft-tissue tumor, a core of tissue is essential. This sample may be obtained by a Tru-Cut core biopsy or an open incisional biopsy. For small, well-circumscribed lesions, an excisional biopsy may be performed to provide an adequate tissue sample for accurate histologic interpretation. If an incisional biopsy is to be performed, the incision should be placed in such a fashion that at the time of the definitive surgical excision, the incisional biopsy site can be encompassed in the surgical specimen. Inappropriate placement of the biopsy incision often can jeopardize definitive surgical treatment and the potential for a curative resection.

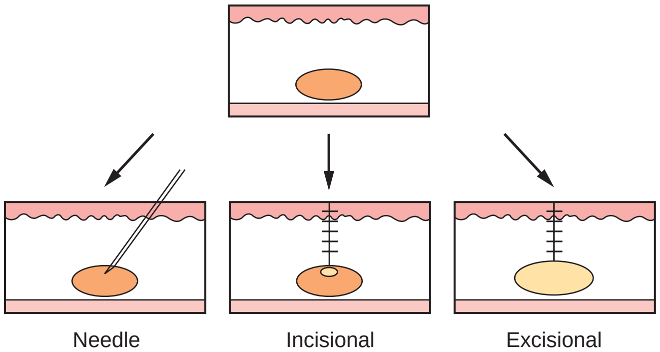

Figure 15.15 Biopsy techniques.

Table 15.2 Newly Revised TNM Staging for Soft-Tissue Sarcomas of the Head and Neck (AJCC Eighth Edition)

T1	Tumor ≤2 cm
T2	Tumor >2 cm and <4 cm
T3	Tumor >4 cm
T4	Tumor with invasion of adjacent structures
T4a	Invasion of orbit, skull base, dura, central compartment viscera, facial skeleton, or pterygoid muscles
T4b	Invasion of brain, prevertebral muscles, carotid artery encasement, or perineural spread to central nervous system
N0	No nodal metastases
N1	Nodal metastases
M0	No distant metastases
M1	Any distant metastases
G1	Total differentiation, mitotic count, and necrosis score of 2 or 3
G2	Total differentiation, mitotic count, and necrosis score of 4 or 5
G3	Total differentiation, mitotic count, and necrosis score of 6, 7, or 8

STAGING

The TNM staging system for soft tissue sarcomas, include anatomic as well as histologic features of the tumor. Thus for T staging, tumor size and local invasion, as well as nodal and distant metastases are included. In addition to the TNM criteria, histologic grade of the primary tumor is added to assign a stage to the sarcoma (Table 15.2). In order to assign stage groupings, the American Joint Committee on Cancer (AJCC) is currently gathering data based on this new classification.

FACTORS AFFECTING CHOICE OF TREATMENT

Surgical excision is the mainstay of treatment for all soft-tissue tumors. Benign neoplasms are adequately excised, preferably in a monobloc fashion, by an appropriate surgical approach depending on the size and anatomic location of the tumor. Highly vascular lesions are best managed with preoperative embolization when feasible to minimize blood loss. For malignant soft-tissue tumors, on the other hand, various factors that influence eventual prognosis must be considered. These factors are related to the histologic type and grade of the tumor as well as the size and location of the sarcoma. Clearly en bloc three-dimensional resection of the tumor with adequate soft-tissue margins is the hallmark of surgical treatment of soft-tissue sarcomas in any part of the body. However, because of the proximity of vital organs and structures in the head and neck region, the broad principles of soft-tissue sarcoma surgery elsewhere in the body cannot be adhered to rigidly in the head and neck region. Often surgical excision must be tailored to avoid unnecessary sacrifice or injury to uninvolved contiguous vital structures to secure adequate margins. In general, small, low-grade lesions carry an excellent prognosis. On the other hand, patients with large, high-grade lesions have a high incidence of local recurrence and distant metastases and have a poor prognosis. Regional lymph nodes usually are not treated electively.

ROLE OF RADIOTHERAPY

The need for adjunctive radiation therapy should be considered in patients with tumors of high-grade histology and for whom the margins are unsatisfactory or close. External radiotherapy or brachytherapy may be used with equal efficacy. The choice of treatment modality depends on the site, histology, and size of the field to be treated. Although enhanced local control is achieved with adjunctive radiation therapy, improvement in survival is not noted.

PREOPERATIVE PREPARATION

In most patients who require surgery for soft-tissue tumors, no specific preoperative preparation is required. However, when a massive resection is to be undertaken and significant blood loss is anticipated, sufficient quantities of blood should be available in reserve to replace operative blood loss. As mentioned earlier, highly vascular lesions are best managed with preoperative embolization when appropriate. If resection of the carotid artery is anticipated, then preoperative testing with balloon occlusion is required to assess the adequacy of cerebral blood flow from the opposite side. An arterial bypass graft may be necessary in certain circumstances. Appropriate reconstructive surgery should be planned preoperatively based on the size, extent, and location of the surgical defect anticipated from resection of the tumor, and reconstruction may involve microvascular free tissue transfer. When tumors approach or involve the skull base, neurosurgical assistance is required and should be planned preoperatively. Similarly, sarcomas extending into the mediastinum or the chest may need assistance from thoracic surgeons to carry out a safe and complete resection. When sarcoma resection requires that the visceral compartment be entered, preoperative antibiotics should be administered to reduce the risk of postoperative sepsis.

TUMORS OF ADIPOSE TISSUE

Lipoma of the Neck

Lipomas in the head and neck region may present as simple subcutaneous lesions or as complex deep-seated tumors. Several examples are presented here to demonstrate the spectrum of head and neck lipomas. The patient whose CT scans with contrast are shown in Fig. 15.16 has a large lipoma involving the lateral compartment and retroesophageal/prevertebral region. She presented with a long-standing history of an ill-defined fullness in the anterior compartment of the neck on the left-hand side and a retropharyngeal bulge in the oropharynx. The axial views of the CT scans at the level of the oropharynx and lower cervical region show a homogeneous well-defined nonenhancing mass

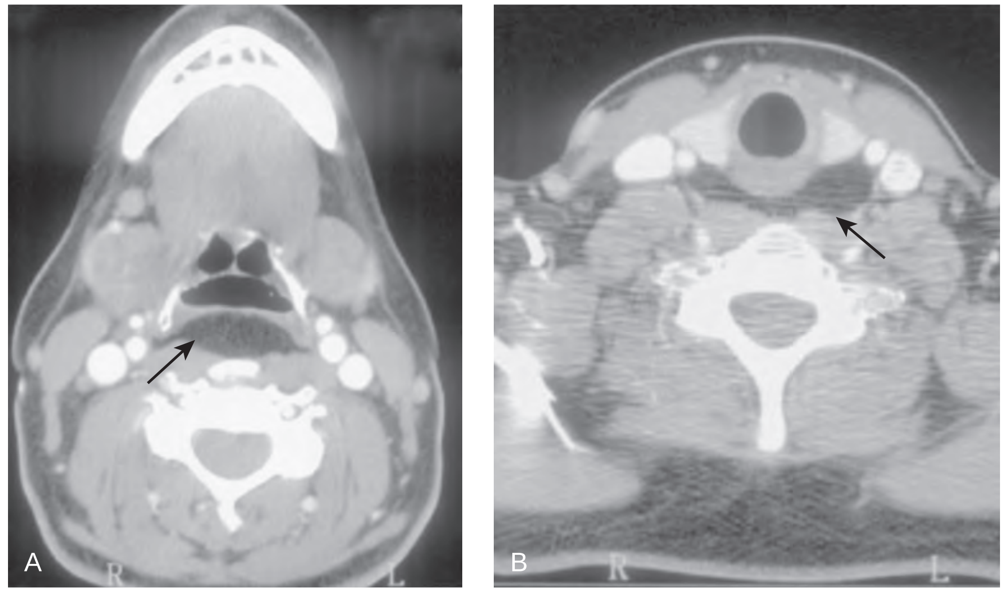

Figure 15.16 Contrast-enhanced computed tomography scan of the neck at the level of the epiglottis (**A**) and in the lower part of the neck (**B**) showing a lipoma in the prevertebral space (*arrow*).

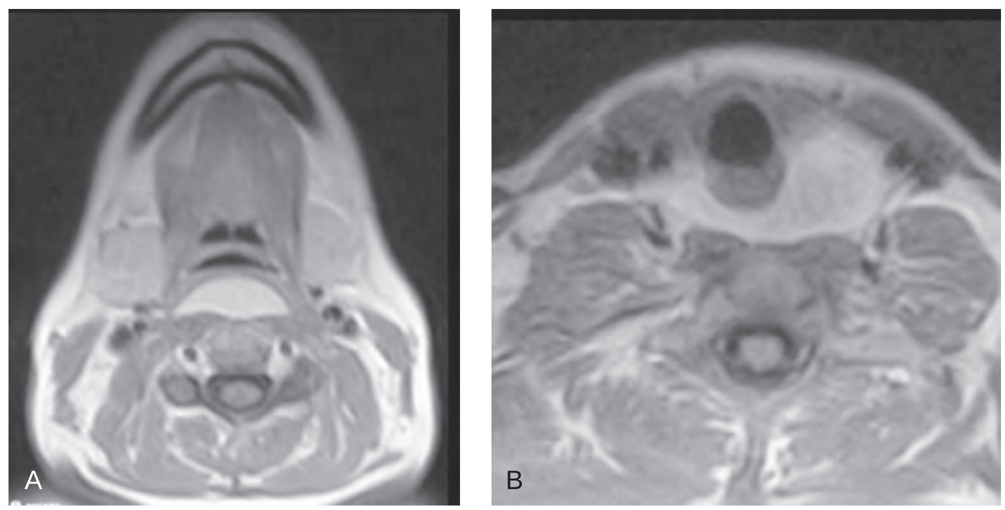

Figure 15.17 T1-weighted magnetic resonance images at the level of the epiglottis (**A**) and lower part of the neck showing a lipoma in the prevertebral space (**B**).

in the prevertebral space, similar to subcutaneous fat consistent with a radiologic diagnosis of lipoma (see Fig. 15.16). Axial views of the T1-weighted MRI scans at the same levels as the CT show a similar well-defined mass of fatty consistency (Fig. 15.17). Surgical excision of this lesion requires a simple transverse incision along a midneck skin crease of sufficient length to gain adequate exposure. The skin incision is deepened through the platysma, and the fascia overlying the sternocleidomastoid muscle is incised to gain exposure of the tumor. By alternate blunt and sharp dissection, the sternocleidomastoid muscle is freed from the underlying tumor and retracted laterally to show the carotid sheath (Fig. 15.18). A well-encapsulated yellowish smooth tumor is seen clearly. By alternate blunt and sharp dissection, the tumor is mobilized carefully, paying attention to the superior laryngeal nerve at the upper end and recurrent laryngeal nerve at the lower end. The superior thyroid artery had to be divided to get the necessary dissection. The superior laryngeal nerve had to be retracted cephalad. In some situations even the inferior thyroid artery may need to be divided. The tumor could be mobilized thereafter, keeping it intact (Fig. 15.19). The feeding blood vessels to the tumor are relatively small vessels that are clamped, divided, and ligated. The specimen is delivered in a monobloc fashion (Fig. 15.20). Drainage of the surgical field usually is not necessary. The skin incision is closed in layers.

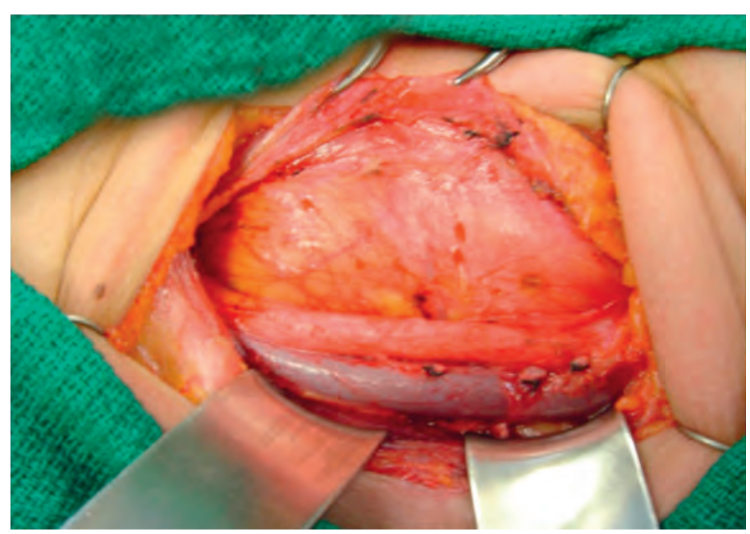

Figure 15.18 The sternocleidomastoid muscle is retracted laterally to expose the lipoma of the prevertebral space.

Lipomas may arise in any part of the head and neck region and occasionally may present adjacent to or within the substance of a major salivary gland. The patient shown in Fig. 15.21 presented with a mass in the tail of the parotid gland that was soft to palpation. The differential diagnosis in this clinical setting

Figure 15.19 All lobulations of the lipoma are dissected and delivered out.

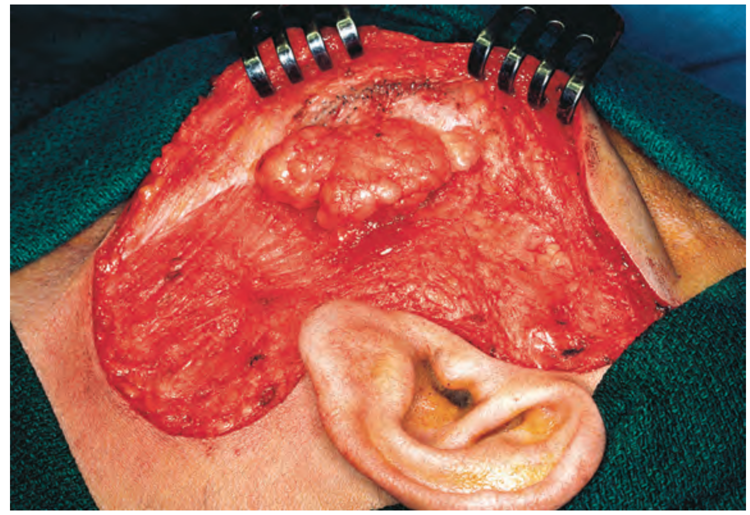

Figure 15.22 A lipoma overlying the tail of the parotid gland.

Figure 15.20 Surgical specimen showing complete excision of the lipoma with an intact capsule.

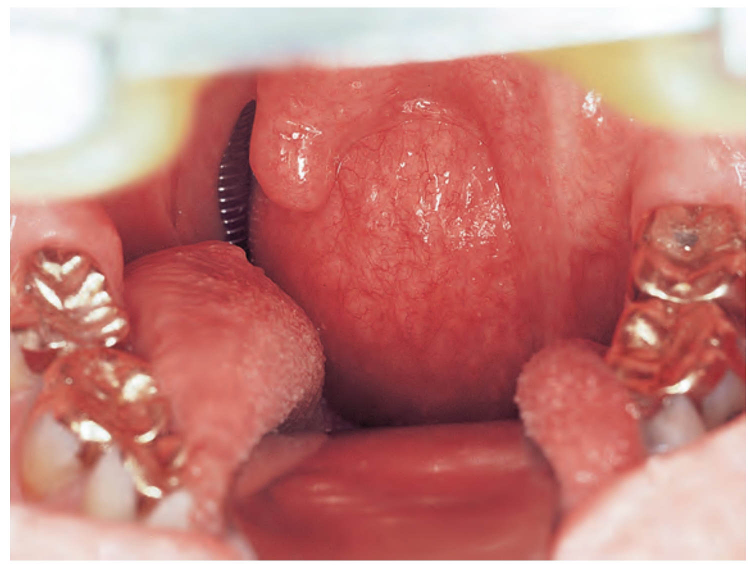

Figure 15.23 An intraoral view showing the submucosal bulge on the left posterolateral pharyngeal wall with the uvula pushed over to the opposite side.

Figure 15.21 A patient with a soft mass at the tail of the parotid gland.

is a parotid tumor, a lipoma, or a vascular lesion in the parotid gland. Imaging studies suggested this to be a lipoma. Surgical exposure of a lesion in the parotid gland requires a standard parotidectomy incision with elevation of the skin flap deep to the platysma. The skin flap is elevated while remaining close to the platysma muscle to avoid injury to peripheral branches of the facial nerve as they exit from the parotid gland. The lesion in this patient is readily visible in Fig. 15.22 after elevation of the skin flap. By alternate blunt and sharp dissection, the lesion is excised, remaining close to the capsule of the tumor to avoid injury to the intraparotid branches of the facial nerve. The skin incision is closed in layers with placement of a small Penrose drain that usually can be removed within 24 hours.

On rare occasions, lipomas may occur in the deep parapharyngeal space and the prevertebral space. The patient whose oropharynx is shown in Fig. 15.23 had increasing difficulty with swallowing and a sense of a narrowed swallowing passage. Examination of the oropharynx through the open mouth showed a significant bulge of the posterior and posterolateral pharyngeal wall on the left-hand side that caused compromise of the airway and the swallowing passage. Upon palpation this lesion felt

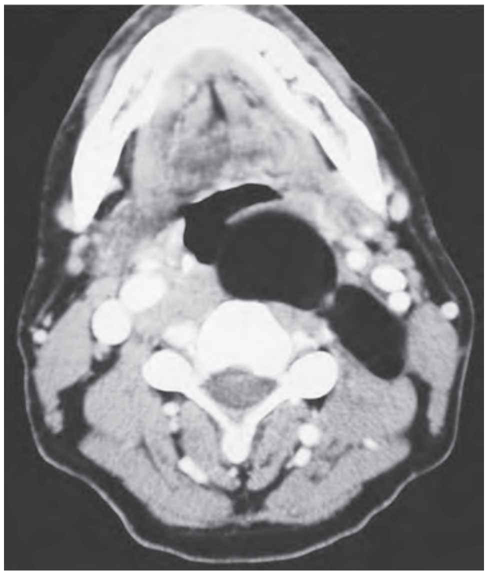

Figure 15.24 An axial view of the computed tomography scan showing the left prevertebral multilobulated tumor extending posterior to the carotid sheath into the parapharyngeal space.

Figure 15.25 A coronal view of the magnetic resonance imaging scan showing the craniocaudad extent of the tumor.

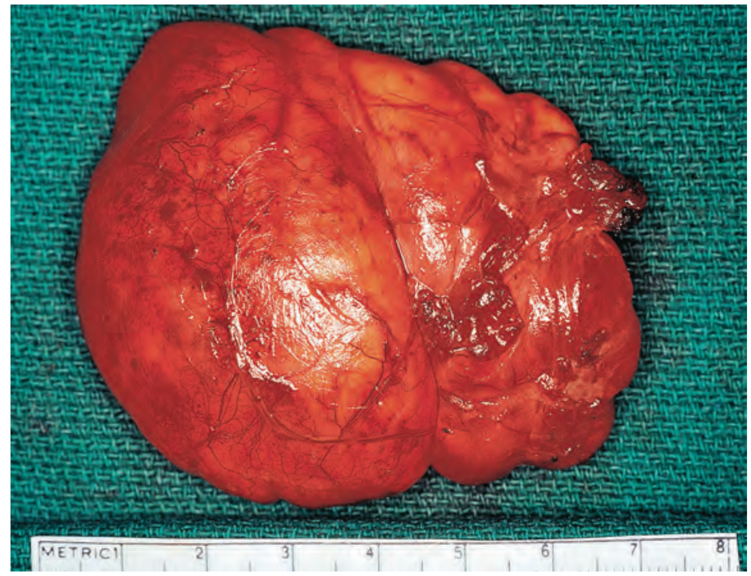

Figure 15.26 The surgical specimen.

Figure 15.27 A patient with progressive swelling on both sides of his face and neck from Madelung disease.

soft and extended from the nasopharynx behind the soft palate cephalad to the lateral wall of the pyriform sinus caudad. The lesion extended well beyond the midline in the prevertebral space, pushing the posterior pharyngeal wall and the tonsil anteriorly. An axial view of the CT scan with contrast through the upper part of the neck vividly demonstrates a multilobulated lipoma in the prevertebral space extending into the parapharyngeal space behind the carotid sheath on the left-hand side (Fig. 15.24). An MRI scan in the coronal plane demonstrates the cephalocaudad extent of this tumor with displacement of the posterolateral pharyngeal wall (Fig. 15.25).

The surgical approach for excision of this lesion required a midcervical incision with careful dissection deep to the sternomastoid muscle and medial to the carotid sheath, with mobilization and delivery of the multilobulated lipoma from the parapharyngeal space laterally and the prevertebral space medially. The superior thyroid artery was divided and ligated. The superior laryngeal nerve was retracted cephalad to gain exposure. The laryngopharyngeal complex was retracted medially and the carotid sheath was retracted laterally to gain exposure and excise the tumor in a monobloc fashion without rupturing its capsule. The surgical specimen shown in Fig. 15.26 demonstrates complete excision of this massive lipoma of the prevertebral/parapharyngeal space.

Madelung disease is a clinical condition in which diffuse infiltration of fat occurs in all compartments of the neck, including the supraclavicular fossae and the submandibular and periparotid regions. This condition is often seen in men of Mediterranean origin. The patient shown in Fig. 15.27 presented with progressive swelling on both sides of his face and neck from Madelung disease. Surgical excision of this abnormal fatty infiltrate is indicated only for cosmetic reasons. The operative procedure is very tedious and time-consuming. The surgical procedure is akin to a modified neck dissection with preservation of all the vital structures including the sternocleidomastoid muscle, the internal jugular vein, the accessory nerve, the submandibular salivary gland, and the peripheral cutaneous branches of the cervical plexus to minimize anesthesia of the skin of the neck. Because of diffuse infiltration of the fat into the anatomic spaces and fascial compartments, dissection is not easy, and tissue planes generally do not separate readily. It is advisable to perform the surgical procedure on both sides of the neck in stages to avoid

Figure 15.28 The patient's postoperative appearance after staged excisions.

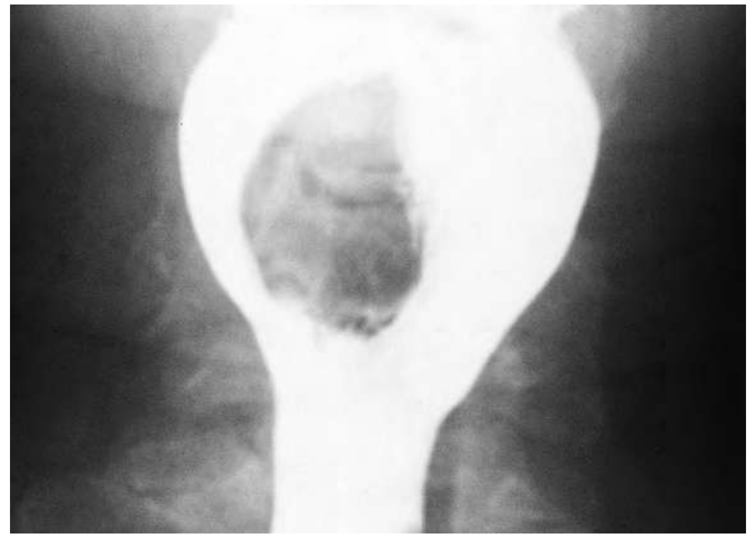

Figure 15.30 A barium swallow showing a filling defect in the left pyriform sinus.

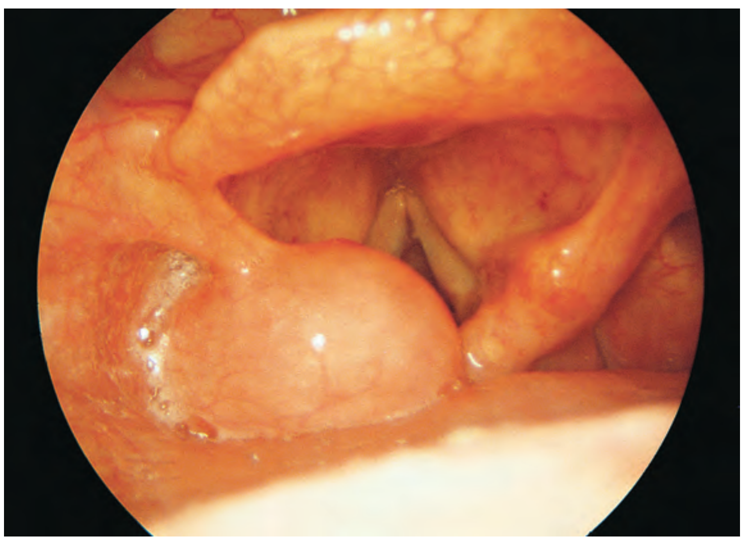

Figure 15.29 An endoscopic examination of the hypopharynx showing a smooth submucosal lesion.

Figure 15.31 The surgical specimen.

excessive blood loss and to reduce the length of the operative procedure. The postoperative appearance of the patient 1 year following bilateral neck surgery is shown in Fig. 15.28.

Low-Grade Liposarcoma (or Atypical Lipomatous Tumor) of the Hypopharynx

Liposarcomas may arise in the fascial or visceral compartments of the head and neck region and present as a soft-tissue tumor. The extent of surgical resection clearly depends on the anatomic location, size, and histologic grade of the primary lesion. The patient shown here presented with slight discomfort in the throat of several months' duration. Flexible fiberoptic nasolaryngoscopy examination of the hypopharynx and larynx showed a smooth submucosal mass involving the medial wall of the left pyriform sinus, as shown in Fig. 15.29. No mucosal ulceration was present, and the lesion did not extend up to the apex of the pyriform sinus. A barium swallow examination shown in Fig. 15.30 clearly demonstrates a smooth-lined mass in the postcricoid region causing partial obstruction of the cervical esophagus. Endoscopy under general anesthesia showed that the lesion was pedunculated and freely mobile over the underlying musculature of the larynx and postcricoid region.

Most malignant lesions in this location would require an open pharyngotomy and adequate resection. However, this patient's tumor was small, well demarcated, and pedunculated, and therefore an endoscopic excision could be performed in a monobloc fashion. The patient is placed under general endotracheal anesthesia, and a wide Jako laryngoscope is introduced and the larynx is suspended. Alternatively a bivalve laryngoscopy can be used for wide exposure of the hypopharynx. After adequate exposure of the lesion is obtained, the operating microscope is brought into the field to provide proper visualization of the lesion to facilitate the operative procedure. With use of endoscopic microlaryngeal instruments, the lesion is excised with an intact capsule from its pedunculated base. Alternatively, the lesion can be excised through its pedicle with a CO_2 laser, remaining clear of the tumor. The surgical specimen shows a lesion that grossly appears to be like a well-encapsulated lipoma and is adequately excised in toto (Fig. 15.31). Histologic analysis of this specimen, however, showed that this lesion was a low-grade liposarcoma. Because of the malignant nature of this lesion and a relatively limited excision, this patient received postoperative external radiation therapy to enhance local control at the surgical resection site.

In contrast to well-differentiated liposarcomas, high-grade liposarcomas are infiltrative lesions with ill-defined and often

diffuse margins. In this category of high-grade lipomatous tumors are dedifferentiated liposarcoma, myxoid liposarcoma, and pleomorphic liposarcoma. Up to 10% of well-differentiated liposarcomas may progress to high-grade, dedifferentiated liposarcomas. Surgical resection for high-grade liposarcomas therefore entails a radical monobloc resection, working through normal tissue planes, around the clinically palpable, grossly demonstrable, and radiologically identified extent of the tumor. Such a radical resection entails traversing through various tissue planes and sacrificing soft tissues, muscles, and other neurovascular structures as deemed necessary. If adequate clearance of the tumor with negative margins is not achieved, then consideration should be given to interstitial implantation of residual tumor with after-loading catheters. The radiation source used in that clinical setting may be ^{192}Ir or ^{125}I. On the other hand, if gross total clearance of the tumor is achieved and concern exists about the margins or the possibility of microscopic extensions of tumor, then external irradiation as adjunctive treatment will provide disease control comparable with that achieved by interstitial radiotherapy. In general, high-grade sarcomas and other sarcomas exceeding 5 cm in diameter are candidates for consideration of adjunctive postoperative radiotherapy. Local control of disease is enhanced with adjunctive irradiation, although long-term survival is not affected.

TUMORS OF FIBROUS TISSUE

Fibromas and Benign Fibrous Tissue Tumors

Benign fibrous tumors of the head and neck region are relatively uncommon. However, tumors of fibroblastic origin may present either as a benign fibroma, a calcified fibroma, or a simple benign fibrous tumor. A somewhat more aggressive benign fibromatous tumor is the solitary fibrous tumor, which has a higher potential for local invasiveness and a higher risk of local recurrence. Surgical treatment of these lesions requires a complete excision in an extracapsular fashion with negative margins, without sacrificing any vital structures. The patient shown in Fig. 15.32 presented with a firm mass adjacent to the lamina of the thyroid cartilage in the right side of the neck that had been present for several years. He reported local discomfort in that area and a history of increasing size of the mass. A CT scan without contrast, shown in Fig. 15.33, demonstrates a calcified tumor in the central compartment of the neck located posterior to the upper pole of the thyroid lobe. Surgical excision of this tumor required a midcervical incision with adequate mobilization of the adjacent tissues and excision of the tumor in a monobloc fashion.

Dermatofibrosarcoma Protuberans

Dermatofibrosarcoma protuberans (DFSP) is a low-grade malignant tumor of fibrous tissue origin most commonly seen in the head and neck area. However, it also can present in the region of the shoulder or trunk or, rarely, on the extremities. The tumor arises from the dermal layer of the skin and often presents as a multinodular lesion (Fig. 15.34). The patient described here presented with a history of having felt several dermal nodules on her forehead for the past 3 years. Most patients do not show local invasion of deeper tissues at initial presentation. Therefore excision of a generous portion of the involved skin and the underlying soft tissues is deemed adequate as definitive treatment.

The extent of surgical resection for this patient is shown in Fig. 15.35. Note the multiple, palpable nodules of this tumor located several centimeters apart, which required a wide excision of the skin of the forehead and underlying soft tissues up to the pericranium. The tumor nodules were mobile over the underlying pericranium without involvement of the bone, and

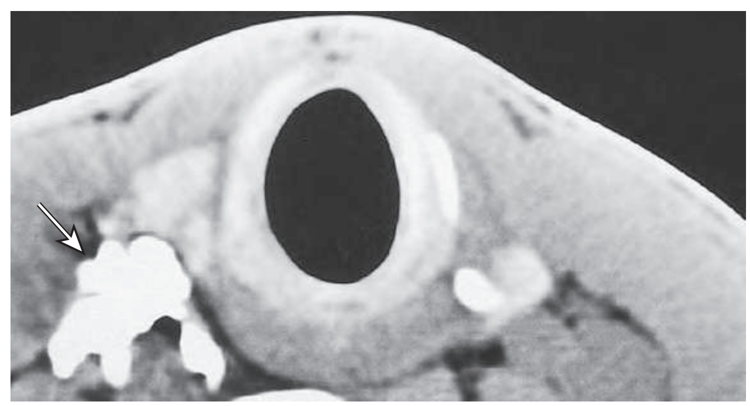

Figure 15.33 An axial view of a non–contrast-enhanced computed tomography scan shows a calcified tumor in the central compartment of the neck (*arrow*).

Figure 15.32 The outline of the firm mass adjacent to the right thyroid cartilage.

Figure 15.34 Dermatofibrosarcoma protuberans presenting as a multinodular lesion on the forehead.

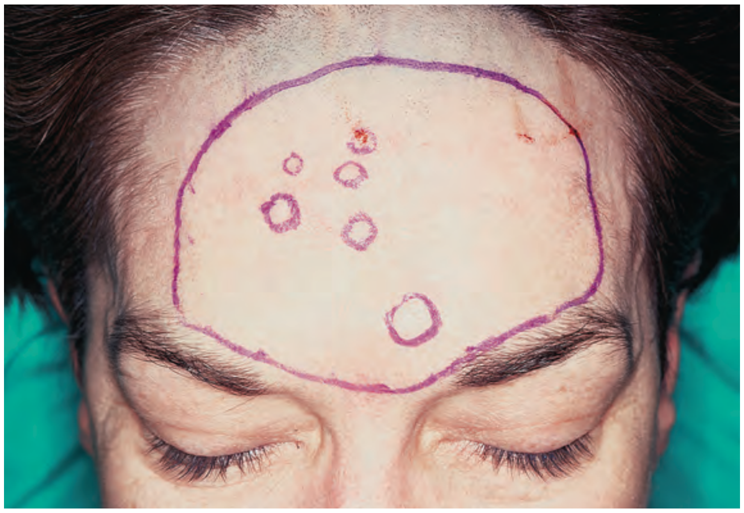

Figure 15.35 The extent of skin resection is outlined.

Figure 15.36 The appearance of the patient 2 years after surgery.

therefore full-thickness excision of the skin, subcutaneous tissue, the underlying occipitofrontalis muscle, and the pericranium was believed to be satisfactory. The surgical defect resulted in a bare surface of the frontal bone, which required vascularized soft tissue and skin for reconstruction. Repair of the surgical defect in this patient was accomplished with use of a radial forearm free flap. The postoperative appearance of the patient 2 years following surgery shows a satisfactory aesthetic and functional result (Fig. 15.36).

Excision of Dermatofibrosarcoma Protuberans of Scalp and Reconstruction With a Latissimus Dorsi Muscle Free Flap and Skin Graft

The patient presented here has a large, nodular, protuberant, neglected dermatofibrosarcoma protuberans of the scalp on the forehead at the hairline (Fig. 15.37). This lesion had been present for more than 7 years. The lesion was mobile over the underlying pericranium and did not involve the calvarium. Imaging studies failed to show any bone erosion. Surgical resection of this tumor required a wide three-dimensional excision including the underlying pericranium as the deep margin. A generous portion of the scalp is resected, exposing the underlying frontal and parietal bones. Reconstruction of such a surgical defect requires free tissue transfer. In this patient, a latissimus dorsi muscle flap was used to provide coverage over the bare bone and to provide soft tissue support for a split-thickness skin graft. The recipient vessels were anastomosed to the superficial temporal artery and vein on the left-hand side. The appearance of the patient approximately 6 weeks after surgery is shown in Fig. 15.38A. Note that the skin graft has taken 100% over the underlying muscle. With passage of time, the grafted area assumes the color and texture of the adjacent scalp and gives an excellent aesthetic outcome (Fig. 15.38B). It is crucial to emphasize that a wide, three-dimensional resection is required as initial surgical treatment for long-term control of this tumor.

Figure 15.37 A large nodular dermatofibrosarcoma of the scalp.

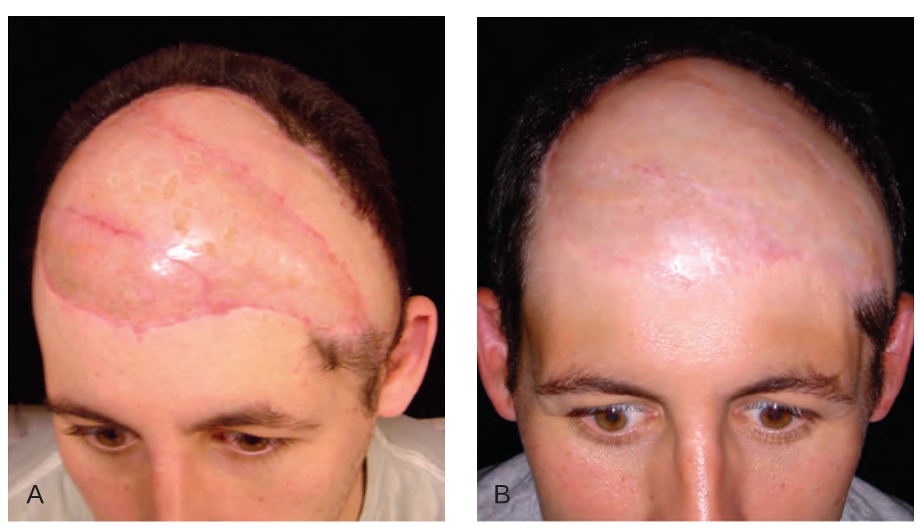

Figure 15.38 The patient's appearance after resection and reconstruction at 6 weeks (**A**) and 1 year (**B**).

Fibroosseous Lesion of the Neck (Gardner's Syndrome)

Benign fibroosseous lesions are quite common in patients with Gardner's syndrome. These lesions are often multiple and on occasion can get massive with local invasion. In spite of extensive local growth and invasion, they are histologically benign and do not have the potential to metastasize. The patient shown in Fig. 15.39 is a 12-year-old boy who has Gardner's syndrome with multiple colonic polyposis, for which he underwent colectomy. In addition he has multiple fibromatous lesions in various parts of his body that are asymptomatic. However, the tumor in the upper part of the neck on right-hand side has shown significant growth over the past 4 years, causing grotesque facial deformity. Imaging studies showed this to be an extensive soft-tissue tumor, with pressure effect on the body of the mandible, causing developmental growth deformity (Fig. 15.40).

Surgical excision was warranted to address the facial deformity and permit normal growth of the body of the mandible in this child. Excision of a generous portion of the skin over the tumor is planned for a satisfactory skin closure to achieve facial symmetry (Fig. 15.41). Although these tumors appear to be relatively avascular on imaging studies, they do have profuse microcirculation causing bleeding from small vessels during surgery. The crucial point in this particular patient is identification and preservation of peripheral branches of the lower division of the facial nerve. Once the facial nerve is identified, dissection proceeds along soft-tissue planes around the tumor (Fig. 15.42). A monobloc resection of the tumor is achieved. The large dead space from surgery requires a suction drain. The wound is closed in the usual fashion. The postoperative appearance of the patient 6 months following surgery shows excellent restoration of the facial contour and symmetry (Fig. 15.43).

Figure 15.39 Extensive fibroosseous tumor in a patient with Gardener's syndrome.

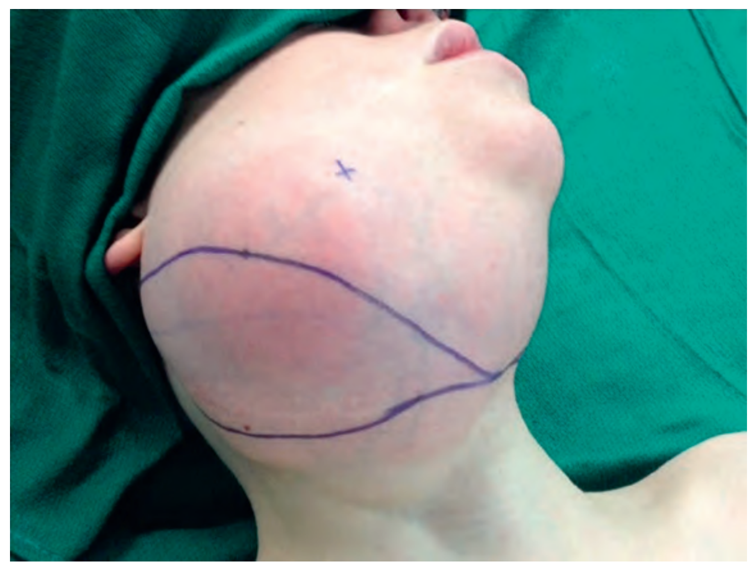

Figure 15.41 Plan of surgical excision with sacrifice of a segment of overlying skin.

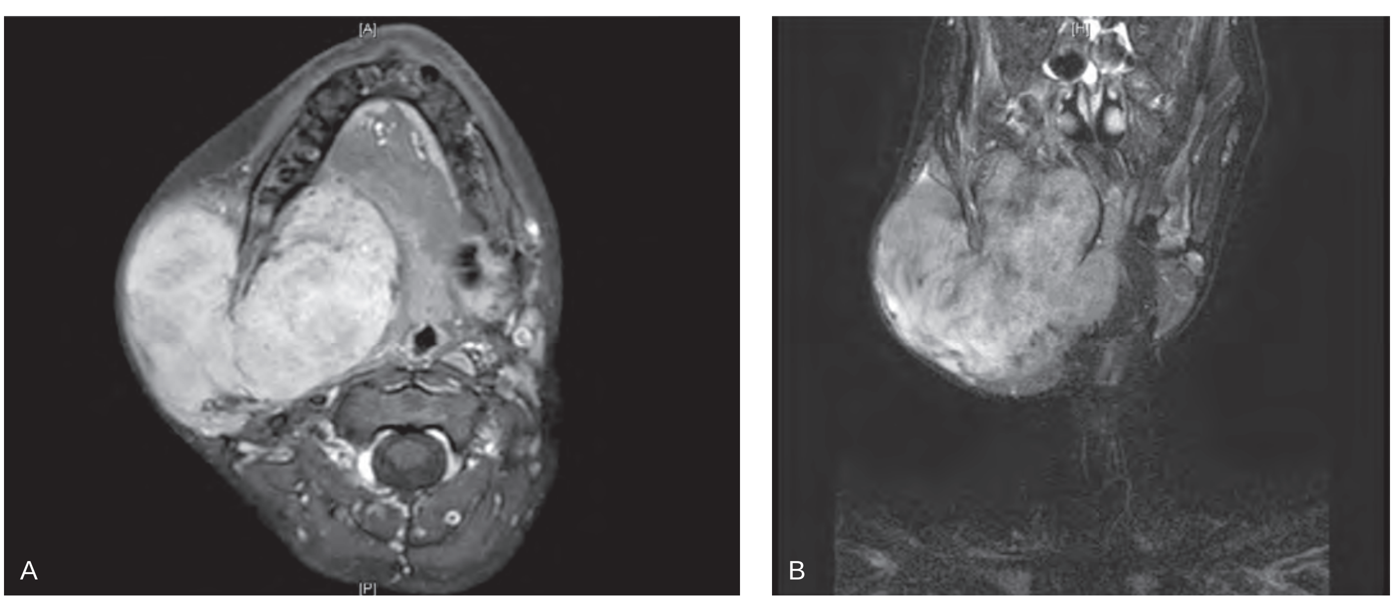

Figure 15.40 T1-weighted magnetic resonance images show extensive tumor surrounding the body of the mandible. **A**, Axial view. **B**, Coronal view.

Figure 15.42 The tumor is circumferentially mobilized after dissection of the facial nerve.

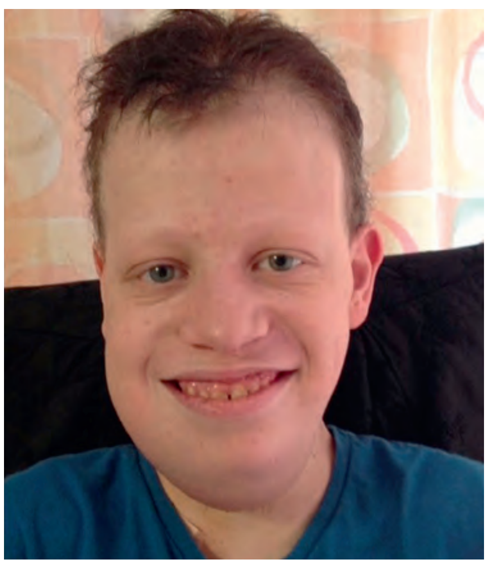

Figure 15.43 Postoperative appearance of the patient 6 months following surgery.

Solitary Fibrous Tumor (Hemangiopericytoma) of the Occipital Region

A solitary fibrous tumor (formerly known as hemangiopericytoma) is a low grade malignant tumor of fibroblastic origin. Although it is known to be locally aggressive, metastases are infrequent. The term *solitary fibrous tumor* is employed for these lesions when they occur in the pleural cavity, and the term *hemangiopericytoma* is often used for lesions involving the meninges, to reflect its aggressive behavior. There is, however, a significant debate among pathologists regarding the exact nomenclature for these locally aggressive tumors. The patient shown in Fig. 15.44 presented with a mass on the left-hand side of her neck in the suboccipital region. An open incisional biopsy was performed elsewhere to establish a histologic diagnosis. Upon clinical examination, the mass, which measured 5 cm, was smooth and fleshy and immobile over the deeper structures. A vascular bruit could be heard on auscultation over the surface of the tumor.

A contrast-enhanced CT scan of the upper part of the neck shows an enhancing lesion in the paraspinal region at the level of the second cervical vertebra (Fig. 15.45). This well-circumscribed lesion is situated over the transverse processes and posterior arch of the upper cervical vertebrae. An arch aortogram showed that the major blood supply of this tumor is derived from the left vertebral artery. A selective left vertebral angiogram in a lateral projection shows a highly vascular lesion in the suboccipital region (Fig. 15.46). The tortuous part of the vertebral artery near the transverse process of the second cervical vertebra is partly surrounded by this highly vascular tumor.

An anteroposterior projection of the left vertebral angiogram confirms the close relationship of the vertebral artery to this very vascular lesion (Fig. 15.47). Preoperative embolization of the lesion was not possible, because the feeding vessels were very small although abundant, and selective catheterization through the vertebral artery was not feasible. No intraspinal or intracranial extension of the tumor could be demonstrated with radiographic studies.

Figure 15.44 A patient with a mass on the left-hand side of her neck in the suboccipital region.

Surgical excision of this highly vascular lesion situated in a difficult location requires a well-planned operation. Ample supplies of blood should be available before surgery. Because of the proximity of the tumor to the upper cervical vertebra, bone instruments should be available. Fogarty balloon catheters also should be available in the event of uncontrolled hemorrhage from the vertebral artery.

The patient is placed in the prone position under general endotracheal anesthesia. The head is fixed in flexion with neurosurgical tongs (Fig. 15.48). An inverted U-shaped incision is made beginning in the midline at the spinous process of the seventh cervical vertebra. It extends cephalad up to the upper part of the occipital region and then curves back downward and laterally to encompass the scar of the previous biopsy and further down along the lateral aspect of the neck parallel to the trapezius muscle. The skin incision is deepened through the underlying soft tissues, and the inferiorly based skin flap is elevated as shown

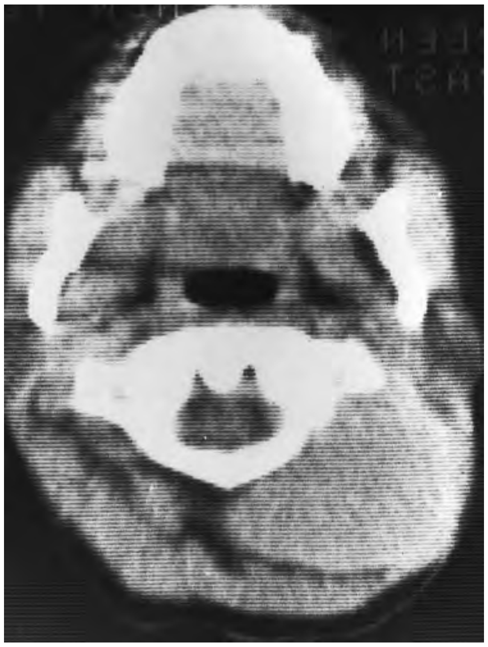

Figure 15.45 An axial view of the computed tomography scan showing a contrast-enhancing mass in the paraspinal region.

Figure 15.46 A selective left vertebral angiogram on a lateral view shows a highly vascular lesion.

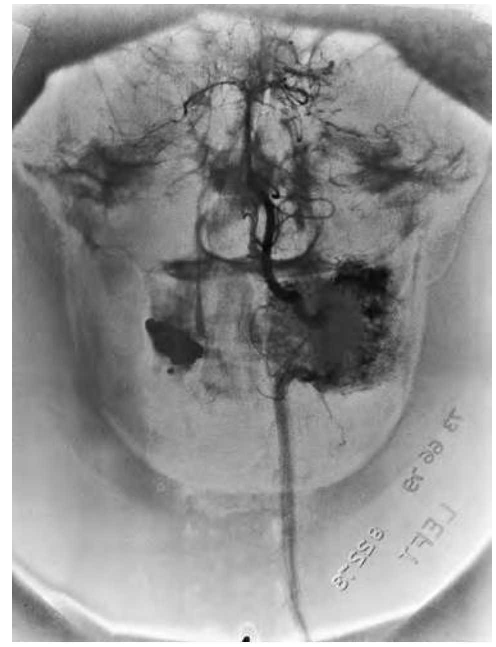

Figure 15.47 An anteroposterior view of the left vertebral angiogram shows the close relationship of the vertebral artery to this very vascular lesion.

Figure 15.48 The patient's head is fixed in flexion with neurosurgical tongs, and the skin incision is outlined.

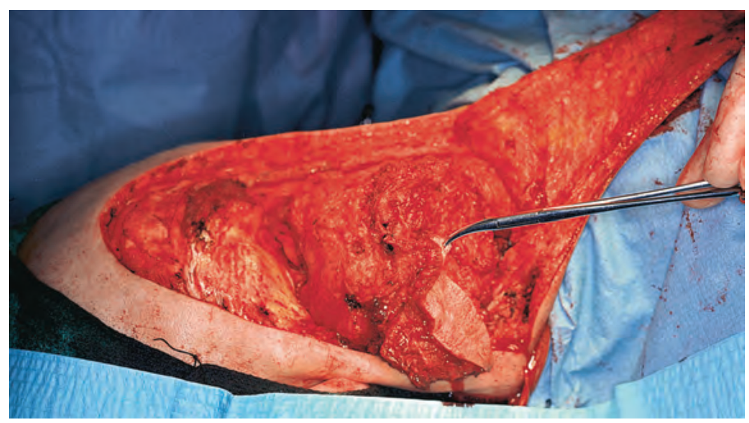

Figure 15.50 The attachments of the suboccipital muscles are detached from the lower border of the occipital bone.

in Fig. 15.49. Brisk hemorrhage from the scalp in the occipital region should be expected but is easily controlled with electrocautery. The skin flap is elevated down to the midcervical region to facilitate adequate exposure of the cervical vertebrae.

Mobilization of the tumor begins in the occipital region with detachment of the attachments of the suboccipital muscles from the lower border of the occipital bone, as shown in Fig. 15.50. This maneuver will permit exposure of the suboccipital region, leaving the soft tissues attached to the pseudocapsule of the tumor. An incision is now made in the soft tissue overlying the spinous processes in the midline, and dissection proceeds laterally, leaving the paraspinous muscles attached to the tumor.

The paraspinous muscles of the left side are divided inferior to the lower border of the tumor. Further dissection on the undersurface of the tumor will permit its rotation anterolaterally to expose the posterior laminae of the cervical vertebrae and the posterior aspect of the transverse processes. This dissection should be done meticulously, gently, and with extreme caution to avoid inadvertent injury to the tortuous part of the vertebral artery (Fig. 15.51). Branches from the vertebral artery providing blood supply to the tumor are carefully isolated, individually divided, and ligated.

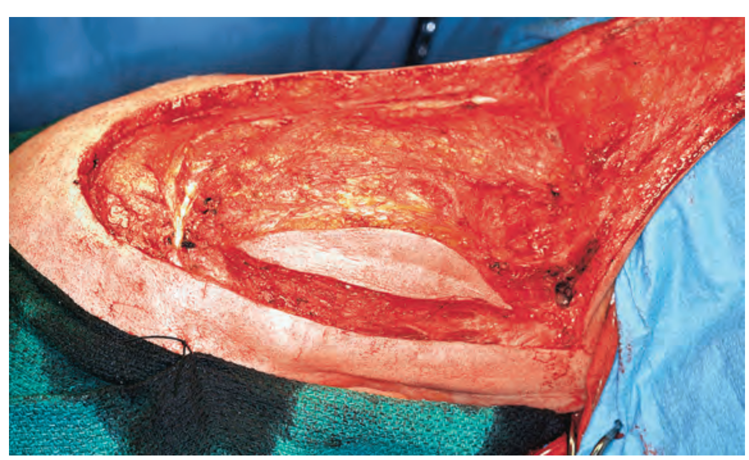

Figure 15.49 The inferiorly based skin flap is elevated superficial to the muscles.

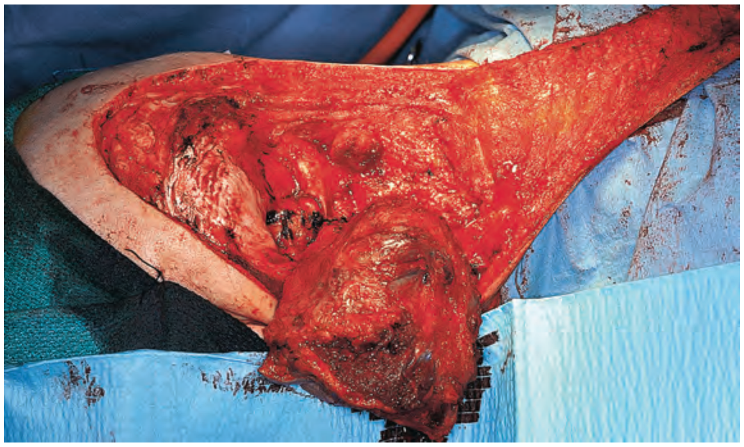

Figure 15.51 The mobilized tumor is reflected laterally by meticulous dissection on the posterior laminae, carefully protecting the vertebral artery.

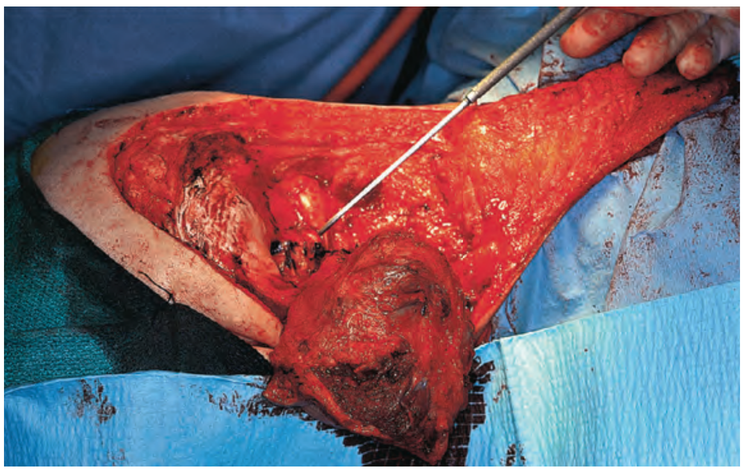

Figure 15.52 The tortuous part of the vertebral artery is dissected off the tumor.

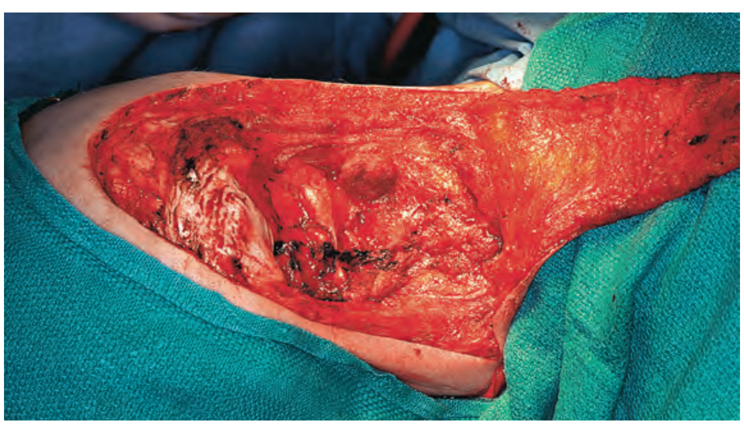

Figure 15.53 The surgical field after excision of the tumor.

Figure 15.54 Wound closure.

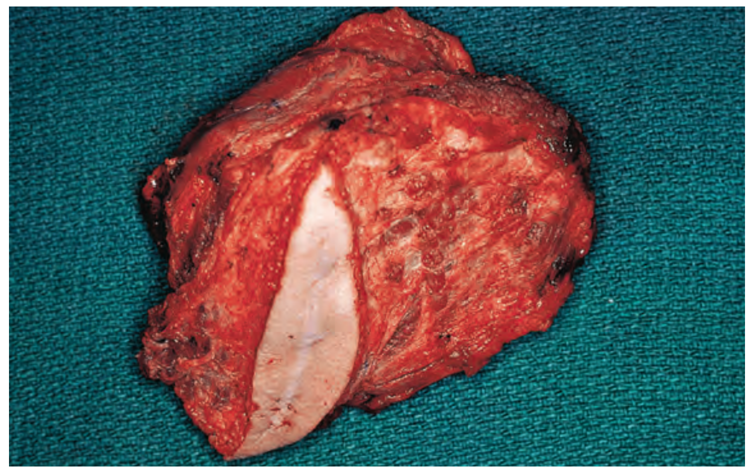

Figure 15.55 The surgical specimen.

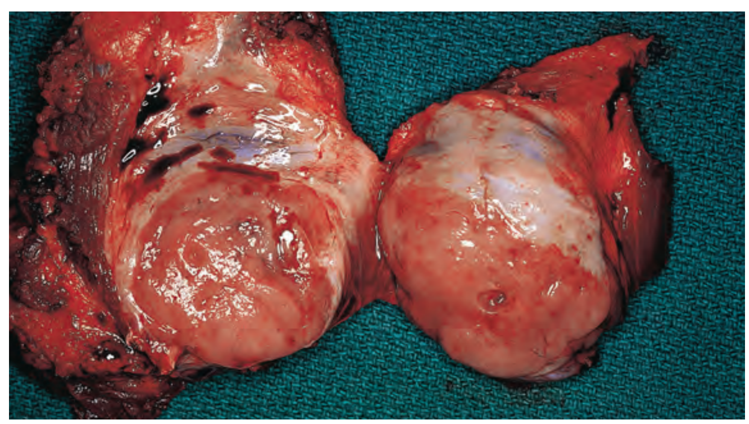

Figure 15.56 The cut surface of the specimen.

With meticulous and slow dissection, the vertebral artery, which is in close proximity to the tumor, is separated as shown with a pointer in Fig. 15.52. The tumor by now is totally mobilized and is ready to be delivered. Minor bleeding during mobilization of the tumor is to be expected. However, major blood loss may occur if rough handling in the region of the extracranial vertebral artery is undertaken. The surgical defect after removal of the tumor shows the bare occipital bone, the transected stumps of the paraspinous muscles, the transverse processes, and the spinous processes of the midcervical vertebrae along with the tortuous portion of the vertebral artery, which remains intact (Fig. 15.53). Absolute hemostasis must be secured before closure of the incision begins.

A Penrose drain is inserted after irrigation of the wound, which is closed in two layers (Fig. 15.54). Pressure dressings are applied because of the large raw area and the potential for oozing from the cut muscles. Immobilization of the cervical spine is unnecessary, because the vertebral column is intact. Although the suboccipital group of muscles and a portion of the paraspinous muscles in the upper part of the neck are resected, the stability of the cervical spine remains intact.

The specimen shows the excised scar of a previous biopsy with an en bloc excision of the tumor and its surrounding soft tissues (Fig. 15.55). The cut surface of the specimen (Fig. 15.56) shows a fleshy, homogeneous, well-circumscribed tumor, which

Figure 15.57 The appearance of the patient 3 months after surgery.

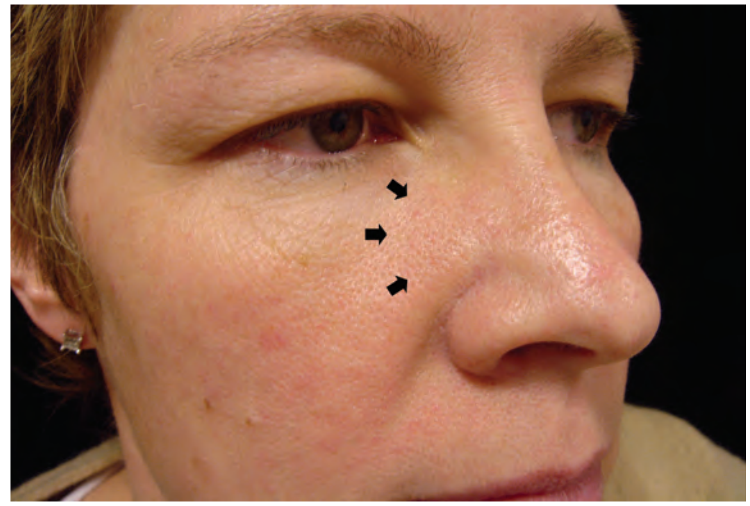

Figure 15.58 The preoperative appearance of a patient with a palpable mass in the right nasolabial region. *Arrows* indicate the extent of palpable mass.

on histologic examination confirmed the diagnosis of solitary fibrous tumor. The postoperative appearance of the patient is shown in Fig. 15.57. Although a significant soft-tissue deficit is present at the site of the resection of the tumor in the posterior triangle of the neck, the stability of the cervical spine remains intact and the movements of the head and neck are unaffected.

Undifferentiated Pleomorphic Sarcoma (Malignant Fibrous Histiocytoma)

Undifferentiated pleomorphic sarcoma (UPS; previously referred to as *malignant fibrous histiocytoma [MFH]*) may arise in any part of the head and neck region. The characteristics of this tumor are manifested by local invasion of adjacent soft tissues and bone, depending on the site of origin. This aggressive malignant tumor of the soft tissues requires a radical surgical resection with generous peripheral and deep margins in all three dimensions.

Undifferentiated Pleomorphic Sarcoma of the Nasolabial Region

The patient shown in Fig. 15.58 has a soft-tissue tumor adherent to the underlying nasal process of the maxilla along the right nasolabial region. An MRI scan in axial and coronal planes shows a well-demarcated tumor eroding the nasal process of the maxilla and the very lower end of the junction between the alar cartilage and the lower end of the nasal bone on the right-hand side. The mass was not readily visible on nasal endoscopy but could be palpated easily in the region of the right nasolabial fold. A needle biopsy of the mass revealed that it was a high-grade malignant tumor of fibrous origin. A lateral rhinotomy incision is marked around the nasal subunits of the ala and dorsum of the nose as landmarks (Fig. 15.59). The MRI scan shown in Fig. 15.60 demonstrates a well-circumscribed mass on the anterolateral wall of the right nasal cavity involving the subcutaneous soft tissues and extending up to the submucosal plane.

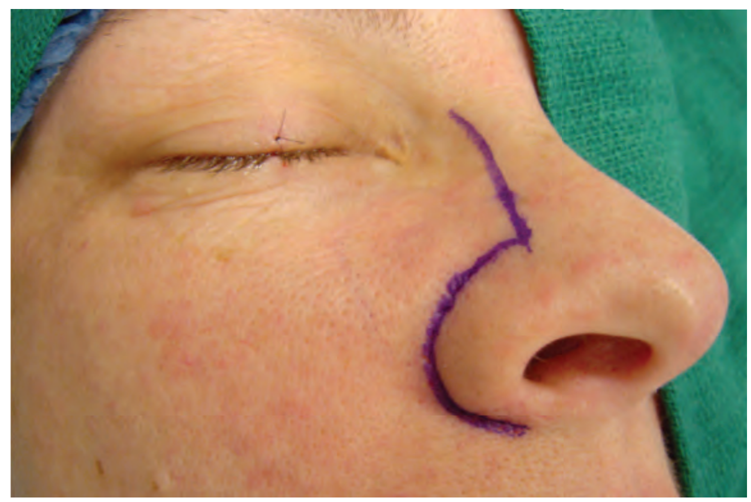

Figure 15.59 The lateral rhinotomy incision is marked along nasal subunits.

The skin incision is made with a scalpel, and the remainder of the operative procedure is continued with an electrocautery. The skin flaps are elevated in the subcutaneous plane, keeping a generous margin of soft tissues around the palpable tumor. The upper flap is elevated up to the anterior wall of the maxilla laterally, the lower end of the nasal bone cephalad, the premaxillary region inferiorly, and the mucosa of the nasal cavity medially. The mass is thus completely exposed, and a monobloc excision of the mass, including the cartilaginous lateral wall of the nasal cavity, is performed (Fig. 15.61). The surgical field following excision shows a through-and-through defect in the lateral wall of the nasal cavity (Fig. 15.62). Hemostasis is secured with electrocautery. Because of the small size of the surgical defect, no specific reconstructive effort is necessary. The surgical specimen is removed in a monobloc fashion with sufficient soft-tissue margins (Fig. 15.63). Nasal packing is introduced, and the surgical incision is closed in two layers (Fig. 15.64). Final histopathologic examination confirmed the diagnosis of a benign fibrous histiocytoma. The patient's appearance 7 weeks after surgery shows an excellent aesthetic outcome with a barely visible surgical scar (Fig. 15.65). With the passage of time, this incision will merge with the skin lines and should be imperceptible.

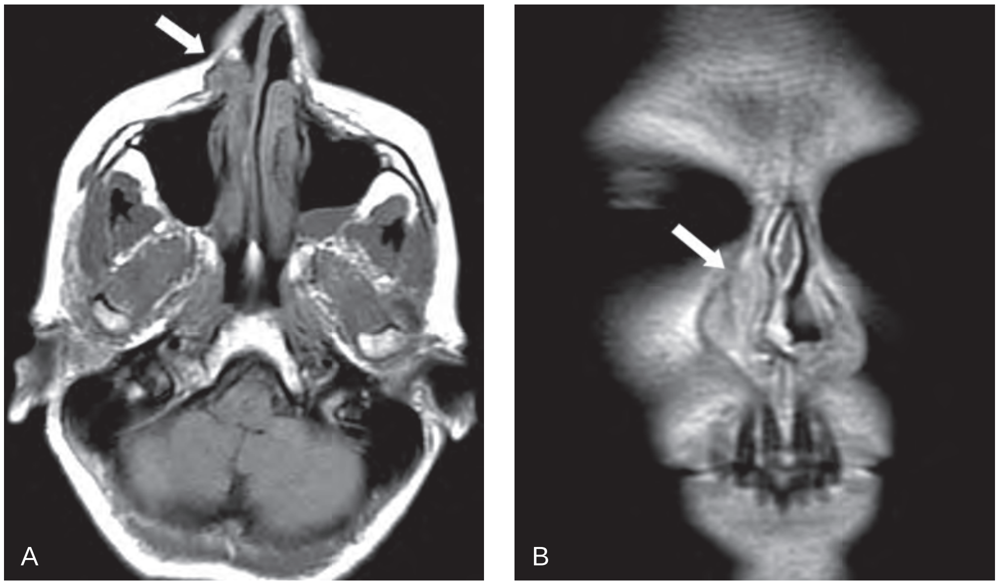

Figure 15.60 **A**, An axial magnetic resonance imaging scan showing a well-circumscribed mass on the anterolateral wall of the right nasal cavity. **B**, A coronal view showing the cephalocaudad extent of the tumor.

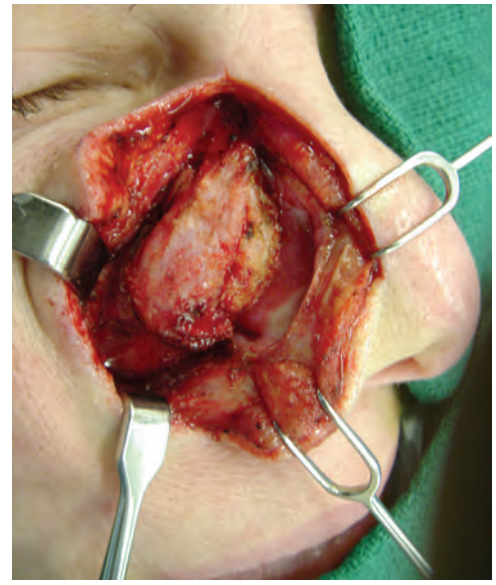

Figure 15.61 Elevation of the flaps allows complete exposure of the tumor.

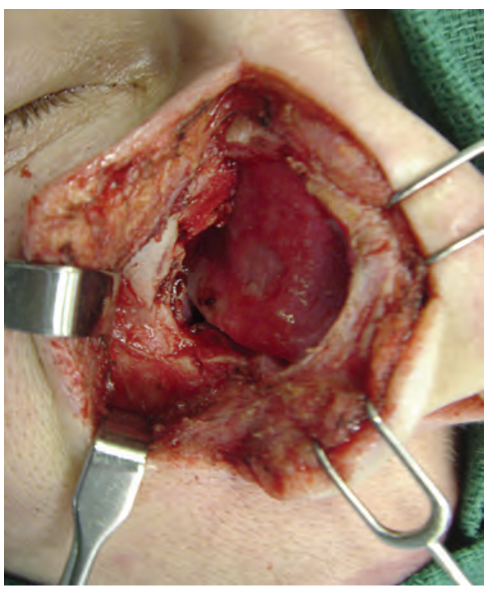

Figure 15.62 The surgical defect after excision of the tumor.

Figure 15.63 Monobloc excision of the tumor with adequate margins.

Figure 15.64 The skin incision is closed in layers.

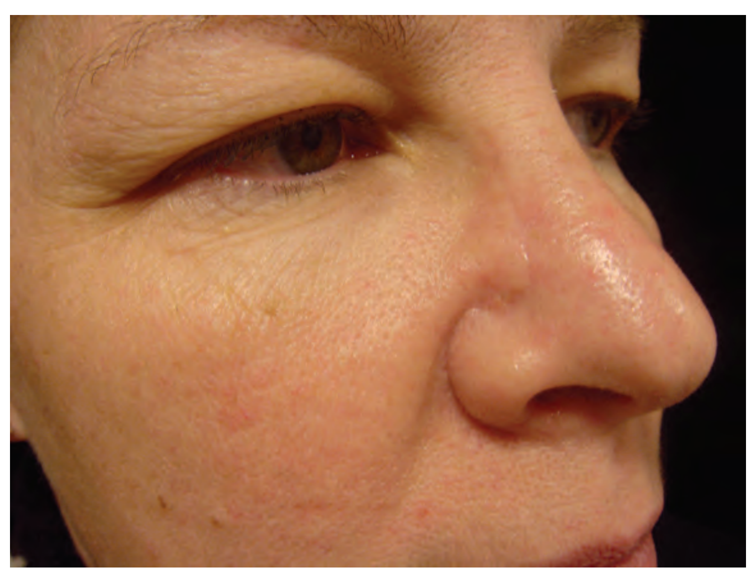

Figure 15.65 Postoperative appearance of the patient 7 weeks following surgery.

Undifferentiated Pleomorphic Sarcoma of the Zygomatic Region

The patient shown in Fig. 15.66 previously had undergone local excision of this lesion, followed by radiation therapy. Prompt

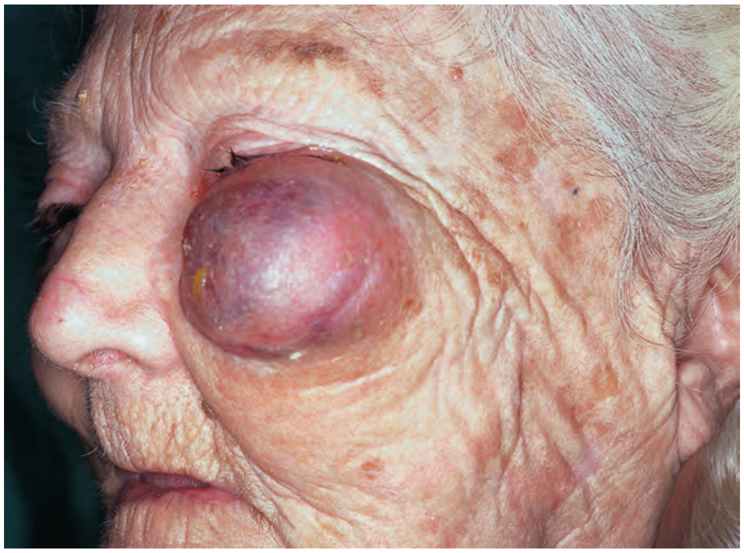

Figure 15.66 An undifferentiated pleomorphic sarcoma that recurred after local excision and radiation therapy.

Figure 15.67 The early postoperative appearance of the patient after resection and reconstruction.

recurrence of the tumor required a radical surgical resection of the tumor with immediate reconstruction. The surgical resection required excision of the skin, adjacent soft tissues (including the lower eyelid), and the anterior surface of the zygomatic process. Reconstruction of the defect was accomplished with use of a Mustardé flap and a composite mucoperichondrial graft from the nasal septum. A postoperative photograph of the patient 1 year following surgery, shown in Fig. 15.67, depicts an acceptable result.

Undifferentiated Pleomorphic Sarcoma of the Pterygomaxillary Region

The patient whose CT scan is shown in Fig. 15.68 had a diagnosis of UPS confirmed by a core biopsy under CT guidance. She was treated with induction chemotherapy elsewhere before presentation. At the conclusion of induction chemotherapy, the tumor

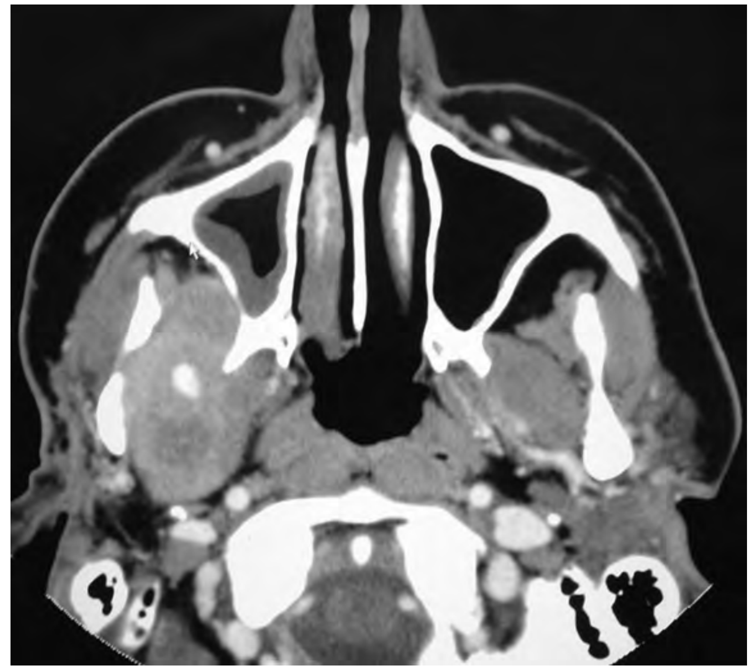

Figure 15.68 An axial view of a contrast-enhanced computed tomography scan shows a well-circumscribed tumor in the right pterygomaxillary region.

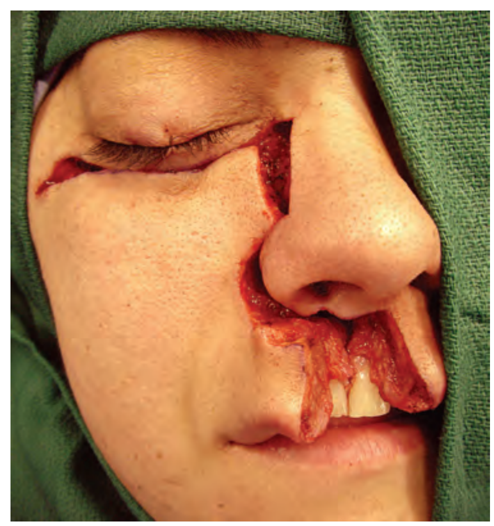

Figure 15.69 A modified Weber-Ferguson incision for the maxillary swing approach.

had shown only modest shrinkage. The gross extent of the tumor as seen on the CT scan occupies the pterygomaxillary region of the infratemporal fossa. The tumor is located between the lateral pterygoid plate anteromedially and the ascending ramus of the mandible laterally. Surgical exposure for resection of this tumor is best achieved with a maxillary swing approach. A modified Weber-Ferguson incision with a subciliary extension is utilized. (For step-by-step details of the maxillary swing procedure, please refer to Chapter 6.) The skin incision is deepened through the soft tissue to expose the underlying bone (Fig. 15.69). The anterior surface of the maxilla, the nasal process of the maxillary antrum, and the infraorbital region are exposed without elevating the cheek flap.

Appropriate osteotomies are made between the central incisor teeth in the premaxilla and then along the infraorbital region, the nasal process of maxilla, and through the zygoma to mobilize the maxilla. Once the maxillary swing is accomplished, the pterygomaxillary region comes into view, providing wide exposure of the tumor to facilitate a three-dimensional resection

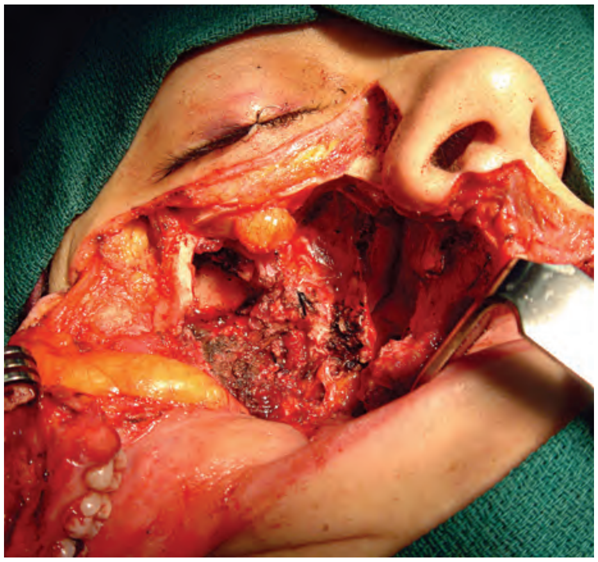

Figure 15.70 Exposure of the tumor. Note that the maxilla is swung to the right-hand side and is pedicled on the cheek flap.

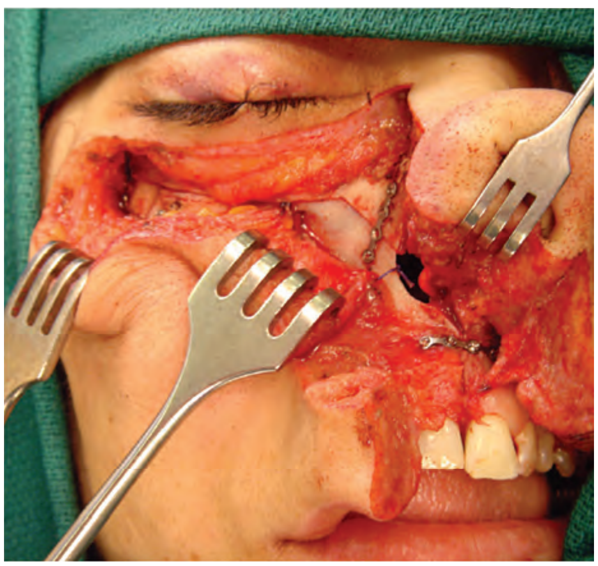

Figure 15.71 Miniplates are used for fixation of the repositioned maxilla.

(Fig. 15.70). Complete hemostasis is secured in the pterygoid space after resection of the tumor. No special reconstructive effort is necessary. The maxilla is repositioned in its normal location and is stabilized by fixation with miniplates and screws to the zygoma, the nasal bone, and the premaxilla (Fig. 15.71). Additional immobilization is achieved by wiring a previously fabricated dental obturator to the upper dentition. Resections such as this by necessity have close margins around the soft tissues in the pterygomaxillary region, and therefore this patient will need postoperative radiation therapy.

FIBROSARCOMAS OF THE CERVICAL REGION

Soft-tissue sarcomas in the head and neck region may occur in any area as a mass lesion. Symptoms usually are a result of local pressure on adjacent tissues. Thus the presence of a mass lesion may cause a visible deformity or pain due to compression of nerves, or it may compromise the airway or swallowing passage as a result of obstruction. The histologic grade is an important feature that determines the local aggressiveness of the tumor and thus guides the extent of surgical resection. Solitary fibrous tumors, low-grade fibrosarcomas, and desmoid tumors usually are well demarcated and may even present with a pseudocapsule around the tumor. In contrast, high-grade fibrosarcomas usually are infiltrative and require a much more radical surgical resection.

Low-Grade Fibrosarcoma

The patient described here had noticed a mass in the floor of the posterior triangle of the neck on the right-hand side for 8 months. A CT scan at the level of the thyroid cartilage demonstrates a homogeneous, slightly irregular soft tissue mass in the posterior triangle of the neck on the right-hand side (Fig. 15.72). Note that the mass is relatively well demarcated and is surrounded by normal fatty tissue. Clinical examination showed the mass to be somewhat mobile over the deeper soft tissues. A core biopsy from the mass had confirmed the diagnosis of a low-grade fibrosarcoma.

The plan of surgical resection in this patient required a three-dimensional resection to secure adequate soft-tissue margins around the tumor. A transverse incision is planned along a lower neck skin crease with the patient in supine position on the operating table (Fig. 15.73). The extent of the palpable mass is demarcated. The plan of the operation is to preserve all vital structures, including the spinal accessory nerve, the vagus nerve, and the carotid artery and jugular vein if technically feasible without compromising oncologically safe surgical

Figure 15.72 An axial computed tomography scan showing a well-circumscribed tumor in the posterior triangle of the right-hand side of the neck (*arrow*).

Figure 15.73 The palpable extent of the tumor depicted on the patient.

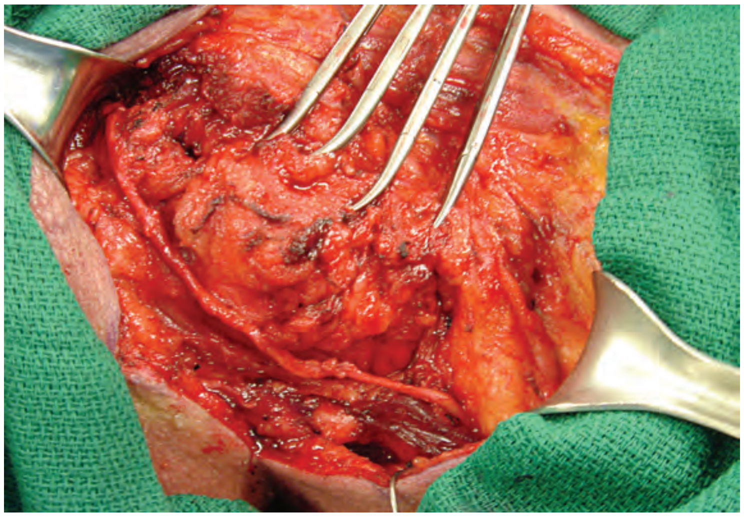

Figure 15.74 Exposure of the posterior aspect of the tumor with preservation of the accessory nerve.

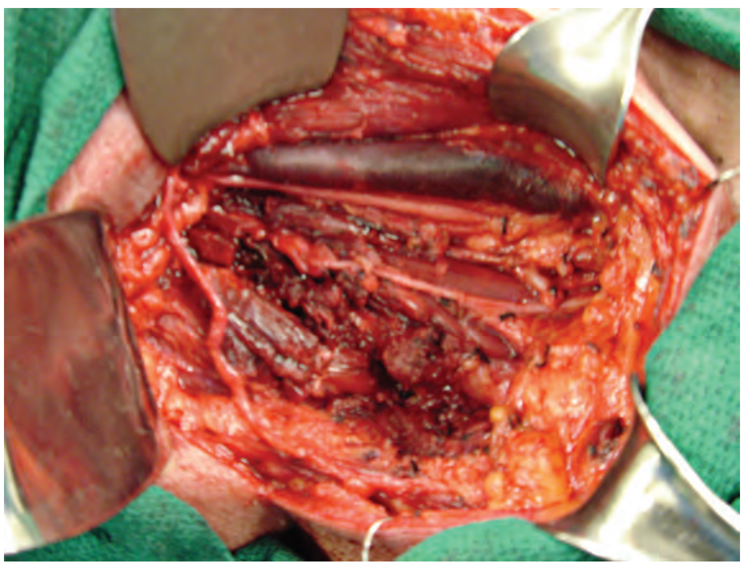

Figure 15.75 The surgical field after resection of the tumor.

resection. The skin incision is deepened through the platysma, and upper and lower skin flaps are elevated. The surgical procedure begins from the posterior aspect of the tumor, with identification of the anterior border of the trapezius muscle and the accessory nerve, which was preserved (Fig. 15.74). Dissection then proceeds medially in the posterior triangle, keeping generous soft-tissue margins in all directions. To that end, the operative procedure is similar to a modified comprehensive neck dissection, whereupon the cutaneous branches of the cervical plexus are sacrificed, preserving the phrenic nerve and the contents of the carotid sheath.

As the dissection proceeds medially, it becomes apparent that the tumor originates from the attachments of the levator scapulae muscle to the transverse processes. Thus the upper end of the attachments of the levator scapulae muscle and portions of the scalene muscles are excised to achieve a monobloc resection. The surgical defect after resection of the tumor is shown in Fig. 15.75. Note the preserved spinal accessory nerve as well as the phrenic nerve, vagus nerve, carotid artery, and jugular vein with loss of portions of the muscles of the floor of the posterior triangle. The surgical incision is then closed in two layers with suction drains. The surgical specimen shows monobloc resection of the tumor with its pseudocapsule intact.

Figure 15.76 The surgical specimen showing monobloc resection with the pseudocapsule of the tumor intact.

The cut surface of the tumor shows a typical pale white fibromatous tumor that is relatively avascular (Fig. 15.76).

Dendritic Cell Sarcoma

Follicular dendritic cell sarcoma is a rare tumor that usually occurs in lymph nodes. The histologic diagnosis is made by specific immunohistochemical staining. These tumors are locally aggressive and have a high potential for distant dissemination. The patient described here had a mass in the lower part of the neck on the right hand side for 4 months. Findings of an initial needle biopsy were not conclusive, and therefore an open biopsy was performed that confirmed the diagnosis of dendritic cell sarcoma. In the axial view of the contrast-enhanced CT scan, a well-demarcated tumor is seen just posterolateral to the carotid sheath in the right side of the neck (Fig. 15.77). The tumor is well circumscribed and lies deep to the sternocleidomastoid muscle. Coronal reconstruction of the CT scan shows that the common carotid artery is displaced medially and the internal jugular vein is displaced laterally by this well-circumscribed tumor (Fig. 15.78). The plan of surgical excision required a

Figure 15.77 A contrast-enhanced axial view of the computed tomography scan shows a well-circumscribed tumor deep to the sternomastoid muscle and lateral to the carotid artery on the right-hand side of the neck.

Figure 15.78 A coronal view of the computed tomography scan shows displacement of the carotid artery medially and the internal jugular vein laterally by the tumor.

Figure 15.79 The palpable extent of the tumor is demarcated on the patient.

transverse incision along the scar of the previous open biopsy. The palpable mass measured 5 by 8 cm (Fig. 15.79).

The operative procedure is very similar to that of a comprehensive modified neck dissection type I, in which the spinal accessory nerve and the contents of the carotid sheath are preserved. However, the sternocleidomastoid muscle is resected. The procedure begins in the posterior part of the neck along the anterior border of the trapezius muscle, with careful identification of the spinal accessory nerve up to the posterior belly of the digastric muscle (Fig. 15.80). Dissection then proceeds along the floor of the posterior triangle of the neck, remaining superficial to the muscular plane. The cutaneous branches of the cervical plexus are sacrificed, but the phrenic nerve is preserved. Dissection then proceeds along the carotid sheath, with identification of the vagus nerve and the common carotid artery (Fig. 15.81). The internal jugular vein is divided at its upper and lower end, and the surgical specimen is delivered in a monobloc fashion. The surgical defect shows the preserved spinal accessory nerve; the carotid artery; and the hypoglossal, vagus, and phrenic nerves (Fig. 15.82). Suction drains are placed, and the incision is closed in layers.

The bisected surgical specimen shows a well-circumscribed tumor, which probably arose in a deep jugular lymph node. A generous cuff of soft tissue is excised surrounding the tumor,

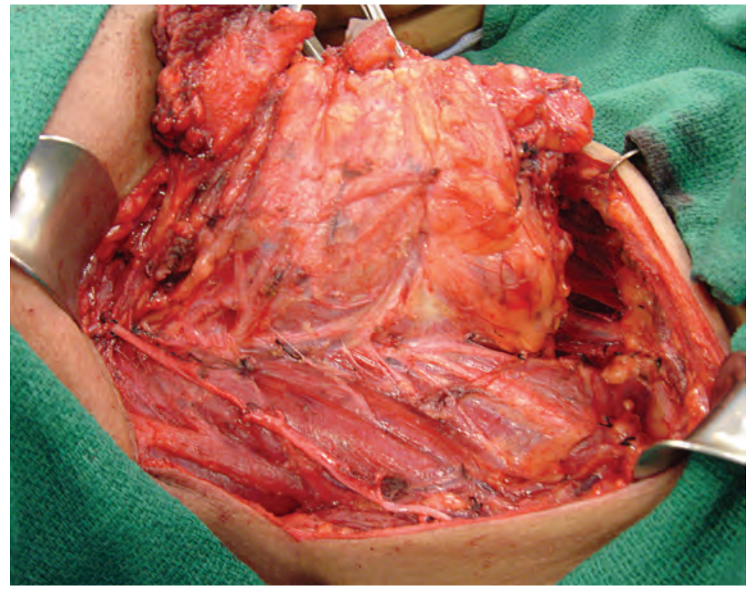

Figure 15.80 Dissection of the tumor in the posterior triangle of the neck is completed, preserving the spinal accessory nerve. Note the roots of the cervical plexus, phrenic nerve, and brachial plexus in the surgical field.

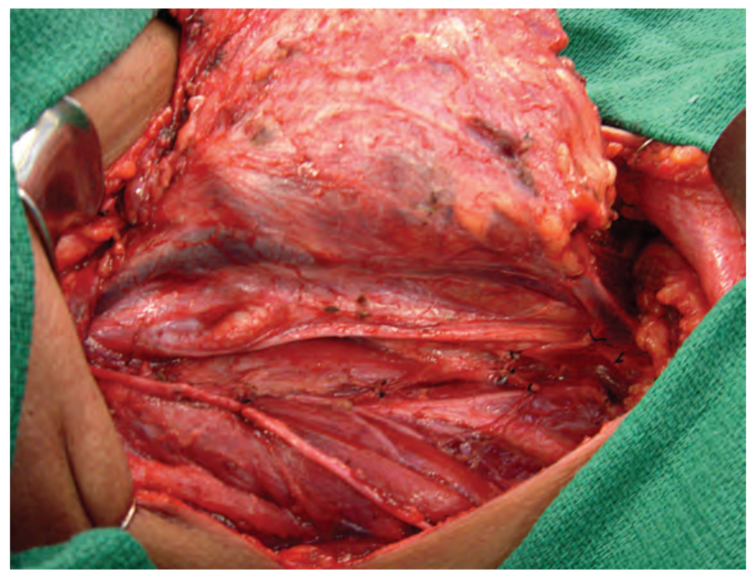

Figure 15.81 The tumor is dissected off the carotid artery, but the internal jugular vein is resected.

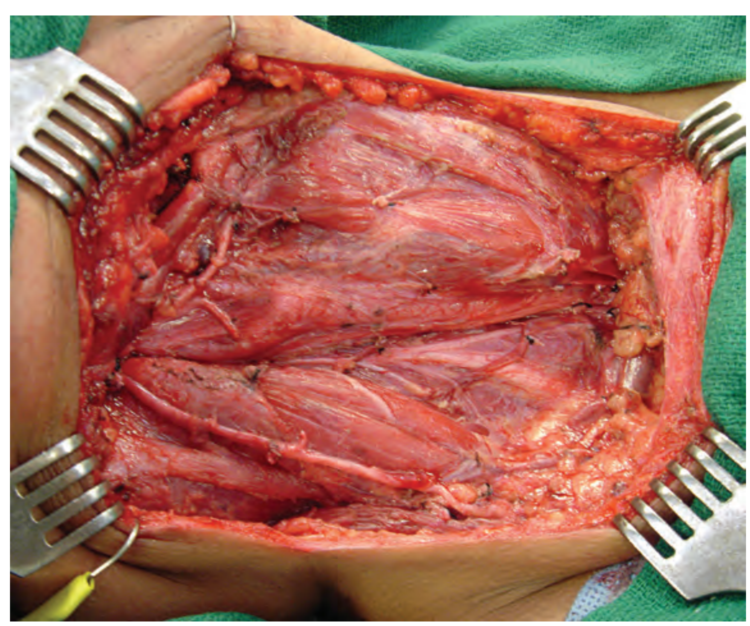

Figure 15.82 The surgical defect after excision of the tumor.

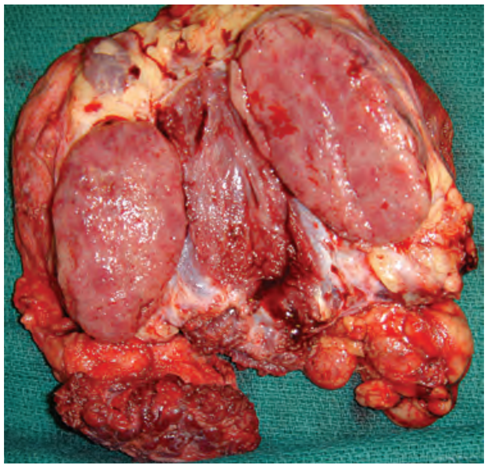

Figure 15.83 The surgical specimen showing a well-circumscribed tumor with generous soft-tissue margins.

Figure 15.85 An axial view of the computed tomography scan shows involvement of the outer cortex of the adjacent occipital bone and mastoid process (*arrow*).

thus securing adequate margins (Fig. 15.83). This patient will require adjuvant postoperative radiation therapy, and consideration should be given to systemic chemotherapy as well, with the intent of reducing the risk of distant metastases.

High-Grade Fibrosarcoma

As indicated earlier, a fibrosarcoma may arise anywhere in the head and neck region as a mass lesion and can progress with local extension to adjacent soft tissues and even bone. The patient shown in Fig. 15.84 presented with a mass lesion in the left postauricular region with increasing pain and discomfort. Upon clinical examination the mass was felt to be firm and fixed to the underlying mastoid process and the adjacent soft tissues of the mastoid region and causing invasion of the overlying skin. A CT scan with contrast demonstrates a soft-tissue tumor involving the outer cortex of the occipital bone and the adjacent mastoid process (Fig. 15.85). The tumor extends from the cortical bone on its deep margin up to the skin on its superficial extent. Wide three-dimensional resection is required to accomplish a monobloc excision of this tumor.

The surgical procedure begins with a circular incision around the area of the involved skin in the postauricular region and the mastoid process. The skin incision is deepened through the soft tissues up to the calvarial bone, and in the upper part of the neck it requires division of the upper end of the sternomastoid muscle, the trapezius muscle, and the splenius capitis muscles. The operative procedure is shown in progress in Fig. 15.86. At this juncture, the outer cortex of the occipital bone is resected in a monobloc fashion with the tumor, and a mastoidectomy is performed. A fine burr is used to create a kerf in the outer cortex of the bone, after which a right-angle saw is used to mobilize the cortical bone superficially. A mastoidectomy is performed in the usual fashion. Osteotomes are then used to separate the outer table of the skull and the tip of the mastoid process, which remain as a deep margin of the tumor.

Figure 15.84 A patient with a firm postauricular mass that was adherent to the overlying skin.

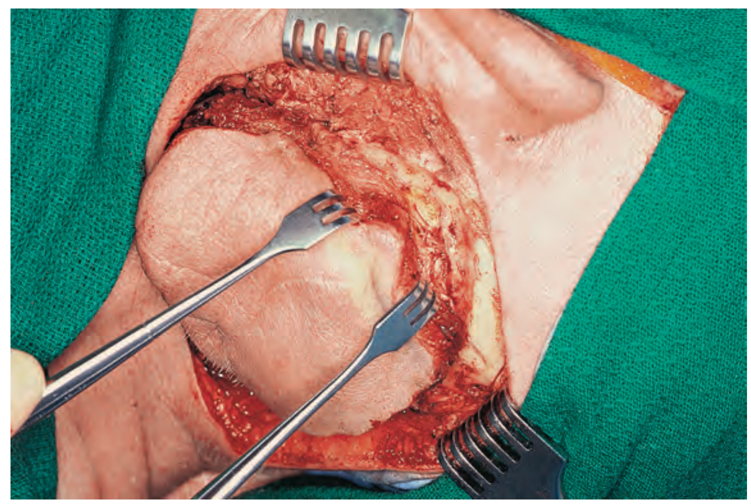

Figure 15.86 The circular incision around the tumor is deepened down to the underlying bone.

Having divided all the soft tissues circumferentially, the specimen is removed in a monobloc fashion. The surgical defect shown in Fig. 15.87 demonstrates removal of the outer cortex of the calvarium with the defect of the mastoidectomy and a generous three-dimensional soft tissue resection in the upper part of the posterior triangle of the neck. The surgical specimen shown in Fig. 15.88 demonstrates a monobloc resection of the tumor with wide three-dimensional margins. The bisected specimen shows a fibrous tumor contained well within the center of the surgical specimen.

Adequate surgical resection of high-grade fibrosarcomas in the head and neck region requires a wide three-dimensional excision that may include the overlying skin, the underlying soft tissues, and bone, as indicated by the local extension of the tumor. Intraoperative brachytherapy may be considered in situations in which complete resection is not feasible or is not desirable because

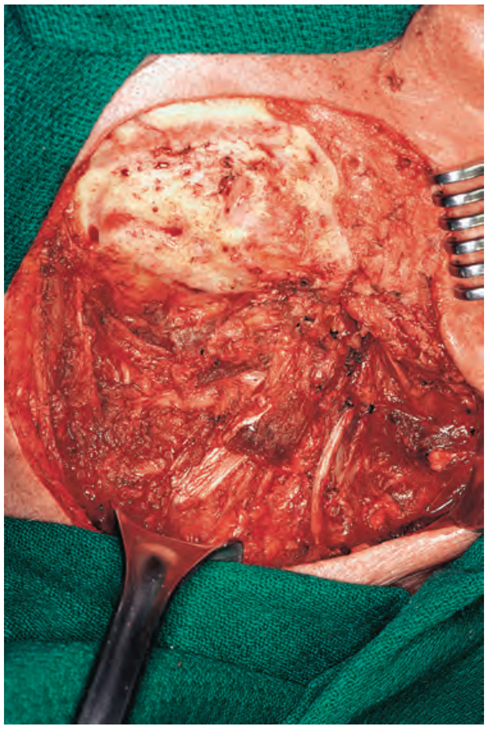

Figure 15.87 The surgical defect showing the mastoidectomy and excision of the outer table of the adjacent calvarium.

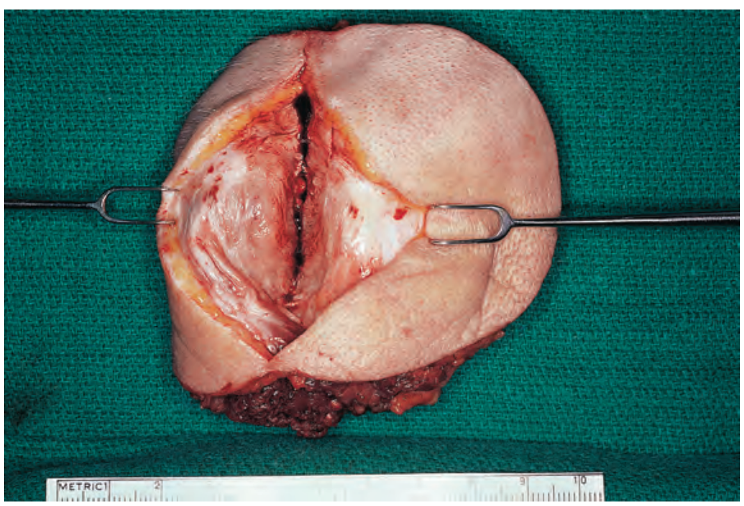

Figure 15.88 The surgical specimen.

of the invasion of vital structures. Appropriate coverage of the surgical defect may require a regional myocutaneous flap or a composite free flap. The surgical defect in this patient was repaired with use of a pectoralis major myocutaneous flap.

Resection of soft-tissue sarcomas of the head and neck requires familiarity with a variety of surgical techniques that may need to be used in different areas of the head and neck. The operative procedure must be devised and tailored to the local extent of the tumor, depending on its size, anatomic location, and histologic grade.

TUMORS OF VASCULAR ORIGIN

Capillary and Cavernous Hemangiomas

Hemangiomas may arise in patients of any age and provide challenging problems for clinicians. In general, infantile hemangiomas seldom require surgical intervention. The patient shown in Fig. 15.89 was born with a massive capillary/cavernous hemangioma involving the lower third of the face, lower lip, chin, and

Figure 15.89 An infant with a capillary/cavernous hemangioma of the lower face and neck.

the skin of the upper part of the neck. Spontaneous regression of lesions such as this is to be anticipated as the child grows. In most instances, by the time the child reaches puberty, the lesions have regressed nearly completely and leave very minimal aesthetic or functional debility. The only indications for surgical intervention in patients with infantile hemangiomas are when compromise of vital organs or function is at risk. Examples of such instances are massive hemangiomas that occlude the palpebral fissure of the eye and require intervention to open the eyelids; hemangiomas that obstruct the larynx, pharynx, trachea, or the oral cavity; and hemangiomas that cause obstruction of the nasal passages or the ear canal. In all other situations, the parents require reassurance, and the child is kept under continued surveillance. As years go by, spontaneous regression is to be expected, and a satisfactory functional and aesthetic outcome is seen in most instances.

Nonsurgical management of hemangiomas in the pediatric population includes systemic therapy with propranolol. Excellent regression is achieved in a majority of cases, without the need for any surgical intervention. An example of a hemangioma of the trachea in an infant is shown here. A postcontrast T1-weighted MRI scan shows a well-defined lesion in the trachea, causing partial airway compromise (Fig. 15.90). Four months following treatment with propranolol, significant regression of the lesion is noted (Fig. 15.91). The propranolol dosage and cardiac

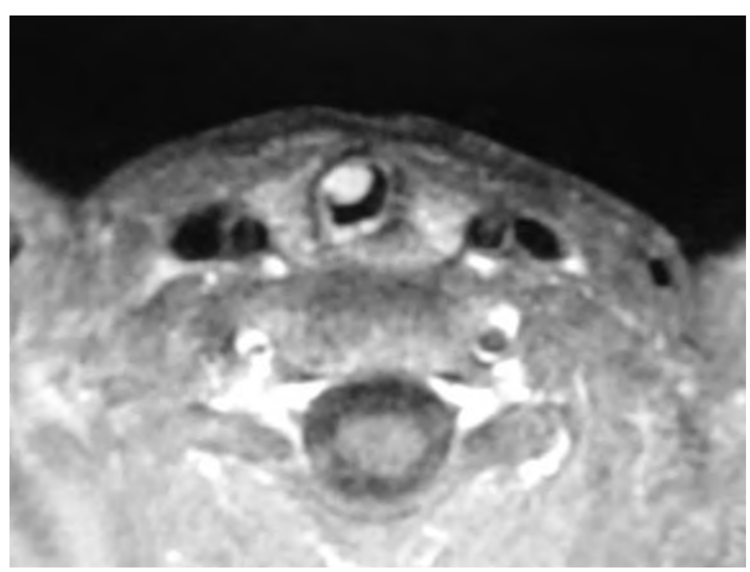

Figure 15.90 Axial view of magnetic resonance imaging scan in an 18-month-old child showing hemangioma of the trachea.

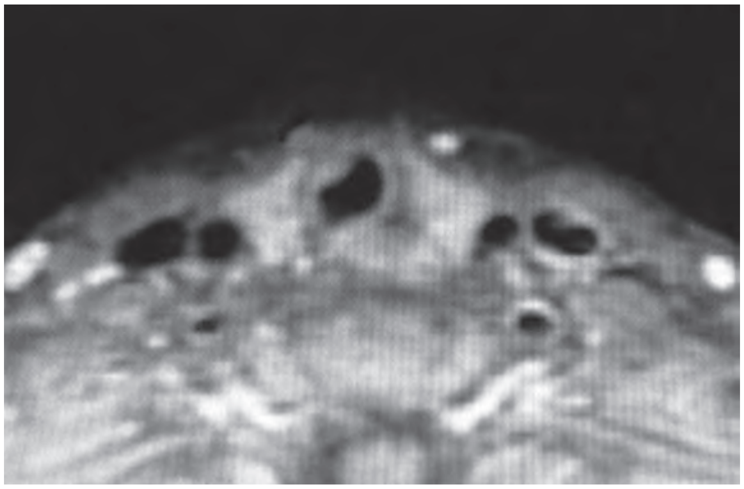

Figure 15.91 Axial view of a magnetic resonance imaging scan 4 months following treatment with propranolol showing regression of hemangioma.

monitoring should be handled by a pediatric cardiologist in consultation with the head and neck surgeon.

Capillary and Cavernous Hemangiomas in Adults

Patients with superficial capillary hemangiomas involving the skin of the head and neck region generally present because of aesthetic concerns. The patient shown in Fig. 15.92 has a deep-seated cavernous hemangioma in the lower part of the central compartment of the neck with a combination of dermal capillary hemangioma showing discoloration of the skin. Although spontaneous regression is observed in children nearly all the time, it is rarely observed in adults. The patient shown in Fig. 15.93 presented 12 years before the time this photograph was taken with a lesion involving the skin of the left side of the cheek without any history of hemorrhage or growth during the previous several years. Other than the aesthetic debility resulting from discoloration, this patient had no other symptoms. Surgical intervention in this clinical setting is rarely indicated. Surgical excision and reconstruction with free tissue transfer is

Figure 15.92 A combination of deep-seated cavernous hemangioma with an overlying dermal capillary hemangioma of the lower part of the neck.

Figure 15.93 Spontaneous regression of a hemangioma of the face in a patient who otherwise has been asymptomatic for 12 years.

Figure 15.94 A cavernous hemangioma of the left side of the forehead and temple and the left eyelid.

Figure 15.95 A cavernous hemangioma involving the tongue, floor of the mouth, buccal mucosa, and lower lip.

easy but will result in loss of facial expression on that side of the face, and there will always be skin color discrepancy. In some patients, spontaneous changes with disappearance of the lesion may be observed with the passage of time. Nonsurgical options, including systemic propranolol therapy or topical timolol may also be tried, but both have side effects. Use of these agents requires close monitoring by a cardiologist.

In contrast to capillary hemangiomas, cavernous hemangiomas present different problems. The patient shown in Fig. 15.94

presented with a nodular, spongy, encrusted lesion involving the skin of the forehead, the temple, and the upper eyelid and had a history of frequent episodes of bleeding from the lesion. Because of his symptoms of bleeding and the external appearance of the lesion, treatment was warranted. Treatment in this clinical setting generally is aimed at inducing thrombosis in the cavernous spaces in the tumor, thus producing shrinkage and aesthetic improvement as well as preventing recurrent episodes of hemorrhage. Thrombosis within the cavernous space may be induced by injection of a variety of thrombogenic substances, including sodium morrhuate, absolute alcohol, boiling water, or any other substance producing an inflammatory response in the endothelium of the blood vessels in the tumor. Occasionally, bleeding from ulcerated hemangiomas can be controlled by using low-dose external radiation therapy. In contrast to symptomatic cavernous hemangiomas, asymptomatic cavernous hemangiomas seldom require surgical intervention. The patient shown in Fig. 15.95 has a cavernous hemangioma involving the tongue, floor of the mouth, buccal mucosa, and lower lip. She has not had any history of hemorrhage from the lesion since childhood, and she does not have functional debility with mastication or speech. In this setting, only clinical surveillance is recommended without surgical intervention.

Hemangioma of the Submental Region

Hemangiomas in adults are benign soft-tissue tumors that may be capillary or cavernous in nature. In fact, many hemangiomas manifest a combination of both capillary and cavernous components. In contrast to a hemangioma, which is a true neoplasm, some patients present with an arteriovenous malformation that usually is congenital in nature.

The patient shown in Fig. 15.96 gave a history of a slowly enlarging submental mass over a period of 3 years. She had been aware of the presence of a submental fullness for several years before the onset of the increase in its size. An MRI scan performed in sagittal and coronal planes (Figs. 15.97 and 15.98) shows a multiloculated infiltrating lesion involving the submental region with extension into the root of the tongue through the mylohyoid muscles in the floor of the mouth. The clinical findings and radiographic appearance on the MRI scan were indicative of a hemangioma, and therefore bilateral selective external carotid angiography was performed to assess the true extent of the lesion and to proceed with preoperative embolization.

The arterial phase of the left lingual artery infusion study shows significant filling of the hemangioma through the left lingual artery (Fig. 15.99). Terminal branches of the lingual artery were selectively catheterized and embolized to reduce the blood flow to the lesion. In Fig. 15.100, the angiographic picture after selective embolization of the branches of the lingual artery on both sides shows a well-embolized extensive hemangioma of the submental region.

Surgical excision of this lesion is performed under general endotracheal anesthesia with the patient in the supine position with the neck extended (Fig. 15.101). The dotted line shows the outline of the palpable extent of the lesion. A transverse skin incision is placed in a natural skin crease in the region of the thyrohyoid membrane. The upper skin flap is elevated deep to the platysma to expose the lesion in the submental region (Fig. 15.102). Note that the mylohyoid muscle is bulging between the anterior belly of the digastric muscles on both sides as a result of the underlying hemangioma.

Meticulous dissection of the hemangioma is now undertaken with the electrocautery, carefully remaining outside the lesion and sacrificing only minimal amounts of adjacent normal tissues. Resection of this lesion required its delivery from within the musculature of the root of the tongue. Adequate exposure is

Figure 15.96 A patient with a submental mass that had enlarged slowly over a 3-year period.

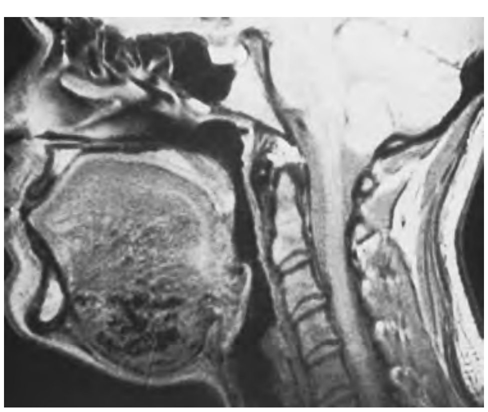

Figure 15.97 A sagittal view of a magnetic resonance imaging scan showing a spongy lesion in the deep muscles of the tongue.

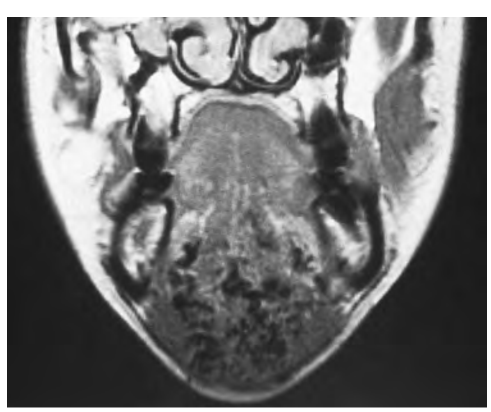

Figure 15.98 A coronal view of the magnetic resonance imaging scan showing a spongy lesion with large vascular spaces in the root of the tongue.

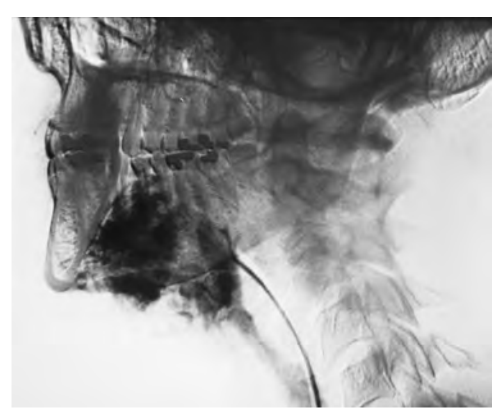

Figure 15.99 Selective lingual artery angiography shows a highly vascular lesion.

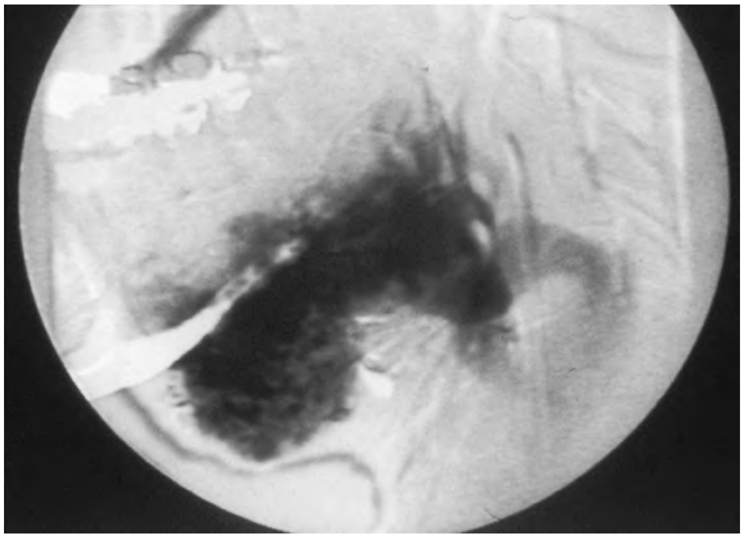
Figure 15.100 A postembolization radiograph.


Figure 15.101 The extent of the lesion is depicted and the incision is outlined.

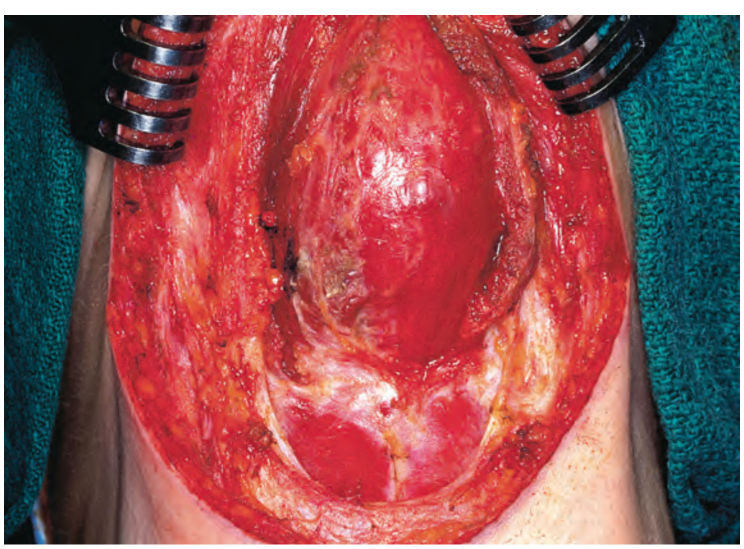
Figure 15.102 Exposure in the submental region shows the lesion bulging through the mylohyoid muscles.

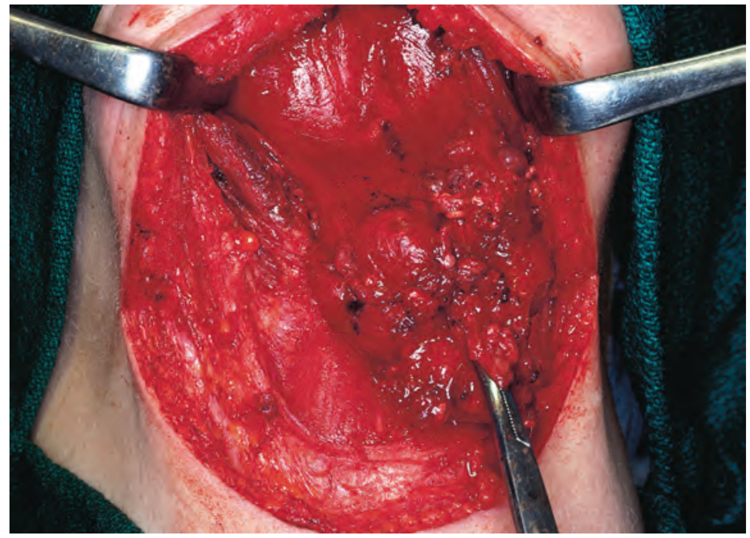
Figure 15.103 The lesion is dissected out from the deep muscles of the tongue.

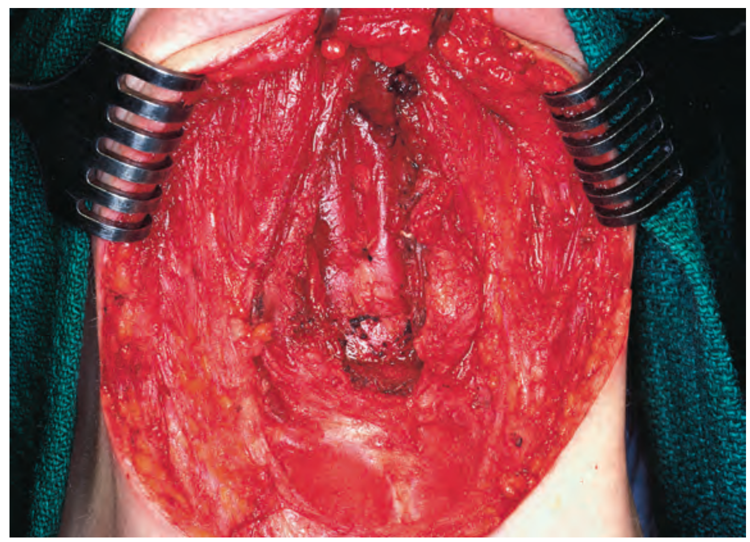
Figure 15.104 The surgical field after total excision of the hemangioma.

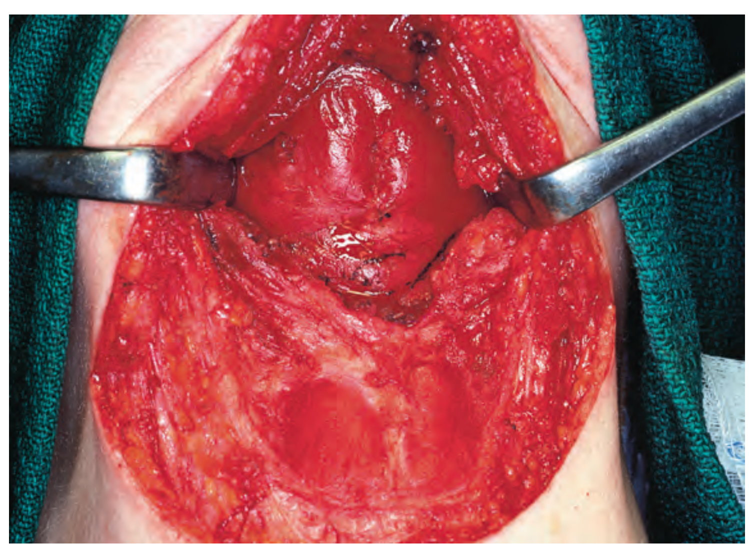
Figure 15.105 The mylohyoid muscles are reapproximated in the midline.

obtained by placement of deep right-angled retractors to separate the musculature of each side of the tongue to permit delivery of the lesion (Fig. 15.103). Each loculus of the lesion is carefully resected without leaving any residual tumor behind.

The surgical field following total excision of the hemangioma is shown in Fig. 15.104. After absolute hemostasis is secured, the mylohyoid muscles are reapproximated in the midline (Fig. 15.105). A suction drain is placed deep to the platysma muscle between the anterior belly of the digastric muscles, and the skin incision is closed in layers (Fig. 15.106). The surgical specimen shown in Fig. 15.107 demonstrates a multilobulated spongy tumor mass with thrombosed vascular spaces within the lesion resulting from preoperative embolization. Preoperative embolization clearly minimizes the blood loss, facilitates performance of the surgical procedure, and increases the safety of the operation.

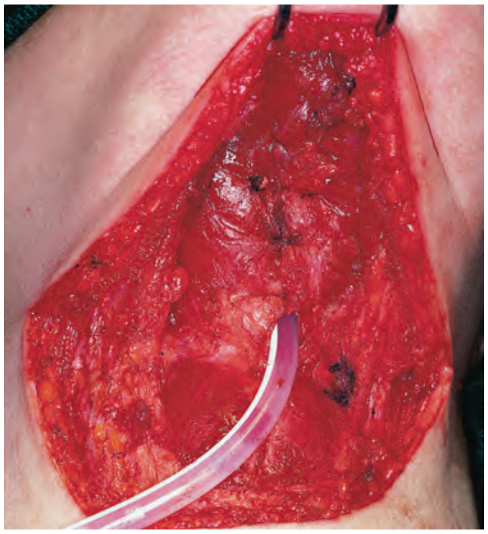

Figure 15.106 A suction drain is placed and the incision is closed in layers.

Figure 15.107 The surgical specimen.

Intermuscular Hemangioma

The patient described here reported vague discomfort and a progressive ill-defined mass in the left suprascapular region deep to the trapezius muscle. Clinical examination showed an ill-defined soft mass with no signs of skin or nerve invasion. The axial view of the contrast-enhanced T1-weighted MRI shows a well-circumscribed enhancing tumor in the suprascapular region located deep to the trapezius muscle (Fig. 15.108). The tumor is located in the tissue planes between posterior compartment muscles but does not infiltrate into the muscles. A sagittal view of the MRI shown in Fig. 15.109 demonstrates an intermuscular well-circumscribed vascular lesion.

Surgical resection of this tumor required a transverse incision along a skin crease in the lower part of the neck overlying the trapezius muscle. The spinal accessory nerve is identified as it enters the trapezius muscle deep to its anterior border (Fig. 15.110). After this nerve is identified, the vertical fibers of the trapezius muscle are separated to create a plane through the trapezius muscle into the deeper soft tissues. The split fibers of the trapezius are retracted to expose the hemangioma, which now comes into view (Fig. 15.111).

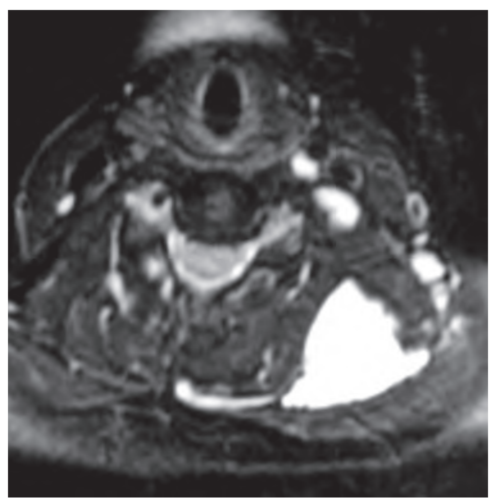

Figure 15.108 An axial view of a T1-weighted magnetic resonance imaging scan shows a bright lesion in the posterior compartment of the left-hand side of the neck.

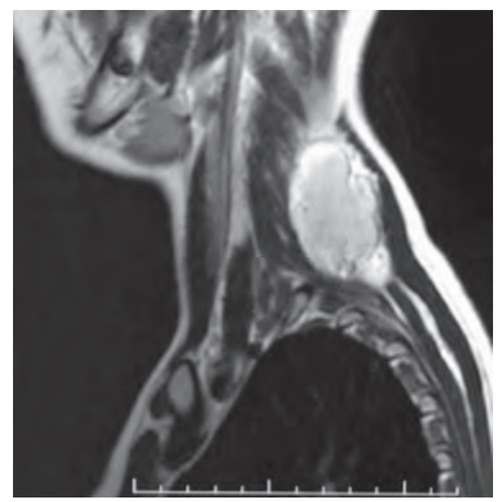

Figure 15.109 A sagittal view of the magnetic resonance imaging scan shows a well-circumscribed lesion deep to the trapezius muscle.

Meticulous dissection is undertaken in a tissue plane around the pseudocapsule of the lesion, securing hemostasis as the dissection proceeds. Major feeding vessels are identified, divided, and ligated. As dissection proceeds, the hemangioma becomes smaller in its dimensions because of a lack of perfusion, and therefore further dissection becomes easier. Eventually the entire lesion is removed in toto and intact with its pseudocapsule. Complete hemostasis is secured. The split fibers of the trapezius muscle are reapproximated with interrupted chromic catgut sutures. A suction drain is placed in the dead space at the site of the tumor, and this drain is brought out through a separate incision. The remaining incision is closed in layers. The bisected specimen shows a spongy lesion with areas of phleboliths resulting from thrombosis within the vascular spaces (Fig. 15.112). Complete surgical excision is usually curative, and the patient is relieved of her symptoms permanently.

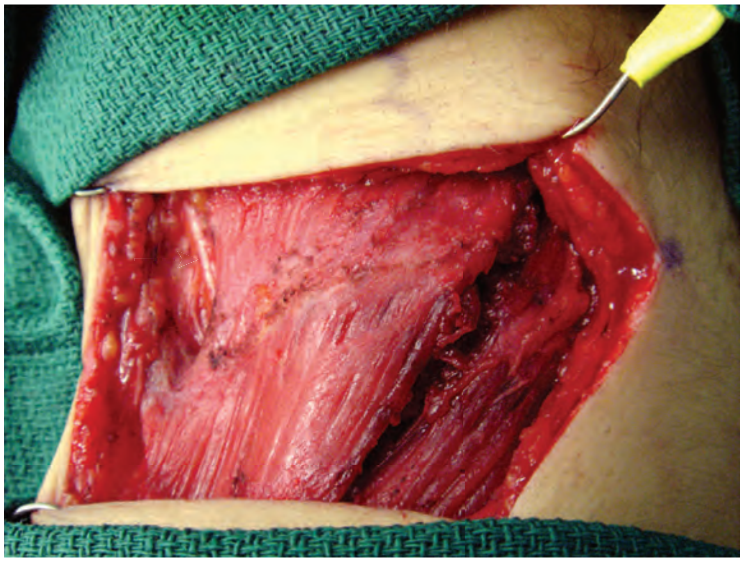

Figure 15.110 The spinal accessory nerve is identified (*arrow*), and the vertical fibers of the trapezius muscle are separated to facilitate exposure of the lesion.

Intramuscular Hemangioma of the Masseter Muscle

Intramuscular hemangiomas often present as mass lesions of the involved muscle with the history of fluctuating dimensions and occasionally are accompanied by pain. The patient shown in Fig. 15.113 had a painful mass in the left parotid region with a history of increase and decrease in the size of the lesion. Clinically this appeared like a parotid tumor. However, a postcontrast T1-weighted MRI in axial and coronal planes clearly showed the lesion to be in the masseter muscle and not in the parotid gland (Fig. 15.114). Surgical excision of this lesion requires a standard parotidectomy approach with dissection, identification, and preservation of the lower division of the facial nerve (Fig. 15.115). The lower division of facial nerve is identified and lifted off the masseter muscle along with the superficial lobe of the parotid gland. It is important that the patient's blood pressure be maintained at normal levels or even slightly higher than normal to identify the extent of the hemangioma. If patient has hypotension, then sometimes the hemangioma collapses and may not be identifiable within the muscle. After elevation of the facial nerve and the parotid gland, the hemangioma of the masseter muscle comes into view (Fig. 15.116). Meticulous dissection is now undertaken to excise the lesion in toto, remaining outside its pseudocapsule in the masseter muscle. The surgical specimen shows monobloc excision of the lesion (Fig. 15.117). The defect in the muscle is repaired with chromic catgut sutures, and the wound is closed in the usual fashion. A Penrose drain is inserted and can be removed in 48 hours.

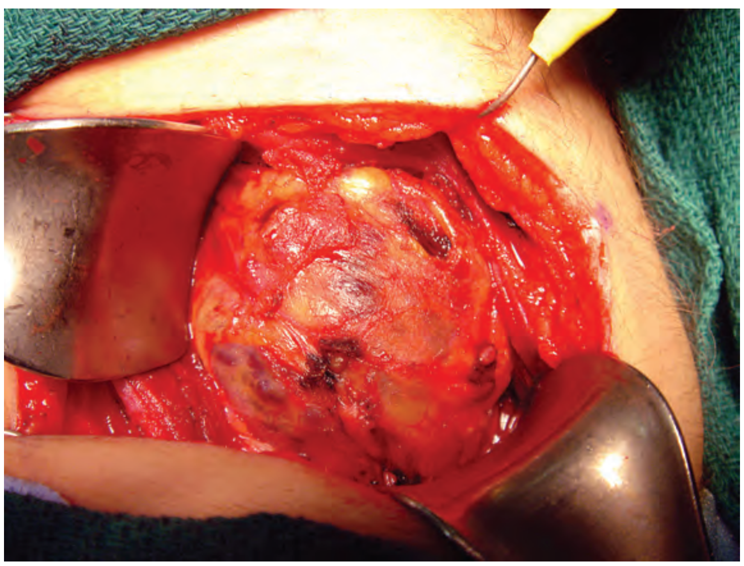

Figure 15.111 The vascular lesion with its pseudocapsule is mobilized circumferentially.

Figure 15.113 A palpable fluctuant mass in the parotid region.

Figure 15.112 The surgical specimen shows a spongy lesion with phleboliths.

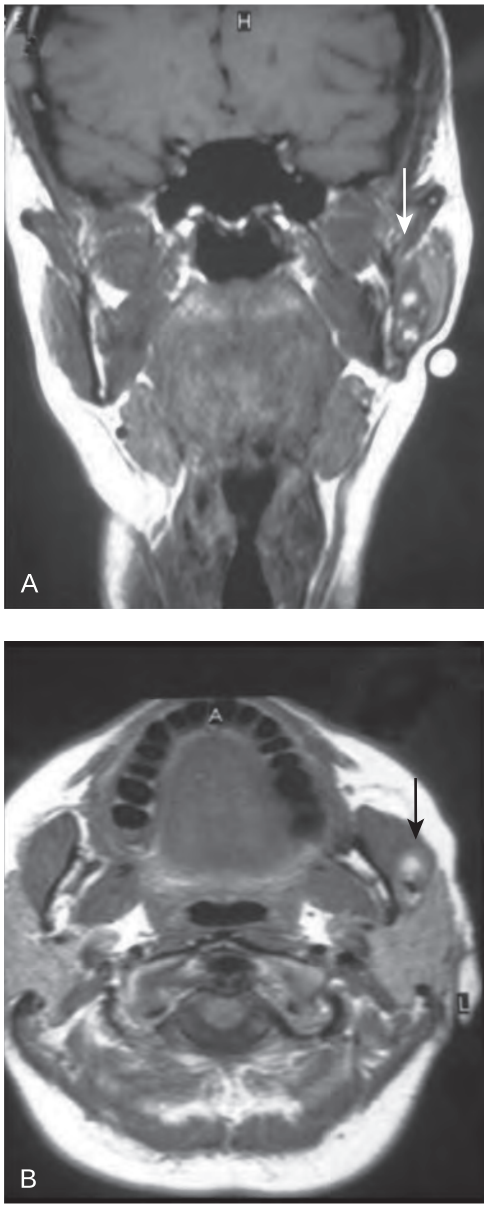

Figure 15.114 Postcontrast T1-weighted magnetic resonance imaging in coronal (**A**) and axial (**B**) views showing the hemangioma in the masseter muscle (*arrow*).

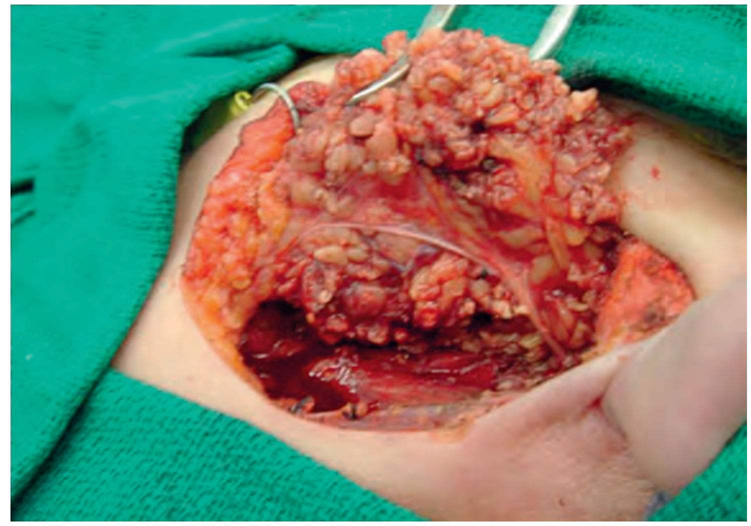

Figure 15.115 Dissection of the lower division of the facial nerve.

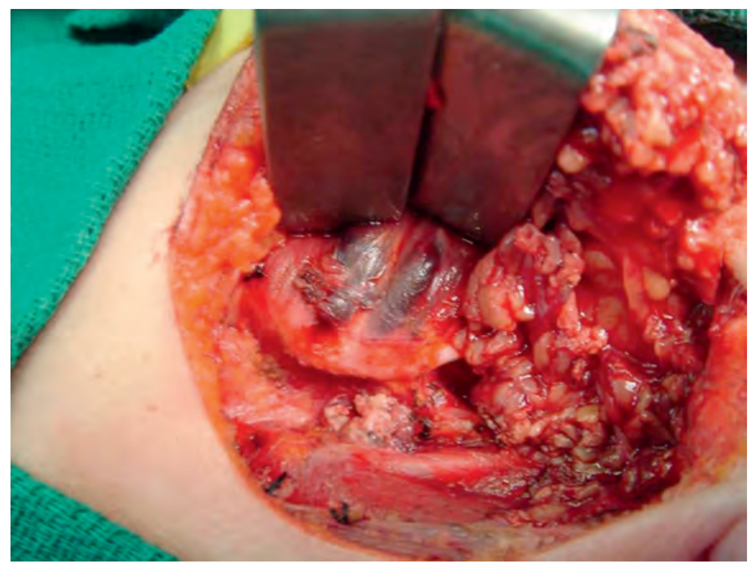

Figure 15.116 Exposure of the masseter muscle with retraction of the parotid gland.

Figure 15.117 Surgical specimen.

Hemangioma of the Parotid Gland

Hemangiomas occasionally occur adjacent to or within the salivary glands. The parotid is the most common site for hemangiomas in the salivary glands. A T2-weighted MRI scan in axial and coronal planes of a patient with hemangioma involving the deep lobe of the parotid gland is shown in Fig. 15.118. The tumor is multilobulated and appears to involve both the superficial and deep lobes of the parotid gland. This patient had previously undergone an attempted resection of this lesion, but without success. The surgical procedure requires a standard parotidectomy approach through a tragal incision (Fig. 15.119). The crucial step is the identification of the main trunk of the facial nerve. Once that is identified, dissection proceeds peripherally to trace out each of its branches (Fig. 15.120). It becomes apparent at this point that the entire lesion is located in the deep lobe, medial to the facial nerve. Meticulous dissection of the facial nerve is completed and the superficial lobe of the parotid gland is removed. Now, with the nerve in view, delicate dissection of the tumor from the deep lobe proceeds teasing out each of its loculations, with retraction of the branches of the facial nerve. The specimen is removed in a monobloc fashion with all its loculi removed. The surgical defect after removal of the hemangioma shows intact facial nerve and complete removal of the tumor (Fig. 15.121). A Penrose drain is inserted in the surgical defect, and the incision is closed in layers in the usual fashion.

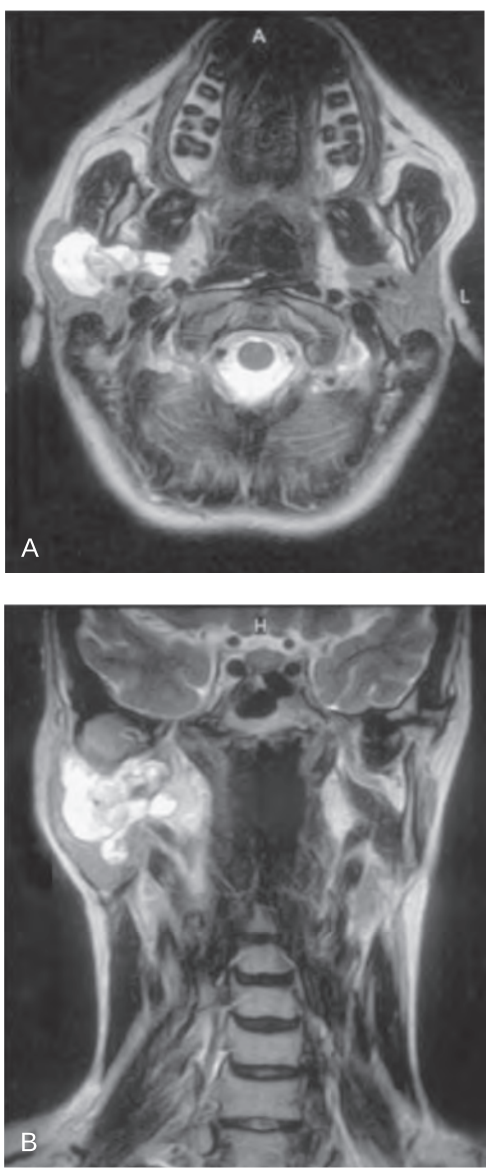

Figure 15.118 A T2-weighted magnetic resonance imaging scan in axial (**A**) and coronal (**B**) views showing a multilobulated hemangioma involving the superficial and deep lobe of the parotid gland.

Figure 15.119 Tragal incision for dissection of the facial nerve and excision of a hemangioma.

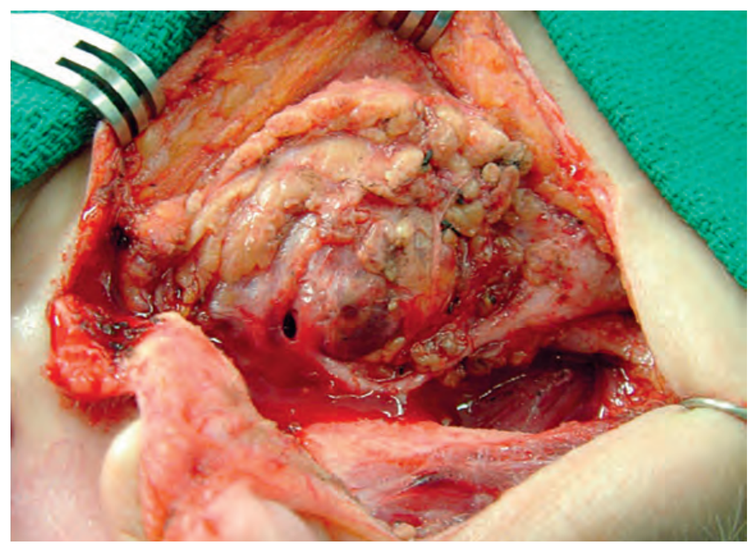

Figure 15.120 Deep lobe hemangioma extending to the superficial lobe between the upper and lower division of the facial nerve.

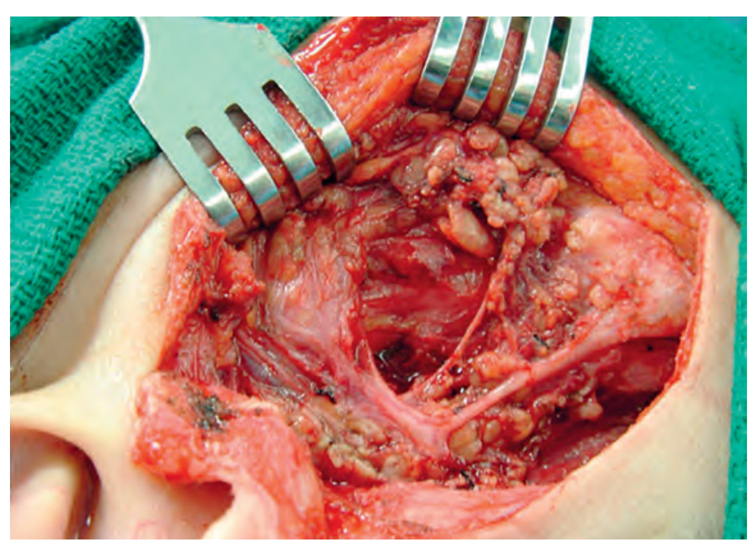

Figure 15.121 Surgical field following complete excision of the hemangioma and preservation of all branches of the facial nerve.

Massive Recurrent Hemangioma of the Chin

The patient shown in Fig. 15.122 had undergone several treatment modalities for an ulcerated bleeding hemangioma of the chin during the course of the previous 8 years. She previously had undergone three surgical procedures, external beam radiation therapy, and two attempts at embolization of this lesion through external carotid arteries bilaterally. In spite of these measures, because excision was incomplete in previous procedures, a massive, recurrent, fungating, ulcerated, bleeding hemangioma developed that involved the skin, underlying soft tissues, the musculature of the tongue, and the mandible.

Figure 15.122 A massive recurrent ulcerated bleeding hemangioma of the chin.

Preoperative radiographic studies included CT and MRI scans. A CT scan with contrast showed a massive soft tissue lesion of the chin anterior and posterior to the mandible in the floor of the mouth (Fig. 15.123). The bone window of the CT scan clearly demonstrates extension of this lesion into the mandible through its anterior cortex (Fig. 15.124). A sagittal MRI scan clearly shows extension of the lesion from the ulcerated skin

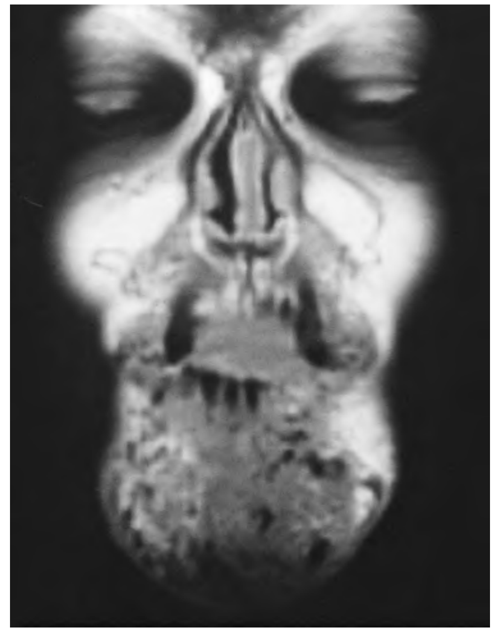

Figure 15.126 A coronal view of the magnetic resonance imaging scan shows a massive tumor of the chin.

through the underlying soft tissues and mandible, well into the musculature of the tongue (Fig. 15.125). Coronal MRI scans through the anterior soft tissues of the face shows a multiloculated spongy lesion involving the soft tissues of the chin from the skin to the musculature of the tongue (Fig. 15.126).

Surgical treatment of massive symptomatic hemangiomas such as this requires a through-and-through surgical resection to include the overlying skin, all the underlying soft tissues, the mandible, and a portion of the floor of the mouth and tongue to achieve a satisfactory and "complete" resection. Unless such a procedure is performed, the probability that the residual tumor will recur is exceedingly high. This patient underwent resection of this tumor, which entailed excision of a generous portion of the skin of the chin and upper part of the neck in continuity with the underlying soft tissues, resection of the mandible from the molar region on one side to the molar region on the opposite side, and amputation of the anterior half of the tongue to encompass the entire lesion in a monobloc fashion (Fig. 15.127).

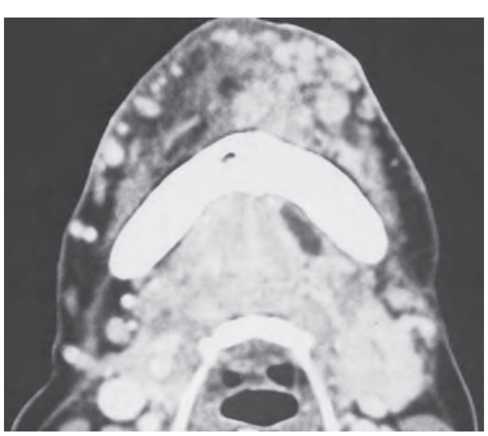

Figure 15.123 A computed tomography scan with contrast shows a multiloculated vascular lesion anterior and posterior to the mandible.

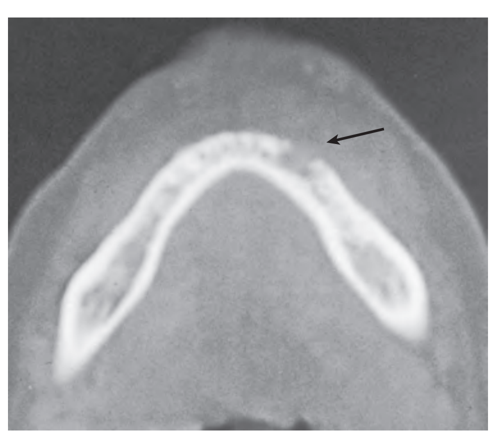

Figure 15.124 The bone window of the computed tomography scan showing invasion of the mandible by the tumor.

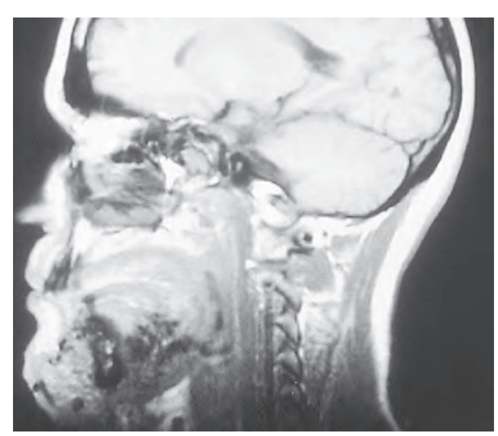

Figure 15.125 A sagittal magnetic resonance imaging scan showing involvement of the skin, soft tissues, mandible, and tongue.

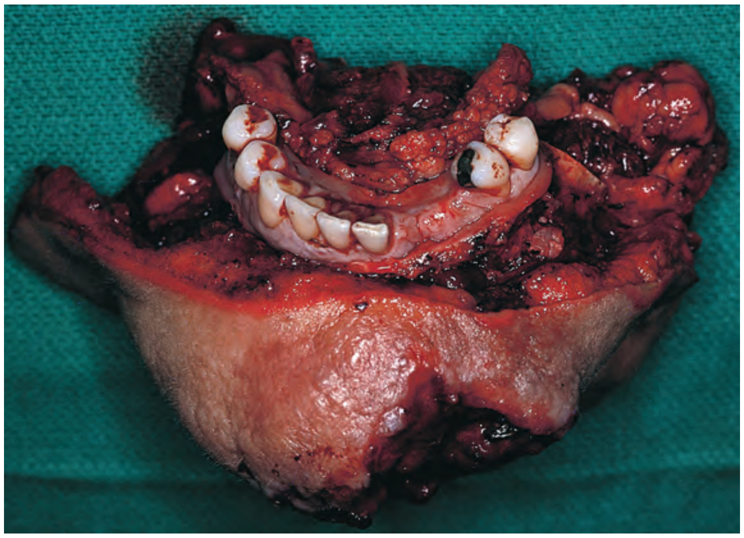

Figure 15.127 The surgical specimen of the tongue, mandible, and chin.

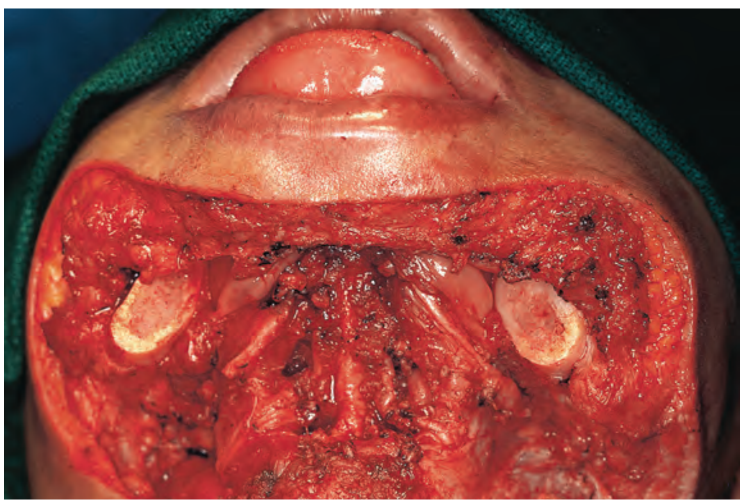

Figure 15.128 The surgical defect.

Figure 15.129 Postoperative appearance of the patient 3 months following surgery.

The surgical field shows a through-and-through defect from the skin to the posterior third of the tongue with stumps of the mandible on both sides (Fig. 15.128). Reconstruction of a surgical defect of this magnitude clearly requires microvascular free tissue transfer for reconstruction of the mandible and repair of the soft tissue and skin defects. This patient required two separate microvascular composite free flaps. A microvascular free fibula flap with soft tissue was harvested for reconstruction of the mandible and tongue, and a rectus abdominis musculocutaneous free flap was harvested for repair of the soft tissue and skin defect.

The appearance of the patient 3 months following surgery shows a well-healed rectus free flap overlying a reconstructed mandible with the fibula free flap (Fig. 15.129). This patient will need further surgery to improve her aesthetic appearance and the function of the resected portion of the tongue. She also required prosthetic support with fabrication of an obturator for the floor of the mouth to reduce the dead space and improve the clarity of her speech and her ability to swallow by mouth.

Angiosarcomas of the Skin

An angiosarcoma is a highly malignant lesion of vascular endothelial origin that most commonly affects the skin of the scalp. However, the lesion may arise in any part of the head and neck region and may present either as a nodular localized lesion or as a diffuse ecchymotic lesion involving the skin. The patient shown in Fig. 15.130 has a nodular lesion involving the skin of the nose with reasonably definable margins. Lesions such as this are suitable for surgical intervention and often will require radical resection, which may entail amputation of the nose. Adjuvant postoperative radiation therapy usually is recommended for improved local control.

In contrast, most angiosarcomas of the head and neck region present as diffuse ecchymotic areas involving a large surface of the scalp, temple, or forehead. The lesion usually has indistinct margins and often has skip areas with the appearance of a subdermal/subcutaneous hematoma. The lesion progresses in a circumferential fashion and advances from the vertex of the scalp inferiorly toward the temporal region and eventually to the skin of the forehead, periorbital region, cheek, chin, and neck.

The patient shown in Figs. 15.131 through 15.133 demonstrates progressive growth of angiosarcoma of the scalp leading to eventual death. The role of the surgeon in the management of this tumor is to establish tissue diagnosis by appropriate biopsies to map out the lesion. Treatment is generally nonsurgical and consists of either radiation therapy alone or in combination with chemotherapy. Chemotherapeutic agents such as paclitaxel, docetaxel, vinorelbine,

Figure 15.130 A nodular angiosarcoma of the dorsum of the nose.

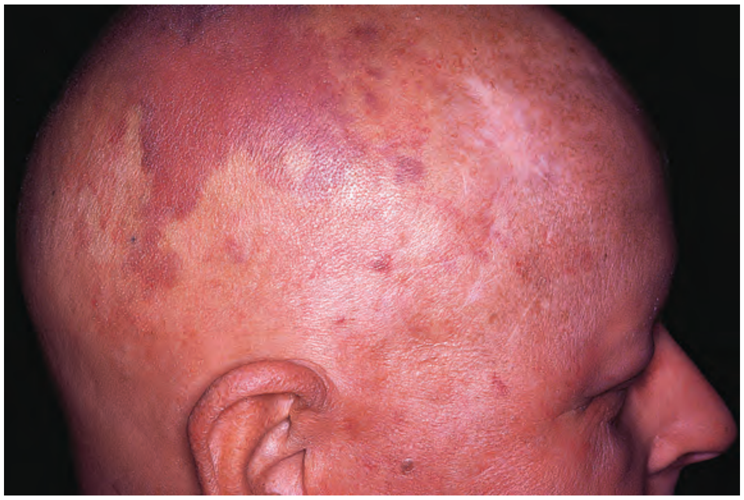

Figure 15.131 An ecchymotic angiosarcoma of the scalp.

Figure 15.132 The same patient as depicted in Fig. 5.133 2 months later.

Figure 15.133 Massive progression of the tumor in the same patient depicted in Figs. 15.131 and 15.132 over the subsequent year with involvement of the face and neck.

sorafenib, and bevacizumab have been shown to have activity against angiosarcoma. Major responses have been reported with pazopanib in selected patients with alterations in *VEGFR2* and *VEGFR3* genes. A very complex treatment plan is required with multiple electron fields to cover a large area of the scalp for radiotherapy. In spite of aggressive concurrent chemotherapy and radiotherapy, the overall prognosis for this highly malignant vascular tumor is poor.

TUMORS OF LYMPHATIC ORIGIN

Cystic Hygroma in a Child

Cystic hygromas and lymphangiomas are spongy multiloculated cystic lesions of the lymphatics that are congenital in nature. They usually present in early childhood but occasionally may manifest in adults. Excision of these lesions is indicated when a large lesion presents with obvious deformity or if a lesion causes compromise of function because of encroachment upon the airway or swallowing passages. The patient shown in Fig. 15.134 has a large cystic lesion occupying the upper part of the neck with extension to the parapharyngeal space, causing difficulty in swallowing. Imaging assessment of the lesion with either a CT scan or MRI is valuable in evaluating extension of this disease process in soft tissues.

Surgical excision of this lesion is performed under general endotracheal anesthesia. A transverse incision is taken through an upper neck skin crease (Fig. 15.135). The incision should be generous enough to provide adequate exposure to facilitate excision of all the loculations of the lesion. The skin incision is deepened through the platysma, carefully avoiding inadvertent entry into the underlying cystic spaces (Fig. 15.136). Meticulous attention should be paid to slow and delicate dissection during elevation of the skin flaps. Inadvertent entry into the loculations of the lesion will result in spillage of fluid and collapse of the cystic spaces, making its subsequent dissection difficult. Separation of the tissues with an electrocautery and traction on the skin flaps with sharp retractors open up a plane of dissection between the platysma and the lesion (Fig. 15.137). The upper and lower skin flaps are elevated far enough to expose the entire lesion.

Excision of the lesion begins by dissection over its surface, carefully separating it from the adjacent normal anatomic structures. If the loculations of the cystic lesion are too tense, then some fluid may be aspirated from the large loculus and the lesion made softer for ease of dissection. As dissection proceeds in a deeper plane, fibrous adhesions between the internal jugular vein and the loculations of the lymphangioma become apparent (Fig. 15.138). These adhesions are sharply divided. Minor venous communications between the internal jugular vein and the cystic spaces require clamping and ligation. During mobilization of the specimen, it should be borne in mind that the lesion has a tendency to extend through the intermuscular planes and to the parapharyngeal space. Thus it is important to proceed with patience to dissect out all of its loculi from all aspects of the lesion to accomplish total excision. Blood loss is usually minimal, because the lesion is relatively avascular.

The surgical field after complete excision of the cystic hygroma is shown in Fig. 15.139. Clearance of the soft tissues and the tumor overlying the carotid sheath has exposed several hyperplastic deep jugular lymph nodes, which are best left undisturbed. The wound is irrigated with a solution of Bacitracin in saline solution. A Penrose drain is inserted and the wound is then closed in two layers (Fig. 15.140). The surgical specimen shows a thin-walled multiloculated cystic lesion that contains brownish-yellow fluid (Fig. 15.141). The cystic spaces are lined by smooth, glistening epithelium. The postoperative appearance of the patient 1 year following surgery shows a well-healed scar (Fig. 15.142).

Figure 15.134 A patient with a large cystic lesion in the neck.

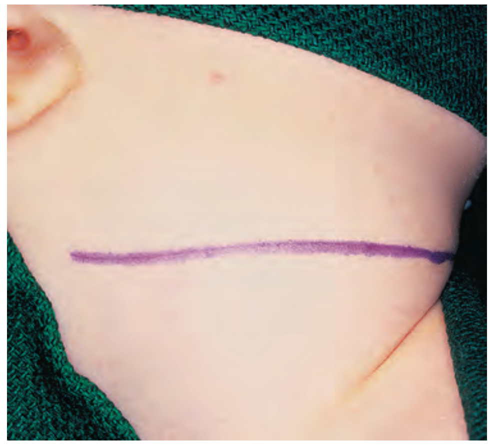

Figure 15.135 The incision is outlined.

Figure 15.136 The incision is deepened through the platysma.

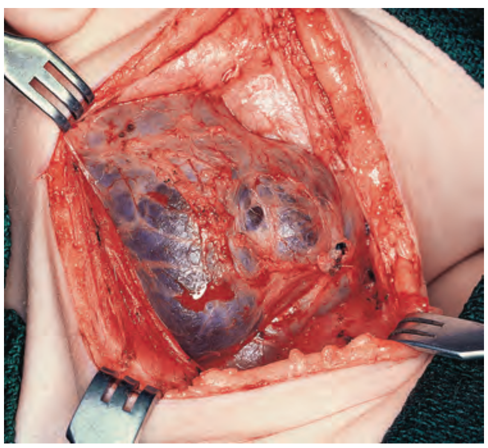

Figure 15.137 A plane of dissection is opened up between the platysma and the lesion.

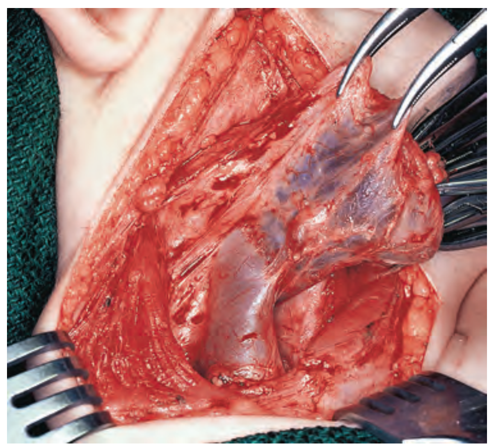

Figure 15.138 Fibrous adhesions between the internal jugular vein and the loculations of the lymphangiomatous process.

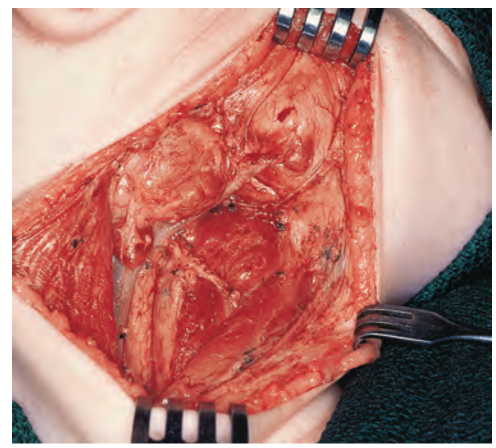

Figure 15.139 The surgical field after complete excision of the cystic hygroma.

Figure 15.140 The incision is closed in layers.

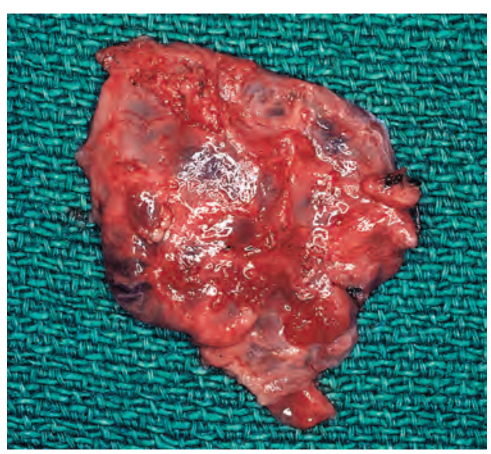

Figure 15.141 The surgical specimen.

Figure 15.142 Postoperative appearance of the patient 1 year following surgery.

Lymphangioma in an Adult

Lymphangioma is a benign tumor of the lymphatic system characterized by abnormal endothelial-lined vessels. These lesions may be frequently seen in the head and neck.

The patient described here previously had undergone two surgical procedures for excision of a cystic lesion in the upper part of the neck. However, it appears that each time the surgical excision was incomplete, leading to further recurrence of the tumor of larger dimensions. An axial view of the T2-weighted MRI scan shows a well-demarcated multiloculated cystic lesion involving the anterior triangle of the upper part of the neck on the right-hand side (Fig. 15.143). Note the bright white appearance, indicating the presence of fluid in the cystic lesion. Radiologic imaging with an MRI scan is crucial in these lesions to identify the extent of multiple loculations interdigitating within muscular planes and thus

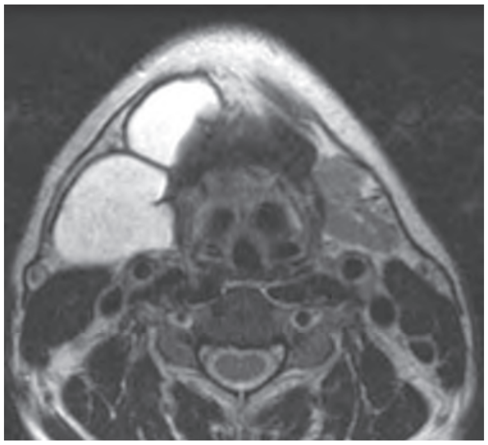

Figure 15.143 An axial view of a T2-weighted magnetic resonance imaging scan shows a multiloculated lymphangioma characterized by a bright white appearance.

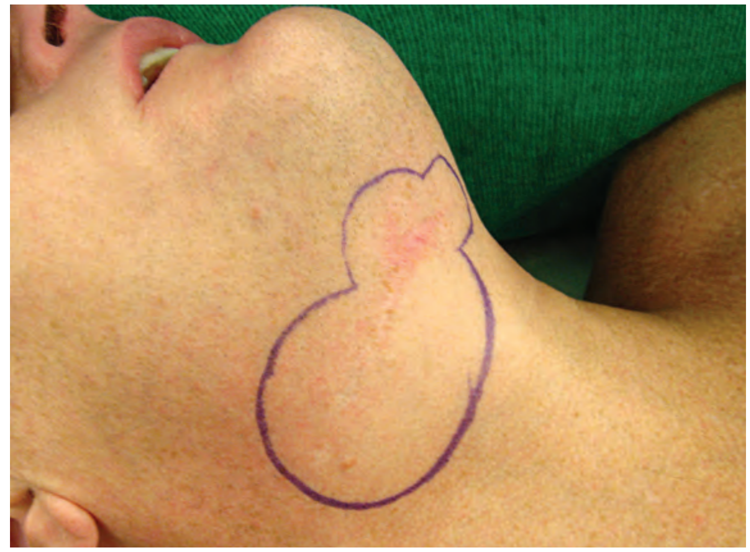

Figure 15.144 The palpable extent of the lesion is outlined on the patient.

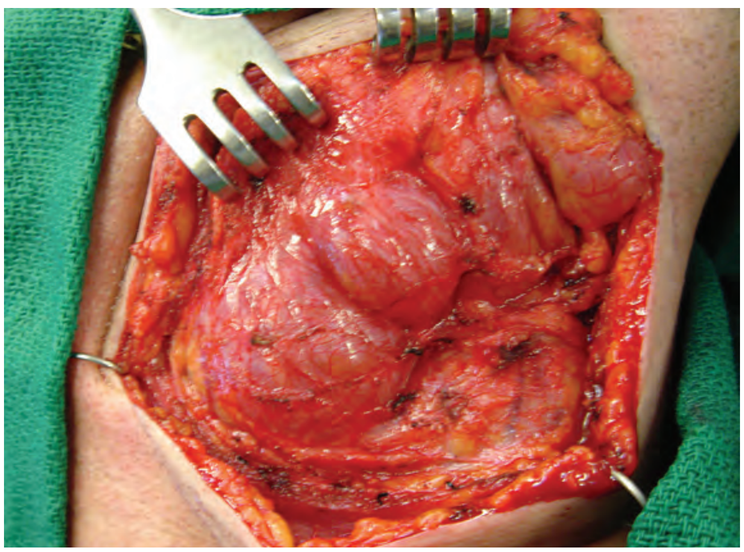

Figure 15.145 The surgical field showing a multiloculated lymphangioma.

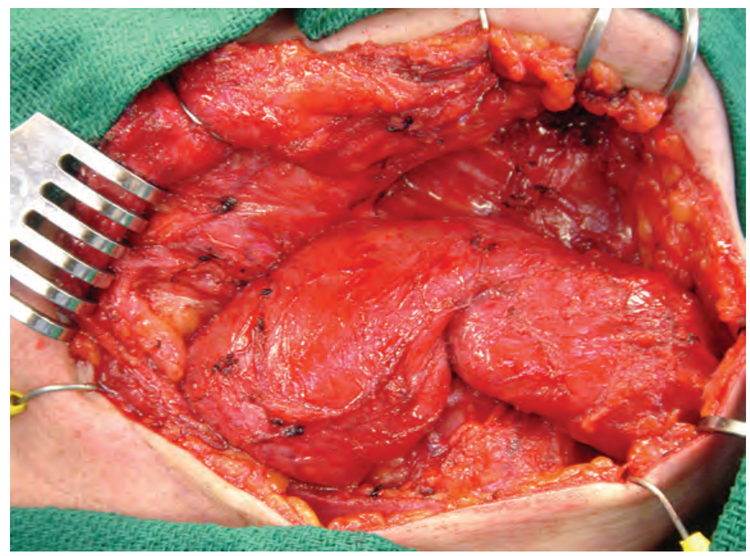

Figure 15.146 All loculi of the lymphangioma are dissected.

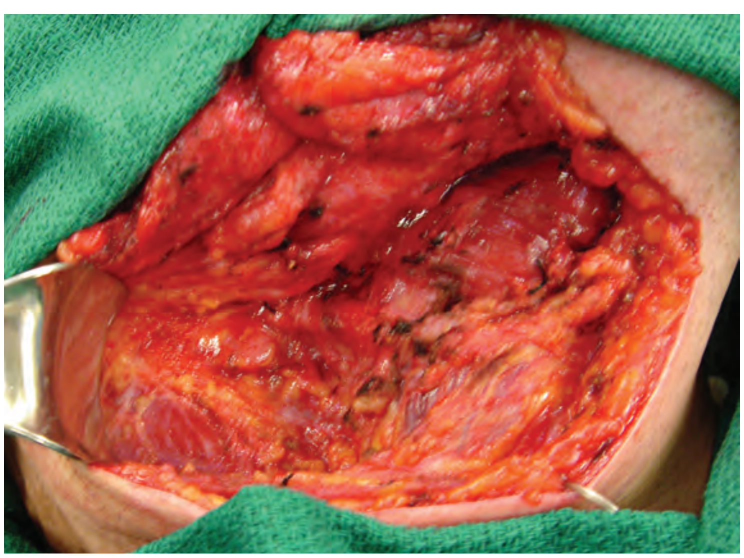

Figure 15.147 The operative field after complete excision of the lymphangioma.

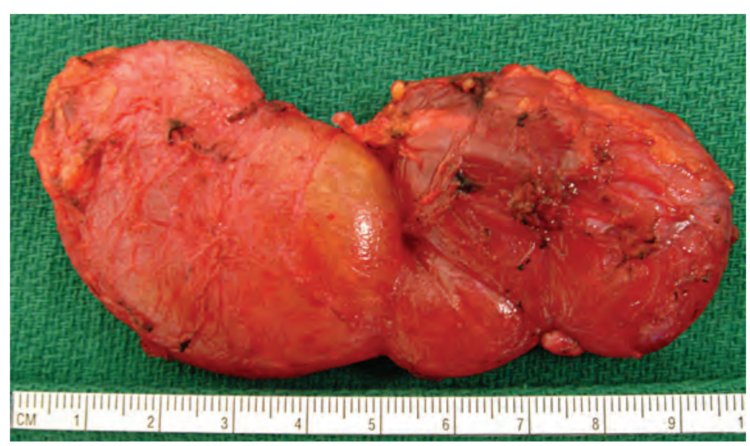

Figure 15.148 The surgical specimen showing an intact multiloculated cystic lymphangioma.

facilitating complete excision of the lesion without leaving any loculi or segments of the cyst wall behind.

The extent of the palpable lesion is depicted on the patient before surgery (Fig. 15.144). The surgical excision is performed through a transverse incision in the upper part of the neck, encompassing the scar of his previous surgery. The skin incision is deepened through the platysma, and upper and lower skin flaps are elevated. In elevating the skin flaps, it is crucial to be gentle and meticulous so as not to rupture the cystic lesion. Rupture of the lesion makes dissection of all the loculi of the multiloculated cystic process difficult and often leads to incomplete excision and eventual recurrence. Therefore extreme care should be exercised in preserving the integrity of the cyst wall to facilitate a complete excision.

As dissection proceeds, the loculated lesion comes into view (Fig. 15.145). Meticulous dissection then proceeds in tissue planes around the cystic lesion, gradually mobilizing each of its loculi and bringing it into the surgical field (Fig. 15.146). After all the loculi of the lesion are dissected out, it is removed in a monobloc fashion. The surgical defect shows complete clearance of the multiloculated cystic lesion (Fig. 15.147). Suction drains are placed and the skin incision is closed in layers. The surgical specimen shows a multiloculated cystic mass that is removed intact, ensuring its complete removal and thus permanent control (Fig. 15.148). Meticulous attention to detail for excision of all the loculations of the lymphangioma is essential for permanent control. Local recurrence of the lymphangioma is quite common if residual cyst lining is left behind.

TUMORS OF SMOOTH MUSCLE

Both benign and malignant tumors of smooth muscle origin arise in the head and neck region. Leiomyomas may present most frequently in the esophagus and pharynx, whereas leiomyosarcomas can arise in any part of the head and neck region. The surgical treatment for these lesions requires total excision of the tumor with adequate margins. Leiomyomas generally require a relatively conservative excision with total resection of the tumor, whereas leiomyosarcomas, which may be low or high grade, require a radical resection with adequate soft tissue margins.

Leiomyoma of the Cervical Esophagus

The patient whose barium swallow is shown in Fig. 15.149 has a smooth indentation in the lateral wall of the esophagus as a result of the presence of an intramural tumor. This patient presented with vague symptoms of difficulty in swallowing solid foods. Esophagoscopy failed to show any mucosal lesion in the lumen of the esophagus, but a smooth displacement of the esophageal wall was appreciated. The radiologic and endoscopic diagnosis of a leiomyoma was entertained.

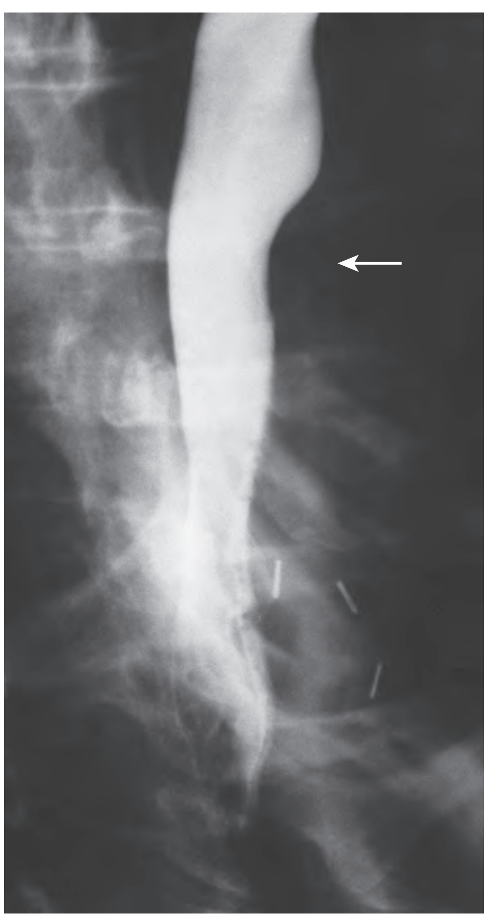

Figure 15.149 A barium swallow showing a smooth indentation from an intramural esophageal tumor (*arrow*).

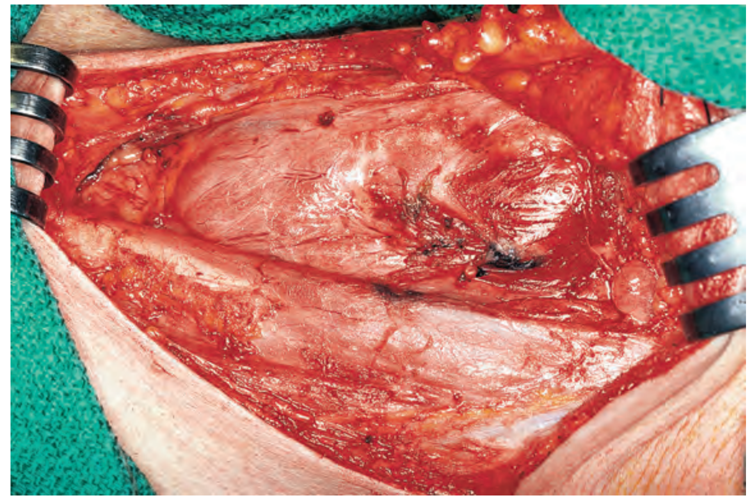

Figure 15.150 Division of the strap muscles on the left-hand side allows adequate exposure.

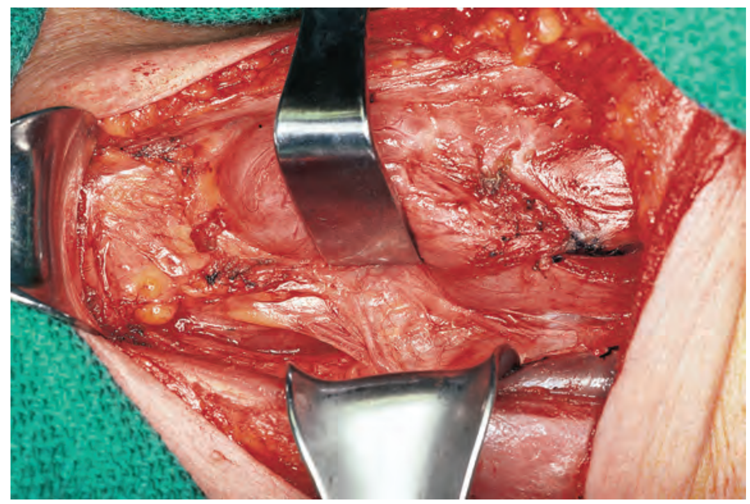

Figure 15.151 The prevertebral region is exposed.

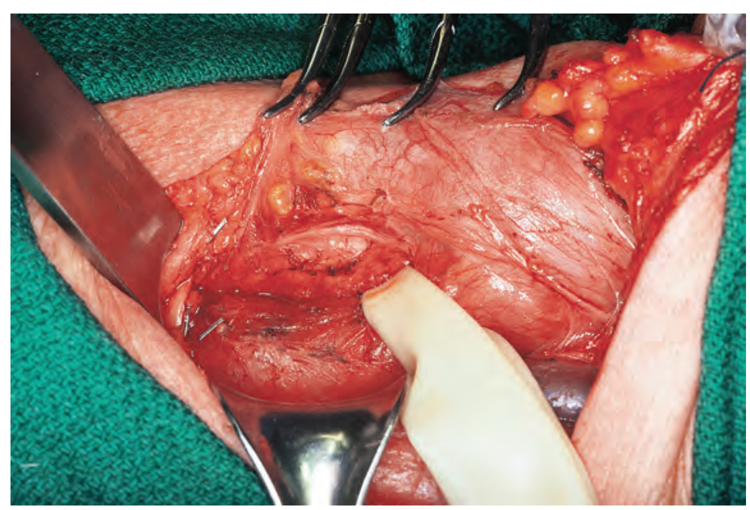

Figure 15.152 The esophagus is mobilized circumferentially.

Surgical exposure required a transverse incision at the level of the cricoid cartilage. The lesion presented on the left-hand side of the patient, and therefore the sternohyoid muscle on the left-hand side was excised to get better exposure (Fig. 15.150). After division of the middle thyroid vein and the capsular vessels of the thyroid gland,

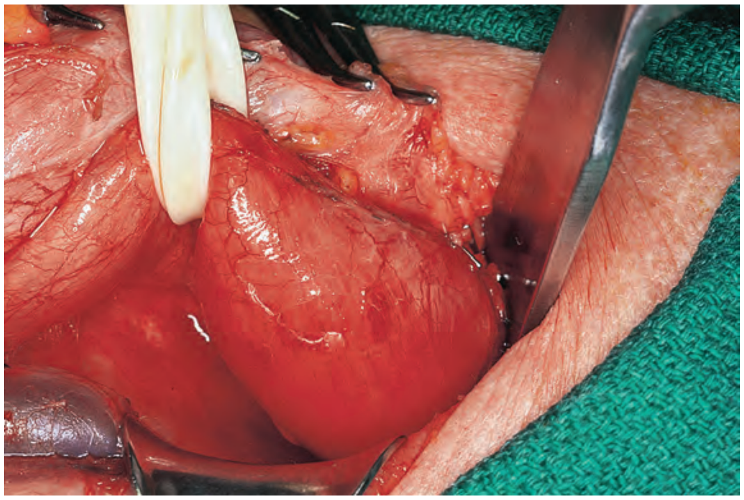

Figure 15.153 The cervical esophagus with the tumor is delivered into the wound.

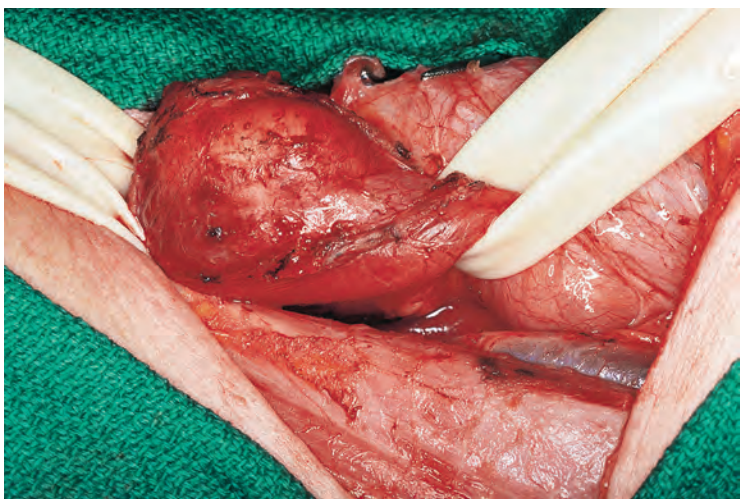

Figure 15.154 The pseudocapsule of the tumor is exposed.

the left thyroid lobe is retracted medially to expose the prevertebral region. The surgical field of the lower cervical region in the central compartment is shown in Fig. 15.151. The carotid sheath and the sternocleidomastoid muscle are retracted laterally. The lower skin flap is retracted caudad and the left thyroid lobe, larynx, and trachea are retracted medially. By alternate blunt and sharp resection, the esophagus is mobilized circumferentially (Fig. 15.152). Extreme care must be exercised in preserving the parathyroid glands and the recurrent laryngeal nerve during mobilization of the esophagus.

Once the esophagus is mobilized circumferentially, a Penrose drain is passed around it at its upper end near the cricoid cartilage to permit traction on the esophagus. By alternate blunt and sharp dissection, the upper thoracic esophagus is mobilized circumferentially and retracted cephalad to bring the tumor-bearing lower cervical and upper thoracic esophagus into the surgical field (Fig. 15.153). A smooth enlargement of the esophagus at the site of the tumor in a fusiform fashion can be appreciated easily. Care must be exercised during digital mobilization of the esophagus to avoid excessive manipulation and trauma to the esophagus.

An electrocautery is used to make a longitudinal incision along the long axis of the esophagus in its musculature. Careful, sharp dissection now is undertaken through the muscular wall of the esophagus up to the plane of the pseudocapsule of the tumor (Fig. 15.154). Once that plane is reached, adequate mobilization of the tumor is accomplished with sharp dissection using Metzenbaum scissors. The tumor can be enucleated easily

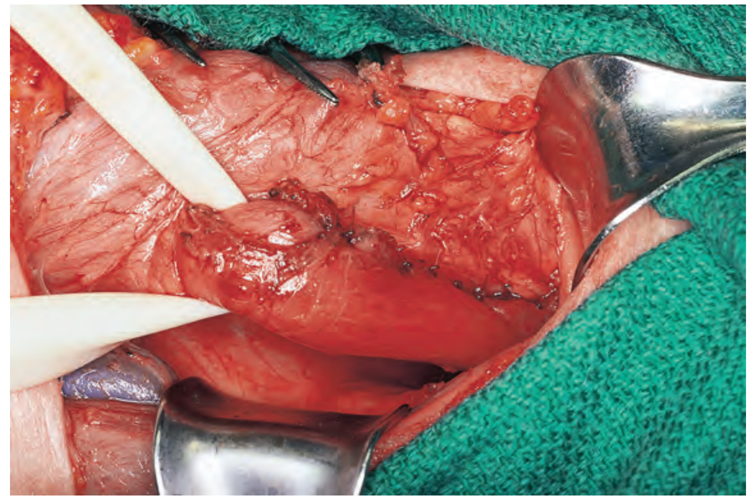

Figure 15.155 The esophageal mucosa prolapses through the muscular wall after excision of the tumor is complete.

Figure 15.156 The surgical specimen.

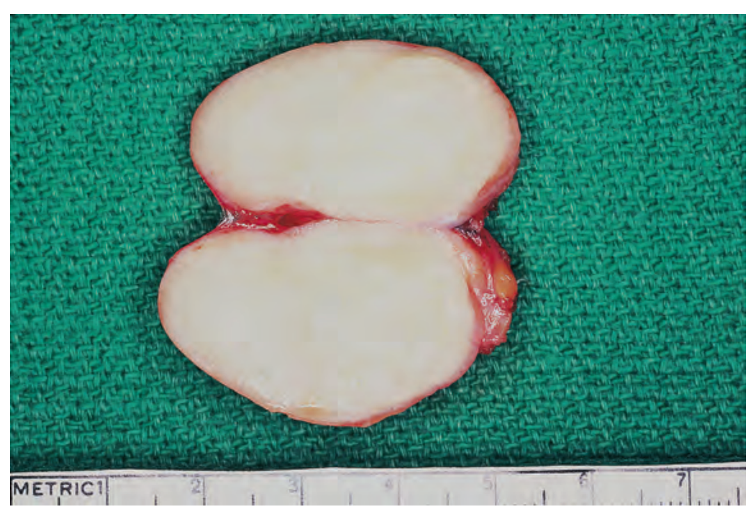

Figure 15.157 The cut surface of the tumor.

and safely from the muscular wall of the esophagus without injury to the mucosa. Meticulous attention is required to avoid entering the mucosa of the esophagus.

Once circumferential mobilization of the tumor is accomplished, it is excised in a monobloc fashion. The surgical defect shows prolapsing mucosa at the site of enucleation of the tumor and the incised and mobilized muscular wall of the esophagus (Fig. 15.155). The muscular wall of the esophagus is now repaired using 3-0 chromic catgut interrupted sutures. A nasogastric

feeding tube is inserted through the nasal cavity. A suction drain is placed into the wound, and the incision is closed in layers. The surgical specimen shown in Fig. 15.156 shows a complete monobloc excision of the leiomyoma of the esophagus with its intact pseudocapsule. Upon bisecting the specimen, a rubbery, white, pale tumor is seen, which is a characteristic appearance of this benign neoplasm (Fig. 15.157).

Postoperative care is relatively simple. The patient is not allowed to take anything by mouth for 1 week. Nasogastric tube feedings can begin as early as 24 hours after surgery. The suction drain is removed from the wound when drainage ceases. The risk of fistula formation is minimal, particularly if the mucosa is not violated. Because this tumor is benign, complete excision of the tumor is usually curative.

TUMORS OF STRIATED MUSCLE

Primary neoplasms of the striated muscle are rare. Benign rhabdomyomas are exceedingly uncommon and are rarely seen in the head and neck region. On the other hand, rhabdomyosarcomas are relatively common in the head and neck region in children, in whom they present as embryonal rhabdomyosarcoma (ERMS). ERMS is rarely seen in adults, in whom alveolar rhabdomyosarcomas are more common. The role of surgery in patients with ERMS is limited to excision of the residual or recurrent tumor after chemotherapy and radiation therapy have been administered.

Benign Rhabdomyoma

Although rhabdomyomas are rare in the head and neck area, they may be seen in the muscles of the floor of the posterior triangle of the neck or very rarely in the deep musculature of the tongue. The patient described here has a well-defined tumor in the base of the tongue just to the left of the midline. An axial view of the contrast-enhanced T1-weighted MRI scan shows that the multilobulated tumor is entirely submucosal and located within the deep musculature of the tongue (Fig. 15.158). A coronal view of the MRI scan shows that the tumor occupies a good part of the base of the tongue, extending from its lateral border at the glossotonsillar sulcus and crossing the midline to the right-hand side of the base of the tongue (Fig. 15.159). The tumor is well circumscribed with distinct margins. On palpation the tumor occupies the base of the tongue from the circumvallate papillae anteriorly up to the glossoepiglottic fold posteriorly. Laterally it extends up to the glossotonsillar sulcus and infiltrates into the musculature of the base of the tongue across the midline to the right-hand side.

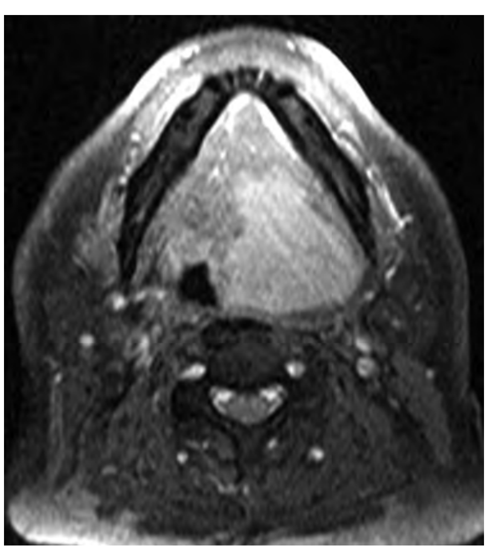

Figure 15.158 An axial view of a contrast-enhanced T1-weighted magnetic resonance imaging scan shows a large tumor in the base of the tongue.

Figure 15.159 A coronal view of the magnetic resonance imaging scan shows the tumor extending well beyond the midline of the base of the tongue.

Figure 15.160 A midline lower lip–splitting incision is planned.

The surgical approach for resection of this tumor requires a median labiomandibular glossotomy (Trotter's operation). This approach preserves the blood supply and nerve supply to the lip, mandible, and tongue on both sides but provides wide exposure for en bloc excision of the multilobulated tumor of the base of the tongue. A midline lower lip–splitting incision is placed and extended up to the level of the hyoid bone (Fig. 15.160). The skin incision is deepened through the labial mucosa up to the mandible, leaving a short cuff of approximately 8 mm at the gingivolabial sulcus. Short cheek flaps are elevated, lifting off the lower lip from the anterior cortex of the mandible on both sides but remaining medial to the mental foramina. An angled osteotomy is performed between the two lower incisor teeth, carefully preserving the sockets of both teeth, with use

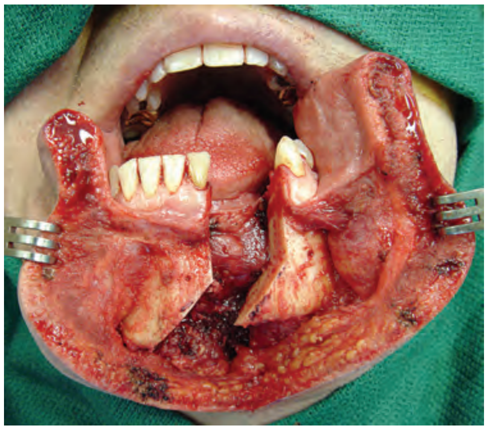

Figure 15.161 An angled mandibular osteotomy is performed.

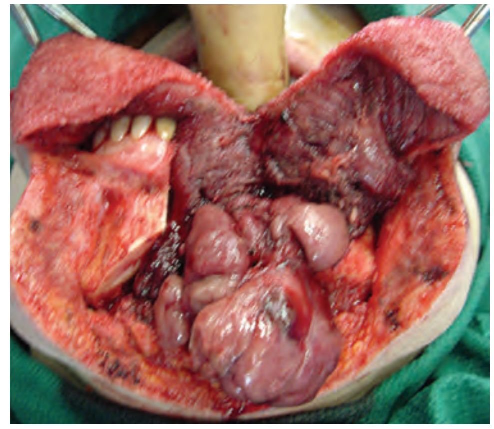

Figure 15.163 The tumor is delivered into the wound by digital pressure on the base of the tongue.

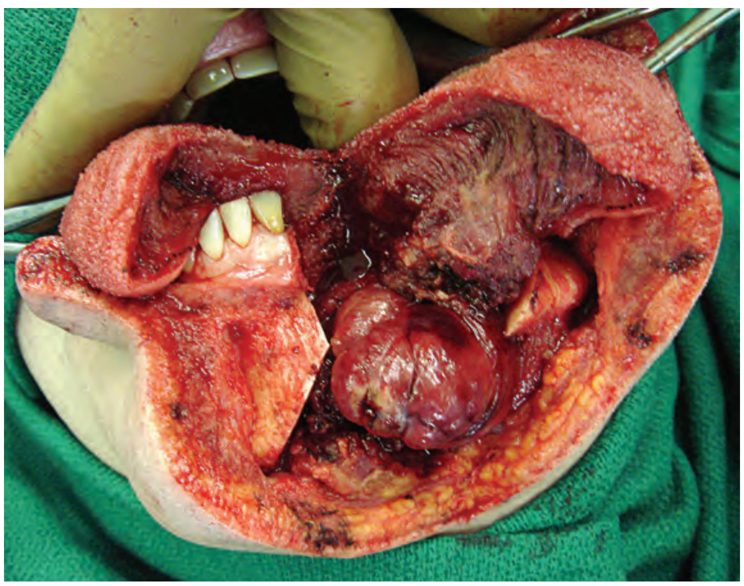

Figure 15.162 A midline glossotomy brings the tumor into view.

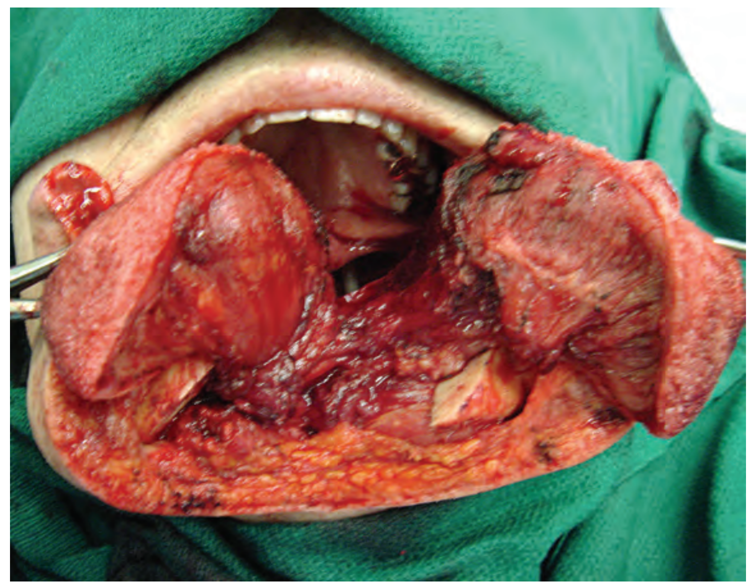

Figure 15.164 The surgical defect after removal of the tumor.

of a fine sagittal saw. The osteotomy is performed in an angled fashion to prevent cephalocaudad displacement of the mandible.

Once the bone is completely divided, bone wax is used to secure hemostasis through the cut ends of the bone. Dissection now proceeds exactly in the midline, remaining between the openings of Wharton's ducts on both sides. A mucosal incision is made from the attached gingiva along the frenulum of the tongue in the midline, keeping the opening of Wharton's ducts intact on both sides. The mucosal incision is deepened to expose the underlying muscles of the floor of the mouth (Fig. 15.161). The mucosal incision in the floor of the mouth is now extended farther to the undersurface of the anterior third of the tongue up to the tip of the tongue. The tongue is now divided exactly in the midline through a mucosal incision on its dorsum up to the circumvallate papillae, splitting the two halves through the midline along the fatty plane between the deep musculature of the tongue. The two halves of the tongue are retracted laterally, exposing the anterior surface of the well-encapsulated tumor (Fig. 15.162).

Extreme caution should be exercised to ensure that the pseudocapsule of the tumor is not breached, allowing it to be removed in an intact fashion. Dissection of the tumor is further facilitated by pushing the tumor out into the surgical field with the index finger of one hand, pushing the mucosa of the base of the tongue in its posterior third anteriorly to facilitate delivery of the tumor (Fig. 15.163). Meticulous dissection is undertaken through the deep muscles of the tongue, remaining around the pseudocapsule of the tumor, to deliver each of its lobules to facilitate complete excision. The intact tumor is excised in a monobloc fashion.

After excision of the tumor, the surgical defect shows the dead space in the deep muscles of the tongue, with the two halves of the tongue remaining completely viable and neurologically intact (Fig. 15.164). A two-layered closure is performed to reapproximate the deep muscles of the tongue and the mucosa of the tongue from the glossoepiglottic fold posteriorly up to the tip of the tongue anteriorly. Similarly, the mucosa of the floor of the mouth is closed with interrupted chromic catgut sutures. The mandibulotomy is repaired with miniplates and screws applied in two planes. One four-hole plate is used on the lateral cortex of the mandible, and another four-hole plate is used on the undersurface of the mandible at the site of the mandibulotomy. A Penrose drain is inserted between the anterior bellies of the digastric muscle in the deep muscular space of the mylohyoid muscle, and this drain is brought out through the skin incision in the submental region.

Figure 15.165 The appearance of the patient 1 year after surgery shows excellent healing of the scar, retained complete dentition, and mobility of the tongue.

The appearance of the patient 1 year following surgery shows an excellent aesthetic result with a barely visible midline lower lip–splitting scar (Fig. 15.165). The patient's ability to open his mouth and protrude his tongue out of the oral cavity remains normal. His speech, mastication, and swallowing are completely restored. A median labial mandibular glossotomy provides excellent exposure for removal of intramural lesions of the deep musculature of the tongue. Because a rhabdomyoma is a benign tumor, a long-term cure is expected in this patient.

Rhabdomyosarcoma

Malignant tumors of the striated muscle such as rhabdomyosarcoma and ERMS are more common than benign rhabdomyomas. ERMS generally affects patients in the pediatric age group and presents as a rapidly growing soft tissue mass lesion in any part of the head and neck region. The face, the periorbital region, the cheek, and the parotid region are common sites (Fig. 15.166). ERMS tumors also occasionally occur in adults.

Tissue diagnosis generally is accomplished with an open biopsy, whereby adequate tissue is harvested for accurate histopathologic diagnosis. Alternatively, a Tru-Cut biopsy also is sufficient for accurate tissue diagnosis in most instances. In the pediatric age group, surgery is not the preferred treatment. Initial treatment consists of multidrug chemotherapy, followed by radiation therapy. Surgery is only considered for disease that is persistent or residual after definitive treatment with chemotherapy and radiation therapy. In the adult population, the response to chemotherapy and radiation therapy is not as good as that observed in the pediatric age group. Therefore surgery often is necessary and is considered to be the definitive treatment in the adult population. Principles of soft-tissue sarcoma surgery should be used for resection. However, in the head and neck region, the extent of surgical resection often is dictated by the proximity of structures such as the orbit, skull base, temporal bone, carotid artery, and cranial nerves that affect vital functions.

TUMORS OF NERVE CELL ORIGIN

Tumors of nerve cell origin arise anywhere in the head and neck area. Both benign and malignant neurogenic tumors may present as solitary or multiple lesions. Neurogenic tumors of lower cranial nerves and neurovascular tumors are discussed in Chapter 14. Benign neurofibromas in patients with neurofibromatosis type I (von Recklinghausen disease) are quite common and usually do not require surgical intervention unless they impinge on vital functions, are painful, or are aesthetically disfiguring. However, these patients can also develop malignant peripheral nerve sheath tumors (MPNST), which are very aggressive. Neurofibromatosis type 2 is characterized by bilateral vestibular schwannomas, meningiomas, ependymomas, and cataracts. Schwannomas usually are solitary and may occur in the head and neck region, arising from the lower cranial nerves and cervical or brachial plexus. These tumors grow very slowly and often are asymptomatic. Therefore the need for surgical intervention must be carefully weighed against the functional impact of neurologic deficit after surgery.

Neurofibromas

Neurofibromas present as either solitary or multiple subcutaneous tumors. They may present as a solitary lesion, or they may

Figure 15.166 An embryonal rhabdomyosarcoma of the right cheek.

Figure 15.167 A solitary neurofibroma of the right external ear.

Figure 15.168 A multifocal plexiform neurofibroma.

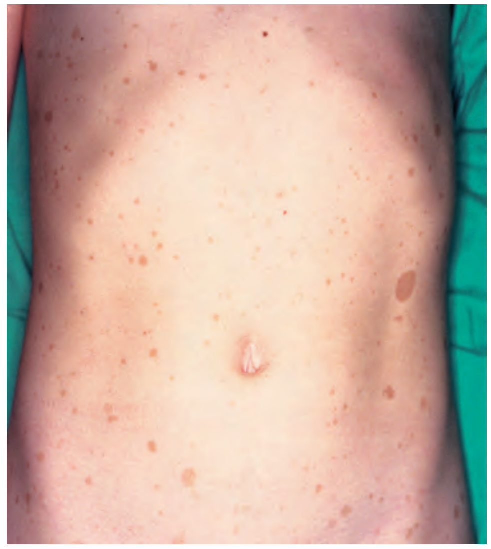

Figure 15.169 Café au lait spots on the trunk in a patient with von Recklinghausen disease.

Figure 15.170 A 3-year-old patient with a massive plexiform neurofibromatosis of the right-hand side of the face and neck.

present as multiple tumors in patients with von Recklinghausen disease. The patient shown in Fig. 15.167 is a child with a solitary neurofibroma involving the right external ear and partially obstructing the external auditory canal. The tumor involves the overlying skin but does not cause any destruction of the underlying cartilage. Surgical excision is indicated in this patient for preservation of the patency of the auditory canal and for aesthetic reasons. Simple surgical excision with skin graft reconstruction is satisfactory in this setting.

Plexiform neurofibroma is a variant of neurofibroma that presents in a diffuse manner, virtually pathognomonic for NF1, sometimes involving large areas of the skin and soft tissues of the head and neck region. The patient shown in Fig. 15.168 has a multifocal plexiform neurofibroma presenting in the periorbital region and forehead on the right-hand side. These lesions are soft in consistency and involve the overlying skin but usually are mobile over the deeper soft tissues and facial skeleton. Conservative local excision generally provides satisfactory control of the tumors. However, with large and multifocal lesions, total excision may not be achievable and subtotal excision with preservation of vital organs and structures to preserve or improve function or aesthetic appearance is acceptable.

Patients presenting with neurofibromas should have a complete history and physical of the entire body to look for multiple lesions. Presence of café au lait spots confirms the diagnosis of von Recklinghausen disease (Fig. 15.169). Large plexiform neurofibromas presenting in the pediatric age group are managed with significant caution, care, and judgment regarding the need and timing for surgical intervention. Lesions compromising the airway or vision or obstructing the pharyngoesophageal passage should be addressed on an urgent basis to retain function. On the other hand, larger lesions that are not compromising any vital structures or functions may simply be observed, and surgery should be considered at an appropriate time when it is safe to proceed with a major surgical resection.

The patient shown in Fig. 15.170 was born with a plexiform neurofibroma involving the lower half of the face and the upper part of the neck on the right-hand side. She required a tracheostomy to maintain a satisfactory airway at the age of 9 months. She is shown here at age 3 years with normal growth but with significant aesthetic deformity in the lower part of the face and neck on the right-hand side. Because no vital functions were

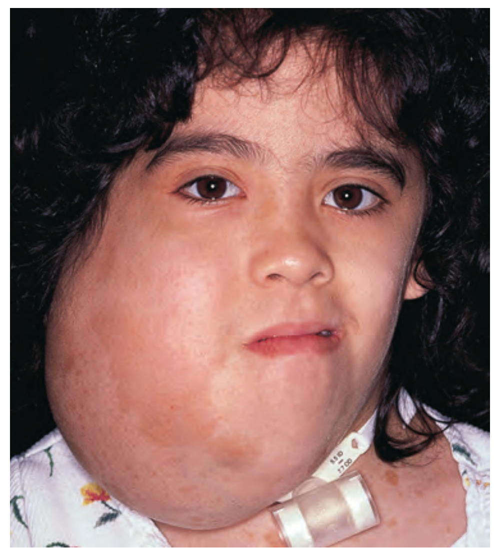

Figure 15.171 The same patient depicted in Fig. 15.139 5 years later showing considerable progression of the lesion.

compromised and because she had normal growth and the ability to swallow normally, surgical intervention was not entertained at that age. The patient remained under clinical surveillance with annual radiologic studies.

Surgical intervention was planned at age 8 years because of increasing peer pressure at school and a somewhat rapid growth of the tumor observed in the previous year (Fig. 15.171). An MRI scan in the coronal plane shows a massive tumor involving the right side of the face, right parapharyngeal region, parotid region, infratemporal fossa, skull base, and extension to the middle cranial fossa. The internal carotid artery is encased by the tumor on the right-hand side (Fig. 15.172). An axial view of the MRI scan again demonstrates a massive tumor literally occupying the right half of the craniocervical junction (Fig. 15.173).

The planned surgical procedure included subtotal resection of the tumor without compromise of cranial nerves or the carotid artery to reduce as much of the tumor volume as possible and thus improve the contour of the face in this child. The patient is shown on the operating table in Fig. 15.174. Note the pigmentation of the skin overlying the tumor with the presence of the tumor through the auditory canal and the region of the parotid

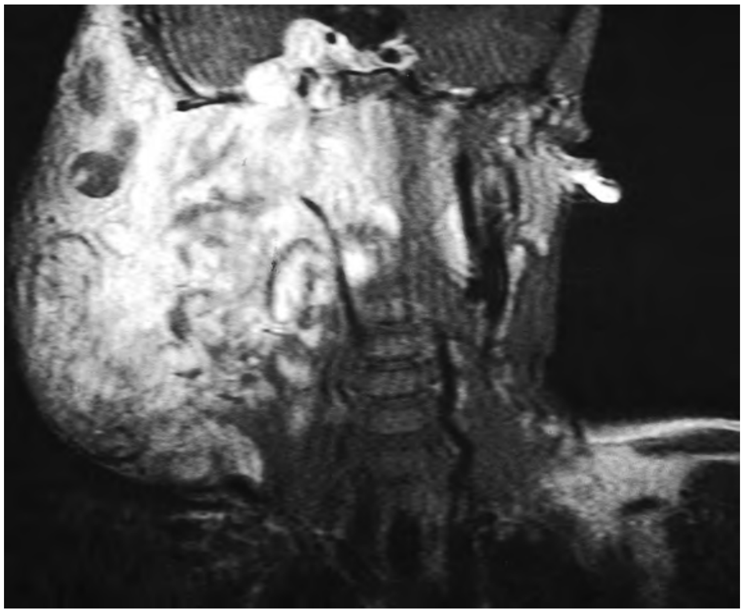

Figure 15.172 A coronal view of the magnetic resonance imaging scan demonstrating intracranial extension of the massive tumor that encased the internal carotid artery.

Figure 15.174 The tumor also involved the auditory canal, parotid region, and retromandibular area.

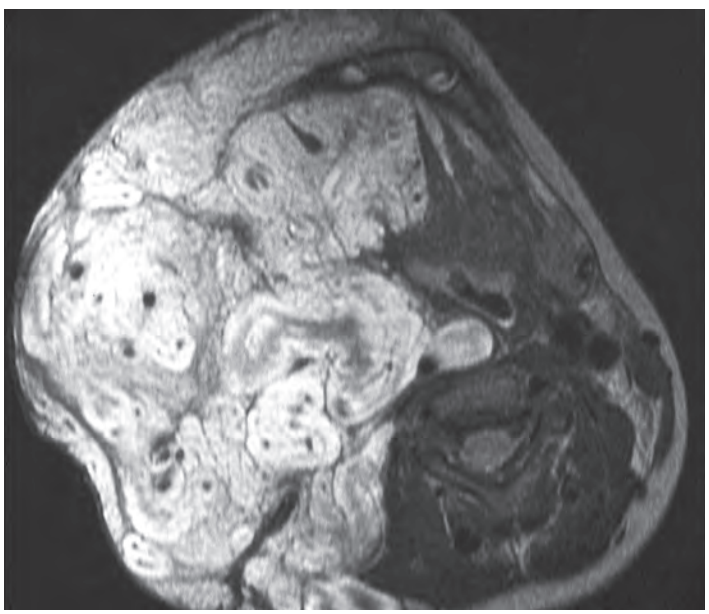

Figure 15.173 An axial view of the magnetic resonance imaging scan.

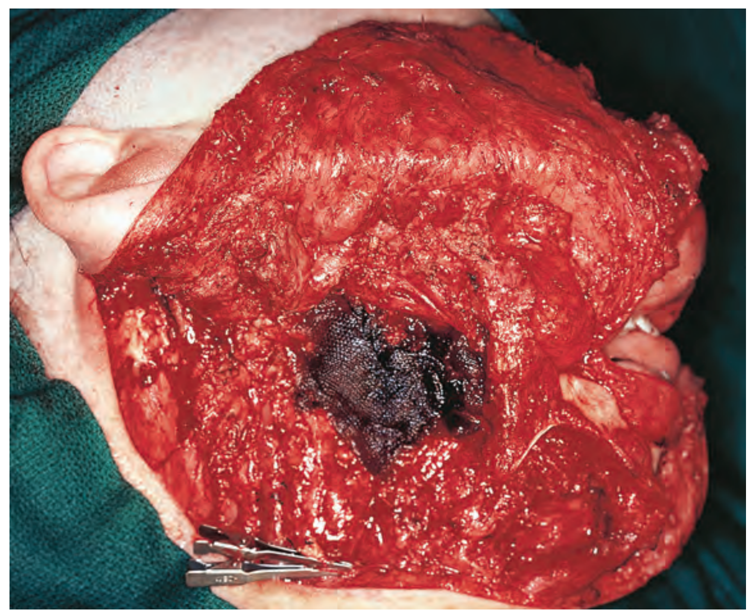

Figure 15.175 The surgical defect after subtotal excision of the tumor.

bed and the retromandibular area as well as the entire craniocervical junction. The surgical procedure entailed resection of a generous portion of the skin overlying the tumor along with excision of the tumor but preserving vital structures. A rectus abdominis muscle free flap was used to fill the dead space created by removal of the tumor to restore facial contour.

During surgery it became apparent that the tumor had involved multiple cranial and cervical nerves, with the cutaneous branches of the cervical plexus measuring as much as 5 to 7 mm in diameter. The great auricular nerve measured 6 mm in diameter, and the lower divisions of the facial nerve each measured approximately 4 mm in diameter. Extremely tedious dissection had to be undertaken to preserve the facial nerve and other lower cranial nerves in the neck. Volume reduction of the tumor by subtotal excision was accomplished (Fig. 15.175). Note that the angle of the mandible and the posterior part of the body of the mandible were scalloped with a concave deformity because of compression from the tumor that occupied that space.

The surgical specimen shown in Fig. 15.176 demonstrates a multilobulated tumor with numerous subcutaneous nerves, each of which measures several millimeters in diameter. A postoperative MRI scan shows residual tumor encasing the internal carotid artery on the right-hand side, as well as the rectus abdominis muscle flap used to fill the dead space and restore contour (Fig. 15.177). The final pathology report of the surgical specimen confirmed the diagnosis of a benign plexiform neurofibroma. The appearance of the patient 5 years after surgery is shown in Fig. 15.178. In spite of preservation of the facial nerve, function of its lower division did not return. This patient may require further surgical intervention as she grows older, depending on the presenting symptoms and physical findings.

Schwannoma of the Cervical Plexus

Schwannomas (also referred to as *neurilemmomas* in the past), like neurofibromas, present as rubbery, nodular, solid tumors that may

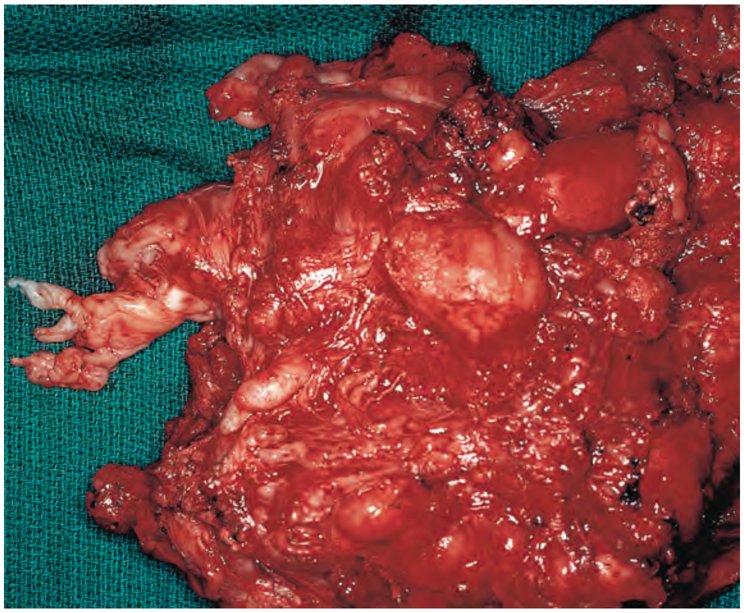

Figure 15.176 The surgical specimen.

be well defined if they are superficial or may be less well defined if they are deeply situated. Schwannomas of the cranial nerves and peripheral nerves are relatively common benign neoplasms that usually are discovered on routine physical examination. Rarely, these lesions are symptomatic, with symptoms related to nerve involvement leading to paresthesias, pain, or muscle weakness.

The patient described here has an ill-defined firm mass with reduced mobility in the left supraclavicular region that was discovered accidentally during a routine physical examination. A contrast-enhanced CT scan shows a well-encapsulated tumor that does not enhance well with contrast and shows areas of central necrosis (Fig. 15.179). A needle biopsy of the tumor showed spindle cells, suggestive of a neurogenic tumor. The nerve and the site of origin are difficult to assess from imaging studies, although this tumor may be a neurogenic tumor from the cervical plexus or the brachial plexus.

The plan of surgical excision required a transverse incision in the floor of the posterior triangle of the neck on the left-hand side. The extent of the palpable abnormality is depicted on the patient (Fig. 15.180). The skin incision is deepened through the platysma, and the upper and lower skin flaps are elevated. It soon becomes apparent that the tumor is located deep to the posterior border of the sternocleidomastoid muscle (Fig. 15.181). Meticulous dissection is undertaken around the tumor to mobilize it from adjacent structures (Fig. 15.182). As dissection proceeds medially, it becomes apparent that the tumor is arising from the cervical plexus. Meticulous dissection proceeds proximally as far as the exit of the involved cervical root from the neural foramen at the lateral aspect of the vertebral column (Fig. 15.183). Dissection of the tumor continues medially beyond its medial margin until a cervical root of normal dimension is identified.

Because this tumor is arising from the cervical plexus, no neurologic deficit is anticipated other than anesthesia of the skin of the neck, and therefore the cervical root is transected, allowing delivery of the tumor intact. The surgical defect after removal of the tumor shows the transected stump of the cervical root posterior to the carotid sheath exiting from the neural foramen (Fig. 15.184). Complete hemostasis is secured, and the wound is closed in two layers after placement of a suction

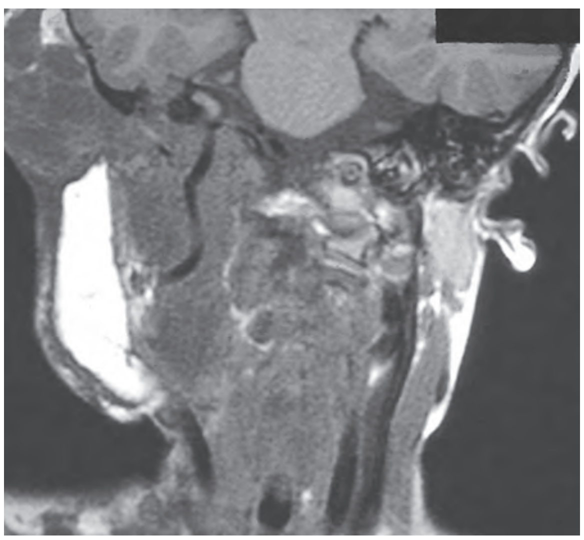

Figure 15.177 A coronal view of the postoperative magnetic resonance imaging scan shows the viable rectus abdominis flap and the extent of the residual tumor.

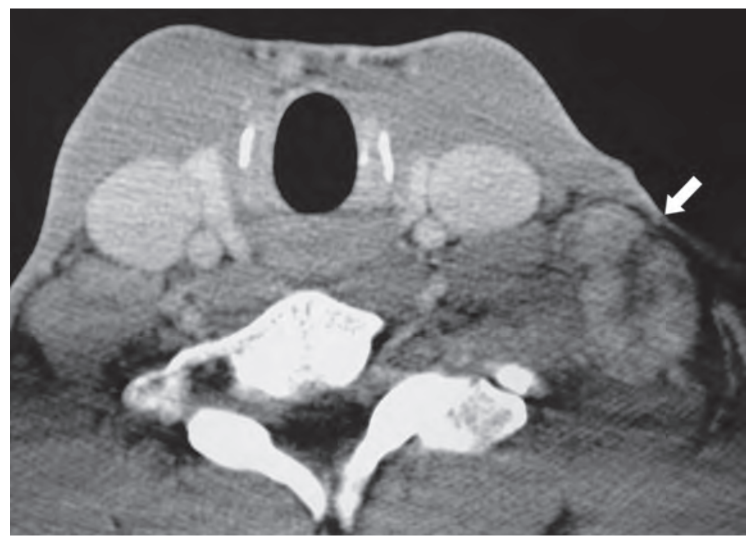

Figure 15.179 A contrast-enhanced axial view of the computed tomography scan shows a relatively avascular tumor with areas of central necrosis (*arrow*).

Figure 15.178 The appearance of the patient 5 years after surgery.

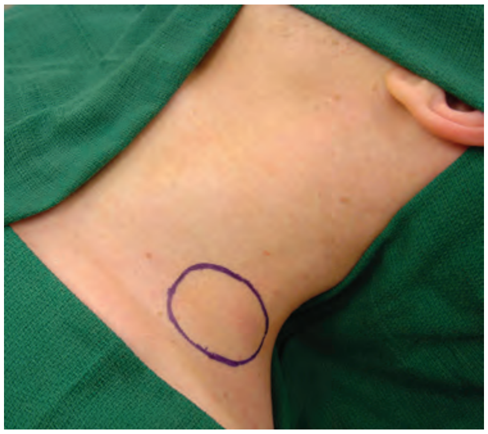

Figure 15.180 The palpable extent of the tumor is demarcated on the patient.

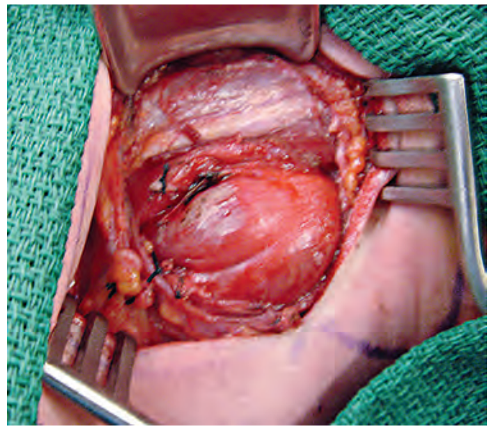

Figure 15.181 The tumor is located deep to the posterior border of the sternocleidomastoid muscle.

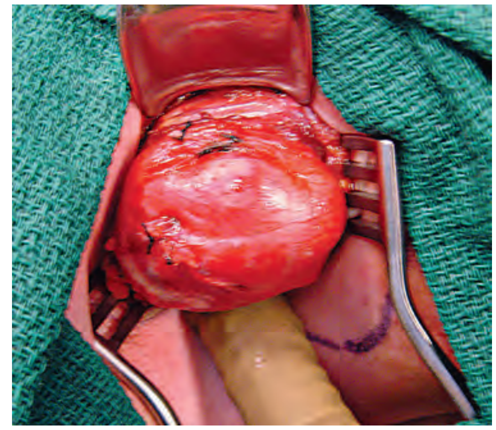

Figure 15.182 The tumor is mobilized circumferentially, maintaining an intact capsule.

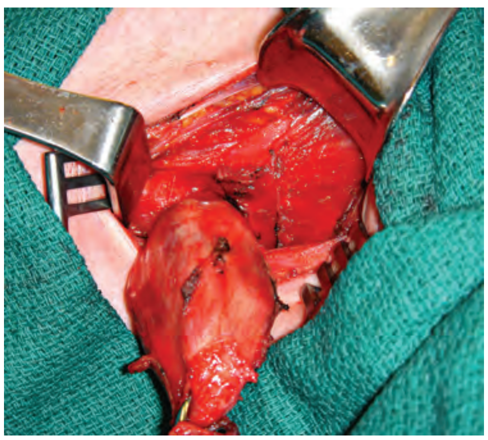

Figure 15.183 Medially the tumor is seen arising from a root of the cervical plexus.

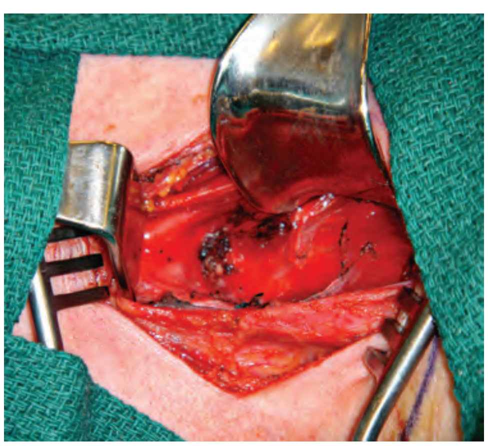

Figure 15.184 The surgical defect showing a transected cervical root at the neural foramen.

drain. The bisected surgical specimen shows a spindle-shaped tumor that is pale with hemorrhagic areas, typical of a neurogenic tumor (Fig. 15.185). Histologic analysis of the tumor confirmed the diagnosis of a benign schwannoma.

Schwannoma of the Brachial Plexus

The patient described here was found to have a right supraclavicular mass during a routine physical examination. The mass

Figure 15.185 The bisected surgical specimen shows the characteristic appearance of a schwannoma.

was firm in consistency and mobile over the deeper soft tissues in an anteroposterior plane. A fine-needle aspiration biopsy of the mass confirmed the presence of spindle-shaped cells, suggestive of a tumor of neurogenic origin. An axial view of the MRI scan shows a well-circumscribed tumor that is bright on the T2 sequence (Fig. 15.186). The location of the tumor between the scalene and posterior compartment muscles is suggestive of a neurogenic tumor of the brachial plexus. A coronal view of the MRI scan confirms a spindle-shaped tumor along the course of the roots of the right brachial plexus (Fig. 15.187). The extent of the palpable lesion is depicted on the patient in Fig. 15.188.

Surgical exposure for this lesion requires a transverse incision along a skin crease in the lower part of the neck. The skin incision is deepened through the platysma, and upper and lower skin flaps are elevated. Dissection is now focused on the posterior triangle of the neck, from which the fibrofatty tissue and lymph nodes overlying the brachial plexus are excised to facilitate exposure of the brachial plexus (Fig. 15.189). The tumor is densely adherent to the nerve roots of the brachial plexus. Meticulous sharp dissection is now undertaken to peel each of the layers of the nerve fibers surrounding the tumor in the manner of "peeling the skin of the onion." Several layers

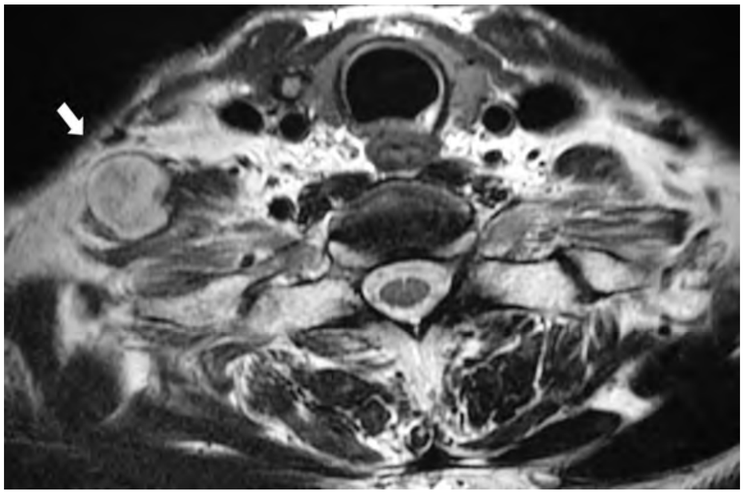

Figure 15.186 An axial view of a T2-weighted magnetic resonance imaging scan showing an encapsulated tumor (*arrow*) with areas of necrosis.

Figure 15.187 A coronal view of the magnetic resonance imaging scan shows a spindle-shaped tumor (*arrow*) along the course of the roots of the brachial plexus.

Figure 15.188 The extent of the palpable lesion is demarcated on the patient.

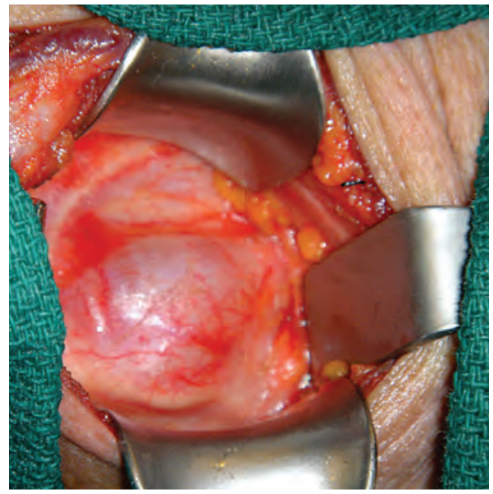

Figure 15.189 The tumor is densely adherent to the roots of the brachial plexus.

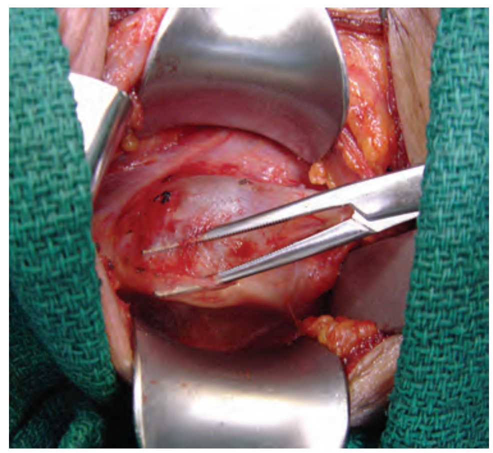

Figure 15.190 The stretched nerve fibers are peeled off the tumor one layer at a time.

of nerve fibers are stretched over the tumor, and each of these fibers need to be meticulously incised along the long axis of the nerve, separated with a hemostat, and peeled away from the tumor. The nerve bundles are separated sharply to preserve as much nerve function as possible (Fig. 15.190). Absolute hemostasis is secured with use of a bipolar cautery to electrodesiccate the minor blood vessels along the nerve fibers to facilitate a bloodless dissection of the tumor (Fig. 15.191).

As dissection continues, more and more layers of the stretched nerve fibers become apparent over the pseudocapsule of the tumor. Thus continuous and tedious dissection should proceed, retracting away the nerve fibers stretched over the capsule of the tumor to preserve function (Fig. 15.192). Eventually, no more nerve fibers remain to be dissected off the tumor and the pseudocapsule of the tumor comes into view, allowing its excision in an intact fashion (Fig. 15.193). The surgical defect after removal of the tumor demonstrates preserved nerve roots from which the tumor was shelled out (Fig. 15.194). The surgical specimen shows an intact tumor removed in toto with its pseudocapsule preserved and showing complete excision (Fig. 15.195).

Meticulous dissection of the schwannoma from functionally important nerves is crucial for retention of nerve function. This patient did not have any postoperative sensory or motor neural deficit. The success of adequate excision of a schwannoma is

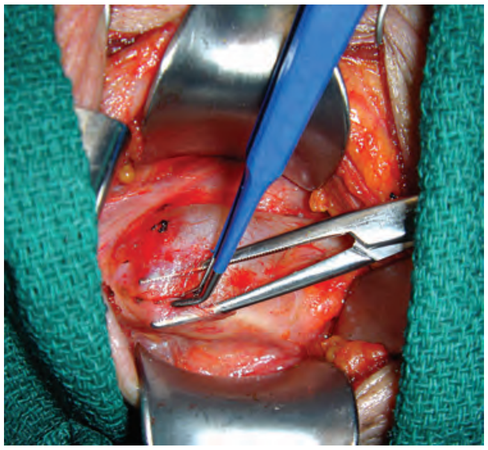

Figure 15.191 Absolute hemostasis is secured with bipolar cautery.

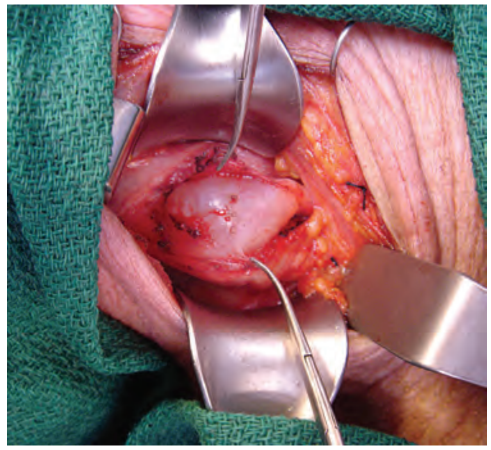

Figure 15.192 The nerve roots are dissected off the tumor.

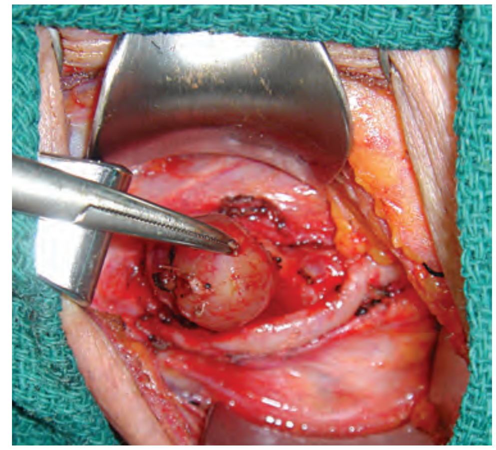

Figure 15.193 The encapsulated tumor is circumferentially mobilized.

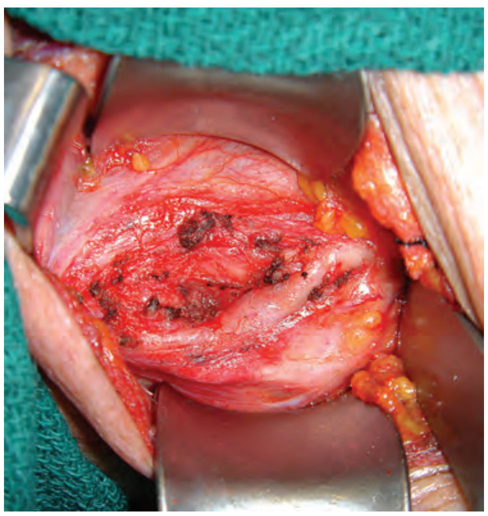

Figure 15.194 The surgical defect after removal of the tumor shows preserved nerve roots.

Figure 15.195 Monobloc excision of the tumor with an intact capsule.

measured by the preservation of nerve function after removal of the tumor.

Surgical resection for malignant neurogenic tumors, such as MPNSTs, requires a wide three-dimensional resection, as is done for any high-grade sarcoma. In general, MPNSTs are considered to be similar to high-grade sarcomas and require surgical management followed by postoperative radiation therapy.

MISCELLANEOUS SOFT-TISSUE TUMORS

Synovial Sarcoma of the Pharyngeal Wall

Soft-tissue sarcomas in the head and neck region may also arise in the visceral compartment and the upper aerodigestive tract. The patient shown in Fig. 15.196 presented with the history of a sore throat and difficulty swallowing of several months' duration. She had no palpable cervical lymphadenopathy. Examination of the oropharynx showed a lobulated, firm, sessile, exophytic tumor mass arising from the right lateral pharyngeal wall, projecting in the oropharynx and partially obscuring the view of the supraglottic larynx (Fig. 15.197). A telescopic examination of the hypopharynx and larynx shows the tip of the epiglottis with the remaining laryngeal vestibule totally obstructed by the multilobulated exophytic tumor mass of the right lateral pharyngeal wall (Fig. 15.198). Endoscopy and biopsy of the lesion confirmed the diagnosis of a synovial sarcoma.

A contrast-enhanced CT scan of the neck at the level of the tip of the epiglottis shows a solid tumor mass occluding the laryngeal vestibule (Fig. 15.199). The tumor has a heterogeneous radiographic appearance with focal areas of necrosis. An axial view of the CT scan through the region of the hyoid bone further demonstrates the lobulated tumor mass, which is producing near-complete obstruction of the supraglottic larynx (Fig. 15.200). The surgical procedure for resection of this tumor will require a mandibulotomy for access. The tumor of the pharyngeal wall will be excised, and the defect will be repaired by primary

Figure 15.196 This patient presented with a history of a sore throat and difficulty in swallowing of several months' duration.

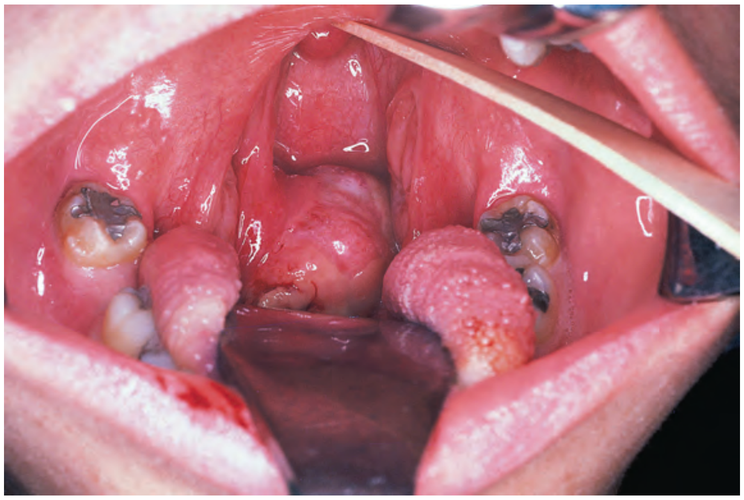

Figure 15.197 A lobulated, firm, sessile, exophytic tumor mass arising from the right lateral pharyngeal wall.

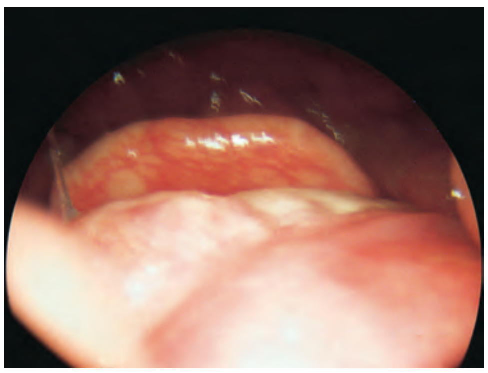

Figure 15.198 Telescopic examination showed the supraglottic larynx obstructed by the pharyngeal wall tumor.

Figure 15.199 A computed tomography scan of the neck showing the tumor arising from the lateral pharyngeal wall.

closure. A supraomohyoid neck dissection is performed to assess the histologic status of the first echelon lymph nodes. A preliminary tracheostomy is carried out under local anesthesia.

A right supraomohyoid neck dissection is performed through a transverse incision in the upper part of the neck extending from the mastoid process up to the midline of the neck. The lymph nodes are dissected en bloc, clearing the supraomohyoid triangle, as shown in Fig. 15.201. The cervical incision is then

Figure 15.200 A computed tomography scan through the region of the hyoid bone shows the pedunculated tumor in the laryngeal vestibule.

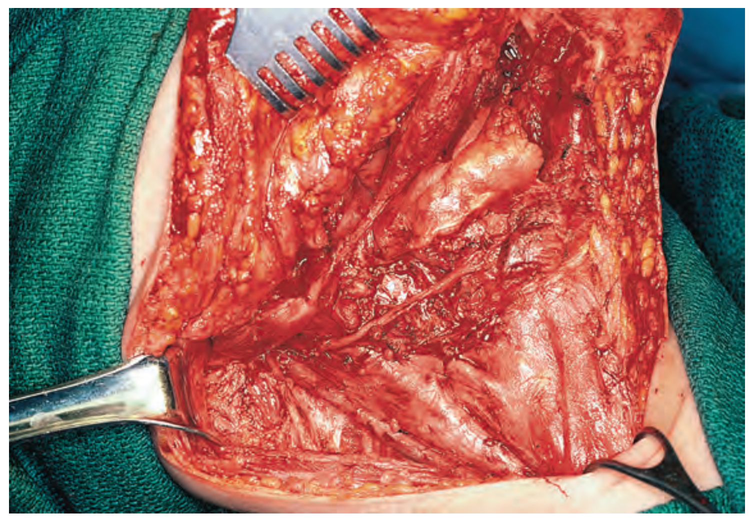

Figure 15.201 A supraomohyoid neck dissection is completed.

extended cephalad in the midline, dividing the chin and the lower lip. A mandibulotomy is now performed, in the paramedian location between the lateral incisor and canine teeth. A right-sided paralingual incision through the mucosa of the floor of the mouth is carried back up to the glossotonsillar sulcus. The mylohyoid muscle is divided, which permits mandibular swing, providing exposure of the oropharynx (Fig. 15.202). The two halves of the mandible are retracted laterally, with large loop retractors exposing the base of the tongue.

Further exposure of the tumor requires extension of the floor of the mouth incision to the soft palate and retraction of the base of the tongue medially (Fig. 15.203). Satisfactory exposure of the lobulated tumor mass is thus obtained. Under direct vision, the tumor is excised with a generous cuff of peripheral mucosa and full thickness of the pharyngeal musculature in a monobloc fashion. Resection of this tumor required excision of the right half of the hyoid bone and sacrifice of the right superior laryngeal nerve, but the right hypoglossal nerve could be preserved (Fig. 15.204).

A close-up view of the surgical defect shows the hypoglossal nerve and the exposed prevertebral fascia (Fig. 15.205). A three-dimensional monobloc resection of the tumor is thus

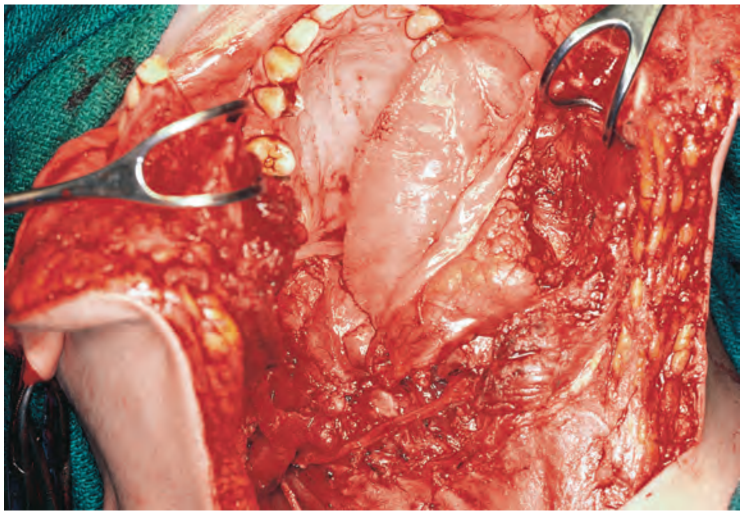

Figure 15.202 A paramedian mandibulotomy with a mandibular swing exposes the oropharynx.

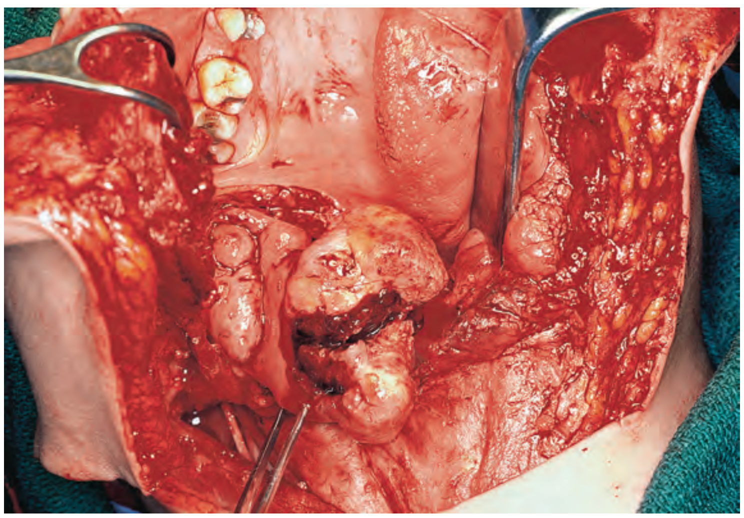

Figure 15.203 The tumor is exposed by medial retraction of the base of the tongue.

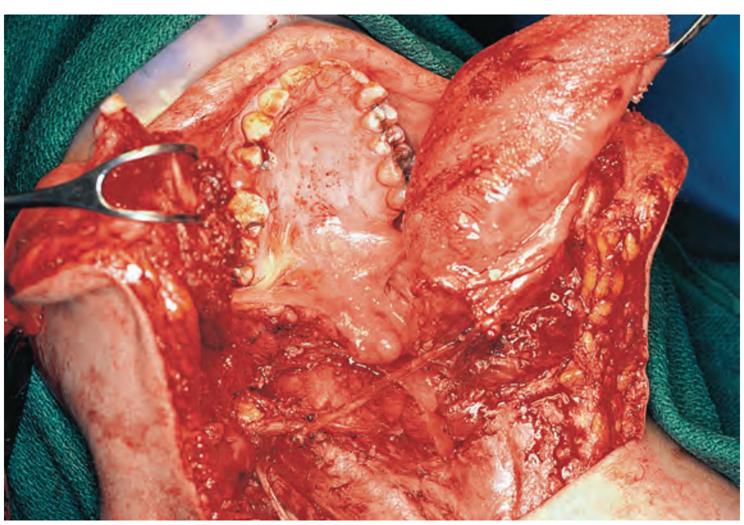

Figure 15.204 The tumor is resected with generous mucosal and soft-tissue margins.

accomplished. The surgical defect is closed by mobilization of the posterior pharyngeal wall and the base of the tongue. Complete closure of the pharyngeal defect could not be achieved because a small area had to be left open to granulate and heal by secondary intention. Remaining closure of the oral cavity

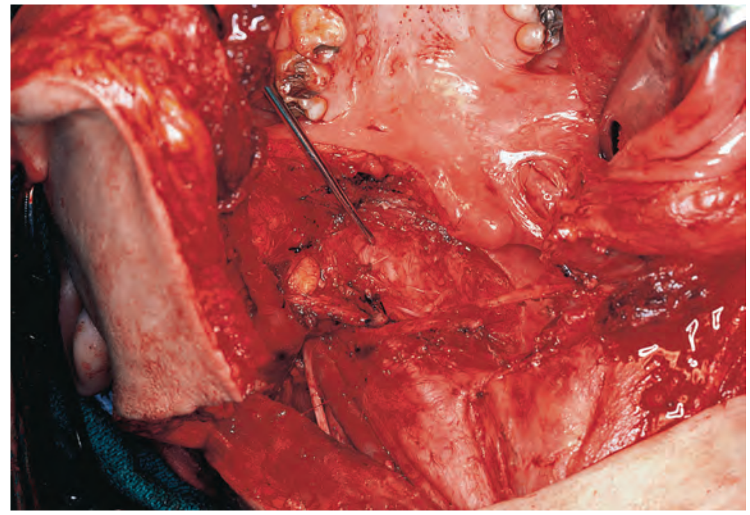

Figure 15.205 A close-up view of the surgical defect.

Figure 15.206 The surgical specimen.

and the mandibulotomy is performed in the usual manner. (For details of the steps of mandibulotomy and repair, see Chapter 8.)

The specimen, shown in Fig. 15.206, is a nodular, multilobulated, firm tumor mass arising from the pharyngeal muscles with superficial necrosis and ulceration. This patient needed a nasogastric feeding tube and a tracheostomy for several weeks. Postoperative radiation therapy further delayed removal of the

Figure 15.207 The postoperative appearance of the patient 1 year following surgery.

nasogastric feeding tube and the tracheostomy. However, within 8 weeks of surgery, the patient was able to tolerate most foods by mouth, and the tracheostomy tube could be removed. The postoperative appearance of the patient 1 year following surgery shows a well-healed scar with minimal aesthetic deformity (Fig. 15.207).

Resection of a soft-tissue sarcoma of the upper aerodigestive tract requires an appropriate surgical procedure designed for that tumor depending on its histologic diagnosis, size, and location. Thus familiarity with a variety of surgical techniques and their applicability is essential. Anticipation and understanding of the functional consequences of such resection is vitally important to plan reconstruction and rehabilitation for a successful outcome.

Cervical Chordoma

Chordomas are tumors of neural crest origin arising from the remnants of the notochord. The most frequent sites of origin of the chordoma are the craniocervical and sacral regions of the spine. However, they may arise in any part of the central axis. The patient described here presented with a retropharyngeal mass and obstruction to the nasopharynx with slight discomfort on flexion of the cervical spine. Clinical examination of the oral cavity showed a submucosal, smooth, firm, retropharyngeal mass extending from the level of the tip of the epiglottis caudad and up to the nasopharynx behind the soft palate cephalad. Laterally it extended from the posterior pillar on one side to the posterior pillar on the opposite side of the pharyngeal wall. The overlying mucosa and musculature of the pharyngeal wall were not adherent to the mass.

The intraoral view shown in Fig. 15.208 demonstrates that the mass has displaced the posterior pharyngeal wall anteriorly and is almost abutting the posterior surface of the soft palate and the uvula. Radiographic studies included a high-kV lateral film of the cervical spine, shown in Fig. 15.209, which clearly demonstrates a smooth, prevertebral, retropharyngeal mass at the level of the first, second, and third cervical vertebrae. The mass partially destroys the anterior portion of the body of the second cervical vertebra, which most likely is the site of origin of this chordoma. No intraspinal extension of this tumor could be demonstrated on a myelogram. A contrast-enhanced MRI would be a preferred study to accurately assess the exact extent of the tumor in relation to the spinal canal.

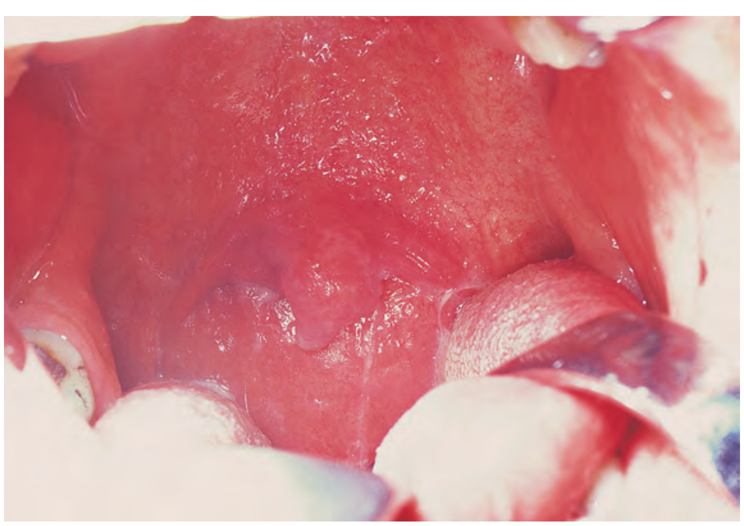

Figure 15.208 An intraoral view of a retropharyngeal submucosal mass in the oropharynx.

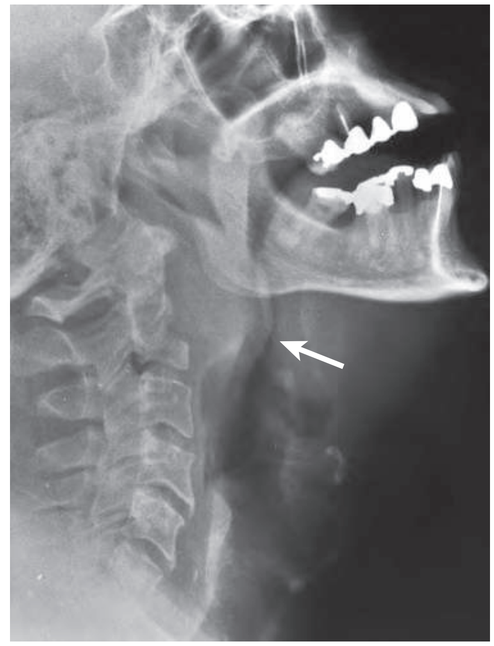

Figure 15.209 A high-kV lateral film of the cervical spine shows a prevertebral mass anterior to C1 and C2.

Surgical resection of this lesion will require a multidisciplinary approach, with the head and neck surgical team providing exposure of the lesion and a neurosurgical team proceeding with appropriate resection, while carefully protecting the anterior surface of the spinal cord. Exposure to this midline lesion is accomplished through use of a classic median labiomandibular glossotomy, described by Trotter. The patient is placed under general endotracheal anesthesia after a preliminary tracheostomy is performed under local anesthesia. The neck is extended, and a vertical midline incision splitting the lower lip and chin up to the hyoid bone is marked (Fig. 15.210). The skin incision divides the lower lip and the soft tissues of the chin up to the anterior surface of the mandible. Short cheek flaps are elevated on both sides of the midline to expose approximately 3 cm of the symphysis of the mandible (Fig. 15.211). A midline mandibulotomy is performed through the socket of a central incisor tooth. The mandibulotomy cut in the bone is angled to prevent cephalocaudad movement.

The floor of the mouth, the frenulum of the tongue, and the entire tongue are bisected in the midline from the tip of the tongue down to the hyoid bone and up to the glossoepiglottic fold (Fig. 15.212). Because the blood supply to the tongue is from the lingual artery on either side, minimal bleeding is encountered when the tongue is divided exactly in the midline. The two halves of the oral cavity and the mandible are now retracted laterally to expose the oropharynx (Fig. 15.213). Note the tip of the epiglottis at the posterior end of the glossotomy and the bulging posterior pharyngeal wall pushing the soft palate anteriorly.

At this point the soft palate is also divided in the midline from the tip of the uvula up to the junction of the soft and hard palate, and the two halves of the soft palate are retracted laterally. A self-retaining retractor is now introduced and positioned to provide exposure of the posterior pharyngeal wall from the level of the arytenoids up to the nasopharynx (Fig. 15.214). Note that the two halves of the tongue are retracted laterally, exposing the lingual surface of the epiglottis in the lower part of the surgical field and the retracted halves of

Figure 15.210 A vertical midline incision splitting the lower lip and chin up to the hyoid bone is outlined.

Figure 15.211 Exposure of the symphysis of the mandible.

Figure 15.212 The floor of the mouth, the frenulum of the tongue, and the entire tongue are bisected in the midline.

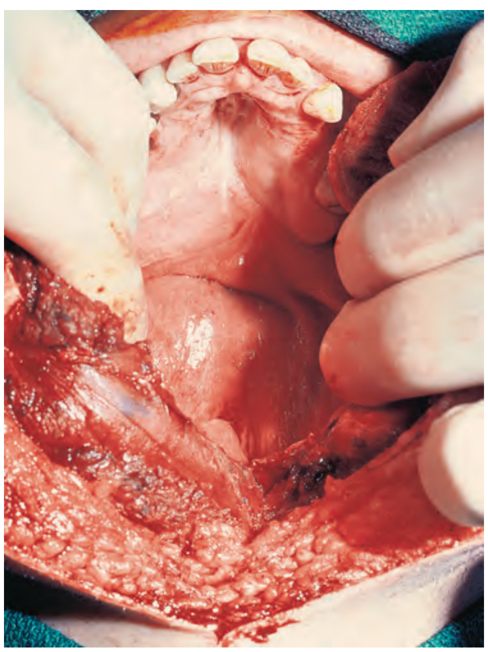

Figure 15.213 Exposure of the oropharynx by lateral retraction of the two halves of the tongue and mandible.

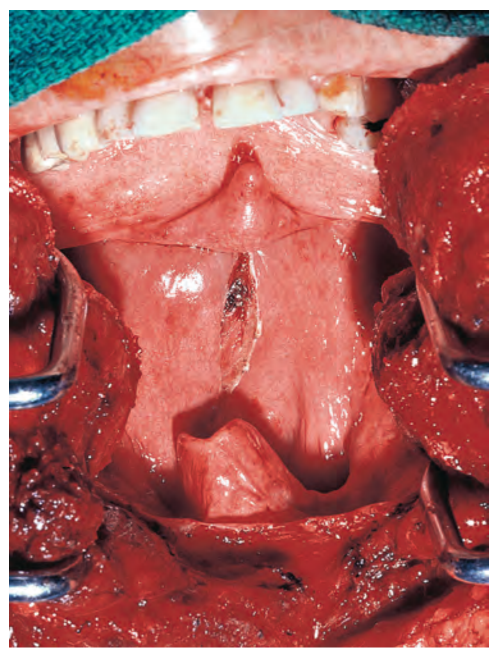

Figure 15.214 Exposure of the posterior pharyngeal wall from the nasopharynx up to the hypopharynx.

the soft palate seen posterior to the upper teeth, exposing the posterior pharyngeal wall. A vertical midline incision is now placed on the mucosa of the posterior pharyngeal wall. The pharyngeal incision is deepened through the full thickness of the pharyngeal musculature to expose the prevertebral fascia. Adequate mobilization of the pharyngeal wall is undertaken over the prevertebral fascia to gain wide exposure of the stretched prevertebral fascia by the tumor (Fig. 15.215).

At this juncture, the neurosurgical team takes over the operative procedure for a monobloc resection of the tumor. The prevertebral fascia is incised in the midline, and with use of dural elevators and dissectors, mobilization of the tumor is begun from within the body of the second cervical vertebra. Meticulous attention to detail is required, particularly during mobilization of the posterior aspect of the tumor, which may be adherent to the dura. In this patient, the dura was not involved by the tumor. If the dura is violated, it should be repaired immediately. If any portion of the dura of the anterior aspect of the cervical spine must be resected, a dural graft should be placed to repair the defect and prevent leakage of the cerebrospinal fluid.

In Fig. 15.216, the surgical defect is shown after gross total excision of the tumor from within the body of the second and third cervical vertebrae. Meticulous hemostasis must be secured with bipolar cautery. Oozing from the cut ends of the bone can be controlled with the use of Gelfoam or bone wax. After absolute hemostasis is secured, the posterior pharyngeal wall is closed with interrupted 2-0 chromic catgut

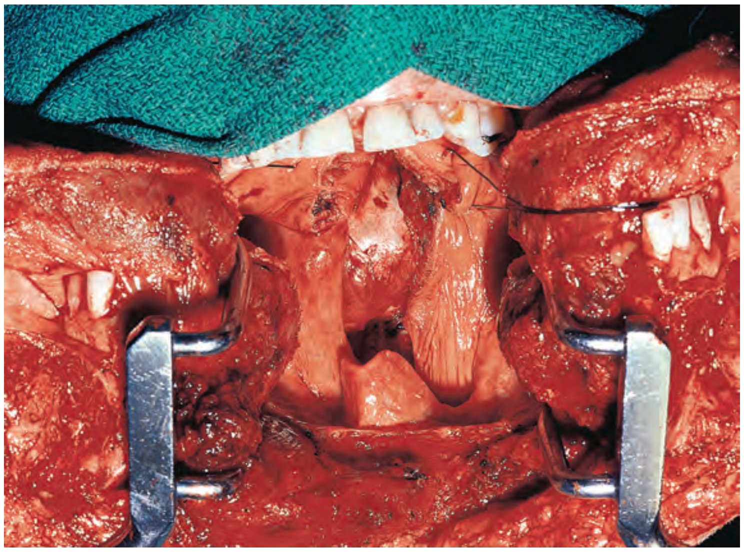

Figure 15.215 Exposure of the stretched prevertebral fascia through a vertical incision in the posterior pharyngeal wall.

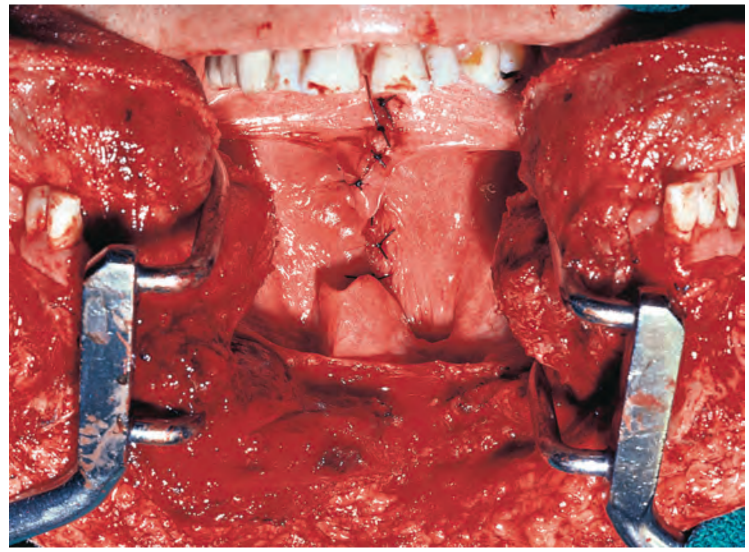

Figure 15.217 Closure of the posterior pharyngeal wall.

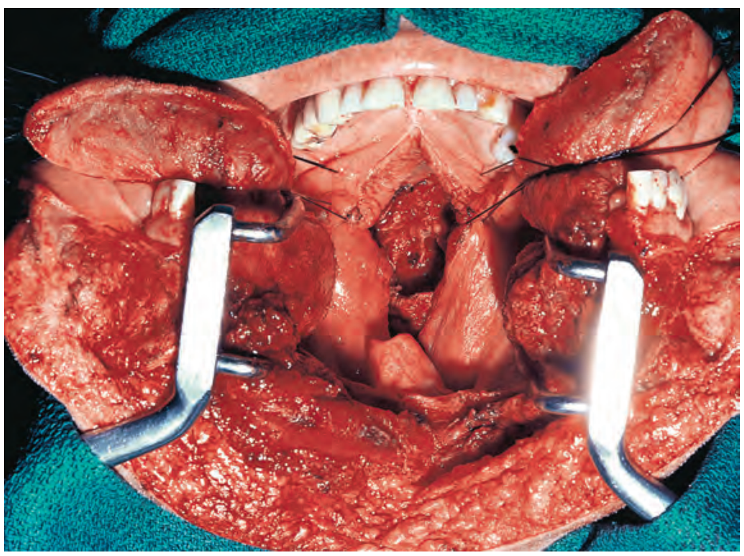

Figure 15.216 The surgical defect.

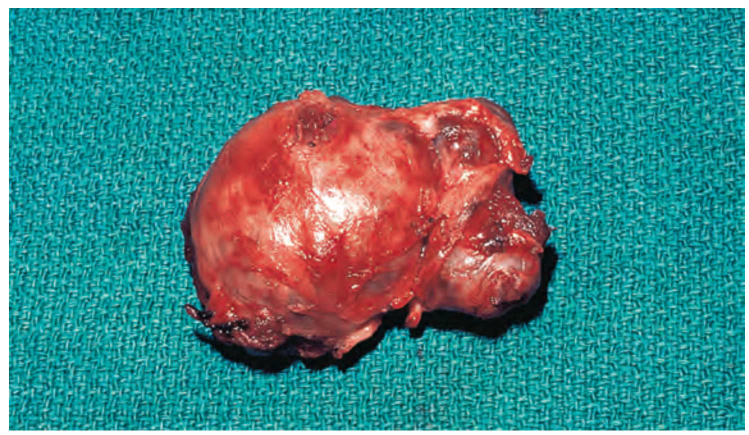

Figure 15.218 The surgical specimen.

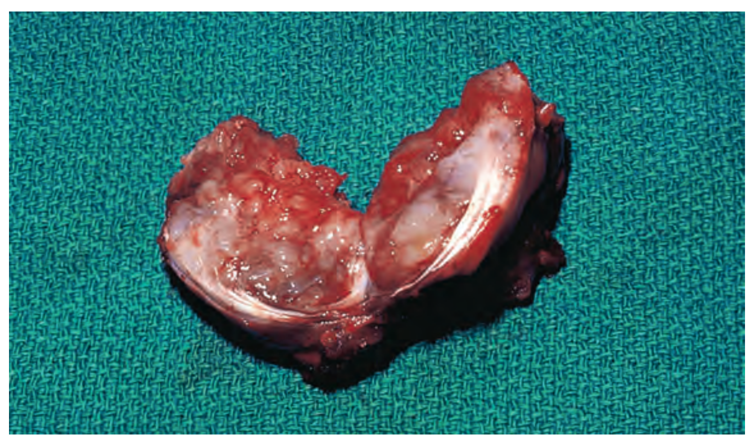

Figure 15.219 The cut surface of the specimen.

sutures (Fig. 15.217). A watertight closure must be secured to prevent leakage of saliva into the prevertebral space. After closure of the posterior pharyngeal wall, a nasogastric feeding tube is introduced and the soft palate is reapproximated accurately in the midline in two layers with interrupted 3-0 chromic catgut sutures.

Following this procedure, closure of the glossotomy is begun, which is accomplished in three layers. The deep layer of the musculature of the tongue is approximated from side to side to restore anatomic continuity of the musculature of the tongue. Closure of the mucosa of the dorsum of the tongue is then undertaken with interrupted 2-0 chromic catgut sutures, accurately aligning the two halves of the tongue. Meticulous attention to accurate approximation is required as the closure approaches the tip of the tongue, because the clarity of speech will depend on accurate reapproximation at this point. Mucosal closure of the tongue continues on its undersurface on the anterior third and then the floor of the mouth up to the midline of the lingual gingiva anteriorly. The mandibulotomy is then repaired with miniplates and screws. Accurate alignment of the two halves of the mandible must be secured with stability. The remaining skin incision is closed in two layers, and a Penrose drain is brought out from the submental region.

Because the bony integrity of the cervical spine is not disturbed, immobilization of the craniocervical region is not required. A simple cervical collar is sufficient to provide support to the cervical spine. The surgical specimen excised in toto in a monobloc fashion is shown in Fig. 15.218. Note a glistening pseudocapsule of the bilobulated tumor on the surface. The cut surface of the specimen shows areas of hemorrhage and a firm, nodular, rubbery, compact tumor (Fig. 15.219).

The appearance of the patient 3 months following surgery shows a well-healed midline incision of the lower lip and chin

Figure 15.220 Postoperative appearance of the patient 3 months following surgery.

Figure 15.222 The reconstructed soft palate and a well-healed incision in the posterior pharyngeal wall in the oropharynx.

Figure 15.221 An intraoral view showing accurate reapproximation of the mandible and the tongue.

Figure 15.223 A postoperative high-kV soft tissue radiograph of the cervical spine showing a soft-tissue defect in the prevertebral space at the site of tumor resection.

with accurate reapproximation of the vermilion border and the contour of the chin (Fig. 15.220). The intraoral view shown shows accurate realignment of the tongue with restored configuration of the oral tongue, particularly at its tip, to ensure clarity of speech and mastication (Fig. 15.221). Upon depressing the tongue, the reconstructed soft palate and a well-healed incision in the posterior pharyngeal wall is shown (Fig. 15.222). A postoperative high-kV soft-tissue radiograph of the cervical spine shows complete excision of the retropharyngeal tumor mass from the anterior aspect of the vertebral column and the craniocervical region (Fig. 15.223). Monobloc resection of a small chordoma of the cranio-cervical region is thus accomplished in a satisfactory manner through a median labiomandibular glossotomy.

OUTCOMES

Local recurrence after excision of benign soft-tissue tumors in the head and neck region is seldom observed unless the tumor is incompletely excised. Complete excision is particularly important in patients who undergo excision of a hemangioma or a lymphangioma, because incomplete excision is likely to be complicated by the development of local recurrence, which often is exceedingly difficult to treat and may lead to significant morbidity from further surgery.

The prognosis in patients with malignant soft-tissue tumors is dependent on the stage of disease, which is determined by the TNM criteria and the histologic grade of the tumor. Survival also is affected by adequacy of resection, signified by negative margins of resection. Local control with the use of postoperative radiation therapy when appropriate is expected in more than 70% of patients who undergo surgical excision of soft-tissue sarcomas in the head and neck region. The long-term outcomes in a consecutive series of 310 patients treated on the head and neck service of Memorial Sloan Kettering Cancer Center over a 30-year period are shown in Fig. 15.224, using the AJCC/International Union Against Cancer (UICC) seventh edition criteria. The 4-year overall survival, disease-specific survival, and recurrence-free survival are 72%, 76%, and 71%, respectively. However, staging for soft-tissue sarcomas of the head and neck is revised in the most recent iteration of the AJCC/UICC staging manual (eighth edition). No data is available as of yet to report outcomes using the eighth edition criteria. The prognosis is

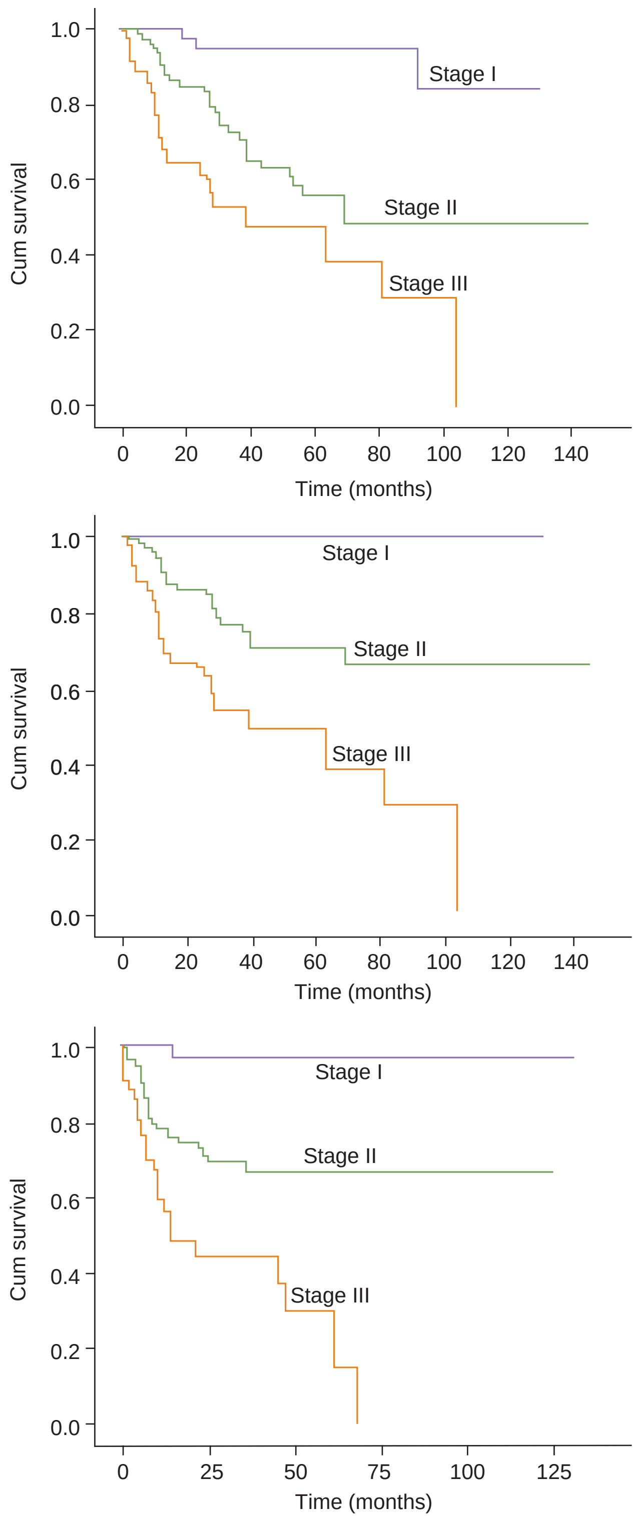

Figure 15.224 Long-term survival for soft-tissue sarcomas in the head and neck by stage of disease (AJCC/UICC seventh edition criteria). **A**, Overall survival. **B**, Disease-specific survival. **C**, Recurrence-free survival. Memorial Sloan Kettering Cancer Center data on 319 patients 1982-2012. *(From Shuman AG et al. Soft tissue sarcoma of the head & neck: nomogram validation and analysis of staging systems. J Surg Oncol 111(6):690-695, 2015.)*

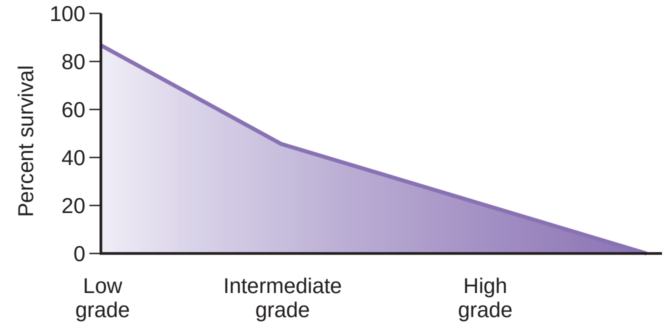

Figure 15.225 Survival in relation to the histologic grade of the sarcoma.

excellent for patients with low-grade sarcomas such as DFSP; intermediate for patients with UPS/MFH and fibrosarcomas; and poor for patients with high-grade sarcomas such as angiosarcomas and rhabdomyosarcomas (Fig. 15.225).

CHAPTER 16

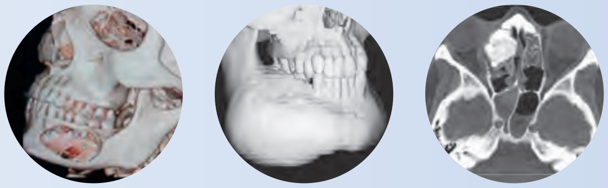

Bone Tumors and Odontogenic Lesions

Bone consists of a solid mineral phase and a matrix of osteoid phase that contains osteoclasts (bone-resorbing cells), osteoblasts (bone-forming cells), and osteocytes (osteoblasts that become incorporated into the matrix). Although bone tumors are rare in the head and neck region, they span a wide spectrum of neoplasms. Primary bone tumors arise from either cellular matrix or lymphoreticular and myeloid cells in the marrow spaces. Occasionally, embryonic sequestered elements also may be the source for a primary neoplasm (e.g., salivary rests giving rise to "central" salivary neoplasms in the mandible or maxilla). Neoplasms also may arise from odontogenic elements in the maxilla and mandible. Generalized disorders of bone turnover and remodeling such as Paget's disease also may increase the risk of development of malignant tumors within the involved bones. Exposure to ionizing radiation, particularly at a young age (e.g., in children with a retinoblastoma) significantly increases the risk of the subsequent development of malignancy, such as osteosarcoma. Metastatic tumors from other sites also can present in the craniofacial skeleton.

Primary benign neoplasms of the craniofacial skeleton consist of osteomas, osteochondromas, and osteofibromas. Occasionally, benign tumors of vascular origin such as hemangiomas are also seen in the craniofacial skeleton. These are often asymptomatic and found incidentally. However, the most common benign bony lesions in the head and neck region are developmental malformations at the site of embryonic fusion lines, such as the torus palatinus. Osteomas typically are asymptomatic and may arise on the calvarium and in the paranasal sinuses. Osteomas usually appear after puberty and require intervention only if they are symptomatic. Malignant transformation is uncommon but occasionally may be associated with Gardner syndrome. Osteoid osteomas (ivory osteomas) are smaller lesions, whereas osteoblastomas are thought to be their larger, more aggressive counterparts. Osteoid osteomas typically present in children and young adults, are usually solitary, and are associated with pain that may be out of proportion to size. Local excision is adequate treatment. In contrast, osteoblastomas are rarely painful, involve long bones, and have a small tendency to progress to an osteosarcoma.

Benign tumors of cartilaginous origin include osteochondromas, chondromas, chondroblastomas, and chondromyxoid fibromas. Osteochondromas (exostoses) are benign, cartilage-capped, bony outgrowths. These tumors usually are solitary but can be multifocal in patients with familial osteochondromatosis. Solitary lesions usually involve the mandible or skull base. Chondromas (enchondromas) are tumors of the hyaline cartilage that frequently arise within the bone. They are thought to be derived from remnants of epiphyseal cartilage. These tumors usually are solitary but can be multiple in persons with Ollier disease (enchondromatosis), which is a nonhereditary spontaneous disorder. A familial variant also exists (Maffucci syndrome) in which chondromas occur in conjunction with cutaneous hemangiomas. Although solitary tumors have very low risk for malignant transformation, multiple, familial tumors progress to chondrosarcomas in up to 50% of cases.

Chondroblastomas usually arise along the epiphyseal region of long bones. Although rare in the head and neck skeleton, they may occur in the temporal bone, mandible, or parietal bone. These lesions are histologically benign and may have radiologic features similar to those of malignant lesions. Chondromyxoid fibromas typically involve long bones but may arise in the mandible, although this presentation occurs rarely. These lesions are benign and require surgical intervention only if they are symptomatic.

Cystic lesions of the bone are common in the head and neck region and most frequently are of odontogenic origin. Nonodontogenic bony cysts typically are fissural cysts that may be lateral (nasolabial or globulomaxillary), medial (nasopalatine or median palatal), or median mandibular (Fig. 16.1). Nasolabial cysts (Klestadt cysts) arise from epithelial rests remaining from the "fusion" of the glabellar process with the lateral nasal process and the maxillary process, or due to the persistence of epithelial remnants from the nasolacrimal duct extending between the

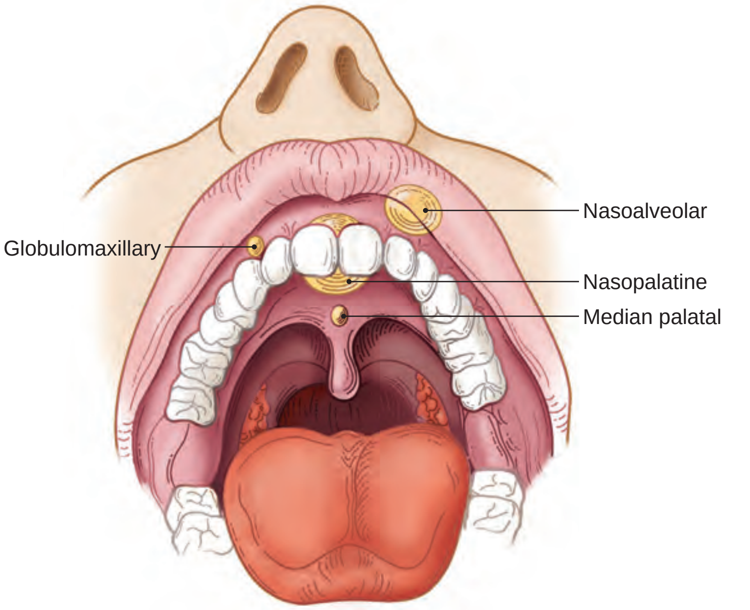

Figure 16.1 Classification of fissural cysts.

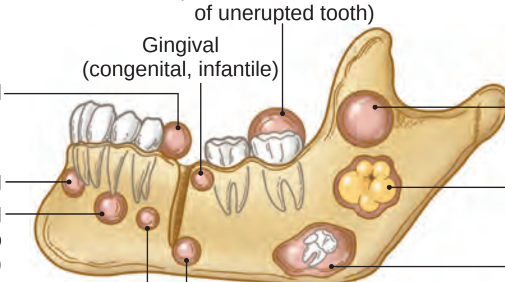

Figure 16.2 Odontogenic cystic lesions of the mandible.

lateral nasal process and the maxillary prominence. These lesions have a predilection for females (75%) and are found near the base of the nostril. They can be bilateral in up to 10% of cases.

Nasopalatine cysts are developmental lesions that are thought to arise from epithelial remnants of embryonic nasopalatine ducts within the incisive canal. They are the most common nonodontogenic cysts and have a predilection for males. Globulomaxillary cysts arise from epithelial elements trapped in the embryonic fusion line between the glabellar process of the frontonasal bone and the maxillary process of the palatine bone. Odontogenic cysts are thought to be derived from remnants of dental lamina or from enamel organ. They can be periodontal (apical, lateral, or residual), dentigerous, gingival, primordial, or keratinizing and calcifying (Fig. 16.2). Periapical or radicular cysts account for more than 50% of cystic lesions. Radicular cysts are thought to arise from an inflammatory process of the epithelial cell rests of Malassez. Dentigerous cysts are developmental cysts that arise from the enamel or dental lamina of an unerupted tooth. They are epithelium-lined sacs that involve the crown of unerupted teeth. Dentigerous cysts arise most commonly from the third molars but also may arise from the bicuspid, cuspid, or canine teeth.

Gingival cysts that arise from remnants of the dental lamina are located in the corium below the surface epithelium. They typically present as multiple nodules on the alveolar ridges of newborn or young infants. These cysts generally are asymptomatic and usually resolve spontaneously. Lateral periodontal cysts generally arise from epithelial rests in the periodontal ligament. Primordial cysts develop in place of a tooth when the dental follicle undergoes cystic degeneration. They also may arise from a supernumerary tooth bud. The treatment is surgical enucleation or curettage with preservation of adjoining teeth.

In 2005, the World Health Organization (WHO) changed the terminology of the lesion previously referred to as *odontogenic keratocyst (OKC)* to *calcifying cystic odontogenic tumor (CCOT)*. The rationale for the name change was genetic data demonstrating alterations in the *PTCH1* gene and the potential for aggressive behavior of these lesions. However, the 2017 WHO classification reverts to the usage of the terminology "odontogenic keratocyst." Furthermore, the 2017 WHO classification states that CCOT is now synonymous with "calcifying odontogenic cyst," a simple cyst lined by an odontogenic ameloblastoma-like epithelium, with associated ghost cells. The rationale for these additional changes is unclear; however, it is important to understand that regardless of "terminology de jour," this entity encompasses a spectrum of clinical behaviors. Odontogenic keratocysts most commonly involve the mandible in the region of the third molar and can extend into the ascending ramus. These lesions are distinguished from other odontogenic cysts by the presence of a keratinizing epithelial lining. They may vary from cystic to solid, and OKCs may involve the crown of a tooth but also can represent a keratinizing variant of the lateral periodontal cyst. Multifocal OKCs are associated with nevoid basal cell carcinoma syndrome. Small lesions may be effectively treated with enucleation. However, enucleation is inadequate for larger lesions with thin wall and satellite cysts. In the presence of multiple cystic lesions (osteitis fibrosa cystica), hyperparathyroidism should be ruled out.

Fibrous dysplasia is a rare, idiopathic primary bony lesion that is characterized by progressive replacement of medullary bone with proliferating, haphazardly arranged isomorphic fibrous tissue. Fibrous dysplasias can be monostotic (70%–75%) or polyostotic, which rarely can be associated with skin pigmentation and endocrine dysfunction (Albright syndrome). The head and neck region is not a common site for fibrous dysplasias (<1%), but when present, they most commonly involve the mandible, maxilla, frontal bone, or calvarium. These lesions tend to be progressive and cause symptoms by compression of local structures. Intervention is usually required to control symptoms or for cosmetic reasons. Less than 1% of these lesions may undergo malignant degeneration.

Giant cell tumors (GCT) of bone are lesions most commonly seen in long bones, but they also can occur in the head and neck region (e.g., in the temporal bone, sphenoid, and larynx). These tumors arise in young adults and have a locally aggressive course, with a high rate of recurrence after incomplete excision. A small proportion of these tumors undergo malignant degeneration and metastasize to distant sites. These tumors should be distinguished from giant cell reparative granulomas (epulis) that arise in the mandible and maxilla and have similar histopathologic features but no inherent malignant potential. In GCT, the giant cells overexpress the RANK receptor, a key mediator in osteoclastogenesis. Stromal cells secrete a cytokine RANKL, which stimulates the RANK receptor, contributing to bone resorption by the tumor. The United States Food and Drug Administration (FDA) has approved the use of Denosumab, a monoclonal antibody that specifically binds RANKL, preventing activation of RANK. This interaction, in turn, inhibits osteoclast formation, function, and survival, subsequently decreasing bone resorption. Currently, Denosumab is in use for inoperable or metastatic GCT, as well as neoadjuvant treatment before surgery. Further clinical trials are needed to establish optimal clinical utilization and long-term outcomes.

Ameloblastomas are the most common tumor arising from the odontogenic epithelium. They are seen most frequently in the mandible (Fig. 16.3). The vast majority of these lesions are loculated, but they may present as a unicystic lesion, and rarely,

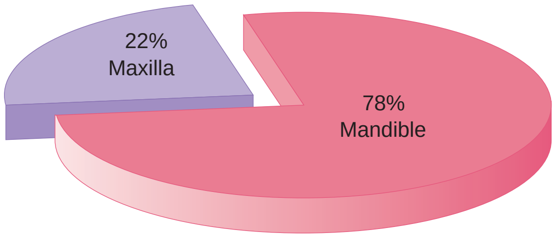

Figure 16.3 Distribution of ameloblastomas of the jaws.

Figure 16.4 The classic "soap-bubble" appearance of an ameloblastoma on a radiograph of a segmental mandibulectomy specimen.

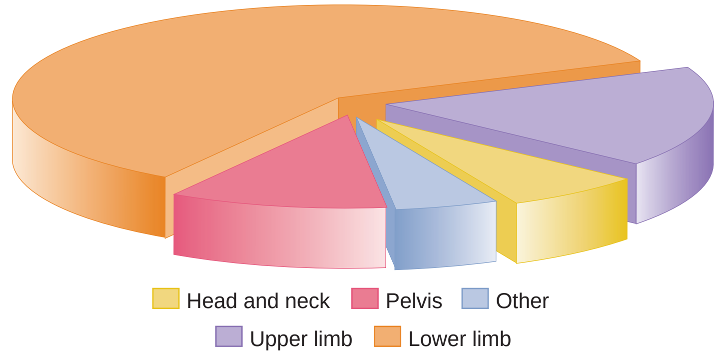

Figure 16.5 Site distribution for osteogenic sarcomas in the human body.

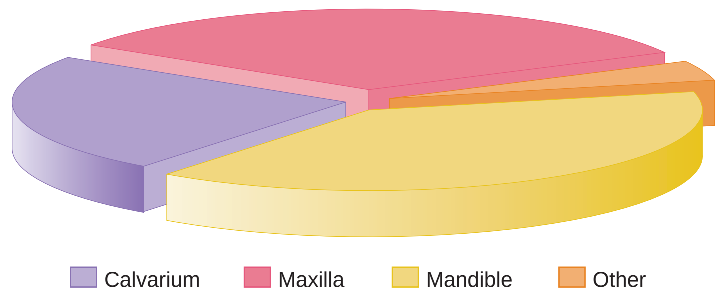

Figure 16.6 Site distribution for osteogenic sarcomas of the head and neck.

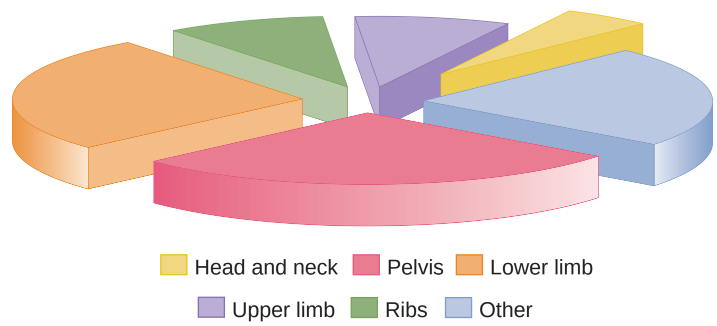

Figure 16.7 Site distribution for chondrosarcomas.

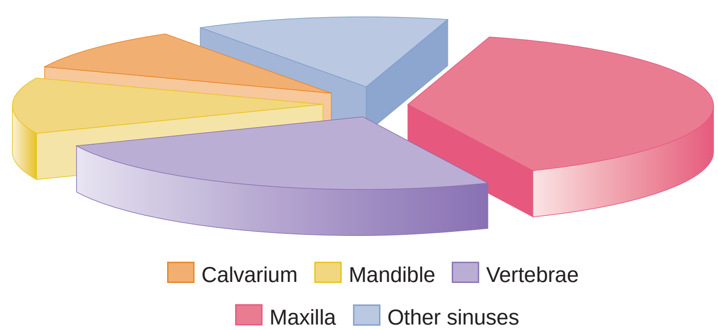

Figure 16.8 Site distribution for chondrosarcomas of the head and neck.

they may be extraosseous in origin. The classic appearance of an ameloblastoma on a plain radiograph is that of a multiloculated, expansile lesion with a "soap-bubble appearance" (Fig. 16.4). Although histologically benign, these tumors can be locally invasive. A small proportion of these tumors can degenerate into ameloblastic carcinomas. Small, benign ameloblastomas can be treated by enucleation, but this method is ineffective for larger lesions and results in a high rate of local recurrence. Multifocal recurrence with involvement of soft tissues may occur after inadequate initial treatment. For larger lesions of the mandible, segmental mandibulectomy is required for local control.

Primary malignant tumors of bone in the head and neck region are of osteogenic origin (osteosarcomas), chondrogenic origin (chondrosarcomas), hematopoietic origin (myelomas and lymphomas), or of unknown cellular origin (e.g., Ewing sarcomas, malignant giant cell tumors, and adamantinomas). Secondary involvement can occur from metastases from other sites.

The most common malignant tumor of the craniofacial skeleton is osteosarcoma, which may arise de novo (primary), in an area of a preexisting condition (e.g., fibrous dysplasia or Paget's disease, or as a result of carcinogenic exposure [ionizing radiation]). Primary osteosarcomas generally develop in long bones in children and young adults (Fig. 16.5). Head and neck involvement is less common (<10% of cases overall). The mandible followed by the maxilla is the most common site of involvement (Fig. 16.6). Secondary osteosarcomas are seen most commonly in patients with Paget's disease and retinoblastomas, but they also can occur in patients with Bloom, Li-Fraumeni, and Rothmund-Thomson syndromes. Exposure to external beam radiation is also associated with the development of osteosarcomas, especially in patients with inherited retinoblastomas. These tumors typically present as a mass lesion that may be painful.

Chondrosarcomas can occur de novo (in approximately 75% of cases) or in association with preexisting conditions such as multiple enchondromatosis (Maffucci or Ollier syndromes), exostoses, and rarely, chondroblastomas. Overall, these tumors involve the head and neck region in fewer than 10% of cases (Fig. 16.7). The maxilla, cervical spine, and mandible are the most common sites for chondrosarcomas in the head and neck (Fig. 16.8). The majority of patients present with a painless mass, and diagnosis is established by imaging or biopsy. Surgery is the mainstay of treatment for these neoplasms. Outcome generally is excellent and is dependent on the extent of disease at presentation, the tumor grade, and the completeness of resection. The histologic subtype also influences outcome, with the clear cell subtype (malignant chondroblastoma) having a

better outcome than the myxoid, mesenchymal, or dedifferentiated subtypes.

Multiple myeloma and lymphoma arise from hematopoietic cells of the bone marrow and may present as solitary or multifocal bony lesions. Multiple myelomas often arise from a precursor condition (monoclonal gammaglobulinopathy of uncertain significance or smoldering myeloma). These tumors are of plasma cell origin and can be solitary (plasmacytoma) or widespread. Multiple myelomas cause systemic effects such as anemia and immunodeficiency because of progressive replacement of bone marrow with myeloma cells. Other symptoms arise from circulatory problems, renal dysfunction due to monoclonal gammaglobulinopathy, or hypercalcemia due to osteoclastic bone destruction. Multiple myeloma can be diagnosed by serum electrophoresis. Evaluation of the extent of disease requires imaging studies, bone marrow biopsy, peripheral blood counts, and renal function. Although plasmacytomas may benefit from surgery, curative treatment of multiple myeloma involves systemic chemotherapy and bone marrow transplantation.

Ewing sarcoma is a malignant round-cell tumor that shares a common translocation with peripheral primitive neuroectodermal tumors, and thus a continuum is considered to exist between these entities. The t(11;22)(q24;q12) translocation brings about fusion of the *FLI1* gene on 11q24 and the *EWS* gene on 22q12. The presence of this translocation can be established by conventional cytogenetics or by molecular studies and is pathognomonic for these entities. These tumors typically arise from the pelvis, femur, humerus, and ribs; primary involvement of the head and neck region is seen in fewer than 5% of cases. The most common sites for Ewing sarcoma in the head and neck region are the calvarium and mandible. Extraosseous Ewing sarcomas can also occur in the head and neck region.

EVALUATION

Clinical Evaluation

The most frequent mode of presentation of a bone tumor is a mass lesion or symptoms that result from pressure on contiguous neurovascular structures or viscera or the adjacent dentition. However, many small lesions are discovered incidentally on imaging studies performed for other reasons. Symptoms also may arise for tumors of the maxilla as a result of compression of the orbit, or displacement of the orbital contents, or obstruction of the nasal passages. Thorough radiographic evaluation and tissue diagnosis, is mandatory for surgical treatment planning.

Imaging

Accurate assessment of the anatomic extent of a lesion of the craniofacial skeleton requires its evaluation in all three dimensions. Plain films of the mandible and skull are used rarely. A panoramic radiograph (orthopantomogram) of the mandible provides an overview of the dentition and architecture of the mandible (Fig. 16.9). However, for more detailed assessment of the mandible, a computed tomography (CT) or magnetic resonance imaging (MRI) scan is required. A CT scan is excellent for bony architecture, whereas assessment of the soft tissues and bone marrow and inferior alveolar nerve in the mandible is better with MRI. Whenever a CT scan is requested for evaluation of a neoplastic process with invasion of bone and soft tissue, the scan should be obtained with contrast enhancement, and both soft tissue and bone windows should be carefully scrutinized.

Figure 16.9 A panoramic radiograph of the mandible showing a large cystic lesion.

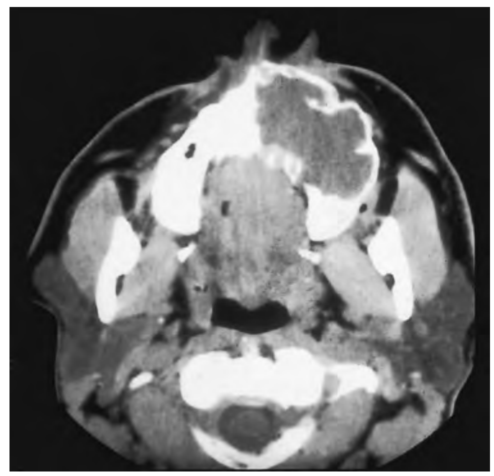

Figure 16.10 A soft-tissue window of an axial computed tomography scan through the upper alveolus demonstrating a hypodense, expansile, bone-destructive lesion.

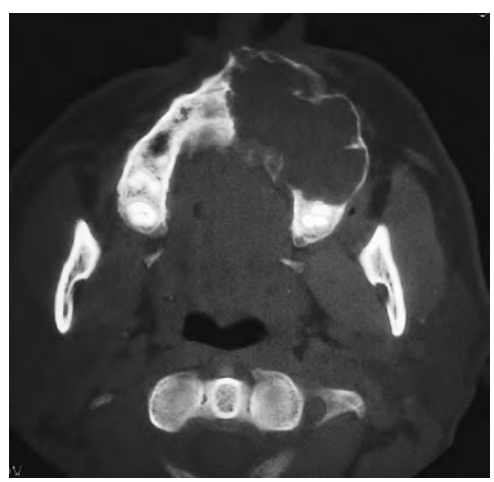

Figure 16.11 A bone window of the axial computed tomography scan of the patient shown in Fig. 16.10 demonstrating the expansile bone-destructive lesion of the upper alveolus.

The patient whose CT scans of the upper alveolus are shown in Figs. 16.10 and 16.11 has a myxoma of the alveolus extending into the maxilla. The soft-tissue window shown in Fig. 16.10 gives excellent soft-tissue detail, but the fine architectural detail of the bone is obscured. On the bone window shown in Fig. 16.11, the soft-tissue detail is obscured and the fine architecture of the bone and the lesion are clearly seen. Thus for adequate evaluation of bone invasion by a neoplastic process, both soft tissue and bone windows of the CT scan are required. An axial

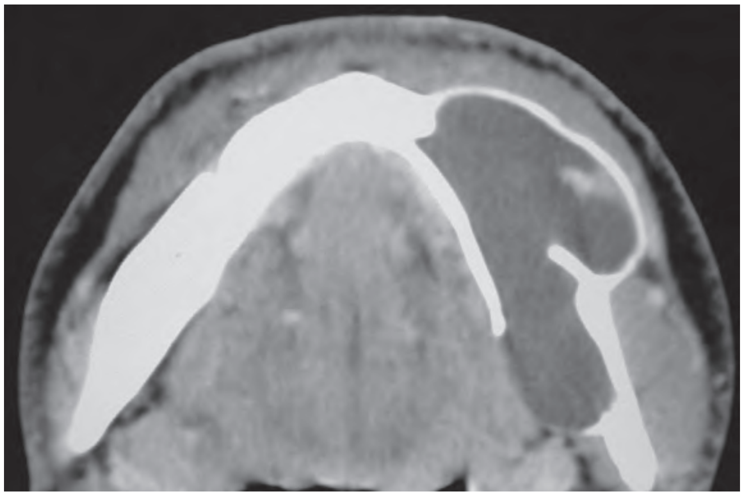

Figure 16.12 An axial view of the computed tomography scan of the patient shown in Fig. 16.9 reveals an expansile cystic lesion of the body of the mandible.

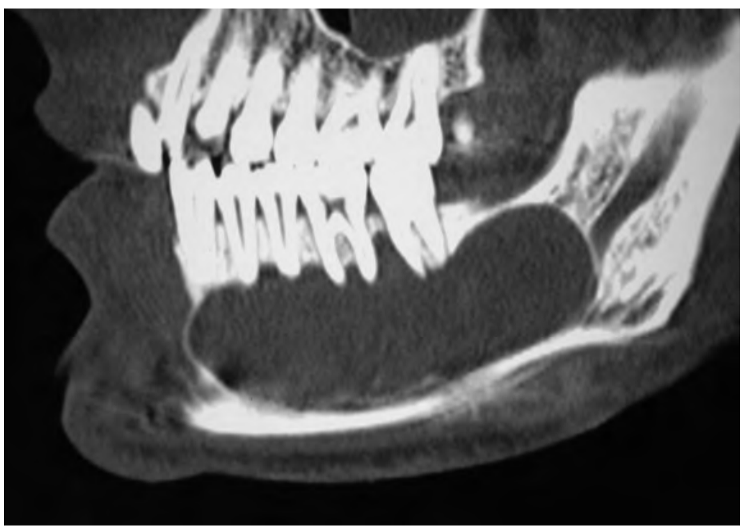

Figure 16.13 The sagittal view of the computed tomography scan of the patient shown in Fig. 16.9 reveals the anteroposterior extent of the lesion and its relation to the dental roots.

view of the CT scan of a patient with a massive expansile cystic lesion involving the body of the mandible on the left-hand side with significant expansion of the lateral cortex of the mandible is shown in Fig. 16.12. The lesion has a uniform ground glass appearance without any bone destruction or new bone formation. The reconstructed sagittal view of the CT scan

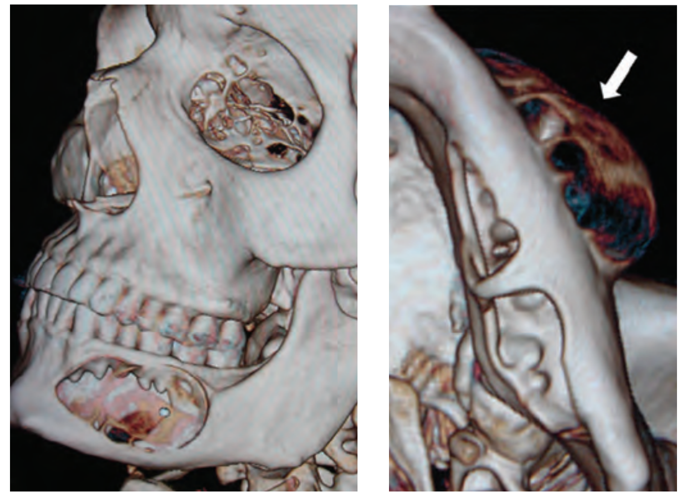

Figure 16.14 The lateral and inferior views of the three-dimensional reconstruction of the computed tomography scan of the patient shown in Figs. 16.9 through 16.11 showing the expansile lesion (*arrow*).

shown in Fig. 16.13 demonstrates a large, unilocular cystic space extending from the region of the retromolar trigone posteriorly up to the lateral incisor anteriorly. The cystic space has clear content and a smooth margin that is well defined. The roots of the teeth are within the cystic space. Three-dimensional reconstruction of the CT scan images clearly demonstrate the large expansile cystic lesion with bone loss in the body of the mandible (Fig. 16.14).

Three-dimensional reconstruction of CT images are very helpful in surgical treatment planning for resection and reconstruction. Three-dimensional computer-aided design/computer-aided manufacturing (CAD-CAM) models can also be fabricated with computer software, which provides three-dimensional printed guides for bone resection and reconstruction, thus facilitating the ability of the reconstructive surgeon to accurately fabricate a graft or flap to achieve exact contour and symmetry (see Chapters 17 and 18). A three-dimensional reconstruction of the mandible of a young patient with fibrous dysplasia of the mandible is shown in Fig. 16.15. Note the shape and dimensions of the lesion of the mandible in relation to the remaining facial skeleton. In a posterior view of the reconstructed CT scan, the thickness of the mandible involved by fibrous dysplasia is vividly demonstrated (Fig. 16.16). An axial view of the CT scan of the same patient shows thickening of the cancellous bone with thinning out of the mandibular cortex. The normal architecture of the cancellous bone is lost and is replaced by a ground glass appearance due to fibrous dysplasia (Fig. 16.17).

Figure 16.15 A three-dimensional computed tomography reconstruction showing an expansile lesion of the mandible.

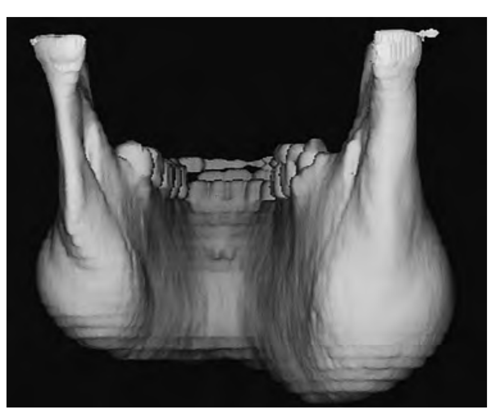

Figure 16.16 The posterior view of the three-dimensional computed tomography reconstruction demonstrates the full-thickness involvement of the mandible.

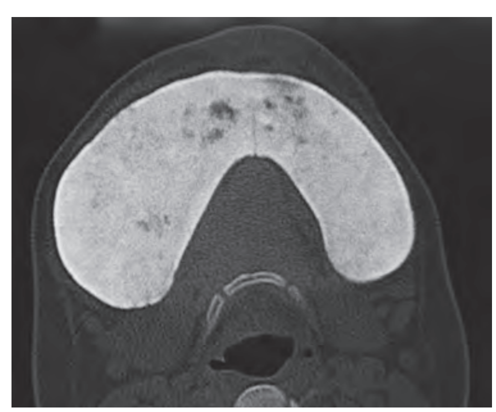

Figure 16.17 An axial view of the computed tomography scan (bone window) shows the featureless "ground glass" appearance of the pathologic bone.

Paget's disease of the craniofacial skeleton has a characteristic appearance on a CT scan with thickened bones with an irregular ground glass patchy appearance. Malignant transformation in a bone involved with Paget's disease clearly shows a punched-out demarcation with the sarcoma in the involved bone, while the remaining bone shows the Paget's disease in the background (Fig. 16.18). The radiographic appearances of several other bone lesions are shown later in this chapter as the surgical procedures are described. Many tumors and tumorlike conditions have characteristic radiographic appearances that almost pinpoint the diagnosis. However, tissue diagnosis is mandatory before implementation of therapy.

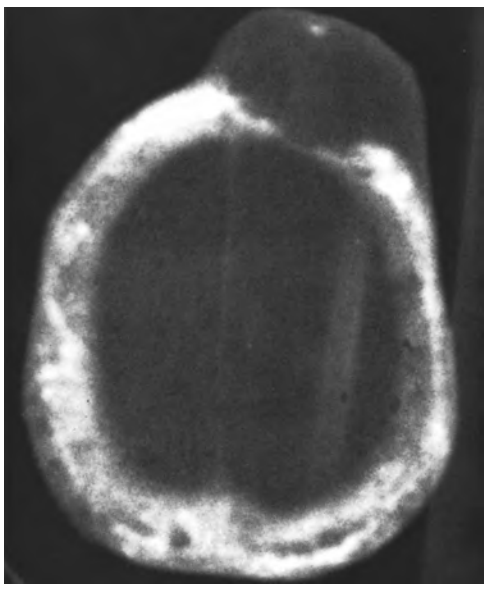

Figure 16.18 Axial view of CT scan of the skull in bone window shows the entire calvarium involved by Paget's disease, and a bone-destructive sarcoma in the frontoparietal region.

Pathology

It is vitally important that accurate tissue diagnosis be established before definitive surgical treatment in patients who present with lesions suspicious of being a neoplastic process involving the facial skeleton. Several bone lesions are benign or of a low-grade malignant histology, and their treatment is significantly different than for high-grade malignant tumors. Because needle biopsy is often not satisfactory, an open biopsy with a generous volume of representative tissue should be submitted for pathologic analysis. Frozen section diagnosis is generally not possible and should not be requested when a bone tumor is suspected. Extraction of a tooth near lesions of the upper or lower jaw should be avoided, and a biopsy from an adjacent area should be obtained to prevent implantation of malignant tumor into the marrow cavity of the affected bone, which would increase the risk of tumor dissemination.

The World Health Organization (WHO) histologic classification of bone tumors is shown in Table 16.1.

Soft-tissue chondromas (synonyms: fibrochondroma, myxochondroma, osteochondroma, chondroma of soft parts, extraskeletal chondroma) are benign cartilaginous tumors that, on rare occasion, may arise in the larynx and craniofacial bones, including the palate. These benign tumors may also occur extraskeletally, whereby they are referred to as *soft-tissue chondromas*. They present as well-circumscribed, nodular masses and may be particularly difficult to differentiate histologically from low-grade chondrosarcoma, particularly on small biopsy samples. These tumors are composed of mature hyaline cartilage with a lobular pattern of growth and cells that are immunoreactive for S-100 protein. Although they do not generally dedifferentiate to chondrosarcoma, incomplete excision of these tumors may lead to local recurrence.

Chondrosarcoma is the malignant counterpart to chondroma and is defined as a malignant tumor of hyaline cartilage. Like chondromas, these are rare neoplasms of the head and neck, but when they occur, they most commonly arise in the maxilla, mandible, larynx, and nasopharynx, in decreasing order of frequency. These tumors are composed of nodules of myxoid and hyaline cartilage, with neoplastic chondrocytes displaying varying degrees of atypia (Fig. 16.19). The severity of atypia

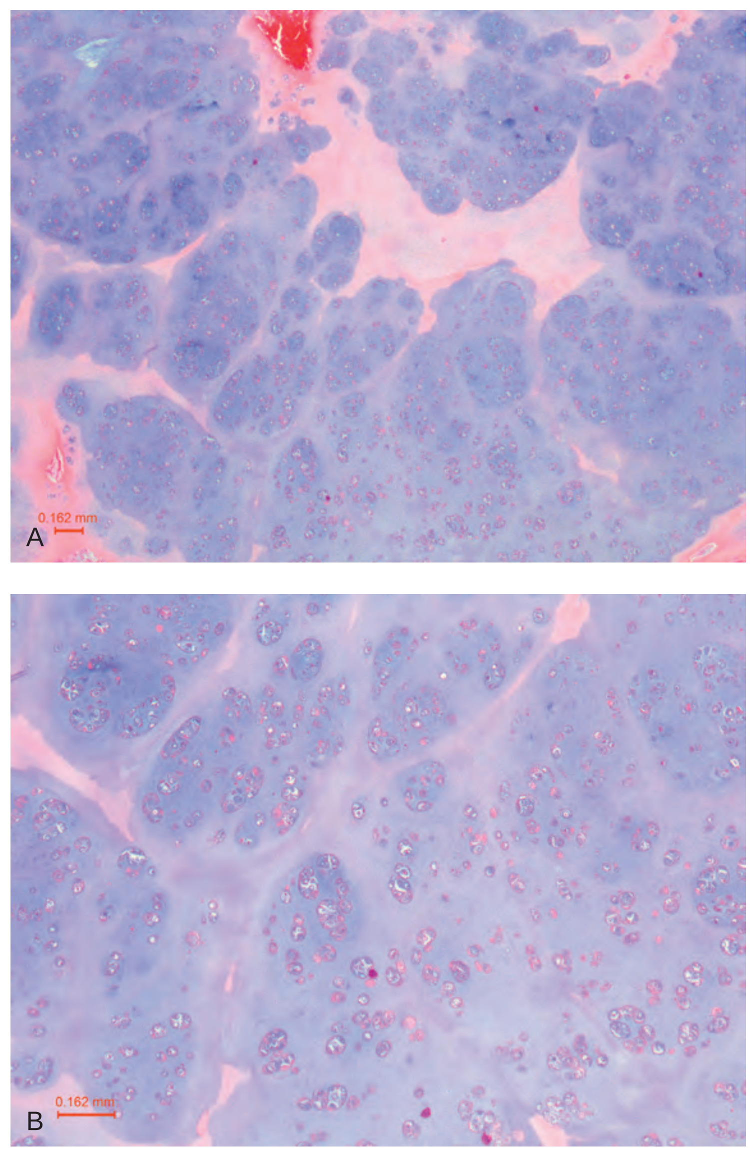

Figure 16.19 **A**, The nodular growth of this laryngeal chondrosarcoma is readily appreciated on low-power view (25×; H&E). **B**, At slightly higher magnification (50×; H&E), multiple abnormal chondrocytes crowded within lacunar spaces are seen.

Table 16.1 The histologic classification of nonodontogenic bone tumors (WHO, 2013) (abbreviated)

TISSUE OF ORIGIN	BENIGN	MALIGNANT
Cartilage	Osteochondroma Chondroma Chondroblastoma Chondromyxoid fibroma	Chondrosarcoma
Osteogenic	Osteoid osteoma Osteoblastoma	Osteosarcoma
Fibrogenic	Desmoplastic fibroma	Fibrosarcoma
Fibrohistiocytic	Fibrous histiocytoma	Malignant fibrous histiocytoma
Primitive neuroectodermal		Ewing sarcoma
Hematopoietic		Plasma cell myeloma Malignant lymphoma
Giant cell	Giant cell tumor	Malignant giant cell tumor
Notochord	Chordoma	
Vascular	Hemangioma	Angiosarcoma
Smooth muscle	Leiomyoma	Leiomyosarcoma
Lipogenic	Lipoma	Liposarcoma
Neural	Neurilemmoma	
Miscellaneous tumors	Adamantinoma	Metastatic malignancy
Miscellaneous lesions	Aneurysmal bone cyst Simple cyst Fibrous dysplasia Osteo fibrous dysplasia Langerhans cell histiocytosis Erdheim-Chester disease Chest wall hamartoma	
Joint lesions	Synovial chondromatosis	

defines tumor grade in a three-tiered grading system. Increasing grade is characterized by increasing pleomorphism, mitotic activity, abnormal mitotic figures, and binucleation. Differentiating grade III chondrosarcoma from chondroblastic osteosarcoma is of prognostic significance, because the former has a much better outcome. Ancillary studies are not generally necessary for diagnosis; rather, the absence of osteoid allows distinction of high-grade chondrosarcoma from the chondroblastic osteosarcoma. Metastases are infrequent, with an 83% 5-year survival for grade I chondrosarcoma and 53% combined 5-year survival for grades II and III.

Osteoid osteoma (synonym: osteoma) is a slowly growing, hamartomatous or developmental lesion composed of cortical bone. It has no malignant potential and may indeed regress in size over time. There is some association between multiple osteomas and Gardner's syndrome. Osteomas most commonly arise from the metaphyses of long bones. In the head and neck, they generally involve the frontal bone, calvarium, mandible, or sinonasal bones. They present as small lesions, 1 to 2 cm in size, with a central nidus of proliferating cells that appear less dense than the adjacent bone on radiographic imaging. Histologically, these are bland proliferations of dense bony spicules, morphologically similar to the surrounding bone, rimmed by osteoblasts, and surrounded by fibrous tissue with an abundance of vessels (Fig. 16.20). Sclerotic bone may surround the lesion.

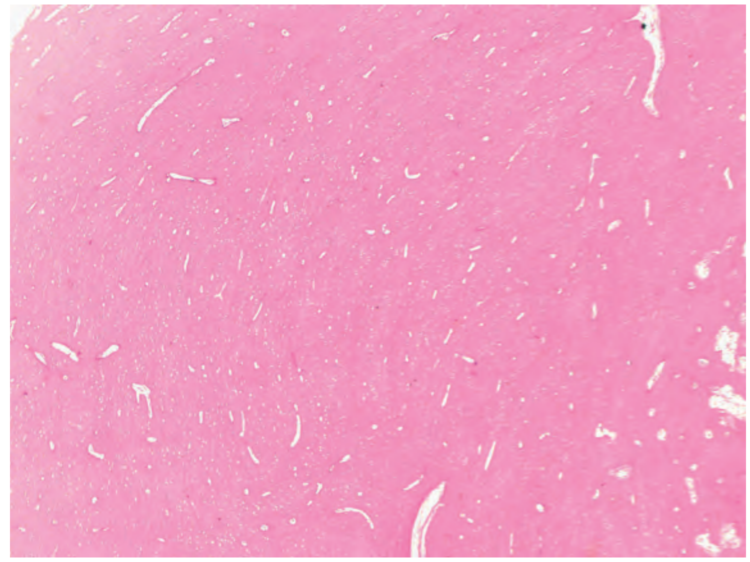

Figure 16.20 Osteoid osteoma (10×; H&E) shows abundant dense eosinophilic cortical bone. *(Photograph courtesy Dr. Mark Edgar, Emory University.)*

Osteosarcoma (synonyms: osteogenic sarcoma, osteoblastic sarcoma, chondroblastic osteosarcoma, medullary osteosarcoma) is a malignant tumor defined by neoplastic bone formation. The WHO classification includes several morphologic variants (e.g., chondroblastic, fibroblastic, telangiectatic, small cell), as well as variants based on the site from which the tumor arises (e.g., periosteal versus endosteal). Grossly, these are hard, destructive osseous neoplasms, which, in the head and neck, are most commonly intraosseous in location. The mandible is the most common primary site, followed by the maxilla and the skull. Histologically, these are matrix-producing tumors whose neoplastic osteoblasts produce bone. These malignant osteoblasts are usually highly pleomorphic and may be plasmacytoid, spindled, epithelioid, or round or have a mixture of these features (Fig. 16.21). Approximately half of all lesions are high grade. Ancillary studies are generally not used in the pathologic diagnosis of osteosarcoma. If a patient has been treated with preoperative chemotherapy, histologic grading of therapeutic response should be reported because it is an important predictor of outcome.

Plasmacytoma (synonyms: plasma cell myeloma, solitary plasmacytoma of bone, myeloma) is a malignant primary neoplasm of bone composed of plasma cells. When present as a single, localized mass, defined by a proliferation of clonal, terminally differentiated B cells (plasma cells), the lesion is a called a *plasmacytoma*. When there are multifocal, lytic bone lesions, this malignant proliferation of plasma cells is termed *multiple myeloma*. Histologically, these tumors are made up of a uniform population of lymphoid cells with eccentric nuclei, which are round to oval, demonstrating a pattern of chromatin distribution referred to as "clock face chromatin." When there is marked nuclear pleomorphism, with increased and abnormal mitoses, the tumors may be referred to as "undifferentiated"

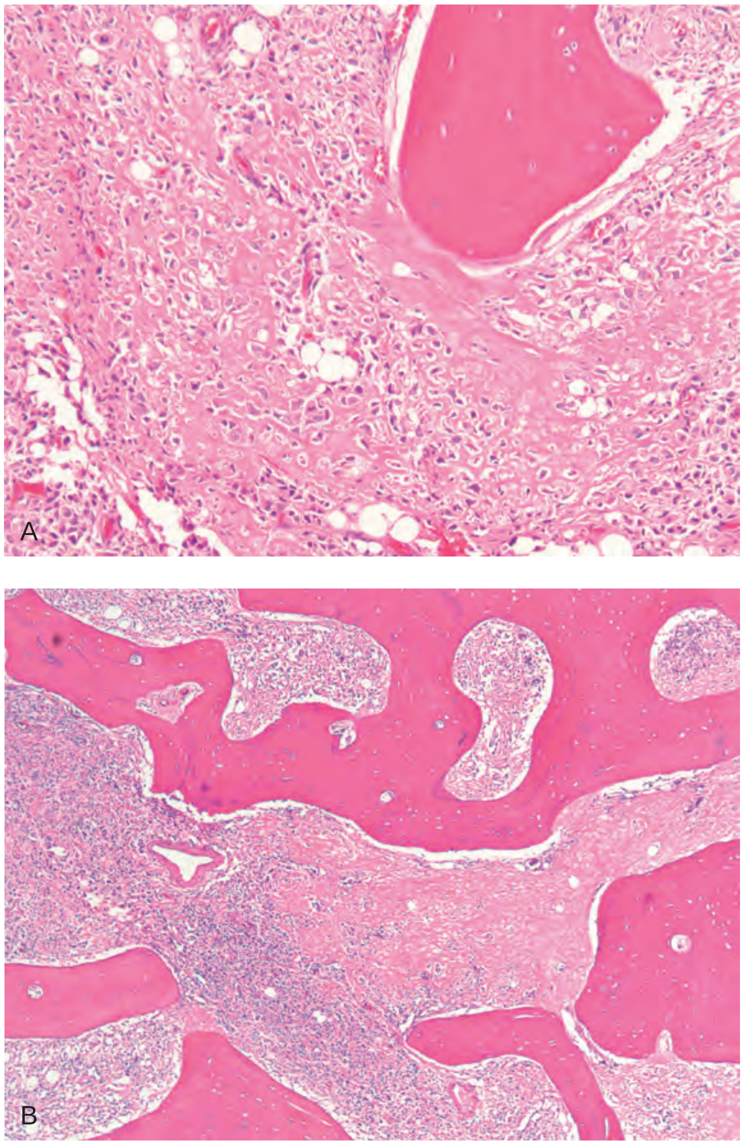

Figure 16.21 High-grade osteosarcoma of the mandible showing neoplastic bone formation, surrounding normal cortical bone (**A**) and numerous mitoses and marked nuclear atypia (**B**). *(Photograph courtesy Dr. Mark Edgar, Emory University.)*

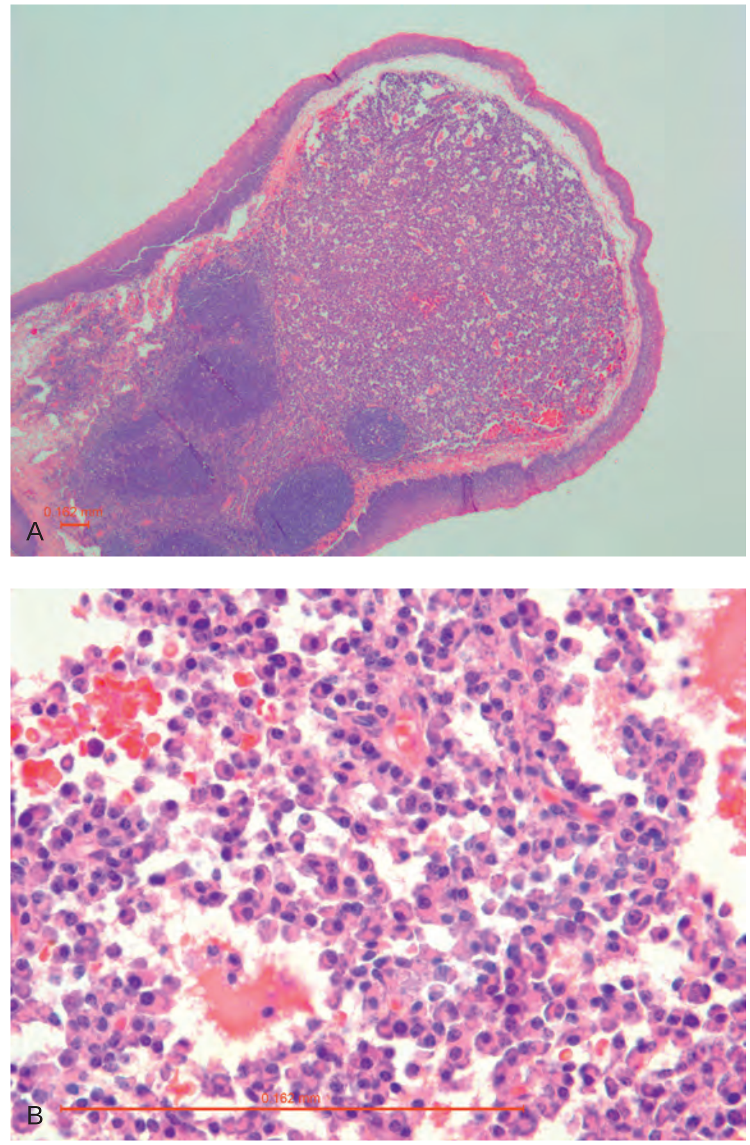

Figure 16.22 Kappa light chain restricted CD138 plasma cell neoplasm of the larynx. **A**, This submucosal proliferation of neoplastic plasma cells formed a small nodule beneath the respiratory mucosa of the ventricle in the larynx (25×; H&E). **B**, Higher magnification (400×; H&E) demonstrates the eccentrically located nuclei of these CD138-positive plasma cells in the patient with widely disseminated multiple myeloma.

or "anaplastic" or "poorly differentiated." The malignant plasma cells demonstrate immunoreactivity to antibodies against CD138, CD79a, and vimentin, whereas LCA (leukocyte common antigen) and CD20, which are both normally expressed by mature B cells, are negative. These tumors can also occur in soft tissue, as shown in this patient with a laryngeal plasmacytoma (Fig. 16.22). Plasmacytomas often also demonstrate light chain restriction, either kappa or lambda. Prognosis depends on stage, with systemic disease defined by high mortality rates at 3 years and an approximately 10% 10-year survival.

Giant cell granuloma (synonyms: giant cell reparative granuloma, solid aneurysmal bone cyst, brown tumor, central giant cell lesion) is an osteolytic, poorly defined intraosseous lesion of the jaw defined by an abundance of osteoclast-type giant cells that can be seen irregularly distributed throughout a background of proliferating reactive blood vessels and fibroblasts and often with associated hemorrhage. In the past, these lesions were deemed purely reactive, but there appears to be some recent molecular evidence that they may be related to aneurysmal bone cysts, with associated identical translocations. The exact same histologic appearance may also be seen in hyperparathyroidism, and the lesion is then called a *brown tumor,* although the molecular aberrations are distinct from giant cell granuloma. Microscopically, it is unencapsulated and has nests of multinucleated osteoclast-type giant cells in a fibrovascular stroma (Fig. 16.23). Ancillary studies are not necessary in the diagnosis, although it is important to evaluate serum calcium levels and parathyroid hormone to exclude hyperparathyroidism. It is also important to differentiate this lesion from giant cell tumor of bone, as behavior, prognosis, and treatment can be different.

Giant cell tumor of bone is a benign, but potentially aggressive neoplasm, which on rare instances may be seen in the craniofacial bones. On radiographic imaging, it has poorly defined borders and presents as a destructive, lytic lesion. Histologically, giant cell tumors share many morphologic features with giant cell granuloma; however, there is also a proportionate abundance of mononuclear cells and the giant cells are often very large, with 50 to 100 nuclei. Although mitotic activity is common, abnormal mitoses are not seen. These tumors can recur, can be very locally destructive, and do metastasize infrequently.

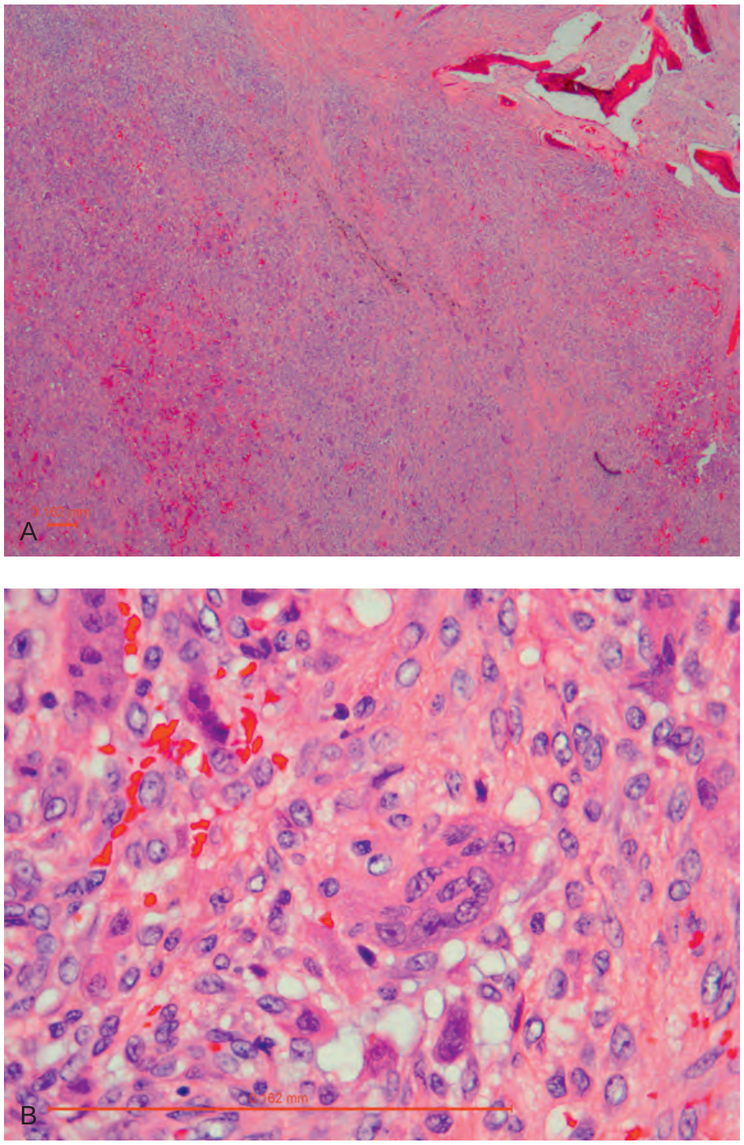

Figure 16.23 Giant cell reparative granuloma of the mandible, which radiographically presented as a lytic lesion in a patient with hyperparathyroidism. **A**, Histologic appearance at 25×; H&E. **B**, Benign, reactive multinucleated giant cells are seen at 400×; H&E.

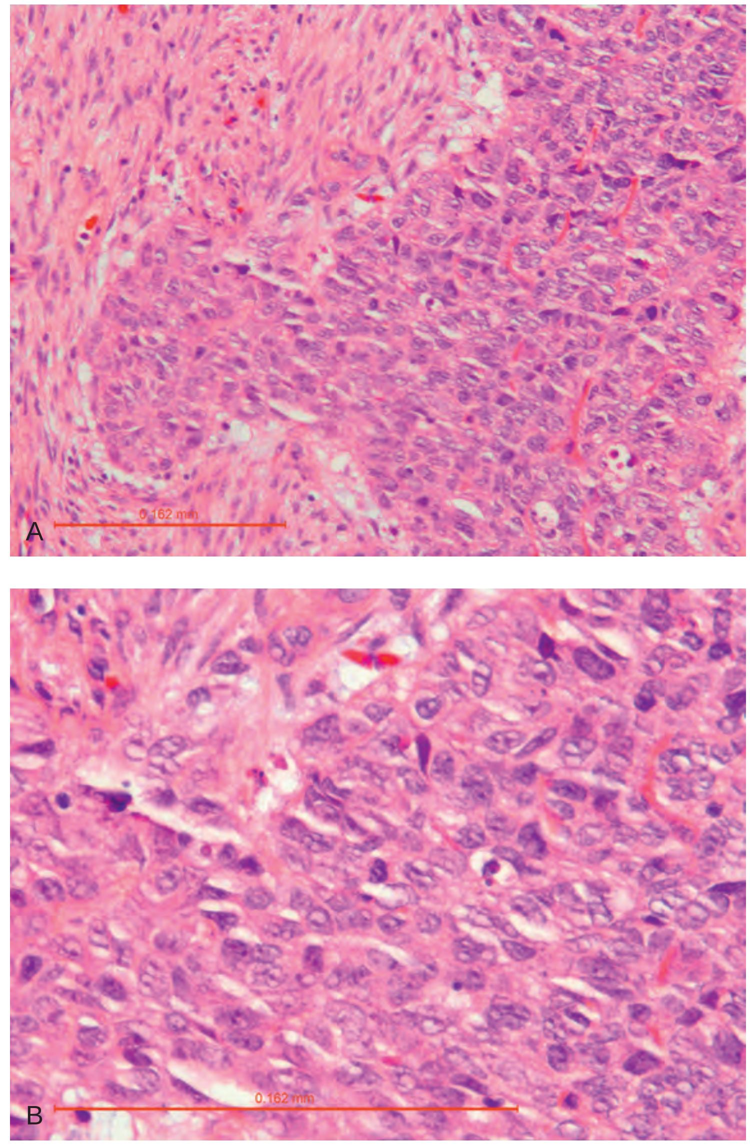

Figure 16.24 Sinonasal Ewing sarcoma demonstrates marked nuclear pleomorphism and an epithelioid appearance with 200× (**A**) and 400× (**B**); H&E.

Ewing sarcoma and primitive neuroectodermal tumor (synonyms: primitive neuroepithelioma; ES/PNET, EWS) is a malignant "small round blue cell tumor" of bone and soft tissue, composed of undifferentiated cells of neuroectodermal origin. Almost 10% of Ewing sarcomas arise in the head and neck, most commonly in the mandible, followed by the maxilla. It may have a bimodal age distribution, with a higher frequency peak in children, and then a second, much smaller peak in older adults. On rare occasions, Ewing sarcoma may be metastatic to the jaw. Histologically, these tumors are high grade by definition and are composed of primitive, small, round uniform cells, which may form rosettes and fibrillary processes (Fig. 16.24). Tumors in the ES/PNET group are characterized by a EWS-FLI fusion, t(11;22) (q24;q12), with several variants of this translocation producing other fusion products. The particular translocation and the corresponding fusion transcript directly affect the outcome, and long-term survival may be as high as 85%.

Undifferentiated pleomorphic sarcoma (UPS) (synonyms: malignant fibrous histiocytoma, MFH, xanthosarcoma, malignant fibrous xanthoma, fibroxanthosarcoma, malignant histiocytoma) is a high-grade malignant neoplasm of soft tissue or bone and is essentially a diagnosis of exclusion. It is a malignant storiform neoplasm arising from histiocytes (Fig. 16.25) or from cells capable of histiocytic differentiation. Because this tumor's immunophenotype is nonspecific and the diagnosis is made by excluding other neoplasms, immunohistochemistry is used to rule out other spindle cell neoplasms of definable lineage.

Extrapleural solitary fibrous tumor (SFT; synonyms solitary fibrous tumor; hemangiopericytoma (obsolete); giant cell angiofibroma) is categorized by the WHO (2017) as a mesenchymal neoplasm of fibroblastic type that forms staghorn-patterned or "hemangiopericytoma-like vascular patterns, which are most commonly benign, although there is a malignant SFT as well. The tumor cells are positive for CD34, bcl2, and CD99; 20% to 30% show variable immunoreactivity for EMA and SMA. More than 70% of these tumors are benign, and histology is not necessarily predictive of behavior, although those with marked mitotic activity, necrosis, and nuclear pleomorphism are more likely to metastasize.

Odontogenic Tumors

The WHO (2017) classification of odontogenic tumors divides these pathologic entities into malignant odontogenic tumors

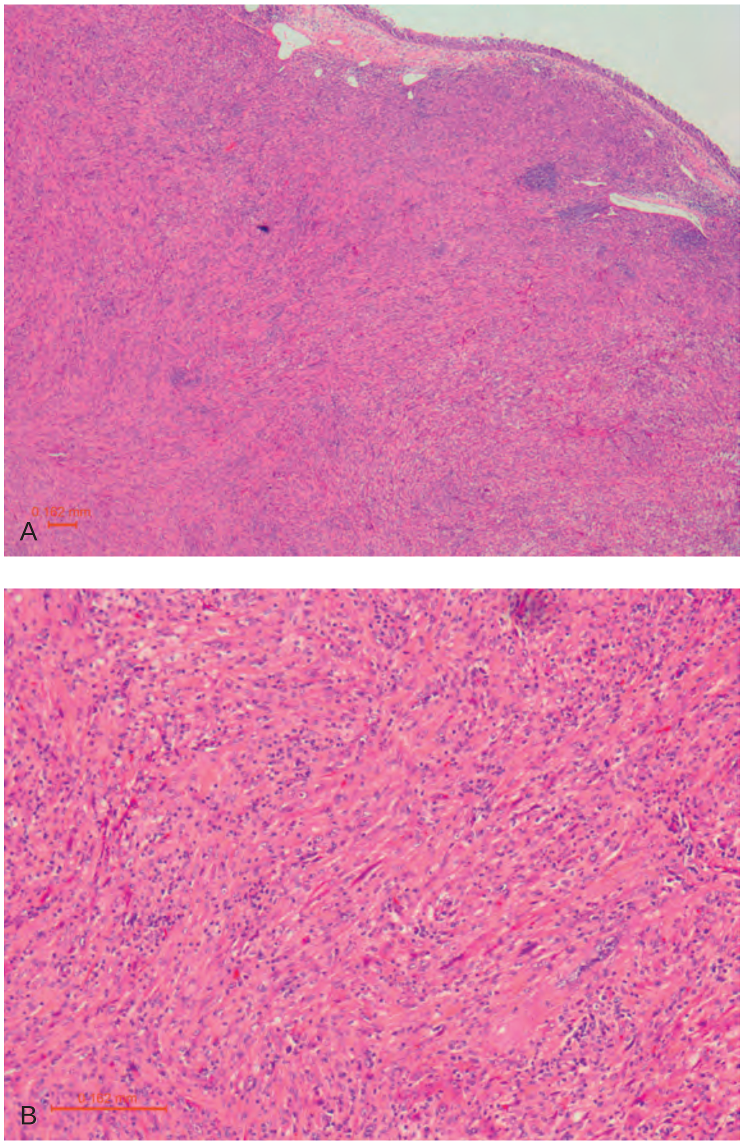

Figure 16.25 Undifferentiated pleomorphic sarcoma (UPS), malignant fibrous histiocytoma (MFH) of the larynx seen as a high-grade, pleomorphic mitotically active malignant spindle cell neoplasm (25× [**A**] and 100× [**B**]; H&E). Immunohistochemical studies were negative for melanoma markers (HMB45, S-100 protein), cytokeratins (CAM 5.2, 34Be12, and AE1:AE3), and muscle markers (HHF-35, SMA, and Desmin).

(carcinomas and sarcomas), benign odontogenic tumors (epithelial, mesenchymal, and mixed origin), and odontogenic cysts (developmental or inflammatory) (Table 16.2).

Ameloblastoma is a benign tumor of ameloblasts, which essentially recapitulates the development of the early tooth-forming apparatus without the formation of enamel or its precursors. As a group, 20% are seen in the maxilla, and 80% occur in the mandible, distributed as follows: 70% molar and ascending ramus, 20% premolar region, and 10% incisor region. They are divided into unicystic ameloblastoma, multicystic or solid ameloblastoma, peripheral ameloblastoma, and malignant ameloblastoma. The pathologic classification further defines ameloblastoma into four varieties: (1) conventional, (2) unicystic, (3) extraosseous/peripheral, and (4) malignant (metastasizing) ameloblastoma. Histologically, these tumors contain nests and islands of odontogenic epithelium with central stellate reticulum-like cells surrounded by peripheral tumor cells that most commonly have subnuclear vacuoles (Fig. 16.26). *Unicystic ameloblastoma* is unilocular and cystic with an epithelial lining consisting of ameloblastoma cells. This entity is seen to arise

Table 16.2 WHO classification (2017) of odontogenic tumors and cysts

TISSUE OF ORIGIN	BENIGN	MALIGNANT
Epithelial	Ameloblastoma Squamous odontogenic tumor Calcifying epithelial odontogenic tumor Adenomatoid odontogenic tumor	Ameloblastic carcinoma Interosseous (NOS) Sclerosing odontogenic carcinoma Clear cell odontogenic carcinoma
Mixed epithelial-mesenchymal	Ameloblastic fibroma Primordial odontogenic tumor Odontoma Dentinogenic ghost cell tumor	Ghose cell odontogenic carcinoma Odontogenic carcinosarcoma Odontogenic sarcoma
Mesenchymal	Odontogenic fibroma Odontogenicmyxoma/ myxofibroma Cementoblastoma Cemento ossifying fibroma	
Odontogenic cysts/ developmental	Dentigerous cyst Odontogenic keratosis Lateral periodontal Botryoid odontogenic cyst Gingival cyst Glandular odontogenic cyst Calcifying odontogenic cyst Orthokeratinized odontogenic cyst	
Odontogenic cysts/ inflammatory	Radicular cyst Collateral inflammatory cyst	

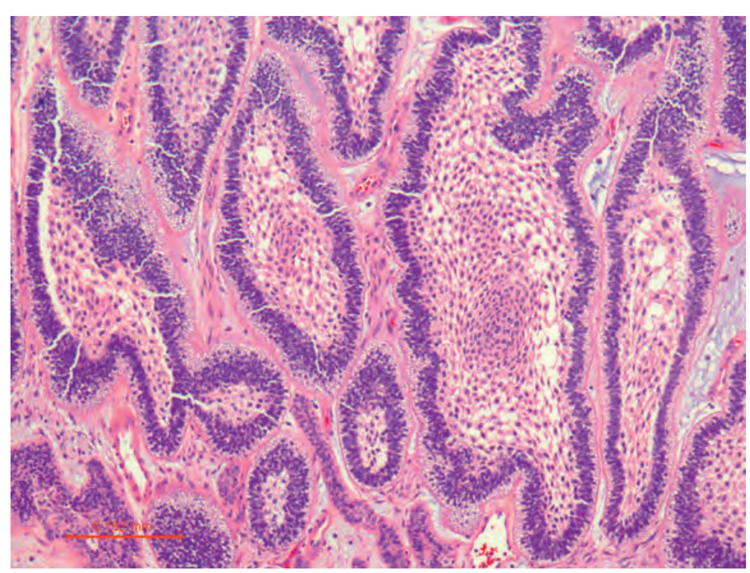

Figure 16.26 Ameloblastoma of the maxilla (100×; H&E) showing subnuclear vacuoles, giving the periphery of the tumor a "picket fence–like" appearance.

in young adults, almost exclusively in the mandible, with more than two-thirds of the lesions in the molar-ramus region. These are thought to be less aggressive than *multicystic ameloblastoma*. Unfavorable prognostic indicators for ameloblastoma include maxillary location in an older adult and extension of tumor from bone into adjacent soft tissue. Marked mitotic activity, nuclear pleomorphism, tumor necrosis, and evidence of metastasis would indicate a diagnosis of malignant ameloblastoma.

OKCs are cystic lesions that may be associated with the roots of teeth or impacted teeth and represent 5% to 15% of all odontogenic cysts. In up to almost 80% of cases of Gorlin-Goltz syndrome (also known as *nevoid basal cell carcinoma syndrome*), the diagnosis of OKC may be the first diagnostic indicator of the underlying genetic disorder. Histologically, these lesions typically display a stratified squamous epithelium of six to eight layers with a corrugated parakeratinized surface layer (Fig. 16.27). These lesions may be locally aggressive, with recurrence rates reported around 30%. Local recurrence has been correlated with the presence of islands of odontogenic epithelium in the cyst wall. There are rare case reports of squamous cell carcinoma arising in these lesions, but that is the exception and not the norm.

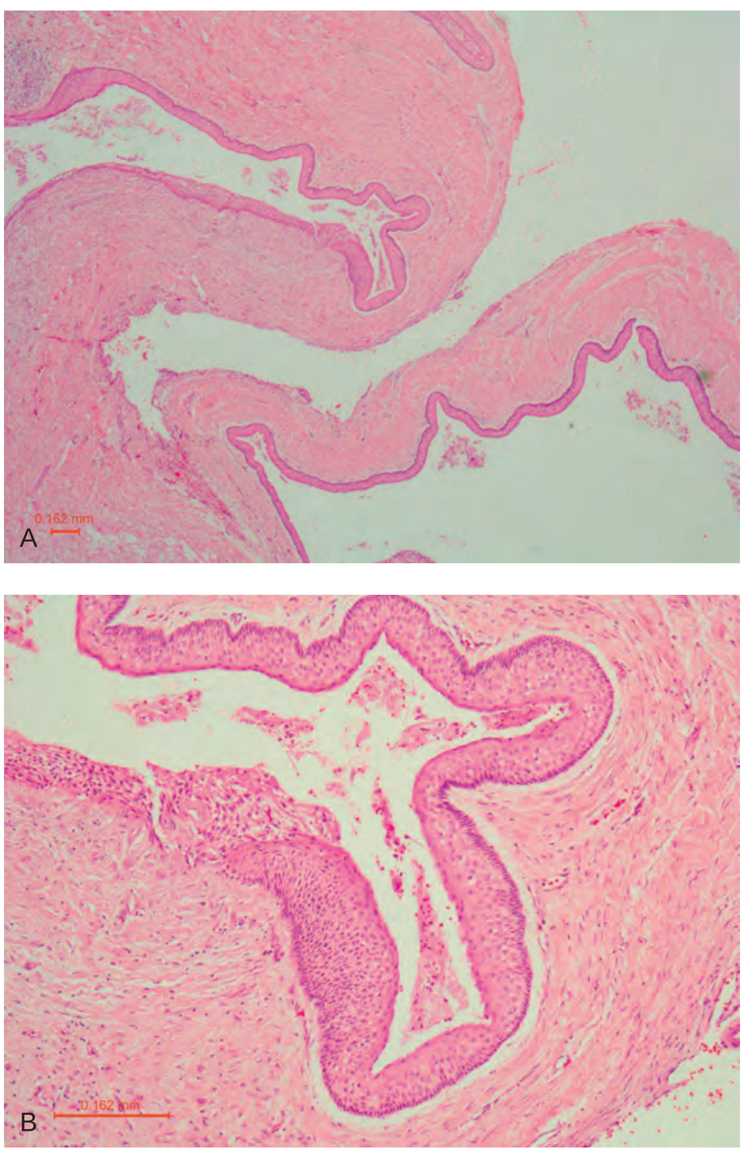

Figure 16.27 A, Odontogenic keratocyst showing squamous epithelial lining of the cyst wall. There are typically no odontogenic epithelial nests within the cyst wall (25×; H&E). **B**, At higher magnification (100×; H&E), the absence of cytologic atypia is apparent.

TREATMENT

Principles and Goals of Treatment

Surgical excision is the preferred modality of therapy for nearly all bone tumors arising in the head and neck region. Most symptomatic benign lesions can be treated adequately by a relatively conservative excision but preferably in a monobloc fashion depending on the size and location of the tumor. In a similar fashion, low-grade malignant tumors such as a low-grade chondrosarcoma and low-grade fibroosseous lesions also are managed by a relatively conservative surgical resection. On the other hand, high-grade malignant tumors require an aggressive surgical approach for satisfactory resection with adequate bone and soft-tissue margins. Histologically aggressive tumors require multimodality treatment to improve local control and reduce the risk of local recurrence or distant metastases. Solitary, symptomatic metastatic tumors to the craniofacial skeleton from primary carcinomas of the kidney, thyroid, lung, and breast occasionally may require surgical resection. Some lesions such as fibrous dysplasia are polyostotic. Involvement of multiple bones clearly would influence the decision for surgical treatment. Appropriate workup therefore should be undertaken to rule out multiple bone involvement.

Lesions of odontogenic origin usually are managed in a conservative fashion. An ameloblastoma is a locally invasive process that usually is treated by "complete excision" to avoid local recurrence. Small, localized ameloblastomas may be suitable for a relatively conservative excision, but larger tumors require complete resection that may include a segmental mandibulectomy or a maxillectomy. Similarly, small cystic ameloblastomas can be treated by curettage and marsupialization, but larger lesions require more aggressive resection. Curettage for larger lesions is unlikely to be successful and almost uniformly results in recurrent disease.

Neoadjuvant multidrug chemotherapy followed by surgical resection has become the standard of care for treatment of osteosarcoma of the extremities in the pediatric age group. The efficacy of this approach in head and neck osteosarcomas in the adult is however unproven. Thus primary surgical resection followed by adjuvant radiation therapy currently is recommended as the most effective treatment for head and neck osteosarcomas. Chondrosarcomas and other rare variants of bone sarcomas generally are treated with appropriate surgical resection. Proton beam radiation therapy for chondrosarcomas in an adjuvant setting has shown improved local control compared with conventional radiation therapy with photons. Treatment options for Ewing sarcoma have improved with the use of multidrug chemotherapy and radiation therapy, reserving salvage surgery for residual disease. A plasma cell tumor generally is managed with radiation therapy, keeping surgery in reserve for salvage. Treatment for multiple myeloma and lymphoma is systemic chemotherapy with or without radiation therapy.

Preoperative Preparation

Most patients requiring surgery for tumors of the craniofacial bones do not need any specific preoperative preparation other than imaging studies and accurate tissue diagnosis. If a massive resection is contemplated where significant blood loss is anticipated, then sufficient quantities of blood should be available to replace operative blood loss. Highly vascular lesions may be considered for preoperative embolization before surgical resection.

If the upper alveolus or maxilla is to be resected, then preoperative consultation from the maxillofacial prosthetic department should be obtained for preoperative dental impressions and fabrication of a dental obturator. If surgical resection entails orbital exenteration or resection of a major portion of facial bones, then preoperative photographs and facial moulage should be obtained for fabrication of facial/orbital prostheses. On the other hand, if bone reconstruction is planned after resection of the tumor, then CAD-CAM planning and modeling is strongly recommended to reduce operating time in designing an appropriate free bone flap to achieve accurate reconstruction. (See Chapter 17 for details.) Similarly, if a mandibulectomy is planned, then a microvascular free flap reconstruction from an appropriate donor site, generally from the fibula, should be planned with assistance of CAD-CAM modeling.

Lesions involving the calvarium or the skull base require neurosurgical consultation for a combined craniofacial approach for adequate surgical resection. In patients requiring craniofacial resections, antibiotics and steroids should be administered preoperatively to reduce the risk of postoperative sepsis and brain edema. Surgical resection of vertebral bodies requires adequate stabilization of the spine, which may require either neurosurgical or orthopedic consultation for posterior stabilization of the spine or to ascertain the availability of a halo splint for postoperative immobilization.

The operative procedures in this chapter are not discussed by tissue of origin, as was done in the chapter on soft-tissue tumors. Instead, the management of osseous tumors is described by the bones of origin, starting from the calvarium, skull base, maxilla, mandible, and cervical spine.

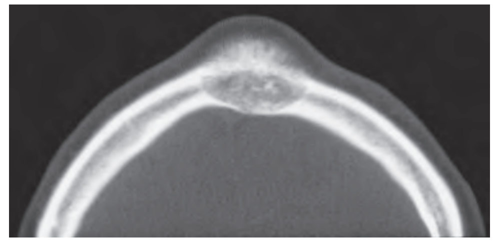

Figure 16.28 An axial view of the computed tomography scan (soft-tissue window) demonstrating the well-demarcated defect in the outer table with a "honeycomb" appearance.

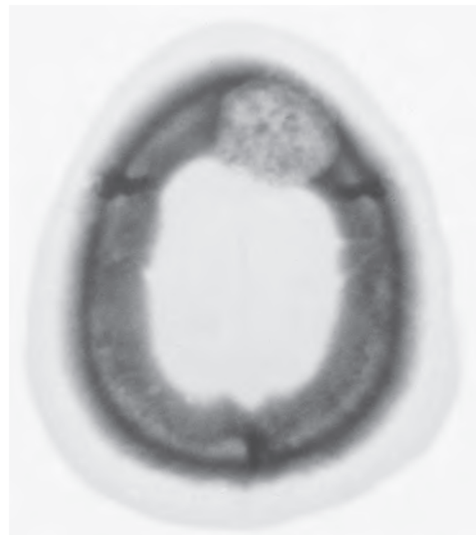

Figure 16.29 The bone window of the computed tomography scan of the same patient as in Table 16.1 shows the punched-out defect in the frontal bone.

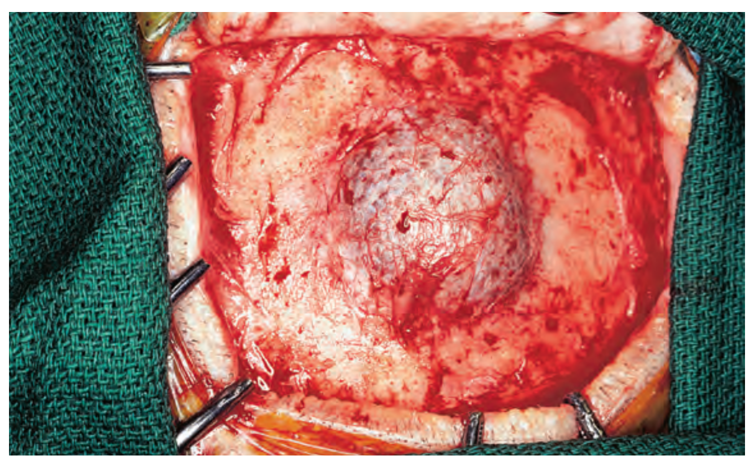

Figure 16.30 The scalp flap is elevated to expose the hemangioma.

Tumors of the Calvarium

Primary bone tumors of the calvarium are exceedingly rare. The benign lesions most frequently seen are osteomas and hemangiomas. The malignant tumors most frequently seen are osteogenic sarcoma, chondrosarcomas, other sarcomas, and metastatic lesions. The indications for surgery are related to histologic diagnosis and symptoms. Some benign lesions are asymptomatic and may simply be kept under observation.

Hemangioma of the Frontal Bone

Hemangiomas of the craniofacial skeleton are usually asymptomatic and present simply as a bony mass. On occasion the lesions get large and produce a skeletal deformity that requires surgical intervention. In addition, because of the progressive growth of the lesion, some patients have symptoms that warrant surgical intervention. A hemangioma in a stress-bearing bone may require surgical intervention to avoid a pathologic fracture. The most common site of hemangiomas in the craniofacial skeleton is the calvarium. The CT scan of a patient with a hemangioma of the parietal region is shown in an axial view (Fig. 16.28). Note the well-demarcated bony defect and the honeycomb appearance of the involved outer cortex of the calvarium. The bone window of the CT scan demonstrates a punched-out area of the frontoparietal region involved by the hemangioma (Fig. 16.29). The lesion had shown growth over the course of a year and was symptomatic with local pain at the site.

Surgical excision of the lesion requires a full-thickness craniectomy and an appropriate cranioplasty. The entire operative procedure is extradural. The patient is placed under general endotracheal anesthesia, and the scalp is shaved and prepared in the usual fashion. A U-shaped incision is made over the scalp around the palpable tumor, with the pedicle of the flap based anteriorly. The scalp flap is elevated deep to the pericranium, exposing the outer cortex of the frontoparietal region (Fig. 16.30). Note the purplish color of the hemangioma involving the bone. Two burr holes are made, one anterior and the other posterior to the lesion. With use of appropriate dural elevators, the underlying dura is separated from the inner cortex of the bone to free the area of bone involvement. A Midas Rex side-cutting power saw is used to complete the craniectomy by connecting the burr holes around the visible and palpable tumor. The surgical specimen is removed in a monobloc fashion

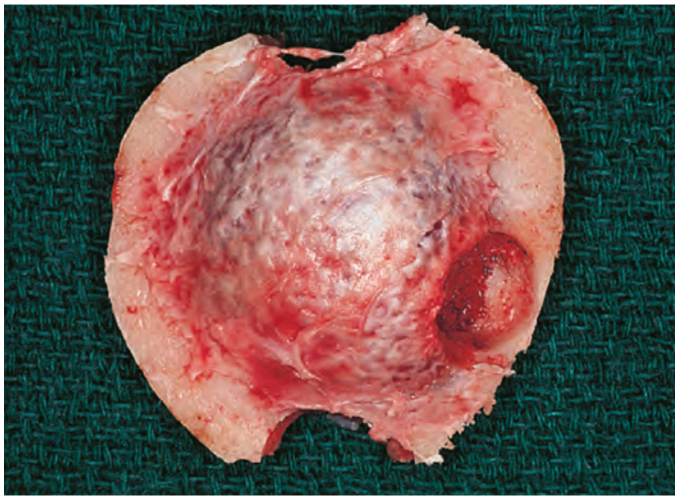

Figure 16.31 The surgical specimen.

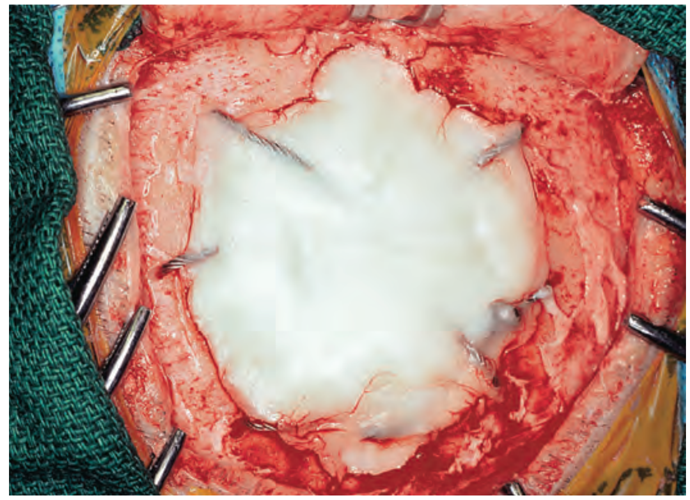

Figure 16.33 The wire acts as a matrix over which the bone cement is placed to provide a shell to repair the craniectomy defect.

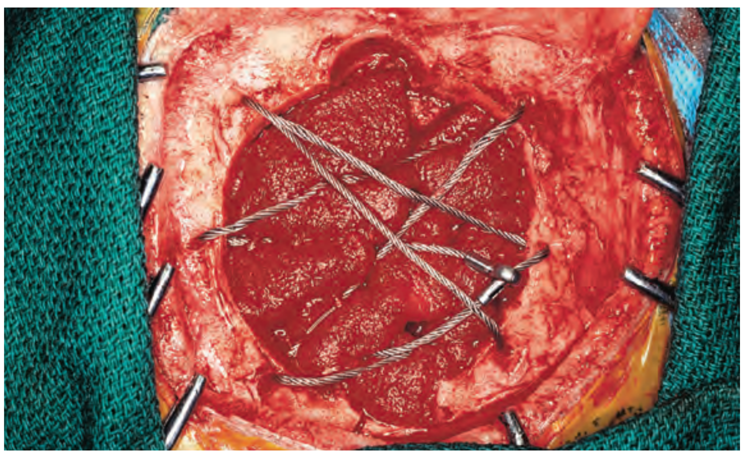

Figure 16.32 Braided wire is crisscrossed between the edges of the surgical defect.

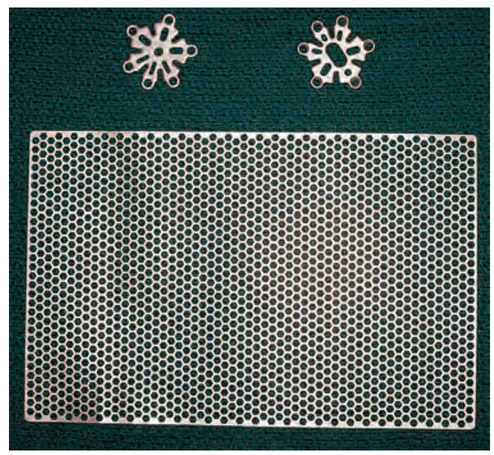

Figure 16.34 A titanium mesh or cranioplasty plate can be used to reconstruct the craniectomy defect.

(Fig. 16.31). Accurate hemostasis is secured by using bipolar cautery for control of bleeding from the dura and bone wax over the cut edges of the calvarium.

A cranioplasty of the craniectomy defect can be performed with a variety of different techniques. The simplest technique is to use a braided wire and bone cement. The wire is crisscrossed between the edges of the surgical defect, and bone cement is used to fill the surgical defect. The wire acts as a matrix over which the bone cement is spread to provide a shell to repair the craniectomy defect (Figs. 16.32 and 16.33). Alternatively, a titanium mesh can be used to provide a matrix of support for the bone cement, or special cranioplasty plates may be used without the bone cement to repair small surgical defects (Fig. 16.34). On the other hand, a computer-assisted cranioplasty prosthesis can be fabricated from Porex. The scalp incision is then closed over the cranioplasty in the usual manner.

Sarcoma of the Frontal Bone

Malignant tumors of the calvarium that are adherent to the overlying scalp and underlying dura require through-and-through monobloc resection. However, when these tumors involve the anterior cranial fossa, a craniofacial resection becomes necessary. If the tumor involves one orbit, then orbital exenteration in conjunction with a formal craniectomy and en bloc excision is indicated.

The patient described here has Paget disease involving the skull. He presented to a local surgeon with an enlarging mass on his forehead of approximately 6 months' duration. A generous open biopsy was performed with a transverse incision in the skin of the forehead, which confirmed the diagnosis of osteogenic sarcoma (Fig. 16.35).

A CT scan of the head in an axial plane with a soft-tissue window shows significant intracranial extension of disease with displacement and/or involvement of the dura and the frontal lobe on the left-hand side (Fig. 16.36). A representative axial view of the CT scan with a bone window shows the entire skull involved with Paget's disease (Fig. 16.37). The tumor involves the frontal bone on the left-hand side with extension of disease to involve the medial part of the frontal bone on the right-hand side. Significant soft-tissue extension is present in an extracranial fashion. A coronal view of the CT scan shows direct extension of the tumor in the orbit through its roof, displacing the globe inferiorly and laterally (Fig. 16.38). However, the tumor does not extend to involve the contents of the nasal cavity.

The operative procedure in this clinical setting requires involvement of two surgical teams. A neurosurgical team will begin with the craniotomy, and the head and neck team will accomplish the facial aspect of the procedure and reconstruction of the surgical defect with appropriate scalp flaps. A third surgical team for microvascular free tissue transfer may be required if

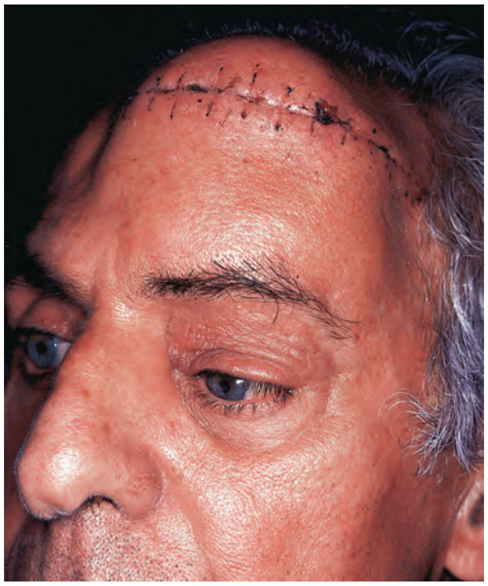

Figure 16.35 A patient with a bony lesion on the forehead. The scar of an open biopsy is visible.

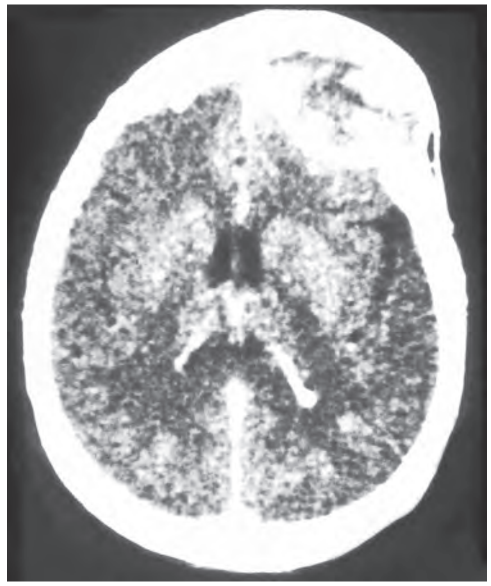

Figure 16.36 An axial computed tomography scan with a soft tissue window showing a massive tumor with intracranial and extracranial extension.

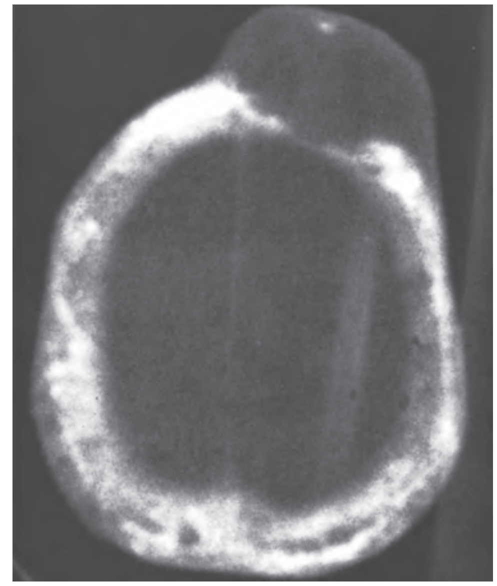

Figure 16.37 An axial CT scan of the head with a bone window showing the bone-destructive tumor and involvement of the cranium with Paget's disease.

Figure 16.38 A coronal view of a computed tomography scan showing extension of the tumor into the orbit.

Figure 16.39 An artist's rendering of the proposed extent of surgical resection.

free flap reconstruction of the surgical defect is planned. The technical details of craniofacial resection are discussed in Chapter 6. An artist's rendering of the extent of the tumor resection is shown in Fig. 16.39.

The surgical specimen shows the orbit, the frontal bone with the tumor, and the overlying skin excised in a monobloc fashion (Fig. 16.40). The posterior view of the specimen shows the excised portion of the dura and the frontal lobe (Fig. 16.41). The surgical defect of the craniectomy is continuous with the lower half of the orbital socket and the contents of the frontal fossa with exposed brain in that region. A close-up view of the surgical defect shows exposed brain of the left frontal lobe with a large dural defect due to its resection with the specimen (Fig. 16.42). Laterally, the stump of the temporalis muscle is visible in the temporal region.

A large segment of the periosteum from the posterior aspect of the skull is now excised and used as a free graft to repair the

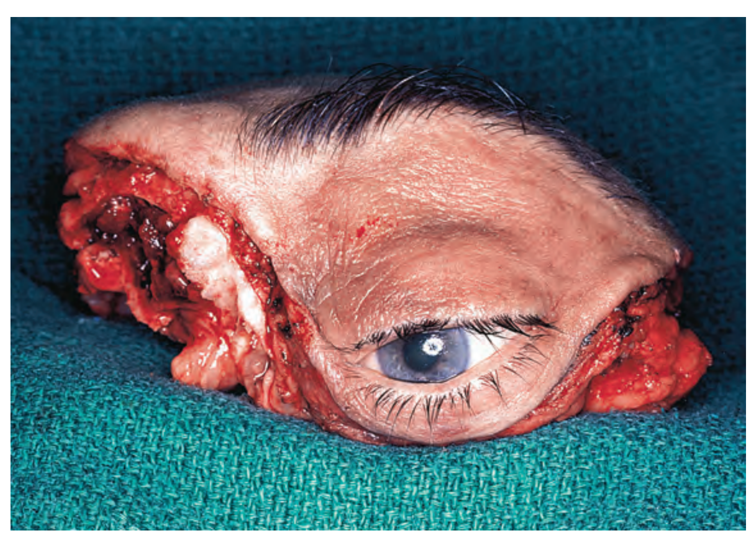

Figure 16.40 The anterior view of the surgical specimen.

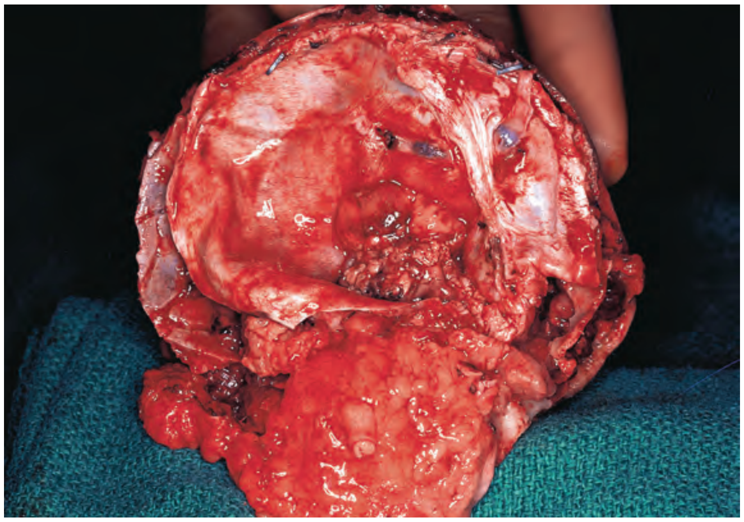

Figure 16.41 The posterior view of the specimen showing the intracranial tumor and the resected portion of the dura.

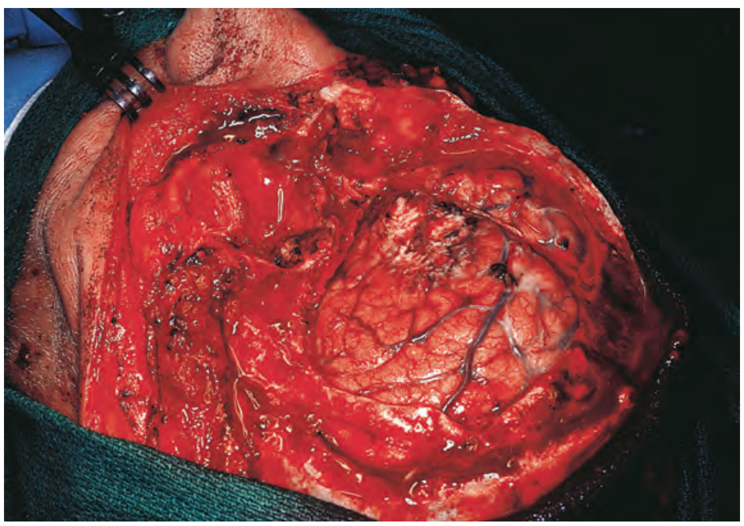

Figure 16.42 A close-up view of the surgical defect showing the exposed brain and the dural defect.

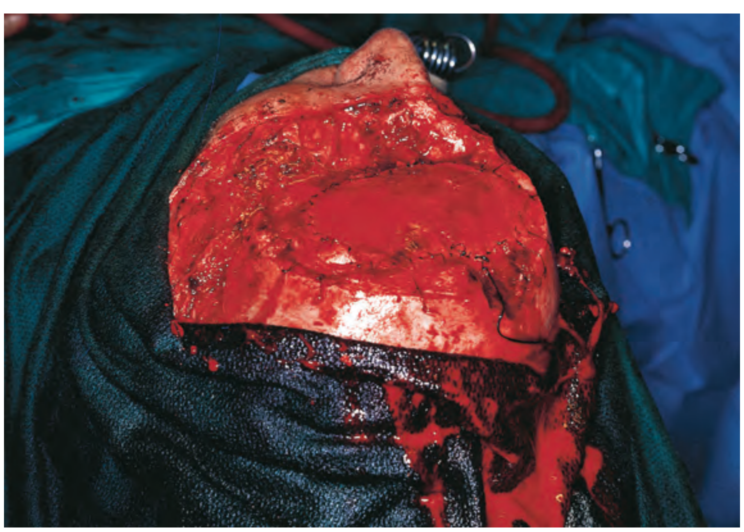

Figure 16.43 A watertight closure is obtained.

defect in the dura. The periosteum is sutured to the dura with 4-0 Nurolon sutures. A watertight closure is obtained to prevent any cerebrospinal fluid (CSF) leakage (Fig. 16.43).

A massive defect such as this is best reconstructed with a computer-assisted Porex prosthesis for bone reconstruction and soft tissue and skin free flap for coverage. A postoperative CT scan demonstrates total excision of the tumor of the frontal region with satisfactory margins (Fig. 16.44).

Figure 16.44 A postoperative computed tomography scan.

Metastatic Tumor to the Calvarium

Tumors of the calvarium that involve the overlying scalp require a through-and-through resection, often including the underlying dura. Primary tumors of the scalp invading the skull and primary tumors or symptomatic metastatic tumors of the calvarium warrant this type of surgical resection.

The plain radiographs of the skull demonstrate a bone-destructive lesion involving the cranial vault in the parietooccipital region on the right-hand side (Figs. 16.45 and 16.46). The soft-tissue windows of the CT scan of the patient shown here clearly demonstrate a bone-destructive lesion, which involves the overlying scalp with extension through the cranium to involve the underlying dura (Fig. 16.47). The extent of bone destruction is shown by a punched-out area of the calvarium on the bone window (Fig. 16.48). A needle aspiration biopsy of this lesion confirmed the diagnosis of metastatic renal cell carcinoma that was a solitary metastasis.

The patient is placed under general anesthesia in the supine position on the operating table with the left parietal region of

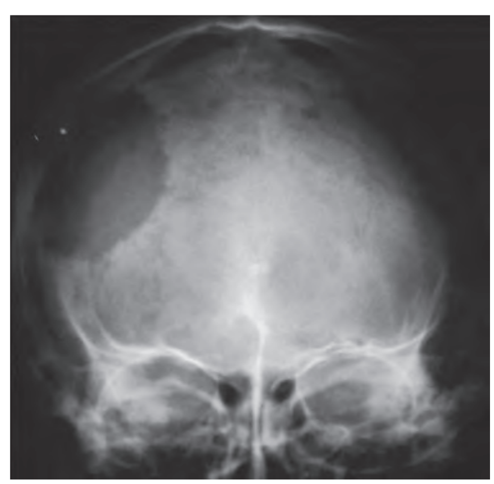

Figure 16.45 The anteroposterior view of the plain radiograph of the skull.

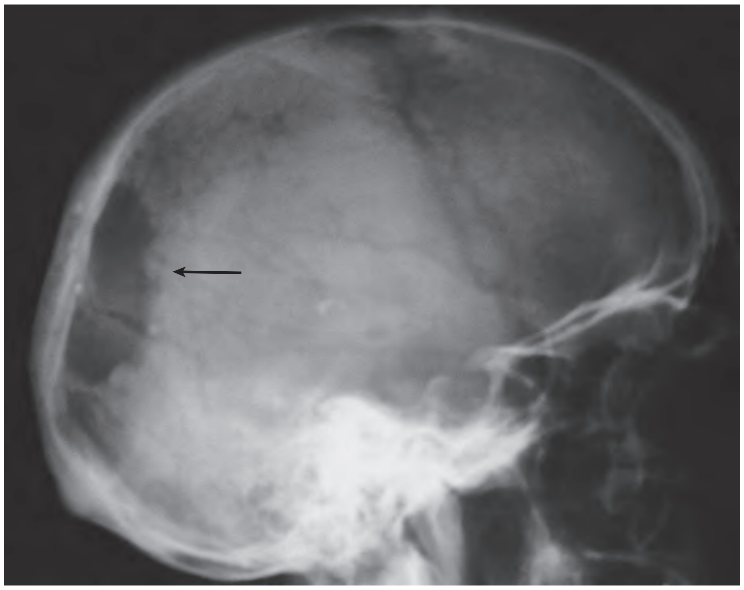

Figure 16.46 The lateral view of the plain radiograph of the skull showing the osteolytic lesion (*arrow*).

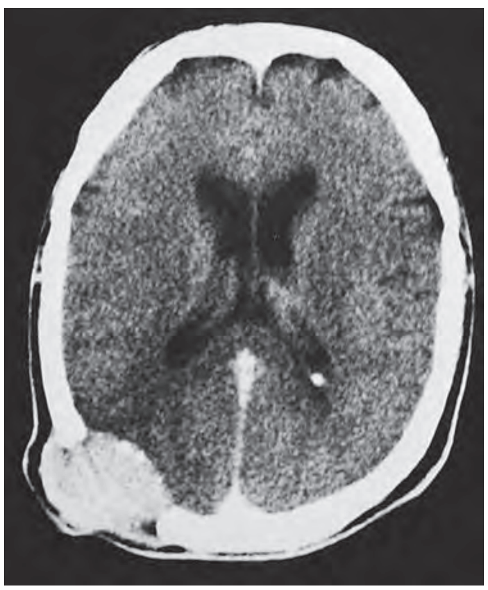

Figure 16.47 A computed tomography scan of the skull with a soft-tissue window shows the extracranial and intracranial component of the tumor.

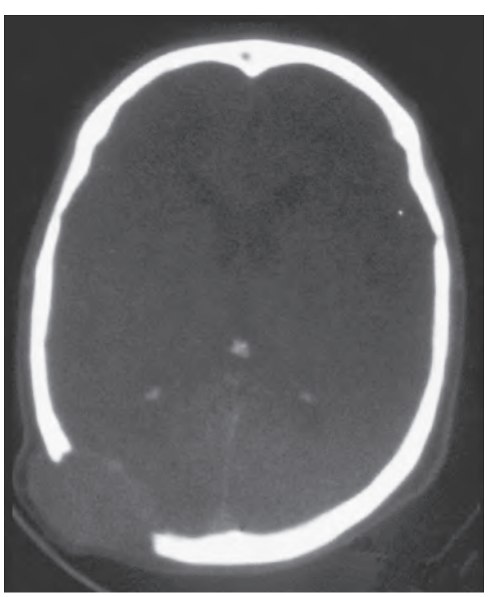

Figure 16.48 A computed tomography scan of the skull with a bone window shows a punched-out area of bone destruction.

Figure 16.49 The patient in position for surgery.

Figure 16.50 The incisions are outlined on the scalp.

the head resting on a standard U-shaped head rest (Fig. 16.49). The shaved scalp clearly shows the gross dimensions of the lesion. An indwelling spinal catheter is placed to monitor CSF pressure and to facilitate withdrawal of CSF to slacken the brain if necessary.

The incisions are outlined on the scalp (Fig. 16.50). The extent of the scalp that will need to be sacrificed to resect the tumor is shown. A parietal scalp flap is outlined; this scalp flap is based on the left-hand side, with the entire scalp elevated from the pinna of the ear on the right-hand side all the way up to the pinna of the ear on the left-hand side (Fig. 16.51). The blood supply to this flap is derived from the superficial temporal, posterior auricular, and occipital arteries of the left-hand side. The scalp flap is elevated all the way up to the pinna of the ear and the mastoid process on the left-hand side. The flap is elevated in a subgaleal plane, remaining superficial to the pericranium, which will be used later to repair the defect.

A circumferential incision now is made through the periosteum, remaining at least 1.5 to 2 cm away from the edges of the portion of the scalp that is to be sacrificed with the specimen (Fig. 16.52). The skull is now exposed subperiosteally in a circumferential fashion around the tumor. Multiple burr holes are made, and a craniotome is used to complete a circumferential craniectomy around the gross tumor (Fig. 16.53). The plane of dissection is still extradural. While making burr holes, care and

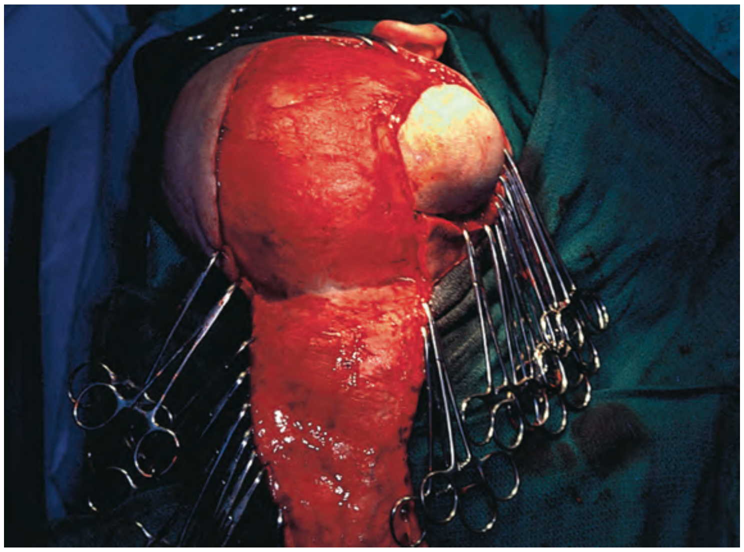

Figure 16.51 The parietal scalp flap is elevated in a subgaleal plane, remaining superficial to the pericranium.

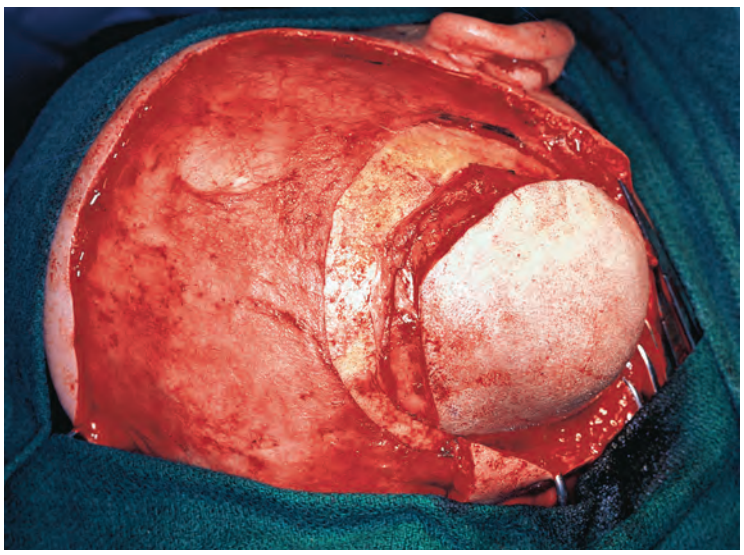

Figure 16.52 A circumferential incision is made in the periosteum around the tumor.

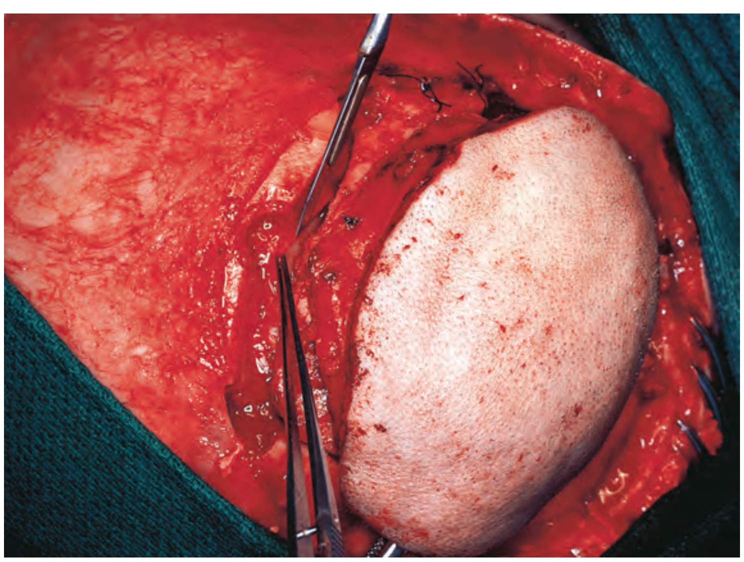

Figure 16.53 A circumferential craniectomy is completed through multiple burr holes, and the dura is opened.

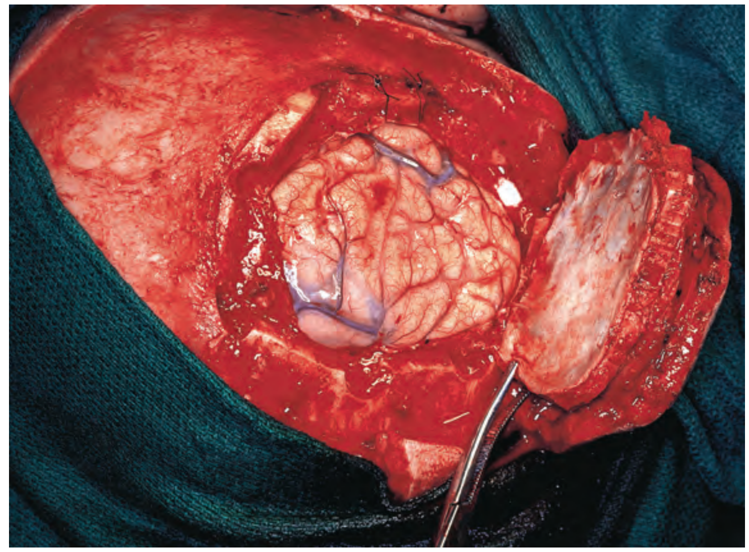

Figure 16.54 The surgical specimen is reflected posteriorly with the dura as its deep margin.

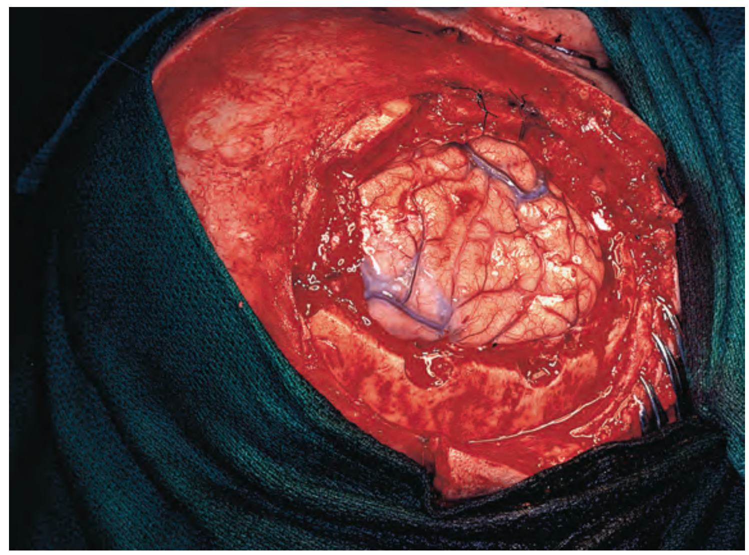

Figure 16.55 The surgical defect after removal of the specimen.

caution must be exercised to stay well away from the gross tumor to avoid compromising the adequacy of the resection.

A dural dissector is used to attempt to elevate the dura from the undersurface of the parietal bone. However, because the dura is adherent to and involved by the tumor, it must be resected, and it is entered by making an incision with a scalpel. Scissors are used to excise it circumferentially around the tumor to facilitate a monobloc resection. As the dura is incised, the surgical specimen becomes more mobile, permitting it to be rotated externally to further facilitate exposure of the remaining dural attachments and their division.

The surgical specimen is now reflected posteriorly with the dura attached to the tumor and exposing the underlying brain (Fig. 16.54). During this phase of the operation it is necessary to withdraw approximately 30 to 40 mL of CSF to slacken the brain and prevent CSF leakage. Bleeding from the dural vessels is controlled easily with a bipolar cautery.

The specimen is now removed, showing the surgical defect (Fig. 16.55). The brain is exposed as a result of sacrifice of the dura. Complete hemostasis must be secured at this point before closure of the dural defect is begun. Bleeding from the edges of the craniectomy defect is controlled with the use of bone wax.

The previously elevated scalp flap is now elevated further posteriorly to expose the left occipital region. The periosteum covering the skull in the occipital region on the left-hand side is thus exposed (Fig. 16.56). A generous portion of the periosteum of the skull over the occipital region from the left side is now elevated and excised to be used as a free graft for repair of the dural defect. The periosteum from the parietal region is not removed because that will be necessary to support the skin graft. A sufficient periosteal graft should be harvested to repair the dural defect. This periosteal graft is sutured to the edges of the dura with 4-0 Nurolon suture (Fig. 16.57). A watertight closure must be secured to prevent CSF leakage.

After satisfactory repair of the dural defect, the sharp edges of the craniectomy defect are smoothed out. Depending on the size and location of the craniectomy defect, a decision should be made regarding the need to reconstruct the bony defect. The previously elevated scalp flap is now rotated posteriorly to cover the craniectomy defect (Fig. 16.58). Closure of the scalp edges is performed in two layers with use of interrupted chromic catgut subcutaneous sutures and 3-0 nylon sutures for the skin. The donor site defect in the scalp of the parietal region still has its periosteum intact (Fig. 16.59). A split-thickness skin graft harvested from the thigh is now applied to the exposed periosteum. The skin graft is secured with continuous absorbable sutures to the edges of the scalp. It is retained in position with a bolster dressing.

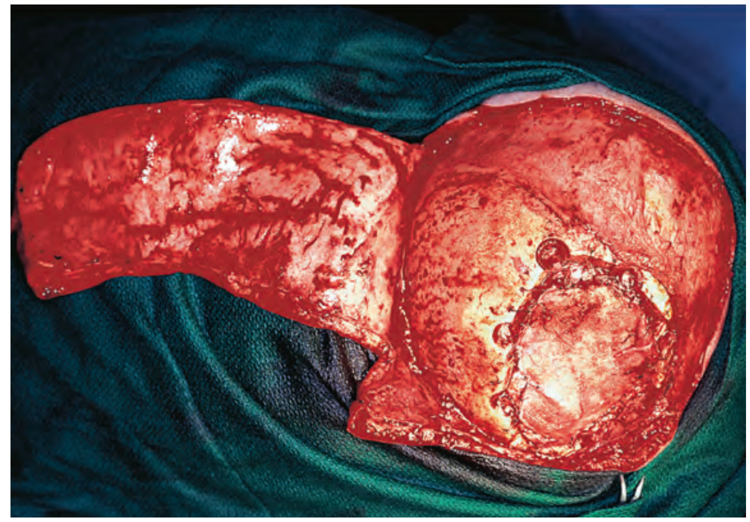

Figure 16.58 The scalp flap is rotated posteriorly to cover the craniectomy site.

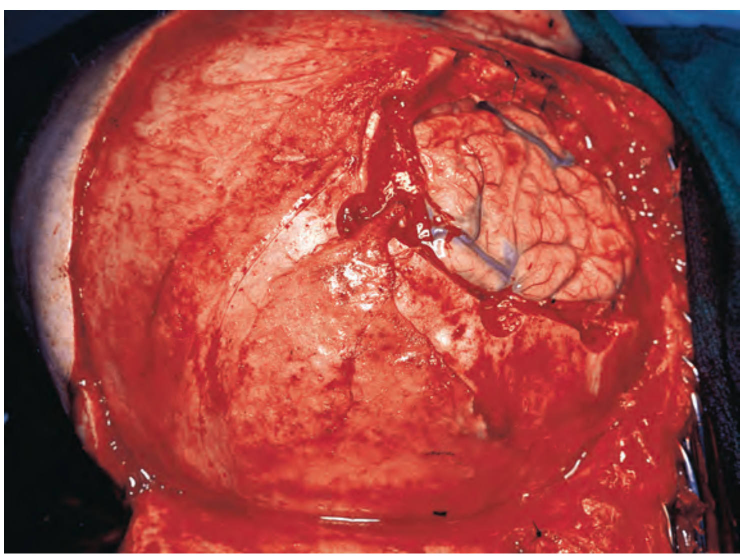

Figure 16.56 The periosteum covering the skull in the occipital region is exposed, and a pericranial graft is harvested.

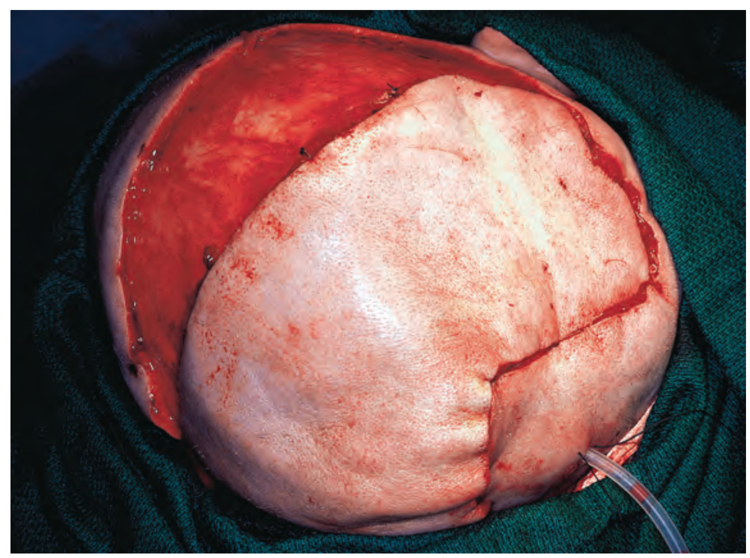

Figure 16.59 The donor site defect has its periosteum intact, over which a split-thickness skin graft is applied.

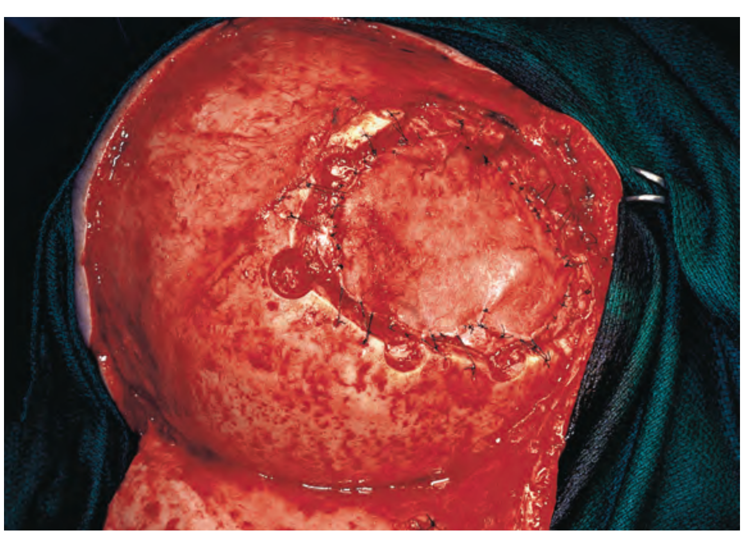

Figure 16.57 This periosteal graft is sutured to the edges of the dura.

Figure 16.60 The surgical specimen.

Figure 16.61 The deep surface of the surgical specimen.

Figure 16.62 The appearance of the patient 9 months after surgery.

A suction drain is placed beneath the rotated scalp flap. The surgical specimen shows the intact portion of the scalp resected with the tumor (Fig. 16.60). Its deeper surface shows intact dura, providing a monobloc resection of the tumor (Fig. 16.61).

The appearance of the patient 9 months following surgery shows satisfactory restoration of the scalp defect (Fig. 16.62). Although no bony support is present at the site of the craniectomy, the defect is covered with full-thickness scalp, and the split-thickness skin graft covers the skull at the donor site of the rotated scalp flap. A scalp flap rotated in this fashion provides very satisfactory coverage of craniectomy defects after resection of primary or metastatic tumors of the calvarium.

Tumors of the Facial Skeleton and Paranasal Sinuses

The most frequently seen benign tumors of the facial skeleton and paranasal sinuses are osteomas and fibroosseous lesions. Osteomas are seen most frequently in the frontal/ethmoid sinuses. Occasionally hemangiomas can develop in the facial skeleton. Chondrosarcomas and osteogenic sarcomas are the most predominant malignant lesions of this region.

Osteoma of the Facial Skeleton

An osteoma is a benign tumor of osseous origin that can arise in any facial bone. The mandible is the most commonly involved bone. Among the paranasal sinuses, the frontal and ethmoid sinuses are involved most frequently. Patients present with symptoms as a result of obstruction of the involved sinus cavity with secondary mucocele formation or occasionally an expansile lesion with distortion of the facial contour. Surgical treatment requires total excision via an appropriate surgical approach depending on the site of presentation. Osteomas grow very slowly, and small lesions often are not symptomatic. In some patients, osteomas present as a component of Gardner's syndrome. Patients with multiple osteomas of the facial skeleton therefore should be investigated for Gardner's syndrome in particular. Small osteomas may be left alone, but larger lesions or symptomatic lesions require surgical treatment.

The CT scan of a patient with an osteoma of the ethmoid sinus is shown in Figs. 16.63 and 16.64. An axial view with bone window demonstrates a bony lesion involving the right

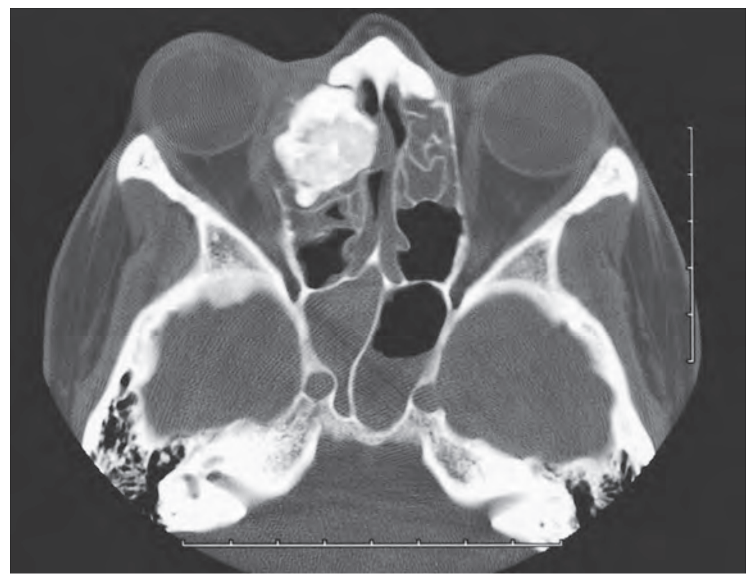

Figure 16.63 An axial view of the computed tomography scan (bone window) shows a dense lesion of the right ethmoid sinus pushing the globe anteriorly.

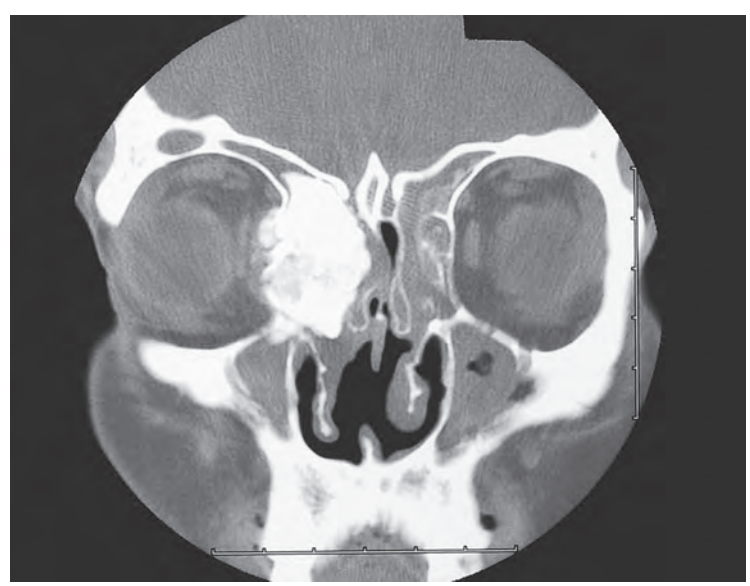

Figure 16.64 A coronal view (bone window) shows that the tumor displaces the right lamina papyracea laterally without involvement of the globe.

ethmoid region with displacement of the left globe anteriorly. The scan does not show any soft-tissue invasion or bone destruction, but it does show an expansile lesion filling up the ethmoid complex with displacement of the lamina papyracea of the right orbit. The coronal view shows that the tumor is completely replacing the right ethmoid complex with displacement of the right orbital contents as a result of displacement of the lamina papyracea. The tumor extends into the floor of the frontal sinus on the right-hand side, but no intracranial extension is present.

The surgical approach for this lesion required an external ethmoidectomy approach via a lateral rhinotomy with a Lynch extension. The medial wall of the orbit and the nasal bone are exposed. A facial disassembly is performed by removing the nasal bone and the medial wall of the orbit, which will be used later for reconstruction. After removal of these structures, adequate exposure of the ethmoid region and the floor of the frontal sinus is obtained. Adequate exposure is a key to the success of this surgical procedure.

The osteoma is inspected and its pedicle is identified. With use of a high-speed burr, the pedicle of the tumor is burred down to a very narrow margin. Eventually small osteotomes are used to fracture the tumor from its remaining attachments, allowing it to be removed in a monobloc fashion. The surgical defect demonstrates complete excision of the tumor (Fig. 16.65). The surgical specimen shows a multilobulated osteoma arising from the frontoethmoidal region that has been removed in a monobloc fashion (Fig. 16.66). The previously disassembled facial bones are repositioned in their proper place and fixed with microplates and screws (Fig. 16.67). The appearance of the patient 3 months following surgery shows satisfactory healing of the skin incision with repositioning of the globe and restoration of binocular vision (Fig. 16.68). A postoperative CT scan shows the extent of the bony resection and complete removal of the tumor (Fig. 16.69).

Ossifying Fibroma of the Ethmoid

The patient shown in Fig. 16.70 is an 11-year-old boy who previously had undergone a lateral rhinotomy and attempted excision of an obstructing lesion from the left nasal cavity that, upon histologic analysis, was diagnosed as an ossifying fibroma. Some residual lesion was left behind, and the patient was asked

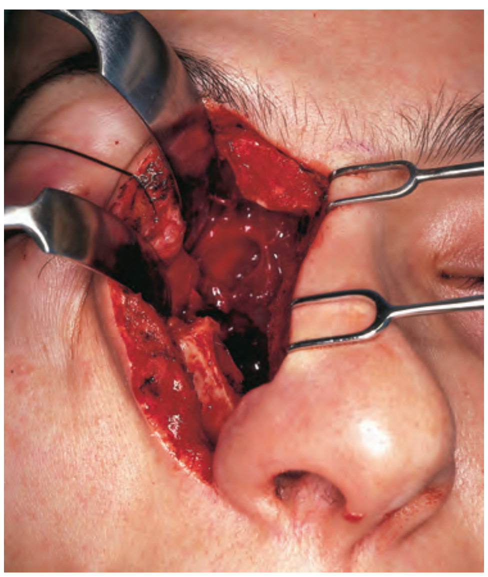

Figure 16.65 The surgical defect after the tumor has been excised through a right lateral rhinotomy and facial disassembly procedure.

Figure 16.66 The surgical specimen.

Figure 16.67 The facial bones are repositioned with the use of microplates and screws.

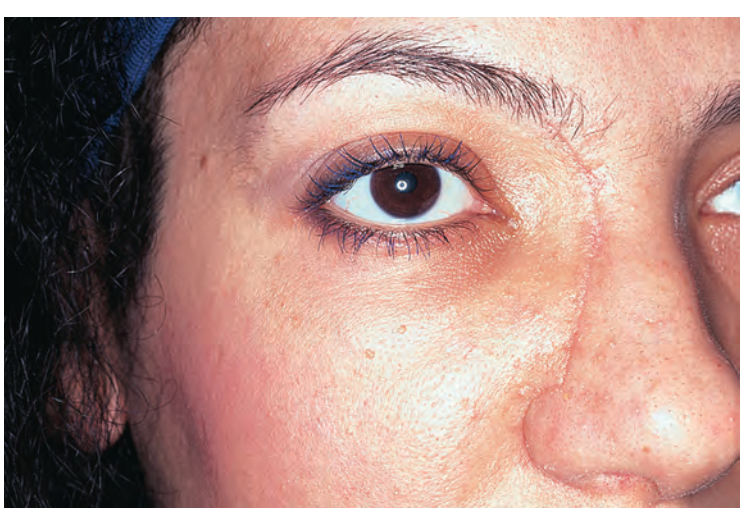

Figure 16.68 An early postoperative view of the patient shows the healed incision and the normal position of the right globe.

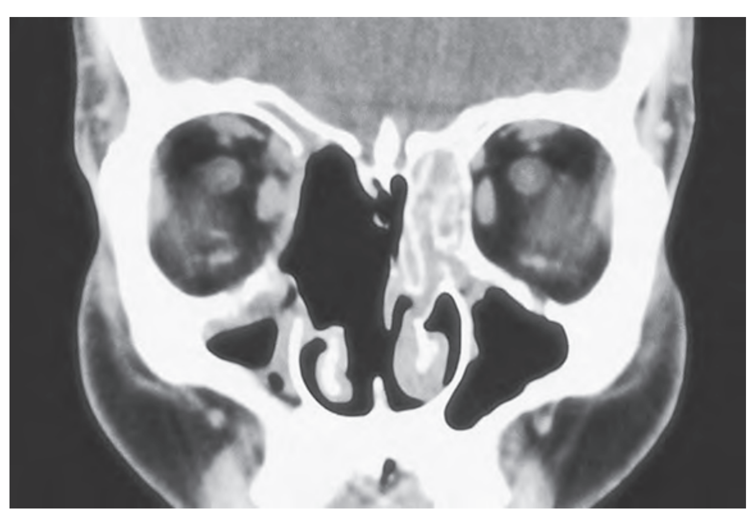

Figure 16.69 A coronal view of the postoperative computed tomography scan shows complete excision of the tumor.

Figure 16.70 This patient previously had undergone a lateral rhinotomy for excision of an obstructing lesion from the left nasal cavity.

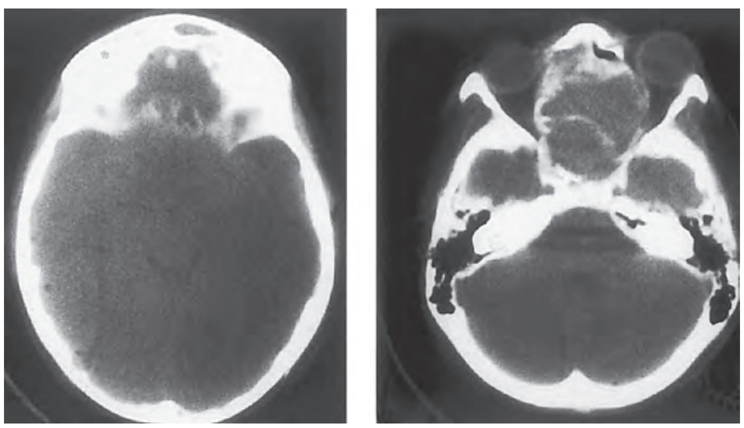

Figure 16.71 Axial computed tomography scans show a hypodense fibroosseous lesion of the ethmoid sinuses.

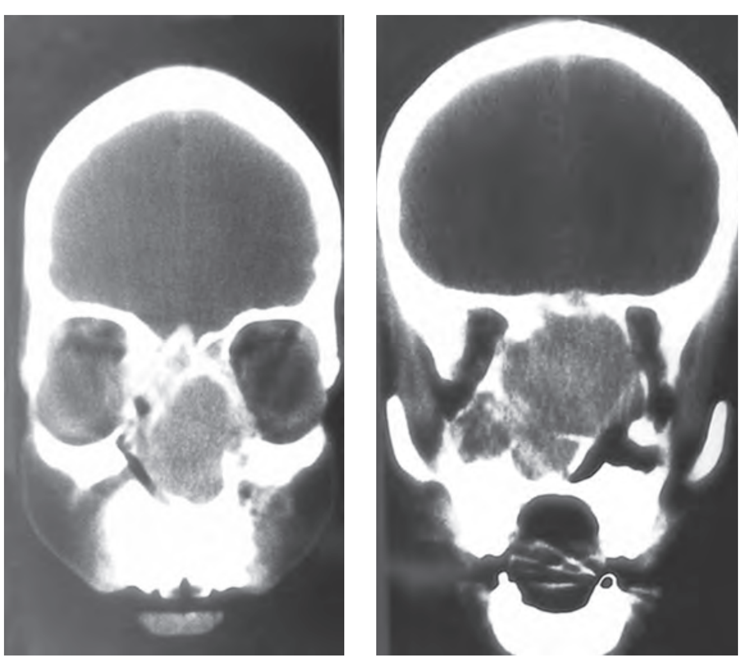

Figure 16.72 Coronal views of the computed tomography scans show the tumor extending up to the cribriform plate and into the sphenoid sinus.

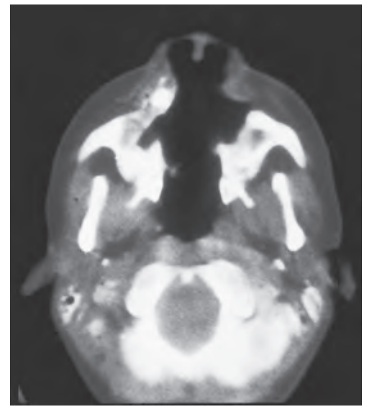

Figure 16.73 A postoperative computed tomography scan through the maxillae shows complete removal of the tumor from the nasal cavity.

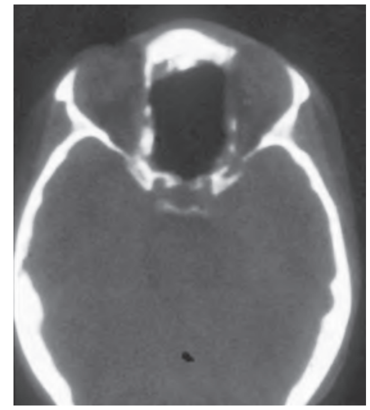

Figure 16.74 A computed tomography scan through the orbits shows complete clearance of the tumor from the ethmoid sinuses.

to seek further consultation for definitive treatment. CT scans in axial and coronal planes demonstrate a bone-destructive expansile lesion filling up the entire nasal cavity and extending from the cribriform plate cephalad to the floor of the nasal cavity caudad (Figs. 16.71 and 16.72). A lesion of this magnitude requires a craniofacial approach for total removal. The technical details of craniofacial resection are described in Chapter 6. Postoperative CT scans of the same patient (Figs. 16.73 and 16.74) demonstrate complete removal of the tumor.

Hemangioma of the Nasal Bone

All hemangiomas of the craniofacial skeleton do not require surgical intervention. However, they must be monitored clinically as well as radiologically for symptoms, growth, or any other changes on imaging studies raising suspicion for malignancy. The patient shown in Fig. 16.75 has a bony hard mass on the upper aspect of the left nasolabial region, of several years duration. He has no other symptoms. Initial MRI scan with contrast in a sagittal view clearly shows a well-defined lesion with a honeycomb architecture, diagnostic of a hemangioma. A follow-up CT scan in axial, coronal, and sagittal views with bone windows several years later shows a stable lesion, with no changes in the size or characteristics of the tumor (Fig. 16.76).

Figure 16.75 External appearance of a bony hard mass in the left nasolabial region.

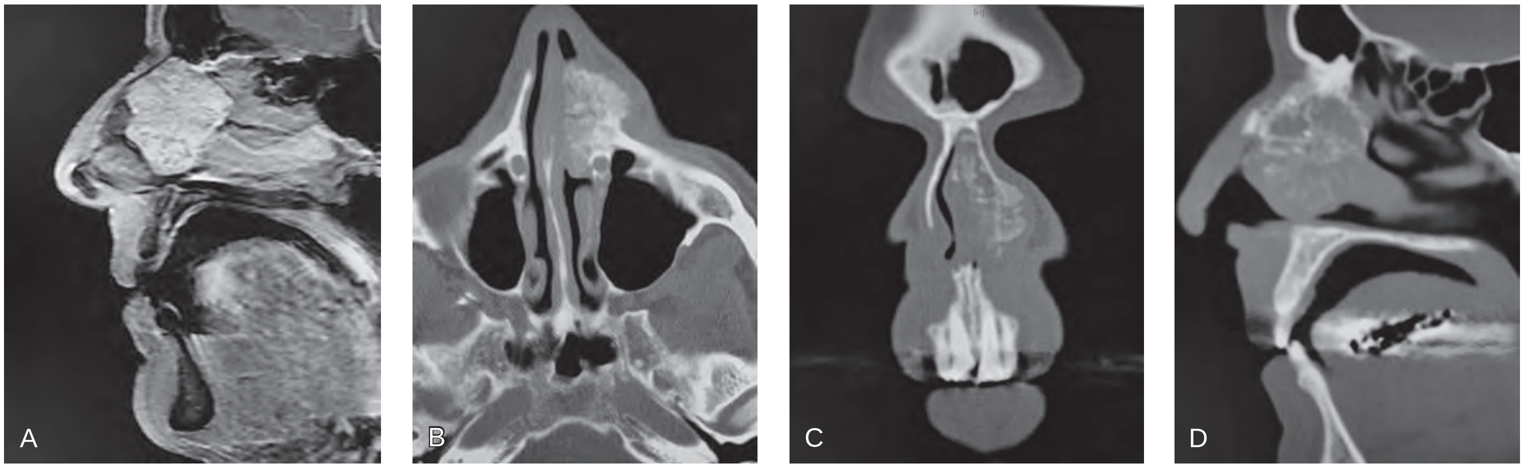

Figure 16.76 **A**, Sagittal view of a magnetic resonance imaging scan shows a well-circumscribed hyperintense lesion in the nasoethmoid region. A computed tomography scan with bone windows in axial (**B**), coronal (**C**), and sagittal (**D**) views show a characteristic honeycomb appearance of the hemangioma.

Osteogenic Sarcoma of the Ethmoid

The patient whose CT scan is shown in Fig. 16.77 had an osteosarcoma of the ethmoid region. Resection initially was attempted elsewhere with a lateral rhinotomy approach. An incomplete resection was performed, after which the patient underwent chemotherapy and radiation therapy. In spite of these treatments, the tumor progressed, and the patient presented with a massive tumor filling up the nasal cavity, the left maxillary antrum, and the ethmoid region, with extradural extension into the anterior cranial fossa. The tumor had infiltrated the periorbita of the left-hand side and had displaced the globe in the right orbit.

A craniofacial resection with orbital exenteration was performed in a monobloc fashion. For technical details of the operative procedure, please refer to Chapter 6. A standard bifrontal craniotomy was performed, and the floor of the anterior cranial fossa was approached in an extradural fashion. Because the tumor had invaded the dura, the dura of the frontal fossa was resected. The surgical defect shows a massive cranioorbital resection with excision of the dura at the floor of the anterior cranial fossa in conjunction with orbital exenteration, maxillectomy, and exenteration of the nasal cavity (Fig. 16.78).

The surgical specimen from the anterior view shows the left orbit and the skin of the frontal region resected with the tumor en bloc (Fig. 16.79). The posterior view of the surgical specimen shows the intracranial component of the tumor with a craniectomy of the frontal bone and the floor of the anterior cranial fossa accomplished in a monobloc fashion (Fig. 16.80). The surgical defect in this patient was reconstructed with use of a rectus abdominis myocutaneous free flap. The appearance of the patient 3 months following surgery shows satisfactory primary healing of the wound (Fig. 16.81). Although the aesthetic appearance of the patient is not optimal, the massive surgical defect has been repaired in a single-stage operation with primary healing. Further reconstructive efforts and restoration of the contour of the face will be required. Eventually an external facial prosthesis may be fabricated for aesthetic rehabilitation of the face.

Figure 16.77 A coronal view of the computed tomography scan shows a massive tumor filling up the nasal cavity, the left maxillary antrum, and the ethmoid region, with extradural extension into the anterior cranial fossa.

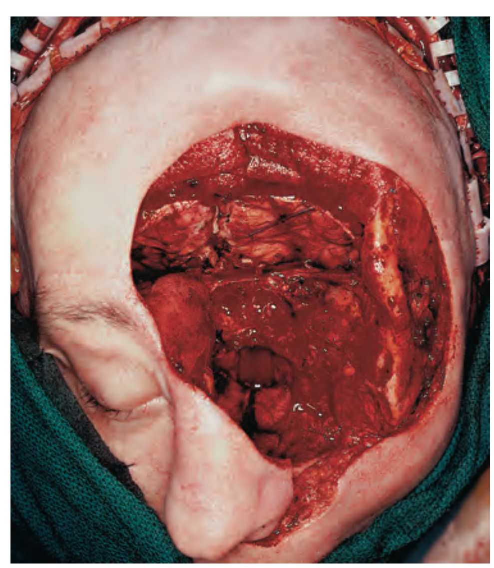

Figure 16.78 The defect after surgical excision of the tumor.

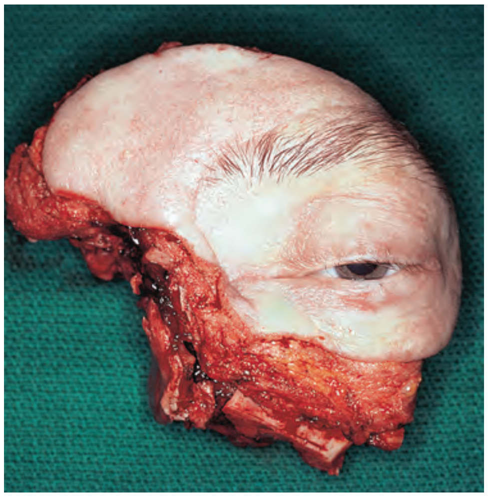

Figure 16.79 The anterior view of the surgical specimen.

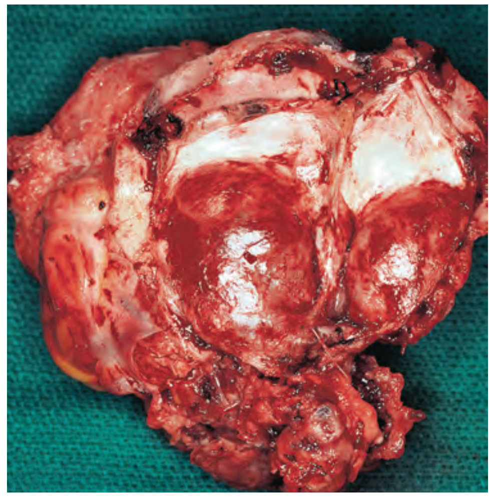

Figure 16.80 The posterior view of the surgical specimen.

Figure 16.81 The appearance of the patient 3 months following resection and reconstruction with a rectus abdominis myocutaneous free flap.

Low-Grade Chondrosarcoma of the Nasal Cavity

The patient whose MRI scan is shown in Fig. 16.82 presented with a 6-month history of progressive nasal obstruction and slight proptosis on the right-hand side. MRI scans in the axial, sagittal, and coronal planes demonstrate a well-demarcated bone-destructive lesion with speckled calcification occupying the entire nasal cavity and the right maxillary antrum, approaching the floor of the orbit and the cribriform plate at the base of the skull (Figs. 16.83 and 16.84). Tissue diagnosis of a low-grade chondrosarcoma was secured with a biopsy performed through the nasal cavity. Surgical resection for a lesion of these dimensions and in this location requires a craniofacial approach. The details of the technique of craniofacial resection are described at length in Chapter 6.

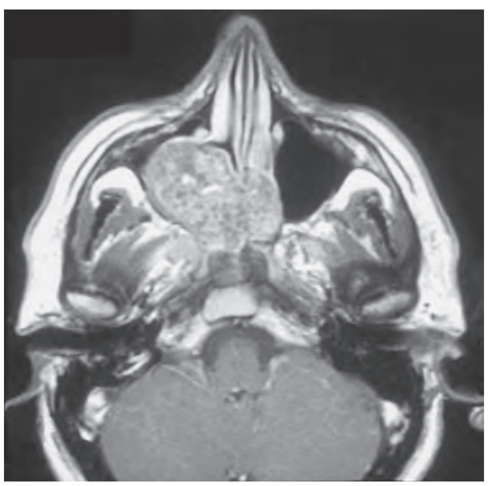

Figure 16.82 An axial view of the magnetic resonance imaging scan shows a honeycomb-like tumor in the nasal cavity and right maxilla.

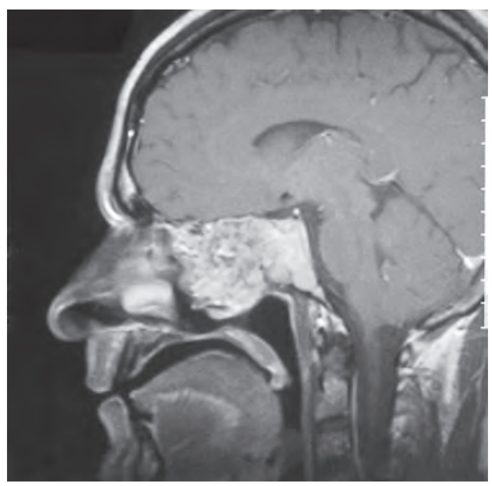

Figure 16.83 A sagittal view of the magnetic resonance imaging scan shows the tumor extending up to the cribriform plate.

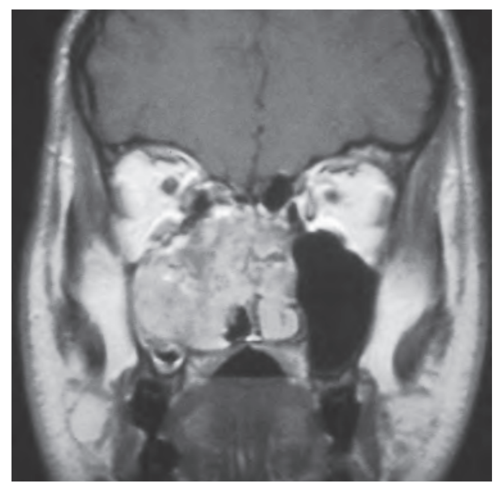

Figure 16.84 A coronal view of the magnetic resonance imaging scan shows a tumor of the nasal cavity and maxilla extending up to the skull base.

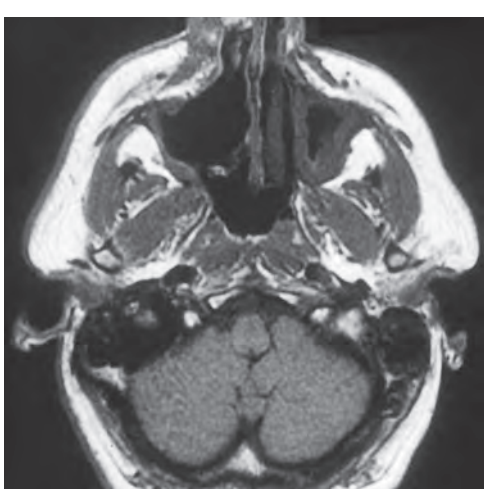

Figure 16.85 An axial view of the postoperative magnetic resonance imaging scan.

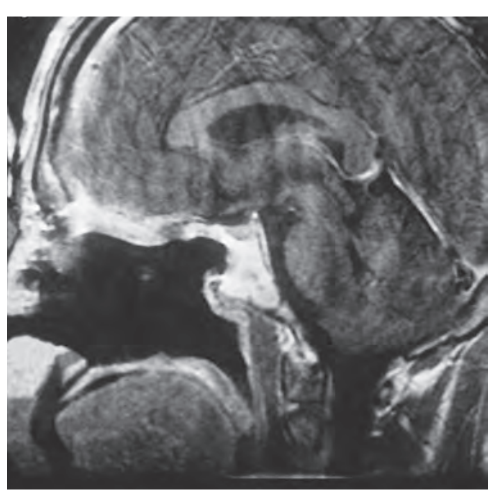

Figure 16.86 A sagittal view of the postoperative magnetic resonance imaging scan.

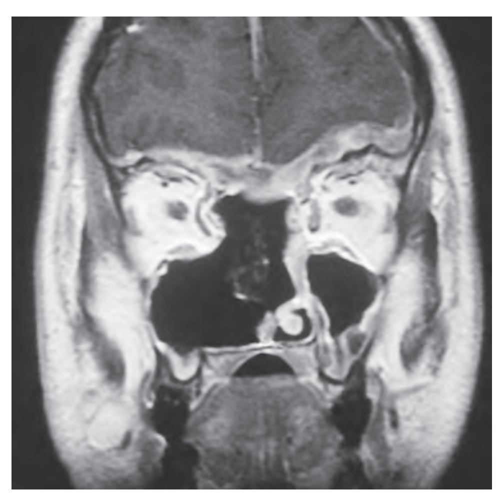

Figure 16.87 A coronal view of the postoperative magnetic resonance imaging scan.

Postoperative MRI scans of the same patient in the axial, sagittal, and coronal planes demonstrate total resection of the tumor from the nasal cavity and right maxillary antrum all the way from the base of the skull cephalad to the floor of the nasal cavity caudad (Figs. 16.85 through 16.87). Because this lesion is low grade, no additional treatment is necessary.

High-Grade Chondrosarcoma of the Orbit

The patient shown in Fig. 16.88 had previously undergone a conservative surgical approach for excision of a chondrosarcoma of the frontal ethmoid region through a supraorbital incision, but the tumor promptly recurred. A biopsy of the excised tumor proved that it was a high-grade chondrosarcoma. An axial CT scan through the level of the midorbit clearly shows a massive tumor involving the medial portion of the left orbit with extension into the nasal cavity (Fig. 16.89). This patient required a craniofacial resection with orbital exenteration and resection of a portion of the frontal bone and the roof of the orbit to excise the tumor in a monobloc fashion. The surgical specimen is shown in Fig. 16.90. Technical details of the surgical procedure of craniofacial resection are discussed at length in Chapter 6.

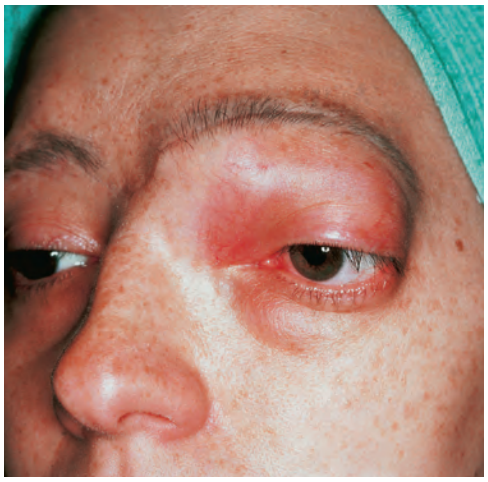

Figure 16.88 This patient previously had undergone an attempt at surgical excision of a chondrosarcoma of the frontal ethmoid region through a supraorbital approach.

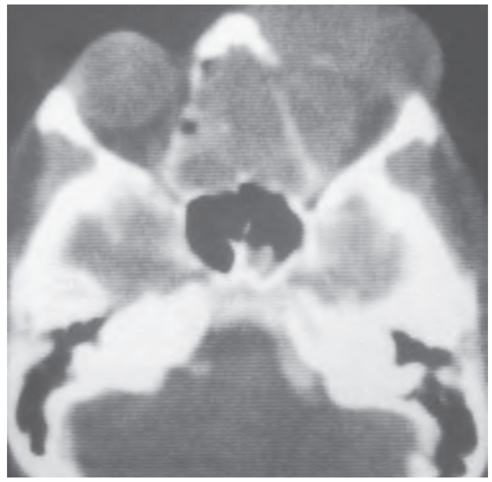

Figure 16.89 An axial computed tomography scan showing a tumor in the ethmoid sinuses and orbit.

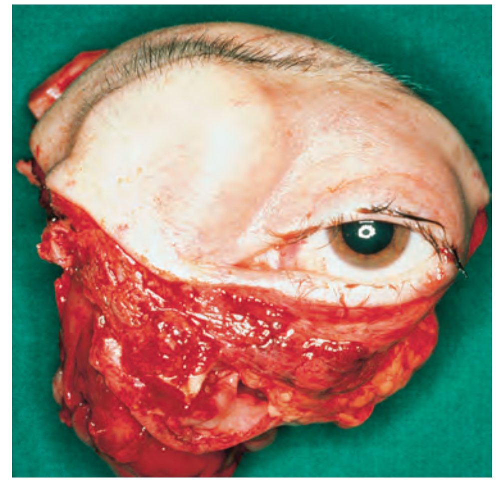

Figure 16.90 The surgical specimen.

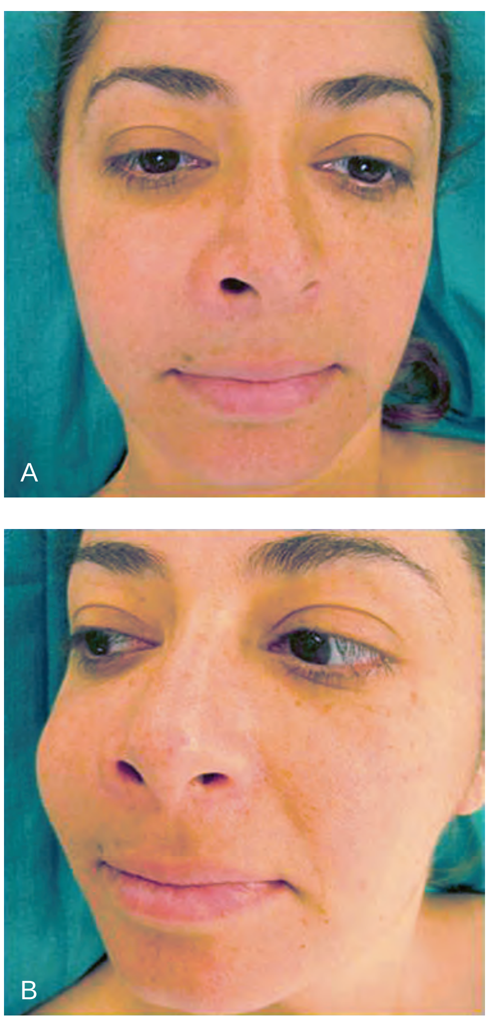

Figure 16.91 Preoperative appearance of the patient with a bony hard mass in the soft tissues of the cheek, anterior to the maxilla.

Benign Tumors of the Maxilla

Benign lesions of the maxilla include fibroosseous lesions such as an ossifying fibroma or osteoma, as well as tumors of vascular origin. Giant cell tumors also occur in the maxilla. In addition, tumors and cysts of dentoalveolar origin also can occur in the maxilla, although less frequently than the mandible. These lesions are locally progressive but histologically benign. Therefore conservative but complete excision is required to prevent recurrence.

Giant Cell Granuloma

The patient shown in Fig. 16.91 noticed a progressive swelling in her right cheek over a period of 8 months. There were no other associated symptoms. An axial view of a noncontrast CT scan of the sinuses shows a well-demarcated cystic lesion with an eggshell thin bony wall arising from the anterior wall of the maxilla causing swelling and displacement of the soft tissues of the right nasolabial region (Fig. 16.92). An attempt was made elsewhere to treat this lesion with an intraoral excision

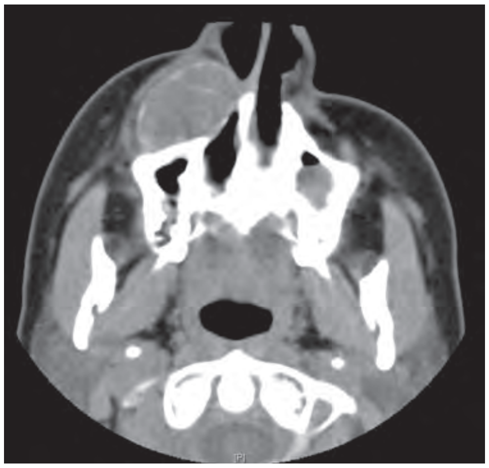

Figure 16.92 Axial view of a noncontrast computed tomography scan of the sinuses shows a mass anterior to the right maxilla in the soft tissues of the cheek. Note the eggshell-thin bony wall of the cystic lesion.

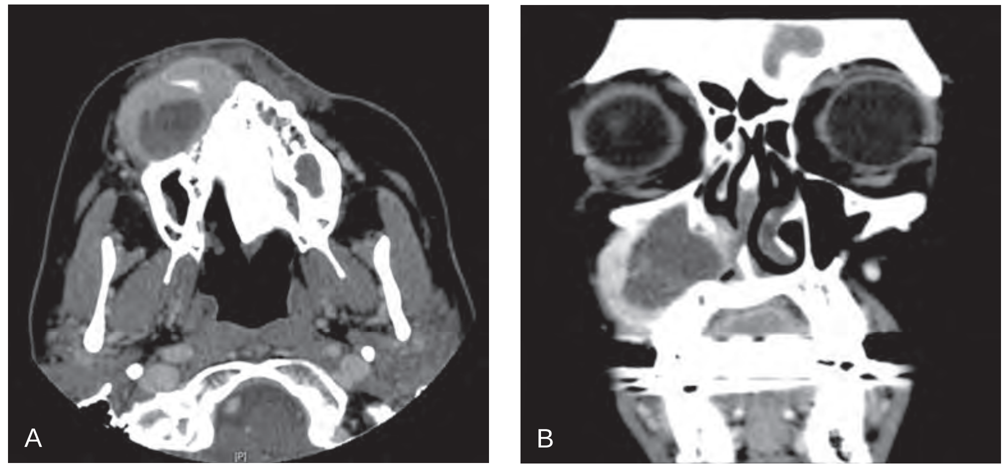

Figure 16.93 A contrast-enhanced computed tomography scan of the sinuses in axial (**A**) and coronal (**B**) views showing a thick wall, cystic lesion following previous attempted excision.

and curettage. However, that was unsuccessful, and the lesion promptly recurred. Repeat CT scans with contrast now show a thick-walled cystic lesion anterior to the maxilla and involving the alveolar process (Fig. 16.93). Surgical resection of this lesion was performed through an upper lip splitting incision with lateral rhinotomy approach. A monobloc excision of the lesion was performed with upper alveolectomy, without entering the maxillary sinus. The surgical specimen shows a monobloc resection of the tumor. On the cut surface of the specimen a cystic lesion filled with brownish chocolate-colored fluid was seen. The lesion extended into the alveolar process of the maxilla (Fig. 16.94). The intraoral view shows a well-healed surgical defect of the upper alveolectomy without any communication with the maxillary sinus (Fig. 16.95). She wears a partial upper denture to replace the lost teeth. The postoperative appearance of the patient 1 year following surgery shows a well-healed scar and aesthetically acceptable appearance (Fig. 16.96).

Figure 16.95 Postoperative intraoral view showing loss of the right upper alveolus.

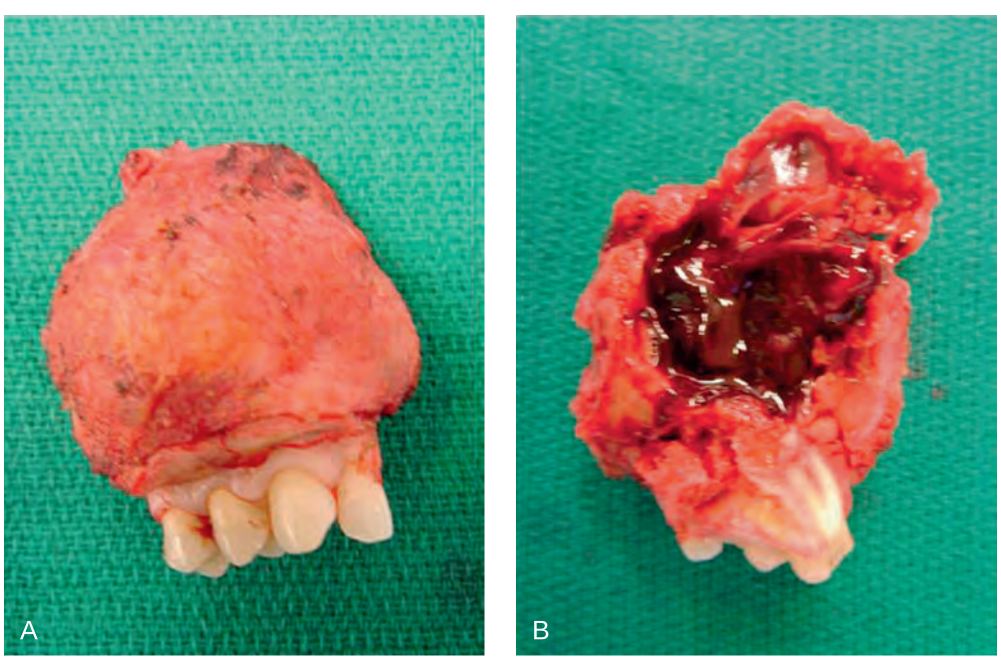

Figure 16.94 Surgical specimen of a monobloc resection in anterior view (**A**) and cross section (**B**) showing a thick walled, cystic lesion, totally excised.

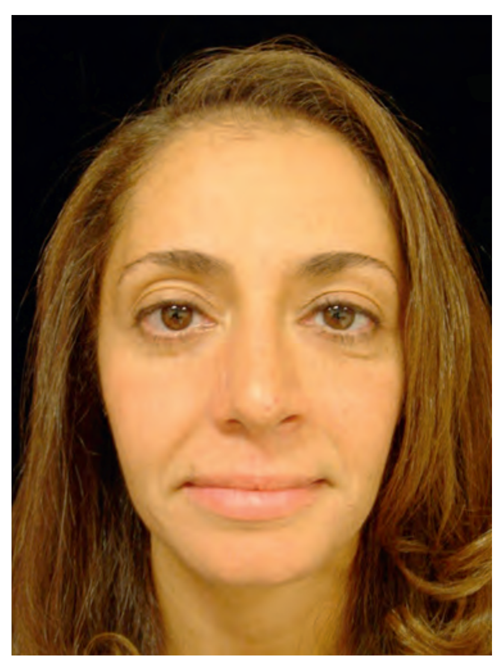

Figure 16.96 Postoperative appearance of the patient 1 year following surgery.

Low-Grade Chondrosarcoma of the Premaxilla

The patient whose upper alveolus is shown in Fig. 16.97 had a firm nodular lesion arising from the midline of the upper alveolus in the premaxillary region. The lesion had been present for several years but had shown recent growth. The patient was unable to wear her upper denture because of the presence of this lesion. An open biopsy of the lesion showed that it was a low-grade chondrosarcoma. A preoperative CT scan of the patient (Fig. 16.98) demonstrates a bone-destructive lesion of the premaxilla with a honeycomb-like appearance that is classic for a chondrosarcoma.

This patient's tumor was excised through a peroral approach with resection of the premaxilla and upper alveolus with satisfactory bony and soft-tissue margins in all three dimensions. The surgical defect was left open to heal by secondary intention because it did not communicate with the nasal cavity or maxillary antrum on either side. The postoperative appearance of the patient approximately 6 months after surgery is shown in Fig. 16.99. Note the absence of the alveolar process in the anterior half of the upper alveolus. This patient required a specially fabricated upper denture to provide protrusion of the upper lip to fill the defect created by the surgical resection. Alternatively, this patient would be a good candidate for dental implants for a fixed permanent denture.

Figure 16.97 The upper alveolus showing a multilobulated hard tumor.

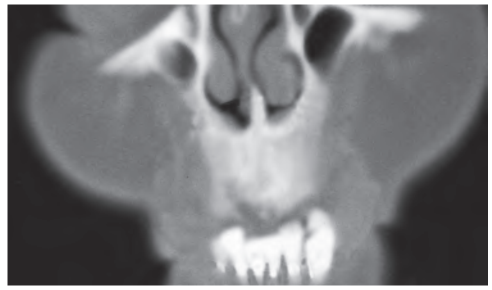

Figure 16.98 A preoperative computed tomography scan showing a bone-destructive lesion of the premaxilla.

Figure 16.99 The upper alveolus 6 months after surgery.

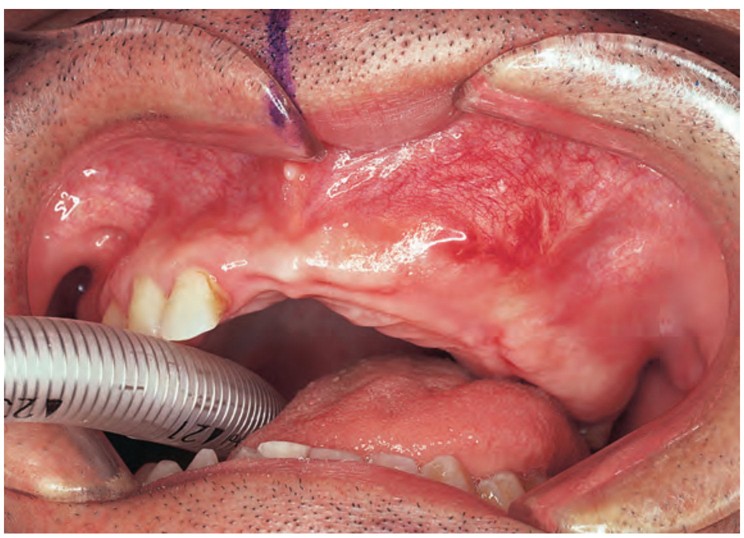

Figure 16.100 The upper alveolus showing an expansile lesion.

Myxoma of the Maxilla

Myxomas and fibromyxomas are benign lesions of the facial skeleton that usually present as expansile lesions with a minimal soft-tissue component. The dentition at the site of the tumor usually is loose or the teeth have spontaneously extruded. The patient whose upper alveolus is shown in Fig. 16.100 presented

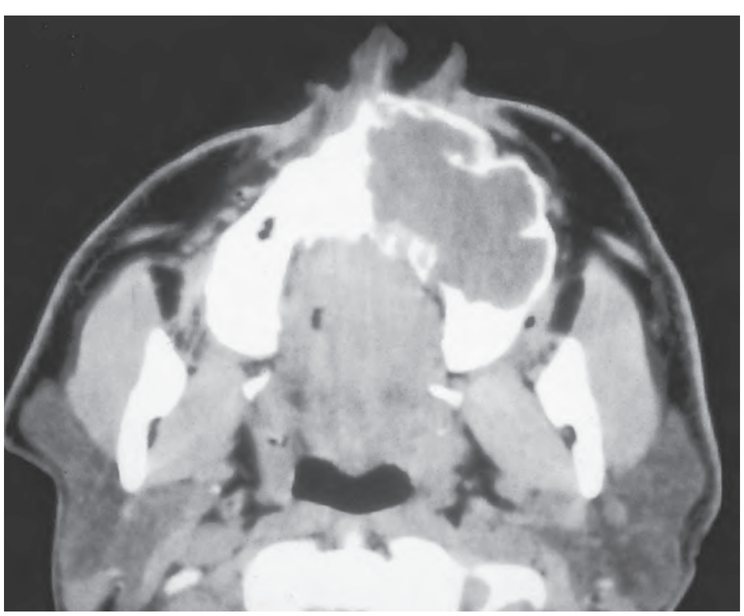

Figure 16.101 An axial view of the computed tomography scan showing an expansile lesion with bone destruction.

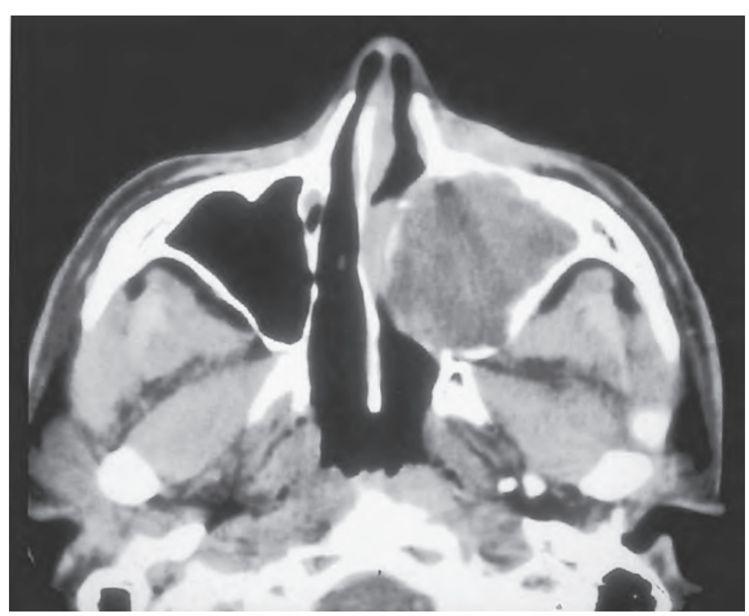

Figure 16.102 An axial view of the computed tomography scan showing displacement of the medial wall of the maxilla into the nasal cavity.

Figure 16.103 A coronal view of the computed tomography scan showing destruction of the alveolus and the lateral wall of the maxilla.

Figure 16.104 A coronal view of the computed tomography scan showing the tumor confined to the maxilla, with its lateral wall intact.

with a fullness of the left cheek and spontaneous extrusion of the upper teeth on the left-hand side. CT scans of the paranasal sinuses in the axial and coronal planes demonstrate a homogeneous tumor mass causing expansion of the alveolus with minimal bone destruction (Figs. 16.101 through 16.104). The lesion extends into the maxillary antrum, and its expansion produces obstruction of the left nasal cavity and displacement of the contents of the orbit cephalad without any soft tissue invasion by the tumor. Although histologically this tumor is benign, because of its dimensions, a total maxillectomy is required for treatment. A patient such as this would be a candidate for consideration of maxillary reconstruction with a free bone flap and use of the CAD-CAM technology for accurate reconstruction. This is also a situation where immediate dental implants can be placed in the vascularized free bone flap.

Osteogenic Sarcoma of the Maxilla

The maxilla is the second most frequent site of origin for osteogenic sarcomas in the craniofacial skeleton. The patient whose oral cavity is shown in Fig. 16.105 is a 19-year-old man who noted pain, discomfort, and swelling of the posterior part of the left upper gum for 3 months. He also reported a loosening of his molar teeth at that site. CT scans of the paranasal sinuses in the axial and coronal planes show a bone-forming and bone-destructive expansile lesion of the left maxilla (Figs. 16.106 and 16.107). The lesion appears to be contained within the confines of the maxillary antrum with a minimal soft tissue component anterolaterally. Surgical treatment for an osteogenic sarcoma of the maxilla requires a true total maxillectomy. The resection includes the entire maxilla, including the left half of the hard palate, the floor of the orbit, the zygomatic process, and the pterygoid plates as well as the nasal process of the maxilla and the lateral wall of the nasal cavity.

Figure 16.105 An intraoral view showing a tumor of the left maxilla, causing expansion of the left upper alveolus.

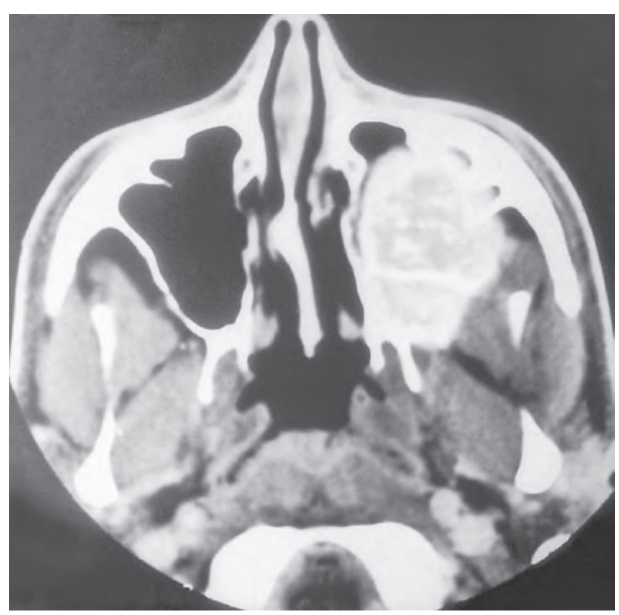

Figure 16.106 An axial view of the computed tomography scan shows an expansile bone-forming tumor of the left maxilla.

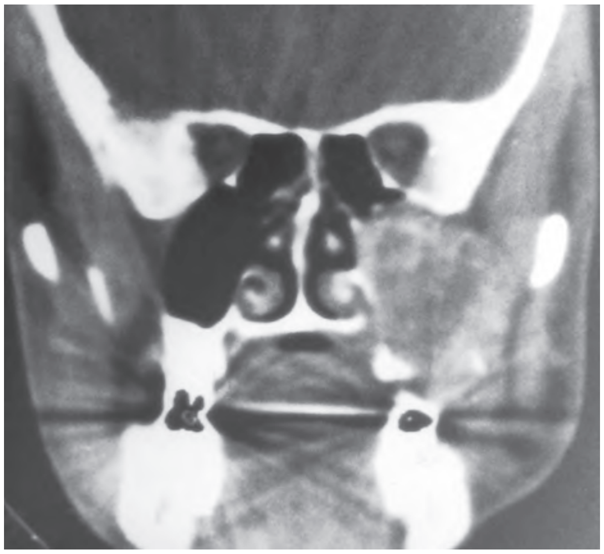

Figure 16.107 A coronal view of the computed tomography scan shows a well-circumscribed tumor of the left maxilla without soft-tissue involvement.

When a maxillectomy is undertaken for a sarcoma, in contrast to an epithelial carcinoma, very generous true en bloc total resection of the maxilla should be undertaken and generous soft-tissue margins should be maintained around the maxilla in all directions. Every attempt must be made to achieve monobloc excision of the tumor to ensure that the resection is adequate. During the course of the operation, extreme care is required to avoid fracture of the specimen and piecemeal removal of the tumor. Removal of the tumor in a piecemeal fashion significantly increases the risk of leaving residual tumor behind. Because this tumor is a neoplastic lesion of osseous origin, its monobloc removal is not that difficult. The total maxillectomy technique is described in Chapter 5.

The lateral view of the specimen shows the transected zygoma and intact posterolateral wall of the maxilla (Fig. 16.108). The medial view of the specimen shows the transected hard palate and lateral wall of the nasal cavity (Fig. 16.109). The left half of the hard palate forms the inferior margin of the specimen (Fig. 16.110). The anterosuperior view of the specimen clearly shows the tumor contained in the maxillary antrum (Fig. 16.111). This patient will need a dental obturator to obliterate the maxillectomy defect and facilitate his ability to speak and swallow by mouth.

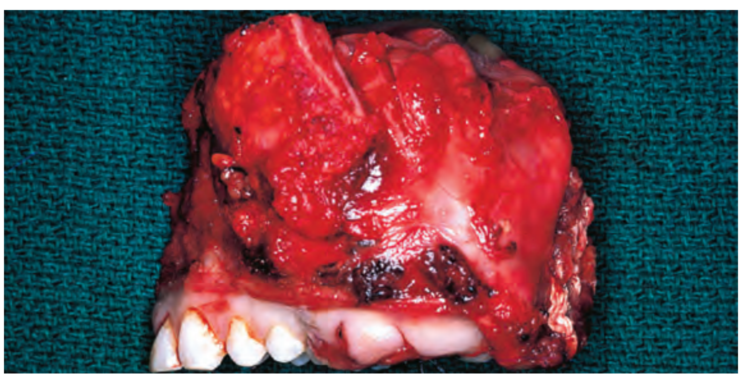

Figure 16.108 The lateral view of the specimen shows the transected zygoma and intact posterolateral wall of the left maxilla.

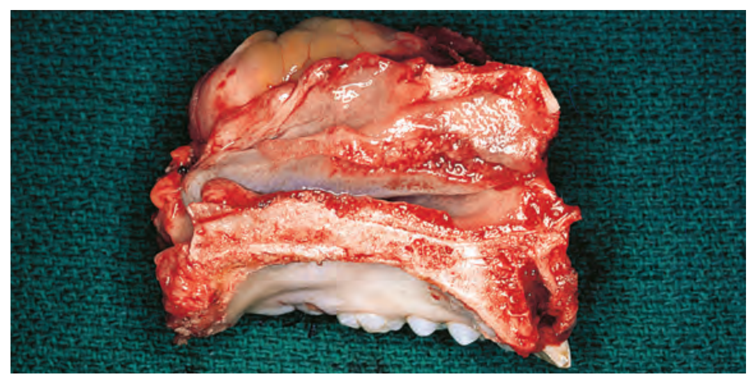

Figure 16.109 The medial view of the specimen shows the intact lateral wall of the nasal cavity.

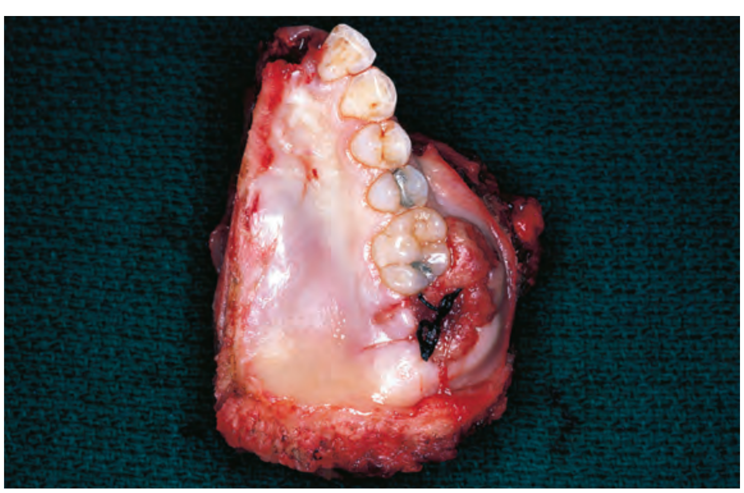

Figure 16.110 The palatal surface of the specimen shows the intact hard palate with an expansile lesion of the alveolus.

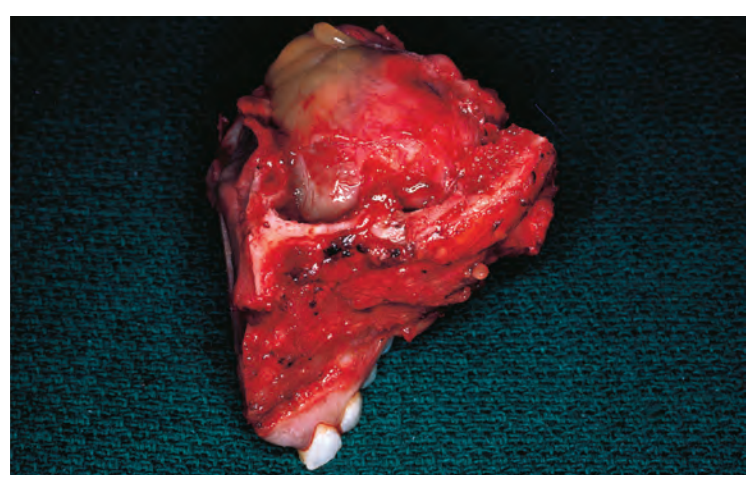

Figure 16.111 The anterosuperior view of the specimen shows the upper border of the tumor in the maxillary antrum.

Tumors of the Mandible

The mandible is the most frequent site of odontogenic and nonodontogenic tumors of bone in the head and neck region. The most frequent nonodontogenic benign tumors are fibroosseous lesions. Osteogenic sarcomas and chondrosarcomas are the most common malignant tumors. Ameloblastomas are the most common odontogenic tumors seen in the mandible. Compared with the maxilla, the mandible is more often involved by ameloblastomas. A variety of odontogenic cystic lesions also are seen more commonly in the mandible than in the maxilla. Common among these are odontogenic keratocysts, dentigerous cysts, and calcifying odontogenic cysts. Occasionally, central salivary tumors are seen in the mandible from buried salivary epithelial cells during development of dentition.

Ossifying Fibroma of the Mandible

Histologically, it is difficult to distinguish between monostotic fibrous dysplasia and an ossifying fibroma of the mandible. A decision regarding treatment, therefore, should be based on physical findings, the patient's symptoms, and the radiographic appearance of the lesion. The patient shown in Fig. 16.112 is a 14-year-old boy who presented with the history of fullness on the left side of his face that was noted by his parents several years ago. He had experienced intermittent discomfort on the left side of the mandible with progressive tenderness and pain within the past year. A plain radiograph of the mandible (Fig. 16.113) demonstrates a periosteal reaction over the ascending ramus of the mandible on the left-hand side, signifying an active neoplastic process. A panoramic radiograph of the mandible (Fig. 16.114) demonstrates an irregular osteolytic lesion involving the ascending ramus and the posterior part of the body of the mandible. Because of progressive symptoms of pain and discomfort, surgical excision of the lesion was recommended.

Because this lesion is benign and is truly a subperiosteal process, exposure of the lesion is obtained through an upper neck incision through a skin crease, remaining deep to all the soft tissues and directly over the periosteum of the mandible (Fig. 16.115). The mandible is exposed from the temporomandibular joint to the mental foramen on the left-hand side. Soft-tissue attachments, including the masseter muscle and the temporalis and pterygoid muscles, are detached with use of an electrocautery. The mandible is divided just posterior to the mental foramen on the left-hand side, and the temporomandibular joint is disarticulated. The surgical specimen is shown in Fig. 16.116. A sagittal section through the mandible demonstrates the fibrous nature of the lesion that is replacing bone in the entire involved hemimandible (Fig. 16.117). A surgical defect of this magnitude requires mandible reconstruction with a fibula free flap, with the added consideration that this patient is a growing child and probably will require further revision surgery as he grows. For complete dental rehabilitation, dental implants should be considered in the reconstructed mandible in this patient, since it is a benign tumor and the long-term prognosis is excellent.

Figure 16.112 This patient presented with a history of pain and fullness on the left side of his face.

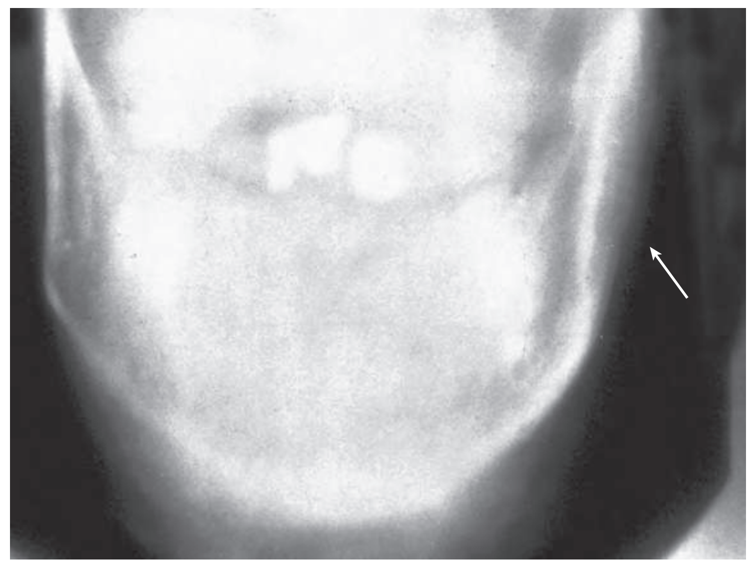

Figure 16.113 A plain radiograph of the mandible shows a periosteal reaction (*arrow*).

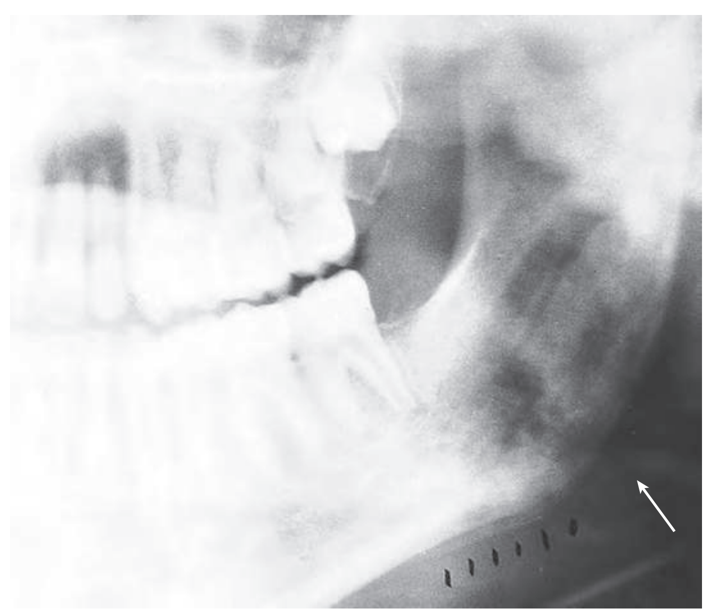

Figure 16.114 A panoramic radiograph of the mandible shows an ill-defined osteolytic lesion (*arrow*).

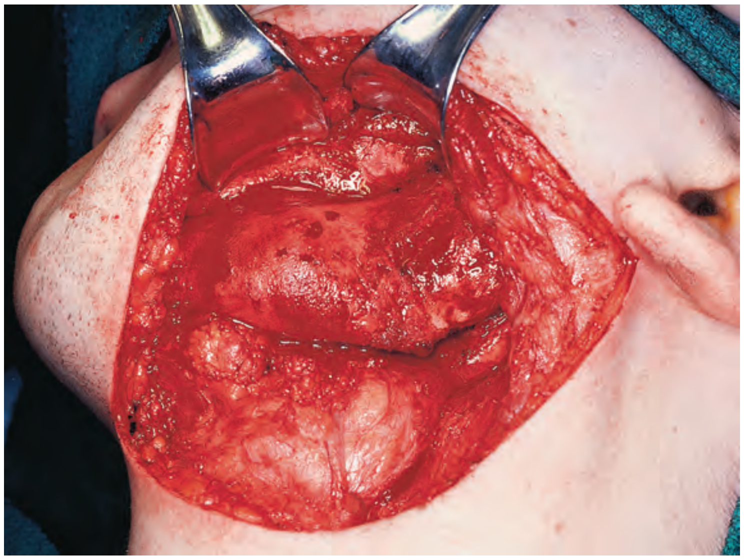

Figure 16.115 The upper neck incision with exposure of the mandible.

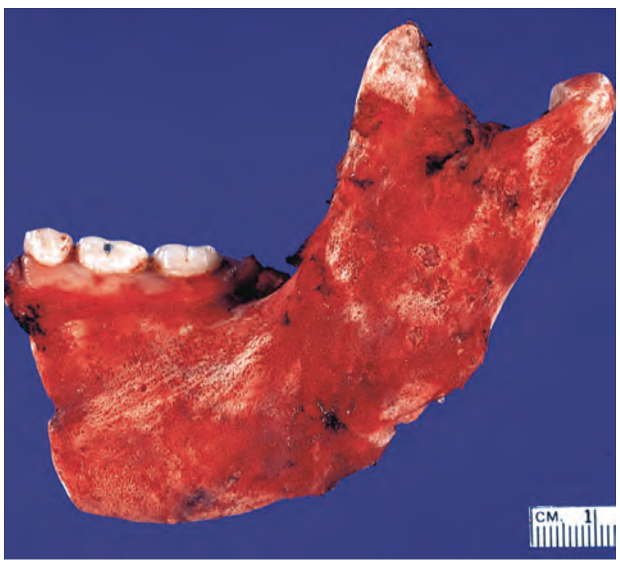

Figure 16.116 The surgical specimen of a left hemimandibulectomy.

Figure 16.117 The whole organ section showing a dysplastic fibrous lesion.

Low-Grade Osteogenic Sarcoma of the Mandible

Osteogenic sarcomas may be endosteal, parosteal, or periosteal. Histologically they also may be low-grade lesions or high-grade tumors. The patient shown in Fig. 16.118 presented with the history of a slowly enlarging bony mass near the angle of the mandible on the left-hand side for 8 months. Physical examination revealed a bony hard mass involving the region of the angle of the mandible with expansion of the lateral cortex and overlying soft tissues. The patient had anesthesia of the skin of the chin on the left-hand side. Intraoral examination showed the presence of a granular polypoid lesion adjacent to the retromolar gingiva in the gingivobuccal sulcus (Fig. 16.119). A biopsy of this lesion through the oral cavity confirmed the diagnosis of a low-grade osteogenic sarcoma. A panoramic radiograph of the mandible shows bone destruction in the edentulous mandible on the left-hand side (Fig. 16.120).

Figure 16.118 This patient had a slowly enlarging bony mass near the angle of the mandible.

Surgical treatment for a low-grade osteogenic sarcoma requires total excision of the clinically palpable and radiographically demonstrable tumor, which can be achieved through a segmental mandibulectomy. This patient underwent a segmental resection of the entire ascending ramus of the mandible from the condyloid process cephalad up to the midbody of the mandible anterior to the mental foramen on the left-hand side. The surgical specimen is shown in Fig. 16.121. Reconstruction of the mandible after such a resection is desirable. However, in this older man, with an edentulous mandible, a microvascular free flap reconstruction was not undertaken because of medical contraindications.

Figure 16.119 An intraoral view shows a polypoid lesion near the retromolar gingiva.

High-Grade Osteogenic Sarcoma of the Mandible

The preoperative appearance of a patient with a high-grade osteosarcoma of the mandible is shown in Fig. 16.122. The patient presented with a 3-month history of an enlarging mass in the lower gum on the right-hand side with friable tissue causing intermittent hemorrhage. Over the course of 3 months the lesion had rapidly progressed, causing visible fullness along the right side of the face. Intraoral examination showed a fleshy, nodular, friable lesion involving the lower alveolus, extending from the left lateral incisor up to the second premolar tooth on the right-hand side (Fig. 16.123). The lesion had a significant soft tissue component on the lateral surface of the alveolar process and the anterior cortex of the midline of the mandible. The extension in the floor of the mouth was minimal. The teeth in the vicinity of the lesion were mobile, indicating destruction of the sockets of the teeth by the tumor process. A biopsy from the projecting soft-tissue mass confirmed the diagnosis of an osteogenic sarcoma.

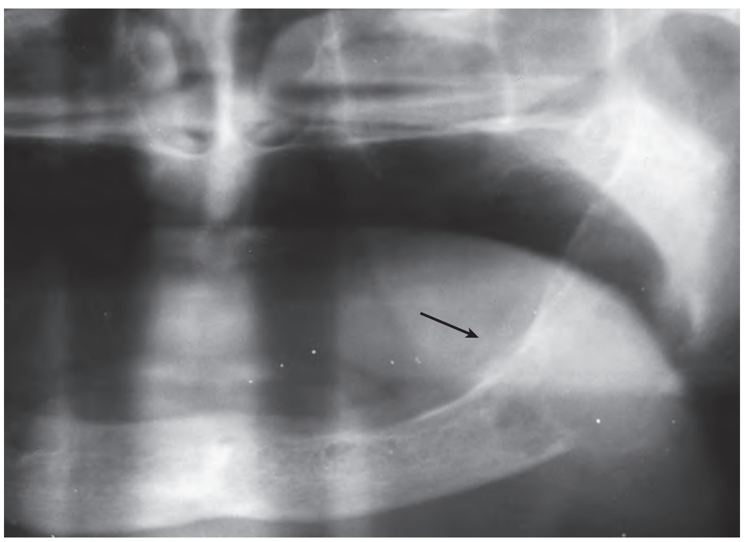

Figure 16.120 A panoramic radiograph showing a bone-destructive lesion (*arrow*).

Figure 16.122 The external appearance of a patient with an osteosarcoma of the mandible showing swelling of the lower lip.

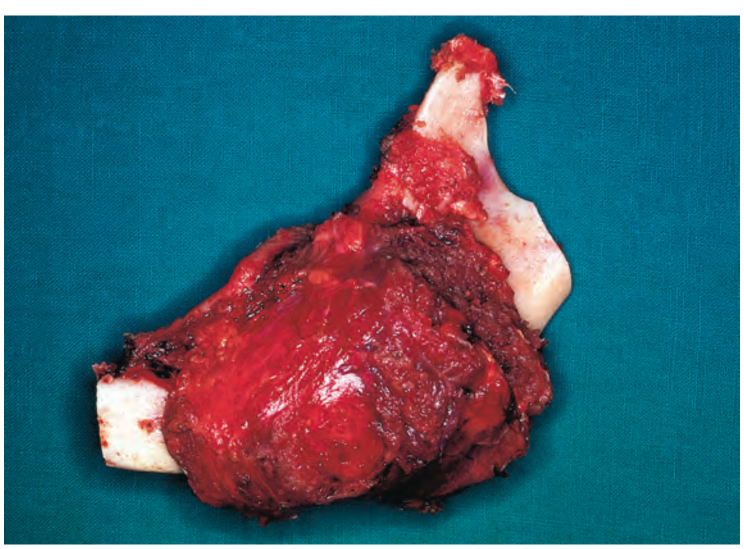

Figure 16.121 The surgical specimen of a segmental mandibulectomy with generous soft tissue margins.

Figure 16.123 An intraoral view shows a cauliflower-like exophytic lesion of the alveolus.

Imaging studies for accurate assessment of the intraosseous extent of this lesion require a contrast-enhanced CT scan with soft tissue and bone windows as well as a contrast-enhanced MRI scan with postcontrast T1- and T2-weighted sequences. Representative axial views of the CT and MRI scans are shown in Fig. 16.124. Note the extent of bone destruction and displacement of teeth from the alveolar process on the CT scan. The axial view of the mandible on a T2-weighted MRI scan shows the extent of bone destruction by the tumor. The axial view of the mandible in a postcontrast T1-weighted MRI scan clearly shows the extraosseous extent of the disease in the subcutaneous soft tissues and the floor of the mouth.

Surgical removal of this tumor required resection of the anterior arch of the mandible, remaining anterior to the second molar teeth on both sides. This surgical resection was accomplished through a transverse incision along an upper neck skin crease and through a visor flap approach. The visor flap approach in this patient is preferred to avoid a midline lower lip–splitting incision. The numbness of the skin resulting from elevation of the visor flap is unavoidable in this patient in whom the anterior arch of the mandible is to be resected, and thus both mental nerves will be excised with the surgical specimen. Thus the visor flap will not leave any additional sequela because of denervation of the skin of the chin. Reconstruction of the resected mandible is performed with a composite fibula free flap to restore the arch of the mandible and provide soft tissue and lining in the oral cavity.

Figure 16.124 Axial views of computed tomography (*left*) and magnetic resonance imaging scans (*middle* and *right*) showing the extent of bone destruction and the extraosseous extent of an osteosarcoma of the mandible (*arrows*).

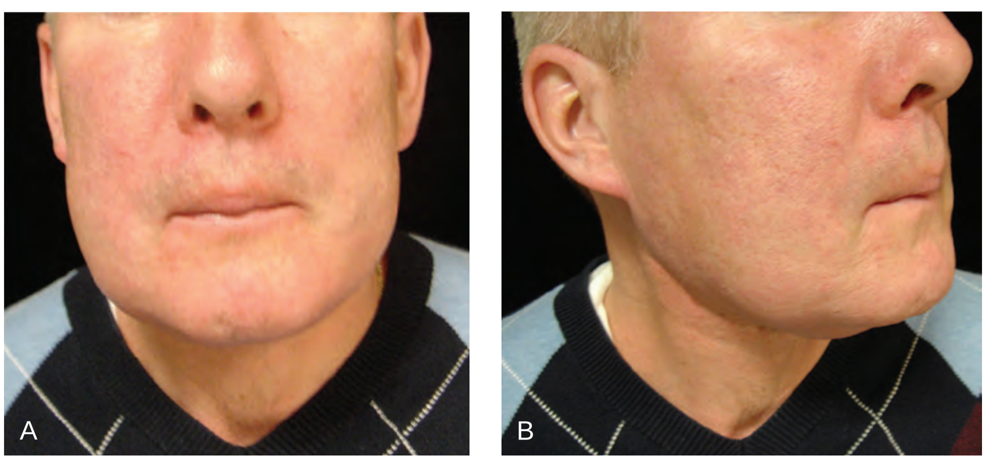

Figure 16.125 The appearance of the patient 6 months after completion of treatment. **A**, Anterior view. **B**, Lateral view.

Figure 16.126 An intraoral view shows the reconstructed alveolar process with the skin of the fibula flap.

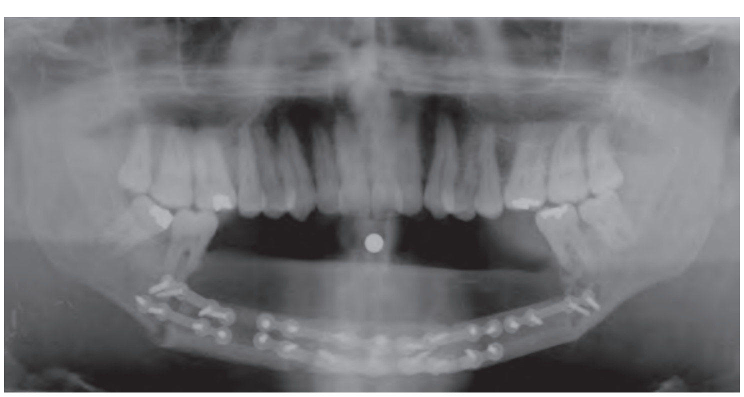

Figure 16.127 A postoperative panoramic radiograph showing the reconstructed mandible.

The appearance of the patient 6 months following surgery and postoperative radiation therapy shows an excellent aesthetic outcome with restoration of the contour of the face (Fig. 16.125). The intraoral view of the patient shows the fibula free flap with the skin island providing coverage over the newly restored alveolar process (Fig. 16.126). A postoperative panoramic radiograph of the mandible shows complete restoration of the arch of the mandible with a fibula free flap (Fig. 16.127).

Chondrosarcoma of the Mandible

High-grade chondrosarcomas are aggressive malignant tumors, the second most common sarcomas occurring in the craniofacial skeleton. The patient shown in Fig. 16.128 had a chondrosarcoma involving the medial aspect of the ascending ramus of the mandible on the left-hand side. She had received previous neoadjuvant chemotherapy with only a modest response in the tumor. The alopecia occurred as a result of the cytotoxic chemotherapy. Her preoperative CT scans with bone windows in axial and coronal planes clearly show a well-demarcated tumor on the medial aspect of the posterior part of the body and ascending ramus of the mandible (Fig. 16.129). The plan of treatment is to do a segmental mandibulectomy, with resection of soft tissues from the masticator space, immediate reconstruction with a vascularized free flap of bone and soft tissues and postoperative radiotherapy.

The extent of the tumor on the mandible is marked out on the skin before surgery (Fig. 16.130). The resection of the left hemimandible was performed through a transverse upper neck incision in a skin crease, and the flap was elevated over the lateral aspect of the mandible without splitting the lower lip. The surgical specimen shown in Fig. 16.131 shows en bloc resection of the left hemimandible with a monobloc resection of the tumor. The masseter muscle is the lateral soft-tissue margin, and the stumps of the resected pterygoid muscles are the soft-tissue margins on the medial aspect. The bone defect in the mandible was reconstructed with an iliac crest free flap. The immediate postoperative appearance of the patient, 3 weeks following surgery, shows good symmetry of the face, although there is a fair amount of soft-tissue swelling at the surgical site (Fig. 16.132). The postoperative MRI scan shows excellent alignment of the iliac crest flap in the reconstructed mandible (Fig. 16.133). The postoperative appearance of the patient 1 year following surgery shows excellent aesthetic outcome (Fig. 16.134). At this time the patient wears a removable partial denture. However, she will be a candidate for consideration of dental implants and a permanent fixed denture.

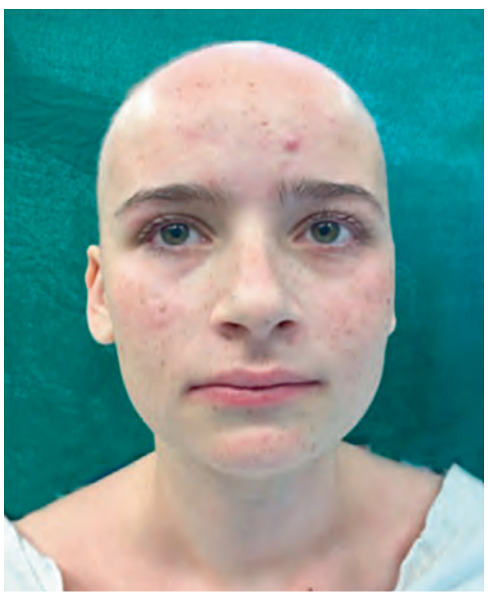

Figure 16.128 Preoperative appearance of the patient following induction chemotherapy.

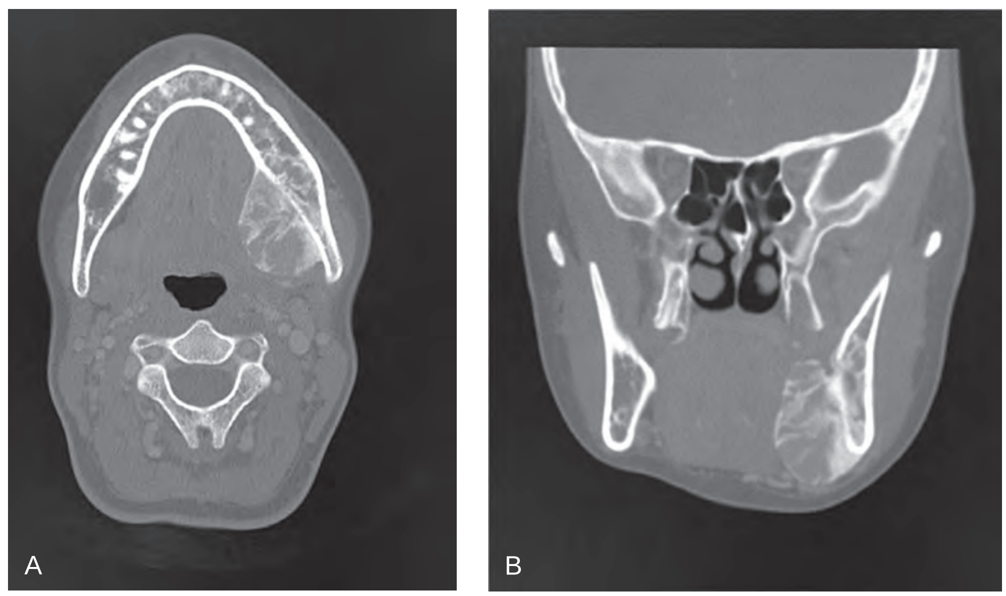

Figure 16.129 Bone windows of the CT scan in axial (**A**) and coronal (**B**) views show a well-demarcated tumor arising from the medial cortex of the mandible, extending into the masticator space.

Figure 16.130 The location and extent of the tumor in relation to the mandible are outlined on the patient.

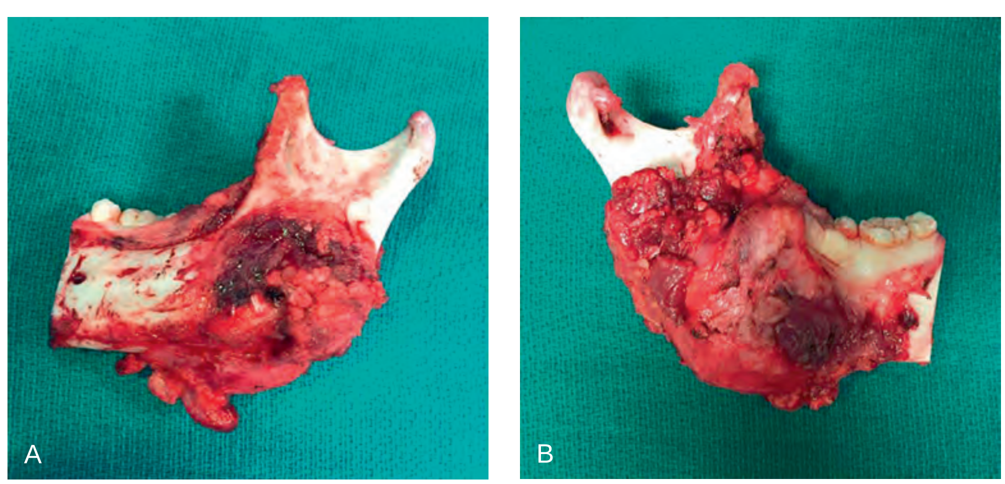

Figure 16.131 Surgical specimen of left hemimandibulectomy, lateral view (**A**) and medial view (**B**), showing en bloc resection with soft tissues and pterygoid muscles covering the tumor.

Figure 16.132 Postoperative appearance of the patient 3 weeks following surgery shows good symmetry of the reconstructed mandible but persistent soft-tissue swelling.

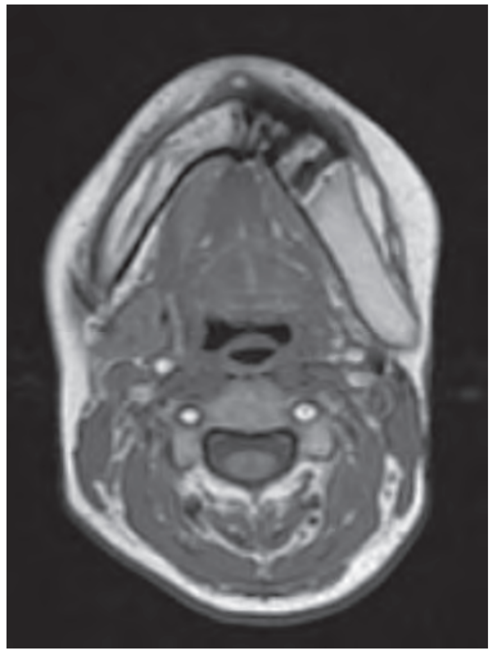

Figure 16.133 Postoperative MRI scan showing excellent alignment of the iliac crest free bone graft.

Figure 16.134 Postoperative appearance of the patient 1 year following surgery.

Ameloblastoma of the Mandible

An ameloblastoma is an epithelial odontogenic tumor that is benign histologically; however, biologically it is aggressive. The lesion is seen most often in the mandible, but it also may arise in the maxilla. The distribution of various sites of origin in the mandible is shown in Fig. 16.135. The surgical treatment of ameloblastoma requires its total excision if a cure is to be achieved. Very small localized lesions can be excised through the oral cavity with a marginal mandibulectomy or, occasionally, by peroral excision by curettage. However, lesions of any significant size are seldom cured by intraoral curettage, because local recurrence invariably develops, which requires a more aggressive surgical resection later. Therefore the optimal treatment for an ameloblastoma is its total excision at initial presentation. The patient whose recurrent ameloblastoma is described here vividly demonstrates the inadequacy of conservative intraoral resection and the need for an eventual mandibulectomy of a larger segment of the mandible as a result of local recurrences.

This patient's history included spontaneous extrusion of her lower premolar and first molar teeth as a result of a bone-destructive lesion 8 years before this presentation. The panoramic radiograph at that time showed a bone-destructive lesion in the body of the mandible on the right-hand side (Fig. 16.136). An intraoral excision and curettage were attempted, but the lesion recurred 3 years later. At that point a second surgical procedure was undertaken intraorally with curettage and placement of a nonvascularized bone graft (Fig. 16.137). Although it appeared that the bone graft had healed, a recurrent lytic lesion was noted 2 years after the last surgical procedure in the body of the mandible (Fig. 16.138). By the time the patient presented for treatment, further bone destruction had developed, which extended across the midline to the body of the mandible

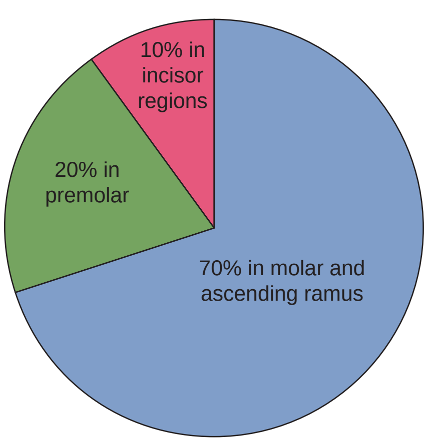

Figure 16.135 Distribution of the site of origin of ameloblastoma in the mandible.

Figure 16.136 A panoramic radiograph showing a lytic lesion of the mandible on the right-hand side (*arrow*).

on the left-hand side (Fig. 16.139). Intraoral examination demonstrated an ulcerated granular exophytic expansile lesion near the symphysis of the mandible with expansion of both the labial and lingual cortices (Fig. 16.140).

Surgical resection of this tumor required excision of the anterior arch of the mandible from the first molar tooth on the left-hand side to the first molar tooth on the right-hand side. The surgical specimen is shown in Fig. 16.141. The lesion did not extend beyond the bone, and thus there is minimal soft-tissue loss in the oral cavity or the chin. The surgical defect is shown in Fig. 16.142. Reconstruction of the anterior arch of the mandible in this patient will require a microvascular fibula

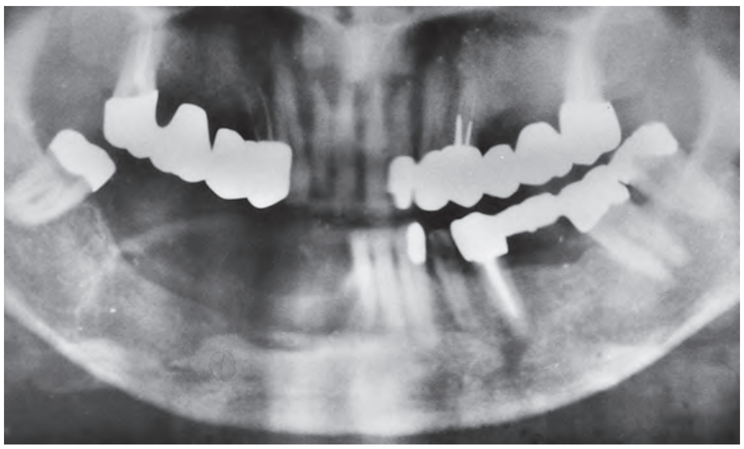

Figure 16.137 A panoramic radiograph after reexcision for recurrence and placement of a nonvascularized bone graft.

Figure 16.138 A panoramic radiograph showing further local recurrence (*arrow*).

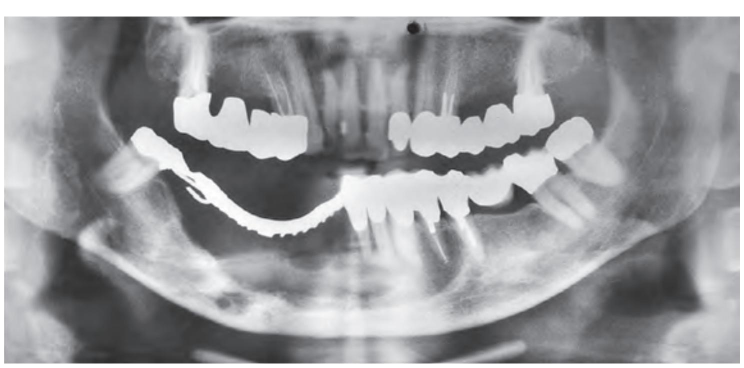

Figure 16.139 Progressive bone destruction of the mandible.

Figure 16.140 An intraoral view shows an expansile lesion at the symphysis of the mandible.

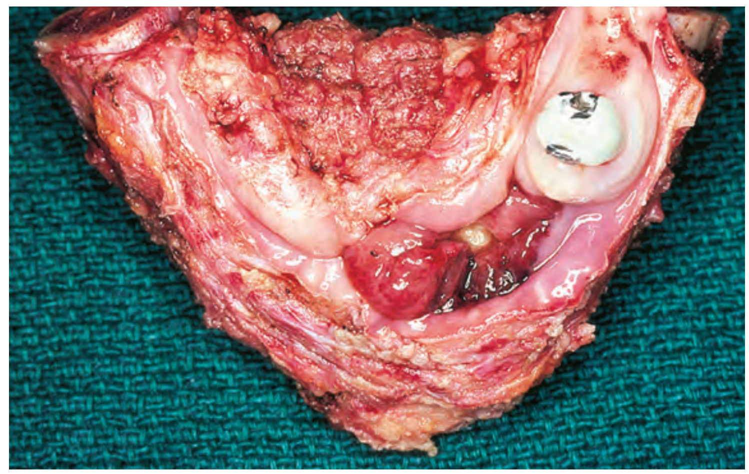

Figure 16.141 The surgical specimen from resection of the anterior arch of the mandible.

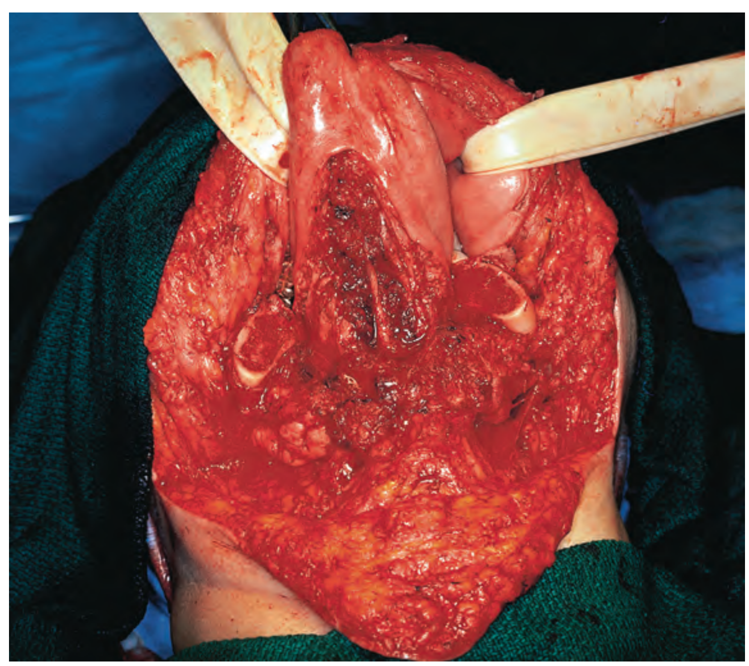

Figure 16.142 The surgical defect after resection of the arch.

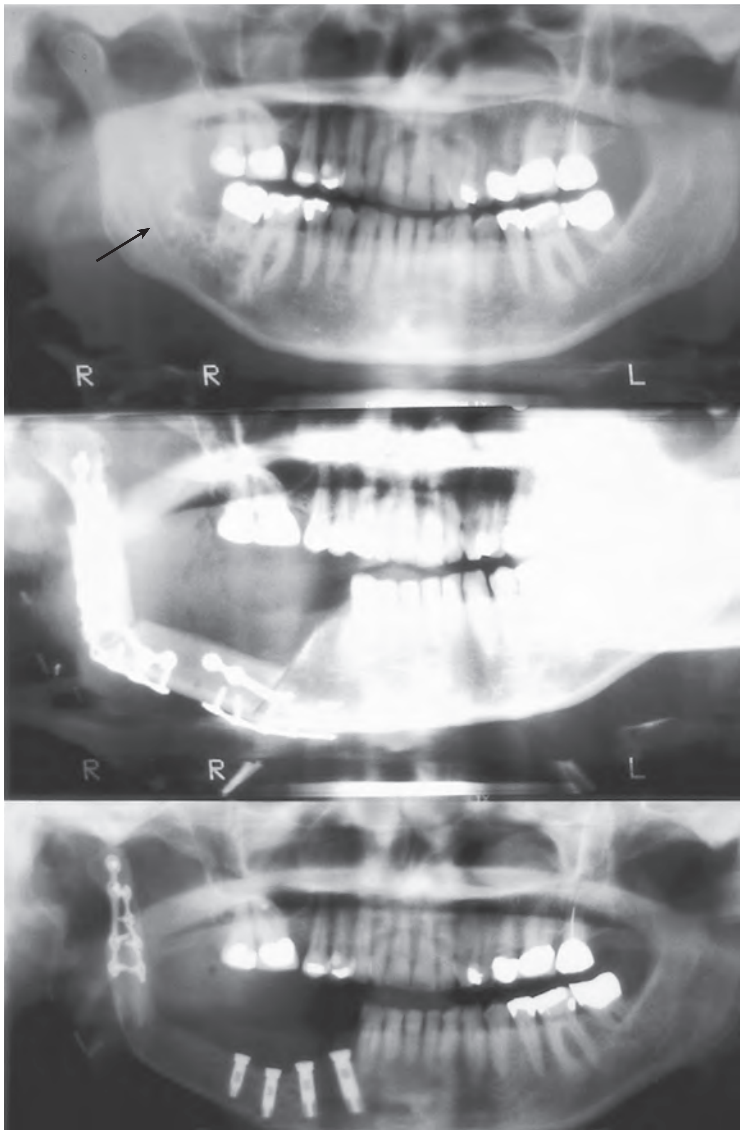

Figure 16.143 Serial panoramic radiographs of a patient who underwent a segmental mandibulectomy for ameloblastoma (*arrow*) and fibula free flap reconstruction followed approximately 1 year later by placement of osseointegrated implants for dental rehabilitation.

free flap with appropriate osteotomies to recreate the shape, size, and configuration of the resected mandible. The technical details of mandible reconstruction are discussed in Chapter 17.

Serial panoramic radiographs of another patient who underwent a hemimandibulectomy, reconstruction with a fibula free flap, and eventual osseointegrated implants for dental rehabilitation are shown in Fig. 16.143. Note the ameloblastoma presenting in the region of the body and retromolar trigone of the right-hand side of the mandible. A segmental mandibulectomy up to the lateral incisor tooth was necessary for resection of this tumor. Reconstruction of the resected mandible was performed with a fibula free flap. The fibula required multiple osteotomies and fixation with several miniplates and screws. Approximately 1 year after reconstruction, the screws and plates in the anterior aspect of the reconstructed body of the mandible were removed, and osseointegrated implants were placed for dental rehabilitation. The postoperative appearance of the patient 2 years following initial surgery is shown in Fig. 16.144. Excellent aesthetic reconstruction of the right hemimandible is achieved, and endosseous implants offered complete dental rehabilitation.

Figure 16.144 The postoperative appearance of the patient 2 years following surgery.

Odontogenic Cysts and Tumors

The surgical treatment for cystic lesions of odontogenic origin is usually conservative. If the etiology is inflammatory in nature, then the inflammatory process should be appropriately addressed. In other situations, the cystic lesion usually is approached intraorally and is widely opened for curettage and complete removal of its epithelial lining. The surgical defect occasionally requires a bone graft but usually is packed open and allowed to heal by secondary intention. Most odontogenic tumors are benign and have characteristic clinical features and a characteristic radiographic appearance. However, a final histologic analysis is necessary to confirm the diagnosis.

Odontogenic Cyst of the Upper Alveolus

The patient shown in Fig. 16.145 is a 21-year-old man who presented with a 4-year history of fullness of the right cheek.

Figure 16.145 This patient presented with fullness of the right cheek.

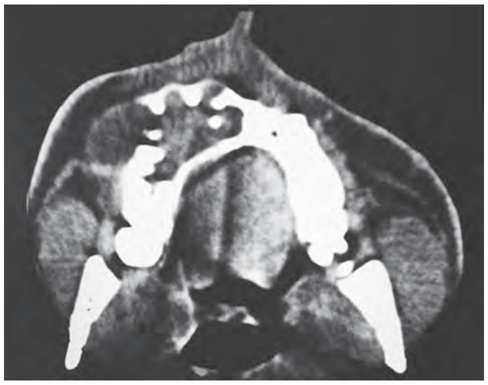

Figure 16.146 An axial computed tomography scan through the upper alveolus shows a thin-walled, expansile, bone-destructive lesion.

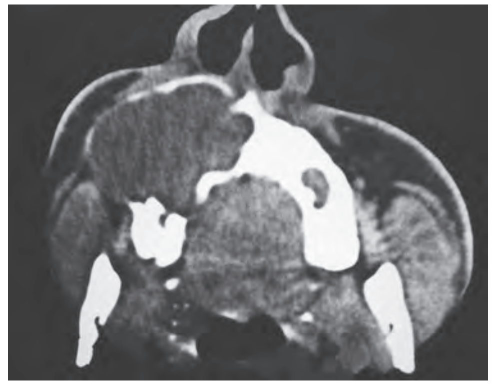

Figure 16.147 An axial computed tomography scan showing expansion of the anterior wall of the maxilla.

Figure 16.148 An axial computed tomography scan showing further expansion of the maxilla.

Sensations of the skin of the cheek were normal. However, upon physical examination a bony hard mass could be palpated on the upper alveolus and anterior wall of the maxilla. CT scans in an axial plane clearly demonstrate an expansile lesion of the upper alveolus extending into the anterior wall of the maxilla, with a hypodense lesion signifying a fluid-filled cystic process (Figs. 16.146 through 16.148). Excision of the cystic lesion by bone resection (maxillectomy) is not necessary; however, marsupialization with removal of the epithelial lining of this cystic lesion is necessary, which is accomplished through an intraoral approach. The bony defect is packed open and the patient uses a temporary dental obturator until reorganization and filling of the cavity with new bone formation takes place. Because the cystic lesion is opened in the oral cavity, the defect after curettage of its lining epithelium has gravity-dependent drainage, and therefore the cystic space initially fills in with soft tissue (granulation tissue) from the roof of the antrum up to the alveolar process. Thus eventually the whole cavity is obliterated, and eventually the soft tissue reorganizes and forms dense fibrosis with new bone formation.

If significant bone destruction of the alveolus has taken place, an oroantral fistula may be persistent for a long time after curettage and marsupialization. In such an event, the patient will require a dental obturator.

Odontogenic Keratocyst of the Mandible

The patient shown in Fig. 16.149 is a 67-year-old woman who presented with a 6-year history of a slowly expanding mass in the region of the angle of the mandible on the left-hand side. She had no symptoms from this mass. A panoramic radiograph of the mandible shows an expansile, multiloculated, smooth, thin-walled, cystic lesion involving the ascending ramus of the mandible (Fig. 16.150). The sensations of the skin of the chin and the tongue were normal. This lesion is approached intraorally through an incision in the mucosa of the retromolar gingiva to expose the anteromedial cortex of the ascending ramus of the mandible. The cyst wall is entered into with an osteotome, and its epithelial lining is carefully elevated with a periosteal elevator and excised. Meticulous attention is required to completely excise all the epithelial lining of the cyst wall. If segments of the lining wall are left behind, then local recurrence is likely to develop. The surgical defect thus created is left open to heal by secondary intention. If the periosteum and lateral or inferior cortex of the mandible is intact, then a bone graft is not required. A simple Xeroform gauze packing is packed into the surgical defect in the ascending ramus and body of the mandible.

Figure 16.149 A patient with a slowly expanding mass of the left cheek.

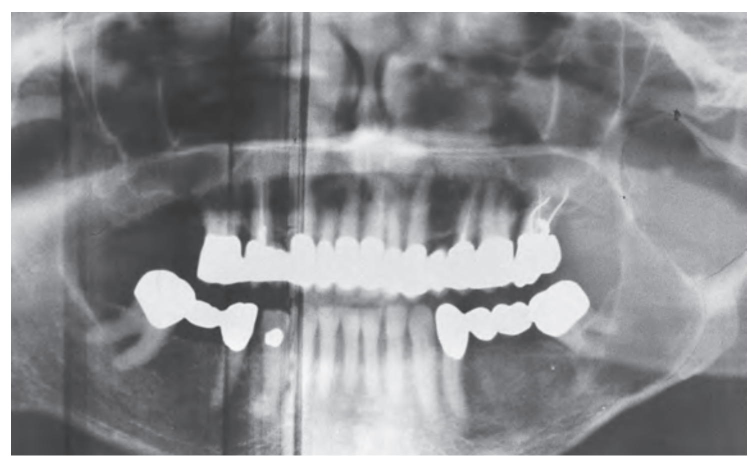

Figure 16.150 A panoramic radiograph of the mandible shows a multiloculated cystic lesion of the left-hand side of the mandible.

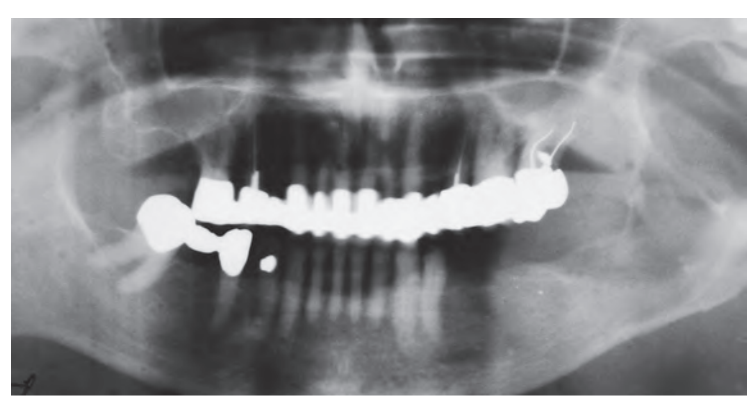

Figure 16.151 A panoramic radiograph 6 weeks following surgery.

A postoperative panoramic radiograph 6 weeks after surgery shows a large defect in the posterior part of the body of the mandible and the ascending ramus of the mandible (Fig. 16.151). The patient required regular packing and irrigations of the defect for nearly 3 months. At that time, secondary healing had completely obliterated the cystic space. A follow-up panoramic radiograph 1 year following surgery shows adequate filling of the defect with new bone formation of the ascending ramus and posterior part of the body of the mandible (Fig. 16.152).

Figure 16.152 A follow-up panoramic radiograph 1 year after surgery shows good healing with new bone formation.

Management of odontogenic cysts in the teeth-bearing part of the mandible also is conservative and is similar to that provided for the patient just described. However, if the teeth are mobile or nonvital, they may need to be extracted. The patient whose photograph of the lower half of the face is shown in Fig. 16.153 shows slight fullness in the region of the body of the mandible and the angle of the mandible on the left-hand side. Sensations of the skin of the chin were normal. An intraoral examination showed expansion of the lateral cortex of the mandible on palpation, and the teeth were immobile and had normal sensitivity.

Figure 16.153 The clinical appearance of a patient with a large odontogenic cyst of the body of the mandible on the left-hand side.

A panoramic radiograph of the mandible shows a well-defined cystic lesion in the posterior portion of the body of the mandible on the left-hand side. Note that the roots of the teeth are projecting into the cystic lesion (Fig. 16.154). An axial view of the CT scan shows a massive expansile cystic lesion involving the body of the mandible on the left-hand side with an intact lingual cortex of the mandible but significant expansion and thinning out of the lateral cortex of the mandible, which is intact (Fig. 16.155). The cystic space has a uniform ground glass appearance without any bone destruction or new bone formation. The reconstructed sagittal view of the CT scan shown in Fig. 16.156 demonstrates a large, unilocular cystic space extending from

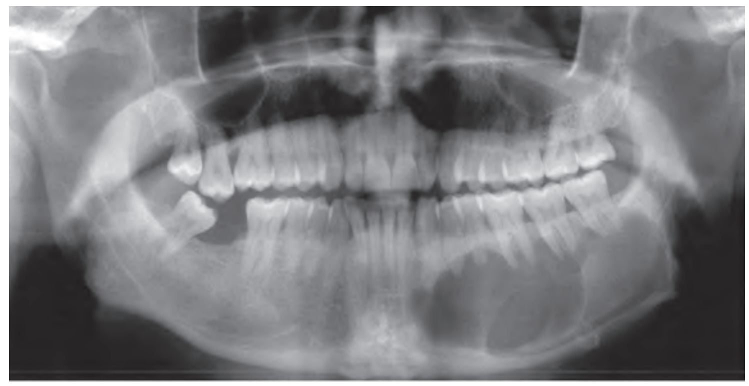

Figure 16.154 A panoramic radiograph showing a large cystic lesion in the body of the mandible on the left-hand side.

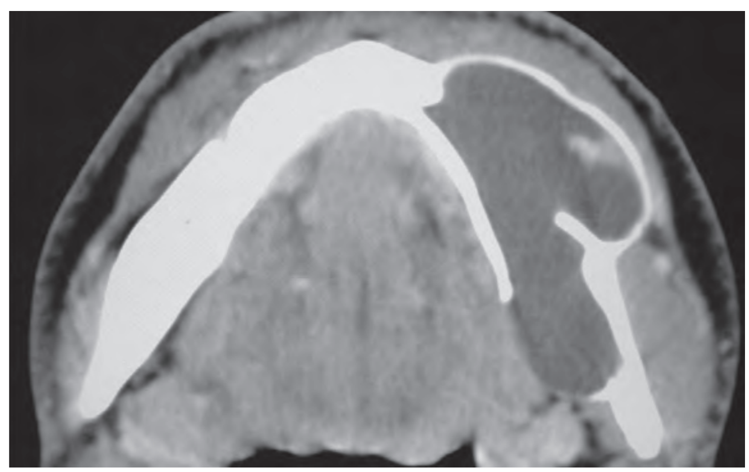

Figure 16.155 An axial view of the computed tomography scan showing an expansile lesion of the body of the mandible with thinning of the lateral cortex.

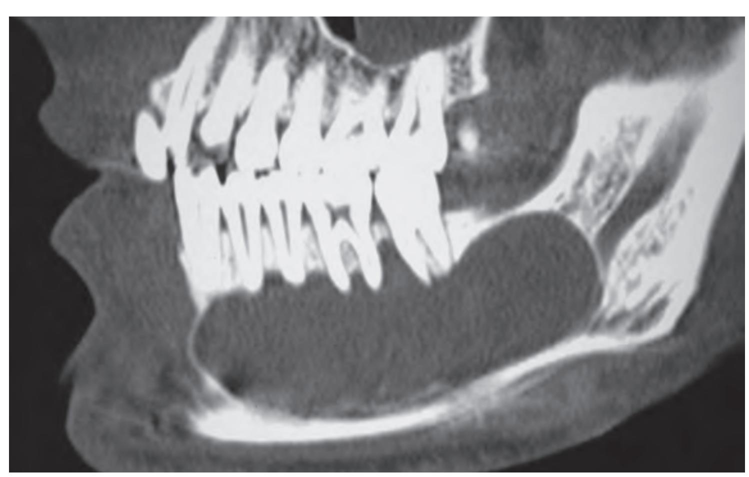

Figure 16.156 A sagittal view of the computed tomography scan showing a uniform cystic lesion in the body of the mandible with roots of the teeth projecting into the cystic space.

the region of the retromolar trigone posteriorly up to the lateral incisor tooth anteriorly. The cystic space has a smooth wall and a sharp margin, which is well defined. The roots of the teeth are within the cystic space. A three-dimensional reconstruction of the CT scan vividly demonstrates the large cystic space in the body of the mandible (Fig. 16.157).

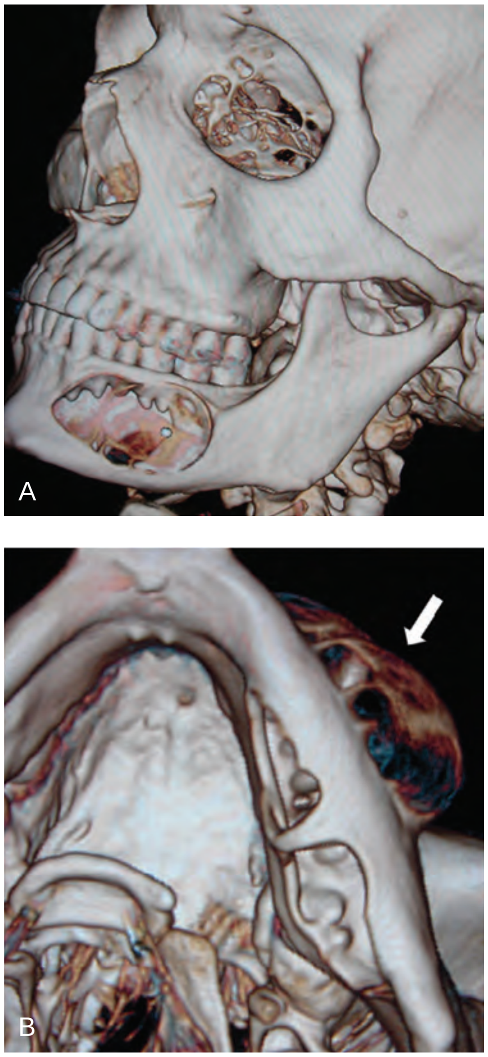

Figure 16.157 A three-dimensional reconstruction of the computed tomography scan demonstrates a large cystic space in the body of the mandible (*arrow*).

This lesion was approached intraorally through the gingivobuccal sulcus. The mucosa is incised, and a periosteal elevator is used to elevate the lateral periosteum. Entry is made through the superior part of the lateral cortex of the mandible in the cystic lesion to gain wide access into the cystic space. Complete curettage of the mucosa of the cystic space is performed, meticulously preserving the inferior alveolar nerve, which is located in the floor of the cystic space. After hemostasis is achieved, the surgical defect is packed with iodoform gauze. The cystic space is left open and will be allowed to granulate during the course of the next several months. The patient is taught how to pack the surgical defect several times a day and is instructed to keep the mouth clean with frequent irrigations. It is anticipated that this surgical defect will heal initially with granulation tissue, which subsequently will show new bone formation, restoring anatomic continuity of the mandible without any surgical sequelae. Postoperative panoramic radiographs 6 months and 1 year following surgery show progressive obliteration of the bone defect with new bone formation at the site of the cystic lesion (Fig. 16.158).

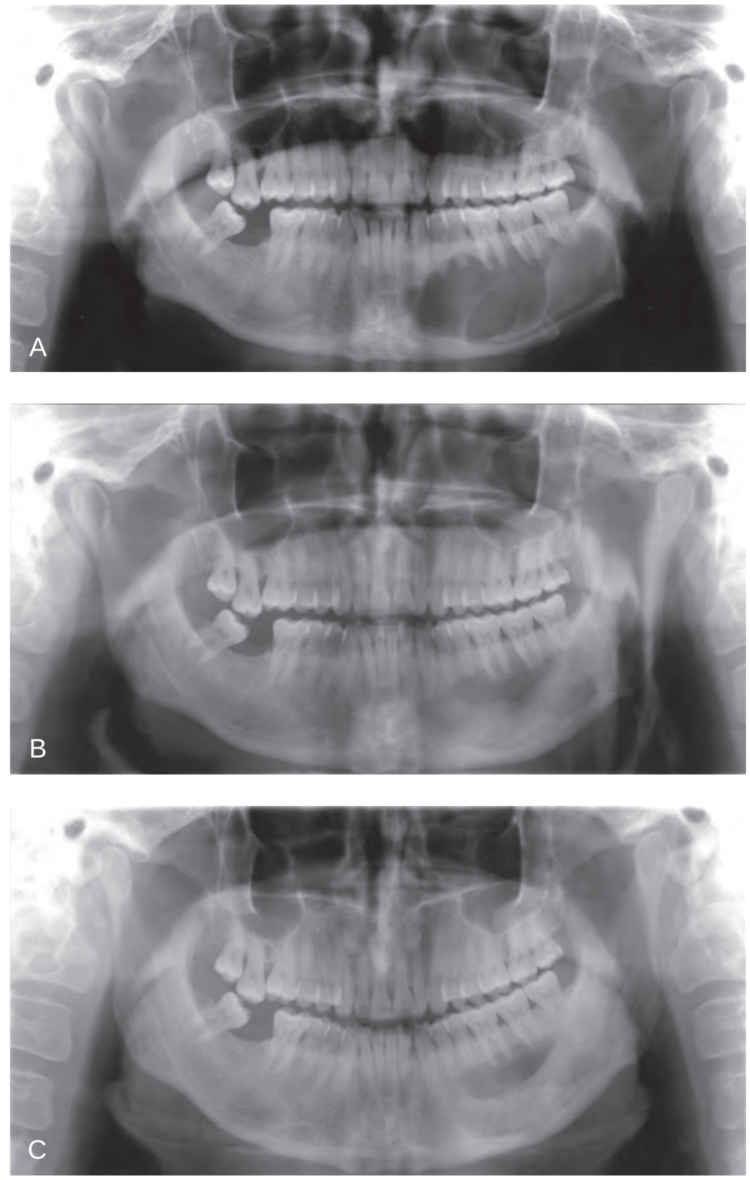

Figure 16.158 Serial panoramic radiographs before surgery (**A**), 6 months following surgery (**B**), and 1 year following surgery show new bone formation with obliteration of the cystic space (**C**).

Dentigerous Cyst

A dentigerous cyst is a developmental cystic lesion around an unerupted tooth that is lined by epithelium. The radiographic appearance is similar to that of an odontogenic cyst, but the characteristic presence of an unerupted tooth in the cystic lesion

Figure 16.159 A panoramic radiograph shows a multiloculated cystic lesion with an unerupted tooth.

confirms the diagnosis. The panoramic radiograph of a patient with a dentigerous cyst involving the ascending ramus and the body of the mandible on the right-hand side is shown in Fig. 16.159. Surgical treatment for a dentigerous cyst is similar to that for an odontogenic cyst. The lesion is approached intraorally.

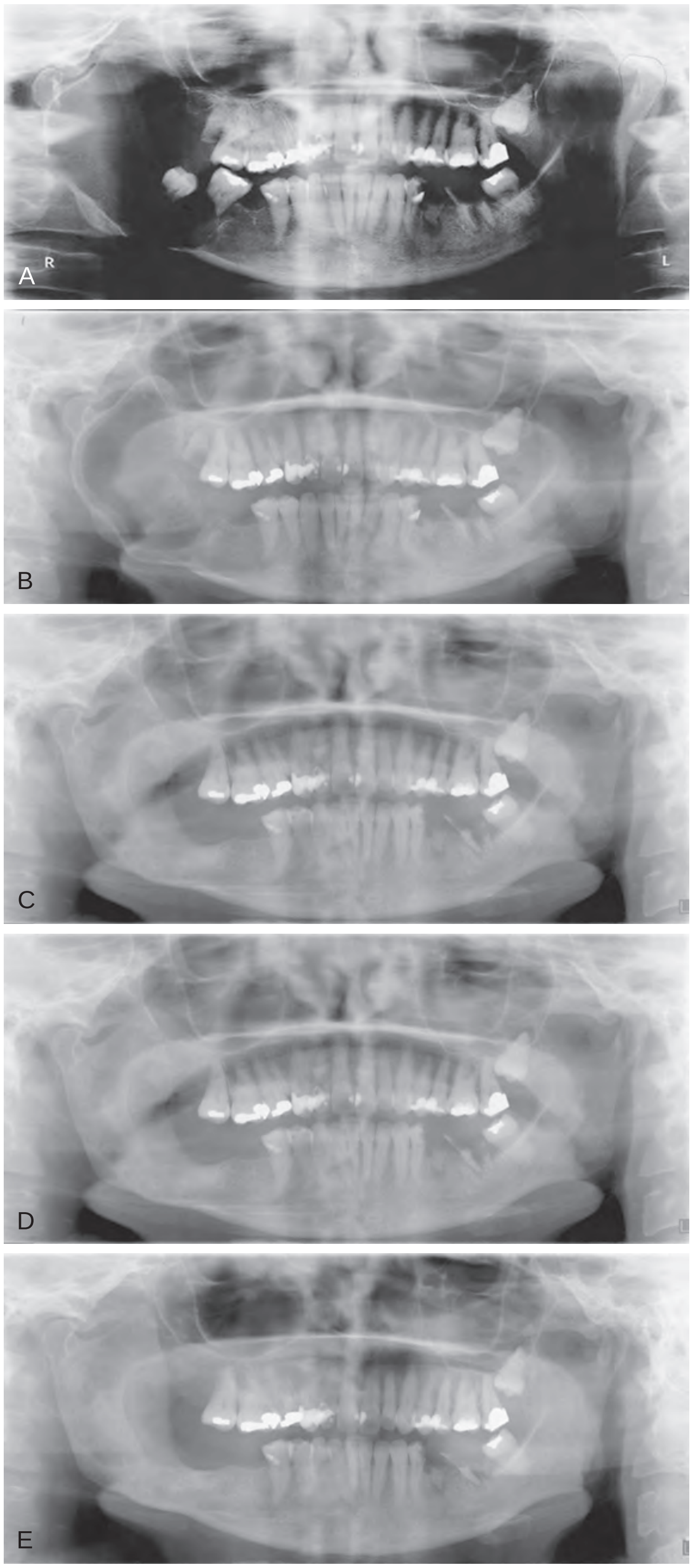

Figure 16.160 Serial panoramic radiographs showing a large dentigerous cyst of the ascending ramus of the mandible on the right-hand side and progressive new bone formation (**A**). Follow-up panoramic x-rays at 1 month (**B**), 6 months (**C**), 12 months, (**D**), 18 months, and (**E**) following surgery.

The unerupted tooth is extracted at the time of curettage and marsupialization of the cyst. Postoperative management is similar, with daily packing of the surgical defect until adequate obliteration of the dead space takes place by healing with secondary intention.

Sequential panoramic radiographs of another patient with a large dentigerous cyst involving the entire ascending ramus of the mandible are shown in Fig. 16.160. The lesion was approached intraorally with curettage and marsupialization of the large cystic space. The cavity was packed, and the patient was instructed to change the packing twice a day until the entire space was filled with soft tissue up to the surface. Sequential panoramic radiographs show gradual filling of the defect initially with soft tissue and subsequently with new bone formation over the course of 18 months.

Conservative management of cystic lesions of the mandible, such as a dentigerous cyst or odontogenic keratocyst, offers excellent control of the disease process, retains the normal contour of the mandible, and avoids the need for external incisions or reconstruction of the mandible.

Giant Cell Reparative Granuloma

Giant cell reparative granuloma is a bone-destructive, rapidly expanding lesion that usually is seen in young patients. It is a self-limiting lesion, and it may regress spontaneously. The classic appearance of a giant cell reparative granuloma is shown in Fig. 16.161. The clinical, radiologic, and histologic differential diagnosis rests between a giant cell granuloma and a giant cell tumor of the bone. The latter occurs in adults, does not show spontaneous regression, and often recurs after treatment. These lesions must also be differentiated from the "brown" tumor of hyperparathyroidism. These lesions primarily involve the bone

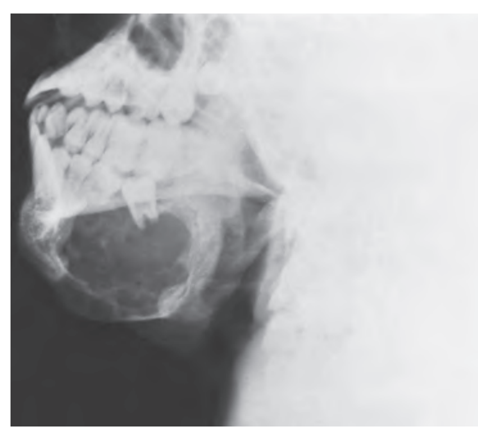

Figure 16.161 A giant cell reparative granuloma.

but may extrude from the bone and present intraorally, giving the appearance of a neoplasm (Fig. 16.162). A panoramic x-ray and CT scan of the mandible show a bone-destructive process from hyperparathyroidism (Fig. 16.163). Therefore, when a lesion of this nature is present in the mandible, appropriate tissue diagnosis should be supplemented with studies for serum calcium, parathormone, and a skeletal survey to rule out involvement of other bones. Surgical treatment for giant cell granuloma usually is undertaken by an intraoral approach with curettage and marsupialization. The surgical defect is left open and is allowed to heal by secondary intention.

Figure 16.162 A brown tumor of primary hyperparathyroidism presenting as an exophytic cauliflower-like growth on the lower alveolus.

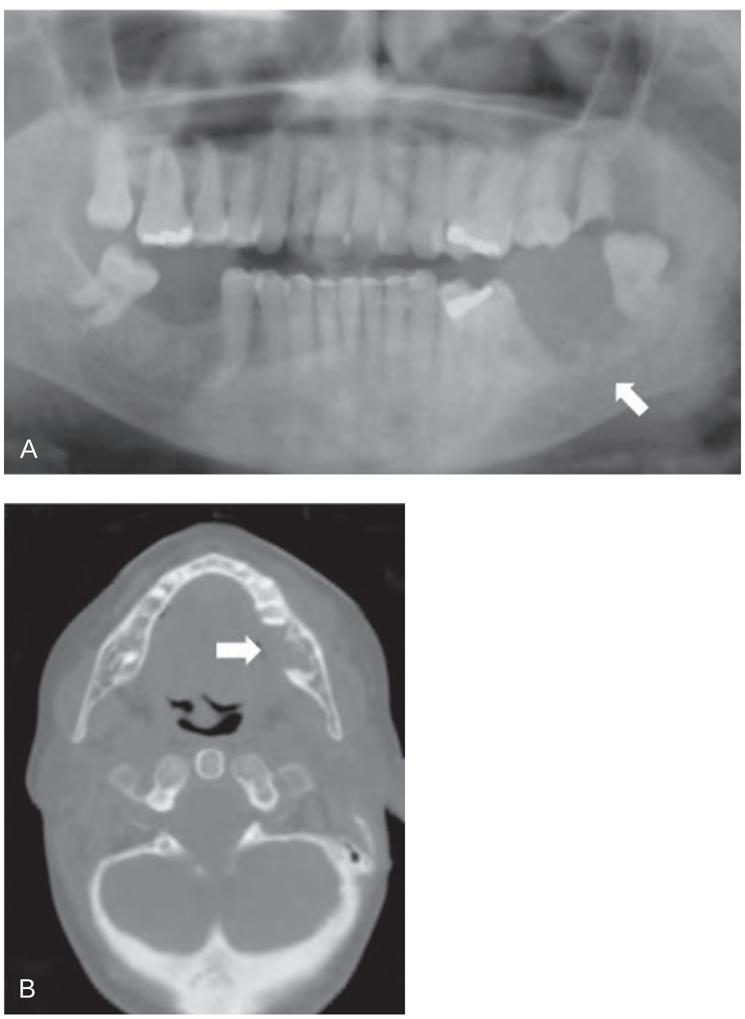

Figure 16.163 Brown tumor of hyperparathyroidism in the mandible showing a bone-destructive process on a panoramic x-ray (**A**) and CT scan (**B**) of the lesion shown in Fig. 16.162.

An intraoral view of the right lower gum of a patient with a giant cell granuloma is shown in Fig. 16.164. Note the granular fleshy lesion arising from the alveolar process of the mandible. This patient had a slightly painful lesion at that site. A CT scan of this patient demonstrates an osteolytic lesion in the posterior part of the body of the mandible on the right-hand side (Fig. 16.165). Surgical treatment for this lesion is accomplished via a peroral approach. A circular incision is placed on the mucosa of the right lower gum around the primary tumor (Fig. 16.166). The mucosal incision is deepened down to the underlying bone. Thereafter, using appropriate periosteal elevators and curettes, the lesion is excised as far as possible in a monobloc fashion. This approach usually is possible for small lesions; however, larger lesions may not be able to be excised in one piece.

The surgical defect after excision of the lesion shows a well-demarcated area of bone destruction (Fig. 16.167). Hemostasis

Figure 16.164 This patient presented with a slightly painful, granular, fleshy lesion of the right lower gum.

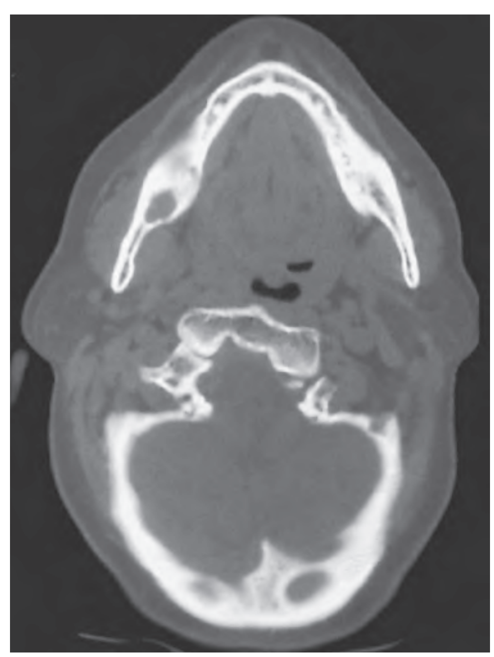

Figure 16.165 An axial view of the computed tomography scan (bone window) demonstrates an osteolytic lesion in the posterior part of the body of the mandible on the right-hand side.

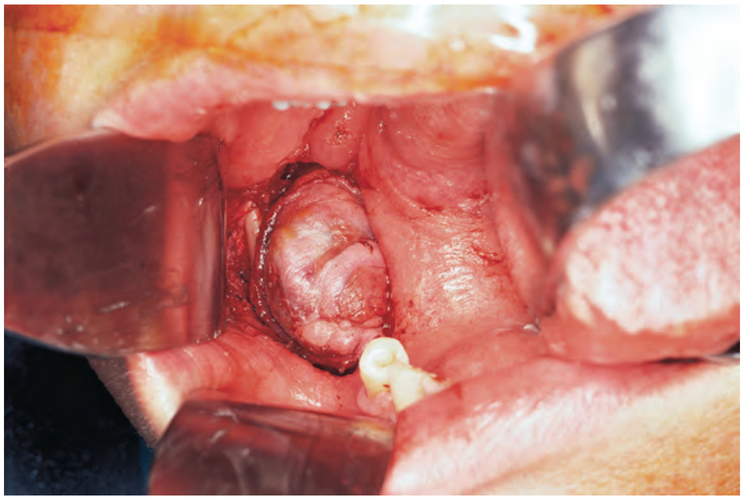

Figure 16.166 The mucosa around the tumor is incised circumferentially.

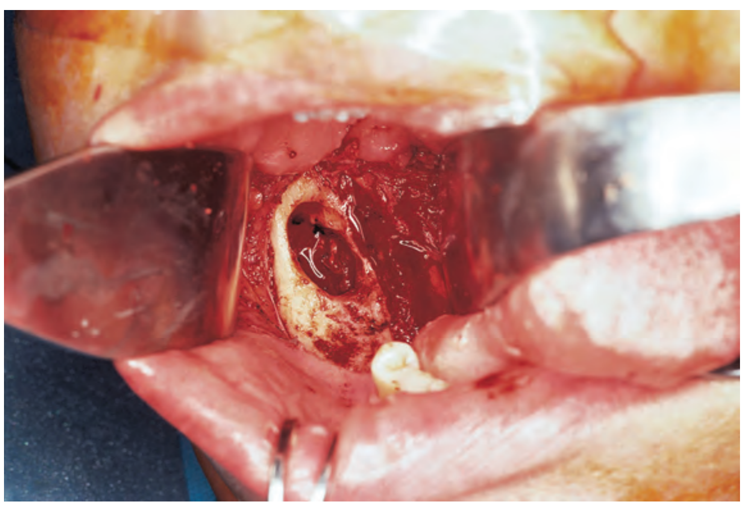

Figure 16.167 A well-demarcated bony defect remains after surgical excision of the tumor.

is secured with electrocautery and bone wax. Xeroform gauze packing is applied snugly to ensure hemostasis in the immediate postoperative period. The mucosal incision is not closed but is left open to heal by secondary intention. The Xeroform gauze packing is removed in 48 hours, and irrigations of the surgical defect are begun with a solution of baking soda and salt in warm water. The patient is instructed to repack the defect at least twice a day on a daily basis for several weeks. The healing of the defect begins from the floor of the surgical defect, eventually leading to filling of the bony defect with granulation tissue and epithelialization over the soft tissues. The surgical specimen of the giant cell granuloma, which was removed in a monobloc fashion, is shown in Fig. 16.168. The mucosal surface shows the previous biopsy site and irregular nodularity on the alveolar process. Upon bisecting the specimen, a fleshy, granular lesion is seen that is consistent with the pathologic diagnosis of a giant cell granuloma (Fig. 16.169).

Figure 16.168 The surgical specimen.

Figure 16.169 A fleshy, granular surface on bisection is consistent with the pathologic diagnosis of a giant cell granuloma.

Cementifying Fibroma

A cementifying fibroma is a benign neoplasm of fibrous origin with calcium deposition that usually presents in adults in the molar region of the mandible (Fig. 16.170). Surgical treatment for symptomatic lesions consists of local excision of the lesion, which usually is performed through a peroral approach. Incidentally found asymptomatic lesions may be left alone.

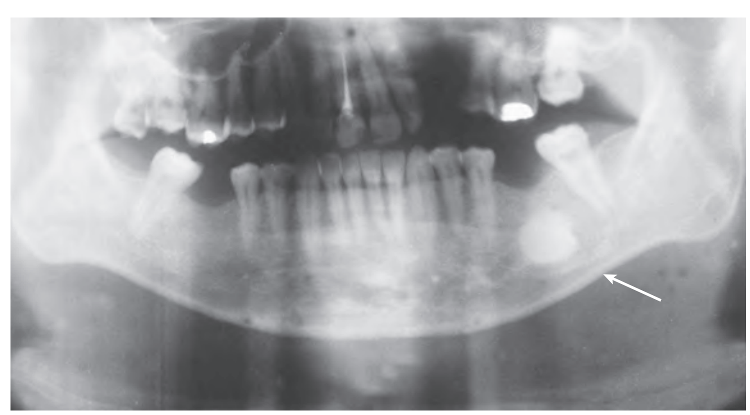

Figure 16.170 A cementifying fibroma of the left side of the mandible (*arrow*).

Surgical Access to Cervical Vertebral Bodies

Surgical access to the vertebral column in the cervical region is indicated in patients who require excision of primary tumors or metastatic tumors to the vertebral bodies. The surgical approaches described in this chapter are all anterior approaches for access to the vertebral column. Standard posterior approaches for a decompression laminectomy or exposure of the spinal cord are not described in this chapter. Anterior exposure of the vertebral column is required sometimes for resection of tumors involving the vertebral bodies or soft-tissue tumors secondarily extending to the vertebral column. These procedures usually are performed in collaboration with a neurosurgeon.

Primary benign or malignant tumors and occasionally metastatic tumors to the vertebral bodies that produce neurologic symptoms require surgical treatment. A posterior laminectomy often is adequate for decompression and immediate relief of symptoms. However, it does not address the problem of the presence of an intraspinal tumor anteriorly or of progressive destruction of the vertebral body, which leads to recurrent spinal cord compression and/or the risk of a compression fracture and an unstable spine. Resection and replacement of the involved vertebral body not only provides decompression of the spinal cord but achieves removal of the intravertebral tumor and allows immediate stabilization of the vertebral column. The surgical approaches to cervical vertebral bodies can be described under three categories, based on the level of involvement: (1) the craniocervical junction for lesions of the clivus and the first two cervical vertebrae; (2) the midcervical region for vertebral bodies C3 to C6; and (3) the cervicothoracic junction for lesions of the lower cervical and upper thoracic vertebral bodies.

Surgical Approach to the Craniocervical Junction and Upper Cervical Vertebrae

Lesions of the craniocervical junction and the first two cervical vertebrae present very special surgical challenges with regard to approach and exposure. Small lesions can be approached through the open mouth. A patient with a craniocervical chordoma presented with the only physical finding of a bulging of the posterior pharyngeal wall. An MRI scan in the sagittal plane shows the lesion arising from the region of the first and second cervical vertebrae (Fig. 16.171). This lesion is approached through the oral cavity under general endotracheal anesthesia. A Dingman mouth retractor is used to open the oral cavity and expose the region of the oropharynx (Fig. 16.172). The soft palate is divided in the midline to get exposure of the posterior wall of the oropharynx and nasopharynx (Fig. 16.173). Retracting sutures are applied to the two halves of the soft palate, and lateral retraction provides satisfactory exposure. Alternatively, Cloward retractors may be used to retract the two halves of the soft palate to expose the posterior pharyngeal wall.

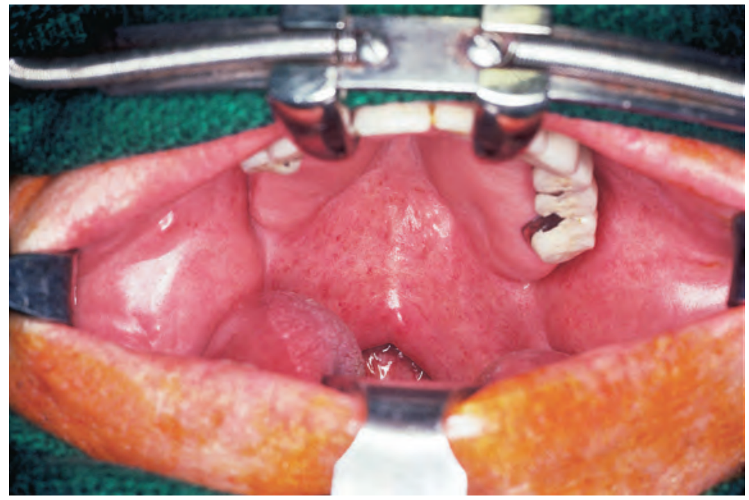

Figure 16.172 A Dingman mouth retractor is used to open the oral cavity and expose the oropharynx.

A vertical incision is made in the posterior pharyngeal wall, beginning at the roof of the nasopharynx and extending caudad up to the region of the arytenoids. The mucosal incision is deepened through the pharyngeal muscles to expose the prevertebral fascia. The prevertebral muscles are similarly incised in the midline, and the vertebral bodies are exposed (Fig. 16.174). Appropriate resection of the vertebral bodies is then undertaken to expose the tumor, which is resected in a monobloc fashion. This procedure generally is conducted in cooperation with a neurosurgical team that will assume the responsibility for the surgical procedure at this juncture. Thus a two-team surgical approach to craniocervical chordomas and similar tumors of the craniocervical junction is desirable for safety and completeness of the surgical resection. The head and neck team provides the necessary exposure for the neurosurgical team to accomplish resection of the tumor. If, however, adequate exposure is not achieved through this approach, then a mandibulotomy should be considered for wider exposure. A detailed description of a mandibulotomy approach for excision of a craniocervical chordoma is presented in Chapter 15.

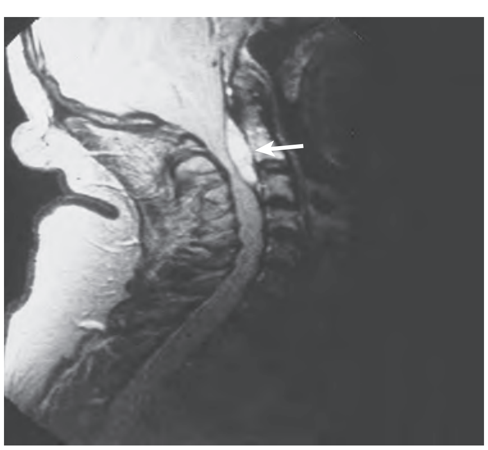

Figure 16.171 A magnetic resonance imaging scan in the sagittal plane shows the chordoma arising from the region of the first and second cervical vertebrae (*arrow*).

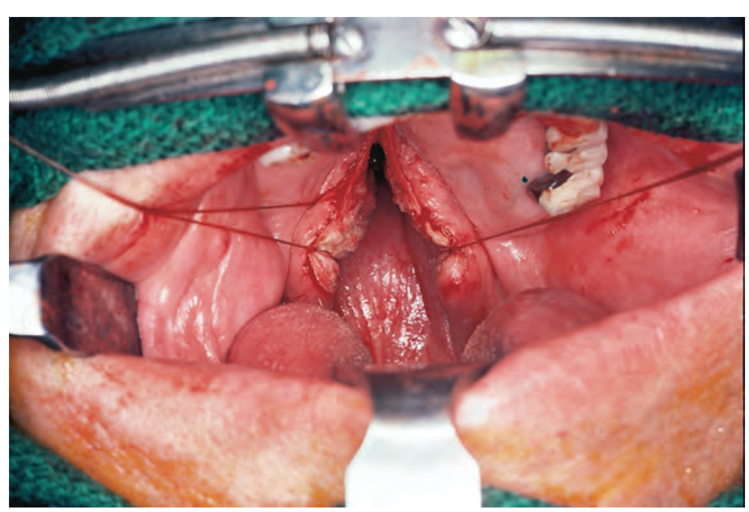

Figure 16.173 Division of the soft palate in the midline.

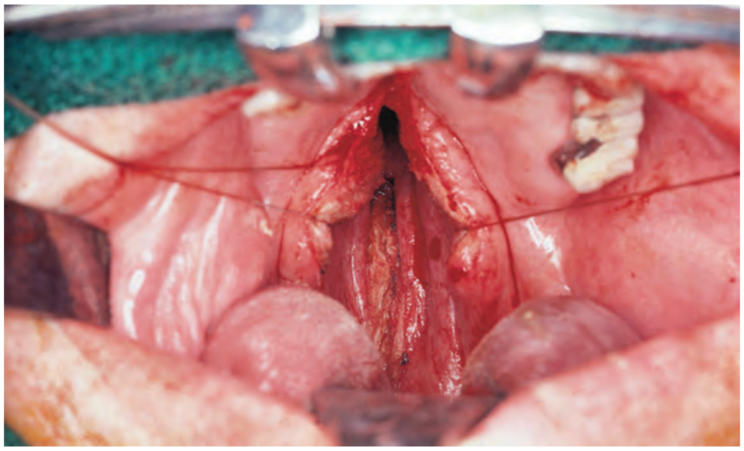

Figure 16.174 The vertebral bodies are exposed by incising the prevertebral fascia and muscles.

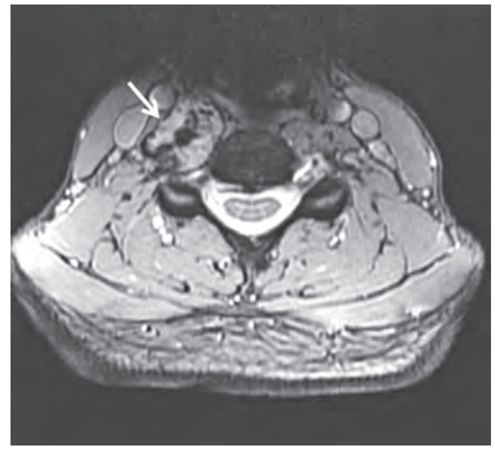

Figure 16.175 An axial view of a T2-weighted magnetic resonance imaging scan shows a tumor arising from the anterior surface of transverse process of the cervical vertebra (*arrow*).

Surgical Approach to Midcervical Vertebrae

Lesions of the midcervical vertebrae are easily approached through a transverse midcervical incision along an upper neck skin crease at the level of the upper border of the thyroid cartilage. The surgical approach differs depending on whether the lesion involves the vertebral body or the transverse process. If the lesion involves the vertebral body or requires resection of any part of the vertebral body, then an anterior approach is required. The following three structures, which cross the central and lateral compartments of the neck, need to be deliberately divided: (1) the superior thyroid artery, (2) the middle thyroid vein, and (3) the omohyoid muscle. The superior laryngeal nerve is at risk of being divided or injured as a result of stretch neuropraxia secondary to its retraction cephalad to gain exposure. So, extreme care should be exercised to avoid excessive stretch on the nerve. Similarly, fibers of the sympathetic chain are at risk of injury in the prevertebral plane. The sympathetic chain therefore should be carefully dissected and retracted laterally along with the carotid sheath. Injury to the sympathetic chain will lead to the development of Horner's syndrome. The larynx and esophagus are retracted medially and the carotid sheath is retracted laterally to expose the tumor. The prevertebral muscles, thus exposed, are incised vertically and dissected off the anterior surface of the vertebral bodies, providing the necessary exposure. If, however, the lesion involves the transverse process or the lateral aspect of the vertebral column, a lateral approach is required through the posterior triangle of the neck.

The patient whose MRI is shown in Fig. 16.175 presented with an ill-defined firm to bony mass in the midcervical region on the right-hand side and with the complaints of discomfort and pain in the right upper arm. The axial view of the T2-weighted MRI image shows the presence of a well-defined irregular heterogeneous lesion in the midcervical region posterolateral to the carotid sheath and contiguous with the transverse process of the cervical vertebra. The sagittal view of the MRI scan clearly shows a pedunculated lesion arising from the anterior aspect of the transverse process of the fifth cervical vertebra (Fig. 16.176). The clinical and radiologic diagnosis of an osteochondroma was made. The tumor did not extend into the epidural space. Surgical resection of this tumor is indicated with the goal of relief of pressure on the cervical roots and thus symptomatic relief of pain in the right upper extremity.

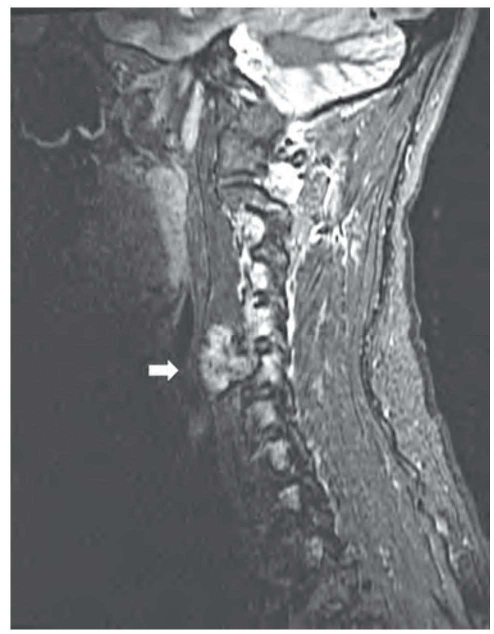

Figure 16.176 A sagittal view of the T2-weighted magnetic resonance imaging scan shows a tumor arising from the fifth cervical vertebra (*arrow*).

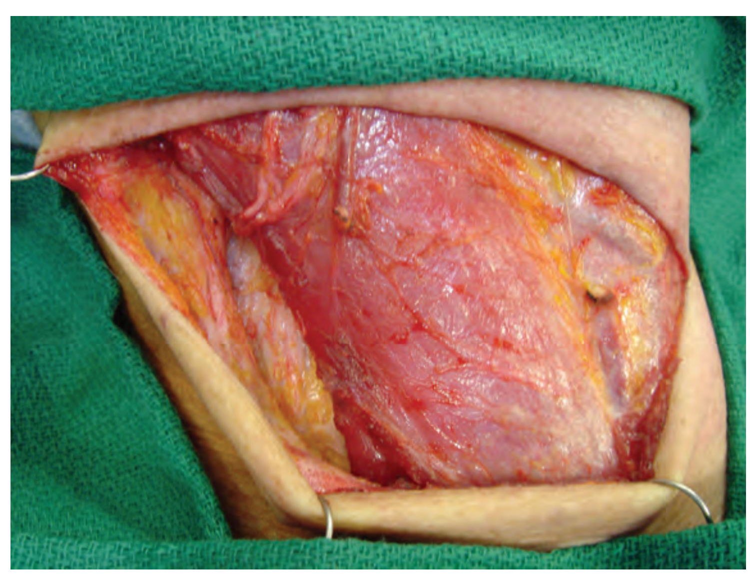

Figure 16.177 The posterior border of the sternocleidomastoid muscle is exposed through a transverse cervical incision.

A transverse incision is placed along the skin crease in the midcervical region, extending from the anterior border of the trapezius muscle posteriorly up to the midline of the neck anteriorly. The skin incision is deepened through the platysma, and upper and lower cervical flaps are elevated. The sternocleidomastoid muscle is identified, and its posterior border is defined to permit its retraction anteriorly to expose the carotid sheath and the prevertebral region (Fig. 16.177). Careful dissection is undertaken in the tissue plane posterior to the sternocleidomastoid muscle to identify, retract, and protect the spinal accessory nerve. Anterior retraction of the sternocleidomastoid muscle with loop retractors shows the contents of the carotid sheath and anterior displacement of the vagus nerve, as well as the roots of the cervical plexus and the phrenic nerve (Fig. 16.178).

Meticulous dissection is now undertaken in the fascia overlying the prevertebral muscles lateral to the carotid sheath. A vertical incision is made along the long axis of the scalene muscles, and the fibers of the scalene muscles are retracted to expose the underlying bony mass (Fig. 16.179). Meticulous dissection is now undertaken, remaining on the pseudocapsule of the bony tumor and carefully preserving all the neurogenic structures in the surrounding soft tissues to expose the tumor (Fig. 16.180). Complete exposure of the tumor in all directions up to its origin from the transverse process of the cervical vertebra is completed. Once complete exposure of the tumor is accomplished, its pedicle at the site of origin from the transverse process is exposed. A high-speed drill with a fine burr is used to amputate the tumor from its site of origin. A circumferential bone cut is made with the fine burr, and then an osteotome is used to excise the tumor. The sharp edges of the transected stump of the bone are smoothed out, protecting the integrity of the underlying vertebral canal and the epidural space (Fig. 16.181). Complete hemostasis is secured. A suction drain is placed and the wound is closed in layers.

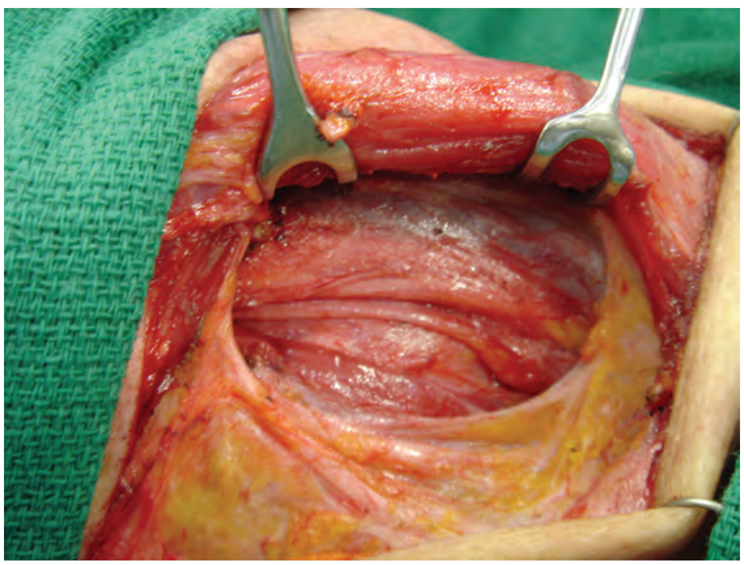

Figure 16.178 The carotid sheath and sympathetic chain are identified. Note the preserved spinal accessory nerve in the lower part of the surgical field.

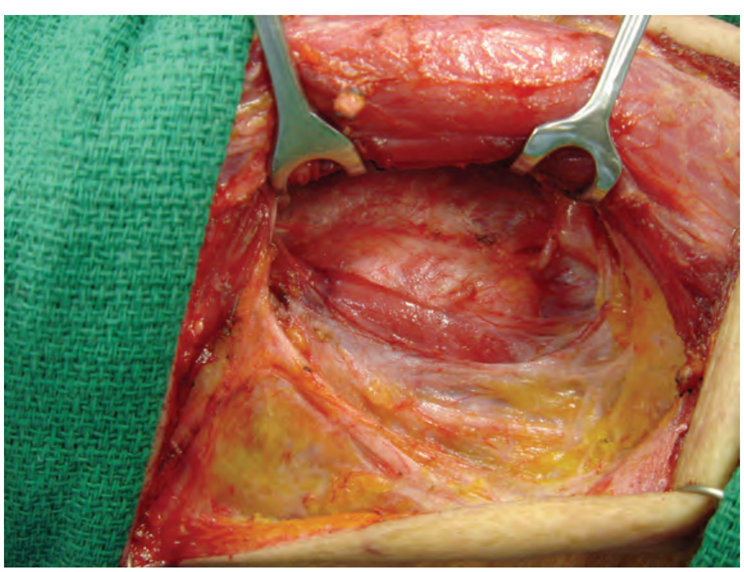

Figure 16.179 The carotid sheath is retracted medially and the scalene muscles are separated to expose the tumor.

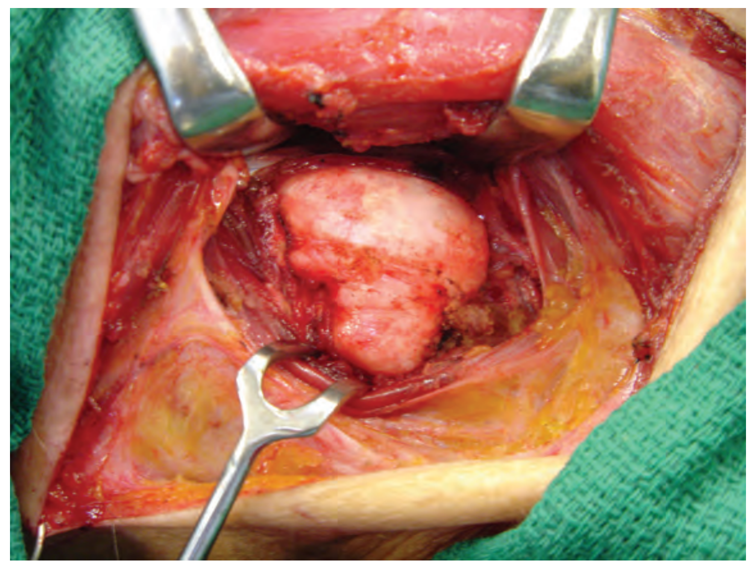

Figure 16.180 The tumor is exposed circumferentially.

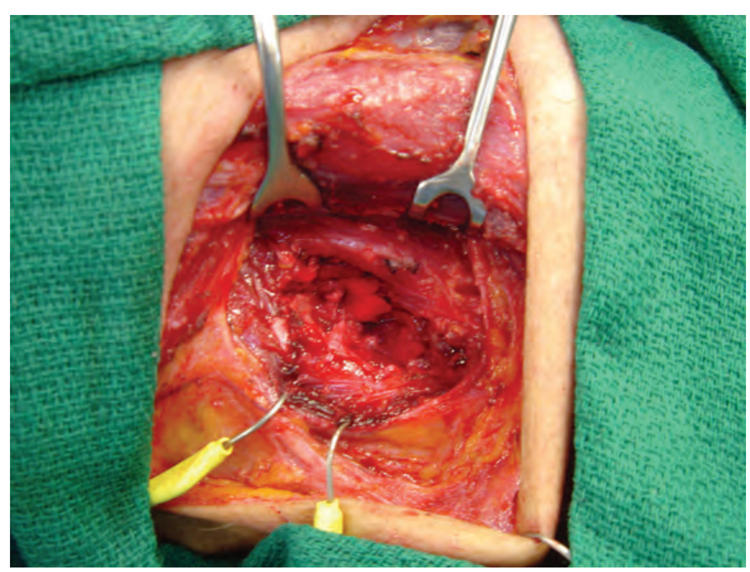

Figure 16.181 The surgical defect after excision of the tumor shows that it has been removed completely.

Surgical Approach to Lower Cervical and Upper Thoracic Vertebrae

Special technical considerations are necessary for the cervicothoracic junction because of the confined space of the thoracic inlet and the presence of major neurovascular structures as well as the trachea and esophagus. The details of the operative procedure are discussed here.

A patient with a bone-destructive lesion of the lower cervical and upper thoracic spine from a metastatic tumor presented with symptoms suggestive of potential spinal cord compression. A myelogram in an anteroposterior projection shows complete spinal block at the level of the involved vertebral body (Fig. 16.182). The surgical approach for exposure and resection of this vertebral body requires two surgical teams: a head and neck surgeon for exposure of the vertebral column and a neurosurgeon for resection and replacement of the vertebral body.

The surgical incisions necessary for exposure are shown in Fig. 16.183. A T-shaped incision with its transverse component extending from the posterior triangle of one side of the neck to the posterior triangle of the other side is necessary. The vertical incision is in the midline extending from the transverse incision over the sternum. The patient is shown on the operating table under general endotracheal anesthesia in the supine position (Fig. 16.184). Upper and lower skin flaps are elevated to expose the strap muscles in the midline and the sternocleidomastoid muscles, as depicted in Fig. 16.185. The lower skin

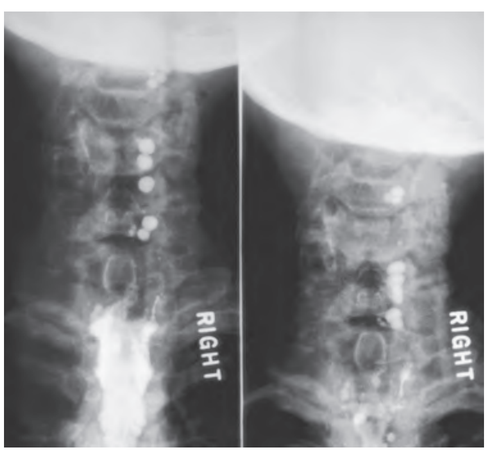

Figure 16.182 A myelogram (anteroposterior projection) shows blockage at the T1 level.

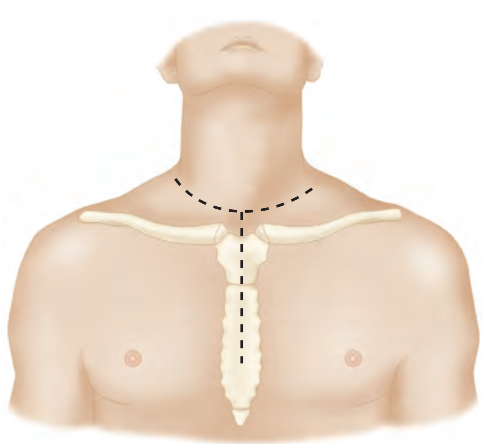

Figure 16.183 The surgical incisions necessary for exposure of the cervicothoracic vertebral column.

Figure 16.184 The incisions are outlined on the patient.

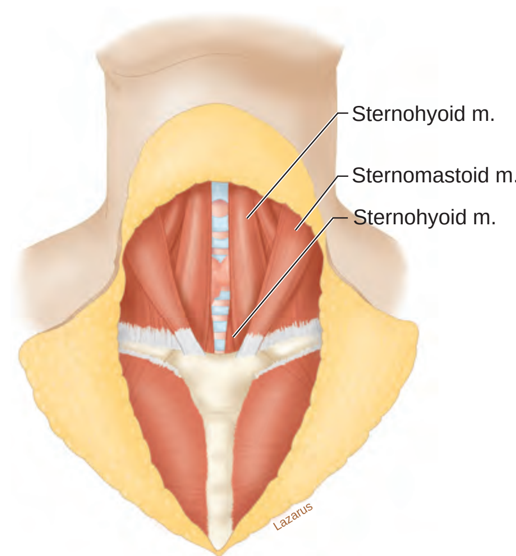

Figure 16.185 Elevation of upper and lower skin flaps. *m.,* Muscle.

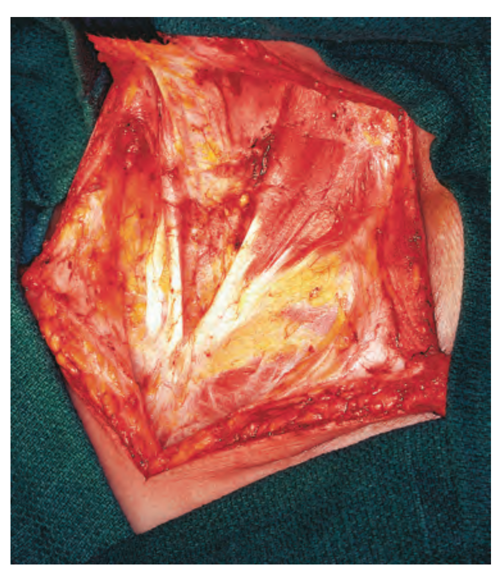

Figure 16.186 The surgical field after elevation of the skin flaps.

flaps should be elevated enough to expose the entire manubrium. Use of an electrocautery expedites clearance of the anterior surface of the sternum by detaching the origin of the pectoralis major muscle from the manubrium. The surgical field that has been exposed up to this point is shown in Fig. 16.186.

The left sternocleidomastoid muscle is now detached from its insertion on the manubrium and the clavicle and is allowed to retract cephalad. Likewise, the strap muscles on the left-hand side are divided close to the sternum and are allowed to retract cephalad. The exposure thus obtained is depicted in Fig. 16.187. The actual surgical field exposed by dividing the sternomastoid muscle and the strap muscles is shown in Fig. 16.188. The internal jugular vein can be seen deep to the sternomastoid muscle. The middle thyroid vein and the inferior thyroid artery are thereafter doubly clamped, divided, and ligated. The thyroid gland, larynx, trachea, and esophagus now can be retracted toward the right-hand side and the carotid sheath can be retracted toward the left-hand side (Fig. 16.189).

The medial third of the clavicle is now cleared circumferentially of all its muscular and ligamentous attachments. The periosteum of the medial third of the clavicle is incised and elevated circumferentially. A power saw is used to divide the clavicle at the junction of its medial and middle thirds. The sternoclavicular joint on the left-hand side is opened by incising its capsule, and the medial third of the clavicle is disarticulated

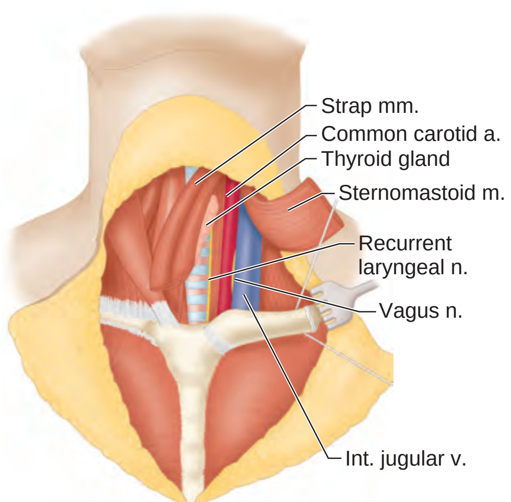

Figure 16.187 The sternomastoid muscle is detached, and the strap muscles on the left side are divided. The clavicle is now ready to be divided. *a.,* Artery; *Int.,* internal; *m.,* muscle; *mm.,* muscles; *n.,* nerve; *v.,* vein.

and preserved for subsequent use as a bone graft. Removal of the medial third of the clavicle requires division of the dense capsule of the joint, the intraarticular disc, and the costoclavicular ligament on the lower border of the clavicle. This maneuver is best done with an electrocautery. Now, with use of a high-speed drill with an olive-shaped burr, the manubrium is scored along its periphery, coring through its anterior cortex and the cancellous part of the manubrium up to its posterior cortex. Finally, a Lebsche knife is used to excise the manubrium to gain exposure of the superior mediastinum, as shown in Fig. 16.190. The excised cancellous bone from the manubrium is also preserved for subsequent use as a bone graft. The surgical exposure up to this point is shown in Fig. 16.191.

The larynx, trachea, and esophagus are mobilized by blunt dissection, paying careful attention to the recurrent laryngeal nerve, to get into the prevertebral plane. The mobilized larynx,

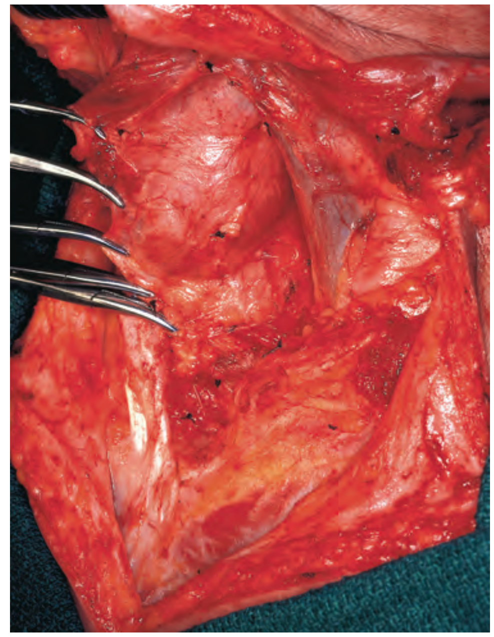

Figure 16.188 The strap muscles and the sternomastoid muscle on the left side are divided.

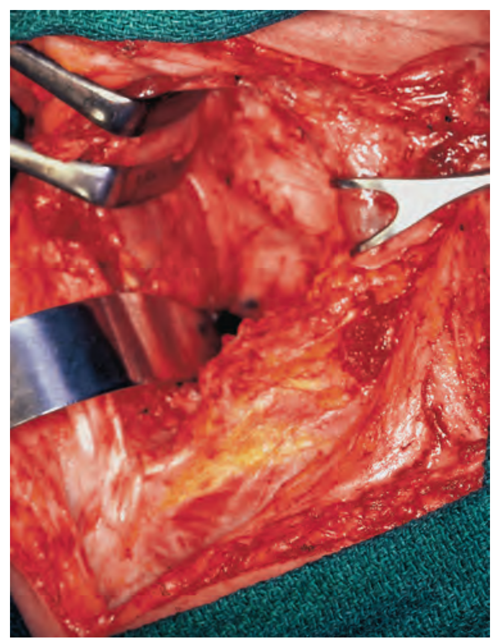

Figure 16.189 The thyroid gland, larynx, trachea, and esophagus are retracted toward the right-hand side, and the carotid sheath is retracted toward the left-hand side.

trachea, and esophagus are retracted to the right-hand side. Similarly, the common carotid artery and internal jugular vein are mobilized from the prevertebral fascia and are retracted laterally, exposing the vertebral column at the root of the neck, as shown in Fig. 16.192. A self-retaining Cloward retractor is used to keep the anterior surface of the vertebral column exposed for further work of resection of the vertebral body (Fig. 16.193). The accurate placement of the Cloward retractor is depicted in Fig. 16.194. The operative procedure beyond this point may be taken over by the neurosurgical team.

The neurosurgical aspects of the operative procedure are described here briefly. Excision of the involved vertebral body generally is performed in a piecemeal fashion with use of

appropriate rongeurs and curettes, as depicted in Fig. 16.195. If the surface of the vertebral body in question does not show any abnormality, then appropriate localization films should be obtained to ensure that the vertebral body exposed is indeed the one involved by the disease process and not the one cephalad or caudad. This determination is vitally important, because accurate localization of the involved vertebral body sometimes can be difficult in the surgical field. The involved vertebral body is completely curetted out to remove all grossly abnormal bone. If the dura is involved by the tumor, or if an intraspinal tumor is present, it is removed at this time and the spinal dura is repaired appropriately. After complete curettage of the involved vertebral body and "excision" of all gross tumor, the surgical defect is irrigated with an antibiotic solution. Complete hemostasis must be secured before reconstruction of the vertebral column begins. The surgical defect after excision of the vertebral body is shown in Fig. 16.196. In this patient, the vertebral

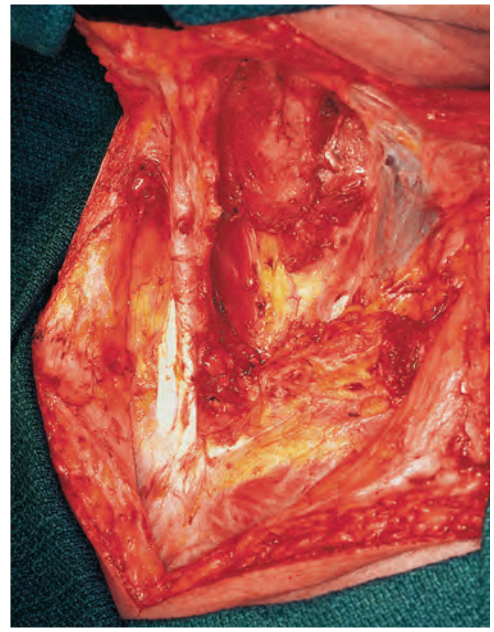

Figure 16.190 Exposure of the superior mediastinum.

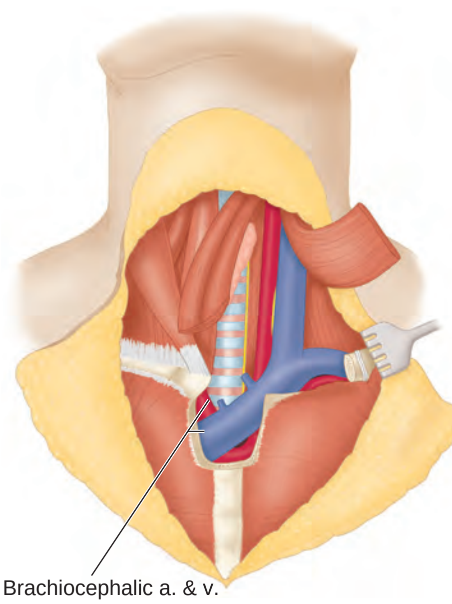

Figure 16.191 The surgical exposure of the mediastinum after resection of the manubrium. *a.*, Artery; *v.*, vein.

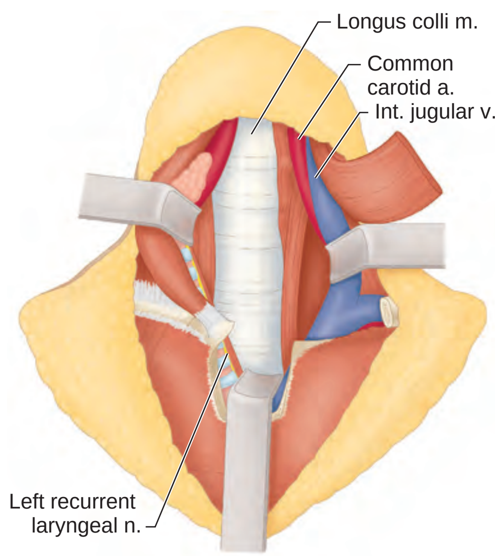

Figure 16.192 Exposure of the vertebral column at the root of the neck. *a.*, Artery; *m.*, muscle; *n.*, nerve; *v.*, vein.

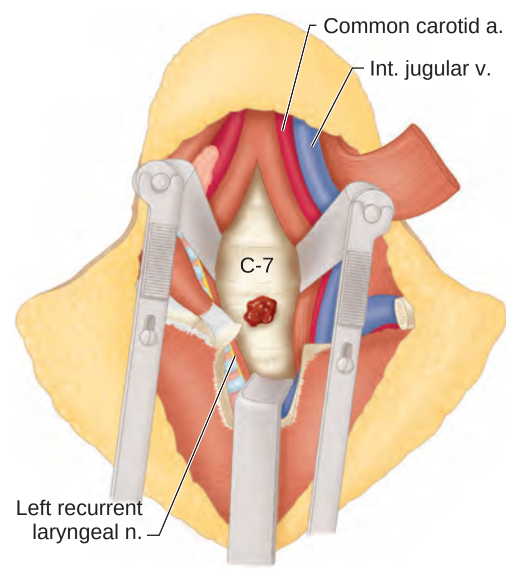

Figure 16.193 Placement of the Cloward retractor. *a.*, Artery; *n.*, nerve; *v.*, vein.

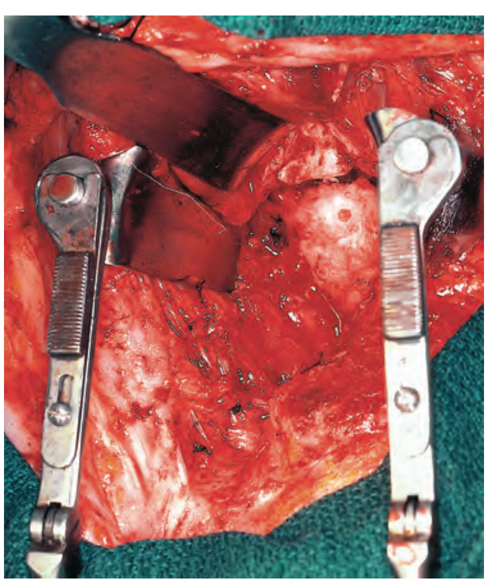

Figure 16.194 The anterior surface of the vertebral column is exposed.

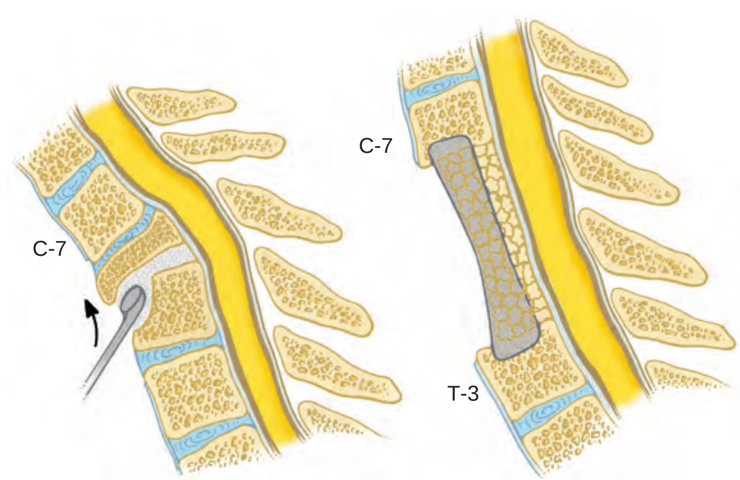

Figure 16.195 Excision of the involved vertebral body and placement of a bone graft.

bodies of T1 and T2 were resected because of involvement by the tumor.

Reconstruction and internal stabilization of the spine require insertion of stainless steel wires or pins in the healthy vertebral body above and below. After this procedure is completed, the remaining surgical defect created by the resection of the vertebral bodies is filled with bone cement (methyl methacrylate) as depicted in Fig. 16.197. Alternatively, the previously harvested bone grafts (a segment of the clavicle and cancellous bone from the manubrium) may be used additionally to complete the reconstruction. Extreme caution must be exercised to prevent excessive projection of the reconstructed vertebral column posteriorly, or else it may create impingement on the spinal cord. The reconstructed vertebral column is shown in Fig. 16.198. The upper part of the surgical field shows the upper border of the bone cement aligned against the undersurface of the vertebral body of the seventh cervical vertebra. Further retraction caudad in the mediastinum shows adequate alignment of the reconstructed vertebral column with the third thoracic vertebra. The wound is irrigated at this point with Bacitracin solution. Suction drains are placed in the field, and the incision is closed in layers (Fig. 16.199).

Postoperative care requires bed rest until satisfactory healing of the wound is achieved. Because the vertebral column is internally stabilized, external immobilization usually is not necessary. A lateral view of the postoperative radiograph of the reconstructed vertebral column shows the metallic wires in position with the bone cement replacing the resected vertebral bodies (Fig. 16.200). Resection and replacement of the lower cervical and upper thoracic vertebral bodies causing spinal cord

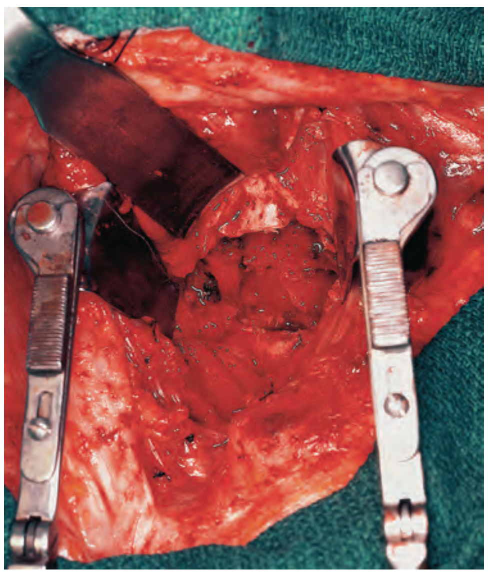

Figure 16.196 The surgical defect after excision of the vertebral body.

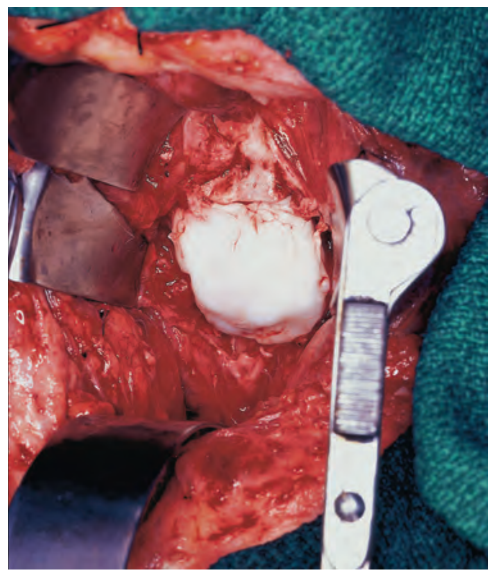

Figure 16.197 The vertebral column is reconstructed with methyl methacrylate.

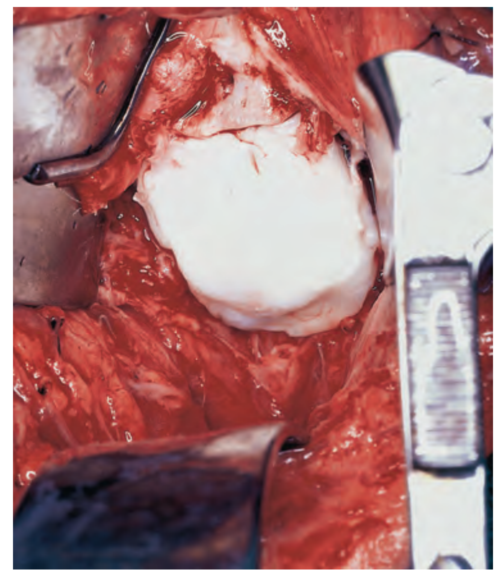

Figure 16.198 A close-up view of the reconstructed vertebral column.

Figure 16.199 Closure of the incision with suction drains in place.

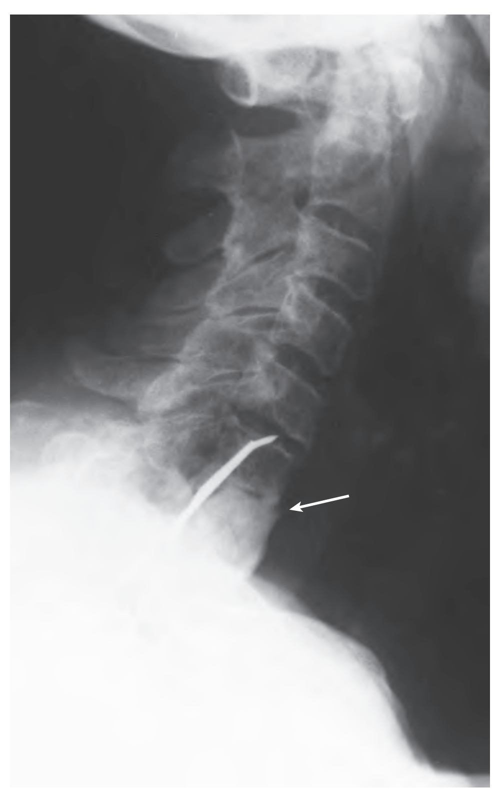

Figure 16.200 A postoperative radiograph (lateral view) showing the reconstructed vertebral body (*arrow*).

compression thus can be performed adequately through this approach. Tumors of the vertebral bodies that are likely to produce an unstable spine also optimally are treated by resection and replacement of the vertebral body as described. The surgical procedure ideally should be undertaken as a team effort with cooperation between a head and neck surgical team and a neurosurgical team.

Miscellaneous Bone Tumors

Extraosseous Osteogenic Sarcoma

Osteogenic sarcomas generally arise from bones, but these tumors occasionally can arise from soft tissues. The natural history of extraosseous osteogenic sarcomas is similar to that of osteosarcomas of osseous origin. The patient shown in Fig. 16.201 has a soft-tissue tumor arising in the superior mediastinum presenting at the root of the neck. The palpable extent of the tumor is shown in the patient, along with its relation to the innominate artery, the common carotid artery, and the subclavian artery (see Fig. 16.201). A coronal view of the MRI scan of the patient demonstrates the lesion with a tumor thrombus in the innominate vein (Fig. 16.202). An axial view of the CT scan at the level of the superior mediastinum demonstrates the classic appearance of an osteogenic sarcoma with areas showing osteolytic and osteoblastic features. The tumor is situated anterior to the trachea and the great vessels (Fig. 16.203).

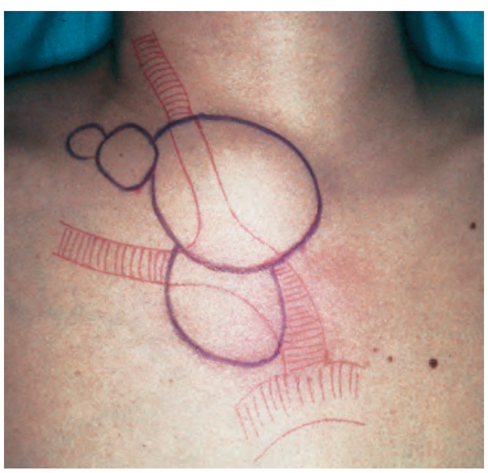

Figure 16.201 The palpable extent of the tumor is shown along with its relation to the innominate artery, the common carotid artery, and the subclavian artery.

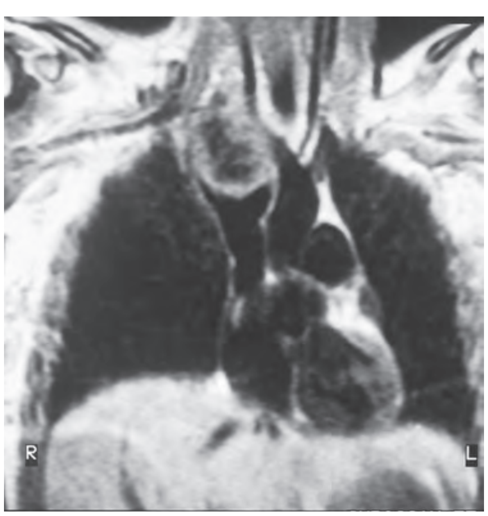

Figure 16.202 A coronal view of the magnetic resonance imaging scan demonstrates the lesion with a tumor thrombus in the innominate vein.

Figure 16.203 An axial view of the computed tomography scan at the level of the superior mediastinum.

The surgical approach to this tumor requires a T-shaped incision. The transverse incision is taken along a lower neck skin crease extending from the anterior border of the trapezius muscle on the right-hand side up to the clavicular head of the sternocleidomastoid muscle on the left-hand side. The vertical incision is in the midline overlying the manubrium sterni. The skin incision is deepened through the platysma, and upper and lower skin flaps are elevated (Fig. 16.204). The sternocleidomastoid muscle on the right-hand side is detached from the manubrium and the clavicle. The strap muscles are resected, which provides exposure of the superior surface of the tumor at the thoracic inlet. At this juncture a "clam-shell" thoracotomy is performed, dividing the manubrium sterni just medial to the left sternoclavicular joint up to the manubriosternal junction. A lateral extension of the sternotomy is taken up to the second intercostal space on the right-hand side (Fig. 16.205). Retraction of the divided manubrium provides satisfactory exposure of the superior mediastinum. By alternate blunt and sharp dissection, the tumor is carefully mobilized from the great vessels in the superior mediastinum.

Figure 16.204 The exposure obtained after elevation of the skin flaps of the T-shaped incision.

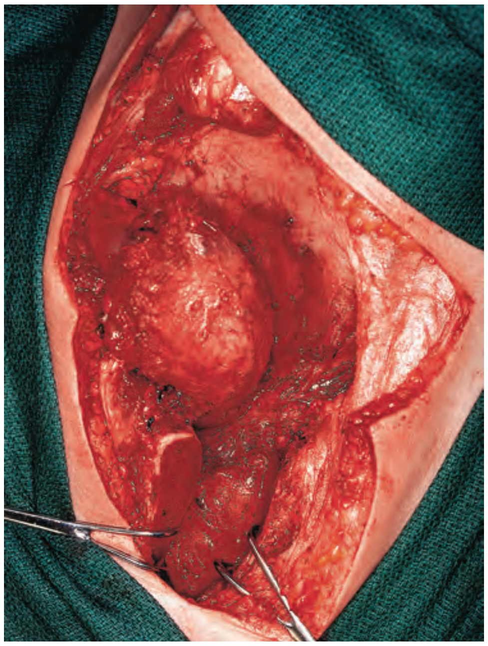

Figure 16.205 The manubrium sterni is divided just medial to the left sternoclavicular joint, and a lateral extension of the sternotomy is taken up to the second intercostal space on the right-hand side.

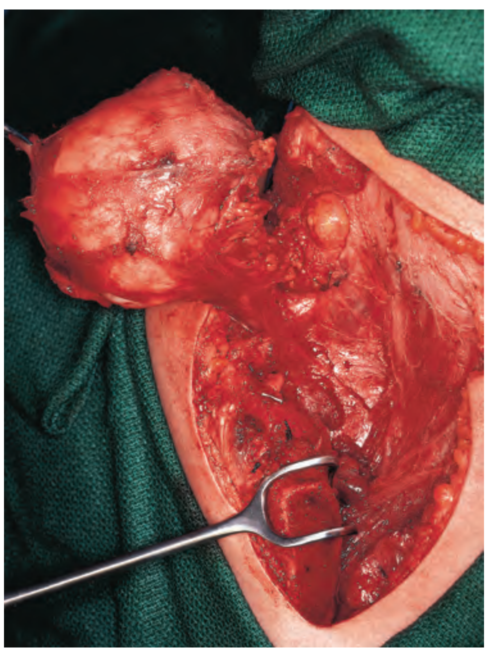

Figure 16.206 A contiguous tumor thrombus is seen in the innominate vein on the right-hand side.

At this juncture it becomes apparent that a contiguous tumor thrombus is present in the innominate vein on the right-hand side (Fig. 16.206). Therefore a segment of the innominate vein on the right-hand side is resected in a monobloc fashion. The surgical specimen shown in Fig. 16.207 demonstrates monobloc resection of the intact tumor along with tumor extension into the innominate vein. The bisected specimen clearly shows the tumor growing through the wall of the innominate vein and presenting in the lumen as a tumor thrombus (Fig. 16.208). The surgical field after excision of the tumor demonstrates the internal jugular vein and the subclavian vein with the stump of the resected innominate vein on the right-hand side (Fig. 16.209). After complete hemostasis, suction drains are placed, and the wound is closed in layers.

As demonstrated in this procedure, resection of osteogenic sarcomas of skeletal origin or extraosseous origin requires a wide three-dimensional resection with adequate soft tissue and bone margins. Wide exposure is essential for the surgical resection to be performed safely, and as many vital structures as possible should be preserved without compromising a satisfactory oncologic resection.

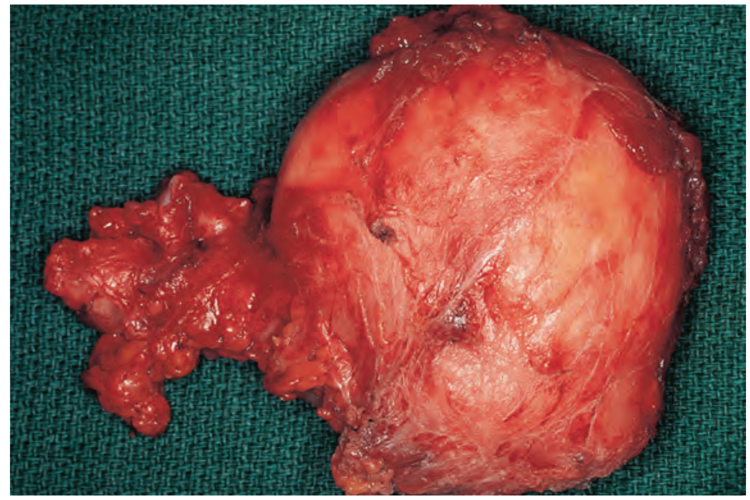

Figure 16.207 The surgical specimen showing monobloc resection of the tumor and the thrombus in the innominate vein.

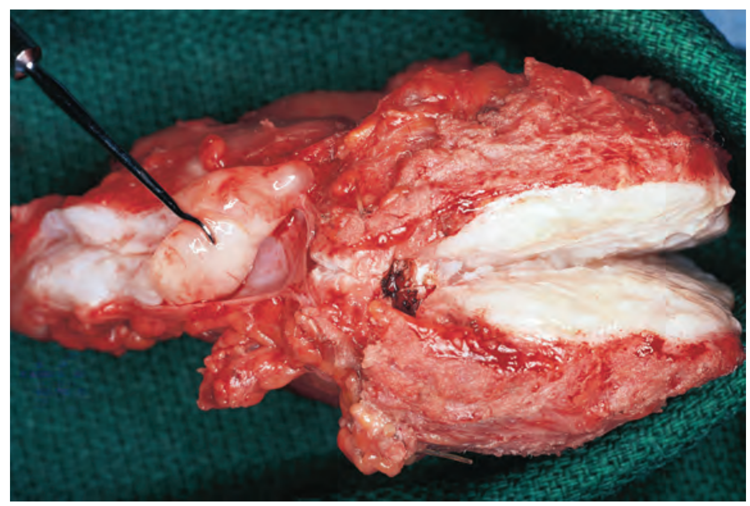

Figure 16.208 The bisected specimen clearly shows the tumor growing through the wall of the innominate vein and presenting in the lumen as a tumor thrombus.

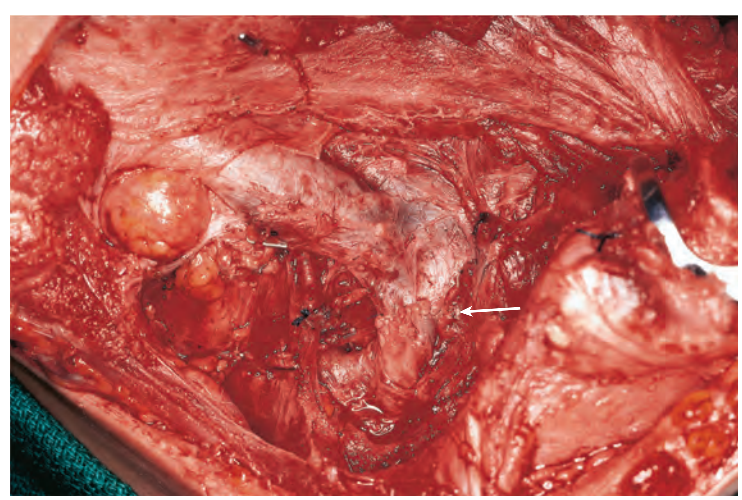

Figure 16.209 The surgical defect demonstrates the internal jugular vein and the subclavian vein with the stump of the resected innominate vein on the right-hand side.

RESULTS OF TREATMENT

Nearly all benign cystic or solid lesions of the cranial-facial-cervical skeleton are cured by adequate total resection. Incomplete removal often is followed by local recurrence, making subsequent surgical undertaking hazardous and much more debilitating. Complete removal is particularly important in tumors with a high potential for local recurrence. Ameloblastomas of the mandible and maxilla generally are cured by initial adequate total excision. Curettage, however, is doomed to failure and results in an unacceptably high rate of local recurrence. Subsequent resection is successful in a high proportion of patients but requires sacrifice of a larger segment of the mandible or maxilla. Long-term control of osteogenic sarcomas of craniofacial bones is not as good as that seen in osteogenic sarcomas of the extremities. Similarly, the long-term prognosis in adults with osteogenic sarcomas is not as good as that observed in children. The cure rates for osteogenic sarcomas of the mandible, maxilla, and other cranial bones are shown in Fig. 16.210. Chemotherapy is not as effective in adults with osteogenic sarcomas of the head and neck region as it is in those with osteogenic sarcomas of the extremities in the pediatric age group. Significant predictors of local control include a tumor size smaller than 4 cm and negative margins of surgical resection; positive margins are the only predictors of disease-specific survival.

Prognosis in chondrosarcomas of the craniofacial bones depends on the histologic grade of the lesion and the status of the margins of the resection (Fig. 16.211). Low-grade chondrosarcomas, if adequately excised, offer excellent control rates. On the other hand, high-grade chondrosarcomas and lesions that are incompletely excised with positive margins recur in a significant number of patients. The risk of local recurrence is very high in patients with high-grade chondrosarcomas and those who have positive margins. Disease-free survival is greater than 85% at 5 years and 70% at 10 years for patients presenting with chondrosarcomas.

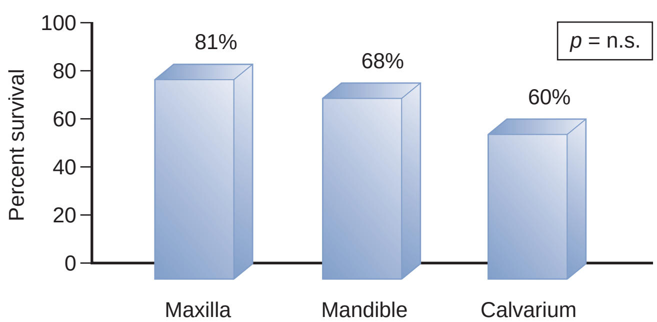

Figure 16.210 Five-year overall survival rates for osteogenic sarcomas of the head and neck by site.

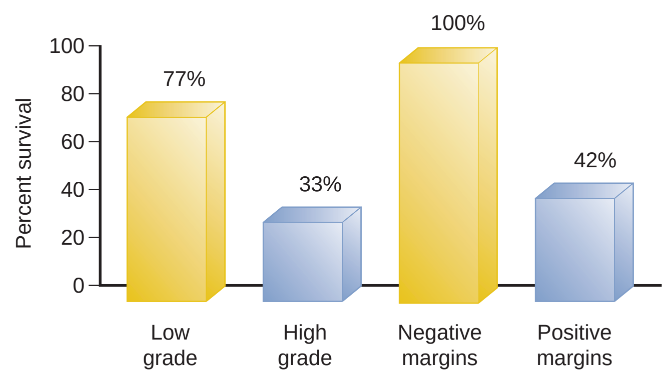

Figure 16.211 Five-year survival rates for chondrosarcomas of the head and neck by histologic grade and margins.

CHAPTER 17

Reconstructive Surgery



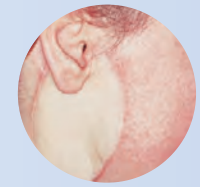

The impact of major ablative surgery for cancer in the head and neck region can be devastating for the patient, aesthetically and often functionally. Reconstruction of oncologic defects is necessary to restore function and appearance in an effort to achieve total rehabilitation (Fig. 17.1). Psychosocial, vocational, and emotional counseling may also be necessary for total recovery. Examples of aesthetic considerations include contour, appearance, and expression of the face. Restoration of oral competence also is necessary for patients who have undergone major surgery of the oral cavity and oropharynx. Functional concerns that warrant consideration include speech, mastication, and deglutition.

Ablative surgery to treat cancer leads to loss of soft tissue and bone (Fig. 17.2). Soft tissue defects include missing epithelial (dermal or mucosal) lining as well as loss of volume of underlying soft tissues. Before any replacement of tissues takes place, the reconstructive surgeon must first prioritize the functional and aesthetic concerns, and then decide what tissue must be replaced or repaired. An assessment of available tissue donor sites then ensues. Ideally, like tissues should be replaced with like. For example, missing bone should be replaced with an osseous reconstruction; however, the need for bone reconstruction depends on the site and extent of bone resection and may not be possible or necessary in all instances. Special consideration is also required for reconstruction of resected nerves, blood vessels, and cartilage.

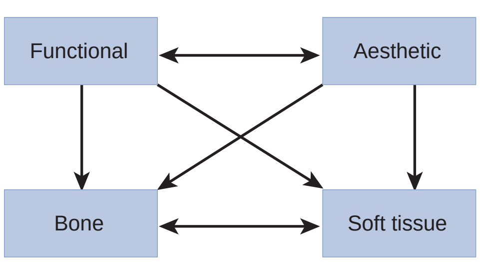

Figure 17.1 Planning for reconstructive surgery.

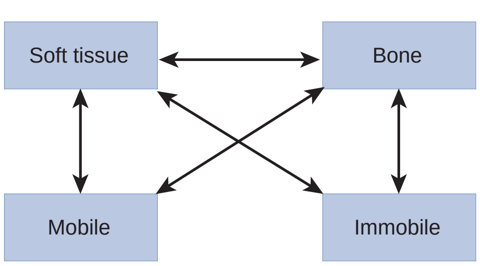

Figure 17.2 The extent of tissue loss from cancer ablative surgery relates to the loss of soft tissue and bone.

The surgical defect created by resection of either a primary or a metastatic tumor in the head and neck region can often be repaired by primary closure if the tissue loss is modest. However, if primary closure is not feasible, then viable tissue should be introduced to repair the surgical defect. Such tissue may be mobilized as a local or regional flap, transferring adjacent tissues from the head and neck region. Alternatively, reconstruction may require free tissue transfer from a distant donor site. Therefore flaps available for reconstruction of defects in the head and neck region may be classified as local, regional, or distant depending on their relationship to the area being reconstructed.

The viability of any flap depends on its type of blood supply. In general, axial flaps are more reliable because they are perfused by a predictable, named vascular pedicle. The width-to-length ratio of an axial flap may be as much as 1:5 or more depending on the particular flap chosen and its associated blood supply. In contrast, random flaps are less reliable because they are perfused by a smaller subdermal plexus of vessels. The narrower the base of the flap, the less likely a random pattern of circulation can support the tissue.

A better understanding of vascular anatomy, regional circulation, and the angiosome concept has resulted in the increase in availability and dependability of flaps with a wide range of applications in reconstruction of various defects. Flaps are most reliable when based upon a known vascular pedicle (i.e., axial pattern). As a result, muscle and myocutaneous flaps used for reconstruction are based on named vessels or their perforating branches, whether used as a pedicled regional flap or as a distant free flap. Microsurgery has evolved significantly, and the use of free flaps has become routine with the advent of operating microscopes and microsutures.

Special considerations are required for reconstructive surgery in each specific region of the head and neck. As such, these topics are approached individually.

ANATOMIC CONSIDERATIONS

Scalp, Skin, and Soft Tissues of the Face and Neck

The skin of the scalp, face, or neck can often be replaced easily with a skin graft or local flaps. However, when extirpation involves the underlying soft tissues with creation of surgical dead space, more complex reconstructive efforts with pedicled or free flaps are required. The use of regional muscle/myocutaneous flaps, such as the pectoralis major flap, is a common solution. Alternatively, free flaps applicable in these situations include the radial forearm, omentum, anterolateral thigh, latissimus dorsi, scapula, rectus abdominis, and groin flaps.

Figure 17.3 Reconstruction with a rectus abdominis free flap for a composite three-dimensional defect after radical temporal bone resection and amputation of the pinna.

Figure 17.4 The overall cosmetic result is greatly enhanced by use of a prosthesis for the external ear in the patient shown in Fig. 17.3.

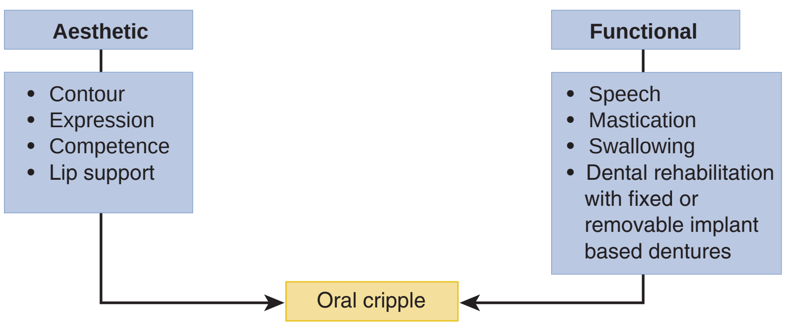

Figure 17.5 The functional and aesthetic impact of ablative surgery for oral cavity cancer.

Paranasal Sinuses, Orbit, and Skull Base

Following major resections of the paranasal sinuses, orbit, or skull base, certain situations mandate reconstruction. For example, dura and intracranial contents should be separated from the nasal cavity after skull base surgery. Likewise, support of the globe should be planned whenever the orbital floor is resected. In addition, replacement of soft tissue bulk and overlying skin is the standard management of major three-dimensional composite defects. Repair of the skull base can be performed without bone by using galeal pericranial or a free flap. Reconstruction of the floor of the orbit may be accomplished with use of a free osteocutaneous flap or by combining a bone graft with a soft tissue free flap, depending on the circumstances. If alloplastic material such as titanium mesh is used to repair the floor of the orbit, then adequate soft tissue coverage should be provided to avoid exposure and extrusion of the alloplastic material. Preoperative planning requires consultation with a maxillofacial prosthodontist for appropriate prosthetic support. Consideration should be given to the use of computer-aided design/computer-assisted manufacturing (CAD-CAM) technology where complex bone reconstruction is required. Examples of these are mandible reconstruction and maxillary reconstruction. On occasion, rehabilitation is accomplished by prostheses alone instead of reconstructive surgery to achieve the desired result (Fig. 17.3 and Fig. 17.4).

Oral Cavity

The goals of oral cavity reconstruction include both functional and aesthetic restoration. Major ablative surgery in the oral cavity may result in an oral cripple if appropriate efforts are not made to reconstruct the surgical defect and rehabilitate the oral cavity with restoration of removable or fixed implant-based dentation (Fig. 17.5). The components of functional restoration are oral competency, clarity of speech, mobility of the tongue, mastication/occlusion, bolus transport, lip support, as well as prevention of nasal regurgitation and aspiration. Aesthetic considerations include restoration of facial height, soft tissue contour, chin prominence, and lip support.

Major ablative surgery for tumors of the oral cavity may result in loss of mucosa, submucosal soft tissues, underlying musculature, overlying skin, and/or adjacent bone. Small, superficial defects of the mucosa and underlying soft tissues in the oral cavity can in some cases be repaired by primary closure, a local mucosal/musculomucosal flap, or a split-thickness skin graft. More complex or extensive resections require tissue transfer with regional or distant flaps.

Resection of the upper alveolus may be satisfactorily reconstructed with a dental prosthesis. However, if permanent obliteration of the communication between the oral cavity and nasal cavity or maxillary antrum is needed, then a free flap is the best option. In reconstruction of the upper alveolus/palatal

defects, CAD-CAM technology should be utilized if bone reconstruction is planned for accurate restoration of the contour of the face and alveolar arch. Resection of the lower alveolus with a marginal mandibulectomy does not typically require replacement of bone. However, dental rehabilitation is difficult, and implants are impossible following marginal mandibulectomy. On the other hand, a segmental mandibulectomy, requires reconstruction of the resected bone with a composite free flap. Here again, CAD-CAM technology is very applicable for accurate and expeditious reconstruction with a free bone flap.

Pharynx

The need for immediate reconstruction of pharyngeal defects cannot be overstated. The goal should be to restore the ability of the patient to resume oral alimentation as soon as possible after resection of the tumor. Reconstruction of the surface lining of the pharyngeal wall resulting from transoral excision of superficial mucosal lesions does not require any major reconstructive effort. In these cases, the surgical defect is left open to heal by secondary intention. On the other hand, full-thickness resection of the pharyngeal wall requires reconstruction with use of a regional myocutaneous flap or a free flap, keeping in mind that the eventual goal of such a reconstruction should be to restore deglutition without aspiration or airway obstruction.

When a laryngectomy is undertaken in addition to pharyngectomy, the reconstructive choices depend on whether there is partial or total loss of the hypopharyngeal circumference. Partial hypopharyngeal defects can be repaired with a pectoralis major myocutaneous flap, a supraclavicular fasciocutaneous flap, or a free flap. When circumferential resection of the hypopharynx is undertaken, the choice of flaps depends on the length of the resected segment. A short, circumferential hypopharyngectomy segment limited to the cervical region is reconstructed with either a free segment of jejunum or a tubed fasciocutaneous free flap. However, when the hypopharyngeal resection extends to include the cervical esophagus, then the options are colon interposition, free flap, or gastric pull up. Complication rates of up to 15% are reported following gastric transposition. Clearly, the goals of reconstructive surgery in this setting are to recreate a satisfactory alimentary conduit, prevent stricture formation, and avoid functional obstruction caused by redundant soft tissue.

RECONSTRUCTION WITH SKIN GRAFTS

Small superficial defects of the mucosa or skin that are not amenable to repair by primary closure or rearrangement of adjacent tissue are considered for reconstruction with either a split-thickness or a full-thickness skin graft. Full-thickness skin grafts tend to have a better cosmetic appearance and less secondary contracture than split grafts; however, they are limited in size. Common full-thickness donor sites for head and neck defects include the retroauricular and supraclavicular areas. Split-thickness grafts are abundantly available but can undergo significant contracture, which can limit movement of functional areas such as the eyelids or tongue. Because split grafts are thinner, including only portions of the dermis, the metabolic requirement for healing is less than that for full-thickness grafts. As such, for poorly vascularized areas, split grafts are preferred. In general, for external skin coverage, skin grafts are best applied to the parts of the scalp or face that are relatively immobile. Thus skin grafts are most suitable for defects of the scalp, temple, nasal bridge, external ear, and postauricular region. A typical example is excision of a

Figure 17.6 A full-thickness defect of the left nasal sidewall after removal of a melanoma before secondary application of full-thickness skin graft.

Figure 17.7 The postoperative appearance of the patient seen in Fig. 17.6 1 year following surgery showing complete healing and an excellent aesthetic outcome with a full-thickness skin graft.

superficial melanoma from the skin of the bridge of the nose. Generally, surgical defects after excision of melanoma are not repaired immediately until the final paraffin section report from pathology shows clear margins. In the interim, the surgical defect is covered with hemostatic dressings, such as Surgicel (Fig. 17.6). Cheek skin was advanced over the lateral portion of the defect, and a full-thickness skin graft from the posterior triangle of the neck was used to close the remaining defect (Fig. 17.7). Occasionally, a full-thickness skin graft may be used, even on mobile parts of the face, if resection of a lesion leads only to skin loss that cannot be repaired in a more aesthetic manner (Fig. 17.8).

Skin grafts similarly may be used in the oral cavity when the mucosal defect is either too large to heal by secondary intention or is likely to cause contracture and functional disability. This situation is particularly true in the case of superficial defects of the anterior floor of the mouth or buccal mucosa. When used in the oral cavity, it is quite common for portions of the skin graft to slough in the immediate postoperative period, but as long as the deeper layers of the skin graft remain viable, eventual epithelialization occurs with excellent functional results. Lesions suitable for skin graft repair in the oral cavity are shown in Figs. 17.9 through 17.12.

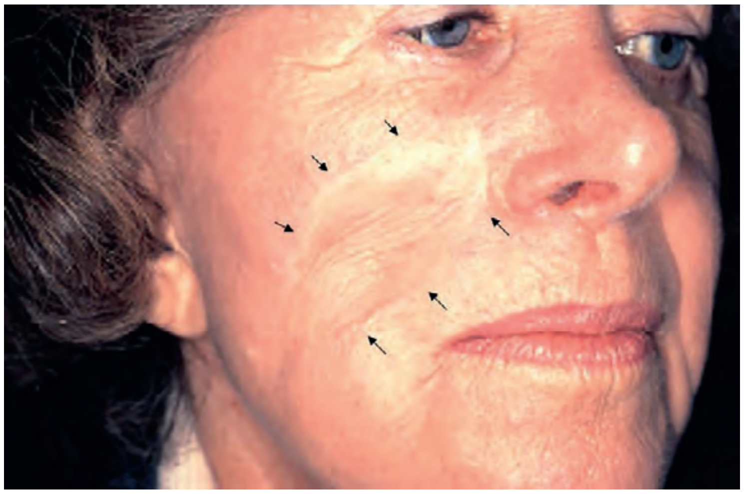

Figure 17.8 The postoperative appearance of a patient after full-thickness skin graft repair of a skin defect of the cheek (*arrows*).

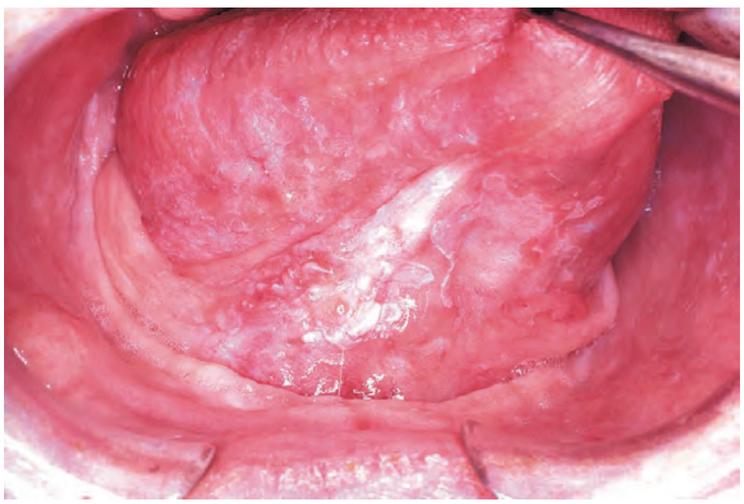

Figure 17.9 A superficially invasive carcinoma of the anterior floor of the mouth.

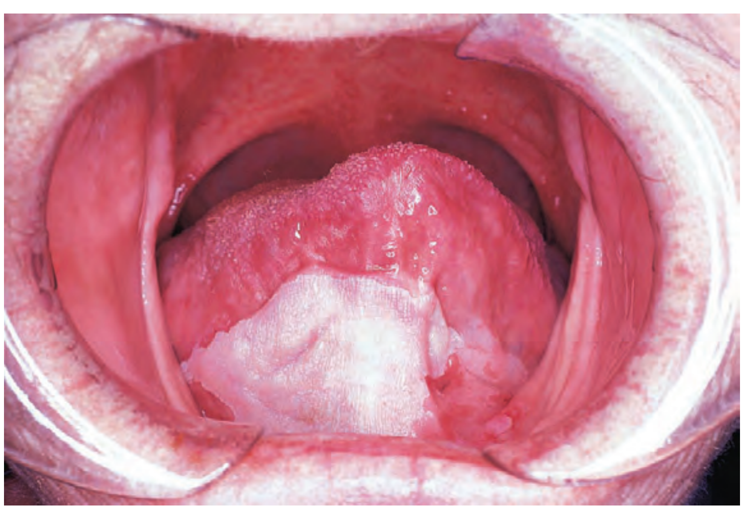

Figure 17.10 The postoperative appearance of the skin graft 3 months following surgery.

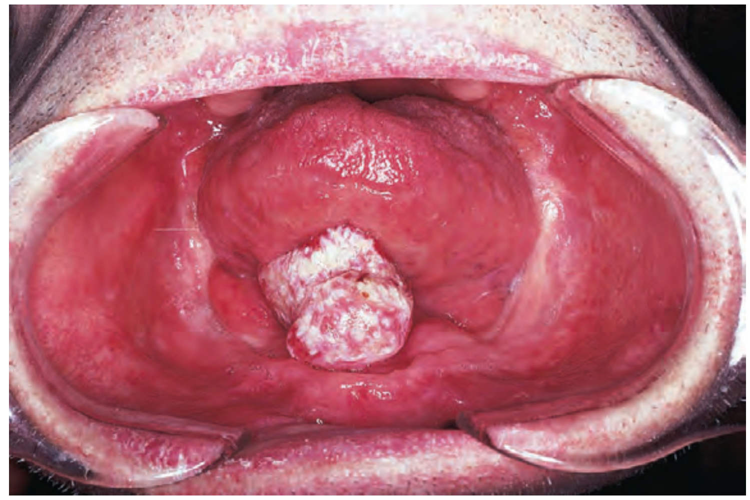

Figure 17.11 A squamous cell carcinoma of the lower gum and adjacent floor of the mouth in an edentulous patient.

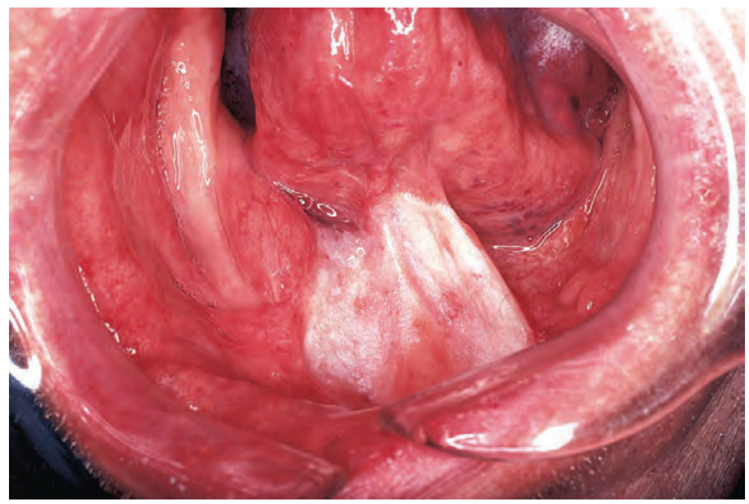

Figure 17.12 The postoperative result 3 months following surgery shows a healed split-thickness skin graft with excellent mobility of the tongue.

RECONSTRUCTION WITH CUTANEOUS FLAPS

Adjacent tissues may be elevated to reconstruct small surgical defects that cannot be repaired primarily. Also known as a local flap, adjacent tissues may be mucosal or cutaneous, depending on the location and the tissue requirements. Examples of mucosal flaps for intraoral repair are the tongue flap, the pharyngeal wall, and facial artery musculomucosal (FAMM) flap. However, because these flaps have a limited number of specific applications, surgeons are often unfamiliar with technical aspects of harvest, and these options may be perceived as unreliable. On the other hand, a palatal mucoperiosteal flap that derives its blood supply from the palatine artery is quite reliable in the repair of small through-and-through palatal defects or for the repair of a postsurgical oronasal fistula.

Many local cutaneous flaps are available for repair of surgical defects of the scalp and skin of the face and neck. Local flaps are preferable for repair of skin and soft tissue defects on the face because of superior color match and skin texture. The nasolabial flap is a commonly used axial local skin flap. Adjacent tissue transfer of skin flaps with a random blood supply (e.g., using cheek advancement, rhomboid, or bilobed flaps) is often useful for small defects of the face and neck when adjacent mobile skin is accessible (see several examples of local flaps in Chapter 3). A few regional fasciocutaneous flaps are available

in the head and neck region for coverage of surgical defects that cannot be repaired by either primary closure or adjacent tissue transfer. Frequently used regional flaps include the deltopectoral, supraclavicular, cervical, and forehead flaps.

With the availability of free flaps, the popularity of regional cutaneous and myocutaneous flaps has declined, except for specific indications, such as the forehead flap for nasal reconstruction. Often the aesthetic and functional morbidity resulting from regional cutaneous flaps in head and neck reconstruction can be avoided by the use of free flaps. Regional flaps are easy to elevate, and the surgical defect can be reconstructed expeditiously. Consideration should be given to the availability of regional flaps before planning reconstruction with a free flap.

Regional Cutaneous Flaps

Regional cutaneous flaps are skin flaps that are available in the head and neck region for transfer from one area to another to cover a surgical defect that cannot be repaired by primary closure or by advancement of local tissues or local flaps. The most frequently used regional cutaneous flaps are the anterior or posterior cervical flap, the deltopectoral flap, the forehead flap, and the supraclavicular artery flap. The forehead flap is rarely used because of its significant donor site aesthetic morbidity. The blood supply to the forehead flap is axial, and the blood supply to the cervical flap is random. The blood supply to the deltopectoral flap is axial in its proximal part and random in its distal part. The blood supply to the supraclavicular artery island flap is axial from a branch of the transverse cervical artery.

Cervical Flap

The cervical flap is a regional flap with a random pattern blood supply. The width-to-length ratio therefore is 1:2, or at most 1:3, and thus, only a limited amount of skin is available. If a cervical flap of large width is used, a skin graft may be required to cover the donor site. The flap may be based superiorly or posteriorly and thus may be oriented vertically or transversely. When the skin of the anterior aspect of the neck is used, it is called the *anterior cervical flap,* and when the skin of the posterior aspect of the neck is used, it is called the *posterior cervical flap* or *Mutter flap*. The cervical flap generally is used to cover defects of the skin and soft tissues of the face and neck.

Reconstruction of a Preauricular Skin Defect. The patient shown in Fig. 17.13 has a metastatic carcinoma in the left parotid region fungating through the skin with palpable cervical lymph nodes. The primary tumor, which was a squamous cell carcinoma of the skin of the left temple, was excised previously, and at this time, no evidence exists of recurrence at that site.

Figure 17.13 Incisions are outlined for a patient with a metastatic carcinoma in the left parotid region.

The surgical procedure planned is a modified neck dissection in conjunction with a subtotal parotidectomy and excision of the skin of the preauricular region to remove metastatic lymph nodes in a monobloc fashion. The incisions encompass the area of skin to be excised in conjunction with the outline of the transverse cervical flap and the remaining incision for completion of a neck dissection.

The cervical flap is elevated first, and then the remainder of the skin flaps are elevated. In Fig. 17.14, the elevated cervical flap is shown, with its blood supply derived from the posterior aspect of the skin of the neck. Although this flap is random, its width-to-length ratio is almost 1:3. The distal part of the flap may be trimmed off and discarded to fit the surgical defect.

The cervical flap is now rotated cephalad (Fig. 17.15). The tip of the flap is brought up to the upper margin of the skin defect in the preauricular region. The flap is appropriately trimmed to fit the surgical defect. The donor site defect in the upper part of the neck is closed primarily by mobilizing the skin of the cheek and the skin of the lower part of the neck.

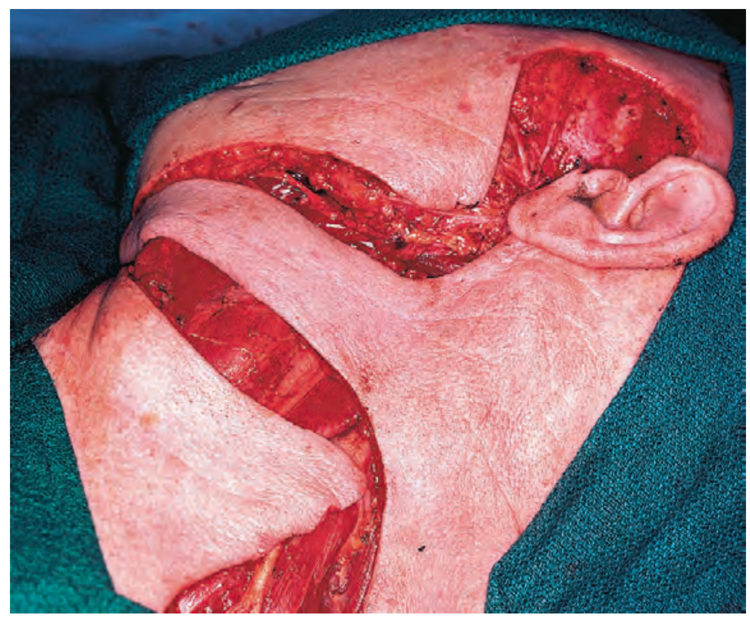

Figure 17.14 The elevated cervical flap.

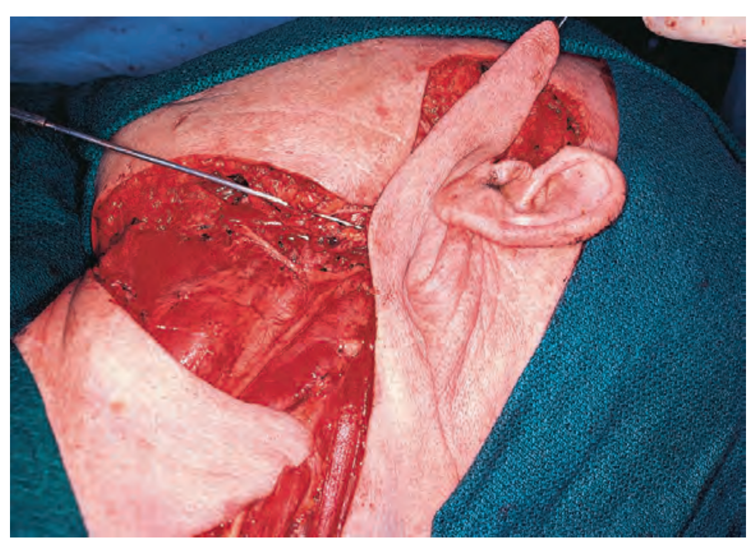

Figure 17.15 The cervical flap is rotated cephalad.

Completed closure is shown in Fig. 17.16. A satisfactory closure of the skin defect in the preauricular region is thus accomplished by the posteriorly based transverse cervical flap. Note the presence of a skin fold at the point of rotation of the cervical flap, producing a "dog ear." In time this fold of skin usually flattens out and in most cases does not require revision.

The postoperative appearance of the patient is shown approximately 3 months following completion of postoperative radiation therapy (Fig. 17.17). The flap not only provides excellent coverage but has a very satisfactory color match, giving an acceptable aesthetic appearance.

Another patient with a multifocal recurrent benign mixed tumor of the right parotid gland involving the overlying skin is shown in Fig. 17.18. A superiorly based cervical flap was planned to correspond with the incisions for a parotidectomy with sacrifice of the overlying skin. The appearance of the patient 1 year following surgery shows excellent coverage of the skin defect in the parotid region (Fig. 17.19).

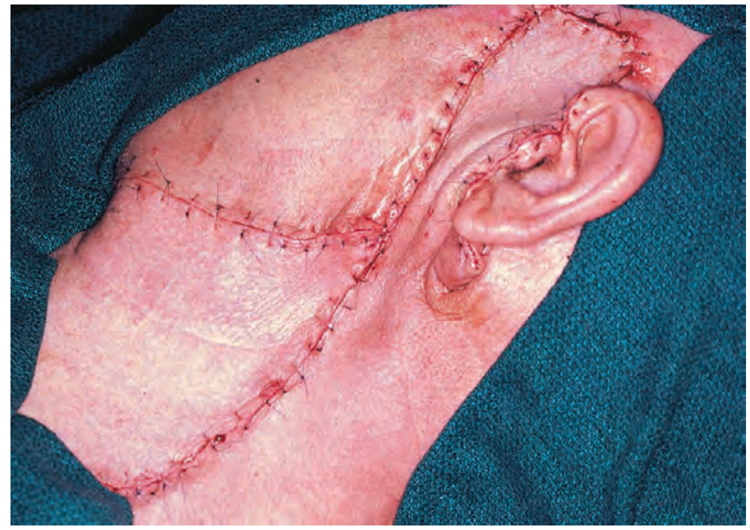

Figure 17.16 The completed closure.

Figure 17.17 The appearance of the flap 3 months after surgery.

Figure 17.18 A patient with a multifocal recurrent benign mixed tumor of the right parotid gland involving the overlying skin.

Figure 17.19 The appearance of the patient 1 year after surgery.

Posterior Cervical Flap (Mutter Flap). A superiorly based posterior cervical flap derives its blood supply from the occipital artery and the posterior auricular artery. Although these vessels are identifiable, the blood supply to the distal part of the flap is random.

In Fig. 17.20, a schematic diagram of the posterior cervical flap and its anterior rotation is shown. The base of the flap should be kept wide enough to include the blood supply derived from the posterior auricular and the occipital arteries. However, the width-to-length ratio of this flap should not exceed 1:3. The donor site in the suprascapular region requires a split-thickness skin graft for coverage.

The patient shown in Fig. 17.21 has a recurrent metastatic carcinoma in the posterior aspect of the right side of the neck following previous neck dissection and radiotherapy. The recurrent cancer involves the skin of the neck and underlying subcutaneous soft tissues, although it is mobile over the deeper soft tissues. The area of skin excision and the planned flap are outlined (Fig. 17.22). Note that the base of the flap extends from the mastoid process to the occiput. A wide three-dimensional excision of the recurrent tumor is performed with a generous margin of skin and underlying muscles from the floor of the posterior triangle of the neck as its deep margin. The flap is elevated and rotated anteriorly to cover the surgical defect, protecting the carotid vessels. The donor site in the suprascapular region is covered with a split-thickness skin graft.

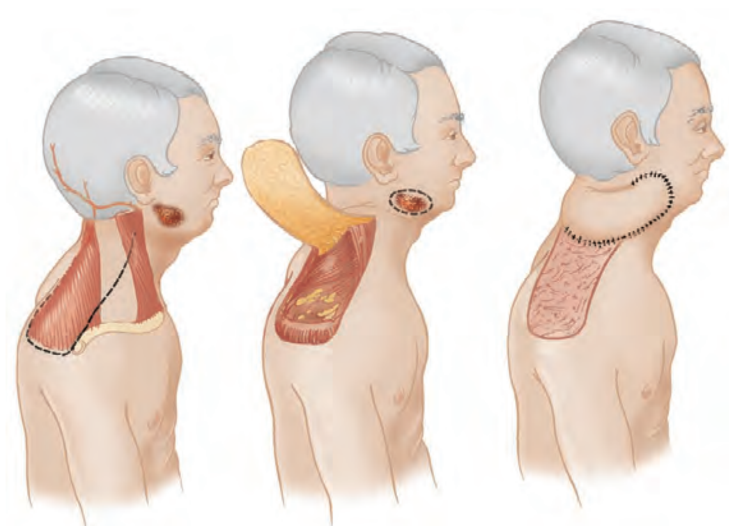

Figure 17.20 A schematic diagram of the posterior cervical flap and its anterior rotation.

Figure 17.21 This patient had a recurrent metastatic carcinoma.

The postoperative appearance approximately 2 weeks following surgery shows primary healing of the skin flap (Fig. 17.23). The postoperative appearance of the patient 3 months following surgery shows excellent coverage of the surgical defect and an acceptable aesthetic result (Fig. 17.24). This cervical flap has provided excellent coverage of the surgical defect with adequate soft tissues over the carotid vessels. The posterior cervical (Mutter) flap is a readily available regional flap for coverage of skin defects in the lateral aspect of the neck and the retromandibular area. However, it must be borne in mind that the flap has random pattern circulation in its distal part, and therefore its length is somewhat limited. It also requires a split-thickness skin graft for coverage of the donor site and thus produces some degree of aesthetic deformity.

Another patient with radionecrosis of the retromandibular skin and soft tissue is shown in Fig. 17.25. The area of excision and outline of the flap are shown. Wide excision of the necrotic area is performed, and a superiorly based posterior cervical flap is rotated to cover the surgical defect. A small split-thickness skin graft is applied to the donor site (Fig. 17.26). The appearance

Figure 17.22 The skin incisions are outlined.

Figure 17.23 The patient 2 weeks after surgery.

Figure 17.24 The appearance of the flap 3 months after surgery.

Figure 17.25 Radiation necrosis of the skin and soft tissues of the retromandibular region. The area of resection and the outline of the posterior cervical flap are shown.

Figure 17.26 The flap is rotated to cover the surgical defect, and a skin graft is applied at the donor site.

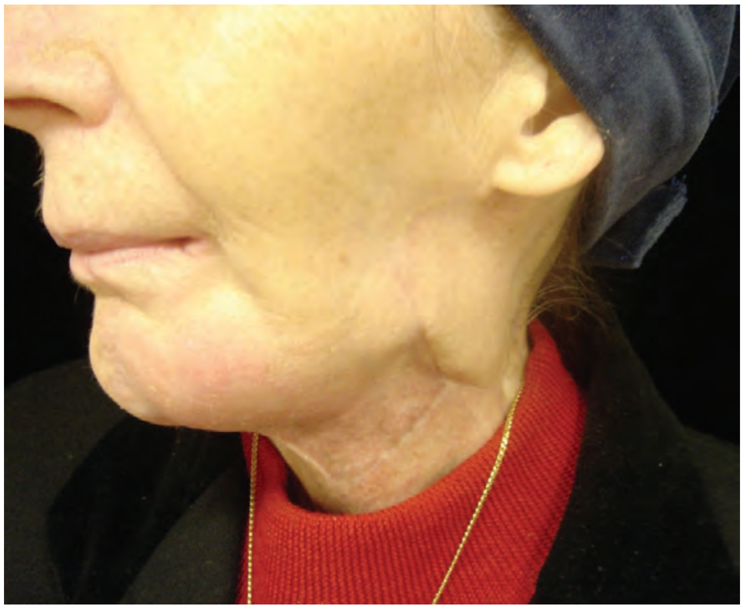

Figure 17.27 The appearance of the patient 18 months after surgery.

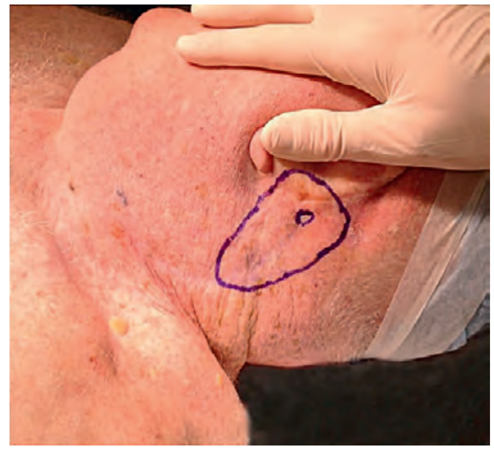

Figure 17.28 Patient with recurrent melanoma in situ of the skin of the postauricular region. The proposed excision is outlined.

of the patient 18 months after surgery shows excellent healing with an acceptable aesthetic result (Fig. 17.27).

The design of the posterior cervical fasciocutaneous flap, originally described by Mutter in 1842, has evolved due to more recent anatomic studies of the supraclavicular artery angiosome. The supraclavicular artery island (SCAI) flap is based on this vessel that originates from the transverse cervical artery and passes through the supraclavicular triangle (bounded by the superior border of the clavicle, the external jugular vein, and the posterior border of the sternocleidomastoid muscle). Its vascular territory extends from the lateral base of the neck to the anterior deltoid region.

The patient shown in Fig. 17.28 has recurrent melanoma in situ of the postauricular region. Following resection, the defect measures 7 by 11 cm (Fig. 17.29). A supraclavicular artery island flap is mobilized up to the origin of its pedicle at the base of the neck (Fig. 17.30) and rotated into the defect (Fig. 17.31). The final result is shown in Fig. 17.32. The postoperative appearance 1 year following surgery shows excellent reconstruction of the contour and an acceptable aesthetic outcome (Fig. 17.33).

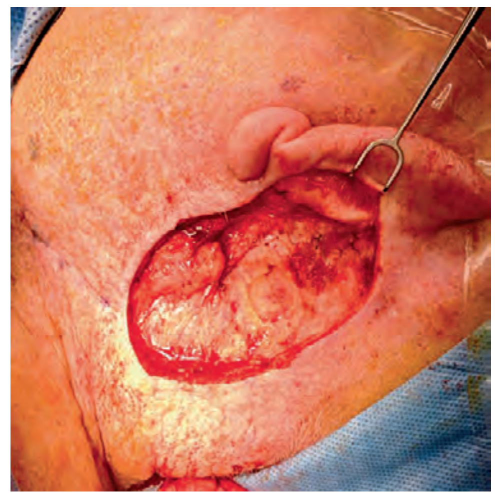

Figure 17.29 A full-thickness skin defect on lateral neck.

Figure 17.30 A mobilized supraclavicular artery island flap.

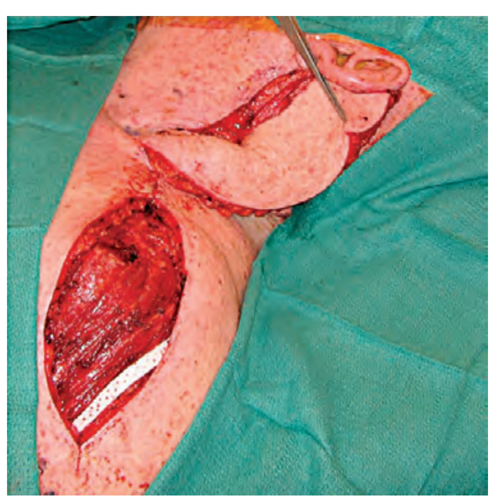

Figure 17.31 A supraclavicular flap rotated into the neck defect.

Figure 17.32 The defect and donor site are closed.

Figure 17.33 The patient is shown at late follow-up.

An elderly patient with a large mucosal and soft-tissue defect of the floor of the mouth and posterior tongue is shown in Fig. 17.34 following resection and neck dissection. A SCAI flap was raised to repair the intraoral defect, as shown in Fig. 17.35. The flap is tunneled and reaches the defect without tension (Fig. 17.36). The flap is inset, showing the anterior aspect of the cutaneous island replacing the missing oral mucosa (Fig. 17.37).

These two examples demonstrate different applications of the supraclavicular flap. In one instance the skin paddle is deepithelialized, creating an island to repair a small intraoral defect. In the other example, the entire skin paddle is preserved to resurface larger areas of missing skin.

Figure 17.34 A 78-year-old with oromandibular cancer following resection and neck dissection with a 2- by 2-cm oral defect. A supraclavicular island flap is planned.

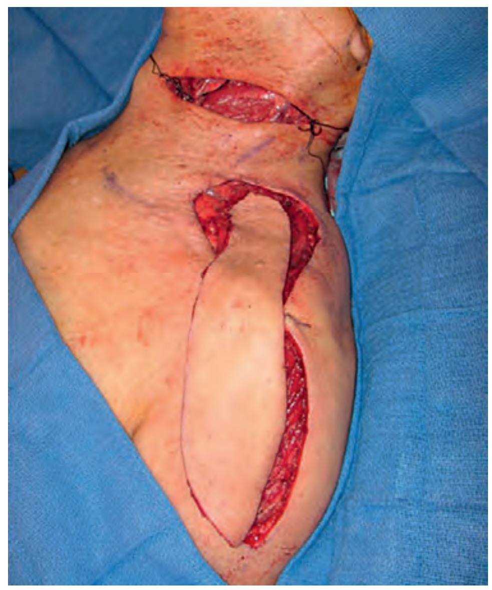

Figure 17.35 The flap is mobilized up to the origin of its pedicle.

Figure 17.36 The flap is tunneled and shown to reach the defect without tension.

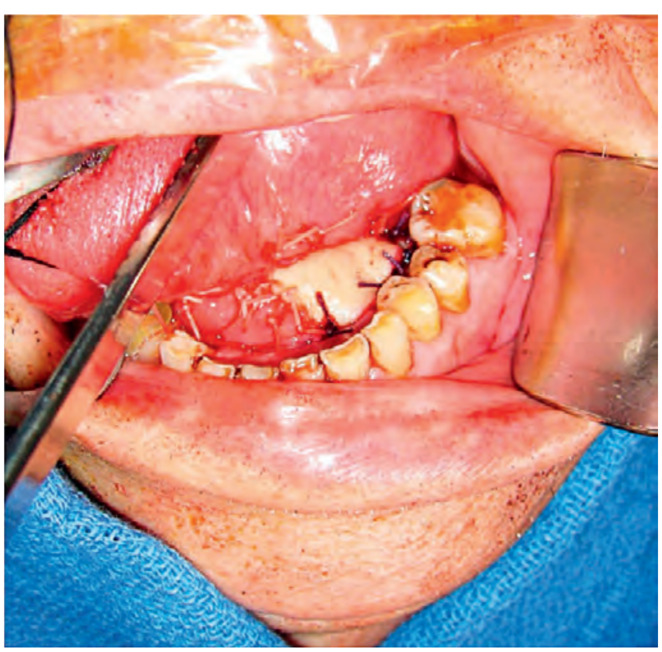

Figure 17.37 The flap inset is completed with a cutaneous island replacing missing oral mucosa.

Deltopectoral Flap

In the past, the medially based deltopectoral fasciocutaneous flap was considered a workhorse for reconstruction of oropharyngeal and pharyngoesophageal defects. The flap derives its primary blood supply from the perforating branches of the internal mammary artery through the second, third, and fourth intercostal spaces. The proximal part of the flap therefore has an axial blood supply; however, the distal third is random, with perfusion relying upon the subdermal plexus (Fig. 17.38). With better understanding of perforator anatomy, the deltopectoral flap has been revisited as the internal mammary artery perforator (IMAP) flap. Advantages of this variant include harvest of a smaller flap enabling primary donor site closure and greater arc of rotation because of the flap's narrow base around a single perforator.

The deltopectoral flap was popularized by Bakamjian in the mid-1960s and remained popular for reconstruction of oropharyngeal and hypopharyngeal defects. However, because of the unreliable blood supply to the distal third of the flap, high complication rate, and need for multiple stages, the flap is no longer routinely used for oral and pharyngeal defects. In contrast, the deltopectoral flap remains an excellent means of reconstruction for resurfacing skin defects in the cervical region. Therefore

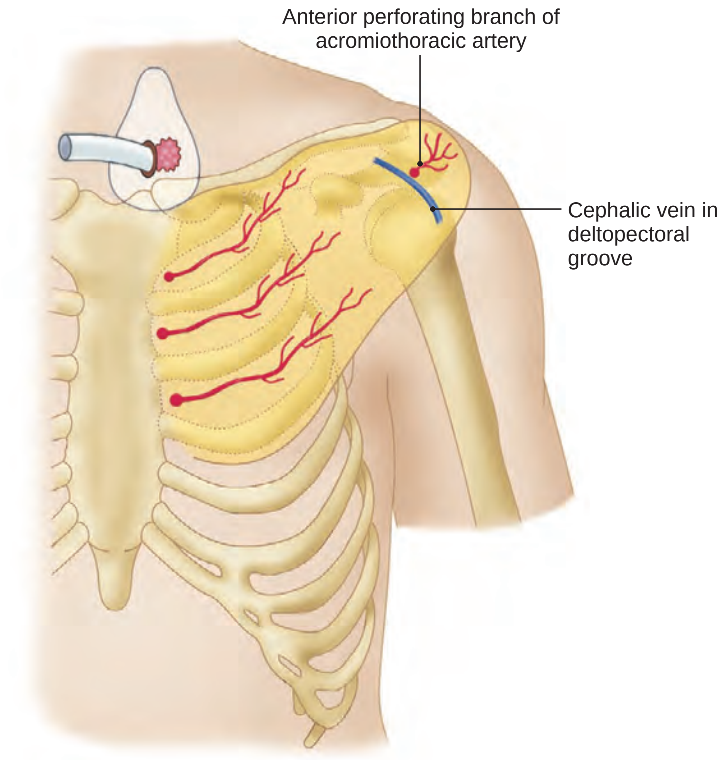

Figure 17.38 A diagrammatic representation of the arterial supply of the deltopectoral flap.

Figure 17.39 Skin necrosis with exposure of the carotid artery after neck dissection in a previously radiated neck.

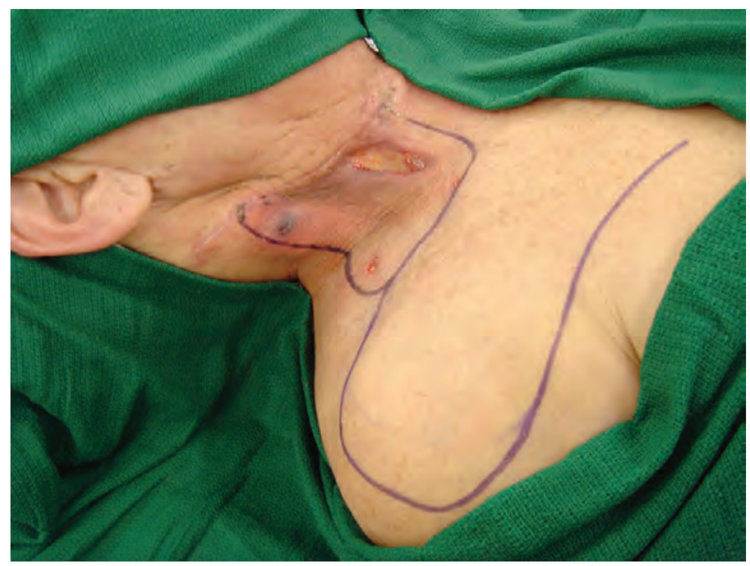

Figure 17.40 The outline of the skin excision and the deltopectoral flap.

Figure 17.41 Necrotic skin is excised and the deltopectoral flap is elevated.

the deltopectoral flap should remain in the armamentarium of the head and neck reconstructive surgeon, particularly for skin and soft-tissue defects involving the lower two-thirds of the cervical region. The deltopectoral flap is an ideal choice for coverage of the skin defects of the lateral aspect of the neck. The patient shown in Fig. 17.39 was previously treated with radiation to the neck. He underwent salvage neck dissection for persistent disease and developed skin necrosis with exposure of the carotid artery. The area of compromised skin covers nearly the entire lateral aspect of the neck. The outline of the deltopectoral flap merges with the lower end of the skin excision of the neck (Fig. 17.40). The skin is excised, and all necrotic tissue is debrided (Fig. 17.41). The flap is elevated, preserving its blood supply from the perforating branches of the internal mammary artery (Fig. 17.42). The flap is rotated cephalad to cover the skin defect in the neck. This is a tension-free closure (Fig. 17.43). The donor site overlying the deltoid muscle is covered with a split-thickness skin graft (Fig. 17.44). Excellent coverage of healthy skin and soft tissues is achieved in this manner.

Another patient with a melanoma of the skin of the lower part of the neck is shown in Fig. 17.45. Wide excision of the skin and underlying soft tissues resulted in a full-thickness defect measuring 9 by 13 cm. This was repaired with a medially based deltopectoral flap (Fig. 17.46). A portion of the flap donor site required skin graft. Therefore the deltopectoral flap should remain in the armamentarium of the head and neck reconstructive surgeon, particularly for skin and soft-tissue defects involving the lower two-thirds of the cervical region.

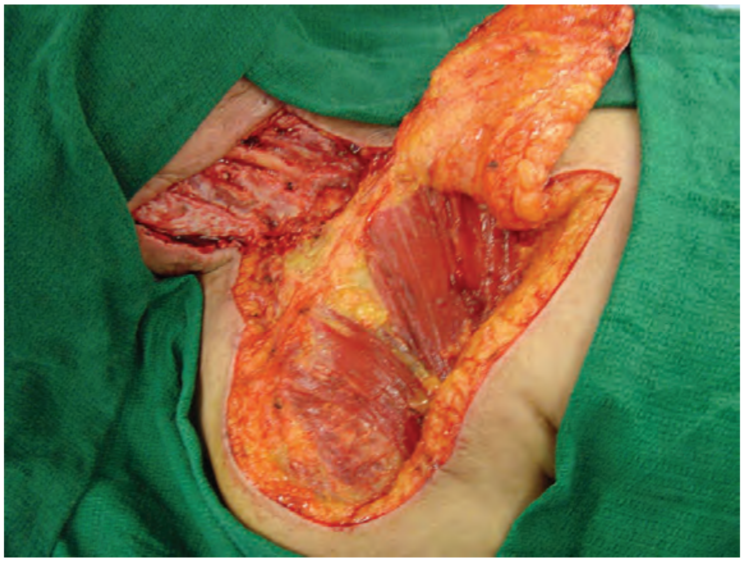

Figure 17.42 The blood supply from the internal mammary artery is preserved.

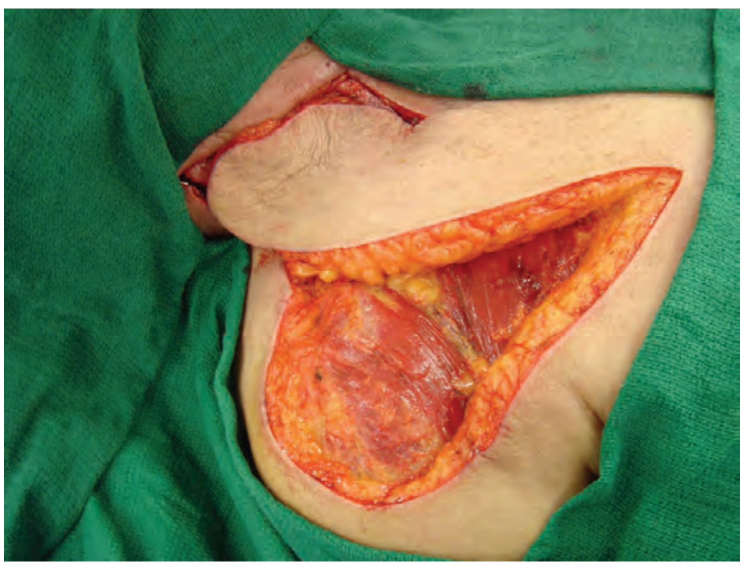

Figure 17.43 The flap is rotated to cover the surgical defect.

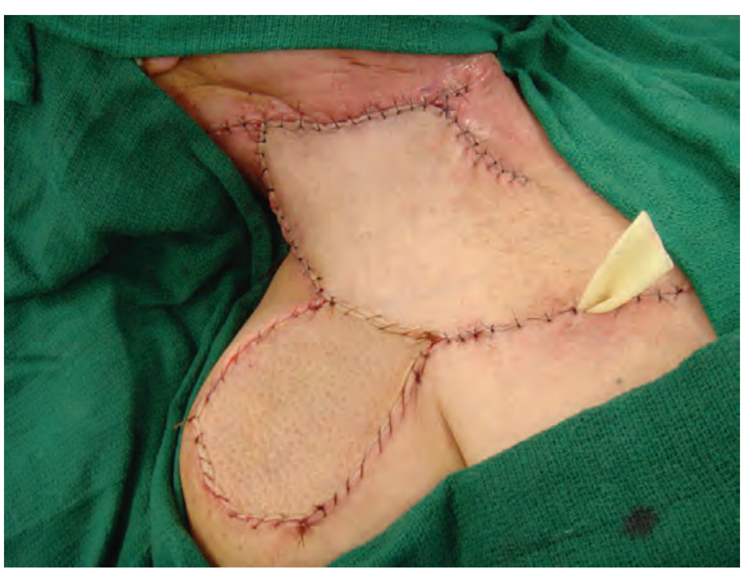

Figure 17.44 A split-skin graft is applied to the donor site.

Figure 17.45 An elderly patient with melanoma of skin of the lower part of the neck.

Figure 17.46 The surgical defect is reconstructed with a deltopectoral flap. A portion of the donor site is skin grafted.

RECONSTRUCTION WITH MYOCUTANEOUS FLAPS

The description of myocutaneous circulation in the mid-1970s led to the development of several regional pedicled myocutaneous flaps that provide an excellent means of reconstruction of defects in the head and neck region, particularly when free tissue transfer capabilities are not available. The pectoralis major, the trapezius, and the latissimus dorsi myocutaneous flaps have been described for reconstruction in the head and neck region.

The pectoralis major myocutaneous (PMMC) flap is readily available for reconstruction of a variety of defects in the head and neck region.

The advantages of this flap include:

- Technical ease of flap elevation
- Generous amount of skin and soft tissue available
- Consistent and reliable blood supply
- Arc of rotation that is adequate for most oropharyngeal and skin and soft tissue defects up to the skull base
- Ability to provide both internal and external lining (using two skin islands on the same muscle)

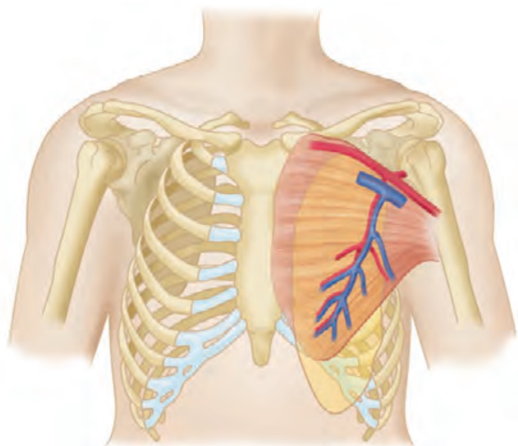

Figure 17.47 The anatomic features of the pectoralis major myocutaneous flap.

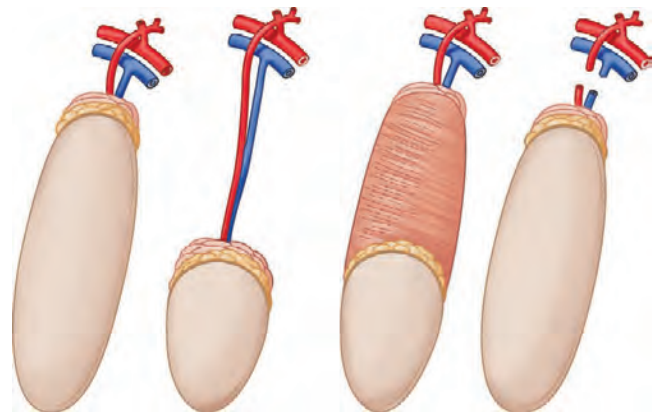

Figure 17.48 Varieties of pectoralis major myocutaneous flaps.

- Utility as a muscle flap alone to buttress the pharyngeal suture line in patients undergoing salvage surgery after radiotherapy
- Robust muscular component of the flap to protect exposed neck vessels
- Ease of primary closure at the donor site

The disadvantages of the PMMC flap are:

- It is bulky, especially in women with large breasts. The bulkiness of the flap in some cases limits its use for oral cavity reconstruction.
- When used for oropharynx or floor of mouth reconstruction, the flap tends to dehisce due to the downward pull of the tissues
- Inadequate arc of rotation for upper facial and maxillary defects
- Donor site aesthetic concerns due to distorted symmetry
- Unreliability of the skin on the distal part of the flap

The anatomic features of the pectoralis major myocutaneous flap are depicted in Fig. 17.47. The blood supply of the pectoralis major myocutaneous flap is derived from the descending branch of the thoracoacromial artery, as shown on the left-hand side in the diagram. This artery runs directly on the undersurface of the pectoralis major muscle. The thoracoacromial artery originates from the subclavian artery at about the midclavicular point and runs directly caudad toward the nipple. Thus a line joining the midclavicular point to the nipple is recommended for the surface marking of the vessel. One or two veins usually accompany this artery. The flap can be raised in a variety of different configurations, depending on the surgical defect to be reconstructed. Thus the size of the skin island is variable, and similarly, the extent of the transposed muscle is also variable (Fig. 17.48).

The technical details of flap elevation are discussed here. The outline of the flap is drawn on the skin (Fig. 17.49). The lined area on the distal part of the flap may be discarded so as to match the shape of the defect. The length and width of the myocutaneous flap skin island and the length of its pedicle are determined by the site, size, and shape of the surgical defect. The pivot point of flap rotation corresponds roughly to the midclavicular point. A tape is used to measure the distance from this point up to the most distal portion of the surgical defect. This measurement is the distance from the midclavicular point up to the distal tip of the flap, which is marked. The approximate width and length of the flap then are estimated to match the defect, and the proposed flap is drawn on the

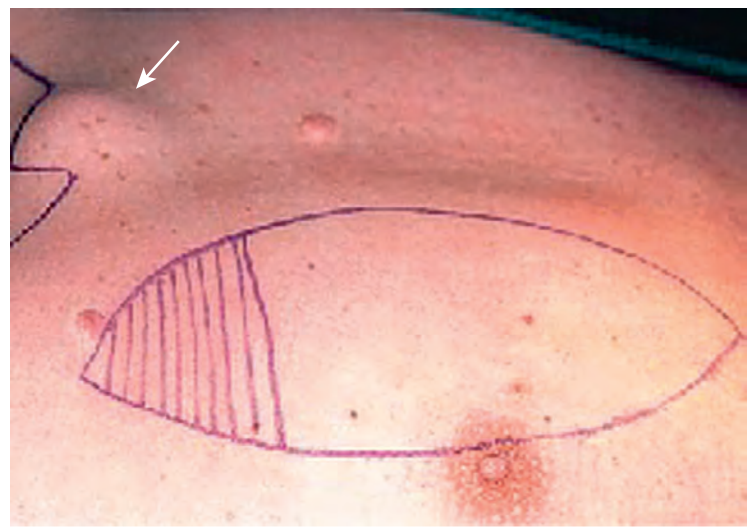

Figure 17.49 The anterior chest wall of a patient in whom a laryngectomy is completed, showing the outline of left pectoralis myocutaneous flap to be used for pharyngeal closure. The xiphial sternum is on the left side (*arrow*).

skin of the anterior chest wall. Elevation of the flap should never occur before resection of the tumor and assessment of the surgical defect. The exact dimensions and configuration of the defect are confirmed to match the outline of the flap. Any adjustments to the length and width of the skin island of the myocutaneous flap, or the length of its pedicle, are performed at this point, before the flap is elevated.

Elevation of the flap begins on its medial aspect first. The skin incision is deepened through the subcutaneous tissues and fat circumferentially around the skin island until the underlying pectoralis major muscle is visualized. From the proximal end of the skin island, an additional incision is taken up to the midclavicular point. The lateral and medial skin edges are elevated over the pectoralis to expose a generous area of muscle to be transferred with the myocutaneous flap (Fig. 17.50).

The fingers of one hand are now inserted deep to the pectoralis major muscle in a plane between the pectoralis major and pectoralis minor muscles, as shown in Fig. 17.51. Because this plane contains only loose areolar tissue, the pectoralis major is easily separated from the pectoralis minor muscle and the ribs. The pectoral nerve that travels between the pectoralis minor and pectoralis major muscles in this plane

Figure 17.50 A circumferential skin incision isolates the skin island. The skin incision is extended up to the clavicle, and medial and lateral skin flaps are elevated to expose the pectoralis muscle.

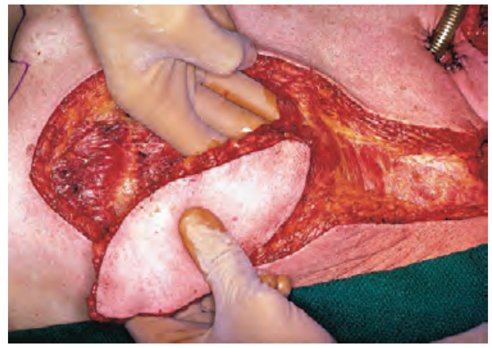

Figure 17.51 The fingers of one hand are inserted deep to the pectoralis major muscle.

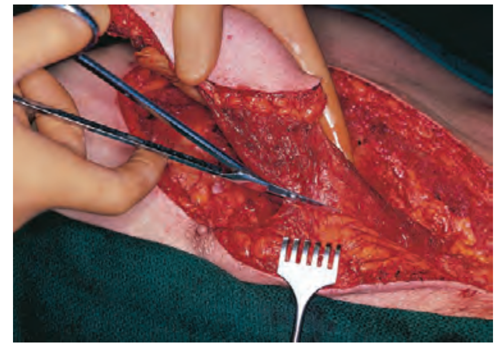

Figure 17.52 The muscle is divided, maintaining an even width of tissue around the vascular pedicle.

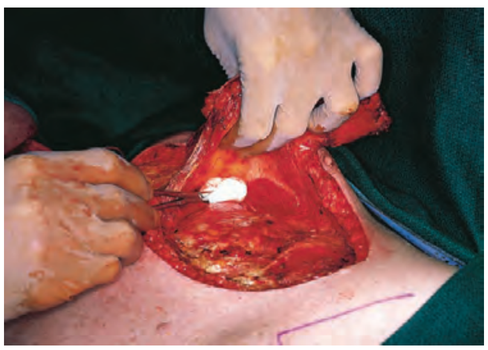

Figure 17.53 The thoracoacromial vessels seen from the right side of the patient.

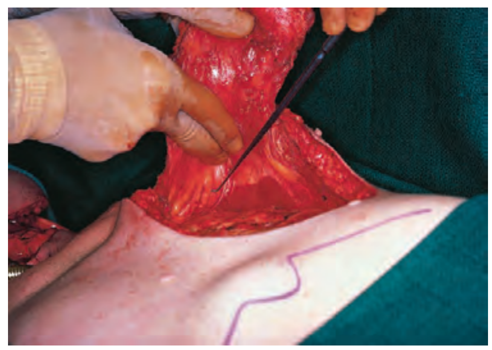

Figure 17.54 The vascular pedicle.

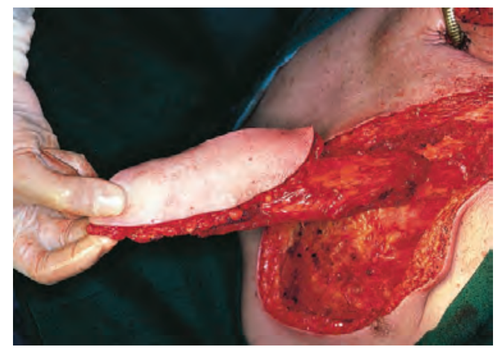

Figure 17.55 The pedicle, the muscle paddle, and the myocutaneous component of the entire flap are fully mobilized.

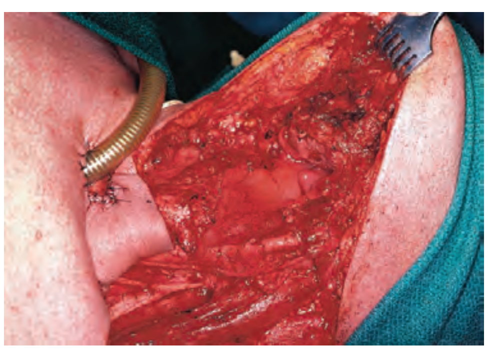

Figure 17.56 The mucosal defect after a pharyngolaryngectomy shows the preserved posterior pharyngeal wall.

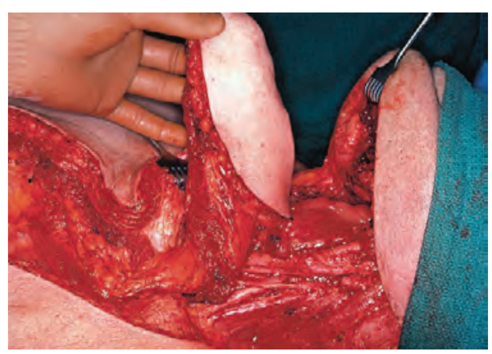

Figure 17.57 The flap is flipped 180 degrees to bring the skin surface inside.

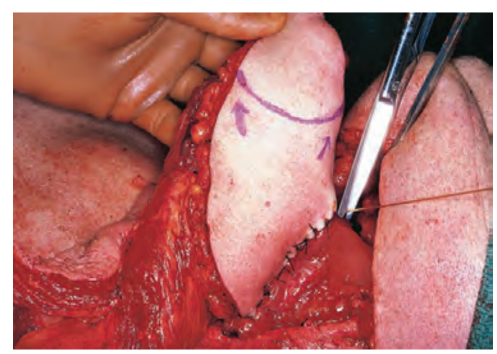

Figure 17.58 Excess skin on the distal end of the skin island is marked for excision. Suturing of the flap to the pharyngeal mucosa begins at its lower end.

is divided. The undersurface of the pectoralis major muscle is mobilized up to the clavicle, freeing up its entire posterior surface. This maneuver enables identification of the thoracoacromial vessels at about the midclavicular point. Using a serrated scissors, the pectoral muscle is divided medial and lateral to the vascular pedicle up to the clavicle (Fig. 17.52). The isolated portion of the myocutaneous flap is now lifted to expose the undersurface of the pectoralis major muscle to show the vascular pedicle, which is viewed from the right-hand side of the patient in Fig. 17.53. A close-up view of the vascular pedicle is shown in Fig. 17.54.

A 4-cm strip of muscle is routinely maintained over the pedicle. During this phase of the operation, several perforating branches of the internal mammary artery will be encountered, which are ligated and divided. The pedicle, the muscle, and the myocutaneous component of the whole flap fully mobilized are shown in Fig. 17.55. If the skin surface of the flap is to be used for pharyngeal repair, then the flap is flipped 180 degrees. On the other hand, if the skin is to be used for surface coverage, then the flap is rotated radially up to 90 degrees. After the flap is rotated, the venous component of the vascular pedicle must be checked to ensure that blood is flowing freely through the veins. If the veins are twisted and collapsed or the skin paddle appears congested, the pedicle should be released further to address pedicle kinking.

The mucosal defect after a pharyngolaryngectomy is shown in Fig. 17.56. Note the absence of the anterior pharyngeal wall, which will be replaced by the rotated PMMC flap, as shown in Fig. 17.57. The proximal portion of the skin island of the flap is at the lower end of the hypopharyngeal defect, and the distal part of the skin island approximates the upper end of the hypopharyngeal defect at the base of the tongue. Redundant skin and subcutaneous fat to be excised from the distal portion of the skin island are marked out (Fig. 17.58). Suturing of the

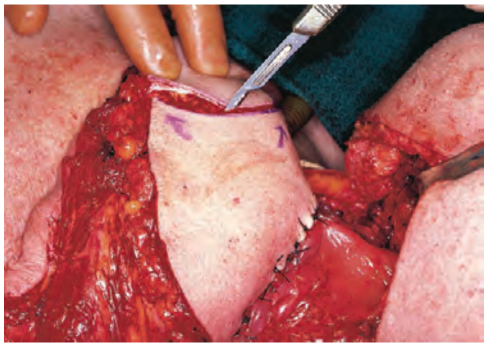

Figure 17.59 Excess skin from the distal part of the skin island is excised.

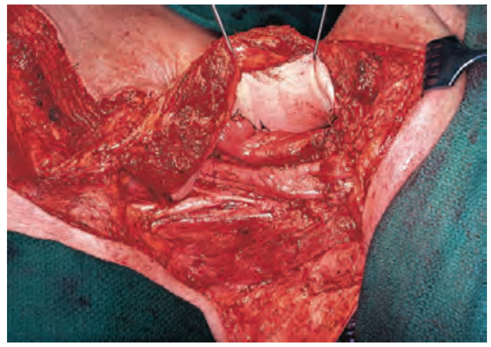

Figure 17.60 Closure of the pharynx is completed circumferentially.

Figure 17.61 A patient with a massive basal cell carcinoma of the skin of the neck.

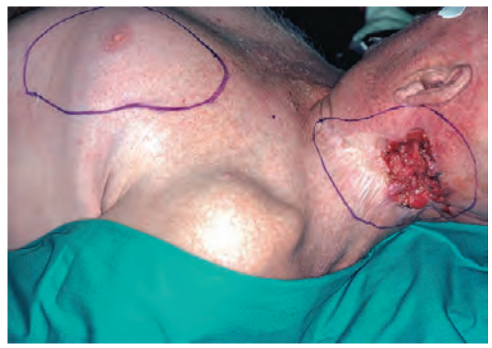

Figure 17.62 The outline of the skin incisions for resection of the tumor and for the pectoralis major myocutaneous flap.

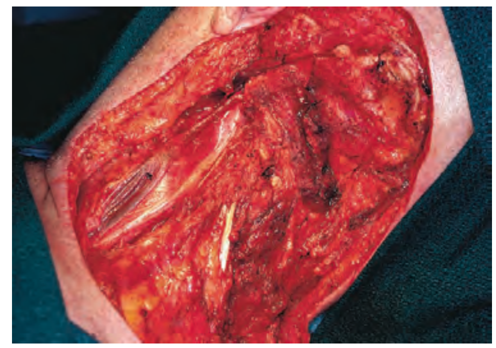

Figure 17.63 The surgical defect.

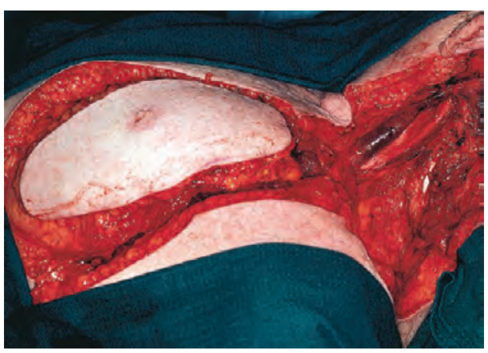

Figure 17.64 Elevation of the pectoralis major myocutaneous flap.

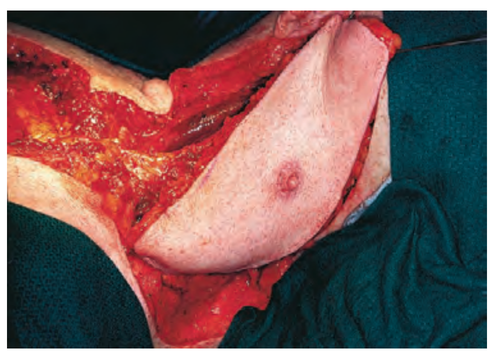

Figure 17.65 The flap is radially rotated 180 degrees.

Figure 17.66 The surgical defect is reconstructed, and the donor site is closed primarily.

skin island to the pharyngeal mucosa begins at its lower end. Excess skin from the distal part of the skin island is now excised (Fig. 17.59). The closure of the hypopharynx is completed circumferentially with interrupted 2-0 absorbable inverting sutures (Fig. 17.60). A nasogastric feeding tube is inserted before complete closure of the suture line.

The muscle paddle is splayed to cover and protect the common carotid artery. The PMMC flap has thus provided complete restoration of the mucosal lining of the pharyngeal defect, and its muscle paddle has provided protection of the carotid artery. The neck wounds are now closed as usual after placing suction drains. The donor side defect on the anterior chest wall also needs suction drains, which are placed away from the vascular pedicle of the flap. The skin defect of the anterior chest wall is closed primarily in layers.

The PMMC flap as shown here provides an excellent one-stage method of reconstruction of partial pharyngeal defects. Several examples of other applications and uses of the PMMC flap are demonstrated in the following sections.

Resurfacing of a Large Skin and Soft-Tissue Defect of the Neck. The patient shown in Fig. 17.61 has a massive basal cell carcinoma of the neck skin, involving the underlying soft tissues up to the transverse processes of the midcervical vertebrae. Surgical resection requires removal of a generous portion of the posterior and lateral neck skin, in conjunction with a posterior neck dissection and resection of underlying musculature as well as a portion of the transverse processes of the third and fourth cervical vertebrae. The skin incisions for removal of this tumor are outlined in Fig. 17.62. The surgical defect involves significant skin and soft-tissue loss (Fig. 17.63). The surface dimensions and depth of this surgical defect require a large, three-dimensional flap for satisfactory reconstruction. A PMMC flap is elevated as previously described (Fig. 17.64). The dimensions and soft-tissue bulk of this flap are adequate to reconstruct the defect. The flap is rotated 180 degrees radially on its vascular pedicle to fill the surgical defect (Fig. 17.65). After appropriate inset and trimming, this flap is used to close the defect satisfactorily without tension. The donor site defect

Figure 17.67 Postoperative appearance of the patient 6 months following surgery and excision of the nipple from the flap.

Figure 17.68 A patient with a recurrent carcinoma of the larynx.

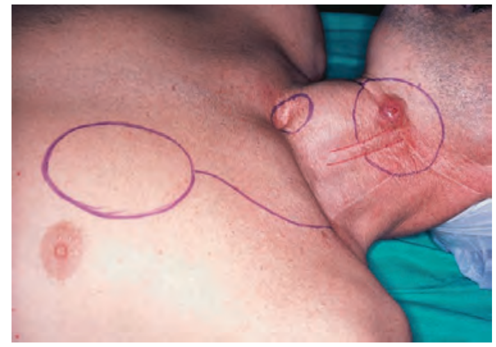

Figure 17.69 The outline of the area of the skin of the neck to be excised.

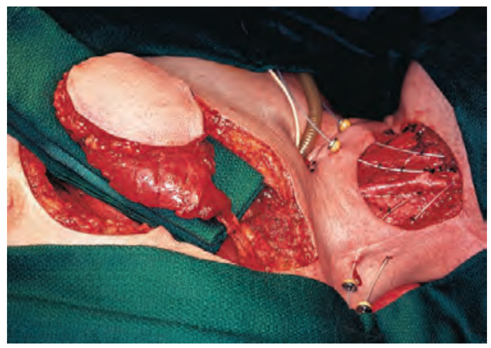

Figure 17.70 The surgical defect with afterloading catheters for brachytherapy and the isolated skin island of a pectoralis major myocutaneous flap.

Figure 17.71 The postoperative appearance of the patient 6 months following surgery.

on the anterior chest wall is closed primarily following undermining of the medial and lateral skin edges (Fig. 17.66). Note that even a donor site defect of 15 by 22 cm on the anterior chest wall can be closed primarily by mobilizing the medial and lateral chest skin. Coverage of the donor site defect with a skin graft is rarely necessary. The nipple was left in place on the myocutaneous flap because of its size. Excision of the nipple was performed under local anesthesia 2 months later. The postoperative appearance of the patient 6 months following surgery shows satisfactory repair of the skin surface and contour of the neck (Fig. 17.67).

Pectoralis Major Myocutaneous Flap in Radiated Tissues. The PMMC flap is usually out of the radiation field in patients with a previous history of radiation for previous head and neck cancer. Therefore it is useful to repair defects in radiated tissues, enabling transfer of healthy, well-vascularized, nonirradiated tissues. Thus the flap provides new circulation, which enhances the healing process. Further, it has the ability to tolerate additional radiation required in patients with recurrent tumors. The patient shown in Fig. 17.68 has soft-tissue recurrence involving overlying skin in a previously operated and radiated neck. He had previously undergone partial laryngectomy with neck dissection and postoperative radiation therapy. Due to the extent of soft-tissue disease, he requires resection of the recurrent tumor in conjunction with total laryngectomy. Presence of extensive soft-tissue disease adjacent to the carotid artery required the need for brachytherapy to deliver a therapeutic dose to the high-risk area. The area of skin of the neck to be excised around the recurrent tumor, the PMMC flap, and the permanent tracheostome are outlined (Fig. 17.69). The common carotid artery adjacent to the recurrent tumor is also shown here.

The surgical defect following total laryngectomy in conjunction with resection of the recurrent tumor along with a generous portion of the overlying skin was done in a monobloc fashion (Fig. 17.70). The external carotid artery has been sacrificed. The recurrent tumor had to be peeled off from the common carotid artery and the internal carotid artery in a subadventitial plane. Because of the close proximity of the recurrent tumor to the carotid artery, afterloading catheters for brachytherapy are inserted. The radiation source selected is ^{192}Ir, and the empty catheters are afterloaded with the radiation source in the postoperative period.

The PMMC island flap is rotated 180 degrees in a radial plane and tunneled beneath the bridge of skin of the lower part of the neck to fill the surgical defect overlying the brachytherapy catheters. The patient received additional 4000 cGy with ^{192}Ir catheters over 5 days through an afterloading implant. The PMMC flap tolerated this radiation dosage without any problems and manifested primary healing. The postoperative appearance of the patient 6 months following surgery is shown in Fig. 17.71.

The PMMC flap is also an excellent choice for repair of pharyngocutaneous fistulae following salvage pharyngolaryngectomy for previously irradiated cancers. The patient shown in Fig. 17.72 developed a fistula 2 weeks following pharyngolaryngectomy and neck dissection. The heavily irradiated skin has significant induration and edema, and a large amount of skin was lost around the fistulous opening, although the mucosal loss was minimal. The remaining skin on the periphery of the ulcerated area is also quite tenuous.

The skin incisions for resection and reconstruction are outlined in Fig. 17.73. A generous portion of the skin of the anterior aspect of the neck was sacrificed. The mucosal edges of the fistulous tract are freshened, and primary closure of the pharynx could be performed. The muscle surface of the PMMC flap will provide support to the mucosal suture line and replace skin loss in the neck.

Figure 17.72 A patient with a pharyngocutaneous fistula with skin loss in a previously irradiated neck.

Figure 17.73 The outline of the skin incisions.

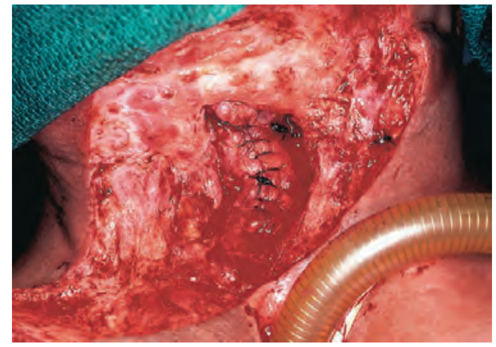

Figure 17.74 The surgical field after excision of the skin of the neck and primary closure of the anterior pharyngeal wall defect.

Figure 17.75 The pectoralis major myocutaneous island flap shows its vascular pedicle over the green towel.

Figure 17.76 The flap fills the surgical defect without tension.

Figure 17.77 The postoperative appearance of the patient 1 month following surgery.

The surgical field after excision of the skin of the neck and primary closure of the pharynx is seen in Fig. 17.74. The pharyngeal closure must be watertight and without tension. The PMMC island flap is now ready for transfer to the neck. Note the vascular pedicle isolated over the green towel to deliver a true PMMC island flap (Fig. 17.75). The PMMC flap is rotated radially to repair the skin and soft-tissue defect in the neck. The flap is of sufficient length and width to fill the surgical defect without tension (Fig. 17.76). The postoperative appearance of the patient 1 month following surgery shows primary healing between the PMMC flap and the skin of the irradiated neck (Fig. 17.77).

Trapezius Myocutaneous Flap

The vertical trapezius myocutaneous flap is dependent on the descending branch of the transverse cervical artery deep to the trapezius muscle. Although the feeding artery is reliable, its venous drainage is not constant and sometimes is inadequate. One disadvantage of this reconstructive option is that the patient must be positioned laterally or prone to elevate the flap. Under ideal conditions, this flap provides a generous amount of soft tissue and a large skin island for repair of major surgical defects, including those in the mastoid and occipital regions.

The patient shown in Fig. 17.78 has a recurrent carcinoma of the parotid gland with cervical lymph node metastases, as well as skin nodules in the left side of the face and the upper neck in the retromandibular region. Surgical resection required left radical neck dissection in conjunction with excision of a generous portion of the skin, radical total parotidectomy, segmental mandibulectomy, partial amputation of the external ear, and partial temporal bone resection. The flap of appropriate dimensions is outlined in Fig. 17.79.

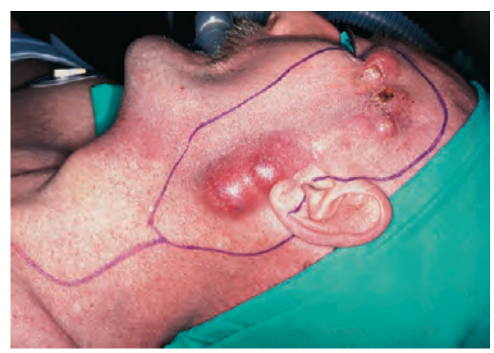

Figure 17.78 A patient with a recurrent carcinoma of the parotid gland.

Figure 17.79 The outline of the flap.

The technical steps of elevation of the trapezius myocutaneous flap are similar to those described for the PMMC flap. The vascular pedicle is usually identified in the region of the nape of the neck, where delicate handling of the flap is required to avoid injury to the blood vessels, particularly the draining veins. To cover the surgical defect, the flap requires radial rotation of its pedicle to permit satisfactory placement of the flap in the

Figure 17.80 Closure of the surgical defect.

Figure 17.81 Secondary repair of a wound dehiscence in the midline of the back with loss of skin and soft tissue following spinal surgery, repaired with a trapezius myocutaneous flap.

surgical defect. A tension-free closure of the surgical defect could be achieved, replacing soft tissues, as well as the large area of skin loss up to the forehead (Fig. 17.80). The donor site defect is closed primarily. Another patient, with a dehiscence of a cervical spinal wound 2 weeks after intramedullary spinal tumor dissection, required secondary reconstruction for a 5- by 12-cm defect in the midline of the back. A left trapezius myocutaneous flap provided excellent closure of the defect with primary healing (Fig. 17.81).

MICROVASCULAR FREE TISSUE TRANSFER

Microsurgical free tissue transfer has been used routinely for the past 30 years and has become the primary method of reconstruction for the majority of large or complex defects in the head and neck area. Today a multidisciplinary head and neck team is considered incomplete without a microvascular reconstructive surgeon. Although the applicability of microvascular techniques is universal, some degree of discretion, restraint, and experience is required before microvascular free tissue transfer is chosen for reconstruction.

The success of microvascular free tissue transfer depends on multiple factors, including appropriate patient selection, adequate recipient vessels, quality donor tissue, recipient site, and the technical proficiency of the microsurgeon. If the head and neck surgeon is inadequately trained in microsurgery or has not maintained his or her technical competence in the field, then it is advisable to call upon a well-trained surgeon to assume the responsibility for the microsurgical reconstructive portions of the procedure. Ideally, the patient requiring major ablative surgery for cancer and reconstruction with microsurgical free tissue transfer is best served by two surgical teams working simultaneously: an ablative surgical team for resection of the tumor and a reconstructive surgery team planning and harvesting the required free tissue transfer.

Resection of head and neck tumors may result in loss of skin, soft tissues, mucosa, bone, cartilage, or any combination of these. Free flaps are available with a variety of tissue type combinations and should be thoughtfully selected based upon the defect. The free flaps used most commonly in the head and neck region are the radial forearm, anterolateral thigh, rectus abdominis, fibula, jejunum, scapula, and iliac crest flaps.

In clinical situations where local or regional tissues are unavailable or inadequate and the application of locoregional tissues would result in significant functional loss or aesthetic deformity, reconstructive surgery with free tissue transfer should be considered. Several patient factors influence the choice of free tissue transfer for reconstruction. It is essential to perform an adequate preoperative evaluation of the patient to assess the risk of a prolonged operative procedure, which may take many hours. Very elderly patients, particularly those with a poor cardiopulmonary status, are poor candidates for microvascular surgery. Patients with atherosclerotic disease of small vessels in peripheral arteries (especially for the fibula free flap) are also suboptimal candidates for microvascular surgery. Microvascular free tissue transfer may be considered for all other patients who are able to withstand a long operative procedure and who have appropriate indications for reconstruction of a major surgical defect in the head and neck area. Several examples are shown to demonstrate the application of a variety of free flaps in the head and neck region.

Radial Forearm Free Flap Reconstruction of Skin and Soft Tissues of the Face

The patient shown in Fig. 17.82 has a recurrent sweat gland carcinoma of the skin of the lateral aspect of her face and the preauricular region. Because she had undergone multiple surgical procedures previously, local or regional skin flaps were not felt to be suitable for reconstruction of the resulting surgical defect. Surgical resection in this patient required sacrifice of a generous portion of the skin and underlying soft tissues of the face, as well as a portion of the zygomatic arch due to adherence of the tumor to the bone. The surgical specimen is shown in

Figure 17.82 The incision for resection and neck dissection is outlined.

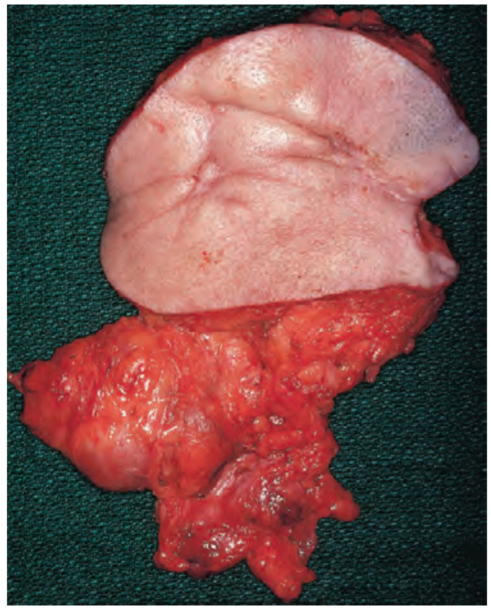

Figure 17.83 The surgical specimen consists of the primary tumor, underlying soft tissues, and contents of the neck.

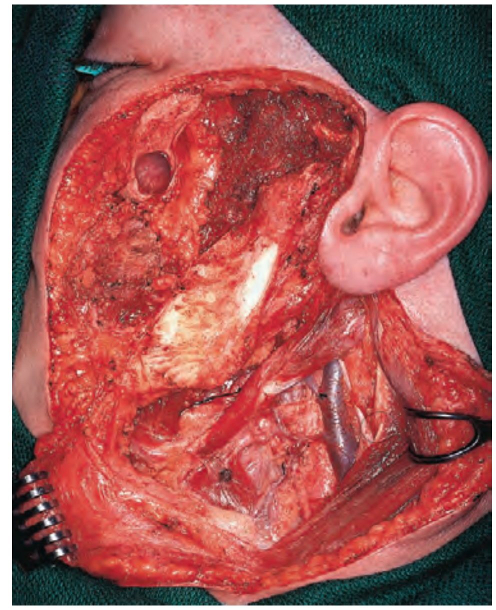

Figure 17.84 The surgical defect shows the lateral aspect of the ascending ramus of the mandible and the maxillary antrum due to resection of the zygoma.

Fig. 17.83. A subtotal parotidectomy with sacrifice of the upper division of the facial nerve was necessary to encompass a monobloc resection with clear margins. A facial nerve graft to animate the eye sphincter would not be of benefit, because a portion of the orbicularis oculi muscle had to be resected to encompass the recurrent tumor. The surgical defect is shown in Fig. 17.84.

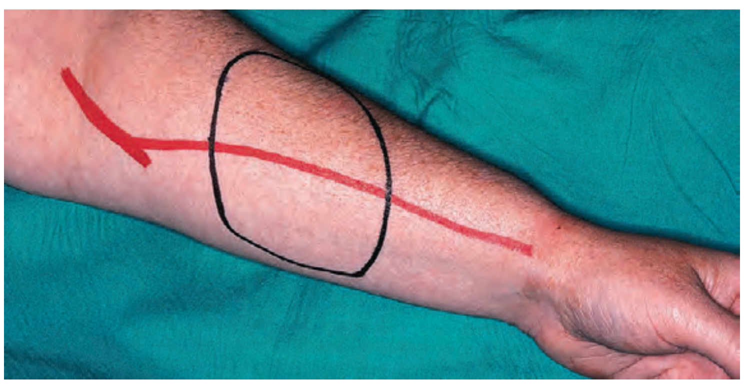

Figure 17.85 The outline of a radial forearm free flap.

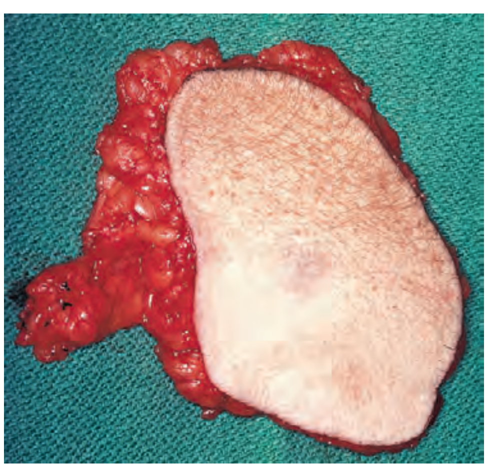

Figure 17.86 The radial forearm fasciocutaneous free flap.

Figure 17.87 The postoperative appearance of the patient 1 year following surgery.

A radial forearm free flap with its vascular pedicle is outlined. The radial artery and its vena comitantes will be anastomosed to the facial artery and one of the tributaries of the internal jugular vein (Fig. 17.85). The harvested free flap provides generous skin and sufficient underlying soft tissues to achieve a three-dimensional repair (Fig. 17.86). A satisfactory repair of the surgical defect of the skin and underlying soft tissues of the face was accomplished. Minor revisions and adjustments of the skin flap are sometimes required to improve the patient's aesthetic appearance, as seen in Fig. 17.87, 1 year following completion of postoperative radiation therapy. Several other examples of a radial forearm free flap for reconstruction of facial defects are shown in Figs. 17.88 through 17.90. The anterolateral thigh (ALT) fasciocutaneous flap, described later, is also an option in similar

Figure 17.88 A radial forearm free flap used for a skin defect of the parotid region.

Figure 17.89 A radial forearm free flap used for a skin and soft-tissue defect of the cheek after excision of a melanoma.

Figure 17.90 Radial forearm free flap reconstruction of a nasolabial defect after resection of a fibrosarcoma.

Figure 17.91 Squamous cell carcinoma of the oral tongue, requiring partial glossectomy, leaving a defect of 8 by 4.5 cm.

Figure 17.92 A well-healed skin graft at the donor site.

Figure 17.93 The postoperative appearance of the reconstructed glossectomy defect.

Figure 17.94 A radial forearm flap reconstruction of a left hemiglossectomy defect.

Figure 17.95 A radial forearm free flap reconstruction of the anterior floor of the mouth and an oral tongue defect.

situations. An advantage of its use is that it eliminates the donor site morbidity on the forearm. The choice between radial forearm free flap or anterolateral thigh flap depends on the size of the skin paddle, color match, presence of hair, and thickness of the flap (subcutaneous fat).

The radial forearm free flap is a workhorse for reconstruction of mucosal defects in the oral cavity, oropharynx, and even hypopharynx. The laxity of the flap permits contouring of the tongue, floor of mouth, and oropharynx. A patient with squamous cell carcinoma involving the middle third of the lateral border of the tongue is shown in Fig. 17.91. Partial glossectomy left a defect measuring 8 by 4.5 cm. Reconstruction of this defect was done with a radial forearm free flap. The donor site required a split-thickness skin graft (Fig. 17.92). The reconstructed oral tongue 6 months following surgery is seen in Fig. 17.93. Several other examples of the use of the radial forearm free flap to reconstruct the lateral and anterior oral tongue and lateral wall of the oropharynx are shown in Figs. 17.94 through 17.96. As illustrated, the radial forearm free flap is considered a workhorse flap for reconstruction of mucosal and soft-tissue defects in the oral cavity and pharynx.

Reconstruction of Skin and Soft Tissues With a Rectus Abdominis Free Flap

The rectus abdominis free flap provides abundant soft tissue and skin. Thus it is an ideal flap where large soft-tissue defects result from resection of massive tumors. The patient shown in Fig. 17.97 has a large, neglected, recurrent squamous cell carcinoma of the skin. The tumor has caused extensive destruction of the skin of the face, upper lip, nose, and lower eyelid, with deep infiltration into the underlying soft tissues and involving the anterior wall of the maxilla and hard palate. A computed tomography (CT) scan of the patient at the level of the maxillary antrum shows an extensive soft-tissue tumor adherent to and involving the anterior wall of the maxilla (Fig. 17.98).

A radical resection of this tumor was performed, which required midface resection with amputation of the nose; exenteration of the left orbit; and resection of the upper lip, the oral commissure, and a portion of the lower lip, along with

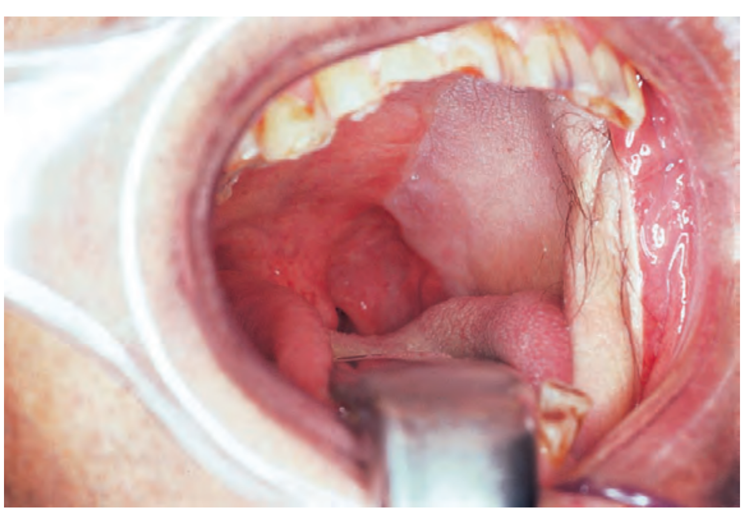

Figure 17.96 A radial forearm free flap reconstruction of the left lateral wall of the oropharynx.

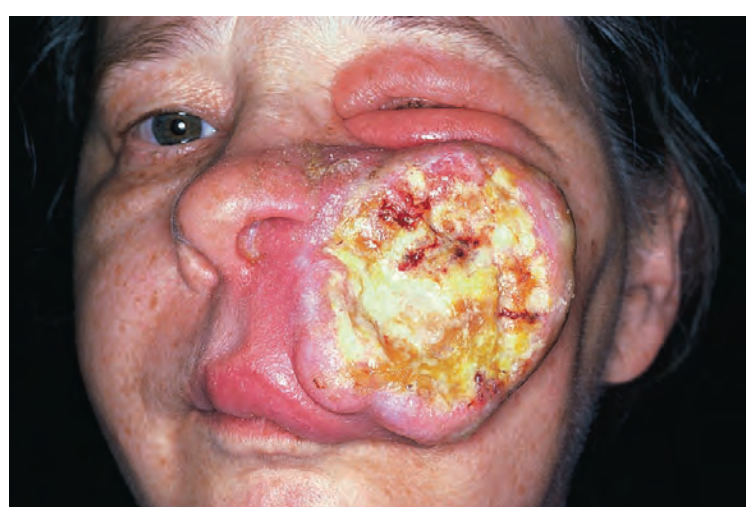

Figure 17.97 A patient with a large, recurrent squamous cell carcinoma of the skin of the face.

Figure 17.98 An axial view of a CT scan shows massive soft-tissue disease with invasion of the maxilla.

Figure 17.99 The surgical specimen shows monobloc three-dimensional resection.

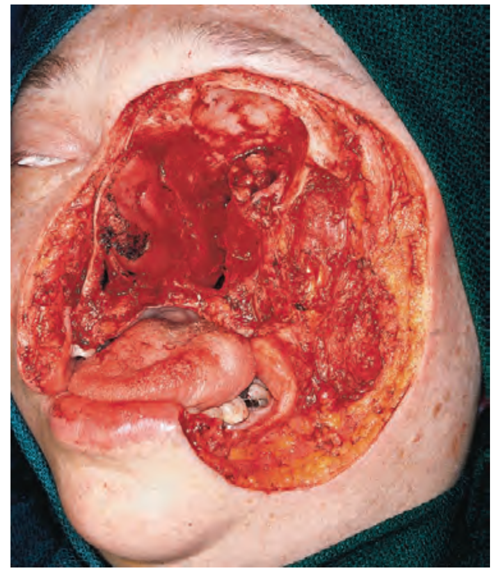

Figure 17.100 The surgical defect shows resection of the contents of the orbit, lateral wall of the nasal cavity, hard palate, and large area of skin and soft tissues.

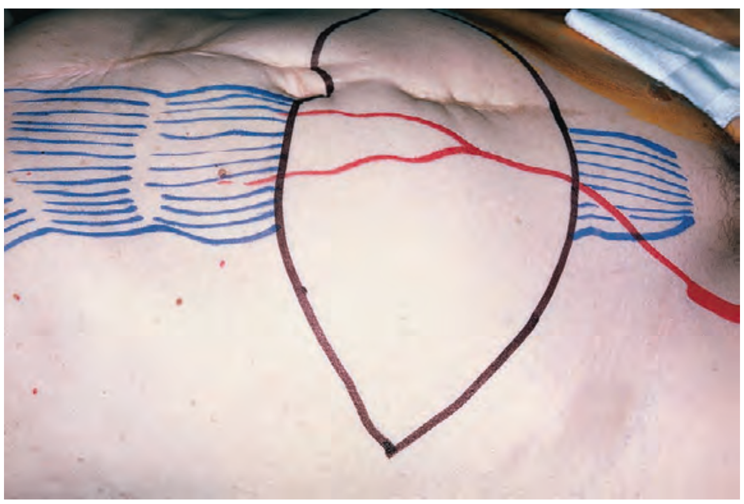

Figure 17.101 Outlines of the rectus abdominis free flap.

partial maxillectomy. The anterior view of the specimen shows the ulcerated surface of the tumor with the amputated nose and the contents of the left orbit (Fig. 17.99). The surgical field after removal of the specimen shows a massive composite defect of the midface with exposure of the nasal cavity, oral cavity, and orbit with loss of soft tissues and skin of the cheek (Fig. 17.100). The reconstruction of this surgical defect required skin lining for the palate, nasal cavity, and skin of the face, as well as soft tissues to fill the hollow space.

The rectus abdominis myocutaneous free flap provided all the essential ingredients necessary for reconstruction of this defect (Fig. 17.101). The blood supply of the flap is derived from the inferior epigastric artery via its perforating branches traversing through the rectus abdominis muscle. The muscle bulk provides soft tissue to fill the hollow space. Three islands of skin were created on this flap to provide lining in the nasal cavity, oral cavity, and external skin coverage. The immediate postoperative appearance of the patient shows a well-healed free flap that has met the immediate goals of the reconstructive procedure (Fig. 17.102). This patient required additional revision procedures to debulk the flap and improve her facial contour. A facial prosthesis provided further improvement of her appearance (Fig. 17.103).

Figure 17.102 The postoperative appearance of the patient 2 months following surgery.

Figure 17.103 A facial prosthesis provided improvement in aesthetic appearance.

Figure 17.104 A patient with extensive carcinoma of the lower gum involving overlying skin, requiring a through-and-through resection with hemimandibulectomy and partial maxillectomy.

Figure 17.105 The postoperative appearance of the patient 1 year following reconstruction with a folded rectus abdominis flap showing a well-healed skin island.

Figure 17.106 The external appearance 2 years following surgery and after debulking and fat grafting to improve appearance.

An additional example of the versatility of the rectus abdominis free flap is that it can be folded over with two islands of skin to provide mucosal and external skin coverage. The patient shown in Fig. 17.104 had squamous cell carcinoma of the right lower gingiva with invasion of the overlying skin. Surgical resection required a through-and-through resection with right hemimandibulectomy and right partial maxillectomy. No bone reconstruction was planned. He was reconstructed with a folded rectus abdominis myocutaneous free flap to repair the oral mucosa and external skin defect (Fig. 17.105). He subsequently underwent staged debulking of the flap and fat grafting to improve contour (Fig. 17.106).

Scalp Reconstruction With a Rectus Abdominis Free Flap or Latissimus Dorsi Free Flap

Massive defects of the scalp require a large area of skin and underlying soft tissues for reconstruction. Such massive surgical defects can be reconstructed with large free flaps, namely, the rectus abdominis myocutaneous, anterolateral thigh fasciocutaneous, or latissimus dorsi muscle flaps (the latter requires a split-thickness skin graft over the muscle). The patient shown in Fig. 17.107 has previously undergone multiple surgical procedures and two courses of external beam radiation therapy for recurrent multifocal basal cell carcinomas arising on the scalp with invasion of the underlying galea. Although the scalp

Figure 17.107 A patient with recurrent multifocal basal cell carcinomas of the scalp following multiple surgical procedures and two courses of radiation therapy.

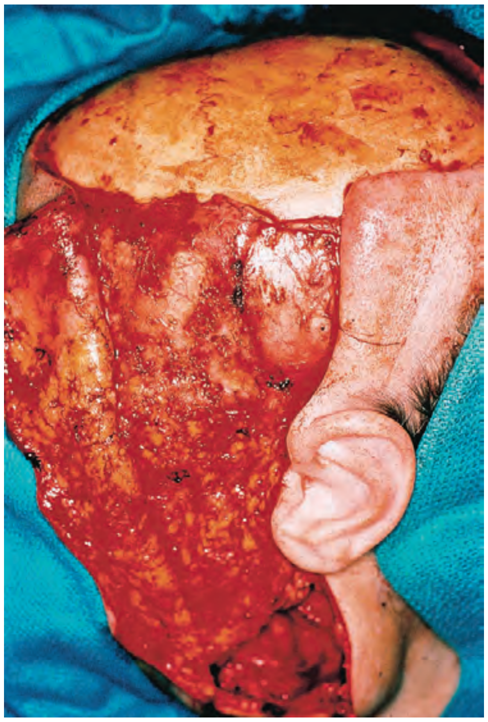

Figure 17.108 The extent of exposed bone after surgical resection.

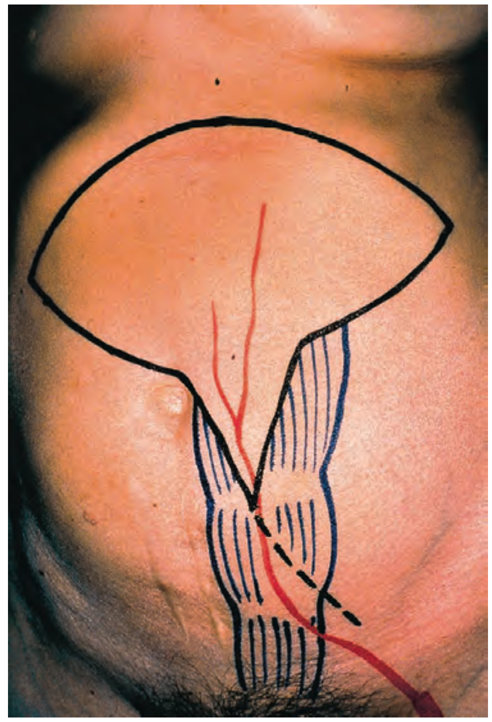

Figure 17.109 The outline of the rectus abdominis free flap.

Figure 17.110 The immediate postoperative appearance of the patient.

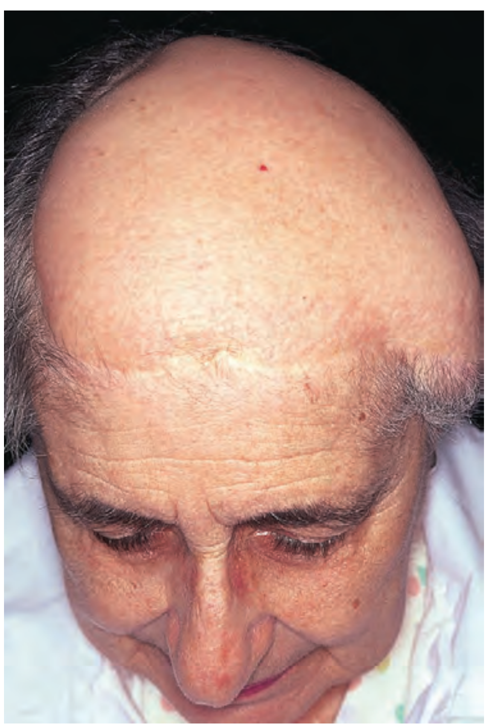

Figure 17.111 Postoperative appearance of the patient 1 year following surgery shows a well-healed flap providing excellent reconstruction. Excess soft tissue in the left temporal region can be debulked at this time.

was mobile over the calvarium, the surgical resection required sacrifice of the pericranium as the deep margin to the tumor. The exposed bone is shown in Fig. 17.108. A vertical preauricular skin incision is used, extending from the left lateral aspect of the surgical defect up to the upper part of the neck, exposing the cervical donor vessels and creating space to inset the rectus abdominis free flap. The free flap is outlined on the anterior abdominal wall (Fig. 17.109). Note that the flap is oriented transversely such that its vascular pedicle will be in the middle of the flap paddle. The immediate postoperative appearance of the patient is shown in Fig. 17.110. This patient wears a wig to camouflage her alopecia, but most importantly, the rectus abdominis free flap has provided excellent and protective reconstruction of the scalp protecting the underlying calvarium (Fig. 17.111).

Other Applications of the Rectus Abdominis Free Flap

For patients undergoing a near-total glossectomy, the rectus abdominis flap also provides excellent bulk and surface lining to replace the resected tongue (Fig. 17.112). This patient has a remnant of the base of the tongue on the left side with hypoglossal innervation intact, preserving some motor function in the reconstructed tongue. To achieve effective swallowing, the patient required a palatal drop prosthesis.

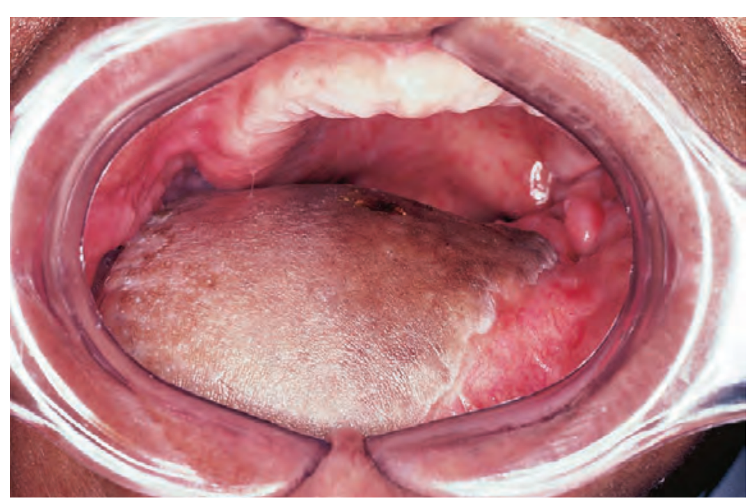

Figure 17.112 Rectus abdominis myocutaneous free flap reconstruction in a patient who underwent a near-total glossectomy.

Figure 17.113 A large dermatofibrosarcoma of the scalp.

Figure 17.114 The postoperative appearance of the patient 3 months following reconstruction with a latissimus dorsi muscle free flap and skin graft.

Figure 17.115 The aesthetic appearance of the patient 1 year following surgery demonstrates excellent restoration of contour.

Scalp Reconstruction With a Latissimus Dorsi Free Flap

If the rectus abdominis myocutaneous flap is too bulky because of excessive donor tissue subcutaneous fat, or a thick muscle, then it is not a good choice for scalp reconstruction. In that setting, a free anterolateral thigh fasciocutaneous flap or free latissimus dorsi muscle flap with split-thickness skin graft will provide better contour for large scalp defects. The patient shown in Fig. 17.113 has a large dermatofibrosarcoma protuberans of the scalp. Surgical resection required excision of a large area of scalp, including the underlying pericranium. Reconstruction of this surgical defect was performed with a latissimus dorsi muscle free flap and a split-thickness skin graft. The postoperative appearance of the patient 3 months after surgery shows well-healed skin grafts and excellent restoration of contour (Fig. 17.114). Approximately 1 year after surgery, the scalp reconstruction offers an excellent aesthetic outcome (Fig. 17.115). For further aesthetic improvement, this patient may use a hairpiece or wig over the reconstructed scalp.

Reconstruction Using an Anterolateral Thigh Flap

The ALT is a versatile fasciocutaneous flap that can provide a large amount of skin for resurfacing. In certain patients, the flap can be quite thin and thus may be used as an alternative to the radial forearm flap for resurfacing when minimal soft-tissue

Figure 17.116 A patient with locally advanced squamous cell carcinoma of the skin of the right cheek with facial nerve paralysis.

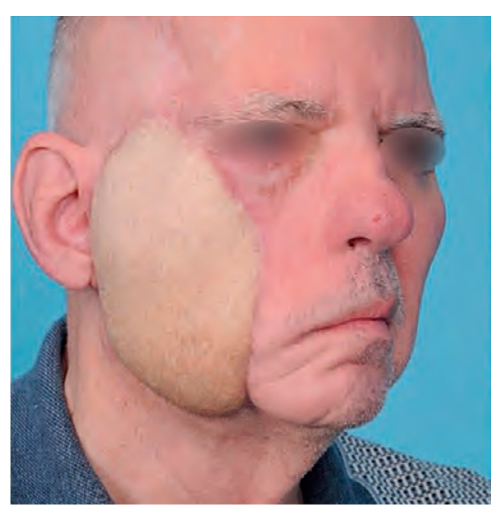

Figure 17.117 The three-dimensional defect was reconstructed with an anterolateral thigh (ALT) free flap and bone graft for the orbital floor.

bulk is required. The arterial blood supply to the ALT flap consists of perforators derived from the descending branch of the lateral femoral circumflex artery, which, in turn, arises from the profunda femoris artery. Fig. 17.116 shows a patient with locally advanced squamous cell carcinoma of the right cheek causing facial nerve paralysis. He required wide excision of the skin with parotidectomy, maxillectomy, and resection of the zygomatic arch, temporalis muscle, and coronoid process of the mandible. The surgical defect measured 20 by 13 cm. An ALT flap was used for reconstruction, along with a bone graft to reconstruct the zygoma and provide support to the orbital contents (Fig. 17.117). Donor sites larger than 8 by 25 cm usually require a skin graft to cover the raw area.

RECONSTRUCTION OF THE MANDIBLE

Reconstruction of the mandible involves several important functional, anatomic, and aesthetic considerations to achieve the goal of restoration of form and function as close to normal as possible. The functional concerns are restoration of oral competence, lip support, mastication, dental occlusion, speech, and deglutition. Anatomic components of mandibular reconstruction are restoration of the interincisor opening, maintenance of the interarch distance and interarch alignment, restoration of teeth if feasible by dental implants, and adequate soft tissue replacement. Clearly, excessive tissue bulk that would compromise the airway should be avoided. The aesthetic considerations include restoration of facial symmetry and lower facial contour, projection of the chin, and avoidance of unnecessary facial incisions.

Previously employed options for mandible reconstruction such as nonvascularized bone, pedicled composite osteomyocutaneous flaps, metallic plates with local flaps, and metallic plates with regional myocutaneous flaps are considered suboptimal and should only be considered under select circumstances when free flap reconstruction is not feasible. The current standard of care for mandible reconstruction consists of free flaps of bone with or without soft tissue and skin. Defects of the posterior aspect of the body of the mandible near its angle or of the ascending ramus may be left alone without consideration of any major bone reconstructive effort in elderly or poor-risk patients. It should be kept in mind that resection of the ascending ramus of the mandible causes loss of ipsilateral pterygoid muscle function and thus causes deviation of the mandible leading to malocclusion (Fig. 17.118). Resection of the anterior aspect of the body of the mandible, and particularly the anterior arch, produces unacceptable functional and aesthetic morbidity that mandates an appropriate reconstructive effort to restore form and function (Fig. 17.119). A very short (up to 3 cm) segmental defect in the mandible without previous or future exposure to radiotherapy can be repaired with a nonvascularized bone graft, which usually is harvested from the iliac crest.

Free flap mandible reconstruction clearly provides significant advantages in that it is highly successful, a nearly unlimited volume of tissue is available, and the harvested tissue can be fabricated to provide an ideal configuration for restoration of the surgical defect. The only disadvantage is that the procedure is technically more challenging than soft-tissue flaps requiring additional resources of operating room time, personnel, and technical sophistication. The currently available free flap choices for mandible reconstruction are the fibula, iliac crest, scapula, and radial forearm. Ideally, microvascular mandibular reconstruction should be accomplished at the time of tumor resection, because immediate reconstruction allows for greater precision and alleviates the need for a second stage operation with an intervening period of temporary deformity. The characteristics, advantages, disadvantages, and indications for various free flaps in mandibular reconstruction are further discussed in this chapter.

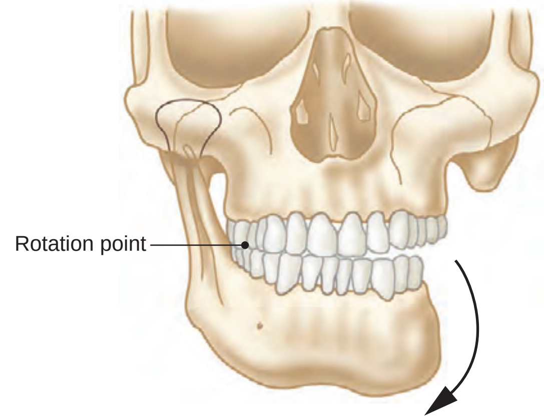

Figure 17.118 Resection of the posterior mandible allows unopposed action of the intact contralateral muscles on the remnant mandible, which tends to rotate around a fulcrum in the region of the molar teeth.

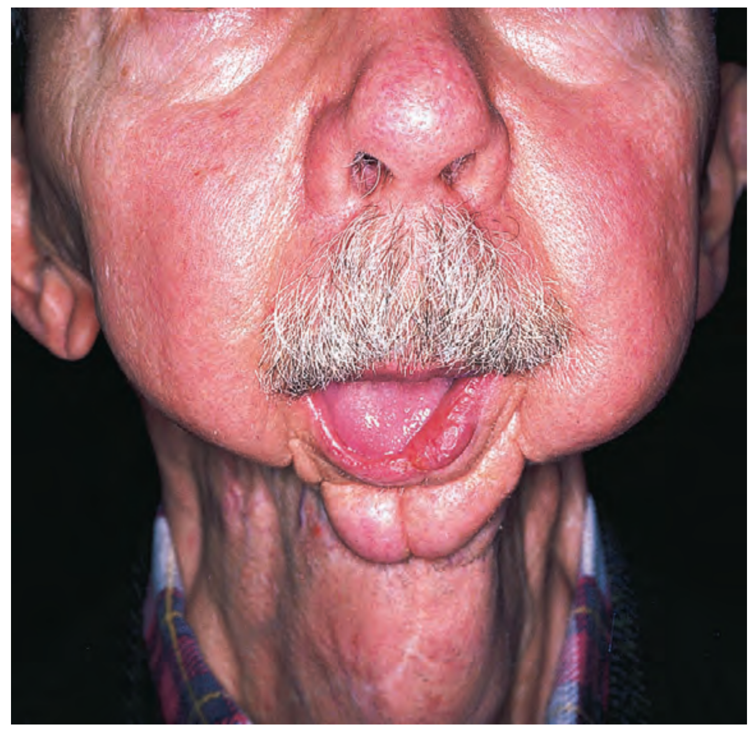

Figure 17.119 Resection of the anterior arch of the mandible produces significant functional debility and an unsatisfactory aesthetic appearance (Andy Gump deformity).

Reconstruction With Radial Forearm Osteocutaneous Free Flap

The radial forearm osteocutaneous free flap offers excellent skin and soft-tissue characteristics. The thickness of the skin is ideal, with a pliable, abundant surface area and an excellent blood supply. However, the length of bone available is limited, and only half of the circumference of the cortex of the bone can be harvested as part of the flap. The bone is not sturdy enough to perform osteotomies and for anchoring of dental implants. The blood supply to the bone is nonsegmental, and thus osteotomies for contouring shape and curvature of the mandible

is not possible. This flap has the potential for significant morbidity if a fracture of the donor site bone occurs; therefore prophylactic plating of the remaining radius bone should be performed by an orthopedic colleague. The skin-grafted appearance of the forearm is an aesthetic disadvantage. The tendons in the forearm sometimes become exposed due to skin graft failure, and prolonged immobilization to prevent fracture may result in a stiff hand and wrist. Clearly, the advantage of the radial forearm flap is its ideal skin paddle and lengthy, reliable vascular pedicle, while its disadvantage is the limited bone stock. With these characteristics in mind, the indications for a radial forearm osteocutaneous free flap are limited to surgical defects in which a large mucosal or skin surface needs to be covered with only a short segment of bone replacement. Non–load-bearing areas such as the maxilla or ascending ramus of the mandible are suitable defects for this flap.

Figure 17.120 Metastatic carcinoma from the lip involving the skin and body of the mandible.

An example of a radial forearm osteocutaneous free flap is shown in a patient who presented with a recurrent carcinoma of the lower lip and involved prevascular facial lymph nodes fungating through the skin that were adherent to the lateral cortex and undersurface of the body of the mandible (Fig. 17.120). The operative procedure included a left neck dissection in conjunction with a segmental mandibulectomy and excision of a generous portion of overlying skin in a monobloc fashion. The surgical defect is shown in Fig. 17.121. A radial forearm osteocutaneous flap is outlined in Fig. 17.122. The postoperative appearance of the patient 6 months following reconstruction of the defect with the radial forearm osteocutaneous free flap is shown in Fig. 17.123. It is important to reiterate, however, that the radial forearm osteocutaneous free flap leads to significant morbidity at the donor site and has a very limited bone stock not suitable for osteotomies or reconstruction of large defects. Thus it has a very limited application under very select circumstances.

Reconstruction With Scapula Free Flap

The scapula free flap is an ideal "chimeric" flap, because it provides abundant soft tissue with separate skin and bone components stemming from a common vascular pedicle. The blood vessels are reliable, and there is minimal donor site morbidity. However, the bone stock of this flap is less than ideal, because the thickness is inadequate for osseointegrated implants, and the maximum length that can be harvested is limited. Blood supply to this segment of bone is not segmental, and therefore multiple osteotomies to fabricate the appropriate shape of the mandible pose a problem. The soft-tissue characteristics are ideal, with an almost unlimited potential skin island size. However, the skin is thick for intraoral reconstruction, and the color match is poor for replacement of the external facial skin. Another disadvantage of this flap is the need for lateral positioning of the patient during surgery, which mandates sequential, rather than simultaneous, resection and

Figure 17.121 The surgical defect following composite resection of the skin and a short segment of the body of the mandible.

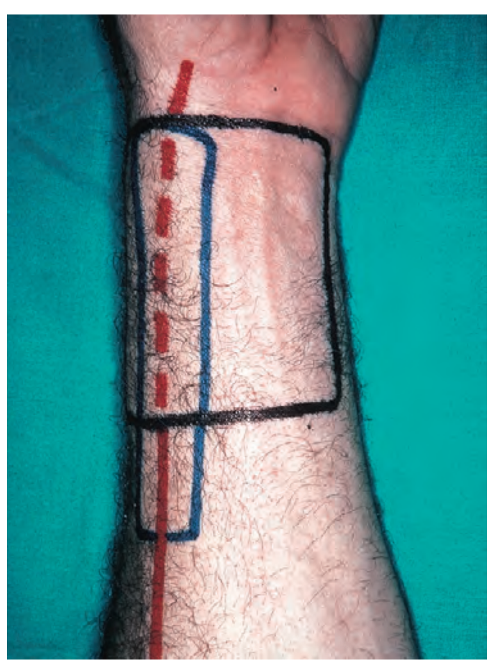

Figure 17.122 The outline of the radial forearm osteocutaneous flap.

Figure 17.123 The postoperative appearance of the patient 6 months following reconstruction.

Figure 17.124 The incisions for composite resection of the cheek and mandible with neck dissection are outlined.

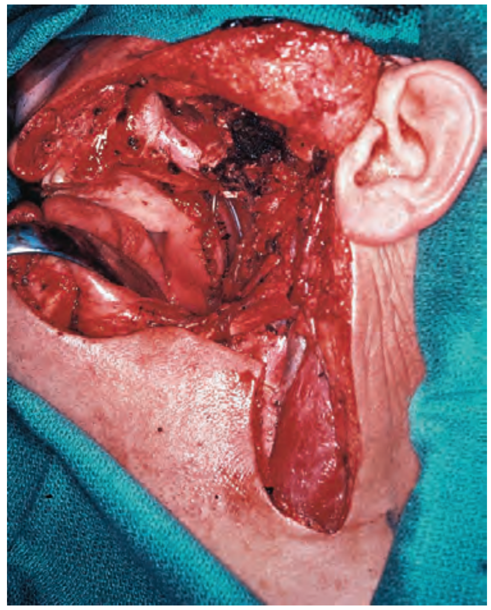

Figure 17.125 The surgical defect of through-and-through resection of the cheek with mandible and neck dissection.

Figure 17.126 The outline of the scapular free flap showing a large skin island, required bone segment, and the vascular pedicle.

reconstruction. The indications for this flap are surgical defects for which massive soft-tissue replacement is the priority.

An example of such a case is a patient who had a sarcoma of the left cheek with invasion of the underlying mandible. The surgical resection required a segmental mandibulectomy with a three-dimensional through-and-through resection of the left cheek, including the overlying skin (Fig. 17.124). The surgical defect is shown in Fig. 17.125. Reconstruction of this surgical defect requires replacement of the resected segment of the mandible in addition to soft-tissue volume, lining of the buccal mucosal, and skin of the cheek. The scapula free flap is outlined on the patient who has been placed in the right lateral recumbent position. The markings indicate the dimensions of the skin island as well as the underlying soft tissues and the segment of bone to be harvested for reconstruction (Fig. 17.126). The scapula free flap showing the new mandibular angle, vascular pedicle, and skin island with underlying soft tissues is shown in Fig. 17.127. The skin island is deepithelialized in the middle, and the flap is folded over to provide inner lining of the cheek and external skin coverage of the face. The postoperative appearance of the patient demonstrates satisfactory restoration of cheek contour and adequate replacement of external skin (Fig. 17.128).

A short segment of edentulous atrophic mandible (pipestem mandible) can be very adequately reconstructed with a scapula free flap. The vascularized bone has an excellent capacity for complete integration with the native mandible. The panoramic radiograph of an elderly patient who required segmental mandibulectomy and reconstruction with a scapula free flap is shown in Fig. 17.129 in the immediate postoperative period. A follow-up panoramic radiograph 1 year following surgery is shown in Fig. 17.130. Significant osteosynthesis has taken place with complete union of the bone ends.

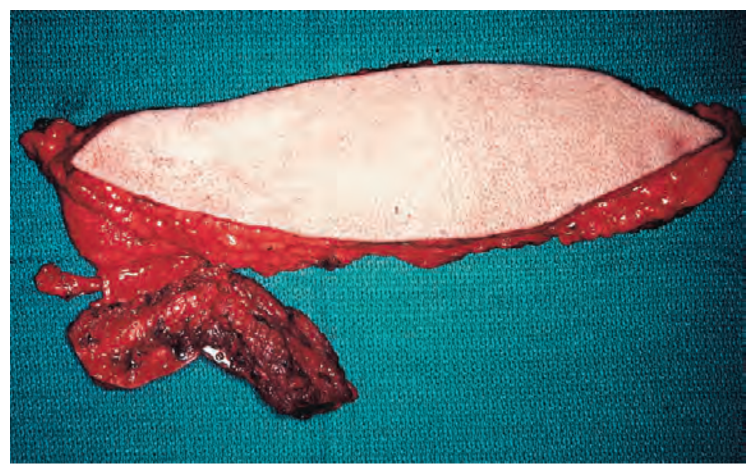

Figure 17.127 The composite scapula free flap with reconstructed angle of the mandible.

Figure 17.128 The postoperative appearance of the patient 1 month following surgery shows satisfactory restoration of volume and coverage of the skin of the cheek.

Reconstruction With an Iliac Crest Free Flap

A composite flap of ilium with the overlying skin (the iliac crest free flap) is often of limited value in mandible reconstruction.

Figure 17.129 A panoramic radiograph of an elderly edentulous patient with "pipestem" mandible reconstructed with a free scapular osteocutaneous flap and miniplates.

Figure 17.130 A panoramic radiograph of the patient shown in Fig. 17.100 showing complete osteosynthesis 1 year following reconstruction.

Figure 17.131 The outline of the iliac crest composite free flap.

Although the amount of the bone available is virtually unlimited, the shape has fixed characteristics and therefore is unfavorable (Fig. 17.131). Blood supply to the bone is nonsegmental, and the overlying skin may be bulky, immobile, and often unreliable. In addition, significant morbidity occurs at the donor site because of a difficult closure with associated pain, leading to delayed ambulation. In some patients a hernia develops at the donor site. Despite these limitations, some reconstructive surgeons prefer the iliac crest free flap for mandible reconstruction, particularly for lateral mandibular defects (Fig. 17.132).

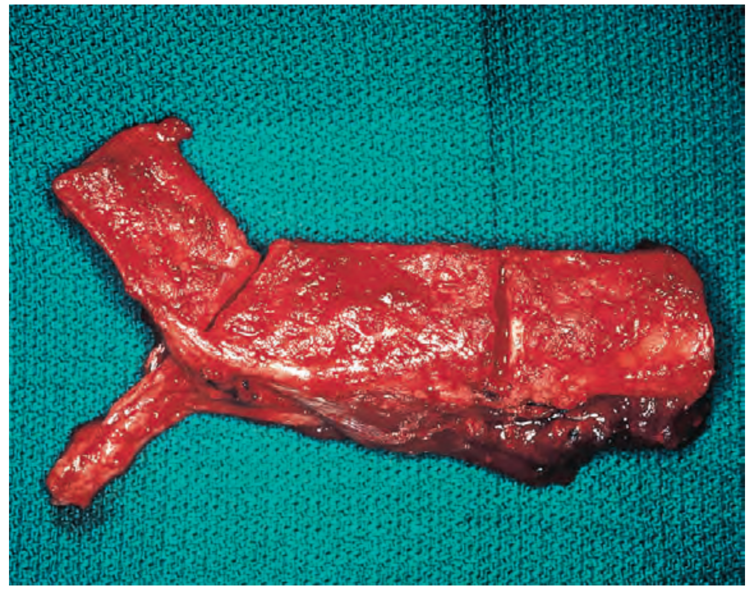

Figure 17.132 The iliac crest bone flap with two osteotomies.

Reconstruction With the Fibula Free Flap

The fibula free flap is the workhorse for mandible reconstruction because of its reliability, excellent bone stock, overlying protective muscle, and optional skin paddle, as well as the acceptable donor site morbidity. Bone lengths up to 25 cm are available. The bone flap consists of circumferential cortical bone, and it has segmental blood supply, which makes multiple osteotomies feasible and safe. Because of these anatomic characteristics, replication of the shape, angulation, and curvature of the mandible can be achieved for all types of mandibular defects. In addition, the donor site is at a distant location, and therefore ablative surgery and harvest of the bone flap can be performed simultaneously by two surgical teams, reducing the length of the operation. An absolute contraindication to use of the free fibula is lower extremity arterial disease that would potentially cause limb compromise with sacrifice of the peroneal artery.

Primary tumors of the mandible that require resection of a segment of bone with minimal or no soft-tissue loss typically require an osseous free flap. The patient shown in Fig. 17.133 has an ossifying fibroma of the mandible that requires a right hemimandibulectomy. The tumor had progressed over time and was causing increasing pain, prompting surgical intervention. A preoperative panoramic radiograph of the mandible shows diffuse patchy bone destruction involving the right hemimandible (Fig. 17.134).

To resect the right hemimandible, a transverse incision is placed through an upper neck skin crease. The right lower cheek flap is elevated in the manner of a visor flap through an incision in the gingivolabial and gingivobuccal sulcus, providing adequate exposure of the right hemimandible (Fig. 17.135). The mandible is divided just to the right of the midline anteriorly and is disarticulated from the right temporomandibular joint. Optimal reconstruction of the resected hemimandible is performed with the fibula free flap. The blood supply to the fibula is derived from the peroneal artery (Fig. 17.136). A segment of the fibula with its attached musculature and feeding vessel is isolated. The fibular composite flap is then contoured and formed into the shape of the resected mandible ex vivo.

Multiple osteotomies are performed in the bone flap, and they are appropriately positioned to match the shape of the resected mandible (Fig. 17.137). Ultimate precision is exercised

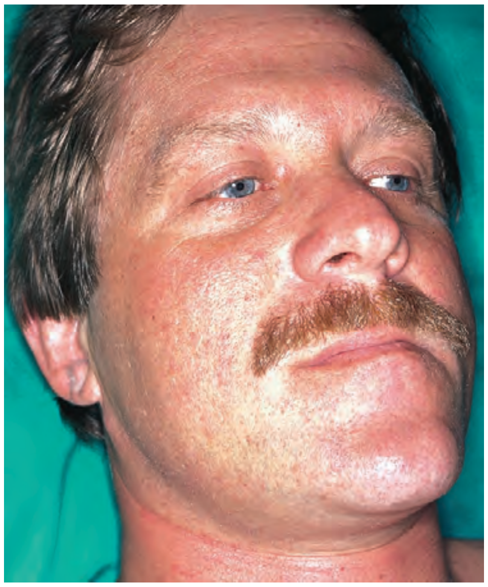

Figure 17.133 The preoperative appearance of a patient with an ossifying fibroma of the mandible.

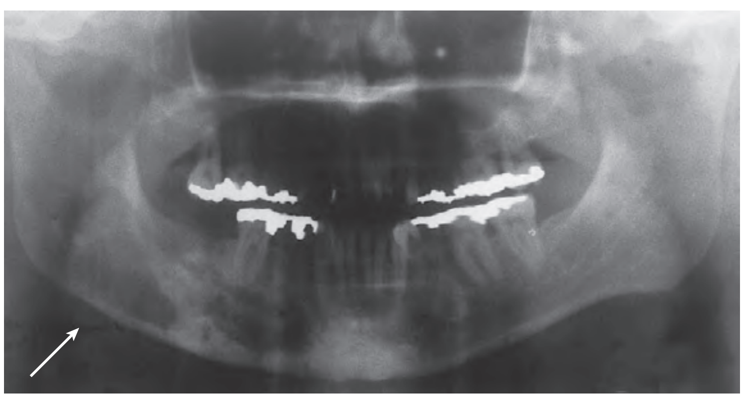

Figure 17.134 A preoperative panoramic radiograph showing an ill-defined, bone-destructive lesion of the right hemimandible (*arrow*).

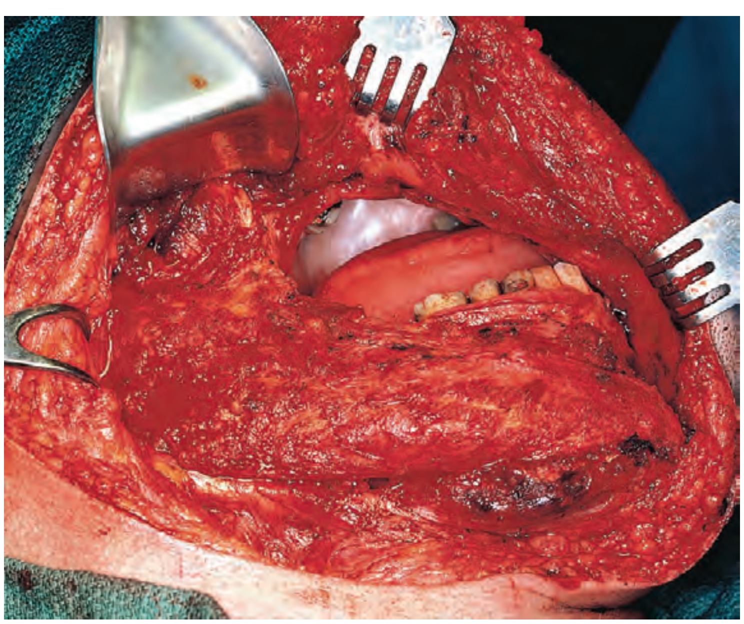

Figure 17.135 The right hemimandible is exposed by retraction of the lower cheek flap.

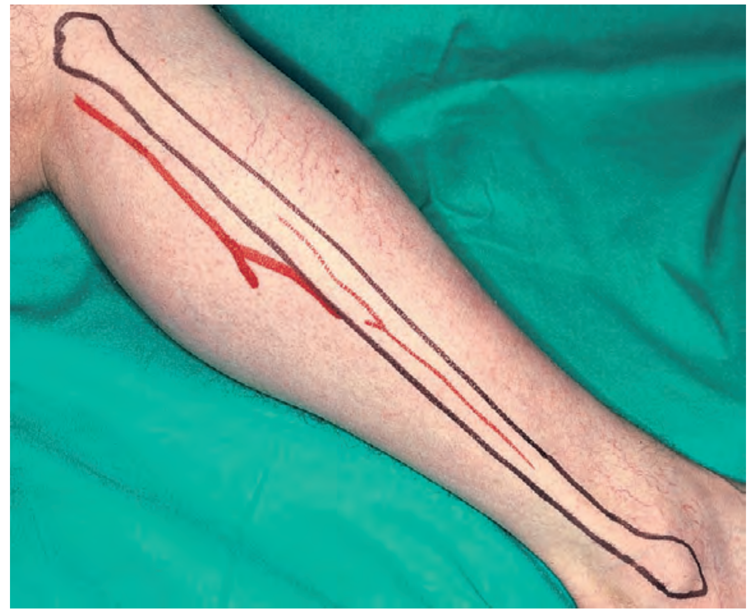

Figure 17.136 The outline of the fibula and peroneal artery.

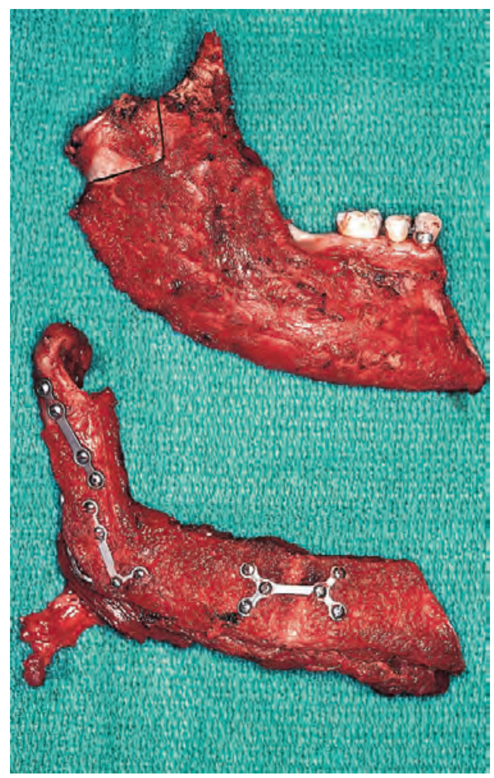

Figure 17.137 The surgical specimen and the preshaped bone flap.

during these osteotomies so the blood supply to the bone is not disturbed. The shape and contour of the osteotomized fibula are maintained with the use of miniplates and screws. The condyle of the resected mandible if uninvolved in the disease process is amputated and attached to the fibula free flap with a miniplate to allow reconstruction of the temporomandibular joint. The patient is kept in intermaxillary fixation with elastic bands to maintain occlusion as the condyle is anchored to the temporomandibular joint, and the flap is plated to the remaining hemimandible. The microvascular anastomoses are then completed.

A postoperative panoramic view of the mandible shows that the bone flap is well aligned (Fig. 17.138). The postoperative appearance of the patient approximately 8 weeks following surgery shows a well-healed incision with a very gratifying

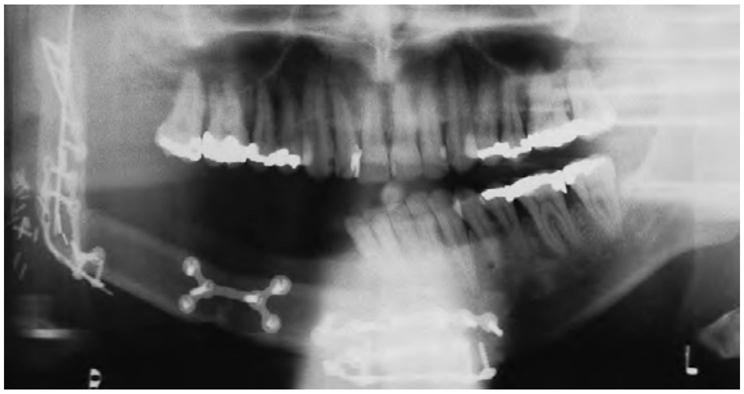

Figure 17.138 A postoperative panoramic radiograph showing the reconstructed hemimandible.

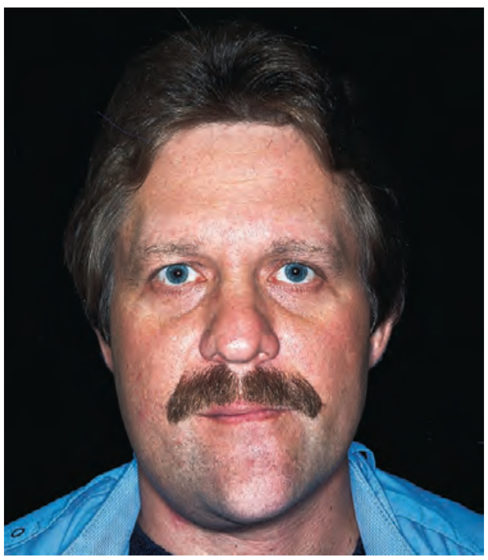

Figure 17.139 The postoperative appearance of the patient 6 weeks following surgery.

aesthetic result (Fig. 17.139). This patient's ability for oral consumption of food and mouth opening is now restored. Note that excessive soft-tissue bulk is avoided in this type of reconstructive procedure because minimal soft tissue is lost after tumor resection. The aesthetic reconstruction of the hemimandible is complete at this point. Full restoration of function requires secondary osseointegrated implants for fixed dentures in the future.

The intraoral photograph of a patient with a locally advanced carcinoma of the lower gingiva involving the molar region is shown in Fig. 17.140. A composite resection with a hemimandibulectomy is performed to resect the primary tumor with adjacent soft tissues in continuity with a right neck dissection. The surgical specimen is shown in Fig. 17.141. A composite free flap is fabricated with appropriate osteotomies in the fibula to create the shape of the mandible with attached soft tissues and overlying skin for restoring lining in the oral cavity (Fig. 17.142). The postoperative appearance of the patient shows restoration of the contour and the continuity of the mandible (Fig. 17.143). A panoramic radiograph of the mandible shows that the fibula free flap has been inset and attached to the remaining mandible with miniplates and screws (Fig. 17.144). If the mucosal defect in the oral cavity is minimal, then a skin island on the composite free flap is not required. Simple primary closure between the mucosa of the cheek and the floor of the mouth is quite satisfactory under those circumstances.

Figure 17.140 An intraoral view of a locally advanced carcinoma of the right lower gingiva.

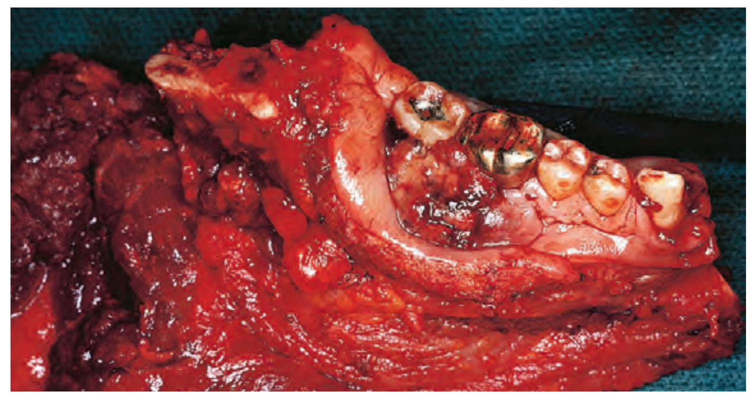

Figure 17.141 The surgical specimen.

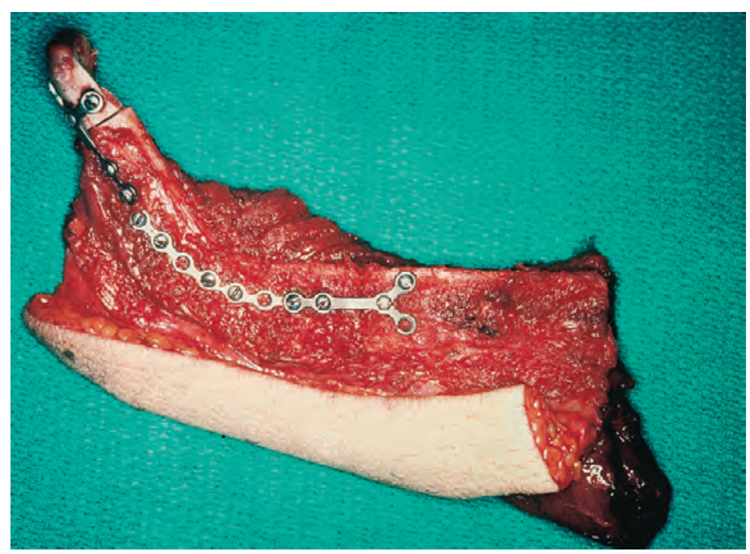

Figure 17.142 The composite fibula free flap preshaped for reconstruction of the surgical defect.

Another patient who underwent a left hemimandibulectomy for squamous cell carcinoma of the lower gingiva invading the retromolar region is shown in Fig. 17.145. Excellent restoration of facial contour and dental occlusion is achieved with fibula free flap reconstruction of a hemimandibular defect. The facial symmetry has been restored and the external contour of the face remains balanced with the unaffected side. An intraoral view of this patient shows the skin island providing coverage over the newly reconstructed left hemimandible, while occlusion of the remaining teeth on the right side is maintained. The fasciocutaneous component of the composite fibula free flap

Figure 17.143 The postoperative appearance of the patient 6 months following surgery.

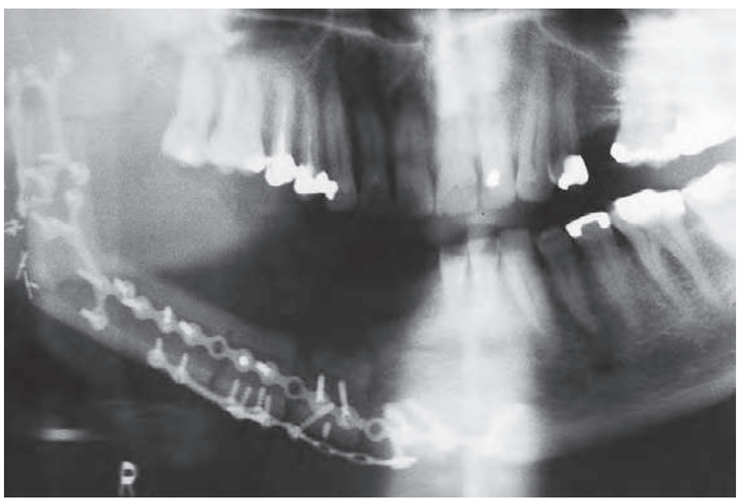

Figure 17.144 A panoramic radiograph of the reconstructed hemimandible.

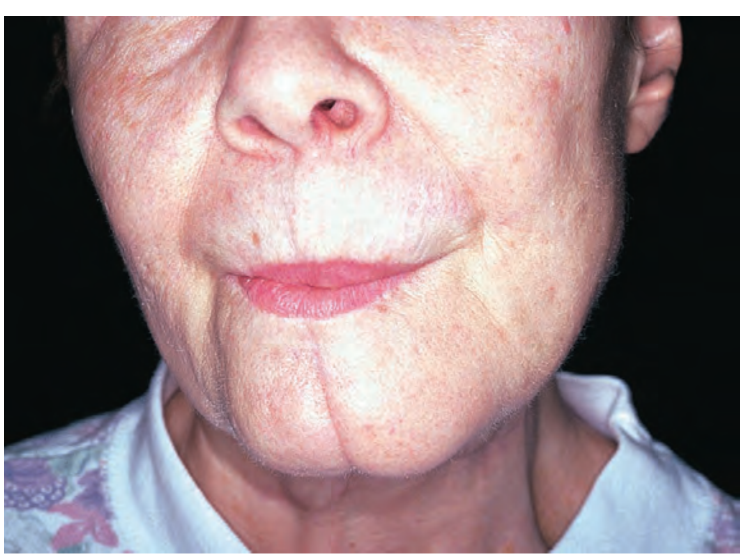

Figure 17.145 Restoration of facial contour after fibula free flap reconstruction of a hemimandibulectomy defect.

Figure 17.146 An intraoral view showing the well-healed cutaneous component of the flap.

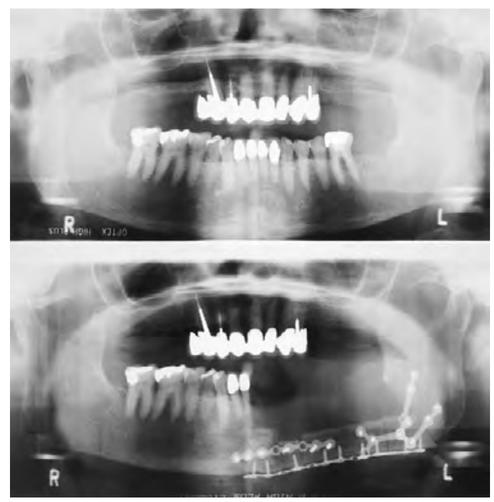

Figure 17.147 Preoperative and postoperative panoramic radiographs show excellent restoration of the contour of the mandible.

provides satisfactory coverage of lining in the oral cavity and allows normal mobility of the tongue (Fig. 17.146). A postoperative panoramic radiograph of the mandible of this same patient compared with the preoperative radiograph demonstrates excellent restoration of the angulation and curvature of the mandible with the fibula free flap (Fig. 17.147).

The free fibula flap can also be used to replace necrotic bone following infection or osteoradionecrosis where bone grafts are much less likely to succeed. Fig. 17.148 shows the panoramic radiograph of a 64-year-old man with osteoradionecrosis and pathologic fracture after radiation treatment for a squamous cell carcinoma of the soft palate. Fig. 17.149 shows a follow-up panoramic radiograph after bone resection and reconstruction with a fibula free flap and miniplates.

The patient whose surgical defect after composite resection is shown in Fig. 17.150 had a locally advanced carcinoma of the oral tongue with extension to the floor of the mouth and fixation to the lingual plate of the mandible that required a hemiglossectomy in conjunction with a hemimandibulectomy and right neck dissection. A harvested fibula free flap contoured to restore the mandible is shown in Fig. 17.151. Multiple osteotomies are made in the bone flap to recreate the missing segment of mandible. The reconstruction is completed by first plating the bone flap to the native mandible (Fig. 17.152). The soft tissue and skin transferred with the flap provided coverage for the floor of the

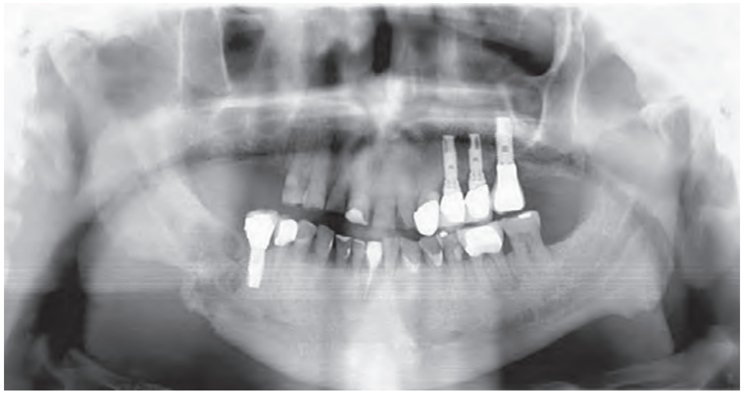

Figure 17.148 A panoramic radiograph of a 64-year-old man with osteoradionecrosis and pathologic fracture of the right mandible following radiation treatment for a soft palate squamous cell carcinoma.

Figure 17.149 A panoramic radiograph of the patient following right partial mandibulectomy and reconstruction with a free fibula bone flap and miniplates.

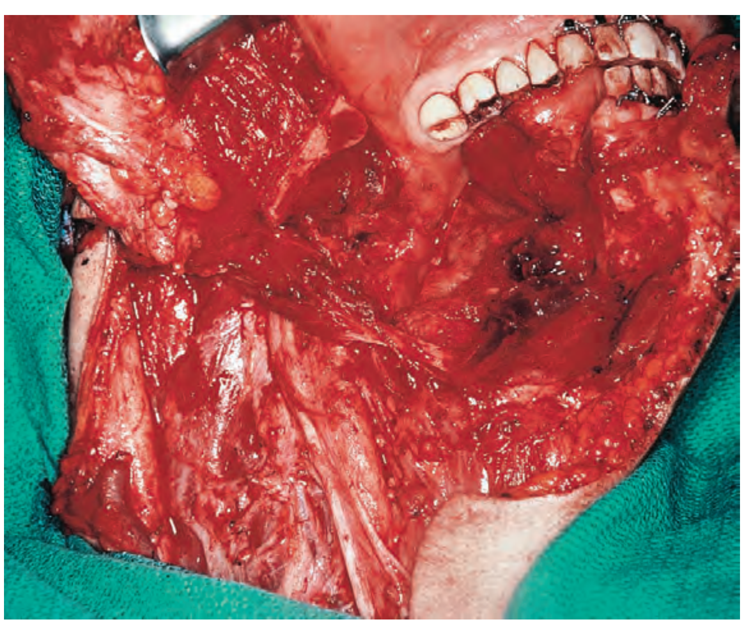

Figure 17.150 The surgical defect after a hemiglossectomy and hemimandibulectomy.

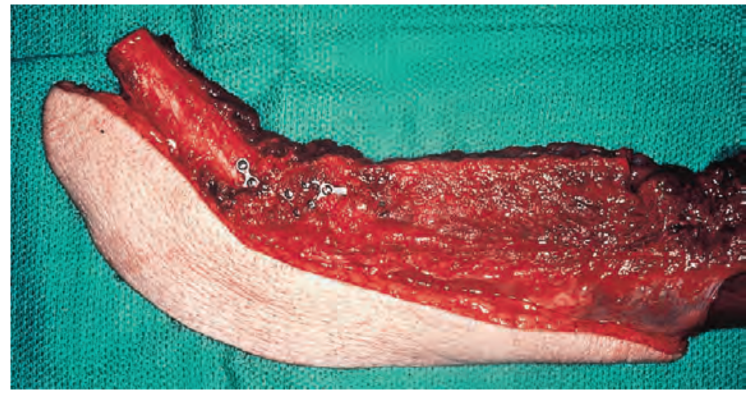

Figure 17.151 The fibula free flap with multiple osteotomies to match the contour of the mandible.

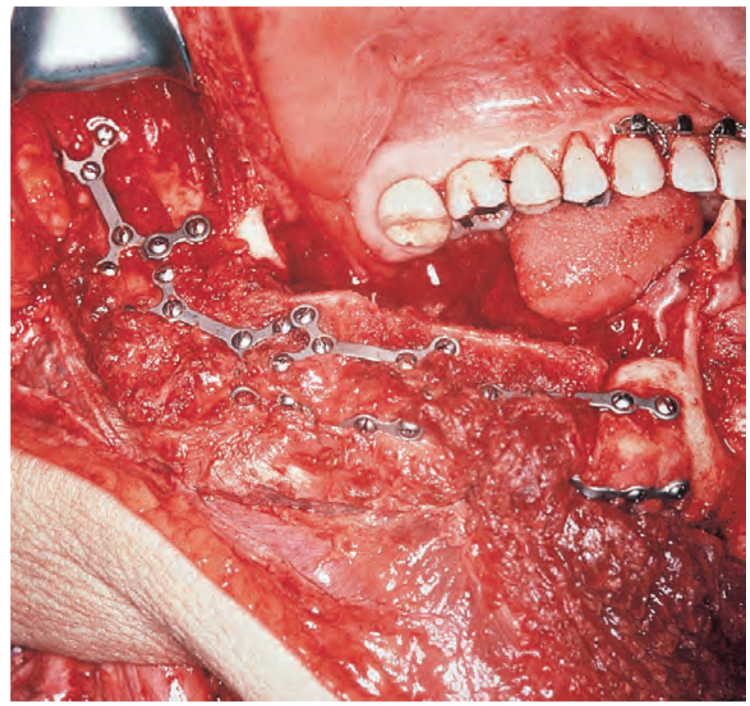

Figure 17.152 Fixation of the flap to the native mandible.

mouth and for reconstruction of the resected right half of the tongue (Fig. 17.153). The intraoral view of the patient 1 year following surgery shows the reconstruction with restored mobility and shape of the tongue (Fig. 17.154). The postoperative appearance of the patient 1 year following surgery shows restoration of the contour and continuity of the mandible (Fig. 17.155). The postoperative panoramic radiograph demonstrates accurate alignment of the reconstructed mandible (Fig. 17.156).

A preoperative photograph of a young patient with a tumor of the anterior arch of the mandible is shown in Fig. 17.157. The CT scans in coronal and axial planes show an intraosseous lesion with a honeycomb-like appearance (Fig. 17.158). A biopsy of this lesion confirmed this to be a low-grade chondrosarcoma. Resection of the anterior arch of the mandible was performed, extending from the right first molar to the left second premolar tooth through a visor flap approach. The surgical specimen consists of a monobloc resection of the anterior arch of the mandible (Fig. 17.159). The bone defect was reconstructed using a fibula free flap with multiple osteotomies. The postoperative appearance of the patient 6 months following surgery shows perfect restoration of the contour and shape of the face and projection of the chin (Fig. 17.160). A comparison of the

Figure 17.153 Reconstruction of the resected half of the tongue.

Figure 17.154 An intraoral view showing the reconstructed tongue.

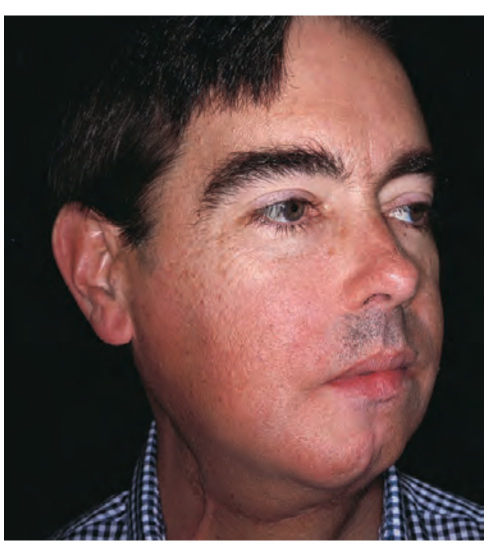

Figure 17.155 The postoperative appearance of the patient.

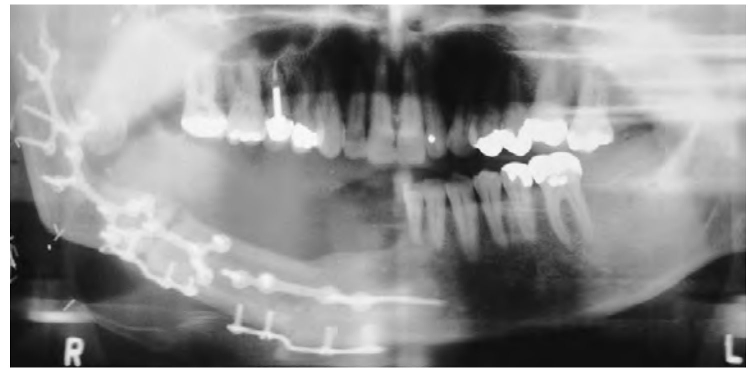

Figure 17.156 A postoperative panoramic radiograph.

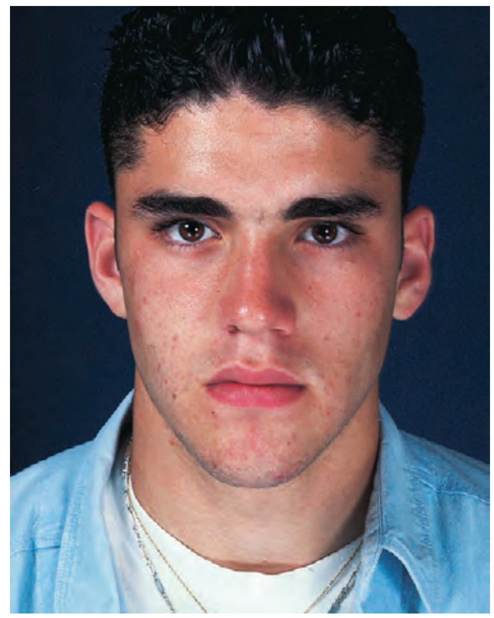

Figure 17.157 The preoperative appearance of the patient.

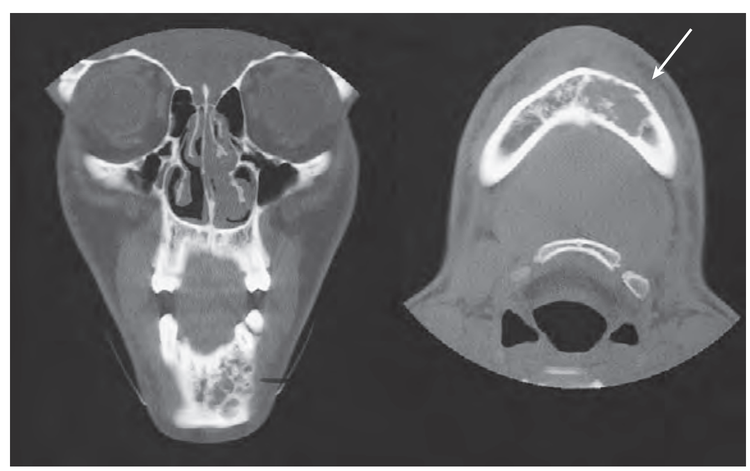

Figure 17.158 Coronal and axial CT scans showing the honeycomb appearance of the tumor (*arrow*).

preoperative and postoperative panoramic radiographs of the mandible shows exact reconstruction of the anterior arch of the mandible (Fig. 17.161).

Through-and-through defects of the oral cavity that require resection of mucosa, intervening mandible, and overlying skin need a major reconstructive effort with a composite flap to provide bone, soft tissue, and skin. The patient shown in Fig. 17.162 has recurrent lymphoma of the soft tissues of the chin that failed to respond to radiation therapy and two courses of chemotherapy. The tumor at this point involves the overlying skin, the mandible,

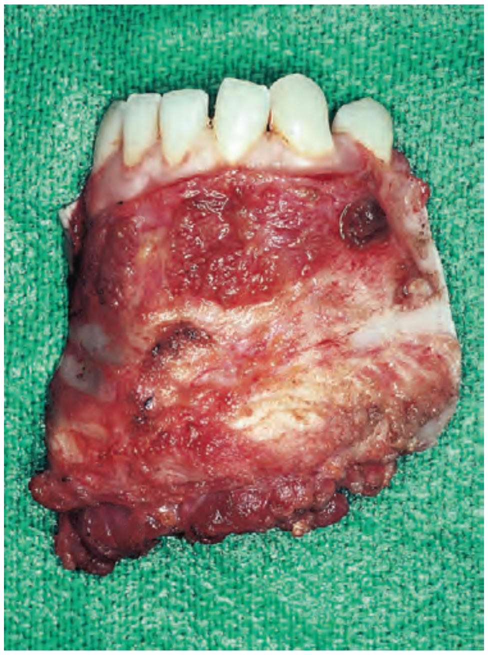

Figure 17.159 The surgical specimen.

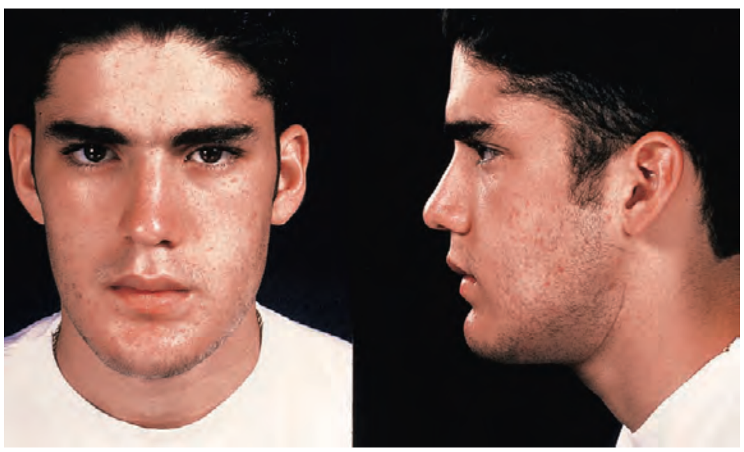

Figure 17.160 Postoperative appearance of the patient 6 months following surgery.

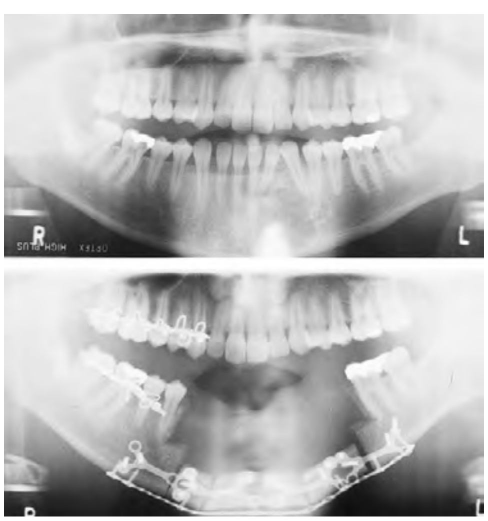

Figure 17.161 Preoperative and postoperative panoramic radiographs showing accurate reconstruction of the mandible.

and the mucosa of the gingivolabial sulcus, and the floor of the mouth. The arch of the mandible is resected in a monobloc fashion in conjunction with the involved skin, soft tissues, and mucosa of the floor of the mouth, creating a through-and-through defect. The specimen is shown in Fig. 17.163.

Figure 17.162 A patient with recurrent lymphoma involving skin of the chin, mandible, and oral mucosa.

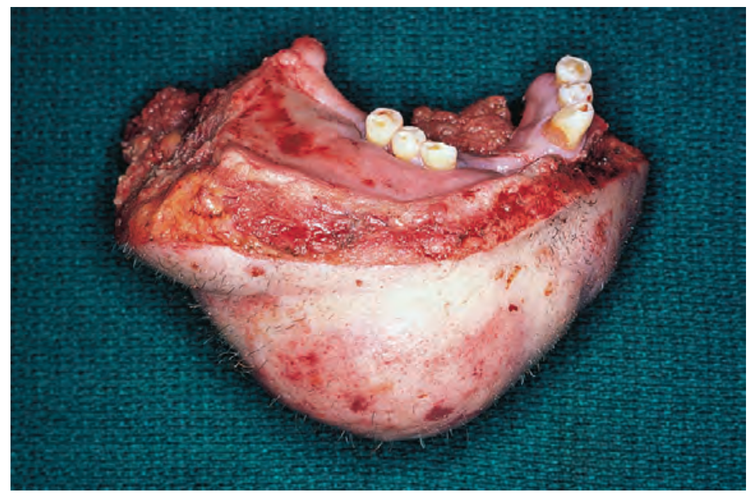

Figure 17.163 The surgical specimen of through-and-through resection of the anterior arch of the mandible.

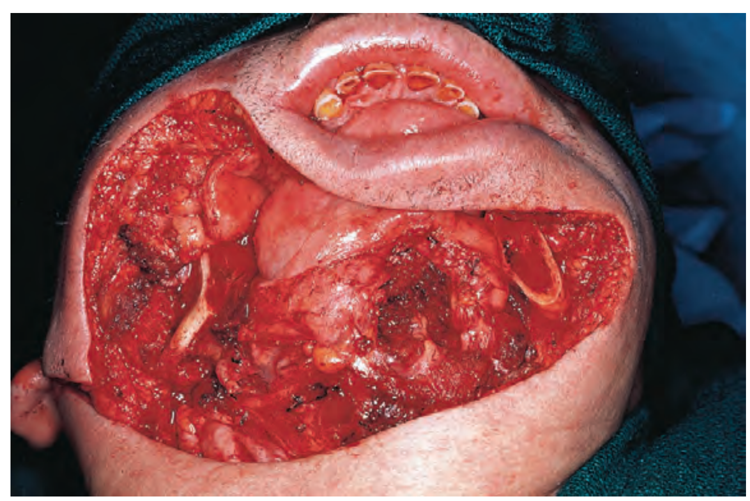

Figure 17.164 The surgical defect showing loss of mucosa, bone, soft tissues, and skin.

The surgical defect after removal of the specimen shows a large area of skin and soft tissue loss, along with the stumps of the native mandible on both sides (Fig. 17.164). The mucosa of the undersurface of the tongue is seen in the surgical defect. The vermilion border of the lower lip was preserved on the right side. A composite free flap is harvested from the leg, which includes a segment of the fibula, attached flexor hallucis longus muscle, and the overlying fasciocutaneous skin paddle (Fig. 17.165). This flap is used to reconstruct the defect in the

mandible and the soft tissues and skin. The mucosal defect in the oral cavity could be repaired by primary closure. The postoperative appearance of the patient several months following surgery shows a well-healed free flap, which provides satisfactory contour, appearance, and function after the major through-and-through resection (Fig. 17.166). Despite an excellent early aesthetic result, atrophy of both the bone and soft tissue is to be expected with the passage of time. A photograph of the patient 10 years after surgery shows significant soft tissue and bone atrophy (Fig. 17.167).

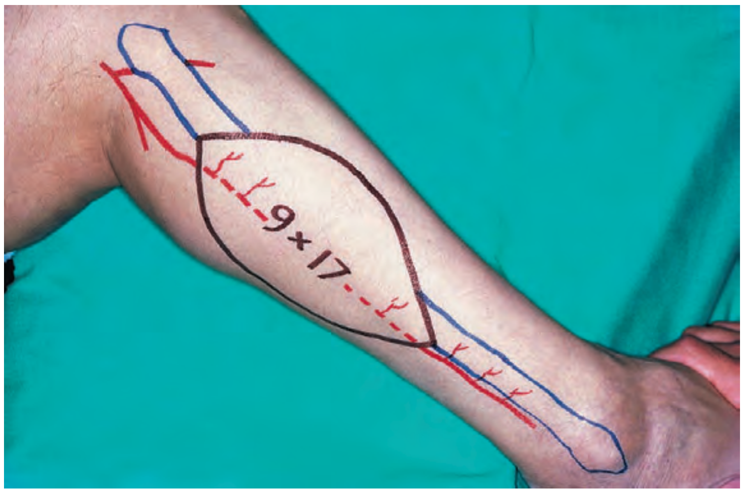

Figure 17.165 The outline of the composite fibula free flap.

Figure 17.166 The postoperative appearance of the patient 1 year following surgery.

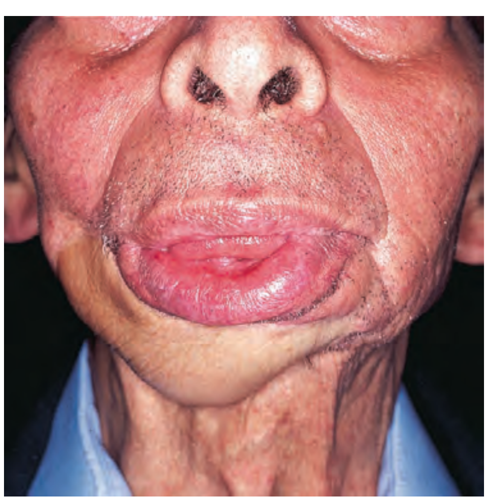

Figure 17.167 Soft tissue and bone atrophy in the patient shown in Fig. 17.166 is evident 10 years after fibula free flap reconstruction of the mandible.

Osseointegrated Implants in a Reconstructed Mandible

The obvious advantages of osseointegrated implants for dental restoration in the reconstructed mandible are improvements in the aesthetic appearance of the patient as well as restoration of clarity of speech, oral competence, and mastication. The requirements for successful osseointegration of implants include the availability of adequate bone stock and pliable soft tissue covering the bone. The vertical height of the bone should be at least 10 mm, and the width of the bone should be at least 5 to 6 mm. The best candidates for dental rehabilitation are patients who are free of disease and have accurate reconstruction of the resected mandible. Patients with defects of the anterior arch of the mandible and those in whom no skin island is required for lining in the oral cavity are ideal candidates.

The availability of CAD-CAM has greatly facilitated accurate fabrication of the fibula free flap for perfect alignment in reconstructing the mandible. This technology further allows the surgeon to plan placement of fixation plates and screws in locations so as to facilitate immediate placement of dental implants at desired locations in the fibula free flap. Clearly, there are advantages and disadvantages to consider immediate dental implants at the time of fibula free flap reconstruction. The distinct disadvantages are that (1) occlusion may not be ideal, (2) the implants may shift during healing of the bone, (3) the presence of the implants adds additional burden to the healing fibula flap, and (4) postoperative radiation therapy may create hot spots around the metallic implants with potential risk of extrusion of the implants. On the other hand, there are several advantages to consider immediate implant placement: (1) The time to complete oral rehabilitation is reduced significantly. (2) Accurate placement of implants is feasible with the use of CAD-CAM technology. (3) Titanium implants do not add significant “metallic burden” on the bone since the hardware to reconstruct the mandible is already there. (4) There is significant reduction in cost and morbidity of multiple surgical procedures required for secondary implant placement. (5) Patients are able to enjoy total oral rehabilitation in just a few months. Therefore immediate or delayed placement of implants in a reconstructed mandible should be discussed in the multidisciplinary team considering all tumor- and patient-related factors.

The preoperative CT scan of a patient with an ameloblastoma of the mandible is shown in Fig. 17.168. Note an expansile bone-destructive lesion involving the region of the angle of the mandible on the right side. This patient underwent a segmental mandibulectomy extending from the mandibular notch up to the central incisor teeth on the right side. Serial panoramic radiographs in Fig. 17.169 show (1) the preoperative appearance, (2) the immediate postoperative appearance of the reconstructed mandible with screws and miniplates, and (3) a delayed view after removal of the screws and plates and insertion of osseointegrated implants. A postoperative intraoral view of the patient shows perfect restoration of the dentition over the osseointegrated implants and restoration of dental occlusion (Fig. 17.170). Mobility of the tongue remains normal, and the patient’s ability to chew is restored. Her speech is excellent, and the external appearance of the patient shows preservation of contour and symmetry of the face (Fig. 17.171). As demonstrated, the ideal reconstruction of the resected mandible is achieved with the use of a fibula free flap.

Figure 17.168 A preoperative CT scan of the patient with ameloblastoma of the mandible showing an expansile, destructive lesion on the right side (*arrow*).

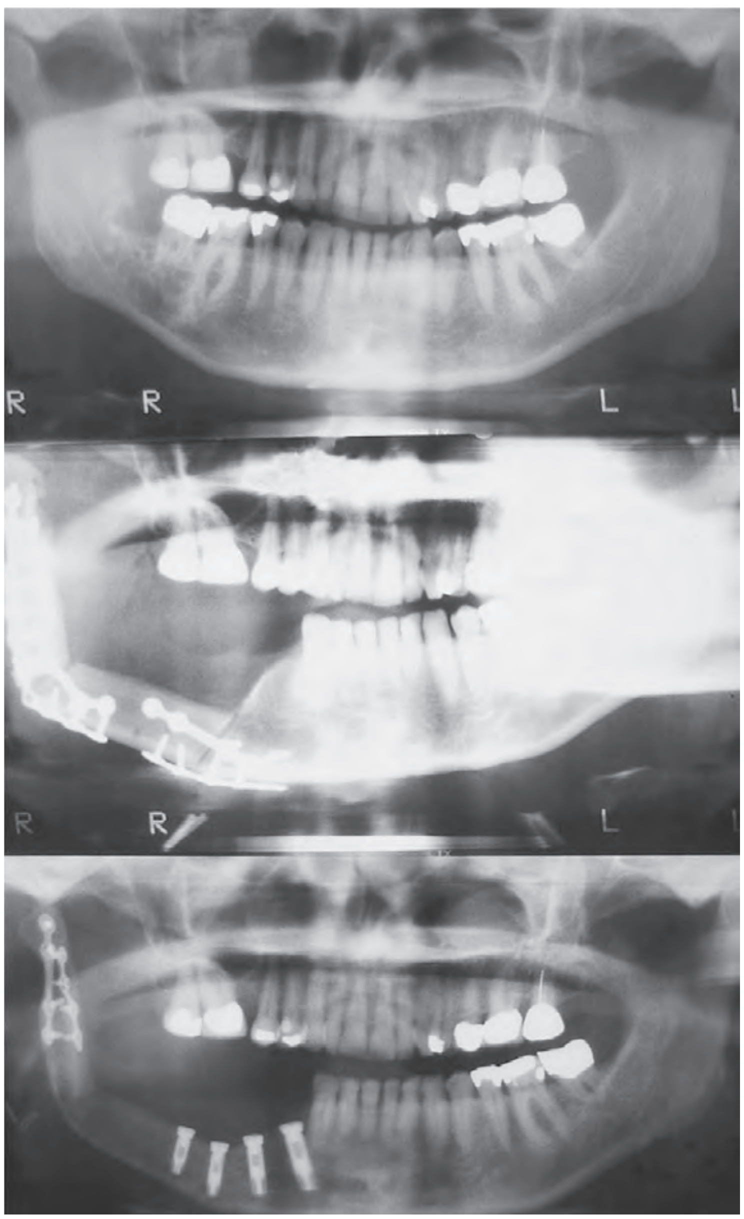

Figure 17.169 Serial panoramic radiographs show the preoperative extent of the lesion (*top*), the reconstructed mandible with fibula free flap (*middle*), and the final appearance after removal of mandibular hardware and placement of osseointegrated implants (*bottom*).

Figure 17.170 Intraoral view of the patient showing reconstructed fixed denture with implants.

Figure 17.171 The postoperative appearance of the patient 1 year following implant-supported restoration of dentition.

Reconstruction of the Maxilla With CAD-CAM Design for Fibula Free Flap

The availability of CAD-CAM models has greatly facilitated preplanning of the proposed reconstruction of bone. CAD-CAM creates a model and prepares predesigned guide planes to precisely perform osteotomies in the free bone flap to create a desired reconstruction. This technology is now routinely used in mandible reconstruction (see Chapter 18 for details). This technology is also extremely useful in maxillary reconstruction to achieve precise restoration of facial contour and also permits placement of dental implants in the reconstructed maxilla at the desired locations.

The patient shown here had previously undergone infrastructure partial maxillectomy for a low-grade myxofibrosarcoma of the maxilla. This procedure was done through a modified Weber-Ferguson incision, respecting the nasal subunits and with the subciliary extension in the infraorbital skin crease. The

Figure 17.172 The preoperative appearance of the patient (**A**) with a planned modified Weber-Ferguson incision (**B**) and the postoperative appearance of the patient 6 months following surgery (**C**).

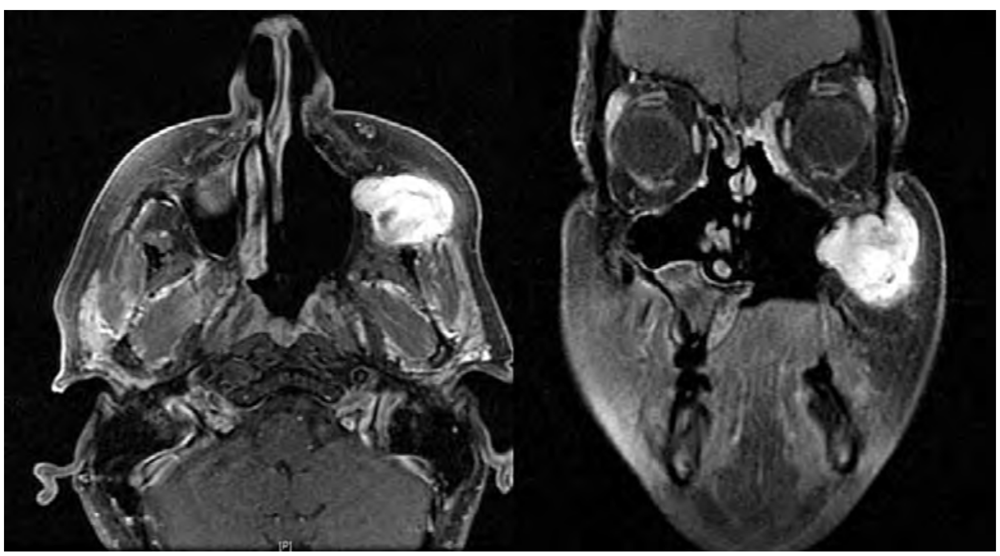

Figure 17.173 Preoperative magnetic resonance imaging in axial and coronal planes shows the recurrent tumor confined to the masticator space and involving the zygoma.

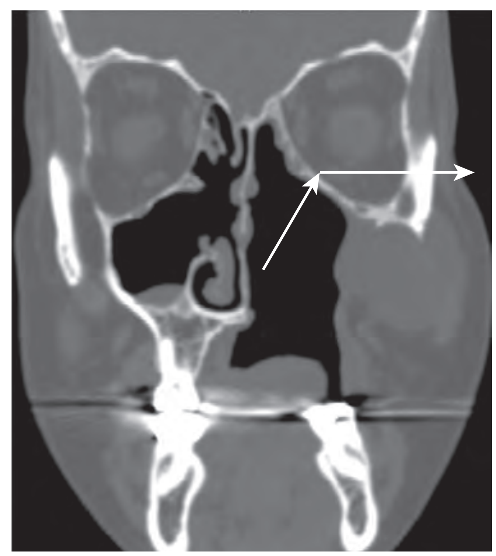

Figure 17.174 Coronal view computed tomography in bone windows shows the plan of resection of the lateral orbital wall and the floor of the orbit.

patient's preoperative appearance, planned modified Weber-Ferguson incision, and ultimate aesthetic result of this modification of skin incision gave an excellent outcome (Fig. 17.172). Three years following surgery, however, the patient developed local recurrence involving the undersurface of the zygoma in the masticator space. A T1 postcontrast magnetic resonance imaging (MRI) scan showed the tumor confined to the masticator space and extended to involve the zygoma (Fig. 17.173). A coronal view CT scan in bone windows shows the planned extent of resection of the recurrent tumor, including the zygoma, lateral floor of the orbit, and lateral orbital wall (Fig. 17.174). The extent of resection is demonstrated on a skull (Fig. 17.175). The extent of bone resection and the plastic flange guides to make the bone cuts are shown on the computer model in Fig. 17.176. The planned bone cuts on the fibula are shown in a diagram, and the plastic flange guides to make the bone cuts on the fibula free flap are also shown in Fig. 17.177. The CAD-CAM model of planned reconstruction shows the osteotomized segments of the fibula free flap with the fixation plate in position (Fig. 17.178). A lateral view of the CAD-CAM model shows the position of the fibula free flap and the location of dental implants so as not to conflict with the fixation screws for the fibula free flap (Fig. 17.179).

The surgical procedure required elevation of the cheek flap through the scar of the previously employed modified Weber-Ferguson incision (Fig. 17.180). Circumferential mobilization

Figure 17.175 Extent of resection outlined on a skull.

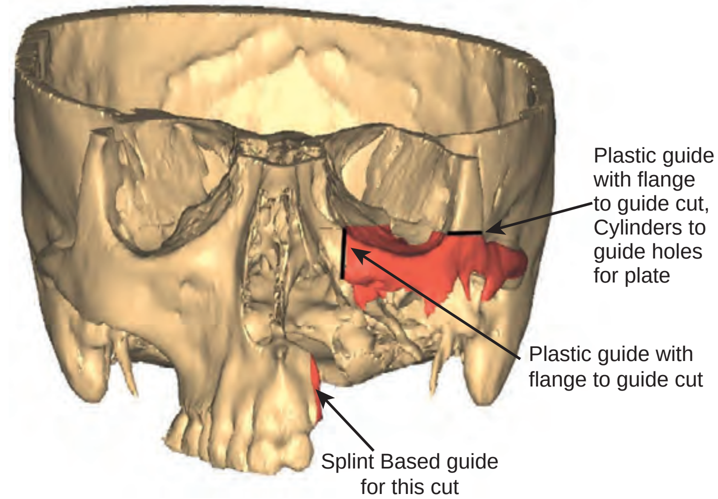

Figure 17.176 Computer model showing the extent of bone resection and the positions of plastic flange guides for bone cuts.

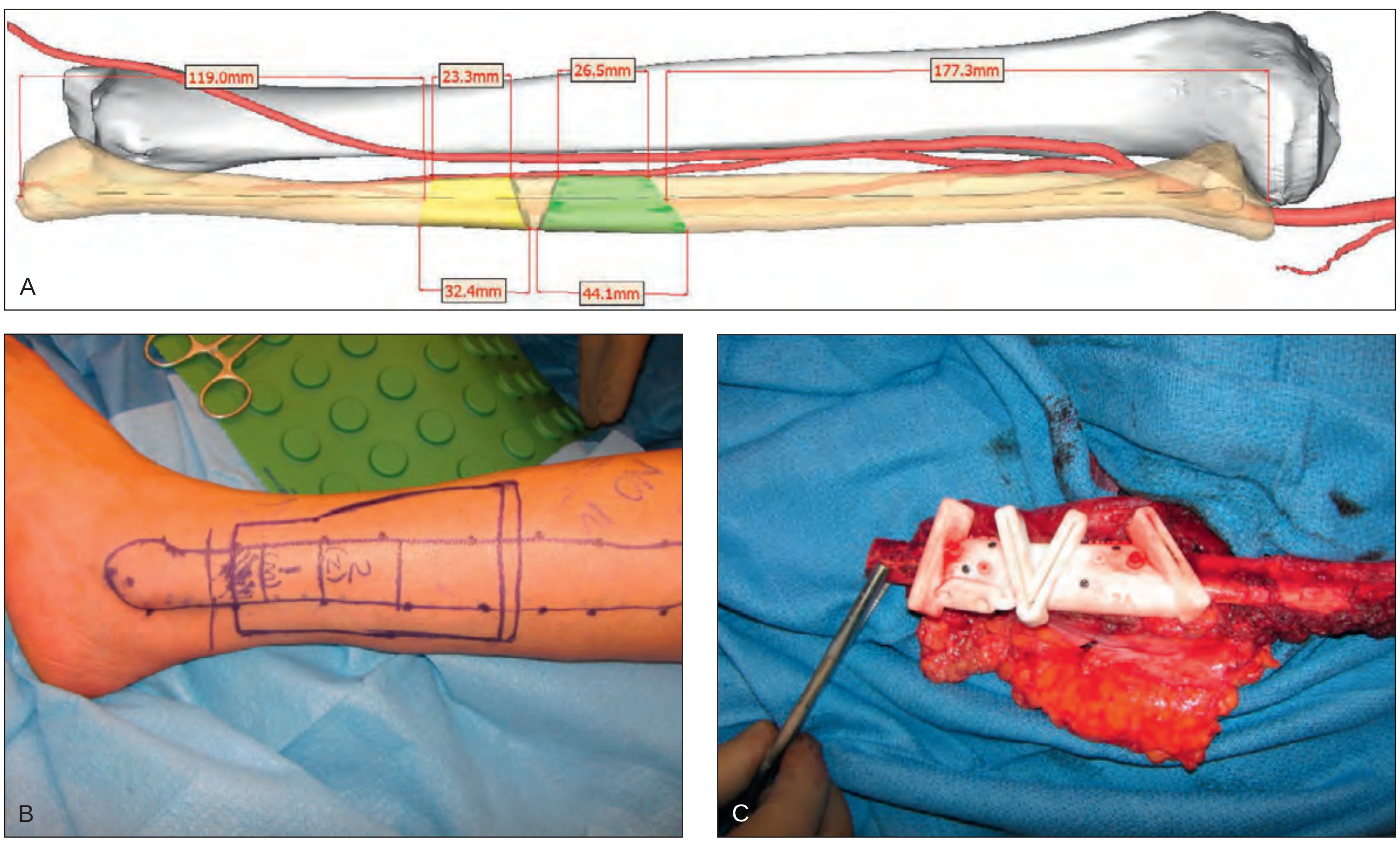

Figure 17.177 Computer-aided design/computer-assisted manufacturing (CAD/CAM)-guided bone cuts (**A**) on a model, drawn on the patient (**B**), and plastic flange guides to make the osteotomies (**C**).

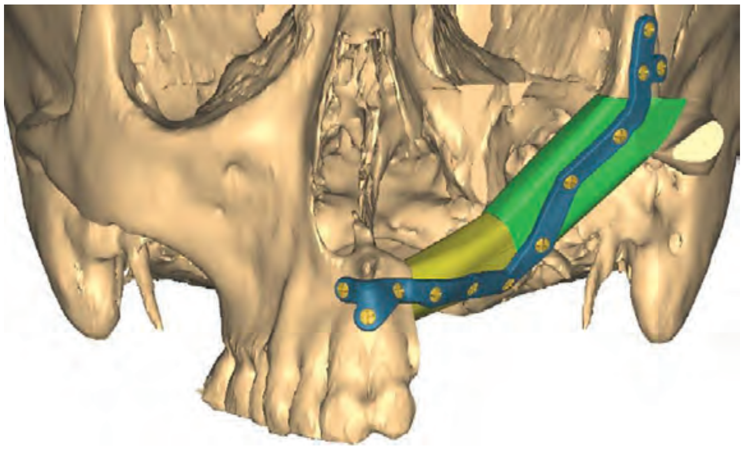

Figure 17.178 A computer-aided design/computer-assisted manufacturing model of the proposed fibula free flap reconstruction and the fixation plate.

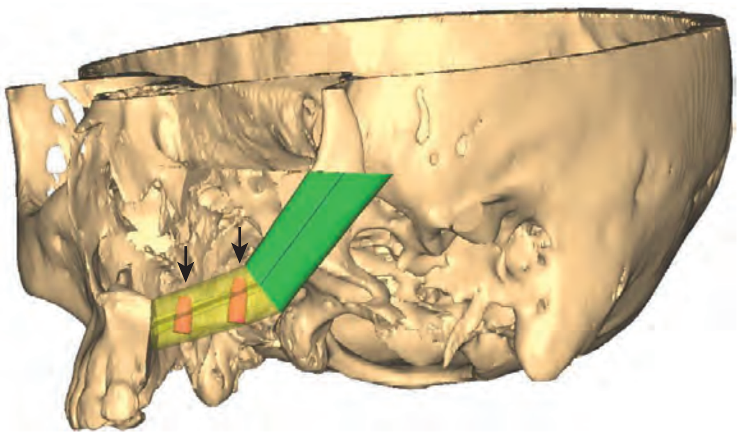

Figure 17.179 A lateral view of the computer-aided design/computer-assisted manufacturing model shows the positions for placement of dental implants (*arrows*) so as not to conflict with fixation screws of the metallic plate.

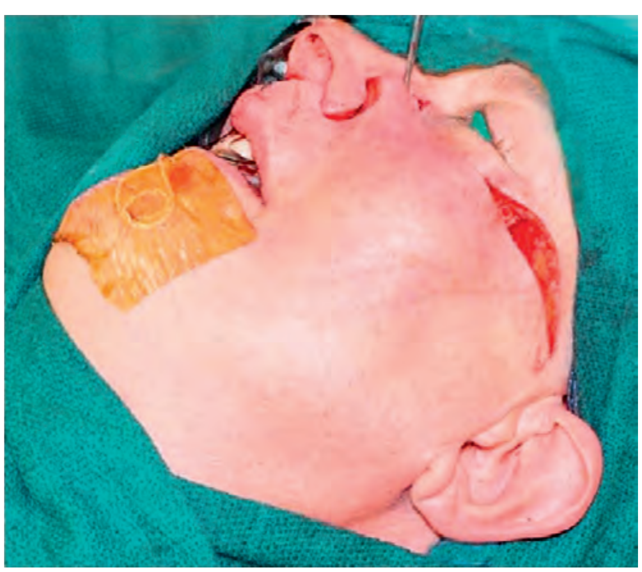

Figure 17.180 A cheek flap elevated through the modified Weber-Ferguson incision.

Figure 17.181 The tumor is circumferentially mobilized after osteotomies of the orbital walls and zygomatic arch guided by the plastic flanges of a computer model.

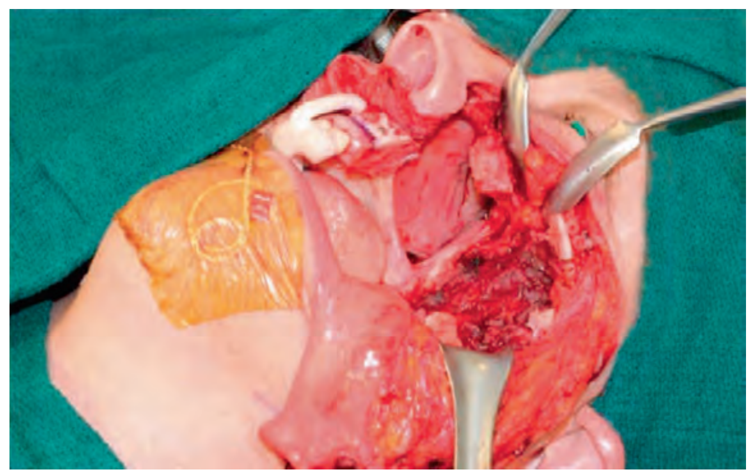

Figure 17.182 The surgical field after removal of the specimen shows the computer-aided design/computer-assisted manufacturing guide planes at recipient bone sites.

of the tumor to achieve a monobloc resection required osteotomies in the lateral wall of the orbit, floor of the orbit, and the zygomatic arch guided by the plastic flanges. The surgical field shows completed osteotomies with the mobilized tumor in situ (Fig. 17.181). The surgical defect and the previously fabricated plastic guide planes on the lateral wall of the orbit and premaxilla are seen in Fig. 17.182. These will guide the surgeon for accurate apposition of the fibula free flap to the recipient bone sites. The composite fibula free flap is fabricated in its preplanned shape at the donor site. The metallic plate holds the osteotomized segments in accurate position (Fig. 17.183A). The prefabricated composite flap is now transposed to the recipient site, and the bone segments are anchored to the recipient bone ends (Fig. 17.183B). The soft-tissue component of the flap is rotated over to cover the bone and the metallic plate. The skin island is positioned to close the defect in the palate (Fig. 17.184). Postoperative 3D reconstruction of the

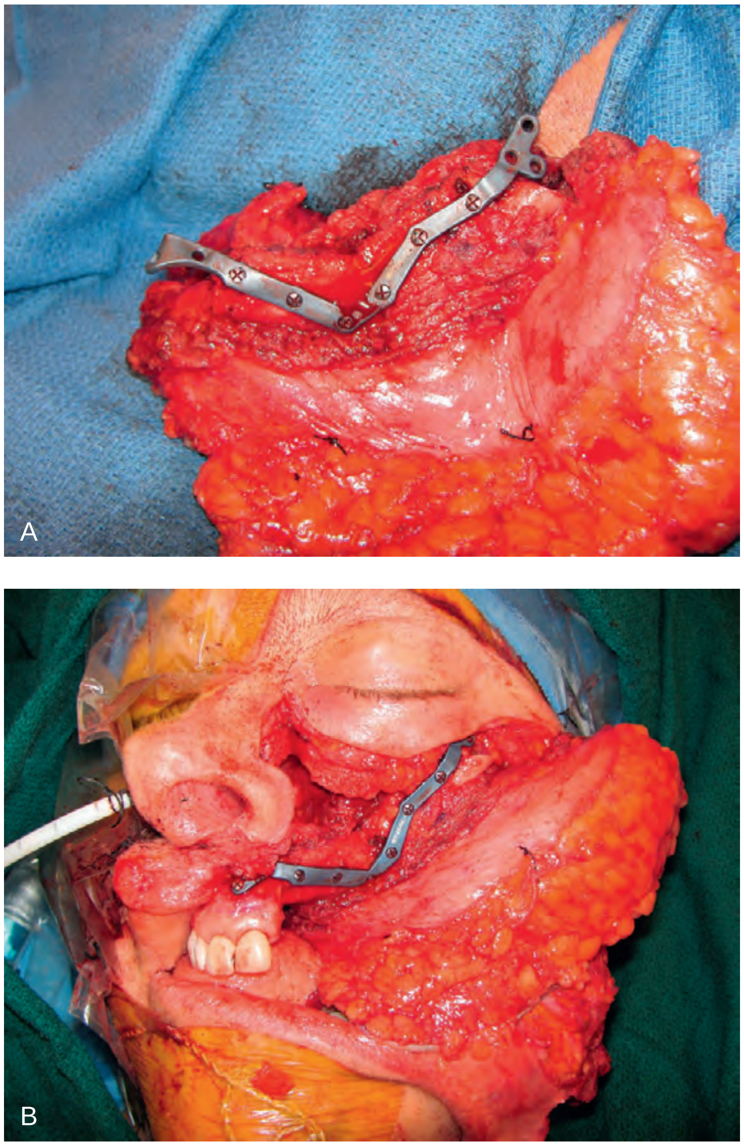

Figure 17.183 **A**, The preplanned fibula free flap is fabricated at the donor site and the bone segments are held in position with the metallic plate. **B**, The composite flap is transposed to the recipient site.

Figure 17.184 Soft tissue of the composite flap is rotated to cover the bone and the metallic plate, and the skin island is positioned to cover the defect in the palate (*arrow*).

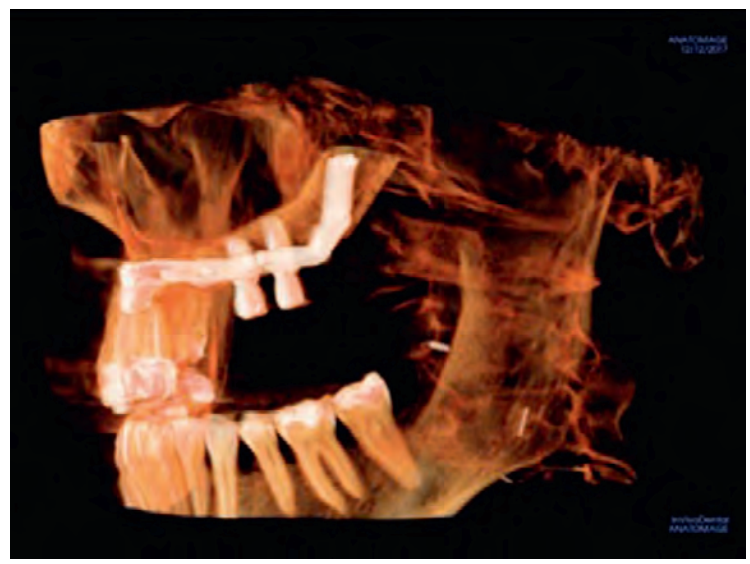

Figure 17.185 Postoperative three-dimensional reconstruction of the cone-beam computed tomography scan shows the position of the flap and dental implants.

cone-beam CT scan shows perfect alignment of the bone flap and the dental implants (Fig. 17.185). The postoperative appearance of the patient 1 month following surgery shows primary healing at all sites with excellent restoration of facial contour and minimally visible surgical scar (Fig. 17.186). Edema of the lower eyelid will subside over the next few months. The intraoral view shows complete closure of the palatal defect (Fig. 17.187). This patient will receive postoperative radiation therapy, and the dental implants will be exposed following recovery from radiation therapy for placement of crowns.

Figure 17.186 The postoperative appearance of the patient 6 weeks following surgery shows excellent restoration of the facial contour.

Figure 17.187 Intraoral view of the patient 6 weeks following surgery showing complete closure of the palatal defect.

CHAPTER 18



Oncologic Dentistry, Maxillofacial Prosthetics, and Implants

Patients in need of treatment for head and neck or oral tumors, whether benign or malignant, require a multidisciplinary team approach, including the head and neck surgeon, prosthodontist, dental oncologist, speech and language pathologist, radiation oncologist, medical oncologist, highly skilled nursing, dieticians, psychiatrists/psychologists, and nurse navigators to coordinate their care. The expertise and collaboration of these individuals can greatly contribute to quality of life issues, such as eliminating or decreasing the intensity of dental disease and/or complications of cancer treatment, along with restoration of oral defects and facial deformities. Maxillofacial prostheses can rehabilitate compromised function after surgical resection of structures essential for speech, mastication, and swallowing nearly to a presurgical level, thus restoring the patient's life. Similarly, prostheses can effectively improve the facial appearance of patients who have undergone major resections such as a rhinectomy or an orbital exenteration, allowing patients to face their family, friends, and the working world with confidence that life after cancer is no different than before the diagnosis.

EVALUATION OF PATIENTS UNDERGOING RADIATION AND/OR CHEMOTHERAPY

Patients planned for nonsurgical treatment, such as radiation and/or chemotherapy, should be evaluated by a dental professional before treatment to screen for potential sources of dental infection. Such sources of dental infection are extensive dental caries, periapical pathology, and periodontal disease, which should be treated before initiating cytotoxic treatment. Ideally, a period of at least 2 weeks should be permitted for soft-tissue healing following dentoalveolar surgery so that mucosal integrity is restored before commencement of oncologic treatment. It must be emphasized that dental extraction in the proximity of the tumor opens up a route for invasion through the bony cortex and thus should be avoided. Additionally, subsequent bleeding through this route can be challenging to manage and should therefore be avoided unless a management strategy has been determined.

The initial dental evaluation of the patient is focused to establish a baseline against which subsequent examinations can be compared. Measures to enhance and maintain oral hygiene are explained to the patient and must be reinforced during and after treatment (Table 18.1). It is critical that the patient fully understand that their hygiene from this point on must be impeccable, and the use of fluoride supplementation, either through dentifrice or otherwise, and other anticariogenic supplements is crucial to the maintenance of the health of their teeth. Additionally, these measures are critical to avoid rampant caries in a hyposalivating patient following radiotherapy. This is equally true for patients taking bisphosphonates, bevacizumab, denosumab, or other bone-stabilizing drugs. Failure to comply with these treatment recommendations increase the likelihood of the patient experiencing undesirable treatment complications, which may include osteonecrosis of the jaw secondary to dentoalveolar surgery (e.g., dental extractions, gingival surgery, dental implants, etc.). The patient's awareness and compliance, along with appropriate counseling and motivation, are crucial to the success of preventive dental strategies and should be reiterated by the entire team of caregivers and documented well for the protection of all involved.

The mucosal surfaces of the oral cavity are exposed to significant doses of radiation therapy during treatment of most tumors except those of the larynx, hypopharynx, and thyroid. Inclusion of the upper neck (i.e., levels I and II) in the radiation portals also places the oral cavity at risk. When examining patients before radiation therapy, whether as single modality or in the postoperative setting, the age, diagnosis, fields, and prescription of radiation should be taken into consideration before making dental treatment recommendations. The effects of radiation on the dentition, periodontium, and mucosal surfaces are listed in Table 18.2. Indirect effects on these structures also can result from exposure of the parotid and submandibular glands to radiation, with consequent alteration of saliva production. Lastly, it is important to remember that patients who are planned for radioactive iodine (RAI) treatment should be seen for dental screening before therapy as well. RAI treatments can have a profound effect on the salivary glands, and

Table 18.1 Self-Care Instructions for Patients to Enhance and Maintain Oral and Dental Hygiene

- Floss daily.
- Brush teeth after *every* meal, including liquid nutritional supplements.
- Gargle frequently with salt and baking soda solution, especially after every meal.
- Use neutral sodium fluoride gel/paste at least once daily, preferably before bed.

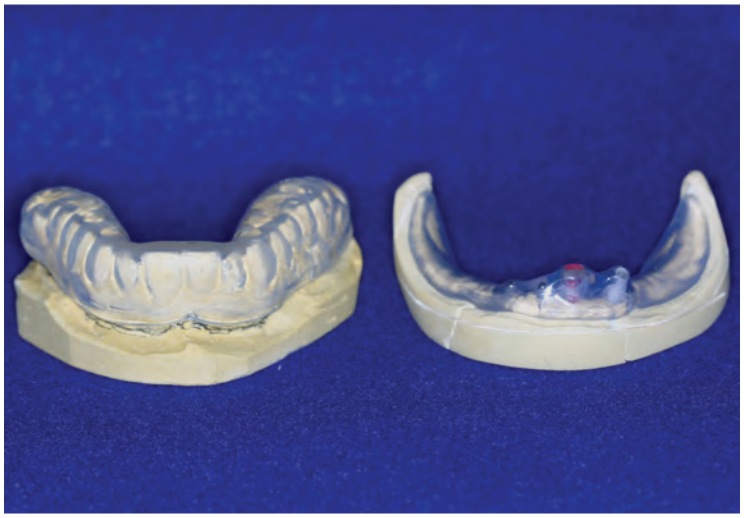

Figure 18.1 Customized mouthguards for a dentate patient (*left*) and an edentulous patient with implants (*right*).

Table 18.2 Acute and Long-Term Effects of Radiation on the Oral Cavity

ACUTE SIDE EFFECTS	LONG-TERM SIDE EFFECTS
Mucositis	Xerostomia
Dysgeusia	Caries
Dysphagia	Periodontal disease
Ropey saliva	Trismus
	Osteoradionecrosis

Table 18.3 Indications for Dental Extraction Before Radiation Therapy

- History of generalized poor dental compliance indicated by poor oral hygiene and multiple missing or decayed teeth
- Nonrestorable dental caries
- Advanced/symptomatic periodontal disease, especially with bone loss, mobility,root furcation involvement
- Residual root tips not fully covered by alveolar bone
- Symptomatic impacted or incompletely erupted teeth not fully covered by alveolar bone

the secondary effect of this xerostomia can be devastating to the teeth.

Patients who have extensive metallic restorations, including restorations made of zirconia that appear tooth colored, require custom mouthguards to reduce scatter that causes mucositis in the surrounding tissues (Fig. 18.1). These guards should be fabricated in time for them to be delivered before the radiation simulation appointment. Table 18.3 lists the indications for dental extraction in patients who are scheduled to undergo radiation therapy. As previously mentioned, all extractions should be completed in time for mucosal healing to occur. If possible, the mucosa of the gingiva at the extraction site should be closed with sutures.

The general practicing dentist and hygienist can use the interval between the initial screening appointment and commencement of radiation therapy to complete oral hygiene procedures such as scaling, polishing, subgingival root planning, and curettage. Overhanging and faulty restorations can be removed and replaced as needed, and ill-fitting dentures should be corrected.

Home care should include effective daily plaque removal and use of soft toothbrushes with application of a fluoridated dentifrice. Factors such as the type of fluoride used or the modality of its application are less important to outcome than is daily compliance in using high-potency fluoride for the remainder of the patient's life. Patients are instructed to floss daily and brush their teeth after every meal, which includes liquid supplements, because they contain cariogenic carbohydrates. A toothpaste or gel that contains neutral 1% sodium fluoride is preferred over stannous fluoride, which has an unpleasant taste and adverse effects such as sensitivity of the teeth and gingiva. The toothpaste can be used with a brush every night for 2 minutes; the patient may expectorate as much as desired but should not rinse, thus leaving a thin film of fluoride on the teeth while sleeping.

Although commonly used chemotherapeutic agents such as cisplatin, 5-fluorouracil, and methotrexate have the potential to cause acute mucositis on their own, their combination with each other and/or with radiation therapy can result in treatment-limiting stomatitis. Current regimens for the treatment of head and neck cancer in general result in less severe oral complications than those seen with treatment of hematologic disease. Chemotherapy-related adverse effects can include mucositis and ulceration, oral candidiasis, and bacterial and/or viral infections of the oral mucosa. In addition to their direct effects, these problems can cause a severe reduction in dietary intake with all the sequelae of malnutrition. As with patients scheduled to have radiation therapy, these patients also should be evaluated at least 2 weeks before chemotherapy is begun. The review should include a discussion of the hematologic status, that is, total white blood cell and neutrophil count, platelet counts, and clotting parameters. The patient is carefully screened for potential sources of bacteremia such as periodontal disease, and appropriate therapy is undertaken if needed. Endodontic treatment or dental extractions are considered for symptomatic teeth with periapical lesions, and third-molar pathology is addressed. As previously described, patients are instructed regarding home care hygiene and caries control. Oral hygiene during treatment should include frequent rinsing with a salt and baking soda solution and brushing of the teeth.

Patients with very advanced cancer may be managed less aggressively, keeping their overall status and prognosis in mind. Asymptomatic teeth may be retained and managed conservatively even in the presence of active chronic dental disease. Abutment teeth for a removable prosthesis should be preserved if possible. Definitive restorations with crowns, fixed bridges, and onlays for control of carious teeth may be delayed until completion of treatment and provisionally restored with use of intermediate restorative material.

MANAGEMENT OF LONG-TERM ADVERSE EFFECTS OF RADIATION THERAPY

Xerostomia is probably the most common long-term sequela of radiating the oral cavity. The severity of xerostomia depends on the total dose of radiation, the source, the fractionation, and the portals of delivery. Radiation results in atrophy of salivary glandular elements, causing cessation of saliva production. The problem is compounded if the patient receives chemotherapy concomitantly with radiation. Anecdotally, patients who have undergone RAI can have profound xerostomia and should thus be evaluated and managed as appropriate.

Apart from the adverse impact on quality of life because of difficulty with eating, oral comfort, fit of prostheses, and speech, xerostomia also increases the risk of caries, periodontal disease, and ultimately osteoradionecrosis (ORN) if the extent of tooth breakdown leads to extraction. Pharmacologic agents such as

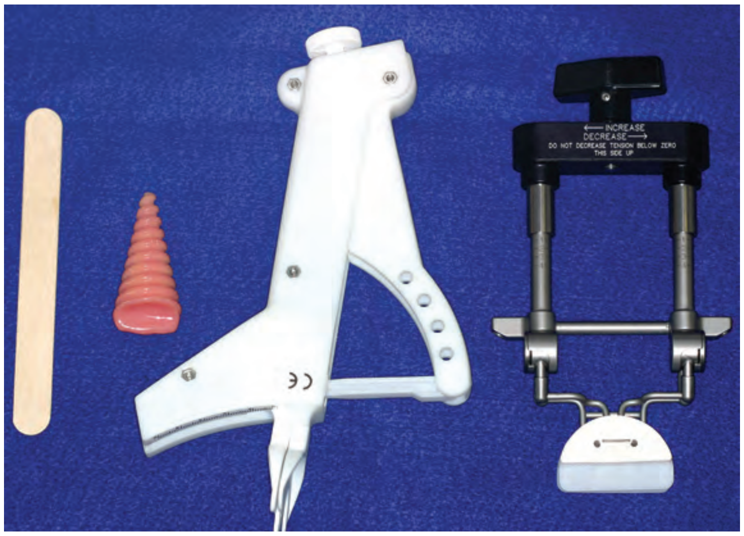

Figure 18.2 Devices for prevention of trismus. Left to right: tongue blades taped together in a stack, an acrylic resin "corkscrew," a Therabite, and a Dynasplint.

Figure 18.3 An intraoral view of a patient with osteoradionecrosis of the mandible.

pilocarpine and amifostine have been investigated with mixed results for relief of xerostomia. However, most patients obtain symptomatic relief through frequent use of water.

Other long-term sequelae are related to effects on soft tissue, bone, or blood vessels. Irradiation of the muscles of mastication can produce fibrosis that leads to trismus over time. Regular stretching exercises of these muscles can mitigate the effects of this complication. Patients should begin to perform these exercises before radiation therapy commences, and if the exercises are stopped during treatment, they must be resumed as soon as the acute side effects of radiation therapy have subsided. The exercises should be performed in multiple cycles throughout every day and can be assisted with appliances such as an acrylic resin corkscrew, tongue depressors taped together, or a commercially available device (Fig. 18.2). Alternatively, patients may be instructed to use their thumb and fingers to forcefully open the mouth to the point of tolerance. It is crucial for the clinician to reinforce the importance of preventing trismus at every opportunity, because difficulty in opening the mouth not only affects quality of life but also interferes with adequate post-treatment monitoring for recurrent or new cancer and providing routine dental care.

The risk for ORN of the jaw increases if the bone is irradiated with more than 55 Gy. The mandible is more commonly affected because of endothelial damage to the relatively sparse intraosseous blood vessels. The maxilla has a richer blood supply, and therefore ORN of this bone is less common. The process can take many months or even years to develop, and patients are at risk for the development of ORN for the remainder of their lives. Bone exposure or exposed retained roots are a common cause for initiation of ORN (Fig. 18.3). Dental caries and periodontal disease leading to extractions are the most common inciting factors. A series of computed tomography (CT) images of a patient who experienced ORN of the mandible after dental extraction in a previously irradiated mandible is shown in Fig. 18.4. However, a third of ORN cases occur spontaneously. Prevention of this complication by rigorous oral hygiene is crucial, because conservative measures such as antibiotics, debridement, and curettage are effective only in early disease. Advanced ORN of the mandible with exposed intraoral bone generally requires segmental resection and reconstruction.

The role of hyperbaric oxygen (HBO) in the management of ORN is controversial. It is important for the clinician to

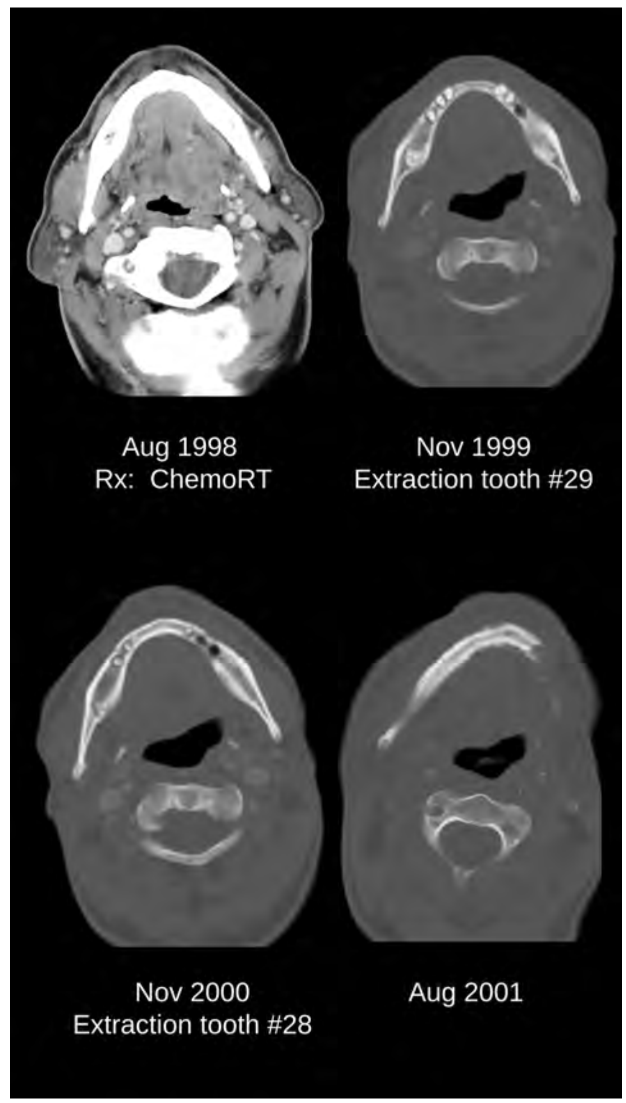

Figure 18.4 Serial computed tomography scans showing the initiation and progression of osteoradionecrosis after dental extraction.

realize that HBO cannot revitalize dead, necrotic bone, for which the only definitive remedy is a sequestrectomy. The major concern in using HBO for ORN revolves around whether replenishing oxygen in the affected tissues can lead to activation of cancer cells that otherwise were dormant. Although no systematic study of this question and other questions regarding the use of HBO in patients with ORN has been conducted,

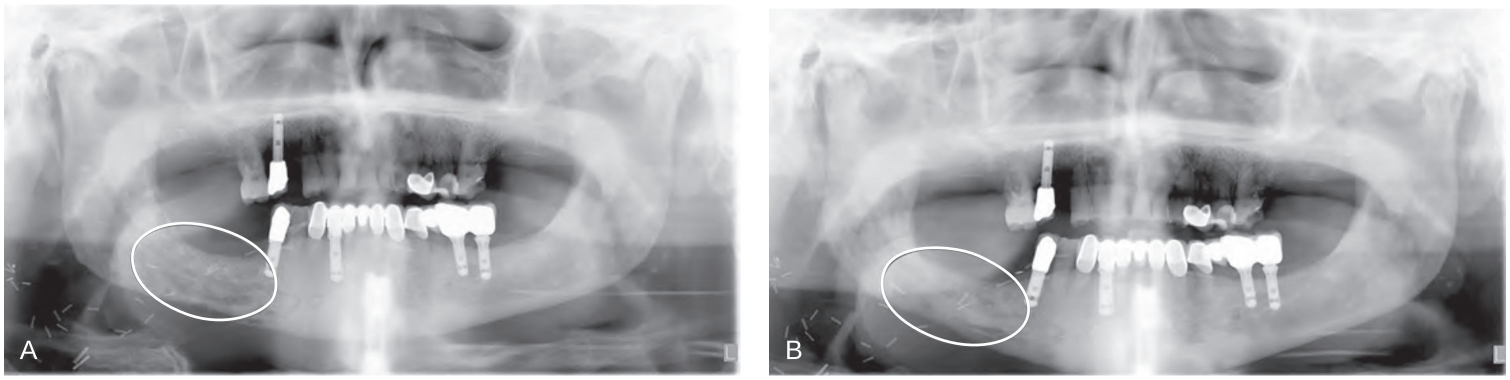

Figure 18.5 **A**, A panoramic radiograph of a patient with osteoradionecrosis of the jaw before pentoxifylline treatment. **B**, A panoramic radiograph of same patient 2 years later after pentoxifylline treatment, with an increase in bone density and fill of the defects.

anecdotal instances of the reactivation of a tumor in this setting certainly exist. Therefore HBO should be used with caution, especially if any doubt exists about the cancer status of the patient. There are increasing reports of the successful use of pentoxifylline and alpha-tocopherol for management of both ORN and MRONJ (medication-related osteonecrosis of the jaws). Pentoxifylline has been long used for the treatment of intermittent claudication. Pentoxifylline increases blood flow to the affected microcirculation. Alpha tocopherol is used for its antioxidant properties. Although the precise mechanism of action is not well defined, blood viscosity is lowered, erythrocyte flexibility is increased, leukocyte deformability is increased, and neutrophil adhesion and activation are decreased. Overall, tissue oxygenation is significantly increased. Because of its interaction with antiplatelet and anticoagulant medications, the use of pentoxifylline in patients taking such drugs should be discussed with the patient's physician. Although there have not been large-scale studies on the effectiveness of pentoxifylline/alpha-tocopherol in the treatment of ORN/MRONJ, current reports appear promising (Fig. 18.5).

MAXILLOFACIAL PROSTHETICS

Maxillofacial prosthetic rehabilitation forms an integral component of a comprehensive treatment program for patients undergoing surgical resection of head and neck cancer. The common goals of rehabilitation are restoration of speech, mastication, and swallowing; control of saliva; and restoration of facial deficits. Preoperative communication and discussion between the head and neck surgeon and the prosthodontist is crucial for optimal planning and achievement of a good functional and aesthetic outcome at various stages of treatment (Table 18.4). The head and neck surgeon should be aware of the functional sequelae from loss of the structures being resected so that the patient's rehabilitation is planned even before the actual surgical procedure is undertaken. The use of diagnostic records, either from direct dental impressions or digital three-dimensional images, can greatly aid both the surgeon and prosthodontist in treatment planning.

Maxillary Defects and Obturators

Surgical resection of the palate and/or maxilla can result in functional and cosmetic sequelae, depending on the dimensions and location of the defect (Table 18.5). Prosthodontic rehabilitation of patients with palatal defects is based on the principle of reestablishing the separation between the oral and nasal cavities so that normal speech and swallowing can be restored. In addition, the maxillary obturator prosthesis improves the cosmetic appearance of the patient by providing support for the upper lip and cheek.

Successful fabrication of a functional maxillary obturator is based on the principles of retention, stability, and support. The head and neck surgeon should be familiar with several important issues that are relevant to palatal resection in order to maximize functional outcome (Table 18.6). Specifically, retention of as much hard palate/alveolus as possible, sparing as many teeth as possible, the use of skin grafts to provide adequate tissue beds to support the prosthesis, and the placement of implants at the time of resection will facilitate a more favorable prosthetic outcome. Conventionally, patients are rehabilitated in phases

Table 18.4 The Role of the Maxillofacial Prosthodontist in the Rehabilitation of Head and Neck Surgical Patients

Preoperatively
- Impression for surgical obturator
- Evaluation of patients undergoing segmental mandibular resection and reconstruction
- Evaluation for extraoral prostheses

Intraoperatively
- Placement of surgical prostheses/obturator
- Intermaxillary fixation for free flap mandible reconstruction
  - Placement of dental implants
  - Dental extractions

Early Postoperative Period
- Interim maxillary prosthesis
- Speech bulb prosthesis
- Palatal augmentation prosthesis

Late Postoperative Period
- Definitive maxillary prosthesis
- Mandibular resection prosthesis
- Lingual splint for unstable mandibulotomy
- Osseointegrated implants
- Fabrication of facial prosthesis

Table 18.5 Common Sequelae of Surgical Resection of the Palate and Maxilla

- Hypernasality and unintelligible speech
- Difficulty chewing
- Difficulty swallowing
- Nasal regurgitation
- Desiccation of nasal mucous membranes
- Difficulty controlling nasal and/or sinus secretions
- Facial disfigurement

Figure 18.6 An intraoral view of squamous cell carcinoma of the hard palate.

Figure 18.7 A panoramic radiograph before a maxillectomy demonstrates the need for planning to section dental bridges and determine the location of implants.

Table 18.6 Modifications in Surgical Technique That May Enhance the Functional Outcome of Palatal Rehabilitation

- Split-thickness skin grafting of maxillary defect
    - Provides keratinized surface to support prosthesis
    - Scar contracture forms undercut to provide lateral support
- Keratinized mucosal coverage of medial cut margin of hard palate
    - Preserves portion of medial palatal mucosa if possible
    - Mucosal coverage decreases ulceration at this margin and increases comfort and usability of prosthesis
- Retain as much premaxilla as possible
    - Provides better support and increases retention of prosthesis
- Place bony resection lines through socket of an extracted tooth that will be sacrificed in the resection
    - Avoids exposure and loss of retained adjacent teeth
- Resect any posterior, nonfunctioning band of soft palate
    - Prevents access to the nasopharynx for effective obturation

to accommodate for healing and configurational changes of the defect. The maxillary obturator prostheses that are used during these phases are termed *surgical, interim,* and *definitive* obturator prostheses.

The maxillofacial prosthodontist evaluates the patient before surgery to obtain impressions and participates in surgical planning of the resection for the surgical obturator (Figs. 18.6 and 18.7). When possible, the head and neck surgeon will mark the anticipated margins of resection on the dental cast (Figs. 18.8 and 18.9). The maxillary surgical obturator usually is fabricated from polymethyl methacrylate acrylic resin and is sterilized for use in the operating room at the completion of the surgical resection. Intraoperatively, the surgical obturator is ligated to the remaining teeth by threading 24-gauge prestretched stainless steel wires between the teeth or, in the edentulous patient, through the alveolar ridge and palatal shelf (Figs. 18.10 and 18.11). If the patient is edentulous, endosseous implants can also be placed to aid in retention and stability of the interim maxillary obturator (Figs. 18.12 through 18.14).

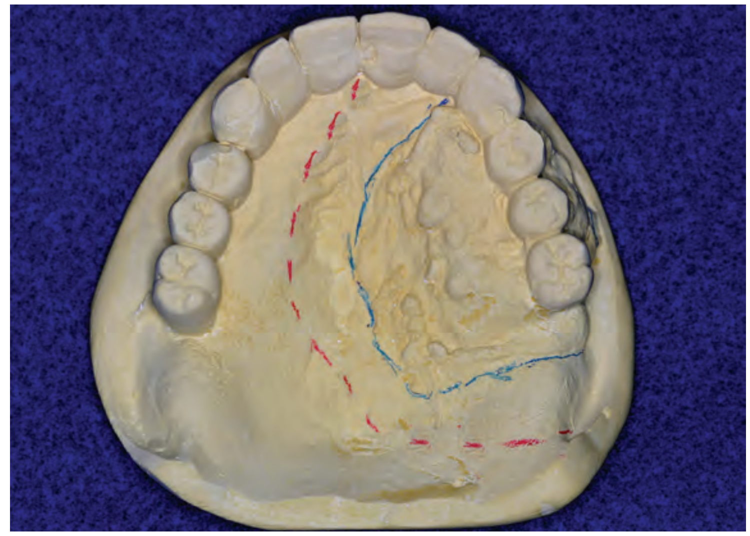

Figure 18.8 A cast with proposed margins outlined by a surgeon.

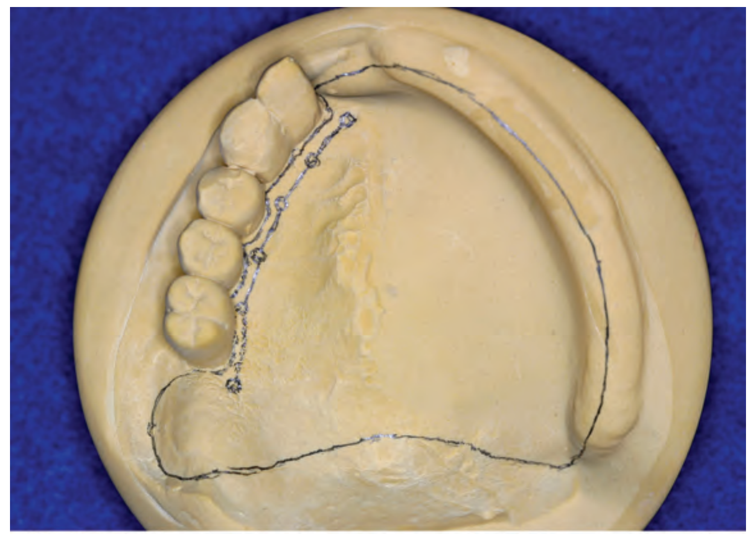

Figure 18.9 A cast prepared for the fabrication of a surgical obturator.

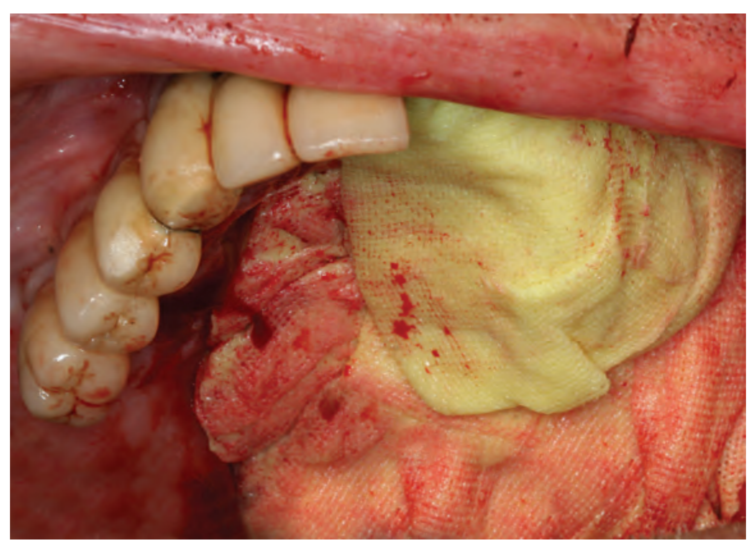

Figure 18.10 An intraoperative view of packing after a maxillectomy.

Figure 18.11 An intraoperative view of a surgical obturator wired into place.

Figure 18.12 Mini dental implants (MDI, IMTEC Corp., Ardmore, OK) with O-ball and straight wall attachments.

Figure 18.13 The early postoperative view of a patient who had two mini dental implants placed at the time of a maxillectomy.

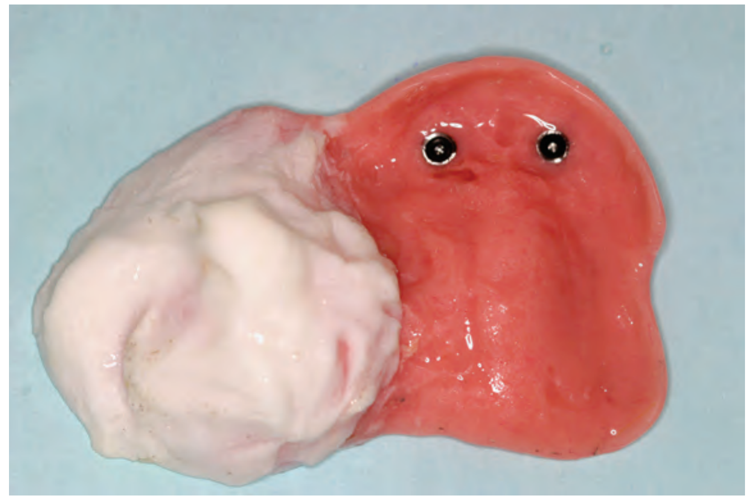

Figure 18.14 An interim obturator with O-rings to fit the implants for improved stabilization.

Figure 18.15 An interim obturator demonstrating conventional clasps around the remaining teeth.

The surgical obturator provides support for the surgical packing, isolates the wound from contamination, and allows the patient to speak and swallow so that nasogastric tube feeding generally is not necessary. The surgical obturator is kept in place until the packing is ready to be removed in about 7 to 10 days after surgery and is replaced immediately with an interim maxillary obturator prosthesis. If the maxillofacial prosthodontist is not present at the time of surgery to place the surgical obturator, it is imperative that the head and neck surgeon verifies the extent of resection and teeth removed for accurate fabrication of the interim prosthesis. This prosthesis may bear teeth and a flange for supporting the lip and cheek and is held in place by wrought-wire clasps that engage the remaining teeth and/or the implants placed at the time of resection (Fig. 18.15). The obturator portion of the prosthesis is fashioned with use of a soft resilient lining material around the defect, and as healing progresses and the configuration of the defect changes, the obturator is relined every other week for the first 6 to 8 weeks after surgery (Fig. 18.16).

Once healing is complete, usually about 4 to 6 months after surgery, a definitive maxillary obturator can be fashioned. Patients treated with postoperative radiation therapy may need to wait longer for the defect to stabilize. The definitive obturator should extend as high as possible along the lateral wall of the

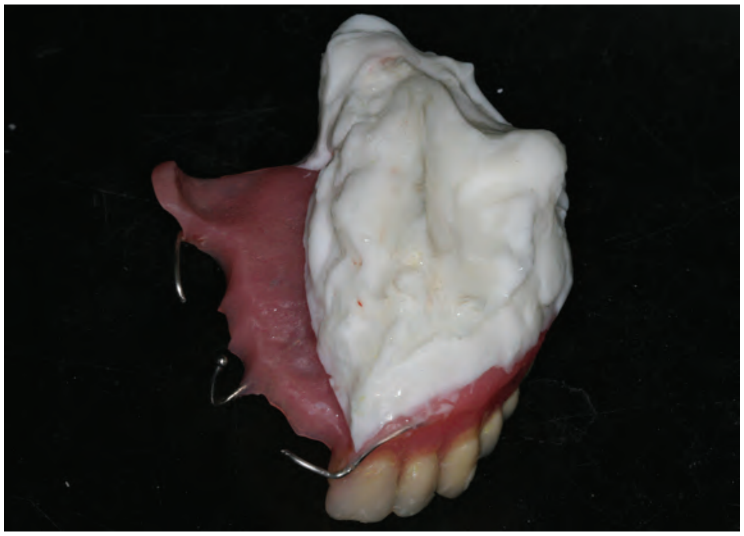

Figure 18.16 An interim prosthesis with the obturator portion formed from resilient lining material (which appears white).

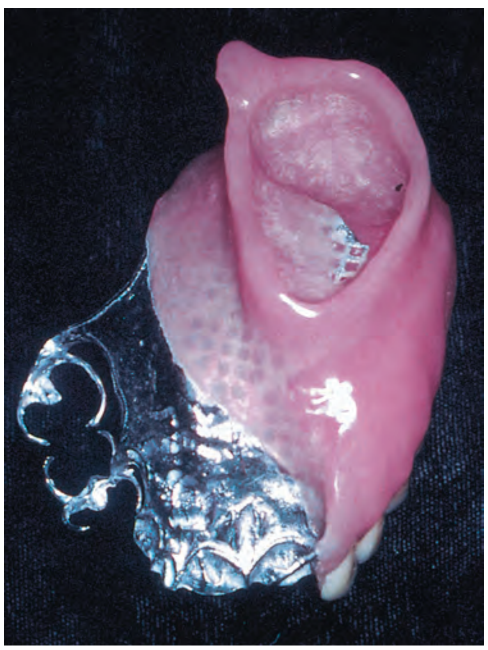

Figure 18.17 A definitive obturator fabricated from a cast alloy framework and acrylic resin.

defect to provide maximum stability and retention (Fig. 18.17). At this stage, if conventional two-piece implants have osseointegrated, the process for designing attachments that will retain or support the maxillary obturator prosthesis will commence. The implants will provide a superior physical attachment, especially in edentulous patients, allowing the definitive obturator to have maximum retention, stability, and function. A well-healed maxillary defect lined with a skin graft (Fig. 18.18) that has been rehabilitated with use of a definitive obturator is shown in Fig. 18.19. Routine care of the prosthesis requires that it be removed several times daily and cleaned with soap and water; in addition, excellent oral hygiene must be maintained for the remaining teeth or implants.

Alternative treatment options beginning with the surgical obturator in brief would be to suture packing in place. If there is no prosthodontic support for an obturator, use gutta percha or layers of polyvinylsiloxane into the defect and form a surgical obturator that doubles as the interim, or place a flap to obliterate the defect altogether. The advantage of suturing the packing to place is ease, less anesthetic time for the patient, and reduced

Figure 18.18 A mature maxillary defect lined with a well-healed skin graft.

Figure 18.19 A definitive obturator results in excellent functional and cosmetic restoration of the patient.

cost. The disadvantage to this alternative is decreased comfort, difficulty in cleaning after meals, and if the packing becomes unraveled it is a potential choking/aspiration risk. The advantage of using layered gutta percha or polyvinylsiloxane is that the defect can be filled completely, thus giving greater control to maintain facial symmetry with complete support of the lateral wall of the defect. The disadvantages to this alternative is longer anesthetic time at tumor ablation, the need to return to the operating room to remove the “custom” packing, and the increased risk of infection, because no seal is airtight, and as this custom packing remains in place for several weeks the risk of postoperative infection increases. Lastly, by obliterating the defect with a flap, the advantage is that the patient does not have a defect that allows leakage. The disadvantage is that the voice may be negatively affected (hyponasal), and flap geometry could make wearing a prosthesis to replace the missing teeth impossible.

Soft Palate Defects and Speech Bulb Prostheses

Restoration of function after resection of soft palate tumors is one of the most challenging intraoral situations that will confront a maxillofacial prosthodontist. Surgical excision of a part of or the entire soft palate (Fig. 18.20) alters normal palatopharyngeal closure, causing hypernasal speech and nasal regurgitation. A speech aid obturator (Fig. 18.21) allows palatopharyngeal closure in these patients by allowing the lateral and posterior walls of the nasopharynx to contract against the prosthesis (Fig. 18.22). The obturator therefore must be sized appropriately to allow unimpeded nasal breathing and should not interfere with the tongue during swallowing and speech.

The patient is referred before surgery and evaluated, and an impression for a surgical obturator is completed. If the surgeon

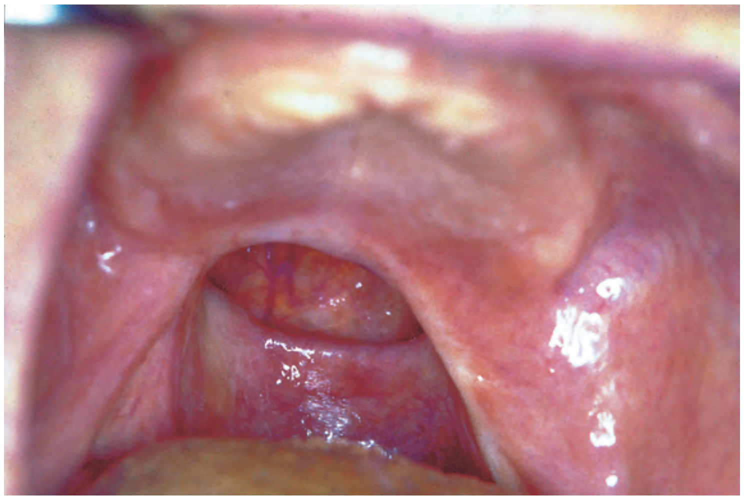

Figure 18.20 A defect of the soft palate.

Figure 18.21 A soft palate speech bulb prosthesis.

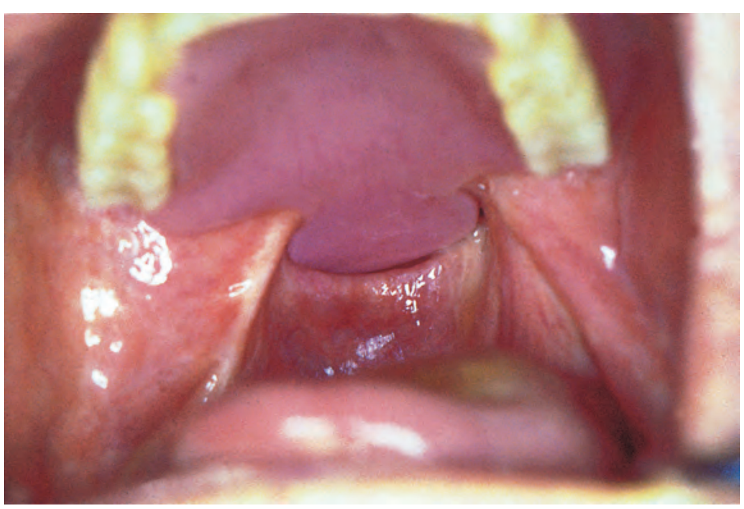

Figure 18.22 Palatopharyngeal closure is achieved when the lateral and posterior walls of the nasopharynx contract against the bulb of the prosthesis.

Figure 18.23 A surgical obturator for soft palate resection.

Figure 18.24 A surgical obturator is wired into place after soft palate resection.

Figure 18.25 A modified cast used after soft palate surgery in preparation for the interim obturator.

does not wish to use a surgical obturator, then fabrication of the interim soft palate prosthesis can be completed for insertion postoperatively at the surgeon's discretion. Figs. 18.23 through 18.28 demonstrate preoperative planning, fabrication of a surgical and interim speech aid, and postoperative insertion. Many soft palate defects are reconstructed laterally with use of a myocutaneous flap, so that the speech aid must be placed posterior and superior to the flap in the nasopharyngeal cavity. It is important to ensure that minimal contact occurs between the flap and the speech aid, which should be shaped and sized to allow the lateral and posterior pharyngeal musculature to contract around it. Although the prosthesis may provide adequate palatopharyngeal closure, the quality of speech is affected by various factors such as the location of the defect, the extent of adjacent

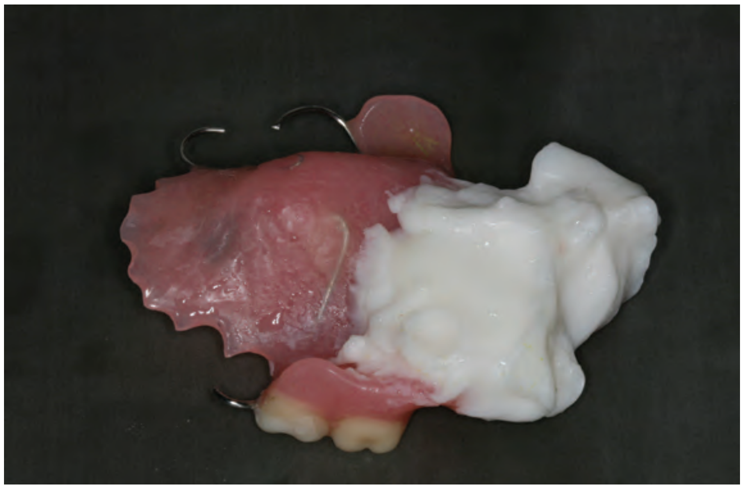

Figure 18.26 An interim soft palate obturator formed from resilient lining (which appears white).

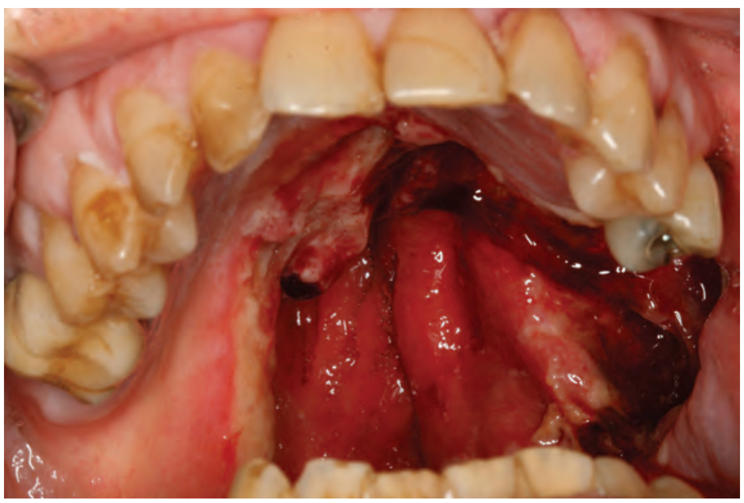

Figure 18.27 Removal of the surgical obturator 1 week after soft palate resection.

Figure 18.28 Placement of the interim obturator with use of a clasp around the remaining teeth.

structures that have been resected, the mode of reconstruction, the amount of fibrosis, the mobility of the tongue, and even the head position. Some of these factors are liable to constant change, and good long-term outcome therefore depends on continued evaluation and modification of the prosthesis.

Figure 18.29 A partially edentulous patient with a soft palate defect.

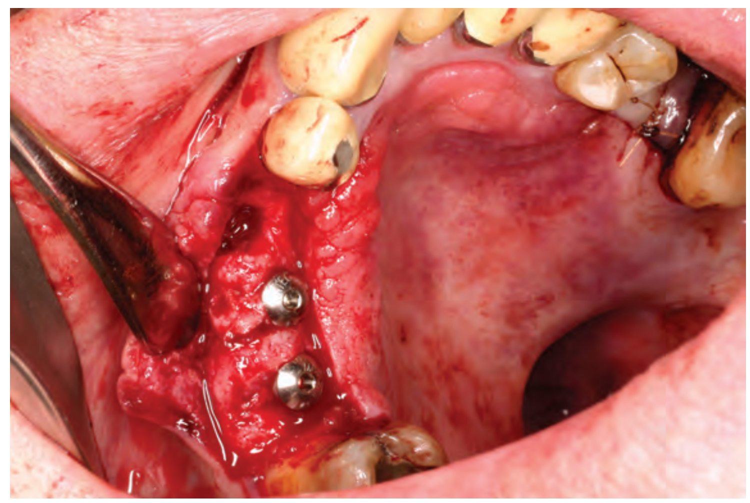

Figure 18.30 Surgical placement of dental implants to retain a soft palate obturator.

Partially dentate and edentulous patients benefit from the use of osseointegrated implants. Dental implants can greatly affect the success of a speech aid by providing a retentive force to counteract the dislodging movement of the functioning pharyngeal sphincter. Figs. 18.29 through 18.34 demonstrate a partially edentulous patient with 75% of his soft palate resected; three dental implants with locator attachments are used to augment conventional clasping in order to thoroughly improve the successful outcome of his speech aid prosthesis. Because implants are directly integrated into the bone, more force can be placed on them compared with natural teeth. Therefore the clasping apparatuses used in the prosthesis can be tighter than those designed for the remaining natural dentition.

The alternative treatment to a prosthesis would be a flap to close the nasopharynx defect. There are several surgeons who promote this, as fabricating and wearing a prosthesis is seen as less than ideal. With several thousand muscle patterns generated by the lateral and posterior walls in conjunction with the soft palate elevation, it is difficult to decide truly which treatment is better. The flap and the prosthesis both provide nearly the same seal when swallowing. The prosthesis however can be adjusted to allow for air flow and swallowing, whereas the flap cannot easily be adjusted without going back to the operating room. Lastly, the surgeon is able to perform direct visual examination of the defect with prosthetic rehabilitation rather

Figure 18.31 An interim soft palate obturator with implant attachments and no clasps.

Figure 18.33 An intraoral view of the implant attachments.

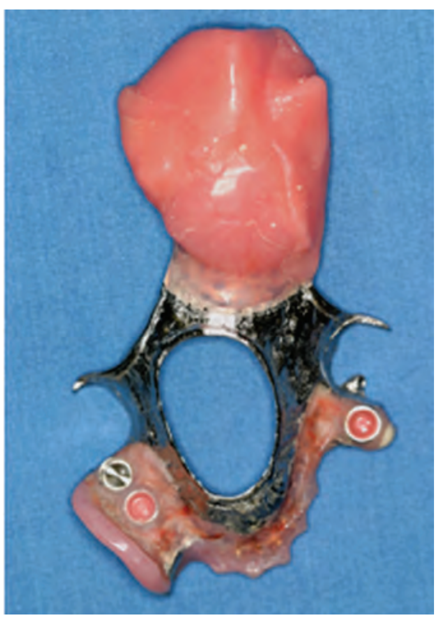

Figure 18.32 A definitive soft palate obturator fabricated from cast alloy and acrylic resin.

Figure 18.34 An intraoral view of the definitive obturator.

than relying on endoscopy and imaging, as is required in the case of the flap reconstruction.

Palatal Augmentation Prostheses for Defects of the Tongue

Surgical resection of the tongue with significant loss of volume and/or mobility produces impairment of both speech and swallowing. Although reconstruction with pedicled or free flaps can restore volume to a certain extent, this reconstruction may not be enough to allow palatoglossal contact in many patients. A palatal augmentation prosthesis provides volume against which the dorsum of the remnant tongue can abut (Fig. 18.35). In dentate patients this prosthesis is retained by the patient's maxillary dentition, and in edentulous patients this prosthesis is retained by the patient's residual maxillary arch. An acrylic resin base is fabricated on the maxillary arch with an inferior extension that abuts against the dorsal surface of the tongue remnant or flap (Fig. 18.36). The approximation or

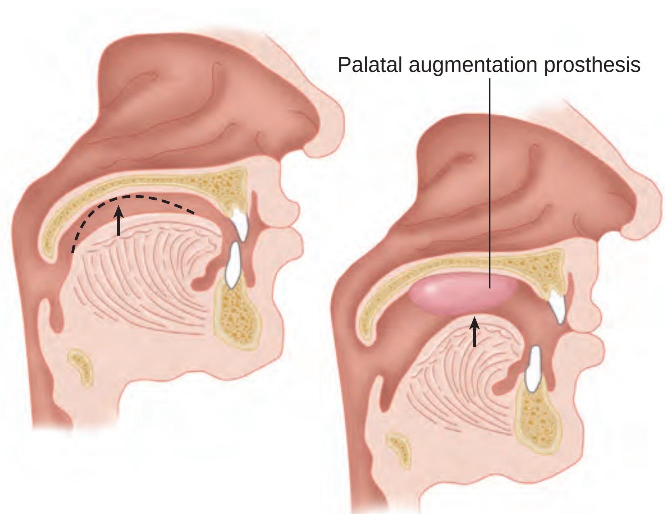

Figure 18.35 A palatal augmentation prosthesis provides volume that abuts against the remnant tongue.

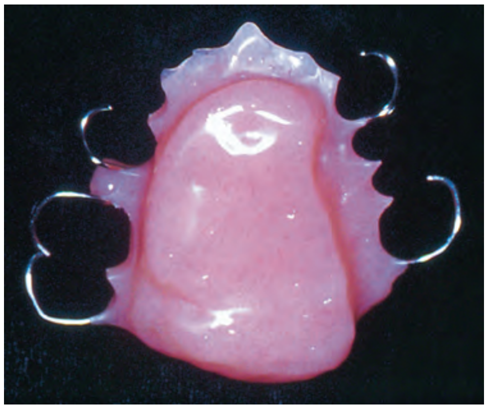

Figure 18.36 The palatal augmentation prosthesis.

Figure 18.37 A palatal augmentation prosthesis improves speech and facilitates swallowing in this patient, who has undergone a near-total glossectomy.

valving of the tongue remnant against this surface can provide improved intelligibility of speech and better control of food and liquid transit in swallowing (Fig. 18.37). Apart from the function of the residual tongue and the extent of resection of adjacent structures, factors such as trismus and the patient's motivation also influence the ultimate functional outcome. It should be noted that the palatal augmentation prosthesis can aid in oral transit of the food bolus during the oral phase of swallowing but will be ineffective for problems in the pharyngeal and esophageal phases. Indeed, better oral transit can promote aspiration in patients with inadequate pharyngeal swallowing, and coordination with the swallowing team is often necessary.

MANDIBULAR DEFECTS

Mandibular defects can be described as marginal or segmental depending on the amount of resection necessary to clear disease. In a marginal defect the continuity of the mandibular arch is not altered; therefore the restoration of this type of defect is more straightforward. These deficits can typically be restored with removable prosthetics or with implants, provided the amount of mandible resected will not lead to impinging on the inferior alveolar nerve or fracture of the remaining mandible due to extensive resection. The segmental resection causes a discontinuity defect as the entire piece of the mandible from superior to inferior cortical plate is removed. Patients who are anticipated to have this type of defect should have preoperative treatment planning by a multidisciplinary team to maximize the outcome for postoperative rehabilitative success. After segmental

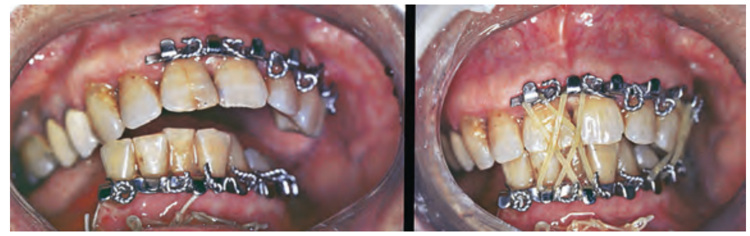

Figure 18.38 Intermaxillary fixation and elastic band immobilization of the remnant mandible after a hemimandibulectomy.

Figure 18.39 A desmoid tumor of the right buccal mucosa.

resection, a nonreconstructed mandible with a discontinuity defect undergoes deviation toward the resected side and causes a deformity that can result in significant functional and cosmetic debility. In modern practice, most patients undergo some form of bone reconstruction after a segmental mandibulectomy. However, if for any reason mandibular continuity is not restored, then measures should be undertaken to minimize mandibular deviation. The use of intermaxillary fixation with elastic bands (Fig. 18.38) for a short period postoperatively acts as a training device to aid in maintaining dental occlusion while allowing mobility of the remaining jaw. Alternatively, the patient may initiate jaw exercises at the surgeon's discretion as soon as possible after surgery, manually guiding the mandible toward the nonresected side. The aim of these exercises is to decrease scar contracture and trismus and improve the maxillomandibular relationship. The patient's progress can be measured to provide positive feedback, and the earlier mandibular guidance is initiated, the greater the chance for success.

A mandibular guide flange prosthesis may be used for patients who retain dentition in their remnant mandible and maxilla. This appliance can be used only in patients who have healthy dentition with adequate bony support to withstand diagonal forces. Additionally, patients must not have fibrotic muscles or soft tissues that would preclude movement in the desired direction to restore normal maximal intercuspation of the dentition. As the guide flanges engage the maxillary buccal tooth surfaces during initial mouth opening and closure, the mandible is directed to the appropriate intercuspal position. Definitive mandibular guidance appliances are used when healing is complete, and therefore their use may be delayed for several months in patients who undergo postoperative radiation therapy.

The patient shown in Fig. 18.39 had a desmoid tumor of the right buccal mucosa that required a segmental resection of the ipsilateral hemimandible in addition to soft tissue. The defect was repaired with use of a rectus abdominis myocutaneous

Figure 18.40 A mandibular guide flange prosthesis.

Figure 18.41 An open mouth with a guide flange prosthesis in place.

free flap without bone reconstruction, and thus the remnant hemimandible was subject to significant deviation. An interim guide flange prosthesis was fabricated (Fig. 18.40) that allowed the patient to maintain alignment of the hemimandible during mouth opening (Fig. 18.41) and occlusion (Fig. 18.42).

In current practice, the ideal rehabilitation of a patient undergoing segmental mandible resection includes immediate free flap reconstruction with dental reconstruction using osseointegrated implants. The implants can either be placed at the time of reconstructive surgery or may be delayed until healing of the free flap is complete. In an oncology setting it is ideal to place the implants during the initial ablative and reconstructive surgery to permit osseointegration before any planned adjuvant therapy. Endosseous implants can then be uncovered during a second stage surgery before the start of adjuvant therapy and assessed, and provisional prosthetic teeth can be provided to the patient. This approach mitigates the risk for development of osteonecrosis of the jaw, which is more likely in patients who undergo dentoalveolar surgery in a radiated field. With current surgical planning software, the free flap

Figure 18.42 Dental occlusion with a guide flange prosthesis in place.

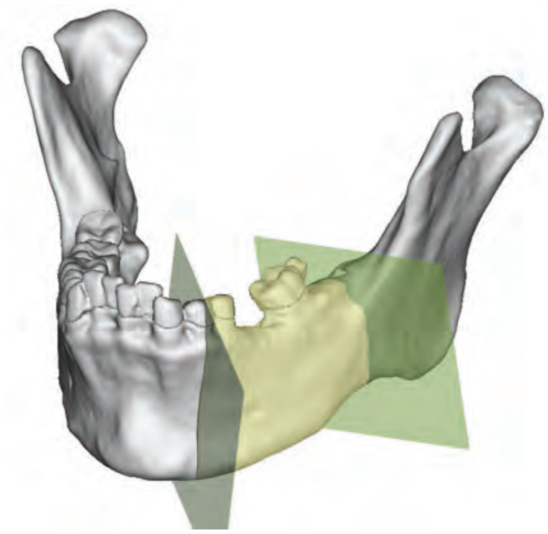

Figure 18.43 Computerized software is used to plan the mandibular osteotomies and fabricate a surgical guide.

reconstruction positioning can be driven by optimal aesthetic outcomes, giving the patient facial symmetry and outstanding occlusal function and aesthetics (Figs. 18.43 and 18.44). As previously mentioned, endosseous implants can be used to support intraoral rehabilitative options, such as fixed dental resection prostheses, or can aid immensely in stabilization of the removable resection prosthesis. The planning and surgical approach for this treatment is demonstrated in Figs. 18.45 through 18.49. The workflow for fabrication of a definitive fixed prosthesis designed with the use of computer-aided design/computer-aided manufacturing (CAD-CAM) is shown in Figs. 18.50 through 18.55. This approach is a huge advance from the past, when outcomes of success were merely measured by successful healing of the flap and the outward appearance of the patient.

Alternatives for patients with soft-tissue reconstructed mandibular discontinuity defects are limited. These patients will either struggle with a conventional removable mandibular resection prosthesis or will not be rehabilitated with an intraoral prosthesis. In either surgery, marginal or segmental, the tissue bed the removable prosthesis uses for support has been severely altered and many times will not allow a prosthesis to be fabricated due to obliteration of vestibules, obliteration of the lingual space due to utilization of the tongue to close the defect, or the flap that is too bulky and does not support the forces

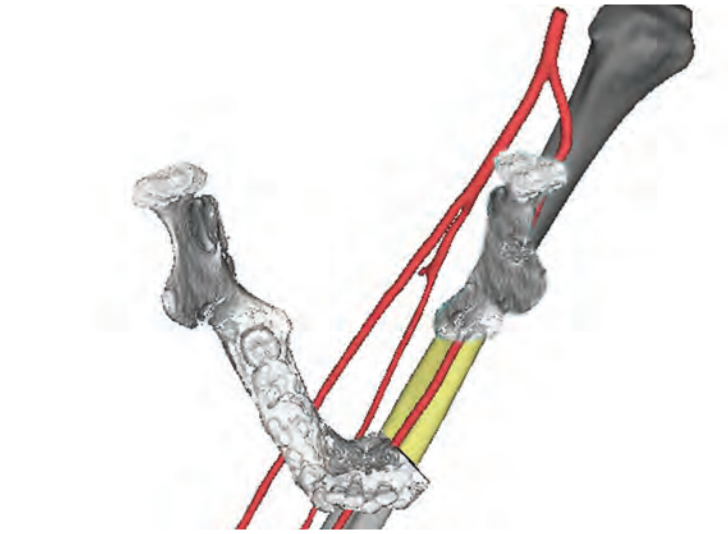

Figure 18.44 Computerized planning software using reconstructed three-dimensional images from a computed tomography angiogram of the fibula and a computed tomography scan of the mandible shows the desired segment of fibula for reconstruction.

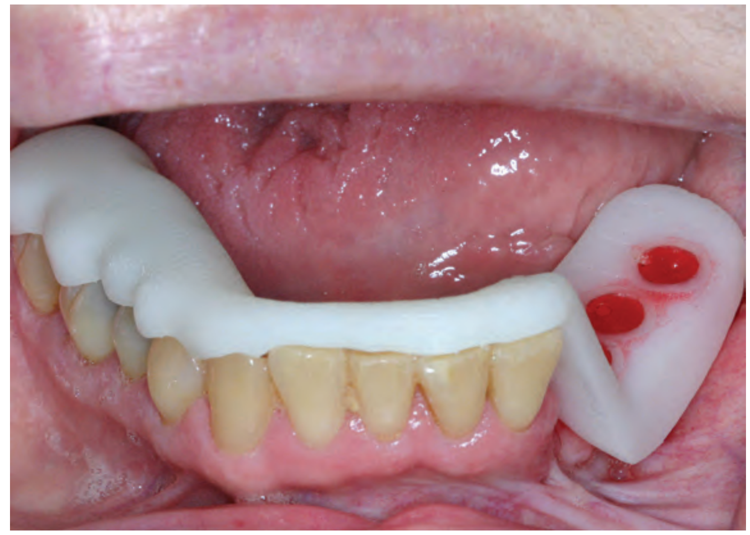

Figure 18.47 A surgical guide is used for flapless placement of implants into the fibula.

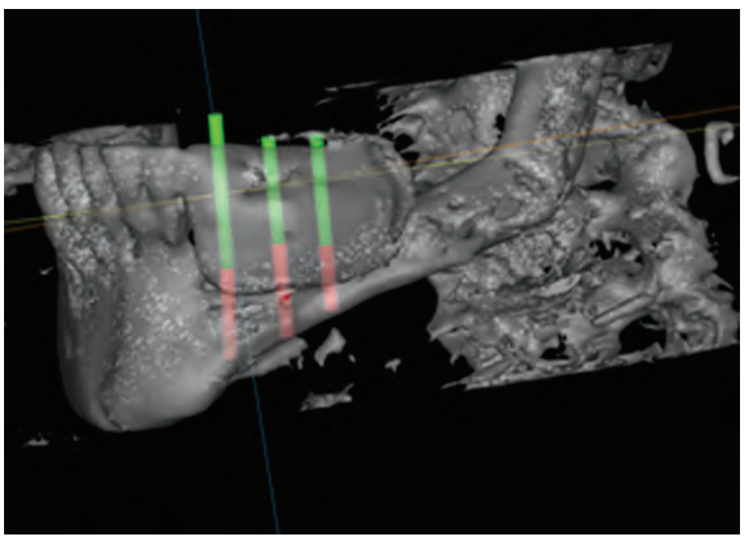

Figure 18.45 Computerized planning software is used to plan the placement of three implants in the healed fibula.

Figure 18.48 Flapless placement of three mini dental implants.

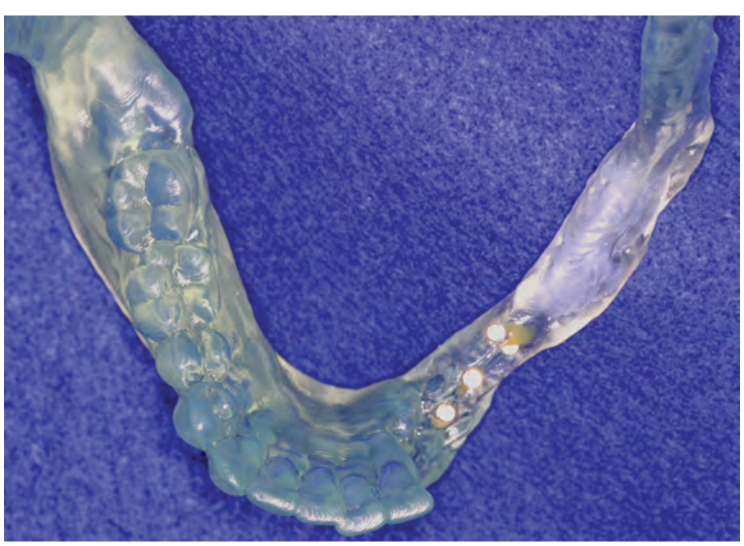

Figure 18.46 A model of the reconstructed mandible with the fibula that will be used to create a surgical guide for implant placement.

Figure 18.49 The postoperative appearance 1 week after the placement of implants.

Figure 18.50 Impression copings (white caps) on implants.

Figure 18.51 The cast of the implants for fabrication of a bridge.

Figure 18.52 An interim acrylic resin bridge is cemented in place.

Figure 18.53 A custom computer numeric controlled (CNC)–milled titanium abutment and framework for the final prosthesis.

Figure 18.54 Custom abutments are cemented to mini dental implants.

Figure 18.55 The final prosthesis cemented in place restores the patient's mandibular arch.

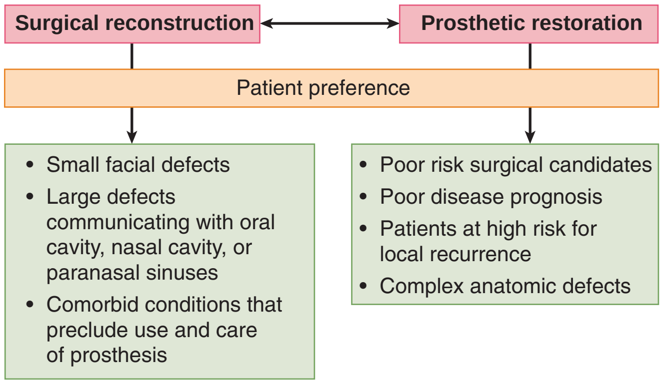

Figure 18.56 Factors influencing the method chosen for facial rehabilitation.

Figure 18.57 An irreversible hydrocolloid (alginate) facial moulage.

Figure 18.58 A wax sculpture of a nasal prosthesis on a stone cast.

Figure 18.59 A patient with a partial rhinectomy defect.

Table 18.7 Methods for Retention of Facial Prostheses
• Skin adhesives • Undercuts in defect • Mechanical (glasses, straps, magnets, clips) • Osseointegrated implants

of occlusion on the prosthesis. It is important to remember that a nonreconstructed defect or a defect reconstructed with soft tissue alone will compromise the retention, stability, and support required for a successfully functioning prosthesis. Even if an osteocutaneous or soft-tissue flap is used for reconstruction, surgical expertise is required to place and form the reconstruction in such a way that will allow utility during the intraoral prosthetic phase of care.

REHABILITATION OF FACIAL DEFECTS

Defects of the head and face present unique challenges for both the reconstructive surgeon and the maxillofacial prosthodontist. Reconstructive efforts for substantial facial defects are limited by the qualities of donor tissue such as texture, color, and availability. The efforts of the maxillofacial prosthodontist, on the other hand, are limited by the prosthetic space available for rehabilitation; the mobility of the tissue bed in the face, which causes problems with regard to the retention of prostheses; and the difficulty in matching the permanence and the natural feel and texture of replaced tissue. The choice between these two options is not always straightforward, and indeed in some situations the two methods may be used to complement each other in the same patient. Apart from the factors outlined in Fig. 18.56, the preference of the patient should be taken into account.

When prosthetic restoration of a facial defect is planned, a presurgical physical moulage (Fig. 18.57), digital image, or laser scan is useful. Irreversible hydrocolloid, vinylpolysiloxane, or plaster can be used to obtain an accurate impression of the patient's face, or a medical model is produced from digital data capture. The contours of the missing anatomy then are sculpted in wax or clay on the cast and on the patient (Fig. 18.58). Appropriate contouring, coloring, and placement of margins are some of the many considerations that contribute to a successful outcome. The physical characteristics of prosthetic materials such as silicone elastomers play an important role in the ultimate outcome, but the skills and resourcefulness of the maxillofacial prosthetic team are probably the most crucial factors.

Another factor that determines whether a prosthesis is utilized is its ease of placement and retention. A variety of retention techniques have been used (Table 18.7). Lack of retention contributing to poor patient compliance or acceptance of a facial prosthesis can be overcome with skin adhesives (Figs. 18.59 and 18.60), design of the prosthesis into undercuts, and mechanical means (i.e., attachment to glasses, straps, and craniofacial implants with clips/magnets) (Figs. 18.61 and 18.62). Decisions regarding the selection of the type of retention technique are made on the basis of the complexity of the prosthesis, skin hygiene, type of skin (i.e., oily, dry, or irradiated),

Figure 18.60 A nasal prosthesis retained with skin adhesive.

daily activity (e.g., sweat and movement), the dexterity of the patient, and other handicaps such as blindness or missing appendages. Prosthesis hygiene is crucial to the lifespan of a silicone prosthesis, which can be expected to be 12 to 24 months. Evaluation of these patients on a semiannual basis ensures that instructions for prosthesis maintenance are reinforced and adjustments such as additional tinting for continued color match are undertaken.

Craniofacial implants have utility in the retention and stability of extraoral prosthetics, especially in prosthetics for the orbit, nose, and ear, which can be difficult to restore with conventional means. The patient shown in Fig. 18.63 had a recurrent basal cell carcinoma of the nose, for which she underwent a total rhinectomy and an anterior upper alveolectomy. A year after her resection, when the defect had matured, implants were placed in the frontal bone. The implants were activated 6 months later (Fig. 18.64). The patient uses a midfacial appliance based on the implants along with magnets on the intraoral maxillary obturator to keep the facial prosthesis in place (Fig. 18.65).

Figure 18.61 A well-healed rectus abdominis flap for an orbitocranial resection.

Figure 18.62 An orbital prosthesis is retained with skin adhesive and the patient's turban.

Figure 18.63 A patient with a recurrent basal cell carcinoma of the nose.

Figure 18.64 Osseointegrated implants and a bar placed in the frontal bone.

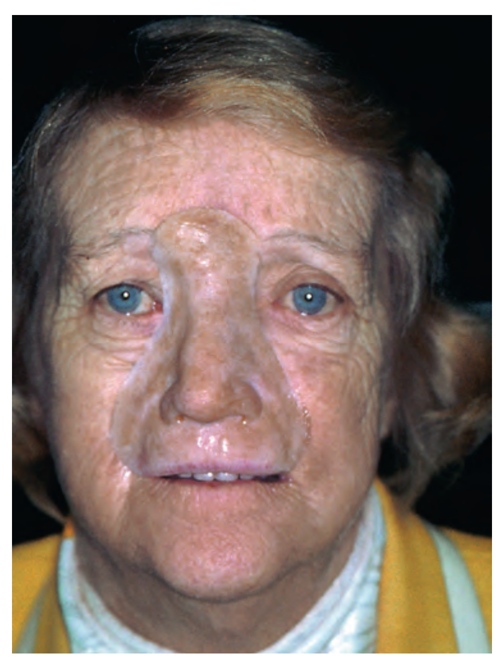

Figure 18.65 Restoration of the patient's appearance with the midfacial prosthesis.

Figure 18.66 Osseointegrated implants in place for an external ear prosthesis.

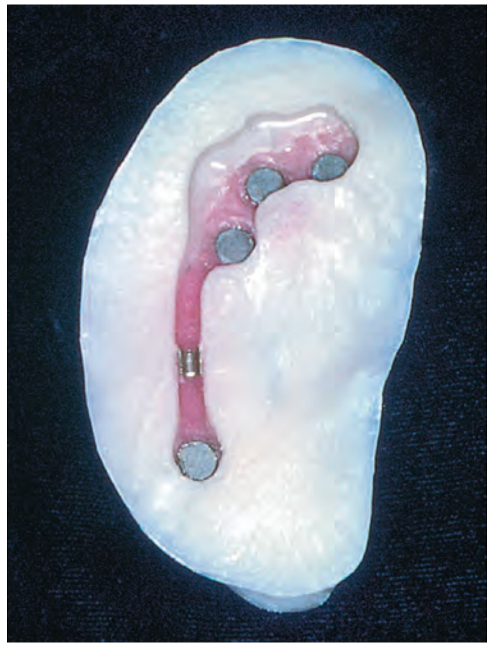

Figure 18.67 The medial surface of the external ear prosthesis showing magnets.

Figure 18.68 The patient's appearance after placement of the external ear prosthesis.

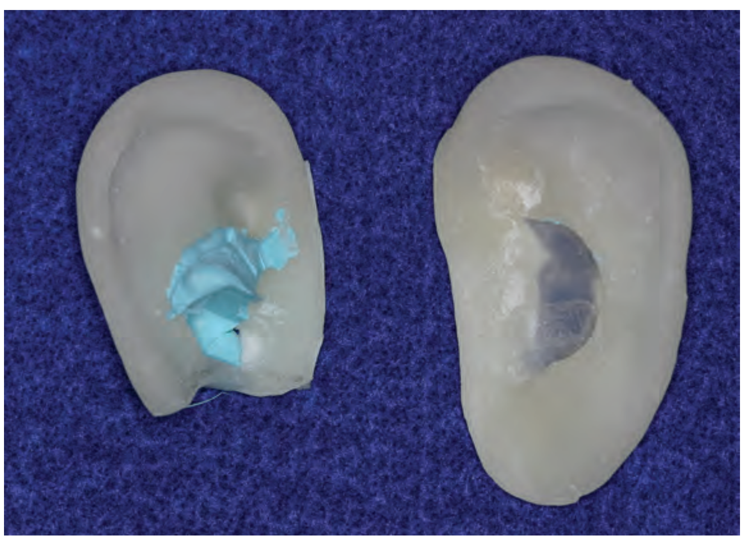

Figure 18.69 Barium sulfate–impregnated auricular prostheses to wear during a computed tomography scan.

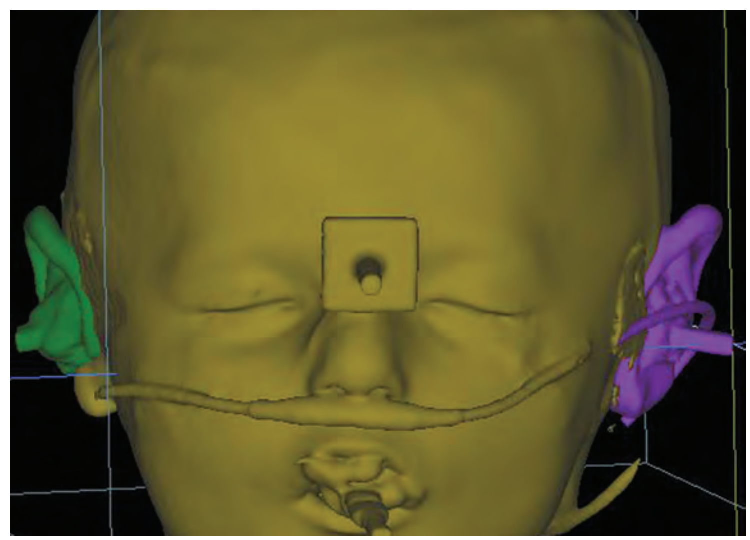

Figure 18.70 Implant planning software for craniofacial implants for bilateral auricular prostheses.

Another patient underwent rehabilitation with osseointegrated implants and an external ear prosthesis (Figs. 18.66 through 18.68).

Advances in imaging and planning software continue to make craniofacial implant surgery and prosthetic rehabilitation safer and more reliable than in the past. Patients now usually undergo imaging with CT while wearing a proposed rendition of the prosthesis that is impregnated with a radiopaque material, such as barium sulfate, to aid in preoperative implant planning (Fig. 18.69). The captured image is formatted and the implant planning is completed (Fig. 18.70). A surgical guide is fabricated and sterilized for use in the operating room (Fig. 18.71). For this specific patient, only a tissue punch was used for placement of the implants rather than a full-thickness flap with a skin graft because of his age and future surgeries that were planned for correction of his hemifacial microsomia and facial reanimation (Figs. 18.72 through 18.74). After 2 months of healing, an impression of the area was made, a wax sculpture derived from the previous scan prosthesis was verified for fit and aesthetics,

Figure 18.71 A computer-manufactured surgical guide for craniofacial implant placement.

Figure 18.72 Intraoperative marking of implant sites.

Figure 18.73 Implant sites are marked and the guide is removed.

Figure 18.74 An 8-mm punch is used to place the implants without a flap.

Figure 18.75 A bar is fitted 3 months after the placement of implants.

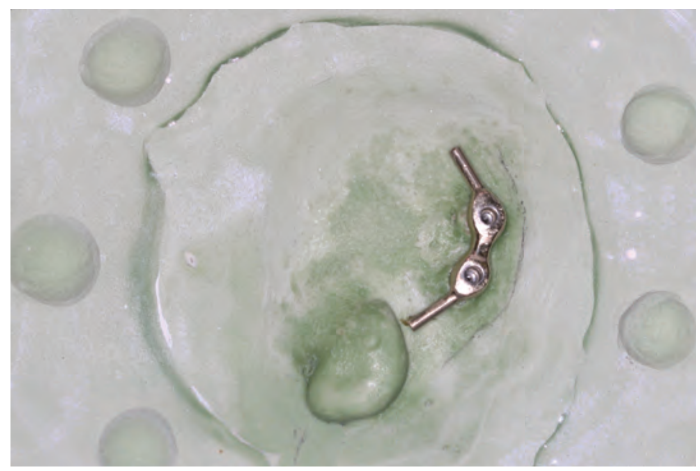

Figure 18.76 A bar on a stone cast for fabrication of an auricular prosthesis.

in this case a gold bar with clips was fabricated, and the bilateral auricular prostheses were tinted to match with facial skin (Figs. 18.75 through 18.79). The prostheses allow the young patient to attend school without the stigma of missing ears and support his glasses, which are necessary for reading, while allowing future surgeries to take place without compromising soft-tissue planes with grafted areas (Fig. 18.80).

COMPUTER-AIDED DESIGN AND COMPUTER-AIDED MANUFACTURING FOR MODELING AND PROSTHESIS FABRICATION

CAD-CAM technology has been evolving since the 1960s for industrial products. Recently great interest has been expressed in developing this technology for medical applications such as drug development, delivery mechanisms, medical models, and custom implants. A technician with an engineering degree works with a physician to produce better prostheses, and this teamwork will improve the standards of prosthetic rehabilitation.

Several methods of "rapid prototyping" can be used to fabricate the product that has been designed on the computer. Although it is termed "rapid," the process can be quite lengthy, depending on the size and complexity of the object being fabricated (Table 18.8). The process for developing a medical model requires an

Figure 18.77 A wax sculpture of the auricular prosthesis.

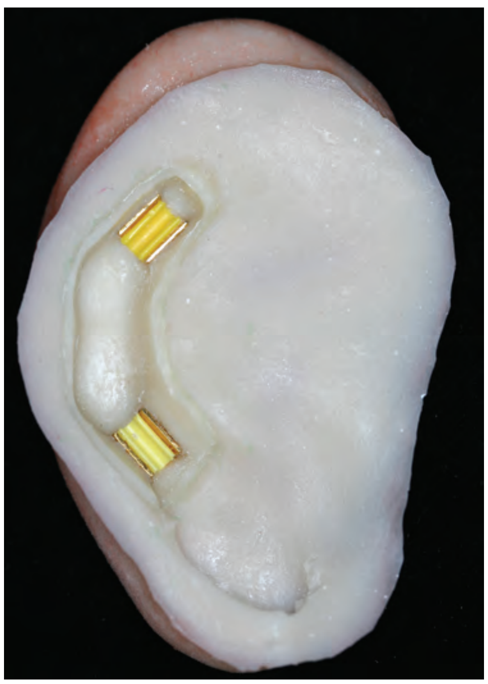

Figure 18.78 The medial surface of the auricular prosthesis showing the clips.

image of the surgical defect, software to manipulate the image, and one of the pieces of hardware previously mentioned. A CT scan, MRI scan, CT/MR angiography, or cone-beam CT of the patient is completed. This image is saved in a digital imaging and communications in medicine (DICOM 3) format, allowing upload of these data via the Internet to a modeling facility. The image is then formatted with use of a variety of commercially available proprietary software packages used at the modeling facility and manipulated according to the surgeon's instructions. Artifacts and extraneous data are removed for a "clean" scan so the model will be high quality. This clean scan is saved in a format that can be used by one of the aforementioned machines to create the model or product needed.

Software manufacturers are revolutionizing the viewing and planning software available at a record pace. It is now possible to view the patient's scan in three dimensions, add motion (e.g., a heartbeat and blood flow), plan the surgical approach, and have custom implants and cutting guides available. Patients who will undergo a segmental mandibulectomy with fibula

Figure 18.79 The external view of the completed auricular prosthesis.

Figure 18.80 The auricular prostheses provide cosmesis as well as functional support for glasses.

Table 18.8 Methods of "Rapid Prototyping" for Fabrication of a Prosthesis

Stereolithography (SLA)	• Liquid resin is polymerized by a laser to form solid objects • Very accurate • Limited colors are available to match surrounding skin
Fused deposition modeling (FDM)	• Plastic from a coil is extruded from a heated nozzle to form solid objects
Selective laser sintering (SLS)	• Uses powdered material and a laser to "tack weld" the material together to form a solid object
Electron beam melting (EBM)	• Powdered metal is fully melted with a laser, yielding a more dense object
Three-dimensional printing	• Process similar to FDM • Photopolymer similar to that used in SLA is used • Multiple hard and soft materials (bone and soft tissue) can be built in one production run

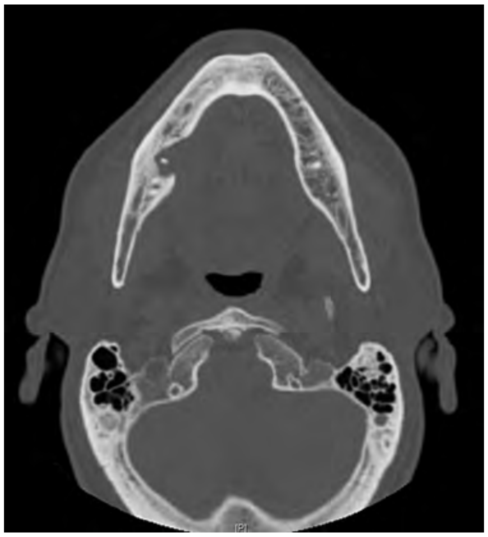

Figure 18.81 Preoperative computed tomography of the mandible in the bone window of a patient with squamous cell carcinoma of the lower gum.

Figure 18.82 The computed tomography images in a three-dimensional reconstruction show the lateral profile of the mandible for accurate planning of resection and fabrication of a model by computer-aided design/computer-aided manufacturing technology.

Figure 18.83 A computer-aided design/computer-aided manufacturing model of the planned reconstruction of the mandible with a fibula free flap showing the exact locations of osteotomies in the fibula and the accurate locations for implant placement in the nonosteotomized segments.

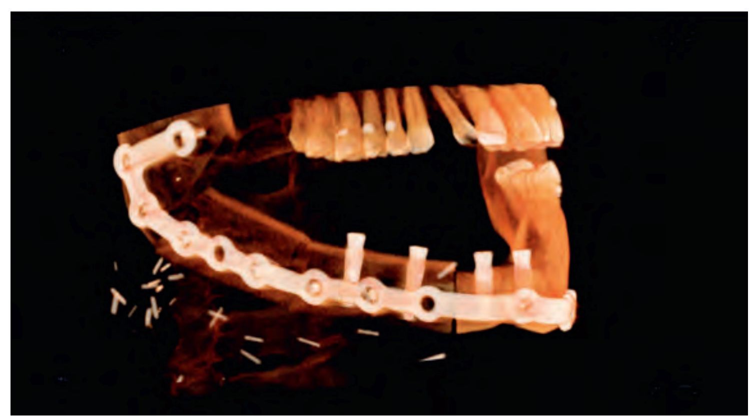

Figure 18.84 The postoperative view of the reconstructed mandible showing the metallic plate supporting the osteotomized fibula and the location of dental implants avoiding the screws and plate used to stabilize the fibula segments.

free flap reconstruction can have the entire surgery virtually planned and performed before entering the operating room. Osteotomy guides for the mandibular resection are made, along with a corresponding fibula osteotomy guide for precise resection and reconstruction. All of these guides are made as a team with the engineer, head and neck surgeon, plastic and reconstructive surgeon, and maxillofacial prosthodontist. Dental implant rehabilitation can also be planned before surgery by the prosthodontist on the team with the goal of immediate accurate placement of implants in the fibula free flap so as not to conflict or overlap with the screws and plates used for stabilization of the osteotomized fibula. Clearly, this effort will reduce the total oral/dental rehabilitation time for the patient and improve the quality of life outcomes. Thus virtual planning can allow for implant placement to be completed during the primary ablative and reconstructive surgery. A preoperative CT scan of a patient with carcinoma of the lower gum is shown in Fig. 18.81. Note the extent of bone destruction in the body of the mandible. The CT scan in three-dimensional reconstruction shows the lateral profile of the mandible and allows for accurate CAD-CAM fabrication of a model (Fig. 18.82). In discussion with the surgical team, the extent of mandible resection is planned out, and a computer model is created to allow accurate placement of dental implants in the nonosteotomized segments of the fibula free flap (Fig. 18.83). Postoperative CT imaging shows the reconstructed mandible with osteotomized fibula free flap achieving accurate shape and curvature of the mandible with immediate placement of dental implants. This plan of preoperative CAD-CAM technology achieves perfect reconstruction of the mandible and accurate placement of immediate implants in the desired locations (Fig. 18.84). In addition, these technologies have been used for prebending and shaping reconstruction plates before surgery as well as fabricating custom reconstruction plates. Ultimately, these technologic advancements will continue to proceed at a rapid pace, and as the financial constraints are diminished, the use of custom devices and models will become the mainstay in medicine. Because of the ease of file transfer, production, and shipping of the finished products, persons in even the most remote locations will be granted access to this type of care within a short period. This type of CAD-CAM capability opens a new era for medicine and for improvements in patient outcomes.

CHAPTER 19

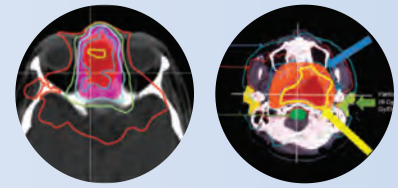

Radiation Therapy

The use of ionizing radiation in the treatment of cancer has evolved during the past century since the discovery of x-rays in 1895 by Wilhelm Conrad Roentgen, a German physicist. Professor Wilhelm Alexander Freund demonstrated the disappearance of a hairy mole with the use of x-rays in 1897, suggesting a potential role for x-rays in treating human disease. Antoine Henry Becquerel is credited with the discovery of radioactivity when he found that uranium salts emitted rays that resembled x-rays in their penetrating power. He inadvertently performed the first radiobiology experiments in 1901, after discovering damage to his own skin from a container with radium in his vest pocket.

Marie Skłodowska-Curie was fascinated by Becquerel's findings and, along with her husband Pierre, initiated her landmark work on radioactivity, leading to the discovery and isolation of radium and polonium (a breakdown product of radium). Pierre Curie validated Becquerel's radiobiological experiment by deliberately producing a radium burn on his own forearm. In 1903 Pierre and Marie Curie and Antoine Henry Becquerel were awarded the Nobel Prize in physics for "joint work concerning investigations of the radiation phenomena described by Henri Becquerel." Marie Curie received a second Nobel Prize in chemistry in 1911, "in recognition of her services to the advancement of chemistry by the discovery of the elements radium and polonium, by the isolation of radium and the study of the nature and compounds of this remarkable element." Marie Curie's contributions included the standardization of radioactivity by quantifying the effects of accurately weighed quantities of pure radium salt in 1911, which continues to serve as the standard to determine the amount of radioactivity in each source.

During the next few decades, improved understanding of radiobiology led to the realization that radiation response is dependent on oxygenation and that fractionation of the radiation dose is required for improved efficacy and better tolerance. In the latter half of the 20th century, new sources of ionizing radiation were discovered, and treatment delivery systems increased in sophistication. In the past 20 years, computerized treatment planning and delivery systems have become the standard of care.

Cell death resulting from ionizing radiation can occur through different mechanisms. The most common cause of cell death is deoxyribonucleic acid (DNA) damage leading to double-stranded breaks. Radiation-induced DNA damage occurs either directly or indirectly by the generation of highly reactive free radicals. The living cell can repair many of these radiation-induced DNA breaks, particularly single-stranded breaks, but tumors cannot, eventually leading to cell death. This damaging effect of radiation may not be evident immediately, but it occurs when the cell attempts to divide. Clinically, the effect of radiotherapy depends on the complex interaction of a multitude of factors. The therapeutic efficacy of ionizing radiation in tumors at most head and neck sites has been well documented. Although control and cure of the disease should be the paramount considerations in choosing the type of therapy, these factors must be balanced against the functional compromise and impact on quality of life. As always, a multidisciplinary approach with close cooperation, not only among the treating team but also with the patient and the family, is crucial in choosing therapeutic interventions. The key factors that influence choice of treatment are shown in Table 19.1.

In general, patients with tumors that require extensive surgical resection with sacrifice of organs such as the larynx or the base of tongue are now considered candidates for organ-preserving approaches with use of chemoradiation therapy, reserving surgery for salvage. Tumors, especially skin cancers, that are located in areas that are technically difficult to reconstruct also may be treated with primary radiation to achieve optimum posttreatment cosmesis. For early-staged tumors (T1 or T2), single-modality treatment (either surgery or radiation therapy) is chosen for both the primary tumor and the neck (limited low-volume neck metastases) if appropriate. For advanced tumors, surgery combined with radiation and/or chemotherapy or primary chemoradiotherapy are the preferred treatment modalities (Fig. 19.1). The principles of radiation therapy presented here are intended to serve as a guide for the surgeon involved in multidisciplinary care of patients with head and neck cancer.

RADIOBIOLOGY

Teletherapy (External Beam Radiation Therapy)

Therapeutic radiation is delivered by two main methods: (1) electromagnetic radiation (photons) in the form of x-rays and gamma rays and (2) particulate radiation in the form of electrons, neutrons, and protons. Ionizing radiation deposits energy at a constant rate as it travels through matter, defined as *linear energy transfer (LET)*. Each unit of absorbed radiation is called *one gray (Gy)*, which is equivalent to one joule per kilogram of tissue. One Gy is also equal to 100 centi-Gy (cGy) or 100 rads. (The *rad [radiation absorbed dose]* is the previous name for the absorbed dose unit.) Gamma rays are produced within the nucleus of materials, such as cobalt-60, that undergoes radioactive decay, resulting in the emission of gamma ray photons.

Sparsely ionizing or low LET radiation, such as x-rays or gamma rays, deposit their energy less densely per unit length of tissue. On the other hand, high-LET or densely ionizing

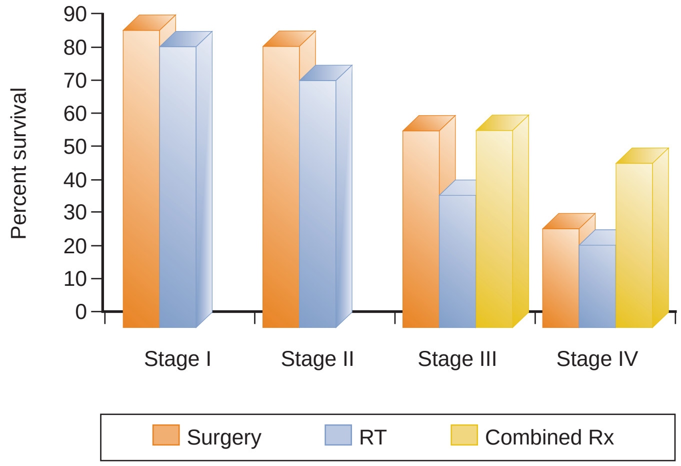

Figure 19.1 Single-modality treatment is adequate for early-stage tumors, but more advanced cancers benefit from combination treatment. *RT,* Radiation therapy; *Rx,* treatment.

Table 19.1 Factors Influencing the Choice of Treatment
Patient Factors • Age • Pulmonary status • Medical comorbidity • Psychological status • Motivation • Capability of self-care • Family support • Rehabilitation potential • Logistic considerations (e.g., proximity and access to radiation facility)
Tumor Factors • Anatomic site • Tumor stage • Topography (exophytic vs. infiltrative) • Proximity to vital structures (e.g., optic nerves, brain, spinal cord) • Tumor extent (e.g., presence of bone invasion) • Histologic type (e.g., squamous cell carcinoma, melanoma, salivary gland carcinoma) • Previous treatment with radiation therapy

radiation, such as neutrons, is composed of particles of higher mass that deposit their energy very densely per unit length of tissue. Equal doses of radiation of differing LET do not produce the same biological response in tissues. The relative biological effectiveness (RBE) is a measure of the ability of radiation with different LETs to produce the same biological effect under the same conditions. A 250-kV x-ray beam generally is used as the reference source for comparison. For example, if a 50% cell kill is achieved with 600 cGy of 250-kV x-rays and 200 cGy of neutrons under similar experimental conditions, the RBE of neutrons is 3. In other words, the test radiation (neutrons) is three times as effective as the reference (x-rays). The depth of penetration required is the main criterion used in choosing which energy or teletherapy unit to use. Superficial (40–100 kV) and orthovoltage (250 kV) x-rays have a limited range of penetration and are effective for more superficial lesions, as is electron particulate radiation. Supervoltage (1.25 MV, cobalt-60) gamma rays and megavoltage (4–25 MV, linear accelerator) x-rays, on the other hand, are more penetrative and are used for deep-seated tumors (Fig. 19.2).

Sources used for teletherapy include photons, electrons, neutrons, protons, α particles (i.e., helium atoms, uranium, thorium, radium, and radon), and heavy charged ions (i.e., carbon, neon, silicon, and argon). In patients with head and neck cancer in whom tumors are not deeply seated, the 6-MV photon is used most commonly. Very superficial skin lesions can be treated with electrons and, depending on the size and depth, different energy sources can be used. For recurrent tumors, brachytherapy can be used. Examples of energy sources for brachytherapy are cesium-137, iridium-192, iodine-125, gold-198, americium-24, palladium-103, samarium-145, and ytterbium-169. The typical amount of electromagnetic radiation energy used to treat head and neck cancer is 6 MV.

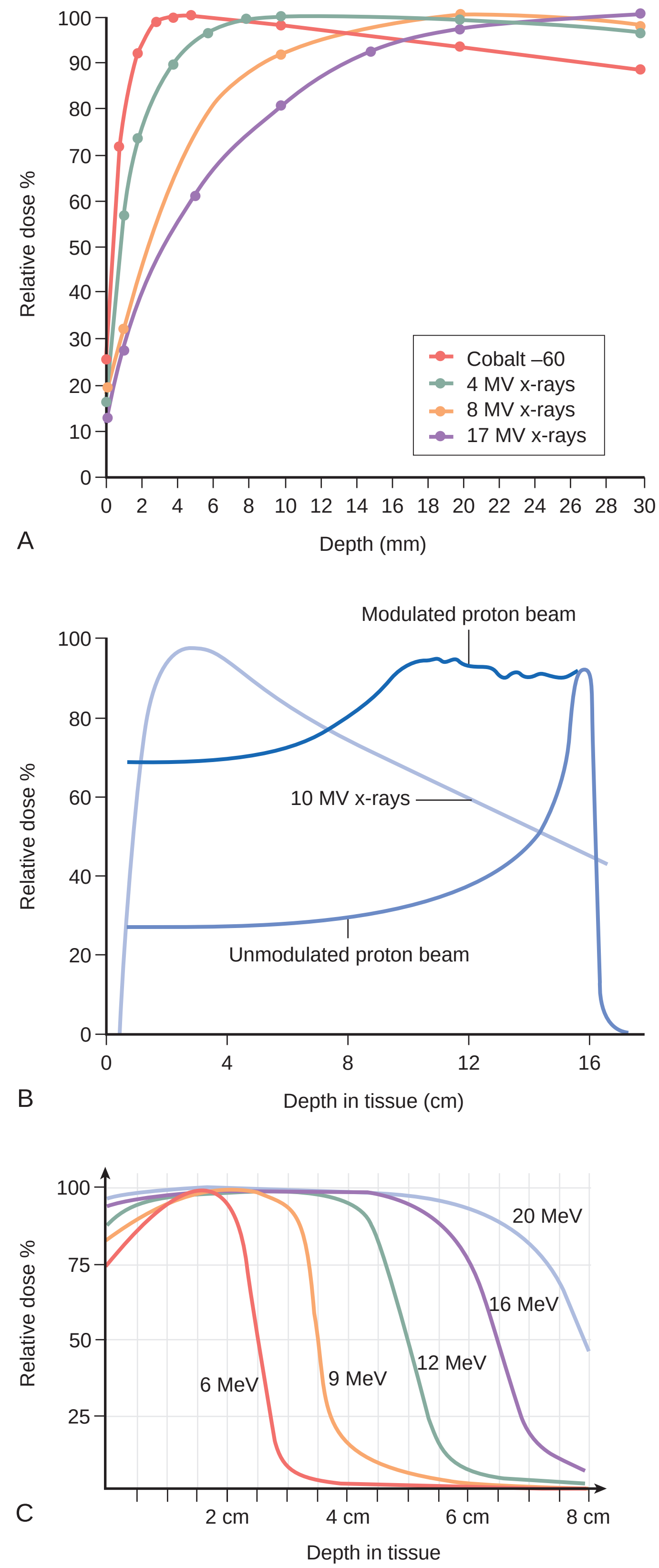

Figure 19.2 The relative depth of tissue penetration for commonly used radiation sources. **A**, Cobalt and photons. **B**, Protons. **C**, Electrons.

For particulate radiation, electrons are commonly used to treat head and neck cancers. Electrons are produced in linear accelerators and generally range from 6 MeV to 20 MeV, depending on the depth of penetration desired. Specific examples of the use of electrons in the head and neck region include treatment for skin cancers and sites in proximity to the spinal cord. Neutrons are produced by cyclotrons and can have a maximum energy of 50 MeV. Although they have no dose distribution advantages over photons, neutrons have a higher RBE. Although this higher RBE may be an advantage in treating malignant cells, potentially major complications can result because of their effect on normal tissues. At the present time, their role is primarily in the treatment of unresectable primary and recurrent salivary gland tumors. Due to limited availability, neutron therapy is not routinely recommended in the treatment of head and neck cancer.

Until recently, proton therapy was not available in most institutions. However, due to technologic advances that have allowed for reduction in cost and downsizing of treatment hardware, many proton therapy centers have now opened or are under development. Use of this technology is becoming more widespread and being advocated with the goal of further minimizing normal tissue toxicity, potentially minimizing the risk of the development of second primary tumors as a result of radiation injury to normal tissues and allowing for safer delivery of higher radiation doses to the tumor volume. Protons are positively charged atomic particles that are also produced in cyclotrons. Although protons and photons have roughly equivalent RBE, the characteristic dose distribution of protons allows significantly better control of the depth of penetration. This control can be a major advantage in some situations, such as the treatment of tumors at the base of skull, well-lateralized tumors that only require unilateral treatment of the head and neck, or tumors that have previously been treated with photon radiation. While numerous dosimetry studies have demonstrated superiority in dose distributions with proton plans, recent retrospective data have also suggested improvements in toxicity among well-selected patients. Multiple clinical trials are ongoing to investigate the toxicity profile and appropriate patient populations that stand to benefit most from proton therapy.

During the past several decades, treatment delivery schemes have also evolved. When sophisticated radiation machines were not available, tumors often were treated with a single radiation port using superficial x-rays. However, the depth of penetration of superficial x-rays to a centrally located tumor was not sufficient. With machines that allowed deeper delivery of radiation and the need to ensure delivery of an adequate dose to centrally located tumors, parallel opposed radiation portals were used more often. Wedge pairs also were used to ensure delivery of an adequate dose to the ipsilateral tumor while sparing the contralateral normal tissue.

The introduction of conformal radiation therapy (CRT) followed by intensity-modulated radiation therapy (IMRT) in the early 1990s further minimized the radiation dose to surrounding normal tissues. With advances in computer technology, IMRT has the unique ability to minimize the dose delivered to all surrounding normal tissues while delivering a therapeutic dose to the tumor. Image-guided radiation therapy (IGRT) ensures daily accurate tumor localization while delivering the complex IMRT treatment plans for a given tumor. This involves two-dimensional or three-dimensional images that are acquired at the treatment machine to ensure accurate patient positioning and delivery of the intended radiation plan.

The percentage of cells that survive a given dose of radiation depends on many factors: the type of radiation (low LET versus high LET), dose size, the use of radiosensitizing systemic therapy, environmental conditions (oxygenated versus hypoxic tissue), and underlying tumor biology. The sensitivity of a cell to radiation also depends on its phase in the cell cycle. Cells are most sensitive to radiation-induced damage during the G2 and M phases of the cycle. A tumor consists of cells that are in different phases of the cell cycle and are dividing asynchronously. After exposure to ionizing radiation, surviving cells undergo partial synchronization as a consequence of G2 arrest, which delays cells in a more radiosensitive phase.

Another important factor that affects the ability of ionizing radiation to cause biological change is the amount of oxygen present in the tissue environment; cells in a 100% oxygen environment are three times more radiosensitive compared with completely anoxic cells. Malignant cells within the center of bulky tumors are relatively hypoxic and therefore are relatively radioresistant by virtue of the fact that they are more than 150 μm away from a blood vessel, which is the maximum diffusing distance of oxygen from a capillary. With the delivery of each fraction of radiation therapy, the better oxygenated cells closer to the periphery of the tumor are preferentially killed and, as the tumor shrinks, the centrally located hypoxic cells are brought closer to the blood vessels. This progressive reoxygenation of certain tumor areas may take a few hours or up to a few days to occur. Advanced imaging techniques such as [18F]fluoromisonidazole positron emission tomography (f-miso PET) are under investigation to measure changes in hypoxia during the course of radiotherapy.

Clones that can proliferate during a course of fractionated radiation therapy exist within tumors as well as normal tissue. Proliferation of these cells within tumors can reduce the net effect of treatment and cause local failure. Conversely, within normal tissues, repopulation during treatment is beneficial to the process of healing. Depending on the cell cycle characteristics of the particular tumor, redistribution can either increase or decrease the percentage of sensitive cells. As previously mentioned, cancer cells are also typically less capable of efficiently repairing DNA damage induced by radiation compared with normal tissues, which also contributes significantly to the selectivity of radiation-induced cell death. Factors such as the size and histology of the tumor and radiobiological characteristics such as cell cycle fractions and repopulation therefore are vital to designing effective treatment and form the basis of techniques such as hyperfractionated and hypofractionated schedules.

Fractionation

The technique of administering radiation therapy in fractions instead of in a single high dose originated in 1927. The underlying principle of fractionation is that a high total dose can be delivered to the tumor while sparing adjacent normal tissue. Generally, the total dose of radiation, the size and number of fractions, and the duration of treatment are determined by the type of tumor and the tolerance characteristics of normal tissue in the treatment field. The conventional fractionation schedule that entails use of 180 to 200 cGy per fraction, one fraction per day, 5 days per week for 6 to 7 weeks for a total dosage of 6500 to 7000 cGy has evolved empirically over many years. Based on both laboratory and clinical research, it is now apparent that the conventional fractionation scheme may not be the best approach for all tumors, particularly in the head and neck region.

Three important areas form the foundation for the evolving use of altered fractionation: (1) tissue response; (2) duration of treatment; and (3) fraction size and number. Acutely responding tissues are rather active in ongoing cellular proliferation. Most tumors (except perhaps prostate cancer, breast cancers, and melanoma) and some normal tissues such as skin, mucous membranes, and gastrointestinal epithelium share this characteristic. These tissues are most affected by the overall treatment duration rather than by the size or number of fractions used. Late-responding tissues have a low proliferative rate and include the spinal cord, brain, bone, and cartilage. These tissues are most affected by the size and number of fractions rather than by treatment duration and therefore are spared by decreasing the dose per fraction of radiation delivered.

Because most tumors consist of rapidly dividing cells, local tumor control is strongly dependent on the overall treatment duration rather than on the size or number of fractions. When squamous cell carcinoma of the head and neck is exposed to radiation, the less radiosensitive cells within the lesion can undergo rapid proliferation approximately 3 to 5 weeks after treatment commences. This accelerated repopulation can overwhelm the ongoing treatment effects of radiation, which ultimately can lead to local failure. The clinical significance of this phenomenon is that even with significant regression of the primary tumor mass, local failure still ultimately could result from proliferation of these resistant clones. Therefore it is essential to complete treatment in as short a time as possible so that accelerated repopulation is minimized, increasing the chance for local control. For this reason, split-course radiation which incorporates a treatment break during the course of radiotherapy is not recommended.

Based on the aforementioned principles, the goal of altered fractionation schemes is to improve the therapeutic ratio by maximizing the tumoricidal effect and minimizing acute and late toxicities while using readily available low-LET radiation. Two major categories of altered fractionation schemes exist: hyperfractionation and accelerated fractionation. They share basic radiobiological principles yet have their own particular features (Table 19.2). Accelerated fractionation is the strategy of choice for rapidly proliferative tumors, whereas hyperfractionation is preferred for slowly proliferating tumors. Hyperfractionation improves the therapeutic ratio primarily through (1) redistribution of tumor cells into more radiosensitive phases as a result of multiple fractions and (2) differential sparing of late-responding normal tissues because of a decrease in the size of the dose per fraction. Accelerated fractionation is based on the concept that the shortened overall treatment time would reduce the opportunity for accelerated repopulation effectively.

A randomized study by radiation therapy oncology group (RTOG) 90–03 evaluated the use of low-LET radiation alone with four fractionation schemes for the treatment of squamous cell carcinoma of the head and neck. Patients included in this trial underwent radiation therapy as a single modality, without the use of chemotherapy. The sites included the oral cavity, oropharynx, hypopharynx, and supraglottic larynx. The stages were limited to III and IV (with no distant metastases); however, the base of the tongue and the hypopharynx subsites included stage II patients as well. The four arms were as follows: (1) conventional fractionation; (2) hyperfractionation; (3) accelerated fractionation with split; and (4) accelerated fractionation with a concomitant boost. A significantly improved 2-year locoregional control and disease-free survival rate occurred with accelerated fractionation with a concomitant boost compared with conventional fractionation and accelerated fractionation with a split. Patients treated with hyperfractionation also had a trend toward improved results. However, a phase III Groupe Oncologie Radiotherapie Tete et Cou cooperative trial did not show a benefit when altered fractionation was combined with chemotherapy. In fact, patients treated with accelerated fractionation with concurrent chemotherapy experienced more toxicities than did patients treated with conventional fractionation with concurrent chemotherapy.

The RTOG 99-14 trial asked the same question about whether chemotherapy given concurrently with concomitant boost radiation can further improve on locoregional control. Because of the encouraging preliminary results, RTOG 01-29 was conducted to answer the question of whether altered fractionation should be used in the setting of chemotherapy. The results of this two-arm prospective randomized trial of more than 700 patients was just recently reported, showing that when chemotherapy is given concurrently with radiation, there is no added benefit of using altered fractionation compared with standard once-daily radiation. Furthermore, the long-term grade 3 to 4 late toxic effects of chemotherapy from RTOG 99-14 with concomitant boost radiation was extremely high at 42%. Gastrostomy tube dependence rates anytime during follow-up, at 1 year, and at 2 years were 83%, 41%, and 17%, respectively. However, it should be mentioned that these patients were treated with older, conventional nonconformal radiation techniques, such as Cobalt 60. Since the introduction of IMRT, which allows for significant reduction in radiation dose to normal tissues, treatment-associated toxicities have improved. Three randomized studies comparing conventional radiation technique versus IMRT for head and neck cancer have indeed shown that there are lower late complications with IMRT. Furthermore, there is no evidence that IMRT causes compromise in locoregional control.

Hypofractionation is the administration of high-dose-per-fraction (HDPF) radiation, in which only one or two fractions are given per week. This technique has evolved for the treatment of malignant melanoma, which generally is perceived as being

Table 19.2 Salient Features of Altered Fractionation Schemes

HYPERFRACTIONATION	ACCELERATED FRACTIONATION	HYPOFRACTIONATION
• Smaller fraction size (115–120 cGy) compared with conventional fractionation (180–200 cGy) • BID to TID fractionation • Larger total dosage (7440–8460 cGy) than conventional fractionation (7000 cGy) • Similar overall treatment duration as conventional fractionation	• Similar fraction size as conventional fractionation (180–200 cGy) • BID to TID fractionation • Similar total dosage as conventional fractionation • Shortened overall treatment duration compared with conventional fractionation	• Larger fraction size (600–800 cGy) compared with conventional fractionation (180–200 cGy) • Fractions delivered several days apart • Lower total dosage (2100–3200 cGy) than conventional fractionation (7000 cGy) • Shortened overall treatment duration compared with conventional fractionation

BID, Twice a day; *TID,* three times a day.

radioresistant. Conventional fractions of 200 cGy delivered 5 days a week allow normal tissues and tumor cells to recover during the intervals between fractions. Experimental in vitro data have shown that malignant melanoma cells are better at repairing radiation-induced sublethal damage compared with other cells. This finding may explain the long-standing notion that melanoma is intrinsically "radioresistant." HDPF regimens deliver higher doses of radiation per fraction (600 cGy twice a week or 800 cGy once weekly) with the aim of overcoming the reparative capacity of the tumor cells by increasing the damage per fraction. In retrospective analyses, response rates have been shown to correlate with dose per fraction but not with the total dose delivered. However, a prospective randomized trial (RTOG 83–05) found no therapeutic advantage in a comparison of HDPF (800 cGy once a week up to a total dose of 3200 cGy) and conventional fractionation (250 cGy daily, 5 days a week, for a total of 5000 cGy). Although no therapeutic advantage was seen, the shorter delivery time of HDPF radiation allows earlier initiation of systemic therapies if applicable. Moderately hypofractionated radiation (225 cGy per fraction), however, has demonstrated superior results for early-stage larynx cancers treated with radiotherapy alone and is currently considered the standard of care in this setting. Additionally, a regimen commonly referred to as *quad shot*, which was originally developed for advanced pelvic tumors, is sometimes applied for palliation of tumors in the head and neck. This involves cycles of a 1480 cGy course of radiotherapy delivered in four fractions over the course of 2 days, which can be repeated multiple times over a period of weeks or months depending on the treatment response. Aside from the demonstrated efficacy of this regimen, it also allows significant advantages in terms of patient convenience in the palliative setting.

Radiation therapy can also be delivered with use of a single fraction. Intraoperative radiation therapy (IORT) is a form of brachytherapy in which radiation is given to the target area while the patient is under anesthesia. It is often used to treat recurrent tumors that have previously been treated with radiotherapy. Stereotactic radiosurgery is a technique whereby radiation is delivered with use of stereotactic principles, primarily established for brain tumors. However, stereotactic body radiosurgery increasingly is being used to treat tumors of the lung, pancreas, liver, spine, prostate, and other sites. Gamma knife radiosurgery using cobalt sources has limited utility, because it is used to treat brain metastases or benign conditions such as trigeminal neuralgia. Gamma knife radiosurgery can be used to treat isolated skull base metastasis.

Dose, Ports, and Beam-Modifying Devices

Although physicists measure a radiation dose as the amount of ionization that it produces in air (roentgens, or R), it is the absorbed radiation dose in tissue that is of clinical relevance. Because performing this measurement is difficult and impractical, the rad is a derived value. One roentgen of exposure in air is equal to approximately a 0.95 cGy absorbed dose in tissue. In contemporary radiation oncology, a dose is expressed as the amount of energy absorbed per unit mass of absorbing material, or cGy, which is equal to 100 ergs absorbed per gram.

Portals or fields used for directing the beams of treatment are designated depending on the direction of entrance into the patient's body (Fig. 19.3). Port films are critical for verifying the field of treatment and are obtained at the start of treatment and at daily or weekly intervals thereafter. Treatment units

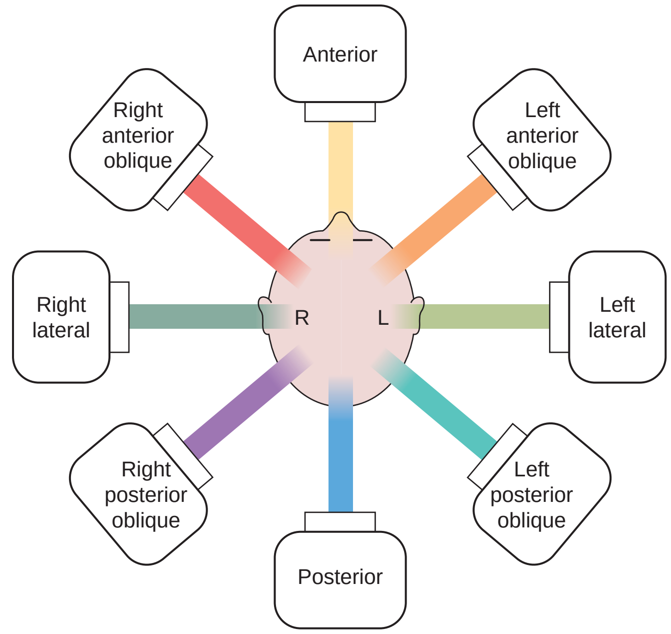

Figure 19.3 Designation of treatment fields (ports).

produce fields that are square or rectangular and deliver a consistent dose across a plane perpendicular to the central ray of the beam. Therefore the beam needs to be shaped and modified according to the configuration of the anatomy and the shape of the tumor.

Shielding blocks, made from Cerrobend lead, generally achieve this goal because their shape and thickness can be varied according to the energy of the beam. The shape and position of the blocks are verified on the port films before treatment is started. A bolus is a material such as petroleum jelly–impregnated gauze, water bags, paraffin wax, and other devices that have interactions with the radiation beam similar to those of tissue. The bolus generally is used to minimize underdosage of superficially situated tumors and scars. For example, filling the postoperative defect of a maxillectomy with petroleum jelly–impregnated gauze improves the homogeneity of dosing to the target.

Compensators are filters positioned within the head of the treatment unit that modify dose distributions. These filters generally are made of copper, brass, Lucite, or lead. When multiple treatment volumes are oriented adjacent to each other, the isodose curves may overlap, resulting in an increased dose at the junction. Depending on the situation, a junction block or creation of a gap between the two adjacent areas may be necessary, especially over the spinal cord. Wedges function to change the angle of the isodose curve of a particular field relative to the beam axis at a specified depth so that the dose distribution can be evened out.

In the modern era, treatment machines typically utilize multileaf collimators that have the capability of not only static but also dynamic shaping of the beam during treatment, which avoids the need to manually change the blocks required for differing fields. Three-dimensional CRT involves treatment with multiple fields that enter the patient from different directions and are designed to avoid normal organs while delivering the desired dose to the tumor volume. IMRT builds on this approach by shaping the radiation beam continuously during treatment delivery with the use of moving multileaf collimators. IMRT is considered to be "inverse planned," meaning that the tumor and organ volumes are contoured manually by the physician and computer software is used to generate a radiation plan

with optimal characteristics in terms of tumor coverage and organ sparing. Volumetric arc therapy, or VMAT, is a more recent iteration of IMRT that involves continuous delivery and shaping of the radiation beam as the treatment gantry rotates around the patient. This technique allows for significantly reduced treatment times and improvements in dose distribution in some scenarios.

Brachytherapy

In contrast to teletherapy, brachytherapy uses selected radioisotopes and specialized instruments to administer radiation directly to a tumor or its bed. The radiation sources are placed either adjacent to the surface of a tumor mass or tumor bed or inside the tumor itself. The treatment may involve permanent implantation of radioactive sources (e.g., permanent ^{125}I seeds injected into a recurrent nasopharyngeal mass) or only a temporary exposure, after which the source is removed (e.g., intracavitary insertion of ^{125}I seeds for a localized recurrent nasopharyngeal carcinoma or temporary interstitial catheter implantation for afterloading with ^{192}Ir sources for a neck mass or tumor bed).

Brachytherapy radiation travels only a short distance to the desired target region, and its dose intensity falls off rapidly with distance according to the inverse square law. This phenomenon permits a sharp decrease in the dosage to the surrounding normal tissue so that the radiation dose is delivered to a relatively small, well-defined volume. Low-dose-rate (LDR) brachytherapy delivers continuous radiation at a rate of 40 to 200 cGy per hour, whereas high-dose-rate (HDR) brachytherapy delivers in excess of 1200 cGy per hour. In radiobiological terms, LDR brachytherapy can be likened to fractionated radiation with an infinite number of small individual doses. The theoretical advantage of this approach is that it allows redistribution of the tumor cell within the cell cycle, resulting in a greater percentage of malignant cells in the more radiosensitive phases. It also allows time for reoxygenation of hypoxic cells during the treatment and thus results in an increase in their radiosensitivity.

LDR brachytherapy favors late-responding normal tissues relative to tumors, and repopulation does occur, but unfortunately it benefits tumors more than normal tissues. HDR treatments have a higher risk for complications involving late-responding tissues. Therefore HDR brachytherapy needs to be well fractionated to deliver only one to three fractions per week. The isotopes most commonly used in head and neck cancer treatments are ^{125}I and ^{192}Ir. The implants can be planar (single plane) or volumetric (more than one parallel plane separated by 1–1.5 cm).

Head and neck tumor sites commonly considered suitable for brachytherapy include the lip, floor of mouth, oral tongue, base of tongue, buccal mucosa, tonsillar region, nasopharynx, skull base, and neck. The size and volume of the primary lesion, the anatomic extent, the topography, adjacent vital organs, any prior therapy, and the medical condition of the patient must be critically evaluated when considering a case for possible brachytherapy intervention. In the oral tongue and floor of mouth regions, T1 and T2 lesions can be treated with brachytherapy alone or in combination with external beam radiation therapy with good results. However, the risk of possible complications from treatment such as soft tissue or bone necrosis must be weighed against consideration of a primary surgical approach with its low complication rate. When the radioactive sources are in close proximity to the gum and bone, the risk of complications (such as bone exposure and necrosis) greatly increases. Other contraindications include an inability to encompass the tumor with adequate margins or inadequate access to the tumor. This form of therapy therefore is ideal as an adjunct to surgery or external beam radiation therapy.

PRETREATMENT REQUISITES

Patient Evaluation and Prevention of Complications

A comprehensive pretreatment evaluation is essential for all patients for whom radiation therapy is planned. If the radiation treatment fields are to include major salivary glands or the oral cavity, a dental evaluation is mandatory. Carious teeth that are not salvageable should be extracted. If postoperative radiation therapy is planned, the appropriate extractions can be carried out either before or during the definitive surgical procedure to obviate such a situation. However, it is important to avoid dental extraction in the vicinity of a tumor before surgery, because extraction in this area increases the risk of tumor implantation by providing the tumor with direct access to the mandible or maxilla and may increase the required extent of surgical resection (Fig. 19.4).

Patients with a significant number of dental fillings should use a customized mouth guard with a lead shield to decrease the chances of adjacent mucositis from the scatter effect of radiation. Fluoride prophylaxis is essential to prevent long-term dental decay and the development of caries. For effective delivery of fluoride, customized dental trays are prepared after obtaining impressions of the patient's dentition. Alternatively, patients may use toothpaste that includes a high concentration of fluoride. The importance of lifelong fluoride use should be emphasized to the patient. Routine periodic follow-up dental appointments are scheduled during and after the completion of radiation therapy to ensure continuing care.

When radiation is administered to the neck, the development of hypothyroidism is a risk, and thus thyroid function tests should be monitored both before and after treatment. Significant anemia has been suggested to adversely affect the efficacy of radiation therapy in patients with head and neck cancer, and therefore the hematocrit level of patients being treated with curative intent should be brought to greater than 30%. A baseline ophthalmologic evaluation is indicated in patients who have tumors of the nasopharynx, nasal cavity, and paranasal sinuses,

Figure 19.4 Extraction of teeth in the immediate proximity of the tumor should be avoided before surgery.

in whom the radiation portals include a portion of the orbits. Evaluation of the patient's nutritional status and aggressive management of problems such as weight loss, dysphagia, odynophagia, and trismus need to be appropriately addressed. Dietary consultation must be obtained, which may result in the prescription of appropriate dietary supplements. Placement of a percutaneous endoscopic gastrostomy tube should be considered in patients in whom significant swallowing difficulties are anticipated, such as those with tumors of the hypopharynx and cervical esophagus. This symptom is exaggerated in patients who undergo concurrent chemoradiation therapy. However, a potential risk of pharyngeal stricture remains in these patients because of the absence of the effort of swallowing during treatment. Consultation with speech and swallow specialists before radiation therapy is valuable to mitigate swallowing issues during the course of treatment. Patients who continue to smoke and abuse alcohol require counseling for cessation and more intense supportive care because they are prone to more severe adverse effects of radiation therapy.

Simulation

Simulation is the first step in radiation planning. A plain radiograph (two-dimensional treatment planning) or, more frequently in the modern era, computed tomography (CT)–assisted (three-dimensional treatment planning) approach is used to determine the fields of treatment around the primary tumor site, lymph nodes, and adjacent tissues that are at risk.

Conventional simulation with two-dimensional treatment planning is performed with the use of fluoroscopy to determine the portal margins under the direction of the radiation oncologist. Simulation films are special radiographs with cross-hair wires marking the isocenter and delineator wires at the perimeter noting the portal margins. Graticule marks are placed 2 cm apart, creating a grid of dots approximately 3 mm in diameter that serve as reference markers (Fig. 19.5). Patients undergoing primary radiation therapy for visible, palpable, and accessible lesions in the oral cavity or oropharynx undergo implantation of gold seeds at strategic points along the perimeter of the tumor for radiographic visualization on the simulation films. A topical anesthetic is sprayed over the tumor region, and a seed injector is used to interstitially implant one or several gold seeds to a depth of approximately 1 cm. All incisional scars, strategic anatomic locations, and masses are marked or outlined with appropriate material for radiographic visualization. Block positions are drawn on the films with a wax pencil to shield structures such as the larynx, spinal cord, and any other areas that do not require radiation. Custom-fabricated Cerrobend blocks then can be mounted on the treatment unit head during therapy. After conventional simulation is completed, Polaroid pictures are taken to show the patient setup. Tattoos are strategically and discretely placed on the skin of the patient to delineate the setup reference points. Beam films are obtained at this point, and treatment is initiated.

The patient is placed in a supine position on the simulation table and properly adjusted with use of an appropriate head holder to position the head at the desired angle. A shoulder pull board is sometimes used to maximally bring the shoulders into a caudad position, with the patient gripping straps that wrap around the soles of the feet. A bite block made of thermoplastic material with a lead wire placed in the longitudinal direction allows separation of the maxillary region from the mandible to spare it from radiation. If dental guards are necessary, they should be placed into position. A thermoplastic face mask is fabricated to firmly hold the head in the proper position (Fig. 19.6).

Three-dimensional CRT or IMRT are now the standard methods of treatment planning. Simulation involves CT scanning followed by a complex course of treatment planning. If indicated, intravenous contrast is administered with use of an infusion pump. Images are obtained in 3-mm slices, and the radiation oncologist determines the superior and inferior margins of the field on the CT images. This process permits the determination of the isocenter, which is marked on the patient through the use of tattoos or markers placed on the thermoplastic mask for future setup reference points. The computerized data then are transferred to a digital treatment planning system, where contours of the tumor; lymph node basins at risk; and vital organs such as the spinal cord, major salivary glands, brainstem, optic nerves, optic chiasm, and orbits are digitized on the CT slices. These data then are used for either three-dimensional conformal radiation treatment or IMRT planning.

Three-dimensional CRT uses CT simulation computer data to develop noncoplanar beam arrangements that conform to the

Figure 19.5 A simulation film from a right lateral aspect of a patient for whom treatment of a T1N2b squamous cell carcinoma of the left tonsil is planned.

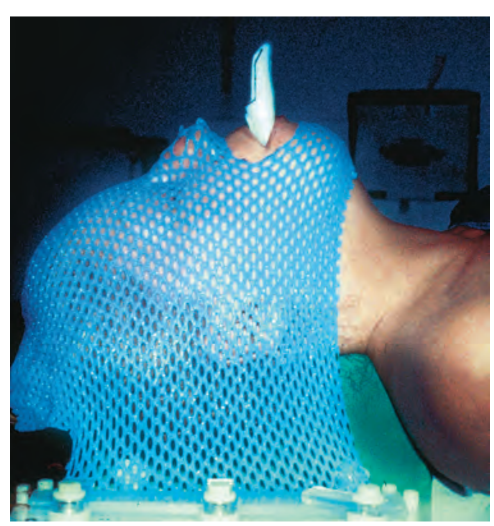

Figure 19.6 A thermoplastic face mask and bite block.

target in three dimensions. Contrary to conventional simulation and two-dimensional treatment planning, a computer-based "virtual simulation" is carried out. A beam's-eye view perspective is created via digitally reconstructed radiographs. Port films of the patient are taken to verify the treatment setups through comparison with the digitally reconstructed radiographs. Complicated three-dimensional dose calculations allow for accurate determination of the dose to the target regions and the adjacent normal critical structures based on the computer-generated isodose curves. Dose-volume histograms are available to the radiation oncologist for determining the three-dimensional dose distribution to both the tumor and vital structures (Fig. 19.7).

IMRT is an advanced form of three-dimensional conformal treatment planning that involves the use of the most sophisticated computer-generated treatment planning and clinical linear accelerators. This technique is especially useful in the treatment of lesions in complex anatomic areas that are adjacent to vital structures such as the spinal cord or brainstem, because it improves the therapeutic ratio by optimizing the dose to the tumor target while limiting the dose given to the surrounding normal tissues. This approach creates multiple nonuniform beam profiles to modulate the intensity of the beam for each unique port. Many small beams with different intensities thus are created, resulting in a beam intensity that will vary across the treatment field. Conceptually, this process involves using the inverse planning technique whereby the target and adjacent vital organ doses are first determined. Then the process works backward through the computerized inverse planning algorithm to generate the appropriate delivery parameters that would result in the preset, idealized dose distributions. The clinical application of IMRT requires a sophisticated linear accelerator with a computer-driven dynamic multileaf collimator capability (Table 19.3). If available, IMRT is the preferred treatment modality for all tumor sites within the head and neck.

IGRT refers to advanced imaging techniques that can be used *during* radiation treatment. IGRT allows daily monitoring of patient setup on the treatment machine. In addition, by using a kilovoltage imaging device on the treatment machine, acquisition cone-beam CT images on the treatment machine allows the visualization of the soft-tissue structures as well as the tumor target volume. This method involves simultaneous kilovoltage projection imaging and immediate image reconstruction to produce a three-dimensional image of the patient position during treatment that can immediately be overlayed on the treatment plan. Therefore it is a valuable tool for daily monitoring of patient setup as well as soft-tissue visualization. IGRT is also useful for treating patients with head and neck cancer because it can direct the need for replanning should the patient's

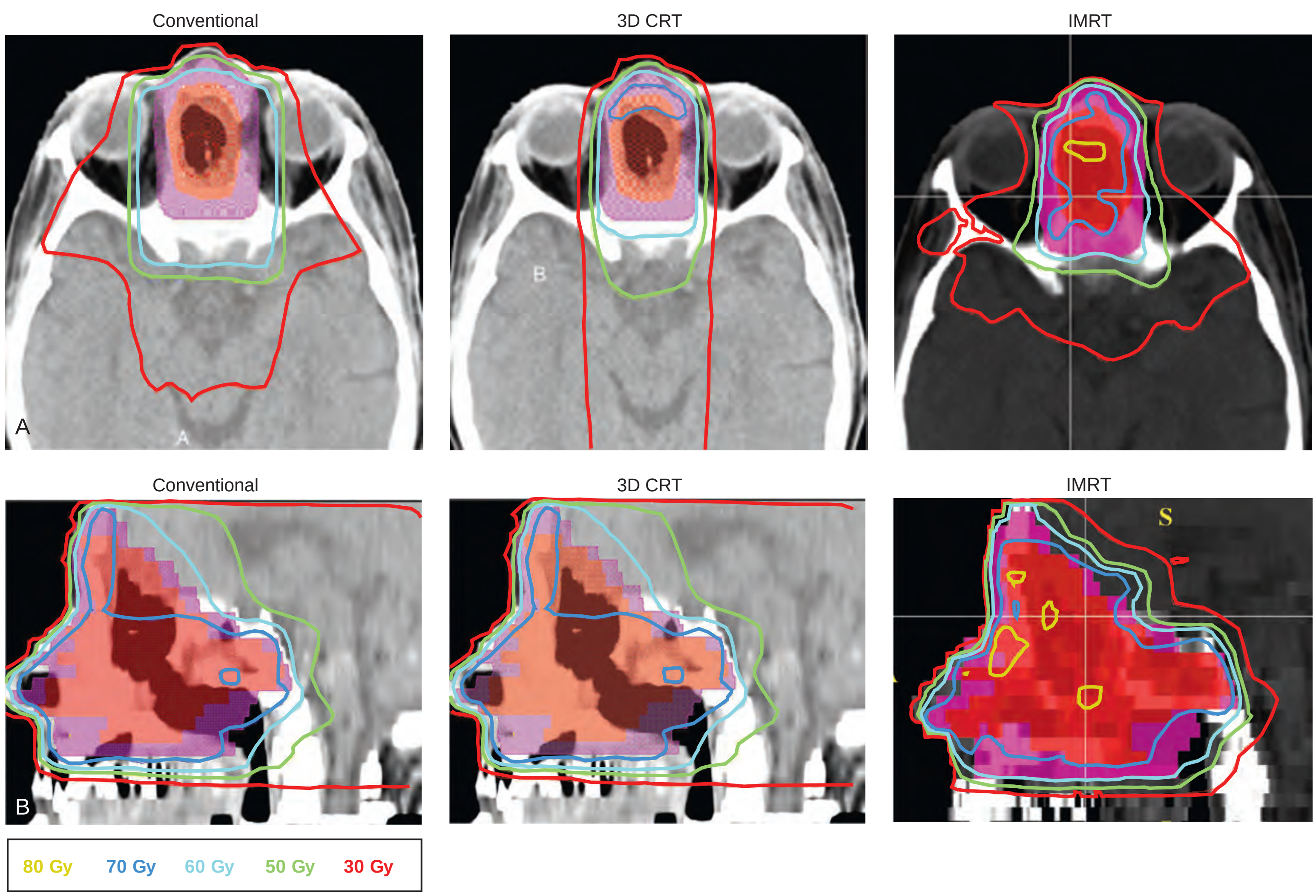

Figure 19.7 Isodose curves comparing conventional delivery, three-dimensional conformal radiation therapy, and intensity-modulated radiation therapy for cancer involving the paranasal sinuses. **A**, Axial view. **B**, Sagittal view. *3D CRT,* Three-dimensional conformal radiotherapy; *IMRT,* intensity-modulated radiation therapy. *(Modified from Figure 1 of Huang D, Xia P, Akazawa P, et al. Comparison of treatment plans using IMRT and 3D CRT for paranasal sinus cancer. Int J Radiat Oncol Biol Phys 56:158–168, 2003.)*

Table 19.3 Dose-Volume Distribution Comparing Conventional Delivery, Three-Dimensional Conformal Radiation Therapy, and Intensity-Modulated Radiation Therapy for Cancer Involving the Paranasal Sinuses

	CONVENTIONAL	3D CRT	IMRT
% GTV >70 Gy	0%	82%	95%
% CTV >60 Gy	94%	98%	96%
1% of chiasm	62 Gy	54 Gy	50 Gy
1% of optic N	64 Gy	49 Gy	54 Gy
1% of brainstem	44 Gy	55 Gy	37 Gy

3D-CRT, Three-dimensional conformal radiotherapy; *CTV,* clinical tumor volume; *GTV,* gross tumor volume; *IMRT,* intensity-modulated radiation therapy; *N,* nerve. (Modified from Table 1 of Huang D, Xia P, Akazawa P, et al. Comparison of treatment plans using IMRT and 3D CRT for paranasal sinus cancer. Int J Radiat Oncol Biol Phys 56:158–168, 2003.)

anatomy change as a result of tumor shrinkage or patient weight loss. A megavoltage imager can also be used to obtain images during radiation treatment, but the soft-tissue resolution is suboptimal compared with kilovoltage imaging.

TREATMENT INTENT

Curative

Radiosensitive tumors such as squamous cell carcinomas of the nasopharynx and oropharynx can be effectively controlled and cured with the use of definitive radiation or chemoradiation therapy. Similarly, early-staged carcinomas of the larynx are suitable for curative radiation therapy. Basal cell carcinomas and superficial squamous cell carcinomas of the skin also can be controlled effectively with radiation therapy. The choice of radiation therapy versus surgery as the definitive modality requires consideration of various tumor and patient factors. Radiation therapy is also commonly administered adjuvantly following surgery in high-risk cases. In most instances, therapeutic doses of radiation exceed 6000 cGy and may be more than 7000 cGy depending on the site, histology, and stage of the tumor.

Palliative

Radiotherapy is an effective means of palliation of symptoms in patients with incurable cancers of the head and neck. Control of pain can be achieved as a result of tumor shrinkage or necrosis by relieving pressure on neural structures. Lesions that obstruct the airway can be palliated effectively when tumor shrinkage is achieved with radiation therapy. Control of hemorrhage from bleeding tumors is another indication for the palliative use of radiation therapy. Palliative radiation involves use of lower doses than are administered in the curative intent setting.

TREATMENT SELECTION

Preoperative Radiation Therapy

The theoretical basis for using preoperative radiation therapy is that tumor cells are in their maximal state of oxygenation and hence are more radioresponsive. In general, the preoperative dose of approximately 5000 cGy using conventional fractionation of 180 to 200 cGy per fraction is delivered 5 days per week for a total of up to 5 weeks. A 4- to 6-week period of recovery is required for the patient to have the acute inflammatory reaction subside before surgical intervention.

Table 19.4 Advantages and Disadvantages of Preoperative Radiation Therapy

Advantages
- No surgery-related delay in delivering radiotherapy
- Allows time for supportive therapy for subsequent surgery: nutritional, pulmonary, cardiac
- No alteration in blood supply to the tumor from scarring reducing tissue oxygenation
- May reduce tumor volume in borderline operable cases
- Reduction in marginal recurrences
- Controls subclinical disease at the primary site and in the lymph nodes

Disadvantages
- Delays definitive surgery
- May adversely affect postoperative wound healing
- Dose limitations, due to potential wound-healing problems
- Complete pathologic information is not available regarding the extent of primary tumor, margin status, and nodal metastases
- Potential noncompliance by patient, in the event of excellent tumor response and refusal of surgery

The advantages and disadvantages of preoperative radiation are shown in Table 19.4. An important factor in preoperative radiation is dose limitation. Because of the increased risk of surgical complications with increasing doses of preoperative radiation, it is no longer recommended. At this time, preoperative radiation therapy is used rarely and only under select circumstances.

Definitive Radiation Therapy

The use of radiation is well established in the definitive treatment of several head and neck cancers, such as early-stage tumors of the nasopharynx, oropharynx, larynx, and hypopharynx. The role of definitive radiation therapy for various sites in the head and neck is discussed in each respective chapter. However, oropharyngeal and nasopharyngeal carcinomas require special consideration and are discussed here.

Oropharyngeal Carcinoma

In the last 2 decades, the incidence of oropharyngeal carcinoma (OPC) has increased substantially as a result of proliferation of human papillomavirus (HPV) infection and its identification as an etiologic factor in tumorigenesis. Patients with HPV-positive OPC demonstrate superior oncologic outcomes compared with their HPV-negative counterparts, with longer survival and an improved response to chemoradiation therapy. Five-year overall survival rates are 80% to 90% for patients with HPV-positive disease and 50% to 70% for patients with HPV-negative disease. The standard approach to locally advanced OPC is definitive chemoradiation with concurrent high-dose bolus cisplatin (100 mg/m^2 every 3 weeks). Areas of gross disease are treated with 7000 Gy while surrounding areas at risk and elective volumes in the neck are treated to a lower dose of 3000 to 6000 cGy, which is considered sufficient for eradication of microscopic disease. With this approach, locoregional control rates are typically greater than 90%. OPC associated with HPV displays marked sensitivity to radiation therapy, and significant clinical responses can often be observed early within the course of therapy, often by the third week. Given the improved treatment response of this disease, ongoing investigation is aimed at deescalating therapy to improve the toxicity profile while maintaining high cure rates. Multiple approaches to personalization of therapy and deescalation are currently being evaluated, including reduction in radiation dose, elimination of systemic therapy, or use of cisplatin alternatives and the integration of transoral

robotic surgery into the multidisciplinary approach. Surveillance following definitive chemoradiation therapy typically incorporates follow-up PET scans; the practice of planned neck dissection has been found to be unnecessary and has largely been abandoned. Salvage neck dissection is now considered in patients with persistent residual or progressive neck disease, particularly if it is PET positive or clinically evident. Patients with HPV-positive disease are typically younger and healthier. This, combined with improvements in radiation precision and supportive care, has made the need for percutaneous gastrostomy feeding tubes uncommon in this cohort as well.

Nasopharyngeal Carcinomas

Radiation therapy is the definitive treatment for nasopharyngeal carcinomas, which are highly radiosensitive tumors. In particular, nasopharynx tumors associated with Epstein-Barr virus (EBV) infection have been found to be especially responsive to radiation therapy. Surgery is used in selected patients with persistent or recurrent cancers. Regional lymph node metastases are present in 75% to 90% of patients. The lymph nodes at risk are levels V and II and retropharyngeal nodes. Lymph node metastases frequently are bulky and are bilateral in up to 50% of cases. Therefore it is important to include bilateral neck nodes, as well as the retropharyngeal nodes, in the radiation fields.

The current standard of care for patients with a locoregionally advanced nasopharyngeal carcinoma is chemotherapy given concurrently with radiation therapy. High-dose cisplatinum–concurrent chemotherapy with radiation is the standard of care. Cisplatinum is administered on days 1, 22, and 43 of radiation therapy. Adjuvant cisplatinum and 5-fluorouracil often are given after the completion of concurrent chemoradiotherapy. In contrast to other head and neck sites, even bulky lymph node metastases from nasopharyngeal cancers usually can be controlled with this treatment approach. Neck dissection is rarely required and should be considered for persistent disease at least 3 months after the completion of radiation therapy. Five-year survival rates between 60% and 75% have been reported for N0- to N1-stage disease, and 5-year survival rates between 40% to 50% have been reported for N2- to N3-stage disease.

Modern techniques, such as CT simulation and IMRT treatment planning, are far superior and permit a more homogeneous dose distribution to the primary tumor and involved lymph nodes while reducing the dose to important adjacent structures (Fig. 19.8). Patients undergo a simultaneous integrated boost IMRT plan. The gross tumor with adequate margins that account for setup errors receives 7000 cGy, whereas the high-risk subclinical region receives a dose of 5940 cGy. Control rates reported from multiple single institutions are in excess of 90%, including patients with T3 to T4 tumors. These results also have been reproduced by an RTOG cooperative trial. Despite efforts at improving local progression-free rate, distant metastasis remains an issue. Adjuvant chemotherapy is currently recommended following chemoradiation. The current NRG HN001 trial is assessing whether response of circulating EBV DNA can be used to guide decision making for adjuvant chemotherapy.

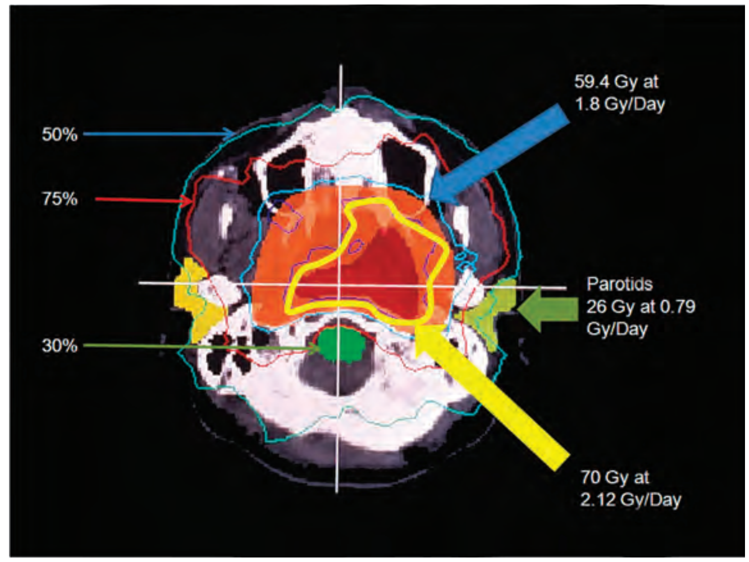

Figure 19.8 Intensity-modulated radiation therapy treatment plan for cancer of the nasopharynx showing isodose curves.

Table 19.5 Indications for Postoperative Radiotherapy and Chemoradiotherapy

Primary Tumor Factors
- Locally advanced T3 or T4 lesions
- High-grade histology
- Presence of perineural or vascular invasion
- Concern with respect to the adequacy of the procedure irrespective of the histologic status of the surgical margins
- Infiltrating rather than pushing borders of the tumor
- *Positive or close margins of surgical resection

Cervical Nodal Factors
- N stage higher than N1 (in selected patients)
- Surgical contamination (e.g., excisional or incisional biopsy) before definitive surgery
- *Presence of gross extranodal extension

*Chemoradiation therapy is recommended for these high-risk features.

Table 19.6 Advantages and Disadvantages of Postoperative Radiation Therapy

Advantages
- No treatment-related delay in surgery
- No limitations to the dose of radiation
- Allows complete surgical, histopathologic, and biological evaluation of the tumor and lymph nodes
- Residual microscopic disease can be effectively sterilized with improved local and/or regional control

Disadvantages
- Potential for delay in initiation of radiation therapy if recovery from surgery is complicated by fistula or other wound problems
- Scarring and vascular modifications from surgery may decrease tissue oxygenation and thus adversely affect radiation tumor cell kill

Postoperative Radiation Therapy

Postoperative radiation therapy (PORT) is indicated when the estimated risk of locoregional recurrence of disease is at least 20%. Although its efficacy in improving locoregional control has never been directly validated in a randomized clinical trial, the role of PORT is well accepted in selected circumstances based on good retrospective data. The indications for using PORT are listed in Table 19.5. A randomized trial comparing preoperative versus postoperative radiation therapy for advanced operable squamous cell carcinoma of the head and neck (RTOG 73–03) demonstrated significant improvement in locoregional control in favor of PORT and no difference in the complication rates between the two approaches. The advantages and disadvantages of PORT are shown in Table 19.6.

The timing for initiation of PORT has never been tested in a randomized trial. In general, however, PORT should be initiated

within 6 weeks of surgery to maximize the benefits of this combined approach. It has been shown, however, that a delay in initiating PORT does not influence local recurrence at the primary site, but a strong temporal correlation has been demonstrated between a delay in starting PORT and subsequent failure in the cervical lymph nodes. Some data suggest that the benefit of PORT can be seen even when it is given 3 months after surgery. Level I evidence is available, showing that the optimal PORT radiation dose for the primary tumor site and/or the neck region using conventional fractionation consists of a 180 to 200 cGy fraction per day administered 5 days per week up to a total dose of 6000 to 6600 cGy to the high-risk areas and 5000 to 5400 cGy for elective nodal irradiation.

Randomized trials by the European Organization for Research and Treatment of Cancer (EORTC) (trial 22931) and the RTOG (trial 95–01) demonstrated that the addition of concurrent chemotherapy with PORT improved locoregional control compared with PORT alone for patients with positive surgical margins at the primary site or extra-nodal extension of disease. However, this benefit is also accompanied by significant high-grade acute toxicity.

Reirradiation

Management of recurrent disease after previous radiation therapy given definitively or in an adjuvant fashion is a complex clinical problem. In general, surgical resection of recurrent disease is the treatment of choice if it is technically feasible. However, if adequate salvage surgery is not feasible or if concerns exist about margins after salvage surgery, then reirradiation may be considered. The important factors that have an impact on the feasibility of reirradiation are (1) previous dose, volume, and tumor response; (2) tolerance of normal tissues to additional radiation; (3) radiation dose to adjacent vital structures; (4) the feasibility of delivering a tumoricidal additional dose of radiation; and (5) the need for bringing in nonirradiated vascularized tissue to protect vital structures. Reirradiation may require consideration of brachytherapy versus IMRT or proton therapy with complex treatment planning. Close cooperation between the surgeon and the radiation oncologist and a detailed review of previous factors used in the initial radiation are crucial to the feasibility and success of reirradiation.

One frequently encountered situation is recurrent metastatic disease in a previously irradiated neck requiring salvage neck dissection. In this setting, tumor invasion of the carotid sheath is quite common. Traditionally, these patients have been treated with brachytherapy with use of either afterloading catheters or placement of ^{125}I Vicryl sutures into a Dexon mesh technique (Fig. 19.9). The radiated skin of the neck is at risk of necrosis because of compromise of the blood supply that accompanies elevation of the flaps at surgery, predisposing the patient to carotid exposure and rupture. This radiated skin therefore needs to be excised and replaced by vascularized tissue. Brachytherapy with placement of afterloading catheters with iridium-192 offers delivery of high-dose radiation to the target area without excessive radiation to the adjacent tissues. This technique is illustrated in Figs. 19.10 through 19.13. For reconstruction of the surgical defect, a pectoralis major myocutaneous flap, or a soft-tissue free flap is used to protect the carotid artery and resurface the skin.

More recently, IORT has been used for these situations at some institutions. Careful consideration of various factors is required, including the volume of residual tumor, the adequacy of exposure, whether the area is technically suitable for IORT, and whether any vital structures are within the proposed treatment field. A CT scan of the neck of a patient who previously was treated with chemoradiotherapy for a carcinoma of the tonsil with nodal metastasis demonstrates persistent disease in the neck (Fig. 19.14). The proximity and involvement of the carotid sheath creates a situation in which IORT is indicated. Gross clearance of all disease is accomplished with a radical neck dissection. However, microscopic disease persists on the

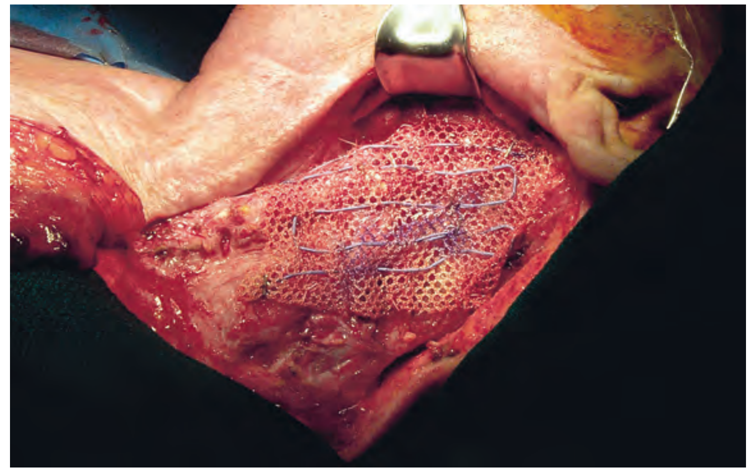

Figure 19.9 125I Dexon mesh for residual disease over a carotid artery.

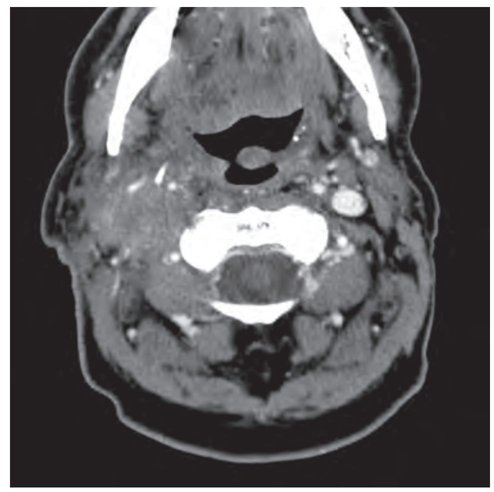

Figure 19.10 A computed tomography scan of a patient with a recurrent metastatic carcinoma in the right side of the neck close to the carotid artery.

Figure 19.11 The extent of skin resection is outlined.

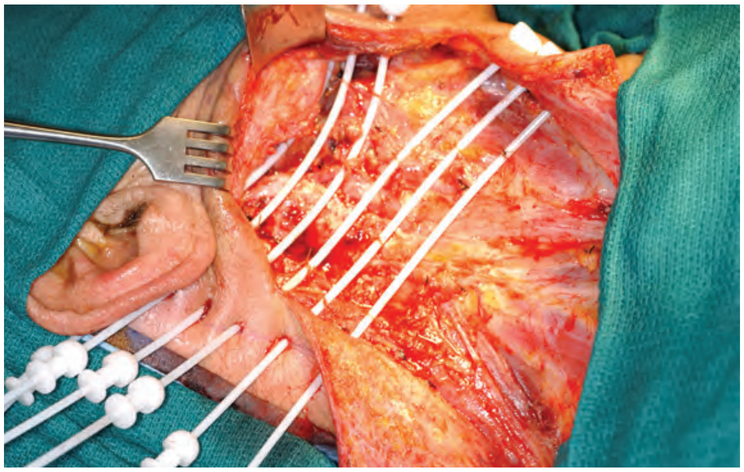

Figure 19.12 ^{192}Ir afterloading catheters are placed over the residual disease on the carotid artery.

Figure 19.13 Reconstruction of the surgical defect with a pectoralis major myocutaneous flap.

wall of the carotid artery and the carotid space up to the skull base. It is essential to determine the dimensions of the treatment area so that the appropriate applicator can be configured.

The applicator consists of parallel afterloading catheters embedded 1 cm apart within a thin slab of silicone-based rubber that can be trimmed to the specifications of the planar treatment field and positioned against the treatment area (Fig. 19.15). The previously radiated skin flaps and vital structures in the area are either moved out of the field or protected by placement of small lead shields. The applicator is then attached to a high-dose rate ^{192}I treatment unit for delivery of IORT. Alternatively, a linear accelerator can be used to deliver electrons through an electron cone. A single fraction generally is used to deliver 1500 cGy (1250–1750 cGy) to the planar treatment area. The isodose curves demonstrate dose distribution to the target field (Fig. 19.16). The obvious advantage of this method is that the previously irradiated skin is protected from further exposure and therefore does not need to be excised and replaced by a flap.

CARE OF THE PATIENT DURING RADIATION THERAPY

A radiation oncologist should perform weekly status checks of patients undergoing radiation therapy. At that time, a pertinent interval history should be obtained with special reference to a sore mouth or throat, dysphagia, hoarseness, altered taste, xerostomia, skin reactions, and ear symptoms. A complete examination should include the tumor status with measurements or photographs when appropriate. The patient should be checked for mucositis (Fig. 19.17), oral candidiasis (Fig. 19.18), and dermal reactions (Fig. 19.19). The general condition, body weight, and complete blood cell count should be monitored.

Over-the-counter skin moisturizing and lubrication products may be used to treat minor to moderate skin burns. RadiaCare Gel pads also are used to soothe skin burns. To treat mouth sores, patients should irrigate their mouth and gargle with a salt and baking soda solution as often as they can. Lidocaine mouth rinses are useful to combat painful mouth sores. It also

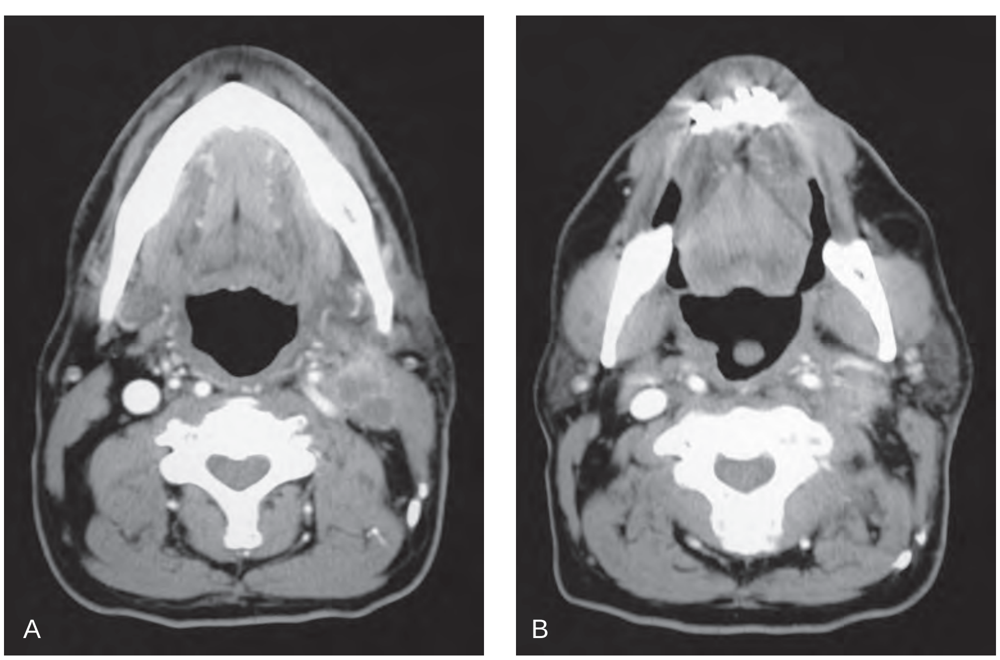

Figure 19.14 A contrast-enhanced computed tomography scan of the neck showing (**A**) recurrent metastatic disease adjacent to the carotid bifurcation and (**B**) involvement of the distal carotid artery.

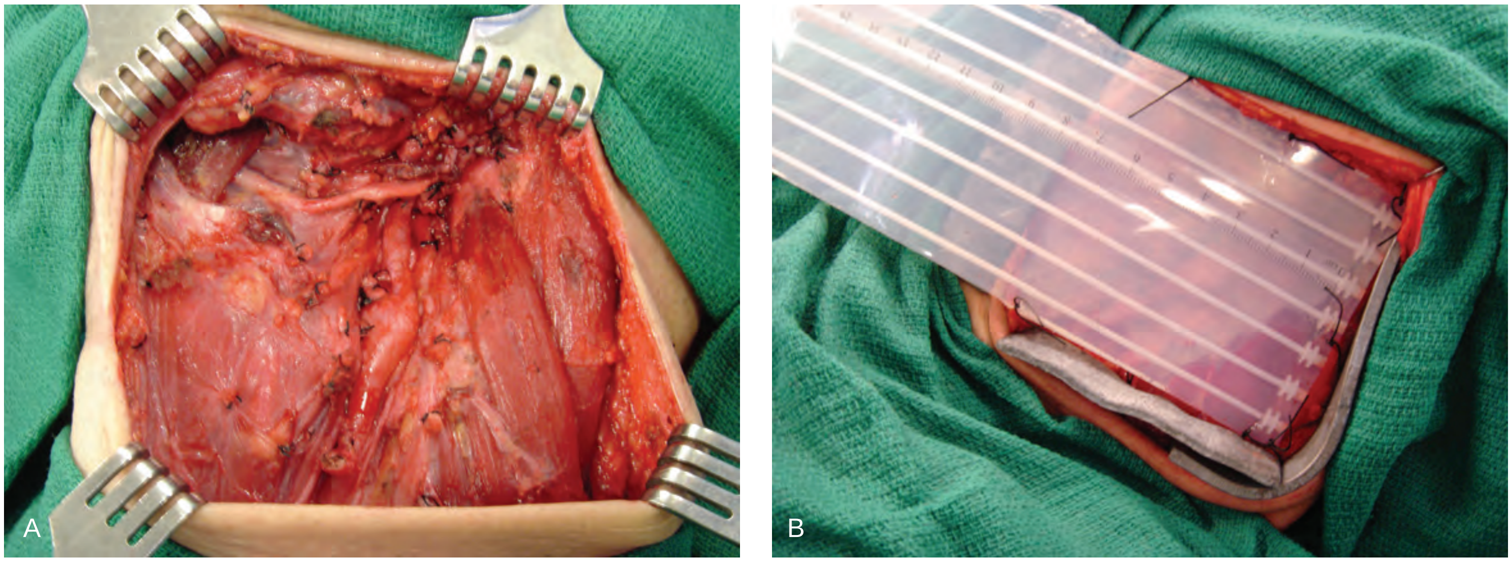

Figure 19.15 **A**, The surgical field after a radical neck dissection clearing all gross disease. **B**, A Harrison-Anderson-Mick applicator is placed against the treatment area, and intraoperative radiation therapy is delivered from a high-dose rate 192I treatment unit.

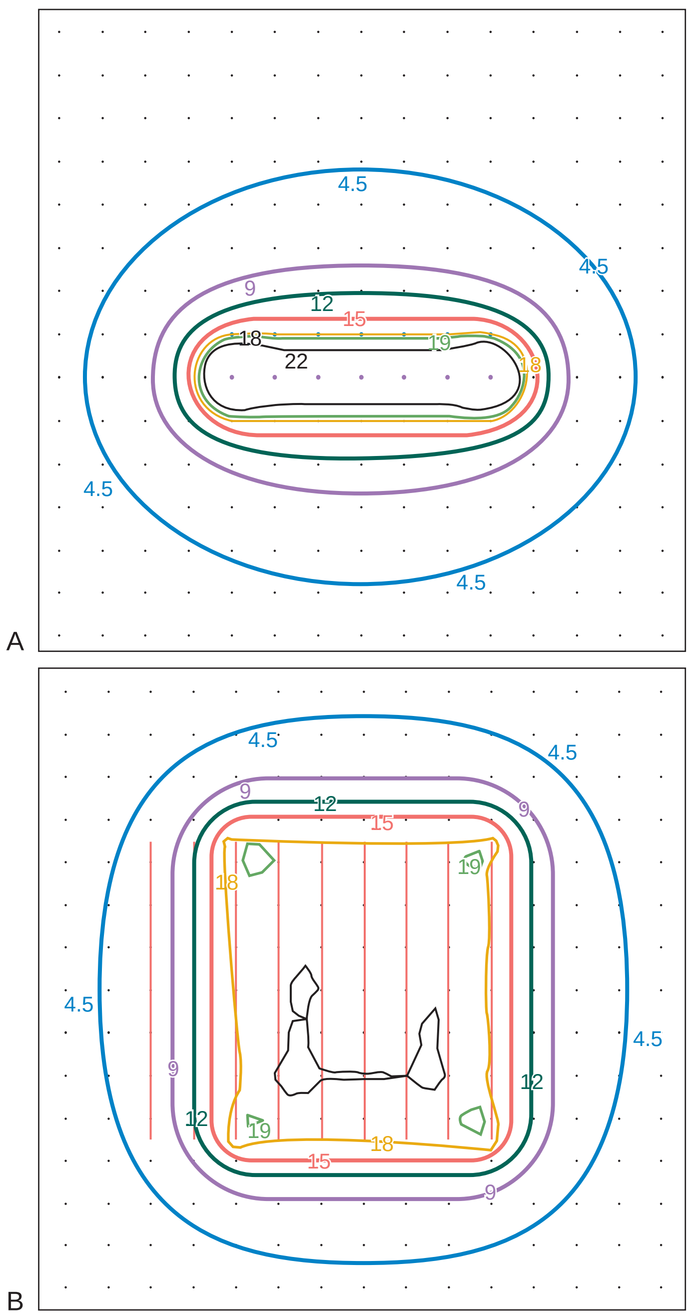

Figure 19.16 Two-dimensional isodose curves with intraoperative radiation therapy. **A**, Cross-sectional view. **B**, Planar view.

Figure 19.17 Radiation mucositis.

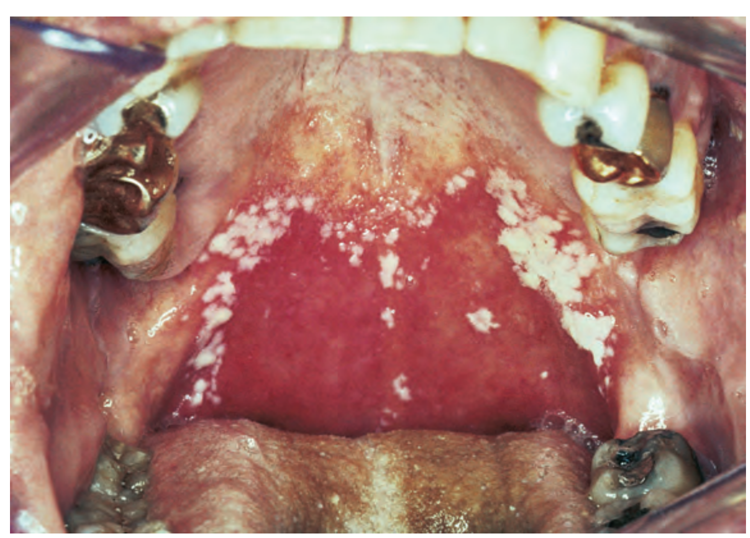

Figure 19.18 Oral candidiasis.

Figure 19.19 A skin reaction from radiation therapy.

Figure 19.20 Wet desquamation of the skin during radiation therapy.

is recommended that patients use a humidifier to prevent desiccation of the mucosa of the upper airway. Pain medications, including gabapentin and opiates, are prescribed as necessary.

Occasionally acute parotitis develops, which can occur within the first 12 hours after initiation of irradiation to portals including the parotid gland. Acute parotitis occurs as a result of an acute inflammatory reaction. Patients with this symptom report parotid swelling, localized pain, and sometimes a low-grade fever. Acute parotitis is a self-limited problem that usually resolves spontaneously after several hours, but the patient may benefit from a nonsteroidal antiinflammatory drug and reassurance.

Some patients, especially those undergoing concurrent chemoradiation, can experience progressive weight loss and dehydration by the fourth to fifth week of treatment. Initial intravenous hydration on an outpatient basis may be sufficient, but use of a percutaneous endoscopic gastrostomy tube may become necessary. Acetaminophen (paracetamol) with codeine either in tablet or liquid form can soothe the symptoms of mucositis initially, but the medication often must be advanced to a long-acting morphine sulfate or fentanyl patch with immediate-release morphine sulfate for rescue. Gabapentin is useful for minimizing mucositis pain and reducing opiate requirements. An oral *Candida* infection occasionally can occur and may be asymptomatic, or it may present as an acute exacerbation of a sore mouth or throat or as an abnormal taste. Antifungal medication is usually effective.

SEQUELAE, COMPLICATIONS OF RADIATION THERAPY, AND POSTTREATMENT FOLLOW-UP

Although radiation is an effective modality of treatment for head and neck cancers, it also affects the surrounding normal tissues. Radiation treatment–related complications can be divided into those that occur acutely (during or shortly after radiation) and those that occur later. These late effects may begin as early as 3 months after the completion of treatment and may occur any time during the patient's life. Typically, acute injury is related to toxic effects of radiation treatment on rapidly dividing cells, whereas late injury manifests itself in slowly dividing tissues such as connective and neural tissues. In addition, concurrent use of chemotherapy can increase the frequency and severity of radiation-related sequelae. The RTOG has published an elaborate acute and late treatment–related toxicity scoring system. The toxicities are scored from 0 to 4, with 0 having no change over baseline and 4 being severe. For example, in the case of skin, grade 4 is ulceration, hemorrhage, and necrosis.

Acute Sequelae

Acute toxicity from radiation typically affects mucous membranes, skin, and salivary tissues. Although in the orthovoltage era radiation doses were limited primarily by skin toxicity, this issue is no longer a concern because of high-energy radiation sources, which spare the skin unless a bolus is used as part of treatment. Radiation primarily affects the basal proliferating layer in the epidermis. At lower levels of exposure to the basal layer, erythema and hyperpigmentation of the skin can be seen. As the radiation effect on the basal layer intensifies, dry desquamation may result, and peeling and scaling of the skin (due to the buildup of dead cells) may be seen. With higher doses of radiation exceeding the tolerance of the basal layer, wet desquamation develops because of the lack of repopulation of epidermal cells (Fig. 19.20). In severe cases the epidermis completely sloughs off, exposing the dermis. To prevent radiation sequelae, skin care should be started before the initiation of radiotherapy. Local care with skin moisturizers and antiseptic creams can help accelerate recovery.

As with the skin, the mucus membranes are sensitive and show dose-dependent acute toxicity. At lower doses, mucosal erythema develops, which progresses to pseudomembranous-like mucositis because of the accumulation of dead cells, fibrin, and inflammatory infiltrate. Areas prone to the development of early radiation–associated mucositis include the soft palate and tonsillar pillars, the buccal mucosa, and the pharyngeal walls. Specific attention must be given to patients with metallic dental restoration, which causes radiation scatter that leads to significant mucositis, typically in the adjacent buccal mucosa and the lateral border of the tongue (Fig. 19.21). With increasing doses of radiation, the acute effects intensify, and areas of mucositis become confluent and ulcerate (Fig. 19.22). Occasionally, soft-tissue necrosis or laryngeal necrosis may be seen, particularly at radiation doses higher than 7000 cGy. Acute serous otitis media occurs in nearly all patients when the base of the skull is included in the radiation fields, such as in patients with tumors of the nasopharynx and paranasal sinuses. Symptomatic

Figure 19.21 Mucositis of the lateral border of the tongue due to radiation scatter from adjacent metallic dental fillings.

Figure 19.23 Telangiectasia, loss of elasticity, and fibrosis of the skin after radiation therapy.

Figure 19.22 Confluent mucositis of the oral cavity.

patients may require a myringotomy and drainage tubes to alleviate pain and improve hearing.

Salivary tissues are exquisitely sensitive to radiation exposure, resulting in a change in the volume and composition of saliva. The viscosity of saliva is increased consequent to radiation with a propensity to dryness of the mucous membranes and the formation of crusts. These areas can be a nidus for infection and should be addressed with oral irrigation with use of a solution that contains baking soda and salt. Alteration in taste occurs as a result of the direct effect on taste buds, as do changes in the biochemical composition of saliva.

Patients usually report a bland and metallic taste; however, the sense of taste spontaneously recovers over time. Acute radiation sequelae can severely impair oral intake of regular food. Dietary modification and nutritional supplements must be provided. Nasogastric or gastrostomy tube feeding should be considered as a last resort. Analgesic drugs, steroids, and antifungal medications also may be required to alleviate acute manifestations of radiation mucositis.

Late Sequelae

The exact mechanism underlying late sequelae remains to be defined. However, a combination of vascular endothelial damage, fibrosis from scarring, and muscle atrophy along with death of the parenchymal cellular network creates a milieu for late complications.

In the skin, late sequelae include atrophy and the development of telangiectasias (Fig. 19.23). Telangiectasias are seen more commonly after treatment with electron therapy. Late radiation effects also can lead to subdermal fibrosis and contracture, as well as very late development of skin carcinomas. Fibrosis, soft-tissue atrophy, and contractures are late phenomena that continue to progress over years (Fig. 19.24). Surgical procedures in previously irradiated fields have an inherent risk of delayed healing and/or skin and soft-tissue necrosis (Fig. 19.25). This risk is dose dependent, and therefore surgical planning should include excision of heavily irradiated skin and reconstruction of the surgical defect with nonirradiated vascularized tissue.

The extent of xerostomia varies and is not particularly dose dependent. Xerostomia leads to difficulty in swallowing and increased risk of dental caries, and it indirectly affects the patient's quality of life. At present, no therapeutic agents are available to effectively treat xerostomia, but commercially available salivary substitutes may afford some relief. Prevention of xerostomia with agents such as amifostine has shown limited benefit. Regular, frequent oral irrigation with a weak solution of salt and sodium bicarbonate is recommended. High humidity in inhaled air, particularly during the winter when the heating of homes tends to make the air dry, is essential to alleviate discomfort from xerostomia.

Continued dental care is essential to minimize the development of caries and the risk of osteoradionecrosis. Lifelong fluoride prophylaxis is essential. Endodontic work and dental extraction may precipitate the initiation of radiation necrosis, and therefore appropriate dental measures should be instituted by a dentist familiar with treating irradiated patients. Exposed bone or septic teeth require vigorous oral hygiene to prevent progressive bone loss and the development of full-fledged radionecrosis (Figs. 19.26 and 19.27). Hyperbaric oxygen

Figure 19.24 Skin soft tissue and bone atrophy progress with time after radiation therapy. **A**, Postoperative view of a patient with a through-and-through resection of the mandibular arch and chin and reconstruction with a fibula free flap 1 year after surgery and postoperative radiation therapy. **B**, Atrophic changes at 4 years following surgery are seen in skin, soft tissue, and bone. **C**, Progressive atrophic changes are seen at 7 years following surgery.

Figure 19.25 Necrosis of the skin and soft tissues after neck dissection in a previously irradiated field.

Figure 19.26 Osteoradionecrosis of the mandible seen in a panoramic x-ray of the mandible in a patient who has undergone previous marginal mandibulectomy and radial forearm free flap reconstruction followed by postoperative radiation therapy.

Figure 19.27 A sequestrum at the site of exposed mandible, in a patient with osteoradionecrosis, shown in Fig. 19.26.

may be of help in the prevention of radionecrosis, but it does not provide any benefit once the bone has already become necrotic.

Thyroid function tests including thyroid-stimulating hormone (TSH) are monitored in all patients who have been treated with radiation in the central compartment of the neck. Although symptomatic clinical hypothyroidism develops in only 5% of adults who are treated with radiation in the thyroid region, subclinical biochemical hypothyroidism is observed in a significant number of patients and approaches an incidence of 66% if the patient has had a previous hemithyroidectomy. Thyroid hormone replacement therapy is started if the TSH level rises above the normal range, irrespective of the T3 and T4 values, which may be within normal limits. If the hypothalamic–pituitary axis has been exposed to radiation, a complete endocrine screening should be obtained.

Fibrosis and muscle atrophy can lead to development of motor dysfunction, contracture, and strictures. Chronic dysphagia may develop as a result of fibrosis, and muscular atrophy may develop as a result of prolonged inactivity, especially in patients who have been treated with high-dose radiation therapy with or without chemotherapy for pharyngolaryngeal cancers. The presence of a pharyngoesophageal stricture is amenable to repeated dilations for relief of dysphagia. Rarely, surgical resection and reconstruction are required for complete strictures. Fibrosis of the muscles of mastication leads to the development of trismus. No effective treatment exists to correct established trismus. Therefore the management of trismus is prevention, with jaw-stretching active and passive exercises instituted soon after the completion of therapy and continued until satisfactory jaw opening is achieved. Postradiation fibrosis and scarring also may hamper shoulder movement, and it is crucial to emphasize the importance of regular daily range-of-motion exercises for the neck and shoulders.

Site-specific late toxicity also must be identified and addressed. Chronic serous otitis media is an intractable and difficult problem to treat. Continued management by an otologist is necessary to manage this long-term complication of radiation therapy. Lhermitte syndrome may develop in some patients whose cervical spinal cord is exposed to radiation. This syndrome is characterized by symmetric shooting pain like an electrical shock radiating down the spine and extremities with flexion of the neck. This benign, self-limiting myelopathy is thought to be due to demyelination that can appear from 1 to 3 months after radiation therapy and can last for up to 9 months or more. There are no other associated neurologic problems. However, if these symptoms develop for the first time 9 to 12 months after radiation therapy, the more likely diagnosis is radiation myelitis, which is a more serious problem.

Other site-specific sequelae can result from the effects of radiation on cartilage and bone, leading to impairment of growth in children, atrophy, and occasionally radiation chondritis or osteonecrosis. Radiation necrosis of the larynx, which was seen in the past, is rarely observed with contemporary techniques of delivering radiation. Patients have a 0.1% to 0.5% risk of a radiation-induced second cancer in the irradiated field. These second tumors typically are squamous cell carcinomas of the skin and high-grade sarcomas that may be difficult to treat. The risk for development of radiation-induced cancers increases with time. Accordingly, use of radiation as a treatment modality in younger patients with a long life expectancy needs to be weighed carefully against the increasing risk of second primary malignancies.

GLOSSARY OF RADIATION TERMINOLOGY

Terminology/Definition

Absorbed dose The energy imparted to matter by ionizing radiation per unit mass of irradiated material

Beam's-eye view (BEV) Used as an interactive tool to define portal/field entry angles that exclude nonirradiated critical structures while fully encompassing the target volume

Blocks Objects made of Cerrobend material that can protect the tissue so it does not receive radiotherapy

Bolus A material that can be placed on the patient to mimic actual tissue

Boost An area that needs to receive extra radiation in addition to the amount already received

Brachytherapy A term that refers to short-range radiation

Cell kill The mechanism by which radiation destroys a tumor, causing double-stranded or single-stranded deoxyribonucleic acid breaks

Chemoradiotherapy (CRT) A term referring to the combined modality treatment of chemotherapy and radiotherapy

Clinical tumor volume (CTV) The volume encompassing the gross tumor volume and all areas of tumor spread

Collimator A device placed on the gantry of the linear accelerator to modulate or change the radiation beams

Compensators A device used to compensate for the missing tissue during radiotherapy

Cone A device that can be placed on the linear accelerator to shape the radiation beam

Digital reconstructive radiograph (DRR) A reconstructive radiograph that enables treatment fields to be visualized in relation to the patient's anatomy

Dose Physical quantity with the units of gray or rad

Dose volume histogram (DVH) A plot that describes the dose delivered to a given target in relation to its volume

Field A term used in conformal radiotherapy that encompasses a given area receiving radiotherapy; multiple fields can combine to complete a treatment plan

Gantry The head of the linear accelerator where the radiation is delivered to the patient

Geographic miss A term used during highly conformal radiotherapy that describes missing the tumor target

Gray (Gy) The unit of ionizing radiation that is defined to be an energy absorption of 1 joule/kg; 1 Gy also equals 100 rads or 100 centigray (cGy)

Gross tumor volume (GTV) The actual clinically defined gross tumor

High-dose rate (HDR) A type of internal radiation treatment in which the radioactive source is removed between treatments; also called *high-dose-rate remote radiation therapy* and *remote brachytherapy*

Image-guided radiation therapy (IGRT) A term referring to the delivery of radiation under image guidance on the treatment machine

Intensity-modulated radiation therapy (IMRT) A highly conformal radiation therapy technique

Isodose curves A plot displaying the curve(s) that encompasses the same dose of radiation

Linear energy transfer (LET) The way in which ionizing radiation deposits energy at a constant rate as it travels through matter

Low-dose rate (LDR) A type of internal radiation treatment in which the radioactive source stays in the patient permanently

Penumbra The edge of the radiation beams where the dose of radiation sharply drops from 80% to 20%

Photons Packets of energy

Planning target volume (PTV) This volume encompasses the gross tumor volume and the clinical target volume with a margin to account for tumor movement and daily patient set-up errors on the treatment machine

R or r Also known as *roentgen;* a unit of radiation exposure; the dose of ionizing radiation that will produce 1 electrostatic unit of electricity in 1 cc of dry air

Rad The former unit for absorbed dose; 1 rad = 0.01 Gy

Radiation ports or fields The number of fields or areas receiving radiation

Relative biological effectiveness (RBE) A ratio of the absorbed dose of a reference radiation to the absorbed dose of a test radiation to produce the same level of biological effect, other conditions being equal

Simulation The beginning of the planning process before starting radiation therapy

Target dose Desired radiation dose for cell kill

Target volume The volume of tissue receiving radiation

Teletherapy Radiation therapy delivered externally

Treatment planning The work done by a medical physicist or dosimetrist to achieve the best possible treatment plan for the patient undergoing radiation

CHAPTER 20

Systemic Therapy

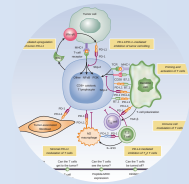

The role of systemic therapy in the treatment of head and neck cancer has increased in recent decades. Randomized clinical studies of integrated chemotherapy/radiotherapy programs have demonstrated improvements in locoregional control, organ preservation, and overall survival. However, high-grade acute toxicity and long-term sequelae of treatment remain a significant problem.

In contemporary multimodality therapy, chemotherapy may be given before surgery or concurrently with radiation therapy. For patients who undergo primary surgery for a disease that carries a poor risk of recovery, concurrent administration of high-dose cisplatin with postoperative radiation therapy often is recommended. The prognosis for patients with recurrent or metastatic disease remains poor in most cases, but treatment options are expanding with the development of novel targeted therapies that are based on a gradual improvement in the understanding of the molecular pathology of the disease and harnessing the power of the immune system to mediate tumor rejection. It is also now well appreciated that human papilloma virus (HPV) status of tumors favorably influences the prognosis for patients with newly diagnosed disease amenable to localized, combined modality therapy (Ang et al., 2010). The significant impact of HPV on clinical outcomes is now reflected in the revised staging system for head and neck cancers (eighth edition of the American Joint Committee on Cancer staging manual [Amin et al., 2017]). While decisions regarding standard of care treatment for head and neck cancers are currently not informed by HPV status, the evaluation of new treatment paradigms for HPV-positive head and neck cancer is currently a strong research focus that potentially could influence practice in the years to come.

ACTIVE CYTOTOXIC AGENTS IN HEAD AND NECK SQUAMOUS CELL CANCER

Platinum agents, taxanes, and antimetabolites all have clinical activity against some head and neck cancers (Table 20.1). Cetuximab, a chimeric monoclonal antibody directed against the extracellular domain of the epidermal growth factor receptor (EGFR), was more recently added to the list of systemic therapies for head and neck cancer. Other drugs such as ifosfamide, vinca alkaloids, hydroxyurea, and bleomycin also have some activity in this disease but are less commonly used in clinical practice.

Cisplatin (*cis*-diamminedichloroplatinum), the agent with the most data to support its use in the combined modality setting, is a platinum coordination complex that cross-links with deoxyribonucleic acid (DNA) and also can cross-link proteins with DNA. Cisplatin was discovered serendipitously in 1965 when it was observed that a substance produced by platinum electrodes was toxic to bacteria in laboratory experiments and was subsequently shown to have significant activity against a variety of human tumor cell lines. Cisplatin is now a standard therapeutic agent for patients with a wide range of malignancies, including head and neck squamous cell cancer. Renal toxicity is the dose-limiting toxicity. It is now widely understood that safe administration of cisplatin requires extensive intravenous hydration before and after the cisplatin infusion.

As with other cytotoxic chemotherapies, cisplatin causes transient myelosuppression, during which time the patient may be at increased risk of infection. Cisplatin is potently emetogenic, but cisplatin-induced emesis usually can be well controlled or prevented with contemporary antiemetic medications. Permanent peripheral neuropathy and ototoxicity (most typically, high-frequency hearing loss) may occur with use of cisplatin. As with most cytotoxic chemotherapies, fatigue tends to worsen with cumulative treatment cycles. Carboplatin appears to have the same general mechanism of action as cisplatin, but the adverse effect profile differs in that carboplatin is less nephrotoxic but more myelosuppressive than cisplatin. Carboplatin has not been studied as extensively as cisplatin in persons with head and neck cancer, but the available evidence suggests that carboplatin has a lower antitumor efficacy than cisplatin in persons with this disease.

Paclitaxel and docetaxel have significant activity against head and neck cancer. Paclitaxel was isolated from the bark of the Pacific yew tree in 1971, and docetaxel is a semisynthetic taxane. Taxanes work by binding to microtubules as cells attempt to divide, thereby causing cell cycle arrest in the M phase. Common adverse effects of taxanes include fatigue, alopecia, myelosuppression, and peripheral neuropathy. Taxanes are significantly

Table 20.1 Main Classes of Active Cytotoxic Chemotherapeutic Agents for Head and Neck Squamous Cell Carcinomas

CLASS OF AGENT	EXAMPLES	MAIN MECHANISM OF ACTION
Platinum	Cisplatin, carboplatin	Form DNA cross-links
Taxane	Paclitaxel, docetaxel	Stabilize microtubules to block M-phase
Antifolate (antimetabolite)	Methotrexate	Inhibit dihydrofolate reductase (DHFR) during S-phase
Fluoropyrimidine (antimetabolite)	5-Fluorouracil	Inhibit thymidylate synthase (TS) during S-phase

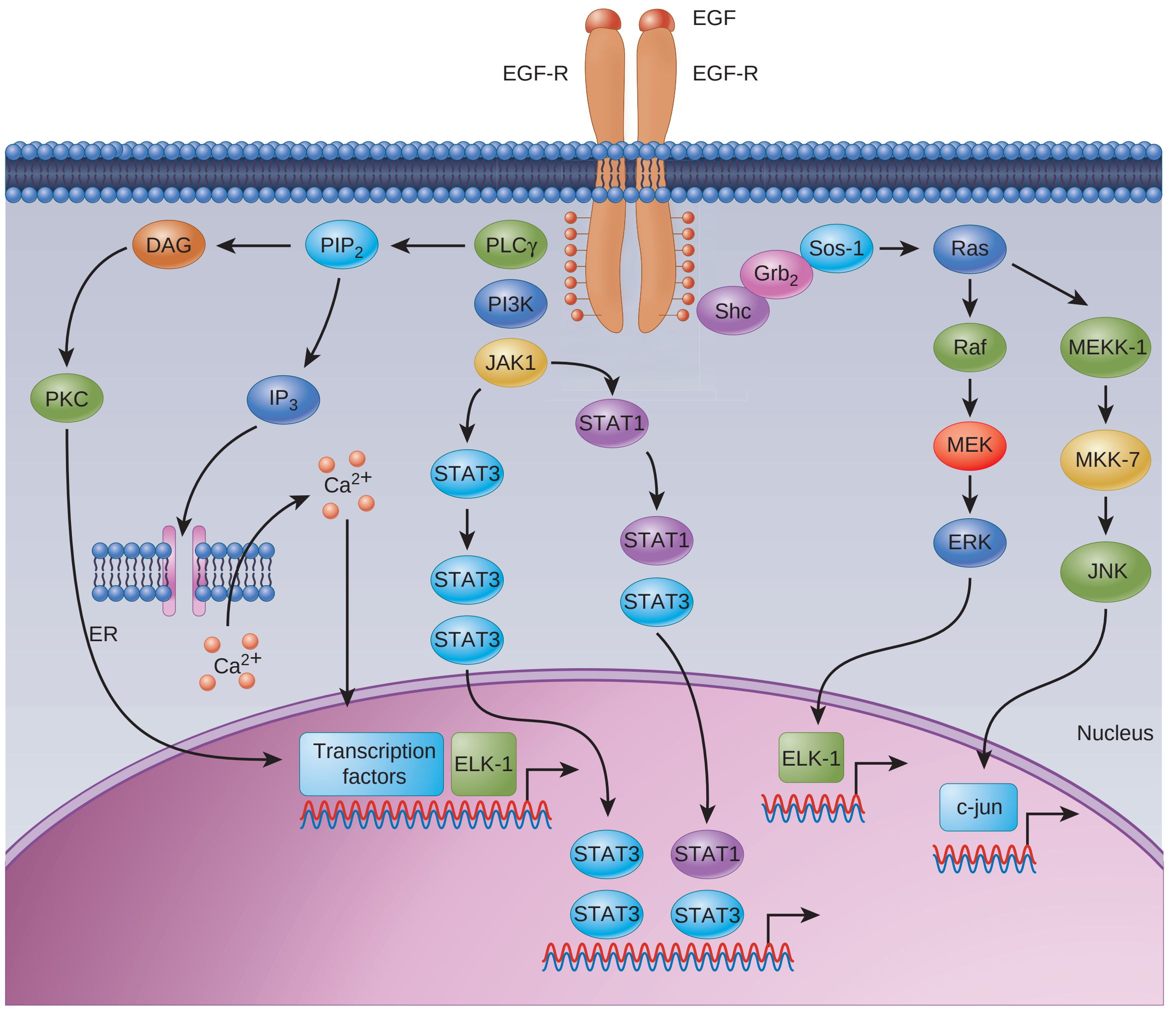

Figure 20.1 A schematic illustration of epidermal growth factor receptor (EGFR) signaling pathways in head and neck squamous cell carcinomas.

less emetogenic than cisplatin, and the peripheral neuropathy is more likely to be reversible. Taxanes are metabolized in the liver, and these drugs generally are not administered to patients with significant liver dysfunction. Patients must receive steroid premedications to reduce the risk of an anaphylactic reaction to components of the lipid solvent in which paclitaxel is administered. As with platinum compounds, taxanes can serve as radiosensitizers in the treatment of patients with head and neck cancer at the cost of increased mucositis in the radiation field.

Methotrexate and 5-fluorouracil (5-FU) are antimetabolites that can yield clinically useful activity against head and neck cancer. Methotrexate was developed in the 1950s and inhibits dihydrofolate reductase (DHFR), the enzyme that catalyzes the production of tetrahydrofolate. The resulting intracellular folate deficiency limits DNA synthesis and cell division. Methotrexate typically is administered to patients with advanced head and neck cancer as a palliative agent at low doses, and it is generally well tolerated in this setting. Low-dose palliative methotrexate may be associated with myelosuppression, fatigue, nausea, and mucositis. The drug 5-FU inhibits thymidylate synthase, thereby interfering with DNA synthesis and cell division. In head and neck cancer treatment, 5-FU most commonly is administered as a continuous infusion over 4 to 5 days in combination with other chemotherapy and/or radiotherapy. Common adverse effects of 5-FU are bone marrow suppression, diarrhea, and mucositis. Patients with low levels of dihydropyrimidine dehydrogenase, the enzyme that catabolizes 5-FU, can increase the risk of severe toxicity when treated with 5-FU.

Cetuximab is a chimeric monoclonal antibody therapy that targets the extracellular domain of the EGFR (Fig. 20.1) and is approved for the treatment of head and neck cancer. Almost all head and neck squamous cell cancers express EGFR, which is the prototype of the erb-B/HER family of type I receptor tyrosine kinases. Dysregulation of EGFR signaling activity appears to contribute to the malignant phenotype in a significant percentage of head and neck cancers, although it is unclear if the clinical efficacy of this therapeutic antibody is linked to inhibiting EGFR signaling or mediating antibody-dependent cell-mediated cytotoxicity. Cetuximab possesses modest activity as a single agent and can be an effective radiosensitizer in head and neck cancer. The most common adverse effect of cetuximab is an acne-like rash. A small risk exists of a severe allergic infusion reaction during a patient's first exposure to cetuximab.

Of these agents, cisplatin is the drug with the most data to support its use in combination with curative-intent radiotherapy. For patients with medical comorbidities that render them suboptimal candidates for treatment with cisplatin concurrent with radiation therapy, other options such as concurrent cetuximab may be preferable. Combination chemotherapy regimens have significant activity in the induction chemotherapy setting for previously untreated patients, although the activity of these drugs is lower in patients with recurrent disease. In the palliative treatment setting, the choice of combination

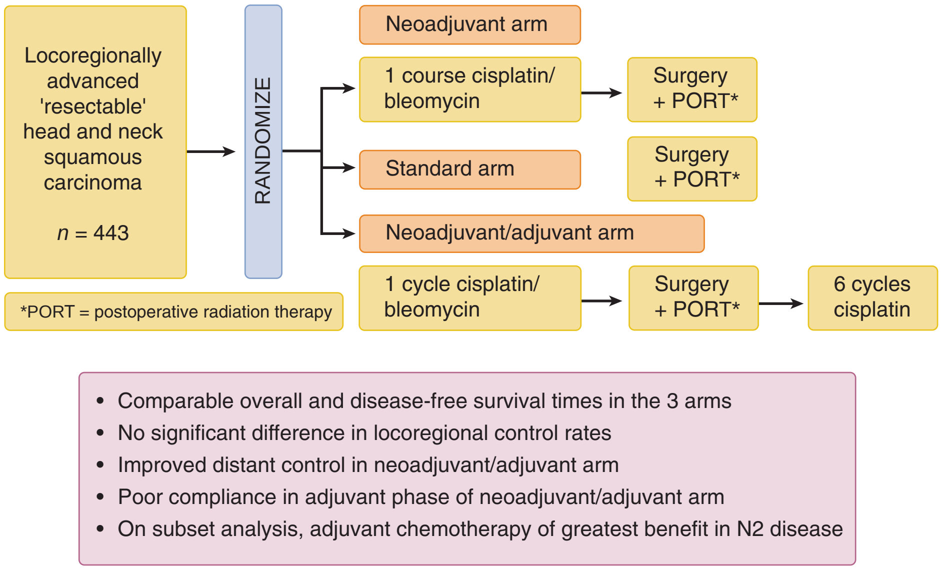

Figure 20.2 Design and results of the Head and Neck Contracts Program Trial. *(Adapted from the Head and Neck Contracts Program. Adjuvant chemotherapy for advanced head and neck squamous carcinoma: final report of the Head and Neck Contracts Program.* Cancer *1987;60:301–311.)*

chemotherapy versus monotherapy must be individualized, balancing quality of life issues against the goal of tumor control.

The remainder of this chapter will review the clinical literature that guides the selection of systemic therapies for patients with head and neck cancer.

INDUCTION CHEMOTHERAPY

The initial proof-of-concept for induction chemotherapy for this disease dates back to The Head and Neck Contracts Program Trial, the first large-scale study to evaluate the role of sequential chemotherapy in the management of advanced, resectable squamous cell cancer of the head and neck (Fig. 20.2). No significant differences could be demonstrated in locoregional control or 5-year disease-free and overall survival times among the three arms of the study. However, patients treated with neoadjuvant/adjuvant chemotherapy had a lower rate of distant recurrence. Of note, only 9% of patients received all six cycles of single-agent cisplatin adjuvant therapy, potentially contributing to the lack of observed survival benefit. Upon subsequent multivariate analysis, only patients with N2 disease had a significant survival benefit with the neoadjuvant/adjuvant chemotherapy. The neoadjuvant arm demonstrated the feasibility of administering primary chemotherapy in patients with head and neck cancer but failed to demonstrate a significant impact of induction chemotherapy on clinical outcome.

In the 1980s, the combination of cisplatin plus 5-FU (PF) emerged as the standard induction chemotherapy regimen. In a randomized phase III study, Paccagnella compared the PF induction chemotherapy regimen (cisplatin, 100 mg/m^2 on day 1 plus 5-FU, 1000 mg/m^2/day with a 24-hour infusion on days 1–5 administered every 21 days for four cycles) before locoregional therapy versus locoregional therapy alone for patients with stage III or IV disease without distant metastases. Patients with either operable or inoperable disease were eligible. Although no significant difference in overall survival between the two treatment groups was found when all patients were considered, a modest survival advantage was associated with induction chemotherapy in a subgroup analysis restricted to patients with inoperable disease.

The Veterans Affairs Laryngeal Cancer Study Group established the larynx preservation paradigm using the PF regimen. Dramatic responses were seen in a significant number of patients with preservation of a functional larynx (Fig. 20.3). As Fig. 20.4 shows, patients were randomly assigned to standard treatment (i.e., primary laryngectomy followed by radiotherapy) or organ preservation therapy (i.e., induction chemotherapy with cisplatin and 5-FU, followed by radiotherapy). The overall and median survival rates were not significantly different between the two arms, but larynx preservation was reported in 66% of the survivors in the induction chemotherapy arm. Induction PF also was used in a study of the larynx-preservation approach for squamous carcinoma of the hypopharynx, which was conducted by the European Organization for Research and Treatment of Cancer (EORTC) (Fig. 20.5). Disease control and survival rates were comparable between the two arms, and the larynx could be preserved in 35% of patients in the chemoradiation arm.

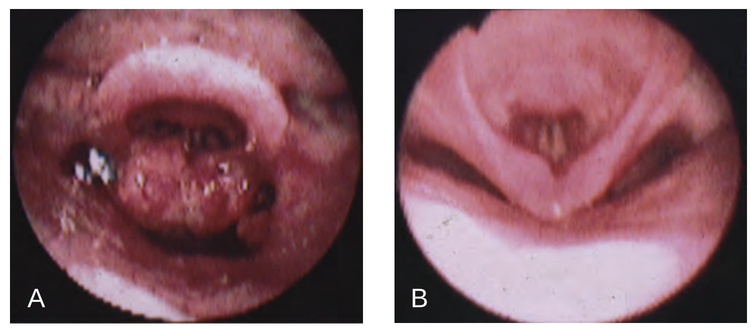

Figure 20.3 **A**, Squamous cell carcinoma of the supraglottic larynx involving both arytenoids that would have required a total laryngectomy. **B**, Complete response with preservation of the larynx after induction chemotherapy and radiation therapy.

The addition of taxanes to PF induction chemotherapy for patients with stage III or IV disease with no distant metastases yields superior outcomes compared with PF alone. The TAX 323 and TAX 324 studies randomly assigned patients to three cycles of PF versus three cycles of TPF (PF plus docetaxel, 75 mg/m^2 on day 1). In both studies, the total dose per cycle of 5-FU was reduced in the TPF regimens compared with the PF regimens. TAX 323 was restricted to patients with unresectable disease. Subtle differences in the dose and schedule of cisplatin and 5-FU existed in the TPF regimens in these two studies (Figs. 20.6 and 20.7). After induction chemotherapy, patients received definitive radiation therapy alone in TAX 323 or with concurrent weekly carboplatin (area under the curve of 1.5) in TAX 324.

Both studies demonstrated superior outcomes with TPF compared with PF. In TAX 323, overall response rates after

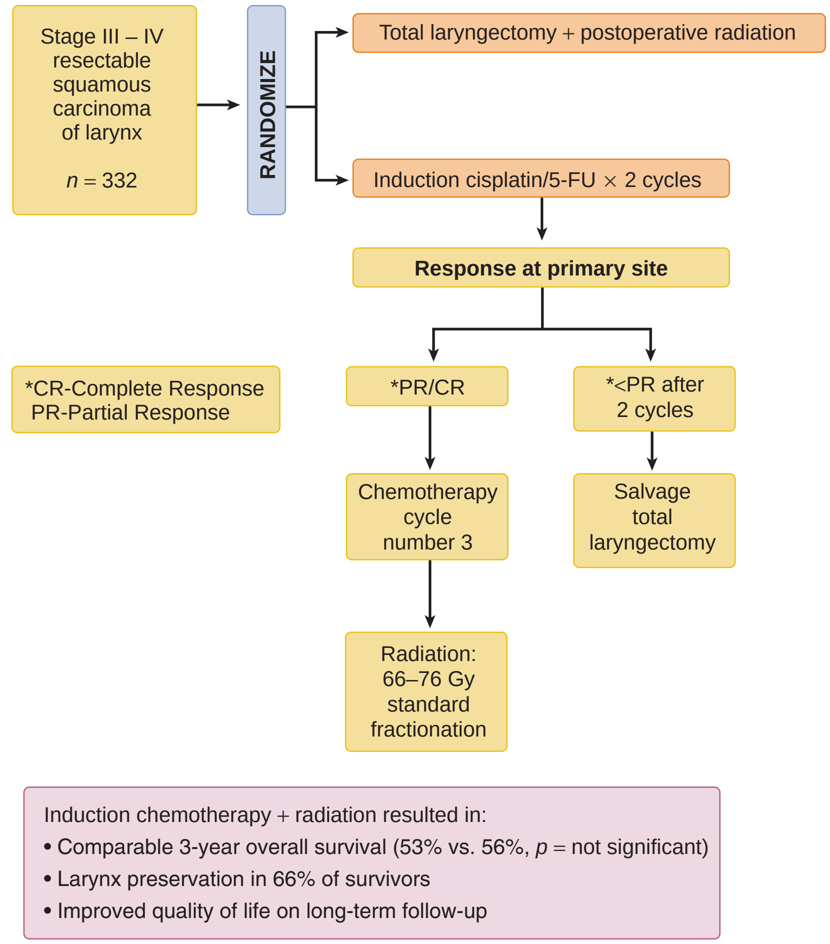

Figure 20.4 Design and results of the Veterans Affairs trial on induction chemotherapy and radiation for larynx preservation. *5-FU,* 5-fluorouracil. *(Adapted from The Department of Veterans Affairs Laryngeal Cancer Study Group. Induction chemotherapy plus radiation therapy compared with surgery plus radiation therapy in patients with advanced laryngeal cancer.* N Engl J Med *1991;324: 1685–1690 and Wolf G, Wolf GT, Fisher SG, et al. VA Laryngeal Cancer Study Group.* Proc Am Soc Clin Oncol *1993;12:277 [Abstract #892]).*

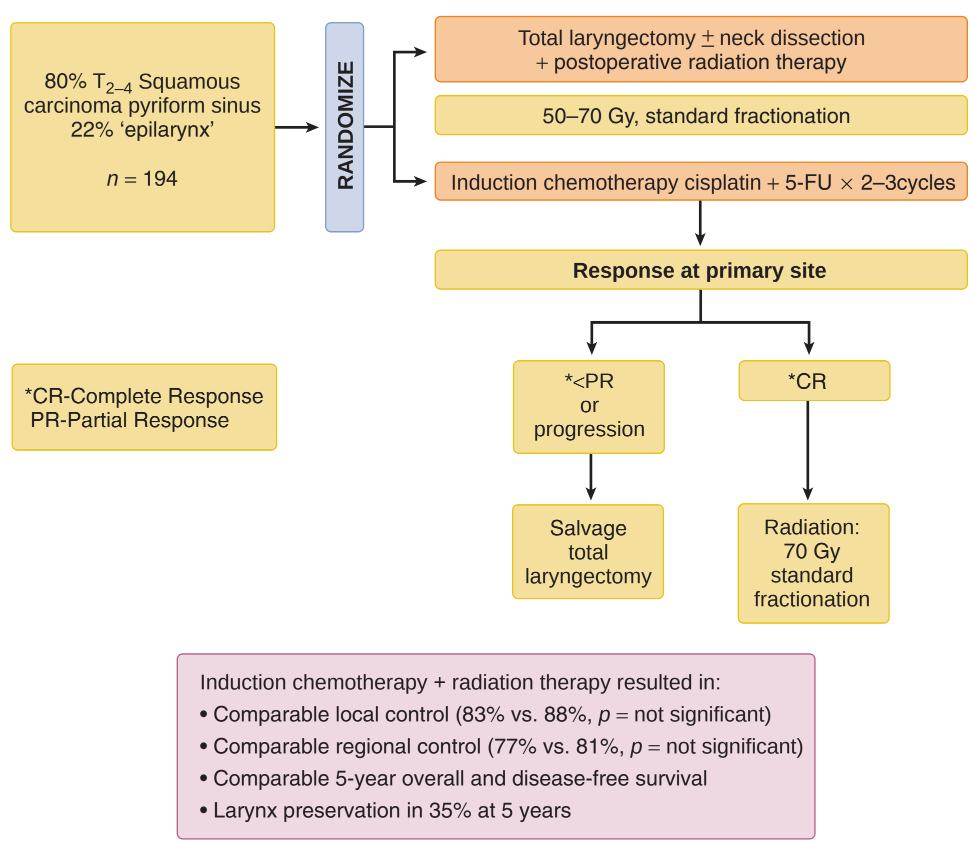

Figure 20.5 Design and results of the European Organization for Research and Treatment of Cancer trial on larynx preservation in hypopharyngeal carcinoma. *5-FU,* 5-fluorouracil. *(Adapted from Lefebvre JL, Chevalier D, Luboinski B, et al. Larynx preservation in pyriform sinus cancer: preliminary results from a European Organization for Research and Treatment of Cancer phase III trial. EORTC Head and Neck Cancer Cooperative Group.* J Natl Cancer Inst *1996;88:890–899.)*

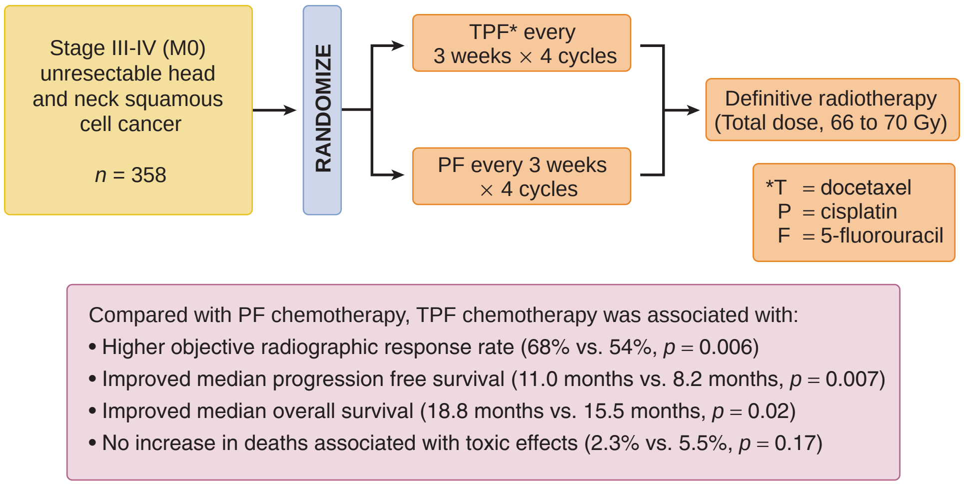

Figure 20.6 Design and results of the TAX 323 induction chemotherapy trial. *(Adapted from Vermorken JB, Remenar E, van Herpen C, et al. Cisplatin, fluorouracil, and docetaxel in unresectable head and neck cancer.* New Engl J Med *2007;357: 1695–1704.)*

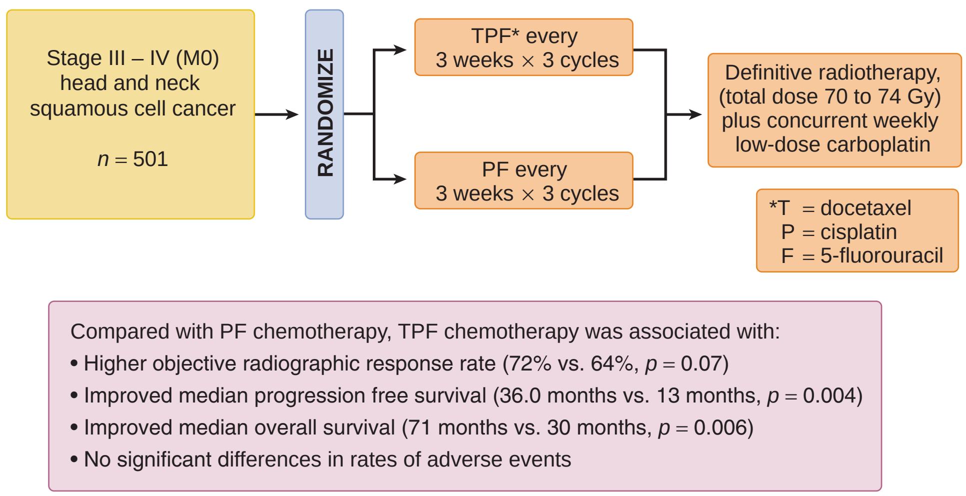

Figure 20.7 Design and results of the TAX 324 induction chemotherapy trial. *(Adapted from Posner M, Hershock DM, Blajman CR, et al: Cisplatin and fluorouracil alone or with docetaxel in head and neck cancer.* New Engl J Med *2007;357:1705–1715.)*

induction chemotherapy (68% versus 54%) and 3-year overall survival (37% versus 26%) were significantly higher for patients treated with TPF versus PF. Similarly, in TAX 324, the overall response rates after induction chemotherapy (72% versus 64%, p = .07) and 3-year overall survival were superior for the TPF group (62% versus 48%). These results are consistent with those of a randomized trial reported by Hitt and colleagues that evaluated the addition of paclitaxel to cisplatin and 5-FU in patients with stage III or IV disease without distant metastasis. The addition of paclitaxel yielded a significant improvement in response rate to induction chemotherapy and a trend toward improvement in overall survival.

These trials, however, were not designed to compare the strategy of induction chemotherapy followed by chemoradiation versus primary chemoradiation. Several phase III randomized clinical trials that followed failed to demonstrate a significant efficacy advantage with this sequential approach (Cohen et al., 2014; Haddad et al., 2013; Hitt et al., 2014). The negative results in the PARADIGM and DeCIDE trials have been attributed to poor accrual and unexpected favorable outcomes in the control arms (Cohen et al., 2014; Haddad et al., 2013), and the Spanish Head and Neck Cancer Cooperative Group (TTCC) study has only been reported with relatively short follow-up (Hitt et al., 2014). The only positive phase III clinical trial demonstrating superior outcomes with TPF induction followed by chemoradiation over chemoradiation alone was reported in abstract form by Italian investigators from Gruppo di Studio Tumori della Testa e del Collo (GSTTC). Taken together, these results suggest that more investigation is required to better elucidate the benefit of induction chemotherapy, and perhaps more importantly better defining the patient population who benefits from the sequential approach.

PRIMARY CONCURRENT CHEMOTHERAPY AND RADIATION

Primary treatment with concurrent chemotherapy and radiation has been accepted widely as a standard of care since the publication of the Meta-Analysis of Chemotherapy on Head and Neck Cancer in 2000. This meta-analysis was later updated in 2009, involving an analysis of 50 trials that showed an absolute survival benefit of 6.5% at 5 years associated with administering chemotherapy concurrently with radiation.

Bolus cisplatin (100 mg/m^2 on days 1, 22, and 43) concurrent with radiation therapy has been extensively studied and may be considered the standard to which other chemotherapy regimens are compared in clinical research. The intergroup trial conducted by Adelstein and colleagues was influential in establishing this regimen as a standard of care (Fig. 20.8). In a three-arm randomized phase III trial of 295 patients with locally advanced stage M0 head and neck squamous cell carcinoma, the treatment groups were radiation therapy alone (70 Gy) versus identical radiation plus concurrent cisplatin (100 mg/m^2 administered intravenously on days 1, 22, and 43) versus a split course of radiation with cisplatin plus 5-FU. With a median follow up of 41 months, the concurrent cisplatin/radiation arm had a significant advantage in survival at 3 years compared with radiation alone (37% versus 23%, p = .014).

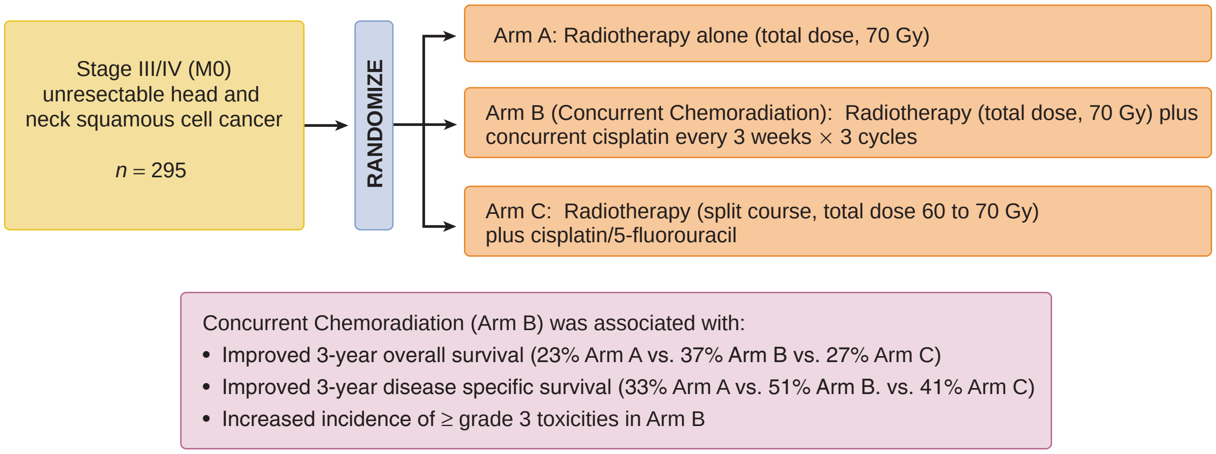

Figure 20.8 Design and results of an intergroup trial. *(Adapted from Adelstein DJ, Li Y, Adams GL, et al. An intergroup phase III comparison of standard radiation therapy and two schedules of concurrent chemoradiotherapy in patients with unresectable squamous cell head and neck cancer.* J Clin Oncol *2003;21:92–98.)*

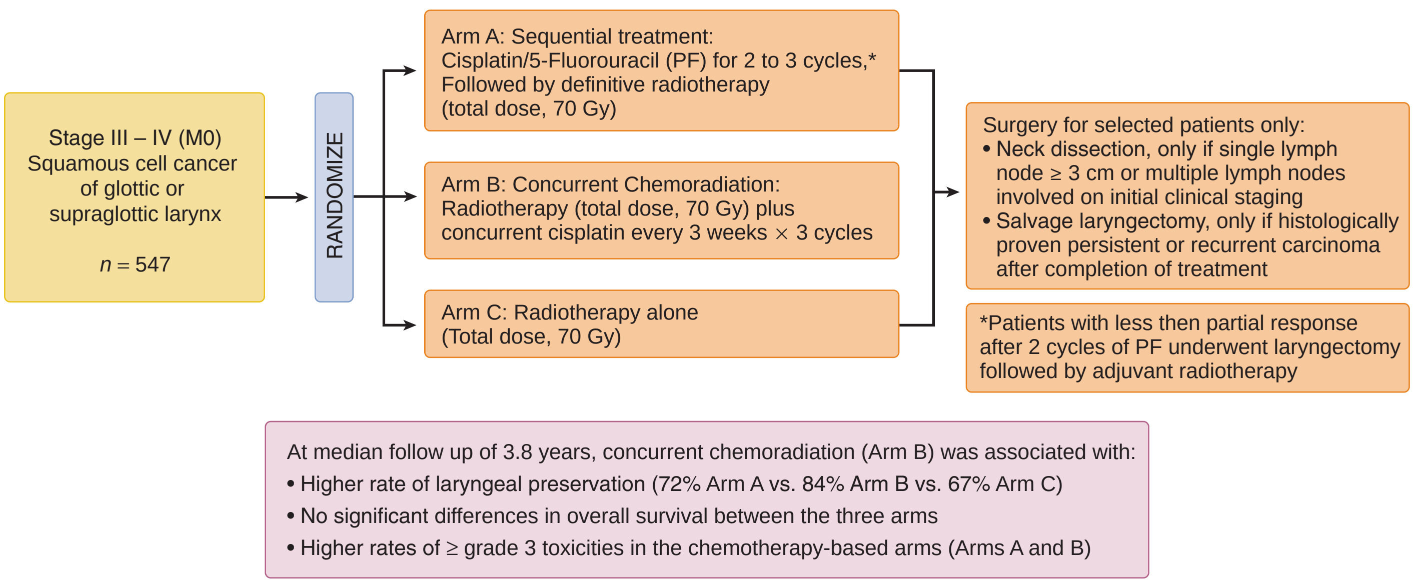

Figure 20.9 Design and results of Radiation Therapy Oncology Group trial 91–11. *(Adapted from Forastiere AA, Goepfert H, Maor M, et al. Concurrent chemotherapy and radiotherapy for organ preservation in advanced laryngeal cancer.* N Engl J Med *2003;349:2091–2098.)*

Survival in the split-course concurrent arm (27%) was not significantly better than that in the radiation arm. This improved efficacy comes at the cost of an increased incidence of acute toxicities, including mucositis and nausea/vomiting. Four toxic deaths occurred among 95 patients enrolled in the cisplatin chemoradiation arm.

The intergroup Radiation Therapy Oncology Group (RTOG 91–11) trial for advanced larynx cancer (Fig. 20.9) established concurrent bolus cisplatin with radiation as a standard of care. The study was open to patients with squamous cell carcinoma of the glottic or supraglottic larynx. Patients with T1 disease or large-volume T4 disease were excluded. Patients were randomly assigned to one of three larynx preservation strategies: induction cisplatin plus 5-FU followed by radiotherapy, radiotherapy with concurrent cisplatin, or radiotherapy alone. The dose of radiotherapy to the primary tumor and clinically positive nodes was 70 Gy in all treatment groups. Severe or life-threatening mucositis in the radiation field was almost twice as common in the concurrent treatment group compared with either the radiotherapy alone group or the sequential treatment group. The primary endpoint of the study was preservation of the larynx.

The rate of laryngeal preservation was 84% for patients receiving radiotherapy with concurrent cisplatin versus 72% for patients receiving induction chemotherapy followed by radiation and 67% for patients receiving radiation therapy alone at a median follow-up of 3.8 years (Fig. 20.10). Distant metastases were reduced in patients who received either concurrent chemoradiotherapy or induction chemotherapy followed by radiotherapy compared with patients who received radiotherapy alone. Overall survival was not significantly different among the three treatment groups. The lack of an overall survival difference between the three groups may be due to the contribution of salvage laryngectomy in all groups, as well as a 2% increase in the incidence of death that may have been related to treatment in the concurrent chemoradiotherapy group compared with the other two treatment groups. It is important to recognize that the primary endpoint of the study was larynx preservation, not overall survival. The current standard of care for larynx preservation remains concurrent high-dose cisplatin and radiation for patients who fit the eligibility criteria that were used in RTOG 91–11. Beyond laryngeal cancer, The Groupe d'Oncologie Radiotherapie Tete et Cou trial is important because it evaluated the concomitant approach in patients with

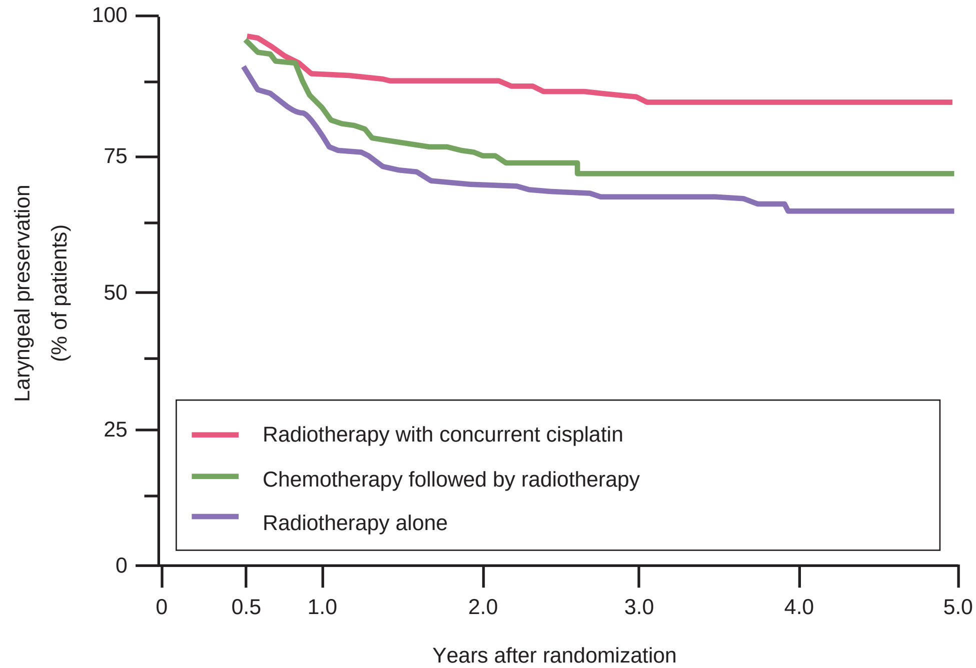

No. at Risk

Chemotherapy followed by radiotherapy	158	94	20
Radiotherapy with concurrent cisplatin	154	107	28
Radiotherapy alone	146	87	20

Figure 20.10 Radiation Therapy Oncology Group trial 91–11: Rates of laryngeal preservation according to the treatment group. *(Adapted from Forastiere AA, Goepfert H, Maor M, et al. Concurrent chemotherapy and radiotherapy for organ preservation in advanced laryngeal cancer.* N Engl J Med *2003;349:2091–2098.)*

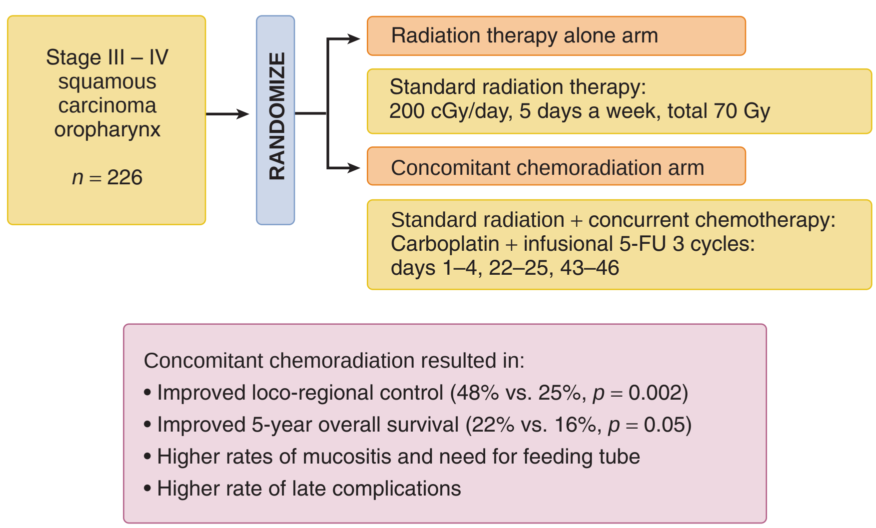

Figure 20.11 Design and updated results of the Groupe d'Oncologie Radiotherapie Tete et Cou trial. *5-FU,* 5-fluorouracil. *(Adapted from Calais G, Alfonsi M, Bardet E, et al. Randomized trial of radiation therapy versus concomitant chemotherapy and radiation therapy for advanced-stage oropharynx carcinoma.* J Natl Cancer Inst *1999;91:2081–2086 and Denis F, Garaud P, Bardet E, et al. Final results of the 94-01 French Head and Neck Oncology and Radiotherapy Group randomized trial comparing radiotherapy alone with concomitant radiochemotherapy in advanced-stage oropharynx carcinoma.* J Clin Oncol *2004;22:69–76.)*

oropharynx cancer only (Fig. 20.11). A total of 226 patients were randomly assigned to either radiation therapy alone (70 Gy) or radiation therapy (70 Gy) with concurrent carboplatin and infusion 5-FU. Significant benefits in 5-year overall survival (22% versus 16%, p = .05) and locoregional control (48% versus 25%, p = .002) were noted in the combined treatment arm. Complete responses were observed in a significant number of patients, thus avoiding the sequelae and short-term morbidity of surgical resection (Fig. 20.12). Phase II trials also support the feasibility of administering other chemotherapy regimens concurrently with radiation therapy for patients with locoregionally advanced head and neck cancer, including but not limited to cisplatin plus paclitaxel, cisplatin plus infusional 5-FU, 5-FU plus hydroxyurea, carboplatin plus paclitaxel, and paclitaxel, 5-FU, and hydroxyurea.

The role for cetuximab in combined modality therapy was established when Bonner and colleagues randomly assigned 424 patients with locoregional advanced head and neck squamous cell cancer to treatment with radiation therapy alone or radiation therapy with concurrent weekly cetuximab (Fig. 20.13). Investigators were required to choose between one of three radiotherapy fractionation regimens, with a total dose of 70 to 76.8 Gy. With a median follow-up of 54 months, the combined treatment group had significantly improved 3-year locoregional control (47%

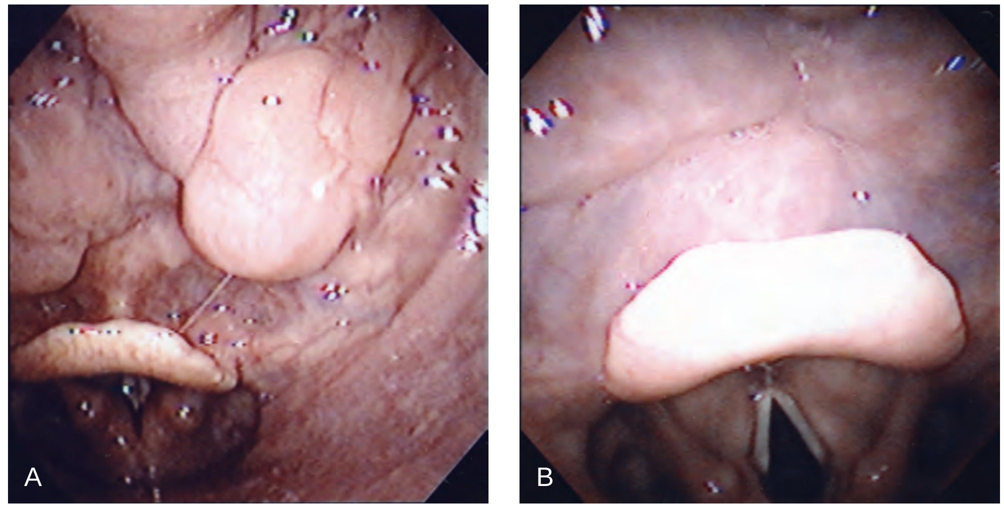

Figure 20.12 **A**, Squamous cell carcinoma of the oropharynx (base of the tongue). **B**, Complete response with preservation of function after concurrent chemoradiation therapy.

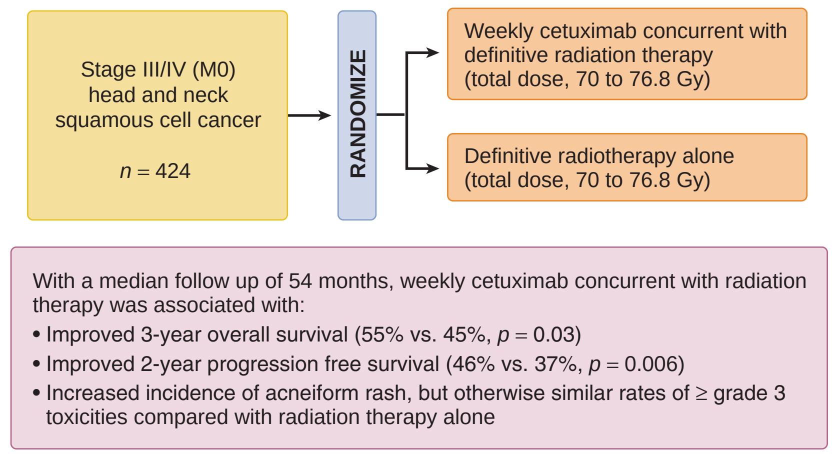

Figure 20.13 Design and results of the Bonner trial. *(Adapted from Bonner JA, Harari PM, Giralt J, et al. Radiotherapy plus cetuximab for squamous-cell carcinoma of the head and neck.* N Engl J Med *2006; 354:567–578.)*

versus 34%, $p < .01$) and 3-year overall survival (55% versus 45%, $p = .05$) compared with the group that received radiation therapy alone. Cetuximab was associated with an increased risk of severe acneiform rash (17%) and severe infusion reaction (3%). While cetuximab and radiotherapy is a valid treatment option for this patient population, retrospective studies have suggested that cetuximab may be associated with inferior outcomes compared with cisplatin and carboplatin plus infusional 5-FU (Riaz et al., 2016; Shapiro et al., 2014). Recently, two randomized phase III trials were conducted to test if cetuximab may serve as a non-inferior and less toxic alternative to cisplatin in combination with radiation for patients with localized HPV-positive oropharyngeal carcinomas (which possess superior clinical outcomes with cisplatin chemoradiation compared to HPV-negative patients; Ang et al., 2010). The De-ESCALaTE HPV trial restricted enrollment to low risk HPV-positive patients (<10 pack-year smoking history) and observed a significantly superior 2-year overall survival with cisplatin over cetuximab (97.5% versus 89.4%; hazard ratio 5.0 [95% CI 1.7-14.7]; p=0.001; Mehanna et al., 2018). RTOG 1016 also demonstrated that among HPV-positive oropharyngeal cancer patients cetuximab failed to meet the pre-specified non-inferiority criteria for overall survival compared to cisplatin (estimated 5-year overall survival of 77.9% [95% CI 73.4-82.5] with cetuximab versus 84.6% [95% CI 80.6-88.6] with cisplatin; Gillison et al., 2018). Both trials also demonstrated that toxicity rates were not significantly lower with cetuximab. Taken together, these prospective data argue strongly for prioritizing the use of cisplatin in these clinical settings and reserving the use of cetuximab with radiation in those who are not cisplatin-candidates.

ADJUVANT CHEMORADIOTHERAPY

In many scenarios, single-modality radiation therapy is a historical standard intervention after primary surgery for stages III and IV head and neck cancer. Intergroup study 0034 (RTOG 8503), which randomly assigned patients with resected head and neck squamous cell carcinoma to receive postoperative radiation therapy alone or postoperative cisplatin (100 mg/m^2 once every 3 weeks) plus 5-FU (1000 mg/m^2/day in a continuous infusion for 120 hours every 3 weeks) followed by radiotherapy failed to show significant differences in outcomes between the two treatment groups. A retrospective analysis did identify subsets of patients with high-risk features on surgical pathology and suggested that clinical studies of postoperative concurrent chemoradiation should be conducted for patients with high-risk disease.

Bachaud and colleagues conducted a randomized trial for patients who had undergone primary surgery for head and neck cancer and had high-risk disease, defined as extracapsular spread of malignancy in resected lymph nodes (Fig. 20.14). Eighty-three patients were randomly assigned to receive postoperative radiotherapy alone or postoperative radiotherapy with concurrent cisplatin (50 mg administered intravenously once a week in a flat dose). Overall survival and disease-free survival were significantly better in the combined modality group; the improvement in the locoregional control rate approached statistical significance in favor of the combined modality group.

Cisplatin plus radiotherapy in the postoperative setting was evaluated in the EORTC 22931 and RTOG 95–01 randomized clinical trials (Figs. 20.15 and 20.16). Both studies were limited

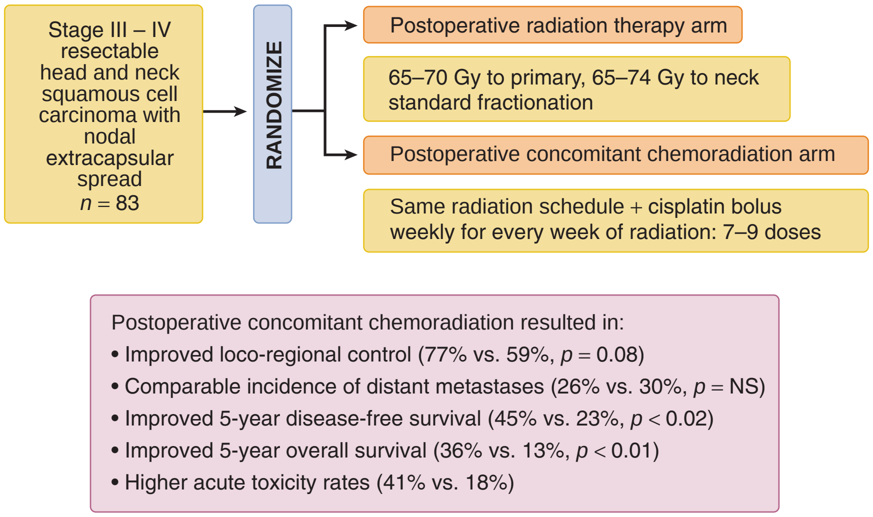

Figure 20.14 Design and results of a trial of postoperative concurrent chemoradiation for locally advanced head and neck carcinoma. *(Adapted from Bachaud JM, Cohen-Jonathan E, Alzieu C, et al. Combined postoperative radiotherapy and weekly cisplatin infusion for locally advanced head and neck carcinoma: final report of a randomized trial.* Int J Radiat Oncol Biol Phys *1996;36:999–1004.)*

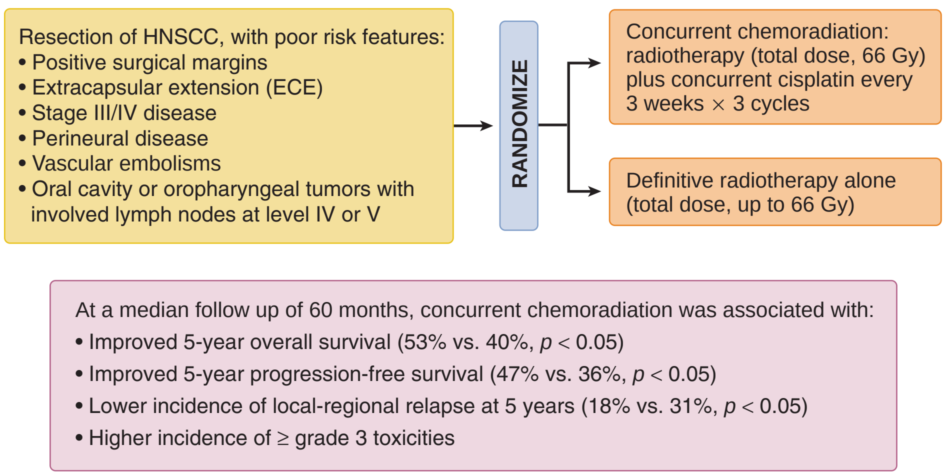

Figure 20.15 Design and results of European Organization for Research and Treatment of Cancer trial 22931. *HNSCC*, Head and neck squamous cell carcinoma. *(Adapted from Bernier J, Domenge C, Ozsahin M, et al. Postoperative irradiation with or without concomitant chemotherapy for locally advanced head and neck cancer.* N Engl J Med *2004;350:1945–1952.)*

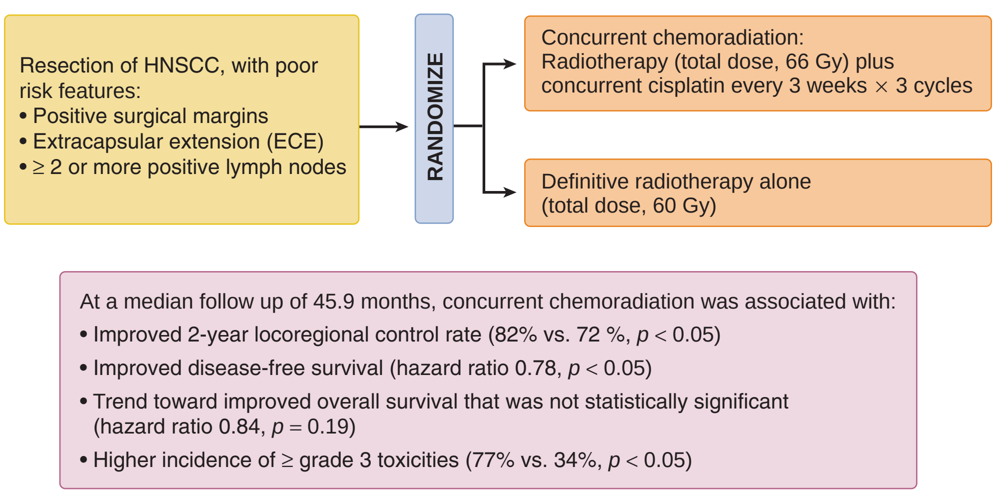

Figure 20.16 Design and results of Radiation Therapy Oncology Group trial 95–01. *HNSCC*, Head and neck squamous cell carcinoma. *(Adapted from Cooper JS, Pajak TF, Forastiere AA, et al. Postoperative concurrent radiotherapy and chemotherapy for high-risk squamous-cell carcinoma of the head and neck.* N Engl J Med *2004;350:1937–1944.)*

to patients who had high-risk features in the surgical pathology, although the studies differed slightly in the high-risk features that were used for eligibility. In EORTC 22931, *high risk* was defined as positive or close surgical margins (≤ 5 mm), extracapsular extension of nodal disease, involvement of lymph nodes at level IV or V from oral cavity or oropharynx primary sites, perineural disease, and/or vascular embolism. RTOG 95–01 defined *high risk* as positive surgical margins, extracapsular extension, and/or involvement of two or more lymph nodes. In both studies, patients were randomly assigned to radiation alone or radiation plus concurrent cisplatin (100 mg/m^2 on days 1, 22, and 43).

The estimated 5-year overall survival from the EORTC 22931 trial was 53% in the combined modality group and 40% in the radiotherapy group ($p < .05$). Progression-free survival and locoregional control also were significantly improved in the combined modality group. With a median follow-up of 45.9 months, RTOG 95–01 demonstrated significant improvements in locoregional control and disease-free survival for the cisplatin plus radiation group, but the improvement in overall survival for this group did not reach statistical significance.

Bernier and colleagues performed a pooled analysis to compare eligibility criteria and outcomes in the two trials. When the analysis was restricted to patients with high-risk disease according

to criteria that were used in both studies (positive surgical margin and/or extracapsular extension), a significant improvement in overall survival was seen for the group of patients that received concurrent cisplatin and radiation therapy (Fig. 20.17). As such, postoperative radiation plus concurrent administration of high-dose cisplatin is a widely accepted standard of care for fit patients with either of these high-risk features on surgical pathology.

SYSTEMATIC THERAPY FOR RECURRENT AND/OR METASTATIC DISEASE: CHEMOTHERAPY, TARGETED AGENTS, AND IMMUNOTHERAPY

After patients with recurrent and/or metastatic squamous cell carcinoma of the head and neck have exhausted the options of surgery and/or radiation, the likelihood of cure diminishes substantially with a median survival historically being less than 1 year. In this group, systemic therapy administered with palliative intent is the treatment of choice. Single agent therapy can produce objective responses in 10% to 30% of patients. Table 20.1 lists the factors that may influence response rates to chemotherapy. Single agents that typically are used in this setting include cisplatin, taxanes, methotrexate, 5-FU, and cetuximab. Vinorelbine, bleomycin, ifosfamide, and pemetrexed also have shown clinical activity against advanced head and neck cancers. The durability of response to chemotherapy alone generally is measured in weeks to months, not years. An early, randomized trial reported by Morton provided evidence that cisplatin treatment prolonged survival by approximately 10 weeks in patients with advanced head and neck cancer, compared with best supportive care.

There are no striking efficacy differences among cytotoxic chemotherapy agents in the recurrent disease setting. Hong and colleagues compared cisplatin versus methotrexate as palliative therapy for 44 patients with head and neck cancer that had recurred after surgery and/or radiation. Patients had not received prior chemotherapy. The median survival was approximately 6 months in both arms, although methotrexate seemed to be somewhat better tolerated. Similarly, in a randomized study of 100 patients with advanced inoperable head and neck cancer that compared cisplatin versus methotrexate, Grose and colleagues did not detect any significant differences in survival between the two treatment groups.

Taxanes yielded encouraging response rates as first-line therapy for patients with recurrent disease. Forastiere's group observed a response rate of 40% among 34 patients treated with paclitaxel, and Dreyfuss and colleagues reported a response rate of 42% among 31 patients treated with docetaxel. In a randomized phase II trial that compared docetaxel versus methotrexate among 57 patients with advanced head and neck cancer, no difference in overall survival was found between the two groups, although the response rate was significantly better for the docetaxel group (27% versus 15%).

Combination chemotherapy regimens appear to be associated with increased response rates and often with increased toxicities, but generally not with increased survival. In 1985 Vogl reported the results of a prospective study in which 163 patients were randomly assigned to receive methotrexate monotherapy or methotrexate plus bleomycin plus cisplatin. Objective responses were more frequent in the combination chemotherapy group, but median survival was 5.6 months in each group. A three-arm randomized study of 249 patients with advanced head and neck cancer that was reported by Jacobs and colleagues compared the cisplatin plus 5-FU doublet versus cisplatin monotherapy versus 5-FU monotherapy. The objective response rate and hematologic toxicities were highest with the doublet regimen, but median survival was approximately 5.7 months for all groups. Taken together, these studies suggest that combination chemotherapy regimens may be appropriate for patients with good performance status if objective tumor response is believed to be necessary for palliation of advanced head and neck cancer.

No combination chemotherapy regimen appears to be superior to another in terms of survival for patients with advanced head and neck cancer. A Southwest Oncology Group study reported by Forastiere randomly assigned 277 patients with advanced head and neck cancer to treatment with cisplatin plus 5-FU, carboplatin plus 5-FU, or methotrexate monotherapy. In the comparison of the doublet regimens, cisplatin plus 5-FU yielded a higher response rate than did carboplatin plus 5-FU (32% versus 21%, p = .05). However, median survival times were similar in all three treatment groups in the study. Gibson reported a randomized comparison of cisplatin plus 5-FU (CF) versus cisplatin plus paclitaxel (CP) for 218 patients with advanced head and neck cancer. The response rate (27% in the CF group and 26% in the CP group) and median survival (8.7 months in the CF group and 8.1 months in the CP group) did not differ significantly.

Cetuximab represents the first biologic agent to enter routine clinical practice as a palliative agent for patients with advanced head and neck cancer. In a phase II study of 103 patients with recurrent and/or metastatic head and neck cancer with documented disease progression within 30 days after a minimum of two and a maximum of six platinum-based chemotherapy treatments, Vermorken reported that the response rate was 13% and the median time to progression was 70 days. Treatment was generally well tolerated, and the most common adverse event was a rash.

Cetuximab can also be combined with other cytotoxic chemotherapeutic agents to achieve therapeutic advantage for some patients with advanced HNSCC. In a phase III study by Burtness for patients with recurrent or metastatic disease who

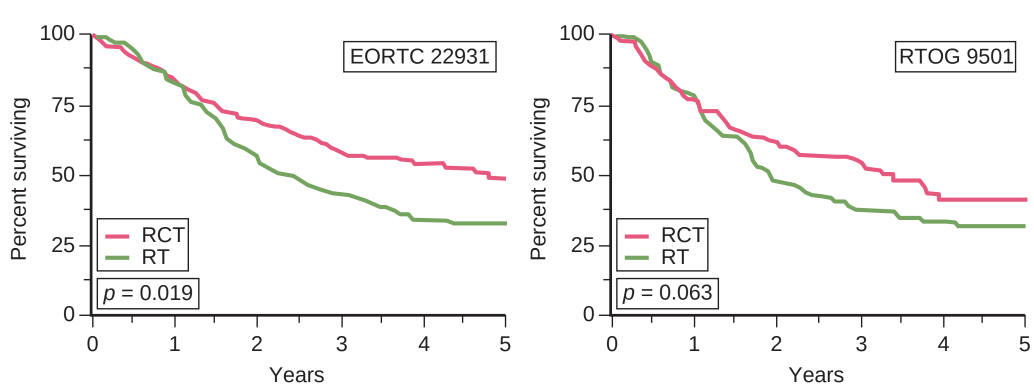

Figure 20.17 Impact of adjuvant chemoradiation on survival in the presence of extracapsular extension and/or positive surgical margins in the European Organization for Research and Treatment of Cancer and Radiation Therapy Oncology Group trials. *RCT*, Radiochemotherapy; *RT*, radiotherapy. *(Adapted from Bernier J, Cooper JS, Pajak TF, et al. Defining risk levels in locally advanced head and neck cancers: a comparative analysis of concurrent postoperative radiation plus chemotherapy trials of EORTC (#22931) and RTOG (#9501).* Head Neck *2005;27:843–850.)*

had not received any prior palliative chemotherapy, 117 subjects were randomly assigned to receive cisplatin plus cetuximab versus cisplatin plus placebo. The objective response rate was higher for cisplatin plus cetuximab (26% versus 10%, $p = .03$), but no significant difference in survival was found between the two groups. The investigators noted that in the cetuximab plus cisplatin group, objective responses were more frequent in patients who experienced skin toxicity, although the number of subjects was too small to establish a statistically significant correlation between dermatologic toxicity and response.

The EXTREME trial randomized 442 patients with untreated recurrent or metastatic head and neck cancer to platinum (cisplatin or carboplatin) plus infusional 5-FU alone for a maximum of 6 cycles with or without cetuximab. Patients randomized to the experimental arm (with cetuximab) with at least stable disease were continued on cetuximab alone after combination therapy. The objective response rate (20% versus 36%, $p < .001$), progression-free survival (3.3 versus 5.6 months, $p < .001$), and overall survival (7.4 versus 10.1 months, $p = .04$) all favored the experimental group. The lack of crossover in the study design leaves open the question of whether similar improvements in overall survival could be achieved with sequential treatment with the platinum doublet followed by cetuximab, or vice versa. However, the study does further establish the platinum/5-FU plus cetuximab as a standard first-line palliative option for patients with advanced head and neck cancer.

One of the most exciting areas of progress for head and neck cancer research is the emergence of immunotherapeutic approaches for this disease, led by the integration of therapeutic antibodies targeting the T cell immune checkpoint PD-1 (programmed death 1) into clinical practice (Fig. 20.18). The activity observed with these drugs established the critical proof of principle that the immune system can be pharmacologically harnessed to produce clinically significant responses in head and neck cancer patients. CHECKMATE-141 was a randomized

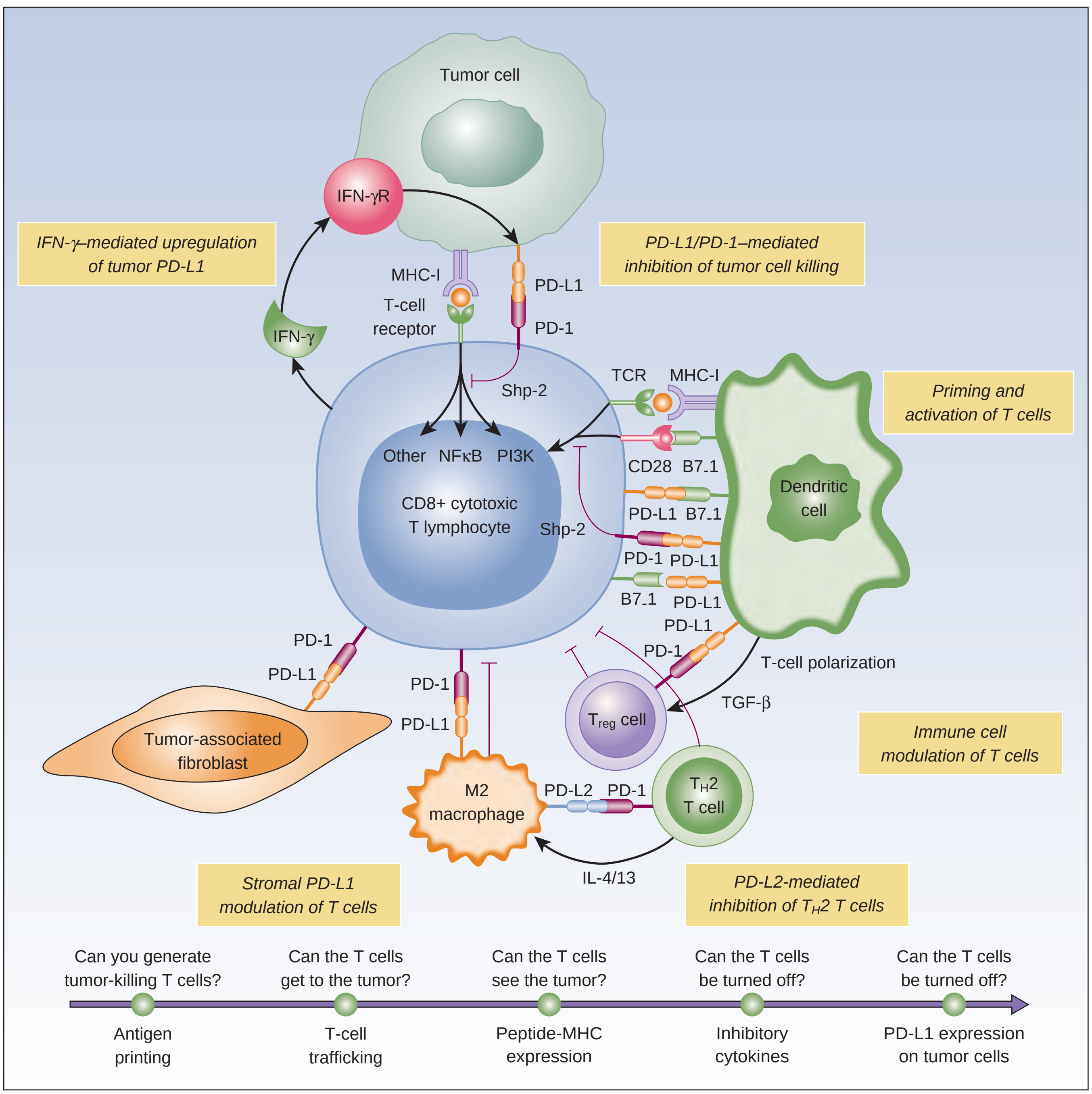

Figure 20.18 PD1 and PDL1 pathway in tumor immune microenvironment.

phase III clinical trial comparing the efficacy of nivolumab, a monoclonal antibody directed against PD-1, to investigator's choice chemotherapy (methotrexate, docetaxel, or cetuximab) in recurrent/metastatic patients with tumor progression or recurrence within 6 months after the last dose of platinum-containing chemotherapy (Ferris et al., 2016). The trial demonstrated a survival benefit with nivolumab over chemotherapy with a median overall survival of 7.5 months versus 5.1 months and a 1-year overall survival of 36% versus 16.6%, respectively. The response rate with nivolumab was 13.3% versus 5.8% with chemotherapy. KEYNOTE-012 was a multicohort phase 1b trial evaluating the efficacy of another PD-1–directed antibody pembrolizumab in a variety of different malignancies, including recurrent/metastatic head and neck cancer. Among 60 head and neck cancer patients whose tumors expressed PD-L1 (the ligand for PD-1), pembrolizumab elicited an 18% response rate and a median overall survival of 13 months (in an intent to treat analysis) (Seiwert et al., 2016). Another expansion cohort in KEYNOTE-012 enrolled 132 recurrent/metastatic head and neck cancer patients regardless of PD-L1 status, reporting an 18% response rate and median overall survival of 8 months (Chow et al., 2016). While KEYNOTE-012–enrolled patients who had received any number of lines of prior chemotherapy for recurrent/metastatic disease (including treatment-naïve patients), KEYNOTE-055 was a single-arm phase II trial designed to evaluate pembrolizumab in patients who experienced progression of disease within 6 months of platinum and cetuximab therapy (Bauml et al., 2017). The reported response rate was 16% with a median overall survival of 8 months. Both nivolumab and pembrolizumab have been FDA-approved for the treatment of recurrent/metastatic head and neck cancer patients with disease progression on or after progression with platinum-containing chemotherapy, establishing a new standard for second-line treatment. After the approval of pembrolizumab in this setting, the results of a randomized, open-label phase III trial comparing the efficacy of pembrolizumab to investigator's choice chemotherapy (methotrexate, docetaxel, or cetuximab) in platinum-refractory recurrent/metastatic patients, or locally advanced disease patients with recurrence or progression within 3-6 months of definitive platinum-based therapy, were reported (KEYNOTE-040; Cohen et al., 2018). For the primary endpoint of overall survival, pembrolizumab was superior compared to standard therapies, but the degree of benefit (hazard ratio [HR] for death 0.80 [95% CI 0.65-0.98; one-sided p = 0.0161] failed to meet the goals pre-specified for the study [HR of 0.70 or better with one-sided a of 0.025]. The authors speculated that the 13% of standard arm patients who received immune checkpoint inhibitor therapy after trial completion could have confounded this survival analysis. Still, most agree that the observed improvements in survival with pembrolizumab, as well as its superior safety profile compared to standard chemotherapies, justifies its use in this setting. More broadly speaking, the smaller margins of benefit observed for nivolumab or pembrolizumab compared to chemotherapy in unselected head and neck cancer patient populations argues for the need to develop predictive biomarkers that will allow identification of those who are most likely to benefit from PD-1/PD-L1 pathway targeting.

ACUTE TOXICITY AND LONG-TERM SEQUELAE

In the curative intent setting, concurrent chemoradiation is associated with risk of severe acute and long-term toxicities. The combined results of four prospective trials indicate that the rate of acute treatment-related death for standard cisplatin-based chemoradiation for locally advanced head and neck squamous cell carcinoma is approximately 4% (22 treatment-related deaths among 545 patients). Acute mucositis (Fig. 20.19) in the radiation field can compromise nutritional intake severely, and placement of a percutaneous gastrostomy tube often is an effective strategy to improve nutrition in this setting. Dermatitis in the radiation field varies in severity among patients (Fig. 20.20). This issue has received increasing attention since the 2006 Food and Drug Administration approval for the use of cetuximab concurrent with radiation therapy for persons with head and neck squamous cell carcinoma.

Long-term complications of chemoradiation can include xerostomia, hypothyroidism, trismus, pharyngeal stricture, and osteoradionecrosis. Although xerostomia remains a common long-term symptom after treatment, the incidence of xerostomia with intensity-modulated radiation therapy appears to be lower than the incidence associated with three-dimensional conventional radiotherapy. Regarding hypothyroidism, in a review of 118 patients who participated in phase I/II trials of sequential chemotherapy and radiation for stage III/IV head and neck cancer, elevated levels of thyroid-stimulating hormone were detected in 45% of patients at a median of 24 months after radiation therapy. Stricture requiring pharyngoesophageal

Figure 20.19 Acute grade IV mucositis in a patient receiving concurrent chemoradiation therapy.

Figure 20.20 Acute skin erythema and an acneiform reaction in a patient receiving cetuximab and radiation therapy.

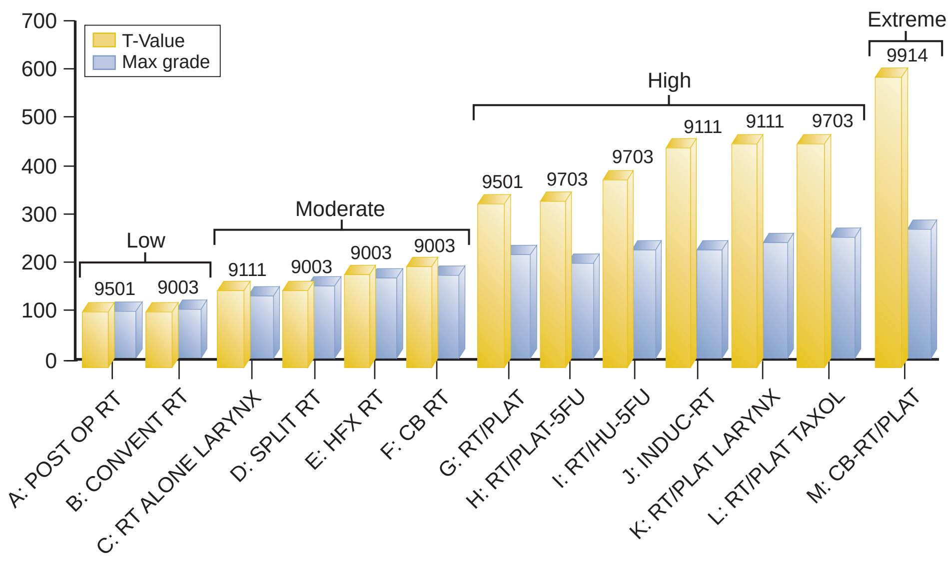

Figure 20.21 Risk groups defined by treatment type and acute toxicity burden. *CB,* Concomitant boost; *CONVENT,* conventional; *5FU,* 5-fluorouracil; *HFX,* hyperfractionated; *HU,* hydroxyurea; *INDUC,* induction; *PLAT,* platinum; *POST OP,* postoperative; *RT,* radiation therapy; *TAXOL,* paclitaxel. *(Adapted from Trotti A, Pajak TF, Gwede CK, et al. TAME: development of a new method for summarising adverse events of cancer treatment by the Radiation Therapy Oncology Group.* Lancet Oncol *2007;8:613–624.)*

dilation may occur in up to 21% of patients who receive definitive radiotherapy, and the primary tumor site in the hypopharynx or oropharynx has been identified as a risk factor for pharyngeal stricture in retrospective studies. Fibrosis of the muscles of mastication as a consequence of chemoradiation may result in trismus, although the retrospective nature of this data has limited the ability to clearly establish risk factors for trismus.

For patients receiving combined modality therapy, accurate and comprehensive measurement of treatment-associated adverse events is challenging. In clinical trials, traditional methods of toxicity reporting describe the frequency and severity of cumulative adverse events during the treatment interval. The National Cancer Institute Common Toxicity Criteria for Adverse Events is a widely used method for toxicity reporting of this nature. However, it is recognized that traditional methods probably do not fully summarize the extent and magnitude of acute and long-term adverse events. To address these concerns, a new reporting system ("TAME") designed to account for the multiplicity and time dimensions of adverse events has been developed. In a retrospective analysis of five trials for patients with head and neck cancer that was performed by the RTOG, the newer method appeared better able to distinguish between the acute toxicity burdens among treatment groups compared with traditional methods for summarizing adverse events. Fig. 20.21 shows that the T values (T = acute toxicity relative risk value) were higher than traditional toxicity summarization values ("Max grade value") in most head and neck cancer treatment groups and that these differences were more apparent in high-intensity treatment programs.

CHEMOPREVENTION OF HEAD AND NECK SQUAMOUS CELL CARCINOMAS

Recent advances in our understanding of the molecular biology of head and neck squamous cell carcinomas have built upon the original concept of "field cancerization" proposed by Slaughter more than half a century ago. The etiologic association of tobacco and/or alcohol is integral to the concept of the multistep model of head and neck carcinogenesis. The concept of multistep carcinogenesis has attracted interest in chemoprevention strategies to interrupt the process in patients at risk for head and neck cancer. Various natural or synthetic compounds have been used, most often based on epidemiologic evidence. The most commonly evaluated compounds include vitamin A and its analogs, especially the natural (e.g., all-*trans*retinoic acid) and the synthetic (e.g., 13-*cis*-retinoic acid) retinoids. These agents modify and modulate cell growth, differentiation, proliferation, and apoptosis through a variety of mechanisms. High-dose isotretinoin reverses oral leukoplakia but has not been demonstrated to reduce the risk of invasive squamous cell cancer.

Because patients who have been treated for head and neck cancer are at high risk for second primary tumors, this patient population has been the focus of most chemoprevention work. Large randomized clinical trials of retinoids and antioxidant vitamins have not demonstrated efficacy in terms of preventing second primary head and neck cancers, as reported by Khuri and by Bairati. Other abnormal signaling pathways in premalignant lesions have been described in chemoprevention research. For example, cyclooxygenase-2 expression is increased in the oral mucosa of active smokers. With the increasing understanding of the molecular biology of premalignant lesions in the head and neck, novel biologic agents have entered chemoprevention research. At present, the only strategy known to decrease the risk of second primary tumors in patients with head and neck cancer is smoking cessation.

FUTURE DIRECTIONS

Ongoing clinical trials are addressing key questions in the multimodality management of patients with head and neck cancer. One of the key challenges that must be addressed is how therapeutic approaches may be better tailored to the biologic heterogeneity of head and neck cancer. For example, tumors associated with the human papillomavirus (HPV, most commonly subtype 16) represent a clinical and biologic entity that is distinct from tobacco-associated and/or alcohol-associated head and neck cancer. HPV-associated head and neck cancer tends to arise in younger persons who typically do not have a significant history of tobacco or alcohol use. HPV-associated head and neck cancer appears to be associated with a more favorable prognosis compared with tobacco-related and alcohol-related disease. It is clear that our approaches to HPV-positive disease need to be distinct from HPV-negative, and future trials will be critical for providing guidance in this regard. Beyond HPV

status, the increasingly routine clinical application of genomic technologies to provide a personalized, molecular profile of each patient's disease is also empowering research approaches dedicated to developing molecularly targeted approaches that selectively abrogate oncogenic alterations in tumors (e.g., activating PIK3CA pathway alterations, *HRAS* mutations, CDK activation, etc.) to induce tumor regressions.

Intense research activity is now dedicated to building upon the exciting advances in immunotherapy for head and neck cancer. Current efforts include investigating how PD-1/PD-L1 targeting agents may be integrated in other clinical management settings, such as definitive chemoradiation and first-line therapy for recurrent/metastatic disease. Novel combinations are also being explored with other immunotherapeutic agents, chemotherapy, and radiation. In conjunction with these efforts are attempts to identify the cellular, molecular, and clinical markers that better define the patient populations that will benefit from these approaches.

For all the excitement regarding recent advances in head and neck cancer management, most encouraging is the recognition that the development of biologically based approaches can only be optimally executed if informed by a sophisticated understanding of the disease biology and how novel therapeutic approaches affect these systems. In this regard, the field has made significant strides, and a continued commitment to this approach provokes optimism for developing new, effective therapeutics for head and neck cancer patients.

SYSTEMIC THERAPY FOR RECURRENT/METASTATIC, RADIOIODINE-REFRACTORY FOLLICULAR CELL–DERIVED THYROID CANCER

Differentiated thyroid carcinomas (DTCs) of follicular origin include papillary thyroid cancer and follicular thyroid cancer. Poorly differentiated thyroid cancer represents a more aggressive, less differentiated subtype of DTC. While localized disease is potentially curable with surgery with or without radioiodine (RAI), recurrent/metastatic thyroid cancer is often incurable and can be managed with surgery, radiation, RAI, and/or systemic therapy. Systemic therapy is a relevant treatment option for patients whose tumors are no longer responsive to RAI, known as *RAI-refractory (RAIR) disease*. For these patients, drug therapy is administered with palliative intent and is reserved for patients with symptomatic and/or progressive disease. Several decades ago, doxorubicin was designated as the only FDA-approved drug for the treatment of RAIR thyroid cancer. However, recent insights into the biology of the disease, and the development of molecularly targeted agents have led to an exponential increase in the clinical research geared toward identifying new, effective therapies for these patients.

This research activity led to the conduct of the first two randomized phase III clinical trials ever performed for RAIR, progressive, recurrent/metastatic thyroid cancer. DECISION and SELECT evaluated the efficacy of the multitargeted tyrosine kinase inhibitors (TKIs) sorafenib and lenvatinib, respectively, compared with placebo. Both trials met the prespecified progression-free survival (PFS) endpoint, leading to FDA-approval for each of these drugs for progressive, recurrent/metastatic RAIR thyroid cancer. While cross-trial comparisons should always be undertaken with caution, the clinical outcomes in lenvatinib versus placebo (PFS: 18.3 vs. 3.6 months; response rate: 64.8% vs. 1.5%) were notably superior to those observed on DECISION with sorafenib (PFS: 10.8 vs. 5.8 months; response rate: 12.2% vs. 0.5%). While each drug targets vascular endothelial growth factor receptor (VEGFR), these TKIs inhibit multiple kinase targets, and the key kinase or combination of kinases that must be blocked for drug activity has not been delineated.

One of the most critical discoveries in thyroid cancer biology was the identification of the BRAF V600E mutation as the most frequently altered gene in papillary thyroid carcinomas (~45%). BRAF mutations carry significant therapeutic implications given the development of clinical drug inhibitors of this target. A phase II trial of the BRAF inhibitor vemurafenib in BRAF mutant, RAIR thyroid cancer reported a 38.5% response rate and 18.2 month median PFS for TKI-naïve patients, and a 27.3% response rate and 8.9 month median PFS for patients previously treated with a TKI (Brose et al., 2016). This study provided the critical proof of principle that mutant BRAF is a viable therapeutic target. Future and ongoing studies are focused on developing rationale therapeutic combinations with BRAF inhibitors, including the use of these agents to "redifferentiate" thyroid tumors to enhance RAI activity. The efficacy of molecularly targeted approaches to other potential oncogenic drivers identified through recent genomic studies is also an active area of research (e.g., *RAS* mutations, *PIK3CA* mutations, *PTEN* alterations, *RET* and *NTRK* rearrangements, etc.). Such progress is leading the field toward personalized oncologic therapies, tailored to the specific biology of each patient's tumor.